КОЛЛОИДНЫЙ
ЖУРНАЛ

COLLOID JOURNAL

(KOLLOIDNY ZHURNAL)

IN ENGLISH TRANSLATION

VOL. 18 NO. 5

CONSULTANTS BUREAU, INC.
227 WEST 17TH STREET, NEW YORK 11, N. Y.
an agency for the interpretation of international knowledge

COLLOID JOURNAL OF THE U.S.S.R. IN ENGLISH TRANSLATION

September-October, 1956

TABLE OF CONTENTS(Continued)

	Page	Russ. Page
18. Dependence of the Flow Curves and Viscosity Characteristics of Bitumens on the Temperature. S. Ya. Shalyt and N. V. Mikhailov	607	609
19. Alteration of the Structural Properties of Some Colloidal Porous Materials During Drying. V. V. Shcherbatenko and V. V. Smirnova	613	615
20. Investigation of Structure Formation in Concentrated Suspensions by the Electrical Conductivity Method. B. Ya. Yampolsky	619	621

Discussion

	Page	Russ. Page
21. Some Questions Concerning the External Friction of Rubber. G. M. Bartenev	623	626

Review

	Page	Russ. Page
22. Monograph by F. M. Shemyakin, E. S. Mitselovsky, and D. V. Romanov "Chromatographic Analysis (Introduction to Theory and Practice)" (State Chemical Press, 1955).	629	632

RUSSIAN CHEMICAL RES[illegible] IN COMPLETE ENGLISH TRANSLA[illegible]

[illegible] survey of [illegible] major [illegible]

Covers the [illegible] prepared by leading Soviet chemists [illegible] applied chemistry, [illegible]

JOURNAL OF GENERAL CHEMISTRY OF THE USSR ([illegible] per year)	$170.00	[illegible] SECTION OF [illegible] SCI. USSR ([illegible] issues per year, [illegible])	[illegible]
JOURNAL OF APPLIED CHEMISTRY OF THE USSR ([illegible] pp. per year)	95.00	CHEMISTRY SECTIONS OF [illegible] SCI. ([illegible] issues per year, [illegible]) Chemistry Section Chemical Technology Section [illegible] Section [illegible] Section All four sections [illegible]	[illegible]
JOURNAL OF ANALYTICAL CHEMISTRY OF THE USSR ([illegible] per year)	80.00		
BULLETIN OF THE ACADEMY OF SCIENCES [illegible] ([illegible] per year)	150.00	COLLOID JOURNAL ([illegible] per year)	[illegible]
[illegible] CHEMISTRY SECTION OF PROC. ACAD. SCI. USSR ([illegible], [illegible] issues per year, published [illegible])	[illegible]	JOURNAL OF ATOMIC ENERGY ([illegible] pp. per year)	[illegible]

and SOVIET RESEARCH IN CATALYSIS, Chemistry Collection [illegible]

Covers all aspects of catalysis, selected from papers in all journals translated by Consultants Bureau 1949-195[illegible].

Sections may be purchased separately as follows:

I.	[illegible] and Sundry Associated Effects	[illegible] pages	[illegible]	[illegible]	[illegible]	[illegible] pages	[illegible]
IIa.	General	[illegible] pages	[illegible]				
IIb.	General	[illegible] pages	[illegible]	[illegible]	[illegible]		
IIc.	[illegible] Fischer-Tropsch	214 pages	[illegible]		[illegible]	[illegible] pages	[illegible]
[illegible]	[illegible]	[illegible] pages	[illegible]				

The Collection, comprising [illegible] pages, [illegible] may be purchased as a unit for [illegible]

SYMPOSIUM ON RADIATION CHEMISTRY

Part I: Action of Radiation on Water and Aqueous Solutions [illegible]

Part II: Action of Radiation on Individual Organic Compounds and High Polymers [illegible]

Both parts are available [illegible]

All Consultants Bureau translations [illegible]

NOTE: [illegible]

COLLOID JOURNAL OF THE USSR IN ENGLISH TRANSLATION

November-December, 1956

TABLE OF CONTENTS

	Page	Russ. Page
1. Investigation of Plastic Disperse Systems in Conditions of Uniform Stress. G. V. Vinogradov, V. G. Lebedev and V. A. Protodyakonov	631	633
2. X-ray Structure Investigations of Peat Bitumens and Waxes. M. P. Volarovich and K. F. Gusev	639	643
3. The Electrochemistry of High-Polymer Dispersions. Effect of Dilution on the Electrokinetic Potential of Synthetic Latex Globules. S. S. Voyutsky and R. M. Panich	645	647
4. Nature of the Solvation of Cellulose Ethers in Solvent Mixtures. S. A. Gluckman and L. A. Root	653	656
5. Influence of Intermolecular Forces and Temperature on the Relative Elongation of Vulcanizates at Break. V. E. Gul and I. I. Farberova	657	660
6. Types of Structure Formation in Clay Suspensions. M. M. Gurvich	663	666
7. A Study of the Properties of Concentrated (Spinning) Solutions of Acrylonitrile—Vinylidene Chloride Copolymer. Z. A. Zazulina, Z. A. Rogovin and G. V. Vinogradov	671	674
8. Mechanism of High-Polymer Plasticization-Structure of Gels. 8. Effect of the Nature of the Plasticizer on the Swelling Kinetics and the Viscosity of Dilute Solutions of Divinyl-Styrene Rubber. P. I. Zubov and M. P. Zverev	677	679
9. Peculiarities of the Deformation Behavior of Gelatin Gels. L. V. Ivanova-Chumakova, P. A. Rebinder and G. I. Krus	681	682
10. Phase Separation in High-Polymer Solutions. L. E. Kalinina, V. I. Alekseenko and S. S. Voyutsky	689	691
11. A Thermomechanical Investigation of Epoxide Resins. B. M. Kovarskaya, L. I. Golubenkova, M. S. Akutin and G. L. Slonimsky	695	697
12. Investigation of the Viscosity of Dilute Polyacrylonitrile Solutions. V. E. Kotina and V. S. Klimenkov	701	703
13. Influence of the Structure of Rubber on Inhibitor Diffusion. A. S. Kuzminsky, S. A. Reitlinger and E. V. Shemastina	705	707
14. Effect of Hydrophilic Substances on the Diffusion of Direct Dyes into Cellulose Fibers. B. N. Melnikov and P. V. Moryganov	709	711
15. Investigation of the Structure and Properties of Carbon-Chain Polymers in Dilute Solutions. 1. Solutions of Polyvinyl Chloride and Polyacrylonitrile. N. V. Mikhailov and S. G. Zelikman	715	717
16. Stability of Metal Sols in Presence of High-Molecular Compounds. E. M. Natanson and N. N. Kozachek	723	724
17. Peculiarities of thermal Expansion of Gels and Solutions of High Polymers. 4. The Volume Effect of Gelation. R. E. Neiman	729	731
18. Swelling of Vulcanized Rubber in α-Pinene in Presence of Oxidation Inhibitors E. N. Novikova	733	735

TABLE OF CONTENTS (Continued)

	Page	Russ. Page
19. Increase of the Hydrophilic Properties of Capron Fiber by Hydroxyethylation. B. V. Petukhov and A. B. Pakshver	739	741
20. Adsorption of Surface-Active Substances (Depressants) on Paraffin Wax. P. I. Sanin, N. V. Melentyeva and Yu. M. Zelenova	743	745
21. Investigation of Structures in Carbon-Black Suspensions. Effect of Temperature and Additions of Surface-Active Substances on Structure Formation in Carbon-Black Suspensions. U-Shu-Tsyu, B. Ya. Yampolsky and S. S. Voyutsky	747	748
22. The Compatibility of High Polymers. A. G. Shvarts	753	755
23. Errata.	761	767
24. Notice.	761	768

THE RELATIONSHIP BETWEEN THE STRUCTURE OF EMULSIFIER OF THE ALKYL-AROMATIC SULFONIC ACID TYPE AND THE POLYMERIZATION OF UNSATURATED COMPOUNDS

3. INFLUENCE OF ANIONS ON THE POLYMERIZATION PROCESS

N. P. Apukhtina and A. M. Lyagalova

The univalent cations Li^+, Na^+, K^+, Rb^+ and NH_4^+ were previously shown to have a regular influence on the polymerization of unsaturated hydrocarbons [1] in the presence of anion-active emulsifiers – alkylnaphthalene sulfonates – and it was shown that the polymerization rate depends both on the nature and the concentration of the electrolytes. It was shown that at low concentrations these cations somewhat increase the polymerization rate to a maximum, the position of which depends on the nature of the electrolyte and emulsifier. The inflexion in the curve is followed by a sharp decrease of the polymerization rate, ions with the greatest radius having the greatest effect.

The influence of the nature of the anions on the polymerization process and on some colloido-chemical properties of the anion-active emulsifier studied is also of considerable theoretical and practical interest. It is known that electrolytes affect the critical micelle concentration of surface-active substances and the solubilization of hydro carbons in emulsifier solutions.

Debye [2] and Klevens [3] consider that the critical micelle concentration decreases appreciably only as a function of the concentration of the ions bearing a charge with sign opposite to the micelle charge. Hence the critical micelle concentration of anion-active emulsifiers changes only under the influence of cations (gegenions). The same conclusion was reached by Goddard and his co-workers [4]. The information in the literature concerning the influence of anions on the solubilization of hydrocarbons in aqueous solutions of anion-active emulsifiers is contradictory. McBain and Green [5] consider that sulfates and chlorides have the same influence on the solubilization of the dye Orange OT in potassium laurate solution. Klevens [3] and Steams [6] demonstrated the influence of anions on the solubilization of various hydrocarbons in aqueous solutions of fatty acid soaps. These authors reached the conclusion that chlorides increase solubilization to a greater extent than sulfates.

Stearns and his co-workers also studied the influence of halide ions on the solubilization of ethyl benzene in aqueous potassium laurate solutions, and established that univalent anions increase solubilization in the following sequence:

$$Cl^- > F^- > Br^- > I^-.$$

The influence of electrolytes on the polymerization rate of unsaturated hydrocarbons has not been adequately investigated. Fryling and John [7], in an investigation of the effect of electrolytes on the copolymerization rate of divinyl with styrene at low temperatures, came to the conclusion that only cations have an influence in systems containing anion-active emulsifiers (fatty acid soaps, alkyl sulfonates, rosin soaps, etc.). For example, sodium chloride, fluoride, and sulfate in equivalent concentrations have the same effect on the polymerization. These authors showed that the monomer conversion in given time as a function of electrolyte concentration passes through a maximum, the position of which does not depend on the nature of the anion.

EXPERIMENTAL RESULTS AND DISCUSSION

We studied the influence of the equivalent concentration of halide ions and also of the SO_4^{2-} ion on polymeriza tion rate of divinyl with α-methylstyrene in the presence of sodium sec-butylbenzene and naphthalene sulfonates, and determined the solubilization of α-methylstyrene in aqueous solutions of these emulsifiers in the presence of potassium sulfate and chloride.

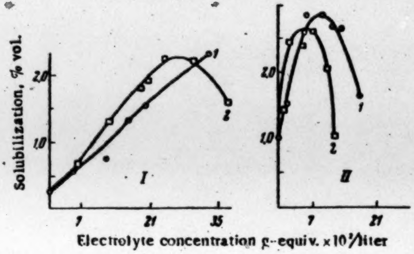

Fig. 1. Influence of electrolytes on the solubilization of α-methylene; I) emulsifier tri-BP (0.0732 g-equiv./liter); II) emulsifer tri-NP (0.044 g-equiv./liter); 1) K_2SO_4; 2) KCl.

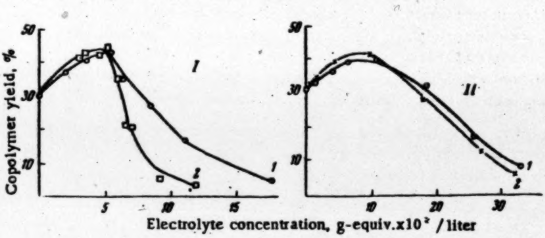

Fig. 2. Influence of electrolytes on the yield of divinyl-α-methylstyrene copolymer; I) emulsifier tri-BP (0.046 g-equiv./liter); II) emulsifier di-NP (0.046 g-equiv./liter); 1) K_2SO_4; 2) KCl.

Fig. 1 shows that the curves for the solubilization of α-methylstyrene as a function of the equivalent concentrations of potassium sulfate and chloride pass through a maximum, the influence of Cl^- and SO_4^{2-} ions being practically equal at low concentrations. Beyond the maximum, the solubilization falls more rapidly in presence of Cl^-.

The curves for the polymerization rate of divinyl with α-methylstyrene as a function of the anion concentration (Fig. 2) are similar in appearance; at low concentrations the presence of the Cl^- ion results in a slightly greater increase in the copolymer yield than in the presence of the SO_4^{2-} ion, but the reverse is true at higher electrolyte concentrations: Cl^- ion has a greater retarding effect on the polymerization reaction than SO_4^{2-} ion. At high concentrations the nature of the halide anions has a strong influence on the polymerization rate (Fig. 3).

At low concentrations, F^- and Br^- ions have no appreciable influence on the polymerization rate, the Cl^- ion produces some increase in the rate, while the I^- ion has a strong retarding effect on polymerization over the whole range of concentrations studied. It must be pointed out that the special influence of the I^- ion may also be the result of its interaction with potassium persulfate which was used as polymerization initiator.

The influence of anions on the polymer yield with increasing concentration becomes greater after the inflexion on the curves. All the univalent ions lower the polymerization rate, and may be placed in the following series of decreasing influence:

$$I^- > Br^- > F^- > Cl^-.$$

It is likely that the influence of halide ions, like that of univalent cations, on the polymerization process is closely related to solvation of the ions.

The Table shows the radii and the heats of solvation (H) of halide ions, taken from Mishchenko's paper [8].

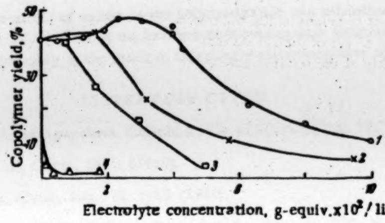

Fig. 3. Influence of anions on the yield of divinyl-α-methylstyrene copolymer in the presence of tri-NP (0.046 g-equiv./liter); 1) NaCl; 2) NaF; 3) NaBr; 4) NaI.

TABLE

Heats of Solvation and Radii of Halide Ions

Ion	F^-	Cl^-	Br^-	I^-
Radius in A	1.345	1.86	1.955	2.18
H, kcal./mole	113	79	72	63

The influence of these anions on the polymerization process evidently increases with increasing radius. Fluorine is an exception; probably as the result of its electronegative character, more pronounced than that of the other halogen ions. It is known that solutions of fluorides, unlike those of other halides, hydrolyze to a considerable extent. In this connection it is interesting to compare our findings with those of Stearns [6], who found that the nature of the halide ions had an analogous influence on the solubilization of ethylbenzene in aqueous potassium myristate solutions. Fig. 4 shows the yields of divinyl – α-methylstyrene copolymer and the solubilization of ethylbenzene as functions of the halide ion radius. The copolymer yields (in percentages) are based on our data obtained in the copolymerization of divinyl with α-methylstyrene in aqueous sodium tri-sec-butylnaphthalene sulfonate (0.046 g-equiv./liter) in the presence of sodium halides (0.033 g-equiv./liter). The solubilization of ethylbenzene (in grams hydrocarbon per 100 g of soap solution) is taken from the data of Stearns *et al.* [6], obtained for aqueous sodium myristate solutions (0.1 molar) in the presence of potassium halides (1.383 molar). It is seen that the maxima on both curves correspond to chloride ions.

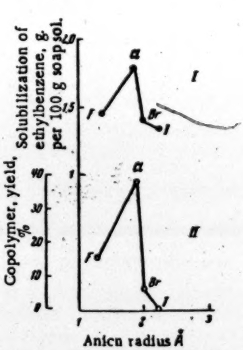

Fig. 4. Solubilization of ethylbenzene (I) and yields of divinyl – α-methylstyrene copolymer (II) as a function of halide ion radius; I) Stearns' data; II) our data.

These results show that the same factors account for the influence of the nature of the anions on the polymerization process and on hydrocarbon solubilization. Thus, it may be concluded that both cations and anions have a strong influence on the polymerization rate, which is associated with the position of the ions in the lyotropic series.

SUMMARY

1. It is established that anions, like cations, influence the emulsion polymerization of hydrocarbons. The effect of anions on the polymerization rate of unsaturated compounds depends on the nature and concentration of the anions, and also on the structure of the emulsifiers.

2. In very dilute solutions the influence of anions on the rate of emulsion polymerization is slight. Increase of the halide ion concentration decreases the polymer yields. The halide ions form the following series according to their retarding effect on the polymerization rate:

$$I^- > Br^- > F^- > Cl^-.$$

The SO_4^{2-} ion has less effect than the Cl^- ion on the polymerization rate.

3. It seems likely that the effect of anions on the polymerization and solubilization of hydrocarbons is associated with solvation of these ions. The effect of the halide ions increases with increasing ionic radius. An exception is provided by the fluoride ion, probably as the result of its strongly electronegative nature.

LITERATURE CITED

[1] N. P. Apukhtina and A. M. Lyagalova, Colloid J., 17, 415 (1955) (T.p. 399) *.

[2] P. Debye. J. Phys. Coll. Chem. 53, 1, (1949).

[3] H. B. Klevens. J. Am. Chem. Soc., 72, 3780 (1950).

[4] E. D. Goddard, O. Harva and T. G. Jones, Trans. Faraday Soc., 49, 980 (1953).

[5] J. W. McBain and A. A. Green, J. Am.Chem. Soc., 68, 1731 (1946).

[6] R. S. Stearns, et. al., J. Chem. Phys., 15, 496 (1947).

[7] C. F. Fryling and W. M. John, Ind. Eng. Chem., 42, 2164 (1950).

[8] K. P. Mishchenko, J. Phys. Chem., 26, 1736 (1952).

Received August 17, 1954

The S. V. Lebedev Research Institute for
Synthetic Rubber, Leningrad

---

* T.p. = C. B. Translation pagination

EFFECT OF THE VALUE OF THE INITIAL MOLECULAR WEIGHT OF RUBBER ON THE STRENGTH AND FATIGUE OF VULCANIZATES

G. M. Bartenev, A. S. Novikov, and F. A. Galil-Ogly

In recent studies of the strength and fatigue of rubber, considerable attention has been paid to the influence of vulcanizate structure on changes of these properties. There have been studies of the influence of the type of bonds in the vulcanizate on fatigue [1] and also of the effect of the initial molecular weight of the rubber on the strength and dynamic fatigue resistance [2]. The analogy which has been established [3] between the dynamic and static fatigue of rubber, which have the same statistical nature and follow the same experimental laws, is important for an understanding of the mechanism of the dynamic fatigue of rubber under repeated deformation.

Thus, in addition to the known influence of oxidative processes, activated by mechanical deformations, on dynamic fatigue [4], this phenomenon also depends on purely physical factors and the structure of the rubber [1,3, 5]. In this connection it is of interest to examine the influence of the initial molecular weight of the rubber on the dynamic fatigue and strength of vulcanizates. Earlier investigations [2] suffered from considerable defects, as the initial molecular weight of the rubber was disturbed during preparation of the mixtures, and the influence of molecular weight on the vulcanizate structure was not considered.

In the present investigation a study was made of the dynamic fatigue resistance (endurance under repeated deformation) and tensile strength of vulcanizate prepared from fractions of butadiene – styrene rubber SKS–30A without disturbance of the initial molecular weights of the fractions. The rubber was separated into 6 fractions by decreasing the temperature of a solution of the rubber in the presence of a small amount of precipitant. The molecular weight was calculated from viscosimetric data with the aid of the formula previously established by Novikov and Khaikina [2] for this rubber: $[\eta] = 2.96 \cdot 10^{-4} M^{0.71}$. The molecular weights of the fractions are shown in the table.

In order that the molecular weights of the rubber fractions should remain unchanged, the films for vulcanization were prepared by drying of benzene solutions of the rubber mixture till the solvent was completely removed. In the first series of experiments the composition of the mixture was the same for all fractions:

	Parts by weight
Rubber	100
Sulfur	3
Mercaptobenzothiazole	1
Zinc oxide	5
Stearic acid	2
Phenyl-β-naphthylamine	1

The films were vulcanized in a hydraulic press at 143°.

In the preceding communication [6] it was shown that the kinetics of sulfur addition does not depend on the molecular weight of the fraction, and that the start of formation of a continuous spatial rubber network during the vulcanization process is determined by the initial molecular weight of the rubber and the amount of combined sulfur, which is greater as the molecular weight of the fraction is less.

There is a "critical" value for the molecular weight of rubber, about 1000 thousand, at which the formation of a single spatial vulcanizate network commences at once in the process of sulfur addition. For rubbers with molecular weights below the "critical" value, the first amounts S_0 of the vulcanizing agents added are consumed in bonding and enlargement of the molecular chains to form longer chains and branched or partly cross-linked structure

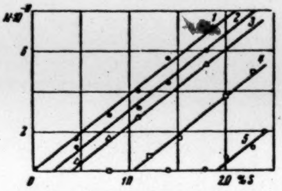

Fig. 1. Variation of the number of chains per cubic centimeter of the spatial network in rubber with the amount of combined sulfur for different fractions. The numbers on the curves represent the numbers of the fractions (see table).

When molecular formations which are of the same magnitude as the "critical" value of the molecular weight are reached, they join into a single spatial network. From that instant the rate of formation of the vulcanizate network, determined by the rate of cross-link formation in the network, does not depend on the value of the initial molecular weight of the rubber. This is confirmed by the equal slopes of the graphs in Fig. 1, in which the ordinate axis shows the number of chains per 1 cm^3 of the spatial network in the vulcanizate of a given fraction, and the abscissa axis shows the amount of sulfur combined during the vulcanization process *. The number of chains in the vulcanizate was calculated by means of the formula [7]: $N = CE_{\infty}^{3/2}$, where N is the number of chains in the spatial network in 1 cm^3 volume of the rubber (equal to twice the number of cross-links), E_{∞} is the equilibrium modulus in kg/cm^2, and C is a constant for the given rubber, equal to $1.3 \cdot 10^{18}$ according to Vishnitskaya [7].

Thus the vulcanizates obtained industrially from low-molecular and high-molecular rubbers, with the same formulations, differ both in the amounts of combined sulfur and its distribution in the vulcanizate, and also in the nature of the structural formations which enter the spatial network.

For studies of the influence of the initial molecular weight of the rubber on the dynamic fatigue resistance (endurance) and tensile strength of the vulcanizates, vulcanizates were prepared from the different rubber fractions both with the same accelerator – vulcanizing agent composition, given above, and with vulcanizing compositions specially selected for each fraction so as to give vulcanizates with equal concentrations of sulfur cross-links, that is, with the same equilibrium modulus.

In order to obtain vulcanizates from low-molecular rubbers with the same equilibrium modulus as those from high-molecular rubbers, it is necessary to add larger amounts of sulfur and to increase the vulcanization time. This is seen from the data in the table.

Fig. 2 shows the influence of the molecular weight of the rubber on the strength** of unfilled vulcanizates, both with the same vulcanizing composition (equal amounts of added sulfur, 2.05 % for all fractions) and with the same equilibrium modulus, but with different amounts of combined sulfur, which are greater with lower molecular weight***.

The strength of vulcanizates with the same amount of combined sulfur varies with the value of the initial molecular weight up to a molecular weight of 500 thousand; further increase has no appreciable influence on the strength. A similar variation of the strength with the initial molecular weight of SKS-30A rubber has been found for rubbers filled with carbon black [2]. The molecular weight has very little influence on the strength of vulcanizates from different rubber fractions with the same equilibrium modulus.

The dynamic fatigue resistance of rubbers is characterized by the time required for destruction of a specimen (endurance) under repeated extension. The frequency of the extensions in our experiments was 256 cycles per minute ****. The temperature of the specimens was maintained at 30°. The two most usual sets of test conditions were used: 1) given maximum deformation, ϵ= const and 2) given maximum load or conditional stress, f= const.

---

* For fraction 6, with molecular weight 56 thousand, a spatial network was not formed with the formation used.

** The tensile strength calculated for the actual cross-section at break; the relationship between the strength and the equilibrium modulus is complex, and is represented by a curve with a maximum [8].

*** At an equilibrium modulus of 13 kg/cm^2 for all fractions, which corresponds to the following amounts of combined sulfur: 1.8% for the high-molecular fractions, and about 4% for the low-molecular fractions.

**** The influence of frequency, extent of deformation, and load on the dynamic fatigue resistance is reported in the paper [3].

For the first set of conditions, the amplitude of the instrument was kept constant; residual deformations accumulated in the specimen in the course of the test. The second set of conditions was achieved by the use of a device which made it possible, after each extension cycle, to select the residual deformation in such a way that the load range was constant in the course of the tests (from 0 to f, where f is the arbitrary stress equal to the maximum load per unit original cross-section of the specimen).

Under the first set of conditions the maximum deformation of the specimen was 100%; under the second, maximum load corresponded to 7.6 kg/cm^2. This was chosen so that the initial deformation during the first extension cycle was 100 % for vulcanizates based on high-molecular fraction.

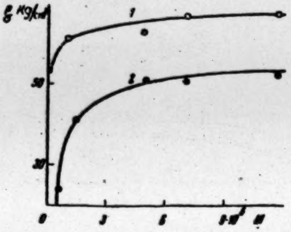

Fig. 2. Effect of molecular weight on the true strength of vulcanizates (by tensile strength tester) from rubber fractions: 1) with equilibrium modulus 13.0 kg/cm^2; 2) with 2.05% combined sulfur.

TABLE

Characteristics of Vulcanizates from Rubber Fractions

Fractions	Molecular weight	Contents, in parts by weight per 100 parts by weight of rubber		Vulcanizing time, min.	Equilibrium modulus E_∞ in kg/cm^2
		of sulfur	mercaptobenzothiazole		
1	1 170 000	3	1	35	13.3
2	700 000	3	1	40	13.0
3	500 000	3	1	45	12.8
4	140 000	4	1	60	13.0
5	100 000	4	2	80	13.5
6	56 000	6	3	100	13.0

Fig. 3 shows the variation of the dynamic endurance with the initial molecular weight for vulcanizates with equal amounts of combined sulfur (2.05%). While under the first test conditions the dynamic endurance decreases, under the second conditions it increases with increasing molecular weight.

The high value of the dynamic endurance of rubbers of low molecular weight under the first test conditions is explained by the fact that vulcanizates based on low-molecular fractions have a low equilibrium modulus and a less dense spatial network (with more free chain ends not in the network) than vulcanizates based on high-molecular rubber fractions. This results in the development of large "residual" deformations during the tests, which in turn lowers the stress and results in milder test conditions.

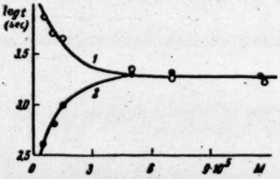

Fig. 3. Effect of molecular weight of the fraction on the dynamic endurance of vulcanizates with equal contents of combined sulfur (2.05%) and different values of equilibrium modulus (17.2; 16.2; 15.2; 8.0; 3.6 kg/cm^2); 1) tests with ϵ = const; 2) tests with f= const; t) time to destruction.

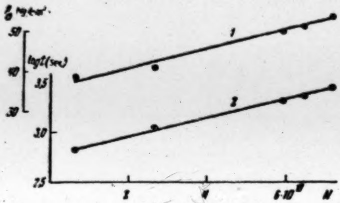

Fig. 4. True strength (1) as tested by the tensile tester, and dynamic fatigue resistance (2) at f = const. for vulcanizates based on different fractions of rubber with equal amounts of combined sulfur, but with different values of N, the number of chains in 1 cm³ on the spatial network.

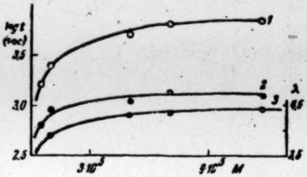

Fig. 5. Effect of molecular weight on the dynamic fatigue resistance of vulcanizates from fractions (1-5) with equal amounts of cross-links: 1) tested at ϵ = const.; 2) f = const; 3) relative extention $\lambda = L_{break}/L_0$ in dynamic tests.

Under the second conditions, the development of large residual deformations leads to harsher test conditions. The residual deformations lead to an increase in the maximum deformation of the specimen; with the final load constant, this increases the true stress in the specimen during the test.

From a molecular weight of 500 thousand and higher, the dynamic endurance of vulcanizates is the same under both sets of test conditions, as practically no residual deformations arise during the fatigue of these high-modulus rubbers (E_∞ = 15-17 kg/cm²). Analogous relationships between the dynamic fatigue resistance and the initial molecular weight of the rubber were obtained for rubbers with carbon black.

Thus it follows that variations of the strength and dynamic endurance of vulcanizates from different rubber fractions with equal amounts of combined sulfur are mainly determined by the influence of the molecular weight of the rubber on the structure of the vulcanizate formed. This is clearly illustrated by Fig. 4, which shows the variations of the dynamic endurance and tensile strength with the number of chains per unit volume of these vulcanizates.

Fig. 5. shows the influence of molecular weight on the dynamic endurance of vulcanizates from different rubber fractions with the same equilibrium modulus (13 kg/cm²) under the two sets of test conditions.

The dynamic endurance of these vulcanizates with the same equilibrium modulus increases under both sets of test conditions with increase of the initial molecular weight of the rubber *. The slight increase (instead of the expected constancy) of the dynamic endurance of the vulcanizates with increasing molecular weight is here due, firstly, to the fact that the molecular chains in vulcanizates based on low-molecular fractions are less mobile because of the greater intermolecular action in consequence of the larger amount of sulfur combined with the rubber; and secondly, to the fact that the low-molecular fractions have a more branched structure and a larger number of free molecular chains which do not form part of the network. All this results in considerable microheterogeneity of the material, lowering its strength.

Thus, the variation of the dynamic fatigue resistance of vulcanizates from different fractions of SKS-30A rubber with the same equilibrium modulus is mainly determined by structural differences of the vulcanizates based on low and high molecular weight fractions of rubber.

It is seen from Fig. 5 that the dynamic relative extension of the vulcanizates increases together with the dynamic fatigue resistance at f = const. This indicates that dynamic modulus and internal friction are higher in low-molecular than in high-molecular fractions, despite the fact that the equilibrium moduli are equal. This, in conjunction with the peculiarities of the structure of vulcanizates based on low-molecular fractions already noted, results in a decrease of the dynamic fatigue resistance.

---

* The different course of the curves for the condition ϵ = const. (Figs. 3 and 5) is explained by the fact that in Fig. 5 the modulus is constant along the curve, while in Fig. 3 it falls rapidly with decrease of mol. wt. of the fraction.

SUMMARY

1. The decrease of strength with decrease of the initial molecular weight of the rubber is rapid for vulcanizates with equal amounts of combined sulfur, but slight for vulcanizates with equal equilibrium moduli (equal densities of cross-links in the spatial network).

2. In repeated dynamic extension tests, the fatigue resistance or endurance of vulcanizates: a) with equal amounts of combined sulfur, depends greatly on the test conditions if the initial molecular weight of the rubber on the equilibrium modulus is low, and is practically independent of them if the initial molecular weight or equilibriu modulus is high; b) with the same equilibrium modulus, increases with increase of the initial molecular weight of the rubber irrespective of the test conditions (given maximum load, given maximum extension, etc), and reaches a practically constant value at high molecular weights.

3. The significiant influence of the initial molecular weight of the rubber on the strength and dynamic fatigu resistance of vulcanizates with equal amounts of combined sulfur is due to a lag in the formation of a spatial network in low-molecular rubbers during vulcanization, which results in the formation of a thin spatial network with considerable numbers of molecular chain ends which do not enter the network. For this reason, large residual deformations develop during tests on vulcanizates based on low-molecular rubbers.

LITERATURE CITED

[1] B. A. Dogadkin and Z. N. Tarasova, Proc. Acad. Sci., USSR, 85,5 (1952); A. S. Kuzminsky and L. I. Lyubchanskaya, Proc. Acad. Sci., USSR, 93, 519 (1953).

[2] A. S. Novikov, M. B. Khaikina et al., Colloid J., 15, 51 (1953) (T.p. 55)*; W. S. Penn, India Rubber J., 69, 64 (1950); P. Vanko, J. Polymer Sci., 4, 576 (1948); P. Flory, Ind. Eng. Chem., 38, 417 (1946).

[3] G. M. Bartenev and F. A. Galil-Ogly, Proc. Acad. Sci., USSR, 100, No. 3 (1955).

[4] A. S. Kuzminsky, N. N. Lezhnev, and M. G. Mayzels, Proc. Acad. Sci., USSR, 71, 2 (1951); Le Bras and A. Solvetti, Rubber Chem. Tech., 22, 374 (1949).

[5] G. L. Slonimsky, V. A. Kargin, et al., Proc. Acad. Sci., USSR, 93, 523 (1954).

[6] A. S. Novikov, G. M. Bartenev, and F. A. Galil-Ogly, Proc. Acad. Sci., USSR, 94, No. 2, 253 (1954).

[7] G. M. Bartenev, J. Tech. Phys., 22, 1154 (1952); Vulcanization of Rubber (Trans. Conf. on Vulcanization 1953), pp. 196-207, State Chemical Press (1954); L. A. Vishnitskaya, Trans. Inst. Rubber Ind., 1, 53 (1954).

[8] G. M. Bartenev and G. I. Belostotskaya, J. Tech. Phys., 24, 1773 (1954).

Received February 11,1955

Research Institute of the Rubber Industry

---

* T.p. = C. B. Translation pagination

COAGULATION OF LYOPHOBIC SOLS BY THE ACTION OF MIXTURES OF ELECTROLYTES

Yu. M. Glazman and I. M. Dykman

Lyophobic colloids consist of three-component ionically stabilized systems [1, 2], the intermicellar liquid of which as a rule contains stabilizing electrolytes in considerable concentrations [3]. Studies of the laws of coagulation of lyophobic sols by electrolyte mixtures are of special interest in this connection, as even in the simplest case, when a single coagulant is added to the colloidal system, coagulation proceeds in reality under the action of at least two electrolytes. This probably explains why the problem of sol coagulation by mixtures of electrolytes has been repeatedly studied by numerous investigators and considerable amounts of experimental data have accumulated on the subject. Despite some contradictions in the literature, the fundamentals of this subject are firmly established. If a mixture of two electrolytes is added to a lyophobic sol, various relationships in the coagulating effect are possible. Fig. 1 shows the experimentally observed relationships; here the axes represent the respective concentrations of the first and second electrolyte in the solution (n^0_{1c} and n^0_{2c} are the concentrations which correspond to their coagulation thresholds).

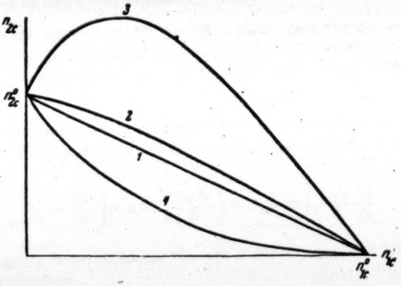

Fig. 1. Experimentally observed relationships in the coagulation of lyophobic sols by mixtures of two electrolytes: 1) additivity of the coagulating action; 2) superadditivity; 3) antagonism; 4) synergism.

It is commonly assumed that the coagulation effect is additive if the electrolytes differ little in their coagulating power (containing oppositely charged ions of equal valency); and accordingly antagonism is assumed to be more pronounced as difference in the coagulating power of the two electrolytes increases. No clear views exist with relation to synergism. It must be stressed that although these views are based on extensive experimental material, they are subject to numerous qualifications and exceptions [4-9]. Even this fact, in our opinion, is a sign of the complex nature of the antagonistic effect and of its dependence on a whole series of factors [9, 2]. It is therefore not surprising that, despite the repeated attempts to explain the observed deviations from additivity of coagulant action, there is still no real theory of antagonism and synergism.

Many investigators [5, 10-13] have related the positive and negative antagonism (synergism) effects to the concept of sol stabilization which occurs as the result of absorption of ions with the same charge as the colloidal particles. Some authors [14,15], on the contrary, attributed the principal role to competition between oppositely charged ions; they tended to consider that the main cause of antagonism is the mutual suppression of adsorption of the coagulant ions by the presence of the other electrolyte (the second component of the mixture) in the solution. It is easy to see that both these and the other authors based their attempts to explain the nature of antagonism on old and generally incorrect views which postulated a purely adsorptional mechanism for the coagulation process. This largely invalidates the treatment of the effect contained in these papers. To this it is necessary to add that the concept of the adsorption of ions with the same charge as the colloid particles, as was shown by one of the present authors [16], is not confirmed experimentally.

At the present time another viewpoint is apparently gaining increasing acceptance; antagonistic relationships in the coagulation of lyophobic colloids are interpreted exclusively in terms of electrostatic action between ions in electrolyte solution [17-21]. It must be pointed out that these theoretical considerations, which explain antagonism is individual instances, are quite imcompatible with the synergism effect. Nevertheless, as has been shown [9] synergism in coagulation is not in the nature of individual exceptions, but is almost as widespread as antagonism.

In order to shed some light on the nature of the phenomena observed when a mixture of two different electrolytes is added to a lyophobic sol, we considered it appropriate to examine the problem on the basis of Deryagin's quantitative theory of lyophobic sol stability [22], which is founded on clear physical concepts of the mechanism of the coagulation process. This was the purpose of the present investigation.

In order to solve the problem, we repeated the calculations carried out by Deryagin and Landau [22] and extended them to the coagulation of a sol by a mixture of two electrolytes. With the initial aim of establishing only general qualitative relationships, we restricted ourselves to a consideration of strongly charged sols and of the simplest system, consisting of two symmetrical electrolytes and fairly large particles with plane surfaces. This choice is justified, on the one hand, by the fact that, as was shown by Deryagin and Landau [22], the form of the adhesion criterion (for the case of a single electrolyte) and the numerical value of its constant change very little with changes in the curvature of the particle surfaces. On the other hand, it is well known from experimental data (and also from theoretical calculations) [22] that the influence of the valency of the secondary ion on the coagulating action of an electrolyte is generally small.

In our calculations, as in the paper cited [22], we will consider only changes in the volume properties in relation to the concentration of the electrolytes in the solution, and will initially ignore any possible changes in surface properties (the potential and chemical nature of the surface, etc.) which result from the addition of electrolytes to the system.

Let unit volume of the solution contain n_1 electrolyte molecules with ion valency z_1 and n_2 molecules with ion valency z_2. The potential ψ at any point within the volume of the solution can be found with the aid of the Debye–Hückel equation:

$$\Delta\psi = \frac{8\pi e}{\varepsilon}\left[n_1 z_1 \operatorname{sh}\left(\frac{e z_1 \psi}{\theta}\right) + n_2 z_2 \operatorname{sh}\left(\frac{e z_2 \psi}{\theta}\right)\right], \tag{1}$$

where e is the electronic charge; ε is the dielectric constant of the solution; $\theta = kT$ is the Boltzmann constant multiplied by the absolute temperature.

If the concentration of colloidal particles in the sol is such that it is sufficient to consider only interactions between pairs of them, then for particles with plane surfaces oriented parallel to each other, Equation (1) is simplified and reduces to an equation which depends only on one coordinate of x (along an axis perpendicular to the particle surface):

$$\frac{d^2\psi}{dx^2} = \frac{8\pi e}{\varepsilon}\left[n_1 z_1 \operatorname{sh}\left(\frac{e z_1 \psi}{\theta}\right) + n_2 z_2 \operatorname{sh}\left(\frac{e z_2 \psi}{\theta}\right)\right]. \tag{2}$$

As will be seen later, this equation is fundamental for determination of the conditions for sol coagulation. Since the individual characteristics of the electrolytes are only reflected in it by their ion valencies, this leads to the conclusion that coagulation by a mixture of two chemically different electrolytes with equal values of the ion valency z does not differ from the action of a single electrolyte at the aggregate concentration.

The first integral of Equation (2) is found direct; it determines the square of the field strength (E^2) and is

$$E^2 = \left(\frac{d\psi}{dx}\right)^2 = \frac{16\pi\theta}{\varepsilon}\left[n_1 \operatorname{ch}\left(\frac{ez_1\psi}{\theta}\right) + n_2 \operatorname{ch}\left(\frac{ez_2\psi}{\theta}\right) - C\right], \qquad (3)$$

where C is the integration constant. Equation (2) must be solved separately for the region of the space limited by the plates, and for the region outside the plates. Therefore, the values of the constant C for these regions must also be found separately.

Let the distance between the plates be h, and their coordinates be $x_1 = -h/2$ and $x_2 = +h/2$ respectively. The plates are charged to the same potential ψ_1. It is obvious from the condition of symmetry that in the central plane at $x = 0$ the field strength is zero. Therefore, by equating $d\psi/dx$ to zero in Equation (3), and denoting the value of the potential at $x = 0$ by ψ_0 (this will be defined below), we obtain the following expression for the constant C_1 in the inner part of the space:

$$C_1 = n_1 \operatorname{ch}\left(\frac{ez_1\psi_0}{\theta}\right) + n_2 \operatorname{ch}\left(\frac{ez_2\psi_0}{\theta}\right). \qquad (4)$$

In the outer part of the space the value of the constant C_2 is determined from the condition that the potential ψ and the field strength E tend to zero when $|x| \to \infty$; this gives:

$$C_2 = n_1 + n_2. \qquad (5)$$

Thus, the field strength has different values on different sides of each of the plates. Hence it follows that a mechanical force is applied to the plates. The numerical value of this force (repulsion) calculated per unit area, is determined by the formula:

$$P = \frac{\varepsilon}{8\pi}(E_2^2 - E_1^2), \qquad (6)$$

where E_1 and E_2 are the respective field strengths at the plate surfaces in the inner and outer regions.

Let us substitute Equations (3), (4), and (5) into Formula (6). Since the potential on both sides of the plates has the same value, the terms containing ψ (after the above substitution) will cancel. The force of repulsion acting per unit area of each of the plates will be:

$$P = 2\theta(C_1 - C_2) = 2\theta\left[n_1\left(\operatorname{ch}\frac{ez_1\psi_0}{\theta} - 1\right) + n_2\left(\operatorname{ch}\frac{ez_2\psi_0}{\theta} - 1\right)\right]. \qquad (7)$$

It is seen from Equation (7) that the force P at given values of n_1 and n_2 depends on ψ_0. In order to find the relationship between P and the distance h between the particles, it is necessary to establish the functional dependence of ψ_0 on h. For this, we find the second integral of Equation (2).

In the subsequent calculations we confine ourselves to the case when $z_2 = 2z_1$, which corresponds, for example, to coagulation of a sol by a mixture of 1–1–and 2–2–valent electrolytes. This choice is justified, on the one hand, by the fact that such a combination of symmetrical ions is most frequently met in experimental investigations of coagulation, and on the other, by the relative simplicity of the calculation.

Substitution of (4) into the Formula (3) gives:

$$\frac{d\psi}{dx} = \pm\left(\frac{16\pi\theta}{\varepsilon}\right)^{1/2}\left[n_1\left(\operatorname{ch}\frac{ez_1\psi}{\theta} - \operatorname{ch}\frac{ez_1\psi_0}{\theta}\right) + n_2\left(\operatorname{ch}\frac{2ez_1\psi}{\theta} - \operatorname{ch}\frac{2ez_1\psi_0}{\theta}\right)\right]^{1/2}. \qquad (8)$$

Since, as was already pointed out, when $x = 0$ the derivative $d\psi/dx = 0$, different signs must be taken in Equation (8) for the regions $-h/2 \leqslant x \leqslant 0$ and $0 \leqslant x \leqslant h/2$. If the potential of the plates is positive, then $\psi_0 < \psi_1$, and when $0 \leqslant x \leqslant h/2$ the value of $d\psi/dx > 0$. We note that the force P, as can be seen from Equation (7), does not depend on the sign of ψ_0 and therefore also on the sign of ψ_1.

Let us introduce the dimensionless potential

$$u = \frac{ez_1\psi}{\theta} . \tag{9}$$

and let $u_1 = \frac{ez_1\psi_1}{\theta}$ and $u_0 = \frac{ez_1\psi_0}{\theta}$. All the subsequent calculations will refer to strongly charged sols, when $u_1 \gg 1$.

If we substitute Equation (9) into Equation (8), and , for clarity, take the potential as positive, we have:

$$\frac{du}{dx} = \left(\frac{16\pi e^2 z_1^2}{\varepsilon\theta}\right)^{1/2} [n_1(\operatorname{ch} u - \operatorname{ch} u_0) + 2n_2(\operatorname{ch}^2 u - \operatorname{ch}^2 u_0)]^{1/2} \quad (0 \leqslant x \leqslant h/2). \tag{10}$$

If we put

$$n_1/4n_2 = f, \tag{11}$$

then, from Equation (10), we have:

$$\frac{1}{2}\varkappa_2 h = \frac{1}{2}\varkappa_1 h f^{-1/2} = \int_{u_0}^{u_1} \frac{du}{[\operatorname{ch}^2 u - \operatorname{ch}^2 u_0 + 2f(\operatorname{ch} u - \operatorname{ch} u_0)]^{1/2}}, \tag{12}$$

where

$$\varkappa_2 = \left(\frac{32\pi e^2 z_1^2 n_2}{\varepsilon\theta}\right)^{1/2}; \quad \varkappa_1 = \left(\frac{8\pi e^2 z_1^2 n_1}{\varepsilon\theta}\right)^{1/2} \tag{13}$$

the reciprocal thicknesses of the ionic atmospheres in a solution containing only one of the electrolytes in question.

Because of the very rapid (exponential) decrease of the integrated function, the upper integration limit in Formula (12), when $u_1 \gg 1$, may be substituted by infinity. In this form, Formula (12) determines the relationship between the potential u_0 in the plane of symmetry and the distance $\underline{h}$. This formula is simplified by substitution of

$$\sin^2\varphi = \frac{(\operatorname{ch} u - \operatorname{ch} u_0)(\operatorname{ch} u_0 + 2f + 1)}{2(\operatorname{ch} u - 1)(\operatorname{ch} u_0 + f)},$$

when the integral in Formula (12) can be reduced to an elliptic integral of the first kind. As a result we have:

$$\frac{1}{2}\varkappa_2 h = \frac{k}{(\operatorname{ch} u_0 + f)^{1/2}} \int_0^{\varphi_1} \frac{d\varphi}{(1 - k^2\sin^2\varphi)^{1/2}}, \tag{14}$$

or

$$\frac{1}{2}\varkappa_1 h = \frac{kf^{1/2}}{(\operatorname{ch} u_0 + f)^{1/2}} \int_0^{\varphi_1} \frac{d\varphi}{(1 - k^2\sin^2\varphi)^{1/2}}, \tag{14'}$$

where the upper integration limit φ_1, is determined by the equation:

$$\sin^2\varphi_1 = \frac{\operatorname{ch} u_0 + 2f + 1}{2(\operatorname{ch} u_0 + f)}, \tag{15}$$

and the modulus of the elliptic integral by the equation:

$$k^2 = \frac{4(\operatorname{ch} u_0 + f)}{(\operatorname{ch} u_0 + 1)(\operatorname{ch} u_0 + 2f + 1)}. \tag{16}$$

From these definitions it is seen k^2 and $\sin^2\varphi_1$ are always less than unity irrespective of the values of f and u_0. Only if $u_0 = 0$, k^2 is equal to unity. Here, however, as follows from Equation (15), $\varphi_1 = \pi/2$ and, in accordance with Formula (14) or (14'), h = ∞. This is in full agreement with physical considerations, since the potential in the plane of symmetry is only zero when the distance between the plates is infinitely great.

It can be shown that, if only one electrolyte is present in the solution, Formulas (14) and (14') become the corresponding formula derived by Deryagin and Landau [22]:

$$\frac{1}{2}\varkappa h = k \int_0^{\pi/2} \frac{d\varphi}{(1 - k^2 \sin^2\varphi)^{1/2}} \tag{17}$$

with the value

$$k = \frac{1}{\mathrm{ch}\,(ez\psi_0/2\theta)}. \tag{18}$$

In fact, if only the first electrolyte with ion valency z_1 is present, then $n_2 = 0$ and f ⟶ ∞. Here, as can be seen from Equation (15), $\varphi_1 = \pi/2$ and the Equations (16) and (18), and (14') and (17), coincide.

If only the second electrolyte is present, that is, if $n_1 = 0$, then f = 0. In order to show that in this case also our Equation (14) coincides with Equation (17), we make use of London's transformation [23]

$$\int_0^{\varphi_1} \frac{d\varphi}{(1 - k^2 \sin^2\varphi)^{1/2}} = \frac{1 + k_1}{2} \int_0^{\chi_1} \frac{d\varphi}{(1 - k_1^2 \sin^2\varphi)^{1/2}}, \tag{19}$$

where k_1 and χ_1 are related to k and φ_1 as follows:

$$k^2 = \frac{4k_1}{(1 + k_1)^2} \tag{20}$$

and

$$\sin(2\varphi_1 - \chi_1) = k_1 \sin\chi_1. \tag{20'}$$

A comparison of Equations (20) and (16), for f = 0 shows that $k_1 = 1/\mathrm{ch}\, u_0$ (the root of Equation (20) $k_1 = \mathrm{ch}\, u_0$ must be rejected as meaningless) which again coincides with (18), if it is taken into account that the valency of the ion in this case is $2z_1$. Further, from Equations (15) and (20') we find $\chi_1 = \pi/2$. Thus, the integral in the right-hand side of Equation (19) is a full elliptic integral of the first kind, and therefore Equation (14) coincides with Equation (17).

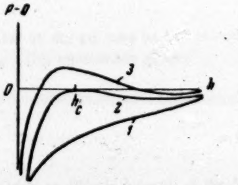

Fig. 2. Possible forms of the relationship between the resultant force of interaction and the distance between the particles: 1) state of instability (coagulation); 2) limit of stability; 3) state of stability.

To obtain the condition for coagulation, we assume, in accordance with Deryagin and Landau [22] that the stability limit of the system is determined by concentrations n_{1c}, n_{2c} at which, at a certain point h_c (that is, at a certain distance h_c between the particles) the electrostatic repulsion force and its derivative with respect to h are respectively equal to the Van der Waals attractive force and its derivative (See Curve 2 in Fig. 2, taken from the paper [22]).

It is known [24] that the potential energy of interaction between two infinitely small volumes dV_1 and dV_2 at a distance r from each other is

$$dU = -A\frac{dV_1\, dV_2}{r^6}, \tag{21}$$

where A is the constant for the mutual molecular attraction *.

From Equation (21) we can find the attractive force Q which acts on unit surface of particles at a distance h from each other. This force (if the particles are assumed fairly "thick" relative to h) is equal to:

$$Q = \pi A / 6h^3. \tag{22}$$

The conditions for the stability limit of the system formulated above

$$P = Q, \; dP/dh = dQ/dh, \tag{23}$$

with the use of Equation (22) may be combined in one equation

$$h/P \cdot dP/dh = -3, \tag{24}$$

which should be regarded as the equation for determination of the "critical" distance h_c. This, on the basis of Equations (14) or (14'), at a given concentration of one of the electrolytes, is a function of f. Therefore it is better to substitute the value of the force P in Equation (24) not in the form of Equation (7) but in the terms of f:

$$P = 4\theta n_2 (\operatorname{ch} u_0 - 1)(\operatorname{ch} u_0 + 2f + 1). \tag{25}$$

It is more convenient to make the further calculations by taking the value of $\alpha = \sin^2 \varphi_1$ as the independent variable, at a fixed value of f. By means of simple transformations it is easy to establish, with the aid of Equations (15), (16), and (25), a relationship between k^2, u_0, P and α, namely:

$$\operatorname{ch} u_0 = \frac{2f(1-\alpha)+1}{2\alpha - 1}, \tag{26}$$

$$k^2 = \frac{2\alpha - 1}{\alpha(f - f\alpha + \alpha)}, \tag{27}$$

$$P = 16\theta n_2 \alpha (1-\alpha) \left(\frac{1+f}{2\alpha - 1}\right)^2 \tag{28}$$

Further, by putting in Equation (24) $dP/dh = dP/d\alpha \cdot d\alpha / dh$, it may be transformed, with the aid of Formula (28), into

$$3 \frac{dh}{d\alpha} = \frac{h}{\alpha(1-\alpha)(2\alpha-1)}. \tag{29}$$

The value of $dh/d\alpha$ may be calculated, for example, from Formula (14), if Equation (26) is substituted into it for ch u_0. This substitution gives:

$$h = \frac{2}{\varkappa_2 (f+1)^{1/2}} (2\alpha - 1)^{1/2} kF(\varphi_1, k), \tag{30}$$

where F(φ_1, k) is an elliptic integral of the first kind:

---

* It must be pointed out, however, that in the limiting case of fairly large distances London's law becomes inapplicable and the energy of interaction becomes proportional to r^{-7} [25, 26]. However, as the critical distance h_c between the particles may be represented by a magnitude of the order of 10^{-6} cm or less, we considered it legitimate to use London's law of molecular interaction in the subsequent calculation.

$$F(\varphi_1, k) = \int_0^{\varphi_1} \frac{d\varphi}{(1 - k^2 \sin^2 \varphi)^{1/2}}.$$

Consequently,

$$\frac{dh}{d\alpha} = \frac{2}{\varkappa_2 (f+1)^{1/2}} \left\{ \frac{k}{(2\alpha - 1)^{1/2}} F(\varphi_1, k) + (2\alpha - 1)^{1/2} \frac{d}{d\alpha} [kF(\varphi_1, k)] \right\}. \tag{31}$$

The last term in Equation (31) is best defined as follows:

$$\frac{d}{d\alpha} [kF(\varphi_1, k)] = F(\varphi_1, k) + k \int_0^{\varphi_1} d\varphi \frac{d}{dk} (1 - k^2 \sin^2 \varphi)^{-1/2} \frac{dk}{d\alpha} + \\ + \frac{k}{(1 - k^2 \sin^2 \varphi_1)^{1/2}} \frac{d\varphi_1}{d\alpha}.$$

Taking into account that:

$$k \int_0^{\varphi_1} d\varphi \frac{d}{dk} (1 - k^2 \sin^2 \varphi)^{1/2} = \frac{1}{1 - k^2} E(\varphi_1, k) - \frac{k^2}{1 - k^2} \frac{\sin \varphi_1 \cos \varphi_1}{(1 - k^2 \sin^2 \varphi_1)^{1/2}} - F(\varphi_1, k),$$

where $E(\varphi_1, k)$ is an elliptic integral of the second kind

$$E(\varphi_1, k) = \int_0^{\varphi_1} (1 - k^2 \sin^2 \varphi)^{1/2} d\varphi,$$

we easily find the right hand side of Equation (31) in explicit form. Here it must be remembered that, in accordance with Equation (27) and the definition of $\alpha = \sin^2 \varphi_1$, we have:

$$\frac{d\varphi_1}{d\alpha} = \frac{1}{2\sqrt{\alpha(1 - \alpha)}} \text{ and } \frac{dk}{d\alpha} = \frac{k}{2(2\alpha - 1)} \left(\frac{2\alpha + f}{2\alpha - 1} k^2 - 2 \right).$$

Substitution of the explicit form of the expression for $dh/d\alpha$ and also of Equation (30) into Formula (29), we obtain the following equation, which is fundamental for the subsequent calculations:

$$F(\varphi_1, k)[1 - 3\alpha(1 - \alpha)] = \frac{3\alpha(1 - \alpha)}{2(1 - k^2)} \left(\frac{2\alpha + f}{2\alpha - 1} k^2 - 2 \right) \left[E(\varphi_1, k) - k \left(\frac{2\alpha - 1}{f + 1} \right)^{1/2} \right] + \\ + \frac{3(2\alpha - 1)^{3/2}}{2k(1 + f)^{1/2}}. \tag{32}$$

Here again it is not difficult to show that in the limiting case of one electrolyte Equation (32) becomes the Deryagin-Landau Equation [22]:

$$\frac{3}{2} \mathrm{E}(k) = \mathrm{K}(k), \tag{33}$$

where K(k) and E(k) are the complete elliptic integrals of the first and second kind, while the modulus $\underset{\bullet}{\underline{k}}$ is given by Formula (18).

It was already pointed out earlier that in the case when f ⟶ ∞, our k coincides with Equation (18), while $\varphi_1 = \pi/2$, that is, $\alpha = 1$. Therefore, by substituting f ⟶ ∞ and $\alpha \longrightarrow 1$ in Equation (32) we have

$$K(k) = \frac{3}{2}\frac{f(1-\alpha)}{1-k^2}k^2 E(k). \tag{34}$$

If we then use Equations (26) and (27), we have

$$\lim_{f\to\infty}\frac{f(1-\alpha)}{1-k^2}k^2 = 1,$$

and therefore Equation (34) or, which is the same thing, Equation (32), becomes Equation (33).

In the second limiting case when f = 0, in order to prove the equivalence of Equations (32) and (33) it is again necessary to make use of the transformations (19) and (20), remembering that the elliptical integral of the second kind is transformed according to the law.

$$E(\varphi_1, k) = \frac{1}{1+k_1}E(\chi_1, k_1) - \frac{1-k_1}{2}F(\chi_1, k_1) + \frac{k_1}{1+k_1}\sin\chi_1. \tag{35}$$

If, in Equation (32) we replace $F(\varphi_1, k)$ and $E(\varphi_1, k)$ by their values in accordance with Formulas (19) and (35), and also if we consider that, (as was shown above), when $f = 0$, $\chi_1 = \pi/2$, $k_1 = 1/\mathrm{ch}\, u_0 = 2\alpha - 1$, it is easily seen that Equations (32) and (33) are identical.

In the general case of the simultaneous action of two electrolytes, the root α_c of Equation (32) (which is a function of f) determines the "critical" values of h_c and P_c. From Equations (22), (23), and (28) we have:

$$16\theta n_2 \alpha_c (1-\alpha_c)\left(\frac{1+f}{2\alpha_c - 1}\right)^2 = \frac{\pi A}{6h_c^3}. \tag{36}$$

From this it is now easy to find the minimum concentration of the second electrolyte n_{2c} (at a fixed value of f) at which coagulation begins. Similarly, the coagulating concentration n_{1c} of the first electrolyte can be determined. If we put in Equation (36), instead of h_c, its value in accordance with Equation (30), we have:

$$n_{2c} = D\frac{k_c^6 F^6(\varphi_{1c}, k_c)\,\alpha_c^2(1-\alpha_c)^2}{2\alpha_c - 1}(1+f); \quad n_{1c} = 4fn_{2c} \tag{37}$$

where $D = \frac{18\varepsilon^3\theta^5}{A\pi^3 e^6 z_1^6}$, and φ_{1c} and k_{1c} are the values of φ_1 and k when $\alpha = \alpha_c$.

The Equations (37) represent the functional relationships of the minimum coagulation concentrations of both electrolytes, in parametric form. It is easily seen that in the limiting cases when $f \to \infty$ and $f = 0$, considered above, the ratio of the concentrations is $n_{2c}^0 : n_{1c}^0 = 1 : 2^6$, which is in full agreement with the findings in [22]. It is also possible to investigate analytically the course of n_{2c} as a function of n_{1c} for the same cases [i.e., $n_{2c} = n_{2c}(n_{1c})$]. It is found that when $f \to \infty$ the derivative dn_{2c}/dn_{1c}, tends to zero, as $f^{-1/2}$. In other words, the curve $n_{2c} = n_{2c}(n_{1c})$ when $n_{2c} = 0$, touches the n_{1c} axis. In the other limiting case when $f \to 0$

$$\lim_{f\to 0}\left(\frac{dn_{2c}}{dn_{1c}}\right) = \left[1 - \frac{1}{4\alpha_c(1-\alpha_c)} + \frac{3(2\alpha_c - 1)}{8(1-\alpha_c)F(\varphi_{1c}, k_c)}\right]_{f\to 0} \approx -0.008 > -\frac{1}{2^6}$$

and the curve $n_{2c} = n_{2c}(n_{1c})$ is slightly above the straight line representing additivity of the action of the two electrolytes, that is, the straight line which joins the coagulation concentration points of the separate electrolytes.

The general form of the curve for the relationship $n_{2c} = n_{2c}(n_{1c})$ is shown in Fig. 3, in which the coagulation concentrations of the first and second electrolytes are taken in arbitrary units along the axes. For clarity, the scale of the ordinate axis (the n_{2c} axis) has been enlarged 64 times. The curve was obtained as the result of numerical solution of Equation (32). The roots α_c of the equation for different values of f are shown in the Table. The values of k_c^2 and $F(\varphi_{1c}, k_c)$ are determined together with α_c during the solution of Equation (32); the values of the coagulation concentrations n_{1c}/D and n_{2c}/D were calculated from Equation (37). For illustration, the Tabl gives values of n_{2c}/D (for corresponding values n_{1c}/D) which should have been obtained if the action of the two electrolytes followed the additivity law, and deviations from this law in percentages. The Table shows that in the initial region (in the region of very low n_{1c} values) the $n_{2c} = n_{2c}(n_{1c})$ curve is above the additivity line, althoug very slightly (the difference cannot be seen on the scale used in Fig. 3).

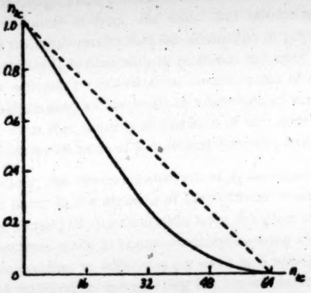

Fig. 3. Relationship between the coagulation concentrations in the action of a mixture of two electrolytes: continuous curve is the theoretical curve; the dotted line is the additivity line.

Our results show that if the coagulation process is not complicated, as is assumed in Deryagin's theory, by additional phenomena (adsorption, chemical action, etc.), the addition of two electrolytes which differ in the valencies of the coagulating ions to the sol should generally result in a clearly defined synergism (at least for mixtures of 1-1- and 2-2-valent electrolytes). In reality, as is known, this is far from always true in practice; often the opposite effect, more or less clearly defined antago ism, is observed. In our opinion, important conclusions may be drawn from this.

Firstly, it is necessary to point out the valuable results obtained by application of B. V. Deryagin's theory to the coagulation of lyophobic colloids by mixtures of electrolytes. As can be seen from the above results, with the aid of this theory it has become possible to explain for the first time the frequently observed phenomenon of synergism, which previously had no rational explanation. At the same time, however, another fact is noted. Such a widespread effect as ionic antagonism in the coagulation of lyophobic sols by electrolyte mixtures is not explained by this theory, at least when applied to the case considered above. The probable reason for this is the fact that the nature of antagonism is complex and, which is most important, that it is not directly related to the purely electrostatic mechanism of coagulation. Antagonism between electrolytes is probably the result of just those secondary effects during coagulation which are not considered in the original form of Deryagin's theory. Thus, antagonism in general cannot be explained merely on the basis of mutual electrostatic effects between ions in electrolyte solutions with complete neglect of sorptional action between the ions and the surface of the colloidally disperse phase.

TABLE

Calculated Values of Coagulation Concentrations in the Action of Two Symmetrical Electrolytes

f	α_c	k_c^2	$F(\varphi_{1c}, k_c)$	$\frac{n_{1c}}{D}$	$\frac{n_{2c}}{D}$	$\frac{n_{2c}}{D}$ add	Deviation from additivity (in %)
0	0.8870	0.9838	1.728	0	0.3294	0.3294	–
0.1	0.8917	0.9734	1.734	0.1314	0.3286	0.3274	+ 0.37
0.5	0.9068	0.9411	1.754	0.6392	0.3196	0.3195	+ 0.03
1	0.9191	0.9120	1.771	1.232	0.3081	0.3102	– 0.68
2	0.9352	0.8741	1.791	2.232	0.2790	0.2946	– 5.30
5	0.9570	0.8149	1.822	4.404	0.2202	0.2606	–15.50
10	0.9711	0.7698	1.845	6.640	0.1660	0.2257	–26.45
15	0.9779	0.7463	1.857	8.016	0.1336	0.2042	–34.57
20	0.9818	0.7298	1.866	9.088	0.1136	0.1875	–39.41
30	0.9865	0.7089	1.877	10.56	0.08797	0.1645	–46.52
50	0.9910	0.6872	1.889	12.25	0.06125	0.1381	–55.65
100	0.9950	0.6640	1.903	14.11	0.03527	0.1090	–67.64
200	0.9973	0.6455	1.914	15.96	0.01994	0.08016	–75.12
1000	0.9994	0.6172	1.928	18.60	0.00465	0.03883	–88.02
∞	1.000	0.5990	1.949	21.09	0	0	–

In this connection it must be pointed out that Wo. Ostwald's assertion that ionic antagonism coagulation is a property of the dispersion medium appears to us totally unfounded both in the light of available experimental data [2] and from the theoretical standpoint. While Wo. Ostwald's "law of constant activity coefficients" [27], which was given a theoretical basis by Deryagin and Landau [22], may be regarded as a more or less correct empirical rule for the coagulation of sols by individual electrolytes, Wo. Ostwald's extension of his "law" to the coagulation of sols by electrolyte mixtures [19] must be considered, on the basis of our results, as devoid of physical meaning.

We therefore conclude that antagonism is apparently in some way connected with adsorptional action which occurs when coagulating electrolytes are added to the sol. Thus, despite the fact that a purely adsorptional mechanism for the coagulation process is known to be incorrect, we do not consider it possible to agree with the opposite viewpoint of some authors, who assert that adsorption only accompanies coagulation but does not determine it [28]. It follows from our results that the adsorption of gegenions is very important in some coagulation phenomena. In this connection it is necessary to point out the need for further development of Deryagin's theory of the stability of lyophobic colloids by quantitative consideration of the possibility of a variation of the particle surface potential during coagulation, as the result of adsorption of electrolytes added to the system, and of other secondary phenomena. We must stress that there is no question of any revision of Deryagin's theory, but only of its development, which in no way disturbs its basis of theoretical concepts and physical ideas.

Finally, the above considerations by no means exclude the possibility that in special isolated cases antagonism may also occur in the absence of adsorptional action between the ions and colloidal particles. In fact, as has been shown by Vester [18] recalculation from the gross concentrations of the electrolytes to activities of the coagulating ions sometimes leads to complete disappearance of the maximum on the antagonism curve, resulting in a straight line corresponding to additivity (or even in a synergism curve). Vester's explanation for this was that since the activity of a multivalent coagulating ion is considerably lowered by the action of another electrolyte in the solution, the concentration of this gegenion must be considerably increased in the presence of the second salt. The paper cited [18] gives such data for the negative AgI sol and mixtures of $Al(NO_3)_3 + K_2SO_4$ and $Th(NO_3)_4 + Na_2SO_4$.

According to available literature data [29] the charge density on the negatively charged surfaces of the AgI colloidal particles is relatively low, and the exchange capacity of gegenion absorption in the outer layer of the electric double layer is correspondingly small. This probably explains the fact that the coagulation of negatively charged silver iodide sol by electrolytes proceeds mainly by an electrostatic mechanism [30], while cation sorption appears in this instance to be unimportant for coagulation [30]. Nevertheless, in the electrolyte systems examined by Vester [18] the effect of activity decrease is, naturally, very pronounced because of the high valency of the component A cation (Al^{3+}, Th^{4+}), on the one hand, and because of the bivalent anion of component B (SO_4^{2-}) on the other. It is probable that in this particular case the antagonistic effect is really caused mainly by purely electrostatic action between ions in a solution of two coagulating electrolytes. This probably accounts for Vester's results obtained by recalculation of the experimental data on the coagulation of AgI sol by mixtures of electrolytes. It is possible, and even highly probable, that for such combinations of electrolytes a calculation based on Deryagin's theory, even though it ignores possible adsorptional action between the electrolytes and the colloidal particles, would nevertheless lead to results opposite to those obtained in the present paper, that is, to an antagonistic curve. This supposition follows from the fact that in the Debye-Hückel equation, which is the starting point of all calculations with the aid of Deryagin's theory, the mutual electrostatic influence of the ions on their activity is already automatically considered. In addition, analysis of the data given above provides a certain basis for this assertion. As has already been pointed out, the theoretical curve for the coagulating action of a mixture of two electrolytes in its initial region (at low n_{1C} values) lies above the additivity line, and only passes into the synergism curve at $f \approx 0.5$. Hence it follows that probably two opposing factors are always superposed: on the one hand, synergism, which is the consequence of the electrostatic mechanism of the coagulation process, and on the other, the mutual effect of the ions on each other's activities. Both these factors are reflected in Deryagin's theory. The aggregate result of a theoretical calculation will evidently depend on which of these two factors predominates. In the case examined in the present paper, the latter factor is weak, as the presence of a 1-1-valent electrolyte has a relatively small influence on the activity of a bivalent coagulating ion of the second component of the mixture. This results in synergism, and the curve lies somewhat above the additivity line only at the earliest stages. With other relationships between the electrolytes, when the suppression of the multivalent ion activity is considerable, this effect may mask the synergism, and therefore in such a case it is possible to obtain a theoretical curve corresponding to antagonism. In our view, this is of undoubted interest, and therefore further similar general calculations are desirable.

It must be remembered, however, that irrespective of the possible results of such calculations the explanation of antagonism in terms of the decrease of the activity of the coagulating ions in solution applies only to particular cases, when adsorption of the electrolyte ions is not significant for the coagulation process. However, as is seen from the results in this paper, this probably plays an important part. In fact, as was shown above, a calculation in which adsorption of the coagulating ions by the colloidal particles is neglected does not reflect the antagonism which is frequently observed in the coagulation of lyophobic sols by mixtures of 1-1-and 2-2-valent electrolytes.

In conclusion, it is the authors' pleasant duty to express their gratitude to Associate Member of the Academy of Sciences USSR B. V. Deryagin for his interest in the work, for much valuable advice, and for discussion of the results.

SUMMARY

1. The coagulation of lyophobic sols by the action of electrolyte mixtures has been examined on the basis of B. V. Deryagin's theory of lyophobic sol stability. The calculations made by B. V. Deryagin and L. D. Landau for the case of one electrolyte were extended to the coagulation of a sol by a mixture of two electrolytes (1-1 + 2-2).

2. It is shown that, if coagulation is not complicated by secondary phenomena, when two symmetrical electrolytes differing in the valencies of the coagulating ions (1-1 + 2-2) are added to a sol, synergism should occur over almost the entire region of electrolyte concentrations.

3. The possible causes of the antagonistic effect in the coagulation of sols by mixtures of electrolytes are discussed.

LITERATURE CITED

[1] N. P. Peskov, Physico-Chemical Bases of Colloid Science, United Sci.-Tech. Press (1932).

[2] Yu. M. Glazman, Colloid J., 8, 387 (1946); 15, 225 (1953) (T.p. 231)* .

[3] V. A. Kargin and G. V. Klimovitskaya, J. Phys. Chem., 5, 969 (1934); 6, 842 (1935); V. A. Kargin and N. A. Ogandzhanova, J. Phys. Chem., 10, 782 (1937).

[4] S. Ghosh, A. K. Battacharya, N. R. Dhar, Koll.-Z, 38, 141 (1926).

[5] A. I. Rabinerson, Koll.-Z, 42, 50 (1927).

[6] V. A. Dorfman, Koll. -Z,46, 186 (1928).

[7] H. Freundlich, H. Tamchyna, Koll.-Z, 53, 288 (1930).

[8] A. Basinski, Roczniki Chem., 15, 430 (1935).

[9] Yu. M. Glazman, Colloid J., 8, 299 (1946).

[10] S. Oden, Der Kolloide Schwefel, Nova Acta Ups (IV) 3, 66 (1912); cited through W. Pauli, E. Valko, Electrochemie der Kolloide (1929).

[11] K. C. Sen, Koll. -Z, 39, 324 (1926); J. Phys. Chem., 29, 517 (1925); Z. anorg. Chem., 149, 139, (1925); K. C. Sen, M. R. Mehrotra, Z. anorg. Chem., 142, 345 (1925).

[12] S. Ghosh, N. R. Dhar, J. Phys. Chem., 29, 435, 659 (1925).

[13] H. R. Kruyt, P. C. van der Willigen, Proceed. Kon. Akad. van Wet., 34, 1240, (1925); cited through C. I, 2443 (1926).

[14] H. Freundlich, H. Pape, Z. phys. Chem., 86, 458 (1914); H. Freundlich, P. Scholz, Koll.-Beih., 16, 267, (1923); cited through: C. II, 920, (1924).

[15] H. B. Weiser, J. Phys. Chem. 25, 665, (1921); 28, 232 (1924); 29, 955 (1925).

[16] Yu. M. Glazman, D. N. Strazhesko, and B. E. Tartekovskaya, Colloid J., 15, 161 (1953) (T.p.161)* .

[17] W. Pauli, E. Valko, Elecrochemie der Kolloide (1929).

[18] C. F. Vester, Dissertation (1935); cited through H. R. Kruyt, Kon. Akad. Wet., 38, 464 (1935).

---

* T.p.= C. B. Translation pagination

[19] Wo. Ostwald, K. Hoffmann, Koll.-Z. 80, 186 (1937).

[20] L. K. Lepin and A. V. Bromberg, J. Phys. Chem., 13, 71, 82 (1939).

[21] H. R. Kruyt, Coll. Sci., 1 (1952).

[22] B. V. Deryagin, Bull. Acad. Sci., USSR, Chem. Ser., 1155 (1937); Colloid J., 6, 291 (1940); 7, 285 (1941); B. V. Deryagin and L. D. Landau, J. Expt.-Theor. Phys., 11, 802 (1941); 15, 663 (1945).

[23] See, e. g. Yu. S. Sikorsky, Elements of the Theory of Elliptic Functions with Applications of Mechanics, United Sci.-Tech. Press (1936).

[24] R. Eisenschitz, F. London, Z. Phys., 60, 491 (1930).

[25] H. B. G. Casimir, D. Polder, Phys. Rev. 73, 360 (1948).

[26] E. M. Lifshits, Proc. Acad. Sci., USSR, 97, 4, 643 (1954).

[27] Wo. Ostwald, Koll. -Z. 73, 301 (1935).

[28] E. J. W. Verwey, Prog. Chem., 4, 1194 (1935).

[29] E. J. W. Verwey, H. R. Kruyt, Z. phys. Chem., 167 A, 149, (1933).

[30] E. J. W. Verwey, H. R. Kruyt, Z. phys. Chem., 167 A, 312 (1933).

Received January 17, 1955

The Technological Institute for the Light Industry,
Kiev

INVESTIGATION OF CLAYS WITH THE AID OF THE CONE PLASTOMETER

I. M. Gorkova

The most important and widespread bulk characterization of the physical state of clays for geological engineering and structural purposes is by evaluation of their consistency and plasticity. No direct, simple methods with a theoretical basis exist at the present time for the determination of these properties of clays. The existing methods do not give comparable results and only express the plasticity and consistency of clays indirectly.

We have applied the cone plastometer method, developed by Rebinder for studies of the mechanical properties of viscoplastic disperse systems [1], to studies of clays with intact structure and of clay pastes. The form of calculation used in this method makes it possible to express the strength of the structure in disperse systems (their "plastic strength") in terms of the yield stress. With the aid of the cone plastometer it is possible to investigate disperse systems in the structurally-viscous and plastic states, and also at semisolid consistencies, when the usual methods for the determination of resistance to shear are not applicable. For relatively liquid systems, when the paste flows along the surface of the immersed cone, the plastic strength corresponds to the true value of the yield stress. In more solid systems, the crumpling deformation during immersion of the cone results in a regular increase of the strength values. In such cases, the value of the yield stress is conditional or arbitrary.

The following formula was used for determination of the plastic strength of clays:

$$P_m = K\alpha F/h^2,$$

where P_m is the conditional yield stress; F is the force acting on the cone; h is the depth of immersion of the cone (read to an accuracy of 0.1 mm); K is a constant; α is the angle at the cone apex. At values of the angle α equal to 30,45, and 90°, the cone constants are: $K_{30} = 1.108$; $K_{45} = 0.658$; $K_{90} = 0.159$.

The plastic strength of clay pastes in the determination of the flow limit by the cone immersion methods of Vasilyev [2] and Boychenko [3], calculated by this formula, is 84 and 32 g/cm² respectively. Immersion of the cone results in extrusion of the clay mass around it, which leads to error in visual readings of the immersion depth of the cone. Therefore the actual strength of pastes at the flow limit, determined by Vasilyev's method, is on the average 100 g/cm². At the flow limit determined with the aid of the cam-type apparatus the plastic strength of pastes as measured by the cone plastometer is, on the average, 50 g/cm² for clays and 35 g/cm² for loams. The plastic strength of clays at the rolling limit (in rolling into a thread down to 3 mm in diameter or calculated for Boychenko's cone [3]) is 2 kg/cm². When clays are rolled into threads of minimum thickness. their strength rises 3-6 kg/cm².

The plasticity number thus represents a range of moisture variation in which the plastic strength of clay pastes varies within arbitrary limits from 6-2 to 100-32 kg/cm², according to the methods for the determination of the plasticity limits. The established plasticity limits according to the State Standard [4] correspond to paste plastic strengths of 2.0 and 0.1 kg/cm².

Plasticity limit determinations provide a measure of the strength of clays only at two moisture contents. With the aid of the cone plastometer it is possible to obtain a much more complete characterization of clays. Fig. 1 shows the variation of the plastic strength of clay pastes of different mineral types as a function of their moisture content. The different moisture contents were produced by the gradual addition of dry clay to moist clay with thorough mixing, as is usually done in determinations of the plasticity limits of clays. The broken lines represent the values of the paste strengths at the plasticity limits determined according to the State Standard. The numbers indicate the consecutive appearance of certain characteristic properties in the pastes, such as: adhesion to the cone, retention of shape, cessation of adhesion, crack formation on kneading, formation of lustrous surface and internal lustrous planes, etc. These curves are analogous to the curves for the decreasing strength of clays on humidification [5] obtained by us earlier by another method. Two groups of clays are seen in Fig. 1. In one of these the strength changes from 5.50 to 0.05 kg/cm^2 over 80-90% of the moisture change range. These are the more hydrophilic, highly disperse clays, containing colloidal minerals of the montmorillonite and hydrated mica types, with a high absorption capacity (31-66 mg-equiv.) and high plasticity numbers (25-54 by the State Standard). In the other group the plastic strength changes from 2.20 to 0.03 kg/cm^2 over 20-38% of the moisture change range. These clays have low hydrophily, contain kaolinite, and have lower degree of dispersion, absorption capacity (from 8 to 30 mg-equiv.) and plasticity number (from 16 to 19). The positions of the numbers on the curves show that the structural and mechanical properties of the different clays are not the same at equal values of their plastic strength. The more hydrophilic the clays are, the wider are the strength and moisture content ranges in which these consecutive changes of properties take place. Therefore comparative evaluations of clays by their State Standard plasticity numbers, that is, by a conventional strength range which is the same for all clays and loams, are unsuitable. These arbitrary limits contain non-comparable sections of the curves, which correspond to different physical states of the less and more hydrophilic clays. Methods of plasticity determination in which the clays are brought into a similar physical condition (determination of the flow limits by Atterberg's method, by the cam-type apparatus or in Okhotin's modification, determination of the adhesion limit or rolling into a thread to the limit) provide a much more correct evaluation of the clays. An objective characterization of clays in accordance with their nature is provided by the curves for the strength as a function of the moisture content, obtained with the aid of the cone plastometer.

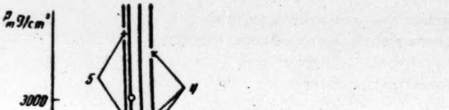

Fig. 1. Plastic strengths of clays of different mineral types as a function of their moisture content; appearance of characteristic properties: 1) adhesion to cone; 2) ability to retain shape; 3) limit of adhesion; 4) crack formation in paste; 5) inner lustrous planes in paste.

With the aid of the cone plastometer it is possible to determine the strength of clays direct in their natural structural state — at their natural moisture content — and also after drying, swelling, and soaking. Fig. 2 shows curves for the strength as a function of moisture content for one sample of clay from Khvalynsk, between the Volga and the Ural rivers, with intact structure, and for a paste of the same clay. The natural structures of the clays studied have much higher strength, while containing up to 15% more water, than the pastes. This shows that the natural structures are more porous and have higher moisture capacity with greater cohesional strength between the particles.

Natural clay structures provide an example of primary, condensational disperse system structures [6] formed during the formation of the deposits and their subsequent diagenesis. The originally formed structures in clay deposits are always porous and contain large amounts of free water in the pores [7, 8]. However, the high moisture content of the natural structures is by no means always a sign of low strength. As a result of aging and syneresis processes characteristic of all disperse systems [9], the hydrate layers at the points of contact between the clay particles become thinner and the boundary phase is "pressed through" in the deposits [10]. This results in high cohesional strength between the particles in the deposit, and makes its structural network rigid and brittle, despite the water retained in the pores. The structures of different clays differ in the degree of porosity and strength according to the ratio between the condensation and strengthening rates in the deposits during diagenesis.

Interaction between the low-hydrated natural clay structures and water in the course of swelling and soaking results in an abrupt increase in the strength of the clay as the result of the disjoining action of the newly formed hydrate layers, which weaken inter-particle cohesion. This is accompanied by an increase in the moisture content of the clay. Mechanical disruption of the natural structures in clays, with retention of the natural moisture content, also leads to the development of hydrate layers from the liberated pore water. The result is the formation of denser, plastic, but much weaker thixotropic structures [6]. The strength values for thixotropic structures obtained by kneading clay at the natural moisture content fit the curve for the paste, and thus confirm Denisov's views on the subject [11].

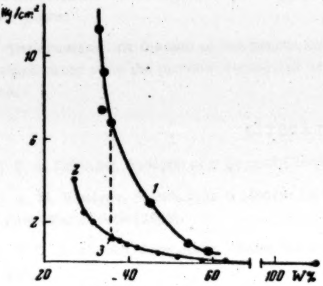

Fig. 2. Strength-moisture content curves for Khvalynsk clay; structures: 1) primary; 2) paste; 3) thixotropic

Since natural clays and pastes differ in the nature of their structure, ratios of the combined and free water, and nature of the deformations and strength at the same moisture contents, it is evident that the accepted method for the evaluation of the consistency of clays by comparison of their natural moisture contents with the plasticity limits of pastes [12] is incorrect. In fact, the plasticity limits of the sample of Khvalynsk clay studied are 22 and 61%; the plasticity number is 39; the natural moisture content of the clay in the natural deposit is 42%. The consistency coefficient is 0.49. The clay in this state might be expected to have a strength of ~ 400 g/cm² (see Fig. 1). However, the strength of the natural structure of the clay at this moisture content is 4 kg/cm², which is double the strength of the paste at the limit of rolling into a thread down to 3 mm, and 10 times the strength which corresponds to the given consistency coefficient. Therefore the indirect method for evaluating the physical condition of the clay gives no idea of the actual strength of the clay in the natural deposit. However, a comparison of the natural moisture content with the curve for the variation of the strength of pastes with the moisture content, and determination of the consistency coefficient, is important in another way, by indicating the strength (consistency) acquired by the clay when its structure is completely disturbed but the natural moisture content is retained.

By comparative investigations of the mechanical properties of natural and thixotropic structures of Khvalynsk clays with the aid of the cone plastometer it proved possible to determine properties of the natural structures. The results are in agreement with the work of Denisov [13], Rosa [14], and others, who established that certain clays and muds, with moisture contents in the natural state above the flow limit, liquefy only when their structure is disrupted and are solids in their natural deposits. These properties of natural structures must be taken into account in the mechanics of clays. The view still prevails in this field that clays containing only firmly bound water are in the solid state, those containing loosely bound water are in the viscoplastic state, and those containing free water form the soil mass [12]. These views are valid only for freshly prepared pastes and for disrupted structures. Clays which consist of aged coagulational structures combine, at their natural moisture content a high porosity and high content of pore water with low degree of hydration and solid-like properties. It is because of this characteristic that clays are dangerous from the engineering and geological viewpoint, as they are subject to swelling and soaking by the action of water, to sagging and condensation under load, and to loss of strength by hydration and disruption of structure.

In conclusion it must be stressed that with the aid of the cone plastometer it is possible to study quantitatively the variation of the strength of clays with changes in their moisture contents and structural state, and also with various additions, by the action of different solutions, on leaching, on swelling and soaking in different media, and during deformation. The cone plastometer is simple and convenient to operate and merits wide application in studies of clays.

SUMMARY

1. With the aid of the cone plastometer it is possible to carry out quantitative investigations of the plastic strength of clays and clay pastes in various structural states as a function of the moisture content.

2. It is shown that natural structures at the natural moisture content are more porous and contain more free water, but the particles are less hydrated at the points of contact, and in consequence they are stronger and more brittle than pastes.

3. The characteristic features of the natural structures in clays have been determined, and the nature of the changes which occur when the moisture contents of natural clays are varied and their structure disrupted has been established.

LITERATURE CITED

[1] P. A. Rebinder, Synopsis of a General Course in Colloid Chemistry, compiled by K. A. Pospelova (1949).

[2] A. M. Vasilyev, Foundations of Modern Methods and Techniques for Laboratory Determinations of the Physical Properties of Soils (1949).

[3] P. O. Boichenko, Symposium "Some Methods for the Determination of Physico-Mechanical Properties of Soils" (1950).

[4] State Standard 5179/49, 5184/49. Soils – Laboratory Determination Methods (1950).

[5] I. M. Gorkova, Colloid J., 10, No 2, 63 (1949).

[6] E. E. Segalova and P. A. Rebinder, Colloid J., 10, No 3, 223 (1948).

[7] M. M. Filatov, Fundamentals of Road Soil Science (1936).

[8] P. A. Rebinder, Symposium "Viscosity of Liquids and Colloid Solutions", p 361 (1941).

[9] S. M. Lipatov, Physical Chemistry of Colloids, Acad. Sci. USSR Press (1948).

[10] B. V. Deryagin and P. A. Krotova, Adhesion (1949).

[11] N. Ya. Denisov, Nature of the Deformation of Clays (1951).

[12] N. A. Tsytovich, Soil Mechanics (1951).

[13] N. Ya. Denisov, Problems of Soviet Geology, 3, No 10, 132 (1934).

[14] S. A. Rosa, Hydrotechnical Construction, No 1, 20 (1950).

Received January 28, 1955

The F. P. Savarensky Laboratory for
Hydrogeological Problems, Academy of Sciences
USSR

DEPENDENCE OF THE EXCHANGE SORPTION OF ORGANIC IONS ON THEIR STRUCTUR

A. T. Davydov and P. F. Skoblionok

In considerations of ion exchange adsorption, which is essentially a heterogeneous reaction, the nature of the adsorbent, of the solvent, and of the exchanged ions must be regarded as the factors which determine the extent and the character of the sorption. The behavior of mineral ions in exchange reactions is primarily determined by their charges and dimensions. There are considerable differences between organic and inorganic ions in their nature and sorption. In organic ions, the charge is concentrated in a definite region and its influence does not extend equally over the whole surface of the ion. This fact must be taken into consideration in evaluations of the behavior of organic ions in exchange sorption. It is therefore interesting from a practical and a theoretical standpoint to study the influence of the structure of organic ions on the extent of exchange sorption and the value of the constants which characterize the exchange; in particular, the influence of the nature and the position of substituents on the behavior of organic ions in exchange reactions. The exchange sorption of the following ions on Ca-sulfocarbon was studied: aniline, ortho-, meta-, and para-toluidine. The hydrochlorides of these amines, which dissolve and dissociate in water, were used.

TABLE 1

Calculation of the Constants in Gapon's Equation

System	Concentration of aniline hydrochloride in solution, in moles		Amount of $C_6H_5NH_3^+$ in mg-equiv. taken up by 10 g of adsorbent	Amount of Ca^{2+} in mg-equiv. desorbed from 10 g of adsorbent	$x = \frac{\sqrt{a/2}}{100c}$	$y = \frac{1}{a}$
	c_0 initial	c equilibrium				
Ca-sulfocarbon + aniline hydrochloride	0.05	0.005	4.5	4.80	3.1750	0.211
	0.10	0.012	8.8	8.48	1.7159	0.121
	0.25	0.110	14.0	12.65	0.2286	0.078
	0.50	0.336	16.4	14.02	0.0788	0.072
	0.75	0.564	18.6	14.46	0.0477	0.070
	1.00	0.797	20.3	15.87	0.0353	0.069

$a_m = 15.3 \pm 0.9$ $K = 0.64 \pm 0.23$ $\sigma_y = 0.003$

The reason for the choice of these ions was that they are very similar in size and basicity, which may therefore be taken as constant. Thus, differences in the ion exchange adsorption of aniline and the different toluidines should be determined by differences in their structure.

0.005-1.00 M solutions of the purified hydrochlorides of aniline, and o-, m-, and p-toluidines were prepared. Weighed quantities of 5 g of Ca-sulfocarbon were placed in special flasks, 50 ml of a solution of the required concentration was added, and the liquid kept for 48 hours with frequent stirring. After 48 hours the flasks with their contents were placed in a thermostat at 25°, and samples for analysis were then taken. The amount of desorbed calcium was determined volumetrically in the equilibrium solutions.

The concentrations of all the equilibrium solutions of the amine hydrochlorides and of the original solutions of the toluidine hydrochlorides were determined by potentiometric titration with sodium nitrite in hydrochloric acid [1].

The experimental results were used to calculate the constants in Gapon's equation [2], which has the following form for the exchange of a bivalent cation by a univalent:

$$\frac{1}{a} = \frac{1}{a_m} + \frac{K}{a_m}\frac{\sqrt{a/2}}{100c}$$

where a is the number of mg-equiv. of the organic ion adsorbed by 10 g, equal to the amount of desorbed Ca^{2+} in mg-equiv.; a_m is the maximum adsorption, calculated for 10 g of the adsorbent; c is the equilibrium concentration of the displacing ion, in mg-equiv. / ml; K is the exchange constant.

TABLE 2

Calculation of the Constants in Gapon's Equation

System	Concentration of toluidine hydrochloride in solution, in moles		Amount of $C_7H_7NH_3^+$ in mg-equiv., taken up by 10 g of adsorbent	Amount of Ca^{2+} in mg-equiv., desorbed from 10 g of adsorbent	$x = \frac{\sqrt{a/2}}{100c}$	$y = \frac{1}{a}$
	c_0 initial	c equilibrium				
Ca-sulfocarbon + + ortho-toluidine hydrochloride	0.0437	0.0037	4.00	4.66	3.8222	0.204
	0.0873	0.0097	7.76	8.23	2.0912	0.142
	0.2183	0.0873	13.10	12.56	0.2871	0.078
	0.4332	0.2740	15.92	13.61	0.0952	0.071
	0.7033	0.5335	16.98	13.73	0.0491	0.070
	0.9457	0.7517	19.40	13.86	0.0352	0.069
	a_m = 14.7 + 2.1		K = 0.52 + 0.04		σ_y = 0.009	
Ca-sulfocarbon + + meta-toluidine hydrochloride	0.0576	0.0048	5.28	4.89	3.2575	0.198
	0.1032	0.0140	8.92	8.92	1.5085	0.125
	0.2544	0.1056	14.88	13.63	0.2472	0.073
	0.5088	0.3312	17.76	14.25	0.0806	0.066
	0.7784	0.5928	18.56	14.86	0.0460	0.065
	1.0560	0.8400	21.60	14.95	0.0325	0.064
	a_m = 15.9 + 0.6		K = 0.66 + 0.09		σ_y = 0.006	
Ca-sulfocarbon + + para-toluidine hydrochloride	0.0505	0.0048	4.57	4.70	3.1938	0.198
	0.0998	0.0120	8.78	8.79	1.7470	0.141
	0.2381	0.0998	13.83	12.14	0.2469	0.082
	0.4579	0.2892	16.87	12.64	0.0869	0.075
	0.7953	0.6025	19.28	12.74	0.0419	0.074
	1.0363	0.8435	19.28	13.10	0.0303	0.073
	a_m = 13.9 + 2.8		K = 0.55 + 0.06		σ_y = 0.013	

The experimental and calculated data are shown in Tables 1 and 2. The values σ_y, a_m, and K were calculated by the method of least squares.

The results show that the same values were found for the maximum adsorption and the exchange constant in all systems. The slight differences may be attributed entirely to experimental error.

The isotherms for the exchange of Ca^{2+} by aniline and o-, m-, and p-toluidine ions coincide, which shows that the nature of the substituent and its position in the ion has no effect on ion exchange sorption.

Comparison of the quantities of sorbed and desorbed ions shows that the amount of sorbed ions is the greater, and at high concentrations this difference is beyond the limits of experimental error. The probable reason is that, in addition to ionic sorption, molecular adsorption also occurs [3].

SUMMARY

1. The exchange sorption of the following organic ions on Ca-sulfocarbon from aqueous solution of their hydrochlorides has been studied: aniline, o-, m-, and p-toluidine.

2. It is shown that Gapon's equation is satisfactorily applicable to the exchange between the mineral and organic ions studied.

3. Equal isotherms for the exchange sorption were found for all the systems studied, showing that the nature and position of the substituent in the ion does not affect ion exchange sorption.

LITERATURE CITED

[1] L. M. Litvinenko and A. P. Grekov, J. Anal. Chem., 10, No. 3, 163 (1955) (T.p. 153)*.

[2] E. N. Gapon, J. Gen. Chem., 3, 145 (1933); 7, 1438 (1937).

[3] N. A. Izmaylov, S. Kh. Mushinskaya, and Yu. V. Shostenko, First Ukrainian Republic Conference on Physical Chemistry (Summaries of Papers), Acad. Sci. Ukrainian SSR, p.108 (1954).

Received February 7, 1955

The A. M. Gorky State University
Kharkov

---

* T.p. = C. B. Translation pagination

THERMOMECHANICAL INVESTIGATION OF THE FORMATION AND STRUCTURE OF INFUSIBLE AND INSOLUBLE p-CRESOL-FORMALDEHYDE RESINS

L. A. Igonin, N. A. Krasulina, and V. A. Kargin

In the previous communication [1] it was shown that, in contrast to linear amorphous polymers, hardened novolac resin can exist in two physical states, the glassy and the high-elastic. The viscofluid region in this case is absent right up to the decomposition temperature of the hardened resins. An increase of the amount of hexamethylenetetramine participating in the hardening process changes the mechanical properties of the hardened resins: the modulus of high-elastic deformation increases sharply, and the glass transition temperature moves into the region of higher temperatures. On the other hand, the addition of low-molecular components such as phenol or dioctyl sebacate to the original resin has a plasticizing effect on the hardened resin; the glass transition temperature decreases and the specimens become increasingly susceptible to high-elastic deformation.

These results led to certain conclusions on the nature of hardened phenolformaldehyde resins: polycondensation of the resins under the action of hexamethylenetetramine results in the formation of linear polymer chains, cross-linked by infrequent chemical bonds. As a result, the viscofluid state is absent and the experimentally observed high elasticity is present. The polymer chains are immersed in a highly viscous medium of low-molecular resin components, and this in turn determines a number of characteristic features in the deformation behavior of the hardened resins.

As a result it appeared of interest to investigate the formation of infusible and insoluble p-cresol-formaldehyde resins. It is known [2] that substituted phenols with the substituents in the ortho or para positions to the hydroxyl group contain two active points in the nucleus and can give rise only to soluble resins of the novolac type. However, under the corresponding conditions p-cresol resins form infusible and insoluble products, and this has not been adequat ly explained.

In the present investigation, the dynamometric balance [3] has been used to study, over a wide temperature range, the mechanical properties of p-cresol-formaldehyde resins of different degrees of polycondensation, obtained by heating mixtures of novolac p-cresol resins with hexamethylenetetramine. The resin used in the study was prepared by the condensation of p-cresol and paraform in the ratio of 2 moles of p-cresol to 1 mole of formaldehyde in the presence of 1 % hydrochloric acid [4]. The condensation was carried out in a flask on a boiling water bath for 80 hours. The resin was purified by molecular distillation at 140°.

As the polycondensation rate of p-cresol resins is much lower than that of phenolic resins, the method used for the preparation of the test samples differed somewhat from that described previously [1]. A mixture of the resin and hexamethylenetetramine was melted with stirring at 120° in a porcelain basin, and then ground to a powder, from which the test specimens were pressed. A mixture of the resin, hexamethylenetetramine, and plasticizer was ground in a porcelain mortar until a dry powder was formed, and kept at 160-170° for 3 hours. The specimens used were cylindrical in shape, 10 mm in diameter and 4-5 mm high, pressed at 180-190° under a specific pressure of 50-60 kg/cm^2 for 20 minutes. In some instances the method used for preparation of the specimens was modified somewhat according to the viscosity of the original resin, and the hexamethylenetetramine and plasticizer contents. In all cases the amounts of the added hexamethylenetetramine or plasticizer were calculated relative to the weight of the resin. The tests with the aid of the dynamometric balance were carried out under the conditions described in the preceding paper [1].

Fig. 1 shows the results of tests of p-cresol resin specimens obtained by polycondensation in the presence of different amounts of hexamethylenetetramine (amounts of hexamethylenetetramine added are indicated by number on the curves). Fig. 1 shows that the glass transition temperature of the original resin lies in the range 50-55°. As the amount of hexamethylenetetramine in the polycondensation increases, the glass transition temperature of the specimens shifts upwards and reached 180-190° for 10% hexamethylenetetramine. The resins obtained with the addition of 10% hexamethylenetetramine retain their fusibility but have restricted solubility in various solvents. The add tion of still greater amounts of hexamethylenetetramine results in the formation of almost completely insoluble resin

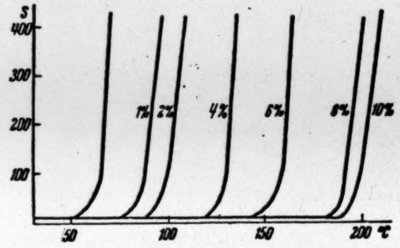

Fig. 1. Thermomechanical curves for a series of p-cresol-formaldehyde resin specimens of different degrees of polycondensation.

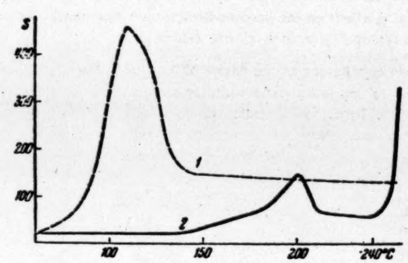

Fig. 2. Thermomechanical curves for phenol-formaldehyde and p-cresol-formaldehyde resins taken during polycondensation under the action of hexamethylenetetramine.

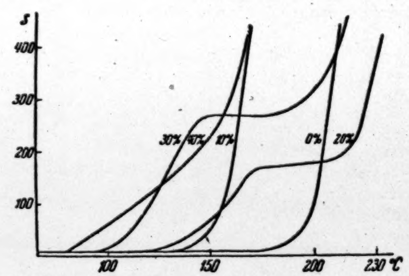

Fig. 3. Thermomechanical curves for a series of plasticized p-cresol-formaldehyde resin specimens after polycondensation in the presence of 10% of hexamethylenetetramine.

with viscofluid transition temperatures beyond the limits of chemical stability. Thus, these specimens are infusible and insoluble products.

If the pressing time of the specimens was not sufficient for all the hexamethylenetetramine to be completely combined, and the specimens retained some thermoreactivity, tests yielded the thermomechanical curves shown in Fig. 2. For comparison, the hardening of a novolac phenol-formaldehyde resin was investigated at the same time (shown by a broken line). The p-cresol resin specimens tested contained 10% hexamethylenetetramine and 20% dioctyl sebacate, prepared as described above. The original mixture was held for 2 hours at 160-170° before pressing. The phenol-formaldehyde resin specimens, containing 5% hexamethylenetetramine and 20% dioctyl sebacate, were prepared in the usual manner [1] except that the pressing was carried out at 130° for 10 minutes.

Fig. 2 shows that polycondensation commences at temperatures at which the viscofluid state of the resin is clearly seen. At the same time, as the result of the chemical reaction which commences, the viscosity of the resin rises sharply and the thermomechanical curve passes through a maximum. By variation of the initial viscosity of the resin by additions of plasticizers, or by preliminary thermal treatment, the maximum may be displaced into the lower or higher temperature regions.

On the other hand, as can be seen from Fig. 1, as the polycondensation reaction proceeds, the glass transition temperature of the resin will increase, and in the case of a highly viscous resin may reach the polycondensation temperature. In that case, because of the sharp increase in the viscosity of the resin, the polycondensation reaction will stop. As has already been noted in the case of polyvinyl chloride [5], the mobility of the reactive groups, which is associated with the macroviscosity of the system, is probably of general signifance for chemical processes in polymers.

Fig. 3 shows thermomechanical curves for a series of p-cresol resins obtained in the presence of 10% of hexamethylenetetramine. Some of the specimens were plasticized by the addition of different amounts of dioctyl sebacate to the original resin (the amounts of added plasticizer are indicated by the numbers on the curves). The specimen of p-cresol resin obtained from a mixture containing 10% hexamethylenetetramine had a glass transition temperature of 180-185°. Addition of 10% plasticizer lowered the glass transition temperature to 140-145°, and the specime had the behavior of a low-molecular glass. Addition of 20% plasticizer to the original resin results in a significant change in the nature of the polycondensation: the final resin exhibits all the three physical states characteristic of amorphous linear polymers. The glass transition temperature is lower than that of a specimen with 10% plasticizer, there is a clearly defined region of high elasticity, and the temperature of viscous flow rises to 220°. Further plasticizer addition produces the usual effects found in the plasticization of amorphous linear polymers [6].

Thus, the polycondensation of unplasticized p-cresol resins under the action of hexamethylenetetramine stops at the stage of low-molecular product formation. A decrease of the viscosity of the original p-cresol resins by the addition of appropriate amounts of plasticizer results in the formation of polymeric glasses, with properties similar to those of linear amorphous polymers.

SUMMARY

1. The mechanical properties of p-cresol-formaldehyde resin specimens obtained by polycondensation in the presence of different amounts of hexamethylenetetramine were investigated with the aid of the dynamometric balance over a wide range of temperatures.

2. It is shown that the formation of infusible and insoluble p-cresol resins with the aid of hexamethylenetetramine consists of the formation of an insoluble linear polymer, the viscofluid transition temperature of which lies above the temperature of its chemical stability.

3. As the polycondensation reaction proceeds, the glass transition temperature of the condensation resins rises continously until the polycondensation temperature is reached. In this case, in view of the sharp increase in the resin viscosity, the polycondensation process ceases and a peculiar "self-freezing" of the resin takes place.

LITERATURE CITED

[1] L. A. Igonin, N. A. Krasulina, and V. A. Kargin, Colloid J., 17, 295 (1955) (T.p. 277)*.

[2] V. V. Korshak, Methods of High-Molecular Organic Chemistry, Vol. I, Acad. Sci., USSR Press, pp. 537, 546 (1953).

[3] V. A. Kargin and T. I. Sogolova, J. Phys. Chem., 23, 530 (1949).

[4] A. A. Vansheydt, A. T. Itenberg, and V. Mikhailov, J. Gen. Chem., 12, 489 (1942).

[5] V. A. Kargin, [illegible], and M. I. Shteding, Chem. Ind., No. 2 (1955).

[6] V. A. Kargin and Yu. M. Malinsky, Symposium "Chemistry and Physical Chemistry of High-Molecular Compounds," Acad. Sci. USSR Press (1952).

Received July 4, 1955

Research and Projects Institute for Plastics and
The L. Ya. Karpov Physico-Chemical Research
Institute

---

* T.p. = C.B. Translation pagination.

VISCOSITY OF STARCH SAMPLES IN AQUEOUS AND ALKALINE SOLUTIONS

M. I. Knyaginichev and T. M. Shchinnikova

Viscosity is a characteristic property of starch solutions; its value depends on a number of factors, including the molecular weight and the nature of the polymer, and its contents of ash, phosphorus, and amylopectin [1, 2]. However, we have shown [2] that the viscosity of starch solutions depends on the presence and properties of the starch grain coating, by which we mean the part of the starch grain which is insoluble in 30% sodium salicylate solution.

It was previously observed [3] that the viscosity of starch grain coating solutions is considerably higher than the viscosity of solutions of the starch substance (the inner contents of the starch grains, soluble in 30% sodium salicylate), and also that the viscosity of the starch substance from different starch samples differs by relatively small amounts (in comparison with the viscosity of the membranes). In this connection it is of great interest to study the changes in the viscosity of starch solutions in different solvents, which destroy the starch grains in different ways, and for different samples of starch. This question is not only of theoretical but also of practical interest, as starch is very important in the food, textile, and other industries.

EXPERIMENTAL

The materials used in the work were potato starch samples prepared by the method described earlier [4]. The relative viscosity was determined with the aid of the Ostwald viscosimeter at 20°, two solvents being used for the preparation of the pastes: water, and aqueous caustic soda solutions of different concentrations.

The well-known difficulties in starch viscosity determinations, owing to poor reproducibility, were met in the course of the work. Our observations showed that the poor reproducibility is the consequence of heterogeneity of the solutions due to the presence of coatings, which do not easily dissolve in water even on prolonged boiling. In view of this, the usual technique for viscosity determination had to be modified so that homogeneous solutions could be obtained.

A sample of the air-dry starch, equivalent to 0.3 g of the bone-dry substance, was weighed out on an analytical balance. The sample was covered with 3-5 ml of water, about 50 ml of boiling water was added, and the paste formed was boiled from 5 to 30 minutes. After cooling, the paste was transferred to a 100 ml measuring flask, made up to the mark, and the contents mixed. For the viscosity measurements 5 ml of the paste was transferred into an Ostwald viscosimeter (with an efflux rate of 10 sec at 20° for water). Table 1 shows some of our experimental results.

Table 1 shows that the efflux rate of pastes made from the same starch sample but boiled for different times varies within very wide limits. With such divergences it is not possible to compare different starch samples because of the poor reproducibility. However, the external appearance of the paste does not disclose its inhomogeneity; the solution appears as a completely homogenous mass of opalescent liquid, with no inclusions visible to the eye. Only after prolonged standing it is sometimes possible to see clots, of almost the same degree of clarity as the solution, at the bottom of the vessel; these consist of the remains of the starch grain coatings which are not completely hydrated. Therefore it was necessary to use a stronger influence than boiling on the starch grains in order to produce a stable homogenous system in water.

The pastes were stirred mechanically after being boiled in order to obtain homogeneous solutions. As the result of experiments with the use of a mechanical shaker, the following procedure for the determination of the viscosity of aqueous starch solutions was adopted. The paste was boiled for 5 minutes, transferred hot (~60°) into a measuring flask, and made up to the mark with warm water to give a temperature of about 50°. The paste was then poured into a warm glass jar and shaken for 15 minutes on the mechanical shaker at 350-400 oscillations per minute. After cooling (after the shaking the starch temperature was ~35-38°) to room temperature, 5 ml of the solution was withdrawn with a pipet and transferred to the viscosimeter; when the temperature fell to 20°, the viscosity was determined. Table 2 shows some of the experimental results.

TABLE 1

Reproducibility of Starch Viscosity Determinations

Duration of boiling, minutes	Efflux rate of 0.3% starch paste, in seconds, in three experiments		
	1	2	3
10	56.9	42.9	47.4
10	12.7	23.6	26.8
30	25.0	12.0	17.2
30	32.2	25.6	26.5

Table 2 shows that the variations between separate determinations of the viscosity of the same solutions are small, while the reproducibility in different experiments is fairly good. Thus, by mechanical action it is quite possible to obtain homogeneous solutions of starch in water, so that reproducible viscosity data can be obtained.

The homogeneity and stability of colloidal solutions are associated with the hydration of high-polymer molecules. The views developed by Dumansky [5] concerning the non-dissolving volume and the solvated shell, provide a satisfactory explanation of the observed effects. A starch paste becomes homogeneous when, as the result of boiling and mechanical action, the polar groups of the starch molecule become accessible to hydration. The arguments put forward by some authors [6] against this viewpoint have been explained. Dumansky [7] showed that the thickness of the layer of water absorbed by a starch particle with considerable evolution of heat is approximately 3 A. This corresponds to the dimensions of the water molecule. However, the thickness of a liquid layer having shear modulus is 800 A, which is evidence of the multilayer nature of the solvent. It is probable that, in solvation, the number of layers can vary from one to many according to the nature of the substance, the solvent, and external factors. For the production of homogeneous and stable starch solutions it is necessary to destroy the coatings so that they can be hydrated with the formation of stable sols.

TABLE 2

Reproducibility of Starch Viscosity Determinations with the Use of a Mechanical Shaker and Higher Solution Temperatures

Experiment	Efflux rate of starch paste in seconds in 5 determinations of the viscosity of the same potato starch sample						Relative viscosity
	1	2	3	4	5	Mean	
1	30.0	30.0	29.0	29.0	29.4	29.50	2.95
2	30.0	30.0	30.0	29.8	29.8	29.9	2.92
3	29.6	29.6	29.6	29.6	29.4	29.5	2.95

We must refer in this connection to the detailed investigations carried out by Nazarov [8], who showed that the disintegration of starch grains (during paste formation in water) is accompanied by absorption of heat. He attributes this to disruption of the starch grain structure, and to rupture of bonds between groups of micelles and between individual micelles.

In addition to studies of starch viscosity in aqueous solution, studies of the viscosity in alkaline solutions without the use of high temperatures are of interest. There are indications in the literature [9] that the viscosity of alkaline starch solutions can provide a measure of the degree of hydrolysis of the starch molecule. The alkaline solution itself has no hydrolyzing action on this polysaccharide. Satisfactory results were not obtained by the use of random concentrations of caustic soda in aqueous solutions. With the object of obtaining homogeneous starch solutions at room temperatures, we studied the effect of the alkaline solutions of the following concentrations on the viscosity of starch: 0.1; 0.25; 0.50; 1.0; 5.0 and 10.0 N.

All the concentrations tested result in different degrees of destruction of the starch grains, and the solutions obtained have different degrees of homogeneity. As a result, the viscosities were different, and the reproducibility varied.

Without quoting numerical data, we note that when 10 N (40%) alkali solution was used, microscopic examination showed the presence of starch grains which were only deformed by not destroyed. An examination of the solution by transmitted light by the naked eye showed particles which settled out on the third day, while the solution over the sediment was quite clear, without any opalescence. Microscopic examination of the sediment showed the presence of starch grains deformed to various extents.

TABLE 3

Reproducibility of Starch Viscosity Determinations in 1 N NaOH Solution

Efflux rate of 0.3% starch solution, in seconds, for solutions from the same starch sample							Relative viscosity
1	2	3	4	5	6	Mean	
25.6	25.2	25.4	25.2	25.0	25.6	25.26	2.18
25.6	25.2	25.4	25.4	25.6	25.8	25.60	2.21

TABLE 4

Variation of Viscosity of Starch in 1 N NaOH Solution on Standing

Efflux rate of 0.3% starch solution, in seconds, at 20°						
19/III	20/III	21/III	22/III	23/III	24/III	25/III
30.5	30.0	28.6	27.4	27.1	27.0	25.0
30.3	30.5	28.5	28.0	27.0	26.1	25.4

Approximately the same state of affairs was found with the use of 5 N alkali. The difference was that in 5 N alkali the solution was turbid, the particles were smaller and did not form a homogeneous sediment even after very long standing. The liquid remained inhomogeneous.

Starch dissolved very readily in 1 N caustic soda solution, with the immediate formation of a homogeneous colloidal solution which was extremely stable on standing. Homogeneous solutions were not obtained with the use of alkali solutions below normal in concentration. Determinations of the viscosity of starch solutions in 1 N caustic soda solution gave quite reproducible results, as is seen in Table 3.

Table 3 shows fairly good agreement between the individual readings, and between the average values of the relative viscosity. These results indicate that the starch grain membranes are easily soluble in 1 N alkali solution, yielding homogeneous solutions. Microscopic examination of these solutions did not reveal even destroyed membranes.

The results of experiments on the stability of starch solutions in 1N alkali are shown in Table 4.

The data in Table 4 show that the viscosity of the starch solutions decreases with time, indicating hydrolysis of the starch.

The results of the experiments with alkaline starch solutions can only partially be explained by hydration effects. The strong dependence of the properties of the starch solutions on the alkali concentration must be noted. It is seen that starch grains are resistant to high concentrations (40%) of alkali. The explanation is that in 40% NaOH solution water is in a bound state, forming hydrates with the caustic soda molecules. As a result the starch grains cannot swel prior to disintegrating and forming a homogeneous starch solution. The forces between the molecules of water and caustic soda at 40% concentration are greater than the forces which arise during swelling and disintegration of the starch grains. Therefore homogeneous solutions are not formed.

When the concentration of caustic soda solution is decreased to 5 N, part of its water remains free, but its volume is insufficient for normal hydration of the starch grains. There is only enough water to swell the grains and to hydrat the starchy material (the inner contents of the starch grains, soluble in 30% sodium salicylate solution); many of the starch grains disintegrate in the process.

In 1 N NaOH solution sufficient free water is available for complete hydration of the starch. The result is a stabl homogeneous colloidal solution. It is known that hydration of the polar groups of high polymers stabilizes colloidal solutions.

Caustic soda solutions weaker than 1 N have a weaker effect than boiling water on the starch grains; they contain sufficient free water, but the room temperature and the low alkali concentration are inadequate for complete destruction of the starch grains and normal hydration of the starch. Most of the starch grains are destroyed, the starchy substance is dissolved, while the grain coatings only swell, and in some cases form a loose sediment of gelatinous appea ance, or fill nearly the whole volume of the liquid.

The optimum alkali concentration (1 N solution) is determined by the presence of sufficient water for hydration of the molecules or micelles in the starch grain. As regards the role of the alkali at the optimum concentration this can hardly be satisfactorily explained at present. It is assumed that hydrogen bonds are of great importance in starch. It is then necessary to assume that the hydrogen bond energy is greater in the starchy material than in the coatings, which is unlikely. It is possible that the action of caustic soda consists of the saponification of some yet unknown bonds, less stable than the 1,4 and 1,5 bonds. The formation of the starch grain membrane and of waxy forms of starch is due to these unknown bonds; the action of boiling water alone is not sufficient for their disruption, and mechanical action or the presence of the required concentration of caustic soda is necessary. In the presence of the necessary volume of water and of alkali, these bonds (which form the coating) are saponified at room temperature, to yield homogeneous solutions.

The reaction involved in the disintegration of starch grains in water (during starch paste formation) proceeds with absorption of heat. It seems likely that more heat will be absorbed during the disintegration of starch grains in alkali solutions than during paste formation in water [8]. The problems which arise can only be solved by further investigations of the coatings, the properties of which are obviously inadequately known.

After the conditions for the preparation of starch solutions in aqueous and alkaline media had been determined and some of their properties studied in different solvents, it was of interest to compare the viscosities of starch pastes based on potato starch samples of different origin *. Table 5 shows the results of viscosity determinations carried out on aqueous and alkaline starch solutions.

TABLE 5

Viscosity of Various Starch Samples in Aqueous and Alkaline Solutions

Potato type	Viscosity of aqueous solution		Viscosity in 1 N NaOH solution	
	relative viscosity	efflux time, sec.	relative viscosity	efflux time, sec.
Berlichingen	3.22	32.2	2.63	30.5
Cobbler	3.26	32.6	2.95	34.3
Solanum Kesselbrenneri	3.21	32.1	2.95	34.4
S. Andigenum	3.86	38.6	2.81	32.6
S. Pureha	3.13	31.3	2.84	32.8
S. Molinae	3.01	30.1	2.88	33.4
S. Leptostigma	2.74	27.4	2.34	27.1
S. Schreiteri	3.29	32.9	2.54	29.5
S. Demissum	3.21	32.1	2.58	30.0
S. Gibberulosum	3.23	32.3	2.65	30.6
S. Antipoviczii	2.73	27.3	1.56	29.7

Table 5 shows that the relative viscosity of starch is lower in alkaline than in aqueous solution. This shows that the starch grains are disintegrated to a greater extent in alkaline solution. This disintegration must be mainly attributed to the coatings, as the starchy material of different starch samples shows much smaller differences [6]. These results also show that Potter and Hassid's view [9] that alkaline solutions do not affect the viscosity of starch is subject to doubt. Probably the differences between the viscosities of pastes prepared in aqueous and alkaline solutions will vary according to the properties of the coatings, type of starch, and the conditions of paste preparation.

The highest viscosity in aqueous solution was found for starch from S. Andigenum, and the lowest, for starch from S. Leptostigma from wild potato tubers. Veselovsky [1] also found that starch from wild Andigenum potatoes had the highest viscosity.

SUMMARY

1. Although starch grains are disintegrated during boiling in water, the coatings are not sufficiently hydrated in such conditions and the solutions obtained are not homogeneous.

2. A method is described for the preparation of aqueous and alkaline starch solutions, which yields fairly homogeneous solutions giving quite reproducible results in viscosity determinations.

---

* We are greatly indebted to Prof. S. M. Bukasov for selecting and supplying the potato specimens from which the starch samples were prepared.

3. The most homogeneous solutions are obtained by the use of normal caustic soda at room temperature; lower and higher alkali concentrations do not yield homogeneous solutions.

4. Alkaline solutions of starch have lower viscosity than aqueous solutions, because of the greater dispersion of the starch grain coatings.

5. Solutions of starch from potatoes of different origins differ widely in viscosity.

LITERATURE CITED

[1] Kavtsits, cited through S. M. Prokoshev, Biochemistry of the Potato, Acad. Sci. USSR Press (1947); L. A. Veselovsky, Proc. Lenin Acad. Agric. Sci., No. 5-6 (1939).

[2] M. I. Knyaginichev, Yu. R. Bolkhovitina, and T. A. Maksakova, Biochemistry, No. 10, 116 (1954).

[3] M. I. Knyaginichev, Biochemistry, 10, No. 5-6 (1945); M. I. Knyaginichev, Proc. Acad. Sci. USSR, 23, No. 1 (1939); Colloid J., 5, No. 10 (1939).

[4] M. I. Knyaginichev and T. M. Gorelkina, Proc. Acad. Sci. USSR, 19, No. 1-2 (1938).

[5] A. V. Dumansky, Colloid Science (1948); Colloids in the Food Industry, No. 2 (1949).

[6] A. A. Tager, Solutions of High Molecular Compounds, Chem. Press (1951).

[7] A, V. Dumansky, Colloid J., 12, No. 5 (1950); 13, No. 1 (1951).

[8] V. I. Nazarov, J. Appl. Chem., 12, 1745 (1939); Trans. All-Union Conf. Colloid Chem., Kiev (1952).

[9] A. L. Potter, W. Z. Hassid, J. Am. Chem. Soc., 70, 3774 (1948).

Received October 10, 1954

The Technological Institute for the
Food Industry, Leningrad

INVESTIGATION OF THE STRUCTURE OF SYNTHETIC POLYAMIDE FIBERS

6. INTEGRAL HEAT OF SOLUTION OF CAPRON FIBER IN FORMIC ACID*

N. V. Mikhailov and E. Z. Fainberg

As was stated earlier [1, 2, 3], in studies of the structural characteristics of polymers it is necessary to use thermodynamic investigation methods, by means of which the structural changes which occur in polymers may be characterized in thermodynamic terms. With this aim in view we have carried out thermodynamic investigations of oriented and isotropic polycaprolactam fibers (capron).

The results of measurements of the sorption of water and the integral and differential heats of wetting of these types of capron fibers by water were reported previously [1, 2, 3]. In these papers the effect of the structure of capron fiber on the sorption of water and the integral and differential heats of wetting was shown. In subsequent studies by one of the authors [4] infrared absorption spectra of capron fibers were investigated, and different types of intermolecular hydrogen bonds, which determine the structure of synthetic polyamide fibers, were found in polycaprolactam for the first time. These results are in qualitative agreement with at least two of the previously found constant values for the differential heats of sorption of water—by isotropic and oriented capron fibers. However, such energy characteristics as the values of the integral and differential heats of solution were lacking for a complete elucidation of the relationship between the spectral data and the structural features of capron fibers.

This paper contains the results of a study of the integral heats of solution of isotropic and oriented fibers in formic acid. As is known, all spontaneous solution processes take place with change of the isobaric thermodynamic potential. The relationship

$$\Delta Z = \Delta H - T\Delta S, \tag{1}$$

where ΔZ is the change of thermodynamic potential, ΔH is the change of enthalpy, $T\Delta S$ is the entropy term, shows that ΔZ depends both on the change of enthalpy and on the change of entropy. The value of the integral heat of solution, which in this instance represents the enthalpy change in an isobaric process, reflects changes in the intermoleuclar action which occur as the result of any structural change in the polymer.

As is known, the integral heat of solution is the algebraic sum of three quantities:

$$\Sigma E = E_{1,1} + E_{2,2} + E_{1,2}, \tag{2}$$

where $E_{1,1}$ is the energy of interaction of the solvent molecules; $E_{2,2}$ is the intermolecular bond energy of the polymer in the solid state; $E_{1,2}$ is the energy of interaction of the polymer with the solvent. By a comparison of the heats of solution of substances of the same chemical composition and chemical structure in the same solvent, it is possible to reduce the whole difference in the thermal effect to the difference in the structural component $E_{2,2}$ in Equation (2).

---

* Z. N. Zaspinok participated in the experimental work.

The literature contains a small number of papers on measurements of the integral heats of solution of fiber-forming polymers. Most of these deal with cellulose and its derivatives [5]. There are almost no data on the heats of solution and dilution of synthetic polyamide fibers. The only work known is that of Lipatov [5], on the integral heat of solution of polycaprolactam resin in tricresol at 70-90°.

EXPERIMENTAL

The method for determination of the integral heats of solution is similar in principle to the measurement of the integral heat of wetting. Therefore there is no need to describe in detail the technique for carrying out the calorimetric determinations, described in the previous papers [2]. The main modification related to the calorimetric ampoule, which was made of platinum (see figure) and which made it possible for the calorimetric liquid to be stirred mechanically during the main period of the experiment.

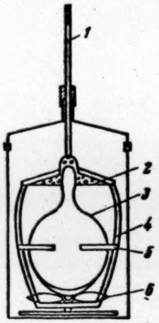

Fig. Platinum calorimetric ampoule: 1) rod, 2) perforated hood, 3) ampoule, 4) stirrer arm, 5) ampoule fixing bracket, 6) stirrer blades.

However, in view of the evolution of considerable amounts of heat during stirring, which is inadmissible with such low experimental heat effects, it was necessary to dispense with mechanical stirring. The solution process was accelerated by means of light stirring by hand. It was shown in special experiments that no appreciable frictional heat was given out during such stirring.

A significant difference from the measurement of the heat of wetting by water is in the length of the main period; instead of the 10-15 minutes in wetting, in measurements of the heat of solution this period lasts 1.5-3 hours. With such a prolonged main period, reproducible results can only be obtained with particularly careful maintenance of adiabatic experimental conditions.

The heat capacity of the calorimeter was determined by heating the calorimetric liquid by an electric current. The energy of the current passed through the calorimeter was measured by a compensation method with the use of a Rapps compensator and a mirror galvanometer. The electrical energy was measured with an accuracy of ± 0.02%.

In contrast to the calorimeter used for measurement of the heat of wetting in a platinum calorimeter, the temperature difference between the calorimeter and the jacket was measured by means of six differential thermocouples; with the aid of a mirror galvanometer it was possible to measure temperature differences to an accuracy of 0.00015°. The heat capacity of the calorimetric vessel was 5.24 cal./degree ± 0.05%.

A necessary condition for carrying out the experiment adiabatically is that the calorimeter should be completely air-tight to prevent evaporation of the formic acid, and this presents considerable operational difficulties. Even slight evaporation of the formic acid may distort the experimental results considerably. For example, evaporation of 0.001 g of formic acid corresponds to approximately 0.12 calorie, which, with a heat capacity of 25 calories for the calorimetric system, corresponds to a temperature rise of 0.005°. With a total rise of 0.1°, the error due to evaporation will be 5%. Various types of cementing materials were tried for sealing the calorimeter. A mixture of natural wax and rosin in a 1:1 ratio, and a specially prepared "plastilin" with very low vapor pressure proved the most suitable. To check the air-tightness, the calorimetric ampoule was weighed on an analytical balance before and after the experiment.

The solvent. Formic acid was used in all the experiments on the integral heat of solution. The original chemically pure 85% formic acid was dehydrated by means of an excess of chemically pure calcined copper sulfate, and then distilled under vacuum under a pressure of 20-25 mm Hg. The concentration of the formic acid obtained in this way was determined volumetrically and refractometrically; both methods gave the same result, 95.01%. Sufficient formic acid was always prepared beforehand for all the experiments, so that acid of the same purity and concentration was always used. The specific heat of the formic acid, determined experimentally, was 0.550 cal./g degree.

The material studied consisted of specimens of oriented and nonoriented capron fibers *. These fibers were obtained from the same resin under the same conditions and differed only in that one of them was preliminarily subjected to 350% cold extraction.

The values obtained for the integral heat of solution of nonoriented and oriented capron fibers are shown in Table 1.

TABLE 1

Integral Heat of Solution of Nonoriented and Oriented Capron Fibers in Formic Acid

Dry weight of sample, g	Heat capacity of system, cal.	Final solution concentration, %	ΔT	Heat of solution in cal./g dry weight
		Nonoriented fiber		
0.310	22.0	1.06	0.187	12.9
0.281	21.5	0.99	0.164	12.3
0.374	21.3	1.36	0.234	13.0
0.353	21.4	1.25	0.212	12.6
0.262	21.6	0.95	0.158	12.6
0.581	22.5	2.03	0.330	12.5
			Mean	12.6 ± 0.2
		Oriented fiber		
0.261	21.1	0.96	0.144	11.2
0.482	21.5	1.76	0.276	11.8
0.332	21.9	1.12	0.178	11.5
0.350	21.7	1.25	0.186	11.2
0.342	21.5	1.23	0.194	11.7
			Mean	11.5 ± 0.2

In studies of integral heat effects, the dependence of the heat effect on the concentration of the solution formed should be taken into account. This is particularly important in the present study, as we are not so much concerned with the absolute values of the heat of solution as with small differences in the value of the integral heat of solution of specimens of different physical structure.

For investigation of the dependence of the integral heat of solution on the concentration, the glass ampoule was filled with an accurately measured quantity of 15% solution; thus, the weight of dissolved substance was known in all the experiments. The ampoule was sealed and placed in a platinum calorimeter which contained the solvent – formic acid. At the correct moment the ampoule was broken and the heat of dilution was determined. By the use of different amounts of solution in the ampoules, it was possible to vary the final solution concentration, which ranged between 0.5 and 2.5% in the experiments.

The results of the measurements of the heat of dilution are shown in Table 2.

Table 2 shows that the values of the heat of dilution are the same in the concentration ranges from 15 to 0.5% and from 15 to 2.5% within the limits of experimental error. This means that in the concentration range from 0.5 to 2.5% the correction for the dependence of the integral heat of dilution on the concentration is zero.

The results obtained show that the heats of solution of isotropic and oriented capron fibers differ by a very small amount, ~ 1.0 cal./g, which is 8% of the total thermal effect. Such a slight enthalpy difference between the oriented and isotropic fibers shows that there are no important differences between the molecular structures of these fibers, and it is not indicative of any phase transitions in the system.

* So that the effect of "age" of the fiber on the value of the integral heat of solution would be eliminated, all the specimens were of "limiting age" [2].

Consequently, the phase transition which occurs during the cold drawing of capron fiber, with recrystallization and reorientation of the crystalline regions, described by Kargin and Sogolova [6], does not lead to the formation of a new crystalline structure in the fiber, and in this sense the main result of our investigation confirms the conclusions in that paper.

TABLE 2

Heat of Dilution of 15% Polycaprolactam Solution in Formic Acid.

Final solution concentration in %	Heat of dilution in cal./g dissolves substance	Final solution concentration in %	Heat of dilution in cal./g dissolves substance
2.46	1.21	1.94	1.27
2.38	1.30	1.96	1.49
2.04	1.22	0.42	1.43

However, since the observed difference in the heats of solution is beyond the limits of experimental error and is invariably reproducible in sign (the heat effect is less for oriented fibers), an explanation is needed. In our view, there can be two explanations for this fact. The first is a simple assumption of possible "healing" of defects in the crystal structure during drawing of capron fiber, along the third branch of the deformation curve for crystalline polymers, as established by Kargin and Sogolova [6]. The cause of such "healing", that is, of a decrease in the defectiveness of the crystal structure without change of lattice parameters, may be a reorientation of the crystalline regions in the polymer.

Another explanation may be based on Lipatov's views [5] on possible differences in crystal packing densities in polymers; the density may either decrease or increase at high orienting stretches, which would lead to a change in the enthalpy of the system. The results of additional experiments should show which of these two explanations is correct.

It should also be pointed out that the differences found between the heats of solution of isotropic and oriented fibers are not characteristic of any essential changes in the magnitude or nature of the intermolecular forces during cold drawing of capron fibers. However, the integral heat of solution cannot be used as a measure of changes in the ratios between the different types of intermolecular forces, established by one of the authors [4]. For this, determination of the differential heats of solution is needed.

The present communication also contains data on the heats of dilution of capron fibers in formic acid. The dilution process is in principle analogous to the solution process, and consists of separation of the polymer molecules from each other, and also of their solvation. In absence of solvation or, more correctly, at low values of solvation, the heat of dilution should be negative. The heat of dilution of cellulose derivatives, determined by a number of authors, is near zero. In our instance the heat of dilution has a finite positive value, which indicates that the solvation effect exceeds the energy required for chain separation. This may be attributed to the flexibility of the caprolactam molecules, because of which less energy is required for chain separation than in the case of rigid molecules, and also to the high polarity of the polymer, which results in a considerable solvational effect.

SUMMARY

1. The integral heat of solution of nonoriented capron fiber is approximately 1 cal./g less than the integral heat of solution of the oriented fiber.

2. The heat of dilution of 15% polycaprolactam solution in formic acid has the same positive value between 1.2 and 1.4 calories in dilution to final concentration from 0.5% to 2.5%.

3. A possible explanation is put forward for the observed change in the enthalpy of capron fibers during cold drawing, based on a decrease in the defectiveness of the crystal structure.

We express our deep gratitude to S. M. Skuratov for advice and valuable help in the course of the work.

LITERATURE CITED

[1]. N. V. Mikhailov, E. Z. Fainberg, and S. M. Skuratov, Colloid J., 15, 271 (1953) (T.p. 279) *.

[2] S. M. Skuratov, N. V. Mikhailov, and E. Z. Fainberg, Colloid J., 16, 58 (1954) (T.p. 65)*

---

* T.P. = C.B. Translation pagination

[3] N. V. Mikhailov and E. Z. Fainberg, Colloid J., 16, 120 (1954) (T.p. 129)*.

[4] D. N. Shigorin, N. V. Mikhailov and S. P. Makaryeva, Proc. Acad. Sci. USSR, 94, No. 4, 717 (1954).

[5] V. A. Kargin and S. A. Papkov, J. Phys. Chem., 7, 483 (1936); A. A. Tager and V. A. Kargin, J. Phys. Chem., 15, 1036 (1941); S. M. Lipatov, Proc. Acad. Sci. USSR, 48, 434 (1945); S. M. Lipatov and S. I. Meerson, Colloid J., 8, 143 (1946); Yu. S. Lipatov, Candidate Dissertation (1954).

[6] V. A. Kargin and T. I. Sogolova, J. Phys. Chem., No. 7, (1953).

Received December 17, 1954

The All-Union Scientific Research Institute
for Artificial Fibers, Moscow

---

* T.p. = C. B. Translation pagination

THERMODYNAMIC INVESTIGATIONS OF COTTON FIBER DYEING

P. V. Moryganov and B. N. Melnikov

Numerous investigations, embracing almost every aspect of this complex physicochemical process, have been devoted to the dyeing of cellulose fibers by direct dyes. In consequence, the conditions in which a dye will dye cellulose fibers are now fairly fully defined. These conditions include the dye and electrolyte concentrations in the dye bath, the dyeing temperature, and the bath ratio. The effects of each of these factors individually on the dyeing process have been studied in considerable detail by a number of authors, including Neale [1], Viktorov [2], Peskov [3], Peskov and Moryganov [4], Sadov [5], and others.

It must be pointed out, however, that theory of the dyeing of cellulose fibers by direct dyes has not been developed to the full. For instance, there is an almost complete lack of data by means of which all the parameters of the dyeing process could be calculated for a given amount of dye on the fiber; and, conversely, the amount of dye on the fiber calculated from given dyeing conditions; in other words, data by means of which the economics of the dyeing process could be calculated without recourse to experiments. These problems can be solved most simply and clearly only by the application of chemical thermodynamics to the dyeing process. The great importance of thermodynamics in application to the dyeing process is seen from the clear and definite way in which it solves one of the fundamental problems of dyeing – the affinity of dye for the fiber.

The term "affinity" was formerly used in a distorted and incorrect sense, and its value was measured by various empirical methods, such as dye bath exhaustion or absorption of dye by the fiber under arbitrarily chosen conditions. Clearly, these methods of affinity determination could lead to error by which slowly diffusing dyes would be assigned lower affinities than dyes with greater diffusion coefficients. The thermodynamical definition of diffusion as the difference between the chemical potentials of the dye in the fiber and in solution in a standard state avoids such inaccuracies and makes it possible to define affinity as the motive force of the dyeing process, on the basis of which it is possible to determine both the economics of the dyeing process and the amounts of electrolyte to be added to the dye bath for a required depth of dyeing.

Despite the importance of the determination of the thermodynamical characteristics of the dyeing process, very little attention is devoted to this problem in the literature. Only a few papers have been published on the subject; these include the work of Willis, Warwicker, Standing, and Urquhart [6], Marshall and Peters [7], and Neale and his co-workers [8].

The purpose of these investigations was to establish a relationship between the basic parameters of the dyeing process and ultimately to solve the question of the possibility of theoretical calculation of the dyeing process. The results obtained by these authors require considerable experimental verification and modification, and, in addition, the value of the results is lowered by the arbitrary choice of dyes without consideration of their structure. It is therefore impossible to determine the influence of various functional groups in a dye on the affinity and therefore to establish any relationship between the affinity of a dye and its structure. The aim of the present work was to determine the thermodynamical characteristics of a number of dyes of different structure, so making it possible to correlate dye structure with affinity, and also to extend and to modify the available experimental data.

In the modern view, direct dyes dissociate almost completely into ions under dyeing conditions, forming true solutions. Only the dye anions can be selectively adsorbed by the fiber, while the sodium cations penetrate into the fiber in order to bring about electrical neutrality.

If we denote the activity of the dye in the fiber and solution by A_f and A_s respectively, we can write that the change ΔZ° of the standard thermodynamic potential during dyeing will be:

$$-\Delta Z^{\circ} = RT \ln K = RT \ln \frac{A_f}{A_s}, \qquad (1)$$

where K is the equilibrium constant for the action between the dye and the fiber; R is the gas constant; T is the absolute temperature.

The activity of the dye in solution can be represented by the product of the ionic concentrations in the solution multiplied by the activity coefficients of the ions, or, if the activity coefficients are neglected as a first approximation, we have

$$A_s = [\mathrm{Na}_s^+]^z \, [R_s^-], \qquad (2)$$

where $[\mathrm{Na}_s^+]$ and $[R_s^-]$ are the sodium and dye ion concentrations in the solution in gram-ions per liter at equilibrium; ; z is the valency of the dye anion.

The activity of the dye in the fiber is a much more complex matter. The amount of dye absorbed by the fiber is usually expressed in mole/kg of the dry fiber, and therefore it would not be quite correct to use this expression for calculation of the dye activity in the fiber.

The reason is that the volume of solid phase accessible to the dye is much less than the total fiber volume. Nevertheless, if we assume that the volume accessible to dye migration is v liters per kg of the dry fiber, and, as a first approximation, that the properties of the dye solution in this volume are similar to those in the dye bath, the activity of the dye in the fiber may be expressed as the product of the dye and sodium ion concentrations relative to the above-mentioned effective volume of the cellulose phase, and then:

$$A_f = \left[\frac{\mathrm{Na}_f^+}{v}\right]^z \cdot \left[\frac{R_f^-}{v}\right] = \frac{[\mathrm{Na}_f^+]^z \cdot [R_f^-]}{v^{z+1}}, \qquad (3)$$

where $[\mathrm{Na}_f^+]$ and $[R_f^-]$ are the concentrations of sodium and dye ions in the fiber in gram-ions per kg of the dry fiber at equilibrium, and v is the effective volume of the cellulose phase.

If the amount of dye absorbed by the fiber and the equilibrium dye concentration in the bath are determined experimentally, then the unknowns in the above equations are the sodium ion concentration in the fiber, $[\mathrm{Na}_f^+]$ and the effective volume of the cellulose phase v. The first of these may be found with the aid of the Donnan equilibrium condition between the dye and the inorganic anions in the fiber and the external solution.

$$\frac{[\mathrm{Na}_f^+] \cdot [\mathrm{Cl}_f^-]}{v^2} = [\mathrm{Na}_s^+] \cdot [\mathrm{Cl}_s^-]. \qquad (4)$$

The condition of electroneutrality of the ions in the fibers gives that

$$[\mathrm{Cl}_f^-] + z\,[R_f^-] = [\mathrm{Na}_f^+]. \qquad (5)$$

By solving Equations (4) and (5) we can calculate the sodium ion concentration in the fiber

$$[\mathrm{Na}_f^+] = \frac{1}{2} \{ z\,[R_f^-] + (z^2\,[R_f^-]^2 + 4v^2\,[\mathrm{Na}_s^+] \cdot [\mathrm{Cl}_s^-]^{1/2} \}. \qquad (6)$$

The second of the unknowns, v, is rather difficult and laborious to determine experimentally, and data available in the literature were therefore used; according to Marshall and Peters, the value of v for cotton fiber is 0.3 liter/kg. It is seen that for determination of the affinity of a dye for the fiber it is sufficient to determine experimentally the equilibrium concentrations of the dye in the fiber and in the solution and to calculate the sodium ion concentration in the fiber.

It should be pointed out that the above formulas for calculating the affinity of a dye for the fiber are only valid for systems in a state of true equilibrium Therefore particular attention was paid to this point in the present investigation, especially as due attention has not previously been paid to this aspect in thermodynamical treatment of the dyeing process, and the equilibrium constants were determined in only one investigation, and only by a direct method.

The best method for demonstration of true equilibrium is an approach to this state from both sides. For this reason, in addition to the equilibrium sorption of direct dyes by cotton fibers, the equilibrium desorption from the fibers was also studied. The affinity was calculated with the aid of the same formulas which were used for equilibrium sorption.

An equally important thermodynamical characteristic of the dyeing process is the standard heat of reaction, which is taken to mean the heat of absorption of 1 mole of the dye bythe undyed fiber from an infinitely dilute solution. The significance of the characteristic of the dyeing process is that, if the affinity of the dye for the fiber is determined at any one temperature, it can be calculated for any other temperature with the use of the heat of reaction. In addition, the value of the heat of reaction between a dye and the fiber provides some measure of information on the mechanism by which the dye is attached to the fiber, and consequently, on the stability of the compound formed by the dye and the fiber.

The heat of reaction between the dye and the fiber may be found with the aid of the equation for the equilibrium constant as a function of the temperature:

$$\frac{d\ln K}{dT} = -\frac{\Delta H^0}{RT^2}. \tag{7}$$

For a narrow range of temperatures we may assume, without undue error, that ΔH^0 = const.

Integration of Equation (7) gives:

$$\ln\frac{K_2}{K_1} = \frac{\Delta H^0}{R}\left(\frac{1}{T_1} - \frac{1}{T_2}\right),$$

By substitution of the value of K from Equation (1), we have

$$\Delta H^0 = \frac{\Delta Z_1^0/T_1 - \Delta Z_2^0/T_2}{1/T_1 - 1/T_2}. \tag{8}$$

With this equation, with a knowledge of the affinity ΔZ_1^0 and ΔZ_2^0 at the temperatures T_1 and T_2, we can determine the heat of reaction between the dye and the fiber.

Although it is possible to determine the heat of dyeing by this method, a knowledge of the affinity and the dyeing mechanism is quite unnecessary for this purpose. The main difficulty in the determination of standard affinity, as has already been stated, is in finding a suitable expression for the activity or effective concentration of the dye in the fiber through values of the measurable dye concentration.

If the activity of the dye in the fiber is represented as an unknown function of the dye concentration (as a first approximation, independent of the temperature), written as $A_f = f[R_f^-]$, while the activity of the dye in solution, with the activity coefficient neglected, is written as $A_s=[R_s^-]$, then Equation (1) takes the form:

$$-\Delta Z^0 = RT\ln\frac{f[R_f^-]}{[R_s^-]}.$$

From a knowledge of the affinity at two temperatures T_1 and T_2 we have:

$$\Delta H^0 = \frac{R\ln(f[R_f^-]_1/f[R_f^-]_2\cdot[R_s^-]_2/[R_s^-]_1}{(T_2 - T_1)/T_1T_2}.$$

If the dyeing conditions are so chosen that the concentrations of the dye in the fiber at T_1 and T_2 are equal, then

$$f[R_f^-]_1 = f[R_f^-]_2$$

and

$$\Delta H^0 = \frac{R \ln [R_s^-]_2 / [R_s^-]_1}{(T_2 - T_1)/T_1 T_2}. \tag{9}$$

It is thus possible to calculate the heat of dyeing from known values for the dye concentration in the solution in equilibrium with one and the same quantity of dye in the fiber at two different temperatures. We carried out such calculations on the basis of the appropriate experimental data. When the affinity of the dye for the fiber ΔZ^0 and the heat of reaction ΔH^0 have been determined, it is possible to calculate the change of the entropy of dyeing ΔS^0 with the use of the relationship:

$$\Delta Z^0 = \Delta H^0 - T\Delta S^0. \tag{10}$$

The entropy of dyeing is taken to mean the entropy change in the transfer of 1 mole of the dye from an aqueous solution with a concentration of 1 mole per liter at $\gamma = 1$, to the fiber with dye concentration of 1 mole per liter of effective fiber volume, at $\gamma = 1$(γ is the activity coefficient).

The entropy of dyeing ΔS^0 is made up of the following entropy changes: of the dye particles, the solvent, and the fiber.

The dye particle become oriented and less mobile in relation to the cellulose macromolecules during the dyeing process, and this leads to a decrease of the entropy of dyeing. The entropy of the cellulose macromolecules changes in the same direction. On the other hand, the simultaneous dehydration of the dye and cellulose particles and the disorientation of the solvent molecules associated with this leads to an increase of the entropy of dyeing. Consequently, the aggregate change of the entropy of dyeing will be determined by the predominant influence of the one or the other factor.

Thus, the value of the change of entropy of dyeing acquires a special significance in comparisons of the behavior of different dyes on the same fiber, and in evaluation of different fibers with respect to the same dye.

EXPERIMENTAL

The experiments on equilibrium dyeing of cellulose fibers were carried out at temperatures from 25 to 100° with the following dyes: Direct Sky Blue K, Direct Violet, Direct Diazo Black O, and chrysophenine. The initial dye bath concentration was varied from 0.1 to 0.5 g/liter. The concentration of the NaCl used as the electrolyte was varied from 0.01 to 0.04 N.

As the electrolyte-sensitive dyes chrysophenine and Direct Diazo Black O were precipitated at 25°, the dyeing experiments with these dyes at that temperature were carried out with decreased concentration both of the dye and of common salt, namely: the dye concentration was varied in the range 0.05-0.15 g/liter, and the salt concentration, 0.005 – 0.015N.

Since the usual commercial direct dyes contain considerable amounts of impurities, both of organic and of mineral origin, the dyes were purified before the experiments by recrystallization from aqueous solution.

The purification was continued until the dyes were entirely free from mineral salts (chlorides and sulfates). The degree of purification was tested by means of silver nitrate and barium chloride. The purity of the dye was determined quantitatively by combustion of a sample of the dye in H_2SO_4. The sodium present in the dye is then converted into Na_2SO_4 In addition, the purity of the dyes was checked by their azo group content, by means of titration with titanium sulfate. One of the dyes, chrysophenine, was also determined by an optical method, as the spectrophotometric curve for a concentration of 0.005 g per liter of the pure dye is known [6].

In the case of Direct Sky Blue K the total nitrogen content was determined by Kjeldahl's method modified for dyestuff analysis. The results are shown in Table 1.

TABLE 1

Analysis of Purified Dyes

Name of Dye	Content of pure dye, in %					Moisture content, %
	by sodium sulfate	by titanium sulfate	by nitrogen content	by optical density	mean	
Direct Sky Blue K	82.1	83.0	81.7	–	82.6	15.3
Chrysophenine	88.3	88.0	87.5	88.1	88.0	9.8
Direct Violet	78.0	82.0	–	–	80.0	14.2
Direct Diazo Black O	84.3	80.1	–	–	82.2	11.2

Equilibrium dyeing procedure. Bleached cotton fabric samples with previously determined moisture content (6.8%) were dyed at a bath ratio of 100 in stoppered flasks in a thermostat at 25, 60, 70, 80, and 90° until equilibrium dye absorption was reached, which was determined by separate experiments. At 100° the dyeing was carried out under reflux. The equilibrium concentration of dye on the fiber and in solution was determined colorimetrically with the aid of the FM universal photometer, both by colorimetry of the residual bath, and of aqueous pyridine solutions after stripping of the dye from the dyed farbic samples. The time required for equilibrium to be established in equilibrium sorption conditions was determined by separate experiments.

For this, the dyeing time was varied in the range from 15 minutes to 35 hours. The dyeing of cotton fiber at 25° was continued for 1750 hours with chrysophenine and Diazo Black O, and 2660 hours for Direct Sky Blue K and Direct Violet.

Fig. 1 shows the kinetics of absorption of Direct Sky Blue K. Analogous graphs were also plotted for the other dyes. The equilibrium dyeing times established from these data are shown in Table 2.

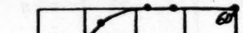

Fig. 1. Absorption of Direct Sky Blue K by cotton fiber with time. Initial dye concentration in bath 0.1 g/liter; NaCl concentration 0.02 N.

The equilibrium desorption of the direct dyes from the dyed fiber was carried out in conditions analogous to those used for equilibrium sorption, for two dyes, Direct Sky Blue K and chrysophenine, at 60 and 80°. The time required for desorption equilibrium to be established was determined from the change in the dye concentration in the desorption liquid. The results of the determinations are shown in Table 3.

The experimental data on equilibrium dyeing and equilibrium desorption were used to calculate the affinity of the dye for the fiber according to the equation

$$\Delta Z^{\circ} / RT = \ln [R_f^-] + z \ln [Na_f^+] - \ln [R_s^-] - z \ln [Na_s^+] - (z + 1) \ln v. \quad (11)$$

The calculated affinities of the four direct dyes studied for cotton fiber in conditions of considerable alteration of the initial dye and electrolyte concentrations are shown in Table 4. Similar results were obtained by calculation of the affinity on the basis of desorption data (these results are not given in this paper).

The average affinity values values shown in Table 4 were used as a basis for calculation of the entropy of dyeing according to Equation (10) and the heat of dyeing according to Equation (8). In addition, the heat of dyeing was determined graphically according to Fig. 2.

TABLE 2

Equilibrium Dyeing Times in Hours

Temperature in C°	Direct Sky Blue K	Direct Violet	Direct Diazo Black O	Chrysophenine
25	2660	2660	1750	1750
60	9	15	17	7
70	6	11	14	5
80	5	7	9	4
90	2	4	7	1.5
100	1	1.5	2	0.75

TABLE 3

Desorption Equilibrium Times

Direct Sky Blue K		Chrysophenine		Direct Sky Blue K		Chrysophenine	
time in hours	optical density	time in hours	optical density	time in hours	optical density	time in hours	optical density
Temperature 60°				Temperature 80°			
$^1/_4$	0.367	–	–	1	0.206	2.30	0.330
1	0.496	1	0.419	$4^1/_4$	0.221	24	0.350
4	0.544	3	0.430	43	0.263	48	0.365
41	0.579	22	0.454	64	0.294	92	0.362
64	0.587	70	0.479	71	0.349	140	0.366
91	0.600	118	0.480	92	0.352	200	0.362
117	0.600	166	0.479	117	0.350	–	–
217	0.600	210	0.480	200	0.350	–	–

Note: The optical density values given allow for decomposition of the dyes during prolonged desorption.

Table 5 shows thermodynamical characteristics for the four direct dyes studied.

For determination of the heats of dyeing without calculation of affinity, experiments were performed on the equilibrium dyeing of cotton fiber by Direct Sky Blue K and chrysophenine from baths with high electrolyte contents. The results of the dye absorption determinations are shown in Figs. 3 and 4.

In these graphs the broken line parallel to the abscissa axis represents equal contents of dye in the fiber at different temperatures. The intersections of this line with the graph lines, projected onto the abscissa axis, represent the dye concentrations in the solution which are in equilibrium with the given content of dye in the fiber. The equilibrium dye concentrations in solution were used to calculated the heat of dyeing according to Equation (9). The results of the calculations are shown in Table 6.

DISCUSSION OF RESULTS

The tables of the Experimental section of this paper show that the affinity of a dye for the fiber, determined at different dye and electrolyte concentrations in the dye bath, is constant within the limits of experimental error. In other words, the experimental results fully confirm the view that the affinity of a dye for the fiber is a purely energetic characteristic of the dyeing process, which depends only on the dyeing temperature and not on such factors as the initial concentration of the dye and electrolyte in the bath. The affinity of a dye for the fiber decreases with

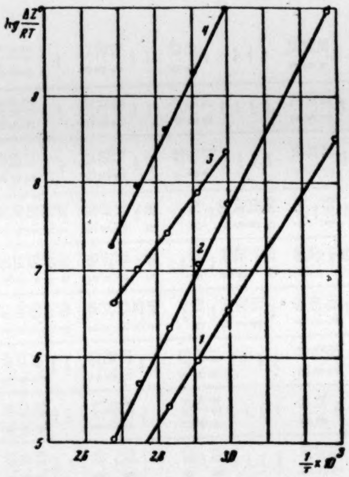

Fig. 2. Variation of the equilibrium constant with temperature: 1) chrysophenine; 2) Direct Sky Blue K; 3) Direct Violet; 4) Direct Diazo Black O.

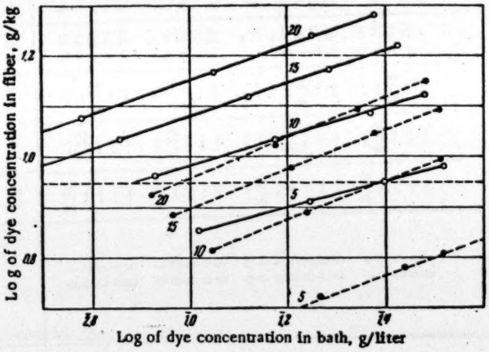

Fig. 3. Adsorption isotherms for Direct Sky Blue K at 60° – continuous lines, and at 80° – dotted lines; 5,10,15,20 - NaCl concentrations in g/liter.

rise of temperature, which was to be expected on molecular kinetic considerations.

Fig. 2 shows that the dependence of the equilibrium constant for both the sorption and the desorption process on the temperature is exactly represented by a straight line over the whole range of temperature changes studied. This type of variation of the equilibrium constants with temperature indicates, firstly, that the assumptions made in the theoretical part of this paper were fully justified, and secondly, that a state of true equilibrium was reached in the experiments.

TABLE 4

Affinities (ΔZ^0) of Dyes for Cotton Fiber in kcal/ mole Based on Experimental Data on Equilibrium Dyeing

Dye	Dye concentration, g/liter	NaCl concentration, g/ liter														
		at 100°			at 90°			at 80°			at 70°			at 60°		
		0.02	0.03	0.04	0.02	0.03	0.04	0.02	0.03	0.04	0.02	0.03	0.04	0.02	0.03	0.04
Direct Sky Blue K	0.1	3.72	—	—	4.39	4.15	4.05	4.43	4.44	4.47	4.84	4.60	4.96	5.25	5.11	5.12
	0.2	—	3.75	—	4.23	4.10	4.05	4.51	4.46	4.43	4.96	4.97	4.78	5.26	5.17	5.11
	0.3	—	—	3.72	4.00	4.20	—	4.55	4.62	4.44	5.05	4.85	4.86	5.15	5.17	5.17
	0.4	—	—	—	4.05	4.00	4.18	—	—	—	4.60	4.87	4.72	—	—	—
	0.5	—	—	—	4.10	4.13	—	—	—	—	4.88	4.80	4.80	—	—	—
Direct Violet	0.1	4.84	—	—	5.30	5.10	4.90	5.23	5.17	5.27	5.38	5.46	5.24	5.67	5.50	5.42
	0.2	—	4.93	—	5.00	5.20	5.10	—	5.25	5.15	5.27	5.29	5.43	5.52	5.35	5.30
	0.3	—	—	4.95	4.90	5.20	5.00	5.25	5.14	5.25	5.48	5.45	5.45	5.45	5.45	5.45
	0.4	—	—	—	5.00	4.90	4.86	—	—	—	5.25	—	—	—	—	—
	0.5	—	—	—	5.20	5.00	5.00	—	—	—	5.45	5.42	5.36	—	—	—
Direct Diazo Black O	0.05	—	—	—	—	—	—	6.20	6.06	6.02	—	—	—	6.68	6.41	6.47
	0.1	5.33	—	—	5.70	5.80	5.85	—	6.10	6.12	6.10	6.20	6.10	6.64	6.51	6.41
	0.15	—	—	—	—	—	—	6.07	6.04	5.97	—	—	—	6.67	6.54	—
	0.2	—	5.37	—	5.75	5.78	5.90	—	—	—	6.50	6.00	6.00	—	—	—
	0.3	—	—	5.54	5.80	5.70	5.65	—	—	—	6.50	6.30	6.30	—	—	—
	0.4	—	—	—	5.50	5.80	5.70	—	—	—	6.10	—	6.10	—	—	—
	0.5	—	—	—	5.68	5.82	5.70	—	—	—	—	6.10	6.50	—	—	—
Chrysophenine	0.1	3.32	—	—	3.58	—	3.45	3.80	3.81	3.81	4.04	4.00	4.04	4.30	4.34	4.34
	0.2	—	3.20	—	3.54	3.62	—	3.80	3.82	3.75	4.00	3.90	—	4.24	4.26	4.28
	0.3	—	—	3.26	3.45	—	3.68	3.75	—	3.72	4.20	—	4.15	4.22	4.28	4.32
	0.4	—	—	—	3.60	3.51	—	—	—	—	—	4.04	—	—	—	—
	0.5	—	—	—	—	3.48	3.48	—	—	—	—	4.15	3.90	—	—	—

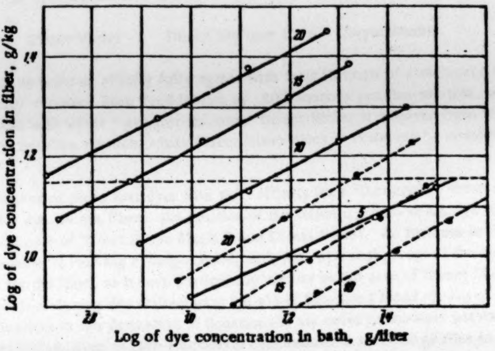

Fig. 4. Adsorption isotherms for chrysophenine at 60° – continuous lines, and at 80° – dotted lines; 5, 10, 15, 20–NaCl concentrations in g/liter.

TABLE 5

Average Thermodynamic Data

Dye	$-\Delta Z^0_{373}$ in kcal./mole	$-\Delta Z^0_{363}$ in kcal./mole	$-\Delta Z^0_{353}$ in kcal./mole		ΔZ^0_{343} in kcal/mole	$-\Delta Z^0_{333}$ in kcal./mole		$-\Delta Z^0_{298}$ in kcal./mole	$-\Delta H^0$ in kcal./mole	$-\Delta S^0$ in kcal./mole
			by sorption	by desorption		by sorption	by desorption			
Direct Diazo Black O	5.40	5.75	6.06	–	6.24	6.56	–	–	16.5	26.80
Direct Violet	4.90	5.05	5.20	–	5.35	5.50	–	–	10.5	14.85
Direct Sky Blue K	3.73	4.10	4.45	4.46	4.80	5.15	5.17	6.25	16.5	34.30
Chrysophenine	3.26	3.52	3.78	3.70	4.04	4.28	4.26	5.22	12.9	24.80

TABLE 6

Heat of Interaction of Direct Dyes with Cotton Fiber from Dyeing Data with High Electrolyte Contents in Dye Bath

Dye	Electrolyte content in bath in g/liter	$-\Delta H^0$ in kcal./mole	Dye	Electrolyte content in bath in g/liter	$-\Delta H^0$ in kcal/mole
Chrysophenine	5	14.40	Direct Sky Blue K	5	13.60
	10	13.75		10	13.50
	15	16.40		15	19.55
	20	16.65		20	15.20
	$-\Delta H^0$ av 15.25			$-\Delta H^0$ av 15.40	

The constancy of the equilibrium constant and of the affinity for a given dye at a definite temperature and with considerable variations in the dye concentration indicates that these values may be calculated with the aid of the formulas given in the theoretical section. At the same time, as the data of Table 5 show, different dyes have different affinities for cotton fiber, and the dyes studied can be placed in the following series in order of affinity:

Direct Diazo Black O > Direct Violet > Direct Sky Blue K > Chrysophenine.

This sequence of the dyes in order of affinity fully agrees with their firmness of attachment to cotton fiber; chrysophenine is easily and completely removed from dyed fabrics by 20% aqueous pyridine solution, while Direct Sky Blue K requires more vigorous treatment with water – pyridine mixture. Direct Violet is removed from the fabric only after repeated treatments with aqueous pyridine solution, while Direct Diazo Black O could not be completely removed from the dyed fabric.

A comparison of the structure of these four dyes with their affinity for a fiber clearly shows the influence of sulfonic groups on the affinity of a dye for the fiber; the position of the sulfonic groups in the dye molecule also has some influence, as can be seen in the case of Direct Diazo Black O and Direct Violet. An increase in the number of groups (OH, NH_2) in the molecule capable of forming hydrogen bonds with the hydroxyl groups of the cellulose macromolecule increase the affinity of a dye for the fiber, as is seen particularly clearly in the case of Direct Diazo Black O and chrysophenine. The fact that the heats of dyeing determined with the aid of Equation (8) and (9) are of the same order of magnitude shows that the simplifications in the derivation of Equation (9) are quite permissible within the limits of experimental error. As was to be expected, even at high electrolyte concentrations up to 20 g/liter in the dye bath the heat of dyeing remains practically constant and, despite the possibility of aggregation of the dye particles in the solution, the mechanism by which the dye interacts with the fiber evidently remains the same. In addition, the fact that the heat effect determined from the affinity ΔZ^0 with consideration of the effective volume of the cellulose phase, on the one hand, and found direct from the equilibrium dye concentrations in the solution on the other, is of the same order of magnitude, shows that the introduction of the value of the effective volume in calculation of the affinity was valid. A calculation of the change of the entropy of dyeing shows that dyeing proceeds with decrease of entropy. This indicates that the governing factor in the change of the entropy of dyeing is orientation of the dye molecules relative to the cellulose macromolecules.

SUMMARY

1. The affinities of four direct dyes for cotton fiber have been determined; the value is a purely energetic characteristic of the dyeing process and does not depend on the concentrations of the dye or electrolyte in the dye bath.

2. The affinity of the dye for the fiber decreases with increase of temperature; the relationship between the equilibrium constants of the sorption and desorption processes and the temperature is represented by an isobaric equation.

3. The affinity of a dye for the fiber is determined by its molecular structure. The influence of sulfonic groups and of groups capable of forming hydrogen bonds on the affinity has been demonstrated.

4. The dyes investigated form the following series in order of their affinity for cotton fiber:

Direct Diazo Black O > Direct Violet > Direct Sky Blue K > Chrysophenine.

5. Thermal effects and entropy changes in the interaction between direct dyes and cotton fiber have been calculated.

In conclusion, it is our duty to express our gratitude to Professor K. B. Yatsimirsky for valuable advice and guidance in the course of the work.

LITERATURE CITED

[1] S. M. Neale, W. A. Stringfellow, Trans. Faraday Soc. 29,1167 (1933); S. M. Neale, A. M. Patel, Trans. Faraday Soc. 30, 905 (1934).

[2] P. P. Viktorov, Bull. Text. Ind., No. 6-7, 73 (1930).

[3] N. P. Peskov, Bull. Text. Ind., No. 5, 25 (1926).

[4] N. P. Peskov, and P. V. Moryganov, Bull. Text. Ind., No. 1, 26 (1929).

[5] F. I. Sadov, Colloid J., 16, No. 1, 51 (1954) (T.p. 57)*.

[6] H. F. Willis, J. O. Warwicker, H. A. Standing and A. [illegible]. Urquhart, Trans. Faraday Soc. 41, 506 (1945).

[7] W. I. Marshall, and R. H. Peters, J. Soc. Dyers Colourists, 63, 446 (1941).

[8] S. M. Neale and E. F. Fishwick, Trans. Faraday Soc. 43, 332 (1947).

Recieved June 7, 1954

Ivanovo Institute of Chemical Technology,
Department of Chemical Technology of Fibrous Materials

---

* T.p. = C. B. Translation pagination

THE COAGULATION RATE OF SILICIC ACID SOL AND THE STRUCTURE OF DRY SILICA GEL

I. E. Neimark, M. A. Piontkovskaya, and I. B. Slinyakova

Numerous studies have been made of the influence of various factors on the gelation rate of silicic acid sol. For example, Okatov [1], Bruns and Kostina and Ferguson and Appelbey [2], who studied the relationship between the coagulation rate and the silicic acid concentration in the sol, found that the time from the commencement of mixing of the reagents to the start of coagulation decreases sharply with increasing silicic acid concentration. The effect of the sol pH on the time from the start of mixing to the start of coagulation has been studied in particularly great detail [1, 3]. It was found that in an acid medium the time before the start of coagulation decreases steadily with rise of pH and becomes a minimum at pH = 7, while at pH > 7 time before the start of coagulation increases again.

The nature of the acid has a considerable effect on the coagulation rate. Oborin, Korneva, and Romanova [3] established that hydrochloric acid coagulates the sol more rapidly than does sulfuric. Turky [3] noted that, of the three acids studied by him, phosphoric acid produces the most rapid coagulation, followed by hydrochloric, and finally, by sulfuric. Oborin [3] established that an increase in the precipitation temperature accelerates coagulation. However, the influence of these factors on the final structure of the silica gel has not been studied sufficiently. According to Okatov [1], an increase of the SiO_2 content in the sol leads to an increase of the adsorptional activity of the silica gel in one case ($t = 10°$), to a decrease in another ($t = 15°$), while in a third case ($t = 25°$) the maximum sorptional volume of the silica gel pores at first increases and then falls with increasing SiO_2 concentration. Such contradictory results are probably the consequence of imperfections in the methods for the determination of adsorptive power, the adsorbents not being completely saturated with the vapor of the adsorbed substance.

The relationship between the sol temperature and the adsorptive power of the silica gel is pointed out only in some patents, where it is stated that increase of temperature results in deterioration of the gel quality, as lumps are formed at high precipitation temperatures. Our own experience shows that lump formation can be avoided by good stirring.

Kharmadaryan and Kopelevich [4] studied the influence of the pH of the medium on the adsorptive power of the silica gel; gels of varying activity were obtained by variations of the reaction of the sol from strongly alkaline to acid. Gels obtained from an alkaline sol had the maximum activity.

According to the literature [5,6], and to our proposed mechanism for structure formation in hydrophilic adsorbents [7, 8, 10], the gel structure is formed during aging and dehydration. The previous history of the hydrogel preparation should have no important influence on the structure of the dry silica gel. Therefore all the factors which influence the coagulation rate of the sol during preparation should have no effect on the final structure of the silica gel. These factors include: the silicic acid concentration in the sol, the residual sol acidity at the time of formation, the nature of the acid used for precipitation, and, finally, the temperature of sol formation. The present paper contains the results of a verification of this view, important in the theory and practice of gel structure formation.

EXPERIMENTAL

Effect of silicic acid concentration •. As already stated, the published data on the adsorption activity of silica gel as a function of the silicic acid concentration in the sol are so contradictory that no definite conclusions can be drawn on the subject. For investigation of this relationship, three series of silica gel samples were prepared from sols with different silicic acid contents; the silicic acid concentration was varied by variation of the ratio of the reacting volumes of sulfuric acid and sodium silicate.

The samples of the first series of silica gels were prepared from sodium silicate and sulfuric acid of specific gravity 1.18. After aging, the hydrogels were washed with distilled water to a negative reaction for SO_4^{2-}, and then dried at 250°.

• R. Yu. Sheinfain participated in this section of the work.

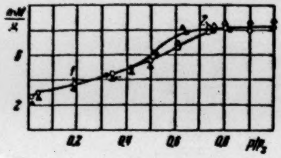

Fig. 1. Isotherm for the sorption of methyl alcohol vapor on silica gels prepared from sols with different silicic acid contents: 1) 7.5 g SiO_2 in 100 ml of sol, 2) 5 g of SiO_2 in 100 ml of sol. The black dots represent desorption.

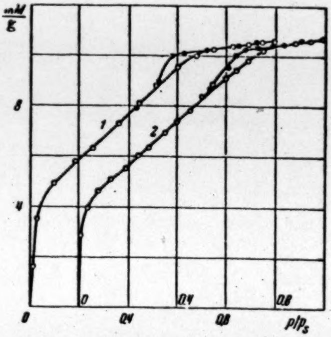

Fig. 3. Sorption isotherms for methyl alcohol vapor on silica gels prepared 1) from $SiCl_4$; 2) from sodium silicate.

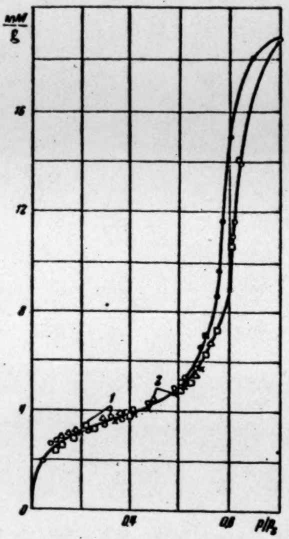

Fig. 2. Sorption isotherms for methyl alcohol vapor on silica gels prepared from sols with different residual acidities: 1) 0.07 N, 2) 0.14 N. The black dots represent desorption

The second series was prepared similarly, but the hydrogels after aging were washed with distilled water at pH 7.84 and dried at 120°. In the third series of experiments, acidified water (pH 2.24) was used for the washing. The residual acidity of the sols was determined by titration of a definite volume of the sol with caustic alkali in presence of phenolphthalein. In addition, the pH of the hydrogel was also determined. The time before the start of coagulation was recorded in all experiments.

Table 1 shows the conditions of the silica gel preparation and the adsorptional and structural characteristics of all the three series of samples, and Fig. 1 shows the sorption isotherm for methyl alcohol on some of these silica gels. Determinations of the apparent specific gravity (δ) of the silica gels showed that its value is not affected either by the time before coagulation, or by the SiO_2 content in the sol; the values found were: at pH 2.2 δ = = 1.42; at pH 6.5 δ = 1.18; at pH 7.8 δ = 0.77.

Table 1 and Fig. 1 show that the adsorptive properties and structure of silica gels are practically independent of the silicic acid concentration in the sol and of the time before coagulation. The sorption isotherms for silica gels prepared from sols with different silica contents practically coincide, which indicates that their porosity is similar in nature.

Therefore the above data show that variation of the silicic acid concentration in the sol greatly varies the coagulation rate, but has no effect on the final structure of the silica gels.

TABLE 1

Preparation Conditions and Adsorptional and Structural Characteristics of Silica Gels Prepared from Sols with Different SiO_2 Contents

Sample series	Solution volumes for sol preparation, in cc			SiO_2 in mg/100 ml of sol	Time to start of coagulation, hours	Wash liquid	pH of hydrogel	Total pore volume in cc/g	Volume of benzene adsorbed in cc/g, in the liquid state at $P/P_s = 1$
	Na_2SiO_3	H_2SO_4	H_2O						
I	200	100	–	10.0	18	Distilled water	6.5	0.39	0.39
	150	75	75	7.5	23.5	"	6.5	0.40	0.40
	100	50	150	5.0	120	"	6.5	0.39	0.42
	100	50	450	2.5	576	"	6.5	0.39	0.45
	100	75	425	2.5	520	"	6.5	0.42	0.45
	150	150	–	7.5	4.5	"	6.5	0.39	0.39
II	150	75	75	7.5	23.5	Ammonia solution	7.84	0.85	0.88
	100	50	150	5.0	120	"	7.84	0.90	0.88
	100	75	425	2.5	576	"	7.84	0.80	0.86
III	150	75	75	7.5	23,5	Acidified water	2.24	0.26	0.28
	100	50	150	5.0	120	"	2.24	0.25	0.29
	100	75	425	2.5	576	"	2.24	0.25	0.26

Effect of residual acidity*. For studies of the effect of residual acidity of silicic acid sols on the final structure of the silica gels, 4 series of samples were prepared: series I had a residual acidity in the range 0.07-0.28 N; series II, III, and IV differed in their precipitation temperatures, which were 1[illegible], 20, and 2[illegible]° respectively. The residual sol acidity was determined by titration of a known volume of the sol with caustic alkali in presence of phenolphthalein, and was expressed in terms of sulfuric acid normality.

Table 2 shows the structural characteristics of these silica gels, and Fig. 2 shows the sorption isotherms of methyl alcohol vapor on some of these samples.

The data in Table 2 and Fig. 2 show that residual acidity of the sol has no noticeable effect on the final structure and sorptional properties of silica gels. The isotherms for the sorption of methyl alcohol vapor on these silica gels practically coincide.

For determination of the influence of the temperature at which the silicic acid sol was prepared on the structure of silica gels, a sol prepared by mixing solutions of sodium silicate and sulfuric acid was divided into 4 parts: one was kept at room temperature, the second was kept in a thermostat at 40°, the third at 60°, and the fourth at 80°. The sols were heated until gelation commenced and were then rapidly cooled to room temperature, and the subsequent aging took place at 20°. The hydrogels were then washed with distilled water and dried at 125°. Table 3 gives the structural characteristics of two series of silica gel samples.

Table 3 shows that the temperature at which the silicic acid sol was prepared also has no influence on the final structure of the dry silica gel.

Effect of the nature of the acid used for coagulation on the structure of silica gels. For determination of the effect of the nature of the acid on the structure of silica gels, 6 samples of silica gels were prepared, precipitated by sulfuric, hydrochloric, nitric, formic, acetic, and phosphoric acids of equivalent concentrations. The silica gels were washed and dried under equal conditions. Table 4 shows the structural characteristics of silica gels precipitated by different acids.

---

* Workers from the Kirovograd Chemical Works, I. M. Gleikhenguaz and V. V. Smirnov, participated in this section of the work.

TABLE 2

Structural Characteristics of Silica Gels Prepared from Sols with Different Residual Acidities

Series	Residual acidity of sulfuric sol, in g-equiv. H_2SO_4	Apparent density in g/cc	Total pore volume in cc /g	Volume of benzene adsorbed, in cc/g, in the liquid state at $P/P_s = 1$
I	0.07	0.76	0.74	0.74
	0.07	0.75	0.73	0.72
	0.14	0.75	0.74	0.73
	0.14	0.76	0.74	0.73
	0.28	0.76	0.74	0.74
	0.28	0.77	0.75	0.74
II	0.05	0.81	0.78	0.75
	0.08	0.81	0.78	0.76
	0.10	0.84	0.74	0.74
	0.15	0.80	0.79	0.74
	0.20	0.83	0.75	0.76
III	0.05	0.89	0.67	0.61
	0.08	0.86	0.71	0.68
	0.10	0.85	0.72	0.66
	0.15	0.83	0.75	0.74
	0.20	0.89	0.67	0.68
IV	0.05	0.84	0.74	0.74
	0.08	0.84	0.74	0.75
	0.10	0.82	0.76	0.76
	0.15	0.87	0.70	0.72
	0.20	0.84	0.74	0.75

TABLE 3

Structural Characteristics of Silica Gels Prepared from Sols Precipitated at Different Temperatures

Series	Precipitation temperature, °C	Time before coagulation, min.	Apparent density in g/cc	Total pore volume in cc/g	Volume of benzene adsorbed, in cc/g, in the liquid state at $P/P_s = 1$
I	20	600	1.29	0.33	0.34
	40	230	1.30	0.32	0.34
	60	90	1.26	0.34	0.36
	80	35	1.26	0.34	0.37
II	20	–	1.26	0.34	0.35
	40	–	1.25	0.35	0.34
	60	–	1.27	0.34	0.35
	80	–	1.25	0.35	0.36

The data in Table 4 show that the nature of the acid used for precipitation has no significant effect on the final structure of the silica gels. An interesting feature is that silica gels which were prepared by different methods but which had the same pH value in the hydrogel stage during aging, had the same structure. Fig. 3 shows sorption isotherms of methyl alcohol vapor in silica gels prepared by hydrolysis of $SiCl_4$ (Curve 1) and from sodium silicate and sulfuric acid (Curve 2); the pH of the hydrogels was 2.2-2.9. Fig. 3 shows that the sorption isotherms practically coincide.

TABLE 4

Effect of the Nature of the Acid Used for Coagulation on the Structure of the Silica Gels

Acid	Apparent density in g / cc	Total pore volume in cc/ g	Pore volume, in cc/ g. filled by benzene in the liquid state at $P/P_s = 1$
Sulfuric	0.80	0.80	0.77
Nitric	0.77	0.85	0.87
Hydrochloric	0.76	0.87	0.87
Formic	0.82	0.77	0.77
Acetic	0.83	0.74	0.76
Phosphoric	0.82	0.77	0.81

Thus, our experimental results show that the coagulation rate of a silicic acid sol has practically no influence on the final silica gel structure. The latter is determined by the subsequent treatment of the hydrogel and the conditions for its dehydration, which is in agreement with our proposed mechanism for the formation of silica gel structure [10].

SUMMARY

1. The influence of silicic acid concentration in the sol, the residual acidity, the temperature of sol formation, and the nature of the coagulant acid on the structure of silica gels prepared from acid media has been studied.

2. It is shown that these factors strongly affect the time of the start of coagulation of the gel, and have practically no influence on the structure of the silica gels formed. Thus, the previous history of the silicic acid hydrogel has no significant effect on the porosity of the final product.

LITERATURE CITED

[1] A. P. Okatov, Colloidal Silicic Acid and Its Adsorptional Properties, The Dzerzhinsky Red Army Academy of Military Technology (1928).

[2] B. P. Bruns and E. A. Kostina, J. Appl. Chem., 8, 1004 (1935); J. Ferguson and M. Appelbey, Trans. Faraday Soc., 26, 642 (1930).

[3] S. N. Nikitin, Silica Gel and Its Application in Ferrous Metallurgy, State Metallurgy, Press (1941); H. A. Fells and J. B. Firth, J. Phys. Chem., 29, 241 (1925); R. Turky, Z. anorg. allg. Chem., 240, 198 (1939); V. I. Oborin, I. K. Koneva, and I. K. Romanova, Trans. Grozny Petroleum Inst., 5, 147 (1948).

[4] M. O. Kharmadaryan and S. L. Kopelevich, J. Chem. Ind., 24, 1484 (1930).

[5] M. V. Polyakov et al., J. Phys. Chem., 2, 799 (1931); 10, 100 (1937).

[6] V. Veselovsky and I. Selyaev, J. Phys. Chem., 6, 117 (1935).

[7] I. E. Neimark, Trans. All-Union Conf. on Catalysis, 298 (1950); I. E. Neimark and R. Yu. Sheinfain, Colloid J., 15, 45 (1953) (T.p. 49)*.

[8] A. V. Kiselev, Colloid J., 2, 17 (1936).

[9] G. K. Boreskov, M. S. Borisova, O. M. Dzhigit and O. A. Likhacheva, J. Phys. Chem., 22, 603 (1948).

[10] I. E. Neimark, Trans. Commission on Analytical Chemistry, Acad. Sci. USSR Press, VI(IX), p. 77 (1955).

Received March 10, 1955

The L. V. Pisarzhevsky Institute of Physical
Chemistry, Academy of Sciences, Ukrainian SSR
Kiev

---

* T.p. = C.B. Translation pagination

VISCOELASTIC CHARACTERISTICS OF MACARONI AND PASTRY DOUGH

B. A. Nikolaev and L. S. Beganskaya

The raw materials and the final products of the food industry have the most varied chemical compositions and structural-mechanical properties. These properties, determined by such viscoelastic characteristics as the elastic shear modulus (E), viscosity (η), relaxation time ($\eta/E = \theta$) and others, are of great theoretical and applied significance. Being an important means for the study of structure, viscoelastic characteristics provide an objective method for the determination of the lyophilic properties of raw materials, and for finding effective means of processing the materials for the production of high-quality finished products; these characteristics augment considerably the method for evaluation of the finished products, and control changes in quality during storage.

The successful development of physicochemical mechanics (rheology) in the USSR and abroad has made possible a wide application of its methods not only in scientific and industrial laboratories, but in automatic regulation of production processes. Despite the existence of a number of papers dealing with the viscoelastic characteristics of raw materials, intermediates, and products of the food industry, their number is still insufficient. However, even the first attempts to apply rheological methods with the aim of improving technological processes in the food industry indicate their great effectiveness [1,2].

It therefore appeared desirable to carry out a preliminary investigation of the viscoelastic characteristics of various food products with the use of a single method of measurement. The viscoelastic and viscoplastic properties of bread, macaroni, and pastry doughs were investigated.

The method used was that proposed by Tolstoy [3] for the measurement of shearing deformation in a plane-parallel gap on an inclined plane. The measurements were carried out with the aid of a special instrument [4] in which small deformations were magnified on a measuring scale in the ratio of the arms of a light balanced pointer in contact with a cover plate on the material under investigation. As some of the materials tested had high viscosity and shear modulus values, a modification of the instrument was used in which the gap width was increased from 5 to 20 mm. Parallel tests with the two instruments showed adequate agreement in their results. The tests were carried out at 20° with 3 minutes deformation time under load and a speed of about 1 mm / minute.

The viscoelastic characteristics (E_0, η av, η/E, elasticity) were determined by means of a technique proposed and developed by Rebinder [5]; the results are supplemented by data on plasticity (measured as the percentage ratio between the residual deformation after removal of the load, and the maximum deformation reached before removal of the load) and on strengthening under deformation, defined in terms of the deformation rates in the third and second minute of deformation (v_3 and v_2) as the relationship $(1 - v_3/v_2) \cdot 100$.

Flour dough for macaroni and pastry differs from bread dough in having lower moisture content and absence of yeast which causes fermentation and volume increase. Macaroni and pastry dough is made from 1st and top grade flour, with a high content of water-insoluble proteins — glutens, with high resilience and elasticity. Macaroni dough is made with a 27-30% moisture content from flour and water without additions of sugar or fat. Pastry dough contains added sugar and fat, which plasticize the dough and lower its viscoelastic values.

The results of tests on macaroni dough are shown in Table 1. The flour used for such dough is derived from hard wheats, characterized by elasticity of their proteins. Ordinary commercial flour is also used. Samples 1-4 in Table 1 and Figs. 1 and 2 represent the results of tests on gluten and dough from hard wheat flour and commercial flour; these results show that the gluten proteins of hard wheat flour have a shearing modulus nearly three times as great, and average viscosity nearly double, those of the gluten from commercial flour.

However, the hydrophilic properties of this gluten are considerably lower (by 3%) than those of commercial flour gluten. Macaroni dough made from hard wheat flour, with a slightly higher moisture content (by 0.6%) than dough from commercial flour, nevertheless had a higher shearing elasticity modulus, higher viscosity, and considerably lower plasticity (percentage ratio between the residual deformation and the maximum deformation attained). Thus, this dough was a more elastic system, more suitable for the manufacture of macaroni products.

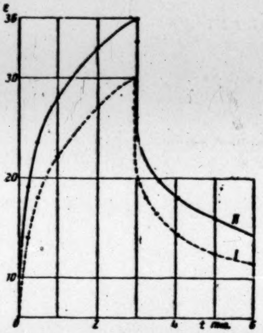

Fig. 1. Shearing deformation curves of 1st grade wheat flour gluten extracted by washing at 30° (see Table 1, Samples 1 and 3): I) from hard wheats, II) from commercial flour.

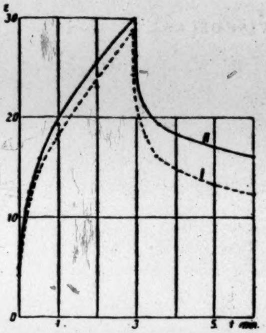

Fig. 2. Shearing deformation curves of 1st grade wheat flour dough (see Table 1, Samples 2 and 4): I) from hard wheats, II) from commercial flour.

TABLE 1

Tests on Macaroni Dough and Flour Gluten

Sample No.	Description of sample	Moisture content, %	Stress, dynes/cm²	E_0, dynes/cm²	η_{av} in poises	$\frac{\eta}{E}$ in sec.	Plasticity, %	Elasticity, %	Strengthening, %
1	Hard wheat gluten	65.0	830	$7.0 \cdot 10^3$	$3.2 \cdot 10^5$	45	38	92	40
2	Dough from hard wheat flour	29.8	6800	$3.4 \cdot 10^5$	$1.0 \cdot 10^7$	29	42	86	20
3	Gluten from commercial flour	68.0	550	$2.6 \cdot 10^3$	$1.8 \cdot 10^5$	70	42	93	40
4	Dough from commercial flour	29.2	6800	$3.0 \cdot 10^5$	$9.5 \cdot 10^6$	32	53	85	20
5	Dough from hard wheat flour	27.7	10500	$7.0 \cdot 10^5$	$3.8 \cdot 10^7$	54	37	67	44
6	Ditto	27.7	10500	–	$5.0 \cdot 10^7$	–	0	63	44
7	Dough from commercial flour	27.0	10500	$6.5 \cdot 10^5$	$4.3 \cdot 10^7$	68	40	97	25
8	Ditto	27.0	10500	–	$5.4 \cdot 10^7$	–	7.0	69	17
9	Dough Sample 5 after 24 hours	28.0	6800	$3.8 \cdot 10^5$	$1.4 \cdot 10^7$	36	63	71	23
10	Ditto	28.0	6800	–	$2.6 \cdot 10^7$	–	14.1	72	–

It is a very interesting fact that the higher elasticity of dough made from hard wheats is evidently explained by analogous properties of its gluten proteins. At the low moisture content of macaroni dough and therefore at incomplete hydration, the individual properties of the gluten proteins apparently come into play even in the high viscosity conditions of such dough.

Macaroni dough (particularly from hard wheat flour) is seen to have high elastic modulus and low plasticity, almost equal to that of gluten proteins. The explanation for this probably lies in the small thickness of the hydrate shells and the strong adsorptional bonding between them and the hydrophilic macromolecules of the proteins, starch, and cellulose forming the dry flour substance. The percentage high-elasticity and the strengthening of macaroni dough are considerably lower than in the gluten. The decreased elasticity should probably be attributed to the decreased moisture and the presence of a starch suspension in the dough, which increase the dimensions of the viscoelastic elements. The decrease of strengthening power is probably caused by the same factors and by the consequent decrease of the ability of the protein fibers to be oriented correctly in the shearing plane.

The high strengthening power of macaroni dough during shearing deformation was already pointed out in the preceding paper [4]. Table 1 (Samples 5-8) shows the results of tests on macaroni dough made from hard wheat and commercial flour with moisture contents about 2% lower than in Samples 2-4. This decrease of the moisture content of the dough resulted in approximate doubling of the shearing modulus and a 3.5-4 fold increase of viscosity.

In a second test of the same samples, of the hard wheat flour dough the instantaneous deformation fell to zero, the viscosity increased and flow properties were completely lost (the plasticity was zero). The elasticity and the strengthening power fell considerably because of the increased viscosity of the system. An interesting fact is that after 24 hours (see Samples 9-10, Table 1) the viscoelastic properties of the dough — the elastic modulus and viscosity — are decreased to less than half of the original values; the plasticity increases considerably. However, in a second test the dough strengthens, and the viscosity and elastic modulus increase again.

Table 2 shows results of tests on pastry flour dough. The dough was made from the same flour by separate additions of sugar and margarine in gradually increasing doses (the amounts are given as percentages on the weight of flour). The moisture content of the dough was ~ 30%. Dough with a moisture content of ~ 20% was also tested with large amounts of sugar and margarine, added separately and together.

TABLE 2

Tests on Dough with Sugar and Fat Additions

Type of dough, and amounts of additions as % of the flour	Moisture content, %	Stress, dynes/cm^2	E_0, dynes/cm^2	η_{av} in poises	$\frac{\eta}{E}$, sec.	Plasticity, %	Elasticity %	Strengthening, %
Control dough	30.2	4600	$3.6 \cdot 10^5$	$1.2 \cdot 10^7$	33	52	65	17
Dough with added sugar —5%	30.6	3520	$1.8 \cdot 10^5$	$4.5 \cdot 10^6$	25	52	68	17
Ditto, 10%	30.4	2450	$7.5 \cdot 10^4$	$2.0 \cdot 10^6$	27	51	69	39
" 20%	30.5	1385	$2.5 \cdot 10^4$	$5.0 \cdot 10^5$	20	55	72	–
" 50%	30.5	230	$3.0 \cdot 10^3$	$1.0 \cdot 10^5$	33	60	88	20
Control dough	30.5	4600	$4.1 \cdot 10^5$	$1.5 \cdot 10^7$	36	51	66	38
Dough with added margarine —5%	30.3	4600	$2.6 \cdot 10^5$	$7.5 \cdot 10^6$	29	55	66	5
Ditto 10%	30.4	3500	$1.4 \cdot 10^5$	$2.5 \cdot 10^6$	18	51	68	36
" 20%	30.4	1920	$9.5 \cdot 10^4$	$3.5 \cdot 10^6$	37	62	75	37
" 50%	30.4	1600	$4.0 \cdot 10^4$	$5.0 \cdot 10^5$	12	90	57	12
Dough with 50% sugar added	20.8	2450	$1.2 \cdot 10^5$	$1.0 \cdot 10^6$	8.0	62	71	–
Dough with 50% margarine added	20.4	2450	$1.6 \cdot 10^5$	$1.2 \cdot 10^7$	76	80	50	–
Dough with 50% sugar and margarine added	20.0	900	$2.0 \cdot 10^4$	$1.5 \cdot 10^6$	75	73	70	64

It is seen from Table 2 that increased additions of sugar and fat progressively decrease the shearing modulus and viscosity. Both these decreases occur to approximately the same extent, and therefore the ratio of the viscosity to the modulus (relaxation time) shows small and irregular changes. It must be pointed out that the greatest decrease of these values occurs as the result of the addition of the first portions (5-10%) of sugar and margarine to the dough. Added sugar has the greater decreasing effect on these values. It is seen that addition of sugar and increasing content of sugar in the dough has very little effect on the plasticity and considerably increases the percentage elasticity. Additions of margarine, particularly in large amounts, appreciably raise the plasticity and lower the elasticity. This is also found for dough with 20% moisture.

Thus, additions of sugar raise the elastic properties of dough, while margarine makes it more fluid-plastic. This must be considered as being of great practical importance for the formation of flour pastry dough products. The so-called "extensible dough", with low contents of sugar (20-30%) and fat (10-20%) has the power of gradually restoring the deformed volume (low plasticity and high elasticity). Sugar dough, and particularly rich pastry dough with high fat and sugar contents, does not have this power, and has high fluidity with a low moisture content.

SUMMARY

1. The specific properties of hard wheat flour and gluten have been studied, and their effects on the visco-elastic properties of macaroni dough investigated.

2. The plasticizing action and the practical importance of additions of sugar and fat to flour dough have been demonstrated. It was established that an increase in the sugar content does not affect the ratio of the viscosity to the modulus, or the plasticity, but appreciably increases the elasticity. Similar additions of margarine appreciably increased the plasticity of the dough.

LITERATURE CITED

[1] M. P. Volarovich, Collected Papers "Colloids in the Food Industry", Food Industry Press, No. 2, p. 40 (1949); G. W. Scott Blair, Foodstuffs, Their Plasticity, Fluidity and Consistency, Amsterdam (1953).

[2] L. E. Chernenko, V. E. Markovich, and L. S. Vetkina, Colloid J., 13, No. 5, 379 (1951).

[3] D. M. Tolstoy, Trans. All-Union Conf. on Friction and Wear in Machines, No. 3, 155 (1949).

[4] B. A. Nikolaev and L. S. Beganskaya, Colloid J., 16, No. 6, 455 (1954) (T.p. 433)*.

[5] P. A. Rebinder, New Methods of Physicochemical Investigation of Surface Phenomena, Acad. Sci. USSR Press (1950).

Received June 17, 1954

Scientific Research Institute for the Baking Industry
Moscow

---

* T.p. = C. B. Translation pagination

THE COLLOID-CHEMICAL ASPECT OF A BIOLOGICAL PROBLEM

S. Papkov

In investigations of systems with high polymer components, great importance attaches to studies of phase equilibrium and, in particular, the physical forms of separation of the system into coexisting phases. While in systems consisting of low molecular components the time for equilibrium to be established is in most cases of the same order as the duration of the experiment *, the most common forms of phase separation in high polymer systems are those in which complete demixing does not occur in finite periods.

In fact, the number of instances of the so-called coacervation demixing characterized by relatively low viscosities of the coexisting phases and correspondingly rapid complete demixing with the formation of a single interphase boundary is very small. In most cases, at the critical point (in the transition from a single-phase to a multiphase system), systems with incomplete demixing are formed – gels with low rates of demixing (syneresis), not comparable with the experimental time.

It is important to note that the properties of the final formations differ significantly according to the physical form of the separation of a one-phase system into two phases. While high polymer coacervates differ little in physical characteristics from the usual viscous liquids, gel formation results in the appearance of peculiar properties among which superelasticity and mechanical form stability ("resilience") should be specially noted.

Without touching upon the various hypotheses of gel and coacervate structure, separate consideration of which is more appropriate, we will point out the exceptionally important role of a correct choice between the two main types of phase separation (coacervation and gel formation) in examination of actual problems. In particular, special interest is presented by biological systems characterized not only by various transformations of a high polymer (for example, protein) as the result of changes in the parameters of the system or of the action of external agents, but also by the direct formation, as the result of synthesis, of the polymer itself. The forms in which the high polymer formed is separated to a great extent predetermine the behavior of the system itself. It appears appropriate in this connection to comment on one of the most complex and interesting problems of biology – the problem of the origin of life. We will naturally restrict ourselves to only the colloido-chemical aspect of the problem, while acknowledging the complexity and variety of the phenomena which comprise this problem as a whole.

Oparin, in a number of publications [1], has developed a hypothesis of the origin of life on Earth. One important point of this hypothesis is the assumption of the special role of protein coacervate particles. The drops of coacervate are regarded as the initial material particles capable of evolution, in the course of which they acquire the power of metabolism and of other complex changes corresponding to the functions of a living organism. Without dealing with the other points of Oparin's hypothesis on the origin of life, and in particular, the undoubtedly correct basic view that the creation of life is the inevitable consequence of further transformations of the chemical substances which are the starting materials for the synthesis of protein molecules, and which arose during the development of the material world, we consider it necessary to make certain comments specifically on the question whether it is legitimate to ascribe to coacervate formations the role assigned to them in Oparin's hypothesis.

The coacervation effect in systems containing high molecular components has been known for a very long time. One of the first examples of this form of separation of a high polymer from solution was the precipitation of gelatin from aqueous solutions by the addition of alcohol, observed by Hardy [2]. Subsequent work by Bungenberg de Jong and his school [3] showed that similar separation of the components in liquid drop form may be observed in a number of systems, including the subsequently most extensively studied system gelatin – gum arabic – water. For long time the view persisted in colloid chemistry that coacervation is a specific phenomenon which does not obey such general laws of physical chemistry as the phase rule.

---

* It should be pointed out that peculiar exceptions (quasi-equilibrium states) also exist for such systems. However, this question requires separate examination.

However, as was shown later by our work [4] among others, the separation of high polymer solutions into two liquid phases fully obeys the phase rule. The complete similarity of these systems to mixtures of low molecular liquids with limited mutual solubility makes it possible to regard the formation of coacervate drops as analogous to the formation of an emulsion when a mixture of two liquids separates into two phases at the critical point. Depending on the presence or absence of stabilizing additions, such an emulsion can either remain as a more or less fine dispersion or be separated into two layers with a common interface.

In systems containing proteins, the drop-like state of the coacervate is partly stabilized by the low-molecular substances and protein hydrolysis products present. However, in these systems also the drops gradually coalesce, and the system thus approaches an equilibrium state, determined by minimum free energy. Thus the drop-like (disperse) state of the coacervate is not stable.

It is also important to note that the coacervate drops in the suspension are spherical only because of surface tension at the interphase boundary. Although this surface is generally small, it has a definite value. But a coacervate, being a liquid in its internal properties, has no "shape elasticity" owing to any structural features, and therefore after removal of the applied external load it does not spontaneously regain its original shape.

Finally, it is not possible to ascribe to coacervate drops any special properties with regard to sorption or desorption of other substances which would distinguish such processes from the usual sorption and desorption effects in heterogeneous systems. From this standpoint there is not, for example, any difference between the absorption of dyes from solution by a protein in the form of a coacervate and dye absorption by wool fibers, leather, or any other form of protein. The process depends on the sorptional properties of the polar groups and the chemical activity of the amino acids which form the protein, and not on any special state of the protein. The coacervate as such does not cause any phenomena which go beyond the limits of normal sorptional equilibrium which depends on the changes in the concentration of the absorbed substance in the external medium.

Thus, the separation of proteins or other high polymers in coacervate form does not create the prerequisites for the appearance of the most characteristic features of living organisms: individualization of the particles, elasticity (stability) of form, and metabolism. As was pointed out earlier, the spontaneous "coalescence" of the particles is an irreversible process, which in principle continues till all the coacervate drops have coalesced into a continuous phase with a common interface, and there are no causes of spontaneous "division" (comminution) of the coacervate particles. The liquid coacervate does not show shape retention in its particles under the action of external loads, which is an important property of a living organism. The sorption and desorption of substances ("metabolism") is of a strictly equilibrium nature, and cannot lead to a continuous assimilation — dissimilation process.

On these grounds it is difficult to assume that the hypothetical appearance of coacervate-type formations during the evolutionary process represented a qualitative jump from non-living to living matter. The necessary prerequisites for the "vivification"* of proteins do not exist in coacervate drops, and this part of Oparin's hypothesis reflects the inadequate development of the theory of coacervation in colloid chemistry rather than an actual discovery of a qualitatively new phenomenon. Incidentally, coacervate formation requires the preliminary accumulation of sufficient concentrations of protein substances, and for this reason alone it is necessary to seek other mechanisms and forms for the natural synthesis of proteins, which are not predetermined by coacervation formations of the protein itself. This makes experimental attempts to create an analog of a living organism on the basis of coacervation systems even more debatable.

A more detailed analysis of the above hypothesis for the origin of life on Earth goes beyond the scope of the present note, but it is necessary to point out that, on the basis of dialectical materialism, it is difficult to assume a sharp separation of form and content for qualitatively new phenomena, and, accordingly, the appearance of a cell prototype (coacervate particle) before occurrence of the determining process — protein synthesis, associated with metabolism.

In order not to restrict ourselves to only a negative criticism of Oparin's coacervation hypothesis of the origin of life, we will briefly consider certain questions associated with the physicochemical aspects of the primary appearance of life processes.

---

* Incidentally, we will note that the term "living matter" has frequently been used in recent biological literature. The use of this term, which is used by geologists and geochemists in a conditional sense, and its adoption in biochemical literature as a direct concept, is quite clearly inadmissible. Nevertheless, Lepeshinskaya and other biologists not only ignore the conditional nature of this concept, but make attempts to isolate such "matter". The concept of "life" should be referred not to a state of matter, but to a definite process (to the process of natural protein synthesis, as will be shown below), which differs qualitatively from any other processes of conversion of matter. The molecules of substances which participate in this process do not thereby become "alive".

The most correct definition of life, and one in accordance with the theoretical views of F. Engels *, is that it is the process of natural protein synthesis. In the course of this process, both as the result of the synthesis and at the same time as its inseparable condition, protein is deposited (separated) in a form which creates the conditions for the unbroken continuation of the synthesis.

The appearance of organic matter at a definite stage in the development of the material world on Earth corresponds to a transition from the formation of the simplest low-molecular compounds of carbon and other elements to the formation of high polymers. The formation of high polymers, and in particular of proteins, differs qualitatively, first in the catalytic nature of the reactions, and second, in the need for a sufficient concentration of the materials required for the synthesis around the catalytic center. The latter is possible only if the catalyst is fixed in a medium in which convection currents are absent, which would otherwise hinder the diffusional access of the starting materials for the synthesis and their accumulation to the concentrations necessary for the catalytic formation of new polymer molecules. This medium must also have shape elasticity, so that the effects of external mechanical influences on the continuity of the synthetic process in the catalytic cell can be avoided.

Such a medium is provided by proteins themselves, which are known to have the property of separation in aqueous media in the form of gels — structural formations with the definite mechanical strength necessary to fix the catalytic center and to prevent the "washing-away" of the initial synthesis products by convection currents. The elastic properties of gels result in individualization of the system and restoration of the original form after removal of accidental external loads. Finally, the fact that gels are formations with a very low content of "skeletal" (polymeric) substance, ensures free diffusion from the external medium to the catalytic center and the reverse diffusional removal of the synthesis by-products. It is known that the rate of diffusion into gels of low concentration hardly differs from the rate of diffusion into the pure medium.

Thus, the medium which is most appropriate to the conditions of protein synthesis is not the coacervate but the gel form of proteins. This is also confirmed by an examination of the structure of all living organisms. From the simplest cells to any complex organisms, proteins are found in the gel-like and not the coacervation state.

Accordingly, the appearance of life on Earth must be regarded as the start of a catalytic process of protein synthesis, for which the necessary prerequisites, including the formation and accumulation of low-molecular carbon and nitrogen compounds, had been created by preliminary evolution of the material world. There is no doubt that among the unlimited possibilities for further transformations of these substances, only those proved stable, and in the greatest accord with the external conditions, in which the primary formation of new complex compounds at the same time created the conditions in which the process could continue and develop. The deposition of the synthesis products in the form of gels, that is, systems with the power of individualization, form retention, and the appropriate diffusional properties, corresponded to such conditions. Other conversion processes of the low molecular compounds could and did arise with the same inevitability as the catalytic synthesis of proteins, but the latter contained all the necessary conditions for becoming the predominant phenomenon of material evolution on Earth.

We may note yet another important property of gel-like depositions of proteins around the catalytic center, namely, the peculiar chemical protection of this center against the action of extraneous substances which could poison the catalyst, effected by chemical and adsorptional incorporation of these substances in the outer layers of the protein molecules in such formations. However, this question, like the question of the cell wall formation, is one of detail.

Such are some of the colloid-chemical aspects of the origin of life processes. It must be pointed out, however, that despite the importance of establishing that proteins in organisms are in the colloidal state, the main problem of the origin of life on Earth, and therefore the main problem of the artificial reproduction of the analog of this process, is still the search for catalytic schemes of protein synthesis in which, simultaneously with the synthesis process and the formation of a gel-like "cell" which favors the uninterrupted continuation of the synthesis, the catalyst is also regenerated. It is easy to see that reproduction of the catalyst, equivalent to the formation of a second catalytic center in the "cell", leads to accumulation of the synthesis products (protein) around two catalytic centers and to "division" of the cell, which is essentially the basis not only for a progressive increase in the

---

* F. Engels wrote in "Anti-Dühring" [5] ". . . The transition from the physics of molecules to the physics of atoms — to chemistry — again takes place by means of a jump; this is true to an even greater extent for the transition from ordinary chemical action to the *chemistry of proteins, which we call life"* (our italics. S.P.).

amounts of substances involved in the biological conversion of matter, but also for further complex transformations (development) of the organic forms. This variation of organic form, up to the creation of the highest form of evolution of matter, capable of exerting an active influence on the further course of evolution, does not alter the fundamental fact that the essence of any manifestation of organic life, from the chemical standpoint, is the natural synthesis of proteins.

SUMMARY

1. Some properties of coacervates, as one of the forms in which high polymers are evolved in the separation of a one-phase system into two phases, have been examined. It is shown that the equilibrium state in coacervates is the formation of a continuous layer, coacervate drops being an intermediate unstable formation. It is noted that coacervate drops do not have elastic properties which would ensure stability of shape under the action of external mechanical loads. The sorption and desorption of substances by coacervates is of a strictly equilibrium nature, and cannot lead to a continuous assimilation – dissimilation process.

2. In view of these properties of coacervates, a special role in the origin of life processes cannot be ascribed to them. The hypothesis put forward by Academician A. I. Oparin concerning the origin of life on Earth is critically examined on this basis.

3. Life processes are defined as processes of natural synthesis of proteins, in the course of which, as the result of the synthesis and as its inseparable condition, a peculiar form of protein deposition – gel formation – arises. It is shown that deposition of proteins in gel form determines such important properties of biological systems as the individualization of particles, shape "elasticity", and protection of the "catalytic center" (cell nucleus) against the action of external influences.

4. It is pointed out that the main problem in the origin of life is not the search for colloidal formations similar in properties to living organisms, but the investigation of catalytic reactions of protein synthesis in the course of which the catalyst is simultaneously regenerated.

LITERATURE CITED

[1] A. I. Oparin, Origin of Life on Earth, 2nd Ed., Moscow (1941); Great Soviet Encyclopedia, 2nd Ed., Vol. 16, p.88.

[2] W. R. Hardy, Proc. Roy. Soc., 66, 95 (1900).

[3] H. G. Bungenberg de Jong, Koll.-Z.,79,223 (1937).

[4] S. Papkov, V. Kargin, and Z. Rogovin, J. Phys. Chem., 10, 157, 607 (1937).

[5] F. Engels, Anti-Dühring, State Political Press, Moscow, p. 63 (1945).

Received March 25, 1955 Moscow

FORMATION OF CRYSTALLINE ICE IN WHEAT GRAINS ON DEEP COOLING

G. B. Radzievsky and Ya. L. Shekhtman

In studies of the mechanism of the radiobiological effect, considerable interest attaches to investigations of the action of radiation during deep cooling (100-190° below zero), since all secondary radiochemical processes are retarded at such temperatures and it becomes possible to study the direct and indirect effects of radiation separately. However, the use of deep cooling in studies of radiobiological effects requires conditions in which the cooling itself would not cause irreversible damage to the living activity of the organism.

According to published data [1], damage to the organism during freezing is associated with the formation of crystalline ice in the organism, while survival after freezing is explained by "vitrification", or the supercooling of the tissue water and its conversion into the glassy state with omission of the crystal phase. All the data available on vitrification relate this effect to the rate of cooling. Vitrification has been observed in very thin objects subjected to rapid, almost instantaneous cooling [1, 2]. Therefore, in studies of the deep cooling method in radiobiology it is necessary to determine:

1. What is the course of ice formation in relatively large objects, such as wheat grains, which were chosen as material suitable for a number of reasons for studies of the mechanism of the radiobiological effect.

2. How does ice formation in wheat grains depend on the moisture content of the grains, and in what moisture content conditions is it possible to work with deep cooling without disturbing the viability of the germ.

Ice formation in plant material can be observed directly only if fairly large crystals are formed. The initial stages of ice formation, the appearance of submicroscopic crystals, can be investigated only by x-ray structure analysis methods. This method has been used by a number of workers for the analysis of the supercooling of water [2,3] and for investigations of ice formation in gelatin [4]. According to Barnes and Matthews [4] the x-ray method is highly sensitive and permits the determination of the presence of ice in gelatin when the ice content is 1% and over. We have therefore used the x-ray method for studying ice formation in wheat grains.

METHOD

Apparatus. As the result of a number of preliminary experiments, a camera was developed which gave reliable and reproducible results (Fig. 1). The camera consists of a Duralium cylinder 86 mm in diameter. The diaphragm is in the form of a cylindrical canal with two openings 0.5 and 0.8mm diameter, and provides a beam 0.5 mm in diameter. A hollow copper tube 6 mm in diameter is fixed in the bottom of the camera, with its upper end, which is inside the camera, widened out into a cone. A detachable conical copper object holder with a central slit fits firmly into this cone.

The camera is first centered exactly in such a way that the beam passes exactly through the middle of the slit in the object holder. The position of the beam is marked on the holder by a graduation line. Before each experiment the object holder is taken out, and a grain prepared as shown in Fig. 1 is inserted into it in such a way that the middle of the germ is exactly opposite the mark on the holder. The holder is then inserted into the conical seating always in the same fixed position. A film is then loaded into the camera, and the apparatus is ready for the photograph. The whole grain fixing procedure takes not more than 1 minute; the grain is in good contact with the copper tube, and the x-ray beam passes exactly through the germ without touching the endosperm.

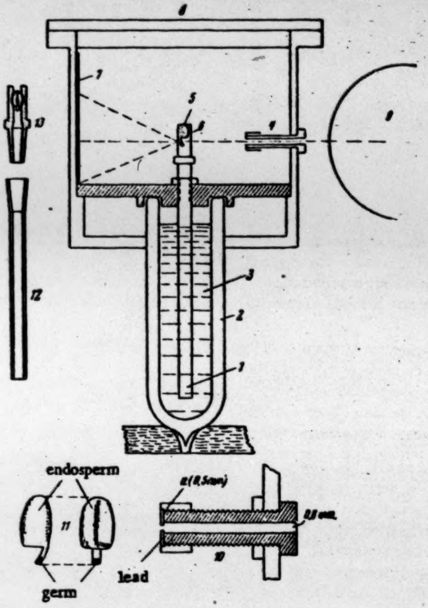

Fig. 1. Diagram of camera for work with deep cooling: 1) copper tube; 2) Dewar flask; 3) liquid nitrogen; 4) diaphragm; 5) grain; 6) holder; 7) film; 8) camera lid; 9) x-ray tube; 10) tube with diaphragm (a); 11) prepared grain; 12) copper tube; 13) object holder.

After the preparation of the camera and object, a Dewar flask containing liquid nitrogen is fixed underneath the camera on a holder with a raising mechanism. As the Dewar flask is raised, the lower end of the copper tube, which protrudes from the bottom of the camera, is immersed in the liquid nitrogen. The nitrogen begins to boil, and vigorous vapor formation throws fine droplets of liquid nitrogen through the tube into the camera and onto the grain fixed in the holder, which rapidly cools the grain (down to −190° and lower in 1-2 seconds). When the copper tube reaches the temperature of the nitrogen, the boiling ceases and the low temperature of the grain is maintained by contact with the metal at a level between −120° and −125°.

In experiments with slow cooling, a stopper was inserted into the tube from below, which prevented the penetration of nitrogen vapor and droplets into the camera. In these cases the required temperature conditions in the germ, as measured by a thermocouple, were established after 5-6 minutes.

In experiments with an open camera, water and air vapors are rapidly condensed around the object, and a frosty layer is formed. Control experiments were carried out to see whether interference rings are produced on the photograph by the external crystals of ice. A cooled dummy grain made of Plexiglas was used for this purpose. No interference rings were found despite considerable frosting. In all the subsequent experiments the camera was covered by a lid. There was then practically no frosting, as the nitrogen vapor displaced the air from the camera.

The photographs were taken with the aid of a BSV-Cu tube for structure analysis at 35 kV maximum. Both α- and β-radiation lines were obtained on the photographs, as filters were not used. The exposure time was ~10-13 minutes.

Temperature measurement. The low temperature measurement was carried out by means of a copper-Constantan thermocouple. The thermocouple was calibrated against the following fixed points:

Boiling point of nitrogen	−195.8°
Freezing point of toluene	− 95.1°
Freezing point of chloroform	− 63.5°
Freezing point of mercury	− 38.9°

The thermoelectromotive force was determined: a) by calculation from the readings of a calibrated galvanometer and from the total resistance of the circuit; b) by a compensation method. The calibration curves for the thermocouple were constructed with the use of standard tables (Adams) for circuit resistances of 700, 800, and 900 ohms. During the measurements one of the junctions of the thermoucouple was maintained at 0° (in melting ice), and the other was inserted into the germ of the wheat grain.

TABLE 1

Variation of Moisture Content with Soaking Time

Soaking of grain				Soaking of endosperm (d = 0.9 mm)	
Soaking time, hours	Moisture content, %			Soaking time, min.	Moisture content, %
	whole grain	whole grain, according to Luyet	germ, according to Luyet		
0	9.6	10.6	10.5	0	9.6
1	18	19.4	28.5	10	21
2	20.4	21.2	34.2	20	29
3	23.2	23	42	30	34
4	25	25.1	50.5	40	36
14	48	–	–	60	37

Moisture determination. The moisture content of the grains as a function of soaking time was determined by weighing the dry and soaked grains. The moisture content of air-dry grains was previously determined. This was found to be 9.6%. The moisture content of the germ was not determined directly, but was calculated according to Luyet's data from the total moisture content of the grain. The endosperm was soaked in thin slices 0.9 mm thick (such slices were used for taking the x-ray photographs after freezing). The results of the moisture determinations on the grain and endosperm are shown in Table 1.

RESULTS OF THE INVESTIGATIONS

X-ray diagrams of the germ and endosperm were taken for different soaking times, from 30 minutes to 39 hours. These diagrams were obtained both after rapid cooling (in 1-2 seconds) and after slow cooling (5-6 minutes). The same interference diagram was obtained in both cases.

In the diagrams obtained (Fig. 2) interference rings for ice appear only at a moisture content ~ 34%, and the intensity of the rings gradually increases with increasing moisture content. Fig. 3 shows microphotograms of the interference rings for different soaking times (from 1 hour 23 minutes to 38 hours). Curve 4 shows only weak indications of the separate interference maxima (they are more pronounced on the negative than in the microphotogram). The height of the peaks, corresponding to individual lines on the x-ray diagram, gradually increases with rising moisture content.

The x-ray diagrams of the endosperm (see Fig. 2, h, i), in contrast to the diagrams of the germ, show separate interference spots and dots on the rings, indicating the formation of larger ice crystals ($10^{-2}-10^{-3}$ cm). In order to confirm that the interference rings obtained are in fact due to ice, control diagrams of frozen 15% gelatin were obtained with the same camera. The lines obtained coincided exactly with the lines in the diagrams for frozen grains (Fig. 2, j).

A comparison was then made between the positions of the observed diffraction rings and the calculated data for the hexagonal crystal lattice of ice with the parameters a = 4.5 A and c = 7.3 A. The quadratic form for a hexagonal system:

$$\sin^2\theta = \frac{\lambda^2}{4a^2}\left[\frac{4}{3}(h^2+k^2+hk)+\frac{a^2}{c^2}\,l^2\right].$$

where λ is the wave length (1.54 and 1.39 A); a and c are the lattice parameters; and h,k, and l are the reflecting plane indexes, was used in the calculation.

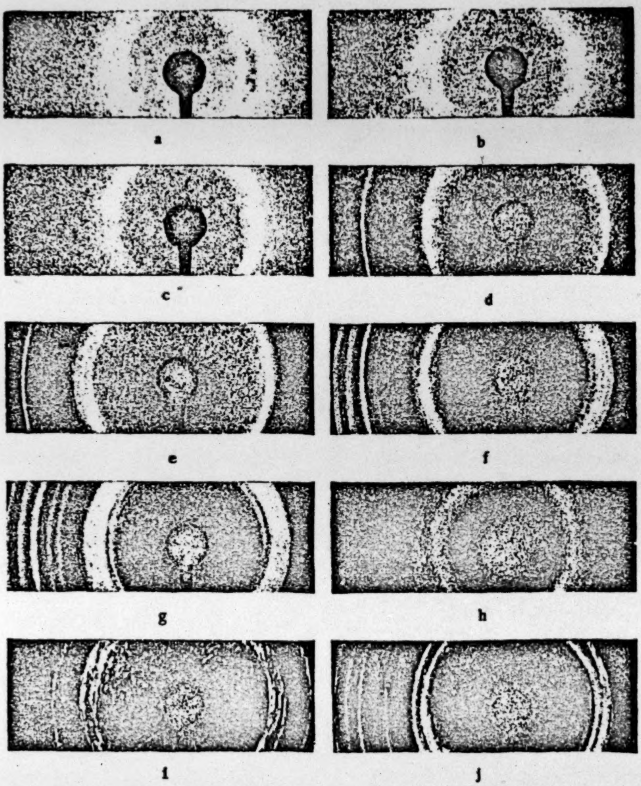

a b c d e f g h i j

Fig. 2. X-ray diagrams of wheat germ: a) air-dry, without cooling; b) ditto, cooled to $-120°$; c) soaked for 30 minutes, 20% moisture, rapidly cooled; d) soaked for 1 hour 55 minutes, rapidly cooled, 35% moisture, ice formed; e) soaked for 2 hours 10 minutes and cooled, ice lines more sharp, 37.5% moisture; f) soaked 4 hours 15 minutes, 50% moisture; g) soaked for 39 hours, moisture over 50%; h) air-dry endosperm (0.9 mm section), starch diffraction rings; i) ditto, soaked for 50 minutes and rapidly cooled, moisture 37%; large(10^{-2} — —10^{-3} cm) ice crystals formed; j) 15% gelatin, rapidly cooled to $-120°$, 85% moisture, large ice crystals formed.

After the introduction of a correction for the absorption of x-rays in the object, according to the formula

$$2r\ \text{corr.} = 2r\ \text{meas.} - \rho(1+\cos 2\theta),$$

where r is the Debye ring radius; ρ is the effective radius of the object, equal to 0.4 mm, good agreement (to the nearest 0.5 %) was obtained between the calculated value of $\sin^2\theta_{\text{calc.}}$ and $\sin^2\theta_{\text{meas.}}$ for the observed lines. The comparative data are shown in Table 2. The positions of the ten observed lines are shown schematically in Fig. 4.

The results of the present investigation may be summarized as follows: 1) on deep cooling of moist wheat grains, crystalline ice forms in the germ when the moisture content of the germ exceeds about 34%; 2) the amount of ice formed gradually increases with rising moisture content; 3) in the presence of less than 34% of water ice is not formed either on rapid (1-2 seconds) or slow (5-6 minutes) cooling; 4) the ice formed in the germ at high moisture contents has a polycrystalline structure; it did not prove possible to determine the dimensions of the separate crystals from the line broadening; it may be assumed that the dimensions of the crystals are less than those of the cell.

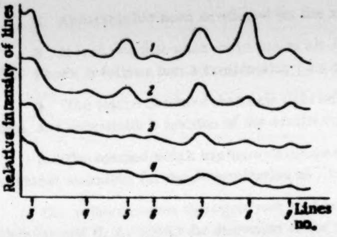

Fig. 3. Differences in diffraction maxima at different moisture contents of wheat grain germ before freezing: 1) 38 hours; 2) 25 hours, over 50% moisture; 3) 2 hours 15 minutes, 37.5% moisture; 4) 1 hour 23 minutes, 30% moisture.

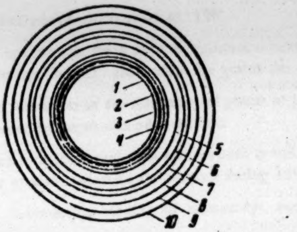

Fig. 4. Diagram of the positions of the ten observed lines for ice.

The results obtained for the dependence of ice formation on the moisture content are in good agreement with the data of Barnes and Matthews on ice formation in gelatin solutions. According to Barnes and Matthews, x-ray investigations of gelatin containing up to 30% of water do not reveal lines for ice either on rapid or on slow cooling.

TABLE 2

Calculation of X-Ray Diagram for Ice

Sequence of lines	Intensity *	Measured ring radius, mm	Corrected ring. radius, mm	$\sin^2\theta$ observed	$\sin^2\theta$ calculated	reflecting plane
1	w	15.8	15.4	0.031	0.031	(100) β
2	vs	17.5	17.1	0.0385	0.0385	(100)
3	m	18.7	18.3	0.0442	0.0441	001 (2)
4	m	20	19.6	0.050	0.0495	101
5	vw	23.3	22.9	0.069	0.067	(102) β
6	w	25.7	25.3	0.083	0.0825	(102)
7	vw	27.5	27.1	0.095	0.094	(110) β
8	m	30.3	29.95	0.116	0.116	(110)
9	w	33	32.7	0.137	0.138	(103)
10	w	35.6	35.3	0.159	0.160	(112)

---

* w) weak; vw) very weak; m) moderate, vs) very strong; s) strong.

As vitrification, or the transition of water into the glassy state without crystallization, is possible only as the result of supercooling, for which a high rate of cooling is necessary (up to 500° per second according to Luyet [5]), our data on rapid (1-2 seconds) and slow (5-6 minutes) cooling lead to the conclusion that at moisture contents up to 34% the water present in the grain does not form ice for reasons which are not related to supercooling. It is probable [6] that this water is in the "bound" state ("intramicellar swelling", according to Katz).

The x-ray structure analysis method developed may be used for biochemical and colloid-chemical investigations of "bound" water if such investigations must be carried out without destruction of the macro- and microstructure of the object studied [7].

SUMMARY

1. The x-ray structure analysis method was used to study ice formation in wheat grains in relation to the moisture content in the grains.

2. Apparatus has been developed for the x-ray structure analysis of wheat germ at –120°.

3. It is shown that when moist grains are frozen ice does not form in them even at moisture contents up to 35%. Hence it follows that a considerable part of the water is in the "bound" state when the grains are swollen.

4. The results obtained shed new light on the role of ice formation in the resistance of plants to low temperatures, and necessitate a revision of the vitrification theory proposed by Luyet and other authors.

5. The method which has been developed for studying ice formation may find applications in colloid and technical chemistry for the determination of "bound" water in various materials and systems during humidification.

The authors express their gratitude to Academician P. A. Rebinder for reading the manuscript, and to G. S. Zhdanov and G. A. Golder for discussion of the x-ray diagrams.

LITERATURE CITED

[1] P. Yu. Shmidt, Anabiosis, Moscow (1948); E. Ya. Graevsky, Progr. Mod. Biol., 25, No. 2, 185 (1949); M. C. Lockett and B. I. Luyet, Biodynamica 7, No. 134, 67 (1951).

[2] E. F. Burton and W. F. Oliver, Proc. Roy Soc., 153, No. 878, 166 (1936).

[3] D. M. Dennison, Phys. Rev. 17, 20 (1921).

[4] W. Barnes and F. Matthews, Biodynamica, No. 49, 1 (1939).

[5] B. I. Luyet and P. M. Gehenio, Biodynamica, 6, No. 110, 93 (1946).

[6] J. R. Katz, Roentgenography of High Polymers, Colloids, Animal and Plant Tissues, Moscow, p. 214 (1937 T. Moran, Proc. Roy. Soc., A, 112, 460, 30 (1926).

[7] E. Kharin, Collected Papers " Technological Processes and Control in the Food Industry", edited by A. V Dumansky, Voronezh, p. 29 (1938); A. G. Kulman, Colloid Chemistry in Bread Baking, Moscow (1953).

Received January 7, 1955

Institute of Biophysics Academy of Sciences
USSR, Laboratory of Radiation Biophysics,
Moscow

SOLVATION OF ALUMINUM HYDROXIDE HYDROSOL IN AQUEOUS ALCOHOL SOLUTIONS

P. V. Rufimsky

The solvation of ions in solution has long been considered as fully proved. However, little information is available on the properties of solvates, with the exception of some rather contradictory determinations of the energy of solvation and of the number of solvent molecules surrounding the ion [1]. Afanasyev and Roginsky [2] attempted to investigate solvation kinetics, but later work [3] did not confirm their results. In 1947, Zaidel and Rotshtein [4] published a paper on the structure of the solvate layers of neodymium ions in aqueous alcohol solutions. The conclusions reached in their investigation may be summarized as follows:

1. The addition of small amounts of water to alcoholic neodymium chloride solution results in replacement of the solvating alcohol molecules by water molecules. Hence the authors conclude that the solvation energy of neodymium ions by water is greater than the solvation energy of neodymium ions by alcohol.

2. The existence of mixed solvates, or neodymium ions solvated by alcohol and water molecules simultaneously, is impossible at low contents of water in the solution. If the amount of water present in solution is insufficient for solvation of all the neodymium ions, the solution contains a mixture of two solvates – purely aqueous, and purely alcoholic.

Popov and Pominov [5] showed in a study of the solvation of ferric ions in aqueous alcohol solutions of ferric chloride that independent solvate layers of purely aqueous and purely alcoholic type exist in such solutions. Bogoyavlensky [6], in a study of the solvation of ferric hydroxide hydrosol in aqueous alcohol solutions, concluded that the "preferential sorption" curve is S-shaped, indicating inversion of the sorption of the components of the mixture; he succeeded in establishing a relationship between the region of the thixotropic gelatin region of the sol and the "preferential sorption" of the aqueous component of the mixture; the author points out that this relationship is not accidental and sheds some light on the mechanism of the thixotropic gelation of a highly disperse ferric hydroxide sol in the presence of alcohol.

METHOD

A necessary and fundamental condition for the determination of the composition of the solvate layer of a micelle is, in our view, that the state of the sol should remain unchanged in the course of any measurement. The best and most reliable method for this purpose would be spectrophotometric analysis, in which no great changes in the state of the sol occur, such as are found in the use of the generally known methods for the determination of solvation (the cryoscopic and ebullioscopic methods, the method involving the solubility of a "third" substance, electrolytic transport of water [7] etc.). However, it was found in preliminary experiments that the region of light absorption by micelles of Al_2O_3 sols lies in the ultraviolet region of the spectrum, which made the experiment difficult to perform in our conditions (absence of a hydrogen lamp). Therefore it was decided to use the "effective" sorption method, used by Vilensky [8] in investigations of alcoholic zein solutions, for studying the solvate layers, since this method has already been tested by Bogoyavlensky [6] in a study of the composition of mixed solvates of Fe_2O_3 hydrosols, with the only difference that instead of equilibrium dialysis he used ultrafiltration of a previously prepared solution, consisting of the sol, alcohol, and water. Mixtures with the components in different proportions were prepared. The ultrafiltration was continued for 24-48 hours, and was accompanied by refractometric determinations of alcohol in the filtrate.

Assume that c_0 is the concentration of component A (alcohol) in per cent by weight in the original mixture, and v and d are the volume and the density of the mixture respectively; then the number of grams q of the component A taken will be:

$$q = \frac{c_0 vd}{100}.$$

If the number of grams of A combined in solvate form with 1 g of colloid is denoted by s, then the total amount of component A bound with m grams of the colloid substance in the mixture will be:

$$x = sm.$$

Let the amount of the component B combined in solvate form with 1 g of colloid be g; then the total weight in grams of the second component bound with m grams of the colloid substance will be

$$y = gm$$

The amount of component A remaining free will be:

$$q - x = \frac{c_0 vd}{100} - sm,$$

and the amount of free mixture will be:

$$z = \frac{vd - (sm + gm)}{100}. \qquad (1)$$

The concentration of the free component A in the free intermicellar liquid will then be:

$$c = \frac{[(c_0 vd/100) - sm] \cdot 100}{vd - m(s + g)}. \qquad (2)$$

The change in the concentration of the component A on simultaneous sorption of the components A and B (alcohol and water) will be:

$$c_0 - c = \frac{(100 \cdot s - sc - gc)\, 100}{vd}. \qquad (3)$$

If the specific change of concentration is denoted by Γ, then we have:

$$\Gamma = (c_0 - c) = \frac{(c_0 - c)\, vd}{100m}. \qquad (4)$$

By analogy with the terms adopted in studies of adsorption from solution, Γ may be termed the "apparent" or "effective" sorption of the component A from a solution consisting of two solvents, A and B. The following expression is readily derived for Γ:

$$\Gamma = s(1 - c/100) - gc/100. \qquad (5)$$

Equation (5) shows that, according to the relative amounts of the components A and B bound, (that is, according to the value of the ratio s/g), Γ may become positive, negative, or zero, thus:

$$\Gamma = 0 \text{ at } s/g = c/(100 - c); \qquad (6)$$

$$\Gamma > 0 \text{ at } s/g > c/(100 - c); \qquad (7)$$

$$\Gamma < 0 \text{ at } s/g < c/(100 - c). \qquad (8)$$

Equation (6) shows that "effective sorption" does not take place if the ratio of components A and B in the solvate layer is equal to their ratio in the intermicellar liquid. Inequality (7) shows that the "effective sorption" has a positive value for component A (alcohol) and that the content of the latter in the solvate layer is relatively high. Inequality (8) gives a negative value for the "effective sorption", indicating predominant sorption of component B (water). Analysis of Equation (4) shows that the composition of the solvate layer around the Al_2O_3 micelle in a mixed alcohol-water solvent may be determined by means of a graph for the "predominant" (effective) sorption over the widest possible concentration range of the aqueous alcohol mixture.

EXPERIMENTAL

A mixture of Al_2O_3 sol of maximum concentration, alcohol, and water was first prepared. The alumina sol was prepared by Crum's method [9]. The maximum concentration of the sol was 9.02 g/liter. The mixture was kept for a while for equilibrium to become established, and then subjected to ultrafiltration through collodion ultrafilters; the latter were previously denitrated by means of an aqueous alcohol solution of ammonium sulfide so that the mixture could not be affected by the collodion. Samples of the ultrafiltrate were tested to establish that the denitrated collodion ultrafilter had not reacted with the aqueous alcohol medium.

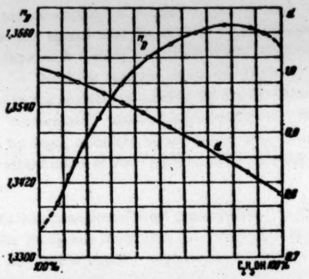

Fig. 1. Refractive index (n_D) and density (d) of aqueous alcohol aluminum hydroxide sols.

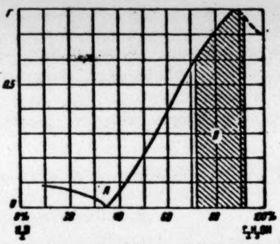

Fig. 2 Curve for the solvation of aluminum hydroxide sol in alcohol – water mixtures; A) predominant alcohol sorption; B) thixotropic gelatin region.

The alcohol content of the ultrafiltrates obtained from mixtures of variable composition was determined refractometrically in the alcohol concentration range up to 50%, and from the density of the ultrafiltrate for more concentrated solutions. This gave the concentration (c) of alcohol in the intermicellar liquid. The value of the "predominant" sorption was calculated from Equation (5). The density d of the mixture, and the other data v, c_0 and m required for the calculation, were determined by the usual methods. The experimental results are shown in the table.

TABLE

Effective Sorption of Alcohol by Al_2O_3 from Aqueous Alcohol Mixtures (Al_2O_3 Concentration 9.02 g/liter)

c_0 of alcohol, %	n_D^{15}	d of mixture (alcohol + ultrafiltrate)	Ultrafiltrate		Γ		
			d of ultrafiltrate	c of alcohol	c_0-c	g/g	moles/g·10^{-3}
93.8	1.365	0.796	0.834	84.2	9.58	0.799	17.3
87.7	1.367	0.831	0.846	74.8	9.92	0.839	18.2
76.1	1.367	0.859	0.877	68.3	7.82	0.685	14.9
65.0	1.366	0.883	0.908	59.6	5.35	0.486	10.5
54.4	1.364	0.910	0.922	51.3	3.08	0.284	6.2
44.3	1.362	0.932	0.932	42.7	1.61	0.150	3.2
34.6	1.357	0.950	0.951	34.6	0.00	±0.000	± 0.0
25.4	1.351	0.966	0.968	25.0	0.46	0.044	0.9
16.6	1.346	0.981	0.980	15.7	0.86	0.084	1.8
8.3	1.339	0.991	0.991	7.3	0.83	0.082	1.8

A reference curve (Fig. 1, Curve n_D) was plotted on the basis of the data obtained in order to determine the nature of the solvation of the sol in aqueous alcohol mixtures of variable composition. The curve shows that the refractive index increases with increasing alcohol concentration in the system and passes through a maximum. The curve for the density as a function of the sol ultrafiltrate concentration has no maxima or minima (Fig. 1, Curve d).

The course of the "preferential" sorption curve was calculated by Vilensky's method with the aid of the experimental data shown in Fig. 1. The results are shown in Fig. 2, in which the composition of the aqueous alcoholic Al_2O_3 sol is shown along the absicissa axis, and values of Γ along the ordinate axis.

An examination of the graph in Fig. 2 shows that, with rising alcohol content in the sol, the "preferential" sorption of water ($\Gamma > 0$) decreases, reaches a minimum at 34.6% alcohol ($\Gamma = 0$), and then rises again. This descent of the curve for the "preferential" sorption of water by the sol may be attributed to the fact that with increasing alcohol content the amount of sorbed water decreases, and the amount of sorbed alcohol correspondingly increases. The increased sorption of alcohol evidently leads to decreased sorption of water. This increase in the sorption of alcohol generally agrees with the state of affairs observed by Bogoyavlensky [6] for a Fe_2O_3 hydrosol. Our experiments did not show such a sharp transition of the "preferential" sorption curve into the region of negative values of ($\Gamma < 0$) as was found for aqueous alcoholic Fe_2O_3 sols, but there was still a decrease in the sorption of water and an increase in the sorption of alcohol by the sol micelles. Thus, a special feature of the behavior of the sol studied is that "preferential" alcohol sorption does not reach $\Gamma < 0$, which may be attributed either to weaker sorption of alcohol by Al_2O_3 micelles, or to the low concentration of the sol studied. The latter was probably the reason for the peculiar course of the "preferential" sorption curve, which, although somewhat "smoothed", still retains its S-shape.

An examination of the "preferential" sorption data in conjunction with the thixotropic properties of aqueous-alcoholic Al_2O_3 sols shows that the thixotropic gelation region is found at 71.1% alcohol concentration, which is the part of the "preferential" sorption curve where a rise in the sorption of water occurs.

SUMMARY

1. A modification of Vilensky's method was used to study the solvation of Al_2O_3 sol of maximum concentration in alcohol-water mixtures over a wide range of compositions.

2. It is shown that the sorption of water varies with changes in the alcohol content of aqueous-alcoholic alumina sols; this is probably the result of an increase in the alcohol sorption.

3. It is established that the region of thixotropic gelation of the alumina sol occurs in the part of the curve for the "preferential" alcohol sorption where increased sorption of water takes place.

4. It is established that the beginning of the thixotropic gelation region of alumina sol does not coincide with the minimum on the curve, but is displaced in the direction of maximum alcohol concentation (71.1 − 92.2%).

Finally, it is my pleasant duty to express my deep gratitude to Professor A. F. Bogoyavlensky for valuable advice and guidance in the course of the work.

LITERATURE CITED

[1] H. Ulich, Hand.u. Jahrb. d. Chem. Phys., 6, IIB, 17-19 (1953).

[2] P. B. Afanasyev and S. Z. Roginsky, Proc. Acad. Sci. USSR, 26, 384 (1940).

[3] A. E. Polesitsky and F. L. Temerlin, Proc. Acad. Sci. USSR, 30, 803 (1941).

[4] A. N. Zaidel and V. Rotshtein, Proc. Acad. Sci. USSR, 57, 587 (1947).

[5] L. V. Popov and I. S. Pominov, Annals State Univ. Kazan, 110, No. 8 (1950).

[6] A. F. Bogoyavlensky, Annals State Univ. Kazan, 110, No. 2 (1950); Trans. All-Union Conf. Colloid Chem. Acad. Sci. Ukrainian SSR Press (1952).

[7] I. S. Tartakovsky, Mem. State Univ. Dnepropetrovsk, Ukrainian SSR, 1,153 (1938).

[8] V. A. Vilensky and V A. Pavlova, Colloid J., 6, No. 7, 607 (1940).

[9] M. Aschenbrenner., Z. phys. Chem. 127, 415 (1927).

Received April 2,1955

The V. I. Lenin State University
Kazan

ION EXCHANGE BETWEEN STREPTOMYCIN AND SODIUM AND CALCIUM IONS ON PERMUTITE

G. V. Samsonov and S. E. Bresler

The ion exchange of complex organic compounds on ionites differs in many ways from the exchange of metal ions. Firstly, in addition to the purely electrostatic action between the ion and the ionite, Van der Waals forces should also have an effect, particularly in the case of organic compounds with different functional groups – carboxyl, hydroxyl, amino, etc. It has been shown by Kressman and Kitchener [1] that the exchange constant is greatly increased as the result of such additional action. In addition, far from all the active centers are accessible to ions with large radii in the exchange of complex ions on the majority of ionites. The exchange capacity of an ionite for complex organic ions is equal to the maximum possible quantity of the complex organic ions absorbed (in mg-equiv./ g of ionite). This value is evidently less than the total exchange capacity of the ionite measured for a usual ion of small radius. In consequence, not all the metal ions present on the ionite can be exchanged by complex ions. In other words, some of the active centers must be excluded from consideration in studies of the laws of complex ion exchange. In the ion exchange equation [2]:

$$\frac{m_1^{1/z_1}}{m_2^{1/z_2}} = K\frac{c_1^{1/z_1}}{c_2^{1/z_2}} \qquad (1)$$

the sorption capacity for complex ions (for example m_1) is equal to the total quantity of the ions of this type adsorbed. The sorption capacity for the second type of ion (m_2), for example, metal ions, in Equation (1) must be calculated as the difference between the exchange capacity of the ionite for the complex ions, m, and the sorption capacity of the complex ions m_1 ($m_2 = m - m_1$).

The exchange of two ions of different valencies is of special interest from the viewpoint of the effect of the concentration of these ions in solution on their sorption capacity by the ionite. Simple analysis of the ion exchange Equation (1) shows that decrease of the ionic concentrations in the solution, with the ratio of the concentrations remaining constant (in simple dilution), leads to an increase in the sorption capacity of ions with the larger charge, and a decrease in the sorption capacity of ions with the smaller charge [3,4,5].

Equation (1), under the condition that $c_1/c_2 = p$ (p is a constant), takes the following form:

$$\frac{m_1^{1/z_1}}{m_2^{1/z_2}} = Kp^{1/z_1}c_2^{1/z_1 - 1/z_2} = A. \qquad (2)$$

If $z_1 > z_2$, then $\lim\limits_{c_2 \to 0} A = \infty$, which can be fulfilled only for $m_2 = 0$ and $m_1 = m$.

The preferential sorption of multivalent ions from solutions of low concentrations is a general law, which is commonly used in water softening and in the extraction of multivalent metals from industrial waste liquors.

The change in the sorption selectivity of ions with different valencies on dilution is easily explained on simple statistical grounds – the decreased probability of the complex collisions necessary for the displacement of one multivalent ion from the ionite by a group of univalent ions.

EXPERIMENTAL

The permutite was prepared by the method described by Kurnakov, Berg and Sveshnikova [6]. 2% solutions of sodium aluminate and silicate were mixed; an aluminosilicate gel was formed after 30-40 seconds. A considerable amount of water separated out during aging for twenty-four hours, and the gel was then dried at 60-65°. The permutite was comminuted to a grain size of 0.10-0.20 mm, and washed with distilled water to remove impurities, after which it was saturated with sodium or calcium by treatment with 10% sodium chloride or calcium chloride solution in dynamic conditions. Finally, the permutite was washed with distilled water and dried at room temperature.

Streptomycin is an organic base; it forms salts the composition of which indicates the presence of three basic groups in the molecule.

A specially prepared sample of streptomycin hydrochloride of a high degree of purity was used for the ion exchange studies. The streptomycin content was 550-600 μg of the streptomycin base per mg (1 unit represents 1 μg of the streptomycin base). In addition to some mannosidostreptomycin, the electrochemical properties of which with respect to ionites do not differ from those of streptomycin, the product also contained 10-20% NaCl. As will be seen later, this amount of sodium could not have any appreciable effect on the ion exchange results obtained.

The streptomycin content in solution was determined by the formation of maltol [7] which gives a violet color in presence of iron salts. The relationship between the extinction and the streptomycin concentration in such solutions obeys the Lambert-Beer law with great accuracy. The light absorption in solution was determined spectrophotometrically at a wave length $\lambda = 525$ mμ.

A study of the equivalence of streptomycin and sodium exchange on permutite by the dynamic method showed that one streptomycin ion displaces three sodium ions. The sorption of streptomycin by permutite is fully reversible, in contrast to the sorption of streptomycin by sulfonic resins and by most molecular adsorbents. Highly concentrated solutions of common salt completely displace streptomycin from permutite.

Potentiometric titration of streptomycin showed that the lower dissociation constant $pK > 7.0$, and therefore at pH 6-6.5 streptomycin is completely dissociated and is present in solution in the form of trivalent cations.

Ion exchange between streptomycin and sodium ions (on sodium permutite) and calcium ions (on calcium permutite) was studied by the dynamic method. A solution of streptomycin hydrochloride and sodium (or calcium) chloride was passed through a column 1 cm in diameter, containing 10 g of permutite until the streptomycin concentration in the percolate reached the streptomycin concentration in the original solution. The solution flow rate was 100 ml/hour. cm^2. The amount of adsorbed streptomycin in equilibrium with the original solution was determined graphically.

The exchange capacity of permutite with respect to streptomycin, determined by the dynamic method, is 0.1-0.2 mg-equiv./liter, which is ~ 5% of the exchange capacity of permutite with respect to calcium (3.8 mg-equiv./liter).

Thus, streptomycin can occupy only a very small part of the active centers in permutite at which exchange of metal ions takes place. Table 1 shows the results of determinations of the exchange capacity of permutite for streptomycin, for various grain sizes.

TABLE 1

Exchange Capacity of Permutite for Streptomycin for Various Permutite Grain Sizes

Grain diameter, mm	Exchange capacity for streptomycin	
	in mg/g	in mg-eqiuv./liter
0.10 – 0.15	45.5	0.234
0.15 – 0.20	44.7	0.230
0.20 – 0.30	43.5	0.224

These results show that streptomycin is adsorbed not only on the grain surface, but within the permutite grains, as the change in the exchange capacity is many times less than the change in the external grain area.

The exchange of streptomycin and sodium ions was studied at high sodium ion concentrations, as otherwise the streptomycin sorption capacity m_1 did not differ sufficiently from the exchange capacity $\underline{m}$. Different specimens of permutite prepared by the same method give appreciably different results (Table 2). The functional relationship (for two specimens of permutite) shown in Fig. 1 confirms the view stated above that only part of the active centers occupied by sodium must be considered.

Despite the fact that the ionic activity coefficients differed from unity because of the high sodium ion concentration in the solutions, Nikolsky's equation is applicable to this system, which contains a highly complex trivalent ion.

Table 3 shows the results of determinations of the sorption capacity of calcium permutite for streptomycin, which show that the exchange of the trivalent streptomycin ion for the bivalent calcium ion obeys Equation (1).

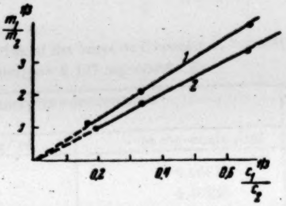

Fig. 1. Exchange of streptomycin and sodium on two specimens of permutite (see Table 2).

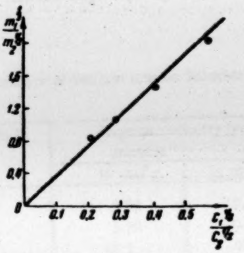

Fig. 2. Exchange of streptomycin and calcium on permutite.

TABLE 2

Sorption Capacity of Permutite for Streptomycin at Various Sodium Ion Concentrations (Streptomycin Concentrtion 0.3 mg/ml, or 0.00155 mg-equiv./ml).

Permutite specimen No.	Exchange capacity for streptomycin in mg-eqiuv /g	Sodium ion concentration in mg-equiv./ml	Sorption capacity for streptomycin		Permutite specimen No.	Exchange capacity for streptomycin in mg-equiv./g	Sodium ion concentration in mg-equiv/ml	Sorption capacity for streptomycin	
			in mg/g	in mg-equiv/g				in mg/g	in mg-equiv/g
2	0.109	0.171	6.2	0.0320	3	0.143	0.171	8.15	0.0421
2	0.109	0.342	1.75	0.0090	3	0.143	0.342	2.17	0.0112
2	0.109	0.684	0.31	0.0016	3	0.143	0.684	0.58	0.0030

TABLE 3

Sorption Capacity of Calcium Permutite for Streptomycin at Various Calcium Ion Concentrations (Streptomycin Concentration 0.00517 mg-equiv./ml)

Calcium concentration in mg-equiv./ml	Sorption capacity for streptomycin		Calcium concentration in mg-equiv./ml	Sorption capacity for streptomycin	
	in mg/g	in mg-equiv./g		in mg/g	in mg-equiv/g
0.0090	12.4	0.0382	0.0360	4.60	0.0155
0.0180	7.20	0.0236	0.0720	1.50	0.0078

Despite the complex nature of the organic ions, their exchange for simple sodium and calcium ions obeys, in the first approximation, the Nikolsky equation (Figs. 1 and 2). The value of the exchange constant (K) is 6.2 and 5.2 for Na-permutite, and 3.7 for Ca-permutite.

The possibility of preferential adsorption of streptomycin, on dilution of the solutions, from solutions containing other ions is of great practical interest. It is possible to show with the aid of Equation (2) and with the use of the exchange constants found above that the adsorption capacity of streptomycin by permutite should very greatly increase on dilution of solutions containing high concentrations of sodium ions.

Table 4 shows the results of measurements of the adsorption capacity of streptomycin from a solution containing streptomycin hydrochloride and common salt, on dilution of the solution.

The sodium ion concentration in the original solution was approximately 300 times as great as the streptomycin ion concentration in terms of molar ratios, and more than 30 times as great in a weight ratio. The streptomycin adsorption capacity in these conditions is very low – 2.18 mg/g. With a tenfold dilution of the solution, despite the unchanged ratio of the ionic concentrations, the streptomycin adsorption capacity increased approximately 10 times, and reached a value rather greater than half the exchange capacity of permutite with respect to streptomycin.

TABLE 4
Variation of the Sorption Capacity of Permutite for Streptomycin in Presence of Sodium Ions on Dilution of the Solution ($m = 0.197$ mg-equiv./g).

Streptomycin concentration		Sodium concentration in mg-equiv./ml	Sorption capacity for streptomycin	
in mg/ml	in mg-equiv./ml		in mg/g	in mg-equiv./g
1000	0.00517	1.50	2.18	0.0112
500	0.00258	0.75	5.52	0.0285
200	0.00103	0.30	16.1	0.0835
100	0.00052	0.15	22.3	0.115

In conclusion, we express our gratitude to L. M. Shuvalova, V. S. Maslennikova, and M. P. Shesterikova for assistance in the experimental work.

SUMMARY

1. It is shown that the exchange of streptomycin ions for sodium and calcium ions on permutite is reversible.

2. In studies of the laws of complex ion exchange it is necessary to consider only that part of the metal ions on the ionite which is available for exchange with the complex ions. Under this condition, the exchange of complex organic ions obeys the Nikolsky equation.

3. Dilution of a solution containing streptomycin and sodium ions results in a great increase in the selectivity of streptomycin adsorption by permutite.

LITERATURE CITED

[1] T. R. Kressman, J. A. Kitchener J. Chem., Soc., 1208 (1949).

[2] B. P. Nikolsky, Doctorate Dissertation, University of Leningrad (1939); B. P. Nikolsky and V. I. Paramonov Prog. Chem., 8, 1535 (1939).

[3] K. K. Gedroits, The Sorptive Capacity of Soils, p. 62 (1932).

[4] E. N. Gapon and A. E. Pryanishnikova, Colloid J., 3, 347 (1937); E. N. Gapon and A. I. Ivanov, Colloid J., 3, 443 (1937); E. N. Gapon and N. I. Gorbunov, Colloid J., 3, 447 (1937).

[5] K. M. Saladze and E. A. Bozhevolnov, Colloid J., 16, 387 (1954) (T.p. 371)*.

[6] N. S. Kurnakov, L. G. Berg, and V. N. Sveshnikova, Bull. Acad. Sci. USSR, Chem. Ser., 6, 1381 (1937).

[7] J. R. Schenk and M. Y. Spielman, J. Am. Chem. Soc., 67, 2276 (1945).

Received March 17, 1955

Institute of High Molecular Compounds Academy of Scienc
USSR, Moscow

---

* T.p. = C. B. Translation pagination

INVESTIGATION OF THE SPECIFIC SURFACE OF INDIVIDUAL CEMENT COMPONENTS AND ITS VARIATIONS IN AN AQUEOUS MEDIUM WITH THE AID OF RADIOACTIVE TRACERS

A. M. Smirnova, N. G. Zaitseva, and P. A. Rebinder

Specific surface determinations of hydrated cements are of great interest, as the magnitude of the active surface primarily determines the rates of the setting and hardening processes. The surface area should change continuously during hydration [1], and should increase sharply at first as the result of spontaneous adsorptional chemical dispersion [2]. In this connection it is very desirable to determine the surface in an aqueous medium at any given instant of hydration, that is, the " instantaneous degree of dispersion".

Up to the present time, however, the specific surface of cements has only been determined in the dry state. The most widely used methods for the determination of specific surface in an aqueous medium have been dye adsorption and surface exchange methods with the use of radioactive atoms (ions), first used by Paneth [3].

In a study of the hydration kinetics of cement clinker components by the radioactive tracer method [4] it was established that the hydration rate is proportional to the active surface of the clinker components, determined from the initial rate of isotope exchange.

An attempt was made in the present investigation to apply the radioactive tracer method to a determination of the specific surface of the three main individual components in cement clinker, in powder form; tricalcium aluminate $3CaO \cdot Al_2O_3$, tricalcium silicate $3CaO \cdot SiO_2$, dicalcium silicate $2CaO \cdot SiO_2$, and Portland cement as a whole, during their reaction with water. The surface of the crystal lattice was determined from the surface of the calcium ions present in it, which gave a conventional value for the specific surface.

The tracers used were calcium-45 ions (ionic radius $r \sim 1A$) in the form of calcium hydroxide and chloride, and also strontium Sr^{89} ($r = 1.27$ A) in the form of strontium nitrate or chloride. The surface of the dry powders was determined by Deryagin's method [5], based on measurement of the resistance offered by a porous body to the passage of rarefied air, and by the nitrogen adsorption method [6].

METHOD

All the materials were investigated in the form of a powder fraction which passed through a 250 mesh sieve, and also characterized by its specific surface in the dry state. A weighed sample of the material was placed in the appropriate labeled electrolyte solution of definite concentration (from 0.18 to 0.045%). A dilute suspension of the material was used (1.25% solid phase) which was advantageous from the experimental viewpoint. All the experiments were carried out at room temperature with continuous stirring at a constant rate. The amount of calcium or other labeled ion passing into the solid phase was determined from the decrease in the activity of the aqueous phase at a given time.

The activity of the solution was determined by means of the apparatus B by a plane face counter. The target was a paper filter of accurately determined dimensions containing the filtered specimen (0.1 cc). Particular attention was paid to careful and rapid separation of the filtrate, for which the filtration was carried out through a dense paper filter with the aid of a water-jet pump. The conventional value of the specific surface S_1 was calculated with the aid of the formula .

$$S_1 = a_m \omega N,$$

where a_m is the number of gram-atoms of the substance bound by 1 g of the solid phase ; ω is the area for each adsorbed or exchanged ion; N is the Avogadro number.

In determinations of specific surface by the surface exchange method, it was necessary to differentiate between the primary (rapid) surface exchange, and secondary exchange within the crystal lattice, which could be achieved by studies of the kinetics of the transition of ions from solution into the precipitate.

EXPERIMENTAL RESULTS

Fig. 1 shows curves for the absorption of calcium by tricalcium aluminate powder, calculated from the decrease of activity as a function of the contact time. Chemical analysis of the solution showed that its calcium content, despite the decreased activity of the solution, remained constant throughout the experiment, which shows conclusively that isotope exchange took place between the calcium ions in solution and in the crystal lattice.

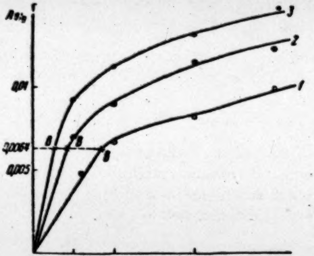

Fig. 1. Absorption of calcium from calcium chloride solution by tricalcium aluminate powder, calculated from the decrease of activity: 1) calcium content in solution 0.045 %; 2) ditto, 0.06%; 3) ditto, 0.09%.

All the curves in Fig. 1 have two characteristic regions: a region of fairly rapid absorption – the proportionality region, and a region of slower absorption, so that the curve shows a fairly sharp inflexion. On the assumption that the proportionality region represents the amount of calcium required to cover the surface, it was reasonable to suppose that the inflexion of the curve at the point B represents the complete filling of the surface. The subsequent slow ascent of the curve must probably be attributed to diffusion of calcium into the particles.

Fig. 1 shows that the time required for complete covering of the surface increases with decreasing concentration of calcium chloride in the solution. Thus, at a concentration of 0.045% calcium, surface ion exchange is practically completed in 1 minute, at 0.06%, in 30 seconds, and at 0.09% in 20 seconds. The ordinate of the point B, however, corresponds to practically the same amount of calcium, 6.4 mg/g, for all concentrations. This value was used in the determination of the conventional specific surface of tricalcium aluminate, which by this method of calculation had the value $S_1 = 3.1\ m^2/g$.

In determinations of the surface of tri- and dicalcium silicate by the use of calcium in labeled calcium chloride solution somewhat different results were obtained, probably as the consequence of structural features of the crystal lattice. The rate of calcium ion exchange on the surface of these substances is practically independent of the calcium concentration in the solution, in the range studied, between 0.18 and 0.045 %. The surface was determined from the amount of calcium exchanged during the first 30-40 seconds of contact between the powder and the calcium chloride solution, probably caused by rapid hydrolytic removal of calcium oxide, and in consequence the calcium which was exchanged during the first minute again passes into solution. The surface exchange reaches a stable state after 5-7 minutes. The surface of tricalcium silicate determined in this way was $S_1 = 3.4\ m^2/g$, and that of dicalcium silicate was $S_1 = 2.26\ m^2/g$.

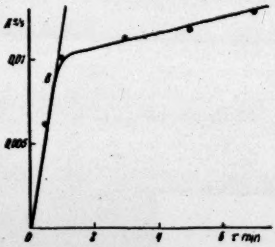

Fig. 2. Absorption of calcium by tricalcium silicate powder from calcium hydroxide solution with a concentration of 0.09% Ca (from activity data).

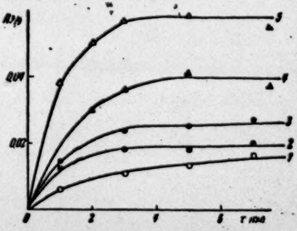

Fig. 3. Absorption of calcium by tricalcium aluminate powder (from activity data) from calcium hydroxide solution; concentrations: 1) 0.023%, 2) 0.03%, 3) 0.045%; 4) 0.06%; 5) 0.09%.

In the determination of the surface of tricalcium silicate by means of calcium ions in labeled calcium hydroxide solution it was found that isotope exchange between the calcium ions in the solution and in the lattice takes place here also. The surface of the compound was determined from the proportionality region of the isotope exchange curve (Fig. 2). The abscissa axis shows the time, and the ordinate axis the amount of calcium passing into the precipitate, in g/g. The curve has a sharp inflexion at the point B, which corresponds to complete covering of the surface. The amount of calcium which passed into the precipitate corresponding to point B was used for calculation of the surface, which in this case was $S_1 = 4.2\ m^2/g$. Less reproducible results were obtained when lower concentrations of calcium hydroxide were used. The surface of cement powder ("Gigant") determined by calcium exchange from calcium hydroxide solution as described for tricalcium silicate had the value $S_1 = 3.0\ m^2/g$.

An attempt to use calcium hydroxide for determination of the surface of tricalcium aluminate gave the curves for calcium absorption in g/g as a function of times for different $Ca^{45}(OH)_2$ concentrations in solution, shown in Fig. 3.

Fig. 3 shows that adsorptional equilibrium is attained fairly quickly after 3-5 minutes at all concentrations, Chemical determination of the calcium ion content in the solution showed, in conjunction with the activity changes, that both isotope exchange and adsorption of Ca from solution take place in this case. Fig. 4 shows curves for the kinetics of the decrease of calcium content in labeled calcium hydroxide solution after contact with tricalcium aluminate powder, based on analytical data (Curve 1), showing the existence of adsorption, and on activity data (Curve 2), where the amount of calcium represents the sum of the adsorbed calcium and the calcium which passed into the precipitate by isotope exchange. From the difference between these two curves the amount of calcium lost from the solution by isotope exchange may be determined. The adsorption and surface exchange processes, as Fig. 4 shows, proceed at a practically equal rate. All this naturally makes the determination of the surface more complicated.

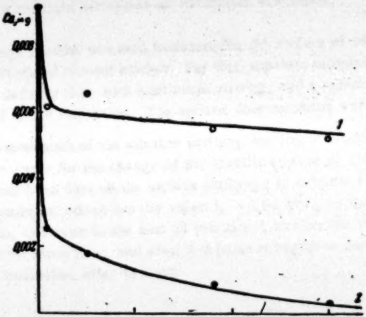

Fig. 4. Loss of calcium from solution after contact with tricalcium aluminate: 1) from analytical data; 2) from activity data.

For the plot of the adsorption isotherm (Fig. 5), the total amount of calcium which entered the precipitate, based on the decrease of the solution activity, was used.

The S-shaped form of the isotherm indicates the complex nature of the processes which occur on the surface of tricalcium aluminate. In this case it appears most appropriate to evaluate the surface from the amount of calcium which passed into the precipitate corresponding to the point A in Fig. 5, found by extrapolation of the central linear portion of the isotherm to zero concentration. This gave the surface as $S_1 = 4.7\ m^2/g$, which was fairly close to the values obtained by other methods.

The use of strontium ions for determination of the surface of cements gave curves for all the clinker components and for cement which were practically the same, and like the curve for the adsorption of calcium from $Ca(OH)_2$ by tricalcium aluminate, discussed above. Adsorptional equilibrium was already reached in the first minute of contact between the powder and the solution. In this instance also the surface could be determined only from the adsorption isotherm, which was S-shaped. The values obtained for the specific surface were very close to the values obtained by other methods (Table 1).

A comparison of the specific surface values in Table 1 shows that similar values were obtained for the separate components by determinations of the surface by the surface exchange from aqueous solution or the adsorption method. The fairly good agreement indicates that this method may be used for specific surface determinations of cements, although the most reliable method must be considered the surface determination with the aid of radioactive calcium from calcium chloride solution, as in this case isotope exchange only occurs, which can be kinetically separated fairly easily from the slower exchange within the crystal lattice.

A comparison of the results obtained by the exchange method in an aqueous medium with the results of surface deteterminations in the dry state (the low temperature nitrogen absorption method, and Deryagin's method) shows that the value of the surface determined by the radioactive tracer exchange method is about 2-3 times as high, which is accounted for by dispersion in the presence of water [2]. It should also be noted that in the dry state the surface of $3CaO \cdot SiO_2$ powder is 1.5-2 times as great as that of $3CaO \cdot Al_2O_3$.

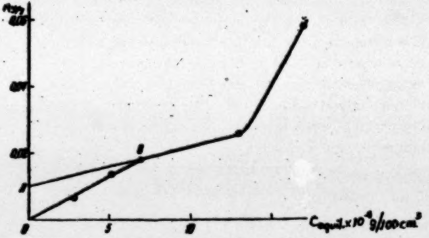

Fig. 5. Isotherm for calcium adsorption on tricalcium aluminate.

The surface exchange method was used to determine the surface of tricalcium aluminate, the most rapidly hydrating component of Portland cement clinker. For this, separate samples of tricalcium aluminate powder were kept in water for a definite time with continuous stirring, and a definite concentration of calcium chloride with Ca^{45} was then added to the suspension. The surface determination was then carried out as described above.

In addition to measurements of the solution activity, the loss of chloride ions was determined by chemical analysis. Fig. 6 shows the curve for the change of the specific surface of tricalcium aluminate as a function of hydration time, calculated from data on the surface exchange of calcium ions. Fig. 6 shows that the specific surface of tricalcium aluminate, which has the value $S_1 = 0.64$ m²/g in the dry state, increases rapidly during the first hour of hydration, and even in the first 30 minutes it reaches the value $S_1 = 11.1$ m²/g. The surface then remains unchanged for some time, and after 2-3 hours it begins to decrease, reaching 3.1 m²/g, the same as in the first minute of hydration, after 48 hours.

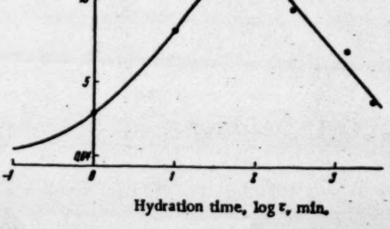

Fig. 6. Variation of the specific surface of tricalcium aluminate during hydration.

The results of chemical analysis showed that the hydration of tricalcium aluminate is accompanied by loss of chloride ions from solution (Fig. 7), but this does not correspond to the loss of calcium as given by activity data. Fig. 7 shows graphs for the kinetics of the transfer of calcium ions from solution into the precipitate: Curve 1 is based on loss of activity and Curve 2 on analytical data (loss of chloride ions).

TABLE 1

Specific Surface of Powdered Cement Clinker Materials in m^2/g

Method of determination	$3CaO \cdot Al_2O_3$	$3CaO \cdot SiO_2$	$2CaO \cdot SiO_2$	Cement
Calcium exchange from calcium chloride solution	3.1	3.4	2.3	3.0
Calcium exchange from calcium hydroxide solution	4.7	4.2	-	3.6
Strontium exchange from strontium nitrate solution	3.4	3.1	2.7	-
Deryagin's method	0.64	1.27	-	0.63
Nitrogen adsorption method	1.1	1.5	-	1.1

Fig. 7 shows that the amount of calcium ions passing into the solid phase is much less according to analytical data (Curve 2) than according to loss of activity (Curve 1). The results indicate that two processes occur simultaneously in the hydration of tricalcium aluminate: calcium chloride adsorption and isotope exchange.

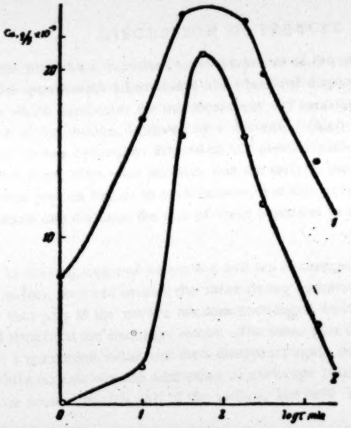

Fig. 7. Transfer of Ca ions from calcium chloride solution into the solid tricalcium aluminate during hydration; 1) from activity data; 2) from loss of chloride in solution.

The adso ption of calcium chloride is represented by Curve 1 while isotope exchange is given by the difference of the ordinates of Curves 1 and 2,, this difference being practically constant throughout the experiment. Fig 7 shows that the amount of calcium which entered the solid phase as the result of calcium chloride adsorption shows a maximum which coincides with the maximum surface development, while no calcium chloride adsorption takes place at all on a nonhydrated surface (a point corresponding to 3-5 minutes of hydration on Curve 2) or on a completely hydrate surface (after 2 days of hydration).

The choice of radioactive tracer used for studying the surface of tricalcium aluminate in the course of hydration is very important; for example, we found that when strontium Sr^{89} (strontium nitrate solution) or Ca^{45} (calcium hydroxide solution) was used as tracer, the loss of activity in the solution during hydration was constant, at a value approximately equivalent to 1 minute of hydration as found by the use of radioactive calcium in calcium chloride solution. In fact, however, the surface increased and the value passed through a maximum, as confirmed by adsorption of the dye indigo carmine, which was used for specific surface determination. The maximum surface in this case corresponded to approximately the hydration time found by means of surface exchange with the use of calcium chloride, 30-45 minutes.

TABLE 2

Transfer of Calcium and Chloride Ions from Calcium Chloride Solution into Solid Tricalcium Aluminate During Hydration

Hydration time	Calcium transferred to solid phase mg/g		Chloride transferred to solid phase, from analytical data, mg/g	Surface in m^2/g
	from activity data	from analytical data		
1 min.	7.7	0	0	3.1
10 min.	17.1	3.3	5.8	8.1
30 min.	23.5	16.1	28.5	11.1
3 hours	231.2	16.1	28.5	10.4
5 hours	19.9	12.9	22.9	9.4
24 hours	14.6	4.8	8.5	6.9
48 hours	8.3	0	0	3.7

DISCUSSION OF RESULTS

The above investigation provides a quantitative development of the concepts put forward by Rebinder and his co-workers [2] concerning the spontaneous adsorptional and chemical dispersion of the surface of tricalcium aluminate by the action of water which penetrates the microcrevices and becomes incorporated in the crystal lattice of the compound. The increase of the surface, followed by a decrease, which has been demonstrated, indicates that two opposing processes occur during hydration: dispersion and crystallization. These processes occur simultaneously, but at first, during the first hour, dispersion prevails, and the surface increases (Fig. 6). Later, after 2 hours of hydration, the recrystallization process begins to predominate, and this accounts for the existance of a maximum. The influence of various factors can displace the rate of these processes in either direction, and this may be studied quantitatively.

The results obtained in investigations of adsorption and ion exchange at the tricalcium aluminate surface lead to the conclusion that this surface does not remain the same during hydration, but acquires qualitatively different properties. It seems likely that part of the surface remains unchanged during hydration, and it is there that isotope exchange and calcium and strontium ion exchange occur. The other part of the surface, formed during the hydration process, which reaches a maximum value and then disappears again on complete hydration, selectively adsorbs calcium chloride, while no calcium ion adsorption or exchange takes place there. This leads to the supposition that no calcium ions are present on this part of the surface, but only Al and OH ions.

SUMMARY

1. A method for the determination of the specific surface of cement materials during hydration wih the aid of radioactive tracers has been developed.

2. It is shown that spontaneous dispersion takes place during hydration, as a result of which the surface reaches a maximum value during the first 30-45 minutes, increasing tens of times. Rapid recrystallization then begins to predominate, resulting in an increase of particle size and hence a decrease of specific surface.

3. It is established that both calcium ion exchange and calcium chloride adsorption take place during hydration of tricalcium aluminate. However, only ion exchange takes place at the nonhydrated and the fully hydrated surface, without any adsorption of calcium chloride.

LITERATURE CITED

[1] A. A. Baikov, Collected Works, Vol. V (1945).

[2] P. A. Rebinder and E. E. Segalova, Nature, No. 12, [illegible] (19[illegible]); E. E. Segalova, P. A. Rebinder, and O. I. Lukyanova, Bull. Moscow State Univ., No. 2 (1954).

[3] F. Paneth, and W. Vorwerk, Z. phys. Chem., 101, 44[illegible], 480 (1922); L. Imre, Koll.-Z. 99, 147, (1942); 106, 39 (1944).

[4] A. M. Smirnova and P. A. Rebinder, Proc. Acad. Sci., 1, 107 (19[illegible]).

[5] B. V. Deryagin, N. N. Zakhavaeva and M. V. Talaev, Apparatus for the Determination of the Specific Surface of Powders and Disperse Substances by Resistance to the Flow of Rarefield Air, Acad. Sci., USSR Press (1953).

[6] S. Brunauer, Adsorption of Gases and Vapors, Foreign Lit. Press, Part 1 (1948).

Received September 20, 1955

Institute of Physical Chemistry
Academy of Sciences USSR, Moscow

INVESTIGATIONS OF POLYVINYL ACETATE FRACTIONS BY THE OSMOMETRIC AND VISCOSIMETRIC METHODS

K. Z. Fattakhov, E. S. Pisarenko, and L. N. Verkhotina

Several papers have been published during the last decade on studies of polyvinyl acetate (PVA) fractions in acetone, benzene, and ethyl acetate by osmometric, viscosimetric, and light scattering methods. As a result of these investigations a relationship was established between the number average molecular weight $\bar{M}_n$ of PVA fractions and the intrinsic viscosity $[\eta]$ in acetone [1]; a comparative evaluation of the thermodynamic interaction between PVA and solvents was carried out [2], and views were put forward on the branching of PVA molecules in relation to the polymerization conditions [3]. In our opinion, some of these results, particularly with reference to branching of PVA molecules, are unconvincing and self-contradictory. The present paper contains the results of osmometric and viscosmetric determinations carried out with solutions of PVA fractions, and a comparison of these results with data obtained by other authors, in order to clarify the question of branching, to generalize experimental data on the relationship between $[\eta]$ and $\bar{M}_n$, and to compare the behavior of solvents (chloroform, benzene, ethyl acetate, acetone) toward PVA.

Polyvinyl acetate samples and their fractionation. The PVA samples denoted by the letters A and C were prepared by polymerization of vinyl acetate in presence of methyl alcohol, in a volume ratio of 1 : 1, at the boiling point of the mixture in presence of 0.1 % benzoyl peroxide calculated on the weight of vinyl acetate. The sample B was a block polymer polymerized at 40° with 0.03% benzoyl peroxide.

The vinyl acetate was distilled over a fractionating column (b.p. 73°) before polymerization in order to remove inhibitor and other impurities. Each sample was divided into 10 fractions on the average, by fractional precipitation by water from 2-4% acetone solution at 20°.

Measurements of the osmotic pressure of PVA fraction solutions in acetone. The osmotic pressure π was determined with the aid of an osmometer described previously [4] by a dynamic method at 20°. The temperature of the water thermostat containing the osmometer was maintained to an accuracy of 0.005° by means of a mercury-toluene thermoregulator and by temperature control of the room. The solutions were made in dried and redistilled chemically pure acetone, and were filtered through No. 3 and 4 glass filters. The original solution was concentrated by evaporation of part of it to constant weight.

Before the start of the determinations, the osmometer filled with the solution and the solvent was kept at constant temperature for 1-2 hours in order to level out any low molecular impurities present and to ensure that the temperature was equal in both cells of the osmometer.

The dynamic method used for the determination of π essentially consisted of establishing the variation with time of the difference of the capillary levels Δh for values of Δh greater and less than the osmotic pressure sought (Fig. 1). Observations of the variation were taken every two minutes with the aid of a microcathetometer to an accuracy of 0.15 mm. In order to shorten the observation time during the approach of the solution-solvent system to equilibrium, the values of Δh chosen differed little from π ($\Delta h \approx \pm 2$ mm). The osmotic pressure was calculated as half the sum of the differences given by $\Delta h \gtrless \pi$ as shown by the graph in Fig. 1.

The accuracy and the reproducibility of the osmotic pressure determinations were checked by the following operations: 1) the value of Δh for the pure solvent, ascribed to the so-called membrane "asymmetry" effect, was determined. The value of Δh for the two osmometers used for the experiments did not exceed the accuracy limits of the readings; 2) the permeability of the membrane (Cellophane) for fractions with relatively low molecular weights was investigated. It was found that the membranes used were practically impermeable to polymer molecules in the molecular weight range studied; 3) osmotic pressure was determined both by the dynamic and static methods at various concentrations. The results agreed within 0.2 mm; 4) the molecular weight of some of the fractions was determined simultaneously in two osmometers and in different solvents. The differences did not exceed 5-10%.

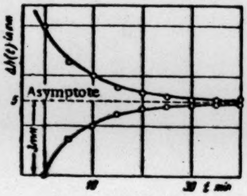

Fig. 1. Illustration of the difference of levels Δh as a function of time.

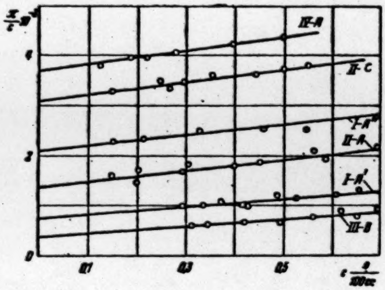

Fig. 2 The $\pi/c-c$ relationship for PVA fractions in acetone.

The results of determinations of the osmotic pressure of PVA fractions in acetone as a function of concentration are shown in Fig. 2.

Fig. 2 shows that in the concentration range 0.001-0.01 g/cc the relationship $\pi/c-c$ is represented by an equation of the form:

$$\pi/c = RT(1/\overline{M}_n + A_2c). \tag{1}$$

Here π/c is in centimeters; $\overline{M}_n$ is the number average molecular weight of the given fraction; A_2 is the second virial coefficient in cc/g. mole.

Extrapolation of the $\pi/c-c$ lines to infinite dilution, and their slopes gave the values of $(\pi/c)_0$, $\overline{M}_n$ and A_2 respectively (Table 1).

The results for fractions I-A' and II-A (Table 1) are averages based on measurements with two osmometers; the deviations of the molecular weight values did not exceed 10%. Fraction II-C was studied in chloroform; the molecular weight of this fraction was found to be $8.1\cdot10^4$ (instead of $8\cdot10^4$ in acetone). The fact that the values of A_2 were higher in chloroform than in acetone indicates the better solubility of PVA in chloroform. A tendency of A_2 to increase with decreasing molecular weight was also found. A similar tendency for A_2 to increase was observed by us previously [7] for polymethyl methacrylate in acetone, in light scattering studies.

Measurements of the viscosity of PVA fraction solutions in chloroform, benzene, ethyl acetate, and acetone. The viscosity measurements were made at 20° with the aid of the usual capillary viscosimeter with an acetone efflux time of 80 seconds, and an average velocity gradient of 2000 sec.$^{-1}$ for acetone.

TABLE 1

Number Average Molecular Weights of PVA Fractions

Fraction	$(\pi/c)_0\cdot10^{-2}$	$\overline{M}_n\cdot10^{-5}$	$A_2\cdot10^{-4}$
III-B	0.37	6.80	2.8
I-A'	0.72	3.50	3.2
II-A	1.35	1.86	4.4
I-A''	2.10	1.20	4.2
II-C	3.10	0.81	5.0
IV-A	3.72	0.68	5.2

A study of the relationship between acetone viscosity and the efflux rate showed that, in the velocity gradient region used in work with acetone solutions, corrections for kinetic energy and other effects may be neglected for practical purposes. The relative viscosities of the solutions were calculated as the ratios of the efflux times of the solution and the solvent, without regard to the slight density differences.

The accuracy and reproducibility of the values obtained for the reduced specific viscosities η_{sp}/c were checked by measurements of the variation of the viscosity of PVA solutions with concentration, with the aid of different viscosimeters (in particular, special viscosimeters, adapted for work with external pressure only, gave results agreeing within 2-3%), and by repeated determinations of the solution viscosities for all the PVA fractions studied. Variations in the values of $[\eta]$ did not exceed 2-3%.

The results of viscosimetric determinations in four solvents are given in the form of $\eta_{sp}/c-c$ graphs in Fig. 3.

In the concentration range 0.1-1 g/100 cc, the experimental relationsip between η_{sp}/c and c, as can be seen from Fig. 3, is represented by the expression

$$\eta_{sp}/c = [\eta] + k'[\eta]^2 c. \qquad (2)$$

TABLE 2

Intrinsic Viscosities of PVA Fractions in Various Solvents

PVA fractions	$\overline{M}_n \cdot 10^{-5}$	Chloroform		Benzene		Ethyl acetate		Acetone	
		[η]	k'	[η]	k'	[η]	k'	[η]	k'
III-B	6.80	3.28	0.36	2.32	0.32	2.20	0.35	2.10	0.38
I-A'	3.50	2.05	0.33	1.40	0.36	1.33	0.37	1.30	0.40
II-A	1.86	1.36	0.31	0.85	0.38	0.85	0.37	0.85	0.33
I-A''	1.20	1.05	0.28	–	–	–	–	0.64	0.36
II-C	0.80	0.67	0.35	–	–	–	–	0.46	0.37
IV-A	0.68	0.55	0.33	–	–	–	–	0.37	0.37
Average k'		0.32		0.36		0.36		0.37	

The values of the intrinsic viscosities [η] and of k' for the fractions studied are shown in Table 2.

The results in Table 2 show that the values for the intrinsic viscosity and k' of PVA fractions in benzene, ethyl acetate, and acetone differ very little. This indicates, on the one hand, that the relationship between [η] and $\overline{M}_n$ may be represented by the same equation for all three solvents, and on the other, that the solubility of PVA in these solvents is the same. This conclusion, based on a comparison of the values of [η], is in agreement with the direction of the change of the thermodynamic parameter A_2 in benzene, ethyl acetate [2], and chloroform.

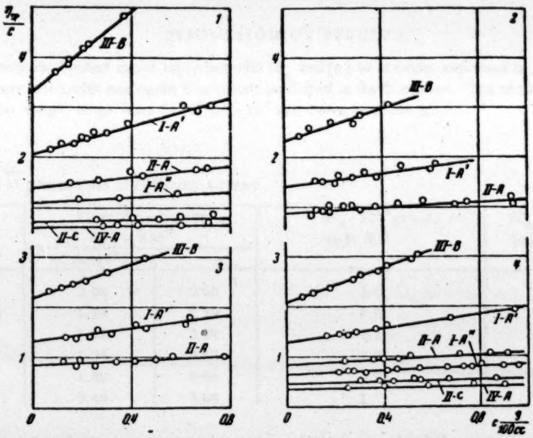

Fig. 3. The η_{sp}/c -c relationship for PVA fractions in the following solvents: 1) chloroform; 2) benzene; 3) ethyl acetate; 4) acetone.

Relationship between $\overline{M}_n$ and [η] for PVA fractions in acetone and chloroform. The relationship between the intrinsic viscosities in acetone and chloroform respectively and the number average molecular weights for the six PVA fractions may be written as follows:

(3)

and

$$[\eta] = 1.58 \cdot 10^{-4} \overline{M}_n^{0.[illegible]}. \qquad (4)$$

For comparison of our experimental results with literature data, Fig. 4 shows a graph for $\log[\eta]-\log \overline{M}_n$ based on data from the papers [1,3] and our own data.

Fig. 4 shows that all these data, in the molecular weight range $3 \cdot 10^4 - 1 \cdot 10^6$, can be approximately represented by the same straight line:

$$[\eta] = 2.09 \cdot 10^{-4} \overline{M}_n^{0.68}. \qquad (5)$$

The Points 4 in Fig. 4 were obtained in ethyl acetate [3]. Within the possible experimental error limits, as was clearly illustrated in the case of polystyrene [5], these results are also in agreement with Equation (5), although the authors of the paper [3] consider that their samples were strongly branched.

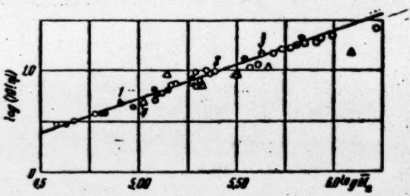

Fig. 4. The relationship $\log \eta - \log \overline{M}_n$ in acetone: 1) our data; 2) Wagner's; 3) Staudinger's; 4) Bosworth, Masson, Melville, and Peaker's.

DISCUSSION OF RESULTS

The relationship established in the study between $\overline{M}_n$ and $[\eta]$ in acetone, expressed in the form of Equation (5), has been compared with analogous expressions published in the literature. The results of this comparison for the molecular weight range from $3 \cdot 10^4$ to $1 \cdot 10^6$ are shown in Table 3.

TABLE 3

Values of k, α and $\overline{M}_n$ from Data of Different Authors

Authors	From the equation $[\eta] = kM^\alpha$		$\overline{M}_n \cdot 10^{-5}$ (calc.) at $[\eta] = 2.5$	$\overline{M}_n \cdot 10^{-5}$ (calc.) at $[\eta] = 2.5$
	$k \cdot 10^{+4}$	α		
General value	2.09	0.68	1.0	3.4
From own data only	1.74	0.70	0.9	3.2
Matthes [1]	1.41	0.67	2.1	7.2
Wagner [1]	1.76	0.68	1.3	4.3
Wagner [1]	1.88	0.69	0.95	3.4
Staudinger [1]	2.43	0.66	1	3.3

Despite the fact that different authors used samples polymerized under different temperature conditions and with different amounts of initiator, did not fractionate them with equal care, there are no contradictions in the relationships between $\overline{M}_n$ and $[\eta]$. The formulas in the literature (with the exception of Matthes's formula) are in satisfactory agreement with the general Equation (5). This means that different PVA samples do not display any specific peculiarities of hydrodynamic and thermodynamic properties in solution.

At the same time, the absolute value of $\alpha = 0.68$, and the root mean square distances $(\overline{h_\eta^2})^{1/2}$, calculated according to [6]: $(\overline{h_\eta^2})^{1/2} = 7.82 \times ([\eta]\overline{M}_n)^{1/3}$ Å $= 7.82(2.09 \cdot 10^{-4}\overline{M}_n^{1.68})^{1/3}$ Å, and also the ratio:

$$(\overline{h_\eta^2})^{1/2} \text{ and } (\overline{h_{free}^2})^{1/2} = 3.08\sqrt{\overline{M}_z/\overline{M}_0} \text{ Å}$$

are in full agreement with the accepted ideas of the structure of linear macromolecules (Table 4).

TABLE 4

Molecular Dimensions of PVA Fractions in Acetone

$\overline{M}_n \cdot 10^{-5}$	$(\overline{h^2_\eta})^{1/2}$ in A	$(\overline{h^2_{free}})^{1/2}$ in A	$(\overline{h^2_\eta}/\overline{h^2_{free}})^{1/2}$ = in α_0
0.68	244	86	2.7
0.84	260	95	2.7
1.20	320	114	2.8
1.86	389	135	2.8
3.50	588	200	3.0
6.8	870	278	3.1
10.0	1060	333	3.2

It must be pointed out that the relationship $(\overline{h^2_\eta})^{1/2} \approx \overline{M}_n^{0.58}$, which is valid for PVA fractions in acetone coincides with the analogous equation for a polymethyl methacrylate fraction in acetone, obtained by the light scattering method [7]. At the same time, the absolute values of $(\overline{h^2_\eta})^{1/2}$ for PVA and $(\overline{h^2_z})^{1/2}$ for polymethyl methacrylate coincide for equal degrees of polymerization. For example, for PVA for $M_n = 1 \cdot 10^6$, $(\overline{h^2_\eta})^{1/2} = 1060$A, and for polymethyl methacrylate for the corresponding degree of polymerization, for $\overline{M}_w = 1.16 \cdot 10^6$, $(\overline{h^2_z})^{1/2} = 1063$ A [7].

SUMMARY

1. Results of osmotic pressure and viscosity measurements of polyvinyl acetate fractions dissolved in benzene, ethyl acetate, and acetone, and data in the literature, have been used to derive a relationship between the molecular weight $\overline{M}_n$ and the viscosity: $[\eta] = 2.09 \cdot 10^{-4} \overline{M}_n^{0.68}$, valid for the molecular weight range $3 \cdot 10^4 - 1 \cdot 10^6$. The same equation can be used with the same degree of accuracy for calculation of M_n from $[\eta]$ in benzene and ethyl acetate. Measurements of the viscosities of solutions of the same fractions in chloroform gave the relationship $[\eta] = 1.58 \cdot 10^{-4} \overline{M}_n^{0.74}$.

2. A comparison of the values of $[\eta]$, A_2, and k' for PVA fractions in different solvents showed parallel behavior: as the solvent power decreases, the values of A_2 and $[\eta]$ decrease, while k' increases.

LITERATURE CITED

[1] H. Staudinger and H. Warth, J. prakt. Chem, 155, 272 (1940); A. Matthes, J. prakt. Chem., 162, 245 (1943); R. Wagner, J. Poly. Sci., 2, 21, (1947); R. Govaerts and G. Smets, J. Polymer Sci., 2, 612 (1947).

[2] C. Masson and H. Melville, J. Polymer Sci., 4, 337 (1949).

[3] P. Bosworth, C. Masson, H. Melville and F. Peaker, J. Poly. Sci., 9, 565 (1952).

[4] I. I. Shukov, I. Ya. Poddubny, and A. V. Lebedev, Colloid J., 10, No. 6, 423 (1948).

[5] International Union of Pure and Applied Chemistry, J. Polymer Sci., 10, 129 (1953).

[6] P. Flory, and T. Fox, J. Am. Chem., Soc. 73, 1904 (1951).

[7] K. Z. Fattakhov, V. G. Tsvetkov and O. V. Kallistov, J. Expt. Theor. Phys., 16, 345 (1954).

Received October 18, 1954

Institute of High Molecular Compounds
Academy of Sciences USSR
Leningrad

X-RAY INVESTIGATION OF THE DISPERSE PHASES OF IRON ORGANOSOLS

V. P. Chaly and E. M Natanson

Metal organosols may be of practical use in various branches of the national economy, and therefore investigations of their properties in relation to the preparation conditions are of definite interest. This paper contains the results of x-ray determination of the primary crystals (clusters) in the disperse phase of iron organosols in xylene, prepared by the electrolytic method [1]. This method is based on the electrolytic formation of the metal from aqueous solutions of its salts in the form of a highly disperse cathode deposit, which is immediately dispersed in the organic medium in the presence of surface-active substances. As is known, certain highly disperse cathode deposits of metals obtained in absence of surface-active substances are unstable, and rapidly change color, volume, and degree of dispersion after cessation of electrolysis [2]. In the electrolytic method for the preparation of metal organosols, the highly disperse cathode deposits are stabilized by surface-active substances at the instant of formation, and aggregative recrystallization processes are almost entirely prevented. For this reason, the influence of current density on the dimensions of the primary crystals should be most clearly defined in such cathode deposits.

The purpose of the present work was to investigate this effect experimentally. The influence of current density on particle size in cathode metal deposits has been studied by numerous workers [3]. However, the cathode deposits investigated were obtained by electrolysis of metal salts in one-layer baths and in absence of surface-active substances. In addition, a different method for forming the deposits was used, and the degree of dispersion was not determined by an x-ray method.

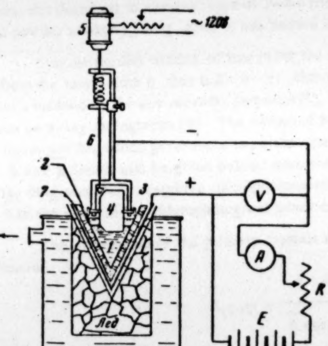

Fig 1 Diagram of apparatus for the electrolytic preparation of iron organosols.

Preparation of organosols. **The apparatus shown diagrammatically in Fig. 1 was used for the preparation of disperse phases of iron organosols in xylene by the electrolytic method.**

The electrolysis was carried out in a two-layer bath. The lower layer 1 was 5% aqueous ferrous chloride solution (30 ml) prepared by dissolving chemically pure metallic iron powder in 3% chemically pure hydrochloric acid. The upper layer 2 was 2% oleic acid solution in xylene (50 ml). The solutions were poured into a glass funnel with a sealed neck. The conical anode 3 was made from Armco sheet iron. The cathode 4 was in the form of a roller 30 mm in diameter and 15 mm long. The cathode was fixed horizontally in the usual form of stand used for electroanalysis. The depth of immersion of the roller cathode into the lower layer of the bath was such that its working surface was 4 cm². The rotary movement was transmitted from the electric motor 5 to the roller cathode by means of the vertical shaft 6. The rotation speed of the cathode was 200-250 revolutions / minute. The anode and cathode compartments were separated by a coarse porous ceramic diaphragm 7.

As the cathode current density was increased from 5 to 75 A/dm², the electrolysis time was decreased

from 60 to 5 minutes in order that the temperature of the electrolyte solution should remain as constant as possible (20°). The electrolyte solution was cooled by ice.

2% solution of ethylcellulose in benzene was added to the iron organosols to give a 0.3% content of ethylcellulose in the organosols. The organosols were dried by shaking them with finely crystalline calcined sodium sulfate powder. The organosols were left to settle, decanted, and then dried at room temperature under a residual pressure of 1 mm Hg.

Determination of degree of dispersion. The specimens were prepared for the x-ray photographs by the method developed previously [4]. The cylindrical specimens 0.68 mm in diameter were placed in the usual camera for powder photographs (cassette diameter 57.3 mm). The camera slits were cylindrical, made of lead, with diameters 0.8 mm (first) and 1.2 mm (second). The photographs were taken with filtered cobalt radiation obtained in an improved dismountable ion tube designed by Solovyev [5], at a voltage of 30 kV, current strength 5 mA, and exposure 1 hour. The exposure was so chosen that the values of the absolute blackening S lay in the linear region of the characteristic curve (for Agfa "Durofilm" x-ray film and Co K_α radiation this corresponded to S from 0.7 to 1.3). The exposures were made to an absolute blackening of 0.8. The values of S were not recalculated in terms of intensity. The characteristic curve was plotted from 13 points on a blackening scale, based on the x-ray tube operating conditions described above. The exposure for the first point was 10 seconds, and this was increased by 1.5 times for each succeeding point. During the blackening point exposures the x-ray film was kept at a distance of ~75 cm from the tube focus. The primary beam was weakened by an aluminum filter 1.5 mm thick. CoK_β radiation was filtered off by means of an iron filter.

All the x-ray photographs were developed simultaneously (by the use of a universal tank) and under the same conditions (fresh D-19 developer [6] at 20° for 5 minutes). Microphotometry of the diagrams was carried out as described previously [4]. The dispersion was calculated from the first (110) line.

The geometric width b of the (110) line was determined from a photograph of a standard specimen under otherwise the same conditions (tube operating conditions, exposure, position of x-ray camera relative to the primary beam, slit diameter in camera, type of x-ray film, and processing of the photographs). The standard used was Armco iron powder made by filing, after it was heated in a vacuum at 500° for 8 hours and cooled.

The diffraction width β of line (110) for the specimens was determined by subtraction of the geometric width b from the total width B, that is $\beta = B - b$. Although this is a less accurate method for the determination of β than Jones's method or the one recently proposed [8], it is quite adequate for our purpose and is recommended in handbooks on x-ray radiography [9]. The values of B and b were determined from microphotometric curves (scale 1 : 100) as linear widths, which gives more accurate results (see also [10]). The numerical values of the linear magnitudes B, b and β which will be given below, were the arithmetical averages of four measurements (both halves of two x-ray diagrams were examined microphotometrically). The maximum differences between separate measurements of B in the scale of the microphotogram never exceeded 1 mm.

The dimensions of the primary crystals in disperse phases of iron organosols were calculated by means of the formula:

$$L_{(110)} = \frac{K \lambda R}{\bar{\beta} \cos \theta},$$

the following values being used: K = 0.94, λ = 1.787 A, R = 28.65 mm, cos θ = 0.897.

RESULTS AND DISCUSSION

First, it must be pointed out that all the x-ray diagrams obtained for disperse phases of iron organosols corresponded to the low-temperature α-modification of iron. In Fig. 2 x-ray diagrams of the disperse phase of iron organosol, 1, obtained at a cathode current density of 12.5 A/dm^2, and a standard iron specimen, 2, are compared.

The results of x-ray determinations of the size of the primary crystals (clusters) in the disperse phase of iron organosols in a direction normal to the (110) face are shown in Fig. 3, Curve 1. Fig. 3 shows that as the cathode current density increases from 5 to 75 A/dm^2, the cluster size in the disperse phase of iron organosols first increases and then decreases. The primary crystals reach maximum size (153 A) at a current density of 37.5 A/dm^2. The peculiar relationship observed between the size of the primary crystals and the cathode current density applies not only to the disperse phases of iron organosols, but also to the loose cathode deposits of iron obtained later by the first of the present authors from 5% $FeCl_2$ solution (Fig. 3, Curve 2). These facts may be explained as follows. At relatively low current densities (up to 37-40 A/dm²), the primary crystals grow mainly in consequence of a gradual increase in the number of metal ions discharged in unit time, and the low degree of passivation of the growth faces of the primary crystals by the iron hydrates deposited on the cathode. On subsequent increase of current density, however, the influence of the passivation factor increases so much that it begins to retard not only the aggregation of the primary crystals, as has been shown by a number of authors [3], but also their individual growth.

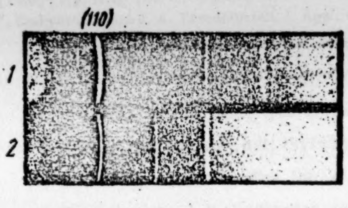

Fig. 2. Photographs of x-ray diagrams; 1) iron organosol; 2) standard iron specimen.

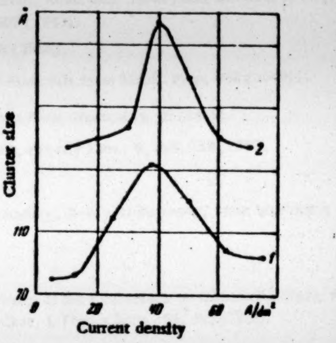

Fig. 3. Variation of cluster size with current density: 1) iron organosol; 2) loose iron deposit.

Our results are of considerable interest, as up to the present time a number of authors [3] reported only a direct relationship between the increase of current density and increased dispersion of the cathodic metal deposits. The effect observed by us can be explained by the considerable differences in the formation and growth conditions of crystals in disperse phase, of metal hydrosols, and of the cathode deposits of metals formed by the usual process of electrolysis. In the first instance the crystals formed are instantaneously transferred into an organic medium, where they are stabilized, while in the second instance their growth takes place on a stationary cathode. Consequently the dimensions of the primary crystals in the disperse phases of organosols should be less than in cathode deposits of metals, which is indeed the case (see Curves 1 and 2, Fig. 3).

It must also be noted that when disperse phase of iron organosols are formed, solution of hydrogen in the metal (see [4]) simultaneously with evolution at the cathode does not occur, as is the case in the formation of compact cathode deposits [11]. Otherwise, the interference lines in the x-ray diagram should become increasingly diffuse as the result of increasing hydrogen evolution with increasing cathode current density, while the primary crystal size should steadily decrease. This was not observed, however. The first of the present authors has proved that broadening of the lines on the x-ray diagrams of loose cathodic metal deposits is caused by their high degree of dispersion; this will be discussed in greater detail in the next communication.

SUMMARY

1. The dimensions of the primary crystals (aggregates) in the disperse phase of iron organosols obtained electrolytically from 5% aqueous $FeCl_2$ solutions at various current densities have been determined by an x-ray method.

2. It is established that the primary crystals first increase and then decrease in size as the current density increases from 5 to 75 A/dm². The primary crystals reach maximum size (153 A) at a current density of 37.5 A/dm². Similar results were obtained for loose cathodic deposits of iron formed from 5% $FeCl_2$ solution with variation of the current density from 10 to 70 A/dm² (Fig. 3, Curves 1 and 2). The maximum aggregate size (244 A) for loose cathodic iron deposits is found at 40 A/dm². The aggregate dimensions are less in the disperse phase of iron organosols than in loose iron deposits at all current densities, which is the consequence of aggregate formation at rotating and stationary cathodes respectively.

3. The peculiar relationship between aggregate size and the cathode current density is explained by the different degrees of passivation of the growth faces of the primary crystals by the iron hydrates formed during electrolysis

LITERATURE CITED

[1] E. M. Natanson, Memoirs Inst. Chem. Acad. Sci. Ukrainian SSR, 7, 311 (1940); Colloid J., 9, 191 (1947).

[2] F. Müllius and O. Fromm, Ber., 27, 645 (1894); W. Kohlschütter and F. Jakober, Z. Elektrochem., 33, 290 (1927); O. K. Kudra and K. N. Ivanov, J. Phys. Chem., 6, 469 (1935); O. K. Kudra, J. Phys. Chem. 9, 286 (1937).

[3] A. I. Levin, J. Appl. Chem., 19, 787 (1946); N. A. Marchenko and A. N. Sysoev, J. Appl. Chem., 23, 493 (1950) (T.p. 515)* ; A. T. Vagramyan, Electrodeposition of Metals, Acad. Sci. USSR Press, Moscow, p. 66 (1950); N. T. Kudryavtsev and E. A. Tereshkovich, J. Appl. Chem., 22, 1302 (1949).

[4] V. P. Chaly, Bull. Acad. Sci. USSR, Phys. Ser., 17, 195 (1953).

[5] F. I. Solovyev, Application of X-rays to Investigations of Materials, State Mach. Press, 386 (1949).

[6] V. Mikulin, Modern Photographic Recipes, State Cinema Press, Moscow, p. 21 (1949).

[7] F. Jones, Proc. Roy. Soc., 166, 16 (1938); G. S. Zhdanov, Factory Labs., 9, 566, 732 (1940).

[8] A. I. Kitaigorodsky, Prog. Phys. Sci., 43, 155 (1951).

[9] Ya. S. Umansky, A. K. Trapeznikov, and A. I. Kitaigorodsky, X-Ray Radiography, State Machinery Press, Moscow, p. 219 (1951).

[10] V. P. Kotov, Factory Labs., 10, 502 (1951).

[11] Yu. V. Baimakov and M. I. Zamotorin, Abstracts of Papers at the Conference on Electrochemistry, Acad. Sci. USSR Press, p. 33 (1950); Yu. V. Baimakov and L. M. Evlannikov, J. Phys. Chem., 25, 483 (1951).

Received March 2, 1955

Institute of General and Inorganic Chemistry
Academy of Sciences Ukrainian SSR
Kiev

---

* T.p. = C. B. Translation pagination

RHEOLOGICAL PROPERTIES OF PRINTING INKS

B. N. Shakhkeldyan

Printing inks are viscous or paste-like pigment suspensions in an oil vehicle. The technological properties of the inks, their behavior in printing and the quality of the prints largely depend on their rheological properties. Therefore studies of the rheological properties of printing inks, and the factors which influence them, present an important theoretical and practical problem.

Printing inks which are at all thick are thixotropic, but the nature of the thixotropic structures varies greatly according to the properties of the pigment and the vehicle. In some inks, structures with more or less definite yield value and elasticity are formed. Such properties are found, for example, in carbon black inks, the thixotropic properties of which have been described in detail by Kazarovitsky and Shalyt [1], and inks based on light fast yellow, phthalocyanine blue, and certain other pigments. Fig. 1 shows the variation of the relative deformation (ϵ) with shearing stress (P), determined with the aid of the Veiler-Rebinder apparatus [2]. An ink based on gas black, previously stirred, has a flat deformation curve which gradually becomes horizontal, indicating flow under constant load, characteristic of viscous systems. Structure formation occurs in the carbon black ink in the course of time, and the deformation curve taken twenty-four hours after stirring shows clearly defined elasticity and a maximum stress representing the yield value.

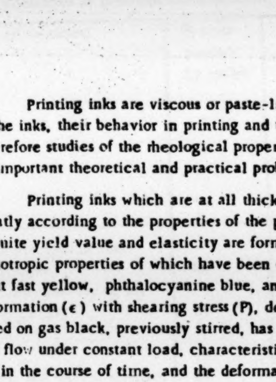

Fig. 1. Variation of deformation with stress for carbon black and Al(OH)$_3$ pastes: 1) carbon black immediately after stirring; 2) ditto, after 24 hours; 3) Al(OH)$_3$ immediately after stirring; 4) ditto, after 24 hours.

In contrast to gas black, ink based on aluminum hydroxide (transparent white) yields a flat deformation curve even after standing twenty-four hours, with the elastic properties masked by viscous flow, and without any yield value. Such properties are found in many inks used in printing, such as those containing Milori, chrome, transparent and printing white, and many inks containing white pigments.

In the printing process the ink is rubbed and spread between the printing rollers, rolled on to the form, subjected to pressure, and is thus placed under strong mechanical stresses which are capable of destroying the strongest ink structure. Therefore, for correlation of the physico-mechanical properties of inks with their printing behavior it is particularly important to study the properties of inks in a condition in which the thixotropic structure has been previously destroyed. In such conditions the principal mechanical characteristic is the viscosity, or, more correctly the structural viscosity, since printing inks have variable viscosity which depends on the deformation rate.

Table 1 contains some data on the viscosity of printing inks during flow under small loads, obtained by measurements of the rate of displacement of a plate in a plane gap. This method, described by Rebinder and Segalova [3] also makes it possible to study elasticity and plasticity, and because of this it proved possible to find a yield value due to structural elements which persisted despite stirring of the specimen before the determination, in some inks. The yield value was determined approximately, as the stress below which no shear was observed in the course of the experiment In cases when the yield stress was other than zero, its value was subtracted from the applied stress, as proposed by Rebinder [3], before calculation of the viscosity.

As Table 1 shows, the viscosity is independent of the stress for some inks over a fairly wide range of stresses, although in general the viscosity, which is high at low loads and shearing rates, decreases with increasing flow rates. The constant viscosity region is fairly wide if it is considered on the scale of the yield value P_k. Ink based on phthalocyanine blue pigment has constant viscosity over a stress range which is nine times the value of P_k, and ink based on light fast yellow, five times.

TABLE 1

Ink Viscosities at Different Rates of Shear

Ink components	% components by weight	Measurements with plane gap apparatus				Measurements with rotational viscosimeter		
		P_k in dynes/cm^2	stress in dynes/cm^2	velocity gradient $\frac{de}{d\tau} \cdot 10^{-4}$	$\eta_1 = \frac{\tau - P_k}{\frac{de}{dr}} 10^{-3}$	average velocity gradient	η_{pl}	$\theta \frac{g}{cm^2}$
Phthalocyanine blue		190	250	0.015	45.0	4.5 – 40	287	8100
pigment	33		500	0.067	46.3			
Polymerized drying oil								
(η_{30} = 37)	67		1100	0.21	43.5			
			1720	0.37	41.4			
			2340	0.87	25.0			
Light fast yellow pigment	38	344	490	0.037	41.0	0.5 – 7.5	940	13800
Polymerized drying oil								
(η_{30} = 37)	62		1100	0.13	57.0			
			1720	0.25	55.0			
			2340	0.73	27.4			
			2960	2.5	10.5			
Gas black	25	0	120	0.025	48.0	3.5 – 17	790	6900
Polymerized drying oil								
(η_{30} = 37)	75		500	0.94	53.0			
			1100	0.56	19.6			
			2340	1.8	13.0			
Chrome No. 570	74	0	25	3.5	0.07	5 – 44	500	1760
Polymerized drying oil			30	7.0	0.04			
(η_{30} = 37)	26		43	12.2	0.035			
			55	32.0	0.017			
White No. 825	55	0	250	18	0.138	2.5 – 7.5	2225	5800
Polymerized drying oil	45		610	98	0.063			

The flow rate at which the viscosity is constant also varies within wide limits. In the case of ink based on light fast yellow it shows at least a 6-fold change, while ink based on phthalocyanine blue has constant viscosity over a 25-fold change of the velocity gradient (from $0.37 \cdot 10^{-4}$ to $0.015 \cdot 10^{-4}$ sec.$^{-1}$).

The absolute deformation rate remains very low, and therefore the structural bonds destroyed during shear have time to be thixotropically restored. This dynamic equilibrium between the destructive action of deformatio and restoration of an equilibrium state accounts, according to Rebinder and Segalova [3] for the constant viscosity at low rates of shear. However, with further acceleration of flow the viscosity decreases sharply, and this is found for all the printing inks studied, irrespective of the existance of a yield value.

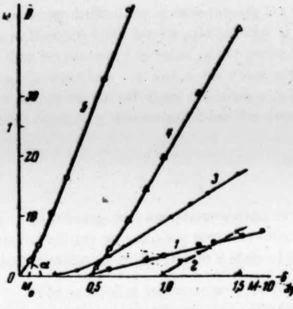

Fig. 2. Flow curves of printing inks: 1) white No. 801; 2) based on light fast yellow; 3) based on gas black; 4) based on phthalocyanine blue; 5) based on chrome No. 570.

The limitations of the plane gap method for studying deformation made it impossible to increase the deformation rate above very small values of the order of 10^{-4} seconds^{-1}. An approximate idea of the course of viscosity variations with increasing shear rates may be obtained if the above results are supplemented by the results of tests on the same inks made with a rotational viscosimeter of the Volarovich type. In these experiments an average velocity gradient D = 5-40 seconds^{-1} was reached, or 10^{-4}-10^{-6} times as great as in the plane gap apparatus. The flow curves in Fig. 2 show that at such rates there is a linear relationship for $\omega = f(M)$, where M is the torgue and ω is the angularvelocity, so that it is possible to calculate the constant plastic viscosity

$$\eta_{pl} = \frac{M - M_0}{\omega} K.$$

Table 1, which also gives the plastic viscosity values, shows that the latter is less by several orders of magnitude than the viscosity determined at low velocities. The viscosity of inks based on gas black, phthalocyanine blue, and light fast yellow decrease by about 10^4 times at the higher velocities, while the viscosity of chrome-based ink and white only decreases by 50.-100 times. The different degrees of viscosity change with increases of shearing rate are explained by the different extents of structurization of these inks. Table 2 shows, for comparison, the yield and viscosity values measured by means of the plane gap apparatus 2 and 10 minutes after stirring. Table 2 shows that the viscosities of inks based on gas black, light fast yellow, and phthalocyanine blue increase sharply in 10 minutes, while the viscosity of white pigment and chrome-based ink remains quite unchanged.

The high viscosity of structurized inks in flow under low loads is the result of formation of relatively stable bonds between the pigment particles. As the stress and the shear rate increase, the structural bonds are broken and the pigment particles become oriented in the stream, with a consequent sharp fall of viscosity.

TABLE 2

Thixotropic Properties of Inks Based on Various Pigments

Pigments	Resting time, min.	Yield value	Viscosity $\eta \cdot 10^{-6}$ poises
Gas black	2	0	19.6
	10	0	64.5
Phthalocyanine blue	2	190	43.0
	10	325	257.0
Light fast yellow	2	344	57.0
	10	420	342.0
White	2	0	0.43
	10	0	0.40
Chrome	2	0	0.035
	10	0	0.037

There are no reasons for presuming the existence of particularly stable bonds in the easily flowing, weakly thixotropic inks based on chrome and white pigments; therefore their viscosity at low rates and stresses is approximately 1000 times less than that of the structurized inks. For the same reason an increase of the stress and shearing rate is not accompanied by any significant changes in their structural nature, and therefore the decrease of viscosity which results is less than in structurized inks. All this is evidence of the complex nature of the rheological properties of printing inks, for the characterization of which the complete flow curve is required.

For some practical purposes it is convenient to simplify the rheological properties of printing inks in view of the fact that the main sharp decrease of viscosity occurs at low rates, clearly very much lower than those found in actual printing conditions. This is particularly applicable to strongly structurized inks. Volarovich [4], in determinations of the viscosities of carbon black inks with the aid of the rotational viscosimeter, used an equation for a viscoplastic body which postulates a sharp change in properties when the yield stress θ is reached. It was possible to determine θ approximately for carbon black inks by determination of the minimum load which caused the viscosimeter to rotate. This method is not applicable to fluid inks because of increasing difficulties in determining the start of rotation. A more suitable method is to plot flow curves at rates sufficiently high for the relationship $\omega = f(M)$ to become linear. The rheological properties of the ink can then be described in terms of the properties of a viscoplastic body, analogous to the ink at high rates of shear, the constants η and θ for which are easy to determine graphically. The value of θ is determined from the value of M_0 cut off along the stress axis by extrapolation of the linear region of the flow curve, while the plastic viscosity is determined from the slope of the linear region (see Fig. 2):

$$\eta_{pl} = K\frac{M-M_0}{\omega}.$$

If printing inks are characterized in this way, it must always be remembered that θ is not the true yield stress but merely an auxiliary constant which defines the type of flow; it can be taken to mean the stress required to maintain in the stream a state of structural disruption in which the system has constant plastic viscosity.

The rotational viscosimeter used in the subsequent experiments used the principle of rotation of the outer cylinder containing the ink, and measurement of the stress from the angle of torsion of the inner cylinder suspended from elastic suspension wire. The rotation speed was varied by a variable gear device and measured by a tachometer.

The tests were carred out at a maximum average velocity gradient of 40-50 seconds^{-1}. Any further increase of the velocity resulted in extrusion of the ink from the gap between the cylinders, which disturbed the determination conditions. At these shear rates the relationship $\omega = f(M)$ was close to linear, although the possibility is not excluded that this linearity is only apparent and that a substantial increase of the rate of shear would result in a continuation of structure disruption and viscosity decrease.

The above method for determination of plastic viscosity was used for an investigation of the effect of oil viscosity on ink properties. Printing inks are made with drying oils obtained by heat polymerization of linseed oil. The drying oil viscosity varies in the range 10-40 poises according to the properties required in the ink; this variation is achieved by the use of different heat treatment times. In contrast to printing inks, dispersions of pigments in raw unpolymerized linseed oil are devoid of printing qualities; they are rolled out badly by the rollers and give an indistinct impression. In order to establish what physicomechanical properties are characteristic for printing inks, we studied inks containing Milori and light fast yellow pigments based on oils of various viscosities, starting from raw linseed oil.

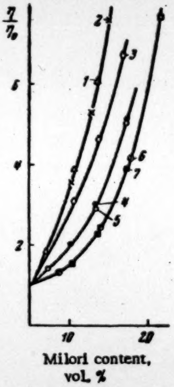

Fig. 3. Effect of concentration of Milori pigment on the relative viscosity of inks based on 1) raw linseed oil (η_0 = 0.33) and various drying oils with viscosities: 2) 0.89; 3) 3.4; 4) 10.8; 5) 23.0; 6) 37.0; 7) 136.0 .

A simple comparison of the absolute viscosities of the inks cannot provide information on the interaction between the different oils and the pigments. From this standpoint it is more correct to compare relative viscosities of the inks in the form of the ratio between the minimum plastic viscosity and the viscosity of the oil on which the given ink is based:

$$\eta_{rel} = \eta_{pl} / \eta_0.$$

The viscosity of each drying oil is taken as unity, which makes it possible to determine the relative thickening when a definite amount of pigment is added to a given drying oil.

Fig. 3 shows the variation of the relative viscosity of the inks with the volume concentration of Milori pigment. The relative viscosity of inks based on drying oils rises comparatively little at first. When the Milori content increases above 10%, thickening is greatly increased so that the points corresponding to concentrated systems (30-40%) fall outside the limits of Fig. 3. The relative viscosity of inks based on raw linseed oil rises sharply at the lowest concentrations, which shows that addition of pigment to raw oil results in much greater thickening than the addition of pigment to drying oil.

The differences between the relative viscosities of systems containing different vehicles with the same degree of filling by volume cannot be attributed to differences in the geometrical form of the particles, as the same pigment was used in all cases. The hypothesis that the volume of the disperse phase increases to different extents as the result of different degrees of solvation in the different oils also cannot explain the observed viscosity behavior. Viscous polymerized drying oils should have the greatest solvation volumes, but in fact they show the least viscosity increases on addition of pigment.

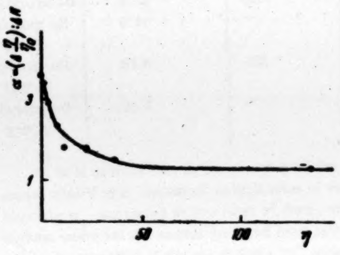

Fig. 4. Effect of the viscosity of drying oils on their stabilizing power.

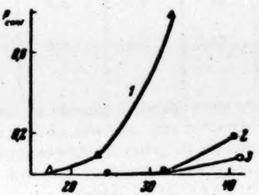

Fig. 5. Effect of the concentration of Milori pigment on the yield value of inks based on: 1) linseed oil ($\eta_0 = 0.33$); 2) drying oil ($\eta_0 = 10.8$); 3) drying oil ($\eta_0 = 23.0$).

The more likely view is that solvation of the polymerized fractions of viscous drying oils stabilizes the pigment particles and protects them from aggregation and formation of agglomerates which increase viscosity. This stabilizing power of viscous drying oils is the reason for the relative lesser thickening of the inks in which they are used; it can be characterized by the slope of the initial linear region of the relative viscosity curve or by the increase of thickening with increasing pigment concentration:

$$\alpha = \frac{\Delta\eta/\eta_0}{\Delta A}.$$

Fig. 4 shows that the stabilizing power changes sharply in the transition from raw oil to drying oil of a very low degree of polymerization. It is noteworthy that the values of α of drying oils with the viscosities generally used (10-40 poises) differ relatively little, although they do decrease with increasing viscosity. The stabilizing action of viscous drying oils is also confirmed by observations of the yield value. Inks with Milori based on the usual drying oils have a low degree of structurization and only acquire a small yield value at high pigment concentrations. In contrast, inks based on raw oil are much more structurized, and at much lower concentrations. In illustration, Fig. 5 shows variations of the conventional yield value P_{conv} in g/cm^2[*] with the concentration of Milori (A) for inks based on linseed oil and two drying oils of different viscosity.

Data on the properties of inks made with light fast yellow pigment lead to the same conclusions. As in the case of Milori, inks made with raw oil show much greater thickening and structure formation than inks with drying oils (Figs. 6 and 7).

---

[*] The conventional yield value was determined as the minimum stress required to produce flow, with the aid of the Veiler-Rebinder apparatus with a spring dynamometer.

The structure formation in inks based on light fast yellow pigment is much more pronounced than in inks based on Milori, and this made it possible to study the influence of drying oil viscosity on the elastic properties and the maximum viscosity of undestroyed structure, found at low deformation rates. The results, obtained by measurements of the displacement of a plate in a plane gap, are shown in Table 3.

TABLE 3

Influence of Drying Oil Viscosity on the Structural-Mechanical Properties of Inks with Light Fast Yellow (Pigment, 31% by vol.; Vehicle, 69%)

Vehicle	Vehicle viscosity η_0 in poises	Plastic viscosity η_{pl} of ink	Relative viscosity $\frac{\eta_{pl}}{\eta_0}$	Maximum viscosity of undestroyed structure	Elastic modulus $E_1 \cdot 10^{-6}$	Elastic modulus $E_2 \cdot 10^{-6}$	Elasticity $\lambda = \frac{E_1}{E_1 - E_2}$
Linseed oil	0.33	23.2	70	246	20	2.5	0.45
Drying oil 40° E	8.64	–	–	10.9	9.8	2.5	0.87
Drying oil 152° E	37.0	425	11.5	5.2	3.0	0.49	0.86
Drying oil 520° E	135.6	–	–	3.7	6.0	0.67	0.90

It is obvious that as the viscosity of the vehicle increases the viscosity of the ink made with it will increase also if it is measured at high rates of shear with disruption of the structure. The undestroyed structural viscosity η_1, measured at low rates of shear, on the contray increases with decreasing oil viscosity, and has the highest value for the system prepared from raw oil. When the dispersion medium has the low viscosity of 0.33 poise, the viscosity of the ink is $246 \cdot 10^6$, which represents a relative viscosity $\eta_1 / \eta_0 = 7.5 \cdot 10^8$. In the case of polymerized drying oil with a viscosity of 37 poises, the thickening is represented by $\eta_1 / \eta_0 = 1.4 \cdot 10^5$ or 5000 times less than when raw oil is used. In inks based on viscous drying oils the structural bonds between the pigment particles are weakened, probably because of adsorption of polymeric fractions of the drying oil. In addition to decreasing the thickening, this also decreases the rigidity of the structure, as can be seen from the values of the elastic modulus E_1.

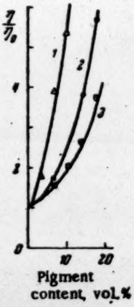

Fig. 6. Effect of the concentration of light fast yellow pigment on the relative viscosity of inks based on: 1) raw linseed oil (η_0 = 0.33); 2) drying oil (η_0 = 23.0); 3) drying oil (η_0 = 37).

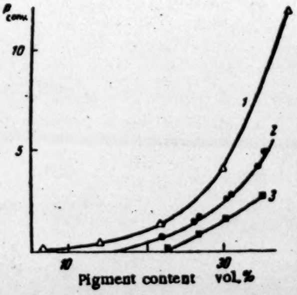

Fig. 7. Effect of the concentration of light fast yellow pigment on the yield value of inks based on: 1) raw linseed oil (η_0 = 0.33); 2) drying oil (η_0 = 37); 3) drying oil (η_0 = 136).

At the same time, the adsorption layers between the pigment particles confer elasticity on the ink, as can be seen from the last column in Table 3, and as has been confirmed by our earlier measurements of the physicomechanical properties of a large number of printing inks. In all cases normal printing inks had high elasticity, of the order of 0.8-0.95, while inks based on raw oil had elasticity of the order of 0.25-0.50.

In addition to the study of the degree of polymerization of drying oils, the mechanical properties of Milori inks based on some other vehicles were investigated. It was found that inks based on oxidized drying oil, and also on solutions of alkyd resins in oxidized drying oil, are structurized to a much greater extent than inks based on polymerized drying oils. This can be seen in Fig. 8, which shows the variation of relative viscosity with Milori concentration for inks based on various vehicles. Particularly great thickening is found in inks with added alkyd resins. When the Milori concentration rises to 40%, which is the approximate working concentration, they are converted into thick solid-like pastes, completely devoid of printing properties, the viscosity of which cannot be determined.

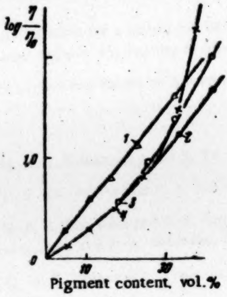

Fig. 8. Effect of Milori pigment concentration on the relative viscosity of inks based on; 1) linseed oil ($\eta_0 = 0.33$); 2) polymerized drying oil ($\eta_0 = 10.8$); 3) oxidized drying oil ($\eta_0 = 1.9$); 4) oxidized drying oil + 30% resin ($\eta_0 = 11.0$).

This resembles the structure formation which occurs in links containing Miloir when they are tritrated with water; small amounts of water convert the easily flowing ink into a brittle solid paste. In practice this occurs in lithographic and offset printing if the ink is rolled on to a moist form. Upon mixing with water and rubbing between rollers of the printer, the ink thickens and then solidifies, disturbing the normal regime of work. Printers, who regard this effect as "drying" of the ink, are well aware that the use of offset printing with inks containing Milori involves considerable difficulties. We assumed that this effect is the result of adsorption of water on the surface of the pigment particles followed by association through the hydrophilic groups, leading to the formation of continuous structural skeleton. It was further postulated that a similar mechanism accounts for the observed abnormally high thickening which is found when Milori is rubbed with oxidized and alkyd drying oils; adsorption of the hydrophilic components of these vehicles, and their subsequent association, binds the pigment particles into aggregates which rise the viscosity. In confirmation of this, Table 4 shows values of the dielectric constant and surface tension at the water interface. Table 4 shows that oxidized drying oil and alkyd resin solutions have higher dielectric constants and much lower surface tension at the water interface than polymerized drying oil, which is an indirect sign of their polarity and affinity for water [*]. It is an interesting fact that inks based on oxidized and alkyd drying oils, which show increased thickening are not structurized by the addition of water, and are only slightly thickened while retaining their fluidity, probably because of emulsification of the vehicle by water.

Thus, adsorption of the polar components of oxidized and alkyd drying oils prevents subsequent penetration of water to the pigment surface and the consequent structurization. Such inks could be used in offset printing if the thickening did not prevent the formation of the high pigment concentration necessary for the required color intensity. However, it proved possible to stabilize the ink by addition, to ordinary polymerized drying oil, of relatively small amounts of oxidized or alkyd drying oils, sufficient to prevent structurization by the action of water but not sufficient to cause serious thickening of the inks themselves.

The results of the above investigation have been used to develop a formulation for an offset printing ink with Milori, which does not thicken by the action of water. This ink proved to be of good quality in large scale tests.

---

[*] We take this opportunity to express our gratitude to M. M. Kusakov for help in the use of the method for determination of surface tension of viscous oils.

TABLE 4

Polar Properties of Drying Oils

Drying oil	Dielectric constant	Surface tension at water interface, dynes/cm
Polymerized	3.3	21
Oxidized	–	10.1 – 10.5
Oxidized,+ 30 % FL-39 resin	4.4	–
Oxidized,+ 40 % FL-39 resin	4.9	8.4
Alkyd	4.5	11.0

SUMMARY

1. The viscosity of printing inks falls sharply as the rate of shear increases from $10^{-6} - 10^{-4}$ second^{-1} to 1-10 second^{-1}. The greatest fall of viscosity is found in inks with a tendency to structurization.

2. The stabilizing power of drying oils can be determined by measurement of the relative viscosity of printing inks.

3. Polymerized linseed drying oils have better stabilizing power than raw linseed oil. Inks based on drying oils have lower relative viscosities and less rigid and more elastic structures.

4. Additions of oxidized drying oil or alkyd resin increase structurization in inks based on Milori pigment. A formulation for a Milori ink has been developed which does not thicken by the action of water, so that it can be used without interruption in offset printing.

We express our thanks to Adademician P. A. Rebinder and to E. E. Segalova for valuable advice and guidance.

LITERATURE CITED

[1] L. A. Kazarovsky and S. Ya. Shalyt, Colloid J., 15, 437 (1953) (T.p.453)*.

[2] S. Ya. Veiler and P. A. Rebinder, Proc. Acad. Sci. USSR, 49, 354 (1945).

[3] P. A. Rebinder and E. E. Segalova, Colloid J., 10, 223 (1948); Proc. Acad. Sci. USSR, 71, 85 (1950); L. A. Kazarovitsky and P. A. Rebinder, Polygraphic Production, No. 6, 31 (1951).

[4] M. P. Volarovich, Trans. Sci. Res. Inst., State United Publishing Houses, 5, 261 (1937).

[5] H. Green, Ind. Eng. Chem., An. Ed. 14, 576 (1942).

Recived December 25, 1954 Moscow

---

* T.p. = C.B. Translation pagination.

DISCUSSIONS

THE PROCESS OF FORMATION OF AGGREGATES FROM BUBBLES AND SOLID PARTICLES IN V. I. KLASSEN'S BOOK "INTRODUCTION TO THE THEORY OF FLOTATION"

Z. V. Volkova

The reply by V. I. Klassen [1] to our comments on the discussion of the formation of flotation aggregates in the book "Introduction to the Theory of Flotation" does not discuss the questions put by us. V. I. Klassen does not deny: 1) the incorrectness, pointed out by us, of the discussion of the work on types of flotation aggregates; 2) the inaptness, both of the kinetic equation of Gründer and Kadur, and of the "simplification" by M. A. Eigeles of our equation for the equilibrium of a particle attached to a bubble surface. The transmission of impulses to the bubble surface by the particle is apparently considered by V. I. Klassen as not necessary for the formation of three-phase boundaries and as improbable.

However, we entirely fail to understand the formalism in V. I. Klassen's approach to the role of the contact angle in the process of attachment of particles on the bubble surface. The value of the contact angle is undoubtedly a function of the degree of hydration of the surface; study of the surface properties of solids is a necessary stage in the development of the flotation theory. However, when a particle adhering to a bubble loses its velocity and acquires the velocity of the bubble which carries it, then: 1) the shape of the bubble which is detached from the particle and 2) the probability of the attachment of the particle in the surface of the bubble, are determined by the value of the contact angle which is established in the given conditions and by the dimensions of the adhesion contour (the particle size). If the contact angle is too small, the particle is detached from the bubble, no matter how the relationship between its value and the degree of hydration of the particle surface is expressed. We therefore completely fail to understand the author's reproach concerning a "contrast of the degree of hydration of a solid surface with its contact angle of wetting", etc.

The development of the physical theory of technological processes forms an important stage in their investigation. The value of a theory depends on confirmation of its conclusions by experiments and practice. Physical theory does not normally embrace the entire complexity of real processes in nature and technology; it is based on certain simplifications and assumptions which were formulated quite precisely in our presentation of the statistical theory of the froth flotation process.

V. I. Klassen lists a number of assumptions alleged to have been made in this theory, although not one corresponds to reality: 1) the theory is not based on the concept of the floatation of each particle by a single bubble, as stated by V. I. Klassen, although an examination of the laws for the formation of such an aggregate is necessary; 2) The particle and bubble velocities were not determined on the basis of Stokes' law in calculation of the probability of mineralization of bubbles of each size. The value of the maximum force for the detachment of a particle from the bubble surface during the fixation process is the same for any bubble velocity in calculations of the resistance of the medium. The differential equation for the motion of the bubble — particle system may be written:

$$v\rho z'' + k(z')^{i} - [V\rho_0 g - v(\rho - \rho_0) g] = 0$$

$$\text{when } t = 0,\ z' = 0 \text{ and } F = V\rho_0 g.$$

In the first instant when the particle is drawn into the motion of the bubble, the force of detachment is equal to the upthrust of the bubble for any value of i. 3) No assumptions are made regarding an ideally regular particle shape. The formation of a flotation aggregate is examined on the assumption that the adhesion angle $\alpha = \theta - \gamma$ where γ is the average shape angle of the particle. 4) The differential equation for the surface of an adhering bubble is based on a consideration of its deformation by pressure in the medium. Why does V. I. Klassen consider that these deformations are not taken into account if the relationship between particle size, bubble volume, and limiting angles of adhesion was derived by integration of this differential equation ? 5) The statistical theory presumes the existence of turbulent motion in the pulp, and does not deny it. We reported in 1946 [2] that in presence of turbulent motion the layers close to the bubble surfaces become stirred, which facilitates adhesion. Turbulent motion ensures a relatively uniform distribution of particles and bubbles in the pulp, on which the calculation of the probability of their mineralization is based.

V. I. Klassen cites the following data from flotation practice in order to contravert the statistical theory. In machines of the mechanical type with an average bubble size 0.8-0.9 mm good flotation of mineral grains up to 200 μ is obtained. Better flotation of large grains has not been observed in pneumatic type machines despite the fact that the average bubble size is double. However, in mechanical type machines the bubble size distribution, according to the size of the average bubble, approaches statistical correspondence for particles up to 400 μ in size. Why, then, did V. I. Klassen expect to find better flotation of large particles in pneumatic type machines ? Further, V. I. Klassen points out that fine slurry grains may be floated by relatively large bubbles, the dimensions of which, in his opinion, do not correspond to our value for the maximum bubble size.

In 1935 we studied [3] the flotation of barytes, chalk, and talc powders by a single frothing agent – isoamyl alcohol. The high wettability of barytes resulted in good separation of fractions down to 75 μ.

We proposed the use of the flotation method for the separation of highly disperse fractions of powders. In 1946, on the basis of a calculation of the maximum bubble dimensions in relation to the floatability of various fractions, we established [4] the formation, in addition to mineralized bubbles and floccules, of a third type of flotation aggregate, consisting of bubbles covered by a continuous coating of particles drawn together by meniscus tension. Such aggregates may be formed in "group" attachment of particles on the bubble surface when, because of the small volume occupied by each of the particles in the pulp, a whole system of them touches the bubble surface simultaneously. Group attachment of particles in the bubble surface is possible with high wettability; it can explain 1) the results of our investigations on the flotation of small particles; 2) the flotation of highly wetted grains up to 200 μ, pointed out by V. I. Klassen; 3) the flotation of slurries by relatively large bubbles. The maximum bubble sizes are relatively large for small particles; for a particle size of 500 μ the diameter of such a bubble is 2.6 mm, and for a particle size of 50 μ, it is 1.35 mm if the limiting adhesion angle is 50°. The maximum bubble size may increase as the result of group adhesion. Group adhesion is probable at a fairly high solid - liquid ratio and at a high content of highly disperse fractions.

It is not clear to V. I. Klassen how the worsening of flotation by very vigorous stirring of the pulp is to be explained. On the basis of the statistical theory this can be explained by an increase of the radial accelerations of the liquid layers in which the particles are fixed in the bubble surfaces, which decreases the range of particle sizes fixed in the surface of a bubble of each given volume, and the range of bubble volumes attached to each particle. Worsening of flotation occurs both in the case of heavy galenite, and of the relatively light coal, which confirms our explanation for the causes of worse flotation as the result of very vigorous stirring.

The facts cited by V. I. Klassen confirm the conclusions of the statistical flotation theory.

LITERATURE CITED

[1] V. I. Klassen, Colloid J., 17, 409 (1955) (T. p. 393)*.

[2] Z. V. Volkova, Acta Physicochim, URSS, 21, 171, 563 (1946).

[3] Z. V. Volkova, Koll.-Z., 72, 83 (1935).

[4] Z. V. Volkova, J. Phys. Chem., 20, 1214 (1946).

Received October 16, 1955

---

* T.p. = C. B. Translation pagination

DETERMINATION OF THE DEGREE OF DISPERSION OF PEAT BY SEDIMENTOMETRIC METHODS

K. K. Lebedev

Sedimentometry is the most widespread method used for determinations of the degree of dispersion [1]. The pipet method, accepted as a standard method for soil suspensions at the International Conference on Soil Science in 1927, has been extensively used also for peat [2]. Even in 1949 the pipet method was recommended in a manual on technical analysis of peat, published by the State Energy Press [3]. The pipet method is still rated highly in soil science [4]. At the same time, the serious defects of this method have been noted repeatedly in the literature. These include inaccuracies in sampling – particles above and below the required level are drawn into the pipet, the finer fractions are taken up preferentially, particle aggregation takes place during settling, errors due to the small weights of the residues after drying are possible, the analysis is lengthy and the apparatus is cumbersome.

Volarovich and Churaev [5] have sought a better technique; finally they developed a method based on a combination of three techniques, namely, sieving for particles larger than 250 μ, sedimentometry for finer particles, and microscopy for particles of size < 1μ. Volarovich and Churaev consider that the use of the sedimentation method for highly disperse fractions involves gross errors because of their sensitivity to convection currents and Brownian movement, and also to particle aggregation which occurs during prolonged settling.

In the new method, after particles larger than 1μ have been settled, further sedimentation is stopped and a sample of the remaining suspension is investigated by means of the electron microscope. There is no doubt that the size distribution of the particles remaining is thereby determined with great accuracy. To that extent the method is faultless. However, the results obtained must be calculated in terms of the weight of the peat used; for this the aggregate weight of all the highly disperse fractions is needed. When the sedimentation is stopped, a special sample is taken from the suspension; according to Volarovich and Churaev, drying of this sample at 105° gives the weight of particles finer than 1μ.

The dispersion medium in all these investigations was water. For some strange reason the authors ignore the fact that an aqueous peat suspension contains dissolved as well as suspended material.

Not only hot but also cold water has a solvent action on peat. We need only think of the so-called "peat water", an aqueous solution of fairly deep color contained in peat deposits. Rakovsky and Rivkina [6] showed that peat water contains a complex material consisting of carbohydrates, uronic acids, bitumens, and nitrogen compounds.

The solvent action of water on peat has also been studied under artificial conditions [7]. The scheme for the group analysis of peat put forward by Thiessen and Johnson [8] commences with infusion of the peat in cold water for 48 hours; they state that 1 to 3% of the air-dry material passes into solution. Stadnikov [9] also determined the substances soluble in cold water. When Sphagnum- cotton grass peat (from Elektroperedacha) was infused for five days, 0.69% of the air-dry mass passed into solution.

The present author has determined the amount of substance which goes into solution when an aqueous suspension of sedge peat from Kosmynino is allowed to settle for thirty days. The suspension, of 1% concentration in distilled water, was settled exactly by Semensky's method [3]. The results are shown in Table 1.

Volarovich and Churaev shortened the settling time to 2.5 days. The solvent action of water during this apparently short time was studied with four varieties of peat. 1 and 0.05% concentrations were used. The settling was continued for exactly 58 hours, without shaking, and the vessels were kept in a dark room. Although distilled water was used in both series of experiments, it was tested for dissolved salts in both cases. The results are shown in Table 2.

The amount of peat which dissolves in water at room temperature is quite appreciable. As was to be expected, the solubility increases at low suspension concentrations in an individual way for each variety of peat. The solubility is an individual feature of each peat variety.

TABLE 1

Aqueous Extract of Sedge Peat

Degree of decomposition, %	Moisture content, %	Ash, % on dry mass	Dry residue of filtrate as % of dry peat	Calcined filtrate residue as % of		
				dry peat substance	mineral content of peat	dry residue
25	84.3	6.6	0.86	0.12	1.85	14.2
35	88.0	7.4	0.79	0.10	1.35	12.6

TABLE 2

Calcined and Dry Residues of Aqueous Extracts of Peat

Origin and varity of peat	Degree of decomposition %	Moisture content, %	Ash, % on dry mass	Concentration of suspension, % of dry material	Color of filtrate	Clarity, Snellen's method, cm	Dry residue of filtrate as % of dry peat	Calcined filtrate residue as % of		
								dry peat substance	mineral content of peat	dry residue
Sukhonogovo, medium	25	87.9	2.8	0.05	–	–	1.76	0.06	2.1	3.4
				1.00	Dark brown	15	1.62	0.06	2.1	3.7
South Alferovo, wood-sedge transitional	40	71.0	9.8	0.05	–	–	2.14	0.13	1.36	6.1
				1.00	Yellow-brown	22	1.39	0.11	1.1	7.9
Galician moss, sedge root	25	85.4	5.9	0.05	–	–	1.20	0.14	2.3	11.5
				1.00	Greyish-brown	25	1.00	0.12	2.0	11.8
Kosmynino, alder	45	77.1	20.2	0.05	–	–	0.48	0.05	0.2	10.0
				1.00	Greyish-green	27	0.45	0.04	0.1	9.0

The ratio of the dry to the calcined residue suggests that the amount of substances passing into solution depends both on the organic and on the mineral components of the peat. These substances are dissolved both out of the large and the small particles. Nevertheless, Volarovich and Churaev ascribe these substances to the fractions < 1μ, while in Semensky's method they enter all the fractions, and so distort the value of each in inverse proportion to its share of the total number of particles.

Beyond a definite threshold, the content of finely dispersed particles in peat becomes progressively less. For example, for a diameter of < 1μ, the amount, according to Volarovich and Churaev [5], does not exceed a fraction of one per cent. The amount of substances dissolved during settling, however, should increase. Thus the distortion of the results, appreciable even for large particles, should progressivly increase in the small particle region, resulting in a picture of size distribution far removed from reality.

It is seen that the pipet method is not suitable. The method of Volarovich and Churaev is less liable to error, but the results obtained by it must be corrected for the dissolved substances.

LITERATURE CITED

[1] N. A. Figurovsky, Sedimentometric Analysis, Moscow-Leningrad, Acad. Sci. USSR Press (1948); F. Hahn Dispersion Analysis, State Chem. Press., Moscow- Leningrad (1940).

[2] E. P. Semensky, Trans. Peat Inst., 11, 24 (1932); E. P. Semensky and Kh. I. Rivkina, Peat Ind., 4, 29 (1932); A. Dumansky, M. Chapek, T. Buravlev, and E. Shurygina, Colloid J., 3, No. 2, 99 (1937).

[3] E. P. Semensky, Technical Analysis of Peat, State Energy Press, Moscow-Leningrad (1949).

[4] V. D. Lomtadze, Methods for the Laboratory Investigation of the Physico-Mechanical Properties of Sand and Clay Soils, Moscow, State Geol. Press (1952).

[5] M. P. Volarovich and N. V. Churaev, Colloid J., 16, 241 (1954) (T.p. 243)* ; 17, No. 3, 200 (1955) (T.p. 185)* ; 16, No. 3, 220 (1954) (T.p. 221)* .

[6] V. E. Rakovsky and Kh. I. Rivkina, Trans. Inst. Peat, Academy of Sciences, Belorussian SSR, 1, 112 (1951).

[7] V. Rudnev, Bull. Petrov Agric. Acad., 12, 2, 11 (1889); R. Hoffmann, J. prak. Chem., 88, 206 (1863).

[8] R. Thiessen and R. C. Johnson, Ind. Eng. Chem., 24, 20, 1190 (1932).

[9] G. Stadnikov and A. Barysheva, Brennstoff Chem., 11, 21 (1930).

Received July 28, 1955

---

* T.p.= C. B. Translation pagination

CONSIDERATION OF DISSOLVED SUBSTANCES IN THE DISPERSION ANALYSIS OF PEAT

M. P. Volarovich and N. V. Churaev

K. K. Lebedev, in his paper "Determination of the Degree of Dispersion of Peat by Sedimentometric Methods" which deals with the interesting problem of the amounts of dissolved substances in peat suspensions, points out the need to apply a correction for the amount of dissolved matter to the results of dispersion analysis of peat.

In principle we agree with K. K. Lebedev. However, as can be seen from his paper, the amount of dissolved matter does not exceed 1-2% of the dry peat. The accuracy of the determination of the contents of the various fractions by dispersion analysis of peat, however, is 3-4%. Since the correction is less than the possible error of the determination there is hardly any purpose in applying it.

Moreover, the value for the dissolved matter obtained by K. K. Lebedev seems to us to be too high. Unfortunately the paper does not give the characteristics of the filter used for separation of the dissolved and the suspended substances. Quite apart from the somewhat arbitrary nature of such a separation, it seems likely that the filtrate contained not only dissolved substances, but also a part of the highly disperse peat fraction. To solve this question an investigation of the filtrate with the aid of the electron microscope would be desirable. For instance, we found considerable numbers of aggregates and particles up to 10-30 μ in size in electron micrographs of optically empty peat water allowed to settle for several months.

Received October 31,1955

REVIEW

F. D. Ovcharenko's book "Development of Colloid Chemistry in the Ukraine" (Acad. Sci. USSR Press, Kiev, 1955).

In view of the dearth of historical literature on colloid chemistry, F. D. Ovcharenko's brochure, intended for workers of institutions of higher education, scientific-research institutions, school teachers, technical school teachers, and technical-engineering workers, merits attention and is of interest. In this work the author rightly stresses the fruitful relationship which existed between scientists who worked in the Ukraine and in other scientific centers of the nation.

The brochure is in two parts. The first part is devoted to the development of colloid chemistry in the Ukraine in the prerevolutionary period. Here the author discusses the substance and importance of the researches of native scientists who carried out their colloid investigations in the Ukraine.

The author aptly concludes the first part with the observation that the researches of scientists who worked in the Ukraine in the prerevolutionary period, – I. G. Borshchov, N. A. Bunge, F. N. Shvedov, G. G. Demetets, A. V. Dumansky, P. I. Kholodny, B. A. Shishkovsky et al. were very important in the development of colloid chemistry and that "the native colloid researchers ... justly occupied a place of honor in this science", and also accurately explains the beneficial influence of the genial Russian scientists – M. V. Lomonosov, D. I. Mendeleev, A. M. Butlerov and their successors on the development of chemistry and, in particular, of colloid chemistry in the Ukraine.

However, despite its merits, the first part suffers from certain flaws; we will cite, in our opinion, the main ones.

The views of M. V. Lomonosov and D. I. Mendeleev in the field of colloids are incompletely discussed. While devoting 6 lines (p.10) to D. I. Mendeleev's views on this subject, in the case of M. V. Lomonosov, the author limited himself to the remark " . . . M. V. Lomonosov already understood the nature of such substances as gelatin, fish glue, gum arabic etc." (p.3). The author should have considered the statements of M. V. Lomonosov with respect to colloids (see "Works of M. V. Lomonosov", Vol. 1 and 2, Acad. Sci. USSR Press, 1950 and 1951). Moreover, the author did not mention the works of Prof. F. I. Gize (1804-1814) of Kharkov University, for example, his "Report on Analysis of Fuller's Earth of the Summer Resorts ... of N. V. Kapnist, Ekaterinoslavskaya Guberniya Aleksandrovsky Uyezd, at Sofievka Derevnya" (Kharkov, 1812), i.e. in particular, he wrote on charcoal adsorption: " . . . when charcoal exhibits its decolorizing, deodorizing and taste-removing action, this may indicate the presenc of substances of an organic nature, which are adsorbed by charcoal" ("General Chemistry", No. 1, Kharkov, 1813, pp 473-475).

The author ignores the researches of biochemists whose main object of investigation was albumins (typical lyophilic colloids), i.e. the works of A. I. Khodnev "Composition of Gelatinous Plant Substances and Their Physiological Importance" (SPb.* 1846); "Course in Physiological Chemistry" (Kharkov, 1847); the work of L. S. Tsenkovsk "Gelatinous Formations of Beet-Sugar Solutions" (Kharkov, 1878); the works of A. Ya. Danilevsky, V. I. Palladin, V. K. Zalessky et al.

The present work also neglects to mention papers on the application of colloid chemistry to medicine (see for example "Importance of Colloid Chemistry in Medicine" by Prof. S. G. Yakushevich and "Physico-Chemical Basis of Colloidal Reactions in Cerebro-Spinal Fluid" by A. P. Ermilov, Acta medica", No. 12, Press "Scientific Thought", Kharkov, 1926).

The author writes on page 14 that, "Prof. I. S. Teletov (Kharkov University) in 1907 determined the rate of catalytic reactions in heterogenous systems (decomposition of hydrogen peroxide with platinum black etc.). "This is inaccurately and rather incorrectly stated, since Prof. I. S. Teletov began to work at Kharkov University, starting in 1936 (which the author mentions on page 24), which contradicts the author's statement that Prof. I. S. Teletov "investigated the kinetics of the decomposition of hydrogen peroxide in the presence of colloidal ferric hydroxide solution" etc. (p. 18) in 1931 at Kharkov University. As we know, the paper of I. S. Teletov on the decomposition of hydrogen peroxide with colloidal platinum was printed in 1907 in the J. Russ. Chem. Soc. (39 No. 7, p. 1145, 1358) while he was at the Riga Polytechnical Institute and only beginning in 1915 did I. S. Teletov start working in Kharkov at the Agricultural Institute where his researches of 1931 were carried out and not at the Kharkov University as the author writes.

---

* SPb. = St. Petersburg

The author should have mentioned several researches in the field of colloids, carried out by memebers of the Kharkov Phys.-Chem. Sci. Soc., for example, the papers of N. D. Pilchinov (1892), A. P. Lidov (1897), P. N. Lyashchenko (1903), G. M. Druzhinin (1912), G. E. Timofeev and V. A. Kravtsov (1915) *.

Insufficient attention is given in the present brochure to the researches of native scientists in regard to practical application of colloid chemistry.

It would have been wise to also discuss those works, which although not carried out in the Ukraine, concern objects of investigation which directly relate to the Ukraine and which were responsible for new investigations in this field, i.e. the papers of P. A. Zemyatchensky "Kaolinite Formations of South Russia (SPb. 1896), his "Absorbtive Properties of Russian Clays" (Pg** 1916); A. M. Skolov "Molecular Decomposition of Kaolinite in First Stages of Firing" (Bull. SPb. Inst. of Technology, 1912), A. E. Fersman "Russian Deposits of Fuller's Earth and Related Substances" (Petrograd, 1919); papers of A. A. Tvalchrelidze *et al.*

In the second part, the author discusses the researches and achievements of Soviet colloid research scientists. The author starts this part well by focussing attention mainly on the works of E. N. Gapon, showing how his work was of prime importance in the initial development of colloid chemistry in the Ukraine during the Soviet period.

The author emphasizes the fact that due to the help of the Communist Party and the Soviet Gov., a great network of institutions of higher education, scientific-research institutes and factory laboratories now exists in our nation in which innumerable investigations are being carried out, some of which concern the field of colloid chemistry. The author cites researches in colloid chemistry conducted in Kharkov, Kiev, Odessa and in other scientific centers of the Soviet Ukraine. However, even this part has some defects. Thus, for example, when discussing the development of colloid chemistry in the Ukraine, it would have been well to discuss the development of the related scholastic and scientific literature, published in the Russian and Ukrainian languages in the USSR during the pre- and postwar years.

Mention also should have been made of the "Colloid Chemistry Circle" at the Kharkov House of Scientists, which united all the colloid researchers of Kharkov and where the research was under the guidance of Prof. I. S. Teletov in the prewar years from 1936 on; during this time more than 30 reports were heard and, moreover, where researches were subjected to review and analysis even as they were being carried out, etc.

Distinguished Soviet scientists such as A. V. Dumansky and P. A. Rebinder also took part in the work of this circle in addition to native Kharkov colloid researchers.

A whole series of works have not been mentioned in the brochure, among which are those of: M. I. Nekrich on white earths (Ukr. Chem. J. 2, Book 4, 1926); and others (J. Phys. Chem. 25, No. 5, 485, 1952; J. Phys. Chem 26, 1317, 1953); A. V. Nagorny on the problem of aging (Koll.-Z. 41,23); "Problem of Aging and Death" Medvidiv (1935); M. A. Egorov on soil dispersion (Agric. Exp. Act 1926-1927); adsorption studies of I. E. Adadurov (J. Phys. Chem. 3, 833, 1930) and of P. Migal (J. Gen. Chem., 5, 6141, 1935); aerosols (J. Phys. Chem. 6, 896, 1936) etc.

Researches carried out at the Mironovsk and Nosovsk agricultural experimental stations (M. N. Yazvitsky, 1928 *et al.*) and researches pertaining to the sugar-beet industry (M. K. Vasilenko, 1926, A. G. Arkhipovich, 1930, 1931, M. R. Kotlyarenko and N. K. Kanibolotsky, 1930 *et al.*) are not mentioned.

Of great importance in the development of chemical science in the USSR and particularly, in the Ukraine was the 6th All-Union Mendeleev Congress and the work of the colloid section of the Congress, Kharkov, 1932.

Colloid chemistry in the Ukraine naturally attained a higher development during the Soviet period than in prerevolutionary times. The second part of F. D. Ovcharenko's work therefore presents a larger number of colloid researchers than does the first. However, F. D. Ovcharenko's method of presentation in the second part merits revision. It seems logical to present the works thematically, first dividing them into two groups: 1) works of theoretical nature and 2) works of an applied nature, accurately citing the years (ex. 1917 1954) and the period (ex.

---

* See papers of the Society of Physico-Chemical Sciences at Kharkov University.

** Pg = Petrograd

"years of the reconstruction", "years of the five-year plans", "postwar years" etc.).

It might have been appropriate to present the material under topic headings, as, for example, "Silica Gel", "Mineralogy of Colloidal Dispersions", "Stability of Colloidal Solutions and Emulsions" etc.; of course, chronological data should not be neglected.

The brochure is not too clear on such matters as the graduation of specialists in colloid chemistry from institutions of higher education, the perfection of industrial processes, based on the application of the latest advances of colloid science, the work of scientific and student scientific organizations, of conferences, seminars, circles etc. on colloid chemistry. The author only superficially touched upon these matters (p. 17, 32).

Historical research on colloid chemistry has been considerably facilitated by "Bibliographic Outline of the Development of Native Colloid Chemistry", Ed. 1 (Kiev, 1952), compiled by A. V. Dumansky. From what has already been stated, it seems F. D. Ovcharenko made poor use of the "Bibliographic Outline".

Accuracy, particularly chronological accuracy, is a prime requisite for a work on the history of chemistry, which F. D. Ovcharenko sometimes neglects in his work. Thus, for example, F. D. Ovcharenko writes that " . . . the usefulness of these (Kharkov – S. K.) clays for the regeneration of transformer oils has been demonstrated" (p. 24). This leads us to believe that this was done recently (1954). However, it is a known fact that the Kharkov tripolite rock "greenstone" was used for industrial purposes as long ago as in July 1941 in Kharenergo on the basis of previously performed experimental research (see conclusion Kharenergo from 5/9/1942; Journal "Electric Stations" No. 2, 1948; J. Phys. Chem. 25, No. 5, 1952); at present methods are being sought for utilizing this Kharkov deposit as a mineral sorbent.

Errors in the spelling of family names are to be found such as V. M. Lezhaev in place of V. M. Lezhoev (p. 21), D. Avdashan in place of D. Avdalian (p. 25), which is also careless. It is also regretable that more illustrations, diagrams and tables were not presented to more explicitly show the development of colloid chemistry in the USSR and in the Ukr. SSR.

The book is written in a popular, clear and concise idiom and the author handles the Ukrainian chemical terminology very well, and, despite the defects mentioned (which should be eliminated in the future), readers will find the book interesting reading.

S. N. Kuzmenko

Ф. Шведов

FEDOR NIKIFOROVICH SHVEDOV

1840-1905

TO THE MEMORY OF FEDOR NIKIFOROVICH SHVEDOV

(On the fiftieth anniversary of his death)

December 12 (old style) 1955 was the fiftieth anniversary of the death of the eminent Russian physicist, founder of the rheology of disperse systems, Professor of the University of Odessa, Fedor Nikiforovich Shvedov [1-4].

F.N. Shvedov was born February 14 (old style) 1840, in the town of Kiliya, Bessarabia province (now the Moldavian SSR). He received his secondary education at the 2nd Odessa Gymnasium, and then entered the Richelieu Lyceum, also in Odessa. However, the teaching at this lyceum was of a low standard. In the words of the famous surgeon N.I. Pirogov, a trustee of the lyceum at that time [3], "the young man who completed the course at the lyceum only increased needlessly the class of those who are incapable of direct application of their knowledge in practice". It was Pirogov who called this lyceum, "a wretched nonentity with pretensions to independence". Dissatisfied with his studies at this lyceum, Shvedov moved in 1859 to St. Petersburg where he entered the physico-mathematical faculty of the University.

Having become interested in physics under the influence of F.F. Petrushevsky, F.N. Shvedov devoted his whole life to this branch of science. After he graduated in 1862, Shvedov was retained at the University and, having attended a special teachers' course, he was sent for 2 years abroad to Magnus' laboratory in Berlin, where Shvedov displayed great independence. Magnus once said reproachfully to him [1], "You are still so young and you are already propounding theories".

Having presented his Master's Dissertation(St. Petersburg, 1898), Shvedov received an offer to become a lecturer in physics at the Novorossiysk University, which was organized in Odessa in succession to the Richelieu Lyceum in 1865; Shvedov replaced the aged professor of physics, V.I. Lapshin. Shvedov spent the rest of his life in Odessa; he was associated with the Novorossiysk University and took an active part in its organization. After his Doctorate Dissertation in 1870 on "The Laws of the Conversion of Electricity into Heat", Shvedov was appointed professor of physics at this University. In 1877-1880 and 1889-1895 Shvedov was Dean of the Physico-Mathematical Faculty, and in 1895-1903 he was Rector of the University. Shvedov died December 12 (old style) 1905. Our noted metereologist, Professor Klossovsky, made a heartfelt funeral oration at his burial [2].

F.N. Shvedov's varied activities left a great impression at the Novorossiysk University. When Shvedov was rector, the Medical Faculty and Library buildings and the buildings of the Law and Philology Faculties were erected at his behest and under his direct supervision. He had a special building put up for the Chemistry and Physics Institutes [5], the latter being one of the first special physics institutes attached to universities in Russia.

When F.N. Shvedov vacated the post of rector in January 1903, his colleagues, members of the Novorossiysk University Council presented him with an address which contained the following words [6]: "Owing to your efforts, the University has greatly flourished during your term of office, its size has more than doubled, and its prosperity has been strengthened. Your name will be linked forever with the great buildings of the Medical Faculty, the Physico-Chemical Institute, and the Library, which have enriched the University in recent years".

The physics demonstration room and the physical laboratory for students' practical work were reorganized by Shvedov. At the time of his move to Odessa there was a special practical physics laboratory for the students, and the physics auditorium seating 250 was also splendidly equipped. De Metz, who attended Shvedov's lectures in 1881, wrote [1], "His lectures were interesting and always attracted a considerable audience; they were distinguished by simplicity of construction, elegance of presentation, and originality of ideas".

Although he devoted much of his time to teaching and organization, Shvedov regularly did scientific work all his life. He published a total of 58 original papers [7] on rheology (shape elasticity and viscosity of colloids), on electrostatics and electric rays, on geophysics (on the form and structure of hail, etc.), and on cosmic physics – on comets and meteorites. Not all of Shvedov's work is of equal value. It cannot be said that all his work on cosmic physics has proved correct. On the other hand, Shvedov's papers on meteorites contain a number of interesting views which have still not lost their value.

However, Shvedov's remarkable work on the elasticity and anomalous viscosity of colloids is still of enormous interest and has retained its significance [8]. These were the first investigations of colloid rheology: they provided the basis for the formation and development of this science.

Shvedov studied relaxation processes in colloid solutions and was the first to demonstrate their anomaly of viscosity and shape elasticity, with the use of 0.5 and 1.0% gelatin solutions as examples [9-11].

Shvedov's work was carried out at a high theoretical level, while for the experimental work he designed and constructed a highly sensitive instrument based on the rotating cylinder principle. This instrument is of original design, is very simple, and at the same time it was provided with a sound theoretical basis by Shvedov [8, 9]. It should be noted that for viscosity measurements the viscosimeter cylinder was rotated by means of an electric motor, which was a very interesting innovation in physico-chemical experiments at that time.

Shvedov measured the elasticity modulus of 0.5% gelatin solution; the value was 0.535 dyne/cm². In a study of stress relaxation in this solution, Shvedov showed that the Maxwell equation [12] for relaxation does not fit the experimental data; the stresses do not completely decay; and therefore Shvedov introduced an additional term into the Maxwell equation. The relaxation time T for this gelatin solution was found to be 13.7 seconds.

Having discovered anomalous viscosity, Shvedov observed that when the rate of rotation of the cylinder was increased to 15 times its original value, the viscosity of a 1% gelatin solution decreased 7 times. The discovery of anomalous viscosity in colloidal solutions is sometimes incorrectly ascribed to Garrett and Du Pre Denning. This is done, for example, by Hatschek [13], though later he gives a detailed description of one of Shvedov's investigations. Since, however, the work of these authors was carried out in 1903, Shvedov's priority is quite evident, as he discovered the effect in 1889, or 14 years earlier. An important fact is that Shvedov deliberately sought this effect on theoretical considerations, discovered it by means of an original method which he developed, and studied it in detail.

In discussing the results of his experiments, Shvedov was the first to write the differential equation for viscoplastic flow in the following form [8, 14]:

$$\eta_a = GT + \frac{\theta}{\gamma}, \tag{1}$$

where η_a is the anomalous (variable) viscosity; θ is the yield stress; γ is the rate of shear or the velocity gradient du/dz. This equation may be transformed [8] into

$$\tau = \theta + \eta_{pl}\frac{du}{dz}, \tag{2}$$

where τ is the shearing stress and η_{pl} is the plastic viscosity.

In Equation (1), Shvedov introduced for the first time the yield stress θ (the flow limit), a value highly characteristic of disperse systems. When $\theta = 0$, the Shvedov equation becomes the Newton equation for viscous flow.

Later, in 1917, a similar equation was put forward by Bingham [15]; a system of equations of this type, analogous to the Navier-Stokes equations in hydrodynamics, was derived by Hencky in 1925 [16], and also, in the most general form by Ilyushin [17, 18].

Shvedov's pupil Veinberg [19] was the first to integrate the Shvedov equation for the case of a rotating cylinder viscosimeter, as early as 1912. On the basis of the derivation used by Petrov [20] for the motion of a true viscous Newtonian liquid in the space between coaxial cylinders, Veinberg obtained the following equation for the torque M, for the case of a viscoplastic substance in accordance with the Shvedov Equation (2):

$$M = \left[-\eta_{pl}\, r\frac{d\omega}{dr} + \theta\right]2\pi r^2 H, \tag{3}$$

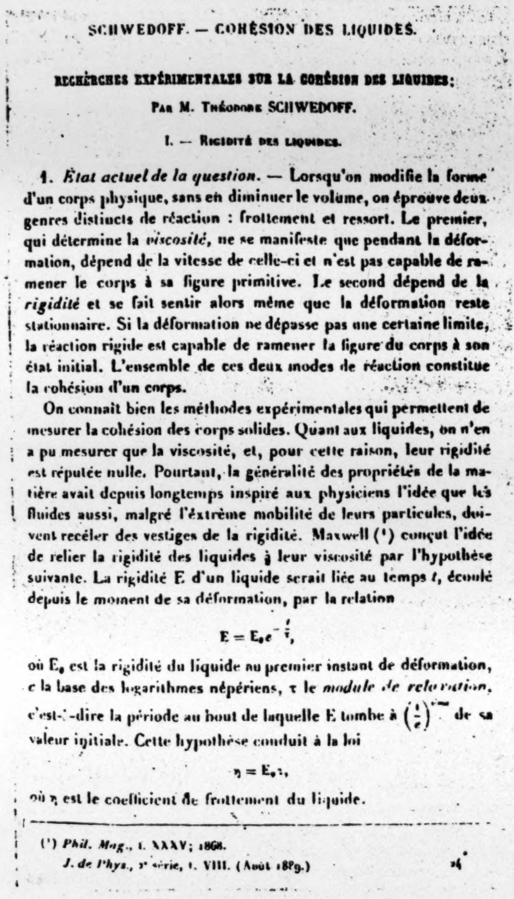

SCHWEDOFF. — COHÉSION DES LIQUIDES.

RECHERCHES EXPÉRIMENTALES SUR LA COHÉSION DES LIQUIDES;

PAR M. THÉODORE SCHWEDOFF.

I. — RIGIDITÉ DES LIQUIDES.

1. *État actuel de la question.* — Lorsqu'on modifie la forme d'un corps physique, sans en diminuer le volume, on éprouve deux genres distincts de réaction : frottement et ressort. Le premier, qui détermine la *viscosité*, ne se manifeste que pendant la déformation, dépend de la vitesse de celle-ci et n'est pas capable de ramener le corps à sa figure primitive. Le second dépend de la *rigidité* et se fait sentir alors même que la déformation reste stationnaire. Si la déformation ne dépasse pas une certaine limite, la réaction rigide est capable de ramener la figure du corps à son état initial. L'ensemble de ces deux modes de réaction constitue la cohésion d'un corps.

On connait bien les méthodes expérimentales qui permettent de mesurer la cohésion des corps solides. Quant aux liquides, on n'en a pu mesurer que la viscosité, et, pour cette raison, leur rigidité est réputée nulle. Pourtant, la généralité des propriétés de la matière avait depuis longtemps inspiré aux physiciens l'idée que les fluides aussi, malgré l'extrême mobilité de leurs particules, doivent recéler des vestiges de la rigidité. Maxwell (¹) conçut l'idée de relier la rigidité des liquides à leur viscosité par l'hypothèse suivante. La rigidité E d'un liquide serait liée au temps t, écoulé depuis le moment de sa déformation, par la relation

$$E = E_0 e^{-\frac{t}{\tau}},$$

où E_0 est la rigidité du liquide au premier instant de déformation, e la base des logarithmes népériens, τ le *module de relaxation*, c'est-à-dire la période au bout de laquelle E tombe à $\left(\frac{1}{e}\right)^{\text{ième}}$ de sa valeur initiale. Cette hypothèse conduit à la loi

$$\eta = E_0 \tau,$$

où η est le coefficient de frottement du liquide.

(¹) *Phil. Mag.*, t. XXXV; 1868.

J. de Phys., 2ᵉ série, t. VIII. (Août 1889.) 24

First page of F.N. Shvedov's paper [11].

where $\frac{d\omega}{dr}$ is the angular velocity gradient; $\underline{r}$ is the radius of an arbitrarily chosen concentric layer in the gap between the cylinders, and H is its height.

In the Veinberg apparatus the rotating cylinder is moved by falling loads (each of weight P) suspended from threads wound on a pulley of radius R. Therefore the moment of the external acting forces was M = 2P · R. In an examination of the boundary conditions Veinberg considered that the bitumens and asphalts which he studied adhered to the cylinder surfaces. Then, in the case when the inner cylinder of radius $\underline{r}$ rotates at constant angular velocity Ω, while the outer cylinder with radius r_1 is stationary, when $r = r_1$, $\omega = 0$, and when $r = r_0$, $\omega = \Omega$.

As a result, Veinberg obtained the following equation for the angular velocity of rotation Ω of the cylinder as a function of the load P:

$$\Omega = \frac{\theta}{\eta_{Fl}} \ln \frac{r_1}{r_0} + \frac{P \cdot R}{2\pi H \eta_{Fl}} \left[\frac{1}{r_1^2} - \frac{1}{r_0^2} \right]. \tag{4}$$

Formula (4) is the first example of integration of the Shvedov equation. This formula is quite identical with the relationships derived later for the case of the coaxial cylinder viscosimeter [21,22], which are widely known in our research work. For the case when $\theta = 0$, Formula (4) becomes the usual Petrov equation for a viscous liquid.

The linear relationship $\Omega = f(P)$ in Formula (4) for a viscoplastic liquid represents the case when the shear of the substance in the gap between the cylinders extends to the end. A second case is found at low loads; the shear then does not extend to the end, and there are two concentric zones: a zone of elastic deformation, closer to the external cylinder, where the stresses τ do not exceed the yield stress value, and a zone of plastic deformation, closer to the inner cylinder, where $\tau > \theta$ This case was not considered by Veinberg; it was examined later by other authors [21,22].

With the use of Equation (4), Veinberg investigated bitumens, asphalts, and other materials. In these experiments he obtained values for the yield stress, of which the following, for asphalt at different temperatures, are an example:

Temperature in °C	15	20	30
Yield stress in dynes/cm²	$7 \cdot 10^2$	$6 \cdot 10^2$	$3 \cdot 10^2$

Veinberg also quotes yield stress values for other substances, namely: wax – $1.3 \cdot 10^5$ dynes/cm²; ice from the Neva river at 0° – $5.5 \cdot 10^5$ dynes/cm²; glacier ice – $0.9 \cdot 10^5$ dynes/cm². Veinberg used the data obtained by Shvedov [9] to calculate the yield stress of 0.5% gelatin solution, 0.009 dyne/cm², and of 1.0% solution, 2.0 dynes/cm². These values are close to the results obtained by modern determination methods [23]. Subsequently Equation (2) was integrated for many particular cases [8].

Among Shvedov's other papers on the rheological properties of disperse systems, the one on the relationship between the elastic and optical properties of colloids [10] is little known. Maxwell [24], Kundt [25], and De Metz [26] observed in the course of their researches that some liquids rotate the plane of polarization of light during deformation; the same liquids lose this property upon removal of the deforming force. Shvedov postulated, and proved theoretically and experimentally, that the ability of disperse systems to rotate the plane of polarization is related to their elastic properties, and in this way he also confirmed the existence of elastic properties in colloids. Using Kundt's data [25] on the viscous properties of collodion, Shvedov showed that the elastic modulus of collodion is 542 dynes/cm². It is because of this property that collodion in the deformed state can polarize light.

Shvedov's classical researches in the field of rheology of disperse systems were many decades ahead of the development of industry, and therefore did not find due application at the time. This is probably the reason why for many years these researches were unjustifiably forgotten, and later attributed to other authors [13,15]. It is now quite evident that priority in the discovery of anomalous viscosity and shape elasticity of colloidal solutions belongs to Shvedov [9-11]. It must also be pointed out in this connection that Shvedov was not only a leading physicist, but took a materialistic view in explaining the laws of Nature.

In Russian science, the name of Professor Fedor Nikiforovich Shvedov occupies an honored place as that of the founder of the rheology of disperse systems, a talented teacher and brilliant organizer, and one of the outstanding workers of the State University of Odessa.

M.P. Volarovich and S.M. Levi

LITERATURE CITED

[1] G.G. De Metz, "To the Memory of F.N. Shvedov", Physical Review, Kiev, 7, No. 1, 1 (1906).

[2] A.V. Klossovsky, "Funeral Oration for F.N. Shvedov", Bull. Exp. Phys., 35, No. 1 (No. 409), 1 (1906).

[3] I.Ya. Tochidlovsky, "To the Memory of Fedor Nikiforovich Shvedov" (Paper read at the Annual Meeting of the Novorossiysk Society of Naturalists, III/17 1907), Bull. Exp. Phys., 35, No. 3 (No. 413), 37 (1906).

[4] Shvedov, Fedor Nikiforovich, Encyclopedic Dictionary, Brokgauz and Efron, 39, 257 (1903).

[5] A.F. Poll, The Physics Department of the Physico-Chemical Institute of the Novorossiysk University, Bull. Exp. Phys., 24, No. 2 (No. 288), 277 (1901).

[6] B.P. Veinberg, "Some Reminiscences of F.N. Shvedov", J. Russ. Phys. Chem. Soc., Phys. Sect., 39, 11 (1907).

[7] List of F.N. Shvedov's published works (compiled by B.P. Veinberg), J. Russ. Phys. Chem. Soc., Phys. Sect., 39, 27 (1907).

[8] M.P. Volarovich, Colloid J., 16, 227 (1954) (T.p. 227)*.

[9] F.N. Shvedov, J. phys., (2), 8, 341-359, (1889); 9, 34 56, (1890); Seance. Soc. Frans. de phys., 134-152, 186-199, (1899).

[10] F.N. Shvedov, J. phys., (3), 10, 49-53 (1892).

[11] F.N. Shvedov, La rigidite de liquides, Rapport Congr. international phys., Paris, 1, 478-486 (1900).

[12] J.C. Maxwell, Phil. Mag., (4), 45, 133 (1888).

[13] E. Hatschek, The Viscosity of Liquids, Translated from English, 2nd Ed., State Tech. Press (1935).

[14] B.V. Deryagin and S.M. Levi, Bull. Acad. Sci. USSR, Div. Tech. Sci., No. 9, 43-52 (1955).

[15] E.C. Bingham, Fluidity and Plasticity, No. 9 (1922).

[16] H. Hencky, Z. angew. Math. Mech., 5, 115 (1925).

[17] A.A. Ilyushin, Trans. Conf. on Plastic Deformations, Acad. Sci. USSR Press (1938).

[18] M.P. Volarovich and A.M. Gutkin, J. Tech. Phys., 16, 321 (1946); A.M. Gutkin, Trans. 2nd Conf. on Friction and Wear in Machines, Acad. Sci. USSR Press, 1, 31 (1947).

[19] B.P. Veinberg, J. Russ. Phys. Chem. Soc., 44, 201 (1912).

[20] N.P. Petrov, Engineering J., 27, No. 1-4 (1883); M.P. Volarovich, Trans. 2nd Conf. on Friction and Wear in Machines, 3,5 (1949).

[21] M.P. Volarovich and D.M. Tolstoy, J. Phys. Chem., 4, 815 (1933).

[22] M. Reiner and R. Riwlin, Koll. Z., 41, 1 (1927).

[23] S.M. Levi, Colloid J., 17, 158 (1955) (T.p. 145)*.

[24] J.C. Maxwell, Pogg. Ann., 1 (1874).

[25] W. Kundt, Wied. Ann., 13 (1881).

[26] G.G. De Metz, Wied. Ann., 35 (1885).

---

*T.p. = C.B. Translation pagination.

EFFECT OF DISPERSE FILLERS ON THE RELAXATION PROPERTIES OF RUBBERS

G.M. Bartenev and L.A. Vishnitskaya

Numerous papers [1-7] deal with investigations of relaxation effects in polymers and materials based on them, which determine the behavior of such materials. In an examination of the molecular relaxation process in linear polymers, Kargin and Slonimsky [3] concluded that two distributions of relaxation times exist. The first distribution of relaxation times for rubberlike polymers [1] is in the region of small times ($10^{-3} - 10^{-6}$ second) and represents orientation of the units in the polymer chain during loading and disorientation during unloading. The second distribution of relaxation times is in a region of much larger times, and is associated with relative displacements of the linear molecules. Orientation of the links in the polymer chain leads to straightening of the molecules and development of high-elastic deformation, while displacement of the linear molecules as a whole leads to viscoplastic flow.

In an approximate examination of relaxation processes in rubbers and vulcanizates, the relaxation time distributions may be replaced by the corresponding average values.

It is known that for structurized polymers (rubbers) [4,5,7,8] the relaxation process at ordinary temperatures may be divided into three parts: 1) orientation of the chain molecule units, which occurs with an average relaxation time of the order of $10^{-3} - 10^{-6}$ seconds; 2) regrouping and slippage of segments, leading to redistribution of stresses in the molecular chains (the usually observed form of relaxation), which lasts for minutes or hours; 3) regrouping of cross-links and chain scission, leading to a slight, approximately linear, decrease of stress, which lasts for months or years.

TABLE

Contents of Fillers in the Rubbers Studied

Code No. of rubber	Chalk content		Code No. of rubber	Carbon black content		Code No. of rubber	Carbon black content	
	Parts by wt. per 100 of rubber	κ in vol. %		Parts by wt. per 100 of rubber	κ in vol. %		Parts by wt. per 100 of rubber	κ in vol. %
MC0	0	0	MC0	0	0	C50	50	20.1
M20	20	6.2	C10	10	4.8	C65	65	24.6
M40	40	11.6	C15	15	7.0	C80	80	28.6
M80	80	20.8	C25	25	11.8	C100	100	33.4
M161	161	34.6	C35	35	15.0	C125	125	38.6

Note: The filler content κ in % by volume was calculated by means of the formula $\kappa = \frac{v}{V} \cdot 100$ where $\underline{v}$ is the volume of the filler, and V is the total volume of the filled rubber.

The third relaxation process is caused by chemical process, and therefore we shall term it chemical relaxation. In distinction, the chain link orientation (the first) and the segment regrouping (the second) processes, we shall term, jointly, chain relaxation. The latter is a purely physical process, the rate of which is determined by the chemical structure of the chains and the forces of interaction between them. Chemical relaxation is determined by chemical processes which occur in the material. It has been shown experimentally [4,5,7,8] that the average time of chemical relaxation is great in comparison with the time of molecular chain relaxation. Therefore these two processes may be separated, although such a separation is conventional.

Technical rubbers are usually rubber vulcanizates containing disperse fillers (various carbon blacks, kaolin, chalk, etc.). Therefore investigation of the relaxation properties of filled rubbers is of direct practical interest. Several investigations [10-13] have been devoted to this problem, and in most of them active fillers were investigated, as being substances which give the greatest reinforcement effect. In these studies it was established that: 1) according to their influence on the strength of the vulcanizates, fillers may be divided into the reinforcing (active) and the inert (inactive); this, however, is a conditional division, as the degree of activity of the same filler depends on the type of polymer; 2) the thixotropic properties of active fillers have a significant effect on the mechanical properties of the filled rubbers; 3) disperse fillers in the filler-rubber system form chains and a continuous network of such chains, under definite conditions; 4) the mechanical properties of filled rubbers greatly depend on their previous deformation history.

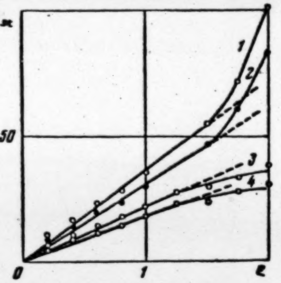

Fig. 1 Extension curves at 22°; 1 and 2) S 50 rubbers; 3 and 4) M 80; 1 and 3) static 10-minute curves; 2 and 4) 24-hour curves.

Because of the complex nature of the systems in question, many aspects of the relaxation process in filled rubbers have not been elucidated.

Our experimental data, presented below and in a previous paper [9], have shown that in filled vulcanizates, in addition to chemical relaxation and chain relaxation, yet another relaxation process occurs, involving the separation of the filler particles from the rubber chains. This process may be conventionally termed the filler relaxation process, since it is accompanied by regrouping of the filler particles.

Method of measurement. Relaxation processes in rubbers are studied by different methods, the most convenient of which is the method of stress relaxation at constant deformation. Results obtained by this method are susceptible to clearer physical interpretation and are directly applicable to rubbers used under conditions of static deformation.

In the absence of chemical processes, stress relaxation in rubbers leads to the establishment of a certain state of equilibrium stress, at which both the deformation and the true stress σ are constant. At low and moderate extensions the equilibrium deformation obeys the following law [5]: $\sigma = E_{\infty}\epsilon$, where E_{∞} is the equilibrium modulus of high elasticity, which depends on the chemical nature of the rubber, the temperature, and the number of cross links in unit volume of the rubber.

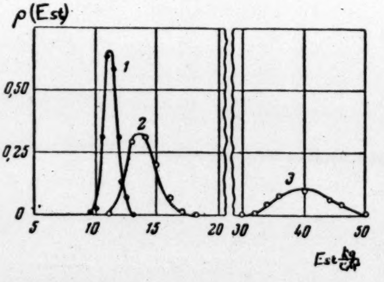

Fig. 2. Distribution curves for the static 15-minute modulus of specimens 20 x 6 x 0.5 mm for the following rubbers: 1 – MC0; 2 – M80; 3 – C50.

Nonequilibrium deformation [4,5] follows more complex laws. For static deformations (ϵ = const) however, for a given observation time, a law analogous to the equilibrium deformation law, with the modulus E_{st} is valid; this modulus depends on the same factors as E_{∞} and also on the time of observation.

By means of the technique used it is possible to determine the static and equilibrium properties of rubbers. The main attention was directed to obtaining $\sigma - t$ curves for prolonged stress relaxation, as prolonged observations are necessary in order to establish the basic laws of practical importance, because rubber articles in the majority of cases remain in a stressed state for prolonged periods during storage and use.

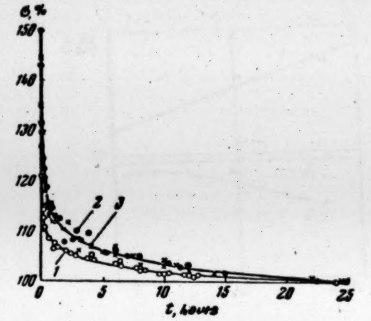

Fig. 3. Relaxation curves in relative stress coordinates (100% is the value of the stress after relaxation for 24 hours) for deformation from 0 to 200% at 25° for the following rubbers: 1 – MC0; 2 – M80; 3 – C50.

The substances studied were rubbers based on SKS-30 rubber with various contents of channel black and chalk, which are typical active and inactive fillers used in the rubber industry. The table shows the weight and volume contents of the fillers in the rubbers studied.

By means of the relaxation curves for various extension deformations it is possible to determine the $\sigma - \epsilon$ relationship, for different observation times. Fig. 1 shows data obtained for specimens which had not been previously subjected to any deformations (nonconditioned specimens) for two observation times. Each point on the graph represents a new specimen tested at the given extension deformation (stress in kg/cm²).

It is seen from these data that filled rubbers obey a proportionality law, but only approximately, as at small deformations the experimental points diverge upward from the curve.* Previous conditioning of the specimens decreases this deviation. In view of this, the applicability of the proportionality law to filled rubbers is restricted. The static modulus may be determined from the slope of the curves in Fig. 1. Irregularities in mixing and vulcanization result in a variation of the modulus values for different specimens of the same rubber. The distribution curves shown in Fig. 2 indicate that this effect must be taken into consideration.

It was shown earlier [4,7] that the curves for stress relaxation obtained at different deformations at normal temperature in the course of twenty-four hours are similar and coincide in relative stress coordinates if the deformation does not exceed 100-200%. This means that the chain relaxation process obeys the following law:

$$\sigma = \varphi(t)\,\epsilon,$$

where, in accordance with the previous notation, $\varphi(t) = E_{st}$. At $t \to \infty$, $\varphi(t) \to E_{\infty}$.

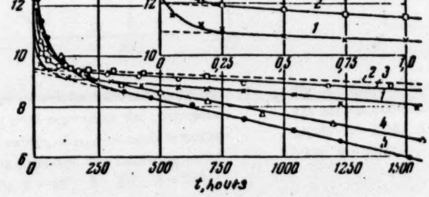

Fig. 4. Curves for brief (a) and prolonged (b) relaxation at 22° and 100% extension, for the following rubbers: 1 – MC 0; 2 – M20; 3 – M40; 4 – M80; 5 – M161.

---

*All the tests carried out in this investigation were on non-conditioned rubbers, as previous deformation (conditioning) produces significant changes in the original structure and mechanical properties of filled rubbers [10,12].

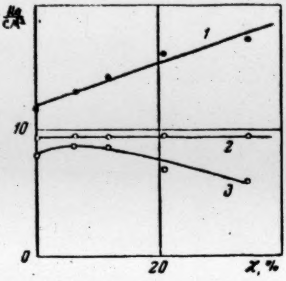

Fig. 5. Variation of: 1) the initial; 2) the equilibrium; 3) the prolonged static modulus with the chalk content of rubber, at 22°.

A similar situation is found in tests on rubbers at high temperatures [7, 8], when the decay of stress is mainly determined by chemical relaxation (the stress falls to zero with time). Hence it follows that the chemical relaxation process obeys the following law:

$$\sigma = \phi(t)\epsilon,$$

where at $t \to \infty$, $\phi(t) \to 0$.

Fig. 3. shows that filled rubbers also display a similarity of relaxation curves, with a certain deviation*. This makes it possible to compare relaxation curves obtained for different deformations, and to confine the investigation to any one deformation value below 200%. In the present study most of the tests were carried out at 100% extension.

Inactive filler. The data in Fig. 4 for rubbers containing various amounts of chalk show that as the chalk content rises there is an increase in the time before the relaxation curve becomes linear, and a slight increase of the initial stress. The curves for brief relaxation (Fig. 4, a) in the course of 1 hour, as is seen by comparison with the curves for prolonged relaxation (Fig. 4, b) indicate apparent equilibrium and the start of a linear relationship. On the other hand, the curves for prolonged relaxation quite distinctly show linear regions over long periods of observation. These linear regions are unconnected with filler relaxation processes, as extrapolation to the ordinate axis gives the same stress value irrespective of the filler content in the rubber.

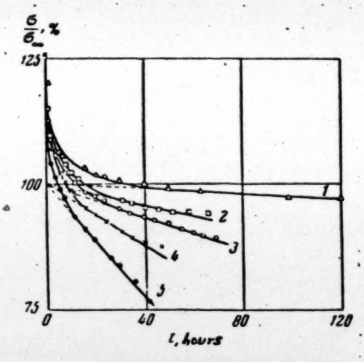

Fig. 6. Relaxation curves for M80 rubber in relative coordinates (100% represents the corresponding extrapolated values of σ_∞ for each temperature) at 100% extension and the following temperatures: 1 – 21°; 2 – 48°; 3 – 60°; 4 – 70°; 5 – 89°.

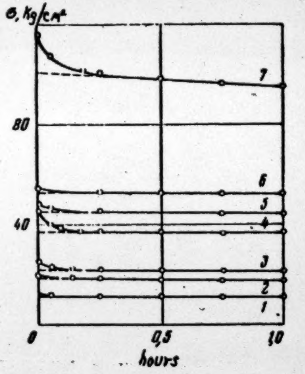

Fig. 7. Brief relaxation curves for rubbers with different carbon contents at 25° and 100% extension: 1 – MC 0; 2 – C10; 3 – C25; 4 – C50; 5 – C65; 6 – C80; 7 – C100.

---

*Deviation at small extensions.

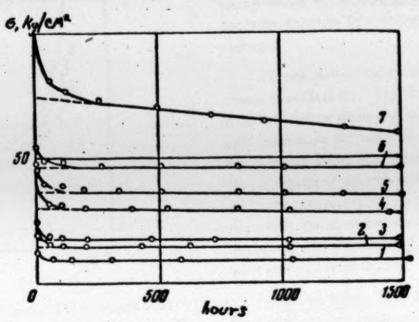

Fig. 8. Prolonged relaxation curves for rubbers with different carbon contents at 25° and 100% extension: 1 – MC0; 2 – C10; 3 – C25; 4 – C50; 5 – C65; 6 – C80; 7 – C100.

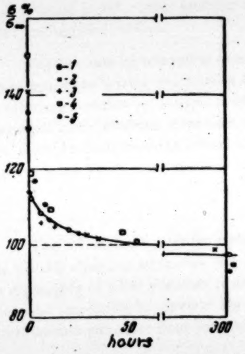

Fig. 9. Relaxation curves in relative stress coordinates at 25° and 100% extension for rubbers with different carbon contents: 1 – MC0; 2 – C50; 3 – C80; 4 – C100; 5 – C125.

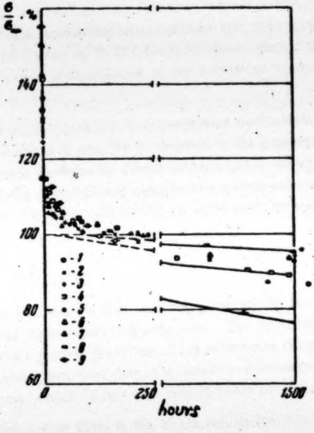

Fig. 10. Relaxation curves in relative stress coordinates at 25° and 100% extension for rubbers with different C contents: 1 – MC0; 2 – C10; 3 – C15; 4 – C25; 5 – C35; 6 – C50; 7 – C65; 8 – C80; 9 – C100 (plotted over 1500 hrs.).

Consequently, the commencement of the linear regions in the relaxation curves corresponds to practically complete chain and filler relaxation. The linear regions represent slow chemical relaxation processes. Hence it follows that extrapolation of the linear regions to the ordinate axis gives the equilibrium stress with respect to the chains and filler. Chemical processes lead to unequal decreases for different degrees of filling.

The modulus values corresponding to the initial* equilibrium and prolonged stresses (1500 hours) for rubbers with different filler contents are shown in Fig. 5. Fig. 5 shows that the initial modulus increases with in-

---

*Determined by extrapolation of the relaxation curve in rectifying coordinates, log σ – t to the ordinate axis.

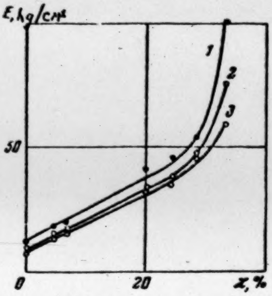

Fig. 11. Variation of the initial (1), conventional equilibrium (2), and prolonged static modulus with the carbon content at 25°.

creased degree of filling, the equilibrium modulus is independent of the filling, while the prolonged static modulus depends in a complex manner on the chalk content.

Temperature increase accelerates chemical processes considerably. Fig. 6 shows relaxation curves for filled rubber at different temperatures. The ordinate axis represents the ratio of the observed stress to the equilibrium value σ_∞, obtained by extrapolation of the linear region of the relaxation curve (σ_∞, different for different temperatures, is taken as 100%). The data show that the time before the linear region is reached decreases and the slope of the linear region increases with rise of temperature.

Active filler. The data in Figs. 7 and 8 for rubbers with various contents of channel black show that with increase of the carbon content: 1) a sharp increase of the initial stress occurs; 2) the decrease of stress is slight in comparison with rubbers containing chalk, but the stress decrease is more rapid when the filler content exceeds 100 parts by weight; 3) extrapolation of the prolonged relaxation curves to the ordinate axis, in contrast to the curves for the inactive filler (Fig. 4) gives stress values which differ for different degrees of filling. This indicates that the extrapolated stress values are not equilibrium values in respect to the filler. They are, however, equilibrium stresses in respect to the chains, as follows from the fact that the relaxation curves in relative coordinates do not depend on the degree of filling up to 300 hours of observation (Fig. 9). The same is found at 70°. More prolonged observations (Fig. 10) show a divergence of the relaxation curves for filled and unfilled rubbers.

The low rate of relaxation processes in rubbers filled with carbon black is confirmed by the data in Fig. 11. Stress relaxation lasting two months at room temperature, when it is possible to determine the conventional equilibrium modulus by extrapolation and the prolonged static modulus by direct measurement, shows that the prolonged static modulus values are not over 10% less, and the conventional equilibrium values are not over 8% less, than the corresponding initial static modulus values for all degrees of filling up to 80 parts by weight. At higher carbon black contents these modulus values differ greatly.

DISCUSSION OF RESULTS

The relaxation curves for rubbers containing disperse fillers show that in rubbers containing inactive filler the usually observed relaxation process consists of chain and filler relaxation processes. The relaxation time due to regrouping of filler particles is of the same order as (rather greater than) the chain relaxation time. It is therefore impossible to separate the chain and filler relaxation processes, but it is possible to separate these two simultaneous processes from the chemical relaxation process, which occurs at a considerably lower rate.

The relaxation usually observed in rubbers containing active filler is the chain relaxation process (when the filler content does not exceed 80-100 parts by weight). The relaxation time due to regrouping of the active filler particles is much greater than the chain relaxation time and is comparable with the chemical relaxation time. Therefore it is impossible to draw a clear distinction between filler particle regrouping and chemical relaxation processes for rubbers containing active filler. In this instance it is possible to separate the latter two simultaneous processes from the chain relaxation process, which occurs at a considerably lower rate.

Thus, the apparent process of stress relaxation in rubbers with inactive filler leads to practical completion of the chain and filler relaxation processes, while in rubbers with active filler (as in unfilled rubber) only chain relaxation is completed. Accordingly, the equilibrium modulus value obtained by extrapolation does not depend on the filler content in the case of an inactive filler, but does depend on it in the case of an active filler.

The equilibrium modulus of rubbers containing inactive filler, and of unfilled rubbers, is a function of the number of chemical cross links formed during vulcanization of the rubber. The equilibrium modulus of rubbers containing active filler depends both on the number of chemical cross links and on the number of adsorptional bonds formed at the rubber–filler particle interfaces.

The change of the equilibrium modulus during aging or any other chemical process which occurs in unstressed rubber and which leads to a change in its structure, is associated with a change in the number of chemical cross links in the case of rubbers with inactive filler, and with the aggregate change in the number of chemical and adsorptional bonds in the case of rubbers with active filler.

The prolonged relaxation curves for rubbers filled with carbon black (Fig. 10) show that: 1) introduction of carbon black retards chemical relaxation processes, in agreement with previous findings [14]; 2) filler relaxation at low filler contents is slower, and at high contents, more rapid, than chemical relaxation; 3) when the filler content exceeds 100 parts by weight the stress relaxation is caused mainly by regrouping of the carbon particles. This is the result of the presence of a relatively large number of weak carbon–carbon bonds and the considerable increase of the extension stresses in rubbers with high filler contents.

In contrast to the results of other investigations [12], in which enforced rearrangement of the structure of filled rubbers took place under brief periodic loadings (several loadings), prolonged static tests were carried out in the present work. Our results represent static conditions of prolonged utilization of rubber, with consideration of the chemical processes which occur. The results of the other investigations [12] represent dynamic conditions for brief operation of rubber articles under periodic loads. Brief operating conditions are rarely met in practice. Relaxation processes under prolonged periodic loads have also been studied [15].

SUMMARY

1. Stress relaxation in filled rubbers consists of three processes: chain relaxation, filler relaxation, and chemical relaxation. These relaxation processes respectively involve orientation of the monomer units and regrouping and slippage of the rubber molecule segments, separation of the filler particles from the rubber chains followed by slippage of the latter, and regrouping of cross bonds and chain scission.

2. The brief stress relaxation curves for rubbers apparently pass into a linear region. Curves for prolonged relaxation (two months) show distinct linear regions. The linear regions of relaxation curves for rubbers containing inactive filler are due to slow chemical processes, while those for rubbers with active filler also involve destruction of rubber–filler particle bonds.

3. In rubbers with inactive filler, the usually observed relaxation process (until the commencement of the linear region) leads to establishment of equilibrium in respect to the chains and filler. The relaxation time for inactive filler is of the same order as the chain relaxation time, but much shorter than the chemical relaxation time. It is therefore possible to separate the chain and filler relaxation processes from the chemical relaxation process.

4. In rubbers with active filler, the usually observed relaxation process leads to establishment of equilibrium in respect to the chains. The active filler relaxation time is comparable with the chemical relaxation time: at low filler contents the regrouping of the filler particles is slower, and at high contents more rapid, than chemical relaxation. In this case it is possible to separate the chain relaxation process from the filler and chemical relaxation processes, which occur simultaneously. Chemical degradation processes are retarded with increasing filler content, in agreement with earlier results.

5. The stresses determined by extrapolation of prolonged relaxation curves to the stress axis in the case of an inactive filler do not depend on the filler content (equilibrium stresses), and do depend on it in the case of an active filler (partially-equilibrium stresses).

LITERATURE CITED

[1] P.P. Kobeko, E.V. Kuvshinsky, and G.I. Gurevich, Bull. Acad. Sci. USSR, Phys. Ser., 3, 329 (1937).

[2] A.P. Aleksandrov and Yu.S. Lazurkin, J. Tech. Phys., 9, 1249 (1939); V.A. Kargin and T.I. Sogolova, J. Phys. Chem., 23, 530 (1949); B.A. Dogadkin, G.M. Bartenev, and M.M. Reznikovsky, Colloid J., 11, 314 (1949).

[3] G.L. Slonimsky, J. Tech. Phys., 9, 1791 (1939); G.I. Gurevich and P.P. Kobeko, J. Tech. Phys., 9, 1267 (1939); V.A. Kargin and G.L. Slonimsky, J. Tech. Phys., 11, 341 (1941); Symposium "Viscosity of Liquids and Colloidal Solutions", Acad. Sci. USSR Press (1941); J. Phys. Chem., 15, 1022 (1941); Proc. Acad. Sci. USSR, 62, 239 (1948); J. Phys. Chem., 23, 563 (1949).

[4] G.M. Bartenev and L.A. Vishnitskaya, J. Tech. Phys., 20, 858 (1950); L.A. Vishnitskaya, Trans. Inst. Rubber Ind., State Chem. Press, 1, 53 (1954); L.A. Vishnitskaya and V.I. Novikov, Trans. Inst. Rubber Ind., State Chem. Press, 2, 27 (1955).

[5] G.M. Bartenev, Colloid J., 12, 408 (1950); J. Phys. Chem., 24, 1210 (1950); J. Tech. Phys., 22, 1154 (1952); Proc. Acad. Sci. USSR, 84, 689 (1952).

[6] B.A. Dogadkin and M.M. Reznikovsky, Colloid J., 12,102 (1950); B.A. Dogadkin and V.E. Gul, Proc. Acad. Sci. USSR, 70, 1017 (1950); V.A. Kargin and V.M. Malinsky, Proc. Acad. Sci. USSR, 73, 967 (1950); Yu. A. Gotlib and M.V. Volkenshtein, J. Tech. Phys., 23, 1936 (1953); L.V. Chumakova and P.A. Rebinder, Proc. Acad. Sci. USSR, 81, 239 (1951).

[7] A.V. Tobolsky and M. Mooney, et al., J. Chem. Phys., 11, 125 (1943); 14, 93, (1946); J. Appl. Phys., 15, No. 4, (1944); 17, 352 (1946); I.R.I. Trans., 112, 181 (1945).

[8] B.A. Dogadkin and Z.N. Tarasova, Proc. Acad. Sci. USSR, 85, 1069 (1952); Colloid J., 15, 347 (1953) (T.p. 355)*; G.L. Slonimsky, V.A. Kargin, G.N. Buiko, E.V. Reztsova, and M. Lyuis-Riera, Proc. Acad. Sci. USSR, 93, 523 (1953); A.S. Kuzminsky and L.I. Lyubchanskaya, Proc. Acad. Sci. USSR, 90, 409 (1953).

[9] G.M. Bartenev, "Vulcanization of Rubbers", Trans. Conf. on Vulcanization, State Chem. Press, p. 196 (1954).

[10] B.A.Dogadkin, K.A. Pechkovskaya, et. al., Colloid J., 8, 31 (1946); 10, 357 (1948); 12, 367 (1950); 14, 250, 346 (1952) (T.p. 375)*.

[11] B.A. Dogadkin and A.I. Lukomskaya, Proc. Acad. Sci. USSR, 88, 1015 (1953); Colloid J., 16, 36 (1954); P.A. Rebinder et. al., Proc. Acad. Sci. USSR, 31, 444 (1941); 52, 235 (1946); A.P. Pisarenko, A.B. Shekhter, and A.I. Echeistova, Proc. Acad. Sci. USSR, 76, 423 (1951).

[12] L. Mullins, Rub. Chem. Techn. 21, 281 (1948); J. Rubber Res.,16, 275 (1947); I.R.I. Trans.,26, 27 (1950); J. Phys. Chem., 54, 239 (1950); M.M. Reznikovsky, L.S. Priss, and B.A. Dogadkin, Colloid J., 16, 211 (1954) (T.p. 213)*.

[13] M.M. Reznikovsky and B.A. Dogadkin, J. Chem. Ind., No.4, 35 (1954).

[14] A.S. Kuzminsky, L.I. Lyubchanskaya, N.G. Khitrova, and S.I. Bass, Proc. Acad. Sci. USSR, 82, No.1, 131 (1952).

[15] G.M. Bartenev and F.A. Galil-Ogly, Proc. Acad. Sci. USSR, 100, 3 (1955).

Received April 13, 1955

Scientific Research Institute for the Rubber Industry
Moscow

---

*T.p. = C.B.Translation pagination

ALKYLPHENOL – ALDEHYDE RESINS AS TACKIFIERS FOR SYNTHETIC RUBBERS

A.G. Belerossova, M.I. Farberov, and V.G. Epshtein

Synthetic butadiene rubbers, in contrast to natural rubber, have very low tackiness. The problem of conferring satisfactory tackiness to these rubbers has not yet been solved satisfactorily, although it has been under investigation here since the start of the wide adoption of synthetic rubber in the rubber industry, in 1934.

Nevertheless, the question of the tackiness of synthetic rubber compositions is of great importance in rubber technology. Tackiness is of particular significance in the construction of rubber–fabric articles, and especially of automobile tires. In addition to the effect on productivity in the assembly operations, lack of tackiness is often the cause of the formation of inner faults ("bubbles") in the finished articles, which may lead to splitting of the latter during use.

A synthetic resin named "Koresin" was produced in Germany during the war; this confers satisfactory tackiness upon synthetic Buna rubber compositions. 5-10% of this resin (calculated on the rubber) is generally added to rubber mixtures and up to 20% to rubber adhesives. A similar product is available in the United States at the present time. Koresin is manufactured by the condensation of tert-butylphenol with acetylene in the presence of zinc naphthenate. The technological process for the production of this resin is carried out under a working pressure of 15-20 atmospheres, and in view of the risk of explosion the equipment is designed to stand 200 atmospheres [1].

It was to be expected that the reaction of acetylene with the phenol would lead to the formation of a vinyl phenyl ether, while the resin is a polymer of this ether, with the Structure I: Le Maistre and Seymour [2], who studied the structure of Koresin, shows that it contains a free phenolic group in each link, and is thus represented by the Structure (II)

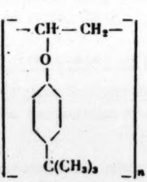

(I)

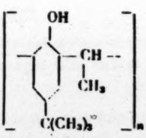

(II)

The substance which corresponds to Structure (II) may be technically produced much more simply than Koresin, by the condensation of m-butylphenol with acetaldehyde in the presence of acid.

The literature contains several publications on the use of alkylphenol–aldehyde condensation products as tackifiers for synthetic rubbers (Smith and Ambelang [3], Marvel et al. [4]). A resin is now being produced in Germany under the name of "Rubresin", which is a condensation product of nonylphenol with formaldehyde in an ammoniacal medium. The aim of our investigation was to determine the structural parameters of these resins as tackifiers for synthetic rubbers.

EXPERIMENTAL

The alkylphenols studied were prepared mainly by alkylation of phenols by means of olefins (propylene, isobutylene, n-butylenes, diisobutylene, methylstyrene, etc.) in the presence of concentrated sulfuric acid [5] in conditions which ensure a maximum yield of the reaction products. Only a few alkylphenols (for instance, n-butylphenol) were prepared by alkylation by means of the corresponding alcohols [6]. The reaction products were fractionated under vacuum and identified. Substances concerning the structure of which there were no doubts were used in the work.

The condensation of alkylphenols with acetaldehyde (paraldehyde) and other higher aldehydes (such as crotonic) was carried out in the presence of 70% sulfuric acid. The condensation of alkylphenols with formaldehyde (35% formalin) was carried out both in the presence of sulfuric acid, and of 20% ammonia. Some of the substances were prepared by condensation in the presence of 10% alkali. The molar ratio of alkylphenol to aldehyde (except when otherwise stated) was always 1:1. The resins were washed with hot water, dried under vacuum, and hardened to the required melting point by heating on an oil bath.

The resins formed were characterized by means of the following determinations: a) melting and softening points; b) molecular weight (cryoscopically); c) total hydroxyl group content by acetylation; d) methylol group content by phthalation [7] (as is known, phenolic hydroxyl groups are not determined by this method).

All the resins were tested for tackiness in rubber compositions of the type used for tires, containing carbon black [8] in a ratio of 5 parts to 100 g of the rubber. The mixes were based on sodium butadiene rubber (SKB) and butadiene–styrene rubber (SKS-30).

The tackiness of the rubber mixtures was determined with the aid of the YaShZ apparatus, which was constructed on the principle of the Behr apparatus [9], and was expressed in kg/cm. For this purpose two strips of fabric coated with the mixture under test are placed on the two disks of the instrument. The disks are then brought into contact and pressed against each other; this is repeated several times. The tackiness is measured by the force required to separate the two disks with the strips. It should be pointed out that the results obtained by this method (as, indeed, by other methods for determination of rubber tackiness) [10]) yield more or less comparable results only for a given series of experiments when the dimensions of the rubber mixture on the strips are accurately maintained; the results are quite unsuitable for comparisons of different series of tests, for example with different synthetic rubbers or with mixtures with different plasticities. It is therefore possible that the results of tests which refer to different experimental series shown in the tables do not agree with each other.

In addition to the tests by this method, considerable importance was attached to organoleptic indications. These were evaluated on a three-point system. The highest rating (5+) represents tackiness found in a mixture of natural rubber (NR) with furnace black; the lowest rating (3) represents the tackiness of mixtures of ordinary types of synthetic rubber with the same carbon black.

Influence of individual structural parameters

The influence of the alkyl group structure in the original phenol was studied with the aid of resins prepared under the same conditions by the condensation of acetaldehyde with various alkylphenols in the presence of acid (Table 1).

The tackiness is only increased in the presence of not less than four carbon atoms in the alkyl group of the phenol. Resins based on p-cresol and isopropylphenol do not confer any appreciable tackiness on rubber. The best tackiness results are obtained with phenols with a tertiary carbon atom in the alkyl group (resins based on various butylphenols). An increase of the number of carbon atoms in the alkyl group above four has a less pronounced effect (resins based on m-butylphenol and octylphenol).

The role of the alkyl group is evidently concerned with an increase of the solubility of the resins in the rubber in the presence of a long and particularly of a branched alkyl group. It is known, for example, that analogous resins based on m-butylphenol have good solubility in oil (100% of resin). Resins based on phenol and m-cresol also confer no tackiness on synthetic rubber. These resins, as is known, have a three-dimensional structure, which is the reason for their complete insolubility in rubber.

Thus, linear structure of the resin and good solubility in rubber, so that the tackifier may diffuse in the adjacent rubber layers, provide the primary requirement for resin tackifiers. This requirement also explains the observation that the tackiness is lower when the resin is added on cold rolls, as compared to when added on hot rolls.

TABLE 1

Effect of the Structure of the Resin Molecule and the Alkyl Group of the Alkylphenol on the Tackiness Conferred by Synthetic Resins on SKB Mixtures (5 Parts by Weight of Resin to 100 of Rubber)

Alkylphenol	Presumed Structure of Resin	Melting point (°C)	Tackiness	
			by YaShZ apparatus in kg/cm	organoleptic grading
Phenol	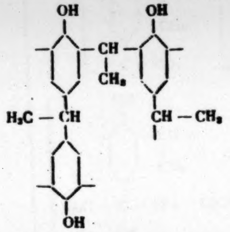	150	–	3
m-Cresol	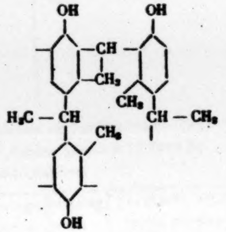	110	–	3
Isopropylphenol	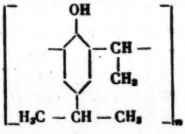	82	–	3
Primary butylphenol	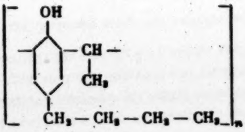	80	0.62	4
Sec-butylphenol	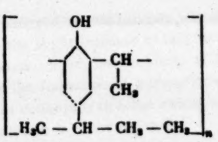	87	0.95	4

TABLE 1 (continued)

Alkylphenol	Presumed Structure of Resin	Melting point (°C)	Tackiness	
			by YaShZ apparatus in kg/cm	organoleptic grading
Tert-butylphenol	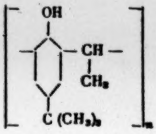	86	1.13	5
Tert-octylphenol	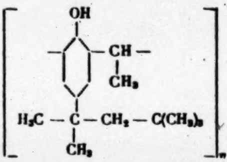	89	1.46	5+
Control mixture		–	0.1	3

TABLE 2

Effect of Various Aldehydes on the Tackiness Conferred by Resins on Synthetic Rubber Mixtures (5 Parts by Weight of Resin to 100 of Rubber)

Aldehyde	Average molecular wt of resin	Melting point (°C)	Tackiness, organoleptic grading	
			SKS-30	SKB
Formaldehyde	947	110	5	–
Acetaldehyde	923	97	5	5
Crotonic	968	86	5	4
Control mixture	–	–	3	3

An increase of the compounding temperature above the melting point evidently results on better solubility of the resin in the rubber mixture.

The nature of the aldehyde used in preparation of the resin, has, under otherwise equal conditions, no appreciable effect on the tackiness conferred by the resin (Fig. 2).

The presence of a free phenolic group in each link is a necessary structural condition for tackifier resins. Blockage of these groups (for example, by acetylation) results in a product which does not appreciably improve the tackiness (Table 3).

To verify this, the prepared resin was acetylated with acetic anhydride.

18 g of the resin dissolved in 50 g of acetic anhydride containing 0.5 g of anhydrous sodium acetate was heated for 30 hours. The reaction mixture was then poured into cold water, the precipitated resin was extracted with ether, and the extract washed with alkali solution and then with water. The product was dried, the ether distilled off, and the acetylated resin was tested in the usual way.

The tackiness conferred by this mixture was only slightly greater than the tackiness of a mixture without resin. In our opinion, the slight increase of tackiness which was found should be attributed to the presence of some free phenolic groups. Thus, the tackiness of the resin is due to the presence of free phenolic groups, and is evidently caused by the formation of intermolecular hydrogen bonds by the hydroxyl groups of the alkylphenol units in the resin. This concept is to some extent supported by the sharp decrease of tackiness conferred by the resins when the temperature is raised to 70-90°.

The alkylphenol–aldehyde ratio must be close to 1:1. An increase of this ratio above 1:1.5 substantially decreases or even entirely destroys the tackiness conferred by the resin (Table 4 and Fig. 1).

These facts are more difficult to explain. It was noted however, that excess of aldehyde in the reaction mixture in all cases leads to a noticeable decrease of the total hydroxyl group content of the resin (sometimes

TABLE 3

Effect of Fhenolic Hydroxyl Groups in the Synthetic Resins on the Tackiness of Mixtures Based on SKB Rubber (5 Parts by Weight of Resin to 100 of Rubber)

Resin	Presumed structure	Average molecular weight	Tackiness	
			by YaShZ apparatus in kg/cm.	organoleptic grading
Condensed in presence of ammonia	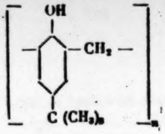	595	1.28	5
Ditto, acetylated	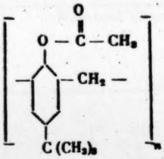	575	0.9	3+
Control mixture	—	–	0.1	3

TABLE 4

Effect of the Ratio of p-tert-Butylphenol to Acetaldehyde on the Tackiness Conferred by Synthetic Resins on Mixtnres Based on SKB and SKS-30 (5 Parts by Weight of Resin to 100 of Rubber)

Moles of p-tert-butylphenol	Moles of acetaldehyde	Melting point in (°C)	Tackiness, organoleptic grading	
			SKB	SKS-30
1	0.5	88	3	3
1	1	90	5	5
1	2	87	4	4
1	3	85	3	3

from 11 to 7% and less), with an increase of the methylol group content. The decrease of the hydroxyl group content may be attributed to the formation of ether linkages [11]. It seems likely that a decrease of the free phenolic group content with an increase of the polarity of the resin (owing to the methylol groups) ultimately leads to worsening of the tackifying properties of the resin. Further special investigation of this problem is, however, needed.

The method of condensation (acid, alkaline, or ammoniacal) has no significant influence on the tackiness of resins prepared from alkylphenols and formaldehyde for a given component ratio (Table 5), although in the alkaline and ammoniacal processes methylol groups are formed, which are entirely lacking in acid condensation resins.

It must be pointed out, however, that this is completely true only for sodium butadiene rubber. The tackiness conferred by acid condensation resins on butadiene—styrene rubber is appreciably higher.

The molecular weight of the resin is one of the most important structural parameters which determine its tackifying effect on synthetic rubber compositions. Neither m-butylphenol itself, nor its condensation product containing two alkylphenol units (molecular weight 300-400), confer tackiness on synthetic rubber. Only resins containing 3-6 alkylphenol units (mol weight 500-900) produce maximum tackiness. A further increase of the

TABLE 5

Effect of the Condensation Method on the Tackiness Conferred by Synthetic Resins on Rubber Mixtures Based on SKB; Alkylphenol and Aldehyde Ratio 1:1 (5 Parts by Weight of Resin to 100 of Rubber)

Condensation method	Melting point (°C)	Average molecular weight	Groups present, %			Tackiness	
			hydroxyl	methylol	phenolic	by YaShZ apparatus in kg/cm	organoleptic grading
Acid	86	666	10.9	0	10.9	1.20	5
Ammoniacal	90	700	13.6	2.5	11.1	1.05	5

TABLE 6

Effect of the Molecular Weight of Synthetic Resins on the Tackiness Conferred by Resins on Rubber Mixtures Based on SKB (5 Parts by Weight of Resin to 100 of Rubber)

Alkylphenol	Presumed structure of resin	Average molecular wt.	Melting point (°C)	Tackiness	
				organoleptic grading	by YaShZ apparatus in kg/cm
p-tert-Butylphenol	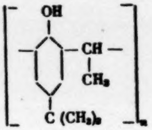	420	–	3	1.4
		464	57	3	1.5
		570	68	5	2.1
		692	82	5	2.2
		870	97	5	2.05
		1038	120	4	1.8
di-tert-Butylphenol	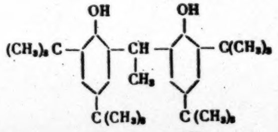	400	63	3	–
di-tert-Butylmetacresol	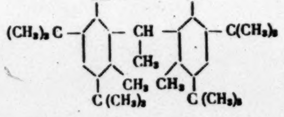	525	68	3	–

molecular weight of the resin (mol. weight > 1000) decreases the tackiness. Resins based on ditertiary butylphenols, in which the ortho and para positions are occupied and which therefore consist of only two alkylphenol units, also do not confer tackiness on synthetic rubber (Table 6). Thus, a tackifier resin should have a definite molecular size, beyond which tackiness is not produced. A possible explanation of the significance of the molecular weight of the resin is given later in this paper.

On the basis of the parameters determined for synthetic rubber tackifier resins, several resins have been developed for this purpose and their production conditions have been established. These resins have been given the general name "Yarresin".

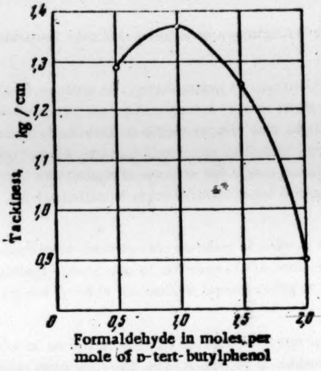

Fig. 1. Effect of the ratio of formaldehyde to p-tert-butylphenol on the tackiness conferred by resins on rubber mixtures based on SKB (5 parts by weight of resin to 100 of rubber).

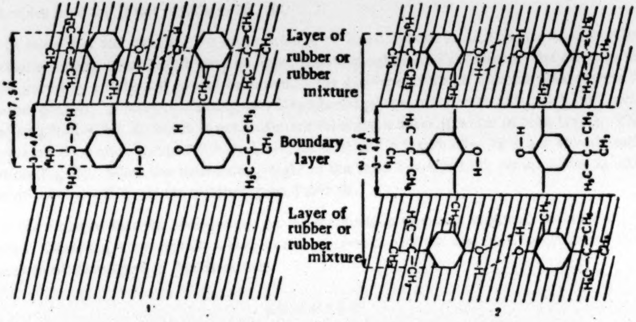
Layer of rubber or rubber mixture
Boundary layer
Layer of rubber or rubber mixture
≈7.5 Å
3–4 Å
≈12 Å
3–4 Å
1
2

Fig. 2. Scheme for the action of synthetic resins; 1) mol. weight 312, two alkylphenol units, no tackiness; 2) mol. weight 474, three alkylphenol units, considerable increase of tackiness.

Discussion of results in the light of modern views on the mechanism of rubber tackiness

The tackiness of rubbers, in the modern view, depends on the degree of autohesion and on the cohesional strength of the material. Zhukov and Talmud [12] were the first to consider the concepts of autohesion, cohesion, and adhesion in relation to the tackiness of rubbers. Autohesion determines the tendency of two surfaces of the same material to coalesce on contact under the influence of an applied force. Cohesion determines the interaction force within a given material, that is, the strength of the material itself. Adhesion determines the bonding power between different substances, such as rubber and metal or fabric, etc.

Numerous investigations have dealt with adhesion of various materials [13]. The tackiness of rubbers, in which autohesion and cohesion effects are prominent, has not been studied sufficiently. According to the views of Mark [14], and also of Voyutsky and Margolina [15], a necessary condition for tackiness in high polymers is coalescence of their surfaces with transfer of molecules from one layer into another and intertwining of the molecular chains.

On the basis of our experimental data it is possible to augment and extend the above by the following considerations.

1. Good tackiness in rubbers capable of crystallization on appropriate stretching (natural and chloroprene rubbers) may be explained as follows: a) the rubbers have a regular structure and also fairly good molecular chain mobility, which allows some chain ends to diffuse readily into adjacent surface layers; b) the ends of the chains which are simultaneously in both adjacent layers can be firmly fixed within them by participation in crystallite formation (in both layers); an attempt to separate the layers probably leads to extension of the surface films, which is known to favor the formation of crystallites oriented in the direction of the extension in crystallizing rubbers.

2. Butadiene rubbers, which have considerable numbers of units in the 1,2 positions in the chains, have lower mobility and a correspondingly lower rate of diffusion of the molecular chains in the adjacent layers. The ends of the molecular chains are not fixed in the surface layers, owing to the lack of crystallizing power in these rubbers.

3. Diffusion of molecules of tackifier resins in the surface layers is possible only if they have good solubility in rubber. Resins with a linear structure, with good solubility in rubbers, may be obtained by the use of alkylphenols with fairly large alkyl groups.

4. The ends of the tackifier molecules are fixed in the two surface layers by interaction of hydroxyl (phenolic) groups with formation of intermolecular hydrogen bonds. This results in the formation of "bridges" between the layers which bind the latter together (Fig. 2).

5. In order that the tackifier molecules should be fixed in both surface layers simultaneously, they should have a definite length. This length may be approximately calculated as follows: the distance between the surfaces to be joined by autohesion cannot be less than the distance at which Van der Waals forces act, or 3-4 Å, but is even rather greater. A resin containing two alkylphenol groups in the molecule (with mol. weight 312) has a molecular length of ~ 7.5 Å, which is not sufficient for simultaneous fixation in both layers. The molecules of a resin containing three such groups (with mol. weight 474) and a length of ~ 12 Å are already sufficiently long for such fixation (Fig. 2). When the molecular weight of the resin exceeds 1000, its solubility in rubber decreases, which has an adverse effect on its tackiness (see Table 6).

It is not claimed that the above views on the mechanism of rubber tackiness embrace the whole complex phenomenon. However, they provide a satisfactory explanation of the observed experimental facts and enable further work to be developed in this direction.

SUMMARY

1. The basic structural parameters of alkylphenol–aldehyde resins as synthetic rubber tackifiers have been determined.

2. The experimental data obtained are discussed in the light of modern views on the mechanism of tackiness. An attempt to extend and amplify these views is presented.

LITERATURE CITED

[1] Kline, Modern Plastics, 23, 151 (1946).

[2] Seymour, Le Maistre, J. Am. Chem. Soc., 70, 1776 (1948).

[3] G. Smith, L. Ambelang, et. al., Ind. Eng. Chem., 38, 1166 (1946).

[4] C.S. Marvel, et.al., J. Pol. Sci., 4, 698 (1949).

[5] V.I. Isagulyants and P.P. Banryantseva, Petroleum Economy, No. 2, 36 (1939).

[6] I.P. Tsukervanik and Z.N. Nazarova, J. Gen. Chem., 7, 623 (1937).

[7] P.I. Elving and B. Warschawsky, Anal. Chem., 19, 1006 (1947).

[8] G.N. Buiko, Trans. Sci.-Res. Inst. Tire Ind., 38 (1947).

[9] Behr, Kautschuk, No. 10 (1944).

[10] W.F. Busse, I.M. Lambert and R.R. Verdery, J. Appl. Phys., 17, 376 (1946).

[11] A.A. Vansheidt, Trans. Session Acad. Sci. USSR on Organic Chem., 71-84 (1945).

[12] I.I. Zhukov and S.L. Talmud, J. Rubber Ind., 12, 1005 (1935).

[13] B.V. Deryagin and N.A. Krotova, Adhesion, Acad. Sci. USSR Press (1949).

[14] H. Mark, Jozefovitz, Ind. Rubber World, 33, 106 (1942); H. Mark, Ind. Eng. Chem., 33, 10 (1943).

[15] S.S. Voyutsky and Yu. L. Margolina, Progr. Chem., 18, 449 (1949).

Received March 25, 1955

The Yaroslav Technological Institute
The Yaroslav Tire Factory

ION EXCHANGE CHROMATOGRAPHY OF STREPTOMYCIN ON PERMUTITE

S.E. Bresler and G.V. Samsonov

The possibility of chromatographic purification of any substance is primarily determined by the reversibility and selectivity of adsorption, and also by a number of other properties of the adsorbent (for example, mechanical strength, chemical stability, etc.). Streptomycin is adsorbed, to some extent irreversibly, by activated carbon and strongly acid cationites. The adsorption of streptomycin is fully reversible on permutite [1] and almost fully reversible on carboxylic cationites. As will be shown in the following paper, adsorption of streptomycin by carboxylic resins is accompanied by a change in the volume occupied by the resin – contraction. A yet greater change in the cationite volume is found on replacement of the streptomycin by acid solutions. In addition, the strongly swelling carboxylic cationites used for adsorption of streptomycin have low mechanical strength. Because of all this, it is difficult to effect true chromatographic separation of streptomycin with the use of carboxylic cationites in long columns because of the low strength of the ionites and because the streptomycin zone formed may undergo appreciable additional dispersion by disturbance of the resin grain packing during contraction.

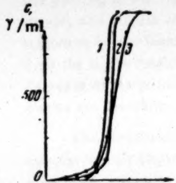

Fig. 1. Curves for the adsorption of streptomycin by permutite: Grain diameters: 1) from 0.10 to 0.15 mm; 2) 0.15 to 0.20 mm; 3) 0.20 to 0.30 mm.

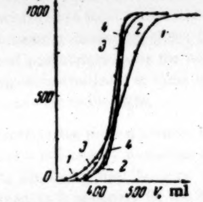

Fig. 2. Curves for the adsorption of streptomycin by permutite: Solution flow rate: 1) 500; 2) 200; 3) 50; 4) 10 ml/cm². hour.

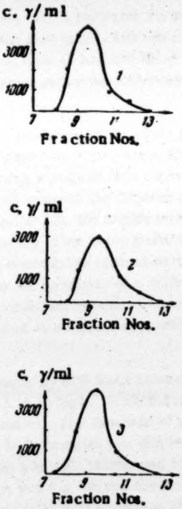

Fig. 3. Curves for the displacement of streptomycin from permutite by 20% NaCl solution at the following initial streptomycin concentrations: 1) 300; 2) 10000; 3) 100000 micrograms/ml.

The most suitable adsorbent for chromatography of streptomycin is permutite, an ionite of great mechanical strength, which does not change its volume in the course of ion exchange.

Ion exchange chromatography must be carried out in such conditions that the zone boundary becomes sharper. As has been shown previously [1], for the exchange of ions of different valencies in dynamic conditions there is a certain critical value of the concentration of the solute ion c_{cr} determined by Equation (1):

$$c_{cr} = mK^{\frac{z_1 \cdot z_2}{z_1 - z_2}} \quad , \qquad (1)$$

where m is the exchange capacity of the ionite, K is the exchange constant, and z_1 and z_2 are the ionic charges.

In equilibrium conditions, on one side of the critical concentration the zone boundary becomes sharper, and on the other, more diffuse. On the basis of our data obtained in a study of the exchange of streptomycin ions for sodium ions under static conditions [1] it is possible to use Equation (1) to calculate the critical conditions for sharpening of the boundary in these systems (see table).

TABLE

Critical Conditions for Narrowing the Front in the Exchange of Streptomycin Ions for Sodium Ions on Permutite

Exchange constants K	Exchange capacity for streptomycin (m), mg-equiv./g	Second ion	c_{cr}	
			mg-equiv./ml Na	micrograms of streptomycin per ml
10.3	0.197	Na+	6.55	$1.27 \cdot 10^6$
6.2	0.109	Na+	1.72	$3.33 \cdot 10^5$
5.2	0.143	Na+	1.69	$2.27 \cdot 10^5$

In the adsorption of streptomycin by sodium permutite in dynamic conditions the streptomycin concentration must be below the critical value. Evidently, this is always true. In fact, as the graphs in Figs. 1 and 2 show, the adsorption of streptomycin by permutite always takes place with the formation of a sharp front. The experiments were carried out in permutite columns 1 cm in diameter, filled with 10 g of permutite. The different nature of the curves is due, on the one hand, to the action of kinetic factors which cause the front to become more diffuse, and on the other, to inhomogeneity of the packing of the ionite grains. At solution flow rates not greater than 200 ml/cm². hour, the curves ascend steeply and remain almost unchanged in form over a wide range of flow rates, which indicates the successful influence of the factors which cause a sharpening of the front. Only when the flow rate is 500 ml/cm²· hour does the lag in establishment of equilibrium cause the adsorbed streptomycin front to become more diffuse. A decrease of the permutite grain diameter leads to some increase of exchange capacity for streptomycin. The curves are therefore shifted somewhat to the right.

The chromatographic purification process consists of adsorption of the substance in the upper part of the column and its displacement at a low rate by a solution which, in ion exchange chromatography, should contain a definite concentration of the displacing ion. In order that a zone containing a considerable concentration of the substance should be obtained, it is necessary for the boundary of the zone between the displaced ion and the displacing ion to become sharpened. According to the theory developed earlier [2], the displacement of streptomycin by sodium ions should take place with sharpening of the zone boundary if the concentration of the displacing ion (sodium), which has a lower charge than the streptomycin ion, exceeds the critical value (see table). The displacement of streptomycin by 1 M solution of common salt leads to the formation of a diffuse streptomycin zone with a very large chromatographic "tail", and therefore in such conditions complete desorption of streptomycin cannot be achieved. When 20% sodium chloride solution is used as eluent, a streptomycin zone of high concentration is formed on all specimens of permutite.

Fig. 3 shows curves for the displacement of streptomycin from permutite by 20% NaCl solution. The process was carried out in stainless steel columns 6.8 cm in diameter and 3.25 m high. In each experiment the column was charged with 10 kg of permutite of 0.1-0.2 mm grain diameter. The flow rate of the eluent solution was 25 ml/cm². hour. The first stage (adsorption of streptomycin by permutite) was different in all three experiments. The streptomycin concentration in the original solution was 300, 10000, and 100000 micrograms/ml. The total amount of adsorbed streptomycin in each experiment was 5 g. In the first experiment (Fig. 3, 1) the culture liquid was used as the original solution, in the second (Fig. 3,2) a solution of partly purified streptomycin, and in the third (Fig. 3,3) a solution of pure streptomycin. At the end of the adsorption process the streptomycin zone occupied different parts of the columns. In the first case the streptomycin occupied almost half the column, and in the last, ~ 5%. Therefore the specific adsorption capacity was about 10 times as large in the third experiment as in the first. Nevertheless, the curves obtained in all three experiments differed little from each other, which indicates that in all cases a steady zone of constant maximum concentration, moving at a constant rate, was formed. The possibility of formation of a steady zone in conditions when the zone boundaries are sharpened was predicted by us earlier [3].

By the use of a true chromatographic process with a permutite column at a low elution rate (25 ml/cm².hour) and with a high column (> 3 m) it is possible to purify streptomycin from the greater part of the organic impurities contained in the culture liquid. A convenient criterion of purification is the number of milligrams of nitrogen per 1000 units of streptomycin. After the chromatographic treatment, the product has a value of 0.169 mg N per 1000 units (micrograms of the base) of streptomycin, which is the theoretical value and which indicates the absence of nitrogenous impurities.

SUMMARY

1. The adsorption of streptomycin by permutite in dynamic conditions proceeds with the formation of a sharp front, in agreement with the previously developed theory.

2. The displacement of streptomycin from permutite during the chromatographic process occurs in conditions when the boundary becomes sharper with the formation of a steady zone at high concentrations of the displacing ion (sodium), in agreement with the theory of equilibrium ion exchange chromatography. At low concentrations of the univalent displacing ion the streptomycin zone becomes diffuse.

3. Chromatography on permutite may be used to purify streptomycin from organic impurities formed during fermentation.

LITERATURE CITED

[1] G.V. Samsonov and S.E. Bresler, Colloid J., 18, No. 1, 88 (1956) (T.p. 83)*.

[2] G.V. Samsonov, Proc. Acad. Sci. USSR, 97, 707 (1954).

[3] S.E. Bresler, Proc. Acad. Sci. USSR, 97, 699 (1954).

Received March 17, 1955

Institute of High Molecular Compounds
Academy of Science USSR, Leningrad

---

*T.p. = C.B. Translation pagination.

BLANK
PAGE

STABILIZATION OF PIGMENT SUSPENSIONS BY DIPHILIC SURFACE-ACTIVE SUBSTANCES

Ya.M. Gurevich

Our previous paper [1] contained a developmentof the view that the surface properties of pigments, which determine their behavior in suspensions containing diphilic surface-active substances, are due to differences in the numbers and ratio of the polar and non-polar active centers on their surfaces.

In the present investigation a study was made of the aggregative stability of the suspensions of two groups of pigments, which differ in the ratio of polar and non-polar groups on their surfaces, in three media of different polarities, in the presence of two diphilic surface-active substances differing in the number of polar groups in the polar part of their molecules.

The following materials were used:

1. Pigments: ocher, umber, Mars brown, Feodosian brown, sienna, zinc oxide, titanium dioxide, red iron oxide, lithopone, chrome yellow. As was shown in our previous paper [1], the first five pigments are rich in polar and poor in non-polar active centers (Group I), while the other five pigments are rich in non-polar and poor in polar active centers (Group II).

2. Dispersion media: lacquer gasoline, butanol, 70:30 water-acetone mixture.

3. Surface active substances: oleic acid R—COOH, and triglycerol fatty acid monoester (emulsifier VNIIZh).

The polar part of the oleic acid molecule consists of one carboxyl group, while the polar part of the emulsifier VNIIZh molecule consists of 7 hydroxyl and ester groups.

The experiments were carried out as follows. 10 ml of suspension containing 2% by volume of the pigment was prepared. For this, the weight of pigment taken was 0.2% of the weight of 1 cc. The pigment was mixed in a porcelain mortar with the surface-active substance to form a thick paste. The paste was then mixed with the dispersion medium. The suspensions were transferred to test tubes and visual observations of settling of the suspensions were made during five days. The time before the appearance of an interphase boundary was noted, or, in the absence of a complete interphase boundary, the time for the pigment to settle on the bottom of the vessel and for the dispersion medium to become completely (or almost completely) clear. A parallel series of suspensions with the dispersion media only was prepared.

The results are shown in the table.

In gasoline suspensions, both the surface-active substances studied, oleic acid and emulsifier VNIIZh, stabilize suspensions of pigments rich in polar active centers, and have a very weak stabilizing effect on suspensions of pigments poor in polar active centers.

In butanol suspensions oleic acid acts as a coagulant for all pigments, both rich and poor in active centers; emulsifier VNIIZh acts as stabilizer in both cases.

In acetone-water and in butanol suspensions of all pigments oleic acid is a still more pronounced coagulant. In suspensions of pigments rich in polar active centers emulsifier VNIIZh acts as a coagulant, while in suspensions of pigments poor in polar active centers it acts as a stabilizer.

TABLE

Time of Settling to Phase Separation or to Complete Settling of Pigment

Medium	Surface-active substance	Pigment group I	Pigment group II
Lacquer gasoline	Pure medium	Instantaneous phase separation	Instantaneous phase separation
	Oleic acid	No settling in 5 days	Settle in 0.1-1 hour
	Emulsifier VNIIZh	Ditto	Ditto
Butanol	Pure medium	Settle in 2-3 days	Ditto
	Oleic acid	Instantaneous phase separation	Instantaneous phase separation
	Emulsifier VNIIZh	No settling in 5 days	No settling in 1-2 days
70:30 Water–acetone mixture	Pure medium	Instantaneous phase separation	Instantaneous phase separation
	Oleic acid	No suspension	No suspension
	Emulsifier VNIIZh	Ditto	No settling in 5 days

DISCUSSION OF RESULTS

In our previous paper on this subject [1], the view was put forward on the basis of the general concepts of the mechanism of the stabilizing action of surface-active substances put forward by Rebinder [2], that surface-active substances are attached by polar groups at polar active centers, and by non-polar groups at non-polar active centers. It was postulated that if the pigment surface is rich in polar and poor in non-polar active centers, then the free groups in the adsorption layer, capable of reacting with the molecules of the medium, will mainly be non-polar. Conversely, if the pigment surface is rich in non-polar and poor in polar active centers, then the free groups in the adsorption layer capable of reacting with the molecules of the medium will mainly be polar.

In the paper cited the following view was also put forward. The dispersing or coagulating action of diphilic surface-active substances on pigment suspensions is a function of the energy affinity of the free ends of the molecules of the adsorption layer for the molecules of the medium: if the affinity is great, the suspensions are dispersed and stabilized, and if it is weak, they are aggregated and coagulated.

The experimental results obtained in that investigation [1] were satisfactorily explained on the basis of these views. However, they do not provide a satisfactory explanation of the experimental results obtained in the present investigation. There is no explanation why two diphilic surface-active substances – oleic acid and emulsifier VNIIZh – produce a different effect in butanol and aqueous acetone suspensions, and the same effect in gasoline suspensions. It is also not clear why emulsifier VNIIZh produces a different effect in two polar media, butanol and aqueous acetone.

These effects are satisfactorily explained if it is assumed that when a diphilic surface-active substance has a long tail consisting of several groups, only a part of them reacts with the active centers of the pigment particle surface, while part remains free and can still interact with the molecules of the medium.

It is also necessary to introduce the concept of the desorbing power of the medium as a function of the affinity of the molecules of the medium for the groups by means of which the molecule of the surface-active substance is attached to the solid surface. The greater the affinity, the greater is the desorbing power.

Let us examine, in the light of these considerations, the course of events in suspensions of pigments of the two groups studied.

Suspensions of Group I pigments. In these suspensions, rich in polar and poor in non-polar active centers, the molecules of oleic acid are attached by their polar groups to the pigment particle surfaces and form an adsorption layer, in which the free ends, capable of interaction with the molecules of the medium, consist mainly of non-polar hydrocarbon groups. The good affinity of the latter for the gasoline molecules and the poor affinity for butanol, water, and acetone molecules explains the stabilizing action of oleic acid in gasoline suspensions and its coagulating action in butanol and aqueous acetone suspensions of this group of pigments.

In suspensions of pigments of this group, the molecules of emulsifier VNIIZh are attached by some of the polar groups on the pigment particle surfaces and form an adsorption layer in which the free ends, capable of interaction with the molecules of the medium, consist of a mixture of non-polar and polar groups. In gasoline and aqueous acetone media the role of the non-polar groups is predominant: their strong affinity for the medium determines the stabilizing action of emulsifier VNIIZh in gasoline suspensions of the first group of pigments, and the lack of affinity for water molecules determines its coagulating action in aqueous acetone suspensions of these pigments.

Butanol occupies an intermediate position between gasoline and water in its affinity for hydrocarbon groups. The aggregate interaction between the butanol molecules and the free hydrocarbon, hydroxyl, and ester groups of the adsorption layer formed by emulsifier VNIIZh is already great enough to produce a stabilizing effect of emulsifier VNIIZh in butanol suspensions of the first group of pigments, in contrast to aqueous acetone.

Suspensions of Group II pigments. In suspensions of Group II pigments, rich in non-polar and poor in polar active centers, the diphilic molecules are fixed on the pigment particle surfaces by weak bonds which act between the non-polar groups of the molecules of the surface-active substance and the non-polar active centers on the pigment particle surfaces. The strength of these bonds depends on the affinity of the non-polar groups of the adsorbed molecules for the molecules of the medium. If the affinity is great, the molecules of the surface-active substance will be desorbed from the surface. This occurs in gasoline suspensions of Group II pigments.

If the molecules of the diphilic surface-active substances were to be fixed by their non-polar groups to the pigment particles, then the free polar groups, owing to their poor affinity for the gasoline molecules, should cause coagulation of the suspension, In reality, however, there is not a decrease but some very small increase of the aggregative stability of the suspension, which is explained by the stabilizing effect of the molecules of the surface-active substances adsorbed by the polar active centers which are present in small numbers on the surfaces of this group of pigments also. The main non-polar part of the pigment particle surfaces does not have an adsorption layer. Aggregation of gasoline suspensions of pigments of the second group in presence of diphilic surface-active substances occurs by direct cohesion of the particles by their solid surfaces, as in the case of gasoline suspensions of pigments which do not contain any surface-active substances.

Because of the poor affinity of the polar molecules of butanol, water, and acetone for non-polar hydrocarbon groups, these media have a weak desorbing power toward molecules attached by their non-polar groups on non-polar active centers of the pigment surfaces, and therefore Group II pigments in butanol and aqueous acetone media retain adsorption layers fairly firmly on their surface, in which the polar groups are free and capable of interaction with the molecules of the medium.

In addition to the polar groups, a part of the non-polar groups also remains free to interact with the molecules of the medium. In the case of oleic acid non-polar groups predominate in the adsorption layer, which determines their coagulating effect in polar media. In the case of emulsifier VNIIZh polar groups predominate in the adsorption layer, which determines their stabilizing effect in polar media.

It also follows from the experimental data that all pigments rich in polar active centers form aggregatively stable suspensions in pure butanol without addition of any surface-active substances to the system, while all pigments which are poor in polar active centers form aggregatively unstable suspensions.

It is commonly assumed that the mechanism of the effects which determine the aggregative stability of suspensions in polar organic solvents is the same as that for aqueous suspensions; that is, that it involves the adsorption of ions and the formation of an electric double layer on the particles of the solid phase, and therefore differs in principle from the mechanism of the effects which determine the aggregative stability of suspensions containing surface-active substances [3]. From the above experimental data it follows that the aggregative stability of butanol suspensions involves adsorption of butanol molecules at the polar active centers of the pigment surface, so that the mechanism is the same as in the adsorption of oleic acid or other surface-active substances, with the distinction that here the medium and the adsorption layer consist of the same kind of molecules.

SUMMARY

1. A study was made of the aggregative stability of suspensions of two groups of pigments differing in the ratio of polar to non-polar active centers on their surfaces, in three media differing in polarity, in the presence of two diphilic surface-active substances, differing in the number of polar groups in the polar part of the molecule.

2. The results make it necessary to assume that molecules with a large number of groups are attached to the active centers of the solid surface by only a part of the groups, while part of the groups remains free and retains its capacity for intermolecular action with the molecules of the dispersion medium. This applies both to polar and to non-polar groups.

3. The view is developed that the desorbing capacity of the dispersion medium is a function of the affinity of the molecules of the medium for those groups in the molecules of the surface-active substances by which they are attached to the solid surface. The greater this affinity is, the greater is the desorbing capacity of the medium.

4. It is shown that pigments rich in polar active centers form aggregatively stable suspensions in butanol, while pigments poor in polar active centers yield aggregatively unstable suspensions.

LITERATURE CITED

[1] Ya.M. Gurevich, Colloid J., 14, No. 4, 233 (1952) (T.p. 259)*.

[2] P.A. Rebinder, Physical Chemistry of Technical Suspensions, Collected Papers (1933).

[3] Yu.M. Glazman, Prog. Chem., 16, No.2, 177 (1947).

Received October 23, 1954

State Research and Project Institute
Ministry of Chemical Industry - Moscow

---

*T.p. = C.B. Translation pagination

CATION EXCHANGE ADSORPTION AS A FUNCTION OF THE DIELECTRIC CONSTANT OF THE MEDIUM

A.T. Davydov and R.F. Skoblionov

For the efficient utilization of different solvents in ion exchange reactions it is necessary to have data on their quantitative relationships in various media, and in particular on changes of adsorption with changes in the composition of the medium. Of the factors which characterize the nature of the medium, the dielectric constant of the solvent was chosen as the determining factor. The reason for this choice was that the solubility of salts, their dissociation, and the behavior of ions in solution are determined by the dielectric constant; therefore it should largely determine the value of the ion exchange adsorption.

In a study of the dependence of adsorption on the dielectric constant of the medium [1] it was established that the exchange value for the weakly hydrated sodium and potassium ions increases considerably with decrease of the dielectric constant of the medium. In the ion exchange reactions $[Ca^{2+}] + Na^+$; $[Ba^{2+}] + Na^+$, $[Ca^{2+}] + K^+$ and $[Ba^{2+}] + K^+$ in various aqueous alcohol media, the exchange value increased with increase of the alcohol content.

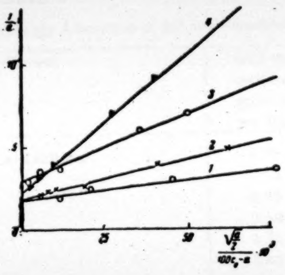

Fig. 1. Gapon equation isotherms: Ca-kaolinite + LiCl in water (1) and in aqueous alcohol solutions with alcohol contents: 2) 50%; 3) 70%; 4) 90%.

Our results on the exchange of Ca^{2+} and Ba^{2+} ions for Na^+ and K^+ ions on glauconite and wolchonskoite from aqueous alcohol solutions agreed with the results of Wigner [2], who studied ion exchange on permutite, and of Kressman and Kitchener [3], who worked with synthetic resins in the same media. It was stated in these papers that the composition of the liquid phase does not affect the exchange adsorption value of the Li ion; however, this conclusion was not confirmed by any data.

In a study of the exchange of Fe^{3+} ions for Mg^{2+} and Al^{3+} ions from aqueous alcohol solutions on sulfonated coal [4] it was shown that the exchange value decreased with decrease of the dielectric constant of the medium. These results were not in agreement with the viewpoint of Wigner and of Kressman and Kitchener concerning Li^+ ion.

In view of the similarity of behavior of the ions studied (Mg^{2+}, Al^{3+}) to that of Li^+ ions in exchange on sulfonated coal, and of their tendency to solvation, it appeared of interest to study the exchange adsorption of the Li^+ ion from aqueous alcohol media by various mineral adsorbents. Adsorbents with different exchange capacities were chosen for the investigation: kaolin [5] (10 mg-equiv.), glauconite [5,6] (40 mg-equiv.), and wolchonskoite [5-7] (100 mg-equiv.). The experiments were carried out in aqueous and aqueous alcohol solutions, with alcohol contents of 50, 70, and 90% by weight, with LiCl concentrations from 0.05 to 1.0 N. The experimental technique was described in a previous publication [1]. The experimental results obtained are shown in Table 1.

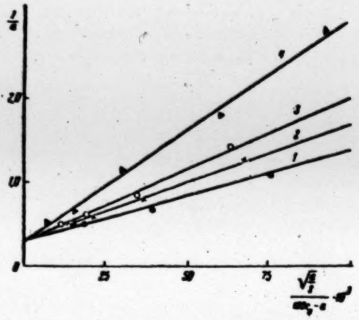

Fig. 2. Gapon equation isotherms; Ca-glauconite + + LiCl in water (1) and in aqueous alcohol solutions with alcohol contents: 2) 50%; 3) 70%; 4) 90%.

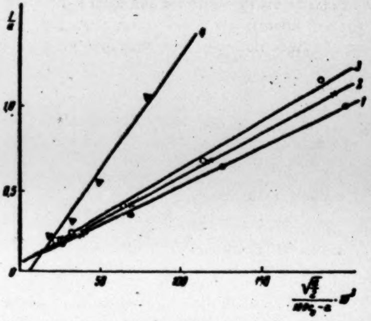

Fig. 3. Gapon equation isotherms; Ca-wolchonskoite + + LiCl in water (1) and in aqueous alcohol solutions with alcohol contents: 2) 50%; 3) 70%; 4) 90%.

The data in this table show that the exchange value decreases with decreasing dielectric constant of the medium. The influence of the dielectric constant on the adsorption value of the Li^+ ion is most pronounced in the region of low concentrations.

TABLE 1

Exchange Adsorption of Li^+ as a Function of the DC of the Solvent

Adsorbent	LiCl concentrations in gram-equiv. per liter	mg-equiv. of Ca^{2+} displaced from 10 g adsorbent at dielectric constant of solvent			
		78.5	49	38	28
Ca-Kaolinite	0.05	0.27	0.20	0.14	0.10
	0.10	0.36	0.28	0.19	0.15
	0.25	0.44	0.40	–	–
	0.50	0.49	0.45	0.28	0.28
	0.75	–	0.49	0.31	0.29
	1.00	–	0.52	0.34	0.33
Ca-Glauconite	0.05	0.61	0.54	0.47	0.36
	0.10	0.94	0.76	0.70	0.58
	0.25	1.50	1.30	1.17	1.01
	0.50	1.98	1.76	1.62	1.35
	1.00	2.34	2.10	2.00	1.74
Ca-Wolchonskoite	0.05	1.08	1.01	0.96	0.60
	0.10	1.73	1.62	1.58	0.97
	0.25	3.18	3.10	2.90	2.12
	0.50	4.72	4.64	4.46	3.46
	1.00	6.55	6.41	6.26	5.54

In order to show the identical nature of the quantitative relationships in aqueous and mixed media, the experimental results were used for calculation of the Gapon exchange adsorption isotherm equation [8]. The Gapon equation has the following form for the case of the exchange of a bivalent cation for a univalent cation:

$$\frac{1}{a} = \frac{1}{a_m} + \frac{K}{a_m} \cdot \frac{\sqrt{a/2}}{100c_0 - a}\,,$$

where a is the number of mg-equiv. of the ion adsorbed by 10 g of adsorbent; a_m is the maximum adsorption calculated for 10 g of adsorbent; c_0 is the initial concentration of the displacing ion in mg-equiv./ml; K is the exchange constant.

The above equation is a linear equation, the free term in which, the intercept cut off at the ordinate $1/a_m$, is the reciprocal of the maximum adsorption. From the angular coefficient of the straight line: K/a_m, we calculate the value of K, the exchange constant. By putting $y = \frac{1}{a}$ $x = \frac{\sqrt{a/2}}{100c_0 - a}$, it is possible to calculate and plot the exchange adsorption isotherms (Figs. 1-3). The values of a_m and K are shown in Table 2.

TABLE 2.

Calculated Data for the Exchange Adsorption of Lithium from LiCl Solutions

Adsorbent	% alcohol by wt.	Dielectric constant	Maximum adsorption a_m	Gapon equation constant K
Ca-Kaolinite	0	78.5	0.56 ± 0.01	13.6 ± 0.9
	50	49.0	0.59 ± 0.01	29.5 ± 2.4
	70	38.0	0.36 ± 0.01	28.8 ± 2.1
	90	28.0	0.42 ± 0.02	68.5 ± 9.2
Ca-Glauconite	0	78.5	3.5 ± 0.2	36 ± 3
	50	49.0	3.0 ± 0.3	40 ± 6
	70	38.0	3.2 ± 0.1	54 ± 3
	90	28.0	3.8 ± 0.6	103 ± 16
Ca-Wolchonskoite	0	78.5	18 ± 1	83 ± 25
	50	49.0	25 ± 5	135 ± 35
	70	38.0	27 ± 6	161 ± 40
	90	28.0	9 ± 3	132 ± 53

The dielectric constant of the medium has no effect on the maximum adsorption value. When the exchange was effected in different aqueous alcohol solvents, the variations of the maximum adsorption values for each adsorbent studied were within the limits of experimental error. The increase of the exchange constant with decrease of the dielectric constant of the medium is explained by the increase of the radius of the lithium ion owing to solvation. The results obtained for variation of the exchange constant K with change of dielectric constant of the medium do not agree with the conclusions drawn by Wigner and by Kressman and Kitchener.

SUMMARY

1. A study was made of the exchange of Ca^{2+} ions for Li^+ ions from aqueous and various aqueous alcohol solutions on adsorbents of different exchange capacities — kaolin, glauconite, and wolchonskoite.

2. The quantitative relationships in exchange adsorption from aqueous and mixed solvents were shown to be identical; it is therefore possible to extend considerably the field of application of ion exchange to the extraction of ions from non-aqueous and mixed media.

3. The exchange adsorption of the lithium ion decreases with decrease of the dielectric constant of the medium. A comparison of the results obtained in the present investigation with earlier data on the exchange adsorption of K^+ and Na^+ ions indicates the strong influence of the solvent and the nature of the ion on the exchange value.

4. The composition of the liquid phase does not affect the maximum adsorption value (a_m).

LITERATURE CITED

[1] A.T. Davydov and R.F. Skoblionok, Trans. Sci.-Res. Inst. Chem., Kharkov State Univ., 10, 195, 205 (1953); 12, 297 (1954).

[2] Jenny Wigner, Koll.-Z., 42, 270 (1927).

[3] R.E. Kressman and J.A. Kitchener, J. Chem. Soc., 1211, 51 (1949).

[4] A.T. Davydov and L.I. Ponirovskaya, Trans. Sci.-Res. Inst. Chem., Kharkov State Univ., 12, 303 (1954).

[5] A.G. Betekhtin, Mineralogy, Vol. I, 839, 849, 863 (1950).

[6] I.Ya. Mikey, Presentation Volume to V.I. Vernadsky for the 50th Anniversary of His Scientific Teaching Activity, Acad. Sci. USSR, 2, 813 (1936).

[7] V.V. Aleksandrov, N.A. Ignatyev, and G.G.Kobyak, Wolchonskoite of the Kama Region, Molotov University Press (1941).

[8] E.N. Gapon, J. Gen. Chem., 3, 145 (1933); 7, 1438 (1937).

Received May 23, 1955

The A.M. Gorky University - Kharkov
Chair of General Chemistry

THE ACTION OF VULCANIZATION ACTIVATORS

B. Dogadkin (Moscow) and I. Beniska (Bratislava)

In modern vulcanization technology metal oxides are widely used as vulcanization activators, especially zinc oxide. Vulcanization activators substantially improve the vulcanization process and the quality of the vulcanizates. However, despite the extensive technical use of activators the mechanism of their action is not sufficiently well understood and the experimental data and the theoretical considerations of various authors in the literature are often contradictory.

The most widely accepted view of the role of vulcanization activators is based on their comparison with promoters in catalytic reactions. It is also believed [1] that metal oxides and accelerators, and in particular mercaptans and dithiocarbamic acids, form saltlike compounds which owing to their better solubility produce high accelerator activity. According to Bruni and Romani [2], and also to Bedford and Sebrell [3], these saltlike compounds react with sulfur to form di- or polysulfides, which evolve sulfur in an active form. Recently it has been shown [4] that zinc oxide participates in reactions which lead to the formation of the vulcanizate spatial network. This aspect of the problem, which is of great theoretical and practical interest, requires further study

Effect of zinc oxide and stearic acid on the kinetics of the addition of sulfur to rubber

The kinetics of the addition of sulfur to rubber was studied in mixtures based on sodium butadiene rubber (SKB) with the following primary composition (in parts by weight): SKB 100, sulfur 3, and Neozone D 2. To this basic composition, the necessary amounts of the other components were added: zinc oxide, stearic acid, and accelerators: mercaptobenzothiazole (MBT) and diphenylguanidine (DPG). The mixing was carried out on microrollers in air; the vulcanization was carried out in a press. Combined sulfur was determined by oxidation of the vulcanizate by a mixture of nitric acid and bromine in presence of magnesium oxide. The ZnS content of parallel samples of the vulcanizates was determined by the amount of H_2S evolved from the sample swollen in ether by the action of concentrated hydrochloric acid in a current of nitrogen. The difference between the total bound sulfur and the sulfur contained in the vulcanizate as ZnS gives the "organic bound sulfur", or the sulfur combined direct with the rubber. The curves shown in this paper represent the kinetics of the addition of organic bound sulfur*.

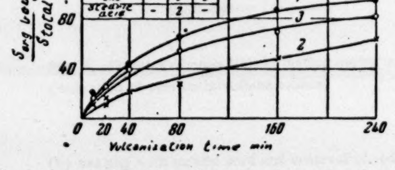

Fig. 1. Kinetics of sulfur addition in mixtures based on technical sodium butadiene rubber (SKB) without accelerator. The composition is given in parts by weight.

The technical SKB used contained 0.56-0.67% alkali calculated as Na_2CO_3. As alkali accelerates the sulfur addition reaction, in order to eliminate this effect some of the experiments were carried out with specially purified rubber, from which the alkali was removed by a method developed by A.V. Dobromyslova

---

*In most published papers on vulcanization kinetics, bound sulfur is taken to mean all the sulfur which is not extracted from the vulcanizate by acetone, including the sulfur contained in the vulcanizate as zinc sulfide. This incorrect method of determination can lead to erroneous conclusions.

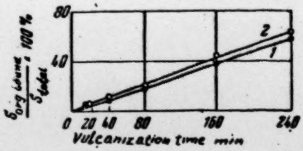

Fig. 2. Kinetics of the addition of sulfur to purified sodium butadiene rubber; composition of mixtures as in Fig. 1.

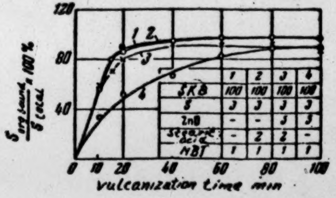

Fig. 3. Kinetics of sulfur addition in mixtures of technical sodium butadiene rubber (SKB) containing mercaptobenzothiazole (MBT) as accelerator.

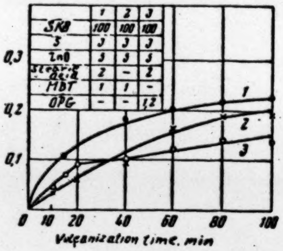

Fig. 4. Kinetics of ZnS formation in mixtures with sodium butadiene rubber (SKB) containing mercaptobenzothiazole (MBT) or diphenylguanidine (DPG) as accelerators: the amount of ZnS is expressed as the S content in % of the bound sulfur.

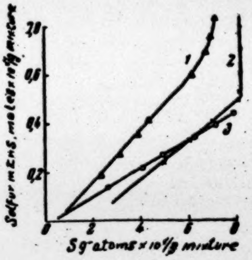

Fig. 5. Variation of the ZnS content with the amount of sulfur added to the rubber: 1) mixture without accelerator; 2) mixture with MBT; 3) mixture with DPG.

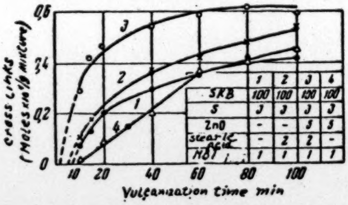

Fig. 6. Kinetics of cross link formation during vulcanization of sodium butadiene rubber.

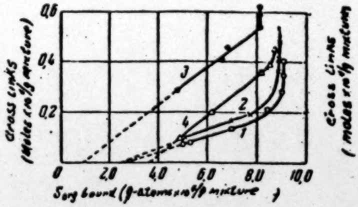

Fig. 7. Variation of the number of cross links with the amount of sulfur combined with the rubber. The compositions of the mixtures are as in Fig. 6.

(by heating with stearic acid and removal of sodium stearate by precipitation of the rubber from benzene solution by methyl alcohol).

As a rule, metal oxides are added to the vulcanization mixture together with fatty acids, usually with stearic acid. It is believed that the activating action of zinc oxide is fully effective only in presence of this acid. Therefore in our experiments wer investigated the action of zinc oxide both separately and together with

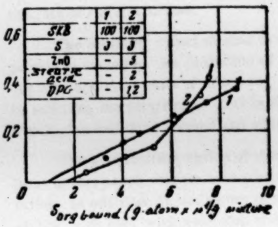

Fig. 8. Variation of the number of cross links with the amount of sulfur combined with the rubber.

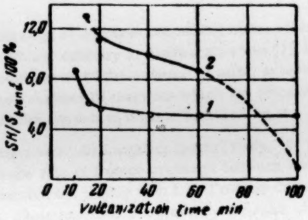

Fig. 9. Variation of the thiol group content during vulcanization of sodium butadiene rubber; accelerator MBT: 1) mixture without ZnO; 2) mixture with ZnO.

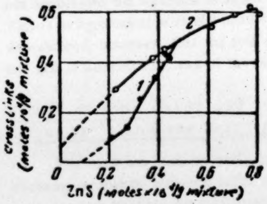

Fig. 10. Variation of the number of cross links with the ZnS content in sodium butadiene rubber vulcanizates; 1) DPG accelerator; 2) MBT accelerator.

the generally used amount of stearic acid (2% on the weight of the rubber).

Fig. 1 represents the kinetics of sulfur addition in mixtures of technical SKB without accelerator. It is seen that in the presence of zinc oxide (5 parts by weight on the rubber) the rate of sulfur addition is somewhat retarded. A greater retardation occurs by the combined action of zinc oxide and stearic acid. The intensification of the retardation effect in the addition of sulfur to rubber by the action of stearic acid may in this case be probably ascribed to neutralization of the alkali contained in the rubber which, as has already been stated, accelerates the addition of sulfur to rubber. In fact, as Fig. 2 shows, a binary mixture of purified alkali-free rubber and sulfur vulcanizes very slowly; zinc oxide and stearic acid have practically no effect on the rate of sulfur addition (the data in Fig. 2 indicate a slight acceleration, which may be attributed to bad reproducibility of the results, largely owing to imperfect mixing of the components).

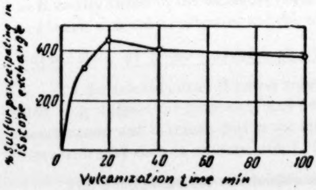

Fig. 11. Isotope exchange of elementary sulfur with vulcanizates containing S^{35}.

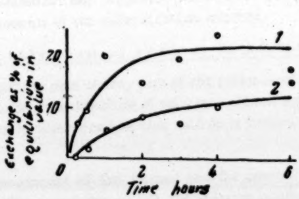

Fig. 12. Kinetics of isotope exchange, with elementary sulfur, of vulcanizates: 1) without ZnO and 2) with ZnO; accelerator MBT.

In mixtures with technical SKB containing mercaptobenzothiazole (MBT) as accelerator, zinc oxide substantially lowers the rate of sulfur addition (Fig. 3). In the presence of stearic acid, and also of stearic acid and zinc oxide, the rate of sulfur addition is practically equal to the vulcanization rate of the original mixture. Since, as was stated earlier, stearic acid neutralizes the alkali in technical rubber, it is evident that stearic acid exerts an accelerating effect in mixtures with MBT.

In mixtures containing diphenylguanidine (DPG) as accelerator, zinc oxide and stearic acid do not change the rate of sulfur addition.

The retarding effect of zinc oxide in the vulcanization of mixtures containing mercaptobenzothiazole is primarily caused by the formation of zinc mercaptide which, contrary to Auerbach's views [1], is, according to our data and the results of others [5], a less active accelerator of the addition of sulfur to rubber than MBT. In addition, the presence of ZnO in the system leads to a number of reactions which are described below, in which zinc sulfide is formed and which therefore lower the content of organic bound sulfur.

The accelerating action of stearic acid in mixtures with MBT requires special study. As will be shown later in this paper, stearic acid substantially increases the rate of isotope exchange between MBT and elementary sulfur. In addition, it was shown in our experiments carried out jointly with I.A. Tutorsky that stearic acid reacts at 140° with MBT with evolution of hydrogen sulfide. These reactions are probably the cause of the activating effect of stearic acid in the addition of sulfur to rubber in the presence of mercaptobenzothiazole.

Thus, the experimental data show that in the sodium butadiene rubber mixtures studied zinc oxide does not accelerate the addition of sulfur to rubber and so cannot be regarded as an "activator" of vulcanization. This is in agreement with the results of the experiments carried out by Dogadkin, Feldshtein, and Orlovsky [15], who showed, however, that the role of zinc oxide (as of other metal oxides) greatly depends on the type of rubber and of accelerator, and of the type of carbon black used as filler.

Effect of zinc oxide and stearic acid on isotope exchange between elementary sulfur (S^{35}) and the thiol group sulfur in mercaptobenzothiazole

The view has been recently put forward in a number of papers [6] that vulcanization reactions and isotope exchange reactions between sulfur and the accelerator have a common mechanism. In this connection it was of some interest to study the influence of vulcanization accelerators on isotope exchange of sulfur with the accelerator studied – mercaptobenzothiazole. The experiments were carried out both in molten sulfur and in a solution in vaseline oil with the aid of a technique similar to that described by Guryanova [6]. The results are shown in Table 1. The results show that zinc oxide sharply retards and decreases the extent of exchange of S^{35} with MBT, while stearic acid has a considerable activating effect on the process. Thus, the influence of ZnO and stearic acid on the exchange reaction is analogous to their influence on the addition of sulfur to rubber in the presence of MBT as vulcanization accelerator. We do not incline to the view that vulcanization reactions consist only of the reactions which occur in the exchange of sulfur with the accelerator [7], but nevertheless it is a significant fact that stearic acid exerts an independent and special action in comparison with zinc oxide both in the addition of sulfur to rubber and in the exchange reaction of sulfur with MBT. This means that stearic acid (and probably other fatty acids) should not be regarded as only a dispersing agent or solvent for zinc oxide, as is usually stated in the technical literature on vulcanization. Apparently it takes direct part in vulcanization, and reacts with the accelerator and the other components of the vulcanization mixture.

Formation of zinc sulfide in the vulcanization of sodium butadiene rubber

In the vulcanization of rubber mixtures containing zinc oxide, part of the sulfur is combined as zinc sulfide. Fig. 4 shows the kinetics of ZnS formation in the vulcanization of mixtures containing MBT and DPG as accelerators, and it is seen that in the initial stages of vulcanization zinc sulfide is formed more rapidly in mixtures with MBT than in mixtures with DPG.

Fig. 5 represents the relationship between the amount of ZnS formed and the content of organically bound sulfur. As was already shown by Hull, Weinlands, Olsen, and France [4], the relative content of sulfur in the form of zinc sulfide is higher in vulcanizates without accelerator than in vulcanizates containing MBT and DPG as accelerators. It is also seen that in the last stage of the process (beyond the vulcanization optimum) mixtures with MBT show a sharp increase of the $ZnS:S_{bound}$ ratio, which indicates the formation of ZnS as the result of reactions with participation of sulfur already combined with the rubber.

The kinetics of ZnS formation and the dependence of the amount of zinc sulfide formed on the composition of the vulcanization mixture indicate that this substance is formed as the result of a series of reactions. It was therefore of interest to find the reactions which may lead to ZnS formation in vulcanization conditions.

It was experimentally shown that zinc sulfide may be formed in the following reactions:

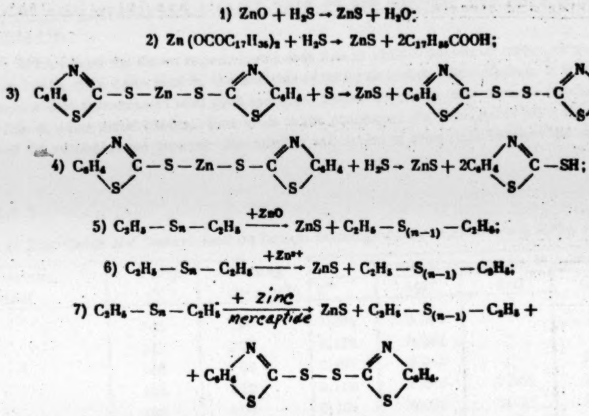

$$1)\ ZnO + H_2S \rightarrow ZnS + H_2O;$$

$$2)\ Zn(OCOC_{17}H_{35})_2 + H_2S \rightarrow ZnS + 2C_{17}H_{35}COOH;$$

$$5)\ C_2H_5-S_n-C_2H_5 \xrightarrow{+ZnO} ZnS + C_2H_5-S_{(n-1)}-C_2H_5;$$

$$6)\ C_2H_5-S_n-C_2H_5 \xrightarrow{+Zn^{2+}} ZnS + C_2H_5-S_{(n-1)}-C_2H_5;$$

$$7)\ C_2H_5-S_n-C_2H_5 \xrightarrow[\text{mercaptide}]{+\text{ zinc}} ZnS + C_2H_5-S_{(n-1)}-C_2H_5 +$$

Reaction 1 was carried out in an aqueous medium, and the others in xylene.

Reactions 1 and 2 proceed at a high rate at room temperature. Reaction 3 (with zinc mercaptide) proceeds slowly at vulcanization temperature (143°); Reaction 4 is fairly rapid in the same conditions. Reactions 5, 6, and 7 correspond to reactions of rubber polysulfides with zinc oxide and zinc salts; they proceed fairly slowly at vulcanization temperature (in 1 hour ~ 50% of the reacting quantity of diethyl polysulfide is decomposed).

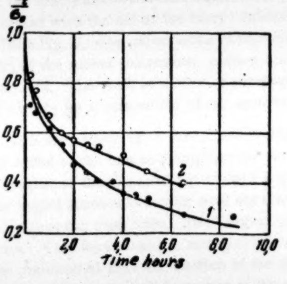

Fig. 13. Stress relaxation of vulcanizates based on sodium butadiene rubber at 126°; 1) mixture without ZnO; 2) mixture with ZnO.

The possibility of zinc sulfide formation as the result of secondary reactions between zinc oxide and rubber polysulfides was also established by direct experiments. For this, a mixture containing MBT as accelerator was vulcanized for 20 minutes and then extracted with cold acetone for 50 hours to remove free sulfur and accelerator. The extracted vulcanizate was then heated again at 142° for 2 hours and analyzed for ZnS.

An analogous experiment was carried out with a sample vulcanized for 100 minutes, when practically all the sulfur was combined with the rubber. In both cases, heating resulted in a further increase of the zinc sulfide content by 32-36% of the initial value, which may be attributed to the reaction between zinc oxide and rubber polysulfides. This reaction is responsible for the previously noted (see Fig. 5) sharp increase of the ZnS:S_{bound} ratio observed during the final stage of the process beyond the vulcanization optimum. As will be shown later, this reaction is significant for structural changes in the vulcanizate.

The hydrogen sulfide necessary for Reactions 1, 2, and 4, as was shown by direct experiments, is formed when the rubber mixture with sulfur is heated, and especially as the result of the reaction between sulfur, MBT, and stearic acid. Thus, the above reactions, which occur to some extent in vulcanization conditions, may lead to the formation of zinc sulfide in the vulcanizate.

These reactions of zinc sulfide formation compete with the primary reaction of the addition of sulfur to rubber, and their occurrence must therefore be regarded as one of the causes of the retarding action of zinc sulfide on this last reaction.

Effect of zinc oxide and stearic acid on the number and type of cross links in the vulcanizate

It follows from the above experimental data that in sodium butadiene rubber mixtures ZnO does not accelerate, but in some cases retards, the addition of sulfur to rubber. Nevertheless, it is known from technological practice that vulcanizates with good technical properties can in most cases be obtained only by the use of zinc oxide or other metal oxides. This leads to the conclusion that zinc oxide has a significant effect on another aspect of the vulcanization process – the number and nature of cross links between the molecular rubber chains [4].

TABLE 1

Effect of Zinc Oxide and Stearic Acid on Isotope Exchange Between Elementary Sulfur and MBT

Experimental conditions	Temp. (°C)	Heating time, min.	Content of components in mixture				Exchange, % of equilibrium
			S^{35}	MBT	ZnO	$C_{18}H_{36}O_2$	
Melt	145	120	0.094	0.055	–	–	73.2
	145	300	0.133	0.062	–	–	90.5
	145	80	0.099	0.049	–	0.227	80.0
	145	120	0.132	0.069	0.264	0.110	1.1
	145	300	0.101	0.055	0.251	0.101	5.6
	150	120	0.144	0.076	0.473	–	6.0
Solution in vaseline oil	143	80	0.115	0.056	–	–	30.0
	143	80	0.123	0.056	–	–	90.0
	143	80	0.109	0.057	0.029	0.011	12.7

For determination of this aspect of the action of vulcanization activators, the number of cross links was determined with the aid of the Flory–Rehner equation from the swelling maximum of the vulcanizates. As is seen from Fig. 6, zinc oxide alone in mixtures containing mercaptobenzothiazole does not accelerate cross linking of the rubber molecules; a sharp acceleration is found with the combined action of zinc oxide and stearic acid. The positive action of activators on the formation of the space structure of vulcanizates is seen more clearly by a comparison of the number of cross links with the amount of sulfur added to the rubber.

It is seen from Fig. 7 that a linear relationship exists between the number of cross links and the amount of sulfur added to the rubber throughout the process up to the moment immediately after the vulcanization optimum. The tangent of the slopes of the straight lines in Fig. 7 represents the "degree of cross linkage", and a comparison of the angles shows that stearic acid accelerates sulfur addition without increasing the fraction of the sulfur which enters the cross links. The "degree of cross linking" increases sharply on the introduction of ZnO into the mixture. This shows that the essential role of zinc oxide as a vulcanization activator consists of the fact that in the presence of ZnO the fraction of the sulfur used for cross link formation in the vulcanizate increases; and it is known that cross link formation is the essential feature of the vulcanization process.

In mixtures containing DPG as accelerator, the role of zinc oxide is less prominent. In this instance ZnO increases the "degree of cross linking" only during the second part of the vulcanization process (Fig. 8). A comparison of Curve 1, Fig. 7 with Curve 1, Fig. 8 shows that in mixtmres without vulcanization activators (ZnO and stearic acid) diphenylguanidine causes a greater cross linking effect than mercaptobenzothiazole.

The formation of sulfur cross links between the rubber molecules in the vulcanizate occurs as the result of a number of chemical reactions. On the basis of our experimental data the following possibilities for the participation of zinc oxide in these reactions, affecting the extent of cross linking, may be considered.

a) The reaction of mercaptobenzothiazole with sulfur occurs through the formation of thiol polysulfide compounds [8] according to the scheme:

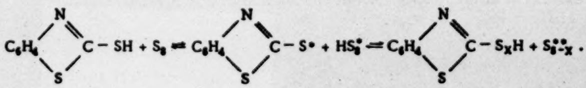

Naylor [9] showed that thiol compounds may form both cross links and intramolecular ring structures. It is possible that reactions of zinc oxide and zinc salts with thiol groups lead, on the one hand, to the formation of ZnS, and on the other, to the formation of sulfur biradicals joining the rubber molecular chains. In the latter case the fraction of sulfur which enters the cross links increases.

b) According to the views of a number of workers [10], thiol groups are formed in the molecular chains of rubber during vulcanization, as the result of reactions between sulfur and α-methylene groups, or of addition of H_2S or $HS^{\bullet}$ at the double bonds. The thiol groups are then oxidized by sulfur (Fischer) or by zinc oxide (Armstrong) to form disulfide cross links between the rubber molecules. However, no direct proof of such a process in the vulcanization of rubber has been obtained*. We attempted with M.A. Vaskovskaya to follow the kinetics of thiol group formation during the vulcanization of mixtures with and without zinc oxides. The vulcanizate was extracted with cold acetone and then ground in a mortar with granulated sugar to a fine state of subdivision. The sugar was leached out of the vulcanizate sample with water, the sample was dried, and covered with ligroine (to swell the particles) and with lead acetate solution. The reaction was continued for 25 hours with continuous shaking. The vulcanizate was then filtered off and successively washed with alcohol–ligroine mixture, pure alcohol, and finally pure water until lead ions were absent from the filtrate. After the washing, the filtrate was treated with an exact amount of 0.5 N sulfuric acid; the unreacted acid was titrated with NaOH solution with phenolphthalein indicator. The thiol group content was determined from the amount of sulfuric acid required to decompose the $R_1-S-Pb-S-R_2$ complex. For a number of reasons this method cannot be regarded as faultless for the accurate determination of thiol groups; it is, however, acceptable for a comparative evaluation of the thiol group content in the mixture at different stages of vulcanization.

Fig. 9 represents the variation of the thiol group content of mixtures with MBT, with and without ZnO. In the first case there is a decrease of the thiol group content during the first 20 minutes of vulcanization; subsequently the thiol group content is practically unchanged, and remains at a level of 6% of the total amount of bound sulfur. In the second case, the initial thiol group content (after 10 minutes of vulcanization) is high, but this decreases gradually, and at the end of vulcanization it reaches a minimum value of ~2% of the bound sulfur. These results indicate that during vulcanization thiol groups are oxidized with formation of cross links, and that zinc oxide participates in this process, probably by the mechanism proposed by Armstrong [4]

$$2RSH + ZnO + S \rightarrow R-S-S-R + ZnS + H_2O.$$

On the basis of model reactions, the cross linkage effect may also be regarded as the consequence of the formation of zinc mercaptide:

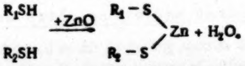

$$\begin{matrix} R_1SH \\ R_2SH \end{matrix} \xrightarrow{+ZnO} \begin{matrix} R_1-S \\ R_2-S \end{matrix} \!\!>\! Zn + H_2O.$$

c) As was described earlier, it was shown in experiments with low-molecular polysulfides and with extracted vulcanizate containing polysulfide groups that zinc oxide and zinc salts react with polysulfides to form ZnS (Reactions 5,6, and 7). The reaction with the polysulfide bonds in the vulcanizate structure evidently follows the scheme

$$R_1-S_x-R_2 \xrightarrow{+\ Zn^{2+}} R_1-S_y-R_2 + ZnS$$

and leads to the formation of cross links with fewer sulfur atoms [11]. The number of cross links can either increase or remain unchanged**. An increase in the number of cross links will occur when part of the polysulfide sulfur is liberated in the form of a new biradical $S_z^{\bullet}$, which reacts with the double bonds (or α-methylene groups) of the molecular chains at another point:

$$R_1-S_x-R_2 + \xrightarrow{Zn^{2+},\ R_3R_4} R_1S_yR_2 + R_3S_zR_4 + ZnS.$$

The number of cross links remains unchanged if the recombination of radicals occurs at the same point:

---

* Hall and others (Rub. Chem. Techn. 20, 649, 1947) and also Bloomfield (Rub. Chem. Techn. 21, 543, 1948) carried out these reactions with model compounds of low molecular weight.

** The case of a regrouping which leads to a decrease in the number of cross links has been examined by Dogadkin and Tarasova [11]; it occurs in the stabilization of radicals as the result of the addition of low-molecular compounds and the formation of intramolecular rings.

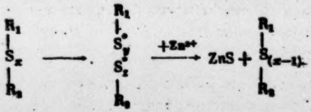

$$\begin{array}{c} R_1 \\ | \\ S_x \\ | \\ R_2 \end{array} \longrightarrow \begin{array}{c} R_1 \\ | \\ S_y^{\bullet} \\ S_z^{\bullet} \\ | \\ R_2 \end{array} \xrightarrow{+Zn^{2+}} ZnS + \begin{array}{c} R_1 \\ | \\ S_{(x-1)} \\ | \\ R_2 \end{array}$$

In the regrouping of polysulfide linkages without the participation of zinc oxide or zinc compounds the probability of an increase in the number of cross links is greater, as the liberated sulfur radicals are not used for the formation of zinc sulfide or polysulfide. This is confirmed by the data shown in Fig. 7. The relative increase of the cross link content which is found after the end of the sulfur addition, and which is primarily explained by regrouping of the polysulfide linkages, is more prominent in mixtures without zinc oxide (the vertical branch of the curves for the variation of the number of cross links as a function of the sulfur combined with the rubber).

The role of zinc oxide and zinc salts in changes of vulcanization structures is seen in the participation of these compounds in side reactions. It is known that H_2S is capable of causing cleavage of polysulfide linkages according to the scheme:

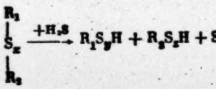

$$\begin{array}{c} R_1 \\ | \\ S_x \\ | \\ R_2 \end{array} \xrightarrow{+H_2S} R_1S_yH + R_2S_zH + S'_{m}$$

The reactions of zinc compounds with the H_2S formed during vulcanization inhibits such processes.

The above experimental data indicate that zinc oxide and zinc compounds participate in different reactions. ZnS may be formed under vulcanization conditions in different ways. Therefore at the present time it is not possible to accept Armstrong's view [4] that ZnS can serve as a measure of the disulfide bond content in a vulcanizate, since it is formed not only by reactions with thiols, but also as the result of the other reactions described above. Moreover, in view of the above considerations the number of cross links in a vulcanizate is not a linear function of the zinc sulfide content, as is confirmed by the data in Fig. 10.

Effect of zinc oxide on isotope exchange of vulcanizates with elementary sulfur*

It was established in the preceding section that ZnO favors an increase in the number of cross links in the vulcanizate and a decrease in the number of sulfur atoms in these cross links. It appeared of interest to confirm this conclusion by an analysis of the vulcanizate structure by the isotope exchange method developed by Dogadkin, Tarasova, and Kaplunov [12]. A vulcanizate prepared with the use of sulfur containing S^{35} was heated, after extraction, with elementary non-radioactive sulfur at 130° for 3 hours. The degree of exchange for various vulcanization times is shown in Fig 11. It is seen that the value rises at first, reaches a maximum at the vulcanization optimum, and then gradually falls. Since the capacity for isotope exchange with elementary sulfur decreases with a decrease in the number of sulfur atoms in the polysulfide bridges [11-13], the existence of a descending branch beyond the vulcanization optimum is a direct confirmation of the regrouping of the polysulfide linkages, as described above, in the direction of an increase in the number of cross links and a decrease of the average number of sulfur atoms per cross link. As was shown by Z.N. Tarasova (Fig. 12) in experiments with butadiene–styrene rubber, the presence of ZnO leads to a decrease of the degree of isotope exchange at all stages of vulcanization, which is also a direct confirmation of the participation of ZnO in reactions in which sulfur bonds with fewer sulfur atoms are formed.

Effect of zinc oxide on the heat stability of vulcanizates

It has been shown [11] that the nature of the vulcanization structures affects the thermal and mechanical stability of vulcanizates and their behavior during aging and fatigue. It was therefore to be expected that vulcanization activators, by influencing the number and the nature of the vulcanization bonds, should also affect their heat stability. For confirmation of this, vulcanizates were prepared from mixtures compounded on micro-rollers mounted in a closet filled with pure nitrogen. Thus, both the mixing and the vulcanization were carried out with exclusion of oxygen. The heat stability of the vulcanizates was evaluated by determination of stress relaxation curves with the aid of a float dynamometer [14] in a nitrogen atmosphere at 126°. Fig. 13 shows the relative stress relaxation in specimens stretched to 100%; a vulcanizate containing MBT, zinc oxide, and stearic acid shows much slower relaxation, with a higher value of quasi-equilibrium stress, than a vulcanizate of the same composition without ZnO. Therefore, the vulcanizate containing ZnO has the greater heat stability. The rate constant of stress relaxation at 126° was, in the first case, $K_{126} = 1.38 \cdot 10^{-3}$ minute^{-1}, and in the second, $K_{126} = 2.52 \cdot 10^{-3}$ minute^{-1}. As stress relaxation in these conditions is due to cleavage and regrouping of chemical bonds [11], the results show that vulcanizates with zinc oxide contain more stable bonds of the type $-C-C-$, $-C-S-C-$, $-C-S-S-C-$, and a relatively lower content of polysulfide bonds of the type $-C-S_x-C-$. Thus, the experiments on stress relaxation are in good agreement with the above data on the effect of vulcanization activators in increasing the number of vulcanization bonds and decreasing the number of sulfur atoms in these bonds.

---

*This and the following section of the work was carried out in consultation with Z.N. Tarasova, to whom the authors express their gratitude.

It is also important to note that the maximum swelling of vulcanizates without zinc oxide decreases, and that of vulcanizates with ZnO increases after relaxation. This difference in the behavior of the vulcanizates under the action of heat and mechanical stress is probably explained by the fact that, as was pointed out earlier, the cleavage of polysulfide linkages in absence of ZnO leads to the formation of new sulfur biradicals, which form additional new cross links. In the presence of zinc oxide and zinc compounds these radicals are "trapped" with the formation of zinc sulfide.

Thus, vulcanization activators have a significant influence not only on the formation of vulcanization structures at the time of vulcanization, but also on changes in them under the action of thermomechanical (and probably oxidative) influences in use.

SUMMARY

1. Zinc oxide and stearic acid do not affect the rate of addition of sulfur to rubber in the vulcanization of pure sodium butadiene rubber in mixtures without accelerators.

2. In mixtures containing diphenylguanidine as accelerator zinc oxide and stearic acid do not affect the rate of addition of sulfur to rubber.

3. In mixtures containing mercaptobenzothiazole zinc oxide retards and stearic acid accelerates the addition of sulfur to rubber.

4. In a similar manner zinc oxide suppresses and stearic acid activates isotope exchange between elementary sulfur and sulfur of the thiol group in mercaptobenzothiazole.

5. Zinc oxide and stearic acid in mixtures with mercaptobenzothiazole increase the rate and degree of cross linking of the molecular chains of rubber; zinc oxide has the greater influence on the degree, while stearic acid has the greater influence on the rate, of the cross linking reaction.

6. In mixtures with diphenylguanidine the influence of vulcanization activators on the degree and rate of cross linking is considerably less pronounced than in mixtures with mercaptobenzothiazole.

7. The kinetics of zinc sulfide formation during vulcanization has been studied and it was established that ZnS is formed as the result of reactions of zinc oxide and zinc compounds with thiol and polysulfide groups in the rubber. Model substances have been used to demonstrate other possible routes for the formation of zinc sulfide during vulcanization. The effect of zinc oxide and stearic acid on the rate and degree of cross linking is associated with participation of these compounds in such reactions.

8. Isotope exchange between radioactive sulfur in the vulcanizate and elementary sulfur was used to follow the formation and changes in the numbers of polysulfide linkages during the vulcanization process. The amount of sulfur participating in isotope exchange as vulcanization proceeds at first increases, passes through a maximum, and then decreases, which indicates a regrouping of the polysulfide linkages with an increase in their number and a decrease of the average number of sulfur atoms per linkage. Zinc oxide decreases the degree of isotope exchange between the vulcanizate and elementary sulfur at all stages of vulcanization.

9. Vulcanization activators, by favoring a decrease in the number of sulfur atoms in the sulfur bonds, increase the heat stability of the vulcanizates. This effect of the activators was demonstrated by kinetic data on stress relaxation in deformed vulcanizates at 125°.

10. The cleavage and regrouping of polysulfide linkages in the presence of zinc oxide and zinc compounds is accompanied by the combination of part of the sulfur as zinc sulfide, which leads to a decrease in the number of newly formed cross links. This effect of zinc oxide is manifested in vulcanization reversion effects and in changes of vulcanizate properties under thermomechanical influences.

11. From the above experimental data the general conclusion may be drawn that the fundamental role of vulcanization activators does not lie in their influence on the kinetics of the addition of sulfur to rubber, but rather in their influence on the nature of the vulcanization structures formed and on changes in them in the course of vulcanization.

LITERATURE CITED

[1] O.A. Zeide and K.D. Petrov, Caoutchouc and Rubber, 2, 53 (1937); I. Auerbach, Ind. Eng. Chem., 45, 1526 (1953).

[2] G. Bruni and E. Romani, India-Rubber J., 62, 63 (1921).

[3] C. Bedford and L. Sebrell, Ind. Eng. Chem., 13, 1034 (1921).

[4] R.T. Armstrong, J.R. Little and K.W. Doak, Rubber Chem. and Technol., 17, 788 (1944); C.W. Hull, L.A. Weinlands, J.R. Olsen and H.C. France, Rubber Chem. and Technol., 21, 553 (1948).

[5] D. Graig, A.E. Juve and W.L. Davidson, Rubber Chem. and Technol., 24, 254 (1951).

[6] G.A. Blokh, E.A. Golubkova, and G.P. Miklukhin, Light Ind., 7, 25 (1952); E.N. Guryanova, Proc. Acad. Sci. USSR, 98, 229 (1954); S.E. Bresler, V.I. Pryadilova, and F.Ya. Khaiman, J. Tech. Phys., 24, 578 (1954).

[7] B. Dogadkin, V. Selyukova, Z. Tarasova, A. Dobromyslova, M. Feldshtein, and M. Kaplunov, Colloid J., 17, 215 (1955) (T.p. 199)*.

[8] B. Dogadkin and I. Tutorsky, Proc. Acad. Sci. USSR (in the press).

[9] R.F. Naylor, Rubber Chem. and Technol., 20, 353 (1947).

[10] H.L. Fischer, Ind. Eng. Chem., 31, 1381 (1939); E.H. Farmer and F.W. Shipley, J. Polymer Sci., 1, 293 (1944).

[11] B. Dogadkin, Z. Tarasova, Colloid J., 15, 347 (1953) (T.p. 355)*; Proc. Acad. Sci. USSR, 85, 1069 (1952).

[12] Z. Tarasova, M. Kaplunov, and B. Dogadkin, Proc. Acad. Sci. USSR, 99, 819 (1954).

[13] E.N. Guryanova, J. Phys. Chem., 28, 67 (1954).

[14] M.M. Reznikovsky, Z.N. Tarasova, and B.A. Dogadkin, Factory Labs., 19, 247 (1953).

[15] B. Dogadkin, M. Feldshtein, and P. Orlovsky, J. Appl. Chem. (in the press).

Received December 31, 1955

M.V. Lomonosov Institute of
Fine Chemical Technology - Moscow

---

*T.p. = C.B. Translation pagination.

COMPATIBILITY OF NITROCELLULOSE WITH BUTADIENE–ACRYLONITRILE COPOLYMERS

2. EFFECT OF THE COMPONENT RATIO IN THE MIXTURE ON THE LOAD–EXTENSION DIAGRAMS

L.E. Kalinina, V.I. Alekseenko, and S.S. Voyutsky

In the previous paper [1] the compatibility of nitrocellulose with some polar high polymers was demonstrated and the view was put forward that the compatibility of two polymers is determined by the ratio of their polarities. The present communication contains an examination of load–extension diagrams of mixtures of nitrocellulose with polybutadiene and butadiene–acrylonitrile copolymers containing various amounts of acrylonitrile. It will be seen that a study of the behavior of a high polymer during the entire stretching process – at the start, during the development of high-elastic deformation, and in the period before break – makes possible a more precise study of the effects in the system undergoing deformation, and of the compatibility of the components.

Nitrocellulose containing ~ 12% nitrogen was used in the work. The second component was polybutadiene with a plasticity value of 0.3, or one of four butadiene–acrylonitrile copolymers, with the following acrylonitrile group contents:

Copolymer	1 – 18.4%	Copolymer	3 – 37.7%
"	2 – 28.6%	"	4 – 44.4%

The films used in the investigation were formed from solutions by the following technique: nitrocellulose in standard mastic form, containing 22% dry residue, 33% ethyl alcohol, 25% ethyl acetate, and 20% benzene, was mixed with 20% solution of the given elastomer in benzene. Both solutions were heated on the water bath to 30° before mixing for better fluidity.

The highly viscous solutions so obtained were diluted with the original solvents so calculated that the dry residue content was 10% in all cases. The proportions between ethyl alcohol, ethyl acetate, and benzene in the final mixtures were kept constant, the solvents present in the initial solutions of the components being taken into account. The solvents were dried by means of calcium chloride and distilled before use.

To ensure complete homogeneity, the viscous solutions obtained were stirred by means of a vertical stirrer for 1½ hours, filtered through a fabric filter, and then warmed on a water bath for 20 minutes at 50° to remove air bubbles. The resulting completely homogeneous transparent solutions were used for casting the films. The films were cast and dried on a plate glass surface in a special laboratory casting apparatus. The casting process was carried out at 50° at a low rate of solvent evaporation so that the process took three days. The films were then dried in air and under vacuum to constant weight. The thickness of all the films was in the range 0.14-0.18 mm.

All the nitrocellulose films containing polybutadiene had very low strength and were highly inhomogeneous in appearance. This can be seen in Fig. 1, which shows photographs of nitrocellulose films containing 20 and 40% of polybutadiene. The heterogeneity of films containing 40% polybutadiene is particularly prominent. In this case the photograph shows white regions of polybutadiene sharply defined on a dark background of nitrocellulose. Films from nitrocellulose and butadiene–acrylonitrile Copolymer 1 did not show macroheterogeneity, but had a characteristic honeycomb structure. This was most prominent when the ratio of nitrocellulose to copolymer was close to 1:1. Nitrocellulose films containing Copolymers 2 and 3 were transparent at all component

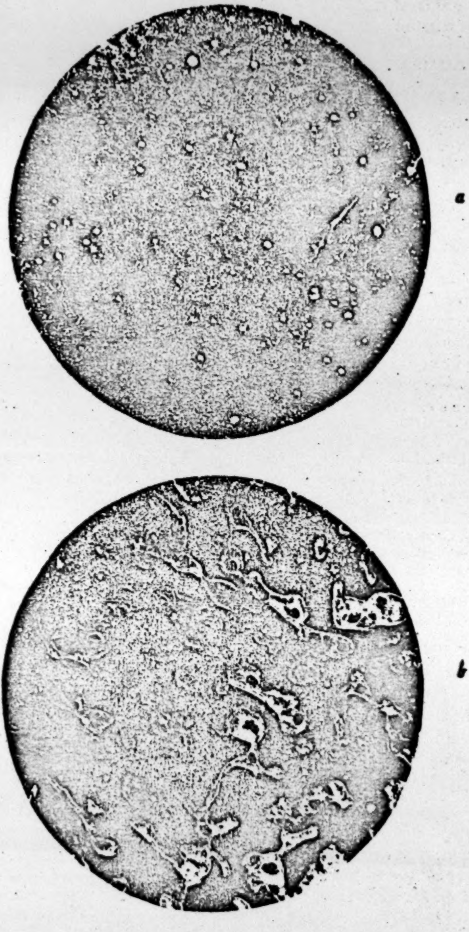

Fig. 1. External appearance of nitrocellulose films containing: a) 20%, b) 40% polybutadiene.

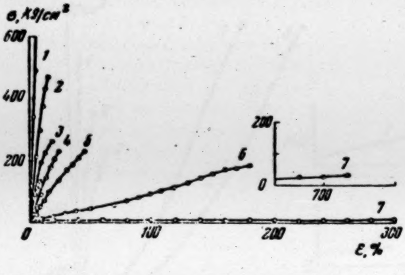

Fig. 2. Load–extension diagrams for nitrocellulose films with different contents of butadiene–acrylonitrile Copolymer 1: 1) without copolymer; 2) with 20%; 3) 40%; 4) 50%; 5) 60%; 6) 80%; 7) 100% copolymer.

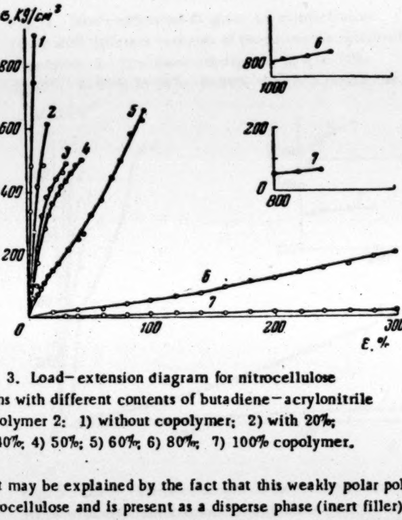

Fig. 3. Load–extension diagram for nitrocellulose films with different contents of butadiene–acrylonitrile Copolymer 2: 1) without copolymer; 2) with 20%; 3) 40%; 4) 50%; 5) 60%; 6) 80%; 7) 100% copolymer.

ratios. When the acrylonitrile content in the butadiene–acrylonitrile copolymer was increased to 44.4%, the films remained transparent, but at medium ratios contained regions with a slightly wavy surface.

The load–extension diagrams for the films were obtained with the aid of a dynamometer of the Polanyi type. The extension was carried out at a constant rate of 7.4 mm/minute at 22 ± 2°. The stress was calculated for the true cross-section by means of the equation

$$\sigma = \sigma_0 (1 + \epsilon),$$

where σ_0 is the stress relative to the original cross-section of the specimen; ϵ is the relative extension.

Figs. 2-5 show the load–extension diagrams for nitrocellulose films with different contents of butadiene–acrylonitrile polymers of various polarities. Load–extension diagrams of films with nitrocellulose and polybutadiene are not shown, as these films had negligible strength owing to their macroheterogeneity.

Fig. 2 shows than an increase of the content of butadiene–acrylonitrile Copolymer 1 in the film up to 40% greatly lowers the film strength with a slight increase of the extension at break. The extensibility modulus, as indicated by the slope of the linear regions of the curves, decreases relatively little. When the copolymer content in the film is increased above 40%, the tensile strength shows only a small decrease but extension rises sharply and the modulus greatly decreases.

The behavior of films with a low butadiene–acrylonitrile Copolymer 1 content may be explained by the fact that this weakly polar polymer does not mix with the relatively highly polar nitrocellulose and is present as a disperse phase (inert filler) in the film. It is clear that an increase of the content of this polymer would lead to a decrease of the strength of the system. With a high content of the same Copolymer 1, the position is reversed – nitrocellulose becomes the disperse phase (filler), and the copolymer is the external medium. Evidently an increase of the nitrocellulose content in the film, which now consists mainly of butadiene–acrylonitrile copolymer, should make the system more homogeneous, should cause a sharp increase of the extension at break, and make the material capable of flow.

The incompatibility of nitrocellulose and Copolymer 1 is also confirmed by the fact that the curves, which approximate to linearity in form, do not show the inflexions characteristic of mixtures of a rigid and a compatible highly elastic polymer. Incompatibility in this case is indicated by the appearance of the films themselves, described above.

Fig. 3, which shows load–extension curves for nitrocellulose films containing butadiene–acrylonitrile Copolymer 2, leads to rather different conclusions. In this case, when the butadiene–acrylonitrile copolymer con-

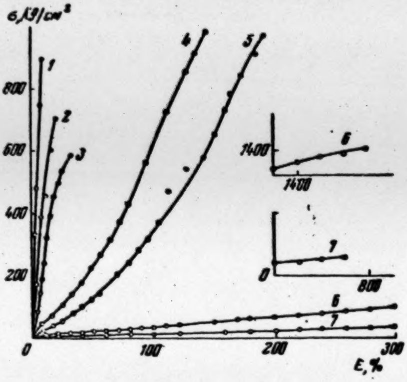

Fig. 4. Load–extension diagram for nitrocellulose films with different contents of butadiene–acrylonitrile Copolymer 3: 1) without copolymer; 2) with 20%; 3) 40%; 4) 50%; 5) 60%; 6) 80%; 7) 100% copolymer.

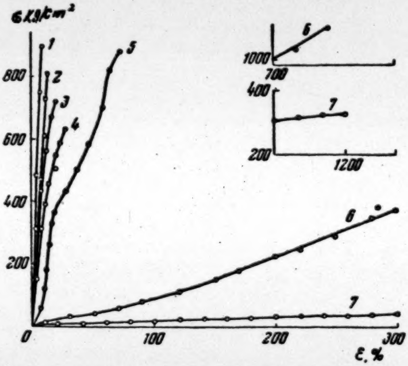

Fig. 5. Load–extension diagrams for nitrocellulose films with different contents of butadiene–acrylonitrile Copolymer 4: 1) without copolymer; 2) with 20%; 3) 40%; 4) 50%; 5) 60%; 6) 80%; 7) 100% copolymer.

tent in the film is 60% and over, the curves are quite distinctly S-shaped, which is typical for load–extension diagrams of highly elastic materials. This indicates that the more highly polar Copolymer 2 has a plasticizing effect on nitrocellulose, and is therefore to some extent compatible with it. The compatibility of the nitrocellulose with the copolymer is indicated by the clarity and homogeneity of the films obtained.

In the case of nitrocellulose plasticized with Copolymer 3, containing 37.7% acrylonitrile groups, even mixtures containing 50% copolymer yield S-shaped load–extension curves with a sharp increase of film strength. This can be seen in Fig. 4. Evidently the plasticizing action of the butadiene–acrylonitrile copolymer is in this case still more pronounced owing to its good compatibility with nitrocellulose. This is also confirmed by the fact that the films from nitrocellulose and Copolymer 3 were quite homogeneous and transparent.

The load–extension curves shown in Fig. 5, which represent the behavior of nitrocellulose films containing Copolymer 4 with 44.4% acrylonitrile groups, again begin to approximate to linearity; the S-shaped bend characteristic of load–extension diagrams of highly elastic substances degenerates. The extensibility modulus, as shown by the linear intercepts of the load–extension curves, increases, while the tensile strength of the films containing 50 and 60% of the elastomer decreases, although it remains higher than that of nitrocellulose films containing butadiene–acrylonitrile Copolymer 1.

The peculiar features of the load–extension diagrams for nitrocellulose films containing butadiene–acrylonitrile Copolymer 4 may be explained by the rigidity of this polymer, and by its consequent lower plasticizing power for nitrocellulose. Another possible explanation is inadequate compatibility of the two components because of the increasing difference in their polarities, which will be discussed in detail later. The inhomogeneity of films containing Copolymer 4, which was noted in some instances, appears to confirm this last view.

The load–extension curves may also be grouped in another way, so that they show the manner in which the mechanical properties of the films are influenced by the addition to the nitrocellulose of equal amounts of butadiene–acrylonitrile copolymers with different acrylonitrile group contents. Fig. 6 shows such an arrangement of the load–extension diagrams for nitrocellulose films containing different amounts (20, 60, and 80%) of butadiene–acrylonitrile copolymers of various degrees of polarity.

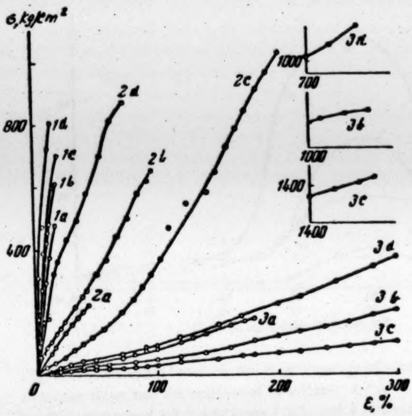

Fig. 6. Load–extension diagrams for nitrocellulose films containing different amounts of butadiene–acrylonitrile copolymers of different degrees of polarity: 1,2,3) films containing 20, 60, and 80% copolymer respectively; a,b,c,d) films with Copolymers 1,2,3, and 4 respectively.

It is seen from Fig. 6 that when the butadiene–acrylonitrile copolymer content in the film is relatively low (20%), the influence of all the copolymers is small and approximately the same. Nevertheless it can be seen that the lower the nitrile group content in the elastomer added to the nitrocellulose, the more it decreases the film strength.

At a 60% content of the butadiene–acrylonitrile copolymers, the curve for films with the weakly polar Copolymer 1 retains its linear character, typical for the curves for films of nitrocellulose alone. This is evidently caused by incompatibility of Copolymer 1 with nitrocellulose. The load–extension diagrams of films containing Copolymers 2 and 3 are quite different in appearance; they are S-shaped curves, typical of highly elastic materials; in the case of Copolymer 3 the S-shape is much more prominent and the films have much better mechanical properties. The load–extension diagram for the film containing Copolymer 4 has a less definite S-shape, and ascends much more steeply than the curves for films containing Copolymers 2 and 3. This was to be expected in view of the greater polarity and greater rigidity of Copolymer 4.

In the case of films containing 80% butadiene–acrylonitrile copolymers the load–extension curves are very flat and at high extensions tend to lie parallel to the abscissa axis, which is a sign of the ability of the material to flow. An interesting feature is that the slope of the curves in this case is greater with decrease in the nitrile group content of the elastomer added to the nitrocellulose. Thus, the effect of polar nitrile groups at high contents of butadiene–acrylonitrile copolymers is opposite to the effect of these groups when the elastomer content of the nitrocellulose is low. Copolymer 4 is an exception.

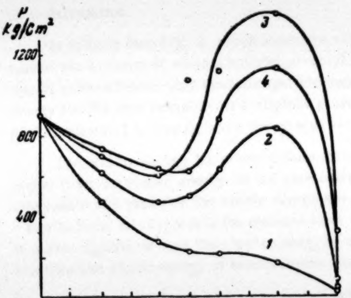

Fig. 7. Relationship between the butadiene–acrylonitrile copolymer content and the tensile strength P of nitrocellulose films; 1,2,3,4) curves for Copolymers 1,2,3,4 respectively.

The experimental data obtained were used to plot curves for the variation of tensile strength and extension at break of the films as a function of the butadiene–acrylonitrile content. These curves, shown in Fig. 7, are in many ways similar to the curves obtained by us both for the same system [1] and for polyvinyl chloride plasticized with butadiene–acrylonitrile copolymers [2]. As was found in the previous investigations, when the components are compatible characteristic inflexions occur at certain points in the curves, the reasons for which were discussed earlier. This indicates that such curves may be successfully used for characterization of polymer compatibility and of the plasticizing action of high molecular softeners.

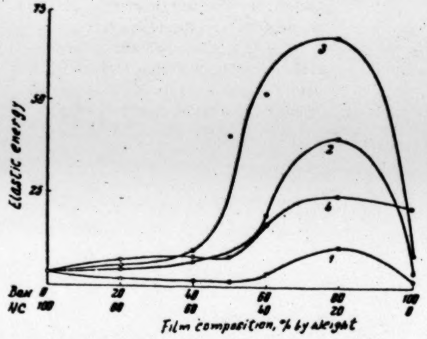

Fig. 8. Relationship between the elastic energy of nitrocellulose films and the content of butadiene–acrylonitrileCopolymers 1, 2, 3, 4 (Curves 1, 2, 3, and 4 respectively).

Fig. 7 leads to the conclusion that the nitrocellulose films obtained in the present investigation have, with a sufficiently high content of polar elastomers, an even higher tensile strength than films of pure nitrocellulose. In addition, the curve for films containing the strongly polarCopolymer 4, shown in the same figure, is noteworthy; it lies below the curve for films containing Copolymer 3, and the inflexion which characterizes the plasticizing action of the high molecular plasticizer is much less prominent. It must be pointed out that a similar effect was found in a study of the plasticizing action of butadiene–acrylonitrile copolymers of different degrees of polarity on polyvinyl chloride [2]. In that case, as here, when the content of polar nitrile groups in the copolymer was excessively increased, there was a tendency for the inflexion to disappear from the curves showing the variation of the tensile strength or the extension at break with elastomer content in the film.

The load–extension diagrams shown in Figs. 2-5 make it possible to calculate the elastic energy of the films, which is an important characteristic, as it represents the work expended on deformation of the material up to destruction.

It follows from Fig. 8, which shows the elastic energy of nitrocellulose films (in arbitrary units) as a function of the contents of various butadiene–acrylonitrile polymers in the films, that the elastic energy for a mixture of nitrocellulose with the incompatible butadiene–acrylonitrile Copolymer 1 is either less than the elastic energy for the pure components or slightly greater, and the elastic energy has a minimum value when the component ratio is 1:1, that is, when the system has maximum heterogeneity.

The elastic energy for nitrocellulose mixtures with the compatibleCopolymers 2, 3, and 4 is, as a rule, higher than the elastic energy for the pure components, and when the films contain 80% of the highly elastic component the values of the elastic energy are particularly high. Evidently, this content of polar butadiene–acrylonitrile copolymers is the optimal from the point of view of the highest strength of the nitrocellulose film. It is also significant that the elastic energy of nitrocellulose films containing the strongly polar Copolymer 4 is less than the elastic energy of nitrocellulose films containing the less polarCopolymer 3.

All the above leads to the conclusion that the compatibility of nitrocellulose with butadiene–acrylonitrile copolymers, and also the plasticizing action of the latter on nitrocellulose, is determined by the ratio of the polarities of the two components. In fact, the non-polar polybutadiene is quite incompatible with the polar nitrocellulose, as shown even by the appearance of the film obtained from a mixture of the two polymers. Very poor, weak films are formed from nitrocellulose in mixtures with the weakly polar Copolymer 1, which contains only 18.4% acrylonitrile groups. Evidently, this content is not sufficient to ensure a uniform distribution of the copolymer in the nitrocellulose, and it collects in microscopic accumulations which are the cause of the optical inhomogeneity of the films. A result of the very poor compatibility of nitrocellulose with Copolymer 1 is the lack of any plasticizing action of this copolymer on nitrocellulose.

Copolymer 2, containing 28.6% acrylonitrile groups, is compatible with nitrocellulose and exerts a plasticizing effect. The films formed are fairly homogeneous and strong. However, to judge by the mechanical properties and external appearance of the films, the best results with nitrocellulose are given by Polymer 3, which contains 37.7% acrylonitrile groups. Evidently, the ratio of the polarities of the two components is the most favorable in this case. The molecules of butadiene–acrylonitrile Copolymer 3 contain enoughpolar groups to ensure its uniform distribution in the nitrocellulose, and at the same time the non-polar regions of its molecules are extensive enough to shield the polar nitro groups and so to produce a strong plasticizing effect.

A further increase of the polar nitrile group content in the butadiene–acrylonitrile copolymer leads, as was seen in the case of Copolymer 4, containing 44.4% acrylonitrile groups, to a decrease of film strength. The plasticizing effect of the highly elastic component also decreases. Both these effects, as was already stated, may be attributed either to increased rigidity of the butadiene–acrylonitrile copolymer with increasing polarity, or to decreased compatibility of the two components owing to increasing difference of their polarities. It seems likely that the polarity of the butadiene–acrylonitrile copolymer with a high content of strongly polar nitrile groups is higher than the polarity of nitrocellulose, and as a result the mutual solubility of the two components is diminished. Only a detailed investigation can show which of the proposed explanations is the more correct.

SUMMARY

1. Load–extension diagrams for nitrocellulose films with various contents of butadiene–acrylonitrile copolymers of different polarities have been examined. It is shown that such diagrams may be used to evaluate the compatibility of high polymers.

2. It is shown that nitrocellulose is not compatible with polybutadiene or with the weakly polar butadiene–acrylonitrile copolymer containing 18.4% acrylonitrile groups. An increase of the acrylonitrile group content to 28.6% results in compatibility of the butadiene–acrylonitrile copolymer with nitrocellulose and produces an appreciable plasticizing effect. Better results with nitrocellulose, however, are given by the butadiene–acrylonitrile copolymer containing 37.7% acrylonitrile groups. An increase of the acrylonitrile group content in the copolymer to 44.4% results in a decrease of film strength and of the plasticizing action of the copolymer on nitrocellulose.

3. It is established that the elastic energy may also be used for evaluation of the compatibility of high polymers and of the plasticizing effect of a highly elastic on a rigid component. It is shown that the highest strength is found in nitrocellulose films containing about 80% of butadiene–acrylonitrile polymer of sufficiently high polarity.

LITERATURE CITED

[1] V.I. Alekseenko, I.U. Mishustin, and S.S. Voyutsky, Proc. Acad. Sci. USSR, 95, 93 (1954); Colloid J., 17, 3 (1955) (T.p. 1)*.

[2] R.A. Reznikova, S.S. Voyutsky, and A.D. Zaionchkovsky, Colloid J., 16, 204 (1954) (T.p. 207)*.

[3] G. Gee, Chemistry of Large Molecules, Vol. 1, Foreign Lit. Press, 137 (1948).

[4] A. Staverman, "Adhesion" (symposium), Foreign Lit. Press, p. 14 (1954).

Received April 19, 1955

Central Scientific Research Institute for
Leather Substitutes - Moscow

---

*T.p. = C.B. Translation pagination.

INVESTIGATION OF THE VISCOSITY OF POLYAMIDE MELTS

T.N. Kokhomskaya and A.B. Pakshver

The formation of a number of synthetic fibers is effected by melt spinning. In such cases the viscosity of the resin melt is the primary factor which determines the parameters of fiber formation.

Flory [1] has studied the viscosity of polymers in the molten state. In investigations of the viscosity of molten polyesters, Flory established a relationship of the following type between the logarithm of the viscosity and the molecular weight:

$$\log\eta = A + cM_W^{1/2}.$$

An analogous relationship applies to polyamides with branched chains [2] and to polyethylene [3]; a linear relationship does not hold for polystyrene [4] or for polyisobutylene [5].

In investigations of the melt viscosity as a function of temperature [1,4-7] it was found that the simple exponential relationship of the type

$$\eta = Ae^{E/RT}$$

is only applicable in a narrow temperature range. For polyisobutylene and for various types of molten glass [8,9], the viscosity–temperature relationship is better described by the equation

$$\eta = Ae^{E/RT^2}.$$

The variation of the viscosity of molten linear polyamides with changes of temperature, molecular weight, and a number of other factors, had not been previously studied. Such an investigation was the purpose of the present work.

Method. The viscosity of polyamide resin melts was determined with the aid of a viscosimeter which employed the principle of the measurement of the rate of fall of a steel ball in a viscous medium. The viscosimeter consists of a cylindrical vessel with an internal channel for holding a test tube with the resin. The lower part of the channel is fitted with sight glasses for observation of the motion of the ball. The heat transfer medium used is a mixture of 26.5% diphenyl and 73.5% diphenyl oxide. The required temperature is attained by electric heating and regulated by the pressure of the vapor of the heat transfer medium in the condenser to an accuracy of ± 0.5°.

The resin sample is held in the apparatus for 30 minutes, in which time the resin melts and the air bubbles are removed. The viscosity of the melt is calculated in absolute units with the aid of the formula

$$\eta = Kt,$$

where η is the viscosity of the melt in poises; t is the time required for the ball to descend between the sight glass marks, in seconds; K is a constant for the instrument. The reproducibility of the viscosity determinations is ± 2%.

The substances studied were polyamide resins based on ϵ-caprolactam and hexamethylene adipamide, and also copolymers of ϵ-caprolactam and hexamethylene adipamide (HA salt) with various component ratios.

In order to eliminate the effect of low molecular substances present in the polycaprolactam resin and in the copolymers of ϵ-caprolactam and HA salt on the viscosity of the melts, these resins were extracted by water or benzene at the boiling point. The resins were dried in a vacuum drier for 24-50 hours at 150-135°. The mole-

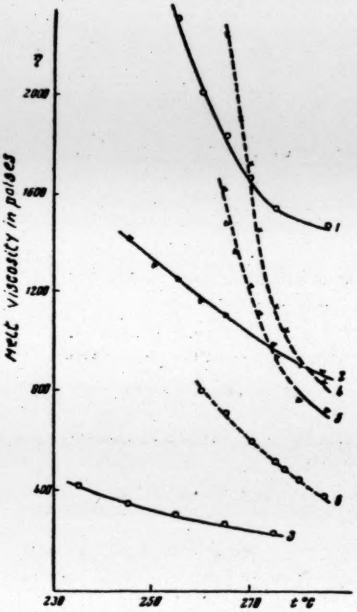

Fig. 1. Variation of melt viscosity with temperature; Capron, mol. weight: 1) 18000; 2) 11500; 3) 2250; Anid, mol. weight: 4) 10500; 5) 9630; 6) 7530.

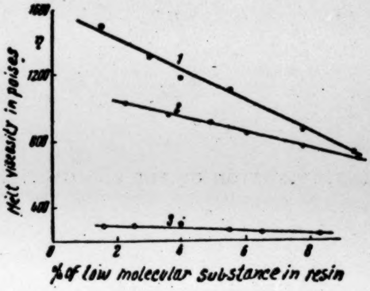

Fig. 2. Variation of the viscosity of Capron resin melts with the content of low molecular weight substances; mol. weight: 1) 18000; 2) 11500; 3) 2250.

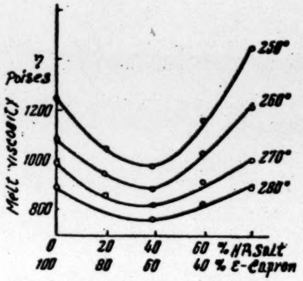

Fig. 3. Variation of the viscosity of melts of the copolymer of caprolactam with HA salt with temperature, for different component ratios.

cular weight of the resins was determined from the equations [10,11]:

$[\eta] = 24 \cdot 10^{-4} M^{0.51}$ for polycaprolactam resin (Capron) in 40% H_2SO_4,

$[\eta] = 11 \cdot 10^{-4} M^{0.72}$ for hexamethylene adipamide (Anid) resin in 85% HCOOH.

EXPERIMENTAL, AND DISCUSSION OF RESULTS

The fiber forming power of polyamide resins is determined both by the thermal extrusion conditions and by the physicochemical properties of the resins. A study was therefore made of the effect of temperature on the viscosity of Capron and Anid resin melts in the range 235-285° (Fig. 1), and of the variation of the melt viscosity as a function of the content of low molecular substances in the resin (Fig. 2). The influence of the chemical structure of the polyamide resins on melt viscosity was studied on copolymers of ε-caprolactam and hexamethylenediamine adipate salt (HA salt) at 245-280°. The results are shown in Fig. 3.

As is known, in the viscous flow of liquids the molecules are displaced from one equilibrium position into another. Since the liquid state is characterized by considerable interaction between the molecules, a definite amount of energy is required for displacement of the molecules in order to overcome intermolecular forces. The

TABLE 1

Activation Energy of Viscous Flow Relative to the Monomer, E_0, as a Function of Molecular Weight

Resin	Capron					Anid		
Molecular weight	18040	11500	8000	4000	2250	10560	9630	7526
E_0, cal./mole	73	71	102	203	361	749	708	549

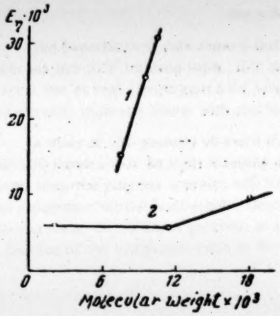

Fig. 4. Variation of the activation energy of viscous flow of polyamide resins with molecular weight: 1) Anid; 2) Capron.

TABLE 2

Variation of the Activation Energy of Viscous Flow with the Ratio of the Components in the Copolymer

Content of HA salt, %	0	20	40	60	80
E_η, cal./mole	6212	4968	4575	6000	10165

. activation energy of viscous flow (E_η) depends on the energy of intermolecular action ΔH and on the change of the macromolecular configuration $T\Delta S$. Therefore E_η may be regarded as a measure of the intermolecular action. It must be pointed out, however, that E_η is not equal to the energy of the intermolecular forces, but is only a certain small fraction of it.

Investigation of the variation of polyamide melt viscosity as a function of the temperature showed that the viscosity of the melt decreases with rise of temperature (Fig. 1). The variation of the melt viscosity with temperature was quantitatively characterized by the equation

$$\eta = Ae^{E/RT}.$$

The experimental data represented as the graph $\log\eta - 1/T$, show that this equation is applicable only in the region of lower molecular weights. Resins of higher molecular weight already begin to show deviations from this equation in the temperature range studied, and the relationship $\log\eta - 1/T$ becomes non-linear. The explanation is that intermolecular action is weakened with increase of the rate of thermal motion of the molecules.

The activation energies for Anid and Capron resins of various molecular weights were calculated. A comparison of the values of E_η for Anid and Capron resins (Fig. 4) shows that E_η is much greater for Anid resins than for Capron resins.

As the number of functional groups per polymer molecule is the same for both resins, the reason for the higher value of E_η is probably that in Capron resin more of the polar amide groups are intramolecularly bound within the same macromolecular chain.

Fig. 5 shows that the nature of the variation of E_η with molecular weight differs for the two resins. While for Anid resin E_η increases continuously with molecular weight, in the case of Capron resin E_η increases only when the molecular weight is > 11500. To determine the cause of this, the values of the activation energy of viscous flow relative to the monomer (E_0) were calculated.

Table 1 shows that the value of E_0 for Capron resin falls rapidly up to a molecular weight of 11500, after which it remains approximately constant. Apparently, as the molecular weight increases, the increased chain flexibility results in a decrease in the number of functional groups on the molecular "surface", and of the interaction energy per monomer unit. Simultaneously, the entropy term $T\Delta S$ increases as the result of increasing flexibility of the macromolecules. These two factors result in a decrease of the value of E_0. After a certain molecular length is reached, the molecular configuration changes little with further increase of the degree of polymerization, and E_0 remains constant.

The value of E_η for Anid resin increases with increasing molecular weight. Evidently in this case the variation of E_η with molecular weight is determined not only by the flexibility of the macromolecules, but also by other factors not yet discovered.

A decrease of polyamide melt viscosity is also found with an increase in the content of substances of low molecular weight in Capron resin. As they have a much lower molecular weight than the polymer, the low molecular compounds act as plasticizers and weaken the resistance to shearing stress.

The variation of viscosity with molecular weight was characterized by the equation

$$\ln\eta = A + cM_W^{1/2}.$$

The experimental data showed that this equation is valid only at lower temperatures: 245-255° for Capron resin and 265-275° for Anid resin. The probable reason for the deviations from this equation at higher temperatures is that at high temperatures the longer molecules become more convoluted than the shorter molecules, and the viscosity increases slower with molecular weight than is shown by the equation.

A study of the viscosity of melts of copolymers of ϵ-caprolactam with hexamethylenediamine adipate salt (HA salt) showed that the melt viscosity varies considerably with the component ratio, and passes through a maximum when the polymer contains 40% HA salt. The reason is that at a 60:40 ratio of ϵ-caprolactam to HA salt the copolymer has the least regular structure, and consequently the intermolecular action is at a minimum and the molecular flexibility is greatest, as is confirmed by the data in Table 2, in which the value of E_η is shown as a function of the component ratio in the copolymer.

SUMMARY

1. The effect of temperature on the viscosity of polyamide resin melts has been studied in the range 235-285°; it was shown that the viscosity of polyamide melts decreases with increase of temperature owing to decreased interaction between the molecules.

2. In the lower molecular weight region the viscosity of melts as a function of the temperature obeys the equation $\eta = Ae^{E/RT}$, where E is the activation energy of viscous flow, which is a measure of changes in the intermolecular action and macromolecular configuration.

3. The viscosity of Capron resin melts decreases with increased content of low molecular weight substances in the resin, and increases with increasing molecular weight, as the total molecular bond energy increases.

4. The variation of melt viscosity with molecular weight, at moisture contents up to 0.1% and temperatures of 245-255° for Capron resin and 265-275° for Anid resin, obeys the equation

$$\ln\eta = A + cM_W^{1/2}.$$

5. For equal molecular weights, the value of E_η for Anid resin is higher than E_η for Capron resin; probably in Capron resin the majority of the polar amide bonds occurs simultaneously within the same chain.

6. The melt viscosity decreases on the introduction into the polymer chain of monomer units different in size from the main monomer unit.

LITERATURE CITED

[1] P. Flory, J. Am. Chem. Soc., 62, 1057 (1940); 62, 3113 (1940).

[2] J.R. Schaefgen and P. Flory, J. Am. Chem. Soc., 70, 2709 (1948).

[3] G. Dienes and H. Klemm, J. Appl. Phys., 17, 458 (1946).

[4] T. Fox and P. Flory, J. Phys. Colloid Chem., 55, 221 (1951).

[5] T. Fox and P. Flory, J. Am. Chem. Soc., 70, 238 (1948).

[6] K. Ueberreiter and H. Orthmann, Koll.-Z., 126, 2/3, 140 (1952).

[7] E. Pieski and A. Zettlemoyer, Ind. Eng. Chem., 45, 167 (1953).

[8] M.M. Skornyakov, A.Ya. Kuznetsov, and K.S. Evstropyev, J. Phys. Chem., 15, 116 (1941).

[9] B.A. Pospelov and K.S. Evstropyev, J. Phys. Chem., 15, 125 (1941).

[10] A. Matthes, J. prakt. Chem., 162, 245 (1943).

[11] G. Taylor, J. Am. Chem. Soc., 69, 635 (1947).

Received March 29, 1955

All-Union Scientific Research Institute for
Artificial Fibers - Mytishchi

INVESTIGATION OF THE COLLOIDAL PROPERTIES OF SOLUTIONS OF SOME SULFONIC DETERGENTS

R.V. Kucher and M.A. Kovbuz

As was stated in our previous papers [1], studies of the size and form of the micelles of soaps and detergents is not only of theoretical but also of practical interest. However, at the present time there is still no finalized theory which would explain fully the diversity of properties of detergents in aqueous solutions. There is no doubt that an explanation of the properties of soaps and detergents must be primarily based on their molecular structure.

Micelle formation in aqueous solutions of soaps is determined, as was shown by Debye [2], primarily by the ratio between the gain in free energy resulting from the removal of the hydrocarbon "tails" of the molecules from water and their union, and the free energy required for approach of the charged ends of the molecules. This is in agreement with the thermodynamic consideration that the gain of free energy which results from the association of molecules into micelles may be calculated from the critical concentration of micelle formation by means of the relationship:

$$w_m = 3kT \ln c_0, \qquad (1)$$

where w_m is the gain of free energy on the association of two molecules; c_0 is the critical concentration of micelle formation (CMC). Thus, the critical concentration may serve as the principal measure of the tendency of a given colloidal electrolyte to micelle formation. Another such characteristic is the micellar weight, which may be determined by the light scattering method. In addition, as was shown by Klevens [3] the micelle size determines in most cases the solubilization of oleophilic substances in aqueous solutions of detergents. This was confirmed by us for certain sulfonic detergents [4].

The present paper describes an investigation of the micellar properties (CMC, micellar weight, micellar dissymmetry factor, solubilization) of some other sulfonic detergents, characterized by structural peculiarities of the hydrophobic portions of their molecules.

EXPERIMENTAL

The substances studied were the dioctyl and dihexyl esters of the sodium salts of sulfosuccinic acid (Aerosols OT and MA). These detergents are characterized by the fact that their hydrophilic group is situated between two hydrophobic portions of the molecule, separating the latter from each other. In addition, the colloidal properties of aqueous solutions of disulfodinaphthylmethylene (Leukanol) were studied. This colloidal electrolyte has two polar groups (sulfo groups) separated in the molecule by an oleophilic group, dinaphthylmethylene. Both Aerosols were chemically pure*. Leukanol – the technical product – was purified from inorganic salts by repeated salting-out by alcohol from aqueous solutions to a constant ash content.

Critical concentration. The critical micelle concentration and the micellar weight were determined by a light scattering method, as described previously [4]. The value of CMC was also determined by measurement of the solubilization of the dye Sudan III in very dilute solutions of the detergents. It was shown in preliminary experiments that electrical conductivity measurements give rather high values of CMC.

In view of the fact that the Aerosols gave faintly turbid solutions in water, which must probably be attrib-

---

*These detergents were kindly supplied by Z.N. Markina.

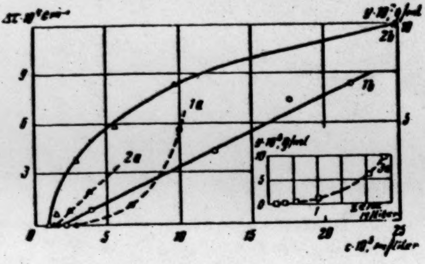

Fig. 1. Solubilization of Sudan III (a) and turbidity (b) in extremely dilute solutions; 1) Leukanol; 2) Aeroiol OT; 3) Aerosol MA.

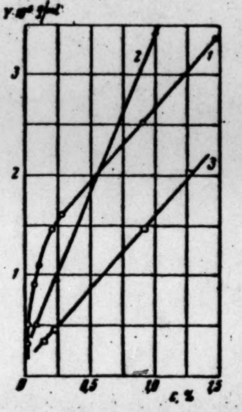

Fig. 2. Solubilization of Sudan III in aqueous solutions of: 1) Leukanol; 2) Aerosol OT; 3) Aerosol MA.

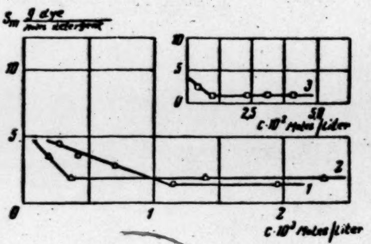

Fig. 3. Molar solubilization of Sudan III in aqueous solutions of: 1) Leukanol; 2) Aerosol OT; 3) Aerosol MA.

uted to partial hydrolysis of the salts, light scattering measurements in these solutions had to be made in the presence of 0.1 g-equivalent of sodium carbonate per liter. This amount of soda suppressed hydrolysis completely and the turbidity of the solutions did not decrease on further addition of electrolyte.

Measurements of the light scattering and the solubilization of Sudan III gave concordant results for the CMC, which are shown in Fig. 1 and Table 1.

A comparison of the values of CMC for the two Aerosols shows that as the hydrophobic part of the molecules increases, in transition to the higher homolog, CMC decreases, which is in agreement with the results of a number of workers [2,3].

Table 1 shows the values of the gain of energy in the removal of the hydrophobic parts of the molecules from water and their association in micelle formation (w_m/kT) calculated from the values of CMC with the aid of Equation (1). This value is essentially the energy of intermolecular action, or the association energy of the hydrophobic parts of the molecules; therefore it may be calculated from the latent heats of evaporation of the corresponding hydrocarbons forming the hydrophobic parts of the detergent molecules. These values are given in the last column of Table 1. The values of the latent heat of evaporation, λ, were taken from tables [5]; in the calculation of w_m/kT for the Aerosols the latent heats of evaporation of octane (9800 cal./mole) and hexane (7100 cal./mole) were used, while for Leukanol the latent heat of evaporation was taken as double the value for naphthalene (9570 cal./mole) plus 1200 cal. This last figure represents the increment of λ for one methylene group in a homologous series of hydrocarbons [2].

The results show that the values for the energy of intermolecular action calculated from the CMC and from the latent heats of evaporation are in agreement. This confirms the validity of the thermodynamical approach to an explanation of micelle formation in soaps and detergents considered as associated colloids.

TABLE 1

Critical Concentration and Energy Gain in Micelle Formation of the Sulfonic Detergents Studied

Colloidal electrolyte	CMC, moles//liter (light scattering)	CMC, moles//liter (solubilization)	$\frac{w_m}{kT}$ from CMC	$\frac{w_m}{kT}$ from λ
Leukanol	$2.05 \cdot 10^{-5}$	$2.67 \cdot 10^{-5}$	32.3	32.7
Aerosol OT + 0.1 N Na_2CO_3 solution	$9.23 \cdot 10^{-6}$	$9.23 \cdot 10^{-6}$	34.7	33.9
Aerosol MA + 0.1 N Na_2CO_3 solution	—	$1.29 \cdot 10^{-3}$	20.0	23.6

TABLE 2

Micellar Weight and Polydispersity of the Micelles of the Sulfonic Soaps Studied

Colloidal electrolyte	0.1 N solution of electrolyte added	Micellar weight M	Degree of micellization	$N - N_0$
Leukanol	—	31800	68.0	2.90
Leukanol	Na_2SO_4	33500	71.8	2.99
Aerosol OT	Na_2CO_3	83400	188.0	4.56
Aerosol MA	Na_2CO_3	10000	25.8	2.56

TABLE 3

Dissymmetry Factors of Sulfonic Detergents

Colloidal electrolyte	Density in g/cc	$D \cdot 10^6$ cm^2//sec.	$\frac{f}{f_0}$
Leukanol	1.445	1.000	1.015
Aerosol OT	1.174	0.747	0.936
Aerosol MA	1.136	1.246	1.121

We must point out, however, that a similar comparison for the previously investigated colloidal electrolyte Nekal (sodium dibutylnaphthalene sulfonate) [1] shows a greater divergence (w_m/kT from the CMC is 24.4; from λ, 32.4) which, as was already stated, must be attributed to the relatively large size of the hydrophobic part of the molecule in comparison with the hydrophilic (sulfo) group. This leads to the conclusion that in addition to the purely thermodynamical approach to an explanation of the tendency of soaps and detergents to micelle formation it is also necessary to consider the structural features of their molecules (size and position of the hydrophobic groups, etc.).

Micellar weight and micelle polydispersity. The micellar weights were determined by light scattering by means of the technique described earlier, with the aid of the equation

$$H \frac{c}{\Delta \tau} = \frac{1}{M} + 2Bc, \qquad (2)$$

where M is the micellar weight; $\underline{c}$ is the concentration of the solution in grams per ml; H is a constant which depends on the refractivities of the solution and the solvent; B is a constant which takes into account deviations from the ideal solution laws.

The micellar weights of the detergents studied are shown in Table 2.

The values of the degree of micellization, or the number of single molecules in the micelle, shown in Table 2, were calculated by division of the micellar weights by the molecular weights of the ordinary molecules. The values of M and of the degrees of micellization are in full agreement with the data in Table 1; a higher micellar weight corresponds to a lower value of CMC.

The values of the polydispersity ($N - N_0$) shown in Table 2 indicate the possible deviations of the degree of micellization from the average value. The polydispersity was calculated with the aid of the equation derived by Debye [2] on purely thermodynamic considerations:

$$N - N_0 = \sqrt{4N_0 \frac{kT}{w_m}}, \qquad (3)$$

where N_0 is the average degree of micellization.

The results of the polydispersity calculations indicate the possibility of only relatively small deviations from the average degrees of micellization. Similar results were also obtained for Nekal ($N - N_0 = 3.09$), sodium dibutylbenzene sulfonate ($N - N_0 = 3.09$) and sodium eicosylbenzene sulfonate (Sulfanole $N - N_0 = 4.77$). These results somewhat contradict McBain's view on the considerable polydispersity of soap micelles in solution [6]; in his view, aqueous solutions contain, in addition to large micelles, very small clusters of soap molecules. However, our results are in good agreement with Debye's data for dodecylamine chloride [2], and also with the results of others who studied the polydispersity of soaps in solutions, for example by the diffusion method [7]. We therefore conclude that sulfonic soaps form relatively monodispese micellar aggregates in aqueous solution.

Characterization of the micelle form. The form or shape of soap micelles in aqueous solutions still presents a controversial problem. Laminar [8], spherical [9], cylindrical, and spheroidal micellar models have been proposed. Certain information on this subject with reference to alkyl derivatives of sulfonated benzene and naphthalene is contained in our preceding paper [10]. It was shown that, in the absence of long aliphatic radicals in the molecules, the micellar shape of these detergents is very close to spherical*.

The micelle form was characterized by the dissymmetry factor – a value directly related to the ratio of the half-axes of the particles in solution. The dissymmetry factor f/f_0 was calculated from the equation:

$$\frac{f}{f_0} = \sqrt[3]{\frac{k'}{MD^3 v}}. \qquad (4)$$

where k' is a constant for a given solvent (for water it is $2.43 \cdot 10^{-14}$); M is the molecular (or micellar) weight of the particles; D is the diffusion coefficient of the dissolved substance; v is its specific volume.

The diffusion coefficient was determined refractometrically, by photographing the scale in the presence of 0.1 N electrolyte solution (sodium sulfate for Leukanol, and sodium carbonate for the Aerosols). It was found that from concentrations a little above the CMC up to several percent the value of D was independent of the concentration. The average value of the diffusion coefficient in this range of concentrations was substituted into the formula. The specific volume in the dry state was calculated from the density, which was determined by the pycnometer method. The values found for the dissymmetry factor are shown in Table 3.

The data in Table 3 show that in all three cases the values of f/f_0 are close to unity in the concentration region from the CMC to several (about three) percent. This indicates that the sulfonic detergents studied have spherical or spheroidal (but nearly spherical) micelles. In any event, it is difficult to accept the existence of considerably elongated or laminar micelles at low detergent concentrations.

Solubilization. As was shown previously [4] the solubilization of oleophilic substances is mainly determined by the detergent micelle size in solution. In this paper we present additional data on the solubilization of Sudan III in aqueous solutions of Leukanol and of Aerosols OT and MA.

As previously, the solubilization of Sudan III was determined photometrically. Fig. 2 shows the results obtained for the variation of the solubility of Sudan III (in grams per 100 ml of solution) as a function of the concentration, in solutions of the detergents studied. The data in this figure and in Table 2 show that variations of micellar weight of the detergents are symbatic with the values for the solubilization of Sudan III. This provides qualitative confirmation of the view that the solubilization of oleophilic substances is related to the micellar weight. Fig. 3 shows the so-called "molar solubilization" of Sudan III, in grams of the dye per mole of the colloidal electrolyte, as a function of concentration. This value is constant and independent of the concentration over a considerable concentration range, especially for Aerosols OT and MA, but also for Leukanol. This indicates that the micelle size remains constant in this concentration region, which is in agreement with the results of diffusion determinations discussed earlier.

SUMMARY

1. The light scattering and solubilization methods were used to determine the critical micelle concentra-

---

*An incorrect value of 4.72 is given in the paper cited for the dissymmetry factor of sodium eicosylbenzene sulfonate (Sulfanole). In fact this value is only 1.67.

tions of the dihexyl and dioctyl esters of sulfosuccinic acid, and of disulfodinaphthylmethylene. Values for the association energy calculated from CMC data are in agreement with data on the latent heats of evaporation, which confirms the validity of the thermodynamical approach to the explanation of micelle formation in aqueous solutions of detergents.

2. Calculation of the polydispersity of these detergents from the experimentally determined degrees of micellization shows that the polydispersity of the micelles is not great, at least at low concentration.

3. At low concentrations, solutions of the sulfonic detergents studied contain micelles close to spherical in shape, as is confirmed by calculation of the dissymmetry factors obtained from diffusion measurements.

4. The results of investigations of solubilization in presence of Leukanol and Aerosols MA and OT are in agreement with data on micellar weights.

In conclusion, the authors consider it their duty to express their gratitude to Professor A.I. Yurzhenko for his guidance in the work.

LITERATURE CITED

[1] A. Yurzhenko and R. Kucher, Proc. Acad. Sci. USSR, 85, 1337 (1952); Colloid J., 14, 219 (1952) (T.p. 243)*.

[2] P. Debye, J. Phys. Coll. Chem., 53, 1 (1949); Ann. N.Y., Acad. Sci., 51, 575 (1949).

[3] H. Klevens, Chem. Rev., 47, 1 (1950).

[4] A. Yurzhenko and R. Kucher, Colloid J., 14, 283 (1952) (T.p. 311)*; 13, 226 (1951).

[5] Lanndolt – Bornstein Tabellen, 3C, 2671; 2B, 1492.

[6] J. McBain, Frontiers in Chem., Vol. 8, N.Y. (1950).

[7] R.Vetter, J. Phys. Colloid Chem., 51, 262 (1947).

[8] J. McBain, Advances in Colloid Sci., 1, 99, (1942).

[9] G. Hartley, J. Chem. Soc., 1968 (1938).

[10] R. Kucher and A. Yurzhenko, Colloid J., 15,442 (1953) (T.p. 459)*.

Received May 10, 1955

The Ivan Franko State University, Lvov
Chair of Physical and Colloid Chemistry

---

*T.p. = C.B. Translation pagination.

HYSTERESIS EFFECTS IN POLYMER SOLUTIONS

S.I. Meerson and E.G. Grimm

A number of investigators have demonstrated the applicability of the phase rule to polymer solutions [1]. Such work was based on studies of the equilibrium in the two-phase system: swollen polymer – polymer solution in a liquid with limited solvent power for the polymer, at relatively low temperatures; or equilibrium in two-phase three component systems: swollen polymer – polymer solution in a mixture of two liquids, one of which has unlimited solvent power for the polymer, while the other only causes limited swelling.

It has been convincingly shown for a number of substances, such as cellulose derivatives, polyvinyl chloride [2], polystyrene, gelatin [3], agar, and others, that this type of equilibrium is a true equilibrium, independent of the method of preparation of the two-phase system (residue–solution). For example, repeated heating and cooling of the system cellulose acetate – methyl alcohol in sealed ampoules resulted in reversible solution of the polymer with the formation of a solution of definite concentration at a given temperature [4]. In some cases a state of equilibrium is not reached for a long time. This leads to the appearance of obligatorily formed polymer solutions which are not, strictly speaking, thermodynamically equilibrium stable solutions, although they exist for very long periods. Such systems are in a state of pseudo-equilibrium. In some cases such supersaturated solutions tend to be stabilized by low-molecular impurities and in consequence become thermodynamically stable.

In the present paper we examine some interesting cases of disturbed equilibrium in one-phase and two-phase systems of three components; polymer, solvent, and non-solvent. We studied polymer solutions obtained by direct dissolution of the polymer in binary mixtures of solvent and non-solvent of definite composition, and also solutions obtained by subsequent addition of the non-solvent to a solution of the polymer in the same solvent. The investigations showed that the method of preparation has a significant influence on the properties of the solution. A detailed description of the relationships found in a study of this problem is given below.

EXPERIMENTAL, AND DISCUSSION OF RESULTS

The materials investigated were polar and non-polar polymers, such as diacetylcellulose, dinitrocellulose, Saniv (a copolymer of acrylonitrile and vinylidene chloride), rubber, and polystyrene. As indicated above, the solutions were prepared by two methods: 1) by solution of the polymer in a mixture of solvent and non-solvent of definite composition, and 2) solution of the polymer in the solvent followed by addition of the non-solvent to form a solution of the same composition as that obtained by the first method.

TABLE 1

Variation of the Viscosity of 20% Diacetylcellulose Solution with the Solution Composition and Method of Preparation

Composition of mixture, %		Ball fall, sec.		
acetone	water	in acetone	first method	second method
100	0	128	–	–
90	10	–	67.5	62.7
80	20	–	114.0	86.0

The effect of the method of preparation on the viscosity, turbidity, heat of coagulation, and osmotic pressure of the solution was studied, and also the effect of the method of dissolving the polymer on its solubility. The viscosity of the solutions was measured in an Ostwald viscosimeter for volatile liquids; before the determinations the solutions were kept in a thermostat. The osmotic pressure was determined with the aid of the osmometer described previously by one of the present authors [5]; the turbidity was determined by means of a photocolorimeter. Acetone was used as the solvent for dinitrocellulose, diacetylcellulose, and Saniv, and

TABLE 2

Variation of the Viscosity of 4% Polystyrene Solutions in Dioxane–Acetone and Benzene–Acetone Mixtures with Composition of the Mixture and Method of Preparation

Composition of mixture, %		η_{rel} 20° C			Composition of mixture, %		η_{rel} 20° C		
dioxane	acetone	in acetone	first method	second method	benzene	acetone	in acetone	first method	second method
100	0	20.9	–	–	100	0	30.1	–	–
40	60	–	10.6	10.9	40	60	–	11.0	10.9
35	65	–	10.7	10.4	35	65	–	12.8	12.4
30	70	–	9.2	8.7	30	70	–	10.6	10.9
25	75	–	Insoluble		25	75	–	Insoluble	

TABLE 3

Effect of Temperature on Viscosity Hysteresis

Polymer and solution concentration	Composition of mixture, %		η_{rel}, first method			η_{rel}, second method		
	acetone	benzene	20°C	40°C	τ %	20°C	40°C	τ %
Saniv, 2% solution	90	10	57.7	45.0	60.2	54.6	42.6	60.0
	80	20	66.5	54.0	60.2	51.0	39.4	60.1
	75	25	75.3	57.6	88.5	55.8	43.7	60.5
	70	30	86.4	(63)	(117)	61.2	(49)	(60)
Dinitrocellulose, 1.5% solution	40	60	33.8*	8.7**	74	17.5*	8.6**	26

*At 16°. **At 50°.

TABLE 4

Effect of Temperature on Reversibility of the Viscosity of 3% Acetylcellulose Solution

Composition of mixture %		η_{rel}, first method			η_{rel}, second method			$\frac{\eta_2}{\eta_1}$ 20°	$\frac{\eta_2}{\eta_1}$ 40°	$\frac{\eta_2}{\eta_1}$ 20° cooling
acetone	water	20°	40°	20° cooling	20°	40°	20° cooling			
80	20	62.5	38.2	65.5	92.4	50.7	96.5	1.48	1.32	1.47

TABLE 5

Effect of Aging on the Viscosity of 2% Saniv Solution; Solution Composition: Acetone 80%, Benzene 20%

Method of preparation	η_{rel} of freshly prepared solutions			η_{rel} after aging 6 months			η_1/η_2 20° for freshly prepared solutions	η_1/η_2 20° after aging
	20°	40°	τ%	20°	40°	τ%		
1	66.5	54.0	60.0	55.0	39.5	80.0	1.31	1.23
2	51.0	39.4	58.0	45.3	30.8	70.2		

water and benzene were used as the non-solvents. Benzene was the solvent, and acetone the non-solvent, for polystyrene and rubber. In addition, the properties of polystyrene solutions in dioxane–acetone mixtures was studied.

TABLE 6

Variation of the Heat of Coagulation of Solutions According to the Method of Preparation

First method					Second method				
m	a	b	Q_1	Q	m	a	b	Q_1	Q
1.1704	1.1310	0.0394	29.1	−42.3	1.1398	1.1014	0.0384	23.0	−223
1.0958	0.9587	0.0371	29.0	−40.1	1.0944	1.0581	0.0363	22.0	−256
0.8966	0.8664	0.0302	23.2	−39.4	1.0118	0.9771	0.0341	22.4	−241
		Average		−40.6			Average		−240

TABLE 7

Solubility Hysteresis of Diacetylcellulose in Acetone−Water Mixture

Composition of mixture, %		Solubility, % of the polymer taken	
acetone	water	first method	second method
80	20	100	100
75	25	95	100
70	30	83.5	100
65	35	43.0	50.7
60	40	16.0	27.5
50	50	5.5	6.7

TABLE 8

Solubility Hysteresis of Saniv in Acetone−Benzene Mixture

Composition of mixture, %		Solubility, % of the polymer taken	
acetone	benzene	first method	second method
90	10	100	100
75	25	100	100
70	30	95	100
60	40	86	100
55	45	57	gel
50	50	36	40
40	60	7	9

Effect of the method of preparation on the properties of the solutions. The effect of the composition of the binary mixture solvent−non-solvent on the viscosity of solutions obtained by the two methods was first studied. The results showed that the solution viscosity depends on the method of preparation. For solutions of polar polymers, in which benzene was the non-solvent, the viscosity of the solutions obtained by the first method was greater than the viscosity of the solutions obtained by the second method, or $\eta_1 > \eta_2$.

The reverse was found with additions of a polar non-solvent (water). In this case $\eta_1 < \eta_2$. The results are shown in Fig. 1, where it is seen that as the benzene content in Saniv and diacetylcellulose solutions increases, the viscosity of the solutions increases also. In addition, an increase of the benzene content in the solution increases the difference between the viscosities of solutions of the same concentration and composition, but prepared by different methods; a viscosity hysteresis effect appears and increases. Similar behavior is shown by dinitrocellulose solutions. Fig. 1 shows that additions of water have a different effect from additions of benzene on the solution viscosity, as increase of the water content in the solutions decreases the viscosity. However, in this case also the viscosity hysteresis increases with an increase of the amount of non-solvent in the solution. It must be noted here that although water exerts a different influence from benzene in the region of low solution concentrations, in the higher concentration region it acts in the same way as benzene, as η_2 again becomes less than η_1. The $\eta = f(c_2)$ curves for solutions of diacetylcellulose in acetone−water mixture prepared by the different methods intersect approximately in the region of 4-5% solutions (Fig. 2). In an investigation of the viscosity of 20% solutions of diacetylcellulose in this mixture by the Stokes method it was found that the viscosity first decreases and then begins to increase with increasing water content in the solution. These changes are accompanied by increasing hysteresis, with $\eta_1 > \eta_2$. The results are shown in Table 1. In an investigation of the effect of the method of solution preparation on the viscosity of non-polar polymer solutions no viscosity hysteresis was found. The viscosity of rubber solutions in benzene−methyl alcohol mixture, and of polystyrene in dioxane−acetone and benzene−acetone mixtures, decreases with increase of the content of non-solvent in the solution but, as Table 2 shows, the method of preparation does not affect the solution properties. Probably in this case in solutions of non-polar polymers another mechanism is operative for the formation of a new phase at the critical point from that found in solutions of polar polymers, as the latter show clearly defined hysteresis.

In order to determine the nature of the observed viscosity anomalies in solutions of polar polymers, a study

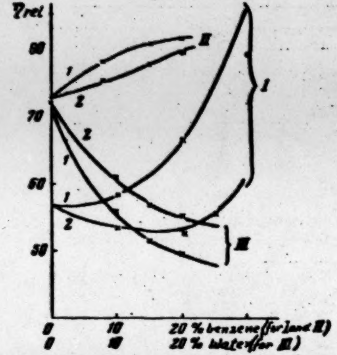

Fig. 1. The relationship η_{rel} = f(composition) for 4% solutions of: I) Saniv, and II) diacetylcellulose in acetone–benzene mixture; III) ditto, for 4% solution of diacetylcellulose in acetone–water mixture; 1 and 2) methods of preparation.

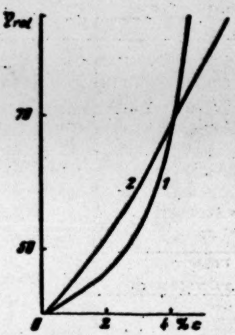

Fig. 2. The relationship η_{rel} = f(c) for solutions of diacetylcellulose in acetone–water mixture; 1 and 2) methods of preparation.

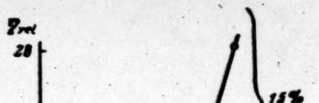

Fig. 3. The relationship η_{rel} = f(composition) for dinitrocellulose solutions of different concentrations in acetone–benzene mixture; 1 and 2) methods of preparation.

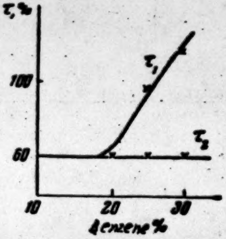

Fig. 4 The relationship τ = f(composition) for Saniv solutions in acetone–benzene mixture; τ_1 and τ_2 are the temperature coefficients of viscosity for solutions obtained by the 1st and 2nd methods.

was made of the effects of solution concentration, temperature, aging time, and nature of the fractions on the viscosity hysteresis of the systems in question. It was found that the hysteresis increases with increasing concentration in all cases. The results are shown in Fig. 3, where it is seen that in the concentration region up to about 1% practically no hysteresis occurs; further rise of concentration increases hysteresis considerably. Therefore, hysteresis may increase both with increase of solution viscosity by the action of a nonpolar addition (acetone–benzene), and with decrease of viscosity by the action of a polar addition (acetone–water). The viscosity changes may be due to changes in the shape and flexibility of the macromolecules, and also to different states of macromolecular aggregation and different structures of the aggregates formed. The viscosity increase in itself may also be the reason why the state of equilibrium in the system, involving redistribution of bonds between the components of the system and the macromolecules, is established very slowly, as the relaxation time for such systems is large.

It appeared of interest in this connection to study the influence of temperature and aging time of the solutions on the hysteresis effects. Rise of temperature should result in destruction of the aggregates, and hence in decrease of hysteresis. A study was made of the effect of temperature on the viscosity hysteresis of 2% Saniv solution in acetone–benzene mixture, and 1.5% solution of dinitrocellulose in the same mixture. The results are shown in Tables 3 and 4.

It is seen from Table 3 that all the solutions studied have a high temperature coefficient of viscosity τ. The values of τ are the same for solutions obtained by the first and second methods, containing small amounts of non-solvent; further increase of the non-solvent content in the solution favors increase of τ. Here $\tau_1 > \tau_2$ (Fig. 4). Thus, increase of hysteresis is proportional to increase of τ, which indicates increasing aggregation in the solutions. As the temperature increases, in some solutions, in which there is clearly defined aggregation, hysteresis practically vanishes (for example, in the system dinitrocellulose–acetone–benzene), and the system attains equilibrium; in other solutions the hysteresis alters little (for example, in the system Saniv–acetone–benzene). Solutions of diacetylcellulose in acetone–water mixture showed decreasing hysteresis with rising temperature, but hysteresis reappeared on subsequent cooling of the solutions.

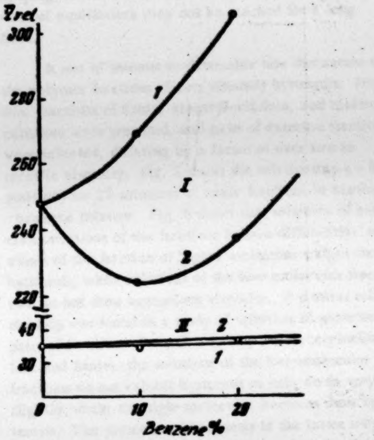

Fig. 5. The relationship $\eta = f(c)$ for 2% solutions of Saniv fractions in acetone–benzene mixture; I) high-molecular fraction; II) low-molecular fraction; 1 and 2) methods of preparation.

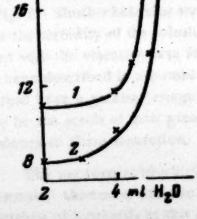

Fig. 6. Variation of the turbidity of Saniv solutions with the amount of non-solvent added to the solution; 1 and 2) methods of preparation.

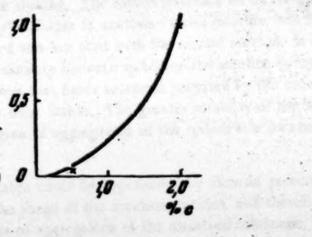

Fig. 7. The relationship $\Delta P = f(c)$ for Saniv solutions in acetone–benzene mixture.

Saniv solutions were kept in sealed ampoules for 6 months, and their viscosity was then measured. Table 5 shows that after prolonged storage the solution viscosity and the viscosity hysteresis decreased slightly, while τ of the solutions increased. Here $\tau_1 > \tau_2$, indicating that Saniv solutions preparedby the first method have a

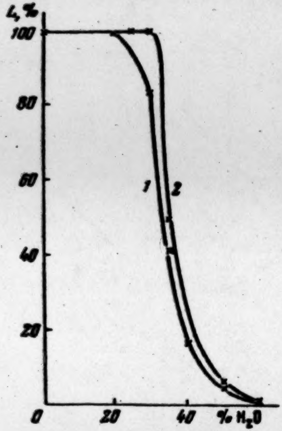

Fig. 8. Variation of the solubility of diacetylcellulose with the composition of acetone–water mixture and the method of dissolving the polymer.

greater tendency to aggregation or lower stability on keeping. In addition, these results indicate that a state of equilibrium may not be reached for a long time.

It was of interest to determine how the nature of the polymer fractions affects viscosity hysteresis. For this, fractions of Saniv, diacetylcellulose, and dinitrocellulose were prepared, and pairs of extreme fractions were selected, differing by a factor of over two in specific viscosity. Fig. 5 shows the relationship η = f(composition) for 2% solutions of Saniv fractions in acetone–benzene mixture. Fig. 5 shows that solutions of equal concentrations of the fractions behave differently: solutions of the fraction of higher molecular weight show hysteresis, while solutions of the low-molecular fraction do not show anomalous viscosity. A similar relationship was found in a study of solutions of extreme pairs of fractions of equal viscosity for diacetylcellulose and Saniv; the solutions of the low-molecular fractions do not exhibit hysteresis or only do so very slightly, while the high-molecular fractions show hysteresis. The presence of hysteresis in the latter may be due both to the greater chain length and to the greater tendency of the macromolecules to aggregation.

The lack of reversibility of the properties of polymer solutions, or the existence of hysteresis, suggests that one of the two solutions studied is less stable. It was decided to determine the "coagulation thresholds" of the solutions prepared by the different methods with the use of the same non-solvent as coagulant as was used in the solution. The changes of solution turbidity produced by additions of increasing amounts of non-solvent to the solution up to complete precipitation of the polymer were studied. The results obtained for Saniv are shown in Fig. 6. Similar behavior was found for solutions of diacetylcellulose in acetone–water mixture, but in this case the turbidity of the solutions prepared by the first method was less than with the second method, in agreement with the viscosity data for these solutions. Such a relationship between turbidity and solution composition has been described in a number of papers [6]. Fig. 6 also shows that Saniv solutions prepared by the second method have a greater "coagulation threshold", and are thus more stable. The greater turbidity of the solutions may be the result of their greater aggregation, while the degree of aggregation of the system is a measure of its tendency to phase separation.

The question as to which of the systems is the more stable could be approached by osmotic pressure measurements. Moreover, osmotic pressure does not depend on the shape of the macromolecules, and therefore the existence of hysteresis in this case indicates different degrees of aggregation of the dissolved substance. The osmotic pressure of Saniv solutions in acetone–benzene mixture was measured, for different methods of preparation of the solution and for different concentrations, with the same composition of the mixture, corresponding to maximum viscosity hysteresis. The results of preliminary experiments, shown in Fig. 7, indicate that the osmotic pressure difference is not large: no hysteresis is found in 0.5 and 1.0% solutions, but in 2% solution the osmotic pressure hysteresis is greater than the experimental error limits. It is seen from Fig. 7 that as the solution concentration increases, the value of $\Delta P = P_2 - P_1$ (where P_1 and P_2 are the osmotic pressures of solutions prepared by the first and second methods) also increases, so that Saniv solutions with lower viscosity, lower turbidity, and a higher "coagulation threshold" have greater osmotic pressure. This corresponds to a greater decrease of free energy in the system, $\Delta F_2 > \Delta F_1$, so that a polymer solution in the binary mixture acetone–benzene prepared by the second method is more stable than a solution prepared by the first method.

To determine whether the macromolecules are in fact aggregated to different extents in solutions prepared by the different methods, the heats of coagulation of 3.3% solutions of diacetylcellulose solutions in a mixture of 80% acetone with 20% water were measured. Water was used as the coagulant. The measurements were made with the aid of an isothermal calorimeter, described previously [7]. The heat of coagulation was calculated by the formula:

$$Q\frac{\text{cal.}}{\text{g polymer}} = \frac{Q_1 m - Q_2 a}{b},$$

where Q_1 is the heat of interaction of the solution with water, per 1 g of solution; m is the weight of solution in grams; Q_2 is the heat of interaction of the pure solvent–non-solvent mixture with water, per 1 g of mixture, equal to 31.6 cal./g; a is the amount of mixture in grams, in m grams of solution; b is the number of grams of polymer in m grams of solution.

Table 6 shows that diacetylcellulose solutions prepared by the first method, which have lower viscosity and lower turbidity, also have a lower absolute value of the heat of coagulation, which is a sign of a lower degree of aggregation of the macromolecules in solution.

Hysteresis of solubility of polymers. By an increase of the content of non-solvent in polymer solutions it is possible to obtain systems exhibiting not only microhysteresis, manifested by a change of properties and hence by a disturbance of equilibrium in a one-phase system, but also macrohysteresis, when systems obtained by the second method consist of supersaturated solutions, while the first method yields a two-phase system (swollen polymer – solution). In other words, it may be said that the addition of non-solvent to a polymer solution does not result in separation of the system into two phases, and at the same time polymers do not dissolve in solvent–non-solvent mixtures of the same composition. This is shown diagrammatically in Fig. 8. Such two systems may in certain cases exist a very long time without appreciably approaching each other, as has been observed by us in the case of Saniv polymer over the course of a year; in other cases one of the systems passes spontaneously into an equilibrium state after one or two weeks, as was observed by us for solutions of diacetylcellulose in a mixture of 75% acetone and 25% benzene, prepared by the second method. For studies of solubility hysteresis, the polymers were placed in ampoules, to which was added either the appropriate mixture of solvent and non-solvent, or at first the solvent only, and then, after the polymer was completely dissolved, the appropriate amount of non-solvent (second method). The ampoules were sealed, and the concentration of the solution over the residue was determined only after prolonged shaking. The solubility hysteresis of Saniv, diacetylcellulose, and rubber was studied. Solubility hysteresis was not found in the case of rubber. Tables 7 and 8 show that in all cases the solutions prepared by the first method have lower concentrations than the solutions prepared by the second method. Change of temperature affects the solubility hysteresis of these polymers in different ways. When the system Saniv–acetone–benzene, containing 40% benzene, is heated, the concentration of solutions prepared by the first and second methods does not change after the solutions are cooled, so that solubility hysteresis persists. However, when the system diacetylcellulose–acetone–water containing 30% water is heated and then cooled, the solubility hysteresis disappears because of the solubility of the precipitate in the system prepared by the first method. Thus, the above investigations showed that the method used for dissolving the polymers affects their solubility.

It is clear from all this that all the factors which favor aggregation of the dissolved substance, such as: increase of solution concentration, increase of the content of non-solvent in the solutions, increase of the molecular weight of the polymer fractions, and decrease of temperature, favor the development of hysteresis effects which are due to changes in the conditions of preparation of the polymer solutions.

SUMMARY

1. The influence of the method of preparation of polymer solutions in binary mixtures of liquids one of which is a non-solvent on the reversibility of the solution properties has been studied.

2. It is shown that the method of preparation of solutions of polar polymers affects the properties of the systems formed; the latter have different viscosities, turbidities, osmotic pressures, and heats of coagulation.

3. The influence of solution concentration, composition of the solvent – non-solvent mixture, temperature, nature of the polymer fractions, and aging time of the solutions, on hysteresis effects has been studied; it is shown that all the factors which favor increased aggregation in solutions lead to appearance of hysteresis.

4. It is shown that the method of preparation of the polymer solutions affects the solubility of the polymers, and polar polymers show solubility hysteresis.

In conclusion, the authors express their gratitude to Member of the Academy of Sciences, Belorussian SSR, S.M. Lipatov, and to Prof. Z.A. Rogovin for their constant interest in the work and for valuable guidance in discussion of the results obtained.

LITERATURE CITED

[1] A.A. Tager, Solutions of High Molecular Compounds, State Chem. Press (1951).

[2] Z.A. Rogovin and L.A. Tsaplina, Colloid J., 7, 171 (1941).

[3] S.M. Lipatov, Problems of the Science of Lyophilic Colloids, Acad. Sci. Belorussian SSR Press, Minsk (1941).

[4] V.A. Kargin, Z.A. Rogovin, and S. Papkov, J. Phys. Chem., 10, 607 (1937).

[5] S.I. Meerson and S.M. Lipatov, Colloid J., 13, 301 (1951).

[6] V.E. Gul and G.S. Klitenik, Colloid J., 16, 171 (1954) (T.p. 179)*.

[7] S.M. Lipatov and S.I. Meerson, Colloid J., 8, 143 (1946).

Received May 30, 1955

The Moscow Textile Institute

---

*T.p. = C.B. Translation pagination.

INVESTIGATION OF THE STRUCTURE OF SYNTHETIC POLYAMIDE FIBERS

7. DIFFERENTIAL HEAT OF SOLUTION OF CAPRON FIBERS IN FORMIC ACID*

N.V. Mikhailov and E.Z. Fainberg

Earlier [1] we determined the differential heats of wetting of Capron fiber by water, when the existence of two constant values of the differential heat of sorption were found, and the view was therefore put forward that at least two types of intermolecular hydrogen bonds exist in polycaprolactam. This view was subsequently confirmed by infrared absorption spectroscopy [2]. Therefore, for a final solution of the question of the intermolecular bonds, it was necessary to study the differential heats of solution of Capron fibers of different degrees of orientation, over a wide range of sorption of the solvent.

Among the literature existing on this subject we must note the paper by Kargin and Papkov [3] on the heats of sorption of acetone and pyridine by cellulose, in which it is shown that a thermal effect occurs during the solution process only in the formation of a monomolecular layer; further absorption of the solvent occurs without a thermal effect, by change of the entropy term. The same conclusion was reached by Lipatov, Preobrazhenskaya, and Putilova [4] after measurements of the differential heat of solution of cellulose acetate in methyl acetate and of gelatin in water. Lipatov and Meerson [5] found, in a study of the influence of temperature on the integral thermal effect of solution of certain polymers, that over a fairly wide temperature range the value of the heat effect is constant. The value of the thermal effect ceases to be constant when the increase of temperature is sufficient for deformation of the bonds, and the heat effect decreases sharply, becoming negative in some cases (for example, when polyvinyl chloride is dissolved in nitrobenzene and dichloroethane).

In our method of measurement of the differential heats of solution of Capron fibers in formic acid, the material was conditioned to a given formic acid content, and the small heats of solution of polycaprolactam containing a definite amount of formic acid were determined.

TABLE 1

Accuracy of Weight Increase Determinations in Separate Experiments

Material	Weight increase in parallel experiments, %		Average weight increase, %	Deviation from average
	1	2		
Oriented fibers	2.59	2.71	2.65	± 0.06
Nonoriented fibers	2.88	2.66	2.77	± 0.11

Conditioning method. The problem of the choice of the method of conditioning was solved in different ways by various workers, according to the purpose of the work. For example, Kargin and Papkov [3] determined the amount of absorbed substance from the change in the refractive index of a mixture consisting of an inert liquid and a solvent. Tager [6] used a simple gravimetric method – small amounts of benzene were absorbed by polystyrene in a desiccator, while large amounts were poured direct into an ampoule containing polystyrene, and weighed by the usual method.

---

*Z.N. Zaspinok participated in the experimental work.

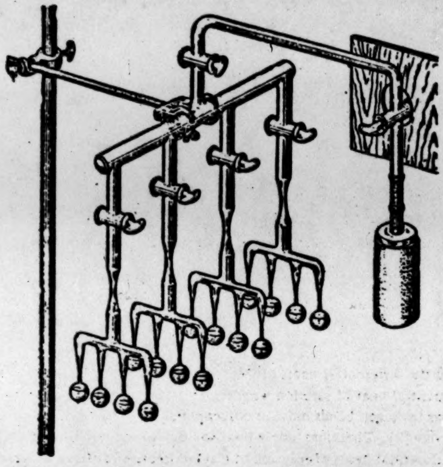

Fig. 1. Conditioning apparatus (description in text).

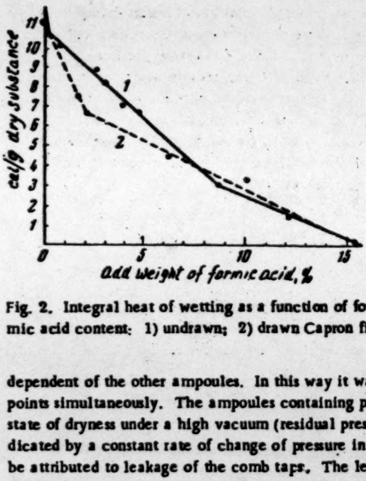

Fig. 2. Integral heat of wetting as a function of formic acid content: 1) undrawn; 2) drawn Capron fiber.

Despite the obvious simplicity of these conditioning methods, we could not use them, as the reproducibility of individual experiments was inadequate for our purpose. We therefore selected the vacuum method of conditioning, which we used in determinations of the differential heat of wetting of Capron fibers by water [1], and which proved free of these defects in the present investigation also.

The vacuum conditioning procedure was as follows. A "comb" with four branches, each closed with a tap, was sealed to a vacuum source. To each branch of the large comb a smaller comb was sealed, also with four branches, to each of which was sealed an ampoule with a weighed sample, so that 16 ampoules were conditioned simultaneously. Each set of four ampoules on one small comb could be shut off by a tap and was independent of the other ampoules. In this way it was possible to prepare for the determination of four sorption points simultaneously. The ampoules containing polycaprolactam were sealed to the combs and brought to a state of dryness under a high vacuum (residual pressure 1.10^{-6} mm Hg). The end of the drying process was indicated by a constant rate of change of pressure in the working part of the system, which in this case could only be attributed to leakage of the comb taps. The leakage of each comb was tested separately. At the end of the drying process the vacuum installation was disconnected from the working part of the system, and formic acid vapor was introduced into the system. The introduction of the formic acid vapor was carried out in the same way as the introduction of water vapor in measurements of the differential heats of wetting of Capron fibers by water [1].

The time taken in adding the formic acid vapor was measured by a seconds clock; it varied from a fraction of a second to 1000 seconds according to the specimen and the required amount of formic acid. After introduction of the formic acid vapor into the ampoules the combs were sealed off and stored for several days (from three to ten days, according to the amount of vapor added). After conditioning of the ampoules, the combs were sealed off. Two ampoules were used for determination of the percentage increase in weight, and two for the calorimetric experiment. The added formic acid in the ampoules was determined gravimetrically. As the increase in weight was small, between 0.0005 and 0.0400 g, it was necessary to introduce a correction for the weight of air in the ampoule. With an accuracy of weighing of ±0.0001 g, and determination of the ampoule volume to an accuracy of ±0.2 cm^3, the error in determining the percentage weight increase of a sample weighing 0.25-0.30 g should be ±0.2%. Special experiments were carried out to check the reproducibility of the determinations of percentage weight increase, and the results did not exceed the above-mentioned error limits (Table 1).

The gravimetric method for the determination of the moisture removed from the fiber was compared with the sorption method. Very good agreement was found between the results obtained by these methods: gravimetric method gave 2.09%, sorption method, 2.03%.

The accuracy of the determination of the weight increase was checked against the results of calorimetric determinations which, for two close sorption points for nonoriented fiber, namely 2.6 and 2.96%, gave values for the heat of solution of 8.63 and 8.01 cal./g respectively.

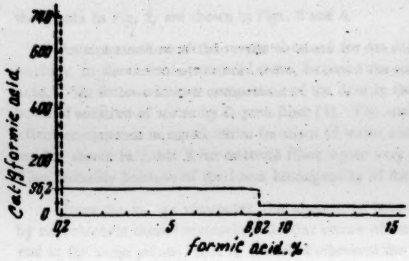

Fig. 3. Differential heat of solution of undrawn Capron fiber in formic acid.

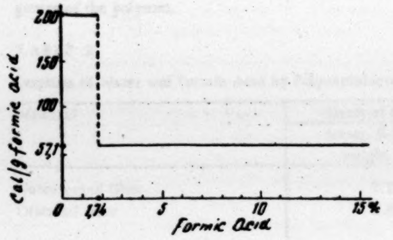

Fig. 4. Differential heat of solution of drawn Capron fiber in formic acid.

The method of measurement of the differential heat of solution of polycaprolactam with a given formic acid content is analogous to that used for determining the integral heat of solution [2].

Materials investigated. The materials investigated were nonoriented and oriented Capron fibers of "limiting age". The specimens were extracted with carbon tetrachloride to remove lubricant and washed with water at 50° to remove monomer. The specimens were then conditioned as described above.

Formic acid was used as the solvent. The purity and concentration of the formic acid were the same as in the experiments on the determination of the integral heat of solution [7].

It was found by special refractometric experiments that the condensed formic acid vapor in the ampoules consisted of 100% formic acid. The experimentally determined refractive index n_D^{20} 1.371 corresponds to anhydrous formic acid. It was not necessary to introduce a correction for the heat of dilution of anhydrous formic acid to a concentration of 95.01%, as measurements showed that this correction does not exceed the experimental error.

RESULTS AND DISCUSSION

The results for nonoriented and oriented Capron fibers are shown in Fig. 2. The curves in Fig. 2 are plotted with allowance for the experimental error both in conditioning and in the calorimetric determinations. The error limits were: in conditioning ±0.2% of the weight increase, in calorimetric determinations ± 0.1 cal.

Within the limits of experimental error, the curves for nonoriented fibers are represented by three linear regions, and for oriented fibers, by two linear regions. The values of the differential heats of solution of nonoriented and oriented Capron fibers in formic acid, calculated from the tangents of the angles of inclination of the graphs in Fig. 2, are shown in Figs. 3 and 4.

An examination of the results obtained for the differential heats of solution of Capron fibers leads to an analogy, in the thermodynamical sense, between the sorption of water and solution of the polyamide in formic acid. This follows from a comparison of the data in the present paper with corresponding data on the differential heats of sorption of water by Capron fiber [1]. The analogy primarily lies in the fact that in both cases zero heat effect corresponds to equal molar fractions of water and of formic acid per mole of polycaprolactam. These results, shown in Table 2 for oriented fiber, agree very closely and differ only slightly in the case of nonoriented fiber probably because of the lower homogeneity of the specimens in the undrawn state.

From the energy viewpoint, this agreement between the data for the sorption of water and of formic acid by caprolactam should represent a similar course of the solvation processes of the active groups in the polyamide, and at the same points; that is, it should represent the rupture of the same types of hydrogen bonds which determine the structure of this polymer in the solid state before it passes into solution. Our values for the differential heats of solution fully confirm this view. As in the case of the heats of sorption of water, the solution of Capron fibers in formic acid involves at least two constant values of differential heat effects, which should also correspond to the cleavage of two types of hydrogen bonds in polycaprolactam in the solvation of the corresponding active groups of the polymer.

TABLE 2

Sorption of Water and Formic Acid by Polycaprolactam

Material	Heats of sorption		Heats of solution	
	water, % by weight	molar ratio	formic acid content, % by wt.	molar ratio
Nonoriented fiber	7.10	0.443	15.30	0.375
Oriented fiber	6.04	0.375	15.24	0.375

Thus, in our view, the analogy in the mechanism of sorption of water and formic acid by polycaprolactam finally confirms the concept that at least two types of hydrogen bonds, differing in their energies, exist in polycaprolactam and determine the structure of Capron fibers. This does not exclude the possibility of the existence of other more stable forms of hydrogen bonds in polycaprolactam, which were detected by one of the present authors by means of infrared absorption spectra, as their detection by the calorimetric method, as Fig. 2 shows, involves the measurement of negative thermal effects. Equally one cannot ignore the possibility of the existence of a small amount of free —CONH— active groups in polycaprolactam; solvation of these groups by the solvent should correspond to large differential heats of solution, which could not be reliably determined in the present instance owing to the low accuracy of weight increment determination in the initial sorption region.

As is seen from Fig. 4, the bond energy values differ by a factor of nearly 3, and redistribution during the cold drawing process can lead to considerable changes in the properties of Capron fibers. From the fact that in the transition from undrawn (nonoriented) to drawn (oriented) fibers the number of bonds corresponding to a high value of the differential heat of solution decreases nearly by 5 times (from 8.82% to 1.74% of sorbed formic acid), it follows that these bonds disappear during the drawing process and pass into other, more stable bonds.

According to an earlier hypothesis [1], confirmed by the work of one of the present authors with the aid of infrared absorption spectra [2], these weak bonds, easily destroyed during the cold drawing of Capron fibers, are intramolecular hydrogen bonds. In this connection it must be stressed once again that in the cold drawing process intramolecular rings formed by such bonds are opened, and the bonds enter the more stable intermolecular bonds, which determine the crystalline structure of polycaprolactam.

The fact that these intramolecular bonds are present in large amounts in undrawn fibers, but also remain in quite appreciable amounts in drawn fibers not only does not contradict existing data on the crystalline structure of these fibers, but confirms the view put forward by V.A. Kargin that their crystalline phase can only be constructed by the selection of the most thermodynamically advantageous bond types.

These conclusions are in good agreement with the fact that the second values of the differential heats of solution for nonoriented and oriented fibers are relatively close together, and should represent the energy of destruction of the crystalline phase in these fibers. The difference between the heat effects must probably be attributed to the fact that it represents the aggregate for two types of intermolecular bonds between −CONH− groups which, as has been shown [2], exist in the cis and trans configurations.

A rather unexpectedly large difference was found between the differential heats for nonoriented and oriented fibers pertaining to the first type of intramolecular hydrogen bonds. It is seen from Figs. 3 and 4 that the differential heat for oriented fibers is double the corresponding value for nonoriented fibers. But it is because as a result of cold drawing this type of bond in the fiber has become less stable, it becomes possible to explain this difference by deformation of the intramolecular bonds remaining in the fiber after reorientation of the crystalline regions during the drawing process, which caused strain in these intramolecular bonds which had not yet been ruptured.

Since, in the above discussion, the possibility was postulated that one type of bond can pass into another during cold drawing of Capron fibers, it appeared of interest to compare the total heats of solvation by formic acid for nonoriented and oriented fibers, given by the area under the curve for the integral heat of solution as a function of the amount of formic acid taken up by the polycaprolactam.

Calculation shows that these total heats of solvation are practically equal, and have the values of 51900 calories for nonoriented fibers, with the omission of the initial sorption region from 0 to 0.2, and 51600 calories for oriented fibers, per mole of formic acid. The corresponding values for the sorption of water by these fibers were also equal at 10800 calories per mole of water.

This agreement does indeed seem to confirm our assumption of the redistribution of bonds in Capron fibers during drawing, and at the same time indicates that from the energy aspect the structure of oriented fibers does not differ significantly from the structure of nonoriented fibers.

This leads to the conclusion that during cold drawing of Capron fibers no change in the phase state of polycaprolactam takes place, as has been already indicated previously in a number of papers [9]. Therefore the physical and mechanical properties of Capron fibers before and after cold drawing are determined not by the phase state, but only by a change in the ratio between the different types of hydrogen bonds. Regulation of this bond ratio by variations of the conditions in the extrusion and drawing of the fibers is a means of modification of the physical and mechanical properties.

SUMMARY

1. A method has been developed for conditioning of polycaprolactam in formic acid vapor, by means of which the amounts of the absorbed formic acid can be determined with a high degree of accuracy, the absorbed substance is uniformly distributed among parallel specimens, and good reproducibility is obtained in calorimetric experiments.

2. The differential heats of solution of nonoriented and oriented Capron fibers in formic acid have been determined; analogously to the differential heats of sorption of water, two constant values were obtained.

3. An explanation is put forward for the difference between the differential heats of sorption and solution for Capron fibers, on the basis of the existence of at least two types of bonds in polycaprolactam, one of which consists of intramolecular hydrogen bonds which become intermolecular during cold drawing.

4. It is shown that equal molar ratios of sorbed water and formic acid per mole of caprolactam correspond to zero heats of wetting and solution of nonoriented and oriented Capron fibers.

5. It is suggested that the physical and mechanical properties of Capron fibers are determined not by their phase state but by the nature of the different types of hydrogen bonds and their ratio in the fiber structure variation of which makes it possible to regulate these properties over a wide range.

LITERATURE CITED

[1] N.V. Mikhailov and E.Z. Fainberg, Colloid J., 16, No.2, 120 (1954) (T.p. 129)*.

[2] D.N. Shigorin, N.V. Mikhailov, and S.P. Makaryeva, Proc. Acad. Sci. USSR, 94, No.4, 17 (1954).

[3] V.A. Kargin and S.A. Papkov, J. Phys. Chem., 9, 631 (1937).

[4] S.M. Lipatov and Preobrazhenskaya, J. Gen. Chem., 4, 59 (1934); S.M. Lipatov and I.N. Putilova, J. Gen. Chem., 4, 73 (1934).

[5] S.M. Lipatov and S.I. Meerson, Proc. Acad. Sci. USSR, 48, 434 (1945); Colloid J., 12, 427 (1950).

[6] A.A. Tager and Zh.S. Dombek, Colloid J., 15, 69 (1953) (T.p. 75)*.

[7] N.V. Mikhailov and E.Z. Fainberg, Colloid J., 18, 44 (1956) (T.p. [illegible])*.

[8] S.M. Skuratov, N.V. Mikhailov, and E.Z. Fainberg, Colloid J., 16, No. 1, 58 (1954) (T.p. 65)*.

[9] V.A. Kargin and T.I. Sogolova, J. Phys. Chem., No. 8 (1953); V.A. Kargin and G.S. Markova, J. Phys. Chem., No. 8 (1953).

Received December 17, 1954

All-Union Scientific Research Institute
for Artificial Fibers

---

* T.p. = C.B. Translation pagination

EXPERIMENTAL INVESTIGATIONS OF LAMINAR SYSTEMS

22. COAGULATION OF COLLOIDAL PARTICLES AT THE LIQUID–GAS INTERPHASE

S.G. Mokrushin and K.G. Potaskuev

One of the authors has shown [1] that addition of a small amount of gelatin favors the migration of colloidal particles to the liquid–gas interphase. Colloidal particles are particularly conveniently transferred to the interphase by means of a current of air blown through the colloidal solution. In order that the area of the liquid–gas interphase should be increased, air was blown through a porous glass partition. The dispersed air consisted of a large number of highly dispersed bubbles, on the surfaces of which the colloidal particles were adsorbed. The aim of the investigation was to determine the kinetics of capture of the colloidal particles by the air bubbles and also the significance of the amount of gelatin added. It was believed that the addition of gelatin (in small amounts) results in the formation of a sensitized colloid. The formation of sensitized particles, consisting of the original colloidal particles and adsorbed particles of gelatin, results in their surface activity, so that they pass spontaneously to the interphase, and are then coagulated there. As the coagulation occurs in the surface layer, it was termed "laminar coagulation", a term introduced by Ermolenko and Plenina in one of their papers [2]. The substances studied were hydrosols of the following metallic sulfides: copper, lead, mercury, silver, cadmium, and bismuth; and also iron and aluminum hydroxides.

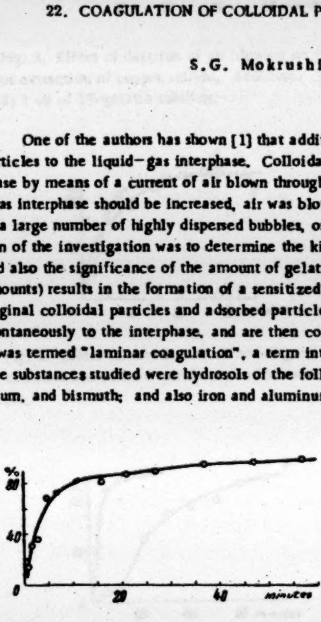

Fig. 1. Effect of duration of air blowing on the degree of extraction of cadmium sulfide.

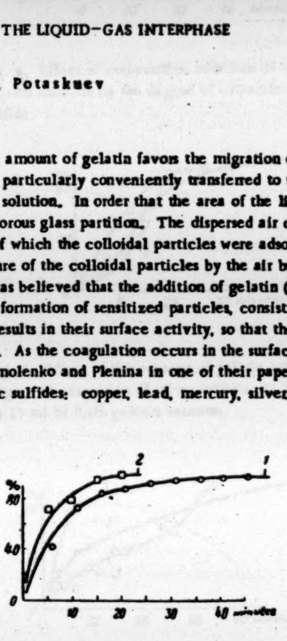

Fig. 2. Effect of duration of air blowing on the degree of extraction of antimony sulfide. Additions: 1) 0.5 ml; 2) 1 ml of 1% gelatin solution.

The method used was as follows: from 0.5 to 10 ml of one per cent gelatin solution was added to 50 ml of the colloidal solution. The colloidal solution containing gelatin was placed in a vertical tube with a porous bottom, through which air was blown at a pressure of 443 mm Hg. The blowing produced a mass of air bubbles which coalesced in ascending the tube to form large bubbles or even disk-like films ("pistons") separated from each other. Thus, a so-called "dry foam" was formed, which contained the coagulated colloidal particles on its surface. In their ascent, these "pistons" reached the upper end of the tube, where they blew out and broke into pieces. In some of the experiments a stirrer was fitted above the tube to break up the foam, and the coagulation products were collected in a funnel fixed coaxially at the top of the tube. The degree of extraction of the colloid was determined colorimetrically (nephelometrically) by means of the Dubosq colorimeter.

The present paper contains experimental data on the percentage extraction of colloid as a function of the air blowing time, the amount of gelatin added, and the addition conditions (in one stage or stepwise). Fig. 1

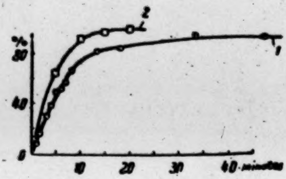

Fig. 3. Effect of duration of air blowing on the degree of extraction of copper sulfide. Additions: 1) 0.5 ml, 2) 1 ml of 1% gelatin solution.

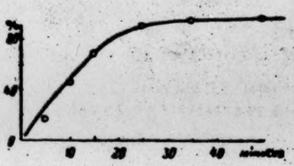

Fig. 4. Effect of consecutive additions of 0.5 ml of 1% gelatin solution on the degree of extraction of copper sulfide.

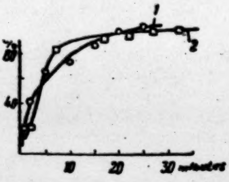

Fig. 5. Effect of duration of air blowing on the degree of extraction of lead sulfide (1) and bismuth sulfide (2).

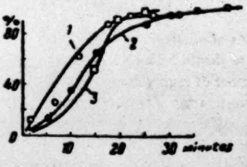

Fig. 6. Effect of the amount of gelatin added on the degree of extraction of silver sulfide: 1) 1 ml, 2) 5 ml, 3) 10 ml of 0.5% gelatin solution.

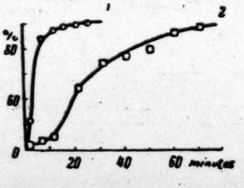

Fig. 7. Effect of the amount of gelatin added on the degree of extraction of mercury sulfide: 1) 1 ml, 2) 10 ml of 1% gelatin solution.

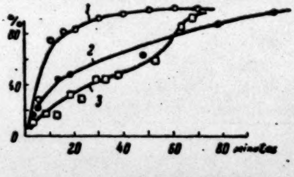

Fig. 8. Effect of the amount of gelatin added on the degree of extraction of iron hydroxide: 1) 1 ml, 2) 3 ml, 3) 5 ml of 1% gelatin solution.

shows the effect of the air blowing time on the degree of extraction of colloidal cadmium sulfide from 50 ml of cadmium sulfide sol to which 0.5 ml of 1% gelatin solution had been added. The air was blown at a pressure of 443 mm Hg.

Fig. 1 shows that 80% of the sulfide is extracted in 10 minutes, while after 1 hour the extraction is complete. Fig. 2 shows the effect of air blowing time and the amount of 1% gelatin solution added on the degree of extraction of colloidal particles of antimony sulfide. Fig. 3 shows the analogous relationships for copper sulfide.

It is seen from Figs. 2 and 3 that the addition of 1 ml of gelatin instead of 0.5 ml accelerated sulfide extraction; the sulfides were completely extracted from the sols after 20 minutes of blowing. In this case the copious foam was broken up by a rubber stirrer at the top of the tube. In order to determine the effect of consecutive additions of gelatin, experiments were carried out in which 1% gelatin solution was gradually added in 0.5 ml portions every 5 minutes, and at the end of the experiment at 10 and 15 minute intervals. A total of 3.5 ml gelatin solution was added; but, as Fig. 4 shows, stepwise addition of gelatin solution does not accelerate but rather retards the extraction of sulfides, as can be seen by a comparison of Figs. 3 and 4. As the result of these experiments it was assumed that the addition (at the beginning of the experiment) of 1 ml of 1% gelatin solution is the optimum for extraction of copper sulfide and antimony sulfide.

Fig. 5 shows data on the extraction of lead and bismuth sulfides, and it is seen that after 25-30 minutes of air blowing complete extraction of the sulfides occurs with additions of 1 ml and 0.5 ml of 1% gelatin solution to the sulfide sols. Fig. 6 shows the effect of excess additions of 0.5% gelatin solution on the extraction of silver sulfide. In these experiments copious formation of gelatin foam occurred, which trapped a considerable amount of solution without specific isolation of sulfide. Only after 20-25 minutes of air blowing, when most of the gelatin had been removed from the solution with the foam, did the foam begin to be enriched with sulfide. It must also be noted that the copious highly disperse foam was almost undestroyed by the stirrer, and therefore much of the solution was removed with the foam.

Fig. 7 shows the same relationship for mercury sulfide, and it is clearly seen that the addition of 10 ml of gelatin solution instead of 1 ml retards the foam extraction of sulfide.

It follows from all the experiments on the influence of the amount of gelatin added on the degree of sulfide extraction that excess of gelatin is detrimental to the extraction process; the foam is enriched by gelatin only, and sulfide is taken up only after most of the gelatin is removed from the solution with the foam.

Similar experiments were performed with iron hydroxide and aluminum hydroxide. The results of the iron hydroxide experiments are shown in Fig. 8, from which it is seen that excess gelatin prevents the passage of the colloidal hydroxide into the foam. In these experiments also copious highly disperse foam is formed first, and extraction of the colloid begins only after the excess gelatin has been removed with the foam.

SUMMARY

1. When air is blown through a colloidal solution with the formation of a gaseous emulsion and foam, the air bubbles entrain the colloidal particles and remove them from the solution.

2. Complete extraction of the colloidal particles from colloidal solutions can be effected by addition of 1% gelatin solution.

3. Excess of added gelatin retards the rate and decreases the degree of extraction of the disperse phase.

4. Optimum extraction of colloid particles in our experiments occurred with the addition of 1 ml of 1% gelatin solution to 50 ml of the colloidal solution.

In conclusion, we acknowledge the participation of student N.N. Samoilova in the experimental work.

LITERATURE CITED

[1] S.G. Makrushin, Report on the Scientific Works of Members of the D.I. Mendeleev All-Union Chemical Society, 2, 26 (1953).

[2] N.F. Ermolenko and G.N. Plenina, Colloid J., 5, 193 (1939).

Received June 16, 1954

The S. M. Kirov Polytechnic Institute, Urals
Sverdlovsk

INFLUENCE OF CATIONS AND THE pH OF SILICIC ACID HYDROGELS ON THE STRUCTURE OF DRY SILICA GELS

I.E. Neimark and I.B. Slinyakova

One of the decisive factors which determines the structure of hydrophilic adsorbents is the degree of hydrophily of the system resulting in different degrees of aggregation of the gel particles into clusters and chains. The degree of aggregation may vary greatly according to the conditions of washing the gel, cation exchange, etc.

Numerous investigators [1] have observed that the pore volume of silica gels is increased if the hydrogels are washed with alkalies, acids, and other electrolytes. In a study of the influence of the nature of the wash liquid on the structure of silica gels, one of the present authors and Sheinfain [2] showed that washing the hydrogels with acidified tap water (pH 3.5) or distilled water (pH 6.5) results in the formation of silica gels of finer porosity than the use of tap water (pH 7.8).

The aim of the present work was a study of the influence of the pH of the washing liquid, over a wide range of pH, on the structure of silica gels prepared from acid and neutral sols.

Preparation of silica gels. Solutions of water glass and sulfuric acid were used for the preparation of silicic acid sols. The required medium for the sol was obtained by variation of the concentrations and proportions of the components. After the solutions had been mixed, the pH of the sol was measured by means of the antimony electrode. After the sol had been coagulated to a gel and aged, it was broken up into lumps, divided into portions, and washed with water of various pH values; the washing liquids were prepared from distilled water. An acid medium up to pH < 7 was produced by additions of various amounts of sulfuric acid to distilled water, and an alkaline medium from pH > 7 up to pH 10.6, by additions of ammoniacal water.

For determinations of the pH of the hydrogels, the antimony electrode was immersed in the sol before conversion of the latter into a gel, and after gelation the electrode was embedded in the lump. The electrode remained in the hydrogel throughout the washing. The washing was considered finished when the pH of the washing liquid and the pH of the hydrogel became equal. The washed hydrogel was dried in a drying oven at 120°.

5 series of silica gel samples were prepared from acid and neutral sols; the pH values of the sols were 1.5, 2.5, 4.0, 5.0, and 7.0 respectively. The hydrogel samples from each series were washed with water having pH from 1.7 to 10.6.

Method of study of the silica gel structure. The following measurements were carried out on the silica gels:

1. Sorption isotherms for methyl alcohol vapor were obtained by means of a vacuum apparatus and a quartz spring balance. The isotherms were used to calculate the specific surface, adsorptional volume, effective pore radius, and the transitional pore volume.

2. The apparent densities were determined and used to calculate the total pore volumes.

3. The static activity in saturated benzene vapor was studied. The method used was described previously [3].

RESULTS AND DISCUSSION

Table 1 shows the adsorptional and structural characteristics of gels obtained from acid and neutral sols, and washed with liquids of different pH values.

TABLE 1

Sorptional and Structural Characteristics of Gels Prepared from Acid and Neutral Sols in Relation to the Hydrogel pH

Series	Samples	pH of original sol	pH of hydrogel after washing	Apparent density δ in g/cc	Total pore volume $V_ε$ in cc/g	Volume of benzene absorbed from saturated vapor, cc/g	$\frac{V_a{}^*}{V_ε}$	Specific surface S in m^2/g
I	1	1.6	2.1	1.37	0.27	0.31	1.0	550
	2	1.6	2.8	1.38	0.28	0.28	—	—
	3	1.6	5.0	1.21	0.37	0.35	0.95	640
	4	1.6	6.0	1.15	0.42	0.43	0.93	585
	5	1.6	6.3	1.10	0.46	0.46	0.78	628
	6	1.6	9.4	0.79	0.81	0.78	—	—
	7	1.6	10	0.78	0.83	0.80	0.19	380
II	8	2.5	1.8	1.33	0.30	0.29	0.87	580
	9	2.5	2.9	1.33	0.30	0.31	—	—
	10	2.5	3.5	1.33	0.30	0.29	—	—
	11	2.5	5.5	1.16	0.42	0,44	0,78	638
	12	2.5	7.2	1.00	0.55	0.54	0,49	698
	13	2.5	7.6	0.87	0.70	0.68	0,37	520
	14	2.5	9.0	0.79	0.82	—	—	—
	15	2.5	9.6	0.81	0.79	0.79	0,24	435
III	16	4.0	3.7	1.30	0.32	0.32	1,00	725
	17	4.0	6.8	1.08	0.47	0.48	0,81	680
	18	4.0	7.3	0.99	0.56	0.57	0,74	695
	19	4.0	9.8	0.78	0.83	0.84	0,25	478
IV	20	5.0	2.2	1.34	0.29	0.30	1.00	585
	21	5.0	2,8	1.28	0.33	0.33	—	—
	22	5.0	6,8	1.04	0.51	0.50	0.72	680
	23	5.0	7,7	0.94	0.61	0.59	0.61	710
	24	5.0	9,0	0.83	0.75	0.75	—	—
	25	5.0	10,0	0.81	0.78	0.79	0.18	376
V	26	7.0	2.7	1.03	0.52	0.52	0.85	550,
	27	7.0	6.3	0.90	0.66	0.70	0.29	405
	28	7.0	9.8	0.80	0.79	0.79	0.29	450

$^*v_a$ is the adsorptional volume.

It follows from the data in Table 1 that when hydrogels prepared from acid sols are washed with water with pH in the range from 1.7 to 4.5-5, the structure of the silica gels formed is practically the same (Specimens 1,2,8,9,10,16,20,21). As the pH of the washing waters changes from 4.5-5.5 to 8.0-9.0, the structure of the silica gels changes, with an increase in the number of the larger pores; the total pore volume increases from 0.30 to 0.80 cm^3/g. When the pH of the washing waters varies from 8.0-9.0 to 10.6, coarsely porous silica gels with equal total pore volumes are formed.

Fig. 1 shows isotherms for the sorption of methyl alcohol vapor on silica gels of Series I and IV, and Fig. 2 shows curves for pore volume distribution by effective pore radius for silica gels of the same series. The analogous sorption isotherms and pore volume distribution curves obtained for silica gels of Series II and III are not reproduced in this paper.

An examination of the sorption isotherms for the silica gel samples shows that, irrespective of the sol pH (up to pH 5) the use of washing waters with pH from 2.1 to 4.5 leads to formation of finely porous silica gels. The sorption and desorption branches of the isotherms for these silica gels coincide, and there is no hysteresis

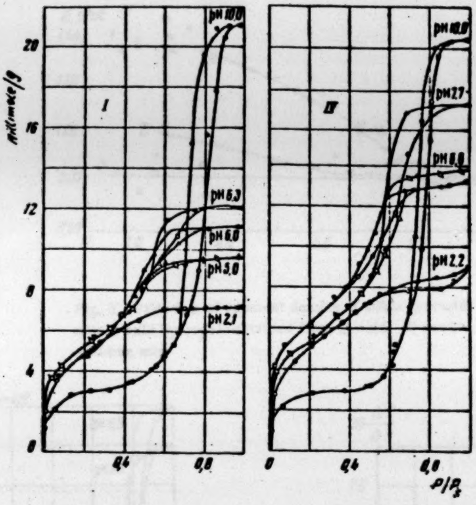

Fig. 1. Isotherms for the sorption of methyl alcohol vapor on samples of silica gel prepared from an acid sol of pH 1.6(Series I) and pH 5 (Series IV) and washed with liquids of various pH values. Black dots represent desorption.

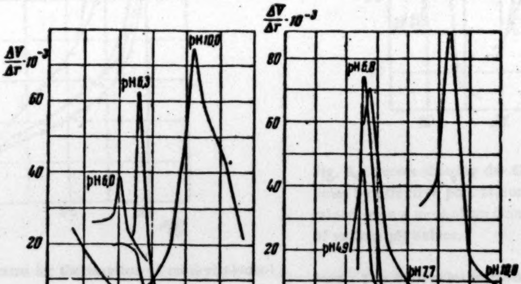

Fig. 2. Curves showing the distribution of pore volumes by effective pore radius for silica gel samples prepared from sols with pH 1.6 (Series I) and pH 5.0 (Series IV) washed with liquids of various pH values.

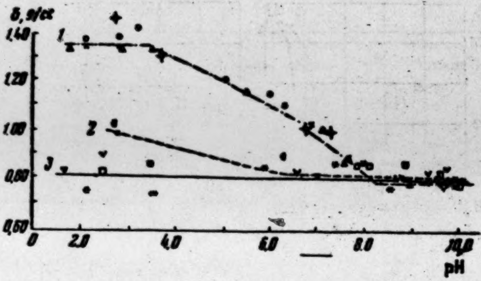

Fig. 3. Variation of apparent density of silica gels with pH of silicic acid hydrogels obtained from 1) acid, 2) neutral, 3) alkaline sols.

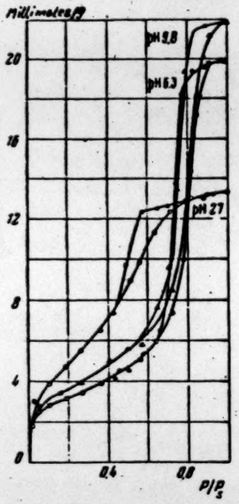

Fig. 4. Isotherms for the sorption of methyl alcohol vapor on samples of silica gel obtained from a neutral medium (pH 7) and washed with liquids of different pH. Black dots represent desorption.

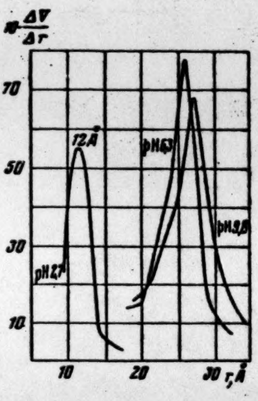

Fig. 5. Curves showing the distribution of pore volumes by effective pore radius for silica gel samples obtained from a neutral medium and washed with liquids of various pH values.

loop. The molecules of methyl alcohol closely fill the whole pore volume in these finely porous silica gels, and capillary condensation is absent. The total pore volume in these adsorbents is equal to the adsorption volume ($v_a/V_\epsilon = 1$). With an increase in the pH of the washing liquid transitional pores develop, their total volume increases, and the maximum sorptional capacity of the silica gels rises. The sorption isotherms show hysteresis due to capillary condensation, and the hysteresis loop widens with increasing pH of the hydrogel. The effective pore radius increases (Fig. 2) while the ratio of the adsorption space to the total pore volume v_a/V_ϵ decreases. The specific surface of the coarsely porous silica gels is nearly twice as small as that of the microporous gels.

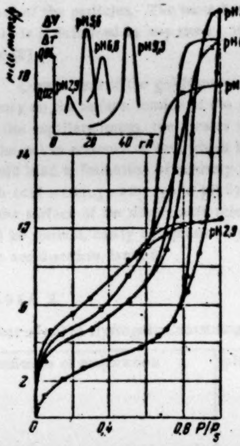

Fig. 6. Isotherms for the sorption of methyl alcohol vapor and curves for the distribution of pore volumes by effective pore radius for silica gels obtained from chemically pure sodium silicate and washed with liquids of different pH. Black dots represent desorption.

The change of the silica gel structure with variation of hydrogel pH is seen more clearly in Fig. 3, which shows the variation of the apparent density of the silica gels with pH of hydrogels obtained from acid, neutral, and alkaline sols. Curve 1, Fig. 3 shows that if the hydrogels are washed with water at pH < 4.5-5.0, finely porous silica gels with a greater apparent density are formed. As the pH of the washing water increases from 4.5 to 8.5, the apparent density gradually falls from 1.35 to 0.76 g/cc.

The points for different experimental series fit well on one curve. Further increase of the pH of the washing liquid from 8.5 to 10.6 leads to formation of silica gels with the same apparent density, 0.78-0.80 g/cc. Thus, the results detailed above show that the structure of acid silica gels does not depend on the pH (up to pH ~ 5) of the original sol, but is determined by the pH value of the silicic acid hydrogel during aging and drying. By varying the pH of the hydrogel it is possible to regulate the porous structure of the resultant silica gels.

The abrupt change of structure observed in acid gels does not occur when hydrogels obtained from neutral sols by waters of different pH (see Table 1, Series V, and Curve 2, Fig. 3). The total pore volume of these silica gels changes only from 0.52 to 0.79 cc/g.

Fig. 4 shows isotherms for the sorption of methyl alcohol vapor on samples of silica gels obtained from neutral sols (pH 7) and washed with waters of different pH values. All the isotherms have a hysteresis loop. The effective pore radius of these silica gels varies from 12 to 27 A (Fig. 5).

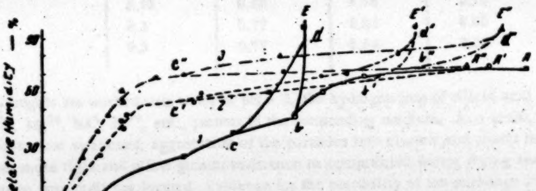

Fig. 7. Tensimetric humidification and dehydration curves: 1) gel washed with acidified water, pH 2.5; 2) tap water, pH 7.8; 3) ammonia solution, pH 8.6.
Points A, A', and A") start of dehydration; B, B', and B") end of the change of the hydrogel volume during dehydration; C, C', and C") points below which dehydration is reversible; F, F', and F") content of structural water in the silica gels.

It was shown in our previous paper [4] that the previous history of the preparation of the hydrogels does not significantly affect the structure of the final product. The structure of silica gels is formed during the aging and drying processes. Aging of the gel results in growth of the primary particles of polysilicic acid and their aggregation into clusters and chains, which are increasingly firmly bound together by chemical bonds by removal of water from hydroxyl groups of particles in contact [5]. The degree of aggregation depends on the hydrophilic nature of the particles. The more hydrophilic are the particles, the more elastic is the framework, and the more easily it is deformed by any stress. Hydrophobization increases particle size and makes the gel framework more rigid [2].

Contraction of the gel framework during dehydration occurs as the result of capillary forces, which depend mainly on the surface tension of the intermicellar liquid. The more elastic is the gel framework and the greater are the capillary forces, the greater will be the compression, and finely porous gels will result. Therefore aging of the gel in presence of ions which block the hydroxyl groups, or drying in presence of surface-active substances, should lead to formation of coarsely porous gels. When hydrogels obtained from technical reagents are washed with acid washing water (up to pH 5), adsorptional processes associated with ion exchange or formation of silicates on the surface of the silicic acid micelles cannot take place. In such cases hydrogels with an elastic framework will be formed, easily compressed by the action of capillary forces during dehydration, and finely porous silica gels are therefore formed.

TABLE 2

Effect of pH of Hydrogels Containing Sodium Ions on Silica Gel Structure

Conditions of preparation	pH of hydrogel	Apparent density in g/cc	Total pore volume in cc/g	Volume of benzene adsorbed from saturated vapor, cc/g	Specific surface in m^2/g
Gelprepared by hydrolysis of $SiCl_4$ in presence of sodium ions	2.25	1.14	0.43	0.42	710
	2.6	1.17	0.40	0.45	–
	4.6	1.13	0.44	0.42	–
	5.2	1.11	0.45	0.42	–
	7.05	0.93	0.62	0.61	494
Gel prepared from pure sodium silicate	2.9	1.13	0.44	0.45	696
	5.6	0.90	0.66	0.64	668
	6.75	0.82	0.76	0.75	565
	8.1	0.77	0.84	0.85	326
	9.3	0.77	0.84	0.86	247

When the hydrogels are washed with water at pH > 5, the hydrogen ions of silicic acid are probably exchanged for the cations Ca^{2+}, Mg^{2+}, Na^{+}, Fe^{3+}, etc., present in the surrounding medium. As a result, the bonds between the micelles and water are weakened, aggregation of the particles into clusters and chains increases, the gel framework becomes more rigid and offers greater resistance to compression during drying and as a result coarsely porous gels with large pore radii are formed. Evidence for the possibility of ion exchange at pH > 5 is provided by the data of Paramonova, Krestinskaya, et al. [6].

Direct experimental confirmation of the existence of ion exchange when the gel is washed with water at pH > 5 is supplied by the experiments of one of the present authors jointly with Yankovskaya and Piontkovskaya [7] by the use of the labeled atom method. Gels washed with water at pH 7.8 in presence of Ca^{45} ions were strongly radioactive after subsequent washing with distilled water until the wash liquors were free from radioactivity, which indicates that calcium was combined in the silicic acid micelles. Such washing yielded a coarsely porous silica gel. When the gels were washed with distilled water to which labeled calcium chloride had been added, the silica gel had negligible radioactivity, and the silica gel produced by such washing was finely porous.

All the above experiments were carried out either in the presence of several ions (Ca^{2+}, Mg^{2+}, Fe^{3+}, Na^{+}) if the silica gels were synthesized from technical water glass, or in the presence of Ca^{2+} ions only when the silica gels were made from pure sodium silicate and washed with water containing Ca^{45}. It was important to determine how the structure of the silica gels is affected when sodium ions only are present when the hydrogel is prepared from different media. For this, silica gels were prepared either by hydrolysis of silicon tetrachloride, or from chemically pure sodium silicate, and the effect of the pH of the silicic acid hydrogel on the structure of the silica gels formed in the presence of sodium ions was studied.

Table 2 shows the conditions of preparation and the structural characteristics of these silica gels.

It is seen from Table 2 that as the hydrogel pH changes up to 5, silica gels with practically the same finely porous structure are obtained. When the pH of the hydrogel is increased above 5, the silica gel structure changes with formation of more coarsely porous samples.

However, the change of the silica gel structure as a function of the hydrogel pH is less when only sodium ions are present in the system than in the presence of other cations(Ca^{2+}, Mg^{2+}, Fe^{3+}). This also follows from the isotherms in Fig. 6 for the sorption of methyl alcohol vapor on silica gels washed with liquids the pH of which was varied between 2.4 and 9.3 in the presence of sodium ions during the aging process. With increasing pH of the washing liquid the pore size of the silica gels increases somewhat, the transitional pore volume increases, and the specific surface decreases. Therefore sodium ions have an effect on silica gel structure which is analogous to (but rather less than) the effect of other cations.

In order to confirm the influence of the nature of the washing water on the degree of hydrophily of the hydrogel particles, we studied the relationship between the vapor pressure over the gel and the water content of hydrogels washed under different conditions. For this, the humidification and dehydration isotherms (Van Bammelen curves) were obtained by the tensimetric method. The hydrogel prepared by precipitation of sodium silicate by sulfuric acid, was divided into three portions, one of which was washed with acidified water (pH 2.5), another with tap water (pH 7.8), and the third with ammonia solution (pH 8.6). The dehydration and humidification of the hydrogels was carried out in dynamic conditions by means of Dubinin's apparatus [8].

Fig. 7 shows the humidification and dehydration isotherms in the coordinates: vapor pressure − water content of the gel in moles per mole silicic acid. It is seen from Fig. 7 that the position of the curves on the diagram depends on the conditions of washing of the hydrogel. At the same atmospheric humidity the water content of a hydrogel washed with acid water is much higher than that of gels washed with tap water or ammonia solution. For example, at the same relative atmospheric humidity of 25%, the molar ratio of water to silicic acid in the hydrogel washed with water at pH 2.5 is 1.44, while for the hydrogel washed by a solution at pH 8.6 the ratio is 0.40, so that the water content of the first hydrogel is 3.6 times as great as that of the second. Similar results are obtained at other vapor pressures. Thus, these results show that variation of the washing conditions of the hydrogels results in different degrees of hydrophily of the systems.

SUMMARY

1. The effect of the pH of silicic acid hydrogels obtained from acid and neutral sols on silica gel structure has been studied.

2. It is shown that variation of the pH of silicic acid hydrogels obtained from acid sols, up to a value of 5, does not affect the structure of the dry silica gel. In the presence of cations, when the hydrogel pH is varied from 4.5-5.0 to 8, the structure of the silica gels formed gradually changes with an increase of the pore size and total pore volume. It is shown that the pore structure of silica gel can be regulated in wide limits by variation of the hydrogel pH.

3. The results obtained are explained in terms of ion exchange between hydrogen ions of the silicic acid micelles and the cations of the surrounding medium in weakly acid, neutral, and alkaline media.

LITERATURE CITED

[1] A.P. Okatov, Colloidal Silicic Acid and Its Adsorptional Properties, Military Academy of the Red Army (1928); M.O. Kharmadaryan and S.L. Kopelevich, J. Phys. Chem., 5, 165 (1934); M.V. Polyakov *et al.*, J. Phys. Chem., 4, 454 (1933); M.S. Golderbiter, Author's Report, Moscow (1952).

[2] I.E. Neimark and R.Yu. Sheinfain, Colloid J., 15, 50 (1953) (T.p. 54)*.

[3] I.E. Neimark, Trans. Conf. on Catalysis, Kiev, 178 (1950).

[4] I.E. Neimark, M.A. Piontkovskaya, and I.B. Slinyakova, Colloid J., 18, 61 (1956) (T.p. 59)*.

[5] R. Signer and G. Cross, Ann., 499, 2, 158 (1932); A.V. Kiselev, Colloid J., 2, 17 (1936); O.M. Dzhigit, A.V. Kiselev, and I.E. Neimark, J. Phys. Chem., 28, 1805 (1954); V.S. Veselovsky and I.A. Selyaev, J. Phys. Chem., 6, 1171 (1935).

---

*T.p. = C.B. Translation pagination.

[6] B.P. Bruns and R.Kh. Burshtein, J. Phys. Chem., 11, 7 (1938); V.I. Paramonova, Soil Science, 6, 65 (1940); V.N. Krestinskaya and N.E. Natanson, Colloid J., 2, 7 (1936).

[7] G.F. Yankovskaya, M.A. Piontkovskaya, and I.E. Neimark, Proc. Acad. Sci. Ukrainian SSR, No. 1, 87 (1955).

[8] M.M. Dubinin and K.V. Chmutov, Physicochemical Bases of Antigas Defense, Moscow (1939).

Received May 13, 1955

The L.V. Pisarzhevsky Institute of Physical Chemistry,
Academy of Sciences, Ukrainian SSR - Kiev

PREVENTION OF VULCANIZATE OXIDATION DURING SWELLING

E.N. Novikova

As is known [1] the swelling of high polymers is a complex process, determined by the temperature conditions, chemical nature, geometric structure, and energy relationships of the components. Moreover, the degree of swelling of a polymer is greatly influenced by additions of polar and non-polar substances, which complicate the swelling process, as they may enter into intermolecular action with the components.

The work of Ermolenko [2] on the action of polar additives (o- and p-nitrophenols, o-and p-toluidines) on the kinetics of swelling of vulcanizates in benzene, and also the work of Gul and Shvarts [3] and others, has shown that the degree of swelling of vulcanizates depends on the polarity of the additives. The influence of various additives in decreasing or raising the degree of swelling is explained by solvation action between the additives and the polar groups of the rubber or the benzene molecules.

The work of Dogadkin [4,5] on structural changes in rubber under the action of molecular oxygen has shown that swelling of a vulcanizate depends not only on its structural characteristics but also on the action of molecular oxygen. In the swelling of vulcanizates in air under normal conditions, the principal swelling period is followed by a stage in which the volume slowly increases owing to oxidative degradation of the hydrocarbon.

Experiments [6] on the action of piperidine and naphthyl mercaptan on the solution rate of vulcanizates have led to the conclusion that the swelling and solution processes are favored by substances which accelerate oxidation, and retarded by substances which inhibit oxidation of rubber. Beatty and Juve [7] also attribute the decreased service life of rubber in contact with oil to the fact that swelling weakens the bonds between the rubber molecules and the unsaturated linkages become more accessible to oxygen.

It follows from the results of these investigations that the swelling of rubber vulcanizates is affected, in addition to other factors, by degradation of the rubber molecules by the action of molecular oxygen.

In this connection it appeared of interest to study the influence of inhibitors of the oxidation of rubber on the swelling of rubber vulcanizates. An equal interest attaches to a study of the influence of the chemical nature and structure of inhibitors of rubber oxidation on their behavior in the swelling of vulcanizates. Such an investigation would permit a closer approach to the nature of the relationship between inhibitors and different types of rubber, which in turn would provide the possibility of choice of inhibitor with a predetermined degree of protective action. The aim of the present study was to investigate the influence of amines and phenols on the degree of swelling of rubber vulcanizates in dipentene.

Vulcanizates based both on natural and synthetic rubbers were studied. The compositions of the vulcanization mixtures are shown in Table 1. The swelling medium was dipentene which had been carefully purified and distilled over metallic sodium, with specific gravity 0.8486 and n_D^{20} 1.474.

In view of the fact that during swelling the solvent may wash out the ingredients of the mixture from the vulcanizate, all the rubber samples were previously washed repeatedly with benzene and then dried in a vacuum desiccator. The vulcanizate samples prepared in this way, 0.1 g in weight, were swollen in 10 ml of dipentene at 20°. The volume and weight of the samples, and the volume of the solution, were constant in all experiments.

The degree of swelling of the vulcanizates was determined gravimetrically. The inhibitor concentrations in the solution are expressed in moles per liter of dipentene. The additives used for retarding the oxidative degradation of the vulcanizates were phenols purified by distillation (pyrocatechol and pyrogallol), β-naphthol, and amines (phenyl-β-naphthylamine or Neozone D and β-naphthylamine), recrystallized from methyl alcohol.

TABLE 1

Composition of Vulcanizates

Vulcanizate components	Mixtures					
	VII	I	III	IV	C-1	C-2
Smoked sheet	100	–	–	–	–	–
SKB	–	200	200	200	–	–
SKN-26	–	–	–	–	309	309
Sulfur	2.75	3	3	3	4.5	4.5
Captax	0.85	3.6	3.6	3.6	2.4	2.4
Zinc Oxide	5	10	10	–	15	15
Stearic acid	1	5	–	–	4.5	4.5
Gas black	40	120	–	–	135	–
Rubberax	5	10	–	–	–	–
Amount of rubber in vulcanizate, %	64.7	56.9	92.8	96.8	65.7	92.2

TABLE 2

Swelling of Vulcanizates in Dipentene

Vulcanizate	Degree of swelling, per 1 g of vulcanizate		Degree of swelling per 1 g of rubber in the vulcanizate; swollen for 29 days
	6 days	29 days	
III	7.44	15.25	16.55
IV	5.92	9.04	9.3
I	2.27	2.43	4.2
C-2	0.85	1.44	1.56
C-1	0.58	0.93	1.42
VII	3.37	3.43	–

The results of our experiments (Table 2) show that the degree of swelling of vulcanizates in dipentene depends both on the nature of the rubber and on the composition of the ingredients in the vulcanizate. Vulcanizates based on SKB show a relatively high degree of swelling in dipentene, while those based on SKN-26 swell considerably less. Vulcanizate VII, containing natural rubber, shows greater swelling than the others in dipentene. Of the three samples containing SKB and the two samples with SKN-26, relatively the least swelling is found in the more highly filled Vulcanizates I and C-1, which contain, in addition to other components, a high percentage of carbon black. We note the different degrees of swelling of two vulcanizates (III and IV) based on SKB under the same vulcanization conditions but differing in zinc oxide content. The presence of zinc oxide in Vulcanizate III results in a much greater degree of swelling in dipentene in comparison with Vulcanizate IV.

The sequence of the vulcanizates according to the degree of swelling is the same whether the degree of swelling is calculated per 1 g of the vulcanizate or per 1 g of the rubber in the vulcanizate.

Influence of additions. The inhibitors of rubber oxidation added to the dipentene have a fairly strong effect in lowering the degree of degradative swelling of the vulcanizates in (dipentene + additive) solution in comparison with the degree of swelling of the same vulcanizates in pure dipentene. Table 3 shows that the percentage decrease of swelling of vulcanizates is 0.05 M phenyl-β-naphthylamine or pyrogallol solution in dipentene, relative to the swelling of the vulcanizates in dipentene, taken as 100, is fairly high for all the samples except I.

The retarding effect of these substances on the degradative swelling of rubber vulcanizates is probably due to a number of causes. Zhukov [8] points out that the presence of unsaturated bonds in the solvent increases the swelling and solution rates of sodium divinyl polymer. In swollen vulcanizates, as was stated above, the rubber itself is more susceptible to the action of oxygen. The view is also held [9] that peroxide type compounds are formed in terpenes after they have been in contact for some time with atmospheric oxygen. It is known from the literature that peroxides have an accelerating effect on the oxidation of a number of substances, including rubber.

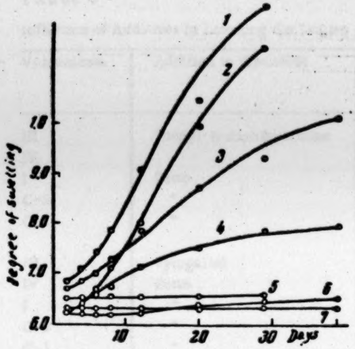

Fig. 1. Effect of additives on the swelling of SKB-III vulcanizate in dipentene: 1) without additions; additives: 2) alcohol; 3) o-toluidine; 4) β-naphthylamine; 5) pyrocatechol; 6) Neozone D; 7) pyrogallol.

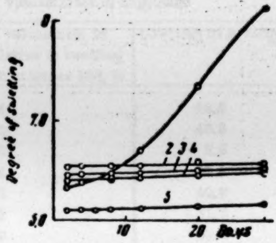

Fig. 2. Effect of additives on the swelling of SKB-IV vulcanizate in dipentene: 1) without additions; additives: 2) pyrocatechol; 3) pyrogallol; 4) toluidine; 5) Neozone D.

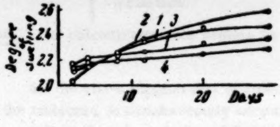

Fig. 3. Effect of additives on the swelling of SKB-I vulcanizate in dipentene: 1) without additions; additives: 2) alcohol; 3) pyrocatechol; 4) pyrogallol.

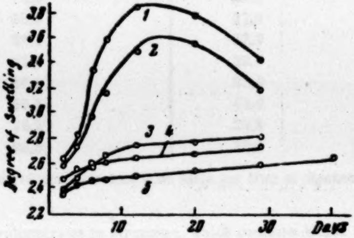

Fig. 4. Effect of additives on the swelling of Vulcanizate VII in dipentene: 1) without additions; additives: 2) alcohol; 3) pyrocatechol; 4) β-naphthylamine; 5) Neozone D.

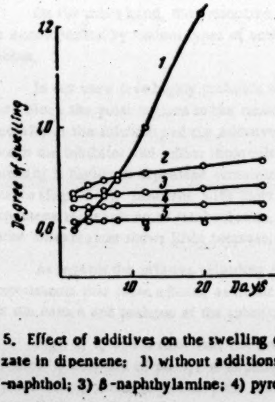

Fig. 5. Effect of additives on the swelling of C-2 vulcanizate in dipentene: 1) without additions; additives: 2) β-naphthol; 3) β-naphthylamine; 4) pyrocatechol; 5) pyrogallol.

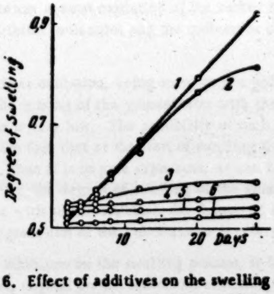

Fig. 6. Effect of additives on the swelling of C-1 vulcanizate in dipentene: 1) without additions; additives: 2) alcohol; 3) β-naphthol; 4) β-naphthylamine; 5) pyrocatechol; 6) pyrogallol.

TABLE 3

Influence of Additives in Lowering the Degree of Swelling of Vulcanizates in Dipentene

Vulcanizate	Addition to dipentene	Swelling of vulcanizate in solution, relative to swelling in dipentene taken as 100, %	Lowering of swelling, %
III	Phenyl-β-naphthylamine	41.4	58.6
IV		59.1	40.9
I	Ditto	97.0	3.0
C-2	"	60.4	39.6
C-1	"	59.1	40.9
		68.3	31.7
III	Pyrogallol	42.0	58.0
IV	Ditto	67.1	32.9
I	"	93.4	6.6
C-2	"	55.9	44.1
C-1	"	57.7	42.1
VII	"	72.3	27.7
IV	Pyrocatechol	68.2	31.8
IV	Pyrogallol	67.1	32.9
IV	β-Naphthylamine	61.2	38.8
IV	β-Naphthol	68.0	32.0
IV	Phenyl-β-naphthylamine	59.1	40.9
IV	o-Toluidine	70.2	28.8
IV	Toluidine	66.9	33.1

Note. The vulcanizates were swollen for 29 days. Additive concentration 0.05 mole per liter of dipentene.

All the above suggests that intensive swelling of vulcanizates in dipentene, which contains double bonds in the molecule, is simultaneously accompanied by oxidation of the rubber present in the vulcanizates. According to Dogadkin, degradation of the rubber occurs even if the amount of oxygen absorbed by it is not large.

The decrease of the swelling of vulcanizates in dipentene when inhibitors of rubber oxidation are added to the latter is probably due to the fact that inhibitors retard the formation of peroxides, as was shown by Ivanov [10] in the case of tetralin peroxide, and they thus protect the rubber against oxidation by oxygen.

On the other hand, the protective effects of the inhibitors against oxidation of the rubber in solution may be accompanied by various types of action between the inhibitor molecules and the molecules of dipentene and rubber.

In our view it is highly probable that inhibitors of rubber oxidation, being more or less polar compounds, may block the polar regions in the rubber and so prevent the mixing of the vulcanizates with the dipentene, especially as the solubility of the additives used in dipentene is very low. The possibility of such interaction between the inhibitor and rubber molecules is confirmed by the fact that at the start of swelling the degree of swelling is higher in dipentene containing added inhibitors, than it is in pure dipentene, as can be seen from the graphs (Figs. 2-6). However, with increased time of swelling, the degree of swelling of the vulcanizates in pure dipentene increases up to total solution, while in dipentene with added inhibitors the degree of swelling of the same vulcanizates shows little increase, as the oxidative degradation of the vulcanizates is retarded.

As regards the relative retarding effects of different inhibitors on the swelling process, it follows from our experiments that these effects, as in the oxidation of rubber, depend on the molecular structure, and particularly on the nature and position of the substituent groups in the inhibitor molecules (Figs. 1 and 2).

Figs. 1, 2, and 4 show that the swelling of Samples III, IV, and VII in dipentene is particularly greatly decreased by addition of phenyl-β-naphthylamine. Of the phenols, pyrogallol is the most effective, followed by pyrocatechol, which is probably the result of the positions of the hydroxy groups in the molecules. o-Toluidine has a weak retarding effect on vulcanizate swelling. The addition of 0.1 mole of ethyl alcohol per liter of dipentene has almost no retarding effect (Figs. 3 and 4).

Our experiments show (Fig. 3) that the filled Vulcanizate I shows little swelling and does not dissolve in dipentene during 50 days. The inhibiting effect of additives on the swelling of Sample I is not large, but the effect is of the same order as in Samples III and IV.

A comparison of the effect of additives on Vulcanizates C-1 and C-2 (Figs. 5 and 6) shows that their retarding effects fall in the same sequence. However, the greatest effect on samples based on nitrile rubber (in lowering the degree of swelling) is exerted by phenols: pyrogallol and pyrocatechol, followed by amines: phenyl-β-naphthylamine and β-naphthylamine. Different retarding effects are produced by naphthalene derivatives: β-naphthylamine and β-naphthol, which is caused by the different chemical nature and the different electronegative character of the substituents NH_2 and OH. As previously, o-toluidine has a weaker retarding effect on swelling than the other additives, but this effect is greater than in the other samples.

SUMMARY

1. The addition of inhibitors of rubber oxidation decreases the degree of swelling of vulcanizates in dipentene.

2. The swelling of vulcanizates is decreased most effectively by phenols (pyrocatechol and pyrogallol), phenyl-β-naphthylamine, and toluidine.

3. o-Toluidine and ethyl alcohol have a slight retarding effect on the swelling of vulcanizates.

LITERATURE CITED

[1] V.E. Gul, Colloid J., 15, No. 3, 170 (1953).

[2] N.F. Ermolenko and L.V. Rabinovich, Annals V.I. Lenin Belorussian State Univ., No. 14, Chem. Ser. (1953); N.F. Ermolenko, Chemistry and Physical Chemistry of High Polymers, Acad. Sci. USSR Press, 182 (1952).

[3] V.E. Gul and A.G. Shvarts, Colloid J., 17, 24 (1955)(T.p. 21)*.

[4] B.A. Dogadkin, Trans. 1st and 2nd Conf. on High Polymers, Acad. Sci. USSR Press (1945).

[5] B.A. Dogadkin and B. Karmin, Colloid J., 9, No. 5, 346 (1947).

[6] B.A. Dogadkin, Z. Bryukhanova, and A. Pasynsky, Trans. M.V. Lomonosov Inst. Fine Chemical Technology, Moscow, No. 1 (1946).

[7] Vitti and Dzhuv, Ref. J., No. 14 (1954).

[8] I.I. Zhukov, S.P. Talmud, and V.A. Zilberman, Synthetic Rubber, No. 6, 4 (1935).

[9] G.V. Pigulevsky, Chemistry of the Terpenes, Lenin State Univ. Press (1949).

[10] K.I. Ivanov, Intermediate Products and Intermediate Reaction of the Autoxidation of Hydrocarbons, State Sci.-Tech Press for Petroleum and Mining Literature (1949).

Received April 23, 1955

The Minsk Medical Institute

---

*T.p. = C.B. Translation pagination.

HEATS OF WETTING OF VISCOSE RAYON

Ya.V. Pak and Kh.U. Usmanov

The demand for artificial and synthetic fibers increases each year, and fiber production is rising also. The greatest output is that of viscose rayon, which raises the primary necessity for exhaustive investigations of its properties and searches for methods of improving its quality.

In addition to textile purposes, viscose rayon is also used in many special manufactures, such as tire cord. Viscose tire cords increase tire life by 48-50% [1]; they have high heat resistance and result in less heat evolution in action. Viscose rayon is a fairly heat-resistant material and readily withstands a temperature of 120-130° [2].

All the methods for viscose thread production are based on the principle of strengthening the fibers with retention of high-elastic properties as the result of a high degree of orientation. The essence of the method is that the freshly spun filament in the form of a cellulose derivative should be stretched in the swollen state under flow conditions, with irreversible displacement of the molecular chains, followed by precipitation of hydrate cellulose, with restoration of flexibility during relaxational shrinkage of the thread by means of complete removal of the stress produced in it.

In recent years a technological process has been developed for the production of viscose yarn with higher tensile strength than cotton fiber. One of the theoretical bases for improvement of viscose rayon quality is increase in its packing density.

METHOD AND RESULTS

The principal measures of the packing density of cellulose are its sorption and heat of wetting. For determination of the heat of wetting, the samples under test were placed in thin-walled glass ampoules which could be easily broken. Each ampoule was fitted with a closely fitting rubber stopper and weighed with four-figure accuracy. The weighed samples (~ 1.0 g) were packed into the previously weighed ampoules, which were then stoppered and weighed again. The air-dry sample weight was found by difference.

The filled ampoules (without the stoppers) were placed in an apparatus for sorption determination, from which air was evacuated for five hours. The apparatus was then filled with dry air, passed through Dreschel flasks with concentrated sulfuric acid, a flask with caustic soda, two U-tubes filled with calcine calcium chloride, and finally through a trap cooled in liquid air. This system completely removed water vapor and carbon dioxide from the air. The ampoules were then removed from the apparatus, carefully closed with the correct stoppers, weighed and sealed. The weight difference before and after the evacuation gave the amount of water removed and the weight of the absolutely dry sample.

The ampoules prepared in this manner were used for determinations of the integral heats of wetting. The differential heats were also found from determinations of the integral heats at various moisture contents. For this, the ampoules with the test material were prepared as described above, but after removal of traces of moisture and reduction of the samples to the dry state, water vapor to the required degree of saturation was introduced into the ampoules. 2-3 hours after equilibrium was established, the ampoules were filled with dry air and held for another hour; they were then stoppered and weighed. The weight of water in the samples was determined by the weight difference before and after humidification. The amount of adsorbed water found in this manner was compared with data obtained from the isotherm for water sorption for the sample and the relative humidity of the air. The results obtained were, as a rule, in agreement.

TABLE 1

Integral and Differential Heats of Wetting of Viscose Rayon

Integral heats of wetting			Differential heats of wetting for Sample 1		
samples	moisture content, %	heat in cal/g cellulose	sorption of water, g	heats of wetting	
				in cal./g	in cal./mole
1	0	24.8	1	250	4500
	1.6	20.4	2	215	3870
	2.8	18.7	3	200	3600
	6.6	10.5	4	175	3150
	7.5	9.0	5	150	2740
	12.8	5.7	6	135	2430
	14.0	5.3	7	125	2250
	0	24.8			
2	0	19.8	8	110	1980
			9	100	1800
3	0	16.3	10	80	1440
			11	75	1350
4	0	20.0	12	72	1296
			13	52	9 6
			14	48	864
			15	40	720

TABLE 2

Data of Foreign Authors on the Heats of Wetting of Viscose Rayon

Authors	Reference	Heats in cal./g	
		integral	differential
Guthrie	[7]	25.2	280
Hermans	[8]	24.4	239-235
Rees	[6]	25.2	–
Wahba	[9]	20.3	270

The heats of wetting were determined in an adiabatic calorimeter [3]. The heat evolved in the system was calculated with the aid of the formula [4]:

$$Q = \frac{(A + W)\Delta t}{g},$$

where W is the heat capacity of the calorimeter; Δt is the temperature change in the calorimeter; A is the amount of water taken for wetting, in grams; g is the weight of the sample in grams.

The differential heats were calculated with the aid of the formula:

$$H = 100\frac{dQ}{dC},$$

where H is the differential heat of sorption; Q is the integral heat of wetting; C is the moisture content of the sample. The differentiation of Q with respect to C was carried out graphically.

4 samples of viscose rayon were taken for calorimetric investigation: 1) viscose rayon (original) without subsequent treatment; 2) the original viscose rayon treated in glycerol for 0.5 hour; 3) viscose rayon treated in glycerol for 5 hours; 4) viscose rayon prepared by spinning into an alkaline bath ("alkaline" sample).

The glycerol treatment was carried out in sealed glass tubes in oil at 250°. Air and moisture were previously pumped out of the glycerol.

The heats of wetting of Sample 1 were determined at different moisture contents, and those of the other samples, in the absolutely dry state (Table 1).

The integral and differential heats of wetting of viscose rayon decrease first rapidly and then more smoothly with increasing moisture content.

For comparison, Table 2 shows data on the heats of wetting of viscose rayon (of the same type as Sample 1) obtained by foreign authors. The discrepancies between our data and those of the foreign authors are probably due to imperfections of technique, and in particular to differences in pretreatment of the samples. Our method for evacuation of the samples is free from these defects and gives reproducible results.

It is seen from Table 1 that the heats of wetting of Samples 2 and 3 (heated in glycerol) are less than that of Sample 1 (unheated), which indicates increased cellulose packing density in viscose rayon (cord) as the result of heating in polar liquids.

Usmanov and Kargin [5] studied the variation of packing density of cellulose materials by determinations of their sorption capacity, and concluded that changes in the packing density of cellulose samples occur as the result of increased flexibility and mobility of the cellulose macromolecules. The heating of hydrate cellulose in polar liquids without access of air produced samples with lower sorptional capacity than the original hydrate cellulose. Our results are in good agreement with this.

These results have great theoretical and practical importance, as all the basic utilizational properties of cellulose threads and films, and also the chemical properties of cellulose, depend on the packing density, while the heats of wetting proved to be the best measure of the packing density of the cellulose chains in the material.

The heat of wetting of the "alkaline" sample of hydrate cellulose (Sample 4) was lower than that of viscose rayon. Therefore the "alkaline" hydrate cellulose has greater packing density than viscose rayon; this is confirmed also by sorption data for these samples. "Alkaline" hydrate cellulose is free from many of the defects of ordinary viscose rayon and approaches native cotton fiber in its properties.

These results provide decisive proof of the continuous gradation of the packing density of all cellulose materials from the strongly oriented natural fibers to completely isotropic hydrate cellulose powders.

SUMMARY

1. The integral heats of wetting of four viscose rayon samples, and the differential heats of wetting of one sample for seven different moisture contents have been determined.

2. The integral heats of wetting are lower for the hydrate cellulose samples heat-treated in glycerol and for an "alkaline" sample than for the original viscose rayon. Consequently, precipitation of cellulose from viscose in weakly alkaline or neutral media, and also heating of hydrate cellulose in polar liquids, increases the packing density of the cellulose samples.

LITERATURE CITED

[1] A.F. Buyanov, The New Fibers, Moscow, p.21 (1953).

[2] A.N. Ryauzov, V.A. Gruzdev, and M.A. Artemenko, Technology of Artificial Fibers, Moscow, 340, 382 (1952).

[3] B.V. Ilyin and A.V. Kiselev, J. Gen. Chem., 4, 498 (1934).

[4] S.M. Skuratov and A.V. Ochkin, Thermochemistry, Moscow University Press, p. 3-7, 31-33 (1951).

[5] Kh.U. Usmanov and V.A. Kargin, Chemistry and Physical Chemistry of High Molecular Compounds, Moscow, p.169-181 (1952).

[6] W. Howard Rees, J. Textile Inst., 11, 351 (1948).

[7] J.C. Guthrie, J. Textile Inst., 8, 489 (1949).

[8] P.H. Hermans, J. Am. Chem. Soc., 68, 2547 (1946).

[9] M. Wahba, J. Phys. Colloid Chem., 54, 1148 (1950).

Received June 9, 1955

Chemical Institute, Academy of Sciences Uzbek SSR,
Tashkent

RHEOLOGICAL INVESTIGATIONS OF THE SETTING OF GYPSUM

V.B. Ratinov, T.I. Rozenberg, G.G. Bogautdinova, and G.D. Stalikova

It was shown by Rebinder and co-workers [1,2] that processes of structure formation in mineral cements may conveniently be studied by rheological methods. The aim of the present work was a rheological study of the system $CaSO_4 - H_2O$, which has an exceptionally high setting rate in comparison with cements. This feature of gypsum plasters was the reason for the choice of the method of study.

The plastic and effective viscosities of the gypsum paste were determined with the aid of Konstantinov's automatic capillary viscosimeter AKV-2 [3]. The operating principle of the visiosimeter is that the gypsum paste loaded into a chamber is squeezed through a capillary. The squeezing is effected by a rod under the pressure of a calibrated spring, the movement of the rod being automatically recorded on paper attached to a drum rotating at an accurately determined speed.

The calculations were made by means of the formulas: .

$$\eta_{\tau}^{\bar{D}} = \tau/\bar{D}; \tag{1}$$

$$\eta_{pl} = (\tau - \theta_g)/\bar{D}, \tag{2}$$

where $\eta_{\tau}^{\bar{D}}$ is the effective viscosity in poises; η_{pl} is the plastic viscosity in poises; τ is the shearing stress in dynes$\cdot$cm^{-2}; $\bar{D}$ is the velocity gradient in seconds^{-1}; θg is the limiting dynamic shearing stesss in dynes$\cdot$cm^{-2}, found by extrapolation of the experimental linear intercept determining theplastic viscosity.

The value of τ was calculated from the equation:

$$\tau = 9.81 \cdot 10^5 \cdot p/2\underline{l}, \tag{3}$$

where $\underline{p}$ is the pressure in the chamber under which the material is extruded at the time instant $\underline{t}$, in kg.cm^{-2}; R is the capillary radius in centimeters; $\underline{l}$ is the capillary length in centimeters.

With a knowledge of the flow rate Q at any instant

$$Q = \pi R_1^2 \omega \tan \alpha \text{ cm}^3 \cdot \text{sec.}^{-1}, \tag{4}$$

(where R is the radius of the rod in centimeters; ω is the rotation velocity of the drum in cm.second^{-1}; α is the angle of the tangent to the curve recorded by the recording instrument at time $\underline{t}$ in degrees), it is possible to find the average shearing velocity gradient:

$$\bar{D} = \frac{4Q}{\pi R^3} = \frac{4R_1^2}{R^3}\,\omega \tan \alpha. \tag{5}$$

In the experiments with the AKV-2 instrument, glass and metal capillaries 0.96-3.00 mm in diameter and 121-150 mm long were used. Immediately after the gypsum hemihydrate was mixed with water, the suspension was stirred vigorously for 30 seconds and charged into the viscosimeter chamber. To determine the influence of stirring on the plastic properties of the system, stirring was also carried out for 15 and 45 seconds; to determine the viscosity changes of the gypsum paste as a function of its age, the paste of calcium sulfate hemihydrate was held for various periods in the viscosimeter chamber before extrusion through the capillary. At the end of the experiments the capillary was immediately detached from thechamber and washed out with water from a syringe.

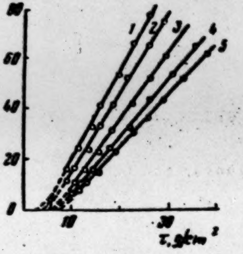

Fig. 1. Velocity gradient as a function of the shearing stress, with variations of the water–gypsum ratio by ± 0.04 of the normal value (N): 1) N + 4%; 2) N + 2%; 3) N; 4) N − 2%; 5) N − 4%.

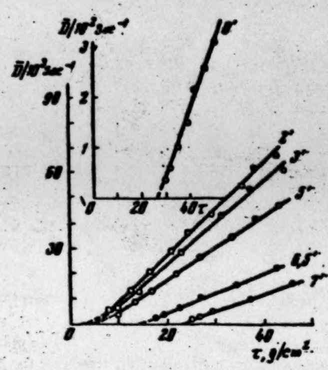

Fig. 2. Typical relationship of the velocity gradient and the shearing rate for different ages of the system.

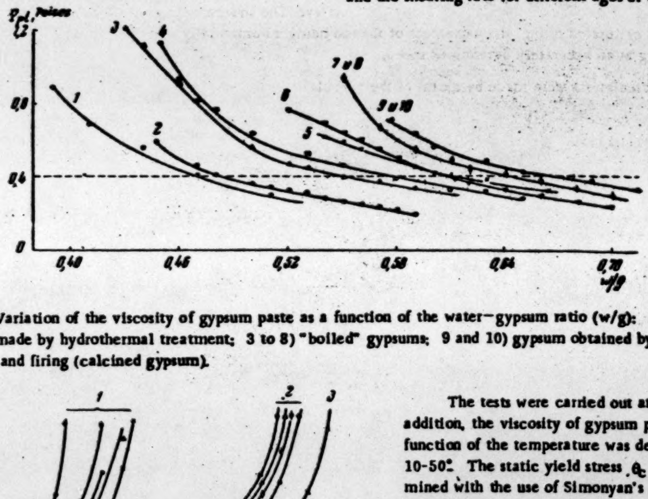

Fig. 3. Variation of the viscosity of gypsum paste as a function of the water–gypsum ratio (w/g): 1 and 2) gypsum made by hydrothermal treatment; 3 to 8) "boiled" gypsums; 9 and 10) gypsum obtained by combined grinding and firing (calcined gypsum).

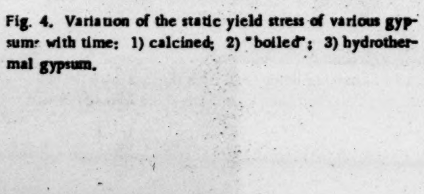

Fig. 4. Variation of the static yield stress of various gypsums with time: 1) calcined; 2) "boiled"; 3) hydrothermal gypsum.

The tests were carried out at 20 ± 1°; in addition, the viscosity of gypsum paste as a function of the temperature was determined at 10-50°. The static yield stress θ_c was determined with the use of Simonyan's apparatus [4], constructed on the following principle; the gypsum paste is packed into a rifled tube; the mass is sheared relative to the portion remaining in the rifling by means of a piston with a calibrated front membrane. The calculation was made by means of the formula

$$\theta_c = \frac{d}{4l}\, p \text{ dynes} \cdot \text{cm}^{-2} \qquad (6)$$

where d is the tube diameter in centimeters; l is the tube length in centimeters; p is the pressure in kg.cm^{-2}.

In determinations of the static yield stress, the instrument was placed vertically and filled with the paste immediately after mixing, through the top of the tube. 0.5-1.0 minutes before the measurement the instrument was placed in the horizontal position. When the region of considerable crystallization was being investigated, a thin (~ 1.0 mm) elastic Formoplast cushion was inserted between the gypsum and the bottom of the piston, to ensure uniform bending of the membrane. Special experiments showed that this lining has practically no influence on the absolute values of the yield stress. The values of θ_c did not vary along the tube (this was verified in the range l = 25 – 170 mm). The deviation of the results from the arithmetic mean was ±5%. After the tube is dismantled, the gypsum is easily removed from the rifling.

The results show that in the first few seconds after calcium sulfate hemihydrate is mixed with normal or large quantities of water, the suspension formed has only a very weak structure (the normal water–gypsum ratio is taken to be Suttard's conventional value for the horizontal spreading of a cake to 120 mm). Later, even after only 1-2 minutes, the gypsum paste is an elastico-plastic body (Figs. 1 and 2) with a low yield stress (lower limit ~ 0.2 g/cm^2). Test results on gypsum plasters by all the usual methods (boiling, autoclave treatment, combined grinding, and calcination of the dihydrate) from gypsum stone of twelve different origins showed that this is true regardless of: 1) the degree of dispersion and the specific surface of the gypsum powder; 2) differences in composition due to the technological schemes and conditions used in the gypsum production; 3) the water–gypsum ratio, over a range of at least ±0.05% of the normal value; 4) the temperature, at least in the range 10-50°; 5) the presence of small amounts of coal, quartz, calcite, and clay, commonly found in the commercial product.

Tests on gypsum paste with the AKV-2 apparatus showed that the paste retains a plastic viscosity value over a wide range of velocity gradients, from $0.5\text{-}1.0 \cdot 10^1$ to $5\text{-}7 \cdot 10^4$ seconds^{-1} in our experiments. In agreement with literature data for other structurized systems [5] turbulent flow of gypsum paste begins at Re < 2400.

It follows from the above that for practical purposes in the early stages of the process it is more convenient to use viscosity characteristics of gypsum pastes, which give a more clear indication of the slow structurization of the system in the low yield stress regions. Statistical treatment of test data on a large number of gypsum samples established that the plastic viscosity of the paste is a linear function of the concentration of the suspension in the range N ±0.05 (where N is the normal water–gypsum ratio). This leads to a nomographic method for the determination of the normal and working mixing consistencies of calcium sulfate hemihydrate, based on measurements of the viscosity of the system at an arbitrarily chosen water–gypsum ratio 2 minutes after the addition of water. This is illustrated by the results in Fig. 3.

With increasing age of the gypsum paste the transition from elastic deformations to flow becomes increasingly sharp and is found at higher values of θ. In the stage of rapid structurization, the changes occurring in gypsum paste are most conveniently observed by the increase of the yield stress (static or dynamic). In these conditions the viscosity is less suitable, and its role in the characterization of gypsum decreases with hardening of the system. The variation of the static yield stress with time for different gypsum plasters is shown in Fig. 4.

Thus, from the rheological viewpoint the setting of gypsum may be divided into two periods: during the whole of the first period the system is an elastico-plastic body, while in the second period the gypsum attains the properties of a brittle solid. Because of the rapid setting, these two periods are fairly sharply distinguished by the loss by the system of the power to flow after disruption, which does not usually coincide with the technological "end of setting" determined by the standard method with the Vicat needle.

The first period, in turn, can also be divided into two phases: in the first, the gypsum paste has a relatively low and slowly changing yield stress, and therefore viscosity is a convenient practical indication of changes in its structural and mechanical properties; in the second phase the system may be characterized both by the viscosity (plastic, effective, and maximum undestroyed structural viscosity) and by the static or dynamic yield stress. The role of these latter values increases with age of the paste.

SUMMARY

1. It is shown that from the rheological viewpoint the setting of gypsum may be divided into two periods: in the first, the system is an elastico-plastic body, and in the second it has the properties of a brittle solid. The two periods are fairly clearly distinguished by the loss of the power of the gypsum to flow after disruption, which does not usually coincide in time with the technological "end of setting".

2. A linear relationship has been found between the viscosity of the suspension and the water–gypsum ratio during the slow structurization stage in the first period; this has been used as a basis for a nomographic method for determination of the normal and working consistencies for the mixing of gypsum hemihydrate.

LITERATURE CITED

[1] P.A. Rebinder and E.E. Segalova, Nature, No. 12 (1952); E.E. Segalova, P.A. Rebinder, and O.I. Lukyanova, Bull. Moscow State Univ., No. 2 (1954).

[2] N.V. Mikhailov, Colloid J., 17, No. 1, 68 (1955) (T.p. 61)*; 17, No. 3, 242 (1955) (T.p. 221)*; N.V. Mikhailov and P.A. Rebinder, Colloid J., 17, No. 2, 107 (1955) (T.p. 99)*.

[3] A.A. Konstantinov and G.V. Vinogradov, Factory Labs., 19, No. 6, 680 (1953).

[4] A.A. Simonyan, Peat Ind., No. 10, 24 (1953).

[5] G.I. Fuks, Colloid J., 10, 155 (1948).

Received October 22, 1954

Scientific Research Institute for Ferroconcrete
and Non-Metallic Materials - Moscow

---

*T.p. = C.B. Translation pagination

MEASUREMENT OF THE VISCOSITY OF PRINTING INKS AT HIGH RATES OF SHEAR

B. N. Shakhdelyan

The viscosity of printing inks has been measured with the aid of the automatic capillary viscosimeter designed by Konstantinov and Vinogradov [1]. By the use of high initial pressures (up to 60 atm.) and fairly wide capillaries for testing such highly viscous systems as printing inks, it proved possible to attain high shearing rates. The average velocity gradient was varied in the range 100-400 seconds^{-1} and higher. On the other hand, measurements of printing ink viscosity with the aid of the rotating viscosimeter used previously [2] already become unreliable at above 40-50 seconds^{-1} as the result of extrusion of the ink from the annular gap and the formation of an air layer between the cylinders. Therefore by the use of the capillary viscosimeter it is possible to extend the flow curves of printing inks into the region of high rates of shear, thus extending the available information on their rheological properties.

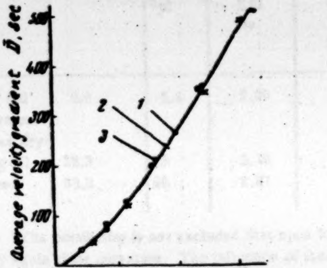

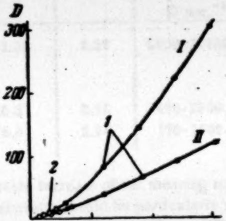

Fig. 1. Agreement between the flow curves for printing ink in a capillary viscosimeter with capillary radius: 1) 0.0954 cm; 2) 0.1494 cm; 3) 2.064 cm.

Fig. 2. Printing ink flow curves [I) offset ink No. 153, II) ink based on Milori] determined by 1) capillary, 2) rotational viscosimeter.

In view of the fact that measurements in conditions of thixotropic breakdown are of considerable interest in the characterization of printing inks, the thermostatic control device of the AKV-2 viscosimeter was modified in order to reduce to a minimum the time the samples were held before testing. In place of the single jacket placed on the apparatus after the chamber had been filled with the material under test, the chamber and capillary were fitted with detachable jackets heated by water circulated from a thermostat, and were kept there before the determinations. The ink samples before testing were stirred on a flat copper plate included in the general circulation system. Thus, the previously stirred and warmed ink was introduced into a chamber which was already thermostatically controlled. This avoids the need for keeping the sample in the apparatus, and enables the test to begin almost immediately after assembly of the apparatus, thus eliminating thixotropic effects.

It was found in the earliest experiments that the capillary radius does not affect the relationship between the velocity gradient and the stress, as it shown in Fig. 1 for one of the model inks consisting of 55% white pigment and 45% drying oil.

The constancy of the flow curves justifies, in the case of printing inks, the calculation of the average velocity gradient by analogy with the flow of a true viscous liquid, and confirms our earlier views on the pseudoplastic nature of printing inks [2]: viscous flow is much more characteristic of them than plastic deformation. This is also demonstrated by the smooth course of the flow curves with increasing rate and shearing stress.

Fig. 2 shows flow curves for typographic ink with Milori pigment and for offset ink No. 153, obtained with the rotational and the capillary instruments. The curves run smoothly from the low velocity region into the region of velocities attained with the capillary instrument; in one case the results obtained with the capillary and the rotational instruments overlap.

The curves show that the constant viscosity region disclosed by determinations with the rotational viscosimeter at rates up to 20-30 seconds^{-1} proves to be only a small part of the rheological curve on the scale used for high rates of shear. The gradual decrease of curvature of the flow curve, with a tendency to straighten over a wide range of high velocities, indicates an approach to constant velocity. Thus, when the velocity increases from 20 to 40-80 seconds^{-1}, the viscosity of ink No. 153 diminishes 2.25 times, while on further increase of the rate to 150-300 seconds^{-1} the decrease is only 20%. The viscosity is almost constant at rates in the range 80-300 seconds^{-1}.

TABLE

Viscosities of Inks Based on Light Fast Yellow Pigment (20% Content)

Vehicle	Viscosity of vehicle, η_0	Determination by rotational instrument			Determination by capillary instrument			$\frac{\eta_{rot.}}{\eta_{capil}}$
		η_{pl}	$\frac{\eta_{pl}}{\eta_0}$	Average velocity gradient $\bar{D}$ sec.$^{-1}$	η_{pl}	$\frac{\eta_{pl}}{\eta_0}$	Average velocity gradient $\bar{D}$ sec.$^{-1}$	
Raw Oil	0.6	5.4	9.00	15-45	1.32	2.20	6000-25000	4.1
Polymerized drying oil	12.3	39	3.16	15-45	26.5	2.15	470-2800	1.47
Ditto	33.5	96	2.87	15-45	75.0	2.24	170-1000	1.28

The possibility is not excluded that upon further considerable increase of the shearing rate the flow curves may again show curvature. The influence of shearing rate on viscosity should be particularly prominent in structurized systems, in which the vehicle has a weak stabilizing effect on the pigment particles.

Pigment suspensions in raw unpolymerized linseed oil are such systems, greatly different in properties from the usual printing inks. We have shown that such systems have a clearly defined flow limit and a much higher relative viscosity than inks with the same pigment content based on polymerized oils.

It was of interest to supplement these observations, obtained by means of the rotational viscosimeter, with results obtained with the capillary viscosimeter. Since the pressure applied to the test samples is always constant in the capillary instrument, the different inks flow out at different rates, which are higher as the viscosity is less. Therefore very high flow rates, of the order of 6000-25000 seconds^{-1}, develop in tests with low-viscosity systems based on raw oil. At such flow rates, destruction of agglomerates and flow orientation of the particles results in a considerable viscosity decrease.

The tabulated data show that the viscosity of ink based on light fast yellow pigment containing oil, when measured at these high rates, is 4 times as low as the viscosity measured in the rotational viscosimeter at low rates, 15-45 seconds^{-1}. The flow rates of inks containing polymerized drying oils in the capillary viscosimeter reach 1000-2800 seconds^{-1}, or 20-60 times the flow rate in the rotational instrument. The viscosity is 1.47-1.3 times less than the value determined by the rotational viscosimeter.

It appears very likely that even if the flow rate could be raised to 20000 seconds^{-1}, 7-20 times higher, the viscosity decrease would still not be as great as in the case of the weakly stabilized structurized system based on raw oil. It is significant that the high relative viscosity of the latter system, indicative of the poor stabilizing power of raw oil, also decreases.

At the high flow rates attained in the capillary viscosimeter the consistencies of all the three inks tend to equalize. This indicates complete breakdown of the structure produced by cohesion between the pigment particles. The stabilizing effect of the vehicle is greater as the minimum flow rate, at which complete breakdown of the structure occurs and at which the plastic viscosity of the system is least, is lower.

We express our gratitude to A.A. Konstantinov and V.V. Sinitsyn for guidance in the use of the capillary viscosimeter.

SUMMARY

1. The automatic capillary viscosimeter AKV-2 was used for measuring the viscosity of printing inks. The flow curves for printing inks were shown to coincide.

2. Much higher flow rates can be attained in the capillary viscosimeter than in the rotational instrument. The rheological curves then enter the constant viscosity region.

LITERATURE CITED

[1] A.A. Konstantinov, Proc. Acad. Sci. USSR, No. 4, 749 (1952); G.V. Vinogradov, Factory Labs., 19, No. 6, 680 (1953).

[2] B.N. Shakheldyan, Colloid J., 18, 111 (1956) (T.p. 105) *.

Received December 25, 1954 Moscow

---

*T.p. = C.B. Translation pagination.

EFFECT OF THE MOLECULAR WEIGHT OF HIGH POLYMERS ON THEIR ADSORPTION BY CARBON BLACK

A.I. Yurzhenko and I.I. Maleev

A restricted number of investigations have dealt with the adsorption of high polymers. At the present time the amount of available data is insufficient for the formulation of a general theory of the adsorption of large molecules. Equally little known is the influence of the type of adsorbent and solvent on the nature of the adsorption of high polymers of different structures and molecular weight. Study of these questions, however, should favor not only the creation of a theory of adsorption of high polymers, but also the solution of a number of other problems. For instance, the problem of the behavior of such active fillers as carbon black in rubber mixtures remains to be solved. On the other hand, differences in the adsorption of separate fractions of high polymers on different adsorbents may serve as a basis for an adsorptional method for the determination of the degree of polydispersity of high polymers. The work of Kolthoff and his co-workers [1,2] on the adsorption of butadiene–styrene rubber on carbon black indicates only very small differences in the adsorption of the different rubber fractions, but the view was put forward that the low molecular polymer fractions are adsorbed at a greater rate than the high fractions. These authors attempted to fractionate butadiene–styrene rubber by the passage of a solution through a carbon black column with the aid of the chromatographic frontal analysis method, and partial fractionation of the material was achieved. Recently [3] two methods were described for the fractionation of butadiene–styrene rubber by selective adsorption on carbon, which yielded semiquantitative results. Several other authors have also studied the adsorption of high polymers [4,5].

TABLE 1

Specific Surface of Carbon Blacks

Type of carbon	Specific carbon in m^2/g
Special	220.6
Furnace	10.0
Channel	89.1

It appeared of interest to study the effect of the mol. wt. of various polymers on the adsorption time of the polymers, and also of their fractions from dilute solutions. Such data may be important for adsorptional fractionation of high polymers and also in all cases when adsorption of high polymers takes place under dynamic conditions. This was the main purpose of the present investigation. In this connection we also studied changes in the molecular weight of the unadsorbed part of the polymers during adsorption from solution. As the adsorption experiments were carried out from different solvents and at different temperatures, it was also possible to determine the influence of these factors on the adsorption rates of high polymers from solutions.

Method of investigation. In order that the influence of substitution of some fractions of the adsorbed polymer by others should be excluded as far as possible, the adsorption experiments were carried out with dilute solutions (polymer concentration not greater than 0.25%) and with the adsorbent present somewhat in excess, until the polymer was practically completely exhausted from the solution.

The materials studied were polystyrene and polyisoprene samples of different molecular weights, obtained by the emulsion polymerization method at +5 and +50°; a series of polystyrene fractions was also obtained by fractional precipitation from methyl ethyl ketone and butyl acetate; methanol was used as precipitant. 20 fractions were obtained by fractionation from methyl ethyl ketone, and 35 from butyl acetate. The intrinsic viscosities of all the polymers and fractions were determined and used for molecular weight estimation. The adsorbent used was carbon black from the Ukhta and Dashava factories, previously washed with ether and dried at 100°. For a comparative characterization of the samples, the specific surface of the carbon black was measured by adsorption of acetic acid from benzene solution. The specific surface values for the carbon blacks are shown in Table 1.

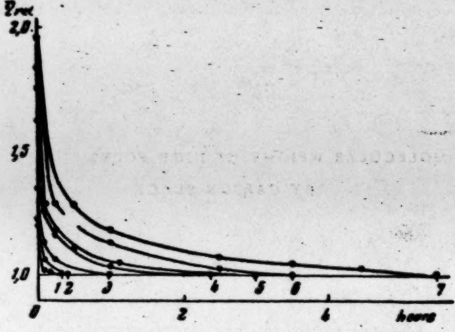

Fig. 1. Variation of the relative viscosity of 25% polystyrene solutions with adsorption time; the intrinsic viscosities of the solutions are: 1) 7.5; 2) 7.7; 3) 14.0; 4) 20.2; 5) 22.6; 6) 23.0; 7) 30.5.

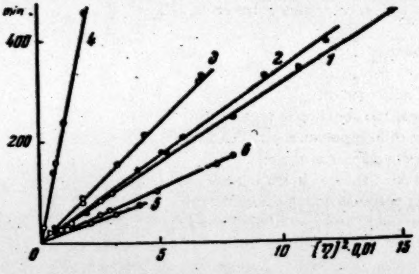

Fig. 2. Variation of the time for total adsorption with the square of the intrinsic viscosity; 1) polystyrene obtained at +50°C (c = = 0.25%); 2) ditto at +5°C; 3) polystyrene fractions (c = 0.25%); 4) polyisoprene (c = 0.1%); 5) polystyrene (c = 0.1%); 6) polystyrene fractions (c = 0.1%).

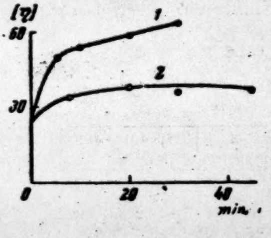

Fig. 3. Variation of the intrinsic viscosity of the unadsorbed portion of polystyrene: 1) from butyl acetate, 2) from benzene.

In addition to those listed, jet blacks, anthracene black and lampblacks were also studied.

The adsorption experiments were carried out at 20° in sealed ampoules, the contents of which were mixed by pouring the liquid from one part of the ampoule into another. The ampoules were filled with 0.50 g of the carbon and 15 ml of 0.1 or 0.25% polymer solution in benzene. The course of adsorption was followed by changes in the relative viscosity of the polymer solution. For each polymer sample a series of ampoules was placed in the thermostat; the ampoules were centrifuged in the sealed state at definite time intervals and opened.

TABLE 2

Total Adsorption Time for Polystyrene from Various Solvents

Solvent	Relatave viscosity of original solution	Adsorption time in minutes	Solvent	Relative viscosity of original solution	Adsorption time in minutes
Butyl acetate	1.169	15	Toluene	1.530	60
Methyl ethyl ketone	1.214	30	Xylene	1.467	90
Benzene	1.641	40	Chloroform	2.771	140

Nearly all the carbon blacks listed formed dark solutions when added to the polymer solutions, and the carbon black was not retained by the filter in filtration of such solutions through paper. It proved possible to obtain transparent solutions by the addition of a special carbon to polymer solutions of low concentration. This carbon had the highest adsorption capacity. In the given conditions, the special carbon was able to adsorb polystyrene, polyisoprene, and SKS-30 rubber completely. The time for complete adsorption was taken to be the time required for complete exhaustion of the polymer from the solution. The other carbon black specimens did not give complete adsorption, and furnace black, which has a lower specific surface, adsorbed polystyrene to a greater extent than did channel black. Thus, in this case the specific surface of the adsorbent is not proportional to its adsorption capacity, which is due to differences in the surface state of the carbon particles, their structure, and other properties of the carbon.

RESULTS OF THE INVESTIGATION

Effect of the molecular weight of high polymers. The molecular weight of the original sample has a great influence on the adsorption rate, and consequently on the time for complete adsorption. The variation of the relative viscosity of polystyrene solutions as a function of the adsorption time is shown in Fig. 1. The data show that the adsorption time of the high polymer increases fairly rapidly with increasing molecular weight of the adsorbed polymer. In the molecular weight range studied, the time for complete adsorption of the high polymer was directly proportional to the square of the intrinsic viscosity; this relationship between the time for total adsorption and the molecular weight of the polymer was found both for the unfractionated polymers obtained at +5 and +50°, and for separate fractions (Fig. 2).

An increase of the adsorption time with increasing molecular weight of the polymer was also found for the other polymers studied, in particular polyisoprene. It was found that, under equal conditions, polyisoprene is adsorbed much more slowly than polystyrene.

For determinations of the intrinsic viscosity of the unadsorbed portion of polystyrene, the latter was isolated in the course of adsorption. The experiments were carried out in a liter ampoule into which was placed 26.6 g of the special carbon black and 800 ml of 0.25% polystyrene solution. The ampoule was placed in a shaker and the ampoule contents were ultracentrifuged at definite time intervals. The resultant clear solutions were concentrated by removal of solvent under reduced pressure, and the polymer was then precipitated by methanol. As Fig. 3 shows, the adsorption of polystyrene from butyl acetate is accompanied by continuous enrichment with the higher fractions. In the case of benzene solutions the enrichment with the high molecular weight fractions is less pronounced, and after prolonged adsorption the intrinsic viscosity of the unadsorbed part of the polymer decreases again, owing to partial replacement of the low molecular by the high molecular fraction. In both cases the experiments were continued to almost complete exhaustion of the polystyrene from solution.

The adsorption time of polystyrene is influenced by the temperature. A temperature increase of 10° results in an increase of the rate of adsorption on the special carbon of about 1.1. This relationship was found to apply in the temperature range from 20 to 100°.

Effect of solvent. The solvent from which adsorption occurs has a significant influence on the time of adsorption. 0.1% polystyrene solutions with an intrinsic viscosity (base-molar) of 46.1 in benzene at 20° were studied. The total adsorption time generally increases in the transition from "poor" to "good" solvents (Table 2).

These results indicate that the adsorption time of the polymer is influenced by the shape of the macromolecules in solution and the degree of solvation, determined by the nature of the solvent.

SUMMARY

1. It is established that in the molecular weight range of polymers and fractions studied the adsorption time of a high polymer on carbon black increases with increasing molecular weight. The time of total adsorption is proportional to the square of the intrinsic viscosity.

2. It is shown that in the adsorption of polystyrene from benzene and butyl acetate on special carbon black the unadsorbed part of the polymer becomes enriched with the higher molecular weight fractions. In the adsorption of polystyrene from butyl acetate the unadsorbed portion is enriched continuously up to complete adsorption of the polymer from solution. In the case of benzene solutions the increase of intrinsic viscosity is less pronounced.

LITERATURE CITED

[1] I.M. Kolthoff and A. Kahn, J. Phys. Colloid Chem., 54, 251 (1950).

[2] I.M. Kolthoff and R.G. Gutmacher, J. Phys. Chem., 56, 740 (1952).

[3] M.A. Golub, J. Polymer Sci., 11, 583 (1953).

[4] R. Simha, H.L. Frisch, and F.R. Eirich, J. Phys. Chem., 57, 584 (1953).

[5] H.H.G. Jellinek and H.L. Northey, J. Polymer Sci., 14, 583 (1954).

Received May 15, 1955

The Ivan Franko State University - Lvov

DISCUSSIONS

THE MOLECULAR NATURE OF THE FRICTION OF RUBBER

G.M. Bartenev

It is now generally accepted that the nature of the deformation of rubber is different from that of solids. With regard to other mechanical properties of rubber, such as external friction, the position is not so clear.

The following two viewpoints, opposed in principle, have been put forward concerning the molecular nature of the friction of rubber (without lubricant*). Deryagin and Ratner [1-5] consider that under external friction rubber behaves as a solid**. This provides the basis for the application of Deryagin's theory of friction [6] to rubber. Schallamach [7] and myself [8] regard the friction of rubber (against rubber or a solid) as a molecular-kinetic process, caused by thermal motion of the molecular chains along the contact surface, in which energy barriers which depend on the molecular adhesion forces are overcome.

On this basis, a theory was developed [8] of the friction of rubber of any degree of roughness against smooth solid surfaces. The relationship for the sliding velocity as a function of the tangential force (or the equivalent frictional force) and the temperature passes under certain conditions into the Schallamach formula, which is evidence in support of the molecular-kinetic view. According to the theory, when the sliding rate tends to zero the frictional force also tends to zero, just as the shearing stress in plastic (disperse and other) systems tends to zero on unlimited decrease of the deformation rate.

The author's theory [8] was developed for friction on smooth solid surfaces, without consideration of mechanical hindrances arising in friction on rough surfaces. However, consideration of the supplementary factor (roughness) is unimportant in a theoretical examination of the molecular nature of rubber friction.

The typical relationship between the frictional force and the load — valid for rubber only for small loads, and for solid elastic bodies at practically any loads — is shown in Fig. 1. This relationship conforms to the Coulomb formula:

$$F = a + bP, \qquad (1)$$

where F is the frictional force, P is the load; a and b are constants determined experimentally.

The proof of the identical nature of the friction of rubber and solids [1-4] is based on the similarity of the relationships between the frictional force and the load. However, this similarity cannot serve as a proof, as the general form of the mathematical relationship between the frictional force and the load in the friction of smooth surfaces is largely determined not by the mechanism of friction, but by the relationship between the frictional force and the area of actual contact S^A (which in turn depends on the load)***

$$F = CS^A. \qquad (2)$$

The physical meaning of the coefficient C, which has been considered for solids [6] and for rubber [10], is determined by the molecular nature of the friction of the materials and the experimental conditions.

---

*It has been shown [9] that the same laws apply to the friction of lubricated rubber as to the friction of lubricated solid surfaces.

**We are not concerned here with rubber in the glassy state, when this assertion becomes trivial.

***In the investigations in question [1-4] the actual contact area was not controlled or measured.

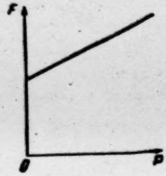

Fig. 1. Effect of load on the frictional force of rubber (at not very high loads).

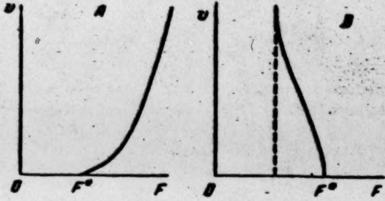

Fig. 2. Effect of tangential force on the sliding rate in the friction of rubber (A) and metal (B) against solid surfaces.

The nature of friction is basically displayed in another property – the kinetics of the friction process. Therefore it is of interest to compare the effects of tangential force on the sliding velocity for rubber and metals. It is known that the velocity as a function of the force increases for rubber and decreases for metals (Fig. 2). The frictional characteristics of rubber, shown in Fig. 2 in the usual terms of sliding velocity, are in agreement with the author's theory [8] but not with Deryagin's theory of the friction of solids [6]*. The coalescence of the curve with the abscissa axis below the conventional sliding limit F* is apparent only; it is due to the rapid rise of the frictional force in the low velocity region beyond the limits of measurement, which gives the impression of the existence of an absolute force of static friction.

The friction of rubber is an effect of the same type as plastic flow. Hence we have the resemblance between the curve characterizing the friction of rubber and the rheological flow curve for plastic bodies. Just as plastic systems do not have an absolute flow limit, so in the friction of rubber there is no absolute sliding limit or a static friction force (the static friction of rubber is a conventional value of the same kind as the plasticity limit). The static frictional force or the conventional sliding limit F* should decrease with increasing temperature. This is confirmed by Schallamach's experiments [7].

In contrast to the above, in the papers [1-5] it is assumed that rubber, like solids, has an absolute static frictional force.

According to [8], the frictional force is directly proportional to the number of chains in contact with the solid surface, and depends on the forces of adhesion across the energy barrier (activation energy). The number of chains depends greatly, and the activation energy slightly, on the load, as the molecular forces of adhesion are far greater than the loads on the actual contact surface of the rubber as used in engineering practice.

According to the Thirion formula [11, 12], the frictional force tends to a constant value with increasing load**, while the coefficient of friction tends to zero, which is possible on the assumption that the load has practically no effect on the adhesion forces (activation energy)***. As the number of chains is proportional to the area of actual contact, we obtain Formula (2). The molecular nature of friction of rubber is implicit in the factor C = C(v, T), which does not depend on the normal load if its influence on the adhesion forces is neglected, but which leads to the dependence of the friction on the temperature and the velocity. The dependence of the friction on the load is mainly implicit in the factor S^A, and is therefore determined largely not by the nature of the friction but by mechanical and geometrical characteristics: the elastic constants of the material, the profile of the contact surface, and the dimensions of the specimen.

---

*According to Deryagin, the coefficient C does not depend on the temperature or the sliding rate; its values are given by $C = \mu_{\infty}(p_0 - p_A)$, where μ_{∞} is a molecular constant, p_0 is the specific adhesion force, and p_A is the pressure on the actual contact area.

**Fig. 1 represents the region of small loads. At high loads the curve deviates from linearity, and practically tends to a constant limit [11, 12]. However, with indefinite increase of the load, because of the effect of the load on the activation energy, the frictional force will still increase, though slowly [10].

***Consideration of the effect of the load on the activation energy [10] leads to the introduction of a correction term, in the form of an additional frictional force proportional to the load, which results in a binomial formula, analogous to the binomial formula for solids, but with a different physical content. For the sake of simplicity this correction term is neglected in the subsequent discussion.

Consequently the search for a mathematical relationship between the frictional force and the load, with neglect of the effect of the load on the adhesion force or the activation energy, is an independent problem, not related to the molecular nature of the friction of this or that substance. Therefore a comparison of the relationships between the frictional force and the load cannot lead to a direct solution of the problem concerning the similar or different nature of the friction of rubber and of solids.

A strict evaluation of the dependence of the area of actual contact on the load is impossible, therefore either the actual surface is substituted by a very simple model, or the evaluation is based on general considerations. The first method, used by Schallamach, did not give satisfactory results for rubber. The second method was used in the paper [10]. If we denote the residual contact area at $P = 0$ by S_0^A, we obtain, at low loads, a linear relationship for the actual contact area, and at high loads, a practically constant value in view of the fact that $S^A \approx S^N$, where S^N is the area of nominal contact.

With consideration of these conditions for small and large loads, it is possible to derive [10] an interpolated relationship for the actual contact area, substitution of which into Equation (2) gives the approximate formula:

$$F = CS^N (S_0^A + \alpha P) / (S^N + \alpha P), \qquad (3)$$

where C is a constant which depends on the adhesion forces (through the activation energy) and on the experimental conditions - the sliding rate and temperature; α is a constant which characterizes the elastic properties and the surface profile of the rubber (the irregularity of the contact surface is not considered, since the friction of rubber against smooth solid surfaces is considered).

This formula is in good agreement with all available experimental data [3-5, 11, 12]. For example, in absence of a residual contact area, when $S_0^A \approx 0$. Formula (3) gives the Thirion experimental formula (for any load). At small loads a binomial formula is obtained(on the assumption that $S_0^A \ll S^N$):

$$F = CS_0^A + C\alpha P, \qquad (4)$$

which coincides with the Coulomb formula.

The law for the friction of rubber at any load assumed in the papers [1-4] was the Deryagin binomial formula derived for solids [6]:

$$F = F_0 + \mu_\infty P, \qquad (5)$$

where F_0 is a value proportional to the adhesion force between the surfaces; μ_∞ is a molecular constant numerically equal to the coefficient of friction at an infinitely large load.

The Formula (4), valid under definite conditions of friction of rubber, only formally coincides with Equation (5). The physical meaning of the two formulas and of the constants in them is different. Moreover, in Formula (5) the frictional force does not depend on the sliding rate or the temperature.

It follows that Formula (5) is not generally applicable to rubber and that the binomial Equation (4) cannot be extrapolated to large loads, as was done by some authors [3, 4]. Therefore, the determination of the coefficient of friction for large loads by extrapolation, as was done in these papers, cannot lead to correct results.

The Thirion formula was considered to be erroneous in the paper [3], as it contradicted the frictional law expressed by Formula (5). However, it had already been shown [5] that the Formula (5) is not applicable to rubber if (as was assumed in the earlier papers by the same authors [3, 4]) F_0 is taken to be constant. In the same paper [5] the authors attempted to improve the agreement between theory and experiment by assuming that

$$F_0 = BP^{1-h}, \qquad (6)$$

where h is the hardness of the rubber in arbitrary units. By substitution of this relationship into Equation (5), the authors obtain, for any load, a formula of the type

$$\mu = \mu_\infty + B/P^h, \qquad (7)$$

where μ is the coefficient of friction; B depends on the adhesion forces and on S^N.

The formula was verified over a limited range of loads. Nevertheless the authors consider that the application of the binomial Formula (5) to the friction of rubber gives useful results. It can be easily shown, however, that the initial Formula (6) is incorrect, if it is remembered that the adhesion force is proportional to the area of actual contact and therefore: $F_0 = C_0 S^A$. Further, comparison with Equation (6) shows that

$$S^A = BC_0^{-1}P^{1-h},$$

where $1 - h > 0$. This means that with increasing load the area of actual contact must increase indefinitely — a result contrary to reality, and in contradiction to the experiments of Thirion, Denny, and the authors themselves.

Consequently, Formula (7) is incorrect, as is the authors' conclusion that with the aid of this formula it is possible to determine the coefficient of friction at large loads.

LITERATURE CITED

[1] B.V. Deryagin, What Is Friction, Acad. Sci. USSR Press, pp 164-180 (1952).

[2] B.V. Deryagin, S.B. Ratner, and M.F. Futran, Proc. Acad. Sci. USSR, 92, 1137 (1953).

[3] S.B. Ratner, Proc. Acad. Sci. USSR, 83, 443 (1952); 93, 47 (1953).

[4] S.B. Ratner and V.D. Sokolskaya, Proc. Acad. Sci. USSR, 86, 121 (1952).

[5] S.B. Ratner and V.D. Sokolskaya, Chem. Ind., No. 1, 27 (1955).

[6] B.V. Deryagin, Proc. Acad. Sci. USSR, 3, 93 (1934); J. Phys. Chem., 5, 1165 (1934).

[7] A. Schallamach, Proc. Phys. Soc., 66, 386 (1953).

[8] G.M. Bartenev, Proc. Acad. Sci. USSR, 96, 1161 (1954).

[9] G.M. Bartenev and L.E. Peregrudova, Proc. Acad. Sci. USSR, 96, 277 (1954); Trans. Inst. Rubber Ind., 2, 48 (1955).

[10] G.M. Bartenev, Proc. Acad. Sci. USSR, 103, No. 6 (1955).

[11] P. Thirion, Rubber Chem. and Technol., 21, 505 (1948).

[12] D.F. Denny, Proc. Phys. Soc., 66, 721 (1953).

Received July 8, 1955 Moscow

Editorial note. After the publication of G.M. Bartenev's article it is proposed to publish discussions on the friction of rubber in subsequent issues.

THE SUBJECT AND PRINCIPLES OF A COURSE IN COLLOID CHEMISTRY

S.S. Voyutsky and P.A. Rebinder

Pasynsky, Vasilyev, and Dogadkin [1] have raised the discussion of the very urgent problem of the subject and principles of a course in colloid chemistry.

The advances of colloid chemistry in the last few decades have indeed been enormous. From an abstract, descriptive, and relatively narrow branch of science, in which individual peculiar phenomena were considered only qualitatively or semiquantitatively, colloid chemistry has become a very large independent section of physical chemistry, outstanding in the importance, breadth, and diversity of its applications.

However, with accumulation of experimental data and the appearance of new views and theories, the subject and problems of colloid chemistry have lost their clarity and precision, and at the present time this science is, in a sense, undergoing a crisis – a crisis of growth. Contradictions and a lack of clarity in the subject and problems of any science are felt most acutely in its teaching and study. It is therefore no accident that the discussion opened in the pages of Colloid Journal has developed mainly around the subject and the principles of a course in colloid chemistry, although there is no doubt that the question is of a far more general significance.

In an examination of the subject of colloid chemistry, the main difficulty, of course, lies in the question of high polymer solutions, the single phase nature of which was established with certainty in recent years.

Several investigators consider that high polymer solutions, despite their one-phase nature, should be considered in colloid chemistry. The arguments in favor of this viewpoint are: a) the dimensions of colloidal particles and macromolecules are similar; b) partly because of this, colloidal and high polymer solutions have a number of features in common; c) a continuous transition in the form of intermediate systems exists between the two types of solutions. Let us examine these arguments one by one.

The idea that high polymer solutions are similar to colloidal solutions in consequence of the similar dimensions of the molecules and the micelles has rarely been explicitly stated, but it can be easily read between the lines in certain articles, monographs, and textbooks. For example, the term "molecular colloids" which has been proposed for high polymers [2] can be understood only in the sense that the dimensions of the molecules of this class of substances correspond to the dimensions of colloidal particles and by this determine their colloidal properties.

This conception is incorrect. Those who assert that colloidal properties are determined only by particle size forget that the main sign of colloid systems in the direct meaning of the term is a di- or multiphase nature and micro- or ultramicroheterogeneity, that is, the presence of a highly developed interphase. This was stressed even in the work of N.P. Peskov.

Pasynsky, Vasilyev, and Dogadkin [1] consider that an intrinsic part of colloid chemistry is the science of high polymer solutions, because of the similarity of properties of colloidal and high polymer solutions. They point out that the two types of solutions have molecular-kinetic, dielectric, optical, and electrochemical properties in common. It is easy to see, however, that the analogies are superficial and formal. Indeed, there does not seem any reason to speak of any special resemblance between the molecular-kinetic properties of colloidal and high polymer solutions, when it is known that these properties are characteristic of any disperse system if its particles are still capable of independent thermal motion. In that case colloidal and macromolecular solutions should be combined with the usual true solutions. It is well known, however, that a natural and healthy tendency in the development of science is differentiation rather than integration of its independent divisions.

Analogous considerations can be put forward with regard to the optical and dielectric properties. As regards the electrochemical properties, here the resemblance between colloidal and macromolecular solutions is even more conventional. For example, is it permissible, in substance and not in form, to say that macromolecules carrying discretely situated ionogenic groups have the same sort of electric double layers as the particles of typical colloids? Here it would be better to draw an analogy with ordinary individual ions surrounded by a Debye ionic atmosphere. On the other hand, it must not be forgotten that even an apparent identity of some electrochemical properties is not an adequate basis for drawing extensive analogies between the systems. As is known, both ordinary ions and colloidal particles are not only transported in an electric field, but even have approximately equal migration rates. Nevertheless, it would be incorrect to identify electrolytic and electrophoretic phenomena and not to see a qualitative distinction between them.

The question of the suitability of consideration of high polymer solutions together with colloid systems must evidently be decided not on the basis of the properties which these systems have in common, but of distinctions between them.

The authors of the paper [1] themselves point out that a distinction of principle exists between colloidal systems and high polymer solutions. The first group contains thermodynamically irreversible, non-equilibrium heterogeneous disperse systems, which require stabilization for an increase of their aggregative stability, while the second group is characterized by thermodynamic stability (a state of equilibrium) typical of true solutions.

It is also necessary to take into consideration a special group of colloidal systems which are formed spontaneously in certain conditions, and which are therefore thermodynamically stable. They are the so-called semicolloids, such as aqueous solutions of soaps or surface-active substances generally, with fairly long hydrocarbon radicals. Of a similar nature are the highly disperse spontaneously formed emulsions of "soluble oils" (hydrocarbon liquids with a high content of surface-active substances) in water. The formation of such emulsions is closely associated with solubilization (colloidal solubility). In this group we may also include emulsions formed close to the critical temperature (the temperature of mixing of two liquid phases). In such systems the surface tension at the interphase is very low, close to zero, with a value less than a hundredth part of one erg/cm^2, as is shown by a simple theoretical calculation [3]. Such highly lyophilic systems (in the sense of a strong molecular affinity between the phases) are transitional between two-phase thermodynamically unstable disperse systems and true solutions (one-phase systems). When the surface tension at the interphase becomes zero (the critical point condition, according to Mendeleev), the phases merge into one. Such systems also include colloidal suspensions of solid phases which spontaneously disperse in water, such as sodium or lithium bentonites [3]. However, these intermediate stages have nothing in common with any transition, non-existent in reality, between colloidal solutions and true solutions of high polymers.

The behavior of colloidal and high polymer solutions also shows enormous differences; a comparison of the methods for preparation of the two systems is sufficient to show this. It is known that colloidal systems may be formed both by dispersion and by condensation methods. High polymers do not require dispersion with the expenditure of work for conversion into solution, as they are capable of spontaneous solution in suitable media, while it is meaningless to speak of the preparation of high polymer solutions by condensation. The attempt to draw an analogy between the formation of colloidal particles by condensation, and the polymerization process [4] is, of course, not justified. In the formation of colloidal systems by the condensation method, molecular aggregates are formed by means of residual Van der Waals forces; in the formation of high polymers from low-molecular substances by condensation or polymerization, typical chemical reactions occur with utilization of principal valencies. In addition, in the first instance we have the synthesis of a system or a new phase in a given medium, and in the second, the synthesis of a new substance. Similar conclusions may be reached by consideration of such typical colloidal processes as peptization and coagulation. Analogous processes do not exist in high polymer solutions.

The third argument in favor of the inevitable inclusion of high polymer solutions in colloid chemistry, namely that transitional systems exist between these two types of systems, also cannot stand up to serious criticism. The existence of transitional systems is typical of any real classification. It is enough to remember the classifications in biology, organic chemistry, and a number of other sciences. However, the existence of transitional intermediate systems or groups in these classifications in no case leads to obliteration of the boundaries between individual classes. On the contrary, the very concept of a transitional system stresses the existence of classes differing significantly from each other. It is also appropriate to point out here that if the existence of intermediate, transitional systems was a serious argument against separation of high polymer solutions from colloidal systems, we would in general not be justified in considering these systems apart from true solutions, as a number of transitional systems exist between solutions of low-molecular substances and colloidal solutions, and between low-molecular and high-molecular solutions.

In contrast to those who consider that the study of high polymer solutions should form an essential part of colloid science, we believe that the time is already ripe for a division of these two branches of physical chemistry, or at least, for a fairly sharp boundary to be drawn between them. This has been stated repeatedly both in a number of lectures and discussions (for example, at meetings of the Moscow Section of the Mendeleev Chemical Society) and in the press [5]. As arguments in favor of this view we may cite not only the essential differences in the fundamental characteristics of the two types of systems which were already noted above, but also the enormous distinctions in the very circle of ideas which form the basis for the interpretation of the experimental facts. Indeed, while colloid chemistry is based mainly on studies of surface phenomena in a wide sense of the term, including, for example, the kinetics of new phase formation, in the interpretation of the specific properties of high polymer solutions the physical chemist mainly relies on the statistics of flexible long chain molecules. Therefore the two types of systems demand a quite different description and interpretation of the phenomena which occur in them.

Another argument in favor of the separation of the study of macromolecular solutions from the field of colloid chemistry is the fact that these solutions cannot be isolated from the study of high polymers as a whole. The inclusion of all high polymer science in modern colloid chemistry, as was proposed by Zhukov [2], on the other hand, is impossible owing to the great extent of this field.

A measure of the value of any idea is its practical utilization. From this standpoint, the validity of the separation of the study of macromolecular solutions from colloid chemistry has been fully confirmed. Independent textbooks on the physical chemistry of high polymers have attained high status both here and abroad. It is significant that even if authors attempt to combine the study of colloidal systems and high polymers in a single book, the book is then inevitably divided into two ill-connected parts. An example is the well known book Colloid Science, edited by Kryut [7]. There is also a tendency to separate journals – in the Soviet Union we have, since 1941, in addition to Colloid Journal, a special publication – "High Molecular Compounds" which, it is true, is at present not issued regularly. In the United States of America, in addition to the Journal of Colloid Science, there is a journal devoted specially to the physical chemistry of high polymers – Journal of Polymer Science. Since 1943 conferences on high polymers have been held in the Soviet Union parallel with conferences on colloid chemistry, and experience has shown this to be very suitable.

Of course, when we speak of the suitability of removing the section on high polymer solutions from courses of colloid chemistry, we do not imply that this separation is to be effected at once and in all cases. The division is obviously appropriate in those higher educational establishments where sufficient time is allocated to the study of colloid chemistry, for example, in the chemical faculties of universities. Where relatively few hours are allocated to colloid chemistry, the section on high polymer solutions can suitably be retained in the colloid chemistry course. However, even in such cases the teacher, in commencing the presentation of the section, should clearly stress the essential difference between colloidal and high polymer solutions and explain that their presence in the same course is due only to a formal resemblance between certain properties of both systems and the existence of some investigation methods common to both.

We will now examine the second important question which arises in a discussion of the subject and principles of a course in colloid chemistry: is it necessary to examine microheterogeneous, that is, the more coarsely disperse systems in colloid chemistry, or do they belong to molecular physics or to the study of surface phenomena?

The paper [1] is muddled in relation to these systems. On the one hand, these systems appear to compose Group IV of the proposed classification. This is indicated by the fact that Group IV also includes simple (?) adsorbents. On the other hand, such typical representatives of microheterogeneous and coarsely disperse systems as foams and emulsions are quite incorrectly placed in Group III – with colloidal systems. Thus, the view of the authors of the paper on this subject is not clear.

To us it seems quite obvious that the study of microheterogeneous systems should be included in colloid chemistry, since these systems have much in common with typical colloidal systems not only in form, but in substance. This deep similarity in properties is due to the fact that both groups of systems are characterized by a highly developed surface, and all the associated specific features. In addition, we believe that much more space should be given to microheterogenous systems in the colloid chemistry course than has been done hitherto. This is also related to the enormous practical significance of microheterogeneous systems. In addition to suspensions, emulsions, and foams, the practical importance of which is generally known, an increasingly large role is played in modern technology by powdered substances (cements, pigments, fillers, carbon black, fertilizers, insecticides and fungicides), porous materials (foam glass, a number of new constructional materials, expanded plastics and rubbers), and fibrous systems (paper, cardboard, insulating materials, leather substitutes). It should be pointed out that soils, with their highly complex physical chemistry, should also be included among the microheterogeneous systems. The modern research chemist, engineer, or teacher of chemistry should also have some idea of the physical chemistry of such processes as flotation, gravitational ore dressing, filtration, silt deposition, impregnation of porous systems, production of articles by powder metallurgy, powder granulation, formation of films from high polymer dispersions, etc. All these are processes characteristic of microheterogeneous systems, and can only be successfully considered in a colloid chemistry course on the basis of modern concepts of protective factors, aggregative stability of disperse systems, mechanism of structure formation, etc.

It is obvious that differences also exist between colloidal and microheterogeneous systems, and it is possible that in the future the science of microheterogeneous systems will develop into an independent discipline. However, at the present time these differences are quantitative in character and do not prevent the examination of both groups of systems in a single course.

In our opinion, on the basis of all that has been said above it is possible to define colloid chemistry definitely as a science [8]. Obviously, the definition of colloid chemistry as the physical chemistry of high molecular and heterogeneous highly disperse systems [1] is too wide. A more correct definition of colloid chemistry would be the physical chemistry of disperse micro- and ultramicroheterogeneous systems and surface phenomena. However, even this definition is too wide — the study of surface phenomena has now quite independent significance. Strictly speaking, colloid chemistry is the physical chemistry of heterogeneous disperse systems, and it includes the consideration of their special properties and processes taking place in them.

LITERATURE CITED

[1] A.G. Pasynsky, P.S. Vasilyev, and B.A. Dogadkin, Colloid J., 15, 466 (1953) (T.p. 483)*.

[2] I.I. Zhukov, Colloid Chemistry, Part I, p. 12, Leningrad State Univ. Press (1949).

[3] P. Rehbinder, Coagulation and Flocculation, Discuss. Faraday Soc., No. 18, 151 (1954); L.A. Abduragimova, P.A. Rebinder, and N.N. Serb-Serbina, Colloid J., 17, No. 3, 184 (1955)(T.p. 171)*.

[4] N.P. Peskov and E.M. Aleksandrova-Preis, A Course in Colloid Chemistry, State Chemical Press, p. 255 (1948).

[5] S.S. Voyutsky and M.I. Prozin, High School Bulletin, No. 5, 46 (1952).

[6] P.A. Rebinder, J. Acad. Sci. USSR, No. 2, 8 (1955).

[7] H.R. Kruyt, Colloid Science, Vol. I, II, Elsevier Publ. Co., (1952).

[8] P.A. Rebinder, "Colloid Chemistry", article in the Great Soviet Encyclopedia, 2nd Ed. Vol. 22, p.5.

Received December 6, 1955 Moscow

---

*T.p. = C.B. Translation pagination.

DEPOSITION OF PARTICLES ON OBJECTS FROM SURROUNDING STREAMS

A. G. Amelin and M. I. Belyakov

The deposition of suspended particles upon objects from streams is met in laboratory practice and in a great variety of industrial processes. In technology, deposition of suspended particles (by filtration of streams of particles) is used for separation of valuable or harmful substances [1], and in the application of economic poisons for the protection of plants from pests and diseases [2]. The icing of airplanes and telegraph cables is caused by deposition of supercooled water droplets from clouds and mists [3]. The growth of raindrops is the result of deposition of fine droplets on larger drops, which move at greater speeds than the fine droplets when falling [4]. In laboratory and research work deposition of particles from streams is utilized in determinations of the degree of dispersion of aerosol systems and of the concentration of a suspended substance in a stream [5]. Numerous other examples could be added to this list.

Despite the great practical importance of the deposition of particles from streams, at the present time there is a lack of sufficiently reliable data for practical calculations on the deposition of particles on objects from surrounding streams.

The first group of published investigations on the deposition of particles from a stream deals with the development of a method for determination of the degree of dispersion of aerosol systems, based on the settling of suspended particles from a stream directed onto a plate [5, 6]. The results obtained in these investigations were not subjected to theoretical analysis, and therefore they have only a narrow applied significance.

The publications of the second group, mainly theoretical in nature [4, 7], consider the deposition mechanism of suspended particles and provide a mathematical description of the process. This work was based on general theoretical considerations with the use of limited experimental data. There are great discrepancies between the results, especially with regard to the minimum size of the particles which can be deposited in given conditions.

Recent publications [8], based on theoretical assumptions, contain calculations of the minimum diameter of the deposited particles and give results of experimental investigations which confirm the general theoretical deductions.

The deposition of suspended particles on a surrounded object is characterized by the collection efficiency E (sometimes also termed the deposition coefficient) which is an expression for the relative number of particles deposited on the object (henceforth the suspended particles are taken to be spherical drops):

$$E = \frac{n}{Nvs\tau}, \tag{1}$$

where E is the collection efficiency; n is the total number of drops of a given size deposited on the object; N is the total number of drops of the given size in unit volume of the aerosol; v is the velocity of the stream away from the object, in cm/second; s is the "midship" section of the object, or the area of a projection of the object along the axis of the stream, in cm²; τ is the time in seconds.

Most investigators express the collection efficiency as a function of the dimensionless quantity K (Fig. 1), where

$$K = \frac{\rho v d^2}{18\mu D}. \qquad (2)$$

where ρ is the density of the drop in g/cc; μ is the viscosity of air in g/cm second; D is the size of the object in cm; d is the diameter of the drop in cm.

For example, Langmuir [4] gives the following expression for a cylinder for the case of potential flow:

$$E = \frac{K^2}{(K + 0.25)^2} \qquad (3)$$

and for viscous flow:

$$E = \left[1 + \frac{0.75 \ln 4K}{2K - 1.214}\right]^{-2}. \qquad (4)$$

The mechanisms of the impaction of suspended particles from a stream on the front (leading) and rear (trailing) sides of the object are not the same. A stream moving with a speed $\underline{v}$ (Fig. 2) on meeting an obstacle changes its direction and flows around the object. Because of inertia forces, the trajectory of a suspended particle which moves with the stream flowing around the object does not coincide with the path of the stream, and if the former crosses the surface of the object the particle is deposited on it.

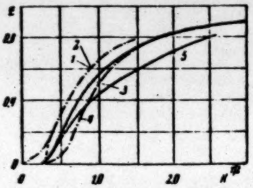

Fig. 1. Variation of the collection efficiency E with the parameter K according to the data of:
1) Albrecht; 2) Sell; 3) Langmuir; 4) Landhal and Herrmann; 5) Ranz and Wong.

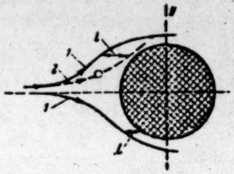

Fig. 2. The motion of a stream and droplet near a surrounded cylinder: 1) stream trajectory; 2) droplet trajectory.

Thus the particles flowing around the object pass through a certain layer $\underline{l}$ of viscous flow owing to inertia forces. Forces of gravity and of interaction between the suspended particles and the object (if such forces exist; for example, in presence of electric charges) influence this process. The general differential equation for the motion of a suspended particle near a surrounded object is complex, as the nature of the motion of the stream near its surface is not sufficiently fully understood. The solution of this equation for the purposes of the present problem involves considerable difficulties. A rational approach is to conduct an experiment and to apply the theory of similarity to the experimental data.

Let us consider the simplest case of impaction of droplets from a stream on a vertical surface, when the force of gravity may be neglected. If it is assumed that there are no forces of interaction between the droplets and the surface, the general equation for the motion of a moving drop may be written as

$$\frac{m dv}{d\tau} = -s, \qquad (5)$$

where m is the mass of the drop in g; s is the resistance of the medium in g·cm/second. The resistance of the medium for droplets 1-60 μ in diameter, when $v < 10^3$ cm/second, may be expressed [4] with an accuracy sufficient for practical purposes by the Stokes equation:

$$s = 3\pi\mu v d. \tag{6}$$

If we substitute the value of s from Equation (6) into Equation (5), and consider that $m = \pi\rho d^3/6$ and $d\tau = dl/v$, where l is the path traversed by the drop on account of inertia forces (Fig. 2), we have:

$$\frac{dv}{dl} = -\frac{18\mu}{\rho d^2} \quad \text{or} \quad l = \frac{\rho v d^2}{18\mu}. \tag{7}$$

For the drop to reach the surface of the object it must travel a certain distance L (Fig. 2); therefore, the equation $l = L$ must be true.

For a particle furthest removed from the axis, the value of L will be greater with increasing size of the object. Therefore, for two such instances, in which an equal degree of drop impaction is reached, we may write

$$l''/l' = D''/D'. \tag{8}$$

From Equations (7) and (8) the Stokes criterion may be derived by the usual method [9]:

$$\frac{\rho v d^2}{\mu D} = \mathrm{St}. \tag{9}$$

It follows from Equations (2) and (9) that

$$K = \frac{\mathrm{St}}{18}, \tag{10}$$

By analogy with heat transfer [10] and diffusion [11] processes, the value of the collection efficiency for the front side of the surrounded object may be represented by the equation

$$E = m(\mathrm{St})^n. \tag{11}$$

where m and n are coefficients which depend on the Stokes criterion. This is the mechanism of particle impaction on the front face of the surrounded object; it obeys different laws on the rear side. In the precritical region of the stream no impaction of droplets occurs on the rear side of the object, as the trajectory of the droplets is in advance of the trajectory of the stream. At sufficiently high Reynolds numbers, eddies are formed at the rear surface; these draw in the suspended particles, which are then deposited on the rear side of the object by the action of centrifugal force. It can be easily shown that in this case also the Stokes criterion is the determining factor, and the collection efficiency can be expressed by Equation (11).

It was stated earlier that all earlier authors report the existence of a critical value $K_{cr} = \mathrm{St}/18$, when $E = 0$ (Table 1). The question of the existence of a critical value for the Stokes criterion is of great practical importance. This can be seen even from the fact that, as is seen from Table 1, droplets of mineral oil less than 40 μ (St < 1.5) in diameter should not be deposited on a vertical leaf of a plant (if it is assumed to be a disk 50 mm in diameter) at a wind velocity of 1 meter/second. This is not in agreement with practical observations.

When plants are treated with toxic agents dissolved in mineral oil, droplets smaller than 10 μ (St = 0.1) are deposited on the leaf surfaces, while the optimum droplet size is ~30μ [2].

TABLE 1

Critical Value of St

Form of object	K_{cr}	St_{cr}	Authors
Sphere	1/24	0.75	Langmuir [4], Levin [8], Ranz and Wong [8]
Cylinder	1/16	1.13	
Circular disk	π/32	1.76	Levin [8]
Plate	1/8	2.25	Levin [8]

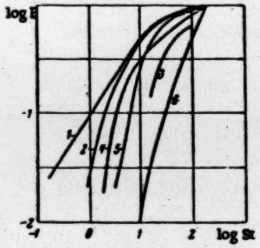

Fig. 3. Settling of droplets on a cylinder, according to the data of: 1) Sell; 2) Langmuir (potential flow); 3) Langmuir (viscous flow); 4) Ranz and Wong; 5) Landhal and Herrmann; 6) Amelin and Belyakov.

The critical value for St has been derived from the laws established for the motion of a stream near an object around which it flows [7, 8]. However, experimental data do not provide a reliable basis for the extension of this to the solution of practical problems.

As is seen from Fig. 3, which shows data obtained by previous authors in the region of low values of the Stokes criterion, the relationship between log E and log St approaches linearity. It follows that the coefficients m and n in Equation (11) change little in this region. The results show also that as St decreases E decreases also, and only when St = 0 does E = 0.

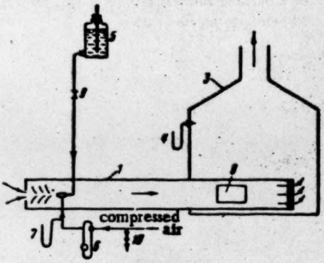

Fig. 4. Diagram of laboratory apparatus.

To determine the values of the coefficients m and n in Equation (11), the deposition of drops of transformer oil from an aerosol stream on cylinders was experimentally studied. The results are presented in this paper.

The laboratory apparatus is shown in Fig. 4. At the entry to the aerodynamic tube 1 the liquid was sprayed by compressed air with the aid of the jet 2. The droplets formed, together with atmospheric air, moved along the tube, the end of which was in the exhaust hood 3. To maintain a constant stream velocity, the rarefaction in the exhaust hood was kept constant; it was measured by the gage 4. The sprayed liquid flowed by gravity from the bottle 5, fixed at some height above the jet. The amount of air entering the jet was measured by the flow meter 6, and its pressure by the manometer 7. The cylinders were placed vertically in the center of the tube through the door 8; 9 and 10 are taps.

The air speed in the aerodynamic tube was measured by means of an indicating vane anemometer; it was varied in different experiments between 100 and 1600 cm/second. The experiments were performed with two aerodynamic tubes, 40 x 40 and 20 x 20 cm, with tube lengths of 350 and 230 cm respectively. The gas flow regime in the aerodynamic tubes, Re_{tu} and near the cylinders, Re_c, was turbulent (turbulent motion near the cylinders is established at $Re_c > 500$ [10]. The volume flow rate of transformer oil was varied from 2 to 3 cc/second in different experiments, and the density of the oil ρ was 0.877 g/cc.

The dispersion and concentration of the aerosol (Table 2) were determined in samples taken from the aerodynamic tube by means of a trap placed in the center of the tube through the door 8 at the place where the investigated objects were put. After impaction of droplets on microscope slides placed on the bottom of the trap, the slides were examined under the microscope [12].

TABLE 2

Dispersion and Particle Concentration of the Aerosol

Droplet diameter, cm	Number of droplets, %
$2.5\cdot10^{-4}$	63.35
$7.5\cdot10^{-4}$	25.64
$1.5\cdot10^{-3}$	8.44
$3\cdot10^{-3}$	2.45
$6\cdot10^{-3}$	0.12
	100.0

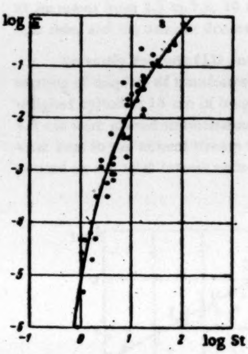

Fig. 5. Settling of drops on a cylinder, front side.

In the earlier investigations the numbers of deposited particles were determined by the increase in weight of the object or by chemical analysis of the substance deposited on the object surface. This gave the total number of particles without discrimination between the front and rear sides of the object. However, the distribution of the droplets on the surface of the object is important not only for determination of the impaction mechanism of particles on surrounded objects, but also for the solution of practical problems. For example, the effective use of economic poisons mainly depends on regular distribution of the particles over the plant surfaces [2].

In the present work, the amount of deposited substance was determined by counting the number of droplets on the cylinder surface and measuring their dimensions. By this procedure it is possible to determine the amounts of substance deposited on the front and rear sides of the cylinders separately and to establish the distribution of the droplets over the whole cylinder surface.

Direct counting of the droplets on the surface involves great difficulties, but gives reliable data at low aerosol concentrations and low values of the collection efficiency E. As has already been pointed out, published data on this are widely divergent, while under practical conditions impaction of particles on objects occurs most often with low values of E.

In view of the difficulty in obtaining an isodisperse aerosol, especially with a large droplet size, a polydisperse aerosol was used.

The results for the front sides of cylinders 1 and 2.5 cm in diameter are shown in Fig. 5. Table 3 shows the values of the coefficients m and n, calculated from these results for values of St from 1 to 170.

TABLE 3

Values of the Coefficients n and m for Front Side of Cylinders

St	n	m	E	St	n	m	E
1	4.90	$5.5\cdot10^{-6}$	$5,5\cdot10^{-6}$	20	1.67	$3.55\cdot10^{-4}$	$5.26\cdot10^{-2}$
2	3.85	$9.12\cdot10^{-6}$	$1.3\cdot10^{-4}$	50	1.39	$9.12\cdot10^{-4}$	$2.10\cdot10^{-1}$
5	2.67	$2.69\cdot10^{-5}$	$1.99\cdot10^{-3}$	100	1.30	$1.29\cdot10^{-3}$	$5.13\cdot10^{-1}$
10	2,05	$1.1\cdot10^{-4}$	$1.23\cdot10^{-2}$	170	1.27	$1.51\cdot10^{-3}$	1,0

In technical calculations, in the range of St from 0.8 to 10, a linear relationship between log E and, log St may be assumed, when $n = 3.5$ and $m = 7\cdot10^{-6}$, and the calculation equation for the front side of the cylinder is:

$$E_{fr} = 7 \cdot 10^{-6} St^{2.3}. \quad (12)$$

A linear relationship in the range St = 10 to 100 may also be assumed; in this case n = 1.85 and m = $3.6 \cdot 10^{-4}$.

The results of experiments to determine the variation of the collection efficiency with the Stokes criterion for the rear side of cylinders 1 and 2.5 cm in diameter are shown in Fig. 6.

In the range of St variations studied, the relationship between log E and log St is close to linear. Here n = 0.54 and m = $2.66 \cdot 10^{-4}$, and the calculation equation for the rear side of the cylinder is:

$$E_{rear} = 2{,}66 \cdot 10^{-4} St^{0.54}. \quad (13)$$

Fig. 7 shows the variations of E with St for both the front and the rear sides of a cylinder. These data show that at the point of intersection of the straight line and the curve, when St = 2.9, equal numbers of droplets are deposited on the front and rear sides of the cylinder. As St increases or decreases, the proportions of the amounts of substance deposited on the front and rear sides of the cylinder vary considerably. For example, as St increases from 2.9 to 7.8, 10 times as much substance is deposited on the front side of the cylinder as on the rear side, and the amount decreases to the same extent when St decreases from 2.9 to 1.29.

To verify Formula (11) and the values of the coefficients n and m, experiments were carried out on the settling of droplets of transformer oil on cylinders of different diameters from an aerosol stream. Ten previously weighed cylinders 15 cm in length and with diameters of 0.006; 0.01; 0.03; 0.1; 0.18; 0.4; 0.8; 1.5; 2.4 and 4.8 cm were placed simultaneously into the aerodynamic tube of the apparatus shown in Fig. 4. The cylinders were kept in the aerosol stream for an equal time; they were then taken out and the weights of the droplets deposited on the total lateral surfaces of the cylinders were determined by a second weighing.

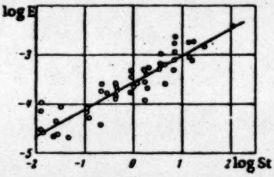

Fig. 6. Settling of droplets on a cylinder, rear side.

The speed of the stream in the aerodynamic tubes was varied from 200 to 1600 cm/second; the flow in the tubes was turbulent, while near the cylinders it varied from laminar to turbulent (Re_c from 2 to 30000).

It is seen from Fig. 8 that the results of different experiments fit reasonably well on a common Curve 1, which represents the variation of log q with log v/D. The nature of the flow near the cylinder has no appreciable effect on the droplet deposition in the range studied. Curve 2 in Fig. 8 is based on data calculated with the use of Formula (11) for the front side of the cylinder. The amount of substance deposited on the rear side of the cylinder was neglected, as Formula (13) shows that it is relatively small in the experimental conditions used.

The calculation was based on the following considerations. The amount of substance deposited from the aerosol stream on the front surface of the cylinder is given by the equation

$$Q = Q_1 + Q_2 + \dots Q_k. \quad (14)$$

where $Q_1, Q_2 \dots Q_k$ are the weights of substance deposited in the form of droplets with diameters $d_1, d_2 \dots d_k$.

For droplets with diameter d_1 on the basis of Equation (1) we may write

$$Q_1 = E_1 N_1 v s \tau \rho \bar{V}_1. \quad (15)$$

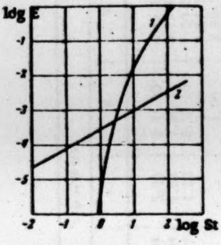

Fig. 7. Settling of droplets on a cylinder: 1) front side; 2) rear side.

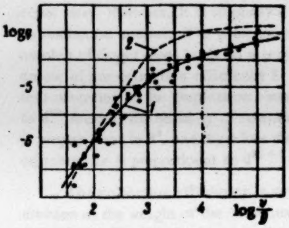

Fig. 8. Settling of droplets on a cylinder: 1) experimental data; 2) calculated data.

where V_1 is the volume of the droplet. Substituting for the droplet volume $V = \pi d_1^3/6$ and remembering that for a cylinder $s = Dl$ (where l is the length of the cylinder) we have, from Equation (15):

$$q_1 = \frac{Q_1}{Dl\tau} = \frac{E_1 N_1 \pi v \rho d_1^3}{6} = \frac{m\pi v\rho}{6}\left(\frac{\rho v}{\mu D}\right)^n N_1 d_1^{2n+3}, \tag{16}$$

where q_1 is the amount of substance deposited on the surface of the obstacle (per unit midship section) in g/cm²·second.

The total quantity of liquid deposited on the front side of the cylinder will be:

$$q = \frac{\pi v\rho}{6}(E_1 N_1 d_1^3 + E_2 N_2 d_2^3 + \ldots E_k N_k d_k^3). \tag{17}$$

The following conditions are assumed in the calculation: v = 100 cm/second; ρ = 0.877 g/cc; μ = 1.83·10^{-4} g·cm/second. The use of this data with Equation (8) gives:

$$\mathrm{St} = \frac{0,877}{1.83\cdot 10^{-4}}\cdot\frac{vd^2}{D} = 4,81\cdot 10^{-8}\cdot\frac{vd^2}{D}.$$

Table 4 shows the calculated results for v/D ratios of 1000 and 10000.

The value of the coefficient E was calculated from the graph in Fig. 5 (for v/D = 1000, Table 4), and from Equation (11) with the use of the coefficients n and m (Table 3). If the graph is available, calculation of E is simplified considerably.

In cases when for some particular droplet diameter the collection efficiency was found to be > 1 (at St > > 170) in Equation (17) it was assumed that E = 1; for example, for droplets with d = 30 and 60 μ at v/D = 10,000 (Table 4).

The increase in the amount of deposited substance on further increase of the v/D ratio occurs as the result of deposition of smaller droplets.

The certain discrepancy between the experimental and calculated curves in Fig. 8 can be attributed to inaccuracies in determination of the droplet size, which greatly affects the weight of deposited liquid (this point is discussed in detail later).

TABLE 4

Weights of Transformer Oil Droplets Deposited on a Cylinder

d_μ	Number of droplets in 1 cc	Total weight of droplets in g per 1 cc	$v/D = 1000$					$v/D = 10\,000$				
			St	log St	log E	E	q	St	m	n	E	q
2.5	1396	$1\cdot10^{-8}$	0.3	—	—	—	—	3	$1.32\cdot10^{-6}$	3.26	$2.74\cdot10^{-4}$	$4.74\cdot10^{-10}$
7.5	565	$1.1\cdot10^{-7}$	2.71	0.433	$\bar{4}.60$	$3.98\cdot10^{-4}$	$4.38\cdot10^{-11}$	27.1	$5.13\cdot10^{-4}$	1.53	$7.99\cdot10^{-2}$	$8.79\cdot10^{-9}$
15	186	$2.88\cdot10^{-7}$	10.8	1.034	$\bar{2}.20$	$1.52\cdot10^{-2}$	$4.58\cdot10^{-9}$	118	$1.32\cdot10^{-3}$	1.29	$5.55\cdot10^{-1}$	$1.60\cdot10^{-7}$
30	53.87	$6.67\cdot10^{-7}$	43.2	1.636	$\bar{1}.23$	$1.70\cdot10^{-1}$	$1.13\cdot10^{-7}$	432	—	—	1,00	$6.67\cdot10^{-7}$
60	2.68	$2.66\cdot10^{-7}$	172.9	2.238	0.00	1,00	$2.66\cdot10^{-7}$	1729	—	—	1,00	$2.66\cdot10^{-7}$

$\Sigma q = 1.34\cdot10^{-6}$ $\Sigma q = 3.84\cdot10^{-7}$ $\Sigma q = 1.120\cdot10^{-6}$

The results obtained are considerably lower than those obtained by other authors; the differences are especially great for low values of the Stokes criterion. This may be due to the fact that the earlier calculations were based on the assumption that all the droplets were of equal size. However, it is impossible to obtain a strictly monodisperse aerosol. The presence of even a very small number of larger drops leads to a very considerable increase of the collection efficiency E: first, the rate of sedimentation of the droplets on obstacles is proportional to d^{2n}; second, the quantity of substance in each droplet is proportional to d^3, and therefore the quantity of deposited substance is proportional to d^{2n+3} (14).

The collection efficiency is usually calculated by division of the weight of the substance deposited on unit area of the object (calculated on the midship section), by the weight of aerosol in unit section of the stream, or

$$E' = q/Q. \tag{18}$$

The results are then plotted in St/18, E or $\sqrt{St/18}$, E coordinates. The droplet diameter, necessary for calculation of St (9) is determined separately, the aerosol being assumed monodisperse.

In the case of a polydisperse aerosol the collection efficiency must be calculated from Equation (1) separately for each droplet fraction. Equation (18) is applicable only to strictly monodisperse aerosols, and if this condition is not satisfied the appropriate correction must be introduced into the equation. It is not possible to determine the correction exactly, as the weights of the settled drops in each fraction are not known. As a first approximation, it can be calculated from Equation (11). For an aerosol which, in addition to droplets of diameter d_1, contains a certain fraction of larger droplets with diameter d_2, the true value of E is given by

$$\bar{E} = E' \frac{(1-\delta)/\delta + (d_2/d_1)^3}{(1-\delta)/\delta + (d_2/d_1)^{2n+3}} \tag{19}$$

where n is the coefficient of Equation (11). If it is assumed that 10% of the droplets in the aerosol have a diameter double that of the rest, so that $\delta = 0.1$ and $d_2/d_1 = 2$, while $n = 3.5$, then we have, from Equation (19):

$$E = E'/60.$$

Thus, in such conditions the results for E are 60 times too high.

With increase of the value of St, this inaccuracy in the relationship $E = f(St)$ (Fig. 3) diminishes, as the largest droplets are gradually deposited completely. At $St = 170$ ($\log St = 2.23$) the inaccuracy due to polydispersity of the aerosol disappears. As is seen from Fig. 3, the curves obtained by different authors coincide at a point corresponding to $E = 1$.

It follows from these considerations that if Equation (19) is applied to the experimental data, then the less monodispese is the aerosol, the more convex will the $\log St = f(\log E)$ curves be.

The results obtained may be used for calculations of the settling of substances from aerosol streams on obstacles under various conditions. At the same time, some practically important conclusions may be drawn from them.

It follows from Equations (12) and (13) that at a wind velocity of 100 cm/second drops of atmospheric mist with diameter $d = 30\mu$ will be deposited on the rear sides of trees and telegraph poles 20 cm in diameter at a rate 2300 times the deposition rate on the front side. In fact, for these conditions $St = 0.25$, and therefore from Equations (12) and (13) we have

$$\frac{E_{rear}}{E_{fr}} = \frac{2{,}66 \cdot 10^{-4} (0.25)^{0.64}}{7 \cdot 10^{-6} (0.25)^{3.5}} = 2300.$$

On stalks of leaves and wires with diameter $D = 0.2$ cm these same droplets will be deposited mainly on the front sides, as in this case $St = 11$, and therefore,

$$\frac{E_{fr}}{E_{rear}} = \frac{7 \cdot 10^{-6} (11)^{3.5}}{2.66 \cdot 10^{-4} (11)^{0.64}} = 32.$$

SUMMARY

1. It is shown that experimental data on the deposition of droplets from an aerosol stream on a cylinder are in agreement with the empirical equation $E = m(St)^n$.

2. The values of the coefficients m and n for the front and rear sides of a cylinder have been determined.

3. It is shown that complete deposition of the droplets ($E = 1$) is reached when the value of the Stokes criterion reaches 170.

The Prof. Ya. V. Samoilov Scientific Institute
for Fertilizers and Insectofungicides, Moscow

Received July 13, 1955

LITERATURE CITED

[1] A. G. Kasatkin, Principal Processes and Equipment of Chemical Technology (State Chem. Press, 1950).

[2] Use of Aerosols in Agriculture, Collected Translations from the Foreign Periodical Literature, edited by Prof. A. G. Amelin (Foreign Literature Press, Moscow, 1955).

[3] N. A. Fuks, Progr. Chem. 19, No. 2, 175 (1950).

[4] I. J. Langmuir, J. Meteorol. 5, 175 (1948)

[5] K. B. May, J. Sci. Instr. 22, No. 9, 187 (1945).

[6] L. S. Sonkin, J. Hyg. Toxicol. 28, 269 (1946).

[7] W. Sell, Forschungshefte UD 1, No. 347 (1931); F. Albrecht, Z. Physik 32, 48 (1931; H. D. Landhal, K. C. Herrmann, J. Colloid Sci. 4, 103 (1949).

[8] L. M. Levin, Proc. Acad. Sci. USSR 91, No. 6, 1929 (1953); W. E. Ranz and I. B. Wong, Ind. Eng. Chem. 44, 1371 (1952).

[9] P. M. Volkov, Symposium, The Theory of Similarity and Modeling (Acad. Sci. USSR Press, 1951).

[10] M. A. Mikheev, Fundamentals of Heat Transfer (State Energy Press, 1950).

[11] D. A. Frank-Kamenetsky, Diffusion and Heat Transfer in Chemical Kinetics (Acad. Sci. USSR Press, Moscow–Leningrad, 1947).

[12] A. G. Amelin and M. I. Belikov, Factory Lab. 1955, No. 12.

INVESTIGATION OF THE DYNAMIC PROPERTIES OF RUBBERS BY THE FREE CONTRACTION METHOD*

G. M. Bartenev, M. M. Reznikovsky, and M. K. Khromov

In earlier investigations [1] a method for studying the free contraction of rubbers was developed and an approximate theory was advanced, with the aid of which the high-elastic and relaxational properties of rubbers could be evaluated from experimental data. The results obtained in studies of a series of rubbers under different conditions of deformation and temperature are presented in this paper. The data shown below confirm the relationships derived previously for free contraction and also somewhat extend our understanding of the nature of internal friction (hysteresis losses) in rubbers and vulcanizates.

Method of Investigation

The instrument described previously [1] was used for investigation of free contraction. The contraction of a stretched rubber strip was recorded on a drum rotating at a high speed (3000 r.p.m.) with the aid of two points (the points x_1 and x_2 shown in Fig. 1) tracing curves of the type shown in Fig. 1 on the drum surface. After release of the stretched specimen, the unloading wave extends from the released to the fixed end and travels through the distance between the points x_1 and x_2 at a certain velocity which can be determined from the slope of the line AB. The contraction rate (the velocity of the points x_1 and x_2 relative to the stationary system of coordinates) is determined from the slopes of the lines AC or BE respectively.

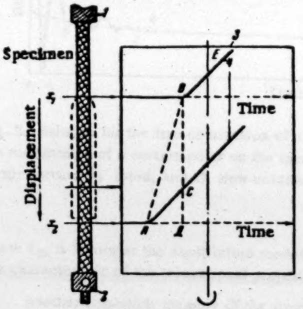

Fig. 1. Scheme for the free contraction process; 1) stationary and 2) moving jaws; 3) drum; 4) contraction curves.

In all cases the contraction curves are close to straight lines. This shows that as soon as the front of the unloading wave reaches any point on the specimen this point travels at a speed equal to the speed of the point x_2 or x_1. This is important, as it makes it possible to determine relatively simply the kinetic energy of the specimen at the end of the contraction.

Analysis of the contraction curves shows that at the instant when the unloading wave reaches the point x_1, the length of the contracted specimen is greater than the initial value (the distance from x_1 to x_2 is taken as the length of the specimen for calculation purposes). The resultant "quasiresidual" deformation (denoted by θ) slowly decreases to zero with time. This deformation is dissipated at a speed several orders of magnitude less than the rate of free (rapid) contraction.

In Fig. 2, the variation of θ with time is represented by the Curve 2, and the rapid contraction with the subsequent extension-contraction cycles is represented by the broken line 1. The quasiresidual deformation θ is caused by slow processes of relaxation which occur in the rubber before the start of rapid contraction (the specimen is held for some time in the stretched state).

---

* The term "free contraction" is equivalent to the term "spontaneous contraction" used in the authors' earlier publications [1].

Thus, the free contraction process comprises two stages: rapid, of a wavelike nature, and slow, when the speed steadily decreases, tending to zero. The total extension deformation ϵ can be divided into two parts: $\epsilon - \theta$, the deformation which disappears during the passage of the unloading wave (10^{-3} second), and θ, the deformation which dissipates slowly. In Fig. 2 the rapid contraction rate is determined by the slope of the straight line AB, and the removal of "quasiresidual" deformation by the slope of the curve OC.

The value of θ, which depends on the method of loading the specimen and the time it is held in the stretched state, can be determined directly from the trace on the drum (by comparison of the initial length of the specimen with the intercept BC), or calculated from the equation:

$$\theta = \varepsilon - \frac{v_k}{v_u}(\varepsilon + 1). \tag{1}$$

where ϵ is the extension deformation; v_k is the contraction rate; v_u is the speed of the unloading wave. Equation (1) is based on the condition that the time of rapid contraction is equal to the time of propagation of the unloading wave through the specimen (the intercept AD in Fig. 1).

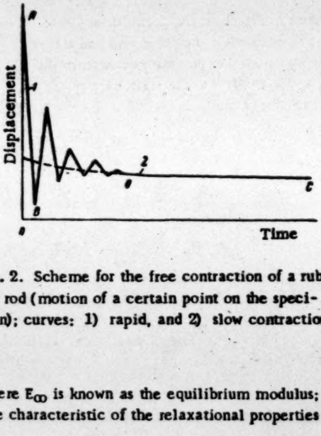

Fig. 2. Scheme for the free contraction of a rubber rod (motion of a certain point on the specimen); curves: 1) rapid, and 2) slow contraction.

In the previous communications [1], the following equation was derived for the high-elastic and relaxational properties of rubbers, from experiments on free contraction:

$$\sigma = E_0' (\varepsilon - \theta). \tag{2}$$

where σ is the true stress; E_0' is the elastic modulus; ϵ is the extension deformation, and θ is the initial "quasiresidual" deformation, determined on free contraction.

In Equation (2) E_0' has the meaning of the dynamic modulus on contraction. This modulus can be represented as the sum of two components.

$$E_0' = E_\infty + E_1. \tag{3}$$

where E_∞ is known as the equilibrium modulus; E_1 is the non-equilibrium part of the dynamic modulus, and is one characteristic of the relaxational properties of rubbers [2].

Another important measure of the mechanical properties of rubber is the internal friction. For its determination in rubber, a quantitative description of the free contraction process is necessary [3]. The latter problem was solved by the use of an approximate method, based on a consideration of the potential and kinetic energy of stretched and contracted specimens [1]. This method is essentially as follows.

It may be assumed that the energy of elasticity stored in the deformed specimen is converted into kinetic energy of motion of the specimen in the process of contraction, and is partially expended in the internal friction of rubber. In absence of external friction losses in the instrument, the potential energy of deformation must be equal to the kinetic energy of motion of the specimen and the energy expended in internal friction.

The specific potential energy of deformed rubber can be represented by:

$$W = E'_0[\varepsilon^* - \ln(\varepsilon^* + 1)]. \qquad (4)^*$$

By analogy, we may write for the dissipated energy

$$\Delta W = K[\varepsilon^* - \ln(\varepsilon^* + 1)]. \qquad (5)^{**}$$

Here $\varepsilon^* = \varepsilon - \theta$; K is known as the modulus of internal friction [4].

Since during contraction the speed of all the points on the specimen is approximately the same (the contraction graph is a straight line), the kinetic energy of unit volume of the specimen can be expressed in the form:

$$W_k = \rho \frac{v_k^2}{2}. \qquad (6)$$

where ρ is the density of rubber. Equating (4) and (6), we have:

$$K = E'_0 - \frac{\rho v_k^2}{2[\varepsilon^* - \ln(\varepsilon^* + 1)]}. \qquad (7)$$

The losses accounted for by the modulus of friction K are due to the existence of rapid relaxation processes during contraction. From Equations (4) and (5) we obtain an expression for the relative hysteresis:

$$\Gamma = K/E'_0 \qquad (8)$$

(previously we used the coefficient γ to characterize internal friction; this is related to the relative hysteresis by the expression $\Gamma = 1 - \gamma^2$).

Thus, by experimental determination of the stress, deformation, contraction rate, and instantaneous quasiresidual deformation θ , it is possible to find the important high-elastic and relaxational characteristics of rubber E'_0 E_1 and K.

EXPERIMENTAL

Effect of the time the rubber is held in the stretched state on the dynamic characteristics. It was shown earlier [1] that for rubbers without fillers an increase of the time during which the rubber is held in the stretched state does not affect the value of E'_0, although the other values (σ, θ, v_k and v_u) change considerably. This confirms the validity of Equation (2).

---

* Equation (4) is obtained if the deformation law is used in the form of Equation (2).

** For small deformations, when the change in cross-section of the specimen may be neglected, we obtain for W and Δ W, by resolution of $\ln(\varepsilon^* + 1)$ into series: $W = E'_0(\varepsilon^*)^2/2$ and $\Delta W = K(\varepsilon^*)^2/2$.

As is seen from Fig. 3, for unfilled rubbers the modulus of friction K is also independent of the time the rubber remains in the stretched state.

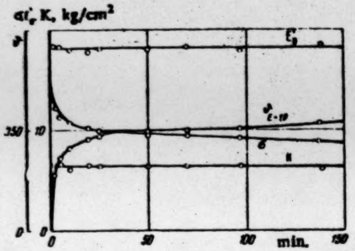

Fig. 3. The stress σ, dynamic modulus E'_θ, modulus of friction K, and the quasiresidual deformation θ as functions of the time the specimen is held in the stretched state (for unfilled rubber based on SKS-30).

A different result is obtained for filled rubbers (Fig. 4). It is seen from Fig. 4 that with increasing time in the stretched state the values of E'_θ and K decrease. The curves for their variation with the time in the stretched state are similar to the stress relaxation curves. The change of E'_θ and K is probably due to the manifestation of thixotropic properties in filled rubbers, when their mechanical properties depend on their previous mechanical history [4].

Influence of the magnitude of deformation. Fig. 5 shows the variation of E'_θ, K, v_k, v_u and θ_∞ with the magnitude of the extension deformation, obtained in experiments in which the equilibrium state had been reached before contraction. Fig. 5 shows that E'_θ and K do not change during an increase of extension to 250%, while v_k and θ_∞ increase in proportion to the deformation. The value of v_u increases linearly from a certain initial value. According to the views advanced earlier, Equation (2) should apply both during changes of the extension ε, and during changes of θ (because of the different time in the stretched state). Fig. 6 shows the variation of σ, v_k and K with ε — θ. Here the value of ε — θ was varied both because of the extension and by the time in the extended state. It is seen from Fig. 6 that the stress increases in proportion to the deformation (ε — θ), and not only the equilibrium, but also the non-equilibrium values of the stress lie on a straight line. The values of v_k also lie on one curve. This confirms the validity of Equation (2), which is a general deformation equation, which describes both the equilibrium and the non-equilibrium states. It is seen from Fig. 6 that the modulus of friction is also independent of the deformation ε and of the time during which the specimen remains in the stretched state.

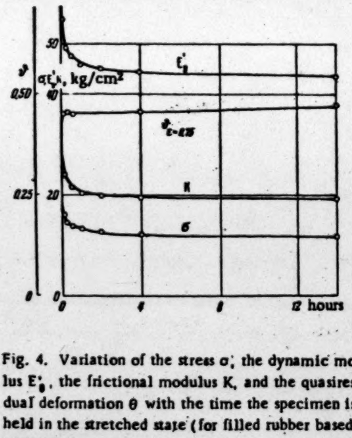

Fig. 4. Variation of the stress σ, the dynamic modulus E'_θ, the frictional modulus K, and the quasiresidual deformation θ with the time the specimen is held in the stretched state (for filled rubber based on SKS-30).

Figs. 7 and 8 show the variations of E'_θ and K with ε — θ for a number of unfilled rubbers. It is seen from Figs. 7 and 8 that E'_θ and K are constant over a considerable range of deformations. At greater deformations these values begin to increase, probably owing to increased rigidity of the polymer molecules on extension. The considerable increase of E'_θ and K for the vulcanizate based on natural rubber (NR) is also probably explained by crystallization on extension.

Fig. 9 shows the variation of the stress σ and the moduli E'_θ and K with the value of ε — θ for a vulcanizate based on SKS-30 filled with channel black. It is seen from Fig. 9 that the stress changes non-linearly with ε — θ. The moduli E'_θ and K first diminish and then begin to increase. It was also noted that the variation of E'_θ and K with deformation becomes more complex with increase of the filler content.

The considerable dependence of the moduli E'_θ and K on the deformation is undoubtedly related to the thixotropic properties of filled rubbers. It has been shown by repeated experiments [4] that the thixotropic properties affect the modulus E'_θ and the modulus of internal friction K to almost the same extent. This is seen from the fact that the ratio K/E'_θ changes little when the magnitude and nature of the deformation is varied*.

The influence of temperature on the dynamic properties was studied for unfilled rubbers. Fig. 10 shows typical graphs for the variation of E_∞, E'_θ, K, v_k, v_u and θ_∞ with temperature changes over a wide range. It is seen from Fig. 10 that the equilibrium modulus E_∞ and the contraction rate v_k increase with temperature, while the other values diminish to various degrees. The initial residual deformation θ_∞ is at its maximum value, equal to the total extension deformation ϵ, at the glass transition temperature. As the temperature rises θ_∞ diminishes sharply and tends to zero at very high temperatures.

It was noticed in the case of natural rubber that the relationship $E'_\theta - T$ has a minimum. The probable reason is that the dynamic modulus is the sum of two components which depend differently on the temperature; the equilibrium modulus, in accordance with the kinetic theory of high elasticity, rises with increase of temperature while the non-equilibrium part of the dynamic modulus decreases because of weakening of intermolecular action.

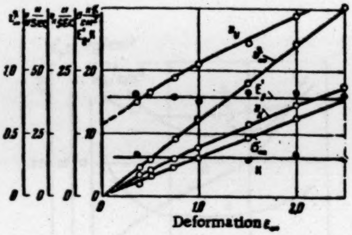

Fig. 5. Variation of the stress σ, the contraction rate v_k, the velocity of the unloading wave v_u, the quasiresidual deformation θ_∞ and the moduli E'_θ and K, with the equilibrium extension deformation ϵ_∞ (for unfilled rubber based on SKS-30).

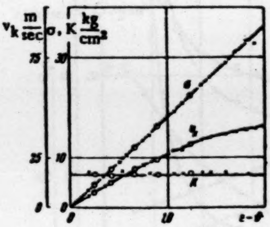

Fig. 6. Variation of the stress σ, contraction rate v_k, and frictional modulus K with the value of $(\epsilon - \theta)$ (for unfilled rubber based on SKS-30); O) equilibrium state; X) non-equilibrium state.

Figure 11 shows the variation of E_1 with 1/T and ln K with 1/T for SKS-30A rubber. It is seen from Fig. 11 that these relationships are linear over a considerable range of temperatures (they deviate from linearity at low temperatures).

Because of the linearity, it is possible to determine the apparent energy of activation of the relaxation processes from the equation:

$$K = K_0 e^{\frac{u}{kT}}. \tag{9}$$

where K is the frictional modulus; K_0 is a constant; $\underline{u}$ is the activation energy; $\underline{k}$ is the Boltzmann constant; T is the absolute temperature.

---

* Here, apparently, we must refer to the ratio K/E'_1, as in the range in question E_∞ does not depend on the deformation. However, as has been shown earlier [4], E_∞ for filled rubbers is close to the corresponding values for unfilled rubbers, and is therefore small relative to E'_θ.

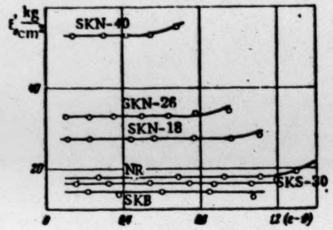

Fig. 7. Variation of the dynamic modulus E'_θ with the value of $(\epsilon - \theta)$ for unfilled rubbers.

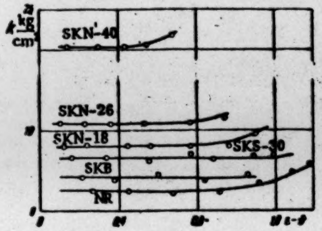

Fig. 8. Variation of the frictional modulus K with the value of $(\epsilon - \theta)$ for filled rubbers.

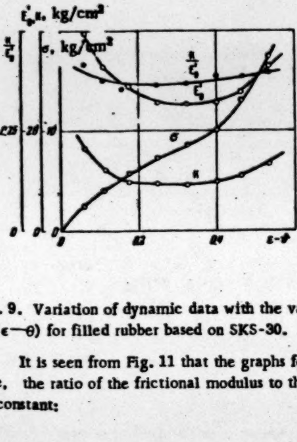

Fig. 9. Variation of dynamic data with the value of $(\epsilon - \theta)$ for filled rubber based on SKS-30.

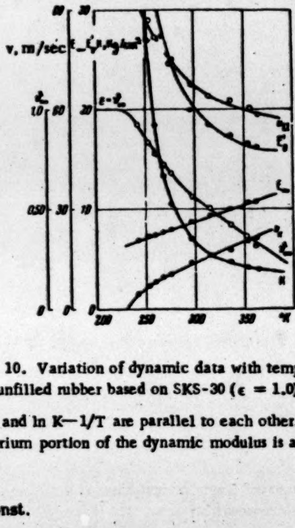

Fig. 10. Variation of dynamic data with temperature for unfilled rubber based on SKS-30 $(\epsilon = 1.0)$.

It is seen from Fig. 11 that the graphs for $\ln E_1 - 1/T$ and $\ln K - 1/T$ are parallel to each other. Therefore, the ratio of the frictional modulus to the non-equilibrium portion of the dynamic modulus is approximately constant:

$$K/E_1 \approx \text{const.}$$

This demonstrates that the relaxation mechanisms responsible for internal friction and dynamic rigidity of rubbers are of a common nature.

By extrapolation of the relationship $\theta_\infty - T$ to the value of full extension deformation it is possible to determine the glass transition temperature for free contraction. Fig. 12 shows the variation of $\ln E_1$ and $\ln K$ with the glass transition temperature T_g, determined in free contraction experiments (the values of E_1 and K are taken at room temperature). It is seen from Fig. 12 that the glass temperature is higher at higher values of E_1 and K. If the results for SKS-30 are ignored, an approximately linear relationship is seen between ln K and the glass temperature T_g. A similar relationship holds for the non-equilibrium portion of the dynamic modulus.

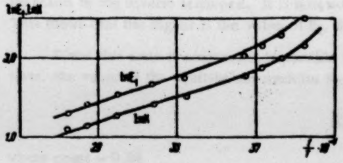

Fig. 11.. Graphs for ln E_1 — 1/T and ln K —1/T for SKS-30.

The relationship established between the glass temperature and the internal friction of rubber may be indirectly interpreted on the basis of modern views on the relaxation mechanism of the glassy state transition in polymers. In fact, transition to the glassy state in polymers occurs when the energy of thermal motion of the molecular chains, which diminishes with decreasing temperature, becomes insufficient to overcome the interaction between them. In other words, the internal friction, which increases with falling temperature, reaches a critical value at the glass temperature, when the development of high-elastic deformation (during the period of loading) becomes impossible.

With the aid of the previously described expression for the frictional modulus as a function of temperature (9), we can write for the glass transition temperature:

$$K_{cr} = K_0 e^{\frac{u}{kT_g}}, \tag{10}$$

where K_{cr} is the critical value of the frictional modulus which determines the glassy state transition and is independent of the individual properties of the polymer; $\underline{u}$ is the activation energy, which depends on the inter- and intramolecular forces in the polymer.

Combining Equations (9) and (10), we have:

$$\ln K = \ln K_0 + \frac{\ln K_{cr} - \ln K_0}{T} T_g, \tag{11}$$

which does not contain the activation energy. In this expression K_0 has the meaning of a constant which characterizes the internal friction of the polymer at an indefinitely high temperature, or when the intermolecular interaction is so small that it may be neglected.

If we assume that K_0, like K_{cr}, does not depend on the individual polymer properties, this expression may be regarded as the analytical expression of the experimentally established linear relationship between the logarithm of the frictional modulus (at T = constant) and the glass transition temperature.

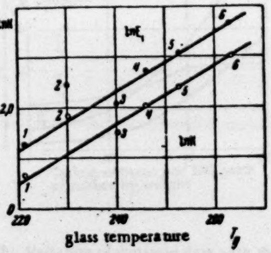

Fig. 12. Relationship between internal friction and the glass transition temperature: 1) natural rubber 2) SKS-30; 3) SKB; 4) SKN-18; 5) SKN-26; 6) SKN-40.

If the experimental data are analyzed with the aid of Equation (11) it is found that K_0 determined from the intercept cut off by the lnK —T_g line along the ordinate axis is of the order of 10^{-4} kg/cm², while K_{cr} determined from the slope of the same line, the absolute temperature, and the previously found value of K_0 is of the order of 10^2 —10^3 kg/cm². This order of magnitude for K_{cr} is, of course, quite reasonable, while the result as a whole may be regarded as some measure of additional confirmation for the relaxation theory of the glassy state of polymers.

Properties of "soft" unfilled rubbers. The table gives values of v_k, v_u, θ_{∞}, E_1, K, K/E_1^{*}, K/E_1, T_g and the apparent energy of activation $\underline{u}$ for soft rubbers based on natural rubber, SKB, SKS-30, SKN-18, SKN-26, and SKN-40. It is seen that the rubbers form the following sequence according to the increasing velocity of the unloading wave v_u, non-equilibrium portion of the dynamic modulus E_1, frictional modulus K, values of θ_∞, and the ratio K/E'_0: natural rubber < SKB < SKS-30 < SKN-18 < SKN-26 < SKN-40. The contraction rate v_k increases in the reverse sequence. It is noteworthy that the ratio K/E_1 is practically the same for all the rubbers. This shows that the higher is the value of E_1, the greater is K.

Since this ratio is constant it is possible to determine, without the necessity of reaching the equilibrium state, the value of the equilibrium modulus E_∞ from dynamic tests with the use of the relationship:

$$E_\infty = E'_0 - K/\mathrm{const}, \tag{12}$$

where const ≈ 0.55

Effect of plasticizer and filler contents on the dynamic properties. Figs. 13 and 14 show the variations of the dynamic properties with the contents of channel black and vaseline oil in the rubbers; it is seen that the moduli E'_0 and K increase with increasing carbon black content and decrease with increasing oil content. The ratio K/E_1, however, remains approximately constant.

Dynamic Characteristics of Unfilled Rubbers with Equal Equilibrium Moduli; E_∞ = = 9 kg/cm² at 20°C

Rubber	Concentration rate v_k at $\varepsilon = 1.0$ in m/sec	Velocity of wave v_u at $\varepsilon = 1.0$ in m/sec	Initial deformation ε_∞ at $\varepsilon = 1.0$	E_1 in kg/cm²	K in kg/cm²	$\frac{K}{E'_0}$	$\frac{K}{E_1}$	T_g in C°	$\bar{u}$ in kcal./mole.
NR	19.5	55.0	0.29	3.7	2.0	0.157	0.54	—50	8000
SKB	16.4	62.0	0.47	8.0	4.5	0.26	0.56	—33	7600
SKS-30	14.5	65.0	0.56	11.5	6.8	0.33	0.56	—43	4200
SKN-18	13.8	81.0	0.65	17.0	8.0	0.31	0.47	—27	7800
SKN-26	12.0	86.0	0.72	23.0	11.0	0.34	0.48	—20	7600
SKN-40	9.5	100.0	0.81	39.0	20.0	0,42	0.51	—10	7000

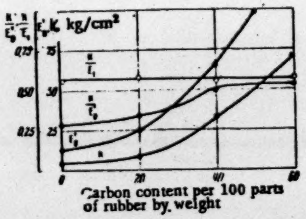

Fig. 13. Variation of dynamic data with the content of channel black in rubber based on SKB.

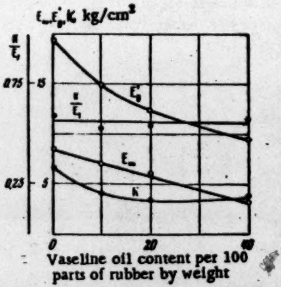

Fig. 14. Variation of dynamic data with the content of vaseline oil in rubber based on SKS-30.

SUMMARY

1. The applicability of the extensibility equation in the form $\sigma = E'_\theta(\varepsilon-\theta)$ to unfilled rubbers has been demonstrated.

This equation is not applicable to filled rubbers owing to their thixotropic properties.

2. A relationship between the frictional modulus K and the glass transition temperature T_g has been found for vulcanizates from different rubbers. It is shown that the glass transition temperature increases with increasing K.

3. It is shown that the ratio K/E_1 depends little on the type of polymer, temperature, fillers, plasticizers, or vulcanization.

Scientific Research Institute for the Tire Industry **Received July 21, 1955**

LITERATURE CITED

[1] M. M. Reznikovsky and M. K. Khromov, Colloid J. 14, No. 3, 177 (1952) (T.p. 199)*; 14, No. 5, 357 (1952) (T.p. 385).*

[2] B. A. Dogadkin, G. M. Bartenev, and M. M. Reznikovsky, Colloid J. 11, 314 (1949).

[3] P. A. Mrowka, S. L. Darth and E. Guth, J. Appl. Phys. 16, 1, 86 (1945).

[4] M. M. Reznikovsky, L. S. Priss, and B. A. Dogadkin, Colloid J. 16, No. 3, 211 (1954) (T.p. 213).*

*** T. p. = C. B. Translation pagination.**

THE ROLE OF DIFFUSION OF POLYMER CHAINS IN THE MECHANISM OF ADHESION AND AUTOHESION OF RUBBERS

B. V. Deryagin, S. K. Zherebkov, and A. M. Medvedeva

The most characteristic feature of autohesion effects in rubber and other polymers is the increase of the adhesion forces with time of contact. Two mechanisms have been used in the interpretation of the observed kinetics of autohesion: a macroscopic mechanism, involving an increase of the total area of true contact owing to relaxation and plastic flow in the zone of contact stresses [2], and a microscopic (molecular) mechanism of diffusional intertwining of adjacent molecular chains, which leads to increasing adhesion in these regions to a value corresponding to cohesion, owing to the disappearance of the physical boundary of separation [1].

The concept of a diffusion mechanism for the autohesion of rubbers was first advanced by Josefowitz and Mark [1] and subsequently developed by Deryagin and Krotova [2] and Voyutsky and his associates [3].

Since relaxation effects also increase with increasing mobility of the chains and their segments, for both mechanisms the rates of cohesion determined by them should vary in a similar manner with the temperature and the type of polymer. Therefore the investigations on autohesion so far carried out do not make it possible to determine the relative significance of the two mechanisms – the chain-molecular and the relaxation-mechanical. An attempt was made in the present investigation to determine the relative importance of the two mechanisms, with the use of two new ideas.

The first idea consists of the measurement of the adhesion forces between two crossed threads, covered with films of the polymers of different thicknesses, including very low values (10^{-6} cm). If the films are very thin, the role of their deformation and relaxation is slight, the contact area is extremely small, and therefore both mechanisms, the macroscopic and the microscopic, which are presumed to form the basis of autohesion kinetics, should not operate, in contrast to the case of fairly thick films.

The second idea is to investigate by some method or other the adhesion not only of similar polymers (rubbers) but different combinations (pairs) of them, and to compare the adhesion results with compatibility data for the rubbers*.

Specifically high values of adhesion for definite pairs in parallel with their compatibilities would indicate the role of a molecular, diffusion mechanism in autohesion and adhesion of polymers. Conversely, with a relaxation mechanism adhesion should not be correlated with compatibility.

Autohesion of Rubbers

For investigation of the autohesion of films of various thicknesses of different types of rubber by the crossed thread method, use was made of the technique developed by Deryagin and Malkina [4], somewhat modified by Moskvitin and Futran [5]. The quartz threads of the instrument were coated with thin uniform films of the rubbers. The films were applied to the quartz threads from solution by the drain-off method proposed by Deryagin [6]. The threads were immersed in a benzene solution of rubber, which was then drained off at a definite rate. The instrument for application of the films, shown in Fig. 1, consists of the following parts: a quartz rod 1, rigidly fixed in a stand, 2, with threads which are coated with the rubber films, a cork float 4, on which a beaker 3 containing the rubber solution is firmly fixed, and a vessel with water 5, rigidly fixed in the stand 9.

The vessel 5 is emptied with the aid of the tube 6, fitted with a micro-tap 7. The turn of the tap in degrees is noted on the scale 8 by means of a pointer attached to the tap. In this way it is possible to set up a required rate of water efflux from the vessel 5, and therefore also the rate of movement of the beaker containing the rubber solution relative to the stationary thread 2. The thickness of the film remaining on the quartz thread depends on the rate of displacement of the beaker with the solution.

---

* This idea was first advanced by us at the conference on adhesion held at the Institute of Physical Chemistry, Academy of Sciences USSR, in May 1955.

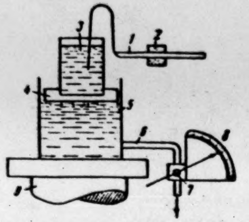

Fig. 1. Apparatus for application of films of definite thickness to threads by the drain-off method.

Quartz threads 150—200 μ in diameter were used; i.e., relatively thick threads, as the autohesion forces for rubbers are very high. The threads were drawn before each experiment, to avoid surface contamination.

The drying time of the threads before application of the rubber films was 30 or 60 minutes, according to the thickness of the films.

The thickness h of the polymer layer applied to the thread was calculated with the aid of the formula [7]:

$$h = 1{,}32\ldots r\left(\frac{\eta u}{\sigma}\right)^{2/3} c, \tag{1}$$

where h is the film thickness in cm; r is the radius of the thread in cm; η is the solution viscosity in poises; u is the drain-off rate of the rubber solution in cm/second; σ is the surface tension in dynes/cm; c is the volume concentration of rubber.

The viscosity of the rubber solutions was determined in an Ubbelohde viscosimeter. The viscosity was calculated from the formula

$$\eta = C\,(P\tau)_{\text{av}},$$

where η is the viscosity in poises; P is the average efflux pressure in cm water column; τ is the efflux time in seconds; $(P\tau)_{\text{av}}$ is the arithmetical average of all the determinations; C is the viscosimeter constant.

Figure 2 shows a diagram of the apparatus used for determinations of autohesion forces. Two freshly drawn quartz threads ~150 μ in diameter were fixed in the beaker A. The thread a was fixed vertically with the thick end held rigidly in a stand; the thread b was fixed horizontally. Thus, the threads met at 90°. The thread b was fixed in a specially designed stand B, the main part of which is a frictionless torsional suspension; this consists of a metal cube N with a hole for the quartz rod and a clamp screw. The cube is fixed in the stand by two steel plates placed crosswise. This method of attachment excludes simultaneously all three forward motions and two rotations, leaving only one degree of freedom – rotation about the vertical axis which passes through the center of the stand. The lever C is connected to the load p by a wire passing over the brass pulley O, which has very low friction. When the lever is moved to one side, a moment of rotation in the opposite direction is set up owing the existence of an elastic attachment. The load p falls or rises, so moving the thread b connected with it, as the vessel D is emptied or filled with water from the upper reservoir E. The supply of water to the vessel is regulated by the micro-tap K.

When water flows out of the vessel D through the lower tube with the tap K_1, the thread b moves, comes into contact with the thread a, and deflects it to a certain (precisely determined) distance from the equilibrium position. At the end of a certain time of contact, as the load p rises (when the vessel is filled from the upper reservoir), the thread b is deflected in the opposite direction. The adhesion force between the polymer-coated quartz threads causes the thread a to move away from the equilibrium position and to follow the motion of the thread b. With this apparatus it is possible to increase the force tending to detach one thread from the other, very slowly and smoothly. The deflections of the thread from the equilibrium position are observed with the aid of a reading mocroscope M with a micrometer eyepiece and vernier scale for measurement of the thread displacement. To make the instrument stable and to prevent distortion of the experimental results by vibrations, it was placed on a shockproof base. The diameter of the quartz threads was determined after application of the films.

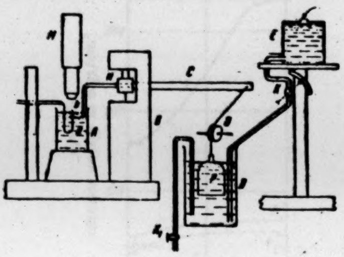

Fig. 2. Diagram of apparatus for measurement of autohesion forces by the crossed thread method.

According to Deryagin's theory [8]:

$$N = \frac{2\pi\sqrt{r_1 r_2}}{\sin\omega} f_\theta, \qquad (2)$$

where N is the force of adhesion *; r_1 and r_2 are the radii of the threads; f_θ is the specific work of separation per unit area; ω is the angle between the axes; for $\omega = 90°$ we have:

$$N = 2\pi\sqrt{r_1 r_2} f_\theta. \qquad (3)$$

Thus, Formula (3) can be used for calculation of the specific adhesion energy f_θ.

The interaction forces between the polymers were determined in dynes by direct readings of the number of divisions of the micrometer eyepiece calibrated in force units.

The rigidity coefficient of the polymer-coated thread was determined by comparison of two vibration periods: T_θ for a free and T_1 for an attached pendulum, as described previously [4]. With a known rigidity coefficient of the thread, the divisions of the eyepiece scale can be expressed in dynes after determination of the value of the eyepiece scale divisions in the mixture with the aid of a micrometer lens.

The first part of this work consisted of a study of the effect of film thickness and contact time on the autohesion energy of different rubbers. Natural smoked sheet rubber and synthetic sodium butadiene rubber were used. The results are shown in Figs. 3 and 4, where the abscissa axes show the film thickness, and the ordinate axes give the specific energy of adhesion (or, more precisely, autohesion).

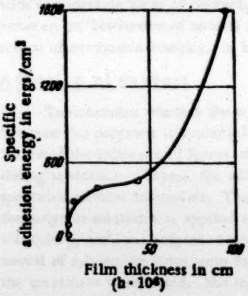

Fig. 3. Autohesion energy as a function of the thickness of a film of natural smoked sheet rubber. Contact time 60 minutes.

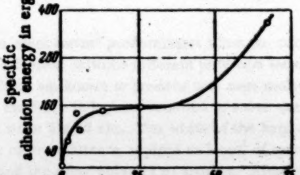

Fig. 4. Autohesion energy as a function of the thickness of a film of synthetic sodium butadiene rubber. Contact time 60 minutes.

To show the effect of film thickness on the kinetics of autohesion, Fig. 5 shows a plot of the contact time, taken along the abscissa axis, against the specific autohesion energy, taken along the ordinate axis. The different curves represent films of different thicknesses.

---

* It is assumed in Formula (2) that N corresponds to point contact, and therefore the values of f_θ calculated with this formula for thick films with an appreciable contact area are conventional.

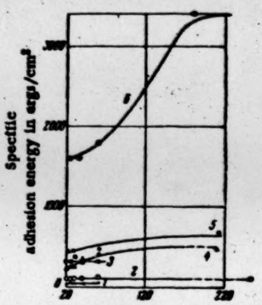

Fig. 5. Kinetics of autohesion for films of different thicknesses: 1) $0.31 \cdot 10^{-6}$; 2) $1.20 \cdot 10^{-6}$; 3) $2.81 \cdot 10^{-6}$; 4) $16.7 \cdot 10^{-6}$; 5) $41.9 \cdot 10^{-6}$; 6) $94.0 \cdot 10^{-6}$ cm.

DISCUSSION OF RESULTS

The above results show that the autohesion energy increases with increase of film thickness from 0.01 to 1μ. In the thickness range from 0.1 to 0.5μ the autohesion energy does not depend on the thickness (plateau on the curves in Figs. 3 and 4). The increase of the autohesion energy in the range from 0 to 0.1μ is probably the result of increasing van der Waals forces between the rubber films; this increase ceases when the thickness of the polymer layer exceeds the radius of molecular action. The increase of the adhesion energy at thicknesses > 0.5μ has a different origin – it is the result of formation of flat areas of contact with the use of thicker films, which are more easily deformed. The formation of such contact areas creates favorable conditions for stress relaxation and coalescence of the contacting films. With film thicknesses up to 0.5μ increase of contact time has little influence on the autohesion energy of rubbers. With film thicknesses > 0.5μ the autohesion energy depends on the contact time (see Fig. 5).

The different adhesion kinetics of thick and thin films of rubber may be explained by the fact that when thin films (< 0.5μ) are applied to quartz threads the contact deformation and the area of contact are both very small. In this case the adhesion force is mainly determined by molecular attraction, which depends, according to Formula (3), on the curvature of the surface, since the contact approximates to point contact; here the effects of contact area and relaxation and chain intertwining processes are unimportant.

On the other hand, with thicker films the contact area becomes fairly extensive, and here intertwining of adjacent chains as the result of intramolecular Brownian movement, and also relaxation and consequent increase of the contact area, may have an influence. In consequence, the autohesion kinetics of quartz threads coated with thick polymer films becomes similar to the autohesion kinetics studied previously by others for flat surfaces with considerable areas of contact. By means of the above method it is also possible to distinguish quantitatively between the autohesion of natural and SKB synthetic rubber, both in the region of molecular adhesion, and in the region of autohesion kinetics. In both regions the autohesion of natural rubber is greater than that of SKB.

Adhesion of Rubbers

To determine whether the relaxation or the diffusion mechanism* predominates when the contact area between two polymers is appreciable, experiments on the adhesion between different polymers were carried out. To avoid the influence of forces of electrostatic origin, which are known to predominate over molecular forces during separation of layers, the adhesion was measured as the force in kg/cm² required to move one part of the specimen relative to another. The specimens were fabric strips 5 x 10 cm. The width of the band onto which the polymer solution was applied was 1 cm. The amount of dry substance applied to 1 cm² of specimen area was 0.03 g/cm², one polymer being applied to one strip, and the other polymer to another. After complete removal of solvent the strips were folded together and placed under a load of 40 g/cm² for 5 minutes, after which the specimens were tested. Not less than five specimens were used in each test, the average value being taken.

The following high polymers were used: natural rubber, SKS-30, SKN-26, SKB, butyl rubber, and Nairit. The method described above was used to determine both the autohesion of these polymers, and their mutual adhesion. The results were compared with data on the compatibilities and polarities of these polymers. Data on compatibility were obtained from the literature [10-13], mainly based on determinations of mechanical properties, and the following method was also used to determine compatibility. Solutions of different polymers in the same solvent were mixed. The mixed solution was thoroughly stirred and observed. If at the end of a definite time the mixture separated out into layers, it was assumed that the polymers are not compatible. Finally, similarity of polarities was taken as the simplest and clearest indication of compatibility.

---

* The concept of the role of a diffusion mechanism in polymer adhesion was advanced at the conference on adhesion held in the Institute of Physical Chemistry, Academy of Sciences USSR, both in our address, which formed the contents of the present paper, and in the paper by Voyutsky et al. [9].

The results of the tests are shown in Table 1, where compatibility is indicated by + and incompatibility by —; the upper sign represents the result of compatibility determination in solution, while the lower, if two are given, represents literature data. In addition, if both polymers are non-polar or both are polar, the sign ⊕ is used, while if one is polar and the other non-polar, the sign ⊖ is given.

TABLE 1

Correlation Between Autohesion and Compatibility

Polymer	Shearing resistance, kg/cm^2					
	Natural rubber	Nairit	SKS-30	SKN-26	SKB	Butyl rubber
Natural rubber	3.20	+ — ⊖ 1.60	+ — ⊕ 1.32	— — ⊖ 0.10	+ + ⊕ 1.14	— ⊕ 1.44
Nairit	+ — ⊖ 1.60	2.0	— ⊖ 0.58	— ⊕ 1.00	— ⊖ 0.30	— ⊖ 1.08
SKS-30	+ — ⊕ 1.32	— — 0.58	1.04	— ⊖ 0.30	+ — ⊕ 0.60	— ⊖ 0.80
SKN-26	— — ⊖ 0.10	— ⊕ 1.00	— ⊖ 0.30	0.48	— — ⊖ 0.28	— ⊖ 0.62
SKB	+ + ⊕ 1.14	— ⊖ 0.30	+ — ⊕ 0.60	— — ⊖ 0.28	0.54	— ⊕ 0.58
Butyl rubber	— ⊕ 1.44	— ⊖ 1.08	— ⊕ 0.80	— ⊖ 0.62	— ⊕ 0.58	0.36

DISCUSSION OF RESULTS

The resistance to shear, which was chosen as the measure of adhesion, may be represented as:

$$T_{12} = S_{12}\tau_{12}, \tag{4}$$

where S_{12} is the area of true or molecular contact of the 1st and 2nd polymers and τ_{12} is their true specific shearing resistance. It is seen that T_{12} depends both on the mechanical properties of the contacting specimens, by virtue of S_{12}, and on their specific interaction, which determines the magnitude of τ_{12}. As a result, a complex situation should be produced in the general case.

A more simple and characteristic situation may, however, be obtained for combinations of polymers for which one of the factors in Equation (4) varies little relative to the other. Let us first suppose that S_{12} varies more strongly. Since S_{12} satisfies the conditions

$$S_{11} \geqslant S_{12} \geqslant S_{22},$$

where S_{11} and S_{22} represent the areas of true contact between identical specimens, Specimen 1 being assumed softer than Specimen 2, then T_{12} in Equation (4) will have a value which does not pass appreciably outside the range T_1, T_2. If the contact is assumed to be elastic and conforming to the Hertz formula, while the elastic moduli of the two specimens are not too widely divergent in order of magnitude, then S_{12} and consequently also T_{12} will be close to the arithmetic means of the corresponding values of S_{11}, S_{22} and T_{11}, T_{22}. If we suppose that the elastic moduli differ greatly or that the contact is determined by plastic deformation, then S_{12}, and therefore also T_{12} will be close to values corresponding to the contact of the softer specimen with a similar one, i.e., $S_{12} \approx S_{11}$, $T_{12} \approx T_{11}$. In any event, irrespective of the mechanical properties of both specimens, S_{12} and T_{12} can never lie outside the ranges of the corresponding values $S_{11} - S_{22}$ and $T_{11} - T_{22}$.

The situation is different if for these combinations of contacting specimens τ_{12} varies much more than S_{12}. Two possible cases must be distinguished here. If the magnitude of τ_{12} is mainly determined by diffusion and intertwining of the chains of the two polymers, which occur more easily as the polymers become more similar in nature, then evidently τ_{12} will vary in parallel with the compatibility of the two polymers and in absence of compatibility τ_{12} may be considerably less not only than τ_{22}, but also in comparison with $\tau_{11} < \tau_{22}$.

There should then be a correlation between compatibility and the ratio τ_{12}/τ_{11}, as in the case of natural rubber and SKN-26 (Table 1). If τ_{12} is mainly influenced by the interaction of charges of the electric double layer at the boundary between the two specimens, then the values of τ_{12} may exceed not only τ_{11} but also τ_{22}, while no parallel should exist between the value of the ratio τ_{12}/τ_{11} and the compatibility (SKB + butyl rubber).

It is easily seen in Table 1 that in the case of adhesion of butyl rubber to other polymers T_{12} is always greater than T_{11}. This indicates that diffusion processes have no appreciable influence, and suggests the possible influence both of the contact area, and of the electric double layer. If the case of butyl rubber is omitted from Table 1, then combinations of all the other polymers show a clear correlation between T_{12} and the compatibilities of the Polymers 1 and 2.

TABLE 2

Correlation Between T_{12}/T_{11} and Compatibility

Polymer pair	T_{11}	T_{22}	T_{12}	T_{12}/T_{11}	Compatibility in solution	Compatibility from literature data	Compatibility from similar polarities
Nairit + NR	2.00	3.20	1.60	0.80	+	+ —	—
SKS-30 + NR	1.04	3.20	1.32	1.27	+	+ —	+
SKN-26 + NR	0.48	3.20	0.10	0.20	—	—	—
SKB + NR	0.54	3.20	1.14	2.11	+	+	+
SKS-30 + Nairit	1.04	2.00	0.58	0.55	—		—
SKN-26 + Nairit	0.48	2.00	1.00	2.08	—		+
SKB + Nairit	0.54	2.00	0.30	0.55	—	—	—
SKN-26 + SKS-30	0.48	1.04	0.30	0.62	—	—	—
SKB + SKS-30	0.54	1.04	0.60	1.11	±	+ —	+
SKN-26 + SKB	0.48	0.54	0.28	0.58	—	—	—
Butyl rubber + NR	0.36	3.20	1.44	4.00	—		+
Butyl rubber + Nairit	0.36	2.00	1.08	3.00	—		—
Butyl rubber + SKS-30	0.36	1.04	0.80	2.22	—		+
Butyl rubber + SKN-26	0.36	0.48	0.62	1.72	—		—
Butyl rubber + SKB	0.36	0.54	0.58	1.61	—		+

With definite incompatibility, $T_{12} < T_{11}$ in all cases, and conversely, which indicates the role of the diffusion mechanism. This is very convincingly confirmed by the correlation between the values of T_{12}/T_{11} and the compatibilities of the corresponding polymers, as shown in Table 2.

The clearest correlation, without any exceptions, is found between the ratio T_{12} / T_{11} and the compatibility index based on the principle of similar polarities. If both polymers are non-polar or both are polar, $T_{12}/T_{11} > 1$, and when one is polar and the other non-polar, $T_{12}/T_{11} < 1$.

The other compatibility indices do not always correlate with the ratio T_{12}/T_{11}. It is noticed, however, that these deviations from the general correlation are always accompanied by contradiction of the respective compatibility indices, which shows that these are doubtful in a number of cases. Consequently, the surface compatibility of rubbers, indicated by their adhesional resistance to shear, is most reliably determined by the characteristic of similar polarities. However, butyl rubber does conform to this rule. In the case of butyl rubber and SKN-26 T_{12}/T_{22} is considerably greater than unity, which may be attributed to specific adhesion due to the electric double layer or van der Waals forces. In the other cases for butyl rubber $T_{22} > T_{12} > T_{11}$, which may be explained by the influence of mechanical properties on the true contact area.

SUMMARY

1. The researches so far published on the autohesion of polymers do not make it possible to isolate the influence of the mechanical properties of rubbers, which determine the true area of contact, from the influence of polymer chain diffusion.

2. Studies of the autohesion of thin films of rubber applied by the drain-off method to quartz threads, in relation to the film thickness and contact time, show that for films less than $3 \cdot 10^{-5}$ cm thick the adhesion force is small and varies very little with contact time. This proves, on the one hand, that in this instance the contact area is small (which is obvious) and does not increase with time, and on the other hand, that diffusion processes play no part in the autohesion of films of this thickness.

3. The effects which depend on mechanical properties and on the specific interaction (per unit area of true contact) between specimens may be separated if the measured values of adhesion between all possible combinations of pairs of rubbers are compared both with their compatibilities, and with their autohesion.

4. The measurements of the adhesional shearing strength of combinations of different pairs of polymers, carried out for this purpose, showed that the results for butyl rubber may be interpreted on the assumption that diffusion processes do not play any appreciable role and that the adhesion strength is determined both by the true contact area, which depends on the mechanical properties of the corresponding polymer specimens, and also by the influence of forces associated with the electric double layer.

5. For the other rubbers the results may be interpreted only on the assumption that diffusion processes play a significant part. For similar polarities, $T_{12}/T_{11} > 1$ and for dissimilar polarities, $T_{12}/T_{11} < 1$.

6. General conclusion: autohesion and mutual adhesion of rubbers is determined both by mechanical properties, which determine the true contact area, and by diffusional properties. The latter are by no means always decisive.

The electric double layer also probably influences the adhesional shearing strength in some instances. It is even more likely to play a role in some cases in measurements of the work of separation of two layers.

Institute of Physical Chemistry
Academy of Sciences USSR
Laboratory of Surface Phenomena and
Scientific Research Institute for the Tire Industry, Moscow

Received April 5, 1958

LITERATURE CITED

[1] D. Josefowitz and H. Mark, Ind. Rub. World. 106, 33 (1942).

[2] B. V. Deryagin and N. A. Krotova, Adhesion (Acad. Sci. USSR Press, 1949), p. 242.

[3] S. S. Voyutsky and Yu. L. Margolina, Progr. Chem. 18,449 (1949).

[4] B. V. Deryagin and A. D. Malkina, Colloid J. 12,431 (1950).

[5] N. I. Moskvitin, M. F. Futran, and B. V. Deryagin, Proc. Acad. Sci. USSR,105,758 (1955).

[6] B. V. Deryagin et al., Trans. II All-Union Conf. on Friction and Wear in Machines (Acad. Sci. USSR Press, 1947),I, pp.96,149; Trans. Inst. Phys. Chem. (Acad. Sci. USSR Press, 1950, No. 1, p. 61.

[7] B. V. Deryagin, Proc. Acad. Sci. USSR 39,11 (1943).

[8] B. V. Deryagin, J. Phys. Chem. 6,1306 (1935); Kolloid-Z. 69, 195 (1934).

[9] S. S. Voyutsky,A. I. Shapovalova and A. P. Pisarenko, Proc. Acad. Sci. USSR 105,1000 (1955).

[10] B. J. Habgood, Trans. Inst. Rub. Ind. 13, 136 (1937).

[11] G. Klebsattel, Ind. Rub. World. 102, 33 (1941).

[12] N. F. Komskaya, Dissertation, "The Physico-Mechanical Properties of Vulcanizates Based on Various Combinations of Raw Rubbers".

[13] I. V. Borodina and A. K. Nikitin, Technical Properties of Soviet Synthetic Rubbers (State Chemical Press, 1952.

THE THEORY OF RUBBER REINFORCEMENT: INTERACTION OF CARBON BLACK WITH SULFUR AND RUBBER

B. Dogadkin, B. Lukin, Z. Tarasova, Z. Skorodumova, and I. Tutorsky

One of the fundamental questions in the problem of rubber reinforcement by active fillers is the nature of the rubber–filler interaction. The commonest view on this question is based on the presumed existence of intermolecular forces at the rubber–filler boundary. Recently, however, evidence has been obtained of the possibility of chemical bonding between rubber and the commonest filler – carbon black. Thus, Stearns and Johnson [1] have shown that the differential heat of adsorption of bromine on the surface of active carbon blacks in the initial period is 28-31 kcal./mole, corresponding to the reaction of bromination of ethylene derivatives. Dogadkin and Feldshtein [2] described as long ago as 1939 the formation of an insoluble and stable rubber–carbon gel on heating a mixture containing carbon black and sodium butadiene rubber. They attributed this to thermo-oxidative structurization processes caused by oxygen and oxygen compounds present in the carbon black. Later a number of investigations of carbon–rubber gels have been made, and Sweitzer, Goodrich, and Burgess [3] have examined the mechanism of the formation from the same standpoint as Dogadkin and Feldshtein [2]. A definite correlation has been established between the reinforcing action of carbon blacks and their ability to combine with rubber. Watson [4] and Garten [5] consider that the formation of a carbon–rubber gel and the reinforcement effect involve the interaction of free radicals formed by the mechanical rupture of the molecular rubber chains and active centers on the carbon black surfaces. In the paper cited above, Stearns and Johnson [1] consider the possibility of bond formation between carbon and rubber in the vulcanizate through sulfur atoms. However, this hypothesis is not supported by the results of Dogadkin and Lukomskaya [6] who showed that the dipole moment of a vulcanizate does not depend on the filler, and is the same both for filled and unfilled rubbers. Thus, the question of the nature of carbon–rubber interaction has not found a generally accepted solution and requires further investigation and discussion. Experimental data directly related to this problem are presented below*.

EXPERIMENTAL

Interaction of carbon black with sulfur in thermal conditions of vulcanization. Two kinds of carbon black were used: channel black from Ukhta, and the same black after hydrogenation.

The purpose of the hydrogenation was to decrease the amount of adsorbed and chemically combined oxygen on the particle surfaces. The process was carried out in a rotary autoclave without the use of a catalyst under an initial hydrogen pressure of 200 atmospheres at 350° (the temperature was raised for 2 hours, held for 3 hours, and lowered for 3 hours.) This treatment decreases the oxygen content of carbon black (Table 1) without appreciable effect on the degree of dispersion.

The carbon blacks were heated with toluene solutions of radioactive sulfur containing S^{35} in sealed tubes at 110, 130, and 150° for 10 hours. In one series of experiments 0.06 g of carbon and 7 ml of a toluene solution containing 7.8 g of sulfur per liter was put into the tubes. In another series, 0.025 g of A100 vulcanization accelerator (condensation product of acetaldehyde and butyraldehyde with aniline) was added to each tube.

---

* Most of the results published in this paper were obtained in 1952-1953 and presented in the report of the Scientific Research Institute for the Tire Industry.

TABLE 1

Characteristics of Carbon Blacks

Carbon black	Elementary composition, %			pH	Colorimetric number	Specific surface in m²/g
	C	H	O*			
Ukhta channel (before treatment	92.69	1.02	4.32	3.87	21	92.2
Ditto, after hydrogenation	96.04	1.25	2.11	7.4	23	92.6

* Determined by the Unterzeicher method

After the heating, the carbon black was filtered off and divided into two portions. The sulfur content in one portion was determined after extraction with chloroform for 80 hours until free (adsorbed) sulfur was completely removed. The completeness of extraction was checked by absence of radioactivity in the solvent. The results gave the amount of chemically combined sulfur. In the other portion sulfur was determined before extraction; the results gave the total sulfur, including the adsorbed sulfur.

The sulfur content of the carbon was determined as follows. A weighed sample of the carbon black was suspended in an alcoholic solution of shellac, placed in the counter cell, and dried to constant weight. The activity of the residue was determined with the aid of a Geiger-Muller counter, and its sulfur content was calculated from a calibration graph plotted from activity data for a residue containing a known amount of S^{35}. As a check, the sulfur content in four samples was determined by the Eschka method as benzidine sulfate. The deviation between the results of the radioactivity method and the Eschka method was in the range of 0.01–0.12%.

The analytical results are shown in Table 2. It is seen from Table 2 that sulfur reacts chemically with carbon black and, as was to be expected, the amount of chemically combined sulfur increases and that of adsorbed sulfur decreases with increase of reaction temperature. The vulcanization accelerator appreciably increases the amount of chemically reacting sulfur.

Figure 1 shows curves for the kinetics of sulfur addition to channel black in the temperature range 110-145° in presence of A100 accelerator. The initial rate of reaction, determined from the tangent at the coordinate origin, varies in conformity with the Arrhenius equation. The apparent activation energy for the addition of sulfur to carbon black, calculated from this equation, is approximately 15000 calories.

TABLE 2

Contents of Total, Adsorbed, and Chemically Combined Sulfur in Different Specimens of Carbon Black Heated at 110, 130, and 150° in Presence and in Absence of Vulcanization Accelerator (as % on the Carbon)

Sulfur content	110°				130°				150°			
	channel black		hydrogenated black		channel black		hydrogenated black		channel black		hydrogenated black	
	without accelerator	with accelerator	without accelerator	with accelerator	without accelerator	with accelerator	without accelerator	with accelerator	without accelerator	with accelerator	without accelerator	with accelerator
Total content (a)	0.07	0.5	0.15	0.40	0.12	0.39	0.22	0.40	0.29	0.57	0.37	0.74
Chemically combined (b)	0.04	0.2	0.09	0.25	0.10 0.09	0.31 0.23	0.18 0.30	0.37 0.41*	0.28	0.54	0.37	0.75
Adsorbed (extracted by chloroform) from the difference (a − b)	0.03	0.3	0.06	0.15	0.02	0.08	0.04	0.03	0.01	0,03	—	—

* Results obtained by Eschka method; accelerator, diphenylguanidine.

It is natural to attribute the increased activity of carbon black toward sulfur after hydrogenation to addition of the latter at the places of reduction of functional oxygen-containing groups. However, we were not able to detect the evolution of measurable amounts of hydrogen sulfide in the reaction of sulfur with hydrogenated carbon black (in a system without accelerator). The possibility of direct addition of sulfur at active sites of the carbon surface is therefore not excluded. This question requires further experimental investigation.

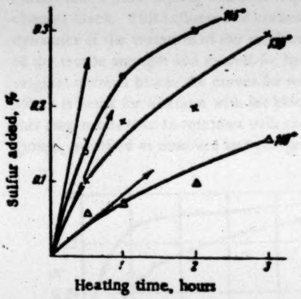

Fig. 1. Kinetics of the addition of sulfur to channel black at various temperatures.

Interaction of carbon black with rubber. Sodium butadiene rubber was mixed in air on laboratory rolls with approximately half its own weight of carbon black. The mixture was heated for an hour at 100 and 180° in air and in nitrogen. The amount of carbon–rubber gel was determined after extraction of the mixture by benzene in a Soxhlet apparatus for 20 hours. The results are shown in Table 3. It is seen that even simple milling in air results in binding of up to 50% of the rubber in a form not extracted by benzene. The amount of bound rubber increases considerably (by about a half) as the result of heating, and heating in air leads to greater structurization of the rubber than heating in nitrogen. It is not possible to draw convincing conclusions concerning the mechanism of carbon–rubber gel formation from the results of these experiments, as the milling was performed in air, in conditions in which structurization of sodium butadiene could occur without chemical action with the carbon black. It is significant, however, that greater structurization of the system occurs on mixing with hydrogenated carbon black than with the original carbon before hydrogenation.

TABLE 3

Effect of Hydrogenation of the Carbon Black on Formation of Carbon–Rubber Gel

Type of carbon black	Conditions of heating the mixture	Weight of carbon in mixture, g	Weight of rubber, g		Combined rubber, %		
			before extraction	after extraction	of the mixture	of total rubber	of carbon black
Ukhta channel black	Without heating	0.2606	0.5212	0.2076	26.5	39.8	79.5
	1 hour in air at 100°	0.4153	0.8307	0.5127	41.2	61.6	123.0
	1 hour in nitrogen at 100°	0.4403	0.8805	0.6035	45.5	68.5	136.8
	1 hour in air at 180°	0.4410	0.8820	0.7980	60.3	90.5	181.0
	1 hour in nitrogen at 180°	0.4108	0.8216	0.7038	57.0	85.5	171.0
Ditto, after hydrogenation	Without heating	0.3112	0.6226	0.3170	34.0	51.0	102.0
	1 hour in air at 100°	0.3210	0.6422	0.4648	48.2	72.2	144.4
	1 hour in nitrogen at 100°	0.3544	0.7088	0.4888	46.3	69.0	138.0
	1 hour in air at 180°	0.3042	0.6084	0.5766	63.2	95.0	190.0
	1 hour in nitrogen at 180°	0.2975	0.5951	0.5325	59.7	89.5	179.0

Effect of hydrogenation of carbon black on vulcanization kinetics and on the mechanical properties of vulcanizates. It might have been expected that the changes produced by hydrogenation in the properties of carbon black, described above, would influence the vulcanization kinetics and the properties of the filled vulcanizates. To confirm this, a mixture of 100 parts by weight of butadiene–styrene rubber SKS-30 and 54 parts by weight of carbon black (accelerator: mixture of benzothiazolyl disulfide and diphenylguanidine) was vulcanized under the usual conditions in a press at 143°. As Fig. 2 shows, the mixture with the hydrogenated carbon reacts more rapidly and adds rather more sulfur than the mixture containing the original untreated channel black. This influence of carbon hydrogenation on the kinetics of sulfur addition is also reflected in the dynamics of the variation of the mechanical properties of the vulcanized mixture. The curves for the variation of the tensile strength and moduli for hydrogenated carbon black lie above the corresponding curves for the original channel black; the curves for relative and residual extension lie in the opposite order (Fig. 3). A similar effect is found for mixtures with jet black before and after hydrogenation (Fig. 4). However, the difference in this case is less than in mixtures with channel black, since jet black has fewer functional oxygen-containing groups, modified or removed by hydrogenation, on the particle surfaces.

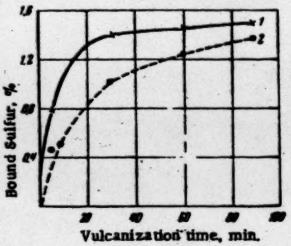

Fig. 2. Kinetics of sulfur addition in the vulcanization of butadiene–styrene rubber in mixtures with hydrogenated carbon black (1) and untreated channel black (2).

It must be pointed out that hydrogenation of carbon black has relatively little influence on the properties of the vulcanizate at optimum vulcanization. The tensile strength in the present instance increases by 15-20 kg/cm² (for channel black). The change of the modulus is greater, which is in good agreement with the change of the combined sulfur content. The differences in the properties are leveled out if the vulcanizates are tested at 100° (Fig. 5). However, an increase of the testing temperature to 100° does not completely eliminate the difference between the properties of mixtures containing untreated and hydrogenated carbon blacks; this indicates that hydrogenation of carbon black influences the number of chemical bonds in the spatial structure of the vulcanizate.

DISCUSSION OR RESULTS

An important result of the present investigation is that the chemical addition of sulfur to channel black has been established by direct experiment. It was found that the chemical activity of channel black increases after hydrogenation.

The reaction between carbon black and sulfur leads to an increase in the dimensions of the carbon black aggregates, determined by the light absorption of suspensions obtained with the aid of ultrasonic vibrations (frequency 10000 cycles/second). The results of determinations by this method are shown in Table 4. It is seen from Table 4 that the aggregates are approximately doubled in size after hydrogenated carbon black has been heated with sulfur. This means either that sulfur reacts with the carbon in the form of a biradical capable of binding separate particles of carbon black together, or that the thiol groups formed in the reaction of sulfur with the functional groups of the carbon black can react with active groups of other carbon black particles. If such structure formation also occurs in the vulcanization of rubber mixtures filled with carbon black, then the resultant structures are a factor in rubber reinforcement, since:

a) They bear part of the tensile stress, the work of rupture of these structures being determined by the chemical bond energy;

b) They may act as sites of adsorptive fixation and orientation of the molecular rubber chains which, according to Dogadkin and Pechkovskaya [7], is the principal factor in the reinforcement of rubber by active fillers.

The possibility is not excluded that sulfur groupings bind carbon black to rubber molecules. We have no direct evidence at present for this reaction; but the observed increase of the moduli of the vulcanizates, parallel with increased contents of bound sulfur in mixtures containing hydrogenated carbon black, makes this reaction highly probable. In such a case the carbon black structures enter into the vulcanization network, being joined to its rubber component by chemical bonds. The extent of formation of such bonds depends both on the extent of

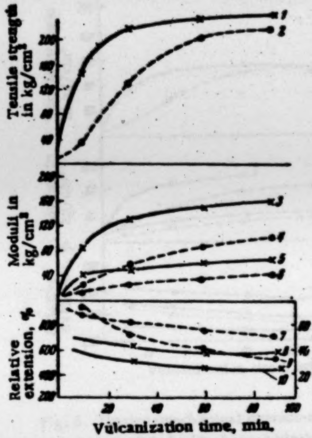

Fig. 3. Variation of the physico-mechanical properties during vulcanization of mixtures of butadiene–styrene rubber filled with channel-black: 1) and 2) tensile strength, 3 and 4) moduli for 400%, 5 and 6) moduli for 200%, 7 and 8) relative extensions, 9 and 10) residual extensions. Continuous lines represent vulcanizates with hydrogenated, broken lines, with untreated, carbon.

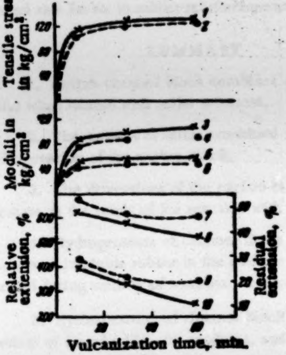

Fig. 4. Variation of the physico-mechanical properties during vulcanization of mixtures of butadiene–styrene rubber filled with jet black: 1 and 2) tensile strength, 3 and 4) moduli for 400%, 5 and 6) moduli for 200%, 7 and 8) relative extensions, 9 and 10) residual extensions. Continuous lines represent vulcanizates with hydrogenated, broken lines, with untreated, carbon.

TABLE 4

Dimensions of Carbon Black Aggregates from Colorimetric Data

Type of carbon black	Color of filter	Optical density	Aggregate radius in μ	Number of primary particles in aggregate	Colorimetric number
Hydrogenated carbon black	Blue Green Red	0.511 0.43 0.351	0.035 0.042 0.051	2	28.2
Ditto, heated in toluene at 150°	Blue Green Red	0.45 0.395 0.30	0.040 0.046 0.060	3	24.8
Ditto, heated with toluene solution of sulfur at 150°	Blue Green Red	0.34 0.278 0.25	0.053 0.065 0.072	4—5	14.9

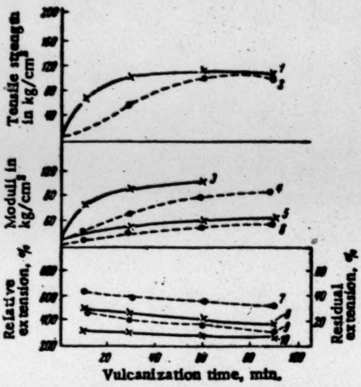

Fig. 5. Physico-mechanical characteristics of vulcanizates filled with channel black, at 100°: 1 and 2) tensile strength, 3 and 4) moduli for 400%, 5 and 6) moduli for 200%, 7 and 8) relative extensions, 9 and 10) residual extensions. Continuous lines represent vulcanizates with hydrogenated, broken lines, with untreated carbon.

the reaction between sulfur and carbon black, and on direct interaction between carbon black and rubber.

The entry of carbon black structures into the composition of the vulcanization network must also be considered as a factor in rubber reinforcement.

SUMMARY

1. Active channel black combines chemically with sulfur when heated with sulfur solutions.

2. The amount of sulfur combined increases after hydrogenation of the carbon black.

3. The dimensions of the carbon black aggregates increase as the result of the reaction with sulfur.

4. Hydrogenation of channel black increases the content of insoluble rubber in the carbon-rubber gel formed during milling of a rubber – carbon black mixture.

5. Hydrogenation of channel black increases the content of bound sulfur, the modulus, and tensile strength, in comparison with vulcanizates containing the original unhydrogenated channel black.

6. These facts suggest that active carbon black enters the composition of the vulcanizate structure, and this is a factor in rubber reinforcement.

Research Institute for the Tire Industry, Moscow

Received November 15, 1955

LITERATURE CITED

[1] Stearns and Johnson, Ind. Eng. Chem. 43, 146 (1951).

[2] B. Dogadkin and Feldshtein, Caoutchouc and Rubber, No. 12,19 (1939).

[3] C. W. Sweitzer, W. C. Goodrich and K. A. Burgess, Rubber Age 65, 651 (1949).

[4] W. F. Watson, Ind. Eng. Chem. 47, 1281 (1955).

[5] V. A. Garten, Nature 173, 997 (1954).

[6] A. I. Lukomskaya and B. A. Dogadkin, Colloid J. 15, 259 (1953) (T.p. 267)*.

[7] B. Dogadkin, K. Pechkovskaya and M. Dashevsky, Colloid J. 10, 256 (1948).

---

* T. p. = C. B. Translation Pagination.

INVESTIGATION OF THE MECHANISM OF EMULSION POLYMERIZATION

E. V. Zabolotskaya, I. G. Soboleva, N. V. Makletsova, and S. S. Medvedev

The view was first developed by Yurzhenko and by Frayling [1], and later by Harkins [2] that emulsion polymerization of water-insoluble monomers, carried out in solutions of colloidal electrolytes (soaps), commences in the emulsifier micelles. Further work by Harkins, Yurzhenko, Medvedev, and Khomikovsky [2-4] established that as the emulsifier passes from solution into the adsorption layers of the growing polymer particles, polymerization proceeds within these particles, containing unpolymerized monomer. However, this concept of polymerization within the polymer particles is not consistent with the observed constant rate of polymerization up to high degrees of conversion [2-4]. Recently Medvedev and Sheinker [5], on the basis of a detailed study of the polymerization kinetics of isoprene in presence of water-soluble initiator, advanced the idea of polymerization reactions occurring in adsorption layers of the emulsifier [5]. This view, based on kinetic investigations, may be confirmed and developed further by detailed topochemical study of the system.

With the aim of a further study of the mechanism of emulsion polymerization – the determination of the reason for the constancy of the polymerization rate and clarification of the mechanism of polymer particle formation – a systematic investigation has been made of the variations of the particle sizes in the polymerization system, starting with micelles of the pure emulsifier, emulsifier micelles with dissolved hydrocarbon, and polymer particles right at the start of polymerization. The stage of polymerization at which the micellar emulsifier passes into the adsorption layers of the forming polymer particles has been determined. The particle sizes were determined by the light scattering method. The instant of disappearance of micellar emulsifier was determined by the change of the surface tension of the latex.

Starting Materials

Isoprene was treated with caustic soda solution, washed with water, dried, and distilled at 34°.

N-cetylpyridinium bromide, used as emulsifier, was synthesized from cetyl bromide and pyridine. The product contained 98% N-cetylpyridinium bromide after precipitation by acetone from dioxane solution.

Hydrogen peroxide, used as initiator, was recondensed under vacuum to remove stabilizer.

Methods of Investigation

Polymerization method and conditions. In view of the use of nephelometry for studying the latex, the polymerization was carried out with gas phase supply of the monomer, as the presence of drops might distort the results of nephelometric determinations. This method of polymerization in aqueous solutions of emulsifier and initiator, continuously saturated with isoprene at constant monomer vapor pressure, can be regarded as modeling the conditions of emulsion polymerization in absence of monomer droplets.

The starting substances were prepared optically pure and were made free from oxygen under vacuum.

The polymerization and saturation of the emulsifier solution by isoprene was carried out at 50° in a rocking vessel shown in Fig. 1*. The solution containing the emulsifier and initiator was in the horizontal bulb 1, and the isoprene in the measuring tube 2. The amount of monomer used for saturation and polymerization was determined from the decrease in the measuring tube. The latexes were analyzed for polymer yield (from the dry residue), surface tension, and the statistical average particle weight.

---

* The design of the vessel was taken from Sheinker [5].

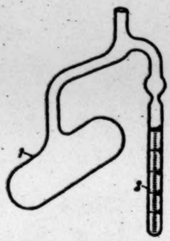

Fig. 1. Polymerization vessel.

The polymerization was performed at two concentrations of N-cetylpyridinium bromide, 5 and 2.5%. The amount of peroxide was 0.45% of the aqueous phase. The consumption of isoprene, in experiments of different duration, was from 1.9 to 16g/100 ml aqueous phase at 5% initial emulsifier concentration, and from 1.4 to 11 g/100 ml aqueous phase at 2.5% N-cetylpyridinium bromide concentration.

Determination of the instant of disappearance of micellar emulsifier during polymerization. The polymerization stage corresponding to the transition of the emulsifier into the adsorption layers of the polymer particles in the given conditions was determined from the surface tension of the latex. This, at the instant of disappearance of micellar emulsifier, was approximately equal to the surface tension corresponding to the critical micelle concentration of the emulsifier. The surface tension was measured at the liquid–air boundary by the depth of immersion of a plate into the liquid [6].

Determination of particle size by light scattering. The weights of the emulsifier micelles and the particles in the polymerization system were determined by the light scattering method [7]. This method was successfully used by Debye [8] for determination of micellar weights of soap solutions. The micellar weights of sulfated emulsifier solutions and dimensions of polymer particles have also been determined with the use of the light scattering method by Yurzhenko and his co-workers [9], and by Bardwell and Sivertz [10]. The measurements of turbidity at various concentrations were made with the use of a nephelometer designed by the Design Bureau of the Karpov Institute.

All the nephelometric measurements of the emulsifier solutions and latexes were carried out for the green line of the mercury lamp at 35°. The maximum concentration of the emulsifier solutions in the turbidity measurements was 2.5%. The latexes were studied in solutions diluted by 0.5% N-cetylpyridinium bromide solution to concentrations of 0.1-0.001 g/100 ml. Freshly prepared latexes were used, without prior degasification. The accuracy of the particle size determination, with all the operations preceding the determination taken into account, can be taken as 12-20%, according to the turbidity.

Experimental Data

Figures 2-4 show experimental data on the kinetics of saturation of N-cetylpyridinium bromide solutions with isoprene.

It was found in determinations of the polymer yield at different stages of the process, at the two emulsifier concentrations studied, that on the average 64% of the total isoprene in the latex is polymerized. Consequently, the isoprene which evaporates from the measuring tube of the apparatus is consumed for saturation of the emulsifier solution, polymerization, and in dissolving in the polymer particles. The saturation limit (solubilization) is 1.75 g of isoprene in 100 ml of 5% emulsifier, and 0.54 g of isoprene in 100 ml of 2.5% solution of N-cetylpyridinium bromide.

The saturation rate of the emulsifier solution considerably exceeds the total rate of isoprene consumption, and therefore entry of the monomer into the latex through the gas phase does not limit the polymerization rate. Only when the isoprene content exceeds 14.2 g/100 ml emulsifier solution (Fig. 3), when the viscosity of the latex increases considerably, is the diffusion of isoprene hindered. The retarded diffusion of the monomer is indicated by a decrease of the rate of transfer of isoprene into the latex from the measuring tube of the vessel, and an increase of the content of polymerized monomer in the polymer particles to 78%. These facts indicate that as a result of gelation of the latex, polymerization occurs mainly in the monomer dissolved in the polymer particles.

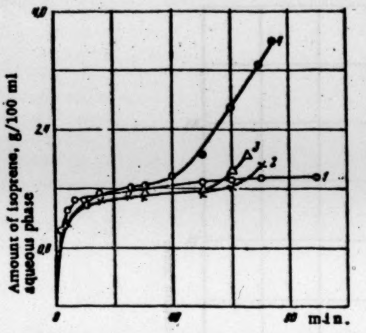

Fig. 2. Amount of isoprene passing into the aqueous phase as a function of time: 1) saturation of 5% N-cetylpyridinium bromide solution; 2 to 4) polymerization; emulsifier concentration 5%.

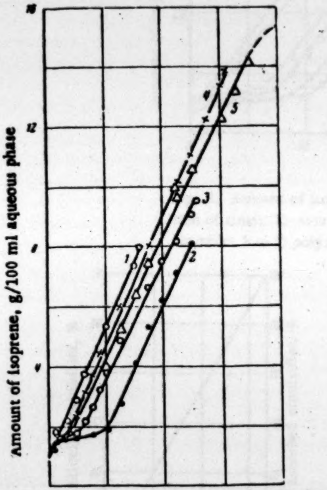

Fig. 3. Amount of isoprene passing into the aqueous phase as a function of time; 1 to 5) polymerization; emulsifier concentration 5%.

The constant ratio of polymer to monomer in the polymer particles indicates that after a short induction period, which is probably to be attributed to the presence of traces of oxygen, the polymerization rate remains constant until gelation of the latex begins (Figs. 3, 4). All the polymerization graphs are straight lines with the same slope, and differ only in the length of the induction period. The polymerization rate in 5% solution is double the polymerization rate in 2.5% solution.

The results of determinations of surface tension of latexes with different isoprene concentrations for the two emulsifier concentrations studied are shown in Table 1.

The surface tension corresponding to the critical micelle concentration, which was found by the light scattering method to be $5.2 \cdot 10^{-4}$ mole/liter, is approximately 42 dynes/cm. Colloidally dispersed isoprene in the unpolymerized and polymerized states does not influence the surface tension of emulsifier solutions.

The results in Table 1 indicate that in the latex with 5% initial emulsifier concentration, micellar emulsifier disappears after absorption of approximately 9 g of isoprene per 100 ml of aqueous phase; in the latex with 2.5% initial emulsifier concentration, micellar emulsifier disappears after absorption of about 5 g of isoprene per 100 ml of aqueous phase. The kinetic curves (Figs. 3 and 4) show that disappearance of micellar soap does not affect the polymerization rate.

On the assumption of a linear relationship between the amount of adsorbed emulsifier and the surface of the polymer particles (which is proportional to the isoprene concentration to the power 2/3), it is easy to determine the amount of free emulsifier in the latex at the early stages of polymerization (Fig. 5). The results obtained can be used to represent graphically the composition of the anhydrous part of the system at various stages of the process (Fig. 6). The main curve, which represents the weight ratio between emulsifier and hydrocarbon in the system with different amounts of isoprene, divides the graph into two parts: the upper represents the hydrocarbon fraction, and the lower, the emulsifier fraction.

The diagram may be divided into three parts along the abscissa axis. The first part, corresponding to isoprene concentrations from 0 to 1.75 g/100 ml of aqueous phase, represents the stage of saturation of the emulsifier solution by monomer. The second part, from 1.75 to 9 g/100 ml, represents polymerization in presence of free emulsifier in the system. The emulsifier is divided into micellar and adsorbed emulsifier according to the data in Figure 5. The hydrocarbon fraction is also divided, by a similarly plotted curve, into monomer forming the polymer particles and the monomer dissolved in the free emulsifier. The third part, from 9 to 16 g/100 ml of aqueous phase, represents polymerization in absence of micellar emulsifier.

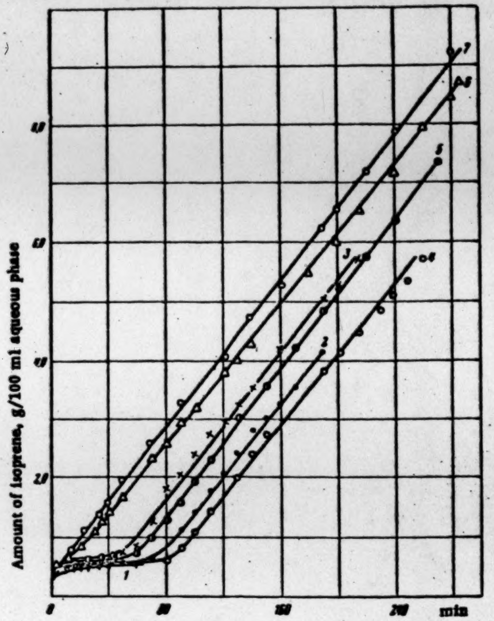

Fig. 4. Amount of isoprene passing into aqueous solution as a function of time: 1) saturation of 2.5% solution of N-cetylpyridinium bromide; 2 to 7) polymerization; emulsifier concentration 2.5%.

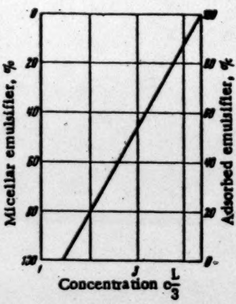

Fig. 5. Distribution of micellar and adsorbed emulsifier; initial emulsifier concentration 5%.

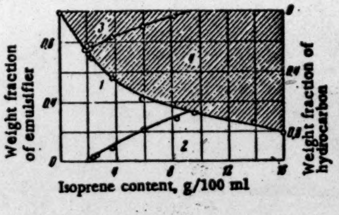

Fig. 6. Graph for the composition of the anhydrous part of the latex, initial emulsifier concentration 5%: 1) micellar emulsifier; 2) adsorbed emulsifier; 3) monomer dissolved in the emulsifier; 4) polymer and unpolymerized monomer in polymer particles.

TABLE 1

Surface Tension of Latexes for Different Isoprene Contents

Amount of isoprene in g/100 ml of aqueous phase (emulsifier concentration 5%)	Surface tension in dynes/cm	Amount of isoprene in g/100 ml of aqueous phase (emulsifier concentration 5%)	Surface tension in dynes/cm
1.90	31.0	1.36	32.6
2.02	32.4	2.51	34.8
3.30	33.6	3.15	35.0
8.05	36.5	4.15	40.0
8.18	38.6	5.70	43.0
9.50	42.2	7.41	49.2
13.80	44.0	8.70	50.6
16.00	49.0	—	—

Figure 6 shows the rate at which the micellar emulsifier is adsorbed by the forming polymer particles, and it can also be used for determination of the composition of the latex particles at all stages of the process.

Since the latex contains micellar emulsifier during the early stages of polymerization, the particle weight determined by nephelometric turbidity measurement, for the total concentration of all the isoprene and emulsifier introduced into the system, is the average of the weights of the polymer particles and the weights of the emulsifier micelles saturated with isoprene ($\underline{m}$). The particle weight found from the total concentration represents the weight of the polymer particles only from an isoprene content of 9 g/100 ml of 5% emulsifier solution, and 5 g/100 ml of 2.5% emulsifier solution, when no micellar emulsifier is present in the latex (the determination of the polymer particle weight at the early stages of polymerization will be described below).

Table 2 and Fig. 7 show that the particle weight gradually increases in presence of micellar emulsifier in the system. In the absence of micellar emulsifier there is a greater increase in the particle weight than at the initial stages of polymerization, indicating "coalescence" of the particles, which is apparently especially prominent after the disappearance of free emulsifier. The particle weight corresponding to the same amount of isoprene is greater for the lower initial emulsifier concentration. This must be attributed to the earlier disappearance of free emulsifier at the lower concentration.

The measured values of the latex particle weights were used to calculate the diameter, number, and total surface area of the particles in 100 ml of the aqueous phase.

Table 2 and Fig. 7 show that the number of particles decreases in the course of polymerization. The initial number of particles is taken to be the number of emulsifier micelles. For the micellar weight which was found to be 12500, the number of micelles in 100 ml of solution is $2.4 \cdot 10^{20}$ for 5% emulsifier concentration, and $1.2 \cdot 10^{20}$ for 2.5% emulsifier concentration.

The total surface of the latex particles is the same for each of the emulsifier concentrations studied, which is a significant fact for an understanding of the topochemistry of emulsion polymerization. The constancy of the total surface of the particles in the polymerization system, in conjunction with the constancy of the polymerization rate, suggests that the polymerization processes occur in the surface layers of the particles, irrespective of whether these particles are the original micelles or polymer particles saturated with monomer or swollen in the monomer. Sheinker and Medvedev [5] reached a similar conclusion. Thus, since polymerization occurs in the surface layers of the latex particles, i.e. in the adsorption layers of the polymer particles and in the emulsifier micelles, transfer of emulsifier molecules from the solution into the adsorption layers does not affect the polymerization rate.

The value of the particle surface should be determined by the amount of emulsifier present in the system. The validity of the views advanced is also confirmed by the proportionality which was found between the polymerization rate, emulsifier concentration, and the total surface of the particles in the polymerization system.

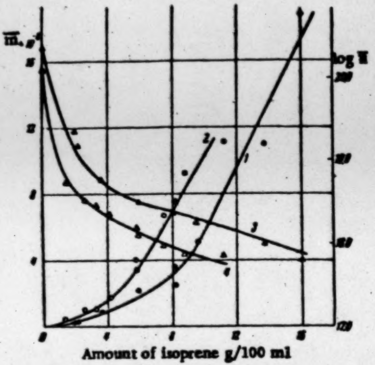

Fig. 7. Weight and number of latex particles as functions of the isoprene content: 1 and 2) particle weight; 3 and 4) numbers of particles. Initial emulsifier concentrations 5 and 2.5%.

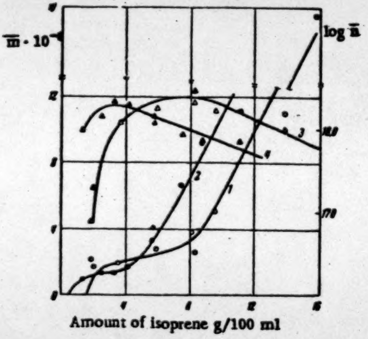

Fig. 8. Weights and numbers of polymer particles as functions of the isoprene content in the latex: 1 and 2) particle weight; 3 and 4) numbers of particles. Initial emulsifier concentrations 5 and 2.5%.

In order to follow the weight variations of the polymer particles in the early polymerization stages, when micellar emulsifier is present in the system, it is necessary to eliminate the influence of the micellar emulsifier on the results of the nephelometric determinations. This was done by subtraction of the micellar emulsifier concentration (Fig. 5) and the amount of the colloidally dispersed isoprene in it, from the total concentration. (The amount of isoprene dissolved in free emulsifier was calculated on the assumption that the micelles are fully saturated during polymerization, since the process took place at constant monomer vapor pressure.) The turbidity caused by the presence of micellar emulsifier is very slight at the latex concentrations used in nephelometric determinations; its magnitude does not exceed the error limits and could be neglected in determinations of the polymer particle size. The free emulsifier turbidity was considerable only in two latex samples with 5% initial emulsifier concentration and with isoprene contents close to the saturation limit of the emulsifier solution; it was then taken into consideration in calculation of the polymer particle weight.

The data obtained on the variation of the dimensions and numbers of polymer particles in the region of the isoprene polymerization process studied (Fig. 8) make it possible to elucidate the mechanism of polymer particle formation.

It is significant that the polymer particle weight at the very start of polymerization, when the amount of isoprene in the latex is at the saturation limit, is greater than the micellar weight of the emulsifier by two orders of magnitude; the number of polymer particles correspondingly decreases by three orders of magnitude relative to the initial number of micelles*. This sharp increase of the polymer particle size relative to the micelle size, and the corresponding decrease of the number of particles, indicate that large numbers of micelles are consumed in the formation of polymer particles, and consequently polymerization does not begin in each micelle.

An approximate calculation, based on the assumption of a monomolecular adsorption layer, and on an assumed average surface area of 50 A^2 for one emulsifier micelle [2], shows that tens of micelles are needed to build a polymer particle at the start of polymerization. The number of micelles forming a polymer particle increases as polymerization proceeds. Several hundreds of micelles are needed for the formation of a polymer particle ~300–400A in diameter. Similar information is given by Harkins [2]. Our data, and also the results reported by Harkins [2], which indicate that the micelles increase in size during solution of hydrocarbon in them, suggest that micelle aggregation commences even before polymerization, during solution of monomer in them, which precedes the

---

* When the isoprene content is 1.9 g/100 ml of 5% solution, the polymer particle weight is 2.2 million, and the number is $0.8 \cdot 10^{17}$.

TABLE 2

Weights, Numbers, and Total Surface of Latex Particles

Isoprene	Emulsifier	Weight $m \cdot 10^{-6}$	Diameter in A	Number $n \cdot 10^{-14}$	Total surface $\Sigma s \cdot 10^{-4}$ cm²
g/100 ml of aqueous phase				g/100 ml of aqueous phase	
1.90	5.28	185	84	23.3	5.15
2.02	4.98	280	94	16.2	4.48
3.60	4.72	870	141	5.75	3.80
5.88	5.00	2100	195	3.10	3.74
8.05	5.30	(3600)	232	2.23	(3.78)
8.18	4.89	2400	204	3.27	4.25
9.50	4.43	5000	280	1.68	3.56
13.80	4.31	11000	340	0.99	3.60
16.00	4.24	(18800)	406	0.65	(3.42)
1.36	2.32	410	113	5.36	2.15
2.51	2.53	950	148	3.20	2.22
3.25	2.40	1110	158	3.05	2.40
4.15	2.18	1670	181	2.28	2.35
5.70	2.36	3300	226	1.46	2.34
5.75	2.10	4000	244	1.18	2.22
7.41	2.52	6700	289	0.89	2.35
8.70	2.66	9200	320	0.74	2.39
11.10	2.50	11100	340	0.74	2.68

polymerization process. Probably the introduction of the hydrocarbon (a second component) into the micelle results in a change in the nature of the forces of interaction, favoring the formation of thermodynamically stable larger aggregates.

By a comparison of the curves for the same emulsifier concentration in Fig. 8, showing the variations of the polymer particle weights and numbers with the isoprene content, it is possible to follow the mechanism of polymer particle formation in the polymerization process.

As has already been pointed out, the jump in the polymer particle weight to 1-2 million indicates formation of polymer particles from several micelles. Polymerization in presence of micellar emulsifier is characterized by a slight increase of particle weight and a sharp increase of the number of polymer particles. Consequently, during this period new polymer particles are initiated in the emulsifier micelles in addition to growth.

After disappearance of the micellar emulsifier, only an increase in the size of the particles already formed is observed. The rapid increase of the polymer particle weight with a decrease of their number in absence of micellar emulsifier indicates that during this stage of the process the particles grow both by polymerization and by coalescence. The coalescence is especially prominent in absence of micellar emulsifier, which is evidently to be explained by incomplete coating of the polymer particle surfaces by the adsorbed emulsifier micelles. The increase of the polymer particle surface as the result of polymerization is compensated by its decrease by coalescence. The existence of these two factors acting in opposite directions is the reason why the surface remains constant.

SUMMARY

1. Isoprene has been polymerized in saturated solutions (with the monomer supplied through the gas phase) at two concentrations of N-cetylpyridinium bromide. The initiator was hydrogen peroxide. The polymerization rate of isoprene is constant in the region studied; it directly depends on the initial emulsifier concentration and does not vary with transfer of the emulsifier molecules from micelles into the adsorption layers of the polymer particles.

2. It is shown that during polymerization the size of the latex particles increases, their number decreases, and the total particle surface remains constant; the latter depends directly on the initial emulsifier concentration.

3. The data obtained on the particle surface, in conjunction with the kinetic data, lead to the conclusion that the polymerization reaction proceeds in the surface layers of the latex particles, irrespective of whether these particles are micelles or polymer particles saturated with monomer.

4. Data on the variation of the number and size of the polymer particles during polymerization indicate that polymerization commences not in all micelles, but only in some, in which initiation occurs. A large part of the micelles containing dissolved monomer participate in the formation of polymer particles.

5. The sharp increase of the polymer particle weight after the disappearance of the micellar emulsifier cannot be attributed to the polymerization process only, but indicates coalescence of the particles, which becomes particularly prominent in the absence of micellar emulsifier.

The views advanced on the layer nature of the polymerization process and on the mechanism of polymer particle formation are probably valid for the polymerization of a large number of water-insoluble monomers under the action of water-soluble initiators.

The L. Ya. Karpov Scientific Research
Institute of Physical Chemistry, Moscow

Received June 9, 1955

LITERATURE CITED

[1] A. I. Yurzhenko, J. Gen. Chem. 16, 1171 (1946); A. I. Yurzhenko and M. Kolechkova, Proc. Acad. Sci. USSR 47, No. 5, 354 (1945); C. F. Frayling and E. W. Harrington, Ind. Eng. Chem. 36, No. 2, 114 (1944).

[2] W. D. Harkins, J. Polymer Sci. 5, 2, 217 (1950); J. Am. Chem. Soc. 69, 1428 (1947).

[3] A. I. Yurzhenko and V. B. Gusyakov, Colloid J., 14, No. 2, 140 (1952); P. M. Khomikovsky, Proc. Acad. Sci. USSR, 60, No. 4, 615 (1948); P. M. Khomikovsky, E. V. Zabolotskaya, and S. S. Medvedev, Proc. 6th Conf. on High Mol. Compounds, Acad. Sci. USSR Press, p. 45 (1949).

[4] G. V. Tkachenko and P. M. Khomikovsky, Colloid J., 13, 217 (1951).

[5] A. P. Sheinker and S. S. Medvedev, Proc. Acad. Sci. USSR, 97, No. 1, 111 (1954); J. Phys. Chem., 29, No. 2, 250 (1955).

[6] A. A. Trapeznikov, J. Phys. Chem., 19, 228 (1944).

[7] P. Debye, J. Phys. and Colloid Chem. 51, 1, 18 (1947).

[8] P. Debye, Ann. N. Y. Acad. Sci. 51, 4, 575 (1949); J. Phys. and Colloid Chem. 53, 1, (1949).

[9] A. I. Yurzhenko and R. V. Kucher, Proc. Acad. Sci. USSR, 85, No. 6, 1337 (1952); A. I. Yurzhenko and V. B. Gusyakov, Proc. Acad. Sci. USSR, 86, No. 1, 129 (1952).

[10] G. Bardwell and C. Sivertz, Can. J. Res. 25B, 255(1947).

ELASTICO-VISCOUS PROPERTIES OF POLYISOBUTYLENE SOLUTIONS

L. V. Ivanova-Chumakova and P. A. Rebinder

Investigations of the mechanical properties of systems of the type of polyisobutylene solutions in hydrocarbon media over a wide concentration range are of great interest, primarily because they provide experimental data for development of the molecular-kinetic theory of the elastico-viscous properties of high polymers. At the same time, such investigations are of great practical importance for a number of industries based on uses of such systems.

Polyisobutylene forms solutions in all proportions in a number of hydrocarbons (toluene, xylene). For investigation of the mechanical properties of solutions over the whole concentration range from pure solvent to pure polyisobutylene it was necessary to select measurement methods which would cover the variation of the mechanical properties over such an extremely wide range. A combination of two instruments [1,2,4], based on measurement of the course of deformation caused by homogeneous pure shear in a narrow gap containing the investigated system, proved very convenient for this purpose. Both instruments were modified in relation to the purposes of our investigation. Instrument A (Fig. 1), in which shear occurs between two plates in a narrow plane-parallel gap [3, 4], was used for determinations on highly concentrated systems, including pure polyisobutylene. Dilute solutions, starting with the pure solvent, could be investigated only with a sensitive apparatus, adapted for systems with low viscosity. Instrument B (Fig. 3), of the Shvedov type [1], is such an instrument.

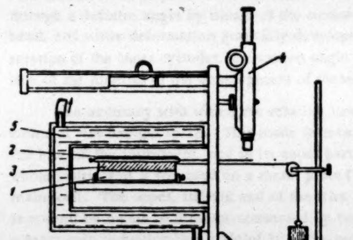

Fig. 1. Instrument A (with two plates) for study of the development of shearing deformation.

The main part of Instrument A (Fig. 1) consists of two riffled plates 1 and 2 50×30×8 mm and 50×30×4 mm in size, made from steel (1) and Duralumin (2); 1 is fixed rigidly to the base of the instrument and is covered with a layer of the investigated material 3 (5 mm thick), and this is covered by the second plate, on which the shearing force F acts. To place polyisobutylene or other rubberlike material into such a gap, it had to be cut out of a piece of the material in an even layer, placed between the plates and then put for a short time in a thermostat while clamped in a small press. At the higher temperature the material flowed into the sharp depressions in the riffled inner surfaces of the plates, and uniformly covered all their surface. This eliminated the possibility of wall slip, especially in view of the good adhesion of the system in question to the plate surface.

When the edges of the pressed layer of material were trimmed, small thin "tongues" 1, 1' (Fig. 2) were left at the sides of the plate faces which moved away from each other during shear; these were turned onto the edges of the plates and held there by the special clamps 2, 3 (see Fig. 2). This prevented separation of the polyisobutylene from the mutually separating edges of the plates, which could lead to some decrease of the actual area of distribution of the shearing force.

Another important feature of the instrument (Fig. 1) is the reading microscope 4, for reliable operation of which it must be rigidly fixed to the working part of the instrument, thus eliminating accidental vibrations relative to the plates. It must be stressed that it should be possible to move this microscope along the plates, as the large total deformation usually exceeds the field of vision of the microscope. In view of the need to conduct the investigations at elevated temperatures (up to 90°) and also at constant room temperature, the working plates were placed in the thermostat 5 – a special metal box with double walls, with a stream of liquid at constant temperature flowing around it from a Hoppler ultrathermostat fitted with a thermoregulator.

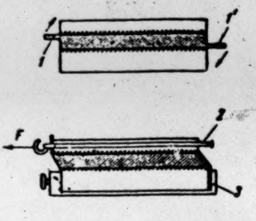

Fig. 2. Attachment of thin "tongues" of the investigated material to the edges of the plates.

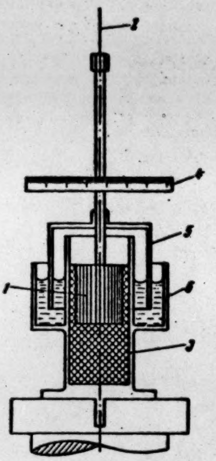

Fig. 3. Instrument B with attachment to protect the system from evaporation and scale for deformation readings.

Instrument B (Fig. 3) consists of two coaxial cylinders; the inner cylinder 1 is suspended by an elastic (tungsten or steel) wire 2, the torsional angle of which is used to measure the stress in the gap. The outer cylinder 3 can rotate at a constant speed, by means of a motor and reducing gear, and the shearing stress which is then set up, by rotating the inner cylinder, causes torsion of the wire. By means of such experiments the effective viscosity in steady flow can be determined as $\eta = \frac{P}{d\epsilon / d\tau}$. The outer cylinder can also remain stationary. The wire is then twisted through a definite angle by means of the torsion head, and while deformation gradually develops by rotation of the inner cylinder, the torsion angle of the wire is kept constant [2]. This corresponds to determination of the kinetics of the development of shearing deformation at a given constant stress $\epsilon = \epsilon(\tau)P$.

The accuracy with which the relative linear displacement of the cylinders could be measured in our instrument was brought to 1μ. This made it necessary to use massive mounting, to exclude all vibrations, both in the base of the instrument, and in its upper part, the torsion head, from which the elastic wire is suspended. The whole instrument is mounted on a metal plate (3 cm thick) which is fixed by screws to brackets built into the main wall. The upper, twisted end of the wire is held in a massive frame. The outer cylinder of the instrument is rotated by means of a motor connected by two gear boxes. The first of these varies the speed continuously, to a maximum reduction in a ratio of 10. The second gives stepwise reductions of speed in ratios of 10,100, 1000, and 10,000. The use of two gear boxes in conjunction, and also application of a torque by twisting of the upper end of the wire, makes it possible to set up shear rates $d\epsilon / d\tau$ from 250 seconds^{-1} to very low values, limited only by the observation time, in the gap of the instrument. The displacement of the cylinders in the instrument is measured by means of the graduated microscope. A number of objectives and eyepieces were used in the experiments, giving various magnifications and therefore permitting observations of the cylinders displaced at various speeds.

The use of a microscope for taking the readings has a number of advantages over other methods, such as a light beam reflected from a mirror onto a large scale. Great accuracy of measurement is attainable with the microscope. Moreover, this method does not restrict the displacement (deformation) region in which the measurements can be made, as the microscope can be rotated about the axis of the instrument and directed at any point of the annular scale 4, connected to the inner cylinder.

For measurement of stresses over a wide range, a series of dynamometers was used – torsion wires of different diameters from 0.050 mm to 1 mm (length of wire 300 mm) with specific torques (corresponding to a torsion angle of 1°) from 0.053 to 8040 dyne. cm/1°.

The thermostat of Instrument B is in the form of a cylindrical jacket divided into halves by a vertical plane. This makes preparation for the experiment easier, as the thermostat can be put into place after the cylinders have been placed in the working position.

The device which protects the system against evaporation is a form of hydraulic seal. A cylindrical hood 5 is firmly fitted on the rod of the inner cylinder; the edges of the hood enter the annular vessel 6, which surrounds the outer cylinder. The annular vessel is filled either with the solvent used in the system under investigation, or a liquid of low viscosity and volatility, which is immiscible with the solvent.

The inertia of the inner cylinder and the additional torque set up in the annular vessel must be determined in separate experiments if the viscosity of the solvent is of the same order as that of the system under investigation. If the latter is greater by several orders of magnitude, the additional effect may be neglected.

The properties of the material were calculated from measurement data obtained with Instrument A by the following formulas:

for the conventional-instantaneous shear modulus [3] $E_1 = \frac{Pb}{20 \cdot 10^{-4} \cdot n_1}$. (1)

for the modulus of elastic after-effects $E_2 = \frac{Pb}{20 \cdot 10^{-4} \cdot n_2}$. (1a)

for the equilibrium modulus of elasticity $E = \frac{E_1 \cdot E_2}{E_1 + E_2}$, (1b)

for viscosity in steady flow $\eta = \frac{Pb\tau}{20 \cdot 10^{-4}}$. (2)

where $20 \cdot 10^{-4}$ is the microscope scale division; n_1 is the absolute deformation of initial elasticity, expressed in microscope scale divisions; n_2 is the absolute deformation of elastic after-effects; $\underline{b}$ is the distance between the plates; P is the stress, equal to F/S (F is the shearing force, S is the plate area); τ is the time of residual displacement per division (after elastic equilibrium has been established).

These formulas are derived by substitution of the instrument constants and experimental data into the expressions for Hooke's and Newton's laws:

$$E = \frac{P}{\varepsilon} \text{ and } \eta = \frac{P}{d\varepsilon / d\tau}.$$

Analogous formulas, in which the effective viscosity is the ratio of the stress $M / r_1 \cdot 2\pi r_1 h$ in the cylindrical gap to the velocity gradient $2\pi r_2 n / b$, were used for Instrument B:

$$\eta = \frac{M \cdot b}{4\pi^2 r_1^2 r_2 hn}. \quad (3)$$

The formula

$$\eta = \frac{M}{8\pi^2 hn} \left(\frac{1}{r_1^2} - \frac{1}{r_2^2} \right), \quad (4)$$

known since the time of Margules [5], which is generally used for the calculation of viscosities of true Newtonian liquids, cannot be used in the present instance, as simple integration is not applicable to a gap containing a liquid which is not truly Newtonian, where both the stress and the velocity gradient, and therefore the viscosity, vary from layer to layer. True values of effective viscosity will be obtained in this case if the flow conditions in the cylindrical gap approximate to conditions of homogeneous shear in a plane-parallel gap. For this the radius both of the inner and of the outer cylinder should be great relative to the difference between them. Formula (4) then becomes Formula (3), which takes the form [6, 7]

$$\eta = \frac{Mb}{4\pi^2 h n r^3},$$

if the calculation is based on the average radius $r = (r_1 + r_2)/2$. In these formulas M is the torque; n is the number of revolutions of the rotating cylinder per second; r_1, r_2 and h are the dimensions of the cylinders.

The end effect in type B instruments is usually eliminated because the torque is measured with the narrow gap filled to two different levels and the viscosity is calculated from the difference of these torques and the difference of the liquid heights in the instrument. This method, satisfactory for determinations of liquid viscosity in steady flow, cannot be used if the kinetics of the development of deformation is being determined; i.e., not only the established steady-state values, but all the intermediate values, which cannot be regarded for certain as the difference of the results of two experiments. In such cases the end effect can be limited by having the end distance between the inner and outer cylinders much greater (by one order of magnitude or more) than the distance between the vertical walls (20 and 2 mm in our instrument). In this way the deformation kinetics is studied in the region of constant viscosity. However, with increase of the velocity gradient and with transition into the region of decreasing viscosity the fraction of the torque which arises at the end increases, as lower velocity gradients at the end correspond to greater viscosities.

The annular gap instrument can be made free from this fault if the inner cylinder 1 is made hollow, without a bottom, and the cylindrical gaps 2, 2' are situated on either side of the inner cylinder, both on the outside and on its axis side (Fig. 4). The wall of the inner cylinder is made as thin as possible, which not only diminishes the annular end area, but decreases the moment of inertia of the cylinder. This variant of the instrument type B was also used in our work. The large surface of the inner cylinder (188 cm² with a diameter of 10 cm and a height of 3 cm) makes it possible to determine viscosities of such liquids as water, toluene, and xylene, which were used to verify the instrument readings. The viscosity values obtained agreed with tabulated data [8]. As the wall thickness of the inner cylinder is finite, its moment of inertia is considerable and inertia forces play an appreciable part in its motion. Therefore, for studies of the kinetics of development of deformation it is more appropriate to use an inner cylinder of small diameter, which was used in the first variant of Instrument B (diameter 1.6 cm, height 2 cm). Use of the second variant is quite legitimate for measurement of viscosity in steady flow.

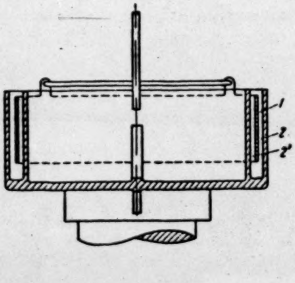

Fig. 4. Instrument with double coaxial gap.

RESULTS

Viscosities of both the pure components and of solutions of various concentrations were first measured in the region of fairly low velocity gradients (maximum viscosities). Figure 5 shows that the variations of viscosity with polymer concentration cover a wide range of 13 orders of magnitude. In addition to the above-mentioned check of Instrument B by means of liquids of known viscosities, the reliability of the results was verified by comparison of the results obtained with both the instruments in that intermediate region of medium concentrations in which this was possible. Very good agreement was obtained. The viscosities were determined at extremely low deformation rates. As has already been reported in a number of papers [2, 6, 9], the highest viscosity is thereby attained, which retains a constant value in the region of fairly low shearing rates. Use was made of the possibility, provided by our instrument, of varying the shearing rate over a wide range to examine the behavior of polyisobutylene solutions, and the results confirmed this view. Figure 6 shows that the viscosity remains constant over a fairly wide range of low velocity gradients, and then decreases with increasing shearing rate.

The elastic behavior of the solutions studied is interesting. In accordance with the well-known general scheme for the growth of shearing deformation with time under constant stress, an elastic "jump" should be found at the initial stage (conventional-instantaneous deformation), followed by a retarded growth of deformation, ending in the establishment of a constant deformation rate. However, polyisobutylene solutions at concentrations up to 40% did not exhibit this behavior in the initial experiments. Figure 7 shows curves characteristic of these experiments. They show a practically constant deformation rate throughout the experiment. No decrease of the resultant deformation was found after removal of the load in these experiments. All this appeared to indicate absence of elasticity in the solutions. However, elastic properties were detected when the experiments were conducted in somewhat modified conditions with the use of greater torques (shearing stresses) and therefore of greater shearing rates. If, as is usual, the stress is set up by means of a previously twisted wire, then the growth of deformation under constant stress can be observed only at a relatively low rate of movement, which permits the operator to rotate the torsion head attached to the upper end of the wire through the additional angle to follow the turning lower end. When the applied stress, and therefore the deformation rate, become too great, it is impossible to proceed in this manner, and if the purpose of the experiment is only to measure the viscosity, it is possible to use the method in which the outer cylinder is rotated at constant velocity, with measurement of the torsion angle of the inner cylinder. This was inadequate for our experiments, and another procedure was therefore used.

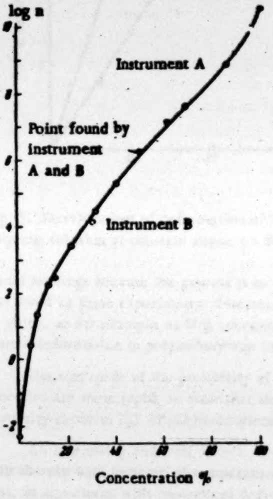

Fig. 5. Variation of constant maximum viscosity with concentration of polyisobutylene in the solution, t = 20°.

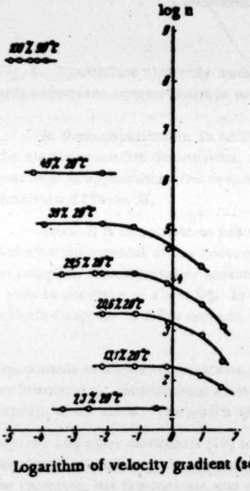

Fig. 6. Variation of the viscosity of polyisobutylene solutions of various concentrations with velocity gradient.

The inner cylinder was disconnected from the elastic wire; the resultant cavity was used to bring its weight to the required value by calculation (in conditions of hydrostatic equilibrium the ratio of the weight of the inner cylinder and its attached parts to the volume of the immersed portion is equal to the density of the liquid). In this free position the inner cylinder floated sufficiently stably in the system, retaining its coaxial position relative to the outer cylinder. The inner cylinder was rotated by means of a pair of loads suspended from a silk thread wound on its rod and with its ends passing over pulleys of very low friction. On removal of the loads, when the inner cylinder was made entirely free of any external load, it was possible to observe an elastic after-effect – elastic recoil – consisting of rotation in the opposite direction. The corresponding elasticity moduli were calculated from the results of measurements at different concentrations, with the use of loads varied in a 1:5 ratio (Fig. 8). It was found that the moduli diminish much less than the viscosity with decreasing concentration. This also explained why elastic properties were not detected in the first experiments. In fact, for a modulus with the value of $9.6 \cdot 10^3$ dynes/cm^2 at 30% concentration, at the greatest stress of those shown in Fig. 8, the value of the possible elastic deformation is very small, $\epsilon_m = 5 \cdot 10^{-4}$, or only 0.3% of the total deformation, 99.7% of which is therefore residual. The higher stresses set up by the suspended loads produced greater elastic deformations, which could be easily detected and studied.

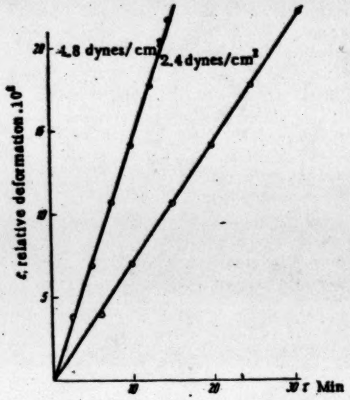

Fig. 7. Development of deformation of 30% polyisobutylene solution at constant stress, t = 20°.

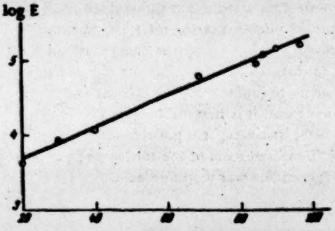

Fig. 8. Equilibrium elasticity modulus as a function of polyisobutylene concentration in solution. t = 20°.

In these experiments, in addition to the values of the elastic reversible deformation, the times for its practical disappearance after removal of the load were determined (Table 1).

Since it is impossible to follow the kinetics of deformation removal at low concentrations by simple visual readings because the process is so rapid, the time for complete development or removal of the deformation was noted in these experiments, determined conditionally with an accuracy of about 5%. In contrast to solutions in which, as for example at 20% concentration, the after-effects disappear in a few seconds, the development of elastic deformation in polyisobutylene lasts several days.

Use was made of the possibility of conducting the experiments at higher temperatures, when deformation processes are more rapid, to show that the elastic properties (viscosity η_0, instantaneous elasticity modulus E_1, elasticity modulus E_2) of polyisobutylene at 90° are independent of the stress. The results are shown in Table 2.

An interesting and well-known property of polyisobutylene and other elastomers [10] is that the viscosity falls sharply with increase of temperature (Fig. 9) while the elasticity modulus remains unchanged. It is possible that, in agreement with theoretical deductions [11], it even increases, but this increase was masked by experimental error.

The deformation rate also increases sharply with rise of temperature, as has already been reported previously [12].

TABLE 1

The Time for Development of Elastic Deformation τ_m as a Function of the Concentration c% of Polyisobutylene in Xylene or Toluene

c%	20	30	40	50	60	80	83	95	100
τ_m	10	1	4	29	2.2	8.5	16	3.5	11.5
	Seconds	Minutes			Hours			Days	

TABLE 2

Properties of Polyisobutylene in the Stress Range from 3 to 34 Thousand dynes/cm² at 90°

P dynes.cm^{-2}	3 270	6 540	13 080	19 620	26 160	33 680
$E_1 \cdot 10^{-6}$ dynes.cm^{-2} .	1.4	1.4	1.4	1.5	1.7	1.4
$E \cdot 10^{-5}$ dynes.cm^{-2} . .	0.98	0.94	1.12	—	0.98	0.98
$\eta_0 \cdot 10^{-8}$ poise . . .	2.9	3.0	2.9	2.7	2.2	2.6

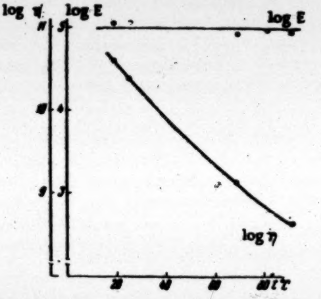

Fig. 9. Variation of the elasticity modulus E in dynes.cm^{-2} and maximum viscosity η_0 in poises, with temperature.

SUMMARY

1. By the combined use of two measurement methods the elastico-viscous properties of polyisobutylene solutions in xylene and toluene have been determined at concentrations from 0 to 100%.

2. The constant maximum viscosity of true flow has been determined; its values cover a range of 13 tenth-powers over the concentration range studied.

3. The equilibrium elasticity modulus is shown to be dependent on the concentration. The elastic properties of solutions at concentrations from 20 to 50% were studied by the floating inner cylinder method, in which it is possible to remove the stress instantaneously and to follow the decrease of elastic deformation after the development of considerable total and elastic deformation.

4. The time of decrease of elastic deformation becomes much greater with increase of the polyisobutylene content in the solution from low concentrations to the pure polymer.

5. The properties studied – maximum viscosity and the equilibrium elastic and conventional instantaneous elastic moduli – are shown to be constant for pure polyisobutylene and its solutions over a wide range of stress variations.

Institute of Physical Chemistry
Academy of Sciences USSR
Division of Disperse Systems, Moscow

Received April 7, 1956

LITERATURE CITED

[1] F. N. Shvedov, J. Phys. 8,341 (1889).

[2] A. S. Kolbanovskaya and P. A. Rebinder, Colloid J. 12,194 (1950).

[3] N. V. Mikhailov and P. A. Rebinder, Colloid J. 17,107 (1955) (T. p. 99)*.

[4] B. P. Veinberg, J. Russ. Phys.-Chem. Soc. 36,47 (1904); 44,3 (1912); D. M. Tolstoi, Colloid J. 10,133 (1948).

[5] Margules, Sitzber. Akad. Wiss. Wien 83, 11, 588 (1881).

[6] W. Philippoff, Viskositat der Kolloid (Dresden – Leipzig, 1942).

[7] V. P. Pavlov, Trans. Third All-Union Conf. on Colloid Chemistry (Acad. Sci. USSR Press, Moscow, 1956).

[8] Landolt – Bomstein, Phys.-Chem. Tables (1923), 126.

[9] A. A. Trapeznikov and V. A. Fedotova, Proc. Acad. Sci. USSR 82,97 (1952).

[10] V. A. Kargin and T. I. Sogolova, J. Phys. Chem. 23,540,551 (1949).

[11] G. M. Bartenev, Colloid J. 12,81,241 (1950); J. Tech. Phys. 20,461, 858 (1950).

[12] L. V. Chumakova and P. A. Rebinder, Proc. Acad. Sci. USSR 81,239 (1951).

---

* T. p. = C. B. Translation Pogination

INVESTIGATION OF THE ELASTICO-VISCOPLASTIC PROPERTIES OF BLACK PRINTING INKS

T. N. Malova

Numerous investigations of the rheological properties of black printing inks, which are highly concentrated structurized systems, have been reported both in the Soviet Union and abroad [1]. A number of authors consider that the printing properties of inks are mainly determined by their elastico-viscoplastic or deformation properties, and also by their adhesive and cohesive characteristics. However, no definite relationship has yet been found between the deformation properties and the behavior of the ink in printing.

A great defect of some printing inks is their lack of mobility [2] or "rotation" in the inking mechanism of the machine. This disturbs the regular feeding of the inking system and lowers the quality of the print. Research workers have attempted for a number of years to explain the nature of this effect and to correlate it with the deformation properties. Deryagin suggested that the defect is to be explained by the thixotropic properties of black printing inks. Volarovich pointed out the connection between the lack of mobility of the ink in the inking mechanism and the wall slip effects studied by Tolstoi [3]. Berezin [4] explained the absence of rotation in printing inks by the existence of wall slippage. Kozarovitsky and Rebinder [1] relate the immobility of printing inks to their thixotropic properties, and attribute it to the disruption of the continuous structure of the ink in a thin layer adjacent to the wall.

An attempt was made in the present investigation to correlate the mobility of printing inks with their viscoplastic characteristics. The elastico-viscoplastic and thixotropic properties of model printing inks, and also of industrial inks of different mobilities were studied. The rotation viscosimeter method of Volarovich [5], the Rebinder conical plastometer method [6] and the tangentially displaced plate method in the Veiler–Rebinder apparatus [7] were used.

The thixotropic reinforcement of the ink structure in time was studied by measurement of the maximum shearing stress P_m (yield stress) in a conical plastometer. For investigation of the kinetics of thixotropic structure formation the paints were stirred thoroughly and P_m was then determined at definite time intervals until the strength of the ink ceased to vary with time. The Veiler–Rebinder apparatus was used to determine the variation of the shear P with the deformation of the system 10 minutes and 2 hours after breakdown of the structure. The Volarovich rotational viscosimeter RV-7 was used to determine the yield stress θ immediately after breakdown of the structure, and this was followed by measurement of the plastic viscosity. The yield stress in this case characterizes a partially broken down structure of the system.

Two commercial ink specimens were used for the investigations: No. 54, made with glyptal vehicle, mobile, and No. 53, made with polymerized linseed oil, with low mobility. In addition, model black printing inks with various components were made: gas channel black, specially oxidized gas channel black, polymerized linseed oil, glyptal resin modified with sunflower oil, lacquer bitumen solution in machine oil, and rosin glycerol ester in machine oil.

The composition and properties of the inks are shown in the table. Fig. 1 shows curves [$P_m = f(\tau)$, where τ is time] for the structure reinforcement of inks in the course of time, plotted from data obtained by means of the conical plastometer data. It is seen from Fig. 1 that all the inks, irrespective of their mobility, are structurized systems. The thixotropic structure formation in inks is completed approximately two hours after breakdown of the structure. The greatest strength increase P_m is found for the low-mobility ink No. 53 and the mobile ink No. 54, and the least, for the ink containing furnace black.

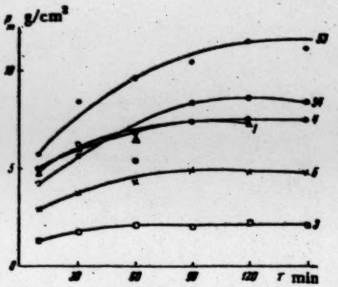

Fig. 1. Structure reinforcement of printing inks with time; the curves show the code numbers of the inks.

Figures 2 and 3 show the variation of the shearing stress as a function of the deformation of the system, determined by means of the Veiler–Rebinder apparatus 10 minutes and 2 hours after breakdown of the structure. It is seen from Figs. 2 and 3 that for a given deformation the least shearing stress 10 minutes after structure breakdown is found in the ink based on furnace black, and the greatest, in the low-mobility ink No. 53. All the inks show a decrease of the shearing stress P two hours after stirring. The increase of P is especially great for the low-mobility ink No. 53 and the mobile ink No. 54. The least increase of shearing stress is found for the ink containing furnace black. These results show that all inks, irrespective of their mobility in the inking mechanism of the printing machine, have very pronounced thixotropic properties.

Rheological data on all these inks are given in the table. The yield stress for the conical plastometer was calculated from the Rebinder formula, while for the Veiler–Rebinder apparatus the maximum value of the stress was taken from the curves shown in Fig. 3. The values so found for the yield stress (which may be termed static values) by means of the conical plastometer and the Veiler–Rebinder apparatus practically coincide, and considerably exceed the dynamic yield stress values obtained with the rotational viscosimeter.

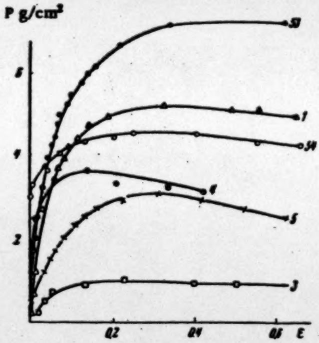

Fig. 2. Variation of the shearing stress of printing inks with deformation of the system 10 minutes after breakdown of the structure; the numbers of the inks are indicated on the curves.

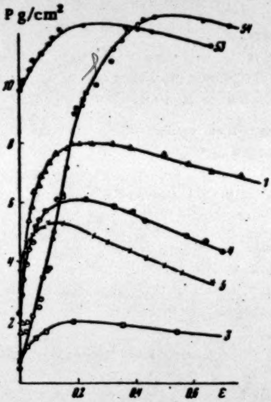

Fig. 3. Variation of the shearing stress of printing inks with deformation of the system 2 hours after breakdown of the structure; the numbers of the inks are indicated on the curves.

The separate values of the yield stress and plastic viscosity do not characterize the mobility of the inks in the inking mechanism of printing machines. However, a definite relationship can be established between the property of "rotation" of the inks and the data determined by means of the Volarovich viscosimeter. Volarovich [8] as the result of studies of various disperse systems including clays, derived an expression for their plasticity.

TABLE

Composition and Plastico-Viscous Properties of Black Printing Inks

Ink No.	Type of carbon and % content	Type of vehicle and % content	Colors and % content	Siccative %	Yield stress after 2 hours, in g/cm^2		Plastic viscosity η in poises	Yield stress θ in $dynes/cm^2$	$\psi = \frac{\theta}{\eta}$
					conical plastometer	Rebinder-Veiler apparatus	RV-7 rotational viscosimeter		
53*	Channel, 20	Polymerized linseed oil, 47	Milori 8, basic violet lacquer 5	20	11.5	11.9	286	3190	11.2
54		Glyptal resin, 50	Basic blue lacquer 7; basic violet lacquer 3	20	8.6	12.3	469	310	0.66
1*		Polymerized linseed oil, 80	ditto	—	7.4	8.0	275	311	1.13
5		Glyptal resin, 80	"	—	4.9	5.3	356	218	0.61
6		Bitumen dissolved in machine oil, 80	"	—	—	—	650	85.7	0.13
4*		Rosin ester dissolved in machine oil, 80	"	—	7.5	6.3	238	2570	10.8
7	Oxidized, 30	Polymerized linseed oil, 70	"	—	—	—	212	106	0.50
3	Furnace, 35	Polymerized linseed oil, 65	"	—	2.2	2.0	140	63.8	0.45

---

* Inks of low or no mobility.

based on the Bingham equation and Maxwell's definition of a plastic body. According to Volarovich, plasticity is determined by the ratio $\phi = \theta/\eta$. This is derived as follows: a plastic body (for example, clay) should retain its shape under the action of small forces, and this property is more pronounced for higher values of the yield stress θ; on the other hand, a plastic body should be easily deformed beyond the flow limit, and this should occur more easily at low values of plastic viscosity. According to Volarovich, the plasticity formula in the general form may be used for comparing the plasticities of various disperse systems.

Our experiments showed (see table) that the mobility of inks in the inking mechanism of printing machines can also be characterized by the plasticity value ϕ. A high value of the yield stress θ hinders mobility of the ink, while the plastic viscosity η, on the contrary, favors transmission of the shear to the whole mass of the ink and therefore assists its mobility. Easily mobile inks have values of plasticity ϕ less than unity; for inks of low mobility the value of ϕ may reach 10.

SUMMARY

1. The elastico-viscoplastic and thixotropic properties of black printing inks which differ in their degree of mobility in the inking mechanism of printing machines have been studied.

2. It is shown that all inks, irrespective of mobility, show thixotropic structure build-up in time.

3. An inverse relationship has been found between the mobility or "rotation" of printing inks and the plasticity, expressed as the ratio of the yield stress to the plastic viscosity. For mobile inks this ratio is less than unity.

All-Union Scientific Research Institute
for the Polygraphic Industry and Technology, Moscow

Received July 12, 1955

LITERATURE CITED

[1] M. P. Volarovich, Trans. Sci. Res. Inst. (United State Press, 1937), No. 1, 261; L. A. Kozarovitsky and R. E. Kaganova, Collected Papers All-Union Sci. Res. Inst. Polygraphic Ind. Technol. 1953, No. 6, 52; L. A. Kozarovitsky and S. Ya. Shalyt, Colloid J. 15, No. 6,437 (1953) (T.p. 453)* ; A. Voet, Am. Ink Maker 1952; L. A. Kozarovitsky and P. A. Rebinder, Polygraphic Industry 6,31 (1951).

[2] T. N. Malova and B. I. Berezin, Polygraphic Industry 2,21 (1952).

[3] D. M. Tolstoi, Colloid J. 10, No. 2, 133 (1948).

[4] B. I. Berezin and L. A. Zagarinskaya, Polygraphic Materials (Moscow, 1955), p. 424.

[5] M. P. Volarovich, Factory Lab. 11, No. 9, 831 (1945).

[6] P. A. Rebinder and N. A. Semenenko, Proc. Acad. Sci. USSR 6,835 (1949); P. A. Rebinder and B. Ya. Yampolsky, Colloid J. 10, No. 6, 466 (1948).

[7] S. A. Veiler and P. A. Rebinder, Proc. Acad. Sci. USSR 49, No. 5, 354 (1945).

[8] M. P. Volarovich, Trans. Inst. Econ. Mineral. 1934, No. 66,19; Colloid J. 7,557 (1936).

---

* T. p. = C. B. Translation pogination

EFFECT OF COOLING ON THE EMULSIFYING POWER OF PROTEINS

V. M. Martynov

Proteins are good stabilizers for emulsions of the oil/water type [1]; very stable emulsions containing 90-95% disperse phase can be obtained with their use [2]. Changes in the emulsifying power of proteins after heat treatment of their solutions (consecutive cooling and heating) have apparently never been studied, although several investigations have been made of the changes in other properties of lyophilic colloids, including proteins, after freezing and subsequent cooling [3].

Apart from its theoretical importance, the question of the effect of cooling on emulsifying power has a definite practical significance, as for example in the preparation of emulsions of low-boiling liquids, which is possible only on cooling of the original components of the system. The rate, duration, and extent of cooling may influence the quality of the emulsion formed, and also the limiting phase ratio in the resultant system.

Investigations of protein-stabilized emulsions of hydrocarbons showed that preliminary cooling followed by heating of the dispersion medium results in a sharp decrease in the emulsifying power of the stabilizer. For example, an emulsion of heptane in 8% casein solution with a 91% content of disperse phase by volume can easily be obtained if the solution is not previously cooled. However, if the solution is cooled to − 15° and held at that temperature for 2 hours or more, and then again warmed to room temperature, it is hardly possible to obtain an emulsion containing 73.5% of the hydrocarbon in the same emulsification conditions. This observation prompted a more detailed study of the effect of cooling on the emulsifying power of proteins.

The table shows some experimental data on casein, solutions of which were made in a weakly alkaline medium. The amounts of alkali, including ammonia, taken were such that the final solution had an almost neutral reaction. Thus, an 8% solution after ten-fold dilution with water had pH 6.8 determined by the Michaelis indicator method. The emulsification was carried out in an emulsifier of the circulating type. The time and rate of stirring were such that the emulsion reached the state of maximum concentration, which, according to Kremnev and Soskin [4] means "an emulsion in which the emulsifier solution is extended into protective layers of a critical minimum thickness, which is attained at different volumes of the dispersed liquid according to the degree of dispersion of the system". The average degree of dispersion of emulsions (average droplet size) depends on the intensity of the mechanical treatment [5] and the time of stirring [6].

The state of maximum concentration is seen to be reached by the commencement of destruction of the emulsion, a characteristic sign of which is a change of external appearance: instead of white and dull, the emulsion surface becomes glossy. A further increase of the stirring time or speed leads to progressive destruction of the emulsion with separation of heptane as a macrolayer.

The resultant highly concentrated emulsion was subjected to dispersion analysis by means of the Figurovsky balance, and the distribution curves were used to determine the specific surface of the dispersion medium, i. e. the surface occupied by 1 ml of the stabilizer solution in an emulsion at maximum concentration. The reciprocal of the specific surface was taken as a measure of the critical thickness of the film of dispersion medium. It must be noted that "the minimum layers of the dispersion medium are not capable of extension" [7] and tear when their area is increased.

TABLE

Effect of Cooling on the Emulsifying Power of Solutions

Casein concentration in solution, wt. %	Nature of solution	Phase volume ratio in emulsion V_{solv}/V_{hept}	Specific surface of dispersion medium $S \cdot 10^{-4}$ cm²/ml	Critical thickness of film $\delta_{cr} \cdot 10^{6}$ cm
4.0	Uncooled	1 : 8.6	1.92	0.52
4.0	Cooled to −15°	1 : 4.3	1.08	0.93
4.0	Ditto, to −72°	1 : 3.3	0.73	1.38
8.2	Uncooled	1 : 10.5	1.43	0.70
8.2	Cooled to −15°	1 : 2.7	0.65	1.54
8.2	Ditto, to −72°	1 : 2.0	0.48	2.07
10.1	Uncooled	1 : 11.3	1.64	0.61
10.1	Cooled to −15°	1 : 2,2	0.51	1.98

It is seen from the table that preliminary cooling significantly decreases the specific surface, and therefore also the emulsifying power of the stabilizer. Greater cooling produces a greater change. An interesting fact is that, as a rough approximation, the specific surface and the critical thickness of the film of the dispersion medium in an uncooled solution are independent of the casein concentration, at least in the range from 4 to 10%; the specific surface is approximately $1.7 \cdot 10^{-5}$ cm/g (the corresponding critical thickness is $0.59 \cdot 10^{-5}$ cm). Cooling of the casein solution with subsequent warming to room temperature approximately doubles or trebles the critical film thickness, according to the temperature of cooling.

Thus, the emulsifying power of casein solutions, evaluated by the Kremnev and Soskin method [4], decreases on consecutive cooling and warming, the decrease being stepwise: the critical film thickness after cooling is a whole multiple of the thickness of a film obtained from uncooled solution. It was necessary to determine whether the increase of critical film thickness is a consequence of casein particle aggregation or whether it is due to other causes. No external changes (color, mechanical homogeneity) were seen in the casein solution after thawing. Even microscopical investigations did not reveal any appreciable changes in the homogeneity of the solution, in contrast to the observations of Bobertag et al. [8], who found structural changes (formation of large aggregates) in solutions of gelatin, fish glue, agar, and certain other substances after freezing. However, viscosity determinations definitely indicate partial aggregation as the result of cooling with subsequent warming. For example, the viscosity of an 8% solution before cooling was 19.3 centipoises at 20°, while after cooling and subsequent warming the viscosity at 20° rose to 22.3 centipoises. The specific rotation of polarization is also different before and after cooling: before cooling $\alpha_D = -86.3°$; after cooling to − 15° $\alpha_D = -98.0°$. These results definitely show that particle aggregation occurs under the action of low temperatures.

It may be incidentally noted that if the solution is cooled until ice crystals appear, which occurs at about − 1.5°, subsequent warming fully restores the emulsifying power of casein. Both the viscosity and the specific rotation return to their initial values, 19.46 centipoises and − 86.5°, as compared with the initial values of 19.3 centipoises and −86.3°. Thus, relatively slight cooling does not produce appreciable aggregation of the casein particles.

In addition to the viscosimetric and optical investigations, the rate of cooling of casein solutions was determined. It was found that below the freezing-out point for water the solution cools more slowly than pure water; above this point the cooling curves for the two systems practically coincide, as can be seen from the figure, which shows cooling curves for 10.1% casein solution and pure water. The course of the curves shows that more heat is evolved during freezing of protein solution than during freezing of pure water, i. e. exothermic processes, probably associated with irreversible aggregation of the particles, occur in the protein solution. At temperatures close to the freezing point of water no aggregation occurs, or its rate is extremely low, and therefore the emulsifying power of casein solutions remains practically unchanged.

Thus, the decrease of the emulsifying power of casein after strong cooling of its solutions is primarily the result of particle aggregation, which causes the formation of thicker critical films of dispersion medium, and therefore results in a lower saturation point for the emulsion.

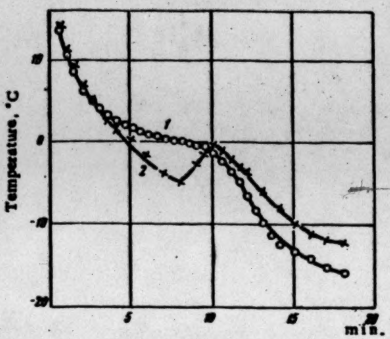

Rate of cooling of water and of casein solution: 1) water, 2) 10.1% casein solution.

SUMMARY

1. It is shown that the emulsifying power of proteins (casein) decreases after prolonged cooling followed by warming to 20°.

2. The decrease of emulsifying power is the result of irreversible aggregation of the protein particles, which proceeds exothermically, with an increase of viscosity and a change of the specific rotation.

In conclusion, I express my sincere gratitude to Academician P. A. Rebinder for valuable advice given during inspection of the manuscript.

All-Union Scientific Research Institute
for Petroleum and Gas Processing and the
Production of Synthetic Liquid Feul, Moscow

Received September 17, 1955

LITERATURE CITED

[1] W. Clayton, Emulsions (Translation edited by P. A. Rebinder) (Foreign Literature Press, Moscow, 1950), p. 224.

[2] L. L. Zhukov and N. N. Bushmakin, J. Russ. Chem. Soc. 59,1061 (1927); S. E. Bresler, M. Kats, and L. Ya. Kremnev, J. Phys. Chem. 5,602 (1934); A. L. Bromberg, Colloid J. 8,281, 377 (1946); see also W. Clayton [1].

[3] K. Lyubavin, J. Russ. Phys. Chem. Soc. 21,397 (1889); A. Lottermoser, Z. physik. Chem. 60,462 (1907); S. I. Dyachkovsky, J. Phys. Chem. 1,964 (1931); Colloid J. 1,513 (1935; 2,793 (1936); 7,139 (1941).

[4] L. Ya. Kremnev and S. A. Soskin, Colloid J. 9,269 (1947).

[5] L. Ya. Kremnev and S. A. Soskin, J. Gen. Chem. 16,2000 (1946).

[6] V. M. Martynov, Colloid J. 10,218 (1948).

[7] L. Ya. Kremnev and S. A. Soskin, Colloid J. 11,24 (1949).

[8] O. Bobertag, K. Feist and H. W. Ficher, Ber. 41, 3675 (1908).

THE DEPENDENCE OF THE HEAT OF SOLUTION OF POLYMERS ON THEIR PHYSICAL STATE

S. I. Meerson and S. M. Lipatov

Our original studies [1] of the heats of solution and swelling of polymers over a wide range of temperatures showed that the thermal effect of the process depends on the temperature, the nature of the dependence being determined by the nature of the polymer, the molecular weight of the fraction, nature of the solvent, and other factors.

The nature of the variation of the thermal effect with temperature in polymers which dissolve spontaneously at elevated temperatures and which exhibit limited swelling at relatively low temperatures can be represented in general form by Fig. 1. This form of dependence was observed in studies of gelatin, agar, and starch [2].

For some polymers (thermolyzed gelatin, rubber, dispersed starch) which dissolve spontaneously in the temperature range studied, the heat effect is independent of the temperature, while in other cases (nitrocellulose, acetylcellulose) the heat of solution decreases with increase of temperature, as shown in Fig. 1.

However, in spontaneous solution, the heat of solution is not always independent of the temperature at relatively low temperatures: this depends both on the nature of the solvent and on the nature of the polymer. Recently two papers [3] have been published, describing studies of the effect of temperature on the heat of solution of polystyrene in benzene. The results show that the heat of solution decreases with rise of temperature but ceases to depend on it beyond a certain temperature. These results are in agreement with our findings and with our quantitative data. Our subsequent investigations of the nature of the observed effects showed that the temperature above which the heat of solution again ceases to be greatly influenced by the temperature, designated by us as the "critical temperature" of solution, in a number of cases closely agrees with the glass transition temperature of the polymers, T_g. Some new data have been obtained for a more complete investigation of this relationship, permitting a more thorough discussion of the temperature coefficient of the thermal effect.

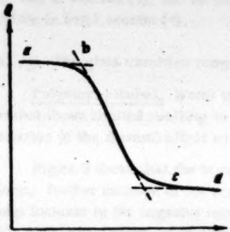

Fig. 1. Variation of the heat of solution of polymers with temperature.

EXPERIMENTAL

An isothermal calorimeter, described previously [4], was used for measurement of the heat effects. The materials studied were polystyrene, polyvinyl acetate, polybutyl methacrylate, polyvinyl alcohol, and also low-molecular substances: δ-valerolactone and phenolphthalein. Data on the variation of the heats of solution of these substances in different solvents with temperature are presented below.

Polystyrene. The solution of polystyrene was studied in benzene, toluene, and dioxane. Polystyrene dissolves spontaneously in these solvents, and the solution process is completed before the end of the calorimetric experiment. Between 6 and 85° the heat of solution diminishes practically linearly with increase of temperature, and depends little on the solvent used (see Fig. 2, Curves 1, 2, and 3). According to the literature [5] the glass transition temperature of polystyrene is 81°. It is noteworthy that the heat effect depends on the temperature even at relatively low temperatures.

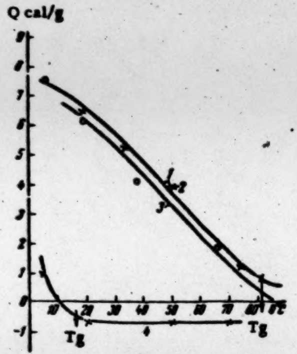

Fig. 2. Variation of heat of solution with temperature for polystyrene in benzene (1), in toluene (2), and in dioxane (3); and for polybutyl methacrylate in butyl acetate (4).

Polybutyl methacrylate. Figure 2 shows the variation of the heat of solution of polybutyl methacrylate in butyl acetate, with the temperature (Curve 4). Polybutyl methacrylate dissolves spontaneously in this solvent. At 5° the heat of solution is positive, while above 15° it has a small negative value and is practically independent of the temperature. The glass transition temperature of polybutyl methacrylate is 16° [6].

Polyvinyl acetate. The heat of solution of polyvinyl acetate in butyl acetate, in which it is spontaneously soluble, is practically independent of the temperature over the entire temperature range studied. Thus, at 20° the heat of solution is zero, while at 40 and 60° it is − 0.4 cal./g. The glass transition temperature of polyvinyl acetate, according to Boyer and Spencer, is 28°. Thus, in this instance the heat effect ceases to depend on the temperature at temperatures a little below T_g.

Rubber. In the case of rubber, as in the previous instance, the heat of solution is independent of the temperature over the whole temperature range. It was found by us earlier that the heat of solution of rubber in benzene at 5 and 20° is − 2.8 cal./g, and at 45 and 65°, − 2.6 cal./g. The glass transition temperature of rubber is in the negative region.

Polyvinyl alcohol. Water was the solvent used for polyvinyl alcohol. At room temperatures polyvinyl alcohol shows limited swelling in water, and dissolves spontaneously at higher temperatures. Accordingly, the variation of the thermal effect with temperature is of the type shown in Fig. 1.

Figure 3 shows that the temperature coefficient of the heat effect is very small at relatively low temperatures. Further increase of the temperature increases the solubility of the polymer and accordingly produces a sharp increase in the negative temperature coefficient, which again becomes very small at temperatures above 85°. This temperature, according to Boyer and Spencer [5], corresponds to the glass transition temperature of polyvinyl alcohol. It follows from these results that at temperatures above T_g the heat of solution is almost independent of the temperature, as is also the case at relatively low temperatures, when only limited swelling occurs. Similar results were obtained by us for gelatin, agar, and starch, and also by Lipatov and Akhmedov [8] for polyvinyl chloride.

The difference between these polymers is seen in the different absolute values of the heat effects, and also in the fact that the Q = f (T) curve lies either in the region of positive heat effects (gelatin), or in the negative and positive regions (polyvinyl alcohol, polyvinyl chloride).

Data for polyvinyl chloride are shown in Fig. 3 (Curve 2). At temperatures below 30° polyvinyl chloride dissolves in dichloroethane with great difficulty, and mostly swelling takes place. At higher temperatures the solubility improves, and this is accompanied by a decrease of the heat effect, which is practically independent of the temperature above 70°. The glass transition temperature of polyvinyl chloride is 75° [5].

It is stated by Boyer and Spencer that T_g for nitrocellulose is 52.6°, and for cellulose acetate, 68.6°. If these figures are considered in relation with our data [9] on the variation of the heat of solution of these polymers with temperature, it is seen (see Table 1) that in relatively bad solvents (butyl acetate) the heat effect ceases to depend on the temperature at temperatures close to T_g, while in relatively good solvents (methyl alcohol, acetone) the heat effect begins to be independent of the temperatures at temperatures below T_g.

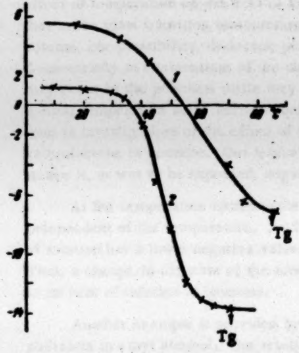

Fig. 3. Variation of the heats of swelling and solution with temperature: 1) for polyvinyl alcohol in water; 2) for polyvinyl chloride in dichloroethane.

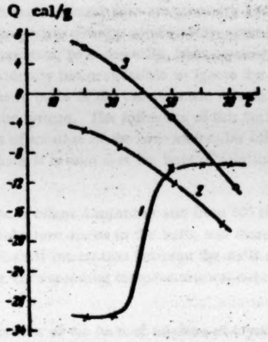

Fig. 4. Variation of heat of solution with temperature: 1) for δ-valerolactone in benzene; for phenolphthalein in ethyl alcohol: 2) crystalline, and 3) amorphous.

TABLE 1

Variation of the Heat of Solution of Nitrocellulose in Different Solvents with Temperature

T° C	Q cal./g butyl acetate	 ethyl acetate	 acetone	 methyl alcohol
20	17.8	18.2	18.0	16.4
25	17.8	18.0	17.6	13.4
30	17.6	16.4	14.4	$\overline{12.0}$
35	17.0	14.6	12.3	12.0
40	15.6	12.9	$\overline{12.0}$	12.0
45	14.0	$\overline{12.0}$	12.0	12.0
50	12.8	12.0	12.0	12.0
55	$\overline{12.0}$	12.0	12.0	12.0

DISCUSSION OF RESULTS

To establish the causes which determine the nature of the variation of the heat of solution of polymers with temperature, the following questions should be considered: 1) on what do the decrease of the heat effect with increase of temperature, and the broadening of the temperature range in which the heat effect decreases, depend; 2) in what cases is the heat effect seen to be independent of the temperature on Q = f(T) curves in the region of relatively low temperatures; 3) what is the reason for the existence of a temperature above which the heat effect is independent of the temperature, and on what does its absolute value depend; 4) on what do the value of ΔQ and the absolute heats of solution depend?

All the foregoing data and also earlier researches indicate convincingly that the heat of solution depends on the physical state of the polymer and the nature of the solvent. Before these investigations little attention was paid to the changes in polymer properties during heating in the course of calorimetric experiments on the effect of temperature on the heat of solution. However, much experimental data are presently available to show that at the glass transition temperature a number of polymer properties change considerably, namely: specific volume, compressibility, dielectric properties, mechanical properties, heat capacity, heat conductivity, etc. Consequently in explanations of the observed behavior it is evidently not permissible to ignore the changes which may occur in the polymers while they remain in the calorimetric bulbs in the calorimetric system at the experimental temperature until thermal equilibrium is attained in the system. The influence of this factor is clearly seen in investigations of the effect of temperature on the heat of solution of the low-molecular substance δ-valerolactone in benzene. Our results are shown in Fig. 4, where it is seen that the heat of solution of this substance is, as was to be expected, negative.

As the temperature increases the negative value of the heat effect diminishes and from 50° it becomes independent of the temperature. At this temperature δ-valerolactone melts in the bulb, and therefore its heat of solution has a lower negative value; it corresponds to the heat of interaction between the melt and the solvent. Thus, a change in the state of the substance in the bulb at the corresponding temperature was naturally reflected in its heat of solution in benzene.

Another example is provided by the results of determinations of the heat of solution of crystalline phenolphthalein in ethyl alcohol. Our results are shown also in Fig. 4. When this substance, like δ-valerolactone, is dissolved, a negative heat of solution is found, typical of low-molecular crystalline substances. However, the negative heat effect increases with increasing temperature. The melting point of phenolphthalein is 240°. Zhurkov and Levin [10] showed in a study of the absorption spectra of amorphous phenolphthalein that its glass transition temperature is 80°. We determined the heat of solution of amorphous phenolphthalein, obtained by rapid cooling of a melt. The results, shown in Fig. 4, indicate that this substance has a positive heat of solution. Increase of temperature decreases the heat of solution, which becomes negative. As melting of amorphous phenolphthalein was not observed at temperatures above 80°, it is possible that in this case, when the substance was contained in the calorimetric bulb in the glass transition range, structural compression of the substance took place, which brought it near to a state of equilibrium at that temperature. It is evident that the solution of such a specimen should be accompanied by additional absorption of heat.

These examples show convincingly that the heat of solution depends on the physical state of the substance. It might seem that the observed decrease of the heat of solution of polymers with increasing temperature could also be explained by structural compression in the T_g range, as an increase in the rate of relaxation processes with increase of temperature should favor an increase of packing density and the formation of new intermolecular bonds. However, very little experimental data are to be found in the literature, indicating the existence of structural compression in studies of the effect of temperature on the volume or heat capacity. There is only the graph in Alfrey's book [11], which indicates an anomalous dependence of polymer volume on the temperature near T_g for a rapidly cooled and then slowly heated specimen, and also Uberreiter's data [12].

To answer some of the questions posed above, we turn to Kirchhoff's law. It is well known that according to this law the relationship between the heat effect and the temperature is represented by the equation

$$dQ/dT = \Sigma C_{\text{initial}} - \Sigma C_{\text{final}}.$$

It follows from this equation that the sign and the absolute value of the temperature coefficient of the heat effect depend on the absolute values of the sums of the heat capacities of the substances in the initial and final states. The initial state is determined, in the cases under consideration, by the heat capacity of the polymer in the bulb and by the heat capacity of the solvent at the experimental temperature.

Data are presently available on the dependence of the heat capacities of polyvinyl acetate, polyisobutylene, polyvinyl chloride, rubber, and polystyrene on the temperature [13]. The relationship between heat capacity and temperature is non-linear for all these polymers. A sharp change of heat capacity is found in the T_g range as the result of absorption of heat to overcome some intermolecular forces in the course of molecular reconstruction.

A discussion of the reasons for this effect of temperature on heat capacity may be found in the paper [14]. The heat capacities of solvents vary linearly in the temperature range studied. Therefore the sum of the initial heat capacities of the polymer and solvent also changes non-linearly with temperature. The final state in cases of spontaneous solution in calorimetric experiment conditions at all temperatures is a solution. In the case of limited swelling, at relatively low experimental temperatures, the final state is a swollen polymer, and at high temperatures, a solution.

Unfortunately, no data are available on the variation of the heat capacities of polymer solutions in good and bad solvents with the temperature over a wide concentration range. We may refer here to the work of Skuratov [15] who determined, at one temperature only, the heat capacities of solid gelatin and starch in the hydrated and anhydrous states, and also the heat capacity of diacetylcellulose in acetone, in which it is spontaneously soluble. In the first instance the heat capacity of the system was composed additively from the heat capacities of the components. The measurements were made at 20°, when the heats of solution of different fractions of these polymers differ little, and are independent of the temperature at room temperatures. The heat capacity of a solution of diacetylcellulose in acetone was higher than the value given by the additivity rule. The above data on the heat capacities of polymers and their solutions may be used to explain the decrease of the heat of solution with increase of temperature.

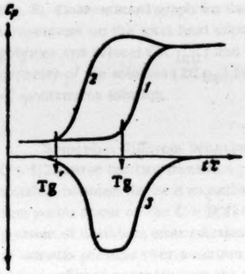

Fig. 5. Conventional graph for the effect of temperature on the total heat capacity of polymer and solvent ΣC_{init} (1), the heat capacity of the swollen polymer ΣC_{fin} (2), and dQ/dT (3). T_g = glass transition temperature of the polymer; T_g' = glass transition temperature of the swollen polymer.

Let us first consider the case when the polymer swells at room temperature and dissolves on increase of temperature.

The Q = f(T) curve for polymers with limited swelling has, as is seen in Fig. 1, two characteristic transition points, represented by b and c. Probably the transition point at the higher temperature c represents T_g for the polymer, while the transition point at the lower temperature b corresponds to T_g', the glass transition temperature for the swollen polymer. Data on the relationship Q = f(T) can be used to calculate the value of dQ/dT and to determine the dependence of dQ/dT on the temperature. The relationship dQ/dT = f(T) determined in this manner is represented by Curve 3 in Fig. 5. Since $dQ/dT = \Delta C$, where $\Delta C = \Sigma C_{init} - \Sigma C_{fin}$, then $\Sigma C_{fin} - \Sigma C_{init} = -dQ/dT$. Hence it follows that if ΣC_{init} and the relationship $\Sigma C_{init} = f(T)$ are known, it is possible to find ΣC_{fin} and the relationship $\Sigma C_{fin} = f(T)$. Since the nature of the dependence of the heat capacity of polymers on the temperature is known (Curve 1 in Fig. 5), the value of ΣC_{fin} and $\Sigma C_{fin} = f(T)$ may be found by graphical addition. The results so obtained are represented by Curve 2 in Fig. 5.

The heat capacity ΣC_{fin} varies non-linearly with the temperature. In the region of relatively low temperatures, when $dQ/dT = 0$, only limited swelling of the polymer occurs, since, according to Skuratov's data, $\Sigma C_{fin} = \Sigma C_{init}$. This means that in this temperature range the heat effect should be independent of the temperature, which is found experimentally to be so.

As the temperature increases, energy is expended to disrupt a certain number of intermolecular bonds during solution of the polymer, and this is accompanied by an increase of the heat capacity ΣC_{fin} and of dQ/dT; further increase of temperature, starting from T_g, produces an increase of the polymer heat capacity ΣC_{init} and in consequence dQ/dT begins to decrease, since less heat is expended for solution of the polymer. This means that ΣC_{fin}, having passed through a small maximum, begins to decrease and at a certain temperature becomes equal to or rather greater than ΣC_{init}.

Thus the decrease of the heat effect with increase of temperature is explained by the expenditure of energy to overcome intermolecular forces in the transition from solid polymer to solution. Above T_g, when some of the bonds have already been broken, less energy must be expended for dissolving the polymer, and in the final analysis the heat effect is independent of the temperature. Let us now consider another case, when the polymer dissolves spontaneously over the whole temperature range in question. If the calorimetric experiments are carried out at temperatures above T_g for the polymer, then, as experimental results show, the heat effect is independent of the temperature (rubber, polybutyl methacrylate, etc.). On the basis of the foregoing reasoning it can be said that this can occur only when the heat capacity of the solution formed is strictly additive, when $\Sigma C_{fin} = \Sigma C_{init}$ and $dQ/dT = 0$. It does not follow from this, however, that the absolute value of the heat effect will be zero.

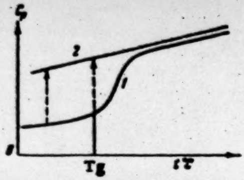

Fig. 6. Conventional graph for the effect of temperature on the total heat capacity of polymer and solvent (ΣC_{init}) and the heat capacity of the solution (ΣC_{fin}) for the case of spontaneous solution.

We may say that if the heat capacity of the spontaneously formed solution varies linearly with temperature, while the heat capacity of the polymer changes abruptly in a certain temperature range, in the transition from the glassy into the high-elastic state, then the Q = f(T) curve should show only one transition point c, corresponding to T_g for the polymer. In Fig. 6, Curve 1 represents the dependence of ΣC_{init}, and Curve 2, of ΣC_{fin}, on the temperature. The difference between the ordinates of the curves represents $\Delta C = dQ/dT$. It is seen from Fig. 6 that up to the glass temperature $dQ/dT < 0$, since $\Sigma C_{fin} > \Sigma C_{init}$ and has a practically constant absolute value. Above the glass temperature $[dQ/dT]$ begins to decrease, and becomes zero. Accordingly, the heat effect decreases at first, and beyond T_g becomes independent of the temperature. A similar state of affairs is probably also found for the solution of polystyrene in benzene.

Somewhat different behavior is found in some cases in the spontaneous solution of cellulose esters, as the Q = f(T) curve has two transition points b and c [15]; in our view, this is the consequence of a non-linear relationship between the heat capacities of the solutions formed and the temperature. Only then could two transition points occur on the Q = f(T) curve. Our earlier determinations of the effects of temperature on the osmotic pressure of cellulose ester solutions [16] showed the existence of an anomalous positive temperature coefficient of osmotic pressure over a certain temperature range. It is possible that this is connected with an anomalous change of heat capacity over the same range. However, these suppositions require direct experimental verification. Since $\Sigma C_{fin} > \Sigma C_{init}$, then $dQ/dT < 0$ and the heat of solution decreases with rise of temperature. The greater is the difference between ΣC_{fin} and ΣC_{init}, the greater is the absolute value of $[dQ/dT]$ and consequently the greater is the slope of the linear region of the curve abcd (see Fig. 1). In this case the decrease of the heat effect occurs in a narrower range of temperatures. It follows, incidentally, that with a knowledge of $[dQ/dT]$, it is possible to find ΔC, or the change of heat capacity on transition from the solid polymer to its solution. The values of ΔC calculated from our data are shown in Table 2.

Unfortunately only the ΔC values for polystyrene can be compared with the results of other workers, as analogous values for other polymers are not known. The ΔC values given here for polystyrene are in good agreement with published data [17,14].

With a knowledge of ΔC it is possible to calculate, with the aid of Kirchhoff's law, the heat effect at any temperature below T_g for the polymer. Above T_g the heat effect is independent of the temperature. However, if in the region of relatively low temperatures the heat effect is independent of the temperature or has a different temperature coefficient, then additional restrictions may be introduced in a number of cases. In the temperature region in which the heat effect varies linearly with the temperature, the heat effect can be calculated from Kirchhoff's law. As an example, we give the approximate calculation for polyvinyl alcohol. If $T_g = 85°$ and $\Delta C = 0.25$, then at 40° we have: $\Delta Q = 0.25 \times (85-40) = 11.25$ cal./g. Figure 3 shows that $\Delta Q = 10$ cal./g. Similarly, for polystyrene we have at 20° $\Delta Q = 0.1 \times (81-20) = 6.1$ cal./g. Such calculations give correct results only when the glass transition temperature is not appreciably depressed by the action of the solvent. The not very good agreement between the calculated and experimental data for polyvinyl alcohol indicates that such an effect has occurred, owing to solvation of the polymer by the solvent. If a corrected glass transition temperature is used in the calculation (this is found graphically from the point of intersection of the linear

TABLE 2

Values ΔC in different polymers

Polymer	Solvent	ΔC in cal/g · degree
polyvinyl alcohol	water	0.25
gelatin, unfractionated	water	0.8
gelatin, 15° fraction	water	0.5
Polyvinyl chloride, difficulty-soluble fraction	dichloroethane	0.8
Ditto, readily-soluble fraction	dichloroethane	0.4
Nitrocellulose	butyl acetate	0.3
Ditto	Acetone	0.6
Polystyrene	Benzene	0.1

region of the $Q = F(T)$ curve and a straight line drawn through the values of the heat effects above T_g), good results are obtained. If we take T_g as 81°, we have $\Delta Q = 0.25\ (81-40) = 10.25$ cal./g; thus the calculated value is in good agreement with the experimental value.

The influence of the nature of the solvent on the depression of the glass transition temperature (ΔT) for nitrocellulose ($T_g = 53°$) is shown by the following values:

	ΔT°C		ΔT°C
Butyl acetate	1	Acetone	18
Ethyl acetate	7	Methyl alcohol	25

The existence of a glass temperature depression makes it necessary to introduce certain corrections into the views put forward above, so that the initial state must evidently be regarded as the state which arises on instantaneous interaction of temperature-activated polymer with a liquid which displaced T_g into the region of lower temperatures. The final state, according to the system and temperature in question, is the state of the equilibrium-swollen polymer or solution. Thus, to explain the dependence of the heat effect on the temperature it is necessary to take into account the changes which the glassy polymer, solvated polymer, and the resultant solution undergo on heating.

SUMMARY

1. The temperature dependence of the heat of solution has been studied for polyvinyl acetate, polystyrene, polybutyl methacrylate, polyvinyl alcohol, δ-valerolactone, and phenolphthalein.

2. It is shown that the heat of solution of a polymer depends on its physical state and is related to T_g. The heat of solution at temperatures above T_g is independent of the temperature of the polymer, while at temperatures below T_g it decreases with increase of temperature. The lower is the experimental temperature relative to T_g, the greater is the heat of solution.

3. The view is advanced that in some cases the heat capacity of polymer solutions may vary non-linearly with the temperature, as otherwise there could not be two transition points on the curve for the variation of the heat effect with temperature for the case of spontaneous solution.

4. It is shown that the nature of the solvent may result in a depression of the glass transition temperature, which must be taken into consideration in calculations of the heats of solution of polymers.

5. For comparisons of heats of solutions of polymers the experiments must be carried out in conditions in which the polymers are in the same physical state.

Moscow Textile Institute
Chair of Physical Chemistry

Received March 6, 1956

LITERATURE CITED

[1] S. M. Lipatov, Proc. Acad. Sci. USSR 48,434 (1945); S. I. Meerson, Dissertation (Moscow Textile Institute, Moscow, 1945); S. M. Lipatov and S. I. Meerson, Symposium, Colloids in the Food Industry, (Food Industry Press, 1946).

[2] S. M. Lipatov, B. A. Kartsovnik, and L. V. Babich, Colloid J. 10, No. 5, 349 (1948).

[3] K. Gunner and G. V. Schulz, Naturwissenschaften 40, No. 5, 164 (1953); V. Z. Schulz, Z. physik. Chem. 4, 192, 211 (1955).

[4] S. M. Lipatov and S. I. Meerson, Colloid J. 8,163 (1946).

[5] R. F. Boyer and R. S. Spencer, Chemistry of Large Molecules (Foreign Literature Press, Moscow, 1948), Vol. 2.

[6] E. I. Barg, Technology of Synthetic Plastics (State Chemical Press, Leningrad, 1954), p. 337.

[7] S. M. Lipatov and S. I. Meerson, Colloid J. 8, No. 4, 233 (1946).

[8] S. M. Lipatov, Proc. Acad. Sci. USSR 48, No. 6, 434 (1946); Bull. State Univ. Central Asia 28,17 (1949).

[9] S. M. Lipatov and S. I. Meerson, Colloid J. 12, No. 2, 122 (1950); 12, No. 6, 427 (1950).

[10] S. I. Zhurkov and B. Ya. Levin, Proc. Acad. Sci. USSR 67, 89 (1949).

[11] T. Alfrey, Mechanical Behavior of High Polymers (Foreign Literature Press, Moscow, 1952), p. 160.

[12] K. Uberreiter, H. J. Orthmann, Koll.-Z., 132, 2/3, 61, 1953.

[13] S. I. Zhurkov and B. Ya. Levin, Symposium for the 75th Birthday of Academician A. F. Ioffe (Acad. Sci. USSR Press, 1950), p. 260; P. P. Kobeko, Amorphous Substances (Acad. Sci. USSR Press, 1952), p. 187; S. Alford and M. Doll, J. Am. Chem. Soc. 77, 18 (1955); K. Uberreiter and Otto-Lanpenmuhen, Z. Naturforsch 8a, No. 10, 664 (1953).

[14] K. Uberreiter and Otto-Lanpenmuhlen, Z. Naturforsch 8a, 10,664 (1953).

[15] S. M. Skuratov, Colloid J. 9, No. 2, 133 (1947).

[16] S. I. Meerson and S. M. Lipatov, Colloid J. 13, No. 4, 301 (1951).

[17] E. Inckel and K. Gorke, Z. Naturforsch. 7a, 9, 630 (1952).

Moscow Textile Institute
Chair of Physical Chemistry

Received March 6, 1956

THE STRUCTURE OF COPOLYMERS AND POLYAMIDE MELTS

N. V. Mikhailov and V. O. Klesman

Synthetic fibers have, in addition to their high mechanical and physicochemical qualities, significant defects which restrict their field of application in technology. These defects include flow or brittleness of the fibers at high and low temperatures, structural and optical inhomogeneity, etc.

Much attention is being devoted at the present time to the problem of production of synthetic fibers and films with predetermined properties appropriate to various requirements of production and use. This problem may be solved in two ways. The first is purely chemical – changes in the structure and properties of the molecule itself occur as the result of chemical action between different original monomers. The second way is by production of polymer mixtures from a common solvent or melt, a molecular mixture of polymers being formed. A paper by one of the present authors [1] dealt with this new trend in modification of synthetic fiber properties by production from mixtures of polymers different in chemical nature and structure.

The present communication contains the results of studies of the structure and certain properties of mixtures of synthetic polyamides obtained from melts. Studies of polymer melts have largely begun only recently and are still at an early stage. Ayers [2] characterized the "equilibrium" state of polyamide melts by means of partition chromatography in order to establish a difference between physical mixtures of 6,6 and 6,10 nylon-type polyamides and copolymers prepared from these polymers by heating together. It was considered that a copolymer is already formed after the mixture has been heated for 2 hours. Fuller [2], found that x-ray diagrams of similar polyamides showed interferences corresponding to the pure polymers. His results contradict the results of Kargin and Markova [3], who showed that the structure of polyamides does not depend on the molecular parameters, i. e., the regularity of the repeat and the dimensions of the hydrocarbon regions in the molecular polymer chain.

Kudryavtsev and Bernadskaya [4] studied the properties of melts of mixed capron and nylon resins by variations of the melting points and viscosities of polymer mixtures obtained from melts; they showed that a copolymer is formed after 25-30 hours of heating, i. e. chemical action takes place with formation of a new compound.

Korshak et al. [5] showed in studies of polyamide mixtures with different chain lengths that transamidation and exchange reactions occur when such mixtures are heated, leading to formation of new molecules of a mixed copolymer polyamide. Mark [6] considers that a compound similar to a eutectic mixture is formed by copolymerization of monomers.

EXPERIMENTAL

The materials studied were polyamide copolymers and polymer mixtures of the same composition, taken in the following proportions by weight:

$$\frac{\text{Caprolactam}}{\text{AH salt}} : \frac{\text{Polycaprolactam}}{\text{Polyhexamethylene adipamide}} = 50{:}50;\ 60{:}40;\ 75{:}25;\ 80{:}20.$$

The polymer mixtures were made from the powdered substances by heating them together for 1 to 20 hours in a nitrogen atmosphere at 275°.

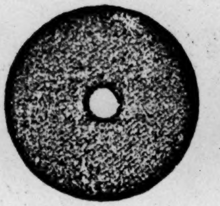

Fig. 1. x-Ray diagram of polyamide copolymer obtained by extrusion of a melt into cold water (1:1 ratio).

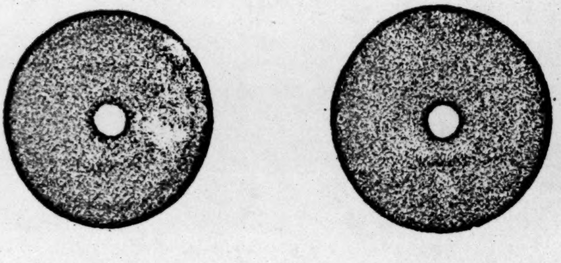

Fig. 2

Fig. 3

Figs. 2 and 3. x-Ray diagrams of polyamide copolymers obtained by free evaporation of the solvent from copolymer solution: 1:1 ratio (Fig. 2); 8:2 ratio (Fig. 3).

For investigation of the structural characteristics, the materials were obtained under different formation conditions (rapid and slow cooling of the melt, or evaporation of the solvent from a solution of the copolymer or polymer mixture). It was necessary to determine the effect of structural regularity of the polymer chain on the structure both of the copolymer and of the polymer melts.

The work of Korshak and Kudryavtsev [4, 5] shows that when polymer mixtures are heated the rates of chemical change in them are very low. Therefore in the course of some particular time interval the fusion of polymers should not be accompanied by appreciable chemical changes. Polymer mixtures obtained by brief heating were mainly studied. The principal investigation methods used were the x-ray and thermographic methods, described previously [7]. Structural differences in the materials studied could be detected and structural changes in them followed, by the use of these methods in conjunction.

Figure 1 shows an x-ray diagram of polyamide copolymers obtained by extrusion of their melt into cold water. This diagram shows a typical picture of an amorphous substance. The x-ray diagrams of polyamide copolymers for other proportions of the components are not shown, as they are quite identical with that given.

Formation of the same copolymers in conditions which favor crystallization (slow cooling of the melt, slow evaporation of solvent from solution) resulted in a different structure, as shown in the x-ray diagram in Fig. 2. The diffraction diagrams of copolymers made in this way showed more interference rings (four or more). With increasing regularity of the copolymer structure (for example, specimens with 8:2 copolymer ratio) the crystallization power increased for otherwise equal conditions, as is shown by the x-ray diagram in Fig. 3. When such specimens were reheated and then cooled rapidly, an amorphous structure was obtained, similar to that shown in Fig. 1.

It is seen in a comparison of the x-ray diagrams of polyamide copolymers made under different conditions that copolymers, like the pure polymers and even to a greater degree, have a tendency to supercooling. It seems likely that the formation of various modifications of the copolymers, and their mutual transitions, are related not only to the kinetics of the copolymer structure formation, but also the regularity of the molecular structure. Certain distinctions in the structure of melts and copolymers were found when copolymers were modeled by formation of melts of pure polymers of the corresponding chemical composition. When polymer mixtures were heated for 1, 2, 3, and 4 hours, products were obtained the x-ray diagrams of which differed from the x-ray diagrams of the pure copolymers. The structure of such mixtures only approximated to the structure of copolymers of the corresponding chemical composition after the polymer mixture had been heated for a long time (5 hours or more).

Thermographic curves for polyamide copolymers are shown in Fig. 4, a and b, an examination of which shows that the temperature regions of transition on the heating and cooling curves depend on the copolymer composition. The relevant data are shown in Table 1.

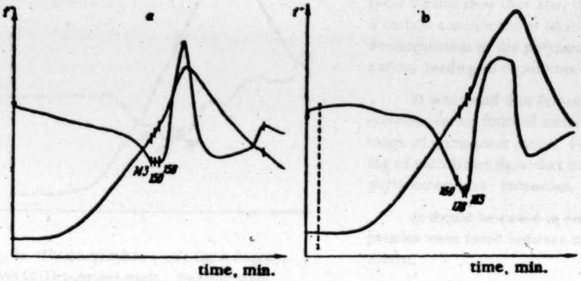

Fig. 4. Thermographic curves for polyamide copolymers: a) 1:1 ratio; b) 8:2 ratio.

The thermographic curves for polymer mixtures in any proportions (obtained by brief heating of the polymers) are close to the curves for the pure polymers and, in addition, show at least one other peak (Fig. 5). The appearance of this endothermic effect may be due to the formation of a new structural modification when the polymers are melted together. For polymer mixtures heated for considerable periods the heating curves are different in character. These curves are close to the heating curves for the corresponding copolymers.

In our opinion, the endothermic effects on the heating curves for supercooled copolymers and polymer melts are explained in the same way as for "pure" amorphous modifications of polycaprolactam, as detailed in a previous paper [7].

Thus, it must be stressed that copolymer structures may be modeled by polymer mixtures after prolonged heating. After brief heating of the melts, the polyamide polymer molecules still retain their individual properties. The most characteristic property of such polymer mixtures is the power of separate crystallization, represented by the appearance of two exothermic effect on the cooling curve for the mixture. Similar "separate" crystallization of the molecules, leading to formation of relatively independent crystalline structures, was also observed by Rylov [9].

TABLE 1

Temperature Regions of Fusion and Crystallization of Polyamide Copolymers

Ratio of components	Final temperature, °C	
	fusion regions	crystallization regions
5:5	156	135
6:4	169	—
7,5:2,5	174	139
8:2	179	146

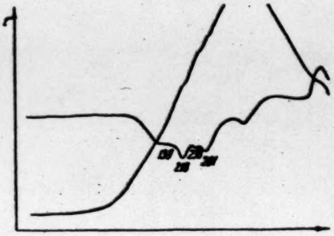

Fig. 5. Thermographic curve for a capron:nylon (1:1) polymer melt. Heating time ~ 2.5 hours.

This physical heterogeneity of polymer mixtures does not allow of their classification with eutectic mixtures. However, it does not exclude the possibility of prolonged coexistence of such products. The formation of eutectics from polymer mixtures is possible in principle, but probably only in a very narrow range of temperatures and compositions, as can be seen when a mixture of polymers in a 60:40 ratio is heated (see the thermogram in Fig. 6).

The viscosities of solutions of the polymer mixtures are given below:

	η
Polycaprolactam	0.265
Polyhexamethylene adipamide	0.24
Mixture of polymers (1:1) after heating for 2.5 hours	0.22
Ditto, after heating for 4 and 5 hours	0.14
Ditto, after heating for 11 and 20 hours	0.12
Ditto, after heating for 45 hours	0.126

These figures show that after the polymer mixture is heated, a certain equilibrium is established between the thermal decomposition of the polymers and secondary polymerization, leading to copolymer formation.

It was found that formation of fibers from polymer mixtures in the form of melts is possible over a wide range of component ratios. Preliminary tests on the spinning of such fibers show that they have fairly satisfactory physicochemical properties, as shown in Table 2.

It should be noted in conclusion that some discrepancies were found between the x-ray and thermographic results.

As follows from the work of Kargin and his associates [3], pure synthetic polyamides of any chemical composition have the same crystal lattice parameters. Nevertheless, the heating curves of solid melts of such polymers show two (and sometimes even more) endothermic effects, indicating a multiphase nature of the polymer melts.

TABLE 2

Physico-Mechanical Properties of Fibers Obtained from Polymer Mixtures in the Form of Melts

Component ratios, wt.%	Stretch, %	Metric No.	Breaking length, km	Dry extensibility, %
Capron:nylon 1:1	365	176	34.3	21.0
Nylon:capron 3:1	365	166	31.4	17.7
Capron:nylon 3:1	354	202	39.0	18.8

Thus the thermodynamic picture of structural inhomogeneity is not in agreement with x-ray data indicating inhomogeneity of the structure of these substances by the molecular parameters. This contradiction may probably be explained on the basis of V. A. Kargin's data on the absence of a three-dimensional geometrical structure in crystalline polymers.

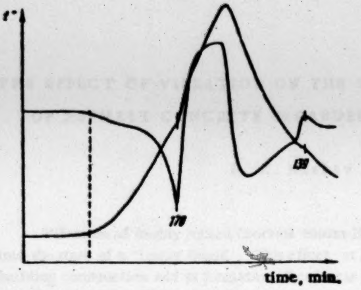

Fig. 6. Thermographic curve for a melt of capron: nylon (6:4) polymers.

SUMMARY

1. Structural and thermochemical data are used to confirm the view that mixing of polymers by fusion passes through at least two stages. In the initial stage of heating a polymer melt is formed in the form of a molecular mixture. Further heating produces a chemical compound with the properties of a copolymer.

2. The formation of a eutectic from a polymer mixture heated for a short time was observed only at a 6:4 ratio of the components.

3. Structure formation in polyamide copolymers is determined by the kinetics of the process, and also by the chemical structure of the substance.

Synthetic fibers of various physicochemical properties may be obtained from polymer melts with a wide range of component ratios.

In conclusion, we take this opportunity of expressing our gratitude to x-ray technologist P. M. Larionov for assistance.

All-Union Scientific Research Institute
for Synthetic Fibers

Received February 15, 1955

LITERATURE CITED

[1] N. V. Mikhailov et al., Textile Industry, 1954, No. 9, 11.

[2] Ayers, J. Appl. Chem., 1954, 444; Fuller, cited by Ayers.

[3] V. A. Kargin and G. S. Markova, J. Phys. Chem. 27, No. 8 (1953).

[4] G. I. Kudryavtsev and Bernadskaya, Symposium, Synthetic Fibers (1952), No. 3,88.

[5] V. Korshak and T. Frunze, Proc. Acad. Sci. USSR 97, No. 4, 675 (1954).

[6] H. Mark, Ind. Eng. Chem., 1952, 2110.

[7] N. V. Mikhailov and V. O. Klesman, Colloid J. 16, No. 3, 191 (T.p. 195)*; 16, No. 4, 272 (T.p. 269)*.

[8] N. V. Mikhailov and V. O. Klesman, Proc. Acad. Sci. USSR, 91, No. 1,99 (1953).

[9] E. E. Rylov, Candidate's Dissertation (Karpov Institute, 1953).

---

* T. p. = C. B. Translation Pogination

BLANK
PAGE

THE EFFECT OF VIBRATION ON THE STRUCTURAL AND MECHANICAL PROPERTIES OF ASPHALT CONCRETE REGARDED AS A THIXOTROPIC COLLOIDAL SYSTEM

S. K. Noskov and N. V. Mikhailov

Vibration of freshly mixed concrete causes liquefaction of the mix and its conversion from a soft state into the state of a "heavy liquid. . This effect, as is known, is widely used for packing down concrete in building construction and in formation of concrete articles. Similar "liquefaction", caused by a decrease of the frictional forces between individual particles, is produced by vibratory treatment of free-flowing materials such as sand, gravel and soil, and this is also widely used for technical purposes.

Desov [1] was the first to study the effects of vibration on the viscosity of cement pastes and mixes; his technique and special instrument (vibroviscosimeter), based on the floating ball principle, were used to study the variations of cement paste viscosity in different vibration conditions.

In contrast to cement-based concrete, asphalt concrete is a highly viscous structurized system with a considerable flow limit [2]. The maximum plastic viscosity of sanded asphalt concrete, even at 85°, was found to be 5.10^8 poises, which is more than 7 orders of magnitude greater than the viscosity of cement paste; the conventional yield stress of asphalt concrete at this temperature was found to be ~ 10 g/cm^{-2}.

The effective viscosity of conventional plastic solidlike bodies [3], which include asphalt concrete, at stresses a little above the conventional flow limit, is greater than the maximum plastic viscosity by about one order of magnitude, while the maximum limiting viscosity is greater by at least 4 orders of magnitude [4].

Despite such high viscosity, asphalt concrete mixes are liquefied by vibration, and the filler particles are then easily displaced by small pressures, and assume a denser packing.

In view of the foregoing, studies of the effect of vibration on the structural and mechanical properties of asphalt concrete are of great importance, since, on the one hand, the most favorable vibration conditions cannot be selected without knowing which of them have the greatest effect on viscosity. On the other hand, with a knowledge of the most effective vibration parameters, it is easy to design vibration conditions.

The floating ball method used by Desov for studying the viscosity of cement pastes during vibration is not suitable for asphalt concrete mixes because of their high viscosity. We used the vibroplastometer (Fig. 1)*, based on the principle of longitudinal displacement of a cylindrical layer of material between two coaxial cylinders [5], for studies of high-viscosity systems. The load was applied to the inner cylinder, which moved along its axis. The cylinder surfaces in contact with the test material were provided with a screw thread 3 mm deep to prevent slip of the wall layer of material against the cylinder surfaces [6], and so to ensure [illegible] shear occurring only within the material. The systems were vibrated at definite frequencies and amplitudes by means of the plate 1 with a variable debalancer 2, which was rotated by a flexible shaft 3 driven by a commutator motor. The motor was fed through a voltage stabilizer to ensure stable vibration conditions; by regulation of the voltage the frequency could be varied between 2000 and 6000 vibrations per minute.

The deformation of the sample in the vibroplastometer was measured by the displacement in the inner cylinder 4, the measurement being made to an accuracy of 0.01 mm with the aid of a dial attached to the outer cylinder.

---

* Designed by S. K. Noskov.

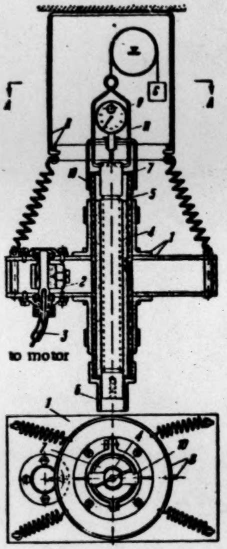

Fig. 1. Scheme and design of the vibroplastometer.

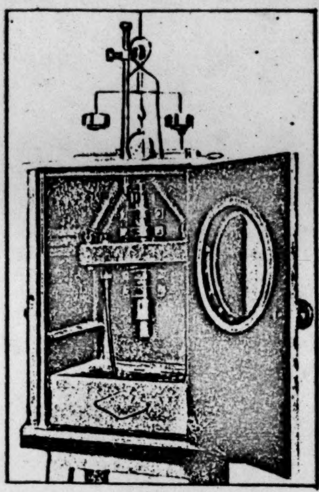

Fig. 2. General view of the installation.

The length of the outer cylinder 5 was 250 mm; the inner effective diameter of this cylinder was 40 mm. The inner cylinder 4 had an external diameter of 30 mm; the thickness of the layer of test material was 5 mm. The inner cylinder was placed in the caps 6 and 7, with the aid of directing sleeves, coaxially with the outer cylinder, while the friction in these sleeves was measured previously and taken into account in the calculations.

Thermostatic control of the sample was effected by means of an ordinary thermostatic oven, the whole instrument being suspended in the oven by the support 8 (Fig. 2). The dial 9, fixed in a special holder 10, and the pulling bracket 11, intended for balancing of the inner cylinder by a load over a pulley, projected from the top of the oven.

The end of the loading rod, passing through the floor of the oven, was screwed into a threaded socket in the lower end of the inner cylinder; different weights were placed on the rod plate for varying the load on the inner cylinder.

First the growth of deformation with time under different loads was followed at a given temperature without the use of vibration, and the E (τ) diagram for p = constant was used to determine the maximum plastic viscosity and the yield value (flow limit) of the material. Then, at the same temperature and for definite predetermined vibration parameters, the course of growth of the deformation of the vibrated sample was studied at different loads; the effective viscosity of the material during vibration was determined from these results. The maximum plastic viscosity η_0^* in poises was calculated with the aid of the modified formula of Pochettino [7]:

$$\eta_0^* = K\frac{G_0 - G_{cr}}{v}, \qquad (1)$$

where G_0 is the load which causes steady flow, in grams; G_{cr} is the critical load at which no flow is found, in grams; v is the rate of flow (speed of the inner cylinder) in cm/second; K is a constant for the instrument;

$K = 981 \frac{\ln \frac{R}{r}}{2\pi H}$, where R and r are the radii of the inner surface of the outer cylinder and of the outer surface of the inner cylinder, in cm; H is the effective height of the displaced layer, in cm.

The critical load G_{cr}, corresponding to the yield value, was determined from the load – plastic flow rate diagram $G_0(v)$ by continuation of the initial linear region of the rheological curve to its intersection with the load axis. For cases in which $G_{cr} = 0$ (no yield value), the effective viscosity was calculated from the formula:

$$\eta_0 = K \frac{G_0}{v}. \qquad (2)$$

The materials studied were highly viscous mixtures of bitumen with ground limestone and sanded asphalt concrete with 8.4% bitumen.

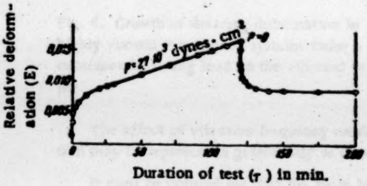

Fig. 3. Growth of shearing deformation in highly viscous structurized systems under a continuously acting load.

The growth of deformation with time under a constantly acting load was of the form shown in Fig. 3, with instantaneous-elastic deformation followed by slow growth of elastic deformation and then by steady flow.

The measure adopted for the effectiveness of vibration was the decrease of viscosity on vibration compared with the viscosity in static conditions. The effect of viscosity on the structural and mechanical properties of highly viscous systems is seen very clearly. A very slight load applied to the inner cylinder during vibration results in its displacement throughout the vibration period. No such displacement occurs in asphalt concrete even with loads 100 times as large in absence of vibration or after the vibration has ceased. It is clear that these results can be obtained only in the event of complete disappearance of the yield value and considerable decrease of viscosity, both of which are restored when the vibration ceases.

The curve for the growth of shearing deformation of sanded asphalt bitumen under a constant load of 288 dynes·cm^{-2} acting on the inner cylinder is of a different nature, as shown in Fig. 4. It is seen that deformation begins some time after the start of vibration, while displacement of the inner cylinder does not cease immediately after the vibration stops. In the deformation of vibrated highly viscous structurized systems, as in the deformation of these systems in static conditions, elastic after-effects are observed, followed by a regular displacement of the cylinder characteristic of steady flow of the system.

The delayed displacement of the cylinder after the start of vibration, and also the delayed cessation of this displacement after the end of vibration, indicate that vibration destroys the structural bonds not instantaneously but gradually, and that the restoration of these bonds is also gradual. The breakdown and buildup times of the structure of the vibrated system depend primarily on its viscosity. In addition, they depend on the magnitude of the acting load and on the vibration parameters – the greater is the load and the higher are the frequency and amplitude, the more rapid is the breakdown and the slower is the buildup, and conversely.

Figure 5 shows that the rate of viscous flow decreases when vibration stops, in consequence of an increase in the viscosity, rapid at first, and then slower. This is in all probability due to orientation processes, which are retarded as the viscosity increases.

Variations of the viscous flow rate with the load for asphalt concrete and for mixtures of bitumen and limestone are represented by straight lines passing through the coordinate origin for all the vibration parameters tried (Fig. 6). This shows that asphalt concrete flows like a true highly viscous liquid during vibration, and the flow rate under a given load increases with increasing frequency and amplitude of the vibrations; the viscosity of the mixture decreases with increasing frequency and amplitude. The maximum plastic viscosity of a sanded asphalt concrete mixture at 100° in static conditions, according to our data, is $1.7 \cdot 10^{8}$ poises; on vibration the effective viscosity decreases: at a frequency of 2000 vibrations per minute to $2.0 \cdot 10^{7}$ poises, and at a frequency of 6300 vibration per minute, to $7.5 \cdot 10^{5}$ poises.

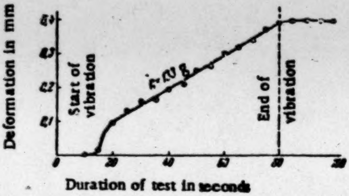

Fig. 4. Growth of shearing deformation in highly viscous structurized systems under a continuously acting load on the vibrated sample.

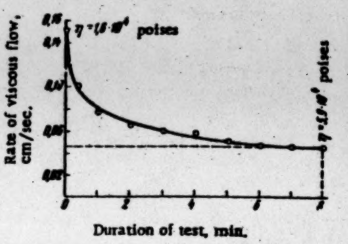

Fig. 5. Variation of the viscous flow rate under constant load (increase of viscosity) after cessation of vibration.

The effect of vibration frequency on the relative viscosity decrease during vibration at an amplitude of 0.25 mm may be represented graphically as shown in Fig. 7.

It must be pointed out that the more highly structurized systems containing large grains, such as sanded asphalt concrete, show much greater viscosity decreases under the same vibration conditions. A similar relationship is found if the vibration amplitude is varied in the vibration of highly viscous systems.

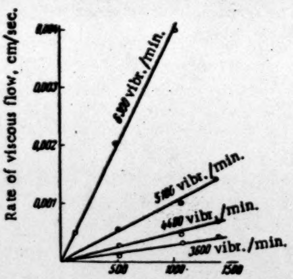

Fig. 6. Effect of a constant load on the rate of viscous flow of a vibrated highly viscous system.

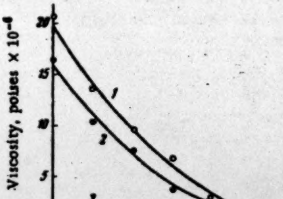

Fig. 7. Effect of vibration frequency on the relative viscosity decrease in a vibrated asphalt concrete mixture: 1) sanded asphalt concrete at 100°, 2) ditto, at 120°, 3) mixture of bitumen with limestone at 60°.

Temperature has an enormous influence on the effect of vibration on highly viscous systems. The structural and mechanical properties of such systems as asphalt concrete vary very greatly with change of temperature. The temperature has a particularly strong influence on the viscosity of bituminous materials, on which the vibration effect largely depends (see table).

TABLE

Effectiveness of Vibration of Sanded Asphalt Concrete at Various Frequencies and Temperatures (Vibration Amplitude 0.25 mm)

Temperature, deg.	η_{st} poises	Viscosity during vibration η_{vibr} in poises, and its relative decrease η_{st}/η_{vibr} at various frequencies							
		2000 vibr./min.		3600 vibr./min.		5100 vibr./min.		6300 vibr./min.	
		$\eta_{vibr.}$	η_{st}/η_{vibr}	$\eta_{vibr.}$	η_{st}/η_{vibr}	$\eta_{vibr.}$	η_{st}/η_{vibr}	$\eta_{vibr.}$	η_{st}/η_{vibr}
60	$5.0 \cdot 10^9$	$1.6 \cdot 10^9$	3.1	$1.4 \cdot 10^9$	3.6	$6.5 \cdot 10^8$	7.7	$3.0 \cdot 10^8$	16,6
80	$1.5 \cdot 10^9$	$1.8 \cdot 10^8$	8.3	$8.5 \cdot 10^7$	18.7	$4.0 \cdot 10^7$	37.5	$1.2 \cdot 10^7$	125
100	$1.7 \cdot 10^8$	$2.0 \cdot 10^7$	8.5	$9.6 \cdot 10^6$	17.7	$3.0 \cdot 10^6$	56.7	$7.5 \cdot 10^5$	227
120	$2.5 \cdot 10^7$	$1.5 \cdot 10^7$	1.7	$1.7 \cdot 10^6$	14.7	$2.6 \cdot 10^6$	9.6	$8.8 \cdot 10^5$	28,4

The table shows that the effect of vibration is always more pronounced at high frequencies. The viscosity of an asphalt concrete mixture vibrated at 100° at a frequency of 6300 vibrations/minute is decreased by a factor of more than 200. This effect, measured by the ratio of the maximum plastic viscosity of the mixture in static conditions, η_{st}, to the effective viscosity of the same mixture during vibration, η_{vibr}, depends on the initial maximum plastic viscosity of the system η_{st} (Fig. 8). The maximum vibration effect at all the frequencies tested corresponds to a viscosity of $2 \cdot 10^8$ poises.

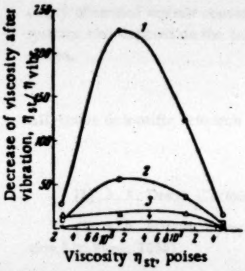

Fig. 8. Effectiveness of vibration of asphalt concrete mixtures at frequencies: 1) 6300; 2) 5100; 3) 3600; 4) 2000 vibrations/minute with different initial viscosities.

An asphalt concrete mixture at 80° and higher is a loose system, consisting of mineral grains of various sizes, weakly held together but surrounded by bitumen. This loose mixture can be easily pressed into a monolithic structure formed by closer packing of the mineral grains and closer cohesion between their bitumen coatings at points of contact. As the system is cooled its strength increases still more, as the viscosity and elasticity of bitumen rise rapidly.

An examination of the structure of asphalt concrete reveals the existence of a primary and secondary structure in it. The primary structure is the structure of the bitumen itself, while the secondary structure is an elastic skeleton of rigid mineral grains held together by very thin layers of bitumen at their points of mutual contact.

The bitumen present on the layers between the grains differs from the bitumen in the main bulk in being much more highly structurized, first, as the result of adsorptive interaction with the mineral grain surfaces, and second, by interaction and closer packing of the solvate layers as the grains are packed closer together. Structurized bitumen has much higher viscosity and elasticity than the bulk bitumen which fills the pores between the grains. When asphalt concrete undergoes deformation, the properties of the bitumen in the layers between the grains at the points of contact are clearly revealed by the higher values for the elasticity and viscosity of the mixture. When the mineral grains are brought closer together during packing of the system, the number of contacts per unit volume increases and the layers between the grains become thinner, which produces a strength increase in the asphalt concrete.

The role of the bulk bitumen in asphalt bitumen during deformation consists of damping all the elastic deformations which arise in the thin layers between the grains.

When the system is vibrated, all the mineral grains receive definite impulses which confer a vibratory motion to them. The vibrations of the grains, in turn, set up velocity gradients, which depend on the mass of the grain, the vibration frequency and amplitude, the thickness of the bitumen layers at the points of contact, and the structural and mechanical properties of these layers. The velocity gradients and the degree of structurization of the system determine the viscosity decrease during vibration.

The more large grains are present in unit volume of the vibrated system, and the larger these grains are, the greater is the viscosity decrease.

These conclusions are confirmed by a comparison of the results for asphalt concrete and for bitumen–limestone mixtures (Fig. 7).

SUMMARY

1. A description is given of the vibroplastometer and of a method for determination of structural and mechanical properties by means of which vibrated highly viscous systems may be studied. Such studies are very important for selection of vibration conditions for packing of structurized systems.

2. Vibration of highly viscous structurized systems destroys their conventional yield value and greatly lowers the viscosity, so that the system acquires the properties of a true liquid; after cessation of the vibration the viscosity and the yield value of the system are thixotropically restored [8], and increase if the grains of the rigid framework have become more closely packed.

3. The maximum viscosity serves as an objective measure of the structural and mechanical properties of a vibrated asphalt concrete mixture. The effectiveness of vibration may be evaluated by the relative decrease of viscosity of the system.

4. The most effective parameters for the vibration of highly viscous systems lie in the region of high frequencies and amplitudes. A frequency of 6300 vibrations/minute and an amplitude of 0.25 mm reduce the viscosity of sanded asphalt concrete by a factor of over 200. The effectiveness of the vibration of highly viscous systems also depends on the initial viscosity of the vibrated system and on the number and size of the constituent grains.

All-Union Scientific Research Institute for Building, Moscow

Received July 28, 1955

LITERATURE CITED

[1] A. E. Desov, Colloid J. 13,346 (1951).

[2] S. K. Noskov, Symposium, Materials and Constructions for Water and Heat Insulation (State Construction Lit. Press, 1955).

[3] N. V. Mikhailov and P. A. Rebinder, Colloid J. 17, No. 2,107 (1955) (T. p. 99)*.

[4] N. V. Mikhailov, Colloid J. 17, No. 3, 242 (1955) (T. p. 221)*.

[5] M. P. Volarovich, Trans. Polygraphic Inst. (United State Press, 1937), 5,299.

[6] D. M. Tolstoi, Colloid J. 9,450 (1947); 10,133 (1948).

[7] A. Pochettino, Nuovo cimento 8, 77 (1914).

[8] P. A. Rebinder (London), Discussion on Coagulation, Sept. 1954.

---

* T. p. C. B. Translation Pogination.

INVESTIGATION OF THE STRUCTURE OF SILVER SOLS

I. M. Ratner, T. A. Koretskaya, and V. A. Kargin

Kargin, Berestneva, and Koretskaya [1] have described a method consisting of simultaneous electronographic and electron-microscopic investigation for investigations of the structures of particles. This method was used by the authors for investigations of the aging kinetics of various sols, and it was shown that particles of freshly prepared sols are always formations with amorphous structure. As the sol ages, its particles pass into the crystalline state. Among the sols studied, the kinetics of the aging of gold sols [2] obtained by the reduction of gold chloride by white phosphorus was investigated. In this sol the lifetime of the particles in the amorphous state at room temperature was 5-10 minutes.

It appeared of interest to apply the method to a study of the change of structure during aging of silver sol particles. Apart from its general scientific significance, this question may be of considerable importance in the solution of a number of problems in the theory of heterogeneous catalysis, and in particular, in the theory of the photographic process.

Sols prepared by reduction of silver oxide by white phosphorus, hydrazine, and formaldehyde were used in the investigation. The starting solution for sol preparation was a saturated solution of silver oxide, prepared by prolonged shaking (for 100 hours) of powdered silver oxide with redistilled water.

The reduction with phosphorus was performed as described in the literature [3]. Reduction by hydrazine and formaldehyde is usually carried out in an alkaline medium (in presence of soda), but this method is unsuitable for electron microscopy, as the soda would distort the observed picture by crystallizing on the object holder. We were able to show that silver oxide may be reduced, although less vigorously, by hydrazine hydrate and formaldehyde in a neutral medium, rather higher concentrations of the reagents being required.

The preparation of the objects and application of the sols to the diaphragms was carried out by means of the methods described in the papers cited above. Collodion films were used as substrates. The same object was used for the electron-micrographs and the electron diffraction diagrams.

Figures 1 and 2 show, respectively, electron micrographs and electron diffraction diagrams representing the aging kinetics of silver sols, prepared by reduction of silver oxide with white phosphorus. The sol was prepared and aged at 20°, and the micrographs were taken at magnifications of 15000.

It is seen from Fig. 1 that electron micrographs of particles of a freshly prepared sol reveal the presence of large and apparently amorphous formations. However, the corresponding electron diffraction diagram shows rings characteristic of silver crystals. Similar experiments were performed several times, and the diffraction picture for the freshly prepared sol was not always well reproduced, although in most cases it was of the type shown in Fig. 2. When the sols were kept for 5-10 minutes at 20° the form of the large amorphous formations remained practically unchanged, while the electron diffraction diagrams invariably indicated an amorphous structure in the particles. In view of this, it is our opinion that the diffraction rings corresponding to a crystalline state which are found in the electron diffraction diagrams for freshly prepared sols are explained by the fact that the loose amorphous silver particles which form in the first instant after preparation of the sol are easily converted into a crystalline state by the action of the electron beam during exposure, so that it is very difficult to obtain the true diffraction picture. Further, the electron micrographs show that approximately 15 minutes after preparation of the sol fine crystals begin to form within the large particles, but their numbers are still very small, and therefore the electron diffraction diagrams do not reveal a crystal structure. A noticeable

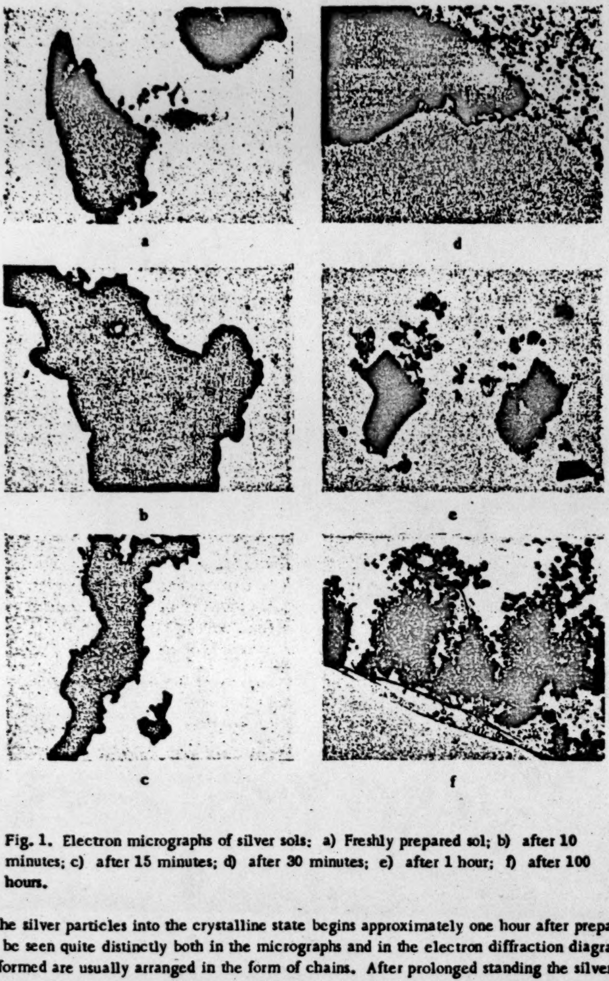

Fig. 1. Electron micrographs of silver sols: a) Freshly prepared sol; b) after 10 minutes; c) after 15 minutes; d) after 30 minutes; e) after 1 hour; f) after 100 hours.

conversion of the silver particles into the crystalline state begins approximately one hour after preparation of the sol, which can be seen quite distinctly both in the micrographs and in the electron diffraction diagrams. The silver crystals formed are usually arranged in the form of chains. After prolonged standing the silver crystals decrease in size, but retain their characteristic crystalline form.

We also studied the aging kinetics of silver sols prepared at other temperatures (both lower and higher). Variation of temperature, as was to be expected, changes the crystallization rate of the particles, but the nature of the process remains unchanged in all cases. The same is found in studies of sols prepared by other methods.

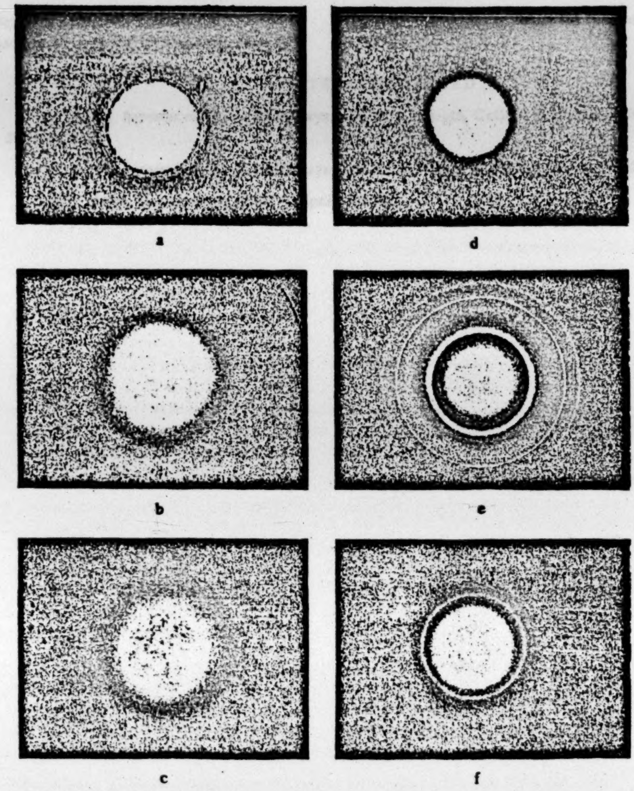

Fig. 2. Electron diffraction diagrams of silver sols: a) Freshly prepared sol; b) after 10 minutes; c) after 15 minutes; d) after 30 minutes; e) after 1 hour; f) after 100 hours.

SUMMARY

1. The formation and aging of colloidal silver particles has been studied by means of the electron microscope and electron diffraction.

2. It is shown that particles of freshly prepared silver sols have an amorphous structure. The particles pass into the crystalline state in the course of aging.

3. It is shown that the rate of conversion into the crystalline state increases with increase of temperature.

4. It is shown that the mechanism of aging (transition into the crystalline state) is the same for silver particles as for the analogous process in gold sols.

Scientific Research Institute for
Motion Pictures and Photography, Moscow

Received February 15, 1956

LITERATURE CITED

[1] Z. Ya. Berestneva, T. A. Koretskaya, and V. A. Kargin, Colloid J. 12, No. 5, 338 (1950); 13, No. 5, 323 (1951).

[2] Z. Ya. Berestneva, T. A. Koretskaya, and V. A. Kargin, Colloid J. 14, No. 6, 395 (1952) (T.p. 427)*.

[3] J. Voigt, Das Kolloide Silber (Leipzig, 1929).

---

* T. p. C. B. Translation Pogination

THE SORPTION AND CHROMATOGRAPHY OF AUREOMYCIN

G. V. Samsonov, S. E. Bresler, and N. A. Rosentsveig

Aureomycin is a tetracyclic compound, the chemical structure of which has been fully established [1]. Aureomycin is an amphoteric substance with two acid and one basic functional groups, with dissociation constants pK of 3.4, 7.4, and 9.2 respectively [2]. The presently available chromatographic methods for the purification of aureomycin [3] are based on the use of mineral cationites at one stage of the process. The low capacity and the poor reversibility of the sorption of aureomycin, as is shown below, suggested that these methods are not the best of the possible chromatographic methods for the purification of this antibiotic.

In view of the amphoteric nature of aureomycin it was desirable to study the conditions of its sorption on cationites, anionites, and molecular adsorbents. The sorption and desorption of aureomycin were determined by the static method. 1 g of the adsorbent in the form of a powder with grain size 0.1-0.2 mm was shaken for 20 minutes with 20 ml of an aqueous solution of aureomycin hydrochloride at a concentration of 500 micrograms/ml (1 microgram of aureomycin base corresponds to one unit). The desorption was carried out three times with 10 ml lots of solution. The results are shown in Table 1.

Aureomycin concentration may be determined by colorimetric or spectrophotometric methods [4]. The following procedure was used. The aureomycin solution (4 ml of aureomycin solution in 2 ml of 5 N HCl) was heated on a boiling water bath for 4 minutes with formation of a yellow color. The solution was cooled and the color intensity was determined spectrophotometrically at λ = 450 mμ. The Lambert–Beer law is followed with great accuracy in this method. The aureomycin concentration is expressed as micrograms of aureomycin base (units) per milliliter of solution, or in terms of normality. Of the molecular adsorbents, the use of aluminum oxide is worthy of attention owing to the good reversibility, despite the low sorption capacity. Among the anionites, resin NO is of the greatest interest.

Chromatography of aureomycin on aluminum oxide. The adsorptive properties of aluminum oxide depend on the method of preparation [5]. Technical specimens of aluminum oxide showed a great diversity of adsorptive behavior toward aureomycin. The adsorption capacity, determined by the dynamic method at an aureomycin concentration of 200 micrograms/ml in the solution, varied from 0 to 10 mg/g for different specimens. The adsorption capacity of aluminum oxide for aureomycin increases as the result of ignition.

Ignition temperature of aluminum oxide in °C .	100	200	400	600
Adsorption capacity in mg/g	2.9	5.2	5.1	5.6

The adsorption capacity before ignition was 0.

The adsorption capacity of aluminum oxide for aureomycin is greatly diminished in presence of various organic substances. Salts of inorganic acids, on the other hand, practically do not decrease the capacity. Therefore quite different results are obtained when aureomycin is adsorbed in dynamic conditions from culture fluids formed during growth in presence of small and large amounts of organic substances respectively (Fig. 1). The experiments were carried out in a column 1 cm in diameter containing 5 g of aluminum oxide, at a flow rate of 100 ml/hour.

The adsorption capacity of aluminum oxide for aureomycin is already considerable at low equilibrium aureomycin concentrations (4-5 mg/g) and subsequently increases only slightly. Therefore aureomycin cannot be desorbed by water. Desorption of aureomycin with almost complete yields may be effected by solutions of hydrogen chloride in methyl alcohol, or by hydrochloric acid solutions. The yield curves obtained for the

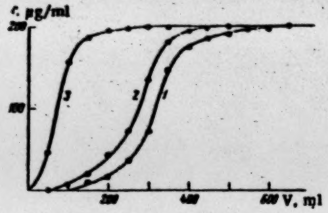

Fig. 1. Curves for adsorption of aureomycin on aluminum oxide: 1) aureomycin hydrochloride solution (sample containing 900 units/mg); 2) aureomycin culture fluid with a low content of organic impurities; 3) ditto, with a considerable content.

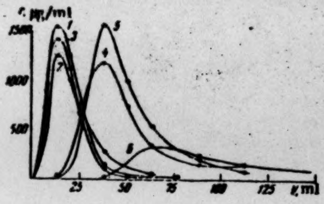

Fig. 2. Yield curves for aureomycin desorption under various conditions: 1 – 1N HCl; 2–0.5N HCl; 3–0.25N HCl; 4–pH 1; 5 – pH 2; 6 – pH 3

desorption of aureomycin under various conditions from a column containing 5 g of aluminum oxide are shown in Fig. 2. A decrease of the amount of hydrogen chloride in the solution does not change the maximum concentration or yield of aureomycin up to pH 2, but only displaces the position of the peak – aureomycin is found in the later effluent fractions. The concentration and yield of aureomycin fall sharply only at pH 3 (Table 2).

TABLE 1

Sorption of Aureomycin by Various Materials

Adsorbent	Sorption capacity in mg/g	Reversibility of sorption, %	Conditions of desorption (displacement)
Molecular adsorbents			
Active carbon	10	0	0.1 *N* HCl in CH_3OH
Silica gel	0.88	48.8	0.5 *N* HCl
Quartz sand	4.20	35.7	0.5 *N* HCl in CH_3OH
Kaolin	9.60	66.7	0.5 *N* HCl in CH_3OH
Brown coal	4.32	42.2	0.5 *N* HCl
Aluminum oxide	3.60	90.0	0.5 *N* HCl in CH_3OH
Anionites			
NO	4.96	100	0.1 *N* HCl in C_4H_9OH
MN	1.36	20.5	20% Na_2SO_4, pH2
MMG-1	0.24	13.3	20% Na_2SO_4, pH2
Espatite TM	3.92	0	20% Na_2SO_4, pH2
Amberlite IR-4	0.16	—	20% Na_2SO_2, pH2
Cationites			
Permutite	6.40	45.3	20% $CaCl_2$
Infusorial earth	9.40	11.9	20% NaCl
Oxycellulose	8.14	49.1	20% NaCl
Sulfocarbon	6.94	0	0.5 *N* HCl
KMT (Na)	8.70	100	0.5 *N* HCl in CH_3OH
KFU (Na)	10.0	100	0.5 *N* HCl in CH_3OH
RF (H)	10.0	100	0.5 *N* HCl in CH_3OH
RBS-1 (H)	7.76	100	0.5 *N* HCl in CH_3OH
SSF (H)	10.0	100	0.5 *N* HCl in CH_3OH
SN (H)	10.0	100	0.5 *N* HCl in CH_3OH
SNF (H)	10.0	100	0.5 *N* HCl in CH_3OH
SkhB (H)	2.6	100	0.5 *N* HCl in CH_3OH

The high content of impurities found in the eluate, containing a considerable proportion of aluminum salts, is noteworthy. If a pure aureomycin solution is initially used, the eluate has exactly the same aluminum content and the same low content of aureomycin after being dried as in the adsorption of aureomycin from culture fluid. Control experiments showed that when aluminum oxide is washed with hydrochloric acid solutions under the same conditions, without preliminary adsorption of aureomycin, the amount of aluminum obtained is 50-100 times as small as after adsorption of aureomycin. This shows that aureomycin combines chemically with aluminum.

TABLE 2

Desorption of Aureomycin from Aluminum Oxide in Dynamic Conditions

Desorption conditions	Yield, %	Relative content of aureomycin in product, in µg/mg
1 *N* HCl . . .	91	50
0,5 *N* HCl . .	88	81
0,25 *N* HCl . .	88,7	101
pH 1	93	189
pH 2	91	214
pH 3	47	460

For the use of aluminum oxide for chromatographic purification of aureomycin, it is necessary to solve the problem of separation for aluminum from aureomycin. The use of oxalic acid, which forms complexes with aluminum, was not successful, as addition of oxalic acid to the solution hinders precipitation both of aluminum and of aureomycin.

Aureomycin was separated from aluminum by extraction with butyl alcohol, which dissolves only aureomycin. Aureomycin can be isolated from butyl alcohol by addition of hexane to the butanol solution. The solubility of aureomycin is then sharply decreased (Fig. 3), and it passes completely into the small volume of aqueous layer, from which aureomycin base is precipitated on neutralization.

Chromatography of aureomycin on NO anionite. The sorption capacity of NO anionite for aureomycin in dynamic conditions is 16 mg/g. This is considerably higher than the sorption capacity of aluminum oxide for aureomycin. The best eluant for aureomycin from NO resin is a solution of hydrogen chloride in butyl alcohol. Figure 4 shows the yield curve for the desorption of aureomycin by 0.1 N HCl solution in butyl alcohol from a column 5 cm in diameter, containing 300 g of NO resin. The yield in this experiment was 98%. Aureomycin can be separated from butyl alcohol as described above.

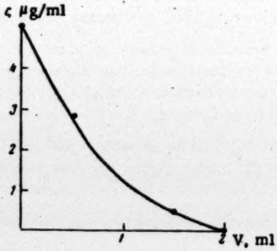

Fig. 3. Solubility of aureomycin in aqueous butyl alcohol with various additions of hexane; V is the volume of hexane (in ml) added to 1 ml of aureomycin solution in aqueous butyl alcohol.

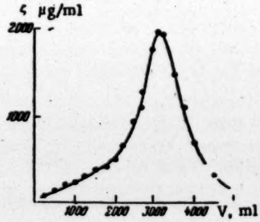

Fig. 4. Yield curve for desorption of aureomycin by 0.1 N HCl in butyl alcohol.

Most of the impurities present with aureomycin in the culture fluid may be removed by chromatographic separation on aluminum oxide and NO resin. The resultant aureomycin base contains 600 µg of the base per mg if the process is carried out by each of the two methods described above.

SUMMARY

The adsorption of aureomycin on 23 adsorbents has been studied in static conditions, and methods have been developed for chromatographic purification of aureomycin on aluminum oxide and NO anionite resin.

Institute of High Molecular Compounds
Academy of Sciences USSR, Leningrad

The Leningrad Chemico-Pharmaceutical Institute

Received June 29, 1956

LITERATURE CITED

[1] M. M. Shemyakin and A. S. Khokhlova, The Chemistry of Antibiotics (1953).

[2] C. R. Stephens, L. H. Conover, F. A. Hochstein, P. P. Regna, F. J. Pilgrim, K. J. Brunings and R. B. Woodward, J. Am. Chem. Soc. 74, 4796 (1953); P. P. Regna, J. Solomons, A. Timreck, K. J. Brunings, W. Lazier, K. Mura, J. Am. Chem. Soc. 73, 4211 (1951).

[3] B. Duggar, U. S. Patent 2 482 055 (1949); A. Saltman, J. Lab. Clin. Med. 35, 123 (1950).

[4] D. Hiscox, J. Am. Pharm. Assoc., Sci. Ed. 40, 237 (1951); E. M. Savitskaya, Symposium on Antibiotics (1953), 34, 29.

[5] H. Brockman and H. Shodder, Ber. 74, 73 (1941); N. A. Fuks, Factory Lab. 16, 878 (1950).

STATICS AND DYNAMICS OF AUREOMYCIN AND TERRAMYCIN ION EXCHANGE WITH HYDROGEN AND SODIUM IONS ON CATIONITES

G. V. Samsonov, L. M. Shuvalova, M. P. Shesterikova, S. F. Lavrentyeva,
V. S. Maslennikova, A. A. Kononova, and V. V. Bokareva

Aureomycin and terramycin are tetracyclic compounds of very similar chemical structure and properties.

Both are amphoteric compounds with two acidic and one basic functional groups(pK for aureomycin: 3.4, 7.4, and 9.2; pK for terramycin: 3.5, 7.6, and 9.2 [1]). Both the antibiotics are less stable in the alkaline than in the acid region. It follows that the use of cationites is more promising than the use of anionites in work with these antibiotics. Carboxylic cationites are capable of ion exchange in neutral and alkaline solutions, i. e. in conditions when aureomycin and terramycin cannot be present in solution in cationic form, since they have weak basic properties.

The best conditions for the sorption of aureomycin and terramycin should be present when they are adsorbed by strongly acidic cationites from acid solutions. Experimental investigation showed that both these antibiotics are adsorbed on carboxylic cationites with capacities many times less than the capacity of sulfonic resins for aureomycin and terramycin.

Exchange capacity of strong cationites for aureomycin and terramycin. The sorption of aureomycin and terramycin by cationites is reversible. The total amount of the adsorbed antibiotic may be displaced from the resin by other ions. Ion exchange with participation of aureomycin and terramycin leads to a definite thermodynamic equilibrium. The sorption of aureomycin by RF resins with phosphate groups, as well as by all the sulfonic resins studied, results in the displacement of an equivalent quanity of hydrogen ions (Fig. 1). Hence it follows that aureomycin (and terramycin) are adsorbed in the form of univalent ions.

The exchange capacity of aureomycin and terramycin on ion exchange resins was determined by the dynamic method. A solution containing 400 µg of aureomycin (or terramycin) base per 1 ml (400 units per 1 ml) was passed at a speed of 200 ml/cm^2 per hour through a column containing 0.25-1 g of resin at pH 2.5. Resin with 0.1-0.2 mm grains was used in the experiments.

The constants for the exchange of aureomycin and terramycin ions and hydrogen ions which are given below show that hydrogen ions at pH 2.5, within the limits of experimental error, do not compete with aureomycin ions for places on the resin, and do not lower the exchange capacity. All the work on determinations of the physicochemical properties of aureomycin and terramycin was carried out with crystalline preparations containing ~900 µg of the antibiotic base per 1 mg of the preparation.

The aureomycin concentration in the eluate was determined by the method described earlier [2]; the determination of terramycin was also based on spectrophotometry [3]. It was found that the most accurate results in the determination of terramycin are obtained by light absorption measurements in a spectrophotometer at a wavelength λ = 375 mµ after 5 ml of terramycin solution had been heated with 1 ml of concentrated sulfuric acid.

The results of determinations of the exchange capacity of sulfonic resins with respect to aureomycin and terramycin for different swelling coefficients are shown in Fig. 2. As in the sorption of streptomycin on carboxylic resins [4], a sharp rise of the exchange capacity occurs with increased swelling of the resins. Special interest attaches to strongly swelling sulfonic resins, for which the relative exchange capacity, or the degree of utilization/of the capacity in comparison with all the available functional groups on which metal ion exchange occurs, reaches 90-95%, which was impossible to attain in the sorption of streptomycin. This may be explained by the fact that in the sorption of univalent complex ions the fulfillment of the conditions necessary for the sorption of multivalent complex organic ions is not required. It was already noted previously [4] that the trivalent streptomycin ion cannot be bound, for steric reasons, by each of even the most accessible functional groups of ion exchange resins.

The exchange of aureomycin and terramycin ions with hydrogen and sodium ions on ion exchange resins was studied in order to verify the applicability of the ion exchange equation:

$$\frac{m_1}{m_2} = K\frac{c_1}{c_2},$$

which is valid for uni-univalent ion exchange.

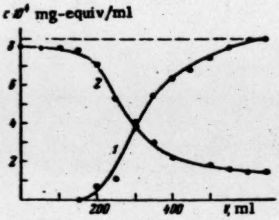

Fig. 1. Exchange of aureomycin ions for hydrogen ions on RF resin. Ion yield curves: 1) aureomycin; 2) hydrogen.

Resins in the H form were used for determination of the sorption capacity for aureomycin and terramycin from solutions of various degrees of acidity, and in the Na form in the case of solutions containing sodium ions. The results obtained in studies of the exchange of aureomycin ions for hydrogen and sodium ions on sulfonated resins SNF, SBS, SM-12, and SSF are shown in Table 1.

As previously [4], in the exchange of ions of substances with large molecular weights, it was found necessary to take into consideration only those hydrogen and sodium ions bound with the resin which could be exchanged for the large organic ions. Only then is Equation (1) (Fig. 3) applicable. The magnitudes of the exchange constants are themselves of interest (Table 2). If the aureomycin or terramycinion is regarded as the first ion, then the exchange constants are of the order of 100-1000. Such large values of the exchange constants and the resultant selectivity of aureomycin and terramycin ion sorption by ion exchange resins can only be explained by additional molecular interaction between the organic ions and the ion exchange resins. The previously found large values for the exchange constants in the exchange of ions of quaternary ammonium compounds of various degrees of complexity from tetramethylammonium to phenylbenzyldimethylammonium for ammonium ions [5] were from 3.67 to 44.4, far below the values found by us. The exceptionally strong action of aureomycin and terramycin with ion exchange resins is probably a consequence of their cyclic structure – the presence of four condensed six-membered rings. A comparison of the exchange constants of aureomycin ions with hydrogen and sodium ions (Table 2) shows that the selectivity of aureomycin ion sorption is far greater for hydrogen ions than for sodium ions. Fig. 4 shows graphs which indicate how Equation (1) is obeyed by the exchange of aureomycin and terramycin ions for hydrogen ions on the same specimens of phosphate resin RF (Fig. 4a) and sulfonic resin SNF (Fig. 4b). (Resins with relatively low coefficients of swelling, 1.9 and 2.5, were used.) Aureomycin ions are adsorbed much more selectively than terramycin ions by the resins.

Dynamics of the sorption and desorption of aureomycin and terramycin on cationites. In accordance with the theory advanced earlier [6], the adsorption of aureomycin and terramycin occurs with formation of a sharp front (Fig. 5), as ions of the same valency are exchanged, when the exchange constants are considerably greater than unity (the first ion is the displacing ion).

By means of these results it is possible to estimate in advance the possibility of displacement of aureomycin and terramycin by acids from sulfonic cationites and RF cationite. The exchange constants for this process are reciprocals of the values given in Table 2 (the displacing ion is regarded as the first ion [6]); their magnitude is of the order of $10^{-2} - 10^{-3}$.

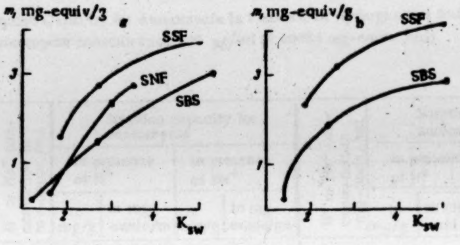

Fig. 2. Exchange capacity of sulfonic resins as a function of the coefficient of swelling: a) Resins SSF, SNF, and SBS (sorption of aureomycin); b) Resins SSF and SBS (sorption of terramycin).

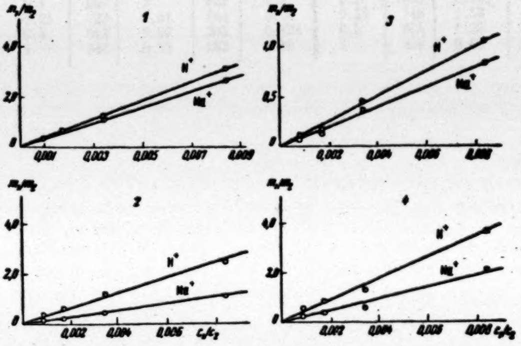

Fig. 3. Exchange of aureomycin ions for hydrogen and sodium ions on resins: 1) SNF; 2) SBS-3; 3) SM-12; 4) SSF.

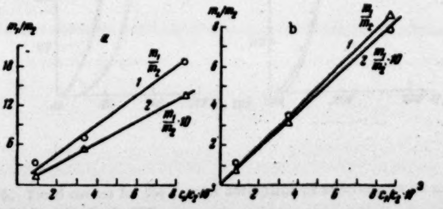

Fig. 4. Exchange of aureomycin and terramycin ions for hydrogen ions on RF phosphate resin (a) and SNF sulfonic resin (b): 1) aureomycin; 2) terra cin.

TABLE 1

Sorption Capacity for Aureomycin in Presence of Hydrogen and Sodium Ions
Aureomycin concentration 400 μg/ml (0.00084 mg-equiv./ml)

H^+ or Na^+ concentration in mg-equiv./ml	Sorption capacity for aureomycin				H^+ or Na^+ concentration in mg-equiv./ml	Sorption capacity for aureomycin			
	in presence of H^+		in presence of Na^+			in presence of H^+		in presence of Na^+	
	in mg/g	in mg-equiv/ml	in mg/g	in mg-equiv/ml		in mg/g	in mg-equiv/ml	in mg/g	in mg-equiv/ml
Sulfonic resin SNF with K_{sw} = 3.1					Sulfonic resin SM-12 with K_{sw} = 8.1				
0.1	1027	2.15	751	1.58	0.1	980	2.05	605	1.26
0.25	744	1.56	548	1.15	0 25	597	1.25	344	0.74
0.5	512	1.07	411	0.86	0.5	285	0.596	154	0.32
1	343	0.71	264	0.55	1	128	0.268	133	0.28
Sulfonic resin SBS with K_{sw} = 5.1					Sulfonic resin SSF with K_{sw} = 2.7				
0.1	967	2	622	1.3	0.1	1031	2.15	741	1.55
0.25	723	1.51	364	0.76	0.25	748	1.56	401	0.84
0.5	513	1.07	203	0.424	0.5	604	1.26	311	0.65
1	346	0.72	183	0.38	1	459	0.95	226	0.472

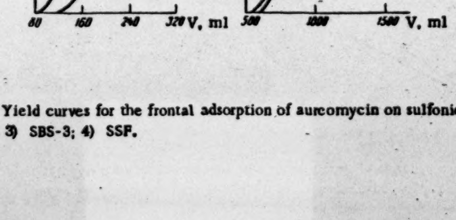

Fig. 5. Yield curves for the frontal adsorption of aureomycin on sulfonic resins: 1) SNF; 2) SSF; 3) SBS-3; 4) SSF.

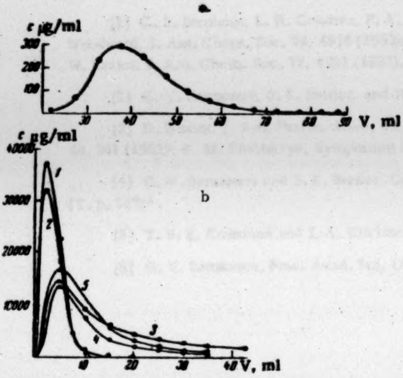

Fig. 6. Displacement of: a) Aureomycin by 1 N HCl solution from SSF resin; b) aureomycin by 1 N solution of HCl in methyl alcohol from ion exchange resins: 1) KFU; 2) RF; 3) SN; 4) SSF; 5) terramycin by 1 N solution of HCl in methyl alcohol from SSF resin.

TABLE 2

Exchange Constants for Aureomycin Ions and Hydrogen and Sodium Ions on Sulfonic Resins

Resin	Swelling coefficient	Aureomycin exchange constant	
		with hydrogen	with sodium
SSF	2.7	425	220
SNF	3.1	370	312
SBS-3	5.1	316	137
SM-12	8.1	130	100

Therefore, it is to be expected (and is actually found) that the front becomes more diffuse in the displacement of aureomycin and terramycin by hydrogen ions (acid solutions) and sodium ions. Solutions of very low concentrations are obtained, only 20-40% of the total substance being found in the peak of the zone with any appreciable concentration. This is followed by an aureomycin (or terramycin) zone with very low concentration, the "chromatographic tail" (Fig. 6, a).

Displacement of aureomycin (or terramycin) from sulfonic resins, RF resin, and carboxylic resins in total yield may be effected by hydrogen chloride solution in methyl alcohol (Fig. 6, b). The use of methyl alcohol instead of water as solvent gives better displacement of aureomycin and terramycin because in presence of methyl alcohol the large ions are held less strongly by the resin than small ions, such as hydrogen ions. A decrease of solvation has an especially strong intensifying effect on the action between the resin and smaller ions. It is possible that this effect is increased because of the lower degree of dissociation of aureomycin and terramycin in methyl alcohol in comparison with the degree of dissociation of acids.

SUMMARY

1. The exchange capacity of sulfonic resins with respect to aureomycin and terramycin increases with increased swelling of the resin, reaching 1.5-2 g/g of resin for the most strongly swelling resins, which corresponds to almost complete replacement of hydrogen or sodium ions.

2. The adsorption of aureomycin and terramycin by sulfonic resins proceeds reversibly.

3. The exchange between aureomycin ions and hydrogen and sodium ions obeys the usual equation of uni-univalent ion exchange, if only the hydrogen and sodium ions on the resin which are capable of substitution by aureomycin ions are taken into account.

4. The dynamics of adsorption and elution of aureomycin and terramycin is in agreement with the theory of the sharpening of the chromatographic front.

Institute of High Molecular Compounds
Academy of Sciences USSR, Leningrad

Received June 29, 1955

LITERATURE CITED

[1] C. R. Stephens, L. H. Conover, F. A. Hochstein, P. P. Regna, F. Y. Pilgrim, K. Brunings and R. B. Woodward, J. Am. Chem. Soc. 74, 4976 (1953); P. P. Regna, I. Solomons, K. Mura, A. Timreck, K. Brunings and W. Lazier, J. Am. Chem. Soc. 73, 4211 (1951).

[2] G. V. Samsonov, S. E. Bresler, and N. A. Rozentsveig, Colloid J. 18, No. 4, 470 (1956 (T. p. 461)*.

[3] D. Hiscox, J. Am. Pharm. Assoc. 40, 237 (1951); T. Monastero and J. Means, J. Am. Pharm. Assoc. 40, 241 (1951); E. M. Savitskaya, Symposium on Antibiotics (1953), 34, 29.

[4] G. V. Samsonov and S. E. Bresler, Colloid J. 18, No. 1, 88 (1956) (T. p. 83)*; 18, No. 3, 337 (1956) (T. p. 327)*.

[5] T. R. E. Kressman and J. A. Kitchner, J. Chem. Soc. 1949, 1208.

[6] G. V. Samsonov, Proc. Acad. Sci. USSR 97, 707 (1954).

---

* T. p. = C. B. Translation pagination.

A METHOD FOR MEASUREMENT OF THE DIELECTRIC CONSTANTS OF CONDUCTING LIQUIDS IN ULTRA HIGH FREQUENCY FIELDS

E. M. Fradkina

Measurements of the dielectric constant (DC) of conducting liquids and disperse systems in ultra high frequency fields involve a number of difficulties, which confine the possibility of determination to relatively low conductivities. In particular, the determination of DC of conducting liquids by Drude's second method is limited by the fact that with increasing conductivity the resonance curves become very flat, so that it is impossible to determine on them the position of the maximum necessary for calculation of the DC of the substance in question. In addition, after a certain value of the conductivity σ, "negative displacements" appear [1].

No strict theory of the method with consideration of negative displacements is available. Malbaum's paper [2] on this subject cannot be regarded as exhaustive, while his formulas are cumbersome and highly inconvenient for calculations. Moreover, the theory derived by him was not subjected to systematic experimental verification.

Measurements of the DC of substances with considerable conductivities are of very great interest in relation to electrical methods for determination of the moisture contents of various materials (mineral oils, petroleum and petroleum products, flour, starch, coal, peat, cotton, wood, etc.). The water present in these substances contains salts, and is thus essentially a solution of electrolytes, often at very considerable concentrations. Thus, electrolyte solutions form an important component of most natural disperse systems, including those of animal origin (blood, muscle and bone tissues, etc.) Measurements of the DC of concentrated electrolyte solutions are therefore required for the solution of purely practical problems associated with moisture measurements on a number of materials, studies of the action of ultra high frequencies on living tissues, high frequency heating, etc. In addition, such measurements are necessary for the development of a theory of concentrated electrolyte solutions, which is far from perfect at the present time.

The foregoing considerations led to the development of a method for the determination of DC of conducting liquids in ultra high frequency fields.

In the condensers commonly used, the electrodes are in direct contact with the liquid under investigation. In our design this direct contact is eliminated, so that negative displacements are prevented even with the use of strongly conducting liquids, such as electrolyte solutions at high concentrations, up to saturation.

The equivalent scheme of our condenser [3] is shown in Fig. 1, where C_2 is the working capacity of the condenser; C_1 and C_0 are ballast capacities, determined by the capacity of the condenser walls and the leads. Calculation gives the following formula for the total capacity C of the condenser:

$$C = C_0 + \frac{\varepsilon C_1 C_2}{C_1 + \varepsilon C_2}, \qquad (1)$$

where ϵ is the dielectric constant of the substance.

The capacity of the condenser is determined from the Coolidge formula

$$C = \frac{\lambda}{2}\,\frac{\sin \alpha d}{\sin \alpha a \,\sin \alpha (a+d)}, \qquad (2)$$

where $\alpha = 2\pi/\lambda$, in which λ is the wave length generated; $\underline{d}$ is the displacement; $\underline{a}$ is the distance from the end of the line to the condenser.

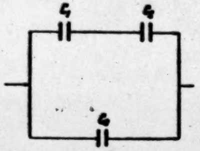

Fig. 1. Equivalent condenser scheme: C_1 and C_0 are ballast capacities; C_2 is the working capacity of the condenser.

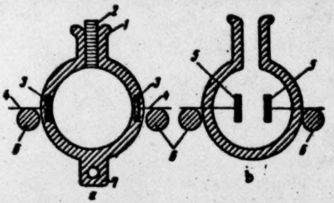

Fig. 2. Condenser types: a) proposed by the author; b) generally used.

To find the DC of a substance in the condenser by means of Formula (1) it is necessary to determine the condenser constants C_0, C_1, and C_2. This can be done with the use of standard liquids.

Our condenser is in the form of a spherical bulb (d = 9 mm) with a small neck 1, which can be closed by a ground glass stopper 2 (see Fig. 2,a). The electrodes are circular platinum plates 3, 3.5 mm in diameter, centrally welded to platinum leads 4, ~8 mm long and 0.5 mm in diameter. The electrodes are totally sealed into the glass walls of the bulb, which prevents their direct contact with the liquid and, if conducting liquids are used, prevents the circuit becoming closed through the condenser. In addition, this design, in contrast to that generally used (Fig. 2,b), in which only the leads are sealed into the walls, ensures that the electrode positions are quite invariable. This is especially important for work with viscous liquids (for example, petroleum emulsions with high moisture contents), which may cause a change in the relative positions of the electrodes when poured into the condensers of the usual type. The leads of the condenser rest on the conductors 6, so that its electrodes lie in the plane of the conductors of the measurement system, where the field is at its maximum value. The absence of special suspensions obviates the need for considering their effect [1] and eliminates an additional source of variability of the condenser parameters.

To give a good contact between the condenser leads and the circuit conductors, and to confer stability to it, a small load is suspended from a glass lug 7 fused to the underside of the condenser.

Calibration curves for the condenser are shown in Fig. 3. The abscissa axis shows the DC values for standard liquids, and the ordinate axis shows the displacements obtained for the same positions of the condenser in the circuit.

The course of the calibration curves depends on the position of the condenser in the circuit (a) and the wave length (λ). If the values of the condenser capacity C are taken along the ordinate axis, then, as Fig. 3 shows, a single calibration curve (C) is obtained, regardless of the position of the condenser and the wave length of the generator. The curve obeys Equation (1), in which the constants C_0, C_1, and C_2 are respectively 4.90, 44.10 and 1.11 cm.

TABLE 1

Characteristic Data for the Standard Liquids

Substance	Temperature, °C	ε	d, cm	C, cm
$\lambda = 166$ cm, $a = 8$ cm				
Air	18.0	1.0	0 172	5.97
Benzene	18.0	2.28	0.217	7.49
Chloroform	18.0	4.81	0.286	9.80
86% aqueous dioxane solution	20.5	8.76	0.376	12.75
Amyl alcohol	20.5	10.00	0.440	14.81
76% aqueous dioxane solution	25.0	13.0	0.468	15.70
Acetone	20.0	21.80	0.620	20.44
Methyl alcohol	18.0	33.70	0.773	25.07
50% aqueous ethyl alcohol solution	18.0	48.20	0.885	28.34
Water	28.1	77.0	1.058	33.26
Water	18.0	81.0	1.067	34.29
Formamide	18.0	119.8	1.273	39.13
$\lambda = 99$ cm, $a = 5$ cm				
Air	20.5	1.0	0.183	5.70
Benzene	20 5	2.28	0.232	7.16
Chloroform	25.8	4.81	0.327	9.93
Methyl alcohol	23.1	33.7	0.931	25.49
Nitrobenzene	20.6	35.8	0.943	25.76
66% aqueous ethyl alcohol solution	18.2	66.6	1.231	32.14
Water	24.0	78.6	1.312	33.80
Water	17.5	81.0	1.321	34.02
Formamide	19.0	108.0	1.492	37.45

Figure 3 shows that the experimental points fit well into a single calibration curve (C). The characteristic data for the liquids studied are shown in Table 1. The values of ε in Table 1 are based on our measurements by Drude's second method with the use of a condenser described previously [4].

TABLE 2

DC of NaCl Solutions, $\lambda = 166$ cm, $a = 8$ cm

NaCl concentration, N	Temperature, deg	d, cm	C, cm	ε
0	18.0	1.067	34.29	81.0
0.05	21.4	1.110	34.69	84.0
0.075	21.0	1.154	35.91	94.0
0.15	20.7	1.308	40.06	148
0.23	20.5	1.415	42.86	218
0.50	20 5	1.485	44.66	322
1.00	19.5	1 507	45.22	364
2.00	20.0	1.517	45.47	386
3.00	20.9	1.523	45.63	404
4.00	20.9	1.528	45.75	418

It must be pointed out that the position of a point on the calibration curve C (Fig. 3) does not depend on the conductivity of the substance. For example, the values for DC of benzene, amyl alcohol, and water, the conductivities of which differ sharply, lie on the same calibration curve. Formamide was used as a substance with a high DC, but with a conductivity not so high as to prevent the use of Drude's second method. Only 3 papers [4-6] deal with the DC of this interesting liquid. The specimen which we studied at a wave length $\lambda = 99$

cm, boiled at 114° under 18 mm Hg. Its dielectric constant was found to be 108, and for a second specimen, $\epsilon = 118$. Our values were in agreement with those reported by earlier workers.

The method described above was used for making the first systematic determinations of the DC of concentrated electrolyte solutions. The results are shown in Table 2. The values are in agreement with our earlier values [7] for DC of solutions up to 0.4 N, and with Maibaum's data [8], who found $\epsilon = 1000$ for saturated KCl solution.

Analysis of the experimental errors shows that the least error is obtained if the DC is determined from a calibration curve which shows d as a function of ϵ at constant a (Fig. 3). For a = 8 cm with $\lambda = 166$ cm for substances with DC up to 10, such as petroleum emulsions with a high moisture content, the relative error in DC determinations is ~1%. For substances with DC ~80 (water), the error is 2%. At DC > 300 (concentrated electrolyte solutions) the experimental error is greatly increased and reaches ~10%.

For improving the accuracy, the calibration curve should be plotted as exactly as possible, which requires the use of DC determinations for the largest possible number of standard liquids. An increase of the generator power is also important; in this way it is possible to increase a and therefore, according to Formula (2), the displacement d. This results in increased accuracy. The maximum accuracy is obtained if the condenser is placed in the vibration antinode of the electric vector, so that $a = \lambda/4$.

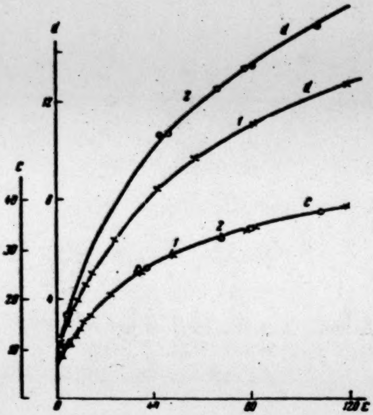

Fig. 3. Calibration curves for the condenser: 1) at $\lambda = 166$ cm; a = 8 cm; 2) at $\lambda = 99$ cm; a = 5 cm.

SUMMARY

1. A method is described for determination of dielectric constants of conducting liquids and disperse systems in ultra high frequency fields, in which negative displacements do not occur, and a measuring condenser is described.

2. The dielectric constants of concentrated NaCl solutions have been measured.

3. The experimental errors are analyzed and means of improving the accuracy are indicated.

Moscow

Received July 28, 1955

LITERATURE CITED

[1] E. M. Fradkina, J. Exptl. Theoret. Phys. 9,1379 (1939).

[2] B. Maibaum, J. Exptl. Theoret. Phys. 10,115 (1940).

[3] E. M. Fradkina, J. Exptl. Theoret. Phys. 20,1011 (1950).

[4] E. Vasenko, J. Phys. Chem. 21,361 (1947).

[5] G. Burdun and P. Kantor, Proc. Acad. Sci. USSR 67,985 (1949).

[6] R. Gordon and Leader, J. Chem. Soc. 73, 856 (1951).

[7] E. M. Fradkina, Dissertation (Moscow, 1941).

[8] B. Maibaum, J. Exptl. Theoret. Phys. 12, 231 (1942).

ADHESION OF HIGH POLYMERS

2. DEVELOPMENT OF A METHOD FOR DETERMINATION OF THE MUTUAL ADHESION OF HIGH POLYMERS

A. I. Shapovalova, S. S. Voyutsky, and A. P. Pisarenko

The present communication deals with a problem of great practical importance – determination of the adhesion of a high-molecular adhesive to a high-molecular substrate. A solution of this problem is important for the footwear, rubber, paper, wood processing, and cardboard box industries, and in a number of other branches of technology. Together with the development of a method for determination of adhesion, we attempted to determine more precisely the influence of certain factors on the mutual adhesion of high polymers.

As is known the adhesion of a high polymer to a substrate can be characterized by: 1) the adhesion pressure, which is the minimum force required to detach the adhesive simultaneously over its total area of contact with the substrate, or 2) the work expended in a gradual stripping of the adhesive from the substrate.

In the development of a method for determination of mutual adhesion of high polymers, the second method of evaluation was chosen, for the following reasons: 1) we are mainly concerned with the strength of adhesion of thin films of high polymer to a hard substrate; in this case the adhesion strength is better characterized by the work of adhesion [1, 2]; 2) in determinations of the work of adhesion exact centering of the detaching force is not needed, while this is necessary in determinations of adhesion pressure; 3) stripping tests give much more reproducible results than tearing tests [3].

The adhesive used was butadiene–acrylonitrile copolymer, containing 37.7% acrylonitrile. The adhesion of this copolymer to the substrates used was not too high, so that the peeling apart of the joints was always adhesive in nature.

The substrates used were models of plant and animal fibers – thin, mirror-smooth films of regenerated cellulose (Cellophane) and hardened and unhardened gelatin. It has been shown in a number of recent investigations that roughness of the substrate surface can have a great effect on adhesion [2, 4, 5].

Great importance was attached in this work to obtaining perfect contact between the adhesive and the substrate. A special technique was developed for producing a layer of adhesive from a solution of fairly low viscosity on the substrate surface for this purpose. The method used for determination of the work of adhesion did not differ in principle from the usual method of adhesion measurement by the pulling apart of a specially prepared joint with the aid of a recording dynamometer.

Preparation of joints. The joints with cellulose substrate were made as follows: standard Cellophane 30 μ thick was washed free of glycerin, stretched in the wet state on some smooth, horizontal surface, and then dried in air. A closely fitting cardboard frame was placed on the dried Cellophane film, and a definite quantity of 8% solution of butadiene – acrylonitrile copolymer in pure benzene was then poured into it. After the solvent had partially evaporated, a layer of very fine cotton percale fabric was placed on the surface of the forming film. This fabric, which adhered to the outer surface of the adhesive layer, served as a reinforcement or base which prevented deformation of the adhesive layer when it was being peeled off the substrate. When the solvent had completely evaporated, the frame was removed and the joint was cut into strips of the required width. Complete contact between the adhesive and substrate was ensured by this method.

McLaren [6], who also used Cellophane as substrate, used a somewhat different technique. To obtain the joints he coated technical Cellophane (not washed to remove glycerin) with adhesive solution, allowing the solvent to evaporate from the film surface, and then joined two layers of film under pressure at a temperature 30° above the softening point of the adhesive. This method has a number of serious faults, one of which is the presence of glycerin, which undoubtedly affects adhesion, in the Cellophane; the possibility of incomplete coalescence of the polymeric adhesive layers during the relatively short contact time; the effect of heat on the properties of the substrate and adhesive, etc.

The preparation of joints with a gelatin substrate was much more complicated. In this case solutions of both components had to be used. Prolonged experimental work showed that the following procedure was the most suitable for the preparation of such joints. A cardboard frame was placed on a mirror-smooth surface of a polyvinyl chloride film (PVC lacquer), and 2% aqueous solution of edible gelatin (All-Union Standard 98) was poured into the frame in sufficient quantity to form a film about 50μ thick. This thickness gave a gelatin film of adequate strength and high clasticity.

When the gelatin film was completely dry, 8% solution of butadiene—acrylonitrile copolymer in benzene was poured over it. After some time, when the benzene had partly evaporated, a layer of fabric (percale) was carefully placed on the forming layer of adhesive. After final drying and removal of the joint from the support it was cut into strips of the required width.

When hardened geltin films were used, a solution of basic chromium salts with a basicity of 41.5%, to give 1 g of Cr_2O_3 per 100 g of air-dry gelatin, was added to the gelatin solution before it was poured into the frame.

EXPERIMENTAL

The joints were peeled apart in a dynamometer, the jaws of which moved horizontally. Thus the stripping was effected at an angle of 180°. The dynamometer was equipped with reducing gear to make it possible to separate joints at different speeds. A diagram for the stripping force as a function of specimen length could be obtained by means of the recording device. A general view of the adhesiometer is shown in Fig. 1.

The specific work of adhesion Ad was calculated from the equation:

$$Ad = \frac{P2lg}{lb} = \frac{2Pg}{b},$$

where P is the average force of separation, found from data for a number of points 1 cm apart on the adhesion diagram; l is the length of the effective part of the joint; b is the width of the joint; g is the acceleration due to gravity.

Since the substrate film and the fabric-reinforced adhesive film were both thin and very flexible, and did not undergo irreversible deformations during the separation, no corrections were applied for the work of deformation of the films. The nature of the contacting surfaces of adhesive and substrate were always examined after separation.

It was assumed that the values obtained characterized adhesion only if both surfaces were mirror-smooth. When the substrate surface after separation was covered with a thin film of adhesive, while the adhesive surface was dull and uneven, it was assumed that the separation took place in the adhesive and that forces of cohesion had been overcome. In many cases mixed separation occurred – in some parts of the joint the separation was adhesive and in others, cohesive. All the values for adhesion given below are average results for 8-10 parallel determinations.

Effect of separation rate on the work of adhesion. It is reported in a number of publications [1, 2, 4, 7-9] that the nature of the separation and the work of adhesion depend on the speed with which the adhesive film is separated from the substrate.

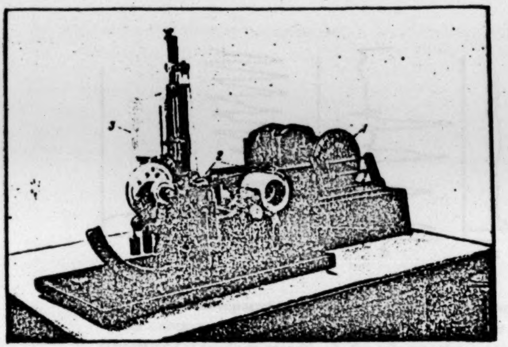

Fig. 1. General view of adhesiometer used for separation of the joints: 1) variable speed gear; 2) adhesiometer jaws; 3) recording device.

It was important to determine the influence of the separation rate on adhesion in the conditions of our experiments. Joints of chrome-tanned gelatin and butadiene–acrylonitrile copolymer were separated for this purpose at speeds from 0.083 to 0.3 cm/second. The gelatin film thickness in these experiments was 47μ (or 0.0058 g gelatin per 1 cm^2), and the thickness of the adhesive film was 218 μ (0.0215 g/cm^2). The width of the joint was 4 cm, and its effective length 10 cm. The results of the experiments are shown in Table 1.

TABLE 1

Effect of the Speed (v) on the Specific Resistance to Separation (P) and the Specific Work of Adhesion (Ad)

v in cm/sec	Type of separation, and P in g/cm			Ad in $ergs/cm^2$
	adhesive	mixed	cohesive	
0.083	—	381	451	—
0.166	74.3	237	—	145780
0.250	78.6	—	—	154210
0.300	76.3	—	—	149700

Table 1 shows that, in full agreement with literature data [1, 2], mixed and cohesive types of separation occur only at low speeds, of the order of 0.083-0.166 cm/second. At higher speeds the separation was purely adhesive in character. The reason is that during slow separation, when the deformation rate is less than the relaxation rate, the adhesive behaves as a liquid. In consequence the joint is broken when the cohesive forces of the adhesive are overcome. At high separation speeds, however, the adhesive behaves as a solid with a high modulus of elasticity and the separation occurs along the interface. No increase was found in the value of the work of adhesion with increasing separation rate in our experiments.

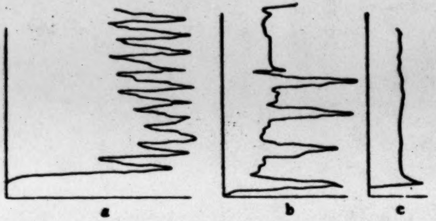

Fig. 2. Typical separation resistance – joint length curves: a) for cohesive separation (at low speeds); b) for mixed separation (at medium speeds); c) for adhesive separation (at high speeds).

An interesting feature is that in the case of purely cohesive separation at low speeds the separation curve is of zigzag form. This is seen in Fig. 2, which shows adhesion diagrams typical of cohesive, mixed, and purely adhesive separation (the ordinate axes show the distance from the start of the working part of the joint, and the abscissa axes give the corresponding separation force). Figure 2 also shows that in the adhesion diagram for the mixed type of separation the maximum values of the resistance to separation correspond to cohesive separation. These peaks alternate with regions of purely adhesive separation, parallel to the ordinate axis.

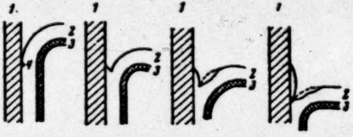

Fig. 3. Scheme for the transition from adhesive to cohesive types of separation, and back: 1) substrate; 2) adhesive; 3) reinforcing fabric; 4) fault on the surface of the adhesive layer.

The transition from adhesive separation to the cohesive form, less advantageous from the energy standpoint, is probably explained by weak spots on the adhesive surface and by the fact that after a tear is formed the stress is concentrated in its lower part. As a result, further separation proceeds not along the interface (where the resistance to separation is less) but along the adhesive layer. This separation will continue until for one reason or another the tear reaches the adhesive–substrate interface. This is clearly seen in the scheme in Fig. 3. It is still not clear why, with purely cohesive separation, there is a distinct periodicity in the fluctuations of the separation force. As the speed increases, the periodicity of the adhesive separation also begins to increase and at sufficiently high speeds a curve corresponding to purely adhesive separation is obtained. Since a speed of 0.3 cm/second always ensured adhesive separation in our conditions, all the subsequent experiments were performed at this speed.

Effect of the width of the joint on adhesion. As we found in one of our investigations that in determinations of autohesion the results may be influenced by the contact area [10], experiments were carried out to determine the effect of joint width on the specific work of adhesion.

The substrate in these experiments was a film of chrome-tanned gelatin ~50μ thick. The layer of adhesive, butadiene–acrylonitrile copolymer, was ~250 μ thick. The length of the working part of the joints was 10 cm in all cases, and the width was varied between 1 and 5 cm. The separation of the joints was carried out at the same speed of 0.3 cm/second. The results of the experiments are shown in Table 2.

The results in Table 2 show that the specific work of adhesion does not depend on the width of the specimen. In the subsequent experiments joints 2 cm wide were used in all tests; the length of the working part of the joint was always 10 cm.

TABLE 2

Effect of Joint Width on the Specific Resistance to Separation (P) and the Specific Work of Adhesion (Ad)

Width of specimen, cm	P in g/cm			Ad in ergs/cm^2
	minimum	maximum	average	
1	115.0	120.0	118.7	232 800
2	99.0	117.0	108.2	212 300
3	109.6	126.0	116.0	227 600
4	108.8	118.8	111.8	219 300
5	104.0	124.0	111.2	218 100

Effect of thickness of the adhesive layer on adhesion. It has been shown by McBain [11] and a number of others [12-18] that the adhesive strength always increases with decreasing thickness of the adhesive layer. Several theories have been advanced to explain this effect [13-15].

However, they all explain the increased adhesive strength with decreasing thickness of the adhesive layer in terms of the properties of the adhesive substance itself. In addition, most of these theories are only applicable when the joint is broken along the layer of adhesive. In this situation, in an investigation the aim of which was to develop a method for the evaluation of the adhesive power of high polymers, it was necessary to determine the influence of layer thickness on adhesion proper, determined by the peeling method.

Experiments for this purpose were carried out with joints in which chrome-tanned gelatin was used as substrate. The preparation and separation of the joints was carried out according to the standard procedure, except that the thickness of the layer of adhesive was varied between 152 and 557 μ, corresponding to 0.015 to 0.055 g of adhesive per 1 cm^2 of substrate. The results are shown in Table 3.

Table 3 shows that the specific work of adhesion is practically independent of the thickness of the adhesive layer. This is possibly explained by the fact that the layers of adhesive used in our experiments were not thin enough. There are indications in the literature that in certain cases the adhesive strength increases appreciably only with very thin layers of adhesive [16]. In our view, however, another explanation is more probable, namely that adhesion proper is independent of the thickness of the layer of high molecular adhesive.

All the subsequent experiments were carried out with an adhesive layer thickness of 253 μ, which corresponds to 0.025 g of adhesive per 1 cm^2 of substrate.

Effect of the pressure applied to the joint on the work of adhesion. When two unlike solid surfaces are brought into contact, the force of adhesion, as a rule, depends on the contact pressure. The usual explanation for this is that increase of pressure increases the area of true contact by changing the shape of the surface.

It was desired to determine the effect of pressure on the work of adhesion in our conditions, when the adhesive was applied to the substrate in solution form. Experiments were therefore carried out in which joints made by the usual method were subjected to various pressures for 40 minutes and immediately separated. Cellophane was used as the substrate.

The experiments showed that the work of adhesion is not changed by increase of pressure on the joint, but practically retains its initial value. Probably application of the adhesive to the substrate surface in solution form ensures complete contact between the surfaces of the two polymers, and further increase of contact area by the action of additional pressure cannot occur in this case.

TABLE 3

Effect of the Thickness of the Layer of Adhesive on the Resistance to Separation (P) and Specific Work of Adhesion (Ad)

Thickness of adhesive layer, µ	P in g/cm	Ad in ergs/cm^2
152	100	196 200
253	135.5	265 850
354	113	221 600
456	105	206 000
557	113	221 000

Effect of heat treatment of the joint on the work of adhesion. Voyutsky and Zamazy [17] showed that heat treatment of the joint has a very strong effect on autohesion of high polymers. We therefore studied the effect of heating the joint on the adhesion of a high molecular adhesive to a high molecular substrate.

Cellophane was used as the substrate in these experiments. The joints were prepared as described above, with the exception that the film of adhesive was formed by evaporation of the solvent in a cold room at a temperature close to zero.

The joints were heated for 40 minutes at 25, 50, 75, and 100° under a pressure of 100 g/cm^2, cooled, and held to constant weight in the cold in an atmosphere with 30% relative humidity before separation. Joints obtained at 0° and not heated were also tested. The results are shown in Table 4.

It is seen from Table 4 that heating of the joint sharply increases the work of adhesion. After heating to 75 and 100°, the adhesion increases so much that separation of the joint assumes a mixed character. In some regions of the joint the separation proceeds along the interface, and at others in the adhesive, leading to a sharp increase of the difference between the maximum and minimum values of the resistance to separation. This indicates that in such cases the magnitude of the adhesion is close to the cohesive strength of the adhesive.

TABLE 4

Effect of Heat Treatment of the Joint on the Specific Resistance to Separation (P) and Specific Work of Adhesion (Ad)

Heating temperature. °C	P in g/cm			Ad in ergs/cm	Type of separation
	minimum	maximum	average		
Without heating	115	121	117	229 550	Adhesive
25	119	134	126	247 210	Ditto
50	128	154	146	286 450	"
75	118	400	183	359 040	Mixed
100	160	455	250	490 500	Ditto

The increase of adhesion as the result of heating of the joint cannot be explained here by an increase of the true area of contact between adhesive and substrate, since when the adhesive is used in solution form this area is at its maximum and is close to the area of nominal contact. In our opinion the positive influence of heat on adhesion between two high polymers is due to the same causes as the influence of heat on autohesion. Thermal motion is increased as the result of increased temperature and molecules of the adhesive, or separate regions of them, diffuse into the substrate. It is possible that at sufficiently high temperatures partial diffusion of the substrate molecules into the adhesive may also occur. Both these processes lead to disappearance of a sharp boundary between adhesive and substrate, to formation of a firm weld between the two high polymers, and therefore to an increase in the strength of the adhesive joint.

Quite obviously, mutual diffusion of molecules from two layers of high polymers brought into contact can occur only if these polymers are mutually soluble. Therefore the increase of adhesion as the result of heat treatment of the joint can also be regarded as the result of increased mutual solubility of the polymers on heating (see [19]).

Another explanation of the increased adhesion as the result of heating the joint may be based on the fact that heating leads to a more rapid redistribution of intermolecular bonds and facilitates orientation of molecules of the adhesive, or separate regions of them, at the substrate surface. The molecules of the adhesive can be regarded as joined together at their polar groups. This, of course, will hinder their orientation at the substrate surface, which is necessary for the formation of a firm adhesive joint. As the result of increased thermal motion on heating, these bonds are broken and the polar regions are more easily orientated at the substrate surface, forming bonds with the polar groups at that surface. This will naturally result in increased adhesion.

However, this theory, advanced by McLaren and his associates [6, 18], hardly seems valid in the present instance, as the adhesive layer was formed from solution, in conditions when orientation of the molecules of adhesive at the substrate surface is not hindered in any way.

Effect of the time of contact between adhesive and substrate on the work of adhesion. In studies of the influence of various factors on adhesion it was noticed that the force of adhesion of a high molecular adhesive to a high molecular substrate varies with time. This fact is undoubtedly important, as it indicates, in the same way as the influence of temperature on the strength of the adhesive joint, a similarity between adhesion and autohesion.

Special experiments were carried out on the influence of the contact time on the work of adhesion, Cellophane and chrome-tanned gelatin being used as substrates. Before separation, the joints were kept for various times in an atmosphere at 30% relative humidity when the substrate was Cellophane, and at 60% relative humidity when the substrate was gelatin.

The results of these experiments are shown in Table 5.

TABLE 5

Effect of the Time of Contact Between Adhesive and Substrate on the Specific Resistance to Separation (P) and Specific Work of Adhesion (Ad)

Contact time, days	P in g/cm			Ad in ergs/cm	P in g/cm			Ad in ergs/cm
	minimum	maximum	average		minimum	maximum	average	
	Joints with Cellophane substrate				Joints with tanned gelatin substrate			
7	100	115	107	209 930	61	71	68	133 410
15	120	154	138	270 750	78	88	83	162 850
31	150	150	150	294 300	106	112	109	213 860
60	155	188	170	333 540	120	148.	125	245 250
90	178	189	185	362 970	165	193	180	353 160
120	163	190	173	339 420	177	238	217	425 750

Table 5 shows that the work of adhesion increases with increasing contact time. This, like the increase of adhesion as the result of heat treatment, may be explained by diffusion of the adhesive into the substrate and of the substrate into the adhesive. However, the work of adhesion does not reach the values attained when the joints are heated even after very long contact times. Moreover, the values of the adhesion tend to a definite limit with increasing contact time, while no such limit is found with the use of heat. This may be explained on the grounds that increase of temperature not only favors accelerated diffusion, but raises the mutual solubility of the polymers.

SUMMARY

1. A simple and fairly accurate method for determination of adhesion between two high polymers has been developed, based on separation of the joints by a peeling method.

2. It was found, in agreement with data available in the literature, that the manner of separation of the joints changes with variations of the speed of separation. At low speeds, separation of polymer – polymer joints is cohesive in character, at moderate speeds it is mixed, and at high speeds it is purely adhesive. No increase of the work of adhesion with increasing speed of separation was found.

3. It is shown that the width of the joint does not affect the results of the adhesion determinations.

4. It was found that in the limits studied (from 150 to 550μ) the thickness of the polymeric adhesive layer does not affect the value of the specific work of adhesion.

5. It is shown that if the layer of high molecular adhesive on the substrate is formed from solution, the pressure to which the joint is subjected after it is made does not affect the adhesion.

6. It was found that heat treatment of the joints considerably increases adhesion.

7. It is shown that adhesion increases and tends to a definite limit with increasing time of contact between a high molecular adhesive and a high molecular substrate.

8. It is suggested that the increase of adhesion by heat treatment and by increased contact time is caused by diffusion of molecules of the adhesive into the substrate and vice versa, which leads to disappearance of the interphase boundary and to formation of a stronger adhesive joint.

Central Scientific Research Institute
for the Leather Substitutes Industry, Moscow

Received May 14, 1955

LITERATURE CITED

[1] B. V. Deryagin and N. A. Krotova, Symposium on Adhesion (Acad. Sci. USSR Press, 1949).

[2] G. R. Hammond and R. C. Moakes, Trans. Inst. Rubber Ind., 25, 179 (1949).

[3] Solomon and Schonlan, Symposium on Adhesion (Foreign Literature Press, 1954), p. 442.

[4] E. M. Borroff and W. C. Wake, Trans. Inst. Rubber Ind., 25, 190, 199, 210 (1949).

[5] R. Thoman, H. Gilman, Trans. Inst. Rubber Ind., 25, 105 (1949).

[6] A. D. McLaren, J. Polymer Sci. 3, 652 (1948).

[7] R. S. Rivlin, Paint Technol. 9, 215 (1944).

[8] W. F. Busse, J. Lambert and R. B. Verdery, J. Appl. Phys. 17, 376 (1946).

[9] J. O. Hendriks, G. F. Lindner and F. J. Wehmer, Rubber Age (London) 32, 327 (1948).

[10] A. I. Shapovalova, N. A. Tsvetkova, and S. S. Voyutsky, Sci. Res. Reports of the Central Sci. Res. Inst. Leather Substitutes (State Light Industry Press, 1953), Vol. V, p. 58.

[11] J. W. McBain and W.B. Lee, J. Phys. Chem. 31, 1674 (1927).

[12] V. P. Konstantinova, Acta Physicochim. URSS 1, 286 (1934-1935).

[13] J. J. Bikerman, J. Soc. Chem. Ind. 60, 23 (1941).

[14] K. Mylonas and N. De Bruyne, Symposium on Adhesion (Foreign Literature Press, Moscow, 1954), p. 108; N. De Brugne, Symposium on Adhesion (Foreign Literature Press, Moscow, 1954), p. 528.

[15] O. Hoekstra and K. Fritzius, Symposium on Adhesion (Foreign Literature Press, Moscow, 1954), p. 43.

[16] I. W. Maxwell, Trans. Am. Soc. Mech. Engrs. 67, 104 (1941).

[17] S. S. Voyutsky and Z. M. Zamazy. Colloid J. 15,407 (1953) (T. p. 421)* .

[18] A. D. McLaren and C. H. Hofrichter, Paper Trade J. 125, 96 (1947); C. H. Hofrichter and A. D. McLaren, Ind. Eng. Chem. 40, 329 (1948).

[19] S. S. Voyutsky, A. I. Shapovalova, and A. P. Pisarenko, Proc. Acad. Sci. USSR 105,1000 (1955).

---

* T. p. = C. B. Translation pagination.

TO THE MEMORY OF A. F. TYULIN

(1885-1955)

Professor Aleksandr Fedorovich Tyulin, the eminent Soviet agricultural chemist and soil scientist, distinguished scientific worker, Doctor of Agricultural Sciences, died suddenly in Moscow, November 6, 1955.

A. F. Tyulin was born June 20, 1885, in a peasant family in the village of Mstera, Vladimir province; he started his working life at the age of 11, worked tenaciously to educate himself, and passed his matriculation examination when an adult. In 1907 A. F. Tyulin entered the Peterburg University, where he graduated with distinction in the Physico-Mathematical Faculty in 1912. After working for 2 years as an assistant in the Vologda Dairy Institute, A. F. Tyulin entered the Moscow Agricultural Institute (now the TSKhA), where he graduated in 1920.

After graduation at the Agricultural Institute, A. F. Tyurin was retained for postgraduate work in D. N. Pryanishnikov's laboratory until 1924; here he conducted his first valuable researches on liming and on the dynamics of humus and nutrients in soil; here, under the influence of the scientific ideas of D. N. Pryanishnikov and K. K. Gedroits, A. F. Tyulin formed his range of scientific interests, to which he devoted many years of creative labor.

In 1925 A. F. Tyulin was appointed professor at the University of Perm where he, jointly with D. A. Sabinin, organized the faculty of agriculture and soil science, and an experimental station.

In 1928 A. F. Tyulin was sent abroad to study the organization of higher agronomical education and agrochemical research in Germany, Holland, and Switzerland.

His activity became highly fruitful after he had been invited in 1932 to join the K. K. Gedroits All-Union Institute of Fertilizers, Soil Science, and Agricultural Engineering, where he organized and took charge of the Soil Colloids Laboratory. Here he developed a theory of the origins of soil structure and methods for its determination, and of the influence of sesquioxides and humus on the stability of aggregates and the absorption of the soil. A. F. Tyulin successfully led work on colloido-chemical studies of soils and on the creative development of the teachings of K. K. Gedroits in the USSR; he studied the organic colloids and organo-mineral gels of soils, introduced the concept of free and film-bound soil colloids, and proposed a new method of fractional peptization for qualitative and quantitative studies of soil colloids, which is used extensively here and abroad. A. F. Tyulin advanced the idea of the organic matter in the absorbing complex as a basis for practical soil classification, developed a theory of the critical zones of ion sorption in the soil, and carried out some very valuable research on the chemical improvement of turfy podzol soils from the colloido-chemical viewpoint. A. F. Tyulin commenced experiments, due to be continued for many years, on soil improvement at the Moscow Fruit Station and the experimental station in Sochi; in these experiments he demonstrated the variations in the absorbing complex of soils under various agricultural conditions and devised a method for chemical improvement of subtropical podzols, which proved highly effective in production after trials (by A. P. Dragovtsev).

His work during the war years on studies of the colloido-chemical composition and agricultural properties of chernozems of Western Siberia and of some regions of the European part of the Union laid the basis of differential application of mineral fertilizers and helped to eliminate the existing routine system of fertilizer application without consideration of the agricultural properties and colloidal composition of the soil. His theoretical and experimental researches are described in his book "Colloido-Chemical Study of Soils for Agricultural Purposes" (Trans. All-Union Inst. Fertilizers, Soil Science, and Agricultural Engineering, No. 27, 1946).

When the Soil Colloids Laboratory at the Institute was closed down, A. F. Tyulin was forced to transfer to the Forestry Institute of the Academy of Sciences USSR in 1950. Here, in a new field, he was able to apply his wide experience in fruitful investigations of material transfer between forest vegetation and the soil. Simultaneously with these studies, Tyulin advanced valuable scientific generalizations on the origin and dynamics of soil structure in forests, associating these with variations of the groupings of colloidal particles in the soil.

A. F. Tyulin was a man of great culture, with an expert knowledge of the latest achievements of agricultural chemistry, soil science, biology, physical and colloid chemistry, and related branches of science. He generously shared his wealth of experience and scientific and experimental knowledge with his pupils and colleagues.

As a scientist and as a man, A. F. Tyulin was distinguished by intellectual honesty, high principles, and rectitude; he never reconciled himself with false authorities, monopolists, and dogmatists in science. When Tyulin appeared, the audience was always enlivened; his sharp tongue and clear mind introduced a stimulating stream and helped to solve the most complex problems.

A. F. Tyulin's scientific heritage (he published about 100 papers) is a great contribution to agricultural chemistry, soil science, and the science of soil colloids; it will aid the advances of Soviet science, by rendering great assistance in the further progress of our socialist agriculture.

E. I. Shkonde

DISCUSSION

SOME IDEAS ON, AND METHODS OF INVESTIGATION OF MECHANICAL PROPERTIES OF STRUCTURIZED COLLOID SYSTEMS

A. A. Trapeznikov

[Reply to N. V. Mikhailov's paper, Colloid J., 17, 68, (1955)]

In 1952-1953 the Institute of Physical Chemistry conducted a discussion on the structural and mechanical properties of colloid systems, at which Trapeznikov in his paper put forward a number of views, some already published [1-5] which indicated the need for a revision of many established rheological ideas. Without dealing with all the controversial questions, which will be discussed in greater detail later, we will consider here a number of statements made by Mikhailov, who later attempted to refute our views [6].

The fundamental concept on which Mikhailov bases all his views and his criticism of our work is the assertion of the unusually important role of dynamometer rigidity in measuring the strength of colloid systems.

Having found that the instrument which he used, despite its great complexity, has the commonest defect – low rigidity of the dynamometer – Mikhailov made the a priori assumption that our work suffered from the same defect, assuming that only non-rigid dynamometers were always used in this work (in reality this is far from true) and that therefore all the conclusions drawn from it are erroneous.

It is interesting to note that Mikhailov criticized only our work, although, had he wished to clarify the essence of the problem, he should have examined the work of other authors (Rebinder [7], Vinogradov [8]), in which the rigidity of the dynamometer used for determinations of strengths of colloid systems was never stated, and all these investigations (to speak objectively) might also have been carried out with non-rigid dynamometers, and then, according to Mikhailov, all the results obtained by these authors on the strength of colloid systems would be erroneous and devoid of physical meaning.

In passing to Mikhailov's critical comments on our work, we will note the following.

The question of non-rigidity of the dynamometer, resulting in an inconstant deformation rate during the first stages of deformation in the method in which Ω = const (at the start of the $P(\tau)$ curve) was already considered by us a long time ago*, when a special compensation method was devised, by means of which a constant deformation rate could be maintained over the whole $P(\tau)$ curve. In this method, the inner cylinder (of the coaxial cylinder instrument), suspended from an elastic wire, is kept in the initial position with "zero" displacement from the start-up of the outer cylinder, while the stress which increases with time (for deformation at a constant rate, ϵ = const), is measured by torsion of the wire in the opposite direction by means of the torsion head. Subsequently, this method was used by myself jointly with Fedotova in a number of variations:

---

* For this reason we did not use the $P(\tau)$ curves (abnormally extended), obtained by the Ω = const method, for calculation of the relaxation time θ of the system, but this was done for the compensation method and the results obtained for θ were compared with the values of θ obtained by Shvedov's method [5].

with manual regulation, and with automatic compensation by a motor regulated by a photoelectric relay (unpublished). Recently the same method (with manual compensation) was used by us jointly with Shalopalkina [9] to obtain P (ϵ) curves of a new type.

In our earlier [3-5], and especially in more recent (unpublished) joint researches with Fedotova, a wide range of dynamometers of different rigidities was used in such a way that dynamometers representing 5-fold variations of rigidity overlapped the ends of the deformation rate ranges in which each of the dynamometers was used. The strength and maximum deformation results obtained by two such dynamometers were similar to each other.

Nevertheless, in our recent joint investigation with Shalopalkina on naphthenate gels of somewhat different composition, detailed P (ϵ) curves were obtained: 1) by Ω = const method (constant rotation rate of the inner cylinder), and 2) by $\dot{\epsilon}$ = const method (compensation method) with different wires,* so that it was possible to determine the role of the inconstant deformation rate, resulting from non-rigidity of the dynamometer. Before presentation of these results, we will consider Mikhailov's views on the influence of dynamometer rigidity.

Mikhailov's fundamental assertion is expressed in the form of curves for increase of stress and velocity gradient with time, shown in Fig. 1 (Fig. 4 of [6]). According to these curves, Mikhailov associates the increase of P from zero to P_s or to P_y only with an increase of $\dot{\epsilon}$ from zero to a constant steady value:" equilibrium stress P_s on the curves without maximum is established when the given angular velocity of rotation ω of the inner cylinder is reached [3]", and further, "the maximum, the yield point P_y, is reached in a time which corresponds to the establishment of the given velocity gradient" ([6], p. 70)**. This is incorrect. Despite the fact that the absolute value of P depends on $\dot{\epsilon}$ (and this was shown in our publications [3-5]), increase of P from zero to P_s or from zero to P_y does not esentially bear any relation to the establishment of a constant value of $\dot{\epsilon}$, and therefore it is not correct to associate the instant when P_y is reached only with the establishment of constant $\dot{\epsilon}$. This primarily follows from Equation (1), which was discussed by us previously [5, 10], and which takes into account the stress relaxation of a Maxwell body in conditions of a constant value of $\dot{\epsilon}$, fixed from the start:

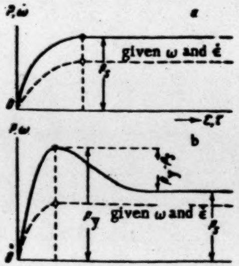

Fig. 1. Relationship of P (τ) and ω (τ) curves (according to N. V. Mikhailov [6], Fig. 4).

$$P = P_s(1 - e^{-\tau/\theta}) = P_s(1 - e^{-\epsilon/\dot{\epsilon}\theta}). \tag{1}$$

It follows from this equation that the exponential nature of the development of P (ϵ) and P (τ), and also the position of P_y, which for an ideal Maxwell body coincides with P_c (when $\dot{\epsilon} > \dot{\epsilon}_c$), have no connection with the establishment of constant. $\dot{\epsilon}$.

Further, if we take into consideration the inconstancy of $\dot{\epsilon}$ during deformation in the Ω = const method, which results from the non-rigid nature of the dynamometer, then for a P (τ) curve with a maximum (Curve 1, Fig. 2) the actual course of $\dot{\epsilon}$ (τ) will be approximately represented by Curve 2 (Fig. 2), and thus will be much more complex than that shown in Fig. 1.

---

* In these measurements the radius of the external cylinder R_2 = 1.5 cm, and the radius of the inner riffled cylinder R_1 = 1.42 cm. In [9], R_2 should be corrected to 1.42 cm.

** C. B. Translation page 63.

The explanation is at the start the inner cylinder moves practically together with the outer cylinder, and $\dot{\epsilon}$ (the velocity difference between the two cylinders) is very small. With increasing torsion of the wire the motion of the inner cylinder is retarded and the velocity gradient increases. When the yield value is approached, the inner cylinder stops and the gradient tends to a constant (predetermined) value. However, beyond the strength limit the inner cylinder moves back, and the gradient therefore increases rapidly, and then, as the inner cylinder moves more slowly, the gradient decreases again and finally, as P approaches P_s, it becomes constant.

For Curve 3 without a maximum (at low values of Ω) the relationship $\dot{\epsilon}(\tau)$ is represented by Curve 4 (Fig. 2).

These general considerations of the course of Curve 2 of Fig. 2, and also the comparison of the form of the $\dot{\epsilon}(\epsilon)$ and $P(\epsilon)$ curves for the methods $\dot{\epsilon}$ = const and Ω = const with a non-rigid dynamometer, were verified with the use of experimental data obtained by Shalopalkina.

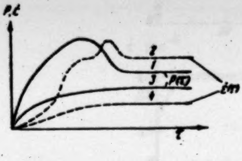

Fig. 2. Relationship between $P(\tau)$ and $\dot{\epsilon}(\tau)$ curves with and without maximum.

Figure 3 shows a $\varphi(\theta)$ curve, for a rotation speed of the outer cylinder $\Omega = 0.0138$ radian/second and $\dot{\epsilon} = 0.257$ cm^{-1} *, obtained with a wire having $C_\varphi = 101,300$ dynes. cm/radian. The values of φ represent the torsion angle of the inner cylinder in degrees, and the values of θ, the angle of rotation of the outer cylinder in degrees. This is the primary curve obtained experimentally by the Ω = const method. To determine the significance of dynamometer rigidity in this method for measurement of the strength of the system, and to find the true $\dot{\epsilon}(\epsilon)$ relationship, on the basis of Curve 1, the differential $\dot{\epsilon}(\epsilon)$ curve was plotted, where $\dot{\epsilon} = 1/k' (\Omega - \Delta\varphi/\Delta\tau)$. (Curve 2 in Fig. 3). The same Fig. 3 shows, for comparison, Curve 3 for $\dot{\epsilon}(\epsilon)$, for the compensation method, which shows a constant value of $\dot{\epsilon}$ along its entire length. It is seen that in the Ω = const method, owing to insufficient rigidity of the wire, as was to be expected, $\dot{\epsilon}$ is not constant over the entire length of the curve; it varies greatly during the first stages of deformation up to $\epsilon \sim 700\%$, then remains almost constant up to $\epsilon = 6700$–7000%, and only slightly lower than the predetermined value, then it begins to exceed the predetermined value of $\dot{\epsilon}$ by ~5%, and finally falls to the predetermined value, coinciding with the same value $\dot{\epsilon}$ = const in the compensation method.

Figure 3 shows the general $P(\epsilon)$ curve for three measurements: for the method Ω = const (plotted from the lower $\varphi(\theta)$ curve with $\dot{\epsilon}$ calculated as $\dot{\epsilon} = k'(\Omega\tau - \varphi)$ and for the method $\dot{\epsilon}$ = const (compensation method) with the use of two wires, with $C_\varphi = 101300$ and $C_\varphi = 16400$ dynes. cm/radian. These curves show that not only the height of the maximum P_y, but the whole course of the $P(\epsilon)$ curve coincides for the methods Ω = const and $\dot{\epsilon}$ = const, and consequently the deviation of the deformation rate $\dot{\epsilon}$ from a constant value which is observed in this case with the Ω = const method, and which reaches ~35%, in the initial "most dangerous" region, does not produce any substantial distortion of the form of the curve or the value of P. We must point out that Mikhailov "takes into account" deviations of $\dot{\epsilon}$ down to 1% and less in his "strict" demands for a constant value of $\dot{\epsilon}$.

We see further that the course of the $\dot{\epsilon}(\epsilon)$ curve in the Ω = const method corresponds to Curve 2 in Fig. 2; namely, up to the maximum P_y, $\dot{\epsilon}$ lags behind the predetermined $\dot{\epsilon}_{st}$ and exceeds it after passing the maximum P_y.

Figure 4 shows the analogous curves for the same oleogel, but deformed at 6 times the value of $\dot{\epsilon} = 1.71$ second^{-1} compared with the previous, and with the use of the same wire with $C_\varphi = 101,300$ dynes. cm/radian. This means that because of the increased $\dot{\epsilon}$, the value of P and with it of φ, also increases, which is equivalent to a considerable decrease of the dynamometer rigidity. In fact, Curve 1 of Fig. 4 already shows that φ_y, instead of ~12°, reaches ~40°, which should lead to a greater deviation of $\dot{\epsilon}$ from the predetermined value. A comparison of the two $\dot{\epsilon}(\epsilon)$ curves (Curves 2 and 3) in Fig. 4 shows that in the method Ω = const $\dot{\epsilon}$ already deviates by 41% from the predetermined value and remains lower by ~18% for a long time before the maximum P_y, while after the maximum P_y $\dot{\epsilon}$ exceeds the predetermined value of $\dot{\epsilon}$ to the same extent. In this instance the total change of $\dot{\epsilon}(\epsilon)$, as before, corresponds to the diagrammatic Curve 2, Fig. 2.

---

* The velocity gradient given in [9] as $\dot{\epsilon} = 0.264$ second^{-1} should be corrected to $\dot{\epsilon} = 0.257$ second^{-1}.

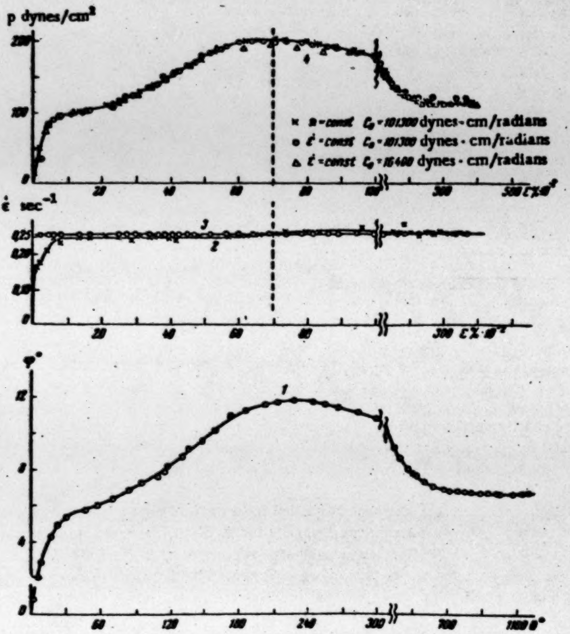

Fig. 3. Curve 1) $\varphi(\theta)$ for the method Ω = const (corresponding to $\dot\epsilon$ = 0.257 second^{-1}); Curves 2 and 3) $\dot\epsilon(\epsilon)$ for the methods Ω = const (2) (calculated from Curve 1, $\varphi(\theta)$ and $\dot\epsilon$ = const (3); Curve 4) P ($\dot\epsilon$) for the methods Ω = const (based on Curve 1, $\varphi(\theta)$ and $\dot\epsilon$ = const (compensation method) for 2% aluminum napthenate gel (experimental works batch No. 24) in vaseline oil.

At the same time, a comparison of Curves 4 and 5 in Fig. 4, which refer to the $\dot\epsilon$ = const and Ω = const methods, shows that these curves differ, but relatively little. The observed differences in the values of P may be attributed to the rather lower value of $\dot\epsilon$ in the method of Ω = const required to reach $P = P_y$, than in the method of ϵ = const.

Comparison of the P (ϵ) curves obtained by the two methods, ϵ = const and Ω = const, provides complete experimental confirmation of the general views presented above, according to which the course of the P(ϵ) curve should not by its nature coincide with the course of the $\dot\epsilon(\epsilon)$ curve, and the instant when $P = P_y$ is reached is not directly related to the instant when $\dot\epsilon$ = const is reached. In fact, the position of the P_y maximum on the ϵ axis is almost the same for the $\dot\epsilon$ = const and Ω = const methods, regardless of the fact that in the compensation method $\dot\epsilon$ is established constant practically right from the start of the motion of the cylinder, while in the method Ω = const $\dot\epsilon$ is finally established only when $P = P_s$ is reached (in some cases $\dot\epsilon$ may become practically constant long before $P = P_y$) (Fig. 3).

Thus, the position of P_y is not essentially related to the moment when $\dot\epsilon$ = const is established, and so to the rigidity of the dynamometer; it is determined (mainly) by the attainment of a certain critical shearing deformation ϵ_y.

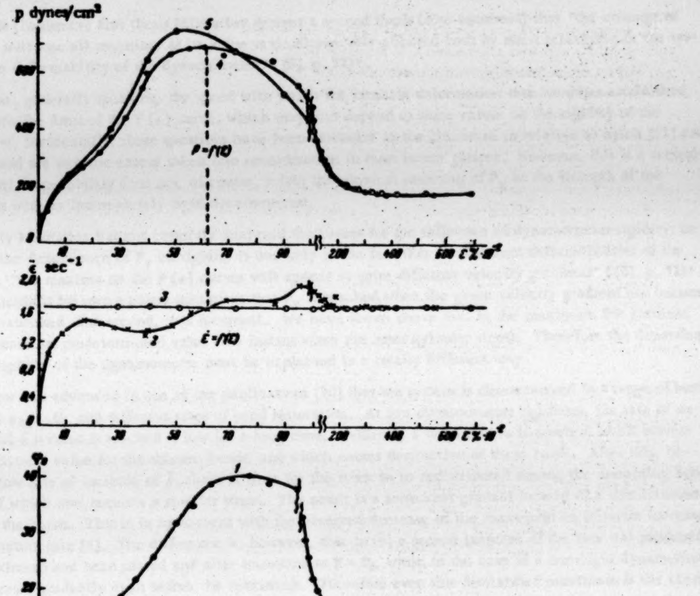

Fig. 4. Curve 1) $\varphi(\theta)$ for the Ω = const method (corresponds to $\dot{\varepsilon} = 1.71$ second^{-1}); Curves 2 and 3) $\dot{\varepsilon}(\varepsilon)$ (C_θ = 101,300 dynes. cm/radian) for the methods Ω = const (2) [calculated from Curve 1, $\varphi(\theta)$] and ε = const (3); Curves 4 and 5) $P(\varepsilon)$ for the methods Ω = const (4) [plotted from Curve 1, $\varphi(\theta)$] and $\dot{\varepsilon}$ = const (5) (compensation method) for 2% aluminum naphthenate gel (experimental works batch No. 24) in vaseline oil.

It is clear from all the above that even if Mikhailov did attempt to demonstrate the nature of the inconstancy of $\dot{\varepsilon}$ in the usual Ω = const method, he did so incorrectly. Moreover, our data demonstrate fully the incorrectness of Mikhailov's views concerning the enormous role of dynamometer rigidity in all cases, and the direct dependence of the position and magnitude of the maximum of P_y only on the instant when $\dot{\varepsilon}$ = const is reached.

We will incidentally point out that the $P(\tau)$ curves for dynamometers of different rigidities, shown in Mikhailov's Fig. 7 [6] seem to be purely schematic and not experimental; in particular, no values for dynamometer rigidities, stress, or deformation are given; and therefore even for the bitumen systems discussed by Mikhailov there is no certainty that the value of P_y depends so greatly on the rigidity of the dynamometer.

From this (incorrect) first thesis Mikhailov derives a second thesis (also incorrect) that "the concept of yield point P_y will lose all meaning, as its value is simultaneously affected both by stress relaxation in the system and by the deformability of the dynamometer" ([6], p. 71)*.

Of course, generally speaking, the speed with which the constant deformation rate becomes established should influence the form of the $P(\epsilon)$ curve, which may this depend to some extent on the rigidity of the dynamometer**. Incidentally, these questions have been discussed in the literature in relation to nylon [11] and also to steel, and are to some extent taken into consideration in most investigations. However, this is a second-order effect and its possibility does not, of course, refute the physical meaning of P_y as the strength of the structure, even with an incompletely rigid dynamometer.

In reality Mikhailov has not correctly analyzed the causes for the influence of dynamometer rigidity; he believes that the dependence of P_y on rigidity is due only to the fact that for different deformabilities of the dynamometer "the maxima on the $P(\epsilon)$ curves will appear at quite different velocity gradients" ([6], p. 71)*. First, this contradicts his own earliest statement that P_y is reached when the given velocity gradient has become practically established, and second, it is incorrect. We have shown above that at the maximum the gradient must always reach its predetermined value (the instant when the inner cylinder stops). Therefore the dependence of P_y on the rigidity of the dynamometer must be explained in a totally different way.

The view was advanced in one of our publications [10] that the system is characterized by a range of bonds with different ϵ_{ci}, θ_i and different rates of bond restoration. At low dynamometer rigidities, the rate of deformation until $\dot{\epsilon}$ = const is reached is low for a long time. Evidently a deformation is reached which corresponds to the critical value for the shortest bonds, and which causes destruction of these bonds. After this, because of the low rate of increase of $\dot{\epsilon}$, there is time for the stress to be redistributed among the remaining bonds, the rupture of which now requires a smaller stress. The result is a somewhat gradual instead of a simultaneous disruption of the bonds. This is in agreement with the observed decrease of the maximum on stepwise increase of the deformation rate [4]. The difference is, however, that in [4] a second increase of the rate was produced after the maximum had been passed and after transition to $P = P_s$, while in the case of a non-rigid dynamometer the rate increases gradually even before the maximum. Therefore even this diminished maximum is the strength limit of the structure; its difference from the maximum value, corresponding to a completely constant value of $\dot{\epsilon}$, is only that it relates to deformation at inconstant $\dot{\epsilon}$. Therefore, to obtain a more definite value of P_y it is necessary to select the conditions such that $\dot{\epsilon}$ = const as strictly as possible, which should be the case by virtue of the very meaning of the method.

In practice this may be achieved either by the compensation method [at not very high values of $\dot{\epsilon}$, and the advantage of this method is the fact that in principle it may be used with dynamometers of any degree of rigidity, even fairly low, which ensures a greater accuracy in plotting the whole $P(\dot{\epsilon})$ curve, if of course the dynamometer (wire) itself is perfectly elastic in operation and if the operator has time to twist the wire through large angles] or by the use of a rigid dynamometer (in the Ω = const method). In the latter case, however, the accuracy of measurement of small values of ΔP may prove insufficient, and it is then natural to use a less rigid dynamometer. It must be pointed out that even with the use of a completely rigid dynamometer (in the Ω = = const method) the deformation rate, according to Curve 2 in Fig. 2, will not be quite constant.

---

* C. B. Translation p. 63.

** The influence of inconstancy of the rate of deformation $\dot{\epsilon}$ on the form of the $P(\dot{\epsilon})$ curve and on the value of P_y may vary for different systems; it is related to a complex aggregate of properties of the system, determined by the range of bonds with ϵ_{ci} and θ_i, and the rate of restoration of different structural elements. This influence is probably seen more clearly in systems which have low critical deformations, and this is because inconstancy of $\dot{\epsilon}$ (in the Ω = const method) which is especially great in the early stage of deformation, in the range of small deformations, corresponds to the "shortest" bonds, which largely determine the strength of the structure in such systems.

In addition it must be stated that rigid dynamometers should be used for far from all measurements of mechanical properties. In a number of cases a weaker dynamometer proves to be more accurate. This applies, for instance, to investigations of deformation by the P = const method, when increase of deformation with time results in contraction of the dynamometer spring and a decrease of P. Thus, selection of the dynamometer should be guided by the type and conditions of deformation. In particular, our multiple instrument provides for a very wide range of dynamometers for various measurement methods and ranges of shearing stresses and deformation rates.

Finally, the fact that the value of P_y in the Ω = const method may depend on the rigidity of the dynamometer C_s, does not mean that maxima of P_y should also occur when $P < P_c$. The dependence of P_y on C_s shows only that with the use of more rigid dynamometers the values of P_y in the region $P > P_c$ would be greater, so that the strength would be expressed in a more pronounced manner.

In addition, N. V. Mikhailov puts forward another extreme view (which in essence completely contradicts his own previous assertions). He states that "the absence of a maximum on the $P(\epsilon)$ curves is a consequence of the deformability of the dynamometer" and further, that "if the dynamometer is absolutely rigid, then at all shear velocity gradients, no matter how small, maxima will always arise which characterize the yield point of the structure".

First, this assertion concerning any small velocity gradients is without any foundation and remains to be specially proved. It was natural to expect that Mikhailov would have carried out all his own experiments with an absolutely rigid dynamometer, and that he would prove experimentally that strength maxima exist at any values of $\dot{\epsilon}$, no matter how small, in the region of constant viscosity with a completely restored structure, at stresses below the lower flow limit (at $P < P_c$ in our notation, which is quite illogically and in a deliberately muddled manner denoted by Mikhailov by P_y, which was used to denote the upper flow limit in a number of our publications). Neither was done, however, and it seems likely that Mikhailov would hardly have been successful in producing such a proof (this probably explains the absence of such an attempt).

It is clear that at low values of $\dot{\epsilon} < \dot{\epsilon}_c$ (see [1-5, 10]) every system, owing to relaxation according to Equation (1), will be represented only by a steady curve without a maximum. On the other hand, in an attempt to refute our views, Mikhailov again takes the opposite extreme view in proving that in our studies, and also in his own ([6], Fig. 1) no maximum was found, and could not be found not only when $P < P_c$ but even when $P > P_c$, while our maxima close to P_c (at $P > P_c$) are attributed by Mikhailov to experimental error.

Of course, experimental errors may cause variations in the values of P and may sometime lead to false maxima; this, naturally, was borne in mind. However, despite this, in our experiments under similar measurement conditions the $P(\tau)$ curves showed maxima at $P > P_c$, while no maxima were found at $P < P_c$ [3]. Even if it is considered, as Mikhailov suggests, that the maximum value of P_y in our experiments [3] is clearly seen only at P_s 3 times as great as P_c, and not 1.5 times, as was actually the case, there is still no basis for the assertion that no maximum at all should exist when $P_c < P_s < 3P_c$. It is clear that if, when $P_s = 3P_c$, the maximum is so large that it is obviously greater than the experimental error, it can also be found when $P_c < P_s < 3P_c$, but smaller in magnitude. Therefore Mikhailov's assertations are illogical.

On the other hand, if the rate of deformation of the system is less than the rate of relaxation and restoration of the most slowly restored bonds, the system should flow with constant viscosity, corresponding to a completely undisrupted structure (a structure fully restored in flow). In this case the $P(\epsilon)$ curve cannot have a maximum when $\dot{\epsilon} < \dot{\epsilon}_c$ and $P < P_c$. It must be noted that $\dot{\epsilon}_c$ can be attained in reality only in fluid-plastic systems [10]. Most colloid systems, fluid at sufficiently high $\dot{\epsilon}$, are in reality solid-plastic. For all such systems $\dot{\epsilon}_c$ is very small and therefore for many of them maxima on the $P(\dot{\epsilon})$ curves will be found even in the region of very small values of $\dot{\epsilon}$, although greater than $\dot{\epsilon}_c$. This behavior is foreseen in our comparative scheme for the behavior of fluid-plastic and solid-plastic systems [4, 5].

The question of a maximum P_y when $P > P_c$ is much more complex. First, in many systems P_y may be small in its absolute magnitude relative to P_s even at high values of $\dot{\epsilon}$, and the possibility of its detection is then determined by the sensitivity of the instrument. Such systems include systems with highly viscous dispersion media, or systems thickened by molecularly dispersed components (for example, sugar syrups or high-molecular oils) which, in addition, contain very small amounts of structure-forming components which form a very weak network. It is evident that in such cases the disruption of a very small number of bonds, producing P_y, on the background of a high P_s for the viscous component, may give a negligibly small $\Delta P = P_y - P_s$. Therefore in such cases breakdown of the structure is revealed much more sensitively by anomalous viscosity, which appears at different values of $\dot{\epsilon}$ and which therefore proves that P_c has not yet been reached. However, this in no way controverts our view that it is theoretically possible for P_y to appear in such cases, and does not refute the concept of P_c.

Second, the existence of P_y depends on the form of distribution function of the bonds with respect to ϵ_{ci} and θ_i. If the given function lies in a narrow range of ϵ_{ci} and θ_i, then as soon as the given $\dot{\epsilon} > \dot{\epsilon}_c$ is reached, a large number of bonds will be broken at once and a sharp maximum will be seen on the $P(\epsilon)$ curve. If the function is diffuse, then, as some value of ϵ on the $P(\epsilon)$ curve is reached, only a small number of bonds will be broken, after which the stress P will be distributed over the remaining bonds, with greater ϵ_{ci} and smaller θ_i, and consequently there will not be a maximum. The maximum will appear when longer bonds will start to be broken with increase of $\dot{\epsilon}$.

Our recent joint investigations with Shalopalkina show that even among gels of the aluminum naphthenate type there are systems in the deformation of which P_y appears on the $P(\epsilon)$ curve at values of P far above P_c (which is extremely small and difficult to attain).

An examination of data on various aluminum naphthenate gels, obtained in our laboratory, shows that P_y may appear in explicit form both at P_s 3 times (or less) as large as P_c, and at P_s 30 or more times as large as P_c. It follows that it is quite possible that systems may be found for which P_y will be found at values of P very slightly above P_c. This is in principle generally true for bonds which are destroyed immediately above P_c, and this destruction would be seen in the appearance of P_y if this effect was not obscured by other factors.

Let us now consider the question of the nature of the $P(\tau)$ curve. We held that the maximum P_y reflects the strength of the structure and represents its fundamental instant of destruction, but we never stated that below P_y (on the ascending branch) breakdown of the structure is impossible or that only the descending branch of the $P(\tau)$ curve represents structural breakdown. Therefore what has been ascribed to us by Mikhailov in this respect is incorrect.

On the contrary, we especially pointed out in a number of papers [1, 2, 12] that when $P > P_c$ plastic flow comes into play on the $P(\epsilon)$ curve with a viscosity η_2, which, as was clearly shown later, reflects structural breakdown processes. In addition, and in accordance with our fundamental thesis that structural breakdown begins when $P > P_c$, we always asserted that even in ordinary investigations of the deformation properties of solids it is necessary to consider that while destruction of the specimen as a whole occurs at P_y, the start of structural breakdown, including the formation of microcrevices, should be attributed to much lower values of P, theoretically at $P \geq P_c$ (which is on the ascending branch of the $P(\epsilon)$ curve).

As regards the descending branch of the $P(\epsilon)$ curve beyond the maximum P_y, here, in addition to other processes, continuing structural breakdown may be presumed. There is nothing impossible in this. It is natural that in the deformation of any body, the destruction which occurs mainly when the so-called temporary resistance is reached will also continue under a subsequently decreasing load owing to excess stress on the remaining part of the body. In particular, tearing tests on rubber strips [13] showed that beyond the maximum P there was a more or less gradual (or stepwise) decrease of P owing to incomplete rupture of the film at the maximum value.

Moreover, we have recently shown in direct experiments that structural breakdown occurs both on the ascending and the descending branch of the $P(\epsilon)$ curve for aluminum naphthenate gel. Therefore Mikhailov's assertion, that structural breakdown along the descending branch of the $P(\epsilon)$ curve is impossible, is unfounded.

At the same time Mikhailov misunderstands completely the nature of relaxation processes. He states ([6], p. 75)* that "with a rigid dynamometer the value of the deformation which corresponds to the maximum stress on the $P(\epsilon)$ curve will correspond to the elastic or fully reversible". On the other hand, in the following paragraph it is stated that: "the descending branch of the $P(\epsilon)$ curve is the consequence of a purely relaxational process which is not completed before the given velocity gradient becomes established". First, Mikhailov is absolutely wrong in associating the relaxation process only with the establishment of the given value of $\dot{\epsilon}$, without making any analysis of the relaxation process itself. Second, it follows from the second paragraph that Mikhailov appears to take into account relaxation before P_y, and then it is not possible to claim that maximum P_y will correspond to fully reversible deformation (even for high rigidity of the dynamometer). It was pointed out in our papers that at values of $\dot{\epsilon}$ a little in excess of $\dot{\epsilon}_c$, despite the appearance of P_y, there is time for relaxation to occur, and therefore deformation before P_y is not necessarily fully reversible. On the other hand, the deformation will be practically fully reversible at high $\dot{\epsilon} >> \dot{\epsilon}_c$, when relaxation becomes almost impossible. Thus, the extent of reversibility of the deformation is determined not by rigidity of the dynamometer, but by the ratio between the deformation rate and the relaxation rate of the system.

---

* C. B. Translation page 67.

Further, no purely relaxation process can produce a maximum on the P (ϵ) curve, and therefore it cannot be said that the relaxation is "completed" on the descending branch. In accordance with Equation (1), because of relaxation in the condition $\dot{\epsilon}$ = const, P can increase only to a certain value of $P = P_s$ (of course, for real bodies the nature of the P (τ) curve cannot be strictly exponential). Therefore the maximum on the P (τ) at $\dot{\epsilon}$ = const points to structural breakdown. The descending branch of the P (ϵ) curve from P_y to P_s represents a number of processes: continuing structural breakdown, contraction or relaxation of destroyed structural elements (this relaxation cannot be combined with relaxation of the undestroyed elements when $P < P_y$), and also of structural elements which remain undestroyed.

Further, in accordance with our concepts of the range of bonds with different ϵ_{ci} and θ_i structural breakdown along the ascending branch (when $P > P_c$) occurs for bonds with low $\epsilon_{ci} < \epsilon_y$. We have now proved this by certain additional experiments.

The views put forward by Mikhailov (and some other authors) that "the descending branch of the P (ϵ) curve with a maximum is the consequence of a purely relaxational process ([6], p. 75)* are incorrect, and are probably the result of a confusion with the fact that Maxwellian relaxation in deformation when $\dot{\epsilon}$ = const can produce a descending P (τ) curve, but only in the condition $P = P_0$ when $\tau = \tau_0$, and not P = 0 when $\tau = 0$, as is the case in our experiments. For the case $P = P_0$ when $\tau = 0$ the equation for the descending curve, according to Maxwell [14] is

$$P = E\theta\dot{\epsilon} + Ce^{-\tau/\theta} = E\theta\dot{\epsilon} + (P_0 - P_s)e^{-\tau/\theta}. \tag{2}$$

In experiments carried out similarly to ours in the condition P = 0 when $\tau = 0$, the cause of the appearance of a descending branch of the P (ϵ) curve can only be the destruction of some structural elements. In this lies one of the favorable aspects of our method and of the views put forward.

Because of the incorrect ideas on the role of the rigidity of the dynamometer, on which Mikhailov bases all his consideration of the structural and mechanical properties of colloid systems, he also draws completely erroneous conclusions concerning the structure and properties of various oleophilic systems. For example, we have shown that a characteristic feature of highly elastic aluminum naphthenate gels in hydrocarbon liquids is enormous elastic deformation, of many thousand percent*, and yet Mikhailov attributes these results, and the idea of the high elastic deformation of such gels, to deformability of the dynamometer ([6], p. 75)*. However, we have shown in our preliminary experiments with Fedotova, more recently in quantitative determinations with Shalopalkina, and also with the aid of a new instrument (elastorelaxometer) specially designed for this purpose by Trapeznikov (with the assistance of technician Glebov), that aluminum naphthenate oleogels do in face have enormous elastic shearing deformations of the order of many thousands per cent. Thus, here also Mikhailov's conclusions are quite erroneous.

---

* C. B. Translation page 67.

* In our earliest experiments [3] the value ϵ_{rm} = 9000%, was possibly somewhat high, but this was in no way connected with rigidity of the dynamometer, as the most rigid dynamometers were used for high values of $\dot{\epsilon}$, but was due to a not quite correct evaluation of the deformation rate owing to start-up of the motor, so that the deformation rate in the initial stages was actually a little lower than the established rate. This was later corrected by the use of a special clutch.

Further, Mikhailov accuses me of denying flow orientation of micelles at low values of P on the ascending branch of the P (τ) curve up to P_y. These accusations are absolutely without foundation. It is obvious that every elastic deformation, which was taken into consideration for all values of P, corresponds to a certain elongation or orientation of the particles. In fact, we were the first [3-5] to draw attention specially to the fact that particle orientation occurs not simply in flow, as was stated in purely viscosimetric papers, but in the course of development of elastic deformation until P_y is reached (with some subsequent elastic contraction of the particles after rupture at P_y), which is at the initial stages of deformation.

It is interesting to note that Mikhailov claims these views on the role of orientation on the ascending branch "in contrast" to our views. It should also be noted that Mikhailov quite erroneously identifies orientation with bond rupture (pp. 71, 75)*. Finally, Mikhailov carried out experiments on thixotropic breakdown which were quite analogous to ours [5], and in an attempt to prove that all breakdown of structure occurs only on the ascending branch of the P (τ) curve gave P (τ) curves which were quite reproducible when the experiment was repeated ([6], Fig. 9). This experiment, however, can prove nothing beyond the fact that the system rapidly restores its structure, as structural breakdown both on the ascending and the descending branches during the first deformation of the system would result in lack of reproducibility of the curves upon second deformation.

In another of Mikhailov's experiments ([6], Fig. 10), with a more viscous bitumen, the maxima on the P (ϵ) curve are lower after the second and third deformation than after the first. This merely indicates partial restoration of the structure in the interim period, but does not in any way show on which of the branches the structure was destroyed. Hence it follows that Mikhailov proved absolutely nothing by his experiments. A totally different method must be used to investigate the extent to which structural breakdown occurs along the whole P (ϵ) curve.

In general, Mikhailov [6] holds quite wrongly that "the degree of disruption of the structure depends only on the velocity gradient" (Fig. 7, p. 72)**.

In reality, as we have shown [1-3, 10] breakdown of structure (continuous network) depends not only on the velocity gradient but on the deformation ϵ (for a given $\dot{\epsilon}$). Recently we have provided additional proof for this.

Finally, Mikhailov has not understood the significance of the maxima on the P (ϵ) curves. On the basis of the fact that hysteresis loops may be obtained for bitumens [15, 6], Mikhailov attempts to prove that curves with and without maxima do not differ in principle. However, the possibility of hysteresis loop formation in no way diminishes the special role of the maximum on the P (ϵ) curves, as was established by our joint work with Shalopalkina on the thixotropy of printing inks. If structural breakdown in general is being considered, it is of course immaterial what curves are used to describe it. There is no doubt, however, that the maxima are not produced by fortuitous circumstances; they are especially clear and characteristic for some particular systems, and their appearance, in principle, is totally unrelated to dynamometer rigidity. Our joint paper with Shalopalkina introduces the concept of two types of thixotropy – strength thixotropy, characterized by destruction of the continuous network, and viscosity thixotropy, characterized by changes of P_s and by hysteresis loops which reflect further fragmentation of the structural elements and desaggregation of the particles (including the orientational fraction of the thixotropy).

Thus, this question is solved not by exclusion of some parameter which reflects structural breakdown, but, on the contrary, by the combined consideration of both types of parameters, which reflect different types of structural breakdown.

In contrast to earlier views that systems with P (ϵ) curves which pass through zero stress have no flow limit and do not undergo structural breakdown, we showed [3] on the basis of the maxima that such systems undergo structural breakdown and have flow limits. Mikhailov denies the role of the maxima, but makes full use of these concepts of the disruption of structure at $P > P_c$, for which he should have no direct basis, as hysteresis loops, generally speaking, may also be a consequence of particle orientation. Thus Mikhailov, while criticizing our views, actually uses them himself, which is inconsistent. We must also point out that the P ($\dot{\epsilon}$) curves which, according to Mikhailov, form a hysteresis loop ([6], Fig. 6), are not linear. Therefore the constant viscosity region had not been reached and Mikhailov's hysteresis loop corresponds to the $P > P_C$ region and not to the $P < P_C$ region.

---

* C. B. Translation pages 63, 67.

**C. B. Translation page 64.

It follows from all the above that Mikhailov's attempted criticism of our publications has no experimental basis: it is itself internally contradictory and illogical; it could even be ignored if many, even eminent, rheologists did not use it to defend obsolete ideas.

Received April 29, 1956

LITERATURE CITED

[1] A. A. Trapeznikov, Colloid J. 12, 67 (1950).

[2] A. A. Trapeznikov, Trans. 2nd All-Union Colloid Conf. (Kiev, 1952).

[3] A. A. Trapeznikov and V. A. Fedotova, Proc. Acad. Sci. USSR 81, 1101 (1951); 82, 97 (1952).

[4] A. A. Trapeznikov and V. A. Fedotova, Proc. Acad. Sci. USSR 85, 95 (1954).

[5] A. A. Trapeznikov and V. A. Fedotova, Paper at the 3rd All-Union Colloid Conference (Minsk, 1953).

[6] N. V. Mikhailov, Colloid J. 17, 68 (1955) (T. p. 61)*.

[7] S. A. Veiler and P. A. Rebinder, Proc. Acad. Sci. USSR 49, 5 (1945); P. A. Rebinder and N. N. Serb-Serbina, Colloid J. 9, 381 (1947); E. E. Segalova and P. A. Rebinder, Colloid J. 10, 223 (1948).

[8] G. V. Vinogradov and K. I. Klimov, Proc. Acad. Sci. USSR 57, 911, 58, 1677 (1947); J. Tech. Phys. 18, 355 (1948).

[9] A. A. Trapeznikov and T. G. Shalopalkina, Colloid J. 17, 471 (1955) (T. p. 457)*.

[10] A. A. Trapeznikov, Proc. Acad. Sci. USSR 102, 1177 (1955).

[11] J. Miklowitz, J. Colloid Sci. 2, 193 (1947).

[12] A. A. Trapeznikov, Collected Papers, New Methods of Physicochemical Investigation of Surface Phenomena (1950), 1, 20.

[13] A. A. Trapeznikov, Proc. Acad. Sci. USSR 22, 84 (1939).

[14] J. C. Maxwell, Phil. Trans. 157, 49 (1867).

[15] M. P. Volarovich and M. F. Nikishina, Colloid J. 12, 169 (1950).

---

* T. p. = C. B. Translation pagination.

CURRENT EVENTS

VIIIth CONFERENCE ON GENERAL QUESTIONS OF THE CHEMISTRY AND PHYSICS OF HIGH POLYMERS

The Division of Chemical Sciences and the Institute of High Molecular Compounds of the Academy of Sciences USSR held the VIIIth Conference on General Questions of the Chemistry and Physics of High Polymers from January 25 to January 28 in Leningrad. More than 600 delegates from scientific institutions and industrial undertakings in Moscow, Leningrad, Kiev, Kazan, Yaroslavl, Tashkent, and other towns of the Soviet Union took part in the Conference.

The purpose of the Conference was to acquaint a wide range of scientists with the main results and achievements in the field of polymer chemistry and physics both in the USSR and abroad. The basic review papers read at the Conference were previously published in the journal Progress of Chemistry No. 7, 1955. In addition, several papers on more narrow topics, in which the results of experimental investigations were presented, were read at the Conference. The present review deals mainly with the questions raised in the main papers and in the discussions on them.

M. M. Koton (Institute of High Molecular Compounds, Academy of Sciences USSR) presented an extensive review of methods for the preparation of new polymers. In addition to the information published in Progress of Chemistry, M. M. Koton noted that the most valuable polymers have been prepared in various countries as the result of extensive use of the copolymerization method. Still greater possibilities arise in this direction owing to the creation of new types of copolymers: "block" and "graft" polymers, by the methods described by Mark, Melville, Norrish, and others. Polymers of this type have a number of valuable properties, such as high tensile strength and specific impact viscosity, etc. Copolymerization reactions of ethylene with carbon monoxide are of great scientific and practical interest. It is possible to obtain, at high temperatures and pressures, polyalcohols, polyketones, polyacids, and other high polymers by these reactions. The speaker drew attention to the possibilities of catalytic polymerization. New discoveries in this field, especially the production of crystalline high polymers from alpha-olefins (Ziegler, Natta) and also the preparation of polyethylene under low pressures, put this field among the most promising for the theory and practice of polymers. M. M. Koton also briefly reported on the investigations made in his laboratory on polymers containing aromatic nuclei in the principal chain. It has been shown, in particular, that polymers of various structures: linear, saturated, unsaturated, and even three-dimensional, can be obtained from the same monomer and catalyst according to the polymerization conditions (temperature, nature of the solvent).

Some participants at the Conference reported practical data on the production of new vinyl polymers. Z. A. Rogovin compared the prospects for the development of different methods of polymer production; he noted, in particular, that the block polymerization method held little promise for the synthesis of heterochain polymers, mainly because technological processing (at high temperatures) results in bond redistribution in the polymer and its properties change. No bond rupture is found in carbon chain polymers, and therefore the block polymerization method is of considerable interest in this case. Z. A. Rogovin recommended that serious attention should be paid to methods of plasticization and processing of polymer mixtures. The papers by E. M. Lavrentyeva and E. P. Melnikova referred to the development of research on reactions in polymer chains. After noting the very promising nature of the catalytic polymerization method, B. A. Dolgoplosk put forward the view that the specific properties of low-pressure polyethylene are due not so much to the initiation method as to the decreased polymerization temperature, and that a similar effect could probably be obtained even in the radical process carried out at low temperatures. In a discussion with Z. A. Rogovin, S. A. Dolgoplosk pointed out the need for work on the synthesis of block polymers, and also of polymers with aromatic nuclei and other ring structures in the principal chain, in particular for the production of thermostable plastics and elastomers.

A. Ya. Berlin also referred to the need for serious attention to be paid to the synthesis of polymers with aromatic nuclei and even with condensed systems, and he stressed the importance of studies of reactions in polymer chains, which are of special significance for solving the problem of aging of polymers and of their stability in various conditions. These reactions can also be used for the synthesis of new polymers.

A. A. Konkin reported on a new method of synthetic fiber production (polymerization of acrylonitrile in aqueous salt solution). The polymerization directly yields the spinning solution, the technological process is simplified, and the use of costly solvents is avoided. N. V. Mikhailov noted the value of the method for production of polymers with improved properties by formation of molecular polymer mixtures in a common solvent or melt, and reported on the actual results and laws governing the processes, studied in the Institute of Synthetic Fibers.

V. A. Kargin and G. L. Slonimsky (the L. Ya. Karpov Institute) developed new concepts of the crystalline state in polymers. They raised the problem of examination of the specific behavior of crystalline polymers, which determines the combination of properties characteristic of crystalline and amorphous systems, and stressed the inadequacy of structure analysis for determination of the nature of crystalline polymers. They noted, in particular, that the existence of a high degree of orientation in a cellulose fiber does not mean that it is crystalline; the same applies to all synthetic fibers. The phase state of crystalline polymers is specific – they are single-phase in respect to macromolecules, but two-phase with respect to their individual links. All evaluations of the degree of crystallinity are considered to be formal, and they should be re-examined after the nature of polymer crystals has been clarified.

The number of controversial questions raised in the paper resulted in a lively exchange of opinions both for and against some of the views advanced. A. I. Kitaigorodsky pointed out that the presence of three-dimensional diffraction on the x-ray diagram is clear evidence of remote order and therefore of the presence of crystalline regions; the crystalline regions in polymers are, of course, defective, but this is not an exclusive property of polymers only; the peculiarity of crystalline polymers lies in the fact that the same polymer molecule can pass through several ordered regions. It is not possible, as is proposed by V. A. Kargin and his associates, to speak of the presence of crystals of the plate or needle type on the basis of structural data. V. I. Kasatochkin disagreed with the view put forward in the paper on the deviation of the thermodynamic and structural factors, which leads to the conclusion that the structure of a substance does not determine its thermodynamic state; he pointed out that the same x-ray diagram may indicate the presence, in a polymer specimen, both of crystalline and of liquid regions, and even highly disordered, "gaseous" regions. The x-ray diagrams of oriented specimens show a pyramidal and two prismatic interferences. The x-ray diagrams of isotropic cellulose specimens also show two rings with periods of 4.6 and 4.2 A, which are the result of intermolecular interference and which differ from prismatic atomic planes. This, in V. I. Kasatochkin's view, leaves no doubt that cellulose contains fairly extensive crystalline regions with three-dimensional order. V. N. Nikitin associated himself with this opinion. M. V. Volkenshtein pointed out that a necessary and sufficient criterion of crystallinity is three-dimensional long-range order, the presence of which can be determined with certainty by the methods of structure analysis. In M. V. Volkenshtein's opinion, a polymer crystal is a defective polycrystal, similar in structure to crystals of long-chain low molecular compounds, which are also considerably defective. M. V. Volkenshtein cast doubt on the concept of laminar crystals, drawing attention to the inadequacy of the experimental data cited by the authors, as in his opinion these data were not subjected to the appropriate treatment. M. V. Volkenshtein, and O. B. Ptitsyn who followed him, pointed out that a fundamental defect of the paper was that kinetic laws were neglected, although a crystalline polymer is not an equilibrium system. M. V. Volkenshtein and O. B. Ptitsyn consider that the concept of a phase is not applicable to crystalline and amorphous regions of the polymer separately; a crystalline polymer as a whole can therefore be regarded as a one-phase system.

G. L. Slonimsky drew attention to the peculiar fact that the aggregate of data on the behavior of crystalline polymers, from which their phase can be established, is highly contradictory. Therefore the concept of the crystalline state must be developed in such a way that the actual experimentally proved inner contradiction of the properties can be understood with the aid of appropriate theoretical views. Crystalline polymers, like many other systems, may be examined from the thermodynamic viewpoint, but it is necessary to take into account the peculiar features manifested in the duality of their properties.

N. V. Mikhailov pointed out that the participants in the discussion essentially disagreed on the following questions: 1) Is geometry alone sufficient for characterization of the crystalline state of polymers; that is, is a divergence between the structural and thermodynamic criteria admissible; 2) Are polymer crystals one-phase or two-phase; 3) What is the structural picture of polymer crystals? He further noted that experiments on the sorption of water vapor by the amorphous and crystalline modifications of polyamides showed that these two modifications had equal equilibrium moisture contents; this, together with other experimental data, confirms the conclusions drawn by V. A. Kargin et al. The lack of any difference between the heats of solution of cellulose samples with different degrees of orientation provides new and independent proof of the absence of phase transitions over the entire orientation range, although the x-ray picture suggests the contrary. The acceptance of a one-phase nature of crystalline polymers, in N. V. Mikhailov's view, is hindered by the undue importance attached by some scientists to the kinetic difficulties which arise in the crystallization of polymers. N. V. Mikhailov also reported that needlelike crystals of caprolactam di- and trimers have been obtained. Data on heats of solution, and the absence of a qualitative diffraction picture in the transition of cellulose from the isotropic into the oriented state indicate that cellulose is an amorphous substance.

The same conclusion was drawn by Kh. U. Usmanov on the basis of his studies of cotton cellulose.

In opposing this view, S. E. Bresler pointed out that the similarity between the sorption isotherms may be the result not of an absence of crystalline and amorphous phases in stretched and unstretched rubber, but of the fusion of crystals on introduction of a low-molecular adsorbent (hexane). Data on the mechanical work of deformation and simultaneously on the thermal effect in non-crystallizing rubber show that the two are similar. In the case of crystallizing rubber there is a large difference between these two values. This shows that these are properties with a low sensitivity, and others with a high sensitivity, to crystallization, and the latter should be used for detection of the crystalline phase.

A review paper entitled "Strength and Tearing Mechanism of Polymers" was presented by G. M. Bartenev (Sci. Res. Inst. Rubber Industry); he defined the state of the problem, noting a number of features which distinguish between the behavior of polymers and simple substances on destruction, and stressing the need for consideration of a number of factors (molecular weight, structure of the polymer, time, temperature, surface-active medium, etc), in studies of strength problems. A specific factor with a great influence on the strength of high polymers is molecular orientation, the influence of which is particularly strong on fibrous and film materials. G. M. Bartenev devoted special attention to questions of the mechanism and kinetics of defect formation in polymer materials, pointed out the need for an extension of theoretical work on the strength of polymers, and indicated the principal directions of future work on the strength properties of polymers. The paper produced a lively discussion.

E. V. Kuvshinsky showed that there is much confusion even in the concepts of "strength" and "destruction", and in the division of polymers into brittle, elastic, and plastic, and that this hinders a scientific approach to the problems in question; he noted that the old view of the destruction process as a critical process (with the existence of a critical stress) is now being replaced by the view that destruction is a process which depends on time.

V. E. Gul stated, in contrast to G. M. Bartenev's views, that the rupture of polymers should be regarded as a continuous process, and the activation energy of this process may be equated to the cohesional strength of the material.

K. Z. Zakharov, G. A. Lebedev, Yu. S. Zuev and others described a number of experimental investigations on questions of the strength and behavior of high polymers under load.

In debating with G. M. Bartenev on some points in his paper, A. G. Epshtein stated that a detailed examination of all the types of rubber used in the tire industry led to the conclusion that there is no correlation between the magnitude of the break and any strength property of the polymers. The presence of two destruction zones is not a basic feature which determines the strength. It is more correct to divide the tearing process into two stages – the formation of a primary site of destruction, and its growth.

G. P. Mikhailov (Institute of High Molecular Compounds) presented a paper on "Dielectric Losses and Polarization of Polymers". After an examination of the theoretical bases for studies of the dielectric properties of high polymers, Mikhailov gave an account of the extensive experimental data available in this field. The method of dielectric polarization and dielectric losses of relaxational nature is especially promising for the solution of a number of problems of polymer structure. It is, for example, possible to estimate the nature of the thermal motion or the mobility of the macromolecules in the glassy and elastic states. The speaker concluded that dielectric loss relaxation is related to the thermal motion of the macromolecules in the form of segmental motion. When units which have a dipole moment are attached to the macromolecular chain, it is possible to solve problems relating to stereoisomerism and hindered rotation of individual atomic groups in the chain.

In the course of the discussion of this paper a number of delegates reported on new experimental data on the dielectric properties of polymers.

The paper by B. A. Dogadkin and M. M. Reznikovsky (Sci. Res. Inst. for the Tire Industry) dealt with methods and special features of the production of polymers with spatial networks (with the exception of monomer polymerization and polycondensation). It was stated that free radicals formed in the decomposition of disulfides accept mobilie hydrogen from the methyl groups of the rubber polymer chains, converting these chains into polymeric radicals. Recombination of these radicals leads to formation of spatial polymers. This process largely involves internal double bonds of the polymer chain, but the number of such steps is very limited – not more than 6 per primary radical. The paper also included a consideration of those physical properties of polymers which are determined by the presence of cross links, and their dependence on the density of the network, its regularity, and nature of the bonds.

In the discussion on this paper B. A. Dolgoplosk pointed out that interaction of radicals with internal double bonds arising in the polymer is highly improbable, and cross linkage of the chains cannot be attributed to this process. In this connection oxidative processes must not be confused with purely radical processes; the latter, in contrast to the former, are mainly directed at hydrogen atom removal and addition to vinyl or isopropenyl groups, and not to internal double bonds. B. A. Dolgoplosk then advanced a scheme for the mechanism of sulfur vulcanization with participation of accelerators, in which initation of vulcanization was considered as an oxidation–reduction process. The role of many vulcanization accelerators is determined by the fact that they are hydrogen donors in the reaction with sulfur, which leads to formation of hydrogen disulfide and its subsequent decomposition by a chain reaction scheme, analogously to the decomposition of hydrogen peroxide.

In A. Ya. Drinberg's address the main attention was devoted to consideration of the reactions of saturated polymers during aging. By control of the reaction conditions in a solid film it was possible to show that the formation of a network polymer could be, in the main, achieved and degradation could be reduced to a minimum. Certain physical and mechanical properties of the film change abruptly in the course of structurization. A. Ya. Drinberg put forward certain practical recommendations on the use of polymers as protective coatings, based on studies of the influence of the structure of vinyl polymers and copolymers on structurization.

In the discussion on B.A. Dogadkin's paper, G. A. Patrikeev raised a number of questions of interest to workers in the rubber industry. He also pointed out that there is a fundamental distinction between the mechanical properties of vulcanizates and raw rubber, since the mechanical properties of vulcanizates are determined by elastic deformations of the polymer molecules. Another feature which distinguishes the structure of a vulcanizate from the structure of rubber is the "contour" which results from the formation of stable bonds between the molecules. Such an "elastic network" (or "skeleton") in G. A. Patrikeev's opinion, takes a considerable part of the external load.

In a paper on "The Aging of Polymers", A. S. Kuzminsky (Sci. Res. Inst. Rubber Industry, reviewed research into fundamental problems related to the influence of polymer structure on their stability to thermal, oxidative, and light aging, and also to the influence of mechanical stresses on the development of chemical processes in polymers. The inadequate theoretical investigation of a number of problems related to polymer aging was noted. For example, little is known about the elementary stages in the course of different types of polymer aging. Not enough work has been done on the relationships between structure and reactivity of polymers, between molecular structure of inhibitors and their protective action, etc. The speaker noted that the resistance of polymers to degradation under the action of light, heat, and especially radiation is not directly related to the bond energy in the polymer chains. Polymers resistant to one form of aging may be quite useless in other conditions. The stability of polymers to ionizing radiations may be considerably improved by introduction of certain chemical groups (such as phenyl nuclei) into their molecules. The high molecular polymer fractions of polymers enter chemical processes more rapidly than the low molecular. A. S. Kuzminsky also described the procedure and apparatus developed by himself and his associates for accelerated aging of polymers.

In the discussion on this paper, V. L. Karpov considered a number of questions related to the action of nuclear radiations on polymers. It has become possible to use such action to confer a number of desirable properties on polymers: heat resistance can be improved, unsaturation produced, vulcanization brought about, etc. Aging under the action of high-energy ionizing radiations differs from other aging processes, mainly in the magnitude of the acting energy. Each collision of an electron with an atom results in the evolution of an amount of energy which is greater than the bond energy. However, this does not always cause bond rupture, as the possibility of energy redistribution among the bonds exists in the molecule, especially in presence of phenyl nuclei.

M. M. Koton pointed out that it is now most important to determine the influence of the structure of polymers which have high heat stability on their resistance to aging. Laboratory investigations showed that polymers containing phenyl groups are more resistant to heat aging and also to ultraviolet and ionizing radiation. However, the effect of a combination of factors (oxygen, moisture) is still not clear. Serious research is necessary on the selection of stabilizers and stable plasticizers.

Yu. S. Zuev presented a series of experimental results on the protective action of photosensitizers in the aging of raw and vulcanized rubber, and noted, in particular, the strong stabilizing effects of certain luminophores. In determining the relationship between the photoprotective action of inhibitors and their structure it is necessary to be able to distinguish between their optical and chemical action.

A. Ya. Drinberg drew attention on the great economic importance of increasing the service life of polymers (in particular, protective coatings) and the consequent importance of research on the problem of their aging. However, the position is not satisfactory, as there are no unified methods for accelerated aging tests. A. Ya. Drinberg stressed that in simulation of atmospheric aging it is necessary to introduce pressure variations, as this factor, according to laboratory data, plays an important part.

Kh. U. Usmanov reported some new data on the aging of cellulose; he pointed out that it is especially important to find means for protecting cellulose against the action of light, as it was found that after the cotton boll is opened the degree of polymerization of cotton cellulose greatly decreases and the fiber strength falls, leading to a decrease of cellulose quality.

Papers on more specialized questions, presenting new experimental research results, were also read at the Conference.

S. E. Bresler (Institute of High Molecular Compounds) reported on studies of vulcanization and polymerization reactions by the labeled atom method; he showed that free radicals may be quantitatively studied in polymerization reactions with the aid of radioactive mercury.

The paper by S. N. Zhurkov (Leningrad Institute of Physics in Technology, Academy of Sciences USSR) dealt with the influence of the time and temperature factors on polymer strength; the primary importance of the time factor was demonstrated. The variation of strength as a function of time was studied experimentally in the range from thousandths of a second to 2-3 months, and the activation energy of rupture in a number of polymers was estimated.

L. G. Tokareva (All-Union Sci. Res. Inst. for Synthetic Fibers) reported new data obtained jointly with N. V. Mikhailov and V. S. Klemenkov on the stabilization of chlorinated vinyl polymers; she examined the results of thermal decomposition reactions in chlorinated vinyl polymers in the pure state and in mixtures, obtained from a common solvent, with added cellulose derivatives and certain other polymers. The stabilizing influence of such additions was noted; this was attributed to an inter-molecular mechanism of C–Cl bond stabilization.

The paper by Yu. S. Lazurkin and G. P. Ushakov (Academy of Sciences, USSR) dealt with cold drawing of glassy and crystalline polymers. This paper noted the need for separate investigations of cold drawing in isothermal and non-isothermal conditions.

The paper by G. L. Slonimsky, V. A. Kargin, and L. I. Golubenkova entitled "Physicochemical Investigations of Resol Resins" included the results of a thermomechanical study of resol resins over a wide range of temperatures with the aid of the dynamometric balance. It was concluded that at all three stages of hardening of resol resins, physical bonding (of the hydrogen bond type) between the molecules plays a very important part; in the first stage it leads to formation of long chains, in the second it forms spatial networks, and only in the third (resite) stage do chemical bonds begin to play an appreciable part. Elastic properties were found to be present at the resite stage.

S. A. Subbotin (All-Union Sci. Res. Inst. for Synthetic Rubber) examined new data on the aging of rubbers, and in particular on the stability of divinyl–styrene rubbers in storage in relation to their production conditions. The adverse effect of iron salts, introduced to accelerate heat plasticization, was noted, as they subsequently have a harmful influence on the rubber from the aging aspect; the use of phenolic compounds is recommended for this purpose.

A resolution on a number of organizational questions was adopted at the Conference. It was proposed to hold the IXth Conference, devoted to unpublished work, at the end of 1956. It was proposed to hold the meetings of the IXth Conference sectionally, to cover more fully the numerous questions of polymer chemistry and physics.

Four meetings devoted to individual questions of topical interest will be arranged in 1956 by the Commission on High Molecular Compounds.

V. A. Kropachev

REVIEWS

A. V. Dumansky, A Bibliographical Review of the Development of the National Colloid Chemistry (1936-1941) (Academy of Sciences Ukrainian SSR Press, Kiev, 1955), Vol. 2.

This book is intended for a wide circle of chemist readers: scientists and technologists, teachers in universities and colleges, postgraduate and senior students of chemical faculties.

The monograph consists of two complementary sections: in the first the substance of the works cited is briefly presented, while the second section consists of a bibliographical historical chronological catalog of the most important publications on colloid chemistry during the period under consideration. In our view, the choice of a chronological order is apt, as it enables the chemist reader to correlate, quickly and accurately, the subject matter of the cited research with the economic development of the country, especially from the chemical aspect.

A. V. Dumansky's bibliographical review not only contains a bibliography of the most important theoretical investigations, but of research, directly related to colloid chemistry, on colloid processes and materials in a number of branches of technology, agriculture, soil science, and plant and animal biochemistry.

The second volume of the bibliographical review contains 2000 references to publications by scientists of the Soviet Union during the period in question, a brief description of many of these publications, and accounts of the development of the theory, investigation methods, and practical applications of colloid chemistry in many branches of the national economy.

Therefore the "Bibliographical Review of the Development of the National Colloid Chemistry", Volume 2 (just as Volume 1, Acad. Sci. Ukrainian SSR Press, 1949), in covering the development of colloid chemistry from its inception to the start of the Great Patriotic War in 1941, is an original work of great value and topical significance, and has a great scientific, practical, and educative value for a wide circle of readers.

By 1936 extensive experimental and theoretical material on lyophilic colloids was already available— these are high-molecular organic compounds, and analysis of the material showed that the old views on the properties of lyophilic and lyophobic systems were in principle incorrect. For this reason, the development of the national colloid chemistry from 1936 to the start of the Great Patriotic War and also during the subsequent period was primarily characterized by successful research directed at clarifying the basic decisive distinctions between high-molecular organic compounds and their solutions and disperse colloidal systems which are characterized by the existence of an interphase with the medium. An integral component of this problem is the question of the interaction between the colloid particles and the medium. Other problems successfully studied during this period, such as surface phenomena, stability and coagulation of colloid systems, and the structural and mechanical properties of high polymers and their solutions, are analyzed in detail. The author has also included investigations in which colloido-chemical views have been applied in technology, agriculture, soil science, and biochemistry. The development of colloid chemistry is illustrated by brief descriptions of the most important theoretical work in these fields. The most important literature sources are cited. In the case of problems which have been studied in detail, a more complete description is given of the solutions which have followed from the investigations during the period in question. In cases of contradictory data, researches in which different results were obtained are cited.

The literature on the most important investigations which is cited by the author gives a full description of the status of the problem. Investigations of an applied nature are cited to demonstrate the practical significance of colloido-chemical methods of investigation and of the theoretical attainments of colloid science.

Much attention is devoted to the question of bound water, which is of enormous importance in relation to the frost resistance of plants and in other instances.

The investigations of an applied nature cited by A. V. Dumansky cover a fairly wide range of practical applications of colloid chemistry in the national economy, to which the author has devoted, and is devoting his attention both in his own work and in the work of the scientific institutions of which he was and is in charge.

It would be very desirable if the next volume of the bibliographical review contained first an account of the status of the principal problems of colloid chemistry, and then a description of the further development of these problems over a definite period. This method of presentation would be very helpful to our young scientists in their work. It would also be very desirable to include a subject index in the next issue.

The division of the researches into theoretical and applied, as done by the author in this review, is necessary. All the work of theoretical importance can be divided into two groups; a) one group should, step by step, reveal the nature of the given problem and generalize the results obtained; b) the second group, at a given stage of our knowledge and with the given methods of investigation should consist of an accumulation of factual experimental data, so that it may subsequently become the basis for generalization. In our opinion these requirements should be taken into consideration in the next issue of the bibliographical review. Some, less important, investigations are not mentioned by the author. However, on the whole the book covers the main directions of our national colloid chemistry.

Despite our comments, this bibliographical review has great significance for the general development of theoretical and applied colloid chemistry, and specialists in this field will undoubtedly greet this work with great satisfaction.

M. P. Kotov

MODELING OF A SPARK DISCHARGE BETWEEN REGIONS OF SPACE CHARGE CONCENTRATION

V. I. Arabadzhi

It has been known since Branley's time [1] that metal powders are capable of momentarily changing their electrical resistance if a spark discharge occurs in the vicinity. Glagoleva-Arkadyeva [2] used particles of a metal powder suspended in oil for excitation of electrical vibrations similar in frequency to molecular radiations. Macky [3] showed that in predischarge electric field of the order of 8-13 kV/cm water drops with radius 0.085-0.26 cm became unstable and formed fine threads of water in the direction of the field. The drops also became luminous in the direction of their polarization poles. After a spark has passed through a drop, the drop assumed various unstable shapes. English [4] studied corona formation on drops and determined the ratio between the field potential and the pressure for a discharge gap containing droplets. Unfortunately, these facts represent our total knowledge of the relationship between a colloidal medium and a spark discharge. Investigation of this field, however, is of great importance.

Especially important among such effects is the development of a lightning discharge in clouds. Lightning discharge in clouds occurs between regions of space charge concentration on aerosols. The conditions for the development of such discharge differ from the conditions of discharge between metal electrodes; to elucidate some of its features we attempted to bring about a discharge of a similar kind in a model under laboratory conditions. On the basis of Snoddy and Beams' results [5] we introduced into the flames of two spirit lamps the electrodes of a Ruhmkorff coil with an ohmic resistance of 20 kΩ in the secondary winding. When a direct current was fed into the coil, the discharge between the flames was as shown in Fig. 1,a. Smooth, thick streamers with bright heads emerged from the edge of the positive flame and, after describing a curved trajectory, terminated in the air without reaching the edge of the negative flame in absence of overpotential; with an overpotential, the streamers bridged the gap. If the coil was operated by an alternating current, the discharge was of the type shown in Fig. 1,b. The streamers originated alternately from the two electrodes. A comparison of the duration of the discharge impulses showed that with metallic electrodes in our conditions an impulse lasted 40 μ seconds, and with flame electrodes, 60 μ seconds. The increased duration of the discharge impulses with flame electrodes, in our opinion, is largely explained by increased resistance of the path owing to extension of the discharge trajectory into an arc. The vibration frequency of the electromagnetic radiation emitted from the working Ruhmkorff coil was determined at a distance of several meters from the electrodes with the aid of an antenna and oscillograph; it was practically the same with metallic and flame electrodes, as it was largely determined by the contour parameters and not by the electrode properties.

A model of a section of a thundercloud was then devised with the use of photographic paper with droplets of water sprayed from an atomizer settled on it. A spark discharge was then effected on the surface of this paper. Examination of the results showed that the spark-discharge streamers which passed along the paper sometimes stopped and formed spherical luminous regions at the ends of their paths. The discharge passing along the paper was frequently of an intermittent nature (Fig. 2,a). Isolated small regions of illumination found near the discharge channel probably arose by the action of neighboring droplets of water which focused the radiation from the channel. A spark discharge between accumulations of coal dust on photographic paper simulated, in laboratory conditions, lightning discharge between clouds. The discharge was seen to be intermittent between individual particles of coal dust and smooth along the paper surface free from dust (Fig. 2,b).

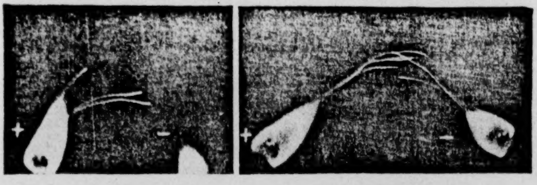

Fig. 1. Discharge between two burner flames with direct (a) and alternating (b) current passing through the coil. The signs + and – in Fig. 1,b indicate that owing to the somewhat different electrode configurations the resistances to the discharge are in this case not the same in opposite directions.

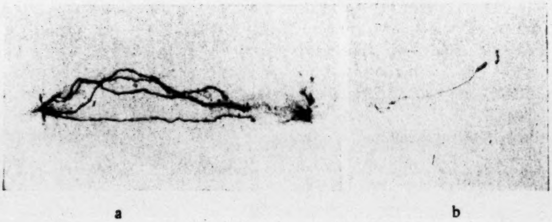

Fig. 2. Spark discharge along the surface of photographic paper between droplets of water (a) and accumulations of coal dust (b).

Fig. 3. Interaction of a spark with a droplet in its path.

If we regard a colloid particle as a conducting droplet in an external electric field E, then according to electrostatic theory [6] we should have a field 3E at the poles of this droplet. A spark through an aerosol system consisting of many such droplets should be propagated in the direction of their polarization poles. In this connection it was necessary to determine how the spark would interact with the droplets lying in its path. On one hand, one might expect that the spark should pass around the droplet, since spark discharge is a discharge in a gas. On the other hand, a spark may interact with the droplet as with a conductor. The droplets would then form breaks in the trajectory of the spark. In our experimental conditions the spark passed along droplets of radius ~3 mm which emerged from a dropper and fell onto a water surface. The second hypothesis was confirmed (Fig. 3).

SUMMARY

1. The lightning discharge which develops in a cloud between one region of charge concentration and another should be, at least in the initial stage, intermittent in nature, similarly to a spark discharge between accumulations of coal dust or droplets on photographic paper.

2. Strongly charged droplets in a cloud can, by corona formation, provide a path for the discharge, as is done by the coal-dust particles or droplets in the photographs shown.

3. The emergency of a streamer from a region of space-charge concentration in a cloud may resemble the situation shown in Fig. 1,a, since a flame in an electric field is a region of space charge-concentration.

LITERATURE CITED

[1] A. S. Popov, Meteorol. Bull. 1891, No. 3.

[2] A. A. Glagoleva-Arkadyeva, Annals Moscow State Univ. 77, No. 3 (1945).

[3] W. A. Macky, Proc. Roy. Soc.(London A 133, 565 (1931).

[4] W. N. English, Phys. Rev. 74, 179 (1948).

[5] L. B. Snoddy and I. W. Beams, Phys. Rev. 57, 63 (1940).

[6] Ya. I. Frenkel, Theory of Atmospheric Electric Phenomena (1949).

Received December 1, 1955

The A. M. Gorky State Pedagogic Institute,
Minsk

PLASTICIZATION OF POLYVINYL CHLORIDE BY BUTADIENE – ACRYLONITRILE COPOLYMER

5. INVESTIGATION OF THE COMPATIBILITY OF THE POLYMERS IN SOLUTIONS

S. S. Voyutsky, A. D. Zaionchkovsky, and R. A. Reznikova

The principal requirement of any high-molecular plasticizer is compatibility with the polymer to be plasticized. In our previous studies the compatibility of butadiene-acrylonitrile copolymer with polyvinyl chloride was evaluated by the mechanical [1-3] and optical [4] properties of films of mixtures of the two polymers. The present paper deals with the compatibility of the two polymers in solutions. Apart from its theoretical importance, this question is of practical interest, as mixed-polymer solutions will undoubtedly become widely used in industry.

The compatibility of high polymers in solutions can be evaluated by the heat effect, the osmotic pressure, and a number of other criteria. In the present investigation viscosity was used as a measure of compatibility of high polymers. As is known, viscosity is a property of polymer solutions which is highly sensitive to the state of the macromolecules in solution and to the changes undergone by that state.

Viscosities of mixtures of polymer solutions have been repeatedly investigated. The relationships have been found to be particularly simple for dilute solutions, when the high-polymer molecules are mutually independent kinetically and their action is additive, leading to proportionality between viscosity and concentration. For such cases, Bungenberg de Jong and his associates [5] established the following formulas for a mixture of solutions of two polymers:

$$\eta_{sp\,m} = x\eta_{sp\,1} + (1 - x)\,\eta_{sp\,2}\,; \tag{1}$$

$$[\eta]_m = x\,[\eta]_1 + (1 - x)\,[\eta]_2; \tag{2}$$

$$\eta_{sp\,m} = x\,[\eta]_1 c_1 + (1 - x)\,[\eta]_2 c_2, \tag{3}$$

where x and (1 – x) are the respective fractions of the first and second polymer in the mixture, while the other designations are those commonly used in viscosimetry [6], the subscripts 1, 2, and m referring to the corresponding characteristics of solutions of the first and second components and of the mixture.

For mixtures of concentrated high-polymer solutions, when the relative viscosity is no longer proportional to the concentration, the relationships between the viscosities of the original and final solutions are far more complex, and it becomes necessary to use one of the known concentration formulas.

Kumichel [7], the first to study the viscosity of mixtures of concentrated high-polymer solutions, attempted to use an exponential formula put forward by Duclaux and Wollman for the concentrational dependence of colloidal systems. Kumichel was not successful in applying this formula to mixtures of high-polymer solutions.

Atsuki and Ichiwara [8], who studied the viscosity of solutions of various nitrocellulose fractions in acetone, showed that the Baker formula was applicable in this instance. Schimoda and Kamihara [9] later reached similar conclusions.

Philippoff [10] repeated the investigations on the viscosity of concentrated solutions of high-polymer mixtures; he came to the conclusion that only hydrodynamic interaction occurs between the macromolecules in polymer solutions, and specific forces are absent. On this basis, Philippoff considers that the following equation is applicable to solutions containing two or more high-molecular components:

$$[\eta]_m = \sum_{i=1}^{\infty} [\eta]_i x_i. \tag{4}$$

It should be pointed out, however, that Philippoff used substances of different molecular weights which differed relatively little in their nature, so that specific interactions could have remained undetected in these experiments.

The question of viscosities of mixtures of not very concentrated solutions has been studied in detail by Krigbaum and Wall [11]. They used the following polymer pairs: natural rubber – polystyrene; natural rubber – ethyl cellulose; ethyl cellulose – polyethylene glycol. The solvent was benzene in all cases. The equation used by Krigbaum and for the viscosity – concentration relationship was

$$\eta_{sp} = [\eta]_c + bc^2. \tag{5}$$

As is known, it is usually considered that in this equation the value of the reduced viscosity at infinite dilution $[\eta]$ is a measure of polymer – solvent interaction, while the term with the coefficient b represents interaction between the polymer molecules at finite concentrations. The total interaction between the high-polymer molecules can evidently be represented in the form of the expression $c_1(c_1b_{11} + c_2b_{12})$ for polymer type 1 and $c_2(c_1b_{12} + c_2b_{22})$ for polymer type 2, where b with the corresponding subscripts represents the constants for the interaction between molecules of the same polymer or between molecules of different polymers. Evidently, the following equation may be written to represent the specific viscosity of a mixture of high-polymer solutions in the light of the above.

$$\eta_{sp\,m} = [\eta]_1 c_1 + [\eta]_2 c_2 + b_{11} c_1^2 + 2b_{12} c_{12} + b_{22} c_2^2. \tag{6}$$

Krigbaum and Wall showed that the experimentally determined viscosities of the mixtures of high-polymer solutions which they studied differed from the ideal values calculated from Equation (6), and they calculated the interaction constants for the polymers. It was found that the value of the constant b_{12} for the nonpolar polymers natural rubber and polystyrene is somewhat higher than the ideal value found from the equation $b_{12} = (b_{11}b_{22})^{1/2}$. The reason for this deviation was not clear. A considerable negative deviation was found for the mixture natural rubber – ethyl cellulose, which was to be expected owing to the different chemical nature of these polymers. Finally, a considerable positive deviation was found for the mixture ethyl cellulose – polyethylene glycol. Attraction between the molecules of ethyl cellulose and polyethylene glycol probably occurs as the result of hydrogen bonding, leading to increased interaction in the mixture and to increased viscosity.

The problem of the viscosity of mixtures of high-polymer solutions was investigated very recently by Cragg and Bigelow [12]. They used the slope constant in the well known Huggins equation [13] instead of the intrinsic viscosity as a measure of the interaction of high polymers in solution. This constant has considerable advantages as a criterion of intermolecular interaction, as the molecular weight of the components has little effect on it. The above authors studied the viscosity of the system polystyrene – polymethyl methacrylate – xylene, and showed that negative deviations are found in this case. These deviations were attributed either to repulsion between the polystyrene and polymethyl methacrylate molecules, or to the fact that polystyrene molecules hinder association of polymethyl methacrylate molecules.

Method and materials used. It follows from the above that there are several viscosimetric methods by means of which intermolecular action of high polymers in solutions may be evaluated. However, these methods have considerable defects: first, they are based on concentration formulas of an empirical or semiempirical nature, which do not always describe with sufficient accuracy the variation of viscosity with the polymer content in the solution. Second, these methods are applicable only to more or less dilute solutions, in which structural viscosity is absent or very small. However, it is concentrated solutions which are of the greatest interest to the research worker, since only they are likely to have practical applications and since intermolecular interaction should be most pronounced in such solutions.

For the foregoing reasons, we restricted ourselves in the present investigation to a simple comparison of the specific viscosities of relatively concentrated solutions in relation to variations of their polymer contents, polymer ratios, temperature, and presence of polar additions. As will be seen, this method provides certain information on the molecular interactions of polymers in solutions, and can therefore lead to conclusions concerning the compatibility of the components.

The main material for investigation was the ternary system polyvinyl chloride – butadiene-acrylonitrile copolymer – dichloroethane. The butadiene-acrylonitrile copolymer contained 36.9% acrylonitrile. Both the high-polymer components were described in detail earlier [1]. The dichloroethane was thoroughly purified. The mixtures of high-polymer solutions for the investigation were made by mixing definite quantities of solutions of the components of known concentrations.

The original solutions were prepared as follows. The polyvinyl chloride was allowed to swell in dichloroethane for twenty-four hours and the swollen polymer was then heated on the water bath until completely dissolved. The solution was filtered, its dry solids content was determined by drying a sample to constant weight at 70-75°, and diluted with dichloroethane to the required concentration.

The butadiene-acrylonitrile copolymer was milled for a short while and allowed to swell for twenty-four hours in a small amount of dichloroethene, and the resultant solution was then diluted with the rest of the solvent. The subsequent procedure was as for polyvinyl chloride.

The mixture of high-polymer solutions was held in jars with ground-glass stoppers for twenty-four hours with periodic shaking before the viscosity determinations. The viscosities of the solvent, polymer solutions, and mixtures of the solutions were measured with the aid of an Ostwald viscosimeter immersed in a water thermostat controlled to the nearest ± 0.1°.

Effect of the component ratio on the viscosity of mixtures of high-polymer solutions. Fig. 1 shows curves for the specific viscosity variations at 20° of mixtures of polyvinyl chloride and butadiene-acrylonitrile copolymer solutions with the component ratio, with 1, 2 and 2.5% total solids in the mixtures.

As Fig. 1 shows, Curve 1 is very slightly convex toward the concentration axis, and approximates a straight line. Similar curves were obtained by others [11] for mixtures of dilute solutions of polar polymers. The reason for this shape is probably the fact that specific interaction between the polymer molecules is absent or very slight in this case. Curve 2 has a totally different character – it is clearly S-shaped. In our opinion this shape is due to interaction between the molecules of the two components by their polar groups. It is known in physicochemical analysis that a steady composition – property curve indicates absence of interaction between the components. Conversely, the presence of maximum or minimum points always indicates the existence of such interaction.

Curve 3 (Fig. 1) retains the S-shape, but the experimental points fit it much less satisfactorily. In general it must be pointed out that the reproducibility was very bad for mixtures with a total dry solids concentration over 2.5%, and the experimental results depended very strongly on the previous history of the solution. This indicates that mixtures of such concentrations have considerable structural viscosity.

Another important conclusion can be drawn from the relative positions of the initial and final points corresponding to solutions of pure polymers in Fig. 1. When the dry solids content of the mixture is 2% or lower, polyvinyl chloride solutions have a lower viscosity than butadiene-acrylonitrile solutions of equivalent concentrations, while the reverse is true for solutions with 2.5% dry solids. The probable reason is that the intermolecular forces are greater in polyvinyl chloride, and aggregates are formed to a greater extent in its solutions with increasing concentration.

It was therefore desired to verify whether Equation (1) is applicable to this system; in other words, to determine to what extent the specific viscosity of a mixture of polymer solutions represents the sum of the specific viscosities of the solutions of the two components. This question was investigated for solutions containing 2% dry solids. Such mixtures, as

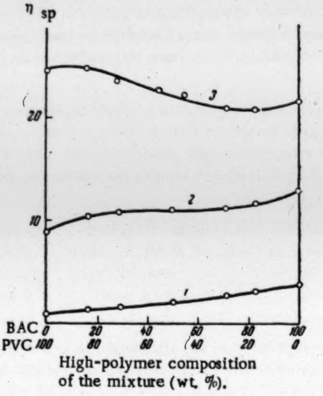

Fig. 1. Variation of specific viscosity of mixtures of polyvinyl chloride and butadiene-acrylonitrile copolymer solutions with the component ratio. Total solids contents of mixtures: 1) 1%; 2) 2%; 3) 2.5%.

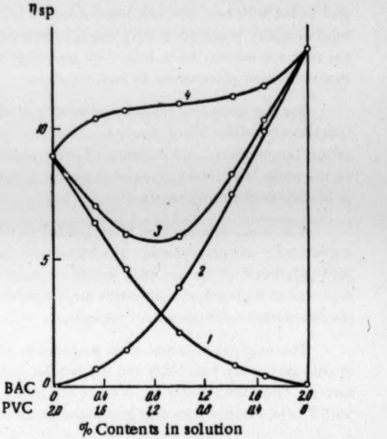

Fig. 2. Variation of specific viscosity with changes in the concentration of each individual component and of the component ratio in a mixture containing a total of 2% solids; 1) curve for polyvinyl chloride; 2) ditto, for butadiene-acrylonitrile copolymer; 3) additive curve for the mixture; 4) experimental curve for the mixture.

We have seen, do not yet have a considerable structural viscosity and give quite reproducible results; on the other hand, they are fairly concentrated and interaction between the polymer molecules in them is sufficiently strong to reveal any nonadditivity of the specific viscosity. Fig. 2 shows curves for the variation of specific viscosity with the concentration of each individual component in the pure state; Curve 3 was obtained by geometric addition of the specific viscosities for the two solutions, and Curve 4 was obtained experimentally. It is seen that the graph based on the assumption of additivity is steady but strongly convex toward the abscissa axis, while the experimental curve has a distinct S-shape. This shows an absence of additivity in this case, evidently due to specific interaction between the molecules of the two components.

An important fact is that the deviation of the experimental curve from additivity has the highest positive value at a 60 : 40 ratio of polyvinyl chloride to the butadiene-acrylonitrile copolymer. This suggests that at a certain excess of polyvinyl chloride relative to the copolymer, either the maximum number of aggregates is formed, or the aggregates have the highest stability.

This is interesting in conjunction with the fact that, as was shown in another paper [2], films made from mixtures of polyvinyl chloride and butadiene-acrylonitrile copolymer have maximum strength at the same component ratio. Thus there is a direct relationship between structure formation in polymer solutions and the mechanical properties of films from solutions of these polymers. The reason for this relationship is, of course, that structurization of solutions and film strength are both due to the same cause – interaction between the polymer molecules.

Effect of temperature on the viscosity of mixtures of polymer solutions. Fig. 3 shows a graphical representation of the relationship between the specific viscosity of 2% solutions of polyvinyl chloride and butadiene-acrylonitrile copolymer, and the temperature. It is seen that the specific viscosity of the polyvinyl chloride solution decreases appreciably more than that of the copolymer solution with increase of temperature. This confirms the greater tendency for formation of macromolecular aggregates in polyvinyl chloride solutions than in butadiene-acrylonitrile copolymer solutions. The considerable forces which arise between the molecules in polyvinyl chloride solutions are evidently associated with the frequency of the polar chlorine atoms along the chain molecules of this polymer.

Fig. 4 shows curves for the variation of the specific viscosity of mixtures of the polymer solutions with the component ratio at various temperatures. The total dry solids content of the final mixture was, as previously, 2%.

It is seen that as the temperature rises, not only does the viscosity of the mixtures decrease, but the nature of the curves themselves changes. At 50-60° the curves change from S-shaped to almost linear, slightly convex toward the abscissa axis. The increase of temperature evidently leads to a breakdown of the aggregates and makes the properties of concentrated high-polymer solutions nearer to the properties of dilute systems.

The curves corresponding to 30-40° are of interest. Their left-hand portions retain curved regions, convex toward the ordinate axis, corresponding to a high proportion of polyvinyl chloride. The right-hand side of the curves, however, has become linear. This also shows that the most stable aggregates are formed in mixtures with an excess of polyvinyl chloride molecules.

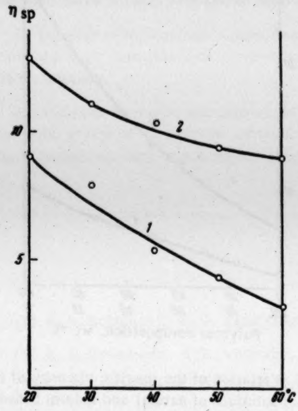

Fig. 3. Variation of the specific viscosity of 2% polymer solutions with temperature: 1) polyvinyl chloride solution; 2) butadiene-acrylonitrile copolymer solution.

Effect of polar additions on the viscosity of mixtures of polymer solutions. It has been reported in the literature that small amounts of extraneous polar substances have a highly characteristic influence on solutions containing macromolecules with polar groups [14]. Such substances, if they have two or more polar groups, can favor aggregate formation by cross-linking the molecules. On the other hand, extraneous molecules with single polar groups can block the polar groups of the macromolecules and thus prevent association.

To verify our view that considerable interaction occurs between polyvinyl chloride and butadiene-acrylonitrile copolymer molecules in solution, it was of interest to study the influence of extraneous polar substances on the viscosity of mixtures of these polymer solutions.

The polar additions used were ethyl alcohol and acetone, which have been used by others to block polar groups of macromolecules.

Fig. 5 shows curves for the variation of the specific viscosity of mixed solutions of polyvinyl chloride and butadiene-acrylonitrile copolymer with the component ratio, in presence of 1% alcohol or acetone in the mixture. The total polymer concentration in the mixture was 2%.

As was to be expected, the introduction of polar additions decreases the viscosity of the system and causes the S-shape of the curves for specific viscosity as a function of the component ratio to become less prominent and even to vanish completely. Alcohol, having more active polar groups, has a stronger action than acetone.

Study of the specific viscosity of mixtures of solutions of nonpolar high polymers. To confirm our view that solution viscosity is influenced by interaction between two polar polymers, experiments were carried out to determine the viscosities of mixed solutions of two nonpolar polymers. The polymers used were natural and sodium butadiene rubber, which are mutually very compatible. The solvent was a volatile ligroine fraction. The original solutions and mixtures were prepared in the same way as in the case of the polar polymers, and the same methods of determination were used.

As Fig. 6 shows, curves for the variation of η_{sp} with the component ratio are quite steady without any signs of an S-shape when the mixture contains 2% or even 3% solids. This indicates the absence of any specific interaction between the nonpolar polymer molecules and confirms the validity of the views advanced by us.

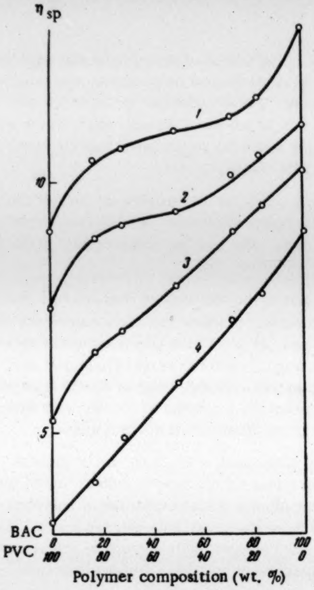

Fig. 4. Variation of the specific viscosity of mixtures of polyvinyl chloride and butadiene-acrylonitrile copolymer solutions with the polymer ratio. Temperature: 1) 20°; 2) 30°; 3) 40°; 4) 60°.

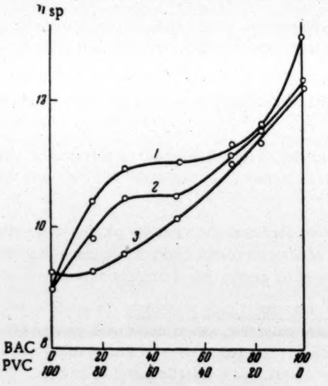

Fig. 5. Variation of the specific viscosity of mixtures of solutions of polyvinyl chloride and butadiene-acrylonitrile copolymer with the component ratio: 1) Without additions; 2) on addition of acetone; 3) on addition of ethyl alcohol.

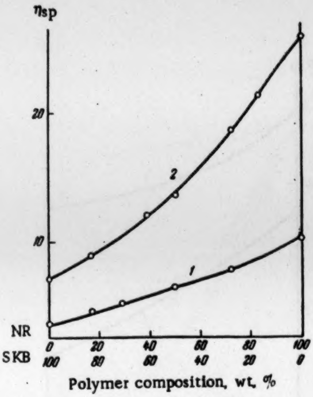

Fig. 6. Variation of the specific viscosity of mixtures of solutions of natural and sodium butadiene rubbers with the component ratio. Total dry solids content in mixture: 1) 2%; 2) 3%.

SUMMARY

1. For mixed solutions of polyvinyl chloride and butadiene-acrylonitrile copolymer containing 36.9% acrylonitrile, with a total solids content below 1%, the η_{sp} – component-ratio curve is smooth and slightly convex toward the abscissa axis. This is a sign of absence of any specific interaction between the molecules of the two polymers at these concentrations. For solutions of higher concentrations the curve is S-shaped, which is probably due to interaction between the molecules by their polar groups and formation of aggregates increasing the viscosity of the system.

2. For mixtures of solutions of natural and sodium butadiene rubber, the η_{sp} – component-ratio curve has a steady course at all concentrations, and resembles the corresponding curve for dilute high-polymer solutions. This is probably explained by absence of any specific interaction between molecules of nonpolar polymers in solution.

3. The specific viscosity of mixtures of fairly concentrated solutions of such polar polymers as polyvinyl chloride and butadiene-acrylonitrile copolymer is not equal to the sum of the viscosities of the initial solutions, which is to be explained by specific interaction between the molecules of the two components.

4. The maximum positive deviation of the η_{sp} – component-ratio curve obtained experimentally from the additive curve is found at a 60 : 40 ratio of polyvinyl chloride to butadiene-acrylonitrile copolymer.

5. Increase of temperature causes destruction of aggregates in mixed-polymer solutions and in consequence the η_{sp} – component-ratio curve loses its S-shape and assumes the steady form typical of such curves for dilute solutions.

6. Addition to mixed solutions of polar polymers of low-molecular polar substances capable of blocking the polar groups of the polymer molecules lowers the viscosity of the mixtures and favors the transition of the η_{sp} – component-ratio curve from S-shaped to a steady course, typical for dilute solutions.

LITERATURE CITED

[1] R. A. Reznikova, A. D. Zaionchkovsky, and S. S. Voyutsky, Colloid J. 15, 108 (1953) (T.p. 111).*

[2] R. A. Reznikova, S. S. Voyutsky, and A. D. Zaionchkovsky, Colloid J. 16, 204 (1954) (T.p. 207).*

[3] R. A. Reznikova, A. D. Zaionchkovsky, and S. S. Voyutsky, J. Tech. Phys. 25, 1045 (1955).

[4] S. S. Voyutsky, A. D. Zaionchkovsky, V. A. Kargin, and R. A. Reznikova, Proc. Acad. Sci. USSR 94, 1093 (1954).

[5] H. G. Bungenberg de Jong and W. A. L. Dekker, Biochem. Z. 212, 318 (1929); see also H. G. Bungenberg de Jong and Gwan Sian, Biochem. Z. 221, 166 (1930); H. G. Bungenberg de Jong and W. A. L. Dekker, Kolloid-Beih. 43, 143 (1935).

[6] G. L. Slonimsky, S. S. Voyutsky, and Yu. L. Margolina, Colloid J. 9, 116 (1949).

[7] W. Kumichel, Kolloidchem. Beih. 26, 161 (1928).

[8] K. Atsuki and M. Ichiwara, J. Soc. Chem. Ind. Japan 33, 508, B (1930); cited through [10].

[9] I. Schimoda and S. Kamihara, Cellulose Ind. 13, 13 (1937) cited through [10].

[10] W. Philippoff, Viscositat der kolloide Verl. T. Steinkopff (Dresden-Leipzig, 1942), p. 330.

[11] W. R. Krigbaum and F. T. Wall, J. Polymer Sci. 5, 505 (1950).

[12] L. H. Cragg and C. C. Bigelow, J. Polymer Sci. 16, 177 (1955).

[13] M. L. Huggins, J. Am. Chem. Soc. 64, 2756 (1942).

[14] A. Tager, Solutions of High-Molecular Compounds (Moscow-Leningrad, 1951), pp. 70, 169.

Received September 9, 1955

Central Scientific Research Institute
for the Leather Substitutes Industry

---

* T.p = C. B. Translation pagination.

VOLUME EFFECTS OF DILUTION OF HIGH-POLYMER SOLUTIONS

S. A. Glikman and L. A. Root

We showed earlier [1] that dilution of high-polymer solutions in a certain relatively narrow range of low concentrations (for example, from 0.4 to 0.2%) results in fairly pronounced volume effects. For some systems these effects constitute up to 20-30% of the integral volumetric effect of solution of the high polymer.

On the hypothesis that the decrease or increase of the volume of the system when a solution is mixed with a separate solvent is a measure of intermolecular interaction, the view was advanced that in the region of low concentrations corresponding to the observed effects there is a change in the internal structure of the solution, consisting of a more or less sharp transition from a random and more or less uniform distribution of the high-polymer molecules (at concentrations below the limiting value) to a discrete system of aggregates of these molecules. Both states are thermodynamically stable. The aggregates are regarded as short-term molecular associations of statistical origin, formed by hydrogen, dipole, or other intermolecular bonds. The lifetime of such bonds is very short and the role of such association is slight in systems of low-molecular substances, but it becomes significant in high-polymer solutions. If for two linear polymer molecules having hundreds of active atomic groups capable of mutual association there are, on the average, even 2-3 such short-lived bonds, then these two molecules should be associated for much longer periods, as the formation of new bonds between high-polymer molecules in close proximity is statistically more probable than if they are uniformly distributed in the solution. However, at higher dilutions, when statistically there are not two, but one or less bonds between two polymer molecules, the existence of aggregates or molecular groups with a longer life period than the life of an individual bond is practically excluded.

It is evident that for an equal probability of bond formation between analogous functional groups the critical concentrations of solutions of polymer homologs should decrease with increasing degree of polymerization.

The earlier experimental data [1] have been supplemented by studies of a number of systems, including solutions of polyvinyl butyral in alcohol (Fig. 1) and ethyl cellulose in dibutyl phthalate (Fig. 2). Table 1 shows our results for the total volume effects of dilution in the critical-concentration region for a number of polymer solution systems.

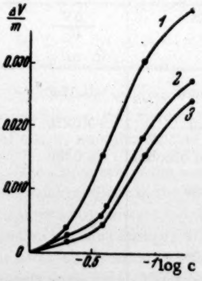

Fig. 1. Volume effects of dilution of polyvinyl butyral solutions in alcohols: 1) benzyl; 2) ethyl; 3) methyl.

The positive volume effects observed for most of the systems studied are explicable in the light of the views advanced above: for such systems the energy of intermolecular cohesion is evidently greater than the energy of solvation, or $E_{22} > E_{12}$. However, if the functional groups which bring about association of polymer molecules are solvated by the solvent when the aggregates are broken down by dilution, then even if the difference between the energy of cohesion and energy of solvation is great, $E_{22} \gg E_{12}$, the positive volume effect should not be large, as the aggregates are not formed by all of the corresponding functional groups present in the polymer molecules. Such systems are ethyl cellulose – benzene, ethyl cellulose – ethyl acetate, and nitrocellulose – ethyl acetate. In these systems the molecular aggregates are probably formed mainly by means of the ester or ether groups, which are considerably more numerous than the hydroxyl groups. Moreover, the formation of bonds between the more prominent ether groups is more likely on steric grounds than the formation of bonds between hydroxyl groups, in view of the relative rigidity of ethyl cellulose molecules.

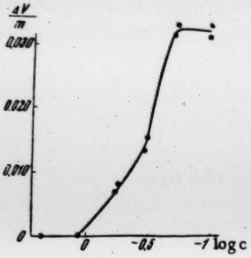

Fig. 2. Volume effects of dilution of ethyl cellulose solutions in dibutyl phthalate.

The volume effect should be even smaller and even close to zero if the value of E_{22} is close to that of E_{12}, as is the case in the systems pectin – water and nitrocellulose – dioxane.

The positive volume effect is considerably greater for the system ethyl cellulose – dibutyl phthalate than for the system ethyl cellulose – benzene. This is explained by the fact the first of these systems at temperatures below 40° is not a true solution but a dilute gel [2]. It is evident that the intermolecular bonds are in this case much more stable, the structure is denser, and the increase of volume on dilution and breakdown of the aggregates should be greater. It is true that ethyl cellulose solutions in benzene cannot be regarded as entirely true solutions, but the gel structure in this instance is less pronounced than in the system ethyl cellulose – dibutyl phthalate.

The volume effect for solutions of polyvinyl butyral in alcohols should be very pronounced, since the molecules of polyvinyl butyral do not contain ring groups and aggregate formation is also possible through all three types of functional groups (hydroxyl, acetate, and butyral), and intermolecular bonds may be formed not only between like but also between unlike groups. It is clear that breakdown of the aggregates should produce a large volume effect if only because the relative number of intermolecular bonds is much larger here than, for example, in the system ethyl cellulose – benzene (or ethyl acetate). The rather lower effect with ethanol as solvent, and the still lower effect with methanol, in comparison with benzene, is to be explained by the greater mobility of the small molecules of these alcohols. This is of great importance, since association is a statistical effect.

The negative volume effect of dilution of benzyl cellulose solutions in benzene may be explained by the fact that the bond energy between the benzyl groups in benzyl cellulose is less than their bond energy with benzene, that is, $E_{22} < E_{12}$, while the role of the hydroxyls in the formation of aggregates is very small, as hydroxyl group association is hindered by the steric factor. As regards the predominant solvation energy of the benzyl groups, the system in question is analogous to the system polystyrene – benzene, for which we showed earlier that the solvation energy is predominant [3].

TABLE 1

Volume Effects of Dilution of High-Polymer Solutions in the Critical Concentration Region

Polymer	Solvent	$\frac{\Delta V}{m}$ in ml/g	Polymer	Solvent	$\frac{\Delta V}{m}$ in ml/g
Nitrocellulose	Acetone	−0.0480	Polyvinyl butyral	Methanol	+0.0240
	Ethyl acetate	+0.0100		Ethanol	+0.0275
Benzyl cellulose	Benzene	−0.0074		Benzyl alcohol	+0.0380
Ethyl cellulose	Benzene	+0.0070	Polystyrene	Benzene	0
	Ethyl acetate	+0.0070	Pectin	Water	0
	Dibutyl phthalate	+0.0320	Nitrocellulose	Dioxane	0

Negative volume effects might be expected for the system polystyrene – benzene. It is quite probable that they might have been detected if the method used had allowed the determination of volume effect of dilution at concentrations below 0.1%, where the absolute values of these effects are very small. The reason is that the molecular weight of the polstyrene sample used (of the order of 600,000) is much higher than the molecular weight of the benzyl cellulose sample (74,000). According to the views on the nature of the association of polymer molecules advanced above, breakdown of aggregates should occur at lower concentrations with increasing molecular weights of the polymers.

TABLE 2

Volume and Heat Effects of Swelling and Solution of Polymers

Polymer	Solvent	$\Delta V/m$ in ml/g	Q in cal./g	$\frac{\Delta V/m}{Q} \cdot 10^4$
Nitrocellulose	Acetone	-0.1162	$+17.0$	63
Benzyl cellulose	Benzene	-0.0123	$+2.5$	48
Rubber	Benzene	$+0.3260$	-2.8	116

The high negative volume effect of dilution for introcellulose in acetone are difficult to explain. These effects are found in a concentration region of the same order as for the system nitrocellulose – ethyl acetate and in solutions of other polymers with molecular weights of the same order as that of the nitrocellulose sample studied (M ~ 40,000); it therefore seems natural to suppose that in this system also these effects are due to breakdown of aggregates. However, the high values of the volume effects and their negative sign evidently require special interpretation. It is possible that in addition to breakdown of aggregates and the possibility of solvation of the liberated ester groups in nitrocellulose, changes in the keto – enol tautomeric equilibrium occur.

In general, our proposed explanations for the nature and the differences in the volume effects of dilution for various systems are a first approximation only, since we did not take into consideration the role of possible changes in the interaction between the solvent molecules.

As regards the relatively high values of the volume effects, which in some systems reach 25 and even 40% of the integral effect of dilution, it must be remembered that they are by no means evidence of relatively equally high heat effects.

It was shown by Katz [4] that the heat of solvation stands in a definite quantitative relationship to the volume change which occurs in the process. Katz determined the heat of swelling in water and the volume change of the system for various high polymers. (proteins and carbohydrates). It was found that the ratio of these two values is constant, independent of the degree of swelling, and has values from $10 \cdot 10^{-4}$ to $30 \cdot 10^{-4}$ for different systems. Moreover, Katz obtained identical graphical relationships to the degree of swelling for both these values, expressed by analogous formulas. The decrease in the volume of a system was found to correspond to liberation of heat, which occurs in bond formation, for example in solvation. The reverse effect corresponds to bond breakdown. Katz did not study swelling of polymers in organic solvents. However, having determined the ratio between the volumetric and heat effects for the system xylene – aniline, for which the value $\Delta V/Q = 40 \cdot 10^{-4}$ was obtained, Katz advanced the view that a similar relationship should hold for the swelling of polymers in organic solvents.

We found the value of this ratio for three systems: nitrocellulose – acetone, benzyl cellulose – benzene, and rubber – benzene (Table 2).

The heats of solution were determined calorimetrically, and the results obtained were close to those obtained by others for the same systems. The volume effects of solution of nitrocellulose and benzyl cellulose, and of swelling of rubber, were determined with the aid of the dilatometer described previously [1].

The difference in the values of $\Delta V/Q$ for different systems obtained by Katz, and also found by ourselves, is understandable. Even in the simplest case, when the volume and the energy effects are the results of one phenomenon only, for example solvation only, or breakdown of molecular aggregates only, the value of this ratio must greatly depend on the bond energy. If the bond energy E is large, as in the case of electrostatic dipole interaction, then the value of ΔE on solvation or on breakdown of aggregates will be large. If the bond energy E is small, then ΔE will be relatively small also. The energy of intermolecular bonding is inversely proportional to the sixth power of the distance between the molecules. Therefore the values of ΔE must differ greatly according to whether the molecules which were, for example, 3 A apart, are brought together to distances of 1.8 or 1.7 A. However, this difference in the distance will have little influence on the volume effect. On the other hand, when molecules which were 4 and 3 A apart are brought together to a distance of 1.7A the volume effects will differ greatly, while the energy effects will differ little. It is therefore evident that $\Delta V/Q$ or, which is the same thing, $\Delta V/\Delta E$ should be small if ΔE is large, and conversely. Since in aqueous systems in the presence of hydrogen bonds both E and ΔE are large, the ratio $\Delta V/\Delta E$ for these systems is also small. According to Katz, it is between $10 \cdot 10^{-4}$ and $30 \cdot 10^{-4}$. For organic substances, however, as we saw earlier, these ratios are greater, and are still more so when the intermolecular forces are predominantly dispersional. Indeed, we saw that for the system rubber – benzene $\Delta V/\Delta E$ has the value $116 \cdot 10^{-4}$. The bond energy can obviously be large or small according to the nature of the bond and steric and other factors, and may differ greatly in two systems despite a very small difference in the volume effects, since a small change in the distance between the bound molecules has little effect on ΔV, while it has an appreciable effect on ΔE, since ΔE varies in proportion to the sixth power of the distance between the molecules, while ΔV is only proportional to the difference of the third powers of this distance.

It is clear that, with high volume effects of dilution, the heat effects can be very small, if the polymer molecules in the aggregates are not sufficiently close together. However, the volume effects are in themselves very significant; their appearance on dilution of solutions of various high polymers in a certain narrow region of low concentrations definitely indicates an abrupt change in the nature of the molecular association, and therefore in the structure of solutions in this concentration region.

SUMMARY

1. The results of a dilatometric study of volume dilution effects in a number of high-polymer solutions in various solvents in the concentration range from 20 to 0.1% are given. It is shown that many systems show a positive or negative volume effect, considerably greater than the volume effect of dilution of concentrated solutions of the same polymers, in a narrow region of low-polymer concentrations (of the order of 0.2-0.4%).

2. The differences of magnitude and sign of the effects found for different systems may be explained on the basis of views concerning the nature and role of different functional groups in the polymer molecules, and their possible interaction with each other and with the solvent molecules.

3. The appearance of considerable volume effects of dilution in a certain narrow region of concentrations is regarded as a sign of an abrupt change in solution structure in this concentration region. However, high volume effects need not necessarily be accompanied by equally high heat effects if the polymer molecules in the aggregates are insufficiently close together.

LITERATURE CITED

[1] S. A. Glikman and L. A. Root, Proc. Acad. Sci. USSR 65, 701 (1949); J. Gen. Chem. 21, 58 (1951) (T.p. 63).*

[2] S. A. Glikman and O. G. Efremova, Proc. Acad. Sci. USSR 81, 1089 (1951).

[3] S. A. Glikman and L. A. Root, Trans. All-Union Conf. Colloid Chem. (Acad. Sci. USSR Press, 1952), p. 296.

[4] J. Katz, Ergeb. exakt. Naturw. 3, 316 (1924); 4, 154 (1925).

October 9, 1955

The N. G. Chernyshevsky State University,
Saratov

---

* T.p = C. B. Translation pagination.

REINFORCEMENT OF RUBBER IN LATEX

B. A. Dogadkin, L. G. Senatorskaya, V. I. Guseva,
A. V. Suslyakov, and P. I. Zakharchenko

The principal obstacle to the development of the technology of production of rubber articles from latex (natural and synthetic) up to the present time has been the absence of a rubber reinforcement effect in latex, and the consequent impossibility of obtaining strong rubbers by direct introduction of fillers into latex, Active fillers (carbon black, colloidal silicic acid, zinc oxide, kaolin, etc.) when added to latex either lower the strength of the latex vulcanizates or yield mixtures the strength of which falls far short of the values found for mixtures made by the usual (but energy-consuming) method of addition of fillers to the dry rubber on rolls or in mixers. In consequence only unfilled rubbers are now made directly from latex, which greatly restricts the range of possible applications of latex technology and its further development.

A number of workers [1] have attempted to solve the problem of reinforcement of rubber in latex. However, as Table 1 shows, these attempts have not led to the desired results.*

The authors of the present paper ** have succeeded for the first time in determining the conditions for obtaining butadiene – styrene SKS-30 latex mixes with carbon black which have strength characteristics (in the vulcanized state) not inferior practically to the usual mixes from the same rubber. This opens up new possibilities for the production of filled latex mixes for the solution of technical problems.

The idea of the investigation. In our opinion there are three main reasons for the insufficient reinforcement effect of rubber in latex mixes. First, active fillers (carbon black, zinc oxide, colloidal silicic acid) are distributed in the latex not as primary particles but as more or less large aggregates. The nature of these aggregates varies with the type of filler, its concentration in the latex, and the protective substances used for dispersion [2].

The first cause of the low strength of latex rubber mixes is the insufficiently fine distribution of the filler in the latex, so that insufficient contact area is developed between the rubber and filler particles.

The second cause is that in a latex mix, even if the disperse phase particles are finely and uniformly distributed, they are not deposited simultaneously during formation of the deposit (film), whether by evaporation of water, by coagulation, or by application of the latex mix to a water-absorbing material. The reason for this nonsimultaneity may be a) varying density of the disperse phase particles; b) different values of the electrokinetic potential and different rates of its variation by the action of the precipitant (electrolyte) or on change of concentration (in the evaporation of water); c) different surface activity and stability of the protective layers on the particle surfaces; and finally d) varying anisometry of the particles, which also influences sedimentation kinetics. Nonsimultaneous deposition of the particles from a latex mix leads to an inhomogeneous, stratified distribution of the film components and hence to low strength in the filled vulcanizates obtained from latex mixes.

The third cause for the absence of a reinforcement effect is the presence of a protective surface coating on the latex globules and carbon particles, which prevents direct contact between the rubber and the filler after removal of the aqueous phase.

---

* In a recent paper by Maron (J. Polymer Sci., 19, 29 (1956) it is stated that reinforcement of rubber in latex is impossible and it is therefore recommended to introduce carbon black into the monomer emulsion before polymerization for the production of filled latex mixtures. It is quite obvious, however, that this procedure is technically more complex than the introduction of filler into the prepared latex.

** The work was initiated by P. I. Zakharchenko and A. V. Suslyakova.

TABLE 1

Comparative Strength Data on Vulcanized Filled and Unfilled Latex Mixes

Latex type	Filler	Filler content per 100 wt. parts mixture	Tensile strength in kg/cm²	Relative elongation, %	Authors
Revertex	Bentonite	0	164*	755	A. Van Rossem,
		5	346*	815	J. A. Plaizier [1]
Natural latex	Askangel	0	242*	690	B. Dogadkin and R.
		30	416*	580	Uzina [1]
Butadiene – styrene latex (Igetex S-3)	Channel black	0	16	560	R. Uzina and M.
		15	53	210	Dostyan [1]
Butadiene – styrene (GR-S)	Channel black	0	22	–	Conover [1]**
		45	127	–	

---

* These values were obtained in two-dimensional tensile tests by the Flint instrument; they are considerably higher than the usual tensile data obtained by the Schopper dynamometer.

** Conover's review gives numerical data only, without indication of the methods used for preparation or testing of the filled latex mixes.

The views advanced above are confirmed by direct experiments. If channel black is added to butadiene–styrene latex in the form of a very fine dispersion, then the strength of the vulcanized films containing 40 parts by weight of carbon per 100 parts of rubber is about 12 kg/cm². The same latex mix after milling and vulcanization in a press has a strength of 136 kg/cm². This effect of the milling can be explained on the grounds that milling produces uniform distribution of the components and homogenizes the system to such an extent that direct contact is established between the rubber and the carbon-particle surfaces, and also between the carbon particles without a weakening protective layer between.

This is in full agreement with the theory of rubber reinforcement advanced by one of us [3] and also with the latest data of Garten [4] and Watson [5] on the radical mechanism of rubber – carbon interaction.

Thus, for the production of filled latex mixes of high strength it is necessary to ensure:

a) a high degree of dispersion of the fillers and other ingredients added to the latex;

b) simultaneous precipitation of the particles from the latex mix;

c) conditions which result in direct contact between the rubber and filler particles, without intermediate layers of protective substances which lower the rubber – filler interaction energy.

It is also evident that protective substances, intermediate layers of which do not diminish the rubber – filler interaction energy and which do not prevent the formation of chemical vulcanization bonds between the latex globules, may be used without significant detriment to the strength of the latex mixes.

Our experiments were therefore based on the foregoing considerations.

Composition and methods of preparation of the latex mixes. The material for investigation was SKS-30 butadiene – styrene latex containing Nekal (sodium dibutylnaphthalene sulfonate) as emulsifier.

Ukhta channel black was added to the latex in the form of a fine dispersion made in a colloid mill with Leukanol (condensation product of sodium β-napthalene sulfonate with formaldehyde) as stabilizer. The vulcanization ingredients were Accelerator 226 (a mixture of Captax sodium salt and triethanolamine), zinc oxide, and sulfur. The zinc oxide and sulfur were dispersed in a ball mill with Leukanol as stabilizer. After addition of all the ingredients, the latex mix was stirred together in a blade mixer, filtered through gauze, and poured into glass cells. The drying was first carried out in air, and the films were then dried in a desiccator over sulfuric acid. The resultant films, ~0.5 mm thick, were vulcanized in a press at 143°.

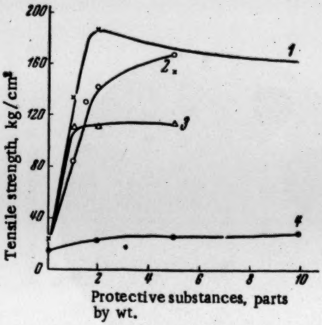

Fig. 1. Effect of additions on the tensile strength of latex vulcanizates containing 40 parts of channel black by weight: 1) Casein; 2) gelatin; 3) sodium alginate; 4) casein without channel black.

Effect of casein and other protective substances. As Fig. 1 shows, latex films filled with channel black (40 parts by wt.) have a strength of ~ 25 kg/cm² at optimum vulcanization. The strength rises sharply, reaching 190 kg/cm², if casein is added in the form of ammonium caseinate. Gelatin and sodium alginate have a similar effect but to a smaller degree (Fig. 1). The maximum reinforcement effect of casein in carbon black mixes is found at a content of ~2% on on the rubber. At the same time, addition of casein to latex without carbon black (in various amounts, up to 10% on the rubber) does not produce any significant increase in the strength of vulcanized latex films (Fig. 1, curve 4). Thus, the influence of these substances involves a change in the nature of the interaction between the components of the carbon – latex mix.

Addition of casein results in thickening and at the same time to destabilization of carbon – latex mixes. This is seen from the microphotographs of the mix before and after addition of casein (Fig. 2,a, and 2,b). The mixture with casein shows large aggregates consisting of rubber and carbon particles after dilution with water, while in the mixture without casein the disperse phase is uniformly distributed. A similar situation (Fig. 2,c, and 2,d) is found on addition of ammonium caseinate to a dispersion of carbon black alone. The destabilization effect is also seen in the sedimentation kinetics of diluted carbon – latex mixes.

As Fig. 3 shows, the sedimentation rate of the suspended particles becomes about 7 times as high on addition of 2% casein (Curve 2) compared with the sedimentation rate in mixes without casein (Curve 1).

The destabilization of the carbon – latex mixture on addition of casein may be attributed to interaction between casein and the protective substances on the surfaces of the carbon particles and the latex globules (Nekal, Leukanol). We believe that this interaction leads to partial desorption of the protective substances from the surface of the particles in the disperse phase and to formation of coacervates – an effect repeatedly described in papers on destabilization of colloid systems. The carbon particles and latex globules, from which the protective surface layer has been to some extent removed, form structures in which direct contact is established between the carbon and the rubber.* This, as was noted above, is one of the conditions for rubber reinforcement. At the same time, the introduction of casein and similar substances, by favoring the formation of secondary structures consisting of rubber globules and carbon black, ensures their simultaneous precipitation in film formation. In other words, another condition for reinforcement is fulfilled – coprecipitation of the components and their uniform distribution in the mix.

The connection between formation of secondary structures in carbon – latex mixes and vulcanizate strength is confirmed by the following experiments. If varying amounts of stabilizer OP-10 (a reaction product of ethylene oxide and an alkyl phenol) are added to the carbon – latex mix, followed by casein, then the stability of the mix rises with the OP-10 content (Fig. 3). However, this is accompanied by a decrease of vulcanizate strength, and there is an inverse linear relationship between the content of OP-10 in the mixture and the tensile strength of the vulcanizate (Fig. 4).**

The destabilization effect can evidently be positive only if it occurs in a well-distributed mixture of carbon particles and latex globules (Fig. 5). Only then can redistribution of protective substance between particles of the disperse phase lead to the formation of a fine structure in a filled latex film with high-strength characteristics.

Effect of vulcanization conditions. The existence of protective coatings on the latex globules is a significant obstacle to the formation of chemical vulcanization bonds between them. It is possible to visualize the existence

---

* According to Voyutsky[6] the surface of the globules in SKS-30 latex is not completely covered by a protective layer of emulsifier.

** The mechanism of the action of various stabilizers requires further careful study for the development of a correct theory of rubber reinforcement in latex mixes.

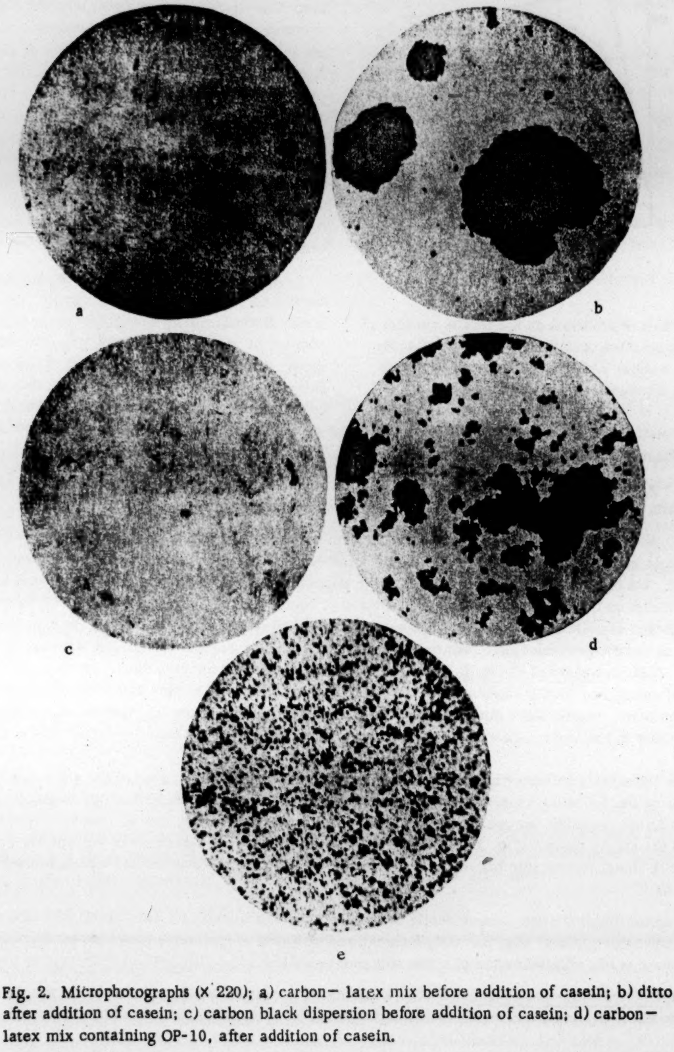

Fig. 2. Microphotographs (× 220); a) carbon– latex mix before addition of casein; b) ditto, after addition of casein; c) carbon black dispersion before addition of casein; d) carbon–latex mix containing OP-10, after addition of casein.

of such layers between the latex globules as would completely prevent the interaction between the vulcanizing agent (sulfur) and rubber. In such cases the vulcanization effect or a due reinforcement effect would not occur. In cases when direct contact takes place in the latex mix between the globules and the filler particles without an intermediate

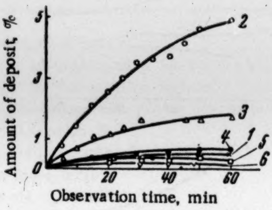

Fig. 3. Sedimentation kinetics of latex mixes containing 40 parts of channel black by weight: 1) Without casein; 2) with casein; 3) ditto with 1 wt. part OP-10; 4) ditto with 2 wt. parts OP-10; 5) ditto with 3 wt. parts OP-10; 6) ditto with 4 wt. parts OP-10.

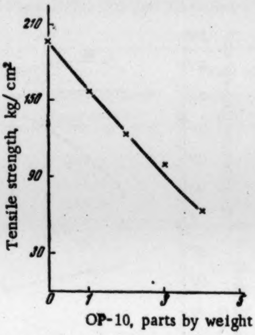

Fig. 4. Effect of the content of OP-10 on the tensile strength of latex vulcanizates containing 40 parts of channel black and 2 parts of casein by weight.

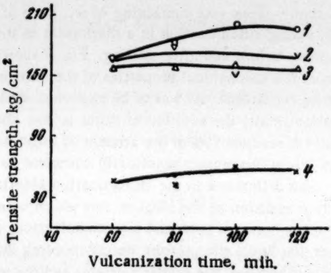

Fig. 5. Effect of conditions for the production of carbon black dispersions on the tensile strength of vulcanized latex mixes (40 wt. parts of channel black); carbon black dispersed by: 1) Colloid mill; 2) ball mill for 48 hours; 3) shaking in a flask for 48 hours; 4) carbon black without mechanical treatment.

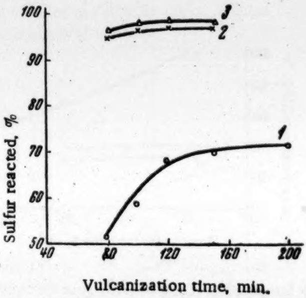

Fig. 6. Kinetics of sulfur addition in films from carbon – latex mixes (40 wt. parts of channel black) according to vulcanization conditions: 1) In air; 2) in press; 3) in press, after preliminary milling.

layer of protective substances, the vulcanization effect would be as pronounced as in ordinary mixes compounded on rolls. Between these two extremes there are a number of real intermediate states in which the vulcanization kinetics and the final degree of development of vulcanization structures depends on the composition of the protective substances, the relative extent of the regions of direct contact between the rubber globules, the thickness of the protective layers, rate of diffusion of sulfur through them, and a number of other factors.

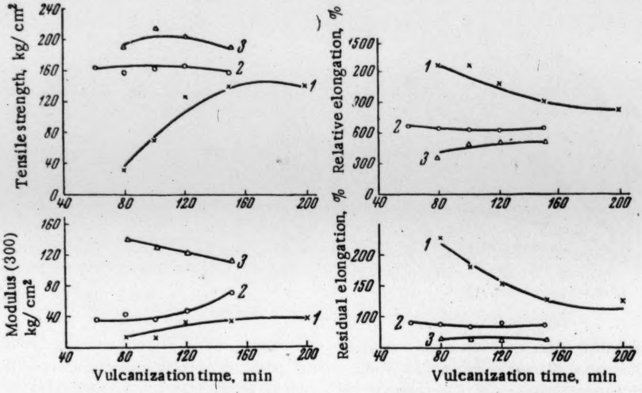

Fig. 7. Effect of vulcanization conditions on the mechanical properties of latex mixes with 40 wt. parts of channel black; vulcanization: 1) In air; 2) in press; 3) in press after preliminary milling.

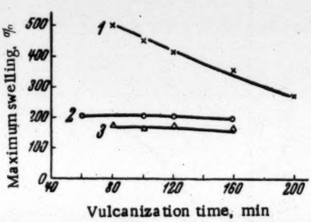

Fig. 8. Kinetics of swelling of latex mix vulcanizates with 40 wt. parts of channel black in relation to the vulcanization conditions: 1) In air; 2) in press, 3) in press after preliminary milling.

Fig. 6 shows the kinetics of sulfur addition in films from a carbon– latex mix containing 40 wt. parts of channel black, during vulcanization in a thermostat in the air, and in a press, before and after milling. Fig. 7 shows the variations of the mechanical properties of the vulcanizates for the same conditions. As was to be expected, during vulcanization in air, the addition of sulfur is slow and in 160 minutes it reaches 70% of the amount of sulfur added. Vulcanization in the press is practically complete in 60 minutes. This difference in the vulcanization kinetics is explained, in addition to the usual factors which determine the differences between press and air vulcanization, also by the fact that hydraulic pressure during molding increases direct contact between the rubber particles and the vulcanization components. Accordingly, the strength of films vulcanized in air (140 kg/cm²) is lower than the strength of films vulcanized in the press (~170 kg/cm²). The highest strength, as already stated, is found in mixtures of the same composition after milling.

A direct measure of the smaller number of chemical cross links in vulcanizates obtained in air is provided by their greater maximum swelling in xylene in comparison with press-vulcanized products (Fig. 8). This suggests that the choice of a more active vulcanization system might yield filled latex mixes which would have strength properties after air vulcanization similar to those of press vulcanizates.

Effect of electrolytic coagulation. If a filled latex mixture is coagulated by an electrolyte and the resultant coagulum is vulcanized in a press, the vulcanizate strength is higher than that of latex films obtained by the drying method (see Table 2). This strength increase is apparently primarily due to the fact that a part of the protective substances of the latex mix remains in the serum after coagulation. It is also possible that the removal of the charge from part of the disperse phase favors the formation of coagulation structures in which more complete contact is effected between the rubber and filler, and also between the filler particles.

TABLE 2

Physical and Mechnical Properties of Vulcanizates with 40 Weight Parts of Gas Channel Black Based on Latex and on SKS-30 Rubber.

Properties	Based on SKS-30 latex		Based on SKS-30 rubber compounded on rolls
	drying method	electrolytically coagulated	
Tensile strength in kg/cm²	214.2	257.5	297.3
Modulus at 100% elongation, kg/cm²	22.2	38.0	12.1
Modulus at 300% elongation, kg/cm²	66.5	102.0	52.3
Relative elongation, %	660	572	748
Residual elongation, %	40.4	25.8	30.4
Tearing strength, kg/cm²	41.9	43.3	47.1
Shore hardness, units	84	–	66
Rebound elasticity at 20°, %	35	–	40

Coagulation of filled latex mixes can be used for the production of granulated rubber mixtures for the manufacture of pressed articles.

Mechanical properties of vulcanizates obtained from filled latex mixes. Fig. 9 shows variations of the mechancial properties of vulcanizates with the amount of Ukhta channel black. Table 2 shows data on the mechanical properties of vulcanizates obtained from latex mixes by the drying and coagulation methods, and of vulcanizates of the same composition made by the usual method of compounding on rolls. It is seen that the principal strength properties of these products are similar. There is no doubt, however, that the different nature of vulcanizate structure cannot fail to show itself in a number of properties, such as the modulus, hardness, etc. Nevertheless we believe that our results open up definite possibilities for the production of technically valuable filled vulcanizates directly from latex, and therefore for the development of new technological methods.

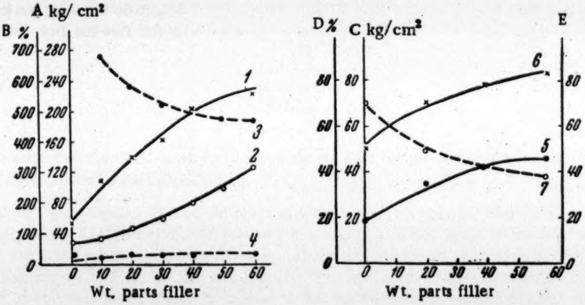

Fig. 9. Effect of the channel black content on the mechanical properties of latex rubber mixes (SKS-30): 1) Tensile strength (A); 2) modulus at 300% elongation (A); 3) relative elongation (B); 4) residual elongation (B); 5) tearing strength (C); 6) Shore hardness (E); 7) rebound elasticity at 20° (D).

SUMMARY

1. Conditions for the production of strong vulcanizates by direct addition ofchannel black to SKS-30 butadiene-styrene latex have been determined.

2. Rubber reinforcement by carbon black in latex mixes occurs on addition of such substances as casein, gelatin, and alginic acid to the mixture.

3. Experimental data are cited to show that the rubber reinforcement effect in the presence of the above substances is due to; a) their destabilizing action and the formation of structures in which the carbon and rubber particles are in direct contact; b) conditions in which the latex components are precipitated simultaneously (coprecipitation effect).

4. Electrolytic coagulation of carbon– latex mixtures results in increased vulcanizate strength.

5. Vulcanization of filled latex mixes proceeds at a lower rate than that of ordinary rubber mixes of the same composition.

LITERATURE CITED

[1] A. Van Rossem and J. A. Plaizier, Rev. Cen. Caoutchouc. 134, 19 (1937); T. S. Conover, Rubber Age N. Y. 58, 207 (1945); B. Dogadkin and R. Uzina, Colloid J. 9, 97 (1947); R. Uzina and M. Dostyan, Colloid J. 14. 197 (1952) (T.p. 221).*

[2] B. A. Dogadkin and R. V. Uzina, Colloid J. 9, 97 (1947).

[3] B. A. Dogadkin and A. I. Lukomskaya, Trans. III All-Union Conf. Colloid Chem. (Minsk, 1953); B. A. Dogadkin, K. A. Pechkovskaya, and M. Dashevsky, Colloid J. 10, 257 (1948).

[4] V. A. Garten, Nature 173, 997 (1954).

[5] W. F. Watson, Ind. Eng. Chem. 47, 128 (1955).

[6] S. S. Voyutsky, Colloid J. 18 (1956).

Received May 6, 1956

Scientific Research Institute
for the Tire Industry, Moscow

---

* T.p = C. B. Translation pagination.

ADSORPTION OF CARBOXYMETHYLCELLULOSE ON CLAYS

N. A. Zavorokhina and V. G. Benkovsky

High concentrations of electrolytes in the aqueous phase of drilling fluids used for oil well drilling result in considerable electrolytic coagulation, with consequent deterioration of the technological properties of the fluids and frequent breakdowns in drilling.

Zhigach et al. [1,2] have developed a technique for the use of sodium carboxymethylcellulose (CMC) as a drilling fluid stabilizer. Industrial trials in a number of oil well regions have shown that CMC is a completely satisfactory stabilizer for drilling fluids even with 15-20% salts in the aqueous phase.

It follows from numerous papers by Rebinder et al. and other workers [3-6] that CMC is adsorbed on the clay particles and forms structurized protective films which prevent coagulation. It was therefore necessary to study the adsorption of CMC on the natural clays of the Emba region, which show poor dispersion in water and have a high content of water-soluble salts, and also to study the effect of various salts (NaCl, $MgCl_2$, and $CaCl_2$) on the adsorption of CMC by clays.

The material used was a chemically pure CMC sample obtained from the technical product by precipitation as the copper salt, followed by treatment with 5-10% HCl and then with 0.1 N NaOH solution. The adsorbents used were Kulsary, Novobogatinskoye, and Makat clays (natural and dialyzed), previously ground and shifted through a 0.25 mm sieve. The CMC concentration in solution was determined by the method given by Zhigach et al. [1-2], based on the precipitation of CMC as the copper salt and iodometric back titration of the excess copper ions in solution. The adsorption was calculated from the formula:

$$a = \frac{(c_0 - c)\,V}{1000 \cdot m}$$

where $c_0 - c$ is the difference of the CMC concentrations in the solution before and after adsorption; m is the weight of adsorbent; V is the volume of solution in milliliters.

In experiments on the adsorption of CMC on clays as a function of its concentration in the solution, the clay was both placed directly in the CMC solution, and soaked previously in distilled water for twenty-four hours with subsequent addition of the CMC solution. In experiments on the effect of salts on adsorption of CMC their concentration was varied in the range 0.1; 0.25; 0.5; 1; 2; 3 and 4 N. The influence of these salts on aqueous solutions of CMC without addition of clay was first studied. It was found that the volumetric method of CMC determination gives low values for the CMC concentration, depending on the concentration of NaCl, $MgCl_2$, $CaCl_2$. The greatest deviations are found on addition of the first small amounts of the salts (up to 1 N) while further additions of the salt have almost no effect on the value for the CMC concentration. The reason is probably that in presence of NaCl, $MgCl_2$, $CaCl_2$ the copper salt of CMC is not completely precipitated; this is confirmed by the partial solubility of CMC copper salt in aqueous solutions of these salts.

Fig. 1 shows that the adsorption of CMC on Kulsary and Novobogatinskoye clays increases with increasing CMC concentration (see Curves 3, 5). In the case of Makat clay, the curve passes through a maximum and on further increase of the CMC concentration the adsorption not only decreases but reaches a negative value after passing through zero (Curve 1). This "negative adsorption" may be explained as follows. In adsorption from concentrated solutions the mass of the solvent cannot be taken as constant, as adsorption of the solvent as well as of the solute

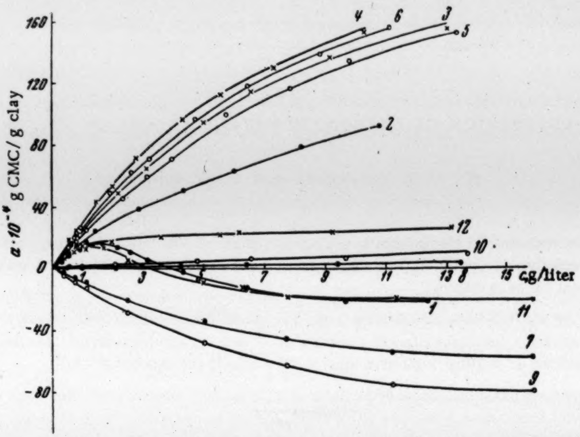

Fig. 1. Variation of the adsorption of CMC on clays with the CMC concentration in solution: 1,3,5) natural clays: Makat, Kulsary, and Novobogatinskoye without soaking; 2, 4, 6) the same clays, soaked; 7,9,11) dialyzed Makat, Kulsary and Novobogatinskoye clays, without soaking; 8,10,12) the same clays, soaked.

must be taken into account. Adsorption of the solvent becomes more pronounced with decreased adsorbability of the solute [7,8]. The adsorption of CMC on Makat clay (Curves 1 and 2) is low in comparison with adsorption on Kulsary (Curves 3 and 4) and Novobogatinskoye (Curves 5 and 6) clays.

To exclude the influence of adsorption of the solvent, a series of experiments was carried out in which the clay was previously soaked in water (Curves 2,4,6). The adsorption of CMC as a function of the reagent concentration in the solution increases in this case for all clays, and the curves lie above those obtained when the clay was placed directly into the CMC solution. However, even in this case the amount of CMC adsorbed by the clays was from 10-15% (on Makat clay) to 20-25% (on Kulsary clay).

Fig. 1 (Curves 7, 8, 9, 10, 11, 12) shows isotherms for the adsorption of CMC on dialyzed clays as a function of the CMC concentration in solution. The isotherms for adsorption of CMC on Makat and Kulsary clays without preliminary soaking all lie in the region of negative adsorption (Curves 7, 9), so that the adsorption of CMC, even it is occurs, is very slight in comparison with adsorption of the solvent. The curve for adsorption of CMC on Novobogatinskoye clay passes through a maximum (Curve 11). The adsorption increases at first, with a positive value, and then decreases and passes into the negative region. If previously soaked dialyzed clays are used, the adsorption isotherms are positive (Curves 8,10, 12) but the values for the adsorption are very low in comparsion with adsorption on native clays.

Fig. 2 shows the variation of CMC adsorption on clays as a function of concentrations of NaCl, $MgCl_2$, and $CaCl_2$. The adsorption of CMC on native clays increases with increasing NaCl concentration (Curves 1,4,7). In presence of $MgCl_2$ and $CaCl_2$ the adsorption isotherms pass through a maximum which is found at salt concentrations of 0.25-0.5 N (Curves 2,3,5,6,8,9). In the adsorption of CMC on dialyzed Kulsary clay the isotherms for all three salts pass through maxima, but the maxima are less sharp and correspond to higher values of adsorption than the maxima on the corresponding curves for adsorption on native clays (Curves 10,11,12).

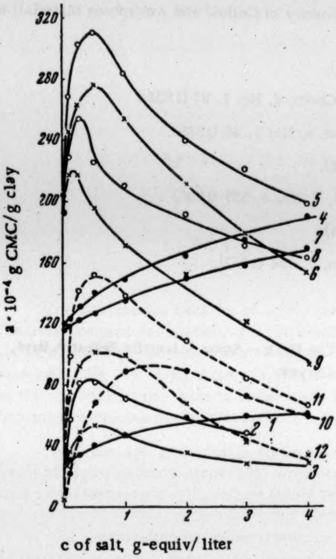

Fig. 2. Variation of adsorption on clays in presence of NaCl, $MgCl_2$, and $CaCl_2$ in solution; 1,2,3) Makat clay; 4,5,6) Kulsary clay; 7,8,9) Novobogatinskoye clay; 10,11,12) dialyzed Kulsary clay.

The initial increase of adsorption can be attributed to surface salting-out [9,10,11,12,13]. On further increase of the electrolyte concentration (past the coagulation threshold), coagulation of the clay occurs, and adsorption therefore decreases (in the case of $CaCl_2$ and $MgCl_2$). In the case of NaCl the coagulation threshold is not reached and therefore the adsorption increases steadily, owing to surface salting-out of CMC.

It is seen from Fig. 1 that practically no adsorption of CMC takes place on dialyzed clays. However, clay suspensions made from these clays and treated with CMC are not inferior in any respect to suspensions made from the corresponding native clays, which do adsorb CMC. It therefore seems likely that the stabilizing effect of CMC consists not only of formation of a structurized protective film, but also of the creation of a highly viscous medium [14].

There is reason to believe [15] that the active adsorption groups in carboxymethylcellulose are alcohol hydroxyls.

SUMMARY

1. The adsorption of carboxymethylcellulose is much greater on native than on dialyzed clays.

2. The nature of carboxymethylcellulose adsorption on native Makat and all the dialyzed clays studied changes sharply under the influence of the solvent (water).

3. The adsorption of carboxymethylcellulose on clays as a function of calcium and magnesium chloride concentrations passes through a maximum, while in presence of sodium chloride it increases steadily.

4. The stabilizing effect of carboxymethylcellulose is explained not only by the formation of adsorbed protective layers, but also by the formation of highly viscous aqueous solutions in which water is bound to the carboxymethylcellulose macromolecules, favoring the retention of the solid phase particles in a suspended state.

LITERATURE CITED

[1] E. G. Kister and K. F. Zhigach, Advances in Petroleum Technology, Petroleum Ind. USSR 6, 3 (1953).

[2] E. G. Kister and D. E. Zlotnik, Advances in Petroleum Technology, Petroleum Ind. USSR 9, 12 (1952).

[3] P. A. Rebinder and A. A. Trapeznikov, Proc. Acad. Sci. USSR 18, 7, 421 (1938); P. A. Rebinder and A. A. Trapeznikov, J. Phys. Chem. 12, Nos. 5-6, 573 (1938).

[4] A. A. Trapeznikov and P. A. Rebinder, Proc. Acad. Sci. 18, No. 3, 185 (1938); A. A. Trapeznikov, Collected papers: Viscosity of Liquids and Colloidal Solutions (Acad. Sci. USSR Press, Moscow-Leningrad, 1941), ibid., (1943), II.

[5] S. E. Bresler and P. F. Pokhil, Bull. Acad. Sci. USSR, Chem. Ser., 1937, No. 2, 413.

[6] D. L. Talmud and S. E. Bresler, Surface Phenomena (State Tech. Press, Moscow-Leningrad, 1934).

[7] I. I. Zhukov, Colloid Chemistry (Leningrad, 1949), p. 209.

[8] W. Lewis, L. Squires, and G. Broughton, Industrial Chemistry of Colloid and Amorphous Materials (Moscow, 1948), p. 101.

[9] V. K. Semenchenko, J. Appl. Phys. 7, No. 4, 75 (1930).

[10] V. K. Semenchenko and E. A. Davidovskaya, J. Phys. Chem. 6, No. 1, 37 (1935).

[11] V. K. Semenchenko and A. F. Gracheva, J. Phys. Chem. 6, No. 1, 45 (1935).

[12] V. K. Semenchenko, Progr. Chem. 3, No. 5, 710 (1934).

[13] N. F. Ermolenko and N. A. Abramchuk, J. Phys. Chem. 7, No. 4, 587 (1936).

[14] V. G. Levich, Proc. Acad. Sci. USSR 103, 3, 453 (1955).

[15] R. S. Hansen and V. W., Fackler, J. Phys. Chem. 57 No. 7, 634 (1953).

Received October 20, 1955

The Urals – Emba Scientific Research Base,
Guryev

LAWS GOVERNING THE DEVELOPMENT OF SHEARING DEFORMATION AND STRESS RELAXATION IN ELASTOMERS AND THEIR SOLUTIONS

L. V. Ivanova-Chumakova and P. A. Rebinder

The deformation behavior of highly elastic bodies under load with time is highly complex. The most complex. The most complex and interesting is the kinetics of elastic deformation (deformation of elastic deformation (deformation of elastic after-effects) which cannot be described by the simplest classical equations (of the type of the Kelvin equation). This led many authors [1,2] to abandon the consideration of general laws with a small number of constants for the material for such kinetic deformation processes. Instead use is made of the concept of the system as a combination of numerous hypothetical elastic elements forming a complex relaxation spectrum.

Such concepts are valuable for consideration of the initial, rapid relaxation processes which are studied by means of high-frequency stresses [3]. However, for a study of the subsequent slow development of deformation or stress relaxation, simple relationships should be sought to represent the process as a whole [4-6].

Our investigation has made it possible to establish a definite relationship with polyisobutylene as example, for the development of elastic deformation under constant load, valid also for the decay of deformation after removal of the load, in the form of a relation between the elastic deformation and the time of its development with the use of only one characteristic, which according to our experimental data is a constant over a wide range of deformation and time.

Polyisobutylene, which is a typical elastomer in its mechanical properties, is chemically highly resistant to external influences, and in addition, its molecular chains do not exhibit strong intermolecular action because of the absence of unsaturated bonds and polar groups.

Great importance was attached in the present investigation to the method and conditions of deformation, whereby the effect could be observed in pure form. Of the two best known methods: the development of deformation at constant stress, and stress relaxation at a constant predetermined deformation; the first was chosen as the main method, as it is then possible to use, for calculation of the characteristic measured (η; E) the simplest forms of Newton's and Hooke's laws:

$$P = \eta \frac{d\varepsilon_\eta}{d\tau}; \qquad P = E\varepsilon,$$

where P is the stress; ε is the relative elastic shear; $d\varepsilon_\eta / d\tau$ is the rate of development of relative residual deformation.

The simplest and the most correct method for investigation of deformation behavior is based on studies of the development of pure shearing deformation [7]. One favorable characteristic of this method is that it permits observations under truly constant stress, as the area of application of the load remains constant. This area is indeed always constant in deformation in an annular gap. In the case of shear between two plane-parallel plates of finite area the area of load distribution may be regarded as constant up to a certain limit of relative displacement of the plates. Moreover, this method is equally applicable to studies of shape elasticity and viscosity, both of solids and of liquids, and is therefore especially convenient if both states of the material enter the course of the investigation.

The duration of deformation in polyisobutylene in our experiments was determined by the time necessary for complete development of high-elastic deformation. Only if this condition was obeyed could the experimental results be used later for clarification of the laws of deformation.

If neither the acting stress nor the other conditions (temperature, structure of the specimen) are changed during the development of deformation, then flow in such a specimen proceeds at a constant rate; at first it proceeds parallel with the development of elastic deformation, and when the limit of the latter is reached it remains the only type of deformation. The value of the elastic deformation found after removal of the load from the decay, corresponds to the value of the elastic deformation developed to the limit in the loading cycle of the experiment. Complete agreement with this was found in our experiments if they were of sufficient duration. The experimental relationship between the developed (ϵ_e) or vanished ($\epsilon_m - \epsilon_e$) elastic deformation and the time does not obey the Kelvin equation. However, it was shown by calculation that this relationship does satisfactorily obey this same Kelvin equation

$$\frac{d\varepsilon_e}{d\tau} = \frac{\varepsilon_m - \varepsilon_e}{\theta_3},$$

modified by substitution of a variable for a constant period of elastic after-effects

$$\frac{1}{k}\,\varepsilon_e = \theta_3$$

for loading:

$$\frac{d\varepsilon_e}{d\tau} = k\,\frac{\varepsilon_m - \varepsilon_e}{\varepsilon_e}; \qquad k = -\frac{\varepsilon_m \ln\dfrac{\varepsilon_m - \varepsilon_e}{\varepsilon_m} + \varepsilon_e}{\tau}, \tag{1}$$

for unloading:

$$-\frac{d\varepsilon_e'}{d\tau} = k\,\frac{\varepsilon_e'}{\varepsilon_m - \varepsilon_e'}; \qquad k = -\frac{\varepsilon_m \ln\dfrac{\varepsilon_e'}{\varepsilon_m} + \varepsilon_m - \varepsilon_e'}{\tau}. \tag{1'}$$

These relationships are experimentally valid for polyisobutylene at all the temperatures [8] (in the range from 20 to 90°) and stresses (from 3 to 33 thousand dynes/cm^2) studied.

Experiments on stress relaxation may serve as proof that this relationship holds for development of deformation. As was stated earlier, stress relaxation cannot yield such clear and convenient data for studying and discovering the laws as can the process of development of deformation, since because of the inconstant load, the residual deformation cannot be found from the simple law $\epsilon_\eta = \frac{P}{\eta}\tau$, and is excluded from the total deformation. However, as an additional check on the validity of the already existing views concerning the relationship between the variables in the development of relaxation, stress relaxation can serve as a convenient independent method of investigation.

The process of stress decrease with time while constant deformation is maintained will be regarded as the result of compensation, at each time instant, of infinitesimal increments of high-elastic deformation $d\epsilon_e/d\tau$ and flow deformation $d\epsilon_\eta/d\tau$ by a corresponding decrease of the initially developed "instantaneous-elastic" deformation $d\epsilon_H/d\tau$.

$$-\frac{d\varepsilon_H}{d\tau} = \frac{d\varepsilon_e}{d\tau} + \frac{d\varepsilon_\eta}{d\tau}. \tag{2}$$

TABLE 1

Variation of k with the Stress P for Polyisobutylene at t = 90°

P dynes·cm^{-2}	6540	13080	33680
k min.$^{-1}$	$3.6\cdot10^{-4}$	$7.2\cdot10^{-4}$	$2.1\cdot10^{-3}$
$\frac{k}{P}$ $\frac{\text{cm}^2}{\text{dynes-sec}}$	$9.2\cdot10^{-10}$	$9.2\cdot10^{-10}$	$10.4\cdot10^{-10}$
1/a poises	$1.1\cdot10^9$	$1.1\cdot10^9$	$0.90\cdot10^9$

To determine each of the terms, we use known and newly found relationships

$$\frac{d\varepsilon_{\text{и}}}{d\tau}=\frac{dP}{d\tau}\frac{1}{E_1};\quad \frac{d\varepsilon_{\eta}}{d\tau}=\frac{P}{\eta};\quad \frac{d\varepsilon_e}{d\tau}=k\frac{\varepsilon_m-\varepsilon_e}{\varepsilon_e}.$$

where E_1 is the modulus of "instantaneous" elastic deformation, and η is the flow viscosity. Since k is directly proportional to P (Table 1) we accordingly put k = aP; ε_m, the maximum elastic deformation for each stress, is conveniently written as P/E_2 (E_2 is the elasticity modulus). Finally, the elastic deformation is none other than the difference between the predetermined deformation ε_0 and those values of the residual and "instantaneous" elastic deformation which can be found in the specimen at a given time instant τ.

$$\varepsilon_e=\varepsilon_0-\frac{P}{E_1}-\int\limits_0^{\tau}\frac{P}{\eta}\,d\tau.$$

Substitution of the above into Equation (2) gives

$$-\frac{dP}{d\tau}\frac{1}{E_1}=aP\frac{\frac{P}{E_2}-\left(\varepsilon_0-\frac{P}{E_1}-\int\limits_0^{\tau}\frac{P}{\eta}\,d\tau\right)}{\varepsilon_0-\frac{P}{E_1}-\int\limits_0^{\tau}\frac{P}{\eta}\,d\tau}+\frac{P}{\eta}. \tag{3}$$

The differential Equation (3) and the integral relationship which can be found by solving it, take into account both possible kinds of relaxation: true relaxation by transition of elastic into residual deformation, and elastic relaxation by elastic after-effects. However, if because of the extremely high viscosity of true flow, when $\eta\to\infty$, the process of true relaxation is very slow or practically nonexistent, Equation (3) may be written in the contracted and simplified form:

$$-\frac{dP}{d\tau}\frac{1}{E_1}=aP\frac{\frac{P}{E_2}-\left(\varepsilon_0-\frac{P}{E_1}\right)}{\varepsilon_0-\frac{P}{E_1}}. \tag{4}$$

In the case of polyisobutylene, in which flow will occur under any applied load, Equation (4) will be valid in the first period of time, when no appreciable residual deformation has yet had time to develop.

We solve Equation (4), introducing a new variable x:

$$\frac{1}{x}=\frac{P}{E_2}+\frac{P}{E_1}-\varepsilon_0.$$

Substitution into Equation (4) and rearrangement gives

$$-\frac{dx}{x}\frac{E_2}{E_1+E_2}+\frac{dx\varepsilon_0}{1-\varepsilon_0 x}=aE_1 d\tau \tag{5}$$

and after integration we have

$$-\frac{E_2}{E_1+E_2}\ln x+\ln(\varepsilon_0 x+1)=aE_1\tau+c. \tag{6}$$

Returning to the original variable and carrying out all the necessary operations, we have

$$-\frac{E}{E_1+E_2}\log\left[\frac{P}{P_0}\left(1+\frac{E_2}{E_1}\right)-\frac{E_2}{E_1}\right]+\log\frac{P}{P_0}=D=\frac{aE_1\tau}{2.3}. \tag{7}$$

For brevity, we denote the left-hand side of this equation by D. Equation (7) does not give the relationship between P and τ in explicit form. Nevertheless, the same relationship in the reverse order, being the result of simple and accessible operations, may be easily verified by calculation and comparison with experimental data. Table 2 shows such a calculation based on experiments on stress relaxation in polyisobutylene at 25° ($P_0 = 54$ and 74 g/cm²).

TABLE 2

Stress Relaxation in Polyisobutylene at 25°.
($E_1 = 2.3\cdot10^6$ dynes/cm²; $E_2 = 1.1\cdot10^5$ dynes/cm²; $a = 1.3\cdot10^{-9}$ cm²/dyne.min.)

Time τ in min.	Stress P in g/cm²	$\frac{D}{\tau}\cdot10^4$	$\frac{aE_1}{2.3}$	Time τ in min.	Stress P in g/cm²	$\frac{D}{\tau}\cdot10^4$	$\frac{aE_1}{2.3}$
	$P_0 = 54.0$ g/cm²				$P_0 = 74.3$ g/cm²		
0	54.0			0	74.3		
1.2	39.0	8		1.0	59.0	10	
2.2	32.0	13		2.0	47.2	10	
4.0	29.0	10		3.5	42.5	11	
5.3	26.0	13		8.0	35.4	9	
8.5	23.7	11	$13\cdot10^{-4}$	12	30.7	8	$13\cdot10^{-4}$
11	22.4	11		15	28.3	10	
17	19.2	10		24	23.6	8	
20	18.3	10		28	21.2	11	
26	16.5	9					

As is seen from Table 2, D/τ, equal to the product of the constants $aE_1/2.3$ according to Equation (7) does in fact remain constant and numerically equal to the value found from other independent measurements.

However, as was to be expected, as relaxation proceeds, the polyisobutylene specimen exhibits a residual deformation not accounted for by Equation (7). By the time at which Table 2 ends, this deformation already reaches ~0.1 of ϵ_0, and therefore subsequent calculations according to Equation (7) no longer give the expected value of D/τ. In order to allow at least approximately for the development of residual deformation, we replace, in Equation (3), the integral $\int_0^\tau \frac{P}{\eta}\,d\tau$ by the sum $\frac{1}{\eta}\Sigma P\cdot\Delta\tau$ the value of which we calculate at each time instant and substract from the constant value of ϵ_0 used. Solution of Equation (3) with this correction gives the following expression:

$$-\frac{E_1}{E_1+E_2-E_2/a\eta}\ln\frac{P\frac{E_1+E_2-E_2/a\eta}{E_1E_2}-\left(1-\frac{1}{a\eta}\right)\left(\varepsilon_0-\frac{1}{\eta}\Sigma P\Delta\tau\right)}{P_0\frac{E_1+E_2-E_2/a\eta}{E_1E_2}-\left(1-\frac{1}{a\eta}\right)\left(\varepsilon_0-\frac{1}{\eta}\Sigma P\Delta\tau\right)}+$$
$$+\ln\frac{P}{P_0}=B=\frac{E_1}{\eta}(a\eta-1)\,\tau. \tag{8}$$

For brevity, we will denote the left-hand side of the equation by B. This is a rather complicated equation. In addition to the quantities determined directly in the stress relaxation experiment: P_0, P, ϵ_0 and τ, it contains four other constants; these are characteristics for the material and are found from independent experiments on the development of deformation under constant stress.

Inaccuracy in the preliminary determinations of these constants may lead to considerable divergences, much larger than shown in Table 3.

TABLE 3

Stress Relaxation in Polyisobutylene at 83.5°.
(P_0 = 39 g/cm^2; E_1 = 1.3 · 10^6 dynes/cm^2; E_2 + 1.0 · 10^5 dynes/cm^2; a = 6.5 · 10^{-10} cm^2/dyne!sec; η = 6.4 · 10^8 poises)

Time τ in sec.	Stress P in g/cm^2	$-\frac{B}{2.3\,\tau}\cdot 10^4$	$-\frac{E_1(a\eta-1)}{2.3\,\eta}$
0	39	—	$5.1\cdot 10^{-4}$
15	30	3.3	
36	22	3.9	
66	18	3.6	
72	16	3.9	
108	14	3.6	
144	12	5.2	
205	9	3.2	
272	7	3.4	
314	6	3.4	
423	4	3.9	
665	2	4.7	
		3.9 (mean)	

If the minuend and subtrahend in the numerator of the $\frac{E_1 + E_2 - (E_2/a\eta)}{E_1E_2}$ are approximately equal, then the final result of the calculation according to Equation (8) depends entirely on the error in determinations of $E_1 + E_2$ and $E_2/a\eta$. A source of error here may be insufficient duration of the experiments to determine these constants, which would give inaccurate results for three magnitudes at once: E_2, η and a. In addition, these values may depend very strongly on the temperature for some materials, and lack of constancy of the temperature, owing to long duration of the experiments, is then a source of error.

We may say, to summarize, that the proposed equation for stress relaxation at a given constant deformation, despite its cumbersome nature, has the obvious advantage that it contains no arbitrary constants and includes only known characteristics of the deformed material, which have a definite physical meaning. No arbitrary assumptions especially associated with the relaxation process are made in the derivation of this equation. On the contrary, the derivation is based on processes, associated with the nature of the material, which are found during development of deformation at constant stress and under the action of a diminishing stress, when the initial predetermined deformation remains constant.

For a particular case, when the viscosity of true flow is sufficiently high, stress relaxation will occur in a fairly short time, definitely less than η/E, owing only to development of elastic deformation, that is, according to Law (7), which follows from Equation (8). A constant stress value P_L, forming a definite fraction α of the initial P_0, would then be reached:

$$P_L = \alpha P_0; \quad \alpha = E/E_1 = 1 - \lambda;$$

in complete agreement with the law of elastic stress relaxation derived from the simplest Kelvin– Hooke mechanical model [7], where $\lambda = E_1/(E_1 + E_2)$ is a measure of the elasticity and $1/E = 1/E_1 + 1/E_2$.

When this limit P_L is reached, the stress does continue to relax further to P = 0, but, in practice, at an infinitely low rate, determined by the true fluidity (the value of $1/\eta$).

The instrument which was designed for studies of the stress relaxation process is shown in the figure.

The part of the instrument specially intended for the relaxation experiments consists of the spring 1 and the graduated rod 2 (100 divisions per 0.3 mm). The rod moves axially inside the sleeve 3, thus extending or contracting the spring, corresponding to variations of the force applied to the plate 4 on the spring side. Before the start of an experiment, the rod scale is set to the zero position; in order to retain this position, but at the same time to apply the necessary tension to all the connections, (the rigid thread 6, and the spring 1); to reach the start of extension of the latter, the sleeve 3 is moved inside the socket 7 to the left until the plate 4 begins to move. The scale readings are taken with the aid of the objective 8' (magnification × 3.7) taken from an ordinary microscope. The distance be-

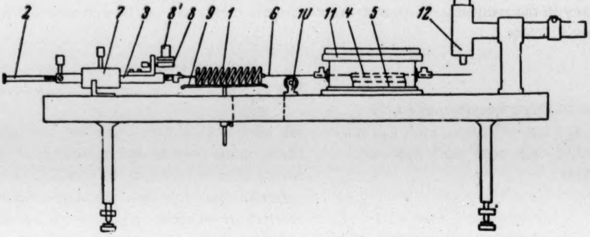

Instrument for determination of stress relaxation.

tween the objective and the scale is regulated by the device 8. To exclude the action of the spring's own weight on the plate, the spring rests on a special table 9, and sliding of the coils of the spring along this is assisted by tapping of the table. If a constant and not a variable stress is used in an experiment, then the stress is transmitted to the upper plate from a load suspended from a flexible thread passing over the pulley 10. The box 11, in which all the openings to the outside are sealed with liquid, serves to protect the material under test from evaporation. The microscope 12 through which the rod connected to the movable plate 4 is observed, acts as the reading device for measurement of the deformation. The instrument has a thermostat, not shown, in which the plates and protective box are housed. After a certain interval the temperature becomes constant and remains so throughout the experiment.

SUMMARY

1. The law governing the development of elastic deformation (elastic after-effects) under constant stress, and the decay of this deformation after removal of the load, has been established for polyisobutylene. The relationship established between deformation and time includes a single characteristic of the system, which is practically constant over the entire range of development and recovery of deformation, and is independent of the stress.

2. An equation is derived for stress relaxation at a given constant deformation. This equation agrees well with experimental data; it is based on the assumption that stress relaxation at constant deformation consists of an increase of elastic deformation and deformation of viscous flow, equal to the decrease of the conventional instantaneous-elastic deformation, while the elastic deformation develops according to the relationship which has been established.

LITERATURE CITED

[1] T. Alfrey, Mechanical Behavior of High Polymers (New York-London, 1948).

[2] W. Kuhn, O. Kunzle, and A. Preissman, Helv. Chim. Acta 30, 307, 464, 487, 839 (1947).

[3] E. R. Fitzgerald, L. D. Grandine, and J. D. Ferry, J. Appl. Phys. 24, 650, 911 (1953).

[4] B. A. Dogadkin, G. M. Bartenev, and M. M. Reznikovsky, Colloid J. 11, 314 (1949).

[5] Yu. S. Zuev, Proc. Acad. Sci. USSR 73, 755 (1950).

[6] S. I. Sokolov, ed. Structure and Physico-Mechanical Properties of Rubber, etc., Collected Papers of the Sci. Research Inst. Rubber Ind. (1937).

[7] P. A. Rebinder, Collected papers: New Methods for Physicochemical Investigations of Surface Phenomena,

Trans. Inst. Phys. Chem. (Acad. Sci. USSR Press, 1950), 1, 5; E. E. Segalova and P. A. Rebinder, Colloid J. 10, 233 (1948).

[8] L. V. Chumakova and P. A. Rebinder, Proc. Acad. Sci. USSR 81, 239 (1951); Colloid J. 18, 429 (1956) (T.p 421).*

Received April 7, 1956

Institute of Physical Chemistry Academy
of Sciences USSR, Moscow

---

[*] T.p = C. B. Translation pagination.

APPLICATION OF LUMINESCENCE MICROSCOPY AND OF RADIOACTIVE ISOTOPES FOR DETERMINATION OF THE DEGREE OF COATING OF MINERAL PARTICLES BY BITUMEN

A. S. Kolbanovskaya

Hydrophobic ash, a material used for insulation against heat and water in building, is made by treatment of ash from power stations with a solution of bitumen in green oil or kerosene, heated to 150-200° [1,2]. This material acquires its hydrophobic properties from the bitumen film which coats the ash particles and prevents the ash becoming soaked in use.

The wetting of bitumenized hydrophobic ash which has sometimes occurred in practice suggests that the bitumen does not cover the ash particles completely, but only in separate regions, and therefore the surface structure of the hydrophobic ash particles is of a "mosaic" nature. The distribution of the bitumen over the ash particles is undoubtedly affected by the quantity of bitumen solution used for the treatment, and also by the presence in it of surface-active substances of an acid character.

The purpose of this investigation was to develop a method for determining the extent of the "mosaic structure" of bitumenized hydrophobic ash, with the object of finding methods for more complete coating of the ash particles by the bitumen film.

Study of the Distribution of Bitumen over the Surface of Ash Particles by the Luminescence method

Determination of the distribution of bitumen on the surface of hydrophobic ash particles involves certain experimental difficulties. Because the ash and the bitumen are black, the oridnary optical methods are unsuitable for observation of the bitumen film on the ash surface. It proved possible to detect and to study the distribution of bitumen on ash particles by means of luminescence microscopy. As is known, bitumens, like other petroleum products, have luminescent properties. The fluorescence method has been widely used [3-5] for detection and study of bitumen in minerals.

Meisel [6] has developed the bases for the application of fluorescence microscopy. Fluorescence effects make it possible to distinguish individual details of the object under examination owing to their different luminescence colors under the influence of ultraviolet or short wave visible light. The rays which excite luminescence are concentrated onto the object and induce visible luminescence of the parts capable of showing the effect. The remaining regions remain dark. As bitumen has the property of fluorescence while ash remains black in ultraviolet and short blue light, the distribution of bitumen over each particle can be studied. Fluorescence was studied with the aid of the Reichart luminescence microscope in visible short wave blue light. Bitumen films, asphaltenes obtained from the bitumen, tars, oils, and the green oil and kerosene used as solvents were first examined under the luminescence microscope. The materials were distinguished by their luminescence colors (Table 1).

An examination of a hydrophilic ash sample showed complete absence of luminescence; the ash particles were fairly large and no aggregation was observed. An examination of bitumenized hydrophobic ash under the luminescence microscope confirmed the view that the bitumen film does not cover the power completely, as dark particles were present in addition to particles exhibiting a greenish yellow luminescence. Most of the particles showed only isolated luminescent regions. Results of an examination of ash treated with various amounts of bitumen solution in green oil or kerosene are summarized in Table 2.

TABLE 1

Luminescence Colors of the Materials Examined

Material	Luminescence color	Material	Luminescence color
Bitumen	Greenish yellow	Oils	Yellow
Asphaltenes	Brown	Green oil	Yellow-green
Tars	Orange	Kerosene	Pale green

TABLE 2

Appearance of Ash Particles Under the Luminescence Microscope

Amount of bitumen solution as % of weight of ash	Appearance under luminescence microscope
	40% solution of bitumen in green oil
3	Numerous dark particles. Occasional particles with isolated yellow-green luminous regions on the surface.
5	Increasing numbers of particles with individual luminescent regions. Size of these regions and luminous intensity vary. Absolutely dark particles occur.
10	Many particles with luminescent regions. A few particles completely luminescent, occasional dark particles.
15	Nearly all particles have luminous regions, mainly at corners and edges. Some aggregation of particles into large clusters. Some particles completely luminescent.
	40% solution of bitumen in kerosene
3	Nearly all particles black, very rare individual luminescent regions. Occasional particles surrounded by a green halo.
5	Some particles have regions with a greenish luminescence; many dark particles.
10	Increasing number of particles with luminescent regions. Green halo around particles.
15	Nearly all particles have luminous regions, mainly at corners and edges. Some particles completely luminescent with a yellow-brown color.

It should be pointed out that ash treated with bitumen solution in green oil has a much larger surface with a yellow-green luminescence than ash treated with bitumen dissolved in kerosene. Addition of surface-active agents, 1% acidol or oleic acid, to the solution used for treating the ash increases the number of luminescent regions on the ash surface.

It should be noted that the fraction of luminous surface in all the examined samples of hydrophobic ash was generally not large (Fig. 1). This may be attributed largely to the mosaic structure of the particle surfaces. However, the possibility is not excluded that some regions are covered with a bitumen coating so thin that it cannot be distinguished by the luminescence method. Moreover, only one plane of the particles is visible in the microscope field.

Fluorescence studies of bitumenized hydrophobic ash show that the bitumen does not cover the ash surface completely; in addition to particles which have no bitumen coating at all, there are numerous particles partially coated with bitumen, with the bitumen preferentially situated at the particle corners and edges. Very few of the particles are completely covered with a bitumen film. An increase of the amount of bitumen solution used for treatment of the ash increases considerably the area of the particles coated with the bitumen film.

Introduction of surface-active agents, acidol and oleic acid, into the bitumen solution makes the coating of the ash more uniform, apparently favoring the distribution of the bitumen over a large area.

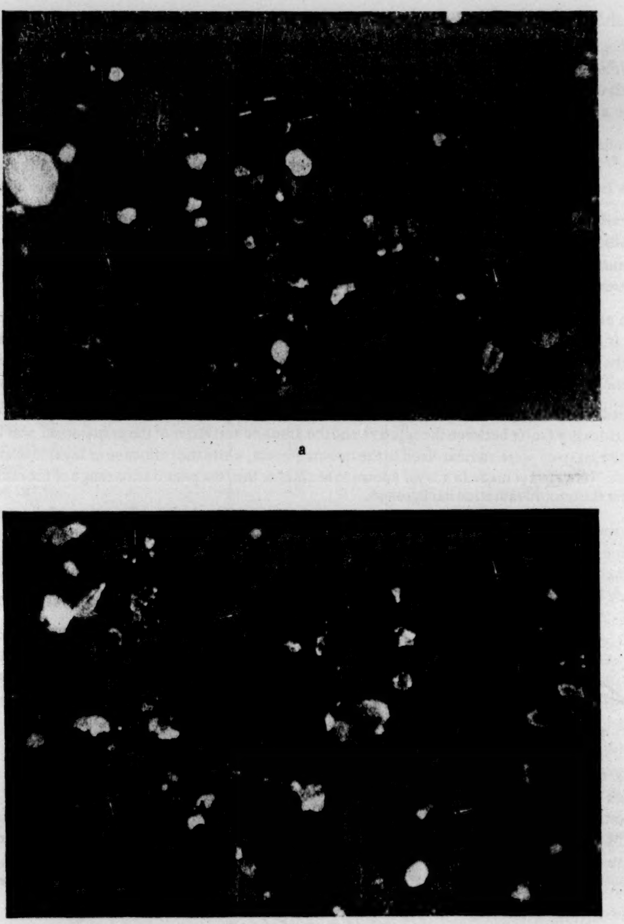

a

b

Fig. 1. Luminescence microphotographs of ash treated with bitumen solutions in green oil: a) 10%, b) 15%.

Treatment of the ash with a solution of bitumen in green oil gives a better distribution of the bitumen over the ash surface; this is probably to be explained by the action of highly aromatic hydrocarbons which are predominantly present in green oil and which make it a good solvent for bitumen; moreover, such hydrocarbons peptize asphaltenes and are adsorbed on them, and are therefore not removed completely during the preparation of hydrophobic ash.

Determination of the Relative Area of the Ash Coated with a Bitumen Film by the Labeled Atom Method

Although studies of the luminescence of bitumenized ash give, in the main, a correct picture of the distribution of bitumen over the ash surface, a quantitative evaluation by this method is difficult. A quantitative estimate of the relative area of the ash surface coated by the bitumen film can be obtained by the selective adsorption method, whereby the adsorbate is adsorbed only by the ash surface and not by the bitumen-coated surface.

Foremost among substances selectively adsorbed by the ash surface are salts of bivalent metals, including Sr^{2+} and Co^{2+}. Adsorption of radioactive isotopes of these metals can be measured very simply and accurately. Radioactive isotopes have been used repeatedly for investigation of surfaces and adsorption effects [7-12].

The radioactive method of adsorption measurement is based on the establishment of adsorption equilibrium between the adsorbent and a solution containing the labeled adsorbate. As small quantities of radioactive materials are easily measured, the adsorption can be determined from the decrease of radioactive material in the solution or from its presence on the adsorbent.

When adsorption equilibrium is reached $E_S/E_V = I_S/I_V$, where E_S is the total quantity of stable isotope on the surface; E_V is its content in the solution I_S is the total quantity of radioactive isotope on the surface, and I_V is its content in the solution. The total surface area of the powder is found by multiplication of E_S by the area (H) occupied by one gram-atom of the substance in the surface.

The radioactivity was detected and measured by means of a Geiger counter. The count coefficient β, which is the proportionality factor between the relative and the absolute activities of the preparation, was 2.5. The area and position of the preparation were standardized in the measurements, while the influence of layer thickness was excluded as the measurements were always made in a layer known to be thicker than the penetration range of the radiation. Corrections were made for the cosmic radiation background.

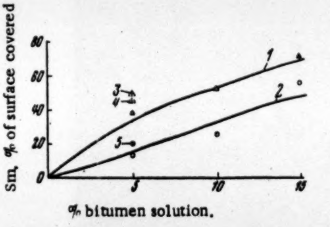

Fig. 2. Area covered by bitumen film as a function of the amount of 40% bitumen solution (found from the adsorption): 1) In green oil; 2) in kerosene; 3) in green oil + 1% oleic oil; 4) in green oil + 1% acidol 5) in kerosene + 1% acidol.

The degree of coating of the ash surface by bitumen film was determined from the adsorption of strontium from an aqueous solution of stable $Sr(NO_3)_2$ to which a small quantity of the active Sr^{89} isotope had been added; the concentration of active Sr^{89} was very low and was neglected.

Equal weights of ash, untreated and treated with various quantities of bitumen, were placed into equal volumes of the $Sr(NO_3)_2$ solution. The ash and solution were shaken on a shaker for 1 hour. Adsorption equilibrium was reached during this time; the ash was then filtered off and dried.

The activity of the preparation was determined in the solid phase. As a small weight of ash (0.05 g) was contained in a large volume of solution (20 ml), the initial concentration of $Sr(NO_3)_2$ could be regarded with sufficient accuracy as the equilibrium concentration. The adsorption was calculated from the formula

$$q = cI_2/I_1m \quad \text{mg Sr/g ash},$$

where c is the initial and equilibrium concentration of the solution in mg/ml; I_1 is the activity of the original solution without the background activity, in pulses/min·ml; I_2 is the activity of the ash after adsorption, without background activity, in pulses/min.

The area of the ash coated by the bitumen film can be calculated from the value for the adsorption on the surface of hydrophilic ash, completely uncoated. The ratio between the adsorption of strontium by hydrophobic ash to the adsorption by hydrophilic ash gives the proportion of "open ash" surface $S_n = q_n / q_0 \cdot 100\%$.

The proportion of the ash surface coated by the bitumen film is $S_m = 100 - S_n$.

Table 3 shows the results of the adsorption determinations and the calculated values of the proportion of the ash surface coated by the bitumen film.

Fig. 2 shows the relationship between the relative area coated by the bitumen film and the amount of bitumen solution added to the ash in treatment. The results show that the proportion of coated surface increases with increasing amount of bitumen solution added. Bitumen dissolved in green oil results in a considerably higher proportion of coated surface than bitumen dissolved in kerosene. Additions of surface-active substances – acidol and oleic acid – to the bitumen solution also produce some increase in the coated area.

TABLE 3

Area of Ash Particles Coated by Bitumen, According to Adsorption Measurements.

Composition of bitumen solution used, %	Amount of bitumen solution, %	Adsorption q, mg Sr/ g ash	Open surface, %	Surface coated with bitumen film, %
Without solution	0	32	100	0
Bitumen 40 + kerosene	5	27.3	86	14
Bitumen 40 + green oil 60	5	19.7	61.5	38.5
Bitumen 40 + green oil 59 + acidol 1	5	17.3	54	46
Bitumen 40 + green oil 59 + oleic acid 1	5	16.0	50	50
Bitumen 40 + kerosene 59 + acidol 1	5	25.6	80	20
Bitumen 40 + kerosene 60	10	24	75	25
Bitumen 40 + green oil 60	10	15.5	48.5	51.5
Bitumen 40 + kerosene 60	15	17.5	54.6	55.4
Bitumen 40 + green oil 60	15	9.4	29.4	70.6

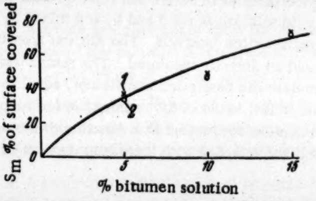

Fig. 3. Variation of the area coated with a bitumen film with the method of adding the bitumen solution (measured by adsorption): 1) In several stages; 2) at once.

The method used for ash treatment (simultaneous or gradual addition of the bitumen solution) has practically no influence on the extent of adsorption, and therefore on the calculated values of the relative proportion of the coated surface (Fig. 3). In addition to selective adsorption of strontium ions, the degree of coating of the ash by the bitumen film can be estimated from the unequal desorption of previously adsorbed strontium from the surface of untreated ash and ash coated with a bitumen film. The ash was first treated with a solution of strontium nitrate containing radioactive Sr^{89} isotope (solution concentration c = = 2 mg/ ml; activity I = 41.64 pulses/ ml) by mixing in a shaker. When adsorption equilibrium had been reached, the ash was filtered off, dried, and treated with a solution of 40% bitumen in green oil.

It was assumed that desorption of Sr^{2+} occurs only at regions of the ash surface not covered with the bitumen film, or the "open" regions. However, in view of the fact that migration of strontium ions from under the bitumen film, and some diffusion of water through the film can occur, the desorption of strontium from the coated regions of the surface may be merely retarded. The kinetics of Sr^{2+} desorption from various ashes was therefore studied. It was intended to carry out the desorption in a solution of stable strontium nitrate, where ion exchange should occur. However, our measurements showed that there was practically no desorption of active strontium even for the surface of hydrophilic ash. The absence of desorption in a solution of stable strontium suggested the existence of a more

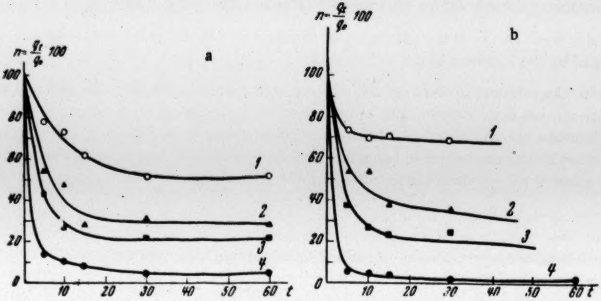

Fig. 4. Kinetics of the desorption of strontium from hydrophobic ash in solution: a) pH 5; b) pH 3; ash treated with: 1) 15%; 2) 10%; 3) 5% bitumen solution; 4) untreated.

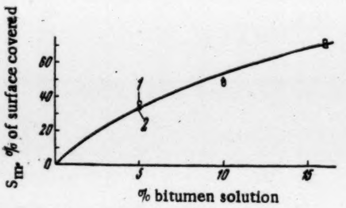

Fig. 5. Variation of the area coated with a bitumen film with the amount of bitumen solution (before desorption) 1) pH 3; 2) pH 5.

stable bond between the adsorbed Sr^{2+} and the ash then is generally the case in physical adsorption. Desorption of Sr^{2+} from ash in the case of physical adsorption, or destruction of a weak chemical complex formed during adsorption, may occur in an acid medium, and a study was therefore made of the desorption of strontium from the ash surface in an acid medium at two pH values. It was previously shown that an acid medium does not destroy the bitumen film and that the hydrophobic properties of the ash are completely retained.

Weighed samples of active ash (0.05 g) were placed into nitric acid solution at pH 3 and 5, and mixed in a shaker for various time intervals. The ash was then filtered off, dried, and its activity measured. The results were used to calculate the desorption coefficient, equal to the ratio of the adsorption of Sr^{2+} by the ash in any time interval, to the initial value of Sr^{2+} adsorption for the given material. The results are shown in Fig. 4 as the variation of the desorption coefficient as a function of the desorption time. Fig. 4 shows that desorption is considerably decreased and retarded with increasing amount of the bitumen solution used for treatment of the ash.

On the assumption that the quantity of desorbed strontium at the initial moment is proportional to the open surface area of the ash, we can calculate the proportion on the ash surface coated with the bitumen film; it is equal to the ratio of the quantity of strontium desorbed from the surface of hydrophobic ash during 5 minutes of shaking, to the quantity of strontium desorbed in the same time from the surface of untreated ash.

Fig. 5 shows the variation of the relative ash area coated with bitumen film, with the amount of bitumen solution (in green oil) taken for treatment of the ash. Fig. 5 shows that the values of the relative ash surface coated with bitumen in the range pH 3-5 are practically equal for the given ash, and depend only on the amount of bitumen solution taken for the treatment.

The results of the desorption measurements are in full agreement with the results obtained by adsorption determinations. Identical results are obtained by those totally different experiments for the relative ash surface coated with bitumen film (Table 4).

TABLE 4

Relative Area of Ash Particles Coated With Bitumen, From Adsorption and Desorption Measurements

Experiment	Percentage surface coated with bitumen, ash treated with		
	5% bitumen solution	10% bitumen solution	15% bitumen solution
Adsorption from solution, c = 1 mg/ml	38.5	51.5	70.6
Ditto, c = 2 mg/ml	33.5	46.5	71
Desorption from ash, solution pH 3	34	51.5	72.6
Ditto, solution pH 5	36.4	48.5	74.8

Adsorption of strontium from aqueous strontium nitrate solution, studied by the radioactive isotope method, showed that strontium is readily adsorbed on the untreated ash surface and is not adsorbed on the bitumen-coated surface. Our calculations of the relative area of the ash coated with bitumen were based on the assumption that the adsorption of strontium is proportional to the "open" surface of the ash. The degree of coating depends, in the first instance, on the amount of bitumen solution taken for the treatment of the ash. A much larger proportion of the surface is covered if ash is treated with bitumen dissolved in green oil than in kerosene. The presence of surface-active agents – acidol and oleic acid – in the bitumen solution increases the degree of coating of the powder by bitumen film.

The rate and extent of desorption of strontium from the ash in an acid medium depend on the degree of coating of the ash surface with bitumen. Strontium is desorbed almost completely from the surface of untreated ash even in the first few minutes, while the desorption of strontium from the surface of hydrophobic ash is very slow. Our calculations of the relative area of the ash coated with bitumen were based on the assumption that the desorption of strontium at the initial instant is proportional to the "open" surface of the ash.

Identical values for the relative surface covered with bitumen film were obtained in experiments on adsorption of strontium on the ash surface and on its desorption.

The results obtained by the adsorption methods for the influence of the solvent and of surface-active agents, and of the method of addition of the bitumen solution, agree qualitatively with the results of similar investigations by the luminescence method.

SUMMARY

1. A simple and reasonably clear method for obtaining a qualitative picture of the distribution of bitumen on the surface of ash particles is the study of luminescence of hydrophobic ash. This method has been used to determine the influence of various factors on the apparent increase of the ash area coated with the bitumen film.

2. The relative proportion of the ash surface coated with the bitumen film can be determined by selective adsorption of radioactive Sr^{89} isotope by the hydrophilic surface of the ash, and also from the difference in the rates of desorption of this ion from a hydrophilic surface and a surface coated with a bitumen film.

3. A study of the distribution of bitumen over the ash surface, made by the luminescence and selective radioisotope adsorption methods, showed that bitumen does not cover the particles completely, but is mainly situated at the corners and edges of the ash particles.

4. The ash surface are coated with the bitumen film primarily depends on the amount of bitumen solution used for treatment of the ash. The coated area increases with increasing amounts of bitumen solution.

5. Treatment of ash with bitumen dissolved in green oil results in a much larger proportion of the area being covered, than treatment with bitumen dissolved in kerosene.

6. Addition of surface-active substances to the bitumen solutions increases the degree of coating of the powder by the bitumen film.

7. A variation of the hydrophobization procedure by gradual addition of bitumen solution to the ash does not produce a significant increase of the degree of coating, but prevents cohesion of the particles at high bitumen concentrations.

Head of the Laboratory, N. V. Mikhailov participated in the work.

LITERATURE CITED

[1] N. V. Mikhailov and A. S. Panin, Roof and Hydroinsulation Coatings (State Building and Architecture Press, 1952).

[2] A. S. Panin, A. S. Kolbanovskaya, and G. A. Mesropov, Roofing with Hydrophobic Ash (Inst. Inform. Econ. Technol., 1954).

[3] A. F. Fioletova, Bull. Acad. Sci. USSR, Phys. Ser. 13, No. 2 (1949).

[4] V. M. Florovskaya, Bull. Moscow Univ. 1949, No. 2.

[5] F. M. Efendiev, Proc. Acad. Sci. Azerbaidzhan SSR 5, (1949).

[6] M. N. Meisel, J. Microbiol. 16, Nos. 1-6, 19, 7 (1948).

[7] F. Paneth, Radio-Elements as Indicators (New York, 1928).

[8] V. G. Khlopin, J. Phys. Chem. 13, 1282 (1939).

[9] O. Hahn, Applied Radiochemistry (State Chem. Press, 1947).

[10] A. I. Brodsky, Isotope Chemistry (Acad. Sci. USSR Press, 1952).

[11] S. E. Bresler, Radioactive Elements (1949).

[12] S. Brunauer, Adsorption of Gases and Vapors (1948).

All-Union Scientific Research Insitute for Building

Received September 19, 1955

DECOMPOSITION RATE OF ISOPROPYLBENZENE HYDROPEROXIDE (CUMENE HYDROPEROXIDE) IN AQUEOUS SOLUTIONS OF EMULSIFIERS

R. V. Kucher and A. I. Yurzhenko

Aqueous solutions of soaps may serve as preferential locations for the occurrence of a number of important chemical processes, such as the emulsion polymerization of hydrocarbons [1]. The successful course of this reaction (which is a chain process) requires the presence of initiators capable of originating the reaction chains. Organic alkyl and alkyl-aryl hydroperoxides are now widely used as initiators [2]. Under certain conditions (for example, at high temperatures) these compounds can decompose to form free radicals, which initiate the chain process. Tertiary peroxides are especially active in this respect [3].

There is no doubt that the initiation activity of peroxides is associated with the mechanism of their decomposition, which may vary under different conditions. The thermal decomposition of organic hydroperoxides has been studied mainly in organic media [4], and it was shown that a significant role is played by the nature of the peroxide itself, and also of the solvent [5]. Very little information is available in the literature on the decomposition of hydroperoxides in aqueous media. However, hydroperoxides are used in aqueous emulsions as polymerization initiators. The question of the decomposition of hydroperoxides in an aqueous medium is therefore of considerable interest.

Kharash et al. [6] studied the decomposition of isopropylbenzene hydroperoxide and showed that it is catalyzed by strong acids. The decomposition reaction is considerably accelerated in an aqueous medium in presence of acids, the main products being phenol and acetone. An ionic decomposition mechanism is assumed. On the other hand, if other substances are added to the reaction medium, decomposition of isopropylbenzene hydroperoxide proceeds by a radical mechanism with formation of the $C_6H_5(CH_3)_2CO$ radical at the first reaction stage.

Recently Yurzhenko and Grobshtein [7] studied the decomposition of tertiary butyl hydroperoxide in an aqueous medium; they showed that the decomposition rate is greatly influenced by the presence of soaps (emulsifiers) in the reaction mixture, and this influence depends both on the nature of the emulsifier and on the pH of the medium. Since emulsifers are inevitably present with peroxides when the latter are used as initiators of emulsion polymerization, the importance of such investigations is obvious.

The present paper deals with a study of the decomposition rate of a known initiator of the emulsion polymerization of hydrocarbons— isopropylbenzene hydroperoxide (cumene hydroperoxide)— in aqueous solutions of certain emulsifiers. In our opinion such an investigation would assist considerably in elucidation of the mechanism of emulsion polymerization.

EXPERIMENTAL

Materials and methods. Cumene hydroperoxide (CHP) was obtained from the technical product by purification as described in the literature [5]. CHP was converted into its salt by addition of 100 ml of the hydroperoxide to 300 ml of 25% caustic soda solution. The salt crystals were filtered off and washed several times with benzene. The salt was then suspended in 100 ml of distilled water and the hydroperoxide liberated by addition of 4 N HCl to pH 7.5; it was separated from the aqueous phase by extraction with ligroine, which was then driven off under vacuum at a temperature not higher than 40°. The purity of the product was found by analysis to be 99.2% active CHP.

The decomposition rate of the hydroperoxide was studied in the presence of the following emulsifiers: Nekal (sodium dibutylnaphthalene sulfonate), sodium oleate, potassium stearate and laurate. The Nekal was purified to remove inorganic salts by a method described previously [8]. The other emulsifiers were obtained by neutralization of the corresponding acids by sodium or potassium alcoholates [9]. The electrolytes used – soda, sodium sulfate, and sulfuric acid – were chemically pure.

The thermal decomposition of CHP in aqueous solutions was carried out in sealed glass tubes in an atmosphere of pure nitrogen. The tubes were immersed in a thermostat at 98.5°, removed at definite time intervals, opened, and the contents were analyzed for hydroperoxide.

The analytical determination of CHP was carried out as follows [10]. A sample of the solution (1 ml) was dissolved in 50 ml of boiling absolute alcohol; 1 ml of glacial acetic acid and 1 ml of saturated potassium iodide solution were added simultaneously. The mixture was boiled for 5 minutes and then cooled; the liberated iodine was titrated with 0.01 N thiosulfate solution. The titration was carried out potentiometrically to zero, that is, until zero difference of potential was established between the platinum microelectrode and the saturated calomel electrode. The potential difference was measured by means of a galvanometer with a sensitivity of 10^{-6} A. The accuracy of the method is 2%.

Since CHP is predominantly an oil-soluble peroxide, it should be solubilized in aqueous solutions of emulsifiers, so that the emulsifier micelles act as the solvent. This must undoubtedly influence the rate and mechanism of decomposition of the hydroperoxide. Therefore, before studying the decomposition rate, we studied its solubilization at different concentrations of Nekal and other emulsifiers.

To determine the solubilization, the solutions were saturated with the hydroperoxide, the undissolved CHP was separated by centrifuging, and the active hydroperoxide content of the solution was then determined. These experiments were performed at 20°.

Solubilization of CPH in aqueous emulsifier solutions. The solubilization of CHP was studied at various emulsifier concentrations and pH values. The pH was varied by addition of 0.1 N soda or sulfuric acid solutions, and measured by means of the glass electrode.

The results of determinations of the solubilization of CHP in aqueous solutions of Nekal are shown in Fig. 1. It is seen that the solubility of the hydroperoxide is increased in presence of Nekal at 11 pH values, indicating solubilization. A similar result is found for the other emulsifiers.

Thus, both the peroxide in true solution (solubility 1.4%) and the peroxide present in the emulsifier micelles will participate in the thermal decomposition of CHP in aqueous solutions of emulsifiers. This may lead to a change in the decomposition rate, and this must undoubtedly be taken into account in explaining the results of experiments on the kinetics of hydroperoxide decomposition.

Effect of pH of the medium on the decomposition rate of CHP. The rate of decomposition of CHP in aqueous solutions was studied, without electrolytes (pH of original solution 5.8), in presence of 0.1 N soda solution (pH 9.9), and in presence of 0.1 N sulfuric acid solution (pH ~ 0.9). The results are shown in Fig. 2. It is seen from Fig. 2 that the decomposition rate of CHP in pure water at pH 5.8 (due to the peroxide itself) is very low. The stability of the hydroperoxide is appreciably decreased on addition of soda. A particularly large acceleration of the decomposition of CHP is found in an acid medium. This is in full agreement with Kharash's results [11], and is caused by the catalytic action of hydrogen ions. The sharp differences in the decomposition rate of CHP at differen pH values are probably a sign of a different mechanism for the decomposition of hydroperoxide in alkaline, neutral, and acid media. This is confirmed by the differences in the decomposition products in an acid and alkaline medium (see below); in this connection it is necessary to take into account the conversion of the hydroperoxide into its salt in an alkaline medium, which results in the formation of other reaction products.

The decomposition of hydroperoxide in the above instances is a first-order reaction, as shown by the linear nature of the log $c = f(t)$ graphs. It is therefore possible to calculate the values of the reaction rate constants from the kinetic equation for a reaction of the first order. The values of the rate constants are shown in Table 1.

Effect of emulsifiers on the decomposition rate of CHP. The effect of the nature of the emulsifier on the decomposition rate of CHP in an aqueous medium is shown in Figs. 2-4. These results show that in an acid and neutral (pH 5.8) medium Nekal accelerates decomposition of CHP. On the other hand, in an alkaline medium the decomposition of CHP is slower in presence of Nekal than in its absence. This poses the question whether the action of Nekal is associated with its colloidal nature or whether its action here is that of an electrolyte.

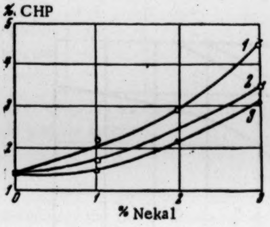

Fig. 1. Solubilization of CHP in aqueous Nekal solutions at pH 5.8 (1), 0.9 (2), and 9.9 (3).

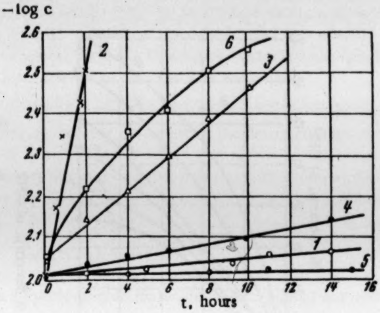

Fig. 2. Decomposition of CHP in an aqueous medium at 98.5°C: 1) pH 5.8; 2) pH 0.9; 3) pH 9.9; 4) 3% Nekal solution (pH 5.8); 5) 0.1 N solution of Na_2SO_4 (pH 5.8); 6) 3% Nekal solution containing solubilized methylstyrene (pH 5.8).

TABLE 1

Rate Constants for the Decomposition of CHP ($k \cdot 10^3$ min.$^{-1}$) in an Aqueous Medium at 98.5°.

pH	$k \cdot 10^3$ min.$^{-1}$ in various media					
	water	1% Nekal solution	2% Nekal solution	3% Nekal solution	0.1 N H_2SO_4 solution	Solubilized benzene in 3% Nekal solution
~0.9	11.4	27.7	30.5	31.4	–	59.0
5.8	0.183	0.196	0.222	0.336	0.029	0.361
9.9	1.57	1.11	1.01	0.974	2.26	1.25

To settle this point, we carried out experiments on the decomposition of CHP at pH 5.8 and 9.9 in presence of sodium sulfate, an ordinary electrolyte with a composition similar to that of the polar group in Nekal. Curve 6 in Fig. 3 and Curve 5 in Fig. 2 show that addition of sodium sulfate does not influence the decomposition rate of the hydroperoxide in the same way as Nekal. There is no doubt that the action of Nekal depends on its colloidal nature in aqueous solutions.

As regards the action of other emulsifiers, it is seen from Fig. 4 that fatty acid soaps, in contrast to Nekal, produce an acceleration in the decomposition of CHP in all cases. The increase in the decomposition rate is particularly sharp in presence of sodium oleate. It should be noted that the rate constants calculated from the first-order equation are different in this case. This indicates that the nature of the decomposition of CHP changes in the presence of sodium oleate. Moreover, the rate constant for the decomposition of the hydroperoxide in presence of sodium oleate depends on the CHP concentration. All this suggests that the reaction is not a simple decomposition of the hydroperoxide, but a chemical reaction occurs between the CHP molecules and the sodium oleate molecules owing to the unsaturated nature of the latter. This view was advanced by one of us [7] in a study of the decomposition of tertiary butyl hydroperoxide in similar conditions. It is possible that the other soaps also accelerate the decomposition of CHP, partly owing to the presence of unsaturated acids as impurities.

To determine the possibility of the reaction of CHP with the organic parts of the micelles, we first saturated the Nekal micelles with hydrocarbons. In these experiments the Nekal solutions were previously saturated with chemically pure benzene or methylstyrene for twenty-four hours. The residue of undissolved hydrocarbon was removed by centrifuging, so that a solubilized solution was obtained. The results of these experiments at pH 9.9 and ~0.9 are shown in Figs. 2 and 3. It is seen from Figs. 2 and 3 that solubilized benzene somewhat

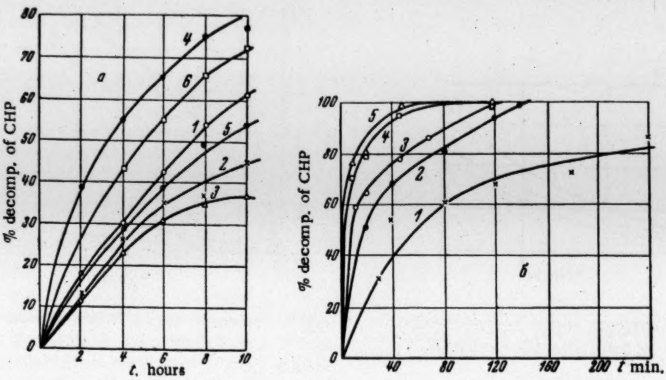

Fig. 3. Effect of Nekal on the decomposition rate of CHP at pH 9.9 (a) and pH 0.9 (b) at 98.5°: 1) In absence of Nekal; 2) 1% Nekal solution; 3) 3% Nekal solution; solubilized methylstyrene solutions – 4a), 5b) and benzene – 4b), 5a); 6) 0.1 N Na_2SO_4 solution.

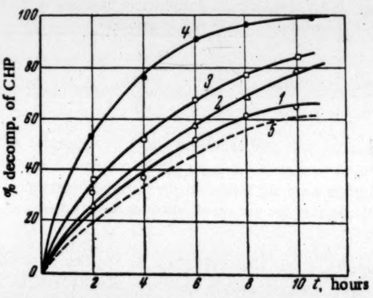

Fig. 4. Effect of emulsifiers on the decomposition rate of CHP at pH 9.9 (t = 98.5°C): 1) 3% potassium laurate solution; 2) 0.5% potassium stearate solution; 3) 0.4% sodium oleate solution; 4) 3% sodium oleate solution; 5) without added emulsifier.

increases the decompositon rate of CHP both in an acid and in alkaline medium. This is probably associated with the role of the interphase in the decomposition of the hydroperoxide, which is a surface-active substance [7]. When the CHP micelles are adsorbed on the surfaces of micelles saturated with hydrocarbon, more favorable conditions are evidently created for their decomposition.

Solubilized methylstyrene increases the decomposition rate of CHP considerably, especially at pH 5.8. It should be noted that the rate constant calculated from the first-order equation does not have a constant value. Apparently in this instance, as in the presence of sodium oleate, a reaction occurs here between the unsaturated compound and the hydroperoxide.

Products of the decomposition of CHP in an aqueous medium. To identify the decomposition products of CHP in an aqueous medium at various pH values, qualitative tests were carried out for the presumed reaction products after the kinetic experiments. The following qualitative reactions were carried out [12]: 1) for phenol, with bromine water; 2) for carbonyl group, with phenylhydrazine; 3) with Schiff's reagent, to distinguish between aldehyde and ketone groups; 4) with Denige's reagent (solution of mercuric oxide in concentrated sulfuric acid) for tertiary alcohols. Aqueous solutions of CHP at pH 5.8, 9.9, and ~0.9 in absence and presence of Nekal were studied. The presence of this emulsifier in the solution did not change the character of the reaction products. The results of these experiments are shown in Table 2.

Moreover, all the acid solutions with the decomposed hydroperoxide had a pronounced odor of phenol. The alkaline solutions had an odor of acetophenone, not found in an acid medium. Thus it follows that the principal

TABLE 2

Decomposition Products of CHP in Aqueous Media

Reaction	Aqueous CHP solution at pH		
	~0.9	5.8	9.9
Bromine water	+ +	+	−
Phenylhydrazine	+	+	+
Schiff's reagent	−	−	−
Denige reaction	−	+	+ +

Convention: − negative reaction; + positive reaction; + + strongly positive reaction.

decomposition products of CHP in presence of acid are phenol and acetone. This is in full agreement with Kharash's results [11]. In an alkaline medium dimethylphenyl carbinol, acetophenone, and also possibly acetone are formed. In absence of electrolytes (pH 5.8), all the above reaction products are formed.

Certain conclusions may be drawn from the foregoing, concerning the nature of the decomposition of CHP in an aqueous medium in presence of emulsifiers. Primary thermal decomposition of CHP occurs at the O−O peroxide bond; as a result, two radicals are formed:

$$C_6H_5(CH_3)_2CO-OH \rightarrow C_6H_5(CH_3)_2CO\cdot + OH. \qquad (1)$$

Subsequently the first of these radicals can react with a hydroperoxide molecule to form phenol and acetone:

$$C_6H_5(CH_3)_2CO\cdot + C_6H_5(CH_3)_2CO-OH \rightarrow C_6H_5(CH_3)_2CO\cdot + C_6H_5OH + (CH_3)_2CO. \qquad (2)$$

Such decomposition of CHP occurs in an acid medium. This type of hydroperoxide decomposition leads to recombination of the free radicals and it is therefore inactive with respect to initiation of the emulsion polymerization reaction. It is in fact found [13] that the emulsion polymerization of styrene and other hydrocarbons proceeds extremely slowly in an acid medium.

Acetophenone may be formed in an alkaline medium by removal of a CH_3 group from a $C_6H_5(CH_3)_2CO\cdot$ radical. The methyl group can then combine with an OH radical to form methyl alcohol. Some formation of dimethylphenyl carbinol may also occur by interaction of both radicals formed in Reaction (1).

Finally, the influence of emulsifiers on hydroperoxide decomposition is probably associated with their hydrophilic nature, a measure of which is provided by their surface activity [14]. The more hydrophilic the emulsifier is, the more it protects the hydroperoxide molecules against decomposition or stabilizes them. In this instance the emulsifiers form the following series according to their hydrophily: Nekal > K laurate > K stearate.. The influence of these emulsifiers on stabilization of CHP follows the same sequence. Thus, the more hydrophobic an emulsifier is, the better it catalyzes the hydroperoxide decomposition.

It must also be taken into account that the influence of emulsifiers on the decomposition rate of hydroperoxides may be associated with solubilization of the latter. The molecules of the solubilized hydroperoxide are probably arranged parallel to the emulsifier groups in the micelles, with the CO−OH peroxide group on the micelle surface. This may give rise to conditions which favor decomposition. The situation may be more complicated if the hydroperoxide forms a salt (in an alkaline medium), where the emulsifier retards decomposition of the hydroperoxide. Thus, colloidal factors undoubtedly influence the decomposition of CHP, because of the surface-active nature of the hydroperoxide, owing to which its molecules may be adsorbed in the surface of the colloidal particles of the emulsifier.

SUMMARY

1. The solubilization of cumene hydroperoxide in aqueous Nekal solutions at various pH values of the medium has been studied. It is shown that the solubility of the hydroperoxide increases with Nekal concentration.

2. The rate of thermal decomposition of CHP in an aqueous medium depends on the pH. Additions of acid or of soda accelerate the decomposition, which indicates that hydrogen and hydroxyl ions have a catalytic effect on the reaction rate. A particularly sharp increase of the rate is found in an acid medium, in which the decomposition mechanism is not the same as in an alkaline medium, which was confirmed by a study of the decomposition products of CHP.

3. Addition of Nekal accelerates the thermal decomposition of the hydroperoxide in an acid medium, and retards it in an alkaline medium. Potassium stearate and laurate and sodium oleate increase the rate of de-

compositon of CHP. A particularly sharp increase is found in the presence of sodium oleate, where a reaction occurs between the hydroperoxide and the unsaturated soap molecules.

4. Benzene solubilized in aqueous Nekal solutions somewhat increases the decomposition rate of the hydroperoxide. A chemical reaction occurs between the hydroperoxide and solubilized methylstyrene.

5. The view is advanced that the influence of emulsifiers on the decomposition rate of CHP varies with the hydrophobic nature of the emulsifiers, and is related to the solubilization and the surface activity of the latter.

LITERATURE CITED

[1] A. I. Yurzhenko, J. Gen. Chem. 16, 1171 (1946).

[2] G. A. Razuvaev, Yu. A. Oldekop, and E. P. Fedotova, Progr. Chem. 21, 379 (1952).

[3] T. I. Yurzhenko, G. N. Gromova, and V. B. Khaitser, J. Gen. Chem. 16, 1505 (1946).

[4] K. I. Ivanov, Intermediate Products and Intermediate Reactions in Hydrocarbon Autoxidation (State Fuel Tech. Press, Moscow, 1949).

[5] I. L. Fordham, and H. L. Williams, Can. J. Research 27 B, 943 (1949).

[6] M. Kharasch, A. Fono, and W. Nudenberg, J. Org. Chem. 15, 763 (1950); Seubol and W. E. Vaughan, J. Am. Chem. Soc. 75, 3790 (1953).

[7] A. I. Yurzhenko and F. I. Grobshtein, Ukrain. Chem. J. 20, 373 (1954).

[8] A. I. Yurzhenko and R. V. Kucher, Colloid J. 13, 226 (1951).

[9] W. D. Harkins, J. Am. Chem. Soc. 51, 1675 (1929).

[10] V. R. Kokatnur and M. Jelling, J. Am. Chem. Soc. 63, 1432 (1941).

[11] M. Kharasch, A. Fono, and W. Nudenberg, J. Org. Chem. 15, 748 (1950).

[12] R. Shriner and R. Fuson, Systematic Identification of Organic Compounds (Moscow, 1950).

[13] A. I. Yurzhenko and N. S. Tsvetkov, Proc. Acad. Sci. USSR 85, 1099 (1952).

[14] E. M. Spivakova, Colloid J. 17, 50 (1955) (T.p. 45).*

Received October 19, 1955

The Ivan Franko State University, Lvov

---

* T.p = C. B. Translation pagination.

EFFECT OF VACUUM ON THE SORPTION OF DYES BY FIBERS

S. M. Lipatov and N. D. Ilyashuk

Dyeing processes, to which increasing attention is being paid, are still little understood from the theoretical side. This probably explains why there have been no important advances in dyeing technology although important changes have taken place in the theory of dyeing in recent years. It is to be expected that they will influence dyeing technology.

Attempts have been made in recent years to relate substantivity to the molecular structure of dyes [1], to explain the affinity of dyes for fibers on thermodynamical grounds [2], and also to make a kinetic and thermodynamical approach to the problem of dye fastness [3]. However, these questions cannot be solved without a detailed study of the properties of dye solutions and also of fiber properties.

The properties of dye solutions are significant because adsorption of dyes by the fibers will take a different course according to whether the dye is in a molecular-ionic or an aggregated state. Our investigations show that many dyes are present in solution in a state of aggregation [4]. As is well known, addition of common salt to the dye bath results in the formation of numerous aggregates, but subsequent heating breaks them down almost completely and the dyeing is effected by a solution in which aggregates are largely or almost completely absent. Studies of the properties of pure dye solutions in water at room temperature, and of solutions in presence of NaCl at a high temperature, show that in a number of instances these solutions show practically no differences and therefore dyeing may be carried out by aqueous solutions of dyes at room temperature. In practice this possibility is restricted, first, by the low solubility of many dyes at room temperature, and second, by their low adsorbability. The present paper deals with an examination of these two questions.

Dye Solubility

As has already been stated, many dyes have very low solubilities at room temperature, but the solubilities rise sharply with temperature, and the dye solutions made a high temperatures do not separate into precipitate and saturated solution on cooling [5]. Thus supersaturated solutions are formed, which can retain their concentration for such long periods that their practical utilization is quite possible. Fig. 1 shows solubility curves for one dye (Direct Brown KKh), although similar curves are obtained for other dyes studied by us (Pure Blue, Direct Violet, etc.)

In Fig. 1 the general Curve ab represents the solubility of the dye as a function of temperature. If the dye is dissolved at 30° and then cooled, then after a day we have the Curve cd; if the solution is made at 40, 50, 60, 70°, we get the Curves ef, gh, ik, bl respectively. Thus, the heating and cooling curves do not coincide, and this fact can be used for preparation of dye solutions of required concentrations. It must be stressed, however, that in solutions of dyes obtained by heating, for example, to 40°, followed by cooling, a part of the dye, for example oa, is present in the form of molecules and ions, and another part of consists of aggregates or "swarms", comprising the dye which can be deposited under favorable conditions. Therefore an equilibrium between aggregates, molecules, and ions exists in the solution. We have shown that if such a solution is brought into contact with any adsorbent, including a fiber, two possibilities exist: 1) the aggregated portion may be adsorbed when the equilibrium in the system is evidently not disturbed while the aggregates as a phase are present in the system; 2) the molecular and ionic portion may be preferentially adsorbed, and in this case the equilibrium in the system will not change, as the existing equilibrium will be shifted in the direction of formation of molecules and ions.

If the aggregates constitute a phase, then the first is a temperature and the second a concentrational equilibrium. If the aggregates do not form a phase, them both equilibria are governed by the mass-action law. In the latter case contact between solution and fiber leads to a shift of equilibrium. The question can therefore only be answered by a determination of the number of these aggregates in solution.

If the first case is true and the aggregates constitute a phase, then the electrical conductivity will not change on dilution of the solutions or on sorption of the aggregates from the solution, while the aggregates still exist in the solution. At the same time the diffusion coefficient will increase, as the number of aggregates diminishes. This is completely confirmed by experiment. Thus, by studies of the properties of solutions or of sorption from solution it is possible to determine also the type of equilibrium which exists in the solution.

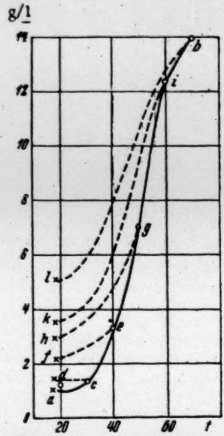

Fig. 1. Solubility curves of the dye Direct Brown KKh in distilled water.

Effect of Vacuum on the Sorption of Dyes by Fibers

Sorption of dyes by fibers at room temperature is not used in practice only because transfer of dye from solution to fiber at ordinary temperatures is very slow. It must be noted that much attention is devoted to the role of diffusion processes in modern theories of dyeing [6]; many authors consider that the affinity of dyes for fibers may be determined from the diffusion coefficients. The fact is completely ignored that a fibrous material, like a powdered adsorbent, may contain air both in a sorbed and in an occluded state. It is obvious that in these conditions penetration of dye into the fiber may be dependent on the competition between air and dye molecules for places on the adsorbent surface. On the assumption that this is possible, dyeing could be expected to occur under vacuum conditions in which diffusion effects would not play a decisive role. This is confirmed by experiment. First we must point out that unbleached yarn, which contains waxes and pectins and is not wetted by water in normal conditions, is wetted completely under vacuum. For a more detailed study of this point, normal yarn was treated with paraffin wax and then immersed in a dye bath. Under vacuum conditions the waxed yarn was dyed in the same way as the original yarn, and both had the same percentage sorption of dye. Thus, in vacuum conditions the fiber is dyed practically instantaneously without preliminary diffusion.

The apparatus shown in Fig. 2 was used for studying sorption of dyes under vacuum. A weighed sample of fiber was fixed in the cylindrical vessel A on the hook E, the vessel was evacuated through the open tap D, the pressure in the vessel being recorded by the manometer C (residual pressure 10 mm Hg), and a solution of dye was drawn in through the tap B. Study of the course of the sorption process showed that equilibrium is reached in the system after 5-10 minutes, while in the ordinary dyeing method the process is completed after about 48 hours.

Fig. 3 shows curves for the kinetics of dye sorption under normal conditions and under vacuum. The curves show the difference in the dye sorption time, and it is also clear that the maximum quantity of dye taken up by the fiber is the same in both cases, but equilibrium in the system is reached after a different period of time.

The Table shows data on the sorption of dyes by fibers under various conditions.

It is seen that in vacuum conditions equilibrium is practically established after 10 minutes, while under normal conditions several hours are needed. Consequently, the diffusion processes under normal dyeing conditions are not associated with fiber structure or the necessity for the dye molecules to penetrate into the fibers, but only with the need to remove air molecules from the pores and from the fiber surface. To eliminate any suspicion that under vacuum conditions the dye is taken up only by the fiber surface, sections of fibers dyed under vacuum and under normal conditions were cut; the fibers were completely dyed through in both cases [7].

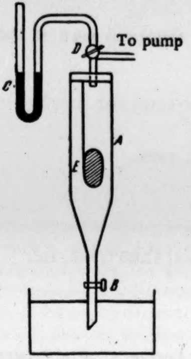

Fig. 2. Apparatus for studying dye sorption under vacuum.

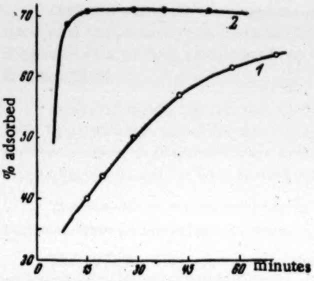

Fig. 3. Kinetic dye sorption curves: 1) in normal conditions; 2) under vacuum.

TABLE

Sorption of Dyes by Fibers Under Various Dyeing Conditions

Dye	Vacuum		Normal conditions	
	10 minutes	60 minutes	10 minutes	60 minutes
Chrysophenine	72	73.4	43.6	64.6
Direct Violet	68	68.9	17	32.1
Direct Brown KKh	39.8	–	4.8	–

The rubbing fastness was also the same as for ordinary dyeing, and in some cases even higher.

In modern theories of dyeing much attention is also paid to the role of the charge on the fiber and dye. As both the fiber and the adsorbed part of the dye are negatively charged, the charges must be diminished by addition of some salt to the solution to increase the interaction between the dye and the fiber. It was also necessary to study the influence of NaCl on dye adsorption because under normal conditions the amount of salt is such as might salt out the dye at room temperature. Investigation of this question showed that the amount of sorbed dye increased from 74% (without addition of salt) to 84% (on addition of 15% salt to the solution); when the amount of salt was increased to 32%, however, the sorption fell to 61%. Thus, addition of salt to the dye bath in vacuum dyeing does not greatly increase sorption, and therefore vacuum dyeing can be effected at a higher zeta-potential, so that the same dyeing effect can be obtained under vacuum as under ordinary conditions.

In our view, the influence of the salt is not so much to decrease the zeta-potential as to lower the stability of the dye solution and thus to increase the sorption of dye by the fiber.

The experimental observations and theoretical considerations presented briefly in the foregoing have led to the development of a new accelerated method of dyeing, both for cellulose and for woolen goods at 25-40° [8].

SUMMARY

1. The solubility of dyes at low temperatures has been studied, and their tendency to form stable supersaturated solutions is shown.

2. The conditions for aggregation of dye particles in solution are considered.

3. Adsorption of dyes by fibers is many times more rapid under vacuum than in normal conditions; the equilibrium state is the same in both cases.

LITERATURE CITED

[1] P. M. Bogoslavsky, Doctoral Dissertation (Moscow Textile Inst., 1952).

[2] W. Marshall and R. Peters, J. Soc. Dyers Colourists 63, 446 (1947); P. V. Maryganov and B. N. Melnikov, Colloid J. 18, 49 (1956) (T.p. 47).*

[3] B. Kramer, Melliand Textilber. 35, 518, 651 (1954).

[4] S. M. Lipatov and G. V. Lipatova, Colloid J. 14, 52 (1952) (T.p. 55).*

[5] S. M. Lipatov, Colloido-chemical Bases of Dyeing (Ivanovo-Voznesensk, 1929).

[6] B. Kramer, Melliand. Textilber. 35, 651 (1954).

[7] N. D. Ilyashuk, Candidate's Dissertation (Moscow Textile Inst. 1955).

[8] S. M. Lipatov and N. D. Ilyashuk, Author's Certification No. 76136 (1948); 82369 (1949), etc.

Received May 18, 1956

Moscow Textile Institute Chair of Physical Chemistry

---

* T.p = C. B. Translation pagination.

DIFFUSION OF DIRECT DYES INTO CELLULOSE FIBERS

B. N. Melnikov and P. V. Moryganov

The process of dyeing with water-soluble dyes comprises at least four stages: external diffusion, adsorption on the surface, internal diffusion, and fixation of the dye on the fiber. Adsorption of the dye on the fiber surface and its fixation on the fiber generally occur much more rapidly than the two diffusion stages. Diffusion within the fiber is slower than diffusion in aqueous solutions, owing to the strong mechanical obstacles formed by the network of the chain molecules in the fiber, and also to the interaction between the dye and the fiber. Therefore the dye will pass onto the fiber surface more rapidly than it is able to diffuse inward from the surface. Thus it may be assumed that dyeing, from the kinetic standpoint, can be regarded as essentially diffusion within the fiber of dye previously adsorbed on the fiber surface. This view was first advanced by Neale et al. [1], and experimentally confirmed by exact measurements of the rate of adsorption of a dye by a Cellophane film, and also by Boulton et al. [2], who carried out similar experiments on viscose yarn.

As the result of these and other experiments it was conclusively shown that internal diffusion is the stage which determines the rate of dyeing as a whole.

Diffusion within the fiber depends on many factors, including the state of the dye and fiber in the dye bath, the dyeing temperature, concentrations of dye and electrolytes, and the chemical nature of the dye. The influence of each of these factors has been studied in considerable detail, principally by the English school of chemists [3-5].

However, despite the fact that many researches have been devoted to the study of internal diffusion, very little is known about certain aspects. Foremost among these are the influence of temperature and of the state of the dye solution. It is seen from the available literature data that diffusion into cellulose fibers over a wide range of temperatures has been studied only for four direct dyes [6,7].

The aim of the present work was to study the influence of temperature on the diffusion of certain dyes into cellulose fibers in conditions of considerable variation of the electrolyte concentration in the dye bath.

The diffusion coefficients (D) of the dyes within the fibers were determined with the aid of the Fick equation for nonsteady state diffusion:

$$-\frac{dc}{dt} = D\frac{d^2c}{dx^2}, \tag{1}$$

where c is the dye concentration at a distance x from the fiber surface at time t.

A solution of this equation for the particular case of the dyeing of a cylindrical fiber from a dye bath of constant composition has been given in the form of an infinite series by Hill [8]:

$$\frac{c_t}{c_\infty} = 1 - 0.692\,(e^{-5.785Dt/r^2} + 0.190\,e^{-30.5Dt/r^2} + 0{,}0775\,e^{-74.9Dt/r^2} + \\ + 0.0415\,e^{-139Dt/r^2} + 0.0258\,e^{-223Dt/r^2} + \ldots) \tag{2}$$

or, in general form

$$\frac{c_t}{\infty} = 1 - Ae^{-BK} - Ce^{-FK} - Ge^{-HK} - \ldots, \quad (3)$$

where A, B, C, F, G, H are constants and $K = Dt/r^2$, c_t is the concentration of dye in the fiber at time t; c_∞ is the equilibrium dye concentration in the fiber. By taking arbitrary values for K it is possible to calculate the corresponding values of c_t/c_∞ and to plot a graph for c_t/c_∞ as a function of K. Further, when experimental values of c_t/c_∞ have been found, it is easy to find from this graph the values of K, and hence the diffusion coefficient.

As in the dyeing of cellulose fibers by direct dyes we are essentially dealing not with free diffusion but with activated diffusion with adsorption; a definite fraction of the dye molecules is always retained during the diffusion process near the active centers of the fibers until they accidentally attain a definite critical energy for random exchange with neighboring molecules. They are then in an activated state and are able to overcome the resistance of the surrounding medium and to advance further. The number of molecules capable of diffusing at any given time instant is proportional to the concentration of dissolved substance and to the factor $e^{-E/RT}$, wher E is the value by which the energy of the activated molecules exceeds the mean energy of the dissolved molecules.

From this viewpoint the Fick equation is applicable only to activated molecules, the concentration of which cannot be measured directly, but since it is proportional to $ce^{-E/RT}$ (where c is the total concentration of dissolved substance), the Fick equation can be applied to the observed concentration gradient if the term $e^{-E/RT}$ is included in the diffusion coefficient.

Such a diffusion process obeys the usual law for the rate of a chemical reaction

$$D_T = D_0 e^{-E/RT}, \quad (4)$$

where D_T is the observed diffusion coefficient at temperature T; D_0 is a constant. In logarithmic form this equation is

$$\ln D_T = \ln D_0 - E/RT. \quad (5)$$

Therefore if the logarithms of the observed diffusion coefficients at various temperatures are plotted against the reciprocal of the absolute temperature, the points should lie along a straight line with a slope of E/2,3R, from which the activation energy of diffusion can be calculated.

EXPERIMENTAL

The experiments on diffusion into cellulose fibers were performed with four direct dyes: Direct Blue K (Color Index 406), Direct Diazo Black C (C. I. 401), Direct Violet (C. I. 394) and Direct Diazo Black O (C. I. 395). The main reason for the choice of dyes was that they have different stabilities to electrolytes, rapidly diminishing from Direct Blue K to Direct Diazo Black O. This makes it possible to evaluate more clearly the influence of changes in the state of the dye in the bath on its diffusion. The dyeing was carried out at temperatures from 40 to 100°; the electrolyte concentration in the dye bath was varied from 0.1 to 15 g/liter according to the stability of the dye to electrolytes and the dyeing temperature; the dye concentration in the bath was 0.1 g/liter for Direct Violet and 0.5 g/ liter for all the other dyes. In addition, in the case of Direct Violet and Direct Diazo Black O several experiments were carried out with dye baths containing leveling agent OS-20 at a concentration of 0.01 g/ liter.

The dyes were carefully purified by recrystallization from aqueous solutions until completely free from mineral salts. The degree of purification was checked by silver nitrate and barium chloride tests. The purity was estimated quantitatively by various methods [9]. Analytical results for the purified dyes are shown in Table 1.

TABLE 1

Analysis of Purified Dyes

Dye	Content of pure dye, %					Moisture, %
	by sodium sulfate	by titanium sulfate	by nitrogen content	by optical density	Average	
Direct Blue K	84.5	85.9	83.4	–	84.6	11.0
Direct Violet	78.0	82.0	–	–	80.0	14.2
Direct Diazo Black C	–	–	–	84.6	84.6	10.0
Direct Diazo Black O	84.3	80.1	–	–	82.2	11.2

The experiments were performed with cuprammonium staple fibers, which were scoured before the experiments for 1 hour at 80° in a soap solution containing 3 g/ liter, rinsed in warm water to remove residual soap completely, and dried. The thickness of the individual fibers, determined microscopically, was 20μ.

The cuprammonium fiber samples prepared as described above, 0.05 g in weight, were immersed in previously prepared solutions of predetermined composition. The bath ratio was 2000 in all cases. Before the start of an experiment the flask was heated for 15 minutes in a thermostat to the required temperature. During the entire dyeing process the dye liquid was continuously stirred at the same speed in all cases (dyeing at 100° was carried out in flasks under reflux).

The following dyeing times were used for the different temperatures:

Dyeing temperature, °C	Dyeing time	Dyeing temperature °C	Dyeing time
100	From 5 min. to 2 hr.	70	From 30 min. to 12 hr.
90	" 5 min. to 3 hr.	60	" 30 min. to 24 hr.
80	" 10 min. to 10 hr.	40	" 30 min. to 36 hr.

After definite time intervals the samples were removed from the flasks, pressed between sheets of filter paper, and then dried in air. The dye concentration in the fibers was determined by stripping the dye from the dyed fiber by 25% aqueous pyridine solution, followed by photometric determination with the FM universal photometer. The experimental results were used to calculate the diffusion coefficients of the dyes by means of Hill's equation. The results for the four dyes are shown in Table 2.

DISCUSSION OF RESULTS

The experimental data in Table 2 show that the internal diffusion coefficients of all the direct dyes studied depend very strongly on the electrolyte concentration in the bath. At low electrolyte concentrations the diffusion coefficients first increase with rising salt concentration, then gradually decrease. This question has been repeatedly discussed in the literature, and it has been shown that this form of relationship between the internal diffusion coefficent and the electrolyte concentration is explained by the existence of like charges on the dye anions and the cellulose fibers, and also by aggregation of the dye particles at high electrolyte concentrations.

We found in a study of the influence of temperature on the internal diffusion coefficients over a wide range of temperatures and electrolyte concentrations that the characteristic maxima on the curves for the variation of diffusion coefficients with electrolyte concentration are shifted at low temperatures into the region of lower electrolyte concentrations. The largest shift is found for Direct Violet and Direct Diazo Black O, which are the dyes most sensitive to electrolytes. For example, for Direct Violet in the high temperature range (100-60°) the maximum diffusion coefficient corresponds to a salt concentration of 2 g/ liter in the dye bath, while at 40° the maximum diffusion coefficient is found at a concentration of 1 g/ liter NaCl. In the case of Direct Diazo Black O in the temperature range from 100 to 60° the maximum diffusion coefficient corresponds to an electrolyte concentration of 1 g per liter, while at 40° a maximum for the diffusion coefficient could not be found even at an electrolyte concentration of 0.1 g/ liter, as diffusion coefficient falls continuously and gradually from (0.098 to 0.057) · 10^{-8} cm^2/ minute as the electrolyte concentration changes from 0.1 to 1 g per liter.

TABLE 2

Average Values of Diffusion Coefficients

NaCl concentration g/liter	Diffusion coefficient · 10^8 cm^2/min					
	40°	60°	70°	80°	90°	100°
Direct Violet						
0,25	0.156	—	—	—	—	—
0.50	0.180	0.85	—	—	—	—
1.0	0,240	1.09	2.05	3.44	5,30	9.61
2.0	0.160	1.22	2.56	4.45	7,03	11.3
3.0	—	0.676	1.85	3.60	6,84	—
4.0	0.102	0.631	1.60	2.75	4,65	8.30
5.0	—	0.398	1.12	2.35	4,32	7.29
10,0	—	—	—	1.17	2.70	5.62
Direct Diazo Black C						
1.0	—	0,74	1.63	3.37	6.26	12.38
5.0	—	—	2,11	3.88	8.13	15.00
10.0	—	—	1.03	2.51	5.30	11,30
15.0	—	—	0.588	1.41	3.50	8.33
Direct Diazo Black O						
0.1	0.098	0.338	—	—	—	—
0.25	0.077	0,386	—	2.26	4.50	—
0.5	0.067	0.550	1.36	2.60	5.60	8.80
1.0	0.057	0.602	1.82	3.62	7.63	13.53
2.0	—	—	0.924	2.18	5.90	12.47
3.0	—	—	0.525	1.41	4.47	11.50
4.0	—	—	—	—	—	10.73
Direct Blue K						
1.0	0.236	1,06	1,76	3,84	7.60	14,00
5,0	0.290	1,27	2.42	4.46	9,40	16,50
10.0	0.178	0.80	1,57	3.61	6,32	12,30
15.0	—	0,283	0.676	1,73	3.71	8,00
Direct Diazo Black O + 0.01 g/ l leveling agent OS-20						
0.25	—	0.483	1.57	2.51	5.35	—
0.5	—	0.794	1.86	3.40	6.37	—
1.0	—	0.739	1.95	3.99	8.37	—
Direct Violet + 0.01 g/ l leveling agent OS-20						
1.0	—	1.70	2.82	4.87	8.18	—

For Direct Blue K and Direct Diazo Black C, less sensitive to electrolytes, such displacements of the maximum coefficient of diffusion could not be found in the temperature and electrolyte concentration range studied. The probable explanation is that for these dyes a sharp change in the state of the solution occurs at lower temperatures. This is supported by the presence of a break in plots of the logarithm of the internal diffusion coefficient against the reciprocal of the absolute temperature for Direct Diazo Black O and Direct Violet.

Thus, it can be seen in Figs. 1 and 2, in which this relationship between the diffusion coefficient and the absolute temperature is plotted, that instead of straight lines with a constant slope for all the temperature range studied, we have straight lines with sharp breaks, the position of which gradually shifts into the region of higher

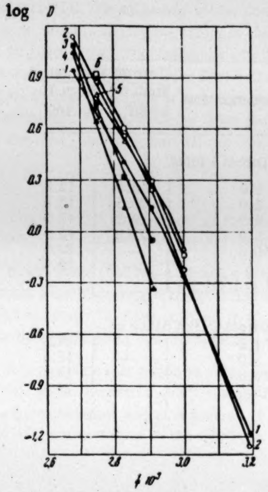

Fig. 1. Logarithm of the diffusion coefficent as a function of 1/T for Direct Diazo Black O: 1) 0.5; 2) 1.0; 3) 2.0; 4) 3.0 g/liter NaCl; 5) 0.5 g/liter NaCl + 0.01 g/liter OS-20; 6) 1.0 g/liter NaCl + + 0.01 g/liter OS-20.

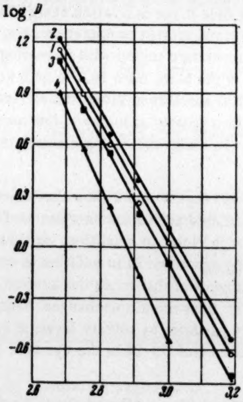

Fig. 3. Logarithm of the diffusion coefficient as a function of 1/T for Direct Blue K: 1) 1.0; 2) 5.0; 3) 10.0; 4) 15.0 g/liter NaCl.

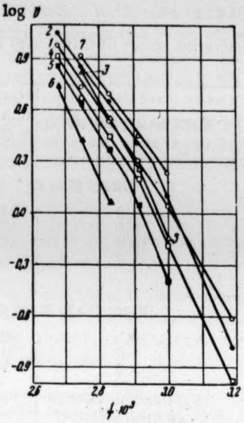

Fig. 2. Logarithm of the diffusion coefficient as a function of 1/T for Direct Violet: 1) 1.0; 2) 2.0; 3) 3.0; 4) 4.0; 5) 5.0; 6) 10.0 g/liter NaCl; 7) 1.0 g/liter NaCl + 0.01 g/liter OS-20.

temperatures with increasing electrolyte concentration in the bath. For example, for Direct Diazo Black O (Fig. 1) at a NaCl concentration of 0.5 g/liter the break is found between 60 and 70°, while at an electrolyte concentration of 1 g/liter it corresponds to 70°. At higher electrolyte concentrations the diffusion coefficients could not be determined at 40 and 60°, as the dye coagulates in these conditions. In the case of Direct Violet (Fig. 2) the breaks are found at 60° for electrolyte concentration of 1 g/liter, between 60 and 70° at 2 g/liter, at 70° at 3 and 4 g/liter, and over 70° at 5 g/liter. As in the case of Direct Diazo Black O, it was not possible to study the diffusion of the violet dye in the temperature range between 40 and 60° at electrolyte concentrations over 5 g/liter, owing to coagulation of the dye. The plots for the other two dyes, Direct Blue K and Direct Diazo Black C (Figs. 3 and 4) show no breaks over the entire temperature range studied, which indicates that no abrupt change of the state of the dye takes place in solution. It should be noted, however, that at an electrolyte concentration of 15 g/liter, the slope of the lines for these two dyes increases considerably, but without showing breaks in the temperature range from 100 to 60°. The probable explanation is a gradual change in the degree of dispersion of these two dyes with decreasing temperature and increasing electrolyte concentration. In the high temperature region (from 70 to 100°) such a gradual change of the solution state with increasing electrolyte concentration in the dye

TABLE 3

Activation Energy of Diffusion of Direct Dyes

NaCl concentration in g/1	Temperature range from 40 to 60°	Temperature range from 70 to 100°
Direct Blue K		
1.0	16.1	16.1
5.0	15.8	15.8
10.0	16.5	16.5
15.0	—	20.5
Direct Diazo Black O		
0.5	22.0	16.0
1.0	24.0	16.5
2.0	—	21.0
3.0	—	25.0
0.5 + 0.01 g/1 OS-20	—	15.5
1 + 0.01 g/1 OS-20	—	16.7

NaCl concentration in g/1	Temperature range from 40 to 60°	Temperature range from 70 to 100°
Direct Violet		
1.0	15.0	12.8
2.0	20.5	12.5
4.0	19.2	14.0
5.0	23.0	15.5
10.0	—	20.8
	—	12.6
1 + 0.01 g/1 OS-20		
Direct Diazo Black C		
1.0	—	16.8
5.0	—	16.5
10.0	—	19.7
15.0	—	21.8

bath is also found for the dyes Direct Diazo Black O and Direct Violet, as shown by a gradual increase of the slope of the lines with increasing electrolyte concentration.

The activation energies for all the studied direct dyes, calculated according to Equation (5) from the slopes of the lines in Figs. 1,2,3, and 4, are shown in Table 3; they demonstrate that this value depends on the state of the dye solution. Thus, for Direct Blue K the activation energy has the same value both at low and at high temperatures, but it increases in the high temperature region with increasing electrolyte concentration in the bath, from 16.1 to 20.5 kcal./ mole. For direct Diazo Black O and Direct Violet the activation energy of diffusion differs greatly at high and low temperatures, and increases in both cases with increasing electrolyte concentration in the bath.

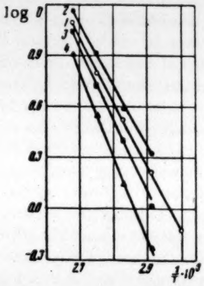

Fig. 4. Logarithm of the diffusion coefficient as a function of 1/ T for Direct Diazo Black C: 1) 1.0; 2) 5.0; 3) 10.0; 4) 15.0 g/ liter NaCl.

Tables 2 and 3 and Figs. 1 and 2 show the diffusion coefficients and the calculated activation energies for Direct Diazo Black O and Direct Violet in conditions when the dye bath contained leveling agent OS-20 in addition to common salt. In all the experiments of this series the internal diffusion coefficients increase while the activation energies and the character of the lines remain unchanged. This in all probability indicates that by replacement of the hydrate layers on the dye particles by solvate layers of leveling agent OS-20 the affinity of the dye for the fiber is decreased, but the presence of OS-20 in the dye bath does not produce any significant change in the solution state of the dye.

It must be pointed out that the activation energies of diffusion of Direct Blue K, Direct Diazo Black C, and Direct Diazo Black O at high temperatures (from 70 to 100°) and fairly low electrolyte concentrations have very similar values. At first sight this does not seem quite normal, as Direct Diazo Black O, which contains two sulfo groups in the molecule, should have a lower electric charge and consequently a lower activation energy than Direct Blue K, and Direct Diazo Black C, which have four and three sulfo groups respectively. The explanation for the same order of magnitude of the activation energy in this case is that, apart from the charge, the value of the activation energy is also greatly influenced by the affinity of the dye for the fiber, and since Direct Diazo Black O has a higher affinity than Direct Blue K and Direct Diazo Black C (5.75, 4.10, and 3.93 kcal./ mole at 90° respectively), the influence of the charge on the activation energy is compensated by the influence of affinity on it, and the aggregate effect of these two factors is to give similar values for the activation energies of diffusion for these dyes. The influence of affinity on the activation energy is most pronounced in the case of Direct Violet; this dye, like Direct Diazo Black O, has two sulfo groups, but the former has a lower affinity, and therefore its activation energy is less than that of all the other dyes. At high electrolyte concentrations, even at high temperatures, the influence of these factors is considerably complicated by variations in the degree of aggregation of the dyes, and therefore all the dyes studied have different activation energies in these conditions.

SUMMARY

1. The diffusion coefficients of four direct dyes have been determined at 40, 60, 70, 80, 90, and 100° with the electrolyte concentration in the dye bath varying between 0.1 and 15 g/liter.

2. It was found that the activation energy for Direct Diazo Black O and Direct Violet increases sharply in the transition from high temperatures to the temperature range of 40 to 60°, while in the case of Direct Blue K the activation energy remains constant over the entire temperature range studied. In all cases the activation energy gradually increases with increasing electrolyte concentration in the dye bath.

3. A tentative explanation is advanced for this nature of the variation of activation energy of diffusion for various dyes, on the basis of a sharp change in the solution states of Direct Diazo Black O and Direct Violet on decrease of temperature, and of a gradual change in the degree of dispersion of all the dyes with increasing concentration of the electrolyte in the dye bath.

LITERATURE CITED

[1] S. M. Neale and W. A. Stringfellow, Trans. Faraday Soc. 29, 1167 (1933).

[2] J. Boulton, A. E. Delph, F. Fothergill and T. H. Morton, J. Textile Inst. 24, 113 (1933).

[3] V. M. Garvie and S. M. Neale, Trans. Faraday Soc. 34, 335 (1938).

[4] V. M. Garvie, L. H. Griffiths and S. M. Neale, Trans. Faraday Soc. 30, 271 (1934).

[5] L. H. Griffiths and S. M. Neale, Trans. Faraday Soc. 30, 395 (1934).

[6] J. Boulton, and T. H. Morton, J. Soc. Dyers Colourists 56, 145 (1940).

[7] S. M. Neale, J. Soc. Dyers Colourists 52, 252 (1936).

[8] T. Vickerstaff, The Physical Chemistry of Dyeing (London, 1954), p. 131.

[9] B. N. Melnikov and P. V. Moryganov, Colloid J. 17, No. 2, 99 (1955) (T.p. 93).*

The Ivanovo Institute of Chemical Technology
Laboratory of the Chemical Technology of
Fibrous Materials

Received October 3, 1955

---

* T.p = C. B. Translation pagination.

EFFECT OF AIR IONIZATION ON THE DISPERSE PHASE OF AEROSOLS

K. M. Merzhanov, N. I. Peterimova, and N. S. Smirnov

According to the modern theories [1-7] the condensation of water vapor and the growth of the disperse phase particles of an atmospheric aerosol system depend on the electric charge of the droplets and consequently on air ionization. It was therefore desired to study experimentally the effect of air ionization on the disperse phase of a natural aerosol. No quantitative data on this subject were found in the literature.

Ultraviolet radiation, x-rays, and β-particles were used for ionization of the atmospheric air. The ionization of the air in the experiments did not exceed 10^6 ip/cc (ip = ion pair). The experiments were performed in ordinary aerosol chambers from 0.8 to 2 m^3 in volume. The air in the chambers was moist and not purified (relative humidity ~100%). In no case was there any supersaturation of water vapor in the chambers. The contents of ultramicroscopic particles in the air before and after ionization were determined by means of a flow ultramicrophotometer [8].

TABLE 1

Effect of Air Ionization on the Concentration of Ultramicrosopic Particles in Humid Air

Air ionization source	n, number of ultramicroscopic particles in 1 cc		% increase of number of particles
	before ionization $n \cdot 10^3$	after ionization $n \cdot 10^3$	
Ultraviolet radiation	0.05	0.17	340
	0.08	0.20	250
x-rays	0.02	0.08	400
	0.08	0.27	340
	0.07	0.33	470
β-radiation	0.02	0.04	200
	0.07	0.16	230
	0.23	0.51	220

About 1000 experiments were carried out in these conditions. In all cases an increase in the number of ultramicroscopic particles in the air was found after irradiation by ionizing radiations. Table 1 shows the most typical data for all the radiation sources.

It follows from Table 1 that increased ionization of the air results in a 2 to 4 fold increase of the concentration of ultramicroscopic particles.

The effect of ionization time on the number of ultramicrosopic particles was studied by irradiation of the air by ultraviolet and x-ray radiations for various times (the most typical data are shown in Table 2).

To determine the effect of air ionization on the concentration of ultramicroscopic particles, experiments were carried out on the irradiation of air with x-rays of varying intensities, regulated by the current strength in the tube. As is known, x-ray intensity increases with current strength, and the degree of ionization of the air in the chamber increases accordingly. Table 3 shows the results of experiments with x-rays of various intensities.

Tables 2 and 3 show that the irradiation time and the degree of ionization of the air are important factors which influence the concentration of ultramicroscopic particles in humid air.

TABLE 2

Effect of Air Ionization (Irradiation) Time on the Concentration of Ultramicroscopic Particles

Air ionization source	Irradiation time, min.	Number of ultramicroscopic particles in 1 cc		% increase of number of particles
		before ionization, $n \cdot 10^3$	after ionization, $n \cdot 10^3$	
Ultraviolet radiation	15	0.06	0.11	180
	20	0.08	0.24	300
	25	0.05	0.21	420
x-rays	5	0.02	0.04	200
	10	0.02	0.05	220
	20	0.02	0.08	400

TABLE 3

Effect of Degree of Ionization of Air by X-rays on the Concentration of Ultramicroscopic Particles

Current strength in tube, mA	Particle concentration in 1 cc		% increase of number of particles
	before ionization, $n \cdot 10^3$	after ionization, $n \cdot 10^3$	
2.4	0.16	0.21	130
9.0	0.21	0.91	430
70.0	0.11	1.07	970

TABLE 4

Effect of Air Ionization on the Maximum Radius of the Ultramicroscopic Particles

Air ionization source	Particle size*	
	before ionization	after ionization
Ultraviolet radiation	12	50
x-rays	56	72
	52	70
	48	60
	60	74

---

* The particle sizes are given in scale divisions of the Deryagin – Vlasenko instrument.

With the aid of S. V. Vavilov's extinction principle and of Deryagin and Vlasenko's principle of flow ultramicroscopy [8], forming the basis of the flow ultramicrophotometer, it is possible not only to determine rapidly the particle concentration of aerosols, but to observe the variations of size of the particles in the disperse phase. Thus it was possible to show by direct measurements that the size of the ultramicroscopic particles increases as the result of increasing ionization of the air (Table 4).

It follows from the data in Tables 1-4 that artificial increase of the natural ionization of ordinary moist air increases the particle concentration and the dimensions of the ultramicroscopic particles of the disperse phase of aerosols.

To determine the effect of ionization on the highly disperse particles of aerosols, measurements of the submicroscopic fraction – the condensation nuceli – were carried out. The concentration of these condensation centers before the action of ionizing radiations and after irradiation was determined with the aid of the usual Scholz counter for condensation nuclei [9]. The condensation nuclei have submicroscopic dimensions of the order of 10^{-6} cm. They are not detected by the ultramicrophotometer, which permits the counting of particles of the order of 10^{-5} cm in size.

These experiments were carried out in the same way as the preceding ones, but in many cases the concentrations of the condensation nuclei and of the ultramicroscopic particles were determined simultaneously. It was found in all these experiments that the concentration of the condensation nuclei is increased by an increase of the natural ionization of ordinary humid air. As the results in Table 5 show, the concentration of the condensation nuclei is considerably increased after ionization of the air.

TABLE 5

Effect of Ionization on the Concentration of Condensation Nuclei

Air ionization source	Concentration of condensation nuclei in 1 cc		% increase of condensation nuclei
	before ionization $n \cdot 10^3$	after ionization $n \cdot 10^3$	
Ultraviolet radiation	5.6	55.0	980
x-rays	2.0-2.5	15.0-17.0	700-800
β-Particles	0.4	1.7	425
	0.4	2.3	575

Finally, experiments were carried out on the ionization of air completely free from ordinary condensation nuclei. These experiments were performed as follows. The air in the chamber of the Scholz counter was cleared of condensation nuclei by means of several expansions (they were deposited as droplets on the floor of the chamber, and further expansions of the air showed no condensation nuclei in the field of the counter). After this, β-particle sources of various activites were brought close to the window of the chamber, covered by a thin rubber film. The duration of irradiation of the air was from 10 minutes to several hours. The contents of condensation nuclei were determined after the irradiation.

It was found in this series of experiments that at ion concentrations from $1 \cdot 10^4$ to $7 \cdot 10^6$ ip/cc, no condensation nuclei are formed in the counter chamber even after prolonged irradiation (several hours). It appears that the purity of the air is very important in relation to the formation of condensation nuclei and ultramicroscopic particles in the experimental conditions described above.

It proved possible to determine the limit of air ionization below which condensation nuclei were not found in our apparatus. According to a preliminary estimate, this limit lay between concentrations of $1.2 \cdot 10^7$ and $1.32 \cdot 10^7$ ip/cc.

The influence of the duration of irradiation of the air in the chamber on the number of condensation nuclei was also determined. At $1.3 \cdot 10^7$ ip/cc, after 10 minutes of irradiation, 324 condensation nuclei were found in 1 cc of air; after 100 minutes, the concentration rose to $0.95 \cdot 10^3$ nuclei per 1 cc, and after 150 minutes, to $2.4 \cdot 10^3$ nuclei per 1 cc.

The observed increase in the concentration and size of aerosol particles on ionization of humid air may be the result of at least three processes.

The mechanism of the first process follows from Thomson's theoretical work [2] on the influence of electric charges on the vapor pressure of aerosol particles. These theoretical views have been considered in detail by Obolensky [3], DasGupta and Ghosh [5], Leontovich [6], and Amelin [7], who showed that the formation of electric charges on water droplets lowers the water vapor pressure and so favors their growth by condensation.

The mechanism of the second process for the origin and growth of the particles is determined by the chemical action of ionizing radiations. It was shown in numerous investigations [1, 10, 11] that atomic oxygen, hydrogen peroxide, ozone, and nitrogen oxides are formed by irradiation of humid air. Submicroscopic water droplets may form and grow on molecules of these substances in humid air. The possibility of such formation of condensation nuclei in upper layers of the atmosphere has been pointed out by Frenkel [11]. Similar processes probably took place in our experiments.

In addition to the above processes, the possibility of growth of the elementary particles by coagulation must also be taken into account. Since the coagulation rate greatly depends on the particle concentration, while an increase of the degree of ionization of the air increases the primary particle concentration, the rate of formation of secondary and larger aerosol particles should increase with the degree of ionization. This third possible process of coagulational growth of the particles should evidently play an important role at high ionizations, as was the case in a number of our experiments.

SUMMARY

1. It is shown that increased ionization of the dispersion medium increases the particle concentration of the disperse phase of aerosols.

2. At concentrations of up to $10^6 - 10^7$ ions pairs/cc in ordinary air at a relative humidity not greater than 100% the concentration of ultramicroscopic particles increases by a factor of 3-4, and the number of condensation nuclei by a factor of over 10.

LITERATURE CITED

[1] C. T. Wilson, Trans. Roy. Soc. (London) 192, 403 (1899); 193, 289 (1899).

[2] J. J. Thomson, Conduction of Electricity Through Gases (1906).

[3] V. N. Obolensky, J. Geophysics 4, 90 (1934).

[4] M. Volmer, Kinetik der Phasenbildung, (Leipzig, 1939).

[5] N. Das Gupta and S. Ghosh, The Wilson Chamber and its Use in Physics (Foreign Lit. Press, Moscow, 1947).

[6] M. A. Leontovich, Introduction to Thermodynamics (State Chem. Press, 1951).

[7] A. G. Amelin, Theoretical Basis for Mist Formation in Chemical Industries (State Chem. Press, 1951).

[8] B. V. Deryagin and G. Ya. Vlasenko, Author's Certification No. 325665 (1944); Proc. Acad. Sci. USSR 63, 155 (1948); New Ideas in the Study of Aerosols (Acad. Sci. USSR Press, 1949).

[9] H. Landsberg, Erg. Kosmisch. Phys. B. 3, 333 (1938).

[10] T. J. M. Farley, Proc. Roy. Soc. 207, 527 (1951).

[11] Ya. I. Frenkel, Bull. Acad. Sci. USSR, Geophys. Ser. No. 2, 191 (1953).

Received September 12, 1955

Geophysical Institute Academy
of Sciences USSR, Moscow

STUDY OF THE KINETICS AND MECHANISM OF THE THERMAL DECOMPOSITION OF CHLORINATED VINYL POLYMERS

I. METHODS AND RESULTS FOR POLYVINYL CHLORIDE

N. V. Mikhailov, L. G. Tokareva, and V. S. Klimenkov

In the production of synthetic fibers from carbon-chain compounds, wide use is made of polymers and copolymers based on polyvinyl chloride, which, in addition to their high chemical resistance have the valuable technical property of nonflammability.

One of the important defects of chlorinated vinyl polymers is their poor resistance to the action of light and heat. The resultant decomposition is accompanied by liberation of hydrogen chloride and a deterioration of the mechanical properties of the polymer. The effect of heat on chlorinated vinyl polymers has been studied by Drinberg and Bocharova [1], Berlin and Denker [2], and others. A more detailed investigation of the thermal decomposition of polyvinyl chloride was made by Kirillova [3].

The foreign literature also contains a number of papers [4] on the thermal decomposition of chlorinated vinyl polymers both in solution and in the solid phase, but most of these deal mainly with practical aspects of aging and stabilization of chlorinated vinyl polymers, while theoretical investigations dealing with the mechanism of the thermal decomposition are relatively few. Moreover, almost all the researches in this field were performed, as a rule, with some one type of chlorinated vinyl polymers. However, the behavior of chlorinated vinyl polymers of different chemical composition on heating has much in common. Therefore a study of each polymer separately is necessary and important, but, in our view, it is not sufficient for a description of the process of thermal decomposition of these compounds.

The aim of the present work was a study of the kinetics of thermal decomposition of chlorinated vinyl polymers differing in molecular structure and chemical composition. The principal method used was the chemical method of studying the decomposition, based on the hydrogen chloride split off at various temperatures in nitrogen and oxygen.

A special high-vacuum thermooxidation apparatus (Fig. 1) was designed for studying the kinetics and mechanism of thermooxidative processes and their influence on certain properties of the polymers; its design was essentially based on the work of Kuzminsky [5] on the aging of rubber. With this apparatus it is possible to heat polymers in the range of 25 to 250° under a high vacuum, in oxygen, or in an inert gas.

As Fig. 1 shows, the apparatus comprises the reaction vessels 1,2, and 3, of which 1 and 3 may be connected alternately, while vessel 2 with a spring balance may be connected in parallel with either vessel. The reaction vessels are connected to two parallel traps 4 to catch volatile decomposition products by freezing them by means of liquid oxygen. Owing to their parallel arrangement, the traps can work alternately. Beyond the traps is a circulating pump 5, by means of which the hydrogen chloride is removed from the reaction vessel and condensed at low temperatures.

In experiments in a medium of oxygen, constant pressure is maintained and the oxygen flow regulated by the buret 7, connected with a leveling device 8 and a Huygens manometer 9. The other branch of the manometer is connected to a manostatic vessel 10, contained in the thermostat 11 which also contains the reaction vessels. The temperature in the thermostat is regulated to the nearest ± 0.2°.

In order to set up the required pressure in the manostatic vessel, it is connected to the rest of the system by the tap 12 before the experiment, and the tap is then closed for the duration of the experiment. To prevent

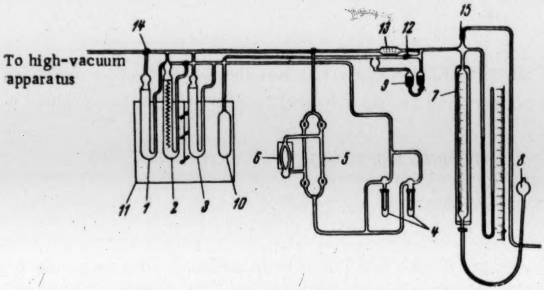

Fig. 1. Thermooxidation apparatus.

the entry of mercury vapor into the reaction vessels, a tube 13 containing gold-coated pumice is inserted in the path of the gases. The system can be connected to a high-vacuum apparatus by the tap 14, and it can be filled with any gas through the tap 15. Variations of the weight of the polymer can be observed by means of the spring balance.

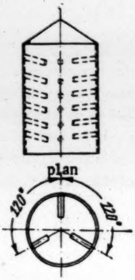

Fig. 2. Rack.

Powdered specimens of the polymers under investigations were uniformly distributed in glass basins which were placed on a glass rack (Fig. 2), previously weighed together with the basins. The rack was then weighed together with the powder and placed into the reaction vessel.

The reaction vessel was connected with the rest of the apparatus through ground-glass joints, and a preliminary reduction of pressure was brought about in the whole system, including the vessels, after which the high-vacuum pump was turned on. As soon as a high vacuum was attained, the taps to the high-vacuum pump were closed, and the apparatus was filled with purified nitrogen. To ensure purer experimental conditions, the apparatus was again evacuated to a high degree of vacuum. The taps to the high-vacuum pump, the taps in the reaction vessel, and the corresponding taps in the rest of the apparatus were closed, the reaction vessel was removed, and the thermostat heater was switched on.

After the required temperature of the oil in the thermostat had been reached and the vessel and apparatus had been filled with purified nitrogen, the reaction vessel was immersed in the thermostat and connected to the system, the circulation pump was switched on, and the trap was immersed in liquid oxygen. After definite time intervals (0.5; 1; 1.5; 2; 2.5; 3; 3.5; 4 hrs.) the traps, which contained condensed volatile decomposition products of chlorinated vinyl polymers, were alternately removed from the apparatus. The traps, described by Kuzminsky et al. [6], are so designed that the normal operation of the apparatus is not disturbed by their disconnection and removal. As has already been noted, the main volatile decomposition product is hydrogen chloride. The hydrogen chloride frozen out in the trap was dissolved in water and titrated argentimetrically by the Volhard method.

Under strictly constant experimental conditions, and with thorough purification of the polymers and of the nitrogen in which the experiments were performed, good reproducibility of the results on the liberation of hydrogen chloride were obtained, as is shown in Fig. 3, where the ordinate axis shows the amounts of liberated HCl calculated in millimoles of Cl_2 per mole monomer unit, and the abscissa axis shows the time in hours. The advantage of such plotting is that it at once shows the number of decomposed units per 1000 such units in the polymer.

The thermooxidative decomposition of chlorinated vinyl polymers was studied at 140, 150, 160, and 170°. The upper and lower limits of this temperature range were determined in preliminary experiments which showed that the use of lower and higher temperatures was unsuitable.

The following chlorinated vinyl polymers of different composition and structure were studied:

	Content of Cl_2 in %
Polyvinyl chloride (PVC)	56.8
Chlorinated PVC (CPVC)	64.2
Vinyl chloride – vinylidene chloride copolymer CP(VDC + VC) with an 89.2:10.8 molar ratio of vinylidene chloride to vinyl chloride monomer units	71.44
Polyvinylidene chloride (PVDC)	72.3

The chlorine content of the polymers was determined by the perborate method of the All-Union Research Institute for Synthetic Fibers [7]. All the materials, with the exception of PVDC, were thoroughly purified by reprecipitation from cyclohexanone and acetone. In the case of PVDC, for which there is no suitable solvent, carefully distilled vinylidene chloride was polymerized under the purest possible conditions. The present communication gives the experimental results for PVC.

In a study of kinetics of the liberation of hydrogen chloride as a function of temperature it was found that PVC begins to split off hydrogen chloride at above 140°, and the rate increases with the temperature.

When PVC is heated for 4 hours at 150°, 3.2 millimoles of Cl_2 is split off per mole of monomer, while at 170° the amount of hydrogen chloride split off is nearly 10 times as large (Table 1).

The decomposition rate of PVC remains constant with time. Thus, when PVC is heated for 0.5 hour at 150°, 0.2 millimole of chlorine is split off per PVC monomer unit, while in 4 hours the amount of hydrogen chloride split off is nearly 10 times as much.

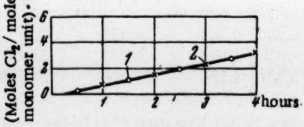

Fig. 3. Liberation of hydrogen chloride by PVC at 150°: 1) First experiment; 2) second experiment.

Fig. 4 shows the effect of heating time on the liberation of hydrogen chloride by PVC at various temperatures. The amount of chlorine remaining in the polymer was determined by the perborate method, and, as a check, was compared with the difference between the chlorine content of the original sample and the amount of chlorine calculated from the HCl in the traps. The results of chlorine determination by these two methods are shown in Table 2.

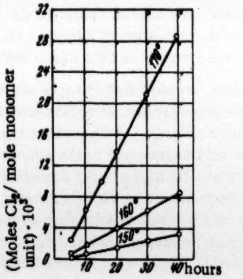

Fig. 4. Liberation of hydrogen chloride by PVC at 150, 160, and 170°.

Table 2 shows that the results are within the error limits of the perborate method of chlorine determination.

The course of the graph in Fig. 4 shows that liberation of hydrogen chloride by PVC proceeds at a constant rate at each of the temperatures studied. Since the kinetic graph shows a simple proportionality between the amount of hydrogen chloride split off and the time, the reaction of PVC decomposition may be regarded as zero-order reaction in the sense of formal kinetics, although by its mechanism it should be a reaction of the first order. (This difference was found in this instance probably because our determinations applied mainly to the initial decomposition stage, and therefore the "initial concentration" of chlorine in the polymer changed very little. For example, at 170° and a maximum time of 4 hours, the maximum liberation of hydrogen chloride by PVC was 28.2 millimoles of Cl_2 per mole of PVC monomer, which corresponds to the removal of chlorine from 56 units per 1000 of the PVC chain, and this represents a decrease of only 5.6% of the "initial concentration" of chlorine in the polymer).

TABLE 1

Liberation of Hydrogen Chloride by PVC at Different Temperatures and Heating Times

Heating temperature, °C	Amount of hydrogen chloride split off, in millimoles of Cl_2 per mole of PVC monomer, in heating time in hours						
	1.0	1.5	2.0	2.5	3.0	3.5	4.0
150	0.608	1.000	1.470	1.900	2.354	2.800	3.218
160	1.696	2.800	4.000	5.100	6.236	7.300	8.500
170	6.000	9.500	13.400	17.000	21.000	25.000	28.200

TABLE 2

Liberation of Hydrogen Chloride by PVC at Different Temperatures and Heating Times

Temperature, °C	Amount of hydrogen chloride split off, as % Cl_2 on the weight of sample, in heating time in hours								Cl content in polymer after heating, %	
	0.5	1.0	1.5	2.0	2.5	3.0	3.5	4.0	calculated by difference	by perborate method
150	0.024	0.069	0.108	0.158	0.207	0.257	0.302	0.347	56.453	–
160	0.064	0.193	0.322	0.450	0.679	0.807	0.936	1.064	55.736	55.840
170	0.423	0.846	1.269	1.692	2.115	2.538	2.961	3.384	53.416	53.300

TABLE 3

Rate Constants for the Reaction of Hydrogen Chloride Liberation From PVC

Temperature, °C	k	$\frac{k_t + 10}{k_t}$	E, kcal/ mole
150	0.22	2.70	36.500
160	0.58		
170	1.58		

The data for the liberation of hydrogen chloride were used to calculate the reaction rate constants (k) which, in accordance with the zero order of the reaction, are given by the tangent of the angle of inclination of the straight line. The calculated results are shown in Table 3.

These results were used to calculate the activation energy E for the liberation of hydrogen chloride from PVC; this was found to be 36.5 kcal./ mole.

To elucidate the chemical changes which occur in PVC during heating, the solubility of PVC (previously heated at various temperatures) in cyclohexanone was determined. The solubility of PVC was determined with the aid of special extractors (of the Soxhlet type) designed for vacuum work (Fig. 5). The determination essentially consisted of measurement of the amount of polymer which passed into solution, or of the residue after the solution. The solubility of PVC decreases considerably with increase of temperature and heating time. After PVC has been heated at 170° for 4 hours, only 7% of the polymer dissolves. This decrease in the solubility of PVC may be the result of formation of spatial structures in which individual monomer units of the PVC molecules are cross-linked, as has been shown in other publications, by saturation of the double bonds formed when hydrogen chloride is split off. The viscosity of the soluble polymer fraction decreases considerably with increase of the heating temperature, probably as the result of degradation of some of the polymer molecules. The specific viscosity (η_{sp}) of 0.2% solutions of the soluble PVC fraction after heating for 4 hours at 150 and 160° was 0.04 poise, and at 170°, 0.03 poise, while the viscosity of the original PVC solution was 0.238 poise.

The insolubility of the PVC and the considerable decrease of the viscosity of the soluble fraction of the heated polymer show that two processes occur simultaneously – structurization and degradation, as is well known in the case of other polymers such as rubber.

SUMMARY

1. A method for studying the kinetics of thermal decomposition of chlorinated vinyl polymers has been developed; this may be applied to studies of the thermal decomposition of other fiber-forming polymers.

2. The kinetics of the liberation of hydrogen chloride from PVC at 150, 160, and 170° in a nitrogen atmosphere has been studied.

3. It is shown that two processes occur simultaneously in the action of heat on PVD – structurization and degradation.

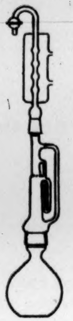

Fig. 5. Vacuum extractor.

LITERATURE CITED

[1] A. Ya. Drinberg and A. M. Bocharova, J. Appl. Chem. 26, No. 10, 1056 (1953) (T.p. 983).*

[2] A. A. Berlin and I. I. Denker, J. Appl. Chem. 24, No. 3, 308 (1951) (T.p. 339);* 24, No. 12, 1311 (1951) (T.p. 1479).*

[3] E. I. Kirillova, Dissertation (The Lensoviet Technological Institute, Leningrad, 1954).

[4] L. Jackson, J. Soc. Chem. Ind. (London) 68, 247 (1949); R. B. Mesrobian and A. V. Tobolsky, J. Polymer Sci. 2, 463, 1947; R. F. Boyer, J. Phys. Colloid Chem. 51, 80, (1947); E. I. Arlman, J. Polymer Sci. 12, 543 (1954); G. P. Mack, Industrie plastiques mod. (Paris) 5, No. 4, 43 (1953).

[5] A. S. Kuzminsky, Dissertation, Sci. Research Inst. Rubber Ind. (1950).

[6] A. S. Kuzminsky et al., Colloid J. 9, No. 5, 374 (1948).

[7] B. E. Geller, Factory Lab. (USSR) 3, 266 (1950).

Received June 25, 1955

Scientific Research Institute for
Synthetic Fibers

---

* T.p = C. B. Translation pagination.

THE PROTECTIVE ACTION OF CERTAIN SUBSTANCES IN THE IRRADIATION OF PROTEIN SOLUTIONS

T. E. Pavlovskaya and A. G. Pasynsky

When ionizing radiation acts on aqueous solutions, OH and O_2H radicals, hydrogen peroxide, and other strongly oxidizing substances are formed in them. The ionization products of water in solutions of proteins, enzymes, nucleoproteins, and other biologically important substances may produce chemical changes in them, and these are among the important factors in the biological action of radiation. In the presence of some biological substances (such as cysteine, glutathione, etc.) this effect of x-rays is appreciably weakened [1, 2] which is, of course, of great interest.

To elucidate the mode of action of protective substances in protein solutions, it appeared important to obtain direct proof that, in the presence of protective organic substances, chemical changes in the functional groups of proteins (which occur during irradiation in pure aqueous solutions) are prevented; this has not been done previously. Main attention was devoted in this investigation to changes in the thiol group content of proteins, in view of the biological importance of these groups [3,4].

An aqueous 2% solution of crystalline egg albumin was used. The organic substances were cysteine hydrochloride, ascorbic acid, and thiourea (all chemically pure).

The x-ray irradiation was effected by means of a BF close-focus tube (90 kW, 10mA, distance 1 cm) at an average wavelength of ~0.6 A; the irradiation dose was 150-300 thousand roentgens, at a dose rate of 20 thousand roentgens/ minute; the irradiated object was cooled in running water, and the irradiation temperature did not exceed 20-22°.

The thiol group content of the protein was difficult to determine in some of the experiments because the protein was present in solution together with cysteine; it was therefore necessary to evolve a special titration technique, which was also used for the other substances studied, including pure protein solutions (without added organic substances).

In this procedure 0.5 ml of 2% protein solution was diluted with water up to 9 ml, and the protein was then precipitated by addition of 1 ml of 20% trichloroacetic acid. The precipitate was centrifuged off, washed with 2% trichloroacetic acid (if protective substances were present in the solution the washing was continued until a negative reaction was obtained for these substances), dissolved in the minimum amount of 0.5 N NaOH, and the solution was made up to 0.5 ml. 3 drops of phosphate buffer (1 M; pH 6.8) and 0.7 g of guanidine hydrochloride were added to the solution, the presence of the latter being necessary for complete titration of the thiol groups. The mixture was held at 37° for 30 minutes, and the solution was then diluted to 1.5 ml with water. A series of 0.2 ml samples were taken from the solution, various amounts of 0.0005 N $K_3Fe(CN)_6$ were added to these from a microburet, and the solutions were left at 37° for 3 minutes. The presence or absence of thiol groups was estabblished qualitatively in each sample by the nitroprusside reaction (we did not consider this reaction reliable for independent quantitative determinations and it was therefore only used as an indicator). The samples were cooled to between 0 and +2°, and 2 drops of freshly prepared 5% sodium nitroprusside solution and 2 drops of 25% ammonia were added to each. The transition from the bright red or bright pink to yellow in the series of samples was fairly sharp, and could be used for an exact estimate of the amount of ferricyanide necessary to oxidize the thiol groups.

The results of thiol group determinations in egg albumin in the various systems studied are shown in Table 1.

TABLE 1

Variation of the Thiol Group Content of Egg Albumin on x-ray Irradiation.

System	Irradiation dose, thousand roentgen	SH group content in mg cysteine per 1 g protein
Egg albumin	0	5.7
(2%)	150	3.4
Egg albumin	0	5.7
(2%) + cysteine	150	5.7
(0.5%)	300	5.7
Egg albumin	0	5.7
(2%) + ascorbic	150	5.7
acid (0.5%)		
Egg albumin	0	5.7
(2%) + thiourea	150	3.4
(0.5%)		

TABLE 2

Variation of the Thiol Group Content of Egg Albumin on Ultraviolet Irradiation

System	Irradiation dose, billion ergs per 5 ml solution	SH group content in mg cysteine per 1 g protein
Egg albumin	0	5.7
(2%)	20	1.2
Egg albumin (2%) + cysteine (0.5%)	20	5.7
Egg albumin (2%) + ascorbic (0.5%)	20	5.7

It is seen that although after irradiation of pure aqueous solution of egg albumin (Table 1) the thiol group content falls sharply (from 5.7 to 3.4 mg/g), in the presence of cysteine and of ascorbic acid the added substances are oxidized (the total SH group content decreases in a mixture of cysteine and protein) while the thiol groups of the albumin remain intact and their content constant. In contrast to these substances, thiourea does exert a protective effect on the thiol groups of the albumin.

In addition to x-rays, we also studied the effect of ultraviolet radiation on the thiol group content of the protein. The irradiation by ultraviolet rays was carried out by means of a PRK-2 quartz lamp at a distance of 25 cm for 2 hours, with the irradiated solution cooled in ice; a total of 5 ml of solution was irradiated. The irradiation intensity was ~ 1 million ergs/cm^2·min., and the total dose was ~ $2 \cdot 10^{10}$ ergs. The results of the experiments are shown in Table 2.

Thus, it is seen that cysteine and ascorbic acid protect the thiol groups in albumin during ultraviolet irradiation also.

The ion yield in the x-ray irradiation of egg albumin in pure aqueous solution was calculated as follows. As 1 roentgen at 0.5-1.0 A forms ~$1.6 \cdot 10^{12}$ ion pairs in 1 g [5], then a dose of 150 thousand roentgens corresponds to $1.5 \cdot 10^5 \times 3.2 \cdot 10^{12} = 4.8 \cdot 10^{17}$ ions per 1 g; on the other hand, the number of molecules of egg albumin (M = 40,000) in 1 ml of 2% solution is $3 \cdot 10^{17}$, so that there are ~ 2 radicals for each albumin molecule. The molecule of egg albumin contains a total of 5 SH groups [6], of which, to judge by the change in the titer from 5.7 to 3.4 mg/g (Table 1), or of 40%, 2 SH groups are oxidized, which is in good quantitative agreement with the number of free radicals. Therefore the ion yield of SH group oxidation in egg albumin during x-ray irradiation of pure aqueous solutions of the protein is ~ 1.

The quantum yield in the oxidation of SH groups of the protein by ultraviolet irradiation of egg albumin solutions is considerably lower than the ion yield. With a total dose of $2 \cdot 10^{10}$ ergs or $2.9 \cdot 10^{21}$ quanta per 5 ml of 2% aqueous solution containing $1.5 \cdot 10^{18}$ protein molecules for 1 molecule there are $(2.9 \cdot 10^{21})/(1.5 \cdot 10^{18}) =$ = 2000 quanta, resulting in the oxidation of 80% of the SH groups in the albumin (fall of the titer from 5.7 to 1.2 mg/g in Table 2), or 4 SH groups. Consequently, the oxidation of one SH group of the protein requires ~ 500 quanta, which gives a quantum yield of ~ $2 \cdot 10^{-3}$ for this reaction.

Incidentally it may be noted that the irradiated egg albumin solutions remained quite transparent in presence of cysteine or ascorbic acid, while without these they became rather turbid. It seems that the oxidation of thiol groups in pure protein solutions is accompanied by formation of disulfide bridges between the protein molecules, and aggregation of the latter, while in presence of cysteine and ascorbic acid the thiol groups of the albumin are not oxidized and no aggregation occurs (for greater detail, see [7]).

These results of the action of ionizing radiations on protein solutions in presence of other organic substances are essentially the consequence of two additive effects. On one hand, in multicomponent solutions a statistical distribution of the active radicals formed in water takes place between the solution components in accordance with their molar concentrations; in solutions of proteins together with organic substances, because of the greater molar concentration of the latter, this concentrational effect in itself results in partial protection of the protein molecules. On the other hand, the protective effect is to a considerable extent determined by the relative effectiveness of interaction of the molecules of the solution components with the active radicals, which is directly related to the specific chemical structure of the reacting substances. The ratio between the concentrational and the chemical factors can be calculated by means of Lea's formula [5], which can be modified to the following form:

$$\frac{S_1}{S_2} = 1 + \frac{c_2 Z_2 P_2}{c_1 Z_1 P_1}, \qquad (1)$$

where, in the present instance, S_1 is the number of protein molecules which have reacted in the given irradiation conditions in 1 ml of pure aqueous solution, S_2 is the corresponding value in presence of another substance; c_1 is the molar concentration of protein; Z_1 is the number of collisions between active radicals and protein molecules, and P_1 is the effectiveness of deactivation of the radical on collision with a protein molecule; the same designations with the subscript 2 refer to molecules of the added substance.

In our experiments (Table 1) the concentration of egg albumin (M = 40,000) was 2%, and therefore $c_1 = 5 \cdot 10^{-4}$; Z_1 for egg albumin (see [5], page 53) is $4 \cdot 10^{12}$; the concentration of cysteine hydrochloride (M = 156) was 0.5%, and therefore $c_2 = 3.3 \cdot 10^{-2}$ and $Z_2 = 3 \cdot 10^{11}$. If the protective action depended only on the concentrational effect, that is, only on the factors $\underline{c}$ and Z, and if both substances (protein and cysteine) deactiviated the radicals with equal effectiveness ($P_1 = P_2$) then in the given irradiation conditions we should find that

$$\frac{S_1}{S_2} = 1 + \frac{3.3 \cdot 10^{-2} \cdot 3 \cdot 10^{11}}{5 \cdot 10^{-4} \cdot 4 \cdot 10^{12}} = 6,$$

so that the number of protein molecules to react should be 6 times as small in presence of cysteine. It follows from Table 1 that the change of the SH group titer in the presence of cysteine should then decrease from 5.7 − 3.4 = 2.3 mg/g to approximately 0.4 mg/g, so that the SH group titer should become ~ 5.7 − 0.4 = 5.3 mg/g, whereas in fact the SH group titer in presence of cysteine was 5.7 mg/g. Thus, the protective action of cysteine in our experiments was predominantly concentrational or statistical in character; the small difference of 0.4 mg/g can be either attributed to experimental error (and in this case $P_1 = P_2$) or, if it has partly a real meaning, it shows that $P_2 > P_1$, so that the effectiveness of reaction of the SH groups of cysteine is rather higher than that of the SH groups of the albumin, which is in accordance with other known facts [8]. Similar results are obtained for solutions of egg albumin with ascorbic acid (Table 1).

In the case of thiourea, on the other hand, with a molar concentration of the components similar to that in the preceding systems (similar values of $\underline{c}$ and Z), the protective effect is close to zero, and instead of $S_1/S_2 \sim 6$, it is found experimentally (Table 1) that $S_1/S_2 = (5.7 - 3.4)/(5.7 - 3.4) = 1$, from which it follows, according to Equation (1), that $P_2/P_1 \sim 0$. Thus, the relative effectiveness of interaction of thiourea with oxidizing radicals is much less than that of the thiol groups in albumin, which is to be expected from the chemical viewpoint. However, thiourea may be a more active substance and exert a protective effect with respect to other less sensitive groups in proteins, or to other substances such as carbohydrates [9].

Our calculations based on certain published data confirm the above conclusions. For example, Anderson and Harrison [10] studied the action of x-rays on the oxidation of ascorbic acid in presence of serum albumin, and they found that the albumin had no protective effect. In their experiments (the subscript 1 refers to ascorbic acid and 2, to the albumin) $c_1 = 3.5 \cdot 10^{-5}$, $Z_1 = 3.5 \cdot 10^{11}$, $c_2 = 5 \cdot 10^{-4}$ and $Z_2 = 9 \cdot 10^{12}$ (for 2.5% solution of serum albumin with M = 700,000) from which it follows that the ratio S_1/S_2, determined by the concentrational factor, for the condition $P_1 = P_2$, should be:

$$\frac{S_1}{S_2} = 1 + \frac{5 \cdot 10^{-4} \cdot 9 \cdot 10^{12}}{3.5 \cdot 10^{-5} \cdot 3.5 \cdot 10^{11}} = 370,$$

whereas it was experimentally found that $S_1/S_2 \sim 1$ (the albumin had no protective effect). It follows that the effectiveness of the reation between the serum albumin molecules and the radicals must be very much less than in the case of ascorbic acid (we should have $P_2/P_1 < 10^{-4}$), and therefore the serum albumin concentration of 2.5 % was quite insufficient for protection of 10^{-5}M ascorbic acid, in agreement with Anderson and Harrison's results [10]. Conversely, for the same reason ascorbic acid should be a good protective agent in the oxidation of protein molecules during irradiation, and in fact in our experiments 0.5% ascorbic acid effectively protected the SH groups in 2% albumin from oxidation. Thus, despite the difference in the proteins used and the aims of the work, the two investigations are in good agreement.

This result demonstrates the conventional nature of the concept of protective action, and the possibility under certain specified conditions of converting the protected substance into a protective agent and vice versa. For example, it was shown by Forssberg [2] that some organic acids (maleic, tartaric, levulinic and others) in 0.1 M concentration can protect catalase at a concentration of 3.7 mg/ ml against the action of x-rays, that is, at $c_1 = 1.5 \cdot 10^{-8}$ (our calculated values for S_1/S_2 from Forssberg's data are from 1.75 to 1.16). Omitting intermediate values, we will only note here that for these systems $P_2/P_1 \sim 10^{-6}$, so that the catalase molecules are immeasurably more sensitive to the radicals than the molecules of the above mentioned acids. Hence it follows that additions of even small concentrations of catalase should have an appreciable protective effect on solutions of these acids, and this was experimentally verified for the system catalase – pyruvic acid.

4.5 ml of 0.1% pyruvic acid solution was irradiated in a bicarbonate buffer (pH 7.5) by a dose of 300 thousand roentgens; 3 ml of concentrated KOH and 1.5 ml of 2% salicylic aldehyde solution were then added to 3 ml of the solution [11]; the mixture was held at 37° for 10 minutes, cooled for 1 minute, and analyzed colorimetrically (the accuracy was ~ 2-3%). In the experiments with catalase; 0.2 mg/ ml of a catalase preparation extracted from ox liver was added to the irradiated solution of pyruvic acid. The relative change of the pyruvic acid content after irradiation in pure solutions was 0.873, after addition of catalase it was 0.930, and in presence of catalase inactivated by boiling for 10 minutes, 0.880. Thus, the addition of small amounts of catalase exerts a protective action against the effects of irradiation on pyruvic acid solution, which is an inversion of the Forssberg effect. If the protective effect of catalase is explained by its action in decomposing the hydrogen peroxide formed in the irradiation, then it is seen from the relative decrease of the effect of irradiation (1.00-0.93): (1.00-0.87) that about 50% of the effect should form the share of hydrogen peroxide.

In the paper by Shekhtman, Krasnovsky, and Vereshchinsky [12], Fig. 4 contains data on the protective effects of glycerol, glucose quinone, and hydroquinone on the fading of methylene blue under the action of x-rays. It is seen from these data that a 50% protective effect (in our notation, $S_1/S_2 = 2$) was found when the concentrations of the added substances were of the order of 10^{-4}, near to the concentration of methylene blue (that is, at similar values of c_1 and c_2); the same applies to the values of Z_1 and Z_2 in Equation (1), in view of the similar molecular weights of the substances. It follows from Equation (1) that for the systems tested by these authors $P_2/P_1 \sim 1$, and consequently methylene blue should also exert a protective effect on the oxidation of the added substances under the given conditions.

This was also confirmed experimentally by us for the system methylene blue – glucose, in which the protective effect of the first component in the oxidation of glucose during irradiation was studied. 6 ml of 0.01% glucose solution was irradiated with a dose of 50 thousand roentgens; 3 ml of concentrated H_2SO_4 [13] was added per 0.5 ml of the solution, the mixture was heated for 4 minutes on a boiling water bath, cooled, and the absorption of the solution in the 480-580 mμ region (maximum at 520 mμ) was measured with an SF-4 spectrophotometer. Similar measurements were made at 520 mμ on an irradiated solution of a mixture of 0.01% glucose and 0.01 % methylene blue (the absorption maximum for the pure dye is found at 660-670 mμ). Upon irradiation of a pure glucose solution the value of ϵ at 520 mμ fell from 0.062 to 0.053, while in presence of methylene blue this decrease did not occur, which confirmed the protective action of the dye.

Thus, in both the systems studied (pyruvic acid – catalase and glucose – methylene blue) the two components exert mutually protective effects, and the main effect observed depends only on their molar concentration ratio and their reactivity coefficient ratio P_2/P_1 in solution.

Most of the available experimental results, fully examined above (as is seen, still not numerous) are not adequate for exact calculations of the values of P_2/P_1 with respect to proteins, which is necessary to establish the relationship between the molar concentration of the added substance and its protective effect. We note incidentally that it seems to us more conveinent to use the coefficient:

$$K = 1 - S_2/S_1, \quad (2)$$

as a measure of the protective action, as in the transition from no protective action ($S_1 = S_2$) to complete protection ($S_2 = 0$) the value of K changes from 0 to 1, while the function S_2/S_1 changes in the opposite direction (from 1 to 0) while the function S_1/S_2 in Equation (1) changes from 1 to ∞, which is inconvenient in use.

In conclusion it must be noted that determinations of the presence or absence of protective action (and of the corresponding values of P_2/P_1) with respect to definite functional groups in proteins for different mixtures of proteins with individual chemical substances may serve as a general method for the quantitative evaluation of the relative reactivities of the functional groups of native proteins to chemical influences.

SUMMARY

1. The thiol group contents of egg albumin after x-ray and ultraviolet irradiation in pure aqeuous solutions and in presence of certain organic substances have been found by direct chemical determination. Cysteine and ascorbic acid protect the thiol groups of albumin against oxidation during irradiation, while thiourea does not have this effect.

2. The ion yield of the oxidation of SH groups in albumin during x-ray irradiation (equal to unity) and the quantum yield of this reaction during ultraviolet irradiation (equal to $2 \cdot 10^{-3}$) have been determined.

3. The ratio of the concentrational and chemical factors in the protective action of various organic substances (cysteine, organic acids) on proteins has been calculated. The systems catalase – pyruvic acid and glucose – methylene blue have been used to show that the concept of protective action is conventional, and that it is possible under definite conditions to convert the protected into the protective substance and vice versa.

LITERATURE CITED

[1] H. Patt, D. Smith, et al., Proc. Soc. Exp. Biol. Med. 73, 18, 198 (1950); W. Chapman and C. Cronkite, ibid. 75, 318 (1950); 76, 396 (1951); Z. Bacq and A. Herke, Brit. J. Radiol. 24, 617 (1951).

[2] A. Forssberg, Nature 159, 308 (1947).

[3] Kh. S. Koshtoyants, Proteins, Metabolism, and Neuroregulation (Acad. Sci. USSR Press, 1951).

[4] E. Barron, Advances in Enzymol. 11, 202 (1951).

[5] D. Lea, Action of Radiations on Living Cells. (1946).

[6] G. Tristram, Advances in Protein Chem. 5, 137 (1950).

[7] A. G. Pasynsky, Symposium: Proteins, Their Specific Properties (Acad. Sci. Ukrain. SSR Press, Kiev, 1955), p. 152.

[8] A. G. Pasynsky, and R. S. Chernyak, Biochemistry (USSR) 17, 198 (1952).

[9] E. Rice, Science 115, 92 (1952).

[10] R. Anderson, and B. Harrison, J. Gen. Physiol. 27, 69 (1943).

[11] N. P. Meshkov and S. E. Severin, Manual of Animal Biochemistry, Soviet Science (Moscow, 1950), p. 178.

[12] Ya. L. Shekhtman, A. A. Krasnovsky, and I. V. Vereshchinsky, Proc. Acad. Sci. USSR 74, 767 (1950).

[13] F. D. Snell, Colorimetric Methods of Analysis (1937), Vol. II, p. 475.

Received August 26, 1955

The A. N. Bakh Institute of Biochemistry
Academy of Sciences USSR, Moscow

EFFECT OF SODIUM CHLORIDE AND ETHYL ALCOHOL ON THE MECHANICAL PROPERTIES OF ALUMINUM OXIDE SOL

P. V. Rufimsky

It was shown in our previous communication [1] that aluminum oxide sol undergoes thixotropic gelation on addition of electrolyte (NaCl) and of ethyl alcohol, and its structure can be broken down repeatedly by shaking. In view of the fact that the existence of a structure confers on a disperse system characteristic mechanical properties which depend on the chemical nature of the substances which compose the system, and which are determined by the molecular forces holding the structural elements together, it was desired to study the rheological properties of aluminum oxide sols, since an analogous study has already been made on ferris hydroxide sol [2], which differs in nature from alumina sol.

EXPERIMENTAL

There has been no generally accepted scientifically based method for evaluation of the mechanical properties, which are their most characteristic properties, of structurized disperse systems. The methods which have hitherto been available are largely qualitative. These include all the test tube methods of determination of gelation rates, the quantity of water required for gelation, etc. [3, 4].

Later, numerous workers [5,6] used viscosimetric methods for evaluation of thixotropy, in which variations of "conventional" viscosity or flow in time were studied. However, it was shown by Rebinder et al. [7,8] that viscosimetric methods alone are not sufficient for characterization of structurized systems, and that it is necessary to measure direct mechanical properties of the system – yield stress, creep, elasticity modulus, and relaxation.

The aim of the present work was to study the mechanical properties of alumina sols (static yield stress and thixotropic gelation time). The method used was the one used by Serb-Serbina [9] in studies of structure formation in aqueous colloidal clay suspensions. The principle of the method is as follows. A dry and clean capillary 1 (0.0052 cm in diameter in our experiments) was fixed exactly horizontally on a table (Fig. 1) and a column on the sol was drawn into it. The length of the column was measured by the millimeter scale 2.

To avoid changes of the sol in the capillary as the result of evaporation of alcohol (isothermal distillation), a bent tube 3 containing the sol in aqueous alcohol was connected to each end of the capillary, and a vacuum was created through the tube 4, and measured by the water manometer 5. The bent tube served as a buffer between the capillary space filled with the vapor of the aqueous alcohol mixture, and the outer space, free from this vapor. This buffer decreases evaporation of alcohol from the sol. The rate of evacuation of the system was 0.1 cm water column per second, with a sol column 10 to 12 cm long. No slip at the capillary walls, and any consequent "breakthrough" of the sol was observed within the limits of our determinations. The pressure P at which the column of sol began to move was read off on the barometer. In order to detect the instant at which the sol column began to move, the manometer was shut off by the tap 6, and simultaneously the capillary was opened to the air. The pressure P was used to calculate the static yield stress θ from the usual formula

$$\theta = rP / 2\underline{l}\,.$$

The thixotropic gelation time was found from the graphs for θ as a function of the time the liquid remained in the capillary. The horizontal region ab indicates the time (τ_{max}) for thixotropic gelation.

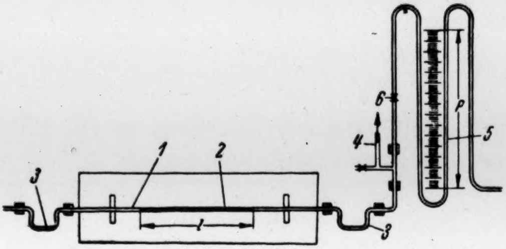

Fig. 1. Apparatus for determination of the mechanical properties of sols.

TABLE

Static Yield Stress of Al_2O_3 Sol in Presence of Electrolyte or Alcohol. (Capillary Radius 0.0052 cm)

Composition of mixture in wt. %				Length of sol column in cm	Static $\theta_{max} \times \sqrt{10^{-3}}$ in cm	Time, min	Type of sol
Al_2O_3	NaCl	C_2H_5OH	H_2O				
0,87	0.45	—	98.68	10.4	6.0	21	Thixostable
0.86	1.71	—	97.43	10.4	4.0	14	Thixolabile
0.82	5.75	—	93.43	10.2	0.5	4	Thixostable
0.71	2.64	—	96.65	10.3	0.7	5	Thixolabile
0.68	0.45	—	98.87	12.2	4.5	23	Thixostable
0.21	5.78	—	94.01	12.1	4.7	12	"
0.48	0.45	—	99.07	10.4	3.4	11	"
0.43	1.01	—	98.56	10.7	1.7	8	Thixolabile
0.24	—	77.86	21.90	10.2	11	50	Thixostable
0.14	—	87.31	12.55	11.1	4.2	21	"
0.08	—	80.28	19.64	12.4	0.8	6	"
0.13	—	75.64	24.33	10.7	3.5	12	"
0.19	—	71 12	28.69	10.3	5.8	19	"

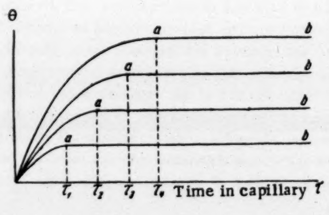

Fig. 2. Curves for the variation of θ with the time in the capillary for various sols; ($\tau_1 - \tau_4$) times for thixotropic gelation.

Thixotropic Al_2O_3 sols obtained in presence of electrolyte (NaCl) and ethyl alcohol were used for the static yield stress determinations. The Table shows the results (average values for four parallel measurements).

SUMMARY

1. The static maximum shearing stress (yield stress) and thixotropic gelation time of aluminum hydroxide sols in presence of electrolyte (NaCl) and ethyl alcohol have been determined by means of a horizontal plastometer of the capillary type.

2. Thioxtropic Al_2O_3 sols prepared in presence of sodium chloride and of alcohol have different me-

chanical strengths. The strength of Al_2O_3 sols made in presence of alcohol is higher than that of sols made in presence of sodium chloride.

3. It is shown that thixotropic Al_2O_3 sols made in presence of alcohol have characteristically stable properties while sols formed by the action of electrolyte often exhibit clearly labile properties; this is probably to be explained by the more harsh action of the electrolyte, leading to syneresis of the sols and decrease of their mechanical strength.

4. The sols containing alcohol show a gradual increase of yield stress, which reaches a maximum in two hours. The sols with electrolyte show an increase of the yield stress only at first (after 15 minutes), but later the strength of their structure decreases and they become less stable.

I express my deep gratitude to Professor A. F. Bogoyavlensky for valuable advice in the course of the work.

LITERATURE CITED

[1] P. V. Rufimsky, Colloid J. 18, 332 (1956) (T.p. 323).*

[2] A. F. Bogoyavlensky, Colloid J. 11, 371 (1949).

[3] H. Freundlich, Kolloid-Z. 45, 384 (1928); 46, 298 (1928); 52,37 (1930).

[4] Winkler, Kolloid-Beih.. 48, 4, (1938).

[5] V. L. Valdman, Factory Lab. 11, 1077 (1943); Colloid J. 9, 175 (1947).

[6] A. I. Rabinerson, Problems of Colloid Chemistry (Leningrad, 1937); Progr. Chem. 7, 1433 (1938).

[7] S. Ya. Veiler and P. A. Rebinder, Proc. Acad. Sci. USSR 49, 354 (1945).

[8] P. A. Rebinder, article in: A. I. Tsurinov, Clays and Muds Used in Oil Well Drilling (State Fuel Tech. Press, 1940).

[9] N. N. Serb-Serbina and S. A. Nikitina, Colloid J. 8, Nos. 1-2, 63 (1946).

Received September 17, 1955

The V. I. Ulyanov-Lenin University, Kazan
Laboratory of Inorganic Chemistry

---

* T.p = C. B. Translation pagination.

EFFECT OF THE DEGREE OF SWELLING OF ION-EXCHANGE RESINS ON THE SELECTIVITY OF SORPTION OF AUREOMYCIN, TERRAMYCIN, AND STREPTOMYCIN IONS BY CATION EXCHANGE RESINS

G. V. Samsonov

The swelling power of ion-exchange resins plays a very important role in the sorption of organic ions [1-4]. Strongly cross-linked resins are insufficiently permeable to ions of large molecular weight. The theory of ion exchange on swelling resins should take into consideration factors neglected in the theory of ion exchange on nonswelling resins [5]. The work of Gregor [6] has made it possible to evaluate the role of resin swelling in ion exchange for the simplest systems. For the exchange of univalent ions of similar properties, Gregor derived the ion-exchange equation

$$RT \ln \frac{\overline{a}_1 a_2}{a_1 \overline{a}_2} = p(V_2 - V_1), \tag{1}$$

where p is the swelling pressure; V_1 and V_2 are the specific volumes of the ions in the resin; a_1 and a_2 are the activities of the ions in solution; $\overline{a}_1$ and $\overline{a}_2$ are the activities of the ions on the resin), in which only the work of swelling is considered as the energy factor, and the differences of the energy of interaction of different ions with the resin are neglected. Consequently, Gregor's theory is not applicable to the exchange of ions with different properties, especially ions of different charge.

Replacement of one ion on the resin by another changes the degree of swelling of the resin. The volume occupied by the resin either increases or decreases. A certain amount of solvent penetrates into the resin or leaves it in the process. The introduction of a strongly solvated multivalent ion decreases the degree of swelling of the resin, owing to decreased solvation of the resin which results from the strong electrostatic interaction between the ion and the resin. A similar situation occurs when hydrogen ions are introduced into carboxylic cationic resins. The sorption of ions by resins with high selectivity is always accompanied by shrinkage of the resins. This occurs also when large ions – ions of organic substances with high molecular weight – are adsorbed. Thus, from the thermodynamic standpoint, the ion exchange-process on swelling resins is characterized by a change of free energy as the result of transfer of A_1 ions from the solution to the resin and simultaneous transfer of A_2 ions into solution, and a change of free energy as the result of passage of the solvent from the solution into the resin or, conversely, from the resin into the solution. Ion exchange can be represented by Equation (2), which represents shrinkage of the resin in the ion-exchange process

$$\frac{1}{z_1} A_1 + \frac{1}{z_2} \overline{A}_2 + n_s \overline{S} \rightleftarrows \frac{1}{z_1} \overline{A}_1 + \frac{1}{z_2} A_2 + n_s S, \tag{2}$$

where $\overline{A}_1$ and $\overline{A}_2$ are ions bound with the resin; S and $\overline{S}$ is the solvent in the solution and in the resin grains; n_s is the number of moles of solvent transferred in the exchange of one milliequivalent of the ions; z_1 and z_2 are the ionic charges.

For the exchange of one equivalent of ions on the resin, the change of thermodynamic potential is calculated from the equation

$$\Delta\Phi = \frac{1}{z_1}\bar{\mu}_1 + \frac{1}{z_2}\mu_2 - \frac{1}{z_1}\mu_1 - \frac{1}{z_2}\bar{\mu}_2 + n_s\Delta\Phi_s, \tag{3}$$

where μ_1, μ_2, $\bar{\mu}_1$ and $\bar{\mu}_2$ are the chemical potentials of the ions in the bound state in the resin; $\Delta\Phi_s$ is the change of thermodynamic potential as the result of transfer of solvent.

The chemical potential of ions of a definite kind in solution is related to the ionic activity by the expression

$$\mu_i = \mu_i^0 + RT\ln a_i. \tag{4}$$

It may be assumed that the chemical potential of the ions in the bound state in the resin can be calculated from an anlogous expression (the ions in the resin are mobile)

$$\bar{\mu}_i = \bar{\mu}_i^0 + RT\ln \bar{a}_i, \tag{5}$$

where $\bar{a}_i$ is the activity of the ion in the resin.

In equilibrium conditions ($\Delta\Phi_{m,p} = 0$) the equation for the ion exchange isotherm, in accordance with Equations (3, 4, 5) has the form:

$$RT\ln\frac{\bar{a}_1^{1/z_1}a_2^{1/z_2}}{a_1^{1/z_1}\bar{a}_2^{1/z_2}} = r - n_s\Delta\Phi_s \tag{6}$$

($\underline{r}$ is a constant) or

$$\frac{\bar{a}_1^{1/z_1}}{\bar{a}_2^{1/z_2}} = \frac{a_1^{1/z_1}}{a_2^{1/z_2}}\,e^{(r-n_s\Delta\Phi_s)/RT}. \tag{7}$$

In dilute solutions the activities of the ions may be replaced by their concentrations, as the interaction between the sorbed ions with one another is much weaker than the interaction between the ions and the resins. The approximate equation for ion exchange on swelling resins than has the form:

$$\frac{m_1^{1/z_1}}{m_2^{1/z_2}} = \frac{c_1^{1/z_1}}{c_2^{1/z_2}}\,e^{(r-n_s\Delta\Phi_s)RT}, \tag{8}$$

where m_1 and m_2 are the numbers of milligrams of ions adsorbed on 1 g of the resin.

The term $e^{(r-n_s\Delta\Phi_s)/RT}$ undoubtedly depends on the ratio of the exchanged ions in the resin. However, as a first approximation, we may regard the function

$$K = e^{(r-n_s\Delta\Phi_s)/RT} \tag{9}$$

as constant with change of concentration.

To a not very high degree of accuracy, the isotherm for ion exchange on swelling resins is in agreement with Nikolsky's isotherm [5], derived for ion exchange on nonswelling resins:

$$\frac{m_1^{1/z_1}}{m_2^{1/z_2}} = K\frac{c_1^{1/z_1}}{c_2^{1/z_2}}. \tag{10}$$

With the aid of Equation (8) we can consider the effect of swelling of resins on the selectivity of sorption of different ions. We may assume that in the exchange of ions of two definite types on resins made from the same starting material under the same conditions, but with different contents of binding groups, that is, with different coefficients of swelling, r will have a constant value. This constant represents the sum of the chemical potentials of the exchanged ions in standard states $\left(\frac{1}{z_1}\overline{\mu_1^0} + \frac{1}{z_2}\mu_2^0 - \frac{1}{z_1}\mu_1^0 - \frac{1}{z_2}\overline{\mu}_2^0\right)$. Therefore the exchange constant K should depend on the term $n_s \Delta \Phi_s$ for a number of resins with different degrees of swelling. Since $n_s\Delta\Phi_s > 0$, if sorption of the ions is accompanied by shrinkage of the resin, it would follow from Equation (8) that the exchange constant K should decrease with increasing swelling. In other words, the selectivity of ion adsorption should decrease with increasing swelling. This is a general conclusion; it is applicable to any system of ions, including the exchange of ions of different valencies Examination of Gregor's Equation (1) shows that both p and $V_2 - V_1$, should change, but in different directions, with the degree of swelling. Therefore the Gregor equation (derived for a special, simplest case of ion exchange on swelling resins) cannot be used to determine the direction of the change of selectivity of ion adsorption with increasing degree of swelling of the resins. A change in the selectivity of ion sorption with the degree of swelling of the resin has been experimentally found by a number of workers [2,7].

EXPERIMENTAL

The effect of the degree of swelling on the ion-exchange constant was studied in the ion systems aureomycin – hydrogen and terramycin – hydrogen for exchange on sulfonic resins, and in the system streptomycin – sodium for exchange on KMT carboxylic resin. The exchange laws were studied by determination of the sorption capacity of the resins for the antibiotics by a dynamic method (the methods have been described in detail previously [3,4,8]).

The concentrations are in every case given in normalities, and the sorption capacities in mg-equivalents per gram. The results, shown in Figs. 1 and 2 and in the Table, show that the exchange constant decreases and the selectivity of ion sorption diminishes with increasing swelling in all systems. This applies both to the exchange of uni – univalent ions in the case of aureomycin and terramycin, and to the exchange of trivalent streptomycin ions for univalent hydrogen ions, and is in agreement with the theory advanced above, since sorption of aureomycin, terramycin, and streptomycin is accompanied by shrinkage of the resins.

The increased accessibility of the inner portions of the resin grains to large ions [1-4] with increased degree of swelling, can, in accordance with the foregoing, be set against the decreased selectivity of sorption of the ions. The two factors operate in opposite directions; their combined effect may be examined by determination of the variation of the sorption capacity for ions of a given type, in presence of ions of another type, with the degree of swelling of the resin. For low-swelling coefficients, when the role of swelling is unimportant, the increased accessibility of the active centers to large ions should have a particularly strong effect. At high-swelling coefficients, when the accessibility changes little, the decreased selectivity of ion sorption should play an important role. Accordingly, the curves for the variation of sorption capacity with the degree of swelling from solutions containing ions of another kind should have a maximum. Such a relationship is shown in Fig. 3 for the sorption of aureomycin from solutions of different acidity by SSF sulfonic resins with different swelling coefficients. The aureomycin concentration was 400 μg/ml in all experiments. At low acid concentrations the decisive role is played by the accessibility of the inner parts of the resins to the aureomycin ions, and the curves do not have a maximum. Curves 3 and 4 in Fig. 3, for systems containing 0.5 and 1 N hydrochloric acid, show a maximum. This represents the superposition of the two factors discussed above.

TABLE

Variation of the Exchange Constants of Aureomycin Ions with H^+ With Degree of Swelling of Sulfonic Resins

Resin	Coefficient of swelling	Exchange constant for aureomycin and H^+
SSF	2.7	425
	5.0	300
SBS	2.0	1280
	5.3	316
SM-12	4.8	300
	8.1	130
SN-2	1.4	650
	3.0	375

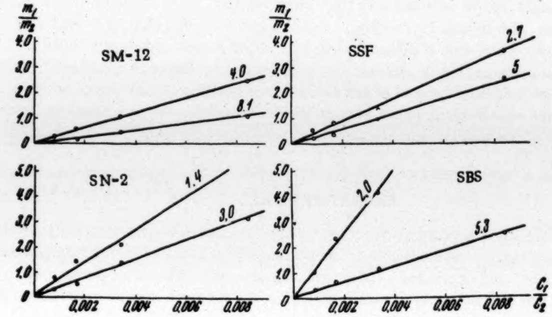

Fig. 1. Exchange of aureomycin ions for hydrogen ions on sulfonic resins SM-12, SSF, SN-2, and SBS (the numbers on the lines represent values of K_{sw}).

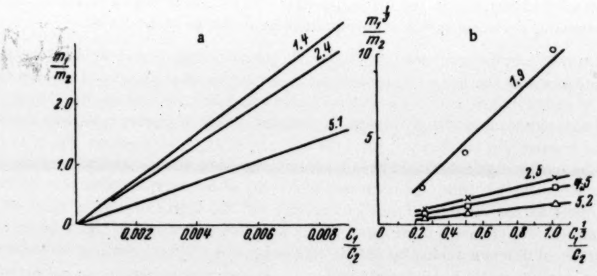

Fig. 2. Exchange of ions: a) terramycin and hydrogen on SBS sulfonic resins; b) streptomycin and sodium on KMT carboxylic resins (the numbers on the lines represent values of K_{sw}).

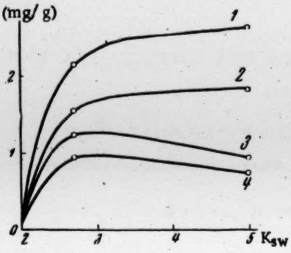

Fig. 3. Variation of the sorption capacity of SSF resin for aureomycin (concentration 0.00084 mg-equiv./ / liter) with the swelling coefficient of the resin, for solutions with different concentrations of HCl: 1) 0.1 N; 2) 0.25 N; 3) 0.5 N; 4) 1N.

SUMMARY

1. A theory of ion exchange on swelling ion-exchange resins is put forward.

2. It is shown theoretically that the selectivity of sorption of ions should decrease with increasing swelling of the resins.

3. The sorption selectivity for aureomycin and terramycin decreases in comparison with the sorption of hydrogen ions with increasing swelling for all the sulfonic resins studied.

4. The sorption selectivity of KMT carboxylic resin for streptomycin decreases with increasing swelling of the resin.

5. The sorption capacity for streptomycin by SSF resin from solutions with high acidity as a function of the degree of swelling is represented by a curve with a maximum.

I acknowledge the assistance of V. V. Bokareva, A. A. Kononova, S. F. Lvarentyeva, V. S. Maslennikova, M. P. Shesterikova, and L. M. Shuvalova in the experimental work.

LITERATURE CITED

[1] S. M. Partridge, R. C. Brimley and K. W. Pepper, Biochem. J. (London) 46, 334, 1950.

[2] R. Kunin and R. J. Myers, Discussions Faraday Soc. No. 7, 114 (1949).

[3] G. V. Samsonov and S. E. Bresler, Colloid J. 18, 88 (1956) (T.p. 83).*

[4] G. V. Samsonov, L. M. Shuvalova et al., Colloid J. 18, 474 (1956) (T.p 465).*

[5] B. P. Nikolsky, Doctoral Dissertation, Leningrad Univ. (1939); B. P. Nikolsky and V. I. Paramonova, Progr. Chem. 8, 1535 (1939).

[6] H. G. Gregor, J. Am. Chem. Soc. 70, 1293 (1948).

[7] H. F. Walton, in Ion Exchange (F. C. Nachod, ed.) (1951), p. 19.

[8] G. V. Samsonov and S. E. Bresler, Colloid J. 18, 470 (1956) (T.p 461).*

Received June 29, 1956

Institute of High Molecular Compounds
Academy of Sciences USSR, Leningrad

---

* T.p = C. B. Translation pagination.

STUDY OF THE KINETICS AND MECHANISM OF THE THERMAL DECOMPOSITION OF CHLORINATED VINYL POLYMERS

2. RESULTS FOR POLYVINYLIDENE CHLORIDE, VINYLIDENE CHLORIDE – VINYL CHLORIDE COPOLYMER AND CHLORINATED POLYVINYL CHLORIDE

L. G. Tokareva, N. V. Mikhailov, and V. S. Klimenkov

The previous paper [1] contained a description of the method used for studies of the thermal decomposition of chlorinated vinyl polymers, and the results of these investigations in the case of polyvinyl chloride (PVC).

The present paper is a continuation of this work, for other chlorinated vinyl polymers: polyvinylidene chloride, (PVDC); copolymer of vinylidene and vinyl chlorides, CP (VDC + VC); and chlorinated polyvinyl chloride (CPVC) with the use of the previously described method. The paper contains experimental data on the kinetics of thermooxidative decomposition of these compounds, and the results are jointly considered in the light of a possible common mechanism for the first stage of the removal of chlorine in the chlorinated vinyl polymers studied, with due consideration of differences in their chemical composition and molecular structure.

EXPERIMENTAL

Polyvinylidene chloride, PVDC. Fig. 1 represents the kinetics of hydrogen chloride liberation from PVDC at different temperatures. These results show a linear variation of the amount of hydrogen chloride split off with the heating time for all the temperatures used: 140, 150, 160, 170°.

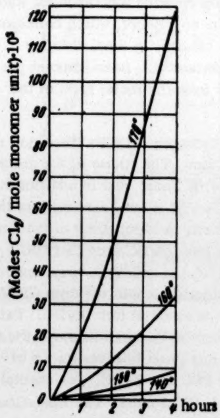

Fig. 1. Liberation of hydrogen chloride by PVDC at 140, 150, 160 and 170°.

The kinetics of thermal decomposition of PVDC presented a similar picture to that of PVC, with the only difference that the rate of decomposition of PVDC is considerably greater than that of PVC. For example, when PVDC is heated at 150°, the quantity of HCl split off in 4 hours is 3 times as large as from PVC.

Table 1 shows comparative data for the chlorine remaining in the polymer, determined by the perborate method, and the chlorine calculated by difference between the chlorine in the original sample and the chlorine calculated from the amount of HCl present in the traps. The results of the chlorine determinations by these two methods agree within the error limits of the perborate method of chlorine determination. It follows from these results that the thermal decomposition of PVDC is considerably accelerated by increase of temperature; for example, while at 140° only 2.7 monomer units are decomposed out of every 1000 ($-CH_2-CCl_2-$) units, at 170°, 126.3 units, or more than 40 times as many, are decomposed.

The data obtained on the kinetics of hydrogen chloride liberation from PVDC were used to determine the rate constant (K) for the reaction of HCl liberation, and the activation energy (E) for the initial stage of PVDC decomposition (Table 2).

An attempt to determine the solubility of PVDC, which had been heated to 150, 160, and 170°, proved unsuccessful, as these specimens did not dissolve in dimethylformamide even when heated to 120°, while we found that the original PVDC dissolved at 100°.

TABLE 1

Liberation of Hydrogen Chloride at Different Temperatures and Heating Times.*

Heating temperature, °C	Amount of hydrogen chloride split off								Cl_2 content in polymer after heating, %	
	% Cl_2				moles Cl_2/mole monomer unit				calculated by difference	determined by perborate method
	heating time, hours									
	1	2	3	4	1	2	3	4		
					PVDC					
140	0.038	0.09	0.14	0.19	0.53	1.2	2.0	2.7	72.1	—
150	0.081	0.24	0.44	0.67	1.10	3.3	6.1	9.1	71.6	71.2
160	0.028	0.82	1.60	2.58	3.86	11.3	21.9	35.2	69.7	70.1
170	—	3.12	5.83	8.84	19.40	48.1	85.3	126.3	63.4	64.2
					CP(VDC+VC)					
140	0.43	0.91	1.29	1.71	5.4	11.3	16.1	21.3	70.6	70.0
150	0.81	1.72	2.54	3.35	10.1	21.4	31.6	41.8	68.9	68.3
160	1.94	4.12	6.22	8.32	24.3	51.2	77.2	103.2	64.0	64.0
170	4.13	10.48	16.6	21.30	55.3	134.3	217.3	275.3	51.3	52.4

---

* For brevity, only some of the determinations, made at 1-hour intervals, are given, and the intermediate points are omitted.

TABLE 2

Rate Constants for the Reactions of Hydrogen Chloride Liberation from PVDC and CP (VDC + VC)

Temperature (°C)	K	$\frac{K_{t+10}}{K_t}$	E, kcal/mole
	PVDC		
140	0.083	2.5	33.6
150	0.21		
160	0.53		
170	1.33		
	CP(VDC+VC)		
140	0.210	2.5	30.0
150	0.525		
160	1.300		
170	3.300		

These results suggest that the decomposition of PVDC is accompanied mainly by structurization or cross linking of the polymer molecules.

Vinylidene chloride – vinyl chloride copolymer, CP (VDC + + VC). A sample containing 74.44% chlorine was taken for studies of the thermal decomposition of the copolymer, which corresponds to an 89.2 : 10.8 ratio of vinylidene chloride to vinyl chloride monomer units. The amount of liberated Cl_2 in millimoles per mole of copolymer was calculated from the molar ratio of the components in the copolymer.

Fig. 2 shows the kinetics of hydrogen chloride liberation by CP (VDC + VC) at various temperatures. The course of the process, as in the case of polyvinyl chloride, is linear, and in addition it is interesting to note that CP (VDC + VC) is less heat-resistant than the corresponding individual polymers. A comparison of the data on hydrogen chloride liberation by PVC, PVDC, and CP (VDC + + VC) shows, for example, that at 150°, and under the same conditions, 13 times as much hydrogen chloride is split off from CP (VDC + + VC), as from PVC, and 3.5 times as much as from PVDC. Table 1 shows the results of experiments on the thermal decomposition of CP (VDC + VC), which illustrate this lower heat resistance of CP (VDC + VC) in comparison with PVC and PVDC. For example, at 140° in 4 hours, out of every 1000 units 21.3 units are decomposed, and at 170°, 275.3 units. The liberation of chlorine from PVC at 170° in 4 hours was 56 units per 1000 monomer units of the PVC chain.

On the assumption of a zero reaction order, the rate constants for the decomposition of CP (VDC + VC) and the activation energy for this process were calculated (see Table 2).

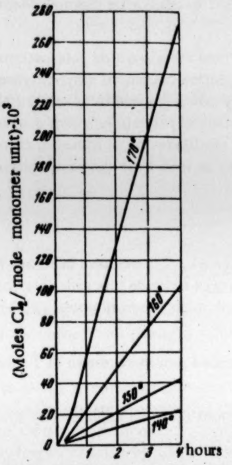

Fig. 2. Liberation of hydrogen chloride by CP(VDC + + VC) at 140, 150, 160 and 170°.

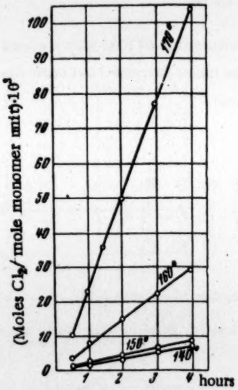

Fig. 4. Liberation of hydrogen chloride by CPVC at 140, 150, 160 and 170°.

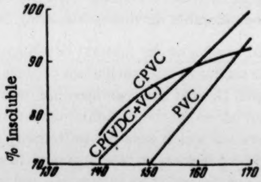

Fig. 3. Solubilities of chlorinated vinyl polymers in cyclohexanone after heating at various temperatures.

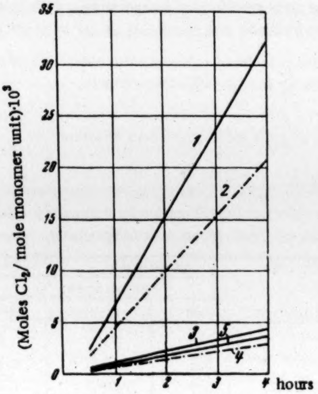

Fig. 5. Liberation of hydrogen chloride by: 1) CP(VDC+ + VC) in oxygen; 2) ditto, in nitrogen; 3) PVDC in oxygen; 4) ditto, in nitrogen; 5) PVC in oxygen.

As Fig. 3. shows, the solubility of CP (VDC + + VC) in cyclohexanone decreases with rise of heating temperature, and at 170° a totally insoluble product is obtained, which suggests that a three-dimensional polymer is formed by a process similar to that found for PVC and PVDC. However, in the case of CP (VDC + VC) a considerable fall in the viscosity of the soluble fraction of the polymer was also found, which suggest a simultaneous degradation process.

Chlorinated polyvinyl chloride, CPVC. Fig. 4 shows the kinetics of hydrogen chloride liberation at various temperatures. The kinetic graphs are linear in this case, similar to those for the other polymers.

The solubility of CPVC in acetone also decreases with increase of heating temperature, as Fig. 3 shows. As in the case of CP (VDC + VC), the viscosity of the acetone-soluble CPVC fraction after thermal decomposition shows a considerable decrease, indicating degradation.

Effect of oxygen on the thermal decomposition of the polymers. There are almost no publications dealing specially with studies of the mechanism of the action of oxygen on the chlorine content of vinyl polymers. However, it is known [2] that the decomposition rate of chlorinated vinyl polymers is greater in an oxygen atmosphere. As the result of our experiments, which did not constitute an exhaustive study of the problem over a wide range of temperatures and which were not sufficiently accurate, it appears that the liberation of hydrogen chloride by chlorinated vinyl polymers at 140° is greater in presence of oxygen, as can be seen from the comparative graphs for the heating of the polymers in nitrogen and in oxygen (Fig. 5).

DISCUSSION OF RESULTS

An examination of all the experimental data shows that the investigated polymers have different resistances to the action of heat. Our experiments showed that the liberation of hydrogen chloride proceeds at a constant rate and with a fairly high temperature coefficient, in good agreement with other reported results [3], obtained by other methods, and apparently at the same time as our work.

Our calculated values for the mean rate of decomposition of chlorinated polymers, shown in Table 3, vary considerably for the different polymers.

The different behavior of the polymers under the action of heat is probably to be explained by specific features of their molecular chain structure.

TABLE 3

Average Rates of Cl_2 Liberation by Polymers in Millimoles Cl_2 per Mole Monomer Unit per Hour.

Polymer	In nitrogen		In oxygen
	Temperature, °C		
	140	170	140
PVC	–	6.0	0.8
PVDC	0.5	19.4	0.9
CP (VDC + VC)	5.4	55.3	8.0

In our opinion, some information which would explain the different behavior of these polymers during thermal decomposition can be obtained by an examination of the initial stages of the process, including the initiation, from the viewpoint of the reactivity of the radicals formed.

The decomposition of PVC may proceed with formation of the rather inactive allyl radical according to the scheme:

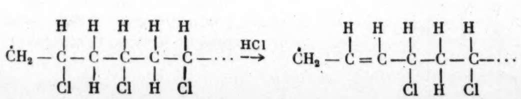

$$\dot{C}H_2 - \overset{H}{\underset{Cl}{C}} - \overset{H}{\underset{H}{C}} - \overset{H}{\underset{Cl}{C}} - \overset{H}{\underset{H}{C}} - \overset{H}{\underset{Cl}{C}} - \cdots \xrightarrow{HCl} \dot{C}H_2 - \overset{H}{C} = \overset{H}{C} - \overset{H}{\underset{Cl}{C}} - \overset{H}{\underset{H}{C}} - \overset{H}{\underset{Cl}{C}} - \cdots$$

The reactivity of allyl polymer radicals has been considered in a number of papers [4-7].

By analogy with PVC, the decomposition of PVDC should yield the less active chloroallyl radical, and the decomposition would proceed according to the scheme:

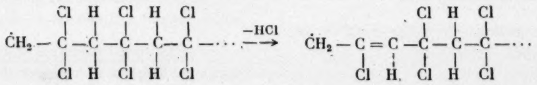

$$\dot{C}H_2 - \overset{Cl}{\underset{Cl}{C}} - \overset{H}{\underset{H}{C}} - \overset{Cl}{\underset{Cl}{C}} - \overset{H}{\underset{H}{C}} - \overset{Cl}{\underset{Cl}{C}} - \cdots \xrightarrow{-HCl} \dot{C}H_2 - \underset{Cl}{C} = \underset{H}{C} - \overset{Cl}{\underset{Cl}{C}} - \overset{H}{\underset{H}{C}} - \overset{Cl}{\underset{Cl}{C}} - \cdots$$

In the case of the copolymer, the still less active dichloroallyl radical may be formed, with a similar course of the decomposition process:

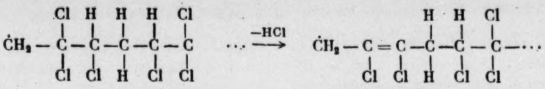

$$\dot{C}H_2-CCl_2-CHCl-CH_2-CHCl-CCl_2 \cdots \xrightarrow{-HCl} \dot{C}H_2-CCl=CCl-CH_2-CHCl-CCl_2-\cdots$$

Liberation of hydrogen chloride by CP (VDC + VC) most probably occurs at the bonds between the vinylidene chloride and the vinyl chloride units, as regions containing unstably linked chlorine are thereby formed:

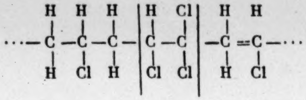

$$\cdots-CH_2-CHCl-CH_2-\,|\,CHCl-CCl_2\,|\,-CH_2=CHCl-\cdots$$

It is known that the hydrogen – carbon bond is considerably weakened in the presence of chlorine, and therefore the removal of hydrogen chloride from CP (VDC + VC) under the influence of heat is easier at these points.

The rather anomalous behavior of CPVC on heating should be noted; on the basis of its chemical composition its chlorine content suggests that CPVC should occupy an intermediate position between PVC and PVDC in its rate of thermal decomposition. However, as the comparative kinetic graphs in Fig. 6 show, the rate of liberation of hydrogen chloride by CPVC in the inital stage is close to or rather higher than the rate of PVDC. Subsequently, the decomposition rate of PVDC on heating exceeds the decomposition rate of CPVC, and the intersection of the kinetic curves occurs earlier at higher heating temperatures. Since the rate at which hydrogen chloride is liberated by CPVC in the initial stage of thermal decomposition is close to the corresponding rate for PVDC and considerably higher than the rate for PVC, it must be assumed that at this stage the liberation of hydrogen chloride by CPVC proceeds predominantly by a mechanism similar to that for the decomposition of PVDC.

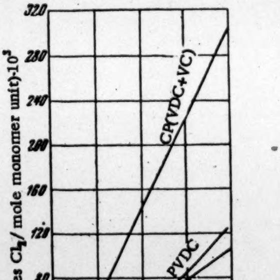

Fig. 6. Liberation of hydrogen chloride by chlorinated vinyl polymers on heating (t = 170°).

Experiments in a medium of oxygen show that oxygen favors the liberation of hydrogen chloride by chlorinated vinyl polymers, as has been reported by other authors [3], whose work was probably simultaneous with ours. It is not possible to discuss the mechanism of thermooxidative decomposition at the present time. There is no doubt, however, that decomposition in presence of O_2 proceeds through the formation of intermediate oxygen-containing compounds, in which the lability of chlorine may be considerably increased. The reaction of oxygen with PVC and CP (VDC + VC) is confirmed by the results of elementary analysis. PVC heated for 4 hours at 170° in oxygen contained 2% oxygen, and CP (VDC + VC) contained 5%, and therefore oxygen enters the composition of the PVC and CP(VDC + VC) molecular chains*. This confirms the hypothesis that when these polymers are heated in oxygen, a reaction between the polymers and oxygen takes place.

Thus, on the basis of our experimental data and the results of other researches the view may be advanced that the thermal decomposition proceeds by a chain radical mechanism.

SUMMARY

1. The kinetics of the liberation of hydrogen chloride by PVDC, CP (VDC + VC), and CPVC at 140 to 170° in oxygen and in nitrogen can be represented by straight lines, so that the reaction of hydrogen chloride liberation can be formally regarded as a reaction of zero order. The activation energy for the liberation of hydrogen chloride by PVDC and CP (VDC + VC) is 33.6 and 30 kcal / / mole respectively.

2. Oxygen was shown to accelerate the decomposition of chlorinated vinyl polymers.

3. The view is advanced that the thermal decomposition of chlorinated vinyl polymers proceeds by a radical chain mechanism. A probable scheme for the start and development of the chain process of the decomposition of chlorinated vinyl polymers is suggested.

LITERATURE CITED

[1] N. V. Mikhailov, V. S. Klimenkov, and L. G. Tokareva, Colloid J. 18, No. 5, 578 (1956) (T.p 573).*

[2] A. Rosenberg, Kunststoffe 42, No. 2, 41 (1952).

[3] E. I. Arlman, J. Polymer Sci. 12, 543 (1954).

[4] B. A. Dogadkin and I. G. Soboleva, J. Phys. Chem. 26, No. 1, 72 (1952).

[5] A. D. Abkin, Proc. Acad. Sci. USSR 75, No. 3, 403 (1950).

[6] Kh. S. Bogdasaryan, J. Phys. Chem. 23, No. 11, 1375 (1949).

[7] N. N. Semenov, Some Problems of Chemical Kinetics and Reactivity (Acad. Sci. USSR Press, 1954).

Received June 25, 1955

Scientific Research Institute for Synthetic Fibers

---

* T.p = C. B. Translation pagination.

VARIATION OF THE DIELECTRIC CONSTANT OF EMULSIONS WITH TIME

E. M. Fradkina and S. F. Khmunin

Much attention is being devoted at the present time to the development of electrical methods of moisture determination in various materials (mineral oils, petroleum products, flour, starch, paper, coal, peat, wood, etc. An evaluation of these methods [1] shows that the most convenient method of moisture determination is based on measurement of the dielectric constant (DC) of the system.

In a study of petroleum emulsions [2], we found that their DC increased with time. This has also been observed by others [3,4]. The need to explain this effect and to allow for it in the use of electrical methods of moisture determination led us to carry out a detailed study of the dependence of DC on time. Emulsions in which the dispersion medium was heavy mineral lubricating oil or mazut were used. Mazut was chosen as a medium of especially high viscosity. The disperse phase was distilled water or 2N NaCl solution.

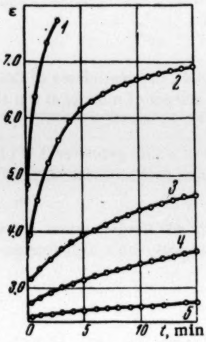

Fig. 1. Variation of the DC of water / /oil emulsions with time (λ = 300 m); 1) 19.8; 2) 14.8; 3) 9.8; 4) 5.8; 5) 2.9% H_2O.

The behavior of these emulsions was studied in an ultrahigh frequency field at wavelengths λ = 1.66 m, 1 m, and 28 cm by Drude's second method, and also by the method of beats at a wavelength of 300 m by means of the "dielcometer." In both cases the DC was found to increase with time; this was especially pronounced in emulsions with a high water content, and the DC – time relationships at λ = 300 m and in an ultrahigh frequency field proved to be entirely different.

In investigation of the DC of emulsions by means of the dielcometer, the readings of the instrument changed very rapidly; the readings for the limits of the silence zone, from which the DC was determined, changed in a fraction of a minute. The speed at which the instrument readings changed was appreciably greater in measurements of emulsions of salt solutions than of emulsions in which distilled water was the disperse phase (Figs. 1, 2). After the condenser plates had been extracted and shaken, as described by Vargaftik, Golubtsov, and Stepanenko [3], and the condenser then connected into the vibration circuit, the original instrument readings were reproduced.

The observed effects may be explained by the effect of the electric field in which the DC measurements were made, on the emulsions. An electric field causes chains of disperse phase droplets to be formed in the emulsion similar to the conducting bridges in suspensions of conductors or semiconductors in dielectrics found by Frenkel and his associates [5]. This accounts for the rapid changes of DC in emulsions of salt solutions in which the droplets have a high conductivity favoring chain formation.

The action of the electric field on the emulsion also explains why the dependence of DC on time of emulsions with viscous mazut (Fig. 3) was always less pronounced than that of oil emulsions. The different nature of the dependence of the DC of emulsions on the time they are exposed to the electric field is also explained on these grounds. Thus, emulsions with distilled water as the disperse phase showed a very rapid increase of DC immediately after the condenser with the sample was connected; this slowed down gradually but persisted for a fairly long time, especially in emulsions with a relatively low volume content of water. In emulsions of salt solutions

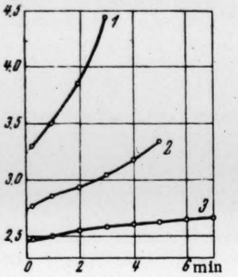

Fig. 2. Variation of the DC of emulsions of 2N NaCl in water with time (λ = 300 m); 1) 9.7; 2) 5.8; 3) 2.95% N solution of NaCl.

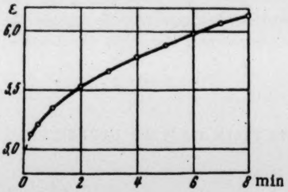

Fig. 3. Variation of the DC of 25.7% water/ /mazut emulsion with time (λ = 300 m).

the rate of increase of DC rose with time so that the beats could be heard only for the first 3-4 minutes and then ceased completely owing to short-circuiting of the measuring condenser vessel by formation of chains from droplets of conducting solutions

In measurements of the DC of oil emulsions in very high frequency (VHF) fields, the dependence of DC on time was much less pronounced – the changes were observed over periods of hours and not of minutes as was the case in measurements with the dielcometer.

In studies of the effect of time on the DC of an emulsion placed in the field of a VHF generator (λ = 1 m) for a long time, and the same emulsion placed in the field for the immediate time of determination only, no difference was found (Table 1).

The variation of DC with time was in most cases linear or very nearly so (Fig. 4). Deviations from linearity were usually found 3-4 hours after preparation of the emulsions, and mainly in emulsions with a high disperse phase content.

TABLE 1

Effect of Time on the DC of Water / Oil Emulsions Held for Long Times on High Frequency Fields, and of the Same Emulsions Placed in the Fields. For the time of direct measurement only (λ = 99.0 cm).

Volume content of disperse phase, %	Temperature, °C	Time from end of stirring	DC	Change of DC		Notes
				absolute	relative, % in 1 hour	
26.0	18.2	2 hr, 10 min.	5.034	0.37	2.67	In the field
	18.0	4 hr. 55 min.	5.404			
	18.0	4 hr. 55 min.	5.404	0.226	2.88	Outside the field
	18.2	6 hr, 25 min.	5.630			
25.0	18.2	3 hr. 0 min.	4.70	0.25	0.89	In the field
	18.2	9 hr, 0 min.	4.95			
	18.15	2 hr, 8 min.	4.88	0.24	0.94	Outside the field
	18.15	7 hr. 21 min.	5.12			

It was therefore possible to determine with adequate accuracy, the DC of the emulsions at the initial time instant at the end of the mixing by extrapolation. Studies of the dependence of the DC of emulsions on time in VHF fields show that it is not influenced by the field. This is explained by the inertia of the macroscopic droplets, which does not allow the necessary degree of dipole interaction between them at such high frequencies. Another explanation of the dependence of the DC on time must therefore be sought.

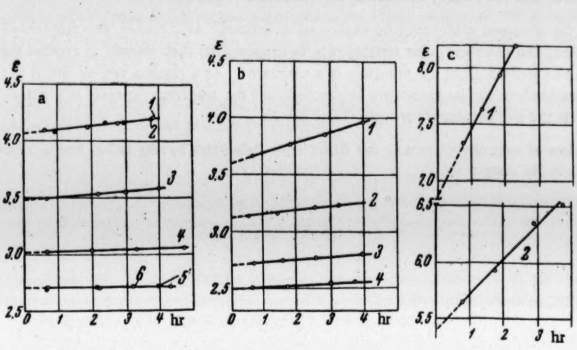

Fig. 4. Variation of DC with time (λ = 99.0 cm); a) Water/ oil emulsion: 1) 19.8; 2) 19.7; 3) 14.8; 4) 9.8; 5) and 6) 5.8% H_2O; b) emulsions of 2 N NaCl/ oil (condenser No. 6): 1) 14.7; 2) 9.7; 3) 5.8; 4) 2.95% 2 N NaCl solution; c) emulsions of 2 N NaCl/ oil (condenser No. 8): 1) 31.05; 2) 25.46% 2 N NaCl solution.

TABLE 2

Effect of Time on the DC of Water/ Oil Emulsions at Various Temperatures

Volume content of disperse phase, %	Temperature, °C	Time from end of stirring	DC	Change of DC	
				absolute	relative, % in 1 hour
30	24.0	1 hr, 5 min	5.90	–	–
	24.6	8 hr, 10 min	9.63	3.73	8.9
27	18.0	1 hr, 5 min	5.11	–	–
	19.7	9 hr, 0 min	6.01	0.90	2.2

TABLE 3

Effect of Time on the DC of Emulsions With Mazut as the Dispersion Medium

Composition of emulsion	Volume content of disperse phase, %	λ in cm	Temperature, °C	Time from end of stirring	DC	Change of DC	
						absolute	relative, % in 1 hour
2 N solution of NaCl/ mazut	28.47	99	17.4	1 hr, 2 min.	5.73	0.01	0.06
	28.47	99	18.05	4 hr,	5.74		
	35.56	99	17.85	1 hr, 9 min.	7.10	0.04	0.14
	35.56	99	17.7	5 hr, 2 min.	7.14		
	19.86	99	17.7	1 hr,	4.51	0.02	0.11
	19.86	99	18.0	5 hr,	4.53		
Water/ mazut	20.89	27.9	17.7	40 min.	4.36	0.01	0.08
	20.89	27.9	18.9	4 hr, 30 min.	4.35		
	34.68	99	18.0	12 min.	6.12	0.04	0.36
	34.68	99	18.0	2 hr,	6.16		

We found that the dependence of DC on time is significantly influenced by the temperature, viscosity of the dispersion medium, and the density difference between the two phases.

Accordingly, the observed effect may be explained as follows. As is known, the droplets of disperse phase grow in size with time, and therefore their settling rate is increased (if their density is greater than that of the dispersion medium) and separation of the emulsion is accelerated. As a result, a system forms in the measuring condenser which is equivalent to two capacities in parallel, and the resultant capacity is greater than that of a disperse system with the same component ratio (f and 1 − f).

If two condensers of capacity C_0 and C_1 are filled with dielectrics having DC ϵ_0 and ϵ_1 respectively, the resultant capacity C of the system is

$$C = \varepsilon_0 C_0 + \varepsilon_1 C_1.$$

The effective DC of the system ϵ is then

$$\varepsilon = \frac{\varepsilon_0 C_0 + \varepsilon_1 C_1}{C_0 + C_1}. \quad (1)$$

For a two-phase disperse system, the DC, as we have shown [1] is given by the Bruggeman formula:

$$1 - f = \frac{\varepsilon_1 - \varepsilon}{\varepsilon_1 - \varepsilon_0} \sqrt[3]{\frac{\varepsilon_0}{\varepsilon}} \quad (2)$$

or by Fradkina's formula

$$\varepsilon = \varepsilon_0 \frac{(1-f)^{3/2} + 2fx^3}{(1-f)^{3/2} - fx^3}, \quad (3)$$

Where $x = \frac{\epsilon_1 - \epsilon_0}{\epsilon_1 + 2\epsilon_0}$, ϵ_0 is the DC of the dispersion medium, ϵ_1 is the DC of the disperse phase, and f is the volume concentration of the disperse phase.

For our emulsion of water in petroleum, containing 30% water, $\epsilon_0 = 2.3$; $\epsilon_1 = 80$; $f = 0.3$. For a plane condenser with plates totally immersed in the dielectric ($C_0 = 0.7C$; $C_1 = 0.3C$), the DC according to Formula (1) is given by $\epsilon = 25.9$. For an emulsion with the same contents of the components, Formulas (2) and (3) give $\epsilon = 5.80$ and 5.54 respectively. Thus, the DC of an emulsion should increase as it separates out.

Of course, complete phase separation of the emulsions, corresponding to the above simplified scheme, did not occur in our experiments, but even a tendency to such separation is sufficient to produce the observed increase of dielectric constant.

The above interpretation of the dependence of DC on time in VHF fields also explains the observed fact that after an emulsion sample in the condenser is stirred, the values of DC found in subsequent measurements are appreciably lower than the values found before stirring. For example, the DC of an emulsion of 2N NaCl solution in oil with ~ 35% disperse phase by volume was found to be $\epsilon = 8.70$. After the emulsion in the condenser had been carefully stirred, the value $\epsilon = 7.60$ was obtained. In further measurements (without stirring) the values obtained for DC again increased with time.

If the dependence of DC on time is due to separation of the emulsion, the value should decrease with decreasing settling rate, for example, on decrease of temperature, resulting in increased viscosity of the dispersion medium. This is confirmed by results of measurements at $\lambda = 166.5$ cm, shown in Table 2.

By suitable choice of emulsion it is possible to eliminate the effect of time on DC almost completely, or, more correctly, to reduce it to a minimum. This can be done by the use of a dispersion medium of high viscosity, and by choosing the two components so that their densities are similar. The coagulation and settling of the disperse phase droplets, which assist phase separation of the emulsion, then become very slight. We studied the effect of time on the DC of emulsions of water and 2N NaCl solution in mazut (density $\rho = 0.902$) of high viscosity. As the results (Table 3) show, the DC was practically constant in these cases.

SUMMARY

1. The variation of the DC of petroleum emulsions with time was studied by the method of beats at a wavelength $\lambda = 300$ m and in VHF fields by Drude's second method. The dependence of the DC on time differed in the two cases.

2. It is suggested that the change of DC with time at not very high frequencies is the result of formation of chains from the disperse phase droplets, while under the action of VHF, when chain formation is hindered by inertia of the macroscopic droplets, it is caused by breaking of the emulsion.

LITERATURE CITED

[1] S. F. Khmunin, Dissertation, Lomonosov Institute of Fine Chemical Technology (Moscow, 1954).

[2] E. M. Fradkina, J. Exptl.-Theoret.Phys. 20, 1011 (1950).

[3] N. B. Vargaftik, V. A. Golubtsov and N. N. Stepanenko, Electrical Method for Moisture Determination in Petroleum Products (State Tech. Press, Moscow, 1947).

[4] Tarkhanov, Rapid Method for Moisture Determination in Petroleum, Report of the Central Institute of Aviation Oils and Fuels (1936).

[5] L. P. Gindin, Ya. I. Frenkel, and O. A. Shpanskaya, J. Tech. Phys. 20, 937 (1950).

Received July 28, 1955

The S. Ordzhonikidze Institute of Aviation,
Moscow

The M. V. Lomonosov Institute of Fine
Chemical Technology

DEPENDENCE OF THE FLOW CURVES AND VISCOSITY CHARACTERISTICS OF BITUMENS ON THE TEMPERATURE

S. Ya. Shalyt and N. V. Mikhailov

Bitumens, both of natural origin and made artificially by oxidative polymerization, are widely used constructional materials; they belong to the high-molecular colloidally structurized lyophilic systems, and are extensively used for insulation against water, for roofing, and for road surfaces. The variability of the structural-mechanical (elastico-plasticoviscous) properties of bitumens, the great dependence of these properties on the temperature, and the possibility of varying these properties over wide ranges by addition of active mineral fillers and diluents make bitumens exceptionally valuable model systems for scientific investigation.

Despite the existence of a number of papers on rheology of bitumens, their structural-mechanical properties are not sufficiently well understood. Such properties are presently studied by various diverse and largely empirical methods, and the results, expressed in arbitrary units which depend on the design of the apparatus and the experimental conditions, are not comparable. For example, viscosity is measured by the depth of penetration of a standard needle or by the time of efflux from a vessel of known capacity, in seconds; fluidity is measured by the softening temperature in degrees, measured by the ring and ball method, etc.

Absolute values for viscosity can be obtained by the use of rotational viscosimeters. Credit for the adoption of such methods is due to Volarovich [1]. Nevertheless, no data have been available hitherto on the elastic, high-elastic, and relaxation properties of bitumens, or data for the construction of complete rheological curves for the deformation rate against steady shearing stress.

We have made a detailed study of the structural-mechanical properties of petroleum bitumens over a wide temperature range. The bitumens used were oxidized bitumens grades III, IV, and V from the Gorky works, made from Artemovsk petroleum with sp. gr. 0.930, initial boiling temperature 202°, sulfur content 0.28%, with 1.5% distilling up to 225°, 18% to 300°, and 22% to 315°. The asphalts obtained from this petroleum were oxidized by air blowing under excess pressure of ~0.3 atm. at a temperature of 260-265° maintained throughout the process, with an air rate of 3.5 to 6.8 cubic meters per hour. The asphalt used for oxidation had sp. gr. 0. 979 and a sulfur content of 0.42%. The bitumens studied, obtained by the same oxidation process, differed in the oxidation times (12 hours for bitumen III, 20 hours for bitumen IV, and 32 hours for bitumen V).

TABLE 1

Group Composition of Bitumens, %

Bitumen grade	Oils	Tars	Asphaltenes	Total
III	55.29	30.12	15.39	100.80
IV	53.90	23.41	22.97	100.28
V	44.69	28.85	27.66	101.20

According to modern views [2] petroleum bitumen has the structure of a colloidal system in which oils are the dispersion medium, asphaltenes the disperse phase, and tars serve as surface-active agents. Table 1 shows the group composition of the bitumens, determined by the method of the Road Building Scientific Research Institute [3].

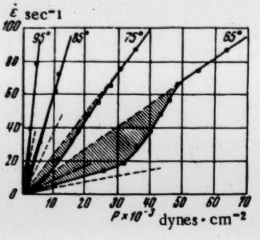

Fig. 1. Complete rheological $\dot{\epsilon}$(P) curves for bitumen III. at t = 65° $\eta_0 = 415 \cdot 10^3$; $\eta_m = 0.73 \cdot 10^3$; S = 685.5 · 10^3; at t = 75° $\eta_0 = 1.25 \cdot 10^3$; $\eta_m = 0.4 \cdot 10^3$, S = 200 · 10^3; at t = 85° $\eta_0 = 0{,}47 \cdot 10^3$, $\eta_m = 0.16 \cdot 10^3$, S = 50 · 10^3; at t = 95° $\eta_0 = 0.20 \cdot 10^3$; $\eta_m = 0.05 \cdot 10^3$, S = 15 · 10^3.

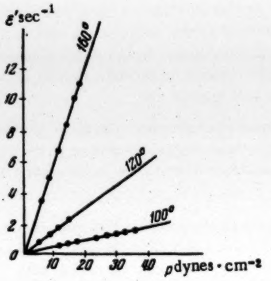

Fig. 2. Rheological $\dot{\epsilon}$(P) curves for bitumen III at 100, 120, and 160°.

The rheological properties of the bitumens were studied by means of the electronic selsyn elastoviscosimeter developed at the Scientific Research Institute for Building [4]. The instrument uses the principle of pure shear of the material in a narrow gap between coaxial cylinders, with automatic recording of the deformation – stress curves. The following methods may be used with this instrument:

a) at constant shearing stress, P = const., study of the course of deformation with time, and kinetics of the decrease of deformation after removal of the stress;

b) at a given constant deformation rate $d\epsilon / d\tau = \dot{\epsilon} = \mathrm{const}$, study of the course of shearing stress with time in relation to the magnitude of the deformation.

In our experiments the constant velocity gradient $\dot{\epsilon}$ = const method was used, the increase of shearing stress to a constant value was observed.

A constant rate of deformation was established by the use of a direct-current variable speed motor, and a gear box with seven gear ratios from 1 to 10^{-6}, by means of which the velocity gradients could be varied from $5 \cdot 10^{-4}$ to 120 seconds^{-1}, or in a range of 1 : 250,000.

The bitumen to be studied was previously dehydrated and filled into the gap between interchangeable coaxial cylinders with various side areas. The shearing stress could be varied from 50 to $50 \cdot 10^4$ dynes · cm^{-2}. The coaxial cylinders with the bitumen were placed in a thermostat where they were heated to 95°, and then cooled at a constant (low) rate to the experimental temperature, at which they were held for an hour, to allow the system to recover completely from structural breakdown which occurred during the filling. The torque for the given deformation rate was recorded on oscillograms, and the shearing stress was calculated for each type of coaxial cylinder.

The bitumens studied belong to the fluidlike systems in the temperature range 40-160°, and therefore by studies of the equilibrium shearing stress resulting from a given deformation rate, constant for each experiment, it is possible to obtain complete $\dot{\epsilon}$(P) rheological curves.

For bitumen III, these $\dot{\epsilon}$(P) rheological curves were obtained at 40, 55, 65, 75, 85, 95, 100, 120, 140 and 160°.

It was found that the curves for 65, 75, 85, and 95° (Fig. 1) are S-shaped and lie within the angle formed by two straight lines passing through the origin – the initial tangent to the curve at the point P = 0; $\dot{\epsilon}_0 = P/\eta_0$; corresponding to the maximum viscosity η_0 of the practically intact structure, and the final tangent $\dot{\epsilon}_m = P/\eta_m$, which corresponds to the minimum viscosity η_m for the structure broken down to the limit. The maximum viscosity η_0 of the bitumen is its principal physicochemical (rheological) constant, which clearly characterizes the features of undisrupted structures in bitumen systems. The importance of characteristics of undisrupted disperse and high-molecular structures has been established by the work of Rebinder and his associates [5].

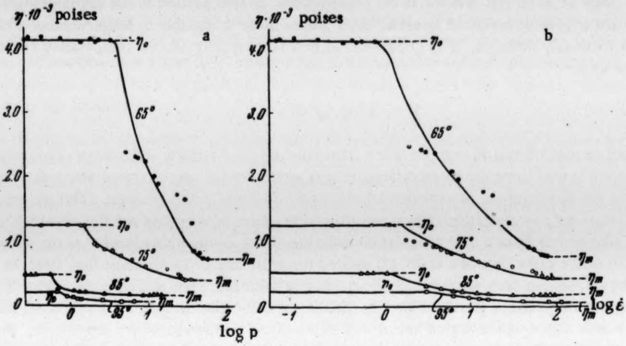

Fig. 3. The effective viscosity η as a function of: a) shearing stress (log P) and b) velocity gradient (log $\dot{\epsilon}$) for bitumen III; at t = 65° $\eta_0 = 4.15 \cdot 10^3$, $\eta_m = 0.73 \cdot 10^3$; at t = 75° $\eta_0 = 1.25 \cdot 10^3$, $\eta_m = 0.4 \cdot 10^3$; at t = 85°, $\eta_0 = 0.47 \cdot 10^3$, $\eta_m = 0.16 \cdot 10^3$; at t = 95° $\eta_0 = 0.20 \cdot 10^3$, $\eta_m = 0.05 \cdot 10^3$.

If bitumens are characterized by their effective viscosities which correspond to equal but arbitrarily chosen velocity gradients, then even if these gradients are small, the corresponding viscosities have no absolute meaning if they do not fall into the region of practically constant initial viscosity for the systems being compared.

In addition to the values of η_0 and η_m, which are the most clearly defined characteristics, the complete rheological curve can be used to determine, for a given temperature, the apparent strength limit of the structure above which the effective viscosity ceases to be practically constant and begins to decrease, and the stress P'_m which corresponds to the entry into the final tangent [6]. It is also possible to determine the velocity gradients $\dot{\epsilon}_r$ and $\dot{\epsilon}_m$ which correspond to these critical stresses. With a knowledge of these values, of which four (η_0, η_m, $\dot{\epsilon}_r$, $\dot{\epsilon}_m$), are independent, it is possible to characterize (schematically) the rheological curve to a first approximation. The region of practically constant (maximum) viscosity $\eta = \eta_0$ is clearly seen in these curves. The corresponding boundary velocity gradients $\dot{\epsilon}$ rise continuously and sharply with the temperature in the investigated range of 40-95°, by a factor of more than 1000, from $2 \cdot 10^{-3}$ to 3.14 seconds^{-1}. The Volarovich RV-7 instrument was used for determinations of the rheological curves at temperatures above 100°, when the systems approximate to true viscous liquids (Fig. 2).

These curves were used to calculate the values of the effective viscosity for various shearing stresses or deformation rates, and the relationships η(log P) and η(log $\dot{\epsilon}$) (Fig. 3,a and 3,b) were plotted.

Our results show that there are three different viscosity regions which characterize the structural-mechanical properties of bitumens, depending on the shearing stress P or velocity gradient $\dot{\epsilon}$. At low values of P and $\dot{\epsilon}$ the bitumen behaves as a true viscous Newtonian liquid and here the value of η_0 remains practically constant. Because the flow is very slow, the relatively slight breakdown of the structural network, which is inevitably associated with flow, has time to be practically completely restored. Further increase of P (or $\dot{\epsilon}$) produces first an abrupt and then a more smooth decrease of effective viscosity up to values of P and $\dot{\epsilon}$ at which the effective viscosity reaches its lowest value and subsequently remains constant. In this region, maximum structural breakdown occurs in the course of flow with only slight restoration because of the high velocity gradients. Here the bitumen again behaves as a Newtonian liquid with structure broken down to the limit.

Our results show that the maximum viscosity η_0 for the practically intact structure in strongly structurized liquids, such as bitumens at sufficiently low temperatures, falls much more rapidly with increase of temperature than in the case of Newtonian liquids of the same viscosity. This is the result of an additional sharp decrease of viscosity owing to structural breakdown when the temperature of the system is raised.

Because of this abrupt fall of viscosity with temperature, $\eta_0 - t°$ curves cannot cover any large temperature range, such as the range of 20 to 160° studied in our experiments. Graphs plotted in the semilogarithmic $\log \eta_0 - t°$ coordinates are of greater practical interest. Such graphs make it possible to judge whether a bitumen is sensitive to heat or thermally unstable. The coefficient of thermosensitivity (K, the temperature coefficient of viscosity) is defined as

$$K = -d \log \eta_0 / dT.$$

Our investigations showed that K remains practically constant over a fairly wide range of temperature. A very interesting feature is that there are three different states which depend on the temperature: the first state (region A) represents the development of additional fairly rigid structures in the bitumen. This occurs at fairly low temperatures, below 40°, by crystallization of paraffins in the form of very fine needles on which the dispersion medium is adsorbed to form a new coagulation structure which considerably reinforces the system as a whole. Investigation of the same bitumen at 20° [7] showed the existence of an apparent flow limit in the conventional-elastic region, so that such systems can be regarded as solidlike. The second state (region B) in the range 40-140° represents structurized fluidlike systems, and in the third state (region C) the bitumen behaves as a Newtonian true viscous liquid. Each region has its own value of the thermosensitivity coefficient. For bitumen III in state A, $K = 25.0 \cdot 10^{-2}$, in state B, $K = 4.5 \cdot 10^{-2}$, and in state C, $K = 0.12 \cdot 10^{-2}$ (Fig. 4).

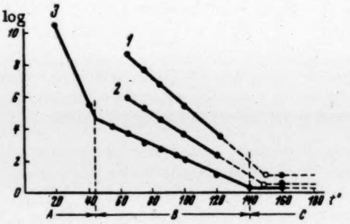

Fig. 4. Variation of the maximum viscosity ($\log \eta_0$) of bitumens III (3), IV (2), and V (1) in the temperature range 20-160°.

For bitumens IV and V, the initial regions of the rheological $\dot{\epsilon}$ (P) curves have been determined at 65, 75, 85, 100, 120 and 160°, and the values of effective viscosity for different shearing stresses and velocity gradients calculated. Table 2 shows the variation of the maximum initial viscosity with temperature.

Fig. 4 shows that the thermosensitivity coefficient in region B increases progressively from bitumen III to bitumens IV and V, the values being $4.50 \cdot 10^{-2}$; $7.60 \cdot 10^{-2}$ and $9.15 \cdot 10^{-2}$, respectively.

Table 2 shows that the thermosensitivity coefficient is greater for the higher grade bitumens, indicating the greater sensitivity of the more stable structures to changes of temperature. A comparison of the values of η_0, and, for clarity, of $\log \eta_0$ for bitumen III, IV, and V at 65, 75, and 85°, respectively shows that in this temperature range (region B) as we pass from one bitumen to the next (in the sequence of bitumen III, IV, and V), the viscosity of the practically intact structure increases by two orders of magnitude, by a factor of 100-300 (Table 2).

TABLE 2

Variation of Maximum Initial Viscosity With Temperature for Bitumens III, IV, and V.

Temperature, °C	η_0 in poises		$(\log \eta_0)_{IV} - (\log \eta_0)_{III}$	η_0 in poises, bitumen V	$(\log \eta_0)_V - (\log \eta_0)_{IV}$
	bitumen III	bitumen IV			
65	$4.15 \cdot 10^3$	$9.4 \cdot 10^5$	2.45	$3.0 \cdot 10^8$	2.51
75	$1.25 \cdot 10^3$	$1.63 \cdot 10^5$	2.01	$3.9 \cdot 10^7$	2.47
85	$0.47 \cdot 10^3$	$2.8 \cdot 10^4$	1.78	$4.5 \cdot 10^6$	2.20

SUMMARY

1. At temperatures below 40° oxidized petroleum bitumen III is in a solidlike pseudoplastic state: at 20° its conventional [6,7] flow limit is $P_{k_1} \sim 10$ g/cm², blow which the practically constant (maximum) viscosity η_0 ($2.5 \cdot 10^{10}$ poises) is greater by 4 orders of magnitude than the plastic viscosity ($\sim 3.9 \cdot 10^6$ poises) above the flow limit, practically constant over a large range of shearing stresses (this range is $\sim 4 P_{k_1}$). In the temperature

range 40 to 140° the bitumen is in the state of a structurized liquid. This state is marked by a gradual fall of the effective viscosity (by a factor of 3-4) with increasing velocity gradient as the structure is broken down in the flow process. At temperatures above 140° bitumen has the behavior of a Newtonian liquid with constant viscosity which is independent of the velocity gradient. This corresponds to practically complete breakdown of the structural network in the bitumen.

2. In the region of the liquid structurized state, the complete rheological $\dot{\epsilon}(P)$ curves for steady flow of the bitumens are S-shaped. These curves lie within an angle contained between two straight lines (asymptotes) which pass through the coordinate origin and which correspond to two constant limiting viscosity values: maximum limiting viscosity of the practically intact structure η_0, and the minimum limiting viscosity of the structure broken down to the limit, η_m. Increase of temperature, by destroying the spatial structure in the bitumen, narrows the stress region which corresponds to practically intact structure.

3. The above temperature limits for the transition from one structural state to another were established from the nature of the variation of the maximum values for the logarithm of the viscosity of the bitumen with the temperature. For a given state of the bitumen, $\log \eta_0$ decreases linearly with increase of temperature, so that the thermosensitivity coefficient $K = -\, d \log \eta_0 / dT$ is practically constant; this value changes fairly sharply in the transition from one state of the bitumen to another, and therefore breaks in the $\log \eta_0 = f(t)$ graphs can be used to determine the boundaries of the structural states of the bitumen.

4. The maximum viscosity η_0 and the thermosensitivity coefficient K are fundamental physicochemical absolute constants for a bitumen, which define the behavior of the undestroyed structures, or the utilizational qualities of the bitumen, while the minimum viscosity η_m at a given temperature represents its technological behavior — its ease of application.

LITERATURE CITED

[1] N. N. Korotkevich, Symposium: Viscosity of Liquids and Colloid Solutions (Acad. Sci. USSR Press, 1941). 1, pp. 4, 57; M. P. Volarovich and M. F. Nikishina, Colloid J. 12, 3 (1950); M. F. Nikishina, Symposium: Study of Organic Binders and Physicochemical Properties of Asphalt Mixtures, (Road Ind. Press, 1949); N. V. Mikhailov, Roof and Hydroinsulation Coatings (Machinery Constr. Press, 1950); S. K. Noskov, Dissertation, Moscow (1952); Symposium, Investigations of Hydro- and Heat-Insulating Materials and Constructions, Moscow (1955).

[2] I. P. Pfeiffer and R. N. Saal., Lab. N. V. de Bataafsche Petroleum Maatshapij, Amsterdam, Holland, 7 (1939); R. Saal and J. Labut, J. Phys. Chem. 44, 2, 149 (1940); P. Walter, Korrosion und Metallschutz (1942), p. 6; N. V. Mikhailov, Roof and Hydroinsulation Coatings, Machinery Constr. Press (1950).

[3] A. I. Lysikhina and L. N. Yastrebova, Symposium: Study of Organic Binders for Road Building Materials (Road Ind. Press, 1947); N. Markuson, Asphalt (Soviet Petroleum Ind. Press, Moscow-Leningrad,1926).

[4] E. E. Kalmykova and N. V. Mikhailov, Colloid J. 16, No. 5, 350 (1954). (T. p. 339).*

[5] E. E. segalova and P. A. Rebinder, Colloid J. 10, 3 (1948); Proc. Acad. Sci. USSR 71, 85 (1950); A. S. Kolbanovskaya and P. A. Rebinder, Colloid J. 12, 194 (1950); L. V. Chumakova and P. A. Rebinder, Proc. Acad. Sci. USSR 81, 2 (1951).

[6] N. V. Mikhailov and P. A. Rebinder, Colloid J. 17, No. 2 (1955).

[7] N. V. Mikhailov, Colloid J. 17, No. 3 (1955).

Received October 28, 1955

Scientific Research Institute for Building
Ministry of Building USSR, Moscow

---

* T.p = C. B. Translation pagination.

ALTERATION OF THE STRUCTURAL PROPERTIES OF SOME COLLOIDAL POROUS MATERIALS DURING DRYING

V. V. Shcherbatenko and V. V. Smirnova

It is found in studies of the drying of such colloidal porous bodies as products made from flour dough with a low moisture content, and grains of rice, rye, corn, and other cereals, that the structural and mechanical properties of the material vary according to the drying conditions. The above bodies consist mainly of proteins and starch, the structural-mechanical properties of which determine to a large extent the mechanical strength, swelling, and softening of the material in water. Starch probably plays the principal role in this. The more the bonds between the structural units of starch are weakened, the lower is the mechanical strength of the material and the greater is its tendency to impregnation and softening by water. These properties are very important signs of the quality of flour dough products with a low moisture content, such as rusks, cracknels, and macaroni.

It has been observed that "mild" drying conditions, with a low moisture gradient in the material, results in the formation of a dense structure with a hornlike fracture, producing high strength and low swelling in these products. "Harsh" drying conditions, with a considerable moisture gradient in the material at the instant when it becomes brittle, lead to the formation of a loose structure with a dull, fractured appearance, which leads to low strength and a high-capillary imbibition rate.

On the basis of Lykov's theory of drying [1] and of Shcherbatenko's data [2] a hypothesis has been advanced to explain the influence of various drying conditions on the structural-mechanical properties of flour dough products and on some properties of grain.

A shrinkage gradient is established in a material during drying owing to the moisture gradient which forms across the thickness of the product. If deformation of the elementary layers of material is restricted by a fairly strong surface layer on the article, the shrinkage gradient sets up a state of volume stress in the material. During the first stages of drying, when the material still has a fairly high moisture content and consequently high elasticity and plasticity, the stresses are quickly relaxed and do not cause any appreciable changes in the structure. Later in the drying process a time is reached when the material passes into the brittle state. If at this time the moisture gradient and the associated shrinkage gradient in the elementary layers of material produce stresses which exceed the strength limit, then the material is fractured and becomes filled with microcrevices and pores throughout its volume, which lower its strength and confer a high capillary imbibition on it. Such a material shows a dull surface on fracture. If the moisture and shrinkage gradients are sufficiently low, the stresses which arise do not exceed the strength limit of the material, microcrevices and pores are not formed, and shrinkage of the material, which condenses its structure, confers a characteristic hornlike appearance in fracture. Such condensed material has high strength and poor water permeability.

Our experimental investigations have confirmed these views. It was found that the material of flour dough products which are first heated by baking and then dried, passes into a brittle state when a moisture content of about 8-12 % is reached.

The graph for the normal stress P_N plotted against the deformation ϵ, based on experimental data (Fig. 1), shows that the material obeys Hooke's law and is typically brittle, as the yield point is reached before the limit of direct proportionality between P_N and ϵ. It was found experimentally that destruction of the material occurs at normal stresses of the order of 40-60 kg/cm^2 and tangential stresses of the order of 4-8 kg/cm^2.

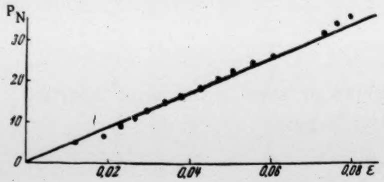

Fig. 1. Relationship between normal stress P_N and deformation ϵ for a flour dough material.

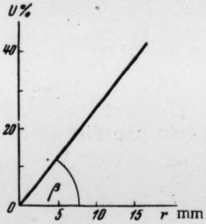

Fig. 2. Moisture distribution in a cracknel material under "harsh" drying conditions; r is the distance from the center of the product.

Fig. 2 shows the moisture distribution (U%) in a cracknel material under "harsh" drying conditions in the baking oven. The moisture gradient under "mild" drying conditions (in a desiccator over calcium chloride) is practically zero.

The experiments showed that at the final stages of drying the distribution of moisture across the thickness of rusks and cracknels is fairly close to linear. Thus the moisture gradient can be assumed to be constant.

$$dU/dr = \tan \beta = \text{const}$$

The change in the linear dimensions of the material during drying as a function of its moisture content is represented by the equation

$$l = l_0 (1 + \alpha U), \tag{1}$$

where l is the length of the material at moisture content U; l_0 is the length of the absolutely dry material; α is the linear shrinkage coefficient, which is approximately 0.005-0.006 for the material in question.

The shrinkage gradient in the material can be defined as

$$dl/dr = \alpha \tan \beta = \tan \varphi. \tag{2}$$

Assuming that the shrinkage gradient is equal to the relative extension deformation in the elementary layers of the material, we have

$$l = l_0 + \epsilon r. \tag{3}$$

If we pass from relative deformation to normal stresses (which will arise if the deformation of the elementary layers of material is restricted by a fairly strong surface layer), and if we assume, as an approximation, that the modulus E is constant since the moisture content of the material fluctuates within relatively narrow limits at the end of the drying, we have

$$dU/dr = \tan \beta = P_N / E_N \cdot \alpha. \tag{4}$$

As a first approximation it may be assumed that Hooke's law is also obeyed in the case of shearing deformation, and then we have for tangential stresses

$$dU/dr = \tan\beta = P_t/E_t \cdot \alpha. \qquad (5)$$

With a knowledge of the maximum normal and tangential stresses we can determine the moisture gradient which corresponds to the destruction of the material and the formation of pores and microcrevices. A calculation of this moisture gradient on the basis of experimentally determined yield stresses gave a value of the order of 20-30 cm^{-1} for normal stresses and 6-8 cm^{-1} for tangential stresses.

Thus, the formation of a loosened structure in the material depends on the maximum shearing stress, which occurs at much lower moisture gradients. It is not possible in practice to determine the drying conditions by the moisture gradients. Experiments showed that under relatively similar conditions of harsh drying, when the materials in question passed into the brittle state, the moisture gradient changed little; this makes it possible to judge whether the material has acquired any given properties from the average moisture content of a sample, which can be easily found under production conditions from changes in the weight of the product if their moisture content and weight before drying are known. With a knowledge of the maximum tangential stress for the material, and with the value of the moisture gradient (tan β) found from Equation (5), it is possible to calculate the integral "critical" moisture content of the product. For products of rectangular section this "critical" moisture content can be calculated from the formula

$$W_{cr} = \frac{\tan\beta}{R}\int_0^R \frac{r}{2}\,dr = \tan\beta\,\frac{R}{4}, \qquad (6)$$

where R is the thickness of the product.

For products of round cross section the "critical" moisture content can be calculated from the formula

$$W_{cr} = \frac{2\tan\beta}{R_1^2}\int_0^{R_1} r^2\,dr = \frac{2}{3}\tan\beta\, R_1, \qquad (7)$$

where R_1 is the radius of the cross section of the product.

The structural-mechanical properties of a material can be predicted by a comparison of its average moisture content at the end of drying carried out under "harsh" conditions with the "critical" moisture content. If the average moisture content at the end of drying is below the "critical" (W_{cr}), then the material will have a loose structure and will be easily impregnated with water. If intensive drying of the material is ended before the critical moisture content is reached, so that the equilibrium moisture content will be acquired by the material during storage, at a very low moisture gradient, the material will be dense, strong, and will not swell easily in water. This critical moisture content for rusks 25 mm thick, as determined by Equation (6), will be ~6%; correspondingly, for round cracknels (7) with a diameter of 20 mm, the value is 8%. Good agreement is obtained between the experimental and calculated values for the critical moisture contents of rusks and round cracknels.

It is seen from Table 1 that when rusks are dried to an average moisture content of 3.8%, and cracknels to 8.4%, the forces required to destroy the samples decrease sharply, while the water imbibition increases considerably. The imbibition was determined by immersion of a piece of the material in water at 60° for 5 minutes, and was expressed as the ratio of the weight of the swollen sample to its original weight.

The changes in the structual-mechanical properties of flour dough products with drying conditions are to a considerable extent reversible. A product with a loose structure is strengthened by repeated humidification and drying at a low moisture gradient. The dense, horny structure can be made more loose by humidification and repeated drying under harsh conditions. These changes of structural-mechanical properties are illustrated by the experimental data presented in Table 2.

For a more complete study of structure formation in cracknels during drying, Shcherbatenko and Chizhova [2] investigated the effects of drying on the two principal components of cracknel dough, which differ considerably

TABLE 1

Changes in the Strength and Imbibition According to Drying Conditions

Product	Drying conditions	Moisture, %	Strength P_N in kg/ cm^2	Breaking force in kg	Imbibition
Rusks	Harsh	11.0	5.2	–	3.1
	"	3.8	0.7	–	4.6
	Mild	13.0	7.7	–	2.1
	"	6.0	3.8	–	2.4
Cracknels	Harsh	19.5	–	29.0	2.3
	"	13.6	–	21.7	2.2
	"	8.4	–	11.2	3.8

TABLE 2

Changes of the Structural-Mechanical Properties of Rusks by Humidification and Repeated Drying

Sample and production conditions	Moisture, %	Strength P_N in kg/ cm^2	Imbibition
Made under mild drying conditions	10.0	9.1	1.24
Same sample stored for 2 days in a desiccator over water, then dried at 130° and stored for 2 more days at room temperature	6.6	3.6	2.2
Made under harsh drying conditions	3.8	0.72	4.6
Same sample alternately humidified in a desiccator over water and dried over calcium chloride for 8 days	12.6	1.8	2.8

TABLE 3

Effects of Gluten and Starch on the Imbibition of Cracknel Products After Heat Treatment at Different Temperatures

Experimental conditions	Gluten models			
	with starch		with inert filler	
Oven temperature, °C	200	260	200	260
Duration of heating, min.	25	14	25	14
Moisture, %	14.2	8.07	11.8	6.21
"Capillarity" (rate of rise of liquid in vertically fixed ring in mm/ min.)	0.5	1.7	15	14
Imbibition in water (at 60°) in 5 min	Almost unsoaked	70% of the mass soaked	Completely soaked	

in their physical properties – gluten and starch. Two model doughs were made: from gluten with added wheat starch, and from gluten with quartz dust as an inert filler. Both samples were similar to cracknel dough in their mechanical properties. The molded cracknel rings were then heated and dried in the bakery oven at 200 and 260°. The results of these experiments are shown in Table 3.

It is seen from the data in Table 3 that the imbibition of cracknels made from gluten and starch directly depended on the heating conditions. The cracknels baked at 200° contained almost no capillaries – water almost did not rise in them. The cracknels made from gluten and filler were very rapidly and completely soaked irrespective of the heating conditions. Most of the water is held mechanically in this case; of the total quantity of water imbibed by the cracknel ring, 70% could be removed by pressing. The cracknels made from gluten with filler had a fine reticular structure because of the considerable shrinkage of the gluten during denaturation and drying.

Experiments were also performed with the object of following changes in the structure of starch at various heating temperatures and drying rates. Sticks of filter paper lined with starch paste were made. These sticks, in the form of tight rolls, were dried in various ways – in a drying cabinet at 102° and in an oven at 190°, to a moisture content of ~8-10%. These specimens differed very considerably. The sticks dried at 190° clearly showed a layer structure in cross section, while the sticks dried at 102° were compacted. The difference in the structure of these two cracknel models was particularly prominent when they were soaked in water at 60° for 5 minutes.

The above experiments showed quite clearly that the formation of capillaries, layers, and microcrevices depends largely on changes in the physical properties of starch during heat treatment and drying. The views which have been put forward on the influence of drying conditions on the technological properties of flour dough products can evidently be extended to other colloidal porous materials. For example, the bursting of corn, rice and other cereal grains on rapid heating is to be explained, in our view, by the rapidly developing tangential and normal stresses in the grain as the result of formation of moisture and shrinkage gradients. This is confirmed by the fact that this effect can be produced only with grain of low moisture content, which ensures its brittleness. Our investigations of the physico-mechanical properties of dough made from flour ground from burst grain confirm this view.

Thus, the drying process in a number of food industries may be regarded, on one hand, as a means for preservation of the food for a long time, and on the other, as a means for conferring the necessary structural-mechanical properties on the products.

SUMMARY

1. Various conditions of drying of colloidal porous materials, such as flour dough products and cereal grains, confer different structural-mechanical properties on them.

2. In mild drying conditions with a low moisture gradient in the material, the shrinkage gradient which results produces only small tangential stresses at the time when the material becomes brittle. This results in a dense structure with a hornlike fracture, and the products have high mechanical strength and poor water imbibition.

3. Under harsh drying conditions, when the material reaches a moisture content below the critical value, a considerable moisture gradient is set up in the material, with a consequent considerable shrinkage gradient and large tangential stresses, which exceed the yield stress for the material. The resulting microcrevices give the products a loose structure with a dull fracture, of low mechanical strength and high water imbibition.

4. In a number of food industries the drying process is not only a means of preservation, but also a method of conferring required structural-mechanical properties on the materials.

LITERATURE CITED

[1] A. V. Lykov, Theory of Drying (State Power Press, 1950).

[2] V. V. Shcherbatenko and K. N. Chizhova, Trans. All-Union Sci. Research. Inst. Baking Ind. 6, 22 (1955).

All-Union Scientific Research Institute
for the Baking Industry

Received October 26, 1955

INVESTIGATION OF STRUCTURE FORMATION IN CONCENTRATED SUSPENSIONS BY THE ELECTRICAL CONDUCTIVITY METHOD

B. Ya. Yampolsky

An important problem in modern physical chemistry of disperse systems is the problem of stability and structure formation in concentrated suspensions. The properties of suspensions may be regulated by the introduction of small amounts of stabilizing additions. The formation and development of structures in disperse systems confers characteristic solidlike properties on them. In such systems the disperse phase particles are held together by molecular forces in a single spatial skeleton, which is capable of retaining mechanically a considerable volume of the dispersion medium.

According to the theories advanced by Rebinder and his associates [1], two types of disperse structures, broken down reversibly by the action of external mechanical forces, may be formed:

a) loose coagulation structures, formed by cohesion of the particles with very thin layers of the dispersion medium remaining at the points of contact between them; in the case of anisodiametric particles, such structures can be formed even at low disperse phase concentrations, when the cohesion occurs at the least lyophilic regions – at the corners or edges of the particle surfaces.

b) compact structures, in which layers of the dispersion medium between the particles are retained; although these layers are thin, they are sufficient for the particles to be completely mobile relative to one another, so that considerable volume concentrations of disperse phase can be obtained in stabilized suspensions. Such structures are formed mainly in lyophilic systems, and only at fairly high concentrations of the disperse phase.

Structure formation in disperse systems has been studied mainly by changes in their mechanical properties, on the appearance of solidlike properties [1]. These methods are based on measurements of the deformational behavior of the system and often involve modification or destruction of the structure of the specimen. The conductometric method has considerable advantages, as with it structure formation in disperse systems can be studied without any modification or breakdown of the structure, the kinetics of the process can be continuously observed, thixotropic changes in the structure can be followed, etc. The electrical conductivity of disperse systems has been studied by a number of workers [2]. McDowell and Usher [3] determined the conductivity of carbon black suspensions in hydrocarbon media and found that nonstabilized suspensions have considerable conductivity, probably in consequence of direct contact between the particles. Carbon black suspensions protected by nitrocellulose exhibited no measurable conductivity. Dogadkin et al. [4] made a detailed study of the electrical conductivity of rubber mixes with conducting fillers. At a definite content of the filler (carbon black) in the mixture, netlike conducting structures are formed, the nature of which determines the physical and mechanical properties of the mixture.

Voyutsky, Zaionchkovsky, Kargin, and Rubina [5] made a conductometric study of structure formation in carbon black suspensions and showed that the conductivity of a suspension increases on formation of a structure in it, owing to the formation of contacts between the individual particles.

Since 1948 investigations have been in progress in our laboratory* of the influence of surface-active substances on structure formation in suspensions, by the conductometric method, with parallel determinations of the strength of the structure (yield stress) by the tangentially displaced plate method (the Veiler – Rebinder method). Suspensions of graphite and reduced metal powders (copper and aluminum) were studied; however, because of their ease of oxidation the metal suspensions were not sufficiently stable and reliably reproducible results could not be obtained with them.

---

* Students of the Chemical Faculty of the Moscow State University, N. N. Matorina and V. N. Vaisman, have taken part in the work.

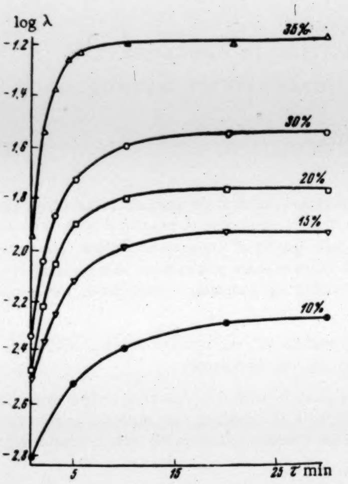

Fig. 1. Kinetics of the variation of the electrical conductivity λ of graphite suspensions of various concentrations in benzene.

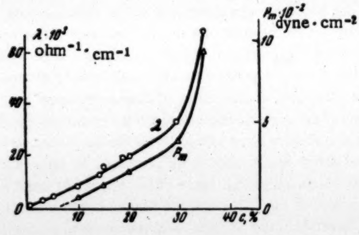

Fig. 2. The conductivity λ_m and strength P_m of the deposit in a graphite suspension in benzene, as functions of the graphite concentration.

All the subsequent determinations were carried out with pure, previously heated graphite, with average particle size ~10μ. The dispersion media were carefully purified benzene, toluene, nonpolar vaseline oil, and kerosene. The measurements were made in cylindrical glass vessels, both with vertical and horizontal electrodes fused into the bottom of the vessel, with the aid of an alternating-current bridge with a tube indicator. The accuracy of the measurements was ±5% with satisfactory reproducibility.

Check determinations of the electrical conductivity (λ) by the direct-current bridge method gave values close to those obtained with the use of an alternating current in nonpolar media only. In polar dispersion media the values of λ were unstable owing to polarization of the electrodes.

A definite volume of the thoroughly stirred suspension was placed in the cell with the electrodes and the first determinations of the conductivity λ were made after 1 minute; this was followed by a determination of the complete curves for the variation of λ with time. Similar vessels (without electrodes) were used for parallel determinations of the strength or the yield stress P_m of the deposits, by means of ribbed metal plates immersed to the bottom of the vessel.

The sedimentation structure of the deposit formed by settling of the graphite particles becomes stronger with time, corresponding to increases of λ and P_m. Fig. 1 shows $\lambda = F(\tau)$ curves for suspensions of graphite in benzene with graphite contents of 35, 30, 20, 15, and 10%. The values of λ and P_m became constant in the layer of deposit near the bottom of the vessel within 10-15 minutes from the start of the experiment. These maximum values λ_m and P_m were subsequently used to characterize the properties of the system. It must be noted that if the vessel is shaken or even moved, breakdown of the structure results in a sharp decrease of λ and P_m, but the values are restored in time.

Both the rate at which constant values of λ and P_m are reached, and the rate of their restoration after breakdown of the structure, are proportional (within certain limits) to the concentration of solid phase in the suspension owing to the deposit becoming denser under its own weight.

The electrical conductivity and yield stress increase with increasing concentration of the suspension because of increased density of the deposit, and of the consequent increasing number of contacts between the particles (Fig. 2); here λ_m increases approximately in proportion to the concentration starting from low concentrations, in contrast to P_m, measurable values of which correspond to a certain minimum concentration (~8%). At greater

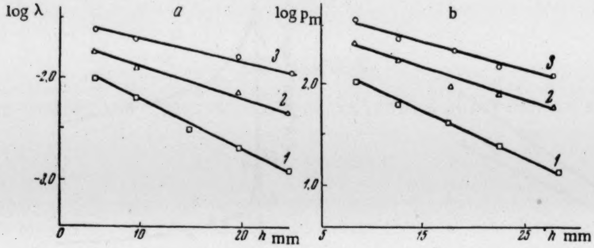

Fig. 3. The conductivity (a) and strength P_m (b) of the deposit in a 30% graphite suspension in benzene for various depths of immersion of the electrodes after sedimentation of the suspension for: 1) 2 minutes; 2) 5 minutes; 3) 20 minutes; n is the distance between the center of the electrodes (for a) and the center of the plate (for b) from the bottom of the vessel.

concentrations ($c > 20\%$) there is a sharp increase both of λ_m and P_m, which may be attributed to a further condensation of the deposit with a rapid increase of the number of contacts between the particles.

Over a certain range of solid phase concentration (which depends on the degree of dispersion and the properties of the medium) the conductivity λ_m of the deposit is proportional to the strength of its structure, represented by the yield stress P_m (Fig. 2). The strength and the conductivity of the deposit increase with depth in the deposit layer approximately according to a logarithmic law (Fig. 3,a and 3,b).

The use of more viscous liquids — kerosene and vaseline oil — as dispersion media retards the establishment of constant values of l and P_m, and sharply decreases their absolute values.

Conductivity measurements on a deposit in a 10% graphite suspension in toluene at temperatures from −40° to +70° showed that the λ_m of the deposit increases considerably with temperature (Fig. 4), approximately according to a logarithmic law. An increase of the conductivity of carbon black suspensions with temperature was also found by Voyutsky, Kargin, et al. [5]. The probable reason for this is accelerated coagulation structure formation as the result of a decrease of the viscosity of the medium with increase of temperature, which makes the deposit considerably denser and facilitates contact of the particles. This is confirmed by the fact that the time for a constant value of λ_m of the deposit to be established is considerably increased with decrease of temperature.

Addition of surface-active agents sharply decreases the conductivity of the suspensions and weakens the action of temperature on the conductivity (Fig. 4, Curve 2) because of the formation of adsorbed layers on the particle surfaces and a general increase in the viscosity of the layers of medium between the particles. When a sufficient amount of surface-active agent has been added to the dispersion medium, the adsorbed layers hinder direct contact between the particles and thus decrease the conductivity of the suspension. Fig. 5 shows the decrease of the deposit in 1.5 and 11.5% suspensions of graphite in toluene, with increased concentration of surface-active agent — oleic acid. The strength of the structure in the deposit, however, is changed little by the addition of surface-active agents. Small quantities of oleic acid, of the order of 0.01%, even slightly increased the strength and density of the deposit; a further increase of the oleic acid content had very little effect on the P_m value of the structurized deposit in the graphite suspension. This is probably due to the formation of mechanically strong layers of the medium between the particles, and to absence of peptization. In such a structurized deposit all the particles are held together by gel-like layers, which results in a considerable strength; at the same time these layers, which have low conductivity, produce a decrease of the total conductivity of the system. In the presence of surface-active substances adsorbed on the particle surfaces, the relationship between λ and P_m is disturbed, so that the system may be fairly strong but a bad conductor.

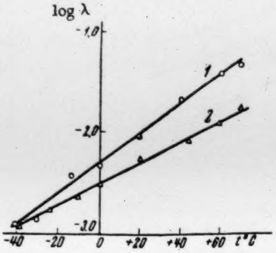

Fig. 4. Variations of the conductivity of 10% graphite suspension in toluene with temperature: 1) without surface-active agent; 2) with 0.1% oleic acid.

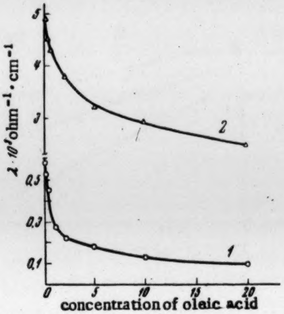

Fig. 5. Effect of additions of oleic acid on the conductivity of the deposit in: 1) 1.5%; 2) 11.5% graphite suspension in toluene.

SUMMARY

1. Structure formation in concentrated suspensions of graphite in nonconducting dispersion media has been studied by the conductometric method.

2. It is shown that the conductivity of structurized deposits in graphite suspensions depends on the concentration of the disperse phase and on the properties of the dispersion medium, and is evidently determined by the number of contacts between the particles. Breakdown of the sedimentation structure by shaking or stirring sharply decreases the conductivity of the deposit, which is then restored with time.

3. Parallel determinations of the strength of the deposits, measured by the yield stress P_m, showed that within certain limits the conductivity of a deposit increases with its strength.

4. Addition of surface-active agents considerably decreases the conductivity of the deposits owing to formation of adsorbed layers which hinder direct contact between graphite particles.

5. The conductometric method has a number of advantages, and may be used in conjunction with other methods for studies of structure formation and thixotropic effects in various disperse systems.

LITERATURE CITED

[1] S. Ya. Veiler and P. A. Rebinder, Proc. Acad. Sci. USSR 49, 354 (1945); B. Ya. Yampolsky and P. A. Rebinder, Colloid J. 10, 466 (1948); E. E. Segalova and P. A. Rebinder, Colloid J. 10, 223 (1948); M. P. Volarovich, Conference on Viscosity of Liquids and Colloid Solutions (1944), 2, 192; D. M. Tolstoi, Colloid J. 10, 133 (1948).

[2] A. V. Dumansky, Z. physik. Chem. 60, 553, (1907); W. Pauli and E. Valko, Elektrochemie der Kolloide (1929); J. Duclaux, Kolloid-Z. 3, 126, (1908); Compt. rend. 140, 1468, 1905; V. Hevesy, Kolloid-Z. 21, 136, (1917).

[3] C. M. McDowell and F. L. Usher, Proc. Roy. Soc. A. 131, 564 (1931).

[4] B. Dogadkin, K. Pechkovskaya, and V. Kupriyanova, Studies of the Physics and Chemistry of Rubber (State Chem. Press, 1950).

[5] S. S. Voyutsky, A. D. Zaionchkovsky, V. A. Kargin, and S. I. Rubina, Colloid J. 13, 333 (1951); Factory Lab. 17, 1229 (1951).

The M. V. Lomonosov State University, Moscow
Laboratory of Colloid Chemistry

Received October 2, 1955

5

DISCUSSION

SOME QUESTIONS CONCERNING THE EXTERNAL FRICTION OF RUBBER

G. M. Bartenev

On the subject of my paper "The molecular nature of the friction of rubber" [1], a paper has been published by Ratner [2], which contains errors, numerous incorrect quotations, and inaccuracies. The present paper is a reply and a further discussion of some questions concerning the friction of rubber.

The analogy between friction and viscous flow. In my paper [3] on the theory of the friction of rubber an analogy between the friction of rubber and viscous flow was seen only in a common molecular mechanism of thermal motion – the overcoming of the energy barrier by the kinetic units. Ratner reduces this analogy to identity, and this explains why 1) he does not take into account the distinction that in internal friction the area of actual contact coincides with the area of nominal contact, and in external friction it does not; 2) instead of my formula for the friction of rubber, Eyring's formula for viscous flow is given. As a result of the first error it is not understood that the main reason why the frictional force of rubber and other bodies depends on the load is that the area of actual contact depends on the load, while the second error leads to a distortion of the theory of the friction of rubber.

It was necessary to substitute Eyring's formula for the relationships derived, in order to assert that "load . . . is ignored in Formula (5) for viscous flow, which Bartenev applies without foundation to friction" (?!). From this it is clear why Ratner sees the main defect of the theory [3] in the fact that in his opinion the frictional force is not considered to depend on the load. In reality, our formula incorporates this dependence, which has been examined in detail in a paper [4] on the laws of the friction of rubber.

The absolute or the conventional nature of the static friction of rubber. One of the basic problems for discussion is a correct understanding of the so-called static friction of rubber. In our view, based on the theory [3], rubber has no static friction in the absolute sense, and it must be regarded as a conventional value which depends on the method of measurement and test conditions.

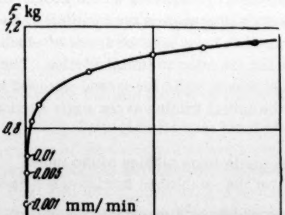

Fig. 1. The frictional force of natural rubber against steel as a function of the sliding velocity under steady friction conditions (30°).

As an illustration of the conventional nature of static friction, Fig. 1 shows a graph obtained by Z. E. Styran for the variation of the friction of rubber with the sliding velocity on steel under steady-state conditions. The graph shows that the frictional force tends to zero with unlimited decrease of the velocity.

Although in theory, if chemical processes between the rubber and the support are excluded, the force of friction tends to zero with unlimited decrease of the sliding velocity, this does not mean that use cannot be made of the force of "static" friction as a conventional value, which has the same practical meaning as the flow limit of solids. The experiments of Ratner and Lavrentyev [5] are of interest because they emphasize the possibility of using static friction as a practical magnitude. However, the results of such experiments on "static friction" must be explained by the very slow tendency of the frictional force to zero with decreasing sliding velocity, and also by possible chemical aging processes on prolonged contact between the rubber and the metal.

In our publications [1,3,4,6] no attempt is made to refute the use of static friction of rubber as an engineering quantity, and only the physical meaning of this concept is modified. Ratner's conclusion that the question of the nature of rubber friction can be regarded as finally settled in favor of the existence of an absolute static friction is not correct.

Initial and established friction. Friction is a single process, and static friction should be a particular case which follows from the theory of friction. Nevertheless, kinetic and static friction is contrasted in Ratner's paper [2], on the assumption that kinetic friction depends on the sliding velocity, and static friction, on the time of previous contact.

The source of the error is that kinetic friction is regarded as independent of the time of previous contact. However, the friction during the first instants of sliding (to which we will refer as the initial friction) is kinetic friction which depends both on the sliding velocity and on the time of previous contact. Only the friction which has become established during the sliding process will be independent of the time of previous contact. This distinction between initial and established friction can be seen from the data [7] graphically shown in Fig. 2.

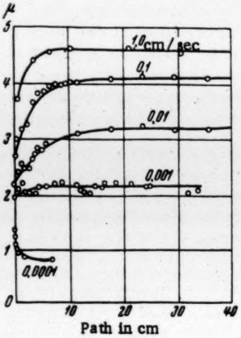

Fig. 2. Variation of the coefficient of friction of rubber on glass with sliding distance (path) at various speeds (in cm/sec) from data in [7].

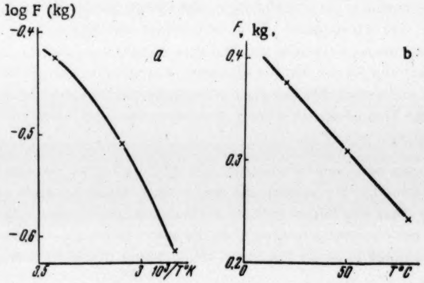

Fig. 3. Friction of SKBM synthetic rubber as a function of temperature, under a load of 1 kg/cm^2, from Ratner's data [11], in different coordinates: a) log F, 1/T; b) F,T.

Ratner did not analyze experimental data on the friction of rubber, obtained both by various other workers and by himself. Such an analysis shows that two methods have been used, one of which corresponded to established and the other to initial friction. The first method was used by Schallamach, Hurry and Prock, Thirion, myself, and others, while the second was used by Thirion, Ratner and Sokolskaya and others. In his experiments Ratner took the initial friction as the static friction of rubber [8-10].

The measured friction in his experiments [9, 10] also depended on the preliminary rubbing of the rubber specimens against the surface, which was to be expected, as the initial and not the established friction was measured.

The effect of temperature on the friction of rubber. An important fact, which indicates the conventional character of the static friction of rubber is that, in contrast to solids, the friction of rubber (both initial [11] and established [12]) is clearly dependent on temperature. According to the theory, in the conditions which apply to the usual experiments the experimentally determined frictional force [12] is related to the temperature by the expression $F = a - bT$, where the constants depend on the sliding rate, normal load, etc.

In considering the effect of temperature, Ratner [2, 11] recommends the formal use of the relationship $F = A\exp(U/RT)$, where U is the activation energy of an unknown process. The proposed formula is not in agreement with his own experimental data [11], as Fig. 3,a shows (a curve is obtained rather than a straight line). However, these data are in good accord with the theory, as shown by Fig. 3,b.

An interesting fact is that, in contrast to his earlier publications in the paper [2], Ratner now admits that the dependence of friction on temperature is proof that the nature of the friction of rubber and of solid bodies is different. It is difficult to reconcile this with the fact that he treats the experimental data [2] on the basis of Deryagin's theory, according to which frictional force is independent of temperature.

The law of the friction of rubber. One of the basic postulates of our publications [1,4] is that the analytical form of the relationship between frictional force and load (the law of friction) in friction at smooth solid surfaces is mainly determined not by the molecular mechanism of friction, but by the dependence of the friction on the area of actual contact which, in turn, depends on the load, the elasticity of the material, and the outline of the contact surface. In addition, the frictional force depends on the effect of the normal load on the forces of adhesion and on the energy barrier, but this relationship is introduced as a correction factor.

It follows from Deryagin's [13] and our own work [4] that if roughness and mechanical obstacles are neglected, a binomial law of friction holds for all bodies:

$$F = AS^f + BP, \qquad (1)$$

where F is the frictional force; S^f is the actual contact area; P is the normal load; A and B are constants which depend on the molecular friction mechanism and the experimental conditions (temperature, contact time, duration and rate of sliding, etc.), while the constant B also depends on the effect of the load on the forces of adhesion or on the energy barrier.

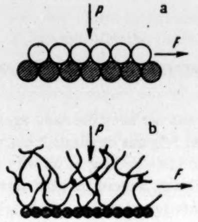

Fig. 4. Friction models: a) solids according to Deryagin [14], b) a cross-linked polymer (rubber) on a solid surface.

In the case of rubber [4] the formula is not applicable when $P \to \infty$, as it is a linear approximation of a more general relationship (in the case of loads used in practice, the second term is a correction).

For rubber [4] the constants are mutually independent, while for solids, according to Deryagin [13, 14] they are related by the expression $A = p_0 B$, where p_0 is the specific adhesion.

The physical meaning of the constants in Formula [1] is not the same for rubber as for solids. For example, according to Deryagin [13, 14] the constant B represents molecular roughness, a model of which is shown in Fig. 4,a this, however, is only applicable to simple solids and has nothing in common with the molecular model of rubber friction (Fig. 4,b) proposed by myself [3], based on the chain structure of rubberlike polymers and chain flexibility. In this model the molecular roughness which is considered in Deryagin's theory does not play an important role because of the great flexibility and mobility of the polymer chains. The constants in Formula (1) are in this instance determined by the nature of the thermal motion of the rubber chains at the polymer – solid boundary.

Evidently Deryagin's formula should be applied only to those molecular models for which it was derived. However, one of the defects of Ratner's work [2] is an uncritical approach to the question of the applicability of Deryagin's formula to rubberlike polymers. For example, it is not clear why Ratner regards as acceptable the model (Fig. 4,a) which represents the contact of two crystal lattices. It is also difficult to see how Deryagin's theory and Schallamach's work can be reconciled if their molecular approach to friction is different in principle. In the same way, the application to rubber of Deryagin's formula, which does not take into account the influence of temperature and the sliding velocity, factors which significantly affect the frictional process, cannot be regarded as well founded.

Earlier [8, 9] Ratner had shown that Deryagin's formula is not applicable to rubber; in other papers [10,11] he contradicts this, and explains the mutual independence of the constants in Formula (1) by the influence of the roughness of the solid support (without noting that such an extension of Deryagin's formula to the friction of rough surfaces was first made by I. V. Kragelsky). However, it follows from our theory [3,4] that the constants in Formula (1) are also independent in the case of the friction of rubber on smooth solid surfaces. Therefore it is not sufficient to attribute the inapplicability of Deryagin's formula in the case of rubber only to roughness of the support.

In his paper [2] Ratner devotes much space to an examination of my paper [4], and makes numerous errors in so doing. It is asserted, for example, that in my paper the law of friction is considered when $P \to \infty$, which is incorrect, as the law of friction was derived as a linear approximation in a limited load range. It must be pointed out that this inadmissible step was in fact taken by Ratner [8-10] who, for example, determined the constant $B = \mu_\infty$* by extrapolation to infinite load, which we have already criticized [1,4].

According to Ratner, our formula is based on Bowden's idea (?!) that the frictional force of solids is strictly proportional to the area of actual contact. This is inaccurate. The proportionality of the frictional force to the actual contact area follows from the molecular model Fig. 4,b) according to which the frictional force is proportional to the number of chains in contact with the solid, and it is therefore a consequence of the theory, and not an extension of the law of solid friction to rubberlike polymers.

The assertion that Kragelsky [20-22] disproved the proportionality of the frictional force to the actual contact area is incorrect. Kragelsky derived a law for the friction of solids with rough surfaces, while our paper derives the law for the friction of rubber on smooth surfaces. Ratner considers that proof is provided by experiments in which the two terms in Formula (1) can be varied independently. However, as we have seen, this is a direct consequence of the theory of rubber friction, while in the case of solids it is a consequence of the fact that Kragelsky took the surface roughness and mechanical obstructions into consideration.

Ratner, while denying the existence of proportionality between frictional force and the area of actual contact, at the same time makes use of Deryagin's formula, which includes this proportionality:

$$F = BS^f (p_0 + p_f),$$

where p_0 is the specific adhesion; p_f is the specific pressure on the actual contact area, determined by the relationship $P = p_f S^f$.

Some other comments must be made. Ratner asserts that our law of friction has not been checked against experimental data. This is not true. The comparison was made not with individual "figures or points," but with the experimental laws for the friction of rubber. Ratner considers that Denny's data have nothing to do with the matter, since they refer to friction with a lubricant. This is a misunderstanding. Denny showed that the same law is derived for the friction of rubberlike polymers with lubricants as in the dry friction of rubber. This is convincing proof that the analytical expression of the law of friction is determined fundamentally not by the molecular mechanism of friction, but by other factors. This is also supported by Deryagin [14, p. 180] who writes: "the binomial law of friction has proved strictly valid both in presence of a layer of lubricant formed by a solid or liquid, and in dry friction."

Was our criticism of Ratner's formula well-founded? In his paper [10] Ratner gives the formula $\mu = \mu_\infty + B'/P^h$, derived on the assumption that $F_0 = B'P^{1-h}$. However, he did not perform any direct experiments to determine F_0. An examination of the paper [10] shows that this assumption includes the possibility that when the load $P \to \infty$ the area of nominal contact $S^N \to \infty$. However, this is contrary to the fact [15] that no appreciable spreading of rubber over the supporting surface under normal load is observed during periods considerably greater than the time required to determine the frictional force. Therefore in experiments on the dry friction of rubber we may ssume that S^N is approximately constant. In addition, his experimental data were obtained in conditions in which changes of S^N were excluded, as the rubber specimens were placed in metal nests in such a way that spreading of the specimens under normal load was practically excluded. This shows that the constancy of S^N is not invented by me, but is a consequence of the method used by Ratner.

In addition, Ratner asserts that rubber flows under load. A raw rubber mix flows but (vulcanized) rubber can slide relative to a solid surface. If it is assumed that rubber slips under load, this leads to two-dimensional extension. This changes the conditions of friction at the surface in a way which has not yet been considered either experimentally or theoretically.

---

* Recently [2,5] Ratner has introduced the qualification that μ_∞ represents the properties of rubber at infinite load not in the literal sense. At the same time, in one of his papers [8] it is stated ". . .μ_∞ is the minimum value of the coefficient of friction at $P \to \infty$." Ratner's error consists of the fact that he theoretically regards this constant as the coefficient of friction at $P \to \infty$.

Thus, the conclusion that the derivation of the formula in question was erroneous is still valid. The formula can be merely regarded as one of many empirical formulas, and moreover as limited in application. This is confirmed by the author's own data. For example, in one set of experiments [10] in the load range of 0.1 to 10 kg/cm^2 the constant $\mu_\infty \approx 0.5$; while in other experiments with the same rubbers [5] in the load range of 3 to 200 kg/cm^2 the same constant now has the value $\mu_\infty \approx 0.1$. This shows that over a wide load range μ_∞ and B' are not constant, but depend on the load. Thus, the proposed formula is much worse than Thirion's formula, which covers a wider range of loads.

In conclusion, Ratner [2] formulates assertions which are ascribed to me; since they are not taken from my papers but are formulated by Ratner, it is necessary to examine them briefly. We will consider them in the order in which they occur in the paper [2].

a) I did not assert that the influence of velocity on frictional force is "always in principle" different for rubber and solids. In [1] it is stated: "it is known that the velocity as a function of the force increases for rubber and decreases for metals'." Thus, the statement refers not to all solids, but to metals, and only to the known decreasing friction of metals [16, 19].* It is known [23] that increasing friction is found in the case of a number of solids, such as fibrous materials.

As regards the existence of maxima in the frictional characteristics of certain metals, the data of Barwell and Rabinovich cited in [2], although of interest, contain a number of obscure points and bear no direct relation to the problem in question.

b) The statement ascribed to me by Ratner that "the static frictional force of rubber is zero" [2] is incorrectly quoted. My claim is that absolute static friction in the strict sense is zero for rubber, while the conventional static friction, like the conventional flow limit for solids, is not zero.

c) Ratner's statement that the "frictional force is strictly proportional to the actual contact area" is cited without reference to actual experimental conditions and is therefore meaningless. This statement is Ratner's and not mine. In [1] I state that "the general form of the mathematical relationship between the frictional force and the load in the friction of smooth surfaces is largely determined not by the mechanism of friction, but by the relationship between the frictional force and the area of actual contact."

d) The assertion that roughness of the support influences the friction of rubber only by increasing the contact area was never made by me, and is in itself incorrect (see Kragelsky, [22, 20]).

e) My statement that Ratner has assumed the friction of rubber and of solids to be of identical nature is in agreement with the facts, as can be seen from Ratner's publications and from his paper [2] in which the law of friction for solids and the concept of molecular roughness are formally extended to the friction of rubberlike materials.

f) Ratner's formula, which contains three empirical constants, is erroneous not because it covers experimental data over a relatively narrow range of loads, but because its derivation is based on false physical assumptions.

Ratner's scientific views are self-contradictory, as while he acknowledges in words the "fertility of Schallamach's ideas" in fact he applies the frictional model and the law of friction for solids to rubber. His assertion, that our theory of the friction of rubber [3] is a formal extension of the equations for viscous flow to external friction, is not true, as can be seen in an examination of the paper [3].

It follows from this discussion that in consideration of the laws of friction for rubberlike polymers their structure may not be ignored, and the molecular model for the friction of rubber cannot be assumed to be identical with that for solids.

---

* Some formulations and statements are distorted in the paper [2]. For example, Ratner states that it is asserted in our papers that the frictional force (of solids) always decreases with increase of velocity; a little later the statement is attributed to us that the influence of velocity on friction is always different in principle for rubber and for solids. The words underlined are not found in our statements.

LITERATURE CITED

[1] G. M. Bartenev, Colloid J. 18, 249 (1956) (T.p239).*

[2] S. B. Ratner, Colloid J. 18, 373 (1956) (T.p 363).*

[3] G. M. Bartenev, Proc. Acad. Sci. USSR 96, No. 6, 1161 (1954).

[4] G. M. Bartenev, Proc. Acad. Sci. USSR 103, No. 6, 1017 (1955).

[5] S. B. Ratner and V. V. Lavrentyev J. Tech. Phys. (USSR) 26, No. 4 (1956).

[6] G. M. Bartenev and L. E. Peregudova, Trans. Inst. Rubber Ind. 1955, No. 2.

[7] F. L. Roth, R. L. Driscoll, and W. L. Holt, Rubber Chem. and Technol. 16, 155 (1943).

[8] S. B. Ratner, Proc. Acad. Sci. USSR 83, 443 (1952).

[9] S. B. Ratner and V. D. Sokolskaya, Proc. Acad. Sci. USSR 86, 121 (1952).

[10] S. B. Ratner and V. D. Sokolskaya, J. Chem. Ind. 1955, No. 1, 27.

[11] S. B. Ratner, Proc. Acad. Sci. USSR 93, 47 (1953).

[12] A. Schallamach, Rubber Chem. and Technol., 27, 234,(1954);Kolloid-Z. 141, 165,(1955).

[13] B. V. Deryagin, Proc. Acad. Sci. USSR 3, 93 (1934); J. Phys. Chem. 5, 1165 (1934).

[14] B. V. Deryagin, What is Friction (Acad. Sci. USSR Press, 1952).

[15] G. M. Bartenev, Factory Lab. 1951, No. 4, 12.

[16] S. E. Khaikin, Mechanics (State Tech. Press, 1947).

[17] S. E. Khaikin, L. P. Lisovsky, and A. E. Solomonovich, Symposium: Friction and Wear in Machines (1939), Vol. 1, p. 480.

[18] N. F. Kunin and G. D. Lomakin, J. Tech. Phys. (USSR) 24, 1361 (1954); 24, 1367 (1954).

[19] G. D. Lomakin, J. Tech. Phys. (USSR) 26, 857 (1956).

[20] I. V. Kragelsky, Symposium: Investigations in the Field of Mechanical Engineering (Acad. Sci. USSR Press, 1944), p. 130.

[21] I. V. Kragelsky and I. E. Vinogradova, Frictional Coefficients (State Machinery Press, 1955).

[22] I. V. Kragelsky, "Machine parts", in Symposium: Calculation and Design Data (edited by Prof. N. S. Acherkan), (State Machinery Press, 1953), Vol. 1.

[23] I. V. Kragelsky, Friction of Fibrous Materials (State Light Industry Press, 1941).

Received June 16, 1956

---

* T.p. = C. B. Translation pagination.

REVIEW

Monograph by F. M. Shemyakin, E. S. Mitselovsky, and D. V. Romanov

"Chromatographic Analysis (Introduction to Theory and Practice)"

(State Chemical Press, 1955)

Chromatographic analysis is becoming increasingly used both in research and in applied science, and is now one of the most widely used methods for the investigation of complex systems. After its discovery in 1903 by the Russian scientist M. S. Tsvet, the method was forgotten and it only became widely used and extensively developed during the last ten years. In these few years an enormous number of publications has appeared in this field, and a systematization and critical survey of this work has become an urgent matter. The fact that this is so is confirmed by the almost simultaneous appearance in 1955 of two monographs on the subject:

1) N. F. Ermolenko, "Chromatographic Adsorption Analysis and Its Development," Acad. Sci. Belorussian SSR Press, Minsk (1955);

2) F. M. Shemyakin, E. S. Mitselovsky, and D. V. Romanov, "Chromatographic Analysis (Introduction to Theory and Practice)," State Chemical Press, Moscow (1955).

N. F. Ermolenko's small book consists of a summary of various methods and fields of application of chromatographic analysis. This makes it useful to a very wide circle of readers.

The book by F. M. Shemyakin and his co-authors is a valuable detailed handbook of chromatographic analysis, which includes not only an extensive review of the work in this field, but a detailed examination of the theory of the method. The book consists of seven chapters, which cover all sections of chromatographic analysis.

The first chapter ("Introduction") details the individual stages in the development of the science of adsorption and the development of the chromatographic method in the work of our national scientists.

The second chapter presents the theoretical basis of the chromatographic method – the types of sorption processes (molecular and ionic) and the corresponding types of chromatographic analysis: liquid, partition, and precipitation chromatography.

The third chapter acquaints the reader with the principal apparatus and materials used in chromatography, while chapter four gives details of various modifications of the chromatographic method.

The last three chapters are especially important; these deal with analysis of inorganic substances (chapter five), analysis of organic substances (chapter six), and the uses of chromatography in industry (chapter seven).

The monograph covers all types of chromatographic analysis and in this it compares favorably with other monographs on the subject, and in particular, with O. Samuelson's book, "The Use of Ion Exchange in Analytical Chemistry" which was published almost at the same time. F. M. Shemyakin and his co-authors have made many contributions to the development and adoption of this method in our country, and this is reflected not only in the fact that the Soviet Literature is critically covered very fully in the book, but also in the large amount of detail of practical value contained in the book.

The criticism may be made that a number of publications by foreign workers (Brunauer, Wicke, Wilson, Gregor, Kerr, and others) are not considered. It is true that this work is dealt with in a number of reviews used by the authors. However, a more detailed presentation of this work would have made the book more complete and useful.

The Russian literature is covered up to 1954, and the foreign, up to 1950.

It should be pointed out, however, that chromatography has extensive applications in various fields and the compilation of a monograph on the subject is a very complex task not only because the author must be a specialist with a wide range, but also because the abundance of the literature on various aspects makes selection very difficult. This difficulty was encountered by the authors. An examination of the pages which deal with the use of chromatography in inorganic analysis and in technology shows that many pages are necessarily of reference value. It was therefore necessary either to omit the omit the work, or merely to mention a series of publications, or to restrict the presentation to brief references. The authors chose the latter, more correct way.

The number of minor slips and obscure sentences in the book will not be discussed here; these will no doubt be eliminated in a new edition, which has already become necessary.

S. M. Lipatov

INVESTIGATION OF PLASTIC DISPERSE SYSTEMS IN CONDITIONS OF UNIFORM STRESS

G. V. Vinogradov, V. G. Lebedev, and V. A. Protodyakonov

The work of Vinogradov [1], Pavlov [2], and some associated studies, have established the importance of studying the mechanical properties of disperse systems in a state of uniform stress. Only in such conditions is it possible to use experimental results directly to give the true rheological characteristics of disperse systems both in the region of viscous flow, and especially in plastic deformation and imperfect elasticity (elastic after-effects, etc.). The elastic properties (shearing modulus, etc.) may in many cases be easily determined on the basis of the theory of elasticity and of tests of disperse systems in nonuniform stress conditions. However, investigation of the mechanical properties of plastic disperse systems in conditions of uniform stress presents considerable difficulties.

Materials Studied and Methods of Investigation

The elastoviscosimeter shown in Fig. 1 was constructed for studing the mechanical properties of plastic disperse systems over a wide range of temperatures and shearing stresses. Our aim was to ensure a definite and highest possible degree of uniformity of the stress in this apparatus.

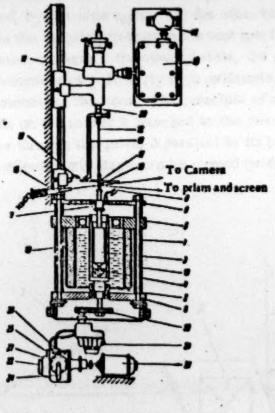

Fig. 1. Elastoviscosimeter

The main working parts of the instrument are: a steel cylinder 1 with a shaft 2 built into it, and, coaxial with this, a metal cylindrical core 3 (steel or duralumin) carrying at its lower end a tempered steel needle which enters the interior of the miniature thrust bearing 4, fitted to the center of the shaft of the outer cylinder. The surface of the core 3 may be smooth or riffled; the space between it and the cylinder 1 is filled with the tested material. The outer cylinder with its shaft is retained by two sets of ball bearings fitted firmly in sockets of the crossbeams 5 and 6. The upper end of the core is centered by means of an air bearing 7, situated in a socket in the crossbeam 8. Air is supplied to the bearing at a pressure of 0.5-1.0 atm. through the nipple 9. The crossbeams 5,6, and 8, together with the vertical cylindrical rods 10, form the framework of the instrument. The bearing sockets and the holes in the crossbeams were bored to the same setting.

The torque is applied to the core or to the outer cylinder. In the first case, the loading head 11 is used, from which the torque is transmitted to the core through the calibrated steel torsion wire 12. The spindle of the torsion head can be rotated by hand or through the multistage reducing gear 13 by the synchronous electric motor 14. Angular displacement of the core was recorded by deviation of a beam of light directed from the source 15 onto a mirror 16, fixed to the core shaft. In addition, large angles of rotation were measured by means of the graduated disk 17 fixed to the core, and the pointers 18 and 19, of which the pointer 19 is stationary while the pointer 18 rotates with the spindle of the torsion head 20. Thus, the pointer 19 shows the angle of rotation of the core, and the pointer 18, the angle of rotation of the upper part of the torsion wire. From this it is easy to find the torsion angle of the wire, and hence the torque applied to the material. When viscous flow is established in the material, the pointer 18 and disk 17 rotate at the same speed. The operation of the loading head and automatic recording of deformations were described earlier [3].

The torque is applied to the outer cylinder by means of a hydraulic drive, which consists of the electric motor 21, hydraulic pump 22, and hydraulic motor 23. The speed of the hydraulic motor is regulated by the hydraulic pump lever 24, which controls the amount of liquid entering the motor from the pump. The hydraulic drive provides variable control over a wide range of speeds, and retains a constant torque on the hydraulic motor shaft irrespective of its shaft speed. Smooth variation of the hydraulic motor shaft and control of constant speed is achieved by means of the knob 25 rigidly coupled to the worm 26 which engages with the worm wheel 27. The hydraulic motor shaft is coupled to the outer cylinder of the instrument through the reducing pinion gear 28. To the large pinion of this gear a stroboscopic disk is attached for measuring the rotation speed of the outer cylinder. The hydraulic drive is used for viscosimetric experiments. The outer cylinder of the elastoviscosimeter is enclosed in an insulated thermostatic jacket. Liquid can be circulated in the space between the cylinder and the jacket. This space can also be used as an independently operating thermostat. The core and air bearing were of the type described by Oldroyd et al. [4]. Both smooth and riffled surfaces of the cores and outer cylinders were used. The internal diameters of the cylinders were 31.6 and 35.5 mm, their heights were 70 ± 0.1 and 35 ± 0.1 mm, and the gaps between them and the cores 0.20 and 0.25 mm. If triangular riffling was used, the depth was 0.35 mm.

As is known, in elastic deformation of a medium in the gap between two coaxial cylinders the angular displacement (γ) of the inner cylinder (core) in radians is given by

$$\gamma = \frac{\tau}{2G}\left[1-\left(\frac{r_0}{r_1}\right)^2\right],$$

where τ is the shearing stress at the core surface; G is the shearing modulus; r_0 and r_1 are the core and outer cylinder radii, respectively. It is seen that in the region of elastic deformations the maximum angle of rotation of the core is determined, first, by the value of the ratio τ_f/G, where τ_f is the flow limit (yield value), and second, by the ratio r_0/r_1. On the other hand, uniformity of the stressed state, or the maximum difference between the shearing stresses in the test specimen, is determined by the value of $(r_0/r_1)^2$. Hence it follows that the more uniform the stressed state, the closer r_0/r_1 to unity, and the lower the value of γ. Therefore measurement of γ at fairly high uniformity requires a highly sensitive method for recording the angular displacements of the core. The principle of our method is illustrated by Fig. 2. A ray of light from the source 1 falls on the mirror 2 attached to the core of the elastoviscosimeter. The ray is reflected by the mirror and passes through the prism 3 parallel to its base. The prism is fixed on the micrometric stage 4 of a microscope. The micrometric stage can be moved (with an accuracy of 5 μ) in a direction perpendicular to the ray passing through the prism. A white screen 5 is placed behind the stage prependicular to the ray of light passing through the prism. In the initial position, the ray of light which passes through the prism and over the prism forms, on the screen 5 placed behind the prism, two bright lines (ab, cd) along one vertical line. When the mirror turns, the ray of light passing over the prism is displaced in the direction of the turn of the mirror (position a'b'), while the ray passing through the prism is displaced in the opposite direction (position c'd'), thus intensifying considerably the effect of the ray displacement. By movement of the micrometric stage the initial position ab, cd of the light ray can be restored. From the readings of the micrometric scale which determines the position of the stage, it is possible to find the displacement which corresponds to the distance b'c', that is, to the angle of rotation of the core. The sensitivity of this method is ~0.002°; the maximum angle of rotation which can be measured conveniently is ~0.1°.

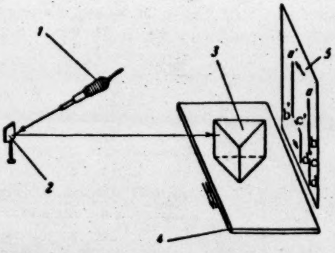

Fig. 2. Optical method for measurement of elastic deformations in a disperse system.

The accuracy to which the light beam can be set by movement of the prism on the micrometric stage is ± 0.01 mm. Accordingly, the relative error in deformation determinations lies in the range ± (4-2.5%). Otherwise, the accuracy of the elastoviscosimeter does not differ significantly from that described by Vinogradov and Klimov [3], with the exception that in the present method the core is forcibly centered, so that errors caused by noncoaxiality of the cylinders can be ignored.

In the experiments described below, the uniformity of the stressed state was 97%, and the end effect, calculated from the core area, was 10%. In all cases (except when otherwise stated) the systems were obtained from melts at a cooling rate of 0.5 degree/ minute. The materials were then homogenized by rubbing through a 200 mesh sieve.

The principal materials used in this investigation were paraffinic plastic petroleum products and highly concentrated plastic disperse systems consisting of natural solid hydrocarbons (paraffin wax and ceresin) and petroleum oils. Earlier investigations showed that the data for the mechanical properties of such systems have poor reproducibility. Nevertheless, if the preliminary mechanical treatment of the samples is uniform and if they are held in the elastoviscosimeter for a long time (72 hours), their mechanical properties can be determined with adequate reproducibility. For example, six experiments performed at 20° on a control sample consisting of a plastic system containing 20% ceresin in MS-14 petroleum oil, homogenized by rubbing through a sieve of 200 mesh [5], gave the following results: yield value $\tau_f = 9.7 \pm 0.2$ g/ cm², effective viscosity (μ_{eff}) at a velocity gradient (D) of 1 second^{-1}, 4940 ± 85 poises.

Comparison of the Behavior of Plastic Disperse Systems in Uniform and Nonuniform Stress Fields

Studies of plastic disperse systems in conditions of uniform stress are most important in investigations of imperfect elasticity effects and transitions from elastic deformations to plastic flow. The greatest shearing stress in a concentric gap acts at the core surface, and its value varies in a radial direction in inverse ratio to the square of the radius of the layer in question. When the torque increases, the shearing stresses increase to different extents in coaxial layers at different distances from the core axis. In consequence, the yield value or even steady viscous flow may be reached at the core surface, while at the surface of the outer cylinder the sample may be undergoing pure elastic deformation only. If the coaxial rotating cylinder method is used without consideration of uniformity of the stress, only the parameters for ideally elastic deformations (shear modulus) and the parameters which characterize qualitative transitions of the system from one state into another, namely the flow and strength limits, can be determined quantitatively. In such conditions it is usually impossible to determine velocity gradients, viscosities, and similar values, as the thickness of the layer in which flow occurs is not known. It must be pointed out that these simple considerations have been ignored in many fairly well known recent investigations, in which the flow velocity gradients of the materials across the whole gap were calculated, and the viscosities and various rheological parameters were found, although it is quite evident that all this lacks physical meaning and cannot serve as a basis for verification of the theory and for evaluation of the true rheological parameters which determine the properties of plastic disperse systems.

A comparison of stress-deformation curves obtained in conditions of a nonuniform stress field (Klimov's elastometer) and in a uniform stress field with the aid of the elastoviscosimeter described above is shown in Fig. 3. This shows the results of tests of homogenized plastic systems based on MS-14 oil thickened by addition of 20% paraffin wax and ceresin (see [5]). Curve 1 was obtained with the elastometer for a paraffin system, and Curve 2 refers to the same system studied with the aid of the elastoviscosimeter. Curve 3 represents the ceresin system tested in the elastometer; Curve 4 represents the same ceresin system in uniform stress conditions. All the experiments were performed at 20° and a loading rate of $3.6 \cdot 10^{-2}$ g. cm^{-2} second^{-1}. Fig. 3 also shows Curves 1'-4', for a repeated loading of the samples at this rate after the core had been rotated one complete turn. The yield stress (strength limit) values determined in uniform and nonuniform stress conditions differ from each other within the limits of experimental error. A distinctive feature of the curves obtained for deformation of the samples in conditions of uniform stress is a longer initial linear region of the τ (γ) curves, and the fact that τ_f is reached at smaller deformations. This is especially noticeable in curves for the paraffin wax systems. Curve 1, obtained with the elastometer, has almost no linear region, and its whole course reflects the deformation of a typical plastic body, characterized by sharply defined irreversible creep, until τ_f is reached. Curve 2 for the same sample, obtained by means of the elastoviscosimeter, shows after-effects and creep at higher values of τ. Steady viscous flow at the load rate indicated above, is reached in the elastoviscosimeter after the core has rotated through 600° and in the elastometer, after 360°. The reason for this difference lies in the difference between the sizes of the samples tested in the elastoviscosimeter and in the elastometer, and the loading conditions.

This difference is very prominent in the curves for the repeated loading of the samples. The strength limits in a second rotation of the core in the elastometer (Curves 1' and 3') are approximately one half of the values obtained by means of the elastoviscosimeter (Curves 2' and 4'). This is undoubtedly caused by the fact that one complete turn of the core in the elastometer does not produce the same structural breakdown in the samples as one complete turn in the elastoviscosimeter.

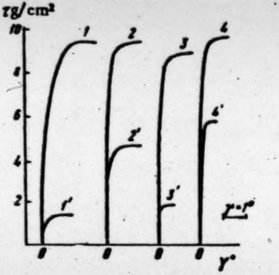

Fig. 3. Stress-deformation curves for nonuniform and uniform stress fields.

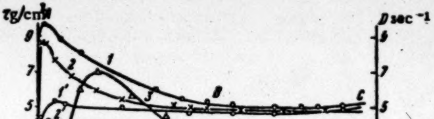

Fig. 4. Deformation-stress curves during continuous loading of a disperse system through an elastic element.

In the case of plastic disperse systems of the pseudogel and paste types, the strength limits, and, still more, established flow conditions, are reached only at very high deformations. A study of the transition beyond the strength limit for systems consisting of MS-14 oil and 20% paraffin wax and ceresin [5] is shown in Fig. 4. The tests were carried out at 20°. The rate of loading was $3.6 \cdot 10^{-2}$ g·cm^{-2}second^{-1}. The deformation of the samples was observed visually. Curves 1 and 2 represent the ceresin and paraffin wax systems respectively. As is seen in Fig. 4, Curve 1 ascends steeply to a maximum at the point A. This initial ascent of the curve represents instantaneous elastic deformation, the subsequent delayed deformation of elastic after-effects, and the start of the structural breakdown and plastic flow of the sample. As the tests were performed in a state of uniform stress, the transition from one kind of deformation to another is fairly sharp. The maximum on the curve corresponds to the strength limit (yield value) which, as was first shown by Vinogradov and Kilmov [6], corresponds to the start of very rapid structural breakdown. Breakdown begins to vary even before the yield value is reached. On the other hand, because of breakdown of the structural skeleton, the deformation rate (D) increases (Curve 3). After the strength limit is passed, the deformations in the samples develop so rapidly that the core rotation speed is sometimes 5-10 times as high as the rate of torsion of the upper end of the torsion wire, and the shearing stress therefore decreases (region AB). Despite this decrease in the stress, the continuing breakdown of the structural skeleton leads to a further increase of the deformation rate, which reaches a maximum and then decreases to a certain constant value (region BC) which corresponds to the equilibrium value of the shearing stress.

Thus, the variation of the deformation rate in the samples proceeds as follows. As the load is applied, the propagation rate of elastic deformation reaches the velocity of sound (elastic deformations). On further increase of the load the propagation rate of elastic deformation is maintained at this high level. Delayed deformation and plastic flow then begin to develop. The rate of this deformation increases, reaches a maximum, and drops to values corresponding to the rate of deformation in steady viscous flow (Curve 3, Fig. 4).

In the torsion method of loading, a definite, usually constant, rate of torsion of the wire is used. These conditions are definite and strictly constant only in the region of pure elastic deformation and of steady viscous flow. In transitional states, when the structural skeleton in the samples is being broken down, the loading conditions are variable. An important feature of the results of tests on plastic disperse systems in uniform stress conditions is that in such cases the maximum is most clearly defined and there is a sharp transition from a constant to a variable loading rate. The course of Curves 1-3 (Fig. 4) depends on the degree of uniformity of the stressed state and on the rate at which the shearing stress increases in the sample.

A correct evaluation of this last question was first described by Pavlov, who showed that rate of increase of the stress is

$$\dot{\tau} = \frac{1}{2\pi} C r^{-2} L^{-1} \dot{\varphi},$$

where r is the radius of the coaxial layer; L is its height; C is a constant for the torsion wire which characterizes its rigidity and which is equal to the torque which must be applied in order to twist its ends through a torsion angle (φ) of 1 radian relative to each other.

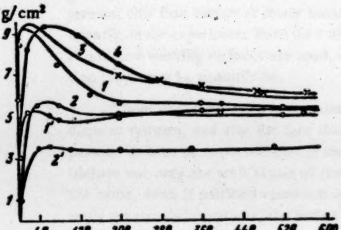

Fig. 5. Influence of the wall effect on the deformation of a disperse system.

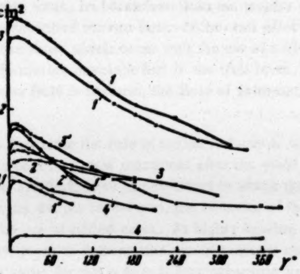

Fig. 6. Influence of wall effect on the nature of the deformation of samples with condensational and disrupted structures.

After steady conditions have been reached, stopping of the loading-head shaft makes it possible to determine the residual shearing stress, which in the given instance was of the order of 2.5 g/cm². Thus, shearing stress in steady flow can be resolved into two components, one of which is the yield value (strength limit) of the structural skeleton of the sample in flow, and the other is related to overcoming the viscous resistance.

In conditions of uniform stress confirmation is found for the special features of the rheological properties of plastic disperse systems which were previously described by Vinogradov and Klimov [7] on the basis of tests of such systems in an elastometer in a sharply nonuniform state of stress. In all cases there is an irreversible change in the strength properties of the samples, as the result of flow orientation of the anisodiametric particles which form the structural skeleton [7].

Role of Macroroughness of the Working Surfaces in Studies of the Deformation of Plastic Disperse Systems.

Despite the fact that the working parts of coaxial viscosimeters are very often riffled, no comparisons have been made between results obtained with and without such riffling. We carried out such experiments in the elastoviscosimeter at 20° on a homogenized system consisting of MS-14 oil thickened with 20% ceresin.

Fig. 5 shows $\tau(\gamma)$ curves for riffled (Curve 1) and smooth (Curve 2) cores. The tests corresponding to Curves 1, 1', 2, 2' were carried out at a loading rate of $3.6 \cdot 10^{-2}$ g. cm^{-2}. second^{-1}.

Fig. 5 shows that when a smooth core is used, the $\tau(\gamma)$ curve has three characteristic features: 1) its initial region is flatter than in curve 1; 2) the maximum is much lower than in Curve 1, while the curve itself is flatter and shifted into the regions of larger deformations; 3) the region of steady flow corresponds to lower shearing stresses than if a riffled core is used.

At the conclusion of these experiments, when the samples ceased to flow and the core stopped, the load was removed and the experiments were repeated under the same conditions. The riffled core gave rise to Curve 1' and the smooth core gave rise to Curve 2'.

Comparison of Curves 1 and 1' with 2 and 2' shows that after initial structural breakdown and flow orientation of the structural elements, the resistance to deformation of the samples during the repeated tests consists mainly of viscous resistance to flow. In these cases the maxima on the $\tau(\gamma)$ curves are less and the curves are flatter, so that the systems show much less structurized behavior than in the first tests.

This behavior of systems in tests with a polished core is explained by the wall effect [8]. During application of the load, deformation develops in the layer nearest to the wall, where the plastic body has a lower structural skeleton strength. Here irreversible plastic deformations readily develop, and in consequence Curve 2 (Fig. 5) is at a considerable angle to the ordinate axis in its initial region. In this region of the $\tau(\gamma)$ curve, elastico-plastic deformations in the wall layer and elastic deformations in the deeper layers of the material are superposed. This accounts for the main peculiarities of the $\tau(\gamma)$ curves in tests of plastic systems in gaps between polished solid surfaces.

Since the structure in the wall layer is relatively weak, its breakdown does not require shearing stresses greatly in excess of those required to maintain the established viscous flow. If the wall effect (W-effect) is present, this flow occurs at lower shearing stresses than those which occur with the use of riffled cores. Consequently, in the experiment described above, flow deformation develops first in the wall layer. It is thus seen that if polished working surfaces are used, even if the stress field is uniform, the field of deformations and deformation rates may be nonuniform.

These experiments have demonstrated for the first time the role of riffled surfaces in studies of plastic disperse systems, and also the fact that the W-effect becomes most prominent after the yield value has been passed. It is to be expected that if such experiments are performed in conditions in which the deformation will include not only the wall layers of the material but the deeper layers also, the behavior of the material will be the same, even if polished cores are used, as with the use of riffled cores. At higher loading rates and correspondingly greater deformations, the resistance of the wall layer to deformation should increase considerably. If this increase becomes sufficiently large and if the yield value for the system is reached within its depth, then evidently, structural breakdown will occur within the volume in the same way as in the experiments with riffled cores. The results in Fig. 5 confirm this.

Curves 3 and 4 in Fig. 5 represent the results of experiments performed with riffled and smooth cores, respectively, at a loading rate of 0.28 $g \cdot cm^{-2} \cdot second^{-1}$. The velocity gradient in steady flow was 1 $second^{-1}$ for Curve 1, and $3 \sim 8$ $second^{-1}$ for Curve 3. Fig. 5 shows that an approximately eightfold increase of the loading rate increases the steepness and height of the $\tau(\gamma)$ curve obtained with the use of a polished core. The initial region of Curve 4 shows a noticeable deviation from the ordinate axis, although this is less than is shown by Curve 2. Here the wall effect plays a part. However, the relative role of the W-effect in this case is less than at low loading rates. Increase of the loading rate causes an increase of the deformation rate in the wall layer, the yield value in it is exceeded, and viscous flow develops in it at lower absolute values of the deformation (angle of rotation of the core). Increased resistance to viscous deformation in the wall layer on increase of the velocity gradients results in transmission of the stress to the inner layers of the material and to structural breakdown in them — the yield value of the depth layers is reached.

These experiments clearly demonstrate that: 1) the W-effect is most prominent at low deformation rates with τ close to τ_f; 2) roughness of the working surfaces of the instrument has an exceptionally strong influence on the $\tau(\gamma)$ curves; 3) W-effects can be very conveniently studied with the use of rotational viscosimeters; 4) there is a qualitative correlation between the results obtained with capillary and rotational instruments; 5) at sufficiently high loading rates the yield values determined by means of instruments with smooth and with macrorough surfaces are similar.

Comparison of the Behavior of Samples With Condensational and Disrupted Structures

Considerable interest attaches to a comparison of the elastic and strength properties of plastic disperse systems in the form of "monolithic" samples with a condensational structure and samples with disrupted structure. For this, samples containing 2% ceresin in MS-14 oil [5] were made from a melt directly in the elastoviscosimeter. All the experiments were performed at 23°. The structural breakdown was effected by rotation of this elastoviscosimeter cylinder at a rate of 80 r.p.m. for 1-1.5 minutes. The results of some of these tests are given in Fig. 6. Here Curves 1 - 1''' represent the results of experiments with the use of a riffled core at a loading rate of $5.6 \cdot 10^{-2}$ $g \cdot cm^{-2} \cdot minute^{-1}$. Curve 1 represents a test on a monolithic sample obtained from a melt cooled at the rate of 10 degrees/minute, after it had been kept at rest for 48 hours. A control experiment with a sample held for 30 minutes only, gave Curve 1'. A comparison of Curves 1 and 1' shows that the formation of a condensational structure is completed fairly rapidly and there is no need for the samples to be held for a long time.

After Curve 1 had been obtained, the sample was broken down and the $\tau(\gamma)$ curve was obtained 30 minutes after breakdown of the sample (1'' in Fig. 6). It follows from an examination of Curves 1 and 1'' and a comparison with earlier findings [5] that the difference between the yield values of samples with condensational and broken-down structures decreases with decreasing concentration of the disperse phase.

After the second breakdown on the sample it was left at rest for 21 hours (Curve 1'''). The sample which gave Curve 1 with the use of a riffled core was obtained again and tested between polished surfaces in the elastoviscosimeter (Curve 2). A control experiment gave Curve 3. All the experimental conditions were the same as for Curve 1.

The sharp distinction of Curves 2 and 3 from Curve 1 is due to the fact that the W-effect is more prominent with the use of a polished core. It is particularly important that the wall slip effect was here detected for the first time for monolithic samples with a condensational structure, whereas it has formerly been studied only in systems with a microgranular structure [8].

After the tests corresponding to Curves 2 and 3 had been carried out, the samples were broken down and again tested after a rest period lasting several dozen hours. The results of these tests are given by Curves 2' and 3'.

It was found that breakdown of samples with the use of smooth cores leads to $\tau(\gamma)$ curves with not only more pronounced but with higher maximums; in other words, the yield value is higher.

This result, astounding at first sight, is easily explained. In cases when the W-effect is most prominent, the deformation affects primarily the wall layer and does not extend to the stronger volume structure of the samples. As a result of the structural breakdown the volume strength of the samples decreases relative to the strength in the surface layer, and deformation can therefore extend more easily into the material. It is consequently found that, in systems of the same nature, the coagulation structure in their volume after breakdown can have higher strength than the condensational structure in the wall layer of monolithic samples.

The experiments described above were repeated with samples obtained from melts cooled more slowly (1 degree/minute). A test with the use of a smooth core gave Curve 4 (Fig. 6), and a test with a riffled core gave Curve 4'. These experiments may be regarded as typical; they show that samples with a weaker condensational structure are obtained from melts as the cooling rate is decreased. However, in this case also there is a very great difference in the behavior of the samples, according to whether they are tested with smooth or riffled cores.

Two practical conclusions in relation to the use of protective greases may be drawn from the above: 1) the coating of machine parts with protective greases from melts should be carried out by brief immersion of the parts into the grease, which should form a thin and strong protective layer on the surface; 2) the best protection of the metal surface can be provided by smearing the surface with a layer of homogenized grease.

SUMMARY

1. The behavior of plastic disperse systems (thick greases and congealed oils) in pure shearing deformation in uniform and nonuniform stress fields, in contact with smooth and macrorough (riffled) surfaces has been compared.

2. The extent of the wall slip effect, which is found when the systems are in contact with smooth solid surfaces, depends on the deformation rate, the smoothness of the surface relative to which the sample moves, the existance of a microgranular or a monolithic structure in the sample, and on the strength of the structural skeleton.

3. The wall slip effect is most prominent in determination of the yield values of plastic systems, but the yield values obtained with smooth and with riffled surfaces may coincide if the loading rate is increased.

The authors express their gratitude to V.P. Pavlov and M.P. Volaravich for discussion of the work and valuable advice.

LITERATURE CITED

[1] G.V. Vinogradov, Investigations of Rheology of Lubricant Greases, Doctorate Dissertation (Petroleum Inst. Acad. Sci. USSR, 1950).

[2] V.P. Pavlov, Trans. 3rd All-Union Conf. Colloid Chem. (Minsk, 1956), p. 144.

[3] G.V. Vinogradov and K.I. Klimov, Trans. 2nd All-Union Conf. on Friction and Wear in Machines (Acad. Sci. USSR Press, 1949), 3, p. 300.

[4] J.G. Oldroyd et al., Proc. Phys. Soc., 64B, 44 (1951).

[5] V.G. Lebedev and G.V. Vinogradov, Colloid J. 17, 38 (1955) (T.p. 35).*

[6] G.V. Vinogradov and K.I. Klimov, Proc. Acad. Sci. USSR 58, 1677 (1947); J. Tech. Phys. 18, 355 (1948); Trans. Military Acad. Armored Forces 1951, No. 11-12 (88-89), p. 35.

[7] G.V. Vinogradov and K.I. Klimov, Proc. Acad. Sci. USSR 71, 697 (1950).

[8] G.V. Vinogradov and V.V. Sinitsyn, Proc. Acad. Sci. USSR 86, 573 (1952); 91, 323 (1953); Colloid J. 17, 255 (1955) (T.p. 233).*

Received December 15, 1955

Military Academy of the Armored Forces, Moscow

---

* T.p. = C. B. Translation pagination.

X-RAY STRUCTURE INVESTIGATIONS OF PEAT BITUMENS AND WAXES

M.P. Volarovich and K.F. Gusev

"Peat bitumens and waxes" is the usual name given to the substances extracted from peats by alcohol – benzene mixtures. According to Rakovsky [1], high-polymer resins (carboids) pass into solution together with bitumens and waxes.

Titov [2] considers that these bitumens, waxes, and resins are formed in peats as the result of reactions between humus substances in the soluble state with various substances, including sugars, aldehydes, amino acids, etc., which are intermediate products of the decomposition of plant tissues. It was desired to make an x-ray study of the structure of these substances by means of a technique developed earlier [3] and to compare the results with known data for normal hydrocarbons from petroleum. As has already been noted in x-ray studies of peats and other solid fossil fuels [4], peats of a high degree of decomposition contain, in addition to the amorphous phase, also a crystalline phase consisting of bitumens and waxes. It has also been shown that the bitumens present in peats, lignites, and sapropels are structurally identical with normal paraffin hydrocarbons from petroleum, which have been studied with adequate accuracy and detail by numerous authors [5].

X-ray structure analysis was carried out on two samples of normal paraffin hydrocarbons from petroleum (Fig. 2, a and b), two samples of waxes (Fig. 2, c and d) and five samples of bitumens from reed peat with degree of decomposition R = 60% (Fig. 3, a), alder peat with R = 40% (Fig. 3, b), Fuscum peat with R = 15% (Fig. 3, c), a complex peat with R = 15%, and spruce – cotton grass peat with R = 50% (Fig. 3, e). All the x-ray photographs were taken with a copper anticathode without a filter with 8 hours' exposure. A camera with flat film of high resolving power [6] was used, with 80 mm distance between the object and the film.

TABLE

Values of the Interplane Distance d_{110} for the Lattice of Normal Paraffin Hydrocarbons from Petroleum, Peat Bitumens and Waxes

Substance	Ring diameter in mm	tan 2θ	d_{110} A°	Intensity
Normal paraffin hydrocarbon from petroleum, No 1*	66.0	0.3882	4.182	Very strong
Ditto, No. 2	62.0	0.3875	4.186	Very strong
Peat wax No. 1	61.0	0.3815	4.246	Very strong
Peat wax No. 2	62.5	0.3900	4.150	Very strong
Bitumen				
Reed Peat	62.7	0.3902	4.160	Strong
Alder peat	62.2	0.3887	4.175	Strong
Fuscum peat	62.5	0.3900	4.150	Strong
Complex peat	62.0	0.3875	4.186	Strong
Spruce – cotton grass peat	61.0	0.3815	4.246	Strong

---

* Diameter of camera 85 mm.

The Table shows the results of the interpretation of the diagrams. It is seen that the interplane distance of the crystal lattice, denoted as d_{110} (and also other interplane distances) corresponding to the shortest distance between the zigzag carbon molecular chains, differs for different samples, varying between 4.150 and 4.248 A. These differences could be detected with the use of the camera, of high resolving power, referred to above. The lattice parameters were calculated graphically, and also by the rhombic lattice quadratic form method in conjunction with the theory of molecular close packing advanced by Kitaigorodsky [5, pp. 24 and 32].

As is known, normal paraffin hydrocarbons have a rhombic lattice, the A-form being regarded as normal; the unit cell parameters are a = 7.4 A; b = 4.93 A; and c = 2.534 A; the valency angle in the zigzag of the hydrocarbon aliphatic chain is 112°. Fig. 1 shows a simplified scheme for the arrangement of aliphatic hydrocarbon chains of normal paraffin hydrocarbons in the cell, on which the graphical calculation was based. The c axis is regarded as perpendicular to the plane of the drawing and, to simplify the figure, hydrogen atoms are not shown. It is possible to calculate what happens to the parameter a of the elementary cell when the interplane distance d'_{110} changes from

$$d'_{110} = 4.150\text{A to } d_{110} = 4.246\text{A}.$$

The value of d'_{110} can be represented by the formula

$$d'_{110} = b \sin(90 - \alpha),$$

which gives

$$\sin(90 - \alpha) = 0.8417.$$

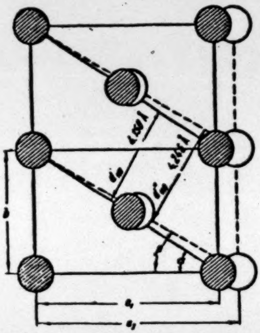

Fig. 1. Aliphatic hycrocarbon chains, in projection along the chain axis. Displacement of chains and change of interplane distance d_{110} (hydrogen atoms not shown).

Then the parameter a_1 of the elementary cell for the least interplane distance d''_{110} becomes $a_1 = b/\tan\alpha = 7.68\text{A}$.

Correspondingly, for the maximum value of the interplane distance $d''_{110} = 4.246$ A we obtain the value of a_2 by an analogous method:

$$d''_{110} = b \cdot \sin(90 - \beta),$$
$$\sin(90 - \beta) = 0.8612,$$
$$a_2 = b/\text{tg}\,\beta = 8.35 \text{ A}.$$

The calculation may also be made with the use of the quadratic form of the rhombic cell for the interplane distance $d'_{110} = 4.150$ A. The quadratic form for d_{hkl}, as is known, has the form:

$$\frac{1}{d^2_{hkl}} = \frac{h^2}{a^2} + \frac{k^2}{b^2} + \frac{l^2}{c^2}.$$

In the present instance:

$$\frac{1}{d^2_{110}} = \frac{1}{a^2} + \frac{1}{b^2}.$$

Calculation gives $a_1 = 7.68$ A. For the interplane distance $d''_{110} = 4.246$ A, we correspondingly have $a_2 = 8.35$ A.

Thus, both calculation methods give the same values of a with great accuracy.

With increasing interplane distance d_{110} in the lattices of normal paraffin hydrocarbons and peat bitumens and waxes, the elementary cell parameters naturally increase also; the structure becomes more loose; the molecular chains are packed less closely. Let us calculate the packing coefficients for the molecular chains for the same two values of the interplane distances: $d'_{110} = 4.150$ A and $d''_{110} = 4.246$ A. Volume increments of the atomic groups can be used for this purpose. For calculation of the volumes of the molecules, it is convenient to calculate the volumes of adjacent atoms and atomic groups. If R is the intermolecular radius of a given atom, and R_i represents the intermolecular radii of atoms joined to it by valency bonds, at a distance d_i from the given atom, then the volume of the increment is calculated as the volume of a sphere less the volumes of the segment cut off from this sphere

$$\Delta V = \frac{4}{3}\pi R^3 - \sum_i \frac{1}{3}\pi h_i^2 (3R - h_i),$$

where the height of the segment h_i is given by the formula

$$h_i = R - \frac{R + d_i^2 - R_i^2}{2d_i}.$$

The volume increment for the CH_2 group calculated by this formula is 16.6 A. The molecular packing density in the crystal will be given by

$$K = \frac{ZV_0}{V},$$

where V_0 is the volume of the molecule (period 4 CH_2); V is the volume of the cell (a · b · c) A^3 and Z is the number of molecules in the cell (number of CH_2 groups).

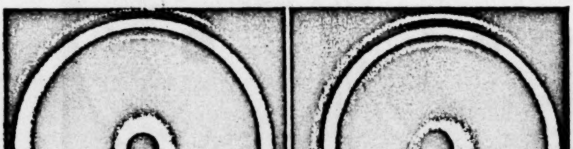

Fig. 2. X-ray diagrams of paraffin hydrocarbons from petroleum (a and b) and peat waxes (c and d).

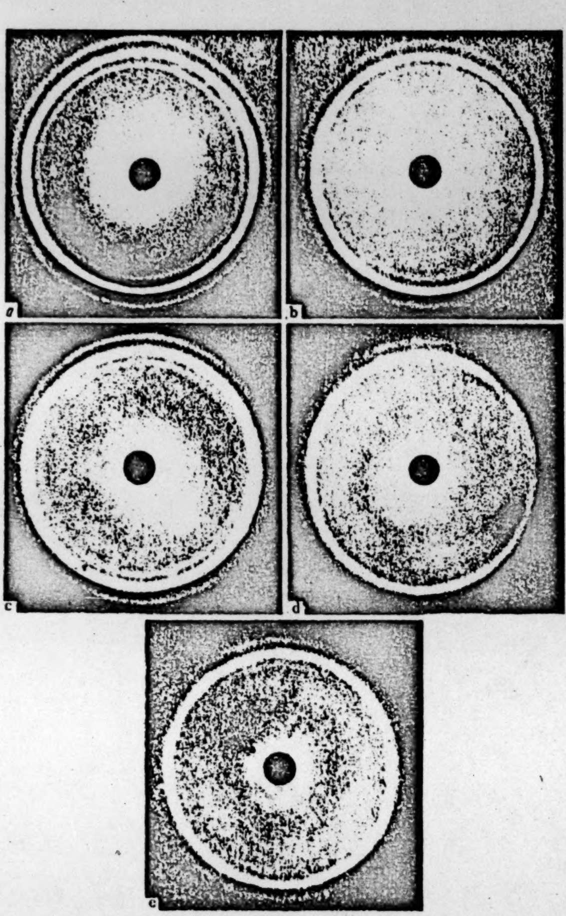

Fig. 3. X-ray diagrams of peat bitumens.

In the first case, for $d'_{110} = 4.150$ A:

$$K = \frac{4 \cdot 16.6}{(7.68 \cdot 4.93 \cdot 2.534)} = 0.691$$

For the second case ($d''_{110} = 4.246$ A) we have :

$$K = \frac{4 \cdot 16.6}{(8.35 \cdot 4.93 \cdot 2.534)} = 0.638.$$

As is known [5, pp. 133 and 221] the packing coefficient of aromatic molecules varies between 0.6 and 0.8. The packing coefficient of normal paraffin hydrocarbons (in the pure state) is 0.72. With a lower value than 0.6 for the packing coefficient, crystal formation is impossible. It seems probable that crystallization of compounds, the molecules of which have large aromatic nuclei with long side chains, is totally impossible.

For our first case, the packing coefficient of 0.691 must be regarded as normal; in the second case the value of 0.638 is low and periodic lattice formation is diffucult. All the peat waxes and bitumens studied, with values of d_{110} intermediate between 4.150 and 4.246 A, should evidently also have packing-coefficient values intermediate between 0.638 and 0.691.

Let us attempt to explain this range of packing coefficients in normal paraffin hydrocarbons. Figs. 3 b, c, d, and e, or the majority of the x-ray diagrams of the peat bitumens studied, show considerable diffuse scattering and an amorphous halo in addition to the interference rings corresponding to normal paraffin hydrocarbons. As was stated earlier, alcohol – benzene mixture dissolves, in addition to waxes, also high-polymer resins (carboids), which evidently have a ring structure with long side chains. Such compounds, as a rule, cannot crystallize or have periodic orientation, and are amorphous substances. The amorphous halo seen in the x-ray diagrams is probably caused by their presence. Contamination of the paraffin hydrocarbons with such impurities leads to an imperfect lattice sturcture and to deviations from the parameters which would be found if the hydrocarbons were pure. Evidence for this is also provided by the small change of the d_{110} interplane distances in the lattices of peat bitumens and waxes, and the associated changes of lattice parameter and packing coefficient.

SUMMARY

1. An x-ray camera of high resolving power has been used to obtain x-ray diagrams of a number of peat bitumens and waxes; these were found to be very similar to the x-ray diagrams of normal paraffins from petroleum.

2. Calculation of the interplane distances d_{110} for the lattice showed that it varies somewhat peat bitumens and waxes, but the value of d_{110} for petroleum paraffins lies within its range.

3. On the basis of a rhombic lattice, the maximum cell parameter $\underline{a}$ was calculated, and was found to lie in the range of 7.68 - 8.35 A; the packing coefficient of the molecular chains varies from 0.691 to 0.638. This variation may be attributed to the presence of cyclic hydrocarbons with long side chains in peat bitumens and waxes.

LITERATURE CITED

[1] V.E. Rakovsky, General Chemical Technology of Peat (State Power Press, 1949).

[2] N.G. Titov, Chemistry and Origin of Solid Fossil Fuels, Features of the Formation of Peats and Brown Coals (Acad. Sci. USSR Press, 1953), p. 356.

[3] M.P. Volarovich and K.F. Gusev, "X-Ray studies of peat," Trans. Moscow Peat Inst. 1954, No. 2; see also N.N. Kulakov, Introduction to the Physics of Peat (State Power Press, 1947).

[4] M.P. Volarovich and K.F. Gusev, "Comparative x-ray investigations of peats, lignites, and sapropels," Trans. Moscow Peat Inst. 1956, No. 5.

[5] A.I. Kitaigorodsky, Organic Crystallochemistry (Acad. Sci. USSR Press, 1955).

[6] K.F. Gusev, Factory Lab. 1953, No. 4.

Received August 8, 1956

The Moscow Peat Institute
Chair of Physics

THE ELECTROCHEMISTRY OF HIGH-POLYMER DISPERSIONS

2. EFFECT OF DILUTION ON THE ELECTROKINETIC POTENTIAL OF SYNTHETIC LATEX GLOBULES

S.S. Voyutsky and R.M. Panich

As has already been reported [1] work has been in progress for a number of years in our laboratory on the influence of some of the most important technological factors on the electrophoresis of synthetic latexes stabilized by soaps. These studies have been accompanied by parallel studies of the influence of the same factors on the aggregative stability of the latexes.

The present communication deals with the effect of dilution on the aggregative stability of synthetic latexes and the zeta-potential of their globules. This problem has been studied very little. There has only been a report that the zeta-potential of natural latex falls sharply on dilution when a certain concentration is reached [2]. The behavior of synthetic latexes in such conditions is not precisely know. Maron and Bowler [3] studied the relationship between the zeta-potential of synthetic latex particles and the solids content of the solution over a very narrow concentration range. Our own investigation, which touched upon the question of variations of particle charge on dilution of synthetic latexes [4] did not take into consideration electrophoretic lag and electrical relaxation, and therefore the values obtained for the zeta-potential cannot be claimed as accurate.

Materials Studied

The two synthetic latexes A and B, investigated previously [1], were used for the electrophoretic studies. In addition to these, latex C was used; this was a product especially made on an experimental scale at one of the synthetic rubber factories. The latex C polymer was obtained by copolymerization of 70 parts divinyl with 30 parts piperylene. The emulsifier was ammonium oleate. In addition to the prepared latex C, we received a sample of the aqueous phase used for its preparation.

Synthetic latexes A and B were, for reasons to be given below, used in a dialyzed state for the electrophoretic investigations. The method used for dialysis was described previously [1].

The analytical characteristics of the latexes used are given in Table 1. The dialyzed latexes are denoted by letters representing the latex type, the letter D to indicate that the latex was dialyzed, and a number to distinguish dialyzates of the same latex.

Method of Determination of the Electrokinetic Potential

The method of microelectrophoresis is not suitable for investigation of the variation of zeta-potential with concentration, as microscopic observation of more or less concentrated colloidal solutions is impossible. Therefore macroelectrophoresis was used in the investigation for determination of the zeta-pontential of synthetic latex particles.

In our previous investigations [4-6], undialyzed latex was subjected to electrophoresis, the auxiliary liquids being buffer mixtures with the same conductivity and pH as those of the latex. An important defect of this method was that the influence of electrophoretic lag and electrical relaxation could not be taken into account in electrophoresis of undialyzed latexes with unknown ionic strengths. Another defect of the method was the difference in the ionic compositions of the latex and the auxiliary liquid, which led to different rates of boundary ascent and descent, and to variation of the potential gradient in the electrophoresis tube in the course of electrophoresis.

TABLE 1

Characteristics of the Latexes Used

Latex	Dry residue content, %	pH	Specific conductivity $\lambda_0 \cdot 10^4$ (at 20° C)	Surface tension in ergs/cm²	Contents, in mg-equiv. per g solid residue		Polymer content*, %	Total content of soap or acid, %	
					soap	organic acid		of the polymer	of the latex
A	24.85	9.0	31.00	44.6	0.436	0	21.6	14.95	3.23
AD1	18.00	5.3	0.42	64.1	0	0.068	17.6	1.96	0.35
AD2	14.00	5.1	0.79	50.6	0	0.156	13.7	4.60	0.68
S	41.50	9.3	52.00	49.4	0.313	0	—	—	—
BD	29.85	8.0	19.00	—	0.151	0.068	—	—	—
C	27.00	8.8	32.00	44.2	0.425	0	23.6	14.5	3.43
Aqueous phase of latex C	3.5	9.5	19.00	30.2	—	—	0	—	3.5

---

* The polymer content was found as the difference between the total solids content and the amount of soap or organic acid.

In the present investigation we used dialyzed latexes diluted with distilled water to a known concentration, and then diluted to double the volume with a buffer solution of known ionic strength. The same buffer solution, correspondingly diluted, was used as the auxiliary liquid in electrophoresis. It may then be assumed that the ionic strengths of the latex and the buffer are practically the same.

The buffer solutions were veronal buffer mixtures with ionic strength 0.2 and pH 7.7 or 8.2.

As was shown previously [1], and as is seen from Table 1, dialysis prior to electrophoresis reduces both the electrolyte and the emulsifier contents of the latex. This is undoubtedly a disadvantage of the method used in this study. However, we regarded it as preferable to have a certain, quite accountable, loss of emulsifier rather than use a method in which the ionic strength of the solution cannot be taken into account.

The electrophoretic mobility was determined by means of the Rabinovich and Fodiman apparatus [7]. The current strength during electrophoresis usually did not exceed 10 ma. The potential was varied according to the conductivity of the solution studied. The potential gradient of the external electric field was calculated from the current strength during electrolysis, the specific conductivity λ_0, and the previously measured cross section of the electrophoretic tube. A microscope with a reading scale was used for observation of the displacements of the latex – liquid boundary. The displacement rate of the boundary was taken as the average of the rates of the ascending and descending boundaries. These rates usually coincided to within 5%. The zeta-potential was calculated from the Henry formula [8]

$$\zeta = \frac{k\pi\eta u}{D}(300)^2,$$

where k is a numerical coefficient, η is the viscosity of the medium, u is the electrophoretic mobility of the latex globules in $\frac{\mu\ /\ \text{second}}{\text{volt/cm}}$, and D is the dielectric constant.

The numerical coefficient in the Henry formula was chosen in accordance with the composition of the buffer solution and with the values of the known criterion κd where κ is the reciprocal of the thickness of the electric double layer, and d is the colloidal particle radius. The viscosity and dielectric constant of the dispersion medium were assumed to be equal to the corresponding values for water.

Effect of Dilution of the Latexes on the Electrokinetic Potentials of their Globules

The first series of experiments to determine the effect of dilution on the electrokinetic potential of latex globules was carried out with latex AD1. In this series of experiments the maximum content of dry residue in the liquid subjected to electrophoresis was 9.0%; the minimum concentration was 0.18%. The numerical coefficient in the Henry equation was chosen with the aid of the diagram given by Overbeek [9] (the ionic strength of the final solution was always 0.1, and veronal buffer contains only symmetrical 1 : 1 electrolytes). The values of the particle radius, necessary for calculation of the criterion κd, were taken from our previous paper [1].

The results of the experiments on the effects of dilution on the zeta-potential of dialyzed AD1 latex are given in Table 2.

TABLE 2

Variation of Zeta-Potential with Dilution of Synthetic Latexes

Latex	Dry residue content, %	pH	Specific conductivity $\lambda_0 \cdot 10^3$ (at 20° C)	$u, \frac{\mu/sec}{V/cm}$ (at 20°C)	ζ in mV
AD1	9.00	7.7	9.5	4.64	72.5
	0.56	7.7	9.5	4.85	76.0
	0.36	7.7	9.5	4.80	75.2
	0.28	7.7	9.5	5.02	78.5
	0.18	7.7	9.5	3.42	53.5
AD2	0.72	8.2	9.8	4.74	76.0
	0.24	8.2	9.8	4.74	76.0
	0.072	8.2	9.8	4.77	76.8
	0.024	8.2	9.8	3.74	60.3
BD1	14.9	8.1	10.2	4.58	71.8
	4.8	8.1	9.8	4.73	73.8
	1.2	8.1	9.8	4.85	76.0
	0.6	8.1	9.6	4.70	73.2
	0.3	8.1	9.3	4.62	72.3

As Table 2 shows, the zeta-potential of the globules first rises somewhat on dilution of AD1 latex, then falls considerably. Since the strong decrease of the zeta-potential was found at low concentrations, it was desired to study in greater detail the effect of dilution on the potential in the region of the lowest concentrations. Latex AD2 was used for this purpose. The method used for the determinations was the same as in the preceding series. All possible steps were taken to improve the visibility of the latex– liquid boundary, which made it possible to use a latex with a content of only 0.024% dry residue. The results of these experiments are also given in Table 2. It is seen that the electrokinetic potential fell at high dilutions in this series of experiments also, but the fall occurred at much lower concentrations. This may be explained by the fact that the stabilizer content was considerably higher in latex AD2 than in latex AD1.

Both the above series of experiments were carried out with dialyzed latex A stabilized by ammonium oleate. It was desired to determine whether the behavior found occurs also in latexes containing stabilizers of a different character. A series of experiments was therefore carried out on the effect of dilution on the zeta-potential of the globules of dialyzed latex B stabilized by ammonium naphthenate. The results are also given in Table 2.

Table 2 shows that a slight increase of electrokinetic potential at not very great dilutions is found for latex BD1 also. No significant fall of zeta-potential was observed on further dilution of BD 1 latex, probably because the maximum dilution in this series was considerably less than the maximum dilution in the experiments with dialyzed latex A.

Effect of Dilution of the Latexes on Desorption of the Stabilizer from the Latex Globule Surfaces

The decrease of zeta-potential of the latex globules which was found to occur at considerable dilutions can be explained most simply by desorption of the stabilizer from the surface of the latex globules. It was therefore considered necessary to determine whether soap passes from the surface of the disperse phase into the solution on dilution of the latex.

The first series of the experiments was performed with latex C and its aqueous phase. The desorption was measured by comparison of changes of surface tension of diluted solutions of the latex and the corresponding stabilizer, with the same initial surface tension.

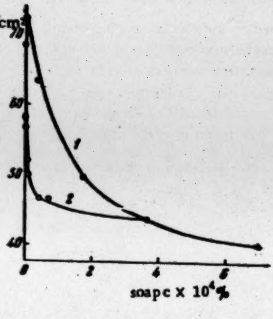

Fig. 1. Surface tension of latex C and its aqueous phase as a function of their soap contents on dilution: 1) Aqueous phase, 2) latex.

The surface tension was determined by the ring detachment method with the aid of a torsion balance. The aqueous phase or latex was diluted to the required concentration by veronal buffer of ionic strength 0.1 and pH 9.3. The resultant solution was poured into a Petri dish and left in an empty desiccator for 12 hours, after which the surface tension was determined. In all cases the first reading only was used. With this procedure the values obtained had quite satisfactory reproducibility.

Fig. 1 shows the variation of the surface tension of the aqueous phase of latex C and of the latex itself with soap content. The curve for the latex was plotted as follows. Since, according to our determinations, the surface tension of the original latex C after twofold dilution by buffer solution was 43.6 ergs/cm², then, according to the curve for the aqueous phase, the free soap content of this latex was $3.55 \cdot 10^{-4}$%. The point corresponding to this concentration was used as the starting point for the latex curve, the soap content of the solution, calculated on the assumption that the system contains free soap only, being taken along the abscissa axis, and the corresponding value of the surface tension along the ordinate axis.

TABLE 3

Ratio of the Amount of Soap Adsorbed on the Globules to the Amount Present in Solution, as a Function of the Dilution of Latex C.

Dilution of original latex	2	10	20	100	200	1000	2000	10000
Dry residue in latex, %	13.5	2.7	1.35	0.27	0.135	0.027	0.0135	0.0027
Total content of soap in latex in % X 10^4	17100	3430	1710	343	171	34,3	17,1	3.43
Free soap content in latex (in the aqueous phase) in % X 10^4	3.55	2.65	2.4	1.7	1.45	0.9	0.8	0.17
Free soap content in latex as % of total soap	0.02	0.08	0.14	0.5	0.85	2.62	4.5	5.0
Content of bound (adsorbed) soap in latex, in % X 10^4	17096	3427.3	1707.6	341.3	169.5	33.4	16.3	3.26
Content of bound (adsorbed) soap in latex as % of total soap	99.98	99.92	99.86	99.5	99.15	97.38	95.5	95.0
Amount of adsorbed soap in g per g polymer	0.145	0.144	0.144	0.144	0.143	0.141	0.139	0.138

A comparison of Curves 1 and 2 in Fig. 1 shows that the curve for the latex lies considerably below the curve for the aqueous phase. The only explanation for this can be that dilution with the buffer solution produces an increase of the total free soap content in the latex by desorption of soap from the latex globule surfaces.

The curves given in Fig. 1 could be used to determine the variations in the ratio of the amount of soap adsorbed on the globules to the amount present in the interglobular liquid in the course of dilution. The results are given in Table 3. In compilation of Table 3 the free soap content was calculated from the value of the surface tension of the latex at a given dilution with the aid of Curve 1 in Fig. 1. The content of bound (adsorbed) soap was found from the difference between the total and free soap. The content of adsorbed soap in grams per 1 g of polymer was calculated by multiplication of the percentage of total soap in the original latex by the percentage of adsorbed soap in the total amount of soap, and division of the result by the percentage of polymer in the latex.

As Table 3 shows, in 13.5% latex practically all the soap is present on the globule surfaces. Desorption occurs on dilution of this latex, but the content of free soap still remains very low relative to the bound soap content. Only on 1000-fold dilution, when the dry content of the latex is 0.027%, does the desorption became appreciable.

An experiment on the desorption of soap from the globules on dilution was also performed with AD2 latex. As this latex does not contain soap, and the stabilizer is oleic acid, the isotherm for the surface tension of the aqueous phase was obtained by the use of a solution prepared by dissolving oleic acid in veronal buffer at pH 8.5 with ionic strength 0.1. The soap formed in such a solution forms the nearest approach to the soap formed when the dialyzed latex and the buffer are mixed. The results of surface-tension determinations on the solution prepared by this method, and AD2 latex, for various soap contents, are given graphically in Fig. 2.

Table 4 shows that in dialyzed latex AD2, with 7.2% solid content, as in latex C, nearly all the soap is adsorbed on the globules. However, in this instance desorption begins to play a significant part at much lower dilutions, which is quite understandable, as the soap content of the dialyzed latexes is low. In the case of latex AD2, the particle size of which had been determined the adsorption as a percentage of the maximum, or the extent to which the globule surfaces were covered with soap molecules, was calculated (Table 4).

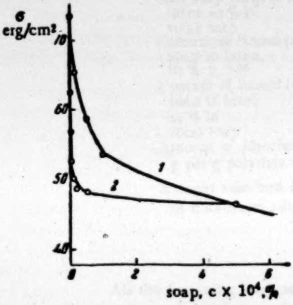

Fig. 2. Surface tension of AD2 latex and solution of oleic acid in buffer solution, in relation to variations of their soap contents on dilution: 1) solution of oleic acid in buffer solution, 2) latex.

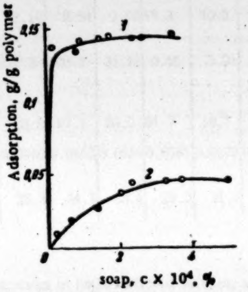

Fig. 3. Isotherms for adsorption of soap in globules: 1) of latex C; 2) of latex AD2.

The data of Tables 3 and 4 were used to plot isotherms for adsorption of soap on the latex globules. These isotherms are given in Fig. 3. As is seen from Fig. 3, the adsorption in the case of latex C is almost treble that of latex AD2. This was to be expected, as the degree of dispersion of latex C, which is undialyzed, is higher than the degree of dispersion of the dialyzed latex AD2.

Effect of Dilution of Latexes on their Aggregative Stability

It was desired to determine whether desorption of stabilizer and decrease of the zeta-potential on dilution of latexes leads to a decrease of their aggregative stability. A measure of the aggregative stability of latexes on dilution, which can be visually estimated easily and accurately, is the so-called dilution threshold. In order to exclude the influence of electrolytes present in the production water, and of changes of pH, veronal buffer with ionic strength 0.02 and pH 8.5 was used for the dilution. Moreover, in order to establish whether the stability of the particles which are not coagulated on dilution of the latexes is the consequence of the presence of still sufficient amounts of soap on the particles, or whether the stability in such cases is due only to the low frequency of collisons between the particles, calcium chloride solution was added to the diluted latexes after they had been kept for 48 hours, and the subsequent changes were observed. The amount of coagulant added was such that the final concentration of calcium chloride was 0.01 N.

No Flocculation or coagulation was found in latex AD2 at any dilutions, no matter how high. No flocculation occurred when the diluted latexes were left to stand for 48 hours. However, addition of calcium chloride to the strongly diluted latexes induced immediate coagulation. Similar results were obtained with the other latexes used in this investigation.

TABLE 4

Ratio of the Amount of Soap Adsorbed on the Globules to the Amount Present in Solution, as a Function of the Dilution of Latex AD2

Dilution of original latex	2	20	60	200	600	2000	6000	20000
Dry residue in latex, %	7.2	0.72	0.24	0.072	0.024	0.0072	0.0024	0.0007
Total content of soap in latex in % × 10^4	3360	336	112	33.6	11.2	3.36	1.12	0.336
Free soap content in latex (in the aqueous phase) in % × 10^4	5	3.7	3.3	2.35	2.05	1.35	0.65	0.25
Free soap content in latex as % of total soap	0.15	1.10	2.94	7.00	18.3	40.3	58.0	74.5
Content of bound (adsorbed) soap in latex, in % × 10^4	3355	332.3	108.7	31.25	9.15	2.01	0.47	0.086
Content of bound (adsorbed) soap in latex as % of total soap	99.85	98.9	97.1	93.0	81.7	59.7	42.0	25.5
Amount of adsorbed soap in g per g polymer	0.0466	0.0460	0.0452	0.0434	0.0381	0.0279	0.0196	0.0119
Amount adsorbed as % of maximum adsorption	35.8	35.3	34.7	33.4	29.3	21.4	15.1	9.1

All the foregoing leads to the conclusion that, even in highly diluted latexes, adsorbed stabilizer molecules are present on the globule surfaces, and that the stability of the diluted latexes is determined not by the kinetic factor, but by adequate protection of the particles. It also follows from these experiments that the dilution threshold as determined in production is not, essentially, a measure of the stability of latexes toward dilution but a measure of the stability of latexes to the action of the salts causing hardness in production water, or of stability to pH changes.

DISCUSSION OF RESULTS

The experiments showed (Table 2) that as concentrated latexes are diluted by buffer solution, the zeta-potential of the globules first increases relatively slightly, and then, at concentrations of the order of 0.02-0.2% solids, falls sharply.

The increase of zeta-potential at the start of the dilution cannot be attributed to a fall in the ionic strength of the interglobular liquid, as the latexes were dialyzed, and were diluted by buffer solution. It is possible that this increase is caused by a decrease of the ionic strength of the whole system owing to a decrease of the number of individual globules, which must be regarded as multivalent ions with a strong influence on the ionic strength of the solution, per unit volume. This assumption seems to us to be quite legitimate. In fact, since even Duclaux had shown that colloidal particles make a contribution to the electrical conductivity of the system, there is no reason for assuming that these particles are to be ignored in calculations of ionic strengths.

The fall of electrokinetic potential on dilution of the latexes to a concentration of 0.02-0.2% solids and lower must undoubtedly be attributed to the desorption of soap from the globules which occurs at these concentrations.

Direct experiments showed that when latexes are diluted right down to 0.02-0.2% solids content, the desorption of stabilizer from the latex globules is negligible. The adsorptivity of the stabilizer is so great that at concentrations of 0.02-0.2% and over, nearly all the soap is present on the globule surfaces. Only at high dilutions does the degree of coating of the globule surface by soap begin to decrease rapidly, and this is also reflected in the zeta-potential of the particles.

Even when the dilution is considerable, the latexes remain fairly stable, as their globules still bear a considerable charge. The stabilizing role of the charge is confirmed by the fact that the system loses its stability and coagulates on addition of calcium chloride.

As has already been noted, earlier we carried out electrophoretic investigations on undialyzed latexes which had not been diluted by buffer solutions, and in which the ionic strength was not taken into consideration [4-6]. In these cases the zeta-potential first rose on dilution, reached a maximum at 14% solids content, decreased, and then began to rise again after a dry solids content less than 1% had been reached. This course of the electrokinetic potential – solids content curve was at the time explained on the grounds that in the concentration range from 14 to 1% desorption of the stabilizer takes place, with significant effect on the electrokinetic potential. However, in the light of our new data on desorption of the stabilizer from the latex globules, this explanation is improbable, as appreciable desorption of soap from the globule surfaces begins at considerably greater dilutions. It is likely that the observed decrease of zeta-potential in the latex concentration range from 14 to 1% is an apparent effect caused by the fact that instead of the Henry equation with a variable coefficient, we used the Smoluchowski equation in the earlier investigations.

All the above once again emphasizes the importance of the method in electrophoretic investigations. It is quite obvious that in determinations of the zeta-potentials of latex globules the latexes must be dialyzed and diluted by buffer solutions, so that the ionic strength of the interglobular liquid can be taken into account.

The foregoing experiments showed that both in undialyzed and in dialyzed latexes nearly all the soap (99.8% and over) is present in the adsorbed state and, as was shown earlier [1], the soap layer on the disperse phase particles is unsaturated. For example, even in the original undialyzed latex A, the globule surfaces were only 68.2% covered with soap.

When the degree of coating of the globule surfaces had been reduced to about 35% by dialysis, the latexes still remain fairly stable – at least, no obvious coagulation occurs. The electrokinetic potential of the globules coated to this extent in a latex diluted by buffer solution, with pH 8.2 and ionic strength 0.2, is 76 mv. It is an interesting fact that latex dialyzed to this degree, despite its lower soap content, proved more stable to the action of electrolytes than the original undialyzed latex, as was shown by determinations of the coagulation threshold of these latexes with calcium chloride [1]. The greater stability of AD2 latex is undoubtedly due to the fact that the zeta-potential increases during dialysis because of the removal of electrolytes from the interglobular liquid.

When the degree of coating of the globule surfaces is decreased to 20% by dialysis, which corresponds to latex AD1 [1], the potential decreases somewhat, reaching ~ 70 mv and the stability of the latex diminishes.

It is evident that in a dialyzed latex which is not diluted by buffer solution, with pH of about 5.0, the electrokinetic potential of the globules is even lower.

In consequence of this, the aggregative stability is diminished. This is confirmed, for example, by the behavior of latex AD1, which was partly coagulated after being left to stand for a month.

SUMMARY

1. It is shown that when dialyzed synthetic latexes are diluted by buffer solutions, the zeta-potential of the globules first increases somewhat, and then, at a solids content of the order of 0.02-0.2%, falls sharply.

2. The initial increase of the electrokinetic potential on dilution of latexes by buffer solutions of constant ionic strength may possibly be attributed to a decrease of the ionic strength of the system because of the decrease

of the number of disperse-phase particles, which must be regarded as multivalent ions, per unit volume. The sharp decrease of the electrokinetic potential when latexes are diluted to a 0.02% solids content must be attributed to desorption of the stabilizer from the globule surfaces.

3. Our method, based on comparison of variations in the surface tensions of the original latexes and stabilizer solution when diluted with buffer solution, has been used to show that both in the original and in dialyzed latexes of sufficiently high concentrations nearly all the soap (over 99%) is present in the adsorbed state, the soap layer on the disperse phase particles being unsaturated.

4. The same method was also used to show that at high dilutions, corresponding to 0.02-0.2% solids in the latex, appreciable transition of soap from the globule srufaces into the interglobular liquid occurs. This confirms the view that the decrease of electrokinetic potential at high dilutions is caused by desorption of the stabilizer from the surface of the disperse phase.

5. Direct observations of the coagulation of latexes with and without additions of coagulant electrolytes showed that the aggregative stability of even very dilute latexes is determined by the presence of soap molecules on the globule surfaces.

6. It is shown that erroneous results may be obtained if the zeta-potential of the globules is determined in undialyzed latexes without dilution by buffer solution, and hence without consideration of the ionic strength of the system.

LITERATURE CITED

[1] R.M. Panich and S.S. Voyutsky, Colloid J. 18, 326 (1956) (T.p. 317). *

[2] W.W. Bowler, Ind. Eng. Chem. 45, 1790 (1953).

[3] T.H. Maron and W.W. Bowler, J. Am. Chem. Soc. 70, 3893 (1948).

[4] S.S. Voyutsky, R.M. Panich, and K.A. Kalyanova, Proc. Acad. Sci. USSR 70, 1013 (1950).

[5] S.S. Voyutsky, R.M. Panich, and K.A. Kalyanova, Collected Papers of the Central Research Institute for Leather Substitutes on the Theory and Practice of Adhesion (State Light Ind. Press, 1952).

[6] S.S. Voyutsky, R.M. Panich, and K.A. Kalyanova, Trans. Lomonosov Inst. Fine Chemical Technology (State Chem. Press, 1953), No. 4.

[7] A.I. Rabinovich and E.F. Fodiman, J. Phys. Chem. 2, 336 (1931); 3, 8 (1932).

[8] D.C. Henry, Proc. Roy Soc. A133, 106 (1931).

[9] J.T.G. Overbeek, Advances in Colloid Science, 3, 97 (1950).

Received January 4, 1956

The M.V. Lomonosov Institute of
Fine Chemical Technology
Moscow

---

* T. p. = C. B. Translation pagination.

NATURE OF THE SOLVATION OF CELLULOSE ETHERS IN SOLVENT MIXTURES

S.A. Glückmann and L.A. Root

As is known, the solubility of polymeric carbohydrates in polar solvents and in mixtures of polar and non-polar solvents is determined to a considerable extent by the energy factor associated with solvation of the polar atomic groups in the polymer. Although, in the limit, there is a stoichiometric relation between the number of polar groups of the polymer and the number of solvent molecules bound by it, as has been demonstrated, for example, by Kargin and Papkov [1] in the case of nitrocellulose and acetone, the nature of solution is essentially monolayer adsorption. This has been demonstrated by Glückmann [2] for cellulose ethers and pectin on the basis of dilatometric and viscosimetric data, and also of data on the effects of temperature on coagulation thresholds with variations of solvent composition. It was shown that the maximum viscosity decrease on addition of alcohol to a solution of benzylcellulose in benzene is reached when the alcohol content in the solvent mixture is more than ten times the molecular alcohol content required to screen all the hydroxyl groups in benzylcellulose; the volume effect (contraction) curve has a form typical for monolayer adsorption. With a considerable excess of alcohol, or on addition of an inert liquid such as hexane to the solvent mixture, the volume effect curve acquires the nature of a desorption curve. In this concentration region of alcohol or hexane, which are diluents for benzene, partial desorption of benzene molecules adsorbed by the benzoxyl groups of benzylcellulose evidently takes place. This causes coagulation. The coagulation thresholds are shifted with change of temperature in the direction a higher or lower diluent concentration as the result of a change in the ratio of the energy of bonding between the polymer molecules to the energy of bonding between the polymer and the solvent. This linear variation of the coagulation thresholds with temperature was not explained at that time. However, a similar relationship, close to linear, between coagulation thresholds and temperature applies to a number of polymer – solvent – diluent systems. In particular, it was noted to apply to the system ethylcellulose – toluene – methanol.

The ethylcellulose chosen for the investigation (degree of substitution 2.4, $[\eta] = 1.6$) is soluble in toluene above room temperature, but the solution coagulates when the temperature is lowered to a certain critical point. Addition of small amounts of methanol displaces the coagulation threshold.

The coagulation point was determined from the curves for the variation of the relative viscosity of dilute (1%) ethylcellulose solutions with temperature (Fig. 1), and from the elastic limit in concentrated (19%) solutions (Fig. 2). The viscosity of dilute solutions and of the corresponding solvent mixtures (toluene and methnol) was measured with the aid of the Ostwald viscosimeter in the temperature range from − 50 to + 30°, and the elastic limits (and other viscoelastic properties) of 19% solutions, by means of an instrument of the Shvedov type by the method developed by Rebinder and Kolbanovskaya [3] at temperatures from − 5 to +20°. Curves for the deformation kinetics and for variations of the deformation rate with shearing stress in a solution containing 1% methanol are given in Figs. 2 and 3. Similar curves were obtained for other solutions, and it was therfore possible to plot a curve for the variation of the depression of the gelation temperature with methanol concentration (Fig. 4). Fig. 4 gives data for 1% ethylcellulose solution.

As is seen in Fig. 4, in the methanol concentration region between 0 and 2% the relationship between the depression of the coagulation (or gelation) temperature and the methanol content is linear in both cases, the depression ΔT per one percent methanol by volume being 13° for 1% solution, and 7.5% for 19% solution.

On the assumption that coagulation or the appearance of an elastic limit represents a state in the system when a certain definite number of stable bonds has been formed between the molecules, we can use, to characterize this state, the Zhurkov equation [4]

$$u = 2nRT^2/(\Delta TN),$$

where u is the bond energy, ΔT is the temperature depression; N is the number of active groups in the polymer; n is the number of solvent molecules absorbed.

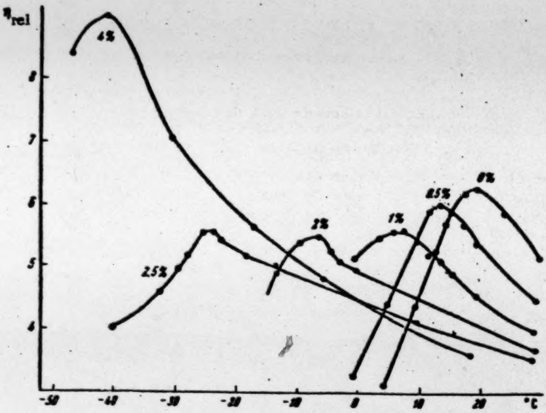

Fig. 1. Variation of the relative viscosity of 1% ethylcellulose solutions with temperature, in mixtures of toluene and methanol (the numbers on the curves represent the methanol concentrations).

Zhurkov based his derivation of the equation on the assumption that the softening point of a polymer corresponds to a definite number of cross-links, which diminishes in accordance with the mass action law when some of the polar groups of the polymer are screened by molecules of the absorbed solvent. We used another criterion to characterize equal structural states of the system; otherwise the reasoning is analogous.

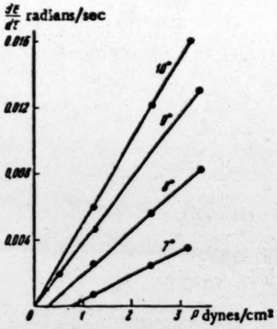

Fig. 2. Variation of the steady flow rate with shearing stress for 19% ethylcellulose solution in toluene – methanol mixture (1% methanol).

However, Zhurkov was able to determine the value of n directly, as in his experiments, at low values of n/N, all the solvent molecules absorbed from the vapor were bound by the polymer. In our case, as it is presumed that solvation is adsorptional in character, there are no grounds for supposing that all the methanol introduced into the toluene solution of ethylcellulose is energetically bonded with it.

Nevertheless, we found a linear relationship between ΔT and the gross methanol concentration in the toluene (c^*). In the case of a 19% solution this may be explained by the almost complete sorption of the methanol by the large quantity of ethylcellulose. If it is assumed that methanol is adsorbed both by the ethoxyl and the hydroxyl groups of ethylcellulose, then complete solvation of ethylcellulose in 19% solutions would require 10 ml of methanol per 100 ml of solution, whereas a linear relationship for the temperature depression was found in the range of 0 to 2.5% methanol by volume. Therefore it may be assumed that the equilibrium concentrations of methanol in the solution were very low, and the amounts of methanol adsorbed by ethylcellulose are proportional to the equilibrium concentrations (c), which correspond to the initial region of the monolayer adsorption curve. The Zhurkov equation was used for approximate calculation of the average bond energy (for ethoxyl and hydroxl groups). Taking $n_1 \sim c^* = 0.79/32$ g methanol per 100 ml of solvent and $\Delta T = 7.5°$ (also for 1 per cent of methanol by volume), we have $u = 4300$ cal /g-equiv , which is higher than the true value; we used $n_1 = c^*$ instead of $(c^* - c)$.

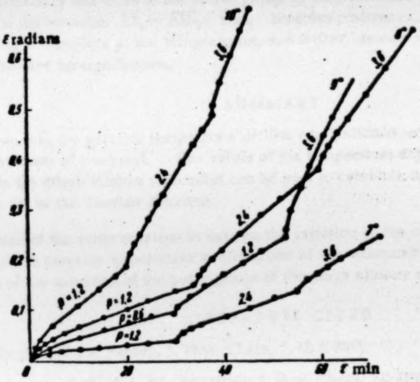

Fig 3. Deformation kinetics of 19% ethylcellulose solution in a toluene – methanol mixture (1% methanol).

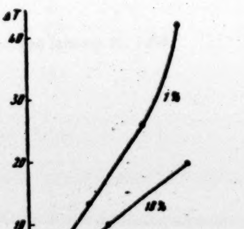

Fig. 4. Variation of the depression of gelation temperature of 19% solutions, and of the depression of the coagulation temperature of 1% solutions of ethylcellulose with the volume concentration of methanol.

In the case of 1% solutions of ethylcellulose there can be no question of nearly complete sorption of methanol from the solutions used, as their methanol contents were equal to or greater than the quantity necessary for saturation of all the active groups in ethylcellulose. If all the methanol was sorbed by the ethylcellulose, the temperature depression would reach the maximum value on the first additions of the alcohol (0.25%). Nevertheless, these solutions also showed a linear relationship between ΔT and the gross alcohol concentration. This may be explained by the fact that the equilibrium concentrations are close to the gross values, that is, that the quantities of methanol n_2 sorbed by the ethylcellulose are relatively small; they should be proportional to the equilibrium (and approximately proportional to the gross) concentrations of methanol, as in this case we also have the initial branch of the monolayer adsorption curve.

On this basis we can calculate n_2 approximately from the Zhurkov equation, taking $u \sim 4300$ cal./g-equiv. and $\Delta T = 13°$ (from the experimental data). The calculation gives $n_2 = 0.0018$ mole/ml, which is 13.7 times less than the quantity of methanol (1 ml) added to 100 ml of solution and 14 times less than the maximum quantity which can be adsorbed by 1 g (0.013 g-equiv.) of ethylcellulose.

---

* As in original-Publisher's note.

Therefore the calculated results show that the assumptions on which the calculation is based, namely that the solvation of ethylcellulose by methanol is adsorptive in character, and that in the system in question (1% ethylcellulose solution) considerable adsorption which corresponds to the initial region of the Langmuir curve takes place, are justified.

The upward bend of the $\Delta T = f(c^*)$ curve at methanol concentrations above 2% may be explained by the fact that when the value $n_2 = 0.0047$ is reached in a solution containing 2% alcohol (or at $n_2/n_\infty = 0.3$), that is, when approximately one-third of the active groups in ethylcellulose have been screened by methanol, the value of $\overline{\Delta H_1}$ in the equation $\overline{\Delta F_1} = \overline{\Delta H_1} - \overline{T\Delta S_1}$ becomes positive or, if it remains negative, is close to zero. The solubility is complete at low temperatures, and further increase of solvation with increasing alcohol concentration should have no significance.

SUMMARY

1. It is shown that the gelation temperature of 19% ethylcellulose solution in toluene is changed by addition of small amounts of methanol. The values of the temperature depression produced by screening of the active groups in the ethylcellulose molecules can be used to calculate the bond energy in cross-links of the gel network by the use of the Zhurkov equation.

2. Application of the same equation to data on the variation of the coagulation temperature of 1% ethylcellulose solutions provides quantitative confirmation of the adsorptive (in the sense of monolayer adsorption) nature of the solvation of the polar groups of the ethylcellulose molecule by methanol.

LITERATURE CITED

[1] V.A. Kargin and I.S. Papkov, J. Phys. Chem. 7, 48 (1936).

[2] S. Glückmann, Kolloid-Z.. 76, 84 (1936); J. Phys. Chem. 11, 492 (1938).

[3] A.S. Kolbanovskaya and P.A. Rebinder, Colloid J. 12, 194 (1950).

[4] S.N. Zhurkov, Trans. 1st and 2nd Conf. on High-Molecular Compounds (Acad. Sci. USSR Press, Moscow –Leningrad, 1945), p. 65.

Received January 30, 1956

The N.G. Chernyshevsky State University
Saratov

INFLUENCE OF INTERMOLECULAR FORCES AND TEMPERATURE ON THE RELATIVE ELONGATION OF VULCANIZATES AT BREAK

V.E. Gul' and I.I. Farberova

Practically important characteristics of vulcanizate strength are the breaking stress, the relative elongation at break, and the time from the start of deformation to the moment of break under the action of a given deforming stress. All these characteristics, in turn, depend on the deformation conditions: temperature, rate and kind of deformation, and also a number of other factors, such as the degree of swelling in vapors and liquids.

The influence of these factors on the tensile strength of vulcanizates has been investigated by a number of workers [1-5]. The influence of a number of factors on the duration of the process from the start of deformation to break has been studied in no less detail [6]. However, such an important practical characteristic of the strength and deformation properties of the material as the relative elongation at break, which will be denoted by ϵ_r, has been studied very inadequately.

The purpose of the present investigation was to determine the relationship between the relative elongation and the intermolecular action and temperature. Moreover, one of us [7] has put forward views on the mechanism of the rupture of vulcanizates, and has derived an analytical relationship between the tensile strength (p), the specific cohesive energy, temperature, deformation rate (v_1) and other factors which influence the tensile strength. For determination of absolute values of tensile strength, the value of p' obtained by this method must be corrected to allow for the fact that the destruction of the material begins only in certain regions [4, 6, 8], to which the relationships between p', T, v, and U are applicable.

The basis of these views is that rupture of vulcanizates proceeds by growth of cracks and tears which we combine under the common name of microcrevices. Growth of the microcrevices occurs at first by elementary ruptures of the chain molecules. The action of chemical affinity bonds and intermolecular forces are overcome in the process. Slow growth of the crevices occurs during the initial deformation stages, until the stress per unit active section reaches a value at which the total resistance of the remaining bonds of both kinds is overcome practically instantaneously. The relationship between the stress which resists the growth of the crevices and the deformation conditions is represented by the equation

$$\ln (p' - p'_x) = \ln v_1^n Ak\tau_0 + \frac{U_0 - ap'}{RT}, \tag{1}$$

where v_1 is the rate of deformation of the specimen; p' is the resistance of the material to rupture, per unit act of rupture; p'_x is the same value in the condition that there is no opposing force of intermolecular action; A and n are constants which determine the ratio of v_1 to the rate of crevice growth v; k is a constant determined by the type of deformation and the properties of the material; τ_0 – is the vibration period of a kinetic unit about a mean position; U_0 is the cohesive energy per unit volume a, in which bond rupture takes place; R is the universal gas constant; T is the absolute temperature.

In accordance with these views, a similar relationship will exist also between $(p - p_x)$, v_1, T, etc., where p is the tensile strength of the specimen as a whole, while p_x is the same value determined in absence of van der Waals forces [3].

In the present paper an attempt is made to use the relationship which has been derived for obtaining a relationship between the relative elongation at break ϵ_r, the specific cohesive energy, temperature, and other factors, and also to compare the results with experimental data.

The materials chosen for the study were nitrile rubber vulcanizates with different contents of polar nitrile groups in the polymer molecular chain, but with approximately the same degree of cross-linking, such as were used in earlier investigations [3]. The specific cohesive energies for SKN-18, SKN-26 and SKN-40 were found to be, respectively: $(8.8)^2$; $(9.0)^2$ and $(9.5)^2$ cal./cc. Since Equation (1), which refers to the specimen as a whole, contains p_x (the tensile strength of the vulcanizate determined by the equilibrium deformation method) the values of p_x for the three vulcanizates were determined.

As in the previous investigation [3], the values of p_x for SKN-18, SKN-26 and SKN-40 were found to be equal to each other. The experimental error relative to the strength values (at a finite rate of deformation) was approximately 1%.

To determine the relationship $\epsilon_r = f(T)$ it was necessary to determine the isotherms for deformation of the vulcanizates at various temperatures. Fig. 1 shows the isotherms at 28° for deformation of the three vulcanizates.

An examination of these results shows that the greatest tensile strength at a finite deformation rate is found in SKN-40 vulcanizate, and the least, in SKN-18. The difference between the values found is ~ 60% of the greatest value. In determinations of the deformation isotherms of the vulcanizates at 40° it was found that, as at 26°, the tensile strength fell with decreasing nitrile-group content in the polymer chains. However, the difference between the absolute maximum and minimum values is less. The difference between the highest and lowest values is 46%.

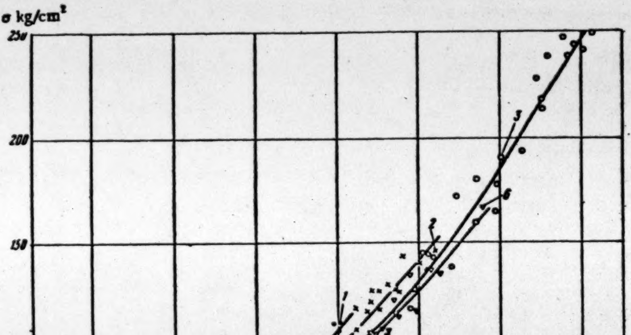

Fig. 1. Isotherms for deformation at a finite extension rate. At t = 26°: (1) SKN-18, 2) SKN-26, 3) SKN-40; at t = 40°: 4) SKN -18, 5) SKN-26, 6) SKN-40.

A similar variation is found when the temperature is further increased to 60°. The absolute difference between the highest and lowest values is less, being ~ 2.5% of the highest value. The deformation isotherms for the vulcanizates studied are given in Fig. 2. This also shows the results of tests on the vulcanizates at 75°. The absolute difference between the maximum and minimum tensile strengths is still less. The results show that the differences in the tensile strengths of the vulcanizates studied decrease with increase of temperature. The explanation is largely that as the temperature rises, the frequency of intermolecular bond ruptures increases as the result of thermal energy fluctuations; the influence of intermolecular forces on tensile strength and deformation properties decreases. All the foregoing considerations concerning the influence of intermolecular action on tensile strength apply also to ϵ_r, as is seen by an examination of the experimental data in Figs. 1 and 2.

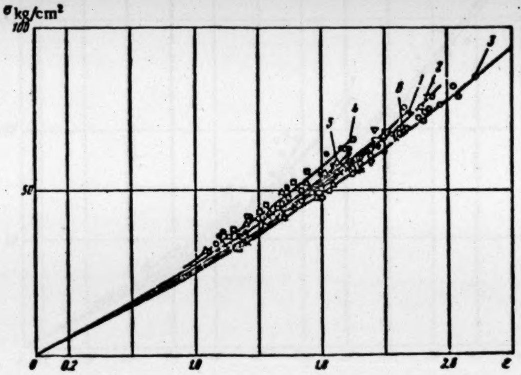

Fig. 2. Isotherms for deformation at a finite extension rate. At t = 60°: 1) SKN-18, 2) SKN-26, 3) SKN-40; at t = 75°: 4) SKN-18; 5) SKN-26; 6) SKN-40.

At 26°, the highest value of ϵ_r is found for SKN-40 vulcanizate, and the lowest. for SKN-18. The difference between the highest and lowest values is ϵ_r ~50 %. The same relative positions of ϵ_r are also found at 40, 60, and 75%, while the differences between the highest and lowest values are ~ 40, 25, and 10% respectively.

Every one of the vulcanizates tested showed a decrease of ϵ_r with increase of temperature. In Fig. 3, isotherms for the deformation of SKN-18 and SKN-40 vulcanizates are compared. Since the theory of vulcanizate rupture with is advanced here is based on the application of Equation (1) to macroscopic aspects of deformation and rupture of the specimens, it was necessary to investigate experimentally the form of relationship which exists between $(p - p_x)$ and T. Fig. 4 shows $(p - p_x)$ as a function of the reciprocal of the temperature.

According to Equation (1), this relationship should be linear. The data in Fig. 4 confirm that there is a linear relationship between $(p - p_x)$ and 1/T.

The next stage in the experimental verification of the theory was the determination of the relationship between p_x and ϵ_r so that the value of ϵ_r could be introduced into Equation (1). The relationship so found could then be verified experimentally. Experimental data derived from the deformation isotherms yielded the relationship:

$$\frac{1}{\sigma} = -\frac{1}{b} + \frac{c}{b}\frac{1}{\epsilon} \qquad (2).$$

where σ is a deforming stress the value of which is close to the breaking stress; ε is the relative deformation close to the value at break; b and c are empirical constants.

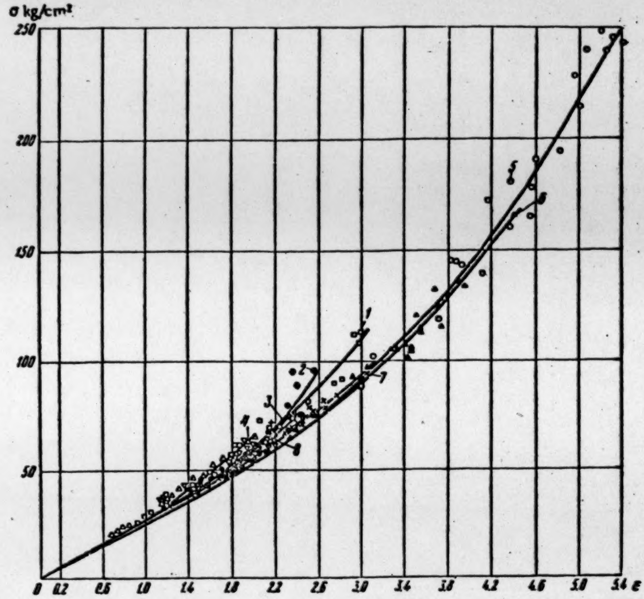

Fig. 3. Isotherms for deformation at a finite extension rate for SKN-18 vulcanizate: 1) 26 ; 2) 40°; 3) 60°; 4) 75°; SKN-40 5) 26°; 6) 40°; 7) 60°; 8) 75°.

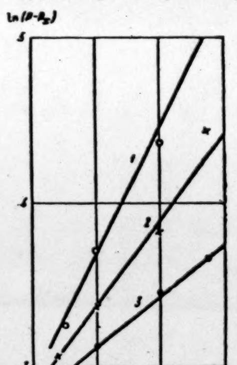

Fig. 4. Variation of $(p-p_x)$ with 1/T; p is the tensile strength; p_x is the tensile strength found by equilibrium deformation method; T is the absolute temperature; 1) SKN-40, 2) SKN-26, 3) SKN-18.

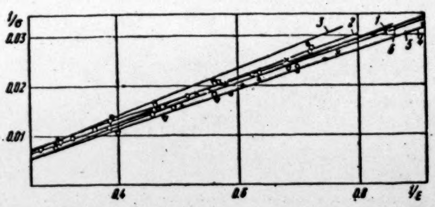

Fig. 5. Variation of $\frac{1}{\epsilon}$ with $\frac{1}{\sigma}$ (σ is the deforming stress and ε is the relative elongation): at 26°: 1) SKN-18; 2) SKN-26; 3) SKN-40; at 75°: 4) SKN-18: 5) SKN-26; 6) SKN-40.

Figs. 5 and 6 represent the results of a verification of Equation (2). The method of least squares was used to determine the values of the constants b and c, shown in the Table.

Substitution of the value of p expressed terms of ϵ_r in Equation (1) leads to the following equation:

$$\ln\left[\frac{\epsilon_r(-b-p_x)+p_x c}{\epsilon_r - c}\right] = \ln k_1 + \frac{U}{R}\frac{1}{T}, \tag{3}$$

where k_1 is a constant in the given experimental conditions. Equation (3) may be verified experimentally. The table shows all the experimental data necessary for verification of Equation (3).

TABLE

Conditions and Results of Experiments on Determination of the Relative Elongation at Various Temperatures

	SKN-18				SKN-26				SKN-40			
P_x	26.62				22.90				24.05			
U/R	1561				2376				3563			
$\ln k$	−1.547				−3.709				−6.962			
	Temperature, °C											
	26	40	60	75	26	40	60	75	26	40	60	75
$\frac{1}{T}\cdot 10^{-3}$	3.34	3.19	3.09	2.88	3.34	3.19	3.09	2.88	3.34	3.19	3.09	2.88
$-b$	182.4	189.7	394.4	197.8	211.0	285.0	416.0	225.7	221.5	267.7	450.3	387.1
$-c$	8.083	8.30	15.38	8.12	9.40	12.1	16.59	9.67	10.25	12.05	18.07	14.80

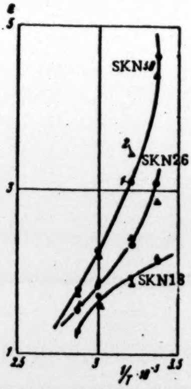

Fig. 6. Relative elongation at break as a function of temperature for SKN-18, SKN-26, and SKN-40 vulcanizates: 1) theoretical values; 2) experimental values.

SUMMARY

1. The previously advanced concepts on the relationship between the tensile strength p and the temperature and deformation rate have been used to derive an equation for the relationship between the relative elongation at break ϵ_r and the temperature.

2. This equation has been verified for butadiene-acrylonitrile rubber vulcanizates with different contents of nitrile groups in the polymer molecules.

In conclusion, the authors regard it as their pleasant duty to express their appreciation to Prof. B.A. Dogadkin for his participation in discussions of this work.

LITERATURE CITED

[1] B.A. Dogadkin and D.M. Sandomirsky, colloid J. 13, 267 (1951).

[2] V.G. Epshtein, Dissertation (Lomonosov Inst. Fine Chem. Technol., 1950).

[3] V.E. Gul, N. Ya. Sidneva, and B.A. Dogadkin, Colloid J. 13, No. 2, 422 (1951).

[4] G.M. Bartenev, Proc. Acad. Sci. USSR 84, 487 (1952); Progr. Chem. 24, 7 (1955); G.M. Bartenev and Belostotskaya, J. Tech. Phys. 24, No. 10, 1773 (1954).

[5] H. Mark, Ind. Eng. Chem. 34, 11, 1343 (1942).

[6] S.N. Zhurkov and E.S. Tomashevsky, J. Tech. Phys. 25, 70 (1955); S.N. Zhurkov and B.N. Narzulaev, J. Tech. Phys. 23, No. 10, 1677 (1953); G.M. Bartenev, Progr. Chem. 24, No. 7, 815 (1955).

[7] V.E. Gul, Proc. Acad. Sci. USSR 96, No. 5, 953 (1954).

[8] A.F. Ioffe, N.V. Kirpicheva, and M.A. Levitskaya, J. Russ. Phys.-Chem. Soc. 56, 489 (1924); G.A. Muller, J. Tech. Phys. 22, No. 3, 461 (1952); T. Kontorova and Ya. I. Frenkel, J. Tech. Phys. 11, 137 (1941); A. P. Aleksandrov and S. N. Zhukov, The Brittle Fracture Effect (State Tech. Lit. Press, Moscow–Leningrad, 1933); A. P. Aleksandrov, Bull. Acad. Sci. USSR 1944, No 7/8, 51.

Received March 27, 1956

The M. V. Lomonosov Institute of
Fine Chemical Technology
Moscow

TYPES OF STRUCTURE FORMATION IN CLAY SUSPENSIONS

M.M. Gurvich

The interesting properties and great practical importance of clay suspensions have attracted the attention of numerous research workers [1]. Among the studies of these systems special attention must be paid to the work of Rebinder and Serb-Serbina [2] on the structural-mechanical properties of bentonite suspensions. They found three types of shearing stress – deformation curves for these systems, which they attributed to three types of structure formation. At the same time, our investigations showed that there are different types of clay suspensions which differ in their external characteristics and utilization properties. The present investigation was performed on clay systems which are used or may be used as drilling muds for oil-well drilling. The work had the following aims:

1. To establish whether the differences in the structural-mechanical properties of clay suspensions are the consequences of different processes of thixotropic structure formation, or whether they are caused by formation of other types of structure, qualitatively different from thixotropic.

2. To determine which structural forms of the systems studied are the most favorable for practical purposes and to find methods for obtaining them.

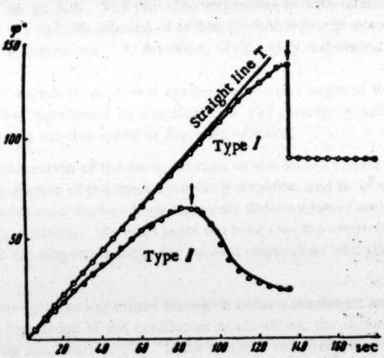

Fig. 1. Types of structural curves for clay suspensions (the arrows indicate the points at which the motor was switched off).

The structural-mechanical properties of clay suspensions were studied by means of the SNS instrument, which is a rotational viscosimeter of the MacMichael type, in which the outer cylinder rotates at a constant low rate of 0.003 revolution per second. The instrument is designed for determination of the static shearing stress of clay suspensions, but, by a suitable technique, it may be used to determine a number of other important characteristics of clay suspensions.

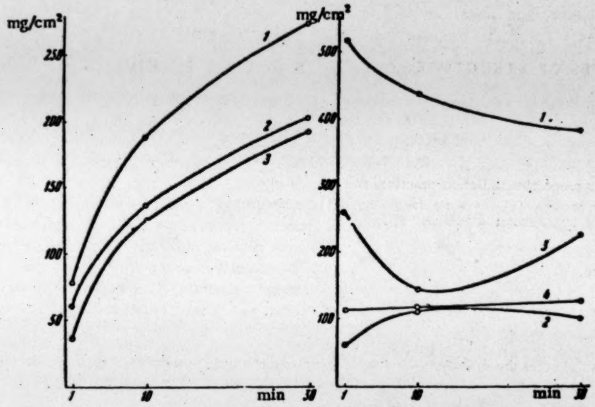

Fig. 2. Examples of curves for variations of structural strength with time in type II clay suspensions (on the left): 1) clay – hematite suspension in 2% solution of sodium humates in sea water, sp. gr. 2.2; 2) the same, sp. gr. 2.0; 3) the same, prepared by a different method; type I (on the right): 1) clay – hematite suspension in sea water, sp. gr. 2.0; 2) Zykh clay suspension in 0.5% solution of NaOH in distilled water; 3) in 0.5% solution of sulfite alcohol liquor in sea water, sp. gr. 2.0; clay–hematite suspension; 4) the same, Zykh clay suspension.

If the time in seconds (t) is plotted against the rotation angle of the cylinders (φ), then the motion of the outer cylinder will be represented by a straight line (T) passing through the coordinate origin. The slope of this line depends on the rotation speed of the outer cylinder.

Because of deformation of the mass, rotation of the inner cylinder lags behind that of the outer. Measurements show that the motion of the inner cylinder is stepwise, and in φ°-t coordinates it is represented by broken line A. The angle between the two lines represents deformation of the mass, and linearity of A corresponds to a constant elasticity modulus. We must point out here that the elasticity modulus was found to be constant over a considerable shearing-stress range for aqueous suspensions of Oglanli clays by Rebinder, Serb-Serbina, and Abduragimova [3].

After the inner cylinder has turned through a certain maximum angle, it begins to move in the return direction. With a knowledge of the coefficient of elasticity, the nominal static shearing stress can be calculated from the value of the maximum angle. If the motor is switched off at this instant, and the plotting of the motion of the inner cylinder is continued, the result is a graph consisting of two branches – ascending and decending. The form of the decending curve is highly characteristic for each type of clay suspension. Suspensions of clays of the first type (I, Fig. 1) show a steep descent from the apex, passing into a high horizontal region. Suspensions of clays of the second type (II, Fig. 1) give smoothly descending curves with a flat summit. Each form of curve corresponds to definite external characteristics of the clay suspensions. We term these curves "structural curves", as they characterize the structure of the system. Intermediate types may be found among clay suspensions. This is reflected in the form of their structural curves. Clay suspensions are considered to be typical thixotropic systems, and it is therefore important to determine their thixotropic characteristics.

TABLE

Effect of the Rate of Stirring of Type I Clay Suspensions on the Rotation Rate of the Cylinder in the RV-4 Viscosimeter

Load, g	Rotation speed, rev/sec		
	Slow stirring by rotation of the cylinder	Rapid stirring by rotation of the cylinder	Vigorous stirring by vertical movements of the cylinder
40.5	1,250	0,965	0.868
42.5	1 389	1.136	1.020
44.5	1.479	1.330	1.208

If the SNS instrument is used to determine the static shearing stress at various time intervals [4] (for different ages of the structure), then type II clay suspensions show a steady increase of the strength of the structure with time, as is shown graphically in Fig. 2, while type I suspensions do not usually show an increase of strength with time.

If type II clay suspensions are stirred vigorously, their structure is broken down completely, or its strength is greatly diminished. In contrast, agitation of type I clay suspensions increases the structural strength. Thus, the two types of clay suspensions exhibit opposite structural properties. The behavior of type I clay suspensions is clearly demonstrated when they are agitated in M.P. Volarovich's RV-4 rotational viscosimeter (see table).

The table shows that the rotation speed decreases as the stirring becomes more vigorous. Thus it may be regarded as established that type I clay suspensions have their structure strengthened by mechanical action. This effect was observed by Volarovich and Erokhin [5] for a suspension of mica in vaseline oil.

A thixotropic system is capable of undergoing spontaneous and isothermal gel – sol conversion by mechanical action. Therefore type I clay suspensions cannot be regarded as thixotropic systems or, more correctly, in such clay suspensions thixotropic structures are absent altogether or are suppressed by predominance of structures of different type.

In further studies of this problem, other characteristic distinctions between the two types of clay suspensions were found. It was of interest to determine how the static shearing stress in the two types of clay suspensions is influenced by the rate at which the load is applied. It is known that the nominal static shearing stress, which is a measure of the structure strength, is not in reality a constant, but depends on the loading rate (or the deformation rate [6]). This has been demonstrated for clay suspensions by Zhigach and Kister [7] and by Abduragimova [8], for oleogels by Trapeznikov and Fedorova [9], and for bitumen by Mikhailov [10].

SNS instruments have only one outer cylinder rotation speed, but with the use of wires of different elasticity coefficients they can also be used for determination of static shearing stress at various loading rates. For this, one instrument was fitted with a wire of elasticity coefficient 2.96; another, of the same type as the first, with a wire of elasticity coefficient 18.75. The ratio of the speeds in the two instruments was 6 : 1. Both instruments were used simultaneously to determine the static shearing stress, the time required to reach P_r (the static maximum shearing stress or yield stress).

The determinations showed that the two types of clay suspensions also show considerable differences in the influence of the rate of application of the stress on the value of the static shearing stress. In type I the effect of the rate of application on the value of the static shearing stress is insignificant, and in a number of instances is not detected at all; in type II, however, it is very considerable (Fig. 3).

Since the influence of the rate of application of the stress on the value of the static shearing stress is related to the relaxation effect, is follows that the two types of clay suspensions differ also in their relaxation properties.

Let us now consider another characteristic distinction between the two types of clay suspensions. The above "structural curves" were obtained with the motor switched off when P_r was reached. If the motor is left on until equilibrium flow is established, and only then switched off, then by plotting the curves as before, with the position of the inner cylinder noted every 5 seconds, we obtain curves of a different character, which may be called "equilibrium curves."

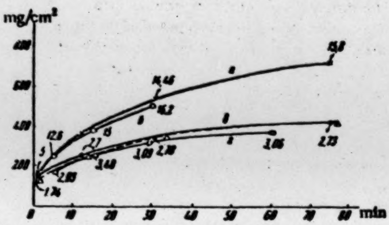

Fig. 3. Variation of structural strength with time in clay suspensions type II for different loading rates. The numbers at the points represent the loading rate in mg·cm^{-2} sec^{-1}. c) and d) Clay-hematite suspension, sp. gr. 2.0. Liquid phase, a 0.5% solution of alkaline sulfate alcohol liquor in distilled water; a) and b) 41.6% suspension of Gekmalin (bentonite) clay. Liquid phase – 2% solution of sodium humates in sea water. a) and b) 2.91; c and d) 18.52 mg/cm² per 1° of torsion of the wire.

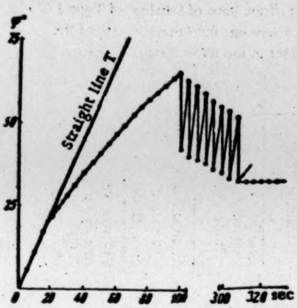

Fig. 5. Equilibrium curve for a type I clay suspension, 23% (by volume) suspension of Zykh clay in 0.05% caustic soda solution in distilled water (the oscillation amplitudes are shown to scale, and the oscillation periods nominally only); P_r = 189-152 mg/cm²; P_0 = 96 mg/cm² (the arrow indicates the instant at which the motor was switched off).

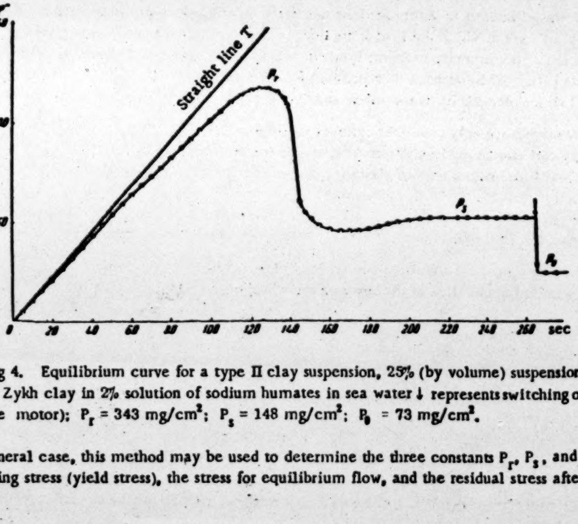

Fig 4. Equilibrium curve for a type II clay suspension, 25% (by volume) suspension of Zykh clay in 2% solution of sodium humates in sea water ↓ represents switching off the motor); P_r = 343 mg/cm²; P_s = 148 mg/cm²; P_0 = 73 mg/cm².

In the general case, this method may be used to determine the three constants P_r, P_s, and P_0 namely the static maximum shearing stress (yield stress), the stress for equilibrium flow, and the residual stress after the motor is switched off.

In type II clay suspensions the transition is smooth and after a certain time the stress becomes constant.

In most type I suspensions, after P_r is reached, oscillation of the inner cylinder begins; this could not be observed until it died down completely in the instrument used, although in some cases the observations were extended to 50 oscillations. The amplitude of the oscillations was fairly considerable, reaching several tens of degrees.

Figs. 4 and 5 give equilibrium curves for type I and II clay suspensions.

Oscillatory motion of this kind has been reported in the literature by Rebinder, Serb-Serbina, and Abduragimova [3], and by Zhigach and Kister [7]. The causes of these oscillations were believed to lie in thixotropic buildup of the structure during its destruction, and according to Zhigach and Kister, also in the action of forces of inertia.

Our observations confirm the significant role of inertia forces in the torsional vibrations of the cylinder. This is supported by the fact that for the oscillatory motion to start it is necessary for the wire to be twisted considerably, irrespective of its rigidity. However, in addition to the action of inertia forces, the oscillatory motion is associated with the properties of type I structures, as type II structures do not show these oscillations.

The available data led us to the conclusion that the oscillatory motion begins with the existence of the following three conditions: Sufficient twisting of the wire (from 40° upward), a high value of the equilibrium flow stress (P_s), and a brittle structure. In most cases oscillatory motion began in these conditions. However, in some instances there were no oscillations despite the existence of these conditions; this shows that other factors, not yet discovered, are also required.

Thus, it has been shown by means of various structural-mechanical characteristics that there are significant differences between the two types of clay suspensions in all the cases examined. In our opinion, these differences must be interpreted as evidence of the existence of two qualitatively different kinds of structure formation in clay suspensions.

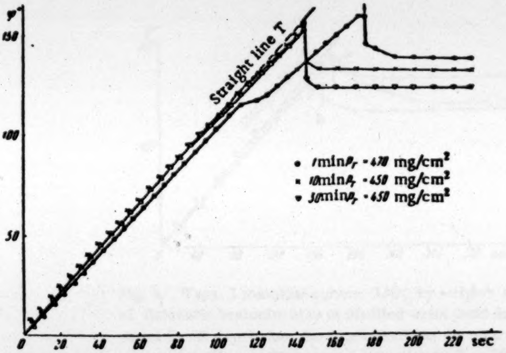

Fig. 6. Type I structural curves: 25% solution of Zykh clay in distilled water (prepared by Tsurinov and Kvirikashvili's kneading method, then kept for 30 days in a closed vessel). The 5.14% of liquid which separated out was decanted off before the determinations. Ages of the suspension: 1, 10, 30 minutes (arrow indicates the moment when the motor was switched off).

Figs. 6-9 show structural curves for both types of structure in two systems of clay suspensions, namely: suspensions of Zykh clay in water, and suspensions of Gekmalin clay (bentonite).

These results show that clay systems with the same solid phase composition can lead to different structural forms with different additions in the liquid phase. As a first approximation it may be assumed that the type of a clay suspension depends on the degree of hydration of the clay. Low hydration gives type I, considerable hydration, type II. If this is so, then it is to be expected that substances which increase hydration of clays should convert type I suspensions into type II.

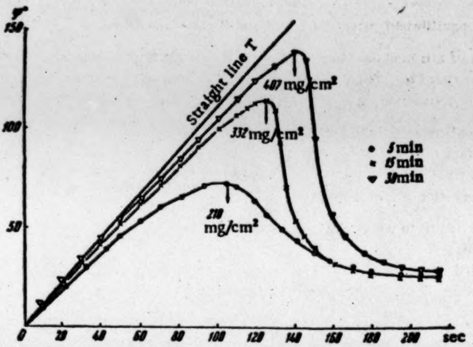

Fig. 7. Type II structural curves: 25% solution of Zykh clay in 2% solution of sodium humates in sea water. Ages of the suspension: 5, 10, 30 minutes (arrow indicates the moment when the motor was switched off).

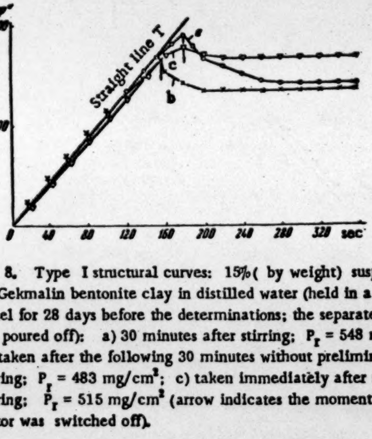

Fig. 8. Type I structural curves: 15% (by weight) suspension of Gekmalin bentonite clay in distilled water (held in a closed vessel for 28 days before the determinations; the separated liquid was poured off): a) 30 minutes after stirring; P_r = 548 mg/cm²; b) taken after the following 30 minutes without preliminary stirring; P_r = 483 mg/cm²; c) taken immediately after subsequent stirring; P_r = 515 mg/cm² (arrow indicates the moment when the motor was switched off).

Our experiments have confirmed this hypothesis. As study of the hydration of Zykh clay in the pure state and with additions of sodium humates and of sulfite alcohol liquor showed that sodium humates increase the hydration of clay several fold, while sulfite alcohol liquor has no effect. It was also found that a suspension of Zykh clay in water, which is of type I, is converted into type II on addition of sodium humates, while addition of sulfite alcohol liquor does not change the type of the system.

These facts are in agreement with Rebinder's views [4, 11] concerning the existance of two types of structure: thixotropic reversible, and condensational irreversible. According to this theory, the formation of one or another type of structure is essentially determined by the extent of the lyophobic regions on the particle surfaces. In thixotropic structures these regions are represented by a small number of centers, mainly at the corners and edges of the particles, at which cohesion between the particles occurs through thin layers of the dispersion medium. Anisodiametric particles give rise to loose, unstable, reticulate formations which penetrate all the original bulk of the mass. In condensational structures the lyophobic regions occupy an appreciable surface of the portion. Direct cohesion of the particles at these regions gives rise to compact, stable formations which are capable of occupying only part of the initial volume, and which therefore give rise to some degree of phase separation in the system. Evidently the magnitude and arrangement of the hydrophobic regions depends on the degree of hydration of the particles. In thixotropic structures the particles are strongly solvated, and in condensational structures are weakly solvated.

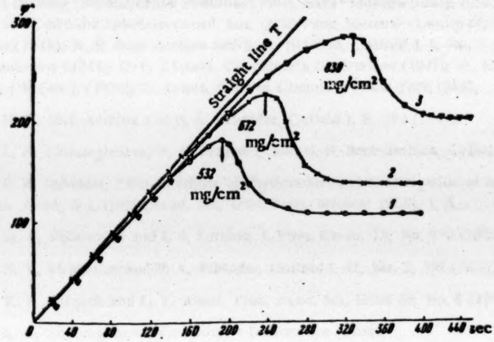

Fig. 9. Type II structural curves: 41.67% (by weight) suspension of Gekmalin clay in 2% solution of sodium humates in sea water (kept for 28 days in a closed vessel before the determinations). The separated liquid was poured off. Ages of the suspensions: 1) 5; 2) 15; 3) 30 minutes (arrow indicates the moment when the motor was switched off).

In the light of this theory and the foregoing facts, it may be concluded that structures of the condensational type predominate in type I clay suspensions. The structural buildup of type I suspensions on stirring, outwardly resembles the emulsification effect. A possible interpretation of the effect is that type I structures are of a flocculational nature, and stirring results in temporary aggregation of the flocculent particles.

SUMMARY

1. Two types of clay suspensions have been studied, differing both in external properties (fluidity) and in structural-mechanical characteristics.

The main differences are seen in the nature of the structural P − t curves obtained with the aid of a rotational viscosimeter. Mechanical action (stirring) strengthens the structure of type I suspensions and destroys the structure of type II suspensions. Increase of the rate of loading does not produce a change of the static maximum shearing stress (yield stress) (P_r) in type I clay suspensions, but P_r for type II clay suspensions increases in these conditions. On passing into a state of equilibrium plastic flow in the rotational viscosimeter after P_r has been reached, type I clay suspensions in most cases produce prolonged oscillations of the inner cylinder of the viscosimeter. Type II clay suspensions show a smooth transition to equilibrium flow with a constant value of P_s.

2. On the basis of these properties the view is advanced that Type I clay suspensions are not thixotropic, or that thixotropic structures in them are suppressed by structurization of another kind, of the condensational type. Type II clay suspensions are typical thixotropic systems.

3. It is shown that the composition of the liquid phase is the main factor which determines the structural type of a system. The composition of the solid phase is less important.

I express my deep gratitude to Academician P. A. Rebinder, M. P. Volarovich, and N. N. Serb-Serbina for their interest in this work and for valuable advice and guidance.

LITERATURE CITED

[1] M. P. Volarovich, Trans. Inst. Appl. Mineralogy 1934, No. 66; M. P. Volarovich and A. M. Tolstoi, Proc. Acad. Sci. USSR 9, 557 (1934); K. A. Tsarevich, R. I. Shishchenko, and B. D. Baklanov, Clay Suspensions in Oil-Well Drilling (Azerbaidzhan Petroleum Press, Baku–Moscow 1935); P. A. Rebinder, Conf. on Viscosity of Liquids and Colloidal Solutions (Acad. Sci. USSR Press, Moscow–Leningrad, 1941) 1; K. F. Zhigach, Doctoral Dissertation (1942); N. N. Serb-Serbina and S. A. Nikitina, Colloid J. 8, No. 1-2, 63 (1946); E. K. Kister, Candidate's Dissertation (1947); D. E. Zlotnik, Candidate's Dissertation (1947); W. K. Lewis, L. Squires and W. L. Thompson, Oil Gas J. (1934); T. Larsen, Colloid Chemistry (New York, 1946).

[2] N. N. Serb-Serbina and P. A. Rebinder, Colloid J. 9, 384 (1947).

[3] L. A. Abduragimova, P. A. Rebinder, and N. N. Serb-Serbina, Colloid J. 17, 184 (1955) (T.p. 171).*

[4] P. A. Rebinder, "New Methods of Physicochemical Investigation of Surface Phenomena," Trans. Inst. Phys. Chem. Acad. Sci. USSR (Acad. Sci. USSR Press, Moscow 1950), 1, 5.

[5] M. P. Volarovich and I. S. Erokhin, J. Phys. Chem. 12, No. 2-3 (1938).

[6] N. V. Mikhailov and P. A. Rebinder, Colloid J. 17, No. 2, 107 (1955) (T.p. 99).*

[7] K. F. Zhigach and E. T. Kister, Proc. Acad. Sci. USSR 69, No. 6 (1949).

[8] L. A. Abduragimova, Candidate's Dissertation (1954).

[9] A. D. Trapeznikov and V. F. Fedotova, Proc. Acad. Sci. USSR 31, No. 6 (1951).

[10] N. V. Mikhailov, Colloid J. 17, 68 (1955) (T.p. 61).*

[11] P. A. Rebinder, Coagulation and Flocculation, General Discussion of the Faraday Society (1954).

Received February 2, 1956

Institute of Chemistry
Azerbaidzhan SSR
Baku

---

*T.p. = C. B. Translation pagination.

A STUDY OF THE PROPERTIES OF CONCENTRATED (SPINNING) SOLUTIONS OF ACRYLONITRILE – VINYLIDENE CHLORIDE COPOLYMER

Z.A. Zazulina, Z.A. Rogovin, and G.V. Vinogradov

It is known that all concentrated spinning solutions used in the production of various types of artifical fibers are strongly structurized systems in which intermolecular action between the dissolved particles occurs. The nature of this interaction has a significant effect on the extrusion conditions and the properties of the fiber. Despite the fact that this view is indisputable and is shared by practically all workers in the field of artificial and synthetic fiber manufacture, there have been practically no systematic investigations of the structure and properties of spinning solutions, and especially of the influence of structure on the extrusion conditions and the properties of the fiber.

The structure of spinning solutions is generally characterized by determinations of the so-called structural viscosity, which represents deviations of the laminar flow of these liquids from the Hagen – Poiseuille law. When structurized solutions flow through a capillary, the ratio Q_1/Q_2 is not equal to p_1/p_2, where Q is the flow rate per second, and p is the pressure difference. The more the efflux behavior of such liquids deviates from the Hagen – Poiseuille equation, the greater is the value of the structural viscosity. This characteristic was used by Pakshver and Bunin [1] and also by Pakshver and Zamilatskaya [2] to study variations in the degree of structurization of viscose solutions during ripening under the influence of various factors. A similar method for determination of the structurization of viscose solutions was used by Ostwald, Nakashima, Herrent [3] and a number of others. This method for investigation of the degree of structurization of solutions gives some idea of the nature of the intermolecular action, but is inadequate for a more detailed study of the process and especially for an understanding of its mechanism. For a given value of structural viscosity, that is, for a given value of the deviation of the rate of laminar flow from the Hagen – Poiseuille equation, the strength of the individual aggregates formed in concentrated solutions, and the possibility of their rapid destruction or repeated formation, cannot be sufficiently well defined. A more detailed characterization of the structure of concentrated solutions is required for elucidation of this question. The necessary data may be obtained by the use of methods used for analogous studies in modern rheology, for investigation of spinning solutions.

Without giving descriptions of these methods, which are presented in details in special monographs [4], we will merely note that they are all based on determinations of the relationships between the velocity gradient (average deformation rate $\overline{D}$) and the shearing stress (τ) over a wide range of τ. At the lower stress limit, flow takes place at constant viscosity ($\tau/D = \text{const}$) and structural breakdown does not occur in the system; at the upper limit of shearing stresses the structure is broken down completely and the solution acquires the properties of a normal Newtonian liquid. In order to realize these conditions, in some instances the velocity gradient must be varied over a range of several orders of magnitude. The flow curves obtained in investigations over such a wide range of shearing-stress variations represent the properties of the systems much more fully than do the methods outlined above for determination of structural viscosity.

Investigations over a fairly wide range of values of D and τ have been carried out on various polymer solutions used in fiber production, such as solutions of acetylcellulose in acetone [5], nitrocellulose in butyl acetate [6], alkaline solutions of cellulose xanthate [7], and a number of other polymers. In recent years systematic rheological studies of concentrated polymer solutions have been carried out by Soviet scientists, including Rebinder [8], Lipatov [9], Dumansky [10], and their associates.

Vinogradov and his co-workers have developed a series of methods which can be used for investigations of viscosity changes in strongly structurized, highly viscous solutions with variations of the velocity gradients over a 10^5 - 10^6 -fold range. The use of the method of Konstantinov and Vinogradov [11] is of considerable interest for evaluation of the degree of structurization of concentrated polymer solutions, and in particular for a more detailed characterization of the properties of spinning solutions. This method is based on determinations of variations of the viscosity of the solution with the pressure difference when the system flows through a capillary. By means of this apparatus it is possible to determine, in one experiment, the dependence of the viscosity over a wide range upon the shearing stress and the deformation rate.

The method developed by Vinogradov and Konstantinov for evaluation of the structural-mechanical properties of lubricants has been used in the present investigation for determining the properties of spinning solutions of acrylonitrile – vinylidene chloride copolymer ("saniv").

In the AKV-2 viscosimeter used, the solution is extruded from a cylindrical chamber into a capillary by means of a calibrated spring connected to a rod. As the spring is released, the pressure difference in the capillary and the efflux rate decrease. In a given experiment the average velocity gradient can be varied by a factor of 10^5 - 10^6. The degree of compression of the spring simultaneously indicates the pressure under which the solution is extruded, and the volume of the solution extruded from the capillary. A recording instrument is used for automatic registration of efflux rates of the solution and the pressure drops in the capillary, from which the average velocity gradients, shearing stresses at the capillary walls, and the effective viscosities may be calculated.

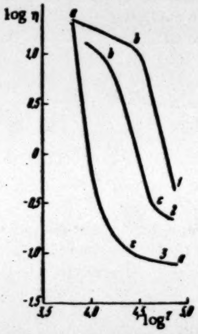

Fig. 1. Effect of molecular weight on the viscosity properties of saniv polymer solutions: 1) M = 130,000, concentration 22%; 2) M = 290,000, concentration 12.5% 3) M = 620,000, concentration 6.5%.

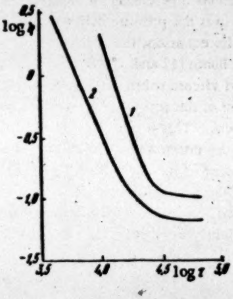

Fig. 2. Effect of polymer concentration on the viscosity properties of saniv polymer solutions; 1) c = 8.5%; 2) c = 7.5%.

This instrument was used to study the influence of molecular weight of the polymer, its concentration, and the temperature, on the viscosity of the solutions. The solvent was acetone.

For investigation of the effect of molecular weight on structural viscosity, polymer fractions I, II, and III were used, with molecular weights 620,000, 290,000, and 130,000 respectively, and polymer concentrations of 6.5, 12.5, and 22%. All these solutions had the same viscosity as measured by the falling ball method. The curves in Fig. 1 represent the course of structure breakdown of flowing spinning solutions for the same variation of shearing stress.

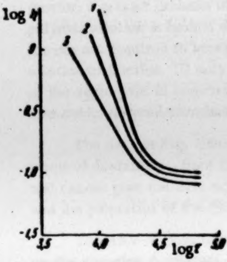

Fig. 3. Effect of temperature on the viscosity properties of saniv polymer solutions: 1) 25°; 2) 35°; 3) 45°.

In Fig. 1, as in Figs. 2 and 3, logarithms of the shearing stress (in dynes/cm²) are taken along the abscissa axis, and logarithms of the effective viscosity (τ/D), which depends on the shearing stress and the velocity gradient, along the ordinate axis.

It is usual to find the values of the shearing stress at the capillary walls ($\tau = p \cdot R/2L$, where R is the radius and L is the length of the capillary, and p is the pressure drop along the capillary) and the average deformation rates ($\bar{D} = Q/\pi R^3$, where Q is the efflux rate per second). These results are then used to plot average flow curves $\tau(\bar{D})$ or effective viscosity curves $\bar{\eta}(\tau)$.

The most correct procedure, however, is to use not the average but the true values of deformation rate and viscosity, which may be calculated by Weissenberg's method (see [12]) from the average values. Since the shearing stresses are usually calculated for the capillary surfaces, the deformation rates (velocity gradients) should also be calculated for the capillary walls. The data are first used to find $\bar{D}$ and τ; the $\tau(\bar{D})$, graph, plotted in logarithmic coordinates, is then used to calculate D, as has been shown by Vinogradov and Pavlov [13], by means of the equation:

$$D = \bar{D}\left(3 + \frac{d \ln \bar{D}}{d \ln \tau}\right).$$

The values of τ and D are used to calculate $\eta = \tau/D$, that is, the effective viscosity of the system at the capillary walls.

The $\eta(\tau)$ or $\eta(D)$ relationship can be used to plot viscosity curves (Figs. 1, 2, 3); their distinctive feature is that they give a constant relationship between the shearing stress and the corresponding effective viscosity irrespective of the capillary dimensions or of the location of the flow zone in the capillary itself. This means that, in conditions of pure shear, there is a constant relationship between effective viscosity and shearing stress which does not depend on the experimental conditions (use of capillary or rotational viscosimeters, etc.).

The greatest interest, in analysis of the results obtained, attaches to three regions of the viscosity – shearing stress curves (see Fig. 1):

a) the region ab, which corresponds to the range of shearing stresses in which the system in steady flow continuously restores its structure as it is broken down;

b) the region bc, which corresponds to the range of shearing stresses in which rapid structural breakdown occurs in the solution;

c) the region cd, which corresponds to shearing stresses at which the structure is broken down considerably, and a gradual transition to flow in accordance with the Poiseuille law takes place.

As Fig. 1 shows, the viscosity curves for the different polymer solutions differ significantly. The polymer of highest molecular weight (Curve 3) forms loose aggregates in the solution of lowest concentration, and these are easily disrupted on application of a relatively small stress. For example, as the shearing stress changes from 7000 to 15000 dynes/cm², or in a ratio of 2.1, the viscosity of the solution decreases in a ratio of 110, in consequence of breakdown of its structure.

At a shearing stress of ~25,000 dynes/cm² the structure in the solution is apparently broken down almost completely. The presence of loose aggregates of this polymer in all probability predetermines the structure of the fiber, as is confirmed by the poor mechanical properties of the fibers obtained from solutions of this polymer [14].

In more concentrated solutions of a polymer of lower molecular weight, the strength of the aggregates is greater; a greater pressure must be applied to break them down. While the structure of the high-molecular polymer solution is broken down completely at a shearing stress of 25,000 dynes/cm^2, much higher shearing stresses are required to break down the structure of solutions of fractions II and III. The structure of the solution of fraction III only begins to break down at shearing stresses above 300,000 dynes/cm^2. The strength of the aggregates in concentrated solutions of fractions II and III, which are polymers of lower molecular weight, also evidently predetermines the stronger structure and mechanical properties of the fibers formed.

The data in Fig. 1 show clearly that evaluation of the degree of structurization of spinning solutions in terms of deviations from the Hagen – Poseuille law is totally inadequate for characterization of the solutions, and cannot give the data necessary to establish a relationship between the viscosity of a structurized solution and the properties of the fiber formed from it.

The AKV-2 viscosimeter was also used to study the influence of temperature and polymer concentration on the viscosity. A polymer with molecular weight 475,000 was used for the investigation.

As the results (Figs. 2 and 3) show, as the temperature increases the strength of the macromolecular aggregates decreases and the shearing stress necessary for breakdown of the structure falls accordingly.

The results which have been obtained in this study of solution structure must be regarded as preliminary. At the present time it is not yet possible to establish a direct relationship between solution structure, extrusion conditions, and properties of the fiber formed. Additional data are required for this. In particular, data are lacking on the shearing stresses and deformation rates in the extrusion of various types of fibers in production conditions. Without such data it is impossible to establish which region of the flow curve corresponds to formation of the fiber in actual conditions. An important task in our further investigations in this field will be to solve this problem, which is of great technological importance.

SUMMARY

1. The structure of concentrated solutions of the synthetic acrylonitrile – vinylidene chloride copolymer ("saniv") has been investigated by studies of variations of the deformation rates of these systems over a wide range of shearing-stress variations.

2. The influence of molecular weight and concentration of the polymer, and of the temperature, on the degree of structurization has been determined. It is shown that in concentrated polymer solutions of equal viscosity, as measured by the falling ball method, the strength of the structure varies considerably. The higher the polymer concentration in the solution, the greater is the strength of the structure in the polymer solution.

3. The direction of further investigations for establishing a relationship between the viscosity properties of concentrated spinning solutions, the extrusion conditions, and the properties of the fibers formed is indicated.

LITERATURE CITED

[1] A.B. Pakshver and M. Bunin, Artificial Fibers 1933, No. 5, 7.

[2] A.B. Pakshver and Zamilatskaya, Artificial Fibers 1935, No. 1, 67.

[3] P. Herrent, S. Morranx and A. Lude, Research 2, 10, 486, (1946).

[4] W. Philippoff, Viskosität der Kolloide J. (1952), p. 112.

[5] B. Rabinowitsch, Z. physik. Chem. 145, 1 (1929); 166, 267 (1933); R. Eisenschitz and B. Rabinowitsch, Ber. 64, 2522 (1931).

[6] W. Philippoff, Kolloid-Z. 71, 1 (1935); W. Philippoff and H. Hess, Z physik. Chem. 31, 237 (1936); Ber. 70, 1808 (1937); 71, 841 (1938).

[7] W. Philippoff and H. Kruger, Kolloid-Z. 88, 215 (1939).

[8] P.A. Rebinder and S. Ya. Veiler, Proc. Acad. Sci. USSR 49, 354 (1945); L.I. Edelman and P.A. Rebinder, Colloid J. 13, 64 (1951); S. Ya. Veiler, V. Likhman, and P.A. Rebinder, Colloid J. 11, 8 (1949).

[9] S.M. Lipatov and S.I. Meerson, Colloid J. 8, 143 (1946); 8, 233 (1946); 12, 123 (1950); 12, 427 (1950), and other papers.

[10] I.A. Dumansky, A.V. Dumansky, and L.V. Khailenko, Proc. Acad. Sci. USSR, 92, 1189 (1953).

[11] A.A. Konstantinov and G.V. Vinogradov, Factory Lab. 1953, No. 6, 680.

[12] W. Philippoff, Viskosität der Kolloide (1952), p. 113.

[13] G.V. Vinogradov and V.P. Pavlov, Symposium, Low-Temperature Properties of Petroleum Products (State Fuel Tech. Press, 1942).

[14] Z.A. Zazulina and A.A. Rogovin, Textile Ind. 1956, No. 1.

Received January 25, 1956

Moscow Textile Institute, Chair
of Synthetic Fibers

MECHANISM OF HIGH-POLYMER PLASTICIZATION — STRUCTURE OF GELS

8. EFFECT OF THE NATURE OF THE PLASTICIZER ON THE SWELLING KINETICS AND THE VISCOSITY OF DILUTE SOLUTIONS OF DIVINYL-STYRENE RUBBER

P. I. Zubov and M. P. Zverev

It is now firmly established that plasticization of high polymers involves a weakening of the interaction between the chain molecules. In a number of cases, however, it has been presumed that mixing of high polymers with low-molecular substances leads to changes not only in the intermolecular but also in the intramolecular interaction [1, 2].

The object of the present investigation was to determine to what extent this is true for divinyl-styrene rubber.

The problem was solved by a comparison of data on the swelling of divinyl-styrene rubber in various plasticizers with data on the viscosity of dilute solutions. In addition, a study of the kinetics of swelling confirmed the earlier conclusion [2] that the mechanism of this process is relaxational in character. The swelling was studied by the gravimetric method with the use of films made from a vulcanizate without carbon black.*

The table gives the values for the equilibrium swelling of carbon-free divinyl-styrene rubber vulcanizate in various solvents at 25°.

TABLE

Equilibrium Swelling of Carbon-Free Divinyl-Styrene Rubber Vulcanizate in Various Solvents at 25°

Solvent	Molecular weight of solvent	Maximum swelling, %	Time to reach maximum swelling, hours
Tetralin	132.20	552.0	17
Toluene	92.13	480.0	9
Benzene	78.11	468.0	7
Green Oil	171.00	425.0	43
Ditolylmethane	196.28	405.0	97
Decalin	138.24	378.0	10
Dicumylmethane	254.38	310.0	53
Dibutyl sebacate	314.45	221.0	162
Dibutyl phthalate	278.34	103.0	140
Diethyl phthalate	222.23	18.0	18
Tricresyl phosphate	368.36	15.5	16

***The mixture had the following composition (in parts by weight): SKS-30A rubber 100, dibenzothiazole disulfide 0.6, diphenylguanidine 0.75, zinc oxide 5, stearic acid 2, sulfur 2. The films were vulcanized at 143°.**

It is seen that the equilibrium swelling depends on the polarity of the plasticizer (solvent). The least swelling is found in polar solvents: tricresyl phosphate, diethyl phthalate, and dibutyl phthalate. In nonpolar solvents the swelling is greater. Maximum effects are found in such solvents as tetralin, toluene, benzene, and green oil. These results lead to the conclusion that the rubber chain molecules have a more coiled configuration in presence of polar than in presence of nonpolar plasticizers. This conclusion is, however, not precise, as both intra - and intermolecular action occurs in swelling.

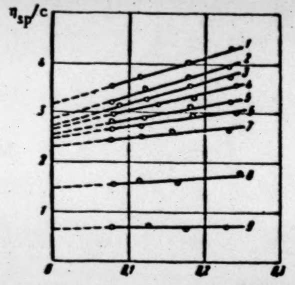

Fig. 1. Variation of the intrinsic viscosity of SKS-30A rubber in various solvents: 1) tetralin; 2) toluene; 3) benzene; 4) green oil; 5) ditolylmethane; 6) decalin; 7) dicumylmethane; 8) dibutyl sebacate; 9) dibutyl phthalate.

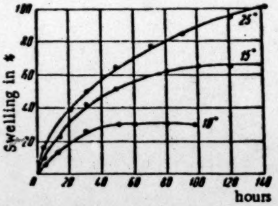

Fig. 2. Swelling of carbon-free SKS-30 rubber vulcanizate in dibutyl phthalate as a function of temperature.

Viscosity data may be used as an indication of changes in the macromolecular configuration when polymers and plasticizers are mixed. In order to exclude the influence of intermolecular forces, the viscosity measurements were made on dilute solutions.

Figure 1 gives experimental data for the reduced viscosity of the polymer plotted against concentration. This figure shows that the nature of the solvent also exerts an influence on the intrinsic viscosity, which, as is known, provides information on the form and asymmetry of the macromolecules and on the swelling process. The greatest asymmetry of the rubber molecules and the greatest values of equilibrium swelling are found in nonpolar plasticizers. In our opinion, it may be definitely concluded from this that swelling is related to changes of macromolecular configuration.

Zubov [2], in a study of the kinetics of gelatin swelling at various temperatures, reached the conclusion that changes in the volume of the gelatin are determined not by the rate of diffusion of the solvent molecules into the mass of the polymer, but by the time required for regrouping of the macromolecules in transition from one equilibrium state into another. It was of interest to determine the extent to which this volume relaxational mechanism comes into effect in the swelling of divinyl-styrene rubber.

A study was therefore made of the kinetics of limited swelling of carbon-free divinyl-styrene rubber vulcanizate in dibutyl phthalate at various temperatures. The experimental results are given in Fig. 2, where it is seen that the swelling curves for the rubber are similar to the curves obtained for gelatin (Fig. 3).* In both instances the time required to reach a state of equilibrium is less at low than at high temperatures, which contradicts the positive temperature coefficient of diffusion. If swelling proceeded by a diffusion mechanism, the equilibrium state should be reached more rapidly at higher temperatures. Nevertheless, experimental data both for rubber and for gelatin show the opposite effect. Thus, in the swelling of rubber, equilibrium is established after 140 hours at 25°, and after 50 hours at 10°. Consequently, the time required for equilibrium swelling both of gelatin and of rubber must be related not to the rate of penetration of the solvent molecules into the bulk of the polymer, but to the rate of regrouping of the macromolecular segments.

In our view, the relaxational mechanism is also supported by data on the swelling of divinyl – styrene rubber in solvents the molecules of which have a fairly similar structure but different molecular weights.

---

*These data are taken from P. I. Zubov's Doctoral Dissertation, and are published for the first time.

The table shows that equilibrium swelling becomes established considerably later in ditolylmethane than in dicumylmethane, although the molecular weight of dicumylmethane is greater than that of ditolylmethane.

Further, if a diffusion mechanism is postulated for swelling, equilibrium swelling should be established later in decalin than in tetralin. However, the experimental data show that the time for equilibrium to be reached is less in decalin than in tetralin. As the table shows, equilibrium is reached considerably earlier in diethyl phthalate than in dibutyl phthalate. This might be thought to support the view that in this instance swelling is not associated with volume relaxation, as the molecular weight of diethyl phthalate is less than the molecular weight of dibutyl phthalate. However, this cannot be so, as the molecular weight of dibutyl phthalate is 1.3 times that of diethyl phthalate, while the time to reach equilibrium is about 8.0 times as great.

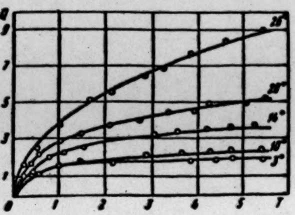

Fig. 3. Swelling of gelatin in water as a function of temperature.

SUMMARY

1. Plasticization of polymers involves not only a weakening of the forces between the chain molecules, but elongation (uncoiling) of the macromolecules.

2. The degree of elongation of molecules of divinyl-styrene rubber increases with decreasing plasticizer polarity.

3. The time to reach equilibrium swelling of divinyl-styrene rubber, as that of gelatin, depends on the rate of macromolecular regrouping. Consequently, swelling, like mechanical deformation of polymers, proceeds by a relaxation mechanism.

LITERATURE CITED

[1] V. A. Kargin and A. A. Tager, J. Phys. Chem. 15, 1029, 1036 (1941); E. M. Frith, Trans. Faraday Soc. 41, 90 (1945); P. V. Kozlov and E. F. Rusakova, High-Molecular Compounds (State Chem. Press, 1952); No. 12, p. 44; B. A. Dogadkin and V. E. Gul, Colloid J. 12, 184 (1950).

[2] P. M. Zubov, Doctoral Dissertation, Mowcow (1949).

The A. Ya. Karpov Scientific Research Institute
for Physical Chemistry

Received June 3, 1956

PECULIARITIES OF THE DEFORMATION BEHAVIOR OF GELATIN GELS

L. V. Ivanova-Chumakova, P. A. Rebinder, and G. I. Krus

The gel formation exhibited by a number of substances (gelatin, agar, pectin, and others), which has been studied in greatest detail for gelatin [1-4], is attributed by a number of authors to formation of local bonds of the crystallization type between macromolecules of these substances when the solution temperature falls below a certain limit. By formation of such bonds, molecules of these substances form a stable network even at low concentrations (from about 1%), which gives rise to the peculiar mechanical properties of such systems. Under relatively small stresses produced by external forces, gels undergo fairly large "instantaneous" – elastic deformations, while residual flow does not develop appreciably, and in some cases it may be assumed that it is practically absent. The slow development of deformations due to elastic after-effects (elastic deformations) is also characteristic. By a detailed investigation of this part of the deformation, after the correct experimental conditions had been found, it proved possible to extend the laws established earlier to such complex materials as gelatin gels, and also to explain some deformation properties of structurized systems.

Sheer elasticity in dilute aqueous (0.5%) gelatin solutions was first discovered and studied by Shvedov [5]. He also discovered the plastico-viscous behavior of such solutions, that is, their flow at stresses above the elastic limit, in accordance with stress relaxation above this limit. However, Shvedov did not discover elastic properties in gelatin solutions, evidently, as will be shown later on the basis of our investigations, because he studied solutions of insufficiently high concentrations (with low viscosities). In subsequent work the elastico-viscous properties of gelatin solutions have not been studied sufficiently well from the quantitative aspect. Such studies are evidently of considerable significance for elucidation of the structural characteristics of gelatin solutions(gels).

As has been stated earlier [6], the time required for the full development of elastic deformation, i. e., elastic after-effects, decreases sharply with decreasing concentration of the substance in solution.

In accordance with this rule, concentrations of 15, 7.5, and 5% were used consecutively in this investigation. The lowest value was determined by the limit of possible investigation of gels of low concentration in an instrument with two plane-parallel plates. This instrument, which has been adapted by us for investigation of elastic systems[6], was subjected to additional modifications for the present work in order to adapt it to the study of systems containing volatile solvents and thus to protect the systems against evaporation during the experiments. For this, the plates 1 and 2 were enclosed in a special metal box 3 with a lid 4, enclosed by a liquid seal 5 (Fig. 1, c). The openings 6 through which the pulling rod 7 for transmitting the external force and the rod 8, which served as an indicator of the displacement of the upper plate, passed were filled with liquid which was retained by capillary forces in the tubes open at both ends.

To eliminate or restrict electrochemical interaction between the gel and the plate material, the plates were made from stainless steel and Plexiglas. Plexiglas was also used as the material for the special mold 9 for making the specimens.

As is seen in Fig. 1, a, the mold is a rectangular vessel in which the two plates, the steel plate 1 and the Plexiglas plate 2, are placed vertically 6 mm apart; they are fixed not on the floor of the mold, but on the lower wall of a special insert 10. The specimen prepared in this manner is inserted into the instrument either immediately or after a preliminary interval.

Since the preliminary intervals and the subsequent tests were very prolonged, it was necessary to

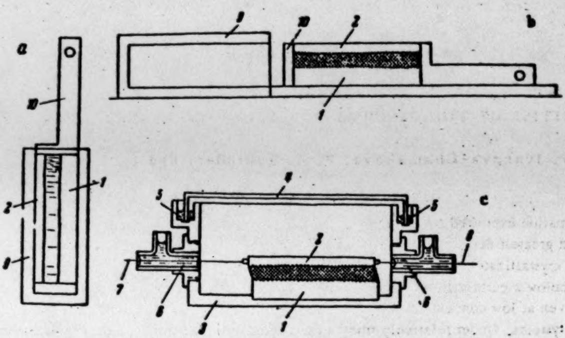

Fig. 1. Mold for making the gel specimens (a, b) and box for protecting the system against evaporation of the liquid phase (c).

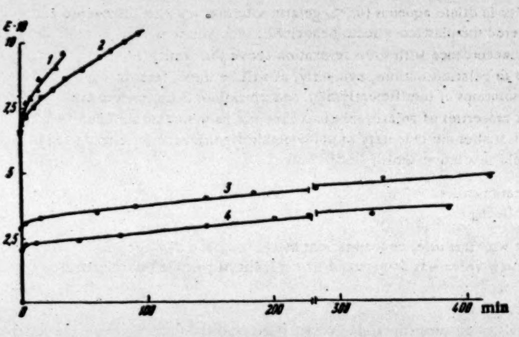

Fig. 2. Deformability of gelatin gels after various aging times: 1) concentration 6.53%, aged 2 days, experimental temperature 22.9°; 2) 5%, 3 days, 22.5°; 3) 7.5%, 6 days, 22.4°; 4) 5%, 50 days, final concentration 6.53%.

protect the specimens against attack by microrganisms. 0.15% of ethylmercury phosphate,* calculated on the dry substance, was used for this purpose. This bactericidal agent proved to be highly effective. The addition had no significant effect on the elastico-viscous properties of gelatin solutions. In view of reports [7, 8] that the mechanical properties, including the viscosity, of gelatin solutions are affected by the action of (ultraviolet) light, light was excluded from the instrument by the use of a protective box; as has already been stated, the capillary seal openings were filled with a dark opaque liquid (water colored with India ink).

The mechanical properties of gels are very greatly influenced by their age and by the temperature at which these properties are determined. The effect of temperature is understandable in view of the fact that the gel structure is formed as the result of cooling, and not at once, but over a certain temperature range. A continuous change of structure evidently goes on beyond the limits of this range, and therefore the temperature, in addition to its usual influence on the mechanical properties by affecting the thermal motion of the molecules, also exerts an additional effect by changing the structure by formation of individual local bonds between the macromolecular chains. The different effects of temperature on gelatin gels and on a material the structure of which is not changed in these conditions, can be seen from a comparison of the following data. In an earlier investigation of polyisobutylene it was found that an increase of temperature from 25 to 90° corresponds to a change of the initial elasticity modulus E_1 from $2.3 \cdot 10^6$ to $1.4 \cdot 10^6$ dynes/cm², and of the equilibrium elasticity modulus E from 1.15 to $0.98 \cdot 10^5$ dynes/cm²; whereas for a 5% gelatin gel (Table 1) these values undergo more than a 2-fold decrease as the temperature increases from 20 to 22.5°.

---

*We are grateful to Prof. N. N. Melnikov for suggesting and providing the ethylmercury phosphate.

Particular attention was paid to investigations of aging of the specimens. It was first established that the gels prepared by the method described tend to lose moisture continuously even when the necessary measures to protect them against evaporation have been taken. It was found that the plates with the gel placed between them came appreciably closer together when left in a desiccator in presence of water vapor, and the distance between them decreased from 6 to 5-4 mm, or even less. To confirm that spontaneous displacement of water occurs in the process by the action of cohesive forces in the gel network – the well-known syneresis effect – a freshly prepared specimen was placed in a Plexiglas box with a lid which was thoroughly sealed with paraffin wax. After some time the floor of the box was found to be covered with water while the weight of the specimen decreased. The dry solid content of the gel correspondingly increased.

A comparison of the mechanical properties of gels of the same concentration (reached after prolonged aging) and gels of the initial value as prepared, showed that changes of mechanical properties as the result of aging cannot be ascribed merely to a simple change of the gelatin content of the gel. Fig. 2 shows the development of deformation under constant stress (1600 dynes/cm² in all cases). These results show that an unaged (or almost unaged) 6.53% gel has similar deformability to that of a 5% gel of approximately equal age (it was rather greater because of the slight increase of temperature from 22.5 to 22.9°, and also because the aging was 2 days instead of 3). The deformability of a gel with an initial gelatin concentration of 5% and a final concentration after 50 days of 6.53%, was even less than that of a 7.5% gel aged for only 6 days. Loss of water, associated with the aging process, was found to proceed, at a diminished but appreciable rate, even after tens of days of aging. For example, similar specimens with initial 5% concentration, aged for 10 and 50 days respectively, had losses of water in the ratio of 1 : 3.

TABLE 1

Elastico-Viscous Properties of Gelatin Gels

Initial concentration, %	Preliminary aging time, days	Average exptl. temp. °C.	$E_1 \cdot 10^{-3}$ in $\frac{\text{dynes}}{\text{cm}^2}$	$E_2 \cdot 10^{-3}$ in $\frac{\text{dynes}}{\text{cm}^2}$	$a \cdot 10^{9}$ in $\frac{\text{cm}^2}{\text{dyne} \cdot \text{sec}}$	$\eta_p \cdot 10^{-9}$ in $\frac{\text{dyne} \cdot \text{sec}}{\text{cm}^2}$	$\eta_c \cdot 10^{-9}$ in $\frac{\text{dyne} \cdot \text{sec}}{\text{cm}^2}$	Loading time, minutes	P in dynes/cm²
5	2	20	4.15	6.50	1.83	0.109	0.058	4,220	327
5	2	22.5	1.90	2.85	11.5	0.055	0.060	700	327
7.5	14	20	14.2	26.5	1.11	1.95	3.9	1,220	3,270
7.5	. 7	22.5	5.60	7.05	1.35	0.82	1.3	1,540	1,595
15	72	22.5	230	35.5	0.047	68	–	40,000	3,270

This property of the gels causes great difficulties in the selection of a method of preparing the specimens for the investigations. On the one hand, correct deformation conditions can be ensured only if the structure of the specimen remains unchanged during the experiment, but on the other hand, the usual method for attaining constant properties—prolonged preliminary aging—is hardly suitable in the present instance, as the structure changes continuously at an almost undiminishing rate, and strengthening of the structure occurs, which is accompanied by a highly undesirable increase of the time required for complete development of elastic deformation.

In view of the above, our procedure for preparing the specimens for the experiments was to some extent arbitrary in character and did not ensure absolute constancy of properties during deformation of the specimens. This probably accounts for some deviations of the deformation behavior of our specimens from ideal behavior in which all the deformation stages (initial elasticity, elastic after-effects, and residual deformation of true flow) along the loading curve for the experiment (development of deformation after application of the load) coincide strictly with the same stages along the unloading curve, which represents the kinetics of removal of the deformation after unloading.

However, when the time for carrying out the experiment, that is, the time for development and decay of the deformation due to elastic after-effects, was reduced to a minimum by suitable choice of conditions (least possible concentration 5% and highest possible constant temperature 22.5° in our conditions), a situation close to ideality was obtained (Fig. 3). The total residual deformation calculated from the flow rate, i. e., from the deformation rate at the end of the experiment, then proved to be approximately equal to the deformation which did not disappear after unloading. The initial jumps during loading and unloading coincided. The deformation due to elastic after-effects, found from the decay of deformation after unloading, was found to be equal to that fraction of the total deformation which remains after deduction of the initial jump and of the flow deformation. Although growth of elastic deformation continues almost up to the end of the loading, as is seen from the duration of the decay of this deformation after unloading, this cannot be detected graphically, as at the end the rate of this process is extremely low comparative to the rate of flow, and the process cannot be observed against total deformation background. The situation is complicated by the fact that, as was found in our numerous experiments, deformation of a gelatin gel is accompanied by jumps in the growth of deformation, so that the time for a given shear range varies. These time fluctuations exceed the retardation which could occur as the result of complete exhaustion of the possibility of elastic deformation. In this connection, a very characteristic feature of the growth of deformation in gelatin gels is the apparent very rapid approach to a linear relationship (for example, as in Fig. 3) although in subsequent unloading it is often found that part of the deformation which developed at the constant rate must be attributed not to residual flow but to elastic after-effects. In such cases the line is not a true straight line, but an intermediate line between points which are scattered, often to a considerable extent.

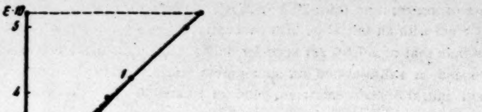

Fig. 3. Growth (1) and decay (2) of deformation of a 5% gel at 22.5°. Preliminary aging 2 days.

Whether the duration of an experiment was sufficient or not, had to be judged on the basis of observations during unloading. An experiment was regarded as correctly performed if the time for development of the deformation was approximately equal to the time of decay of the deformation due to elastic after-effects. It must be pointed out that the relationship established earlier [6] for the development and decay of elastic deformation in gelatin gels was obeyed only in such instances. If the growth of deformation was not sufficiently long, the coefficient calculated from deformation decay data began to decrease toward the end. An increase of the loading time to the necessary limit invariably led to constant values of k being obtained over the entire course of decay of the deformation. Table 2 shows an example of the calculation of decay deformation kinetics by means of the equation

$$k = \frac{\varepsilon_m \ln\frac{\varepsilon_e}{\varepsilon_m} + \varepsilon_m - \varepsilon_e}{\tau}, \tag{1}$$

which shows that this relationship is fully applicable in this instance. The small deviations from a constant value found in Table 2 may be attributed to the above-mentioned continuous variation of the gel structure, and to temperature fluctuations, which in some experiments reached 0.5°. It was not possible to eliminate these fluctuations because the temperature of the building changed sharply several times during experiments lasting several days, and while the thermostatic liquid supplied from the ultrathermostat was at constant temperature, the thermometric readings in the instrument itself were not constant.

TABLE 2

Kinetics of the Decay of Elastic Deformation ε_e After Unloading (in Micrometer Eyepiece Readings); τ – Time in Minutes After Unloading; $k = \frac{\varepsilon_m \ln\frac{\varepsilon_e}{\varepsilon_m} + \varepsilon_m - \varepsilon_e}{\tau}$

5% gelatin gel, aged 2 days, microscope scale division $43 \cdot 10^{-4}$ cm, t = 20°C, P = 327 dynes · cm^{-2}, b (distance between plates) 0.60 cm

τ	0	65	170	430	790	1440
ε_e	7	5	4	3	2	1
$k \cdot 10^4$	—	56	54	48	47	52 average 51)

5% gelatin gel, aged 2 days, microscope scale division $43 \cdot 10^{-4}$ cm, t = 22.5°, p = 327 dynes · cm^{-2}, b = 0.60 cm

τ	0	5.5	11	22	34	50	70	97	137	180	243	312	455	600	810
ε_e	16	14	13	12	11	10	9	8	7	6	5	4	3	2	1
$k \cdot 10^5$	—	26	32	27	29	31	32	32	30	32	31	32	30	32	36 av. 31)

7.5%-gelatin gel, aged 14 days, microscope scale division $43 \cdot 10^{-4}$ cm, t = 20°, p = 3270 dynes · cm^{-2}, b = 0.47 cm

τ	0	1.2	6	17	35	57	85	132	180	250	345	520	600
ε_e	13.5	12.5	11.5	10.5	9.5	8.5	7.5	6.5	5.5	4.5	3.5	2.1	1.5
$k \cdot 10^5$	—	25	30	20	23	22	23	22	23	23	24	27	29 av. 24)

7.5%-gelatin gel, aged 7 days, microscope scale division $43 \cdot 10^{-4}$ cm, t = 22.5°, P = 1595 dynes · cm^{-2}, b = 0.53 cm

τ	0	7.5	23.5	35	49	67	87	140	180	270	395	685	1015	1565	4055
ε_e	28	25	23	22	21	20	19	17	16	14	12	9	7	5	1.5
$k \cdot 10^5$	—	13	15	15	15	15	16	17	17	17	17	16	16	15	13 av. 16)

15%-gelatin gel, aged 72 days, microscope scale division $16 \cdot 10^{-4}$ cm, t = 22.5°, P = 3270 dynes · cm^{-2}, b = 0.40 cm

τ	0	410	1330	1870	2770	3310	4210	5650	11410
ε_e	23	17	14	12	10	9	7,5	6	3
$k \cdot 10^4$	—	24	20	21	22	23	24	25	23 av. 23)

5%-gelatin gel, aged 2 days, microscope scale division $43 \cdot 10^{-4}$ cm, t = 20°, P = 981 dynes · cm^{-2}, b = 0.60 cm

τ	0	2.7	12	27	50	90	125	175	330	765	930	1210	2285	2875
ε_e	20	19	18	17	16	15	14	13	11	8	7	6	3	2
$k \cdot 10^4$	—	95	97	99	92	83	89	94	91	82	86	83	92	97 av. 90)

It is very important to stress that in all these calculations only that part of the deformation which was recorded in our observations as actually decaying with time was taken into consideration. The part which was recorded as disappearing instantaneously was ignored in the calculations. This is especially interesting in view of the fact that, in contrast to polyisobutylene [6], for which the initial elastic deformation was one-tenth of the elastic after-effect, in the present instance it was very pronounced, and was about one and a half times the value of the deformation due to elastic after-effects. Calculations, not shown here, of the factor k, with the sum of the elastic after-effects and initial elasticity effects being taken as the deformation ϵ_e, showed that k was far from constant in this instance. This gives reason for regarding the two parts of the deformation as independent and developing in accordance with different laws.

The values shown in Table 1 were calculated from the Formulas:

$$E_1 = \frac{P \cdot b}{43 \cdot 10^{-4} \cdot n_1}; \qquad (2)$$

$$E_2 = \frac{P \cdot b}{43 \cdot 10^{-4} \cdot n_2}; \qquad (3)$$

$$\eta = \frac{P \cdot b \cdot \tau_1 \cdot 60}{43 \cdot 10^{-4}}; \qquad (4)$$

$$a = \frac{k_{av} \cdot 43 \cdot 10^{-4}}{b \cdot 60 \cdot P}; \qquad (5)$$

where P is the stress in dynes/cm^2; $43 \cdot 10^{-4}$ is the value of a microscope scale division in cm; n_1 and n_2 are the numbers of microscope scale divisions corresponding to conventional instantaneous-elastic deformation and to deformation due to elastic after-effects; b is the distance between the plates; τ_1 is the time for residual displacement per 1 division in minutes; k_{av} is the average value of k calculated by Formula (1), in microscope divisions per minute.

The first line in Table 1 gives values calculated from the results of an experiment the duration of which was sufficient for complete development of elastic deformation. At the same time, the great duration of the experiment led to structural changes in the specimen. Therefore the rate of irreversible flow gradually decreased. Thus the viscosity, η_t, calculated from the rate of growth of the deformation at the end of the loading, represents a property of the gel which has become established after some aging during the experiment. The viscosity η_{av}, however, can be regarded as a kind of average of all the intermediate values observed in course of the loading, as it is found from the average rate, calculated as the ratio of the total irreversible deformation to the time for its development. The duration of the experiments described in Lines 3 and 4 (Table 1) was evidently not sufficient for completion of growth of the elastic deformation, and therefore the rate recorded at the end of the experiment refers not only to irreversible flow, but also to elastic after-effects, and the viscosity value calculated from it is too low.

The constant a in Table 1 is the ratio of the already known factor k to the stress P in the experiment. In contrast to k, which cannot be used in evaluating the material, as it depends on the stress P and varies proportionately with it, the constant a is a perfectly definite characteristic of the material. An interesting fact is that its dimensions are reciprocal to the dimensions of viscosity and, being a value which the reciprocal of viscosity, it varies with the temperature and concentration. Proportionality between k and the applied shearing stress P was demonstrated by us in the case of polyisobutylene [6]. This rule was assumed as established for our investigations of gelatin, as the features of gel behavior made an exact verification of this previously established rule impossible. Experimental data are shown here (Table 2) which indicate approximate proportionality between k and P. Similar investigations were not performed with solutions of other concentrations or at other temperatures, as it would be difficult to find a range of significantly different stresses outside the permissible limits for shear in a gap between two plane-parallel plates. However, in a study of stress relaxation at constant deformation in gelatin gels, we obtained indirect proof that k is proportional to P. Table 3 shows a calculation of stress relaxation in 5% gelatin gel at 22.5° according to the simplified formula.

$$-\frac{E_1}{E_1+E_2}\log\left[\frac{P}{P_0}\left(1+\frac{E_2}{E_1}\right)-\frac{E_2}{E_1}\right]+\log\frac{P}{P_0}=D=\frac{aE_1\tau}{2.3}. \qquad (6)$$

which is derived in the paper [6].

As has already been stated, this derivation is applicable to the case when relaxation due to elastic aftereffects (elasticity) is rapid, but that due to irreversible flow has not yet developed, as is usually the case at the start of an experiment. The use of Equation (6) for verification, against experimental data, of deductions and equations relating to the relaxation process has the advantage that in this case the calculation is less affected by inaccuracies of the previously determined characteristics, owing to its greater simplicity, the absence of viscosity (η) (which cannot be determined with enough precision for gelatin gels) among the characteristics, and the avoidance of subtraction in the operations, which in some conditions can also lead to a result affect by inaccuracies in the values used.

TABLE 3

Stress Relaxation in 5% Gelatin Gel Aged for 2 Days

$E_1 = 1.9 \cdot 10^3$ dynes·cm^{-2}; $E_2 = 2.85 \cdot 10^3$ dynes·cm^{-2}; $a = 1.15 \cdot 10^{-8}$ cm^2·dyne^{-1}·sec^{-1}

$\tau \cdot 10^{-2}$ sec.	$P\ \frac{\text{dynes}}{\text{cm}^2}$	$\frac{D}{\tau} \cdot 10^5$	$\tau \cdot 10^{-2}$ sec.	$P\ \frac{\text{dynes}}{\text{cm}^2}$	$\frac{D}{\tau} \cdot 10^5$
0	975	–	9.12	853	0.77
0.3	949	1.0	16.8	815	0.84
1.02	925	0.88	22.5	790	0.89
2.88	900	0.80	32.4	755	0.99
6.30	875	0.95	36.3	731	1.21

$$\frac{aE_1}{2.3} = 0.95 \cdot 10^{-5}$$

The calculation shows that the left-hand side of the equation remains constant for a considerable time (about an hour); and it is not only constant, but is equal in sign and absolute magnitude to the right-hand side of the equation, which is a product of constants. In general, however, it must be pointed out that calculations with the use of Equation (6), or with the more complex equation published earlier [6], should be performed only if the previously determined characteristics of the system are known with sufficient accuracy, and if the system does not undergo any structural changes in the course of relaxation.

SUMMARY

1. The previously established laws of the growth of elastic deformation ε_e under constant stress P, and its decay after unloading, and also for relaxation of stress at constant deformation, based on the simple differential relationships:

$$\left(\frac{d\varepsilon_e}{d\tau}\right)_P = k\,\frac{\varepsilon_m-\varepsilon_e}{\varepsilon_e}\ (\text{ loading }):\ -\left(\frac{d\varepsilon_e}{d\tau}\right)_{P=0} = k\,\frac{\varepsilon_e}{\varepsilon_m-\varepsilon_e}\ (\text{ unloading }):\ k\approx aP,$$

are applicable to the corresponding processes in the deformation of gelatin gels.

2. The growth and decay of elastic deformation in gelatin gels show that the kinetics of the two processes coincide, which is an important condition for exact determination of the deformation properties of the system. For this condition to be fulfilled, a number of requirements must be carefully satisfied (the duration of deformation under a constant acting stress must be sufficient for complete development of elastic deformation; side processes which alter the gel structure, and drying of the gel during the experiment, must be eliminated).

LITERATURE CITED

[1] P. L. Zubov, Z. N. Zhurkina and V. A. Kargin, Colloid J. 9, 109, 367 (1947); 16, 109 (1954) (T. p. 119);* Proc. Acad. Sci. USSR, 67, 659 (1949).

[2] S. M. Lipatov, Problems of Gelation of Lyophilic Colloids (All-Union Sci.-Tech. Soc. Engineers and Technicians, Moscow, 1937); Problems in the Science of Lyophilic Colloids (Minsk, 1941).

[3] J. E. Eldridge and J. D. Ferry, J. Phys. Chem. 58, 11, 992 (1954).

[4] H. Boedtker, P. Doty, J. Phys. Chem. 58, 11, 968 (1954).

[5] F. N. Schwedoff, J. Phys. 8, 341 (1889).

[6] L. V. Chumakova and P. A. Rebinder, Proc. Acad. Sci. USSR 81, 239 (1951); L. V. Ivanova-Chumakova and P. A. Rebinder, Colloid J. 18, 429, 540 (1956) (T. p. 421).*

[7] S. A. Reitlinger and A. V. Igolkina, Biochemistry (USSR) 4, 23 (1939); S. A. Reitlinger, Colloid J. 4, 679 (1938).

[8] A. Galecki, Badania fizyko-chemiczne nad želatina, Poznan, 1950.

Institute of Physical Chemistry
Academy of Sciences USSR
Division of Disperse Systems
Moscow

Received April 7, 1956

---

* T. p. = C. B. Translation pagination.

PHASE SEPARATION IN HIGH-POLYMER SOLUTIONS

L. E. Kalinina, V. I. Alekseenko, and S. S. Voyutsky

The phase separation into layers of two high polymers in solution is of great interest both theoretically and practically. There is no doubt that a definite relationship must exist between the compatibility of high polymers in solution and their ability to form homogeneous mixtures with one another.

To the best of our knowledge, phase separation of high-polymer solutions (various cellulose derivatives) was first observed by the Soviet scientists Medvedev and Dogadkina [1]. They also showed that phase separation of high polymers in solution is caused by formation of molecular swarms and structures in the system, and that this structure formation is determined by different polarities of the macromolecules.

Later, Dobry and Boyer-Kawenoki [2] studied the separation of 35 pairs of high polymers in various solvents (a total of 78 systems). They concluded that the phase separation of polymer mixtures in solutions is the rule rather than an exception. Phase separation was found only to occur in fairly concentrated systems, when the high-polymer molecules were fairly close together.

It is significant that phase separation in solution proved to be completely reversible – if a concentrated solution was diluted it lost its capacity for phase separation and, conversely, evaporation of solvent caused a homogeneous solution to become turbid and to show signs of separation. It was also shown that the concentration at which separation begins depends not only on the chemical nature of the components, but also on their molecular weights and the shape of the macromolecules. Compatibility of polymers decreases with increasing molecular weights. If two polymers are incompatible in one solvent, then, as a rule, they are also incompatible in other solvents. According to the authors cited [2], the nature of the solvent has a significant influence on the concentration at which separation occurs.

As a result of their observations Dobry and Boyer-Kawenoki concluded that there is no direct relationship between compatibility and chemical nature. A similar structure of the principal chain is insufficient for compatibility between two polymers. Vinyl derivatives are not mutually compatible; the same is true of cellulose derivatives. The presence of the same substituent in the molecules is also not sufficient for compatibility of polymers in solution. For example, polyvinyl acetate is not compatible with cellulose acetate. However, benzylcellulose is compatible with polystyrene.

The demixing of high-polymer solutions has been studied very recently by N. F. Komskaya, G. V. Struminsky, and G. L. Slonimsky. These authors discovered phase separation to occur in solutions of a number of mixtures of rubberlike polymers, and showed that the heat term in the well-known equation $\Delta F = \Delta H - T\,\Delta S$ has a significant influence on the compatibility of high polymer solutions.

The present communication contains some data on the behavior, in solutions, of mixtures of nitrocellulose and butadiene-acrylonitrile copolymers of various polarities. These data, together with the characteristics of the polymers used, from the point of view of their ability to yield homogeneous mixtures [3], lead to certain new conclusions and generalizations concerning the incompatibility of high polymers in solution.

EXPERIMENTAL

One of the components used in the present investigation was nitrocellulose containing ~12% nitrogen. The other component was polybutadiene with plasticity value 0.3, or one of four butadiene-acrylontirile copolymers containing 18.4, 28.6, 37.7 or 44.4% acrylonitrile groups.

The solvent was a mixture of ethyl acetate, benzene, and ethyl alcohol in 4 : 2 : 1 ratio. This mixture is generally used as a solvent for nitrocellulose in production of nitrocellulose varnishes, and was found also to dissolve the other, high-elastic, component of the system.

Experience showed that solutions of moderate concentration are convenient for observing polymer separation. Because of their high viscosity, separation in highly concentrated solutions is extremely slow. On the other hand, in dilute solutions, evidently because of the considerable intermolecular distances, there is no appreciable interaction between the components and no separation into layers occurs. It was found experimentally that solutions containing ~10% solids (by weight) are the most suitable. Solutions of this concentration were used for all the experiments.

To carry out the experiments, mixtures of solutions of the two components taken in definite quantitative proportions were poured into 100 ml cylinders with ground-glass stoppers. The mixtures were thoroughly agitated before being put into the cylinders, and were quite homogeneous in all cases. The filled cylinders were kept in a closed cupboard in the laboratory. Changes in the external appearance of the solutions in the cylinders were observed at intervals. At the end of the observation period the cylinders were opened and, if separation had occurred, films were cast separately from the upper and lower layers and subjected to physicochemical analysis.

In solutions containing nitrocellulose and nonpolar polybutadiene, separation was already observed 12-13 hours after the mixture had been made. Tests of the physical and mechanical properties of films cast from each layer separately showed that the upper layer contained almost pure polybutadiene, and the lower layer, almost pure nitrocellulose. This is in accordance with the fact that polybutadiene is completely incompatible with nitrocellulose. Films made from a freshly prepared unseparated mixture of the two components were extremely weak and very inhomogeneous in appearance. This can be seen in Fig. 1, which gives a photograph of a nitrocellulose film containing 40% polybutadiene.

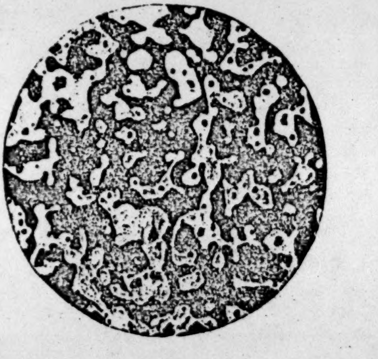

Fig. 1. Photograph of a nitrocellulose film containing 40% polybutadiene.

On the other hand, no separation was observed at all in systems containing nitrocellulose with one of the butadiene-acrylonitrile copolymers containing 28.6% acrylonitrile groups, and over. This also is in accordance with the fact that such fairly polar copolymers are completely compatible with nitrocellulose in all proportions [3].

The most significant experiments were those with a weakly polar butadiene-acrylonitrile copolymer, containing 18.4% acrylonitrile groups, which is only partially compatible with the relatively highly polar nitrocellulose [3]. Solutions containing this polymer and nitrocellulose after a certain time separated into two layers (upper and lower), with at first a weak and then a well-defined boundary between them. Fig. 2 shows curves for the separation kinetics of 10% solutions of mixtures with various contents of nitrocellulose and copolymer containing 18.4% acrylonitrile groups. As the start of each curve shows, the separation becomes noticeable on the second or third day, when a second layer appears in the lower part of the cylinder, the volume of this layer growing at a decreasing rate. Conversely, the volume of the upper layer diminishes correspondingly. After 200-250 days the separation is completed and the volumes of the upper and lower layers become practically constant.

The films obtained from the upper liquid layers in all the cylinders were very similar in external appearance to films made from butadiene–acrylonitrile copolymer. However, it was shown by physical tests that the tensile strength of these films is rather higher, and the extensibility at break rather lower, than of the pure copolymer films. This indicates that the upper layer contains some nitrocellulose in addition to the butadiene–acrylonitrile copolymer.

Similar tests on films made from the lower liquid layers showed that they contain mainly nitrocellulose

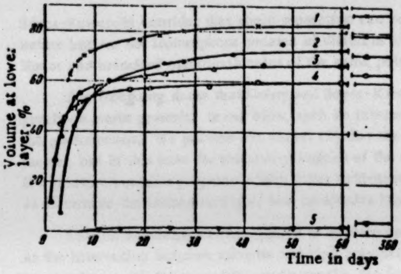

Fig. 2. Curves for the separation kinetics of 10% solutions of mixtures of nitrocellulose and butadiene–acrylonitrile copolymer containing 18.4% acrylonitrile groups. Mixtures contain: 1) 20%; 2) 40%; 3) 50%; 4) 60%; 5) 80% butadiene–acrylonitrile copolymer.

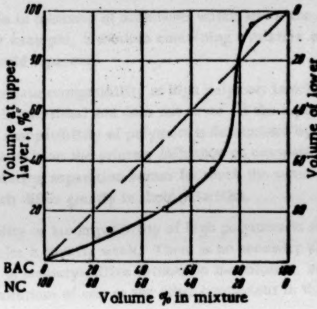

Fig. 3. Variation of the equilibrium volumes of the upper and lower layers with the volume composition of the polymer mixture present in solution.

with an admixture of butadiene–acrylonitrile copolymer. A comparison of the regions of the curves corresponding to the start of the separation shows that the process is slowest when the content of butadiene–acrylonitrile copolymer in the mixture is ~40%. This is probably caused by the high viscosity of the system, which is in turn the result of its maximum microheterogeneity in this instance. Our investigations showed that the heterogeneity of the films is greatest precisely at this ratio of the two polymers.

Figure 3 shows the variations of the equilibrium volumes of the upper and lower layers as a function of the volume composition of the polymer mixture in solution. It is seen that the graph resembles typical vapor–composition curves for binary systems the behavior of which is nonideal. In view of the high complexity of the system nitrocellulose–butadiene–acrylonitrile copolymer–solvent, it is impossible without additional investigations to establish the cause for the deviation of the curve from the diagonal of the square. It seems likely, however, that the curve cuts the diagonal for the same reasons as those which cause this effect in solutions of low-molecular substances, namely, the formation of molecular complexes (aggregates) in solution, probably of variable composition which depends on the component ratio.

DISCUSSION OF RESULTS

Dobry and Boyer-Kawenoki [2] give the following explanation for the compatibility or incompatibility of high polymers in solution.

In a fairly concentrated solution of one polymer, or of a mixture of compatible polymers, interaction occurs between the macromolecules which leads to formation of semicrystalline lattices, which become gradually more perfect with increasing concentration of the solution. Each such lattice, arising in a restricted region, can be regarded as a submicroscopic mesophase, and the whole solution then evidently consists of a large number of such mesophases with different orientation. As a result the whole solution appears homogeneous. Thus, the structure of a high polymer solution is analogous to the structure of a liquid, except that in this instance the size of the particles considerably exceeds the size of the molecules.

The formation of such semicrystalline lattices may occur if the molecules which constitute them are isomorphous. In other words, a condition for the formation of such lattices is the existence of common quasicrystallographic elements in the molecules of both polymers present in the solution. In the absence of such elements microlattice formation is impossible, and this leads to incompatibility of the polymers in solutions of sufficiently high concentrations.

Since, according to Dobry and Boyer-Kawenoki, the basic condition for compatibility is the presence of quasicrystallographic elements in the macromolecules, it is not surprising that two cellulose derivatives can exhibit phase separation in solution despite their apparently great chemical similarity. Moreover, Dobry and

Boyer-Kawenoki consider that phase separation can occur even in mixtures of molecules which are of the same nature but are not isomorphous because of different form. For example, a solution containing a mixture of linear and branched macromolecules of the same polymer should separate.

The foregoing shows that Dobry and Boyer-Kawenoki explain compatibility of high polymers in solution purely on steric grounds. In our view, such an interpretation is one-sided and does not cover all the aspects of the phenomenon. We pointed out earlier [3] that the mutual compatibility of polymers is determined by many factors, but in this case the relative polarities of the components have the primary influence on compatibility. If a mixture contains polymers which differ sufficiently in polarity, separation occurs for much the same reasons as determine the immiscibility of low-molecular liquids which differ greatly in their polarities.

Similar reasoning can be applied to explain compatibility or incompatibility of high polymers in solutions, as the interaction between solvents and high polymer molecules is usually weak. There is no necessity at all to postulate, with Dobry and Boyer-Kawenoki, the formation of semicrystalline lattices in the solution, and it is sufficient to use the concept of microvolumes containing solutions of one or the other component in the common solvent.

The validity of this viewpoint is confirmed not only by our experiments, which showed that compatibility of polar nitrocellulose with butadiene—acrylonitrile copolymers increases with increasing polarity of the latter, but also by the extensive data found in Dobry and Boyer-Kawenoki's paper. In fact, a careful examination of their results will show that compatibility occurs only when the polarities of the components were similar. For example, the strongly polar polyvinyl alcohol, which is still compatible with methylcellulose within certain limits, is not only incompatible with the less polar ethylcellulose, but even has no solvent in common with it. Conversely, the nonpolar natural rubber is compatible within certain limits with the weakly polar polystyrene and ethylcellulose, but has no common solvent with the polar nitrocellulose. Ethylcellulose, which has moderate polarity, has relatively good compatibility in solution with benzylcellulose, polyvinyl acetate, methyl methacrylate (polymer) and other polymers which also have moderate polarities.

Another argument against the view of Dobry and Boyer-Kawenoki that the compatibility of two high polymers is determined only by the presence of quasicrystallographic elements in them is provided by the compatibility, in solution, of methylcellulose with polyvinyl alcohol, or of nitrocellulose with polyvinyl acetate, which have totally different structures. A final argument against the view of Dobry and Boyer-Kawenoki is that their prediction of spontaneous phase separation of high-polymer solutions containing molecules of the same nature but different in form has never been confirmed in practice.

Of course, it by no means follows from the above that steric factors can have no influence on compatibility or leave no mark on the general picture of phase separation. However, as we have already stated, this influence has little significance in polymer solutions in comparison with the influence of the polarity relationships of the components on compatibility.

Certain conclusions concerning the mechanism of phase separation in solutions of high-polymer mixtures can also be drawn from observations of the general process of phase separation and of its kinetics. We may suppose that at the start of the process microseparation of the two polymeric components takes place, with formation of microvolumes containing solutions of one or other of the components. If interaction takes place in the system between the two polymers to give rise to aggregates, then evidently the microvolumes formed can contain such aggregates with one or other component quantitatively predominant. As a result, the microvolumes containing a solution of the less dense polymer or aggregate float up, while the microvolumes with denser contents sink, and two layers are gradually formed. It is seen that this process somewhat resembles the separation of complex emulsions, with the exception of the fact that the polymers are dissolved in a low-molecular solvent, and the microvolumes containing solutions of one or other of the polymers have no clearly defined boundaries. A boundary between the layers is evidently formed only when the separation is fairly advanced and individual microvolumes containing one or other of the polymers have coalesced. Subsequent changes in the volumes of the two solutions probably occur largely as the result of differences in their osmotic pressures. This

---

* Unfortunately, Dobry and Boyer-Kawenoki give no data from which the polarity of the polymers used by them could be evaluated. Therefore only general considerations — molecular structure and the dipole moments of the groups present in the molecules — can be used to estimate the polarities of these polymers. Therefore no quantitative conclusions can be drawn from the data in the paper.

process can be regarded as a syneresis process in the layer of dimishing volume, and as swelling in the layer of increasing volume.

The explanation for the incompatibility of two high polymers in solution which was given above is based on the nature of the intermolecular interaction. It would be of interest, however, to touch briefly on the thermodynamics of this effect.

In the most general case, the separation of two high polymers is the consequence of the low entropy of mixing, insufficient to overcome the negative heat of mixing. The question arises, however, why a solution of two high polymers can show phase separation even at very low concentrations, while solutions of two low-molecular substances only begin to show signs of separation at concentrations close to saturation. The special tendency of high-polymer solutions to phase separation should probably be attributed to the fact that the entropy change per unit volume of solution when their solutions are mixed is very small because of the high molecular weights of the components and of the existence, even in relatively dilute solutions, of intermolecular forces which diminish the number of possible macromolecular configurations. On the other hand, the enthalpy change when solutions of two high polymers are mixed should differ little from the enthalpy change when solutions of two low-molecular substances are mixed, since in both cases a unit volume of the final solution will contain the same number of groups between which the molecular forces act.

In such conditions the compatibility or incompatibility of high polymers in solution will be largely determined by the enthalpy change of the system, and even a small negative heat of mixing of the high-polymer solutions should correspond to phase separation.

SUMMARY

1. Phase separation in solutions of mixtures of nitrocellulose with polybutadiene and butadiene−acrylonitrile copolymers of various polarities in a mixed solvent used for production of nitrocellulose lacquer has been studied. It is shown that polybutadiene is totally incompatible with nitrocellulose, while butadiene−acrylonitrile copolymers containing 28.6% acrylonitrile groups and over are completely compatible with it.

2. A study has been made of the kinetics of phase separation in solutions of nitrocellulose and butadiene−acrylonitrile copolymer containing 18.4% acrylonitrile groups.

3. The curve for the variation of the equilibrium volumes of the upper and lower layers as a function of the composition of the high-polymer mixture in the solution resembles typical vapor−composition curves for binary nonideal systems. The view is advanced that this is caused by formation of molecular complexes (aggregates) in the solution, probably of variable composition which depends on the component ratio.

4. Suggestions as to the causes of phase separation in mixtures of high-polymer solutions are put forward.

Central Scientific Research Institute
for Leather Substitutes
Moscow

Received November 28, 1955

LITERATURE CITED

[1] A. I. Medvedev and N. A. Dogadkina, Artificial Fiber (USSR) 1935, No. 1, 21.

[2] A. Dobry and F. Boyer-Kawenoki, J. Polymer Sci. 2, 90 (1947).

[3] V. I. Alekseenko, I. U. Mishustin and S. S. Voyutsky, Colloid J. 17, No. 3, (1955).

A THERMOMECHANICAL INVESTIGATION OF EPOXIDE RESINS

B. M. Kovarskaya, L. I. Golubenkova, M. S. Akutin, and G. L. Slonimsky

A new kind of synthetic resins, termed epoxide resins, has recently come into extensive use in various branches of industry. These resins, obtained by condensation of diphenols with compounds containing the epoxy group 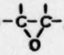 $-\overset{|}{C}-\overset{|}{C}-$ (with O bridging), such as diphenolylpropane with epichlorohydrin, are thermoplastic products with various softening temperatures which depend on the proportions of the starting materials and on the condensation conditions [1]. The molecular weight of such resins lies in the range of 400-4000 [2, 3].

The action of various substances, such as diamines, thermosetting resins, and fatty acids and their anhydrides, can convert epoxide resins into hardening resins with formation of tridimensional structures [2, 4-10].

Papers dealing with investigations of the hardening mechanism of epoxide resins contain indications that the formation of network structures occurs as the result of reactions of the epoxy and hydroxyl groups with the reactive groups of substances added to harden the resin [1]. In particular, it has been stated that reactions between phenol-formaldehyde resoles and epoxide resins occur by interaction of hydroxyl groups of phenol nuclei and methylol groups of the resoles with the epoxy groups of the epoxide resins [1, 3, 5, 11].

The hardening of epoxide resins is not accompanied by evolution of volatile products, as is the case in the hardening of thermosetting condensation resins, and this facilitates their processing considerably. The hardened products have good adhesion to metals, glass, and other materials, high chemical resistance, and good dielectric and mechanical properties.

In the present investigation thermomechanical studies were carried out on epoxide resins with additions of various hardeners (hexamethylenediamine, polyethylene polyamine, phenol-formaldehyde resole) in order to determine the structure and the possible temperature limits for the utilization of these resins.

The material studied was an epoxide resin obtained by condensation of diphenylolpropane with epichlorohydrin (in a molar ratio of 1 : 2.3) in an alkaline medium. This resin was a viscous liquid with a glass point of about 0°C. (Fig. 1). The thermomechanical curve for the original resin was obtained with the aid of Kargin's dynamometric balance [12] (height of specimen 6 mm, duration of stress 10 seconds).

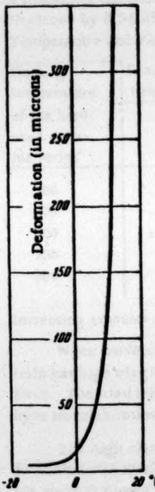

Fig. 1. Deformation of an epoxide resin as a function of temperature (constant applied load $\sigma = 0.07\ kg/cm^2$).

Thermomechanical curves for the resin with added hardeners were determined with the aid of a consistometer [13] in which compressive deformation of polymers can be studied at constant stress in the temperature range from +20 to +250°.

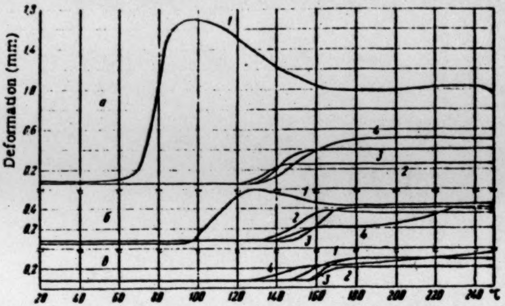

Fig. 2. Deformation-temperature curves ($\sigma = 5$ kg/cm^2) for epoxide resin hardened by 6.5 (a), 10 (b) and 15% (c) of polyethylene polyamine (Curves 1), and after additional heating for 10 hours at 100 (2); 150 (3); 200° (4)

TABLE 1

Variation of the Glass Temperature of Epoxide Resin, Hardened by 6.5% of Hexamethylenediamine, with Temperature and Time of Heating[*]

Heating temperature of the hardened epoxide resin,[*]	Glass temperature, °C after heating time in hours			
	1	5	10	20
100	50	–	65	–
100	70	–	95	–
200	110	120	120	120
250	–	–	105	–
300	85	–	–	–

Hardening of epoxide resins by amines. As hardeners for epoxide resins the substances containing amino groups tested were polyethylenepolyamine (a mixture of homologs from triethylenetetramine to hexaethyleneheptamine with boiling point above 175°) and hexamethylenediamine. Appropriate quantities of the hardeners were added to the epoxide resin warmed to 50°. After the resin had been cooled it was made into specimens (10 mm in diameter and 10 mm high) by by hardening for 10 minutes at 125° under a specific pressure of 250 kg/cm^2. The deformability of the specimens was tested by the action of a stress of 5 kg/cm^2 for 10 seconds.

The thermomechanical curves for the original specimens given in Fig. 2 show that the maximum deformation of epoxide resin not subjected to heat treatment is diminished 5 to 7-fold with increasing amounts of polyethylene polyamine. The glass temperature simultaneously rises by 70°.

When hardened in presence of even a small quantity of hardener, 6.5%, (Fig. 2, a, Curve 1), the epoxide resin has high elasticity, and its original shape is practically completely restored after removal of the deforming force. The elasticity modulus of such resins is 3-3.5 times less than the elasticity modulus of phenol-formaldehyde Novolak resins hardened with 6.5% of hexamethylenetetramine.

The high elasticity of epoxide resins hardened by small quantities of hardener is probably caused by the formation of a spatial network with infrequent and long cross-links. The great length of the cross-links in epoxide resins is caused by the fact that their chains are linked by long molecules (for example, in the case of hexamethylenediamine the cross-link has the structure $-NH-CH_2-CH_2-CH_2-CH_2-CH_2-CH_2-NH-$). Thus, the presence of a structure with infrequent and long flexible cross-links between the chains in hardened epoxide resins results in high elasticity when such specimens are deformed by the action of small stresses.

The behavior of hardened epoxide resins subjected to additional heat treatment is very interesting. Fig. 2

---

[*] These results were obtained with resin specimens with glass temperature 45°.

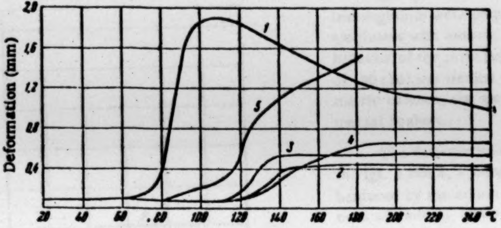

Fig. 3. Deformation-temperature curves (σ = 5 kg/cm²) for epoxide resin hardened by 6.5% of hexamethylenediamine (Curve 1) and after additional heating for 10 hours at 100° (2); 150° (3); 200° (4); and for 1 hour at 280° (5).

and table 1 show that heating of the hardened resins results in a considerable increase in the rigidity of the structure, manifested in an increase of the glass temperature and a decreased maximum deformation. Similar results have been reported in the literature [3]. This effect is especially prominent in resin hardened with 6.5% of polyethylene polyamine or hexamethylenediamine (Fig. 2, a and 3). In the case of hexamethylenediamine, if the hardened resin is heated for 10 hours at 100-150° the glass temperature rises by 60°. Prolonged heating at higher temperatures (150-200°) leads to some degradation of the resin, shown by a slight increase of maximum deformation (Fig. 2, Curves 3 and 4). If the specimen is heated in the range of 250-300° (Fig. 3, Curve 5), considerable degradation occurs,* leading to a sharp fall of the glass temperature (compared to specimens heated at lower temperatures), and destruction of the specimen when tested at the same stress (5 kg/cm²).

The data on degradation of the hardened resin after additional heating are confirmed by data on the solubility of these resins in boiling acetone (Fig. 4). Hardened resins which had been heated for 10 hours at 150-200° have higher solubility than the original resins. Heating for an hour at 300° produces a 4 to 5-fold increase of solubility.

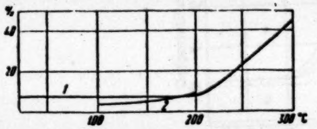

Fig. 4. Solubility in acetone (in %) of epoxide resin hardened by 6.5% of hexamethylenediamine and heated for 1 hour (1) and 10 hours (2).

Heating of a resin hardened with 6.5% of polyethylene polyamine at 100-150° produces the same strengthening as is found in resins hardened with 10-15% of this hardener. Thus, the use of smaller quantities of hardener and additional heat treatmement of the resin may be recommended, as it appears that excess hardener

Epoxide resin hardened by polyethylene polyamine retains its original appearance even after prolonged heating (up to 200°), whereas resin hardened by hexamethylenediamine becomes black and opaque, and cracks, in the same conditions. Thus polyethylene polyamine has advantages over hexamethylenediamine from the point of view of processing technology and of the appearance of the resins after hardening.

Hardening of epoxide resins by phenol-formaldehyde resole. To investigate the hardening of epoxide resin in presence of resole, the specimens were made by mixing different quantities of acetone solutions of the components (ratios of epoxide to resole were 100:10, 100:50, 100:100, 100:150). Acetone was removed from the solutions by distillation, and the resultant resins were dried under vacuum at room temperature to complete removal of acetone.

---

*The occurrence of degradation is quite obvious from the external appearance of the specimen.

The specimens for the thermomechanical investigations were prepared as described for the specimens with amines. The thermomechanical behavior of the resin (with epoxide-resole ratio of 100 : 10) was studied with the aid of dynamometric balance, the specimens being cast in special beakers.

The deformation-temperature curves given in Figs. 5 and 6, a show that the epoxide resin is hardened by the action of resole, as in the presence of amines. However, in presence of small quantities of resole (10%) (Fig. 5) the hardening proceeds very slowly, and the structures formed, even after additional heating, are very soft, and gelatinous at high temperatures. The glass temperature of the hardened epoxide resin is practically unaffected by an increase of the resole content, but the latter makes the system more rigid.

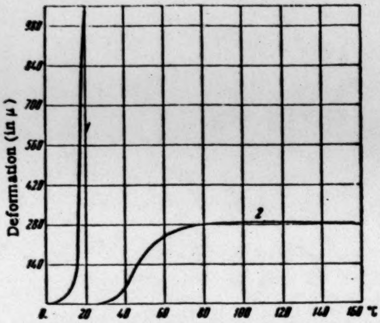

Fig. 5. Deformation-temperature curves (σ = 0.07 kg/cm^2) for hardened epoxide-resole, 100 : 10 (1), and after additional heating at 100° for 10 hours (2).

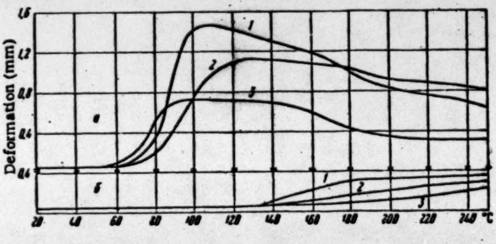

Fig. 6. Deformation-temperature curves (σ = 5 kg/cm^2) for hardened epoxide-resole resins, 100 :50 (1), 100 : 100 (2), and 100 : 150 (3); a) not heated; b) after additional heating for 10 hours at 200°.

As in the case of hardening by amines, when an epoxide resin with added resole is heated, the hardness is increased considerably (Fig. 6, b). However, a resole-hardened epoxide resin is much more stable to heat than the same epoxide resin hardened by amines.* In such resins slight degradation occurs only on heating at 280° for 10 hours (Fig. 7).

The hardened mixed resins have much higher elasticity than hardened phenol-formaldehyde resins (resites)

---

*Addition of hexamethylenediamine to epoxide-resole resins produces a considerable deterioration of the external appearance of the specimens owing to phase separation. It is possible that this separation is caused by the formation of three types of structure—epoxide resin hardened by hexamethylenediamine, epoxide resin hardened by resole, and hardened resole. The formation of such structures is quite probable, as hexamethylenediamine reacts with epoxide resin at room temperature, while the hardening of resole requires high temperatures (of the order of 100° and over). Therefore additional hardener is not required for hardening of mixed (epoxide and resole) resins.

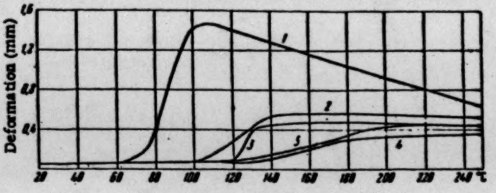

Fig. 6. Deformation – temperature curves (σ = 5 kg/cm²) for hardened epoxide-resole resins, 100:50 (1), 100:100(2), and 100:150 (3); a) not heated; b) after additional heating for 10 hours at 200°.

TABLE 2

Values of Elasticity Modulus of Epoxide Resins Hardened at 200° for 10 hours

Resins and hardener	Elasticity modulus E in kg/cm²	Resins and hardener	Elasticity modulus E in kg/cm²
Epoxide resin and 6.5% polyethylene polyamine	100	Epoxide-resole resin (100 : 50)	140
Epoxide resin and 10% polyethylene polyamine	190	Epoxide-resole resin (100 : 100)	190
Epoxide resin and 6.5% hexamethylenediamine	80	Epoxide-resole resin (100 : 150)	500
		Phenol-formaldehyde resin (resite)	4,300

(Table 2). The equilibrium modulus of elasticity of epoxide resins with added resoles in 100 : 50 ratio is 20 times less than the equilibrium modulus of elasticity of phenol-formaldehyde resites.

Finally it must be pointed out that for a complete investigation of the hardening of epoxide resins, our thermomechanical investigation of elasticity under uniaxial compression must be augmented by studies of other important mechanical characteristics, such as tensile strength, brittleness, etc.

SUMMARY

1. Thermomechanical studies of epoxide resins can be used to reveal differences in the hardening process by the action of different substances, and to determine structural changes which occur in hardening.

2. Hardened epoxide resins are probably tridimensional structures with infrequent long and flexible cross-links between the chains, giving rise to high elasticity. This view, based on studies of the mechanical behavior of the resins, and on the fact that the equilibrium modulus of elasticity was found to be independent of temperature, contradicts the structural formulas for hardened epoxide resins given in the literature.

3. Epoxide resins hardened by amines are less heat-resistant (150-200°) than resins hardened in presence of phenol-formaldehyde resole (250-280°).

4. Hardened epoxide resins are much more elastic than phenol-formaldehyde resites, which makes them suitable for use as lacquers, adhesives, and coatings.

LITERATURE CITED

[1] K. Theile and P. Colomb, Chimia 9, No. 5, 104 (1955).

[2] M. M. Koton, Progr. 24 901 (1955).

[3] H. Jahn, Plaste u. Kautschuk, H. 3 - 4, 50, 83 (1954).

[4] W. J. Marmion, Research 7, No. 7, 351 (1954).

[5] E. S. Narracott, Brit. Plastics 28, No. 6, 253 (1955).

[6] A. I. Lazareva and M. F. Sorokin, Chem. Ind. 954, No. 5, 24 (1954).

[7] J. Zonsveldj, J. Oil and Colour Chemists' Assoc. 37, No. 414 (1954).

[8] A. Bring, Chemicky Prumysl. 5, No. 2, 74, (1955).

[9] W. Fisch and W. Hofmann, J. Pol. Sci. 12, No. 67, 497, (1954).

[10] W. Olechowa, Przemyst.Chem. 10, No. 12, 603, (1954).

[11] R. Wegler, Angew.Chem. 67, No. 19/ 20, 582 (1955).

[12] V. A. Kargin and T. I. Sogolova, J. Phys. Chem. 23, No. 5, 530 (1949).

[13] G. M. Bartenev, J. Phys. Chem. 24, 1210 (1950).

Received March 16, 1956

Scientific Research and Project Institute
for Plastics, Moscow

INVESTIGATION OF THE VISCOSITY OF DILUTE POLYACRYLONITRILE SOLUTIONS

V. E. Kotina and V. S. Klimenkov

Several investigations have been published on the determination of the molecular weight of polyacrylonitrile; the most important of these are the papers by Houtz and by Frind [1]. Houtz published data on fractionation of the polymer. He used the osmotic pressure values for individual fractions to calculate the coefficient K, which depends on the chemical nature of polyacrylonitrile and the dimethylformamide used as solvent, and also the coefficient α, which depends on the form of the macromolecules in solution. Houtz gives the following formula for determination of the molecular weight of polyacrylonitrile from the intrinsic viscosity of the polymer:

$$[\eta] = KM^{a} = 1.75\cdot 10^{-3}\cdot M^{0.\text{[illegible]}}.$$

Frind, who studied the viscosity of polyacrylonitrile and the osmotic pressure of its dilute solutions, found a different value of K for this polymer:

$$[\eta] = 2.50\ 10^{-3}\cdot M^{0.\text{[illegible]}}.$$

Frind states that deviations of K from the value found by him may be attributed to the methods of preparation.

We have found that the variation of reduced viscosity (η_{sp}/ c) with concentration of dilute solutions differs for polyacrylonitrile polymerized by different methods. In view of this, the intrinsic viscosity of polyacrylonitrile found by extrapolation cannot always be used to characterize the polymer, and therefore its use as a basis for molecular weight calculations does not always give comparable results.

However, the variation of η_{sp}/ c gives an indication of the behavior of the molecules in solution.

EXPERIMENTAL

Polyacrylonitrile made by emulsion polymerization in presence of various initiators usually has a high degree of polymerization, and therefore in some instances it is technically unsuitable. The polymerization is therefore carried out in presence of various substances which regulate chain growth, or in presence of oxidation-reduction initiator systems, leading to a decrease of the degree of polymerization of the product.

We have studied viscosity-concentration relationships in dilute solutions of polyacrylonitrile prepared by three different methods. The polymer was obtained by emulsion polymerization: 1) in presence of potassium persulfate; 2) by the same procedure, but in presence of 0.1; 0.5; 0.7; and 1.0% hydroxylamine used as regulator of chain growth (4 samples); 3) in presence of an oxidation-reduction system consisting of potassium persulfate and sodium hydrosulfite (3 samples).

The specific viscosity of the polymers was determined by means of an Ostwald viscosimeter at 25 ± 0.5°. Dimethylformamide was used as the solvent. The concentrations of the solutions used were 0.5; 0.25; 0.125; and 0.062%. The variation of specific viscosity with concentration for all three types of polymer is given in Figs. 1, 2, and 3.

Figure 1 shows that the polymer obtained in the absence of chain growth regulators shows a rapid fall of reduced viscosity with dilution. The variation of reduced viscosity with concentration is considerably less for the polymer obtained in presence of an oxidation-reduction initiator system (Fig. 3).

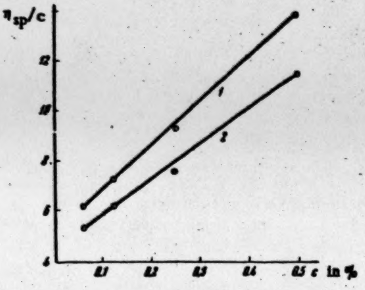

Fig. 1. Variation of η_{sp}/c with concentration of a polymer obtained without the use of chain growth regulators: 1 and 2) sample numbers.

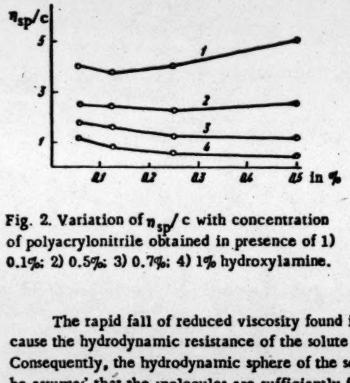

Fig. 2. Variation of η_{sp}/c with concentration of polyacrylonitrile obtained in presence of 1) 0.1%; 2) 0.5%; 3) 0.7%; 4) 1% hydroxylamine.

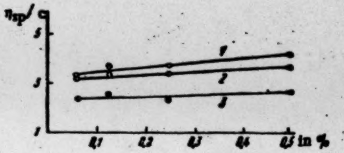

Fig. 3. Variation of η_{sp}/c with concentration of polyacrylonitrile obtained in presence of oxidation-reduction initiator systems: 1, 2, and 3) sample numbers.

The polymer obtained in presence of hydroxylamine (Fig. 2) shows an increase of η_{sp}/c with dilution; this increase is greater with larger amounts of hydroxylamine.

DISCUSSION OF RESULTS

The foregoing data show that determination of the intrinsic viscosity by extrapolation of values of η_{sp}/c to c = 0 may give results which are not comparable, with polyacrylonitrile polymerized by different methods. For example, the intrinsic viscosity of a polymer obtained in presence of potassium persulfate (Fig. 1, Sample 2) is ~4.5 ~4.5; the intrinsic viscosity of a polymer obtained in presence of hydroxylamine (Fig. 2, Sample 1) has approximately the same value. Consequently the two polymers should have similar molecular weights, but at 0.5% concentration their solution viscosities differ considerably. Therefore the value of the molecular weight calculated from the intrinsic viscosity, whatever formula may be used, cannot serve as a technological characteristic of the polymer.

The rapid fall of reduced viscosity found in polyacrylonitrile of a high degree of polymerization occurs because the hydrodynamic resistance of the solute molecules to the flow of liquid decreases appreciably on dilution. Consequently, the hydrodynamic sphere of the solute molecules diminishes also, and in the present instance it may be assumed that the molecules are sufficiently flexible.

Polyacrylonitrile of a lower degree of polymerization shows a considerably smaller variation of η_{sp}/c with solution concentration. In this case the polymer chains are considerably shorter and consequently they lose flexibility; their hydrodynamic radius is more stable. Our observations here are in agreement with data on the relationship between molecular flexibility of polymers and the polymer chain length [2]. Accordingly it may be presumed that the polyacrylonitrile molecule is rigid, and it exhibits flexibility only at high degrees of polymerization.

The same conclusion may be reached from the packing coefficient for polyacrylonitrile, which is calculated from data on the contraction of the molar volume of the monomer during formation of the polymer chain. According to calculations performed by Klimenkov, Kargin, and Kitaigorodsky [3] the contraction value for acrylonitrile is 19.8 cm^3/ mole. For the more flexible polyethylene molecule this value is 88.8 cm^3/ mole for the amorphous form, and 97.65 cm^2/ mole for the crystalline polymer. For the less flexible 2-vinyldibenzofuran the contraction is only 10.0 cm^2/ mole.

The flexibility of the polymer chains was evaluated by these authors from data on the ratio $\Delta V_c/\Delta V_t$, where ΔV_c is the absolute contraction and ΔV_t is its lower limit. For polymers with flexible chains, $\Delta V_c/\Delta V_t \approx 2$; this value diminishes with increasing chain rigidity, and reaches 0.21 for 2-vinylbenzofuran. The ratio $\Delta V_c/\Delta V_t$ for polyacrylonitrile is 0.97. Accordingly, polyacrylonitrile is rather more rigid than polystyrene, for which $\Delta V_c/\Delta V_t = 1$. The rigidity of the polyacrylonitrile chain may be attributed to the high polarity of the nitrile group.

The characteristic increase of reduced viscosity on dilution found in solutions of polyacrylonitrile obtained in presence of hydroxylamine is the consequence of an increase in the hydrodynamic dimensions of the molecule. A similar variation of the viscosity of highly dilute solutions was observed by Umstatter [4] for a number of other polymers.

A combination of several investigation methods must be used to determine the causes of the increase in the hydrodynamic dimensions of the molecules on dilution. It is possible that it may be caused by some degree of uncoiling and straightening of the polymer chains. On the basis of the work of Dargin, Mikhailov, and Elenek [5] it is also to be expected that the polymer chains would be more rigid in this instance.

SUMMARY

1. The relationship between reduced viscosity and concentration of dilute polyacrylonitrile solutions in dimethylformamide differs for polymers prepared by different methods.

2. Molecules of polymers prepared by different polymerization methods have different flexibilities and change their configurations in different ways when the solutions are diluted. In consequence, molecular weight values calculated from the intrinsic viscosities must be regarded as provisional.

LITERATURE CITED

[1] R. C. Houtz, Textile Research. J. 1950, No. 11, 786; H. Frind, Faserforsch and Textiltech. 1954, No. 12, 540.

[2] A. A. Tager, Solutions of High-Molecular Compounds (Chem. Press, 1950), p. 25

[3] V. S. Klimenkov, V. A. Kargin, and A. I. Kitaigorodsky, J. Phys. Chem. 17, No. 8 (1953).

[4] H. Umstätter, Macromol. Chem. 11, 94 (1954).

[5] V. A. Kargin, N. V. Mikhailov, and V. I. Elenek, Proc. 6th Conf. on High Polymers (1949).

Received September 6, 1955

All-Union Scientific Research Institute for
Artificial Fibers

INFLUENCE OF THE STRUCTURE OF RUBBER ON INHIBITOR DIFFUSION

A. S. Kuzminsky, S. A. Reitlinger, and E. V. Shemastina

Various rubbers and vulcanizates can be used for technical purposes only if they are stabilized by inhibitors (antioxidants). It is known that antioxidants are much less effective in the aging of rubber than in the aging of low-molecular hydrocarbons. This specific behavior of antioxidants is due, among other causes, to the special physical conditions in which oxidative processes develop in rubbers. In high polymers the rate of chemical reaction depends significantly on the diffusion of the reactants which is in turn determined by the internal mobility of the polymer molecular chains. It has been shown [1] that the diffusion constants of antioxidants in polymers are approximately one or two orders of magnitude lower than in liquids. The commonest antioxidant in the rubber industry is phenyl-β-naphthylamine (Neozone D). In our earlier investigations [1-3], the solubility and diffusion constants of phenyl-β-naphthylamine in a number of synthetic rubbers were determined.

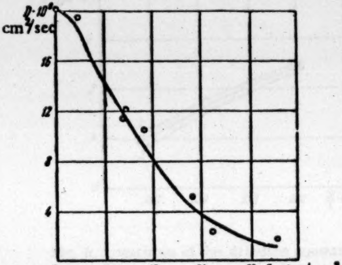

Fig. 1. Variation of the diffusion constant D of phenyl-β-naphthylamine with the equilibrium modulus E_∞ of the rubber at 20°.

It is known that, in contrast to the raw rubber, vulcanized rubbers are polymers with a spatial structure, in most cases containing a highly dispersed filler. In the present investigation the influence of the space structure and filling of rubbers on the diffusion rate of phenyl-β-naphthylamine has been studied in relation to the density of the network and the nature of the filler.

The diffusion constants were determined with the use of rubber plates[*] 20 mm in diameter and 1 mm thick. The plates were previously extracted with acetone in a stream of nitrogen to remove free sulfur and soluble impurities, dried under vacuum and paired with plates of similar size made from SKB vulcanizate containing 2% phenyl-β-napthylamine. The pairs of plates were clamped together and placed in a glass vessel full of nitrogen, which was immersed in an ultrathermostat. To prevent evaporation of the antioxidant, the plates were insulated from the surroundings by cellophane. At the end of a definite period the plates were extracted with acetone, and the contents of phenyl-β-naphthylamine in the extracts were determined colorimetrically. To eliminate edge effects, the concentration of the antioxidant was determined in the middle of the plate only.

The diffusion coefficient D was calculated from the Stefan formula [4] for the contact of two infinite cylindrical columns of solution and solvent.

$$A = a_0 \sqrt{\frac{Dt}{\pi}},$$

---

[*] The formulation, in parts by weight, was: SKB 100; zinc oxide 2.0; stearic acid 2.0; diphenylguanidine 1.0. The sulfur content and the time of vulcanization in the press were varied to obtain networks of different densities.

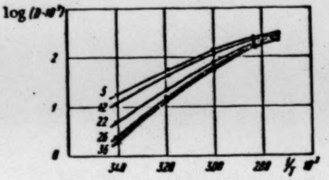

Fig. 2. Logarithm of the diffusion constant (log D) of phenyl - β - naphthylamine in rubbers as a function of the reciprocal absolute temperature (1/T). The numbers on the curves represent the equilibrium modulus E_∞ of the rubber in kg/cm².

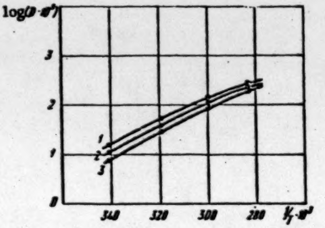

Fig. 3. Logarithm of the diffusion constant (log D) of phenyl - β - naphthylamine in filled rubbers as a function of the reciprocal absolute temperature (1/T): 1) unfilled SKB vulcanizate; 2) SKB + 50 wt. parts chalk; 3) SKB + 60 wt. parts gas black.

where A is the amount of antioxidant, in grams, passed through 1 cm² of the separation boundary; a_0 is the initial antioxidant concentration in the vulcanizate in g/cc; _t_ is the time in seconds. In order to approach the required conditions, the duration of the experiments was so chosen that the inhibitor did not have time to diffuse through more than one-third of the thickness of the rubber plate.

Figure 1 shows the variation of the diffusion constant of phenyl - β - naphthylamine with the density of the spatial network, expressed in terms of the equilibrium modulus of the rubber. Values of the equilibrium modulus E_∞ may be used to calculate N, the number of individual chains in the spatial network per unit volume of rubber, with the use of Bartenev's formula [5].

$$E_\infty \sim N^{2/3} \quad \text{or} \quad [N] \sim E_\infty^{3/2},$$

where [N] is a factor proportional to the number of chains N. Increase of the equilibrium modulus, and therefore of the density of the spatial network, is accompanied by a considerable decrease of the diffusion constant of phenyl - β - naphthylamine in rubber, analogous to the decrease of the diffusion constants of gases in rubbers with increasing content of bound sulfur [6].

The results of investigations of the effect of temperature on the diffusion constant of phenyl - β -naphthylamine in rubbers with spatial networks of different densities, plotted in log D - 1/T coordinates, are shown in Fig. 2. As the equilibrium modulus of the rubber increases, the activation energy of diffusion, calculated from $D = D_0 e^{-E/RT}$ for the temperature range 20-40° increases also (see table).

As the temperature rises, the log D - 1/T curves come closer together, which indicates a decrease of the influence of the density of the spatial network in the diffusion constant. It may be presumed that at temperatures of the order of 150-180° the diffusion rate of the antioxidant will be practically the same in cross-linked and in structureless rubber. It is interesting to note that a similar mobility of the spatial structures of rubber at elevated temperatures was also observed in studies of the mechanical properties of rubbers [7, 8].

In the temperature range chosen for the present investigation, this effect cannot be explained by destruction or regrouping of the spatial network, but is caused by the temperature variations of the thermal motion of the chain molecules.

It seems likely that the action of covalent cross-links extends to neighboring regions of the rubber chain molecules, so favoring an increase in the magnitude of the intermolecular forces by bringing these regions closer together. The density of the structure and the energy of intermolecular interaction would increase with increasing density of the network.

The values of the activation energy of diffusion in rubbers with a spatial structure determined from the slope of the log D - 1/T graphs in Fig. 2, approach with increasing temperature to the values for the activation energy of diffusion in structureless rubber. Increase of temperature favors the destruction of intermolecular bonds, which at 150-180° no longer play a significant part in the formation of the spatial structure of the polymer.

TABLE

Variation of the Activation Energy of Diffusion with the Equilibrium Modulus of the Rubber

Amount of bound sulfur, %	Equilibrium modulus of the rubber in kg/cm² at 20°	[N] a factor proportional to the number of chains	Activation energy of diffusion E_D in cal/mole (20-40°)
1.9	5	11.2	10400
3.4	12	36.7	12100
5.5	22	107	14000
6.3	26	133	17800
8.1	36	215	18400

In addition to the density and the nature of the spatial network, the properties of rubbers used in practice depend significantly on the properties of the fillers added to the rubber.

To determine the effect of fillers, the diffusion constants of phenyl-β-naphthylamine were determined in rubber containing 50 wt. parts of chalk (inactive filler) and 60 wt. parts of gas black (active filler). The data on the temperature relationship of the diffusion constants in Fig. 3 show that introduction of a filler lowers the diffusion constant of the antioxidant, but has practically no effect on the activation energy of diffusion. In this instance the filler has no significant effect on chain flexibility, and its role is that of a "mechanical" rather than an "energetic" action on diffusion [9].

SUMMARY

1. The diffusion rate of antioxidant (phenyl-β-naphthylamine) in rubbers decreases with increasing density of the spatial network and on addition of filler.

2. Increase of the density of the spatial network leads, at 20-40°, to a considerable increase of the activation energy of diffusion in rubbers, but with increase of temperature the activation energies for variously structurized rubbers decrease, and tend in the limit to the value of the activation energy of diffusion of the antioxidant in the original rubber.

3. The view is advanced that the spatial network affects the rate and activation energy of diffusion in cross-linked polymers by the action of additional intermolecular forces, which decrease with increasing temperature.

LITERATURE CITED

[1] A. S. Kuzminsky, S. A. Reitlinger and E. V. Shemastina, Proc. Acad. Sci. USSR 98, 4, 611 (1954).

[2] S. A. Reitlinger and A. S. Kuzminsky, J. Appl. Chem. 27, 2, 214 (1954).

[3] A. S. Kuzminsky, S. A. Reitlinger and E. V. Shemastina, Aging and Fatigue of Rubbers and Increase of Their Stability (State Chem. Press, 1955), pp. 130-140.

[4] Cited through J. Duclaux, Diffusion in Liquids (United Sci.-Tech. Press, 1939), p. 8.

[5] G. M. Bartenev and L. A. Vishnitskaya, J. Tech. Phys. 20, 858 (1950).

[6] R. Barrer and G. Skirrow, J. Polymer Sci. 3, 4, 549 (1948).

[7] B. A. Dogadkin and Z. N. Tarasova, Colloid J. 15, 347 (1953) (T.p. 355).*

[8] G. L. Slonimsky, V. A. Kargin, G. N. Buiko, E. V. Reztsova and M. Luis-Riera, in Symposium: Aging and Fatigue of Rubbers and Increase of Their Stability (State Chem. Press, 1955), pp. 100-119.

[9] J. Amerongen, Kautschuk and Gummi 7, 6, 132 (1954).

Received April 16, 1955

Scientific Research Institute for the Rubber Industry

---

*T.p. = Translation pagination.

EFFECT OF HYDROPHILIC SUBSTANCES ON THE DIFFUSION OF DIRECT DYES INTO CELLULOSE FIBERS

B.N. Melnikov and P.V. Moryganov

It has now been indubitably established that the diffusion rates of dyes within fibers are 1,000-10,000 times as slow as the diffusion rates of the same dyes in water. This great decrease of the rate of internal diffusion is explained by mechanical resistance of the network of chain molecules of the fiber, the like charges of the dye particles and the cellulose surface, and mainly by the existence of affinity forces between the dye and the fiber. To describe the internal diffusion process with interaction between the dye particles and the active centers of the fiber taken into consideration, Crank [1] derived the following differential equation:

$$\frac{\partial c}{\partial t} = D_0 \frac{\partial^2 c}{\partial x^2} - R \frac{\partial c}{\partial t} \quad \text{or} \quad \frac{\partial c}{\partial t} = \frac{D_0}{R+1} \frac{\partial^2 c}{\partial x^2},$$

where R is a constant which represents the distribution of the dye between the fiber and the dye bath, and D_0 is the true diffusion coefficient of the dye within the fiber in conditions such that no adsorption of the dye by the fiber takes place and electrostatic interaction is absent. If the dye – fiber interaction is represented by the factor ΔZ^0, or the affinity of the dye for the fiber, then the relationship between the internal diffusion coefficient and affinity may be represented [2] as:

$$D = C_1 e^{-\Delta H/RT} e^{\Delta S/R} = C_1 e^{-\Delta Z^0/RT}$$

or

$$\ln D = C_2 - \Delta Z^0 / RT \text{ when } C_2 = \ln C_1.$$

Here C_1 is a constant proportional to D_0.

It follows from these equations that, with a gradual decrease of affinity of the dye for the fiber, the internal diffusion coefficient, and consequently the total dyeing rate, should increase. One possible method of decreasing the affinity of the dye for the fiber is the addition of hydrophilic substances to the dye bath, such as polyvinyl-pyrrolidone, various ethylene oxide condensation products such as Dispersol A, and, finally, pyridine.

According to Martin and Standing [3], in sufficiently concentrated solutions these compounds form fairly stable addition products with the dye molecules, and these do not have the power of interacting with the fiber. For example, at a pyridine concentration of ~ 20 –25% it is possible to strip a dye completely from a dyed fiber, which indicates total loss of affinity of the dye for the fiber. At lower pyridine concentrations the dye only partially loses its affinity for the fiber, and this is expressed in decreased adsorption of the dye by the fiber. In view of the existence of this method for regulation of dye – fiber affinity, the object of our work was to study possibilities of a considerable increase of the rate of penetration of the dye through the fiber, and consequently, of an increase in the rate of dyeing. However, by the term "dyeing rate" we do not mean the rate of removal of the dye from the bath, but the rate of its migration from the outside to the center of the fiber. The first hydrophilic addition chosen was pyridine, and our intention was to pass later to cheaper and industrially more convenient additives.

The diffusion coefficients were calculated on the basis of a diffusion equation, solved for the conditions of an infinite dye bath and a fiber of circular section by Hill [4] in the form of the series:

$$\frac{c_t}{c_\infty} = 1 - 0.692\,(e^{-5.785Dt/r^2} + 0.190\,e^{-30.5Dt/r^2} + 0.0775\,e^{-74.9Dt/r^2} +$$
$$+ 0.0415\,e^{-139Dt/r^2} + 0.0258\,e^{-223Dt/r^2} + \ldots)$$

or, in general form:

$$\frac{c_t}{c_\infty} = 1 - Ae^{-BK} - Ce^{-FK} - Ge^{-HK},$$

where A, B, C, F, H, etc. are constants with known values, and $K = Dt, F/r^2$; c_t – is the concentration of the dye in the fiber at time t; c_∞ is the equilibrium concentration of the dye in the fiber. By giving arbitrary values to K, it is possible to calculate the corresponding values of c_t/c_∞ and to plot the relationship between c_t/c_∞ and K. Further, by determining experimental values c_t/c_∞, this graph can be easily used to find values of K, and hence the diffusion coefficients.

Since the diffusion coefficients were calculated from a determination of the total quantities of dye taken up by the fiber, we had to confine ourselves to the use of fairly low concentrations of pyridine in the dye bath, of the order of 10-15 g/liter. At high pyridine concentrations the selective sorption of dyes by the fiber is so low that it becomes impossible to follow the variation of c_t with time, as the dye reaches the fiber center very rapidly and subsequently its concentration does not change with time. In such cases, with high pyridine concentrations in the solution, determination of the internal diffusion coefficients requires the use of the monolayer cellulose membrane method, with treatment of the results by Barrer's method [5] or Neale's method [6]; this we intend to do later.

The experiments were performed on cuprammonium staple fibers, which were scoured before the experiments for an hour at 80° in a solution containing 3 g of soap per liter, rinsed with warm water to remove all traces of soap, and dried. The filament thickness was determined microscopically, and found to be 20 μ. The dyes used were purified direct dyes – Direct Diazo Black C (Color Index 401), and Direct Diazo Black O (Color Index 395). The dyes were purified and analyzed as described previously [7]. The bath ratio was 2000 in all cases. The dye concentration in the fiber was determined experimentally at definite time intervals, that is, c_t was found. The dyeing was then taken to equilibrium and c_∞ was determined. The ratio c_t/c_∞ was used graphically, as described above, to determine the corresponding values of K and hence of D. The calculated diffusion coefficients are given in Table 1.

For comparison, the same table shows the diffusion coefficients of the same dyes, in the same fiber, determined in identical conditions, but without pyridine in the dye bath.

It is seen from the experimental results in Table 1 that the internal diffusion coefficients of both the dyes are always higher when pyridine is present in the dye bath. Diazo Black O, which has a higher affinity for the fiber than Diazo Black C (see Table 2) shows a larger increase of internal diffusion coefficients for the same concentrations of pyridine in the dye bath.

The influence of pyridine is especially pronounced at high electrolyte concentrations and low temperatures. For example, in the case of the dye Direct Diazo Black O at a concentration of 5 g/liter, the diffusion coefficient could not be determined in absence of pyridine. This is to be explained, on the one hand, by the higher affinity at lower temperatures, and on the other, by the fact that in this instance the dye particles are strongly aggregated and the solution is so unstable that at the first stages of the experiment, dye aggregates are deposited on the fiber surface in the form of a multimolecular layer. Subsequently, however, simple redistribution of the dye probably occurs by its migration from the outside to the center of the fiber. Therefore determination of diffusioncoefficients in these conditions involves considerable difficulties. The tendency of the dye particles to aggregate is, again, greater if the thermodynamic affinity is greater, as the forces which act between the individual dye anions are of the same character as the forces acting between the dye anions and the fiber.

TABLE 1

Average Diffusion Coefficients

NaCl concentration in g/liter	Diffusion coefficient $D \cdot 10^{-8}$ cm^2/min at temperatures, °C				
	60	70	80	90	100
Direct Diazo Black C					
1	0,74	1.63	3.37	6.26	12.38
5	—	2.11	3.88	8.13	15.00
10	—	1.03	2.51	5.30	11.30
15	—	0.588	1.41	3.50	8.33
Direct Diazo Black C with addition of 50 g pyridine per liter					
1	1.48	3.15	6.30	12.03	20.1
5	—	4.32	8.20	14.03	24.8
10	1.75	3.72	8.0	14.90	26.2
15	1.11	2.46	5.50	11.23	21.2
Direct Diazo Black O					
0,5	0,550	1.36	2.60	5.60	8,80
1	0,602	1.82	3.62	7.63	13.53
2	—	0.924	2.18	5.90	12.47
3	—	0.525	1.41	4.47	11.50
5	—	—	—	—	—
Direct Diazo Black O with addition of 50 g pyridine per liter					
1	1.83	3.50	6.00	9.80	19.0
2	2.20	4.00	7.12	11.95	21.8
3	2.00	3.56	—	13.00	22.7
5	1.56	3.00	5,25	9.55	20.2

TABLE 2

Affinity of the Direct Dyes Diazo Black O and Diazo Black C for Cotton Fiber

Dye	Affinity in kcal /mole at temperatures, °C				
	60	70	80	90	100
Direct Diazo Black O	6.56	6.24	6.06	5.75	5.40
Direct Diazo Black C	4.40	—	4.08	—	3.78

In the light of the foregoing, the greater influence of pyridine on the diffusion coefficients at low temperatures and high electrolyte concentrations is quite understandable.

The figure shows the relationship between the internal diffusion rate and the temperature in log D − 1/T coordinates. The straight lines found show that the temperature − diffusion rate relationship for the diffusion of direct dyes into cellulose fibers is satisfactorily described by the Arrhenius equation

$$\log D = B - A/T.$$

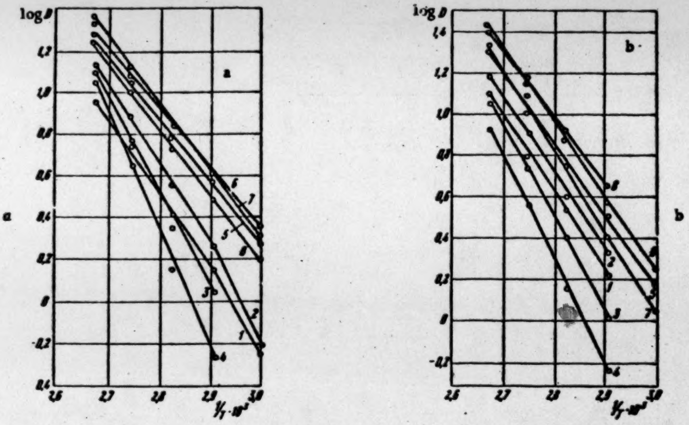

The logarithmic relationship between diffusion coefficients and the reciprocal absolute temperature :
a) Direct Diazo Black O; 1, 2, 3, 4) NaCl concentration in bath 0.5, 1, 2, 3 g/liter, respectively; 5, 6, 7, 8) NaCl concentration 1, 2, 3, 5, g/liter, respectively, and pyridine concentration 50 g/liter;
b) Direct Diazo Black C: 1, 2, 3, 4.) NaCl concentration in bath 1, 5, 10, 15 g/liter, respectively; 5, 6, 7, 8) the same, with 50 g pyridine per liter.

It must be noted, however, that the lines for Direct Diazo Black O in absence of pyridine show breaks in the region of 40-60°. The existence of these breaks, which gradually move into the higher temperature region with increasing electrolyte concentration in the bath, was attributed by us [8] to an abrupt change in the solution state of this dye at temperatures around 40-60°.

As was to be expected, the slope of the lines in the graph varies with the electrolyte concentration in the bath. This is especially prominent in dyeing without pyridine in the dye bath. The increasing slope of the lines at higher electrolyte concentrations is explained by gradually increasing aggregation of the dye particles in the solution, and the consequent increase of the resistance to penetration of the dye into the fiber. It must be pointed out that in presence of pyridine the smallest slope of the lines is found at a certain " optimum" amount of added electrolyte in the dye bath. This is probably caused by the action of the similar electric charges of the fiber and dye anions, and the greater prominence of such action in presence of pyridine is to be explained by the lower hindrance to aggregation in this instance. The activation energy of the diffusion process, calculated from the slopes of the graphs in the figure (see Table 3) is always less for dye baths containing pyridine. This decrease of activation energy, and the consequent easier dyeing, is more prominent for Diazo Black O, which is full accordance with the fact that this dye has a higher affinity for the fiber than Direct Diazo Black C.

It may be concluded from our experimental data that the action of hydrophilic additions in dyeing is analogous to that of an increase of temperature. Therefore, if compounds of such type, suitable for dyeing practice, are found, it would be possible to increase the rate of dyeing considerably, and so to solve the problem of continuous dyeing of cotton fabrics by direct dyes to medium and dark shades without the use of equipment which operates at temperatures above 100°.

TABLE 3

Activation Energy of Diffusion of Direct Dyes in kcal/mole

Electrolyte concentration in g/liter	Temperature range 0-60°	Temperature range 70-100°	Electrolyte concentration in g/liter	Temperature range 70-100°
Direct Diazo Black O			Direct Diazo Black C	
0.5	22.0	16.0	1.0	16.8
1.0	24.0	16.5	5.0	16.5
2.0	—	21.0	10.0	19.7
3.0	—	25.0	15.0	21.8
Direct Diazo Black O with added pyridine			Direct Diazo Black C with added pyridine	
1.0	—	13.9	1.0	15.8
2.0	—	13.3	5.0	14.3
3.0	—	14.7	10.0	16.1
5.0	—	15.2	15.0	17.2

SUMMARY

1. The diffusion coefficients of two direct dyes have been determined over a wide range of temperatures and electrolyte concentrations, with and without addition of pyridine to the dye bath.

2. It is shown that the internal diffusion coefficients of direct dyes increase, and the activation energy of diffusion decreases, on addition of pyridine to the dye bath, and this effect is more prominent for dyes with higher affinity for the fiber.

3. This behavior of dyes in presence of pyridine is explained by the fact that retardation of the diffusion of dyes in fibers is mainly caused by forces of interaction between the dye and the fiber.

LITERATURE CITED

[1] J. Crank, J. Soc. Dyers Colourists, 63, 412 (1947).

[2] S. Glasstones, K.J. Laidler, and H. Eyring, Theory of Rate Processes (New York, 1941), 524. (Cited in T.C. Majury, J. Soc. Dyers Colourists 70, 445 (1954).

[3] J.T. Martin, and H.A. Standing, J. Textile Inst. 40, T671 – 688 and T689 –701 (1949).

[4] T. Vickerstaff, Physical Chemistry of Dyeing (Edinburgh, 1954), p. 131.

[5] R.M. Barrer, Diffusion in and through Solids (Cambridge, 1941)[Russian translation edited by B.D. Tazulakhov (Moscow, 1948), p. 33].

[6] Garvie, Neale, Trans. Faraday Soc. 34, 335 (1938).

[7] B. N. Melnikov and P.V. Moryganov, Colloid J. 17, No. 2, 99 (1955) (T.p. 93)*.

[8] B.N. Melinkov and P.V. Moryganov, Colloid J. 18, No. 5 (1956).

Received February 12, 1956

The Ivanovo Institute of Chemical Technology

---

* T.p. = C.B. Translation pagination.

INVESTIGATION OF THE STRUCTURE AND PROPERTIES OF CARBON-CHAIN POLYMERS IN DILUTE SOLUTIONS

1. SOLUTIONS OF POLYVINYL CHLORIDE AND POLYACRYLONITRILE

N.V. Mikhailov and S.G. Zelikman

The physical properties of polymers in the solid state and in solution are directly related to their chemical structure and the polymer-chain flexibility.

The main laws of polymer solutions have been established by the work of Kargin and his associates, Lipatov and Meerson, Flory, Huggins, Schulz, and others. Spontaneous solution of high polymers occurs with a decrease of free energy and, in the general case, depends both on the energy (ΔH) and on the entropy term ($T\Delta S$)

$$\Delta F = \Delta H - T\Delta S.$$

For rigid polar polymers of the type of cellulose and its derivatives, change of ΔH is the most significant; for non-polar rubberlike polymers increase of entropy plays the dominant role. Molecular flexibility is determined by a number of factors: chemical structure and regularity of the chain, number and nature of functional groups, linear or branched chain structure, and the temperature and nature of the solvent.

A number of methods exist for evaluation of the flexibility and form of molecular chains. The most convenient and widely used methods are measurements of the viscosity and osmotic pressure of the solutions, and combined investigations of these over a wide temperature range.

The object of the present investigation was to determine the relationship between flexibility and molecular structure of carbon-chain fiber-forming polymers.

This paper contains the results of determinations of the viscosity and osmotic pressure of polyvinyl chloride and polyacrylonitrile solutions. Of these compounds, polyvinyl chloride has been studied more extensively. Mead and Fuoss [1] determined the viscosity of polyvinyl chloride in various solvents in the 25-80° temperature range. Staudinger and Schneiders [2] measured the osmotic pressure of technical polyvinyl chloride fractions in tetrahydrofuran and 1, 4-dioxane; Doty and Mischuck [3] carried out determinations in various solvents over a wide temperature range; for solutions of nonfractionated polyvinyl chloride in cyclohexanone Breitenbach and his co-workers [4] obtained the value $\mu = 0.24$. The thermodynamic properties of chlorinated polyvinyl chloride fractions in various solvents have been studied by Bykov [5]. There have been few investigations of the physicochemical properties of polyacrylonitrile. There have been reports on the fractionation [6] and molecular weight determination [7] of polyacrylonitrile.

EXPERIMENTAL

As most synthetic and natural polymers are polydisperse substances, thermodynamic investigation of their properties is impossible without careful fractionation of the materials. Polyvinyl chloride was fractionated as follows: polyvinyl chloride was dissolved in a mixture of equal volumes of chlorobenzene and cyclohexanone at 60-70°. The diluent, acetone, was added to a 1-2 % solution (1 volume of acetone per 1 volume of solvent). The precipitant was methyl alcohol. After precipitation, the flocculent precipitate was removed by decantation and centrifuged. For more complete removal of low-molecular fractions and of traces of chlorobenzene and cyclohexanone, the precipitate was washed with large portions of acetone (2-3 times). An excess of methanol was added in the precipitation of the last fraction.

A method for fractionation of polyacrylonitrile has been described by Houtz [6]: a 1-2% solution of polyacrylonitrile in dimethylformamide was treated with heptane. When the solution was heated to 60° and stirred, partial mixing of solvent and precipitant took place, and the fraction was precipitated in the form of a gel. The solubilities of the different fractions were very similar. Precipitation of the fractions began on addition of 22.3% heptane, and ended at 30.0%.

TABLE 1

Results of Fractionation of One of the Polyacrylonitrile Samples

Amount of precipitant added	Weight of fraction in g	η_{sp} of 0.5% solution
175 ml heptane	0.063	2.12
180 ml heptane	0.111	1.99
185 ml heptane	0.353	1.84
190 ml heptane	1.701	1.50
Excess heptane	0.260	1.41
Excess of 2% $CaCl_2$ solution	2.30	0.99

In a study of this fractionation technique it was found that ~ 40 − 50 % of the polyacrylonitrile is not precipitated by heptane, even if a very large excess of the latter is added. The last fraction can only be isolated by acidification of the solution, or by addition of electrolytes (for example, $CaCl_2$). To obtain white and easily soluble precipitates, the fractions were washed repeatedly with water and dried under vacuum at 80°. The results obtained for one of the samples are given in Table 1.

Viscosities were determined in Ostwald viscosimeters at 20-60°.

The osmotic pressures were determined by the static method with the aid of a modified form of Schulz's osmometer. The membrane was denitrated nitrocellulose made by the method of Montonna and Jilk [8]. After being fixed in the osmometer, the membranes were consecutively treated with alcohol − water mixture, anhydrous alcohol, and dimethylformamide. Three fractions of different viscosities were studied for each material. The variations of viscosity and osmotic pressure with concentration and temperature were studied. Viscosities were determined at 20, 30, 40, 50, and 60°; osmotic pressures at 20, 35, and 50°. In the osmotic pressure determinations the temperature was kept constant in the thermostat to an accuracy of ± 0.01°. At 50° the accuracy decreased somewhat. Measurements of viscosity, and especially of osmotic pressure, are more difficult at higher temperatures because of the considerable increase in the vapor pressure of dimethylformamide.

Results of the Determinations

Polyvinyl chloride. The variation of the reduced viscosity (η_{sp}/c) of polyvinyl chloride with concentration for fractions I and III is given in Fig. 1, where it is seen that (η_{sp}/c) is practically independent of the concentration (c). Variation of η_{sp} with temperature (Fig. 2) is represented by straight lines of increasing slope for higher solution concentrations.

The variation of the reduced osmotic pressure π/c with the concentration c is given in Fig. 3. Variation of osmotic pressure with temperature is given in Fig. 4. The molecular weights of the three polyvinyl chloride fractions, calculated from values of π/c extrapolated to infinite dilution, were found to be 170,000 (fraction I), 137,000 (fraction II), and 47,000 (fraction III). These fractions were used for all the experiments.

Data for osmotic pressure and intrinsic viscosity $[\eta_{sp}/c]_{c \to 0}$ were used to calculate the constants K and α in the equation $[\eta] = KM^{\alpha}$. The values found for polyvinyl chloride were $K = 0.44 \cdot 10^{-3}$; $\alpha = 0.50$. These are approximate values, as the fractions varied over only a 2 to 3-fold range of molecular weight, and the number of fractions studied was not large. A linear relationship between π/c and c is found for polyvinyl chloride; the slope of the lines increases with increasing molecular weight. The slopes of the lines (Fig. 3) were used to calculate the values of the constant μ, which are characteristic for any given polymer − solvent system. The density of polyvinyl chloride in the calculations of μ was taken as 1.41. (from Doty's data [3]).

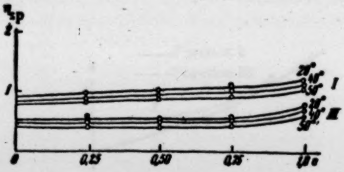

Fig. 1. Reduced viscosity of polyvinyl chloride fractions I and III as a function of solution concentration.

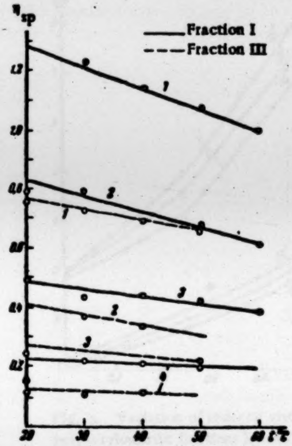

Fig. 2. Variations of viscosity of polyvinyl chloride fractions I and III with temperature, at concentrations: 1) 1.0; 2) 0.75; 3) 0.50; 4) 0.25%.

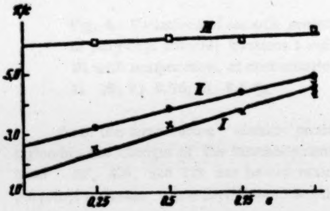

Fig. 3. Reduced osmotic pressure of polyvinyl chloride (I, II, and III represent the fractions).

The values of μ for the three polyvinyl chloride fractions were: fraction I, 0.39 (M = 170,000); fraction II, 0.40 (M = 107,000); and fraction III, 0.48 (M = 47,000). The values of α and μ indicate that polyvinyl chloride is a relatively flexible polymer. The flexibility of the polymer diminishes with decreasing molecular weight, and therefore for the fraction with molecular weight 47,000 μ rises to 0.48.

TABLE 2

Values of the Thermodynamic Functions of the System Polyvinyl Chloride – Dimethylformamide

Fraction	Concentration in g/100 g solution	$-\Delta F_1 \cdot 10^2$ cal /mole			$\Delta H_1 \cdot 10^2$ cal /mole		$\Delta S_{exp} \cdot 10^5$ cal /mole		$\Delta S_{1\,id} \cdot 10^5$ cal /mole
		293°K	308K°	323°K	300,5°K	315,5°K	300,5°K	315,5°K	
I	0.50	0.205	0.240	0.273	0.47	0.44	2.3	2.2	0.32
	0.75	0.496	0.548	0.728	0.52	3.14	3.5	12.0	0.78
II	0.50	0.223	0.248	0.273	0.27	0.21	1.7	1.5	0.55
	0.745	0.496	0.531	0.565	0.19	0 17	2.3	2.3	0.82
	1.00	0.685	0.762	0.890	0.82	1.93	5.1	8.7	1.10
III	0.50	0.505	0.531	0.556	0	0	1.6	1,7	1.56
	0.746	0.753	0.805	0.899	0.26	1.14	3,4	6.3	2.30

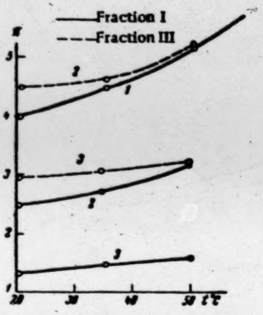

Fig. 4. Variations of osmotic pressure of polyvinyl chloride fractions I and III with temperature, at concentations: 1) 10; 2) 0.75; 3) 0.5 %.

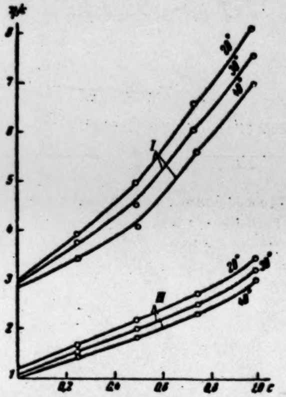

Fig. 5. Variation of reduced viscosity of polyacrylonitrile fractions I and III with solution concentration (at 20, 30 and 40°).

From the temperature – osmotic pressure relationship the changes of the thermodynamic functions ΔF, ΔH, and ΔS can be calculated. The values of the thermodynamic functions for the system polyvinyl chloride – dimethylformamide (characteristic of the solvent) are given in Table 2.

Polyacrylonitrile. The variation of the reduced viscosity with the concentration of polyacrylonitrile solutions in dimethylformamide is given in Fig. 5. The steep rise of viscosity is striking, especially for the first polyacrylonitrile fraction. The deviation from linearity, already found at 0.3-0.4 % concentration, indicates that in these solutions aggregation of polyacrylonitrile molecules begins at very low concentrations.

To determine the solution state of polyacrylonitrile molecules at infinite dilution, the molecular weights of three polyacrylonitrile fractions were measured at different temperatures (Fig. 6). The results are given in Table 3.

Table 3 shows that the molecular weight of polyacrylonitrile is practically independent of the temperature. The slight deviations are within the limits of experimental error. It may be assumed that extrapolation of osmotic pressure to infinite dilution should make it possible to determine the true values of the molecular weight of polyacrylonitrile.

For calculation of μ, the density of polyacrylonitrile was taken as 1.154. The results are given in Table 4. The values of μ decrease with increasing molecular weight and solution temperature, but they are close to 0.5 in all cases.

Changes of the thermodynamic functions for the system polyacrylonitrile – dimethylformamide, calculated per 1 mole of solvent, are given in Table 5.

The influence of functional groups on the behavior of polyvinyl chloride and polyacrylonitrile in solution can be seen from a comparison of the variations of the specific viscosity of these polymers with concentration (Fig. 7). It is seen from Fig. 7 that the viscosity of 0.8% solution of the first polyacrylonitrile fraction (molecular weight 75,000 is 6 times the viscosity of polyvinyl chloride with a molecular weight of 17,000. The increased viscosity in this case is due not to the molecular weight of the polymer but to the different effects of the functional groups Cl and CN. The sharp difference in the temperature coefficients of viscosity should be noted. The specific viscosity is a linear function of temperature over all the temperature range studied (20-60°) both for polyacrylonitrile and for polyvinyl chloride. Therefore the temperature coefficient of viscosity, defined as the increase of viscosity when the temperature is decreased by 10°, is constant over the whole temperature range. The values of the temperature coefficient of viscosity are given in Table 6.

TABLE 3

Variation of the Molecular Weight of Polyacrylonitrile with Temperature

Temperature in °C	Molecular weight		
	Fraction I	Fraction II	Fraction III
20	75,000	70,900	39,100
35	70,000	66,600	38,800
50	69,200	66,100	37,700

TABLE 4

Values of the Coefficient μ for Polyacrylonitrile Fractions

Fraction	Temperature (°C)	μ
I	20	0.46
	35	0.45
	50	0.44
II	35	0.47
III	35	0.485

The temperature coefficient of viscosity for polyvinyl chloride is very small, and changes little with the concentration. The temperature coefficient of viscosity for polyacrylonitrile is several times that of polyvinyl chloride, despite the fact that the molecular weight of the latter is considerably greater. It follows from these results that intermolecular action plays an important part even in 0.8-1.0 % solutions of polyacrylonitrile. This action can be attributed to the presence of the constant CN group dipole and its easy polarizability. These factors are probably connected with certain properties of polyacrylonitrile: poor solubility in most solvents, tendency to structurization in solution, thermoelastic properties, etc. The polarization of molecules with constant dipoles decreases with increasing temperature, leading to a sharp decrease of intermolecular action. In this case the polyacrylonitrile molecules can assume a more coiled configuration, resulting in decreased solution viscosity.

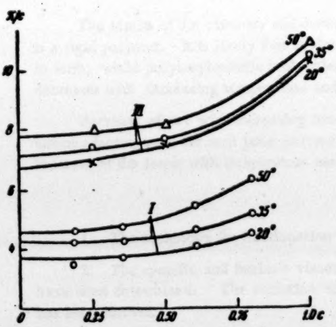

Fig. 6. Variation of reduced osmotic pressure of polyacrylonitrile fractions I and III with concentration (at 20, 35, and 50°).

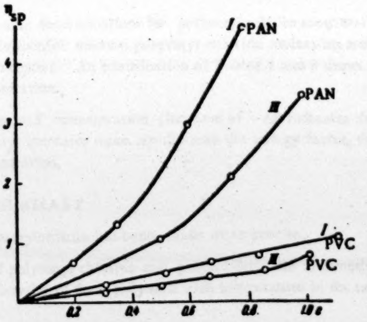

Fig. 7. Variation of the specific viscosity of polyvinyl chloride (PVC) and polyacrylonitrile (PAN) fractions with solution concentration.

TABLE 5

Values of the Thermodynamic Functions of the System Polyacrylonitrile – Dimethylformamide

Fraction	Concentration in g/100 g solution	$-\Delta F_1 \cdot 10^2$ cal /mole			$\Delta H_1 \cdot 10^2$ cal /mole		ΔS_1 exp $\cdot 10^5$ cal /mole		ΔS_1 id $\cdot 10^3$ cal /mole
		293°K	308°K	323°K	300.5°K	315.5°K	300.5°K	315.5°K	
I	0.177	0.111	0.128	0.145	0.19	0.22	1.0	1.1	0.39
	0.350	0.231	0.248	0.282	0.10	0.44	1.1	2.2	0.69
	0.600	0.419	0.488	0.565	0.93	1.09	4.6	5.1	1.19
	0.800	0.616	0.736	0.864	1.72	1.95	8.0	8.8	1.58
III	0.25	0.300	0.335	0.355	0.38	0.07	2.3	1.3	0.96
	0.50	0.633	0.659	0.710	—0.14	0.39	1.7	4.1	1.88
	1.00	—	1.75	1.874	—	0.72	—	8.0	8.77

TABLE 6

Temperature Coefficients of Viscosity for Polyvinyl Chloride and Polyacrylonitrile

Polymer	Molecular weight	Temperature coefficient ($\Delta\eta/\Delta t$) of viscosity at solution concentration	
		1.1–1.0%	0.85–0.75%
Polyvinyl chloride	170,000	0.08	0.07
	47,000	0.05	0.04
Polyacrylonitrile	75,000	—	0,35
	39,100	0.22	0.13

The results of the viscosity and osmotic pressure determinations for polyacrylonitrile show that the latter is a rigid polymer. It is likely that in dimethylformamide solution polyvinyl chloride molecules are globular in form, while polyacrylonitrile molecules are straighter. An examination of Tables 2 and 5 shows that ΔF decreases with increasing temperature and concentration.

Decrease of ΔF with increasing temperature and concentration (increase of −ΔF indicates that the entropy factor, even for such polar polymers, always increases more rapidly than the energy factor, despite the increase of the latter with temperature and concentration.

SUMMARY

1. The technique for fractionation of polyacrylonitrile has been made more precise.

2. The specific and intrinsic viscosities of polyvinyl chloride and polyacrylonitrile in dimethylormamide have been determined. The variation of the viscosity of these polymers with temperature in the range 20-60° has been studied.

3. The osmotic pressure – temperature relationship has been studied, and changes of the thermodynamic functions ΔF, ΔH, and ΔS have been calculated.

4. It is shown that the chain molecules of polyacrylonitrile are less flexible than polyvinyl chloride molecules, because of the different polarities of the functional groups in these polymers.

LITERATURE CITED

[1] D.J. Mead and R.M. Fuoss, J. Am. Chem. Soc. 64, No. 2, 227 (1949).

[2] H. Staudinger and J. Schneiders, Ann. 541, 151 (1939).

[3] P. Doty and Mischuck, J. Am. Chem. Soc. 69, 1631 (1947).

[4] J.W. Breitenbach, E.L. Forster, A.J. Reuner, Kolloid-Z.127, No. 1 (1952).

[5] A.N. Bykov, Dissertation Ivanovo Institute of Chemical Technology, 1952).

[6] R.C. Houtz, Textile Research J. 20, No. 11, 786 (1950).

[7] C.K. Masson and H.W. Melville, J. Polymer Sci. 4, No. 3, 321 (1949).

[8] K.E. Montonna and L.T. Jilk, J. Phys. Chem. 45, 1376 (1941).

Received August 2, 1955

Central Scientific Research Institute for Artificial Fibers

STABILITY OF METAL SOLS IN PRESENCE OF HIGH-MOLECULAR COMPOUNDS

E.M. Natanson and N.N. Kozachek

In our previous studies [1], on the basis of the concepts of structural-mechanical factors in the stabilization of disperse systems and of the formation of structural network, put forward by Rebinder and his school [2], we advanced certain views on changes of stability of disperse systems in presence of high-molecular compounds, which can be stated as follows.

1. Protective action is caused mainly by the ability of a protective high-molecular compound to form an internal structure, or by the formation of such a structure on mixing with a lyophobic sol. The stability of this structure, and its power of rapid restoration when broken down, are the principal factors upon which the aggregative stability of lyophobic sols very often depends.

2. In considering adsorptional interaction between the polymer macromolecules and the metal colloidal particles, we assume that only individual segments of the macromolecules are adsorbed on the surfaces of the latter. The same macromolecules can be attached to a number of other metal colloidal particles, producing chainlike aggregates of such particles in the system. As the result of such interaction a structural network often arises in such systems, where the metal particles are usually in groups, forming chains of various shapes and lengths. At numerous points in such systems the lyophobic colloidal particles also act as cross-links and join sections of different or the same macromolecules. In such systems the lyophobic colloidal particles are contained in a kind of web of threadlike macromolecules of the protective high-molecular compound.

3. The nature of the interaction between the lyophobic sol particles and the macromolecules is also significant in the mechanism of the protective action. The protection is most effective in the case of irreversible adsorption, caused by chemical interaction between the lyophobic particle surface and individual regions of the polymer macromolecules.

4. High-molecular compounds also exert a protective effect at lower concentrations, when a continuous structural network is not formed. In such instances, rare in practice, the protective effect apparently depends on the ratio of the particle concentrations of the polymer and the metal sol. If the particle concentration of the polymer considerably exceeds the concentration of the metal colloidal particles, the protective action is very effective. Most probably in such systems the lyophobic colloidal particles are centers for accumulation of several macromolecules and the formation of branched structural entities, which increases their aggregative stability. Otherwise, destabilization of the metal sol occurs. Thermal motion of individual macromolecules favors coagulation of metal colloidal particles. In such cases the macromolecules of the protective high-molecular compounds bind individual colloidal metal particles together to form large aggregates of metal particles, which are much less stable to sedimentation.

Some of the foregoing views on the mechanism of protection have been confirmed experimentally by us in an investigation of the stability of bismuth organosols in hydrocarbon media [3], and have been provided with a theoretical basis in the recent paper by Simha, Frish, and Eirich [4]. It must also be pointed out that in recent years similar views on adsorptional interaction between hydrophobic colloidal particles and polymer macromolecules have been advanced by some American scientists (Heller and Pugh [5], and Heller and Tanaka [6]), who consider that so-called "steric protection" occurs in the system as the result of such interaction. Unfortunately, these authors make no reference to our prior publications [1].

The present communication contains certain experimenal data obtained in an investigation of the stability of iron organosols in xylene stabilized by rubber, and platinum hydrosols stabilized by agar.

Stability of iron organosols in xylene. We assumed in these investigations that the stability of these organosols depends on the existence of a spatial structure in them. This structure determines a number of mechanical properties of the system, including anomalous viscosity. As is known, anomalous viscosity is not a definite criterion of the existence of a spatial network in sols. However, an abrupt increase or appearance of anomalous viscosity in a system where it was previously slight or absent, is evidence for the reinforcement of formation of a spatial network in such a system.

In this connection, the present communication contains the results of an investigation of the viscosity of iron organosols in xylene, stabilized by rubber, and also the results of yield-stress determinations in these systems and of observations of their stability when exposed to light at room temperature. The organosols used were prepared by the electrolytic method developed by one of us [7].

The viscosities of these organosols and their dispersion media were measured by means of the Höppler falling ball viscosimeter as modified by Goronovsky [8], who introduced a device for varying the slope angle of the viscosimeter. When the angle of the slope down which the ball rolls is varied, the pressure exerted by the ball on the liquid in the tube varies in proportion to the sine of the slope. This makes it possible to measure viscosity in the system under different pressures using the same ball, and thus with the same instrument constants. The measurements were made at 20°. The temperature was kept constant by means of an ultrathermostat.

The viscosimeter was calibrated by means of aqueous glycerol mixture with refractive index 1.426, which corresponds to 68.7% glycerol.

The results of the viscosity determinations are given graphically in Figures 1 and 2.

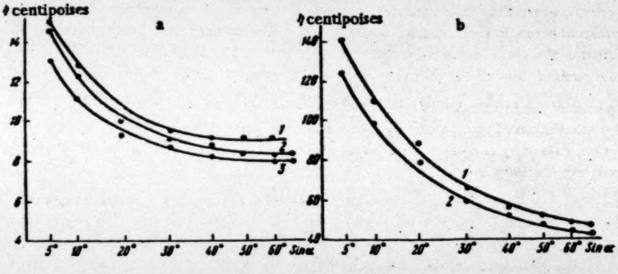

Fig. 1. Viscosity variations of iron organosols in xylene stabilized by a) 0.6% and b) 1.2% rubber; 1) pure solution; 2) with 0.05% Fe; 3) with 0.1% Fe.

An examination of the data in Figures 1 and 2 established the following facts:

1. Solutions of rubber in xylene have anomalous viscosity, which is particularly pronounced at a rubber content of 1.8%. As the rubber concentration increases, the structural region of the curve ascends steeply; for the same range of slope angles from 5 to 70° in the viscosimeter, the values are only 6 centipoises for 0.6% rubber solution, 95 centipoises for 1.2% solution, and 530 centipoises for 1.8% rubber.

2. Highly disperse metallic iron has a strong influence on the viscosity of rubber solutions in xylene. The concentration of the disperse phase of the iron organosol and of the protective polymer (rubber), and the weight ratio of these components in unit volume of sol, are significant. At a rubber concentration of 0.6 and

1.2%. the presence of highly disperse metallic iron in the system produces a viscosity decrease. However, the height of the structural region of the $\eta = f(\sin\alpha)$ curves changes little, and these curves are almost parallel to the corresponding curves for pure rubber solutions over the whole range of slope angles of the viscosimeter (from 5 to 70°). An interesting fact is that when the iron – rubber ratio by weight is doubled, from 1 : 12 to 1 : 6, a further decrease of viscosity occurs. It must be pointed out that the iron organosols formed in these conditions are unstable. The disperse phase in such systems separates out and takes with it a considerable proportion of the rubber, forming a gelatinous precipitate with thixotropic properties. The separation of rubber together with the disperse phase of the iron organosol is the main reason for the viscosity decrease in such systems.

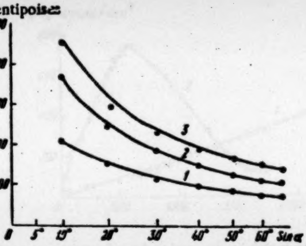

Fig. 2. Viscosity variations of iron organosols in xylene stabilized by 1.8% rubber: 1) pure solution; 2) with 0.05% Fe; 3) with 0.1% Fe.

A totally different picture is seen at a rubber concentration of 1.8%. Here the appearance of disperse iron organosol in the solution produces a considerable viscosity increase. The height of the structural region of the $\eta = f(\sin\alpha)$ curves rises from 550 centipoises for a pure solution of rubber in xylene to 1075 centipoises for an iron– rubber ratio of 1 : 18. This change is especially prominent at small slopes of the viscosimeter, from 10 to 30°. These facts show fairly convincingly that the disperse phase of iron organosols in xylene solutions of rubber causes considerable reinforcement of the space structure, and acts as a kind of active filler in such systems. A similar situation was found in our study of the stability of bismuth organosols [3].

Direct studies of the structural-mechanical properties of metal sols stabilized by high polymers are of great interest. Such investigations may greatly clarify the problem of the relationship between sol stability and the existence of a space structure in the sols. Our investigations of the deformation of iron organosols and their dispersion media at different shearing stresses are of definite importance in the connection.

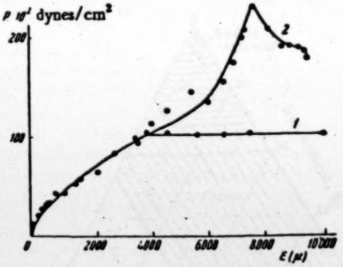

Fig. 3. Variation of deformation with shearing stress for iron organosol in xylene, stabilized by 1.2% rubber: 1) pure solution; 2) with 0.1% Fe.

The measurements of the maximum (static) shearing stress (the yield stress) were carried out by the Veiler and Rebinder method [9]. According to these authors, the method can be used for detection of even the first traces of structure in dilute polymer solutions under the action of active fillers. Some of the results of these measurements are given in Figs. 3 and 4; these show that a yield value is not found in the deformation of rubber solutions in xylene in the concentration range from 1.2 to 1.8%. The absence of a yield value in hydrocarbon solutions of rubber has also been reported by other authors [10].

The presence of highly disperse metallic iron in solutions of rubber in xylene changes their deformation behavior; these systems begin to exhibit a yield value, which is seen especially clearly at rubber concentrations of 1.2 and 1.8%. For the same concentration of iron (0.1% Fe) an increase of the rubber content by 0.6% (from 1.2 to 1.8%) increases the yield value from 230 to 750 dynes/cm², or by a factor of 3.2.

Organosols containing 0.6% rubber and 0.1% iron do not exhibit a yield value, and the curve lies below the corresponding curve for the dispersion medium. It is important to note that these organosols (concentration

0.6%) were the least stable. In such systems the separating disperse phase entrains considerable quantities of rubber, forming, as has already been stated, gelatinous precipitates with thixotropic properties.

The stability of rubber-stabilized iron organosols in xylene as a function of the component ratio is represented in Figure 5 in the form of a triangular diagram for the system xylene – iron – rubber. The criterion of stability in this case was the time until separation of the system took place with formation of a transparent layer of the dispersion medium 1 cm thick. Since the stability region of this system lies in the range of low concentrations of rubber and iron, the compositions of this system over the whole triangle were not investigated.

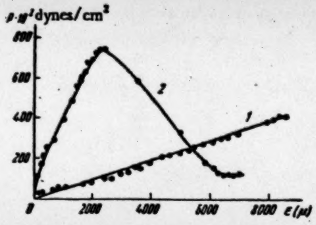

Fig. 4. Variation of deformation with shearing stress for iron organosol in xylene, stabilized by 1.8% rubber: 1) pure solution; 2) with 0.05% Fe.

As the diagram (Fig. 5) shows, organosols containing from 0.3 to 1.0% iron are not stable in a fairly wide range of rubber concentrations, from 0.1 to 1.6%. At iron concentrations up to 0.3% only systems containing from 1.2 to 1.6% rubber were found to be stable. In this instance this very restricted stability region is probably to be explained by the very pronounced interaction between the oxide film on the surface of the colloidal iron particles and individual sections of the rubber macromolecules. At low iron concentrations, this interaction results only in the formation and reinforcement of the internal structure of the iron organosols. The structural network formed consists mainly of intertwined and randomly distributed rubber molecules. Colloidal iron particles act as cross-links at many points of this network. At higher iron concentrations this interaction becomes so pronounced that it leads to appreciable condensation of the internal structure, and in consequence the iron organosols become unstable and fairly soon deposit gelatinous precipitates, which are considerably condensed solvated structural networks of the original organosol, consisting of colloidal iron particles and rubber macromolecules.

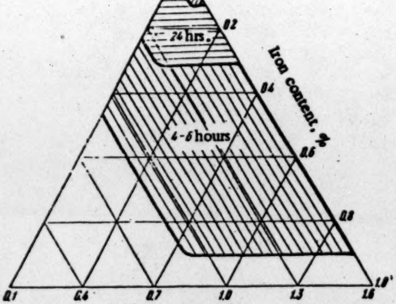

Fig. 5. Stability as a function of the composition of iron organosols stabilized by rubber in xylene.

Stability of platinum hydrosols. Platinum hydrosols were prepared by reduction by means of hydrazine hydrate in an alkaline medium. The protective polymer used as agar, which is typical in this respect. The viscosity variations of these hydrosols were measured by means of an Ostwald viscosimeter with attachments such as are used in studies of viscosity as a function of pressure.

Figures 6 and 7 give the results of determinations of the viscosity and deformation as functions of the shearing stress, for the most stable platinum hydrosols and their dispersion media, kept for several months. An examination of the data in Figures 6 and 7 shows that small concentrations (0.006%) of highly disperse metallic platinum in an alkaline solution of agar produces a considerable increase of viscosity, and the corresponding curve has a well-defined structural region.

Investigations of the variations of deformation of platinum sols and their dispersion media with changes of shearing stress show that the dispersion media of these hydrosols, which are solutions of the hydrolysis products of agar in an alkaline medium, do not exhibit a yield value, and the $P = f(\epsilon)$ curves are more or less smooth. Introduction of highly disperse metallic platinum into these systems again results in reinforcement of the system in comparison with the original dispersion medium.

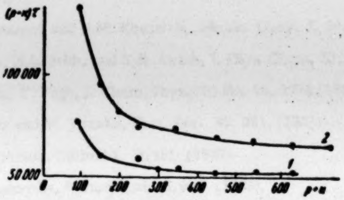

Fig. 6. Viscosity variations of a platinum hydrosol stabilized by 0.5% alkaline agar solution: 1) pure solution; 2) with 0.006% Pt.

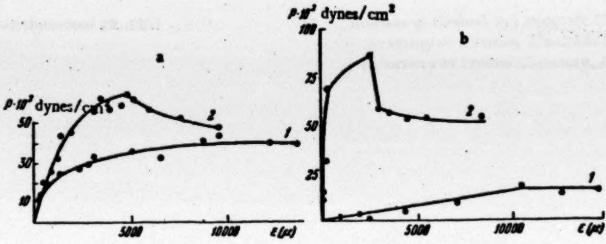

Fig. 7. Variation of deformation with shearing stress in platinum hydrosols stabilized by: a) 0.1% alkaline agar solution; b) 0.25% agar. 1) Pure solution; 2) with 0.006% Pt.

SUMMARY

1. Investigations of the properties of iron organosols in xylene, stabilized by rubber, and of platinum hydrosols stabilized by products of hydrolysis of agar in an alkaline medium, have shown that metal sols which have anomalous viscosity and a yield value are the most stable.

The presence of a highly disperse metal phase in solutions of high polymers results in the appearance or a considerable increase of anomalous viscosity in such solutions, which is evidence of the direct participation of the colloidal metal particles in the formation of the internal structure of stable sols.

3. At low concentrations of rubber in iron sols, the quantitative ratio between the disperse metal phase and the rubber polymer plays an important part. At high values of this ratio the sol usually has low stability and the rubber then acts as a sensitizer (destabilizer).

4. The experimental results presented in this paper confirm our views on the mechanism of stability changes of metal sols in presence of certain polymers, and are of definite importance with regard to the general theory of lyophobic sol stability.

LITERATURE CITED

[1] E.M. Natanson, Proc. Acad. Sci. USSR 74, 517 (1950); E.M. Natanson, Trans. 2nd All-Union Conf. Colloid Chem.(Kiev, 1952) p. 113.

[2] P.A. Rebinder, Bull. Div. Math. Nat. Sci. Acad. Sci. USSR, Chem. Ser. 1936, 5, 639; P.A. Rebinder and S.Ya. Veiler, Proc. Acad. Sci. USSR 31, 444 (1951); Ya. B. Aron and P.A. Rebinder, Proc. Acad. Sci. USSR, 52, 235 (1946).

[3] E.M. Natanson and N.N. Kozachek, Ukrain. Chem. J. 20, 364 (1954).

[4] R. Simha, H.L. Frish, and T.R. Eirich, J. Phys. Chem. 57, No. 6, 584 (1953).

[5] W. Heller, T. Pugh, J. Chem. Phys. 22, No. 10, 1778 (1954).

[6] W. Heller and W. Tanaka, Phys. Rev. 82, 301, (1951).

[7] E.M. Natanson, Colloid J. 9, 191 (1947).

[8] I.T. Goronovsky, Factory Lab. 8, 940 (1953).

[9] S. Ya. Veiler and P.A. Rebinder, Proc. Acad. Sci. USSR 49, 354 (1945).

[10] A.S. Kolbanovskaya and P.A. Rebinder, Colloid J. 12, 194 (1950); A.S. Kolbanovskaya, P.A. Rebinder, and O.I. Lukyanova, Colloid J. 12, 208 (1950).

Received November 19, 1955

Institute of General and Inorganic Chemistry
Academy of Sciences, Ukrainian SSR
Laboratory of Colloid Chemistry, Kiev

PECULIARITIES OF THERMAL EXPANSION OF GELS AND SOLUTIONS OF HIGH POLYMERS

4. THE VOLUME EFFECT OF GELATION

R.E. Neiman

It was shown in the earlier communications [1,2] that gelation of gelatin and agar gels is not accompanied by a volume effect. However, this is not in agreement with earlier published data obtained by some authors, who reached the opposite conclusion. In our opinion, the laws of thermal relaxation of volume of gels and solutions, established in our work [3], allow of a new and more correct evaluation of the results of these authors.

Heymann [4] studied gelation by a dilatometric method. A gelatin solution was heated in a dilatometer until completely homogeneous, and then transferred into a thermostat at 22.5°, where the course of the volume changes until a constant volume was established was observed. Figure 1 gives the results of such an experiment, taken from this paper (Curve 1). Contraction was seen to occur for many hours after the temperature had become equalized. As the solution changed into a gel during the experiment, the author concluded that the observed slow contraction was the volume effect of gelation. This conclusion would appear to be confirmed by the control experiment (Curve 2) in which the dilatometer containing the gel was first placed in an ice bath, and then transferred into a thermostat at 22.5°. A constant volume was rapidly reached in this case. In the second experiment, of course, there was no gel ⟶ sol transition. This confirmed the opinion that the effect observed in the first experiment was a volume gelation effect. However, one important detail was omitted in the description of the second experiment: the time during which the dilatometer with the gel was held in the ice bath was not stated. We shall return to this point later.

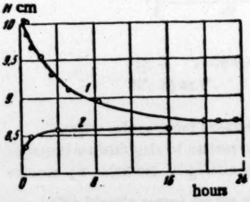

Fig. 1. Kinetics of the establishment of constant volume in a gelatin solution at 22.5°, after Heymann [4]: 1) solution previously held at 50°; 2) the same, at 0°.

Taft and Malm [5] used another method for studying the volume effect of gelation. A hot solution of gelatin was poured into a pycnometer, which was placed in a thermostat at 30°. After equalization of the temperature, the meniscus in the neck of the pycnometer was photographed. After one hour, a second photograph was taken. It was found that the area of the meniscus was rather less in the second photograph than in the first. Since gelation had occurred in the time between the first and second photographs, the authors concluded that the observed small contraction was the volume effect of gelation.

However, an analysis of the experiments, the results of which are presented below, leads to the conclusion that the authors of the papers cited drew erroneous inferences, and that their data are not directly related to gelation.

Figure 2 gives the curves obtained by us for the equalization of temperature and establishment of a final volume in a 20% gelatin gel at 22°. The dilatometer containing the gel was held for not less than twenty-four hours at a temperature 8° below or above the experimental temperature. Equalization of temperature occurred rapidly, and was complete in not more than 30 minutes. The situation with regard to a final constant volume was quite different. The same constant volume was reached perfectly reversibly both from the lower and from the higher temperatures.* However, the process required 400 minutes, after which no further volume changes were observed even when the experiment was continued for several hours.

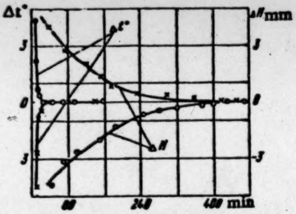

Fig. 2. Curves for the establishment of: ΔH) constant volume, and Δt) constant temperature, in 20% gelatin gel at 22°.

Thus the establishment of constant gel volume is typically relaxational in character. A significant feature, from the viewpoint from which the question is considered here, is that in the transition from 14 to 22° the gel state is preserved throughout. Hence the slow establishment of a constant volume is in no way related to the gelation process. Similar experiments were repeated many times. For example, a 10% gel was held in the dilatometer for 50 hours at 14°, then placed in a thermostat at 22°, and the volume curve was plotted. As Figure 3, a shows, the final volume in this case was reached in nearly 8 hours, and the gel state was retained throughout. Figure 3, b shows a curve for the initial stage of relaxational volume equalization of a 10% gelatin gel at 0°. The dilatometer with the gel was held for 50 hours at 16° and then placed in an ice bath at 0°. After 5 hours there was no clear tendency to a cessation of volume change. Obviously, in this case also, the system was in the gel form throughout.

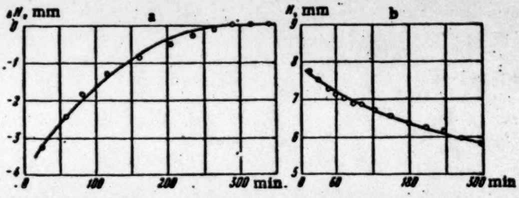

Fig. 3. Temperature relaxation of volume in 10% gelatin gel: a) at 22°; b) at 0°.

Similar relaxational behavior was observed by us in every one, without exception, of our numerous experiments with gels of various concentrations. The table gives the times for the temperature relaxation of volume (τ minutes) of gelatin gels at various temperatures.

The kinetic curves for the establishment of constant volume in a 20% gel, given in Figure 4, illustrate the relaxational nature of this process, which is regularly accelerated on increase of temperature. At temperatures above 40° relaxation of volume can no longer be detected in gelatin solutions.

---

* In the ordinates of the graphs, ΔH is the difference between the final constant mercury level in the dilatometer capillary and the level measured at a given instant; H is the mercury level in the dilatometer capillary.

It is evident in the light of these results that the result of Heymann's control experiment (see Curve 2, Fig. 1) could only have been obtained in one particular instance. We can only assume (the author does not give these details) that the gel, after being taken from the thermostat, was held for only a short time in the ice bath (sufficient, for example, to cool it to 0°). In that case the relaxational process of the establishment of constant volume at 0° would be at its earliest stages. Therefore the volume became established rapidly on return to 22°. The situation in cooling from 50 to 22° is quite different. The temperature relaxation of volume of gelatin solutions is very rapid at 50°. Consequently, the relaxational transition from one state into the other occurs completely during the subsequent cooling.

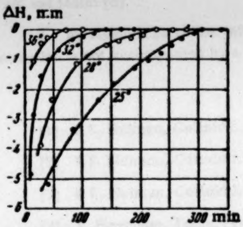

Fig. 4. Temperature relaxation of volume in 20% gelatin gel at various temperatures.

The results obtained by Taft and Malm [5] can also be explained by temperature relaxation of volume. Unfortunately, these authors do not state for how long the pycnometer with the gel was held in the thermostat before the first photograph was taken. In any event there can be no doubt that this time could not have been long, as the first photograph had to be taken before gelation. According to our data however, a final constant volume, for example in 10% gel at 30°, is established only 90 minutes after equalization of the temperature. Therefore it seems very probable that the first photograph was taken at an instant when the temperature relaxation of volume, caused by the transition from a higher to a lower temperature, had not yet been completed. The second photograph (after an hour) recorded the completion of this relaxational shrinkage, which was unrelated to the gelation process.

TABLE 1

Time for the Temperature Relaxation of Volume of Gelatin Gels at Various Temperatures

Temperature (°C)	Time τ for temperature relaxation in volume in min., for gels			Temperature (°C)	Time τ for temperature relaxation in volume in min., for gels		
	10%	20%	40%		10%	20%	40%
22	280	400	—	31	80	145	195
25	200	310	350	32	—	140	180
28	145	220	310	33	35	125	165
29.5	115	—	—	36	—	70	100
30	90	175	—	38	—	35	45

Thus it may be definitely asserted that the authors of both the cited papers were in reality dealing with temperature relaxation of volume of the gels, and erroneously interpreted their observations as proof for the existence of a volume effect of gel formation. The experimental data in these papers give no information on the volume effect of gelation.

In our opinion, the only completely reliable method for investigation of this problem is by plotting reversible thermal expansion curves. Such curves were obtained in our earlier investigations [1, 2]. When the possible influence of temperature relaxation of volume had been excluded, it was found that gelation of gelatin and agar solutions is not accompanied by a volume effect. The effect observed by Taft and Malm was greater by nearly two orders of magnitude than the sensitivity of our dilatometric determinations. If this effect had really been a volume change on gelation, it could not possibly have remained undetected in the conditions of our experiments.

SUMMARY

1. It is shown that the slow establishment of constant volume in a gelatin gel in the transition from one temperature to another is a typical relaxation effect. It was found that this effect is not caused by gel formation, and it occurs both in gels and in sols of gelatin. At the same time, as was shown previously [3], gel formation results in a change of the molecular mechanism of the temperature relaxation of volume.

2. The results obtained provide a correct explanation of the results obtained by Heymann [4] and by Taft and Malm [5].

3. By elimination of the influence of the temperature relaxation of volume it can be shown that gel formation is not accompanied by a volume effect.

LITERATURE CITED

[1] R.E. Neiman, Colloid J. 14, 107 (1952) (T.p. 119).*

[2] R.E. Neiman, Colloid J. 16, 201 (1954) (T.p. 203).*

[3] R.E. Neiman, Colloid J. 16, 280 (1954) (T.p. 275).*

[4] E. Heymann, Trans. Faraday Soc. 32, 462 (1936).

[5] R. Taft and L.E. Malm, J. Phys. Chem. 42, 1187 (1938).

Received December 5, 1955

Voronezh State University
Department of Chemistry

SWELLING OF VULCANIZED RUBBER IN α-PINENE IN PRESENCE OF OXIDATION INHIBITORS*

E.N. Novikova

Swelling of vulcanizates is usually accompanied by oxidation, as the solvents or solutions in which swelling occurs contain oxygen. Studies of swelling in solvents, especially unsaturated hydrocarbons, which contain dissolved oxygen and which are, therefore, themselves subjected to the action of oxygen, are of interest in relation to the mechanism of vulcanizate swelling in oxidation conditions.

It has been shown in a number of investigations [1-4] that swelling and solution of vulcanizates is accompanied by structurization and degradation processes in the rubber, caused by the action of molecular oxygen. Gul, Khodzhaeva and Dogadkin [5] obtained interesting data which showed that kinetic swelling curves for rubber can be used to evaluate the degree of oxidation of the rubber, while swelling can be regarded as a test method for the aging of rubber. From this viewpoint particular interest attaches to studies of the effect of the chemical nature and molecular structure of antioxidants on the swelling of rubber or its vulcanizates in unsaturated hydrocarbons, in which peroxide compounds capable of accelerating oxidative degradation of the rubber are easily formed.

On the basis of the known data [6] that some vulcanization accelerators increase, while antioxidants decrease oxidative degradation of rubber and thus influence the solubility of vulcanizates, we used the vulcanizate swelling method to study the protective effects of antioxidants. In our opinion this method can be used to detect the relative protective effects of antioxidants in relation to their chemical structure and the nature and positions of the functional groups.

As is known, [7], the mobility of antioxidant molecules in films of rubber or vulcanizates can be severely restricted, which leads to a decrease of the antioxidant activity. This fact is one of the most important difficulties in studies of the protective properties of antioxidants of different chemical nature in rubber films oxidized by gaseous oxygen. Conversely, the antioxidant should be more active in swollen films of rubber or vulcanizates, as penetration of the solvent into the vulcanizate medium facilitates access of the antioxidant molecules to the active regions of the rubber macromolecules. Moreover, swelling results in a weakening of the intermolecular bonds in the polymer, which leads to increased mobility of the macromolecular segments and in its turn favors an increase of the oxidation rate.

EXPERIMENTAL

The materials used for the swelling experiments were vulcanizate samples based on natural (NR) and synthetic butadiene (SKB) rubbers.

---

*R. Ekimenkova participated in the work.

Vulcanizate IV

Smoked sheet	100	wt.	parts
Sulfur	2.75	"	"
Zinc oxide	5	"	"
Stearic acid	1	"	"
Captax	0.85	"	"

Vulcanizate III

SKB	200	wt.	parts
Sulfur	3	"	"
Zinc oxide	10	"	"
Captax	3.6	"	"

The vulcanizates were thoroughly extracted, alternately by a mixture of acetone and benzene and by pure acetone, and then dried to constant weight in a vacuum desiccator. The extraction of the samples was necessary in order to remove free and easily removable impurities which might obscure the influence of antioxidants on the swelling kinetics of the vulcanizates. In the study of the mechanism of the action of antioxidants on swelling, groups of substances with a regularly variable molecular structure: phenols, naphthols, primary and secondary aromatic amines, were used rather than individual antioxidants. The amounts added corresponded to 5 millimoles of antioxidant per liter of α-pinene. In addition to the antioxidants, iron palmitate and benzoyl peroxide were used; these, according to the literature [8] exert a considerable effect on the oxidation of hydrocarbons, including rubber. 0.1 g of these substances per 100 ml of α-pinene was taken.

The solvent used was α-pinene with d_4^{20} 0.8576, n_D^{20} 1.4658, b.p. 155-156°, obtained from resin turpentine and twice distilled over a rectifying column. As is known [9], the oxidation of α-pinene yields peroxides

The swelling of rubber vulcanizates in α-pinene at room temperature is slow, and the experiments were therefore carried out at 80° to accelerate swelling. The experiments were performed in tall beakers; 4 ml lots of α-pinene or antioxidant solution in α-pinene were put into these, followed by vulcanizate specimens of the same shape and weight. The beakers containing the solutions and specimens were kept at a definite temperature in an ultrathermostat. Variations of the degree of swelling were determined gravimetrically. The degree of swelling was expressed in grams of absorbed solvent per 1 g vulcanizate.

Effect of temperature on accumulation of peroxide compounds in α-pinene. The degree of swelling of rubber or vulcanizates should be influenced by the amounts of peroxides formed in the α-pinene. These amounts depend on the temperature. To determine the optimum temperature conditions for peroxide formation in α-pinene in presence of atmospheric oxygen, we carried out experiments on the oxidation of α-pinene in the same conditions as those used in the subsequent experiments on swelling. 4 ml lots of α-pinene were placed into 25 ml bulbs, which were heated at the required temperature (in the range of 20-110°) in an ultrathermostat for two hours. The peroxides formed were determined iodometrically, the contents being expressed in milliliters of 0.1 N thiosulfate solution per 100 g of α-pinene.

Our experimental results (Table 1) show that increase of temperature and heating time of α-pinene in presence of atmospheric oxygen favor the accumulation of peroxides in α-pinene.

Swelling of vulcanizate in presence of phenols. It has been shown [5] that phenyl-β-naphthylamine, used as an antioxidant in rubber, influences the swelling of rubber in methyl alcohol containing dissolved oxygen. It was desired to investigate the effects of other similar compounds, including pyrocatechol, pyrogallol, resorcinol, and triacetoxyhydroquinone (Pyrogallol A). The results (Fig. 1) show that the phenols studied decrease th swelling of the vulcanizate in α-pinene at 80°. Pyrogallol and pyrocatechol have the greatest effects.

An examination of the data in Table 2 on the accumulation of peroxide compounds in α-pinene, in conjunction with the course of the kinetic Curve 2 (Fig. 1), which gives the kinetics of vulcanizate swelling in α-pinene without additions, shows a correlation between the peroxide content of α-pinene and the degree of swelling of the specimen.

The course of the kinetic curve for vulcanizate swelling in α-pinene without added phenols shows a slow and continuous increase of swelling, in consequence of the oxidative degradation of the rubber molecular chains. The curves for the swelling kinetics of the vulcanizate in α-pinene in presence of phenol are of a somewhat different character. At first these curves, as those for swelling without additions, show a steep ascent due to diffusional penetration of the solvent into the vulcanizate, and then the curves pass into straight lines almost parallel to the abscissa axis. This course of the swelling curves can be explained on the assumption that phenols inhibit the oxidation not only of rubber, but also of α-pinene, and so prevent formation of peroxides in the latter, which in turn could initiate oxidation of the rubber and so increase its swelling.

TABLE 1

Accumulation of Peroxide Compounds in α-Pinene

Effect of temperature		Effect of heating time	
Experimental temperature, °C	Peroxide content of 100 g α-pinene after 2 hrs. of heating	Heating time at 80°, hours	Peroxide content of 100 g α-pinene oxidized at 80°
20	0	1	12.8
60	4.65	2	19.3
70	10.76	3	26.9
80	18.5	4	48.7
90	23.45	5	69.9
100	29.40	6	77.0
110	33.40	7	97.0
120	38.07	8	131.2
130	32.3		

Note: The peroxide content is expressed as ml of 0.1 N thiosulfate solution per 100 g α-pinene.

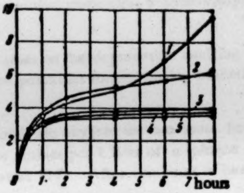

Fig. 1. Effect of phenols on the swelling of NR vulcanizate in α-pinene at 80°: 1) Pyrogallol A; 2) without additions; 3) resorcinol; 4) pyrocatechol; 5) pyrogallol.

The features of the swelling kinetics of the vulcanizate in α-pinene in presence of phenols are related to their molecular structure. Pyrocatechol, which contains two hydroxyl groups in the ortho position in its molecule, effectively inhibits oxidative degradation of the vulcanizate, as was shown earlier by data on the rate of oxygen absorption. Resorcinol has less retarding effect than pyrocatechol on the oxidative degradation of the vulcanizate, as the two hydroxyl groups in its molecules are in the meta position.

Swelling of vulcanizates in presence of naphthalene derivatives. Of the naphthalene derivatives which inhibit the oxidation of vulcanizate III during its swelling, dihydroxynaphthalene, β-naphthol, and α-nitroso-β-naphthol were studied. The experimental data given in Fig. 2 indicate that all three antioxidants retard oxidative degradation of the vulcanizate, but to different extents. The most effective in retarding the degradative swelling of the vulcanizate is dihydroxynaphthalene, followed by β-naphthol, and α-nitroso-β-naphthol is the least active.

An explanation for the more effective antioxidant action of dihydroxynaphthalene is that its molecule already contains two hydroxyl groups in the 2,7 positions [10]. Introduction of a nitroso group in the α-position in β-naphthol decreases its antioxidant effect.

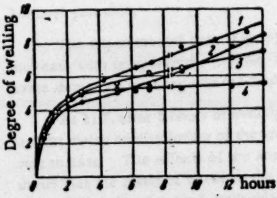

Fig. 2. Effect of naphthalene derivatives on the swelling of SKB vulcanizate in α-pinene at 80°: 1) without additions; 2) α-nitroso-β-naphthol; 3) β-naphthol; 4) dihydroxynaphthalene.

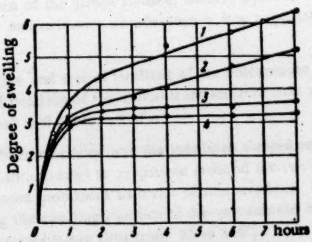

Fig. 3. Effect of secondary amines on the swelling of NR vulcanizate in α-pinene at 80°: 1) without additions; 2) diphenylamine; 3) 1,4-diphenylphenylenediamine; 4) p-hydroxydiphenylamine.

Swelling of vulcanizates in presence of amines. The degree of swelling of vulcanizate III in presence of primary amines: benzidine, tolidine, and dianisidine, was measured. Our experiments showed that primary aromatic amines have practically no inhibiting effect on the swelling of the vulcanizate in α-pinene at 80°.

In contrast to the primary amines, secondary aromatic amines proved to be active inhibitors of the oxidative degradation of vulcanizates III and IV. The experimental data in Fig. 3 show that the secondary amines form the following sequence in order of decreasing protective properties: p-hydroxydiphenylamine, 1,4-diphenylphenylenediamine, diphenylamine.

In order to explain the action of primary and secondary amines on the degradative swelling of rubber vulcanizates in α-pinene, we carried out determinations of the peroxides formed during oxidation of α-pinene in presence of amines.

The oxidation of α-pinene was effected by means of atmospheric oxygen for two hours. Four-ml lots of freshly distilled α-pinene with additions of 4 millimoles of the amines per 1 liter of α-pinene were sealed in 25 ml bulbs. The bulbs were heated in an oil ultrathermostat at 110°. After two hours of heating, the peroxide contents were determined iodometrically.

TABLE 2

Effect of Amines on Formation of Peroxide Compounds in α-Pinene

Antioxidant	Peroxide content expressed as ml of 0.1 N thiosulfate solution per 100 g α-pinene
None	51.2
Benzidine	42.3
Tolidine	46.3
Dianisidine	27.1
1,4-Diphenylphenylenediamine	0
p-Hydroxydiphenylamine	0

Table 2 shows that primary aromatic amines have little influence on peroxide formation in α-pinene in these conditions. It is therefore natural that they do not inhibit the oxidation of vulcanizates during swelling in this solvent.

Additions of 1 millimole per 1 liter of α-pinene of secondary aromatic amines: 1,4-diphenylphenylenediamine and p-hydroxydiphenylamine, hinder formation of peroxides in α-pinene and thereby retard oxidation of the vulcanizate, and so decrease its swelling in α-pinene.

The results of our experiments show that phenols, naphthalene derivatives, and amines form the same sequence with regard to their activities as antioxidants in the swelling of rubber, as with regard to retardation of the oxidation of rubber in solution [11], when the oxidative degradation of the rubber molecular chains was measured in terms of the viscosity of the oxidized rubber solutions.

Effect of temperature on vulcanizate swelling in presence of various substances. In experiments carried out to determine the effect of temperature on the swelling of natural rubber vulcanizates (vulcanizate IV) the antioxidants used were the most effective members of the groups studied, namely pyrocatechol, dihydroxynaphthalene, 1,4-diphenylphenylenediamine, and oxidation accelerators – iron palmitate and benzoyl peroxide.

The experimental data (Fig. 4) show that the degree and rate of swelling of the vulcanizate in α-pinene increase with temperature. While at 25° the degree of swelling of the vulcanizate after 11 days was 5, the same degree of swelling was reached in 4 hours at 90° and in 2 hours at 110°.

At 110°, after 5 hours of swelling, the vulcanizate became sticky and the specimen showed some loss of weight owing to dissolution of the rubber. Addition of antioxidants to α-pinene reduced the swelling of the vulcanizate. The effects of the antioxidants became more prominent with rise of temperature. Figure 5 shows that the distance between the curves representing the swelling kinetics of the vulcanizate in pure α-pinene and with added antioxidants increases as the temperature rises from 25 to 110°.

The individual characteristics of the antioxidants, due to their chemical nature and molecular structure, become more pronounced with increase of temperature.

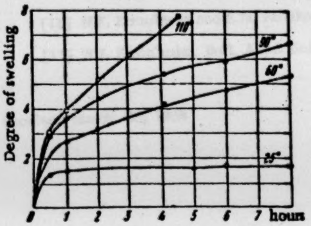

Fig. 4. Effect of temperature on the swelling of natural rubber vulcanizate in α-pinene.

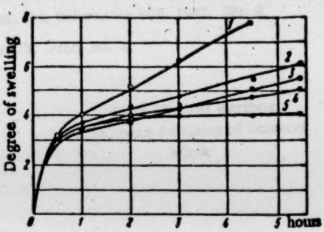

Fig. 5. Swelling of natural rubber vulcanizate in presence of antioxidants at 110°: 1) without additions; 2) iron palmitate; 3) pyrocatechol; 4) dihydroxynaphthalene; 5) 1,4,-diphenylphenylenediamine.

At 60°, pyrocatechol, 1,4-diphenylphenylenediamine, and dihydroxynaphthalene all retard the swelling of the vulcanizate to practically the same extent. At 90° dihydroxynaphthalene retards the swelling of the vulcanizate to a greater extent than does pyrocatechol.

SUMMARY

1. Determinations of swelling kinetics have been used to demonstrate a relationship between accumulation of peroxides in α-pinene and increase of the degree of swelling of rubber vulcanizates in α-pinene.

2. Phenols, naphthalene derivatives, and aromatic amines retard peroxide formation in α-pinene and thus decrease oxidative degradation of rubber, and accordingly diminish the swelling of rubber vulcanizates in α-pinene in the range of 60-110°.

3. Naphthalene derivatives form the following sequence in their ability to decrease the swelling of rubber vulcanizates in α-pinene at 80°: dihydroxynaphthalene > β-naphthol > α-nitroso- β-naphthol.

4. Secondary aromatic amines (1,4-diphenylphenylendediamine, hydroxydiphenylamine) are more active retarders of the swelling of rubber vulcanizates in α-pinene than primary amines (benzidine, tolidine, and anisidine).

LITERATURE CITED

[1] B.A. Dogadkin, Trans. 1st and 2nd Conf. on High-Molecular Compounds (Acad. Sci. USSR Press, 1945).

[2] B. Dogadkin and B. Karmin, Colloid J. 9,348 (1947).

[3] B. Dogadkin, Yu. Bryukhanova and A. Pasynsky, Trans. Moscow Inst. Fine Chem. Technol. 1948, No. 1.

[4] A.S. Kuzminsky, Colloid J. 10, No. 1 (1948).

[5] V.E. Gul, L.V. Khodzhaeva and B.A. Dogadkin, Colloid J. 16, No. 6, 412 (1954) (T.p. 393)*.

[6] B.A. Dogadkin and Z.I. Tarasova, J. Gen. Chem. 17, No. 8, 1401 (1947).

[7] L.B. Morgan and W.J.S. Naunton, Kautschuk 1939, No. 11, 186.

[8] A.S. Kuzminsky, Trans. Moscow Inst. Fine Chem. Technol. 1948, No. 1.

---

* T. p. = C. B. Translation pagination.

[9] G. Pigulevsky, Chemistry. of the Terpenes (Leningrad State University Press, 1949).

[10] N.F. Ermolenko and E.N. Novikova, Bull Acad. Sci. Belorussian SSR 1952, No. 4.

[11] N.F. Ermolenko, Bull. Acad. Sci. Belorussian SSR 1955, No. 3.

Received March 23, 1956

State Medical Institute
Belorussian Academy of Sciences
Minsk

INCREASE OF THE HYDROPHILIC PROPERTIES OF CAPRON FIBER BY HYDROXYETHYLATION

B.V. Petukhov and A.B. Pakshver

It is known that polyamide fibers and films react with ethylene oxide on heating, the latter being added to the amide nitrogens in the form of polyoxyethylene chains [1]. Changes in the hydrophilic properties of polyamide fibers on hydroxyethylation have not, however, been studied.

EXPERIMENTAL

Notes on the method. Oriented capron fibers in the form of threads of metric number 34 were treated with ethylene oxide or mixtures of ethylene oxide with other substances in sealed glass bulbs placed in an air thermostat at temperatures from room level to 160°. After the bulbs had been opened, the contents were treated with hot water to remove side products. Isotherms for the sorption of water vapor at 20° were determined for all the specimens by means of the vacuum sorption balance. The change in the hydrophilic properties of capron fibers was represented by ΔH, the increase of the moisture sorption of the fiber at 65 % relative humidity as a percentage of the sorption of untreated capron fiber. The kinetic data were used to determine the integral diffusion coefficient D, calculated from the diffusion equation [2]:

$$\left(\frac{Q_\tau}{Q_\infty}\right)^2 = \frac{16}{\pi} D \frac{\tau}{r^2}.$$

The mechanical properties of the fibers were represented by means of load – extension diagrams, which were used to determine the elasticity modulus M_5, taken to be the load on the thread in g/mm² at 5% extension. The twisting rigidity of the fibers was determined by means of Petrov's torsion pendulum [3]. The nitrogen content of the polymers was determined by the Kjeldahl method.

As Fig. 1 shows, treatment of capron fiber by ethylene oxide at 17° for 120 hours decreases its water vapor sorption over the whole humidity range. If oriented capron fiber is heated with ethylene oxide at 100° for 20 hours, the sorption isotherm is slightly lower in the monomolecular sorption region, but increases in the region of high relative humidities.

The sorption isotherm for a specimen heated at 120° for 20 hours shows a considerable increase of hydrophilic properties in the humidity region above 40%, and an appreciable decrease of sorptive power at low water vapor pressures; for this specimen, ΔH = 55 %. Fibers heated with ethylene oxide at 117° for 4 hours have ΔH = −5.0%, for 12 hours, ΔH = 1.7%, and for 20 hours, ΔH = 17 0%. However, as nitrogen determinations showed (see table), addition of ethylene oxide also occurs during the first 4 hours. Probably the decreased sorption in experiments with short heating times (or low reaction temperatures) is caused by the fact that at low degrees of substitution the new side groups are not numerous enough or large enough to influence the polyamide structure. At the same time, the side groups themselves, by filling the intermolecular pores, decrease sorption.

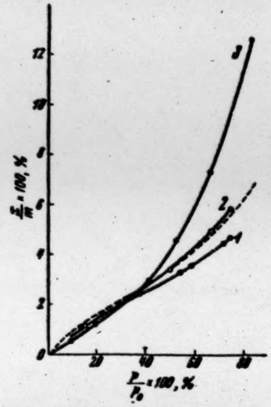

Fig. 1. Isotherms for water vapor sorption at 20° by capron fibers treated with C_2H_4O: 1) at 17° for 120 hours; 2) at 100°, 20 hours; 3) at 126°, 20 hours. The broken line represents the original oriented fiber.*

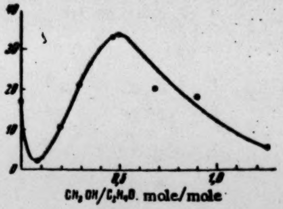

Fig. 2. Variation of the hydrophilic properties of capron fiber (heated for 20 hours at 117°) as a function of the CH_3OH : C_2H_4O ratio in the reaction medium.

All the fibers treated with ethylene oxide alone were colored orange to red. Careful purification of the ethylene oxide to remove possible impurities such as aldehydes, passage of nitrogen through the bulbs, and addition of the simplest antioxidants (hydroquinone, p-aminophenol, α-naphthol) to the reaction mixture did not reduce the color of the modified fibers. Colorless fibers are obtained only if methyl alcohol is added to the ethylene oxide. As Fig. 2 shows, the greatest increase in hydrophilic properties is obtained if the fibers are treated with a mixture of 0.5 mole methyl alcohol to 1 mole of ethylene oxide. Curves of this type most frequently indicate the simultaneous occurrence of several independent processes. In the present instance the addition of methyl alcohol, on the one hand, decreases the concentration of ethylene oxide by formation of glycol monoethers and polyoxyethylenes, as shown by the minimum in the left-hand side of the curve; on the other hand, the swelling of polycaprolactam is increased in the presence of methyl alcohol, and, in addition, breakdown of ethylene oxide aggregates is probably increased, and this is reflected by the appearance of a maximum at a methyl alcohol – ethylene oxide ratio of 0.5 mole/mole. The subsequent descent of the curve is caused by a further decrease of the ethylene oxide content in the reaction mixture, and also by side reactions.

The table shows that addition of methyl alcohol to the reaction mixture in the ratio of 0.5 mole/mole considerably accelerates the addition of oxyethyl residues. For example, capron fibers treated with ethylene oxide alone at 117° for 20 hours, add 10% C_2H_4O groups; after treatment with a mixture of methyl alcohol and ethylene oxide the amount of ethylene oxide added increases to 17.8%. ΔH correspondingly increases from 17.0 to 33.5%. This clearly shows the role of methyl alcohol as an agent which causes breakdown of ethylene oxide aggregates and swelling of the polyamide.

The hydrophilic properties of hydroxyethylated capron fibers are found to be greater than those of acetate yarn; this is illustrated by Fig. 3, which shows the sorption isotherm for capron fiber hydroxyethylated at 117° for 20 hours in a methyl alcohol – ethylene oxide mixture in a ratio 0.47 mole/mole. ΔH for this specimen is 33.0%, and the absolute value for water sorption at 97.7% relative humidity is 19%, while for the original capron fiber it does not exceed 10%. The sorption isotherms for hydroxyethylated derivatives of polycaprolactam are not S-shaped and are characterized by an infinite growth of the sorption as the vapor pressure approaches saturation.

---

* The numerical values are reproduced as in the original, although there appears to be a discrepancy between the text and the figures.—Translator's note.

TABLE

Analytical Data for Capron Fibers Hydroxyethylated at 117°

Reaction medium	Reaction time, hours	Nitrogen content, by Kjeldahl, in % N	Weight content of C_2H_4O groups, from % N	ΔH in %
C_2H_4O	4	12.08	2.6	−5.0
	12	11.77	5.2	1.7
	20	11.18	10.0	17.0
$CH_3OH : C_2H_4O = 0.5$	5	11.72	5.6	6.0
	12	11.23	9.6	24.5
	20	10.25	17.8	33.5

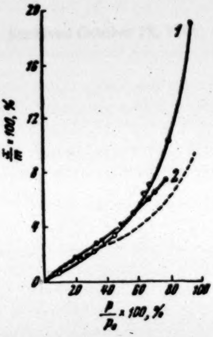

Fig. 3. Isotherms for water vapor sorption at 20°: 1) by hydroxyethylated capron fiber; 2) by acetate yarn. Broken line represents sorption by oriented capron fiber.

Capron fibers containing over 10% hydroxethyl residues are soluble in warm methyl alcohol and all the usual polyamide solvents. Despite the considerably increased hydrophilic properties, the melting point of hydroxyethylated capron fibers remains high. For specimens with ΔH = 33% the melting point was still ~ 200° (the melting point of capron fiber is 212-216°). This is an undoubted advantage of hydroxyethylation over other known methods for modification of polyamide fibers to make them more hydrophilic. The tensile strength of the fibers is decreased by 10-40% after hydroxyethylation. For example, at ΔH = 10.5% the breaking length is 47 km, and at ΔH = 33.5% it is 41 km (the breaking length of the original fiber is 58 km). The extension at break is almost unchanged. The elasticity modulus M_s decreases from 14.5 to 4-6 kg/mm². The wet strength of the fibers is 90 to 60% of the dry strength, and diminishes with increasing ΔH. The fibers become condsiderably softer to the touch. The twisting rigidity decreases from 4.35 to 3.98 arbitrary units for the specimen with ΔH = 33.0%.

As the result of heating of hydroxyethylated fibers at 110 and 142° the sorptive power decreases somewhat, but the initial sorption is restored after treatment of the fibers with hot water. Thus it may be assumed that hydroxyethylated capron fibers are quite thermostable up to 142°. This is an especially valuable property if it is compared with the behavior on heating of methylol derivatives of polyamide resins, in which cross-linking of the macromolecules is produced by very brief heating at 110° with an acid catalyst and at 140° without catalysts.

Hydroxyethylated capron fiber is dyed more strongly than untreated fiber by acid dyes, and considerably less time is required to reach a deeper shade. The depth of shade of ordinary capron fiber dyed for 2 hours is considerably less than that of modified fiber held in the same dye bath for 5 minutes.

The diffusion coefficient of water vapor in oriented capron fiber is $4.0 \cdot 10^{-10}$ $cm^2 \cdot sec^{-1}$. Hydroxyethylation increases the diffusion coefficient to $7.7 \cdot 10^{-10}$ $cm^2 \cdot sec.^{-1}$ (for a specimen with $\Delta H = 15.5\%$). This indicates a less dense packing in hydroxyethylated caprolactam.

Calculation showed that the sorption corresponding to the filling of a monomolecular layer is 3.1% for a specimen with $\Delta H = 33.5\%$, while for the original capron fiber the value is 2.0%.

Therefore it may be assumed that increased sorption after hydroxyethylation is the result both of an increase in the number of active sorption centers (hydroxyl and ether groups) and of decreased packing density of the polycaprolactam.

SUMMARY

1. Hydroxyethylation of capron fibers results in a considerable increase of the hydrophilic properties, water vapor sorption rate, softness, and dyeability of the fibers.

2. Colorless hydroxyethylated capron fibers are obtained if the reaction is carried out in a mixture of methyl alcohol and ethylene oxide; addition of methyl alcohol accelerates hydroxyethylation.

LITERATURE CITED

[1] H.C. Haes, S.G. Cohen, A.C. Oglesby and S.R. Karlin, J. Polymer Sci. 15, 427 (1955).

[2] R. Barrer, Diffusion in and Through Solids. (Foreign Lit. Press, Moscow, 1948).

[3] G.N. Kukin, A.N. Solovyev, F. Kh. Sadykova, and A.G. Monastyrsky, Laboratory Manual for the Course on Fibrous Materials (Light Ind. Press, Moscow, 1952).

Received October 12, 1955

The Ivanovo Institute of Chemical Technology

ADSORPTION OF SURFACE-ACTIVE SUBSTANCES (DEPRESSANTS) ON PARAFFIN WAX

P.I. Sanin, N.V. Melentyeva, and Yu. M. Zelenova

The few investigations of the mechanism of the action of pour point depressants (surface-active substances which increase the fluidity of paraffinic petroleum products) give reason to believe that this mechanism is adsorptional [1-8]; apparently it may be manifested either in the crystallization of paraffins from oil solutions (changes of crystal shape and size, stabilization of the crystalline phase) or in the structure-formation process in absence of a crystalline phase (decrease of supermicellar structure formation).

Although the adsorptional nature of the mechanism of depressant action is accepted by the majority of authors, including the authors of the present paper [9], experimental data providing a quantitative basis for such a mechanism are almost totally lacking.

For elucidation of the adsorptional mechanism of depressant action it is important to prove that depressants can be adsorbed on the crystals of paraffin hydrocarbons in the hydrocarbon oil medium. Several workers have qualitatively confirmed the possibility of such adsorption.

For quantitative experiments which would prove the adsorptional character of depressant distribution between the liquid and crystalline phases, it is necessary to determine quantitatively the contents of the depressant in both the liquid and the crystalline phases. The depressants known at the present time, which are complex mixtures of not always definite composition, are not suitable for such quantitative determinations. This also applies to paraflow, the molecules of which, moreover, do not contain chemically active groups.

The adsorption determinations were carried out with a purified fraction of Grozny paraffin: m.p. 53.0° (Zhukov's method); sp. gr. 0.7794 (d_4^{60}); the average molecular weight was 366, corresponding to the hydrocarbon $C_{26}H_{54}$. The solvent in all the experiments was isooctane: b.p. 99.3°; d_4^{20} 0.6902; n_D^{20} 1.39144. The depressant used was "paraffin-phenol" (average molecular weight 767 [8, p. 262]. The synthetic paraffin-phenol consisted of a mixture of dialkyl derivatives of phenol and was convenient to use because its quantitative distribution between the liquid and solid phases could be easily determined by determination of the hydroxyl-group content by the Chugaev – Tserevitinov method. The following method was used for determination of adsorption.

3.2 g of the paraffin wax and the necessary amount of paraffin-phenol (from 0.2 to 5.0 g) were weighed out into a 100 cc flask. 40 ml of isooctane was added to the flask and the mixture was heated at 50° until the paraffin and depressant were completely dissolved. The solution was allowed to cool to room temperature and was then cooled slowly in a cryostat to 4° with periodic stirring, and was then held at that temperature for 40 minutes.

The precipitated crystalline paraffin was quantitatively transferred together with the solution to a special filter funnel, also kept in the cryostat at 4°. The glass filter of the funnel was covered with a layer of purified asbestos before filtration. The filtrate, the weight of which was determined, consisted of a mixture of paraffin wax and depressant in isooctane. The isooctane was distilled off and the hydroxyl group content of the residue was determined. The results were used to calculate the content of the depressant, paraffin-phenol, in the filtrate, and the paraffin wax and isoctane contents were found by difference. The residue on the filter, in addition to the adsorbed depressant, also contained a certain amount of solution, which was greater at lower contents of depressant in the solution; this is explained by the fact that when the depressant is adsorbed on the paraffin, the latter is more easily separated from the solvent. As the depressant concentration increases, instead of a gelatinous mass, difficult to filter, a suspension of paraffin wax in the solvent is formed, which separates readily and is easy to filter. As the depressant content increased from 0.2 to 5.0 g, the amount of solution retained by the paraffin decreased from 5.5 to 1.0 ml. After removal of the solvent, the quantitative contents of depressant and paraffin were determined in the precipitate as described above. A correction for the depressant and paraffin wax in the solution retained by the precipitate on the filter was applied to the results.

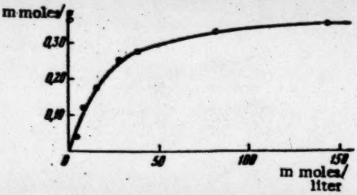

Isotherm for the adsorption of paraffin-phenol on paraffin wax at 4°; solvent – isooctane.

TABLE

Adsorption of Paraffin-Phenol on Paraffin Wax; Solvent–Isooctane; Temperature 4°.

Equilibrium concentration of depressant		Amount of depressant adsorbed by 1 g of paraffin wax	
in g/liter	in millimoles/liter	in g	in millimoles
3.64	4.8	0.030	0.039
6.24	8.1	0.093	0.121
11.25	14.7	0.134	0.175
21.24	27.7	0.194	0.253
29.27	38.2	0.213	0.278
62.66	81.7	0.253	0.330
110.46	144.0	0.268	0.349

The conditions for adsorption on paraffin wax must be so chosen that any possibility of precipitation of the depressant during precipitation of the paraffin is completely eliminated. For example, the first experiments with o-hydroxysterophenone at 4° gave a linear relationship between the equilibrium concentration of o-hydroxystearophenone in isooctane and the amount of it adsorbed on 1 g of paraffin wax. Adsorptional saturation could not be reached in this instance because of the insufficient solubility of the depressant in isooctane, and at concentrations close to saturation not only adsorption of the depressant, but its crystallization together with the paraffin wax took place.

Paraffin-phenol has a high solubility in isooctane (over 124 g per ml of isooctane at 0°) and it could not be precipitated at 4°. The amount of paraffin wax precipitated was 1.8 g in all the experiments.

The results of the experiments on the adsorption of paraffin-phenol on paraffin wax are shown in the table and figure.

The figure shows that the variation of the amount of paraffin-phenol adsorbed by 1 g of paraffin (in millimoles per 1 g) with the equilibrium concentration of paraffin-phenol in solution (millimoles per liter) is represented by a typical adsorption isotherm.

Complete saturation of the adsorption layer is reached at depressant concentrations above 150 millimoles/liter (115 g) of the solvent; 1 g or 2.7 millimoles of crystalline paraffin wax adsorbs 0.37 millimole (0.28 g) of depressant. At complete saturation of the adsorption layer the molar ratio between the paraffin wax and the paraffin-phenol adsorbed on it was 7:1.

From the results it is easy to calculate the depressant concentrations with respect to paraffin wax in the solid and liquid phases. The ratio of these concentrations is not constant, but varies more than three fold in different experiments according to the depressant concentration in the solution. This also shows that in conditions of paraffin wax crystallization the crystalline paraffin wax formed cannot be regarded as a solvent for the depressant.

SUMMARY

1. It has been shown with an alkyl phenol as an example that depressants are surface-active substances which can be adsorbed on paraffin wax during its crystallization from hydrocarbon solutions.

2. The relationship between the amount of depressant adsorbed on the paraffin wax and the equilibrium concentration of depressant in solution is represented by a typical adsorption isotherm.

LITERATURE CITED

[1] L. G. Gurvich, Scientific Fundamentals of Petroleum Processing (Soviet Petroleum Ind. Press, Moscow – Leningrad, 1925), pp. 243, 255.

[2] N.I. Chernozhukov, Petroleum and Shale Economy 1925, No. 4, 640.

[3] G.H. Davis and Y.C. Zimmer, The Science of Petroleum, (London – New York, 1938), Vol. 4, p. 2673.

[4] K.S. Ramaiya, Anomalous Viscosity of Oils and its Influence on Friction in Machines (Machinery State Press, Moscow, 1949), No. 55, p. 96.

[5] P.A. Rebinder, N.A. Boguslavskaya, and V.B. Moklevsky, Symposium, Viscosity of Liquids and Colloidal Solutions (Acad. Sci. USSR Press, Moscow – Leingrad, 1944), Vol. 2, p. 173.

[6] T.P. Zhuze, Investigation of Structure Formation in Hydrocarbon Media in Relation to the Setting of Paraffinic Petroleum Products, Dissertation (Moscow, 1949), p. 127.

[7] G.I. Fuks, Symposium, Additions to Lubricants (State Fuel Tech. Press, Moscow – Leningrad, 1946), p. 37.

[8] P.I. Sanin, Structural-Mechanical Properties of Lubricant Oils and the Influence of Surface-Active Substances on Them, dissertation (Moscow, 1952), pp. 69, 352, 364.

[9] P.I. Sanin, Symposium, Low-Temperature Properties of Petroleum Products, (State Fuel Tech. Press, Moscow, 1949), p. 28.

Received December 25, 1955

Institute of Petroleum
Academy of Sciences, USSR
Moscow

INVESTIGATION OF STRUCTURES IN CARBON - BLACK SUSPENSIONS

2. EFFECT OF TEMPERATURE AND ADDITIONS OF SURFACE-ACTIVE SUBSTANCES ON STRUCTURE FORMATION IN CARBON-BLACK SUSPENSIONS

U-Shu-Tsyu, B. Ya. Yampolsky, and S.S. Voyutsky

Investigations of the disperse structures formed in concentrated carbon-black suspensions in hydrocarbon media, serving as models of filled rubber compounds, are of great importance for the theory of the action and for the technology of the application of active fillers.

Rebinder and his co-workers [1-6] have studied the influence of active and inactive fillers on the properties of rubber solutions, and have shown that a space structure develops even at relatively low volume concentrations of the active filler particles, which act as centers of structure formation. The formation and reinforcement of such space structures in the polymer with the aid of the filler particles are intensified by additions of surface-active substances, which activate the filler particles by their oriented adsorption layers.

Later, the electrical conductivity method was used for investigation of structure formation processes in systems with conducting particles in the disperse phase [7, 8]. Dogadkin [9, 10] used this method for studying rubber mixtures filled with carbon black.

The peculiar influence of temperature on the electrical conductivity of carbon-black suspensions, studied over a relatively narrow temperature range, has already been reported [7, 8]. When the system was heated, the electrical conductivity increased considerably rather than diminshed. The probable explanation of this is that in this instance increase of temperature assists the formation of coagulation structures. Yampolsky [8] found that additions of surface-active agents appreciably decrease the conductivity of graphite suspensions.

The aim of the present work was to study in greater detail the influence of temperature and of surface-active substances on the electrical conductivity and hence on structure formation in carbon-black suspensions in hydrocarbons. The influence of carbon-black concentration on the conductivity of the suspensions was studied at the same time.

The disperse phase used in our experiments was type A lamp black from the Kudinovo works. This black contained 0.09% moisture and 0.06% ash. The volume of 1 g of the black was 60 cc in air and 22 cc in ligroine. As is known [12] lamp black has relatively large particles, the primary round particles being welded together into more or less branched rigid chains. This form is probably explained by the simultaneous growth of contiguous primary particles during formation. The dispersion medium was highly purified petroleum jelly ("Vaseline oil"). Treatment of this oil by active carbon did not change its surface tension, showing the absence of surface-active impurities. The viscosity of the oil at 20° was 143.5 centipoises.

The electrical conductivity of the carbon-black suspensions was measured by means of a bridge with an electric-lamp indicator fed by alternating current. A direct current was used in some experiments. At low voltages the same results were obtained with direct and alternating current.

The freshly prepared carbon-black suspension was put into a glass beaker 35 mm high and 25 mm in diameter. Stainless steel electrodes in the form of rectangular plates 1.4 cm^2 in area were introduced into the vessel in a glass frame which kept them at a constant distance (4 mm) apart. The conductivity λ_0 of the suspension was calculated by means of the equation $\lambda_0 = k\lambda$, where λ is the measured conductivity and k is the cell constant determined by previous calibration with the aid of calcium chloride solution of known concentration.

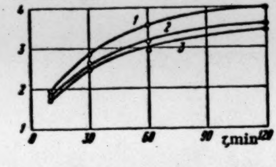

Fig. 1. Kinetic curves for the electrical conductivity of 5% suspension of lamp black in a nonpolar Vaseline oil, obtained with the use of electrodes placed at various heights; 1) electrodes 0.5 cm from the bottom of the vessel; 2) the same, 2.5 cm; 3) the same, 4.5 cm.

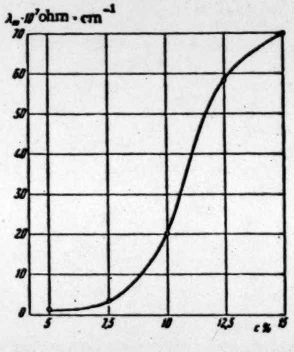

Fig. 3. Variation of maximum conductivity λ_m of carbon-black suspensions with carbon-black concentration in %.

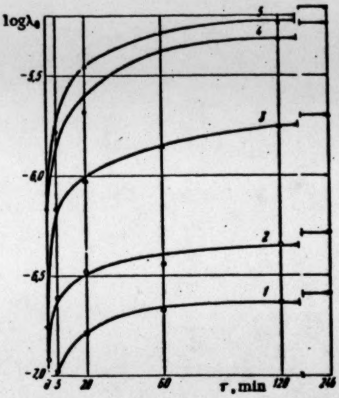

Fig. 2. Variation of log λ_0 with τ for carbon-black suspensions of various concentrations: 1) suspension containing 5% carbon black; 2) ditto, 7.5%; 3) ditto, 10%; 4) ditto, 12.5%; 5) ditto, 15%.

The experiments showed that the method of preparation of the carbon-black suspension has an important influence on the results. Reproducible results were obtained when the suspension was ground in a motar by rubber pestle for not less than 5 minutes. All the results given below were obtained with carbon-black suspensions prepared by this method.

When carbon-black suspensions are left to stand, structure formation is accompanied by sedimentation of the disperse phase. Special experiments were carried out to determine the extent to which this sedimentation can influence the results of the conductivity determinations.

Fig. 1 gives kinetic curves for the electrical conductivity of 5% carbon-black suspension, obtained with the electrodes immersed to various depths in the system. As all the curves are close to each other even for a suspension of low concentration, in which sedimentation should be particularly rapid, it may be assumed that the effect of sedimentation of carbon black on the electrical conductivity of its suspensions in Vaseline oil is relatively small. However, in order to exclude the effect of sedimentation on the results as much as possible, the electrodes were always placed half-way up the vessel, where concentrational changes caused by sedimentation should have least effect.

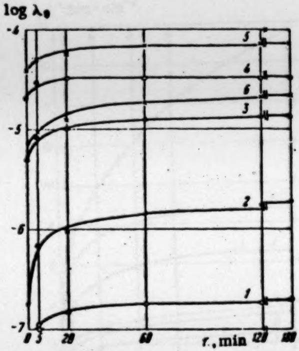

Fig. 4. Variation of log λ_0 with τ for 10 % carbon-black suspension at various temperatures: 1) 0°, 2) 20°, 3) 40°, 4) 60°, 5) 80°, 6) 110°C.

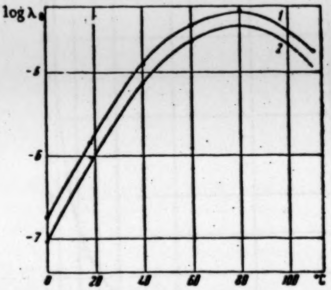

Fig. 5. Variation of log λ_m with t° for 10% carbon-black suspensions without (1) and with (2) 0.5% oleic acid.

EXPERIMENTAL

Effect of concentration on the electrical conductivity of carbon- black suspensions. Fig. 2 gives the variation of log λ_0 with structurization time τ at 20° for suspensions with various carbon-black contents.

Fig. 3 gives the variation of the maximum conductivity λ_m, reached in the suspension 2-3 hours after the end of the stirring, which corresponds to completion of the structurization process, with concentration of the disperse phase (c). The form of the characteristic S-shaped curve suggests that the optimum concentration range of the solid phase, in which the system is most highly structurized, is between 10 and 12 %. Similar curves were obtained by Dogadkin [7].

In examination of Curves 2 and 3 and of all the kinetic curves given in this paper it must be taken into account that the log $\lambda_0 = f\ (\tau)$ curves are plotted in such a way that the abscissa axis shows, not the time from the end of the mixing of the suspension, but the time from the first conductivity determination. As the first determination was usually carried out one minute after the suspension had been made (the time required to pour the viscous suspension into the cell), it is evident that the conductivities corresponding to zero time on the graphs are higher than conductivities for the freshly made suspensions. Unfortunately, the latter values could not be determined by the method adopted.

As Fig. 2 shows, the increase of conductivity during standing of the suspension proceeds at a diminishing rate, and the conductivities tend to a definite limiting value. This character of the log $\lambda_0 = f\ (\tau)$ curves may be attributed to a gradual increase of the number and area of contacts between the carbon particles in the suspension in the course of formation of a coagulation structure. The higher the concentration of the carbon black suspension, the higher is the maximum conductivity (Fig. 3), because of the increased number of conducting chains of carbon particles in the more concentrated suspensions.

Effect of temperature on the electrical conductivity of carbon-black suspensions. Fig. 4 gives the variation of log λ_0 with the structurization time τ of a 10% carbon-black suspension at various temperatures. Increase of temperature to 80° increases the conductivity, in full agreement with the results of the previous investigation [7]. Further increase of temperature, however, leads to a fall of conductivity. The maximum conductivities are reached earlier at higher temperatures, as increase of temperature always favors more rapid establishment of equilibrium in the system.

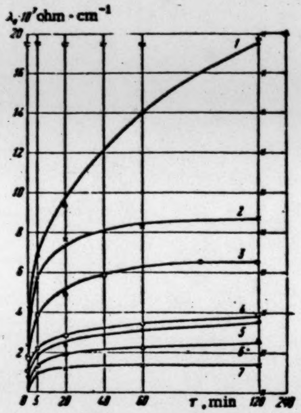

Fig. 6. Variation of λ_0 with τ for 10% carbon-black suspensions with various amounts of added oleic acid: 1) suspension without oleic acid, and suspensions with oleic acid: 2) 0.05% (0.5% on the carbon); 3) 0.1% (1% on the carbon); 4) 0.15% (1.5% on the carbon); 5) 0.3% (3% on the carbon); 6) 0.5% (5% on the carbon); 7) 0.7% (7% on the carbon).

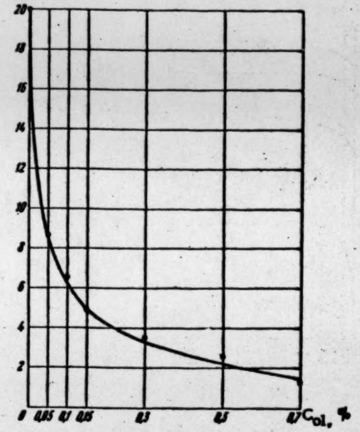

Fig. 7. Variation of the maximum conductivity λ_m of 10% carbon-black suspension with concentration of surface-active addition (oleic acid) in %.

The fact that the conductivity – temperature curve passes through a maximum is clearly seen in Fig. 5, which gives the variation of log λ_0 with temperature for a 10% carbon-black suspension structurized for different times. These results confirm the earlier view [7] that increase of temperature leads to the formation of coagulation structures with increased number and area of contacts between the particles. The fall of conductivity with rise of temperature above 80° is probably due to partial breakdown of the structure as the result of more intense Brownian movement of the disperse-phase particles.

Effect of additions of surface-active substances on the electrical conductivity of carbon-black suspensions. Fig. 6 gives curves for the variation of conductivity with time for 10% carbon-black suspensions containing different amounts of oleic acid. In contrast to the preceding graphs, values of λ_0 and not of log λ_0 are taken along the ordinate axis in Fig. 6. The determinations were carried out at 20°. Fig. 7 gives the maximum (established) conductivity of 10% carbon-black suspension as a function of the concentration of the added surface-active agent, oleic acid (in % on the weight of the system).

Small additions of surface-active material, in full agreement with Yampolsky's findings [8], produce a sharp fall of conductivity in the systems. Further increase of the concentration of the surface-active agent in the suspension also lowers the conductivity, but to a lesser extent. The cause of the decreased conductivity of carbon-black suspensions on addition of a surface-active substance probably lies in adsorption of the latter on the disperse-phase particles. The adsorbed layers formed on the particle surfaces hinder contact between the particles and so lower the conductivity of the suspension.

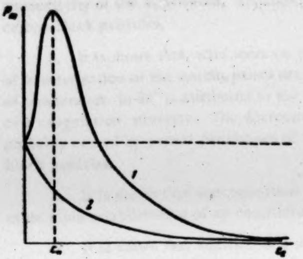

Fig. 8. General scheme showing the influence of surface-active additions on the strength of the coagulation structure in suspensions: 1) if peptization (dispersion) is possible; 2) with stabilization only. P_m) Strength of the structure; c_a) concentration of the active addition.

A comparison of the nature of the conductivity-time curves for suspensions with different oleic acid contents leads to the conclusion that the speed with which the maximum conductivity is reached increases with oleic acid concentration. This effect may be attributed to a lowering of the structural viscosity of the suspension.

The effects of surface-active substances on conductivity of carbon-black suspensions were also studied in suspensions containing 5 and 15% carbon black. In both cases the relationships were analogous to those obtained in experiments with 10% suspensions.

It was of interest to determine the influence of temperature on the electrical conductivity of carbon-black suspensions with surface-active substances. The results of such experiments, carried out with 10% carbon-black suspension containing 0.5% oleic acid, are given in Fig. 5, which also gives the results of experiments with a suspension without oleic acid. It is seen that the conductivity passes through a maximum with increase of temperature both in presence and in absence of oleic acid in the system. However, as was to be expected, the presence of the surface-active substance somewhat lowers the conductivity of the suspension because of its stabilizing action.

Dogadkin and his co-workers [9,10] advanced the view that introduction of a peptizing agent into a rubber–carbon-black mixture should increase the conductivity of the system as the result of breakdown of the carbon-aggregates into primary particles and the consequent formation of a larger number of conducting chains. It is well known from the work of Rebinder and his associates [13,14] how surface-active additions at various concentrations influence structure formation in suspensions in hydrocarbon media. At low concentrations peptization is predominant and, in consequence, structure formation reaches a maximum. At higher concentrations the stabilizing action prevails, leading to total liquefaction of the system – structural breakdown. This means that at low concentrations of the surface-active substance the predominant process is an increase of the number of individual primary particles – kinetic elements, per unit volume of the system. As their surface is not completely covered by adsorption layers, such particles form a loose structural network by the action of cohesion forces at the less protected regions. The increase of the number of particles in consequence of peptization (adsortional dispersion) results in increased strength in the structure (Fig. 8). Further increase of the concentration of the surface-active substance then leads to a sharp decrease of structurization, with a fall of the strength of the structure to zero in consequence of the total stabilization of the particles by adsorption layers. This was the effect found in our experiments, in which additions of oleic acid (from 0.5 to 5% calculated on the carbon black) to the suspensions sharply lowered their conductivity.

The data of the authors cited [9,10] refer to the same region of fairly high concentrations, in which, according to the views put forward above, the stabilizing action of the surface-active substances should predominate; this is found in practice. For example, a careful comparison of Figures 3 and 6 in [9] shows that the conductivity of the mixtures was always lower if stearic acid had been added to the mixtures. In the same way, Fig. 7 [9] clearly shows that the electrical resistance of mixtures containing stearic acid was higher than that of the control mixtures without stearic acid.

SUMMARY

1. The influence of various factors (concentration of the disperse phase, temperature, addition of surface-active substances) on structure formation in carbon-black suspensions in a hydrocarbon medium (nonpolar Vaseline oil) has been studied by measurements of the variation of the electrical conductivity with time.

2. It is shown that increase of the disperse-phase concentration favors structurization and increases the conductivity of the suspensions, apparently as the result of an increase in the number of conducting chains of carbon-black particles.

3. It is shown that, with increase of temperature, the electrical conductivity, and therefore the degree of structurization of the system, passes through a maximum at ~ 80°. The increased conductivity with rise of temperature to 80° is attributed to the fact that in this instance increase of temperature favors the formation of a coagulation structure. The decrease of conductivity when the temperature is increased above 80° is probably caused by partial breakdown of the structure owing to intensified Brownian movement of the carbon-black particles.

4. It is shown that structurization is completed more rapidly at higher temperatures, because of the more rapid establishment of an equilibrium state in the system at higher temperatures.

5. It is shown that addition of a surface-active substance considerably lowers the conductivity of carbon-black suspensions, evidently because of the stabilizing effect – formation on the particle surfaces of protective adsorption coatings which prevent coagulation of the particles and formation of a conducting structural network.

LITERATURE CITED

[1] P.A Rebinder and V.B. Margaritov, J Rubber Ind. 12, 991 (1935).

[2] V.B. Margaritov, Physical Chemistry of Rubber (State Chem. Press, Moscow, 1941).

[3] P.A. Rebinder, Bull. Div. Math. Nat. Sci. Acad. Sci. USSR, Chem. Ser. 1936, 5, 639.

[4] P.A. Rebinder, G.A. Ab, and S. Ya. Veiler, Proc. Acad. Sci. USSR 31, 444 (1941).

[5] Ya. B. Aron and P.A. Rebinder, Proc. Acad. Sci. USSR 52, 235 (1946).

[6] A.S. Kolbanovaskaya, P.A. Rebinder, and O.I. Lukyanova, Colloid J. 12, 208 (1950).

[7] S.S. Voyutsky, A.D. Zaionchkovsky, V.A. Kargin, and S.I. Rubina, Colloid J. 13, 333 (1951).

[8] B. Ya. Yampolsky, Colloid J. 18 (1956).

[9] B. Dogadkin, K. Pechkovskaya, and V. Kupriyanova, Investigations of the Physics and Chemistry of Rubber (State Chem. Press, Moscow, 1950).

[10] K. Pechkovskaya, Ts. Milman, and B. Dogadkin, Colloid J. 14, 250 (1952) (T.p. 275).*

[11] N.A. Figurovsky and M.M. Fainberg, Proc. Acad. Sci. USSR 31, 342 (1941).

[12] V.V. Keltsev and P.A. Tesner, Carbon Black (State Fuel Tech. Press, 1952).

[13] E.E. Segalova and P.A. Rebinder, Colloid J. 10, 223 (1948).

[14] V.B. Mokievsky and P.A. Rebinder, Proc. Acad. Sci. USSR 26, 47 (1940); J. Phys. Chem. 14, 1507 (1940).

Received March 12, 1956

The Moscow State University
Chair of Colloid Chemistry

---

* T. p. = C. B. Translation pagination.

THE COMPATIBILITY OF HIGH POLYMERS

A.G. Shvarts

The use of formulations based on mixtures of rubbers and synthetic resins in the rubber and plastics industries has provided the solution to a number of important practical problems. For example, addition of resins to rubber mixtures improves abrasion resistance; butadiene – acrylonitrile resins can be used as plasticizers for polyvinyl chloride. Vulcanizates of new properties can be obtained from mixtures of different rubbers.

The question of correct methods for selection of such systems has not yet been solved theoretically. The few investigations on this problem show that the best strength and fatigue properties are found in systems with compatible components [1-3].

In practice, the compatibility of polymers is usually determined experimentally. The possibility of assessing polymer compatibility by calculation is considered in this paper.

The compatibility of two components is understood to mean the ability to form a thermodynamically stable homogeneous one-phase system. The formation of a one-phase system of two components (mixing, mutual solubility of two components) at constant temperature and pressure occurs with a decrease of the free energy of the system

$$\Delta F = \Delta H - T \cdot \Delta S, \tag{1}$$

where ΔF is the change of free energy or thermodynamic potential of the system; ΔH is the change of enthalpy on mixing; ΔS is the change of entropy on mixing; T is the absolute temperature of the mixture.

In the mutual solution of high polymers, the component molecules differ little in size, and therefore the molar change of entropy on mixing should be close to the ideal. Because of the high molecular weight of high polymers, the entropy change per 1 cc of mixture is small relative to the corresponding change when low-molecular liquids are mixed. This may be illustrated as follows: if the molar volume of an ordinary low-molecular liquid is taken as 100 cc, and the molar volume of a polymer as 100,000 cc, then, according to Gee [4], in the mixing of 1 cc of one low-molecular liquid with 1 cc of another, the value of $T \cdot \Delta S = 8.3$ cal/2 cc. For the mixing of 1 cc of a polymer with 1 cc of a low-molecular liquid, $T \cdot \Delta S = 4.5$ cal /2 cc, and for the mixing of 1 cc of one polymer with 1 cc of another polymer $T \cdot \Delta S = 0.0083$ cal /2 cc. At the same time, according to recent data, the enthalpy change in the mixing of two polymers per 1 cc of the mixture will be of the same order as in the mixing of two low-molecular liquids of the same composition and structure (several calories per 1cc). It is assumed that the change of enthalpy on mixing does not influence the molecular chain flexibility, that is, it does not affect the change of entropy on mixing.

It follows from the above that the possibility of mutual solution of polymers is primarily determined by the change of enthalpy on mixing, or by the sign of the heat effect. Studies of the mixing of polymer solutions of equal concentrations [1,5,6] have shown that of 58 solutions of different polymer pairs only 9 mixtures do not separate into phases, so that only 9 combinations of polymers out of 58 proved truly compatible. Investigations of the heats of mixing of polymers, carried out by Struminsky [5] have shown the existence of a negative heat effect for the mixing of a number of polymers.

Thus, most binary polymer mixtures are nonequilibrium systems, which can exist only by virtue of their high viscosity, which prevents phase separation. Therefore, although no macroscopic separation into phases occurs in such systems, an interphase boundary exists of the same order of magnitude as the segments of the polymer molecules. This is due to an increase of the enthalpy of the system when the polymers are mixed.

The enthalpy change of a mixture depends on the partial enthalpy changes of its components

$$\Delta H = n_1\Delta\overline{H}_1 + n_2\Delta\overline{H}_2, \qquad (2)$$

where ΔH is the enthalpy change on mixing (the heat of mixing taken with the opposite sign); ΔH_1 and ΔH_2 are the changes of partial molar enthalpies of the first and second components; n_1 and n_2 are the number of moles of the first and second components in the mixture.

For the mixing of two liquids in which the intermolecular forces are of similar character, accompanied by heat absorption, the changes of the partial molar enthalpies can be calculated [7] from the following equations:

$$\Delta\overline{H}_1 = V_1 (\sqrt{E_1/V_1} - \sqrt{E_2/V_2})^2 v_2^2, \qquad (3)$$

$$\Delta\overline{H}_2 = V_2 (\sqrt{E_1/V_1} - \sqrt{E_2/V_2})^2 v_1^2, \qquad (4)$$

where V_1 and V_2 are the molar volumes of the first and second components; v_1 and v_2 are the volume fractions of the first and second components in the mixture; E_1/V_1 and E_2/V_2 are the cohesive energy densities of the first and second components (the energy of intermolecular action per 1 cc of the first and second component, respectively). The factor $(\sqrt{E_1/V_1} - \sqrt{E_2/V_2})^2$ is usually represented by the parameter β [8].

Thus, for the enthalpy change on mixing of two components we have the expression:

$$\Delta H = n_1V_1\beta v_2^2 + n_2V_2\beta v_1^2, \qquad (5)$$

$$\Delta H = \beta (V_1' v_2^2 + V_2' v_1^2), \qquad (6)$$

where V_1' and V_2' are the volumes of the first and second components in the mixture. It is assumed that no volume change occurs in the system on mixing.

It follows from Equation (6) that the increase of enthalpy on mixing of two polymers depends on the parameter β. The lower the value of this parameter, the greater is the possibility of formation of a homogeneous mixture. Let us now calculate at what values of β the increase of enthalpy is less than the increase of the entropy term, $\Delta H < T\Delta S$, i.e., when the polymers are mutually soluble. Let us assume that we mix 1 cc each of two polymers with a similar character of intermolecular action (for example, two polymers of low polarity). The enthalpy change (from Equation (6)) is:

$$\Delta H = \beta\ (0.5^2 + 0.5^2) = 0.5 \cdot \beta \text{ cal/2 cm}^3. \qquad (7)$$

For compatible polymers, when $\Delta F < 0$ and $\Delta H > 0$

$$\Delta H < T\Delta S. \qquad (8)$$

If we take the molar volume of the polymers to be 100,000 cc, then on mixing, as stated above, $T\Delta S =$ $= 0.0083$ cal/2 cc.

In this case the polymers are compatible when

$$\beta < \frac{0.0083}{0.5} < 0{,}0166. \qquad (9)$$

Comparison of Equations (6) and (9) shows, first, that with decreasing molecular weights of the polymers, compatible polymers will be those with greater differences in their cohesive-energy densities (ΔS increases, while ΔH is unchanged), and second, with increasing differences in the nature of the intermolecular forces the difference between the cohesive-energy densities of the polymers, which ensures compatibility, decreases as ΔH increases, while ΔS is almost unchanged.

Determination of the parameter β for mixtures of different polymers. With known values of the cohesive energy density, the parameter β is calculated, as stated above, as follows:

$$\beta = (\sqrt{E_1/V_1} - \sqrt{E_2/V_2})^2. \tag{10}$$

For ordinary liquids the cohesive energy density at a given temperature is defined as the energy of evaporation of the liquid, at constant temperature and volume, per 1 cc of the liquid. As all polymers decompose at temperatures considerably below their boiling points, their cohesive-energy densities are calculated from data on swelling, differential heats of solution in various solvents, etc.

Table 1 gives the square roots of the cohesive-energy densities for a number of polymers at 25°, calculated by us or taken from the literature. Most of the values are averages of different data.

TABLE 1

Square Roots of Cohesive-Energy Densities of Polymers

Polymer	$\sqrt{E/V}\left(\frac{cal}{cc}\right)^{1/2}$* at 25°
Cellulose	15.65
Polyamides	15.05
Nitrocellulose (11.83% nitrogen)	14.85
Acetylcellulose (56% acetyl groups)	13.60
Ditto, 48%	13.29
Benzylcellulose	12.33
Polymethyl methacrylate	12.84
Polyvinyl alcohol	12.60
Polyvinyl acetate	11.05
Polyvinyl chloride	10.10
Polystyrene	9.33
Divinyl–acrylonitrile rubber (40% acrylonitrile)	9.83
Ditto, 26%	9.50
" 18%	9.30
" 12%	9.10
Thiokol F**	9.40
Polychloroprene	9.00
Butadiene–styrene rubber (40% styrene)	8.55
Ditto, 30%	8.48
" 25%	8.45
" 15%	8.40
" 10%	8.37
Polybutadiene	8.35
Natural rubber	8.22
Polyisobutylene	7.85
Polyethylene	7.70
Dimethyl silicone rubber	7.35

---

* The values of $\sqrt{E/V}$ represent the cohesive energy densities of the polymers in the amorphous state.

** Product of reaction between sodium tetrasulfide and dichlorodiethyl ether and dichloroethane.

The calculations were based on:

1. Heats of solution and solvation of nitrocellulose in acetone, methyl ethyl kentone, and methyl propyl ketone [5, 9]; of acetylcellulose in acetone, chlorofoform, and methyl acetate [5, 9]; of benzylcellulose in cyclohexane and chloroform [5], and of polymethylmethacrylate and polyvinyl acetate in acetone [5].

2. Osmotic pressure data for polyvinyl chloride in methyl ethyl ketone and dioxane, and for polyisobutylene in toluene and benzene [10].

3. Equilibrium swelling data for rubber vulcanizates [11-15], apart from those indicated below, by calculation with the aid of a method similar to that used by Scott and Magat [11].

4. Thermodynamic comparison of data on the swelling of divinyl– acrylonitrile rubbers containing 18 and 12% nitrile, and of butadiene – styrene rubber containing 10 and 30% styrene, with data on the swelling of divinyl – acrylonitrile and butadiene – styrene rubbers with known values of cohesive-energy densities.

5. The cohesive-energy densities for cellulose, polyamides, Thiokol F, polyvinyl alcohol, and dimethyl silicone rubber are taken from the literature [16,17].

Table 1 shows that the greater the polarity of a polymer and the denser its molecular packing, the higher is its cohesive-energy density.

The most exact data are those for the rubbers, as they are based on swelling data in more than fifty solvents. It should also be pointed out first that the discrepancies in the values of $\sqrt{E/V}$, obtained for the same polymer on the basis of different data are less in all cases, with the execption of polystyrene and acetylcellulose with 50% acetyl groups, than the fifferences between the values of $\sqrt{E/V}$ for two neighboring polymers in Table 1. Second, the variation of the cohesive energy density in the series from cellulose to polymethyl silicone is in good agreement with known data on intermolecular interaction of polymers [16].

Determination of the relationship between the compatibility of two polymers and the difference between their cohesive-energy densities, or the absolute value of the parameter β. Let us compare the results (Table 2) obtained by Komskaya [1] for the mixing of 5 % rubber solutions with the values of the parameter β calculated from the data in Table 1.

TABLE 2

Effect of the Compatibility of Polymers on the Behavior of Solutions of Equal Concentration on Mixing

Rubber mixtures	Parameter β, cal /cc	Behavior of solutions
SKN-18 + NR	1.085	Separation into two phases
SKN-18 + SKB	0.904	
SKN-18 + SKS-30	0.673	
SKS-30 + NR	0.068	
SKS-30 + SKB	0.017	
SKS-30 + SKS-10	0.017	No phase separation
SKB + NR	0.017	
SKB + DB-2	0.000	

Table 2 shows that mixtures of polymers for which the value of β is low are compatible. The value of β for the compatible rubbers SKB and NR, SKS-30 and SKS-10, is 0.017, which is of the same order as the value of β calculated from Equations (7-9).

Let us also consider Struminsky's data on polymer mixing [5], and compare them with the values of the parameter β found from Table 1.

Of the polymer systems studied [5], the only compatible polymers were those the mixing of which is accompanied by evolution of heat. Examination of the data in Table 3 shows that the enthalpy increase of the system diminishes with decreasing difference of the cohesive-energy densities of the two mixed polymers. Only systems containing highly polar polymers (such as nitrocellulose or acetylcellulose) do not obey this rule. Polymers which have high intermolecular interaction (170-180 cal /cc and over) have loose molecular packing. When they are mixed, the molecular chain flexibility may be changed as the result of polar group interaction [18]. Therefore Equations (3) and (4), which do not take account of volume contraction as the result of changes in the molecular packing density, are not applicable to such systems.

TABLE 3

Effect of Compatibility of Polymers on the Behavior of Solutions of Equal Concentration on Mixing

Polymer mixtures	Parameter β in cal/cc	Change of enthalpy on mixing ΔH cal/2cc	Behavior of solutions
Acetylcellulose (56 and 48% acetyl groups)	0.24	8.0	Separation into two phases
Acetylcellulose (56% acetyl groups) and polyvinyl acetate	6.52	2.9	•
Benzylcellulose and polystyrene	9.00	2.6	•
Polymethyl methacrylate and polymethyl acrylate	–	2.5	•
Polymethyl methacrylate and polyvinyl acetate	3.22	1.0	•
Polystyrene and polybutadiene	0.96	−0.45*	•
Polybutyl methacrylate and polybutyl acrylate	–	0.6	•
Polyvinyl acetate and polybutyl acrylate	–	0.5	•
Polymethyl methacrylate and polybutyl methacrylate	–	0.3	•
SKS-30 + NR	0.068	0.3	•
SKS-30 + polybutadiene	0.017	−0.03*	•
Polybutylmethacrylate and polymethyl acrylate	–	0.0	•
Polybutadiene + NR	0.017	−0.3	No phase separation
Nitrocellulose and polyvinyl acetate	–	−0.9	•
Nitrocellulose and acetylcellulose (56% acetyl groups)	–	−5.9	•

---

* As was shown by Struminsky [5], the negative heat of mixing of polybutadiene with polystyrene is the result of a large volume contraction on mixing, and not of intermolecular interaction between the components.

Effect of the parameter β on the microheterogeneity and physical and mechanical properties of polymer mixtures. As was stated above, the more heat absorbed during mixing of the polymers, the greater is the microheterogeneity of the resultant mixtures, and the worse are the strength and fatigue properties. Let us consider the properties of mixtures of polyvinyl chloride [2] and nitrocellulose [3] with various rubbers of approximately the same strengths, but with different cohesive-energy densities (Table 4).

TABLE 4

Tensile Strengths of Polymer Mixtures in Relation to their Compatibilities

Second component		Parameter β cal./cc	Tensile strength calculated on the section at break in kg/cm²	Second component		Parameter β cal./cc	Tensile strength calculated on the section at break in kg/cm²
Designation	Contents, %			Designation	Contents, %		
Principal component – nitrocellulose (~ 12% nitrogen)				Principal component – polyvinyl chloride			
—	—	—	660	SKN-50	50	0.0009	830
SKN-40	50	24.7	489	SKN-37	50	0.090	545
SKN-28	50	28.2	434	SKN-28	50	0.325	86.5
SKN-20	50	30.4	214	SKN-20	50	0.670	28.3
SKN-12	50	33.2	168	SKN-12	50	1.000	18.0
SKS-30	44	40.6	23				

Table 4 shows that the strength of mixtures of nitrocellulose and polyvinyl chloride with various rubbers falls sharply with increase of the parameter β for the system, that is, with increased microheterogeneity of the system. Thus, in practical formulation of polymer mixtures such as those given in Table 4, a preliminary comparison of the cohesive-energy densities of the components eliminates the need for numerous experiments to determine the compatibilities of the components. A decrease in the value of β in the transition from one mixture to another favors an improvement of the physicomechanical properties.

SUMMARY

1. It is shown that the compatibility of polymers can be determined by calculation with the aid of known thermodynamic equations.

2. Values for the cohesive-energy densities of 19 polymers in the amorphous state, calculated on the basis of literature data, are given.

3. The compatibility of high polymers with cohesive-energy densities not greater than 160-170 cal/cc in the amorphous state is determined by the ratio of the cohesive-energy densities of the components.

4. At molar volumes of 100,000 cc and over, polymers for which the value of the parameter $\beta < 0.017$ cal/cc are mutually soluble.

This is the reason for the small number of thermodynamically compatible polymers.

5. The physicomechanical properties of a mixture depend on the difference between the cohesive, energy densities of the components. The greater this difference is, the lower the strength of the mixture, other conditions being equal.

The author expresses his deep gratitude to Doctor of Chemical Sciences G.L. Slonimsky for help and valuable comments.

LITERATURE CITED

[1] N.F. Komskaya, Dissertation (Karpov Institute of Physical Chemistry, 1952).

[2] R.A. Reznikova, A.D. Zaionchkovsky, and S.S. Voyutsky, Colloid J. 15, 108 (1953)(T.p. 111).*

[3] V.I. Alekseenko, N.U. Mishustin, and S.S. Voyutsky, Colloid J. 17, 3 (1955) (T.p. 1).*

[4] G. Gee, Quart. Revs. 1, 26 (1947).

[5] G.V. Struminsky, Dissertation (Karpov Institute of Physical Chemistry, 1953).

[6] A. Dobry, F. Boyer-Kawenoki, J. Polymer Sci. 2, 90 (1947).

[7] J.H. Hildebrand, Solubility of Nonelectrolytes (State United Sci.-Tech. Press, Moscow, 1938).

[8] G.Gee, Chemistry of Large Molecules, (Foreign Lit. Press, Moscow, 1948), Vol. 1.

[9] A.A. Tager and V.A. Kargin, J. Phys. Chem. 15, 1036 (1941).

[10] A.A. Tager, Solutions of High-Molecular Compounds (State Chem. Press, Moscow – Leningrad, 1951).

[11] R. Scott and M. Magat, J. Polymer Sci. 4, 555 (1949).

[12] G. Gee, Trans. Inst. Rubber Ind. 18, 266 (1943).

[13] F. Rostler et al., Rubber Age 59, 299 (1946).

[14] F. Rostler, R. White, Rubber Age 61, 313 (1947).

[15] G. Whitby, A. Evans, D. Pasternack, Trans. Faraday Soc. 38, 269 (1942).

[16] H. Mark, Ind. Eng. Chem. 34, 1343 (1942).

[17] R. Boyer, J. Appl. Phys. 20, 540 (1949).

[18] P.V. Kozlov and E.F. Russkova, Proc. Acad. Sci. USSR 95, 583 (1954).

Received November 26, 1955

Scientific Research Institute for
the Tire Industry
Moscow

---

* T. p. = C. B. Translation pagination.

ERRATA

I. The paper by B. Dogadkin, B. Lukin, Z. Tarasova, Z. Skorodumova, and I. Tutorsky, "The Theory of Rubber Reinforcement: Interaction of Carbon Black With Sulfur and Rubber ", Colloid J. 18, No. 4, 413 (1956)* contains an error. The quantities of sulfur shown in Table 2 were calculated on the total weight of the precipitate and not on the carbon-black present in the precipitate. Therefore, the figures in Table 2 should be multiplied by approximately 4, and Table 2 should be as follows:

TABLE 2

Contents of Total, Adsorbed, and Chemically Combined Sulfur in Different Specimens of Carbon-Black Heated at 110, 130, and 150° in Presence and in Absence of Vulcanization Accelerator A 100, (as % on the Carbon-Black)

Sulfur content	110 °C				130 °C				150 °C			
	Channel black		Hydrogenated black		Channel black		Hydrogenated black		Channel black		Hydrogenated black	
	without accelerator	with accelerator	without accelerator	with accelerator	without accelerator	with accelerator	without accelerator	with accelerator	without accelerator	with accelerator	without accelerator	with accelerator
Amount of sulfur	0.28	1.8	0.52	1.72	0.48	1.52	0.88	1.16	1.16	2.28	1.48	2.98
Amount of chemically bound sulfur	0.16	0.8	0.36	1.00	0.36	1.24	0.72	1.48	1.04	2.16	1.48	3.00
Amount of adsorbed sulfur (extracted by chloroform	0.12	1.0	0.16	0.72	0.12	0.28	0.16	0.12	0.12	0.12	—	—

II. In the paper by N.V. Mikhailov and E.Z. Fainberg "Investigation of the Structure of Synthetic Polycaprolactam Fibers. 8. Heats of Solution of the Crystalline and Amorphous Modifications of Polycaprolactam", Colloid J., 18, No. 3, 315 (1946);** the caption under Fig. 1 should read "X-ray diagram of polycaprolactam: A) crystalline, B) amorphous.

NOTICE

The Commission on High-Molecular Compounds of the Division of Chemical Sciences, Academy of Sciences, USSR announces that the IXth Conference on High-Molecular Compounds, Convened by the Academy of Sciences, USSR jointly with the Ministry of Higher Education, USSR, will be held in Moscow from January 28 to February 2, 1957.

The Conference will be devoted to new experimental work on the theory of the synthesis of high-molecular compounds, chain reactions and chemical properties of polymers, the structure and physicomechanical properties of polymers, aging processes, and applications of polymeric materials.

The papers will be discussed in the appropriate sections. Summaries of the papers will be circulated by the Organizing Committee together with the program and invitation tickets before January 1, 1957 on application from institutions and undertakings interested in the work of the Conference.

Applications for invitations should be accompanied by lists of delegates and sent in good time to the Organizing Committee (Moscow, B. Kaluzhskaya, 14, corp. 2, Division of Chemical Sciences, Academy of

---

* C. B. Translation page 407.

** C. B. Translation page 305.

Sciences, USSR, for the Organizing Committee of the IXth Conference on High-Molecular Compounds) with an indication of the address to which the invitations are to be sent.

Hotel requirements should be indicated in the applications.

Commission on High-Molecular Compounds
Division of Chemical Sciences
Academy of Sciences, USSR

RUSSIAN CHEMICAL RESEARCH IN COMPLETE ENGLISH TRANSLATION

A comprehensive survey of most major Russian chemical journals

Covers the most advanced Soviet research, including papers by leading Soviet chemists on both theoretical and applied chemistry, with wide industrial applications.

JOURNAL OF GENERAL CHEMISTRY OF THE USSR (12 issues, 3,600 pp. per year)	$170.00
JOURNAL OF APPLIED CHEMISTRY OF THE USSR (12 issues, 1,800 pp. per year)	95.00
JOURNAL OF ANALYTICAL CHEMISTY OF THE USSR (6 issues per year)	80.00
BULLETIN OF THE ACADEMY OF SCIENCES USSR (12 issues per year)	150.00
PHYSICAL CHEMISTRY SECTION OF PROC. ACAD. SCI. USSR (Doklady, 36 issues per year, published in 6)	160.00
BIOCHEMISTRY SECTION OF PROC. ACAD. SCI. USSR (Doklady, 36 issues per year, published in 6)	$65.00
CHEMISTRY SECTIONS OF PROC. ACAD. SCI. (Doklady, 36 issues per year, published in 6)	
Chemistry Section	95.00
Chemical Technology Section	15.00
Agrochemistry Section	15.00
Geochemistry Section	15.00
All four sections of Proc. Acad. Sci. USSR cited above may be purchased as a unit for	125.00
COLLOID JOURNAL (6 issues per year)	80.00
JOURNAL OF ATOMIC ENERGY (12 issues, 1,200 pp. per year)	75.00

and SOVIET RESEARCH IN CATALYSIS, Chemistry Collection III

Covers all aspects of catalysis, selected from papers in all chemistry journals translated by Consultants Bureau 1949-1955.

Sections may be purchased separately as follows:

I.	Theoretical and Sundry Associated Effects	262 pages	$50.-	
IIa.	General	250 pages	50.-	$125.-
IIb.	General	250 pages	50.-	
IIc.	General: Reduction-Oxidation and Fischer-Tropsch	214 pages	50.-	
III.	Hydrogenation Dehydrogenation Cracking	294 pages	50.-	
IV.	Isomerization Alkylation Dehydration	274 pages	$50.-	
V.	Polymerization Friedel-Crafts Zeigler	128 pages	30.-	

The Collection, comprising 1,672 pages, 262 papers may be purchased as a unit for **$200.00**

SYMPOSIUM ON RADIATION CHEMISTRY

PART I:	ACTION OF RADIATIONS ON WATER AND AQUEOUS SOLUTIONS	$75.00
PART II:	ACTION OF RADIATIONS ON INDIVIDUAL ORGANIC COMPOUNDS AND HIGH POLYMERS	65.00
	Both parts are available for	100.00

All Consultants Bureau translations are by scientists who are specialists in each field, equally familiar with Russian, and the technical vocabulary. All material is translated cover-to-cover, it is clearly reproduced by the multilith process, staple bound, and includes all diagrams, photographs, and tabular matter integral with the text. Issues are mailed to subscribers upon publication. Single articles are available. Write for free Tables of Contents, specifying publication desired.

NOTE: *Consultants Bureau is still seeking scientist translators.*

CONSULTANTS BUREAU, INC.

227 WEST 17th STREET, NEW YORK 11, N.Y. — U.S.A.

Telephone: ALgonquin 5-0713 • Cable Address: CONBUREAU, NEW YORK

COLLOID JOURNAL

Journal of Theoretical and Applied Physics and Chemistry of Colloids

VOLUME XIX (1957)

A PUBLICATION OF THE ACADEMY OF SCIENCES OF THE USSR

IN ENGLISH TRANSLATION

Copyright, 1959

CONSULTANTS BUREAU, INC.
227 West 17th Street
New York 11, N. Y.

Printed in the United States

Annual Subscription $80.00
This index 5.00

Note: The sale of photostatic copies of any portion of this copyright translation is expressly prohibited by the copyright owners.

COLLOID JOURNAL OF THE U.S.S.R. IN ENGLISH TRANSLATION

January-February, 1957

TABLE OF CONTENTS

	Page	Russ. Page
1. Calculation of the Limiting Shear Stress (Yield Value) of Disperse Systems in Experiments with the Cone Plastometer. N. N. Agranat and M. P. Volarovich.	1	3
2. Theory of the Cone Immersion Method for Determination of the Yield Values of Disperse Systems. N. N. Agranat and M. F. Shirokov.	9	9
3. An Electron Microscope Study of Structure Formation in Loess. 1. Influence of the Dispersion Medium. E. Aripov, Z. Ya. Berestneva and V. A. Kargin	15	14
4. An Electron Microscope Study of Structure Formation in Loess. 2. Influence of Loess Components on Structure Formation. E. Aripov, Z. Ya. Berestneva and V. A. Kargin	19	17
5. The Effect of Air Ionization on the Disperse Phase of Aerocolloids. I. I. Belyaeva, A. E. Mikirov and N. S. Smirnov.	25	24
6. Intermolecular Structure of High Polymers. Communication 22. Modification of the Molecular Structure of High Polymers by the Inclusion Method. A. N. Bykov and A. B. Pakshver.	29	27
7. Equilibrium of a Viscoplastic Disperse System on a Rotating Disk. A. M. Gutkin.	33	31
8. Investigation of the Structure and Properties of Carbon Chain Polymers in Dulute Solutions. 2. Solutions of Vinyl Chloride – Acrylonitrile Copolymer. S. G. Zelikman and N. V. Mikhailov.	37	35
9. Distribution of a Weak Electrolyte in the Double Layer. I. G. Ivanter.	43	41
10. Compatibility of Nitrocellulose with Butadiene – Acrylonitrile Copolymers. 3. Dependence of the Glass Transition Temperature and Flow of Nitrocellulose Films on their Contents of Various Butadiene – Acrylonitrile Copolymers. L. E. Kalinina, V. I. Alekseenko and S. S. Voyutsky	57	51
11. Thixotropic Structure Formation and Elasticoplasticoviscous Properties of Askangel Suspensions. E. I. Kobakhidze and M. E. Shishniashvili	65	59
12. Gelatinized Emulsions. 13.O/W Type Emulsions of Maximum Concentration with a Thixotropic Dispersion Medium. L. Ya. Kremnev.	75	68
13. Investigation of Structurized Suspensions. E. F. Kurgaev.	79	72
14. The Effect of Surface-Active Substances on the Specific Viscosity of Gelatin Solutions. S. M. Levi.	85	78
15. Effect of Hydrophilic Plasticizer Additions on the Properties of Concentrated Cement Suspensions. O. I. Lukyanova, E. E. Segalova and P. A. Rebinder	89	82
16. Preparation of Ferric and Zirconium Hydroxide Organosols. V. N. Maslov	97	90

COLLOID JOURNAL OF THE U.S.S.R. IN ENGLISH TRANSLATION

January-February, 1957

TABLE OF CONTENTS (continued)

Page — Russ. Page

17. Experimental Investigations of Laminar Systems. 23. Kinetics of the Formation of Hydroxide Films on the Surface of Cupric Ammine Solutions. S. G. Mokrushin and G. A. Kitaev 99 93

18. The Relationship Between the Affinity and Structure of Direct Dyes. P. V. Moryganov and B. N. Melnikov 105 100

19. Structure of High Polymers. Communication 18. Strengthening of the Molecular Structure of Tire Yarn. A. B. Pakshver, L. S. Gerasimova and Kh. N. Kozlovskaya 109 104

20. Molecular Structure of High Polymers. Communication 17. Investigation of the Intermolecular Structure of Thermoplastic Fibers. A. B. Pakshver, E. E. Natan and I. F. Katushkina 115 109

21. The Electrochemistry of High-Polymer Dispersions. 3. Effect of pH on the Electrokinetic Potential of Globules in Synthetic Latexes. R. M. Panich and S. S. Voyutsky 119 113

22. The Fractional Composition of Fine Cellulose Fibers. S. L. Talmud, A. N. Turzhetskaya and A. A. Kuleshova 125 118

Discussion

23. Characterization of the State of High-Polymer Gels. A. V. Nikolaev, R. E. Neiman and O. V. Neiman 129 121

Letter to the Editor

24. Coagulation of Atmospheric Condensation Nuclei on Dust Particles. M. L. Mikhelson. 133 125

Tribute

25. The Seventieth Anniversary of the Birth and Fifty Years of the Scientific Activity of Grigory Semenovich Petrov. M. S. Akutin 137 127

COLLOID JOURNAL OF THE U.S.S.R. IN ENGLISH TRANSLATION

March-April, 1957

TABLE OF CONTENTS

	Page	Russ. page
1. On the Fiftieth Birthday of Valentin Alekseevich Kargin	139	129
2. The Structure of Linear Polymers. V. A. Kargin, A. I. Kitaigorodsky, and G. L. Slonimsky	141	131
3. Molecular Configuration and Structure Formation in Polyacrylate Solutions. V. A. Kargin and N. F. Bakeev	143	133
4. The Formation of Crystalline Aluminosilicates. Z. Ya. Berestneva, M. B. Konstantinopolskaya, and V. A. Kargin	149	138
5. Study of the Transition of Amorphous and Crystalline Polymers from the Solid into the Fluid State on Addition of Substances of Low Molecular Weight. V. A. Kargin, G. L. Slonimsky, and L. Z. Rogovina	153	142
6. Adsorption of Polystyrene Latexes in Relation to the Sign of the Particle Charge and the Sorbent. E. M. Aleksandrova and N. S. Razumikhina	159	148
7. The Relationship Between the Structure of Emulsifiers of the Alkylaromatic Acid Type and the Polymerization of Unsaturated Compounds. 4. Salts of Di-Sec-Butylnaphthalenesulfonic Acid with Univalent Cations. N. P. Apukhtina and A. M. Lyagalova	165	154
8. Investigation of the Aqueous Properties of Peat by Means of Radioactive Isotopes. M. P. Volarovich, N. V. Churaev, and B. Ya. Minkov	171	159
9. Heats of Swelling and of Solution of Nitrocellulose. D. I. Galperin and L. I. Moseev	179	167
10. Investigations of the Physical Chemistry of Agar. 1. Method for the Determination of the Intrinsic Viscosity of Agar. S. A. Glikman and I. G. Shubtsova	183	172
11. Aggregative Stability of Pigment Suspensions in Hydrocarbons, Alcohols, and Esters of Low Molecular Weight. Ya. M. Gurevich	189	178
12. Dependence of the Exchange Adsorption of Ions on their Structure. 2. Adsorption of Bivalent Amines. A. T. Davydov and R. F. Skoblionok	193	183
13. The Influence of Structure on the Chemical Activity and Vulcanizability of Butadiene Polymers. B. A. Dogadkin, A. V. Dobromyslova, F. S. Tolstukhina, and N. G. Samsonova	199	188
14. The Use of High Frequency Analysis in Colloidochemical Investigations. V. I. Ermakov, V. N. Maslov and O. G. Stolyarov	207	198
15. The Structure of Gels. 9. Effect of the Nature of the Plasticizer on the Physicomechanical Properties of Divinyl-Styrene Rubber. M. P. Zverev and P. I. Zubov	211	201
16. The Hardening Mechanism of Thermosetting Plastics (Molding Powders). I. F. Kanavets, L. G. Batalova, and A. G. Romashova	215	204

COLLOID JOURNAL OF THE U.S.S.R. IN ENGLISH TRANSLATION

March-April, 1957

TABLE OF CONTENTS (continued)

	Page	Russ. page
17. Electron Microscope Studies of Colloids. 1. Minerals of the Kaolinite-Halloysite Group. M. I. Kuadzhe	229	219
18. The Mechanism of Protein Denaturation. 10. Effect of Fatty Acid Anions on the Stability of Globular Proteins to Denaturation. A. L. Loseva and A. S. Tsyperovich	233	222
19. Gelation of Latexes on Porous Forms. D. M. Sandomirsky	239	228
20. The Thixotropic Properties of Certain Printing Inks. A. A. Trapeznikov and T. G. Shalopalkina	243	232
21. Effect of an Active Filler and a Solvent on the Structural and Mechanical Properties of Bitumens. S. Ya. Shalyt, N. V. Mikhailov, and P. A. Rebinder	253	244
Letter to the Editor		
22. Possible Differences in the Composition and Viscosity Ratio of a Two-Sided Film and a Surface Layer of a Soap Solution. A. A. Trapeznikov	259	252

COLLOID JOURNAL OF THE U.S.S.R. IN ENGLISH TRANSLATION

May-June, 1957

TABLE OF CONTENTS

	Page	Russ. page
1. Heats of Swelling and Solution of Polymers in Relation to Molecular Weights and Temperature. K. S. Akhmedov and S. M. Lipatov	263	257
2. Two Stages of the Network Formation Process in Polymers. G. M. Bartenev	267	261
3. The Electrochemistry of High Polymer Dispersions. 4. Influence of Cations of Different Valencies on the Electrokinetic Potential of Synthetic Latex Globules. S. S. Voyutsky and R. M. Panich	273	268
4. Adhesion of High Polymers. 3. Effects of the Size, Shape, and Polarity of High Polymer Molecules on Their Adhesion to Cellophane. S. S. Voyutsky, A. I. Shapovalova, and A. P. Pisarenko	279	274
5. Studies of the Physical Chemistry of Agar. 2. Theory and Practice of Agar Fractionation. S. A. Glikman and I. G. Shubtsova	285	281
6. The Effect of Swelling on the Strength of Vulcanizates. B. A. Dogadkin, D. L. Fedyukin, and V. E. Gul	291	287
7. Elastic Deformation of Wood. Yu. M. Ivanov	297	293
8. Thixotropic and Structuromechanical Properties of Askangel Suspensions in Relation to the Composition of the Exchange Complex. E. I. Kobakhidze, M. E. Shishniashvili, and N. N. Serb-Serbina	303	299
9. Properties of Thin Layers of Liquid Between Mica Plates. G. A. Korchinsky	311	307
10. Investigation of the Mechanical Properties of Plastic Disperse Systems in Conditions of Uniaxial Extension and Compression. E. P. Mosikhin and G. V. Vinogradov	315	311
11. Electron Microscope and X-ray Investigations of Disperse Phases in Organosols of Lead–Tin Alloys. E. M. Natanson, V. P. Chalyi, N. N. Kozachek and A. P. Kaban	323	319
12. Production of Titania–Silica Gels and Their Porous Structure. I. E. Neimark, A. I. Rastrenenko, and M. A. Piontkovskaya	329	324
13. Phase Equilibria in Colliod Systems. 1. Separation of A Homogeneous Solution Into Two Phases and the Gel Formation Process. S. P. Papkov	337	333
14. Investigation of the Structuromechanical Properties of Ethylcellulose Solutions and the Effect of Oxidation on These Properties. T. I. Samsonova and L. V. Ivanova-Chumakova	345	343
15. The Theory of Flow of Plastic Disperse Systems. N. V. Tyabin and G. V. Vinogradov	353	352
16. An Electrochemical Study of Bentonite Suspensions. 1. Action of Sodium Hydroxide on Suspensions of Electrodialyzed Askangel. I. A. Uskov and E. T. Uskova	361	361

COLLOID JOURNAL OF THE U.S.S.R. IN ENGLISH TRANSLATION

May-June, 1957

TABLE OF CONTENTS (continued)

Page Russ. page

17. Action of the Basic Salt Aluminum Oxychloride on the Structuromechanical (Thixotropic) Properties of Askangel Suspensions. E. D. Uznadze and M. E. Shishniashvili 367 368

18. Evaluation of Rubber–Solvent Interaction. A. G. Shvarts 375 376

19. Investigation of the Adsorbability of Carbohydrate Solutions By a Polarographic Method. M. S. Shulman 383 384

20. Industrial Unit for Production of Emulsions by Means of An Ultrasonic Liquid Whistle (Jet). S. I. Sinkova and S. A. Puzyrev 387 387

Discussions

21. The Equilibrium State of High Polymer Gels. (On the Subject of the Comments by A. V. Nikolaev, R. E. Neiman, and O. V. Neiman, Colloid J. 19, 129(1957)) S. M. Lipatov and S. I. Meerson 391 390

22. Problems Relating to the Mechanism of the Friction of Rubber. S. B. Ratner 395 394

23. Concerning the Discussion on the Friction of Rubber. G. M. Bartenev 399 397

24. Applicability of the Binomial Law of Friction to the Friction of Rubber. B. V. Deryagin 401 398

Letter To The Editor

25. Use of Ion Exchange Resins for Purifying Quartz Suspensions. K. V. Chmutov and O. G. Larionov 403 399

26. List of Abbreviations 405

5

COLLOID JOURNAL OF THE U.S.S.R. IN ENGLISH TRANSLATION

July-August, 1957

TABLE OF CONTENTS

	Page	Russian page
Changes in the Structure, Degree of Dispersion and Yield Value of Peats as the Result of Complete Freezing. M.P. Volarovich, K.F. Gusev, S.N. Markov and V.P. Tropin.	407	401
Investigation of Electroosmosis in Capillary Systems of Different Charge and Structure. O.N. Grigorov and K.P. Tikhomolova	411	406
Investigation of Adhesion Effects in Bonding Rubber to Metal by Leukonat Adhesive. A.M. Medvedeva, B.V. Deryagin and S.K. Zherebkov	417	412
Effect of Mercaptobenzothiazole on Structural Changes in Rubber on Oxidation, Heating and Plasticization. B. Dogadkin, A. Dobromyslova, L. Sapozhkova and I. Tutorsky	425	421
The Structure of Gels. 10. Globulization of Rubber Under the Action of Nonsolvents Added to Solutions. P.I. Zubov, Z.N. Zhurkina and V.A. Kargin	435	430
Sedimentation Volumes of Polydisperse Suspensions of $Ca_3(PO_4)_2$ in Electrolyte Solutions. G.G. Kandilarov.	439	435
Gelatinized Emulsions. 14. Ethylcellulose as a Stabilizer of Emulsions of the W/O Type. L.Ya. Kremnev and G.A. Shadrin	443	440
Colloidochemical Processes in Reactions of Tetraalkoxysilanes with Aqueous Aluminate Solutions. A.P. Kreshkov, L.V. Myshlyaeva and L.M. Khananashvili.	449	446
Study of the Colloidal Properties of Sulfosuccinic Acid Esters. 1. Esters of the Lower Aliphatic Alcohols. R.V. Kucher, A.A. Yavorsky and M.A. Kovbuz	457	454
Heat Evolution in the Initial Period of Hydration of Cement with Plasticizing Additions. O.I. Lukyanova, E.E. Segalova and P.A. Rebinder	461	459
Effect of Temperature on the Magnitude and Rate of Swelling of Agar. V.P. Mishin and N.D. Verderevskaya	467	472
Investigation of the Structure and Properties of Carbon Chain Polymers in Dilute Solutions. 3. Mixtures of Polyvinyl Chloride and Polyacrylonitrile. N.V. Mikhailov and S.G. Zelikman	473	465
Alteration of the Intermolecular Structure of Capron Fiber as the Result of Heat Treatment. L.I. Pokrovsky and A.B. Pakshver.	479	478
Periodic Deformation of Collagen in Solutions of Electrolytes and Tanning Agents. A.G. Pasynsky and A.M. Tongur.	483	483
Effect of Atmospheric Turbulence on the Kinetics of Aerosol Coagulation. O.M. Todes and A.A. Chekunov	489	490
Settling of Aerosol Particles on the Walls of an Enclosed Space. I. Todorov and A. Sheludko.	495	496
Application of the Method of Approximations to Calculations of Flow of Disperse Systems. N.V. Tyabin and G.V. Vinogradov.	505	505
Effect of Electrolytes on the Structuromechanical Properties of Bentonite Suspensions. I.A. Uskov	511	511
Relationship Between the Intrinsic Viscosity and Molecular Weight of Buna S Rubber. Chien Jen-Yuan, Ching Wen and Cheng Yung-Shih	515	515

TABLE OF CONTENTS (continued)

	Page	Russian page
Letters to the Editor		
The External Friction of Rubber. V.V. Lavrentyev.	523	522
Current Events		
Ninth Conference on Compounds of High Molecular Weight. Yu.M. Malinsky.	527	524

COLLOID JOURNAL OF THE U.S.S.R. IN ENGLISH TRANSLATION

September-October, 1957

TABLE OF CONTENTS

	Page	Russ. Page
1. Development of Colloid Chemistry in the USSR	531	529
2. Antifrictional Properties of Disperse Phases of Metal Organosols. M. L. Barabash and E. M. Natanson	535	534
3. Modification of Polyamide Properties by the Inclusion Method. A. N. Bykov, M. I. Ivanova and A. B. Pakshver	543	542
4. Studies of Electroosmosis in Binary Powder Mixtures Consisting of Particles of Different Chemical Nature. O. N. Grigorov and K. P. Tikhomolova	549	548
5. The Influence of Intermolecular Interaction on the Properties of Rubber Solutions. V. E. Gul and V. A. Berestnev	553	552
6. The Possibility of Surface Activation and Passivation of Nuclei in Water Vapor Condensation. G. I. Izmailova, P. S. Prokhorov and B. V. Deryagin	557	556
7. Adsorption of Water Vapor by Silica and Hydration of its Surface. A. V. Kiselev and G. G. Muttik	563	562
8. Influence of Pore Size and Surface Hydration of Silica on Adsorption of Nitrogen Vapor. A. V. Kiselev and E. V. Khrapova	573	572
9. The Specific Heat of Bound Water. O. D. Kurilenko	585	584
10. Variations of the Specific Volume of Rubber During Stretching. A. B. Kusov, V. I. Trofimova and Yu. I. Nilova	587	587
11. Effect of the Nature of the Emulsifier on the Thermal Decomposition of Cumene and 1,1-Diphenylethane Hydroperoxides in an Aqueous Medium. R. V. Kucher and S. D. Kazmin	591	592
12. The Structure of Thin Copper Sulfide Films at the Solution–Gas Interface. S. G. Mokrushin, Yu. D. Tkachev and O. K. Shabalina	595	597
13. The Effect of Structure on the Viscosity of Butadiene–Styrene Rubbers. A. S. Novikov and F. S. Tolstukhina	599	599
14. Dependence of the Elastic Constant of a Vulcanizate on the Molecular Weight of the Original Rubber. L. S. Priss	607	607
15. Reciprocal Displacement of Components in Ion Exchange Chromatography. G. V. Samsonov and V. A. Orestova	615	615
16. Investigation of the Structure of Branched Polystyrene by the Light Scattering Method. I. G. Soboleva, N. V. Maktletsova and S. S. Medvedev	619	619
17. The Effect of Plasticizers on the Hydrogen Permeability of Polyvinyl Chloride. S. I. Sokolov, S. A. Reitlinger and R. I. Feldman	625	624
18. Specific Heats of Aqueous Solutions of Some Soaps. V. I. Solnyshkin	629	629
19. Light Scattering by a Coagulating Aerosol. O. M. Todes and A. A. Chekunov	633	633

COLLOID JOURNAL OF THE U.S.S.R. IN ENGLISH TRANSLATION

September-October, 1957

TABLE OF CONTENTS (continued)

Page — Russ. Page

20. Orientation of Clay Particles During Deformation of a Clay Body. V. S. Fadeeva 641 640

21. Effects of the Types of Rubber and Carbon Black on the Formation of Carbon–Rubber Gels Z. V. Chernykh and V. G. Epshtein 645 644

22. The Structure of Gels. 11. Effect of the Formation Conditions of Gelatin Films on Bonding Strength. S. A. Shreiner and P. I. Zubov 651 651

Letter to the Editor

23. The Tensile Strength of Mixtures of Polyethylene and Polyisobutylene. R. I. Feldman and A. K. Mironova 655 654

COLLOID JOURNAL OF THE U.S.S.R. IN ENGLISH TRANSLATION

November-December, 1957

TABLE OF CONTENTS

	Page	Russ. Page
1. The Coagulation Mechanism of Butadiene–Styrene Latex. S. A. Glikman and E. P. Korchagina	657	657
2. Analysis of the Forms of Moisture Bonding in Porous Adsorbents With the Aid of Drying Thermograms. M. F. Kazansky	661	662
3. Study of Gelation Processes in Fruit Candy Masses by Means of the Cone Plastometer. L. S. Kuznetsova and A. L. Sokolovsky	667	668
4. The Adsorptive Activity of Cadmium Hydroxide in Relation to the Conditions of its Formation. S. A. Levina and N. F. Ermolenko	671	673
5. A Study of Changes in the Structural and Mechanical Properties of Photographic Emulsions During Drying. L. A. Lepilkina	677	678
6. The Swelling of Ion Exchange Resins and the Nature of Their Selectivity. V. P. Meleshko and O. N. Myagkoi	683	684
7. The Solution State of Direct Dyes and Their Diffusion in a Cellophane Film. B. N. Melnikov and P. V. Moryganov	687	689
8. Electron Microscope Study of the Structure of Aluminosilicate Hydrogels by the Replica Method. Ya. V. Mirsky	695	696
9. General Principles of Formation of Metal Alloy Organosols at the Cathode in a Two-Layer Bath. E. M. Natanson and N. N. Kozachek	697	698
10. Influence of the Reaction of the Precipitation Medium and of the pH of the Wash Water on the Structure of Chalky Silica Gels. I. E. Neimark and I. B. Slinyakova	705	706
11. Gelatin–Glycerol Gels as Materials For Studying Stresses by the Optical Polarization Method. D. N. Osokina	713	713
12. The Selection of Plasticizers For High Polymers. S. P. Papkov	721	722
13. Exchange of Sodium and Calcium Ions on Swelling Sulfonic and Carboxylic Resins. G. V. Samsonov, A. A. Vasilyev and V. A. Orestova	729	730
14. Hydrates of the Calcium Salts of Certain Fatty Acids. V. I. Solnyshkin	735	736
15. The Shrinkage of Collagen. N. N. Stefanovich and A. N. Mikhailov	741	741
16. The Hydrophilic Properties of Clays of the Kaolinite Group. E. T. Uskova	747	747

Discussion

	Page	Russ. Page
17. More on the Subject of Thermomechanical Curves. E. I. Regirer and M. S. Kalantarova	751	752

Letters To The Editor

	Page	Russ. Page
18. Kinetics of the Spraying of Water Drops in an Electric Field. V. I. Arabadzhi	755	756
19. The Development of a Kinetic Theory of Gelation. I. F. Efremov and S. V. Nerpin	756	757

COLLOID JOURNAL OF THE U.S.S.R. IN ENGLISH TRANSLATION

November-December, 1957

TABLE OF CONTENTS (continued)

	Page	Russ. Page
20. The Nature of the Chromatographic Method. S. G. Mokrushin.	758	759
21. The Role of Filler Grain Structure in the Formation of Structures in Bitumen Suspensions. L. S. Terletskaya	760	760

AUTHOR INDEX

1957

Agranat, N.N., and M. F. Shirokov. Theory of the cone immersion method for determination of the yield values of disperse systems, 9.
Agranat, N.N., and M.P. Volarovich. Calculation of the limiting shear stress (yield value) of disperse systems in experiments with the cone plastometer, 1.
Akhmedov, K.S., and S.M. Lipatov. Heats of swelling and solution of polymers in relation to molecular weights and temperature, 263.
Akutin, M.S. The seventieth anniversary of the birth and fifty years of the scientific activity of Grigory Semenovich Petrov, 137.
Aleksandrova, E.M. and N.S. Razumikhina. Adsorption of polystyrene latexes in relation to the sign of the particle charge and the sorbent, 159.
Alekseenko, V.L., see Kalinina, L.E.
Apukhtina, N.P., and A.M. Lyagalova. The relationship between the structure of emulsifiers of the alkylaromatic acid type and the polymerization of unsaturated compounds. 4. Salts of di-sec-butylnaphthalenesulfonic acid with univalent cations, 165.
Arabadzhi, V.I. Kinetics of the spraying of water drops in an electric field, 757.
Aripov, E., Z.Ya. Berestneva and V.A. Kargin. An electron microscope study of structure formation in loess. I. Influence of the dispersion medium, 15.
Aripov, E., Z.Ya. Berestneva and V.A. Kargin. An electron microscope study of structure formation in loess. 2. Influence of loess components on structure formation, 19.

Bakeev, N.F., see Kargin, V.A.
Barabash, M.L., and E.M. Natanson. Antifrictional properties of disperse phases of metal organosols, 535.
Bartenev, G.M. Concerning the discussion of the friction of rubber, 399.
Bartenev, G.M. Two stages of the network formation process in polymers, 267.
Batalova, L.G., see Kanavets, L.F.
Belyaeva, I.I., A.E. Mikirov and N.S. Smirnov. The effect of air ionization on the disperse phase of aero colloids, 25
Berestnev, V.A., see Gul, V.E.
Berestneva, Z.Ya., see Aripov, E.
Berestneva, Z.Ya., M.B. Konstantinopolskaya and V.A. Kargin. The formation of crystalline aluminosilicates, 149.
Berestneva, Z.Ya., and G.L. Slonimsky. On the fiftieth birthday of Valentin Alekseevich Kargin, 139.
Bykov, A.N., M L Ivanova and A.B. Pakshver. Modification of polyamide properties by the inclusion method, 543.
Bykov, A.N., and A.B. Pakshver. Intermolecular structure of high polymers. Communication 22. Modification of the molecular structure of high polymers by the inclusion method, 29.

Chalyl, V.P., see Natanson, E.M.
Chekunov, A.A., see Todes, O.M.
Chernykh, Z.V., and V.G. Epshtein. Effects of the types of rubber and carbon black on the formation of carbon-rubber gels, 645.
Chmutov, K.V., and O. G. Larionov. Use of ion exchange resins for purifying quartz suspensions, 403.
Churaev, N.V., see Volarovich, M.P.

Davydov, A.T., and R.F. Skoblionok. Dependence of the exchange adsorption of ions on their structure. 2. Adsorption of bivalent amines, 193.
Deryagin, B.V. Applicability of the binomial law of friction to the friction of rubber, 401.
Deryagin, B.V., see Izmailova, G.L
Deryagin, B.V., see Medvedeva, A.M.
Dobromyslova, A., see Dogadkin, B.
Dobromyslova, A.V., see Dogadkin, B.A.
Dogadkin, B., A. Dobromyslova, L. Sapozhkova and I. Tutorsky. Effect of mercaptobenzothiazole on structural changes in rubber on oxidation, heating and plasticization, 425.
Dogadkin, B.A., A.V. Dobromyslova, F.S. Tolstukhina and N.G. Samsonova. The influence of structure on the chemical activity and vulcanizability of butadiene polymers, 199.
Dogadkin, B.A., D.L. Fedyukin and V.E. Gul. The effect of swelling on the strength of vulcanizates, 291.
Dumansky, A.V. Development of colloid chemistry in the USSR, 531.

Efremov, I.F. and S.V. Nerpin. The development of a kinetic theory of gelation, 759.
Epshtein, V.G., see Chernykh, Z.V.
Ermakov, V.I., V.N. Maslov and O.G. Stolyarov. The use of high frequency analysis in colloidochemical investigations, 207.
Ermolenko, N.F., see Levina, S.A.

Fadeeva, V.S. Orientation of clay particles during deformation of a clay body, 641.

Fedyukin, D. L, see Dogadkin, B.A.
Feldman, R.I., and A.K. Mironova. The tensile strength of mixtures of polyethylene and polyisobutylene, 655.
Feldman, R.I., see Sokolov, S.I.

Galperin, D.L., and L.I. Moseev. Heats of swelling and of solution of nitrocellulose, 179.
Gerasimova, L.S., see Pakshver, A.B.
Glikman, S.A., and E.P. Korchagina. The coagulation mechanism of butadiene styrene latex, 657.
Glikman, S.A., and I.G. Shubtsova. Investigations of the physical chemistry of agar. 1. Method for the determination of the intrinsic viscosity of agar, 183.
Glikman, S.A., and I.G. Shubtsova. Studies of the physical chemistry of agar. 2. Theory and practice of agar fractionation, 285.
Grigorov, O.N., and K.P. Tikhomolova. Investigation of electroosmosis in capillary systems of different charge and structure, 411.
Grigorov, O.N., and K.P. Tikhomolova. Studies of electroosmosis in binary powder mixtures consisting of particles of different chemical nature, 549.
Gul, V.E., and V.A. Berestnev. The influence of intermolecular interaction on the properties of rubber solutions, 553.
Gul, V.E., see Dogadkin, B.A.
Gurevich, Ya.M. Aggregative stability of pigment suspensions in hydrocarbons, alcohols, and esters of low molecular weight, 189.
Gusev, K.F., see Volarovich, M.P.
Gutkin, A.M. Equilibrium of a viscoplastic disperse system on a rotating disk, 33.

Ivanov, Yu.M. Elastic deformation of wood, 297.
Ivanova, M.I., see Bykov, A.N.
Ivanova-Chumakova, L.V., see Samsonova, T.I.
Ivanter, I.G. Distribution of a weak electrolyte in the double layer, 43.
Izmailova, G.I., P.S. Prokhorov and B.V. Deryagin. The possibility of surface activation and passivation on nuclei in water vapor condensation, 557.

Chien Jen-Yuan, Ching Wen and Cheng Yung-Shih. Relationship between the intrinsic viscosity and molecular weight of Buna S rubber, 515.

Kaban, A.P., see Natanson, E.M.
Kalantarova, M.S., see Regirer, E.I.
Kalinina, L.E., V.I. Alekseenko, and S.S. Voyutsky. Compatibility of nitrocellulose with butadiene-acrylonitrile copolymers. 3. Dependence of the glass transition temperature and flow of nitrocellulose films on their contents of various butadiene-acrylonitrile copolymers, 57.
Kanavets, I.F., L.G. Batalova and A.G. Romashova. The hardening mechanism of thermosetting plastics (molding powders), 215.
Kandilarov, G.G. Sedimentation volumes of polydisperse suspensions of $Ca_3(PO_4)_2$ in electrolyte solutions, 439.
Kargin, V.A., see Aripov, E.
Kargin, V.A., and N.F. Bakeev. Molecular configuration and structure formation in polyacrylate solutions, 143.
Kargin, V.A., see Berestneva, Z.Ya.
Kargin, V.A., A.I. Kitaigorodsky and G.L. Slonimsky. The structure of linear polymers, 141.
Kargin, V.A., G.L. Slonimsky and L.Z. Rogovina. Study of the transition of amorphous and crystalline polymers from the solid into the fluid state on addition of substances of low molecular weight, 153.
Kargin, V.A., see Zubov, P.I.
Katushkina, I.F., see Pakshver, A.B.
Kazansky, M.F. Analysis of the forms of moisture bonding in porous adsorbents with the aid of drying thermograms, 661.
Kazmin, S.D., see Kucher, R.V.
Khananashvili, L.M., see Kreshkov, A.P.
Khrapova, E.V., see Kiselev, A.V.
Kiselev, A. V., and E.V. Khrapova. Influence of pore size and surface hydration of silica on adsorption of nitrogen vapor, 573.
Kiselev, A.V., and G.G. Muttik. Adsorption of water vapor by silica and hydration of its surface, 563.
Kitaev, G.A., see Mokrushin, S.G.
Kitaigorodsky, A.I., see Kargin, V.A.
Kobakhidze, E.I., and M.E. Shishniashvili. Thixotropic structure formation and elasticoplasticoviscous properties of askangel suspensions, 65.
Kobakhidze, E.I., M.E. Shishniashvili and N.N. Serb-Serbina. Thixotropic and structuromechanical properties of askangel suspensions in relation to the composition of the exchange complex, 303.
Konstantinopolskaya, M.B., see Berestneva, Z.Ya.
Korchangina, E.P., see Glikman, S.A.
Korchinsky, G.A. Properties of thin layers of liquid between mica plates, 311.
Kovbuz, M.A., see Kucher, R.V.
Kozachek, N.N., see Natanson, E.M.

Kozlovskaya, Kh.N., see Pakshver, A.B.

Kremnev, L. Ya. Gelatinized emulsions. 13. O/W type emulsions of maximum concentration with a thixotropic dispersion medium, 75.

Kremnev, L.Ya., and G.A. Shadrin. Gelatinized emulsions. 14. Ethylcellulose as a stabilizer of emulsions of the W/O type, 443.

Kreshkov, A.P., L.V. Myshlyaeva and L. M. Khananashvili. Colloidochemical processes in reactions of tetraalkoxysilanes with aqueous aluminate solutions, 449.

Kuadzhe, M.I. Electron microscope studies of colloids. 1. Minerals of the kaolinite-halloysite group, 229.

Kucher, R.V., and S.D. Kazmin. Effect of the nature of the emulsifier on the thermal decomposition of cumene and 1,1-diphenylethane hydroperoxides in an queous medium, 591.

Kucher, R.V., A.A. Yavorsky and M.A. Kovbuz. Study of the colloidal properties of sulfosuccinic acid esters. 1. Esters of the lower aliphatic alcohols, 457.

Kuleshova, A. A., see Talmud, S.L.

Kurgaev, E.F. Investigation of structurized suspensions, 79.

Kurilenko, O.D. The specific heat of bound water, 585.

Kusov, A.B., V.I. Trofimova and Yu. I. Nilova. Variations of the specific volume of rubber during stretching, 587.

Kuznetsova, L.S. and A. L. Sokolovsky. Study of gelation processes in fruit candy masses by means of the cone plastometer, 667.

Larionov, O. G., see Chmutov, K.V.

Lavrentyev, V.V. The external friction of rubber, 523.

Lepilkina, L.A. A study of changes in the structural and mechanical properties of photographic emulsions during drying, 677.

Levi, S.M. The effect of surface-active substances on the specific viscosity of gelatin solutions, 85.

Levina, S.A., and N. F. Ermolenko. The adsorptive activity of cadmium hydroxide in relation to the conditions of its formation, 671.

Lipatov, S.M., see Akhmedov, K.S.

Lipatov, S.M., and S.I. Meerson. The equilibrium state of high polymer gels. On the subject of comments by A. V. Nikolaev, R. E. Neiman and O. V. Neiman, Colloid J. 19, 121 (1957), 391.

Loseva, A. L., and A.S. Tsyperovich. The mechanism of protein denaturation. 10. Effect of fatty acid anions on the stability of globular proteins to denaturation, 233.

Lukyanova, O.I., E.E. Segalova and P.A. Rebinder. Effect of hydrophilic plasticizer additions on the properties of concentrated cement suspensions, 89.

Lukyanova, O.I., E.E. Segalova and P.A. Rebinder. Heat evolution in the initial period of hydration of cement with plasticizing additions, 461.

Lyagalova, A.M., see Apukhtina, N. P.

Makhletsova, N.V., see Soboleva, I.G.

Malinsky, Yu.M. Ninth conference on compounds of high molecular weight, 527.

Markov, S.N., see Volarovich, M.P.

Maslov, V.N. Preparation of ferric and zirconium hydroxide organosols, 97.

Maslov, V.N., see Ermakov, V.I.

Medvedev, S.S., see Soboleva, I.G.

Medvedeeva, A.M., B.V. Deryagin and S.K. Sherebkov. Investigation of adhesion effects in bonding rubber to metal by leukonat adhesive, 417.

Meerson, S.I. , see Lipatov, S.M.

Meleshko, V.P., and O.N. Myagkoi. The swelling of ion exchange resins and the nature of their selectivity, 683.

Melnikov, B.N., and P. V. Moryganov. The solution state of direct dyes and their diffusion in a cellophane film, 689.

Melnikov, B.N., see Moryganov, P.V.

Mikhailov, A.N., see Stefanovich, N.N.

Mikhailov, N.V., see Shalyt, S.Ya.

Mikhailov, N.V., and S.G. Zelikman. Investigation of the structure and properties of carbon chain polymers in dilute solutions. 3. Mixtures of polyvinyl chloride and polyacrylonitrile, 473.

Mikhailov, N.V., see Zelikman, S.G.

Mikhelson, M.L. Coagulation of atmospheric condensation nucei on dust particles, 133.

Mikirov, A.E., see Belyaeva, I.I.

Minkov, B.Ya., see Volarovich, M.P.

Mironova, A.K., see Feldman, R.I.

Mirsky, Ya. V. Electron microscope study of the structure of aluminosilicate hydrogels by the replica method, 697.

Mishin, V.P., and N.D. Verderevskaya. Effect of temperature on the magnitude and rate of swelling of agar, 467.

Mokrushin, S.G. The nature of the chromatographic method, 761.

Mokrushin, S.G., and G.A. Kitaev. Experimental investigations of laminar systems. 23. Kinetics of the formation of hydroxide films on the surface of cupric ammine solutions, 99.

Mokrushin, S.G., Yu.D. Tkachev and O.K. Shabalina. The structure of thin copper sulfide films at the solution-gas interface, 595.
Moryganov, P.V., and B.N. Melnikov. The relationship between the affinity and structure of direct dyes, 105.
Moryganov, P.V., see Melnikov, B.N.
Moseev, L.I., see Galperin, D.L.
Mosikhin, E.P., and G.V. Vinogradov. Investigation of the mechanical properties of plastic disperse systems in conditions of uniaxial extension and compression, 315.
Myshlyaeva, L.V., see Kreshkov, A.P.
Muttik, G.G., see Kiselev, A.V.
Myagkoi, O.N., see Meleshko, V.P.
Natan, E.E., see Pakshver, A.B.
Natanson, E.M., see Barabash, M.L.
Natanson, E.M., and N.N. Kozachek. General principles of formation of metal alloy organosols at the cathode in a two-layer bath, 699.
Natanson, E.M., V.P. Chalyl, N.N. Kozachek, and A.P. Kaba. Electron microscope and x-ray investigations of disperse phases in organosols of lead-tin alloys, 323.
Neiman, O.V., see Nikolaev, A.V.
Neiman, R.E., see Nikolaev, A.V.
Neimark, I.E., A.I. Rastrenenko and M.A. Piontovskaya. Production of titania-silica gels and their porous structure, 329.
Neimark, I.E., and I.B. Slinyakova. Influence of the reaction of the precipitation medium and of the pH of the wash water on the structure of chalky silica gels, 707.
Nerpin, S.V., see Efremov, I.F.
Nikolaev, A.V., R.E. Neiman and O.V. Neiman. Characterization of the state of high-polymer gels, 129.
Nilova, Yu.I., see Kusov, A.B.
Novikov, A.S., and F.S. Tolstukhina. The effect of structure on the viscosity of butadiene-styrene rubbers, 599.

Orestova, V.A., see Samsonov, G.V.
Osokina, D.N. Gelatin-glycerol gels as materials for studying stresses by the optical polarization method, 715.

Pakshver, A.B. see Bykov, A.N.
Pakshver, A.B., L.S. Gerasimova and Kh. N. Kozlovskaya. Structure of high polymers. Communication 18. Strengthening of the molecular structure of tire yarn, 109.
Pakshver, A.B., E.E. Natan and I.F. Katushkina, Molecular structure of high polymers. Communication 17. Investigation of the intermolecular structure of thermoplastic fibers, 115.
Pakshver, A.B., see Pokrovsky, L.I.
Panich, R.M., and S.S. Voyutsky. The electrochemistry of high-polymer dispersions. 3. Effect of pH on the electrokinetic potential of globules in synthetic latexes, 119.
Panich, R.M., see Voyutsky, S. S.
Papkov, S.P. Phase equilibria in colloid systems. 1. Separation of a homogeneous solution into two phases and the gel formation process, 337.
Papkov, S.P. The selection of plasticizers for high polymers, 723.
Pasynsky, A.G., and A.M. Tongur. Periodic deformation of collagen in solutions of electrolytes and tanning agents, 483.
Pionotovskaya, M.A., see Neimark, I.E.
Pisarenko, A.P., see Voyutsky, S.S.
Pokrovsky, L.I., and A.B. Pakshver. Alteration in the intermolecular structure of capron fiber as the result of heat treatment, 479.
Priss, L. S. Dependence of the elastic constant of a vulcanizate on the molecular weight of the original rubber, 607.
Prokhorov, P.S., see Izmailova, G.I.
Puzyrev, S.A., see Sinkova, S.I.

Rastrenenko, A.I., see Neimark, I.E.
Ratner, S.B. Problems relating to the mechanism of the friction of rubber, 395.
Razumikhina, N.S., see Aleksandrova, E.M.
Rebinder, P.A., see Lukyanova, O.I.
Rebinder, P.A., see Shalyt, S.Ya.
Regirer, E.I., and M.S. Kalantarova. More on the subject of thermomechanical curves, 753.
Reitlinger, S.A., see Sokolov, S.I.
Rogovina, L.Z., see Kargin, V.A.
Romashova, A.G., see Kanavets, I.F.

Samsonov, G.V., and V.A. Orestova. Reciprocal displacement of components in ion exchange chromatography, 615.
Samsonov, G.V., A.A. Vasilyev and V.A. Orestova. Exchange of sodium and calcium ions on swelling sulfonic and carboxylic resins, 731.
Samsonova, N.G., see Dogadkin, B.A.
Samsonova, T.I., and L.V. Ivanova-Chumakova. Investigations of the structuromechanical properties of ethylcellulose solutions and the effect of oxidation on these properties, 345.

Sandomirsky, D.M, Gelation of latexes on porous forms, 239.
Sapozhkova, L., see Dogadkin, B.
Segalova, E.E., see Lukyanova, O.I.
Serb-Serbina, N.N., see Kobakhidze, E.L
Shabalina, O.K., see Mokrushin, S.G.
Shadrin, G.A., see Kremnev, L.Ya.
Shalopalkina, T.G., see Trapeznikov, A.A.
Shalyt, S.Ya., N. V. Mikhailov and P.A. Rebinder. Effect of an active filler and a solvent on the structural and mechanical properties of bitumens, 253.
Shapovalova, A.L., see Voyutsky, S.S.
Sheludko, A., see Todorov, I.
Shirokov, M.F., see Agranat, N.N.
Shishniashvili, M.E., see Kobakhidze, E.L
Shishniashvili, M.E., see Uznadze, E.D.
Shreiner, S. A., and P.I. Zubov. The structure of gels. 11. Effect of the formation conditions of gelatin films on bonding strength, 651.
Shubtsova, I.G., see Glikman, S.A.
Shulman, M.S. Investigation of the adsorbability of carbohydrate solutions by a polarographic method, 383.
Shvarts, A.G. Evaluation of rubber-solvent interaction, 375.
Sinkova, S.L., and S. A. Puzyrev. Industrial unit for production of emulsions by means of ultrasonic liquid whistle (jet), 387.
Skoblionok, R.F., see Davydov, A.T.
Slinyakova, I.B., see Neimark, I.E.
Slonimsky, G.L., see Berestneva, Z.Ya.
Slonimsky, G.L., see Kargin, V.A.
Smirnov, N.S., see Belyaeva, I.I.
Soboleva, I.G., N.V. Maktletsova and S.S. Medvedev. Investigation of the structure of branched polystyrene by the light scattering method, 619.
Sokolov, S.L., S.A. Reitlinger and R.I. Feldman. The effect of plasticizers on the hydrogen permeability of polyvinyl chloride, 625.
Sokolovosky, A.L., see Kuznetsova, L.S.
Solnyshkin, V.I. Hydrates of the calcium salts of certain fatty acids, 737.
Solnyshkin, V.I. Specific heats of aqueous solutions of some soaps, 629.
Stefanovich, N.N., and A.N. Mikhailov. The shrinkage of collagen, 743.
Stolyarov, O.G., see Ermakov, V.L
Talmud, S.L., A.N. Turzhetskaya and A.A. Kuleshova. The fractional composition of fine cellulose fibers, 125.
Terletskaya, L.S. The role of filler grain structure in the formation of structures in bitumen suspensions, 763.
Tikhomolova, K.P., see Grigorov, O.N.
Tkachev, Yu. D., see Mokrushin, S.G.
Todes, O.M., and A.A. Chekunov. Effect of atmospheric turbulence on the kinetics of aerosol coagulation, 489.
Todes, O.M., and A.A. Chekunov. Light scattering by a coagulating aerosol, 633.
Todorov, I. and A. Sheludko. Settling of aerosol particles on the walls of an enclosed space, 495.
Tolstukhina, F.S., see Dogadkin, B.A.
Tolstukhina, F.S., see Novikov, A.S.
Tongur, A.M., see Pasynsky, A.G.
Trapeznikov, A.A. Possible differences in the composition and viscosity ratio of a two-sided film and a surface layer of a soap solution, 259.
Trapeznikov, A.A., and T.G. Shalopalkina. The thixotropic properties of certain printing inks, 243.
Trofimova, V.I., see Kusov, A.B.
Tropin, V.P., see Volarovich, M.P.
Tsyperovich, A.S., see Loseva, A.L.
Turzhetskaya, A.N., see Talmud, S.L.
Tutorsky, I., see Dogadkin, B.
Tyabin, N.V., and G.V. Vinogradov. Application of the method of approximations to calculations of flow of disperse systems, 505.
Tyabin, N.V., and G.V. Vinogradov. The theory of flow of plastic disperse systems, 353.

Uskov, I.A. Effect of electrolytes on the structuromechanical properties of bentonite suspensions, 511.
Uskov, I.A., and E.T. Uskova. An electrochemical study of bentonite suspensions. 1. Action of sodium hydroxide on suspensions of electrodialyzed askangel, 361.
Uskova, E.T. The hydrophilic properties of clays of the kaolinite group, 749.
Uskova, E.T., see Uskov, I.A.
Uznadze, E.D. and M.E. Shishniashvili. Action of the basic salt aluminum oxychloride on the structuromechanical (thixotropic) properties of askangel suspensions, 367.

Vasilyev, A.A., see Samsonov, G.V.
Verderevskaya, N.D., see Mishin, V.P.
Vinogradov, G.V., see Mosikhin, E.P.
Vinogradov, G.V., see Tyabin, N.V.
Volarovich, M.P., see Agranat, N.N.

Volarovich, M.P., N.V. Churaev and B.Ya. Minkov. Investigation of the aqueous properties of peat by means of radioactive isotopes, 171.
Volarovich, M.P., K.F. Gusev, S.N. Markov and V.P. Tropin. Changes in the structure, degree of dispersion, and yield value of peats as the result of complete freezing, 407.
Voyutsky, S.S., see Kalinina, L.E.
Voyutsky, S.S., and R.M. Panich. The electrochemistry of high polymer dispersions. 4. Influence of cations of different valancies on the electrokinetic potential of synthetic latex globules, 273.
Voyutsky, S.S., see Panich, R.M.
Voyutsky, S.S., A.I. Shapovalova and A.P. Pisarenko. Adhesion of high polymers. 3. Effects of the size, shape and polarity of high polymer molecules on their adhesion to cellophane, 279.
Wen, Ching, see Jen-Yuan, Chien.
Yavorsky, A.A., see Kucher, R.V.
Yung-Shih, Cheng, see Jen-Yuan, Chien.

Zelikman, S.G. and N.V. Mikhailov. Investigation of the structure and properties of carbon chain polymers in dilute solutions. 2. Solutions of vinyl chloride – acrylonitrile copolymer, 37.
Zelikman, S.G., see Mikhailov, N.V.
Zherebkov, S.K., see Medvedeva, A.M.
Zhurkina, Z.N., see Zubov, P.I.
Zubov, P.I., see Shreiner, S.A.
Zubov, P.I., Z.N. Zhurkina and V.A. Kargin. The structure of gels. 10. Globulization of rubber under the action of nonsolvents added to solutions, 435.
Zubov, P.I., see Zverev, M.P.
Zverev, M.P., and P.I. Zubov, The structure of gels. 9. Effect of the nature of the plasticizer on the physicomechaniaal properties of divinyl-styrene rubber, 211.

SUBJECT INDEX

1957

Acid, di-sec-butylnaphthalenesulfonic, salts of, with univalent cations, as emulsifiers, relationship between structure of, and polymerization of unsaturated compounds, 165;

–Polyacrylic, and salts, molecular configuration of, and structure formation in, determined by electron microscopy, 143;

– Sulfosuccinic, esters of, see esters.

Acids, alkylaromatic, emulsifiers, see emulsifiers;

– fatty, anions of (C_4-C_9 sodium caprylate type), effect on the stability of globular proteins to denaturation, 233;

– (stearic, oleic, richinoleic), formation of hydrates of calcium salts of, 737.

Acrylonitrile polymers, see high polymer chemistry;

Acrylonitrile - vinyl chloride copolymer, see high polymer chemistry.

Adhesion. Effect of formation conditions of gelatin films on bonding strength, 651;

– of high polymer molecules to cellophane, influence of size, shape and polarity on, 279;

– of rubber to metal, using leukonat adhesive, effect of type of filler, sandblasting of metal surface on the strength of the bond, 417.

Adsorbents, porous, (silica gel, activated charcoal), analysis of forms of moisture bonding in, with the aid of drying thermograms, 661.

Adsorption, by cadmium hydroxide, in relation to its conditions of formation, 671;

– of nitrogen vapor, influence of pore size and surface hydration of silica on, 573;

– of polystyrene latexes in relation to the sign of the particle charge and the sorbent, 159;

–of water vapor, by silica, and hydration of its surface, 563;

– exchange, of ions, dependence on their structure, adsorption of bivalent amines, (o-, m- and p-phenylenediamines on sulfocarbon -Ca and Espatite-Ca), 193.

Aerocolloids, see colloids.

Aerosols, coagulating, light scattering by, 633;

– Effect of atmospheric turbulence on kinetics of coagulation of, 489;

– Settling of particles of, on the walls of an enclosed space, influence of particle size, temperature, radius of enclosed spherical space, adhesion coefficient, viscosity of gas, 495.

Agar, effect of temperature on the magnitude and rate of swelling of, 467;

– Method for determination of the intrinsic viscosity of, effect of mineral salt concentrations on viscosity, 183;

– Physical chemistry of, theory and practice of fractionation, 285.

Agricultural chemistry. The hydrophilic properties of clays of the kaolinite group, 749.

Air ionization, see ionization.

Alloys, lead-tin, electron microscope and x-ray investigations of disperse phases in organosols of, 323;

– Metal, organosols, see organosols.

Aluminate solutions, aqueous alkaline, reactions with tetraalkoxysilanes, colloidochemical processes in, 449.

Aluminosilicate hydrogels, see hydrogels.

Aluminosilicates, crystalline, mechanism of formation from aluminum hydroxide and silicic acid sols or aqueous suspensions of quartz or silica gel, 151.

Aluminum oxychloride, effect on the structuromechanical (thixotropic) properties of askangel suspensions, 367.

Amines, bivalent (o-, m-, p-phenylenediamines exchange adsorption on sulfocarbon-Ca and Espatite-Ca, 193.

Amines, cupric solutions, kinetics of growth of hydroxide films on the surface of, in relation to concentration, temperature and blowing rate, 99.

Analytical chemistry. Exchange of sodium and calcium ions on swelling sulfonic and carboxylic resins, 731;

– Reciprocal displacement of components in ion exchange chromatography, 615;

– The nature of the chromatographic method, 761;

– The swelling of ion exchange resins and the nature of their selectivity, 683;

– The use of high frequency analysis in colloidochemical investigations, 207.

Antifrictional properties of disperse phases of metal (iron, bismuth, etc.), organosols, 535.

Askangel suspensions, see suspensions.
Atmospheric condensation, see condensation.
Bentonite suspensions, see suspensions.
Benzothiazole, mercapto, effect of, on structural changes in rubber on oxidation, heating and plasticization, 425.
Biochemistry. Periodic deformation of collagen in solutions of electrolytes and tanning agents, 483.
Bitumen suspensions, see suspensions.
Bitumens, effect of an active filler (slakedlime powder) and a solvent (green oil) on the structural and mechanical properties of, 253.
Butadiene polymers, see rubber chemistry, high polymer chemistry.
Cadmium hydroxide, adsorptive capacity of, in relation to conditions of formation, 671.
Calcium phosphate suspensions, see suspensions.
Calcium salts, of fatty acids, see acids.
Candy, fruit, study of gelation processes in, by means of the cone plastometer, 667.
Capillary systems, see systems.
Carbohydrate solutions (dextrins, starch, paste, dispersed starch glucose, maltose arabinose), adsorption, study by a polarographic method, 383.
Carbon black, and types of rubber, effects on the formation of carbon-rubber gels, 645.
Carbon rubber-gels, see gels.
Cellophane, adhesion of high polymers to, influence of size, shape and polarity on, 279.
Cellulose, ethyl; as a stabilizer of emulsions of the W/O type (water in toluene), 443;
– Solutions, structuromechanical properties of, and the effect of oxidation on these properties, 345.
Cellulose fibers, see fibers.
Cellulose nitrate, heats of swelling and of solution, determined with dibutyl phthalate and acetone, respectively, 179;
– Films, dependence of glass transition temperature and flow of, on contents of various butadiene-acrylonitrile copolymers, 57.
Cement, with plasticizing additions, heat evolution in the initial period of hydration of, 461.
Cement suspensions, see suspensions.
Ceramic chemistry. Orientation of clay particles during deformation of a clay body, 641.
Chromatography, principles of, 761;
– Ion exchange, reciprocal displacement of components in, 615.
Clay bodies, plastic, orientation of clay particles during deformation of, 641.
Clay particles, see particles.
Coagulation, aerosols, effect of atmospheric turbulence on kinetics of, 489;
– of atmospheric condensation nuclei on dust particles, with reference to precipitation studies and dust removal, 133;
– of butadiene-styrene latex, mechanism of, 657.
Collagen, periodic deformation of, in solutions of electrolytes and tanning agents, 483;
– Shrinkage on heating, determination of heat of shrinkage, 743.
Colloid chemistry, development in the USSR, 531.
Colloids, aero, effect of air ionization on the disperse phase of, 25.
Condensation, of water vapor, possibility of activation and passivation of nuclei (NaCl and SiO_2), in, mechanism of effect, 557;
– Nuclei, atmospheric, coagulation on dust particles, with reference to precipitation studies and dust removal, theoretical and experimental results, 133.
Cone immersion method, for determination of the yield values of disperse systems, theory of, 9.
Cone plastometer, see plastometer.
Conference, ninth, on compounds of high molecular weight, held in Moscow, Jan. 28th – Feb. 1st, 1957, 527.
Copper hydroxide films, growth on surface of cupric ammine solutions in relation to concentration, temperature and blowing rate, 99.
Copper sulfide films, see films.
Cumene hydroperoxide, see hydroperoxides.
Curves, thermomechanical, discussion on plotting of, 753.
Diffusion, of direct dyes in a cellophane film in presence of dispersing agents, and in solution over a wide range of temperatures and electrolyte concentration, 689
Disperse systems, see systems.
Divinyl-styrene rubber, see rubber chemistry.

Drops, water, kinetics of spraying in an electric field, 757.
Dyestuffs chemistry. The relationship between the affinity and structure of direct dyes, 105;
– The solution state of direct dyes and their diffusion in a cellophane film, 689.

Elasticity, of rubber vulcanizates, dependence on the molecular weight of the original rubber, 607.
Electrochemistry. An electrochemical study of bentonite suspensions. Action of sodium hydroxide on suspensions of electrodialyzed askangel, 361;
– Distribution of a weak electrolyte in the double layer, 43;
– Electrochemistry of high-polymer dispersions. Effect of pH on the electrokinetic potential of globules in synthetic latexes, 119;
– Electrochemistry of high polymer dispersions. Influence of cations of different valencies on the electrokinetic potential of synthetic latex globules, 273;
– General principles of formation of metal alloy organosols at the cathode in a two-layer bath, 699;
– Investigation of electroosmosis in capillary systems of different charge and structure, 411;
– Kinetics of the spraying of water drops in an electric field, 757;
– Periodic deformation of collagen in solutions of electrolytes and tanning agents, 483.
Electrolytes (calcium and sodiumchlorides and sulfates), effect on the structuromechical properties of bentonite suspensions (askangel), 511;
– Weak, theory of distribution in the double layer, 43.
Electroosmosis, see osmosis.
Emulsifiers, effect of the nature of, on thermal decomposition of cumene and 1,1-diphenylethane hydroperoxides, in an aqueous medium, 591;
– of the alkylaromatic acid type, relationship between the structure of and polymerization of unsaturated compounds. Salts of di-sec-butylnaphthalenesulfonic acid with univalent cations, 165.
Emulsions, industrial unit for production of, by means of an ultrasonic liquid whistle (jet) 387;
– Gelatinized. Ethylcellulose as a stabilizer of emulsions of the W/O type (water in toluene), 443;
– O/W type of maximum concentration with a thixotropic dispersion medium, (sodium oleate), structure formation in, 75;
– Photographic, changes in structural and mechanical properties of during drying, 677.
Esters, of sulfosuccinic acid, of lower aliphatic alcohols, surface tension isotherms, micelle formation, solubilization of Sudan III in, 457.
Ethane, 1,1-diphenyl hydroperoxides, see hydroperoxides.
Ethylcellulose, see cellulose.
Equilibria, of high polymer gels, 391;
– Phase, in colloid systems, separation of a homogeneous solution into two phases and the gel formation process, 337.

Ferric hydroxide organosols, see organosols.
Fibers, artificial, thermoplastic (nitron, celluloseacetate, khlorin), intermolecular structure of, 115;
– (viscose, capron), strengthening the molecular structure of, (heat stretching, swelling in alkali, use of lactam as plasticizer), 109;
– Capron, alteration of the intermolecular structure as a result of heat treatment, 479;
– Cellulose, fine, fractional composition of, determined by microscopical analysis, 125.
Filler, role of grain structure of, in the formation of structures in bitumen suspensions, 763.
Films, copper sulfide, thin, structure at the solution-gas interface, 595;
– Gelatin, effect of formation conditions of, on bonding strength, 651;
– Two-sided, soap and similar, and surface layer of a soap solution, possible differences in the composition and viscosity ratio of, 259.
Friction, of rubber, applicability of the binomial law of friction to, 401;
– Discussion on, 399;
– Problems relating to, 395.
Gelatin films, see films.
Gelatin-glycerol gels, see gels.
Gelatin solutions, effect of surface active agents on the specific viscosity of, 85.
Gelation, development of a kinetic theory of, 759;

– of latexes, on porous forms, influence of latex concentration, duration of contact with the porous surface, temperature, 239.
Gel formation, considered as separation of a homogeneous solution into two phases, with particular reference to low-molecular (mainly inorganic) substances and high polymers, 337.
Gels, structure of. Effect of the formation conditions of gelatin films on bonding strength, 651;
– Effect of the nature of the plasticizer on the physicomechanical properties of divinylstyrene rubber, 211;
– Globulization of rubber under the action of nonsolvents added to solutions, 435;
– Study of gelation processes in fruit candy masses by means of the cone plastometer, 667;
– Carbon-rubber, effects of the types of rubber and carbon black, on the formation of, 645;
– Glycerol-gelatin, as materials for studying stresses by the optical polarization method, 715;
– High-polymer, characterization of the state of, discussion, 129;
– Equilibrium state of, 391;
– Silica, chalky, influence of the reaction of the precipitation medium and of the pH of the wash water on the structure of, 707;
– Titania-silica, production and porous structure of, adsorption, influence of conditions and composition, 329.
Glycerol-gelatin gels, see gels.

Halloysite-kaolinite minerals, study by the electron microscope, 229.
Hardening, mechanism of, of thermosetting plastics (molding powders), 215.
Heat evolution, of cement with plasticizing additions, in the initial period of hydration, 461.
Heats, of swelling and of solution, of nitrocellulose, determined with dibutyl phthalate and acetone, respectively, 179;
– of polymers, (PVC and chlorinated PVC and ftorlon in relation to molecular weight and temperature, 263.
High polymer chemistry. Adsorption of polystyrene latexes in relation to the sign of the particle charge and the sorbent, 159;
– Characterization of the state of high polymer gels, 129;
– Dependence of the glass transition temperature and flow of nitrocellulose films on their contents of various butadiene-acrylonitrile copolymers, 57;
– Effects of size, shape and polarity of high polymer molecules on their adhesion to cellophane, 279;
– Effects of the types of rubbers and carbon black on the formation of carbon-rubber gels, 645;
– Evaluation of rubber-solvent interaction, 375;
– Exchange of sodium and calcium ions on swelling sulfonic and carboxylic resins, 731;
– Heats of swelling and solution of polymers in relation to molecular weights and temperature, 263;
– Investigation of the intermolecular structure of thermoplastic fibers, 115;
– Investigation of the structure and properties of carbon chain polymers in dilute solutions. Solutions of vinyl chloride – acrylonitrile copolymer, 37;
– Investigation of the structure and properties of carbon chain polymers in dilute solutions; mixtures of polyvinyl chloride and polyacrylonitrile, 473;
– Investigation of the structure of branched polystyrene by the light scattering method, 619;
– Modification of polyamide properties by the inclusion method, 543;
– Modification of the molecular structure of high polymers by the inclusion method, 29;
– Molecular configuration and structure formation in polyacrylate solutions, 143;
– Ninth conference on compounds of high molecular weight, 527;
– Phase equilibria in colloid systems. Separation of a homogeneous solution into two phases and the gel formation process, 337;
– Relationship between the intrinsic viscosity and molecular weight of Buna S rubber, 515;
– Structure of high polymers. Strengthening of the molecular structure of tire yarn, 109;
– Studies on electroosmosis in binary powder mixtures consisting of particles of different chemical nature, 549;

High polymer chemistry (continued)
– Study of transition of amorphous and crystalline polymers from the solid into the fluid state on addition of substances of low molecular weight, 153;
– The coagulation mechanism of butadiene-styrene latex, 657;
– The effect of plasticizers on the hydrogen permeability of polyvinyl chloride, 625;
– The electrochemistry of high polymer dispersions. Influence of cations of different valencies on the electrokinetic potential of synthetic latex globules, 273;
– The equilibrium state of high polymer gels. (On the subject of the comments by A. V. Nikolaev, R. E. Neiman and O. V. Neiman, Colloid J. 19, 121 (1957), 391;
– The external friction of rubber, 523;
– The hardening mechanism of thermosetting plastics (molding powders), 215;
– The influence of intermolecular interaction on the properties of rubber solutions, 553;
– The influence of structure on the chemical activity and vulcanizability of butadiene polymers, 199;
– The relationship between the structure of emulsifiers of the alkylaromatic acid type and the polymerization of unsaturated compounds. Salts of di-sec-butylnaphthalene-sulfonic acid with univalent cations, 165;
– The selection of plasticizers for high polymers, 723;
– The structure of gels. Effect of the nature of the plasticizer on the physicomechanical properties of divinyl-styrene rubber, 211;
– The structure of linear polymer, 141;
– The swelling of ion exchange resins and the nature of their selectivity, 683;
– The tensile strength of mixtures of polyethylene and polyisobutylene, 655;
– The use of ion exchange resins for purifying quartz suspensions, 403;
– Two stages of the network formation in polymers, 267.
Hydrogels, aluminosilicate, electron microscope study of, by the replica method, 697;
Hydrogen permeability, see permeability.
Hydroperoxides, cumene, 1,1-diphenylethane rate of thermal decomposition in an aqueous medium, effect of nature of emulsifier on, 591.
Inclusion, modification of molecular structure of high polymers by, to increase reactivity, (cellulose, acetylcellulose, polyamides), 29.
Inclusion method, for modification of properties of polyamide fibers, using benzene as inclusion substance, 543.
Inks, printing, thixotropic properties of (strength and viscosity), 243.
Interaction, molecular, influence on the properties of rubber solutions (divinyl-acrylonitrile), with particular reference to viscosity and light scattering and swelling of vulcanizates, 553.
Ion-exchange resins, see high polymer chemistry.
Ionization, air, effect on the disperse phase of aerocolloids, 25.
Ions, dependence of exchange adsorption of, on structure, adsorption of bivalent amines (o-, m-, p-phenylenediamine) on sulfocarbon-Ca and Espatite-Ca), 193.

Kaolinite clays, effect of the ratio between ions of different valencies in the exchange complex, on the hydrophilic properties of, 749.
Kaolinite-halloysite minerals, study by the electron microscope, 229.
Kargin, Valentin Alekseevich, fiftieth birthday of, 139.

Latexes, polystyrene, adsorption in relation to the sign of the particle charge and the sorbent, 159;
– Rubber, gelation on porous forms, influence of latex concentration, duration of contact with the porous surface, temperature, 239;
– Synthetic, effect of pH on the electrokinetic potential of globules in, 119.
Leather chemistry. Periodic deformation of collagen in solutions of electrolytes and tanning agents, 483.
Leukonat adhesive, see adhesion.
Light, scattering, by a coagulating aerosol, 633.
Liquids, properties of thin layers of, between mica plates, results for disjoining pressure of water and aqueous solutions of acetic, propionic and butyric acids, 311.
Loess, electron microscope study of structure formation in, influence of the dispersion medium, 15;

– Influence of loess components on, 19.

Metal, adhesion to rubber, using leukonat adhesive, influence of type of filler, sandblasting of metal surface, on the strength of the bond, 417.
Metal organosols, see organosols.
Metallurgical chemistry. Electron microscope and x-ray investigations of disperse phases in organosols of lead-tin alloys, 323.
Mineralogical chemistry. Electron microscope studies of colloids. Minerals of the Kaolinite-halloysite group, 229;
– The formation of crystalline alumino-silicates, 149.
Moisture, bonding, in porous adsorbents (silica gel, activated charcoal), analysis of the forms of, with the aid of drying thermograms, 661.
Molding powders, theory of mechanism of hardening of, influence of various factors on kinetics of, 215.
Nitrogen vapor, influence of pore size and hydration of silica, on adsorption of, 573.

Organosols, ferric and zirconium hydroxide, in benzene and toluene, preparation, 97;
– Metal, (iron, bismuth, etc.), antifrictional properties in ordinary lubricating oils, technology of preparation, 535;
– Metal alloy, general principles of formation at the cathode in a two-layer bath, 699;
– Lead-tin alloys, electron microscope and x-ray investigations of disperse phases in. 323.
Osmosis, electro, in binary powder mixtures, consisting of particles of different chemical nature (pure polystyrene and polystyrene with additions of Sudan III dye), 549;
– in capillary systems of different charge and structure (quartz and polystyrene powder), 411.

Particles, clay, orientation of, during deformation of a clay body, 641.
Peat, study of aqueous properties of, by means of radioactive isotopes (S^{35} in the form of $Na_2S \cdot O_4$), 171;
– Changes in structure, degree of dispersion and yield value of, as a result of complete freezing, 407.
Permeability, to hydrogen, of polyvinyl chloride, effect of plasticizers on, 625.
Petrov, Grigory Semenovich, sevenieth anniversary of the birth of and fifty years of scientific activity of, 137.
Phase equilibria, see equilibria.
Photographic chemistry. A study of changes in the structural and mechanical properties of photographic emulsions during drying, 677.
Pigment suspensions, see suspensions.
Plasticizer, effect of the nature of, on the physicomechanical properties of divinyl-styrene rubber, 211;
– Effect on the hydrogen permeability of polyvinyl chloride, 625;
– General principles for selection of, for high polymers, in relation to phase equilibrium in the plasticizer-polymer system, 723;
– Hydrophilic, (lignosulfonates), effect on properties of concentrated cement suspensions, (adsorption, stabilization, structure formation, hydration, crystallization structure), 89.
Plastometer, cone, calculation of the limiting shear stress (yield value) of disperse systems with, 1;
– Use for study of gelation processes in fruit candy masses, 667.
Polarography, use in a study of the adsorbability of carbohydrate solutions, (dextrins, starch paste, dispersed starch, glucose, maltose, arabinose), 383.
Polyethylene, see high polymer chemistry.
Polyisobutylene, see high polymer chemistry.
Polymerization of unsaturated compounds, and relationship with the structure of emulsifiers of the alkylaromatic acid type (salts of di-sec-butylnaphthalene-sulfonic acid with univalent cations), 165.
Polymers, amorphous and crystalline, transition from the solid into the fluid state on addition of substances of low molecular weight, 153;
– Linear, amorphous, and crystalline, new model proposed for molecular structure of, 141.
Polystyrene, see high polymer chemistry.
Polyvinyl chloride, see high polymer chemistry.
Powder mixtures, binary, consisting of particles of different chemical nature (pure polystyrene and polystyene with additions of Sudan III dye), electroosmosis in, 549.

Printing inks, see inks.
Proteins, globular, effect of fatty acid anions on stability of, to denaturation, 233.

Quartz suspensions, see suspensions.

Radiochemistry. Investigation of the aqueous properties of peat by means of radioactive isotopes, 171.
Resins, ion-exchange, see high polymer chemistry.
Rheology. Application of the method of approximations to calculations of flow of disperse systems, 505;
- Calculation of the limiting shear stress (yield value) of disperse systems in experiments with the cone plastometer, 1;
- Dependence of the glass transition temperature and flow of nitrocellulose films on their contents of various butadiene acrylonitrile copolymers, 57;
- Effect of an active filler and a solvent on the structural and mechanical properties of bitumens, 253;
- Effect of electrolytes on the structuromechanical properties of bentonite suspensions, 511;
- Equilibrium of a viscoplastic disperse system on a rotating disk, 33;
- Investigation of the mechanical properties of plastic disperse systems in conditions of uniaxial extension and compression, 315;
- The theory of flow of plastic disperse systems, 353;
- Theory of the cone immersion method for determination of the yield values of disperse systems, 9.
Rubber, adhesion to metal, using leukonat adhesive, influence of type of filler, sandblasting of metal surface, on strength of the bond, 417;
- Applicability of the binomial law of friction to the friction of, 401;
- Discussion on friction of, 399;
- External friction, theory of, influence of temperature, 523;
- Natural and synthetic, globulization of, under the action of nonsolvents added to solutions, (solvent-carbon tetrachloride, nonsolvent-methyl alcohol), 435;
- Review of problems relating to the mechanism of friction of, 395.
Rubber chemistry. Dependence of the elastic constant of a vulcanizate on the molecular weight of the original rubber, 607;
- Effect of mercaptobenzothiazole on structural changes in rubber on oxidation, heating and plasticization, 425;
- Effects of the types of rubber and carbon black on the formation of carbon-rubber gels, 645;
- Electrochemistry of high polymer dispersions. Influence of cations of different valencies on the electrokinetic potential of synthetic latex globules, 273;
- Evaluation of rubber-solvent interaction, 375;
- Gelation of latexes on porous forms, 239;
- Influence of intermolecular interaction on the properties of rubber solutions, 553;
- Relationship between the intrinsic viscosity and molecular weight of Buna S rubber, 515;
- The coagulation mechanism of butadiene-styrene latex, 657;
- The effect of structure on the viscosity of butadiene-styrene rubbers, 599;
- The effect of swelling on the strength of vulcanizates, 291.
- The influence of structure on the chemical activity and vulcanizability of butadiene polymers, 199;
- The structure of gels. Effect of the nature of the plasticizer on the physicomechanical properties of divinyl-styrene rubber, 211;
- Two stages of the network formation in polymers, derivation of formula, application to vulcanization, 267;
- Variations of the specific volume of rubber during stretching, 587.

Sedimentation volumes, of polydisperse suspensions of $Ca_3(PO_4)_2$ in electrolyte solutions,(NaOH, Na_2CO_3, Na phosphate, HCl, $AlCl_3$), 439.
Shear stress, calculation in disperse systems using the cone plastometer, 1;
- of disperse systems, theory of the cone immersion method for determination of, 9.
Silanes, tetraalkoxy, see silicon organic compounds.
Silica, adsorption of water vapor by, and hydration of its surface, 563;
- Influence of pore size and surface hydration of, on adsorption of nitrogen vapor, 573;
- Gels, see gels;
- -titania gels, see gels.

Silicon organic compounds. Colloidochemical processes in reactions of tetraalkoxysilanes with aqueous aluminate solutions, 449.
Soap solution, (sodium palmitate and oleate) possible differences in the composition and viscosity ratio of a two-sided film and a surface layer of, 259.
Soaps (sodium oleate and ricinoleate), specific heats of aqueous solutions of, 629.
Solution, heat of, see heat;
– Homogeneous, separation into two phases and the gel formation process, 337.
Solvents, evaluation of the influence of the nature of intermolecular forces of, on the swelling of rubber, 375.
Specific heat, of bound water, calculation of, 585.
Specific heats, of aqueous solutions of soaps (sodium oleate and ricinoleate), 629.
Specific volume, of rubber, variations during stretching, 587.
Spraying, of water drops in an electric field, kinetics of, 757.
Stresses, study by the optical polarization method, use of gelatin-glycerol gels, 715.
Structure, influence on the chemical activity and vulcanizability of butadiene polymers, 199.
Surface active agents, effect on the specific viscosity of gelatin solutions, 85.
Suspensions, askangel, action of the basic salt aluminum oxychloride on the structuromechanical (thixotropic) properties of, 367;
– Effect of electrolytes (calcium and sodium chlorides and sulfates) on the structuromechanical properties of, 511;
– Thixotropic and structuromechanical properties of, in relation to the composition of the exchange complex, 303;
– Thixotropic structure formation and elasticoplasticoviscous properties of, in relation to equilibrium pH on treatment with NaOH solution, 65;
– (askangel), bentonite, electrodialysed, action of sodium hydroxide on electrical properties of, 361;
Suspensions, bitumen, role of filler grain structure in the formation of, structures of, 763;
– $Ca_3(PO_4)_2$, polydisperse, sedimentation volumes in electrolyte solutions, (NaOH, Na_2CO_3, Na phosphate, $AlCl_3$, HCl), 439;
– Cement, concentrated, effect of hydrophilic plasticizer additions (lignosulfonates) on properties of, (adsorption, stabilization, structure formation, hydration, crystallization structure), 89;
– Pigment, in hydrocarbons, alcohols and esters of low molecular weight, aggregative stability of, 189;
– Quartz, use of ion exchange resins for purification of, 403;
– Structurized, (hydroxides and carbonates), new method for determining density, strength in normal uniaxial compression, amount of water immobilized by structural network, cohesive forces, 79.
Swelling, effect on the strength of vulcanizates, 291;
– Heat of, see heats;
– of ion exchange resins and the nature of their selectivity, 683;
– of sulfonic and carboxylic resins, exchange of sodium and calcium ions on, 731.
Systems, capillary, (polystyrene and quartz powders), of different charge and structure, electroosomosis of, 411;
– Colloid, phase equilibria in, separation of a homogeneous solution into two phases and the gel formation process, 337;
– Disperse, (greases, bitumens), application of the method of approximation to calculations of flow of, 505;
– Calculation of the limiting shear stress (yield value) of, in experiments with the cone plastometer, 1;
– Theory of the cone immersion method for determination of the yield values of, 9;
– Plastic, mechanical properties of, in conditions of uniaxial extension and compression (solidol greases), 315;
– (solidol) theory of flow of, 353;
– Viscoplastic, equilibrium on a rotating disk, theory of, and experimental results, 33;
– Nitrocellulose-dibutyl phthalate-acetone, heats of swelling and solution of, 179;

Tensile strength, of mixtures of polyethylene and polyisobutylene, 655.
Textile chemistry. Alteration of the intermolecular structure of capron fiber as the result of heat treatment, 479;
– Investigation of the intermolecular structure of thermoplastic fibers, 115;
– Modification of polyamide properties by the inclusion method, 543;

- Structure of high polymers, strengthening the molecular structure of tire yarn, (viscose, capron), 109;
- The fractional composition of fine cellulose fibers, 125.

Thixotropy. Action of the basic salt aluminum oxychloride on the structuromechanical (thixotropic) properties of askangel suspensions, 367;
- O/W type emulsions of maximum concentration with a thixotropic dispersion medium (sodium oleate), 75;
- The thixotropic properties of certain printing inks (strength and viscosity), 243;
- Thixotropic and structuromechanical properties of askangel suspensions in relation to the composition of the exchange complex, 303;
- Thixotropic structures formation and elasticoplasticoviscous properties of askangel suspensions, 65.

Titania-silica gels, see gels.

Ultrasonics; industrial unit for production of emulsions by means of an ultrasonic liquid whistle (jet), 387.

Vinyl chloride — acrylonitrile copolymer, see high polymer chemistry.

Vinyl chloride polymers, see high polymer chemistry

Viscosity, of butadiene-styrene rubbers, influence of structure on, 599;
- Specific, of gelatin solutions, effect of surface active agents on, 85.

Vulcanizability, of butadiene polymers, influence of structure on, 199.

Water, bound, calculation of the specific heat of, 585.

Water vapor, adsorption of silica by, and hydration of its surface, 563;
- possibility of surface activation and passivation of nuclei (NaCl, SiO_2) in condensation of, mechanism of the effect, 557.

Wood, elastic deformation, characteristics of, 297.

Yield value, see shear stress.

Zirconium hydroxide organosols, see organosols.

CALCULATION OF THE LIMITING SHEAR STRESS (YIELD VALUE) OF DISPERSE SYSTEMS IN EXPERIMENTS WITH THE CONE PLASTOMETER

N. N. Agranat and M. P. Volarovich

The yield value θ is an important rheological parameter of plastic disperse systems, the determination of which is necessary for characterization of the structuromechanical properties of such systems. There are several methods for determination of θ in disperse systems [1-11]; the relative accuracy obtained in determinations by each of these is of the order of several percent. A greater accuracy in determination of θ is difficult to obtain because, like any other yield value, it depends to some extent on the experimental conditions, such as the time during which the force acts [12],etc. Until recently, however, few investigations have dealt with comparative tests of different methods for determination of θ [3,13,14]. It was therefore important to determine θ simultaneously by different methods in some definite disperse systems, such as lubricant greases, and to compare the results.

We have determined θ for several greases with the use of six different instruments: the RV-4 rotational viscosimeter [1], a vertically moving plate [7] and cylinder [5,6], Tolstoi's cone instrument [9], Simonyan's capillary type instrument [10], and Rebinder's cone plastimeter [8]. Fairly good agreement was found between the values of θ measured by all these methods. However, the values of θ calculated from the results of measurements with the cone plastometer by Rebinder's approximate formula [8] were 1.5-2.5 times as large as the values obtained by other methods. This was also found in other investigations [15]. We advanced the view, jointly with M. F. Shirokov, that the reason for the discrepancy was the fact that in derivation of the formula only the shearing stress acting along the cone surface was taken into account, and extension of plastic deformations into the volume near the cone was ignored; this last effect has been established experimentally by means of X-ray transmission [16]. In this investigation the cone has been considered as an axially symmetrical punch pressed into the plane boundary of the plastic medium. Examples of the solution of such problems by the construction of a network of slippage lines for complete plasticity conditions are contained in publications by Sokolovsky [17] and Ishlinsky [18]. Hencky [19] and Puchkov [18] have shown that problems of this type can be solved to a sufficient degree of accuracy by construction of slippage lines for the corresponding plane problem. We have applied this method to the cone, the basis adopted being the fact that at limiting equilibrium of the system the pressure P acting on the punch from the side of the plastic medium becomes equal to the external acting force G, i.e., P = G.

The pressure force P was determined by two methods. First, Puchkov's approximate method [18] was used. In this case the total pressure force of the plastic medium on the cone can be represented by the formula:

$$P = p_A F + \frac{p_O - p_A}{h} V, \qquad (1)$$

where p_O and p_A are the pressures at points O and A (Fig. 1), the point A being very close to the apex of the cone; F is the cross section of the cone at the surface of the plastic medium; V is the volume of the immersed portion of the cone; h is the maximum immersion depth.

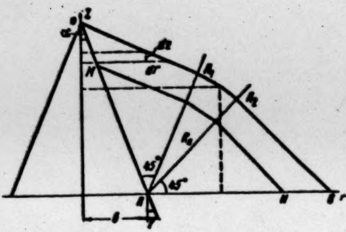

Fig. 1. Slippage lines for the plane problem (conical punch).

The pressure p_A and p_O were calculated from the formula

$$p_M = \sigma_S\left(1+\gamma_M+\frac{1}{2}\ln\frac{r_N}{r_M}-\frac{1}{2}\int_M^N\frac{dz}{r}\right), \quad (2)$$

where σ_S is the maximum normal stress, equal to the flow limit in extension; γ_M is the angle formed by the tangent to the cone at the given point and the negative direction of the z axis (Fig. 1); M and N are points at the cone surface and the surface of the plastic medium respectively, belonging to the given slippage line; r, z, and ϕ are cylindrical coordinates [8]. By the Mises conditions, in this case $\sigma_S = 2\tau_{max}$, where τ_{max} is the flow limit in shear, i.e., $\tau_{max} = \theta$. Therefore Equation (2) may be written as follows:

$$p_M = \theta\left(2+2\gamma_M+\ln\frac{r_N}{r_M}-\int_M^N\frac{dz}{r}\right). \quad (3)$$

According to Fig. 1, for the slippage line OA_1A_2B

$$p_0 = \theta\left(2+2\alpha+\ln\frac{r_B}{r_0}-\int_0^B\frac{dz}{r}\right) \quad (4)$$

here r_0 is the radius of curvature of the cone apex (in practice r_0 is never 0), and α is half the vertical angle of the cone. The pressure at the rounded apex may be neglected, as projection of it on a very small area gives a negligible value.

From Fig. 1 we have

$$\int_0^B\frac{dz}{r} = \int_0^{A_1}\frac{dz}{r}+\int_{A_1}^{A_2}\frac{dz}{r}+\int_{A_2}^{B}\frac{dz}{r}. \quad (5)$$

Putting for each of the regions z = f (r), we have

$$\int_0^B\frac{dz}{r} = -\left[\mathrm{tg}\left(\frac{\pi}{4}-\alpha\right)\ln\frac{r_{A_1}}{r_0}+\ln\frac{r_B}{r_{A_2}}+\int_{A_1}^{A_2}\frac{r-b}{r\sqrt{R_A^2-(r-b)^2}}\,dr\right]. \quad (6)$$

Substituting Equations (6) and (3) into Equation (4) and calculating $p_A = \theta\,(2 + 2\,\alpha)$, we find, in accordance

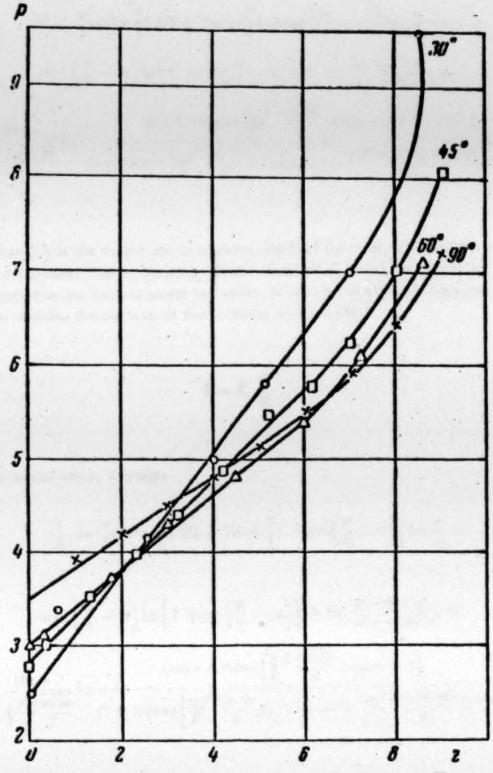

Fig. 2. Pressure distribution over the surface of a conical punch for cones of different vertical angles.

with Equation (1), the total pressure P of the plastic medium on the punch, after first expressing all the quantities in the formula in terms of α and h

$$P = \frac{\pi}{3}\tan^2\alpha \left\{6.69 + 7\alpha + \left[1 + \tan\left(\frac{\pi}{4} - \alpha\right)\right]\ln\frac{h}{r_0} - \right.$$
$$-\tan\left(\frac{\pi}{4} - \alpha\right)\ln\left[1 + \tan\left(\frac{\pi}{4} - \alpha\right)\right] + \ln\frac{(1+\sin\alpha)^2}{\cos\alpha + \sin 2\alpha} +$$
$$\left. + \frac{\sin\alpha}{\sqrt{\frac{\cos 2\alpha}{2}}}\ln\frac{(\cos\alpha + \sin\alpha)\left(\sqrt{\frac{\cos 2\alpha}{2}} + \sin\alpha + 1\right)}{(1 + 2\sin\alpha)\left[\sqrt{\frac{\cos 2\alpha}{2}}(1 + \sin 2\alpha) + \frac{\cos 2\alpha + \sin 2\alpha + 1}{2}\right]}\right\}\theta h^2. \tag{7}$$

It was found that if h is the maximum immersion depth of the cone, and θ is the yield value, equal to the flow limit of the system, then at limiting plastic equilibrium, when the pressure P of the medium on the punch becomes equal to the force G under the action of which the punch is immersed, the relationship between these values remains the same as in the Rebinder formula [8], i. e.,

$$\theta = K\frac{P}{h^2}. \tag{8}$$

However, K has a different value, namely:

$$\frac{1}{K} = \frac{\pi}{3}\tan^2\alpha \left\{6.69 + 7\alpha + \left[1 + \tan\left(\frac{\pi}{4} - \alpha\right)\right]\ln\frac{h}{r_0} - \right.$$
$$-\tan\left(\frac{\pi}{4} - \alpha\right)\ln\left[1 + \tan\left(\frac{\pi}{4} - \alpha\right)\right] + \ln\frac{(1+\sin\alpha)^2}{\cos\alpha + \sin 2\alpha} +$$
$$\left. + \frac{\sin\alpha}{\sqrt{\frac{\cos 2\alpha}{2}}}\ln\frac{(\cos\alpha + \sin\alpha)\left(\sqrt{\frac{\cos 2\alpha}{2}} + \sin\alpha + 1\right)}{(1 + 2\sin\alpha)\left[\sqrt{\frac{\cos 2\alpha}{2}}(1 + \sin 2\alpha) + \frac{\cos 2\alpha + \sin 2\alpha + 1}{2}\right]}\right\}. \tag{9}$$

Formula (1), put forward by V. V. Puchkov, gives somewhat low values of P (and therefore low values of K), as the relationship between p_M and z_M can be regarded as linear only over a restricted region, and linearity is disturbed as the vertex is approached (Fig. 2). Formula (9) contains the term, ln h/r_0, where r_0 is the radius of curvature of the cone vertex. This means that K depends not only on the cone angle 2α, but also on the ratio h/r_0.

There is also a graphical method for calculation of the total pressure P of a plastic medium on a punch [17]. It is easy to show that

$$P = \int_0^b 2\pi p_m r_m dr_m. \tag{10}$$

This integral can be replaced by a sum

$$P = \int_{0}^{b} 2\pi\, p_m r_m\, dr_m = 2\pi\theta\Sigma \overline{pr}\, \Delta r, \qquad (11)$$

where

$$\overline{pr} = \frac{1}{2\theta}(p_{i-1} r_{i-1} + p_i r_i).$$

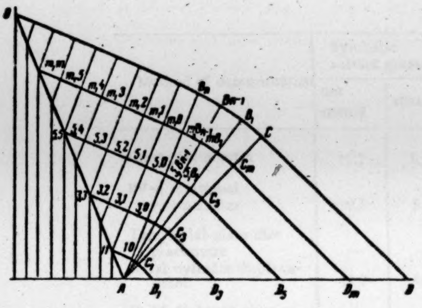

Fig. 3. Network of slippage lines for the immersion of a cone into a plastic medium.

By constructing the network of slippage lines (Fig. 3) (for greater calculation accuracy the drawing must be considerably larger than the actual dimensions of the punch) it is possible to find, in accordance with Equation (2), the pressures p_m at different points of the cone surface and by measuring r_m, to calculate P from Equation (11). We found the values of P for conical punches with different angles 2α. Since $\theta = K \frac{P}{h^2}$ by measuring on the diagram the immersion depth h, the equation

$$K = \frac{h^2}{2\pi\Sigma \overline{pr}\, \Delta r} \qquad (14)$$

was used to find the values of the constant K for cones with different vertical angles 2α. These values are given in Table 1.

TABLE 1

Values of the Constant K for Cones With Different Vertical Angles 2α

2α	Value of K	
	found graphically	analytical solution
30°	0.949	0.959
45°	0.416	0.416
60°	0.217	0.214

Agranat and Shirokov [21] determined the total pressure of a plastic medium on a conical punch by an analytical method. A formula for the constant K was derived. The values so found for the constant for cones with different vertical angles are also shown in Table 1.

It is seen from Table 1 that the graphical method gives values close to those found by the analytical method.

We determined experimental values of the yield stress θ for a number of greases by means of a number of instruments of different types, including the cone plastometer, for which the value of θ was calculated from experimental data with the use of values of K calculated by the analytical (and also the graphical) method. The experimental results are given in Table 2.

It is seen from Table 2 that the values obtained for θ with the cone plastometer coincide with the values found by means of other types of instruments. Rebinder and Segalova [22] showed that, for systems with yield values of the order of 1 g/cm² and less, in calculations with the aid of Formula (8) the expression $K = \frac{1}{\pi} \cot \alpha \cos^2 \alpha$ may be used. This also gives good agreement with yield values found by other methods. We did not test such systems.

TABLE 2

Yield Values (g/cm^2) of Greases, Determined by Different Methods

Method of determination	Synthetic solidol grease		1-13 grease		Gun grease	
	not stirred	stirred	not stirred	stirred	not stirred	stirred
Cone plastometer	11.7	5.1	22.9	12.3	30.7	17.9
RV-4 rotational viscosimeter	10.5	5.8	21.2	12.5	27.0	19.8
Tangential plate displacement	—	—	24.1	10.4	29.5	—
Axial cylinder displacement	11.7	6.0	25.1	11.1	—	—
D. M. Tolstoi's cone instrument	—	5.1	23.3	10.8	35.0	17.5
A. A. Simonyan's capillary type instrument	—	—	—	10.5	28.0	—

SUMMARY

1. P. A. Rebinder's cone plastometer must be regarded as the most convenient instrument for measurement of θ, as it is possible to measure yield values over a wide range of θ and to repeat the experiments many times, with good agreement between the results. The instrument is simple to construct and operate.

2. The values of the constants K given in Table 1 should be used for measurements on systems with yield values greater than 1 g /cm^2 by means of the cone plastometer.

3. If, in addition to θ, it is also necessary to determine the plastic viscosity of a disperse system, the rotational viscosimeter should be used.

The Moscow Peat Institute
The S. Ordzhonikidze Institute of Aviation, Moscow
Chair of Physics

Received August 8, 1956

LITERATURE CITED

[1] M. P. Volarovich, Tran. Inst. Mineral Raw Materials, No. 66, 1 (1934).

[2] P. A. Rebinder, Trans. Conf. on Viscosity of Liquids and Colloid Solutions, 1, 361 (1941); 2, 173 (1944).

[3] M. P. Volarovich, Colloid J., 16, No. 3, 227 (1954).

[4] M. P. Volarovich and N. N. Kulakov, Bull. Acad. Sci. USSR, No. 10, 1331 (1935).

[5] D. M. Tolstoi, J. Phys. Chem., 5,28 (1934).

[6] M. P. Volarovich, Trans. Polygraphic Inst. State United Press, No. 5 (1937); M. P. Volarovich and D. M. Tolstoi, Colloid J., 6, No. 5, 409 (1940).

[7] P. A. Rebinder and S. Ya. Veiler, Proc. Acad. Sci. USSR, 49, No. 5, 354 (1945).

[8] P. A. Rebinder and B. Ya. Yampolsky, Colloid J., 10, No. 6, 466 (1948); P. A. Rebinder and N. N. Semenenko, Proc. Acad. Sci. USSR, 64, No. 6, 835 (1949).

[9] D. M. Tolstoi, Proc. Acad. Sci. USSR, 77, No. 5, 847 (1951).

[10] A. A. Simonyan, Peat Ind., No. 10, 24 (1953).

[11] K. I. Klimov, Factory Labs., 21, No. 4, 491 (1955).

[12] R. Houwink, The Yield Value, Amsterdam (1938).

[13] N. N. Kulakov, Colloid J., 3, No. 3, 217 (1937).

[14] N. P. Volarovich and E. P. Loshakova, Colloid J., 8, No. 3, 127 (1946).

[15] E. E. Segalova, Trans. All-Union Conf. Colloid Chem., Kiev (1950).

[16] M. P. Volarovich and S. N. Markov, Factory Labs., 17, No. 12, 1461 (1951).

[17] V. V. Sokolovsky, Theory of Plasticity, State Tech. Press (1950).

[18] A. Yu. Ishlinsky, J. Appl. Math. Mech. 8, 3 (1944).

[19] G. Hencky, in Symposium "Theory of Plasticity" edited by Yu. N. Rabotnov, Leningrad – Moscow (1948).

[20] A. A. Ilyushin, Plasticity, State Tech. Press (1948).

[21] N. N. Agranat and M. F. Shirokov, Colloid J., 19, 9 (1957).

[22] P. A. Rebinder and E. E. Segalova, Colloid J., 10, No. 3 (1948).

THEORY OF THE CONE IMMERSION METHOD FOR DETERMINATION OF THE YIELD VALUES OF DISPERSE SYSTEMS

N. N. Agranat and M. F. Shirokov

A widely used method for determination of the yield values of disperse systems, proposed by Rebinder [1], is based on the immersion of a cone into a viscoplastic medium under the action of a constant force. The method depends on the relationship

$$\theta = K\frac{G}{h^2}, \tag{1}$$

where θ is the yield value; G is the force causing immersion of the cone; h is the maximum depth of immersion; K is a constant which, according to [1], should be calculated from the formula

$$K = \frac{1}{\pi}\cos^2\alpha\cot\alpha, \tag{2}$$

where α is half the vertical cone angle.

It has been found, however, that values of θ for disperse systems calculated from Formulas (1) and (2) from experimental data on the immersion of a cone are 1.5-2.5 times as large as the values of θ found by other methods [2, 3]. It is likely that the reason for this is that in derivation of Formulas (1) and (2) the spread of plastic deformation into the volume around the cone was not taken into consideration. In fact the medium around the cone is in a state of elasticoplastic deformation. Therefore the cone can be regarded as an axially symmetrical punch pressed into the plane surface of a plastic medium. The general theory leads to the following expression for the pressure p_M at a given point M in the surface [4]

$$p_M = \sigma_S\left(1 + \gamma_M + \frac{1}{2}\int_M^N \frac{dr - dx}{r}\right), \tag{3}$$

where σ_S is the maximum normal stress; γ_M is the angle between the tangent to the cone surface and the negative direction of the X axis; r, x, φ are cylindrical coordinates of the point on the slippage line joining the points M and N in the surface and in the medium, lying in the meridianal plane (Fig. 1).

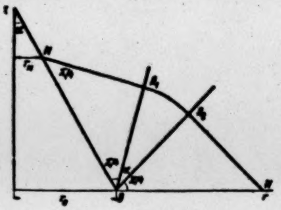

Fig. 1. Slippage line for the penetration of a conical punch into a plastic medium.

Methods for construction of the slippage lines have already been developed [5-7]. The force P which acts from the direction of the medium upon the surface of the punch in contact with it in the direction of the X axis is given by the expression

$$P = \int p_M n_x \, df,$$

where n_x is the vector component of the normal $\bar{n}$, external relative to the medium, to an element df of the cone surface area. It is evident that $n_x \, df = -2\pi r_M dr_M$.

Consequently,

$$G = P = + \int_0^{r_0} p_M \, 2\pi r_M \, dr_M. \tag{4}$$

Substituting into this the value of p_M from Equation (3), and remembering that for a cone $\gamma = \alpha$, we have:

$$G = \sigma_S \int_0^{r_0} \left(1 + \alpha + \frac{1}{2} \int_{r_M}^{r_N} \frac{dr - dx}{r} \right) 2\pi r_M \, dr_M$$

or

$$G = \sigma_S \int_0^{r_0} \left(1 + \alpha + \frac{1}{2} \ln \frac{r_N}{r_M} - \frac{1}{2} \int_M^N \frac{dx}{r} \right) 2\pi r_M \, dr_M \, . \tag{5}$$

According to Fig. 1

$$\int_M^N \frac{dx}{r} = \int_M^{A_1} \frac{dx}{r} + \int_{A_1}^{A_2} \frac{dx}{r} + \int_{A_2}^{N} \frac{dx}{r}.$$

The arc $A_1 A_2$ may, without much error, be replaced by a chord, and then

$$\int_M^N \frac{dx}{r} = -\left[\cot\left(\frac{\pi}{4}+\alpha\right)\ln\frac{r_{A_1}}{r_M} + \cot\left(\frac{\pi}{4}+\frac{\alpha}{2}\right)\ln\frac{r_{A_2}}{r_{A_1}} + \ln\frac{r_N}{r_{A_2}}\right]$$

and Equation (5) assumes the form

$$G = \sigma_S \int_0^{r_0} \left[2 + 2\alpha + \ln\frac{r_N^2}{r_M r_{A_2}} + \cot\left(\frac{\pi}{4}+\alpha\right)\ln\frac{r_{A_1}}{r_M} + \right. \tag{6}$$

$$\left. + \cot\left(\frac{\pi}{4}+\frac{\alpha}{2}\right)\ln\frac{r_{A_2}}{r_{A_1}}\right]\pi r_M \, dr_M$$

or

$$G = \sigma_S \pi r_0^2(1+\alpha) + \sigma_S \pi \left[\int_0^{r_0}\left(\ln\frac{r_N^2}{r_M r_{A_2}}\right) r_M \, dr_M + \right.$$

$$\left. + \cot\left(\frac{\pi}{4}+\alpha\right)\int_0^{r_0}\left(\ln\frac{r_{A_1}}{r_M}\right) r_M \, dr_M + \cot\left(\frac{\pi}{4}+\frac{\alpha}{2}\right)\int_0^{r_0}\left(\ln\frac{r_{A_2}}{r_{A_1}}\right) r_M \, dr_M\right]. \tag{7}$$

On the basis of Fig. 1 we may write: $r_N = r_0 + R_M \sqrt{2}$ where $K_M = OA_1 = OA_2$, and since $R_M = \frac{r_0 - r_M}{\sqrt{2}\sin\alpha}$,

then

$$N \quad \frac{r_0(\sin\alpha + 1) - r_M}{\sin^{\alpha}}. \tag{8}$$

In the same way we find

$$r_{A_1} = \frac{r_0 \cot\left(\frac{\pi}{4} - \alpha\right) - r_M}{2/(\cot\alpha + 1)}; \tag{9}$$

$$r_{A_2} = \frac{r_0(2\sin\alpha + 1) - r_M}{2\sin\alpha}. \tag{10}$$

By partial integration, we have

$$\int_0^{r_0}\left(\ln\frac{r_N^2}{r_M r_{A_2}}\right) r_M \, dr_M = \left[\frac{r_M^2}{2}\ln\frac{r_N^2}{r_M r_{A_2}}\right]_0^{r_0} - \int_0^{r_0}\frac{r_M^2}{2} d\left(\ln\frac{r_N^2}{r_M r_{A_2}}\right) =$$

$$= -\int_0^{r_0}\frac{r_M^2}{2} d\left(\ln\frac{r_N^2}{r_M r_{A_2}}\right). \tag{11}$$

since

$$\left[\frac{r_M^2}{2}\ln\frac{r_N^2}{r_M r_{A_0}}\right]_0^{r_0} = 0.$$

Similarly we have

$$\int_0^{r_0}\left(\ln\frac{r_{A_1}}{r_M}\right) r_M\, dr_M = -\int_0^{r_0}\frac{r_M^2}{2}\, d\left(\ln\frac{r_{A_1}}{r_M}\right); \tag{12}$$

$$\int_0^{r_0}\left(\ln\frac{r_{A_2}}{r_{A_1}}\right) r_M\, dr_M = -\int_0^{r_0}\frac{r_M^2}{2}\, d\left(\ln\frac{r_{A_2}}{r_{A_1}}\right). \tag{13}$$

Putting the values of (8), (9), and (10) into Equation (7), taking into account Equations (11), (12), and (13), and remembering that according to the Mises condition $\sigma_S = 2\tau_{max}$ where σ_S in the present case can be assumed equal to the flow limit in extension, and τ_{max}, the maximum tangential stress, is equal to the flow limit in shear, or the yield value θ, we have

$$\begin{aligned} P = {} & \pi\theta(2+2\alpha)r_0^2 + \pi\theta\left\{2\int_0^{r_0}\frac{r_M^2\, dr_M}{r_0(\sin\alpha+1)-r_M} + \right.\\ & + \int_0^{r_0} r_M\, dr_M - \int_0^{r_0}\frac{r_M^2\, dr_M}{r_0(2\sin\alpha+1)-r_M} + \cot\left(\frac{\pi}{4}+\alpha\right)\times\\ & \times\left[\int_0^{r_0}\frac{r_M^2\, dr_M}{r_0\cot\left(\frac{\pi}{4}-\alpha\right)-r_M} + \int_0^{r_0} r_M\, dr_M + \right.\\ & \left.\left. + \cot\left(\frac{\pi}{4}+\frac{\alpha}{2}\right)\left[\int_0^{r_0}\frac{r_M^2\, dr_M}{r_0(2\sin\alpha+1)-r_M} - \int_0^{r_0}\frac{r_M^2\, dr_M}{r_0\cot\left(\frac{\pi}{4}-\alpha\right)-r_M}\right]\right]\right\}. \end{aligned} \tag{14}$$

We calculate the definite integrals and carry out the permissible simplifications remembering that $r_0 = h\tan\alpha$; then we have:

$$\begin{aligned} P = {} & \pi\theta h^2\tan^2\alpha\left\{2\alpha - 2(\sin\alpha+1)^2\ln\frac{\sin\alpha}{\sin\alpha+1} + \right.\\ & + \left[1-\cot\left(\frac{\pi}{4}+\frac{\alpha}{2}\right)\right](2\sin\alpha-1)^2\ln\frac{2\sin\alpha}{2\sin\alpha+1} + \\ & + \left[\cot\left(\frac{\pi}{4}+\frac{\alpha}{2}\right)-\cot\left(\frac{\pi}{4}+\alpha\right)\right]\cot^2\left(\frac{\pi}{4}-\alpha\right)\ln\frac{2}{\cot\alpha+1} + \\ & \left. + \cot\left(\frac{\pi}{4}+\frac{\alpha}{2}\right)\left[\cot\left(\frac{\pi}{4}-\alpha\right)-(2\sin\alpha+1)\right]\right\}. \end{aligned} \tag{15}$$

Thus we see that the relationship between θ, G, and h derived by P. A. Rebinder is retained. However, the value of the constant K is determined by an expression different from Formula (2), namely

$$\frac{1}{K}=\pi\tan^2\alpha\Big\{2\alpha-2(\sin\alpha+1)^2\ln\frac{\sin\alpha}{\sin\alpha+1}+$$
$$+\Big[1-\cot\Big(\frac{\pi}{4}+\frac{\alpha}{2}\Big)\Big](2\sin\alpha+1)^2\ln\frac{2\sin\alpha}{2\sin\alpha+1}+$$
$$+\Big[\cot\Big(\frac{\pi}{4}+\frac{\alpha}{2}\Big)-\cot\Big(\frac{\pi}{4}+\alpha\Big)\Big]\cot^2\Big(\frac{\pi}{4}-\alpha\Big)\ln\frac{2}{\cot\alpha+1}+$$
$$+\cot\Big(\frac{\pi}{4}+\frac{\alpha}{2}\Big)\Big[\cot\Big(\frac{\pi}{4}-\alpha\Big)-(2\sin\alpha+1)\Big]. \tag{16}$$

This formula was used to calculate values of K for cones with different vertical angles (excluding the value $\alpha = \pi/2$), some of which are given in the table.

Values of the Constant K Calculated From Equation (16)

2α	30°	45°	60°	89°20'
K	0.959	0.416	0.214	0.073

For the angle $2\alpha = 90°$ Equation (14) assumes the form

$$P=\pi\theta(2+2\alpha)r_0^2+\pi\theta\Big[2\int_0^{r_0}\frac{r_M^2\,dr_M}{r_0(\sin\alpha+1)-r_M}+$$
$$+\int_0^{r_0}r_M\,dr_M-\int_0^{r_0}\frac{r_M^2\,dr_M}{r_0(2\sin\alpha+1)-r_M}+\cot\Big(\frac{\pi}{4}+\frac{\alpha}{2}\Big)\int_0^{r_0}\frac{r_M^2\,dr_M}{r_0(2\sin\alpha+1)-r_M}\Big]. \tag{17}$$

Therefore for a cone with this vertical angle

$$P=\pi h^2\tan^2\alpha\cdot\theta\Big\{1+2\alpha-2(\sin\alpha+1)^2\ln\frac{\sin\alpha}{\sin\alpha+1}+$$
$$+\Big[1-\cot\Big(\frac{\pi}{4}+\frac{\alpha}{2}\Big)\Big](2\sin\alpha+1)^2\ln\frac{2\sin\alpha}{2\sin\alpha+1}-\cot\Big(\frac{\pi}{4}+\frac{\alpha}{2}\Big)\Big(\frac{3}{2}+2\sin\alpha\Big)\Big\} \tag{18}$$

and the constant K is given by the equation

$$\frac{1}{K}=\pi\tan^2\alpha\Big\{1+2\alpha-2(\sin\alpha+1)^2\ln\frac{\sin\alpha}{\sin\alpha+1}+$$
$$+\Big[1-\cot\Big(\frac{\pi}{4}+\frac{\alpha}{2}\Big)\Big](2\sin\alpha+1)^2\ln\frac{2\sin\alpha}{2\sin\alpha+1}-$$
$$-\cot\Big(\frac{\pi}{4}+\frac{\alpha}{2}\Big)\Big(\frac{3}{2}+2\sin\alpha\Big). \tag{19}$$

Figure 2 shows K plotted against the cone angle 2α.

The yield values calculated from experimental data by means of Formula (1) with the use of the constant K given by Formula (16) are in good agreement with values of θ determined experimentally by other methods for a number of disperse systems, in the range of 5 to 100 g/cm² [7].

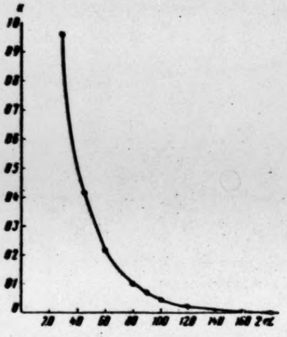

Fig. 2. Constant K as a function of the cone angle.

SUMMARY

1. A theory of the cone plastometer is developed on the basis of the properties of viscoplastic media; this leads to P. A. Rebinder's known formula, but with a different coefficient K.

2. A formula for calculating the coefficient K is derived, and the values of K for cones with different angles are found.

The S. Ordzhonikidze Institute of Aviation, Moscow Received August 2, 1956

LITERATURE CITED

[1] P. A. Rebinder and N. N. Semenenko, Proc. Acad. Sci. USSR, 64, No. 6 (1949).

[2] P. A. Rebinder and E. E. Segalova, Colloid J., 10, No. 3 (1948).

[3] D. S. Velikovsky, Petroleum Economy, No. 2 (1950).

[4] A. A. Ilyushin, Plasticity, State Tech. Press (1948).

[5] G. Hencky, in Symposium "Theory of Plasticity", translation edited by Yu. N. Rabotnov, Foreign Lit. Press (1948).

[6] V. V. Sokolovsky, Theory of Plasticity, State Tech. Press (1950).

[7] N. N. Agranat and M. P. Volarovich, Colloid J., 19, 3 (1957).*

---

* Original Russian translation. See. C. B. translation.

AN ELECTRON MICROSCOPE STUDY OF STRUCTURE FORMATION IN LOESS

1. INFLUENCE OF THE DISPERSION MEDIUM

E. Aripov, Z. Ya. Berestneva, and V. A. Kargin

Electron microscopy has been used by many workers as an analytical method for qualitative investigations of the mineralogical composition of soils. Sedletsky and Ananyev [1] used the electron microscope to study the mineralogical composition of loess of various origins. The specimens were investigated in the form of aqueous suspensions. Vikulova [2] made a more detailed study of particle size in aqueous soil suspensions in relation to the sedimentation time.

For studies of soils by means of the electron microscope, the specimens are usually prepared from aqueous or amyl alcohol suspensions of clays not subjected to preliminary treatments, or from aqueous suspensions of clays previously treated with hydrochloric acid, hydrogen peroxide, or acetic acid, or from separate fractions of aqueous suspensions (separated by the sedimentation method). In all these methods the water-soluble salts present in the material are first removed by decantation of the clear liquids from the suspensions. Repeated decantation of the top liquid layer followed by dilution results in peptization of the clay particles; some authors [2] recommend the addition of ammonia (until a faint odor is apparent) as stabilizer.

These methods may be used in studying the structure of soil or loess particles, but for studying structure formation processes, in which all the components of the loess probably participate, it is necessary to investigate not only the particle structure of the mineral components of the loess, but also their behavior in various media.

It is known that both soils and loesses swell in water, and therefore it is of interest to study, by means of the electron microscope, the influence of the medium on the structure of loess particles. Loess specimens were prepared for this purpose, both by powdering loess in the dry state, and also in the form of aqueous and alcoholic suspensions. Loess of the Tashkent region was used for the work. The investigations were performed with the aid of the EM-3 electron microscope with direct electrono-optical magnification (8000-12000) followed by photographic enlargement.

The specimens were prepared as follows. Copper gauzes with hole diameter not exceeding 0.1 mm were used as supports. These were coated with collodion films 100-150 A thick. The films were made from a solution of collodion in amyl acetate. The films were dried in air under a glass cover to protect them against dust and other contamination. A drop of the suspension to be investigated was then applied to the film and then carefully removed by a piece of filter paper. It was necessary to remove the drops in our investigation because, during slow drying of the drops, structure formation or coalescence of the individual particles due to slow evaporation of the water could occur. This would interfere with interpretation of the results. Removal of the drop results in almost instantaneous evaporation of the remaining moisture. The prepared specimens were stored in Petri dishes placed under a glass cover to protect them against contamination.

The dry loess specimens were made by pulverization of the loess in a dessicator at the bottom of which gauzes with collodion films, serving as supports, were placed. The aqueous and alcoholic suspensions were made by stirring 5-10 g of loess with 200-300 ml of distilled water or ethyl alcohol.

In our electron microscope investigations of loess suspensions, the particles seen in the microphotographs are referred to as "loess particles", irrespective of whether they are clearly defined particles of individual minerals contained in the loess, or amorphous formations consisting of different minerals and salts which are components of the loess.

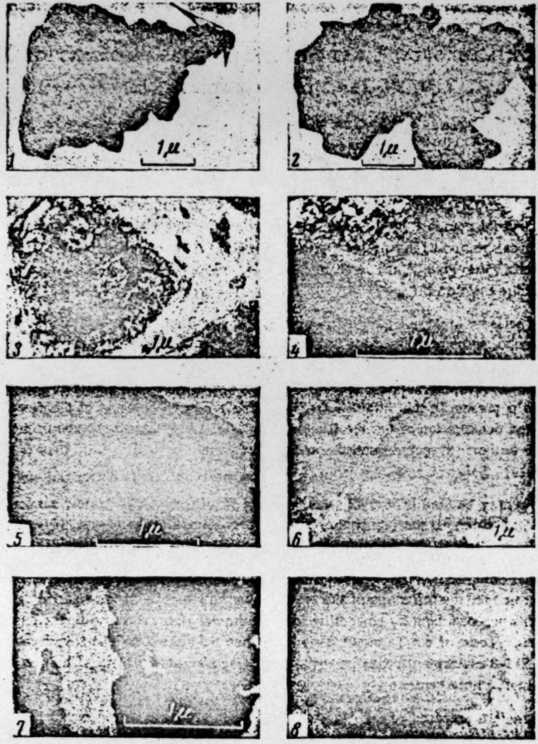

Figs. 1-8. Microphotographs of loess in various media (explanation in text).

Fig. 1 is a microphotograph of specimens prepared by pulverization. The particles consist of scales with dense formations and clear outlines. Loess particles from an alcoholic suspension (Fig. 2) are similar under the electron microscope to specimens prepared by pulverization.

Figs. 3 and 4 are microphotographs of aqueous loess suspensions. The particles retain their external form almost completely but contain pores (Fig. 3). The presence of such pores in loess in aqueous suspensions may be caused by swelling of the loess particles and the consequent formation of a fine porous structure; on the other hand, these porous formations may arise as the result of solution of the easily soluble salts which are always present in loess. In the latter case the formation of a fine porous structure in the loess particles will be irreversible, as the dissolved salts are removed with the water. If the pores are formed as the result of swelling, the effect should be reversible, i. e., pores should be formed during swelling of the loess in water and disappear on drying.

To determine the causes of the formation of a porous structure in loess particles in aqueous suspensions, the structure of the loess particles was studied in aqueous suspensions under the electron microscope, and the water in the suspension was then replaced by ethyl alcohol. Dehydration of the loess by ethyl alcohol was assumed to be permissible as identical electron micrographs are given by loess particles obtained by pulverization and in alcoholic suspensions. The water – alcohol change of medium was performed 5-6 times with the same loess specimen.

It is seen in Fig. 5 that, after the first dehydration, scales with dense formations and sharp edges appear again. This microphotograph is quite similar to those shown in Figs. 1 and 2. When this alcoholic suspension was converted into an aqueous suspension, porosity appeared again, as can be seen in Fig. 6.

Repeated hydration and dehydration of the loess showed that the formation and disappearance of the pores was completely reversible. After the fifth hydration of the suspension a porous structure appeared again (Fig. 7). After the sixth dehydration, dense formations with sharp outlines were again visible (Fig. 8). The reversibility of this process in the transitions between aqueous and alcoholic suspensions indicates that pore formation is caused by swelling of the loess, and not by solution of the salts which are usually present in loess; otherwise the formation and disappearance of the pores would be irreversible.

Water-soluble salts, which may cause the formation of fairly strong surface structures, penetrate to the surface and accumulate on it through the pores formed during swelling in water, by capillary action. This question will be examined separately in the next article.

SUMMARY

1. The structure of loess particles from the Tashkent region has been studied in different media by means of the electron microscope.

2. It is shown that a finely porous structure, which disappears on drying, is formed in an aqueous medium.

3. The process of pore formation and disappearance is reversible, which may be attributed to swelling of the clay mineral particles in loess in water.

The loess specimens were kindly supplied by Prof. Yu. A. Skvortsov, to whom we are grateful.

The L. Ya. Karpov Physicochemical Institute
Moscow

Received September 7, 1956

LITERATURE CITED

[1] I. D. Sedletsky, Proc. Acad. Sci. USSR, New Series, 81, No. 5, 109 (1951); 86, No. 4 (1952); 89,339 (1953); New Series, 70, No. 2, 27 (1953); 96,375 (1954); Sci. Mem. Rostov State Univ., Geol.-Geograph. Faculty, 23, No. 5, 115 (1954); V. P. Ananyev, ibid., 23, No. 5 (1954); I. D. Sedletsky and V. P. Ananyev, Proc. Acad. Sci. USSR, 90, 651 (1953); paper in Symposium "Prevention of Water Filtration in Loess Soils", Acad. Sci. Ukrainian SSR, Kiev (1954).

[2] M. F. Vikulova, Soviet Geol., No. 39,121 (1949); Trans. All-Union Geol. Inst., No. 2 (1950); Electron Microscopy of Clays, State Chem. Press, Moscow (1952).

AN ELECTRON MICROSCOPE STUDY OF STRUCTURE FORMATION IN LOESS

2. INFLUENCE OF LOESS COMPONENTS ON STRUCTURE FORMATION

E. Aripov, Z. Ya. Berestneva, and V. A. Kargin

Loess is a finely granular, porous, loose sedimentary mineral material of a gray-yellow or straw color. Loesses not only serve as parent minerals in soil formation, but are valuable materials used in building, engineering geology, etc. Characteristic properties of loess which distinguish it from other sedimentary rocks are the porosity and looseness of its structure; moreover, the surfaces of loess strata may carry dense formations analogous to the crusts formed on soil surfaces. Geological data relate the loose and porous structure of loess to the deposition conditions, while the question of the influence of mineralogical and mechanical composition on the structure of loess is usually not considered in geological investigations [1].

Most studies of the formation of soil structure in relation to agriculture, dealing with the origins of a lumpy granular (agricultural) structure, associate this with the mineralogical composition of soils [2]. However, such investigations do not deal with causes of formation of a loose and porous structure in loess. In studies of the origins and properties of crusts on soil surfaces [3], these effects are also related to the mineralogical and mechanical composition of soil and the interaction of soil aggregates when the soil is humidified.

The purpose of our investigation was to study the mechanism of structure formation in loess in relation to its mineralogical composition, as the formation of a loose, porous structure and of dense layers on loess is probably primarily associated with its mineralogical composition. Structure formation in disperse systems can be studied by various methods, the most common of which are methods for studying the viscosity and mechanical properties of colloidal solutions and suspensions. Experimental data in this field indicate that structure formation in disperse systems already occurs in the suspensions. themselves [4].

The most widely accepted theory of structure formation in disperse systems is the theory developed by Rebinder [5], which has been extensively confirmed by experimental investigations. According to this theory, the formation of secondary structure in disperse systems is attributed to cohesion between the disperse phase particles by means of chemical or van der Waals forces. With this type of cohesion between particles in suspensions, the structures formed are retained after removal of the dispersion medium. Because of this it is possible to study the mechanism of structure formation in aqueous loess suspensions by means of the electron microscope. It is extremely important in the use of this method that the structures formed in the suspensions should persist after removal of water, as the photographs are taken under a high vacuum.

Since the major part of loess is highly disperse in mechanical composition, aqueous suspensions of loess were used for studying processes of structure formation. Electron microscopy was used in our investigations, whereby it is possible to observe changes of shape, dimensions, and relative positions of the loess particles directly, and therefore to study processes of structure formation.

In addition to clay minerals (montmorillonites, kaolinites, etc.), loess contains fairly large amounts of calcium and magnesium carbonates, relatively small amounts of calcium sulfate, and humates. To elucidate the mechanism of structure formation in loess it was necessary to study separately all the loess components as well as their mutual influence on structure formation.

The mechanism of structure formation in loess was studied with the aid of the EM-3 electron microscope with direct electrono-optical magnification (7,000-12,000) followed by photographic enlargment. Loess specimens from the Tashkent region were used for the experiments. Ammonium humates obtained from alkaline extracts of chernozem soil were used. Alkali extracts of humic acids contain excess alkali which may influence structure formation in loess. Humic acids were therefore precipitated from the alkaline extracts by addition of concentrated hydrochloric acid. The precipitate was transferred to a filter and washed with distilled water to a negative reaction for chloride ions. The humic acids were then dissolved in ammonia, excess of which can be easily evaporated. The concentration of the ammonium humate solutions was determined gravimetrically, the drying being carried out at 105°. All the samples for investigation were made from freshly prepared suspensions or mixtures of these, and subsequently at various time intervals.

As a check of the reproducibility of the results, each sample to be studied was prepared a number of times; 150 to 250 photographs were taken of each sample. All the samples, with the exception of natural loess, were prepared in the same way: the suspensions and mixtures made from them were shaken before samples were taken for applying the drops to the supports. In this way particles of all sizes present in the suspension were obtained in the specimens. In the case of natural loess the samples were taken from the upper layer of a settled suspension so that very large particles, which might mask the field of vision, could be avoided. However, in this case also control experiments were carried out, in which suspensions of natural loess were diluted and shaken before sampling. It was found that the structure of the larger particles was of the same character as previously (in settled suspensions). Thus the results are based on completely reproducible data.

Natural loess, as is known, consists of many components: clay minerals, various salts (mainly of calcium and magnesium), and remains of plants and microorganisms in the form of humus. These components probably influence structure formation processes in loesses. It was therefore desirable first to study the influence of such surface-active substances as humic acids on the structure of crystals of calcium and magnesium carbonates and calcium sulfate which are present in loess.

It is known that surface-active substances influence the form and dimensions of crystals, and therefore structure formation processes in structurized systems. Ammonium humates, calcium and magnesium carbonates, and calcium sulfate were therefore studied separately under the electron microscope, and then mixtures of these in various proportions were studied.

According to electron microscope data, ammonium humates consist of fine particles, a few hundredths of a micron in size, joined into large flocculent aggregates. Electron micrographs of aqueous calcium carbonate suspensions show that calcium carbonate consists of aggregates of very fine particles of various sizes (but no larger than 0.05-0.07 μ). Magnesium carbonate also consists of aggregates of semitransparent particles 0.2 –0.4 μ. in size.

A study of the interaction of ammonium humates with calcium and magnesium carbonates showed that ammonium humates have practically no effect on the structure of calcium and magnesium carbonate particles irrespective of the proportions in which these salts and ammonium humates are taken and of the time elapsing after preparation of the mixtures.

A totally different situation is found in the interaction between ammonium humates and calcium sulfate. According to electron microscope data, calcium sulfate particles in aqueous suspensions are needle-like in shape, reaching 0.8 μ in length and several hundredths of a micron in width. The particles are generally joined into aggregates. Ammonium humates have a considerable effect on the form and dimensions of the calcium sulfate particles. Additions of 0.4 and 1.3% of ammonium humates at once result in recrystallization of the calcium sulfate, the particles of which become progressively larger. As the ammonium humate concentration increases from 6.9 to 17.6%, the calcium sulfate particles are first peptized, and subsequently recrystallization occurs in the mixture, accompanied by considerable growth of the crystals. When the ammonium humate concentration reaches 31.8%, peptization of the calcium sulfate particles first takes place, and subsequently, owing to the blocking effect of the ammonium humates, the recrystallization of the calcium sulfate is retarded.

Recrystallization of the calcium sulfate which occurs in ammonium humate — calcium sulfate mixtures is due to presence of ammonium humates in the mixture, as a pure aqueous suspension of calcium sulfate, allowed to stand 120 days under ordinary laboratory conditions, yields the same electron micrographs as freshly prepared aqueous suspensions of calcium sulfate.

In order to study the effects of calcium and magnesium carbonates, calcium sulfate, and humic acids on structure formation in loess it was first necessary to study loess from which these components had been removed. Removal of calcium and magnesium carbonates from loess was effected by treatment of the loess with 1% acetic acid solution, while the calcium present in the loess was removed by treatment with 0.5% barium chloride solution. It may be assumed that prolonged washing of the loess with water also removed the water-soluble humic acids.

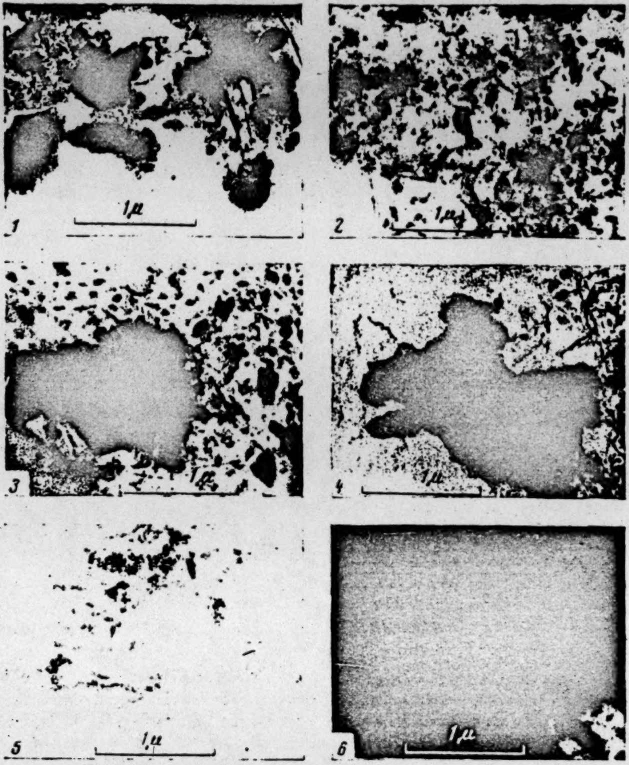

Figs. 1-6. Microphotographs showing variations in the structure of loess under the action of additions.

In our electron microscope investigations of suspensions of loess or of their mixtures with other components, the particles seen in the microphotographs are referred to as " loess particles," irrespective of whether they are clearly defined particles of individual minerals contained in the loess, or amorphous formations consisting of different minerals and salts which are components of the loess. According to electron microscope data, particles of natural loess (Fig. 1) are aggregates 1 to 2 μ in size, consisting of smaller particles.

Acetic acid treatment causes dispersion of the loess, with formation of fine particles of irregular shapes, a few hundreths of a micron in size, and needlelike particles 0.5 – 0.7 μ in length. These needlelike particles have sharp outlines (Fig. 2) in contrast to the particles with a loose structure and indistinct outlines. Loess particles remain practically unchanged after treatment with barium chloride solution (Fig. 3).

The nature of the interaction between loess and calcium and magnesium carbonates is quite different from that between loess and calcium sulfate. Calcium and magnesium carbonate are evidently substances which bind the mineral particles in loess, as dispersion of the loess occurs after removal of the carbonates. Removal of calcium sulfate has practically no effect on the size of the loess particles.

To confirm this hypothesis of the cementing (binding) effect of calcium and magnesium carbonates on loess and to determine the nature of the interaction between calcium sulfate and loess, and also between humates and loess, studies were made of the influence, first of the individual components, and then of their mixtures in various proportions, on structure formation processes in loess. As far as possible, the mixtures consisting of loess, humates, calcium and magnesium carbonates, and calcium sulfate, were made up in the proportions corresponding to natural loess. Loess treated with acetic acid was used. The influence of the individual components and their mixtures was studied with freshly made preparations, and subsequently at various time intervals, in order to observe the course of structure formation in loess. For studies of the effect of calcium carbonate on structure formation in loess, a number of mixtures was prepared consisting of aqueous suspensions of loess with increasing amounts of calcium carbonate. The interaction of loess with calcium carbonate first results in slight aggregation of the loess particles. Subsequently (after 4 days) the aggregates become considerably larger, reaching 2 μ and over (Fig. 4). Structure formation in loess is intensified by the combined action of humates and calcium carbonate, large rapidly growing amorphous particles being formed. Addition of calcium carbonate to aqueous suspensions of clay minerals also causes aggregation in these systems.

The interaction of magnesium carbonate with loess is similar to that of calcium carbonate, with the difference that the aggregation processes are considerably slower in the former case.

A study of the combined action of humates and magnesium carbonate on structure formation in loess showed that magnesium carbonate does not exert the cementing action in presence of humates which is found in the case of pure magnesium carbonate. The humates in the mixture, however, also do not influence structure formation in loess, while addition of humates only to loess suspensions causes some aggregation of the loess particles. This suggests that in a mixture consisting of magnesium carbonate, ammonium humates, and loess, magnesium carbonate reacts chemically with the humates to form insoluble magnesium humates, so that the individual components do not exert their influence on structure formation in the loess.

Calcium sulfate in the pure state also has no effect on structure formation in loess, irrespective of time and concentration. Figure 5 shows a microphotograph of a mixture of aqueous suspensions of calcium sulfate and loess washed with acetic acid. Particles can be seen characteristic of loess treated with acetic acid, as seen earlier in Fig. 2.

In the loess — calcium sulfate — humate mixture, according to electron microscope data, aggregation occurs, accompanied by an increase in the density of the aggregates and considerable increases in their size (Fig. 6). This is probably caused by the binding properties of calcium sulfate which are effective in presence of humates, as pure calcium sulfate has no influence on loess, while recrystallization of calcium sulfate occurs in its aqueous suspensions in presence of humates, with increase of crystal size. In this case the rapidly growing calcium sulfate crystals may "seize" the smaller loess particles. Simultaneous addition of the main loess components (carbonates, humates, calcium sulfate) to washed loess induces aggregation processes with formation of rapidly growing aggregates.

Electron micrographs of loess particles washed free from calcium and magnesium carbonates indicate that in this case the loess particles are small (a few hundredths of a micron) and are incapable of forming dense aggregates, while gradual addition to aqueous suspensions of washed loess, first of calcium and magnesium carbonates, calcium sulfate, and humates separately, and then in mixtures of 2 and 3 components, and finally of all these components in a mixture, showed that loess particles are aggregated in presence of these components. Therefore, structure formation in loesses primarily depends on their mineralogical composition. Consequently, the size of the loess particles, the loose and porous nature of its structure, and the formation of dense crusts on surfaces of loess strata, are all associated with the presence of calcium and magnesium carbonate, humic substances, and calcium sulfate in the loess.

DISCUSSION OF RESULTS

The main property which distinguishes loess from other sedimentary minerals is the loose and porous nature of its structure, which persists through practically the whole stratum. The chief mechanical component of loess is fine dust, of which up to 70% is present. It is also known that loesses have a high carbonate content. Therefore it seems likely that carbonates, by binding together the fine loess particles, play the main part in the formation of the loose and porous structure of loess.

In fact, a comparison of electron micrographs of natural loess and of loess washed with acetic acid to remove carbonates showed that the particles in natural loess are aggregates up to 1-2 μ in size, consisting of smaller particles, while treated loess is seen to contain very small randomly scattered particles a few hundredths of a micron in size.

Addition of calcium and magnesium carbonates to aqueous suspensions of loess previously washed free from carbonates induces aggregation of the loess particles, large aggregates being again formed; the loose structure of loess is due to the manner in which these are packed.

The study of the effect of calcium sulfate on loess showed that when it is removed from natural loess the loess particles remain practically the same as before the removal. Addition of pure calcium sulfate to aqueous suspensions of the treated loess has no effect on the loess structure, irrespective of concentration or time. Therefore calcium sulfate in the pure form plays no part in the formation of loess structure. However, in presence of humates recrystallization occurs in aqueous calcium sulfate suspensions, accompanied by rapid growth of the calcium sulfate crystals. Evidently, in presence of humates, calcium sulfate can influence structure formation in loess. In fact, if calcium sulfate is added together with humates to aqueous suspensions of treated loess, structure formation occurs in the loess and very large aggregates are formed.

Simultaneous addition of the principal components of loess (carbonates, humates, etc.) results in aggregation, with growth and condensation of the aggregates. It is known that the surfaces of loess layers with a porous and loose structure may become covered with dense formations similar to the soil crusts formed on cultivated land in Central Asia.

As was shown earlier [6], when loess is humidified the particles swell and small pores form in them, through which water-soluble salts may rise by capillary action and accumulate on the surface. In fact, an aqueous extract of natural loess obtained by ultrafiltration contains dissolved calcium sulfate and magnesium and calcium bicarbonates. Increase of the contents of these substances on the surfaces of loess strata, and especially of the calcium sulfate content, may result in the formation of the dense crusts.

It is known that carbonates and calcium sulfate are present throughout the thickness of the loess stratum, the carbonate contents sometimes reaching 50%, and the calcium content 2%. Therefore an increase of the carbonate content in the surface layer (where it is already high) should not play any important part in the formation of dense crusts on the loess surface, while an increase of the calcium sulfate concentration may have an important effect on structure formation in the loess. In the presence of the humates which are always found in loess, recrystallization of calcium sulfate takes place, with very rapid crystal growth. This favors the formation of large aggregates which create a dense and fairly strong structure on the loess surface.

Since sierozem soils formed on loess deposits have almost the same composition and properties as loess, the mechanism of formation of loose and porous structures and surface crusts on loess strata may also apply to processes of lump and crust formation in sierozem soils of Central Asia.

SUMMARY

1. Structure formation in loesses has been studied by means of the electron microscope.

2. It is shown that ammonium humates added to aqueous suspensions of calcium and magnesium carbonates have practically no effect on their structure, but addition of these humates to aqueous calcium sulfate suspensions results in recrystallization and rapid growth of the calcium sulfate crystals.

3. Calcium and magnesium carbonates influence structure formation in loess, causing formation of aggregates, the nature of the packing of which is the cause of the loose structure of loess.

4. Calcium sulfate in the pure form has practically no effect on structure formation in loess. In presence of humates, recrystallization of calcium sulfate occurs, with rapid growth of its crystals which, by binding the loess particles together, can form either large dense aggregates or structural frameworks which give rise to dense formations on the loess surface.

The alkaline extract of humic acids used in this investigation was kindly provided by Prof. S. N. Aleshin, to thom we express our gratitude. We also thank Prof. I. N. Antipov-Karataev for supplying samples of clay minerals.

The L. Ya. Karpov Physocochemical Institute
Moscow

Received September 7, 1956

LITERATURE CITED

[1] V. A. Obruchev, Trans. II International Conf. Assoc. for Studies of the Quaternary Period of Europe, No. 2, 115 (1933); Trans. V. V. Dokuchaev Soil Inst., 27, 23 (1948); L. S. Berg, Nature, No. 6, 445 (1947); No. 2, 107 (1929); Trans. II. International Conf. Assoc. for Studies of the Quaternary Period of Europe, No. 1, 68 (1932); S. S. Neustruev, Nature, No. 1-3, 47 (1925); I. P. Gerasimov, Bull. Acad. Sci. USSR, Geol.-Geophys. Ser., No. 1, 97 (1939); N. Ya. Denisov, Conctructional Properties of Loesses and Loesslike Loams, State Building and Architecture Press, Moscow (1953).

[2] R. V. Vilyams, Fundamentals of Soil Cultivation, 4th div. gen. Agric. Press, Moscow (1946); K. K. Gedroits, Selected Works, 1, 241 (1955); A. N. Sokolovsky, Pedology, No. 1, 3, (1933); Soil Physics, 5, 9 (1936); A. F. Tyulin, Pedology, No. 3, 9 (1940); Colloidochemical Studies of Soils for Agricultural Purposes, Agric. Press, Moscow (1946); I. N. Gorbunov, The Absorptive Capacity of Soil and Its Nature, Agric. Press, Moscow (1948); I. N. Antipov-Karataev, V. V. Kellerman, and V. V. Khan, Soil Aggregates and Methods of Their Investigation, Acad. Sci. USSR (1948); P. V. Vershinin and V. P. Konstantinova, Physicochemical Principles of Artificial Soil Structure, Agric. Press, Moscow-Leningrad (1935); G. Ya. Rozen, Nature, No. 5, 88 (1956); Z. S. Filippovich, Pedology, No. 2, 16 (1956); E. O. Sushko, Chemical Melioration of Soils, Agric. Press, Moscow-Leningrad (1936).

[3] A. N. Izyumov, Pedology, No. 10, 00 (1938);* I. A. Kaspirov, Pedology, No. 7, 60 (1940); Soil Crust and Its Prevention, Agric. Press, Moscow-Leningrad (1951); N. I Gorbunov and N. E. Bekarevich, Cotton Growing, No. 7, 52 (1951); Soil Crust in Cotton Irrigation, Acad. Sci. USSR Press, Moscow (1955); N. K. Balyabo, Increase of Soil Fertility in the Irrigated Cotton Zone of the USSR, Agric. Press, Moscow (1954); M. I. Lomonovich, Loess in Kazakhstan and Its Significance in the National Economy, Acad. Sci. Kazakh SSR Press, Alma-Ata (1955).

[4] I. N. Putilova, Practical Manual of Colloid Chemistry, Chem. Press, Moscow (1947); P. A. Rebinder, Synopsis of a General Course in Colloid Chemistry, Moscow State Univ. Press, Moscow (1950).

[5] Rebinder P., Disc. Far. Soc., No. 18, 151, 1954; E. E. Segalova, P. A. Rebinder, and O. P. Lukyanova, Bull. Moscow State Univ., 2, 17 (1954); N. V. Mikhailov and P. A. Rebinder, Colloid J., 17, 107 (1955).

[6] E. Aripov, Z. Ya. Berestneva, and V. A. Kargin, Colloid J., 19, 14 (1957).

---

* As in original — Publisher's note.

THE EFFECT OF AIR IONIZATION ON THE DISPERSE PHASE OF AEROCOLLOIDS

I. I. Belyaeva, A. E. Mikirov, and N. S. Smirnov

It was shown in the previous comunication [1] that artificial increase of air ionization by ultraviolet and X-rays and β-particles results in a 3-4 fold increase of the concentration of ultramicroscopic particles and a more than 10-fold increase of the number of condensation nuclei. Wilson [2] observed mists in pure moist air without water vapor supersaturation upon irradiation by "strong ultraviolet." M. Curie [3] introduced radon into small chambers (30-55 cc) and observed the formation of mists in air of relative humidity from 100 to 7 %; she noted that the mists were visible for 10-20 days after introduction of radon into the chambers and disappeared only when the radon concentration in the chamber fell considerably as the result of disintegration. Finally, Strieder et al. [4] irradiated pure moist air by X-rays and obtained mists at a relative humidity of ~ 100 %. Our object in the present work was to study the scattering power and stability of such mists.

EXPERIMENTAL

The optical system used in the experiments in shown in Fig. 1. Rays from the light source S, passing through the condenser K, the diaphgram D, and the objective O_1 are rendered parallel. The light then passes through the objective O_2 and reaches the screen E situated at the focus of the objective O_2 giving a real image of the diaphgram D of natural size. The screen is 3 × 3 mm. A photomultiplier type FEU-1 is situated behind the screen. The aerosol cell a-c, 1.6 liter in capacity with plane-parallel sides, was placed between the objectives O_1 and O_2. Thus, if no optical inhomogeneities are present between the objectives O_1 and O_2 (with the cell empty) no light reaches the photocathode, and the microammeter in the photomultiplier circuit registers the dark value of the current (I_0).

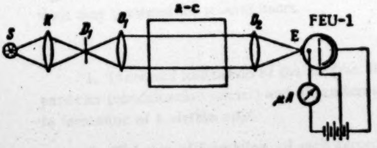

Fig. 1. Optical diagram of the experiments.

When an aerosol forms in the cell, the light scattered by the particles will pass around the black screen and reach the photocathode, and as a result current (I) will flow through the microammeter. The magnitude of this current is a measure of the scattering power of the mist, and depends on the concentration and size of the particles.

The optical diagram shows that the indicatrix of light scattering by the particles is rationally utilized. As is known [5], most of the light (80%) scattered by a particle is directed forward and is contained in an angle of 45-50°. This made it possible to measure fairly accurately variations of the scattering power of turbid media with time.

Ionization of the air in the cell (chamber) was effected by α-particles from Po^{210} of different activities by introduction of the sources into the chamber.

Results of Determinations. In all cases in which air of relative humidity not greater than 100% was ionized by a α-particles, a visible mist was formed, the rate of formation of which depended on the activity of the source. The mists were very stable in these humidity conditions, and were destroyed very slowly after removal of the radioactive source.

The increase of the light scattering power of the mist with the time of irradiation by sources differing in activity by one order of magnitude is given in Table 1.

TABLE 1

Light Scattering by Mist Formed as the Result of Irradiation of Moist Air by α-Particles

Activity of source 200 mcurie		Activity of source 20 mcurie	
Irradiation time, min.	Scattering power I/I_0	Irradiation time, min.	Scattering power I/I_0
00	1.00	00	1.00
20	1.02	30	1.00
45	1.09	70	1.01
50	1.12	85	1.03
55	1.22	115	1.06
60	1.37	130	1.08
65	1.42	160	1.12
		175	—

TABLE 2

Variation of Light Scattering by a Mist With Age

Age of mist in minutes	Scattering power I/I_0	Age of mist in minutes	Scattering power I/I_0
00	1.38	205	1.22
15	1.38	220	1.12
55	1.37	—	—
175	1.31	—	—

The same apparatus was used to determine the stability of the mists by the changes of their light scattering power with time.

After the radioactive source had been removed from the chamber, the scattering power of the mist decreased, and usually after several hours I/I_0 became practically equal to unity. The results of such a determination are given in Table 2.

The results of our experiments confirm the visual observations of Wilson [2], M. Curie [3], and Strieder et al. [4].

Moreover, our experimental data show that artificial increase of the ionization of moist air of relative humidity not over 100% not only increases the concentration of the submicroscopic condensation nuclei) and ultramicroscopic fractions of the disperse phase of aerocolloids [1], but produces a visible stable mist. Measurements of the light scattering power of such mists showed that it increases with irradiation time and source activity. For example, on irradiation by a source of 200 mcurie, a mist was formed in 5-10 minutes, and after 65 minutes its light scattering was 42% greater than that of the same air before irradiation. The action of a 20 mcurie source produced a mist visible after 20 minutes, and 175 minutes after irradiation the light scattering was 12% higher than before the irradiation. It was shown experimentally that such mists are stable; i. e., in our conditions they persisted for several hours.

SUMMARY

1. Increased ionization of the air (the dispersion medium) increases the concentration of submicroscopic particles (condensation nuclei) and ultramicroscopic fractions in the disperse phase of aerocolloids and results in formation of a visible mist.

2. The rate of formation of such aerocolloids depends on the activity of the ionizing radiation source, and therefore on the rate of formation and the concentration of ions in the dispersion medium.

3. Such mists are stable in the conditions studied, and increase light scattering by 12-40%, according to the activity of the source and the time of irradiation.

Geophysical Institute, Acad. Sci. USSR
Moscow

Received May 5, 1956

LITERATURE CITED

[1] K. M. Merzhanov, N. I. Peterimova, and N. S. Smirnov, Colloid J., 18, No. 5, 574 (1956).

[2] C. T. R. Wilson, Phil. Trans. Roy. Soc., London, Ser. A. 192, 403, 1899.

[3] M. Curie, C. r.*145, 1145, 1907.

[4] F. Strieder et al, Ann. Phys. 46, H−7, 989, 1915.

[5] See, e. g., K. S. Shifrin, Light Scattering in Turbid Media, GITTL (1951).

---

* C. r. = Comptes rend. − Publisher's note.

INTERMOLECULAR STRUCTURE OF HIGH POLYMERS.

COMMUNICATION 22. MODIFICATION OF THE MOLECULAR STRUCTURE OF HIGH POLYMERS BY THE INCLUSION METHOD

A. N. Bykov and A. B. Pakshver

Inclusion can serve as one of the methods for modifying the molecular structure of high polymers. By inclusion of molecules of an inert substance in the molecular structure of a polymer previously loosened by a substance which causes swelling, it is possible to preserve the loose structure. In this way it is possible to increase the reactivity of high polymers (cellulose, polyamides, acetylcellulose, etc.) in solution, dyeing, and sorption of acids and bases.

Only a few investigations, relating to hydrate cellulose fibers, and cellulose, have so far dealt with inclusion in high polymers. Nikitin [1], in a study of the esterification of cotton linters, noted that after preliminary swelling in water and treatment with pyridine (inclusion) cellulose is much more rapidly esterified. Hydrate cellulose treated with pyridine remained highly reactive even after drying.

Rogovin [3] attributes the increased reactivity of cellulose containing included substances to impossibility of removing the included substances for steric reasons. Because of the presence of the included substance within the fibers the distance between the macromolecules increases and formation of hydrogen bonds between adjacent macromolecules is hindered. Krässig [4] included various organic liquids: benzene, acetone, pyridine, etc., in cellulose swollen in water. The reactivity of the cellulose increased, and it reacted readily with hexamethylene diisocyanate, combining with up to 0.25 mole of hexamethylene diisocyanate per 1 mole of glucose residue. The result of inclusion treatment of cellulose depends both on the molecular size of the included substance, and on the degree of preliminary swelling of the cellulose or hydrate cellulose fibers.

No publications have yet appeared on inclusion in synthetic polymers, although Scharf [5], who studied the action of mineral and organic acids on polyamide fibers, was in fact dealing with inclusions in polyamides. The increased sorption of dye anions in the regions damaged by acid can only be explained by inclusions in the polyamide.

The present paper is the first communication on a series of investigations on modification of the molecular structure of high polymers by the inclusion method in order to increase their reactivity.

EXPERIMENTAL

The inclusion treatment was carried out as follows. A sample of the fiber, cellulose, or flake $\sim$2g in weight was treated with a substance causing swelling of the polymer and weakening the forces between the macromolecules. For polyamides, phenol solutions (15, 20, and 25 g/liter) and 15% H_2SO_4 solutions; for cellulose, 5 and 10% NaOH solutions; and for acetylcellulose, 10, 30 and 40% aqueous acetone solutions and 20% HCOOH solution were used for this purpose. The samples were pressed out after the treatment and the swelling liquid was replaced by the inclusion substance: benzene, acetone, alcohol, ether, or water (in the case of capron and acetylcellulose). The replacement was performed consecutively, for example:

Phenol (or NaOH) → water → alcohol → benzene (or ether)
Phenol (or NaOH) → water → acetone → benzene (or alcohol)
Acetone (or HCOOH) → water → alcohol → benzene (or ether)

The inclusion treatment time was 30 minutes for polyamides and 60 minutes for acetylcellulose and cellulose. The treatment temperature was 20°. The treated polymer was dried at 50° for 1 hour.

Various methods were used to evaluate the influence of inclusion on the polymer properties: sorption rates of dyes, acetic acid, and phenol; also, for polyamides, the time required for solution, the rate of dye sorption for acetylcellulose, and the rate of dye sorption and viscose filtration blockage coefficient for cellulose.

An acid brown dye was used for polyamide dyeing (pH 3: dyeing time 10 minutes). Acetic acid was used at 0.01 N concentration. The phenol used as the sorbed substance after inclusion had a concentration of 8 g/liter; the sorption time was 10 minutes. The amount of substance sorbed was determined from the concentrations in solution before and after treatment. The solubility of capron resin was determined in concentrated solution of calcium chloride in methyl alcohol at 60°.

The dye used for acetylcellulose was Acetoquinone Blue. The sulfite cellulose was previously shredded and treated with NaOH solution to remove hemicellulose.

Cellulose reactivity before and after the inclusion treatment was determined by the method of the All-Union Scientific Research Institute for Artificial Fibers [6], i. e., by the retardation of the filtration rate of viscose solution, and also by the rate of dye sorption (Congo Red, dyeing time 10 minutes, dye concentration 0.5 g/liter). The capron resin was reprecipitated from solution in 88% phenol. Ethyl alcohol was used to precipitate the resin from this solution.

The tensile strength and extensibility of the fibers were determined with the aid of a recording dynamometer.

Tables 1 and 2 give the results of studies of the effects of inclusion of various substances on the properties of polyamides (flake and fibers), cellulose, and acetylcellulose. The properties of the original polymers are taken as 100% in all cases.

These results show that polymer reactivity can be increased by inclusion in all cases. The sorption of dyes and acids by capron resin and fibers is increased by a factor of 1.4-2.2, and the sorption of phenol, nearly 4-fold. The solution time of carpon resin is decreased by 30%. Cellulose and acetylcellulose take up 1.2-1.8 times more dye after inclusion treatment.

The viscose-making properties of cellulose are also improved, and filtration blockage rate is considerably decreased. All this is explained by the fact that preliminary treatment of the polymer by the swelling agent causes rupture of intermolecular bonds and weakening of molecular interaction. This change of structure becomes fixed by incorporation of the included substance, the presence of which prevents re-intensification of the weakened forces between the macromolecules. The higher the concentration of the substance causing swelling of the high polymer, the greater is the inclusion effect and the reactivity of the treated polymer.

It is true that an increase of acetone concentration above 10% in the treatment of acetylcellulose somewhat lowers its reactivity (dye sorption). However, this is probably caused by removal of the more active low molecular portion of the acetylcellulose, soluble in 30-40% acetone solutions.

Some increase in the reactivity of the inclusion-treated polymer also occurs with increasing molecular weight of the inclusion substance. Sorption of dyes and acids increases somewhat, polyamide solution time decreases, and the viscose filtration blockage rate is lowered. It seems that an included substance of higher molecular weight, on incorporation between the polymer macromolecules, creates greater obstacles to the restoration of the molecular bonds broken during swelling.

Reprecipitation of capron resin leads to a sharp increase of reactivity, as the reprecipitated resin has a looser structure with fewer molecular bonds, and the active polyamide groups become more accessible to dyes and acids. The solution time of such resin is also considerably less. The physicomechanical properties of drawn capron yarn are changed by inclusion treatment: the fiber strength is decreased by 10-25%, and the extension at break increases by 25-30%.

TABLE 1

Effects of the Inclusion of Various Substances on the Properties of Capron Resin and Fibers

Substance studied	Swelling solution	Method of evaluation	% Change after inclusion (for 60 min. at 20°) of			
			benzene	acetone	ethyl alcohol	water
Capron resin	20 g/liter phenol	Dye sorption	163	138	138	—
		Solution time	68	65	71	—
Ditto, after reprecipitation*	20 g/liter phenol	Dye sorption	803	711	710	—
		Solution time	43	49	49	—
Undrawn capron yarn	25 g/liter phenol	Dye sorption	187	—	—	—
		Sorption of acetic acid	172	148	—	—
	15 g/liter phenol	Dye sorption	172	145	—	—
		Sorption of acetic acid	135	133	—	—
Ditto, drawn	Sorption of acetic acid	Sorption of phenol	390	329	—	245
		Tensile strength	81	71	—	79
		Extension at break	125	131	—	128

---

* After reprecipitation, capron flake without inclusion takes up 636% of dye and the solution time decreases to 57%.

TABLE 2

Effects of the Inclusion of Various Substances on the Properties of Cellulose and Acetylcellulose

Substance	Swelling solution	Method of evaluation	% Change after inclusion (for 60 min. at 20°) of			
			benzene	acetone	ethyl alcohol	ether
Sulfite cellulose*	5% NaOH	Filtration blockage rate	—	78	—	—
		Dye sorption	—	122	—	—
	10% NaOH	Filtration blockage rate	78	91	100	113
		Dye sorption	188	186	130	170 (вода)
Acetylcellulose	10% acetone	Dye sorption	154	—	—	—
	30% acetone	Ditto	128	—	—	130
	40% acetone	» »	99	—	—	—
	20% formic acid	» »	137	—	—	116

---

* All the data refer to sulfite cellulose from which hemicellulose had been removed by treatment with 17.5% NaOH solution. This treatment increases the filtration blockage rate to 158% and dye sorption to 115%.

SUMMARY

1. Inclusion treatment increases the reactivity of high polymers, considerably raising the sorption rates of dyes and acids by polyamides, and of dyes by acetylcellulose and cellulose.

2. The viscose-making properties of cellulose are improved and the solution times of polyamides are decreased.

3. The greater the preliminary weakening of the high polymer structure, the greater is the effect produced by the inclusion and the higher is the polymer reactivity.

LITERATURE CITED

[1] N. I. Nikitin, Paper Ind., No. 3, 38 (1941).

[2] H. Staudinger, W. Döhle, J. Heick, Prakt. Chem. 161, 191, 219, 1942; Staudinger H., Döhle W., Makr. Chem. 9, 2, 188, 1953.

[3] Z. A. Rogovin, High Molecular Compounds, No. 9, 1 (1949); Z. A. Rogovin and N. N. Shorygina, Chemistry of Cellulose and Associated Substances, State Chem. Press, p. 87 (1953).

[4] H. Krässig, Makr. Chem. 10, I, 1953; H. Krässig, E. Schroft, Bull. Inst. text. France, No. 49,47, 1954, Makr. Chem. 13, 2/3, 179, 1954.

[5] R. Scharf, Textil and Faserstoff, 5, No. 10, 573, 1955.

[6] All-Union State Standard 5982-51, Group K-51, Refined Viscose Cellulose, p. 10.

EQUILIBRIUM OF A VISCOPLASTIC DISPERSE SYSTEM ON A ROTATING DISK

A. M. Gutkin

Tyabin, Shklyar, Mosikhin, and Vinogradov [1] have described a centrifugal method for studying the rheological properties of greases, based on investigations of the equilibrium and flow of a thin layer of grease on a rotating disk. This method can be used for studying any viscoplastic disperse system. However, the theory of the method as put forward by the authors cannot be accepted as correct. The defects of the theory are largely due to the fact that it is based on the "general equation for the flow of a viscoplastic medium," proposed by M. V. Tyabin. Comments on this equation and on its practical applications have already been published [2].

The problem of equilibrium in a layer of a viscoplastic disperse system on a rotating disk is considered below. Since the case of the flow of the medium is not discussed, plastic viscosity does not enter the solution of the problem. This then reduces to the problem of the elasticoplastic equilibrium of the disk, differing in boundary conditions from the problem of elasticoplastic equilibrium of rotating disks which was examined by Sokolovsky [3]. The difference in boundary conditions significantly influences the method and solution of the problem.

Suppose that a layer of viscoplastic medium of thickness $\underline{h}$ lies on a disk rotating with angular velocity ω. It is assumed that adhesion takes place between the disk and the grease layer, i. e., that the displacement $\underline{u}$ of the medium on the disk surface is zero: $u_z = 0$ and $u_r = 0$ when $z = 0$. With these boundary conditions the problem can be solved in terms of deformations.

In the elastic deformation region the components of the stress tensors in a cylindrical system of coordinates are expressed as follows:

$$\sigma_r = -p + 2G\frac{\partial u_r}{\partial r}, \quad \sigma_\varphi = -p + 2G\frac{u_r}{r}, \quad \sigma_z = -p + 2G\frac{\partial u_z}{\partial z};$$

$$\tau_{rz} = G\left(\frac{\partial u_r}{\partial z} + \frac{\partial u_z}{\partial r}\right); \quad \tau_{r\varphi} = 0; \quad \tau_{z\varphi} = 0, \tag{1}$$

where G is the shearing modulus, $p = -{}^1/_3\ (\sigma_r + \sigma_\varphi + \sigma_z)$.

The equations

$$u_\varphi = 0; \quad \frac{\partial u_r}{\partial \varphi} = 0; \quad \frac{\partial u_z}{\partial \varphi} = 0$$

are a consequence of circular symmetry.

In the given conditions the equilibrium equations have the form:

$$\frac{\partial \sigma_r}{\partial r} + \frac{\partial \tau_{rz}}{\partial z} + \frac{\sigma_r - \sigma_\varphi}{r} + \rho\omega^2 r = 0; \tag{2}$$

$$\frac{\partial \tau_{rz}}{\partial r} + \frac{\partial \sigma_z}{\partial z} + \frac{\tau_{rz}}{r} = 0. \tag{3}$$

In addition to Equations (2) and (3), the equation for continuity of displacements must be satisfied:

$$\frac{\partial u_r}{\partial r} + \frac{u_r}{r} + \frac{\partial u_z}{\partial z} = 0. \qquad (4)$$

In order that Equation (4) should be satisfied identically, we introduce a certain function ψ, such that

$$u_r = -\frac{1}{r}\frac{\partial \psi}{\partial z}; \quad u_z = \frac{1}{r}\frac{\partial \psi}{\partial r}. \qquad (5)$$

Replacing the stress tensor components in Equations (2) and (3) by their expressions in the form of (1) where displacements are first expressed in terms of ψ, we have:

$$-\frac{\partial p}{\partial r} = \frac{G}{r}\frac{\partial}{\partial z}\Delta\psi - \rho\omega^2 r; \qquad (6)$$

$$\frac{\partial p}{\partial z} = \frac{G}{r}\frac{\partial}{\partial z}\Delta\psi, \qquad (7)$$

where Δ denotes the operator

$$\Delta = \frac{\partial^2}{\partial r^2} - \frac{1}{r}\frac{\partial}{\partial r} + \frac{\partial^2}{\partial z^2}. \qquad (8)$$

Eliminating p from Equations (6) and (7), we have a differential equation for ψ:

$$\Delta\Delta\psi = 0. \qquad (9)$$

Differential Equation (9) must be solved for the boundary conditions:

$$\frac{1}{r}\cdot\frac{\partial \psi}{\partial r} = 0, \ \frac{1}{r}\frac{\sigma \psi}{\partial z} = 0, \qquad \text{when } z = 0; \qquad (10)$$

$$\tau_{rz} = G\left(\frac{\partial u_r}{\partial z} + \frac{\partial u_z}{\partial r}\right) = 0, \ \sigma_z = 0, \qquad \text{when } z = h. \qquad (11)$$

The medium is assumed to be unlimited in the direction r. The function ψ is found to be:

$$\psi = r^2(az^3 + bz^2).$$

The constants a and b are to be determined from the boundary conditions (11), which have not yet been satisfied.

Since $\frac{\partial u_z}{\partial r} = 0$ everywhere, it follows from the first boundary condition in (11) that

$$\frac{\partial u_r}{\partial z} = -r(6az + 2b) = 0, \quad \text{when } z = h,$$

and hence

$$6ah + 2b = 0 \tag{12}$$

The second boundary condition in (11) may be transformed into

$$\frac{\partial p}{\partial r} = 0, \text{ when } z = h \tag{13}$$

From Equation (6) it follows that

$$-\frac{\partial p}{\partial r} = r(6aG - \rho\omega^2).$$

To satisfy Condition (13), the following equation must be true:

$$6aG = \rho\omega^2. \tag{14}$$

From Equations (12) and (14) the constants a and b can be found. Thereby the function ϕ and the values of u_r, u_z, τ_{rz} are also found.

The pressure p is found to be

$$p = \rho\omega^2 (z - h)^2. \tag{15}$$

The boundary of the elastic deformation zone is found from the condition

$$\frac{1}{6}[(\sigma_r - \sigma_z)^2 + (\sigma_z - \sigma_\varphi)^2 + (\sigma_r - \sigma_\varphi)^2] + \tau_{rz}^2 = \theta^2, \tag{16}$$

i. e., by equating the tangential stress intensities to the yield stress.

Equation (16) leads to equation for the boundary surface separating the elastic and plastic deformation regions:

$$\rho^2\omega^4 [3z^2 (z - 2h)^2 + r^2 (z - h)^2] = \theta^2. \tag{17}$$

If the thickness of the layer is small, the first term in the square brackets may be neglected, and Equation (17) is simplied to

$$\rho\omega^2 r (h - z) = \theta. \tag{18}$$

Thus, the region of plastic deformation approaches most closely to the axis of the disk at the periphery

$$z = 0, \; r_0 = \frac{\theta}{\rho\omega^2 h}. \tag{19}$$

If r_0 is known, θ can be found:

$$\theta = \rho\omega^2 r_0 h. \tag{20}$$

If the radius of the layer is less than or equal to r_{θ}, the medium will not flow.

The solution found for this case is not exact, as the medium is assumed to be unlimited in the direction of the axis $\underline{r}$. The boundary conditions for the lateral surface of the layer of medium therefore did not enter into the formulation of the problem. However, the error introduced if the boundary conditions at the lateral surface are not satisfied cannot be large, because the height of the layer is small.

If the radius of the layer is greater than r_{θ} the medium will flow and the position of the elastic zone boundary will depend not only on θ, but also on the viscosity and flow rates. Formula (20) can be used to find θ experimentally, by studying the behavior of the medium on a rotating disk. The formula gives the most accurate results if the layer of medium with radius R is applied and the angular velocity is then gradually increased until the medium begins to flow.

Let us determine the yield value of a lubricant grease by means of Formula (20) on the basis of the experimental results described in [1]. The results treated in this way are given in the table.

Table of Yield Values

Revolutions of disk per min.	Radius of elastic zone in cm	Height of grease layer in elastic zone, in mm	θ calculated from Formula (20), in dynes/cm²
400	5.6	3	3000
500	4.3	3	3000
600	3.75	3	4500
700	3.4	2.8	5000
800	2.8	2.8	5000
900	2.5	2.5	5000
1200	1.75	2.3	6400
1600	1.15	1.8	5900

The values of θ found from the results of the first three experiments must be considered low, as the radii of the elastic zone in these experiments were less than the radii calculated from Formula (20). The reason for this was that, in addition to its plastic properties, the viscous properties of the grease also influenced its behavior, as in these experiments the viscoplastic grease covered the whole disk and was in a state of flow on it before the measurements were made.

The last five experimental determinations give values for the yield stress of the grease which are in fairly good agreement with each other. These values are close to the yield value (6000 dynes /cm²) which, as is noted by the authors [1], was obtained by K. I. Klimov for this grease by another method.

SUMMARY

1. Deformation and stress distributions in a layer of a plastic medium in equilibrium on a rotating disk have been determined.

2. A relationship has been derived between the limiting radii of the medium in the equilibrium state and the yield value.

3. The formula has been used to calculate yield values from the experimental results of N. V. Tyabin, L. A. Shklyar, E. P. Mosikhin, and G. V. Vinogradov.

The Molotov Institute of Power Engineering
Moscow

Received March 26, 1957

LITERATURE CITED

[1] N. V. Tyabin, L. A. Shklyar, E. P. Mosikhin, and G. V. Vinogradov, Trans. S. M. Kirov Inst. Chem. Tech., Kazan, No. 16, Tatar State Press, Kazan (1951).

[2] M. P. Volarovich and A. M. Gutkin, Colloid J., 15, No. 2 (1953).*

[3] V. V. Sokolovsky, Theory of Plasticity, State Tech. Theoret. Press, Moscow–Leningrad (1950).

---

* Original Russian pagination. See C. B. translation.

INVESTIGATION OF THE STRUCTURE AND PROPERTIES OF CARBON CHAIN POLYMERS IN DILUTE SOLUTIONS

2. SOLUTIONS OF VINYL CHLORIDE – ACRYLONITRILE COPOLYMER

S. G. Zelikman and N. V. Mikhailov

Copolymerization is one of the most widely used methods for the production of polymers with a great variety of properties. Copolymers are becoming increasingly important in the production of synthetic fibers. At the present time fibers based on caprolactam and AH salt copolymers (trelon, efrelon), acrylonitrile and vinyl acetate, acrylonitrile with small amounts of other monomers, etc., are widely used.

Synthetic fibers made from vinyl chloride – acrylonitrile copolymer have certain specific properties which distinguish them advantageously from most other types of carbon chain fibers. These properties include high stability to heat and light, easier dyeing, stability in many organic solvents, absence of shrinkage, and high strength in the wet and dry states. Because of the good fiber properties and wide availability of the raw materials, this is one of the most promising copolymers [1].

The present paper describes a study of the properties of vinyl chloride – acrylonitrile copolymers. The properties of the pure polymers were described previously [2].

EXPERIMENTAL

Three copolymers were used for the study, with the following ratios of acrylonitrile to vinyl chloride: 40:60, 29:71, and 13:87% by weight. The physicochemical properties of these copolymers and methods for their fractionation have not been described in the literature.

The 40:60 and 29:71 copolymers were fractionated from acetone solutions. The solvent used for the copolymer containing 13% acrylonitrile was a 5:1 mixture of acetone with dimethylformamide.

The fractionation procedure for the 40:60 copolymer was as follows: a mixture of methanol and acetone (10:13) was added dropwise with stirring to a 2% solution of the copolymer in acetone until a flocculent precipitate was formed. After settling and decantantion the precipitate was washed with methanol and dried. These operations were repeated to precipitate the following fractions. The last fraction was precipitated by an excess of pure methanol. The copolymers containing 29 and 13% acrylonitrile were precipitated by a 3:1 mixture of acetone and water. The last fraction was precipitated by an excess of water. Three fractions, differing in specific viscosity, were isolated from each of the copolymers. These fractions were used for studying the viscosity and osmotic pressure of the copolymers. The nitrogen contents of the fractions were determined by the Kjeldahl method. It was found that the fractions of a given copolymer, while differing in molecular weight, had equal nitrile group contents. The differences between the fractions corresponded to ~ 0.5% nitrile groups, which is within the error limits of the nitrogen determination.

The variations of viscosity with concentration in the 0.25-1.0% range, and also variations of viscosity with temperature (from 20 to 60°) were studied for all the copolymers. The osmotic pressure was determined at 20, 35, and 50°. To determine molecular weights, π/c graphs were used and the reduced osmotic pressures were extrapolated to zero concentration. The methods of viscosity and osmotic pressure determinations were described previously [2].

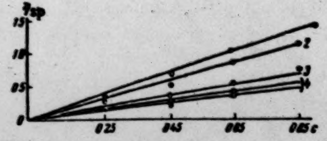

Fig. 1. Variation of specific viscosity with concentration of copolymer solutions: 1) fraction I of 40:60 copolymer; 2) fraction I of 29:71 copolymer; 3) fraction I of 13:87 copolymer; 4) fraction III of copolymers of all compositions.

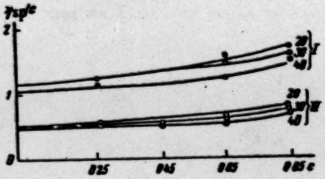

Fig. 2. Variation of reduced viscosity at 20, 30, and 40° with concentration of 40:60 copolymers: I) fraction I, mol. wt. 54,000; III) fraction III, mol. wt. 30,000.

TABLE 1.

Molecular Weights of Copolymer Fractions at 20,35, and 50°

Copolymer	Fraction	Molecular weight of copolymer at temperature, °C		
		20	35	50
Copolymer 40 : 60	I	54 000	53 000	48 000
	III	30 000	30 000	30 000
Copolymer 29 : 71	I	53 000	52 000	51 000
	III	33 000	32 000	32 000
Copolymer 13 : 87	I	55 000	55 000	52 000

The variations of specific and reduced viscosity with concentration for copolymers of different composition are shown in Figs. 1,2, and 3.

The variation of viscosity with temperature for fraction I of the 40:60 copolymer is shown in Fig. 4. In the temperature range studied, the variation of specific viscosity with temperature was linear for all the copolymers. The slope of the $\eta_{sp} - t$ curves depends on the molecular weight of the fractions and the solution concentration: the slope increases with increasing molecular weight and concentration.

As is seen from Figs. 2 and 3, the relationship between reduced viscosity and concentration is practically linear for all the copolymers in the concentration region 0.25 – 0.85%. Figure 5 shows the variation of reduced osmotic pressure with concentration for the two extreme fractions (I and III) of all the copolymers at 20, 35, and 50°. The molecular weights of the copolymers are given in Table 1.

Table 1 shows that the molecular weights of any given copolymer fraction practically coincide at different temperatures. The molecular weight variations with the temperature are very small, and are within the limits of experimental error.

Thus, like the pure polyvinyl chloride and polyacrylonitrile polymers, their copolymers W of various compositions form true solutions at infinite dilution, and no molecular aggregation occurs. The absence of aggregation is also indicated by the linear course of the $\eta_{sp} - c$ curves. A comparison of the copolymer properties shows that the viscosities of the copolymers of all compositions practically coincide at low molecular weights (fraction III). Some differences are found for the fractions of higher molecular weight (Fig. 6).

The curve shows that copolymer viscosity increases with increasing nitrile group content. Small deviations from additivity are found even for dilute solutions (0.65%). To evaluate the flexibility of the copolymers studied, the values of μ were calculated (Table 2).

A comparison of the values of μ for polymer fractions of approximately equal molecular weight shows that the 40:60 polymer has the greatest flexibility. The flexibility of copolymers with lower nitrile group contents approaches the flexibility of polyvinyl chloride. Variations of μ with composition (for fractions of similar molecular weight) are shown in Fig. 7.

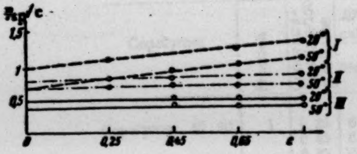

Fig. 3. Variation of reduced viscosity at 20 and 50° with concentration: I) fraction I of 29:71 copolymer; II) fraction I of 13:87 copolymer; III) fraction III of 29:71 and 13.87 copolymers.

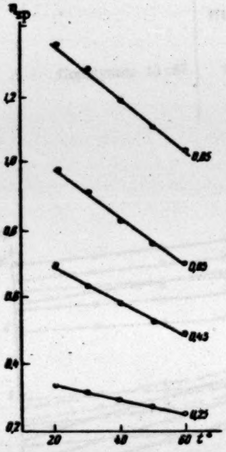

Fig. 4. Variation of specific viscosity of 40:60 copolymer with temperature at different concentrations.

TABLE 2

Values of μ for Copolymers of Different Compositions

Copolymer	Molecular weight of fraction	μ
Copolymer 40:60	54 000 30 000	0.38 0,46
Copolymer 29:71	53 000 33 000	0.41 0.47
Copolymer 13:87	55 000	0.44

This leads to the conclusion that copolymer flexibility decreases with decreasing molecular weight. Copolymers of all compositions with molecular weight ~ 30,000 fraction III), and polyacrylonitrile, consist of rigid molecular chains. These results agree with the findings of Flory [3] and Lang and Münster [4] that the second virial coefficient of osmotic pressure depends on the molecular weight of the polymer.

The temperature – osmotic pressure relationship was used to calculate the changes in the thermodynamic functions (free energy ΔF, enthalpy ΔH, and entropy ΔS); the results are given in Table 3.

The appreciable differences between the properties of the copolymers and the pure polymers can probably be explained if the dipole interactions of the CN and Cl groups are taken into account. Both polyvinyl chloride and polyacrylonitrile are polar polymers. The dipole moment of Cl^- (for example, in 1,3-dichloropropane) is $2.5 \cdot 10^{-18}$, and the dipole moment of nitrile group is $3.5 \cdot 10^{-18}$. In the case of copolymers a decrease of polymer polarity caused by intramolecular action between Cl and CN groups can probably be assumed. In fact, introduction of CN groups into the polyvinyl chloride molecule disturbs the regular arrangement of the chain segments, which favors easier coiling of the molecules into globules. If a Cl group is then found close to a nitrile group carbon, dipole attraction will prevail over repulsion.

In presence of such intramolecular saturation, the polarity of the molecules should decrease somewhat, and this should lead to increased polymer flexibility, decrease of intermolecular interaction, increased solubility, etc. Similar views on dipole interaction within molecular polymer chains were advanced earlier by Mikhailov [5].

This view is confirmed by studies of the properties of mixtures of pure polymers, in which fairly stable (CN – Cl) bonds are formed between the molecules, leading to considerable changes in the behavior of such mixtures in solution and in the solid state.

TABLE 3

Changes of the Thermodynamic Functions for Copolymers of Various Compositions (dimethylformamide solvent)

Copolymer	Fraction	Concentration in g/100 g solution	$\Delta F_1 \cdot 10^3$ cal./mole			$\Delta H_1 \cdot 10^3$ cal./mole		$\Delta S_{1\,exp} \cdot 10^3$ cal./mole		$\Delta S_{1\,id} \cdot 10^3$ cal./mole
			293° K	308° K	323° K	300,5° K	315,5° K	300,5° K	315,0° K	
Copolymer 40 : 60	I	0.25	0.213	0.231	0.274	0.14	0.65	1.2	2.8	0.65
		0.45	0.394	0.428	0.496	0.27	0.95	2.3	4.5	1.20
		0.65	0.565	0.625	0.736	0.60	1.65	4.0	7.4	1.75
		0.85	0.907	0.981	1.113	0.54	1.73	2.3	11.2	2.30
	III	0.25	0.385	0.411	0.428	0.12	0.06	1.7	1.1	1.20
		0.45	0.702	0.753	0.796	0.30	0.13	3.4	2.8	2.16
		0.65	1.044	1.096	1.164	0.03	0.30	3.6	4.5	3.17
		0.85	1.370	1.438	1.506	—0.05	—0.03	4.5	4.5	4.55
Copolymer 29 : 71	I	0.25	0.231	0.240	0.257	0	0.10	0.6	1.1	0.69
		0.45	0.411	0.445	0.487	0.25	0.45	2.2	2.9	1.29
		0.65	0.605	0.659	0.727	0.45	0.56	3.6	3.9	1.70
		0.85	0.976	1.079	1.198	1.04	1.37	6.9	8.0	2.35
	III	0.25	0.342	0.368	0.394	0.17	0.17	1.7	2.3	1.10
		0.45	0.608	0.651	0.719	0.05	0.75	4.6	4.5	1.98
		0.65	0.873	0.913	1.027	—0.23	1.38	6.3	6.3	2.90
Copolymer 13 : 87	I	0.25	0.184	0.223	0.257	0.49	0.47	2.3	2.3	0.64
		0.45	0.351	0.411	0.462	0.82	0.64	4.0	3.4	1.20
		0.65	0.514	0.599	0.676	1.15	0.98	5.7	5.1	1.69
		0.85	—	0.907	1.027	—	1.56	—	8.0	2.25

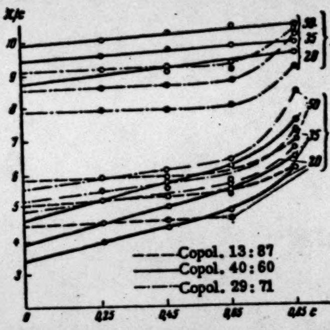

Fig. 5. Variation of reduced osmotic pressure with concentration; I) fraction I of all copolymers; III) fraction III of all copolymers.

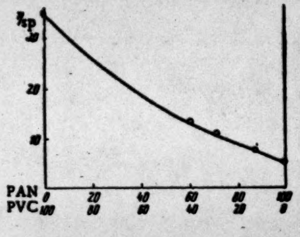

Fig. 6. Specific viscosity of 0.65% solutions as a function of the composition (PAN = polyacrylonitrile, PVC = polyvinyl chloride).

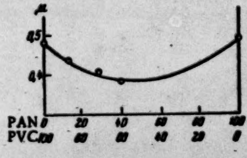

Fig. 7. Values of the constant μ as a function of the composition for polymers of similar molecular weight.

SUMMARY

1. The variation of the viscosity of vinyl chloride — acrylonitrile copolymers of various compositions with temperature has been studied in the range 20-60°; the specific and intrinsic viscosities of the copolymers in dimethylformamide have been determined.

2. The molecular weights of copolymer fractions have been determined at 20, 35, and 50° (by the osmotic method) and the changes in their thermodynamic functions have been calculated.

3. The view is put forward that the differences in the copolymer properties (increased solubility and molecular flexibility, decreased solution viscosity, change in the heat stability) are explained not only by the irregular structure of the copolymers, but also by intramolecular interaction between polar groups; in this instance, between chlorine and carbon of the nitrile groups.

All-Union Scientific Research Institute
for Artificial Fibers, Mytishchi

Received August 2, 1955

LITERATURE CITED

[1] Z. A. Rogovin, Chemistry and Technology of Artificial Fibers, State Light Industry Press (1952).

[2] N. V. Mikhailov and S. G. Zelikman, Colloid J., 18, No. 6, 717 (1956).

[3] P. Flory, J. Chem. Phys. 13, 453, (1945).

[4] X. Lang, A. Münster, Naturwissenschaft. 3, 68 (1946).

[5] G. P. Mikhailov, Progr. Chem., 24, No. 7, 875 (1955).

DISTRIBUTION OF A WEAK ELECTROLYTE IN THE DOUBLE LAYER

I. G. Ivanter

The existing theory of strong electrolytes [1] is based on the assumption that a self-consistent field may be used. • The distribution of positive and negative ions is therefore purely Boltzmann in character. It is natural to assume that the existence of a relationship between the dissociation constant and the field strength must influence this distribution in some way [2]. The derivation of this distribution must be based not on the existence of a self-consistent field, but on the general Gibbs method.

Debye and Hückel applied the idea of a self-consistent field [2] to calculating the deviations from ideality of the thermodynamic functions of dilute solutions of strong electrolytes. Fowler [3] derived the condition for the applicability of the self-consistent field to dilute neutral solutions of strong electrolytes. Kramers [4] calculated the statistical integral and found the deviations of the thermodynamic functions from ideality without using the self-consistent field concept. Although the self-consistent field method can be applied to neutral solutions only at very low concentrations, it has been used by various authors for calculations of interactions in the ionic double layer, where the ionic concentrations can by no means be regarded as low. In establishing the applicability of this method to ionic double layers, Frenkel [5] pointed out that the slow decrease of the field with distance (in proportion to $1/r$) should result in small fluctuations, and thus make the use of the self-consistent field legitimate. However, at first sight Fowler's work appears to contradict this. Moreover, the view is widely held that the self-consistent field may be used up to concentrations at which the interaction between two particles is less than the thermal energy, i. e., until $e^2/r_{ij} \ll kT$.

It will be shown that Fowler's calculations are applicable only to neutral solutions, •• and that when repulsive forces are predominant the self-consistent field may in any case be used up to concentrations at which intermolecular forces begin to operate.

Application of the Fowler Method to Double Layers of Strong Electrolytes

Fowler considers the statistical integral (partition function)

$$B(T) = \int \ldots \int e^{-U/kT} \, d\Gamma \text{ •••}$$

• The self-consistent field method is an approximate method in which the interaction energy between particles is replaced by the sum of the interaction energies of one particle with the others. The latter set up a force field with the property that the probability distribution of each particle in this field is $\sim e^{-e\varphi/kT}$ and with this density distribution the particles themselves create this field, which is termed self-consistent.

•• Here and subsequently this refers to the electric charge and not acidity.

••• U is the potential energy of particle interactions as a function of their coordinates, the product of the differentials of which is expressed conventionally as $d\Gamma^d$.

and, if U contains long-range forces, he formally introduces the function W, defined by

$$Ce^{-W/kT} = \int\ldots\int e^{-U/kT}\,d\Gamma'^{i}, \tag{1}$$

where the integral is not taken over the coordinates of the i-th particle.

In a double layer of strong electrolytes, in the absence of specific adsorption forces, U represents the interaction energy of the charged particles among themselves and with the external field

$$U = e^2 \sum_{ij} \frac{Z_j Z_i}{r_{ij}} + \sum_i e Z_i \varphi_0,$$

where φ_0 is the external field.

Differentiating Equation (1) with respect to x_i,

$$\frac{\partial W}{\partial x_i} \cdot Ce^{-\frac{W}{kT}} = \int\ldots\int e^{-U/kT} \frac{\partial U}{\partial x_i}\, d\Gamma'_i$$

or

$$\frac{\partial W}{\partial x_i} \cdot Ce^{-W/kT} = \frac{\partial W}{\partial x_i} \int\ldots\int e^{-U/kT}\, d\Gamma'_i = \int\ldots\int e^{-U/kT} \frac{\partial U}{\partial x_i}\, d\Gamma'_i. \tag{2}$$

Fowler [3] points out that W in Equation (2) can be interpreted as the average energy of the i-th particle.

After differentiating again, performing the same operations with respect to y_i and z_i, and adding the three equations, we have:

$$\begin{aligned} &\left[\Delta W - \frac{1}{kT} \sum_{\alpha=1}^{3} \left(\frac{\partial W}{\partial x_{i_\alpha}}\right)^2\right] \cdot \int\ldots\int e^{-U/kT}\, d\Gamma^{i'} = \\ &= \int\ldots\int e^{-U/kT} \left[\Delta_i U - \frac{1}{kT} \sum_{\alpha=1}^{3} \left(\frac{\partial U}{\partial x_{i_\alpha}}\right)^2\right] d\Gamma^{i'}. \end{aligned} \tag{3}$$

Fowler notes that the electrostatic energy U_i always satisfies Laplace's equation

$$\Delta_i U_i = -\frac{4\pi\rho e_i}{D},$$

and therefore

$$\Delta W + \frac{4\pi\bar{\rho}e_i}{D} = \frac{1}{kT}\sum_{\alpha=1}^{3}\left[\left(\frac{\partial W}{\partial x_{i_\alpha}}\right)^2 - \overline{\left(\frac{\partial U}{\partial x_{i_\alpha}}\right)^2}\right], \tag{3a}$$

from which we can find the root mean square deviation of the force acting on the i-th particle.

In evaluating the applicability of the Debye–Hückel theory, Fowler assumed that the deviations will be small if $\frac{\partial W}{\partial x_i}$ is mainly determined by a constant field which does not depend on the particle distribution. However, this evaluation cannot be applied to a charged electrolyte. As will be shown, the field formed by the particles distributed in it is stable in a number of cases. This is because the root mean square deviation of the derivative of the energy from its mean value will be much less than the mean value itself, if it is possible to divide the region of the double layer into a large number of layers, in each of which the difference between the space-average of the density at any time and its time-average is much less than the latter. A more exact evaluation may be obtained directly from Equations (3) and (3a).

For simplicity, we consider the one-dimensional case:

$$\left[\left(\frac{\partial W}{\partial x_i}\right)^2 - \overline{\left(\frac{\partial U}{\partial x_i}\right)^2}\right] = \overline{\left[\frac{\partial W}{\partial x_i} - \frac{\partial U}{\partial x_i}\right]^2} = e^4\,\overline{\left[\int_0^x \{\bar{f}(\xi) - f(\xi)\}\,d\xi\right]^2}. \tag{4}$$

But, since the greatest density deviations occur when the deviations are independent and the numbers of particles are not related in a way such that an increase of their number in one region results in a decrease in another, we have

$$\int_0^x [\bar{f}(\xi) - f(\xi)]\,d\xi = \int_0^{\Delta x} [\bar{f}(\xi) - f(\xi)]\,d\xi = [\bar{f}(\xi^*) - f(\xi^{**})]\,\Delta x \tag{4a}$$

ξ^* and ξ^{**} lie between 0 and Δx. It is assumed that the greatest deviations exist in the neighborhood of 0; here Δx is a layer for which it is still permissible to introduce an average density.

However, for the particle density we have, according to Equation (4), $\overline{(f - \bar{f})^2} = \frac{\bar{f}}{d\Gamma}$ and hence

$$\overline{[f(\xi^*) - f(\xi^{**})]^2\,(\Delta x)^2} = \frac{\bar{f}\,(\Delta x)^2}{d\Gamma}. \tag{4b}$$

Here f is normalized to the density in the volume d Γ. Substitution of Equation (4b) into Equation (4) gives

$$\left[\left(\frac{\partial W}{\partial x}\right)^2 - \left(\frac{\partial U}{\partial x}\right)^2\right] = \frac{e^4\,\bar{f}\,(\Delta x)^2}{d\Gamma}\,.$$

By comparing the terms in Equation (3a), we can formulate the condition:

$$\bar{f}e^2 4\pi \,/\, D > \bar{f}e^4\,(\Delta x)^2 \,/\, d\Gamma kT$$

or

$$1 > De^2\,(\Delta x)^2 \,/\, 4\pi\, d\Gamma\, kT. \tag{5}$$

However, to satisfy Equation (4a) it is necessary that f (ξ •) differ little from (ξ •'), otherwise it is necessary to consider large values of Δx, i. e., Δx may be decreased so long as the deviations of the density from the mean are small. In other words, the approximation in question becomes increasingly valid if we can increase the number of parts into which we can divide the whole space interval over which the potential changes; these parts must however, be such that in each one the deviation of the particle density is small, i. e., $\sqrt{(\bar{f} - f)^2} \ll \bar{f}$

We shall use the Boltzmann distribution for the evaluation; f (ξ •') and f (ξ•) should not differ greatly. Primes denote average values at a given interval. We require that

$$f(\xi^{*}) - f(\xi^{*\prime}) = B\left(e^{-e\varphi^{*}/kT} - e^{-e\varphi^{*\prime}/kT}\right) < Be^{-\varphi^{*}e/kT}$$

or

$$1 - e^{-(\varphi^{*\prime} - \varphi^{*})/kT} < 1, \text{ i. e., } \varphi^{*} - \varphi^{*\prime} < \frac{kT}{e}\,. \tag{6}$$

On the other hand, it is also necessary that

$$\overline{f(\xi)^2} > \overline{[f(\xi) - \overline{f(\xi)}]^2} \doteq \frac{\bar{f}(\xi)}{d\Gamma} = \frac{\bar{f}(\xi)}{\Delta x\,\Delta y\,\Delta z} = \frac{\bar{f}(\xi)\,\varphi'_x}{\Delta y\,\Delta z\,\Delta\varphi} = \frac{\bar{f}(\xi)\cdot\varphi'_x}{\Delta y\,\Delta z\,\rho kT/e}\,. \tag{7}$$

But, from the first integral of the Laplace – Boltzmann equation we have:

$$\varphi'_x \sim \left(\sqrt{\Lambda cK}\, kT\right)^{1/2} \cdot e^{-\varphi e/2kT}; \tag{8}$$

the number of particles is

$$dn = \sqrt{cKA}\, e^{-\varphi e/kT}\, dx\, dy\, dz \tag{8a}$$

where $\sqrt{cKA}$ is the density in the volume. Substituting the values of the densities $f(\xi) = Be^{-\varphi e/kT}$ and $f(\xi') = Be^{-\varphi' e/kT}$ into Equation (7), taking into account (8) and (8a), we have

$$e / \sqrt{kT}\, p\Delta y\Delta z < (cKA)^{\frac{1}{4}} \cdot e^{-\varphi e/2kT}, \tag{9}$$

where 1/p is the number of subdivisions. Condition (9) is satisfied even for very small values of p.

$$P_{\text{lim}} = \frac{e \exp(\varphi e / 2kT)}{\sqrt{kT}\, \Delta y\, \Delta z.(cKA)^{1/4}};$$

$$\Delta x_{\text{lim}} = \frac{pkT}{e\varphi'_x} = \frac{1}{\Delta y\, \Delta z}\, \frac{1}{f(\xi)} = \frac{1}{\Delta y\, \Delta z}\, \frac{1}{\sqrt{cKA}}\, e^{-\varphi e/kT}; \tag{10}$$

where A is Avogadro's number; K is the dissociation constant. Thus by the set of Equations (6) and (10) we have shown that application of an average self-consistent field to strong electrolytes is quite legitimate for double layers of sufficient extent. This has been demonstrated here for a plane double layer, but it must be pointed out that the proof may be extended to cases involving several variables with the condition that sufficiently large electrodes are considered. It must be pointed out that fluctuations decrease with increasing ion concentration in the double layer. The above considerations, however, do not apply if it is not possible to select a macroscopic volume $d\Gamma$, or exact $\Delta y\Delta z$, which is the case for neutral solutions, for which Fowler's reasoning is valid.

Distribution of a Weak Electrolyte in the Double Layer

As for strong electrolytes, we consider the statistical integral

$$B(T) = \int \cdot \cdot \cdot \int e^{-U/kT}\, d\Gamma. \tag{11}$$

Since the dissociation energy plays an important role in consideration of weak electrolytes, we introduce intramolecular energy and forces into our reasoning. The average values of these forces may depend on the surrounding medium.

We shall consider ions only, and a distinction is made between their situation within and outside the molecular volume. The energy of the system will be given by the sum of the energies of all the ions. We first consider a binary 1:1 electrolyte. The energy U of the whole system is

$$U = \sum_{ij} \left\{ \left[Z_i \frac{e^2 Z_j}{D r_{ij}} + e Z_i \varphi_0 \right] (1 - \bar{\delta}_{r_{ij}}) + W_{\text{mol}} \bar{\delta}_{r_{ij}}, \right.$$

where $\bar{\delta}_{r_{ik}} = 1$, if $Z_k = Z_i$, r_{ik} within the molecular volume,

$x\bar{\delta} r_{ik} = 0$, if $Z_k = Z_i$,

$\delta_{r_{ik}} = 0$, is outside the molecular volume.

A function of this type was used by Kramers [4] for calculation of deviations of thermodynamic functions from ideality; this was required in order to make the integral convergent.

We first determine the probability (P_{lm}) of the l-th positive ion forming a molecule with the m-th negative ion. This is the same as finding the probability of the l-th positive ion being in the volume of the m-th negative ion, and we must integrate along the coordinate of the m-th negative ion

$$P_{lm} = \frac{1}{B(T)} \int dV_m \int d\Gamma^{*ml} \left(\exp \left[\frac{1}{kT} \sum_{ij}^{ml} \ldots \right] \right) \int e^{-1/kT} W_{\text{mol}\, lm}\, dV_l.$$

The integration with respect to $d\Gamma^*$ is performed for all the volumes except the molecular volume of the m-th ion, and with respect to dV_l, for the molecular volume of the m-th ion. The sum of the probabilities that all the particles will be in the molecular state or, after appropriate rearrangement, the average number of molecules at the point $\vec{r}$ is given by

$$N_{\text{mol}\,(\vec{r})} = \frac{N_0 d\vec{r}}{B(T)} \int d\Gamma^{*ml}\, (iden) \int\limits_{\substack{\text{molecular volume} \\ \text{around } \vec{r}}} e^{-1/kT} W_{\text{mol}\, lm}\, dV_l, \qquad (12)$$

where the integration is performed as stated above; N_0 is the total number of molecules.

The probability of the i-th ion being in the unbound state is:

$$P_i = \frac{1}{B(t)} \int dV_i \int \exp \left\{ - \frac{1}{kT} \left[\sum_{qs} \left(\frac{Z_q Z_s}{D r_{qs}} + e r_q \varphi_0 \right) (1 - \bar{\delta}_{r_{qs}}) + W_{\text{mol}}\, \bar{\delta}_{r_{qs}} \right] d\Gamma'^i. \right. \qquad (13)$$

Correspondingly, the average number of ions around a certain point $\vec{r}$ will be obtained if in Equation (13) integration over the whole volume of the i-th ion is replaced by integration around a fixed point only, followed by multiplication by the total number of ions.

As was done by Fowler, we formally introduce the function ω_{mol}, defined by the following equation:

$$Ce^{-\omega_{mol}/kT} =$$

$$= \int \ldots d\Gamma^{*ij} e^{-\sum_{kn}^{*ij} (W_{kn\,electr} + W_k + W_{kn\,mol})} \int\limits_{around\ \vec{r}_j} e^{-W_{ij\,mol}/kT}\, dV_i .$$

It is easily shown by differentiation that ω_{mol} is the average energy. It must be noted that the average value with respect to the inner integral is the most important $W_{kn_{mol}}$ represents the sum of the energies of interaction between the k-th and n-th particles and between each of these and each of the others, with the condition that they are all in direct proximity. In some important cases it is possible to neglect, in this sum, the terms which represent interaction with molecules.

We apply the term average intramolecular energy $\tilde{\omega}_{ij\,mol}$

$$\tilde{\omega}_{ij\,mol} = \int\limits_{around\ \vec{r}_j} W_{ij\,mol} \exp[-W_{ij\,mol}/kT\, dV_i].$$

Here $\tilde{\omega}_{ij\,mol}$ will depend on the coordinates of all the other particles. We shall assume, since this interaction is of a purely statistical nature, that it may be reduced to interaction with a certain average field. This field will be mainly determined by the ion distribution; the influence of molecular distribution will be slight, and therefore the estimates of the fluctuations given previously should be of the same order of magnitude as before. Introduction of this average field is therefore permissible. It must be pointed out, however, that the field will not be self-consistent in the sense of satisfying the Laplace – Boltzmann equation, as molecules will also influence this field.

Consequently, if fluctuations are not taken into account, $\tilde{\omega}_{mol}$ may be regarded as function of the strength of an average field (the strength because the molecular dimensions are small in comparison with the thickness of the double layer). In other words, interaction of the dipole type is taken into consideration, and hence

$$\tilde{\omega}_{mol} = \tilde{\omega}_{ij\,mol}[\vec{F}(\vec{r}_j)].$$

We determine the ion distribution by means of perturbation theory, assuming as a first approximation that the energy of interaction of ions with molecules is much less than the energy of interaction with ions. Then after suitable rearrangement, we may remove $-\frac{1}{kT}\sum_{ks} W_{mol\,ks}\,\tilde{\delta}_{ks}$ in Eq. (13), but this gives an expression coinciding with the probability for strong electrolytes, and therefore we have $n_{\pm} = n_0 K_{\infty} e^{\pm e\varphi/kT}$. On the other hand, $n^+ n^- = Kn_{mol}$ by definition of the dissociation constant. The possibility that the latter may depend on the field strength (according to Onsager [2]) must be taken into account, but

$$n^{+}n^{-} = K_{10\infty}\, n_{\mathrm{mol}\,10\infty}\,, \tag{14}$$

$$\frac{K(\infty)}{K(x)} = \frac{n_{\mathrm{mol}}(x)}{n_{\mathrm{mol}}(\infty)}\,. \tag{15}$$

On the other hand, we have from Equation (3)

$$\frac{n_{\mathrm{mol}}(x)}{n_{\mathrm{mol}}(\infty)} = e^{[-\omega_{\mathrm{mol}}(x) + \omega_{\mathrm{mol}}(\infty)]/kT}, \tag{16}$$

and hence

$$\ln \{K(x)/K(\infty)\} = \frac{\omega_{\mathrm{mol}}(x) - \omega_{\mathrm{mol}}(\infty)}{kT} \tag{17}$$

or

$$\Delta \ln K(x) = \Delta\omega_{\mathrm{mol}}(x)/kT. \tag{18}$$

This last expression is a generalization of a well known thermodynamical expression of the case when K depends on the field. In order to obtain the second approximation and an equation for the electrostatic field, we assume that

$$\tilde{\omega}_{\mathrm{mol}\,ij} = kTK(x_j)\,\bar{\delta}_{r_{ij}}. \tag{19}$$

This is equivalent to replacing the electrostatic forces by their average field in their action on a molecule.

To find the distribution of the ions, we again use Fowler's theory:

$$Ce^{-W/kT} = \int d\Gamma' e^{-U/kT}, \tag{20}$$

where W is the average interaction with all the molecules and ions (as may be shown by differentiation of the integral), as in [3]. Differentiation with respect to x_i gives for the derivative of the total energy

$$\frac{\partial W}{\partial x_i} - \frac{\partial \overline{W}_{\text{ion}}}{\partial x_i} = \frac{\partial}{\partial x_i} \sum_{kn} \overline{\omega}_{kn} (Exn). \tag{21}$$

We note that averaging $\frac{\partial}{\partial x_i} \sum_{kn} \overline{\omega}_{kn}$ has given the last term of Equation (21); it may be written in the form $\frac{\partial}{\partial x_i} = \epsilon_{\text{mol}}$:

$$\epsilon_{\text{mol}} = \int \tilde{\omega}(x)\, n_{\text{mol}}(x)\, dV, \tag{22}$$

where ϵ_{mol} is the total energy of all the molecules or, introducing the average electrostatic field,

$$\epsilon_{\text{mol}} = \int \tilde{\omega}(\varphi'_{(x)})\, n_{\text{mol}}(\varphi'_{(x)})\, dV, \tag{23}$$

and hence

$$\frac{\partial}{\partial x_i} \epsilon_{\text{mol}} = \int \frac{\partial \tilde{\omega} n}{\partial \psi'(x)} \frac{\partial \psi'(x)}{\partial x_i} dV. \tag{24}$$

Equation (24) may, as a first approximation, be written as

$$\int f(x) \frac{\partial \psi'(x)}{\partial x_i} dV \rightarrow \int f_1(x)\, dx \cdot q,$$

where q is the charge of one particle.

Thus, integration with respect to x gives the average value of the expression

$$\frac{\partial (\tilde{\omega} n)}{\partial \psi'(x, x_i)} \cdot q.$$

By its physical meaning this must be the derivative of the total energy of interaction of the i-th ion with the molecules.

Let us now calculate directly the energy of interaction of the i-th ion with the molecules. Suppose that the i-th ion is introduced at some point of the space. Suppose that before this a field ψ' was given in all space; then the total energy of the molecules was

$$\varepsilon_{\mathrm{mol}} = \int \tilde{\omega}(\psi')\, n_{\mathrm{mol}}(\psi')\, dV. \tag{25}$$

After introduction of the i-th ion at the point (x_i, y_i, z_i) the field was changed, and the energy of the system becomes:

$$\dot{\varepsilon}_{\mathrm{mol}} = \int \tilde{\omega}(\psi' + \psi_i')\, n_{\mathrm{mol}}(\psi' + \psi_i')\, dV.$$

The difference between these two energies is the required energy of interaction

$$\dot{\varepsilon}_{\mathrm{mol}} - \varepsilon_{\mathrm{mol}} = \int [\tilde{\omega}(\psi' + \psi_i')\, n_{\mathrm{mol}}(\psi' + \psi_i') - \tilde{\omega}(\psi')\, n_{\mathrm{mol}}(\psi')]\, dV. \tag{26}$$

If ψ_i' is small relative to the whole field, the expression under the integral may be replaced by $\frac{\partial(\tilde{\omega}n)\,\psi_i'}{\partial\psi'}$

Here the expression $\frac{\partial(\tilde{\omega}n)}{\partial\psi'}$ does not depend on the i-coordinate, i. e., Equations (24) and (26) are in agreement.

Consequently, the total energy given in Equation (20) is

$$W = W_{\mathrm{ion}} + \int \frac{\partial(\tilde{\omega}n)}{\partial\psi'}\, \psi_i'\, dV. \tag{27}$$

Introducing the average field concept, we obtain Laplace's equation

$$\Delta_i \psi = -\frac{4\pi}{D}\rho,$$

where ρ is taken to be the density of the ions only. The dipole correction is taken into account only in Equation (28). For the densities of the ions we have:

$$n_{\pm} \sim e^{\pm \frac{\psi z e}{kT}}\, e^{\pm \frac{1}{kT} \int \frac{\partial(\tilde{\omega}n)}{\partial\psi'} \psi_{ki}'\, dV}. \tag{28}$$

Returning to Equations (14) and (15), we have the condition that Equation (28) must not contradict Equation (15). There will be no contradiction if the factor is small or if it vanishes (the corrections for(−) and (+) ions balance out). However, it will vanish only if the distribution itself does not depend on the sign of the charge.

In considering the range of applicability of the above theory it is first necessary to note that introduction of an average field strength is permissible only if the influence of the field set up by the nearest ion is considerably less than the influence of the total field at the point under consideration. This can only be the case if the charge distribution is fairly continuous. The sign of the charge of the ion is immaterial if charges of one sign predominate over charges of the other sign (this is due to the fact that the field of a plane is finite, and that of a point is infinite at the point).

The following is the condition for the applicability of the theory: the interaction of one ion with all the molecules must be much less than the interaction of all the ions with one molecule, as only then are the approximations (16), (18), and (28) valid.

The first interaction is of the order

$$\frac{\int W(x)\,n(x)\,dx}{\int n_{\mathrm{ion}}(x)\,dx} \sim \frac{\overline{W} n_{\mathrm{mol}}}{n_{\mathrm{ion}}}, \tag{29}$$

where $\overline{W}$ is the total energy of interaction of the molecules with the ions. It is therefore sufficient that $\frac{n_{\mathrm{mol}}}{n_{\mathrm{ion}}} \ll 1$.* (The concentrations refer to the double layer region. Therefore our equations can always be applied at sufficiently high potentials. However, we are concerned not with abstract values of n, but with those corresponding to the limiting concentrations: $n_\infty \ll 1/V_m$, where V_m is the volume of a gram-molecule. For these conditions we may use the results of the theory of double layers of strong electrolytes, and substitute the appropriate expression into Equation (15). Integration over the whole depth of the layer gives the total negative adsorption (desorption). However, this value is not of as much interest as it might appear, as it is small in comparison with the positive adsorption of ions, and its influence on surface tension will be slight. Nevertheless, such negative adsorption may be significant in reactions at electrodes, as neither molecules themselves nor definite parts of them may be found at one of the electrodes (for example, if we are dealing with organic acids, neither the undissociated acid nor its negative ions will be found at one of the electrodes). Possibly this may be related to some forms of catalysis.

We write in explicit form the relationship between concentration and potential

$$n = n_\infty / F \tag{30}$$

where F is the Onsager function [2]

$$F = 1 + \bar{b} + \sum_{k=r}^{\infty} \frac{(2\bar{b})^k}{k!\,(k+1)!}, \text{where } \bar{b} = \frac{\psi' e^3}{2Dk^3T^3}; \tag{30a}$$

---

* It would be formally possible to use a method analogous to (16–28) to consider the reverse case $n_{\mathrm{mol}}/n_{\mathrm{ion}} \gg 1$ thus obtaining the change of the ion distribution, but in view of the necessity pointed out above, for the space charge to be fairly continuous, this cannot be done. This is because replacement of the dipole (ionic—molecular) interaction by an interaction with an average field is inadmissible, because of the prevailing role of fluctuations. In particular, the form of the formula for the capacity is quite obscure in this case.

It is known from the theory of the double layer [1] that

$$\psi' = (\sqrt{n_\infty K_\infty A})^{1/2} e^{\left|\frac{e\varphi}{kT}\right|} \qquad (30b)$$

(If the influence of ions of the opposite sign is ignored; this is necessary, as our theory is not applicable to the region in which this cannot be done).

A second result of the theory is that, at sufficiently high potentials, the theory derived for strong electrolytes is applicable to double layers of weak electrolytes. It must be emphasized that we have throughout considered the case of a double layer in absence of appreciable amounts of strong electrolytes. In conclusion, we must draw attention to the close connection between the change in the energy of molecules along the thickness of the double layer, if the dissociation constant depends on the field (and therefore on the coordinate), and the Onsager principle of microscopic equilibrium.

In fact, it can be shown that equilibrium can be established by a noncyclic process, with a dissociation constant which varies along the thickness of the double layer, only under the condition that the activity coefficient also varies with the coordinate. In the present instance this is equivalent to the molecule-field interaction varying with the coordinate, and it also indicates that this interaction is not small relative to kT.

SUMMARY

1. Electric field strength fluctuations in the double layer at electrodes of sufficiently large size are small, and introduction of the average field is permissible. Conditions are derived for which deviations of the field strength from the average value are small.

2. In the double layer region, where the number of molecules is much less than the number of ions (in practice, for dilute solutions, throughout the double layer if the potential differences are not too small), it is permissible to apply all the consequences of the double layer theory of strong electrolytes, including those relating to capacity, if the values of the concentration and the dissociation constant in the depth of the solution are taken.

3. It is shown that the distribution of neutral molecules varies in inverse proportion to the dissociation constant. The relationship between the distribution and the field has been derived in explicit form for cases to which Onsager's theory of dissociation of weak electrolytes is applicable.

4. Decrease of the number of neutral molecules at the electrode surface may be of importance in the occurrence of chemical and electrochemical reactions at the electrode surfaces.

I express my gratitude to Prof. V. G. Levich for proposing the problem and for criticism of the first version of the paper, and to Academicians M. A. Leontovich, V. I. Kogan, and I. Z. Fisher for their interest, discussions, and valuable advice.

The Minsk Tractor Works Mechanical Laboratory,
Central Factory Laboratory

Received December 15, 1955

LITERATURE CITED

[1] A. N. Frumkin et al., Kinetics of Electrode Reactions, Moscow (1952).

[2] H. Harned and B. Owen, Physical Chemistry of Electrolytic Solutions, Foreign Lit. Press, Moscow (1952).

[3] R. H. Fowler, Proc. Cambridge Philos. Soc. 22, 861, 1925; Statistical mechanics, 1929 (cited through B. Falkenhagen, Electrolytes, United Sci.-Tech. Press, Theoret. Chem., 1935).

[4] H. A. Kramers, Proc. Royal Acad. Sci. Amsterdam 30, 145, 1927 (in Russian in V. K. Semenchenko, Physical Theory of Solutions, ONTI, Moscow–Leningrad (1941).

[5] I. Ya. Frenkel, Statistical Physics, Moscow – Leningrad (1948).

COMPATIBILITY OF NITROCELLULOSE WITH BUTADIENE – ACRYLONITRILE COPOLYMERS

1. DEPENDENCE OF THE GLASS TRANSITION TEMPERATURE AND FLOW OF NITROCELLULOSE FILMS ON THEIR CONTENTS OF VARIOUS BUTADIENE – ACRYLONITRILE COPOLYMERS

L. Z. Kalinina, V. I. Alekseenko, and S. S. Voyutsky

Studies of the changes of deformation of polymer mixtures in relation to the component ratios and temperature extend our knowledge of the compatibility of polymers and of the plasticization of rigid polymers by high-molecular softeners. Moreover, determination of the effects of butadiene – acrylonitrile copolymers on the transition temperatures of nitrocellulose is important from the practical standpoint, as it provides information on the behavior of such systems in use under various temperature conditions.

The studies were performed on films made from solutions of nitrocellulose and butadiene – acrylonitrile copolymers with the following acrylonitrile group contents:

Copolymers	1	2	3	4
Acrylonitrile group content, %	17.6	28.0	37.7	44.4

The preparation of the films is described in one of our previous communications [1].

The deformability of the films over a wide temperature range was determined by means of V. A. Kargin's modified thermomechanical balance, in which the specimens were subjected to periodic extension at a gradually increasing temperature. The temperature was raised uniformly during the test by approximately 1° per minute. The deformation of the specimens was measured at 5-10° intervals; the load was 15 kg/cm². The specimens were strips of standard size. The width of each specimen was 5 mm, and the length of the working section was 20 mm. The deformation was always read off 5 seconds after application of the load.

Figure 1 shows the thermomechanical curves obtained, which represent variations of extension deformation with temperature under constant load, for nitrocellulose films containing various amounts of different butadiene–acrylonitrile copolymers.

It follows from Fig. 1, which refers to experiments with copolymer 1, that the relative extension of nitrocellulose itself is very small, and increases very little with temperature. Addition of from 20 to 60% of the weakly polar copolymer 1 produces relatively slight increases of deformation. With higher contents of copolymer 1 in the films the deformation–temperature curve is shifted in the direction of lower temperatures. The sharp inflections in the curves for films with high contents of copolymer 1 indicate that in this case there is a direct transition from the glassy to the viscous-flow state with increase of temperature, at temperatures below zero. The absence of regions corresponding to a state of high elasticity on the curves can be taken as indicating mutual insolubility of the two components, and therefore incompatibility of copolymer 1 and nitrocellulose.* The system is evidently heterogeneous at all the component ratios studied, and probably consists of microinclusions of one phase dispersed in the other, the mechanical properties of the film being, of course, determined mainly by the properties of the external phase. From this viewpoint, the different deformations of films with low and high contents of butadiene – acrylonitrile copolymer must be attributed to the fact that in the first case the external phase is nitrocellulose (or, more accurately, a dilute solution of butadiene – acrylonitrile copolymer in nitrocellulose) and in the second, butadiene – acrylonitrile copolymer (or, more

COMPATIBILITY OF NITROCELLULOSE WITH BUTADIENE–ACRYLONITRILE COPOLYMERS

3. DEPENDENCE OF THE GLASS TRANSITION TEMPERATURE AND FLOW OF NITROCELLULOSE FILMS ON THEIR CONTENTS OF VARIOUS BUTADIENE–ACRYLONITRILE COPOLYMERS

L. E. Kalinina, V. I. Alekseenko, and S. S. Voyutsky

Studies of the changes of deformation of polymer mixtures in relation to the component ratios and temperature extend our knowledge of the compatibility of polymers and of the plasticization of rigid polymers by high-molecular softeners. Moreover, determination of the effects of butadiene – acrylonitrile copolymers on the transition temperatures of nitrocellulose is important from the practical standpoint, as it provides information on the behavior of such systems in use under various temperature conditions.

The studies were performed on films made from solutions of nitrocellulose and butadiene – acrylonitrile copolymers with the following acrylonitrile group contents:

Copolymers	1	2	3	4
Acrylonitrile group contents, %	18.4	28.6	37.7	44.4

The preparation of the films is described in one of our previous communications [1].

The deformability of the films over a wide temperature range was determined by means of V. A. Kargin's modified dynamometric balance, in which the specimens were subjected to periodic extension at a gradually increasing temperature. The temperature was raised uniformly during the tests, by approximately 2° per minute. The deformation of the specimens was measured at 5-10° intervals; the load was 15 kg/cm^2. The specimens were always of standard size. The width of each specimen was 5 mm, and the length of the working section was 20 mm. The deformation was always read off 3 seconds after application of the load.

Figure 1 shows the thermomechanical curves obtained, which represent variations of extension deformation with temperature under constant load for nitrocellulose films containing various amounts of different butadiene–acrylonitrile copolymers.

It follows from Fig. 1, which refers to experiments with copolymer 1, that the relative extension of nitrocellulose itself is very small, and increases very little with temperature. Additions of from 20 to 60% of the weakly polar copolymer 1 produce relatively slight increases of deformation. With higher contents of copolymer 1 in the films the deformation – temperature curve is shifted in the direction of lower temperatures. The sharp inflections in the curves for films with high contents of copolymer 1 indicate that in this case there is a direct transition from the glassy to the viscofluid state with increase of temperature, at temperatures below zero. The absence of regions corresponding to a state of high elasticity on the curves can be taken as indicating mutual insolubility of the two components, and therefore inability of copolymer 1 to elasticize nitrocellulose. The system is evidently heterogeneous at all the component ratios studied, and probably consists of microvolumes of one phase dispersed in the other, the mechanical properties of the film being, of course, determined mainly by the properties of the external phase. From this viewpoint, the different deformations of films with low and high contents of butadiene – acrylonitrile copolymer must be attributed to the fact that in the first case the external phase is nitrocellulose (or, more accurately, a dilute solution of butadiene – acrylonitrile copolymer in nitrocellulose) and in the second, butadiene – acrylonitrile copolymer (or, more

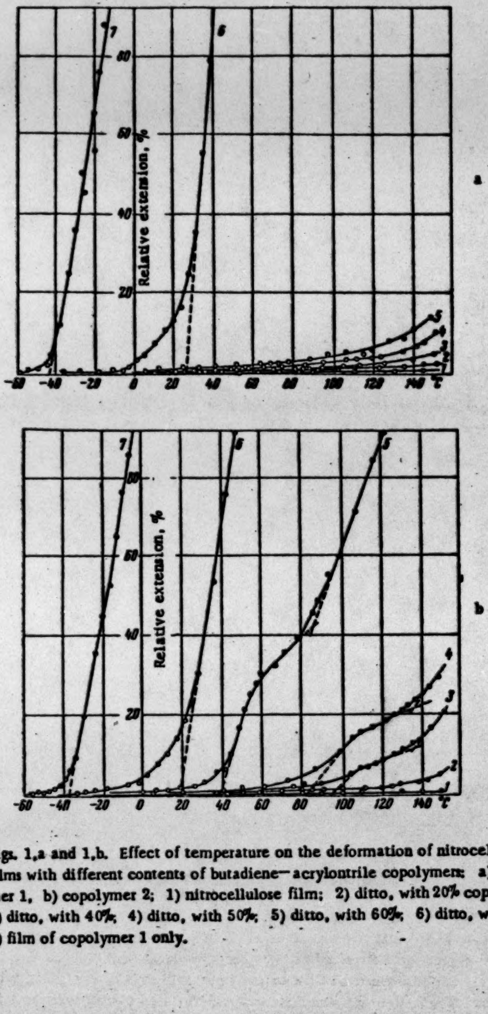

Figs. 1,a and 1,b. Effect of temperature on the deformation of nitrocellulose films with different contents of butadiene—acrylontrile copolymers: a) copolymer 1, b) copolymer 2; 1) nitrocellulose film; 2) ditto, with 20% copolymer; 3) ditto, with 40%; 4) ditto, with 50%; 5) ditto, with 60%; 6) ditto, with 80%; 7) film of copolymer 1 only.

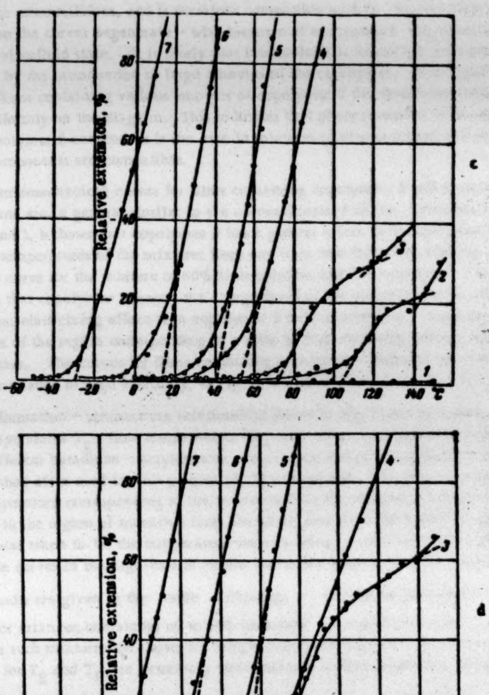

Figs. 1,c and 1,d. Effect of temperature on the deformation of nitrocellulose films with different contents of butadiene–acrylonitrile copolymers: c) copolymer 3; d) copolymer 4); 1) nitrocellulose film; 2) ditto, with 20% copolymer; 3) ditto, with 40%; 4) ditto, with 50%; 5) ditto, with 60%; 6) ditto, with 80%; 7) film of copolymer 1 only.

accurately, a dilute solution of nitrocellulose in butadiene – acrylonitrile copolymer). Phase inversion occurs, to judge by the positions of the curves in Fig. 1, when the system contains 60-80% butadiene– acrylonitrile copolymer.

The situation is somewhat different for films containing the more polar copolymer 2. As Fig. 1, b shows, the thermomechanical curves for films with fairly high contents (40-60%) of this copolymer have inflections characteristic of high-elastic materials. This indicates that the butadiene – acrylonitrile copolymer 2 can elasticize nitrocellulose, and is therefore compatible with it. At very high contents of copolymer 2 the inflexions on the curves degenerate – with increase of temperature the material passes directly from the glassy into the viscofluid state. It is likely that intermolecular forces are weakened to a greater extent than intramolecular by the introduction of large amounts of the copolymer. It is significant that in the case of nitrocellulose films containing various amounts of copolymer 2 the thermomechanical curves are arranged much more uniformly on the diagram. This indicates that phase inversion does not occur in the system with increase of copolymer 2 content, as is the case in mixtures of nitrocellulose and copolymer 1. It also confirms that the two components are compatible.

The thermomechanical curves for films containing copolymers 3 and 4 are also situated uniformly on the diagram, and are, in general, similar to the curves discussed above. However, a comparison of the curves in Figs. 1, c and 1, b shows that copolymer 3 has a greater effect than copolymer 2 on the displacement of the transition temperatures of the mixtures from one state into the other, into the lower temperature region. Moreover, the curve for the mixture of 80% nitrocellulose and 20% copolymer 3 is already clearly S-shaped. This indicates that copolymer 3 lowers the energy level of the potential barrier of rigid molecules; i. e., that it has a stronger elasticizing effect than copolymer 2 on nitrocellulose. However, degeneration of the curve (disappearance of the region corresponding to a state of high elasticity) occurs in this case at a lower content of the copolymer. The curves for films containing copolymer 4 indicate considerably greater extensions in the temperature range of high elasticity, as Fig. 1, d clearly shows.

The deformation – temperature relationships shown in Fig. 1 can be readily used to determine glass transition temperatures T_g, flow temperatures T_f, and differences between these values $T_g - T_f$ for mixtures containing different butadiene – acrylonitrile copolymers and nitrocellulose in various proportions. The graphical method often used for this purpose [2, 3] was applied. The glass transition temperature was taken to be the temperature corresponding to the intersection of the abscissa axis with extension of the linear portion of the curve in the region of transition from the glassy into the high-elastic or viscofluid states. The flow temperature was taken to be the temperature corresponding to the intersection of the extensions of the linear portions of the curves in the high-elastic region and at the beginning of the viscofluid region.

The results are given in the table following. It must be pointed out that T_g and T_f could not be determined for mixtures containing up to 60% butadiene – acrylonitrile copolymer 1, since the inflections on the curves for such mixtures lie above the temperatures investigated. Moreover it should be noted that the values found for T_g and T_f are extremely conventional, as they depend on the methods used for their determination [4, 5].

As the table shows, the maximum difference between T_f and T_g, which represents the temperature range of the high-elastic state, increases with increasing acrylonitrile group content in the copolymers. This indicates that the elasticizing action increases with increasing polarity of the butadiene – acrylonitrile copolymer. Since the rigidity of a high-molecular plasticizer usually increases with polarity, the only explanation of this effect is that the compatibility of nitrocellulose with the copolymer increases with rising acrylonitrile group content.

It also follows from the table that, for butadiene – acrylonitrile copolymers compatible with nitrocellulose, increase of polarity leads to a decrease of the amount required for elasticization. For example, in the case of copolymer 2 an elasticizing effect is found only with 50-60% of the copolymer. In the case of copolymer 4, an elasticizing effect occurs with 20-40% of the copolymer. With higher contents of this strongly polar copolymer the system passes directly from the glassy into the viscofluid state with increase of temperature. This also can only be explained by the better compatibility of strongly polar copolymers with nitrocellulose.

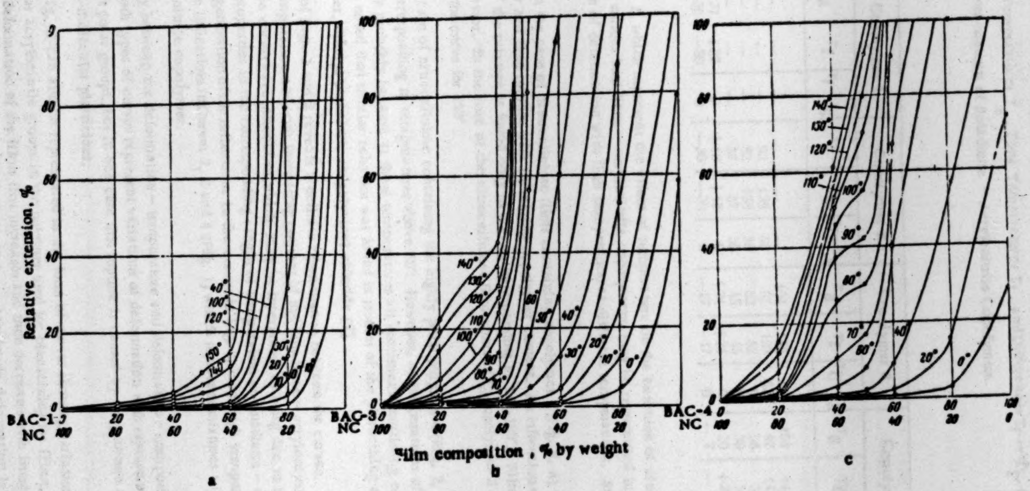

Fig. 2. Dependence of deformation on the contents of butadiene – acrylonitrile copolymers (BAC) in nitrocellulose (NC) films: a) copolymer 1; b) copolymer 3; c) copolymer 4.

TABLE

Glass Transition Temperatures T_g, Flow Temperatures T_f, and Differences $T_f - T_g$ for Nitrocellulose Films with Different contents of Butadiene – Acrylonitrile Copolymers

Copolymer contents, wt. %	Copolymer 1			Copolymer 2			Copolymer 3			Copolymer 4		
	T_g	T_f	$T_f - T_g$	T_g	T_f	$T_f - T_g$	T_g	T_f	$T_f - T_g$	T_g	T_f	$T_f - T_g$
20	—	—	—	—	—	—	104	145	41	104	144	40
40	—	—	—	93	139	46	61	123	62	62	142	80
50	—	—	—	82	138	56	52	52	0	58	58	0
60	—	—	—	37	87	50	45	45	0	50	50	0
80	+27	+27	0	+18	+18	0	+21	+21	0	+20	+20	0
100	–30	–30	0	–30	–30	0	–17	–17	0	– 7	– 7	0

The data in Fig. 1, which represent the effect of temperature on the extension of nitrocellulose films with different contents of various butadiene – acrylonitrile copolymers, may be represented in the form of curves showing the variation of deformation with film composition at different temperatures. Such curves are shown in Fig. 2.

It is seen that in the case of nitrocellulose films containing copolymer 1 (Fig. 2, a) the deformation increases first slowly and then rapidly with increasing copolymer content. An inflection corresponding to a high-elastic state of the mixture is found only in curves corresponding to 140-150°. Films containing copolymer 2 shows similar behavior. In the case of the nitrocellulose film containing copolymer 3 (Fig. 2, b) an inflection is already found on the curve for 120°.

Finally, in the case of nitrocellulose containing the highly polar polymer 4 (Fig. 2, c) inflections are visible on curves corresponding to temperatures above 60°. However, at temperatures of 110° and over these inflections disappear probably because at these temperatures all specimens containing copolymer 4 are capable of flow. It must be noted that similar behavior was found in studies of the plasticizing action of a true low-molecular plasticizer, dibutyl phthalate, on polyvinyl chloride [2].

A comparison of Figs. 1 and 2 reveals a definite resemblance between the curves. Deformation increases both with rise of temperature and with increasing content of the butadiene – acrylonitrile copolymer in the film. Some of these curves have inflections, which may be interpreted as being due to the fact that the mixtures have high-elastic properties in the corresponding ranges of temperature or butadiene – acrylonitrile copolymer concentration. Degeneration of the inflections in the curves in Fig. 2, c for high temperatures corresponds to degeneration of the inflections in Curves 2, 3 and 4 (Fig. 1) which represent mixtures with high contents of the butadiene – acrylonitrile copolymer.

This similarity between the deformation – temperature and deformation – composition curves is quite understandable. Both types of curves represent variations of deformation with rupture of intra - and inter-molecular bonds at polar groups, but in one case this rupture is caused by temperature and in the other by presence of a high-molecular plasticizer.

The data in Fig. 1 can also be represented in the form of curves showing variations of deformation with the content of polar acrylonitrile groups in the polymer used for plasticizing the films. Examination of such curves shows that deformation of the films first increases and then decreases with increasing content of acrylonitrile groups in the copolymer added to the nitrocellulose. Maximum deformation is found in mixtures containing copolymer 3. It seems likely that this copolymer also has the maximum effect on nitrocellulose. This entirely agrees with the result derived by analysis of extension diagrams for nitrocellulose films containing various butadiene – acrylonitrile copolymers [1]. A comparison of these curves also shows that deformation of the films increases sharply with increasing contents of butadiene – acrylonitrile copolymers in the films.

In the case of films of pure butadiene – acrylonitrile copolymers, the curves for deformation as a function of the acrylonitrile group content in the copolymer are of a different character – deformation decreases sharply with increasing polarity of the copolymer.

SUMMARY

1. The nature of the relationship between deformation and temperature for nitrocellulose films with various contents of butadiene – acrylonitrile copolymers indicates that a weakly polar copolymer containing 18.4% acrylonitrile groups is not compatible with nitrocellulose and cannot plasticize it. Copolymers with higher acrylonitrile group contents are compatible with nitrocellulose and can plasticize or elasticize it.

2. The difference $T_f - T_g$, which represents the temperature range of the high-elastic state of nitrocellulose films containing butadiene – acrylonitrile copolymers, increases with increasing acrylonitrile group content in the copolymers. This indicates an increase of the elasticizing action of butadiene – acrylonitrile copolymer on nitrocellulose with increasing polarity.

3. Curves for the variation of deformation with content of butadiene – acrylonitrile copolymer in the nitrocellulose are similar in form to the deformation – temperature curves. It is suggested that this similarity is the consequence of the similar effects of temperature and copolymer addition on the rupture of intramolecular bonds at polar groups.

4. The maximum influence on the deformation of nitrocellulose films is produced by the addition of a butadiene – acrylonitrile copolymer containing 37.7% acrylonitrile groups to nitrocellulose.

Central Scientific Research Institute for Leather Substitutes
Moscow

Received March 17, 1956

LITERATURE CITED

[1] L. E. Kalinina, V. I. Alekseenko, and S. S. Voyutsky, Colloid J.,18, 180 (1956).

[2] R. A. Reznikova, A. D. Zaionchkovsky, and S. S. Voyutsky, J. Tech. Phys., 25, 1045(1955).

[3] A. P. Aleksandrov and Yu. S. Lazurkin, Proc. Acad. Sci. USSR,43, 396 (1944).

[4] G. M. Bartenev, Proc. Acad. Sci. USSR,69, 373 (1949).

[5] G. M. Bartenev and L. A. Lukyanova, J. Phys. Chem., 29, 1486 (1955).

THIXOTROPIC STRUCTURE FORMATION AND ELASTICOPLASTICOVISCOUS PROPERTIES OF ASKANGEL SUSPENSIONS

E. I. Kobakhidze and M. E. Shishniashvili

As is known, thixotropic structure formation and the structural and mechanical properties of bentonite suspensions are among the most important of their varied characteristics. Studies of these properties are, on the one hand, of independent scientific importance in relation to the mechanism and principal laws of structure formation, and, on the other, the structural and mechanical characteristics are used for evaluation of the properties of structurized systems used in various branches of the national economy. In particular, thixotropic bentonite suspensions are extensively used in oil-well drilling, the success of which largely depends on the thixotropic and the structural and mechanical properties of these suspensions [1].

It has been shown in the numerous investigations by Rebinder and his school [1–3] that the process of thixotropic structure formation is completely reversible, and after complete or partial breakdown the thixotropic structure is again fully restored. In such systems, cohesion between the elements of the structural network is effected by van der Waals coagulation forces, weakened by very thin layers of the dispersion medium. The relatively easy breakdown and easy restoration of coagulative cohesion ensures complete reversibility of the system. It has also been shown [4] that completely reversible spatial structures, such as the structures in bentonite clay suspensions, are conventionally solid-like plastic bodies, with conventional flow limits.

The present investigation consisted of a study of the mechanism of thixotropic structure formation and the structural and mechanical properties of askangel suspensions in relation to the equilibrium pH on treatment with 1 N NaOH solution.

Askangel is a highly disperse, strongly swelling bentonite, and it forms thixotropic suspensions with low solid-phase contents. Askangel has very promising applications in various branches of the national economy, especially for drilling processes [5]. Suspensions of natural, and particularly of chemically treated askangel, are high quality suspensions with clearly defined thixotropic properties; they produce a thin but strong crust, not easily permeable to water, on the borehole walls, thus decreasing possibilities of caving. Because of their good thixotropic properties, askangel suspensions satisfactorily retain the cuttings in a suspended state if the circulation in the borehole stops, and eliminate the danger of drill clogging.

It must be pointed out that additions of even small amounts of natural askangel greatly improve the inferior suspensions of clays of other origins, confer thixotropic properties on them, raise their stability, and diminish water loss [5].

The above advantages of askangel suspensions are due to their special physicochemical and especially structural and mechanical properties. Because of this, apart from its independent scientific importance, the present investigation is also of practical value for determining the best methods for the production of drilling muds and for quantitative evaluation of their working properties.

Investigations in our laboratory have shown that high quality clay suspensions, satisfying the demands of complex deep oil-well drilling, must be made from highly disperse fractions of bentonite clays. We therefore isolated highly disperse fractions of natural askangel, in powder form, for the investigation. The highly disperse askangel powders were prepared from dilute (~ 3%) aqueous suspensions which were settled for three days to deposit the coarse fractions, with subsequent evaporation of the settled suspensions on the water bath.

The structural and mechanical properties of 4% suspensions prepared from the powders so obtained were equivalent to the properties of 7% suspensions of the original askangel.

The thixotropic properties of the systems were studied by the increase with time of the yield value P_m, which is conventionally taken to represent the strength of the structure. On the basis of these results, the systems were kept at rest in a dessicator until thixotropic buildup was complete; their elasticoplasticoviscous properties were then studied by Rebinder's method [3], based on investigation of the deformation kinetics at constant shearing stress.

Askangel suspensions were studied with the aid of a Veiler – Rebinder type instrument [6], and askangel pastes with the aid of the Tolstoi instrument [7].

Investigation of the kinetics of thixotropic structure formation in askangel suspensions in relation to the solid-phase concentration showed that the time for thixotropic structure formation increases with increasing solid-phase concentration. Thixotropic buildup of dilute (3, 4, and 5%) askangel suspensions is largely completed in 120-300 hours; the strengthening of askangel pastes (7, 8, and 10%) continues for 20-30 days. However, the coefficient of thixotropy [8]

$$K_T = \frac{P_m - P_0}{P_0}$$

(where P_0 is the original strength of the system, and P_m is the strength after time τ) decreases sharply, probably in consequence of retarded orientation of the particles.

Figure 1 shows a graph of the variation of the coefficient of thixotropy with solid-phase concentration during the time of thixotropic buildup, 120 hours. According to the literature [8, 9] the coefficient of thixotropy of clay suspensions first increases to a maximum and then decreases with increasing solid-phase concentration. Evidently because of the highly disperse nature of the askangel particles, the maximum of the coefficient of thixotropy is displaced into the low concentration regions (<3%), while the decrease of K_T is restricted to a narrow concentration range.

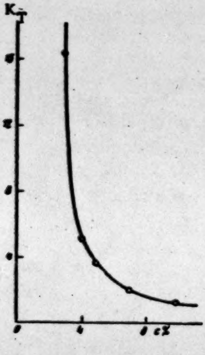

Fig. 1. Variation of the coefficient of thixotropy K_T of an askangel suspension with solid-phase concentration (τ_b = 120 hours).

In studies of the kinetics of structural buildup, the structure was broken down mechanically and its restoration was verified. It was found that the thixotropic structures in askangel suspensions and pastes are eventually converted into thixolabile structures.

Figures 2 and 3 show curves for the kinetics of thixotropic buildup of a 4% suspension and a 7% paste of askangel. It is seen that only a part of the bonds existing between the elements of the structural network is destroyed by mechanical action. In consequence, the rate of restoration of the broken-down structure is higher than the rate of the original thixotropic structure formation. Therefore the strength of the restored structure is considerably increased. With increasing age of the structure, its breakdown becomes less effective, and after several breakdowns the system appears to lose its thixotropic nature.

The formation of thixolabile structures culminates in syneresis of the system. The syneresis is increasingly pronounced with decreasing concentration of the solid phase.

The incomplete reversibility of askangel suspensions and pastes is probably to be explained by their gradual and lengthy buildup and formation of compact aggregates during breakdown, which ultimately leads to loss of thixotropic properties.

For comparison, a study was also made of the kinetics of thixotropic buildup in 10% suspensions of natural Oglanli bentonite. The results are shown graphically in Fig. 4. The thixotropic buildup time and the strength of the structure in 4% askangel suspension (see Fig. 2) are considerably greater ($\tau_b \sim 190$ hours; $P_m = 250$ dynes/cm^2) than in 10% suspension of Oglanli bentonite ($\tau_b \sim 40$ hours; $P_m = 170$ dynes/cm^2).

The viscosity of Oglanli bentonite suspensions does not vary with time. The viscosity of askangel suspensions, on the other hand, increases sharply with time (Fig. 5).* The explanation is that completely reversible thixotropic structures are formed in the first, while in the second the structures are not completely reversible.

For complete quantitative characterization of the structural and mechanical properties of askangel suspensions, $\epsilon = f(\tau)$ curves for the deformation kinetics at various shearing stresses were plotted, with subsequent measurements of the decay of deformation after removal of the load. The elastic, plastic and viscosity parameters were calculated from the results. For illustration, Fig. 6 shows curves for the deformation kinetics of 8% askangel paste. Elasticity, plasticity, and viscosity data for different solid-phase concentrations are given in Table 1.

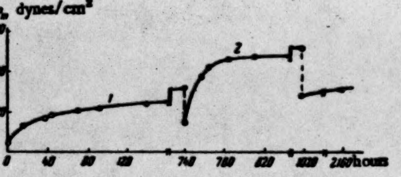

Fig. 2. Kinetics of thixotropic buildup in a 4% askangel suspension (the broken line indicates structural breakdown).

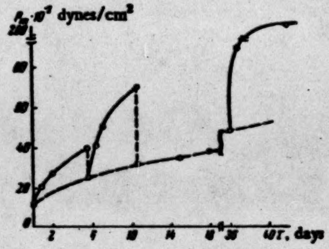

Fig. 3. Kinetics of thixotropic buildup in 7% askangel paste.

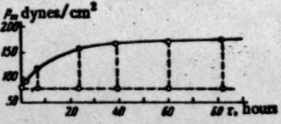

Fig. 4. Kinetics of thixotropic buildup in a 10% suspension of Oglanli bentonite.

These investigations showed that suspensions and pastes of natural askangel have a flow limit P_f which coincides with the elastic limit, below which flow cannot be detected experimentally during any period of time which the experimental technique allows.

The curves in Fig. 6 show that stresses $P < P_f$ produce completely reversible instantaneous-elastic and elastic deformations, which disappear after removal of the load. This region is accordingly characterized by the instantaneous E_1 and elastic E_2 moduli. The elastic viscosity η_2, which determines the rate at which elastic deformation develops, was also calculated.

---

* A Hoeppler viscosimeter was used for measuring the viscosities of the suspensions. The suspensions were vigorously agitated with a stirrer before each determination.

TABLE 1

Elastic, Plastic, and Viscous Properties of Askangel Suspensions with Various Solid-Phase Concentrations

4% askangel, P_f = 76 dynes/cm^2					8% askangel, $P_f = 9.7 \cdot 10^3$ dynes/cm^2					10% askangel, $P_f = 12.5 \cdot 10^3$ dynes/cm^2				
P dynes/cm^2	$E_1 \cdot 10^{-4}$ dynes/cm^2	$E_2 \cdot 10^{-4}$ dynes/cm^2	$\eta_1 \cdot 10^{-8}$ poises	$\eta_2 \cdot 10^{-3}$ poises	$P \cdot 10^{-3}$ dynes/cm^2	$E_1 \cdot 10^{-5}$ dynes/cm^2	$E_2 \cdot 10^{-3}$ dynes/cm^2	$\eta_1 \cdot 10^{-9}$ poises	$\eta_2 \cdot 10^{-9}$ poises	$P \cdot 10^{-3}$ dynes/cm^2	$E_1 \cdot 10^{-5}$ dynes/cm^2	$E_2 \cdot 10^{-5}$ dynes/cm^2	$\eta_1 \cdot 10^{-9}$ poises	$\eta_2 \cdot 10^{-9}$ poises
25	0.86	3.0	–	0.63	4.0	5.8	5.8	–	1.41	5	8.68	8.68	–	2,6
50	0.86	3.0	–	0.63	8.7	5.8	5.8	–	1.53	10	8.66	8.66	–	2.6
67	0.88	2.7	–	0.57	10.7	5.3	4.9	3.0	1.54	15	8.14	8.64	6.2	2.7
85	0.85	2.9	0.92	0.56	15.7	5.5	5.0	4.9	1.43	20	8.0	8.7	7.1	2.7
106	0.9	3.18	1.2	0.65	17.7	5.5	5.5	4.7	1.53	30	8.66	8.66	7.0	2.5
119	0.84	–	–	–	22.7	6.0	5.6	5.0	1.57	35	8.50	9.15	6.5	2.7
135	0.85	–	–	–	24.7	5.4	4.5	4.7	1.27	40	9.0	9.0	7.4	2.7
122	0.81	–	–	–	25.7	4.6	4.6	4.0	1.38	45	7.16	8.1	0.9	1.72

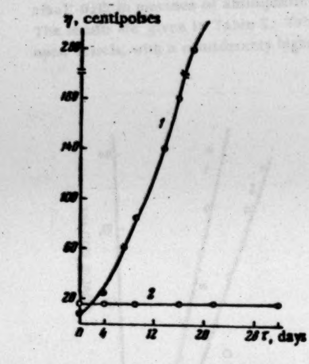

Fig. 5. Viscosity variations with time 1) 4 % askangel suspensions; 2) 10 % Oglanli bentonite suspensions.

Under the action of stresses only slightly greater than the flow limit, flow at a very high and constant viscosity occurs, i. e., when $P > P_f$ flow occurs almost without structural breakdown. Flow at constant viscosity continues over a wide range of shearing stresses, with the instantaneous and elastic deformations fully retaining their original values. Very rapid breakdown of the structural framework occurs only when the limiting deformation is reached, with corresponding decreases in the elasticity and viscosity data.

Rheological $d\epsilon/d\tau = f(P)$ curves (Fig. 7) for these systems consist of straight lines which cut off intercepts on the stress axis equal to the values of P_f determined directly from the curves for the deformation kinetics. Thus, askangel suspensions and pastes are characterized by a flow limit P_f, conventionally-instantaneous elastic modulus E_1 and elastic after-effect modulus E_2, plastic viscosity η_1 and after-effect viscosity η_2.

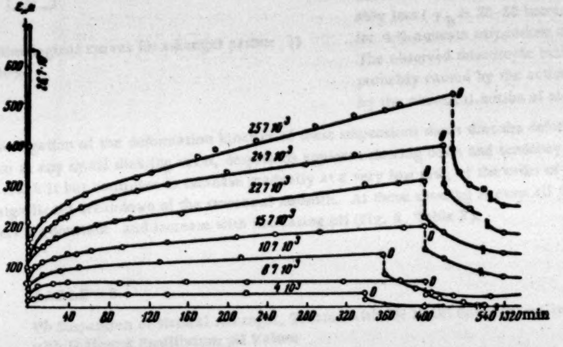

Fig. 6. Deformation kinetics of 8% askangel paste at various shearing stresses P in dynes/cm² (shown on the curves).

The data in Table 1 show that all the elasticity and viscosity characteristics remain constant over a wide range of shearing stresses and increase sharply with increasing concentration of the solid phase. Increase of the concentration from 4 to 10% produces nearly a 100-fold increase of E_1, a 30-fold increase of E_2, a 68-fold increase of η_1, a 44-fold increase of η_2, and a 164-fold increase of P_f.

We also studied the effects of added electrolytes on the thixotropic and rheological properties of askangel suspensions. The suspensions were first treated with 1 N NaOH solution until equilibrium pH was established.

When the suspensions are treated with NaOH solution, some of the alkali is converted into carbonate by the action of atmospheric carbon dioxide; this carbonate may undoubtedly influence the structural and mechanical properties. To investigate the effect of this factor, the askangel suspensions were treated with alkali both in presence of atmospheric carbon dioxide, and in closed vessels in absence of carbon dioxide. The results are given in Table 2. Table 2 shows that a longer time is needed to reach equilibrium pH in open vessels, with a considerably higher alkali consumption.

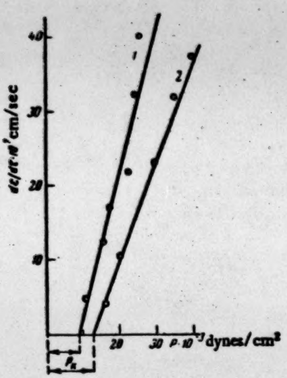

Fig. 7. Rheological curves for askangel pastes: 1) 8%; 2) 10%.

The askangel suspensions differed in viscosity, initial strength of structure, and thixotropic properties, according to the conditions of treatment.

Treatment of the suspensions with NaOH solution in closed vessels resulted in considerable liquefaction (decrease of viscosity and initial shearing stress) caused by the peptizing action of the alkali, resulting in structural breakdown. The liquefaction effect increases with rising pH. At pH 10.5 and 11 thixotropic structure formation does not occur at all. If the suspensions are treated in open vessels, increase of pH increases the viscosity and initial shearing stress, * so that the Hoeppler viscosimeter cannot be used to measure the viscosity.

Studies of the kinetics of thixotropic structure formation at different equilibrium pH values (Fig. 8) showed that thixotropically reversible structures are formed in these suspensions. The thixotropic buildup times and the coefficients of thixotropy are considerably less (τ_b is 20-50 hours; K_T = 1.2-0.6) than for 4 % aqueous suspensions of natural askangel. The observed thixotropic buildup in these systems is probably caused by the action of carbonates, formed by the chemical action of atmospheric CO_2 with the alkali

Investigation of the deformation kinetics of these suspensions shows that the deformation which arises in the system at any small shearing stress, despite its apparent slowing down and tendency to a limit, actually does not reach it but continues to increase gradually at a very low rate, of the order of 10^{-8}-10^{-9} cm/sec, without significant breakdown of the structural network. At these shearing stresses all the elastic and viscous parameters are constant and increase with increasing pH (Fig. 9, Table 3).

TABLE 2

4% Suspension of Natural Askangel, Treated with 1N NaOH Solution to Give Suspensions with Different Equilibrium pH Values

Treatment conditions	pH	Amount of 1 N NaOH consumed, in ml per 100 ml suspension	Time to reach equilibrium, days	Viscosity in centipoises	P_0 dynes/cm^2
In closed vessels	10.0	0.46	12	97.7	100
	10.5	0.65	14	65.7	90
	11.0	1.02	19	45.8	80
In open vessels	9.5	0.65	30	Could not be measured	180
	10.0	1.65	44		550
	11.0	6.49	60		800

---

* The possibility of concentrational changes in the suspensions during the experiments was excluded.

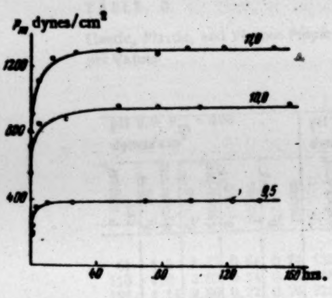

Fig. 8. Kinetics of thixotropic buildup in 4 % askangel suspension at various equilibrium pH values (shown on the curves).

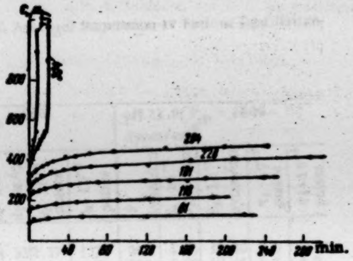

Fig. 9. Deformation kinetics of 4% askangel suspension of pH 9.5, at various shearing stresses P in dynes/cm² (shown on the curves).

It is seen from Fig. 9 that a slight increase of the shearing stress results in very rapid development of structural breakdown processes, so that the viscosity drops suddenly and flow results in decreasing viscosity. It is evident that at these shearing stresses the flow rate exceeds the rate of bond restoration, and the destroyed structures do not have time to be built up again. Accordingly, the rheological curves for these systems (Fig. 10) consist of two regions: the first is linear, corresponding to flow of the suspension at constant viscosity, with the structure still intact, and the second rises steeply. This portion of the curve represents flow of the suspension with partially destroyed structure.

As is known, the shearing stress corresponding to the boundary between the region of flow at high constant viscosity and the region of flow at variable viscosity is regarded as the conventional flow limit P_{cl}. Systems having a conventional elastic region are classified with the solid-like plastic systems [10, 4].

The conventional flow limit of the suspensions studied is much lower than the yield value P_m (the strength of the structure), and increases considerably with increasing equilibrium pH (Fig. 10, Table 3).

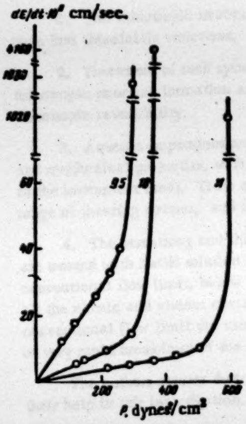

Fig. 10. Rheological curves for 4% askangel suspension at various equilibrium pH values (shown in the curves).

The results of our experiments justify the classification of askangel suspensions with the solid-like plasticoviscous systems.

TABLE 3

Elastic, Plastic, and Viscous Properties of 4% Askangel Suspension at Various Equilibrium pH Values

pH 9.5; P_m = 400 dynes/cm²					pH 10.0; P_m = 960 dynes/cm²					pH 11.0; P_m = 1300 dynes/cm²				
P dynes/cm²	$E_1 \cdot 10^{-4}$ dynes/cm²	$E_2 \cdot 10^{-4}$ dynes/cm²	$\eta_1 \cdot 10^{-9}$ poises	$\eta_2 \cdot 10^{-8}$ poises	P dynes/cm²	$E_1 \cdot 10^{-4}$ dynes/cm²	$E_2 \cdot 10^{-4}$ dynes/cm²	$\eta_1 \cdot 10^{-9}$ poises	$\eta_2 \cdot 10^{-8}$ poises	P dynes/cm²	$E_1 \cdot 10^{-4}$ dynes/cm²	$E_2 \cdot 10^{-4}$ dynes/cm²	$\eta_1 \cdot 10^{-9}$ poises	$\eta_2 \cdot 10^{-8}$ poises
81	1.2	2.77	0.64	0.74	132	1.76	4.52	2.57	1.74	218	4.75	10.46	6.0	5.31
118	1.0	2.83	0.64	0.76	148	1.77	4.44	2.55	1.70	292	5.00	10.01	5.6	4.9
191	1.14	2.86	0.72	0.76	221	1.82	4.80	2.23	1.80	363	5.44	10.89	5.5	5.38
228	1.09	2.74	0.67	0.73	298	1.78	4.45	2.10	1.74	437	5.52	11.00	5.1	5.2
264	1.13	2.64	0.65	0.70	331	1.73	—	0.01	—	510	5.56	10.2	5.1	5.0
304	1.07	—	0.03	—	367	1.75	—	0.008	—	583	5.00	—	0.06	—
337	1.10	—	0.01	—	418	1.73	—	—	—	619	4.64	—	—	—

SUMMARY

1. The thixotropic structures formed in aqueous suspensions and pastes of askangel pass in course of time into thixolabile structures, resulting in syneresis of the system.

2. Treatment of such systems with 1 N NaOH solution in open vessels sharply decreases the time of thixotropic structure formation and the coefficient of thixotropy. The structures formed have complete thixotropic reversibility.

3. Aqueous suspensions and pastes of askangel belong to solid-like plastic systems by their structural and mechanical properties, with flow limits coinciding with the elastic limits (within the sensitivity range of the instrument used). Their elastic, plastic, and viscous characteristics remain constant over a wide range of shearing stresses, and increase sharply with increasing concentration of the solid phase.

4. The less strong and thixotropically completely reversible structures formed when askangel suspensions are treated with NaOH solution are conventionally classified with the solid-like systems. These systems have a conventional flow limit, below which they flow at very high constant viscosities. At these shearing stresses all the elastic and viscous characteristics remain constant, but increase with increasing pH. Above the conventional flow limit the viscosity decreases sharply and flow occurs at variable viscosity as the result of very rapid breakdown of the structural network which develops in the system.

The authors express their deep gratitude to Academician P. A. Rebinder and to N. A. Serb-Serbina for their help in this investigation.

The P. N. Melikishvili Institute of Chemistry,
Acad. Sci. Georgian SSR
Colloid Chemistry Laboratory Tbilisi

Received May 7, 1956

LITERATURE CITED

[1] P. A. Rebinder, Symposium, Viscosity of Liquids and Colloidal Solutions, Vol. 1, Acad. Sci. USSR Press, Moscow-Leningrad, p. 361 (1941); N. N. Serb-Serbina, ibid, p. 381.

[2] N. N. Serb-Serbina and P. A. Rebinder, Colloid J. 9, 381 (1947); N. N. Serb-Serbina and S. A. Nikitina, Colloid J. 8, 63 (1946).

[3] P. A. Rebinder, New Methods of Physicochemical Investigation of Surface Phenomena, vol. 1, Acad. Sci. USSR Press, p. 5 (1950); E. E. Segalova and P. A. Rebinder, Colloid J. 10, 223 (1948; P. A. Rebinder and E. E. Segalova, Proc. Acad. Sci. USSR, 71, 85(1950); E. E. Segalova, P. A. Rebinder, and L. I. Sentyurikhina, Colloid J., 13, 6(1951).

[4] L. A. Abduragimova, P. A. Rebinder, and N. N. Serb-Serbina, Colloid J., 17, 184(1955).

[5] S. Filatov, Symposium, The Bentonite Clays of Georgia and their Use in the National Economy, Acad. Sci. Georgian SSR Press, Tbilisi, p. 27 (1953); E. Pondoeva, ibid, p. 83.

[6] S. Ya. Veiler and P. A. Rebinder, Proc. Acad. Sci. USSR 49, 354 (1945).

[7] D. M. Tolstoi, Colloid J., 10, 133 (1948).

[8] E. M. Tarasova, Candidate's Dissertation, Moscow (1919).

[9] S. A. Kudrina, Candidate's Disseration, Tashkent (1950).

[10] N. V. Mikhailov and P. A. Rebinder, Colloid J., 17, 107(1955).

GELATINIZED EMULSIONS

13. O/W TYPE EMULSIONS OF MAXIMUM CONCENTRATION WITH A THIXOTROPIC DISPERSION MEDIUM

L. Ya. Kremnev

We have demonstrated, by a number of examples, the possibility of greatly increasing the sedimentational and aggregative stability of concentrated emulsions (with disperse phase contents considerably less than 74% of the volume of the system) as the result of thixotropic structure formation in the dispersion medium. Spatial structure formation was induced by addition of small amounts of cetyl alcohol [1] or cholesterol [2] to the dispersion medium – aqueous solution of sodium oleate, stearate, or palmitate. Such solutions have very high rates of thixotropic buildup of the structures broken down in emulsification. This factor is decisive for prevention of coalescence of the droplets incorporated in the spaces of the spatial networks, and for the formation of a highly disperse emulsion.

A thixotropic dispersion medium, both in bulk and in thin layers, has higher structural and mechanical characteristics: elasticity in shear, structural viscosity, and considerable strength. An indication of these properties is given by the results of viscosity determinations by means of the capillary viscosimeter. As an example, Fig. 1 shows the variations of efflux rate $v \approx 1/\tau$ (where τ is the time) of 1 % aqueous sodium oleate solution containing different concentrations of cetyl alcohol. According to Rebinder [3], this behavior of the protective layers on the particle surfaces provides a universal means for an extremely great increase of the aggregative and sedimentational stability of disperse systems. This explains why in our experiments with thixotropically structurized soap solutions [1, 2] the stability of concentrated emulsions was increased by thousands of times.

In the course of our investigations which led to the conclusion that emulsions based on alkali soaps are stabilized by unsaturated adsorption monolayers [4], it was of interest to study emulsions of maximum concentrations with thixotropically structurized dispersion media, and to investigate the state and structure of the protective layers in them. Emulsions of benzene, of maximum concentration, were prepared in aqueous solutions of sodium oleate mixed with cetyl alcohol were prepared for this purpose.

The soap solutions were boiled for 20-30 minutes with weighed quantities of cetyl alcohol in a flask under reflux. The cooled solutions were fairly thixotropic, and were used as dispersion media for the emulsions. The emulsification was carried out by our method by the use of a spiral moving through the system [5]. As usual, the end of emulsification (formation of maximum strength emulsion) was established by the end of absorption of benzene by the emulsion. The emulsions were subjected to complete dispersion analysis by the microscopic method, the emulsion characteristics being based on the results.

Thixotropic solutions are obtained with various proportions of soap and cetyl alcohol, but all such solutions are suitable for emulsification, irrespective of the component concentrations.

The Table gives the characteristics of maximum strength emulsions based on aqueous sodium oleate solutions of three different concentrations, containing 0.025 mole/liter of cetyl alcohol. The Table gives: the maximum volume V_{∞} of emulsified benzene in 1 ml of dispersion medium, the maximum surface S_{∞} of the protective adsorption-solvation layers per 1 ml of the aqueous solution, the minimum thickness δ_{crit} of the layers, and the area S_0 per oleate molecule in the droplet surfaces.

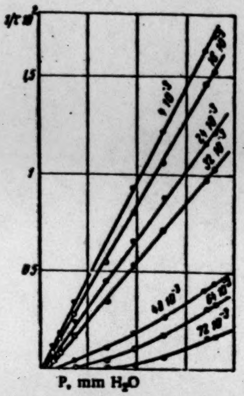

Fig. 1. Effect of cetyl alcohol on structure formation in aqueous sodium oleate solutions (the numbers on the curves represent the concentrations of cetyl alcohol in mole/liter).

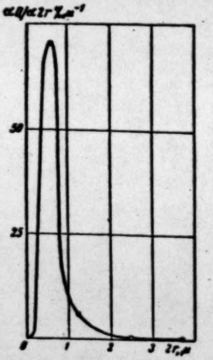

Fig. 2. Differential droplet size distribution curve for a maximum strength emulsion in thixotropic sodium oleate solution.

TABLE

Maximum Strength Emulsions in Thixotropic and Aqueous Solutions of Sodium Oleate

Soap concentration in mole/liter	V_∞ in ml	S_∞, in m^2	S_{crit} in μ	S_0 in A^2
Thixotropic solutions of Sodium Oleate				
0.033	20	146	0.0146	350
0.098	46	150	0.0066	270
0.164	74	250	0.0040	225
Aqueous solutions of Sodium Oleate				
0.032	33	33	0.030	160
0.096	88	69	0.014	115
0.160	140	100	0.010	100

The maximum volume of the disperse phase V_∞ increases with soap concentration in the mixture at a constant content of cetyl alcohol in the dispersion medium, but the values of V_∞ are much lower than in experiments with sodium oleate alone [6] because of greater dispersion of the droplets. Indeed, the degree of dispersion and homogeneity of the emulsions is very high. To illustrate this, Fig. 2 shows a differential curve of droplet size distribution in a maximum strength emulsion in a dispersion medium containing 0.164 mole sodium oleate and 0.025 mole cetyl alcohol per liter.

The maximum on the distribution curve corresponds to a droplet diameter of the order of 0.6 μ, while in maximum strength emulsions based on soap solutions without cetyl alcohol the maximum is always found at a diameter of ~1 μ, which is in accordance with an analysis of the emulsification process [7]. The shift of the maximum in the direction of smaller drop size is due to the thixotropic properties of the dispersion medium, as the spatial structures, being rapidly restored after breakdown, prevent coalescence of the smaller droplets formed during the emulsification. In the emulsions studied the droplet diameter never exceeded 5 μ.

The shift of the maximum in the direction of smaller droplet size results in an appreciable decrease of V_∞ in comparison with the values of V_∞ obtained earlier with sodium oleate.

Returning to the table, we see that the minimum thickness of the protective layer δ_{crit} decreases with increasing soap concentration, while the maximum layer area S_{∞} increases. As regards the packing density of the soap molecules on the droplet surfaces, the values of S_a leave no doubt that the adsorption layers are considerably unsaturated monolayers. It is particularly interesting to note in this connection that the structural and mechanical properties of the protective layers are effective in monomolecularly attenuated adsorption layers.

It is useful to compare the data obtained with the results of a study of maximum strength emulsions in sodium oleate without cetyl alcohol [6]. The table therefore contains some earlier data for maximum strength emulsions in aqueous sodium oleate solutions.

A comparison of the data in the table leads to the conclusion that addition of cetyl alcohol to the soap solution does not produce any radical changes in the characteristics of maximum strength emulsions and protective layers. However, spatial structure formation in the dispersion medium results in a sharp decrease in the thickness of the adsorption – solvation layers which can stabilize the droplets. This is probably to be explained by the higher structural and mechanical properties of thixotropic stabilizer solutions both in a large volume and in thin layers. Accordingly, the surface area S_{∞} of the layers formed from 1 ml of solution increases in proportion to the decrease of their thickness. At the same time the adsorption layers become more attenuated, and the emulsifying power of the sodium oleate, quantitatively represented by the values of S_{∞}, increases.

SUMMARY

1. Maximum strength o/w type emulsions have been prepared in thixotropic sodium oleate solutions. In agreement with Rebinder's views, the main factors determining the stability of such emulsions are the structural and mechanical properties of the protective adsorbed solvate layers.

2. Thixotropic structure formation in the dispersion medium of the emulsion results in an appreciable increase of the emulsifying power of the stabilizer and a decrease of the critical thickness of the protective layers.

3. The protective adsorbed layers are monomolecular and unsaturated.

4. Emulsions with a thixotropic dispersion medium have a very high degree of dispersion and are homogeneous in droplet size.

The Lensoviet Technological Institute
Leningrad

Received April 16, 1956

LITERATURE CITED

[1] L. Ya. Kremnev, Colloid J., 10, 18 (1948); Trans. Leningrad Tech. Inst., No. 17, 73(1950); L. Ya. Kremnev and E. I. Kvit, Trans. Leningrad Tech. Inst., No. 17, 89(1950).

[2] L. Ya. Kremnev and T. A. Volkova, Trans. Leningrad Tech. Inst., No. 21, 50 (1951).

[3] P. A. Rebinder, Introduction to translation of W. Clayton's "Emulsions", Foreign Lit. Press, Moscow (1950).

[4] L. Ya. Kremnev and S. A. Soskin, Colloid J., 9, 269 (1947); L. Ya. Kremnev and R. N. Kagan, Colloid J., 10, 436 (1948).

[5] L. Ya. Kremnev, Proc. Acad. Sci. USSR, 79, No. 4, 655 (1951); Colloid J., 13, 394 (1951).

[6] L. Ya. Kremnev and S. A. Soskin, J. Gen. Chem., 16, 2004 (1946); Colloid J., 9, 269(1947).

[7] L. Ya. Kremnev and A. A. Ravdel, Colloid J., 16, 17 (1954).

INVESTIGATION OF STRUCTURIZED SUSPENSIONS

E. F. Kurgaev

In coagulation and softening of water by the precipitation method a flocculent suspension is formed; the floc particles are independent structurized systems which at a definite concentration unite into a loose spatial structure [1]. Experiments performed by the Veiler – Rebinder method [2] have been used to determine the shearing stress and relaxation time of such structures [3, 4]. At the same time, technological investigations of the operation of water clarification equipment have involved the determination of such parameters of the suspension as its volume concentration in the dispersion medium, compressive strength, density, and the cohesive forces which cause aggregation of the particles and assist the removal of mechanical impurities from the water. The technique of such determinations has been developed by the author; it is based on an analysis, given below, of the results of observations of the kinetics of lowering of the boundary of the suspension allowed to settle simultaneously in several glass cylinders. The suspension in all the cylinders has the same initial concentration, but different layer heights H_0.

Observations show that at the start of the settling the boundary of the suspension layer sinks at a constant rate, independent of the layer height H_0. The rate then decreases, gradually becoming zero, and the boundary becomes stabilized at a certain height H_f. While the boundary sinks at a constant rate, the suspended particles in the layer (with the exception of its lower part, consisting of a zone of settled particles) retain their individual outlines and are in a state of appreciable circulation in various directions. This suggests that collective subsidence of the particles occurs; this is confirmed by a comparison of the calculated rates of such subsidence for different initial suspension concentrations.

The start of the change in the rate of sinking of the layer boundary is accompanied by cessation of particle circulation, and formation of a continuous spatial network. The subsequent sinking of the layer boundary is the result of condensation of this network by contraction of the pores between the particles forming it. This is followed by stabilization of the height of the layer. Similar stages in the process were also observed by Zuev [5].

We have carried out special investigations over a wide range of initial layer heights H_0; it was found up to values below a certain value H_{cr}, the ratio of H_0 to the stabilized height H_f remains constant while after H_{cr} is exceeded this ratio begins to increase. There are no pores between the particles of the suspension when the layer height has become stabilized. This is shown both by visual observations and by the fact, established by special experiments, that the layer is impermeable to water.

There is reason to believe that in the initial height range below H_{cr} the stabilized layer is a structurized system of the same density as the particles of the suspension forming it. At heights greater than H_{cr} the pressure of the layer exceeds the compressive strength of the structure and causes the latter to condense. From this it is possible to determine the volume concentration of the suspension in its original form, i. e., as a disperse phase in a structureless medium, which is the state of the layer of the particles in the suspension at its initial height H_0. This concentration is evidently equal to the ratio of the stabilized height to the initial height of the layer, for values of the latter not exceeding H_{cr}; i. e., $c_0 = H_f/H_0$ when $H_0 < H_{cr}$.

Having determined the weight concentration (c_w) of the solid phase of the suspension in grams per milliliter in the original volume of the layer by the usual method, we can find the solid phase content in unit volume of the suspension structure from the expression $\gamma_1 = c_w/c_0$. Hence we can find the density of the suspension floc from the formula

$$\gamma_2 = 1 + \gamma_1 (1 - 1/\gamma_d) \text{ g/ml}$$

where γ_d is the density of the dry substance contained in the suspension structure, in g/ml.

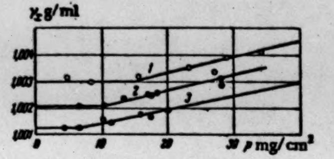

Fig. 1. Variation of suspension density with pressure: 1) 50% $Al(OH)_3$ + 50% $Fe(OH)_3$, p_{cr} = 14 mg/cm²; α = 0.064 cm^{-1}; 2) 75% $Al(OH)_3$ + 25% $Fe(OH)_3$; p_{cr} = 10 mg/cm²; α = 0.059 cm^{-1}; 3) $Al(OH)_3$, p_{cr} = 7 mg/cm², α = 0.052 cm^{-1}.

The amount of water (density of which is unity) relative to the volume of the dry substance in the suspension is $\varphi_0 = (\gamma_d - \gamma_1)/\gamma_1$ and relative to the weight of the dry substance, $\varphi_w = \varphi_0/\gamma_1$.

The above data on the critical layer height H_{cr} and the suspension parameters may be used to calculate the value of its maximum normal uniaxial compressive stress p_{cr} from the formula

$$p_{cr} = c_0 H_{cr} \gamma_1 (1 - 1/\gamma_d) \text{ g/cm}^2$$

or

$$p_{cr} = H_{cr} c_0 (\gamma_2 - 1) \text{ g/cm}^2 .$$

Observed data on the ratios of the initial and final layer heights when $H_0 > H_{cr}$ make it possible to follow the variations of the suspension density, of the amount of water present in its structure, and of the compressive deformation stress as a function of pressure.

Figure 1 shows the variations of density γ_x with pressure p for suspensions formed in coagulation of water by aluminum and iron salts.

It was found experimentally that, for these suspensions, the relationship $\gamma_x = f(p)$ can be represented as

$$\gamma_x = \gamma_2 + (p - p_{cr}) \cdot \alpha \text{ g/ml} .$$

Almost the same value of α (0.06 cm^{-1}) was obtained for different coagulants, which may be a sign that their structural bonds are of the same character.

The amount of water in the suspension structure decreases as p_{cr} is exceeded; the above data may be used to calculate the loss of water from the suspension by increase of the externally applied pressure.

The cohesive forces between the particles may be quantitatively estimated by parallel observations of the condensation kinetics of suspension layers of different initial heights. For this, we determine the rates of condensation of the layers from the instant at which continuous structurized systems are formed in them to the instant at which the density of the system becomes equal to the density of its constituent suspension particles. As has been stated earlier, when $p < p_{cr}$ this state is reached when the height of the layer has become stabilized. The average value of the required rate V can be approximately calculated by dividing the difference between the heights of the layer at the beginning and the end of the condensation period by the duration of the latter.

The average rate can be found more exactly by integration of the relationship between the condensation rate and time, which varies in the course of the process. For this, the $V_{cond} = f(\tau)$ graph is plotted and $\bar{V}$ is then determined from the expression

$$\bar{V} = \frac{1}{T} \int_{\tau_1}^{\tau_2} V_{cond} \, d\tau ,$$

where $1/T = \tau_2 - \tau_1$.

It was found experimentally that the suspension condensation rate increases with increasing initial layer height H_0 and pressure p, the relationship $\bar{V} = f(p)$ being of the form shown in Fig. 2. This relationship, expressed in the form $\bar{V} = ap + b$, shows that condensation of the structurized system is caused not only by gravitational forces, but also by other forces, which may be assumed to be forces of cohesion between the particles of the suspension. This relationship is used to find the magnitude of the cohesion forces from the suspension condensation rate V_a, corresponding to zero value of the pressure p. For this, the pressure increment p_a corresponding to the rate V_a is determined. A simple transformation of the above expression for $\overline{V}$ shows that the required value of p_a corresponds to the ordinate $2V_a$.

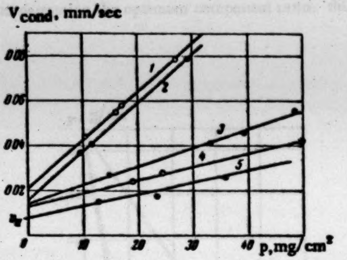

Fig. 2. Variation of the condensation rate of the suspension layer with pressure: 1) 80 % $Al(OH)_3$ +20% $Fe(OH)_3$; p_a = 10.0 mg/cm²; 2) $Al(OH)_3$ p_a = 7.5 mg/cm²; 3) 25% $Al(OH)_3$ + 75% $Fe(OH)_3$; p_a = 18.5 mg/cm²; 4) $Fe(OH)_3$; p_a = 22.2 mg/cm²; 5) 50% $Al(OH)_3$ + 50% $Fe(OH)_3$; p_a = = 17.0 mg/cm².

It must be pointed out that if the observations are made at values of $p > p_{cr}$ for calculation of V_a, the end of the condensation period cannot be taken to be the instant when the height of the layer becomes stabilized, as an additional process is superposed here, due to disturbance of the natural state of the suspension structure as the result of its condensation. However, the results of such experiments can also be used if the period of condensation of the suspensions for a cylinder with the minimum value of p, less than p_{cr}, is taken as equal for all the cylinders. This gives satisfactory agreement with experiments in which $p < p_{cr}$ in all the cylinders.

In addition to the above values, the following were determined: the magnitude of the cohesion forces per unit weight of the dry substance forming the suspension, p_a/γ_1 (which we term the adhesion coefficient K_a), and the critical concentration by weight c_{cr} at which a continuous structural network is formed.

The experimentally determined values of the physical parameters are given in the table.

Quantitative Characteristics of the Suspensions Studied

Composition of suspension	Physical parameters				
	γ_2, g/ml	mg/cm²	$\frac{p_a}{\gamma_1}$	a_w	c_{cr} %
$Al(OH)_3$	1.0012	7.5	3.75	500	0.07
$Fe(OH)_3$	1.0026	22.2	5.94	270	0.15
$Fe(OH)_3$	1.0064	9.6	1.04	109	0.46*
$Fe(OH)_2$	1.0061	11.6	1,33	115	0.43
75% $Al(OH)_3$ + 25% $Fe(OH)_3$	1.0020	10.0	3.13	332	0.13
50% $Al(OH)_3$ + 50% $Fe(OH)_3$	1.0029	17.0	3.98	233	0.17
25% $Al(OH)_3$ + 75% $Fe(OH)_3$	1.0048	18.5	2.65	144	0.32
$Mg(OH)_2$	1.0026	3.5	0.78	222	0.07
25% $Mg(OH)_2$ + 75% $CaCO_3$	1.0300	26.0	0.53	20.4	1.47
15% $Mg(OH)_2$ + 85% $CaCO_3$	1.0860	66.0	0.44	7.2	6.95

---

* After condensation for 40 hours and dispersion of the precipitate by water.

The data in the table show that the particles in the suspension include very large amounts of water, considerably exceeding the dry substance in weight; this quantity is determined by the nature of the structure of the suspension. The suspension densities vary over a wide range, and are not directly related to the density of the dry substance. The critical concentrations also vary over a wide range.

In combined coagulation of aluminum and iron salts the density and subsidence rate of the suspension are higher than for a suspension of aluminum hydroxide alone. The values of the adhesion coefficient are greater in combined coagulation than for ferrous hydroxide, which is usually present in the coagulum in incomplete hydrolysis of iron salts. The quantitative values of these parameters explain the improved water clarification effect and the extension of the range of its optimum ionic composition in combined coagulation with iron and aluminum salts, as compared with coagulation by one of these reagents. Moreover, it is possible to determine the optimum component ratio: this was 1:1 in our experiments.

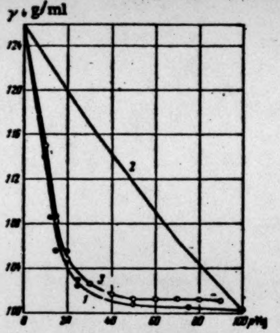

Fig. 3. Densities of suspensions consisting of calcium carbonate and magnesium hydroxide in various proportions: 1) $\gamma_{cm} = f(p_{Mg})$ from experimental data; 2) $\gamma_{cm} = f(p_{Mg})$ calculated for $\gamma_{Ca} = 1.26$ g/ml; 3) $-\gamma_{Ca} = f(p_{Mg})$ from experimental data;

$$p_{Mg} = \frac{Mg(OH)_2}{Mg(OH)_2 + CaCO_3} \cdot 100\%$$

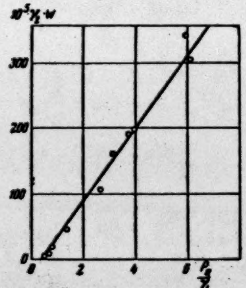

Fig. 4. Variation of the mass of floc particles with the magnitude of the cohesion forces.

Data showing the influence of "aging" and repeated mechanical peptization on the suspension parameters were obtained for ferric hydroxide.

The particle diameters calculated from the values of γ_2 and from the experimentally determined subsidence rates were in agreement with the generally observed dimensions of such particles.

A study of the physical parameters of the suspensions formed in water softening showed that the presence of magnesium hydroxide alters the character of the structure formation in calcium carbonate suspensions. With increasing magnesium content the structure formation passes from the condensation-crystallization to the coagulation type. Calculations showed that this is accompanied by a sharp decrease in the density of the calcium carbonate suspensions (Fig. 3).

Observations by the electron and optical microscopes revealed an approximately 400-fold decrease in the volume of the calcium carbonate crystals and a change in the nature of the structural bonds. Instead of aggregation at the plane faces, the crystals join by their corners (sharp projections) and are coated with magnesium hydroxide. This is in entire agreement with the laws for the effects of surface-active substances on structure formation established by Rebinder and his associates [6].

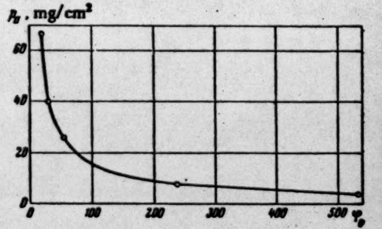

Fig. 5. Relationship between cohesion forces and the amount of water immobilized by the structural network of a suspension consisting of calcium carbonate and magnesium hydroxide.

Our experiments showed that a linear relationship, shown in Fig. 4, exists between the adhesion coefficient and the particle mass $\gamma_2 W$ (here W is the volume of a particle).

Interesting relationships were found between the cohesion forces p_a and the amount of water contained in the structural network. Figure 5 shows such a relationship for a suspension of calcium carbonate and magnesium hydroxide.

SUMMARY

1. A new method has been used to determine the following physical parameters of flocculent suspensions formed in water coagulation and softening processes: density, strength in normal uniaxial compression, amount of water immobilized by the structural network of the suspension, and quantitative values of the cohesion forces causing floc aggregation.

2. A linear relationship exists between the specific cohesion force (coefficient of adhesion) and the mass of a floc particle.

3. When a calcium carbonate suspension is formed in presence of magnesium hydroxide, the character of its structure formation changes and its density alters. With increasing magnesium content the structure gradually passes from the condensation-crystallization to the coagulation type, and the density of the calcium carbonate floc decreases.

4. A relationship, represented by a curve close to a hyperbola, exists between the cohesion forces and the amount of water immobilized in the structural network of a suspension consisting of calcium carbonate and magnesium hydroxide. The vertex of the hyperbola represents transition to a predominant influence of one of the above types of structure formation.

5. In combined coagulation with aluminum and iron salts the suspension has optimum physical properties with equal amounts of aluminum and iron hydroxides.

6. The quantitative data on the physical parameters of flocculent suspensions can be used in the design of equipment for water purification, and the relationships between these parameters, for investigation and control of water coagulation and softening processes.

I express my deep gratitude to Academician P. A. Rebinder for valuable advice and guidance in generalization of the experimental results.

All - Union Scientific Research Institute
for Railroad Transport
Moscow

Received June 23, 1956

LITERATURE CITED

[1] P. A. Rebinder, Bull. Div. Math. Nat. Sci. Acad. Sci. USSR. Chem. Ser., 5, 603 (1936); P. A. Rebinder and E. E. Segalova, Science and Life, No. 5 (1955).

[2] S. Ya. Veiler and P. A. Rebinder, Proc. Acad. Sci. USSR, 49, No. 5 (1946).

[3] E. N. Teterkin and N. S. Lebedeva, Trans. Inst. Water Supply and Hydrogeol. Eng., Inform. Material No. 3, Moscow, p. 23 (1952).

[4] T. L. Baryshnikova, Dissertation, Sverdlovsk Polytech. Inst. Urals (1954).

[5] Yu. S. Zuev, Colloid J., 10, No. 4, 281, No. 6, 431 (1948).

[6] N. N. Serb-Serbina and P. A. Rebinder, Colloid J., 9, 381 (1947); E. E. Segalova and P. A. Rebinder, Colloid J., 10, No. 3, 223 (1948); L. A. Abduragimova, P. A. Rebinder, and N. N. Serbina, Colloid J., 17, No. 3, 184 (1955); P. Rebinder, Faraday Society, Discussion on Coagulation and flocculation, No. 18, 1954.

THE EFFECT OF SURFACE-ACTIVE SUBSTANCES ON THE SPECIFIC VISCOSITY OF GELATION SOLUTIONS

S. M. Levi

Deryagin, Levi, and Koltsov [1] put forward the view, which was experimentally confirmed, that the observed sharp change in the viscosity of gelatin solutions under the influence of small amounts of surface-active substances – the colored components – is explained by "adsorption" of the latter, leading to a change in the shape of the gelatin molecule (elongation). This process is represented by the following equation:

$$\frac{1}{c}\ln\frac{\eta}{\eta_0} = f(\Gamma), \qquad (1)$$

where c is the concentration of the gelatin solution; η_0 is the viscosity of the gelatin solution before introduction of the surface-active substance; Γ is a quantitative measure of the "adsorption"; $f(\Gamma)$ is a certain function of Γ. Since in this instance (gelatin solutions) the magnitude of the adsorbing surface is not known, and even the concept of the gelatin particle – dispersion medium interface is somewhat conventional, we take Γ to mean the adsorption (more correctly, sorption) of surface-active substance (wetting agent) in grams per 1 g gelatin.

In the investigation cited [1], we studied the viscosity change as a function of the ratio of the gelatin concentration c to the colored component c_1, i. e.,

$$\frac{1}{c}\ln\frac{\eta}{\eta_0} = f\left(\frac{c_1}{c}\right), \qquad (2)$$

assuming that

$$K = f\left(\frac{c_1}{c}\right) = f(\Gamma), \qquad (3)$$

where K is the asymmetry coefficient of the particles, equal, according to Einstein, to 2.5 for spherical particles, and having large values, determined by the Simha equation [2], for particles of other shapes.

In our subsequent experiments an attempt was made to determine the value of $f(\Gamma)$ directly by adsorption measurements. The magnitude of adsorption was found from measurements of the surface tension isotherms in aqueous and gelatin solutions of wetting agents. The adsorption was calculated graphically by means of the Gibbs equation and the Langmuir adsorption isotherm [3]. The following assumption was made: the difference between the adsorption (Γ_w) of the wetting agent in aqueous solution and the adsorption (Γ_g) in gelatin solution is a measure of the "adsorption" of the wetting agent by gelatin, which is the cause of the viscosity change, and therefore

$$K = f(\Gamma_w - \Gamma_g), \qquad (4)$$

and it follows from Equation (4) that

$$\frac{1}{c}\ln\frac{\eta}{\eta_0} = f(\Gamma_w - \Gamma_g). \qquad (5)$$

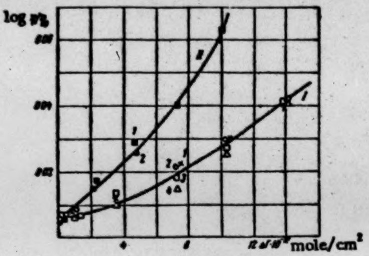

Fig. 1. Effect of adsorption of wetting agent by gelatin on its specific viscosity. I) Wetting agent 2: 1) 4% solution of 30°; 2) ditto, at 35°; 3) 6% solution at 35°; 4) ditto, at 40°; II) wetting agent 3: 1) 4% solution at 35°; 2) 6% solution at 35°.

Equation (5) was tested for the following wetting agents: Dismulgan and octo- and dodecanoglycerides of alkenylsuccinic acids, having the formulas:

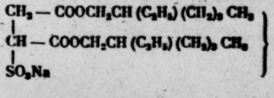

$$\left.\begin{array}{l} CH_2-COOCH_2CH(C_2H_5)(CH_2)_3CH_3 \\ | \\ CH-COOCH_2CH(C_2H_5)(CH_2)_3CH_3 \\ | \\ SO_3Na \end{array}\right\}$$

Wetting agent 1

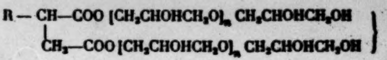

$$\left.\begin{array}{l} R-CH-COO[CH_2CHOHCH_2O]_n\,CH_2CHOHCH_2OH \\ \quad\; | \\ \quad CH_2-COO[CH_2CHOHCH_2O]_n\,CH_2CHOHCH_2OH \end{array}\right\}$$

Wetting agent 2 with 2n = 6

Wetting agent 3 with 2n = 10

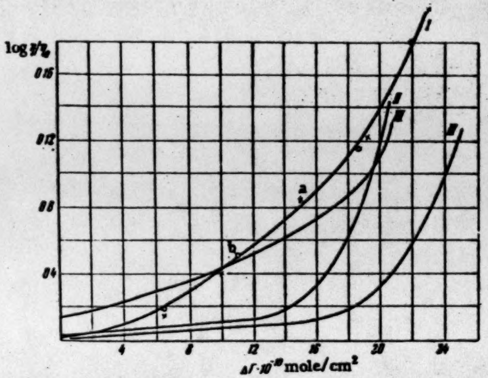

Fig. 2. Effect of adsorption of wetting agent 1 by gelatin on its specific viscosity: 1) 4% (a) and 6% (b) gelatin solutions; II) gelatin I; III) gelatin 2; IV) gelatin

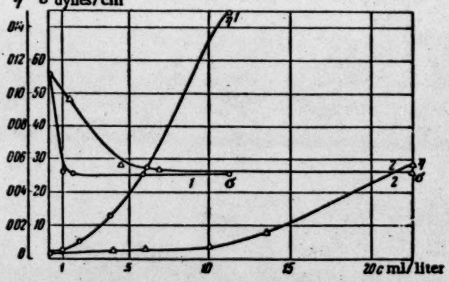

Fig. 3. Effect of additions of wetting agent in different concentrations on the viscosity η (poises) and surface tension σ (dynes/cm) of gelatin solutions; I) wetting agent 1; II) wetting agent 2.

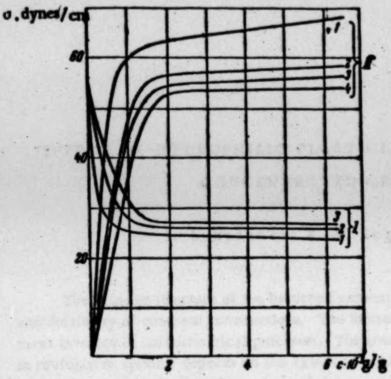

Fig. 4. Surface tension (I) and adsorption (II) isotherms for wetting agent 1 with different gelatin samples (1, 2, 3, and 4).

The Relationship (5) was found from the experimental data given in Figs. 1 and 2 (Curve 1). These figures show that the points for different gelatin concentrations coincided, thus confirming the views put forward. Figure 3 shows the course of the viscosity and surface tension variations with wetting agent concentration. It follows from Fig. 3 that an initial increase of wetting agent concentration produces a considerable decrease of surface tension and a slight change of viscosity. Subsequently, this relationship is reversed, i. e., the surface tension remains almost constant while the viscosity increases considerably. The reason is that initially adsorption occurs mainly at the air interface, and only later at the solvent interface.

Further evidence for the change of viscosity as the result of adsorption is provided by the data in Figs. 2 and 4. Figure 4 shows isotherms for the adsorption and the surface tension σ of wetting agent 1 for aqueous and gelatin solutions (three different gelatins), samples 1, 2, and 3. These results show that the adsorption of the wetting agent by each of the gelatins is different. In Fig. 2 (Curves II, III, and IV), the Relationship (5) is shown for these gelatins; this indicates that the different adsorption by each of the gelatin samples leads to a corresponding change of molecular configuration.

The above data provide direct experimental proof, based on adsorption measurements, of the validity of the views advanced earlier concerning the adsorption mechanism of the influence of surface-active substances on the viscosity of gelatin solutions.

SUMMARY

1. The view is confirmed that the increased viscosity of gelatin solutions on addition of surface-active substances is the result of adsorption of the latter, leading to changes in the shape of the gelatin molecules.

2. A relationship between the change in the specific viscosity of gelatin solutions and the adsorption of surface-active substances is derived and experimentally verified.

Scientific Research Institute for Cinephotography,
Moscow

Received December 29, 1955

LITERATURE CITED

[1] B. V. Deryagin, S. M. Levi, and V. S. Koltsov, Proc. Acad. Sci. USSR 79, 283 (1951).

[2] R. Simha, J. Phys. Chem. 44, 25 (1940).

[3] I. I. Zhukov, Colloid Chemistry, Leningrad State Univ. Press (1952).

EFFECT OF HYDROPHILIC PLASTICIZER ADDITIONS ON THE PROPERTIES OF CONCENTRATED CEMENT SUSPENSIONS

O. I. Lukyanova, E. E. Segalova, and P. A. Rebinder

The disperse structure of the hardened cement in concrete largely determines the mechanical properties and durability of concrete constructions. The formation of this structure in all its stages of origin and development involves colloidochemical processes. The course of hydration reactions of the cement clinker minerals in multiphase systems depends on the extent and qualitative composition of the cement particle surface and also on changes in the specific surface of the cement in the course of hydration.

New phases of the cement hydration products pass through the colloidal state as crystallization nuclei of the most rapidly crystallizing components, such as hydroaluminates and calcium hydroxide, or as slowly crystallizing calcium hydrosilicates, existing for a long time in a submicrocrystalline state.

The formation of a disperse structure as such in the hydration products, including various proportions of still nonhydrated cement grains, is due to bond formation between individual elements of the structure. These bonds may be of the nature of weak coagulation bonds or of crystal coalescence, according to the formation conditions and age of the structure.

It is important for pratical purposes to obtain hardened cement with a compact, monolithic structure, with a low susceptibility to the corrosive effects of the surroundings and a high mechanical strength. This goal is approached by decreasing the total porosity, especially the open (filtering) porosity, caused by evaporation of free water. Effective condensation of the structure is achieved by the combined use of various mechanical and physicochemical methods. Among the substances added to cement pastes and concrete mixes for increasing their density, a special position is held by organic surface-active substances which render the cement particle surfaces hydrophilic. Lignosulfonates in sulfite alcohol wastes (SSB) are most often used for this purpose.

The effects of hydrophilizing plasticizers on cements, caused by the properties of their adsorbed layers, are extremely varied, and are not confined to condensation of the hardened cement structure. It was discovered as early as 1937 [1] that additives of this type have a stabilizing effect on cement suspensions, retard cement hydration, and modify the crystallization rate of the hydration products.

The stabilizing and peptizing effects of SSB on cement suspensions have been discovered in numerous experimental investigations by Soviet [2-6] and foreign [7-9] scientists. The effects of SSB additions on the rate of chemical reaction between cement and water [2, 10], and on modification of the crystallization of cement hydration products and of the individual minerals of cement clinker [11-13] have also been studied. The influence of this plasticizer on the physical structure and mechanical properties of hardened cement has been investigated in detail [2-8].

In the present investigation we have studied some aspects of the influence of SSB lignosulfonates on structure formation in concentrated aqueous suspensions (pastes) of ground Portland cement clinkers during the initial stages of their interaction with water. The materials studied were factory Portland cement clinkers with different tricalcium aluminate contents, as it is known that the principal reactions in the initial period of interaction between Portland cement and water are hydration of the aluminate of the clinker and their interaction with the other cement components [2, 14]. The mineralogical composition of the clinker, calculated from chemical analysis data, is given in the table.

TABLE

Composition of the Portland Cement Clinkers Studied

Factories	Mineralogical composition, %			
	$3CaO \cdot Al_2O_3$	$3CaO \cdot SiO_2$	$2CaO \cdot SiO_2$	$4CaO \cdot Al_2O_3 \cdot Fe_2O_3$
Komsomolets (K)	5	58	18	16
Novorossiyski (N)	8	56	22	13
Gigant (G)	9	53	20	14
Chernovechensky (C)	11	51	22	11

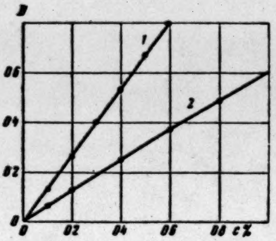

Fig. 1. Optical density of SSB lignosulfonate solutions; 1) pH 6.0; 2) pH < 3.0.

The SSB plasticizer used in our experiments consisted mainly of calcium lignosulfonates, and had a total solids content of 52.32%, including 3.62% calcium and 4.61% reducing substances, inclusive of 2.80% sugars. The small sugar content does not affect the properties of SSB as a cement plasticizer.

The action of calcium lignosulfonates on cement paste, suspensions, or concrete mixes depends largely on their adsorbability on the cement particles. It was therefore necessary to study the behavior of SSB lignosulfonates in cement suspensions during the initial period of interaction between the cement and water. The colorimetric method was used for determining lignosulfonate concentration in aqueous solutions after definite times of contact with the cement. The colorimetric method of lignosulfonate determination is free from error caused by different adsorbability of the lignosulfonates occurring is SSB plasticizers. The same method has been used by Shestoperov and others [2, 9].

In the pH range from 3 to 9 the color intensity of lignosulfonate solutions greatly depends on the acidity of the medium. This is important in relation to cement suspensions, in which large pH variations in the direction of increased alkalinity are possible. Our determinations showed that the optical density (D) of lignosulfonates, measured by the photoelectric colorimeter, greatly diminished with increasing acidity (Fig. 1), reaching a limiting value which does not change on further decrease of pH. Solutions of maximum acidity were therefore used for determinations of the concentration of lignosulfonate solutions. Despite the decreased sensitivity, the accuracy of the determinations is increased by acidification because the aqueous extracts of the cement suspensions do not become turbid in air.

Our experiments showed that adsorption of SSB lignosulfonates in cement suspensions is irreversible over a wide range of additions of SSB to the cement, including adsorbed layers containing 40-50 mg of lignosulfonates per 1 g cement, formed when the system contains more than 5% SSB on the weight of the cement. The adsorption becomes partially reversible at higher lignosulfonate contents in the cement suspensions. When such suspensions are mixed with water, some of the adsorbed substance can pass back into solution.

The irreversibility of the adsorption can be attributed to formation of surface compounds between the lignosulfonates and the clinker minerals, or peculiar denaturation of the former in the surface layers. This latter hypothesis is quite probable, as graphite, which is chemically inert to lignosulfonates, also adsorbs them irreversibly [15].

The formation of adsorbed layers of SSB lignosulfonates is a rapid process, completed within a few minutes. However, the amount of bound lignosulfonates may continue to increase, although at a much lower rate, owing to changes occurring in the system as the result of interaction between the cement and water. The initial adsorption, determined after 5 minutes of contact between the cement and water, or found by extrapolation of the kinetic curves for the binding of the lignosulfonates, comprises the main part of the adsorbed substance, and is a characteristic value. The initial adsorption (a_0) is linearly related to the SSB content of the system (Fig. 2). The linear relationship is also valid for very large additions of SSB, beyond the limits of those used in practice, 8-10% on the cement content. If systems are compared at equal lignosulfate concentrations in the solutions, the results are not independent of the amount of adsorbent (Curves 1,2 and 3,4, Fig. 2). If, however, the basis of comparison is the SSB content of the system relative to the cement content, the values for the adsorption are similar (practically identical) even for systems with an 8-fold difference of the water – cement (w/c) ratio (Curves 5,6, Fig. 2). Therefore, in studying the effects of adsorbed lignosulfonate layers on structure formation in cement suspensions, the SSB concentration in the system should be expressed as a percentage of the cement content.

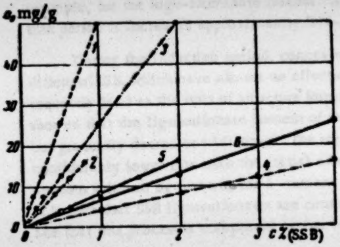

Fig. 2. Initial adsorption of SSB lignosulfonates in cement suspensions: 1, 3, 6 w/c ratio 4.0; 2, 4, 5) w/c ratio 0.5): 1,2) percentage concentration of SSB in solution after adsorption; 3,4) ditto, before adsorption; 5,6) SSB addition as percentage of the cement.

The peculiar character of lignosulfonate adsorption in cement suspensions is probably related to the gel-like nature of the adsorbed layers. The gel-like nature and the stabilizing action of adsorbed lignosulfonate layers in cement suspensions are confirmed, for example, by measurements of the volume of deposits formed in suspensions containing added SSB. The relative volume of the deposit (V) in a stabilized suspension greatly decreases with increasing amounts of lignosulfonates adsorbed by the cement particles, as Fig. 3 shows. This corresponds to increased stabilization of the suspension, i. e., increasingly complete prevention of coagulative structure formation. Complete stabilization of cements ground to medium fineness (with specific surface of 0.2-0.4 m^2/g is reached with additions of 0.5 to 1.0% SSB, on the weight of cement. The initial adsorption (a_0) is 3-5 mg per 1 g cement. The further increase of the volume of the deposit with increasing SSB content in the system is explained by the formation of thick gel-like lignosulfonate layers on the cement particles.

The stabilizing action of SSB on cement suspensions could not be applied in practice for increasing the density of hardened cement if the lignosulfonates did not, in addition, retard processes of cement hydration and crystallization of the newly formed materials. In presence of SSB, a cement suspension remains in its initial stabilized state for a considerable time, which depends on the amount added. The period during which the cement suspension remains in the retarded state may be termed the induction period of structure formation or of hydration.

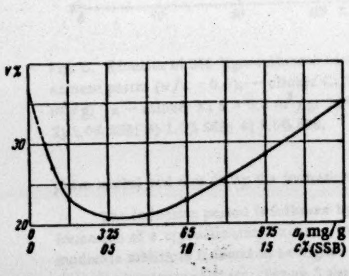

Fig. 3. Relative volume of deposits in cement suspensions stabilized by additions of SSB: $V=v/v_0 \times$ $\times$ 100 where v and v_0 are the volume of the deposit and the total volume of the suspension. Clinker G; S=0.35 m^2/g; w/c= 4.0.

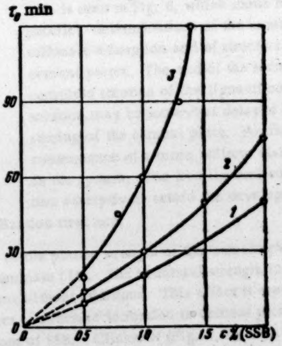

Fig. 4. Duration of the structure formation and hydration induction period (w/c = 0.5) : 1) clinker G; S = 0.5 m^2/g; 2) clinker C; S = 0.35 m^2/g; 3) clinker K; S = 0.5 m^2/g.

The variations in the mechanical properties of cement pastes during the induction period are very slight. The end of the induction period is easily established by the rapid acceleration of structure formation in cement paste, accompanied by an increase of its plastic strength.

The variation of the induction period (τ_0) with the amount of SSB added, for clinkers with different degrees of dispersion and tricalcium aluminate contents is shown in Fig. 4. A comparison of Curves 1 and 3 shows that the clinker with the higher tricalcium aluminate content has the shorter induction period for the same nominal specific surface and with equal amounts of SSB. Curves 1 and 2 represent clinkers with similar tricalcium aluminate contents but differing in specific surface. Comparison of Curves 1 and 2 shows that the clinker with the smaller specific surface has the longer induction period. The duration of the induction period also depends on the concentration of the cement suspension, decreasing with increase of the latter. For example, for the high-aluminate clinker "G", with $S = 0.5\ m^2/g$ (retarded by addition of 0.6% SSB), the induction period is increased approximately five-fold as the water – cement ratio increases from 0.4 to 4.0.

During the induction period, concealed processes occur in cement paste stabilized and retarded by additions of SSB, which have almost no effect on the mechanical properties during this stage, but which subsequently lead to the start of structure formation, the setting of the cement paste. Colorimetric measurements showed that the lignosulfonate content of the aqueous phase of the cement suspension does not remain constant, but gradually decreases with time. The sorption of lignosulfonates from solution by the cement occurs at a considerably lower rate than the initial adsorption. Fig. 5 shows the kinetics of sorption of lignosulfonates from aqueous solution by cement, for a cement paste made from clinkers with high and low aluminate contents. It is seen that SSB lignosulfonates are completely taken up from solution by cement paste in the course of time, and that this process is completed earlier in the high-aluminate cement.

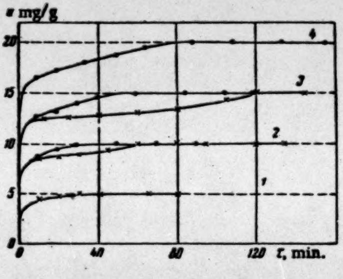

Fig. 5. Kinetics of SSB lignosulfonate adsorption by cement pastes (w/c = 0.5); • – clinker C; $S = 0.35\ m^2/g$; x – clinker K; $S = 0.5\ m^2/g$; 1) 0.5% SSB; 2) 1.0% SSB; 3) 1.5% SSB; 4) 2.0% SSB.

This effect is explained [16, 17] by adsorption of lignosulfonates on the clinker hydration products, the formation of which is greatly retarded in presence of lignosulfonates. Tricalcium aluminate, as the softest and most hydrophilic mineral in cement clinker, undergoes especially strong dispersing action of the adsorbed layers, and is at the same time the most rapidly hydrated mineral in the clinker.

The end of SSB sorption from the aqueous phase of the cement paste coincides with the end of the induction period, and with sharp acceleration of hydration and structure formation in the system. This is seen in Fig. 6, which shows the results of parallel determinations of the kinetics of lignosulfonate adsorption and of structure formation in cement pastes. The end of the induction period and complete sorption of the lignosulfonates from the solution may be somewhat delayed by prolonged stirring of the cement paste. Possibly this is the consequence of a more uniform distribution of SSB in the system. The free lignosulfonates in the solution adsorptively retard the development of new phase nuclei and thus delay the formation of a crystallization structure.

The induction period is followed by a sharp rise of the plastic strength of the cement paste, due to the formation of a crystallization structure in the hydroaluminate [14]. The structural strength in systems with moderate additions is found to be higher than in systems without additions. This effect is especially pronounced in high-aluminate clinkers. Figure 7 shows the kinetics of structure formation in cement pastes made from high-aluminate clinkers (without gypsum) with additions of SSB. Clinker N (Fig. 7, b), with additions of 0.1-0.5% SSB, and clinker G (Fig. 7, a), even with 1 and 2% SSB, show considerably greater increases in the strength of the hydroaluminate structure after the end of the induction period than systems without additions.

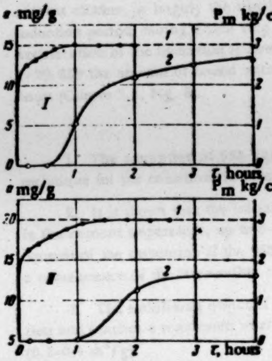

Fig. 6. Kinetics of structure formation and lignosulfonate adsorption in cement pastes (I) 1.5% SSB; II) 2.0% SSB); 1) lignosulfonate adsorption; 2) plastic strength of the cement paste (P_m).

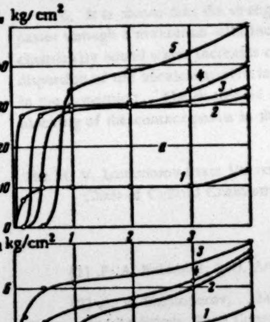

Fig. 7. Kinetics of structure formation in cement pastes made from high-aluminate clinkers (a) clinker G; S = 0.5 m²/g; w/c = 0.25; b) clinker N; S = 0.2 m²/g; w/c = 0.4): 1) without SSB; 2) 0.25% SSB; 3) 0.5% SSB; 4) 1.0% SSB; 5) 2.0% SSB.

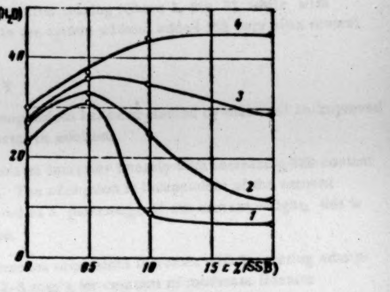

Fig. 8. Contents of chemically bound water (clinker C; S = 0.35 m²/g; w/c = 0.26): 1) 30 minutes after mixing; 2) 1 hour; 3) 3 hours; 4) 7 hours.

The increase of the strength of the structure may be caused by adsorptive dispersion of tricalcium aluminate in the clinker, resulting in an increase of its effective surface and increasing its rate of hydration (solution and therefore crystallization of the hydrate) in presence of SSB additions; this, in turn, results in a more rapid increase of the plastic strength. However, at very high SSB contents structure formation is retarded and the plastic strength of the cement paste is decreased, as can be seen, for example, in Fig. 7,b. This is probably caused by adsorptional blocking of the contacts in the crystallization structure of the hydroaluminate.

Acceleration of the hydration of high-aluminate cements in presence of small amounts of SSB may be observed by means of direct determinations of the kinetics of the chemical binding of water by cement pastes. Figure 8 shows the contents of chemically bound water (W) in cement paste made from high-aluminate clinker C with additions of 0 to 2% SSB, 30 minutes, 1, 3, and 7 hours after mixing of the cement paste. For these determinations the cement paste was treated with alcohol and ether; the resultant powder was dried in a vacuum dessicator and then heated at 1000° to constant weight. A correction for the lignosulfonates, burnt at this temperature, was introduced into the calcination loss values.

It is seen from Fig. 8 that additions of SSB favor an acceleration of chemical action between water and cement clinker, or largely the tricalcium aluminate in it. This acceleration occurs after the end of the induction period, during which very little water is combined. Therefore, in presence of small amount of SSB, acceleration of the hydration is already noticeable 30 minutes after mixing (Curve 1, Fig. 8), while with 1-2% SSB the amount of bound water becomes greater than in the system without added SSB only after several hours (Curves 3,4, Fig. 8).

SUMMARY

1. The adsorption of SSB lignosulfonates by cement suspensions has been studied by means of an improved technique for the colorimetric determination of lignosulfonates in solution.

2. It is shown that the initial adsorption of lignosulfonates increases linearly with increasing SSB content in the cement suspensions, up to 8-10% SSB on the cement. The adsorption is independent of the cement content of the suspension if the SSB concentration is expressed as a percentage of the cement weight; this is a consequence of the irreversible character of the adsorption.

3. The stabilizing effect of SSB lignosulfonates on cement suspensions increases with increasing adsorption and reaches a maximum when the adsorption reaches 3-5 mg/g for cements of moderate fineness (0.2-0.4 m^2/g).

4. The effect of the amount of SSB added on the duration of the induction period of structure formation and hydration has been studied in clinkers of different mineralogical compositions and degrees of dispersion. With equal amounts of SSB the length of the induction period decreases with increasing fineness and tricalcium aluminate content in the clinker, and also with decreasing water content in the suspension. Increase of the amount of SSB added to the suspension lengthens the induction period.

5. The content of SSB lignosulfonates in the liquid phase of the suspension was found to decrease during the induction period; this is caused by binding of the lignosulfonates in the formation of new surfaces during adsorptive dispersion of tricalcium aluminate and in the initial stage of crystallization of the hydroaluminate.

6. It is shown that the strength of the crystallization structure of the hydroaluminate increases and passes through a maximum with increasing amounts of added SSB in the cement suspensions. The amount of chemically bound water increases continuously in the process. This is probably explained by adsorptive dispersion of the tricalcium aluminate, eventually leading to accelerated hydration and structure formation in the suspension. The decreased strength of the structure at very high SSB contents is due to adsorptive blocking of the contact points in the crystallization structure of the hydroaluminate.

The M. V. Lomonosov State University, Moscow
Chair of Colloid Chemistry

Received October 5, 1956

LITERATURE CITED

[1] P. A. Rebinder, Bull. Acad. Sci. USSR, Div. Tech. Sci., No. 4 (1937).

[2] S. V. Shestoperov, M. Ivanov, A. N. Zashchepin, and T. Yu. F. Lyubimova, Cement Concrete With Plasticizing Additions, Road Construction Press, Moscow (1952).

[3] V. I. Soroker, Bull. Building Technol., No. 10 (1947); Plasticizers for Cement Pastes and Concretes, Moscow, Coal Tech. Press (1951); Plasticized Concretes and Pastes, Moscow-Leningrad, State Building and Architecture Press (1953).

[4] Ts. G. Ginzburg, Hydrotech. Construct., No. 4 (1949); Plasticizing Additions to Hydrotechnical Concrete, Moscow-Leningrad, Hydroelectric Power Press (1956).

[5] B. D. Trinker, Use of Plasticized Cement and of Plasticizing Additions to Concrete, State Constructio Press (1952).

[6] Yu. M. Butt and T. M. Berkovich, Cements with Surface-Active Additions (1953).

[7] E. W. Scripture, Eng. News Record, 127, No. 23, (1941;) Pit and Quarry 36, No. 2 (1943).

[8] T. C. Powers, J. Am. Concr. Inst.17, No. 2 (1945).

[9] F. M. Ernsberger, N. G. France, Ind. Eng. Chem. 37, No. 6, (1945).

[10] B. Ya. Yampolsky and E. S. Solovyeva, Trans. III All-Union Conf. Colloid Chem., 42, Acad. Sci. USSR Press, Moscow-Leningrad (1956).

[11] V. V. Stolnikov, Proc. Acad. Sci. USSR, 71, No. 2 (1950); J. Appl. Chem., 23, No. 7 (1950).*

[12] A. B. Shekhter, N. N. Serb-Serbina, and P. A. Rebinder, Proc. Acad. Sci. USSR, 89, No. 21 (1953).

[13] V. A. Tikhonov and L. A. Tikhomirova, J. Appl. Chem., 28, No. 10 (1954).*

[14] P. A. Rebinder, Trans. Conf. on Cement Chemistry, 125, Industrial Construction Press, Moscow (1956); E. E. Segalova and E. S. Solovyeva, ibid., 138.

[15] L. V. Lyutin and G. V. Zakharova, J. Phys. Chem., 4, No. 3 (1933); Colloid J., 4, No. 2-3 (1938).

[16] P. A. Rebinder and E. E. Segalova, Nature, No. 12 (1952).

[17] E. E. Segalova, P. A. Rebinder, and O. I. Lukyanova, Bull. Moscow State Univ., No. 2 (1954); Trans. III All-Union Conf. Colloid Chem., 26, Acad. Sci. USSR Press, Moscow-Leningrad (1956).

---

* Original Russian pagination. See C. B. translation.

PREPARATION OF FERRIC AND ZIRCONIUM HYDROXIDE ORGANOSOLS

V. N. Maslov

The transfer of colloid particles from one dispersion medium to another was observed long ago [1], and has been termed "the Wikkelblech phenomenon" and "pseudoextraction" [2]. The partial coagulation at the interface and within the liquid phases which occurs in the process is now explained [3] by lyophobization of the colloid particle surfaces with respect to both dispersion media.

The preparation of organosols from the corresponding hydrosols by transfer from one medium to another is very rarely used. A definite combination of dehydrating and lyophilizing factors is required for the formation of organosols by this method. For example, by the use of a third liquid which is distributed between the first two, as an auxiliary dehydrator, it proved possible to transfer selectively certain soil colloids from an aqueous into an organic phase [4]. This method has been studied in detail in relation to gold hydrosols and various organic systems [5]. It has also been shown that dissolved electrolytes influence the distribution of colloidal gold between liquid phases [6]. American patents [7] describe the production of organosols by multistage operations, with consecutive introduction of intermediate dispersion media, and including the removal of water by distillation. By replacing water in W, Mo, and Zr coagulates by acetone, and the latter by various hydrocarbon media, it proved possible to obtain organosols of these metals in presence of surface-active stabilizers and rubber [8].

Definite interest attaches to determination of the conditions in which colloidal hydroxides of heavy metals, having great affinity for water, may be transferred into an organic liquid in a single step, without preliminary dehydration of the system.

Colloidal solutions of ferric and zirconium hydroxides, prepared hydrolytically from $FeCl_3$ and $Zr(SO_4)_2$ [9], were used in our work. The iron contents of the aqueous and organic phases were determined by means of radioactive tracers. Benzene and toluene were used as the nonpolar liquids. The following methods were used for intermediate dehydration: 1) separation of the particles at the aqueous solution – air interface; 2) preliminary saturation of the air with vapor of the corresponding organic liquid; and 3) addition of a third liquid (acetone), distributed between the phases. The organosols were stabilized by additions of rubber and oxidized kerosene to benzene or toluene.

The simple apparatus shown in the diagram was used for preparation of the organosols. Each experiment lasted 30 minutes. The volumes of the aqueous phase and organic liquid were 115 ml and 25 ml respectively. Bubbles of air, 3-5 mm in diameter, were bubbled consecutively through the two liquid phases. Only the colloid particles which had been at the aqueous solution – air interface and were thus prepared for transfer into the other phase generally came into contact with the organic liquid. To prevent the ascent of bubbles near the walls, a directing ring was used; its performance was improved considerably by hydrophobizing treatment of its surface in diethyldichlorosilane or phenyltrichlorosilane vapor for 20 minutes [10].

It was found that when air, both with and without organic vapors in it, is bubbled through, no transfer of colloidal ferric and zirconium hydroxide into pure benzene or toluene occurs at all, and the film at the interphase boundary remains very thin and transparent. Additions of up to 4% (on the weight of the organic phase) of oxidized kerosene result in the transfer of accidentally present fine particles (dust, etc.) into the organic phase, and at the end of the bubbling a silvery opalescent film is seen at the interphase boundary. However, no transfer of the colloidal hydroxide occurs in this case either, or on addition of 0.005% rubber. The result is not changed by the presence of up to 4% acetone in the toluene, if rubber or oxidized kerosene are absent.

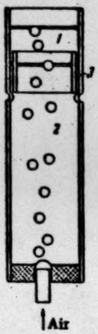

Apparatus for preparation of organosols by means of interphase air bubbling: 1) organic liquid; 2)original hydrosol; 3) directing ring.

Simultaneous addition of 1% oxidized kerosene, 0.005% rubber, and 4% acetone, and the bubbling of air saturated with benzene or toluene vapor, results in appreciable transfer of the hydroxides into the organic phase. Ferric and zirconium hydroxide organosols are quite transparent, but the former has a brownish color. A material balance shows that from 25 to 60% of the colloid taken remains in the films at the separation boundary. It is very helpful to dissolve part of the acetone in water first. In this case up to 40% of the ferric hydroxide was extracted into the toluene, from an initial hydrosol with a concentration of 0.02 g Fe/liter. The ratio of the concentrations of the organosols to the concentrations of the residual hydrosols reached 4-5. The resultant ferric and zirconium hydroxide organosols in benzene and toluene are quite stable to light, heating, and keeping, and may be concentrated by evaporation.

SUMMARY

1. To facilitate the direct transfer of colloid particles from an aqueous into an organic phase, in addition to the usual methods, interphase bubbling of air saturated with vapor of the corresponding organic liquid was used.

2. The resultant organosols of ferric and zirconium hydroxides in benzene and toluene are stable on keeping and may be concentrated by evaporation.

The Mendeleev Institute of Chemical Technology
Moscow

Received April 14, 1956

LITERATURE CITED

[1] K. Wikkelblech, Z. angew. Chem. 19, 1953, (1906).

[2] K. Kharichkov, J. Russ. Chem. Soc., Chem. Section, 52, No. 1-2-3, 96 (1920).

[3] E. M. Natanson, Colloid J., 9, 428 (1947).

[4] N. K. Krupsky, Trans. 3-rd Intern. Congr. Soil Sci., Oxford 1, 46, (1953).

[5] A. Janek, A. Schmidt, Koll.-Z. 66, 296, (1936).

[6] T. R. Bolam, J. Bowden, Rec. trav. chim. 58, 1109, 1939; C. A. 34, 3560⁸.

[7] C. A. 42, P2064 h.

[8] E. M. Natanson, Proc. Acad. Sci. USSR, New Series, 64, No. 6, 831 (1949).

[9] H. B. Weiser, Inorganic colloid chemistry, v. 2, New York, 1935.

[10] I. P. Alimarin and M. N. Petrikova, J. Anal. Chem., 10, No. 4, 251 (1955).

EXPERIMENTAL INVESTIGATIONS OF LAMINAR SYSTEMS

23. KINETICS OF THE FORMATION OF HYDROXIDE FILMS ON THE SURFACE OF CUPRIC AMMINE SOLUTIONS

S. G. Mokrushin and G. A. Kitaev

The spontaneous formation of hydroxide films on the surfaces of solutions of complex ammines of copper and nickel has been studied by one of the authors [1, 2]. The nature of the effect is that when such a solution is left to stand, hydrolysis of the complex salt accompanied by formation of colloidally dispersed hydroxide commences in its surface layers. The hydroxide particles become fixed in the solution surface, forming a very thin invisible film. The thickness of the film increases with time, it acquires interference colors and becomes visible.

The aim of the present investigation was to study the kinetic relationships in the formation and thickness increase of copper hydroxide films on the surface of cupric ammine solutions.

The copper hydroxide films were prepared by the improved technique described by Mokrushin [1], in which air is blown over the surface of a solution contained in a watch glass. In the present investigation a glass thermostat was used instead of the watch glass, while the air blown over the solution surface was heated and saturated with water vapor, so that the temperature of the solution was kept constant both throughout its volume and at the surface, and evaporation was prevented. The glass thermostat was heated by water by means of a Hoeppler circulation thermostat. The cup of the glass thermostat was cleaned by chromic acid mixture and then washed thoroughly with tap and distilled water. To prevent flow of surface-active substances onto the solution surface, a paraffin wax ring was made around the outer wall of the thermostat cup. The ammine solutions were made from copper sulfate solution and poured into the thermostat cup from a buret.

Experiments showed that a copper hydroxide film is not formed on a clean surface of ammine solution. If a monolayer of a nonvolatile surface-active substance is applied to the solution surface, a uniform lustrous hydroxide film is formed, exhibiting interference colors. It was found that a hydroxide film of more uniform thickness is formed on application of a substance which forms a liquid monolayer, such as oleic acid, to the surface of the solution. Substances which form solid films, such as palmitic acid, cetyl alcohol, and cellulose, also assist the formation of hydroxide films, but less uniform in thickness.

In the present communication the results of a study of the kinetics of copper hydroxide film formation on the surface of ammine solutions under a monolayer of oleic acid are discussed. Oleic acid was applied to the solution surface in a quantity sufficient to give a monomolecular layer. Ammoniacal solutions of copper sulfate of the following concentrations were studied: 0.025; 0.05; 0.10 and 0.15 mole/liter, at 10; 20; 30; 40; 50° with air blown at 0.5 and 1.0 liter/minute.

Figure 1 shows the growth of the thickness of hydroxide films on cupric ammine solutions. The thickness of the hydroxide films was determined by comparison of the interference colors of the films with the colors of Newton's rings in an air layer. The refractive index of the films was taken to be $n = 1.66$ [1].

Curve 1 (Fig. 1) represents the growth of a hydroxide film on a solution containing a slight excess of ammonia, while Curves 2 and 3 refer to solutions with ammonia in considerable excess. Comparison of the slopes of Curves 1 and 2 shows that excess ammonia in the solution has practically no effect on the rate of growth of the film thickness, but only affects the time interval before film formation begins. Variation of the rate of air blowing in the range 0.5-1.0 liter/minute has a similar effect. The character of Curves 2 and 3 is explained as follows. During the first 20-25 minutes the air blown over the solution surface removes excess ammonia. When the ammonia content of the solution has decreased enough for hydrolysis of cupric ammine to be possible, formation of the hydroxide film begins. At first isolated islets of the film are formed and the solution surface remains mobile. Gradually the islets become more numerous and finally they fill the whole surface of the solution, coalescing into a continuous immobile colorless film. The thickness of the film then begins to increase. It is easily seen that from 600 A the growth of film thickness is described by a linear equation. The rate of film growth is given by the tangent of the angle this line forms with the time axis.

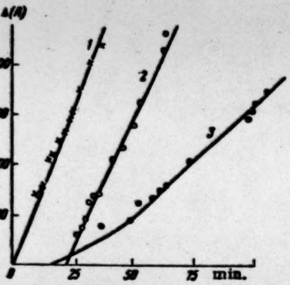

Fig. 1. Growth of the thickness of hydroxide films on cupric ammine solutions with concentration of 0.10 mole/liter (1 and 2) at 30° and 0.024 mole/liter (3) at 20°; air flow rate 0.5 liter/minute.

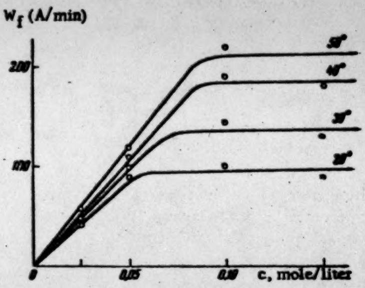

Fig. 2. Variation of the rate of growth of film thickness with concentration of cupric ammine solution at 20, 30, 40, and 50°.

Figure 2 shows the variation of the rate of growth of the film thickness (W) with concentration of the cupric ammine solution (c). The linear character of the initial portions of the curves indicates that the growth of films from solutions up to 0.1 mole/liter in concentration is determined by a process the kinetics of which can be represented by the equation for a monomolecular reaction.

The formation and growth of the film may be divided into several stages. In the first stage the rate of growth is determined by the rate of the reaction of ammine hydrolysis, i. e., by the formation rate of copper hydroxide, the material from which the film is formed. The hydrolysis reaction, for example of the complex ion $[Cu(NH_3)_2]^{2+}$, may be represented by the equation:

$$[Cu(NH_3)_2]^{2+} + 2H_2O = Cu(OH)_2 + 2NH_3 + 2H^+ .$$

Since the hydrolysis is accompanied by liberation of ammonia, the hydrolysis rate is determined by the rate at which ammonia is removed from the reaction zone.

In the second stage, the hydroxide particles become fixed on the solution surface. We regard this as a surface coagulation process, the kinetics of which may be represented by an equation for a reaction of the second order. It is probable that for solutions with a concentration of 1 mole/liter the surface coagulation process does not determine the rate of the aggregate process of hydroxide film growth. Conversely, in solutions of higher concentrations the rate of film growth is determined by the coagulation rate of the primary colloidally dispersed particles of copper hydroxide.

In order to find the rate-determining step, both the kinetics of ammonia evaporation and the kinetics of the hydrolysis reaction were studied. The kinetics of both processes can be described by an equation for a reaction of the first order, of the form

$$\frac{dx}{d\tau} = k(a-x),$$

where k is the reaction rate constant; a is the initial amount of ammonia or ammine complex; x is the amount of ammonia evaporated or ammine reacted in time τ.

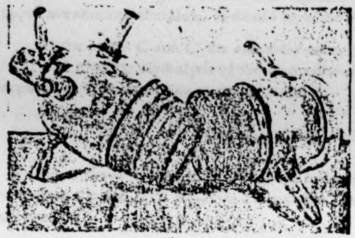

Fig. 3. Thermostat for studying the kinetics of ammonia evaporation and of the hydrolysis reaction (explanation in text).

The glass thermostat shown in Fig. 3 was used for studying the kinetics of these processes. 10 ml of cupric ammine solution with an accurately known ammonia content was put into the lower part 1 of the thermostat. Heated air saturated with water vapor was fed through the central tube 2 of the upper part of the thermostat, and then passed into wash bottles containing sulfuric acid. Ammonia was absorbed in the first wash bottle, containing 50 ml of 0.2 N H_2SO_4; the second contained 50 ml water, to which was added two drops of 0.2 N H_2SO_4 and two or three drops of bromocresol purple or phenolphthalein. The amount of ammonia absorbed was determined by back titration of excess acid by caustic soda solution. The second wash bottle served to check the complete absorption of ammonia in the first. The growth of the film was observed (by the alternation of its interference colors) through the thermostat wall.

The kinetics of ammine hydrolysis was studied in the same thermostat by a potentiometric method with the use of a cathode voltmeter, whereby it was possible to observe continuously variations in the concentration (activity) of the copper ions in solution. A saturated calomel electrode was used as the reference electrode. A copper-plated platinum electrode and an electrolytic switch were introduced through the two side tubes 3 of the glass thermostat (Fig. 3) and securely sealed. In this way it was possible to observe the film growth, variation of Cu^{2+} ion activity, and removal of ammonia from the solution simultaneously.

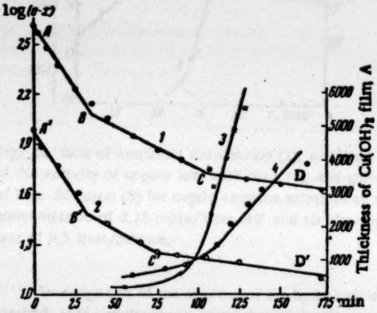

Fig. 4. Rate of ammonia evaporation (1,2) and growth of film thickness (3,4) for cupric ammine solutions with concentrations of 0.15 mole/liter (1) and 0.05 mole/liter (2,4) at 40°.

Figure 4 shows the experimental data for the kinetics of ammonia evaporation and growth of the film thickness at 40°.

The ammonia contents in 10 ml of cupric ammine solutions corresponding to the inflection points B and B' were found to be 120 and 30 mg, and corresponding to the points C and C', 53 and 18 mg. These amounts of ammonia correspond to the calculated amounts necessary for the formation of complex ions: 102 and 34 mg for $[Cu(NH_3)_4]^{2+}$ and 51 and 17 mg for $[Cu(NH_3)_2 \cdot (H_2O)_2]^{2+}$.

The agreement between the calculated and experimental data leads to the following explanation of the process of formation and growth of copper hydroxide films. First, ammonia in excess of the amount stoichiometrically required for formation of the $[Cu(NH_3)_4](OH)_2$ complex and binding of the sulfate ions of the copper is removed. A comparison of the slopes of the regions AB and A'B' of Curves 1 and 2 shows that the rate of ammonia removal does not depend on the amount of it added to the solution. At the instants corresponding to points B and B', hydrolysis of the copper tetrammine complex begins according to the equation

$$[Cu(NH_3)_4](OH)_2 + 2H_2O = [Cu(NH_3)_2(H_2O)_2](OH)_2 + 2NH_3.$$

The rate of ammonia evaporation decreases, and is determined at this stage by the hydrolysis rate of the ammine. Thus, the regions BC and B'C' represent evaporation of the ammonia formed by hydrolysis of the copper tetrammine complex. It should be noted that no film is formed at this stage.

At the points C and C' the ammonia contents of the solution are 53 and 18 mg (the theoretical amounts are 51 and 17 mg). Hydrolysis of the diammine-diaquo complex commences at this point, with formation of copper hydroxide according to the equation:

$$[Cu(NH_3)_2(H_2O)_2](OH)_2 = Cu(OH)_2 + 2NH_3 + 2H_2O.$$

Fig. 4 shows that rapid growth of the hydroxide film commences at the same time. This confirms that the regions CD and C'D' represent evaporation of the ammonia formed by hydrolysis of the diammine-diaquo complex.

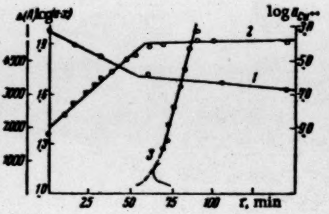

Fig. 5. Rate of ammonia evaporation (1), variation of the activity of copper ions with time (2), and growth of film thickness (3) for cupric ammine solutions at a concentration of 0.15 mole/liter, 40° and air blowing rate of 0.5 liter/minute.

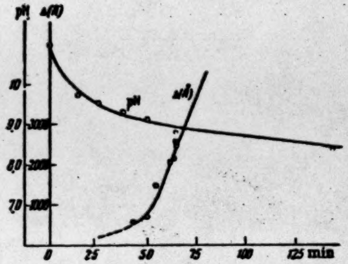

Fig. 6. Dependence of the growth of film thickness on the variation of pH with time for cupric ammine solution of c = 0.15 mole/liter.

Investigation of the kinetics of the hydrolysis of the cupric ammine complex by the potentiometric method, with simultaneous absorption of the liberated ammonia and observations of the growth rate of the hydroxide film, confirmed the mechanism of the process postulated above. As an example, Fig. 5 gives data for cupric ammine solution. The inflection point on Curve 1 corresponds to 52 mg ammonia in the solution, which corresponds to the amount necessary for formation of the diammine-di aquo complex. The inflection on the curve for the variation of cupric ion activity with time (2) coincides in time with the inflection on the ammonia evaporation curve (1). Formation and thickness increase of the film begins at the same time, which indicates the start of hydrolysis of $[Cu(NH_3)_2(H_2O)_2]^{2+}$ and formation of copper hydroxide.

The cupric ion activity at the start of film formation (inflection point on Curve 2, Fig. 5) is $a_{Cu^{2+}} = 10^{-3.9}$ Assuming that his is equal to the concentration, and using the value of the decomposition constant of the diammine complex

$$K = \frac{[Cu^{2+}]\cdot[NH_3]^3}{[Cu(NH_3)_2^{2+}]} = 1.05\cdot10^{-8},$$

When the ammonia concentration in the solution has been determined, it is possible to calculate the solution pH at which hydrolysis of the $[Cu(NH_3)_2]^{2+}$ ion occurs. The ionization constant of NH_4OH is $10^{-4.75}$ [4], and the ionic product for water at 40° is $10^{-13.42}$. Hence the pH is 9.73.

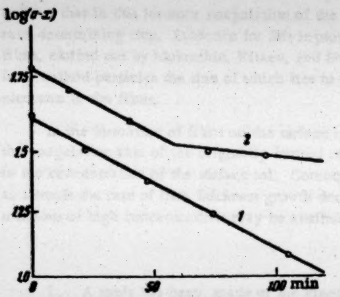

Fig. 7. Rate of evaporation of ammonia from solutions with a clean surface (1) and with surface covered with a monolayer of oleic acid (2).

TABLE

Calculated Values of m_1 and m_2 in mg/min for Cupric Ammine Solution at 40° and Air Blowing Rate of 0.5 liter/min

Solution concentration in mole/liter	$m_2 \cdot 10^{-6}$	$m_1 \cdot 10^{-6}$
0.025	34	34
0.05	68	64,5
0.10	136	97
0.15	204	90

The results of our simultaneous observations of variations of solution pH and film thickness, given in Fig. 6, confirm this approximate calculation. Film growth does in fact occur at pH 9.0. In our opinion, therefore, it may be concluded from the foregoing that rapid film growth coincides with the start of hydrolysis of the diammine-diaquo complex, accompanied by formation of copper hydroxide.

To decide whether ammonia evaporation or hydrolysis of the cupric ammine complex is the rate-determining step, a study was made of the evaporation of ammonia from a solution with a clean surface, i. e., in conditions in which a hydroxide film is not formed. The results of one such experiment are shown in Fig. 7. Hydroxide film begins to form at the point of inflection on Curve 2. The course of Curves 1 and 2 shows that evaporation of ammonia through the hydroxide film is the determining step in the growth of the copper hydroxide film.

The foregoing experimental results indicate that film formation coincides with the start of hydrolysis of the diammine-diaquo complex, and the rate of growth of the hydroxide film is determined by the rate of ammonia evaporation through this film.

Satisfactory agreement may be demonstrated between data for the evaporation of ammonia from the solution and the rate of film growth for solutions of concentrations ≤ 0.1 mole/liter. The film area in our experiments was $S = 15.95$ cm², the density of copper hydroxide $d = 3.37$ g/cc [4]; in one minute the film thickness increases by an amount which numerically corresponds to the film growth rate W in A/minute. Hence the weight increase m_1 of the film in unit time, i. e., the amount of copper oxide passing into the film, is $m_1 = SWd \cdot 10^3$ mg/minute. On the other hand, it is also possible to calculate the amount of copper hydroxide formed in the surface layers of solution in unit time from the rate of evaporation of the ammonia formed by hydrolysis of the complex ion $[Cu(NH_3)_2(H_2O)_2]^{2+}$.

The rate constant for the evaporation of ammonia through the hydroxide film is $K = 1.39 \cdot 10^{-6}$ min⁻¹, and the evaporation rate is evidently Kc_{NH_3} where $c_{NH_3} = a - x$. In accordance with the equation for the hydrolysis of the $[Cu(NH_3)_2(H_2O)_2]^{2+}$ ion, the hydrolysis rate is equal to half the rate of ammonia evaporation, and can be calculated from the expression:

$$m_2 = \frac{1}{2} \cdot \frac{98}{17} k (a - x).$$

An examination of the tabulated values of m_1 and m_2 shows that for solutions with concentrations of 0.025, 0.05, and to some extent 0.5 mole/liter the amount of hydroxide passing into the film is equal to the amount formed in solution $(m_1 \sim m_2)$.

For solutions the concentration of which is > 0.1 mole/liter, m_1 differs considerably from m_2, which indicates that at these concentrations the evaporation rate of ammonia does not determine film growth. We believe that in this instance coagulation of the colloidally dispersed copper hydroxide may be taken as the rate-determining step. Evidence for this is provided by electron microscope investigations of copper hydroxide films, carried out by Mokrushin, Kitaev, and Shabalina [5], who showed that copper hydroxide films are formed from colloid particles the size of which lies in the range 100-200 A. Larger particles cannot act as structural elements in the films.

In the formation of films on the surface of solutions with concentrations greater than 0.10 mole/liter, the coagulation rate of the originally formed copper hydroxide particles probably increases owing to an increase in the concentration of the surface sol. Consequently the number of particles of optimum size decreases, and as a result the rate of film thickness growth decreases also. The horizontal regions of the curves in Fig. 2 for solutions of high concentrations may be attributed to surface coagulation effects.

SUMMARY

1. A study has been made of the kinetics of growth of hydroxide films on the surface of cupric ammine solutions in relation to the concentration, temperature, and air blowing rate.

2. It is shown that $Cu(OH)_2$ films are not formed on clean solution surfaces. The presence of a monolayer of a surface-active substance is a necessary condition for film formation.

3. It is shown that the rate of film growth increases with increasing solution concentration and temperature and does not depend on the air flow rate.

4. On the basis of experimental data on the kinetics of ammonia evaporation and the hydrolysis of the cupric ammine, the process has been divided into the following steps: evaporation of excess ammonia, hydrolysis of the cupric tetrammine, hydrolysis of the diammine-diaquo complex, fixation of the colloidal copper hydroxide particles on the solution surface to form the film.

5. It is shown that for solutions with concentrations < 0.10 mole/liter the step which determines the growth rate of the $Cu(OH)_2$ film is evaporation of ammonia formed by hydrolysis of the diammine-diaquo complex, while for solutions of higher concentrations the rate-determining step is fixation of the hydroxide particles in the solution surface.

The S. M. Kirov Polytechnic Institute, Urals

Received May 28, 1956

LITERATURE CITED

[1] S. G. Mokrushin and P. S. Konyaev, J. Phys. Chem., 6, 1, 95 (1935).

[2] S. G. Mokrushin, J. Phys. Chem., 5, 8, 1082 (1934); Colloid J., 10, 4, 305 (1948).

[3] I. M. Kolthoff and J. J. Lingane, Polarography, State Chem. Press, Moscow-Leningrad, p. 185 (1948).

[4] Chemist's Reference Book, vol. 2, State Chem. Press, Moscow-Leningrad (1951).

[5] S. G. Mokrushin, G. A. Kitaev, and O. K. Shabalina, Proc. Acad. Sci. USSR, 1946, 1109 (1954).

THE RELATIONSHIP BETWEEN THE AFFINITY AND STRUCTURE OF DIRECT DYES

P. V. Moryganov and B. N. Melnikov

It has now been established that the selective takeup of direct dyes by cellulose fibers depends on such factors as linearity and plane structure of their molecules, the presence in the molecules of long chains of conjugated double bonds and groups capable of forming hydrogen bonds, and also a number of other less important factors. In Schirm's view [1], lengthening of the chain of conjugated double bonds between the outside auxochrome groups in the dye molecule leads to an increase in the residual valence forces at the ends of such a chain, and therefore increases the affinity of the dye for cellulose fibers. This readily explains why dyes derived from J acid have greater substantivity than dyes which are derivatives of γ or H acid.

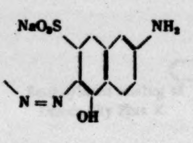

J-acid

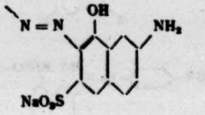

γ-acid

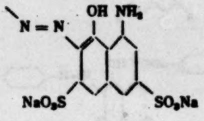

H-acid

The above formulas clearly show that the molecule of J acid has the longest chain of conjugated double bonds. According to Schirm, a dye molecule must contain a chain of not less than eight conjugated double bonds to ensure substantivity for cellulose fibers. Later work [2] has shown that this is not always true, a chain of five double bonds being sometimes quite sufficient. However, the lack of an exact definition of the concept of the affinity of a dye for a fiber delayed further detailed development of the theory of substantivity, as its value has frequently been determined under arbitrarily chosen conditions, making interpretation of the results difficult. Determinations of the affinity of direct dyes for cellulose fibers on a thermodynamic basis reported in a series of publications [3, 4] make it possible to verify and to extend considerably the views advanced earlier.

Accordingly, the purpose of the present work was determination of the thermodynamic affinity of a number of direct dyes of the same type with different lengths of conjugated double bond chains, and also a study of the effect of disrupted conjugation and of benzoylation of the free amino groups of the dyes on the affinity.

The affinity of a dye for the fiber was calculated from the formula:

$$-\frac{\Delta\mu^\circ}{RT} = \ln [D]_f \cdot [\mathrm{Na}]_f^z - \ln [D]_s \cdot [\mathrm{Na}]_s^z - (z+1) \ln V, \qquad (1)$$

where $[D]_\phi$ and $[Na]_\phi$ are the concentrations of dye and sodium ions in the fiber in gram-ions per kilogram of absolutely dry fiber $[D]_\sigma$ and $[Na]_\sigma$ are the concentrations of the same ions in solution in gram-ions per liter; V is the effective volume of the cellulose phase in liters per kilogram of the absolutely dry fiber; z is the valence of the dye anion.

The theoretical derivation of this formula and a detailed description of the equilibrium dyeing method were given in a number of our earlier papers [4-6].

The equilibrium dyeing experiments were performed at 80 and 100° with the following dyes:

Direct Sky Blue K (C. I. 406)

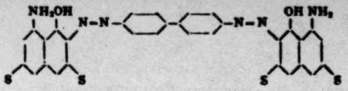

Direct Diazo Black O (C.I.395)

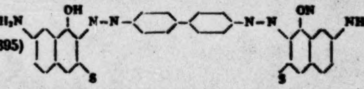

Analog of Direct Sky Blue K

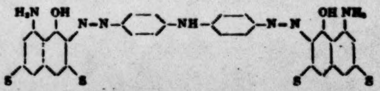

Benzoylated analog of Direct Sky Blue K

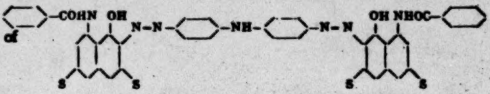

Analog of Direct Diazo Black O

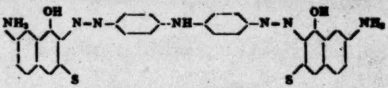

Benzoylated Analog of Direct Diazo Black O

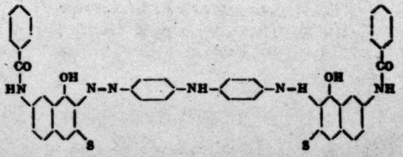

The results of determinations of the affinity of these dyes for cotton fabric are given in the table.

A comparison of the structure and affinities of the dyes studied shows that an increase of the number of sulfo groups in the dye molecule decreases affinity for cotton fiber. A particularly interesting feature is the sharp decrease of affinity in dyes derived from 4,4'-diamino-diphenylamine (analogs of Direct Sky Blue K and Direct Diazo Black O); this is probably largely explained by disruption of conjugation in the molecules of these dyes, and also partly by the fact that the azo groups in these dyes, in contrast to the corresponding dyes derived from benzidine, are separated by a distance greater than the repeat period of the cellulose macromolecule.

Affinities of Certain Direct Dyes for Cellulose Fiber in Relation to Their Structure

Dye	Experimental values in cal./mole		Calculated values in cal./mole	
	$-\Delta\dot{\mu}_{373}$	$-\Delta\dot{\mu}_{353}$	$-\Delta\dot{\mu}_{373}$	$-\Delta\dot{\mu}_{353}$
Direct Diazo Black O	5.40	6.06	—	—
Direct Sky Blue K	3.73	4.45	—	—
Analog of Direct Sky Blue K	2.34	2.56	—	—
Benzoylated analog of Direct Sky Blue K	3.77	4.38	3.85	4.07
Analog of Direct Diazo Black O	3.75	4.12	—	—
Benzoylated analog of Direct Diazo Black O	5.41	6.09	5.26	5.63

Replacement of hydrogen by the benzoyl residue in the amino groups increases the affinity of the dyes for cellulose in both cases owing to formation of carbamide groups, which confer high substantivity.

The higher affinity of benzoylated direct dyes in comparison with the same dyes before benzoylation may be attributed to an increase of the hydrocarbon—water interface by introduction of additional benzene rings into the dye molecule. This viewpoint has recently been developed extensively by Derbyshire and Peters [7].

In the formation of aqueous solutions of dyes, the large hydrophobic surfaces of their molecules cause the separation of water molecules against the action of intermolecular forces. This becomes possible only when the energy liberated in solvation of the sulfo groups present in the dye molecule completely compensates the absorption of energy in the formation of new hydrocarbon—water interfaces. Removal of dye from the solution by fixation in the fiber, and the consequent disappearance of hydrocarbon—water interfaces, results in a return of this energy, which appears in the form of free energy of dyeing. It is assumed that the dye is attached to the fiber by nonpolar van der Waals forces between the cellulose surface and the hydrophobic surface of the dye molecule. The solvated sulfo groups of the dye still remain solvated after the dye has become attached to the cellulose surface, at least until the dyed fiber has been removed from the dye bath and dried. Accordingly, introduction into the dye molecule of additional hydrophobic surfaces, with the same content of groups capable of strong hydration in them, leads to increase in the hydrocarbon—water interfaces, and consequently to decreased solubility on the one hand [8], and an increase of the free energy of dyeing on the other.

The decrease of the absolute value of the free energy of solvation, and therefore the increase of the free energy of dyeing, can be calculated from the formula:

$$-\Delta F = N\sigma\Delta S, \qquad (2)$$

where ΔS is the increase in the molecular surface on introduction of the hydrophobic group R; σ is the free energy per unit R . . . solv. surface; N is the Avogadro number.

Yatsimirsky [8] showed that Equation (2) provides a route to quantitative evaluation of the influence of various groups on the solubilities of organic compounds. Hartley [9] and later Meggy [10], gave the value $\sigma = 30\,\mathrm{erg/cm^2}$ for the C—H . . . H_2O interface; Equation (2) can accordingly be written as:

$$-\Delta F = 0.043\,\Delta S. \qquad (3)$$

In this equation ΔS is in A^2 and ΔF is in kilocalories. Equation (3) would be valid on the condition that all interaction between the separated water molecules ceases when the organic molecules are introduced into the solution. In reality the molecules do not become separated by infinitely large distances, interaction between them continues, and its value, according to Meggy [10], is about a half of the total free energy. Consequently, the free energy decrease resulting from introduction of the hydrocarbon residue into the aqueous solution is

$$-\Delta F = 0.021\,\Delta S. \qquad (4)$$

The surface area of an individual molecule can be estimated from known values for different bond lengths; according to our data, the value for the benzene nucleus is 36 A^2. This value, which represents the increase of the hydrophobic surface of a benzoylated direct dye over that of the nonbenzoylated dye, makes it possible to calculate the expected increase in the affinity of the former dyes in comparison with the latter. The corresponding calculated values for the affinities of benzoylated dyes are shown in the table above.

The reasonably good agreement between the experimental and calculated values suggests that the increased affinity of benzoylated dyes may be attributed not only to the strong substantivizing influence of the carabamide groups, but also to the considerably greater hydrophobic surface of these dyes. Good confirmation of this is also provided by the azotol series; they each contain a single carbamide group in the molecule, but differ very greatly in fiber affinity; this may be explained by the increase of the hydrophobic surface of the azotols with increasing molecular complexity.

SUMMARY

1. The length of the conjugated double bond chain is shown to have a strong influence on the affinity of direct dyes for cotton fiber. Disruption of this chain results in a sharp decrease of affinity, while replacement of one of the hydrogen atoms in the amino group by a benzoyl residue compensates for this decrease, and raises the affinity to the level of that of a nonbenzoylated dye before disruption of the conjugation.

2. It is shown that quantitative calculation of the increase in the affinity of a dye for fibers by introduction of new hydrocarbon—water interfaces into its molecules is possible in principle.

We express our gratitude to S. N. Solodushenkov for providing the dyes, derived from p,p'-diaminodiphenylamine, synthesized by him.

LITERATURE CITED

[1] E. Schirm, J. Prakt. Chem. 144, 69 (1935).

[2] B. M. Bogaslovsky, Dissertation (1946).

[3] W. J. Marshall and R. H. Peters, J. Soc. Dyers Col. 63, 446 (1947).

[4] P. V. Moryganov and B. N. Melnikov, Trans. Ivanovo Inst. Chem. Technol. 5, 121 (1955).

[5] P. V. Moryganov and B. N. Melnikov, Textile Ind. No. 8, 33 (1955).

[6] P. V. Moryganov and B. N. Melnikov, Colloid J. 18, 49 (1956).

[7] A. N. Derbyshire and R. H. Peters, J. Soc. Dyers Col. 71, 530 (1955).

[8] K. B. Yatsimirsky, J. Anal. Chem. 8, 5, 314 (1953).

[9] G. S.Hartley, Koll.-Z. 88, 22 (1938).

[10] A. R. Meggy, J. Soc. Dyers Col. 66, 510 (1950).

Received February 12, 1956

Ivanovo Institute of Chemical Technology

STRUCTURE OF HIGH POLYMERS

COMMUNICATION 18. STRENGTHENING OF THE MOLECULAR STRUCTURE OF TIRE YARN

A. B. Pakshver, L. S. Gerasimova, and Kh. N. Kozlovskaya

Tire yarns made from artificial fibers have high heat endurance (viscose yarn) or high tensile strength (capron). Nevertheless, these fibers, especially capron, have a serious defect: the fibers are very extensible under low loads, and as a result the tires are deformed by the action of small loads (i. e., the tires " swell"). This effect can be explained by the low value of the modulus M. * We have shown [1] that the magnitude of the modulus M depends on intermolecular interaction, which is determined by the existence of dipole bonds between the polar groups of the macromolecules, and it may increase or decrease within wide limits according to the methods for the production and subsequent processing of the fibers. When fibers are stretched, especially in the heated or swollen state, the molecular structure is strengthened considerably; this is manifested in an increase of the modulus M, a decrease of the sorption capacity [1] and rate of sorption of various polar substances [2], retardation of variation of fiber length during swelling [3], and decrease of the heat of solution [4]. It is known [5] that when fibers, especially thermoplastic, are stretched, the strengthening of the molecular structure is accompanied by increase in the heat endurance of the fibers.

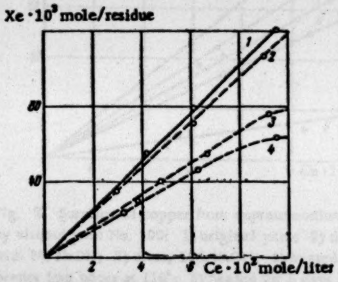

Fig. 1. Sorption of phenol by capron yarn. 1) Original yarn at 17°; 2) heat-stretched at p = 500 g, 17°; 3) ditto, 55°; 4) ditto, 100°.

The stretching of fibers in the heated or swollen state is accompanied by weakening of intermolecular bonds and slipping of the macromolecules in the direction of the stretch. If the cause of the weakening of the intermolecular bonds is then removed, then the intermolecular forces may either increase, or decrease as the result of increasing flexibility of the macromolecules, depending on whether the fibers are cooled or washed in the stretched or relaxed state. In the former case the "rigidity" of the fiber is increased and the modulus M increases considerably; in the latter, the modulus M decreases and the fiber becomes softer. In tire cord production it is particularly valuable to increase the modulus M, by processing the fibers in the stretched state.

To determine the effects of stretching on the physicochemical and physicomechanical properties (values of K_e, D, and M) of viscose and capron

---

* The modulus M is our term for the load on the thread which produces a given extension.

tire yarn, experiments were carried out in which the yarns were stretched in the heated state in a laboratory tube, with definite times, temperatures, and extensions* . The methods described previously [1] were also used to determine values of the modulus M at 5% extension (by means of a recording dynamometer), the rate and equilibrium value of the sorption of phenol by capron fiber, and of copper from cuprammonium reagent [6] and of triethylbenzylammonium base (TEB) from its solutions by viscose fiber. The data so obtained were used to calculate the diffusion coefficients D and the sorption equilibrium constants K_e. Tables 1 and 2 give the values found for M, D, and K_e. Sorption isotherms for the original, stretched, and relaxed fibers are also shown in Figs. 1-3. Figures 4-7 show the influence of heating time, load, initial fiber modulus, and temperature on the modulus of capron yarn. Figures 4 and 7 show that under laboratory conditions the maximum value of the modulus M_5 is reached when capron yarn is heated to 150° for 8 seconds, or to 170° for 1.5 seconds at loads up to 500 g per thread, i. e., at 30% of the breaking load. According to the literature [5] treatment of nylon yarn for use in tire cords requires heating to 180-190° for 7 seconds at 50% of the breaking load. The data in Figs. 4-7 show that when the heating time is increased above the optimum, the modulus again decreases rapidly and the fiber loses strength. The optimum value of the modulus M is reached more rapidly at higher temperatures, greater loads, and with higher values for the initial fiber modulus. In presence of lactam the modulus M increases more rapidly, but storage of capron fibers containing lactam for 2 months leads to a sharp deterioration of the heat stretching process and to decreased values of the modulus M for the same temperatures and times of heating. Thus, lactam acts as a typical plasticizer, but in course of time fibers containing lactam become more brittle, age, and are found to be less suitable for heat stretching.

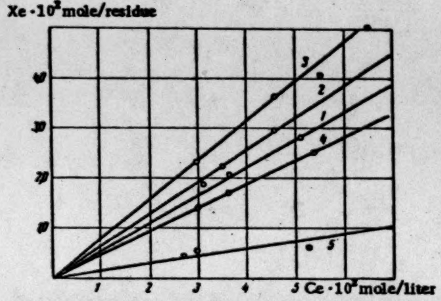

Fig. 2. Sorption of copper from cuprammonium reagent by viscose yarn No. 100: 1) original yarn; 2) treated with 5% NaOH; 3) ditto, 10% NaOH; 4) heated for twenty four hours at 110°; 5) heated for 5 days at 110°.

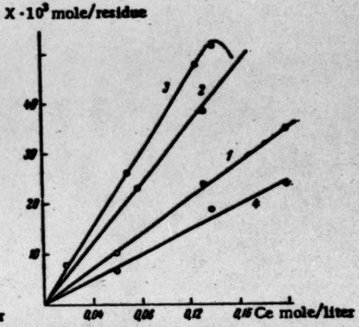

Fig. 3. Sorption of triethylbenzylammonium base (TEB) by viscose yarn No. 100: 1) original yarn; 2) treated with 5% NaOH; 3) ditto, 10% NaOH; 4) heated for twenty four hours at 110°.

Figures 8 and 9 show that the modulus M rises sharply with decreasing rate of diffusion of phenol and decreasing sorption capacity of the fiber. The parameters D and K_e characterize condensation of the molecular structure in heat stretching.

Comparison of the data in Tables 1 and 2 clearly shows the small influence of heat treatment on viscose yarn in comparison with capron. The modulus of viscose yarn is increased by only 10% even by heating under the optimum conditions at 160° for 10 seconds. Similar treatment of capron cord yarn increases the deformation modulus from 280 to 500 g per thread, i. e., by 80%.

---

* The optimum heat treatment conditions vary according to the dimensions of the heating tube; the temperature and duration of heat treatment should increase with increasing size of the equipment used for the treatment.

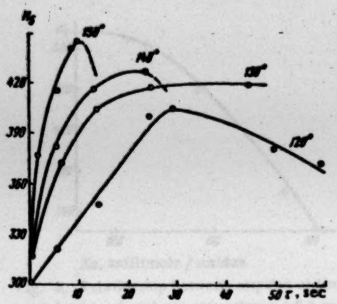

Fig. 4. Effect of heating time on M_s modulus in heat stretching of capron yarn; load p = 200 g per thread.

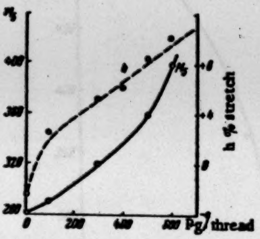

Fig. 5. Effect of load on modulus M_s and stretch h in percent in heat stretching of capron yarn, heated for 1.5 sec at 170°.

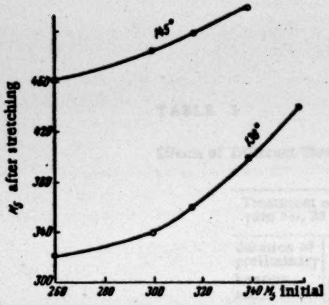

Fig. 6. Effect of initial modulus on increase of M_s in heat stretching of capron yarn for 10 seconds at p = 200 g per thread.

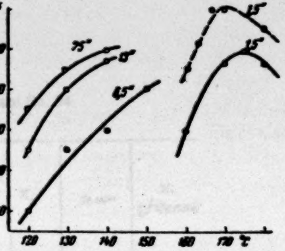

Fig. 7. Effect of temperature on heat stretching of capron yarn at p = 200 g per thread; continuous lines — yarn without lactam; broken line — yarn with lactam.

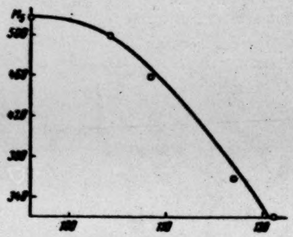

Xe, millimole / residue

Fig. 8. Relationship between sorption of phenol and modulus M; phenol concentration c = 8.5 mole/liter.

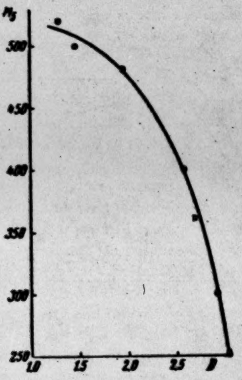

Fig. 9. Relationship between diffusion rate (D × 10^{10}) of phenol and modulus M.

TABLE 1

Effects of Different Treatments of Capron Yarn No. 34

Treatment of capron yarn No. 34		Sorption temperature, °C	K_e	$D\cdot10^{10}$	M, g/thread
duration of preliminary heating, sec.	Heat stretching at 150° under loads in g/thread				
—	—	17	1 35	2 90	280
—	—	55	1 0	—	—
—	—	100	0 6	—	—
—	100	17	—	2 59	—
—	200	17	1 2	1 94	440
—	200	55	0 9	—	—
—	200	100	0 75	—	—
10	200	17	—	.1 47	445
8	500	17	—	—	500

TABLE 2

Effects of Different Treatments on Viscose Yarn

Characteristics of viscose fibers studied	Treatment		K_e at 17° for sorption of		Modulus M_s in g per thread
	heating temperature, °C	heating time	cuprammonium base	triethylbenzylammonium base	
Viscose yarn No. 100	—	—	0,038	0.200	100
Ditto, treated (without tension) with 5% NaOH	—	—	0.060	0.300	85
Ditto, 10% NaOH	—	—	0 068	0.360	72
Ditto, heated dry under tension	110	1 hr.	0.018	0.118	90
	160	10 sec.	—	—	110
	170	10 sec.	—	—	95
Ditto, heated in glycerol (without tension)	180	2 hrs.	0.050	0.255	100
Viscose cord No. 7.3	—	—	0.068	0.267	580
Ditto, heated under tension	160	10 sec.	0.060	0.210	600

SUMMARY

1. Heat stretching increases the modulus M of viscose yarn by 10%, and almost doubles that of capron yarn. The increase of the modulus is accompanied by decreases in the rate and magnitude of sorption, i. e., in the physicochemical data which characterize the strength of the intermolecular structure.

2. Above certain optimum values of temperature, heating time, and load, the quality of the yarn deteriorates.

3. Free swelling of viscose yarn in alkali solution (shrinkage) results in increased softness, decrease of the modulus M, and increased sorption of bases.

4. Lactam acts as a plasticizer in the heat stretching of capron.

LITERATURE CITED

[1] A. B. Pakshver, E. E. Natan and I. F. Katushkina, Colloid J., 19, 109 (1957).*

[2] E. K. Mankash and A. B. Pakshver, Colloid J., 16,451 (1954); V. D. Tetyushkina, A. B. Pakshver, and S. S. Frolov, Colloid J., 17,120 (1955).*

[3] E. K. Mankash and A. B. Pakshver, J. Appl. Chem., 26, 835 (1953).*

[4] E. K. Mankash, Trans. Ivanovo Inst. Chem. Technol., 109 (1954).

[5] Litzler., Mod. Text. Mag. 35, No. 2, 32, (1954).

[6] B. D. Tukhlov, S. S. Frolov, and A. B. Pakshver, J. Appl. Chem., 27, No. 8, 907 (1954).*

Ivanovo Institute of Chemical Technology

Received October 19, 1955

---

* Original Russian pagination. See C. B. translation.

MOLECULAR STRUCTURE OF HIGH POLYMERS

COMMUNICATION 17. INVESTIGATION OF THE INTERMOLECULAR STRUCTURE OF THERMOPLASTIC FIBERS

A. B. Pakshver, E. E. Natan, and I. F. Katushkina

It has been shown in the case of capron fiber that as the intermolecular structure is strengthened by stretching or heat treatment of the fiber, sorption of phenol [1] and hydrochloric acid [2] is retarded, the equilibrium amounts of sorbed phenols are decreased [3], the dyeing rate is diminished [4], and changes of fiber length during swelling are retarded [5]. The decreased coefficients of diffusion of various substances into the fiber, decreased equilibrium amounts of bound phenols or acids, and retardation of shrinkage processes during swelling, characterize the strengthening of intermolecular dipole bonds between the amide groups of the macromolecules. Stretching of polyamide fibers, especially in the heated state, increases the energy of intermolecular interaction and the deformation modulus. Brief heating or swelling of the fibers in the unstretched state, on the other hand, weakens the intermolecular bonds, causing increased sorption of phenols and a decrease of the deformation modulus.

These effects are characteristic for all thermoplastic fibers, in which intermolecular dipole bonds are rapidly weakened by increase of temperature. The most characteristic thermoplastic fibers are fibers made from polyvinyl polymers, such as "khlorin" fibers from chlorinated polyvinyl chloride and "nitron" from polyacrylonitrile, and also acetate fiber. Data on the rate and magnitude of phenol sorption by nitron yarn and on the magnitude of acetone sorption by khlorin and acetate fibers are given below. Phenol was determined by the bromide – bromate method [1], and acetone iodometrically [6]. The diffusion coefficients were calculated by the same method as before. The equilibrium constant K_e was calculated from the sorption isotherms by the formula

$$K_e = \frac{x}{(1-x)\,c_e},$$

where $\underline{x}$ is the amount of sorbed substance in mole/mole; c_e is the equilibrium concentration in solution of the substance being absorbed, in mole/liter.

For the linear portions of the isotherms this equation simplifies to $K_e = \frac{x}{c_e}$. Figs. 1 – 3 show isotherms for the sorption of acetone by acetate and khlorin yarn, and of phenol by nitron yarn. The table gives calculated values of the equilibrium constant K_e and of the deformation modulus M, in kg/mm². Figures 4 and 5 show the effects of temperature, load, and stretching time on the deformation modulus M and give the optimum conditions for the production of fibers with maximum modulus.

The data in the table and Figs. 1-5 show that stretching of thermoplastic fibers increases the modulus of deformation and decreases the equilibrium constant K_e and the diffusion coefficient D. Thus, stretching of these fibers intensifies intermolecular interaction, decreases the sorption capacity of the fibers for substances which solvate the polar groups of the polymers, and makes the fibers more rigid.

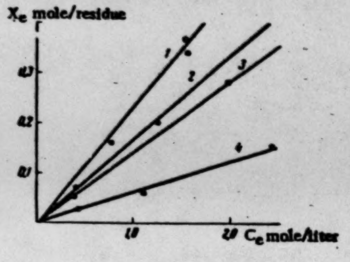

Fig. 1. Sorption of acetone by khlorin: 1) resin; 2) unstretched yarns; 3) yarn after 4-fold stretching; 4) yarn after 4-fold stretching and additional 22% stretch at 60°.

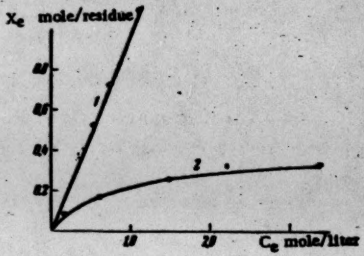

Fig. 2. Sorption of acetone by acetate yarn: 1) original yarn; 2) yarn stretched by 21% at 135°.

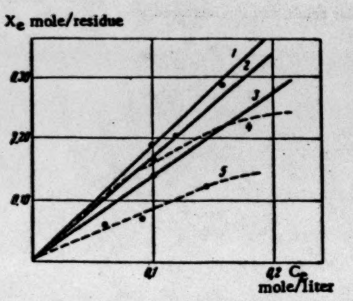

Fig. 3. Sorption of phenol by nitron yarn and resin: 1) nitron resin at 17°; 2) ditto, at 47°; 3) ditto, at 100°; 4) nitron yarn at 17°; 5) ditto, at 55°

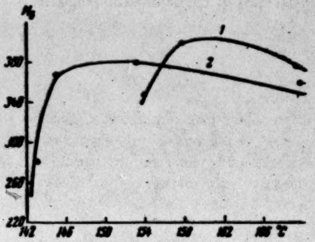

Fig. 4. Heat stretching of nitron yarn: 1) load 25 g per thread, 1.8 sec.; 2) load 10 g per thread, 6 sec.

TABLE

Equilibrium Constants K_e, Diffusion Coefficients D and Deformation Moduli M of Khlorin, Nitron, and Acetate Yarns After Various Treatments.

Type of yarn and treatment	N_m	Sorption temperature, °C	K_e	$D \cdot 10^{10}$	Deformation modulus $M_{1\%}$	Deformation modulus $M_{2.5\%}$
Original khlorin resin	10	17	0 200	—	1.13	5 16
Ditto, spun without stretch	32	17	0 165	—	2 26	—
Ditto, yarn stretched 4-fold at 160°	93	17	0 155	—	7 3	—
Ditto, additional 22% stretch at 60°; 3.5 sec.; load 30 g per thread	100	17	0 065	—	8 0	—
Original acetate yarn	90	17	1 02	—	—	3 1
Ditto, 14% stretch at 125°; 3 sec.; load 20 g per thread	118	17	0 33	—	—	7 16
Ditto, 21% stretch at 135°; 2.5 sec.; load 25 g per thread	134	17	0 19	—	—	11.36
Original nitron resin	—	18	0 205	—	—	—
	—	47	0 177	—	—	—
	—	100	0 133	—	—	—
Ditto, after heating at 160°, 60 min.	—	18	0 113	—	—	—
Original nitron yarn	100	18	0 147	14 6	—	—
	100	53	0 118	—	—	—
	100	95	0 079	—	—	—
Ditto, 10-fold stretch in spinning	100	18	0 254	—	—	—
Ditto, 15-fold stretch	100	18	0 197	—	—	—
Ditto, 20-fold stretch	100	18	0 147	—	—	—
Ditto, 15-fold stretch and additional 13% stretch at 155°	115	18	0 149	7 7	—	—

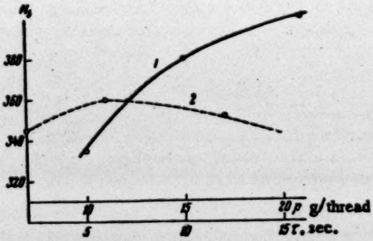

Fig. 5. Heat stretching of nitron yarn: 1) effect of load at 155°, 1.8 sec.; 2) effect of heating time at 155°, load 15 g per thread.

SUMMARY

1. Sorption of phenol by nitron yarn and of acetone by acetate and khlorin yarns decreases with increasing stretch of the fibers.

2. The sorption decreases with increase of temperature, which is characteristic for processes occuring with a decrease of enthalpy.

3. Stretching of acetate, khlorin, and nitron yarns results in decrease of the equilibrium constant K_g, increase of the modulus of deformation M, and decrease of the diffusion coefficient D. All this definitely indicates strengthening of the intermolecular structure.

Ivanovo Institute of Chemical Technology

Received October 19, 1955.

LITERATURE CITED

[1] E. K. Mankash and A. B. Pakshver, Colloid J., 16, No. 6, 451 (1954). *

[2] V. A. Myagkov and A. B. Pakshver, Colloid J., 17, No. 2, 120 (1955).*

[3] V. D. Tetyushkina, A. B. Pakshver, and S. S. Frolov, Colloid J., 17, No. 1, 63 (1955).*

[4] E. K. Mankash and A. B. Pakshver, J. Appl. Chem., 26, No. 9, 976, and No. 11, 1200 (1953).*

[5] E. K. Mankash and A. B. Pakshver, J. Appl. Chem., 26, No. 8, 835 (1953).

[6] A. N. Akhreyanova, K. N. Vanyushina, and B. E. Geller, Factory Labs., No. 12, 1431 (1951).

---

* Original Russian pagination. See C. B. translation.

THE ELECTROCHEMISTRY OF HIGH-POLYMER DISPERSIONS

3. EFFECT OF pH ON THE ELECTROKINETIC POTENTIAL OF GLOBULES IN SYNTHETIC LATEXES

R. M. Panich and S. S. Voyutsky

The effect of pH on the electrokinetic potential (zeta potential) of natural latex particles has been studied by several workers [1-3]. It has been established that the zeta potential of natural latex globules first increases with pH, and then remains constant or even decreases. The increase of zeta potential with increasing pH of the latex is probably caused by the greater ionization of the stabilizer molecules in an alkaline medium. The subsequent fall of zeta potential is probably caused by desorption of proteins, readily soluble in alkaline media, from the globule surfaces, by cation adsorption, and also by increase of the ionic strength of the medium as the result of addition of alkali.

Decrease of pH results in charge reversal in natural latex globules, and the latex passes through the isoelectric point at which it coagulates if special steps are not taken.

Maron and Bowler [4], and also Voyutsky and his associates [5-7] showed that the zeta potential of synthetic latexes changes similarly to that of natural latex with increased pH. Coagulation was observed by all foreign workers in synthetic latexes with decrease of pH. However, in 1950 the present authors showed for the first time that if the latex is sufficiently dilute (not more than 3-4% solids content) and the required amount of acid is added rapidly, the pH can be decreased to 2.5 and less. Qualitative experiments on determination of the charge of the particles in latex acidified with hydrochloric acid showed that in this case the globules are positively charged.

The isoelectric point of undialyzed synthetic latexes was also found, and the nature of the variations of the zeta potential in the region below this point was studied; it was found that the potential first increased and then decreased as acid was added to the latex.

In the present investigation the effect of pH on the zeta potential of globules in dialyzed synthetic latexes at constant known ionic strength was studied. In this way it is possible to take into account the influence of a number of complicating factors in determinations of electrophoretic mobility, and therefore to obtain more correct values for the zeta potential.

Materials studied and methods for determination of electrokinetic potential. Two latexes were studied: latex A, consisting of a dispersion of vinyl chloride – divinyl copolymer in ammonium oleate solution, and latex B, which was a dispersion of a polar polymer in ammonium naphthenate solution. Both latexes were used in the form of dialyzates, denoted by AD2 and BD1 respectively. Fuller details of the original latexes and their dialyzates are given in earlier publications [8, 9].

The zeta potential was determined by means of macroelectrophoresis by a method described previously [9]. In this method the dialyzed latexes were diluted with a buffer mixture of known composition. A suitably diluted buffer mixture was also used as the auxiliary liquid in electrophoresis. Since the electrolyte contents of dialyzed latexes are very low in comparison with those of buffer solutions, it may be assumed that in this instance the ionic strengths of the latex and auxiliary liquid are practically equal. This method had a number of advantages, including the fact that it enabled us to make corrections for electrophoretic lag and electrical relaxation. The determinations themselves were performed in the Rabinovich and Fodiman apparatus [10].

The buffer mixtures used were solutions containing univalent ions only, of different pH values, but with the same ionic strength of 0.02. Buffer mixtures of higher ionic strength caused coagulation of the latexes at low pH values.

Effect of pH on the electrokinetic potential of latex globules. Latex AD2 was diluted with distilled water before the determinations to approximately 1% solids content, and then diluted twofold with buffer mixture. Thus, the values given below for the zeta potential refer to globules in latex with ~ 0.5% solids content. The numerical coefficient in the Henry formula used to calculate the zeta potential was chosen on the basis of the facts that the ionic strength of the final solution was 0.01, the buffer solution contained univalent ions only, and the particle radius of AD2 latex was 210 A [8].

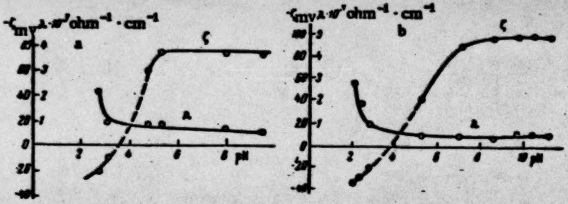

Fig. 1. Variations of the electrokinetic potential (ζ) of the globules, and of the specific conductance (λ_0) of latex AD2 (a) and BD1 (b) with pH.

The results of the experiments on AD2 latex are shown graphically in Fig. 1, a. It is seen in Fig. 1, a that the zeta potential remains unchanged as the pH varies between 10 and 5.3, and then falls sharply with further increase of hydrogen ion concentration, becoming zero at pH of about 3.7, and finally reaching increasing positive values.

The specific conductance, variations of which are also shown in Fig. 1 a, is more or less constant at pH > 3 and increases appreciably only in strongly acid media. This increase must evidently be attributed to the exceptionally high mobility of the hydrogen ion.

The results of experiments on latex BD1 are shown in Fig. 1, b. It is seen that the general character of the variation of zeta potential with hydrogen ion concentration is the same as for latex AD2, but the curve begins to descend at pH 7.

Effect of pH on the aggregative and sorptional stability of synthetic latexes. To determine the effect of pH on the aggregative stability of synthetic latexes, an investigation was made of the change in the particle size in diluted AD2 latex after twofold dilution by buffer mixtures of various pH., but with the same ionic strength of 0.02. The degree of dispersion was determined nephelometrically [11] half an hour, and 25 days after dilution of the latex. The sorptional stability of the resultant systems toward cotton wool was determined at the same time. For this, 20 ml of the latex diluted by the buffer was placed in contact with 0.5 g cotton wool, and after 30 minutes the latex was poured off and its rubber content was determined nephelometrically.

The results of the experiments are given in the table.

It is seen from the table that latexes with 0.375% solids content have considerable aggregative stability at pH above 6.2 – their particle size remains practically unchanged for 25 days, which is quite consistent with the high negative values of their zeta potential.

The particle size does not increase upon reversal of charge when the latex pH is taken to 2.7; however, the resultant latex has low aggregative stability and in the course of 25 days its particle size is increased by about a half. If during the charge reversal the pH is taken to only 3.1, the latex particles increase in size during the process; the size increase continues in the reversed latex and the latex coagulates in twenty four hours. At the isoelectric point, pH 3.9, a stable latex cannot be obtained.

TABLE

Particle Size and Sorptional Stability of Diluted AD2 Latex at Various pH Values

pH	in mv	Particle diameter after dilution, in A		Latex concentration, % solids		Sorption, %
		after 1/2 hour	after 25 days	before sorption	after sorption	
8.3	−72	510	520	0.375	0,334	10.9
6,2	−72	513	520	0.375	0.328	12.5
3.9	(−8)	Coagulation occurred on dilution of the latex by the buffer				
3.1*	+11.4	575	—	0.375	0.093	75.5
2.7	+20.6	486	725	0.375	0.225	40

---

* The latex coagulated after 24 hours.

The table also shows that positively charged latex particles are sorbed much more rapidly than negatively charged particles by cotton fibers.

DISCUSSION OF RESULTS

It has hitherto been believed that reversal of the charge on the globules on acidification is possible only in natural latexes, stabilized by natural proteins, the molecules of which have two functional groups: the amino group, causing the positive charge of the globules in an acid medium, and the carboxyl group, which causes the globules to be negatively charged in an alkaline medium. In the case of synthetic latexes stabilized by soaps,it was considered that in an acid medium the soap is converted into an acid which has no protective properties, and the latex should coagulate.

Our experiments have shown that under certain conditions charge reversal on acidification is also possible in dispersions stabilized by substances which cannot cause a change in the sign of the charge when the reaction of the medium is changed. The cause of this evidently lies in the fact that the latex remains stable at low pH values owing to adsorption of positively charged hydrogen ions by the globules. The hydrogen ion has high adsorbability and in many instances can act as a stabilizer. There are indications in the literature of the possibility of charge reversal, by means of hydrogen ions, of particles in certain colloids and emulsions; including rubber globules, originally stabilized by hydroxyl ions [1].

The graph shows that when the pH is decreased by addition of acid the absolute values of the zeta potential of the globules in AD2 and BD1 latexes first remain constant over a certain pH range, and then begin to decrease after pH 5.3-7 has been reached. This form of the zeta potential – pH curve is in good agreement with the general relationship established by Jordan [2] for natural latex. The decrease of the zeta potential after sufficient acidification is probably the result of conversion of the strongly ionized soap into a weakly ionized acid. Although the latter is adsorbed on the globules, it does not form a protective ionic layer characterized by the zeta potential. Maron and Bowler's explanation [4] of the weaker stabilizing action of acids as being due to lower adsorption by the globules is not, in our opinion, satisfactory. A fatty acid, being less soluble, will always be adsorbed better than soap on rubber globules. The known fact that the surface tension of latexes is decreased on acidification is explained, not by passage of the fatty acid particles formed from the soap into the solution, but by the fact that the acid has higher surface activity than the soap.

If the medium is sufficiently acid, all the soap is converted into an acid devoid of protective properties. This corresponds to the isoelectric state of the system. In accordance with the values found for the isoelectric points, the stabilizers – ammonium oleate and naphthenate soap – present in latexes AD2 and BD1 are evidently converted into the corresponding acids at pH 3.7-3.9. Upon further acidification, hydrogen ions are adsorbed on the polymer globules and confer a positive charge on them. As the pH decreases the adsorption of hydrogen ions increases and the positive zeta potential rises. Nevertheless, the absolute value of the positive potential in an acid medium is considerably lower than the value in an alkaline medium. This is certainly associated with the nature of the stabilizing ion.

The aggregative stability of the latexes also increases with increasing absolute values of the zeta potential. The increase of latex stability with increasing absolute values of the negative zeta potential on addition of alkali is common knowledge. However, we see that this is also true for latexes with positively charged globules. The connection between zeta potential and stability is also confirmed by the fact that latexes with negatively charged particles with high zeta potentials are much more stable than latexes with positively charged particles and relatively low zeta potentials.

The zeta potential – pH curve for undialyzed latexes, determined by us earlier [7] had maxima in the acid and alkaline regions.

The explanation for these maxima should be sought in the fact that while the experiments with dialyzed latexes were performed with solutions of strictly constant ionic strength, this was not the case in the experiments with undialyzed latexes. In the latter case the pH was increased by addition of alkali to the latex, which resulted in an increase of ionic strength, and consequently to compression of the electric double layer and a decrease of the absolute value of the negative zeta potential. In this same way, considerable decreases of pH in this case were produced by additions of large amounts of acid to the latex, which also increased the ionic strength and decreased the value of the positive zeta potential. Similar effects have been reported earlier for dilute mineral oil emulsions [12].

SUMMARY

1. Latex particles stabilized by anion-active soaps can undergo charge reversal on acidification. An essential condition for charge reversal is low latex concentraion and rapid addition of the acid, so that the sign of the particle charge can be reversed before any appreciable coagulation occurs.

2. The zeta potential of latex globules remains constant on acidification over a certain pH range, then decreases as the result of the conversion of soap into undissociated acid, reaches zero (isoelectric point), and then becomes positive in acid media, probably as the result of adsorption of hydrogen ions.

3. When the zeta potential of the globules is close to zero, the latexes completely lose their aggregative stability. It has been found that the isoelectric point of latexes stabilized by soaps is at pH 3.7-3.9.

4. The zeta potential – pH curves for undialyzed latexes have maxima at high and low pH values. The presence of these maxima is probably caused by the increase of ionic strength as the result of addition of large amounts of alkali or acid to confer high or low pH values on the solution.

5. Latexes with reversely charged particles are much less stable than the original latexes; this is due to the lower absolute values of the zeta potential of the particles of such latexes in comparison with the original.

6. The positively charged particles of reversed latexes are actively sorbed by cotton fibers and can therefore be successfully used for impregnating paper, cardboard, andfor similar purposes.

The M. V. Lomonosov Institute of Fine Chemical Technology
Moscow

Received February 12, 1956

LITERATURE CITED

[1] A. R. Kemp, D. F. Twiss, Rubb. Chem. Techn. 9, 551 (1936).

[2] H. F. Jordan, Proceedings of the Rubber Technol. Conference, 1938, p. 111.

[3] W. W. Bowler, Ind. Eng. Chem., 45, 1790 (1953).

[4] S. H. Maron, W. W. Bowler, J. Am. Chem. Soc. 70, 3893 (1948).

[5] S. S. Voyutsky, Yu. A. Smetkin, R. M. Panich, and K. A. Kalyanova, Proc. Acad. Sci. USSR, 70, 1013 (1950).

[6] S. S. Voyutsky, R. M. Panich, and K. A. Kalyanova, Collected Papers of the Central Sci. Res. Inst. for Leather Substitutes on the Theory and Practice of Impregnation, State Light Ind. Press, p. 90 (1952).

[7] S. S. Voyutsky, R. M. Panich, and K. A. Kalyanova, Trans. Lomonosov Inst. Fine Chem. Technol., Moscow, No. 5, State Chem. Press, p. 30 (1953).

[8] R. M. Panich and S. S. Voyutsky, Colloid J., 18, 326 (1956).

[9] S. S. Voyutsky and R. M. Panich, Colloid J., 18, 647 (1956).

[10] A. I. Rabinovich and E. F. Fodiman, J. Phys. Chem., 2, 336 (1931); 3, 8 (1932).

[11] P. Debye, J. Phys. Coll. Chem., 51, 18, (1947).

[12] R. Ellis, Z. Phys. Chem. 78, 321, (1912).

THE FRACTIONAL COMPOSITION OF FINE CELLULOSE FIBERS

S. L. Talmud, A. N. Turzhetskaya, and A. A. Kuleshova

It has been shown by one of the present authors and co-workers [1] that cellulose may be refined by size fractionation of sulfite cellulose fibers; for this, fine cellulose fibers must be removed. For a correct evaluation of the role of fine cellulose fibers and of the possibilities of utilizing them rationally, it was necessary to determine the chemical composition of this fine fraction, and to study the molecular heterogeneity of its constituent cellulose.

The cellulose was fractionated by consecutive solution in phosphoric acid solutions of known concentrations [2, 3]. Akim and Kilkki [4] used this method to show that a definite relationship exists between the fractional composition and the reactivity of sulfite viscose cellulose. According to these authors, a viscose cellulose with good reactivity has a low content of low molecular fractions with degree of polymerization up to 200, and is completely free from high molecular fractions with degree of polymerization above 1200. Thus, consecutive solution of cellulose in phosphoric acid solutions is a convenient method for comparative determinations of the degree of polymerization of different technical cellulose fractions.

We have studied the fine cellulose fibers obtained from sulfite pulp waste waters (fibers present in pitch settling tank effluents). The quantitative proportions of different fractions (by fiber length) were determined by means of a microscope with a micrometer eyepiece, by fiber counts in several fields. The results of the microscopical analysis are given in Table 1.

TABLE 1

Microscopical Analysis of Fine Cellulose Fibers

Fiber length, mm	Content of fraction, as % of total fibers	Fiber length, mm	Content of fraction, as % of total fibers
1.0	2.5	0.3	9.4
0.7	–	0.2	21.0
0.5	2.7	0.1	34.2
0.4	–	0.05	30.2

Table 1 shows that most of the fine fibers, 84.4%, were from 0.05 to 0.2 mm long.

The fine cellulose fibers contained 4% moisture, 1.45% ash, and 16.2% resins and fats (soluble in dichloroethane).

For fractionation of the fine cellulose fibers by molecular weight, it was first necessary to extract resins and fats. However, after thorough extraction of the fine cellulose fibers by dichloroethane, or by ethyl ether and ethyl alcohol, successful fractionation could not be achieved, as phosphoric acid solution had practically no solvent action on the cellulose.

It was noticed that the contents of resins and fats, determined by extractions by the above solvents, steadily decreased during storage of the fine cellulose fibers. Evidently the resins were oxidized and the oxidation products were not extracted by the solvents. In a discussion of this problem, S. S. Malevskaya reported that she had observed similar effects, and that when resins and fats are extracted from cellulose by ethyl ether and acetone, oxidized resin is also extracted.* The content of resins and fats, soluble in ethyl ether and acetone, in the fine cellulose fibers was found to be 18.2%. It proved possible to fractionate the cellulose after extracting the fine cellulose fibers with ethyl ether and acetone to remove unoxidized andoxidized resins and fats.

---

* We are deeply grateful to S. S. Malevskaya for this communication [6, 7].

The results of the fractionation of extracted fine cellulose fibers are given in Table 2. Table 2 gives the average results of at least two parallel determinations for each experiment. If the discrepancies were considerable, the number of parallel determinations was increased to 3-5.

TABLE 2

Molecular Heterogeneity of Extracted Fine Cellulose Fibers

Degree of polymerization of cellulose	Amounts of fractions, wt. %					
	I	II	III	IV	V	mean
Up to 10	3.0	3.8	3.9	2.8	3.4	3.4
10 — 200	2.7	2.8	0.9	3.7	2.5	2.5
200 — 300	2.7	6.7	2.5	0.7	3.0	3.1
300 — 420	31.4	28.5	33.3	34.8	27.9	31.2
420 — 600	0.0	0.0	0.0	1.8	6.3	1.6
600 — 1200	2.9	0.0	0.7	0.0	0.0	0.7
Over 1200 (by difference)	57.3	58.2	58.7	56.2	56.9	57.5

Table 2 shows that extracted fine cellulose fibers contain on the average only 42.5 wt. % of cellulose with degree of polymerization up to 1200; most of the cellulose (57.5%) is insoluble in phosphoric acid and has degree of polymerization above 1200.

The lignin content of the extracted fine cellulose fibers, determined by the sulfuric acid method, was 5.62%.

Analysis of the fine cellulose fibers gave the following results, calculated on the absolutely dry material (in wt. %):

	wt. %
(1) Resins and fats	19.0
(2) Lignin	7.2
(3) Ash	1.5
(4) Cellulose	72.3
(5) Including cellulose with degree of polymerization up to 1200	30.7
(6) above 1200	41.6

This low quality of the cellulose fines is probably due to the morphological structure. These results confirm the possibility and advisability of refining cellulose by removal of the low quality portion, the fine fibers [1].

Cases are known when viscose cellulose, which confirms to various technical specifications, proves to be insufficiently reactive, and the viscose has poor filterability. In our opinion, this may be the result of incomplete removal of the fine cellulose fibers, for example, during bleaching.

The extracted fine cellulose fibers proved to be quite unreactive (with 110% CS_2 and 11% NaOH).

The advantages of cellulose fractionation by fiber length [1] have been confirmed by the work of

Perila [5], who reported that after removal of 12.6% of short fiber material the reactivity of the cellulose is raised and the filterability of viscose solutions is improved.

SUMMARY

1. The chemical composition of fine cellulose fibers (a short fiber fraction of sulfite cellulose) has been determined and the constituent cellulose has been fractionated by molecular weight.

2. It is shown that fine cellulose fibers contain, calculated on the absolutely dry substance: 19.0% resins and fats (soluble in ethyl alcohol and acetone), 7.2% lignin, 1.5% ash, and only 72.3% cellulose. Most of the cellulose (45.8%) in the fine fibers has degrees of polymerization below 200 and above 1200, and only 26.5% of the fine fiber material, with degrees of polymerization between 200 and 1200, is suitable for chemical processing. This low quality of the fine cellulose fiber fraction is probably due to its morphological structure.

3. The results indicate the possibility and suitability of cellulose refining by removal of the low grade portion, the fine fiber fraction.

The V. M. Molotov Technological Institute
Leningrad
Chair of Physical and Colloid Chemistry

Received April 14, 1956

LITERATURE CITED

[1] S. L. Talmud, A. M. Ivanyushkina, L. A. Popova, and L. P. Yanzuvalova, Proc. Acad. Sci. USSR, 92, 2, 397 (1953).

[2] N. I. Nikitin, Chemistry of Wood, Acad. Sci. USSR Press, p. 96 (1951).

[3] Ekenstam, Svensk Papperstidning 45, 61, (1942).

[4] L. E. Akim and V. E. Kilkki, Paper Ind., 10, 5(1953).

[5] O. Perila, Paperi ja Puu, 35, 4a, 139 (1953).

[6] S. S. Malevskaya, V. D. Karnaukhova, and S. D. Kharad, Paper Ind., 9, 14(1955).

[7] S. S. Malevskaya and V. D. Karnaukhova, J. Appl. Chem., 29, 401(1956).

DISCUSSION

CHARACTERIZATION OF THE STATE OF HIGH-POLTMER GELS

A. V. Nikolaev, R. E. Neiman, and O. V. Neiman

The question of the nature of the gelation process has repeatedly been discussed in the literature. This is not surprising, since formation of gels from high-polymer solutions is met fairly frequently and in a number of cases is of definite practical importance.

One cannot fail to agree with Lipatov and Meerson [1] that in a number of cases (dyes and purified polymers) gels have all the signs of thermodynamic instability, and that gelation is merely an intermediate stage on the way to complete separation of the system into two phases. We are therefore dealing with phenomena occurring in systems with limited mutual solubility (limited swelling of the polymer) over a definite temperature range; on heating, this passes into complete miscibility. When such homogenized systems are cooled, their behavior may differ:

a) In some cases phase separation occurs and a state of equilibrium is reached fairly rapidly. One of the phases formed is a partially swollen polymer, i. e., an equilibrium gel of a constant composition for a given temperature, and the other is a solution of polymer in low molecular liquid.

b) In other cases the separation is delayed for indefinite periods. A nonequilibrium, continuous, one-phase gel is formed. The persistence of this nonequilibrium state is aided, as is known, by inhomogeneity of the polymer and presence of impurities in it. Thus, solutions of ordinary gelatin on cooling are converted into gels which do not separate into phases for indefinitely long periods. Nevertheless, as was shown by Tager and Kargin [2], when solutions of highly purified gelatin are cooled they separate fairly rapidly into two layers.

In our opinion the study of nonequilibrium gels is not only of specialized but also of very general interest, since the equilibrium state is in many cases reached through this intermediate stage.

1. The formation of gels directly by cooling solutions of a number of polymers, i. e., case "b" above, was studied by us thermographically [3, 4]. We were not able to detect any heat effect on gelation. We must again stress that this refers to the formation of a gel from the solution, and not to its subsequent phase separation.

Lipatov and Meerson [1], in referring to these studies, regard the result of our thermographic investigation as failure on our part. They see the reason for this failure in the fact that we used nonfractionated materials. However, the data of Lipatov and Feldman [5] can be used to show that this view is incorrect. Indeed, these authors used nonfractionated gelatin and agar, individual fractions of these, mixtures of such fractions, and in a number of cases they also added various electrolytes. In all these cases differential thermograms of the same type were obtained; in the authors' view, these provided evidence for the existence of a heat effect of gelation. The values of these effects varied somewhat with variations of the experiments, but remained of the same order of magnitude. Therefore it is necessary to seek some other cause of the diametrically opposite results obtained in our investigations [3, 4], by Lipatov and Feldman [5], and by Lipatov and Meerson [6].

We must point out that, in numerous repetitions of the thermographic experiments and with careful attention to all the precautions necessary in obtaining differential thermograms, we were never able to detect—within the limits of the fairly high sensitivity of our determinations – any appreciable heat effects on gelation. It is also necessary to bear in mind that these thermographic results of ours are in any event in agreement with the results of our highly sensitive dilatometric determinations [3, 7], in which we did not detect any volume changes in the formation of gels from solutions. Thus, two independent methods gave results which were similar in principle.

We therefore continue to regard our thermographic and dilatometric data as quite reliable.

2. The absence of a heat effect of gelation contradicts, in our opinion, the data of Lipatov and Meerson [8] on the temperature dependence of the heat of solution of polymers. These authors showed that the magnitude of this heat effect decreases in a certain temperature range; in their opinion, this is due to an endothermic process of bond rupture between the polymer chains. This intermediate region is regarded by them as a region of phase transition, completed after rupture of the interchain bonds and solution of the polymer.

The transition from an equilibrium heterogeneous system (partially swollen polymer in excess liquid), on heating, to a homogeneous solution, from the latter on cooling to a nonequilibrium gel, and finally the return to the initial state on phase separation of the gel, may be represented in the form of an energy diagram (Fig. 1).

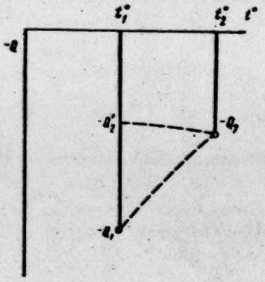

Fig. 1. Energy diagram for the transitions: equilibrium heterogeneous system ($-Q_1$) – homogeneous solution ($-Q_2$) – nonequilibrium gel (Q'_2).

At the lower temperature t_1 a heterogeneous system is formed when the polymer is mixed with the liquid. This process is characterized by the heat effect $-Q_1$. In agreement with Lipatov and Meerson's data [8], the complete solution of the polymer at a higher temperature t°_2 to give a homogeneous solution should correspond to a smaller heat effect $-Q_2$.

The difference $[Q_1 - Q_2]$ determines the heat of phase transition, corresponding to the region of phase transition on Lipatov and Meerson's $Q = f(t^{\circ})$ curve.

If, when the homogeneous solution is cooled from temperature t°_2 to t°_1, a continuous nonequilibrium gel is formed; this means that phase separation is delayed. The system does not return to the initial state in which it was found before it was homogenized by heating. Thus gelation may not be phase transition. Therefore the heat effect corresponding to such transition is absent. The difference between $-Q'_2$ for the nonequilibrium gel and $-Q_2$ for the homogeneous solution is determined only by the temperature term of the heat content. Only on subsequent slow phase separation of the nonequilibrium gel can we expect to find a heat effect corresponding to the difference $-[Q_1 - Q'_2]$. Here transition to a state of equilibrium occurs, and one of the two phases formed is an equilibrium gel of definite composition.

3. Transition of a polymer solution into a nonequilibrium gel without a heat effect or volume change is not a new phenomenon. It has long been known for the melt – glass system. To illustrate this, we give a heating curve, of interest from our point of view, obtained by one of us [9] for a series of borate glasses. When a borate glass is heated (branch $\underline{a}$ of Curve $\underline{t}$ in Fig. 2) at a definite reproducible temperature the molecules become mobile and the glass passes into crystals with evolution of heat (effect 1 on the Curve Δt), and the crystals melt at once with absorption of heat (effect 2). The heat effects 1 and 2, are, of course, of equal magnitude. When the resultant melt is cooled (branch $\underline{b}$), neither absorption nor evolution of heat can be detected by the most sensitive differential recording, although the melt is completely converted into glass. The glass so obtained can be heated again, and the whole cycle can be reproduced repeatedly.

We must emphasize that the analogy between glass and a nonequilibrium gel relates to energy only. The mechanism by which the nonequilibrium state is produced may differ for gels and glasses, but for our purpose (energy analogy) this is immaterial.

4. Our theoretically important modification of the Lipatov and Meerson scheme, like the scheme as a whole in its new form, may be illustrated with the aid of data published a relatively long time ago by one of the present authors [10]. In fact, phenomena occur in the gel which are very similar to phase transitions in their nature and in the accompanying effects, such as the volume effect. Thus, the contraction of a gel on coagulation is accompanied by a volume effect comparable to that for the formation of a gel from a true solution at a low concentration of coagulant. When a 4% solution of ferric chloride is mixed with an equal volume of caustic soda solution, equivalent quantities give a volume increase of + 0.874 cc per 1 g of the ferric hydroxide formed. If the same reaction, with the same amounts and concentrations of ferric chloride and caustic soda, is carried out in 10% or 20% solutions of common salt, the corresponding volume changes will be +0. 559 cc (− 35.3%) and +0.487 cc (− 45%).

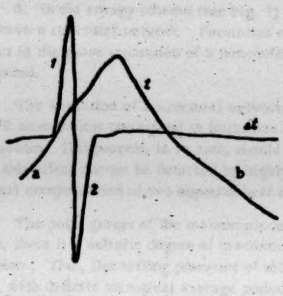

Fig. 2. Heating curve for borate glasses (explanation in text).

In other words, the contraction of a gel by the action of a coagulant is accompanied by a volume effect comparable in magnitude (being 35-45% of the latter) with the effect in such an evident phase transition as the formation of a precipitate in solution.

In the same investigation the volume effect of the transition of a sol into an uncontracted gel was also studied for 4% ferric chloride solution; its value was $^1/_2$ of the value for the phase transition.* This volume effect diminishes with decreasing concentration of the coagulant (concentrations of the solutions being mixed), tending to zero or a very small value at infinite dilution, in the following way:

Volume effect in the sol − gel transition as % of the volume effect in the formation of a sol from a true solution**	−2,43	−3.40	−5,0	−9.6
Concentration of original ferric chloride solution, %	1.0	2,0	3,0	4,0

This variation of the volume effect with concentration must attributed wholly to changes of the gel volume, as the volume effect of sol formation from true solution depends very little on the concentration. The values of this effect without corrections for dilution are:

Concentration of ferric chloride solution, %	2	3	4
Volume effect of sol formation in cc per 1 g Fe $(OH)_3$	0.681	0.687	0.690

Therefore there is no doubt that the volume effect of the sol − gel transition depends very much on the state of the gel: in absence of a coagulant it is equal or close to zero, *** while in the shrinkage of a gel by the action of a coagulant (analogously to syneresis) it may be comparable with the effect in phase transition.

---

* As small as $^1/_{48}$ for 2% solution.

** Without the dilution effect on mixing being taken into account; if this factor is taken into account, the values diminish still further, for example, −9.6% for 4% ferric chloride solution becomes − 8.5% after the correction is applied (see above).

*** This is in good agreement with the thixotropy of a given gel.

We have thus confirmed the validity of our scheme (Fig. 1), but instead of heat effects we used their equivalent volume effects, and instead of syneresis, we considered gel shrinkage by coagulation.

5. In our energy scheme (see Fig. 1) the nonequilibrium gel which has not separated into layers should not have a structural network. Formation of such a network should then be the essential cause of a heat effect in the phase separation of a nonequilibrium gel. However, another hypothesis probably cannot be excluded.

The formation of a structural network in a nonequilibrium gel, while unconnected with phase transition, would nevertheless correspond to formation of a definite number of local bonds between the polymer macromolecules. This process, in its turn, should be accompanied by heat and volume effects. What is the reason that this effect cannot be detected by highly sensitive differential thermograms? We tentatively suggest that mutual compensation of two opposite heat effects may occur in the formation of a structural gel network.

The polar groups of the macromolecules in solution are solvated by the solvent molecules. At the same time, there is a definite degree of macromolecular association, which depends on the temperature, in the solution. Thus, fluctuating processes of solvate and aggregate formation and destruction develop in the solution, with definite statistical average period of their existence corresponding to each given temperature. As the solution is cooled, a definite number of bonds becomes fixed between the most polar groups of the macromolecules and finally the structural gel network is formed. Since, in solution, the polar groups of the macromolecules are blocked by solvating molecules of solvent, it may be assumed that preliminary desolvation is a condition for bond formation between them. Therefore, in the formation of the structural network in the gel, two heat effects opposite in sign and similar but not equal in magnitude may be mutually compensated.

Of the total number of polar groups contained in a macromolecule, only a relatively small part is involved in the formation of the structural gel network. The molar concentrations of polymers in solutions are, however, very low. Thus, for gelatin with molecular weight $5 \cdot 10^4$, a 25% solution corresponds to a concentration of $\sim 5.10^{-3}$ mole/liter. It may be that because of the compensation of the opposite effects and because the number of local contacts is very small, the heat of formation of intermolecular bonds in the structural gel network becomes vanishingly small.

In phase separation of a nonequilibrium gel the number of intermolecular bonds rises sharply, and the small energy difference relative to hydration bonds is then manifested quite clearly in the form of heat and volume effects.

Institute of General and Inorganic Chemistry
Acad. Sci. USSR, Moscow
Voronezh State University
Engineering and Building Institute, Voronezh

Received May 21, 1956

LITERATURE CITED

[1] S. M. Lipatov and S. I. Meerson, Colloid J., 17, 230 (1955).*

[2] A. A. Tager and V. A. Kargin, J. Phys. Chem., 15, 1029 (1941).

[3] A. V. Nikolaev, G. I. Golub, and P. Osetrov, Colloid J., 8, 345 (1946).

[4] R. E. Neiman and O. V. Neiman, Colloid J., 9, 203 (1947).

[5] S. M. Lipatov, N. V. Stepanova, and R. I. Feldman, Colloid J., 3, 703 (1937); R. I. Feldman, Colloid J., 6, 753, 875 (1940); S. M. Lipatov and R. I. Feldman, Colloid J., 6, 805 (1940).

[6] S. M. Lipatov and S. I. Meerson, Trans. Moscow Sci. - Res. Textile Inst., 13, 74 (1954).

[7] R. E. Neiman, Colloid J., 14, 107 (1952); 16, 201(1954).*

[8] S. M. Lipatov and S. I. Meerson, Colloid J., 8, 143 (1946).

[9] L. G. Berg, A. V. Nikolaev, and E. Ya. Rode, Thermography, Acad. Sci. USSR Press (1944).

[10] A. V. Nikolaev and A. G. Kurnakova, Symposium, Protective Films on Salts, Acad. Sci. USSR Press, p. 138 (1944).

---

* Original Russian pagination. See C. B. translation.

LETTER TO THE EDITOR

COAGULATION OF ATMOSPHERIC CONDENSATION NUCLEI ON DUST PARTICLES

M. L. Mikhelson

As was shown earlier [1], one of the main problems which arises in development of the condensation method for the removal of flying dust is the influence of atmospheric condensation nuclei on the growth of the droplets formed on the dust particles.

Critical supersaturation values for some soluble nuclei may be of the same order as for dust particles $\sim 1\mu$ in size. Therefore in some cases atmospheric nuclei may act as competitors which take up a considerable amount of the condensing moisture, thereby decreasing the residual supersaturation. Moreover, being present in air in tens and hundreds of times as high as the usual dust content of mine air, atmospheric nuclei are capable of increasing, in roughly the same proportions, the amounts of energy required to bring about supersaturation in a condensation type dust filter. In this connection, the coagulation of atmospheric condensation nuclei on dust particles which we have discovered is a very favorable factor in the condensation method and is worthy of investigation.

In our experiments, the atmospheric nuclei were detected directly in the condensation filter when air was passed between parallel moist surfaces with different temperatures [2]. The experiments were carried out as follows. The Deryagin – Vlasenko flow ultramicroscope [3] was used to determine the concentration of atmospheric nuclei formed in the apparatus (Fig. 1) before introduction of dust into the dust chamber; its value was $3 \cdot 10^5$/cc. After introduction of coarse dust ($r \sim 10-100\mu$) into the dust chamber to a concentration $n_0 = 10^4$/cc, no atmospheric nuclei at all could be detected after 20 minutes under the same conditions, i. e., conditions determining supersaturation in the apparatus (temperatures of the hot and cold moist surfaces, the distance between them, length of the channel, flow rate). The distance between the moist surfaces $\underline{d}$ was 7 cm. the channel length $\underline{l}$ was 150 cm; the air flow rate $\underline{v}$ was 5 m/second. The same apparatus was then used to determine the concentration of atmospheric nuclei as a function of time (Fig. 2). In order to avoid changes of dust concentration during the experiment by precipitation of the dust particles, the dust used had average particle size $R \sim 1\ \mu$. As Fig. 2 shows, the concentration of the atmospheric nuclei fell, which may be attributed to coagulation of the atmospheric nuclei on the dust particles. In this experiment the initial concentration of the atmospheric nuclei was $N_0 = 7.5 \cdot 10^5$/cc, and the dust concentration $n_0 = 6 \cdot 10^4$/cc.

The coagulation of atmospheric nuclei on the dust particles is probably mainly due to their Brownian movement. The coagulation rate is easily calculated by means of the Smoluchowski equation applied to one absorbing particle of radius R

$$Q = -4\pi DRN, \quad D = kTB, \tag{1}$$

where Q is the number of atmospheric nuclei absorbed in unit time; N is the concentration of the atmospheric nuclei; D is the coefficient of diffusion corresponding to an atmospheric nucleus of radium $\underline{r}$; $\underline{k}$ is the Boltzmann constant; T is the absolute temperature; B is the mobility of the atmospheric nuclei calculated from Formula (8.6) [4, p. 39].

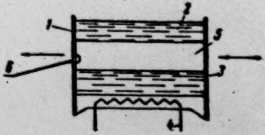

Fig. 1. Apparatus for measurement of the concentration of atmospheric nuclei: 1) body of the apparatus; 2) running water with t = 16°; 3) water with t = 65°; 4) heater; 5) vapor – air channel; 6) branch tube for sampling, by the flow ultramicroscope, from the center of the stream.

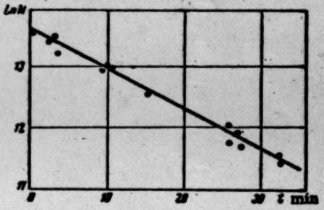

Fig. 2. Variation of the concentration of atmospheric nuclei with time.

If the dust concentration is n_0 and n_0 absorbing nuclei are therefore present, then

$$\frac{dN}{dt} = -4\pi DRNn_0 , \tag{2}$$

or, in integral form

$$\ln N = \ln N_0 - 4\pi DRn_0t . \tag{3}$$

In our experiment $N_0 = 7.5 \cdot 10^5/\text{cc}$, $n_0 = 6 \cdot 10^4/\text{cc}$, $R \sim 1\mu$. To plot the line $\ln N = f(t)$ it is necessary to know the size of the atmospheric nuclei.

The straight line calculated from Formula (3) coincides with the experimental plot at $r = 3.0 \cdot 10^{-6}$ cm. According to Nolan and Guerrini [5], the radius of the atmospheric nuclei $r = 2.85 \cdot 10^{-6}$ cm; the maximum on the size distribution curve for atmospheric nuclei, reported by Kumai [6], corresponds to $2.5 \cdot 10^{-6}$ cm. Thus, the foregoing considerations are confirmed by the linear character of the $\ln N = f(t)$ relationship and the satisfactory agreement of our value for the radius of the atmospheric nuclei with results obtained by other authors.

Coagulation of atmospheric nuclei should probably also occur rapidly on mist droplets, which is very significant in relation to studies of precipitation conditions. In such cases the coagulation process will probably be accelerated or retarded depending on whether the mist droplets undergo condensational growth or evaporation [7].

SUMMARY

1. The effect of coagulation of atmospheric nuclei which has been detected is of meteorological interest in relation to studies of precipitation, and is also important in relation to the condensation method of dust removal. For example, it seems likely that, because of prolonged contact with dusty air, atmospheric nuclei will be totally absent in mine air.

2. The calculated values for the size of atmospheric nuclei, based on experimental results, are in agreement with the data of other authors.

The Scientific Research Mining Institute
Krivoi Rog

Received April 14, 1956

LITERATURE CITED

[1] B. V. Deryagin, S. S. Dukhin, M. L. Mikhelson, and V. M. Kaganer, Silicosis Prevention, Symposium, vol. 2, Acad. Sci. USSR Press, p. 22 (1955).

[2] S. S. Dukhin, B. V. Deryagin, and M. L. Mikhelson, Proc. Acad. Sci. USSR, 105, No. 6 (1955).

[3] B. V. Deryagin and G. Ya. Vlasenko, New Ideas in the Study of Aerosols, Symposium edited by B. V. Deryagin, Acad. Sci. USSR Press (1949); Proc. Acad. Sci. USSR, 63, No. 2 (1948).

[4] N. A. Fuks, Mechanics of Aerosols, Acad. Sci. USSR Press (1955).

[5] J. Nolan, N. Guerrini, Trans. Faraday Soc. 32, 1175, (1936).

[6] M. Kumai, J. Met. 8, No. 3, 151 (1951).

[7] B. V. Deryagin and S. S. Dukhin, Proc. Acad. Sci. USSR, 106, No. 5 (1956).

THE SEVENTIETH ANNIVERSARY OF THE BIRTH AND FIFTY YEARS OF THE SCIENTIFIC ACTIVITY OF GRIGORY SEMENOVICH PETROV

[illegible]

[illegible]

[illegible]

[illegible]

THE SEVENTIETH ANNIVERSARY OF THE BIRTH AND FIFTY YEARS OF THE SCIENTIFIC ACTIVITY OF GRIGORY SEMENOVICH PETROV

October 27, 1956 was noted by the scientific community as the seventieth birthday and the end of fifty years of scientific activity of Professor Grigory Semenovich Petrov, Doctor of Technical Sciences – an eminent scientist, widely known in the USSR and abroad. From 1904 G. S. Petrov carried out a wide series of investigations on the decomposition of fats, and invented his famous "kontakt," obtained by treatment of various petroleum distillates with fuming sulfuric acid or sulfuric anhydride. Kontakt is still widely used in the USSR and abroad, mainly in the fat industry for splitting of fats and in the textile industry as a detergent in place of soap or alizarin oil, etc. In 1911-1914 G. S. Petrov and his associates laid the foundations of the national plastics industry. Being the first to organize the production of phenolic resin in Russia, he is rightly acknowledged to be the founder of the large plastics factory "Karbolit." After the October Socialist Revolution Petrov directed extensive work on the synthesis of carboxylic acids by oxidation of liquid petroleum distillates, carried out in the Karpov Institute. A carboxylic acid plant was installed at the Vakhitov factory as the result of this work.

The main direction of G. S. Petrov's scientific activity, however, has been the synthesis and study of various high polymers obtained by condensation. He has synthesized a large number of high polymers based on various phenols and aldehydes, urea, melamine, and aldehydes, glycols and carboxylic acids, etc. In particular, he determined the differences in the behavior of various substances at high temperatures in relation to the "coke number," and was first to observe that the heat stability of high polymers is increased by introduction of benzene nuclei in the chain. He therefore attached great importance to the condensation products of phenols and aldehydes for the production of plastics used in high-temperature conditions. G. S. Petrov made detailed studies of the formation of high polymers in condensation reactions in relation to the reaction conditions and the use of various catalysts. His work on the compatibility of numerous condensation polymers with polymers having high elasticity, such as rubber, has proved particularly valuable.

Long before the publication of work on block and graft polymers, G. S. Petrov indicated the possibility of, and predicted an important future for, the formation of chemical bonds between various polymeric products. In recent years he has been engaged in extensive work on the oxidation of high polymers, and in particular of phenol–aldehyde condensation products. He has established that oxidized condensation products have increased hardening rates.

G. S. Petrov has written 13 books on the technology of plastics, fats, and petroleum; he has published 85 papers, and has been awarded more than 200 author's certificates for inventions. Many of the inventions have been adopted in industry.

Jointly with Professor L. P. Losev, G. S. Petrov organized the Department of Plastics in the Mendeleev Institute of Chemical Technology, Moscow.

G. S. Petrov is an eminent research worker and teacher, and has trained many pupils who are now working in scientific institutions, factories, and teaching establishments.

M. S. Akutin

ON THE FIFTIETH BIRTHDAY OF

Valentin Alekseevich Kargin

January 23, 1957 was the fiftieth birthday of the eminent Soviet scientist and social worker, Valentin Alekseevich Kargin. The fruitful scientific and organizing activity of V. A. Kargin in the fields of physical and colloid chemistry is well known to the scientific community.

V. A. Kargin began his working life at the age of fifteen. In 1924, as a youth of seventeen, he commenced scientific work in the L. Ya. Karpov Physicochemical Institute, and his first scientific paper, on analytical chemistry, was already published in 1926. Without leaving his research work, V. A. Kargin studied at the Moscow State University, where he graduated in 1930. During the same period V. A. Kargin worked in Academician A. E. Fersman's group on radioactive ores, and also in the laboratory of the "Russian Gems" Trust, and by the time of his graduation he had published more than ten original scientific researches. V. A. Kargin's subsequent activity developed mainly in the fields of colloid chemistry and the physical chemistry of high polymers. Being already at that time an eminent specialist in the field of analytical chemistry, well acquainted with rare minerals, V. A. Kargin took part in the discovery of valuable mineral deposits in his capacity of geochemist to the Pamir expedition in 1932-1934.

In 1936 V. A. Kargin's creative scientific activity was recognized by the award, without presentation of a dissertation, of the degree of Doctor of Chemical Sciences. From 1937 to the present day he has been the head of the Colloid Chemistry Laboratory at the L. Ya. Karpov Physicochemical Institute. In 1946 he was elected an associate member, and in 1953 a full member of the Academy of Sciences USSR. His work has been rewarded by three Stalin prizes and two Bakh prizes. He has received the Order of Lenin and the Order of the Red Banner of Labor.

V. A. Kargin, jointly with his pupils and associates, has published about 200 papers. Kargin's earlier papers mainly dealt with research into hydrophobic colloids. In these papers he demonstrated the erroneous nature of the views, prevalent at that time, on the causes of stability in colloid systems, and proved experimentally the need for studying the chemistry of the phenomena in such systems. He proved that reactions between various colloids occur in true solutions, and not by coalescence of the particles. In addition to this work, V. A. Kargin carried out original research on the preparation of metal organosols and studied the properties of these systems. A large series of his papers dealt with studies of the properties of soil colloids. In recent years he has taken up work on the mechanism of formation of aluminosilicate systems, using the results of his earlier investigations on the mechanism of formation of colloidal particles.

V. A. Kargin made wide use of electrochemical methods for studying colloidal systems and developed a number of new techniques. Among these mention must be made of the use of high-voltage electrodialysis for purification of colloidal systems, multichamber electrodialysis for synthesis of colloidal systems and for separation of different substances, and the development of an electrochemical method for evaluation of anticorrosion coatings.

In the 1930's V. A. Kargin began his research in the field of high polymers. In his earlier papers in this field it was shown that polymer solutions are true equilibrium, thermodynamically stable systems. By using electrochemical methods, he succeeded for the first time in making a detailed study of the chemical composition of viscose, and its changes during the ripening process. By the combined use of X-ray and electronographic methods V. A. Kargin established the amorphous nature of cellulose structure, despite the existing views on its microcrystalline structure. V. A. Kargin's further work on high polymers has been in connection with the relationships between the structure and the mechanical and physicochemical properties of polymers. Of this extensive series of investigations covering many years, mention must be made of the work on the properties of amorphous linear polymers, in which the glassy, high-elastic, and viscofluid states of these polymers were studied in detail and the relationships between these states and the chain structure of the molecules were demonstrated. A further development of this line of investigation has been the extensive study, during recent years, of the properties of crystalline polymers; in this work V. A. Kargin was able to demonstrate the erroneous nature of the application to such systems of the theories developed for low-molecular crystalline substances, and to indicate the future development of the theory of the crystalline state in polymers.

Of the other directions of V. A. Kargin's research on polymer properties we shall mention only the work on the properties of gels, in which the mechanism of gel formation was revealed, and studies of the mechanism of flow of structurized polymer systems, which have provided an approach to studies of polymer processing. V. A. Kargin is carrying out extensive work in organizing research on high polymers, correlating theoretical work in this field with concrete production problems.

V. A. Kargin is directing scientific control over important problems on the production and processing of polymers on an All-Union scale; he is the chairman of the Commission on High Polymers at the Academy of Sciences USSR,; and is closely associated with the chemical institutes of the Academies of Sciences of the Uzbek and Georgian SSR, and a large number of branch institutes. In the technology of production of processing of polymers, V. A. Kargin has shown new and original routes which have led to many important results utilized in our industry.

During the years of V. A. Kargin's scientific activity a group of scientific workers, developing the lines of research created by him, has arisen. The work of V. A. Kargin and his school has exerted a great influence on the development of Soviet physical and colloid chemistry. He organized and directed the Department of High Polymers at the Moscow State University.

In addition to his scientific, teaching, and organizing work, he has numerous social activities, being a deputy at the Moscow City Council of Deputies for several terms, working for many years as a member of the Plenum of the Higher Certification Commission at the Ministry of Higher Education of the USSR, and participating in the work of scientific societies.

V. A. Kargin has been a member of the Editorial Board of Colloid Journal for many years.

With all our hearts we wish our beloved Valentin Alekseevich Kargin health, strength, and creative successes in his varied fruitful activities for the good of our great Fatherland.

Z. Ya. Berestneva and G. L. Slonimsky

THE STRUCTURE OF LINEAR POLYMERS

V. A. Kargin, A. I. Kitaigorodsky, and G. L. Slonimsky

As is known, long chain molecules are flexible and therefore become coiled under the influence of thermal motion. This is the reason for the appearance of high-elastic properties in polymers, and for the anomalies in their physical properties. The ability of chain molecules to change their configuration is especially prominent in orientation effects during deformation of amorphous and crystalline polymers, and during flow of polymer solutions. The hypothesis of the easy coiling of chain molecules has been finally confirmed by the recent investigations of the configuration of chain molecules, by the possibility of obtaining a number of linear polymers in globular form, and by other experimental data. This has provided the basis for the development of modern views on the arrangement of chain molecules in amorphous polymers and on orientation in crystallization of polymers. This has given rise to the concept of polymers as systems of chaotically entangled, coiled chain molecules. However, modern data on the structure of matter lead to the conclusion that the packing of chaotically coiled chain molecules, having flexibility owing to rotation about the C – C bonds, cannot be dense enough to account for the experimentally observed densities of polymers.

On the other hand, electron-microscopic observations show that the arrangement of chain molecules in polymers corresponds in some cases to systems of molecules coiled on themselves into globules, and in others to systems of chain bundles, in which each chain has largely the same neighbors.

Thus the generally accepted picture of the molecular arrangement in amorphous polymers must be reviewed.

In our view, amorphous polymers are composed either of chains coiled into globules, or of packets of uncoiled chains. The mechanical and other physical properties of polymers consisting of packets of chains can be satisfactorily explained by this model because of the inevitable flexibility, with several possible structural mechanisms, of the packets themselves. Examples of such mechanisms may be the untwisting of a region of the packet within which the chains are twisted into spirals, or coordinated rotation of one region of the packet relative to another, about C – C bonds. Further structural investigations of this question are, of course, necessary. It is also necessary to develop a statistical theory of deformation of elastic polymers based on this model. It should be pointed out that the above views on the structure of amorphous polymers refer not only to the high-elastic and glass states, but also to the viscofluid state. Indeed, as is known, liquids consisting of rodlike molecules of low molecular weight contain packets of molecules: each molecule is surrounded by other molecules, predominantly arranged with the same axial orientation. Although these packets (sometimes termed "swarms") are not thermodynamically stable formations, they are nevertheless always present in such liquids. This applies in greater force to polymers. It must be stressed that, in consequence of the well known slow nature of mechanical relaxation processes in polymers, the life of a packet of long chain molecules must be exceptionally long, while in the glassy state the bundles will remain practically unchanged.

These concepts of the structure of amorphous polymers naturally necessitate a revision of the views on the structure of crystalline polymers. The picture, widely accepted at the present time, of the structure of a crystalline polymer as a system of small ordered domains linked by common chains passing successively through regions of oriented and disordered parts of the chains, cannot be valid in the form in which it is usually presented. This follows even on purely geometrical considerations: on the basis of the quite well known dimensions of the ordered domains and the distances between them it is impossible to construct a polymer model in which the chains would leave an ordered domain, become twisted, and then again form an ordered domain. There is no doubt that any one chain passes through several domains of order and disorder. However, the chain does not leave the limits of its packet, and largely retains its same neighbors along its entire length.

In the proposed model, the degree of order of a polymer is determined by the structure of the packets of chain molecules, since all the packets are of the same type. The order of the packet depends on the degree of lateral order of its molecules and on the alternation of ordered and disordered domains along the packet. The latter is associated with the mechanical stresses which invevitably arise within the packet with growth of the ordered domains. These stresses, which oppose further growth of the ordered domains, can be appreciably diminished only by alternation of the domains of order and disorder along the packet. The proposed model for the molecular structure of amorphous and crystalline polymers must be amplified by structural investigations and analysis of various physical properties of polymers. The structure of polymer systems consisting of individual molecules coiled into globules must be considered separately.

SUMMARY

1. Consideration of modern data on the structure of matter and the latest results of polymer research makes it necessary to review the generally accepted views on the arrangement of molecules in amorphous and crystalline polymers.

2. A new model for the molecular structure of amorphous and crystalline polymers is proposed.

The M. V. Lomonosov State University, Moscow
The Institute of Elementoorganic Compounds Acad.
Sci. USSR
Moscow

Received December 28, 1956

MOLECULAR CONFIGURATION AND STRUCTURE FORMATION IN POLYACRYLATE SOLUTIONS

V. A. Kargin and N. F. Bakeev

Determination of the configuration and relative disposition of macromolecules in polymers presents perhaps one of the most interesting and important problems. The existing views on polymer structure are, unfortunately, largely speculative, and not confirmed by direct experimental data. The structure of amorphous polymers is generally regarded as comprising quite randomly and chaotically twisted polymer chains, having the configuration of irregularly coiled globules resulting from their flexibility.

The answer to the question of configuration and relative disposition of macromolecules should in the first instance be sought by the use of structure analysis and direct observations of molecules. The low resolving power of optical microscopy (maximum 2000 A) does not allow of its use for studying the structure of polymers, although their molecules are of enormous size. It is also difficult to determine the arrangement and configuration of a polymer chain molecule along its entire length by means of structure analysis, since the magnitudes of the distances given by structure analysis are not great. Apparently the best method is that of electron microscopy, which has been widely used for studying high polymers. By the use of the electron microscope in high polymer studies it has been possible to see individual macromolecules [1], the dimensions of which proved to be within the resolution limits of the electron microscope, and also to study the elements of "secondary structure" in high polymers.

We have therefore used electron microscopy for studying the configuration of polyelectrolyte macromolecules, and the nature of their aggregation and structure formation in solutions. By a gradual increase in the concentration of the polymer solution, we passed from observations of individual isolated molecules to their aggregates, since use of the electron microscope for investigations of condensed systems of polymers cannot reveal their structure because of the high density of the object under examination.

The materials chosen for the study were polyacrylic acid and its salts: the barium, sodium, cesium, and quaternary ammonium salts. The choice was determined by the known structure of the polyacrylic acid chain and the ease with which its configuration may be varied in different media. The universal electron microscope UEM-100 was used for the investigations. The material was prepared by the method described in the literature [2], by application of a drop of the solution onto a supporting film placed on a gauze. To eliminate the influence of the support, two types of support were used in parallel investigations: collodion and structureless quartz. The electron microscopy was carried out with direct electron-optical magnification of 20,000-25,000 with subsequent photographic enlargement. To test the reproducibility of the results each solution used was prepared a number of times. Numerous electron micrographs (100-150 for each solution) were taken for each series of solutions. The results of this investigation are therefore based on repeatedly checked and completely reproducible data. The polyacrylic acid used was prepared by polymerization of acrylic acid, the molecular weight of the fractionated acid was determined viscosimetrically, using the constant $K_m = 2.9 \cdot 10^{-4}$, found by Staudinger [3] for aqueous polyacrylic acid solutions. The molecular weights found for several samples of polyacrylic acid were within the range of 1,000,000-3,000,000.

A micrograph of pure polyacrylic acid is shown in Fig. 1,1. Single isolated globules of spherical shape, and always symmetrical, can be seen. The size of the individual globules is in the range of 100-150 A. The molecular dimensions were calculated from the molecular weight of the polyacrylic acid used, on the assumption that each chain constitutes a coiled globule and that the density of the globule is equal to the density of the polymer mass. The calculated diameter of such a globule is approximately 100 A. Hence it may be concluded that most of the globules seen in the photographs are individual molecular chains. Formation of "secondary" structures was observed on increase of the acid concentration. These are fairly compact structures, formed by individual symmetrical globules joined together without interpenetration.

Barium polyacrylate (Fig. 1, 2), like pure polyacrylic acid, is characterized by "secondary" structures of a globular type, formed by union of symmetrical globules of molecular globule dimensions (80-100 A). Symmetrical globules which are not involved in secondary structure formation correspond in size to coiled molecular chains. The diameter of such globules are also about 80-100 A.

The analogous behavior of pure polyacrylic acid and of its barium salt, seen in the formation of similar secondary structures and single symmetrical globules, consisting of coiled molecular chains, is explained by the similar configuration of the long chain polyions in solution. Polyacrylic acid is a weak polymeric electrolyte. The weak acid is ionized only partially in the pure solvent (water in this case), and the intramolecular forces of electrostatic repulsion between the ionogenic (carboxyl) groups, covalently linked to the molecular chain, are small and not sufficient to straighten the molecule. The flexible polyion assumes a random ring configuration under the action of thermal forces. Of course, such a polymer globule will have a more diffuse structure than barium polyacrylate, where the thermal forces are augmented by large intramolecular forces caused by the presence of bivalent barium and its interaction with the carboxyl group, pulling the globule into a more dense formation. The viscosities found for polyacrylic acid and barium polyacrylate confirm the more diffuse structure of the molecular globules of polyacrylic acid in comparison with its barium salt.

It appeared of considerable interest to study the molecular configuration of polyacrylic acid after introduction of univalent cations, capable of increasing the degree of dissociation of the carboxyl groups, into its side chains. In this case it is to be expected that intramolecular forces of electrostatic repulsion between the charged segments of the chain should lead to increased rigidity and straightening of the molecular chains. The following salts were studied:polyacrylates of sodium, cesium, and quaternary ammonium bases. The relationship between polyacrylate viscosity and the degree of neutralization was investigated. This relationship could be represented by the type of curve shown in Fig. 2 for all the salts. The viscosity rises sharply on addition of alkali and reaches a maximum at pH 6.5, which corresponds to approximately 80 % neutralization. Further additions of alkali decrease the viscosity, and with excess alkali the viscosity reaches a definite limiting value.

The salts used for the electron microscopy were neutralized to pH 6.5, corresponding to maximum viscosity, and therefore to maximum molecular asymmetry.

Electron micrographs of sodium polyacrylate are shown in Figs. 1, 3, 4 and Fig. 3,1. The micrographs of sodium polyacrylate do not resemble those of pure polyacrylic acid or its barium salt. The secondary structures of sodium polyacrylate have totally different configuration and structure. The structure is unfolded, composed of curved threads of varying density and length; it is a typical fibrillar structure in which the fibrils are joined in the most random manner. The transverse dimensions of the fibrils lie in the range of 60-120 A. These fibrils are apparently formed from several molecular chains joined together in a definite manner into "packets" which participate in that form in the formation of secondary structures. From the dimensions of the molecule of maximum asymmetry, the distances between them (approximately 7.5 A), and the fibril dimensions (60-120 A), we may conclude that from 8 to 16 molecular chains are involved in the formation of one fibril. In dilute solutions, single isolated particles are also found; these are either strongly convoluted isolated "packets" formed from molecular chains, or, as in the case of polyacrylic acid and its barium salt, they are individual symmetrical globules, corresponding in size to single coiled molecular chains (90-100 A).

The secondary structures seen in the case of cesium polyacrylate (Fig. 3,2) are even more unfolded than those in sodium polyacrylate. As in the case of sodium polyacrylate, the structure is formed by convoluted long fibrils which do not penetrate into each other. However, the fibrils participating in the formation of secondary structures of cesium polyacrylate are smaller than those in sodium polyacrylate structures; their transverse dimensions are in the range of 40-80 A. These are not greatly convoluted "worms" but longer and straighter threads. They are probably also formed analogously by union of molecular chains into packets. However, in this case the molecular chains are straighter and join in smaller numbers. The average number of molecular chains joined together to form a fibril is 5-11.

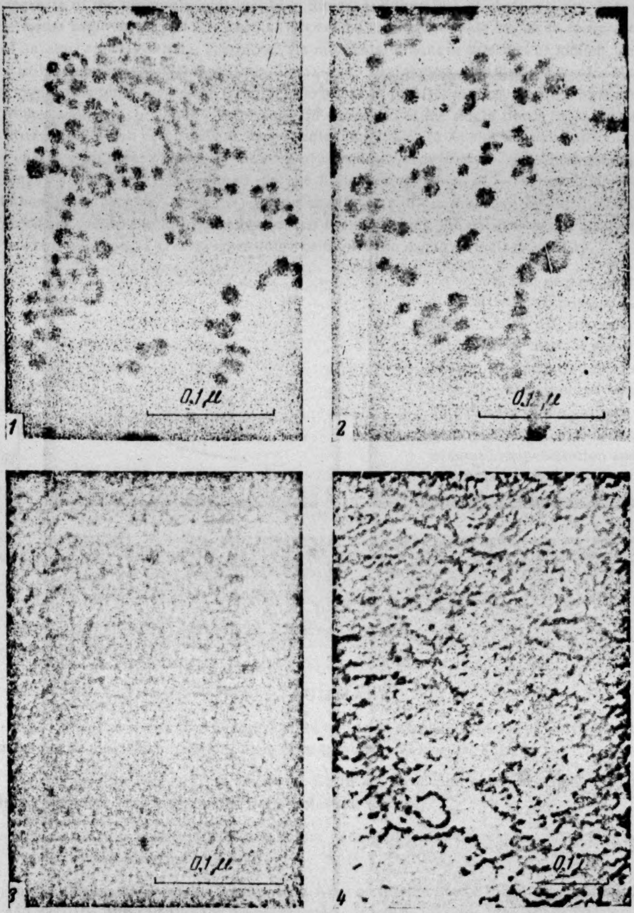

Fig. 1. Electron micrographs: 1) polyacrylic acid (x 250,000); 2) barium polyacrylate (x 250,000) ; 3) sodium polyacrylate (x 250,000); 4) sodium polyacrylate.

Quaternary ammonium polyacrylates (tetramethylammonium, Fig. 3,3 and triethylphenylammonium, Fig. 3, 4) show chain aggregation analogous to that in cesium polyacrylate. The secondary structures formed from chain aggregates are typical fibrillar structures. The individual fibrils, to judge by their transverse size of 40-90 A, are formed from 5-12 asymmetric molecular chains joined in parallel into packets.

The presence of strongly branched secondary structures in sodium, cesium, and quaternary ammonium polyacrylates is to be expected if the configuration of flexible polyions in solution is considered in terms of the relationship between the thermal forces tending to coil the chain into a globule and the electrostatic forces between the charged chain segments, resulting in increased rigidity. In fact, in a weak polymeric

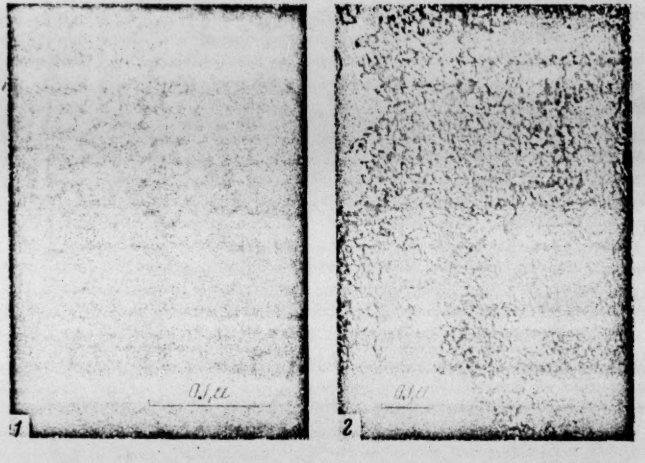

Fig. 3. Electron micrographs of polyacrylates: 1) sodium (x 250,000); 2) cesium (x 100,000); 3) tetramethylammonium (x 250,000); 4) triethylphenylammonium (x 250,000) .

electrolyte (as was shown above for polyacrylic acid in aqueous solution), the molecules of which are only partially ionized, the polyion is in the form of a compact or more or less diffuse globule, since the intramolecular electrostatic repulsion forces are not large, and are not sufficient to straighten the molecule, but merely expand the globule. When cations favoring increased dissociation of the ionogenic group, and therefore also favoring an increase in the effective charge of the chain, are introduced into the weak electrolyte chain, an increase of the intramolecular repulsion forces, and therefore of chain rigidity, is to be expected. When these forces begin to exceed the thermal forces, the molecular chain begins to straighten and attain the form of an elongated rigid rod. Therefore, the molecular chains in solutions of sodium, cesium, and quaternary ammonium polyacrylates will be of maximum straightness. Further, molecular chains with maximum asymmetry form aggregates by joining together in parallel to form fibrils, which interwine to form networks — the secondary structures. The transverse diameters of the single fibrils lie in the range of 40-120 A. From the distances between compactly arranged molecular chains (3 A) and the transverse dimensions of the molecular chains themselves (4.5 A), in the case of maximum asymmetry, when the molecules are in the form of elongated rods, it may be assumed that the fibrils are composed of 5-16 molecular chains joined together in bundles or packets. It should be noted that in very dilute solutions, in which secondary structures are not formed because of the low concentrations of the substances, the packets do not dissociate; they continue to exist, acquiring a greatly convoluted configuration owing to their flexibility.

Solutions of pure polyacrylic acid and of its barium salt contain individual molecular chains, which coil into compact globules by the action of thermal and strong intramolecular forces. Interpenetration of such globules, naturally, cannot occur because of the considerable density of the globular formations. Such symmetrical globules become joined together without interpenetration and form secondary structures of another type, analogous to the globular structures in biological systems.

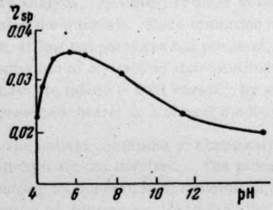

Fig. 2. Viscosity of sodium polyacrylate as a function of the degree of neutralization.

SUMMARY

1. Two types of structure in polyacrylic acid and its salts, the character of which is determined by the configuration of the long-chain polyion, have been established:

a) Typical fibrillar structures, in which the fibrils are molecular chains of maximum asymmetry, formed by parallel aggregation into "packets" of 5-16 molecular chains.

b) Typical globular structures, formed by the joining of molecular chains coiled into symmetrical globules, without interpenetration.

2. In the case of sodium polyacrylates both types of structure were found simultaneously: coiled globular and fibrillar; no intermediate type was found. It seems that this type of aggregation, i. e., coiling of the molecular chain into a globule and further structure formation by cohesion of the globules without interpenetration, and parallel (although not strictly so) joining of straightened chains into flexible packets is the only and the regular type for polyacrylates.

3. The existence of globular and fibrillar structures in biological systems in natural polyelectrolytes and proteins suggests that this type of aggregation and mutual arrangement of polymer chains is of a more general character.

Moscow State University Faculty of Chemistry

Received December 28, 1956

LITERATURE CITED

[1] B. Siegel, D. Johnson, H. Mark, J. Polym. Sci. 5, 111 (1950).

[2] A. A. Lebedev, Electron Microscopy (Tech. Theoret. Lit. Press, 1954).

[3] H. Staundinger, High-Molecular Organic Compounds (State United Sci.-Tech. Press, 1935).

THE FORMATION OF CRYSTALLINE ALUMINOSILICATES

Z. Ya. Berestneva, M. B. Konstantinopolskaya, and V. A. Kargin

It is known that aluminosilicates of various compositions are widely distributed in nature and form the main mass of the soil. The crystal structures of the minerals contained in soils have been studied by means of x-ray analysis. However, in order to understand the nature of soil formation processes, it is necessary to synthesize the minerals. Since formation of soil minerals occurs under normal conditions of the earth's surface, at low temperatures and pressures, aluminosilicates should be synthesized under these conditions also. The formation of crystalline aluminosilicates in alkaline media when aqueous solutions of sodium silicate and aluminate are mixed is well known. By saturating the resultant precipitates with magnesium salts, Sedletsky [1] approached nearer to a neutral medium, but aluminosilicates have not been prepared in a neutral medium.

The natural conditions of aluminosilicate formation are entirely different; large volumes of aqueous salt solutions are not involved. The process of aluminosilicate formation in natural conditions can be regarded as occurring by interaction of minerals of the aluminum hydroxide group with silicic acid. To determine the mechanism of this process, we studied the interaction of aluminum hydroxide both with colloidal silicic acid and with aqueous suspensions of finely ground silica gel and quartz.

The EM-3 electron microscope was used for the investigations.

As is known from the previous paper [2], freshly prepared aluminum hydroxide has an amorphous structure, and crystallization occurs progressively. Both freshly prepared amorphous and crystallized aluminum hydroxide were used for studying the interaction between aluminum hydroxide with silicic acid sol, silica gel, and quartz. The plate shows electron micrographs of aluminosilicates formed by the interaction of freshly prepared amorphous aluminum hydroxide with silicic acid (1), silica gel (2), and quartz (3). All three photographs present practically the same picture – they all show small spherical particles forming cellular structures, and having an amorphous structure in agreement with electron diffraction data. Aluminosilicates prepared from crystallized aluminum hydroxide and silicic acid sol, silica gel, and quartz, are shown in Micrographs 4,5, and 6 respectively. A different picture is seen in this case – crystals of aluminum hydroxide surrounded by silicic acid, constituting cellular structures, are clearly visible. However, here also all three micrographs are similar regardless of whether silicic acid sol, silica gel, or quartz was mixed with aluminum hydroxide.

Thus it is found that in all cases, regardless of the form of the silicic acid (sol, silica gel, or quartz), the results of its interaction with aluminum hydroxide appear the same under the electron microscope. To find the reasons for this, silicic acid sol, and aqueous suspensions of silica gel and quartz, were studied separately. The silica gel and quartz were first ground to a fine dust in an agate mortar. In this case the specimens were subjected to oblique chrome shadowing to increase contrast. The micrographs of silicic acid (7), silica gel (8), and quartz (9) were very similar, although in the case of silica gel and quartz amorphous formations can be seen together with spherical particles.

The only explanation for this is that colloidal silicic acid solution [3], like aqueous suspensions of silica gel [4] and quartz [5] always contain silicic acid in a state of true solution; in aqueous suspensions of silica gel and quartz the colloidal solutions may be formed as the result of evaporation of water and temperature fluctuations, so that in all three cases (sol, silica gel, and quartz) the processes of interaction are of the same nature, consisting of reactions between true silicic acid solution and aluminum hydroxide, and therefore the same result is obtained in each case by electron microscopy.

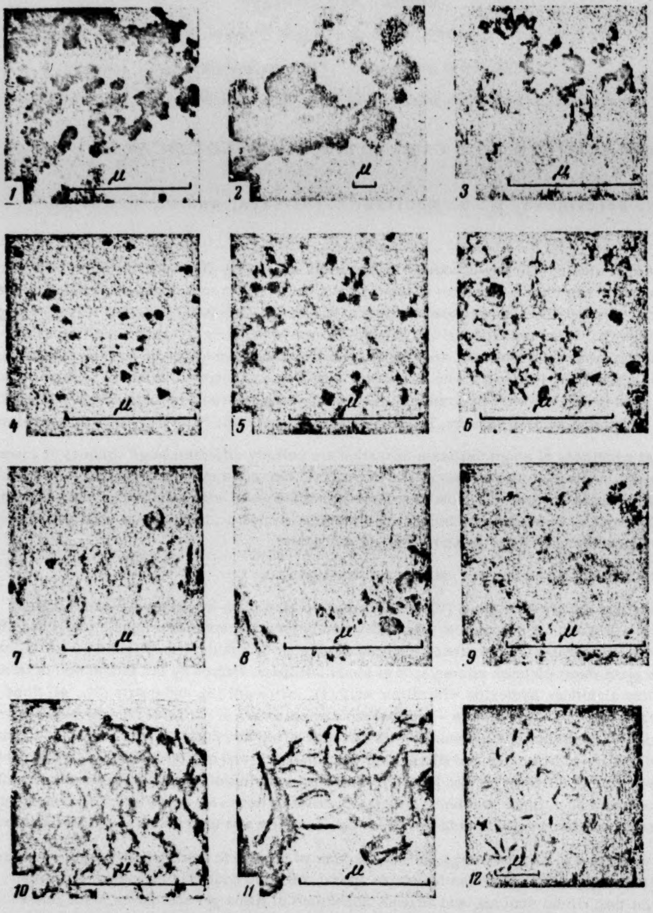

Electron micrographs of aluminosilicates (explanation in text).

Thus, the reaction between colloidal solutions of silicic acid and aluminum hydroxide occurs in true solution, as is the case in a number of other colloidal systems [6]. The rate of aluminosilicate formation when aluminum hydroxide sols react with silicic acid sols or with aqueous suspensions of silica gel or quartz, if the reaction occurs in true solution, will evidently be determined by the diffusion rates of the corresponding ions. However, the amount of substances in true solution in these cases are so small that the formation of aluminosilicates will proceed exceedingly slowly.

The migration of dissolved substances can be accelerated by application of an electric field. We used five-chamber electrodialysis [7] for this purpose.

The central and the two end compartments were filled with redistilled water. The second compartment was filled with silicic acid sol, and the fourth, with aluminum hydroxide sol. On application of an electric field (potential gradient 300-400 v/cm) across the membranes separating the compartments, two streams of ions (aluminum and silicate) move toward each other into the central compartment, interact, and form aluminosilicates.

As the membrane is not permeable to colloid particles, these remain in the second and fourth compartments. Application of an electric field accelerates the formation of aluminosilicates considerably. For example, samples taken from the central compartment after 300-350 hours give an electron micrograph shown in the Figure, 10. This clearly shows the crystalline form of the particles, which have a needlelike structure and form fairly large aggregates. Electron diffraction data also indicate that the particles formed have a crystalline structure.

In our previous investigation [8] we made unsuccessful attempts to obtain crystalline aluminosilicates under normal conditions by mixing 0.1 N true solutions of aluminum nitrate and sodium metasilicate. Neither variations of the $Al_2O_3 - SiO_2$ ratio, nor changes in the pH of the medium, had any effect on the structure of the aluminosilicate gels formed. The gels were amorphous in all cases. Only as the result of prolonged heating at high temperatures was it possible in a few cases to obtain aluminosilicates with a crystalline structure.

It is evident that in this case crystallization is exceedingly slow, as was shown by Sedletsky [1].

The interaction of true solutions of aluminum nitrate with sodium silicate may give aluminum hydroxide sols, silicic acid sols, and mixed aluminosilicate gels. We do not know the kinetics of formation of each of these substances in the given conditions. The electron microscope in this case reveals spherical particles of various sizes, from which the chemical composition of the resultant formation cannot be deduced, while electron diffraction data indicate that the substances formed are of an amorphous structure. The 0.1 N solutions used in the preceding investigation are concentrated relative to the true solutions of silicic acid or aluminum hydroxide which are present in the corresponding sols or suspensions. Experiments were therefore carried out with 0.001 N solutions of aluminum nitrate and sodium metasilicate. Mixing of these solutions at room temperature gave the same results as for 0.1 N solutions. However, if the solutions were mixed at the boiling point an aluminosilicate was formed which gave an electron micrograph quite analogous to that found for the aluminosilicate synthesized by electrodialysis (Micrographs 11 and 12). Further investigations showed that an aluminosilicate of crystalline structure, with $Al_2O_3 - SiO_2$ ratio of 3:1, is formed in the temperature range between 85-90 and 100°. The aluminosilicate gels formed at lower temperatures had amorphous structure and formed spherical particles. Evidently at higher temperatures the rate of formation of aluminosilicates is considerably higher than the formation rate of aluminum hydroxide and silicic acid sols. Micrograph 12 shows that the aluminosilicate crystals formed appear to be enclosed within larger spherical particles. Probably, larger amorphous particles are formed first, and crystallization then takes place within them, but the rate of this process is so high that the original particles can be seen under the electron microscope. The higher crystallization rate is probably the consequence of the higher temperature. Thus aluminosilicates of crystalline structure can be obtained at elevated temperatures in dilute solutions.

SUMMARY

1. It is shown that formation of aluminosilicates in the interaction of aluminum hydroxide with silicic acid sols or aqueous suspensions of quartz or silica gel occurs in true solutions.

2. Aluminosilicate with a crystalline structure has been synthesized by means of five-chamber electrodialysis.

3. From dilute solutions of aluminum nitrate and sodium silicate at high temperatures an aluminosilicate was prepared having a crystalline structure and given the same type of electron micrograph as the aluminosilicate synthesized by means of five-chamber electrodialysis.

The L. Ya. Karpov Physicochemical Institute
Moscow

Received July 12, 1956

LITERATURE CITED

[1] I. D. Sedletsky, Proc. Acad. Sci. USSR, 17,371 (1937).

[2] Z. Ya. Berestneva, T. A. Koretskaya, and V. A. Kargin, Colloid J., 13, 323 (1951).

[3] Z. Ya. Berestneva, T. A. Koretskaya, and V. A. Kargin, Colloid J., 11,369 (1949); H. Brinzinger and B. Troemer, Z. Anorg. Chem. 181, 237 (1929).

[4] V. Lehner, H. Merill, J. Am. Chem. Soc. 39, 2630 (1917).

[5] E. J. King, G. McMurray, Biochem. J. 32, 476 (1938); P. D. Ritchie, P. B. Demster, Nature 169, 538, (1952); D. W. Clellang, W. M. Cumming, P. D. Ritchie, J. Appl. Chem. 2, 31, (1952).

[6] V. A. Kargin and R. E. Chernitskaya, J. Phys. Chem., 9,461, 471, 481 (1937).

[7] V. A. Kargin, T. A. Matveeva, Proc. Acad. Sci. USSR, 105,294 (1955); O. I. Dmitrienko and V. A. Kargin, Colloid J., 13,259 (1951).

[8] Z. Ya. Berestneva and V. A. Kargin, Colloid J., 17,196 (1955).

STUDY OF THE TRANSITION OF AMORPHOUS AND CRYSTALLINE POLYMERS FROM THE SOLID INTO THE FLUID STATE ON ADDITION OF SUBSTANCES OF LOW MOLECULAR WEIGHT

V. A. Kargin, G. L. Slonimsky, and L. Z. Rogovina

In recent years the effects of temperature and molecular weight on the deformation of linear amorphous and crystalline polymers has been studied in detail [1]. In addition, the effects of plasticizers on the glass and flow transition temperatures have been studied [2]. However, no investigations of this type have yet been carried out over a wide range of plasticizer concentrations, covering the transition from a solid (glassy or crystalline) polymer to its dilute solution [*]. Study of this transition was the purpose of the present work.

The materials studied were glassy polymers — polyvinyl chloride and polymethyl methacrylate, and also a crystalline polymer — a mixed polyamide formed by joint polycondensation of caprolactam and salts of hexamethylenediamine and adipic and azelaic acids. Polyvinyl chloride of two different molecular wieghts (80,000 and 120,000) was used, so that it was possible to study the influence of molecular weight on the transition of the polymer into solution. The plasticizer used for both amorphous polymers was dibutyl phthalate, chosen as being the most common plasticizer of low volatility; meta-cresol was used for the polyamide. The mixing of the polymer with the plasticizer was effected by the swelling method at ~140° with stirring. Specimens with little or no plasticizer were molded for the tests; specimens which were in the form of gels or solutions were poured into aluminum basins. The specimens with different plasticizer contents were studied over a wide temperature range (from − 70 to +200°) by means of the dynamometric balance. The deformation produced by uniaxial compression of the specimens in 15 seconds, at constant stress of 0.05 kg/cm^2, was studied as a function of the temperature. In view of the possibility of flow, which can occur especially easily in systems of low concentrations, the measurements were started at low temperatures.

Polyvinyl chloride (PVC). Fig. 1 shows thermomechanical curves obtained by the method outlined above for specimens of PVC containing different amounts of dibutyl phthalate. In agreement with earlier results [4], the original PVC does not show residual deformation at any temperatures, i. e., it does not exhibit true flow; at a definite temperature large deformations are produced in it, which can be easily mistaken for flow (this is seen in the graph in the sharp upward turn of the curve). However, additional investigation showed that these deformations are reversible.

A similar result is found for a system containing 33.5 wt. % of dibutyl phthalate, which is also incapable of flow. However, in this case two temperature regions of softening are found (~40 and 120°). With 50 wt. % the system softens slightly even at -10°, and again at 70-80°. In this case further increase of temperature leads to true flow at 110°. It must be pointed out that the temperature at which flow begins does not coincide with the start of large deformations. Thus, in the case of plasticized PVC there are two softening resions and one flow region, which we shall term the first and second glass (softening) temperatures and the flow temperature respectively. Consequently, when glassy plasticized PVC is heated, elastic deformations arise in the first glass region; the magnitude of these remains constant over a certain temperature range. Then, in the second glass region, the deformability increases sharply, although flow only occurs at still higher temperatures.

---

[*] Chumakova-Ivanova and Rebinder [3] studied the mechanical properties of polyisobutylene and its solutions over a very wide concentration range, but this investigation was confined to the high-elastic and viscofluid states.

Increase of the plasticizer content softens the system and lowers the first and second glass temperatures, and also the flow temperature. At dibutyl phthalate concentrations above 82 wt. % the flow and second glass temperatures coincide. Further dilution of the polymer leads to a contraction of the high elastic region, which vanishes completely at a concentration of ~ 90%. More dilute systems behave as liquids of low molecular weight. It must be stressed that the transition from systems which are elastic gels to fluid systems – solutions – occurs in a very narrow concentration range, from 86 to 90% dibutyl phthalate; at 90% the flow in still accompanied by elastic deformations, but 95% dibutyl phthalate content PVC already forms a true solution, with only one flow temperature. The transition toward solutions for the PVC specimen of higher molecular weight is in general similar to that described.

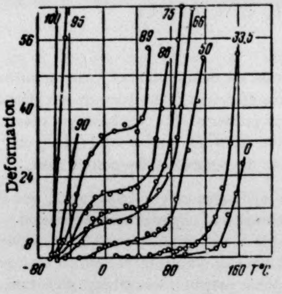

Fig. 1. Effect of temperature on the deformation of polyvinyl chloride with various contents of dibutyl phthalate plasticizer (the numbers on the curves represent dibutyl phthalate concentrations in wt. %).

The features common to both PVC specimens are: 1) displacement of the region of high elasticity into the region of lower temperatures; decrease of the elasticity modulus (elevation of the plateau in the graph); expansion of the temperature range in which elasticity is present at low plasticizer contents, and narrowing of this range, down to complete disappearance, at high plasticizer contents; 2) existence of a considerable region of the gel state, up to very high dilutions, the transition to solution occurring in a narrow range of temperatures and concentrations; 3) existence of two glass (softening) temperatures, not coordinated with transition into the region of high deformations and with appearance of flow.

The differences in the transition to solutions, associated with the molecular weight of the polymer are as follows: 1) transition to solutions in specimens of higher molecular weight is more sharp (thus, with 96% dibutyl phthalate the system is still a gel, and at 98% it is a fluid solution); 2) in the specimens of higher molecular weight there is a greater divergence between the temperature at which residual deformations arise and the temperatures at which large deformations appear.

Polymethyl methacrylate (PMMA). The transition to solutions is much more gradual in PMMA, as can be seen in Fig. 2. The temperatures at which true residual deformations appear and large deformations arise, coincide for all specimens of plasticized PMMA. As was to be expected, the glass and flow temperatures depend on the plasticizer concentration. With 50 and 66% of dibutyl phthalate the specimens are gels over a considerable temperature range. Transition into the solution region begins from 75%, as is shown by the gradual degeneration of the region of high elasticity and the convergence of the glass and flow temperatures. With 90% of dibutyl phthalate the region of high elasticity disappears completely and the system becomes an ordinary fluid solution.

Polyamide (PA). The curves for the crystalline polyamide are given in Fig. 3 . The original polyamide passes directly from the solid into the viscofluid state, and a region of high elasticity is not observed at all. Fusion, as in other crystalline polymers, does not occur at one definite temperature, but over a narrow temperature range (125-140°).

On addition of cresol to the polyamide, in contrast to the amorphous polymers considered above, the system passes into solution at room temperatures even at relatively low plasticizer concentrations, from 50% of cresol. The behavior of the polyamide on addition of 0 to 75% of cresol was therefore studied. On addition of 9% of cresol the thermo mechanical curve is on the whole of the same form as for the original polyamide, but the fusion temperature rises somewhat and the bend in the curve becomes sharper. Moreover, an increase in the PA deformability is seen over a narrow temperature range before fusion, although these deformations are not large enough to make it possible to speak of an elastic state. On additions of 23 and 28% of cresol the fusion temperature decreases correspondingly, the fusion region becomes increasingly diffuse, and a small temperature region of weak elasticity appears, which becomes more prominent on application of greater forces of deformation. Specimens containing 33 and 43% of cresol are elastic at room temperature and become viscous liquids on slight heating. With 50% of cresol the system is a normal but viscous solution even at room temperature. Increase of the cresol content to 75% converts the system into an easily flowing liquid, which thickens at low temperatures.

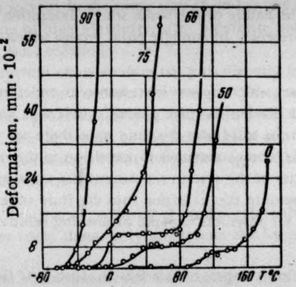

Fig. 2. Effect of temperature on the deformation of polymethyl methacrylate with various contents of dibutyl phthalate plasticizer (the numbers on the curves represent dibutyl phthalate concentrations in wt. %).

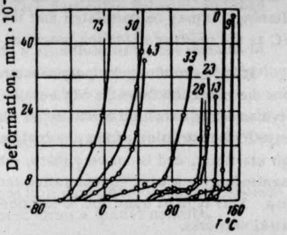

Fig. 3. Effect of temperature on the deformation of polyamide with various contents of m-cresol plasticizer (the numbers on the curves represent m-cresol concentrations in wt. %).

DISCUSSION OF RESULTS

Polyvinyl chloride. First ut must be noted that addition of a substance of low molecular weight has little effect on the properties of the solid polymer up to the softening region. The softening region lies in a relatively narrow concentration range, in which the polymer passes from the solid to the high-elastic state. Thus, the variation in the properties of any polymer on dilution is not uniform, but is analogous to the variation in the polymer properties on heating, and therefore the deformation – concentration graph is of characteristic form (Fig. 4).

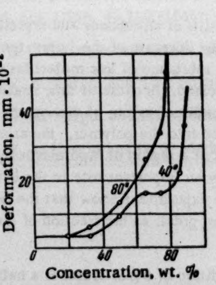

Fig. 4. Deformation of polyvinyl chloride plasticized with dibutyl phthalate as a function of the dibutyl phthalate concentration at 40 and 80°.

The absence of true flow in PVC, the existence of a wide concentration region of gel formation, up to very high degrees of dilution (95-98% of dibutyl phthalate), and the sudden transition to solutions in a very narrow concentration range – all this can only be explained on the assumption that PVC, which is usually regarded as a linear polymer, nevertheless forms a spatial network owing to intermolecular interaction. Structure formation by PVC molecules during heating has been detected previously [5], when it was attributed to the presence of thermoreactive groups, the origin of which is not clear, in PVC.

The second transition temperature in the region of large deformations does not correspond to the temperature at which flow appears, and therefore these large reversible deformations must arise when some other, stronger bonds are overcome at a definite temperature.

Thus, the existence of two glass temperatures indicates that the network is formed by two types of bonds, which are respectively broken at two different temperatures. Bonds of the first type are evidently formed between CHCl and CH_2 groups of two adjacent molecules; they are not very stable and when the energy of thermal motion on increase of temperature becomes comparable to the energy of these bonds the first softening occurs, and the polymer passes into the state of high elasticity. However, during deformation in this state bonds of the second type still retain the molecules in a partially glassy state. On further increase of temperature thermal motion overcomes these bonds also, and the deformation then begins to increase rapidly, corresponding to the second softening region. The question arises, what is the nature of the bonds which determine the second softening. It may be postulated that they are caused by the presence of strongly polar groups which appear in PVC as the result of oxidation processes.

It has been shown for polyisobutylene [3] that in polymers which cannot form networks under any conditions the transition from the high-elastic to the fluid state on dilution is quite gradual. It is seen that not all polymers show transition of this type. When PVC passes from the solid into the fluid state there are two sudden jumps in the variation of the physical properties of the system: one corresponds to transition to the state of high elasticity, and is not very sharp; subsequently the elasticity of the system remains of the same order of magnitude over a wide concentration range, and the second jump in the transition into the fluid state is very sharp. This type of transition to solution is probably found in all polymers capable of forming relatively stable spatial networks.

The discrepancy between the second softening and the flow temperatures arises because PVC flows only when the viscosity of the polymer is low enough; therefore the flow temperature need not be related to the temperature at which rupture of intermolecular bonds of either type takes place.

Polymethyl methacrylate (PMMA). The fairly narrow region of gel formation and the absence of a second softening indicate that PMMA contains only one type of intermolecular bonds, which are easily overcome on heating; this correspond to softening. The transition into the solution region is therefore much more gradual; in this respect PMMA occupies an intermediate position between linear polyisobutylene and polyvinyl chloride, which forms a spatial network.

Polyamide. The appearance of a state of high elasticity in the polyamide on addition of small amounts of the low-molecular substance and the simultaneous small rise in the fusion temperature appear unnatural at first sight. The rise of the fusion temperature suggests that when a crystalline polymer is swollen in a low - molecular substance the polymer crystals become more regular. A similar effect has been discovered recently [6], when it was shown that as the temperature approaches themelting point of a crystalline polymer the reflexions become sharper on the X-ray diagram.

This effect may be explained as follows: a crystalline polymer consists of amorphous and crystalline regions; the nonequilibrium stressed state of the crystals is manifested in the decrease of the fusion temperature and the existence of a fusion region rather than a melting point. When a substance of low molecular weight is added, it is dissolved in the amorphous portion, i. e., the latter is plasticized. Because of this, stresses are diminished both in the amorphous and the crystalline regions, and the crystalline regions of the system therefore become more ordered. Thus, with small amounts of solvent introduced into the polymer, the amorphous regions are changed first. This is in entire agreement with the appearance of a region of high elasticity in this range of solvent concentration: if the amorphous regions begin to play an important role in the behavior of the polymer, its characteristic state of high elasticity will appear. The experiments show that the height and extent of this elasticity plateau on the thermomechanical curve are not great, as the fraction of the amorphous regions is not large.

The observed rise in the fusion temperature of the polyamide on addition of 9% of cresol is a natural consequence of the increased crystal order. With a higher cresol content in the mixture the solubility of the crystals in it increases and as a result the temperature at which the crystals disappear is lower. At high degrees of swelling the crystals dissolve so rapidly on heating that the flow temperature decreases considerably. Thus, while in amorphous polymers the decrease of the flow temperature on plasticization is the result of decreased viscosity of the system, plasticization of crystalline polymers leads to a decrease of the flow temperature owing to loss of the crystalline state by solution of the polymer crystals in the plasticized amorphous portion. In absence of plasticizer, flow begins in the crystalline polymer only after fusion of the crystals.

SUMMARY

1. The transition from the pure solid polymer to its fluid solution has been studied for two glassy and one crystalline polymer, and the characteristics associated with phase state and molecular structure have been demonstrated.

2. The transition of a polymer from the glassy or crystalline state into a fluid solution is effected by addition of a solvent in the same way as on heating; i. e., the solid polymer, with increasing dilution, passes through a state of high elasticity, with a definite concentration region for each particular polymer, and then passes into a fluid solution.

3. Polyvinyl chloride does not pass directly from a high-elastic into a viscofluid state, but remains in gel form over a wide concentration range. Thus, two transitional stages were found during solution of polyvinyl chloride. The appearance of a second transitional stage on dilution of PVC, and also of a second glass temperature, are the results of the existence of two types of intermolecular forces, differing in magnitude, in PVC. It may be assumed that the second type of bonds is formed by strongly polar groups which arise as the result of oxidation of PVC.

4. In the case of polymethyl methacrylate the transition to solutions is intermediate in nature between that found for ideal linear polyisobutylene and for polyvinyl chloride, which forms a spatial network.

5. The characteristics of the transition from a crystalline polymer (polyamide) to its solution depend on the development of crystal order in presence of small amounts of plasticizer, the development and growth of a state of high elasticity within the limits of existence of the crystalline state, and the decrease of flow temperature as the result of increased solubility of the ordered regions (crystals) in the plasticized amorphous portion.

The L. Ya. Karpov Physicochemical Institute
Moscow

Received November 20, 1956

LITERATURE CITED

[1] P. Kobeko, E. Kuvshinsky, and G. Gurevich, Bull. Acad. Sci. USSR, Phys. Ser., No. 3, 329 (1937); A P. Aleksandrov and Yu. S. Lazurkin, J. Tech. Phys., 9,1249 (1939); V. A. Kargin and T. I. Sogolova, J. Phys. Chem., 23,530 (1949); 27,1039, 1208 (1953).

[2] S. N. Zhurkov, Proc. Acad. Sci. USSR, 47,493 (1945); 49,201 (1945); S. N. Zhurkov and R. L. Lerman, Proc. Acad. Sci. USSR, 47,109 (1945); V. A. Kargin and Yu. M. Malinsky, Proc. Acad. Sci. USSR, 73,967 (1950).

[3] L. I. Chumakova-Ivanova and P. A. Rebinder, Colloid J., 18,429 (1956).

[4] V. A. Kargin and T. I. Sogolova, Proc. Acad. Sci. USSR, 108,662 (1956).

[5] V. A. Kargin and M. N. Shteding, J. Chem. Ind., No. 3, 137 (1956).

[6] V. A. Kargin and G. S. Markova, J. Phys. Chem., 29, 1273 (1955).

ADSORPTION OF POLYSTYRENE LATEXES IN RELATION TO THE SIGN OF THE PARTICLE CHARGE AND THE SORBENT

E. M. Aleksandrova and N. S. Razumikhina

The ability of colloidal systems to be adsorbed on extraneous surfaces is of great practical importance in such processes as dyeing, leather tanning, sizing and impregnation. According to Peskov [1], adsorptive fixation of colloid particles is a special form of coagulation (heterocoagulation), differing from ordinary coagulation in that an extraneous phase is required for it. The mechanism of the process is that the extraneous surface adsorbs the stabilizer of the colloidal particles, and the destabilized particles coagulate on the adsorbing surface.

The colloidochemical theory of sizing was developed by Voyutsky [2], the basis being the fact that the fiber and sizing material are colloid systems. The sizing process is regarded as coagulation of the sizing agent on the fiber surface, i. e., as heterocoagulation. Heterocoagulation occurs as the result of destabilization of the colloidal particles by means of some coagulant, or by direct interaction between the surface layers of the fiber and the stabilizer (molecular or micellar).

The heterocoagulation process occurs most effectively if the charges on the colloidal particles and on the adsorbing surface are of opposite sign. If the particles and the surface are similarly charged, heterocoagulation usually does not occur.

It is known that electrolytes are added when fibrous materials are treated with negatively charged latexes. We followed the same procedure, combining positively charged adsorbents and latexes. The need to add electrolytes for the adsorption of colloidal particles has been demonstrated not only for latexes [3]. Considerably earlier, Peskov and Moryganov [4] added electrolytes in studying the adsorption of dyes. Recently Koganovsky and Rovinskaya [5] performed analogous experiments on the adsorption of humic acid micelles on graphite.

The probable explanation for the action of electrolytes is that they cause some desolvation of the colloidal particles, although the system remains aggregatively stable until the adsorbent is introduced.

Considerable interest in relation to impregnation and sizing attaches to the use of positively charged latexes, which have been obtained by charge reversal of negatively charged latexes [2] and directly by emulsion polymerization of styrene [6].

The stability of such latexes was studied by Aleksandrova and Kertes-Mureshan [7]. The colloidochemical properties of latexes, as of other sols, are largely determined by the properties of the stabilizing component.

The stabilizers used by us for preparation of latexes were cation-active colloidal electrolytes.

These substances form semicolloidal systems in aqueous solution. The distribution of the substance between the phases is determined by the temperature and especially by the concentration. Micelles are formed in large amounts only in a relatively narrow range of concentrations –at the so-called critical concentration of micelle formation (CCM).

The stabilizing action of cation-active substances, making them effective stabilizers, depends on their tendency to form colloidal solutions, their structuromechanical properties, and their considerable surface activity.

Two cation-active substances were studied: Leveling Agent A (LA), and octadecyloxymethylpyridinium chloride (OOPC). The cationic agent sold as Leveling Agent A was first synthesized by Lapina [8], and is widely used in the textile industry, in dyeing fur, woolen, and felt goods, and as a detergent; its general formula is

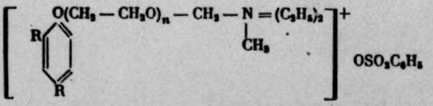

where n can vary from 3 to 30; R is C_8H_{17}.

The molecular weight varies, according to n, over a wide range from M = 634 when n = 3, to M = 1246 when n = 30. We used Leveling Agent A (n = 12.9) the colloidochemical properties of solutions of which has been studied by Kertes [7].

The other stabilizer, octadecyloxymethylpyridinium chloride (OOPC), of molecular weight 397.7, has the structure

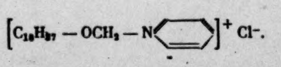

It is sparingly soluble in water at room temperature; 0.1% solutions of OOPC are strongly opalescent; its colloidal properties were also studied by Kertes [7]. The surface activities of both stabilizers are of the same order of magnitude.

Investigations of the adsorption of latexes were preceded by studies of adsorption of the stabilizers themselves. The adsorbent was filter paper, which is negatively charged at the water interface.

The reasons for this choice were the purity of filter paper (ash content 0.01%), its standard quality, relatively high adsorptive activity, and also the practical importance of the adsorption of latex particles on fibrous materials.

The adsorption of LA was also studied on active carbon, which also has a negative surface charge. The degree of adsorption was determined from the decrease of solution concentration. The equilibrium concentrations of LA and OOPC stabilizers were determined by an optical method developed by A. S. Kryukova. The principle of the method is that when the dye Acid Blue K is added to solutions of the stabilizers LA and OOPC, they are colored violet at low concentrations and blue at high concentrations. These solutions obey Beer's law over a definite concentration range. Calibration curves (Figs. 1,2) are obtained by plotting the optical density of the solutions ($D_{\lambda=619}$) against the concentration (c). The optical densities were measured by means of the MF universal photometer.

The results obtained were used to plot adsorption isotherms (Figs. 3,4) the amounts of adsorbed substance in millimoles per gram of sorbent (a) being plotted against the equilibrium concentrations (in millimoles per liter). Both stabilizers are well adsorbed by ashless filter paper and active carbon. The adsorption on carbon reaches almost the same values as in experiments with CH_3COOH or isoamyl alcohol. The adsorption on paper is less, owing to its different structure. The adsorption is, as a rule, reversible.

The experiments show that both stabilizers have considerable surface activity at the adsorbent — aqueous solution interface. There are therefore grounds to expect effective heterocoagulation in latexes stabilized by these cation-active agents.

The latexes were prepared by the emulsion polymerization method described by Mochalov [3] and Kertes [7].

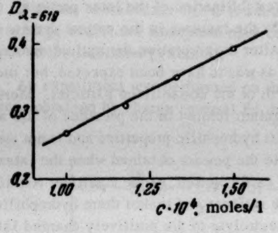

Fig. 1. Calibration curve for determination of the concentration of leveling agent LA from the optical density.

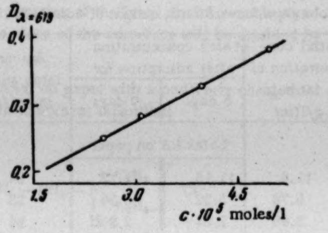

Fig. 2. Calibration curve for determination of the concentration of leveling agent OOPC from the optical density.

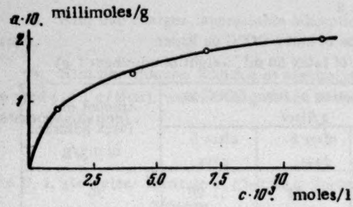

Fig. 3. Adsorption isotherm for LA on carbon.

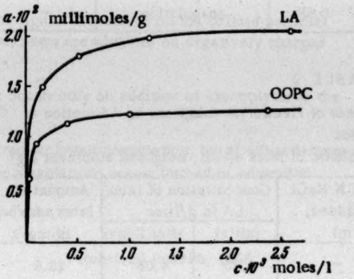

Fig. 4. Adsorption isotherm for LA and OOPC on paper.

Latex with stabilizer LA (latex LA) was stable to dilution and to addition of electrolytes (K_2SO_4, $BaCl_2$, K_3PO_4) even at very high concentrations of the latter. The dry solids content was 168 g/liter. The latex was positively charged; its electrokinetic potential was 42 mv.

Latex with stabilizer OOPC (latex OOPC) was stable to electrolytes in the amounts usually added for coagulation of hydrosols with solvated ion stabilization; its aggregative stability is only destroyed by salting out of the stabilizer on addition of large amounts of electrolytes (KCl – 1 millimole/liter, K_2SO_4 – 0.5 millimole/liter). The dry solids content was 52.8 g/liter; the electrokinetic potential was + 40 mv.

The adsorption of latex LA was studied on ashless filter paper and on active carbon, which has a negatively charged surface at the water interface. The results of the experiments are given in Table 1.

The experiments showed that positively charged latex LA is adsorbed on negatively charged surfaces without addition of electrolyte. As Table 1 shows, not only heterocoagulation but also homocoagulation took place. Particularly strong homocoagulation was observed at low latex concentrations (from 0.5 to 2 g/liter). Stabilizer LA passes almost completely to the sorbent surface, with resultant total destabilization of the latex particles. At latex concentrations between 4 and 12 g/liter mainly heterocoagulation occurs, the extent of homocoagulation being very small. Only some isolated particle aggregates were visible under the microscope.

TABLE 1

Adsorption of Latex LA on Paper and Carbon
(Volume of latex 50 ml, weight of adsorbent 1 g)

Initial concentration of LA latex in g/liter	Latex concentration after adsorption for		Amount of latex adsorbed in mg/g
	5 days	9 days	
	Latex LA on paper		
11.6	11.16	11.12	24
5.76	5.32	5.30	23
2.68	2.24	2.20	24
1.24	coagulation		–
0.68	coagulation		–
	Latex LA on carbon		
8.72	7.4	7.32	70
4.32	3.52	3.48	42
1.04	coagulation		–
0.68	coagulation		–

Both types of coagulation are the result of transfer of the stabilizer from the latex particles to the adsorbent, and destabilization of the latex particles; this is confirmed by the increase in the optical density of the latexes. After the adsorption the optical density did not decrease, as was to have been expected, but increased owing to growth of the destabilized particles. Moreover, the latex coagulum formed in the presence of the adsorbent loses its hydrophilic properties and is not wetted by water, while the powder obtained when the latex is dried in air is easily wetted, as the stabilizer remains on the particle surfaces and makes them hydrophilic. Addition of electrolyte to the positively charged latex LA at a concentration below the coagulation threshold results in a very slight increase of adsorption of the latex on paper (Table 2), but addition of the same electrolyte to a negatively charged latex increases adsorption sharply [3].

In the adsorption of latex OOPC on ashless filter paper with a negatively charged surface the result was quite analogous to that in the adsorption of latex LA on paper and carbon (Table 3).

TABLE 2

Effect of Electrolyte Additions on Adsorption of Latex
(Volume of latex 40 ml, weight of adsorbent 1 g)

0.1 N NaCl added, ml	Concentration of latex LA in g/liter		Amount of latex adsorbed in mg/g
	initial	after 3 days	
–	4.65	4.08	22.8
1	4.65	3.96	27.6
2	4.65	3.90	29
5	4.65	3.90	29

TABLE 3

Adsorption of Latex OOPC on Paper
(Volume of latex 50 ml, weight of adsorbent 1 g)

Concentration of latex OOPC in g/liter			Amount of latex adsorbed in mg/g
initial	after 5 days	after 9 days	
11.8	11.34	11.20	30
8.68	8.12	8.04	32
5.0	4.37	4.36	32
3.32	2.68	2.68	32
1.86	coagulation		–
0.66	coagulation		–

TABLE 4

Effect of Concentration of Stabilizer OOPC on the Adsorption of Latex OOPC
(Volume of latex 50 ml, weight of adsorbent 1 g)

Initial concentration of latex OOPC in g/liter	0.1 N solution of OOPC added, ml	Volume of H_2O, ml	Equilibrium concentration of latex after		Amount of latex adsorbed in mg/g
			4 days	10 days	
4.32	–	10	3.60	3.60	36
4.24	3	7	3.90	3.90	17
4.68	10	3	4.50	4.40	8

TABLE 5

Adsorption of Latexes in Relation to the Sign of the Charge on the Particles and the Adsorbent

Change on adsorbent	Change on latex	Addition of electrolyte	Result
+	+	Required	Heterocoagulation
+	–	Not required	"
–	+	Not required	"
–	–	Required	"

It is seen from Table 3 that latex OOPC undergoes volume coagulation at concentrations from 0.66 to 2 g/liter, while at concentrations from 3 g/liter upward both types of coagulation occur, homocoagulation being slight, and detected only by the slight increase of optical density.

If excess of stabilizer OOPC is added to latex OOPC, the adsorption of the latex diminishes sharply. With a large excess the adsorption may cease altogether, as the surface of the adsorbent will be shielded by a layer of the stabilizer (Table 4).

An experiment was performed on the adsorption of latex OOPC on paper with a positively charged surface, obtained by charge reversal by the use of a cation-active substance, sapamine:

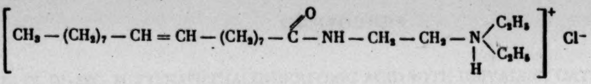

$$\left[CH_3-(CH_2)_7-CH=CH-(CH_2)_7-\overset{O}{\overset{\diagup}{C}}-NH-CH_2-CH_2-\underset{H}{\underset{|}{N}}\begin{matrix} \diagup C_2H_5 \\ \diagdown C_2H_5 \end{matrix} \right]^+ Cl^-$$

The charge on the paper surface was determined by the electroosmotic method.

Positively charged latex OOPC was not adsorbed on the positively charged surface, but addition of electrolytes induced adsorption. The results of experiments on the influence of the sign of the charge on the particles and the adsorbent on the adsorption of polystyrene latexes are given in Table 5.

SUMMARY

1. The adsorption of polystyrene latexes, in relation to the sign of the charge on the colloid particles and latexes, has been studied. It is shown that cation-active stabilizers are adsorbed on negatively charged adsorbents.

2. With like charges, appreciable adsorption of the latex occurs only on addition of electrolytes to the system.

3. With like charges, addition of electrolytes is not required for heterocoagulation, but if dilute latexes are used ($\leqslant 1$ g/liter), volume coagulation of the latexes (homocoagulation) occurs instead of adsorption (heterocoagulation).

The D. I. Mendeleev Institute of Chemical Technology
Moscow

Received June 28, 1956

LITERATURE CITED

[1] N. P. Peskov, Symposium "Modern Problems of Colloid Chemistry and the Leather Industry" (Mendeleev All-Union Chem. Soc. Press, Moscow, 1937).

[2] S. S. Voyutsky, Colloid Theory of Paper and Cardboard Sizing (Light Ind. Press, 1946).

[3] P. V. Mochalov, Dissertation (Moscow, 1952); E. M. Aleksandrova and P. V. Mochalov, Colloid J., 16, No. 3,161 (1954); No. 6, 401 (1954.).

[4] N. P. Peskov, Bull. Textile Ind., No. 5,25 (1926); P. V. Moryganov and V. E. Rostovtsev, Cotton Ind., No. 11,36 (1938).

[5] A. M. Koganovsky and T. M. Rovinskaya, Colloid J., 17, No. 2, 81 (1955).

[6] A. P. Sheinker (Dissertation, Moscow, 1954); E. V. Zabolotskaya (Dissertation, Moscow, 1954).

[7] Yu. Kertes-Mureshan, Dissertation (Moscow, 1954); E. M. Aleksandrova and Yu. Kertes-Mureshan, Proc. Acad. Sci. USSR, 103, No. 2,269 (1955).

[8] P. A. Lapina (Dissertation, Moscow, 1955).

THE RELATIONSHIP BETWEEN THE STRUCTURE OF EMULSIFIERS OF THE ALKYLAROMATIC ACID TYPE AND THE POLYMERIZATION OF UNSATURATED COMPOUNDS

4. SALTS OF DI-SEC-BUTYLNAPHTHALENESULFONIC ACID WITH UNIVALENT CATIONS

N. P. Apukhtina and A. M. Lyagalova

In the previous papers we demonstrated the dependence of the solubilization of α-methylstyrene and of the copolymerization of divinyl with α-methylstyrene on the butyl group contents of alkyl aryl sulfonates [1], and on the contents of univalent cations [2] and anions [3]. It was shown that all these factors have a great influence on the emulsifier properties. It was found [2] that, in presence of alkyl aryl sulfonates with different cations in the same equivalent concentrations, the rates of polymerization are different, both in presence and in absence of salts.

The present study deals with certain colloidochemical properties of alkaline di-sec-butylnaphthalenesulfonates with K^+, Na^+, Li^+ and NH_4^+ cations (di-NP K, di-NP Na, di-NP Li, and di-NP NH_4).

The solubilities in water, the surface tensions of the aqueous solutions, and the influence of these compounds on the solubilization and polymerization of divinyl were determined.

Starting materials. The emulsifiers were prepared by neutralization of di-sec-butylnaphthalenesulfonic acid with potassium, sodium, lithium, and ammonium hydroxides. The compounds obtained were purified to remove mineral salts and hydrocarbons. The purity of the products was determined from the sulfur contents of the emulsifier molecules.

Method of investigation. The solubilities of the emulsifiers were determined from the saturated solutions at 20°. The surface tension was determined with the aid of the Rebinder apparatus from the maximum bubble pressure.

For the solubilization determinations, 25 g of aqueous emulsifier solution was placed in an ampoule fitted with an electromagnetic stirrer. The ampoule was evacuated and joined to a buret containing divinyl; the absorption of the latter was continued, with stirring, to constant volume, at 20° ± 0.2°. The solubilization of α-methylstyrene was determined refractometrically [1,4].

Divinyl was polymerized at 50° with potassium persulfate initiator; the pH of the medium was 11.8-12; the volume ratio of the hydrocarbon and aqueous phases was 1:1.

In the emulsifier solubility determinations it was noted that the saturated solutions differ in appearance according to the cation combined with the alkylnaphthalenesulfonic acid. For example, di-NP K forms turbid solutions, a fine suspension passing through the filter. Di-NP Na gives transparent saturated solutions with a solid phase in the form of loose flakes. Aqueous solutions of d-NP Li gelatinize readily.

The solubilities of the emulsifiers increase with decreasing cationic radius:

Emulsifiers	di-NP K	di-NP NH_4	di-NP Na	di-NP Li
Solubility in water, %	7-9	12-13	20-22	25-27

The absolute values of surface tension of aqueous solutions of the emulsifiers are fairly similar (Fig. 1), and all four $\sigma = f(c)$ curves can be classified as curves of the first type, in McBain's terminology [5]. In all cases the surface tension decreases sharply up to emulsifier concentrations of $4.0 \cdot 10^{-3} \div 4.5 \cdot 10^{-3}$ g-equiv./1000 g; the curves flatten out on further increase of concentration. The surface tension of emulsifier solutions as a function of concentration decreases regularly with increasing heat of solvation of the cations, which form the following lyotropic series in order of surface tension decrease produced:

$$K^+ > NH_4^+ > Na^+ > Li^+ .$$

The results are in agreement with Aickin's observations [6] on the influence of the nature of the cations in the electrolytes added to aqueous solutions of alkyl sulfonate esters.

The solubilization of divinyl was studied over a wide range of emulsifier concentrations in dilute solutions and in saturated solutions (Figs. 2,3). In all cases with the exception of di-NP NH_4 the solubilization gradually increases with emulsifier concentration. In dilute solutions, approximately up to concentrations of 0.2 g-equiv./1000 g, the solubilization of divinyl is practically the same in all these cases. On further increase of emulsifier concentration* the solubilization varies linearly, di-NP K being the most effective, and di-NP Li the least. All the curves pass through a maximum at a concentration of ~0.7 g-equiv./1000 g; the solubilization of divinyl in di-NP Li solution falls sharply. The curve for the variation of divinyl solubilization with di-NP NH_4 concentration is of a different character (Fig. 2, Curve 4); the solubilization diminishes starting with an emulsifier concentration of 0.2 g-equiv./1000 g.

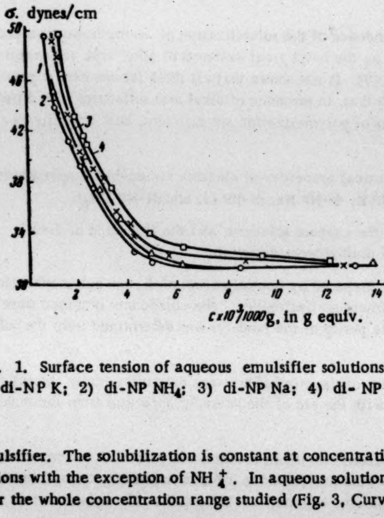

Fig. 1. Surface tension of aqueous emulsifier solutions: 1) di-NP K; 2) di-NP NH_4; 3) di-NP Na; 4) di-NP Li.

In Fig. 3 the solubilization is represented as the ratio of moles of divinyl to moles of emulsifier. The solubilization is constant at concentrations up to 0.6-0.7 g-equiv./1000 g in presence of all the cations with the exception of NH_4^+. In aqueous solutions of di-NP NH_4 the solubilization of divinyl falls steeply over the whole concentration range studied (Fig. 3, Curve 4).

Thus it may be concluded that emulsifier cations influence solubilization in the order of their positions in the lyotropic series: $K^+ > Na^+ > Li^+$; the NH_4 ion is exceptional, as it is the most effective at low concentrations (up to 0.2 g-equiv./1000 g), while on further increase of concentration it goes to the last place in the above series.

Earlier we determined the solubilization of α-methylstyrene as a function of the concentrations of K^+, Na^+, and Li^+ ions, added as chlorides of the univalent metals to an aqueous solution of sodium tri-sec-butylnaphthalenesulfonate. The cations in this case again formed the same lyotropic series [2].

---

* It should be noted that with the exception of di-NP Li the properties of all the emulsifiers were mostly studied in saturated solutions of these colloidal electrolytes, containing different amounts of the solid phase. Thus, in solutions of di-NP K, di-NP Na, di NP-Li, and di-NP NH_4, the solid phase was present at emulsifier concentrations in the water above 0.19, 0.45, 0.7, and 0.35 g-equiv./1000 g of the mixture respectively. Therefore in this paper the term "concentration" of the emulsifier represents its total content in the water both in the dissolved state and as the solid phase.

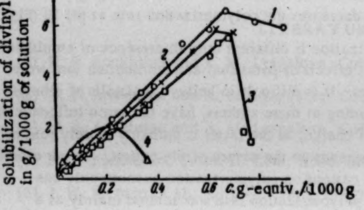

Fig. 2. Solubilization of divinyl in aqueous solutions of emulsifiers: 1) di-NP K; 2) di-NP Na; 3) di-NP Li; 4) di-NP NH_4.

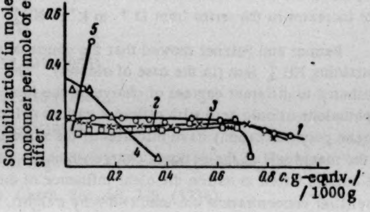

Fig. 3. Solubilization of hydrocarbons in aqueous emulsifier solutions: 1) di-NP K; 2 and 5) di-NP Na; 3) di-NP Li; 4) di-NP NH_4; 1,2,3,4) divinyl; 5) α-methylstyrene.

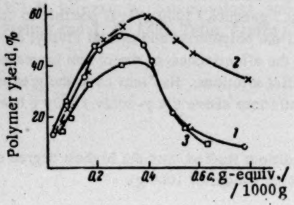

Fig. 4. Influence of emulsifier concentration on conversion of divinyl:
1) di-NP K; 2) di-NP Na; 3) di-NP Li.

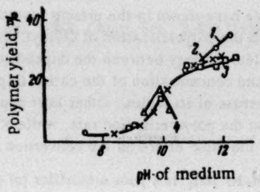

Fig. 5. Influence of the emulsifier cation on the yield of divinyl- α-methylstyrene polymer at different pH values:
1) di-NP K; 2) di-NP Na; 3) di-NP Li; 4) di-NP NH_4.

As has been shown by McBain and his associates [7], the nature of the solubilization curves depends on the emulsifier used and also on the added electrolytes. They showed that in aqueous solutions of emulsifiers of the ionic type (both anion-active and cation-active) aromatic hydrocarbons are solubilized to a far greater extent than aliphatic hydrocarbons, and in some instances the curves for solubilization as a function of concentration also differ in type.

We have also shown that solubilization of α-methylstyrene in aqueous solutions of di-NP Na is considerably greater than that of divinyl (Fig. 3, Curve 5), and that the curve for solubilization as a function of emulsifier concentration is of a different type. The complex character of monomer solubilization suggests the existence of micelles which vary in form and size according to the emulsifier concentration. McBain earlier reached a similar conclusion on the basis of data on transference numbers in laurylsulfonic acid solution [8] and X-ray investigations of highly concentrated solutions of surface-active agents [9].

Polymerization of divinyl. Contradictory data are found in the literature on the influence of cations on the polymerization process. For example, Fermor and Peizner [10, 11] studied the influence of alkyl aryl sulfonate and oleate anions on the polymerization of styrene and concluded that univalent K^+ and Na^+ cations exert an equal influence on the polymerization process, and also on the solubilization of styrene. According to their observations, the nature of the cation in salts of dibutylnaphthalenesulfonic acid does not influence the polymerization rate of styrene over a wide pH range.

We have shown that the polymerization rate of a mixture of divinyl and α-methylstyrene in presence of Li^+, Na^+, and K^+ cations is the same at pH from 7 to 11, while on further increase of pH the polymerization rate increases in the series from Li^+ to K^+; NH_4^+ sharply decreases the polymerization rate at pH 10 (Fig. 4).

Fermor and Peizner showed that the course of polymerization is different only in presence of emulsifiers containing NH_4^+ ions (in the case of oleates). The different effects of potassium and ammonium ions were attributed to different degrees of charge on the ionic micelles. It is difficult to believe that salts of dibutylnaphthalenesulfonic acid with different cations (which, according to these authors, have the same influence on styrene polymerization) have micelles of the same degree of charge, as the latter is probably closely related to the magnitude of the cationic charge which, in its turn, depends on the nature of the cation. In our opinion the authors failed to notice the clear influence of emulsifier cations on polymerization because only one emulsifier concentration was used (~4% by weight), and the polymerization rate was studied mainly as a function of pH at high degrees of conversion of styrene (80-100%).

According to our data, the influence of emulsifier cations on polymerization and certain colloidochemical properties of emulsifier solutions is seen most clearly if the investigations are performed over a wide range of emulsifier concentrations.

It should be noted that some of the authors' data [11] show a clear distinction between the influence of K^+, Na^+, and NH_4^+ ions. However, their conclusions contradict the results of our investigations [2], and the data obtained by others [12].

We have shown in the present investigation that the nature of the emulsifier cation has a significant effect on the polymerization of divinyl. For dilute solutions (up to 0.2 g-equiv./1000 g) it is possible to draw a complete analogy between the dependence of solubilization and of the polymerization rate of divinyl on the nature and concentration of the cation (Figs. 2 and 5); namely, that the effectiveness of the cation increases with increase of its radius. Other laws apply to concentrated emulsifier solutions; Na^+ ions have the greatest effect on the polymerization rate, while K^+ and Li^+ ions at concentrations above 0.4 g-equiv./1000 g have roughly the same effect on the conversion of divinyl.

Di-NP NH_4 is a poor emulsifier for polymerization in the conditions studied, and the highest degree of conversion of divinyl does not exceed 6% (emulsifier concentration 0.05 g-equiv./1000 g).

Polymerization is a more complex process than solubilization of monomers, which is associated with a number of different factors (nature of the monomer, emulsifier, and initiator, pH of the medium, phase ratio, stability of the monomer and polymer emulsions, etc); therefore a complete analogy between variations of polymerization rate and polymerization is hardly to be expected.

It is highly probable that the complex character of the relationship between polymerization rate and the nature of the cations in the region of high concentrations is related to the solubility of colloidal electrolytes in water. Thus, the maxima on the curves for the conversion of divinyl (Fig. 4) in presence of di-NP K and di-NP Na are near the region of maximum solubility of the emulsifiers. The sharp decrease of divinyl conversion in presence of di-NP K at high concentrations is probably caused by a salting-out effect. It is possible that the decreased effectiveness of di-NP Li is associated with the tendency of its solutions to gelation.

SUMMARY

1. The solubilities in water of the emulsifiers studied increase in the following order: di-NP K < < di-NP NH_4 < di-NP Na < di-NP Li.

2. The surface tensions of aqueous solutions of these emulsifiers increase from K^+ to Li^+ in the above series.

3. At emulsifier concentrations up to 0.2 g-equiv./1000 g the solubilization and the polymerization rate of divinyl increase linearly with emulsifier concentration. In this concentration region the cations form the following series according to their effectiveness: $K^+ > Na^+ > Li^+$. The NH_4^+ ion occupies a special position. The solubilization of divinyl, expressed in moles of the monomer per mole of emulsifier, does not change for lithium, sodium, and potassium salts, at concentrations of the latter up to 0.7 g-equiv./1000 g, which

suggest that the micelle structure is also constant in this concentration region.

The S. V. Lebedev Scientific Research Institute
for Synthetic Rubber

Received July 14, 1956

LITERATURE CITED

[1] N. P. Apukhtina and A. M. Lyagalova, Colloid J., 17,337 (1955).

[2] N. P. Apukhtina and A. M. Lyagalova, Colloid J., 17,415 (1955).

[3] N. P. Apukhtina and A. M. Lyagalova, Colloid J., 18,3 (1956).

[4] A. I. Yurzhenko, Trans. III Conf. Acad. Sci. USSR on High Mol. Compounds (Moscow, 1945).

[5] J. W. McBain et al., Koll.-Z. 78, I, (1937); J. Am. Chem. Soc. 58, 379, (1936).

[6] Aickin, J. Soc. Dyers Colorists, 60,36 (1944).

[7] J. W. McBain, K. J. Lissant, J. Phys. Coll. Chem. 55, 655, (1951).

[8] M. E. L. McBain, Phys. Chem. 47, 196, (1943).

[9] J. W. McBain, O. A. Hoffman, J. Phys. Coll. Chem. 53, 39, (1949).

[10] N. A. Fermor and A. B. Peizner, Colloid J., 15,292 (1953).

[11] N. A. Fermor and A. B. Peizner, Colloid J., 15,459 (1953); 16,297 (1954).

[12] K. Berezan, A. Dobromyslova, and B. Dogadkin, Bull. Acad. Sci. USSR, Chem. Ser., 2,409 (1936); C.F. Fryling and T. G. John, Trans. Faraday Soc., 49,980 (1953).

INVESTIGATION OF THE AQUEOUS PROPERTIES OF PEAT BY MEANS OF RADIOACTIVE ISOTOPES

M. P. Volarovich, N. V. Churaev, and B. Ya. Minkov

Ever increasing use is now being made of radioactive tracers in science and technology. In particular, this method has been used in hydrotechnical and melioration research for measurement of the rate and direction of flow [1-6]. In peat technology great importance attaches to the problem of drainage of peat deposits, the successful solution of which involves studies of the aqueous properties of peat. For effective utilization of drainage methods and of open drainage systems used in the peat industry it is necessary to study the motion of water in the deposit, and its relationship to the solid phase in the peat.

After the first investigations by Dumansky and his associates [7], several methods for studying free and bound water in peat have been described [8]. The use of the radioactive tracer method opens up new ways for studying the aqueous properties of peat, and in particular makes it possible to study the movement of moisture in peat, which was not feasible before. For this, it was first necessary to develop techniques for studying the aqueous properties of peat by means of radioactive isotopes.

In developing the methods, it was first necessary to solve the problem of the choice of a suitable radioactive tracer for the water whose motion was to be observed. This was fairly difficult, as there have already been unsuccessful attempts in experiments with soils [6]. After a number of preliminary experiments it was found that the most successful tracer is radioactive sulfur S^{35} (as aqueous $Na_2S^*O_4$) which, as will be shown later, is only slightly adsorbed by the peat particles. The S^{35} sulfur isotope, as is known, disintegrates with the emission of β-particles of 0.16 Mev; the half life of this isotope is 87 days.

The filtration of tagged water through specimens of peat with intact structure was studied in experiments with S^{35} under laboratory conditions. The laboratory apparatus is shown in Fig. 1. The peat specimen 1 cut from the deposit was placed in the glass tube 2 (2.4 cm in diameter) and impregnated with distilled water to constant weight. Tagged water was then poured into the tube over the peat, the level being kept constant by means of the flask 3. The specific activity of the water, tagged with the S^{35} isotope, used in the experiments was 0.005-0.01 μC per 1 ml. The filtrate was collected in the buret 4 with a stopcock and at intervals (when 2 ml had accumulated) was transferred to test tubes fixed in the rotating disk 5. Toward the end of the experiment samples 2 ml in volume alternated with 8-10 ml samples. The time for accumulation of the filtrate in the buret was also noted.

The activity of the filtrate samples was measured by the T-25-BFL window-type counter contained in the universal lead casing IFKh-2, by means of the B-2 type installation. Filtrate samples 1 ml in volume were transferred from the test tubes into brass foil cups and dried under an infrared lamp.

The results of one of the experiments with fuscum peat with degree of decomposition R = 10% are given in Fig. 2. The height of the peat specimen was 6 cm, and the pressure h, 18 cm (see Fig. 1); the relative humidity of the peat, w, was 91.1%. In Fig. 2 the values of the volume V of the filtered liquid in milliliters are taken along the abscissa axis, and the counting rates N for the filtrate in pulses per minute along the ordinate axis. Corrections for radioactive decay and background [9, 10] were introduced in calculation of the counts N. The relative error of the activity determinations, performed under strictly similar conditions, did not exceed 3% [11]. Fig. 2 also shows the variation of the volume V of the filtered liquid with the filtration time τ in minutes. The variation is almost linear, which shows that the filtration coefficient remains constant during the experiment.

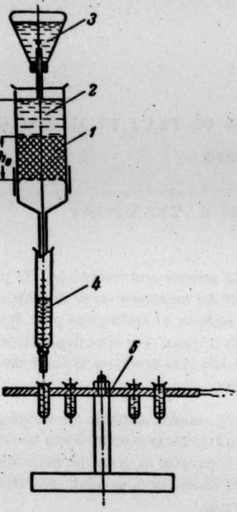

Fig. 1. Diagram of laboratory apparatus for studying the filtration of tagged water through peat.

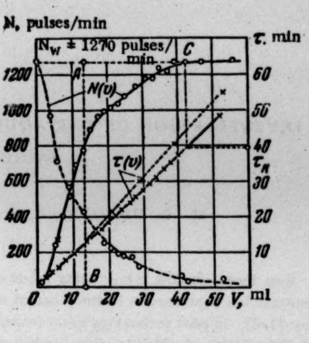

Fig. 2. Results of experiments on the filtration of tagged water through a peat specimen (continuous curves) and subsequent filtration of pure water (broken curves); fuscum peat, R = 10%.

As Fig. 2 shows, the activity of the filtrate samples gradually increases and after a certain time τ_k = 39.5 minutes reaches, at the point C, the value N_w = 1270 pulses/minute, which is the activity of the tagged water entering from above. Analysis of the N – V curve leads to the following suggested mechanism of filtration.

The tagged water moves along the pores in the peat and displaces the free (gravitational) water contained in them. Water is displaced first from the large and then from the finer pores, and finally, at time τ_k, the tagged water fills all the water conduction paths in the peat. After this the activity of the filtrate becomes equal to N_W, the activity of the tagged water. If all the pores in the peat were of the same size, then the N – V graph would be represented by the broken line OBAC in Fig. 2. The deviation of the actual N – V curve from this broken line is a measure of the heterogeneity of pore size in the peat specimen. It must be remembered that this refers only to water-conducting pores along which the filtering liquid moves.

If it is assumed that the paths for the movement of liquid in the peat specimen do not change during the experiment described above, then the N – V curve can be used to plot distribution curves for the amounts of filtering liquid by rates of filtration and dimensions of the water-conducting pores. Pore size distribution in active carbon was determined by Figurovsky [12] from the kinetics of displacement of one liquid from the pores by another.

The calculation data for an experiment with fuscum peat are given in Table 1.

In Table 1 the activity changes Δ N of the filtrate samples have been calculated for different volumes V of the filtered liquid and the time intervals $\Delta\tau$ corresponding to them on the τ – V graph. It is easily seen that in the region OC of the N – V curve (Fig. 2) the activity increment Δ N is proportional to Δ Q, the amount of tagged water, moving at rates from u_n to u_{n+1} where $u_n = h_0/\tau_n$ and h_0 is the height of the specimen, taken to be equal to the length of the liquid path. The fractions of the amount of water for each rate range are given in Table 1 as percentages of the total amount of liquid flowing across all the cross sections of the specimen.

TABLE 1

Calculation of Distribution Curves of the Amounts of Filtering Water by Filtration Rates and Equivalent Dimensions of the Water-Conducting Pores for Fuscum Peat of R = 10%

V in ml	Time intervals Δ_T in min.	ΔN in in pulses/ / min.	ΔQ in %	Rate ranges Δu in cm/min.	Pore size ranges ΔD in μ
0—2 m,	0— 2.0	25	2.0	∞— 3.0	∞—23.1
2—4	2.0— 3.8	45	3.5	3.0 —1.58	23.1—16.8
4—6	3.8— 5.5	160	12.6	1.58—1.09	16.8—13.9
6—8	5.5— 7.2	161	12.7	1.09—0.83	13.9—12.1
8—10	7.2— 9.0	129	10.2	0.83—0.67	12.1—10.9
10—14	9.0—12.5	270	21.2	0.67—0.48	10.9—9.25
14—18	12.5—16.2	160	12.6	0.48—0.37	9.25—8.1
18—32	16.2—29.2	210	16.5	0.37—0.20	8.1 —5.95
32—∞	29.2—∞	110	8.7	0.20—0	5.95—0
		1270	100.0		

By means of Poiseuille's law it is easy to pass from the flow rates to the dimensions of the water-conducting pores (the equivalent diameters D), using the formula

$$D = 4\sqrt{\frac{2\,\eta h_0 \cdot u}{p}}, \qquad (1)$$

where η is the viscosity of the liquid, h_0 is the length of the path (height of the specimen), u is the flow speed of the liquid and p is the pressure difference between the ends of the specimen.

The calculated values of the equivalent diameters are, naturally, far from the true dimensions of the pores, which have highly complex outlines. Despite this, it would be of interest, as is customary in dispersion analysis [13], to make at least an approximate evaluation of the dimensions of the water-conducting pores in peat.

A curve for the distribution of the amounts of filtering liquid by its rates of motion through fuscum peat is given in Fig. 3, where the flow speeds u in cm/minute are shown along the abscissa axis, and values of the distribution function dQ/du along the ordinate axis. The flow speeds vary within wide limits; 75% of the liquid flowing through the specimen moves at speeds from u = 0 to u = 0.9 cm/minute. The mean, most probable speed is u_p = 0.46 cm/minute.

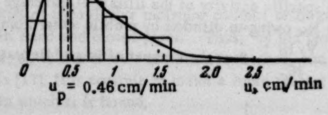

Fig. 3. Distribution of the amounts of filtering liquid by rates of flow in a fuscum peat specimen.

In Fig. 4, the continuous line represents the distribution of the amounts of liquid filtered by sizes of the water-conducting pores. The values of the equivalent diameters D in microns are taken along the abscissa axis. Examination of the distribution curve shows that most of the liquid flows through pores with D equal to 8 – 12μ. The size distribution curve of the water-conducting pores may serve to characterize the peat microstructure, which determined its water-conducting properties.

The procedure described above was tested on a simple disperse system close to ideality, namely, homogeneous fine sand with grain diameter < 0.25 mm. The size distribution curve of the water-conducting pores in sand is shown as a dotted line in Fig. 4. The experiments with sand were performed under the same conditions as with peat. Fig. 5 shows the variation of the activity of filtrate samples for sand.

As Fig. 4 shows, the calculated diameters of the water-conducting pores in sand vary in the range of 30 to 100μ. The values are in good agreement with the actual pore sizes, comparable with the sand grain size (D < 250μ).

As has already been stated, only part of the water present in the water-conducting pores in peat moves during filtration. The amount of immobile (fixed) water is evidently an important physicochemical characteristic of peat, which determines its aqueous properties. Water bound in various ways (according to Rebinder, see Korchunov [14]) with the peat particles: by adsorptive, osmotic, and microcapillary bonding, may be regarded as immobile. Immobile water includes also the part of the fixed water filling the blind and closed pores of the peat.

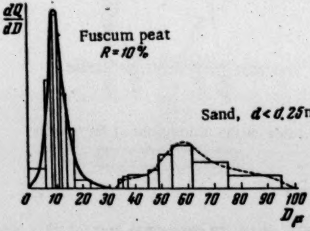

Fig. 4. Distribution of the amounts of filtering liquid by the sizes of water-conducting pores in peat and sand.

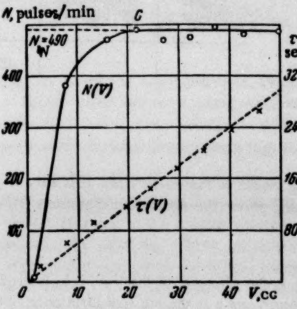

Fig. 5. Results of an experiment on the filtration of tagged water through sand.

It should be pointed out that direct methods for determination of immobile water have not yet been developed [15]. In soil science, the content of fixed water is regarded as being close to the wilting moisture content, corresponding to the limit of mobility of water in the soil [16].

The content of immobile water in peat may be determined from experiments on the filtration of tagged water. As is clear from Fig. 2, the filtrate volume V_f passing through the peat specimen in time $\tau > \tau_k$, contains a part of the tagged water V_t with specific activity N_w, and all the free (mobile) water V_m displaced from the peat during filtration. If the volume of the filtrate in Fig. 2 is represented by a rectangle of height N_w and base V_f, then the volume of mobile water will correspond to the area enclosed between the ordinate axis, the N – V curve, and the broken line (N_w). The specific activity of the filtrate N_f (average for the volume V_f) is lower than the activity of the tagged water N_w owing to dilution by mobile water from the peat. Since the volume of tagged water in the filtrate $V_t = \frac{V_f N_f}{N_w}$, then the amount of immobile water remaining in the peat can be calculated from the formula:

$$V_i = V - V_m = V - V_f + \frac{V_f \cdot N_f}{N_w}, \qquad (2)$$

where V is the total amount of water in the peat specimen.

The amount of immobile water can also calculated from the N – V graph, from the area corresponding to the amount of mobile water.

The results of determinations of immobile water in some types of peat are given in Table 2. Here w and W represent the moisture content of the peat specimen; w_1 and W_1 are the contents of immobile water in the peat.

TABLE 2

Contents of Immobile Water in Some Types of Peat

Type of peat	Degree of decomposition R in %	Relative moisture content, %			Absolute moisture content, %	
			w_H			
		w	by filtration method	by displacement method	W	W_1
Fuscum peat	10	91.1	41.1	40.8	1016	458
Medium peat	10	88.5	38.5	36.9	788	343
Bog sedge	35	90.0	30.2	30.7	892	300

The data in Table 2 show that a considerable amount of water in peat is not involved in filtration. This distinguishes peat from soils, in which the amount of fixed water, determined as water of wilting, does not exceed 10-15% [16]. The active porosity of peat, corresponding to the content of water-conducting pores, with the immobile water taken into account, for fuscum peat, is $n_0 = 51.7\%$. The porosity of the specimen with the immobile water not taken into account is $n = 94.3\%$. From this, the average speed of the water in the peat pores may be calculated:

$$u = \frac{v}{n_0} = \frac{0.246}{0.517} = 0.476 \text{ cm/minute} \tag{3}$$

where $v = 0.246$ cm/minute = the filtration rate, found from the experimental data:

$$v = \frac{Q}{F}, \tag{4}$$

where Q is the amount of filtering liquid and F is the cross section of the specimen. The value found for the average speed is close to the probable speed of the water $u_p = 0.46$ cm/minute (see Fig. 3).

Experiments with filtration of tagged water through sand (D < 0,25 mm), performed for comparison, showed that sand contains practically no immobile water. This is in good agreement with Rode's data [16], who estimated the wilting moisture of sand at some tenths of one per cent. This also accounts for the very great difference in the dimensions of the water-conducting pores in sand and in fuscum peat with R = 10% (see Fig. 4), although they are both coarsely disperse systems. The pore cross sections in peat are constricted by immobile water, while in sand all the pores are water-conducting.

The amount of adsorptively bound water, determined by Dumansky's method of negative adsorption of sugar [7, 8] is given by values of w of 15-20% for fuscum and medium peats with R = 10%. Consequently, up to 20-25% of the relative moisture content belongs to osmotically bound water, microcapillary water, and water in blind and closed pores. Thus, by the proposed method in conjunction with the negative adsorption method, N. S. Kurnakov's tensimetric method, and the Volarovich and Gusev method of x-ray structure analysis [17], it is possible to make a more precise evaluation of the types of water in peat according to the forms in which it is bound.

However, the results of the above experiments are valid only if the peat particles adsorb only small amounts of the radioactive tracer. To elucidate this point, after the filtration of tagged water further experiments were carried out, in which the tagged water which had filled the water-conducting pores of the peat during the first experiment was displaced by pure water. The experiments with filtration of pure water were analogous to the preceding experiments with filtration of tagged water, but in this case the mobile water in the peat was tagged water. The results of one such experiment are given in Fig. 2. The N – V and τ – V curves for the filtration of pure water are represented by dotted lines. The activity of the filtrate in this case decreases from the value N_W for the tagged water, to zero. The symmetrical nature of the N – V curves shows that the experiment is reversible and that no appreciable adsorption of the tracer occurs.

The results of experiments on the displacement of tagged water can also be used to calculate the content of immobile water in peat; this is equal to

$$V_i = V - \frac{V_f \cdot N_f}{N_w}; \tag{5}$$

in the same notation as before.

If the radioactive tracer had been adsorbed by the peat, the amounts of immobile water determined by the filtration method and the displacement of tagged water would be different. It is easily seen that the values for the content of immobile water in peat would be somewhat high in the first case and somewhat low in the second. The results of the experiments are given in Table 2.

Table 2 shows that the values found for w_i differ only slightly; therefore the amount of tracer adsorbed is not large. This is explained by the negative adsorption of Na_2SO_4 at the interphase in an aqueous medium (as in the case of sucrose), which has also been reported by Dumansky [7, 18].

After displacement of tagged water from the peat, the specimen was removed from the apparatus and cut into equal portions along its height. The pieces were dried and made into samples the activity of which was measured with the window-type counter. Self-absorption of radiation in the peat powder was taken into account in the activity measurements. From the amounts of tagged water which passed through the peat and which remained in the peat, it was calculated that not more than 3-4 % of the radioactive tracer is retained in the peat. This may be attributed both to adsorption of the tracer and to its diffusion into blind pores and immobile water.

An attempt to use the P^{32} phosphorus isotope (aqueous $Na_2HP^{*}O_4$ solution) as radioactive tracer for water in filtration experiments was unsuccessful. Radioactive phosphorus is almost totally taken up by the peat (90-95%).

At low filtration speeds, appreciable distortion of the N – V curves, and therefore of the results, may occur owing to diffusion of the given radioactive tracer in the liquid. To study the influence of diffusion, a peat specimen was placed in a horizontal glass tube. Tagged water was put into the left hand side of the tube, and pure distilled water in the right hand side. The ends of the tube were connected to storage vessels. The pressure was the same in both parts of the tube, and therefore the tracer could penetrate through the peat from the right to the left of the tube only by diffusion. The tube and specimen dimensions were the same as in the filtration experiments. 0.5 ml samples were regularly withdrawn from the right and left sides of the tube at the surface of the peat specimen. The samples were dried and their activities determined by means of the window-type counter. The determinations were continued for several weeks, but the tracer was not detected in the samples taken from the left of the tube. This indicates that diffusional transfer of the indicator is insignificant in the conditions of the filtration experiments. Calculations carried out in order to give an approximate estimate of the influence of diffusion of the tracer show that at filtration speeds above 0.1 m per day the influence of diffusional transfer can be neglected for practical purposes.

The results of these experiments, the main object of which was to develop methods for studying the aqueous properties of peat by means of radioactive tracers, may be applied in extensive investigations both in laboratory and in field conditions.

SUMMARY

1. A method for studying the filtration of water through peat with the use of radioactive tracers has been developed.

2. The radioactive tracer for water used in studying the aqueous properties of peat was the radioactive sulfur isotope S^{35} in the form of $Na_2S^{*}O_4$. The adsorption of this tracer by peat does not exceed 3-4 %. Diffusion of the tracer, at the filtration rates used in the experiments with peat, has no appreciable effect on the results.

3. The results of the experiments on the filtration of tagged water through peat specimens have been used to develop a method for determining the dimensions (equivalent diameters) of the water-conducting pores in peat and the liquid flow speeds in them. Curves for the distribution of the amount of filtering liquid by flow speeds and sizes of water-conducting pores in peat and sand have been obtained.

4. A method is described for determination of the amount of immobile water, not involved in filtration, in peat; this is based on displacement of mobile water from peat by water tagged with a radioactive tracer. In conjunction with the negative adsorption method, this method can be used for a more precise classification of water in peat according to type of bonding.

5. The results of the experiments show that peat contains considerable amounts (up to 30-40%) of water which is not involved in filtration.

The Moscow Peat Institute
Chair of Physics

Received October 25, 1956

LITERATURE CITED

[1] A. N. Glazov, Hydrotechnics and Melioration, No. 9, 19 (1956).

[2] A. Montens, GWF, H. 14, 411 (1952).

[3] S. A. Kursin and V. N. Mikhailovsky, Hydrotechnics and Melioration, No. 6, 33 (1956).

[4] A. Montens, Bautechnik, H. 9, 297, (1955).

[5] H. Seligman, Technik, No. 5, 349, (1956).

[6] V. N. Breslav, G. A. Melik-Shakhnazarova, and I. M. Taksar, Bull. Acad. Sci. Latvian SSR, No. 3 (92), 99 (1955).

[7] A. V. Dumansky, Lyophility of Disperse Systems (Voronezh State University Press, 1940).*

[8] N. N. Kulakov, Introduction to the Physics of Peat (State Power Press, 1947).*

[9] V. I. Spitsin et al., Methods of Use of Radioactive Tracers (Acad. Sci. USSR Press, 1955).*

[10] A. V. Sokolov and I. P. Serdobolsky, Use of Phosphorus Isotopes in Agrochemical Investigations (Acad. Sci. USSR Press 1954).*

[11] I. N. Verkhovskaya et al., The Tagged Atom Method in Biology (Moscow University Press, 1955).*

[12] N. A. Figurovsky, Proc. Acad. Sci. USSR, 20, No. 6,453 (1938); J. Phys. Chem., 12, No. 5-6,619 (1938).

[13] N. A. Figurovsky, Sedimentometric Analysis (Acad. Sci. USSR Press, 1948).*

[14] S. S. Korchunov, Investigation of the Physicomechanical Properties of Peat (Symposium, State Power Press, 1953).*

[15] A. I. Budagovsky, Absorption of Water by Soil (Acad. Sci. USSR Press, 1955).*

[16] A. A. Rode, Soil Moisture (Acad. Sci. USSR Press, 1952).*

[17] M. V. Volarovich and K. F. Gusev, Trans. Moscow Peat Inst., No. 2, (State Power Press, 1953) p. 97.*

[18] A. V. Dumansky, The Science of Colloids (State Chem. Press, 1948).*

---

* In Russian.

HEATS OF SWELLING AND OF SOLUTION OF NITROCELLULOSE

D. I. Galperin and L. I. Moseev

The information available in the literature on the heats of interaction of nitrocellulose with solvents is scanty and restricted to a relatively narrow range of systems, in which volatile solvents predominate. Nevertheless considerable interest attaches to heats of interaction of nitrocellulose with solvents of low volatility, "plasticizers", which are widely used in the production of cellulose ester plastics. It is particularly important to study the heats of swelling of nitrocellulose over the entire concentration range, so that it is possible to determine the molar ratio of nitrocellulose to solvent in the energy-saturated solvate layer. Integral heats of interaction in the system nitrocellulose – dibutyl phthalate have therefore been determined over the whole concentration range, and the effects of temperature, varied in the range of 0 to 80°, on the integral heats of swelling and solution of nitrocellulose in certain volatile and nonvolatile solvents have been studied.

The same sample of ground nitrocellulose, of medium viscosity lacquer type, containing 12% nitrogen, was used in all the experiments. The heats of swelling were determined with the aid of a variable temperature calorimeter of the type described previously [1]. The integral heats in the dilute solution region (from 0.5 to 3%) were determined directly, by introduction of small weighed quantities of pure nitrocellulose into 150 ml of solvent. In the concentrated solution region, the following procedure [2], based on the Hess law, was used: nitrocellulose samples previously swollen in a restricted amount of solvent, at different component ratios, were first prepared; the heats of dilution of these samples in an excess (150 ml) of the same liquid were then determined. The required integral heat of swelling was then calculated as the difference between the integral heat of solution of pure nitrocellulose in a large quantity of solvent, and the heat of dilution of the sample.

In the case of acetone, the previously swollen nitrocellulose samples were prepared by absorption of the solvent vapor in a vacuum dessicator at room temperature to a definite weight increase [2]. In swelling in dibutyl phthalate, an exact weight of nitrocellulose was treated with dibutyl phthalate diluted with five times its own volume of pure ethyl ether, which was then allowed to evaporate in air with continuous stirring of the mixture. The residual ether was quantitatively removed by heating the specimen under vacuum at 60° for 2 hours. The heats of interaction in dilute solutions at 25° were, per 1 g of nitrocellulose, 18 cal. for acetone, and 10.9 cal. for dibutyl phthalate. The results of determinations of integral heats of interaction over the whole concentration range are shown graphically in Figs. 1 and 2, the integral heats being expressed in calories per 1 g of solution ($-\Delta H$). The maxima on the curves correspond to the limiting concentration of the solvent, at which and above the heat of dilution is zero. This concentration, which corresponds to the energy-saturated solvate layer, is ~ 34 % for acetone and ~ 53 % for dibutyl phthalate.

The influence of temperature on the integral heats of interaction of nitrocellulose with solvents was studied in dilute solutions (~ 1 %), for acetone, butyl acetate, dibutyl phthalate, and tricresyl phosphate *. The same solvents were used by Lipatov and Meerson [3] in an investigation with the same object in view. The results of the determinations, which are averages for numerous determinations, are given in the table, which shows negative temperature coefficients of the integral heat for acetone and butyl acetate, a small negative coefficient for dibutyl phthalate, and a positive coefficient for tricresyl phosphate.

---

* M. M. Iovleva and L. Ya. Muzheva participated in this section of the work.

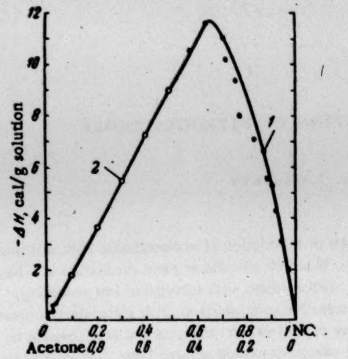

Fig. 1. Variation of integral heats of interaction with solution composition in the system nitrocellulose-acetone: 1) experimental data; 2) calculated data.

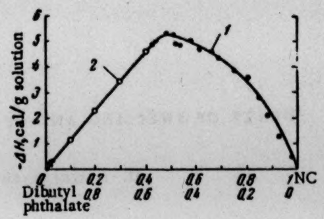

Fig. 2. Variation of integral heats of interaction with solution composition in the system nitrocellulose – dibutyl phthalate: 1) experimental data; 2) calculated data.

TABLE

Integral Heats of Interaction of Nitrocellulose with Solvents at Various Temperatures

(weight taken ~ 1.5 g per 150 ml of liquid)

Temperature in °C	Q in cal/g of nitrocellulose			
	acetone	butyl acetate	dibutyl phthalate	tricresyl phosphate
0	17.9	—	10.7	—
25	18.0	17.5	10.9	3.9
40	15.5	16.0	11.0	6.7
50	12.0	—	—	—
60	—	14.0	10,0	9.9
70	—	13.1	—	10.6
80	—	11.3	—	11.3

DISCUSSION OF RESULTS

Our values for the integral heats of solution of nitrocellulose in acetone for dilute solutions at 25° (18 cal./g of nitrocellulose) agree with the previously published results of Kargin and Tager [4], and also of Lipatov and Meerson [3]. The boundary concentration (34% acetone) at which the solvate layer becomes energy-saturated, corresponds to 1-1.06 mole of acetone per 1 mole of $-ONO_2$ groups, if it is assumed that there are on the average 2.2 $-ONO_2$ groups per each monomer unit in 12% nitrocellulose. This confirms analogous data for acetone, published earlier [1].

The corresponding boundary concentration for dibutyl phthalate (53% by weight) represents a ratio of 1 mole of dibutyl phthalate per 2.2 moles of $-ONO_2$ groups. Thus, in the formation of a monomolecular saturated solvate layer dibutyl phthalate exhibits bifunctional properties in relation to the number of active (ester) groups in its molecule. The above data indicate, moreover, that in the case of dibutyl phthalate only the $- ONO_2$ groups are involved in the formation of the solvate layer. It seems likely that this type of interaction is not universal, but depends on the nature of the active groups in the solvent and the degree of nitration of the nitrocellulose.

As regards the effect of temperature on the integral heats of interaction between nitrocellulose and solvents, our experiments in general (with the exception of dibutyl phthalate) confirm the results of Lipatov and Meerson [3]. However, we cannot agree with the interpretation given by Lipatov and Meerson [3, 5].

It is known that the variation of the heat effect of any process with temperature obeys Kirchhoff's law [6]

$$dQ_p / dT = - \Delta C_p = - (\Sigma C_p \text{ prod} - \Sigma C_p \text{ init.}),$$

where Q_p is the heat effect of the process; C_p prod is the heat capacity of the final products; C_p init is the heat capacity of the initial substances.

In the case of the solution process, Q_p is the heat of solution, $C_{p\ \text{prod}}$ is the heat capacity of the solution, and $C_{p\ \text{init}}$. is the heat capacity of the initial components. If, in any temperature region, the heat capacity of the solution is the sum of the heat capacities of the initial components ($\Delta C_p = 0$), then the heat effect of solution in this temperature region will not vary with temperature. If the heat capacity of the solution is greater than the sum of the heat capacities of the initial components ($\Delta C_p > 0$), then the heat effect will decrease with rise of temperature. If $\Delta C_p < 0$ the reverse is the case.

Very little information on heat capacities of polymer solutions is available in the literature. It is noted in one of Skuratov's papers [7] that, in the systems studied by him, either the heat capacities are additive ($\Delta C_p = 0$), or the heat capacity of the solution is greater than the sum of the heat capacities of the initial components ($\Delta C_p > 0$). He did not find any decreases of the heat capacities of solutions relative to the heat capacities of the initial components ($\Delta C_p < 0$). An increase of heat capacity ($\Delta C_p > 0$) was found for diacetylcellulose solutions. A similar effect is to be expected in the case of nitrocellulose.

In our opinion, the increase in the heat capacity of the system when nitrocellulose passes into solution is the cause of the decrease of the integral heats of solution of nitrocellulose in acetone and butyl acetate with temperature, which was found by Lipatov and Meerson and in our experiments.

We extend this conclusion to solvents of low volatility (dibutyl phthalate, tricresyl phosphate), for which the heats of interaction with nitrocellulose should also decrease with increasing temperature. If this effect does not occur, but even the reverse is found (for dibutyl phthalate and tricresyl phosphate in Lipatov and Meerson's experiments, and only for the second of these solvents in our experiments), this must be the result of a retarded swelling process, the duration of which at ordinary temperatures is outside the limits of the ordinary calorimetric determination, but which decreases rapidly with increase of temperature. This applies especially to tricresyl phosphate, which has particularly high viscosity and a large molecular volume; this gives grounds for attributing only a provisional significance to the heat effects found in experiments with tricresyl phosphate, at least at temperatures between 25 and 60°.

The retarded swelling factor is less prominent in the case of dibutyl phthalate, which has lower viscosity and molecular volume. Therefore, in using ground nitrocellulose, we not only did not find an increase of the heat effect in its interaction with nitrocellulose as the temperature increased from 0 to 60°, but even found some tendency to a decrease (see Table). Thus, in contrast to Lipatov and Meerson, we do not attribute the difference of the signs of the temperature coefficients of the integral heats of solution of nitrocellulose in volatile solvents and in tricresyl phosphate to differences in the type of energy interaction of volatile solvents and " plasticizers" with nitrocellulose, but regard it as the result of the influence of the diffusional kinetic factor. In conditions of a brief calorimetric experiment, the effect of this factor compensates and even exceeds the influence of the true thermodynamic factor of heat capacity increase. Confirmation of this viewpoint was provided by the data, cited above, on the heats of interaction of nitrocellulose with dibutyl phthalate over the entire concentration range, showing that dibutyl phthalate does not in any way differ in principle from acetone in the character of its energy interaction with nitrocellulose. Energy saturation is reached in both cases on interaction of 1 mole of active solvent groups with 1 mole of $- ONO_2$ groups. Any difference in the nature of the energy interaction of nitrocellulose with dibutyl phthalate and butyl acetate is still less to be expected, as both these solvents are esters, i. e., they have active groups of a similar nature.

Neither can we agree with the interpretation given by Lipatov and Meerson [3, 5] of the decrease with temperature of the heat of solution of nitrocellulose in volatile solvents. In this interpretation it is postulated that at normal temperatures the systems nitrocellulose – acetone or nitrocellulose – butyl acetate are not true solutions but gels.

It is known that such solvents are compatible with nitrocellulose in all proportions at all temperatures studied, to form one-phase systems [4, 8]. In relation to these actual systems, especially at low concentrations, one can hardly speak of any critical temperature (within the range in question) of spontaneous transition of a gel into a molecular solution and vice versa. This would be in clear contradiction to experimental results which (in absence of external influences) never show syneresis in such solutions, even if they are cooled to temperatures considerably below the "critical" values. The extensive production experience of many branches of industry in which nitrocellulose solutions are used confirms this.

SUMMARY

1. The integral heats of interaction of 12% nitrocellulose with dibutyl phthalate and acetone over the entire concentration region have been determined. It is shown that the energy-saturated solvate layer corresponds to ratios of one molecule of dibutyl phthalate or of two molecules of acetone per 2 $-ONO_2$ groups. Therefore both ester groups in dibutyl phthalate are involved in blocking the polar groups of nitrocellulose. It was found that only $-ONO_2$ groups enter into energy interaction with these solvents in the formation of monomolecular layers.

2. A negative temperature coefficient of the heat effect has been found for acetone and butyl acetate, a small negative coefficient for dibutyl phthalate, and a positive temperature coefficient for tricresyl phosphate.

In conclusion, the authors express their gratitude to A. A. Tager for participation in discussions of the results of this work.

Regional town of Molotov Received December 10, 1955

LITERATURE CITED

[1] V. A. Kargin and S. A. Papkov, J. Phys. Chem., 7,483 (1936).

[2] A. A. Tager and Zh. S. Dombek, Colloid J., 15,69 (1953).

[3] S. M. Lipatov and S. I. Meerson, Colloid J., 12,122,427 (1950).

[4] A. A. Tager and V. A. Kargin, J. Phys. Chem, 15,1029,1036 (1941).

[5] S. M. Lipatov and S. I. Meerson, Colloid J., 17,230 (1955).

[6] M. Kh. Karapetyants, Chemical Thermodynamics, (State Chem. Press, 1949).(In Russian.)

[7] S. M. Skuratov, Colloid J., 9,133 (1947).

[8] P. I. Zubov, Z. I. Zhurkina, and V. A. Kargin, Colloid J., 9,109 (1947).

INVESTIGATIONS OF THE PHYSICAL CHEMISTRY OF AGAR

1. METHOD FOR THE DETERMINATION OF THE INTRINSIC VISCOSITY OF AGAR

S. A. Glikman and I. G. Shubtsova

As is known, polyelectrolyte solutions are characterized by a sharp rise of the reduced specific viscosity in the low concentration region. This anomalous effect is diminished by additions of mineral salts. The pronounced role of the valency of the added salt led Smoluchowski and Kruyt to advance the theory of the so-called electroviscous effect. Complete suppression of the effect is not always possible because of coagulation. However, even when a linear $\eta_{sp}/c - c$ relationship is attained, extrapolation of the line to zero polyelectrolyte concentration gives different values for η which decrease with increasing salt content. Interpretation of these results presents a fairly difficult problem.

According to modern theories, if groups ionizable in a given medium are present along a polymer molecule, the bulk of the randomly kinked or globularly coiled polymer molecule increases owing to forces of repulsion. The bulk of such a molecule depends on the number of ionizable groups and on their degree of dissociation. It therefore increases with dilution of the polyelectrolyte, decreases with additions of salts, and depends on the composition of the solvent. Intramolecular forces between the polar groups (ionizable and nonionizable), which in their turn depend on the composition of the solvent and on the contents of electrolytes and nonelectrolytes in the solution [1, 2], also play a part.

The object of our work was to develop a technique for finding the true values of the intrinsic viscosity of different agar specimens and fractions with complete suppression of ionization, i. e., values of η_{∞}, corresponding to the behavior of a single randomly kinked molecule devoid of electric charge.

As is known, agar solutions exist in a state of molecular dispersion only above a certain limiting temperature. At lower temperatures they are "gel solutions"; their viscosity greatly depends on the efflux rate, and an elastic limit may be detected in them by sensitive methods.

It was established by preliminary experiments that, of the samples studied (Japanese and domestic Far Eastern agar and their fractions), one of the fractions of the Far Eastern sample * had the highest transition temperature from a true solution to an aggregated system. The approximate value of the critical temperature, 58°, corresponds to the intersection of two straight lines (Fig. 1), expressing the efflux time – temperature relationship for the solutions in the chosen conditions. To obtain comparable results, all subsequent viscosity determinations were performed at 60° ± 0.01. The temperature was maintained constant by means of a well insulated water ultrathermostat.

The aqueous solutions of the samples were prepared as follows. A weighed portion of agar, after 10-12 hours of swelling, was heated on the water bath at 100° for 15 minutes. The hot solution was filtered through a No. 3 glass filter with suction, and then placed in a thermostat at 60° for 30 minutes. 10 ml of the solution was taken out by means of an accurate pipet (kept in an air thermostat at 60°) and transferred to an Ubbelohde viscosimeter of the hanging level type. Viscosity measurements were started after 15-20 minutes. The concentration of the original solution was found from the dry residue. The efflux time for water in this instrument at 60° was 220.8 seconds. The maximum value of the kinetic energy correction for a solution with the lowest specific viscosity $\eta_{sp} = 0.008$ was 0.052%, so that this correction could be neglected.

---

* The fractionation procedure is described in our next communication.

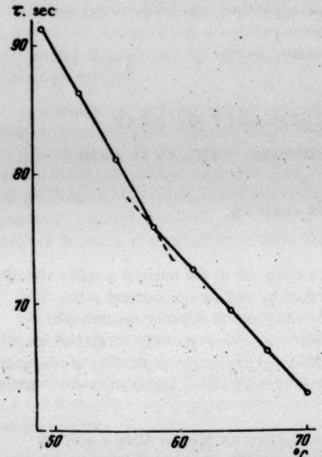

Fig. 1. Effect of temperature on the viscosity of a 0.5% solution of fraction V of Far Eastern agar.

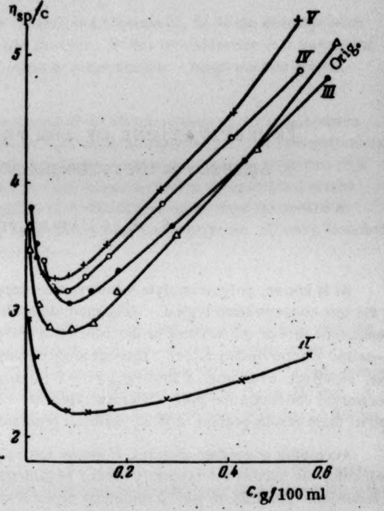

Fig. 2. Effect of concentration on the reduced specific viscosity of fractions (II, III, IV, V, original) of Far Eastern agar.

To prevent evaporation of the solvent during the determinations, the air space of the viscosimeter was closed by joining the ends of its tubes together.

The solutions were diluted in the viscosimeter by the volume method, with the solvent contained in the thermostat at the same temperature. Repeated weighing of the volume of liquid taken up by the same pipet showed that the dilution error does not exceed 0.2%. The accuracy of the specific viscosity found in our experiments depended mainly on the unavoidable error in determinations of the efflux time (within ± 0.1 second). Calculations showed that for most of the solutions studied, even the most dilute, the relative error did not exceed 1%.

Figure 2 shows the effect of concentration on the reduced specific viscosities of fractions of one of the agar samples. It is seen from Fig. 2 that a pronounced electroviscous effect is found in all cases in the low concentration region, and extrapolation to zero concentration is impossible. Minimum values of η_{sp}/c, different for different fractions, were found for agar concentrations of the order of 0.1%. Similar results were obtained for the sample of Japanese agar.

The effects of mineral salt additions on the viscosity of aqueous agar solutions were studied on 0.1% solutions of Far Eastern and Japanese agar fractions. Similar results were obtained for both (Fig. 3).

With increasing valency of the cations in the chlorides added to aqueous agar solutions, the viscosity minimum is shifted in the direction of lower salt concentration c_i ; the decrease of viscosity becomes greater as the region in which η_{sp}/c is constant becomes narrower, while the viscosity increase beyond the minimum is greater.

On the assumption that viscosity depends on the effective volume of the randomly kinked molecule, and that local or complete charge reversal of the polyelectrolyte molecule is possible, all these differences can be explained by the influence of the valency of the cation on compression of the ionic atmosphere, on the adsorbability of the cations (i. e., their attachment to the anionic groups of the polymer molecule), on the intramolecular binding of individual anionic groups, and on repulsion of groups of like charge, with charges reversed owing to adsorption of cations.

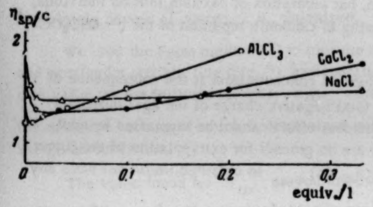

Fig. 3. Effect of electrolytes on the viscosity of 0.1% solutions of fraction II of Far Eastern agar.

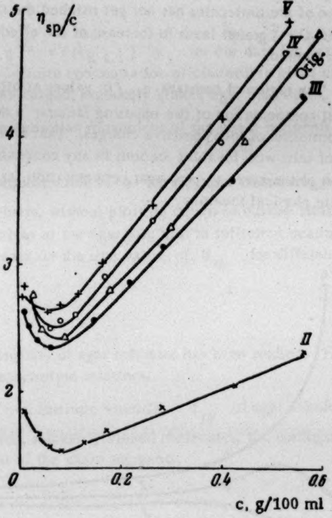

Fig. 4. Effect of concentration on the viscosities of fractions (original, II, III, IV, V) of Far Eastern agar solutions containing 0.01 g-equiv. CaCl$_2$ per liter.

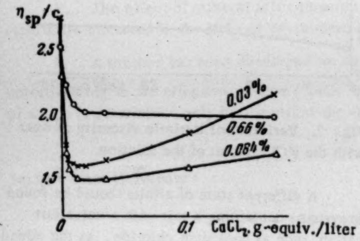

Fig. 5. Effect of CaCl$_2$ on the viscosity of Japanese agar solutions of various % concentrations.

Since agar is essentially the calcium salt of a sulfuric acid ester of a linear polygalactan, to avoid complicating effects (ion exchange), we first studied the influence of calcium chloride on the electroviscous effect. Since, as Fig. 3 shows, the viscosity of 0.1% agar solutions was at a minimum when the solutions contained 0.01 g-equiv. CaCl$_2$ per liter, the viscosities of all the agar solutions were determined at the same calcium chloride content. The data so obtained on the variation of η_{sp}/c with concentration for solutions of Far Eastern agar containing 0.01 g-equiv. CaCl$_2$ per liter are given in Fig. 4. Similar results were obtained for Japanese agar.

Comparison of Figs. 4 and 2 shows that addition of 0.01 g-equiv. CaCl$_2$ to agar solutions results in a considerable viscosity decrease, but does not eliminate the electroviscous effect. The explanation for the latter fact may be that, at low agar concentrations, adsorption of bivalent Ca^{2+} ions on the anionic groups of the agar causes reversal of the molecular charge. This is confirmed by data on the influence of calcium chloride on agar solutions of various concentrations (Fig. 5).

While in the case of 0.66% agar solution the values of η_{sp}/c, after a sharp fall, remain constant over a wide range of CaCl$_2$ concentrations, the curves for agar solutions of lower concentrations show more or less definite maxima. The ascent of the curve after the minimum is the result of partial or total charge reversal of the polymer molecules. Naturally, the role of charge reversal is greater at lower agar concentrations.

Adsorption of bivalent cations on univalent anionic groups of the agar molecules is the reason why the viscosity minimum attained at low calcium chloride concentration is not in any way a measure of the effective volume of the uncharged agar molecule. It is not possible to explain in any other way the higher value of the viscosity minimum for 0.03% agar solution in comparison with the minimum for 0.083% solution. The ionic atmosphere is apparently not yet compressed to the limit, the potential is not yet reduced to zero, the effective volume of the molecules has not yet reached the minimum value, but adsorption of calcium ions on individual ($-OSO_2O-$) groups leads to increase of the effective volume owing to Coulomb repulsion of the $(-OSO_2OCa)^+$ groups formed.

The region of constant η_{sp}/c values at higher calcium chloride concentrations is the consequence of mutual compensation of two opposing factors: a decrease of the total negative charge of the agar molecule and formation of local positive charges. That is why the electroviscous effect cannot be suppressed by additions of salts with bivalent cations in any concentrations. There are no grounds for extrapolation of the linear portion of the curve to zero agar concentration, as the values of $(\eta_{sp}/c)_{c \to 0}$ so obtained would not have any definite physical meaning.

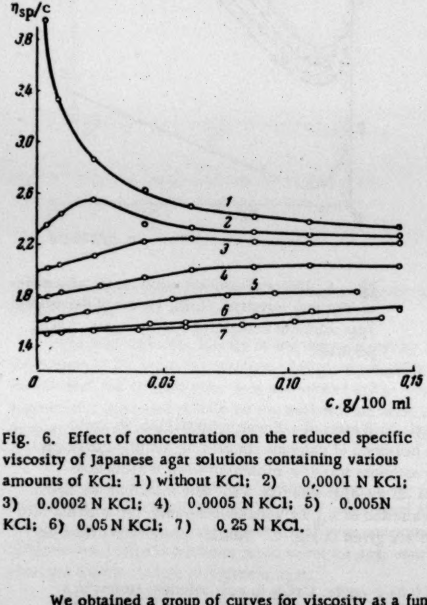

Fig. 6. Effect of concentration on the reduced specific viscosity of Japanese agar solutions containing various amounts of KCl: 1) without KCl; 2) 0.0001 N KCl; 3) 0.0002 N KCl; 4) 0.0005 N KCl; 5) 0.005N KCl; 6) 0.05 N KCl; 7) 0.25 N KCl.

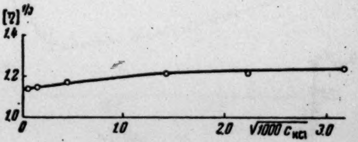

Fig. 7. Variation of intrinsic viscosity of agar with the KCl content of the solution.

A different state of affairs should be found in systems containing a salt with a univalent cation, such as potassium chloride, as the added electrolyte. Here attachment of the K^+ ion to the anionic ($-OSO_2O-$) group cannot lead to charge reversal, but only has an effect on compression of the ionic atmosphere and decrease of the charge on the agar polyanion. The role of K^+ ion adsorption on the hydroxyl groups of the agar molecule at low potassium chloride concentrations is evidently not great. This is shown by the wide range over which η_{sp}/c is constant in presence of various amounts of KCl (Fig. 6).

We obtained a group of curves for viscosity as a function of concentration, for various potassium chloride concentrations from 0.0001 to 0.25 g-equiv./liter, analogous to the curves obtained by Fuoss and Strauss [3] for polyvinylpyridinium bromide, and by Pals and Hermans [4] for sodium pectate, with characteristic maxima which gradually level out with increasing salt contents (Fig. 6). Pals and Hermans [4] attribute the maxima to the relationship between the concentrations of the polyelectrolyte ions and the ions of the added low-molecular electrolyte. At low concentrations of the polyelectrolyte, for example of sodium pectate, the number of its ions is far smaller than the number of NaCl ions. Therefore in the initial region of the curve the ionic strength of the solution (at constant NaCl concentration) varies very little with the polyelectrolyte concentration and therefore the degree of uncoiling of its molecules (their bulk) remains almost constant, while the regions of the η_{sp}/c curve to the left of the maximum, in agreement with the Huggins equation, remain linear.

Extrapolation of the initial linear region to zero concentraion gives a value of η_{∞}, corresponding to the given degree of ionization of the polyelectrolyte. The higher the ionic strength of the solution, the less will be the effective volume of the polyelectrolyte molecule, and the lower the value of η. With excess of added salt, the minimum value of η_{∞} is reached, corresponding to the effective volume of a molecule completely devoid of charge, i. e., unionized.

We used the Fuoss method [3] to plot the relationship $\eta^{1/3} = f(c_{KCl})^{-1/2}$ for our data for agar, and obtained a straight line (Fig. 7), extrapolation of which to infinite concentration of electrolyte gives the true value for the intrinsic viscosity η_{∞} corresponding to uncharged, randomly kinked agar molecules, the effective volume of which is determined only by the micro-Brownian movement of the chain segments in the given conditions.

The value found for η_{∞} proved to be equal to the constant value of η for solutions containing from 0.05 to 0.25 g-equiv. of potassium chloride per liter. On this basis, without plotting groups of curves similar to that shown in Fig. 7 for each fraction, but by adding electrolyte to the agar solutions in sufficient quantities to stabilize the viscosity values, we can obtain quite definite data on the true values of η_{∞} for different agar samples and their fractions.

SUMMARY

1. The effect of mineral salt concentrations on the viscosity of agar solutions has been studied. The results are discussed in the light of the modern theory of polyelectrolyte solutions.

2. A method has been developed for determining the true intrinsic viscosity η_{∞} of agar solutions, corresponding to the effective volume ("bulk") of undissociated, randomly kinked molecules, the configuration of which is determined only by the micro-Brownian movement of the chain segments.

Saratov State University Received September 10, 1955

LITERATURE CITED

[1] H. Kruyt, Colloid Science, vol. 2, Reversible Systems (1949).

[2] A. Katchalsky, J. Polymer Sci., 12, 159 (1954).

[3] R. M. Fuoss, P. Strauss, J. Polymer Sci., 3,602 (1948).

[4] D. Pals, J. J. Hermans, J. Polymer Sci., 3,897 (1948); 5,733 (1950).

AGGREGATIVE STABILITY OF PIGMENT SUSPENSIONS IN HYDROCARBONS, ALCOHOLS, AND ESTERS OF LOW MOLECULAR WEIGHT

Ya. M. Gurevich

It was found in our investigation [1] that if pigment suspensions in gasoline are stabilized by oleic acid these pigments also form aggregatively stable suspensions in butanol. Otherwise, the latter are unstable. It was therefore suggested that the factors which determine stability have the same mechanism in both cases. This mechanism consists of adsorption of stabilizer molecules (oleic acid) on the pigment surface in the one case, and of molecules of the dispersion medium (butanol) in the other.

The validity of this view in relation to other organic media has been tested in the present investigation. The following dispersion media were used: lacquer gasoline, xylene, butanol, ethylene glycol, butyl acetate, dibutyl phthalate, tricresyl phosphate, and mixtures of esters with xylene. Twelve pigments were studied, namely: iron blue, ultramarine, cobalt blue, emerald green, Mars brown, yellow ocher, titanium dioxide, zinc sulfide, red ocher, chrome yellow, cadmium yellow, and vine black (suspensions in 2% concentration by volume).

The stability of the suspensions was evaluated by their sedimentation time until clear. All the pigments used contain a certain proportion of particles of fractions of one micron in size. In the unaggregated state such particles remain in suspension and color the suspension throughout the layer for several days, even in media of low viscosity.

In suspensions with low aggregative stability and fairly high pigment concentrations, all the pigment particles are distributed simultaneously among the aggregates formed, and in consequence the aggregates are of the same size and density and settle at the same rate. When they come into contact at the bottom of the vessel, the aggregates cohere and form a loose continuous structure, which gradually becomes more compact under the force of gravity. In such suspensions, a measure of the aggregative stability can be taken to be the time which elapses from the end of agitation of the suspensions to the start of settling of the aggregates formed, which is indicated by the appearance of a layer of pure dispersionsmedium in the upper part of the vessel.

In suspensions in which aggregates of different sizes, settling consecutively at the bottom of the vessel, are formed, a measure of the aggregative stability is provided by the time for the complete settling of all the pigment particles and clarification of the suspension over the entire layer.

In suspensions of the intermediate type, in which part of the pigment particles forms aggregates of the same size forming a continuous structure at the bottom of the vessel, and part forms smaller aggregates of various sizes remaining in the suspended state, a measure of the aggregative stability can be taken to be the time for complete settling of the pigment and clarification of the suspension in the layer from the top to the boundary of the continuous structure.

A similar method for qualitative evaluation of the aggregative stability of suspensions was used by Rebinder, Serb-Serbina, and Kordyukov [2] in studying the wetting action of surface-active agents.

The results of visual observations on the settling of pigment suspensions are given in schematic form in Tables 1 and 2. Table 1 gives results for pigment suspensions in alcohols and hydrocarbons. Table 2 compares results for suspensions in esters and their mixtures with xylene. Table 1 shows that the aggregative stability of suspensions of all pigments in hydrocarbons is low, and that there is a similarity between the degree of stability in alcohol suspensions and in suspensions in lacquer gasoline stabilized with oleic acid.

The explanation for the low aggregative stability of suspensions in hydrocarbons is that the hydrocarbon molecules, devoid of polar groups, do not saturate the secondary valencies of the polar active centers in the pigment surface when adsorbed on it. Secondary valency forces appear in these centers; under the action of these the pigment particles cohere on collision, and the suspension passes into an aggregated state.

The reason for the similarity between alcohol suspensions and suspensions in gasoline stabilized with oleic acid in the degree of aggregative stability lies in the fact that the polar active centers of the pigment surface, which have an affinity for carboxyl groups, have a similar affinity for hydroxyl groups. Therefore pigments rich in active centers, capable of firmly adsorbing oleic acid molecules, have the same property with regard to alcohol molecules.

Both in the adsorption of oleic acid molecules and in the adsorption of alcohol molecules two effects occur: the secondary valencies of the active centers become saturated and other active centers, situated in the areas occupied by the firmly adsorbed acid or alcohol molecules, become blocked.

TABLE 1

Sedimentation Times of Pigment Suspensions in Hydrocarbons and Alcohols

Pigment	Dispersion medium			
	Hydrocarbons		Alcohols	
	lacquer gasoline, xylene	lacquer gasoline with 3-5% of oleic acid	Butanol	Ethylene glycol
Iron blue	—	+++	+++	+++
Ultramarine	—	+++	++	+++
Cobalt blue	—	+++	++	+++
Mars brown	—	+++	++	+++
Emerald green	—	+++	++	++
Red ocher	—	+++	++	++
Titanium dioxide	—	—	—	—
Zinc sulfide	—	—	—	—
Yellow ocher	—	—	—	—
Chrome yellow	—	—	—	—
Cadmium yellow	—	—	—	—
Vine black	—	—	—	—

Symbols: +++ suspension colored throughout the layer for more than 5 days; ++ pigment settles between 3 hours and 5 days; — — pigment settles or upper zone clarifies in less than 3 hours.

It is seen from Table 2 that as the number of polar groups in the ester molecule increases, the number of pigments forming suspensions of a high degree of stability in these media increases also. Dilution of suspensions of pigments in esters with xylene decreases their stability. The dilution effect depends not only on the amount of xylene added, but also on the properties of the pigment and the ester: it increases in the order of the pigments as given in Table 2, and decreases with increasing number of polar groups in the ester molecule.

This behavior is in agreement with the view that the degree of aggregative stability is determined by the stability of the bonds between the pigment surface and the molecules adsorbed on it.

As the number of ester groups in the molecule increases, there is an increase in the number of polar contacts by which it is attached to the pigment surface, and the degree of saturation and shielding of the pigment particle surface increases accordingly.

Dilution of pigment suspensions in esters by xylene reduces their aggregative stability owing to increased desorption of the ester molecules. The effect of dilution should increase with decreasing stability of the bonds between the adsorbed ester molecules and the pigment surface, and with decreasing number of contacts between them. This is illustrated by Table 2.

To sum up the interpretation of Tables 1 and 2, we may conclude that in all the suspensions studied the degree of aggregative stability is determined by the ratio of the saturated and blocked active centers of the pigment surface to the active centers in this surface in which secondary valency forces are free to develop. This is analogous to P. A. Rebinder's theory [3] of the conditions which determine the formation of thixotropic structurized suspensions.

It must be pointed out that the above considerations are only valid for suspensions in media of low molecular weight. As has been shown in our studies [1, 4], aggregative stability in suspensions containing substances of high molecular weight depends not only on the degree of saturation or blocking of secondary valencies in the pigment surface, but also on the degree of saturation of those secondary valencies of the adsorbed molecules which do not interact with the pigment surface.

TABLE 2

Sedimentation Times of Pigment Suspensions in Esters and Their Mixtures with Xylene

Pigment	Dispersion medium								
	butyl acetate–xylene			dibutyl phthalate–xylene			tricresyl phosphate – xylene		
	100–0	60–40	20–80	100–0	60–40	20–80	100–0	60–40	20–80
Vine black	+++	++	—	+++	+++	+	+++	+++	++
Iron blue	+++	++	—	+++	+++	+	+++	+++	++
Red iron ocher	—	—	—	+++	++	—	+++	+++	+
Chrome yellow	—	—	—	+++	++	—	+++	+++	+
Cadmium yellow	—	—	—	+++	++	—	+++	+++	—
Cobalt blue	—	—	—	+++	++	—	+++	++	—
Emerald green	—	—	—	+++	++	—	+++	++	—
Ultramarine	—	—	—	+++	++	—	+++	++	—
Mars brown	—	—	—	—	—	—	+++	++	—
Yellow ocher	—	—	—	—	—	—	+++	++	—
Titanium dioxide	—	—	—	—	—	—	+++	++	—
Zinc sulfide	—	—	—	—	—	—	+++	++	—

Symbols: +++ suspension remains colored throughout the layer for more than 5 days; ++ pigment settles in 1-5 days; + pigment settles in 3-24 hours; —— pigment settles or upper zone of the suspension clarifies in less than 3 hours.

Some specific conclusions concerning the properties of individual pigments may be drawn from the data in Tables 1 and 2.

Iron blue, ultramarine, cobalt blue, and emerald green have high affinity for carboxyl, hydroxyl, and ester groups. Vine black, red iron ocher, chrome yellow, and cadmium yellow have strong affinity for ester groups and weak affinity for carboxyl and hydroxyl groups.

Mars brown and yellow ocher have strong affinity for carboxyl and hydroxyl groups, and weak affinity for ester groups.

Titanium dioxide and zinc sulfide have weak affinity for carboxyl, hydroxyl, and ester groups.

From the rule that polar regions of the molecules interact with polar groups and nonpolar with nonpolar, it may be assumed that the different affinities of various polar groups of the adsorbed molecules for the active centers of the pigment surface are determined by correspondence of their polarities.

It follows from the experimental results that hydroxyl and carboxyl groups are similar to each other, and differ significantly in polarity from ester groups, and that on the pigment particle surfaces there are active centers of different degrees of polarity, which interact with groups differing in polarity in the adsorbed molecules.

SUMMARY

1. Investigations of the aggregative stability of pigment suspensions in hydrocarbons, alcohols, and esters of low molecular weight show that the degree of aggregative stability of suspensions in these media depends on the stability of the bonds between the pigment surface and the molecules of the medium adsorbed on it.

2. The stability of the bonds between pigment surfaces and adsorbed molecules increases with increasing number of polar groups in the latter.

3. Pigments differ in their affinities for hydroxyl, carboxyl, and ester groups in the adsorbed molecules; this is determined by correspondence between the polarities of the active centers in the pigment surface and of the groups of the adsorbed molecules interacting with them.

State Research and Project Institute
Moscow

Received April 16, 1956

LITERATURE CITED

[1] Ya. M. Gurevich, Colloid J., 18,158 (1956).

[2] P. A. Rebinder, N. N. Serb-Serbina, S. A. Kordyukov, Symposium, The Struggle against Silicosis, vol. 1 (Acad. Sci. USSR Press, 1953).

[3] P. A. Rebinder, Discussions Faraday Soc., No. 18 (1954); A. A. Abduragimova, P. A. Rebinder, and N. N. Serb-Serbina, Colloid J., 7, 184 (1955).

[4] Ya. M. Gurevich, Colloid J., 14,93 (1952).

DEPENDENCE OF THE EXCHANGE ADSORPTION OF IONS ON THEIR STRUCTURE

2. ADSORPTION OF BIVALENT AMINES

A. T. Davydov and R. F. Skoblionok

The numerous investigations on the exchange of mineral ions do not exhaust the whole range of phenomena which determine the nature of their adsorption. Investigations of exchange adsorption of organic ions are of especial theoretical and practical interest because the information available in this field is very restricted. It is known that the relationships established for exchange adsorption of mineral ions are not fully applicable to the exchange of organic ions on modern ion exchange resins. An important difference of the exchange adsorption of organic ions, as compared with mineral ions, is the simultaneous operation of electrostatic and van der Waals forces [1-5]; the significance of the latter increases with increasing size of the organic ions and their concentration in the solution. In studies of the exchange adsorption of organic ions it is natural to assume that their structure should have a greater influence than that of mineral ions. The question of the influence of the structure of organic ions on the extent and nature of their adsorption is of undoubted interest.

The present paper describes a study of the extent and nature of the adsorption of bivalent organic ions in relation to their structure. The substances chosen for the study were the hydrochlorides of ortho-, meta- and para-phenylenediamines, which are readily soluble in water and dissociate in aqueous solution. In earlier investigations we studied the adsorption of univalent amines [5]; the reason for choosing phenylenediamines was that by comparing their adsorption (of ions of different phenylenediamines) with the adsorption of univalent amines from solutions of their hydrochlorides it is possible to estimate the influence of the valency of the ion. Ca-sulfocarbon and Ca-Espatite were used for the investigations. Solutions of ortho-, meta-, and paraphenylenediamine hydrochlorides of various concentrations from 0.05 to 1.00 N were prepared. Five gram samples of the adsorbents were covered with 50 ml each of a solution of the given phenylenediamine of the appropriate concentration. The experimental procedure used is described in the preceding paper [5].

In the study of the adsorption of univalent amines [5] it was found that equivalence between the amount of Ca^{2+} desorbed and the amount of amine adsorbed from the solution was not maintained. Nonequivalence of the exchange began to appear in the region of moderate concentrations, and increased with increasing concentration. To determine whether the number of equivalents of Ca^{2+} desorbed corresponds to the number of equivalents of phenylenediamine adsorbed, the concentrations of the phenylenediamine ions in the original and equilibrium solutions were determined, in addition to the Ca^{2+} concentration in the equilibrium solution. The Ca^{2+} concentration was determined gravimetrically (the volumetric method for Ca^{2+} determination could not be used in presence of colored solutions), and the concentrations of the phenylenediamine ions were determined by potentiometric titration by sodium nitrite in a hydrochloric acid medium [6].

To test for molecular adsorption when the adsorbents were treated with salts or organic ions, the chloride ion concentrations in the original and equilibrium solutions were determined by potentiometric titration with $AgNO_3$ solution. The results are given in Table 1.

The difference between the Cl^- ion concentrations in the original and equilibrium solutions, as was to be expected, was within the limits of experimental error; this shows that molecular adsorption of phenylenediamine hydrochlorides does not take place.

TABLE 1

Desorption of Ca^{2+} Ions by Bivalent o-, m-, and p-Phenylenediamine Ions on Sulfocarbon and Espatite

System	Ion exchange on sulfocarbon				Ion exchange on Espatite			
	amine concentration in solution, normality		amount of amine in mg-equiv. adsorbed by 10 g	amount of Ca^{2+} in mg-equiv. displaced from 10 g	amine concentration in solution, normality		amount of amine in mg-equiv. adsorbed by 10 g	amount of Ca^{2+} in mg-equiv. displaced from 10 g
	initial	equilibrium			initial	equilibrium		
[Ca] + o-phenylenediamine hydrochloride	0.025	0.001	4.8	4.99	0.025	0.0005	4.9	3.57
	0.055	0.002	10.6	7.42	0.055	0.002	10.6	6.99
	0.132	0.027	21.0	11.98	0.132	0.022	22.0	15.26
	0.255	0.125	26.0	13.27	0.255	0.118	27.4	18.69
	0.382	0.245	27.4	13.55	0.382	0.225	31.4	19.26
	0.519	0.367	30.4	13.84	0.519	0.353	33.2	19.54
[Ca] + m-phenylenediamine hydrochloride	0.054	0.001	5.3	4.78	0.054	0.002	5.2	4.07
	0.102	0.007	9.5	7.99	0.102	0.006	9.6	8.13
	0.265	0.092	17.3	12.62	0.265	0.075	19.0	15.30
	0.538	0.345	19.3	12.98	0.538	0.326	21.2	17,19
	0.768	0.550	21.8	13.12	0.768	0.544	22.4	17.69
	1.133	0.811	32.2	13.27	1.133	0.806	32.7	17,97
[Ca] + p-phenylenediamine hydrochloride	0.023	0.001	4.4	5.42	0.023	0.001	4.4	4.57
	0.051	0.005	9.2	8.56	0.051	0.005	9.2	7.70
	0.121	0.051	14.0	12.41	0.121	0.037	16.8	13.55
	0.280	0.187	18.6	14.84	0.280	0.164	23.2	16.69
	0.444	0.350	18.8	15.26	0.444	0.304	28.0	17.83
	0.514	0.420	18.8	15.55	0.514	0.368	29.2	—

As the solution concentrations varied from 0.05 to 1.00 N, the pH decreased from 2.2 to 1.0. The pH values of the original and equilibrium solutions were equal, eliminating the possibility of participation of H^+ ions in ion exchange reactions.

As in the titration of o- and p-phenylenediamines by sodium nitrite, probably only one amino group is diazotized [7] (this can be confirmed by comparing the results of amine and chloride determinations in the original solutions); the values found for the normalities of their solutions are halved. This was taken into account in calculations of the amounts of the amines in milligram equivalents adsorbed by 10 g of the adsorbents (the differences between the number of equivalents in the original and equilibrium solutions of o- and p-phenylenediamines were doubled).

Table 1 shows that the number of equivalents of the amine adsorbed is greater than the number of equivalents of Ca^{2+} desorbed, and this difference is especially great in the region of high concentrations. With a constant concentration of Cl^- in the solution this may be attributed to adsorption of a nonpolar form of the amine. Comparison of the number of equivalents of Ca^{2+} desorbed by various organic cations (aniline, and o-, m-, and p-toluidines, with one amino group [5]) with desorption of Ca^{2+} by bivalent ions (o-, m-, and p-phenylenediamines) from sulfocarbon (Table 1) gave the same results. This behavior of phenylenediamines suggests that, despite the presence of two amino groups, they are present in the form of univalent ions in aqueous solutions. This is confirmed by the difference between the first and second ionization constants of p-phenylenediamine [8]: $K_1 = 1.1 \cdot 10^{-8}$; $K_2 = 3.5 \cdot 10^{-12}$.

The identical behavior of all three phenylenediamine derivatives in adsorption indicates that the difference between the first and second ionization constants is of about the same order, 10^4, for the ortho and meta derivatives. Since the value of the acidity constant of one of the ions is very high, of the order of 10^{-2}, its dissociation is so great that the H^+ ions are not in fact held by the amino group. Our hypothesis is also confirmed by the fact that phenylenediamine sulfates $[C_6H_4(NH_2)_2]_2\ H_2O_2SO_2$ contain univalent phenylenediamine ions [9].

If we are to assume that adsorption of phenylenediamine ions in univalent form occurs owing to hydrolysis of one of the ions, we must also assume that the hydrolysis is complete at all the equilibrium phenylenediamine concentrations studied, in the pH region 1.0-2.2, which is highly improbable. The assumption concerning the influence of hydrolysis is also contradicted by literature data [10] which show that phenylenediamine is hydrolyzed as a univalent ion in aqueous solution.

We have therefore considered, on the basis of our experimental data and information available in the literature, the exchange adsorption of phenylenediamines as the adsorption of univalent ions.

TABLE 2

Calculation of the Gapon Equation Isotherms

Systems	a	$x=\frac{\sqrt{a/2}}{100\ c}$	$v=\frac{1}{a}$	v_{calc}	a_m	K	σ_v
Sulfocarbon-Ca + o-phenylenediamine hydrochloride	4.99	5.2650	0.200	0.194	14.0 ± 0.5	0.33 ± 0.08	0.005
	7.42	3.2102	0.135	0.146			
	11.98	0.4450	0.084	0.082			
	13.27	0.1026	0.075	0.074			
	13.55	0.0531	0.074	0.073			
	13.84	0.0358	0.072	0.072			
Sulfocarbon-Ca + m-phenylenediamine hydrochloride	4.78	5.1533	0.209	0.200	13.8 ± 1.1	0.34 ± 0.07	0.009
	7.99	2.8553	0.125	0.143			
	12.62	0.2730	0.079	0.079			
	12.98	0.0738	0.077	0.074			
	13.12	0.0466	0.076	0.073			
	13.27	0.0318	0.075	0.073			
Sulfocarbon-Ca + p-phenylenediamine hydrochloride	5.42	5.4873	0.185	0.185	14.7 ± 0.4	0.32 ± 0.14	0.005
	8.56	2.0687	0.117	0.116			
	12.41	0.2442	0.081	0.076			
	14.84	0.0728	0.067	0.068			
	15.26	0.0394	0.065	0.067			
	15.55	0.0332	0.064	0.066			
Espatite-Ca + o-phenylenediamine hydrochloride	3.57	13.3600	0.280	0.283	18.8 ± 0.5	0.32 ± 0.03	0.004
	6.99	4.6738	0.143	0.134			
	15.26	0.6424	0.065	0.064			
	18.69	0.1301	0.054	0.055			
	19.26	0.0688	0.052	0.054			
	19.54	0.0433	0.051	0.053			
Espatite-Ca + m-phenylenediamine hydrochloride	4.07	7.1325	0.246	0.238	18.9 ± 1.0	0.49 ± 0.08	0.005
	8.13	3.3602	0.123	0.140			
	15.30	0.3688	0.065	0.063			
	17.19	0.0900	0.058	0.056			
	17.69	0.0551	0.056	0.055			
	17.97	0.0372	0.055	0.054			
Espatite-Ca + p-phenylenediamine hydrochloride	4.57	5.0390	0.219	0.220	17.2 ± 0.6	0.55 ± 0.16	0.003
	7.70	2.1801	0.130	0.128			
	13.55	0.3471	0.074	0.069			
	16.69	0.0883	0.060	0.061			
	17.83	0.0492	0.056	0.059			

For the exchange of bivalent with univalent ions, the Gapon isotherm equation [11] has the form:

$$\frac{1}{a} = \frac{1}{a_m} + \frac{K}{a_m}\sqrt{\frac{a/2}{100c}}\,.$$

where a is the number of mg-equivalents of desorbed cation per 10 g of adsorbent, equal to the number of mg-equivalents of the adsorbed univalent cation: a_m is the maximum adsorption in mg-equivalents per 10 g of adsorbent; c is the equilibrium concentration of the univalent cation in millimoles per 1 ml (in calculations of c the concentration of hydrolyzed ions was not taken into account, as it is very low, of the order of 10^{-5} - 10^{-6} millimole/ml); K is the exchange constant.

TABLE 3

Constants for the Exchange Adsorption Isotherms for Univalent Amines

Systems	a_m	K
Sulfocarbon - Ca + aniline hydrochloride	15.3 ± 0.9	0.64 ± 0.23
" + o-toluidine hydrochloride	14.7 ± 2.1	0.52 ± 0.04
" + m-toluidine hydrochloride	15.9 ± 0.6	0.66 ± 0.09
" + p-toluidine hydrochloride	13.9 ± 2.8	0.55 ± 0.06
" + o-phenylenediamine hydrochloride	14.0 ± 0.5	0.33 ± 0.08
" + m-phenylenediamine hydrochloride	13.8 ± 1.1	0.34 ± 0.07
" + p-phenylenediamine hydrochloride	14.7 ± 0.4	0.32 ± 0.14

The calculated data for this equation, based on our experimental results, are given in Table 2. The small root mean square errors of the average values of the constants and of individual determinations of y = 1/a show that the Gapon equation applies satisfactorily to the systems studied. The values found for y and the calculated constants for the isotherms in the exchange adsorption of o-, m-, and p-phenylenediamine on sulfocarbon and Espatite agree within the limits of experimental error. Consequently, the structure of the ions (the relative positions of the amino groups) has no influence on the extent and nature of the adsorption.

A comparison of the constants for the exchange adsorption isotherms for phenylenediamines with the corresponding constants for univalent amines [5] (Table 3) on sulfocarbon-Ca shows that the differences between them also lie within the limits of experimental error. This confirms the view that o-, m-, and p-phenylenediamines behave as univalent ions in aqueous solution. The somewhat lower values of K for the exchange of phenylenediamine ions are probably the result of somewhat greater effects of van der Waals forces.

SUMMARY

1. The exchange adsorption of o-, m-, and p-phenylenediamines on sulfocarbon-Ca and Espatite-Ca has been studied.

2. Equal exchange adsorption isotherms have been found for all the systems studied on sulfocarbon and Espatite, showing that structure of the phenylenediamines has no effect on ion exchange adsorption.

3. The adsorbents studied do not adsorb phenylenediamine hydrochlorides in molecular form from solution; this is shown by the same concentrations of Cl^- in the original and equilibrium solutions.

4. The amounts of Ca^{2+} desorbed are not equivalent to the amounts of phenylenediamine ions

adsorbed. The number of equivalents of phenylenediamine adsorbed was greater than the number of equivalents of Ca^{2+} liberated in all systems.

5. The exchange adsorption of phenylenediamine ions is of the same magnitude as that of univalent amine ions. The Gapon equation for the exchange of bivalent with univalent ions is applicable to the results obtained.

The A. M. Gorky State University
Kharkov
Chair of General Chemistry

Received May 29, 1956

LITERATURE CITED

[1] T. R. E. Kressman, J. A. Kitchener, J. Chem. Soc. No. 5, 1208, (1949).

[2] T. R. E. Kressman, J. Phys. Chem. 56, No. 1, 118, 1952.

[3] W. H. Slabaugh, J. Phys. Chem. 58, No. 2, 162, 1954.

[4] N. A. Izmailov and S. Kh. Mushinskaya, Proc. Acad. Sci. USSR, No. 1, 101 (1955).

[5] A. T. Davydov and R. F. Skoblionok, Colloid J., 18, No. 1,31 (1956).

[6] L. M. Litvinenko and A. P. Grekov, J. Anal. Chem., 10, No. 3,164 (1955).

[7] M. D. Zhorina, Factory Labs., 7, 10, 1180 (1947).

[8] Yu. Yu. Lurye, Calculation and Reference Tables for Chemists (Moscow, 1947) 193.

[9] H. Hübner, Ann. Chem. 209, 339, 1881.

[10] Victor Herbert, Veley, J. Chem. Soc. 93, 2122, (1908).

[11] E. N. Gapon, J. Gen. Chem., 3,145 (1933); 7,1438 (1937).

THE INFLUENCE OF STRUCTURE ON THE CHEMICAL ACTIVITY AND VULCANIZABILITY OF BUTADIENE POLYMERS

B. A. Dogadkin, A. V. Dobromyslova, F. S. Tolstukhina, and N. G. Samsonova

In polymerization of butadiene and its derivatives, the monomer groups join in various positions. The 4-1 and 2-1 structures are the most common:

$\sim CH_2-CH=CH-CH_2-CH_2-CH=CH-CH_2\sim$;

(4 – 1)

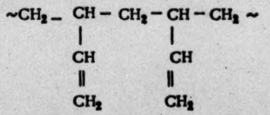

$$\sim CH_2-\underset{\substack{|\\ CH\\ \|\\ CH_2}}{CH}-CH_2-\underset{\substack{|\\ CH\\ \|\\ CH_2}}{CH}-CH_2\sim$$

(2 – 1)

The relative contents of these structures have a significant influence on the physical properties of the polymer (glass transition temperature, degree of orientation, strength, etc). It is also evident that differences in the position and nature of substitution of the double bond cause differences in the chemical activity of the polymers. These differences in chemical activity are also determined by the fact that the 4-1 structure contains methylene groups in the α-position to the double bonds, which therefore have hydrogen atoms with weakened bonds with carbon. In the 2-1 structure there is a hydrogen atom attached to a tertiary carbon atom. The differences in the chemical activities of butadiene polymers were studied in their interaction with perbenzoic acid, iodine chloride, and elementary sulfur.

The materials studied were synthetic butadiene rubbers with various relative contents of 4-1 and 2-1 structures in their molecular chains. The contents of vinyl side chains in the 2-1 structure were determined by the ozonation method, from the amounts of formic acid and formaldehyde split off [1]; the double bond contents of the 4-1 structure were determined from the difference between total unsaturation and the contents of vinyl side chains.

For some of the rubbers the results were confirmed by spectrographic data from the characteristic frequencies of 965 cm^{-1} for double bonds of the 4-1 structure and 909 cm^{-1} for monosubstituted double bonds of the 2-1 structure.

Interaction with perbenzoic acid. The reaction of unsaturated compounds with perbenzoic acid was studied in detail by Prilezhaev [2]. He established that the rate of the perbenzoic acid reaction depends on the positions and nature of the substituents at the double bonds. The chief direction of the reaction is the formation of epoxide groups in the polymer, in amounts equivalent to the benzoic acid formed. Meyer* has proposed the use of the Prilezhaev reaction for determination of the structure of butadiene polymers by calculating the content of 4-1 structural units with the aid of a special diagram, based on the results of titration of model low-molecular hydrocarbons under the same conditions. Our kinetic investigations showed that, in chlorobenzene medium with 0.1 N concentration of the rubber at 20°, both types of double bonds react with perbenzoic acid, but at very different rates. Figure 1 shows the kinetics of the reactions of benzoic acid with solutions of natural rubber, one of the butadiene polymers, and vinylcyclohexene as a model substance containing a disubstituted double bond in the ring and a monosubstituted double bond in the vinyl side chain. The amount of perbenzoic acid consumed was determined by titration with 0.1 N thiosulfate solution. Natural rubber, which contains only the 4-1 structure in its molecules, reacts rapidly, and the total amount of perbenzoic acid decomposed corresponds (to within 2%) to α, the total unsaturation of this compound (Curve 1). The kinetic curve for the oxidation of vinylcyclohexene contains two distinct regions — an initial region of steep ascent, and a final linear region which represents the reaction proceeding at a low constant rate. If the linear region is extrapolated to the ordinate axis, it cuts off an intercept corresponding to 50% of the total number of double bonds in vinylcyclohexene. From this it may be concluded that the linear region represents the oxidation kinetics of the less active vinyl groups, while the steeply ascending region corresponds to rapid oxidation of disubstituted double bonds in the ring. By drawing a horizontal straight line from the point of intersection of the linear region with the ordinate axis, it is possible to find ordinates corresponding to slow oxidation of vinyl groups, for each time instant on the experimental curve, and to plot a theoretical curve representing oxidation of the double bonds in the ring only (Curve 4).

---

* Meyer's work, carried out in the laboratory of the Schkopau works, has not been published; it is mentioned by Weindlein [3].

The kinetic method for the determination of the structure of butadiene rubbers by the perbenzoic acid reaction was developed by Dogadkin and Dobromyslova [4]. Salfer and Johnson [5] consider that this method is applicable only to polymers containing more than 70% of internal double bonds.

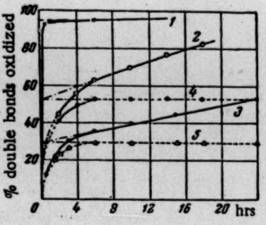

Fig. 1. Kinetics of oxidation of vinylcyclohexene and different rubbers by perbenzoic acid: 1) natural rubber; 2) vinylcyclohexene; 3) butadiene polymer SR-1; 4, 5) kinetics of double bond oxidation in the 4-1 structure of vinylcyclohexene and butadiene polymer SR-1.

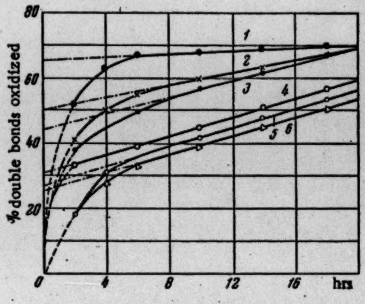

Fig. 2. Kinetics of oxidation of various butadiene rubbers by perbenzoic acid: 1) SR-6; 2) SR-5; 3) SR-7; 4) SR-4; 5) SR-8; 6) SR-9.

The kinetic curves for the reaction of perbenzoic acid with butadiene polymers are of similar form, since the latter contain two kinds of double bonds in their chains (Fig. 2). The double bonds in the vinyl side chains are oxidized very slowly, and therefore at a constant rate, because their concentration does not change significantly during the time of observation. By extrapolating the linear regions of the kinetic curves to the ordinate axis, it is possible to determine the initial contents of double bonds of the 4-1 structure, and to plot the kinetic curve for the oxidation of the 4-1 structure (Fig. 2, Curve 5) as described above.

The validity of this method of segregating the oxidation processes of different types of double bonds, and of their quantitative determination, is confirmed by data on ozonation of the same polymers (Fig. 2 and Table).* The values for the double bonds of different structures in seven grades of synthetic rubber, determined from kinetic data with perbenzoic acid, are in good agreement with the values obtained from ozonation data and data on the reaction with iodine chloride.

Interaction with iodine chloride. Reactions of rubbers with halogens have been frequently studied. The reactions are complex in character, and vary according to conditions, both in their mechanism and in the intermediate steps and final results. In many cases, addition of halogens at the double bonds is accompanied by substitution of hydrogen at the α-methylene groups and formation of intramolecular rings [6].

---

* This table appears at the end of the article.

The structure of the polymer has a significant effect on the course of the reaction. We studied the reaction between iodine chloride and butadiene polymers with various contents of 4-1 and 2-1 structures. The reaction was carried out by mixing 0.05 M (calculated on the unit molecular weight) of the rubber solution in dichloroethane with 0.2 N solution of iodine chloride in the same solvent. The halogen was in 100% excess above the theoretical amount. The course of the reaction was followed by the consumption of iodine chloride (by titration of samples with thiosulfate) and by formation of iodine (titration of samples with potassium iodate).

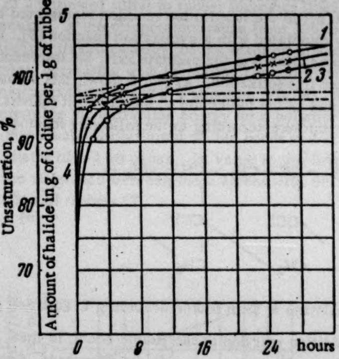

Fig. 3. Kinetics of iodine chloride absorption in the reaction with butadiene polymers: 1) SR-4; 2) SR-5; 3) SR-6.

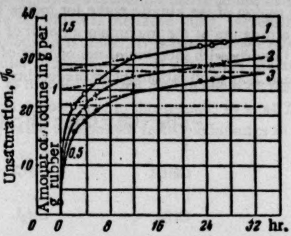

Fig. 4. Kinetics of iodine formation in the reaction of iodine chloride with butadiene polymers: 1) SR-4; 2) SR-5; 3) SR-6.

As Fig. 3 shows, absorption of iodine chloride by the polymer at 20° proceeds at a high rate during the first 6-8 hours; subsequently the reaction slows down and continues for a long time at a low constant rate (linear region of the kinetic curve). The initial region mainly represents the addition of iodine chloride at the double bonds [6] according to the schemes:

$$\sim CH_2-CH=CH-CH_2\sim \xrightarrow{ClI} \sim CH_2-CHI-CHCl-CH_2\sim \qquad (1)$$

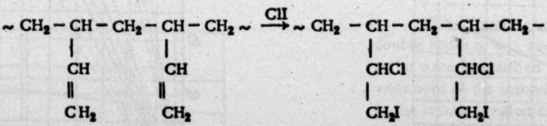

$$\sim CH_2-\underset{\underset{CH_2}{\overset{\|}{CH}}}{\overset{|}{CH}}-CH_2-\underset{\underset{CH_2}{\overset{\|}{CH}}}{\overset{|}{CH}}-CH_2\sim \xrightarrow{ClI} \sim CH_2-\underset{\underset{CH_2I}{|}}{\underset{|}{\underset{CHCl}{\overset{|}{CH}}}}-CH_2-\underset{\underset{CH_2I}{|}}{\underset{|}{\underset{CHCl}{\overset{|}{CH}}}}-CH_2- \qquad (2)$$

The linear region represents the slow reaction of hydrogen substitution, which probably occurs according to the scheme:

$$\sim CH_2-CHI-CHCl-CH_2\sim \xrightarrow{ClI} \sim CHCl-CHI-CHCl-CH_2\sim + HI \qquad (3)$$

As the result of the last reaction, an equivalent amount of iodine is liberated:

$$HI + ClI \rightarrow HCl + I_2 \qquad (4)$$

Since I_2 is titrated by thiosulfate in the same way as ClI, Reaction (4) is not reflected in the kinetic curve for the absorption of iodine chloride. If the linear region of the kinetic curve for the absorption of iodine chloride is extrapolated to the ordinate axis, it will evidently cut off an intercept corresponding to maximum absorption of ClI in the addition reaction, which in its turn corresponds to the content of double bonds in the rubber molecules.

In fact, the unsaturation determined by this method coincides with the unsaturation found as the sum of double bonds of 4-1 structure (by the reaction with perbenzoic acid) and double bonds of 2-1 structure (from the amounts of formic acid and formaldehyde in the ozonation reaction).

The liberation of iodine in the reaction medium is represented by kinetic curves analogous to the kinetic curves for the addition of iodine chloride (Fig. 4). The linear regions of the curves in Fig. 3 and Fig. 4 have the same slope. This proves convincingly that in the last stage of the process iodine is liberated according to Equation (4), and the amount formed corresponds to the HI split off in the substitution reaction represented by Equation (3). The initial rapid liberation of iodine is probably associated with a cyclization reaction [6]. If the linear region of the kinetic curve for iodine liberation is extrapolated to the ordinate axis, the intercept cut off is a measure of the maximum amount of iodine liberated in cyclization. As Fig. 5 shows, this amount increases linearly with increase of the content of the 2-1 structure in the molecules of the different rubbers. This suggests that cyclization occurs predominantly in the 2-1 structure according to the following scheme:

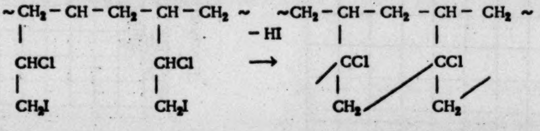

(5)

The liberated hydrogen iodide then reacts with iodine chloride to form iodine according to Equation (4).

Thus, different rubbers show the same behavior in the addition reaction at the double bonds, in the reaction with iodine chloride under the conditions studied. The cyclization process, in the other hand, develops mainly in the structure with vinyl side chains; this may be attributed to steric conditions favorable for six membered ring formation in such structures. The fact that the straight line in Fig. 5 does not pass through the coordinate origin suggests that a similar process may occur also in the 4-1 structure.

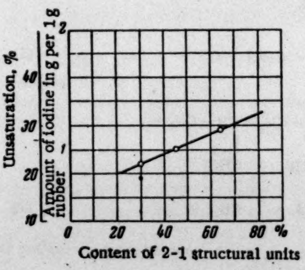

Fig. 5. Variation of the amount of iodine formed in the cyclization reaction with the contents of 2-1 structural units in various polymers.

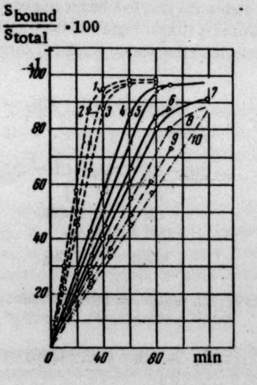

Fig. 6. Kinetics of sulfur addition to rubbers of 4-1 structure in solution in a nitrogen atmosphere at various temperatures: 1,2,3—155° 4,5,6,7, — 142°; 8, 9, 10 — 135°; 1,4,8 — SR-6 — 65%; 2,5 — SR-5 — 50%; 6,9 — SR-7 — 43%; 3,7,10 — SR-4 — 30% of 4-1 structure.

Interaction with sulfur and vulcanization. The interaction of rubber with sulfur is the main reaction in the vulcanization process. The reaction of butadiene polymers with sulfur was studied by heating solutions in toluene in ampoules, with strict exclusion of atmospheric oxygen. The solutions contained ~ 4 g of rubber per 100 ml of solvent; the sulfur content was 2 g per 100 g of rubber. The accelerator was a condensation product of aniline with acetaldehyde and butyraldehyde (Accelerator A-100), and triethanolamine was used as activator. In the conditions described, addition of sulfur to rubber proceeds at a constant rate for nearly the total duration of the reaction (Fig. 6), which may be explained by the large excess of active centers (double bonds and α-methylene groups) in rubber, in relation to the sulfur, and the narrow variation range of the volume concentration of sulfur in the solution during the entire observation time. As Fig. 7 shows, the rate of addition of sulfur to rubber increases linearly with increasing content of the 4-1 structure in the rubber molecules. In the temperature range from 135 to 155° this reaction obeys the Arrhenius equation (Fig. 8). The apparent activation energy of the reaction of addition of rubber to sulfur depends on the structure of the polymer, decreasing with increasing content of the 4-1 structure or, which is the same thing, increasing with increasing content of the 2-1 structure (Fig. 9). Since this relationship is linear, it is possible by extrapolation to determine the activation energy for a polymer of one particular structure, i. e., to determine the activity of sulfur toward disubstituted double bonds of 4-1 structure and to monosubstituted double bonds of the vinyl side chains of 2-1 structure. Its value in the first case is 14 kcal./mole, and in the second, 19 kcal./mole, and the difference between these agrees with the corresponding value determined from the kinetics of thermal oxidation of rubbers [7].

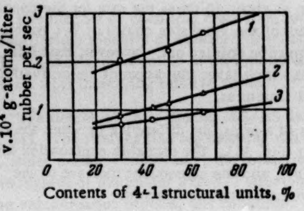

Fig. 7. Rate of sulfur addition as a function of the rubber structure: 1 — 155°; 2 — 142°; 3 — 135°

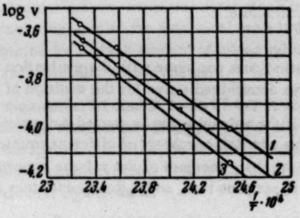

Fig. 8. Rate of sulfur addition to rubbers of 4-1 structure, as a function of the temperature: 1) SR-6, 65%; 2) SR-5, 50%; 3) SR-4, 30%.

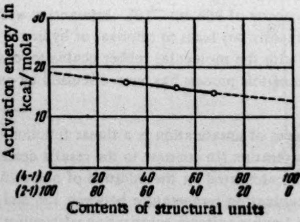

Fig. 9. Activation energy for the addition of sulfur to rubber as a function of the rubber structure.

The different chemical reactivities of double bonds of 4-1 and 2-1 structure toward sulfur were established by direct observation of variations of the intensity of the absorption bands in the infrared region of the spectrum during vulcanization. The technique developed for this was reported by Dogadkin and Klausen at the 10th All-Union Conference on Spectroscopy. Rubbers containing 65 and 50% of double bonds of 4-1 structure were studied. The absorption intensity for the 4-1 structure was measured at a frequency of 965 cm^{-1}, and for the 2-1 structure at 909 cm^{-1}. The vulcanization was carried out in films applied to rock salt plates, and in solution. In the latter case the spectroscopic determinations were made after evaporation of a sample of the solution placed on a rock salt plate. In the vulcanization experiments in solution, changes of unsaturation were also determined by the reaction with iodine chloride; the results so obtained were in good agreement with the spectroscopic data.

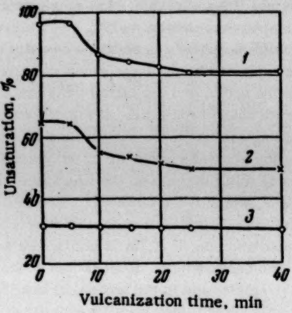

Fig. 10. Variation of the unsaturation of rubber with 65% of 4-1 structural units during vulcanization in film form in a nitrogen atmosphere at 142°; 1) total unsaturation; 2) unsaturation of 4-1 structure; 3) unsaturation of 2-1 structure.

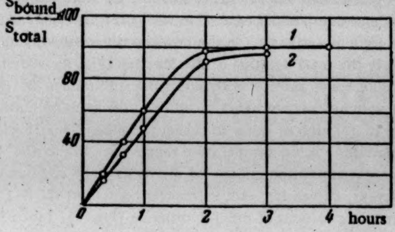

Fig. 11. Kinetics of sulfur addition to technical rubbers of different structure of the same degree of alkalinity in vulcanization without accelerators in a press at 142°; 1) SR-6, 65% of 4-1 structure; 2) SR-4, 30% of 4-1 structure.

As Fig. 10 shows, the double bonds of the 4-1 structure disappear as the result of vulcanization at about 15 times the rate for the double bonds of the vinyl side chains of 2-1 structure. It must be pointed out, however, that this evaluation does not agree with the evaluation based on kinetic data which takes into account the activation energies determined above for the addition of sulfur to 4-1 and 2-1 structures.

If the vulcanization is carried out under technical conditions in a press, the difference between the rates of sulfur addition to rubbers of different structure tends to disappear (Fig. 11). The probable explanation for this is the sharp increase of the volume concentration of double bonds, and the consequent increase of the absolute reaction rate, under these conditions in comparison with vulcanization in solution.

It is also significant that, according to spectroscopic data, there is no decrease in the double bond content at the start of vulcanization (horizontal regions in Curves 1 and 2, Fig. 10). This means that reactions involving α-methylene groups of the 4-1 structure predominate at this stage of vulcanization. The reactions involving the α-methylene groups have different mechanisms. Direct interaction with sulfur leads to formation of thiol groups and displacement of the double bonds into a new position, indicated in the case of natural rubber by the appearance of absorption bands at a characteristic frequency of 965 cm^{-1}[8]. Interaction with molecules of the accelerator (or with radicals formed by their decomposition) leads to removal of hydrogen and formation of polymeric radicals which react with each other or with the molecular rubber chains to form chemical cross bonds of the vulcanization network. The mechanism of this process has been discussed by one of the present authors elsewhere [9].

During the steady state period of vulcanization the total decrease of unsaturation is a linear function of the amount of sulfur added (Fig. 12). It is found that the loss of unsaturation (in contrast to the results described in the literature for natural rubber) is 4-6 times as great as the value calculated for the addition of one sulfur atom per double bond. The loss of unsaturation increases with vulcanization temperature between 135 and 155°. This increase in the loss of double bonds above the value calculated from maximum substitution with sulfur can be attributed either to polymerization processes involving joining of the molecular chains at the double bonds, or thermal formation of intramolecular rings. The latter hypothesis is refuted by the fact that unsaturation is not changed as the result of prolonged heating (for 12 hours) of rubber and its solutions in an inert gas at vulcanization temperatures, as shown both by spectroscopic data and by the iodine chloride reaction. As regards the hypothesis that in these conditions interaction occurs between the sulfur, accelerator, and rubber, inducing polymerization processes analogous to those which occur in the reaction between rubber and benzothiazolyl disulfide [9], this does not agree with the fact that the number of cross links in a vulcanizate (determined from the modulus) is considerably less than the number of atoms of bound sulfur. Further experimental study of this effect is therefore needed.

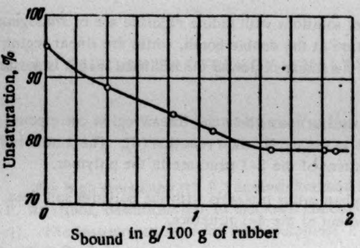

Fig. 12. Variation of the total unsaturation of SR-5 rubber with addition of sulfur during vulcanization in solution, in a nitrogen atmosphere at 142°.

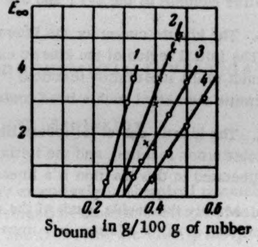

Fig. 13. Equilibrium modulus as a function of the amount of bound sulfur for rubbers with different contents of 4-1 structural units: 1) SR-6, 65%; 2) SR-5, 50%; 3) SR-7, 43%; 4) SR-4, 30% of 4-1 structure.

The number of chemical cross links formed between the molecular rubber chains was determined from the equilibrium modulus of elasticity E which, as is known, is a linear function of the number of cross links. As Fig. 13 shows, the number of intermolecular chemical bonds formed for a given amount of added sulfur increases with increasing relative content of the 4-1 structure in the molecular rubber chains.

The degree of cross linking $\Delta E/\Delta S$ is a linear function of the number of double bonds of 4-1 structure (Fig. 14). The straight line representing this relationship passes through the coordinate origin. This shows that, under certain conditions*, the formation of sulfur bonds in the spatial vulcanization network occurs only in the regions of the chains with 4-1 structure. Since the formation of chemical cross links is the main factor in the vulcanization process, this conclusion is of considerable technical significance.

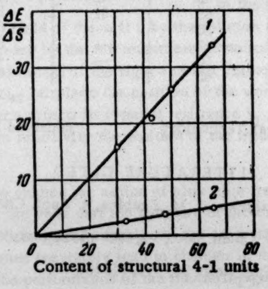

Fig. 14. Effect of rubber structure on degree of cross linking: 1) Mixture with thiuram; 2) mixture with mercaptobenzothiazole and sulfur.

SUMMARY

1. Differences between the chemical reactivities of 4-1 and 2-1 structures of butadiene are found in the reactions with perbenzoic acid, iodine chloride, and sulfur.

---

* These conditions are determined by an average molecular weight of the rubber at which E reaches its final value during the first instants of vulcanization.

2. The interaction of perbenzoic acid with solutions of butadiene polymers is represented by kinetic curves with an initial region of a high rate, mainly corresponding to the reaction of the double bonds of 4-1 structure, and a final linear region of a low rate, characterizing the reaction of the double bonds in the vinyl side chains of 2-1 structure. By extrapolation of the linear region to the ordinate axis it is possible to determine the relative contents of the 4-1 (and hence of the 2-1) structure in the polymer.

3. The kinetic curves for the interaction of the polymer solutions with iodine chloride are of analogous form. The initial region of the kinetic curve represents addition at the double bonds, while the linear region corresponds to the substitution reaction. By extrapolation of the linear region to the ordinate axis it is possible to determine the actual double bond content of the polymer.

4. The kinetic curves for iodine liberation are also of similar form; here the linear region corresponds to the substitution reaction, and the initial region corresponds to the cyclization reaction [6]. The amount of iodine liberated in this reaction is a linear function of the content of the 2-1 structure in the polymer.

5. Mainly the double bonds of the 4-1 structure react when sulfur interacts with the polymer solutions. The total rate of sulfur addition is a linear function of the content of the 4-1 structure.

6. The activation energy for sulfur addition increases with increasing relative content of the 2-1 structure in the polymer.

7. Formation of sulfur cross links in vulcanizates occurs mainly as the result of reactions in the 4-1 polymer structure. In consequence, the degree of cross linking $\Delta E/\Delta S$ is a linear function of the relative content of 4-1 structure in the polymer.

Characteristics of Butadiene polymer double bonds

Type of rubber	Total unsaturation in %, by the ClI reaction	% content of structures			Sum of double bond contents of 4-1 and 2-1 structure by oxidation with perbenzoic acid and ozonation
		4–1	2–1		
		by oxidation with perbenzoic acid	by ozonation	by difference between total unsaturation and contents of 4-1 structure	
SR - 1	87	30	57	57	87
SR - 2	92	49	40	43	89
SR - 3	94	65	31	29	96
SR - 4	94	30	—	64	—
SR - 7	96	43	—	53	—
SR - 5	95	50	—	45	—
SR - 6	96	65	—	31	—

The Moscow Institute of Fine Chemical Technology

Received November 28, 1956

LITERATURE CITED

[1] A. I. Yakubchik, A. A. Vasilyeva, V. M. Zhabina, J. Appl. Chem., 17,107 (1944).

[2] N. Prilezhaev, J. Russ. Phys. Chem. Soc., 42,1387 (1910); 43,609 (1911); 44,613 (1912).

[3] E.R. Weindlein, J. Chem. Eng. News 24, 771, (1946).

[4] B. A. Dogadkin and A. V. Dobromyslova, Trans. Moscow Inst. Fine Chem. Technol., No. 6 (1946).

[5] A. Salfer, B. Johnson, Ind. Eng. Chem. 40, 3, 538, (1948).

[6] T. S. Lee, I. M. Kolthoff, Mary Anne Mairs, J. Polym. Sci. 3, 66 (1948).

[7] A. S. Kuzminsky and N. N. Lezhnev, Proc. Acad. Sci. USSR, 70, 6,1021 (1950).

[8] N. Sheppard, C. B. Sutterland, Rub. Chem. Techn. 21, 799, (1948).

[9] B. A. Dogadkin et al., Colloid J., 17,215 (1955).

THE USE OF HIGH FREQUENCY ANALYSIS IN COLLOIDOCHEMICAL INVESTIGATIONS

V. I. Ermakov, V. N. Maslov, and O. G. Stolyarov

The high frequency (H. F.) analysis method is already used fairly extensively in chemical research for H. F. titrations, determination of unknown concentrations, and measurements of electric constants of solutions [1-4]. The instruments used for these purposes: F-meters, Z-meters, and Q-meters, are usually fairly complicated.

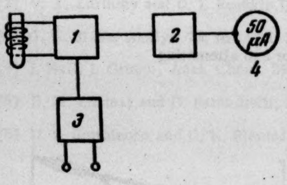

Fig. 1. Block diagram of the installation: 1) measuring generator and alternating current tube voltmeter; 2) universal shunt; 3) stabilized rectifier; 4) microammeter.

We have tested a simple measurement circuit which gives results of good reproducibility. A block diagram of the installation is shown in Fig. 1, and the circuit of the measuring generator and alternating current tube voltmeter in Fig. 2. The measuring generator (tube T_1) is of the three-point circuit type with autotransformer coupling and a high frequency grounded anode. The oscillator circuit formed by the measurement cell L and the capacity C_M is directly connected to the left half of the tube T_2, the grid circuit of which contains a grid leak C_{g_2} and R_{g_2} so that it acts as a grid detector. If the solution under investigation is placed in the measuring cell L, as the result of absorption of the energy of the magnetic field of the coil L by the solution the amplitude of the generator oscillations will decrease. This will be recorded by the microammeter connected in the diagonal of the measuring bridge: R_4, R_5, and R_i (the internal resistances of the right and left halves of the tube T_2). Changes in the oscillation amplitude of the circuit LC_M displace the position of the working point on the anode grid characteristic of the left half of T_2, which in turn affects its internal resistance R_i, causing unbalance of the bridge. It is important to note that for maximum sensitivity the position of the middle point a on the coil should be determined experimentally.

Eristavi and Barnashvili [5], who studied the action of ultra high frequency fields on hydrophobic sols of heavy metal ferrocyanides, advanced the view that the structure of the diffuse layer of the micelles is changed by the action of a high frequency electromagnetic field. On the other hand, changes of the electric double layer in colloidochemical processes must inevitably lead to changes in the nature of the dispersion of conductivity. This, in its turn, will change the performance of the measuring generator circuit and the oscillation amplitude, and therefore also the readings of the tube voltmeter. Satisfactory confirmation of these views is provided by studies of the coagulation of ferric hydroxide sols by the action of electrolytes.

The colloidal ferric hydroxide sol was prepared by the usual hydrolytic method. Coagulation was effected by gradual addition of electrolyte solutions. At relatively high ferric hydroxide concentrations the maximum deflection of the microammeter needle exactly corresponds to the first appearance of turbidity in the solution, while at high dilutions there is a certain lag before the turbidity is detected. This is easily explained if it is remembered that the latent coagulation period increases with dilution. Figure 3 shows variations of the $(NH_4)_2SO_4$ concentration corresponding to maximum deflection of the instrument needle, with the concentration of a ferric hydroxide sol made in redistilled water and not dialyzed. The reproducibility of the curve proved quite adequate for quantitative determination of ferric hydroxide from the concentration of the electrolyte required for coagulation. Special experiments showed that presence of variable amounts of hydrochloric acid does not appreciably influence the results. The same applies to additions of unhydrolyzed $FeCl_3$.

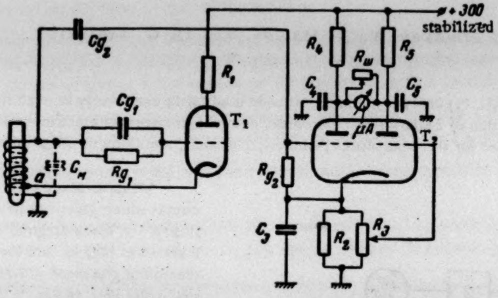

Fig. 2. Circuit diagram of the measuring generator and alternating current tube voltmeter.

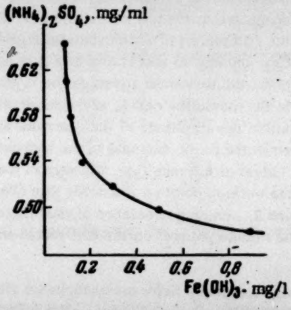

Fig. 3. Effect of dilution of ferric hydroxide sol on its coagulation by the action of ammonium sulfate.

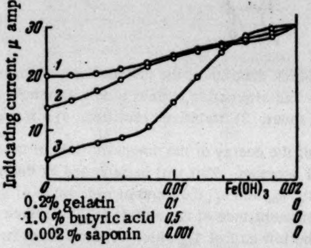

Fig. 4. Diagram of composition vs. indicating current for the following systems: 1) ferric hydroxide-gelatin; 2) ferric hydroxide-butyric acid; 3) ferric hydroxide-gladiolus saponin.

The H. F. analysis method was also used to study adsorptive interaction between colloidal particles of ferric hydroxide and gelatin molecules. Formation of adsorption complexes by the mechanism described by Ermolenko and Plenina [6]

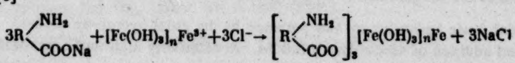

$$3R\begin{matrix}\diagup NH_2 \\ \diagdown COONa\end{matrix} + [Fe(OH)_3]_nFe^{3+} + 3Cl^- \rightarrow \left[R\begin{matrix}\diagup NH_2 \\ \diagdown COO\end{matrix}\right]_3 [Fe(OH)_3]_nFe + 3NaCl$$

implies deep changes in the electric double layer of the particles, which should be reflected in the nature of dispersion of the conductivity. However, the composition – current diagram shown in Fig. 4, where the deflection of the instrument needle is plotted against the composition, shows almost complete additivity of the properties of the solutions studied. However, curves for the systems ferric hydroxide sol – gladiolus saponin and ferric hydroxide sol – butyric acid showed much greater deviations from additivity, which casts doubt on the mechanism, mentioned above, of the interaction of gelatin with colloidal ferric hydroxide.

SUMMARY

1) An instrument was designed for high frequency analysis in which the oscillating circuit of the generator served directly as the measuring cell.

2) With a number of coagulation and adsorption processes as example, it has been shown that high frequency analysis may be used for studying colloid-chemical phenomena associated with changes in the electrical double layer.

The D. I. Mendeleev Institute of Chemical Technology
Moscow

Received May 21, 1956

LITERATURE CITED

[1] O. L. Kaptzan and V. A. Teplyakov, J. Anal. Chem., 8, No. 3,131 (1953).

[2] V. A. Zarinsky and D. I. Koshkin, J. Anal. Chem., 10, No. 2,111 (1955).

[3] G. G. Blake, Analyst 79, No. 935, 108 (1954).

[4] J. Hall, J. Gibson, Anal. Chem. 26, 1539, (1954).

[5] D. M. Eristavi and D. Barnashvili, Proc. Acad. Sci. USSR 25, No. 7,606 (1939).

[6] N. E. Ermolenko and G. N. Plenina, Colloid J., 5, No. 3, 194 (1939).

THE STRUCTURE OF GELS

9. EFFECT OF THE NATURE OF THE PLASTICIZER ON THE PHYSICOMECHANICAL PROPERTIES OF DIVINYL – STYRENE RUBBER

M. P. Zverev and P. I. Zubov

It was shown in the previous communication [1] that plasticization of high polymers, like the swelling process, involves not only weakening of the forces between the macromolecules, but also changes in their form. The greatest plasticization effect in divinyl–styrene rubber was produced by nonpolar plasticizers. The present paper contains experimental data on the influence of the plasticizer structure (polarity) on the physicomechanical properties of SKS-30 A divinyl–styrene rubber and its vulcanizate. The composition of the mix, vulcanization conditions, and plasticizers were the same as before [1]. The effect of the nature of the plasticizer on the temperatures of transition of the polymer from one physical state into another was studied with the aid of Kargin's dynamometric balance [2]. The mechanical strength of unfilled vulcanizates, calculated on the initial cross section, was determined by means of a dynamometer of the Polanyi type. The maximum error was ±5%. The vulcanization optimum was established from the equilibrium modulus [3].

Kargin and Malinsky [4] showed that the magnitude of the plasticizing effect for nonpolar polymers is a linear function of the volume fraction of the plasticizer in the polymer. It was of interest to determine to what extent the volume fraction rule applies to divinyl–styrene rubber.

Table 1 shows the variations of the glass transition temperature of rubber with the volume fraction of the plasticizer.

TABLE 1

Variations of the Glass and Flow Temperatures of Rubber with the Volume Fraction of the Plasticizer

Plasticizer	Amount of plasticizer in volume %							
	5	10	20	30	50	5	10	20
	Glass transition temperature of rubber in °C					Flow temperature of rubber in °C		
Tetralin	—53	—56	—63	—70	—77	146	127	99
Green oil	—53	—57	—65	—72	—78	140	122	92
Ditolylmethane	—55	—58	—66	—76	—85	135	117	84
Dicumylmethane	—54	—58	—68	—77	—85	137	118	85
Dibutyl sebacate	—58	—63	—70	—81	—89	133	110	80
Dibutyl phthalate	—55	—60	—69	—82	—90	134	108	78
Diethyl phthalate*	—55	—60	—68	—	—	130	108	80
	—55	—58	—70	—	—	130	108	78

---

* Only up to 20% of diethyl phthalate and tricresyl phthalate was added to the rubber, as larger amounts of these plasticizers were not compatible with the polymer.

Table 1 shows that at low plasticizer concentrations in the rubber the volume fraction rule is obeyed fairly satisfactorily; the decrease of the glass transition temperature does not depend on the nature of the plasticizer. Deviations from this rule are found at higher concentrations. In such conditions the glass transition temperature is lower in presence of nonpolar than of polar plasticizers.

Table 1 also gives data on the influence of the nature of the plasticizer on the temperature of transition of divinyl – styrene rubber into the viscofluid state; these results show that considerable increases of the flow temperature of rubber are also produced by nonpolar plasticizers. We also investigated the effects of plasticizer structure on the mechanical strength and relative extension of the unfilled vulcanizate. The results are given in Table 2.

TABLE 2

Effect of Plasticizer Structure on the Tensile Strength and Relative Extension of Unfilled Vulcanizate

Plasticizer	Amount of plasticizer in volume %				
	5	10	20	30	50
	Tensile strength in kg/cm²				
Tetralin	16.1	14.3	12.0	9.8	7.8
Green oil	15.8	14.6	11.6	9.2	7.3
Ditolylmethane	15.7	13.9	10.7	8.8	6.5
Dicumylmethane	16.0	14.3	11.4	9.0	6.4
Dibutyl sebacate	15.7	13.6	10.6	8.6	5.8
Dibutyl phthalate	15.6	13.8	10.9	8.4	5.8
Diethyl phthalate	16.1	14.0	10.6	—	—
Tricresyl phosphate	15.8	14.3	10.5	—	—
	Relative extension in %				
Tetralin	570	580	540	530	490
Green oil	600	570	550	520	480
Ditolylmethane	590	570	540	520	450
Dicumylmethane	570	560	540	510	450
Dibutyl sebacate	570	560	550	500	420
Diethyl phthalate	570	580	540	—	—
Tricresyl phosphate	570	570	540	—	—

Table 2 shows that in presence of small amounts of plasticizer in the vulcanizate the decrease of tensile strength and the change of relative extension are practically independent of the plasticizer structure. The effects of molecular structure of the plasticizer become noticeable above 20%. With 50% plasticizer the mechanical strength and the relative extension of specimens plasticized with tetralin or green oil are approximately 25-30%, and the relative extension is 50-60%, higher than the strength and the relative extension of specimens plasticized with phthalate or sebacate esters.

SUMMARY

1. The glass and flow temperatures and the strength and relative extension of rubber depend not only on the concentration of the plasticizer but also on its molecular structure.

2. Divinyl – styrene rubber plasticized with nonpolar plasticizers has higher glass and flow transition temperatures than rubber plasticized with polar substances. The same relationships are found for the strength and relative extension of vulcanizates of this rubber.

3. Nonpolar plasticizers also weaken intramolecular interaction to a greater extent than polar plasticizers.

The L. Ya. Karpov Physicochemical Institute Received June 13, 1956

LITERATURE CITED

[1] P. I. Zubov and M. P. Zverev, Colloid J., 18,679 (1956).

[2] V. A. Kargin and T. I. Sogolova, J. Phys. Chem., 23,530 (1949).

[3] G. M. Bartenev, Investigations of High Molecular Compounds (Acad. Sci. USSR Press, Moscow-Leningrad, 1943) 306.

[4] V. A. Kargin and Yu. M. Malinsky, Chemistry and Physical Chemistry of High Polymers (Acad. Sci. USSR Press, Moscow-Leningrad, 1952) 255.

THE HARDENING MECHANISM OF THERMOSETTING PLASTICS (MOLDING POWDERS)

I. F. Kanavets, L. G. Batalova, and A. G. Romashova

The first place among plastics, in volume of production and diversity of applications, is occupied by thermosetting plastics, and among these, by plastics based on phenol – formaldehyde resins. The conversion of thermosetting resins into the infusible and insoluble state, in the course of which thermosetting plastics acquire all the physicochemical properties necessary for processing into articles and for stability of the products in use, has so far not been sufficiently well investigated.

Thermosetting molding powders, used for the production of plastic articles, are complex compositions consisting of resins, fillers, and other components which influence their technological properties and the mechanical properties of the material in the finished articles. A clear understanding of the nature of this influence is necessary for production of molding powders with the required technological properties.

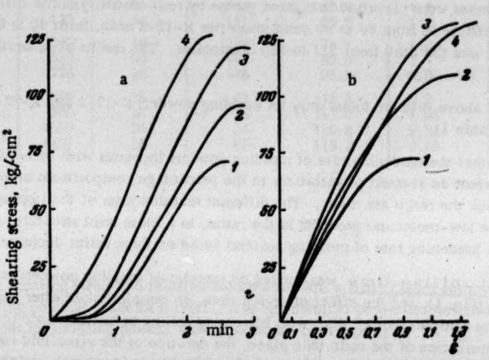

Fig. 1. Kinetics of the hardening at 170° of a molding composition of the Novolak type grade K-18-2 with different rolling times (a), and the mechanical properties for the hardening time corresponding to a stress of 25 kg/cm² (b); 1) rolling for 30 seconds, 2) 2 minutes, 3) 3.5 minutes, 4) 3 minutes 50 seconds.

The study of chemical reactions occurring in resins, and especially in molding powders, is a very difficult problem. A plastometer designed by one of the authors has proved very convenient for this purpose [3, 4]. Determinations of the kinetics of the hardening process by means of this plastometer are based on variations of the shearing stress with time at constant temperature, pressure, and rate of shear. The results are automatically recorded by the instrument in stress – time coordinates (in determinations of the hardening rate), and in stress – relative deformation coordinates for determination of the mechanical properties. The hardening rate is found from the time required to reach a viscosity of $2 \cdot 10^9$ poises or a shearing stress of 25 kg/cm^2. The duration of the viscofluid state is read off along the time axis up to the steep ascent of the curve (Fig. 1, a), and the mechanical properties of the molded material at the given hardening stage are read off the maximum shearing stress and relative deformation at the point at which the curve takes a horizontal course (Fig. 1, b). These are the most characteristic values for evaluation of the quality of thermosetting molding powders, as they are closely associated with the structure of the resins and of the material in the molded article.

The study was carried out with molding powders of the Novolak and resole types, made by the dry rolling method in laboratory and factory conditions from resins differing in chemical nature and degree of condensation. Molding powders made by the dry rolling method were rolled for different periods or treated in a mixer, with samples taken during the rolling, while resole powders made by the emulsion process were heated for different times during drying, also with periodic sampling. In addition, molding powders containing various amounts of additives, both reacting and not reacting with the resins, etc., were studied.

Physicochemical processes occurring during the production of molding powders.

The effects of the degree of condensation of the resins (resins of different viscosities in solution) on the technological properties of the molding powders and the mechanical properties of the molded articles were studied for molding powders based on phenol–, cresol–, and xylenol – formaldehyde resins. These resins varied in viscosity coefficients in the range of 50 to 155 centipoises for Novolaks and from 345 to 776 centipoises for resoles. The investigations showed that increase of the degree of condensation of the resins shortens the time of existence of the viscofluid state, and increases the rate of hardening, the maximum shearing stress, and the relative deformation of the material in the finished articles. This is confirmed by the test results for a large number of production batches, the average values for which are given in Table 1. More than 50 of the batches were classified into three groups by resin viscosity. The first group contains resins with viscosity coefficients from 60 to 90 centipoises (for K-18-2 resin, from 90 to 99 centipoises), the second, from 91 to 120, and the third from 121 to 160 centipoises. The results of laboratory experiments are given in Table 2.

Exceptions to the above rule are found only for molding powders K-17-2 and K-20-2, made from xylenol and cresol resins (see Table 1).

The general law that the hardening rate of molding powders increases with increasing resin viscosity may be disturbed to some extent on account of variations in the percentage compositions of isomeric phenols in the raw materials from which the resins are made. The different reaction rates of the isomeric phenols lead to different contents of the low-molecular products in the resins, to a loose resin structure, and to steric hindrances, and in consequence the hardening rate of molding powders based on these resins decreases.

The effect of rolling time was studied on samples of molding powders taken from the rolls at intervals during rolling (Fig. 1), and the effect of drying time, on samples taken after various times of drying (Fig. 2). Tests of these samples showed that, with increasing rolling or heating time (during drying), polymer chain growth and structurization of the resin take place, the duration of the viscofluid state of the molding powders decreases, the hardening time decreases (or the hardening rate increases), and the maximum shearing stress and relative deformation of the hardened material in the articles increase. Data for molding powders made from resins differing in viscosity and taken at various stages of rolling are given in Table 2.

The mixer method. The following experiment was performed to compare the properties of molding powders made by the rolling and the more up-to-date internal mixer methods: molding powder compositions of grade K-17-2, made from three resin batches ranging in viscosity from 80 to 129 centipoises, were each divided into two portions for processing on rolls and in mixers. The rolling was performed by the factory procedure established for this grade of powder, and the mixing by the factory procedure (I), and by a procedure in which the feed rate into the mixer was halved (II). The results of these trials, including one with the composition without rolling, are given in Fig. 3. Fig. 3, a shows that the technological characteristics of a molding powder rolled for one minute are similar to those of a powder made by the mixer method. As regards the mechanical properties of the mixer material, the maximum shearing stress and relative deformation are lower than in material rolled for one minute. The nonrolled molding composition (Fig. 3,c) has quite low values for maximum shearing stress and relative deformation. Nonrolled molding powders made by the solvent method (solutions of resin and urotropine in alcohol) have the same high values as the rolled. Production batches of molding powders made by the roll and mixer methods are similar in duration of the viscofluid state and hardening rate. The average results are given in Table 3 .

TABLE 1

Technological Properties of Molding Powders Made from Resins of Different Viscosities

Molding power grade	Viscosity coefficient in centipoises	Plastometer data at 170°		Shearing stress at the final hardening stage in kg/cm^2	Mechanical properties	
		duration of viscofluid state in sec.	hardening time in sec.		relative deformation ε	Shearing stress in kg/cm^2
K-18-2	96	35	89	61.2	0.95	65.5
	108	34	90	72.2	1.0	77.7
	127	32	80	82.5	1.1	90.0
K-17-2	86	39	100	78	1.4	78.5
	105	42	107	70	1.2	76.0
	128	58	131	66.5	1.1	75.7
K-15-2	84	39	101	73.5	1.1	73.0
	105	39	97	60.4	1.0	66.2
K-20-2	86	39	106	63.5	1.2	68.0
	108	40	103	65.8	1.1	67.5
	123	44	111	66.8	1.1	71.0
K-21-22	345	48	238	73.1	1.3	56.5
	535	30	188	82.0	1.7	72.4
	776	26	178	85.2	2.0	73.6
"Voloknit"	699	28	62	115.3	0.9	121.5
	900	26	58	113.9	1.05	116.6
	1059	24	54	126.8	0,8	135.5
	1457	28	66	119.2	0,86	129.5

The maximum shearing stress and relative deformation are a little higher for molding powders made by rolling than for molding powders made in mixers . The mechanical properties determined according to the technical specifications for molding powder are the same for both types.

Changes in the properties of Novolak resins on rolling with hexamethylenetetramine. Novolak resins were rolled with additions of 15% hexamethylenetetramine at the same temperature as the molding powders, to convert them into hardening resins. It was found (see Fig. 4) that such resins have considerably lower hardening rates than molding powders made from the same batches: they reach the same value of maximum shearing stress as is found for molding powders after 2 minutes rolling, only after 10-15 minutes. At the initial hardening stage, Novolak resins rolled with hexamethylenetetramine, as a result of greater cross linking than is found in resins rolled with fillers, give hardening curves of the same form as are given by molding powders of the resole type. The well defined horizontal region, characterizing softening of the resin, is lacking in these curves also. The viscosity of resins rolled with urotropine is two to three times as high as the viscosity of the molding powders, as the result of greater structurization during rolling. The same applied to other grades of resin rolled with hexamethylenetetramine .

TABLE 2

Technological Properties of Thermosetting Molding Powders Made with Different Rolling Times

Molding powder grade	Viscosity coefficient in centipoises	Drop temperature, °C	Rolling time, min	Plastometer data at 170°					
				Duration of viscofluid state in sec.	hardening time in sec.	complete hardening time in sec.	shearing stress at final hardening state, kg/cm²	mechanical properties	
								shearing stress, kg/cm²	relative deformation e
K-17-2	76	96	1.0	40	122	272	55.5	—	—
	76	96	1.5	36	112	270	62	50	0.9
	76	96	2.0	36	110	260	56.5	—	—
K-17-2	155	103	1.0	28	84	210	117.5	117.5	1.25
K-20-2	87	95	1.0	54	122	242	58.5	25.4	1.1
	87	95	1.5	50	122	254	71	63.5	1.1
	87	95	2.0	50	112	260	66.5	60.5	1.0
K-20-2	104	99	1.0	46	98	280	86	68.5	1.15
	104	99	1.5	42	92	272	95	68.5	1.05
	104	99	2.0	42	94	254	92.5	81.5	1.20
K-20-2	131	102	1.0	50	108	226	78	82.5	1.2
	131	102	1.5	42	100	210	79	86	1.2
	131	102	2.0	40	100	200	78	93	1.3

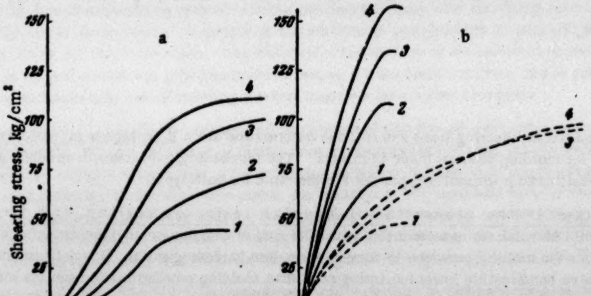

Fig. 2. Kinetics of the hardening at 170° of a molding composition of the resole type grade K-21-22 with different drying times (a), and the mechanical properties for the hardening time corresponding to a stress of 25 kg/cm² (b) (broken lines) and at the final hardening stage (continuous lines): 1) drying for 30 seconds, 2) 1.5 hours, 3) 2 hours, 4) 2.5 hours.

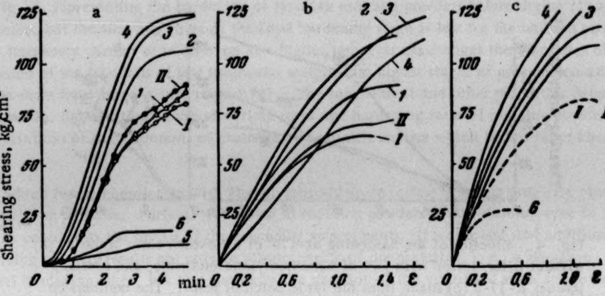

Fig. 3. Kinetics of the hardening at 170° of a molding composition of the Novolak type grade K-17-2 with different rolling times (a), the mechanical properties for the hardening time corresponding to a stress of 25 kg/cm^2 (b), and the mechanical properties at the final hardening stage (c): 1) rolling for 1 minute; 2) 2 minutes; 3) 3 minutes; 4) 4 minutes; 5) not rolled; 6) ditto, heated at 150° for 20 minutes; and I and II) from internal mixer .

TABLE 3

Average Data for Factory Grades of Molding Powders Made by the Roll (r) and Mixer (m) Methods .

Grade	Viscosity in centipoises	Technological properties		Mechanical properties	
		duration of viscofluid state in sec.	hardening time in sec.	shearing stress in kg/cm²	relative deformation, ε
K-18-2 (r)	119	33±8	83±14	86.2±16	1.0 ±0.1
K-18-2 (m)	99	29±3	87±4	61.0±4.5	0.85±0.05
K-15-2 (r)	95	40±5	96±9	68.7±10	1.1 ±0.15
K-15-2 (m)	97	39±6	99±5	67±10,7	0.99±0.1
K-20-2 (r)	97	41±9	106±13	67.7±10	1.1 ±0.15
K-20-2 (m)	101	44±12	109±14	64.5±6.7	1.0 ±0.04
K-17-2 (r)	100	13±10	106±17	74±12.7	1.2 ±0.2
K-17-2 (m)	100	55±14	128±21	67.3±9.7	0.95±0.1
K-17-23	—	71±14	153±14	21.2±3.7	0.65±0.04
K-21-22	552	38±21	189±27	72.2±12.5	1.8 ±0.7
K-211-2	—	92±13	566±81	29.5±5.0	1.0 ±0.07
K-220-23	—	83±6	300±36	29.7±3.2	1.2 ±0.22
K-214-2	—	91±14	208±35	78±12.5	1.6 ±0.4
"Voloknit"	—	28±5	60±6	121.2±11.7	0.86±0.13
K-103-2	—	42±11	117±19	—	—
K-111-2	—	50±9	145±32	—	—
K-15-2	—	67±3	113±6	56.2±8.5	0.95±0.1
K-17-2	—	85±5	140±7	51.2±3.5	0.93±0.02
Aminoplastic	—	60±8	102±8	84.5±16	1.3 ±0.2
K-F-3	—	56±9	79±9	87.0±16,5	0.89±0.17
"Monolit" No. 1	—	40±3	89±4	64.2±6.2	1.05±3.0
"Monolit" No. 7	—	54—60	120—128	45—65	1.0 —1.1
K-77-51	—	180±60	240±20	50±5	0.9 ±0.1

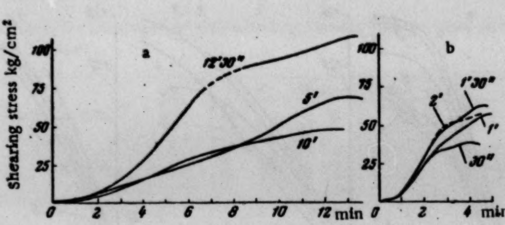

Fig. 4. Kinetics of the hardening at 170° of a Novolak resin grade 17 (a) without filler, rolled with 15% of hexamethylenetetramine, and molding powder K-17-2 (b) made from the same batch of resin. The numbers on the curves are the rolling times.

Variation of the contents of substances extracted by alcohol-benzene mixture in molding powders at different stages of rolling and drying. Thermosetting molding powders undergo changes with increasing rolling and drying times, resulting in a decrease of the duration of the viscofluid state, and a decrease of the content of substances extracted by alcohol-benzene mixture from 58 to 34%. Experimental data show that molding powders after 1 minute of rolling have an extractable content of about 50-58%, and at the last stage of rolling and drying this falls to 34-40%. It should be noted that at the last stage of rolling and drying the molding powders give hardening curves (Fig. 1) which ascend sharply without an appreciable horizontal region corresponding to the viscofluid state, although such powders contain 34-40% extractable matter. It follows from these experiments that a decrease of the amounts of extractable reactive resins in molding powders decreases the duration of the viscofluid state, and conversely.

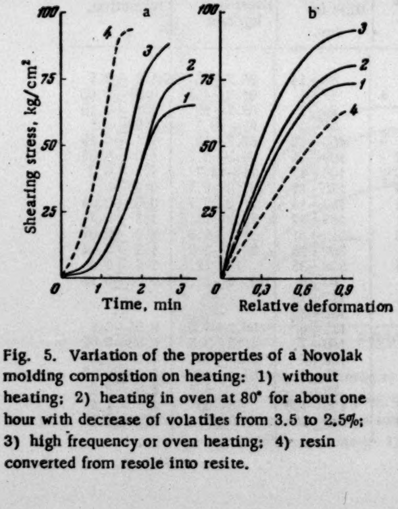

Fig. 5. Variation of the properties of a Novolak molding composition on heating: 1) without heating; 2) heating in oven at 80° for about one hour with decrease of volatiles from 3.5 to 2.5%; 3) high frequency or oven heating; 4) resin converted from resole into resite.

Influence of other components present in molding powders on their quality. Various substances of low molecular weight, such as hexamethylenetetramine, magnesium oxide, lime, organic fatty acids, etc., are added to molding powder compositions; in addition, moisture, free phenol, and resin fractions in the initial stages of polycondensation are introduced into the molding powders with the resins, while moisture and mineral impurities enter the composition with the fillers. To obtain a molding powder with predetermined properties it is necessary to know what effects the various substances present influence its technological properties and the properties of the material in the finished article.

The effects of moisture and volatile matter were studied on Novolak and resole molding powders. The experiments show that variation of the moisture content in the molding powder (from 1 to 12%) has no practical effect on the hardening rate, but the viscosity coefficient at the final hardening stage is approximately halved when the moisture content is increased to 12%. The same is found on variation of the volatile content. Fig. 5 gives data found for molding powders containing 3-3.5% volatiles, and for the same powders after drying for one hour at 70-80°. In the latter case the volatile content of the molding powder decreased by about one per cent. The curves in Fig. 5, representing the hardening of Novolak molding powders before drying (1) and after drying (2), coincide, but the shearing stress at the final hardening stage is less for the undried powders. Stronger heating by high frequency current or in an oven at a higher temperature changes the properties of the resin owing to conversion of the fractions of low molecular weight into higher stages of polycondensation [3], and conversion of the resin from stage A into stage B [4]. The mechanical and other properties deteriorate in the process; consequently, the duration of the viscofluid state and hardening rates of molding powders are practically unchanged by variations of their contents of moisture and volatile matter which do not react chemically with the resins.

Furfural, which reacts chemically with phenol-formaldehyde resins, is a characteristic plasticizer for thermosetting molding powders. Furfural was added to molding powders of the Novolak type in 5, 10, and 15% amounts. In contrast to the results of the preceding experiments, it was found that addition of furfural to Novolak molding powders results not only in plasticization of the material, i. e., a decrease of the shearing stress at the final hardening stage, but also increases the duration of the viscofluid state and retards the hardening rate (see Fig. 6). For example, molding powder K-18-2, after additions of 5, 10, and 15% furfural, has (instead of 50 seconds without additions) durations of the viscofluid state of 55, 60 and 70 seconds respectively, while the time of hardening increases from 90 seconds to 100, 112, and 123 seconds respectively. Thus, furfural and extractable resins, which react chemically with the resin, have a different effect from moisture and other plasticizing additions on the technological properties of molding powders.

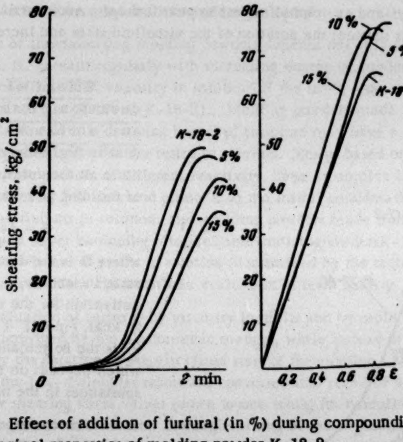

Fig. 6. Effect of addition of furfural (in %) during compounding on the technological properties of molding powder K-18-2.

The effects of hexamethylenetetramine, magnesium oxide, and lime on the technological properties of molding powders based on resins of the resole type are illustrated by the experimental results given in Fig. 7. The molding powder represented by Curve 1 gives Curve 2 on addition of hexamethylenetetramine; this shows an increase of the duration of the viscofluid state and a lower viscosity in the initial hardening stage. Addition of magnesium oxide or lime (Curve 3) increases the viscosity and shortens the duration of the viscofluid state of the molding powder. Molding powders with added magnesium oxide, lime, and hexamethylenetetramine have higher viscosities or greater maximum shearing stresses than molding powders containing smaller amounts of these substances.

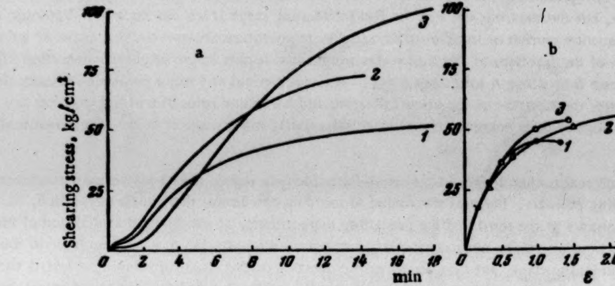

Fig. 7. Variation of technological and mechanical properties during an interval corresponding to a stress of 25 kg/cm² at 170°: 1) resole molding composition K-21-22 without additions; 2) with added hexamethylenetetramine; 3) with hardeners of the magnesium oxide or lime type.

Similar changes in the technological properties of molding powders are found with FFG phenol-furfural resin and the same resin with addition of hexamethylenetetramine. Experiments show that resin FFT, based on peat furfural, has a lower hardening rate than FFG resin based on hydrolytic furfural; probably owing to the presence of ~ 20-25 % of methyl-and oxymethylfurfural in peat furfural. Addition of hexamethylenetetramine to the Novolak molding powders shortens the duration of the viscofluid state and increases the hardening rate and shearing stress.

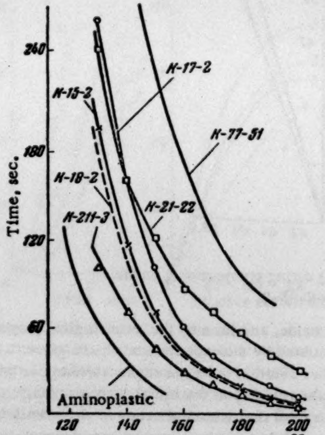

Fig. 8. Effect of temperature on the duration of the viscofluid state.

Effect of temperature on the duration of the viscofluid state and on the hardening rate. The data in Fig. 8 show that the effect of temperature on the duration of the viscofluid state of molding powders conforms to the law

$$\theta = Ae^{-u/kT}, \qquad (1)$$

where θ is the duration of the viscofluid state in seconds; u is the free energy of activation for the polycondensation reaction, in kcal./mole; T is the absolute temperature; k is the Boltzmann constant; A is a factor which depends on the amount of reactive substances in the molding powder.

The course of the hardening reaction with time is represented by the equation

$$\Delta\sigma_t = \frac{\Delta\sigma_f}{1 + e^{-\lambda\theta}}, \qquad (2)$$

where σ_t — is the shearing stress at time t, in kg/cm²; σ_f is the shearing stress at the final hardening stage in kg/cm², and σ_0, at the initial instant, in kg/cm²; $\Delta\sigma_t = \sigma_t - \sigma_0$; $\Delta\sigma_k = \sigma_f - \sigma_0$; $\theta = t - t_m$,

t_m is the time from the start of the experiment to the moment when the maximum hardening rate is reached.

The hardening rate K varies with temperature and time according to the equation

$$K = \frac{A_0 e^{-\lambda\theta}}{(1 + e^{-\lambda\theta})^2} \cdot e^{-u/kT}, \tag{3}$$

where A_0 is a constant, λ is a factor which depends on the resin properties and the temperature, and the remaining symbols are as in Equation (1). Data on the hardening rates and other characteristics of the main grades of molding powders are given in Table 3.

DISCUSSION OF RESULTS

According to the modern theories, hardening of thermosetting resins occurs as the result of chemical reactions between the functional groups in the macromolecular chains. The physicochemical properties of the resultant plastics depend not only on the chemical structure of the reacting molecules but also on the shape and dimensions of the macromolecules formed in the reactions. Good quality thermosetting molding powders should soften but not melt on heating, and should remain for some time in the softened or viscofluid state. This time is used for molding the articles. The softening power is determined by the state of the resin in the molding powder; this should be intermediate between stages A and B*. The duration of the viscofluid state is determined not by the physical properties of the resins, as has been believed hitherto, but by the rate of chemical conversion of low-molecular fractions and reactive substances into products of higher molecular weight. This is shown by the decrease in the content of extractable resins in molding powders with decreased duration of the viscofluid state, and its increase on addition of furfural. If the resin in the molding powder is at stage A, the molding powder is not suitable for conversion into articles owing to extrusion of resin from the filler and faulty external appearance of the articles. If the resin has reached stage B, the molding powder is not suitable because the articles are gray and incompletely molded.

The hardening rate of thermosetting molding powders depends not only on the degree of condensation but on the resin structure; it increase regularly with increasing degree of condensation from 60 to 150 centipoises (measured by the coefficient of viscosity in solution) if the resin, near to linear in structure, has been made from crystalline phenol (see Table 1, K-18-2). Molding powders made from cresol, xylenol, aniline-formaldehyde, and other resins with a complex branched structure may have a lower hardening rate despite a higher average viscosity coefficient for the resins in solution. Resins based on raw materials containing different amounts of isomeric phenols of different reactivity have a complex branched structure and contain large amounts of low-molecular fractions and products at the initial condensation stage. Such resins have high average viscosity coefficients in solution, and molding powders made from them have increased duration of the viscofluid state and a lower hardening rate (see Table 1 molding powders K-17-2, K-20-2, and Table 3). Therefore the viscosity coefficient of resins in solution (determined by the technical specification methods for molding powders) does not provide a characteristic evaluation of resin quality.

A more correct evaluation of resins is by viscosity in melts and by molecular weight distribution. The melt viscosity can be determined by the plastometric method, while instead of molecular weight distribution resins may be evaluated by the duration of the viscofluid state of the molding powders, directly related to the duration of the reaction whereby the low-molecular resins are converted into resins of high molecular weight. Attention must be drawn to the low shearing stress values (down to one tenth) for nonrolled resins with hexamethylenetetramine and for molding powders even after thorough mixing of the ingredients in a ball mill and after rolling on cold rolls. The fact that Novolak resins rolled with 15% of urotropine have a considerably lower hardening rate than molding powders made from the same batches of resins and at the same rolling temperatures confirms that resin quality should be evaluated in molding powder compositions made up by the usual procedure, as the duration of rolling and drying needed to give a molding powder with particular technological characteristics depend on the molecular weight distribution in the resin and the contents of low-molecular fractions. In such experiments carried out by accelerated methods [3, 4] on samples taken during rolling, data are obtained on the resin hardening rate, on the quality of the molding powder, on the rolling conditions, etc., and therefore such evaluation is less laborious and more complete than the procedure adopted at present.

---

* Stage A resins are fusible and soluble, at stage B resins do not melt but soften and swell in solvents, and at stage C they do not melt or dissolve.

The duration of the viscofluid state, the effective viscosity coefficient, and the hardening rate are the most characteristic values for establishing the optimum temperatures and rolling and drying times of molding powders, and also for evaluating the quality of the finished products. An under-rolled molding powder will have a longer, and an over-rolled powder a shorter duration of the viscofluid state (in comparison with the normal). The duration of the viscofluid state gives the most correct evaluation of the state of the resin in the molding composition, ensuring the correct flow properties in the molding powder during processing. This very important characteristic can be determined only by the plastometric method [3, 4]. The exponential decrease of the duration of the viscofluid state with temperature indicates the statistical nature of the law governing the conversion of resin from stage A into stage B in molding powders. The exponential course of the reaction as represented by Equations (1) and (2) is a general law for processes determined by the probability of surmounting potential barriers. We showed earlier [4] that conversion of thermosetting resins from stage B into stage C also obeys a statistical law. It was then pointed out that the kinetics of the hardening of phenol-formaldehyde resins and of molding powders made from them obeys the same law for the conversion from stage B to stage C, and is described by an equation of the form of Equation (2), which applies to degenerate explosion reactions. Therefore molding powders with a low duration of the viscofluid state harden rapidly on contact with the hot mold, which leads to rejects in production owing to grayness.

Because of the polycondensation reaction which takes place at various stages of molding powder production according to a statistical law, the resin gradually becomes less polydisperse or more homogeneous in composition because the lower fractions, being more mobile, react more rapidly than the fractions of higher molecular weight. This accounts for the improved mechanical properties of the material in articles molded from powders taken at later rolling and drying stages. In the experiments described (Figs. 1-3) each successive sample taken during rolling and drying is, in a sense, made from a resin more homogeneous than the preceding one in fractional composition, and of higher molecular weight.

It follows from the theory of reaction rates that the factor which determines the rate of a reaction is not the heat of activation (H) but the free energy of activation (u), which enters Equations (1) and (2).

Taking θ as constant in Equation (3), we find that the rate of the hardening reaction as a function of temperature obeys the Arrhenius law

$$K = Be^{-u/kT}. \tag{4}$$

Korshak [7], on the basis of literature data, gives the activation energy of the chain growth process as 12 kcal./mole for polyesters and 24 kcal./mole for polyamides. For phenol-formaldehyde resins, as determined in molding powders, $\underline{u}$ lies in the range of 7.2-16.6 kcal./mole, H from 18.8 to 23.8 kcal./mole, and the entropy of activation from 17 to 52 cal./mole. degree [1, 3].

In the reactions occurring according to Equations (2 and 4) between complex molecules in resins rolled with urotropine or resins of the resole type in molding powders, considerable redistribution of energy between all the degrees of freedom takes place. This leads to a decrease of the entropy of activation, i. e., a decreased probability of the formation of an activated complex, and hence to retarded hardening. The data in Table 3 show that molding powders of grades K-21-22, K-220-23, and K-211-2, which have more complex structure than Novolak resins, harden more slowly. The complex structure of these resins is confirmed experimentally by the absence of a clearly defined horizontal region on the curve in the initial stage of hardening.

The hardening process may be accelerated in the part of it which depends on the entropy of activation either by the use of resins of less branched structure, or by increase of temperature. In either case the probability of collision between the reacting particles will be increased, favoring acceleration of the hardening reaction.

The influence of steric hindrances, caused by the loose structure of xylenol and aniline-formaldehyde resins, on the hardening rates of molding powders K-112-2 and K-211-2 is confirmed by experiments illustrated by Fig. 9. The hardening rate of these molding powders increases with increase of shearing rate and rise of temperature. We believe that the reason for this is that shearing deformations destroy the loose structure of the resins and so remove the steric hindrances which prevent entry of the unreacted components into the reaction, and not an agitation effect [9, 10, and 11]; if the agitation effect prevailed over destruction, this effect would be greater at lower temperatures and it could be observed by deviations between the curves representing the variation of hardening rate with temperature. The experimental results shown in Fig. 9 indicate that these curves are almost parallel for different temperatures.

The experimental results given above show that, despite the great diversity of the chemical and physical composition of the substances contained in molding powders, they may be divided into two characteristic groups, depending on whether they react chemically with the resins or not. Depending on this, they have different effects on the technological properties of molding powders and the mechanical properties of the materials in the finished articles. The substances which react chemically with the resins influence the duration of the viscofluid state and the hardening rate of molding powders. If they react to form initial or intermediate resin products, the molding powder remains longer in the viscofluid state and has a lower viscosity coefficient, while the hardened material has a higher maximum shearing stress and relative deformation, indicating growth of the polymer chains as the result of the reaction. An example of this effect is provided by hexamethylenetetramine in molding powders of the resole type (Fig. 7), or furfural in Novolak molding powders (Fig. 6). If, however, cross linking of the polymer chains predominates in the reaction, the duration of the viscofluid state decreases, the viscosity coefficient in that state increases, while the maximum shearing stress in the hardened material increases and the relative deformation changes little or diminishes. An example of such cross linking of the polymer chains is provided by the action of magnesium oxide or lime when added to molding powders of the resole type (Curve 2 in Fig. 7 lies above Curve 1 along its entire length). Substances which do not react with the resins only cause an increase in the plasticity of the material at all stages of hardening and have practically no effect on the duration of the viscofluid state or the hardening rate (Fig. 5).

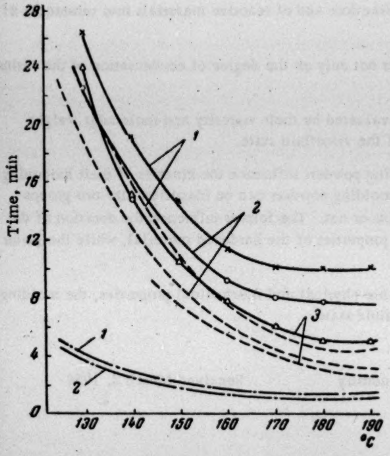

Fig. 9. Effect of shearing rate on the hardening time of molding compositions K-18-2 (dot-dash line), K-112-2 (broken line) and K-211-2 (continuous line): 1) full turn of the mold T = 2698 seconds; 2) T = 1350 seconds; 3) T = 295 seconds.

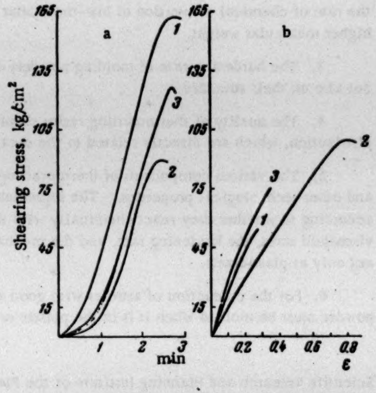

Fig. 10. Kinetics of the hardening reaction (a) and mechanical properties (b) of a Novolak molding powder at 170° made from oxidized resin: 1) molding composition based on oxidized resin; 2) K-18-2 (normal) molding composition; 3) molding composition based on oxidized resin with addition of furfural.

Oxidized resins have a loose structure, and molding powders made from them lose their viscofluid properties in the same rolling time as unoxidized resins (Fig. 10). Shearing deformations produce a strength increase (Curve 1 in Fig. 10, a); the mechanical properties of the material are inferior to those of the normal material (Curve 2, Fig. 10, b). Addition of furfural increases the duration of the viscofluid state and improves the mechanical properties (Curve 3, Fig. 10).

The relationships which have been found between the technological and mechanical properties of molding powders and the nature of the substances present in them can be used for studying the physicochemical processes occurring in resins at various stages in the production and processing of molding powders, and facilitate control of the technological processes. The choice of the optimum technological characteristics of molding powders must be made in relation to the technology of molding them into articles. Molding must take place while the material is in the viscofluid state. For example, despite the fact that a powder rolled for 230 seconds (Curve 4, Fig. 1) has a higher hardening rate (40 seconds) than a molding powder rolled for 210 seconds (63 seconds), it is not suitable for ordinary molding, as it has lost its viscofluid properties and a considerable higher pressure and greater time are required to attain the same density of the material in the finished article as is obtained from samples rolled for a shorter time, in which the duration of the viscofluid state is of the order of 30-40 seconds. Experience shows that molding powders having a viscofluid state lasting 30-40 seconds are of good quality and can be used for production of articles of complex form and large dimensions (radio receiver bodies) if molded with preheating. Small articles can be molded from powders with a lower duration of the viscofluid state. For example, electric bulb sockets of the best heat resistance, electrical properties, and external appearance are molded from powders the duration of the viscofluid state of which is ~ 10 seconds.

SUMMARY

1. The influence of physicochemical factors on the plasticity and reaction kinetics of thermostatting plastics during production of molding powders and their conversion into articles has been studied, and the structural changes occurring in the plastics during these processes have been elucidated.

2. The duration of the viscofluid state in molding powders is determined not by physical factors but by the rate of chemical conversion of low-molecular resin fractions and of reactive materials into substances of higher molecular weight.

3. The hardening rate of molding powders depends not only on the degree of condensation of the resins, but also on their structure.

4. The quality of thermosetting resins should be evaluated by their viscosity and molecular weight distribution, which are directly related to the duration of the viscofluid state.

5. The various components of thermosetting molding powders influence the kinetics of their hardening and other technological properties. The ingredients of molding powders can be classified into two groups according to whether they react chemically with the resins or not. The former influence the duration of the viscofluid state, the hardening rate, and the mechanical properties of the hardened material, while the latter act only as plasticizers.

6. For the production of articles with good and stable physical and mechanical properties, the molding powder must be molded when it is in the plastic or viscofluid state.

Scientifc Research and Planning Institute of the Plastics Industry
Moscow

Received March 2, 1956

LITERATURE CITED

[1] I. P. Losev and G. S. Petrov, Chemistry of Synthetic Resins (State Chem. Press, 1951).*

[2] A. A. Vansheidt, J. Chem. Ind., No. 7 (1954).

[3] I. F. Kanavets, Proc. Acad. Sci. USSR, 95, No. 6 (1954); Org. Chem. Ind., No. 7 (1940).

[4] I. F. Kanavets, Proc. 7th Conf. on High Mol. Compounds (Acad. Sci. USSR Press, 1952). *

[5] P. P. Kobeko, Amorphous Substances (Acad. Sci. USSR Press, 1952).*

[6] S. Glasstone, K. Laidler, H. Eyring, Theory of Rate Processes (Foreign Lit. Press, Moscow, 1948).*

[7] V. V. Korshak, Organic Chemical Methods in the Chemistry of High Polymers (1953).

[8] I. P. Mikheev, Molding Materials Based on Phenol-Formaldehyde Resins (State Chem. Press, Moscow, 1955).*

---

* In Russian.

[9] G. L. Slonimsky, V. A. Kargin, and L. I. Golubenkova, Proc. Acad. Sci. USSR, 93,2 (1953).

[10] L. A. Igonin, N. A. Krasulina, and V. A. Kargin, Colloid J., 17,4 (1955).

[11] G. L. Slonimsky, B. M. Kovarskaya and S. I. Klaz, Colloid J. 16,5 (1954).

ELECTRON MICROSCOPE STUDIES OF COLLOIDS

1. MINERALS OF THE KAOLINITE – HALLOYSITE GROUP

M. I. Kuadzhe

The main mass of finely dispersed clay materials consists of kaolinite, halloysite, montmorillonite, illite, and other closely related minerals. These clay minerals usually compose the fine fractions of clays, muds, soils, etc. (0.005 – 0.001 mm and less), and therefore study of them presents considerable difficulties.

Detailed analysis of clay minerals necessitates the use of a number of modern physicochemical methods of investigation. One such method is electron microscopy, which has been widely used in recent years for studying the mineral composition of various clays [1-3].

Methods of investigation. A 1-3 g sample was soaked in distilled water in a porcelain basin; after kneading with the fingers and stirring it was transferred to a beaker 200-300 ml in capacity. After 24-48 hours the top layer of the suspension (10-15 cc) was carefully poured off and the suspension was diluted with distilled water to a slight opalescence. A drop of the suspension was transferred onto a collodion film on a wire screen fixed in the specimen holder, and dried in air or in a thermostat at 20-25°. The quality of the specimen was checked by examination under the microscope to confirm that the film is suitable for the work, i. e., that it is not too thick, not torn, and not warped. The dried specimen was examined under the electron microscope. After evacuation, an image of the object was examined on a fluorescent screen and characteristic regions of the specimen were photographed.

EXPERIMENTAL DATA

Certain electron micrographs of fine clay fractions are given below; these are mainly of the kaolinite and halloysite groups and their mixtures (the photographs were taken by V. M. Lukyanovich and A. V. Bogdashevsky, to whom the author is deeply grateful).

The plate shows electron micrographs (1, 2, 3, 4, 5) of fine fractions (< 1 μ), of typical kaolinite minerals of Glukhovets, Balai, Kumak, and Prosyanaya clays, which clearly show hexagonal plates of kaolinite of various thicknesses and sizes, with internal angles from 106 to 140°, similar to those found in coarser fractions of kaolinite minerals. Careful examination of the micrographs reveals, in addition to these particles, also mica-like scales of various thicknesses and sizes, irregular in shape, and thinner at the edges. Fragments of kaolinite of these varieties are also seen, with their primary form partly retained and partly lost. Allowing for maximum accumulation of the plates, the thickness of the plates is estimated at about 20 mμ, which agrees with x-ray estimations. The diameter of the plates is 0.1 – 0.5 mμ. Electron micrographs of Kavpov (6), Pologoe (7) and Yantsensk (8) clays show that these clays consist mainly of kaolinite with small amounts of halloysite.

Examination of the electron micrograph of the fine fraction (< 1 μ) of white Zhuravlinsk clay (9) reveals halloysite crystals of acicular form, elongated, narrow and thin plates, and possibly also tubes evenly sheared off at the ends, sometimes grown together as twins at an angle. The specimen of clay (9) examined contained little or no kaolinite, and therefore Zhuravlinsk clay can be regarded as a typical halloysite. This is in good agreement with results obtained by the thermal, x-ray, and other methods of analysis. Thus, visible crystals of halloysite were first found by us in 1948 in Zhuravlinsk, Yantsensk, Pologoe and Karpov clays.

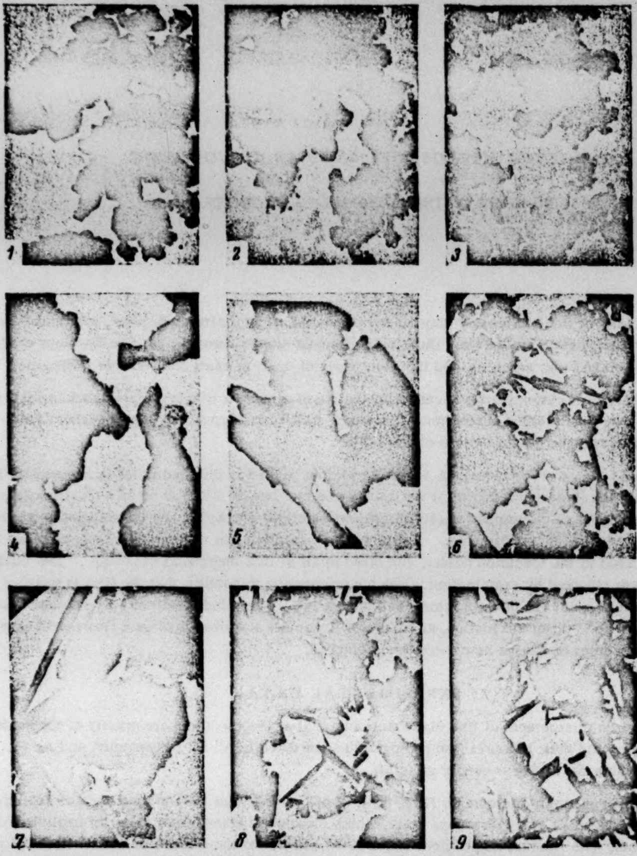

Electron micrographs of fine clay fractions: 1) Glukhovets kaolinite (x 8000); 2) Balai kaolinite (x 8000); 3) Kumak clay (x 8000); 4) Prosyanaya kaolinite (x 17000) 5) ditto, after heating to 700° (x 20000); 6) Karpov kaolinite with halloysite (x 8000); 7) ditto, Pologoye (x 25000); 8) ditto, Yantsensk (x 8000); 9) Zhuravlinsk halloysite (25000).

Halloysite forms clearly defined cryptocrystals,closely resembling nontronite crystals * but differing from the latter in having smooth and even edges. Burton and Kohl [1] report that, under a magnification of 44,000 most of the plates are ~ 1 μ long and 1 / 20 μ wide. This distinguishes halloysite from kaolinite, the crystals of which are hexagonal plates.

Changes of the particle shape of clay minerals on increase of temperature are of considerable interest, as the adsorptive and catalytic properties of clays depend on these to a considerable extent. A typical Prosyanaya kaolin was chosen as an example. The specimens were kept at a definite temperature in a thermostat, and then examined under the electron microscope. It was found that a specimen heated at 200° showed no appreciable changes of particle shape. The same specimen, heated at 700° in a thermostat for

---

* According to Bakulova [2], nontronite consists of a mass of elongated splinterlike thin crystals up to 0.3 μ long with sharp and splitting ends of thicker and larger grains or aggregates of irregular and isometric form with diffuse edges.

4-5 hours (Micrograph 5) changed appreciably, and acquired the shape of montmorillonite particles. The adsorptive and catalytic properties of the substance changed also.

Thus, the electron microscope can be used to distinguish the shape, dimensions, and relative thicknesses of particles and to estimate the degree of homogeneity and dispersion of the substance under investigation. The main grounds for assigning a clay substance to a given mineral class are the particle shape and the sharpness of the particle outlines. Kaolinite and halloysite minerals have particles with sharp contours, while minerals of the montmorillonite group usually have particles with diffuse contours.

Kaolinite, halloysite, montmorillonite and others are relatively easily identified in finely dispersed clay fractions under the electron microscope. It is very difficult to distinguish montmorillonite from beidellite, while the latter may be confused with hydromica, which forms elongated plates.

SUMMARY

1. The specimen of fine Zhuravlinsk clay fraction examined was halloysite. White Karpov, Yantsensk and Pologoe clays consist of kaolinite and halloysite.

2. Specimens of fine fractions of Glukhov, Glukhovets, Prosyanaya, Balai and Kumak clays were found to be typical kaolinites and did not contain halloysite.

3. When Prosyanaya kaolinite is heated at 200° its crystal form is unchanged; heating kaolinite at 700-800° alters its original crystal form and also the adsorptive and catalytic properties.

The M. V. Lomonosov State University
Moscow
Faculty of Chemistry

Received October 19, 1955

LITERATURE CITED

[1] M. Arden, K. Endell, U. Hofmann, Betrich Keram. Gesel., Bd. 21, No. 6, (1940); F. Burton, W. Kohl, The Electron Microscope,(New York, 1942).

[2] B. N. Vertener, Factory Labs., No. 6 (1945); M. F. Vikulova, Soviet Geology, No. 39 (1949); Trans. All-Union Sci. Res. Geol. Inst., No. 2 (1950); Electron Microscopy of Clays (State Geological Press, 1952).

[3] M. I. Kuadzhe, Questions of Petrography and Mineralogy, vol. II (Acad. Sci. USSR Press, Moscow, 1953); Trans. Mineral. Museum, No. 5 (1953); V. T. Bykov, V. M. Lukyuanovich, L. V. Radushkevich, Bull. Acad. Sci. USSR, Div. Chem. Sci., No. 3 (1952).

THE MECHANISM OF PROTEIN DENATURATION

10. EFFECT OF FATTY ACID ANIONS ON THE STABILITY OF GLOBULAR PROTEINS TO DENATURATION

A. L. Loseva and A. S. Tsyperovich

During the last 8-10 years the view has become established in the literature that salts of organic fatty acids with small nonpolar radicals ($C_4 - C_9$), are effective stabilizers of globular proteins, especially serum albumin. There have been several investigations [1, 2] of the stabilizing effects of such salts as sodium caprylate, heptylate, caproate, and valerate on globular proteins. These investigations were related with the need of certain states to provide their armed forces, operating in tropical conditions, with thermostable blood protein preparations [3]. It was found that salts of fatty acids raise the coagulation temperature of serum albumin and prevent viscosity increases and turbidity in its solutions on heating [4]. These observations were directly related to aggregation phenomena, and are therefore not entirely convincing. It was possible, however, that in some instances strengthening of the macromolecular structure of the protein (inhibition of denaturation proper) does occur, as salts of fatty acids decreased the usual viscosity increase produced by 6 M urea in serum albumin, in conditions in which aggregation reactions are improbable [5]. The magnitude of the effect increased with lengthening of the hydrocarbon radical in the salt molecule. These and other facts [6, 7] led to the opinion that fatty acid salts exert a stabilizing effect on proteins.

Subsequently the binding of fatty acid anions by serum albumin was studied by various, including some direct, methods; it has been demonstrated by the ultrafiltration method [8], by the increase of the electrophoretic mobility of proteins in presence of these substances [9], and by equilibrium dialysis, whereby the reversible bonding of small amounts of salts with tagged carbon (C^{14}) in the carboxyl was detected [10]. It was established that the bonding was of a nonpolar character, and its stability increased with increasing length of the anion chain.

The principal defect of these investigations is that the true influence on denaturation was not studied in any of them. Observations of viscosity changes, turbidity, or coagulation in protein solutions would mainly indicate postdenaturation processes. Therefore the true nature of the action of salts on protein stability (on the course of denaturation proper) cannot be regarded as established.

In view of this, it was decided to study the influence of fatty acid anions separately on denaturation proper and on the postdenaturation aggregation of denatured molecules, with special attention to the main phase of the process (denaturation proper). This was the only possible way of determining the true influence of the substances studied on the stability of the macromolecular protein structure.

Materials and methods. Three globular proteins were used for the experiments: serum and egg alumins and edestin. The first two proteins were prepared by Baranovsky's method [11], with double recrystallization; crystalline edestin was prepared by Osborne's method [12]. The proteins were generally used at 2.3-2.8% concentrations in the experiments.

The action of the sodium salts of caproic and nonylic acids on the proteins was studied. The acids were converted into salts by neutralization with caustic soda, by a standard procedure described elsewhere [13]. In the experiments, to 10 ml of the protein solution 0.5 ml of 1 M phosphate buffer at pH 7.4 was added, followed by 0.5 ml of 1 M solution of the fatty acid salt (sodium nonylate). The final salt concentration was 0.045 M.

This corresponded to the concentrations generally used in various investigations for stabilization of serum albumin. The amount of sodium caproate used was 2-3 times as large, to obtain a more pronounced action. The amount of salt to be used was generally determined by preliminary experiments. The same volumes of water were added to control specimens, containing the same amounts of protein and buffer.

The denaturation was effected by heating. The course of the process was determined by isolation of the denatured protein by isoelectric precipitation (denaturation proper) and findingits amount by the biuret reaction. The isoelectric precipitation tests for all three proteins did not differ from the usual tests [14, 15]. Variations in the course of aggregation processes were observed by the viscosity changes measured by means of the Ostwald viscosimeter. After addition of the salt or after its prolonged action on the samples the pH was always checked to determine whether the reaction of the medium had changed.

The experiments were started with studies of the action of salts on serum albumin, as this protein was the main material used in all studies of the stabilizing action of fatty acid anions. The first experiments were with sodium nonylate. The hydrocarbon radical of this salt differs by only one CH_2 group from the more frequently used caprylate. For comparison, a salt of a fatty acid with a shorter hydrocarbon radical, sodium caproate, was used.

After addition of the fatty acid salt, samples were immediately taken from the experimental and control mixtures and their contents of denatured protein determined. This gave the first point on the curve. The experimental and control mixtures were then placed in a water bath and the course of denaturation was followed by taking samples at definite time intervals (15 and 30 minutes, 1 hour, 2 hours, etc).

The basic fact described in all investigations was first reproduced. The experimental and control solutions were heated at various relatively high temperatures (80-90°). The solution containing nonylate remained without visible change, while in the control (without nonylate) the protein was completely denatured. It appeared that addition of the salt increases the stability of the albumin.

The experiment was then performed with mild heating (50°), when neither solution changed in appearance, and the course of denaturation proper was followed by isolation of the denatured part of the protein by isoelectric precipitation. Even the first experiments yielded a clear and apparently unexpected result. It was found that addition of the fatty acid not only does not increase the stability of serum albumin but, on the contrary, diminishes it, sharply accelerating denaturation.

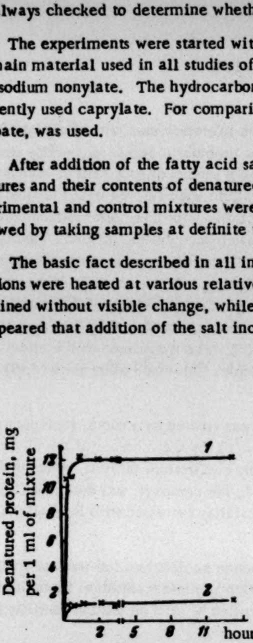

Fig. 1. Denaturation of serum albumin by heating at 50°: 1) with sodium nonylate; 2) without sodium nonylate.

Figure 1 illustrates a typical experiment; this shows that addition of nonylate causes rapid formation of a considerable amount of insoluble protein, which is easily isolated from the outwardly unchanged "stabilized" mixture; it comprises ~ 12 mg of the 25 mg (in 1 ml of solution) taken for the experiment. The salt therefore acts as a denaturant. The reaction occurs only to a slight extent in the control sample.

Figure 2 represents an analogous experiment, but here the temperature was gradually raised, the protein being heated first at 50°, and then at 65, 75, and 85°. It is seen that in the sample with nonylate a considerable amount of denatured protein is formed very rapidly and this gradually increases with rise of temperature. Denaturation in the control sample followed the normal course; the amount of protein passing into the insoluble form increased with increase of temperature.

These results naturally suggest that the fatty acid anion acts on the protein only by preventing or weakenin the aggregation of denatured molecules, i. e., postdenaturation changes. Since aggregation is the main cause of increased solution viscosity, this suggestion was verified by measurements of viscosity increases during denaturation in presence of sodium nonylate and under normal conditions (without the salt). The experimental conditions were chosen so that it was possible to study changes in the protein in solutions in which no coagulation occurred at all (pH ~ 7; temperature 72-75°; protein concentration 2.5%) .

A typical experiment is illustrated by Fig. 3, a, which shows the effect of nonylate on postdenaturation aggregation in serum albumin solutions. There is almost no increase of viscosity in the experimental mixture although, as is already known, denaturation occurs in it very rapidly. In the control (without nonylate) aggregation proceeds normally, and the viscosity increases. Both solutions changed little in external appearance, and only their opalescence increased slightly. On stronger heating (85-95°) the protein in the solution without nonylate coagulated, while in the experimental solution there was no visible change. These observations directly confirmed that the fatty acid salt retards secondary aggregative changes in the denatured particles, preventing or greatly weakening aggregation reactions.

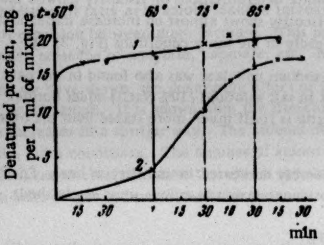

Fig. 2. Denaturation of serum albumin by heating at 50, 65, 75, and 85°: 1) with sodium nonylate; 2) without sodium nonylate.

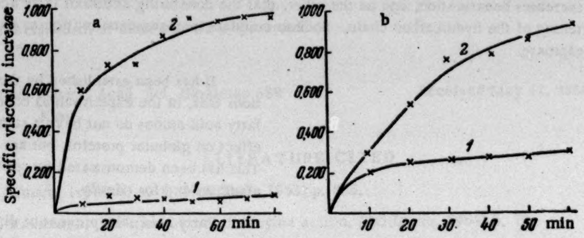

Fig. 3. Effect of sodium nonylate on postdenaturation aggregation in solutions of serum (a) and egg (b) albumins; 1) with nonylate ; 2) without nonylate.

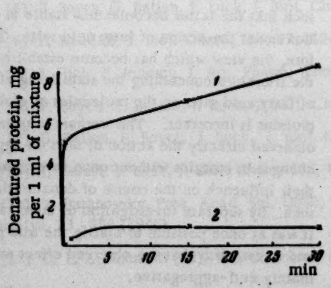

Fig. 4. Denaturation of egg albumin by heating: 1) with sodium nonylate; 2) without sodium nonylate.

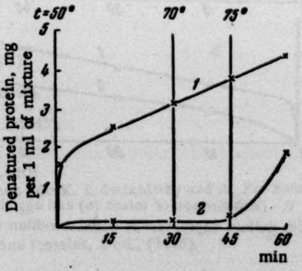

Fig. 5. Denaturation of edestin by heating at 50, 70, and 75°: 1) with sodium nonylate; 2) without sodium nonylate.

The facts established for serum albumin were fully confirmed in studies of the action of fatty acid anions on egg albumin and edestin. Figure 4 shows that denaturation is sharply accelerated immediately after addition of sodium nonylate to egg albumin. The process is so rapid that a considerable amount of denatured protein can be isolated by isoelectric precipitation immediately after addition of the salt solution; the amount increases on further heating. External changes in the experimental and control solutions may not occur if the heating is not very strong (50-55°). However, separate determinations of viscosity showed that the viscosity changes very little in presence of nonylate (the viscosity shows almost no increase throughout the process). The viscosity of the control solution increases rapidly in the same conditions (Fig. 3, b).

A sharp decrease of protein stability under the action of sodium nonylate was also found in the case of edestin. The experiments with this protein were carried out in salt solutions (10% NaCl) under normal conditions [15], but at higher temperatures, as in this case edestin is itself much more stable than the other proteins studied.

Figure 5 shows that addition of the fatty acid salt considerably decreases its stability to heat. Edestin, like the other proteins, was protected from coagulation (the postdenaturation reactions were diminished). The magnitude of this effect depended on the added salt.

The action of a fatty acid salt with a shorter hydrocarbon radical, sodium caproate, was then studied. As has been stated, this salt has appreciably less reactivity toward proteins. It seemed likely that the observed effect – decrease of the stability of the macromolecular structure to denaturation – will be much less pronounced with the use of sodium caproate. This was confirmed by experiments with two proteins.

In the case of serum albumin (Fig. 6, a) the amount of denatured protein after addition of the salt always exceeded the control value; however, it was considerably less than in the action of nonylate under the same conditions. An analogous result was obtained for egg albumin (Fig. 6, b). It was therefore shown, on the one hand, that caproate increases denaturation, and on the other, that the denaturing action of fatty acid salts diminishes with shortening of the hydrocarbon chain. Sodium nonylate increases denaturation to a much greater extent than sodium caproate.

It has been established by these investigations that, in the experimental conditions used, fatty acid anions do not have a stabilizing effect on globular proteins, but are denaturants. This has been demonstrated for serum and egg albumins and for edestin.

Fatty acid salts prevent or diminish secondary (aggregative) changes in denatured molecules, thereby giving the impression of protein stability. Their effect on the macromolecular structure of the protein is, however, such that the latter becomes less stable to denaturation under the action of fatty acid salts. Therefore, the view which has become established in the literature concerning the stabilizing effect of fatty acid salts on the molecules of globular proteins is incorrect. The workers in question observed directly the action of salts on aggregative changes in proteins without once investigating their influence on the course of denaturation as such. By separate investigation of these stages it was at once possible to clarify the true position and to establish that the observed effect was mainly anti-aggregative.

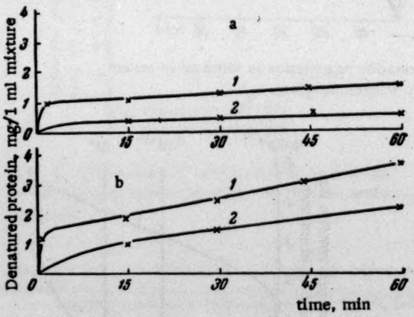

Fig. 6. Denaturation of serum (a) and egg (b) albumin: 1) with sodium caproate; 2) without sodium caproate.

Both effects – the denaturing effect of the salt, and the protection of the denatured protein against aggregation – are apparently fairly easily explained. The anions are bound by the protein and decrease the stability of the macromolecular particle structure as the result of addition of a considerable number of negative charges (COO^- groups of the fatty acid), and also by interaction of the nonpolar radicals with the hydrophobic regions of the protein molecule. The first factor probably results in a stress in the macromolecular structure owing to repulsion of the negative charges, while the second weakens and even ruptures the stabilizing bonds in the hydrophobic regions owing to incorporation of long hydrocarbon chains. There are various possibilities, but it is clear that in any event the action of fatty acid anions must be similar to the action of detergents.

Addition of fatty acid anions leads to increase of the total negative charge on the protein molecules; forces of repulsion between them increase. This probably accounts for the decreased aggregation of the denatured particles in presence of nonylate, caproate, etc. In such cases fatty acid salts act as alkalies.

As we have shown, the denaturing effect of fatty acid salts increases sharply with increasing hydrocarbon radical chain length. It is known from the literature that the stability and extent of anion bonding by the protein increases in a similar way. The amount of butyrate is only 15-20% of the amount of caprylate bound under the same conditions. The number of anions attached to the protein will be much greater in the latter case. It is reasonable to assume that this is the reason for the greater labilizing action of salts containing radicals with longer hydrocarbon chains.

SUMMARY

1. Fatty acid salts ($C_4 - C_9$, of the sodium caprylate type) do not exert a stabilizing effect on serum albumin and other globular proteins.

2. Fatty acid anions decrease the stability of the macromolecular structure of serum and egg albumins and of edestin and intensify denaturation; i. e., they are denaturants, and they weaken the secondary (aggrevative) changes in the denatured molecules.

3. The denaturing action of fatty acid salts increases with the size of the hydrocarbon radical in the anion.

4. The mechanism of these effects is discussed.

Institute of Biochemistry, Acad. Sci. Ukrainian SSR
Kiev

Received May 12, 1956.

LITERATURE CITED

[1] F. Putnam, Proteins, v. 1, (New York, 1953) p. 825.

[2] W. Kausmann, The mechanism of enzyme action, (Baltimore, 1954) p. 70.

[3] J. Edsall, Adv. Protein Chem. 3, 383, (1947).

[4] P. Boyer, F. Lum, G. Ballon, J. Luck, R. Rice, J. Biol. Chem. 162, 181, (1946).

[5] P. Boyer, G. Ballon, J. Luck, J. Biol. Chem. 162, 199, (1946).

[6] F. Kendall, J. Biol. Chem. 138, 97, (1941).

[7] J. Hink, F. Johnson, J. Am. Pharm. Assoc., 40, 537, (1951).

[8] P. Boyer, G. Ballon, J. Luck, J. Biol. Chem. 167, 407, (1947).

[9] G. Ballon, P. Boyer, J. Luck, J. Biol. Chem., 159, 111, (1945).

[10] J. Teresi, J. Luck, J. Biol. Chem. 194, 823, (1952).

[11] T. Baranovsky, Proc. Acad. Sci. USSR, 28, 723 (1940); see also K. I. Strachitsky and A. Yu. Kologrivova, Biokhimiya, 11, 385 (1946).

[12] C. L. A. Schmidt (ed), The Chemistry of Amino Acids and Proteins, 2 ed., (1945).

[13] A. L. Loseva, "Investigation of Some Questions of Stabilization of Globular Proteins", dissertation (Acad. Sci. Ukrainian SSR, Kiev, 1956).

[14] A. S. Tsyperovich, Ukrain. Biochem. J., 20, 108 (1948); 21, 44 (1949).

[15] A. S. Tsyperovich and A. L. Loseva, Biokhimiya, 21, 53 (1956).

GELATION OF LATEXES ON POROUS FORMS

D. M. Sandomirsky

A number of processes for the production of rubber articles from latex are based on the formation of a rubber gel either by slow formation of various cations in the latex (gelation in the true sense) or by diffusion into the latex of cations from the surface of the form coated with a suitable solution (known as ionic deposition), or from a metallic anode (electrodeposition) [1-3].

In addition to these methods another process is used in practice, in which destabilization of the globules by the action of ions is not used. This is the production of articles in porous molds or forms, for example, made of plaster [4-6]. In this method the latex mixture is poured into a dry plaster form the inner cavity of which has the shape of the required article. After some time the latex mixture is poured out, and the gel remaining on the walls of the form is then dried and vulcanized.

The main cause of gel formation in this case is evidently the absorption of the dispersion medium of the latex by the pores of the form. Although the production of latex articles in porous forms is used fairly widely in the rubber industry abroad, it has not so far been systematically studied.

The present communication contains the results of an investigation of the influence of the nature and concentration of the latex, duration of deposition, and temperature, on the course of the deposition and on certain properties of the gel.

EXPERIMENTAL DATA•

The deposition was effected on cylindrical plaster of Paris forms 16-18 mm in diameter and with working portions 45 mm long, made from analytical grade calcium sulfate. Two types of natural latex were studied: unconcentrated latex with 34.6% dry content, and vulcanized "Revultex" concentrate (60.4%). Attempts to obtain deposits from Revertex (concentrate made by evaporation) and SKS-30 butadiene – styrene synthetic latex were unsuccessful owing to the looseness of the gel formed.

The dried plaster form was immersed to a definite depth in the latex and removed after a certain time; the gel was rinsed, removed from the form, weighed, and dried at 80° to constant weight. The amount of rubber deposited per 1 cm^2 of the form surface and the concentration of the gel were calculated. It should be noted that the gels formed on porous forms differ from gels produced by, say, ionic deposition, in being more loose and not having a clearly defined boundary with the latex.

The Figure shows the kinetics of deposition of rubber from Revultex and unconcentrated latex at different temperatures. The amount of rubber deposited and the rate of deposition increase with increasing latex concentration and temperature. It was observed during these experiments that the concentration of the gel formed is independent of the concentration of the original latex, of the duration of deposition, and of the temperature.

To test the effect of latex concentration on the amount and concentration of the gel formed, experiments were carried out on deposition of gel from Revultex, diluted with distilled water to various concentrations, for 15 minutes. The results are given in the Table.

• G. Baibakova and I. Shmurak, students at the Lomonosov Institute of Fine Chemical Technology, assisted in the experimental work.

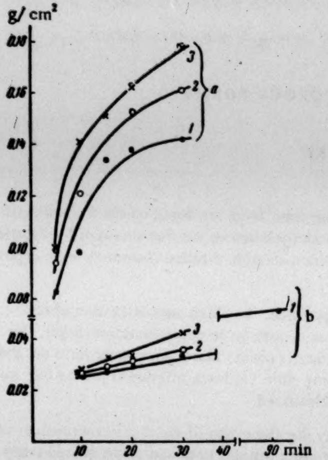

Kinetics of deposition of rubber on a plaster form from Revultex (a) and unconcentrated latex (b):
1) at room temperature; 2) at 40°; 3) at 60°.

DISCUSSION OF RESULTS

The processes which occur when the latex comes into contact with a porous surface (with pores smaller than the latex globules) may be represented as follows. When the latex comes into contact with the porous wall, the latter begins to absorb the dispersion medium. The concentration of the adjacent latex layer gradually increases, and a moment is reached when the globules come into continuous contact. Evidently this limiting concentration will not depend on the initial concentration of the latex, but will be determined by general geometrical considerations.

In fact, as is shown above, gels formed from Revultex at different dilutions and from unconcentrated natural latex differ relatively little in concentration, although the latex concentrations are very different. The gel concentration is close to the degree of space filling in close packing of spheres of equal diameters (74.05%). The absence of any appreciable influence of temperature on the gel concentration is explained by the same considerations. Increase of temperatur accelerates the dehydration process, but the gel is always formed at practically the same concentration.

After a gel layer has been formed directly on the plaster surface, dehydration of the latex layers further from the form proceeds by diffusion of the serum through the gel layer. This retards the process somewhat, as is confirmed by the nature of the kinetic curves. Because of this, there is at any given instant a concentration gradient in the gel, from a greatest value at the form wall to greatest dilution at the opposite surface of the gel. It was stated above that gels formed by dehydration at a porous surface have no sharp boundary with the latex. There is rather a gradual transition from latex through a thick paste to the gel.

Effect of Latex Concentration on the Amount and Concentration of the Gel Deposited

Type of latex	Latex concentration in %	Amount of gel in g/cm²	Gel concentration in %	Average concentration of gel from Revultex, %
Revultex	60.4	0.092	69.0	70.5
	49.8	0.067	73.5	
	40.1	0.058	71.4	
	28.9	0.047	69.9	
Latex	34.6	0.014	64.1	

The above considerations are supported by the fact that the gel concentration decreases somewhat with increasing time of deposition. The existence of a limiting concentration in rubber gels was also found by us in the syneresis, in water, of a gel formed by gelation of a "Nairit" latex by means of zinc oxide [7]. The effect also occurs in the syneresis, in water, of natural latex coagulum in the production of rubber in plantations [8].

Thus the partial destabilization of latex globules, leading to formation of a gel with a network structure, occurs not only as the result of changes in the protective layer by interaction with electrolytes, but also by close contact between the globules. The strength of the gels so formed is a sign of breakdown of the layers and of contact between the rubber contained in the globules at these points. The presence of large amounts of protective substances in the latex (as in Revertex or SKS-30) prevents close packing and formation of a firm gel.

It seems likely that gel formation in consequence of close packing of the globules occurs not only when a rubber gel is dehydrated at a porous surface, but also when films are made from latex by drying the latter. Gel formation is probably the first stage of this process.

SUMMARY

1. The deposition of rubber from latex on a porous surface has been studied.

2. The amount of rubber deposited depends on the concentration of the latex, the duration of contact with the porous surface, and the temperature.

3. The concentration of the gel formed does not depend on the latex concentration or the conditions of deposition, and is close to the degree of space filling in close packing of spheres of equal diameters.

The M. V. Lomonosov Institute of Fine Chemical Technology
Moscow

Received May 31, 1956

LITERATURE CITED

[1] S. S. Voyutsky and B. V. Shtarkh, Physical Chemistry of Film Formation from High Polymer Dispersions (State Light Ind. Press, 1954), p. 110.*

[2] D. M. Sandomirsky and V. V. Chernaya, Trans. Sci. Res. Inst. Rubber Ind., No. 1, 20 (1954).

[3] B. Dogadkin and D. Sandomirsky, Trans. VI Mendeleev Conf., Vol. 2, No. 3 (1933).

[4] S. C. Stokes, Trans. I. R. I. 25, 407, (1950).

[5] N. J. Jarman, Rubber Age 67, 68, (1950).

[6] A. A. Round, Rubber Age a. Synth. 33, 169, (1952).

[7] D. Sandomirsky, in Symposium "Production and Applications of Synthetic Latexes" (State Chem. Press, 1953), p. 33.*

[8] Th. G. F. Schoon, Chem. Abstr. 48, 13255, (1954).

---

* In Russian.

THE THIXOTROPIC PROPERTIES OF CERTAIN PRINTING INKS*

A. A. Trapeznikov and T. G. Shalopalkina

Printing inks are structurized colloidal systems with a complex combination of structural and mechanical properties, including fairly pronounced thixotropy.

These properties, including the thixotropy of disperse systems, have been studied by many workers [1-13]. A number of authors plotted hysteresis loops and evaluated thixotropy from the viscous properties only [4-8]. Others [9-11] studied strength properties only, without consideration of the viscous properties. There have been hardly any investigations covering methods for evaluating the thixotropy of systems at various stages of deformation, both by strength and by viscosity. In consequence, the role of each of these stages in evaluation of the complex combination of thixotropic properties has not been determined.

In work on oleophilic aluminum naphthenate gels [12], both strength and viscous properties were studied; after the maximum on the stress – deformation curve, corresponding to the strength of the structure, had been passed, a constant shearing stress became established, corresponding to steady flow, with a corresponding viscosity value.

Two samples of newspaper inks have been similarly studied in the present investigation. However, owing to some structural characteristics of these systems, their rheological properties were different from the corresponding properties of aluminum naphthenate gels. It was found that the shearing stress reached after the strength maximum (yield value) after not too long a time must be regarded as not a true equilibrium, but only a quasi-equilibrium value, which depends on the velocity gradients to which the system had previously been subjected. These characteristics can be represented by the so-called hysteresis loops. Thus by our investigations it was possible to elucidate more fully the thixotropic characteristics of different systems related to their structural differences, and also to combine methods for evaluating thixotropy based on strength and viscosity determinations.

The two newspaper inks, supplied by the Sci. Res. Inst. of the Polygraphic Industry and Technology, had the following compositions: No. 787 – furnace black 16%, fused induline 16%, black marine oil 68% (ink rated as nondusting); No. 788 – channel black 9%, fused induline 19%, black marine oil 72% (ink rated as dusting).

The structural and mechanical properties were studied by means of a compound elastoviscosimeter [12, 13] further modified in some details. The outer cylinder was rotated at a constant rate Ω = const. Cylinders of the following dimensions were used in systematic determinations: outer cylinder, radius $R_2 = 1.495$ cm, height $L_2 = 12.0$ cm; inner cylinder (longitudinally fluted, with a concave hemispherical base), radius $R_1 = 1.420$ cm, height $L_1 = 7.96$ cm. In some instances an inner cylinder was used with $R_1 = 1.404$ cm, with a thermocouple fixed flush with its fluted side surface for measurement of the cylinder surface temperature. An ultrathermostat was used to regulate the temperature of the instrument ($t = 20° \pm 0.1$). The torque at the inner cylinder arising at different velocity gradients in this series of experiments was measured with the aid of wires with elasticities C_0 from $10.13 \cdot 10^4$ to $12.9 \cdot 10^6$ dynes-cm/radian. This made it possible to measure shearing stresses from 10 to 30,000 dynes/cm^2; the velocity gradient was varied stepwise over a wide range by means of a gear box system. The angle of displacement of the inner cylinder was read off by means of a light spot reflected from a mirror. The outer cylinder was started and stopped by means of an electromagnetic clutch.

---

* The investigation was suggested by the Scientific Research Institute of the Polygraphic Industry and Technology.

RESULTS AND DISCUSSION

Since printing ink is used under high velocity gradients in printing, and undergoes considerable structural breakdown in the process, the properties of the inks were studied at relatively high velocity gradients.

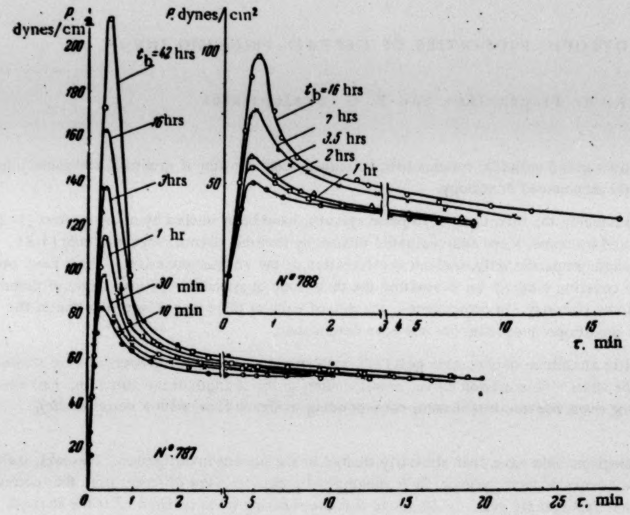

Fig. 1. P – τ curves for inks No. 787 and 788 at C = 0.192 sec. $^{-1}$.

A characteristic property of thixotropic systems is the formation, by the particles of the disperse phase, of structures with resistance to shear, which are broken down by mechanical forces and restored after a period of rest. Increase of the strength of the structure during rest is one of the characteristics of its restoration.

The inks studied in this work have clearly defined resistance to shear, as shown by the stress maxima P_r formed on the stress – time (P – τ), curves plotted for a constant rate of rotation of the outer cylinder[†] (the Ω const. method).

Figure 1 shows P – τ curves for different times of restoration of the structure of inks No. 787 and 788 after prolonged deformation at a velocity gradient G = 0.192 sec. $^{-1}$.

A constant value of the shearing stress after the maximum P = P_r and partial breakdown of the structure ought to correpond to equilibrium established between the structures additionally broken down and restored in flow, and determine the steady flow viscosity. However, it is seen (Fig. 1) that the shearing stress continues to decrease on prolonged rotation of the outer cylinder (τ). This slow decrease of the shearing stress was observed, for example, in ink No. 788 with longer rotation of the cylinder than that shown in Fig. 1 (see Table).

τ, min	1	5	10	30	60	90	120
P_s* dynes/cm²	44.0	39.0	38.4	36.4	35.9	35.4	34.9

[†] In these experiments, for easier measurement of changes of stress for short deformation times with an incompletely restored structure, a wire of relatively low rigidity C_0 = 101300 dynes · cm / radian was used. For this reason the initial regions of the P – τ curves refer to a not quite constant deformation rate, but to one becoming established only gradually.

Therefore a true equilibrium value of P_s is not reached in 2 hours. It is seen from the curves in Fig. 1 that when the system is at rest the increase of P_r is accompanied by increases in the values of P_s^*, which refer to the same periods of rotation of the cylinder, for example, to τ = 5 minutes (which is about 10 times as much as the time required to reach the maximum). These values of P_s^* we shall term quasiequilibrium, in distinction from the true equilibrium P_s. Fig. 2 gives curves representing structural buildup at rest, $P_r - \tau_b$ and $P_s^* - \tau_b$, where τ_b is the time of restoration or buildup of the structure. These curves show that the strength of the structure greatly increases during rest, but does not reach a completely constant value even after 42 hours.

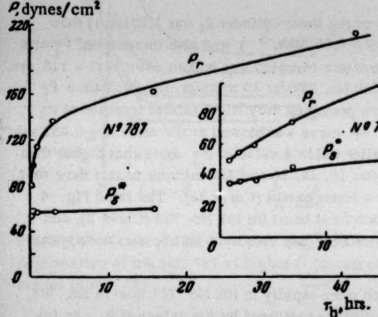

Fig. 2. Variation of P_r and P_s^* with the time of structural buildup in inks No. 787 and No. 788.

The descending part of the $P - \tau$ curve (Fig. 1) represents breakdown of the continuous structural network. The slow decrease of P far beyond the maximum on the $P - \tau$ curve indicates very protracted breakdown of the structure, which should be attributed to breakdown of separate aggregates of particles and fragments of the continuous network. It is natural to suppose that a certain true equilibrium value should be reached with much greater deformation times. At the same time we can obtain values for P_s^* at G = 0.192 sec.$^{-1}$ much lower than the true P_s by breaking down the system by a much greater velocity gradient. Then P_s^* will increase and approach the true value during restoration of the structure even from lower values of P_s^*. This is illustrated by ink No. 788, broken down at G = 433 sec.$^{-1}$, and then measured at G = 0.192 sec.$^{-1}$ or after every 15 minutes of rest (Curve 1, Fig. 3) or with continuous rotation of the outer cylinder (Curve 2, Fig. 3). In the latter case the experiment was continued for only 3.5 hours and during this time P_s^* rose continuously and tended to a certain limit, reaching only 18.2 dynes/cm^2, a value considerably lower than the value of P_s^* reached at the same value of G in 2 hours rotation in a system with an undestroyed structure (34.9 dynes/cm^2)(see Table). Therefore the true equilibrium P_s lies between the values of 34.9 and 18.2 dynes/cm^2, reached during decreasing and increasing P_s^* within this time of rotation.

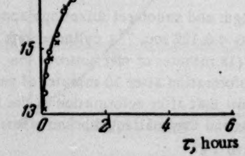

Fig. 3. Restoration of structure in ink No. 788, broken down at G = 433 sec.$^{-1}$ Description in text.

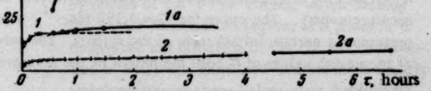

Fig. 4. Restoration of structure in ink No. 787 (1, 1a, and 1b), and No. 788 (2 and 2a). Description in text.

The explanation of the difference between Curves 1 and 2 in Fig. 3 is that during each 15 minutes of rest (Curve 1) the structure is restored appreciably, possibly even to a greater extent than would correspond to the true equilibrium value of P_s. For this reason Curve 1 ascends continuously. Therefore curves of the type of Curve 2 in Fig. 3 are of special significance for finding and establishing the true value of P_s. It is evident that such a curve for structure restoration with continuous rotation in principle represents only the value of P_s^*, as in such conditions of deformation a continuous network, determining P_r, cannot be formed. Any $P-\tau$ curve, however, obtained even after a minimum period of rest and structural buildup in static conditions, could in principle have a maximum P_r, relating to breakdown of the rapidly restoring elements of the structural network.

The curves in Fig. 4 (in these measurements the radius of the inner cylinder R_1 was 1,201 cm) show increases of P_s^* on continuous rotation of the outer cylinder ($G = 0{,}052$ sec.$^{-1}$) and also increases of P_s^* and appearance of P_r after rest in inks No. 787 and No. 788, the structure of which was broken down at $G = 115$ sec.$^{-1}$. Curve 1 shows the increase of P_s^* with continuous rotation of ink No. 787 for 30 minutes, in which time P_s^* reaches an almost constant value (the broken line represents the presumed very slight further increase of P_s^*). After this the system was rested for five minutes, and then a $P-\tau$ curve was plotted at the same $G = 0{,}052$ sec.$^{-1}$. In this case a distinct maximum appears on the $P-\tau$ curve, after which a value of P_s^* somewhat higher than before is reached. Further similar measurements performed after 10, 15, 30 and 120 minutes of rest show that P_r increases especially rapidly (Curve 1b) and P_s^* decreases to a lesser extent (Curve 1a). The same Fig. 4 also shows curves for the increase of P_s^* with continuous rotation for 4 hours for ink No. 788 (Curve 2), and after rests of 30, 60, and again 60 minutes for the same system (Curve 2a). We note that P_r does not appear at all in this ink during this resting time.

This comparison shows that the structure is restored much more rapidly in ink No. 787 than in No. 788, and the formation of a network is more pronounced in ink No. 787, as indicated by the values of P_r. In ink No. 788 P_s^* increases slowly, while P_r probably appears only when the structure has been restored to a considerable extent. It should be noted that here again there is still a considerable difference between the values of P_s^* found in the "down" and "up" curves (35 and 18.2 dynes/cm^2 for ink No. 787, 24 and 8.2 dynes/cm^2 for ink No. 788).

Thus, in farily complex systems, P_r may appear on the $(P-\tau)_G$ curve and may increase during rest to some extent independently of the increase of P_s^* and of the attainent of true P_s. The maximum P_r may be the consequence of the formation of a structural network from a part of especially rapidly restoring elements of the structure. Consequently, the true value of P_s can be correctly determined only from the coincidence of the ends of the $(P-\tau)_G$ curves for a restored and a strongly broken down structure. Hence the maxima of P_r relate to deformation and breakdown of the continuous network, and the increase of P_r during rest to its strengthening. The prolonged decrease of P_s^* during deformation of the undestroyed structure (at a certain value of G) and the prolonged increase of P_s during continuous rotation of the system (at the same G) after considerable structural breakdown, relate to breakdown of network fragments and individual aggregates of particles, and to their restoration respectively. Consequently, the whole thixotropic effect can be regarded as consisting of two parts:, strength thixotropy, relating to breakdown and restoration of the continuous network; and viscosity thixotropy, involving breakdown of network fragments and individual aggregates of particles, and their restoration (this also includes the orientation component of thixotropy). Viscosity thixotropy is associated with the duration of the time required for reduction of the size of the particles in the structure, which depends on their slippage through the liquid medium.

In addition to the experiments described above, the effects of strength and structural thixotropy appear in $P-\tau$ curves (Fig. 5, for ink No. 787) obtained for the same value of $G = 0.192$ sec.$^{-1}$ (cylinder with $R_1 = 1.42$ cm) after deformation of the inks at various higher values of G (10 minutes of rest between the measurements). The curve for $G = 0{,}192$ sec.$^{-1}$, taken for repeated deformation after 10 minutes of rest, represents a certain initial state of the system. The subsequent curves show that after deformation of the ink at increasing values of G both the height of the maximum P_r on the curve and the quasiequilibrium stress P_s^* diminish.

The effect of the magnitude of the "destroying" velocity gradient on the values of P_r and P_s^* is seen in the curves in Fig. 6 . These show that the greatest structural breakdown occurs up to values of G of 50-60 sec.$^{-1}$, which represent a certain critical value of the "destroying" velocity gradient for the given type of structure. Increase of G to 430 sec.$^{-1}$ leads to only a very slight further structural breakdown.

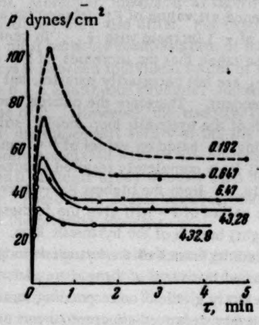

Fig. 5. $P - \tau$ curves for $G = 0{,}192$ sec.$^{-1}$, after deformation of ink No. 787 at higher G (shown on the curves in sec. $^{-1}$).

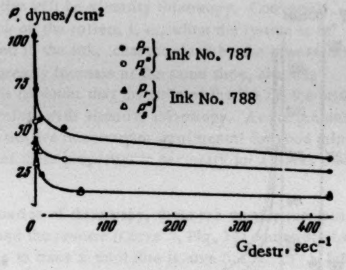

Fig. 6. Variation of P_r and P_s^* at $G = 0.192$ sec. $^{-1}$ with the value of the destroying G (curves based on data in Fig. 5).

The variation of G with P_s gives an idea of the rheological curve (flow curve). Such a curve would be conclusive only for true equilibrium values of P_s, corresponding to true steady flow. However, as we have seen, in practice true values of P_s are difficult to attain at low G. Therefore quasiequilibrium values of P_s^* can be used to plot at least an approximate rheological curve. Fig. 7 shows a rheological curve of this kind, based on values of P_s^* found from $P - \tau$ curves (at different values of G). In conjunction with this curve it is possible to calculate the effective viscosity of the system, curves for which (as a function of P_s^*) are given in Fig. 8 in two different scales. These curves show that a rapid viscosity increase with decreasing shearing stress begins for both inks at $P_s^* \approx 200 - 300$ dynes /cm^2 and at $G \approx 2 - 3$ sec.$^{-1}$.

As we pass from higher to lower values of G, the values of P_s^* obtained are lower than would correspond to a gradual increase of G and even lower than the true equilibrium values of P_s. These values of P_s^*, found for increasing and decreasing G, may be used to plot hysteresis loops, as shown in Fig. 9 for $G < 7$ sec. $^{-1}$ (based on the curves in Fig. 5).

A great variety of conditions has been used in different investigations for plotting hysteresis loops, and therefore none of these loops is quite conclusive. Moreover, often it is not known how steady is the value of the shearing stress used in plotting the hysteresis loop. By means of our $P - \tau$ curves, which include the initial deformation region, it is possible to determine the principle of the correct construction of hysteresis loops and to show more clearly which particular stress values give the widest loop, i. e., show its outermost branches.

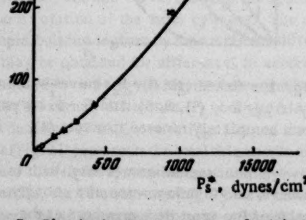

Fig. 7. Rheological $G - P_s^*$ curve for inks No. 787 (1) and No. 788 (2).

Further, these data demonstrate the relationship between the hysteresis loop and the rheological curve, and demonstrate the difference between anomalous viscosity and viscosity thixotropy.

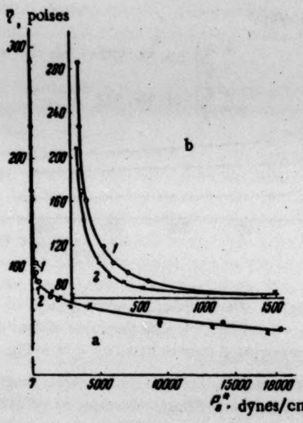

Fig. 8. Viscosity as a function of the shearing stress for inks No. 787 (1) and No. 788 (2): a) on small scale, b) on large scale.

According to Figs. 1 and 2, the $P-\tau$ curves for different τ_b lie one above the other, and hence all values of P_s^* (chosen for any value of τ) increase with τ_b. In general it may be taken that the increases of P_s^* and P_r with τ_b are not necessarily parallel, but may be independent. Therefore the outside, ascending branch of the hysteresis loop should, strictly speaking, be based on values of P_s^* found for each G for a completely restored structure, namely, P_s^* from the highest $P-\tau$ curve. These values of P_s^* will give the furthest (to the right) branch of the hysteresis loop. The left (return) branch of the hysteresis loop should be plotted by means of a rapid transition from the velocity gradient corresponding to a completely destroyed structure (theoretically, from the upper linear region of the rheological curve, but in practice possibly from a smaller gradient) to each given gradient, as shown schematically in Fig. 10 by the curved arrows (a continuous transition from a higher to lower velocity gradients cannot give the correct left branch of the hysteresis loop owing to the continuous restoration of a certain part of the structure during progressive decrease of G).

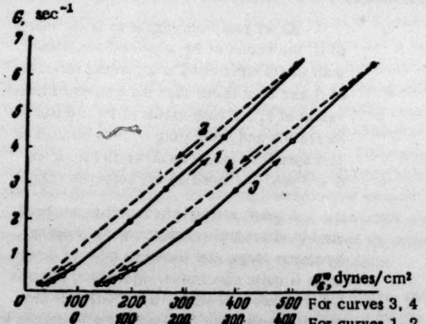

Fig. 9. Examples of hysteresis loops for ink No. 788 (1 and 2), and No. 787 (3 and 4).

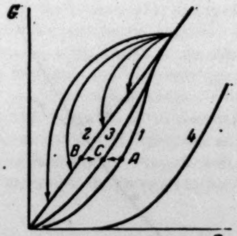

Fig. 10. Schematic $G-P_s$ curves with hysteresis loop (1, 2, 3) and $G-P_r$ curve for a completely restored structure (4).

The choice of the value of P_s^* on the continuous $P-\tau$ curve remains somewhat arbitrary, both in deformation of the undisrupted structure, i. e., in passing "downward", and in deformation of a strongly broken down structure, i. e., in ascent "upward". Clearly, this value of P_s^* must lie somewhere at the end of the steeply descending branch of the $P-\tau$ curve at its transition from the maximum region into the "horizontal" part. In our investigation, the quasiequilibrium P_s^* characterizing the transition from the strength region to the viscosity region was taken to be the value of $P^{\bullet}_{s}$ at a distance $10\tau_r$ (τ_r is the time to reach maximum P_r) from the start of the $P-\tau$ curve. The values of $P^{\bullet}_{s}$ for the left branch of the loop should be taken from the start of the $P-\tau$ curve corresponding to the establishment of the given G after total breakdown of the structure. This arbitrariness, however, does not invalidate the division of thixotropy into strength and viscosity components, as the mechanism and character of the structure which determine them are different. Moreover, the practical significance, and the possibility of the appearance, of each of these kinds of thixotropy may also differ. For example, if the ink is being continuously agitated on the machine rollers, the most probable manifestation of thixotropic properties will be viscosity thixotropy. Conversely, in the intervals between individual stages of rotation of the ink on the rollers, i. e., when the system is at rest (at $G = 0$), a continuous structural network may be formed in the ink, characterized by the appearance and increase of P_r. However, the viscosity component may greatly increase at the same time, and this determines the subsequent ability of the ink to flow. There is no doubt that the state of the ink on the printing form is closely associated with its viscous properties, and therefore with viscosity thixotropy. At the present time it is still difficult to say whether such thixotropic properties are necessary or detrimental for good printing ink quality. There is no doubt, however, that detailed study of these properties is necessary for a better understanding of the printing process.

In all investigations which use hysteresis loops for evaluation of thixotropy, these are usually represented as two branches, representing the forward (Curve 1, Fig. 10) and the reverse (Curve 2, Fig. 10) course of changes in the deformation rate. On the basis of our data it is possible to trace a third line (Curve 3, Fig. 10[†]), lying between the two extreme lines, and corresponding to equilibrium values of P_s, reached both in breakdown of the restored structure on prolonged deformation, and in restoration of a strongly broken down structure during continuous rotation at a given G. In Fig. 10 the horizontal arrows show the variation of $P^{\bullet}_{s}$ with time (during flow at a given G) in the transition from the restored quasiequilibrium (A) and maximally broken down (B) state of the system to the true equilibrium state (C). During rest of the system, restoration results in transition from the state represented by the point B in Curve 2 to the state represented by the point in Curve 1, i. e., a jump across the true equilibrium viscosity to a quasiequilibrium, higher viscosity of the system.

The middle Curve 3 with the point C represents anomaly of viscosity only. Goodeve [2, 3] determined thixotropy from the rheological curve, thus taking anomaly of viscosity to be thixotropy. In that case it would be impossible to distinguish between anomalously viscous and thixotropic systems. Moreover, a characteristic feature of thixotropy is the variation of the rheological properties of the system with time. Thixotropy must therefore be evaluated from changes of the strength and viscosity properties with time. Strength thixotropy is characterized by variation of the strength P_r with time in relation to the quasiequilibrium $P^{\bullet}_{s}$ existing at the given instant of structure restoration. Viscosity thixotropy is characterized by increase, with time, of the quasiequilibrium $P^{\bullet}_{s}$ in relation to the minimum $P^{\bullet}_{s}$ found for conditions of maximum structural breakdown and corresponding to the extreme left branch of the hysteresis loop. The relationship between the strength and viscosity components of thixotropy is illustrated by the diagram for the variation of these quantities during rest (Fig. 11). The lower line, designated $P^{\bullet}_{SB}$, represents the minimum shearing stress, after maximum breakdown, required to maintain a given G at which the strength and viscosity thixotropies are measured (it is interesting to note that measurement of even only the strength component of thixotropy from the values of P_r, as has been done by various workers, must be based on the use of a definite G).

Figure 11 shows curves for the increase of $P^{\bullet}_{s}$ and P_r with time for a certain value of G used in the determination, and the curves showing the approach to a true equilibrium P_s "downward" and "upward" with continuous rotation of the outer cylinder. The difference ($P_r - P^{\bullet}_{s}$) gives the strength thixotropy. Complete thixotropic buildup is given by the maximum difference ($P_r - P^{\bullet}_{s}$), (P_r and $P^{\bullet}_{s}$ const., independent of τ_b). Such curves may be obtained for different G in accordance with the hysteresis loop. It is evident that the greatest difference ($P^{\bullet}_{s} - P^{\bullet}_{SB}$) in Fig. 11 corresponds to the maximum width of the loop for the given G. On the other hand, the maximum difference ($P_r - P^{\bullet}_{SA}$) in Fig. 11 corresponds to the abscissa between the line representing P_r as a function of G (Curve 4, Fig. 10) and the right branch of the loop in the same Fig. 10. The full $P_r - P^{\bullet}_{SB}$ ordinate (Fig. 11) represents the total thixotropic effect, the sum of the strength ($P_r - P^{\bullet}_{SA}$) and viscosity ($P^{\bullet}_{SA} - P^{\bullet}_{SB}$) components. It is clear that if the system has practically no viscosity thixotropy, as is the case for many systems with aluminum naphthenate, the line representing $P^{\bullet}_{s}$ as a function of τ_b in Fig. 11 will be absent, and the system will be characterized by strength thixotropy only, represented by ($P_r - P^{\bullet}_{SB}$), and then $P^{\bullet}_{SB} = P_{SC} = P^{\bullet}_{SA}$. In this case there will be no hysteresis loop (Fig. 10), and only Curve 3, representing anomaly of viscosity, will remain. Systems in which the viscosity component of the structure reaches its equilibrium value practically "instantaneously" on change of G evidently have such properties.

[†] Curve 2 is represented as a straight line in accordance with literature data [6, 7]. However, it cannot be assumed that this branch of the loop must always be linear, even with maximum breakdown.

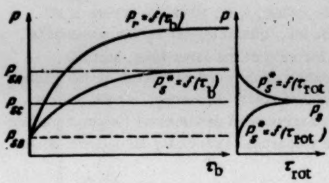

Fig. 11. Variation of P_r and P_s^*, measured at definite G, with the time of structural buildup τ_b (at rest) after maximum (or sufficiently great) breakdown of the structure.

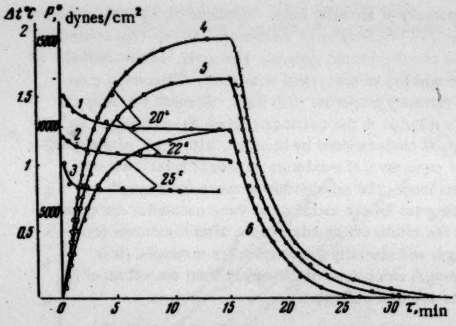

Fig. 12. Curves for $P = f(\tau)$ (Curves 1, 2, and 3) and $\Delta t = f(\tau)$ (Curves 4, 5, and 6) for ink No. 787 at G = 253,9 sec.$^{-1}$ and at initial temperatures of 20, 22, and 25°.

Since, according to our experimental data on printing inks, P_s^* decreased continuously during prolonged deformation, the suggestion arose that this may be related to some extent to a decrease in the viscosity of the system owing to the increase of temperature as the result of rotation. To verify this, the increase in the temperature of the system at the surface of the inner cylinder was measured by means of a thermocouple attached to it. Fig. 12 gives $P = f(\tau)$ and $\Delta t = f(\tau)$ curves for three initial temperatures (20, 22, and 25°) for rotation of ink No. 787 at G = 288.5 sec.$^{-1}$. These curves show that the gradual increase Δt of the ink temperature reaches maximum and constant values after 15 minutes of rotation of 1.94, 1.64 and 1.26° at 20, 22, and 25° respectively.

Consequently, after 15 minutes of rotation of the cylinder thermal equilibrium is established in the system and any further change of viscosity cannot be ascribed to changes of the ink temperature. When the outer cylinder is stopped, the temperature difference falls to zero also in 15-17 minutes. At a low value of G = 0.192 sec.$^{-1}$ there was practically no temperature effect.

In our experiments, in studies of the consecutive influence of large and small values of G, breakdown in the system at large G lasted for not more than 1 minute (30 seconds in a number of experiments), and therefore, according to Fig. 11, the temperature could not rise by more than 0.5°.

Moreover, before measurements at low G (0.192 sec.$^{-1}$), the intervals were 10 minutes, which was evidently quite enough for almost complete equalization of temperature. It follows from these experiments that variation of P_s^* with time can be assumed to be practically independent of the heat effect, and to be the consequence of mechanical breakdown of the structure only.

Mills and Gates [8] found that heat effects may necessitate a certain correction to the hysteresis loop, but did not determine its value.

Thus, the two inks studied, of different composition, are very similar in viscosity at sufficiently high velocity gradients, in the region of almost complete structural breakdown: at G ≈ 433 sec.$^{-1}$ the value for both inks is $\eta \approx 41$ poises (at 20°). However, they show an appreciable viscosity difference in the region of small velocity gradients of thixotropic buildup, and they differ in the properties of the restored structure and in viscosity after extensive breakdown. Thus, the viscosity measured 10 minutes after passing from $G = 433 \text{ sec.}^{-1}$ to $G = 0.192 \text{ sec.}^{-1}$ is 158 poises for ink No. 787, and 63 poises for ink No. 788. Ink No. 787 quickly regains its properties, and has a relatively high structural network strength and higher P_s, especially in the initial resting stages. This shows that the particles in this ink have greater mobility and are able to interact fairly strongly with each other.

SUMMARY

1. The strength and viscosity of two printing inks, studied by means of an apparatus based on the coaxial cylinder principle, are independent and mutually complementary characteristics of the state of their structure, which vary both with variations of the velocity gradient and during rest of the system or during its continuous deformation. These properties are manifested in different ways in the two inks studied.

2. The thixotropic effect of a system is composed of two components: the strength and the viscosity components. The strength component characterizes breakdown and restoration of the structural network in the colloidal system, and is evaluated by the difference between the maximum strength and the quasiequilibrium shearing stress corresponding to quasistationary flow. The viscosity component, which reflects the breakdown and restoration of separate aggregates of particles, is evaluated by the difference between the quasiequilibrium shearing stresses corresponding to deformation of a structure restored to the limit (or partially) and of a structure broken down to the limit (or partially), and determining the complete (or incomplete) width of the hysteresis loop. It is pointed out that viscosity thixotropy is not identical with anomaly of viscosity.

Institute of Physical Chemistry Acad. Sci. USSR
Moscow

Received March 22, 1956

LITERATURE CITED

[1] M. P. Volarovich, Symposium, Physicochemical Principles of Printing Processes and Investigation of Printing Inks, Trans. Sci. Res. Inst. State United Press, No. 5 (1937).

[2] C. F. Goodeve, G. Whitfield, Trans. Far. Soc. 34, 511, (1938).

[3] J. E. Arnold, C. F. Goodeve, J. Phys. Chem. 44, 652, (1940).

[4] H. Green and R. Weltmann, Physical Chemistry of Clay Suspensions (Translated from English) (State Fuel Tech. Press, 1947).

[5] K. F. Zhigach and D. E. Zlotnik, Factory Labs., No. 5, 542 (1949).

[6] M. P. Volarovich and M. F. Nikishina, Colloid J., 12,169 (1950).

[7] V. L. Valdman, Trans. All-Union Conf. Colloid Chem. (Acad. Sci. Ukrainian SSR Press, Kiev, 1952).

[8] C. C. Mills, E. R. Gates, Analyt. Chem. 25, No. 9 (1953).

[9] N. N. Serb-Serbina and P. A. Rebinder, Colloid J., 9,381 (1947).

[10] E. E. Segalova and P. A. Rebinder, Colloid J., 10,233 (1948).

[11] L. A. Kozarovitsky and S. Ya. Shalyt, Colloid J., 15,437 (1953).

[12] A. A. Trapeznikov and V. A. Fedotova, Proc. Acad. Sci. USSR, 81, 1101 (1951); 82, 97 (1952); 95, 595 (1954).

[13] A. A. Trapeznikov and E. M. Shlosberg, Symposium, New Methods of Physicochemical Investigation of Surface Phenomena, Trans. Inst. Phys. Chem. (Acad. Sci. USSR Press, Moscow-Leningrad, 1950) p. 39.

[14] B. N. Shakhkeldyan, Colloid J., 18, 111, (1956).

EFFECT OF AN ACTIVE FILLER AND A SOLVENT ON THE STRUCTURAL AND MECHANICAL PROPERTIES OF BITUMENS

S. Ya. Shalyt, N. V. Mikhailov, and P. A. Rebinder

The preceding paper [1] gave the results of an investigation of the structural and mechanical properties of various oxidized petroleum bitumens in the temperature range of 40-160°. The temperature limits for the transition of the bitumen from one rheological state into another were determined from the relationship between the limiting viscosity values and the temperature. The region of the fluidlike state was studied in particular detail. Complete S-shaped rheological curves were obtained, from which a number of important characteristics could be determined: η_0, the maximum viscosity of the practically intact structure; η_m, the minimum viscosity of the structure broken down to the limit; and values of P_r', the conventional strength limit (the start of appreciable breakdown) and P_m', the limit of maximum structural breakdown.

It was of considerable interest to study the effect of an active disperse filler, which reinforces the bitumen structure, and a solvent which plasticizes it, as we had shown that by additions of filler and solvent in certain proportions it is possible to obtain a new system with a predetermined fairly high maximum viscosity η_0, with a simultaneous decrease of thermosensitivity, i. e., of the temperature coefficient of viscosity. The results of this investigation are presented in this paper.

Effect of active filler. The active filler used was fine calcium hydroxide powder, slaked lime. When anhydrous calcium oxide (quicklime) is made to react with the exact stoichiometric amount of water by the chemical dispersion method [2], the hydration reaction yields highly disperse slaked lime powder; from 2 to 25% of the total volume of this mixture was introduced into the bitumen. The hydrophilic surfaces of the filler particles form surface chemical compounds, calcium soaps, with the asphaltogenic acids of the bitumen; these compounds render the filler surface hydrophobic and improve its wetting by the bitumen. Diffuse structurized bitumen layers are thereby formed around the filler particles (Fig. 1), with highest viscosity in the layer directly adjacent to the particle surface owing to adsorption of the high molecular weight components and adhesion of the colloidal components of the bitumen.

To prepare the mixture, the bitumen was heated to 120-130° until moisture was completely removed, and the lime powder was then introduced into the hot bitumen. The mixture was thoroughly stirred and heated again until its surface became glossy. The hot mixture was poured into the space between the coaxial cylinders.

It was shown in the preceding paper that the maximum viscosity η_0 of the bitumen is its fundamental physicochemical property which reflects the characteristics of the intact structures formed by the bitumen micelles. Therefore we used the values of the maximum initial viscosity η_0 of the undestroyed structure to characterize the structural and mechanical properties of bitumen – filler systems.

For this, the initial regions of the ϵ (P) rheological curves were plotted for temperatures of 65, 75, and 85°. A sharply defined critical degree of volume filling was found (Table 1), evidently corresponding to the formation of a new spatial structure involving the active filler grains [3]. The explanation for this is that, at low filler contents, the particles with the structurized bitumen layers do not interact and no interlayers of more highly structurized bitumen are present between them (Fig. 2a). In such a case the viscosity variation may be represented by a linear equation of the Einstein equation type $\eta_0(\varphi) = \eta_0(0)(1 + \alpha\varphi)$, where $\eta_0(\varphi)$ is the viscosity of the mixture; $\eta_0(0)$ is the viscosity of the medium, α is the shape and solvation factor for the particles, and φ is the volume content of filler in the mixture:

$$100\varphi = \frac{c_1}{D_1} \cdot \frac{100}{100 + c_1/D_1},$$

where c_1 is the amount of filler in grams per 100 g of bitumen, and D_1 is the density of the filler.

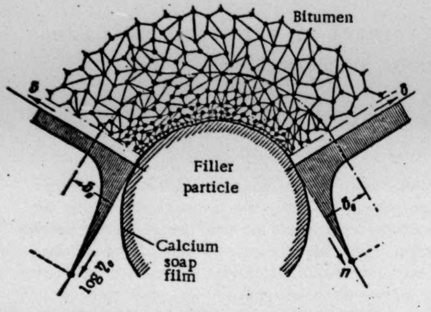

Fig. 1. Formation of a diffuse structurized bitumen layer on a filler particle.

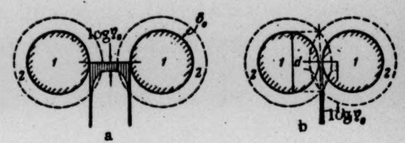

Fig. 2. Interaction of filler particles at low (a) and high (b) contents of filler in the mixture: 1) filler particles; 2) diffuse structurized layers on the filler particles.

TABLE 1

Maximum Viscosity η_0 and Thermosensitivity Coefficient K for a Mixture of Grade III Bitumen with Different Filler Concentrations (c_1 in g/100 g of bitumen) at Various Temperatures

c_1	100φ	65°			75°			85°			$K\cdot10^3$ for 65–85°
		$\eta_0\cdot10^{-3}$ poises	$\log\eta_0$	$\frac{\eta_0(\varphi)}{\eta_0(0)}$	$\eta_0\cdot10^{-3}$ poises	$\log\eta_0$	$\frac{\eta_0(\varphi)}{\eta_0(0)}$	$\eta_0\cdot10^{-3}$ poises	$\log\eta_0$	$\frac{\eta_0(\varphi)}{\eta_0(0)}$	
0	0	4.15	3.62	1.00	1.25	3.11	1.00	0.470	2.67	1:00	4.50
5	2.33	4.76	3.68	1.14	1.58	3.20	1.2[illegible]	0.540	2.73	1.15	4.50
10	4.55	5.30	3.72	1.28	1.78	3.25	1.42	0.610	2.79	1.29	4.50
15	6.68	6.00	3.78	1.44	1.86	3.27	1.48	0.680	2.83	1.44	4.50
20	8.70	6.50	3.81	1.56	2.10	3.32	1.68	0.750	2.87	1.59	4.50
30	12.5	7.95	3.90	1.91	2.69	3.43	2.15	1.02	3.01	2.17	4.50
40	16.0	11.5	4.06	2.77	3.90	3.59	3.12	1.29	3.11	2.75	4.50
50	19.2	25.5	4.41	6.15	8.00	3.90	6.40	2.30	3.36	4.90	5.20
60	22.2	62.0	4.79	4.9	14.0	4.15	11.2	3.00	3.48	6.39	6.50
70	25.0	76.0	5.88	183	115	5.06	92.3	20.4	4.31	43.5	7.80

With a higher content of filler the particles with their structurized bitumen layers interact and a contact region of diameter h, consisting of highly structurized bitumen, is formed between them (Fig. 2,b).

The coefficient α was found to be 7.5 for different bitumens and temperatures (Fig. 3), both because the particles were not spherical and because of solvation – the presence of structurized layers of bitumen on the surfaces.

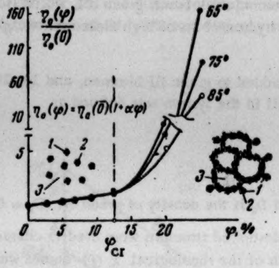

Fig. 3. Change of relative viscosity $\frac{\eta_0(\varphi)}{\eta_0(0)}$ of bitumen as a function of the volume content of Ca $(OH)_2$ filler at temperatures of 65, 75, and 85°: 1) filler particles; 2) diffuse structurized bitumen layers on the filler particles; 3) dispersion medium – bitumen; 4) contact between two filler particles, consisting of highly structurized bitumen.

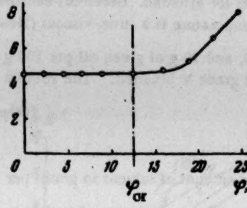

Fig. 4. Thermosensitivity coefficient of bitumen as a function of its volume content of active filler.

Figure 3 shows the variation of the relative viscosity of the mixture of bitumen and filler ($\eta_0(\varphi)/\eta_0(0)$) with the volume content of the filler at 65, 75, and 85°. Fig. 3 shows that at a volume content above the critical value, corresponding to 12.5-16% by volume of the active filler, the viscosity η_0 increases sharply owing to interaction of the active filler particles by their diffuse structurized outer layers (Fig. 2b). A new coagulation structure is formed, with the active filler grains acting as centers of structure formation. The calcium soaps of the asphaltogenic acids, which must be considered as the natural activators of the added filler, evidently play an important part in the formation of the continuous structural network. The structurizing action of the filler, as was to be expected, rapidly weakens with increase of temperature. Thus, with 25% by volume of the filler in the mixture, the viscosity of grade III bitumen is increased 183-fold at 65°, 92-fold at 75°, and 43-fold at 85° (Fig. 3 and Table 1).

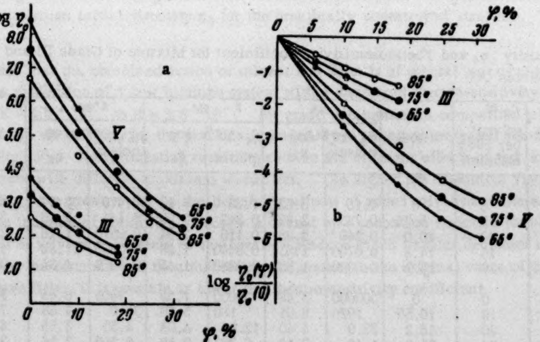

Fig. 5. Variation of maximum viscosity (a) with volume content of solvent in grade III and V bitumens at 65, 75, and 85°, and variation of the maximum relative viscosity $\log\frac{\eta_0(\varphi)}{\eta_0(0)}$ of grade III and V bitumens (b) with content of solvent φ.

The log η_0 (t) relationship found was used to calculate the thermosensitivity coefficients $K = -d \log \eta_0 / dT$. It was found (Table 1 and Fig. 4) that, below the critical degree of filling, the thermosensitivity coefficient does not differ from that for the pure bitumen. Further increase of the filler content produces a sharp increase in the thermosensitivity coefficient owing to formation of a secondary structure. Thus, for grade III bitumen, K increases from $4.5 \cdot 10^{-2}$ to $7.8 \cdot 10^{-2}$, which is a 1.7-fold increase.

Effect of solvent. The effect of a solvent on the structural and mechanical properties of grade III and V bitumens was studied. The solvent used was a nonvolatile technical solvent, green oil, which is the usual plasticizer for bitumen. Green oil consists mainly of aromatic hydrocarbons of high molecular weight, and at room temperature is a true-viscous (Newtonian) liquid.

5, 10, 15, and 20 g of green oil per 100 g of pure bitumen was added to grade III bitumen, and 10, 20, 30, and 40 g to grade V bitumen. The volume content φ of green oil in the system was defined as

$$100\varphi = \frac{c_2}{D_2} \cdot \frac{100}{100 + \frac{c_2}{D_2}},$$

where c_2 is the amount of solvent in grams per 100 g of bitumen, and D_2 is the density of green oil ($D_2 \approx 0{,}90$).

The values of the maximum viscosity η_0 of the practically undestroyed structure were used to characterize the systems. For determination of the values of η_0, the initial regions of the rheological $\dot{\varepsilon}$ (P) curves were studied at 65, 75, and 85°.

The results are given in Table 2. Fig. 5,a shows the variation of the maximum viscosity (η_0) with volume content of filler in bitumens III and V at 65, 75, and 85°. Fig. 5,b shows the variation of the maximum relative viscosity $\left(\log \frac{\eta_0(\varphi)}{\eta_0(0)}\right)$ of bitumens III and V with the amount of solvent present (φ). The effects of the solvent are enormous even with relatively small amounts of solvent present. The viscosity decrease is especially great for the most structurized bitumen (grade V) at lower temperatures (65°). As was to be expected, the solvent effect is greatest for the strongest, i. e., the most viscous, bitumen structures, where this effect is used in practice for plasticization. Thus, addition of 20% of green oil to bitumen produces a 100-fold decrease of viscosity in grade III bitumen and 10,000-fold in grade V bitumen.

The thermosensitivity coefficient of bitumen also falls considerably with increasing solvent content (Fig. 6); for grade III bitumen from $4{,}5 \cdot 10^{-2}$ to $0{,}85 \cdot 10^{-2}$, and for grade V bitumen from $9{,}1 \cdot 10^{-2}$ to $1{,}9 \cdot 10^{-2}$. The variation of the thermosensitivity coefficient with solvent content can be represented by the linear relationship $K(\varphi) = K_0 - \beta\varphi$, where K_0 is the thermosensitivity coefficient of pure bitumen, while the coefficient β, which represents the degree of decrease of K on addition of solvent, can be termed the coefficient of solution.

TABLE 2

Maximum Viscosity η_0 and Thermosensitivity Coefficient for Mixture of Grade III and V Bitumens with Green Oil

Bitumen grade	c_2 of solvent per 100 g bitumen	100φ	65°		75°		85°		$K \cdot 10^2$
			$\eta_0 \cdot 10^{-3}$ poises	log η_0	$\eta_0 \cdot 10^{-3}$ poises	log η_0	$\eta_0 \cdot 10^{-3}$ poises	log η_0	
III	0	0	4.15	3.62	1.25	3.11	0.470	2.67	4.50
	5	5.25	0.783	2.90	0.312	2.50	0.145	2.16	3.70
	10	10.0	0.240	2.38	0.110	2.04	0.0570	1.76	2.90
	15	14.3	0.0700	1.85	0.0460	1.66	0.0330	1.52	1.60
	20	18.2	0.0330	1.52	0.0280	1.45	0.0223	1.36	0.85
V	0	0	300000	8.48	39000	7.59	4500	6.65	9.10
	10	10.50	1020	6.01	180	5.26	36.0	4.56	7.25
	20	18.2	25.0	4.40	12.0	4.08	4.50	3.65	4.55
	30	25.0	1.46	3.16	0.760	2.88	0.360	2.56	3.05
	40	30.1	0.265	2.42	0.150	2.18	0.110	2.04	1.90

Combined effect of active filler and solvent on the structural and mechanical properties of bitumens. The investigations show that it is possible to control the structural and mechanical properties of bitumens by plasticization of the spatial structure by means of green oil followed by structurization by addition of active filler to the previously plasticized system.

We investigated, at 65, 75, and 85°, grade III bitumen diluted with 20% of green oil with subsequent additions of 30, 50, 60, and 70% of lime powder, and grade V bitumen diluted with 40% of green oil with subsequent addition of 20, . 40, and 50% (by weight of the mixture) of lime powder.

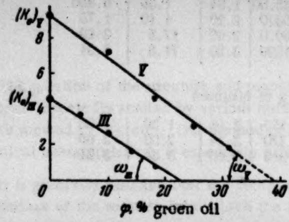

Fig. 6. Variation of the thermosensitivity coefficient of grade III and V bitumens with solvent content.

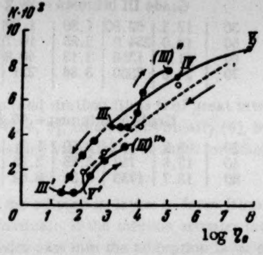

Fig. 7. Variation of the maximum viscosity η_0 and thermosensitivity coefficient by the simultaneous action of active filler and solvent at 75°. Roman numerals indicate the grade of bitumen; primes represent dilution by green oil; double primes represent addition of active filler.

The volume content of active filler in the system was defined as

$$100\varphi = \frac{(100 + c_2)\, c_1'}{D_1} \Big/ \left[100 + \frac{c_2}{D_2} + \frac{(100 + c_2)\, c_1'}{100 D_1}\right],$$

where φ is the degree of filling of the system by the active filler; D_1 and D_2 are the densities of the filler and solvent respectively; c_1 is the amount of filler added per 100 g of the solution of bitumen and green oil; c_2 is the amount of solvent added per 100 g of bitumen.

The initial regions of the rheological curves were investigated, and the systems were characterized by the values of the maximum initial viscosity η_0 for the practically undestroyed structure. The results are given in Table 3.

Thus it is seen that the combined action of solvent and filler is of special practical importance, as it makes possible the production of a new bitumen system with a decreased thermosensitivity coefficient (decreased from $K = 4.5 \cdot 10^{-2}$ to $K = 3.6 \cdot 10^{-2}$ for grade V bitumen) in comparison with pure bitumen and with values of the viscosity η_0 for the practically undestroyed structure increased about tenfold (from 312 to 3340 poises) (Fig. 7). This interesting result depends on the different effects of the solvent on the structures of bitumens with different maximum viscosities. The higher the maximum viscosity of the bitumen system without filler, the greater will be the liquefying effects of added solvent and increase of temperature. However, when the increase of maximum viscosity is caused by a secondary structure formed by the filler particles, additions of solvent or increase of temperature produce much smaller decreases of viscosity. Thus, by adding solvent to the bitumen and then thickening the system to the original value of the maximum viscosity by addition of active filler, it is possible to lower the thermosensitivity coefficient.

TABLE 3

Maximum Viscosity η_0 and Thermosensitivity Coefficient K for Mixtures of Different Grades of Bitumen with Green Oil, at Different Contents of Active Filler

c'_s	100φ	65°			75°			85°			$K \cdot 10^{r}$
		η_0 poises	log η_0	$\frac{\eta_*(\varphi)}{\eta_*(0)}$	η_0 poises	log η_0	$\frac{\eta_*(\varphi)}{\eta_*(0)}$	η_0 poises	log η_0	$\frac{\eta_*(\varphi)}{\eta_*(0)}$	
Grade III bitumen + 20 g of green oil per 100 g of bitumen											
30	12.3	62.50	1.80	1.89	45.00	1.65	1.60	35.00	1.54	1.56	0.850
50	19.0	354.0	2.55	10.7	220.0	2.34	1.85	158.0	2.20	1.10	1.75
60	21.8	1350	3.13	40.9	724.0	2.86	25.8	390.0	2.60	17.5	2.69
70	24.6	7300	3.86	221	3340	3.52	119	1590	3.20	71.8	3.31
Grade V bitumen + 40 g of green oil per 100 g of bitumen											
20	9.2	400	2.60	1.51	227	2.36	1.51	150	2.18	1.36	1.90
40	15.6	750	2.88	2.85	386	2.56	2.57	220	2.34	2.00	2.66
50	18.7	1750	3.24	6.62	759	2.88	5.03	399	2.60	3.64	3.21

SUMMARY

1. When slaked lime powder, an active filler, is added to bitumen, a sharply defined critical region of volume filling is found, corresponding to the formation of a new spatial structure involving the active filler grains. When the degree of volume filling is above the critical value, the viscosity η_0 and the thermosensitivity coefficient both increase sharply with increasing filler content.

2. Addition of green oil solvent to bitumen causes plasticization effects in the spatial structure, opposite to the effects of the active filler, and both the viscosity η_0 and the thermosensitivity coefficient decrease rapidly with increasing solvent content.

3. By combined addition to bitumen of an active disperse filler, which reinforces its structure, and a solvent, which plasticizes it, in definite proportions, it is possible to attain a required high viscosity η_0 with a simultaneous decrease of the heat sensitivity of the mixture.

Scientific Research Institute for Building
Ministry of Construction USSR
Moscow

Received November 28, 1956

LITERATURE CITED

[1] N. V. Mikhailov and S. Ya. Shalyt, Colloid J., 18, No. 5, 609 (1956).

[2] P. A. Rebinder and G. I. Loginov, J. Acad. Sci. USSR, 10, 47 (1951); G. I. Loginov, P. A. Rebinder, and V. P. Sukhova, Proc. Acad. Sci. USSR, 98, 2, (1954).

[3] P. A. Rebinder, G. A. Ab, and S. Ya. Veiler, Proc. Acad. Sci. USSR, 31, 5, 444 (1941); Ya. B. Aron and P. A. Rebinder, Proc. Acad. Sci. USSR, 52, 3, 235 (1946); A. S. Kolbanovskaya and P. A. Rebinder, Colloid J., 12, 3, 208 (1950).

LETTER TO THE EDITOR

POSSIBLE DIFFERENCES IN THE COMPOSITION AND VISCOSITY RATIO OF A TWO-SIDED FILM AND A SURFACE LAYER OF A SOAP SOLUTION

A. A. Trapeznikov

The question of the structure and properties of two-sided soap (and similar) films is of great interest. It has been repeatedly studied by various methods: optically [1, 2, 3, 4, 5], conductometrically [6], by the froth method [7, 8], etc. Our method of measurement of the surface viscosity or strength (or other mechanical characteristics) is especially effective.

It is generally assumed that the composition and structure of the adsorption layers in foam films and in the surface of the solution from which the foam is formed are identical. If the solution contains more than one component, the components with the greatest surface activity pass into the adsorption layer of the solution surface and into the foam. It is usually supposed that such components are transferred equally in both cases, and consequently the composition and properties of the adsorption layers in the foam films and the solution surfaces are assumed to be the same. For example, this assumption is the basis of the frequent verification of the Gibbs equation by analysis of the composition of the destroyed foam from a solution. Similar assumptions are made when the surface tensions of solutions obtained from destroyed foams and the original solutions are compared.

Of interest in this connection are our experiments which show a difference in composition and properties of the adsorption layers in two-sided films and in the surface of the solutions from which the films are formed. The differences are cause by different rates of adsorption and with differences in the kinetics of layer formation from different components.

Differences of surface activity in such cases are seen not only in different degrees of surface tension lowering in equilibrium conditions, which is how surface activity is usually determined, but also in different mobilities of the solution components, and the special ability of some of them, evidently the more mobile, to migrate two-dimensionally and to pass into two-sided films as they become detached. This also shows that the mechanism of formation of a two-sided film involves a natural fractionation of different surface-active components, a sort of filtration of them at the instant when the two-sided film is detached from the solution surface.

A solution of a mixed soap, consisting of sodium palmitate and oleate in 1:9 ratio, was studied. The solution was warmed to 40° and cooled rapidly to 18°. In these conditions, after complete solution of the soap and cooling of the solution, sodium palmitate is held in solution for some time and then begins to separate out as a fine precipitate (apparently as an acid soap, which disappears on addition of alkali).

If, during aging of such a solution, two-sided films and adsorption layers on the solution surface form from such a solution, and their resistance to shear is measured between concentric horizontal platinum wire rings by a method described previously [9], the shearing deformation curves shown in Fig. 1 can be obtained. Here the serial numbers represent the sequence of formation and measurement of the surface layers or films, formed anew each time by raising and lowering the solution level, i. e., after stirring the solution. Therefore consecutive measurements reflect, not the aging of adsorption layers or films, but the aging of the solution in bulk and the precipitation of palmitate from the solution, i. e., changes in the composition of the solution.

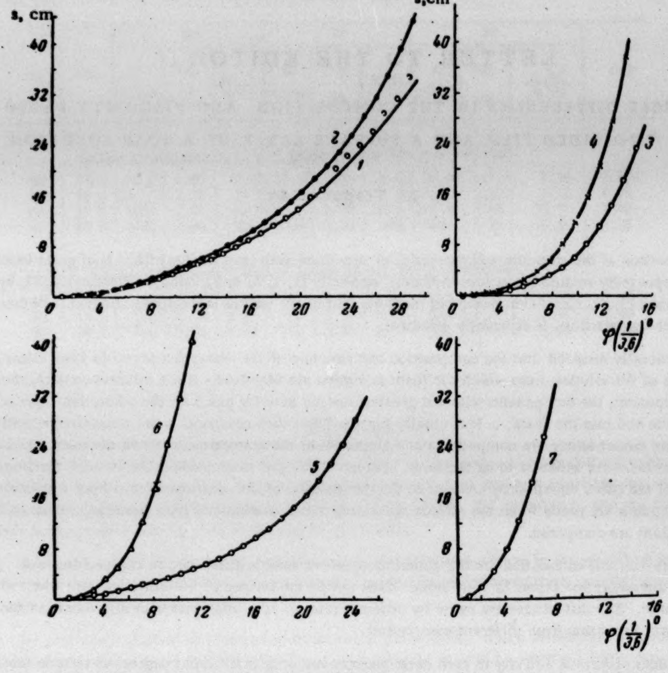

Fig. 1. Deformation S vs. angle of rotation ρ for the solution surface and two-sided films, measured in the sequence shown by the numbers, in a 1:9 palmitate – oleate soap solution; c_{total} = 2.7 millimoles / liter; 1 and 2) surface; 3 and 4) two-sided film; 5) surface; 6) film; 7) surface.

Fig. 2 shows curves for variation of the deformation rate with the torque $dS/d\varphi = f(\varphi - \theta)$. Although these curves are not linear (they indicate the existence of a structure in the films), and were obtained for conditions of not quite steady flow, the viscosity in surface poises (η_s , g / second) can be approximately calculated from their lower regions. The values of η_s are given in the Table and are shown graphically in Fig. 3 in order of the measurements.

It follows from the curves in Fig. 3 that the surface layer of a rapidly cooled solution has a high surface viscosity, ~ 7.0 surface poises, which persists during the first stages of aging of the solution, corresponding to the first 5 measurements (~ 1 hour), after which the high surface viscosity rapidly decreases to negligibly small values [10].

The viscosity of two-sided films (calculated on the full thickness) is even at the start 1.75 times less than the viscosity of the surface layer of solution (it must be remembered that a two-sided film has 2 adsorption layers, and therefore the difference for one layer is a factor of 3.5), while with aging of the solution (increasing number of the determination) it decreases to values of the order of $3 \cdot 10^{-5}$ surface poises.

It is significant that while the viscosity of the surface layer of the solution remains for some time at the same level, the viscosity of the films formed from the same solution decreases fairly rapidly and systematically.

The viscosity of the surface layer decreases extremely rapidly somewhat later, and practically overtakes the film viscosity. Thus, throughout the aging and decomposition of the solution, accompanied by deposition of the precipitate, the ratio of the viscosities of the film and the surface, if it is calculated from the ordinates of the curves, varies continuously. It decreases at first, and then increases again. Thus, for unstable solutions of this type the ratio of the viscosities of the two-sided film and the solution surface is not constant.

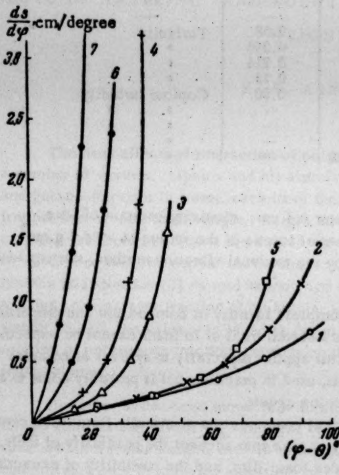

Fig. 2. Curves for the deformation rate as a function of the torque $dS/d\varphi = f(\varphi - Q)$, based on the $S-\varphi$ curves of Fig. 1. Numbering of the curves is the same as in Fig. 1.

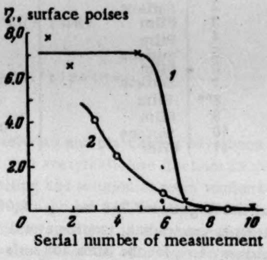

Fig. 3. Variation of the viscosity of the surface layer of solution and the two-sided films in the sequence of measurements, for a 1:9 palmitate – oleate solution.

These results show that the composition of the adsorption layers in two-sided films and at the solution surface may differ. During formation of the film, as it becomes detached from the solution surface, the more mobile components probably pass into it. In this instance they are less viscous and consist mainly of sodium oleate, while the more viscous component – sodium palmitate – remains in the bulk of the solution. However, it cannot be said in general that the less viscous components will always pass into the two-sided film. In a number of cases the reverse probably occurs, when the total viscosity of the 2-sided film is more than double that of the adsorption layer on the solution surface; this difference should be attributed to differences in the composition of the adsorption layer, and not to the additional high viscosity of the intermediate "volume" part of the two-sided film, although the role of this factor is not, of course, excluded in principle. It may be that in the mixed sodium palmitate and oleate soap solution mixed micelles are formed, which persist unchanged at first after the solution is cooled. However, during adsorption these micelles may break up into their components, the process being more intensive in the two-sided film.

These results show that adsorption at the foam films is selective in comparison with adsorption at the solution surface, and that the composition of the adsorption layers in both cases greatly depends on the adsorption kinetics of all the components and probably on the rate of film formation.

The viscosity differences between the film and the surface layer of solution are especially prominent in the case under consideration, when different components are present. In solutions of individual soaps, such as sodium myristate or palmitate, the two-sided film and solution surface differ less in composition and structure [10]. In such cases differences in the adsorption of the solution components may be attributed to formation of dissociated and undissociated soap micelles, formation of free acid or acid soap, etc., with different adsorptions and mobilities in the bulk of the solution and in the surface layer.

Viscosities of Two-Sided Films and Surface layer of a Mixed 1:9 Palmitate – Oleate Soap Solution; c_{total} = 2.7 millimole/liter•

Serial number of measurement	Object of measurement	η_s in surface poises		$\eta_{s\,film}/\eta_{s\,surf}$ calculated from curves in Fig. 3	State of solution
		surface	film		
1	Surface	7.7	—	--	--
2	Surface	6.4	—	---	—
3	Film	--	4.05	0.58	Turbidity
4	Film	—	2.42	0.346	»
5	Surface	7,0	—	0.214	»
6	Film	—	0.75	0.15	»
7	Surface	0.24	—	0.90	Copious turbidity
8••	Film	---	0.0063	--	» »
9	Film	—	0.0005	--	» »
10	Surface	0.00905	—	—	» »
11	Film	—	0.000029	—	» »

• Radii of the rings R_1 = 2.738 cm, R_2 = 2.995 cm; wire diameter 0.1 cm; elasticity constant of wire C_0 = 2.81 dynes•cm/radian, its diameter d = 0.005 cm; moment of inertia of the system M = 84.9 g cm^2.

•• The values of η_s for the films and surface were obtained by the torsional vibration method, starting with measurement No. 8.

It follows from the foregoing that, in the general case, complete identity of composition and properties of the adsorption layers at the solution surface and in two-sided isolated films or in foam cannot be expected, even if their formation time is (macroscopically) the same. This applies especially to systems of complex composition, many of which are good foaming or wetting agents, used in practice, but it probably holds to a certain extent for all cases, even the simplest "individual" foaming agents.

It is often throught that, at concentrations above the critical concentration of micelle formation, complete soap micelles are adsorbed at once. Apparently it is necessary to take into account the possibility of their decomposition in the course of adsorption, especially at a two-sided foam film, and the possibility of extraction of the most surface-active and mobile components from the micelles in the process.

Institute of Physical Chemistry Acad. Sci. USSR
Moscow

Received January 9, 1957

LITERATURE CITED

[1] J. Perrin, Ann. de phys. 10, 160, (1918).

[2] P. V. Wells, Ann. de phys. 16, 39, (1921).

[3] K. S. Jochonott, Phil. Mag. 47, 501,(1899); 11, 716, (1906).

[4] S. Spierer, Koll.-Z. 54, 17, (1931).

[5] B. V. Deryagin and A. S. Titievskaya, Colloid J., 15, 416 (1953).

[6] W. Rikenbacker, Koll. chem. Beih. 8, 139, (1916).

[7] M. E. Laing, Proc. Roy. Soc. A109, 28, (1925).

[8] A. P. Brady, J. Phys. Coll. Chem.53, 56 (1949); A. Brady, and A. Brown, article in Symposium "Monomolecular Layers," translated from English (Foreign Lit. Press, Moscow, 1956).

[9] A. A. Trapeznikov, Symposium, Viscosity of Liquids and Colloidal Solutions, 1,67, 87,(1941).

[10] P. A. Rebinder and A. A. Trapzenikov, Proc. Acad. Sci. USSR, 18, 421 (1938).

HEATS OF SWELLING AND SOLUTION OF POLYMERS IN RELATION TO MOLECULAR WEIGHTS AND TEMPERATURE

K. S. Akhmedov and S. M. Lipatov

The heat effects of interaction of polymers with organic solvents and plasticizers have been studied by a number of workers. Lipatov and his associates [1] established that acetylcellulose fractions in methyl acetate, and gelatin fractions in water, each have the same heats of swelling and solution at room temperature, irrespective of molecular weight. Kargin and Tager [2] showed that the heats of solution of different nitrocellulose fractions in acetone are equal. However, it has also been found that in a number of instances heats of solution or swelling depend on the molecular weight and the strength of the structure of the polymer. Lipatov and Morozov [3] showed as long ago as 1935 that agar fractions have different heats of swelling and solution. For an agar fraction of molecular weight 6050 the heat of swelling was 36.9 cal./g, and for molecular weight 25,380, the value was 44.6 cal./g, or higher by 7.5 cal./g. Recently Schulz [4] found that the heat of solution of polystyrene fractions depends on the molecular weight. Tager [5] obtained a similar result for the same polymer.

However, as has been shown in a number of papers by Lipatov et al. [6], studies of heat effects at room temperature cannot reveal the structural characteristics of different polymers in relation to their chemical structure, molecular weight, etc. In these papers [6] it was established that structural problems can be solved conclusively only by studying variations of the heats of solution with temperature. This approach has been increasingly used in recent years; it was successfully utilized by Schulz [4] in studying the heats of solution of polystyrenes of different molecular weight, and by Tager [2] in studies of the same polymer.

While it was previously believed that problems of polymer structure could be definitely solved by the simultaneous use of X-ray and electron diffraction methods [7], at the present time the calorimetric method can be regarded as a method for studying structure together with these [6, 8]. Thus, the thermodynamic and structural criteria of the phase state not only do not diverge in the case of polymers, as has been asserted quite recently [9], but they are firmly interconnected, as for substances of low molecular weight.

EXPERIMENTAL

Polyvinyl chloride and perchlorovinyl (chlorinated PVC). To study the effect of molecular weight on the heat of solution of polymers at different temperatures, polyvinyl chloride and two of its fractions were used; for this, polyvinyl chloride was fractionated from 4% solution in dichloroethane by additions of various amounts of absolute alcohol. The chlorine contents of the polyvinyl chloride samples were determined by the Carius combustion method; the value for our samples was 56.2% by weight, corresponding to the following composition: $-CH_2-CHCl-CH_2-CHCl-$.

The molecular weights of the polyvinyl chloride samples were determined viscosimetrically from the intrisic $M^{0.67}$ viscosities of their solutions in dichloroethane at 30°, and calculated from the formula

$$[\eta] = 3 \cdot 10^{-4}\ M^{0.67}.$$

The viscosimetric determinations were performed with a capillary hanging level viscosimeter, adapted for use with volatile liquids, convenient for studies of viscosity over a wide temperature range.

The heats of swelling and solution were determined by means of an adiabatic calorimeter, in adiabatic or isothermal conditions depending on the duration of the swelling and solution processes. The tables and graphs give average values for 2-3 parallel determinations. The determinations were accurate to within ± 0.25 cal./g.

TABLE 1

Intrinsic Viscosities and Molecular Weights of Polyvinyl Chloride Samples in Dichloroethane at 30°

Polymer	Intrinsic viscosity in poises	Molecular weight
Nonfractionated polyvinyl chloride	0.75	117 900
Polyvinyl chloride, Fraction I	0.65	95 500
Ditto, Fraction II	1.15	223 100

Polyvinyl chloride. The behavior of Fractions I and II in two solvents – dichloroethane and nitrobenzene – was studied as a function of the temperature. The heats of swelling and solution of the low and high molecular weight fractions of polyvinyl chloride in dichloroethane and nitrobenzene at various temperatures are given in Figs. 1 and 2.

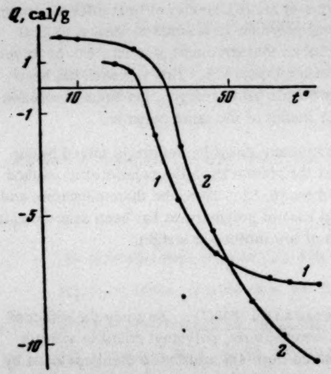

Fig. 1. Variation of the heats of swelling and solution of polyvinyl chloride in dichloroethane with temperature: 1) soluble fraction; 2) insoluble fraction.

It is seen in Figs. 1 and 2 that with increase of temperature the structural differences between the fractions, and the influence of the nature of the solvent on the heat effect and its temperature relationship, become more prominent. Figure 1 shows that the two polyvinyl chloride fractions differ considerably in their behavior in dichloroethane. In the temperature range of 25-50° the first fraction dissolves with a greater negative heat effect than the second, while at temperature above 50-55° a clearly pronounced opposite is seen. Thus, at 70° the first fraction dissolves with absorption of 8 cal./g, and the second, with absorption of 14 cal./g. This is not found with nitrobenzene as solvent (Fig. 2). In the 20-70° temperature range the heats of solution of the two fractions differ sharply, while above 70° they are equal.

Here we have a case in which, for the same packing density, the heat of solution varies greatly at different temperatures according to the nature of the solvent.

Ftorlon.* A similar study was made of the heats of swelling and solution of three fluorinated polymer samples with equal fluorine contents, but with different specific viscosities in 0.25% solutions in acetone** (η_{sp}).

---

* "Ftorlon" derives its name from "ftor", Russian from fluorine, and is one of the fluorinated hydrocarbon polymers.

** The fluorinated polymers with definite characteristics were kindly supplied by Z. A. Rogovin, to whom we express our gratitude.

The heats of solution of the fluorinated polymers in acetone at different temperatures are given in Table 2 and Fig. 3.

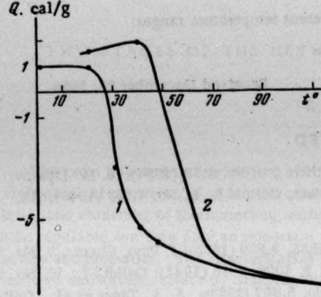

Fig. 2. Variation of the heats of swelling and solution of polyvinyl chloride in nitrobenzene with temperature: 1) soluble fraction; 2) insoluble fraction.

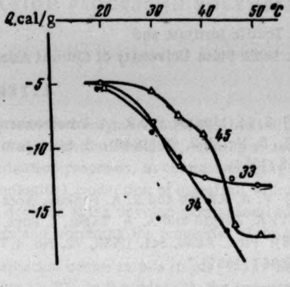

Fig. 3. Variation of the heats of swelling and solution of three fluorinated polymer samples (33, 34, 45) with temperature.

TABLE 2

Heats of Solutions of Fluorinated Polymers (Q cal./g) in Acetone at Different Temperatures

Temperature in °C	Heats of solution in cal./g		
	Sample 33 $\eta_{sp} = 0.26$	Sample 45 $\eta_{sp} = 0.705$	Sample 34 $\eta_{sp} = 0.94$
20	— 5.14	— 5.10	— 5.14
30	— 8.20	— 5.33	— 8.80
35	—11.75	— 7.60	—10.65
40	—12.35	— 9.00	—14.45
45	—12.44	—16.37	—16.5
50	—13.2	—17.0	—22.5

As Table 2 shows, the heats of solution of the fluorinated polymers in acetone in the 20 to 50° temperature range are negative. Samples 34 and 45 show a gradual decrease of the heat effect of solution with temperature, the decrease being greater with higher solution viscosity. Sample 33, with considerably lower solution viscosity, shows a sharp decrease of the heat of solution between 20 and 35°, but from 35° the heat of solution remains constant. These results demonstrate the influence of molecular weight on the heats of swelling and solution as a function of the temperature. However, the influence of the molecular weight greatly depends on the chemical composition and physical state of the polymers.

The heat effect for amorphous polystyrene increases with increasing molecular weight, and the curves lie higher for greater molecular weights [4]. At 20°, despite the molecular weight differences, the heats of swelling of the polymers are equal, but a 50° increase in the molecular weight of the polymer results in an increasing negative value of the heat of solution.

SUMMARY

1. The effect of temperature on the heats of swelling and solution of polyvinyl chloride and ftorlon of different molecular weights has been studied.

2. The increasing negative heat effect cannot be attributed to changes of packing density.

3. The influence of the molecular weight differs in different temperature ranges.

Moscow Textile Institute and
the V. I. Lenin State University of Central Asia

Received December 28, 1956

LITERATURE CITED

[1] S. M. Lipatov and Z. A. Preobrazhenskaya, J. Gen. Chem., 4, No. 1,59 (1934); S. M. Lipatov, Colloid J., 8, No. 1-2, 73 (1946); S. M. Lipatov and S. I. Meerson, Colloid J., 8, No. 4,233 (1946); 12, No. 2,122 (1950).

[2] V. A. Kargin and S. A. Papkov, Acta Physicochim. URSS, 3,839 (1935); J. Phys. Chem., 7, No. 4,483 (1936); V. A. Kargin and A. A Tager, J. Phys. Chem., 15, No. 9, 1029, 1036 (1941); Colloid J., 10, No. 6, 455 (1948); Proc. Acad. Sci. USSR, 72, No. 4,725 (1950); 73, No. 5,967 (1950); A. A. Tager et al., Colloid J., 14, No. 5,367 (1952).*

[3] S. M. Lipatov and A. A. Morozov, J. Gen. Chem., 5, No. 8, 1120 (1935).

[4] G. V. Schulz, Naturwissensch. 40, 164, 1953; Z. phys. Chem. 192, 221, 1955.

[5] A. A. Tager, R. V. Krivokorytova, and P. M. Khodorov, Proc. Acad. Sci. USSR, 100, No. 4, 741 (1955).

[6] S. M. Lipatov, Proc. Acad. Sci. USSR, 48, No. 6,434 (1945); S. M. Lipatov and S. I. Meerson, Colloid J., 8, No. 4,233 (1946); 12, No. 2,125 (1950); S. I. Meerson, Dissertation (Moscow, 1945).

[7] G. L. Slonimsky, Mechanical Properties of Polymers and the Properties of their Solutions (State Light Ind. Press, Moscow, 1951).

[8] N. V. Mikhailov and E. Z. Fainberg, Proc. Acad. Sci. USSR, 109, 1160 (1956).

[9] B. A. Kargin and G. L. Slonimsky, Progr. Chem., 24, 785 (1955).

---

* Original Russian pagination, see C. B. Translation.

TWO STAGES OF THE NETWORK FORMATION PROCESS IN POLYMERS

G. M. Bartenev

The cross linking (structurization) of linear and slightly branched polymers forms the basis of a number of technological processes, of which the most important are: vulcanization of rubber, tanning of collagen and gelatin, and hardening of thermosetting resins. These structurization processes, in contrast to aging processes, can be regulated and they play an important part in the technological production of materials with required structure and properties. The structurization processes which occur in aging develop spontaneously and in most cases have and adverse effect by changing the desired structure and worsening the properties of the materials.

It has been shown that the process of spatial network formation occurs in two stages [1-3]. The two-stage nature of the process was observed in the first two investigations [1, 2]. In the third [3], the importance of the initial molecular weight of the polymer was established. It was shown that the start of network formation corresponds to a certain quite definite amount of bound sulfur, which depends on the molecular weight of the polymer. The first general views on the two-stage nature of the process were probably put forward by Flory [4].

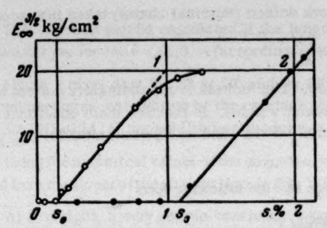

Fig. 1. Relationship between the equilibrium modulus and the amount of bound sulfur (in weight percentages on the vulcanizate): 1) NR (natural rubber); 2) SKS-30A.

The general mechanism of spatial network formation in the structurization of linear polymers, for the case of rubber vulcanization, is discussed below. The chemical aspects of polymer network formation are discussed in a recent review [5].

1. The two-stage nature of the network formation process is seen in Fig. 1, which shows, as an illustration, the variation of the equilibrium modulus (to the power 3/2) with the amount of sulfur bound during vulcanization of an unfilled natural rubber composition (NR), of molecular weight 150,000, modulus at 20°, from N. M. Novikova's data, and a synthetic SKS-30A rubber fraction of molecular weight 140,000, modulus at 70°, from the data of F. A. Galil-Ogly. The choice of the equilibrium modulus to characterize the spatial network [6, 7] is explained by the fact that the equilibrium modulus E_∞ bears a definite relationship to the number of chains in the network N per unit volume. In Fig. 1, values of $E_\infty^{3/2}$, which, according to [6], is proportional to N, are taken along the ordinate axis. If the amount of bound sulfur is proportional to the number of cross links, then the relationship between $E_\infty^{3/2}$ and the amount of bound sulfur must be linear; this is found to be so for all fractions of SKS-30A at the second stage of cross linking [3]. Natural rubber shows a deviation from linearity at the end of the second stage; this is explained by superposition of thermooxidative degradation processes on the vulcanization.

At the first stage a single spatial network is not yet formed, as the equilibrium modulus is zero. At the first stage the material is in a plastic, and at the second, in an elastic state. At the first structurization stage the molecular chains are not yet joined in a single spatial network, but individual molecules are cross-linked into larger formations. Only after these molecular aggregates have reached a definite size does the subsequent cross linking lead to the formation of a continuous spatial network.

2. Let us consider the cross linking of a linear polymer with initial molecular weight M_0, assuming that the cross links have a statistically uniform distribution throughout the volume. Let M be the molecular weight of a chain in the network (segment of a linear molecule between two cross links). Corresponding to these are N_0 and N, the numbers of original molecules and network chains per unit volume; n is the total number of cross links per unit volume of the polymer; ν is the number of cross links per unit volume.

At the first stage of structurization the cross links join individual linear molecules, which results in an increase of the average molecular weight of the polymer. As has been reported [1, 4, 8], network formation begins not at once, but after all (or nearly all) the molecules of the original material have been joined by cross links. At this stage long branched chains are formed, much larger than the original linear molecules. Thus, cross linking of individual molecules leads to formation of long branched chains, the molecular weight M of which increases to values greatly exceeding M

The material remains plastic until enough cross links have been formed to join the original molecules into a spatial network. We shall term this number of cross links per unit volume the "critical" number, and shall denote it by $n_k = \beta N_0$, where β is a coefficient which depends on the molecular weight distribution, and the degree of coiling and intertwining of the molecules in the original material (the meaning of the coefficient β is discussed below).

It is evident that when $n < n_k$, $\nu = 0$; when $n \geqslant n_k$, $\nu = n - n_k$.

The number of chains N determines the equilibrium properties and is included in the formulas of the molecular theory of network polymers. Since each new cross link forms two new chains, $N = 2\nu$, and therefore when $n \geqslant n_k$

$$N = 2(n - nk) = 2(n - \beta N_0), \qquad (1)$$

and when $n < n_k$, $N = 0$.

The Flory formula [4, 8] derived (for $\beta = 1$) with network defects (terminal chains) taken into account

$$N = \frac{\rho_0 N_A}{M}\left(1 - \frac{2M}{M_0}\right)$$

is not suitable for the whole $n \geqslant n_k$ range of network formation. The formula is approximately correct when $M \ll M_0$, that is, for dense networks and high original molecular weights. In practice these conditions are probably satisfied for network polymers with molecular weight $M_0 > 10^5$ and equilibrium modulus E_∞ greater than 10 kg / cm².

The general formula valid over the entire $n \geqslant n_k$ range has the following form

$$N = 2n \Big/ \left(1 + \frac{2\beta\rho M}{\rho_0 M_0}\right),$$

where ρ is the density for the active part of the rubber; ρ_0 is the density for the whole rubber, including the regions of the molecules which did not enter the network. Calculation of ρ is the main difficulty in the use of this formula.

3. To illustrate the application of these relationships, let us consider the vulcanization of butadiene-styrene SKS-30A and natural (NR) rubber. Let j be the number of sulfur atoms per cross link both between different molecules and between parts of the same molecule. The total and "critical" numbers of cross links are expressed in terms of the amount of bound sulfur by the following formulas:

$$n = \frac{\rho N_A}{\mu j}\,\frac{s}{100}; \qquad n_k = \frac{\rho N_A}{\mu j}\,\frac{s_0}{100}, \qquad (2)$$

where $\mu = 32{,}1$ is the atomic weight of sulfur; s and s_0 are the total and "critical" amounts of bound sulfur in percentages by weight (on the vulcanizate).

For the "critical" amount of bound sulfur we have the formula

$$s_0 = \beta j/\mu \cdot 100 \frac{1}{M_0}, \tag{3}$$

which is in good agreement with the data [3] given in Fig. 2.

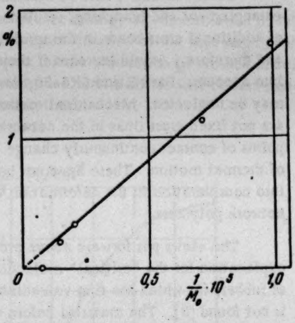

Fig. 2. Relationship between the "critical" amount of sulfur added during vulcanization, and the reciprocal molecular weight of the original polymer (from data in [3]).

The value of s_0 is determined from the intercept cut off (Fig. 1). For NR ; s_0 is 0.15% at M_0 = 150.000, which gives β j = 7. For SKS-30A the value, found from the straight line in Fig. 2, is β j = 50.

It is not possible to determine the number of sulfur atoms in the cross link, j, by the intercept method, as the coefficient β is not known. It is possible to find j from the slope of the straight line in the coordinates of Fig. 1.

From Equations (1) and (2) it follows that

$$N = \frac{2\rho N_A}{\mu j} \frac{\Delta s}{100}, \tag{4}$$

where $\Delta s = s - s_0$.

For further calculations by this formula it is necessary to know the relationship between N and E_∞. For this we use the relationship $N = CE^{3/2}_\infty$ [6], where C is a constant which depends on the physical properties of the polymer molecules and the temperature.

This constant can be calculated if the length of the chain segment in the Kuhn model is known. According to Vishnitskaya, for NR l = 12.0 Å (according to Kuhn l = 13 Å), and for SKS-30A l = 12.6 Å.

Figure 1 gives data for NR at 20° and for SKS-30A (fraction of molecular weight 140,000) at 70°. For these temperatures, calculation of the constant gives the following values: $C = 2.29 \cdot 10^{18}$ for NR, and $C = 1.96 \cdot 10^{18}$ for SKS-30A, if the equilibrium modulus is expressed in kilograms per 1 cm^2.

Using the numerical values of the quantities in Formula (4) $\rho = 0.96$ for NR, $\rho = 0.94$ for SKS-30A vulcanizates), we find from the slopes of the straight lines in Fig. 1 (for NR) and Fog. 3 (for SKS-30A that j ≈ 7 for both rubbers.

At first sight, a very simple conclusion suggests itself: each cross link is formed by the opening of an eight-membered molecular sulfur ring, as in vulcanization without accelerators [9]. However, this cannot be asserted, in view of the possible deviations from the ideal vulcanization process. There are data [9] showing that j should be smaller in vulcanization with an accelerator *.

Network defects (in contrast to the ideal network formed by cross linking of a linear polymer of the maximum molecular weight) include closed loops, end of molecules not included in the network, mechanical entanglement of two chains (according to Flory [4]), cross links in close proximity to each other, and branching of the polymer chains. These "defects" can be taken into account only roughly and qualitatively. It has been shown for NR [6] that the ends of the original rubber molecules which do not enter into the network do not influence the equilibrium modulus if the initial molecular weight is high enough (150,000) and the modulus is not too low. It is evident that defects like ends and closed loops depend on the initial molecular weight. It follows from the data in Fig. 3 that for SKS-30A rubber these defects are not significant, as the initial molecular weight has practically no influence on the equilibrium modulus.

---

* It must be taken into account that part of the added sulfur does not form cross links [1], and this may lead to a decrease of j. From the experimental results given (Figs. 1, 3, 4) it follows that the amount of sulfur which does not form cross links is proportional to the total amount of bound sulfur.

Cross links in close proximity arise with increasing frequency as the spatial network becomes denser and with greater irregularity of distribution of the sulfur molecules through the vulcanizate. Such defects should lead to deviations from the linear relationship shown in Fig. 3 only with high contents of bound sulfur. For thin networks, such as are represented by the data in Figs. 1-3, these defects can probably also be ignored. If ends, loops, and closely situated cross links are taken into account, the value of $\underline{j}$ should decrease (to only a slight extent for the vulcanizates in question).

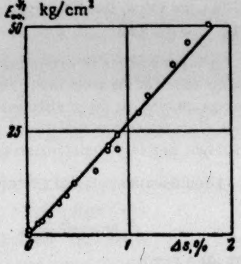

Fig. 3. Variation of equilibrium modulus with the amount of bound sulfur added in the second stage of vulcanization, for different fractions of SKS-30A rubber with molecular weights from 100,000 to 1,170,000, from F. A. Galil-Ogly's data (equilibrium modulus determined at 70°).

Other "defects", such as mechanical entanglement and branching, result in formation of additional cross bonds in the spatial network and therefore $\underline{j}$ would increase if they are taken into account. For NR and SKS-30A branching may be neglected. Mechanical entanglements are not fixed cross links in the network, as the points of contact continuously change because of thermal motion. These have not been taken into consideration in the deformation theory of network polymers.

The views put forward above provide an explanation for the "critical" molecular weight of rubber, for which the first vulcanization stage is not found [3]. The material before vulcanization usually contains a certain number n' of cross links of various origins. With a high enough molecular weight of the rubber this number may reach the critical value, and the critical molecular weight is therefore $M'_0 = \beta \rho N_A / n'$.

The different coefficients for NR and SKS-30A ($\beta = 1$ and $\beta = 7$) were somewhat unexpected. The probable explanation for the difference lies in the technological preparation of the materials for vulcanization. Fractions of SKS-30A rubber were prepared in the form of films from a solution of the rubber and other ingredients in benzene, while the natural rubber mix was made in the usual way on rolls. The same result as for NR ($\beta = 1$), was obtained for SKS-30A and SKS-30 mixes made on rolls. This probably indicates that the molecules become globulized in solution [10], in contrast to processing on rolls, * when the chain molecules become ruptured and entangled.

In a globular structure a considerable proportion of the cross links is used in intramolecular cross linking, and the rest in intermolecular, which prolongs the first structurization stage.

4. In rubber technology attention has been devoted mainly to studies of the vulcanization optimum. The initial stage of vulcanization has been studied only recently. In two investigations [11, 12] the conditions and duration of the initial stage of vulcanization were studied both from the technological and the chemical aspects (chemical kinetics of cross link formation).

The first vulcanization stage determines the correct technological production of molded rubber articles. The flow of the rubber mix and filling of the mold depend on the existence of this stage. The pressure in the vulcanization press and in pressure molding makes for a more rapid filling of the mold. Absence of the first vulcanization stage leads to the undesirable effect known as "scorching", **

---

* In this case the molecular weight M_0 refers not to the original rubber but to the material after treatment on rolls.

** At vulcanization temperatures (130 – 150°, as has been shown [9, 13, 14]), irreversible flow occurs in network polymers also, but the rate of plastic deformation at the second vulcanization stage is low and the mold is filled mainly during the first stage of the process.

The duration of the first vulcanization stage $t = \int_0^{s_0} \frac{ds}{W}$ depends on the sulfur addition rate $W = ds/dt$, critical amount of sulfur s_0, and therefore on the type of accelerator group, vulcanization temperature, technological preparation, and the molecular weight of the starting material. Absence of the first vulcanization stage is a result of the fact that a critical or larger number of cross links is formed in the original material before vulcanization, owing to thermooxidation processes, scorching, and other structurization processes. The existence of a prolonged first vulcanization stage (like its absence) is undesirable, and is caused by a low rate of sulfur addition, low molecular weight, absence of high molecular weight fractions in the rubber, globular structure of the polymer, etc.

Correct technology of vulcanization of rubber mixes in molding presses should correspond to a quite definite optimum duration of the first stage of the process. At present the composition of the technological rubber mixes for the production of molded articles is based on the results of practical experience. Therefore the technological potentialities will be increased by the use of a method whereby the duration of the first stage can be determined.

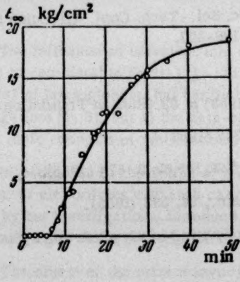

Fig. 4. Variation of the equilibrium modulus with vulcanization time for unfilled SKS-30 rubber, from data in [2].

The duration of the first stage can be determined by measurements of the equilibrium modulus for different times of vulcanization of the mix*. As an illustration of this method, Fig. 4 shows the variation of the equilibrium modulus with vulcanization time for an unfilled mixture made on rolls from SKS-30 rubber with 3 parts of sulfur and 1 part of mercaptobenzothiazole by weight, at a vulcanization temperature of 143°.

At the present time the optimum value of the first vulcanization stage is chosen indirectly – by plasticity tests on the mixes and by selection of rubbers of suitable molecular weight distribution**, by addition of antioxidants, and by suitable selection of vulcanizing groups, mixing conditions, and vulcanization temperature.

The effectiveness of the proposed method should be verified by further investigations on technical rubbers. Applications of the method to studies of structurization processes in gelatin and resins [15, 16] are of undoubted interest.

SUMMARY

1. The two-stage nature of network formation in polymers is discussed, and a formula is derived connecting the number of chains in the network with the initial molecular weight of the polymer and the number of cross links. It is shown that below a certain critical number of cross links a network is not formed.

2. The application of the derived relationships in determination of the number of sulfur atoms in the cross links, the critical molecular weight, and the degree of globulization of the rubber, has been studied in the case of rubber vulcanization.

3. The first vulcanization stage is shown to be of considerable practical importance, as it determines the correct technological conditions for the vulcanization of rubber in molding presses, multilayer articles, etc. For this reason, determinations of the vulcanization optimum in rubber technology must be augmented by studies of the initial stage of the process. A method for determining the duration of the first stage of vulcanization is described.

---

* The nonequilibrium (technological) modulus is unsuitable for this purpose, as it is not zero for the plastic state.

** The simultaneous presence of fractions of low and high molecular weight ensures plasticity of the mixture at the first stage and a high rate of network formation at the second stage.

I express my gratitude to B. A. Dogadkin for discussion of the work.

Scientific Research Institute for the Rubber Industry
Moscow

Received May 4, 1956

LITERATURE CITED

[1] B. A. Dogadkin, G. M. Bartenev, and N. M. Novikova, Colloid J., 10, No. 2,94 (1948).

[2] G. M. Bartenev and G. I. Belostotskaya, J. Tech. Phys., 24, No. 10, 1773 (1954).

[3] A. S. Novikov, G. M. Bartenev, and F. A. Galil-Ogly, Proc. Acad. Sci. USSR, 94, No. 22, 253 (1954).

[4] P. Flory, Chem. Rev. 35, 51, (1944).

[5] B. A. Dogadkin and M. M. Reznikovsky, Progr. Chem. 24, No. 7, 801 (1955).

[6] G. M. Bartenev, J. Tech. Phys., 22, No. 7, 1154 (1952); Proc. Sci.-Tech. Conf. All-Union Sci. Tech. Soc. Rubber Technologists, 1953 (State Chem. Press, 1954) pp. 196-207.

[7] L. A. Vishnitskaya, Trans. Inst. Rubber Ind., 1,53 (1954).

[8] L. Treloar, Physics of Rubber Elasticity (Foreign Lit. Press, 1953) p. 69. [Russian Translation.]

[9] B. A. Dogadkin and Z. N. Tarasova, Colloid J., 15, No. 5, 347 (1953).*

[10] A. S. Novikov, T. V. Dorokhina, and P. I. Zubov, Proc. Acad. Sci. USSR, 105, No. 3, 514 (1955).

[11] B. A. Dogadkin, M. Feldhstein, and D. Pevzner, J. Appl. Chem., 28, 533, (1955).

[12] B. A. Dogadkin, Bond Strength Between the Layers of Rubber-Fabric Multilayer Articles (State Chem. Press, 1956) pp. 16-28.

[13] A. Tobolsky, I. Prettymann, J. Dillon, Appl. Phys. 15, 380, (1944).

[14] G. L. Slonimsky, V. A. Kargin, G. N. Buiko, E. V. Reztsova, and M. Lyuis-Riera, Proc. Acad. Sci. USSR, 93, 523 (1953).

[15] P. I. Zubov, Z. N. Zhrukina, and V. A. Kargin, Colloid J., 16, 109, 345 (1954).*

[16] G. L. Slonimsky, V. A. Kargin, and L. I. Golubenkova, Proc. Acad. Sci. USSR, 93, 311 (1953).

---

* [Original Russian pagination. See C. B. Translation].

THE ELECTROCHEMISTRY OF HIGH POLYMER DISPERSIONS

4. INFLUENCE OF CATIONS OF DIFFERENT VALENCIES ON THE ELECTROKINETIC POTENTIAL OF SYNTHETIC LATEX GLOBULES

S. S. Voyutsky and R. M. Panich

The influence of univalent ions on the zeta-potential of negatively charged latex globules has been studied in considerable detail [1]. In contrast to this, the action of multivalent ions on the electrokinetic potential of latex globules has hardly been studied at all. This question has only been touched upon in our investigations [2, 3], but as the zeta-potential was determined by an imperfect method without allowance for the ionic strengths of the solutions, the results obtained require correction.

Investigation of the action of multivalent cations on the zeta-potential of latex globules is of great interest, as electrolytes with such cations are the usual latex coagulant in industry. Moreover, as was first shown by our investigations, introduction of multivalent cations into the latex results in reversal of the globule charge, which may also be of great practical importance.

The object of the present investigation was a more detailed comparative study of the effects of cations of different valencies on the zeta-potential of synthetic latex globules, with due attention to all the requirements of the experimental technique for determination of electrophoretic mobility. Considerable attention was also paid to charge reversal on the latex particles by means of multivalent ions.

Determination of the thresholds of coagulation of latex by electrolytes.

First, the maximum electrolyte concentrations were determined at which the latex is still stable and does not contain floccules which hinder electrophoresis. The material studied was dialyzed BDl latex, containing ammonium napthenate stabilizer. Fuller details of this latex were given in an earlier communication [4].

TABLE 1

Threshold of Coagulation of Latex BDl by Electrolytes with Cations of Different Valencies

Electrolyte	Coagulation threshold in millimoles/liter	Ratio of coagulation thresholds
NH_4Cl	440	245
$CaCl_2$	6.7	3.75
$AlCl_3$	1.8	1.0

The electrolytes used were ammonium chloride, calcium chloride, and aluminum chloride. The first was chosen because the latex contained ammonium ions; the second, because calcium ions are usually present in industrial water; and the third because, in industry, aluminum salts are generally used for latex coagulation. These electrolytes all had the same anion. The coagulation threshold was determined by mixing equal volumes of latex and electrolyte solutions of various concentrations. The concentration of BDl latex used for the experiments was 1%. The results are given in Table 1, where the concentrations given for calcium and aluminum chlorides correspond to irreversible coagulation, while the aluminum chloride concentration corresponds to reversible flocculation, which disappears on dilution of the latex with water.

Table 1 shows that, for latexes with negatively charged particles, the valency of the cation has a very strong influence on the coagulation threshold; i. e., the Schulze – Hardy rule for lyophobic colloidal systems is obeyed. Table 1 shows also that the coagulation thresholds for uni- and bivalent ions are inversely proportional to the sixth power of the valency, which is in agreement with the formula derived by Deryagin and Landau [6] from the theory of stability of Lyophobic sols, and which is a quantitative refinement of the Schulze – Hardy rule. The deviation from this rule for the trivalent cation may be attributed either to the effects of hydrolysis, or to approach to charge reversal.

Effect of electrolytes on the zeta-potential of latex globules. The experiments to determine the effect of electrolytes on the zeta-potential of latex globules were carried out by the macro-electrophoretic technique described in an earlier communication [5]. The dialyzed BDI latex, diluted with distilled water to 1% solid content, was mixed with an equal volume of buffer solution with ionic strength 0.02 and pH 9.9, to which the required amount of electrolyte had previously been added. In contrast to the experiments described in the preceding section, the electrolyte with a univalent cation was sodium chloride. The auxiliary liquid in the apparatus was a mixture of buffer and electrolyte diluted with an equal volume with distilled water.

The zeta-potential was calculated by means of the Henry formula [7] with corrections for electrical relaxation. The numerical coefficient in the formula was found from the appropriate curves in the diagram given in Overbeek's paper [8], which shows the variation of the coefficient with a certain criterion κa. For sodium and aluminum chlorides, the coefficient was determined from the curve for a uni-univalent electrolyte, and for calcium chloride, from the curve for a bi-univalent electrolyte.

The curve for a uni-univalent electrolyte was used in the case of aluminum chloride because, as has been shown by Nikolsky and Paramonova [9], this salt is hydrolyzed at pH 4 and above to the hydroxide, while the hydroxide is ionized to give univalent ions. At pH > 8, these are mainly the anions $Al(OH)_2O^-$ or AlO_2^-, and at pH < 8, $AlCOH)_2^+$ cations. Trivalent aluminum ions can only appear in solution at pH < 4.

The results of the electrophoretic determinations are given in Table 2.

It is seen from Table 2 that addition of increasing amounts of electrolytes with uni- and trivalent cations leads first to some increase and then to a decrease of the zeta-potential of the latex globules. Increase of the concentration of bivalent electrolyte results in a steady fall of the potential.

As was to be expected, if the results are calculated per unit concentration of the added electrolyte, aluminum chloride lowers the zeta-potential to a greater extent than the other electrolytes, while sodium chloride has the least effect. It is important that coagulation of the latex by aluminum and calcium chlorides began not at the zeta-potential which corresponds to the appearance of floccules on addition of sodium chloride, but at a much higher value.

Charge reversal of the latex globules by addition of aluminum chloride to to the latex. It might have been expected that multivalent cations, having higher adsorption potentials, reverse the charge on latex globules as effectively as hydrogen ions, which are readily adsorbed [9]. In fact, our experiments showed that additions of definite amounts of aluminum chloride solution to 2-4% latexes resulted only in partial coagulation and charge reversal of the globules remaining in the latex. It should be pointed out, however, that in such cases charge reversal took place only when equal volumes of aluminum chloride solution with a concentration of 1 millimole/liter and over were added to the latex. Additions of aluminum chloride at lower concentrations did not result in charge reversal, but merely lowered the electrokinetic potential of the latex globules and decreased the stability of the system.

As is seen in Fig. 1, as increasing amounts of aluminum chloride are added to latex BDI, the zeta-potential of the globules first increases very lightly, then falls, and at a certain not very high electrolyte concentration (~ 1 millimole / liter of the final solution) the latex coagulates. The coagulum so formed is quite unlike the coagulum formed by acidification of the latex, but consists of a fine powder or loose lumps, easily rubbed apart by the fingers. However, the range of aluminum chloride concentrations causing coagulation of the latex is not wide. If this concentration is exceeded slightly, the latex is not coagulated and charge reversal takes place. Still larger amounts of aluminum chloride decrease the positive zeta-potential only slightly. It is significant that on addition of very large amounts of aluminum chloride (46 millimoles/liter and over) the latex again becomes unstable, and coagulates.

TABLE 2

Effect of Electrolytes on the Zeta-Potential of BDl Latex Globules

Electrolyte	Electrolyte concentration, millimoles/liter	pH	Ionic strength	Electrophoretic mobility in $\frac{\mu/\text{sec}}{\text{v}/\text{cm}}$	Coefficient in the Henry equation	Zeta-potential in mv
NaCl	0	9.9	0.01	—4.87	4.9	—83.2
	80	9.8	0.09	—6.05	4.55	—95.5
	170	9.8	0.18	—3.93	4.45	—61.0
	260	9.8	0.27	—2.12	4.35	—32.0
$CaCl_2$	0	9.9	0.01	—4.87	4.9	—83.2
	1.12	9.6	0.013	—3.85	5.7	—76.5
	2.25	9.3	0.017	—3.70	5.55	—71.5
	4.5	9.2	0.026	—2.76	5.3	—51.0
$AlCl_3$	0	9.9	0.01	—4.87	4.9	—83.2
	0.23	9.7	0.011	—5.38	4.9	—92.0
	0.46	9.5	0,018	—5.25	4.9	—90.0
	0.92	9.2	0,015	—4.00	4.7	—65.5

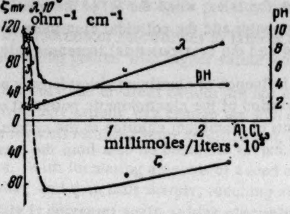

Fig. 1. Variations of the zeta-potential of the globules, pH, and specific conductance (λ) of BDl latex on addition of aluminum chloride.

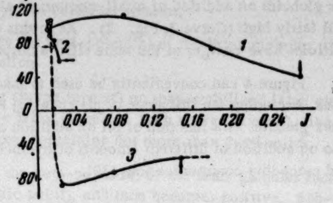

Fig. 2. Effect of ionic strength (J) on the zeta-potential of BDl latex globules on addition of various electrolytes: 1 – NaCl; 2 – $CaCl_2$; 3 – $AlCl_3$

DISCUSSION OF RESULTS

For a clearer picture of the effect of electrolytes on the zeta-potential of latex globules and latex stability, let us examine the curves in Fig. 2, based on the data in Table 2 and Fig. 1. The ionic strengths of BDl latex samples diluted with buffer solution and containing various amounts of electrolytes are taken along the abscissa axis, while the ordinates represent the corresponding electrokinetic potentials of the latex globules. The last points on the curves, indicated by arrows, correspond to the highest electrolyte concentrations at which the zeta-potential could still be determined. These maximum concentrations decrease sharply with increasing valency of the cation.

With increasing sodium chloride content in the latex the zeta-potential first increases somewhat, then begins to fall. An increase of the zeta-potential of latex globules on addition of small amounts of electrolytes with univalent cations has been reported by other investigators [11, 12]. The cause of this effect probably lies in adsorption of the anions present in the system by the globules. The glycine anion in the buffer mixture, or the chloride anion, may habe this effect. The subsequent decrease of the zeta-potential is probably to be explained by compression of the electric double layer.

Addition even of small amounts of calcium chloride to the system results in a sharp decrease of the zeta-potential. Addition of aluminum chloride produces first a slight increase of the zeta-potential, and then a sharp decrease and coagulation. If excess aluminum chloride is added, in certain conditions the latex globules may undergo charge reversal. There are two complicating factors, to which reference was already made earlier, in the action of aluminum chloride on the latex.

1. Then aluminum chloride is added to the latex it is hydrolyzed, and the system therefore becomes more acid. Thus, when aluminum chloride is added, the zeta-potential of the globules is influenced not only by the aluminum ions but also by the change in the solution pH as the result of hydrolysis.

2. From pH 4 and above a colloidal suspension of insoluble aluminum hydroxide is formed in the system, stabilized by ions which may arise during its ionization. The structure of the aluminum hydroxide micelles on each side of the isoelectric point, according to Nikolsky and Paramonova [9], is shown schematically in Fig. 3.

It follows from the foregoing that at pH < 8 latex to which aluminum chloride had been added contains positively charged colloidal particles of aluminum hydroxide. These, in becoming adsorbed on the as yet negatively charged globules, cause, in our opinion, a sharp decrease of the zeta-potential, and in certain conditions also charge reversal. Evidence of the adsorption of aluminum hydroxide by the latex particles is provided by the fact that the coagulum formed in these conditions differs in appearance from the coagulum formed when the latex is acidified. The explanation for the powderlike nature of the coagulum is that a layer of aluminum hydroxide is formed around the globules, protecting them against direct contact and thereby preventing the formation of the usual compact aggregates.

In our opinion, adsorption of colloidal aluminum hydroxide particles, having a high adsorption potential, on the surface of the negatively charged latex globules also accounts for the increase in the zeta-potential of the globules on addition of small amounts of aluminum chloride to the latex, when the pH of the medium is still fairly high (Curve 3, Fig. 2). As in this case the polymer globules and the colloidal aluminum hydroxide particles have charges of the same sign, adsorption is not too rapid and the zeta-potential increases only slightly.

Figure 4 can conveniently be used to take into account the influence of aluminum chloride only on the latex, excluding the influence of pH changes; Fig. 4 shows the variation of the electrokinetic potential of the latex globules as a function of pH on addition of increasing amounts of aluminum chloride to the system, and also on addition of different amounts of hydrochloric acid. These curves are based on data from the present and preceding communications [10].

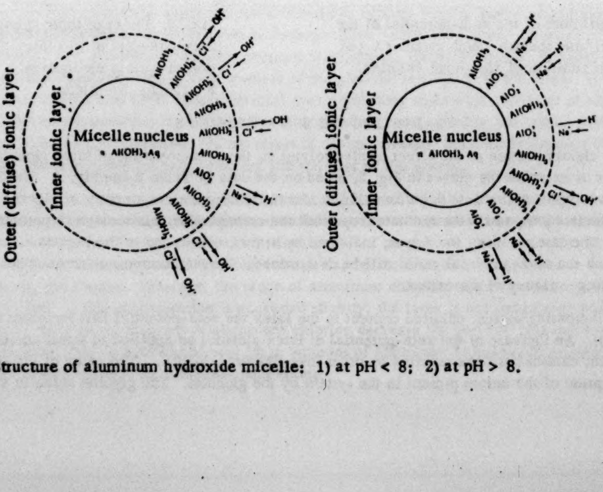

Fig. 3. Structure of aluminum hydroxide micelle: 1) at pH < 8; 2) at pH > 8.

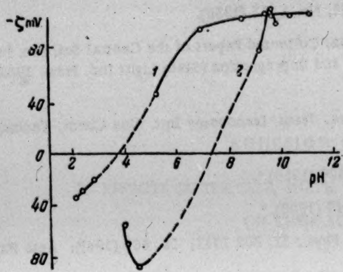

Fig. 4. Zeta-potential of BD1 latex globules as a function of pH in experiments with additions of: 1) hydrochloric acid; 2) aluminum chloride.

Comparison of Curves 1 and 2 (Fig. 4) shows that addition of aluminum chloride to the system shifts the zera-potential – pH curve for the latex in the direction of higher pH values than the curve obtained for the addition of hydrochloric acid. The curve for the addition of aluminum chloride to the latex cuts the abscissa axis at pH ~ 8, which coincides with the isoelectric point of aluminum hydroxide. Evidently the electrical properties of the particles below pH 8 are wholly determined by the aluminum hydroxide layer adsorbed on the globules.

Adsorption of aluminum hydroxide accounts for the certain difference in shape between Curves 1 and 2 in Fig. 4. Curve 2 has a minimum as a result of the fact that on further decrease of pH the hydroxide dissolves, the adsorbed layer of hydroxide on the latex globules becomes less dense, and the positive zeta-potential decreases.

It should also be noted that, for dialyzed latex, the positive zeta-potential is much higher in presence of aluminum chloride than in presence of hydrogen ions, which indicates that the positively charged colloidal aluminum hydroxide particles have a high adsorption potential.

SUMMARY

1. The coagulation of latexes stabilized by soaps, by electrolytes with cations of different valencies entirely conforms to the Schulze – Hardy rule, established for typical colloidal systems.

2. Addition of electrolytes to latexes in general decreases the zeta-potential of the latex globules, the decrease being greater with higher valency of the electrolyte cation.

3. Uni- and divalent cations are not capable of effecting charge reversal on soap-stabilized latex globules, while trivalent cations can change the sign of the charge on the latex globules. Such charge reversal, like the charge reversal resulting from acidification, occurs only in latexes containing not more than 2-4% solids.

4. With increasing amounts of added aluminum chloride the zeta-potential of the latex globules increases somewhat, and then falls sharply, reaching zero (at the isoelectric point), and then becomes positive. Subsequently it decreases again at high electrolyte concentrations in the system. Addition of aluminum chloride to the latex gives rise to two regions of aggregative instability, corresponding to two regions of low zeta-potential.

5. When aluminum salts are added to latexes, the zeta-potential of the globules is influenced not only by the ions formed by ionization of these salts, but also by the pH changes resulting from their hydrolysis. To establish the effect of the aluminum ions only, zeta-potential – pH curves for latex acidified by different amounts of HCl should be compared with similar curves for latex containing different amounts of aluminum chloride.

6. When aluminum chloride is added to latexes, the active ions are apparently not Al^{3+} ions but, at pH > 8, $Al(OH)_2O^-$ or AlO_2^- ions, and at pH < 8, $Al(OH)_2^+$ ions formed from aluminum hydroxide which is produced in the hydrolysis of aluminum chloride. At pH < 8, in latexes to which aluminum chloride has been added, positively charged colloidal particles of aluminum hydroxide are probably formed. These are adsorbed on the latex globules and cause a sharp decrease of the negative electrokinetic potential, followed by charge reversal.

The Moscow Institute of Fine Chemical Technology

Received April 4, 1956

LITERATURE CITED

[1] S. S. Voyutsky and R. M. Panich, Progr. Chem., 25, No. 1, 57 (1956).

[2] S. S. Voyutsky, R. M. Panich, and K. A. Kalyanova, Collected Papers of the Central Sci. Res. Inst. for Leather Substitutes on the Theory and Practice of Sizing and Impregnation (State Light Ind. Press, 1952) p. 90.

[3] S. S. Voyutsky, R. M. Panich, and K. A. Kalyanova, Trans Lomonosov Inst. Fine Chem. Technol., Mosco, vol. 5 (State Chem. Press 1953) p. 30.

[4] S. S. Voyutsky and R. M. Panich., Colloid J., 18, 326 (1956).*

[5] S. S. Voyutsky and R. M. Panich, Colloid J., 18, 647 (1956).*

[6] B. V. Deryagin and L. D. Landau, J. Exp. Theoret. Phys., 11, 802 1941; 15, 662 (1941); Acta Phys. Chim. URSS 14, 633, 1941.

[7] D. C. Henry, Proc. Roy. Soc., 133, 106, (1931).

[8] T. G. Overbeek, Adv. Coll. Sci. 8, 97, (1950).

[9] B. P. Nikolsky and V. I. Paramonova, J. Phys. Chem., 2, 687 (1931).

[10] R. M. Panich and S. S. Voyutsky, Colloid J., 19, 113 (1957).*

[11] E. A. Hauser, M. Bender, Proceedings of the Rubber Technology Conference, 1938, p. 101.

[12] S. H. Maron, D. Turnbull, M. E. Elder, J. Am. Chem. Soc. 70, 582, (1948).

---

* [Original Russian pagination. See C. B. Translation].

ADHESION OF HIGH POLYMERS

3. EFFECTS OF THE SIZE, SHAPE, AND POLARITY OF HIGH POLYMER MOLECULES ON THEIR ADHESION TO CELLOPHANE

S. S. Voyutsky, A. I. Shapovalova, and A. P. Pisarenko

The effects of the nature of high polymers on their adhesive properties have been the subject of several investigations [1-4]. However, the question still remains obscure, as most of the investigations in this direction have been based on faulty methods. In particular, much harm was done in the earlier investigations because it was not strictly determined whether in the tests the joints were broken at the adhesive – substrate boundary or within the adhesive itself; i. e., whether true adhesion or the cohesive strength of the adhesive was being measured. Because of this, a number of experimental investigations of adhesion are rendered valueless, and the development of the physical chemistry of adhesion in general has been slow for this reason.

The present communication contains certain data on the effect of the nature of high polymer adhesives on adhesion to a polymeric substrate, obtained by means of a technique developed by us earlier [5], in which the usual methodological defects have largely been eliminated. This method essentially consists of determination of the force or work expended in gradual peeling-off of a film of adhesive applied in solution form to the substrate. Special attention is paid to determining whether the peeling is adhesive or cohesive in character.

The substrate used in the present investigation was a cellulose model – Cellophane from which the glycerol plasticizer had been washed out. Adhesion of high polymers to cellulose is important in impregnation of tire cords, gluing of paper and board, production of fabric-based leather substitutes, etc. Cellophane is the most convenient of all the cellulose materials because of its mirror-smooth surface, so that it is possible to assume the area of nominal contact equal to the area of true contact, and to determine the character of the peeling visually.

The adhesives tested were several elastomers used in industry. The solvents used in applying the adhesives to the substrate were the solvents generally used in the production of rubber adhesives – gasoline, benzene, dichloroethane.

The joints were made and peeled apart under strictly standardized conditions [5].

Effect of the size of the macromolecules on adhesion. Table 1 contains our data on the force required to peel isobutylenes of different molecular weights from Cellophane.

As Table 1 shows, the peeling resistance of polyisobutylene of molecular weight 7000 is practically zero, and the peeling is purely cohesive, i. e., it occurs in the layer of adhesive. With increase of molecular weight to 20,000 the resistance to separation increases sharply, and the separation is of the mixed type. Evidently in this case the cohesive strength of the adhesive is equal to the force required to peel the adhesive from the substrate. With molecular weights of 100,000 and over, the peeling is purely adhesive; the absolute value of the resistance to separation is the same in all cases, approximately 70 g/cm.

Table 1 also gives the results of experiments on the peeling from Cellophane of polyisoprenes of molecular weight 20,000 – 150,000 (synthetic product) and 150,000 – 300,000 (natural rubber). Here again the polymer of lower molecular weight had considerably greater adhesion. The mixed type of separation of synthetic polyisoprene from Cellophane shows that the cohesive strength of this polymer is approximately equal to the adhesive force.

TABLE 1

Resistance to Separation of Cellophane and Polyisobutylenes of Different Molecular Weight

Adhesive	Molecular weight	Type of separation	Separation resistance in g/cm		
			minimum	maximum	average
Polyisobutylene	7 000	Cohesive	0	0	0
	20 000	Mixed	307	386	369
	100 000	Adhesive	61	70	67
	150 000	Ditto	59	73	67
	200 000	Ditto	60	71	68
Polyisoprene	20 000—150 000	Mixed	1112	1617	1379
	150 000—300 000	Adhesive	13	25	18

At first sight it seems strange that natural rubber had such poor adhesion to Cellophane. It is generally considered that natural rubber is an excellent adhesive. However, poor adhesion of natural rubber to Cellophane has also been reported by others [3].

Table 1 shows that polymer adhesion increases with decreasing molecular weight. However, as the cohesive strength of a polymer decreases with decreasing molecular weight, the optimum gluing powers should probably be found in polymers of moderate molecular weight, which ensures adequate adhesion together with sufficient strength of the adhesive layer.

Effect of the structure and shape of the macromolecules on adhesion. Table 2 gives data on the separation of various nonpolar or weakly polar polymers from Cellophane.

Table 2 shows that adhesion of polybutadiene to cellophane is greater when the elastomer molecule has a more regular structure. Increase of the number of vinyl side chains in the molecule greatly diminishes adhesion. From the nature of the separation in this case it may be concluded that polymers with more regular structure have higher cohesive strength. This is in entire agreement with the modern views on the relationship between the mechanical properties and molecular structure of polymers. Styrene side chains in the butadiene polymer molecule have an analogous influence on adhesion.

A comparison of the adhesion of the copolymer containing 70% butadiene and 30% styrene, and of the copolymer containing 70% butadiene and 30% methylstyrene, to Cellophane shows that adhesion is considerably lower in the latter case. This is probably to be attributed to the presence of a methyl group in the styrene residue.

The adverse effect of methyl groups in adhesion can also be seen from a comparison of the resistance of butyl rubber and polyisobutylene, of similar molecular weight, to separation from Cellophane. The presence in the butyl rubber molecule of even a small number of isoprene groups, containing only one methyl group per four carbon atoms in the main chain, results in a sharp increase of adhesion. However, the increase of adhesion may also be the consequence of the presence of a small content of low molecular weight polymer fractions in the synthetic product.

The general conclusion to be drawn from the data in Table 2 is that the adhesion of a polymeric adhesive to Cellophane decreases with increasing number of short side chains in the molecule.

Effect of the presence of polar groups in the macromolecule on adhesion. The data in Table 3 show how the resistance to separation of Cellophane from butadiene – acrylonitrile copolymers varies with the contents of polar acrylonitrile groups.

Table 3 shows that the resistance to separation for butadiene – acrylonitrile copolymers decreases with increasing contents of polar nitrile groups in the molecule. The type of separation also alters from cohesive to pure adhesive.

TABLE 2

Resistance to Separation of Various Nonpolar or Weakly Polar Elastomers from Cellophane

Adhesives and their characteristics	Type of separation	Resistance to separation in g/cm		
		minimum	maximum	average
Polybutadiene containing 50% butadiene groups in 1,4 position and 50% in 1,2 position	Adhesive	1433	1484	1445
Polybutadiene of the same molecular weight, containing 20% butadiene groups in the 1,4 position and 80% in the 1,2 position	Mixed	498	594	550
Copolymer containing 70% butadiene and 30% styrene	Cohesive	1153	1652	1368
Copolymer containing 50% butadiene and 50% styrene	Adhesive	3	22	14
Copolymer containing 70% butadiene and 30% methylstyrene	Mixed	274	1727	771
Butyl rubber, mol. wt. 60,000-80,000	Adhesive	272	307	298
Polyisobutylene, mol. wt. 80,000-100,000	Adhesive	61	70	67

TABLE 3

Resistance to Separation of Butadiene – Acrylonitrile Copolymers of Different Polarities from Cellophane

Adhesives and their characteristics	Type of separation	Resistance to separation in g/cm		
		minimum	maximum	average
Butadiene–acrylonitrile copolymer containing 18.4% acrylonitrile groups	Cohesive	1380	1735	1638
Ditto, containing 28.6% acrylonitrile groups	Mixed	1144	1717	1382
Ditto, containing 37.7% acrylonitrile groups	Adhesive	125	138	132

DISCUSSION OF RESULTS

Up to the present adhesion has been thought to be caused either by the action of molecular forces [3, 6] or by formation of an electric double layer at the interphase [7-9]. However, as we have shown [10], neither of these viewpoints is valid when both the adhesive and the substrate are high polymers.

It our theory, both adhesion of high polymers to each other and autohesion consists of diffusion of chain molecules or sections of them from one polymer into the other to form a stable bond constituting a gradual transition from one polymer to the other. It is quite obvious that the interdiffusion of two high polymers in contact is none other than mutual solution. Therefore adhesion of high polymers to each other is closely related to their mutual solubilities, which, as we have shown [11], is largely determined by their polarity relationships.

If our diffusion theory of adhesion is correct, the adhesion of high polymers to each other should depend very largely on the ability of the macromolecules to diffuse into solids and on the mutual solubility of the high polymers. Unfortunately, almost nothing is known at the present time about these important characteristics of high polymers, and therefore verification of the views put forward above must be confirmed to finding the relationships between adhesion and molecular structure (molecular weight, form of the macromolecules, presence of polar groups) of the contacting polymers.

In our experiments the same substrate, Cellophane, was used. Cellophane, like cellulose, consists of macromolecules containing polar hydroxyl groups. Because of the size and rigidity of these macromolecules, and the molecular forces acting between them, they are not capable of any appreciable diffusion into elastomers. Conversely, the molecules of the elastomers used in our investigations are fairly flexible and capable of diffusion. Therefore in our case it is sufficient to correlate the adhesion between Cellophane and elastomers with the molecular structure of the latter.

Effect of molecular size and shape of nonpolar elastomers on their adhesion to Cellophane. We have seen that, with the same contact time, the adhesion of polyisobutylene to Cellophane first decreases with increasing molecular weight, and then becomes practically constant. Experiments with polyisoprenes of different molecular weight do not contradict this result. The fact that adhesion ceases to be dependent on the molecular weight after the latter has reached a certain value has been reported by others for other materials [4]. In our theory, this can be explained in the same way as in the case of autohesion [12]: as the molecular weight increases, the number of free ends of molecules, capable of diffusing especially easily, diminishes. When the molecular weight is high, mainly chain segments diffuse, and their penetration into the spaces between the substrate molecules is difficult. Therefore a less stable bond will be formed in a given time between two high polymers in contact, and as the segment size does not depend on the length of the macromolecule, the adhesion ceases to depend on the molecular weight.

Another explanation of the fact that adhesion becomes independent of molecular weight above a certain value is the higher plasticity of the adhesives with lower molecular weight which, of course, favors diffusion. There are reports in the literature [3] that introduction of not too large amounts of plasticizers into high polymer adhesives improves adhesion. It is possible, of course, that the increase of adhesion with diminishing molecular weight is to be explained by the combined action of both these factors.

It should be noted here that the increase of adhesion with decreasing molecular weight does not contradict the observed fact that bond strength increases with increasing molecular weight of the adhesive. The reason is that in most instances the joints are broken not at the adhesive – substrate boundary but within the adhesive layer. In such conditions the resistance to separation will, of course, increase with increasing molecular weight of the adhesive.

Thus, the question of the influence of molecular weight on adhesion needs to be reviewed in the light of the foregoing data. There are adequate grounds for believing that decrease of molecular weight, which decreases the cohesive strength of the substance, favors increased adhesion. This view is quite understandable from the viewpoint of the diffusion theory of adhesion – as the molecular size decreases the capacity of the molecule for diffusion increases, and adhesion should therefore increase also.

We have seen that determination of the adhesion of polybutadiene to Cellophane showed that an increase of the number of butadiene groups in the 1,2 position in the adhesive molecule worsens the adhesion. The probable explanation is that, as the number of butadiene groups in the 1,2 position increases in the molecule, the ability of the molecule to diffuse becomes less on purely steric grounds (increased number of side groups).

Another example of the influence of side groups is provided by the adhesion of butadiene – styrene copolymers, with different proportions of the components, to Cellophane. A small amount of styrene groups in the copolymer increases adhesion, but a large amount produces a decrease. Similar changes of adhesion with different proportions of the components in copolymer molecules have been observed by others [4]. The explanation again is that the copolymer molecules with a low styrene group content are largely regular in structure and therefore diffuse more easily into the substrate. A large number of styrene groups in the copolymer molecule decreases the ability to diffuse because of the presence of a large number of cumbersome side chains in the macromolecule and decreased chain flexibility.

As we have seen, replacement of styrene by methylstyrene groups in the copolymer molecule decreases adhesion. The probable reason for this is the considerable decrease of the diffusion capacity of the macromolecules owing to the presence of additional methyl groups. The results of experiments with polyisobutylene and butyl rubber lead to similar conclusions.

Reference was made earlier to the adverse effect of short side chains in the macromolecule on adhesion. However, if these side chains are long enough, they may act as individual chains which, for steric reasons, diffuse more readily into the substrate than do the middle regions of the molecular chains [12]. This is quite understandable, as the probability of entry of such a molecular end into a space between the substrate molecules is certainly higher than the probability of entry of a middle part of a molecule into the same space. This view is confirmed by the results of McLaren [3], who showed that adhesion to Cellophane increases in the polymethacrylate series from n-methyl methacrylate polymer to n-butyl methacrylate polymer. McLaren also showed that isopropyl and isobutyl methacrylate polymers have considerably lower adhesion to Cellophane than the corresponding normal methacrylate polymers. This is in full agreement with our views on the influence of molecular shape on adhesion.

Effect of polarity of the adhesive on adhesion to Cellophane. First it must be pointed out that it is found experimentally that such nonpolar or weakly polar high polymers as polyisobutylene and polybutadiene have fairly high adhesion to polar Cellophane. The reason, in our view, is the insufficiently close packing of the cellulose molecules, owing to which the flexible and mobile molecules of the adhesive can diffuse into the cellulose. Another interpretation of the effect is that the hydrocarbon chains of the nonpolar adhesive are capable of dissolving in cellulose to a certain extent, thus forming a bond between the adhesive and substrate. Further, it has been found that butadiene – acrylonitrile copolymers have decreasing adhesion to Cellophane with increasing contents of polar acrylonitrile groups in their molecules. Others [3] have also reported that high polymers containing nitrile groups in their molecules have poor adhesion to Cellophane. Since Cellophane molecules are strongly polar, this result seems at first sight incomprehensible – it would seem that the more strongly polar nitrile groups the polymer contains, the better would it dissolve in Cellophane and the stronger would be the bond formed between the adhesive and the substrate. However, the contradiction is easily explained because, with increasing contents of polar groups in the macromolecules of the adhesive, the rigidity of the macromolecular chains increases and therefore their diffusion capacity diminishes. Moreover, adhesion decreases owing to the presence of often cumbersome polar side chains in the molecules, which hinder diffusion for steric reasons. Finally, the polar groups present in the polymer molecules may themselves interact by intermolecular forces, and this would also hinder diffusion.

Thus, the decrease of adhesion with increasing polarity of the adhesive in our experiments must be explained as a purely kinetic effect. It is important that if instead of the polar Cellophane a nonpolar substrate was used, the adhesion would also decrease with increasing polarity of the adhesive. However, the interpretation of this effect would be different – in this case increase of the polarity of the adhesive would result in a decrease of the solubility of the adhesive in the substrate, i.e., it would be explained purely on thermodynamic grounds.

It should be noted that adhesion does not always diminish with increasing polarity of the high polymer. For example, McLaren [3] found that, with increasing chlorine content in chlorinated polyethylene, the adhesion of the polymer to Cellophane first increases, then begins to decrease. McLaren also found that moderate contents of polar groups – chlorine, carboxyl, carbonyl, and hydroxyl – in the macromolecules may improve adhesion to Cellophane. The possible explanation is that, for a moderately polar high polymer, the improvement of adhesion as the result of better solubility exceeds the decrease of adhesion caused by increased rigidity of the molecules and decreased diffusion of the polymer.

SUMMARY

1. The method developed by the authors has been used to study the influence of size, form, and polarity of macromolecules on the adhesion of high polymers to Cellophane.

2. Adhesion of high polymers to Cellophane increases with decreasing molecular weight. However, for maximum bond strength, the cohesive properties of the polymer must also be taken into account.

3. Increase of the number of short side chains in the polymer molecule lowers its adhesion.

4. The adhesion of a polymer to Cellophane decreases with increasing contents of polar groups in its macromolecules.

5. The results are explained on the basis of the diffusion theory of high polymer adhesion developed by the authors.

Central Scientific Research Institute for the Leather
Substitutes Industry, Moscow

Received May 3, 1956

LITERATURE CITED

[1] O. Gerngross, Z. ang. Chem. 44, 33, (1942).

[2] K. Thinius, Kunststoffe 37, 36,(1947).

[3] A. D. McLaren, C. H. Hofrichter, Paper Trade J. 125, 96, (1947); A. D. McLaren, J. Pol. Sci. 3, 652, (1948).

[4] C. J. Seiler, Paper Trade J. 126, 37, (1938).

[5] A. I. Shapovalova, S. S. Voyutsky, and A. P. Pisarenko, Colloid J., 18, 485 (1956).*

[6] J. Remond, Rev. Produits Chim. 57, 469, (1954); 58, 70, (1955).

[7] B. V. Deryagin and N. A. Krotova, Adhesion (Acad. Sci. USSR Press, Moscow, 1949).

[8] B. V. Deryagin, J. Acad. Sci. USSR, No. 7, 10 (1954).

[9] S. M. Skinner, R. L. Savage, J. E. Rutzler, J. Appl. Phys. 24, 438, (1953).

[10] S. S. Voyutsky, A. I. Shapovalova, and A. P. Pisarenko, Proc. Acad. Sci. USSR, 105, 1000 (1955).

[11] V. I. Alekseenko, I. U. Mishustin, and S. S. Voyutsky, Colloid J., 17, 3, (1955)*; Proc. Acad. Sci. USSR, 95, 93, (1954).

[12] S. S. Voyutsky and B. V. Shtarkh, Colloid J., 16, 3, (1954).*

---

* [Original Russian pagination. See C. B. Translation].

STUDIES OF THE PHYSICAL CHEMISTRY OF AGAR

2. THEORY AND PRACTICE OF AGAR FRACTIONATION

S. A. Glikman and I. G. Shubtsova

It is known that agar obtained from different seaweeds and by different technological processes varies greatly in chemical composition (contents of proteins, ash elements, etc.) [1]. The principal component which determines the properties of agar is a polygalactan in the linear molecules of which some of the galactose residues are esterified by sulfuric acid which, in turn, is combined with various cations, mainly calcium and potassium. According to the literature [2, 3], different samples of agar contain on the average from 18 to 57 d-galactopyranose units per sulfate ester group, while in carrageenins nearly every galactose unit is esterified by sulfuric acid [4].

However, the physicochemical properties of different agar samples are evidently determined not only by the average chemical composition of the polysaccharide and its average degree of polymerization, but also by its molecular heterogeneity. Attempts to fractionate agar have not hitherto given the desired results. By washing with cold water, electrodialysis, or precipitation by alcohol – water mixtures [5-8], soluble fractions could be separated from the sparingly soluble portion, but the latter, which comprises more than 70% of the original substance, could not in practice be separated into fractions. An interesting fact is that similar results were obtained by a number of workers [9, 10] in the fractionation of another polyelectrolyte, pectin. In this case also the main part of the material, comprising ~ 70% of the total, could not be fractionated by extraction with mixtures of variable composition.

The method, often used for the fractionation of other high polyners, of solution at increasing temperatures has as yet not been used for agar, because of its supposed instability to the action of heat. However, the literature data on the effects of prolonged heating on the properties of agar solutions are very contradictory [2, 11, 12]. There is reason to believe that only solutions of partially dialyzed agar, containing free sulfate ester groups, are unstable to high temperatures, the agar molecules being hydrolyzed [2]. Our own experiments have shown that when nondialyzed solutions of agar were heated for five hours at 100° their viscosity decreased only slightly (by about 4%).

Two nondialyzed agar samples were used in our investigation: Sample I, Japanese fibrous, extracted from Gelidium seaweed, and Sample II, Far Eastern film agar, obtained from Ahnfeltia plicata seaweed by the freezing process. The fractionation was effected by consecutive extraction with water at 25, 45, 60, 75, 85 and 90°. The material was usually washed four times, until the fraction soluble in the given conditions was completely extracted. All the washings were combined in the one fraction. The durations of the washings were: at 25°, 10 hours, at 45 and 60°, 1 hour, and at 75,85, and 90°, 30 minutes. The solutions were evaporated at 50° and the residues were finally dried at 80°. The high-temperature extracts were not evaporated but were dehydrated by the freezing method.

Most of the water-soluble free impurities of mineral and organic origin were extracted with the first fraction. Therefore the physicochemical characteristics determined for the first fraction must be regarded as provisional. The insoluble impurities remained in the fraction insoluble at 90°, which comprised 3.7% of the weight of Sample I and 11.7% of sample II, and which was not investigated.

Calcium was determined by the Grossfeld method [13], verified for agar by Starostina [7]. The determination of SO_4^{2-} ions by oxidation with HNO_3 was carried out by Pavlov's method [14], and these ions were also determined in a hydrochloric extract of the ash obtained in presence of excess cations [13].

The table shows that the sulfate group content in Sample I and all its fractions (except the 90° fraction) is considerably higher, and the calcium content considerably lower, than in Sample II. The ratio of the equivalents shows that in Sample I not all the sulfate groups are saturated with calcium, while Sample II contains calcium in excess. This is confirmed by qualitative analysis of the ash, which showed that in addition to calcium Sample I contains considerable amounts of other cations (Na^+, K^+, Mg^{2+}, Al^{3+}, Fe^{3+}), while Sample II contains only Na^+, K^+, and Fe^{3+}, the first two being present only in the first two fractions. The ash and SO_4^{2-} contents of the fractions decrease progressively in both samples.

Fractionation Yield and Characteristic Fraction

Samples		Yield of fraction, %	Moisture, %	Ash, % of dry agar	Ash constituents, % of dry agar		Relative numbers of esterified residues	Ratio of $\frac{Ca}{SO_4}$ equivalents	$[\eta]_\infty$
					SO_4^{2-}	Ca^{++}			
Sample I		—	16.6	3.95	3.48	0.75	1 : 16	0.55	1.48
Its fraction at	25°	26.2	18.3	10.72	10.20	1.47	1 : 6	0.34	0.72
•	45°	5.7	15.9	3.96	3.46	0.64	1 : 16	0.44	0.80
•	60°	5.4	—	—	—	—	—	—	0.84
•	75°	14.5	17.0	1.90	1.69	0.48	1 : 34	0.68	0.96
•	85°	16.1	16.7	0.86	1.04	0.26	1 : 58	0.60	1.05
•	90°	16.2	16.9	0.75	0.67	0.24	1 : 88	0.87	1.18
Residue		13.7	—	—	—	—	—	—	—
Sample II		—	14.0	3.89	1.06	1.64	1 : 56	3.73	2.25
Its fraction at	25°	6.9	12.1	24.65	4.36	8.27	1 : 18	4.79	—
•	60°	11.2	17.3	4.10	1.24	2.27	1 : 47	4.28	1.50
•	75°	19.1	17.4	2.33	0.79	1.39	1 : 74	4.24	2.22
•	85°	23.8	17.5	2.02	0.65	0.95	1 : 90	3.50	2.44
•	90°	28.2	17.4	2.05	0.69	0.98	1 : 86	3.40	2.60
Residue		11.7	—	—	—	—	—	—	—

The intrinsic viscosities given in the table were determined by the method described in the preceding communication • from the experimental data in Figs. 1 and 2. For the two samples studied, the values of $[\eta]_\infty$ increase consecutively from the low to the high temperature fractions. The value of $[\eta]_\infty$ for the original Sample II is close to that of its 75° fraction, and for Sample I, it is higher than the value for its 90° fraction. The values found for $[\eta]_\infty$ cannot accurately reflect the relative molecular weights of the fractions, as their chemical composition differs both in the sulfate ester group contents and in the cation contents. For the same molecular weight, the molecules of a polyelectrolyte should become straighter with increasing numbers of sulfate groups in the molecules, and therefore the effective volume (bulk) and viscosity should increase. A decrease in the content of these groups should produce the opposite effect.

It is this effect – a consecutive decrease in the frequency of the sulfate ester groups – that is seen in the transition from the low to the high temperature fractions of Sample I. Therefore the consecutive increase of intrinsic viscosity found for this series of fractions probably does not correspond completely to increasing molecular weights, but is somewhat diminished owing to the lower contents of sulfate groups in the high temperature fractions.

Sample II differs from Sample I by a lower content of sulfate ester groups and a considerably higher calcium content. The decrease in the frequency of sulfate groups in the transition from the low-molecular 25° fraction to the higher fractions is not so rapid in Sample I as in Sample II. Therefore the discrepancy between the molecular weight and viscosity changes is less prominent in Sample I. Indeed, in the case of Sample II the $\eta_{sp}/c - c$ curve and the value of $[\eta]_\infty$ for the original sample are not higher than for all the

---

• Colloid J., 19, 172 (1957). [C. B. Translation, p. 183].

fractions, but are similar to those for the intermediate 75° fraction.

The nature of the cations replacing hydrogen in the acid groups in agar should also have a definite influence on the form of the polyelectrolyte molecule and therefore on the viscosity of the agar. This influence depends on the possibility of formation of intramolecular bonds on replacement of hydrogen by bivalent cations, and also on the different degrees of solvation of the cations in solution. Samples I and II differ considerably in their cation contents and the degree of substitution in the acid groups. In Sample I, on the average, only half the sulfate ester groups are saturated with calcium, and the degree of substitution only reaches 0.85 in the highest 90° fraction. On the other hand, in Sample II the number of calcium equivalents is on the average 4 times as great as the number of sulfate ester groups, and this proportion varies relatively little for the different fractions. With the greater homogeneity of Sample II, both in respect of the sulfate group contents and of cation substitution, its values of $[\eta]_{\infty}$ probably reflect molecular weight differences of the fractions more accurately than in the case of Sample I.

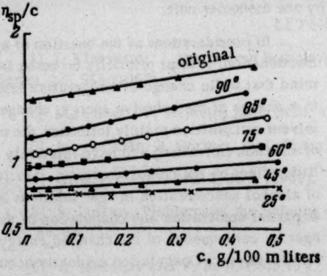

Fig. 1. Viscosity of Japanese agar and its fractions in presence of KCl solution containing 0.1 equiv. / liter.

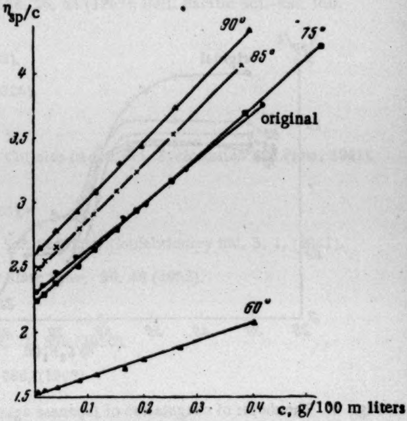

Fig. 2. Viscosity of Far Eastern agar and its fractions in presence of KCl solution containing 0.1 equiv./liter.

To characterize the hydrophilic nature of the fractions and the stability of their aqueous solutions, the thresholds of coagulation of these solutions by alcohol were determined. The method consisted of measurement of the relative viscosities (at 60°) of 0.15% aqueous solutions of the agar and of the same solutions after addition of increasing amounts of alcohol. The curves in Fig. 3 show that the reduced specific viscosity of the solutions remains almost unchanged up to a certain critical alcohol concentration, and then decreases sharply, evidently as the result of coagulation. The critical concentrations of alcohol for the original agar and all the fractions studied are very similar (~ 60% alcohol). This accounts for the failure of attempts to fractionate agar by variations of the solvent composition.

In order to explain the very different effects of two parameters of state – temperature and solvent composition – on equilibrium in the system agar – solvent, it is necessary to consider briefly the modern theories of high polymer fractionation. As is known, the phase equilibrium theory advanced by Gee and Huggins is based on the assumption of a homogeneous force field around the polymer molecule, and does not take into account specific interaction between the different functional groups of these molecules. In the solution and fractionation of polymers containing polar groups, the energy factor plays a greater role than the entropy factor. The Gee and Huggins theory is evidently not applicable to such systems.

The Brønsted equation should provide a better explanation of the observed effects. The applicability of this equation to negative heat effects only does not prevent its use for positive heats of swelling, since the heat of solution, which represents the difference between the heat expended in separating the polymer chains and the heat of solvation, may be negative. If the heat of solution is also positive, it is necessary to take into account that the characteristic which determines the phase equilibrium conditions is not the absolute value of q, but the difference between the heats of solvation of the polymer in a mixture of the given composition (q_x) and in a mixture of optimum composition (q_n), in which all the functional groups of the polymer molecule are solvated to the maximum; this difference $q = q_x - q_n$ will always be negative.

A defect of the Brønsted equation is that it is applicable only to regular solutions. This has been taken into account by Meyer [15], who introduces into the Brønsted equation a correction term for entropy

$$N_2^{sat} = e^{z(q + Ts)/RT},$$

where N_2^{sat} is the mole fraction of the polymer in a saturated solution; $\underline{z}$ is the number of units in the molecule; $s = (\Delta S - \Delta S^{id}/z = \Delta S^{exc}/z$ is the excess of the entropy change over the ideal value, per monomer unit, when a polymer molecule is transferred into another phase. Meyer points out that $\underline{s}$ must be very small, as it represents the difference between two values of S^{exc} corresponding to excesses, over the ideal entropy of solution, of two polymer molecules differing by one monomer unit.

In considerations of the question of agar fractionation, it must primarily be borne in mind that while change of temperature results in a change of the cohesive energy, changes of solvent composition mainly influence the energy of adhesion (solvation) and have relatively little effect on the cohesive energy. Increase of alcohol concentration in agar solutions leads to partial desolvation and coagulation of the agar in consequence of the changed energy relationships. Coagulation evidently occurs when the heat effect $\underline{q}$ of a unit in the polymer chain reaches a negative value greater in absolute magnitude than the entropy effect T_s, as follows from the Brønsted – Meyer equation $N_2^{sat} = \exp[z(q + T_s)/RT]$.

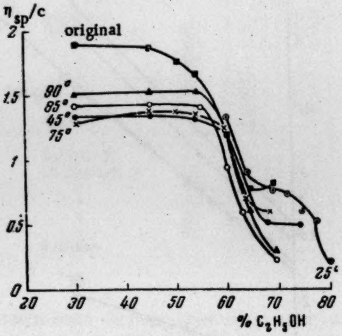

Fig. 3. Thresholds of coagulation of Japanese agar and its fractions by alcohol.

Since the values of q are determined by the difference between the solvation and cohesive energies of all active groups, capable of hydrogen bonding (i.e., mainly hydroxyl groups), in the agar molecules, it naturally follows that the coahulation threshold should be practically the same for all agar fractions differing in degree of esterification or in the nature of the substitution in the sulfate ester groups, if the number of such goups in all the fractions is small relative to the number of hydroxyl groups. As regards the molecular weight differences, if (q + Ts), is similar for all the fractions, only large differences in the degree of polymerization can result in separate precipitation of the fractions.

Variation of the solvent composition affects not only the energy relationship in high polymer solutions, but also the entropy of solution, which should be reflected in a change in the term Ts in the Brønsted – Meyer equation. If this change was at all considerable, then agar fractions differing in molecular weight would be precipitated at different maximum concentrations of alcohol. This is not so, probably because the molecules of agar, as of other polymeric carbohydrates, are greatly extended and fairly rigid. Therefore their flexibility should not greatly change at constant temperature with the solvent composition.

The situation should be different with variations of the solution temperature of agar in a solvent of constant composition or in pure water. In such cases not only the hydration energy but the cohesive energy is changed considerably. Moreover, as the cohesive energy decreases with increase of temperature, even small differences of cohesive energy, depending on the relative contents of sulfate ester groups in the macromolecule, should appreciably influence the magnitude of the aggregate effect. Therefore.fractionation of agar by variation of the temperature is quite feasible, and the fractions so obtained differ both in molecular weight and in chemical composition.

SUMMARY

1. It has been shown for two agar samples that, by consecutive extraction at increasing temperatures (from 25 to 90°), agar can be separated into a series of fractions differing in intrinsic viscosity, sulfate ester group contents, and substituent cations, but differing little in their hydrophilic nature.

2. The results of fractionation by varying the temperature with a solvent of constant composition, and by varying the solvent composition at constant temperature, are explained thermodynamically on the basis of the Brønsted equation as modified by Meyer.

The N. G. Chernyshevsky State University
Saratov

Received September 10, 1955

LITERATURE CITED

[1] I. Kizevetter, J. Far Eastern Branch Acad. Sci. USSR, 26, 53 (1957); Bull. Pacific Sci.-Res. Inst. Fisheries, 36, 265 (1952).

[2] M. Samec, V. Isajevic, Koll. Beih. 16, 285, (1922).

[3] W. Hoffman, R. Gortner, Biol. Chem. 65, 371, (1925).

[4] H. Kruyt, Coll. Sci. 2, 187, (1949).

[5] S. Lipatov, Problems of the Science of Lyophilic Colloids (Acad. Sci. Byelorussian SSR Press, 1941). pp. 53, 84-85.

[6] A. Morozov and V. Rudi, Colloid J., 15, 117 (1953).*

[7] V. Gryuner and K. Starostina, Trans. All-Union Sci. Res. Inst. Confectionery Ind. 3, 1, (1941).

[8] S. Glikman and M. Lipovsky, Sci. Mem. Saratov State Univ. 30, 46 (1952).

[9] G. Schneider, H. Bock, Ber., 70, 1617, (1937.)

[10] S. Glikman and S. Orlov, Proc. Acad. Sci. USSR, 71, 895 (1950).

[11] W. Cooper, B. Cantal, W. Nuttal, Pharm. J. 26, 688, (1908).

[12] S. Levites, Koll.-Z. 2, 237, (1907).

[13] I. Grossfeld, Manual for the Investigation of Food Products (Food Ind. Press, 1937) p. 93.

[14] S. Pavlov, J. Appl. Chem., 5, 877 (1932).

[15] K. Meyer, Natural and Synthetic High Polymers, Second Ed., (New York, 1950), p. 709

---

* [Original Russian pagination. See C. B. Translation].

THE EFFECT OF SWELLING ON THE STRENGTH OF VULCANIZATES

B. A. Dogadkin, D. L. Fedyukin, and V. E. Gul

Data on the influence of temperature, deformation conditions and swelling on the strength characteristics of high polymers are important in relation to the theory of the mechanism of the rupture of these materials. The relationship between the tensile strength of vulcanizates and the temperature and deformation rate [1] indicates the important role of intermolecular interaction in the mechanism of the rupture of high polymers with a spatial structure.

The observed relationships are difficult to explain if it is assumed that the resistance of a material to rupture is determined by principal chemical valency forces only. On the other hand, if the tensile strength of a vulcanizate is regarded as the sum of the principal valency forces P_X and intermolecular forces P_M all the known relationships between strength characteristics and the temperature and extension rate can be interpreted with a certain degree of approximation [2]. To determine the role of intermolecular forces in the mechanism of vulcanizate rupture it was of special interest to study the influence of swelling on tensile strength. This is of great practical as well as theoretical interest. The addition of substances of low molecular weight, known as softeners or plasticizers, to mixtures based on high polymers, is a widely used technological procedure. The substances used as plasticizers or softeners are generally well compatible with the polymers and can swell them.

Various chemical processes can take place between the plasticizers and the other ingredients in the production of a finished article from a raw mixture. In particular, softeners influence vulcanization and oxidation processes. Therefore in most cases a distinction must be made between chemical and physical interaction of plasticizers and the components of the mixture. The present paper deals mainly with the determination of the influence of physical interaction between the plasticizer and high polymer (swelling) on the tensile strength of vulcanizates.

One method whereby intermolecular interaction can be varied is swelling. This method is very convenient as by its means it is possible to vary intermolecular interaction without affecting interaction by the principal chemical valency forces. It is shown [3] that even in one and the same vulcanizate (and still more so in different vulcanizates) chemical and intermolecular bonds differing in nature and intensity are present. Consequently, different solvents should have different effects on the intermolecular interaction of a vulcanizate swollen in them. Therefore the materials chosen for the investigation were carbon-filled vulcanizates based on rubbers differing in chemical composition and structure, namely: natural (smoked sheet), butadiene—styrene (with 70:30 butadiene—styrene ratio), and butadiene—acrylonitrile (with 62:40 butadiene—acrylonitrile ratio); while the solvents used were dimethyl phthalate, dibutyl phthalate, dioctyl phthalate, dibutyl sebacate, dioctyl sebacate, and Vaseline oil. These substances differ both in molecular size and structure, and in polarity.

The swelling was effected by immersion of spade-shaped test specimens either directly into the solvent or into its alcoholic solution. To ensure uniform distribution of the solvent through the vulcanizate at different degrees of swelling, the specimens were kept between sheets of paper for 7-8 days after being extracted from the solvents, before the tensile tests. The degree of swelling was expressed in percentages on the weight of vulcanizate. The tensile and relative elongation tests were carried out according to State All-Union Standard 270-41. The number of parallel tests was not less than 25 in each case. The changes in the specimen dimensions caused by swelling were not taken into account in calculations of the cross section. The results for filled vulcanizates based on natural, styrene (SKS-30) and acrylonitrile (SKN-40) rubbers are given in Figs. 1,2, and 3 respectively. These figures show that the tensile strength varies in different ways for different combinations of vulcanizate and swelling agent. In some cases the often described steady decrease of tensile strength with increasing swelling is observed. This is found for natural rubber vulcanizate swollen in dimethyl and dioctyl phthalates, and for SKS-30 vulcanizate swollen in dibutyl and dioctyl phthalates and in dibutyl and dioctyl sebacates (Figs. 1, 2). In contrast to these typical cases, when filled vulcanizates of natural rubber are swollen in dibutyl phthalate and dibutyl sebacate, of styrene rubber in dimethyl phthalate, and of nitrile rubber in dimethyl, dibutyl, and dioctyl phthalates and dibutyl sebacate, the tensile strength does not change steadily but passes through a maximum at a definite degree of swelling. When natural rubber vulcanizate is swollen in dimethyl phthalate, the tensile strength falls sharply, while SKN-40 vulcanizate swollen in this solvent shows an initial considerable increase of tensile strength. Dimethyl phthalate is the most polar of the solvents used. When natural rubber vulcanizate is swollen in a less polar solvent, dibutyl sebacate, the greatest increase of tensile strength is found. The relative elongation of the vulcanizates varies similarly with the degree of swelling. A steady decrease of relative elongation is found for natural rubber vulcanizate swollen in dimethyl phthalate (Fig. 4) and for butadiene–styrene (SKS-30) rubber vulcanizates swollen in dibutyl phthalate, dioctyl phthalate, dibutyl sebacate, and dioctyl sebacate (Fig. 5). Variation of the relative elongation which passes through a maximum is found for swollen butadiene–acrylonitrile rubber (SKN-40) in all solvents (Fig. 6). The curves in Fig. 7 show that the variations of tensile strength and elongation at break for swollen vulcanizates follow a similar course.

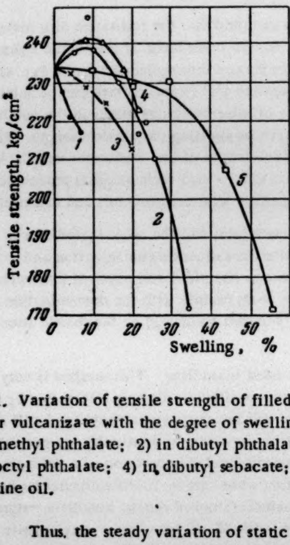

Fig. 1. Variation of tensile strength of filled natural rubber vulcanizate with the degree of swelling: 1) in dimethyl phthalate; 2) in dibutyl phthalate; 3) in dioctyl phthalate; 4) in dibutyl sebacate; 5) in Vaseline oil.

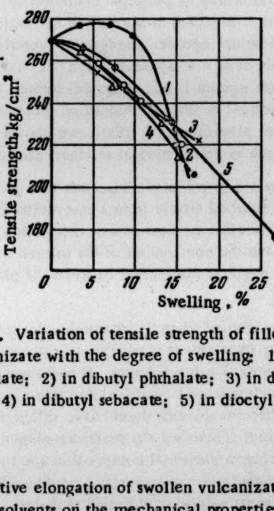

Fig. 2. Variation of tensile strength of filled SKS-30 vulcanizate with the degree of swelling: 1) in dimethyl phthalate; 2) in dibutyl phthalate; 3) in dioctyl phthalate; 4) in dibutyl sebacate; 5) in dioctyl sebacate.

Thus, the steady variation of static strength and relative elongation of swollen vulcanizates, described in the literature, is only a particular case of the influence of solvents on the mechanical properties of vulcanizates. Cases of unsteady variation, with increasing strength at low degrees of swelling, such as described here, are met quite often.

This course of strength and relative elongation variations during swelling of vulcanizates can be explained as follows. Swelling, on the one hand, increases the flexibility of the chain molecules, which facilitates their orientation during extension and therefore increases the tensile strength of the specimen. A direct relationship between the degree of orientation (in the limit, the degree of crystallization) and strength of vulcanizates has been demonstrated in a series of papers [4]. On the other hand, penetration of the solvent molecules during swelling weakens the forces between the molecular polymer chains, leading to a decrease of the vulcanizate strength. The consequence of the superposition of these opposing influences is that, in the general case, the relationship between strength and degree of swelling will show extreme values. If the positive influence of the

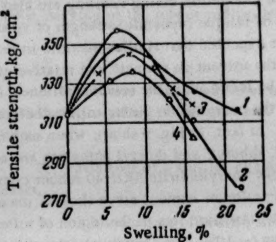

Fig. 3. Variation of tensile strength of filled SKN-40 vulcanizate with the degree of swelling: 1) in dimethyl phthalate; 2) in dibutyl phthalate; 3) in dioctyl phthalate; 4) in dibutyl sebacate.

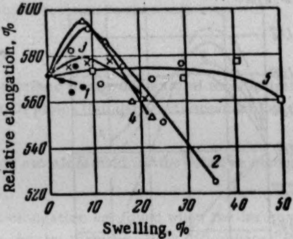

Fig. 4. Variation of relative elongation of filled natural rubber vulcanizate with the degree of swelling: 1) in dimethyl phthalate; 2) in dibutyl phthalate; 3) in dioctyl phthalate; 4) in dibutyl sebacate; 5) in Vaseline oil.

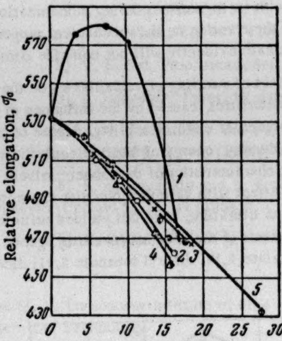

Fig. 5. Variation of relative elongation of filled SKS-30 vulcanizate with degree of swelling: 1) in dimethyl phthalate; 2) in dibutyl phthalate; 3) in dioctyl phthalate; 4) in dibutyl sebacate; 5) in dioctyl sebacate.

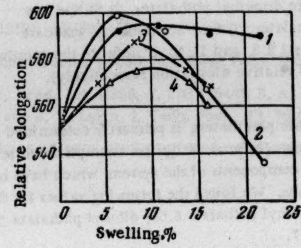

Fig. 6. Variation of relative elongation of filled SKN-40 vulcanizate with degree of swelling: 1) in dimethyl phthalate; 2) in dibutyl phthalate; 3) in dioctyl phthalate; 4) in dibutyl sebacate.

chain flexibility increase prevails, an increase of strength and elongation at break will be found at low degrees of swelling.

In the experiments described this was the case for butadiene-acrylonitrile rubber, the molecular chains of which are less flexible than those of natural rubber, swollen in all the solvents used. In the case of natural rubber the increase in chain flexibility as the result of swelling is slight, and for most solvents the more pronounced effect is decrease of strength owing to decreased energy of intermolecular interaction. Natural rubber vulcanizates show decreases of strength and relative elongation even at low degrees of swelling. Natural rubber has high chain flexibility and the action of solvents on it largely consists of changes in the energy of interaction between the molecular chains.

The effect of changes of molecular chain flexibility on the strength of swollen vulcanizates becomes evident when Figs. 3 and 8 are compared. It is seen that the glass transition temperature, which characterizes molecular chain flexibility, falls up to 12% swelling; further addition of solvent does not lower the glass transition temperature. The strength maximum corresponds to the degree of swelling which gives the lowest glass transition temperature.

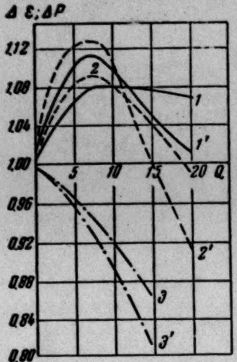

Fig. 7. Relative changes of tensile strength and elongation at break for different degrees of swelling: 1) SKN-40 in dimethyl phthalate; 2) SKN-40 in dibutyl phthalate; 3) SKS-30 in dibutyl sebacate (the symbols 1, 2, 3, and 1', 2', 3' refer to the tensile strength and relative elongation respectively).

It must be pointed out that, as has already been reported by us [5], maximum values of tensile strength and relative elongation during swelling are also found in the case of fatigue (dynamic) strength of vulcanizates. It was to be expected that similar maxima in the influence of the solvent on strength and relative elongation would be found when the solvent (softener) is introduced into the composition during milling before vulcanization. In fact, as Fig. 9 shows, when such softeners as dimethyl, dibutyl, and dioctyl phthalate are added to a butadiene–acrylonitrile SKN-40 rubber composition, the strength–softener content curve shows a maximum. The strength maximum lies in the region of softener concentration (~ 10%) corresponding to the strength maximum for the swollen vulcanizate. Additions of dibutyl and dioctyl sebacate result in steady decrease of strength with increasing softener concentration. Thus, the low molecular compounds act similarly as softeners (plasticizers) and as swelling agents. However, since softeners introduced into the composition may interact chemically with its ingredients during vulcanization, the results of their action on the mechanical properties of the vulcanizate evidently will not coincide completely.

The effect of swelling of vulcanizates on their strength characteristics, caused by the influence of swelling on the molecular chain flexibility, degree of orientation, packing density, energy of intermolecular interaction, and other parameters, is primarily determined by the molecular characteristics of the rubber–solvent (softener) pair. Unfortunately, the attempts to correlate the swelling effect with various molecular characteristics of the components of the system, which have been reported in the literature, have not yielded sufficiently definite results. We found the following values for the dielectric constants of the solvents (swelling agents) studied: dimethyl phthalate 6.56; dibutyl phthalate 5.03; dioctyl phthalate 4.17; dibutyl sebacate 3.71; dioctyl sebacate 3.37.

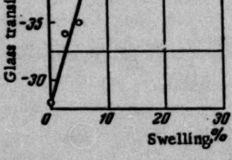

Fig. 8. Variation of the glass transition temperature of SKN-26 vulcanizate with degree of swelling in dibutyl phthalate.

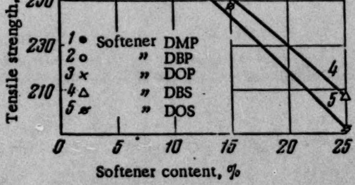

Fig. 9. Variation of tensile strength of butadiene–acrylonitrile rubber vulcanizates with amounts of softener added during milling: 1, 2, 3) dimethyl, dibutyl, and dioctyl phthalates; 4) dibutyl sebacate; 5) dioctyl sebacate.

It is not possible to correlate the dielectric constant of a solvent with the effects of its action on the strength characteristics of swollen vulcanizates [6]. There is no doubt that, in addition to the polarity of the solvent and the magnitude of the cohesive energy, the size and configuration of the solvent molecules which affect the packing of the rubber molecules are also important in relation to these effects.

SUMMARY

1. It is shown that, in addition to the previously described steady decrease of tensile strength of vulcanizates during swelling, there are cases in which the strength passes through a maximum at low degrees of swelling.

2. Variations of a similar character during swelling are also found for the relative elongation of vulcanizates.

3. Such variations of tensile strength and relative elongation are found when the increase of chain flexibility and the associated increased orientation effect is greater than the effect of weakened intermolecular bonding in the polymer caused by penetration of the solvent molecules into the polymer.

4. A strength maximum may also be found if the swelling agent (softener) is introduced into the rubber composition on rolls before vulcanization.

LITERATURE CITED

[1] B. A. Dogadkin and D. M. Sandomirsky, Colloid J., 12, 267 (1950); S. N. Zhurkov and B. N. Narzulaev, J. Tech. Phys., 23, 1677 (1953).

[2] V. E. Gul, Proc. Acad. Sci. USSR, 85, 145 (1952); 96, 953 (1954).

[3] B. Dogadkin, Trans. III All-Union Conf. Colloid Chem., (Acad. Sci. USSR Press, 1953) p. 136.

[4] A. P. Aleksandrov and Yu. S. Lazurkin, Proc. Acad. Sci. USSR, 7, 308 (1944); B. A. Dogadkin and B. K. Karlin, Colloid J., 9, 348 (1947); V. I. Kasatochkin and B. V. Lukin, J. Tech. Phys., 19, 76 (1950).

[5] B. A. Dogadkin and V. E. Gul, Colloid J., 12, 184 (1950); V. E. Gul, V. L. Fedyukin, and B. A. Dogadkin, Colloid J., 15, 11 (1953).*

[6] V. E. Gul, Colloid J., 13, No. 2, 99 (1951).

The M. V. Lomonosov Institute of Fine
Chemical Technology
Moscow

Received May 25, 1956

---

* [Original Russian pagination. See C. B. Translation].

ELASTIC DEFORMATION OF WOOD

Yu. M. Ivanov

A peculiarity of the deformation of wood is that as the stress increases there are two consecutive regions of characteristic deformation [1]: the first is the region of ordinary elasticity, while in the second, after-effect (creep) deformations develop rapidly, accompanied by a decrease of the "instantaneous" deformation modulus. The boundary between these two regions corresponds to the stress σ_{pf}, formerly termed the plastic flow limit.

In the first region the deformation of wood is mainly elastic with a fairly high "instantaneous" modulus of the order of $1-1.5 \cdot 10$ kg/cm^2 (in the air-dry state at room temperature) which remains constant during the development of the elastic-after effect type, the modulus for which is 5-6 times as great as the elastic deformation modulus. When σ_{pf} is exceeded the situation changes abruptly – the rapid development of after-effect deformation is accompanied by a continuous irreversible decrease of the elasticity modulus, which retains a constant decreased value on subsequent application of a force less than σ_{pf}, i.e., in the first region.

These deformation regions are clearly seen in the compression of wood in the direction of the fibers. Micromechanical studies have shown that considerable deformations in the second region do not cause any microscopic changes in the structure of wood, and must be attributed entirely to submicroscopic changes in the secondary walls, consisting mainly of cellulose, which take the main part of the force [2]. A more detailed investigation of after-effect deformations on compression in the second region is of considerable interest. Such an investigation could provide much additional information on the behavior of native cellulose on compression along the direction of the principal anisotropic axis, which cannot be effected in cellulose fibers, the deformation of which in longitudinal extension has been extensively studied [3].

It is possible that the decrease of the elasticity modulus, i.e., an increase in the flexibility of the system, is the result of bond cleavage in the cellulose complex of the secondary walls; if so, this effect should be more prominent as the result of a decrease of the intermolecular interaction, for example in swelling. To verify this view, experiments were performed on swollen wood; the results are detailed below.

Methods. Specimens of beech, oak and larch 20 x 20 x 40 mm in size, with moisture contents above the fiber saturation values, were subjected to compression in the direction of the fiber length at constant temperatures in the range between +15 and +40°. Measures were taken to avoid contact deformation at the end planes of the specimens, which could introduce considerable errors into the results. Metal stops were glued to the opposite end faces of each specimen, with 20-26 mm distance between their axes, i.e., the deformation measurement base. Scales with 0.001 and 0.01 mm divisions were placed on the steel balls of the stops; the former were used for absolute deformations of up to 0.7-0.8 mm, and the latter for larger deformations. The stops were glued to the air-dry wood by means of synthetic glue, either on the cold wood or with heating to not over +60° for 1-2 hours. Then (usually after a day) the specimen was gradually humidified during several days to a state of saturation and tested, immersed in water, by means of the reversing device of the lever testing machine. The general testing procedure was as follows. A load was rapidly applied to the end of the lever and the specimen was left for some time under a constant stress. After the unloading the specimen was completely released, centered again if necessary, and the loading was repeated.

Results of the experiments. Typical deformation–time curves in the second region for beech, oak, and larch wood specimens are given in Figs. 1, 2, and 3. It is seen that the deformation increase rapidly at constant stress; the "instantaneous" deformation on unloading is greater than on loading, indicating increased flexibility of the system. The total deformation Y_2 in the last cycle is 10-20 times as large as the initial "instantaneous" deformation, Y_1 and in other experiments it is 30-45 times as large, reaching 5-8 % of the original length. As the experiments were continued, with the same (or somewhat smaller) load applied to the specimen in the second region, the deformation increased further. For example, one beech specimen tested as described four times at +20° in two months showed a total deformation (including residual) of 11.1%, with an "instantaneous" deformation of 5.5%; another beech specimen tested three times at +38° during 13 days gave a total deformation of 8.9%, with an "instantaneous" deformation of 5%. Despite these large deformations, there were no signs of any damage to the wood structure. The residual deformation was largely restored after the specimens were heated in water at +90° for 4 hours. The equilibrium modulus was about 2 orders of magnitude lower than the initial elastic modulus. The very low values found for the modulus persisted for long periods. For example, repeated tests on beech specimens in the first region (at a stress of 87.5 kg/cm^2) during 7 months, accompanied by periodic drying and wetting of the specimens, gave approximately the same values for the modulus; heating of the specimens in water at +90° for 4-5 hours also had no influence on the modulus.

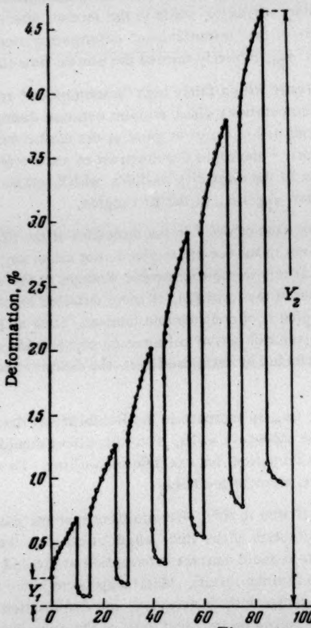

Fig. 1. Deformation–time curves for swollen beech wood compressed longitudinally in the second region; stress 262 kg/cm^2; σ_{pf} = 238 kg/cm^2; temperature +17.6°.

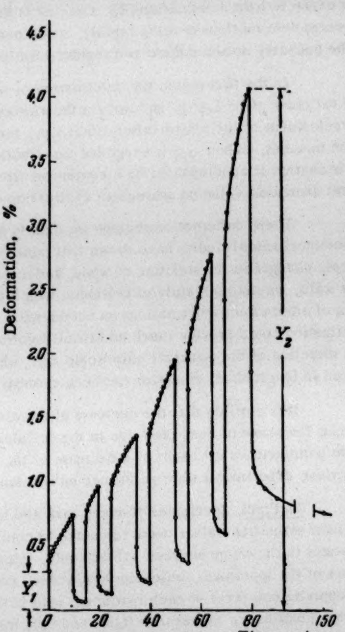

Fig. 2. Deformation–time curves for swollen oak wood compressed longitudinally in the second region; stress 214 kg/cm^2; σ_{pf} = 203 kg/cm^2; temperature +17.6°.

Thus it has been shown that large deformations in the second region can arise in wood; the corresponding low values of the equilibium modulus persist for long periods of time. The excess of the stress over σ_{pf} is significant. This follows from the fact that, for the same conditions of swelling, temperature, and mechanical stress conditions, the deformations in the first region are of a totally different character – the "instantaneous" deformation remains practically constant (Fig. 4, a), the equilibrium elastic modulus is almost 4 times as large as the "instantaneous" equilibrium elastic modulus is almost 4 times as large as the "instantaneous" modulus, while the residual deformation in swollen wood is restored after 1-2 days, without increase of temperature. The deformations remain similarly constant on application of a stress $\sigma < \sigma_{pf}$ to a specimen previously subjected to a considerable deformation – up to 3.5% of the original length in the second region (Fig. 4,b).

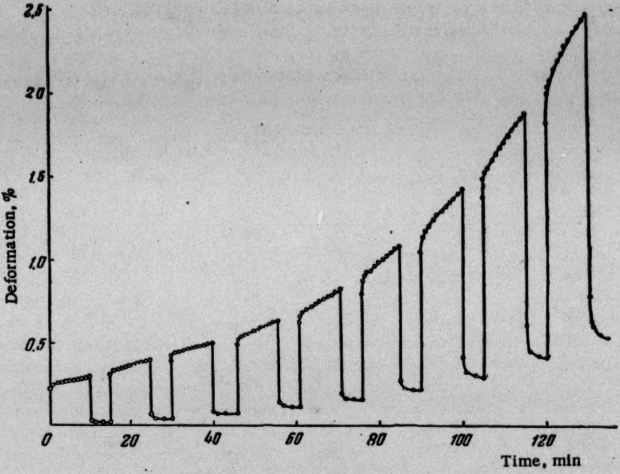

Fig. 3. Deformation–time curves for swollen larch wood compressed longitudinally in the second region; stress 242 kg/cm^2: σ_{pf} = 228 kg/cm^2; temperature + 16.0°.

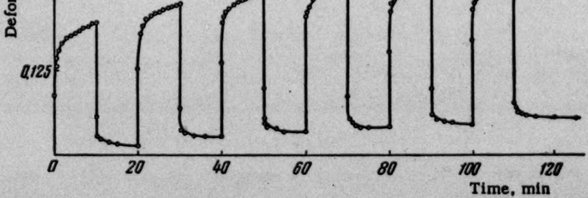

Fig. 4. Deformation–time curves for swollen beech wood compressed longitudinally in the first region: a) natural; stress 180 kg/cm^2; σ_{pf} = 225 kg/cm^2; temperature 16.1 °C; b) previously subjected to 3.5% deformation in the second region; stress 85 kg/cm^2; σ_{pf} = 225 kg/cm^2; temperature 19.0°C.

DISCUSSION OF RESULTS

Analysis of the foregoing results leads to the conclusion that after-effect deformations on compression of wood in the direction of the fibers in the second region are elastic deformations with the characteristic feature that they are accompanied by an irreversible increase in the flexibility of the system. Residual deformations in the second region, which we erroneously considered to be irreversible, are delayed elastic deformations, i.e., reversible by their nature.*

The deformations in the second region are generally similar in character to high elastic deformations of linear polymers, including cellulose fibers; they distinctly show: 1) the relaxation character of the deformations; 2) two principal relaxation time distributions – the first of short times, relating to rapid changes of deformation during loading and unloading, and the second of long times, seen in the slow restoration of deformations after unloading, and 3) a thermoreversible residual deformation of considerable magnitude.

This result is of great theoretical importance, and provides a clear description of the behavior of wood in the two deformation regions, the independent significance of which is emphasized by the above results: these regions differ not only in the magnitude but in the nature of the deformations.

The behavior of wood under stress $\sigma > \sigma_{pf}$, i.e., in the first region, resembles that of polymers in the glassy state. This resemblance is the consequence of the high degree of orientation which is produced in the cellulose of the secondary cell walls during biosynthesis. Strongly polar polymers such as cellulose are characterized by an increase of intermolecular interaction as the result of orientation. Having a fixed structure with almost total loss of high elastic properties, they are in a peculiar form of glassy state [4]. Because of this, deformations in the first region are largely determined by changes in the distances between the particles, and the plasticizing action of moisture influences only the magnitude of the deformation. Under the action of greater stresses in the second region, the state of natural "vitrification" of the cellulose in the secondary cell walls is gradually overcome. This process is effected when intermolecular interaction is weakened by swelling. It seems likely that the molecular mechanism whereby the elastic deformation is irreversibly changed (i.e., increased) consists of an increase of chain mobility owing to rupture of intra- or intermolecular bonds in the cellulose. A gradual increase of chain mobility during isothermal deformation of wood begins from the instant a definite value σ_{pf} of the stress is exceeded, as the result of a lowering of the potential barrier of bond rupture in the force field. The stress σ_{pf}, which is more correctly described as the start of irreversible increase of elasticity σ_{ie}, evidently cannot be a constant quantity, but should decrease not only with increase of moisture content and temperature, but with increased time during which the force acts; this is confirmed experimentally.

The irreversible increase of elastic deformation observed for wood is therefore the result of mechanical activation of an increase of the mobility of the cellulose chains in the secondary cell walls. The high elasticity observed in this case, however, differs from typical high elasticity of polymers in increasing irreversibly in isothermal conditions. Transition of polymers into the state of high elasticity is reversible – a polymer heated above the glass transition temperature T_g passes into the high elastic state, and returns to the glassy state when cooled below T_g. In the present instance the cellulose of the secondary cell walls leaves the natural "glassy" state on application of a force field $\sigma > \sigma_{pf}$, but removal of this field does not result in the loss of the high elastic properties in the cellulose, which does not return to the "glassy" state. On the contrary, the acquired high elasticity is retained for prolonged periods, indicating the irreversible nature of the bond rupture caused by the force field.

Further study is needed to determine the causes of the irreversible transition of the cellulose in the secondary cell walls from the natural "glassy" state. In our opinion, the explanation should be sought in the theory of the amorphous structure of cellulose, which demonstrates the nonequilibrium nature of its highly oriented state [5].

SUMMARY

1. It is shown that under certain conditions, when wood is compressed in the direction of the fibers in the second region, large deformations are produced, reaching 5-10% of the original length. The corresponding low values of the equilibrium modulus persist for a considerable time.

---

* The residual deformations obtained in the second region in longitudinal compression are also prevented in air-dry wood after it has been swollen in water.

2. It is shown that these deformations are reversible; they have the characteristic features of high elastic deformation in polymers – a relaxational character, two main relaxation time distributions, and retarded thermoreversible residual deformation.

3. It is suggested that these large elastic deformations produced when swollen wood is longitudinally compressed in the second region are caused by transition of the cellulose in the secondary cell walls from a natural "glassy" state, owing to increased mobility of the cellulose chains resulting from bond rupture under the action of the force field.

4. These results emphasize the significance of the two regions of the deformation of wood which had been established earlier, as mechanical activation of bond rupture only begins after a certain stress, which can be termed the start of irreversible elasticity increase σ_{ie}, has been exceeded.

In conclusion, the author expresses this deep gratitude to Academician V. A. Kargin, O. P. Golova, and N. V. Mikhailov for valuable comments in the course of discussion of the results of this investigation.

LITERATURE CITED

[1] Yu. M. Ivanov, Proc. Acad. Sci. USSR, 19, No. 6-7, 549 (1938); J. Tech. Phys., 16, No. 11, 1357 (1946); Trans. Inst. Wood Acad. Sci. USSR, 9, 431 (1953).

[2] Yu. M. Ivanov, Trans. Inst. Wood Acad. Sci. USSR, 9, 89 (1953).

[3] N. V. Mikhailov and V. A. Kargin, Trans. IV Conf. High Mol. Compounds, (Acad. Sci. USSR Press, 1949) p. 138.

[4] A. P. Aleksandrov, Trans. 1st and 2nd Conf. High Mol. Compounds (Acad. Sci. USSR Press, 1945) p. 49; V. A. Kargin, N. V. Mikhailov, and V. I. Elinek, Investigations of High Molecular Compounds (Acad. Sci. USSR Press, 1949) p. 315; U. S. Usmanov and V. A. Kargin, Chemistry and Physical Chemistry of High Molecular Compounds, (Acad. Sci. USSR Press, 1952) p. 169.

[5] V. A. Kargin, V. L. Karpov, Yu. S. Lipatov, G. S. Markov, and T. A. Koretskaya, Proc. Acad. Sci. USSR, 101, 707 (1955).

Moscow Received June 22, 1956

THIXOTROPIC AND STRUCTUROMECHANICAL PROPERTIES OF ASKANGEL SUSPENSIONS IN RELATION TO THE COMPOSITION OF THE EXCHANGE COMPLEX

E. I. Kobakhidze, M. E. Shishniashvili, and N. N. Serb-Serbina

One of the most important factors to influence the thixotropic properties of clay suspensions is the composition of their exchange complex, which mainly affects the strength and nature of the thixotropic structure formed in the system [1]. Studies of the influence of the composition of the exchange complex on the thixotropic properties of clay suspensions are both of independent scientific significance in relation to the mechanism and basic laws of this effect, and of practical value for determining the rational conditions for the production of drilling muds with the required structromechanical properties.

Rational production and use of clay suspensions with the necessary structuromechanical properties is important e.g. deep oil drilling. Thus, the main purpose of the present investigation was to carry out a qualitative and quantitative study of the thixotropic and structuromechanical properties of bentonite suspensions in relation to the composition of the exchange complex and to the equilibrium pH values established on addition of alkaline electrolytes.

The material studied was a highly disperse askangel fraction, which was converted into Na- and Ca-askangels, Al (electrodialyzed) askangel, and Na-askangel prepared by replacement of the bases absorbed by the electrodialyzed product by Na ions.

The sodium, calcium, and sodium-substituted electrodialyzed askangels were prepared by the Gedroits method [3], consisting of treatment of the natural and electrodialyzed clays by 1 N NaCl and $CaCl_2$ solutions. The saturated samples were purified by ordinary dialysis in Cellophane bags. Electrodialyzed askangel was prepared by electrodialysis of askangel pastes in three-compartment electrodialyzers at an electrode potential of 600 v (39-37 v / cm). The electrodialysis was continued for about two months and was terminated after the transfer of detectable amounts of electrolyte into the side compartments of the dialyzer, in the form of the corresponding acids or bases, had ceased. According to most investigators [4], electrodialyzed bentonite is to be regarded as "hydrogen bentonite" (H-bentonite), i.e., it is assumed that it contains hydrogen ions only, instead of alkali metal or alkaline earth cations, in the exchange complex. These authors ascribe to H-bentonite the properties of a strong acid.

However, in recent years it has been shown in our laboratory [5] that when askangel is electrodialyzed a considerable decrease of pH of the suspensions occurs in the central compartment of the apparatus, with a simultaneous substantial increase of exchange aluminum in the exchange complex. It has been shown by numerous experiments that electrodialyzed askangel has high exchange acidity and that its exchange capacity is almost entirely determined by exchange aluminum. A similar effect was also found by Shishniashvili and Batsanadze [6] in the purification of aluminosilicate gels by electrodialysis. At low degrees of purification, the aluminosilicate gels contained considerable amounts of exchange aluminum. At high degrees of purification (at electrode potentials of 7000 v), aluminosilicate gels, in contrast to clays, contained no exchange aluminum. Thus, according to the results of our laboratory, electrodialysis of askangel yields Al-bentonite and not H-bentonite.

The samples of askangel derivatives so obtained were made into aqueous suspensions and the following physicochemical characteristics were determined: viscosity, water loss, specific conductance, and pH; the degree of swelling and the swelling kinetics were also determined for all the samples.

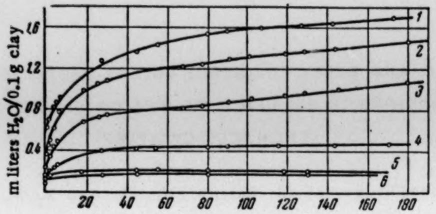

Fig. 1. Swelling kinetics of: 1) Na-askangel; 2) highly disperse fraction of native askangel; 3) native (original) askangel; 4) Oglanli bentonite; 5) Ca-askangel; 6) Al (electrodialyzed) askangel. Time in hours

The viscosities were determined by the falling sphere method by means of the Höppler viscosimeter. Water loss was determined by filtration of the suspensions under vacuum at a residual pressure of 18 mm Hg. In our experiments the standard funnel (d = 9 cm) was replaced by a smaller funnel (d = 5 cm). It was thus possible to carry out experiments with relatively small volumes of suspension (40 ml).

The Freundlich, Schmidt, and Landau method as simplified by Kister [7] was used for studying the kinetics of swelling.

The results of the determinations are given in Table 1 and Fig. 1. For comparison, Table 1 also gives data for suspensions of Oglanli and Na-substituted Oglanli bentonite.

It is seen from Table 1 that the viscosity, water loss, specific conductance, and pH of askangel suspensions greatly depend on the composition of the exchange complex.

The results of studies of the swelling kinetics of askangel and Oglanli bentonite show that Na-askangel has the greatest swelling capacity followed by highly disperse native askangel and then by native (original) askangel. Oglanli bentonite swells considerably less, and Ca- and Al (electrodialyzed) askangels show practically no swelling.

The thixotropic properties of these suspensions were studied by means of the Veiler–Rebinder apparatus [8], by measurement of the increase of the structural strength P_m with time. The results of these measurements were used to plot kinetic curves for thixotropic buildup.

As has been stated, Ca- and Al-askangels do not swell in water, and therefore they form suspensions containing large aggregated particles which show visible sedimentation. Structure formation in suspensions of Ca- and Al-askangels occurs only at a high solid phase content (>30 %), when the particles come into direct contact with one another. The structural strength, for example, of 32% Ca-askangel paste ($P_m = 3.7 \cdot 10^4$ dynes//cm^2), is lower than the strength of 10% native askangel paste ($P_m = 5 \cdot 10^4$ dynes/cm^2).

The properties of Na-askangel are different. Because of its high swelling in water, Na-askangel forms fairly stable, but nonthixotropic suspensions even at a low solid phase content (3%).

These results are in agreement with earlier findings. Serb-Serbina and Rebinder [1] showed that, with increasing contents of Na ions in bentonite clays, structure formation passes through a maximum and then gradually diminishes or ceases completely.

It has been shown in the present investigation that thixotropic structure formation does not occur to any practical extent in suspensions of askangel saturated with Na ions, irrespective of the concentration of the solid phase. It is shown in Figs. 2 and 3 that the shearing stress for Na-askangel suspensions does not vary with time.

Introduction of increasing amounts of Na cations into other bentonites also decreases thixotropic structure formation. However, as has been reported in the literature [9, 10], suspensions of Na-bentonites, such as Na-Oglanli bentonite, do not lose their thixotropic properties. The thixotropic buildup of Na-askangel differs significantly in character from that of Na-Oglanli bentonite, as it is evidently determined by the colloidochemical properties and mineralogical composition of these clays.

TABLE 1

Viscosity, Water Loss, pH, and Specific Conductance of 4% Suspensions of Askangel and 10% Suspensions of Oglanli Bentonite in Relation to the Composition of the Exchange Complex

Sample	Viscosity at 20° in centipoises	Water loss in 30 min., in ml	Specific conductivity at 25° 10^4 ohm^{-1} cm^{-1}		pH	
			suspension	filtrate	suspension	filtrate
Native askangel	7.5	9.0	6.83	4.96	8.95	8.50
Na-askangel	11.3	7.5	3.0	1.04	6.96	7.9
Ca-askangel	Kinetically unstable suspension		1.08	1.06	8.18	7.86
Al (electrodialyzed) askangel	ditto	—	0.29	0.19	3.72	4.82
Na-substituted electrodialyzed askangel	39.5	6.5	1.96	0.71	5.27	7.43
Oglanli bentonite	3.0	12.0	10.82	9.6	8.85	8.27
Na-substituted Oglanli bentonite	5.16	5.5	4.4	2.79	8.9	7.79

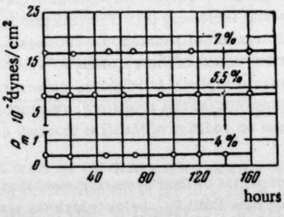

Fig. 2. $P_m - f(\tau)$ curves for Na-askangel suspensions.

We also studied the thixotropic properties of suspensions of Na-substituted electrodialyzed askangel. Figure 4 shows the thixotropic buildup curves for a 7% suspension of Na-substituted electrodialyzed askangel; in contrast to the Na-askangel suspensions, this shows thixotropic buildup. The time of thixotropic buildup for a 7% suspension of Na-substituted electrodialyzed askangel is ~ 70 hours.

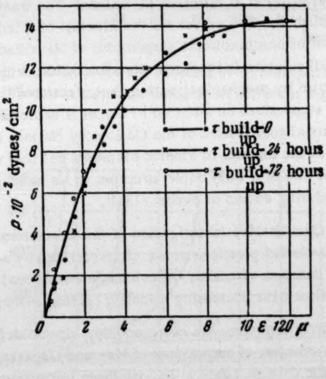

Fig. 3. Variation of shearing deformation with shearing stress in 7% Na-askangel suspensions for different times of thixotropic buildup.

Quantitative investigations of the composition of the exchange complex of Na-askangel and Na-substituted electrodialyzed askangel showed that the total exchange capacity and the amount of exchange sodium are the same for both these materials, but the Na-substituted electrodialyzed askangel has a much lower calcium content, and also contains 3.7 mg-equiv. of exchange aluminum per 100 g (Table 2).

TABLE 2

Composition of the Exchange Complex in Na-Derivatives of Bentonites

Exchange cations	Total exchange capacity in mg-equiv./100 g clay		
	Na-askangel	Na-substituted electrodialyzed askangel	Na-Oglanli bentonite
Sodium	71.75	75.7	56.28
Calcium	14.25	2.78	10.47
Magnesium		Trace	
Aluminum	—	3.72	—
Total exchange capacity	86.0	82.2	66.75

Thus, the thixotropic properties of suspensions of Na-derivatives of bentonites depend not only on the composition of the exchange complex, but also on the conditions of preparation. In particular, thixotropic structure formation in Na-substituted askangel suspensions made from electrodialyzed askangel is probably the consequence of the chemical changes in the particle surfaces which always occur during electrodialysis [5].

For studies of the effect of the equilibrium pH on the thixotropic and structuromechanical properties of askangel, nonthixotropic 4% suspension of Na-askangel and 5% suspension of Ca-askangel were treated with 1 N NaOH solution at different pH values. The treatment of the suspensions was continued until equilibrium pH was established. The curves for the kinetics of thixotropic buildup in these systems are shown in Figs. 5 and 6. Treatment of nonthixotropic suspensions of Na-askangel and of kinetically unstable suspensions of Ca-askangel with NaOH solution induces structure formation, which increases with increasing pH. The structure is completely broken down by mechanical action, but is restored during rest. Formation of a thixotropic structure in Ca-askangel suspensions on addition of NaOH is caused by the dispersing action of this electrolyte, which is the result of partial substitution of the Ca ions by Na ions in the exchange complex. As is known, dispersion, i.e., increase in the number of kinetic elements per unit volume of suspension, favors thixotropic structure formation. The formation of a thixotropic structure in Na-askangel suspensions on addition of NaOH is probably caused by the coagulating action of excess alkali.

Quantitative investigation of the structuromechanical properties of these systems showed that they belong to quasisolid plastic systems, characterized by a conventional flow limit P_{k1}, below which the system flows at a high constant viscosity. Above the conventional flow limit the viscosity falls sharply and the system continues to flow with decreasing viscosity (giving S-shaped curves for the deformation kinetics).

In illustration, the corresponding kinetic deformation curves are shown in Figs. 7 and 8. The elasticoviscous parameters of suspensions of Na- and Ca-askangels at different equilibrium pH values are given in Table 3. From the data in Table 3, P_{k1} for these suspensions is 28.5, 124, and 140 dynes/cm^2 respectively.

At shearing stresses $< P_{k1}$ all the eleasticoviscous parameters are invariant and increase with pH. Evidently, at such stresses either no structural breakdown takes place, or the individual disrupted bonds have time to reform thixotropically during flow.

However, a slight increase of the shearing stress produces an abrupt fall of viscosity as the result of commencing breakdown of the structural skeleton. At such stresses the disrupted bonds do not have time to be thixotropically restored, and breakdown develops rapidly. Thus, structure formation in nonthixotropic Na-askangel

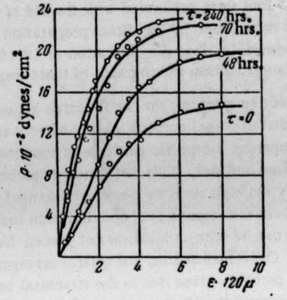

Fig. 4. Variation of shearing deformation with shearing stress in 7% suspensions of Na-substituted electrodialyzed askangel for different times of thixotropic buildup.

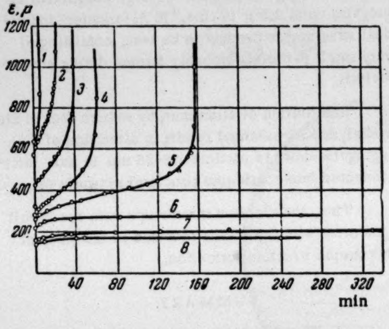

Fig. 7. Curves for the deformation kinetics of 4% suspension of Na-askangel of pH 10.5, for P: 1) 268; 2) 242; 3) 224; 4) 190; 5) 137; 6) 111; 7) 85; 8) 69 dynes/cm².

suspensions and kinetically unstable Ca-askangel suspensions on addition of NaOH consists of the formation of a continuous structure in which the structural elements are held together by weak and labile coagulation forces.

The structure formation process in askangel suspensions in relation to the composition of the exchange complex was also studied by means of the electron miscroscope. Owing to the high resolving power of the microscope, this method allows visual

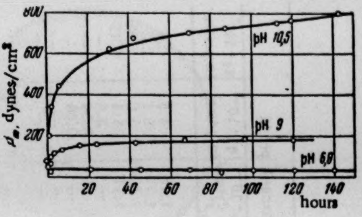

Fig. 5. Curves for the kinetics of thixotropic buildup in 4% Na-askangel suspensions at different equilibrium pH.

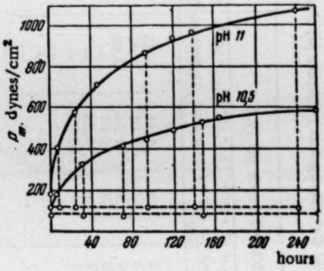

Fig. 6. Curves for the kinetics of thixotropic buildup in 5% Ca-askangel suspensions at different equilibrium pH.

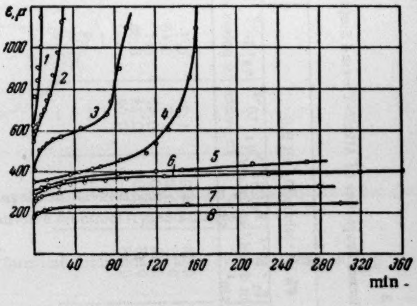

Fig. 8. Curves for the deformation kinetics of 5% suspension of Ca-askangel of pH 11.0, for P: 1) 194; 2) 180; 3) 167; 4) 153; 5) 127; 6) 100; 7) 75; 8) 59 dynes/cm².

TABLE 3

Elasticoviscous Properties of Alkali-Treated Suspensions of Na- and Ca-Askangel at Different pH Values

4% Na-askangel; pH 9.0					4% Na-askangel; pH 10.5					5% Ca-askangel; pH 11				
P in dynes/cm²	$E_1 \cdot 10^{-4}$ in dynes/cm²	$E_2 \cdot 10^{-4}$ in dynes/cm²	$\eta_1 \cdot 10^{-8}$ in poises	$\eta_2 \cdot 10^{-7}$ in poises	P in dynes/cm²	$E_1 \cdot 10^{-4}$ in dynes/cm²	$E_2 \cdot 10^{-4}$ in dynes/cm²	$\eta_1 \cdot 10^{-9}$ in poises	$\eta_2 \cdot 10^{-9}$ in poises	P in dynes/cm²	$E_1 \cdot 10^{-4}$ in dynes/cm²	$E_2 \cdot 10^{-4}$ in dynes/cm²	$\eta_1 \cdot 10^{-8}$ in poises	$\eta_2 \cdot 10^{-7}$ in poises
15	0.18	0.9	1.3	0.7	69	0.59	3.31	1.19	0.63	25	0.4	1.76	4.8	2.8
33	0.17	0.9	1.3	0.65	85	0.63	3.40	1.01	0.65	59	0.38	1.77	5.1	2.2
24	0.19	1.0	0.47	0.7	111	0.60	3.33	1.04	0.63	75	0.36	1.80	5.0	2.25
42	0.18	1.0	0.24	0.69	137	0.63	3.29	0.07	—	100	0.41	1.71	5.1	2.11
48	0.18	—	0.02	—	190	0.62	—	0.03	—	127	0.43	—	3.4	—
—	—	—	—	—	224	0.54	—	0.02	—	153	0.43	—	0.94	—
—	—	—	—	—	—	—	—	—	—	167	0.47	—	0.56	—
—	—	—	—	—	—	—	—	—	—	180	0.37	—	—	—
—	—	—	—	—	—	—	—	—	—	194	0.37	—	—	—

observation of the finest collidal particles in askangel, and of structure formation in askangel suspensions. The investigations were performed with the aid of 100 kv electron microscope by the direct preparation method, with electrono-optical magnification of $13\text{-}15 \cdot 10^3$. Fig. 9 shows electron micrographs of these suspensions.

Electron micrographs (a) of native askangel showed that askangel consists mainly of very small, semitransparent, isometric particles of rounded shape with diffuse outlines. This diffuseness is probably caused by the high swelling power of askangel particles in water. In Micrograph (a) bonds between individual particles can be seen in a number of places, forming kinds of individual chains, the spatial arrangement of which probably gives rise to the structural networks which penetrate the whole volume of the thixotropic suspension.

Particles of Na-askangel (b) also have diffuse outlines, evidently caused by the high degree of dispersion and strong swelling in water. In contrast to native askangel, no structural networks are seen in Na-askangel.

- The particles in Ca-askangel (c) and electrodialyzed Al-askangel (d) consist of large coagulated aggregates up to 2.5 μ in size. In Al-askangel individual structural networks can be seen, consisting of very small particles, probably formed during electrodialysis.

Substitution of aluminum by sodium ions in electrodialyzed Al-askangel results in dispersion of the aggregates down to particles 48-96 mμ in size, interconnected into continuous structural networks (e).

Thus, the electron microscope data are in full agreement with the results obtained in the study of thixotropic structure formation.

SUMMARY

1. The thixotropic and structuromechanical properties of askangel suspensions in relation to the composition of the exchange complex have been studied. It is shown that substitution of the exchange complex of askangel by Na ions causes peptization of the particles, and in consequence a thixotropic structure is not formed in Na-askangel suspensions, irrespective of the concentration of the solid phase.

2. Suspensions of Na-substituted electrodialyzed askangel, in contrast to Na-askangel suspensions, show thixotropic structure formation.

3. Suspensions of Ca- and Al (electrodialyzed)

---

* This part of the work was carried out jointly with Scientific Assistant A. I. Mumladze.

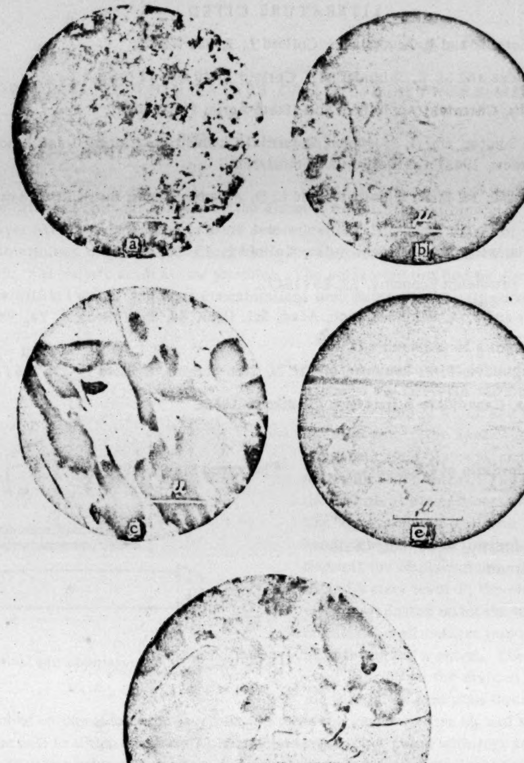

Fig. 9. Electron micrographs: a) native askangel; b) Na-askangel; c) Ca-askangel; d) Al-askangel (electrodialyzed); e) Na-substituted electrodialyzed askangel.

askangel are kinetically unstable, sedimenting suspensions. Structure formation in these systems occurs only with high contents of the solid phase.

4. Treatment of nonthixotropic Na-askangel suspensions and of kinetically unstable Ca-askangel suspensions by 1 N NaOH solution leads to formation of thixotropic structures. Structure formation in Na-askangel suspensions is caused by the coagulant action of excess alkali. Structure formation in Ca-askangel suspensions is the result of the dispersant action of NaOH.

5. Suspensions of Na- and Ca-askangel treated with NaOH solution have the structuromechanical properties of quasisolid or practically solidlike (plasticoviscous) systems.

LITERATURE CITED

[1] N. N. Serb-Serbina and P. A. Rebinder, Colloid J., 9, 381 (1947).

[2] E. L. Kobakhidze and M. E. Shishniashvili, Colloid J., 19 No. 1 (1957).*

[3] K. K. Gedroits, Chemical Analysis of Soil (State Agric. Press, 1929).

[4] W. Lewis, L. Squires, and G. Broughton, Industrial Chemistry of Colloidal and Amorphous Materials (Foreign Lit. Press, Moscow, 1948) p. 216. [Russian Translation.]

[5] S. N. Papuashvili, M. E. Shishniashvili, and L. D. Agladze, Trans. Inst. Chem. Acad. Sci. Georgian SSR, 12,23 (1956).

[6] M. E. Shishniashvili and A. L. Batsanadze, Colloid J., 15, 130 (1953).*

[7] E. G. Kister, Petroleum Economy, 12, 63 (1947).

[8] S. Ya. Veiler and P. A. Rebinder, Proc. Acad. Sci. USSR, 49, 354 (1945); S. Ya. Veiler, Factory Lab. No. 4, 432 (1948).

[9] L. A. Abduragimova, P. A. Rebinder, and N. N. Serb-Serbina, Colloid J., 17, 184 (1955).*

[10] S. A. Kudrina, Canadidate Dissertation (Tashkent, 1950).

The P. G. Melikishvili Institute of Chemistry,
Acad. Sci. Georgian SSR
Tbilisi

Institute of Physical Chemistry, Acad. Sci. USSR
Division of Disperse Systems
Moscow

Received May 7, 1956

---

* [Original Russian pagination. See C. B. Translation.]

PROPERTIES OF THIN LAYERS OF LIQUID BETWEEN MICA PLATES

G. A. Korchinsky

There are different opinions concerning the distance to which the influence of a solid surface on an adjacent liquid layer extends. According to some determinations, it reaches values of the order of one micron [1]. We have determined this distance by measuring the disjoining pressure of water and aqueous solution of acetic, propionic, and butyric acids at low pressures. The acids were purified by distillation. The solutions were made in redistilled water, and their concentrations were determined by titration.

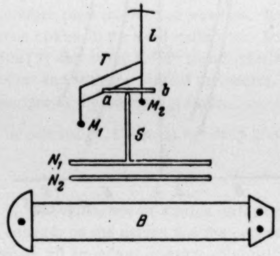

Fig. 1. Diagram of the apparatus.

The thickness of a liquid layer between two mica plates at a definite disjoining pressure was measured by means of the Deryagin and Obukhov apparatus [2] the receiving portion of which had been modified (Fig. 1). The essential part of the apparatus consits of two mica plates, glued onto steel plates N_1 and N_2 (in order to eliminate distortion of the mica). The lower plate N_2 is attached to the bottom of the cell containing the liquid to be studied. The upper plate N_1 is placed on the lower plate beforehand. The rod S, an integral part of plate N_1, serves to transmit the displacements. The receiving portion consists of a steel lever T, the section ab of which was previously graduated under the microscope. The divisions consist of small notches into which the prism-shaped head to the rod S enters. The sensitivity of the instrument depends on the division in which the head of the rod is held. A fine glass thread l, which serves as a pointer, is attached on one side of the lever; on the other side counterpoises M_1 and M_2 are attached to stabilize the system. The cell to which the plate N_2 is attached stands on a frame with legs adjustable by screws; these are used to establish the pointer in the zero position. The values were calculated from the ratios of the lever arms. Additional experiments to determine the influence of side factors were performed and necessary precautions taken as described in the paper cited [2].

The experimental data for water and aqueous acid solutions were used to plot disjoining pressure isotherms (Figs. 2,3). Fig. 2 shows that the distance between the mica plates increases with decreasing disjoining pressure of the liquid up to a maximum value, beyond which the distance remains almost unchanged on decrease of pressure. Consequently, repulsion forces cease to act at this distance, or the influence of the solid surface on the liquid layer in contact with it ceases at half this distance. The repulsion forces measured by this method have an appreciable effect at distances of several microns between the two plane parallel surfaces separated by a liquid layer. This does not mean that all this layer constitutes a special phase. Two layers should be distinguished.

1. A surface layer, in which the molecules are fixed in definite positions and in definite mutual orientation. Thereby they form a kind of crystal lattice. This is confirmed by Trillat's experiments [3]. This layer has been named the multimolecular adsorption layer and, as has been shown [4], can be regarded as a separate phase.

2. The second layer, from a thickness of about 0.3μ, does not form a separate phase, but differs in certain respects from the main bulk of the liquid. Above the multimolecular layer there is an ionic atmosphere,

the density of which probably decreases in a direction away from the surface. Our experimental results may be represented by the equation

$$\alpha P^2 + Ph = \text{const},$$

where P is the disjoining pressure; h is the distance between the plates.

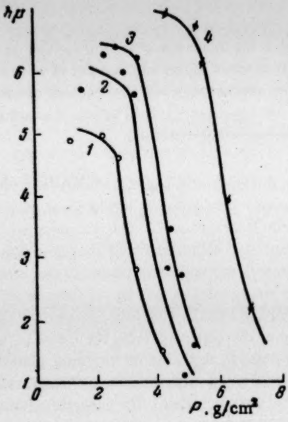

Fig. 2. Disjoining pressure isotherms: 1) water; and aqueous solutions of acetic acid at concentrations: 2) 1.01 mole/liter; 3) 0.505 mole/liter; 4) 0.125 mole/liter.

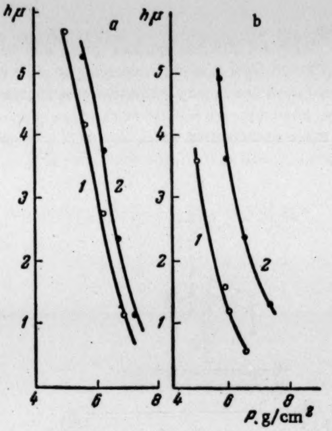

Fig. 3. Disjoining pressure isotherms for aqueous solutions of propionic (a) and butyric (b) acids at concentrations: 1) 0.5 mole/liter; 2) 0.125 mole/liter.

This equation also applies to the data for free films of $2 \cdot 10^{-5}$% undecylic acid solution obtained by Deryagin and Titievskaya [5].

The curves in Figs. 2 and 4 show that, as the concentration of acetic acid increases, the orientation energy and the thickness of the liquid layer first increase and then, at considerable concentrations, decrease. This can be attributed to adsorption induced by the field of force of the mica. Water is present on the mica in an adsorbed state, i.e., a multimolecular adsorption layer is formed, above which ions are arranged in a definite manner, forming an ionic atmosphere.

Acetic acid molecules are adsorbed on mica more strongly than water. This is in accordance with the fact that liquids of lower surface tension, for example at the liquid–air interface, wet solid surfaces better. Water is therefore displaced by acetic acid from the mica surface, and both water and acid molecules are present upon it in the adsorbed state. Here the water molecules are held more firmly than in the case of pure water, because water molecules are additionally bound by mica through acetic acid. The water and acid molecules are probably joined by hydrogen bonds.

It is shown in a number of papers [6] that acetic acid molecules are hydrated in a definite region of solution concentrations. In the present instance the concentration in the main volume of the solution is below this region, but, owing to the fact that acetic acid molecules are more strongly adsorbed on the mica surface, the concentration needed for the formation of such compounds is produced in the multimolecular layer; in consequence the multimolecular adsorption layer is increased and the ionic atmosphere also becomes thicker; this leads to an increase of the disjoining pressure effect.

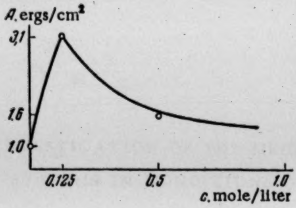

Fig. 4. Variation of particle orientation energy with acetic acid concentration.

On further increase of concentration, acetic acid tends to displace water completely. A kind of hydrophobic surface is formed; i.e., the particles are almost isolated from the force field of the mica, and the multimolecular adsorption layer and the ionic atmosphere both diminish; this ultimately leads to a decrease of the disjoining pressure effect, similarly to the compression of the diffuse layer on increase of electrolyte concentration. The variation of the orientation energy with concentration resembles the variation of zeta-potential with concentration. The variation of orientation energy (Fig. 4) as a function of the concentration of surface active substances indicates variations in the strength of the films separating plane parallel surfaces.

For concentrations of 0.5 mole/liter, the work of orientation of the molecules increases with increasing hydrocarbon chain length in the acids studied (Fig. 4), while at a concentration of 0.125 mole/liter it decreases. The orientation energy varies between 2 and 3 ergs//cm². The explanation is that with decreasing concentration the distances between the solute particles increase, and therefore their interaction weakens. Solute–solvent interaction decreases with increasing length of the hydrocarbon chains in the acid molecules. In general, the structure of the adsorption layer both at the liquid–gas interface [7] and at the solid–liquid interface depends on the nature of interaction of the solute molecules with each other and with the solvent molecules, while the thickness of the ionic atmosphere, in its turn, depends on the structure of the adsorption layer.

In conclusion, I express my deep gratitude to Prof. A. V. Pamfilov for his constant interest in this work.

SUMMARY

1. The influence of a mica surface on an adjoining liquid layer extends to distance up to 4μ; the distance depends on the nature and the concentration of the surface active substance present.

2. The results obtained in measurements of the disjoining pressure of water and aqueous solutions of acetic, propionic, and butyric acids can be represented by the equation $\alpha P^2 + Ph = \text{const}$.

3. The orientation energy of the molecules in water and aqueous acids solutions can serve to characterize the state of a fine layer on a solid surface.

LITERATURE CITED

[1] J. C. Henniker, Rev. of modern Phys. 21, 322 (1949).

[2] B. V. Deryagin and E. Obukhov, Colloid J., 1, 385 (1935).

[3] I. Trillat, Phys. Radium 10, 32, (1929); J. Z. Phys. 6, 191 (1930).

[4] B. V. Deryagin and Z. M. Zorin, J. Phys. Chem. 29, 1755 (1955).

[5] B. V. Deryagin and A. S. Titievskaya, Colloid J. 15, 416 (1953).•

[6] A. N. Glagoleva, J. Gen. Chem. 18, 1005 (1946); S. Ya. Levitman and N. F. Ermolenko, J. Gen. Chem., 18, 1567 (1948).

[7] A. V. Pamfilov, G. G. Devyatykh and L. V. Shirshova, J. Phys. Chem. 24, 292, 1832 (1950).

Chernovits State University

Received June 17, 1956

• [Original Russian pagination. See C. B. Translation.]

INVESTIGATION OF THE MECHANICAL PROPERTIES OF PLASTIC DISPERSE SYSTEMS IN CONDITIONS OF UNIAXIAL EXTENSION AND COMPRESSION

E. P. Mosikhin and G. V. Vinogradov

Because of the existence of a fairly rigid structural framework in such soft plastic materials as clay pastes, solid greases, and similar materials, it is possible to study their mechanical properties by the same methods as are used for typical solids. As the result of investigations carried out by Vinogradov and Klimov [1] on lubricants and congealed oils, considerable success has been attained in the study of the elasticoplastic and strength properties of such plastic disperse systems, test methods have been worked out in detail, and the typical characteristics of these properties have been described. The most important data have so far been obtained in investigations in which pure shear conditions were realized.

The lack of information on the resistance of soft plastic bodies to normal stresses, and on the role of normal stresses in deformation processes in general, is a significant gap, as under actual conditions of use many disperse systems are subjected not only to shearing deformations but are often in a state of complex stress. In such conditions the deformation and destruction processes may be determined not only by tangential but also by normal stresses.

In shearing deformations effected in instruments with concentric gaps visual observation of destruction of the structural framework is difficult, and difficulties therefore arise in defining the conditions in which the yield value is passed. Moreover, in this test method the deformation process may be obscured by the wall effect. The method, described in the present paper, for studying soft plastic bodies in conditions of uniaxial extension and compression is free from most of these defects, and makes possible the determination of the true volume mechanical properties of such materials.

It must be remembered, however, that plastic disperse systems show the properties of solids only at low shearing stresses. Experiments on the extension of plastic disperse systems involve considerable practical difficulties because of their ease of deformation, with the consequent difficulties of suitable design for the clamps, of specimen molding, and a number of other factors. Devices designed for this purpose and some of the results obtained are described below.

A conventional diagram of the simplest proposed apparatus is shown in Fig. 1. The test specimen 1 is molded in the band holders 2 by means of the graduated tube 3. The lower holder, in one piece with the massive stand 4, is stationary. The upper holder is joined by the thread 5 to the balance arm 6. Weights 8 are placed on the pan 7 suspended from the arm.

Molding of the specimen begins with filling the tube with thoroughly homogenized grease. The band holders are then introduced simultaneously into the tube, and the grease is partially extruded through the hole, as shown by arrows in Fig. 1. The position of the graduated tube at this stage in the preparation of the test specimen is shown in Fig. 1 by a dotted line. The movement of the upper holder into the tube stops when the thread has become slightly tensed. To complete the molding of the specimen the graduated tube is slowly lowered onto the base of the stand with the lower holder. Extension of the specimen is determined by displacement of the pointer 9 attached to upper holder (Fig. 1). The readings are taken by means of the measuring microscope 10, to an accuracy of 5 μ. The angles of the slip lines and the planes along which the specimens are destroyed (ruptured) are measured to an accuracy of 1'.

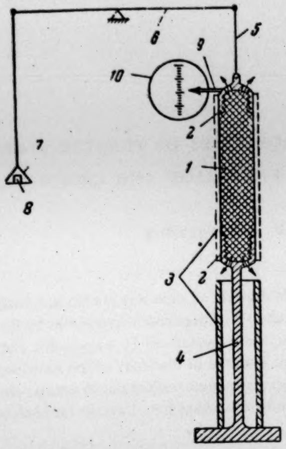

Fig. 1. Simplified apparatus for extension of plastic bodies.

Some results of the use of this apparatus for testing "solidol" grease, a plastic material the rheological properties of which have been studied in detail by Vinogradov, Klimov, and Pavlov [2], are given below. Fig. 2 shows photographs corresponding to different stages of deformation of solidol at a load rate of 2 g/minute. Photograph a shows the original specimen; b shows the beginning of local constriction or neck formation. This stage corresponds to the end of uniform plastic deformation. After a neck has been formed, deformation increases at constant load to failure. Formation and further development of local constriction is accompanied by appearance of slip lines, inclined at about 45° to the specimen axis.

The deformation and destruction of specimens of plastic disperse systems after the formation of a neck differ in some respects from the effects observed in metals which form a neck on extension. In specimens made from homogenized grease the cross section of the neck at right angles to the axis is oval in shape; the neck from the sides of the major and minor axes of the oval is shown in Photographs c and d respectively. A typical specimen after destruction is shown in e. The start of destruction is easily recognized by the appearance of cracks in the region of the neck (Photo f).

The final destruction – separation of the specimen into two parts – is explained in Fig. 3. The rupture surface is an oval (shown in Fig 3 by a shaded area), the plane of which is inclined at 45° to the specimen axis. Figure 3 shows the direction of the shear plane which coincides with the direction of the minor axis of the oval. Thus, destruction of grease specimens occurs in the direction of the greatest tangential stresses. According to Bartenev's classification [3], this is a case of plastic rupture. In all the experiments the neck was formed near the upper holder, which shows that the weight of the specimen itself exerted an appreciable effect.

A typical extension diagram, in nominal stress – relative extension coordinates, is shown in Fig. 4, Curve 1. The linear portion of this curve, starting from the coordinate origin, up to $\sigma = 10$ g/cm^2 (elastic limit) corresponds to purely elastic deformation. In fact, experiments with decreasing loads showed that at stresses less than 10 g/cm^2 the loading and unloading lines for solidol practically coincide. The relative extension in purely elastic deformation is a few tenths of one per cent. Young's modulus is of the order of $3 \cdot 10^3$ g/cm^2. Beyond the region of purely elastic deformation, homogenized greases undergo fairly considerable elongation and show appreciable plasticity. The point K on the diagram represents the nominal strength, which is determined from the ratio of the maximum load sustained by the specimen to its original cross section.

Comparison of the tensile strength σ_t with the maximum shearing strength τ_s, determined by shearing experiments, showed that $\sigma_t/\tau_s \sim 2$. This fact, in the first approximation (because a nominal value of the tensile strength was used), confirms the applicability of the plasticity theory to plastic disperse systems.

Clearly defined hysterisis effects are observed in the plastic deformation region. This is illustrated by the data in Fig. 4, which also shows that the unloading Curves 2 are nearly linear, and that with repeated loadings increase of load results in smaller extensions, i.e., the test specimens exhibit less plasticity. Repeated loadings to values above the elastic limit and below the strength limit produce a decrease of the strength limit – the weakening effect discovered by Vinogradov and Klimov [4] in experiments on greases in conditions of pure shear; this is illustrated by Curve 2 in Fig. 4.

After several loading – unloading cycles the system reached a strength limit at the point E, i.e., the resistance of the specimen to tensile deformation decreased considerably. Rest produced the opposite effect. A specimen which, after the same loading – unloading cycles, was rested for one hour before the last loading,

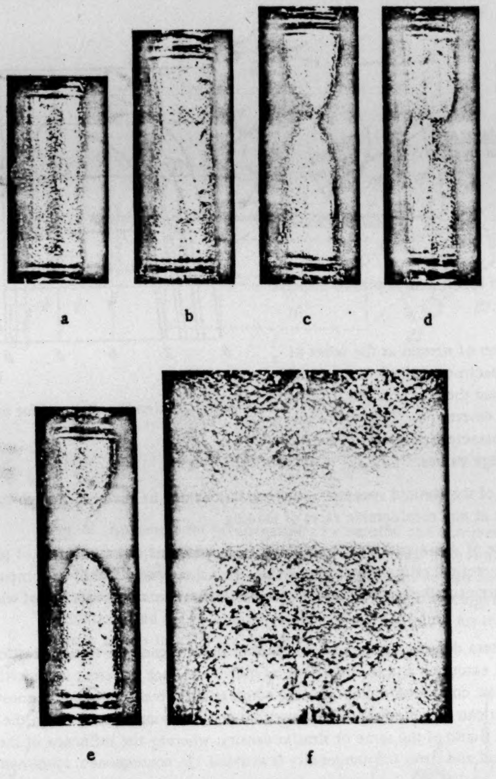

Fig. 2. Photographs of a solidol specimen at different stages of extension: a) original state; b) start of neck formation; c) view of neck in the direction of the major axis of the oval; d) ditto, in the direction of the minor axis; e) after destruction; f) cracks in the neck region.

reached, as the result of thixotropic buildup, a strength limit not at the point E but at the point F, i.e., at higher stresses and accordingly at a greater plastic deformation. The broken region EF of the curve therefore represents the increase of strength as the result of one hour of rest. These results show that the weakening effect and thixotropy in plastic disperse systems may appear not only when the strength limit has been exceeded, but generally as the result of plastic deformations at stresses below the strength limit. The above method for studying soft plastic bodies under uniaxial extension has certain defects.

1. The apparatus, with direct loading, is of the absolutely yielding type and does not record decreased resistance of the specimens to deformation on formation of local constrictions. Therefore loads and extensions should be measured only up to the moment of neck formation.

2. The weight of the specimen itself results in an inhomogeneous stressed state, which is intensified

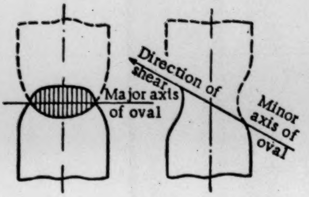

Fig. 3. Destruction of specimens of plastic disperse systems in extension.

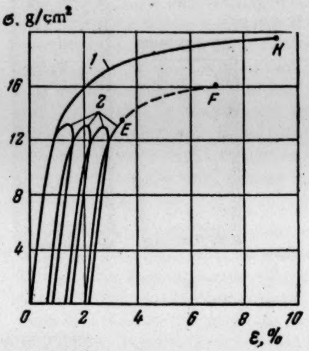

Fig. 4. Extension diagram for solidol.

owing to concentration of stresses at the point of transition from the specimen surface to the inner surface of the tube, and the true strength limit is therefore difficult to determine. Therefore the elastic and plastic characteristics determined by this method are average values.

3. Because of the limited speed at which extensions can be read off through the microscope, tests cannot be carried out at any considerable rates of loading.

4. In the use of this apparatus it is difficult to prepare and test specimens of plastic disperse systems with length (l) — diameter (d) ratio greater than 3-3.6. It is therefore difficult to compare the results of tests on plastic disperse systems with results for such typical solids as metals, specimens of which usually have $l/d = 5$.

In view of these defects, an improved apparatus was designed for testing plastic disperse systems in conditions of uniaxial extension and compression, by means of which different deformation rates can be obtained, the extension (or compression) diagrams are automatically recorded, and thermostatic control is provided. The specimens can be tested either in a vertical or a horizontal position. In the latter case the specimen is contained in a liquid of the same or similar density, whereby the influence of the weight of the specimen is largely excluded and stress inhomogeneity is avoided. In consequence, specimens with $l/d = 5$ can be tested.

The apparatus consists of an electric drive, loading and load measuring mechanisms, recording mechanism, and a bath containing a liquid. The apparatus is shown diagrammatically in Fig. 5.

The bath is a rectangular vessel 340 mm long, 150 mm wide, and 140 mm high; the electric drive consists of a direct current motor 2 and worm reducing gear 3. The speed of the motor shaft is measured by means of a stroboscopic disk 4 and neon lamp 5. A rheostat (not shown) in the shunt winding circuit is used to vary the speed from 50 to 3000 revolutions per minute. The gear ratio of the reducing gear is 60. The loading mechanism consists of a step pulley 6, thread 7, a movable holder 8 with a connecting rod, and a return spring 9. The step pulley is fixed on the shaft by means of a cotter, and can be moved along the shaft, so that the thread can be moved onto any of the steps. The moving holder is in one piece with the rod. The external diameter of the holder is 20 mm, internal — 17 mm, length — 25 mm, internal thread (right hand) pitch — 1.5 mm; The rod diameter is 10 mm, and length 175 mm. The rod can move within the tube. The return spring 9 is used for moving the holder during unloading.

For compressive testing, a reversing device shown separately in Fig. 5,b is screwed into the holders 8 and 12.

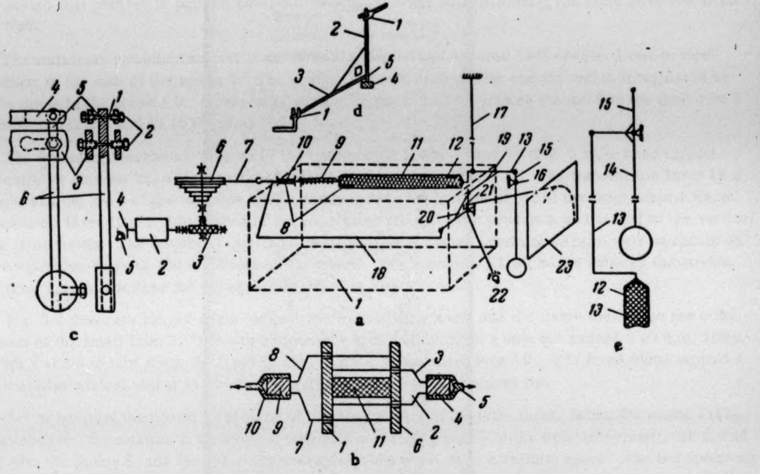

Fig. 5. Apparatus for investigation of extension and compression in plastic disperse systems: a) kinematic scheme; b) reversing mechanism for compressive testing; c) pendulum device for extension and compression tests; d) frame for mirror readings of deformations and loads; e) arrangement of the pendulum for testing plastic bodies in a vertical position.

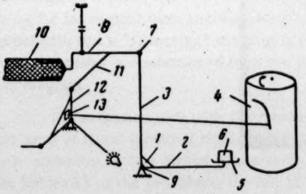

Fig. 6. Diagram of device for automatic recording of deformation—time curves.

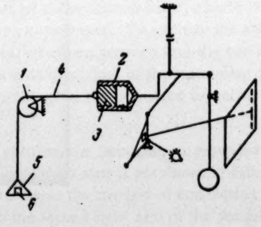

Fig. 7. Diagram of device for constructing the loading scale.

The load measuring mechanism (Fig. 5,a) consists of the holder 12 this holder has a left hand thread and is of the same dimensions as the movable holder) pendulum connecting rod 13, a pendulum consisting of a long arm 14 and a short arm 15, a bracket 16, and a suspension thread 17. The connecting rod 13 joins the holder 12 to the short arm 15 of the pendulum. The suspension thread acts as an additional support. The point of attachment of the thread 17 to the rod 13 is found after this rod has reached equilibrium with the holder in the free state in order to decrease excess pressure on the pendulum supports. When a load is applied to the

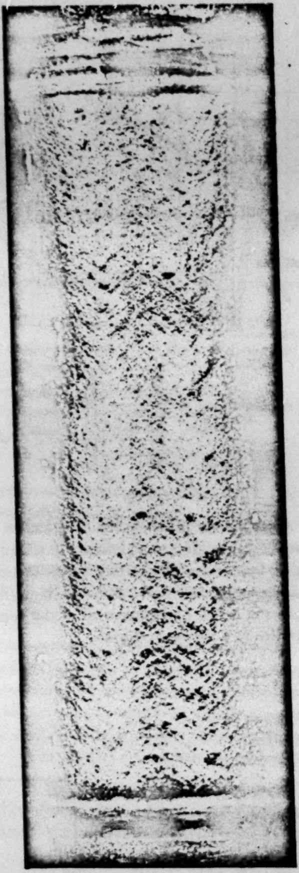

Fig. 8. Slip lines on the surface of a solidol specimen subjected to extension.

specimen, the pendulum connecting rod moves, while the point of suspension of the rod 13 and thread 17 describes an arc of radius equal to the length of the thread; in consequence, the holders are no longer coaxial. To decrease this effect, the suspension thread was 500 mm in length; the suspension point is then displaced by not more than 0.05 mm with a maximum displacement of 3.5 mm of the rod. Interchangeable disks of different weight (from 20 to 150 g) are used for testing specimens with different strength limit.

The reversing device (Fig. 5,b) consists of a plate 1, joined by the connectors 2 and 3 to the bung 4, screwed into the "stationary" holder 5. The plate 6 is joined by connectors 7 and 8 to the bung 9, which is screwed into the movable holder 10 The plates have suitable openings to allow free movement of the connectors 2,3,7, and 8. The specimen 11 is molded between the plates 1 and 6. Because of the right hand internal thread in holder 10 and left hand in holder 5, and corresponding right and left hand external threads on the bungs 9 and 4, the device can be screwed into both holders simultaneously. Thus, with the use of this reversing device it is possible to perform compressive tests, with the holders moving the same direction as in extension tests.

The stationary pendulum support is shown in Fig. 5,c. The tempered steel needles 1 rest in steel conical sockets in the ends of the screws 2. The contact between each needle and the socket is regulated by turning the screw in the bracket 3. A support of similar design is used for joining the rod 6 to the short arm 5 of the pendulum (13,15, and 14 in Fig. 5,a).

The recording mechanism consists of the transmission levers 18 and 19 (Fig. 5,a), a three-support frame 20 carrying a mirror 21, a light source 22, and a photosensitive screen 23. The transmission lever 18 is rigidly linked to the rod 8 of the movable holder and hinged to the horizontal rod of the three-support frame. The transmission lever 19 is rigidly linked to the connecting rod 13 of the pendulum and hinged to the vertical rod of the same frame. The lengths of the frame rods (horizontal 80 mm, vertical 40 mm) were so chosen as to give an extension diagram 200× 200 mm on the screen. The specimen 11 is molded between the holders 8 and 12 (Fig. 5,a) as described for the apparatus shown in Fig. 1.

Fig. 5,d shows the hinged joints between the transmission levers and the frame rods; these are effected by means of the small forks 1. The gap between the rods and the forks 1 does not exceed 0.05 mm, allowing the rods 2 and 3 to turn about the fixed frame support 4 by not more then 14°. The fixed frame support 4 is also a metallic conical socket in which rests a steel needle 5 with a conical tip.

Let us consider the operation of some of the mechanisms of the instrument. When the motor 2 (Fig. 5,a) is switched on, the rotation is transmitted through the reducing gear 3 to the step pulley shaft, the thread is wound onto the pulley 6, and the rod of the movable holder 8 moves at a definite speed. The test specimen 11 is deformed and transmits the load to the short arm 15 of the pendulum through the connecting rod 13, displacement of which deflects the pendulum by a definite angle. The transmission lever 19, which moves together with the rod 13, turns, by means of the fork, the vertical rod of the frame 20 with its attached mirror 21. The ray of light reflected by the mirror moves upward on the screen and records the increase of load on a definite scale. The transmission lever 18 moves together with the movable holder 8, and turns the horizontal rod of the frame by means of the fork. The reflected ray is displaced to the right (if the screen is viewed from the side of the drive) and registers, again on a definite scale, the change in the length of the specimen. In this way an extension (of compression) diagram is recorded in load—extension coordinates. It should be remembered that the total deformation includes the deformation of the specimen itself, elastic deformations of the instrument parts, and displacement of the rod 13 during the experiment. To exclude the elastic deformation of the instrument parts and displacement of the rod, a metal specimen screwed into the two holders is "squeezed"., and a "squeezing" diagram is recorded. The elastic deformations of the instrument parts and the rod displacement are substracted from the total deformation, which gives the corrected extension (or compression) diagram.

For extension tests with the specimen in the vertical position, the pendulum is proveded with two short arms of equal length at right angles to each other (the second short arm is not shown in Fib. 5,a). The whole apparatus is then placed in the vertical position. Fig. 5,e shows the method of connecting the immovable holder 12 to the pendulum, the rod 13 being connected to the second short arm of the pendulum.

To obtain curves showing the deformation kinetics, the pendulum is replaced by a special angle bracket 1 with levers 2 and 3 and a photorecording drum 4 fitted with a clock mechanism (Fig. 6). One end of the horizontal lever 2 carries a pan 5 for weights 6; its other end is connected by means of a point support 7 with the pendulum rod 8. The support 9 of the angle bracket 1 is of the fixed hinge point type. When the load is applied by the weights 6, the lever 2 and the rigidly linked lever 3 turn about the hinge 9. The transmitted force causes deformation of the specimen 10 and therefore displacement of the rod 8. The transmission lever 11, rigidly linked to the rod 8, turns the vertical rod 12 of the frame and with it, the mirror 13. The ray reflected from the mirror moves downward along the slit of the drum and records the deformation of the specimen. The drum 4 with photographic paper attached on it is rotated by means of the clock mechanism, thus provides a time axis on the diagram.

The instrument is calibrated in order to determine the load and extension scales. The holders 8 and 12 (Fig. 5,a) are first set in the zero position, so that the "fixed" holder 12 was not under any load, and the movable holder 8 was 100 mm away from it.

The device shown in Fig. 7 is used to construct the loading scale. It consists of a pulley 1 rotating on needle supports of the type described above. A light bung fitted with a ring is screwed into the "fixed" holder 2. The thread 4 is joined to the ring at one end and to the pan 5 with weights 6 at the other. The position of the point of light corresponding to the zero position of the holders is marked on the screen. The first load is then put on the pan 5, the light spot being thereby displaced upward on the screen; the new position is marked on the screen. A second load is applied and the position of the light spot is again marked, etc. The calibration is continued up to the maximum load (150 g). When the loading scale is completed, and unloading scale is constructed in a similar way. Friction in the pulley bearings 1 (Fig. 7) is allowed for by previous calibration of the pulley itself.

To construct the extension scale, the holder 8 (Fig. 5,a) is moved from the zero position by means of a micrometer, the light spot being displaced horizontally on the screen; its new position is marked. The positions of the light spot are again noted with successive loadings, etc. The points so obtained are used to construct a coordinate grid which is photographed to natural size on sensitive film.

After the testing of each specimen the coordinate grid is photographed onto the paper which is used to record the extension curve (care is taken that the zero points of the curve and coordinate grid coincide). The sensitive paper thus carries an image of the extension curve and the coordinate grid.

To illustrate the use of the extension method, the results of an investigation of a homogenized solidol grease are given. Figure 8 shows a photograph of the specimen after a stress corresponding to plastic deformation has been reached. The photograph clearly shows shearing lines at an angle of 45° to the specimen axis, similar to the lines found after extension of metal specimens.

SUMMARY

1. A new method is described for investigating the rheological properties of plastic disperse systems by testing them in conditions of uniaxial extension and compression. Two instruments designed for such tests are described.

2. Homogenized Ca solidol greases have been used to demonstrate that tensile failure of specimens of plastic disperse systems occurs in the direction of the maximum tangential stress, i.e., by a plastic failure mechanism. Slip lines (Lüders lines) are observed in the direction of the maximum tangential stress. At failure, the neck of the specimen is in the shape of an oval in a direction at right angles to the specimen axis.

3. The uniaxial extension instrument has been used to determine Young's modulus for solidol ($3 \cdot 10^3$ g/cm^2), and it has been shown that in the region of pure elastic deformation the relative extensions comprise tenths of one per cent. The greases showed appreciable plasticity in deformation beyond the pure elastic region.

4. It was found that the ratio of the tensile strength to the shearing strength (determined by means of rotational elastometers) is approximately two. Hysteresis effects in loading and unloading in the plastic deformation region have been examined, and it is shown that plastic disperse systems may exhibit strength loss and thixotropy at stresses below the strength limit.

LITERATURE CITED

[1] G. V. Vinogradov and K. I. Klimov, Proc. Acad. Sci. USSR, 57, 911; 58, 1677 (1947).

[2] G. V. Vinogradov, V. P. Pavlov, K. I. Klimov, and M. M. Gvozdev, Trans. Military Acad. Armored and Tank Forces, No. 11-12 (88-89) 27 (1951).

[3] G. M. Bartenev, Progr. Chem. 24, No. 7, 815 (1955); G. M. Bartenev and G. I. Belostotskaya, J. Tech. Phys. 24, 1773 (1954).

[4] G. V. Vinogradov and K. I. Klimov, J. Tech. Phys., 18, 355 (1948).

The I. V. Stalin Military Academy of
Armored and Tank Forces

Received May 21, 1956

ELECTRON MICROSCOPE AND X-RAY INVESTIGATIONS OF DISPERSE PHASES IN ORGANOSOLS OF LEAD–TIN ALLOYS

E. M. Natanson, V. P. Chalyi, N. N. Kozachek, and A. P. Kaban

Electron microscope investigations of the disperse phases in nonstabilized organosols of lead–tin alloys, made electrolytically [1] from alkaline electrolytes, were carried out in order to study the particle form in these alloys in relation to the component ratio and current density during their formation at the cathode.

The Em-100 electron microscope, giving ~ 18,000 magnification, was used for these investigations. The specimens were prepared by application of microdrops of the organosols onto thin collodion films, which were then dried at 30-40°.

The materials studied were disperse phases of lead and tin organosols and of their alloys, obtained by cathodic deposition with the following atomic ratios of the two metals in the aqueous layer of a two-layer electrolyte: 3: 1, 1: 1, 1: 2, 1: 3 and 1: 7. Cathode deposits were obtained at current densities of 3,5,10,15,20 and 30 amp./dm^2 from each of these electrolyte compositions.

From the results, which are presented in the form of the most typical photographs (see Plate), it is possible to establish certain characteristics relating to the formation of the particles in the alloy organosols.

For the same atomic ratios of lead and tin in the electrolyte, variations of current density have a significant effect on the structure of the highly disperse metal particles formed at the cathode.

This factor is especially prominent in the formation of disperse phases of lead–tin alloy organosols at the cathode in electrolytes with lead–tin ratios of 1: 2, 1: 1, and 3: 1. As the Photographs 1 (D_C = 5 amp./dm^2, electrolyte ratio Pb: Sn = 1: 2) and 2 (D_C = 10 amp./dm^2, electrolyte ratio Pb: Sn = 1: 1) show, at low current densities between 5 and 10 amp./dm^2 the cathode deposits are predominantly microdendritic in structure. The branches of such dendrites are often almost perpendicular to the main axial stem, and separate accumulations of dendrites have a more or less ordered structure. It was noted that the axial dendrites do not have a continuous structure but consist of chains of closely adherent individual crystals. In some instances this structure is fairly loose and the distances between individual crystals can be clearly detected in the field of vision of the electron microscope.

Irregular formations, probably consisting of a mechanical mixture of tin and lead particles, are also seen. Here the lead is deposited on the cathode in the form of microdendrites, and tin in the form of irregular amorphous particles. This is confirmed by electron micrographs of highly disperse cathode deposits formed in two-layer electrolytes in total absence of tin (Micrograph 3, D_C = 10 amp./dm^2) and in total absence of lead (Micrograph 4, D_C = 20 amp./dm^2) at current densities from 3 to 30 amp./dm^2.

At current densities from 3 to 10 amp./dm^2 the cathode deposits consist mainly of lead particles. Tin particles are found much less often in the field of vision. The main reason for this is probably that at low current densities tin, even in a two-layer bath, is deposited in the form of coarse lumps.

At current densities from 10 to 20 amp./dm^2 the tin content of the deposits increases sharply. The dendrites in such deposits have a disoriented structure, seen in Micrographs 5,6, and 7 (D_C=10 and 15 amp./dm^2, atomic ratios of Pb to Sn in the electrolyte 3: 1 and 1: 1). This is especially prominent if the position of the side branches relative to the axial stem is examined, as the side branches of the dendrites begin to disintegrate

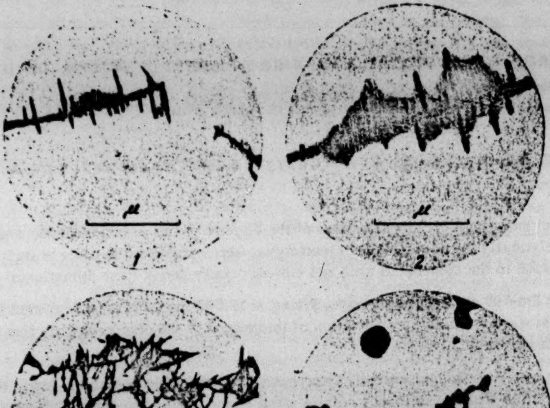

Electron micrographs of the disperse phase of organosols: 1) alloy of Pb: Sn = 63.7: : 37.3%, D_C = 5 amp./dm^2; 2) alloy of Pb: Sn = 60: 40%, D_C = 10 amp./dm^2; 3) lead, D_C = 10 amp./dm^2; 4) tin, D_C = 20 amp./dm^2; 5) alloy of Pb: Sn = 75: 25%, D_C = = 10 amp./dm^2.

from the base. Disintegration of the dendrites is most pronounced in alloys with Pb: Sn = 1: 2 (Micrograph 9, D_C = 10 amp./dm^2). The process is seen particularly clearly when the current density is increased to 30 amp./ /dm^2 (Micrograph 8).

Transition from a dendritic to an amorphous structure in the cathodic particles commences at a current density of 10 amp./dm^2 at Pb: Sn = 1: 2, at current density of 15 amp./dm^2 at Pb: Sn ratios of 1: 1 and 3: 1, and is almost complete at a current density of 20 amp./dm^2. In our opinion this process is the result of formation of a lead–tin alloy at the cathode.

At current densities of 25-30 amp./dm^2 (Micrograph 8, atomic ratio Pb: Sn = 1: 2) no dendrites are seen in the cathode deposits of lead–tin alloy. In all probability, at these current densities the two metals form the alloy at once at the cathode, in the form of fine particles, sometimes joined in large loose amorphous aggregates.

It is also important to take into account that the composition of the lead and tin deposits varies with the current density (see Table).

The Table shows that, with increasing cathode current density, the lead content of the cathode deposits decreases in the range from 3 to 15 amp./dm^2, and then remains almost unchanged on further increase of current density up to 25 amp./dm^2.

Micrographs 3,5,2,9, and 10 show that, at the same current density of 10 amp./dm^2, the structure of the cathode deposits greatly depends on the lead–tin ratio in the electrolyte. At a ratio of Pb: Sn = 1: 0 the particles of the highly disperse lead are of clearly defined microdendritic form. These particles aggregate into very loose accumulations, randomly arranged relative to each other. At ratios of Pb: Sn = 3: 1, 1: 1, and 1: 2 the cathode deposits mainly consist of lead particles of an oriented dendritic structure. Most of the branches of these dendrites are almost exactly perpendicular to the main stem. However, in many cases a transition into an amorphous mass can be seen, probably owing to alloy formation (for example, for Pb: Sn = 1: 1 in Micrograph 2). In this case the cathode deposit is probably a mixture of particles of lead–tin alloy and of pure dendritic lead.

At a ratio of Pb: Sn = 1: 2 (Micrograph 9) alloy formation and transition of dendritic into amorphous particles is still more pronounced. At a lead–tin ratio of 1: 3 in the electrolyte the cathode deposit consists mainly of amorphous particles and contains almost no dendritic particles.

Similar results are seen in electron micrographs of disperse phases of organosols obtained at a current density of 15 amp./dm^2.

These facts suggest that increase of the tin content in the electrolyte favors formation of highly disperse lead–tin alloys at the cathode and decreases the current density at which this process begins. For example, at the ratio of Pb: Sn = 1: 3 there are almost no dendrites in the cathode deposits formed at current densities of 3,5, and 10 amp./dm^2.

In conclusion, it may be noted that for any given lead–tin atomic ratio in the electrolyte there is a definite current density range in which particles of lead–tin alloy are formed at the cathode. In this range, the start of alloy formation is indicated by a sort of "swelling" process in the microdendrites; as the current density increases, this leads to the formation of cathode deposits consisting of almost entirely disintegrated dendrites.

X-ray investigations. Specimens of the disperse phases of lead–tin organosols were studied by the x-ray powder method with iron radiation. An ordinary cylindrical camera with a cassette 57.3 mm in diameter was used. The specimens (0.84 mm in diameter) were prepared as described previously by one of us [2].

To determine the phase composition, standard specimens of spectroscopically pure tin and lead were first taken, and the x-ray diagrams of these were compared with the diagrams of the specimens under investigation.

The results showed that with Pb: Sn ratios of 2: 1, 1: 1, 1: 3 and 1: 5 in the electrolyte, and at the same current density of 10 amp./dm^2, the phase composition of the disperse phase of lead–tin organosols is represented by Pb + β-Sn and does not depend on the Pb: Sn ratio in the aqueous layer of the two-layer electrolyte.

At a ratio of Pb: Sn = 1: 2 in the aqueous electrolyte layer, with a gradual decrease of the cathode current density from 3 to 25 amp./dm^2, the phase composition remains unchanged. At 30 amp./dm^2 the disperse phase of the organosol consists of pure lead.

These results show that the phase composition of disperse phases of lead–tin alloy organosols fully corresponds to the phase diagram for the lead–tin system, in which the components form a eutectic [3].

According to x ray data in the literature [4], at 20° lead dissolves 3.5 atomic % of tin; its crystal lattice parameter decreases as a result. Alloys containing 10-95 atomic % of tin give x ray diagrams showing lines for both metals. With tin contents of 98.6 atomic % and higher, a solid solution of lead in tin is formed, the lattice parameter of the latter being changed only slightly.

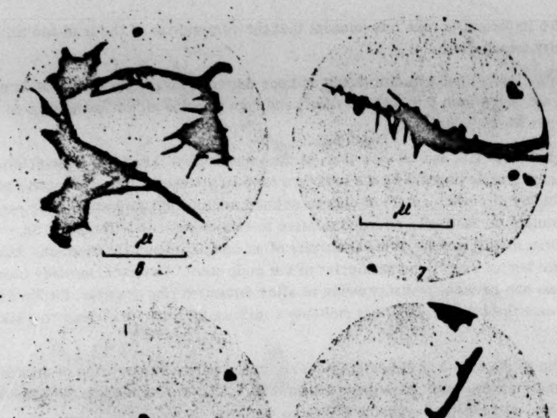

Electron micrographs of the disperse phase of organosols: 6) alloy of Pb: Sn = 48.8: 51.2%, D_c = 15 amp./dm², 7) alloy of Pb: Sn = 72: 28%, D_c = 15 amp./dm², 8) alloy of Pb: Sn = 23.: 77%, D_c = 30 amp./dm², 9) alloy of Pb: Sn = 44.5: 55.5%, D_c = 10 amp./dm², 10) alloy of Pb: Sn = 19.8: 80.2%, D_c = 10 amp./dm².

With increasing tin content in the electtolyte solution the β-Sn lines on the x ray diagrams become more prominent. Increase of current density causes a weakening of th β-Sn lines, and at 30 amp./dm² these lines disappear completely because of the increased degree of dispersion of the tin deposits.

Composition of Cathode Deposits of Lead and Tin Alloys at Different Current Densitites and Component Ratios in the Lower Electrolyte Layer

Atomic Pb : Sn ratio in electrolyte	D_c amp./dm^2	% composition of deposit		Atomic Pb : Sn ratio in electrolyte	D_c amp./dm^2	% composition of deposit	
		Pb	Sn			Pb	Sn
1 : 7	10	16.4	83.6	1 : 2	15	30.0	70.0
	15	12.6	87.4		20	22.0	78.0
	20	6.0	94.0		30	23.0	77.0
	30	5.5	94.5				
1 : 3	3	46.1	53.9	1 : 1	3	70.0	30.0
	5	40.0	60.0		10	60.0	40.0
	10	36.4	63.6		15	48.8	51.2
	15	14.7	85.3		20	40.7	59.3
	20	12.0	88.0		30	30.0	70.0
	30	12.0	88.0	3 : 1	3	79.5	20.5
1 : 2	3	71.4	28.6		10	75.0	25.0
	5	63.7	36.3		15	72.0	28.0
	10	44.5	55.5		20	69.3	30.7
					30	61.5	38.5

In the production of metal organosols by the electrolytic method [1], hydrogen is copiously evolved at the cathode. It was therefore desired to investigate whether it enters into the metal lattices, in particular of lead. The (331) and (420) lines were used to calculate the lattice parameter for lead. The measurements were performed by means of sliding calipers, from the centers of the lines (measurement accuracy was ± 0.05 mm). Arithmetic averages of five measurements were taken for the calculations. The value found for the crystal lattice parameter of pure lead was 4.938 A. This is in good agreement with literature data for very pure lead [5]. Thus, it is confirmed once again [2,6] for alloy organosols that when loose (disperse) metal deposits are formed at the cathode, nonequilibrium solid solutions by incorporation of hydrogen into the metal lattice are not formed.

Our investigations showed that the size of the "blocks" (primary crystallites) of lead in lead–tin alloys remains constant under different conditions of electrolysis (salt concentrations and cathode current density). This is an exception to the general rule (see [6]) and is applicable only to loose cathodic deposits of lead and its alloys, at which hydrogen is evolved at a considerable overvoltage. The average "block" size for all the organosol alloys was 308 A.

SUMMARY

1. Electron microscope investigations showed that the disperse phase particles in lead organosols have a dendritic structure, and the tin particles are of indefinite form and of amorphous structure. It is therefore possible to follow, by means of the electron microscope, the course of formation of the colloidal particles of alloys of these metals under various conditions.

2. For a given atomic ratio of lead to tin in the electrolyte, increase of cathode current density favors simultaneous deposition of these metals in the form of an alloy.

3. At a given current density and different lead–tin atomic ratios in the electrolyte, alloy formation depends on the quantitative proportions of the components. Relative increases of the tin content favor alloy formation.

4. X-ray investigations showed that, when lead and tin are simultaneously deposited on the cathode from two-layer electrolytes, a eutectic alloy is formed. The crystal lattice parameter of lead in the alloys is

4.938 A. The size of the primary crystals ("blocks") in the alloys does not vary with the cathode current density or the ratio of the metals in the electrolyte, and has a value of 308 A.

LITERATURE CITED

[1] E. M. Natanson, Mem. Inst. Chem. Acad. Sci. Ukrainian SSSR 7, 311 (1940); Colloid J. 9, 191 (1947); Trans. All-Union Conf. Colloid Chem.*, (Acad. Sci. USSR Press, 1952), p. 113.

[2] V. P. Chalyi, Bull. Acad. Sci. USSR, Phys. Ser. 17, 195 (1953); V. P. Chalyi and E. M. Natanson, Colloid J. 18, No. 1, 127 (1956).*

[3] Landolt-Börnstein, Tabellen, T. 1 (1923), p. 581.

[4] W. C. Phebus, F. C. Blake, Phys. Rev. 25, 107 (1925); G. S. Zhdanov and Ya. S. Umansky, X-ray Crystallography of Metals, II (State United Sci.-Tech. Press, Moscow-Leningrad, 1938), p. 372. **

[5] B. F. Ormont, Structures of Inorganic Substances (State-Tech. Theoret. Press, Moscow-Leningrad, 1950), p. 334. **

[6] V. P. Ghalyi and S. P. Rozhenko, Summaries of Papers at the 5th All-Union Conference on the Use of x-rays for Investigation of Materials (Leningrad, 1955), p. 45.

Institute of General and Inorganic Chemistry
Acad. Sci. Ukrainian SSSR

Received May 29, 1956

---

* [Original Russian pagination. See C. B. Translation.]

** [In Russian.]

PRODUCTION OF TITANIA–SILICA GELS AND THEIR POROUS STRUCTURE

I. E. Neimark, A. I. Rastrenenko, and M. A. Piontkovskaya

Silicate catalysts occupy a prominent position in organic synthesis and the petroleum industry. It has been conclusively shown [1] that the productivity, activity, and often even the selectivity of a catalyst depends considerably on the character of its porous structure. Therefore the rational utilization of catalysts is directly related to the problem of producing them with the desired microstructure.

Processes of gel and porous structure formation have been studied in greatest detail for silicic acid gels [2]. It has been shown that the porous structure of silica gels is determined by the aging, washing, and drying conditions. Advances in the question of formation of a porous structure in silica gels have made it possible to approach the problem of developing methods for the production of optimum porous structures in gels of technically important hydroxides; these include titania–silica gels. Little work has been done on methods for regulating the porous structure of titania–silica gels during their formation, or on production of gels with a given porous structure. The only information available in the literature relates to the production of titanium catalysts by application of titanium dioxide to already prepared silica gels. For example, Graeber and Cryder [3] have described the production of titania–silica gels by application of titanium tetrachloride in paste form to prepared silica gels. These authors did not study the structural characteristics of the titania–silica gels.

The object of the present investigation was to develop methods for producing titania–silica gels of various structural types and to test the possibility of extending the main concepts of the mechanism of porous structure formation in silica gels to these more complex systems.

Methods for the production and investigation of porous structures in titania–silica gels. Titania–silica gels were prepared by simultaneous precipitation of the respective components. The hydrogels were suitably treated to give titania–silica gels with the required porous structure. The treatment was so designed that the main chemical composition did not vary from specimen to specimen in a given series of catalysts. The starting materials were: water glass of 2.7 ratio, sulfuric acid solution, and titanium dioxide or titanium hydroxide prepared from titanium tetrachloride.

Certain factors which might influence the structure of titania-silica gels were studied, namely: pH of the wash water, drying temperature, nature of the intermicellar liquid, etc. The intermicellar liquid in the hydrogels was replaced by n-butyl or isobutyl alcohols, i.e., liquids which do not dissolve the mixed gel components and which have much lower surface tension than water.

Intermediate structure types were also prepared by a combined method, in which the hydrogels were first dried and then treated with alcohols. In this way micropores were produced in the structure in addition to a considerable volume of larger pores.

By variations of the temperature conditions in drying the hydrogels and alcogels, and in the preliminary drying before replacement of water by alcohols in the hydrogels, and also by variations of the pH of the wash waters, we were able to obtain specimens differing in specific surface, total pore volume, and nature of porosity in each series of gels. Four series of titania–silica gels with different titanium contents were prepared.

Production of titania–silica gels of Series I. Titanium dioxide in the form of a fine powder was added to sulfuric acid (d = 1.18) and made into a fine suspension by means of vigorous stirring for several hours. After this, without interruption of the stirring, a water glass solution with a density of 1.18 g/cc was carefully added to the mixture. The respective proportions of sulfuric acid, water glass, and titanium dioxide were: 1 volume, 2.15 volumes, and 12.5 g/liter. The mixture was warmed to 50° to accelerate coagulation. When syneresis commenced, the hydrogel mass was cut into 1.5-2 cm pieces and divided into two portions: one was washed with acidified tap water at pH 3.5 (Specimen T-1), and the other, with ammoniacal water at pH 8 (Specimen T-2). After washing to remove salts, part of the hydrogel washed with ammoniacal water was treated with isobutyl alcohol and dried at 250° (Specimen T-3).

Production of titania–silica gels of Series II. A silicic acid sol was prepared by mixing one volume of sulfuric acid (d = 1.18) with 2.15 volumes of sodium silicate solution (d = 1.18) with vigorous stirring; to this was added a previously prepared suspension of TiO_2, to give 15 g of dry titanium dioxide per 1 liter of the sol. The mixture was then warmed to 75° with uninterrupted stirring, when coagulation ensued. The coagulated mass was cut into 1.5-2 cm pieces and washed with distilled water to remove salts. After being washed by decantation, the hydrogel mass was divided into four portions for subsequent treatment. One portion was dried at room temperature immediately after the washing (Specimen T-21), the second was dried at 200° (Specimen T-22), and the third was treated with n-butyl alcohol at the boil. Complete replacement of the hydrogel water by butyl alcohol was confirmed by the refractive index of the condensate. The product was dried at 200° (Specimen T-23). Finally, the fourth portion of the washed hydrogel was dried at room temperature for 15 days. The dried gel was treated with n-butyl alcohol, then dried at room temperature for 20 days and at 150° for 4 hours (Specimen T-24).

Production of titania–silica gels of Series III. The original hydrogel mass for production of titania–silica gels of Series III was made by the same method as for Series I. The main difference between the two series was the titanium dioxide content, which in Series III was based on a content of 30 g of TiO_2 per liter of the original silicic acid sol. Specimen T-11 was prepared by drying the hydrosol at room temperature for 20 days and then for 6 hours at 200°. Specimen T-13 was obtained from the hydrogel which was washed, treated with n-butyl alcohol, dried at 100° for about 2 hours, and then at 200° for 3 hours. To remove traces of alcohols, the dried gel was heated at 500° for 1 hour. The hydrogel from which Specimen T-14 was prepared was dried for 6 days at room temperature, treated with n-butyl alcohol, then dried at room temperature for 25 days and finally at 150° for 4 hours. Traces of alcohol were removed at 500° for 1 hour.

Production of titania–silica gels of Series IV. The specimens of this series were prepared by simultaneous precipitation. Different volumes of $Ti(OH)_4$ suspensions were added with vigorous stirring to equal volumes of a silicic acid sol prepared by the usual method. The stirring was continued to coagulation. The mixed gel was aged for 24 hours, then cut into 1.5-2 cm pieces and divided into two portions: one was washed with tap water at pH 7.5, and the other with distilled water at pH 6.0. The washed hydrogels were dried at 160°.

Methods of adsorption and structure determination. The porous structure of the titania–silica gels was characterized by determinations of the total pore volume from the difference between the reciprocals of the apparent and true densities, by study of the adsorption isotherms for methyl alcohol vapor at 20°, determined with the aid of vacuum apparatus with a spring quartz balance, and by calculations of the specific surfaces and effective pore sizes. For additional clarity, the adsorption isotherms were converted into differential adsorption isotherms [4].

Structural and adsorption characteristics of titania–silica gels: results and discussion. The structural characteristics of the titania–silica gels are given in Table 1.

Figures 1 and 2 show the adsorption isotherms and pore radius distributions for the specimens of Series I. The data in Table 1 and the adsorption isotherms show sharp differences between the pore structures of different specimens of this series. The lowest capacity was found for Specimen T-1; its isotherm shows only a slight hysteresis loop, indicating that the intermediate pore volume is small and that micropores predominate.

Specimen T-2 has greater capacity and its isotherm shows a large hysteresis loop. The largest pores were found in Specimen T-3; its porosity was nearly 9 times that of the finely porous Specimen T-1. The distribution of the intermediate pore volume by effective radius (Fig. 1) and differential adsorption isotherms (Fig. 2) give a clear picture of the character of the porous structure of titania–silica gels of Series I: Specimen T-1 is homogeneously microporous, with predominant pore radius < 10 A, while Specimen T-2 has a larger average radius, ~30 A. The average pore radius for Specimen T-3 is in the range 60-70 A.

The preparation conditions of T-1 and T-2 titania–silica gels differed by the use of wash waters of different pH. The dried Specimen T-2, washed with alkaline water at pH 7.5, had larger pores than Specimen T-1, washed with water at pH 6. This agrees with data obtained earlier for silica gels [5].

Replacement of hydrogel water in Specimen T-3 by a liquid of low surface tension resulted in the formation of a very coarsely porous specimen; this is also in good agreement with the influence of the same factor on the structure of silica gels [5].

TABLE 1

Structural Characteristics of Titania–Silica Gels

Series	Specimen	Apparent density in g/cc	Total porosity in cc/g	Maximum sorptive capacity in cc/g	Specific surface in m^2/g	Predominant pore radius in A
I	T-1	1.29	0.33	0.36	465	<10
(10% TiO_2)	T-2	0.78	0.84	0.82	260	30
	T-3	0.30	2.89	2.80	400	65
II	T-21	1.39	0.28	0.33	645	<10
(13% TiO_2)	T-22	1.24	0.37	0.38	686	15
	T-23	0.41	2.0	2.04	652	45
	T-24	0.62	1.17	1.18	625	40
III	T-11	1.32	0.34	0.34	539	<10
(22% TiO_2)	T-12	1.28	0.36	0.38	598	<10
	T-13	0.38	2.21	2.20	598	45
	T-14	0.07	0.51	0.52	569	15
IV	T-3^d	1.28	0.34	0.34	696	<10
(4,6% TiO_2)	T-3^b	0.82	0.76	0.77	580	17.5

The structure and adsorption characteristics of titania–silica gel specimens of Series II are illustrated by the data in Table 1 and Figs. 3 and 4. These data show that the specimens in this series, prepared under different conditions, differ considerably in porous structure. The adsorption and desorption isotherms for methyl alcohol are given in Fig. 3. The volume distribution curves for the intermediate pores by effective radius show that Specimen T-23 has the greatest effective pore radius (~ 40 A), and Specimen T-22 has the least (~ 15 A) (Fig. 3). The figure does not show the curve for the pore distribution by radius for the most finely porous Specimen T-21; its pore size lies in the < 10 A region.

Differential isotherms for titania–silica gels of Series II are given in Fig. 4. As already stated, Specimens T-21 and T-22 differed in the temperature at which the hydrogel was dried; the first was dried at room temperature and the second at 200°. The adsorption and desorption branches of the isotherms for Specimen T-21 coincide over the whole range of relative pressures, while the isotherm for Specimen T-22 shows a hysteresis loop, indicating that some of the pores in this specimen are of the intermediate type. The porosity differences between Specimens T-21 and T-22 arose in consequence of the different contracting action exerted by the capillary forces on the gel skeleton during drying, as the difference between the surface tensions of the intermicellar liquid (water) at 18 and 200° is more than 20 dynes/cm. In consequence the hydrogel dried at room temperature was more finely porous than the hydrogel dehydrated at 200°.

Replacement of the water in the hydrogel by n-butyl alcohol, as in the specimens of Series I, gave Specimen T-23, with a very high adsorptive capacity. Preliminary drying followed by replacement of water by alcohol gave T-24, with a lower capacity. The curves for the volume distribution of the intermediate pores by effective radius also differ for the two specimens. The maximum on the curve for T-24 lies further in the direction of smaller radii. The explanation for the change in the porous structure of Specimen T-24 is probably that the hydrogel shrank somewhat during the preliminary drying. The subsequent treatment with n-butyl alcohol halted the shrinkage.

The conditions for the preparation of titania–silica gels of Series III were similar to those for Series II. The difference lay in the different contents of titanium dioxide in the specimens. The structural and adsorptive characteristics of these specimens, given in Table 1 and Figs. 5 and 6, indicate that the structure relationships found in titania–silica gels of Series II apply also to the specimens of Series III with other titanium dioxide contents.

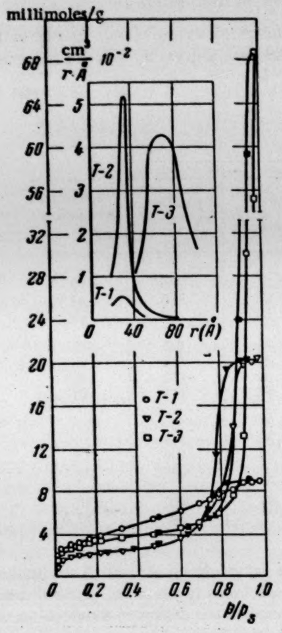

Fig. 1. Isotherms for adsorption of methyl alcohol vapor on titania–silica gel specimens of Series I; black points represent desorption; curves for the volume distribution of intermediate pores by effective radius are shown at the top.

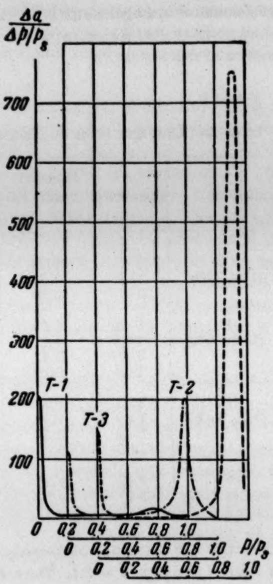

Fig. 2. Differential adsorption isotherms for titania–silica gel specimens of Series I.

The structural characteristics of Specimens T-3^d and T-3^t, washed with water of different pH, differ sharply (Table 1 and Fig. 7). The titania–silica gel washed with water at pH 6.0 is microporous. The isotherm for methyl alcohol adsorption does not show a hysteresis loop. The specimen washed with water at pH 7.5 has larger pores. The isotherm for this specimen has a considerable hysteresis loop.

It is interesting to note that titania–silica gels containing different amounts of titantium dioxide but prepared under the same conditions are almost identical in structure.

Figure 8 shows isotherms for adsorption of methyl alcohol vapor on titania–silica gels with different titanium dioxide contents but washed and dried under the same conditions. It is seen from Fig. 8 that the adsorption isotherms for these specimens practically coincide. The reason is probably the similarity of the chemical and hydrophilic properties of silica and titania.

It was important to determine the influence of some of these factors on the structure of titania gels. The influence of the intermicellar liquid and drying temperature on the porosity of titania gels was studied. Figure 9 gives isotherms for adsorption of methyl alcohol vapor on titania gels, the intermicellar liquid in which was water (Specimen 880^d) and n-butyl alcohol (Specimen 890), respectively. Figure 9 shows that replacement of hydrogel water by a liquid of low surface tension leads to formation of specimens with very large pores.

Increase of the drying temperature, which leads to a decrease of the surface tension of the intermicellar liquid, also results in formation of more coarsely porous gels (Table 2).

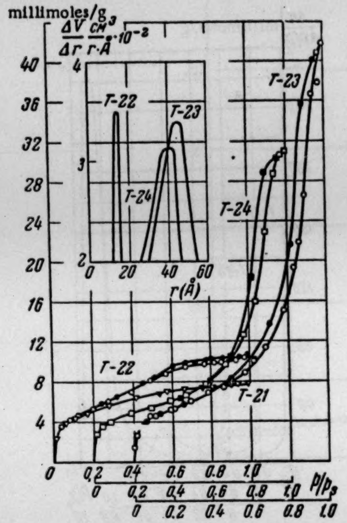

Fig. 3. Isotherms for adsorption of methyl alcohol vapor on titania—silica gel specimens of Series II; black points represent desorption; curves for the volume distribution of pores of effective radius are shown at the top.

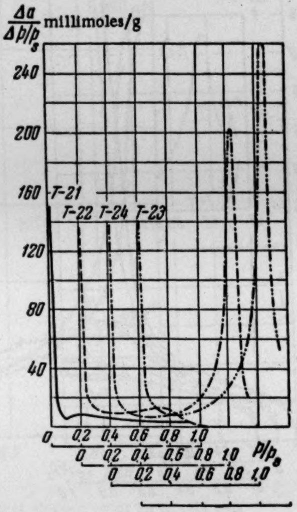

Fig. 4. Differential adsorption isotherms for titania—silica gel specimens of Series II.

These results indicate that the relationships found earlier for the effects of various factors on the structure of silica gels [2, 5, 6] are also applicable to titania—silica gels and titania gels. It is probable that the pore formation mechanism is similar for silica, titania—silica, and titania gels.

TABLE 2

Effect of Drying Temperature on the Structure of Titania Gels

Drying temperature in °C	Apparent density in g/cc	Total pore volume in cc/g	Volume of benzene adsorbed from saturated vapor in cc/g
20	1.78	0.25	0.28
140	1.48	0.38	0.38

An alkaline medium favors ion exchange between the gel hydrogen and the cations of the medium, whereby the bonds between the gel particles and water are weakened, which results in accelerated aggregation of the particles into longer chains and clusters. The framework becomes more rigid and less compressible during drying, and in consequence more coarsely porous titania—silica gels are formed. A weakly acid medium hinders ion exchange, the gel framwork remains hydrophilic and elastic, and this gives a denser packing of the particles when the hydrogels are dried. Decrease of the surface tension of the intermicellar liquid and the associated decrease of capillary forces always leads to formation of coarsely porous specimens.

We have been able to vary the porous structure of titania—silica gels within wide limits on the basis of the theory of the formation of porous structure in silica gels.

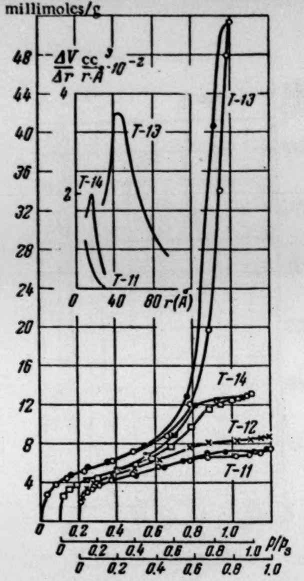

Fig. 5. Isotherms for adsorption of methyl alcohol vapor on titania–silica gel specimens of Series III; black points represent desorption; curves for the volume distribution of the intermediate pores by effective radius are shown at the top.

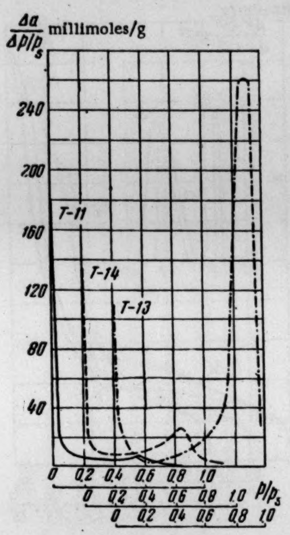

Fig. 6. Differential adsorption isotherms for titania–silica gel specimens of Series III.

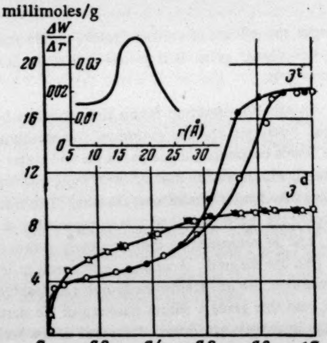

Fig. 7. Isotherms for adsorption of methyl alcohol vapor on titania–silica gels of Series IV; black points represent desorption; curves for the volume distribution of the intermediate pores by effective radius are shown at the top.

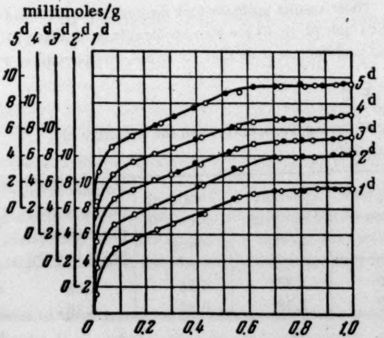

Fig. 8. Isotherms for adsorption of methyl alcohol vapor on titania–silica gels with different titanium dioxide contents; black points represent desorption; 1^d) 2.3% TiO_2; 2^d) 3.4%; 3^d) 4.6%; 4^d) 5.6%; 5^d) 6.7% TiO_2.

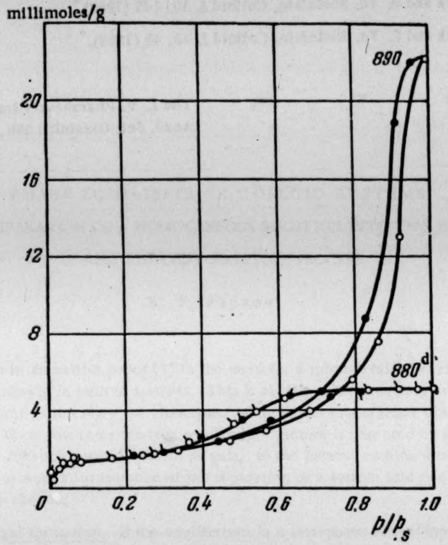

Fig. 9. Isotherms for adsorption of methyl alcohol vapor on titania gels 880^d and 890; black points represent desorption.

SUMMARY

1. Specimens of titania–silica and titania gels of different porous structures have been prepared and their adsorptive and structural properties have been studied in detail.

2. It is shown that the structure and adsorptive properties of titania–silica gels depend on the preparation conditions and are independent of the titanium content (up to 22% TiO_2).

3. On the basis of the parallel influence of preparation conditions on the nature of the porous structure in silica, titania–silica, and titania gels it is shown that our theory of the mechanism of structure formation in hydrophilic adsorbents is applicable to titania gels.

4. Methods have been developed for preparing titania–silica gels with a required porous structure over a wide range of total porosity (from 0.3 to 2.2 cc/g).

LITERATURE CITED

[1] G. K. Boreskov, Chem. Ind. 221 (1947); 257 (1947); I. E. Neimark and R. Sheinfain, J. Phys. Chem. 23, 595 (1949); G. K. Boreskov and V. A. Dzisno, J. Phys. Chem. 24, 1135 (1950); I. E. Neimark, Trans. All-Union Conf. on Catalysis, Kiev (Acad. Sci. Ukr. SSR Press, 1950); I. E. Neimark and L. Kh. Freidlin, Bull. Acad. Sci. USSR, Div. Chem. Sci. No. 3, 311 (1951).

[2] I. E. Neimark, Trans. Commission on Analytical Chemistry 6 (IX) (Acad. Sci. USSR Press, 1955) p. 77; Progr. Chem. No. 6 (1956).

[3] E. G. Graeber and D. S. Cryder, Ind. Eng. Chem. 27, 828 (1935).

[4] V. G. Bykov, Bull. Acad. Sci. USSR, Div. Chem. Sci. No. 6 (1951).

[5] I. E. Neimark and R. Yu. Sheinfain, Colloid J. 15, 145 (1953).*

[6] I. E. Neimark and R. Yu. Sheinfain, Colloid J. 15, 45 (1953).*

Received June 11, 1956

The L. V. Pisarzhevsky Institute of Physical Chemistry,
Acad. Sci. Ukrainian SSR, Kiev

---

* [Original Russian pagination. See C. B. Translation.]

PHASE EQUILIBRIA IN COLLOID SYSTEMS

1. SEPARATION OF A HOMOGENEOUS SOLUTION INTO TWO PHASES AND THE GEL FORMATION PROCESS

S. P. Papkov

Attention was drawn in an earlier paper [1] to the need for a more detailed examination of cases in which equilibrium is established slowly in colloid systems. This is all the more necessary as it is often wrongly concluded that colloidal systems do not obey the phase rule owing to the low rates at which equilibria are established. Moreover, as the result of these low rates the true equilibrium picture is obscured by secondary processes. This is seen especially clearly for such colloid systems as gels. In the present communication an attempt is made to consider gel formation as a specific instance of the separation of a system into two phases, on the assumption that the phase rule is fully obeyed.

General scheme of gel formation. If the equilibrium in a one-phase two-component system is displaced so that the system passes through the critical compatibility point of the components, separation into two phases takes place. The separation passes through the following successive stages: a) formation of nuclei of the new phase; b) growth of these nuclei; c) coalescence of the particles of the new phase owing to the tendency to decrease the interphase to a minimum; and finally, d) hydrostatic (mechanical) equilibrium, as the phases are usually of different densities.

Each of these stages has its own characteristics which depend on the equilibrium composition and physical properties of the coexisting phases. Accordingly the time for complete equilibrium to be established will also differ for different systems.

When gas–liquid or liquid–liquid (with both liquids of low viscosity) phases are formed, the time required for the establishment of complete equilibrium (with respect to the composition and mechanical) is usually short. Completely separated macrophases with a minimum interphase area are formed.

The situation is somewhat different when a liquid solution separates into two phases with formation of a crystalline phase. The time required to reach equilibrium may be relatively long, depending on the number of active centers of crystallization (impurities or spontaneously formed crystal nuclei), and coalescence of the particles of the crystalline phase is generally limited, since natural recrystallization (or crystal growth) depends on the difference of vapor pressures (or solubilities) over crystals of different size. This difference is vanishingly small for large crystals. Therefore systems with crystalline phases are regarded as being practically equilibrium systems even if a microcrystalline precipitate is formed. Hydrostatic equilibrium is usually established comparatively rapidly.

In systems in which the separating phases are amorphous and not crystalline the position is quite different. Such systems include not only most solutions of high polymers, but many solutions of substances of low molecular weight. The peculiar nature of phase separation in such solutions often leads to formation of imperfectly separated systems, with highly disperse phases, with consequent specific physicochemical properties. Such systems are justifiably considered as a separate domain, included in colloid chemistry.

For a clearer picture of the structure of colloids formed in the separation of a one-phase multicomponent system, and for derivation of certain conclusions concerning their specific physicochemical properties, it is necessary to examine in detail the phase separation process leading to formation of amorphous phases in such a system.

Coexisting amorphous phases (in equilibrium with respect to composition) are mutual solutions of the components, differing in concentration. We may arbitrarily call one of the phases a solution of Component B in Component A, and the other a solution of A in B. Restricting ourselves to a consideration of only a particular group of condensed systems, we will for convenience term the substance which has the properties of a solid at normal temperatures Component B, and the substance which has the properties of a liquid (the "solvent") Component A. We shall term a solution of B in A Phase I, and a solution of A in B, Phase II.

In contrast to systems which separate with formation of crystalline phases, Phase II in amorphous systems is never 100% Component B, but contains some Component A in a state of equilibrium. It is important to note that the physical properties of this phase may vary considerably according to the ratio of the components in it. This applies, in particular, to viscosity. At viscosities above 10^{10} poises this phase will have the properties of a solid (it will be brittle under stresses of relatively low frequency). At lower viscosities the second phase is a liquid; i. e., it will change its shape under its own weight in a time comparable with the usual duration of an experiment.

The composition and the corresponding physical properties of Phase II to a great extent determine the course of phase separation in a system, and its structure in incomplete hydrostatic equilibrium. As a rule, Phase I has very low viscosity differing little from the viscosity of Component A ("solvent"), since in most of the systems with which we are concerned the concentration of Component B in it is very low. Therefore Phase I has little influence on the structural characteristics of separating systems.

Let us consider the process of phase separation in greater detail. In the first instant after the change in the parameters of the system (transition through the critical point of total miscibility of the components) nuclei of the new phases are formed. Here attention must be drawn toa point which has generally been neglected. Hitherto, as a rule, the separation only of the "solid" phase (Phase II) from the nonequilibrium solution has been considered. In various investigations [2] the rates of formation and growth of particles of the "precipitated" substance (Component B) have been studied on the assumption that the nonequilibrium solution becomes poorer in Component B as the separation proceeds, and gradually reaches an equilibrium concentration. In this view, the concentration of Component B in the nonequilibrium solution at any instant in the course of precipitation represents the difference between the original amount of Component B and the amount of it present in the "solid" phase formed. However, there are no grounds for assuming that simultaneous separation of equilibrium Phase I does not occur simultaneously, so that the nonequilibrium solution becomes poorer in Component A. Indeed, if formation of stable nuclei of Phase II is possible owing to fluctuation processes, formation and further growth of Phase I nuclei is equally justifiable. These two routes are equivalent from the energy aspect, since either can independently lead to the formation of two equilibrium phases. Therefore we must start with the assumption that displacement of the equilibrium leads to the simultaneous formation of nuclei of Phases II and I.

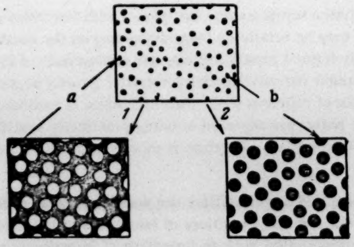

Fig. 1. Separation of a homogeneous solution into two phases. a) Phase I, b) Phase II; 1) growth rate of Phase I nuclei predominates; 3) growth rate of Phase II nuclei predominates.

The next stage is the growth of the nuclei, and the rates of such growth may differ for the two phases. The growth rate of the nuclei depends on many factors, an especially prominent role being played by the mobility of the molecules of the substance which predominates in the composition of the given phase. The greater the difference between the molecular weights of Components A and B, the more probable it is that the Phase I nuclei will grow at the greater rate, since this phase consists mainly of Component A of low molecular weight (the solvent). Certain experimental data lead to the same conclusion.

A system undergoing separation into two phases can be likened to an emulsion, in which the "emulsion medium" is the nonequilibrium solution, and the "emulsified particles" are spherical particles of the new phases. These particles gradually grow, while the volume of "emulsion medium" (the nonequilibrium solution) gradually decreases.

Depending on the relative rates of growth of the particles, the "emulsion medium" (the nonequilibrium solution) will become richer either in Component B or in Component A, gradually approaching the composition of one of the equilibrium phases. For example, if particles of Phase I grow more rapidly, the nonequilibrium solution will become richer in Substance B. When equilibrium with respect to composition is reached, Phase II will have been formed mainly by enrichment of the nonequilibrium solution (emulsion medium) by Component B rather than by growth of its nuclei. The concentration of this, formerly nonequilibrium, solution coincides when equilibrium concentration is reached with the concentration of the particles of the slowly growing phase, and a homogeneous medium is formed, surrounding isolated spherical particles of the rapidly growing phase. Two variants of phase separation of a system are shown schematically in Fig. 1.

The course of the hydrostatic separation and subsequent coalescence of the disperse phase particles will depend on which of the phases is disperse. If both phases are of low viscosity, a completely separated system with a single interface is formed relatively rapidly. If the disperse phase is solid (viscosity greater than 10^{10} poises), a suspension is formed which does not form a continuous layer even on settling, while at very high degrees of dispersion it constitutes a colloidal sol with all its characteristic properties (adsorption processes at the interphase).

In our opinion, the greatest interest attaches to the case in which the disperse phase is a liquid, and the dispersion medium is a solid (with viscosity greater than 10^{10} poises). In such a case a solid continuous framework is formed, consisting of Phase II and containing isolated microregions of liquid Phase I. Both the geometrical form of the microparticles and consequently of the "walls" of the framework, and the physicomechanical properties of the whole system, will vary according to the volumes of the coexisting phases.

If the volume of Phase II (solid) is greater than the volume of Phase I (liquid), Phase I will consist of spherical inclusions separated by thick partitions of Phase II, while the physicomechanical properties of the whole system will differ little from the properties of continuous Phase II. If the volume of Phase II is very small compared with the volume of Phase I, the most probable geometrical configuration of Phase I particles is polyhedral, while the structural "skeleton" consisting of Phase II will resemble a honeycomb structure. This gives a system which is very interesting in its physicomechanical properties, with its framework consisting of thin "walls" of homogeneous composition. Such thin layers of solids, as is known, are capable of elastic bending. With a true elastic deformation of the thin "walls" not exceeding 1-2%, as for any continuous system the total deformation of such a system can reach very high values owing to elastic bending.

Unfortunately, little is known about the mechanics of such systems, consisting of solid thin formations (films, fibers) with very low densities of the substance ("loose" solid systems). Nevertheless, the number of such systems found in practice is very large (paper, leather, cotton, etc.). All these materials behave as "high-elastic" systems at low loads and can undergo large reversible deformations considerably exceeding the elastic deformations of continuous materials.

If, in the separation of a multicomponent solution, the solid phase forms a structural "skeleton" consisting of thin films, the result is a limiting example of a lamellar superelastic system. Such systems are known in colloid chemistry as gels. This mechanism for the formation of gel systems can be extended both to gels of low molecular, including inorganic, substances, and to gels formed by high polymers. Each of these classes has its own specific characteristics, and they are therefore considered separately below.

Gels of low molecular substances. One of the specific characteristics of substances of low molecular weight is their tendency to crystallization. Therefore, before we consider concrete examples of gel formation in inorganic low molecular substances, it is necessary to present briefly certain principles concerning the relationship between crystalline and amorphous equilibria. This is necessary because, as was shown in the preceding section, the gel formation mechanism is based on separation of a homogeneous solution into two amorphous phases.

It is known that many substances are deposited from solution not as crystals but as amorphous formations. Weimarn [2] at one time held the view that external distinctions between the forms in which a solute was deposited are determined only by the degree of dispersion of the crystalline substance. However, Weiser and his associates [3] carried out a series of x-ray investigations of precipitates, in which it was shown that the transition from an amorphous to a crystalline precipitate often requires a long time, sometimes measured in years. After the series of detailed investigations made by Berestneva and Kargin [4] there is no longer any doubt that, at least for sparingly soluble compounds which give rise to colloid systems, primary formation of amorphous particles is characteristic; these particles are subsequently converted into crystalline formations at rates which depend on the nature of the components and the experimental conditions.

It may be assumed that the amorphous and crystalline state are separated by an energy barrier, the magnitude of which determines the practical probability and rate of transition from an amorphous to a crystalline precipitate. This view was put forward in relation to pure substances by Kobeko [5]. It can undoubtedly be extended to multicomponent systems such as amorphous precipitates deposited from solutions.

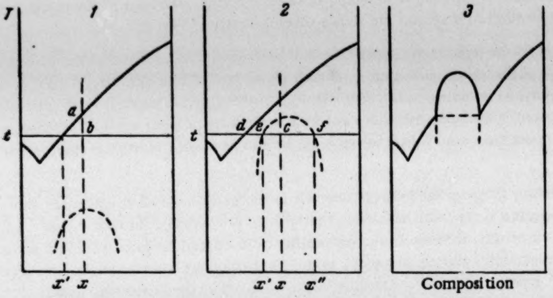

Fig. 2. Crystalline and amorphous equilibrium diagrams.

However, the existence of a potential barrier between the two states in itself indicates that separation of a substance in amorphous form when a one-phase two-component system separates into two phases leads to formation of equilibrium phases such that their composition does not in principle depend on the possibility and rate of a further transition to another equilibrium state with a lower energy level (crystal–solution). Thus, the potential energy minimum of the system, corresponding to amorphous equilibrium, should not depend on the second minimum, which characterizes crystalline equilibrium. This principle of the mutual independence of the two types of equilibrium forms the basis of all the subsequent discussion.

Let us now consider the general equilibrium scheme for a two-component condensed system (with the vapor phase ignored) on the assumption that the rates of transition from one equilibrium state to the other are determined by not very small activation energies of such transitions. In Fig. 2 three variants are given of the relative positions of the curves for crystalline and amorphous equilibrium on composition–temperature diagrams. To simplify the picture, we shall consider only cases in which the crystal–solution equilibrium is not complicated by formation of intermediate molecular compounds.

Figure 2,1 represents the case in which the curve for the equilibrium separation of a two-component solution into amorphous phases lies considerably below the curve for separation into a crystalline phase and a solution over it. If a solution of composition x is cooled, saturation is reached at the point a. Below this point the solution is supersaturated with respect to the crystal-solution equilibrium. For example, at room temperature t (point b) such a solution separates into a crystalline phase consisting of 100% B and a saturated solution of B in A, the composition of which is represented by x'. The rate of this separation is determined by the rates of formation and growth of the crystal nuclei. Amorphous phases cannot be formed at the point b, as the amorphous equilibrium curve lies considerably below the room temperature region and the system is "unsaturated" with respect to such equilibrium. Systems of this kind include many aqueous solutions of highly soluble inorganic salts (sodium chloride, potassium chloride, etc.) and also numerous organic substances of low molecular weight dissolved in organic solvents.

In Fig. 2,2 the amorphous separation curve lies close to the crystal–solution equilibrium curve. When a solution of composition x is cooled down to temperature t, or when substance B is formed, say by an exchange reaction in solution, the system reaches the point c. The solution, supersaturated with respect to crystalline equilibrium, is also supersaturated to amorphous equilibrium. If the potential barrier between the two states is large enough, two stable amorphous phases are formed, with equilibrium compositions x' and x" (Phase I and Phase II).

The "life" of these phases may vary. If the viscosity of Phase II is very high, the rate of crystallization in it may be very low and transition to the crystalline state will occur mainly in Phase I with subsequent gradual crystallization of substance B at the peripheries of the particles in Phase II.

As regards the physical form of the demixing of the system, the considerations in the first section of this paper are applicable. Rapid growth of particles of Phase I leads to formation of a cellular structure, the "framework" of which consists of Phase II, richer in Component B; i. e., a gel is formed. If the total concentration of Component B in the system is very low, the continuous gel structure breaks down and an amorphous "precipitate" is formed, the particles of which are nevertheless of gel form. Similar breakdown of the gel occurs under mechanical action on the system (stirring, convection currents, etc.). These particles, irrespective of the plasticity of Phase II or, more accurately, of the plasticity of the solution which is nonequilibrium at the start of the separation and which approaches Phase II in composition, may assume a rounded shape under the action of surface tension forces; in our opinion this is confirmed by the electron micrographs of precipitates obtained by Shekhter, Roginsky, and Sakharova [6] and similar micrographs given in the papers by Berestneva and Kargin [4].

The lack of quantitative experimental data on amorphous equilibrium curves in the literature is primarily explained by the exceptional difficulties encountered in analysis of the precipitates. Therefore we shall illustrate this type of equilibrium only by certain data reported by Weimarn [2], relating to the water–barium sulfate system. Weimarn gradually increased the initial concentrations of salts forming $BaSO_4$ by a double decomposition reaction, and observed the following characteristic types of precipitation. At very low concentrations of $BaSO_4$, lying within the range of its solubility in water in contact with a crystalline precipitate, a stable aqueous solution is formed (up to the point d on the normal temperature line, see Fig. 2,2). Further increase of concentration leads to formation of a crystalline precipitate, corresponding to the concentrations in the range d–e. At yet higher concentrations (region e–f), the precipitate is no longer crystalline but amorphous, which takes the form of a continuous gel on further increase of concentration, as the "walls" of the gel are already strong enough mechanically. This region corresponds to the region in which the system separates into equilibrium amorphous phases. The relevant data reported by Weimarn are given in the table.

Effect of Total $BaSO_4$ Concentration on the Form of the Precipitate (After Weimarn [2])

Normality	Form of precipitate
$5 \cdot 10^{-5}$–$1.4 \cdot 10^{-4}$	No precipitate formed in course of a year
$1.4 \cdot 10^{-4}$–$1.7 \cdot 10^{-3}$	Slow precipitation
$1.7 \cdot 10^{-3}$–0.75	Crystalline precipitate
0.75–3.0	Rapid formation of amorphous precipitate
3.0–7.0	Transparent gel

These data do not reflect the exact positions of the transition points for the $BaSO_4$ system, but nevertheless the general type and sequence of the transitions in this system conform completely to the diagram in question.

It is likely that for most systems which form sparingly soluble precipitates the crystalline and amorphous equilibrium curves lie close together. At least, gel structures are formed in hydroxides, sulfates, carbonates, and sulfides of multivalent metals. As is shown by the data of Berestneva and Kargin [4], vanadium pentoxide also first forms an amorphous precipitate; this is fully confirmed by the ease with which this substance forms gels. Efremov [7] observed gel formation in the separation of vanadium pentoxide in instances in which crystallization could not proceed far; this also provides indirect evidence that gel formation is directly related to amorphous deposition.

The third type of relative position of the curves for crystalline and amorphous equilibrium (Fig. 2,3) does not lead to formation of more or less stable colloid systems, as the amorphous separation region lies above the fusion curve and this leads to rapid separation of the liquid phases with formation of macroregions of both phases. A well-known example of such a system is the system water–isovaleric acid.

Characteristics of gel formation in high polymer systems. The concept of high polymer gels as imperfectly separated systems, consisting of two equilibrium phases, the honeycomb structural skeleton being formed by the phase with high viscosity, has been discussed earlier [8]. Therefore in the present paper we shall consider only certain characteristics of high polymer gels as compared with gels of substances of low molecular weight.

The main peculiarities of high polymers are the low kinetic mobility of their molecules and their complex configuration. The consequence of the first of these is that the amorphous equilibrium curve is sharply displaced into the region of low concentrations of the polymer, and in many actual instances Phase I may be regarded as the pure solvent. Nevertheless, it constitutes an equilibrium phase, containing a definite if small amount of the high polymer. This is clearly seen in experiments on the osmotic effects of swelling. This fact also provides the basis for high polymer fractionation when the system approaches the upper critical point of complete mutual solubility, at which the high polymer concentration in Phase I becomes quite appreciable. An example of phase equilibrium in high polymers is provided by the previously studied [9] equilibrium in the system acetal cellulose–chloroform.

Because of the high molecular weights of high polymers, Phase II in a separated system is highly viscous and its properties approach those of a solid even at relatively high concentrations of the "solvent" in it. Therefore hydrostatic equilibrium and coalescence of microregions of the phases are generally reached slowly, and gels are therefore formed exceptionally frequently. In fact, as has already been pointed out (see, for example, [1]), instances of liquid coacervation are very rare cases of equilibrium in high polymers.

A consequence of the complexity of configuration of polymeric macromolecules is that the rates of transition of the amorphous into the crystalline phase are so low that the crystalline state is realized exceptionally rarely. The view is advanced in the paper cited earlier [9] and in a number of papers by Kargin and his associates that for many high polymers it is the amorphous and not the crystalline state which is the state of true equilibrium in many high polymers. This view is quite admissible if the complexity of the spatial configuration of certain high polymers with large side chains is taken into account. Regular packing of such macromolecules may be less favorable from the energy aspect than a random disposition. However, even for high polymers for which the ordered state corresponds to lower values of free energy, the activation energy of the transition to an ordered arrangement of the molecules is so high that equilibrium becomes established between the amorphous phases without intervention of the crystallization process. The question of the relationship between the crystalline and amorphous state of high polymers in general should be specially examined. We shall only point out here that the crystalline (ordered) high polymer structures obtained by the action of mechanical forces (stretching) and formed in the course of natural synthesis of the polymer cannot be regarded as more favorable than the amorphous state from the energy aspect.

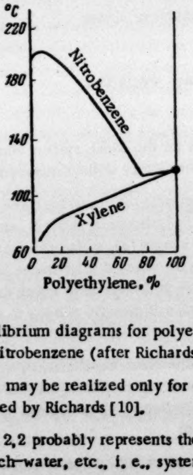

Fig. 3. Equilibrium diagrams for polyethylene with xylene and nitrobenzene (after Richards).

For high polymers with monomer units of simple structure the energy barrier is relatively low, and such polymers crystallize not only from solution but also in the solid state. A good example of this is provided by polyethylene.

It is evident that the relationships between the amorphous and crystalline states represented in Fig. 2 are also applicable to systems containing high polymers. Figure 2,1 corresponds to the case in which the region of amorphous separation into two phases lies in the very low temperature region. Here crystalline equilibrium ought to be attained first. However, polymers which crystallize with difficulty traverse the equilibrium curve without change of the phase state. In the case of deeper cooling, down to the region of amorphous phase separation, separation into two amorphous phases is preceded by vitrification of the system, which makes phase separation impossible in practice. Separation in accordance with Fig. 2,1 may be realized only for crystalline high polymers, as is shown by the behavior of polyethylene in xylene, studied by Richards [10].

Figure 2,2 probably represents the behavior of systems of the type gelatin–water, acetylcellulose–benzyl alcohol, starch–water, etc., i. e., systems in which gel formation occurs in the range of normal temperatures. The true position of the crystalline equilibrium curves for such systems cannot be determined owing to the impossibility of crystallization in practice.

The systems represented by Fig. 2,3 have been studied little, since many high polymers do not melt without chemical decomposition. This applies, at least, to most polymers which have polar groups and are difficult to crystallize. An example of such a system with an easily crystallizable polymer — polyethylene — is provided by the system with nitrobenzene as "solvent," which was also studied by Richards [10].

Richards' data are reproduced in Fig. 3; it is seen that the system polyethylene—xylene corresponds to the case shown in Fig. 2,1 and the system polyethylene—nitrobenzene to the case shown in Fig. 2,3.

In conclusion it must be pointed out that high polymer gels have another important characteristic ; their high deformability may be caused not only by peculiarities in their physical structure (a lamellar system with "elastic walls") which is also found in gels of low molecular substances, but also by the flexibility of the macromolecules. It is known that polymers such as rubber have high elasticity owing to the possibility of more or less free rotation about the individual valency bonds in the chain molecule. Thus, when a mechanical force is applied to a high polymer gel, two mechanisms of elastic extension are superposed. For the polymers described as "rigid" the predominant mechanism is deformation of a lamellar system, while in "flexible" polymers, especially under large loads, the predominant deformation is that caused by straightening of the macromolecules which are coiled when in the equilibrium state.

Calculation of the extension obtainable in the gel model described in this paper shows that the maximum extension is 157% relative to the initial length. In practice the extension at break is considerably less than this. At the same time, rubber-like polymers may show reversible extensions of several hundred per cent.

Therefore it would not be correct to attempt to explain the high elasticity of rubber solely on the assumption that it has a two-phase structure, just as it is not correct to ignore the mechanism of deformation of a lamellar structure for cases in which the system is in a state of imperfect separation into two phases, i. e., when it is in the gel state.

SUMMARY

1. On the principle that the two forms of equilibrium — crystalline and amorphous — are mutually independent, the mechanism of separation of a two-component system into two amorphous phases and of gel formation is considered.

2. A gel is defined as a system with imperfect or uncompleted phase separation, consisting of two phases in equilibrium with respect to composition. One of these phases, which approximates to a solid in its properties, forms a continuous framework which includes isolated regions of the other phase (of low viscosity).

3. The special characteristics of the formation of gels and gel-like precipitates in low molecular (mainly inorganic) substances and in high polymers are discussed.

4. The distinction between the elasticity of gels and the high elasticity of rubber-like polymers is noted.

LITERATURE CITED

[1] S. Papkov, Colloid J. 18, 72 (1956). [Original Russian pagination. See C. B. Translation].

[2] P. Weimarn, J. Russ. Chem. Soc. 38, 263, 466 (1906); 47, 4133 (1915); M. Volmer, Kinetik der Phasenbildung (Dresden-Leipzig, 1939).

[3] See H. B. Weiser, Inorganic Colloid Chemistry, v. 2, 3 (N. Y., 1934) p. 8.

[4] Z. Berestneva and V. Kargin, Progr. Chem. 24, 249 (1955).

[5] P. Kobeko, Amorphous Substances (Acad. Sci. USSR Press, Moscow-Leningrad, 1952).

[6] A. Shekhter, S. Roginsky, and S. Sakharova, Bull. Acad. Sci. USSR, Div. Chem. Sci. 205 (1948).

[7] I. Efremov, Colloid J. 16, 264 (1954). [Original Russian pagination. See C. B. Translation].

[8] S. Papkov, J. Phys. Chem. 18, 546 (1954).

[9] S. Papkov, V. Kargin and Z. Rogovin, J. Phys. Chem. 10, 607 (1937).

[10] R. B. Richards, Trans. Faraday Soc. 41, 127 (1945); 42, 10 (1946).

Received March 27, 1956 Moscow

INVESTIGATIONS OF THE STRUCTUROMECHANICAL PROPERTIES OF ETHYLCELLULOSE SOLUTIONS AND THE EFFECT OF OXIDATION ON THESE PROPERTIES

T. I. Samsonova and L. V. Ivanova-Chumakova

Ethylcellulose – the cellulose ether formed by the reaction of ethyl chloride with alkali cellulose – has good resistance to the effects of low temperatures and to chemical attack by alkalies, salt solutions, and water. However, if it is subjected to the action of oxygen, especially at elevated temperatures, ethyl cellulose is oxidized and develops considerable brittleness. Comparisons of the properties of different grades of ethylcellulose and of changes caused by oxidation are important owing to its very extensive use in industry. In addition to studies of the chemical changes which occur in the oxidation of ethylcellulose [1, 2] and determinations of molecular weight and its distribution [3], considerable interest attaches to investigations of the structuromechanical properties of its solutions, which characterize intermolecular interaction.

The usual method [4] for determination of tensile strength and maximum deformation of films gives sharply different results for oxidized and unoxidized ethylcelluloses, but does not reveal differences in the properties of original unoxidized samples of different degrees of substitution, probably because this method provides a better measure of the bond strengths in the molecular chains than of the intensity of intermolecular interaction. By the methods for studying the mechanical properties of dissolved substances used in the present investigation it is possible to detect differences between the original samples.

The solutions were prepared from two commercial grades of ethylcellulose, K and NI, corresponding to different degrees of hydroxyl group substitution (with ethoxyl group contents of 44.5% for K and 48.5 for NI), but with the same intrinsic viscosity $[\eta] = 2.3$ and average molecular weight of the order of $66 \cdot 10^3$. As the presence of mineral impurities has a great influence on the properties of ethylcellulose, especially in solution [5, 6], the commercial ethylcellulose samples were purified by passage of the dilute solutions through purified active carbon followed by precipitation of the ethylcellulose. The ethylcellulose samples were oxidized by the action of heat in a stream of oxygen: NI at 120° for 3 hours 20 minutes to an intrinsic viscosity $[\eta] = 1.3$ and average molecular weight $41 \cdot 10^3$ (ethoxyl content 46.9%), to give NI of the first degree of oxidation, while to obtain a higher degree of oxidation with $[\eta] = 0.6$ and average molecular weight $25 \cdot 10^3$ (ethoxyl content 35.5%) it was heated at the same temperature for 5 hours, giving NI of the second degree of oxidation.

Ethylcellulose grade K was oxidized by the action of heat at 125° for 2 hours 15 minutes, to give $[\eta] = 0.87$; the average molecular weight was $27 \cdot 10^3$ (ethoxyl content 41.5%).

The solvents used for making the ethylcellulose solutions were benzyl alcohol ($\eta = 0.056$ poise) and dibutyl phthalate ($\eta = 0.206$ poise). Benzyl alcohol is a good solvent for all grades of ethylcellulose; moreover, its volatility is low (b. p. 205.4°), which simplifies its use for filling the liquid seal in the instrument [7].

Because of the low volatility of dibutyl phthalate (b. p. 340°) and the total absence of any film formation on the surface of its solutions after prolonged exposure to air, such solutions could be studied without steps being taken to protect them against evaporation.

The elasticoviscous properties of the ethylcellulose solutions were studied in a rotational instrument with small coaxial cylinders, described in a previous paper [7]. The concentration ranges were from 3 to 10% in dibutyl phthalate, and from 5 to 18.5% in benzyl alcohol. All the experiments were performed at 22.2° ± 0.2.

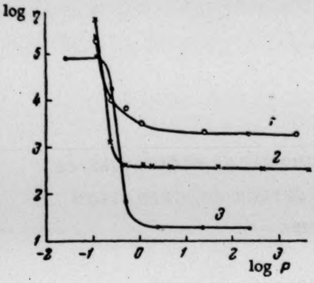

Fig. 1. Variation of effective viscosity with stress for 18.5% solutions of NI ethylcellulose in benzyl alcohol at 22.2°: 1) NI, η_m = 1900 poises; 2) NI of the first degree of oxidation, η_m = 320 poises; 3) NI of the second degree of oxidation, η_m = 9 poises.

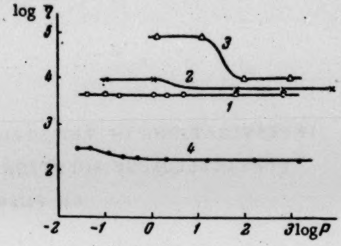

Fig. 2. Variation of effective viscosity with stress for 18.5% solutions of K ethylcellulose in benzyl alcohol at 22.2°: 1) in the first week of aging, $\eta = 4.3 \cdot 10^3$; 2) the same solution after two weeks of aging; 3) the solution after one and a half months of aging; 4) oxidized K, η = 125 poises.

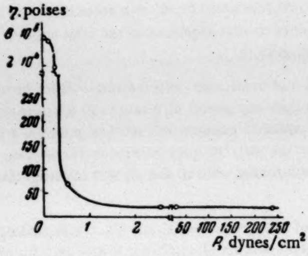

Fig. 3. Variation of effective viscosity with stress for 18.5% solution of NI ethylcellulose, of the second degree of oxidation, in benzyl alcohol at 22.2°.

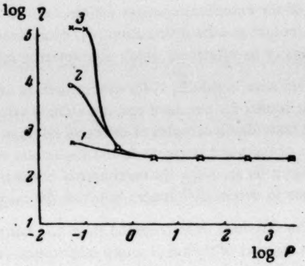

Fig. 4. Variation of effective viscosity with stress for 10% solution of K ethylcellulose in benzyl alcohol at 22.2° after aging for: 1) one day, 2) two days, 3) three weeks.

Measurements were made both of the kinetics of the growth and decrease of the deformation on application and removal of small stresses by rotation of the upper end of the dynamometer thread through a certain angle, and of the equilibrium stresses established in the flowing systems when the outer cylinder was rotated by means of a motor. These measurements were used to plot curves for the variations of effective viscosity in steady flow with the acting stress; these are shown in Figs. 1, 2, and 3 for 18.5% solutions of ethylcellulose in benzyl alcohol. Other concentrations of the same ethylcellulose samples (for example, 10% of K, and 5 and 10% of NI), because of their high fluidity, proved to be less suitable for studies of this relationship, but the results for these in general confirm the other findings. The data presented show that there is a very sharp difference between the behavior of low-substituted (K) and high-substituted ethylcellulose solutions.

The first striking feature is the very different decrease in the viscosities of NI and K ethylcellulose solutions with increase of stress over a certain narrow range: for NI, from $\eta_0 = 1.7 \cdot 10^5$ to $\eta_m = 1.9 \cdot 10^3$ poises (Fig. 1, Curve 1), i.e., by a factor of about 100; and for K, from $\eta_0 = 9.3 \cdot 10^3$ to $\eta_m = 5.8 \cdot 10^3$ poises (Fig. 2, Curve 2), which is less than a two-fold decrease. The similar viscosities at the lower ends of the curves show that the properties of both types of systems become similar after structural breakdown, but the structural buildup during preliminary rest differs. Studies of the changes in the properties of the solutions during prolonged standing in the instrument showed that in the case of NI ethylcellulose, and especially of its oxidation products, maximum structure develops in a relatively short time (~ 2 days), as indicated by constant and high viscosity values, while solutions of K ethylcellulose do not show any significant structural changes in the same period of time. This is convincingly shown by the course of Curve 1 (Fig. 2), all the points on which (η = 4.4 · 10^3 poises) were obtained for the same sample in the course of one week. Repeated experiments on the same sample after 2 weeks, with small stresses of up to 1 dyne/cm^2 revealed the formation of some additional structure, corresponding to an increased viscosity η = 9.3 · 10^3 poises.

Together with the data obtained after the sample had been held for one and a half months in the instrument (Fig. 2, Curve 3; η_0 = 7.8 · 10^4), this shows that structure formation also occurs in solutions of K ethylcellulose, but much more slowly than in NI ethylcellulose. With 10% of K ethylcellulose in the solution (Fig. 4) this process is no longer as slow, probably because of the freer movement of the molecular segments in the less concentrated solution. Curves 1, 2, and 3 (Fig. 4) correspond to different aging times of the samples in the instrument before the start of the experiment, and they show that viscosity in flow with undestroyed structure becomes 17 times as high even on the second day (from η_0 = 5.0 · 10^2 to η_m = 8.8 · 10^3 poises), and after 20 days it reaches 1.4 · 10^5 poises. The fact, revealed by these investigations, that structure buildup in 18.5% solutions of NI ethylcellulose is completed in not more than two days, while in K ethylcellulose it does not develop to any appreciable extent in the same period, was taken into account in studying the characteristics of each individual system (Figs. 1, 2, 3). This is particularly important because each such series of tests was performed on the same sample, kept for a long time in the instrument, since it was not possible either to change the sample before each experiment or to stir it. Such stirring would require additional time before the start of our extremely lengthy experiments, for relaxation of the stresses which would arise. Since the stress was removed in all the experiments after the necessary deformation had been developed and the system reached complete equilibrium, the sample could be used for the next experiment. However, if structural breakdown took place, the system was allowed to age before the next experiment. It must also be pointed out that tests at different stresses were always performed in the sequence from smaller to larger stresses. With this procedure the viscosity increases found on the curves cannot be attributed to structural buildup in the system in the course of time.

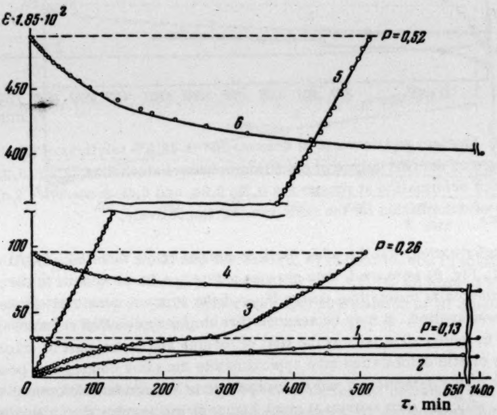

Fig. 5. Increase and decrease of deformations in 18.5% NI ethylcellulose solution in benzyl alcohol at 22.2°: 1,3,5) increase of deformation at stresses P = 0.13, 0.26, and 0.52 dyne/cm^2; 2,4,6) decrease of deformation for the same stresses, respectively.

In addition to this relatively rapid structural buildup and its rapid breakdown in flow under very high stresses, 18.5% solutions of NI ethylcellulose were also found to have structural instability under low stresses. This was shown by the fact that, between low and high stresses, intermediate stresses were found (Figs. 5, 6, Curves 3) at which the properties of the system changed abruptly in the course of the deformation, in the direction of structural breakdown [8]. The two viscosity values, calculated from the flow rates before breakdown and after steady flow has been established in the disrupted structure, coincide with the η(P) curve in the region in which it shows an abrupt, almost vertical drop over a certain fairly narrow range of stresses. Similar breakdown was not found in experiments at higher stresses, but in such experiments the viscosity of the system was close to its lower limit

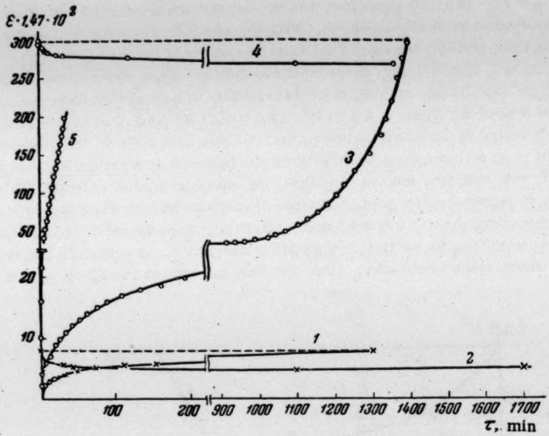

Fig. 6. Increase and decrease of deformation in 18.5% solutions of NI ethylcellulose of the first degree of oxidation in benzyl alcohol at 22.2°: 1,3,5) increase of deformation at stresses P = 0.12, 0.24, and 0.48 dynes/cm^2; 2,4,6) decrease of deformation for the same stresses, respectively.

right at the start of the deformation. On the other hand, if stresses below these intermediate values (0.13 dyne/cm^2, Fig. 5 and 0.12 dyne/cm^2, Fig. 6) were used, then changes took place in the system in the course of the experiments which must be attributed to restoration, during flow, of the structure previously broken down to some extent when the external stress was applied. It may be assumed that abrupt application or removal of a stress equally break down the structure to some extent both at the start of loading and at the start of unloading. If the development and decrease of the elastic deformation take approximately the same course, it is possible from the total time for the development of the deformation and the magnitude of the residual deformation to calculate the average rate of true flow, which in such systems is much higher at low stresses than the rate of flow at the end of loading, i. e., after a time greater than the time required for complete dissipation of the elastic deformation. It must be pointed out that the same effect was found in repeated experiments, performed on the same sample after it had been at rest for some time without any preliminary destruction. The reproducibility of the results obtained for any one stress showed that no significant irreversible changes occur in solutions of NI ethylcellulose in the process. Therefore the discrepancy between the true flow rates at the beginning and end of the development of deformation indicates that the structure may have been broken down at the instant the load was applied.

The data for viscosity calculations in such experiments were based on their final periods, when, after a sharp retardation of the flow rate owing to structure formation in flow, on about the second day of the experiment, a constant flow rate became established, corresponding to a constant time, measured in tens of hours, for displacement by one scale division.

Figures 1 and 2 show that the effective viscosity is much higher for oxidized than the original (unoxidized) ethylcellulose samples, and the minimum viscosity is less for higher degrees of oxidation. This is fully in agreement with molecular weight data [3] indicating that oxidation shortens the chain length. In addition to the lower viscosity limit, $\eta_m' = 19$ poises, an upper limit, $\eta_0' = 7.8 \cdot 10^4$ poises (Table 1, Fig. 3) was determined for NI ethylcellulose of the second degree of oxidation. For the other samples of NI ethylcellulose only a transition into the high viscosity region was found, but the maximum could not be determined because the low rates of flow already reached (one division per day or longer) did not allow of the use of even lower rates and therefore even longer observation periods.

TABLE 1

Viscosity of 18.5% Solution of NI Ethylcellulose (Second Degree of Oxidation) in Benzyl Alcohol

P, dynes/cm^2	0.026	0.13	0.26	0.52	2.55	23.67	239.2
$\frac{d\varepsilon}{d\tau}$, sec^{-1}	$0.33 \cdot 10^{-6}$	$0.18 \cdot 10^{-5}$	$0.15 \cdot 10^{-4}$	$0.77 \cdot 10^{-3}$	0.1239	1.239	12.395
η, poises	$7.8 \cdot 10^4$	$7.2 \cdot 10^4$	$1.7 \cdot 10^1$	67.5	20.6	19.2	19.1

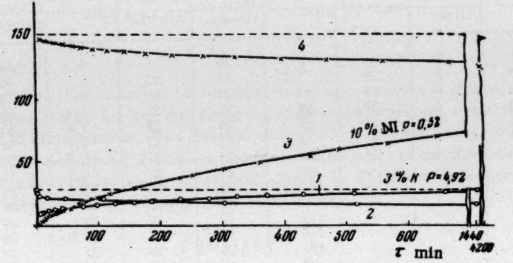

Fig. 7. Increase (1, 3) and decrease (2, 4) of deformation in solutions of ethylcellulose in dibutyl phthalate at 22.2°: 1,2) 3% solution of K ethylcellulose, stress P = 4.92 dynes/cm^2; 3,4) 10% solution of NI ethylcellulose, stress P = 0.52 dyne/cm^2.

The ethylcellulose solutions showed elastic behavior during the unloading part of the experiment; i. e., there were considerable elastic after-effects – a certain decrease of the deformation, as shown in Figs. 5-7. Therefore solution concentrations were chosen [7] at which the deformation would develop and decrease correctly under the experimental conditions used. The optimum conditions were such that, as the solution concentration was increased, a system with an excessively long period of development of elastic deformation should not be obtained, as this would hinder development of the process to completion, but at the same time the degree of molecular interaction in solution should be enough to retard the residual flow to such an extent that it should not greatly obscure the elastic deformation. In a rotational instrument with a dynamometer of the thread type observations of deformation kinetics under constant stress are difficult for systems of low viscosity, as the rapid development of residual deformation makes it impossible to maintain and record the acting stress with a high degree of accuracy. However, the accuracy to which any possible external stresses are removed from the system is important in studying the kinetics of the decrease of elastic deformation. The best conditions are obtained for this if the development of deformation equivalent to 50-100 microscope scale divisions leading to steady flow requires a force provided by rotation of the dynamometer thread (usually the thinnest because of the low concentration) through an angle of not less than 200-300°. This relation between the angle of rotation of the inner cylinder and the thread torsion angle is necessary because any additional twisting [9] may cause errors in determination of the stresses. The magnitude of such an error should not exceed a very small fraction of the given stress. Otherwise it would be difficult, at the end of the fall of deformation, to avoid the action of external stresses giving deformation rates of the same order of magnitude, in addition to the internal elastic after-effect forces in the sample itself.

It did not prove possible to fulfill these optimum conditions satisfactorily in experiments on solutions of different ethylcellulose samples in benzyl alcohol, thereby finding the correct and exact course of the development and decrease of elastic deformation. However, when the solvent was changed to dibutyl phthalate, which resulted in greater interaction between the molecular chains at low concentrations, these conditions were approached, and it proved possible to obtain a fuller and more correct development of the elastic deformation (under strictly constant stress), and also more accurate readings of its decrease, especially at the end of the process.

TABLE 2

Calculation of the Constant k for the Kinetics of Elastic Deformation from Experimental Data on Solutions in Dibutyl Phthalate

3% K; $t = 22°$; $P = 4{,}9$ dynes/cm²			10% NI $t = 22°$; $P = 0.52$ dynes/cm²			10% NI $t = 45°$; $P = 0.52$ dynes/cm²		
Time after unloading min.	Elastic deformation in scale divisions	k in scale divisions in min · 10^3	Time after unloading min.	Elastic deformation in scale divisions	k in scale divisions in min · 10^3	Time after unloading min.	Elastic deformation in scale divisions	k in scale divisions in min · 10^3
0	9	—	0	30	—	0	44	—
48	5	26	7.5	27	21	2	40	9
108	4	21	12	26	23	3.7	33	12
188	3	22	18	25	25	6.1	36	13
303	2	21	26	24	26	7.8	35	13
578	1	23	35	23	27	9.7	34	13
910	0.3	24	46	22	27	11.8	33	13
—	—	—	61	21	27	14.5	32	13
—	—	—	77	20	27	17.5	31	13
—	—	—	95	19	27	21	30	13
—	—	—	119	18	27	25	29	13
—	—	—	148	17	27	29.5	28	13
—	—	—	181	16	26	35	27	13
—	—	—	222	15	26	41.5	26	12
—	—	—	272	14	25	48	25	12
—	—	—	325	13	25	65	23	11
—	—	—	400	12	24	86	21	11
—	—	—	472	11	23	114	19	10
—	—	—	564	10	23	131	18	9
—	—	—	670	9	23	176	16	9
—	—	—	824	8	21	234	14	8
—	—	—	1004	7	20	—	—	—
—	—	—	1234	6	20	—	—	—

Table 2 gives, in accordance with the relationship established previously [10], calculations of the constant k for the kinetics of elastic deformation, based on experimental data for solutions in dibutyl phthalate (Fig. 7),

$$k = -\frac{\varepsilon_m \ln \frac{\varepsilon_e}{\varepsilon_m} + \varepsilon_m - \varepsilon_e}{\tau},$$

where ε_m is the maximum value of the elastic deformation for the given stress; ε_e is the elastic deformation remaining at a given time instant; τ is the time of decrease of the deformation (recovery time).

As is seen from Table 2, the values of k are satisfactorily constant; for convenient calculation from the available data they are given in Table 2 in terms of microscope scale divisions per time in minutes (scale div./min.$^{-1}$). However, for comparison of the values for different samples and temperatures the average value must be expressed as an absolute quantity, and also reduced to a stress of 1 dyne/cm² [10].

The formula for this conversion is

$$a = \frac{k \cdot 0{,}54 \cdot 10^{-2}}{60 \cdot P} \left(\frac{\text{cm}^2}{\text{dyne} \cdot \text{sec}}\right).$$

where a is the absolute constant for the development of elastic deformation with time, independent of the stress; $0.54 \cdot 10^{-2}$ is the relative deformation corresponding to one scale division; 60 is the conversion factor to give the time in seconds; P is the stress acting during development of the deformation, in dynes/cm^2.

Conversion of the data in Table 2 gave the values of a given in Table 3. They are in full agreement with the ordinary influence of temperature, resulting in accelerated deformation with increase of temperature, and also with out data on the greater deformability of NI solutions in comparison with K ethylcellulose solutions, as shown, for example, in Fig. 7. The curves in Fig. 7 for 10% solutions of NI ethylcellulose show that, in a given time, considerably greater deformations, both residual and elastic, develop in such solutions than in 3% solutions of K ethylcellulose, despite the fact that the acting stress in the latter case was almost 10 times the stress used in the case of NI ethylcellulose. The probable reason for this difference in properties is that the greater intermolecular interaction in the original K ethylcellulose prevents solvation of the molecular chains by dibutyl phthalate molecules to a greater extent than in NI ethylcellulose [11]. Therefore the length of the free regions of the chain is less in K ethylcellulose, leading to lower deformability.

TABLE 3

Constant a (Independent of the Stress) for Solutions of K and NI Ethylcellulose Solutions in Dibutyl Phthalate

Solutions in dibutyl phthalate	3% K	10% NI	
Dissolving temperature	22°	22°	45°
a in poises^{-1}	$0.42 \cdot 10^{-6}$	$0.43 \cdot 10^{-5}$	$1.9 \cdot 10^{-6}$

SUMMARY

1. The elasticoviscous properties of ethylcellulose solutions of different degrees of substitution (K and NI) and solutions of oxidized ethylcellulose have been studied.

2. A difference has been found between the rates of structure formation in 18.5% solutions of K and NI ethylcelluloses in benzyl alcohol, resulting in sharply different decreases of the effective viscosities of such solutions, aged for the same periods, over a certain narrow range of stress increases.

3. It is shown that the minimum constant viscosities of such solutions are lower for oxidized than unoxidized samples, and lower for the more highly substituted NI ethylcellulose than for K. This corresponds to the higher molecular weights of K than NI, and of unoxidized than oxidized ethylcelluloses [3].

4. Solutions of ethylcellulose in dibutylphthalate were shown to conform to a relationship previously established [10], by means of which the decrease of elastic deformation with time can be characterized by a single constant.

We offer our sincere gratitude to Academician P. A. Rebinder for valuable advice during discussions of this work, and also to Associate Member of the Academy of Sciences USSR, S. N. Danilov for guidance in selection of the materials.

LITERATURE CITED

[1] L. F. McBurney, Ind. Eng. Chem. 41, 1251, 1256 (1949).

[2] O. P. Kuzmina and V. I. Kurlyankina, Proc. Acad. Sci. USSR 114 (1957).

[3] T. I. Samsonova and S. Ya. Frenkel, Colloid J. 19, 2 (1957).*

[4] P. P. Kobeko, Amorphous Substances (Acad. Sci. USSR Press, 1952).

[5] O. G. Efremova and S. A. Glikman, Sci. Mem. Saratov State Univ. 30, 55 (1952).

[6] E. V. Evans and H. M. Spurlin, J. Am. Chem. Soc. 72, 4751 (1950).

[7] L. V. Ivanova-Chumakova and P. A. Rebinder, Colloid J. 18, 429 (1956).*

[8] A. A. Trapeznikov, Colloid J. 12, 73 (1950).

[9] A. S. Kolbanovskaya and P. A. Rebinder, Colloid J. 12, 194 (1950).

[10] L. V. Chumakova and P. A. Rebinder, Proc. Acad. Sci. USSR 81, 239 (1951); Colloid J. 18, 540 (1956).*

[11] S. M. Lipatov and S. I. Meerson, Colloid J. 12, 2 (1950).

Received November 28, 1956

Institute of Physical Chemistry, Acad. Sci. USSR,
Division of Disperse Systems, Moscow
Institute of High Molecular Compounds, Leningrad

---

* [Original Russian pagination. See C. B. Translation.]

THE THEORY OF FLOW OF PLASTIC DISPERSE SYSTEMS

N. V. Tyabin and G. V. Vinogradov

Numerous flow processes in plastic disperse systems do not directly conform to the Newton and Shvedov–Bingham equations, but a theory of such flow processes has not yet been developed. The lack of such a theory makes impossible even approximate mathematical calculations relating to various deformations of plastic disperse systems in heterogeneous tangential stress fields, to say nothing of flow in the complex stressed state, when normal as well as tangential stresses act on the system.

Experimental viscosimetric data are generally represented in the form of rheological flow curves which show the variation of the average velocity gradient $\overline{D}$ with the shearing stress τ_R at a capillary wall or the inner cylinder in a capillary viscosimeter. As the result of the experimental investigations performed during the last ten years, mainly by Vinogradov, Pavlov, and Sinitsyn, on the flow of plastic disperse systems in capillary and rotational viscosimeters, the nature of the functional relationship $\overline{D} = \varphi(\tau_R)$ for many plastic disperse systems is known over velocity gradient ranges covering 6-8 orders of magnitude. The Weissenberg–Rabinowitsch method, developed for capillary [1] and rotational [2,3] viscosimeters, can be applied to data on the flow of such media in heterogeneous tangential stress fields to calculate the true, characteristic flow curves $D_R = \varphi(\tau_R)$, where D_R is the velocity gradient in a layer of radius R, for example at a capillary wall or at the wall of the cylinder in a rotational viscosimeter. We shall write this last equation in the form: $\overline{D} = \varphi(\tau)$. The functions $\overline{D} = \varphi(\tau_R)$ and $D = \varphi(\tau)$ can be written in polynomial form, such as

$$\tau = a_0 + a_1 D + a_2 D^{n_2} + a_3 D^{n_3} + \ldots + a_n D^{n_n}, \tag{1}$$

where a_i are constant coefficients and n_i are exponents; $0 < n_i < 1$.

However, the constant coefficients and exponents in this equation have no physical meaning. Substitution of values of the tangential stresses found from this equation into the equation for the motion of a continuous medium gives equations for the flow of the medium, in the form of nonlinear differential equations difficult to solve. It is therefore more convenient first to simplify the equation for the flow of a plastic disperse system; this will simplify considerably the solution of the original differential equations, and therefore also the mathematical calculations necessary for the solution of practical problems of flow of disperse systems.

In order to simplify the equation for the flow of a plastic disperse system, i.e., to reduce it to linear equations of the Newton or Shvedov–Bingham type, we shall first evaluate the deviation of the flow Equation (1) from these equations: $\tau = a_1 D$ or $\tau = a_0 + a_1 D$, following from Equation (1). For a given accuracy E% for the calculation of the tangential stress, we can write that, at a certain velocity gradient $D = D_x$ the nonlinear part of the polynomial (1) will be equal to

$$a_2 D_x^{n_2} + a_3 D_x^{n_3} + \ldots + a_n D_x^{n_n} = \frac{\tau_x E}{100}. \tag{1a}$$

Substituting τ_x from Equation (1) for $D = D_x$, we have the equation

$$a_0 + a_1 D_x + \frac{100 - E}{E} a_2 D_x^{n_2} + \frac{100 - E}{E} a_3 D_x^{n_3} + \ldots + \frac{100 - E}{E} a_n D_x^{n_n} = 0, \tag{2}$$

solution of which gives D_x, which is the velocity gradient to which Equation (1) should be approximated in the form of Shvedov–Bingham equations. We shall term D_x the approximation limit. For $D > D_x$ a plastic disperse system obeys the Shvedov–Bingham law within the given limits of accuracy. If $a_0 \leq \tau_x E/100$, the plastic system flows according to Newton's law $\tau = a_1 D$.

We shall now consider an analytical graphical method for approximation of the flow curve to linear functions or chords in the zone in which $D \leq D_x$. Let the graph for the functional relationship $D = \varphi(\tau)$ over a certain range of values of τ and D be represented by the Curve AB (Fig. 1). Through the points $C(\tau_0 - \Delta\tau_0, D_0)$ and $F(\tau_0 + \Delta\tau_0, D_0)$, where $\Delta\tau_0 = \tau_0 E/100$, we draw the Curves CE and EG, the respective equations for which are

$$D = \varphi_1(\tau) \quad (2) \qquad \text{and} \qquad D = \varphi_2(\tau) \tag{3}$$

Curves CE and FG determine the error zone CEFG on the graph. In the error zone we can replace any curve by a linear segment without exceeding the permissible error limits. We replace a section of the curve by a chord, drawn tangentially to one of the curves of the error zone, in this instance the Curve CE. The equation of the tangent to the Curve CE at the point $K(\tau_1, D_1)$ passing through the point $F(\tau_0 + \Delta\tau_0, D_0)$, will be:

$$D - D_0 = \varphi_1'(\tau_1)\,[\tau - (\tau_0 + \Delta\tau_0)]. \tag{4}$$

Simultaneous solution of Equations (2) and (4) gives the coordinates of the point $K(\tau_1; D_1)$. The tangent FM will cut the Curve FG of the error zone at the point $M(\tau_2, D_2)$. By solving Equation (3) and $D_2 - D_0 = \varphi_1'(\tau_1)[\tau_2 - (\tau_0 + \Delta\tau_0)]$simultaneously, we find the coordinates of the point $M(\tau_2, D_2)$ as the positive roots of these equations nearest to the values of τ_1 and D_1. We have thus replaced the curve AB by the chord AM in the first region. By drawing a new tangent from the point M to the left curve of the error zone, and finding by an analogous procedure the coordinates of the point of intersection of this tangent with our curve, we obtain a new chord. By continuing this approximation process over the section of the curve from D to D_x we represent it by sections of linear chords, i.e., we replace the functional relationship $D = \varphi(\tau)$ by a set of linear functions $D = \varphi_i(\tau)$, valid over a definite range of tangential stress variations from τ_i to τ_{i+1}.

The equations for the approximated straight lines or the equations for the tangents to the curve CE the error zone may be regarded as equations for the viscoplastic flow of the medium over a definite range of tangential stresses or velocity gradients, or as Shvedov–Bingham equations: $\tau = \theta_i + \eta_i D$, where, as usual, θ_i represents the tangential stresses cut off by extrapolated straight lines along the abscissa axis, which we shall term the maximum shearing stresses, and η_i are the plastic viscosity coefficients (Fig. 1).

The critical values of the tangential stresses at which the Shvedov–Bingham law for the flow changes (i.e., the constants θ_i and η_i change) in consequence of a transition from one flow zone to another we shall term the boundary shearing stresses τ_{0i}. It is evident that the values of τ_{0i} are determined from the condition: when $D_i = D_{i+1}$, $\tau_i = \tau_{i+1} = \tau_{0i}$, and hence

$$\tau_{0i} = \frac{\theta_i \eta_{i+1} - \theta_{i+1}\eta_i}{\eta_{i+1} - \eta_i} \quad (i = 1, \ldots, n-1). \tag{5}$$

At some definite surface in the flow zone the tangential stresses will be equal to the boundary shearing stresses. In accordance with the foregoing, we shall give the name of the boundary shearing stress surfaces to the surfaces in the flow zone in which the flow law changes. All the flow zone will thus be divided by the boundary shearing stress surfaces into a series of zones, the number of which will be determined by the number of Shvedov–Bingham or Newton equations approximating to the flow equation for the given medium. It must be pointed out that, on the basis of this approximation method, flow may extend over a limited region of the plastic disperse system, and in the rest of the space the medium will be as if in a solid state. The flow zone is separated from the solid zone by a maximum shearing stress surface at which the tangential stress equals the extrapolated value of the maximum shearing stress θ_1. At the boundary and the maximum shearing stress surfaces, the conditions of continuity and equality of the tangential and normal stresses and of the flow velocity components of the medium are satisfied. Thus, the flow of a plastic disperse system will be described by a system of differential equations for the flow of viscoplastic [4] and viscous media.

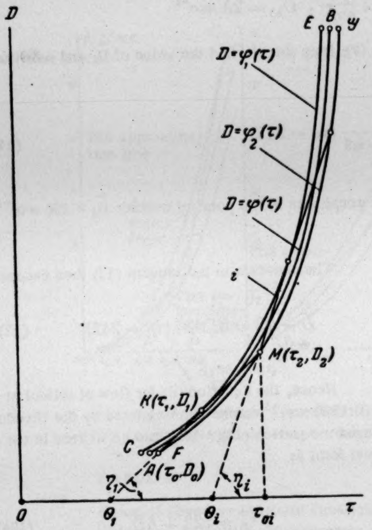

Fig. 1. Approximate representation of nonlinear flow of a plastic disperse system in the form of Shvedov–Bingham equations.

As an application of the proposed method, we shall consider the approximation of the laws of flow for plastic greases, "solidols", the flow of which has been studied by Pavlov [5] in capillary and rotational viscosimeters. The laws for the flow of solidol in a capillary viscosimeter, determined by Pavlov, are given in Table 1, and empirical data for the flow of solidol in a rotational viscosimeter of Pavlov's design are given in Table 2.

Since the experimental data were determined to an accuracy not exceeding 5%, we shall approximate the flow laws with an accuracy of 5%.

Determining the approximation limit of Equation (6) on the basis of Equation (1a), we can write:

$$30\bar{D}_x{}^{1/2} = {}^{5}/_{100}\,(4\bar{D}_x + 30\bar{D}_x{}^{1/2} + 20).$$

Solving this equation, we find the approximation limit for Equation (6): $\bar{D}_x$ = 1700 sec.$^{-1}$; therefore this equation should be simplified in the gradient range from $\bar{D}_0$ = 29 sec.$^{-1}$ to $\bar{D}_x$ = 1700 sec.$^{-1}$. When $\bar{D} > D_x$, the flow equation for the medium will be: $\tau_R = 4\bar{D} + 20$. However, when $\bar{D} = \bar{D}_x$, θ = 20 dynes/cm^2 is ~ 0.3 % of the tangential stress, and therefore when $\bar{D} > \bar{D}_x$ solidol (80°) must be regarded as a viscous liquid, the flow equation for which will be: $\tau_R = 4D$. For analytical approximation of Equation (6) when $\bar{D} < \bar{D}_x$, we find the equations for the Curves CE and FG of the error zone (Fig. 1):

$$\tau_R = 3{,}83\,\bar{D} + 28{,}8\,\bar{D}^{1/2} + 19; \qquad (9)$$

$$\tau_R = 4{,}25\,\bar{D} + 31{,}6\,\bar{D}^{1/2} + 21. \qquad (10)$$

TABLE 1

Laws for the Flow of Solidol, Made with Spindle Oil Distillate, in a Capillary Viscosimeter

t° C	Initial values		Final values		Flow equation	Approximation limit $\bar{D}_x$ sec.$^{-1}$	Equation numbers
	$\bar{D}$, sec.$^{-1}$	$\tau_R \cdot 10^{-3}$ dynes/cm^2	$\bar{D}$, sec.$^{-1}$	$\tau_R \cdot 10^{-3}$ dynes/cm^2			
80	29	0.227	11 750	47.7	$\tau_R = 4\bar{D} + 30\bar{D}^{1/2} + 20$	1700	(6)
20	0.083	4.72	1 170	39.4	$\tau_R = 6\bar{D} + 2800\bar{D}^{1/2} + 3500$	—	(7)
–45	0.032	55.6	13	541	$\tau_R = \bar{D} + 2850\bar{D}^{1/2} + 7200$	1920	(8)

Through the initial point of the Curve FG of the error zone, with the coordinates

$$\tau_{02} = 0{,}23 \cdot 10^3 + \frac{\tau_{02} \cdot 5}{100} = 242 \frac{\text{dynes}/}{\text{cm}^2}; \; D_{02} = 29 \text{ sec}^{-1}$$

we draw the tangent to the curve represented by Equation (9); from this we find the value of $\bar{D}$, and substitute it into equation (4), so obtaining

$$\bar{D} - 29 = \frac{\bar{D}_1^{5/6}}{3{,}83 \bar{D}_1^{1/6} + 9{,}6} (\tau_R - 242). \tag{11}$$

We solve Equations (11) and (9) simultaneously to find the coordinate of the point of contact $\bar{D}_1$ = 166 sec.$^{-1}$, and then, from Equation (9), τ_1 = 813 dynes/cm^2.

TABLE 2

Experimental Data for the Flow of Tallow Solidol in Rotational Viscosimeter at 50°

n r.p.m.	D sec.$^{-1}$	$\tau \cdot 10^{-3}$ dynes/cm^2		
		τ_{exptl}	$\tau + \frac{5}{100}\tau$	$\tau - \frac{5}{100}\tau$
0.192	0.47	0.86	0.90	0.82
0.96	2.35	1.69	1.77	1.60
4.8	11.76	2.71	2.85	2.58
24	58.8	3.27	3.43	3.11
120	294	4.76	5.00	4.52
600	1470	7.95	8.34	7.55

The equation to the tangent (11) then becomes:

$$\bar{D} - 29 = 0{,}242 \;\; (\tau_R - 242). \tag{12}$$

Hence, the Equation (6) for flow of solidol at $\bar{D}$ < 1700 sec.$^{-1}$ can be approximated by the Shvedov–Bingham equation (12), which can be written in the usual form as

$$\tau_R = 122 + 4\bar{D}. \tag{12a}$$

Determining the approximation limit of Equation (6) in the form of this Shvedov–Bingham equation, we write the expression:

$$122 = \frac{5}{100} (122 + 4\bar{D}_{x1}),$$

from which we find $\bar{D}_{x1}$ = 580 sec.$^{-1}$.

Thus, solidol at 80° flows according to the Shvedov–Bingham law in the velocity gradient region $\bar{D} \leq 580$ sec.$^{-1}$, while in the zone in which $\bar{D} \geq 580$ sec.$^{-1}$ it flows according to the Newton law $\tau_R = 4\bar{D}$. We determine the approximation limit of equations (7) and (8) by a similar procedure. Equation (7) should be approximated over the whole range of $\bar{D}$ and τ_R studied.

A much more convenient and rapid method is the graphical method for approximation to a flow curve in the form of linear portions corresponding to the Shvedov–Bingham law. The graphical approximation can be performed with sufficient accuracy on 3-4 graphs for the relationship $\bar{D} = \varphi(\tau_R)$, plotted on different scales chosen so as to cover the whole flow zone without decreasing the accuracy of the method. Figure 2 shows a graphical approximation of the equation for the flow of solidol in a capillary viscosimeter at 20° (7), on three different scales. Table 3 gives approximation data for Equation (7) in the form of Shvedov–Bingham equations. In this case the Shvedov–Bingham equations will be the equations to the tangents, while the abscissas of the points of intersection of the tangents with the second curve of the error zone will give the boundary shearing stresses. The limits within which the given expression for the Shvedov–Bingham law is valid will be termed the upper and lower boundary shearing stresses and the boundary velocity gradients.

A comparison of the analytically derived expressions for the Shvedov–Bingham equation with the equations obtained graphically shows that they coincide completely. Figure 3 gives the graphical approximation of empirical data on the flow of solidol in a rotational viscosimeter (see Table 2), analyzed by the Weissenberg–Rabinowitsch method [2,3].

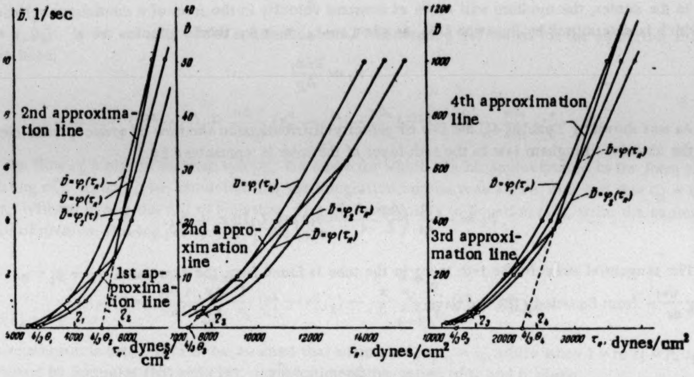

Fig. 2. Graphical approximation of the curve for the flow of solidol in a capillary viscosimeter, on three different scales.

TABLE 3

Group of Shvedov–Bingham Equations Approximating to the Law for the Flow of Solidol in a Capillary Viscosimeter

Lower boundary				Upper boundary	
velocity gradients $\overline{D}$, sec.$^{-1}$	shearing stresses $\tau_R \cdot 10^{-3}$, dynes/cm^2	$\tau_R = \frac{4}{3}\theta + \eta\overline{D}$	$\tau = \theta + \eta D$	velocity gradients $\overline{D}$, sec.$^{-1}$	shearing stresses $\tau_R \cdot 10^{-3}$, dynes/cm^2
0.083	3.68	$\tau_R = 4875 + 1084\,\overline{D}$	$\tau = 3650 + 1084\,D$	2.30	7.73
2.30	7.73	$\tau_R = 7250 + 193\,\overline{D}$	$\tau = 5430 + 193\,D$	31.5	13.4
31.5	13.4	$\tau_R = 1200 + 40.6\,\overline{D}$	$\tau = 9000 + 40.6\,D$	385	27.0
385	27.0	$\tau_R = 22000 + 14.0\,\overline{D}$	$\tau = 16500 + 14.0\,D$	—	—

The proposed method for simplification of the flow equations of plastic disperse systems can be used for calculations relating to various cases of flow of such systems in a heterogeneous field of tangential shearing stresses. Here we shall consider the flow of plastic disperse systems in round cylindrical pipes. This case is of great importance in viscosimetry and technology.

Suppose that a plastic disperse system flows in conditions of pure shear through a tube of radius R and length L under the action of a pressure difference Δp at the ends of the tube. The flowing medium will contain a heterogeneous field of tangential stresses, determined by the expression

$$\tau = \Delta pr/2L. \tag{13}$$

The boundary stress surfaces will be coaxial cylindrical surfaces of radii r_i. These are given by Equations (5) and (13):

$$r_i = \frac{2L\tau_{0i}}{\Delta p} = \frac{2L}{\Delta p}\,\frac{\theta_i \eta_{i+1} - \theta_{i+1}\eta_i}{\eta_{i+1} - \eta_i} \quad (i = 1,\dots,n-1). \tag{14}$$

In the center, the medium will move at constant velocity in the form of a continuous cylinder, the radius r_0 of which is determined by Equation (13), as when $r = r_0$, $\tau = \theta_1$, then

$$r_0 = \frac{2L\theta_1}{\Delta p}. \tag{15}$$

As was shown by Tyabin [4], the law of velocity distributions in the flow of a viscoplastic medium which obeys the Shvedov–Bingham law in the i-th layer of the tube is represented by

$$v_i = -\frac{1}{\eta_i}\left(\frac{\Delta p}{L}\cdot\frac{r^2}{4} - \theta_i r\right) + C_i \ln r + N_i. \tag{16}$$

The tangential stress in the i-th layer in the tube is found from the expression $\tau_i = \theta_i - \eta_i \frac{dv_i}{dr}$. Finding $\frac{dv_i}{dr}$ from Equation (16), we have:

$$\tau_i = \frac{\Delta pr}{2L} - \eta_i \frac{C_i}{r}. \tag{17}$$

Comparison of Equations (13) and (17) shows that the constant C_i in Equation (17) is equal to zero. Before consideration of the general case, we shall examine the flow through a tube of a disperse system the rheological flow curve for which can be approximated in the form of two expressions of the Shvedov–Bingham equation. In this case (Fig. 4) there will be one cylindrical surface of boundary shearing stress, the radius of which will be

$$r_1 = \frac{2L}{\Delta p}\,\frac{\theta_1\eta_2 - \theta_2\eta_1}{\eta_2 - \eta_1}.$$

The velocity distributions in the two viscoplastic layers will be given by Equation (16)

$$v_1 = -\frac{1}{\eta_1}\left(\frac{\Delta p}{L}\frac{r^2}{4} - \theta_1 r\right) + C_1 \ln r + N_1;$$
$$v_2 = -\frac{1}{\eta_2}\left(\frac{\Delta p}{L}\frac{r^2}{4} - \theta_2 r\right) + C_2 \ln r + N_2.$$

In order to find the velocity distribution, it is necessary to find the integration constants in these equations. Assuming that the plastic disperse system adheres to the tube walls, we have for $r = R$, $v_2 = 0$; it follows from the condition of velocity continuity at the boundary shearing stress surface that when $r = r_1$, $v_1 = v_2$. From the condition of continuity of the tangential stresses, as was shown above, we find that the constants $C_1 = C_2 = 0$. Then, determining N_1 and N_2, we have from the boundary conditions:

$$N_1 = -\frac{1}{\eta_2}\left(\frac{\Delta p}{L}\frac{r_1^2}{4} - \theta_2 r_1\right) + \frac{1}{\eta_1}\left(\frac{\Delta p}{L}\frac{r_1^2}{4} - \theta_1 r_1\right) + N_2,$$
$$N_2 = \frac{1}{\eta_2}\left(\frac{\Delta p}{L}\frac{R^2}{4} - \theta_2 R\right).$$

The amount of plastic disperse system flowing through the round tube per second is given by the expression

$$q = \pi r_0^2 v_0 + 2\pi \int_{r_0}^{r_1} v_1 r dr + 2\pi \int_{r_1}^{R} v_2 r dr,$$

where $v_0 = v_1(r_0)$ is the velocity of the continuous core. Substituting the values for the velocities and integrating, we have:

$$q = \frac{\pi\Delta p}{8L\eta_2}(R^4 - r_1^4) + \frac{\pi\Delta p}{8L\eta_1}(r_1^4 - r_0^4) - \frac{\pi\theta_2}{3\eta_2}(R^3 - r_1^3) - \frac{\pi\theta_1}{3\eta_1}(r_1^3 - r_0^3). \qquad (18)$$

For the flow of a plastic disperse system, the curve for which can be approximated in the form of a broken line consisting of n sections, we can determine the integration constants as above, and find that $C_i = 0$ and N_i = const. Without giving the full calculation, we can, analogously to Equation (18), write the expression for the amount of medium flowing per second in the pipe:

$$q = \frac{\pi\Delta p}{8L}\sum_{i=1}^{i=n}\frac{1}{\eta_i}(r_i^4 - r_{i-1}^4) - \frac{\pi}{3}\sum_{i=1}^{i=n}\frac{\theta_i}{\eta_i}(r_i^3 - r_{i-1}^3). \qquad (19)$$

When this expression is used, it must be assumed that when $i = 1$, $r_{i-1} = r_0$, while when $i = n$, $r_i = R$, r_0 and r_i are determined by Formulas (15) and (14). Substitution of the values of r_0 and r_i gives:

$$q = \frac{2\pi L^3}{\Delta p^3}\sum_{i=1}^{i=n}\frac{(\tau_{0i}^4 - \tau_{0i-1}^4) - {}^4/_3\,\theta_i(\tau_{0i}^3 - \tau_{0i-1}^3)}{\eta_i},$$

where for $i = 1$, $\tau_{0i-1} = \theta_1$, and for $i = n$, $\tau_{0i} = \Delta pR/2L$.

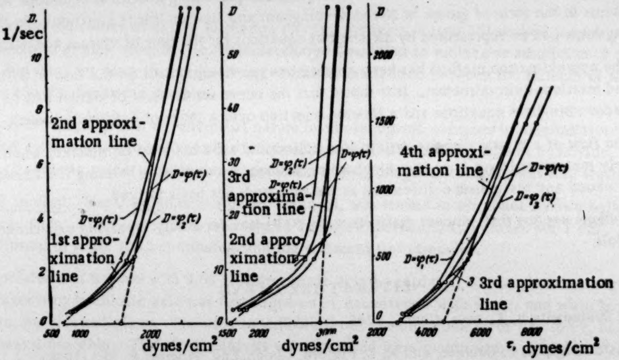

Fig. 3. Graphical approximation of experimental data for the flow of solidol in a rotational viscosimeter, on three scales.

When the curve for the flow of a disperse system is represented by one straight line, i.e., when the disperse system conforms to the Shvedov–Bingham equation, Equation (19) becomes the Buckingham equation for the flow of a viscoplastic medium in a tube. In this case n = 1, and we have:

$$q = \frac{\pi\Delta p}{8L\eta_1}(R^4 - r_0^4) - \frac{\pi}{3}\frac{\theta_1}{\eta_1}(R^3 - r_0^3) = \frac{\pi R^4 \Delta p}{8L\eta_1}\left[1 - \frac{4}{3}\frac{r_0}{R} + \frac{1}{3}\left(\frac{r_0}{R}\right)^4\right].$$

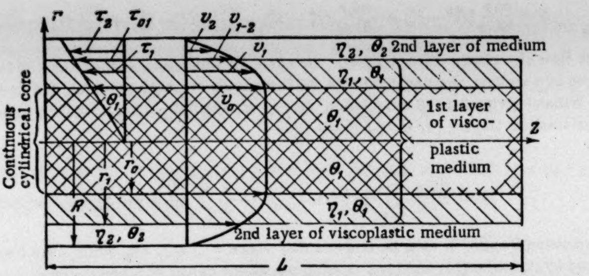
r
τ_2
τ_{01}
τ_1
v_2
v_{1-2}
v_1
v_0
η_2, θ_2 2nd layer of medium
η_1, θ_1
θ_1
θ_1
θ_1
1st layer of visco-plastic medium
z
Continuous cylindrical core
r_0
r_1
R
η_1, θ_1
η_2, θ_2
2nd layer of viscoplastic medium
L

Fig. 4. Flow of a plastic disperse system in a round tube for the case in which the flow curve is approximated by two Shvedov–Bingham equations.

SUMMARY

1. An approximation method has been developed for representing nonlinear equations for flow of plastic disperse systems in the form of groups of Shvedov–Bingham and Newton linear equations. In this way the flow of disperse systems can be represented by differential equations for the flow of viscous and viscoplastic media.

2. The approximation method has been applied to experimental data on the flow of solidol greases in capillary and rotational viscosimeters. It is shown that the curve for the flow of solidol can be represented by several Shvedov–Bingham equations and a Newton equation over a range of 5-6 tenth-powers.

3. The flow of a plastic disperse system in a cylindrical tube has been considered, when the flow can be approximately represented by n Shvedov–Bingham equations. An expression relating the amount of medium flowing per second and the pressure difference at the tube ends has been derived.

The authors express their sincere gratitude to V. P. Pavlov for kindly supplying experimental data on the flow of solidols.

LITERATURE CITED

[1] B. Rabinowitsch, Z. phys. Chem. A145, 1 (1929).

[2] G. E. Alves, D. F. Bourher, and K. L. Pigford, Chem. Eng. Progress 8, 385 (1952).

[3] V. G. Lebedev and G. V. Vinogradoy, Colloid J., 17, No. 1, 38 (1955). *

[4] N. V. Tyabin, Colloid J., 13, No. 1 (1951).

[5] V. P. Pavlov, Candidate's Dissertation (Moscow, 1949); G. V. Vinogradov and V. P. Pavlov, Symposium, Low Temperature Properties of Petroleum Products (Moscow, 1949).

Institute of Petroleum
Academy of Sciences USSR
Moscow

Received July 5, 1956

AN ELECTROCHEMICAL STUDY OF BENTONITE SUSPENSIONS

1. ACTION OF SODIUM HYDROXIDE ON SUSPENSIONS OF ELECTRODIALYZED ASKANGEL

I. A. Uskov and E. T. Uskova

The principal properties of clays greatly depend on the state of the surface of their particles and on the processes which occur in the surface layers of these particles. The state of the surface is largely determined by the electrokinetic potential. Several studies of the electrokinetic properties of clays have been reported [1], but the question is still far from solved. Some workers regard clay as consisting of salts of silicic, aluminosilicic, and ferrisilicic acids [2]. The clay particles then become negatively charged in water owing to dissociation of molecules in the surface layer. Others [3] regard clay as an amphoteric electrolyte, containing sufficiently dissociated acid (silicic acid) and basic (sesquioxide) groups. The particle charge is a certain statistical value representing the aggregate values of the positive and negative charges arising by dissociation of the surface molecules. The view also exists that particles in clay suspensions carry two different double layers simultaneously [4]; one belonging to plane surfaces and the other to fractures and edges. These layers may even differ in sign; this is indicated by electronographs [5] which show that negatively charged gold micelles are adsorbed only at the edges of kaolinite and montmorillonite particles.

To determine the causes of charge formation on clay particles, Kargin [6] studied mixed gels of silicic acid and sesquioxides as clay models. He attributes charge formation to molecular adsorption of electrolyte from solution, but does not deny the possibility of chemical interaction between the surfaces of the disperse phase particles and the dispersion medium.

In the present investigation the chemical nature of the ionogenic complex in electodialyzed bentonite has been studied by means of potentiometric and conductometric titrations by sodium hydroxide. The variation of the electrokinetic potential with the composition of the ionogenic complex was also studied.

Material studied. The Caucasian bentonite, askangel, was soaked in ten times its own bulk of distilled water for several days. The swollen mass was rubbed through a sieve with 4,900 holes per 1 cm^2. A 2% suspension was allowed to settle for 2-3 minutes, and the sediment was discarded.

The suspension was treated with 0.05 N hydrochloric acid by repeated decantation to a negative reaction for calcium. Excess hydrochloric acid was first removed by decantation with water, and when peptization of the sediment began, by electrodialysis. The electrode potential of the electrodialyzer was 160 v, and the central compartment was 6 cm wide. The electrodialysis was continued for a month with overnight breaks. The electrical conductivity of the suspension was $2 \cdot 10^{-6}$ $ohm^{-1}cm^{-1}$.

It was assumed that as the result of this treatment all the exchangeable cations and anions of the bentonite had been replaced by hydrogen and hydroxyl ions respectively, i.e., that hydrogen bentonite had been prepared.

Measurement methods. The hydrogen bentonite was subjected to conductometric and potentiometric titrations. These methods have been successfully used by many workers [7] for determinations of the composition of ionogenic complexes in sols. It was found in preliminary experiments that the electrical conductivity and pH of the suspensions varied appreciably for several days after addition of alkali. The titrations were therefore performed by determinations of the parameters which became established by the seventh day after addition of alkali.

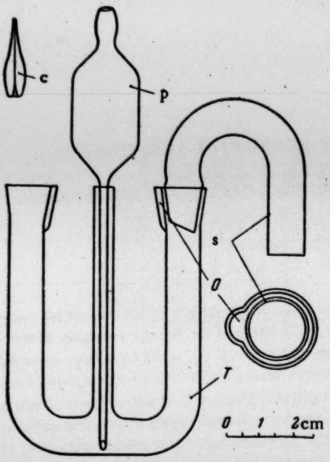

Fig. 1. Electrophoresis apparatus: T) U-tube; S) siphon tube filled with agar gel (second siphon tube not shown); 0) orifice for air outlet; P) pipet for introducing the suspension into the apparatus; C) capillary tube to serve as air brake, joined to the pipet by means of a rubber tube.

The pH measurements were performed with the aid of an antimony electrode; the electromotive force was determined by the compensation method with the "Etalon" potentiometer. The antimony electrode was calibrated against buffer solutions the pH of which had been determined by means of the quinhydrone and hydrogen electrodes. The electromotive force was regarded as constant when the value found did not differ from the previous one by more than 1-2 units in the fourth figure. The readings were taken one minute after stirring of the suspension.

The conductance was determined by the Kohltausch method with smooth platinum electrodes and an alternating current generator; the temperature was maintained at 20° ± 0.05.

The electrokinetic potential was measured by the electrophoretic method in an apparatus based on a similar design described by Chaikovsky [8]. A diagram of the apparatus is given in Fig. 1.

The siphons are connected by means of ground glass joints with grooves for the escape of air displaced from the apparatus by the suspension (introduced by means of a pipet). The use of ground glass joints ensures that the interelectrode distance is strictly constant. The lower end of the pipet is cut obliquely, and the upper end is closed by a capillary so chosen that the time to fill the apparatus is 10-15 minutes. Before each determination the apparatus was treated in hot chromic mixture, washed in running water, and steamed for 15-20 minutes. All the glassware used was cleaned similarly.

As has been shown by one of us [9], the use of agar in saturated potassium chloride solution for filling the siphons is inadmissible, as it results in changes in the conductance of the auxiliary liquid owing to penetration of KCl into it. The siphons were therefore filled with 2% agar solution in distilled water.

Solutions of hydrochloric acid of the same conductivity as the suspension were used as auxiliary liquids. For alkaline suspensions the auxiliary liquid was prepared from sodium hydroxide solutions. The potential gradient in the suspension and auxiliary liquid was calculated with allowance for the potential drop in the siphons. The total resistance R of the circuit was calculated by Ohm's law. The resistance $\underline{r}$ of the siphons was measured separately. The potential drop between the siphons, i.e., in the suspension and auxiliary liquid, is

$$E = V\frac{R-r}{R},$$

where V is the potential at the instrument terminals.

The electrophoretic mobilities were determined by measurements, with the aid of a microscope, of the time required for the boundary between the liquid and the suspension to move through 1 mm. 5-6 such determinations were performed in one direction (without the current being switched off). As a rule the rate of electrophoresis did not vary in the course of an experiment, i.e., while the suspension boundary moved through 5 mm; this can be seen in Fig. 2. All the readings were taken at the rising boundary.

The electrokinetic potential was calculated from the Smoluchowski equation. As reported by Kruyt and Overbeek [10], the Smoluchowski equation is valid for suspensions. Surface conductance and relaxation effects can be ignored in this case.

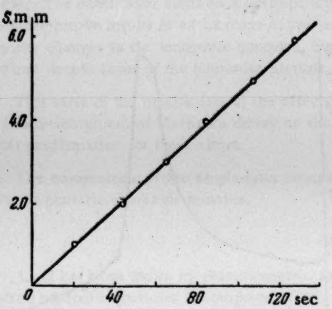

Fig. 2. Displacement of the boundary hydrogen bentonite suspension and auxiliary liquid in the electrophoresis cell.

Results of the Determinations

Potentiometric titrations showed that suspensions of electrodialyzed askangel behave as mixtures of two weak acids (Fig. 3). The stronger of these is neutralized at pH 7.9, and the weaker at pH 10.3; their dissociation constants, calculated from potentiometric titration data, are $7 \cdot 10^{-6}$ and $5 \cdot 10^{-10}$ respectively.

The curve suggests that two different acids, and not one dibasic acid, are present. The suspension contains 650 microequiv. of the first acid and 250 microequiv. of the second per 1 g of the dry material.

The stronger acid is evidently one of the polysilicic acids present in the surface layers of bentonite particles; it dissociates to give hydrogen ions, as is shown by the low pH value of 4 for the electrodialyzed suspension. The dissociation of the second acid is suppressed, as its degree of dissociation is 10^4 times smaller than that of the first.

Nikolsky and Paramanova [11] have shown that aluminate formation occurs at pH 10.0-10.5. Since bentonite contains a considerable amount of alumina and the second acid is neutralized at pH 10.3, there is good reason to believe that this is aluminic acid; evidently aluminum hydroxide, which is converted into aluminate at high pH values, is present on the surfaces of electrodialyzed bentonite particles.

Conductometric titration confirms the hypothesis that two acids are present on the surfaces of electrodialyzed bentonite particles. The conductometric titration curve in Fig. 3 shows three fairly distinct linear regions. The first additions of sodium hydroxide to the hydrogen bentonite suspension produce a slow increase of conductivity. This region corresponds to addition of 0-600 microequiv. of sodium hydroxide per 1 g of dry hydrogen bentonite. The conductivity over the region corresponding to 600-800 microequiv./g increases much more steeply than over the preceding region. Further additions of hydroxide, above 800 microequiv./g, result in a still more rapid conductivity increase. This type of curve is typical of conductometric titrations of mixtures of two weak acids, and is in agreement with the potentiometric titration data. An interesting facts is that the inflexions on the conductometric and potentiometric titration curves almost coincide (Fig. 3).

Results of the electrokinetic potential measurements are shown in Fig. 4. Additions of small amounts of sodium hydroxide produce only a small increase of the electrokinetic potential. From 500 microequiv./g the potential rises steeply, passes through a maximum at 700 microequiv./g, and falls just as steeply to the original values at 830 microequiv./g. Further addition of alkali results in a further decrease of the zeta potential. This complex variation of the electrokinetic potential with the amount of sodium hydroxide added to the suspension can be explained on the basis of the potentiometric and conductometric data.

The surface layer of the particles in the original hydrogen bentonite suspension consists of silicic (or aluminosilicic) acid and aluminum hydroxide. The presence of the acid is indicated by the first break on the conductometric titration curve. The existence of aluminum hydroxide in the surface layer is shown by the second break and inflexion on the same curve. The negative charge of the particles id determined by the dissociation of silicic acid (or the acid groups of the aluminosilicate); dissociation of aluminum hydroxide (or the corresponding groups of the aluminosilicate) accounts for the possibility of a positive charge. The negative value of the zeta potential indicates the predominant significance of the acid in the formation of the electric double layer on the particles.

Addition of small amounts of sodium hydroxide results in substitution of H ions in the outer layer of the double layer by Na ions, and the pH of the suspension increases in consequence. Despite the fact that the very mobile H^+ ions are replaced by the less mobile Na^+ ions, the electrical conductivity not only does not diminish, but even increases. This can only be explained by a considerably higher degree of dissociation of the salt formed, in comparison with the corresponding acid, which makes the outer layer of the double layer more diffuse.

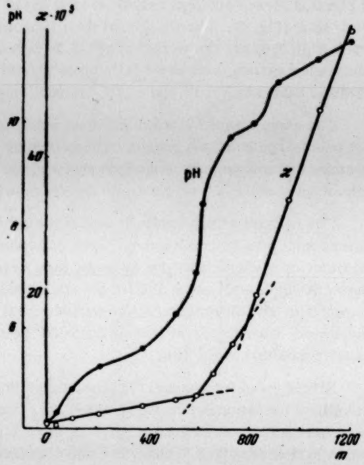

Fig. 3. Curves for potentiometric (pH) and conductometric (κ) titration of 0.55% suspension of hydrogen bentonite with sodium hydroxide; m is the number of microequivalents of NaOH per 1 g dry material.

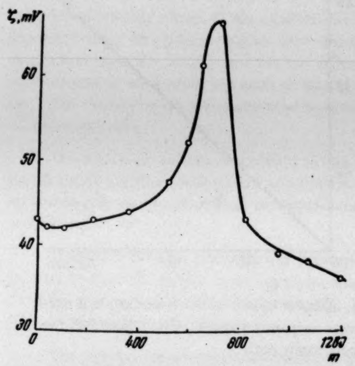

Fig. 4. Variation of the electrokinetic potential of 0.55% bentonite suspension with the amount of sodium hydroxide added.

At the same time the dissociation of aluminum hydroxide, already low, is suppressed; this ultimately results in an increase of negative charge.

The sharp increase of zeta potential coincides with the point at which the acid is neutralized and a salt which dissociates readily is formed, favoring development of the diffuse double layer. However, the zeta potential does not decrease on further addition of sodium hydroxide. On the contrary, it increases even more steeply. This can be explained by the amphoteric nature of aluminum hydroxide. At high pH values sodium aluminate is formed, which dissociates to a greater extent than sodium silicate (see the conductometric titration curve). Formation of aluminate ions on the particle surfaces results in an increase of the positive charge and a rise of the zeta potential.

The increase of potential does not continue up to the formation of the maximum amount of aluminate. It is known that aluminate can exist only in the presence of large amounts of alkali. Excess of electrolyte leads to a sharp increase in the ionic strength of the solution, as shown by the steep ascent of the conductometric titration curve in this region. As a result the diffuse layer is compressed and the electrokinetic potential decreases. However, the "double stabilization" is so strong that even at the high pH values of 10-12 the potential remains considerable (over 35 mv).

A hypothesis concerning the structure of the surface layer of the bentonite particle can be advanced on the basis of these results. The inner layer of the electric double layer in hydrogen bentonite is composed of $HSiO_3^-$ ions and, in much smaller amounts, of $Al(OH)_2^+$ ions. The outer layer contains predominantly hydrogen ions and some hydroxyl ions. The particle as a whole has a negative charge.

In neutral and weakly acid media (pH 7-9), $Al(OH)_2^+$ ions disappear from the inner layer owing to suppression of the main dissociation of aluminum hydroxide. All the silicic acid in the surface layer is converted into its acid sodium salt, dissociation of which results in an increase of the amount of $HSiO_3^-$ ions on the particle surface. The negative charge of the particle greatly increases as the result of the considerable dissociation of this salt. In the outer layer the hydrogen ions are replaced by sodium ions. These are held less strongly than H^+ ions by the particle surface, making the outer layer of the electric double layer more diffuse.

In an alkaline medium (pH 9-10) the inner layer of the double layer of a sodium bentonite particle contains, in addition to $HSiO_3^-$ions, also AlO_2^- ions, which leads to an even greater increase of the charge on the particle. The outer layer contains a corresponding number of sodium ions. Formation of the easily dissociated sodium aluminate results in an increase of the surface charge. Further additions of sodium hydroxide do not cause any changes in the ionogenic complex, but merely compress the diffuse region of the outer layer of the electrical double layer of the bentonite particle.

This view of the mechanism of the effects produced by addition of alkali to suspensions of hydrogen bentonite is a development of Mattson's theory on the ampholytoid structure of clay particles, and provides experimental confirmation for these views.

The composition of the ampholytic complex of the bentonite particle is in reality much more complicated, but its amphoteric character remains.

SUMMARY

1. It has been shown by potentiometric and conductometric titrations that the surface layer of electrodialyzed bentonite particles is composed of 2/3 silicic acid and 1/3 aluminum hydroxide.

2. The electrokinetic potential of electrodialyzed bentonite suspensions as a function of the amount of alkali added has been measured by an electrophoretic method.

3. Small additions of sodium hydroxide produce only a slight increase of the zeta potential of hydrogen bentonite particles. Starting with additions of 500 microequiv./g, the potential rises sharply, passes through a maximum at 700 microequiv./g, and then falls to the original value at 830 microequiv./ g. Addition of sodium hydroxide in excess of this amount causes a further fall of zeta potential. An explanation for the dependence of the electrokinetic potential on the amount of sodium hydroxide added is advanced.

4. The surface layer of the bentonite particle is amphoteric in character. The inner layer of the electric double layer of the hydrogen bentonite particle consists of $HSiO_3^-$ and in part of $Al(OH)_2^+$ ions, while the outer layer consists mainly of H^+ ions with a much smaller amount of OH^- ions. The inner layer of the electric double layer of the sodium bentonite particle consists of $HSiO_3^-$ and AlO_2^- ions, and the outer layer, of sodium ions.

The authors express their deep gratitude to A. V. Dumansky for valuable advice and comments on the manuscript.

LITERATURE CITED

[1] P. Tuorila, Koll.-Z. 44, 11, (1928); I. I. Zhukov and M. N. Sokolova, J. Russ. Chem. Soc., 61, 1081 (1929); A. Buzagh, Koll.-Z. 47, 223, 1949; S. Mattson Soil. Sci. 28, 179, 337 (1929); I. N. Antipov-Karataev, T. F. Antipova-Karataeva, and A. N. Yasinovsky, Colloid J., 1, 333 (1935); E. A. Hauser, A. J. Jonson, J. Am. Ceram. Soc. 25, 223 (1942); E. A. Hauser, Trans. Faraday Soc. 44, 287 (1945); A. H. Beavers, B. L. Larson, Soil Sci. Soc. Am. Proc. 17, No. 1, 22 (1953).

[2] K. K. Gedroits, Selected Works (State Agric. Lit. Press, 1955), 1; N. I. Gorbunov, Sorptive Capacity of Soils and Its Nature (Agric. Press, Moscow, 1948).

[3] S. Mattson, Soil Colloids (Agric. Press, Moscow, 1938).

[4] H. Olphen, Rec. Trav. Chim. Pays-Bas. 69, 1308 (1950).

[5] P. A. Thiessen, Z. Elektrochem. 48, 675 (1942).

[6] M. E. Shishniashvili and V. A. Kargin, Colloid J., 8, 101 (1946); V. A. Kargin and A. L. Batsanadze, Colloid J., 8, 269 (1946).

[7] W. Pauli, E. Schmidt, Z. phys. Chem. 129, 199 (1927); W. Pauli, Koll. Chem. Beih. 17, 256 (1923); W. Pauli, E. Walko, Electrochemie der Kolloide (1932); A. I. Rabinowitsch and R. Burstein, Biochem. Z. 32, 187 (1927); A. I. Rabinowitsch and V. A. Kargin, Trans. Karpov Chem. Inst., 8, 33 (1928); J. Phys. Chem., 1, 65 (1930).

[8] S. Chaikovsky, Colloid J., 5, 131 (1939).

[9] O. D. Kurilenko and E. T. Shechkova, Ukrain. Chem. J., 16, 501 (1950).

[10] H. R. Kryut, Colloid Science (IL, 1955) p. 291.

[11] B. P. Nikolsky and V. I. Paramonova, J. Phys. Chem. 2, 687 (1931).

The T. G. Shevchenko State University
Kiev
Ukrainian Academy of Agricultural Sciences

Received May 15, 1956

ACTION OF THE BASIC SALT ALUMINUM OXYCHLORIDE ON THE STRUCTUROMECHANICAL (THIXOTROPIC) PROPERTIES OF ASKANGEL SUSPENSIONS

E. D. Uznadze and M. E. Shishniashvili

Studies of the mechanism of the action of electrolytes on structure formation in bentonite suspensions are of independent scientific significance, and are also important in relation to the correct utilization of such suspensions in the complex conditions of oil well drilling. The better the structuromechanical and thixotropic properties of a clay suspension used in oil well drilling, the more successful is the elimination of difficulties caused by losses of the suspension through pores in the strata and sand. The structurizing electrolytes used in drilling practice must cause the formation of thixotropic suspensions, increasing both the strength of the structure and the rate of its buildup. Structurizing electrolytes which mainly cause changes in the hydrophilic nature of the clay particles (electrolytes containing the alkali cations K, Na, and Li, or electrolytes containing the multivalent cations Ca, Al, Fe, etc.) do not produce any substantial increase of the thixotropic structure formation in bentonite suspensions and are therefore not very effective in preventing losses of the circulating clay suspension in drilling processes.

The purpose of the present investigation was to seek possible ways of increasing the strength of thixotropic structures in bentonite suspensions, with the ultimate aim of using them in complicated drilling conditions.

A basic aluminum salt — aluminum oxychloride, $[Al_2(OH)_5]Cl$ [1] was used for increasing the structural strength of the suspensions; its effective action on the electrochemical properties of mineral colloidal solutions [2], and also its significant influence on the structuromechanical properties of bentonite suspensions, even when used in very small amounts [3], has been demonstrated.

The existing method for the preparation of this salt is very laborious and requires the expenditure of many chemical reagents with a low yield of the final product. We therefore developed a direct method for preparation of aluminum oxychloride from a readily available raw material — aluminum hydroxide.

Aluminum hydroxide was prepared in an aqueous medium by the following reaction: $2Al(OH)_3 + HCl \rightarrow [Al_2(OH)_5]Cl + H_2O$. It was shown in preliminary experiments that the yield of aluminum hydroxide greatly varies with the degree of dilution of the acid and with variations of the relative proportions of water and aluminum hydroxide. To find the optimum conditions, equal amounts of aluminum hydroxide were dissolved in hydrochloric acid solutions of different concentrations: 1; 0.75; 0.5; 0.2 and 0.1 N. It was found that the purest salt is obtained by treatment of aluminum hydroxide with 0.2 and 0.1 N solutions of HCl; treatment of the gel with 0.5 N HCl gives a less pure salt and a low yield.

The glassy aluminum oxychloride was chemically analyzed to determine its composition.

The concentrations of chloride ions and complex $[Al_2(OH)_5]^+$ cations were determined by potentiometric titration with glass and silver electrodes. The concentrations of the ions, calculated from the inflexions on the curves, showed that the aluminum–chlorine ratio is close to unity.

To determine the composition of the complex cation, the number of hydroxyl groups bound with aluminum in the complex cation was determined, and the number of water molecules combined in a molecule of the glassy aluminum oxychloride was also found. It was shown by a method [4] based on the formation of the salt Na_3AlF_6 by the action of sodium fluoride on the aluminum cation that the complex cation of aluminum oxychloride obtained from aluminum hydroxide contains five hydroxyl groups [3].

The number of water molecules of the glassy aluminum oxychloride was found from the difference between the theoretical content of Al_2O_3 in this salt and the content as given by chemical analysis. This difference, calculated per 1 mole of the salt, corresponds to 6 moles of water [3].

Thus it may be assumed that the aluminum oxychloride molecule contains five hydroxyl groups and has the composition $[Al_2(OH)_5]Cl$; it is probably bound with not more than six molecules of water.

In order to study the structure of this peculiar salt, experiments were carried out to obtain it in the crystalline state. The method used consisted of crystallization of the salt from alcoholic solution with gradual dehydration of the alcohol by metallic calcium.

Microscopical examination of the monocrystals of aluminum oxychloride so obtained showed that the salt crystallizes in the monoclinic system. The crystal structure was confirmed by electron diffraction diagrams.

The material studied was bentonite clay of Askan origin. The experiments were performed on a 3.3% suspension of a highly disperse askangel fraction (enriched askangel) with a water yield W = 8.5 ml and relative viscosity of 25 seconds as determined by the SPV-5 instrument.

The effect of aluminum oxychloride on the structuromechanical properties of askangel suspensions was studied by a method based on model analysis with the aid of the modified Veiler–Rebinder apparatus [5,6]. This method gives the most complete quantitative characterization of the structuromechanical properties of structurized systems.

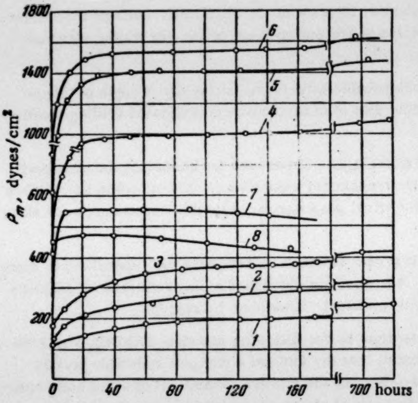

Fig. 1. Kinetics of thixotropic buildup in 3.3% askangel suspension with various contents of aluminum oxychloride: 1) askangel suspension without additions; ditto, with additions of: 2) 0.015%; 3) 0.034%; 4) 0.07%; 5) 0.14%; 6) 0.28%; 7) 0.42%; 8) 0.56% $[Al_2(OH)_5]Cl$.

A study was made of the changes in thixotropic structure formation in askangel suspensions on addition of various amounts of aluminum oxychloride. The question of the reversibility of the thixotropic structure formation process was also studied.

Figure 1 shows kinetic curves for thixotropic buildup in natural askangel suspensions containing from 0.015 to 0.56% of aluminum oxychloride on the volume of the suspension. These curves show that thixotropic strengthening of askangel suspensions increases with increasing amounts of aluminum oxychloride, reaching a maximum value for 0.28% of the electrolyte. On further increase of the amount of added electrolyte the maximum shearing stress of the suspension decreases considerably with time (Fig. 1, Curves 7,8).

Curves 4,5, and 6 (Fig. 1) show that during the first 10-20 hours the maximum shearing stress for the suspension (P_m) increases with time; subsequently the strength of the thixotropic structure remains practically unchanged. Thixotropic buildup in these suspensions is largely completed in 80 hours.

The measure of thixotropy used was the relative strengthening or the coefficient of thixotropy, $K_T = P_m - P_0) / P_0$, where P_m is the maximum shearing stress at a given instant; P_0 is the initial maximum shearing stress or the initial strength of the structure.

The Table (p. 371) gives the experimental data from which the thixotropy coefficients were calculated; the variation of the thixotropy coefficients with the aluminum oxychloride contents in the suspension is shown in Fig. 2.

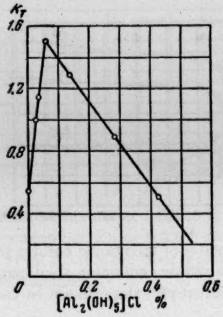

Fig. 2. Variation of K_T with aluminum oxychloride content for a 3.3% askangel suspension.

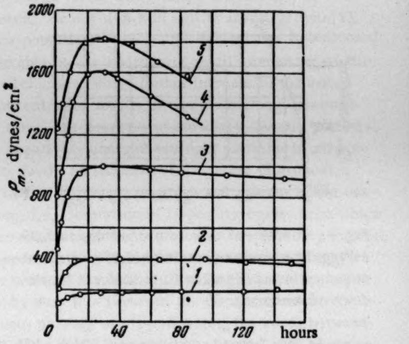

Fig. 3. Variation of the maximum shearing stress for a 3.3% askangel suspension as a function of $AlCl_3$ content: 1) without additions; with additions of: 2) 0.015%; 3) 0.034%; 4) 0.07%; 5) 0.14% $AlCl_3$.

It follows from the Table and Fig. 2 that the coefficient of thixotropy K_T of the askangel suspension first increases with increasing amounts of added electrolyte, reaching a maximum value with 0.07% of aluminum oxychloride in the suspension, and then decreases rapidly.

The variation of K_T is probably caused by changes in the composition of the askangel exchange complex owing to specific adsorption of the complex cation of the basic aluminum salt, causing considerable changes in the electrokinetic properties of the suspension. The structures formed have high thixotropic properties, probably owing to formation of stable coagulation structures.

Coefficient of Thixotropy K_T of a 3.3% Suspension of Natural Askangel as a Function of the Aluminum Oxychloride Content (Buildup time 80 hours)

Suspension studied	P_0 in dynes/cm²	P_m in dynes/cm²	$K_T = \frac{P_m - P_0}{P_0}$
Natural askangel	128	200	0.56
Ditto with 0.015% aluminum oxychloride	140	280	1.00
Ditto with 0.034% aluminum oxychloride	168	365	1.17
Ditto with 0.07% aluminum oxychloride	400	1000	1.50
Ditto with 0.14% aluminum oxychloride	605	1400	1.31
Ditto with 0.28% aluminum oxychloride	840	1570	0.90
Ditto with 0.42% aluminum oxychloride	356	538	0.51
Ditto with 0.56% aluminum oxychloride	470	470	—

For a comparison of the effect of aluminum oxychloride as a structurizing electrolyte, experiments were also carried out with askangel suspensions containing aluminum chloride added in equimolecular amounts in the form of 1 N solutions.

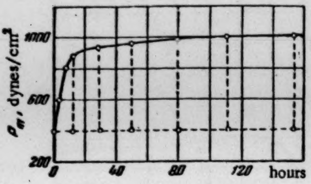

Fig. 4. Kinetics of thixotropic buildup in 3.3% askangel suspension containing 0.07% of aluminum oxychloride (broken lines indicate breakdown of structure).

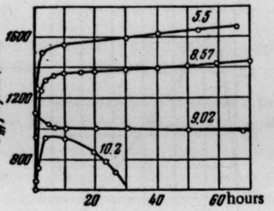

Fig. 5. Kinetics of thixotropic buildup in 3.3% askangel suspension containing aluminum oxychloride, at different pH values (shown on the curves).

As Fig. 3 shows, addition of 0.034% $AlCl_3$ to askangel suspensions produces a slight increase of structural strength. Further increases of the amount of electrolyte added raise the structural viscosity, and the strength of the structure diminishes appreciably with time. Thus, aluminum chloride causes the formation of nonthixotropic structures in askangel suspensions as the result of its hydrophobizing action leading to formation of compact aggregates with visible coagulation of the system.

Experiments on the reversibility of thixotropic structure formation were carried out on a 3.3% suspension of natural askangel, containing 0.07% aluminum oxychloride on the volume of the suspension. During the determinations of the structural buildup with time, the structure was periodically destroyed mechanically and its strength determined.

The structural network in the suspension is totally broken down by mechanical destruction, but it is built up again with time to its maximum value (Fig. 4), indicating the formation of reversible and very stable thixotropic structures in presence of aluminum oxychloride.

As the structuromechanical properties of clay suspensions under the action of various electrolytes depend also on the pH of the medium [6], our next task was to study thixotropic structure formation in askangel suspensions containing aluminum oxychloride at various equilibrium pH values of the suspensions. The original suspensions were treated with 0.1 N solutions of NaOH and HCl to give pH values of 5.5, 9.02, and 10.20 (the pH of a suspension of natural askangel is 8.57). 0.14% of aluminum oxychloride on the volume of the suspension was then added, in the form of 1 N solution.

The maximum shearing stress P_m or the strength of the structure increases considerably with decreasing pH of the suspension (Fig. 5). By decreasing the pH of the suspension it is possible to decrease the consumption of aluminum oxychloride considerably, with a simultaneous increase of the strength of the thixotropic structure. For example, for a suspension of natural askangel containing 0.07% of aluminum oxychloride at pH 8.62, $P_0 =$ $= 400.2$ dynes/cm² and $P_m = 1000.9$ dynes/cm², while for an askangel suspension containing 0.034% of aluminum oxychloride with equilibrium pH 5.5, $P_0 = 450$ dynes/cm² and $P_m = 1370.0$ dynes/cm².

The more effective action of the basic aluminum salt as a structurizing electrolyte at pH 5.5 should be attributedto the fact that this salt is the more stable in these conditions. At lower pH values, and also at pH values of 8.62 and over in the natural askangel suspension, the action of the $[Al(OH)_5]^+$ cation becomes less effective, probably owing to its hydrolysis at high pH and partial decomposition at low pH values.

Figure 6 shows a curve for thixotropic buildup in a 3.3% suspension of natural askangel having pH 5.5 and containing 0.034% aluminum oxychloride. The maximum shearing stress P_m for this suspension is considerably higher than for a suspension containing 0.07% aluminum oxychloride at initial pH 8.62 (Fig. 4). It also follows from Fig. 6 that after mechanical breakdown of this suspension the structural network is completely destroyed, indicating the formation of reversible thixotropic structures.

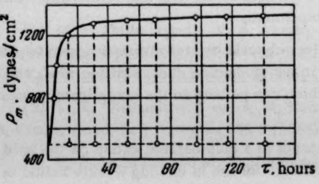

Fig. 6. Kinetics of thixotropic buildup in 3.3% askangel suspension containing 0.034% aluminum oxychloride at pH 5.5 (broken lines represent breakdown of structure).

The action of aluminum oxychloride as a structurizing electrolyte in askangel suspensions apparently consists mainly of a considerable decrease of the electrokinetic factor determining the stability of the suspension. As was shown in earlier investigations [2], the zeta potential of highly purified soil sols is decreased considerably by the addition of small amounts of aluminum oxychloride, while further increase of the added salt concentration results in complete charge reversal in the sols. The decrease of the electrokinetic potential of the negatively charged askangel particles in all probability favors an increase of the forces of attraction between the individual particles and induces latent coagulation, i.e., formation of larger aggregates from which the continuous thixotropic structures are probably formed. The appreciably hydrophilic nature of the $[Al(OH)_5]^+$ cation prevents the individual askangel particles, separated by very thin layers of the dispersion medium, from forming compact aggregates. The formation of a continuous network of clay particles, the bonds between which are weakened by the presence of very thin hydrate shells and also by the presence of larger clay particles, determines the formation of completely reversible thixotropic structures.

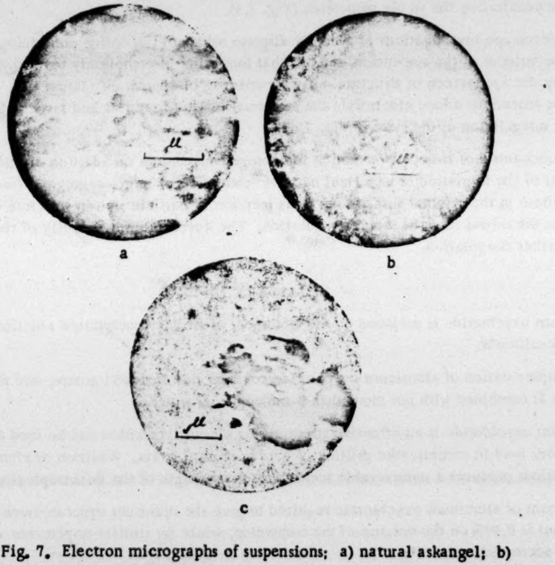

Fig. 7. Electron micrographs of suspensions; a) natural askangel; b) ditto, containing 0.0043% aluminum oxychloride; c) ditto, containing 0.048% aluminum oxychloride.

When the amount of the added electrolyte is increased, the forces of attraction between the particles increase so much, probably owing to charge reversal, that visible coagulation occurs. The compact aggregates formed readily separate from the dispersion medium, and the system gradually loses strength and thixotropic characteristics. When aluminum chloride is added to an askangel suspension, hydrophobization (dehydration) of the particle surfaces occurs in addition to a change in the electrokinetic stability factor. This results in visible coagulation, the structural viscosity greatly increases, and the strength of the structure diminishes. Thixotropic structure formation therefore does not take place in such suspensions.

Thus, the use of aluminum oxychloride as a structurizing electrolyte in natural askangel suspensions leads, on the one hand, to a considerable decrease of clay consumption in the production of the drilling mud, and on the other, to formation of thixotropically reversible suspensions which can be used in the complicated conditions of deep drilling.

As the effectiveness of the structurizing electrolyte used depends to a considerable extent on the acid or alkaline properties of the drilled rock, aluminum oxychloride is suitable for use in drilling weakly acidic or neutral strata. The use of this electrolyte in drilling may be of considerable practical importance.

Thixotropic structure formation in askangel suspensions, and in suspensions treated with aluminum oxychloride, was also studied with the aid of the electron microscope. This method was used for making visual observations of thixotropic structure formation in askangel suspensions. * A highly disperse suspension, prepared by prolonged settling of a dilute suspension of askangel, was used. The concentration of the final suspension was 0.236%.

The electron micrographs (Fig. 7) show clearly that the bentonite particles are not anisodiametric in form, and do not form long chains or plane laminar networks as usually described in the literature. The askangel particles are rather rounded, often with characteristically diffuse outlines, probably because of the high degree of swelling in water. At a number of points in the micrographs bonds can be detected between the finest individual particles, forming types of chains; spatial distribution of these chains probably results in the formation of a structural network penetrating the whole suspension (Fig. 7,a).

Electron microscope investigations of a highly disperse askangel suspension containing 0.0048% of aluminum oxychloride on the volume of the suspension, showed that formation of completely reversible thixotropic structures is accompanied by the appearance of structural chains consisting of appreciably larger clay particles (Fig. 7,b). With 10 times this amount of added electrolyte the structural chains disappear and large aggregates are formed, leading to visible coagulation of the system (Fig. 7,c).

Thus, the mechanism of structure formation in askangel suspensions on addition of aluminum oxychloride essentially consists of the formation of structural networks composed of larger aggregates (secondary formations) of particles than those in the original suspension. This increase of particle size in structure formation in askangel can be regarded as the initial stage of latent coagulation. The appreciable hydrophily of the complex $[Al_2(OH)_5]^+$ cation prevents further coagulation.

SUMMARY

1. Aluminum oxychloride is prepared by the treatment of freshly precipitated aluminum hydroxide with 0.2 and 0.1 N HCl solutions.

2. The complex cation of aluminum oxychloride contains five hydroxyl groups, and the aluminum oxychloride molecule is combined with not more than 6 molecules of water.

3. Aluminum oxychloride is an effective structurizing electrolyte which can be used as an additive to bentonite suspensions used in complicated drilling of acid or neutral strata. Addition of aluminum oxychloride to askangel suspensions produces a considerable increase in the strength of the thixotropically reversible structure.

4. The amount of aluminum oxychloride required to give the optimum structuromechanical properties in askangel suspensions is 0.07% on the volume of the suspension, while for similar suspensions with equilibrium pH 5.5 the amount is decreased to 0.034%.

5. Structure formation in askangel suspensions in presence of aluminum oxychloride mainly consists of the formation of structural networks composed of larger aggregates (secondary formations)of askangel particles.

---

*This section of the work was carried out with the assistance of A. N. Mumladze, scientific assistant at the laboratory.

This increase of askangel particle size should be regarded as the initial stage of latent coagulation.

LITERATURE CITED

[1] M. E. Shishniashvili, V. A. Kargin, and A. L. Batsanadze, Trans. Inst. Chem. Acad. Sci. Georgian SSR 7, 33 (1946); J. Phys. Chem., 21, 3 (1947); Z. Ya. Berestneva and V. A. Kargin, J. Phys. Chem., 10, 533 (1937); V. A. Kargin and N. Ogandzhanova, J. Phys. Chem., 10, 782 (1937).

[2] M. E. Shishniashvili and É. M. Nanobashvili, Report of the Acad. Sci. Georgian SSR, 1-2 (1945); Trans. Inst. Chem. Acad. Sci. Georgian SSR 9 (1948).

[3] E. D. Uznadze and M. E. Shishniashvili, Trans. Inst. Chem. Acad. Sci. Georgian SSR 14 (1956).

[4] V. A. Chernov, The Nature of Soil Acidity (Izd. AN SSSR, Moscow—Leningrad, 1947).

[5] E. E. Segalova and P. A. Rebinder, Colloid J., 13 (1951); S. Ya. Veiler and P. A. Rebinder, Colloid J., 11, 8 (1949).

[6] E. L. Kobakhidze, Candidate's Dissertation (Inst. Chem. Acad. Sci. Georgian SSR, 1955).

The P. G. Melikishvili Institute of Chemistry
Academy of Sciences, Georgian SSR
Laboratory of Colloid Chemistry
Tbilisi

Received June 5, 1956

EVALUATION OF RUBBER – SOLVENT INTERACTION

A. G. Shvarts

It is known that the solution (or swelling) of rubbers is accompanied by a decrease in the free energy ΔF of the rubber–solvent system

$$\Delta F = \Delta H - T\Delta S, \tag{1}$$

where ΔH is the enthalpy change; ΔS is the entropy change, and T is the absolute temperature.

If F decreases continuously during the swelling, the result is unlimited swelling or solution. If F passes through a maximum with increase of swelling, the swelling is limited. This latter case is characteristic of vulcanizates.

The equilibrium swelling can be theoretically calculated from the Flory equation [1]:

$$\ln\left(1 + \frac{1}{Q_\infty}\right) - (Q_\infty + 1)^{-1} - \mu (Q_\infty + 1)^{-2} - \\ - \frac{1}{m_c} [(Q_\infty + 1)^{-\frac{1}{3}} - \frac{1}{2} (Q_\infty + 1)^{-1}] = 0, ^* \tag{2}$$

where Q_∞ is the equilibrium degree of swelling, expressed as the ratio of the volume increase of the swollen specimen to the volume of the dry specimen after swelling; $m_c = M_r/\rho_r V_s$; V_s is the molar volume of the solvent in cubic centimeters per mole; ρ_r is the density of the rubber in grams per cubic centimeter; M_r is the molecular weight of a segment of the molecular chain between adjacent cross links; μ is a parameter characterizing intermolecular interaction between the rubber and the solvent. The enthalpy increment ΔH on mixing increases with increasing μ. The intermolecular interaction parameter μ depends on the ratio of the square roots of the cohesive energy densities for the rubber and the solvent [4,5].

$$\mu = \mu_s + \frac{V_s\,(\delta_r - \delta_s)^2}{RT}, \tag{3}$$

where δ_r and δ_s are the square roots of the cohesive energy densities of the rubber and solvent respectively. These are generally known [4,5] as the solubility parameters. The value of the parameter for the solvent can be calculated from its latent heat of vaporization (ΔH_v) at the given temperature:

$$\delta_s = \sqrt{\frac{\Delta H_v - RT}{V_s}}, \tag{4}$$

---

* Two other equations [2,3] are known which connect Q_∞ with the density of the vulcanization network and a parameter characterizing rubber–solvent interaction. However, Equation (2) is the one most commonly used.

in Equation (3) $\mu_s = 1/\gamma$, where γ is the number of solvent molecules surrounding one segment of the rubber molecule. It is generally assumed that γ is constant for all rubbers [5]. On the basis of literature data it is assumed in the present paper that $\gamma = 4$.

We must point out that Equation (3) is valid for systems with the same nature of intermolecular interaction forces (for example, nonpolar rubber – nonpolar solvent). Equation (2) shows that the interaction of solvents with rubbers and vulcanizates depends on the absolute values of μ and m_c. It should be noted that the parameter μ depends on the chemical nature of the rubber units and is independent of the molecular weight of the polymer, and therefore it characterizes the interaction both of the rubber itself and of its vulcanizates with the solvent.

It has been shown in a number of investigations [6,7] that for limited swelling of unvulcanized rubber, $\mu > 0.5$. Therefore, for a rough evaluation of the solvent power of a particular solvent it is sufficient to compare the values of the solubility parameters for the rubber and the solvent.

Values of the solubility parameters of certain rubbers and solvents, taken from the literature and calculated, are given in Tables 1 and 2.

TABLE 1

Values of the Solubility Parameter δ in $(\text{cal./cc})^{1/2}$ for Various Rubbers

Rubber	Literature data		Calculated
	Gee [5]	Scott [4]	
Natural	7.98	8.35	8.22
Sodium butadiene	—	8.45	8.35
Divinyl–styrene (Buna S type), 15% styrene	—	8.55	—
Ditto, 25%	8.1	8.60	8.45
Ditto, 40%	—	8.70	—
Polychloroprene (Neoprene GN type)	8.2	9.25	9.00
Divinyl – acrylonitrile (Buna N type)	—	9.50	9.70

TABLE 2

Range of Solubility Parameters for Solvents of Different Chemical Classes, Calculated from the Heats of Vaporization at 25°

Solvents	Range of values of $\delta_s (\text{cal./cc})^{1/2}$
Paraffin hydrocarbons	6.75* — 7.55
Low molecular aromatic hydrocarbons	9.15 — 8.80
Ethers	7.90 — 7.45
Esters	10.15 — 8.00
Ketones	9.9 — 7.6
Nitriles	11.9 — 9.4
Monohydric alcohols	16.5 —10.3

---

* The values of δ_s on the left refer to solvents of lower molecular weight.

It follows from Equation (3) that the value of μ decreases, and the solvent power of a given solvent therefore increases, with decreasing absolute difference between the solubility parameters of the rubber and the solvent. However, some classes of solvents, such as hydrocarbons, ethers, and ketones, may have similar solubility parameters (Table 2) but different solvent powers; i.e., Equation (3) is not applicable to the general case of solution of rubbers in different solvents. Gul [8] showed that this is because Equation (3) does not take into account the differences in the intermolecular forces acting between different rubbers and solvents. Some authors [4] propose the introduction of a correction factor K> 1 into Equation (3) for describing the interaction of rubbers with different solvents

$$\mu = \mu_s + \frac{K \cdot V_s (\delta_r - \delta_s)^2}{RT}. \qquad (5)$$

The factor K is to be calculated from experimental values of μ found with the aid of Equation (2) from the degrees of swelling of the same vulcanizate in different solvents. However, this calculation method is laborious and is valid for only a few solvents. In the present paper a method is proposed for graphical determination of μ from Equation (5), applicable to the interaction of a number of rubbers with solvents of different chemical classes. Since the correction factor K takes differences in the nature of the intermolecular forces into account, it is to be expected that K will have the same value for a given rubber and solvents of the same chemical nature.

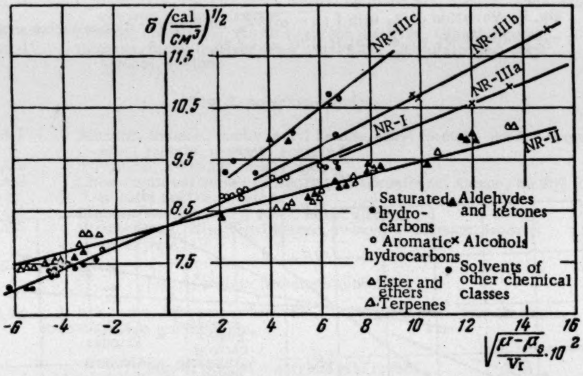

Fig. 1. Variation of δ_s with $\sqrt{(\mu - \mu_s)/V_s}$ for natural rubber; $\delta_r = 8.22$ (cal./cc)$^{1/2}$, $\mu_s = 0.25$.

We write Equation (5) in the form:

$$\delta_s = \delta_r \pm \sqrt{RT/K} \cdot \sqrt{(\mu - \mu_s)/V_s}. \qquad (6)$$

For systems with intermolecular interaction forces of the same character RT/K = const. Therefore for such systems Equation (6) represents a linear relationship between $\sqrt{(\mu - \mu_s)/V_s}$ and δ_s. A line of this type cuts off an intercept numerically equal to the solubility parameter δ_r of the rubber along the ordinate axis.

Data on the swelling of filled and unfilled vulcanizates in a large number of solvents [4,5,9-12] (the solvents are listed in Table 3) were used to calculate values $\sqrt{(\mu - \mu_s)/V_s}$ from Equation (2). The values so found were plotted graphically (Figs. 1-5). It was found that the parameter μ, characterizing intermolecular interaction, is independent of the loading of the rubber. Figure 1 shows points for the swelling of three different filled and three unfilled natural rubber vulcanizates in about 50 solvents. Figure 2 gives data for swelling of three divinyl–styrene rubbers containing 25% styrene (Buna S type) in 28 solvents, and Fig. 3, for three polychloroprene rubbers (Neoprene GN type) in 25 solvents. Figure 4 refers to swelling of one sodium butadiene rubber in 7 solvents, and Fig. 5, to one divinyl–acrylonitrile rubber (Buna N type) in 9 solvent.

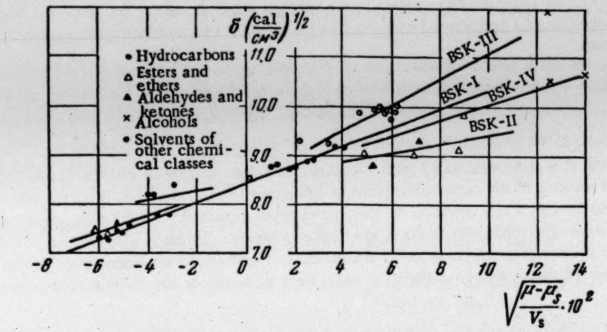

Fig. 2. Variation of δ_s with $\sqrt{(\mu-\mu_s)/V_s}$ for divinyl–styrene rubber with ~25% styrene; $\delta_r = 8.45\ (\text{cal./cc})^{1/2}$; $\mu_s = 0.25$.

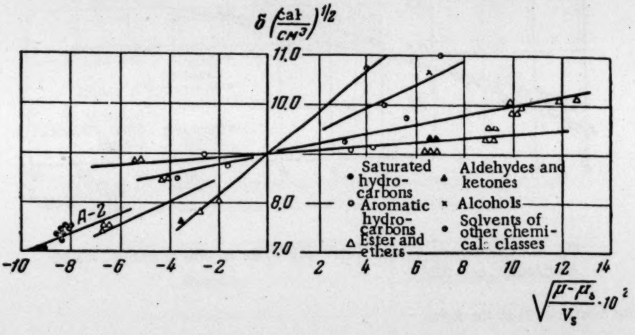

Fig. 3. Variation of δ_s with $\sqrt{(\mu-\mu_s)/V_s}$ for chloroprene rubber of the Neoprene type; $\delta_r = 9.00\ (\text{cal./cc})^{1/2}$; $\mu_s = 0.25$. Designations of the curves (reading downward on the right of the diagram): A-5, A-4, A-3, A-1.

The graphs show that all points corresponding to systems with intermolecular interaction of the same character lie on one straight line. Several lines intersect at one point, thus determining the exact value of the solubility parameter of the given rubber (Table 1).

The accuracy with which the position of the straight lines determining the interaction of rubbers with solvents of different chemical classes is fixed increases with increasing amounts of experimental data used for plotting these graphs (for example, 115 points were plotted for natural rubber in Fig. 1).

TABLE 3

Lists of Solvents Used in Calculations of the $\delta_s - \sqrt{(\mu - \mu_s)/V_s}$ Relationships Shown in Figs. 1-5

Symbol on graph	Solvents
	Fig. 1, natural rubber
NR-I	Saturated and aromatic hydrocarbons
NR-II	Methyl ethyl ketone, diisopropyl ketone, mesityl oxide, methyl formate, diethyl ether, ethyl acetate, n-amyl acetate, propyl acetate, n-butyl acetate, n-butyl n-butyrate, isobutyl n-butyrate, limonene, isoprene, butyraldehyde, acetone
NR-IIIa	Nitriles; alcohols: tertiary butyl, amyl, n-propyl; nitromethane
NR-IIIb	Dioxane, chloroform; alcohols: hexyl, benzyl
NR-IIIc	Alcohols: heptyl, octyl; cyclohexane, dichloroethane, carbon tetrachloride, styrene, acetyl chloride, notrobenzene
	Fig. 2, divinyl — styrene rubber
BSK-I	Saturated and aromatic hydrocarbons; limonene, dichloroethane, carbon tetrachloride
BSK-II	Cyclohexane, cyclohexene, methyl ethyl ketone, mesityl oxide, ethyl acetate, n-amyl acetate
BSK-III	Styrene, chloroform, dioxane, carbon disulfide, benzyl alcohol
BSK-IV	Isoprene, methylcyclohexane, ethyl ether, hexyl alcohol, octyl alcohol, acetone
	Fig. 3, polychloroprene
A-1	Benzene, toluene, methyl ethyl ketone, ethyl formate, methyl acetate, ethyl acetate, n-propyl acetate
A-2	n-Pentane, n-hexane, n-heptane
A-3	Chloroform, carbon tetrachloride, dichloroethane, xylene, methyl formate, n-butyl acetate, acetone
A-4	Dioxane, aniline, ethyl ether, hexyl alcohol
A-5	Nitrobenzene, diisopropyl ketone, n-butyl n-butyrate, isobutyl n-butyrate
	Fig. 4, sodium butadiene rubber
SKB-1	n-Hexane, n-heptane, benzene, toluene, p-xylene, ethylbenzene, carbon tetrachloride
	Fig. 5, divinyl — acrylonitrile rubber
SKN-1	n-Hexane, n-heptane, cyclohexane, benzene, toluene, p-xylene, ethylbenzene, chloroform, carbon tetrachloride

It is seen in Fig. 1 that the points corresponding to saturated and aromatic hydrocarbons lie along one straight line. The points for all the ketones, esters, and ethers given in Table 3 also lie on one straight line. The behavior of alcohols is different.

In the action of alcohols on natural rubber the nature of the intermolecular interaction changes with increasing molecular weight of the alcohol. As a result, the points corresponding to swelling of NR vulcanizates in tertiary butyl, amyl, and n-propyl alcohols lie on one straight line, and the points for n-heptyl and n-octyl alcohols on another.

Of the data used, only the point for the interaction of NR with cyclohexane did not lie on one of these lines for NR. The interaction of polychloroprene rubbers with solvents could not be represented by straight lines specific for given homologous series. Points representing interaction of polychloroprene rubbers with different

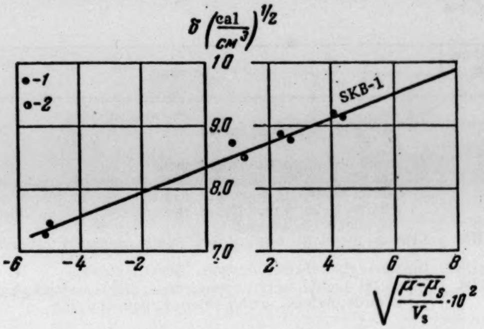

Fig. 4. Variation of δ_s with $\sqrt{(\mu - \mu_s)/V_s}$ for sodium butadiene rubber SKB-I; δ_r = 8.35 (cal./cc)$^{1/2}$; μ_s = 0.25: 1) hydrocarbons; 2) carbon tetrachloride.

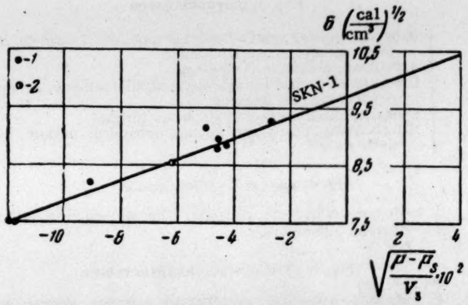

Fig. 5. Variation of δ_s with $\sqrt{(\mu - \mu_s)/V_s}$ for divinyl–acrylonitrile rubber SKN-I of Buna N type; δ_r = 9.70 (cal./cc)$^{1/2}$; μ_s = 0.25: 1) hydrocarbons; 2) carbon tetrachloride.

esters or ethers lay on different lines. The regular transition from one line to another, found for the swelling of NR in alcohols, is not shown in this case. The probable explanation is the insufficient accuracy of the data used. Further investigations are needed for a complete characterization of the behavior of polychloroprene.

The straight lines in Fig. 1 can be used to evaluate the interaction of natural rubber not only with the solvents listed in Table 3, but also with their homologs; the lines for polychloroprene (as given in Fig. 3) can be used only for determining its interaction with the solvents given in Table 3.

The data in Fig. 3 show that for determination of the parameter μ it is not always possible to make use only of the difference between the absolute values of the solubility parameters of the solvent and the rubber. For example, for ethyl formate the solubility parameter δ_s = 9.43 (cal./cc)$^{1/2}$, for isobutyl n-butyrate δ_s = 7.78

$(\text{cal./cc})^{1/2}$, and for polychloroprene $\delta_s = 9.00$ $(\text{cal./cc})^{1/2}$. It seems at first sight that polychloroprene should swell better in ethyl formate than in isobutyl n-butyrate, but it follows from Fig. 3 that μ for the system polychloroprene–ethyl formate is 0.95, and for the system polychloroprene – isobutyl n-butyrate it is 0.46, so that the solvent power of isobutyl n-butyrate is much greater.

Let us consider the swelling of vulcanized SKS-30 rubber (composition in parts by weight: rubber 100, sulfur 0.5, diphenylguanidine 0.3) in solvents of approximately the same molecular volume but with different types of intermolecular forces (Table 4).

TABLE 4

Swelling of SKS-30 Rubber Vulcanizates

Solvents	Molar volume in cc/mole	Solubility parameter δ_s in $(\text{cal./cc})^{1/2}$	Parameter μ	Maximum swelling Q_∞
Carbon tetrachloride	96.5	8.50	0.250	41.0
m-Xylene	123.0	8.80	0.292	34.5
Toluene	107.0	8.90	0.312	34.6
Benzene	89.5	9.15	0.375	31.4
Dichloroethane	78.7	9.75	0.624	21.1
n-Heptane	146.0	7.45	0.648	6.91
n-Amyl acetate	147.0	9.10	0.912	3.30
Ethyl acetoacetate	127.0	10.00	1.550	0.30

It is seen from Table 4 that the maximum swelling of the vulcanizate decreases with increase of μ, and that the different character of the intermolecular forces in n-amyl acetate and benzene leads to quite different values of μ although the values of δ_s for these solvents are approximately the same.

To determine the solvent power of a given solvent at normal temperature it is necessary to:

1) calculate δ_s by means of Equation (4) from tabular data on heats of vaporization at 20-25°;

2) find the value of $\sqrt{(\mu-\mu_s)/V_s}$ in one of the graphs (from a known ordinate on the line for solvents of the appropriate homologous series);

3) calculate μ by the formula:

$$\mu = 0.25 + \left[\left(\sqrt{\frac{\mu-\mu_s}{V_s}}\right)^2 \cdot V_s\right]. \tag{7}$$

When the value of μ is known, Equation (2) can be used to determine the maximum swelling of any vulcanizate, with known density of the spatial network, in the given solvent.

SUMMARY

1. The influence of differences in the nature of the intermolecular forces in different solvents on their solvent powers has been examined.

2. A graphical method is proposed for evaluation of the influence of the nature of the intermolecular forces of the solvent on the maximum swelling of vulcanizates.

3. For a given rubber and a given chemical class of solvents, the relationship between δ_s and $\sqrt{(\mu-\mu_s)/V_s}$ is linear. Lines for different classes of solvents intersect at one point which represents δ_r, the solubility parameter for the rubber.

The author expresses his deep gratitude to Prof. B. A. Dogadkin and to V. E. Gul for guidance and help in the investigation.

LITERATURE CITED

[1] P. Flory, J. Chem. Phys. 18, No. 1, 108 (1949.

[2] P. Flory, J. Chem. Phys. 11, 521 (1943).

[3] Kuhn, Pasternack, Kuhn, Helv. Chim. Acta 30, 1705 (1947).

[4] R. Scott and M. Magat, J. Pol. Sci. 4, 555 (1949).

[5] G. Gee, article in Symposium "Chemistry of Large Molecules" No. 1, (IL, 1948).

[6] J. Hildebrand, and R. Scott, Solubility of Nonelectrolytes, (N.Y., 1950).

[7] V. E. Gul, Trans. All-Union Conf. Colloid Chem. (Kiev, 1950).

[8] V. E. Gul, Colloid J., 13, 99 (1951).

[9] G. Whitby, A. Evans, and D. Pasternack, Trans. Faraday Soc. 38, 259, (1942).

[10] G. Gee, Trans. IRI 18, 266 (1943).

[11] F. Rosbler, and R. White, Rub. Age 61, 313 (1947).

[12] F. Rostler, et al., Rub. Age 59, 299 (1946).

Tire Institute
Moscow

Received June 5, 1956

INVESTIGATION OF THE ADSORBABILITY OF CARBOHYDRATE SOLUTIONS BY A POLAROGRAPHIC METHOD

M. S. Shulman

It is known that the polarographic maxima on current–potential curves are suppressed by adsorbed surface-active substances. The suppression of the polarographic maximum increases with increasing adsorption.

Heyrovsky [1,2] showed that oxygen dissolved in an electrolyte is readily reduced at a dropping electrode, giving two polarographic waves. The first wave is produced by reduction of oxygen to hydrogen peroxide, and the second, an extended wave, is the result of reduction of hydrogen peroxide to water or to hydroxyl ions. The first oxygen wave forms a sharp maximum which is suppressed by surface-active substances.

The suppressing effects of surface-active substances are studied by measurement of the polarographic wave height of oxygen dissolved in potassium chloride solution. Heyrovsky [2] considers that the suppressing power is characterized by the dilution at which the substance suppresses the greatest oxygen maximum in 0.0014 N KCl solution by one half. Frumkin [3] has established a number of laws relating to the formation of maxima on polarographic curves.

Variation of the Height of the Oxygen Wave in 0.02 N KCl Solution on Addition of Carbohydrate Solutions

% of carbohydrate present in 0.02 N KCl solution	Height of oxygen maximum wave in mm after addition of 1% solution						
	starch paste	dispersed starch	dextrin	glucose	maltose	sucrose	arabinose
0	212	212	212	212	112	212	212
0.0004	209	—	198	—	—	—	—
0.0008	203	—	—	—	—	—	—
0.0016	184	189	—	—	—	—	—
0.0032	175	—	—	—	—	—	—
0.0064	138	118	—	—	—	—	—
0.0080	—	—	112	212	122	—	—
0.016	76	74	—	—	—	153	212
0.024	—	—	—	—	118	—	206
0.032	57	55	47	—	115	149	199
0.048	42	—	41	—	—	—	—
0.064	39	—	—	—	—	—	—
0.08	35	—	—	192	97	144	182
0.096	35	35	35	—	—	—	—
0.12	35	—	—	—	92	—	177
0.20	—	—	—	185	86	—	—

The purpose of the present investigation was to study the adsorption of solutions of certain carbohydrates (native and dispersed starch, dextrins, glucose, maltose, and arabinose) by measurement of the oxygen wave height.

The polarograph designed by the State Institute of Nonferrous Metals was used for the investigations. All the determinations were performed on 0.02 N potassium chloride solution; different amounts of 1% solutions of the carbohydrates studied were added to 25 ml quantities of this solution by means of a micropipet.

The potential range was from 0 to 2.4 v. All the determinations were carried out at 18-20°. Galvanometer readings were taken at 0.15 v intervals. The sensitivity of the galvanometer was $^{1}/_{500}$.

The results are given in the Table.

It follows from the results that glucose and arabinose have little effect on the height of the oxygen maximum wave; sucrose has a greater effect, and the action of maltose is still more appreciable.

Carbohydrates of high molecular weight (dextrins, starch paste, and dispersed starch) have the same adsorbability. The diagram shows the changes in the height of the oxygen wave after additions of potato starch to 0.02 N KCl solution. It is seen that maximum adsorption occurs with a starch content of 0.06-0.08% in the solution.

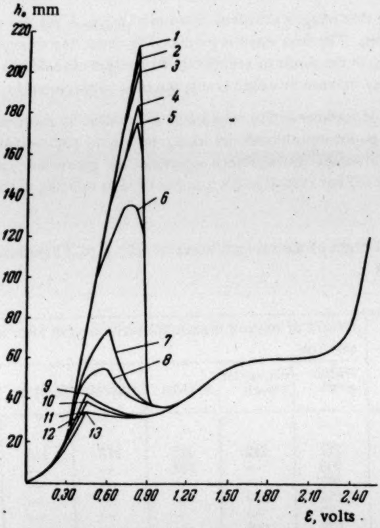

Variation of the maximum on polarographic curves for 0.02 N KCl solution after addition of potato starch solution: 1) no addition; 2) 0.0004%; 3) 0.0008%; 4) 0.0016%; 5) 0.0032%; 6) 0.0064%; 7) 0.016%; 8) 0.032%; 9) 0.048%; 10) 0.064%; 11) 0.08%; 12) 0.096%; 13) 0.12%.

Analogous results were obtained by Sokolov [4], who studied the suppression of the oxygen maximum by additions of normal and disaggregated gelatin. The curves for the suppression of the oxygen maximum by normal and disaggregated gelatin were found to coincide completely, indicating that they were adsorbed equally on mercury.

SUMMARY

1. Polymeric carbohydrates – dextrins, starch paste, and dispersed starch – are adsorbed equally on a mercury surface.

2. Glucose and arabinose have little effect on the height of the oxygen wave; maltose lowers the polarographic maximum appreciably.

LITERATURE CITED

[1] J. Heyrovsky, Trans. Faraday Soc. 19, 785 (1924).

[2] J. Heyrovsky, Polarographic Technique (IL, Moscow, 1951).

[3] A. N. Frumkin, Supplement to Chapter VIII of I. Kolthoff and J. Lingane, Polarography (Goskhimizdat, 1948).

[4] I. Ya. Sokolov, Colloid J., 4, 533 (1938).

All-Union Scientific Research Institute
for the Alcohol Industry
Moscow

Received May 18, 1956

INDUSTRIAL UNIT FOR PRODUCTION OF EMULSIONS BY MEANS OF AN LIQUID WHISTLE (JET)

S. I. Sinkova and S. A. Puzyrev

Various types of equipment are used for the production of emulsions; the commonest are stirrer devices, centrifugal emulsifiers, and colloid mills [1]. All such equipment has various disadvantages, and some of the devices are of complex construction and require the expenditure of considerable amounts of energy for emulsification.

The purpose of the present communication is to describe an ultrasonic unit the operation of which is based on the production of ultrasonic vibrations by means of a liquid jet.

It is known that ultrasonic vibrations have a strong emulsifying effect. However, the practical applications of this effect have been very restricted because piezoelectric and magnetostriction vibrators used for producing ultrasonic vibrations require a high frequency generator. Moreover, with the use of such vibrators the radiating surfaces are rather small (30-100 cm^2) so that only very small volumes of liquid can be treated. The radiating surface in piezoelectric vibrators is limited by the natural dimensions of native quartz crystals. For treatment of large volumes, the radiating surface can be increased by the use of a large number of single crystals. However, because of the high cost of polished crystals, this method cannot be widely used. The use of a large number of magnetostriction vibrators also involves great difficulties. The cost of units using either method is very high. All this accounts for the fact that emulsification by means of ultrasonics has not been adopted industrially.

The production of relatively powerful ultrasonic vibrations in liquids by means of a hydrodynamic vibrator – an ultrasonic liquid jet – is based on the following principle: a liquid stream emerging under high pressure at a high speed through a narrow jet impinges on a metal plate with oblique edges (the "knife") situated in front of the jet and fixed at four points (Fig. 1). The plate vibrates under the impact of the liquid jet; the vibration frequency depends on the velocity of the liquid stream and the distance between the jet and the plate. The distance between the jet and the edge of the plate (l) must be one half of the wave length ($\lambda/2$) of the fundamental vibration emitted by the source, as the vibration nodes must be at the points where the stream emerges from the jet and where it hits the plate

$$l = \frac{\lambda}{2} = \frac{u}{2\nu}, \tag{1}$$

where u is the velocity of sound in the given liquid and ν is the vibration frequency.

For intense ultrasonic vibrations to be produced it is necessary to obtain resonance of the system, for which the fundamental frequency ν' of the plate must coincide with the frequency as defined in Equation (1). The fundamental frequency of the plate is given by the equation

$$\nu' = \frac{\epsilon^2 \pi b}{4\sqrt{3}a}\sqrt{\frac{Eg}{D}}, \tag{2}$$

where ν' is the fundamental frequency of the plate; a is the length of the plate; b is the thickness of the plate; E is Young's modulus; D is the density; g is the acceleration due to gravity; ϵ is a factor (for the fundamental vibration $\epsilon = 0.5969$).

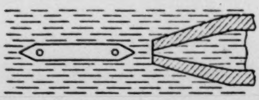

Fig. 1. Diagram of arrangement of jet and "knife".

By varying the dimensions or the length of the plate it is possible to select a definite fundamental vibration frequency of the plate and, by varying the distance between the jet and the plate and regulating the speed of the stream, it is possible to produce resonance in the system. The frequencies of the vibrations produced by the jet are of the same order as the frequencies of magnetostriction vibrators, i e., 20-30 kilocycles/second; the power is 100-180 w.

In contrast to other ultrasonic generators, direct conversion of mechanical into ultrasonic energy is effected by means of the ultrasonic liquid jet.

An emulsification apparatus with the use of a liquid jet has been designed by Pollman and Janovski [2] and was described in detail in the book by Garlinskaya and Bezzubov [3]. The unit used by the present authors differs from the apparatus described by Pollman and Janovski. Different design variations both of the whole apparatus and of the jet were tried, the basic principle being that of the liquid jet. After prolonged researches and trials, the design shown in Fig. 2 was chosen. *

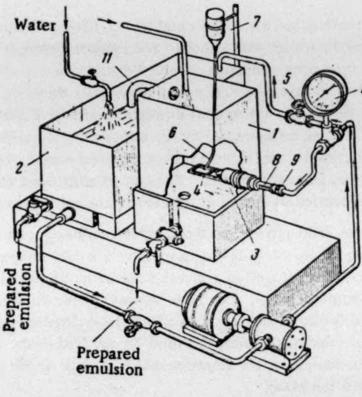

Fig. 2. Ultrasonic liquid jet apparatus for production of emulsions.

The whole unit is a closed system consisting of two reservoirs 1 and 2 connected by pipes through which the liquid is circulated by a pump.

The right tank 1 contains the liquid jet 3. The slit orifice of the jet is 0.5 mm wide and 1 cm long. The speed of the stream leaving the jet is regulated by variation of the pressure by means of the valve 5. The pressure is indicated by the manometer 10. A tube 6 with a clip, through which the liquid for emulsification is fed from the vessel 7, leads to the "knife" 4, formed by the edge of the plate.

---

* The authors express their deep gratitude to S. V. Andreev, A. P. Sviridov, and G. M. Shkarlat for help and advice in designing and constructing the unit.

The distance between the jet and the knife is regulated by means of a screw 9 and the scale 8, situated outside the tank. Before the unit is started up, both tanks are filled with a definite volume of water (20, 60-100 liters), the pump is switched on, and a pressure of 5-12 atmosphere is set up by means of the valve 5, the correct distance between the jet and the knife being adjusted by means of the screw 9. The clip on the inlet tube 6 is then opened and a definite volume of the liquid to be emulsified is let in. The design of the jet is such that the liquid passes through the zone of maximum action of the ultrasound and is instantly emulsified. Very vigorous agitation also occurs in this zone. The concentration of the emulsion formed depends on the volume of water previously put into the tanks, and on the amount of liquid introduced for emulsification. The emulsion formed in the reservoir 1 passes through the pipe 11 into reservoir 2 and again enters the first reservoir through the jet, with continuous addition of the emulsified liquid. Emulsions with concentrations of up to 20% and over can be made in this way.

The emulsions produced are generally finely dispersed (droplet size 0.5–4 μ) and are stable even in absence of emulsifiers. The output of the unit can be increased severalfold by connecting several jets in parallel to the pump, in the same reservoir. The unit can also easily be used for continuous emulsification. For this, fresh water must be fed continuously into the second tank, while the prepared emulsion is continuously removed from the first.

Among the emulsions prepared by means of this unit, emulsions of various organosilicon compounds have been obtained without the use of emulsifiers; some of these cannot be produced with the use of stirrers rotating at 3000 revolutions/minute, even with the use of emulsifiers (gelatin, etc.). An ultrasonic unit with one jet can produce 60-100 liters of emulsions of these compounds in a few minutes.

Because of its high rate of output, simplicity, and cheapness, this unit can be recommended for industrial use.

LITERATURE CITED

[1] W. Clayton, Emulsions (IL, Moscow, 1950).

[2] Pollman, Janovski, Z. ang. Phys., 1, 222 (1948).

[3] E. I. Garlinskaya and A. D. Bezzubov, Ultrasound and its Utilization in the Food Industry.

Central Scientific Research Institute
for Cellulose and Paper Industry
Leningrad

Received June 2, 1956

DISCUSSIONS

THE EQUILIBRIUM STATE OF HIGH POLYMER GELS

(ON THE SUBJECT OF THE COMMENTS BY A. V. NIKOLAEV, R. E. NEIMAN, AND O. V. NEIMAN, COLLOID J. 19, 121 (1957)*

S. M. Lipatov and S. I. Meerson

The problem of gel formation is again becoming very important because several new polymers (polyacrylates, polyvinyl chloride, polystyrene, etc.) of interest for fiber production form solutions only in a small number of liquids and only at high temperatures. On cooling, such solutions form gels in the same manner as has been shown earlier for gelatin, agar, and other natural polymers. The mechanism of gel formation by these new polymers is identical with the mechanism of gelatin gel formation; in both cases the gel at definite concentrations is not in a state of equilibrium, but clearly defined aging of the gel occurs, leading to syneresis – separation of the system into two phases. The analogy between gelation and crystallization developed in our publications over a number of years [1] is now not only confirmed as an analogy, but in a number of papers gelation is identified with crystallization.

Many theories of gelation have existed in the past [2]. Here we may mention two viewpoints, each of which still has its supporters. In our publications we assumed the possibility of complete saturation of the polar groups in the macromolecules by solvent molecules, and the process of structure formation was regarded as interaction between the polymer molecules by means of their polar or generally unsolvated groups [3]. In the other view [4], supported by the authors of the comments on our paper, it is assumed that polar groups may interact with each other in consequence of desolvation of such groups during gelation.

Let us consider the main points put forward by the authors [4].

I. They state that gelation of solutions, and therefore fusion of gels, is not accompanied by heat effect. There are neither theoretical nor experimental grounds for this assertion. Although the authors refer to the care taken in their experiments, the papers [5,6] do not contain experimental data on gelatin gels, while the data on agar are unconvincing. On the assumption that the gelation process consists of two stages: a) gelation without phase separation, the author attribute the absence of a heat effect of gelation to the fact that at the first stage "the nonequilibrium, gel which has not separated into layers should not have a structural network" (p. 132). In this case either there are no bonds between the macromolecules or the bonds are weak and there is no heat effect, while in case (b) phase separation occurs and heat may be evolved.

The authors evidently are not aware that the very first instant of gelation is accompanied by microseparation of the system and interaction between the molecules. Therefore there is no reason for associating the evolution of heat with phase separation in the system. This is also clear from the fact that a 12% solution, which exists as a solution at 40°, forms an equilibrium gel on cooling, which does not separate out in course of time. Earlier we showed that gelation proceeds in stages, each of which is associated with strengthening of the gel structure with time.

1. Solution → gel I + g_1. 2. Gel I → gel II + g_2. Gel II → syneresis + g_3. The total heat effect of the process is equal to the sum of these effects. The authors put forward a scheme according to which the first process is not accompanied by a heat effect, all the heat being evolved at the second stage. They describe this as a new scheme in principle. It is seen from this scheme (p. 130, Fig. 1) that when the solution is cooled from T_2 to T_1 the gel formed has a higher heat content than the solution at temperature T_2 (?). This does not

---

* [Original Russian pagination. See C. B. Translation, p. 129].

correspond to reality, as gelation of solutions below 12% concentration is also accompanied by a heat effect.

The authors themselves realize that the heat effect of gelation which they could not detect must exist. Thus, at the end of the article (p. 132) it is stated that a definite number of local bonds may be formed during gelation; "this process should be accompanied by heat and volume effects." To escape from this confused situation, the authors assume that gelation is accompanied by simultaneous desolvation and interaction between the particles by their desolvated groups.

The desolvation concept is new in principle only in that it is now introduced into the authors' explanations, although quite recently they considered that "there can be no changes in the hydration or structure of the sol and gel, as each of these processes would be accompanied by a heat effect or volume change" (p. 351). It is seen that previously there was no mention of any compensation of two opposing effects. If this veiwpoint is accepted, the conclusions should be quite different from those drawn by the authors. Indeed, if gelation was accompanied by desolvation and formation of bonds between the macromolecules of the desolvated groups, heat absorption should occur, and not compensation of two heat effects. This follows from the fact that hydration and solution of gelatin have a positive heat effect, as in the equation $Q = g - c$, $g > c$. Consequently the reverse process of desolvation and bond formation between the macromolecules should be accompanied by absorption of heat. In reality heat is not absorbed. If it is assumed that $g = c$, as is done by the authors, the formation of very stable bonds must be postulated, as hydrogen bonds are formed in the hydration of gelatin.

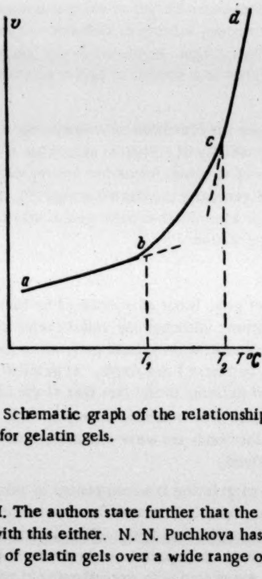

Fig. 1. Schematic graph of the relationship v = = f (T) for gelatin gels.

The authors state further that "in phase separation the number of bonds between the macromoles increase sharply," as a result of which heat should be evolved. The question of the nature of these bonds arises. If desolvation and compensation of two effects is presumed here also, why do the authors assume evolution of heat in syneresis? Or do other groups take part in intermolecular interaction in this case?

It is clear on theoretical grounds that spontaneous gelation should proceed with a decrease of free energy. Since in gelation the large number of possible configurations of the macromolecules is decreased and $\Delta S < 0$ gelation can only proceed spontaneously if $\Delta H < 0$ and $|\Delta H| > |T\Delta S|$. Hence it follows that the gelation process must be accompanied by a heat effect. Finally, if we assume that desolvation occurs spontaneously during gelation, we must assume the existence of two spontaneous processes of opposite sign – solvation (in swelling) and desolvation (in gelation).

Since a gel is formed during gelation and subsequent separation of the system, the composition of which coincides with the composition of the swollen gel, and gelation and syneresis return the system to its original state, the assumption that desolvation occurs in gelation is unfounded. *

II. The authors state further that the gelation process is not accompaned by a volume effect. We cannot agree with this either. N. N. Puchkova has made numerous measurements in our laboratory of the thermal expansion of gelatin gels over a wide range of concentrations.

The results may be schematically represented by Fig. 1. The v = f (T) curve shows two characteristic points. At T_1 the change of gel volume is associated with the start of fusion, which is completed at T_2. If these results are compared with the data published by Neiman [7] on gelatin gels, it is seen that he ignores the

---

* Recently calorimetric studies have been carried out in our laboratory of the solution of gelatin gels of different compositions in urea solutions at 20 and 50°. The results not only confirm that the gelation process is exothermic, but make possible a quantitative evaluation of the heat effect (≈ 9 cal./g for a 20% gelatin gel). The results of these determinations are to be published in the near future.

the volume changes over the intervals ab and cd and considers only the region bc. Two straight lines are drawn in this region, intersecting at 37-39°. The author states that "beyond the limits of the indicated range there is a deviation from linearity, in the direction of both high and low temperatures." It is not clear why the author neglects these "deviations from linearity." However, the erroneous conclusion is drawn from this that no volume change occurs during fusion of a gel. On the basis of our data it can be claimed that the gel–sol transition is accompanied by a volume change at $T_1 - T_2$, and this region always corresponds to fusion of the gel.

Incidentally, the paper [8] contains data for the relationship $\log \tau = f(1/(T))$ where τ is the relaxation time for the gel volume. It is shown that a certain temperature, which the authors call the "melting point" of the gel, corresponds to the intersection of two straight lines, one of which represents the state of the gel, and the other, of the solution. The difference between the activation energies is 42-40 kcal./mole. Even from these data it follows that there should be a heat effect of gelation, and a characteristic point on the $v = f(T)$ curve corresponding to the "melting point."

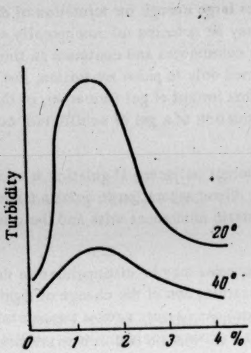

Fig. 2. Variation of turbidity of gelatin gels with concentration.

III. The authors consider two examples in confirmation of their views concerning the absence of heat and volume effects on gelation. One is the thermogram for heating and cooling of borate glass, and the other relates to volume effects in coagulation of $Fe(OH)_3$. The authors assert in the case of the first example that the vitrification of fused glass is not accompanied by a heat effect. However, Botvinkin [9] has shown experimentally that the heat of vitrification of boric anhydride is 26.7 cal./mole. This result is obtained from the heat capacity of glass as a function of temperature. With regard to the second example, it is sufficient to note certain contradictions in the publications by the authors of the discussion paper. For example, it is stated [10] that "coagulation of $Fe(OH)_3$ sol is practically unaccompanied by a volume effect," and the general conclusion is drawn that "volume effects in sol–gel transitions (peptization, coagulation) are zero." However, in the discussion paper we read: "therefore there is no doubt that the volume effect of the sol–gel transition ... while in the shrinkage because of condensation of a gel by the action of a coagulant (analogously to syneresis) it may be comparable with the effect in phase transition". Because of all the foregoing we must disagree with the authors of the discussion papaer and consider their viewpoint to be erroneous.

IV. Mechanism of gel formation. If the force field on the molecules is heterogeneous i.e., if polar and hydrocarbon bonds exist between the macromolecules, solution of the polymer is possible if both types of bond are overcome as the result of interaction with the solvent

$$Q = (g_p - c_p) + (g_n - c_n),$$

where g_p and g_n represent the solvation of polar and nonpolar groups respectively, and c_p and c_n are the bond energies between such groups. If the solvent solvates only one type of group, for example polar, and $g_p > c_p$ while $g_n = 0$, the swelling process is accompanied by evolution of heat, but it is limited, as the energy of the structure, which depends on c_n, has not been overcome. If a quantity of heat equivalent to c_n is supplied to the swollen polymer, a solution is formed which, when cooled to the original temperature, forms either a structurized solution or a gel (depending on the concentration). In either case aggregation occurs in a very short time. The number of aggregates is large, and this can be determined very exactly by light scattering, and also by the heat-effect. Figure 2 shows curves for light scattering at two different temperatures; these curves clearly show the conditions for aggregate formation. As was shown by us in 1936 [11], aggregation precedes gelation only in relatively dilute systems; at gelatin concentrations above 2% aggregation becomes progressively less necessary for gel network formation, as the number of macromolecules becomes large enough for formation of direct bonds between them. As was already stated above, liquid droplets which may be detected microscopically are exuded during the first stages of gel formation, i.e., separation of the system commences and continues in time up to syneresis. It is therefore quite wrong to assume that a network is formed only in phase separation, just as it is wrong to believe that all the heat of gelationis liberated during the first instant of gel formation, or that gelation always leads to complete phase separation of the system with formation of a gel of equilibrium composition.

Gelation proceeds in a complicated manner, differently for different polymers: if gelation is accompanied by chemical effects, as in starch, the phase separation is irreversible. Phase separation in gelatin is completely reversible, while when a polyethylene gel undergoes such separation steric hindrances arise and the system does not return to its original equilibrium state.

The aggregates formed in gelation are fairly stable, and two processes may be distinguished in the fusion of a gel: 1) fusion of the network, and 2) fusion of the aggregates. Examination of the change of light scattering on increase of temperature shows that the aggregates disappear (fuse) over a very narrow temperature range. This and a number of similar facts gives reason to consider gelation as a process analogous to crystallization.

In recent years publications have appeared in which gel formation is regarded as crystallization. Richards [12] showed that when a solution of polyethylene in xylene is cooled, crystallites are formed and aggregate into spherulites. Boedtker and Doty [13] showed, for gelatin solutions, that the aggregates formed are crystallites and their formation has the same origin as gel formation. The presence of crystalline structures in gels is proved not only by the liberation of heat and increase of volume, but by the appearance of sharp rings on X-ray diagrams of gelatin films obtained from gels. Similar effects have recently been found in gels of carboxymethylcellulose and of polyvinyl chloride. Doty stresses that fusion of gels consists of two stages: 1) fusion of the network, accompanied by liberation of the aggregates, and 2) fusion of the aggregates themselves. As was shown by us, formation of not very concentrated gels is preceded by aggregation, and therefore a freshly prepared gel can, in agreement with Doty, be regarded as a precipitate in a weak gel. It follows from the foregoing that stable bonds are formed between macromolecules or their aggregates during gelation, and the authors [4] now admit this, and consider that heat is evolved in the earliest stages of gelation, but it is used to compensate the desolvation process.

It is clear that there are no grounds for assuming desolvation, and therefore the mechanism suggested by the authors to replace ours, which is based on erroneous assumptions, contradicts both experimental data and theory in its very basis.

LITERATURE CITED

[1] S. M. Lipatov, J. Russ. Chem. Soc., 59, 471 (1927); 40-55 (1929); Physical Chemistry of Colloids (Moscow, 1948).

[2] S. M. Lipatov, Problems of Gelation of Lyophilic Colloids, (VSNITO, Zelinsky University, 1937).

[3] S. M. Lipatov, J. Gen. Chem., 3, 694 (1933).

[4] A. V. Nikolaev, R. E. Neiman, and O. V. Neiman, Colloid J., 19, No. 1, 121 (1957).

[5] A. V. Nikolaev, G. I. Golub, and P. Osetrov, Colloid J., 8, 345 (1946).

[6] R. E. Neiman and O. V. Neiman, Colloid J., 9, 203 (1947).

[7] R. E. Neiman, Colloid J., 14, No. 2, 108 (1952). [Original Russian pagination. See C. B. Translation].

[8] R. E. Neiman, Colloid J., 16, No. 4, 281 (1954). [Original Russian pagination. See C. S. Translation].

[9] O. K. Botvinkin, Physical Chemistry of Silicates, (Moscow, 1951), p. 261.

[10] R. E. Neiman and R. I. Sukhorukova, Colloid J., 12, No. 5, 363 (1950).

[11] S. M. Lipatov, Problems of Gelation of Lyophilic Colloids (1937).

[12] R. B. Richards, Trans. Faraday Soc., 42, 10 (1946).

[13] H. Boedtker and P. Doty, J. Phys. Chem. 58, 968 (1954); 17, 89 (1955).

Moscow

Received March 3, 1957

PROBLEMS RELATING TO THE MECHANISM OF THE FRICTION OF RUBBER

S. B. Ratner

Scientific studies of rubber friction are of recent origin and enough data for drawing definite conclusions concerning its mechanism are not yet available. However, since a discussion on the mechanism of rubber friction is already in progress [1-3], it is necessary to point out that it is rational to compare the friction of rubber with three other allied phenomena which are better understood: a) friction of ordinary solids; b) flow of viscous liquids; c) deformation of rubber itself.

Friction of rubber and of solids. In contrast to solids, rubber in the course of friction undergoes high-elastic rather than plastic deformation, and creeps like a caterpillar around projections, "flowing" around them [4]. Despite the reversible character of high-elastic deformation, it resembles irreversible plastic deformation in two respects: the possibility of large displacements and the existence of irreversible energy losses (similar to those accompanying friction). It is therefore not surprising that many factors influence the friction of rubber and of oridnary solids similarly. In relation to the role of the load [5,6] this is not disputed by Bartenev [1]

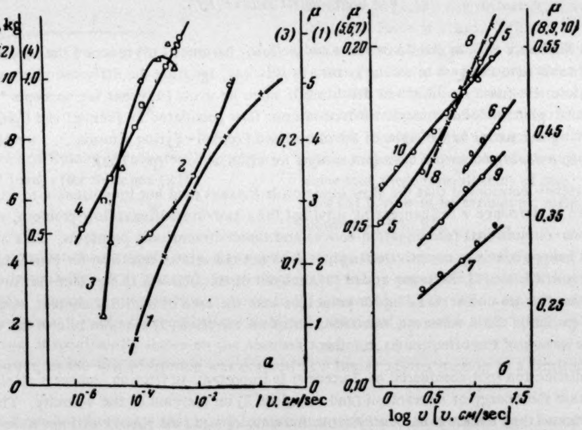

Fig. 1. Variation of the force F (or coefficient μ) of friction with the logarithm of the sliding velocity for rubber (a) and other materials (b) [7]; 1) rubber on glass [9]; 2) on glass [7]; 3) on steel [10]; 4) on steel [3]; 5) pine wood on walnut wood; 6) steel on steel; 7) bronze on steel; 8) leather on steel; 9) the same, after rubbing in; 10) aluminum on steel [7].

However, despite his assertions [1], the influence of sliding velocity v (Fig. 1) is also analogous; the frictional coefficient μ of rubber also generally increases with increasing v (Fig. 1,a), like that of other bodies (leather, wood, metals – Fig. 1,b); often in accordance with the same [7,9] Shallamach–Many equation: $\mu = a + b \log v$. Even cases in which the $\mu - v$ curve passes through a maximum are known both for rubber [10, 11] and for metals [12-14]

These data cover the velocity range from 10^{-12} to 10^{2} cm/second, in which the positions of rubber, wood, and metals are sometimes displaced according to differences in their "relaxation" rates. The data in Curves 2 and 5-11 (Fig. 1), obtained without vibration or heating of the surfaces, are especially reliable. Increase of contact time increases the static friction of rubber and of solids.

Thus, the laws of friction of rubber and of solids are analogous in many respects (the role of temperature is discussed below) which shows that there are similar features in the respective mechanisms.

Friction of rubber and viscous flow. The role of deformation. It is possible, following Schallamach [9, 11], to attempt to demonstrate the analogy between the friction of rubber and the flow of viscous liquids, on the on the assumption that in the sliding of rubber thermal motion RT aids the tractional force F to overcome the activation barrier E. Schallamach presented experimental data which provided the basis for his molecular kinetic theory of rubber friction, represented by the equation

$$v = v_0 \exp\left[-(E - \alpha F)/RT\right].$$

However, in addition to a certain resemblance between the formulas for friction and flow, experience indicates considerable differences between these phenomena These are: absolute static friction [15]; maxima on F−v (see [11]) and also Curve 3 in Fig. 1); minima on F−T curves [16]. Let us consider these effects, found for the friction of rubber and contrary to the mechanism of flow.

Schallamach did not consider his formula valid when v → 0. However, on the basis of his idea (similarity between friction and flow) it is possible to apply the Eyring equation [17] for viscous flow to the friction of rubber:

$$v = v_1 \exp(E/RT) \sinh(\alpha F/RT).$$

Now F = 0 when v = 0, as should be the case in flow. Bartenev [18] reached the conclusion that the static friction of rubber (in contrast to solids) is zero in this way, ignoring the difference between the mechanisms of flow and friction. He formerly admitted this himself when he wrote [18] that his concepts "do not essentially differ from the analogous molecular mechanism of viscous flow postulated by Frenkel and Eyring" (p. 1161), so that "by considering the jumps in the light of the simplified Frenkel–Eyring scheme . . . we obtain a simple but inexact equation analogous to the Eyring equations for viscous flow" (p. 1162).

Thus, Bartenev considered that the flow equation is inexact (and not inapplicable to friction), and therefore he attempted to introduce a refinement by solving [18] a two-dimensional flow problem, whereas Eyring [17] solved the one-dimensional (see equation above) and three-dimensional problems. This mathematical distinction does not bring about any essential change; it does not convert an equation for flow into an equation for friction. After my criticism [2], Bartenev added [3] that the distinction lies in the fact that in friction, i.e., "in internal friction the area of actual contact coincides with the area of nominal contact, and in external friction it does not" (p. 627). This, however, contradicts his own assertion [1] that the role of the contact area bears no relation to the nature of the effect or its kinetics.

Another distinction (not considered by Bartenev) is important: in friction, rubber is displaced as a whole, which may decrease the energy of interaction (and therefore E) on increase of the velocity. Therefore F may reach a maximum and then decrease on considerable increase of v (as the rubber will not have time to come into close contact with the support), in agreement with the experimental data mentioned above [10, 11].

From this standpoint, and also with the deformation of rubber during friction taken into consideration, it is possible to explain other experimental facts not accounted for by the flow mechanism: it is possible to correlate the existence of static friction in rubber with the existence of an equilibrium modulus (in addition to adhesion forces), and the appearance of a minimum on the F(T) curve for the static friction of rubber with competition between increasing deformation and decreasing rigidity with increase of temperature.

The influence of temperature on the force of kinetic friction increases with decreasing E, according to the equation:* $F = E/\alpha$, which follows from the Schallamach equation when $\underline{v}$ = constant. Therefore for rubber, when E is not large, the temperature has a strong influence on friction, in contrast to its weak influence on the firction of solids. A similar conclusion follows from a comparison of the effects of temperature on the deformability of rubber and of solids.

Thus, on the basis of all the known facts, it is inadmissible to ignore the differences in principle between rubber friction and viscous flow. The existence of such facts, and of points of resemblance between the friction of rubber and of solids (and also of the characteristic role played by the deformation of rubber in friction) does not justify the assumption that the phenomena are identical, but poses the task of further comparisons and investigation of their mechanisms on the basis of carefully planned experiments.

Certain Errors in the Discussion Articles [1,3].

a) Bartenev [3] quotes Z. E. Styran's data on the F – v relationship for one sample of rubber and writes: "The graph shows that the frictional force tends to zero with unlimited decrease of the velocity" (p 626). However, this is incorrect, as can be easily seen if the same data are plotted in F – log $\underline{v}$ coordinates (Curve 4, Fig. 1). It is seen from the graph that the Schallamach equation is applicable to these data, which are analogous to other known data. However, it cannot be concluded from Fig. 1,a that $F \rightarrow 0$ when $v \rightarrow 0$ (i.e., when $\log v \rightarrow -\infty$). This is so because, if extrapolation to $F = 0$ is admissible, we have $v \neq 0$, while if it is inadmissible there are no grounds for Bartenev's assertion.

Bartenev [3] accuses me of not noting the fact that the Deryagin formula was first extended by I. V. Kragelsky (p. 628). This is untrue, as our papers [4,19] make appropriate reference to the work of Kragelsky [20].

b) Bartenev writes [3]: "Ratner [2] formulates assertions which are ascribed to me; . . . they are not taken from my papers but are formulated by Ratner" (p. 629). This refers to the following points made by Bartenev in [1,18]: the influence of velocity on the frictional force is always different in principle for rubber and for solids (p. 249); the static friction of rubber is zero (p. 1163); the frictional force is strictly proportional to the actual contact area (p. 250); roughness of the support influences the friction of rubber only by increasing the contact area (p. 250). Lack of space makes it impossible to give quotations which show that these formulations of ours, which Bartenev now [3] admits to be erroneous, reflected his views correctly [1,18,21].

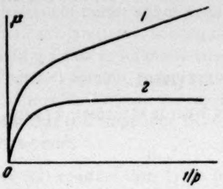

Fig. 2. Frictional coefficient of rubber as a function of the reciprocal load, after Bartenev [21].

We shall consider one example only, Bartenev [3] writes that in examining the paper [1], Ratner [2] made "numerous errors in so doing. It is asserted, for example, that in my paper the law of friction is considered when $p \rightarrow \infty$." (p. 628). However, my assertion is shown to be correct by Fig. 2, which reproduces Fig. 2 from [21], in which Bartenev gives $\mu - 1/p$ curves starting with $1/p = 0$ (zero, and not some other boundary of the load range under consideration, is specifically shown on the abscissa axis), i.e., from $p = \infty$. This, as he now admits himself [3] "is incorrect, as the law of friction was derived as a linear approximation in a limited load range" (p. 628).

It is seen from this discussion that many important questions relating to the friction of rubber are as yet unsolved; their solution requires further collection and generalization of facts.

---

* This equation describes data [16] on static friction over a narrow temperature range, since it passes through a minimum. However, Bartenev [3] takes only some values from our data, ignoring the minimum and the subsequent increase of F; he erroneously asserts that I wrote [16] the equation $F = A \exp(U/RT)$, whereas I used not the total frictional force F but only one term F_0.

LITERATURE CITED

[1] G. M. Bartenev, Colloid J., 18, 249 (1956).*

[2] S. B. Ratner, Colloid J., 370 (1956).*

[3] G. M. Bartenev, Colloid J., 18, 626 (1956).*

[4] B. V. Deryagin and S. B. Ratner, Proc. Acad. Sci. USSR, 103, No. 6, 1021 (1955).

[5] B. V. Deryagin, S. B. Ratner, and M. F. Futran, Proc. Acad. Sci. USSR, 92, No. 6, 1137 (1953).

[6] A. Schallamach, Proc. Phys. Soc. B65, 657, (1952).

[7] C. Many, Am. J. Phys. 20, 203, (1952).

[8] Roth, Driscoll, Holt, Rubb. Chem. Techn. 16, 155, (1953).

[9] A. Schallamach, Proc. Phys. Soc. B66, 386 (1953).

[10] J. Hurry and J. Prock, Ind. Rubb. J. 128, No. 5, 619 (1953).

[11] A. Schallamach, Koll.-Z. 141, No. 3 (1955).

[12] J. Burwell, and E. Rabinowicz, J. Appl. Phys. 24, No. 2, 136 (1953).

[13] P. Konti, Sulla resistenza di Attrito Royal Acad. de Lincei, II, (1875).

[14] I. V. Kragelsky and V. S. Shchedrov, Development of the Science of Friction (Izd. AN SSSR, 1956).

[15] S. B. Ratner and V. V. Lavrentyev, Proc. Acad. Sci. USSR, 108, No. 3 (1956).

[16] S. B. Ratner, Proc. Acad. Sci. USSR, 93, No. 1, 47 (1953).

[17] A. Tobolsky, R. Powell, and H. Eyring in Chemistry of Large Molecules, vol. 2 (IL, Moscow, 1948) p. 206.

[18] G. M. Bartenev, Proc. Acad. Sci. USSR, 96, 1161 (1954).

[19] S. B. Ratner and V. V. Lavrentyev, J. Tech. Phys., No. 4, 147 (1956).

[20] I. V. Kragelsky, Trans. II All-Union Conf. on Friction and Wear in Machines, 3 (1949).

[21] G. N; Bartenev, Proc. Acad. Sci. USSR, 103, No. 6 (1955).

Received October 18, 1956

---

* [Original Russian pagination. See C. B. Translation.]

CONCERNING THE DISCUSSION ON THE FRICTION OF RUBBER

G. M. Bartenev

The article [1] which opened the discussion raised the following problems: 1) the nature of friction, and 2) the law of the friction of rubber, since there is no agreed opinion in the literature concerning the nature of the effect, and some very varied and contradictory laws of friction are put forward.

In Ratner's second article, published in this issue, the molecular mechanisms of the friction of rubber and of the flow of liquids are confused as before. The similarity between friction and viscous flow, pointed out in our paper [2], lies in a common molecular-kinetic activation mechanism for the transition of the kinetic units through the barrier, which is also found for other processes, such as ionic conductance, diffusion, etc. Differences between these processes follow from differences in the structure and in the nature of the thermal motion of rubber and liquids. Therefore the actual mechanisms and the molecular models of these processes are different.

In Fig. 1 in Ratner's paper he compares two graphs for two essentially different friction regions (low velocities for rubber and high velocities for metals), which is inadmissible, since the distinction between the external friction of rubber and of metals, which we emphasized, is found only in the region of low sliding velocities, where no vibration or heating of the surface occur. Ratner states that the author of the paper erroneously extrapolated the data to infinitely large loads. A graph is given (Fig. 2), taken from the paper [3], in which the curve, in Ratner's opinion, is drawn from $1/p = 0$, i.e., from $p = \infty$. It was however, stated in our paper [3] that the relationship between the coefficient of friction and normal pressure was derived for $1/p > 10^{-4}$ cm^2/kg. It is evident that it is impossible to show this on a graph drawn to an ordinary scale for normal pressures from 0.1 to 100 kg/cm^2.

We still consider that: 1) the friction of rubber is a molecular-kinetic activation process, determined by its structure; 2) the static friction of rubber is therefore an arbitrary magnitude which depends on the accuracy of the determinations and the experimental conditions; 3) the analytical form of the law of rubber friction is basically determined by the dependence of the actual contact area on the load; 4) the Deryagin binomial equation cannot be applied to the friction of rubber; 5) the Ratner equation does not represent the dependence of the coefficient of friction on the load.

LITERATURE CITED

[1] G. M. Bartenev, Colloid J., 18, No. 2, 249 (1956); 18, No. 5, 626 (1956).*

[2] G. M. Bartenev, Proc. Acad. Sci. USSR, 96, No. 6, 1161 (1954).

[3] G. M. Bartenev, Proc. Acad. Sci. USSR, 103, No. 6, 1017 (1955).

[4] S. B. Ratner, Proc. Acad. Sci. USSR, 83, 443 (1952); 86, 121 (1952); Colloid J., 18, 272 (1956);* 19, 394 (1957).*

Received April 1, 1957

---

* [Original Russian pagination. See C. B. Translation.]

APPLICABILITY OF THE BINOMIAL LAW OF FRICTION TO THE FRICTION OF RUBBER

B. V. Deryagin

One point made by G. M. Bartenev, which he regards as proved, is that the binomial law of friction is not applicable to the friction of rubber. It is first necessary to stress the danger of confusing two essentially different laws under the name of a binomial law of friction:

1. The law for total friction

$$F = F(N), \tag{1}$$

which relates the frictional force F to the load N; an example of this is provided by Coulomb's empirical law of friction

$$F = AN + B,$$

where A and B are constants.

2. The elementary (elemental, in I. V. Kragelsky's terminology) law of friction, which connects the frictional and adhesion forces per unit area of true contact

$$\frac{F}{S} = \Psi\left(\frac{N}{S}\right). \tag{2}$$

The relationship which usually exists between S and N, and which may depend on the form of the bodies, must be known before it is possible to determine the form of Equation (2) when the form of Equation (1) is known from experimental data.

By suitable choice of the form of the relationship S = S(N) it is possible to obtain most varied forms of Equation (2); for example, as described in [1], a mononomial law of friction F/S = const. It is evident that if the S = S(N) function is chosen differently it is possible to obtain a binomial law $F/S = \mu\,(N/S + p_0)$ or any other elementary law of friction. Conversely, it follows that it is by no means proved by G. M. Bartenev [1] that the binomial elementary law of friction is inapplicable.

As regards positive proofs of the applicability of the binomial elementary law of friction to rubber, this question is discussed by me, with reference to new experimental data, in articles now in the press.

LITERATURE CITED

[1] G. M. Bartenev, Proc. Acad. Sci. USSR, 103, No. 6, (1955).

Received May 15, 1957

Editorial note: In publishing the papers by S. B. Ratner, G. M. Bartenev, and B. V. Deryagin, the editor closes the discussion on the friction of rubber.

LETTER TO THE EDITOR

USE OF ION EXCHANGE RESINS FOR PURIFYING QUARTZ SUSPENSIONS

K. V. Chmutov and O. G. Larionov

Fine quartz suspensions made by vibratory grinding are often contaminated by metallic particles corresponding in chemical composition to the structural parts of the vibratory mill and containing iron, chromium, manganese, etc. Such suspensions must be made free from these contaminations in preparation for laboratory use. Treatment of the ground material with acids followed by washing and decantation takes a great deal of time, as the suspension settles very slowly. Washing on filters is also ineffective, as the quartz particles pass through the filter paper in large amounts.

This last fact, the poor retention by filters, was utilized by us for purification of quartz suspensions. After the metal particles have been dissolved in acid, the suspension together with the dissolved impurities is filtered through a column containing a granular cation exchange resin in the H form. The suspension passes through the column almost completely, while the salt cations remain in the resin layer.

The purification technique was as follows. A quartz suspension containing 100 g of dry material, with a solid–liquid ratio of 1 : 4, was placed in a conical flask containing a mixture of hydrochloric (50 ml) and nitric (10 ml) acids. Part of the acid was removed by 2 hours of boiling. The suspension was diluted to two liters with water and passed through a column containing KU-2 cation exchange resin in the H form. The height of the layer was 20 cm, the diameter of the column was 4 cm, and the resin grain size was 1 mm. After the layer was exhausted (reaction for iron) it was regenerated by 4 N HCl solution and washed with water to a neutral reaction to methyl orange; a new portion of solution was then passed through, etc.

If a coarse suspension is used, the upper layer of the adsorbent may become clogged with settling particles. To avoid this, the solution above the top layer can be agitated by a current of air. The use of the "fluidized layer" principle with the suspension fed in at the bottom of the column is rational, but more complicated technically, and cannot be recommended for purification of small amounts of suspension.

A static method can also be used, the suspension being shaken with a certain amount of cation exchange resin and filtered through a gauze filter on a Buchner funnel. This operation must be repeated several times with fresh portions of resin.

If a dry powder is required, excess hydrochloric acid is removed by evaporation and drying. If the suspension is to be used, it is simpler to remove the acid by similar filtration of the suspension through a column containing an anion exchange resin in the OH form.

Institute of Physical Chemistry
Academy of Sciences USSR
Chromatography Laboratory
Moscow

Received March 3, 1957

SIGNIFICANCE OF ABBREVIATIONS MOST FREQUENTLY ENCOUNTERED IN SOVIET PERIODICALS

FIAN	Phys. Inst. Acad. Sci. USSR.
GDI	Water Power Inst.
GITI	State Sci.-Tech. Press
GITTL	State. Tech. and Theor. Lit. Press
GONTI	State United Sci.-Tech. Press
Gosenergoizdat	State Power Press
Goskhimizdat	State Chem. Press
GOST	All-Union State Standard
GTTI	State Tech. and Theor. Lit. Press
IL	Foreign Lit. Press
ISN (Izd. Sov. Nauk)	Soviet Science Press
Izd. AN SSSR	Acad. Sci. USSR Press
Izd. MGU	Moscow State Univ. Press
LEIIZhT	Leningrad Power Inst. of Railroad Engineering
LET	Leningrad Elec. Engr. School
LETI	Leningrad Electrotechnical Inst.
LETIIZhT	Leningrad Electrical Engineering Research Inst. of Railroad Engr.
Mashgiz	State Sci.-Tech. Press for Machine Construction Lit.
MEP	Ministry of Electrical Industry
MES	Ministry of Electrical Power Plants
MESEP	Ministry of Electrical Power Plants and the Electrical Industry
MGU	Moscow State Univ.
MKhTI	Moscow Inst. Chem. Tech.
MOPI	Moscow Regional Pedagogical Inst.
MSP	Ministry of Industrial Construction
NII ZVUKSZAPIOI	Scientific Research Inst. of Sound Recording
NIKFI	Sci. Inst. of Modern Motion Picture Photography
ONTI	United Sci.-Tech. Press
OTI	Division of Technical Information
OTN	Div. Tech. Sci.
Stroiizdat	Construction Press
TOE	Association of Power Engineers
TsKTI	Central Research Inst. for Boilers and Turbines
TsNIEL	Central Scientific Research Elec. Engr. Lab.
TsNIEL-MES	Central Scientific Research Elec. Engr. Lab.—Ministry of Electric Power Plants
TsVTI	Central Office of Economic Information
UF	Ural Branch
VIESKh	All-Union Inst. of Rural Elec. Power Stations
VNIIM	All-Union Scientific Research Inst. of Meteorology
VNIIZhDT	All-Union Scientific Research Inst. of Railroad Engineering
VTI	All-Union Thermotech. Inst.
VZEI	All-Union Power Correspondence Inst.

Note: Abbreviations not on this list and not explained in the translation have been transliterated, no further information about their significance being available to us. — Publisher.

CHANGES IN THE STRUCTURE, DEGREE OF DISPERSION, AND YIELD VALUE OF PEATS AS THE RESULT OF COMPLETE FREEZING

M.P. Volarovich, K.F. Gusev, S.N. Markov and V.P. Tropin

The physicomechanical and physicochemical properties of moist peat are changed considerably by complete freezing. It is known [1, 2] that frozen peat after thawing gives up water much more easily, but has lower strength and higher moisture absorption in the air-dry state. This is caused by coagulation of the peat during freezing and subsequent thawing. It was of interest to study this effect by a combination of x-ray, dispersion and rheological analysis methods. The x-ray structure analysis was carried out by a procedure described previously [3]. The photographs were taken with the aid of a tube with a copper anticathode in a special x-ray camera of high resolving power [4] over a period of 8 hours, the β-lines not being filtered off. The x-ray diagrams were used to give microphotometric curves with the aid of a "Magnephot" microphotometer obtained from Hungary [5], adapted for this purpose.

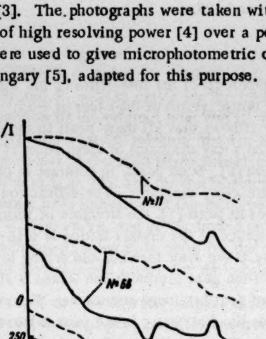

Fig. 1. Microphotometric curves based on x-ray diagrams of upper No. 66 peat and bottom peats Nos. 3 and 11. Continuous lines represent the original peats; the broken lines, after freezing.

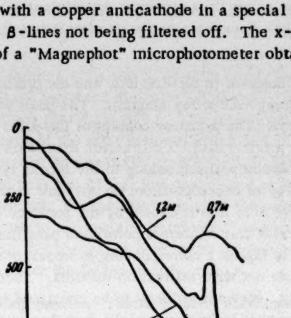

Fig. 2. Microphotometric curves from x-ray diagrams of peats taken from depths of 0.2; 0.4; 0.7 and 1.2 meters.

Figure 1 shows microphotometric curves taken from x-ray diagrams of upper pine – cotton grass peat No. 66 with degree of decomposition R = 65%, and wood – reed No. 3 (R = 50%) and reed No. 11 (R = 35%) lower peats, both in the original states and after freezing. The abscissa axis shows the distances from the center of

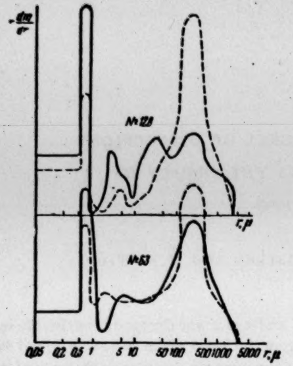

Fig. 3. Particle size distribution curves for peats: bottom No. 63 and upper No. 128. Continuous lines represent the original peats; broken lines represent peats after freezing.

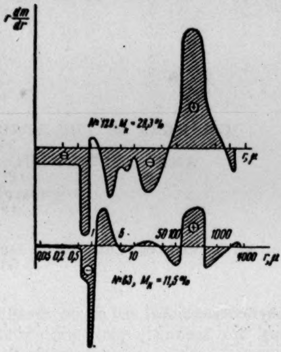

Fig. 4. Curves for dispersability ranges affected by coagulation on freezing, for peats Nos. 63 and 128.

the x-ray diagram in millimeters, and the ordinates represent the reciprocals of the intensities of the light beam passing through the x-ray diagram. The peats were subjected to low temperatures of the order of −15, −25° for several days. The moisture content of the peats was 86-88%. Figure 1 shows that all these peats in the original state give a fairly distinct diffraction maximum at $l = 30.5$ mm. The x-ray diagrams of these peats of a high degree of decomposition belong to the second type in our classification [6]. Such peats, in contrast to peats of a low degree of decomposition, do not show a cellulose structure in the x-ray diagrams. The diffraction maximum at $l = 30.5$ mm is caused by the presence of bitumens and waxes in peats [7], the structure of which is identical with that of normal petroleum paraffins. The interplane distance of the crystal lattice is 4.15-4.25 A. The lines in Figure 1 corresponding to frozen peats (the diagrams were taken after thawing and drying to an air-dry state) do not show diffraction maxima. Therefore, the structure of the peat bitumens and waxes is affected by freezing. Water is unlikely to be contained in the crystal lattice of peat bitumens and waxes. The structural change is probably the result of the fact that at these low temperatures the free water in the peat is frozen, and also the partially bound water, namely part of the physicochemically and physically bound water, in the Dumansky-Rebinder theory. As a result of the freezing large internal stresses arise in the peat, which deform the soft crystals of the peat bitumens and waxes, thus disturbing their crystal lattices.

The above results of laboratory experiments are confirmed by observations relating to peat frozen under natural conditions. Figure 2 shows microphotometric curves based on x-ray diagrams for samples of bottom sedge peat No. 63 (R = 55%) taken from various depths. It is seen that the sharp diffraction maximum at $l = 30.5$ mm is found only for the peat sample taken from a depth of 1.2 meters. The peat sample taken from a depth of 0.7 m has a diffuse maximum at $l = 30.5$ mm, which is almost imperceptible on the curve for the sample taken from 0.4 m. This maximum does not appear on the curve for peat taken from the surface layer (0.2 m). The explanation is that peat deposits usually freeze through down to a depth of 0.5-0.7 m in winter.

Dispersion analysis of the frozen peats was carried out by the method developed previously [8], fractions with equivalent radius greater than 125μ being subjected to wet sieve analysis, while fractions between 125 and 0.5μ were studied by means of the weight sedimentometer [9]. Figure 3 shows particle size distribution curves for bottom alder peat No. 63 (R = 55%) and for upper pinewood-cottongrass peat No. 128 (R = 50%). Electron micrographs were not taken, and therefore the highly disperse fraction ($r < 0.5\mu$) is shown in Figure 3 in the form of a rectangle. The peats were frozen for about three weeks, the minimum temperature reaching −30°.

It is clear from Figure 3 that when peats are frozen through and subsequently thawed out there are changes in their degree of dispersion, caused by coagulation, the effect being most pronounced for peat No. 128. In particular, this peat underwent an abrupt transition from an initial plastic state into a loose coarsely granular system on freezing. An especially clear picture is obtained if coagulation dispersability range curves [8] are plotted, as shown in Figure 4, where the differences between the ordinates of the size distribution curves for each peat in the original and frozen states are shown. Here the finer fractions, which disappeared in course of coagulation, lie below the abscissa axis and are indicated by a minus sign, while the coarser fractions which appeared lie above the abscissa axis and are denoted by a plus sign. It was found that coagulation on freezing affected 11.5% of peat No. 63 and 28.3% of peat No. 128.

It is seen from Figures 3 and 4 that in peat No. 63 only the fraction with radius 0.5-1.5μ coagulated on freezing, while in peat No. 128 the coagulation process covered a wider range of fractions from hundredths of a micron to 60μ. Additional amounts of a coarse fraction, mainly between 100 and 500μ, appeared in both peats as the result of coagulation.

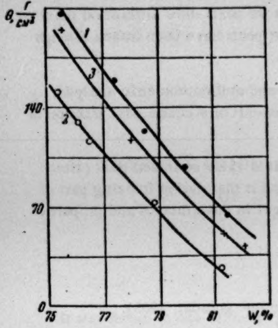

Fig. 5. Variation of yield value with moisture content of peat: 1) not frozen; 2) after thawing; 3) the same, but after two years of storage at positive temperatures.

A comparison of the principal dispersion characteristics of the original and coagulated peats also reveals considerable changes in the degree of dispersion resulting from freezing. For upper peat No. 128, the specific surface (S), calculated by S.G. Solopov's method, of fractions with particle radius $r < 2\mu$ was $S_0 = 4520$ cm²/g for the original peat and $S_n = 3185$ cm²/g for the frozen peat, and the average weighted diameter (d) of the coarsely disperse fraction of the original peat was $d_0 = 495\mu$, and of the frozen peat $d_n = 600\mu$. The inhomogeneity coefficient (f), often used in relation to soils, which represents the ratio of the radii between which 50% of the mass of the particles of the solid phase is included ($f = r_{10}/r_{60}$), underwent an especially pronounced change; for the original peat $f_0 = 275$, and for the frozen peat $f_n = 10$. Bottom peat No. 63 was less coagulated as the result of freezing, as is indicated by the principal dispersion characteristics: the specific surface of the original peat was $S_0 = 3700$ cm²/g, and of the frozen peat $S_n = 3060$ cm²/g, while the average weighted diameter was almost unchanged, being $d_0 = 500\mu$ for the original and $d_n = 520\mu$ for the frozen peat. The inhomogeneity coefficient also changed little; for the original peat $f_0 = 58.8$, and for the frozen peat $f_n = 30.6$.

Part of the bound water in peat becomes free in the freezing process. Therefore after thawing the rheological properties of peat are different from those of the original peat. We determined the limiting shearing stress (yield value) of previously frozen peat by means of a cone plastometer [10] by Rebinder's method [11]. The constant for the cone (with a riffled surface) with an angle of 45° was taken as 0.416, in accordance with the theory developed by Agranat, Volarovich and Shirokov [12].

Figure 5 shows curves for the yield value θ as a function of the moisture content of wood-sedge peat No. 4 of degree of decomposition R = 45%, in the original state (Curve 1) and after freezing (Curve 2). The peat, taken out of the deposits, was subjected to low temperatures during winter. Its yield value was determined after thawing. It is seen that θ for peat decreases considerably (by 30-50%) after freezing. The explanation is that when peat is frozen at low enough temperatures some of the bound water freezes, while after thawing this water becomes free.

However, if peat is kept at positive temperatures for a prolonged time after thawing, its original rheological properties are to some extent restored. Curve 3 in Figure 5, which corresponds to peat kept for two years at positive temperatures after freezing, lies considerably nearer than Curve 2 to Curve 1 for peat which had not been frozen. It seems that after thawing part of the free water again becomes bound by the solid phase of the peat at positive temperatures, and the relative content of free water decreases. The yield value of the peat again increases as a result.

SUMMARY

1. The x-ray diagrams and the corresponding microphotometric curves for peats show diffraction maxima corresponding to peat bitumens and waxes; these maxima disappear after the peats have been frozen through at temperatures of -15 to $-25°$.

2. The particle size distribution curves for peats, determined by sieve and sedimentometric analysis, show that freezing causes coagulation in peat and considerable additional amounts of a coarse peat fraction of particle size 100-500μ are formed.

3. Experiments with the aid of the cone plastometer showed that the yield value of frozen peat (after thawing) is considerably lower than that of the original peat. The explanation is that during freezing part of the bound water in the peat becomes free, and this causes considerable changes in the structure and properties of the peat.

LITERATURE CITED

[1] V.G. Goryachkin, Fundamentals of Peat Production Technology (Gosenergoizdat, 1953).

[2] M.A. Veller et al., Technology of Hydropeat (Gosenergoizdat, 1956).

[3] M.P. Volarovich and K.F. Gusev, Trans. Moscow Peat Inst. No. 2, 97 (1954).

[4] K.F. Gusev, Factory Labs. No. 4, 477 (1953).

[5] M.P. Volarovich and K.F. Gusev, Trans. Moscow Peat Inst. No. 6, 38 (1957).

[6] M.P. Volarovich and K.F. Gusev, Trans. Moscow Peat Inst. No. 5, 31 (1957).

[7] M.P. Volarovich and K.F. Gusev, Colloid J. 18, 643 (1956) (T.p. 639).*

[8] M.P. Volarovich and N.V. Churaev, Colloid J. 17, 200 (1955) (T.p. 185)*; Trans. Moscow Peat Inst. No. 3, 33 (1955); Trans. 3rd All-Union Colloid Conference, Minsk 1953 (1956), p. 258.

[9] N.V. Churaev, Colloid J. 16, 220 (1954) (T.p. 221).*

[10] M.P. Volarovich and S.N. Markov, J. Peat Ind. No. 10, 23 (1951); Factory Labs. 17, No. 12, 1461 (1951).

[11] P.A. Rebinder and B.Ya. Yampolsky, Colloid J. 10, 466 (1948); P.A. Rebinder and N.N. Semenenko, Proc. Acad. Sci. USSR, 64, No. 6, 835 (1949).

[12] N.N. Agranat and M.P. Volarovich, Colloid J. 19, 3 (1957) (T.p. 1)*; N.N. Agranat and M.F. Shirokov, Colloid J. 19, 9 (1957)(T.p. 9).*

Received April 11, 1957

Moscow Peat Institute

---

*T.p. = C.B. Translation pagination.

INVESTIGATION OF ELECTROOSMOSIS IN CAPILLARY SYSTEMS OF DIFFERENT CHARGE AND STRUCTURE

O.N. Grigorov and K.P. Tikhomolova

It was shown in one of our papers [1] that a definite ratio of capillary length to cross section is required for electroosmotic flow to occur in systems of regular geometrical structure composed of capillaries of circular or square cross section. This ratio was not constant for capillaries of different cross section, but varied with the latter and with the potential gradient of the applied electric field. Increase of the capillary cross section resulted in an increase of this ratio, while increase of the potential gradient had the opposite effect.

It was desired to test the results of that investigation on powder capillary systems of various types, more similar in structure to natural materials. It also seemed likely that variation of the effective charge density on the particle surfaces of materials differing in their chemical nature should influence the ratio of capillary length to cross section at which electroosmotic flow can occur.

EXPERIMENTAL

The materials chosen for study were powders consisting of spherical polystyrene particles prepared by emulsion polymerization of styrene, and also quartz powders and powdered melts of polystyrene with MMG-1 anion exchange resin. The polymerization of styrene was carried out in presence of polyvinyl alcohol or polymethacrylic acid as emulsifier and benzoyl peroxide as catalyst, at 80-90°. To vary the charge on the polystyrene particles, a certain amount of dye was added to the styrene during polymerization until a saturated solution was formed. In this way, a series of specimens of polystyrene powders was obtained, with different ζ-potentials in KCl solution. Quartz powder, made by grinding quartz crystals in a steel ball mill, was treated with 10% H_2SO_4 solution with warming, and washed with distilled water to a negative reaction for SO_4 ions. Positively charged powders were made by taking finely powdered MMG-1 anion exchange resin which was melted together with polystyrene and ground in a mortar. The quartz and polystyrene powders were then fractionated by means of Tyler standard sieves. Powders with particle size $< 44\mu$ were fractionated by elutriation in an ascending current of water with cone apparatus. For dispersion analysis of the fractions, micrographs of individual samples of

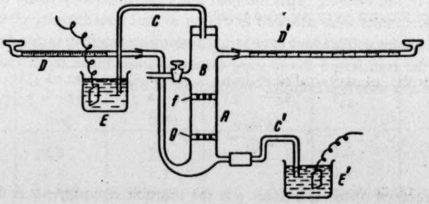

Fig. 1. Diagram of apparatus for measurement of electroosmotic transfer.

TABLE 1

ζ-Potentials of the Materials Used in the Experiments

Details of sample	Specific conductance of KCl solution $\times 10^4$ ohm^{-1} cm^{-1}	ζ in mv	Details of sample	Specific conductance of KCl solution $\times 10^4$ ohm^{-1} cm^{-1}	ζ in mv
Polystyrene (polymethacrylic acid emulsifier)	9.3	−15	Polystyrene with added Sudan III (saturated solution)	9.3	−33
Polystyrene (polyvinyl alcohol emulsifier)	9.3	−10	Quartz powder	3.5	−29
Polystyrene with addition of fat-soluble Brown K (saturated solution)	9.3	− 6	Quartz powder	9.4	−15
			Melt of polystyrene with MMG-1 resin	9.4	+21

the powders were taken and the average particle sizes were determined from these.

Data on the ζ-potentials of the samples used for the experiments in KCl solution are given in Table 1.

Electroosmotic transfer was measured by means of the apparatus shown schematically in Figure 1.

The apparatus essentially consisted of a tube A 1.1 cm in diameter, placed vertically for easier removal of air bubbles, which distort the results, from the powder diaphragm. The powder was pressed between two perforated "Plexiglas" plates f and g. The tube A was joined by two agar bridges C and C' to the beakers E and E', which contained copper electrodes in $CuSO_4$ solution. The volume of the transported liquid was read off by means of the two graduated capillaries D and D'. Current at potentials up to 410 v was supplied from a kenotron, its direction being varied by a commutator.

The apparatus was filled as follows. A suspension of the powder in KCl solution, of known concentration, was introduced into the main tube A of the apparatus onto the lower perforated plate and left to settle there until a column of the required length was formed. The powder diaphragm so formed was compressed between the two plates and the whole apparatus was filled with KCl solution of the same concentration. The constancy of the electrical conductance of the KCl solution in the apparatus was additionally checked after each experiment. To establish equilibrium between the disperse system and the solution, the powder to be studied was first kept in the given solution for not less than three days; this was shown to be necessary by special experiments. After the apparatus had been filled a certain time interval was also necessary before the start of the determinations, for equilibrium to be established in the system. This interval was experimentally found to be 10 to 12 hours. Intervals of 1 hour between experiments were allowed to elapse so that equilibrium, characteristic of the given system in the steady state, could be established between the electroosmotic transfer determinations. Definite and reproducible volumes of the transferred liquid were obtained under these conditions. The electrokinetic potential was calculated from the usual Helmholtz-Smoluchowski equation

$$\zeta = \frac{4\pi\varkappa\eta V}{DI} 9\cdot 10^4, \quad (1)$$

where κ is the specific conductance of the solution; η is the solution viscosity; V is the volume of liquid transferred in cubic centimeters per second; D is the dielectric constant; I is the current strength in amperes, and $9\cdot 10^4$ is the conversion factor to give the ζ-potential in volts.

To find the minimum ratio of the length of the powder column (in other words, the thickness of the diaphragm) to the cross section, at which a definite constant value for the electroosmotic transfer of the liquid becomes established, which we term the "critical ratio," a series of parallel experiments with different lengths of column was carried out.* The results of experiments with powders consisting of spherical particles are shown

---

*In these experiments in a number of cases it was clearly seen that the liquid did not move in the graduated capillary when the length of the powder column was insufficient. With increasing column length a certain region was found in which the liquid was seen to move but the results were inconsistent, and this was followed by a region of constant values corresponding to steady electroosmotic flow. Values corresponding to the critical length (l_{cr}) were determined to an accuracy of 1-2 mm.

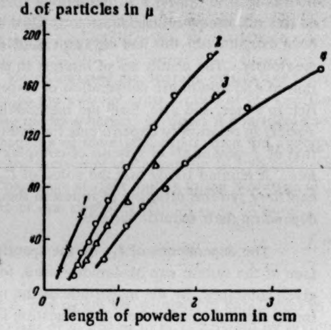

Fig. 2. Variation of the critical length of the powder diaphragm column with dimensions and charge of the spherical particles: 1) $\zeta = -30$ mv; 2) $\zeta = -15$ mv; 3) $\zeta = -10$ mv; 4) $\zeta = -6$ mv.

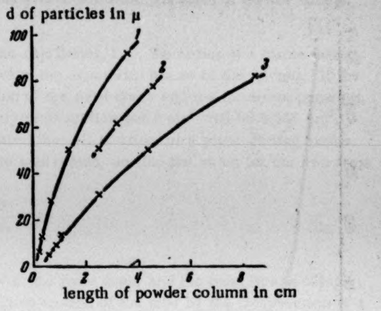

Fig. 3. Variation of the critical length of the powder diaphragm column with dimensions and charge of particles of irregular shape: 1) $\zeta = -29$ mv; 2) $\zeta = +21$ mv; 3) $\zeta = -15$ mv.

in Figure 2.

Examination of the curves in Figure 2 shows that, as was to be expected, the critical length of the powder column depends on the degree of dispersion, and increases with increasing particle size, which is equivalent to increase of capillary radius. Further, the critical column length depends on the surface charge, decreasing with increase of the latter. The differences between critical lengths for systems with different ζ-potentials are fairly large for a given degree of dispersion. For example, for particles 150μ in diameter, the critical length of a column of polystyrene powder with added fat Brown K ($\zeta = -6$ mv) is 3 cm, for polystyrene with ζ-potential −10 mv, $l_{cr} = 2.3$ cm, and for polystyrene with ζ-potential −15 mv, $l_{cr} = 1.9$ cm. A comparison of any two systems shows that, with variation of the particle size in a given system, the ratio of the critical lengths remains approximately constant for the same degree of dispersion. Table 2 gives comparative values of the critical length (l_{cr}) ratios for different diameters of the spherical particles in powders with different electrokinetic potentials.

TABLE 2

Critical Length Ratios for Systems of Spherical Particles with Different Charges

Particle diameter, in μ	l'_{cr} in cm ($\zeta = -6$ mv)	l''_{cr} in cm ($\zeta = -10$ mv)	l'''_{cr} in cm ($\zeta = -15$ mv)	l''''_{cr} in cm ($\zeta = -33$ mv)	$\frac{l'_{cr}}{l''_{cr}}$	$\frac{l'_{cr}}{l'''_{cr}}$	$\frac{l'_{cr}}{l''''_{cr}}$
150	3.0	2.3	1.3	–	1.3	1.6	–
100	1.8	1.5	1.1	–	1.2	1.6	–
50	0.9	0.75	0.6	0.5	1.2	1.5	1.8
20	0.65	0.55	0.45	0.3	1.2	1.4	2.2

Results of experiments with powders with particles of irregular shape are shown in Figure 3.

The results in Figure 3 show that the length of the powder column necessary for steady laminar flow of liquid to be established also increases in these experiments with increasing particle size in a given system, and decreases with increasing ζ-potential for the same degree of dispersion of the powders.

Thus, the results of our experiments for powder capillary systems fully confirm earlier data [1] for glass and polystyrene capillaries of regular geometrical form. Further, the influence of the effective charge density on the occurrence of electroosmotic flow has been established; this had not been studied previously. The results are of interest in relation to electroosmotic dehydration of dispersoids rich in water, and also, from the methodological aspect, in relation to experiments for determination of ζ-potentials of systems of complex structure. It seemed likely that the value of l_{cr} for capillary systems differing in structure should depend on their specific surface.

The dependence of l_{cr} on the specific surface of the system can be demonstrated, for any given substance, by the magnitude of the maximum electroosmotic rise. This question is of independent interest. Very few experiments have been carried out on determination of the maximum electroosmotic rise, and these were performed either in single capillaries in very narrow limits (Quincke [2]) or in heteroporous systems with pores of indeterminate structure, as in Manegold and Solf's experiments [3] with collodion membranes.

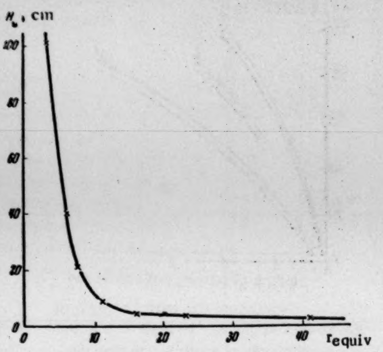

Fig. 4. Variation of the maximum electroosmotic rise with the equivalent capillary radius in a powder diaphragm consisting of spherical particles.

Theoretically, the maximum rise (H_M) is defined by the expression:

$$H_M = \frac{2\zeta ED}{\pi r^2}, \tag{2}$$

where E is the potential gradient at the membrane; D is the dielectric constant; ζ is the electrokinetic potential, and r is the capillary radius. The maximum rise is therefore inversely proportional to the square of the radius.

TABLE 3

Maximum Electroosmotic Rise in Powders of Spherical Polystyrene Particles

Average particle diameter (d) in μ	Equivalent pore radius (r_{equiv}) in μ	Maximum electroosmotic rise (H_M) in cm	$\frac{(H_M)_1}{(H_M)_i}$	$\left[\frac{(r_{equiv})_i}{(r_{equiv})_1}\right]^2$	Current strength in ma
10.15	2.8	105	1.0	1.0	2.9
16.5	4.4	41	2.6	2.5	2.9
26.9	7.4	12	8.7	7.0	2.8
41.5	11.5	3.5	28.5	17.0	2.9
62.6	17.4	2.1	50.0	38.0	2.8
86.5	23.9	1.4	78.0	73.0	2.7
108.5	29.3	1.0	105	109	2.7
152.5	42.0	0.5	210	224	3.0

In Quincke's experiments the maximum rise was found to be inversely proportional to the first power of the radius. In Manegold and Solf's experiments the results for some membranes were close to those required by the above formula, but in many cases there were considerable deviations, probably because of the uncertainty of the structure of the materials used. Their results cannot therefore be regarded as providing complete confirmation of the theory. Experiments for verification of this equation must be carried out for systems of constant structure with variations of capillary radius. Systems of spherical particles, in which the structure depends only on the nature of the packing and is not related to the particle size, are quite suitable for this purpose. Many structural parameters of a system of monodisperse spherical particles can be calculated by analogy with the "fictitious soil," a concept used in hydraulics and soil science in analysis of filtration processes of liquids through porous bodies [4, 5].

We calculated the average equivalent radius r_{equiv} of the capillaries, i.e., the radius of a circle equal in area to the average cross section of the capillary space between the equatorial planes of the spheres. If the packing of the spherical particles is considered as a combination of the most dense and the most free packings, i.e., packing of the eighth order, then the average free capillary cross section per 1 cm^2 will be 0.395 cm^2. The cross section of our apparatus is 0.95 cm^2. On the assumption that all positions of a plane cutting across these packings at right angles to the direction of liquid flow are equivalent, we find the value for the free cross section of one capillary (f)

$$f = \frac{0{,}95 \cdot 0{,}395}{(n_1 + n_2) \cdot {}^1/_2},$$

where n_1 and n_2 are the numbers of capillaries in the section with the most dense and the most free packings. The values of n_1 and n_2 were calculated by dividing the total cross section of the tube by the cross section of a unit gap in the given type of packing. The maximum electroosmotic rise was determined by the Manegold and Solf method [3].

The experiments to determine the maximum electroosmotic rise were performed on a powder of spherical polystyrene particles with ζ-potential of -10 mv. The experimental results are given in Table 3.

It follows from Equation (2) for the electroosmotic rise that the ratio $(H_M)_1/(H_M)_i$, i.e., the ratio of the maximum electroosmotic rises, varies in proportion to the square of the inverse ratio of the radii. The data in Table 3 show that the ratio of the electroosmotic rises is approximately equal to the square of the inverse ratio of the radii. This variation of H_M with capillary radius should be represented by a parabola; this is illustrated in Figure 4.

Thus, the maximum electroosmotic rise depends on the capillary radius in the system, variation of which leads, in its turn, to variation of the specific surface. Differences of the critical lengths of the capillaries (in relation to their radii) for a given substance are determined by differences of the motive electroosmotic forces, which depend on the specific surface of the capillary system and which may be characterized by the electroosmotic rise. Therefore variation of the critical capillary length is ultimately determined by variation of the specific surface of the system.

SUMMARY

1. Steady electroosmotic flow of liquid becomes established in a powder diaphragm at a definite ratio of the length of the powder column to the capillary cross section. This ratio increases with increasing particle size in the powder and decreases with increasing surface charge, which is characterized by the magnitude of the electrokinetic potential.

2. The ratio of the maximum electroosmotic rises for diaphragms with particles of different sizes varies in direct proportion to the inverse ratio of the capillary radii, in agreement with the classical formula.

LITERATURE CITED

[1] O.N. Grigorov and M.G. Leibovich, Colloid J. 12, 175 (1950).

[2] G. Quincke, Pogg. Ann. 107, 1 (1859).

[3] E. Manegold and K. Solf, Koll.-Z. 55, 3, 273 (1931).

[4] V. Zigel, Filtration (GONTI, 1939).

[5] L.S. Leibenzon, Movement of Natural Liquids and Gases in Porous Media (State United Press, 1947).

Received July 6, 1956

The A.A. Zhdanov State University
Leningrad

INVESTIGATION OF ADHESION EFFECTS IN BONDING RUBBER TO METAL BY LEUKONAT ADHESIVE

A.M. Medvedeva, B.V. Deryagin and S.K. Zherebkov

Adhesives based on isocyanates for bonding rubber to metals were first developed and used in Germany during the Second World War [1]. Adhesives, based on isocyanates, for rubber-metal bonding are used in a number of countries under various trade names (HDI, Vulcabond TX, Xylen M, Desmodur R, MD-1). In the USSR, "Leukonat" isocyanate adhesive is widely used. The reasons for the wide use of isocyanate adhesives are that the bonds obtained are the most suitable for general purposes and have a number of valuable properties: heat resistance, frost resistance, resistance to solvents, oils, and water, and good stability to repeated deformation.

There have been numerous investigations [2-5] of the properties of bonds formed by isocyanate adhesives. However, there is still no definite theory concerning the causes of bond formation at the adhesive-rubber and adhesive-metal boundaries. The various viewpoints advanced in the literature are often unsupported by experimental data. For example, in Bayer's paper [1] it is suggested that isocyanates react with the hydroxide layer on the metal surface during bonding of rubber to metal. Bayer also states that isocyanates can polymerize into compounds of high molecular weight under the action of metals or basic compounds.

Proske [6] also states that in rubber-metal bonding by means of isocyanates chemical reactions with the oxygen-containing groups of the rubber may occur.* The suggestion is made in the same paper that the $-N=$ $=C=O$ group is of decisive importance in adhesion of the adhesive film to metal; the rest of the isocyanate molecule, i.e., the hydrocarbon portion, forms a bond with rubber. On the whole it may be said that adhesion phenomena, which include rubber-metal bonding, are not sufficiently well understood. The electrical theory of adhesion put forward by Deryagin and Krotkova [7] is the most fully developed theory of the adhesive bond. The above examples cover all the existing views on the mechanism of rubber-metal adhesion by means of isocyanates.

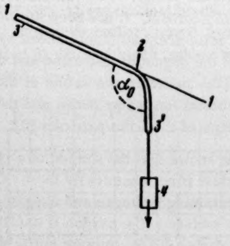

Fig. 1. Deryagin's rotating plate instrument: 1-1') plate; 2) axis; 3-3') film; 4) load.

An attempt is made in the present paper to approach the problem of rubber-metal bonding by means of Leukonat isocyanate adhesive. The isocyanates, as a chemical class, have a number of characteristic properties, such as polyfunctionality (mono-, di-, and triisocyanates exist), and exceptional chemical activity. The formation of isocyanate polymers is based on the fact that the isocyanate group $-N=C=O$ contains a double bond between N and C, at which active hydrogen can be added extremely readily. Bayer [1] arranged compounds containing active hydrogen in the following series by their order of reactivity toward isocyanates: amines > water > alcohols > > acids > urea derivatives > phenols > compounds with active methylene groups.

The present paper gives a description of an investigation of adhesion of rubber to metal by means of Leukonat, which is a 20% solution of triphenylmethane triisocyanate in dichloroethane.

Methods. The strength of the rubber-metal bond was measured in terms of the specific work of peeling the rubber from the metal. Several methods and instruments for this purpose have been described previously [7]. The principle of one of these is illustrated in Figure 1. The specific work of peeling was calculated by the equation:

---

*Proske does not exclude the possibility of electrical forces arising at the adhesive-rubber boundary.

$$A = \frac{P}{b}(1 - \cos \alpha), \tag{1}$$

where P is the weight of the load; *l* is the length of the plate; b is the width of the plate; α is the peeling angle; A is the specific work of peeling. If the plate is horizontal, then

$$A = P/b. \tag{2}$$

Deryagin and Krotova [7] showed that the work of peeling depends on the rate at which the polymer film is peeled from the support.

In the present paper the test results are also shown in the form of adhesion diagrams showing the work of peeling as a function of the rate at which the rubber is peeled from the metal. The peeling rate of the rubber from the metal was varied between 0.001 and 1 cm/second, approximately a 1000-fold range, and the peeling angle was 90°; for this, a special self-regulating device was designed.

The experimental procedure was as follows. The surfaces of steel plates (110 x 25 x 3) were cleaned with No. 100 fine grain emery paper or sandblasted, according to the experimental conditions, and washed with ligroine; the plates were then coated with a thin layer of Leukonat by dipping.* Prepared samples of raw rubber mixes were freshened by solvent, after which the coated plates and rubber samples were placed in a mold and vulcanized in a press under the optimum vulcanization conditions for the particular rubber. The projecting edges of the treated rubber-metal specimens were cleaned off and the specimens were tested as described above.

EXPERIMENTAL

The subject of this paper is a study of the influence of fillers in the rubber on the bonding of rubber to metal by Leukonat adhesive in vulcanization. As is known, fillers play an important part in vulcanized natural and especially synthetic rubbers. The physicomechanical properties of rubbers can be varied over wide limits by addition of various fillers. Fillers may be divided into two groups according to their effects on the physicomechanical properties of the vulcanized products: reinforcing and inert fillers. The commonest fillers used in the rubber industry are various carbon blacks. No single existing theory accounts for all the variety of effects associated with filler reinforcement. It has been shown however, that reinforcement is influenced by such factors as the degree of dispersion and the shape of the filler particles, the nature of the secondary structures formed by them, and the surface properties of the filler particles [9].

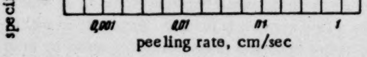

Fig. 2. Work of peeling of rubbers containing different carbon blacks, from steel: 1) gas channel black, adhesive on rubber after peeling; 2) lamp black, adhesive on rubber; 3) jet black, most of the adhesive on rubber; 4) without carbon, most of the adhesive on metal; 5) thermal black, adhesive on metal.

It is now known that the surface of a channel black particle is not chemically inert. Chemical groups containing hydrogen and oxygen are present on this surface. The oxygen is usually present in the carbon black structure entirely in the form of oxygen-containing groups. Several papers have appeared in the literature [10] on the chemical nature of the channel black surface, in which it is stated that the following groups may be present in the surface of channel black

---

* A special device was designed for applying a thin uniform film of adhesive to the metal.

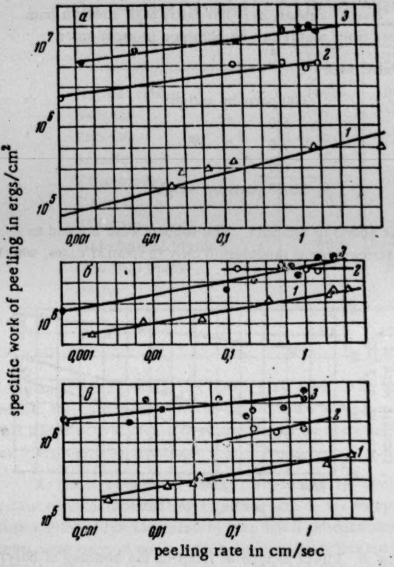

Fig. 3. Work of peeling of different rubbers, containing different fillers, from steel:
a) SKN-26: 1) gas channel black, adhesive on rubber after peeling; 2) without carbon, most of the adhesive on the metal; 3) thermal black, peeling along the rubber, adhesive on the metal;
b) NR: 1) gas channel black, adhesive on the rubber; 2) without carbon, peeling along the rubber, adhesive on the metal; 3) thermal black, rubber torn out in places, adhesive on the metal;
c) SKS-30: 1) gas channel black, adhesive on the rubber; 2) without carbon, rubber torn, adhesive on the metal; 3) thermal black, rubber torn, adhesive on the metal.

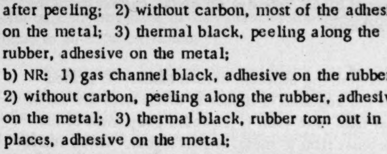

Fig. 4. Effect of heating Leukonat adhesive at 120° on its isocyanate group content.

particles: phenolic, carboxylic, quinone, ketone, aldehyde, peroxide, hydroperoxide, ester, alcoholic, etc. The complex nature of the chemical behavior of the carbon surface is a consequence of this diversity of the chemical groups present.

As is known, the carbon black surface adsorbs rubber and certain ingredients of rubber mixes. The adsorbed ingredients and those dissolved in the rubber participate in different ways in vulcanization, oxidation, or aging. Moreover, catalytic processes should occur at the carbon black surface, activated by condensation of the substances in adsorbed layers and orientation of their molecules [11]. On the other hand, a part of the ingredients adsorbed on the carbon reacts chemically with the carbon surface and is thereby deactivated [12]. There is no doubt that the nature of the carbon surface must play an important role in rubber-metal bonding.

A paper was published in 1952 [13], describing the use of an adhesive containing carbon black (of the channel black type) as an intermediate layer between the material causing adhesion to the metal (brass, and to chlorinated rubber) and the rubber. The adhesive containing the carbon black was made in a mixer from a mix made on rolls and in a ball mill into which the raw rubber and the other ingredients were introduced directly. The greatest bond strength was obtained with the use of the adhesive made in the ball mill. The investigation showed that the adhesive made in the ball mill contained the carbon black particles in the form of floccules, while the flocculation was considerably less in the adhesive made in the mixer. The authors consider that the carbon black particles in the floccules are incompletely wetted by the adhesive and are therefore able to react directly with adjacent surfaces. The effect of the pH of the carbon black added to the adhesive on the rubber-metal bond strength was also studied. It was found that the rubber-metal bond strength increases with decreasing pH of the carbon black. The diversity of the functional groups present on the carbon black surface is, in the opinion of the authors, an adequate explanation of this increase of adhesion.

It was mentioned earlier that isocyanates react very readily with substances containing groups with active hydrogen. In view of this property of isocyanates it was of interest to see how introduction of different kinds of carbon black into the rubber would influence its adhesion to a Leukonat film. The following blacks were tested: gas channel, furnace, jet, lamp and thermal.

The material to which various fillers were added was "Nairit" rubber, as it has fairly high strength both with and without fillers, so that adhesive peeling of the rubber from metal can be obtained in most cases.

Composition of Nairit Mix

Nairit B	100 parts by weight
Zinc oxide	5.0 "
Magnesium oxide	7.0 "
Stearic acid	1.0 "
	113.0 parts by weight

Fifty parts by weight of the different carbon blacks was added to this mix. The rubbers were bonded to steel plates cleaned with No. 100 emery paper. The metal surfaces were sandblasted only in special cases, which will be mentioned.

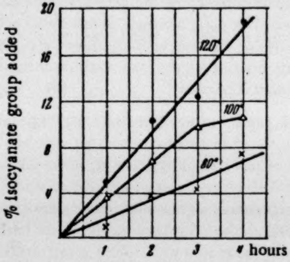

Fig. 5. Variation of the isocyanate group content of Leukonat on heating with channel black at 80, 100 and 120°.

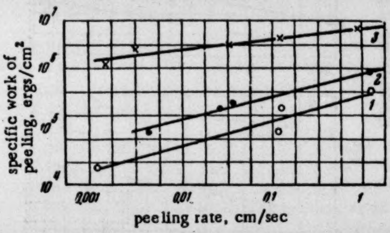

Fig. 6. Effect of type of filler on the bonding of butyl rubber to steel by means of Leukonat adhesive: 1) without carbon, adhesive on metal after peeling; 2) with thermal black, adhesive on metal; 3) with gas channel black, adhesive on metal, carbon particles on adhesive.

Figure 2 shows a series of adhesion diagrams for rubbers containing different carbon blacks. It is seen from Figure 2 that some blacks have a significant influence on the adhesion of rubber to metal with the use of Leukonat. Unfilled Nairit rubber has high adhesion to Leukonat film, but when it is peeled away most of the adhesive remains on the metal, so that the adhesion of the Leukonat film to metal is still higher. When active fillers of the channel black type are added to the rubber, the strength of the rubber-metal bond decreases, and the nature of the peeling changes: the adhesive film is attached to the rubber. Addition of thermal black (a filler of low activity) to the rubber produces some increase of the rubber-metal bond strength, the adhesive remaining on the metal and the peeling being mainly cohesive in character.

It was next decided to test how the same carbon blacks influence the bond strength between metal and other rubbers with Leukonat as adhesive. Two most characteristic types of carbon black — gas channel and thermal — were used for these experiments. Three rubbers were tested: butadiene-acrylonitrile (SKN-26), natural (NR) and butadiene-styrene (SKS-30). The compounding formulas are given in the table.

Figure 3 shows adhesion diagrams for the bond strengths between metal and rubbers based on SKN-26 (Figure 3a) NR (Figure 3b) and SKS-30 (Figure 3c) containing different carbon blacks.

The results given in Figure 3 show that in all cases, irrespective of the type of rubber, the presence of channel black in the rubber results in decreased rubber-metal bond strength, with the adhesive film attached to the rubber, while in presence of thermal black high adhesion of rubber to metal is obtained, and the peeling remains of the same character as with unfilled rubbers, i.e., the adhesive remains on the metal. Therefore the carbon added to the rubber is involved in the mechanism of rubber-metal bonding by means of Leukonat adhesive. To confirm this, in the following series of experiments the interaction of carbon blacks directly with the Leukonat adhesive was studied. The experimental procedure was as follows: 0.16 g of carbon black and 0.6 g

Compounding Formulas for the Rubber Mixes in Parts by Weight

Rubber and ingredients	Mix No.					
	121^{K}	121^{T}	122^{K}	122^{T}	123^{K}	123^{T}
Natural rubber	100.0	100.0	–	–	–	–
SKN-26	–	–	100.0	100.0	–	–
SKS-30	–	–	–	–	100.0	100.0
Stearic acid	0.5	0.5	0.5	0.5	2.0	2.0
Zinc oxide	5.0	5.0	5.0	5.0	5.0	5.0
Captax	0.7	0.7	0.8	0.8	0.6	0.6
Thiuram	–	–	–	–	0.1	0.1
Gas channel black	50.0	–	50.0	–	50.0	–
Thermal black	–	50.0	–	50.0	–	50.0
Sulfur	3.0	3.0	1.5	1.5	2.0	2.0
Total	159.2	159.2	157.8	157.8	159.7	159.7

of Leukonat adhesive was put into a glass tube. The tube was sealed and heated in a thermostat; it was then opened, the carbon was filtered off from the adhesive and repeatedly washed on the filter with dichloroethane until traces of isocyanate could no longer be detected in the washings. The isocyanate content of the solution was determined by titration.

As has already been stated, isocyanates are chemically very active and have a tendency to cyclization in certain conditions, resulting in a decrease of the isocyanate group content. It was therefore necessary to determine whether high temperature may itself produce the changes which occur in isocyanates on heating. Experiments were carried out in which Leukonat was heated by itself (without carbon black) for 1, 2, 3 and 4 hours at 120° (the most severe conditions used in the present investigation). The results of these tests, given in Figure 4, show that when Leukonat is heated at 120° for 4 hours its isocyanate group content is practically unchanged. The results obtained in heating of channel black with Leukonat adhesive at 80, 100 and 120° are given in Figure 5. From these results it was possible to calculate the apparent activation energy of the reaction of channel black with triphenylmethane triisocyanate by means of the Arrhenius equation. The apparent activation energy was found to be 8900 cal/mole.

Experiments in which thermal black was heated in sealed tubes with Leukonat showed that in these conditions thermal black does not react with triphenylmethane triisocyanate, and the isocyanate group content of the adhesive remains practically unchanged. These experiments showed that the nature of the filler present in the rubber influences the bonding of the rubber to metal by means of Leukonat. A comparison of the data on rubber-metal bonding with the results of experiments on the influence of the filler on the properties of the adhesive itself gives rise to the following picture.

Unfilled rubbers of the types studied are firmly bonded to metal by means of Leukonat adhesive. This means that the film of adhesive is bonded equally well to the rubber and to the metal during vulcanization. However, when the rubber is peeled away from the metal most or all of the adhesive (depending on the type of the rubber) remains on the metal, and therefore the adhesion of the Leukonat film is somewhat greater to metal than to rubber.

On addition of an active filler of the gas channel black type to the rubber, the interaction of one of the surfaces (the rubber) with the adhesive film is greatly intensified. The bonding at the adhesive-rubber boundary is now effected not only by interaction between isocyanate and rubber, but also by interaction of the adhesive with groups containing active hydrogen, present on the carbon black surface. The number of active centers with which the isocyanate can interact is increased. The interaction between the metal and the adhesive film remains the same as before. Therefore during the bonding process the isocyanate groups react sooner with the more active rubber surface (the adhesive film is attached to the rubber) and the adhesion to the metal is decreased. Inactive fillers of the thermal black type introduced into the rubber have little influence on the processes occurring at the adhesive-rubber boundary. The peeling in this case remains of the same character as with unfilled rubbers (the adhesive remains on the metal after peeling).

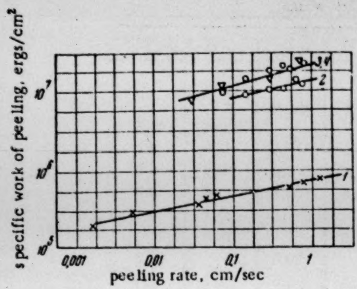

Fig. 7. Effect of treatment of the metal surface on its bond strength with Nairit rubber: 1) with channel black, metal cleaned with emery paper, adhesive on rubber after peeling; 2) with thermal black, metal cleaned with emery paper, large pieces of rubber torn out; 3) with channel black, metal sandblasted, peeling along the rubber; 4) with thermal black, metal sandblasted, peeling along the rubber.

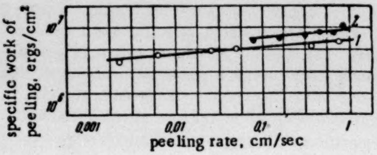

Fig. 8. Effect of treatment of the metal surface on its bond strength with butyl rubber containing gas channel black: 1) metal cleaned with emery paper, adhesive on metal after peeling; 2) metal sandblasted, adhesive on metal.

Experimental data providing further confirmation of these views are presented below. Most of the rubbers studied have fairly good adhesion to Leukonat films, without added fillers. The adhesion of butyl rubber to the Leukonat film is very low (Figure 6). The results of the experiments lead to the following empirical rule: if the rubber-metal bond strength produced by Leukonat is high, this means that both surfaces in contact with the Leukonat film interact with it with approximately the same intensity. This corresponds to the bonding of most unfilled rubbers.

If an active filler is added to such a rubber, one of the surfaces becomes more active, the adhesive becomes attached to it first, and the total bond strength produced is low. When unfilled butyl rubber is bonded to metal, the rubber surface has the lower intensity of interaction with the adhesive film; in this case addition of a filler of the gas channel black type may increase the intensity of interaction between the rubber and the adhesive film, thereby increasing the bond strength between the butyl rubber and the metal. Addition of a filler of the thermal black type to such a rubber should not greatly increase the adhesion of the rubber to the adhesive film. The experimental data in Figure 6 confirm this view. Thus, it is demonstrated once again that carbon black present in rubber is directly involved in bond formation at the adhesive-rubber boundary when rubber is bonded to metal by means of Leukonat.

It is well known from experience in the use of Leukonat adhesive that the metal should be sandblasted to obtain a sufficiently high bond strength between metal and rubber with the aid of this adhesive. It is reported in a number of papers that Leukonat adhesive softens during vulcanization and leaks out of the mold. It was assumed that sandblasting of the metal prevents leakage of the adhesive, thus increasing bond strength. However, as has been shown in the present investigation, good bond strength can be obtained also with smooth metal surfaces if the rubber formulation is suitably chosen (unfilled rubbers of a number of types, rubbers with thermal black). Therefore this is not the sole cause of poor bonding with smooth metal surfaces. It was also believed that sandblasting increases the contact area between the metal and the adhesive film, with greater bond strength as a result. Several experiments were performed to test this; it was found that sandblasting increases the true surface area of the metal by a factor of 1.5-2, while the bond strength becomes 20-100 times as great. Therefore increase of the contact area is also not the main cause of increased bond strength. The probable reason is that a sandblasted metal surface differs qualitatively from a surface which has not been so treated. The interaction intensity of adhesive films with such surfaces increases (Figure 7).

By sandblasting the metal surface we tend to equalize the degree of interaction of the Leukonat film with the metal and the rubber. The test results in Figure 7 show that rubber containing an active filler is bonded fairly firmly to a sandblasted metal surface: the peeling is cohesive in character. Sandblasting is quite ineffective for bonding rubber containing thermal black. As has already been stated, when butyl rubber (with or without fillers) is bonded to metal by means of Leukonat adhesive, the adhesive remains on the metal in all cases. Therefore in this instance it is necessary to seek methods of increasing the activity of the rubber, for improving the bond strength. Sandblasting of the metal does not result in any considerable increase of bond strength.

The slight increase of bond strength is evidently the result of an increase of the contact area of the sandblasted metal (Figure 8).

SUMMARY

1. In bonding of rubber to metal by Leukonat adhesive, the type of filler present in the rubber has a very great influence on the rubber-metal bond strength.

2. Active fillers of the gas channel black type in the rubber mixture increase the interaction of the rubber with the adhesive film.

3. Inactive fillers of the thermal black type have little influence on the interaction of the rubber with the adhesive film.

4. The results of the experiments suggest that Leukonat interacts chemically with active fillers present in the rubber during the bonding process.

5. The following empirical rule is formulated: high rubber-metal bond strength is obtained if the interaction of the adhesive film with the rubber is approximately of the same degree as with the metal. This rule is supported by the experimental data.

6. Sandblasting of the metal surface increases the true contact area by a factor of 1.5-2, while the bond strength is increased 20 to 100 times; this indicates that qualitative changes occur in the surface on sandblasting and that the nature of the metal-adhesive interaction is greatly changed in the process.

It is difficult to explain this other than on the assumption that the charge of the double layer at the metal-adhesive boundary is increased, and in consequence the work of separation of this layer at the boundary is greater.

LITERATURE CITED

[1] O. Bayer, Modern Plastics 24, 10, 149 (1947).

[2] T.J. Meyrick and J.T. Watts, IRI Transactions 25, 3, 150 (1949).

[3] H. Barron, Rub. Plastics Age 35, 1, 40 (1954).

[4] T.J. Meyrick and J.T. Watts, Ind.Rub. J. 72, 13 (1952).

[5] K.S. Zherebkov, Bonding of Rubber to Metals (Goskhimizdat, 1956).

[6] G.E. Proske, Kautsch. u Gummi 10, 153 (1952).

[7] B.V. Deryagin and N.A. Krotova, Adhesion (Izd. AN SSSR, 1949).

[8] A.A. Blagonravova and G.A. Levkovich, Progr. Chem. 24, 1, 93 (1955).

[9] F.F. Koshelev, Rubber Technology (State Tech. Press, 1951).

[10] K.S. Stearns and B.L. Johnson, Ind. Eng. Chem. 43, 146 (1951); M.L. Studebaker, Rubber Age 77, No. 1, 69 (New York, 1955); W.R. Smith and W.D. Schaeffer, Ind. Eng. Chem. 33, 1303 (1941); M.L. Studebaker and J.R. Hultman, Rubber World 132, No. 1, 74 (1955).

[11] N.N. Lezhnev and A.S. Kuzminsky, Proc. Acad. Sci. USSR 110, 1, 108 (1956).

[12] B.A. Dogadkin, B.V. Lukin and Z.N. Tarasova, Colloid J. 18, No. 4, 413 (1956) (T.p. 407).*

[13] G.M. Sheehan, G. Kraus and A.B. Conciatori, Ind. Eng. Chem. 44, 3, 580 (1952).

Received April 26, 1957

Institute of the Rubber Industry, Institute of
Physical Chemistry, Acad. Sci. USSR
Laboratory of Surface Phenomena – Moscow

---

*T.p. = C.B. Translation pagination.

EFFECT OF MERCAPTOBENZOTHIAZOLE ON STRUCTURAL CHANGES IN RUBBER ON OXIDATION, HEATING AND PLASTICIZATION

B. Dogadkin, A. Dobromyslova, L. Sapozhkova[*] and I. Tutorsky

Mercaptobenzothiazole (MBT, Captax) belongs to a class of compounds which, owing to presence of SH groups, are vigorous activators of rubber plasticization.

The first report of the plasticizing action of mercaptans is contained in a paper by Williams and Neal [1]. Subsequently some of these compounds (β-naphthylmercaptan, xylylmercaptan, etc.) were used in technological practice, designated as RPA (Rubber Peptization Agents). This name shows that it was originally believed that the plasticizing action of these compounds consists of peptization of the structural formations in the rubber. However our investigations showed that the acceleration of the plasticization process caused by mercaptans is largely the result of their influence on the interaction between oxygen and the rubber. Other authors [2] reached a similar conclusion. Our principal experimental data on the influence of mercaptobenzothiazole on oxidation and plasticization of rubber are given below.[**]

Effect of mercaptobenzothiazole on oxidation of natural rubber. There were no direct experimental data in the literature on the influence of mercaptans on the oxidation of rubber. We therefore carried out experiments on the kinetics of rubber oxidation in an apparatus of the Kohman type [3], at atmospheric, approximately constant, oxygen pressure, by measurement of the volume of the gas absorbed. The rubber was placed in the absorption vessel in the form of films deposited from solution on glass plates. The films were 0.015-0.02 mm thick. Figure 1 shows that addition of MBT significantly influences the oxidation of rubber, shortening the induction period and increasing the oxidation rate during the principal steady period. The apparent activation energy of oxygen absorption, calculated from data on the principal temperature over the temperature range of 100 to 120°,

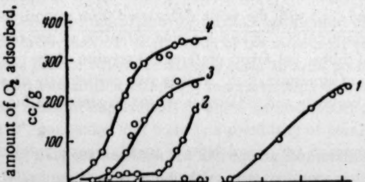

Fig. 1. Kinetics of oxidation of rubber at 100°: 1) without MBT; 2) with 0.31% MBT; 3) with 0.78% MBT; 4) with 1.55% MBT.

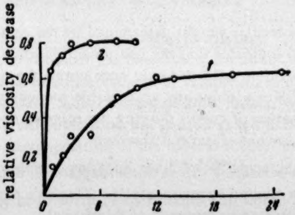

Fig. 2. Variation of the viscosity of rubber solutions as the result of oxidation: 1) without MBT; 2) with 1.55% MBT.

---

[*] Deceased

[**] These results were obtained in 1942-1944 and are given in the reports of the M.V. Lomonosov Institute of Fine Chemical Technology, Moscow, and in L. Sapozhkova's dissertation "Investigation of the Chemical Factors in the Plasticization of Rubber" (Moscow, 1947).

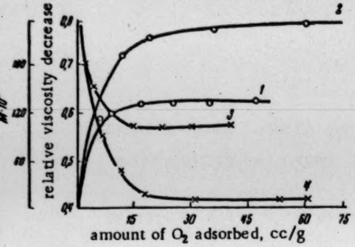

Fig. 3. Variation of the viscosity (1, 2) and molecular weight (3, 4) of rubber with the amount of oxygen absorbed: 1,3) rubber without MBT; 2,4) rubber with 1.55% MBT.

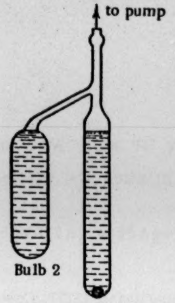

Fig. 4. Tube with ball for determining viscosity of rubber solutions.

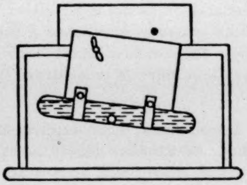

Fig. 5. Apparatus for determination of viscosity from the time of rolling of a ball in rubber solution.

is ~17 kcal/mole for pure rubber, and ~12 kcal//mole for rubber containing 1.55% MBT.

Oxidation of rubber in presence of MBT results in a greater decrease of solution viscosity than that found for rubber without MBT (Figure 2). This viscosity decrease is caused by scission of the molecular chains in the rubber, as is shown by data on the molecular weight of the rubber, determined by the osmotic method [4]. Degradation of the rubber occurs mainly during the initial (induction) period, and after 3 hours of oxidation the average molecular weight already falls from 200,000 to 54,000 (Table 1). A comparison of the molecular weight determined by the osmotic method (M_0) with the value calculated from viscosimetric data (M_V) indicates that the chain configuration remains practically unchanged during oxidation in presence of MBT. Therefore MBT not only accelerates the oxidation of rubber but favors preferential scission of the molecular chains without any appreciable secondary processes of structurization. This is seen particularly clearly in examination of curves showing the relative decreases of viscosity and molecular weight (Figure 3) as functions of the amount of oxygen absorbed.

The accelerating effect of mercaptans on oxidation of unsaturated compounds has not been adequately considered or studied experimentally. Ziegler's paper [5] merely mentions that oxidation of benzodimethylfulvene is accelerated in presence of thiophenol.

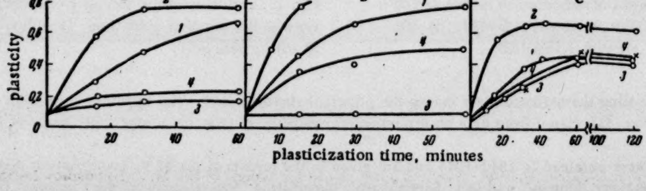

Fig. 6. Plasticization kinetics of natural rubber at 120° (a), at 150° (b) and at 100° (c): 1) in air without MBT; 2) in air with 1.55% MBT; 3) in nitrogen without MBT; 4) in nitrogen with 1.55% MBT.

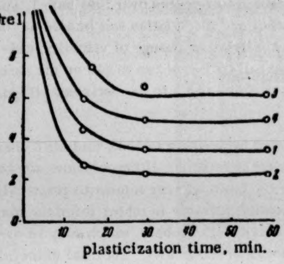

Fig. 7. Viscosity variations in plasticization of natural rubber at 100° (designations as in Figure 6).

In our opinion, MBT may act by the following mechanism. At high enough temperatures a reaction occurs with formation of $HO_2^\bullet$ and $RS^\bullet$ radicals:

$$RSH + O_2 \rightarrow RS^\bullet + HO_2^\bullet.$$

Interaction of $RS^\bullet$ radicals with α-methylene groups in the rubber molecule (KaH) results in regeneration of the mercaptan and formation of a polymeric radical ($Ka^\bullet$) which initiates an oxidation chain:

$$RS^\bullet + KaH \rightarrow RSH + Ka^\bullet;$$
$$Ka^\bullet + O_2 \rightarrow KaOO^\bullet, \text{ etc.}$$

The $HO_2^\bullet$ radical probably reacts with the double bond to form a hydroperoxide group, subsequent decomposition of which results in formation of an epoxide group and oxygen in active form.

TABLE 1

Change of Molecular Weight of Rubber on Oxidation

Rubber	M_v	M_O	M_O/M_v
Smoked sheet before oxidation	106,000	200,000	1.8
Ditto, after oxidation for 3 hours at 120°	33,000	54,000	1.6

The possibility is not excluded that the oxidation may be accelerated by an oxidation chain transfer mechanism as the result of direct interaction of peroxide radicals with MBT:

$$KaOO^\bullet + RSH \rightarrow KaOOH + RS^\bullet;\ RS^\bullet + KaH \rightarrow RSH + Ka^\bullet;\ Ka^\bullet + O_2 \rightarrow KaOO^\bullet.$$

Effect of mercaptobenzothiazole on thermal decomposition of rubber on heating in solution. The possibility of the thermal degradation of the molecular chains of natural rubber has been often discussed. Bolland [6] showed that no structural changes occur in solid purified rubber heated in a vacuum at temperatures up to 200°. We obtained similar results [7] in experiments with sodium butadiene rubber heated to 200°. Later, Watson [8], as the result of experiments in which natural rubber dissolved in chlorobenzene was heated at temperatures up to 120°, concluded that there is a possibility of purely thermal decomposition of the natural rubber molecules, containing a special type of weak bonds, the concentration of which is one bond per $1.3 \cdot 10^4$ monomer units.

The procedure used by Watson was similar to that used by us in earlier experiments,* in which we also found appreciable changes in the viscosity of rubber solutions heated to 100° in a nitrogen atmosphere. As we considered that the procedure used did not ensure complete removal of oxygen from the system,** we worked out a method whereby the action of oxygen was excluded to a greater extent when the rubber solutions were heated. The glass apparatus, shown diagrammatically in Figure 4, was repeatedly evacuated and filled with pure nitrogen in the heated state. A weighed quantity of MBT was then introduced into the bulb 2, followed by redistilled benzene saturated with nitrogen. The bulb 1, which contained a stainless steel ball 4 mm in diameter, was filled with 2% solution of purified rubber, all the purification stages of which (extraction, solution, reprecipitation and drying) were performed in a special apparatus in a nitrogen atmosphere. The apparatus was connected to a pump; after some of the benzene had been pumped out of bulb 2 the remaining benzene was frozen, while the benzene in bulb 1 was pumped out completely on heating to 35-45°. The residual pressure was 3-4 mm.

---

*See L.F. Sapozhkova's dissertation, the Lomonosov Institute of Fine Chemical Technology (Moscow, 1947).

**In Watson's experiments the rubber contained 0.25% of oxygen.

The apparatus was then again filled with pure nitrogen, the benzene in bulb 2 was poured over into bulb 1, and this bulb was then sealed off; the rubber in it was dissolved in the benzene, and the solution was heated to 100° in a thermostat. Structural changes in the rubber were characterized by the relative change of viscosity, calculated by the equation $(T_0 - T_1)/T_0$, where T_0 is the time for the ball to roll (between two marks on the bulb) before heating, and T_1, the time after heating. The bulb was fixed at a definite angle to the horizontal (Figure 5).

Table 2 shows that very little change of solution viscosity is produced by heating to 100°, and MBT does not increase thermal degradation of the rubber. These viscosity changes are reversible; if the solutions are kept in the dark at room temperature the viscosity gradually increases and in 100 hours already returns to practically its original value (Table 3). From this it may be concluded that the viscosity decrease in rubber solutions heated to 100° is to be explained by deaggregation of secondary structural formations in the rubber, which may be associated with the presence of oxygen-containing functional groups in the rubber molecules. Thermal dissociation of the rubber molecules into free radicals evidently does not occur on heating to 100°, since mercaptobenzothiazole and other free radical acceptors do not influence the course of the reversible thermal change of solution viscosity.

TABLE 2

Changes in the Viscosity of Rubber Solutions on Heating at 100° in a Nitrogen Atmosphere

Duration of heating, minutes	Solution without MBT		Solution with 1.55% MBT	
	T_1 sec	$\frac{T_0 - T_1}{T_0}$	T_1 sec	$\frac{T_0 - T_1}{T_0}$
0	67	0	63	0
15	55	0.18	51	0.19
30	–	–	52	0.18
45	56	0.16	–	–
60	–	–	49	0.23
100	50	0.22	–	–
120	–	–	50	0.20
160	53	0.21	51	0.19
180	–	–	51	0.19
300	53	0.21	–	–
360	53	0.21	–	–

TABLE 3

Restoration of Viscosity on Storage of Solutions in the Dark at Room Temperature

2% rubber solution	Initial viscosity in seconds	Viscosity after heating at 100°, in seconds	Viscosity after storage for	
			48 hours	100 hours
Without MBT	67	53	63	64
With MBT	63	50	59	60

Effect of mercaptobenzothiazole on plasticization of natural rubber. The experiments on plasticization of rubber were first performed in a specially constructed closed mixer with Z-shaped blades rotating at 24 and 30 revolutions per minute [9]. Two cocks fitted in the airtight lid were used for evacuation of the mixer and for admission of the required gas (nitrogen, air, nitrogen-oxygen mixture) after the rubber had been put in. The mixer was electrically heated; the temperature in the range of 50-175° was regulated to the nearest ± 2.5°.

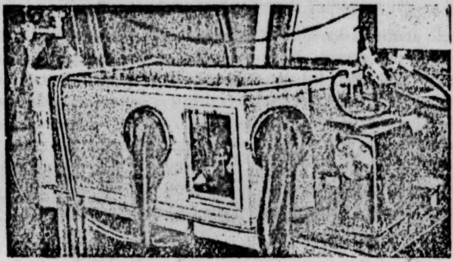

Fig. 8. Photograph of rolls in the "nitrogen" closet.

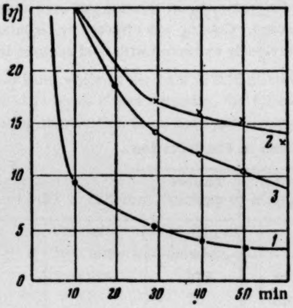

Fig. 9. Variation of the intrinsic viscosity of NR during mastication: 1) in air; 2) in nitrogen containing 0.5% O_2; 3) in nitrogen.

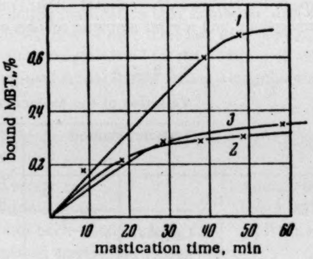

Fig. 10. Kinetics of MBT addition during mastication of NR: 1) in air; 2) in nitrogen containing 0.5% O_2; 3) in nitrogen.

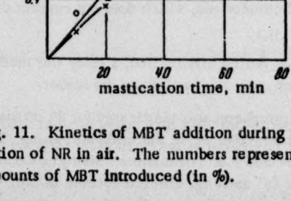

Fig. 11. Kinetics of MBT addition during mastication of NR in air. The numbers represent the amounts of MBT introduced (in %).

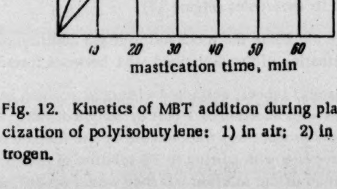

Fig. 12. Kinetics of MBT addition during plasticization of polyisobutylene: 1) in air; 2) in nitrogen.

Nitrogen was made free of oxygen by passing it over copper gauze at 475-525°.

Figure 6 represents the plasticization kinetics of natural rubber in nitrogen and in air at 120°. In both cases MBT increases the rate of the process, and is more effective in plasticization in air. Similar results were obtained in experiments at 100 and 150°. It is important to note that the temperature coefficient of plasticization of rubber in a nitrogen atmosphere (without MBT) is negative and at 150° practically no plasticization occurs. Structural changes in the rubber are characterized by the viscosity variation curves shown in Figure 7. It is seen in Figure 7 and also in Table 4 that mercaptobenzothiazole has a strong effect in decreasing the average molecular weight of the plasticized rubber. Thus MBT is involved both in thermooxidative and in mechanical processes of rubber degradation during mastication. In the latter case the mechanism of its action is probably in accordance with the views advanced by Pike and Watson [10] and other authors.

As has just been stated, mechanical degradation of the molecular chains during plasticization has a negative temperature coefficient. For a clearer determination of the role played by MBT in mechanical plasticization of rubber, experiments were performed at temperatures not exceeding 30°.* Specially designed micro-rolls fitted in a "nitrogen" closet (Figure 8) filled with the required gas (nitrogen, argon, air). The inert gas was passed through the closet until the exit gas was free from oxygen (cuprammonium solution was used as indicator). To prevent leakage of air into the closet, excess gas pressure was used. Cooling was effected by circulation of water through the hollow rolls. Natural rubber (smoked sheet), previously extracted with cold acetone in a nitrogen atmosphere, and several synthetic rubbers of different structures were used.

TABLE 4

Variation of the Molecular Weight of Rubber in Plasticization

Material studied	Plasticization time in minutes	Plasticity	Mol wt 10^{-3}
Original rubber	–	0.08	216
Rubber plasticized in air	30	0.65	57
Ditto, in nitrogen	60	0.10	107
Rubber plasticized with 1.55% MBT in air	15	0.67	35
Ditto, in nitrogen	60	0.44	72

Figure 9 shows that at 30° the plasticization of rubber, as measured by change of intrinsic viscosity, is more rapid in air. MBT is found to combine with the rubber (Figure 10), more rapidly in air than in nitrogen. This addition proceeds by a more complex mechanism than that of a simple bimolecular action, as shown by the consumption of MBT as a function of the concentration (Figure 11). The type of rubber has a significant influence both on the plasticization rate and on the addition of MBT. Table 5 shows that, for a given plasticization time, the amount of MBT added to the rubber increases with increasing contents of 1-4 structure in its molecular chains. Addition of MBT occurs also in plasticization of polyisobutylene, which does not contain double bonds in its molecules (Figure 12).

To elucidate the mechanism of the addition of MBT to rubber during mastication, a study was made of the distribution of the combined MBT between fractions of different molecular weight in the rubber.

Natural rubber, extracted with cold acetone in a nitrogen atmosphere, was masticated for 20 minutes on cold rolls with addition of 1 part by weight of MBT, tagged with radioactive S^{35} in the sulfhydryl group. The masticated product was fractionated by the method of A.S. Novikov and F.S. Tolstukhina. Methyl alcohol was added dropwise with stirring to 1% solution of rubber in benzene at 35° until the solution became turbid. The temperature of the solution was then raised by 2-3° until it became quite clear, and the solution was stirred for

---

*These experiments were performed in 1955.

1 hour at that temperature. The temperature was then again lowered to 35°; the solution was held at that temperature for 24 hours until the liquid above the precipitated fraction became quite clear. The liquid was decanted off, and the precipitated fraction was purified by threefold precipitation by methyl alcohol from benzene solution. Neozone (phenyl-β-napthylamine) was added each time to the solution. The isolated fraction was then dried under vacuum until the solvent was completely removed, dissolved in benzene, and analyzed for MBT by the radiometric method, the radioactivity of the film being determined. The intrinsic viscosities of benzene solutions of the fractions were determined.

TABLE 5

Binding of MBT by Rubbers of Different Structure During Mastication for 20 Minutes in Air

Type of rubber	Content of 1-4 bonds	$\frac{MBT_{bound}}{MBT_{total}}$
NR	100	0.48
SKBM	70	0.25
SKB	30	0.11

The results obtained are given in Table 6. Table 6 shows that the amount of combined MBT increases considerably (up to a certain limit) with decreasing molecular weight of the fractions. This shows that there is a direct connection between the reactions of mechanical degradation of the rubber molecules and of MBT addition. The lower MBT content of the last fraction can be attributed to the fact that this fraction contains the low molecular portion of the original rubber, which is less prone to mechanical degradation under shearing stresses.

From the results given in Table 6, and from the fact that during mastication MBT combines with saturated polyisobutylene, while in the case of unsaturated compounds the addition of MBT increases with increasing contents of diallyl bonds of 1-4 structure, the following mechanism can be postulated for the addition of MBT to rubber during mastication in an inert gas atmosphere. When the mechanical strains arising along the elastomer chains in a field of large shearing forces exceed the energy of the $=CH-CH_2 \downarrow CH_2-CH=$ chemical bond, which is approximately 40 kcal/mole, these bonds are broken to give stable polymeric radicals of the allyl type:

TABLE 6

Contents of MBT in Different Fractions of Masticated Rubber

Fraction No.	Precipitation temperature, °C	Weight of fraction, in g	(η)	Average radiation activity with background correction	I_t/I_0	Amount of combined MBT in moles/liter x 10^3
Not fractionated	–	23	12.0	546	1	–
1	35.3	6	27	29	0.0531	3.21
2	26.7	7	24.5	50	0.0915	5.45
3	20.4	5	10.2	60	0.11	6.22
4	9.5	3	8.0	39	0.0715	4.28

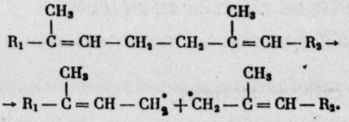

$$R_1-\overset{CH_3}{\overset{|}{C}}=CH-CH_2-CH_2-\overset{CH_3}{\overset{|}{C}}=CH-R_2\rightarrow$$

$$\rightarrow R_1-\overset{CH_3}{\overset{|}{C}}=CH-CH_2^{\bullet}+{}^{\bullet}CH_2-\overset{CH_3}{\overset{|}{C}}=CH-R_2.$$

These radicals react with MBT molecules, saturating their free valencies; this prevents their recombination and causes a sharp decrease of molecular weight:

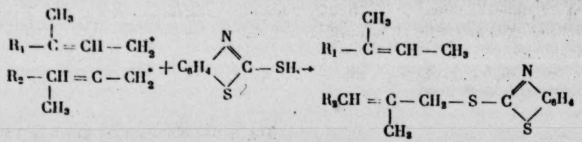

The benzothiazole radical C_6H_4 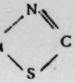 $C - S^\bullet$, formed by removal of an H atom from the MBT molecule, does not initiate a new chain by addition at a double bond in the rubber molecule or removal of an H atom from an α-methylene group, as is the case when rubber is heated with dibenzothiazolyl disulfide [11]. Recombination of the benzothiazolyl and polymeric radicals is more advantageous from the energy standpoint. Moreover, the polymeric radicals formed by mechanical rupture of the macromolecules cannot be removed far apart owing to the high viscosity of the medium, so that the topochemical conditions also favor addition of MBT to two polymeric radicals.

SUMMARY

1. Mercaptobenzothiazole (MBT) accelerates the oxidation of natural rubber and considerably increases the rate of its oxidative degradation.

2. When benzene solutions of natural rubber are heated in an inert gas atmosphere at 100°, no irreversible changes occur in the rubber whether in presence or in absence of MBT.

3. Plasticization of natural rubber in air at 100-150° is intensified in presence of MBT, which is caused mainly by the accelerating action of the latter on the oxidative degradation of rubber.

4. Mercaptobenzothiazole assists plasticization of rubber at low temperatures in an inert gas atmosphere. MBT is consumed in the process, owing to its interaction with the polymeric radicals formed by mechanical rupture of the rubber molecules.

5. The amount of MBT reacting with the rubber increases with increasing contents of 1-4 structure in the rubber molecules.

6. It is shown that different fractions of the masticated product contain different amounts of MBT, indicating that MBT reacts preferentially with the end valencies of the radicals formed by cleavage of diallyl bonds.

7. Reaction schemes for the interaction of MBT with rubber in mechanical and oxidative processes are suggested.

LITERATURE CITED

[1] J. Williams and A.M. Neal, Ind. Eng. Chem. 22, 874 (1930).

[2] W.F. Busse and E.N. Cunningham, Proc. Rub. Techn. Conf (London, 1938), p. 288; D.F. Twiss, Ind. Rub. J. 108, 26 (1945).

[3] G.T. Kohman, J. Phys. Chem. 33, 226 (1929).

[4] B.A. Dogadkin, M.I. Arkhangelskaya and I.G. Soboleva, Investigations of High Molecular Compounds (Izd. AN SSSR, Moscow-Leningrad 1949), p. 253.

[5] K. Ziegler and K. Gänicke, Ann. 551, 213 (1942).

[6] J.L. Bolland and W.J. Orr, Trans. IRI 21, 2 (1945).

[7] B.A. Dogadkin and D.M. Pevzner, Trans. Sci. Res. Inst. Tire Ind. 47 (1950).

[8] W.F. Watson, Trans. IRI 29, 202 (1953).

[9] A.S. Novikov, Dissertation, Moscow Inst. Fine Chem. Technology (1945).

[10] M. Pike and W.F. Watson, J. Pol. Sci. 9, 229 (1952).

[11] B. Dogadkin, V. Selyukova, Z. Tarasova, A. Dobromyslova, M. Feldhstein and M. Kaplunov, Proc. Acad. Sci. USSR 92, 61 (1953); Colloid J. 17, 215 (1955) (T.p. 199).*

Received March 22, 1957

The M.V. Lomonosov Institute of
Fine Chemical Technology,
Moscow

---

*T.p. = C.B. Translation pagination.

THE STRUCTURE OF GELS

10. GLOBULIZATION OF RUBBER UNDER THE ACTION OF NONSOLVENTS ADDED TO SOLUTIONS

P.I. Zubov, Z.N. Zhurkina and V.A. Kargin

It has been shown [1-4] that under certain conditions it is possible to obtain globular structures from ordinary linear polymers. Globulization of the molecules in these cases was induced by formation of intramolecular bonds between active groups which were either present in the molecular chains or were introduced into them in various ways. Globular structures of certain proteins, gelatin, casein and synthetic and natural rubbers were obtained. In a number of properties, namely: solubility, solution viscosity, mechanical properties of films and others, the polymers with "globular" molecular structure differed considerably from the original polymers, evidently because of the difference in the molecular form.

The degree of globulization was determined [1-4] mainly by measurement of solution viscosity. It is known, however, that changes in the composition of the medium also produce changes of solution viscosity in some instances. For example, alcohols are often used in the rubber industry for decreasing the viscosity of rubber adhesives. On the supposition that coiling of the molecules also takes place when nonsolvents are added to rubber solutions, we commenced an investigation of this effect. This study was also of interest because there is a significant difference between globulization of rubber caused by addition of active substances to solutions, and that caused by addition of nonsolvents. In the former case coiling of the molecules is largely the consequence of energy interaction, while in the latter globulization is determined by entropy effects.

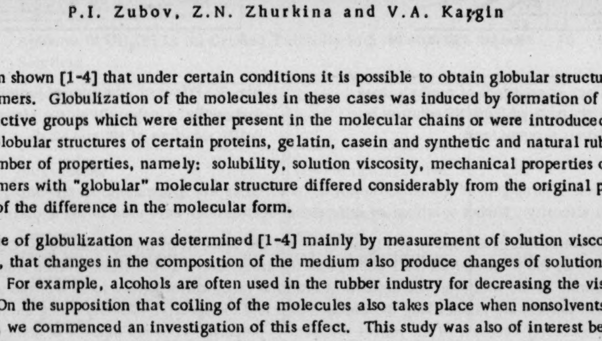

Fig. 1. Effects on the viscosity of 0.25% NR solution (a), 1% NR solution (b), and 0.25% SK-B solution (c), of additions of: 1) methyl alcohol; 2) 10% of bromine; 3) carbon tetrachloride.

The present communication contains data obtained in a study of the influence of added nonsolvents on the viscosity of solutions of different rubbers. The materials studied were natural smoked sheet rubber and synthetic rubbers, mainly of the sodium butadiene type. The solvent used was carbon tetrachloride, and the nonsolvent

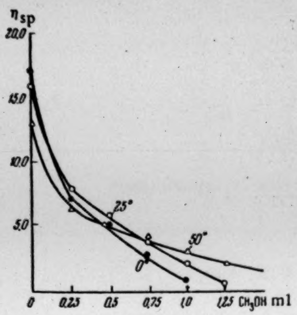

Fig. 2. Effect of additions of methyl alcohol on the viscosity of 0.5% NR solution in CCl_4 at various temperatures.

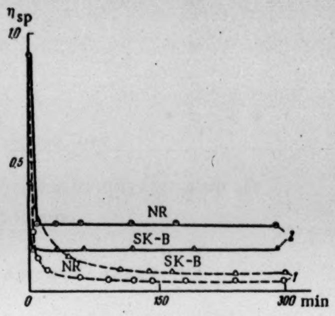

Fig. 3. Effect of additions of bromine (1) and methyl alcohol (2) on the viscosities of 0.16% solutions of NR and SK-B.

was methyl alcohol. The degree of globulization of the molecules was determined, as previously, by measurements of solution viscosity. Rubber solutions of different concentrations were used in the experiments.

The experimental results are shown in Figure 1, where the amounts of methyl alcohol or CCl_4 in milliliters added to 5 ml of the solution (Curves 1 and 3) and the time, Curve 2 (the time is taken from the moment of addition of bromine to the solution; the amount of bromine taken corresponded to 10% of the unsaturated bond content in the rubber) are taken along the abscissa axis and the specific viscosity along the ordinate axis; it is seen that the viscosity decrease of the rubber solutions is proportional to the amount of nonsolvent (methyl alcohol) added, right up to precipitation of the rubber. The limiting value of the viscosity of rubber solutions in presence of the nonsolvent differs little from the viscosity of globular rubber solutions produced by bromination.

Experiments were carried out to determine the effects of rubber solution concentration and temperature on the amount of methyl alcohol required to produce turbidity of the solution. The results show that the amount of methyl alcohol depends to some extent on the solution concentration (Table 1) and to a large extent on the temperature (Figure 2). Figure 2 gives curves for the viscosity variations of 0.5% solution of natural rubber (of a low degree of milling) in carbon tetrachloride on addition of methyl alcohol. The curves in Figure 2 correspond to experimental temperatures of 0, 25 and 50°. The amounts of methyl alcohol in milliliters added to 5 ml of rubber solution are taken along the abscissa axis, and the specific viscosity of the solution along the ordinate axis. Arrows indicate precipitation of the rubber. Figure 2 shows that one and a half times more methyl alcohol is needed at 50° than at 0° to precipitate the rubber.

In dilute solutions (0.16%) of a number of rubbers precipitation of rubber occurs at practically the same contents of methyl alcohol. The only exception is polyisobutylene, which is precipitated at a lower alcohol content than the other rubbers (Table 2).

It may be concluded from these results that globulization of rubbers by addition to the solutions of active substances which react with the rubber molecules (S_2Cl_2 and halogens) and the coiling of rubber molecules by the action of added nonsolvents have the common feature that in both cases the macromolecules assume a globular configuration. Experiments carried out in order to study the kinetics of globulization of the molecules caused by additions of nonsolvents to the rubber solutions showed that on addition of methyl alcohol the viscosity of the rubber solutions falls almost instantaneously and remains constant for a considerable time. In contrast to this, globulization of rubber effected by the action of 20% of bromine (calculated on the unsaturated bonds) is clearly seen to be a function of time (Figure 3).

The following experiments were carried out to investigate the reversability of the globulization of rubber

TABLE 1

Variation of the Amount of CH_3OH in Milliliters Required to Produce Turbidity, with the Concentration of the Rubber Solution

Concentration of NR solution in %	0.1	0.16	0.25	0.4
Specific viscosity of solution	0.68	0.77	2.73	6.77
Amount of CH_3OH in ml to produce turbidity in 5 ml of solution	1.14	1.07	0.52	0.39

TABLE 2

Amounts of CH_3OH in ml Causing Turbidity in 5 ml of 0.16% Rubber Solutions

Type of rubber	Amount of CH_3OH in ml	Type of rubber	Amount of CH_3OH in ml
Butyl rubber	1.25	Low-temperature No. 3	1.20
Low-temperature No. 1	1.25	SKS-30A	1.20
SK-B	1.30	Polyisobutylene	0.75
Isoprene	1.25	Neoprene	1.10
SK-B No. 1, low-temperature	1.30	NR, low mastication	1.10
SK-B No. 3, high-temperature	1.25		

TABLE 3

Effect of Additions of CH_3OH and CCl_4 on the Specific Viscosity of Rubber Solutions

Concentration of original NR solution in %	Specific viscosity			
	of original solution	after addition to 10 ml of the original solution, of 15 ml of		after evaporation of mixture and solution of rubber in CCl_4
		CH_3OH	CCl_4	
0.4	6.95	1.9	–	5.2
0.4	6.95	–	5.3	5.0
1	70.6	9.0	–	32.3
1	70.6	–	42.0	38.0

molecules caused by addition of nonsolvents to solutions. Methyl alcohol was added to a rubber solution the viscosity of which had been determined previously, and after thorough stirring the viscosity was measured again. The solvent was then removed from the mixture at room temperature by means of a vacuum pump. The residual rubber was dissolved in the pure solvent (CCl_4) and the viscosity of the solution was again measured. A comparison of the viscosity of this solution with the viscosity of the original rubber solution before addition of the methyl alcohol gave an indication of the reversibility of the globulization of the rubber molecules caused by addition of the nonsolvent. To allow for the influence of other factors (oxidation, etc.) on the viscosity of the rubber solution, a control experiment was carried out, which differed from the main experiment only by the addition of the same amount of pure solvent (CCl_4) instead of methyl alcohol to the rubber solution. The results of these experiments showed that even on incomplete evaporation of the rubber solution containing methyl alcohol, followed by dilution of the resultant concentrated solution with pure solvent (CCl_4) to the original concentration, the viscosity of the solution increases. Complete removal of the solvent followed by solution of the rubber in CCl_4 results in a greater viscosity increase (Table 3).

It seemed possible that in consequence of the globulizing action of methyl alcohol on the rubber molecules the solubility of rubber in a mixture of CCl_4 and CH_3OH should differ from the solubility in pure CCl_4. Experiments showed that different rubbers dissolve much more rapidly in a mixture of CCl_4 and CH_3OH than in pure CCl_4. The viscosities of solutions of rubbers in the mixture are much lower than the viscosities of solutions in the pure solvent. For example, a 2.5% solution of NR (of a low degree of mastication) in CCl_4 is a nonfluid gelatinous mass, while a 2.5% solution of the same rubber in a mixture of CCl_4 and CH_3OH in 6.7 : 1 ratio is quite fluid, although viscous. An interesting feature is that, in contrast to solution in the pure solvent, solution of rubber in the solvent-nonsolvent mixture proceeds almost without swelling, which, naturally, is associated with globulization of the molecules.

If a low-viscosity solution of rubber containing methyl alcohol is evaporated and the rubber residue is then dissolved in pure CCl_4, the viscosity of the solution so formed differs little from the viscosity of a rubber solution of the same concentration, prepared without the use of methyl alcohol (Table 4).

TABLE 4

Reversibility of the Globulization of Rubber Molecules

Composition of solvent	Specific viscosities of rubber solutions					
	1% NR		1% SKB		2.5% SKB	
	before evaporation	after evaporation and solution in CCl_4	before evaporation	after evaporation and solution in CCl_4	before evaporation	after evaporation and solution in CCl_4
CCl_4	52.3	68.3	4.1	4.0	20.4	16.8
$CCl_4 : CH_3OH = 20 : 1$	31.7	66.1	–	–	–	–
$CCl_4 : CH_3OH = 10 : 1$	25.2	63.7	–	–	–	–
$CCl_4 : CH_3OH = 6.7 : 1$	18.1	60.3	2.1	3.5	9.1	16.1

SUMMARY

1. Addition of nonsolvents to rubber solutions causes globulization of the macromolecules, similar to that occurring on addition of active substances (sulfur monochloride, halogens, etc.) to rubber solutions.

2. The difference between these processes lies in the fact that the coiling of the rubber molecules under the action of methyl alcohol is very rapid.

3. The globular structures in rubbers, produced by addition of nonsolvents to the solutions, in contrast to the stable globules formed in halogenation and vulcanization of rubber solution, are easily broken down and the molecules assume the linear form characteristic of the original rubber.

LITERATURE CITED

[1] P.I. Zubov, Z.N. Zhurkina and V.A. Kargin, Proc. Acad. Sci. USSR 67, 659 (1949).

[2] P.I. Zubov, Z.N. Zhurkina and V.A. Kargin, Colloid J. 16, 179 (1954) (T.p. 185).*

[3] P.I. Zubov, Z.N. Zhurkina and V.A. Kargin, Colloid J. 16, 345 (1954) (T.p. 337).*

[4] P.I. Zubov, Z.N. Zhurkina and V.A. Kargin, Colloid J. 17, 31 (1955) (T.p. 27).*

Received August 7, 1956

The L.Ya. Karpov Physicochemical
Scientific Research Institute

---

*T.p. = C.B. Translation pagination.

SEDIMENTATION VOLUMES OF POLYDISPERSE SUSPENSIONS OF $Ca_3(PO_4)_2$ IN ELECTROLYTE SOLUTIONS

G.G. Kandilarov

Earlier communications dealt with variations of the sedimentation volumes of polydisperse kaolin suspensions in relation to the concentrations of various electrolyte solutions [1, 2]. It was of interest to determine the extent to which the results are applicable to other suspensions, and to study the influence of the electric charge on the particles of a suspension on its sedimentation volume. A study has been made of polydisperse suspensions of calcium orthophosphate in basic and acidic electrolytes with ions of different valencies (sodium hydroxide, normal sodium carbonate, sodium phosphate, aluminum chloride, and hydrochloric acid). Pure normal calcium orthophosphate (analytical reagent grade), previously ground in a mortar, was used for the investigation. It was found by means of electrophoresis that its aqueous suspensions are positively charged. 2 g samples of $Ca_3(PO_4)_2$ were mixed with 10 ml of the given electrolyte solution and shaken during two periods of 2 minutes, with or without the use of a glass rod. The suspensions so formed were left to settle in a thermostat for 24 hours at 25°. The deposit formed generally had a curved surface, which made exact determination of its volume difficult. Despite this, the dependence of the volume of the $Ca_3(PO_4)_2$ sediment on the concentrations of the various electrolytes was fairly well defined.

The results of the observations are shown in Figures 1-4.

Results for $Ca_3(PO_4)_2$ suspensions in NaOH solutions are given in Figure 1a. It is seen that with increasing NaOH concentration in the solution the volume of the $Ca_3(PO_4)_2$ suspensions at first remains approximately constant; at a concentration of ~200 millimoles/liter a minimum is formed, after which the curve begins to ascend. Under the same conditions the sedimentation volume and internal friction curves for kaolin suspensions rise steeply.

Figure 1b shows the results of experiments with $Ca_3(PO_4)_2$ suspensions in solutions of Na_2CO_3. It is seen that with increasing concentration of Na_2CO_3 the volume of the $Ca_3(PO_4)_2$ deposits tends to decrease. In this case also there is a minimum (at a concentration of 500 millimoles/liter), but this is situated somewhat to the right of the corresponding minimum for suspensions containing NaOH. For suspensions in sodium phosphate solutions (Figure 1c) the same tendency to a volume decrease is seen, but the minimum is shifted still further to the right (1000 millimoles/liter).

Finally, the results of experiments with $Ca(OH)_2$ solutions (Figure 2) show the same tendency, although weak, to a decrease of the sedimentation volume of $Ca_3(PO_4)_2$. In this case, however, the curve ends at a low concentration of $Ca(OH)_2$ owing to its low solubility.

A comparison of the curves for the variation of the sedimentation volume of positively charged $Ca_3(PO_4)_2$ suspensions in solutions of these electrolytes [NaOH, Na_2CO_3, sodium orthophosphate, $Ca(OH)_2$] reveals a tendency for the sedimentation volume to decrease with formation of a minimum in all cases. It was shown in earlier investigations [1] that negatively charged suspensions of kaolin in NaOH solutions give steeply ascending sedimentation volume and internal friction curves.

The opposite character of the variations of the sedimentation volumes of $Ca_3(PO_4)_2$ and of kaolin suspensions is probably related to the opposite electric charges of these suspensions. Since the $Ca_3(PO_4)_2$ particles are positively charged, changes of its sedimentation volume in solutions of basic electrolytes must be associated with their anions, i.e., hydroxyl ions. The latter probably neutralize the positive charge of the suspensions,

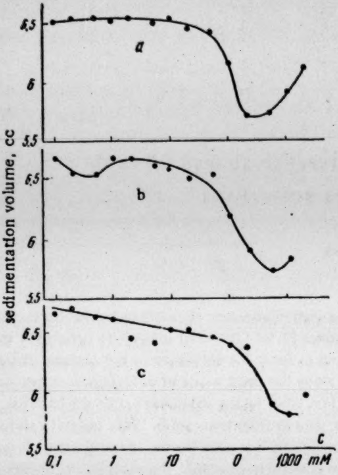

Fig. 1. Variation of the sedimentation volume of $Ca_3(PO_4)_2$ with electrolyte concentration: a) NaOH; b) Na_2CO_3; c) sodium orthophosphate.

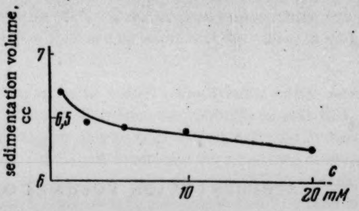

Fig. 2. Variation of the sedimentation volume of $Ca_3(PO_4)_2$ with $Ca(OH)_2$ concentration.

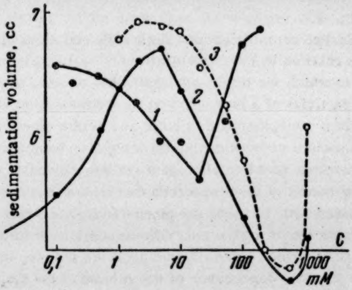

Fig. 3. Variation of the sedimentation volumes of: 1) $Ca_3(PO_4)_2$; 2) Schering kaolin; 3) Senovo kaolin, with $AlCl_3$ concentration.

thereby decreasing their hydration. In consequence the sedimentation volume of $Ca_3(PO_4)_2$ also tends to decrease. In kaolin suspensions, however, irrespective of hydration, hydroxyl ions repel the negatively charged particles (of the suspensions), resulting in a loose packing of the latter, so that the sedimentation volume of kaolin in sodium hydroxide solutions increases.

The charge of the anions also has an influence, seen in the fact that the minimum on the sedimentation volume curve for $Ca_3(PO_4)_2$ suspensions shifts, from a concentration of 200 millimoles/liter for sodium hydroxide, in the direction of higher concentrations for carbonate and phosphate ions, which have double and triple charges respectively.

It is seen in Figure 3 that with increasing concentration of aluminum chloride (which in this case can be regarded as a weak tribasic acid) the sedimentation volume of $Ca_3(PO_4)_2$ suspensions (Curve 1) decreases at first as the concentration changes to about 20 millimoles/liter, and then increases rapidly. At a concentration of 200 millimoles/liter the suspension becomes a mass with thixotropic properties, and the concentration-sedimentation volume curve is interrupted. It is highly probable that the increase of the sedimentation volume at high concentrations is the consequence of considerable hydration of the $Ca_3(PO_4)_2$ suspensions. At a concentration of 200 millimoles/liter the suspension becomes so thick that it resembles a gel, but strong agitation again converts it into a fairly mobile suspension.

At high concentrations of $AlCl_3$ the solubility of $Ca_3(PO_4)_2$ increases. With an $AlCl_3$ concentration of 500 millimoles/liter a turbid suspension is formed, with a deposit 2.25-2.40 cc in volume at the bottom of the vessel. At 1000 millimoles of $AlCl_3$ per liter the suspension becomes more transparent, and the volume of the sediment at the bottom of the vessel decreases to 0.70-0.75 cc.

Comparison of the curve for the variation of the sedimentation volume of $Ca_3(PO_4)_2$ suspensions in alumi-

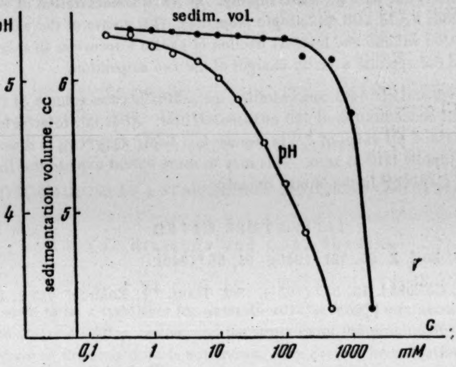

Fig. 4. Variation of the sedimentation volume of $Ca_3(PO_4)_2$ with HCl concentration.

num chloride solutions with the analogous curve for kaolin suspensions [1] (Figure 3, Curves 2 and 3) shows that the curves are opposite in character: with increasing aluminum chloride concentration the sedimentation volume (and the internal friction) of kaolin increases to a maximum at ~5 millimoles/liter, and then decreases rapidly. The sedimentation volume of $Ca_3(PO_4)_2$ suspensions, on the other hand, shows a minimum at a concentration of 20 millimoles/liter. This relative position of the curves is probably connected with the opposite electric charges of the two suspensions.

Figure 4 shows the variations of the pH of $Ca_3(PO_4)_2$ suspensions after exposure to hydrochloric acid for twenty four hours at 25°. The pH values were determined potentiometrically with quinhydrone and calomel electrodes. It is seen from Figure 4 that with increasing HCl concentration the sedimentation volume of $Ca_3(PO_4)_2$ suspensions remains at one relatively constant level up to an HCl concentration of 100 millimoles/liter. However, past this relatively high threshold value, at which the suspension reaches pH 4.2 in twenty-four hours, $Ca_3(PO_4)_2$ begins to be dissolved more rapidly, and the sedimentation volume quickly falls to zero. The relatively high threshold value beyond which rapid solution of $Ca_3(PO_4)_2$ in the acid begins is noteworthy. The concentration-pH curve also shown in Figure 4 indicates that in reality $Ca_3(PO_4)_2$ also dissolves at lower concentrations of hydrochloric acid, but because of its low content in the solution the acid is rapidly consumed in dissolving the salt, and the pH assumes higher values as a result.

In view of the fact that $Ca_3(PO_4)_2$ is present in soils or is added to soil as a phosphate fertilizer, and that it is present in urine (the pH of human urine is 5-7), these findings may shed some light both on the problem of phosphorus retention in the soil, and on the question of the formation of deposits of this salt in the human organism.

SUMMARY

1. The sedimentation volume of positively charged $Ca_3(PO_4)_2$ suspensions tends to decrease with increasing concentrations of NaOH, Na_2CO_3, sodium orthophosphate, and $Ca(OH)_2$, while the sedimentation volume and internal friction of negatively charged kaolin suspensions in sodium hydroxide increase sharply with increasing sodium hydroxide concentration. It may be assumed that this opposite course of the variation of sedimentation volume is associated with the opposite electric charges of the suspensions.

The curves for $Ca_3(PO_4)_2$ suspensions have a minimum which is shifted in the direction of higher concentrations with increase of the anionic charge. For NaOH solutions this minimum lies at ~200, for Na_2CO_3 at ~500, and for Na_2HPO_4 at ~1000 millimoles/liter.

2. With increasing $AlCl_3$ concentration the sedimentation volume of $Ca_3(PO_4)_2$ first decreases ($AlCl_3$ concentration 20 millimoles/liter) and then increases rapidly. At $AlCl_3$ concentration of ~200 millimoles/liter the suspension forms a viscous liquid with thixotropic properties. This course of the variation is opposite to the variation of the sedimentation volume and internal friction of kaolin suspensions in solutions of the same salt, which may be attributed to the opposite electric charges of the two suspensions.

3. With increasing hydrochloric acid concentration the sedimentation volume of $Ca_3(PO_4)_2$ suspensions remains constant up to an HCl concentration of 100 millimoles/liter. After this relatively high threshold value, at which the suspension attains a pH value of 4.2 in twenty-four hours, $Ca_3(PO_4)_2$ is dissolved more rapidly, and the sedimentation volume rapidly falls to zero. This may to some extent explain the fixation of phosphorus in soils and also deposition of $Ca_3(PO_4)_2$ in the human organism.

LITERATURE CITED

[1] G.G. Kandilarow, Koll. Z. 90, 321 (1940); 91, 56 (1940).

[2] G.G. Kandilarov, Colloid J. 13, 357 (1951); Sci. Trans. "V. Kolarov" VSI 1, 1 (1954); Colloid J. 18, 293 (1956) (T.p. 283).*

Received July 19, 1956

Chair of Inorganic, Analytical, Colloid and
Physical Chemistry at VIKhVPROM
Plovdiv, Bulgaria

---

*T.p. = C.B. Translation pagination.

GELATINIZED EMULSIONS

14. ETHYLCELLULOSE AS A STABILIZER OF EMULSIONS OF THE W/O TYPE

L. Ya. Kremnev and G. A. Shadrin

Ethylcellulose is known to be a stabilizer for water-in-oil ("reverse") emulsions. However, no quantitative data are available on its emulsifying action, and the structure of the protective films which stabilize the droplets of the disperse phase in the emulsions is not known. The present investigation deals with these questions. Seven industrial ethylcellulose samples, differing in molecular weight and degree of ethylation, were used for studies of the emulsifying properties. The samples were previously fractionated. Four fractions were isolated by means of ligroine (b.p. 80-90°) from a solution of each sample in toluene; the molecular weights and ethoxyl group contents of the fractions were then determined. The molecular weights were calculated by the equation

$$[\eta] = KM^a,$$

where $[\eta]$ is the intrinsic viscosity; M is the molecular weight of the polymer; K and a are constants. The values of these constants for ethylcellulose were determined by Nikurashina and Glikman [1], and are:

For the high molecular fractions, $K = 11.8 \cdot 10^{-4}$; $a = 0.666$;
For the low molecular fractions, $K = 6.9 \cdot 10^{-4}$; $a = 0.715$.

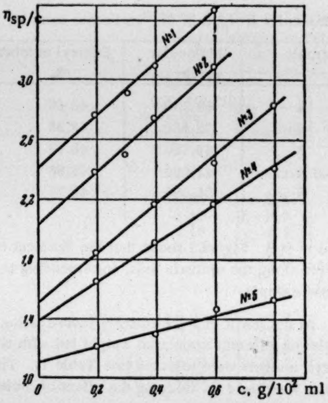

Fig. 1. Variation of reduced viscosity η_{sp}/c with concentration c of ethylcellulose fractions. The numbers correspond to the sample numbers in Table 1.

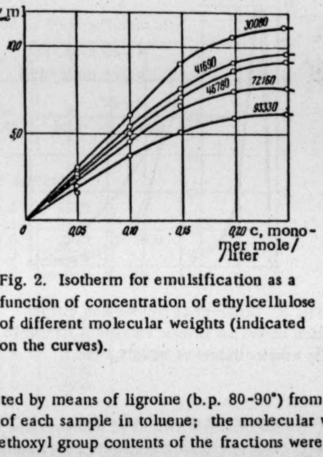

Fig. 2. Isotherm for emulsification as a function of concentration of ethylcellulose of different molecular weights (indicated on the curves).

As in the investigation cited [1], we determined the viscosity of alcohol-benzene solutions of the fractions in a capillary viscosimeter at 20 ± 0.05°. The values of the reduced viscosity η_{sp}/c were used to plot graphs for

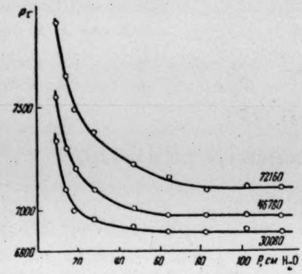

Fig. 3. Viscosities of ethylcellulose solutions of different molecular weights (shown on curves).

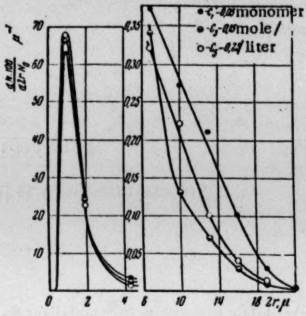

Fig. 4. Differential droplet size distribution curves for inverse emulsions stabilized by ethylcellulose of M = 93,330.

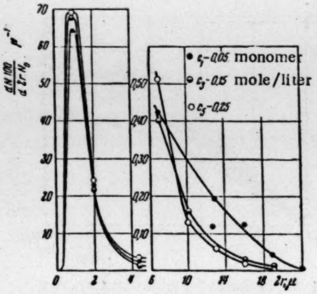

Fig. 5. Differential droplet size distribution curves for inverse emulsions stabilized by ethylcellulose of M = 72,160.

TABLE 1

Molecular Weights of Ethylcellulose Samples

Sample No.	Molecular weight	Ethoxyl number, %
1	93,330	48.66
2	72,160	48.90
3	46,780	48.79
4	41,690	48.86
5	30,080	48.73

$\eta_{sp}/c = f(c)$. Figure 1 shows that the lines cut off intercepts along the ordinate axis, corresponding to $[\eta]$ for each sample.

As the result of a preliminary investigation, five samples of different molecular weight but with similar ethoxyl numbers were selected (see Table 1). These samples were used for studying the effect of molecular weight of the polymer on emulsification.

Emulsions of water in toluene, of maximum concentration ("maximum emulsions") were prepared for the investigation, by our method with the use of a flexible spiral moving in a cylinder [2]. As usual, the end of emulsification was indicated when a successive addition of a small portion of water was no longer absorbed by the highly concentrated emulsion. The emulsions were diluted with xylene and subjected to microscopical dispersion analysis by the usual procedure adopted in our laboratory [3]. The results of this analysis were used to plot differential droplet size distribution curves, and the following were calculated: the thickness δ_{cr} of the protective films on the droplets, the surface S_∞ developed by 1 ml of the dispersion medium in maximum emulsions, and the surface area S_0 per molecule of the polymer in the interphase.

Figure 2 shows emulsification isotherms, representing the maximum volume V_∞ of the disperse phase in 1 ml of the dispersion medium as a function of the concentration c of ethylcellulose of different molecular weights. It is seen from Figure 2 that V_∞ increases with c, the curves being concave toward the abscissa axis; this, as in the other cases studied by us, is in agreement with the emulsification mechanism. The deviations from linearity, which increase with increasing c, are explained by the fact that when each successive portion of the dis-

TABLE 2

Reverse Maximum Emulsions Stabilized by Ethylcellulose of High Molecular Weight

Ethylcellulose concentration		δ_{cr} in μ	S_∞ in m^2	S_0 in $Å^2$	S in $Å^2$
monomer mole/liter	mole/liter × 10^4				
Sample No. 1; M = 93,330					
0.05	1.24	0.71	1.4	1860	15 200
0.10	2.49	0.25	4.0	2660	
0.15	3.73	0.17	5.9	2610	
0.20	4.97	0.16	6.2	2060	
0.25	6.21	0.15	6.5	1750	
Sample No. 2; M = 72,160					
0.05	1.61	0.56	1.8	1840	11 770
0.10	3.22	0.20	5.0	2560	
0.15	4.82	0.14	7.1	2430	
0.20	6.43	0.11	9.1	2330	
0.25	8.04	0.10	10.0	2050	

TABLE 3

Reverse Maximum Emulsions Stabilized by Ethylcellulose of Molecular Weight 30,080-46,780

Ethylcellulose concentration		δ_{cr} in μ	S_∞ in m^2	S_0 in $Å^2$	S in $Å^2$
monomer mole/liter	g mole/liter				
Sample No. 3; M = 46,780					
0.05	2,5	0,39	2,5	1660	7650
0.10	5,0	0,14	7,1	2360	
0.15	7,4	0,10	10,0	2220	
0.20	9,9	0,07	14,3	2380	
0.25	12,4	0,06	16,7	2220	
Sample No. 5; $M = 30,080$					
0.05	3.9	0.29	3.4	1440	4920
0.10	7.7	0.12	8.3	1780	
0.15	11.6	0.07	14.3	2030	
0.20	15.5	0.05	20.0	2130	
0.25	19.4	0.04	25.0	2130	

perse phase is introduced into the system, its emulsification is accompanied by further dispersion of all the emulsion droplets. Thus, the degree of dispersion of the highly concentrated emulsion increases continuously (homogenization occurs) during emulsification, up to the limiting value. Part of the stabilizer is expended in homogenization of the emulsion. Figure 2 shows that V_∞ decreases with increasing molecular weight of ethylcellulose. This influence of the molecular weight of the polymer is associated with the structural features of the protective films in emulsions, which will be discussed later. Another characteristic feature is that, at the limit, ethylcellulose emulsifies much smaller volumes of the disperse phase than typical stabilizers such as alkali soaps. This is also associated with the structure and properties of the protective films.

Table 2 gives details of the protective films in reverse maximum emulsions stabilized by ethylcellulose of relatively high molecular weight. The protective film thickness δ_{cr} decreases with increasing stabilizer concentration, tending to a constant value at high values of c. In this respect, polymeric emulsifiers are similar to the soaps studied previously. The significant difference is, however, that in the case of ethylcellulose stabilization of maximum emulsions is effected by much thicker protective films. It may be noted that in the case of sodium oleate δ_{cr} in direct and reverse emulsions is between 0.006 and 0.01μ at high soap concentrations.

The emulsifying power, quantitatively represented by the magnitude of the film surface S_∞, changes in the reverse emulsions. The emulsifying power of ethylcellulose is not high, and is appreciably lower than that of alkali soaps, as shown by the values of S_∞.

For an indication of the structure of the protective films it is useful to calculate the surface S_0 per molecule of ethylcellulose in the interphase, and to compare it with the surface S which the stabilizer molecule would occupy if it was situated completely at the liquid interface in the emulsion. On the assumption that all the polymer present in the maximum emulsion is adsorbed at the droplet surfaces, we find that the surface S_0 per molecule of No. 1 or No. 2 ethylcellulose is 2000-2500 A^2 (see Table 2).

Further, for an ethoxyl number of ~48.8 the degree of substitution of OH groups in the cellulose molecule is 2.5. In this case the "molecular weight" of the monomer is 232 and its degree of polymerization n = = 402. Then, from x-ray data on the dimensions of the cellobiose molecule [4], we find that the area S of a molecule of ethylcellulose No. 1 is 15,220 A^2. Similarly, S for ethylcellulose No. 2 is 11,770 A^2. Comparison of the values of S_0 and S leads to the highly important conclusion that the protective films of ethylcellulose, in contrast to alkali soaps, are not monomolecular but consist of several layers of polymer molecules.

To determine the principal factors influencing the stability of the emulsions studied, the viscosities of solutions of ethylcellulose of different molecular weights in toluene were measured by means of a capillary viscosimeter at 20 ± 0.05°. Figure 3 shows curves for the viscosities of solutions of three ethylcellulose fractions, at a concentration of 0.1 monomer-mole/liter (0.1 base-molar), for different efflux pressures P. The measure of viscosity is the value of $P\tau$ (τ is the efflux time). It is seen that ethylcellulose solutions have structural viscosity even at relatively low concentrations. The effective viscosity increases with increasing ethylcellulose concentration. Increase of the molecular weight of the polymer acts in the same direction. There is therefore no doubt that the dispersion medium in the emulsions is structurized. The mechanical properties of ethylcellulose solutions can be characterized by the yield value. Moreover, the solutions are thixotropic, and the spatial networks in them which are broken down at high pressures are restored during rest, as shown by the results of repeated viscosity determinations at initial low pressures.

The results indicate that, in full agreement with Rebinder's theory [5], protective films in emulsions consist of two-dimensional gels, greatly solvated by the dispersion medium and having considerable mechanical strength. Such high polymer gel films have a strong stabilizing effect on highly concentrated emulsions and, having peculiar structuro-mechanical properties, they are able to withstand considerable destructive forces for long periods.

The degree of dispersion of the emulsions studied is high; this is illustrated by the differential droplet size distribution curves in Figures 4 and 5.* An interesting feature is that despite the above structural peculiarities of the polymeric stabilizer films, the maximum on the distribution curves always corresponds to a droplet size of the order of 1μ. This is in full agreement with kinetic data on the emulsification process [6]. It should be remembered that stabilization of droplets of such limitingly small size is favored by rapid thixotropic buildup of the structures broken down in emulsification.

Table 3 gives the characteristics of the protective films in maximum emulsions stabilized by two ethylcellulose samples** of lower molecular weight than those described above.

The relationships found for the samples of higher molecular weight are also found for these samples. However the thickness δ_{cr} of the protective films decreases with decreasing molecular weight of the polymer, while the emulsifying power, represented by S_∞, increases (compare the data in Tables 2 and 3). The degree of dispersion of the maximum emulsions stabilized by ethylcellulose of lower molecular weight is also high. Comparison of the values of S and S_0 (Table 3) shows that, as for the polymers of high molecular weight, stabilization of maximum emulsions by ethylcellulose samples Nos. 3 and 4 is effected by means of gel films.

SUMMARY

1. Emulsions of water in toluene, of maximum concentration, have been prepared with ethylcellulose as

---

*For convenience the right hand regions of the distribution curves are shown separately in the diagrams.

**The emulsifying properties of sample No. 4 with M = 41,690 (see Table 1) are very similar to those of No. 3 with M = 46,780, and are therefore not given in the table.

stabilizer.

2. The emulsifying power of ethylcellulose increases and the thickness of the protective films which stabilize the droplets decreases with decreasing molecular weight of the ethylcellulose.

3. Maximum emulsions stabilized by ethylcellulose, like those with other stabilizers, are highly disperse, the maximum on the size distribution curves corresponding to droplets of the order of 1μ.

4. The main factor determining the stability of the emulsions studied is the mechanically strong multimolecular stabilizer gel film at the droplet surfaces.

LITERATURE CITED

[1] I.I. Nikurashina and S.A. Glikman, Sci. Mem. Saratov State Univ. 30, 66 (1952).

[2] L.Ya. Kremnev, Proc. Acad. Sci. USSR 79, 655 (1951); Colloid J. 13, 394 (1951).

[3] L.Ya. Kremnev and S.A. Soskin, Colloid J. 9, 269 (1947).

[4] Meyer and Misch, Helv. Chim. Acta 20, 232 (1937).

[5] P.A. Rebinder, Colloid J. 8, 157 (1946); P.A. Rebinder and K.A. Pospelova, introductory chapter to W. Clayton, Emulsions, translation edited by P.A. Rebinder (IL 1950).

[6] L.Ya. Kremnev and A.A. Ravdel, Colloid J. 16, 17 (1954) (T.p. 19).*

Received July 12, 1956

The Lensoviet Technological Institute

---

*T.p. = C.B. Translation pagination.

COLLOIDOCHEMICAL PROCESSES IN REACTIONS OF TETRAALKOXYSILANES WITH AQUEOUS ALUMINATE SOLUTIONS

A.P. Kreshkov, L.V. Myshlyaeva and L.M. Khananashvili

During the last decade there has been a considerable increase of interest in the organosilicon compounds. This is the consequence of the extension of their uses in industry and modern technology [1].

Particular theoretical and practical importance attaches to studies of reactions of orthosilicic acid esters (tetraalkoxysilanes) with various organic and inorganic compounds [2-7].

The present paper deals with a study of the reactions of tetraalkoxysilanes with aqueous sodium aluminate solutions.

Esters of orthosilicic acid are hydrolyzed by water, with condensation of the hydrolysis products

$$\mathrm{Si(OR)_4 + HOH \rightarrow (RO)_3SiOH + ROH;}$$

$$\mathrm{(RO)_3SiO\boxed{H + HO}Si(OR)_3 \rightarrow (RO)_3SiOSi(OR)_3 + H_2O}$$

etc., up to formation of polymeric compounds corresponding to the formula $\mathrm{(RO)_3SiO[Si(OR)_2O]_nSi(OR)_3}$. With excess water, further alkoxy groups are split off.

Alkalies accelerate the hydrolysis of alkoxyl groups, and give rise to silanolates: $\mathrm{NaOSi(OR)_3}$, $\mathrm{NaOSi(OR)_2OSi(OR)_3}$, etc.

Subsequent hydrolysis produces polydisperse systems containing small amounts of silicic acid in true solution, colloidally dissolved silicic acids, and alkoxypolysiloxanes. Hydrolysis of tetraalkoxysilanes ultimately leads, as has been shown by Grimaux [8], to formation of colloidally soluble silicic acid.

The polydisperse system: true aluminate solution – aluminum hydroxide sol in alkali, is in a state of equilibrium. Decrease of the alkalinity of the medium, change of temperature, and other factors may result in a shift of the equilibrium and coagulation of the $\mathrm{Al(OH)_3}$ sol to a gel. The presence of alcohols in high concentrations also leads to coagulation owing to desolvation of the disperse phase micelles. The rate of each of these reactions depends on various conditions. For example, in highly alkaline media coagulation of $\mathrm{Al(OH)_3}$ is retarded, and ester hydrolysis is accelerated.

The products of hydrolysis and dissociation of tetraalkoxysilanes and aqueous alkaline aluminate solutions interact:

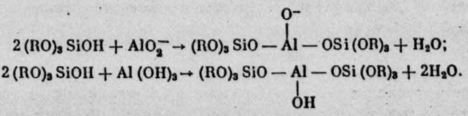

$$\mathrm{2(RO)_3SiOH + AlO_2^- \rightarrow (RO)_3SiO-\overset{\overset{\displaystyle O^-}{|}}{Al}-OSi(OR)_3 + H_2O;}$$

$$\mathrm{2(RO)_3SiOH + Al(OH)_3 \rightarrow (RO)_3SiO-\underset{\underset{\displaystyle OH}{|}}{Al}-OSi(OR)_3 + 2H_2O.}$$

In addition to purely chemical processes, coagulation of sols of $\mathrm{Al(OH)_3}$ and $\mathrm{mSiO_2 \cdot nH_2O}$ present in the reaction mixture also occurs.

Loewenstein's investigations [9] have shown that aluminosilicate crystal lattice, in accordance with the

Pauling rule, cannot contain more than 50% of aluminum. This has been confirmed experimentally by Iskoldsky [10] for the interaction of aqueous solutions of silicates with aluminates. The ratio of SiO_2 to Al_2O_3 in the reaction products varies between 2 and 3.

Nevertheless, we obtained precipitates which, on the basis of the foregoing considerations, cannot be regarded as individual substances, as their contents of aluminum were considerably higher than 50%. Their formation can be explained quite satisfactorily on the basis of colloidochemical concepts. In view of the complex nature of the processes involved, the laws governing them could be determined only by wide variations of the ratios of the reactants, their concentrations, reaction temperature, and other factors. It may be regarded as established that total mutual coagulation of the hydrolysis and condensation products of tetraalkoxysilanes and aqueous alkaline aluminate solutions occurs over a fairly wide range, but is nevertheless restricted by the proportions and concentrations of the reactants. No coagulation occurs at very high or very low molar Al: Si ratios. The reactions were in most cases accompanied by exothermic effects, which may be largely attributed to heat of hydrolysis of orthosilicic acid esters and heat of silicate formation.

The latent and visible coagulation periods were largely determined by the reaction conditions. During the reaction, coagulation apparently began to be accompanied by chemical reactions between the principal components of the system: $Na_2O-Al_2O_3-SiO_2-H_2O$, which were contained in the precipitates formed. Because of the considerable duration of the coagulation, it was possible to establish the sequence of the processes occurring in the reaction mixture by analysis of consecutive samples. It may be regarded as established that the primary process in most instances was coagulation of $Al(OH)_3$ sol. This was followed by deposition of precipitates containing increasing amounts of silicon. In strongly alkaline media at low aluminum concentrations, gelation of the reaction mixture usually took place, probably owing to coagulation of the hydrolysis and condensation products of tetraalkoxysilanes.

The reactions with tetramethoxysilane were very violent, even on considerable cooling, and it was therefore not possible to determine the consecutive stages of the process. On the other hand, the reactions with tetrapropoxy- and tetrabutoxysilane were so slow that it was possible to establish the formation of $Al(OH)_3$ precipitate at room temperature. Precipitation of $Al(OH)_3$ at the interface between aqueous aluminate solution and tetraalkoxysilane may be regarded as an instance of the adsorptive instability of $Al(OH)_3$ sol with respect to tetraalkoxysilanes.

Partial hydrolysis of tetrapropoxy- and tetrabutoxysilanes in strongly alkaline media proceeds with formation of silanolate groups, which results in removal to the stabilizing OH^- ions and coagulation of $Al(OH)_3$ [11]. The reaction with tetraethoxysilane continues for a considerable time in some cases. This is fully explained by the fact that the tendency of orthosilicic acid esters to hydrolysis decreases with increasing size of the organic radical.

Chemical analysis of the liquid phase separated from the precipitate showed that it consisted of an aqueous alcoholic solution of alkali. The solid reaction products contained only very small amounts of alkoxy groups, while the molar Al: Si ratios were the same as the original. The products were optically inhomogeneous. They were purified by repeated extraction in a Soxhlet apparatus, first with absolute ethyl alcohol and then with benzene. This purification considerably decreased the alkalinity and the aluminum contents of the products, probably owing to peptization of $Al(OH)_3$. Analysis of the purified products showed that they were of constant composition. In addition, a crystalline product identified as sodium hydroaluminosilicate was isolated.

To determine whether the solid reaction products are mixtures of gels of alkoxypolysiloxanes and silicic acid with aluminum hydroxide gel, or whether the coagulation processes are accompanied by chemical reactions with formation of alkoxyaluminosilicates or aluminosilicates, the reaction products were studied by physical methods of analysis (spectroscopic, x-ray structure, and optical crystallography). Usually structures are determined from chemical and physical analytical data by analogy with compounds described in the literature. No data are available in the literature on compounds similar to those prepared by us. However, certain structural groups characteristic of these compounds are also characteristic of compounds which have been studied and described in the literature. Calculations of interplane distances on the basis of x-ray data for most of our products showed that their basic structure is that of orthosilicates. On the other hand, samples containing aluminum showed characteristic features of aluminosilicates. It was shown by means of infrared absorption spectroscopy (powder method) that all the products gave absorption maxima characteristic of Si–O and Na–O bonds. The reaction products of tetraethoxysilane and aqueous sodium aluminate solution gave an absorption maximum at

10.2μ (981 cm^{-1}), characteristic of aluminosilicates of the albite and anorthoclase type.

EXPERIMENTAL

Sodium aluminates were prepared by dissolving chemically pure $Al(OH)_3$ in concentrated NaOH [12]. Details of the sodium aluminate solutions are given in Table 1.

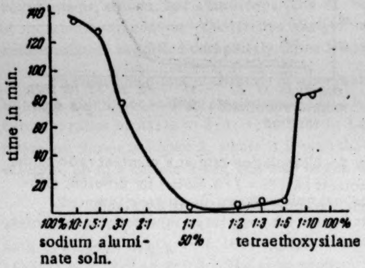

Fig. 1. Coagulation rates with different proportions of the reactants (in moles).

TABLE 1

Composition of Sodium Aluminate Solutions

Aluminate solutions	Na_2O in %	Al_2O_3 in %	Caustic ratio in moles
Sodium aluminate I	30.20	18.00	2.76
Sodium aluminate II	21.05	19.40	1.78

Orthosilicic acid esters were synthesized by methods described in the literature [1]. The reactions between tetraalkoxysilanes and alkaline aluminate solutions were carried out in a three-necked flask fitted with a stirrer and thermometer. Experiments in which it was required to determine the times for visible coagulation were performed in test tubes or cylinders with stirring by hand.

Tetraalkoxysilanes behave differently in their reactions with aluminate solutions. Tetramethoxysilane reacted practically completely within 1-2 minutes, with a high exothermic effect, in experiments with Al: Si ratios from 1 : 10 to 10 : 1, in which the aluminate solution was diluted with water to give aluminate : water ratios of 1 : 0, 1 : 1, etc., up to 1 : 20. The reaction products were gels of various consistencies, from which a liquid phase separated by syneresis; this was found to contain methyl alcohol and alkali in addition to water. With tetrapropoxy- and tetrabutoxysilanes no large amounts of precipitate were formed even after many hours of stirring at room temperature or at 65-70°. Analysis of the precipitate formed with tetrapropoxysilane (ratio of Al: Si = 1 : 1) at room temperature with continuous stirring for 10 hours gave the following results: Na_2O – 2-3%; SiO_2 – traces; Al_2O_3 – 10.15%; with tetrabutoxysilane at the same ratios and under the same conditions the small amount of precipitate contained: Na_2O – 1.96%; SiO_2 – traces; Al_2O_3 – 9.87% (analytical data not recalculated on the dry substance). Consequently, the precipitate consists of aluminum hydroxide with adsorbed alkali.

TABLE 2

Chemical Composition of Reaction Products

Molar Al: Si ratio	Nature of products	Na_2O in %	SiO_2 in %	Al_2O_3 in %	C_2H_5O in %	Molar ratios of Na_2O : SiO_2 : Al_2O_3 : C_2H_5O
1 : 6	Liquid	1.21	26.06	6.53	66.20	0.05 : 1 : 0.15 : 3.4
1 : 6	Solid	28.60	17.42	51.68	2.30	1.59 : 1 : 1.74 : 0.2
1 : 9	Liquid	0.73	23.50	4.33	71.44	0.03 : 1 : 0.1 : 4.15
1 : 10	Solid product, extracted twice	14.52	42.46	40.03	2.99	0.33 : 1 : 0.55 : 0.1

To study the influence of the proportions of the reactants, the original aluminate I solution was reacted with tetraethoxysilane with continuous stirring at room temperature, at different molar Al: Si ratios. The variation of the time for visible coagulation (i.e., turbidity and formation of a precipitate) with the ratio used is shown in Figure 1. It is seen in Figure 1 that coagulation in the system tetraethoxysilane-sodium aluminate solution proceeds at the maximum rate at moderate concentrations of AlO_2 ions. The end of the reaction is easily seen by homogenization of the whole mass, and by subsequent coagulation if it occurs. At Al: Si ratios of

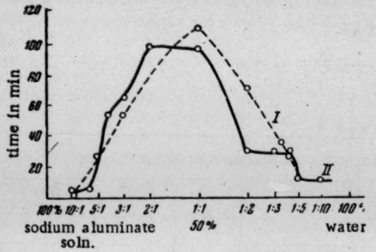

Fig. 2. Coagulation rates at a constant ratio of the reactants (Al: Si = 1:1 molar) at different dilutions of aluminate solutions I and II with water.

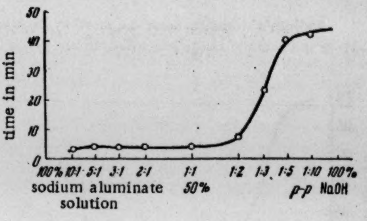

Fig. 3. Coagulation rate at a constant ratio of the reactants (Al: Si = 1:3 molar) for different dilutions of aluminate II solution by alkali.

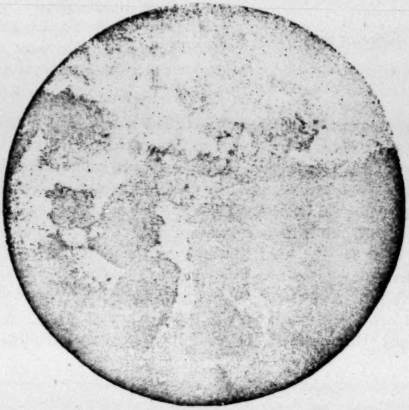

Fig. 4. Micrograph of reaction product of tetraethoxysilane with sodium aluminate solution (Al: Si = 1:3 molar, and aluminate solution:NaOH = 1:10).

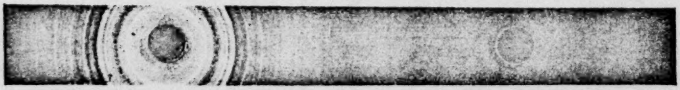

Fig. 5. X-ray diagram of reaction product of tetraethoxysilane with sodium aluminate solution (Al: Si = 1:3 molar and aluminate solution: NaOH = 1:10).

8:1 and over coagulation did not take place.

At Al: Si ratios from 1:6 to 1:10 slight precipitates were formed some time after the mixture became homogeneous. Some of the reaction products were analyzed. Silicon [13] and aluminum [14] were determined gravimetrically. Alkalinity was determined by titration with standard hydrochloric acid against phenolphthalein [14], and alkoxyl groups by Nessonova's modification [15] of Pregl's semimicro method. Analytical data for products with high Al: Si ratios (recalculated on the dry substance) are given in Table 2.

The analytical results showed that the precipitates (after washing with benzene) were practically free of ethoxyl groups; the Al: Si ratio changed in the direction of an increase of the relative amount of aluminum in comparison with the original ratio. The liquid products contained, in addition to small amounts of alkali, alkoxyl groups, silicon, and aluminum. The Al: Si ratio remained almost unchanged, apart from a slight decrease of the aluminum content. Qualitative analysis of the liquid separated out by syneresis in cases in which the reaction mixture solidified completely showed that the liquid consisted of an aqueous alcoholic solution of alkali.

To study the effect of dilution of aluminate solutions with water, aluminate solutions I and II diluted with water to aluminate solution : water ratios of 1 : 1, 1 : 2, etc., up to 1 : 50, were reacted with tetraethoxysilane at constant ratios of Al: Si = 2 : 1; 1 : 1; 1 : 2; 1 : 3 and 1 : 4 at room temperature. The results obtained for these ratios are shown in Figure 2, where it is seen that for both aluminates the reaction rate decreases with increasing dilution, up to a certain limit, and then begins to increase again.

Chemical analysis of the unpurified product formed at a ratio of Al: Si = 2 : 1 with 1 : 3 dilution of the aluminate solution with water gave the following results (recalculated on the dry substance): $Na_2O = 41.70\%$; $SiO_2 = 18.64\%$; $Al_2O_3 = 35.46\%$; $C_2H_5O = 4.20\%$, corresponding to molar proportions of $Na_2O : SiO_2 : Al_2O_3 : C_2H_5O = 2.18 : 1 : 1.1 : 0.3$. The same product, purified by repeated extraction first with absolute ethyl alcohol and then with benzene, contained: $Na_2O - 25.14\%$; $SiO_2 - 63.25\%$; $Al_2O_3 - 10.03\%$; $C_2H_5O - 1.58\%$, corresponding to molar proportions of $Na_2O : SiO_2 : Al_2O_3 : C_2H_5O = 0.38 : 1 : 0.1 : 0.034$.

TABLE 3

Analytical Data for Consecutively Precipitated Reaction Products

Na_2O in %	Al_2O_3 in %	SiO_2 in %	Al : Si in g-molar	Na_2O in %	Al_2O_3 in %	SiO_2 in %	Al : Si in g-molar
Aluminate solution $H_2O = 1:2$				Aluminate solution $H_2O = 1:3$			
7.82	1.89	9.48	5.88	6.68	2.07	5.90	3.35
8.49	1.46	6.46	5.50	6.58	1.84	5.75	3.70
8.31	1.84	8.01	5.10	5.40	2.14	6.14	3.37
7.24	4.16	18.40	5.20	6.14	1.74	5.44	3.67
7.24	2.07	7.50	4.26	5.92	2.14	6.03	3.32
7.82	3.67	13.15	4.22	5.46	2.68	6.42	2.82
5.34	2.07	7.49	4.26	6.00	1.95	3.32	2.00
10.00	1.97	7.82	4.66	6.68	2.16	4.58	2.50
6.93	1.78	5.06	3.34	4.84	1.62	Traces	—

Comparison of the molar proportions of the purified and unpurified products shows that the Al: Si ratio in the purified product was considerably lower. The alkalinity of the purified product was also lower. Similar results were obtained by purification of other solid products. Precipitation extended over a considerable period made it possible to carry out fractional analysis of consecutively precipitated reaction products. Aluminate I was used for the reactions. The analysis was performed for the ratio Al: Si = 1 : 1 and aluminate solution : water = = 1 : 2 and 1 : 3. The analytical results are given in Table 3.

The analytical results show that the precipitates have higher aluminum contents than the original mixture, i.e., that the coagulation of $Al(OH)_3$ sol must be regarded as the predominant process. For the ratio of aluminate solution: $H_2O = 1:3$ the relative content of aluminum in the precipitates is less than for aluminate solution: $H_2O = 1:2$.

To study the effect of amount of alkali in the reaction mixture, a series of experiments was carried out, in which the aluminate was diluted with alkali, so calculated that its concentration in the solution remained constant (i.e., with increasing caustic ratio). Increase of the caustic ratio had the following effects: first the time for the start of visible coagulation decreased in comparison with corresponding experiments on dilution with water; this may be attributed to acceleration of ester hydrolysis (Figure 3). The end of visible coagulation was somewhat retarded.

In a reaction mixture with ratios of Al : Si = 1 : 3 and aluminate solution: NaOH = 1 : 10, the amorphous precipitate initially formed crystallized after prolonged standing in the form of needles and branched crystals (Figure 4). The crystals had the following composition: Na_2O – 44.62%; Al_2O_3 – 7.63%; SiO_2 – 46.45%; C_2H_5O – 1.3%. This corresponds to molar proportions of: $Na_2O : SiO_2 : Al_2O_3 : C_2H_5O$ = 0.93 : 1 : 0.1 : 0.038. The average refractive index of the crystals was 1.483 ± 0.003.

Experiments to determine the effect of temperature on the reaction rate showed that the reaction rate increases considerably with temperature. Table 4 gives the reaction rates, at different temperatures, of tetraethoxysilane with aluminate II at a ratio of Al : Si = 1 : 1 and with the aluminate solution diluted with water in the ratio aluminate solution: H_2O = 2 : 1. The reaction products of tetraethoxysilanes and aqueous sodium aluminate solutions were examined in transmitted polarized light; their average refractive indices were determined by the immersion method. Many of the products had a fine crystalline structure, while some were deposited in the form of large crystals. In some cases study of the crystals was difficult owing to their hygroscopic nature.

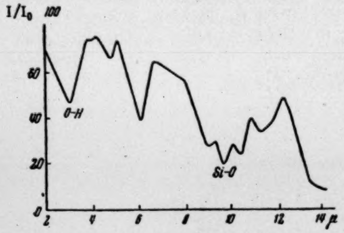

Fig. 6. IR-absorption spectrum of the interaction product of tetraethoxysilane with aqueous sodium aluminate solution (Al : Si = 1 : 2; aluminate solution: H_2O = 1 : 4).

TABLE 4

Coagulation Rates of Reaction Products at Various Temperatures

Temperature, °C	End of visible coagulation	Temperature, °C	End of visible coagulation
0	28 hours	50	25 minutes
10-12	12.5-13 hours	75	5 minutes
20	98 minutes	100	3 minutes

The crystalline product formed in the interaction of tetraethoxysilane with aqueous sodium aluminate solution (Al : Si = 1 : 3; aluminate solution: NaOH = 1 : 10) had the following characteristics. It crystallized in the form of needles and dendrites. The average refractive index N_m = 1.483. The crystals were not pleochroic. The micrograph (Figure 4) shows the crystals under a magnification of 800. The same product was examined by x-ray analysis. This was performed by the Debye method (with the RKD camera). Soft Cuα radiation was used. The interplane distances were calculated from the equation $d = \lambda/2 \sin \theta$. The line intensities were evaluated on a five-point scale. The product had a well defined crystalline structure. A comparison of the calculated interplane distances with literature data for various modifications of SiO_2, sodium silicates, and aluminosilicates leads to the conclusion that the structure of the product contains elements characteristic of albite and kaolin [16]. It is impossible to identify any of the compounds described in the composition of the product. An x-ray diagram of the product is shown in Figure 5.

The product obtained in the interaction of tetraethoxysilane with sodium aluminate solution (Al : Si = = 1 : 2; aluminate solution: H_2O = 1 : 4) was studied by the infrared spectroscopic method. Absorption spectra were obtained by the powder method by means of the IKS-11 infrared spectrograph in the region between 2 and 15μ. The absorption spectra of the products were found to contain absorption bands characteristic of individual functional groups. The absorption spectrum (Figure 6) contained the following maxima: 3.00μ (3333 cm^{-1}), characteristic of the O–H bond in aluminosilicates [17]; 9.6μ (1042 cm^{-1}), for the Si–O bond [18]; 11.4μ (878 cm^{-1}) for the Na–O bond [19], and 10.2μ (982 cm^{-1}) for the albite and anorthoclase structure [20].

SUMMARY

1. Interaction of tetraalkoxysilanes with aqueous alkaline aluminate solutions results not only in chemical processes (hydrolysis of orthosilicic acid esters and formation of aluminoalkoxy- and aluminosilicates), but also in colloidochemical processes (coagulation of $Al(OH)_3$ and $mSiO_2 \cdot nH_2O$ sols and peptization of the corresponding gels).

2. In a number of cases the primary process in the interaction is coagulation of $Al(OH)_3$ sol caused by decrease in the concentration of the stabilizing OH^- ions. This may be regarded as an instance of the adsorptive instability of $Al(OH)_3$ sol with respect to tetraalkoxysilane.

3. It is shown that the nature of the processes taking place differs according to the conditions:

a) at high molar Al : Si or Si : Al ratios precipitates are not formed. The explanation is that the reaction products can form colloidal solutions in the reaction medium;

b) the times for visible coagulation to begin depend considerably on dilution, temperature and other factors.

4. Amorphous and crystalline products have been isolated; these have been shown by chemical and physical analysis to consist of sodium aluminosilicates of the albite and anorthoclase type.

LITERATURE CITED

[1] A.P. Kreshkov, Organosilicon Compounds in Technology, 2nd edition (Industrial Construction Press, Moscow 1956).

[2] A.P. Kreshkov, Proc. Acad. Sci. USSR 59, 723 (1948).

[3] A.P. Kreshkov, A.N. Chivikova, G.D. Nessonova, V.A. Matveev and M.L. Darashkevich, Trans. Mendeleev Inst. Chem. Technology Moscow 17, 15 (1952).

[4] A.P. Kreshkov and L.V. Myshlyaeva, Trans. Mendeleev Inst. Chem. Technology Moscow, 13, 38 (1948).

[5] A.P. Kreshkov, J. Appl. Chem. 23, 545 (1950).

[6] A.P. Kreshkov, J. Gen. Chem. 20, 1415 (1950).

[7] A.P. Kreshkov and G.S. Petrov, J. Chem. Ind. No. 8, 10 (1944).

[8] E. Grimaux, Comptes rendus 98, 1434 (1884).

[9] W. Loewenstein, Am. Mineral 39, 92 (1954).

[10] I.I. Iskoldsky, Chemistry of Solutions in the Aluminum Industry (ONTI, Moscow-Leningrad 1937).

[11] N.P. Peskov and E.M. Aleksandrova-Preis, Course of Colloid Chemistry (Goskhimizdat, Moscow-Leningrad 1948).

[12] Prascott, J. Am. Chem. Soc. 2, 27 (1880) (cited through [10]).

[13] P.N. Grigoryev, Water Glass (Industrial Construction Press, Moscow 1948), p. 185.

[14] W.G. Hillebrand and G.E. Lundell, Applied Inorganic Analysis (ONTI, Moscow 1937).

[15] A.P. Kreshkov, V.A. Bork, L.V. Myshlyaeva and G.D. Nessonova, Analysis of Organosilicon Compounds (Goskhimizdat, Moscow 1954).

[16] J.D. Hanawalt, H.W. Rinn and L.K. Frevel, Ind. Eng. Chem. 10, 469 (1938).

[17] A. Buswell and Dudenbostel, J. Am. Chem. Soc. 63, 2554 (1941).

[18] A.P. Kreshkov, Yu.Ya. Mikhailenko and G.F. Yakimovich, J. Phys. Chem. 28, 537 (1954).

[19] P.N. Ghosh and B.D. Catterjee, Z. Physic. 72, 542 (1931).

[20] G.S. Bachman, Glass Industry 29, 435 (1948).

Received December 1, 1956

The D.I. Mendeleev Institute of
Chemical Technology

STUDY OF THE COLLOIDAL PROPERTIES OF SULFOSUCCINIC ACID ESTERS

1. ESTERS OF THE LOWER ALIPHATIC ALCOHOLS

R.V. Kucher,, A.A. Yavorsky* and M.A. Kovbuz

The colloidal properties of soaps and soaplike substances have great significance in relation to a number of important problems of modern chemistry. These include chemical reactions in emulsions (polymerization, hydrocarbon oxidation). Our earlier publications [1-3] described the colloidochemical properties (micellar weight, critical concentration, etc.) of various sulfonated soaps. Although the substances studied had been purified to remove electrolytes, they could still contain various impurities which might influence the behavior of colloidal electrolytes in aqueous solutions. It was therefore very desirable to investigate the colloidal properties of a number of pure colloidal electrolytes in which the influence of impurities would be excluded. From this standpoint the esters of the sodium salts of sulfosuccinic acid are particularly worthy of attention. Data on the colloidal properties of these substances, which were synthesized by us, will be presented in this and subsequent communications.

Sulfosuccinic acid esters are of considerable theoretical and practical interest. Under the names of Aerosols OT, MA and IB, some of them are widely used as very effective surface active agents. Nevertheless, the literature contains no data on systematic investigations of their colloidochemical properties or on methods for synthesizing these esters. Such investigations are essential for systematic selection of a particular representative of the series for a given purpose.

We have studied the colloidochemical characteristics of a series of completely substituted sulfosuccinic acid esters in aqueous solutions, with different, gradually increasing numbers of carbon atoms in the alkyl chain. The present communication deals with the four lowest representatives of the series – the dimethyl, diethyl, dibutyl, and diisoamyl esters. Very little information on the synthesis of such compounds is given in the literature. The first reports on sulfosuccinic acid esters as wetting agents appeared in 1936 [4]. Subsequently numerous other publications appeared on the subject [5-8]. However, methods of synthesis of individual members of the series are mentioned only very briefly.

The literature cited above contains reports of the production of sulfosuccinic acid esters from maleic acid esters. The preparation of sulfosuccinic acid from maleic acid by bisulfite addition has been described in considerable detail [9-11]. The sulfosuccinic acid esters and a number of other compounds studied in the present investigation were synthesized from the corresponding maleic acid esters by addition of sodium or potassium bisulfite. The conditions for the addition reaction, however, differ considerably for different representatives of the series. Therefore, questions relating to the syntheses will be described in greater detail in a separate communication.

The substances studied, in the form of the sodium salts, were thoroughly purified after synthesis. For this they were recrystallized 2-3 times from water, and then dried under vacuum at a residual pressure of 10 mm Hg over calcium chloride at 100-110° for 12-24 hours; they were then analyzed. The dimethyl and diethyl esters were also azeotropically distilled with toluene and held for 24 hours under vacuum at 40° over paraffin.

The analyses were carried out by the Korshun and Gelman combustion method, with the sulfur combined with metallic silver. The analytical results are given in Table 1.

The present communication describes the results of a study of the colloidochemical properties of aqueous

---

*Deceased.

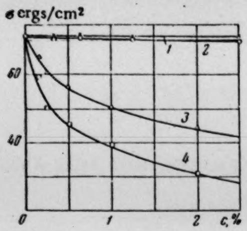

Fig. 1. Surface tension isotherms for aqueous solutions of sodium sulfosuccinate esters at 20°: 1) DME; 2) DEE; 3) DBE; 4) DIAE.

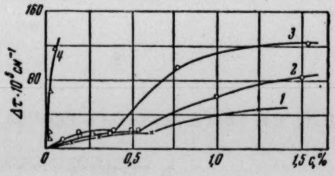

Fig. 2. Turbidity of dilute aqueous solutions of sodium sulfosuccinate esters: 1) DME; 2) DEE; 3) DBE; 4) DIAE.

TABLE 1

Analytical Data on the Dimethyl (DME), Diethyl (DEE), Dibutyl (DBE), and Diisoamyl (DIAE) Esters of Sodium Sulfosuccinate

Compound	Carbon content, %		Hydrogen content, %	
	found	calculated	found	calculated
DME	28.75	28.98	3.55	3.67
DEE	36.12	36.05	4.87	4.92
DBE	42.95	43.32	6.46	6.37
DIAE	44.63	44.66	6.66	6.69

TABLE 2

Colloidochemical Properties of Lower Esters of Sodium Sulfosuccinate in Aqueous Solutions at pH 9.9 (20°)

Compound	CCM moles/liter	W_m/kT	Micellar weight, M	Degree of micellization, N_0	$N - N_0$
DEM	$2.89 \cdot 10^{-2}$	10.6	2330	10.8	2.09
DEE	$2.19 \cdot 10^{-2}$	11.5	4350	17.8	2.49
DBE	$1.28 \cdot 10^{-2}$	13.1	5820	19.4	2.43
DIAE	$3.05 \cdot 10^{-5}$	30.8	71400	217.1	5.31
Aerosol MA	$1.29 \cdot 10^{-3}$	20.0	10000	25.8	2.56

solutions of the four compounds indicated in Table 1.

Figure 1 shows the surface tension isotherms (at 20°) of aqueous solutions of DME, DEE, DBE and DIAE, determined by the maximum bubble pressure method by means of P.A. Rebinder's apparatus. The results show that the first two members of the series (DME and DEE) have practically no surface activity in aqueous solutions. The dibutyl ester produces an appreciable decrease of surface tension in aqueous solution (to 44 ergs/cm² at $c = 2\%$). The diisoamyl ester has even greater surface activity; in this respect it approaches such well known sulfonates as Nekal [1]. Similar results are obtained both in acid (6% HNO_3) and alkaline media (0.1 N soda solution, pH 9.9).

We may conclude from these results that in the series of sodium sulfosuccinate esters surface activity at the water-air interface reaches appreciable values starting with the third member of the series, the dibutyl es-

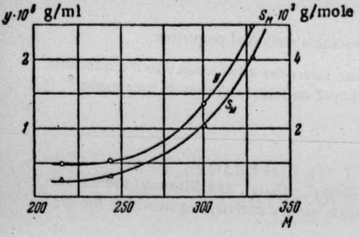

Fig. 3. Solubilization (y) and molar solubilization (S_M) of Sudan III in aqueous solutions of lower esters of sodium sulfosuccinate, in relation to the molecular weight (M) of the colloidal electrolytes.

ter. The hydrophobic radical of the molecule of this compound is large enough to cause considerable surface adsorption. In addition to surface activity, a very important property of colloidal electrolytes is micelle formation in aqueous solutions. This property plays an especially important role when colloidal electrolytes are used as emulsifiers for chemical reactions in emulsions (for example, polymerization or liquid phase oxidation of hydrocarbons). To determine the tendency to micelle formation in the lower esters of sodium sulfosuccinate, we studied their critical concentrations of micelle formation (CCM) and micellar weights. A 0.1 N soda solution was added to all the solutions to give pH 9.9, as it is colloidal behavior in alkaline media which is important in relation to chemical reactions in emulsions, when the aqueous medium usually has pH > > 7. It has recently been shown [12] that the micelle formation of soaps and soaplike substances increases considerably in presence of electrolytes. Micelle formation was studied by the light scattering method described previously [2].

Variations of turbidity with concentration of very dilute solutions of these colloidal electrolytes are shown in Figure 2. By means of these data it is possible to determine CCM from the point at which the turbidity begins to increase. Figure 2 shows that these points are fairly distinct. The values of the CCM for the substances studied are given in Table 2.

The micellar weights of the compounds were determined from the results of turbidity measurements for solutions of higher concentrations (up to 2.5%). The micellar weights given in Table 2 were found by extrapolation of $H(c/\Delta\tau) = f(c)$ to zero concentration, as described previously [2]. The first three members of the series have relatively high CCM and low micellar weights. Therefore, the degree of micellization N_0 (ratio of micellar to molecular weight), and the energy of association, calculated from the equation [13, 14]

$$w_m = -3\,kT \ln c_0$$

(where c_0 is the critical concentration of micelle formation (CCM) and w_m is the association energy of two molecules of the colloidal electrolyte) are also low. Thus, the colloidal nature of these two lowest members of the series under investigation is very weak. The diisoamyl ester, however, has low CCM and a fairly high micellar weight. It is interesting to note that the colloidal properties of Aerosol MA (an imported dihexyl ester of sulfosuccinic acid), data for which [14] are included in Table 2 for comparison, are weaker than those of DIAE, although the hydrophobic portion of its molecule contains two more CH_3 groups than that of the latter compound. It seems that the greater tendency to micelle formation of DIAE as compared with Aerosol MA is related to the iso-structure of the alkyl hydrocarbon chain in the DIAE molecule. It is intended to study this question in greater detail in a later investigation.

We may also note that the polydispersity of the micelle $(N - N_0)$, calculated by the Debye equation [13] is low for all the compounds studied. Finally, as was shown previously [3], the colloidal properties (micellar weight) are closely associated with solubilization of oleophilic substances in aqueous solutions of colloidal electrolytes. Thus, solubilization can also serve as a measure of the colloidal nature of a soaplike substance. Moreover, solubilization is an important factor in chemical reactions in emulsion systems.

We studied the solubilization of the oleophilic water-insoluble dye Sudan III in aqueous solutions of the esters; the solution pH was 9.9. The solubility of the dye was determined photometrically [3]. Figure 3 shows the variation of the solubilization of Sudan III in 2% solutions of the colloidal electrolytes studied with the molecular weight of the latter. The graphs show the solubilization[(y) in g/ml)]and the molar solubilization (S_M in grams of dye per mole of colloidal electrolyte). The solubility of Sudan III in aqueous solutions of the lowest two esters is almost the same. Solubilization is greatly increased in presence of the dibutyl and especially of the diisoamyl ester. This indicates that in this series of compounds colloidal properties first appear in DBE, which must be regarded as the first member of the series to have appreciable colloidal properties.

All this shows that in the series of aliphatic sodium sulfosuccinate esters the alkyl residue in the molecule must contain at least four carbon atoms (butyl and higher) for formation of colloidal solutions in an aqueous medium.

SUMMARY

1. Surface tension isotherms of aqueous solutions of dimethyl, diethyl, dibutyl, and diisoamyl sodium sulfosuccinate have been studied. It is shown that in this series appreciable surface activity begins within the dibutyl ester.

2. Micelle formation in aqueous solution in the first three members of this series of esters is slight, as confirmed by the values of the critical micelle concentration and micellar weight determined by the light scattering method. The diisoamyl ester has definite colloidal properties.

3. The solubilization of Sudan III in aqueous solutions of the lower sulfosuccinate esters begins to increase starting with the dibutyl ester, and is especially high with the diisoamyl ester.

LITERATURE CITED

[1] A.I. Yurzhenko and R.V. Kucher, Proc. Acad. Sci. USSR 85, 1337 (1952).

[2] A.I. Yurzhenko and R.V. Kucher, Colloid J. 13, 226 (1951); 14, 219 (1952) (T.p. 243).*

[3] A.I. Yurzhenko and R.V. Kucher, Colloid J. 14, 283 (1952) (T.p. 311).*

[4] A.O. Jaeger, U.S. Patent 2028091; C.A. 30, 1466 (1936).

[5] F.C. Ross, Amer. Dyestuff Reporter 26, 825 (1937).

[6] C. Caryl and W. Ericks, Ind. Eng. Chem. 31, 44 (1939).

[7] C. Caryl, Ind. Eng. Chem. 33, 731 (1941).

[8] A.O. Jaeger, U.S. Patent 2252401; C.A. 35, 7585 (1941).

[9] H.J. Backer and J.M. van der Zanden, Rec. trav. chim. 46, 473 (1927).

[10] E. Hägglünd and A. Ringbom, Z. anorg. Chem. 150, 231 (1926).

[11] J.M. van der Zanden, Rec. trav. Chim. 45, 242 (1926).

[12] A.N. Mankowich, J. Phys. Chem. 58, 1827 (1954).

[13] P.J. Debye, J.Phys. Colloid Chem. 53, 1 (1949).

[14] R.V. Kucher and M.A. Kovbuz, Colloid J. 18, 193 (1956) (T.p. 185).*

Received August 7, 1956

The I. Franko State University, Lvov
The Ukrainian Scientific Research
Institute for the Polygraph Industry

---

* T.p. = C.B. Translation pagination.

HEAT EVOLUTION IN THE INITIAL PERIOD OF HYDRATION OF CEMENT WITH PLASTICIZING ADDITIONS.

O.I. Lukyanova, E.E. Segalova and P.A. Rebinder

The chemical interaction of water with cement clinker minerals includes exothermic reactions the heat effects of which are fairly high, and which may serve as a sensitive quantitative measure of the cement hydration process. Studies of the exothermal effects in cements are also of independent importance in relation to massive concreting problems, concreting in winter conditions, and to hydrothermal treatment of concrete.

Hydration of Portland cement in the form of paste, suspension, or concrete is a slow process. It has been shown [1-5] by several investigators that cement evolves heat for at least 6 months during hardening, but most of the heat, sometimes up to 80%, is liberated during the first few days after it is mixed with water. Heat evolution by cement is therefore studied by one of the following methods. The heats of hydration at different stages are determined as the differences between the heats of solution of the anhydrous and the hydrated cement. This method has been used to determine the heats of hydration of individual minerals in Portland cement clinker in the form of concentrated aqueous suspensions [1, 6]. The kinetics of heat evolution in the hydration of cement during the first few days can be studied by direct calorimetric [7, 8] or thermometric [9, 10] methods.

The results of such investigations show the existence of two stages in the initial hydration of Portland cement. The first stage, which lasts 1-2 hours after the cement is mixed with water, is characterized by an initially high but rapidly decreasing rate of heat evolution. This stage consists largely of hydration of tricalcium aluminate in the clinker. The rate of heat evolution increases again after 5-14 hours, depending on the mineralogical composition and the degree of dispersion of the cement, on the content of added gypsum, and a number of other factors. The kinetics of heat evolution in the hydration of cement, both in the initial and in the subsequent stages, may be changed considerably by addition of hydrophilic plasticizers.

In our previous investigations we studied the effect of the hydrophilic plasticizer SSB on the properties of concentrated cement suspensions during the initial stages of their interaction with water. The studies included investigation of changes in the kinetics of structure formation in cement paste as the result of additions of SSB resulting from adsorptive retardation of hydration and adsorptive dispersion of tricalcium aluminate in the clinker. Data on the influence of SSB lignosulfonates on the kinetics of the chemical interaction of cement with water were obtained either by an indirect method, or by determinations of the chemically bound water, which is an insensitive although in some cases convenient method.

In the present investigation the influence of the hydrophilic plasticizer SSB on the kinetics of the chemical interaction of cement with water in the initial stage was studied by the course of the evolution of heat in the process. Ground factory clinkers without added gypsum were used for the work. The contents of the principal minerals in the clinker, calculated from analytical data, and the degree of dispersion (by Tovarov's method) are given in the table.

The reasons for the choice of the calorimetric method were: the relatively low heat effect at the first stage of heat evolution, the desirability of carrying out the hydration in a concentrated aqueous suspension (cement paste), and the necessity of making such suspensions directly in the calorimeter. The diathermic method was used, at a variable heat exchange rate and at a low rate of cooling. The calorimetric vessel in which the cement was mixed with water was of the massive calorimeter type, contained an interior glass vessel for water or the solutions to be studied, and was fitted with a special stirrer for mixing the cement (Figure 1). A calorimeter of this type was used by Logginov [11].

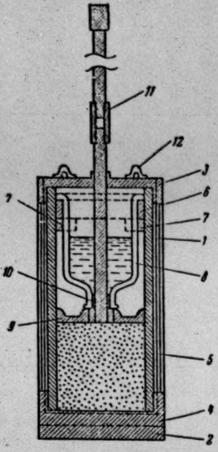

Fig. 1. Calorimetric vessel: 1) brass cylinder; 2) detachable cylinder base; 3) brass lid with gap for stirrer; 4 and 5) grooves for thermistor and leads; 6) seal ring; 7) half-ring supports; 8) inner brass or glass vessel for solutions; 9) stirrer for cement mixing; 10) rubber seal ring; 11) heat insulating collar.

The temperature was measured to the nearest 0.01° by means of a semiconductor resistance thermometer, the MMT-1 thermistor, connected in a Wheatstone bridge circuit. Thermistors are being more and more widely used as resistance thermometers in physicochemical research [12-15]. Our preliminary experiments showed that the MMT-1 thermistor mounted in the calorimeter is stable in operation and gives reproducible readings when standardized against a mercury thermometer (Figure 2, Curve R).

For calculation of the temperature from the thermistor resistance we used the approximate equation:

$$\Delta t = (\log R_2 - \log R_1)/C_{av}, \qquad (1)$$

valid for fairly narrow temperature ranges, derived from the general expression $1/R = C \cdot e^{B/T}$, (2), where C_{av}, C and B are constants determined from the calibration data. Over temperature ranges greater than 4-5°, C_{av} depends appreciably on the temperature (Figure 2, Curve C_{av}).

The cooling rate and the heat capacity of the calorimeter were determined by the usual calorimetric methods [16]. The average specific heat of the cements at room temperature was calculated by a method used for complex silicate systems [17], by summation of the specific heats of the constituent oxides in the cement; it was found to be 0.19 cal/g degree for the clinkers studied.

The kinetics of heat evolution in the interaction of cements (without gypsum) with water and with aqueous solutions of SSB sulfonates was studied in suspensions with water-cement ratio (w/c) of 0.4, so that it was possible to compare the results with data on structure formation in such suspensions. Figure 3 represents the kinetics of initial heat evolution by the high-alumina clinker N with additions of 0.10 to 1.00% SSB, calculated as the dry substance, on the weight of the cement. Curve 1 represents heat evolution during hydration of cement without added SSB; Curves 2-5 represent heat evolution in systems containing increasing amounts of SSB. Curve 3 shows that there is practically no induction period of heat liberation (hydration) in cement pastes without SSB and with small amounts of SSB (less than 0.25% for clinker N).

Mineral Contents and Degree of Dispersion of Clinkers

Factory	Mineralogical composition, in %*				S
	C_3S	C_2S	C_3A	C_4AF	m²/g
Komsomolets (K)	58	18	5	16	0.32
Novorossiisky (N)	56	22	8	13	0.18
Gigant (G)	53	20	9	14	0.28

---

*The clinker minerals are denoted by the usual symbols: C_3S—$3CaO \cdot SiO_2$; C_2S—$2CaO \cdot SiO_2$; C_3A—$3CaO \cdot Al_2O_3$; C_4AF—$4CaO \cdot Al_2O_3 \cdot Fe_2O_3$.

An increase of the amount of SSB to 0.5-1.0% results in the appearance of an induction period, the duration of which increases with the amount of SSB added. Heat evolution during the induction period is very small, thus

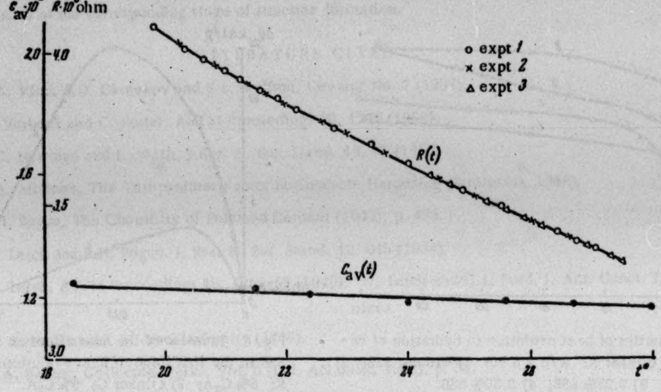

Fig. 2. Variation of the resistance (R) of thermistor MMT-1 with the calorimeter temperature (intervals of 1 month between experiments). Variation of the coefficient C_{av} in the approximate Equation (1) with temperature.

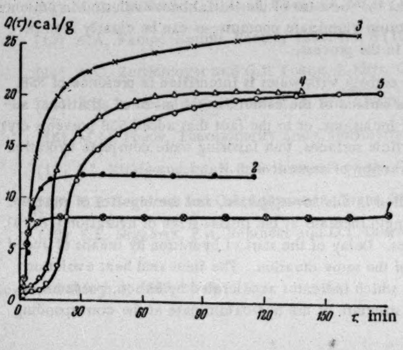

Fig. 3. Kinetics of heat evolution in hydration of cement from clinker N; w/c = 0.40: 1) without SSB; 2) 0.10% SSB; 3) 0.25% SSB; 4) 0.50% SSB; 5) 1.0% SSB.

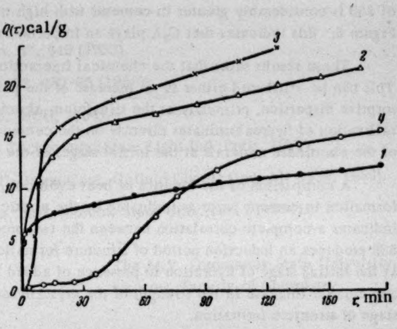

Fig. 4. Kinetics of heat evolution in hydration of cement from clinker G; w/c = 0.40: 1) without SSB; 2) 0.10% SSB; 3) 0.25% SSB; 4) 0.50% SSB.

confirming the previously reported [18, 19] retardation of the hydration of Portland cement by SSB lignosulfonates. The small initial jump on the heat evolution curves probably corresponds to heats of wetting and adsorption, which are small compared with the heat of subsequent hydration. The total heat evolved during the first stage is considerably greater in cement paste with added SSB than without additions.

Similar results were obtained for the other two clinkers, differing in tricalcium aluminate contents, but of similar specific surface (0.3 m^2/g). A great increase of the initial heat evolution in presence of SSB is found for clinker G (Figure 4); the optimum addition of SSB in this respect is 0.25%. Addition of 0.5% SSB, despite the considerable adsorptive retardation of cement hydration which it produces (as shown by the appearance of a noticeable induction period), also produces a certain increase of the initial heat evolution after the end of the induction period. Clinker K, with a lower content of tricalcium aluminate, also shows a noticeable increase of

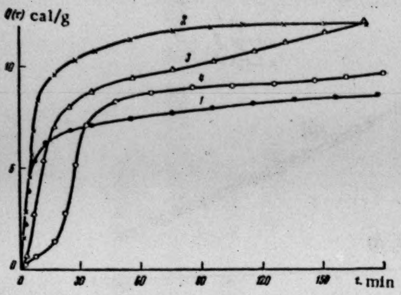

Fig. 5. Kinetics of heat evolution in hydration of cement from clinker K; w/c = 0.40: 1) without SSB; 2) 0.10% SSB; 3) 0.25% SSB; 4) 0.50% SSB.

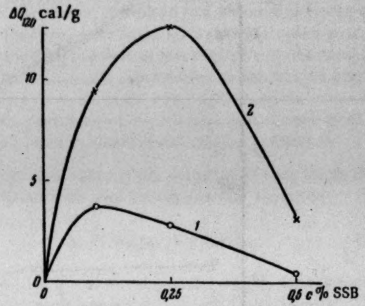

Fig. 6. Increase of the heat effect on addition of SSB in the first stage of heat evolution: 1) clinker K; 5% C_3A; 2) clinker G; 9% C_3A.

initial heat evolution in presence of SSB, the effect being greatest with 0.1% addition (Figure 5).

In comparing these results it is necessary to note that the increase of the initial heat evolution in presence of SSB is considerably greater in cements with high tricalcium aluminate contents, as can be clearly seen in Figure 6; this indicates that C_3A plays an important role in the process.

These results show that the chemical interaction of cement with water is intensified in presence of SSB. This can be attributed either to an increase of the particle surface of the cement as the result of additional adsorptive dispersion, primarily at the tricalcium aluminate inclusions, or to the fact that added SSB prevents crystallization of hydroaluminates directly on the cement particle surfaces, thus favoring more complete hydration of the aluminate minerals at the initial stages of the interaction of cement with water.

A comparison of the kinetics of heat evolution, studied in this investigation, and the kinetics of structure formation in cement paste as indicated by the plastic strength increase at the initial stage of hydration [18, 19], indicates a complete correlation between the two processes. Delay of the start of hydration by means of added SSB produces an induction period of structure formation, of the same duration. The increased heat evolution at the initial stage of hydration in presence of added SSB, which indicates accelerated hydration, produces an appreciable increase in the strength of the crystallization structure of the hydroaluminate at the corresponding stage of structure formation.

This coordination of the structure formation and hydration (heat evolution) processes in gypsumless cements at the initial stage of their interaction with water is found in all cases, if allowance is made for such important factors as the duration of mixing of the cement, which has a strong influence on the kinetics of structure formation, and also heat loss from the system studied, which often distorted earlier data on the heat evolution by cements.

SUMMARY

1. A method has been developed for quantitative study of the initial heat evolution in hydration of cement pastes mixed within the calorimeter.

2. A study has been made of the kinetics of heat evolution in the initial hydration stage of gypsumless cements with various contents of tricalcium aluminate, and of the effects of the hydrophilic plasticizer SSB, added in amounts from 0.1 to 1.0%, on the weight of the cement, on the kinetics of heat evolution.

3. It is shown that the induction period of cement hydration (as indicated by heat evolution) increases with increasing amounts of SSB added, resulting in an induction period of structure formation of the same duration.

4. It is shown that additions of SSB over a wide range result in an increase of the initial heat evolution in comparison with cement pastes without plasticizer; this increases the strength of the crystallization structure of the hydroaluminate at the corresponding stage of structure formation.

LITERATURE CITED

[1] V.A. Kind, S.D. Okorokov and S.L. Volfson, Cement No. 7 (1937).

[2] G. Verbeck and C. Foster, ASTM Proceedings 50, 1235 (1950).

[3] E.C. Newman and L. Wells, J.Res. N. Bur. Stand. 49, 55 (1950).

[4] S.A. Mironov, The Temperature Factor in Concrete Hardening (Stroiizdat, 1948).

[5] R.H. Bogue, The Chemistry of Portland Cement (1947), p. 434.

[6] W. Lerch and R.H. Bogue, J. Res. N. Bur. Stand. 12, 645 (1934).

[7] W. Lerch, ASTM Proceedings 46, 1252-97 (1946); W. Lerch and C.L. Ford, J. Am. Concr. Inst. 19, 745-95 (1948).

[8] W. Swietoslawski, Microcalorimetry (1946).

[9] A.A. Baikov, Collected Works, Vol. 5 (Izd. AN SSSR, 1948), p. 34.

[10] V.A. Tikhonov, Hydrotech. Constr. No. 7 (1953).

[11] G.I. Logginov, J. Acad. Sci. USSR No. 7 (1954).

[12] V.Ya. Mikhelson, J. Anal. Chem. 9, No. 1 (1954).

[13] A.A. Kampe-Nemm, Factory Labs. No. 6 (1954).

[14] A.C. Zettlemoyer and G.I. Young, J. Phys. Chem. 57, 649 (1953).

[15] M.J. Rand and L.P. Hammett, J. Am. Chem. Soc. 72, 287-93 (1950).

[16] M.M. Popov, Thermometry and Calorimetry (Izd. MGU, 1954).

[17] I.I. Kitaigorodsky, K.S. Evstropyev, et al., Glass Technology (State Light Ind. Press, 1939).

[18] E.E. Segalova and O.I. Lukyanova, Trans. 3rd All-Union Conf. Colloid Chem. (Izd. AN SSSR, 1956).

[19] E.E. Segalova, P.A. Rebinder and O.I. Lukyanova, Bull. Moscow State Univ. No. 2 (1954).

Received March 3, 1957

The M.V. Lomonosov State University,
Moscow, Faculty of Chemistry

EFFECT OF TEMPERATURE ON THE MAGNITUDE AND RATE OF SWELLING OF AGAR

V.P. Mishin and N.D. Verderevskaya

Data on the influence of temperature on the magnitude and rate of swelling are of interest not only in relation to the complex problem of the temperature coefficient of swelling of high polymers, but also in connection with the submicroscopic structure of the latter. However, the literature contains very few publications dealing with the influence of temperature on the magnitude and rate of swelling.* By using an improved technique for measurement of swelling, and various media in which the solubility of the swelling substance could be varied within certain limits, we set out to show that when the solubility of a swelling substance remains practically unchanged at different temperatures, the degree of swelling increases with increasing temperature, but otherwise it should pass through a maximum which shifts in the direction of lower temperatures in the transition to media in which the temperature coefficient of solubility progressively increases.

The substance used was finely divided domestic fibrous white agar purified by prolonged treatment with water containing ethyl ether in the cold. The washed agar was dried at 40°; particles 0.5-1 mm in diameter were sieved off for the experiments. The ash content of the agar after treatment was 1.87%, and the moisture content (at 110°) was 17.8%. The swelling media were redistilled water and aqueous solutions of potassium sulfate and thiocyanate (extreme members of the lyotropic series). The temperature in the experiments was varied between 0 and 50°. In addition to swelling, the solubility of agar was determined gravimetrically.

The increase in volume on swelling was taken as the measure of swelling. Most investigators use the weight increase as a measure of swelling. It must be pointed out that there is no direct proportionality between the weight and volume changes of a substance on swelling, and the functional relationship between the two has not been accurately established [2]. An automatic recording instrument of our design was used for measurements of the volume increase (Figure 1). The main part of the apparatus consists of a cylindrical glass vessel a with a perforated bottom. The substance to be studied is placed in the vessel, and on this is placed a light (7.75 g) hollow glass cylinder b 1.50 cm in diameter with a perforated bottom. The small vessel a is fixed in a vessel A, contained in a thermostat and filled at the right moment with the swelling liquid. The upper part of the movable cylinder b is connected to a long glass tube e, which is a lever with unequal arms, with one end slightly bent and drawn out into a capillary. The capillary and part of the tube are filled with ink and brought into contact with millimeter squared paper on a drum rotated uniformly by means of a Warren motor. By this apparatus it is possible to measure the swelling of small amounts of substance in large volumes of solution, so that the concentration of the latter remains practically constant throughout the experiment. In all the experiments the agar-liquid volume ratio was 1:200, the weight of agar was 0.2500 g, and the average volume of the loose material was 1.06 cc. After the pen had been put into position and the drum started, the zero reading line was drawn. The liquid was then introduced into the vessel a by displacement of the bottle B from position d' into position d". As the substance swells, the pen e is displaced and traces a curve. The experiment is continued until the pen follows its own trace. With the aid of a calibration curve, the experimental curves were used to determine the volume increments at various time intervals; the results were used to plot swelling-time curves.

The calibration curve was plotted by measurement of definite volumes of mercury introduced into the small vessel and of the corresponding displacements of the pen from the zero line. The average error was ~3%.

---

* A detailed critical analysis of the literature is given in [1].

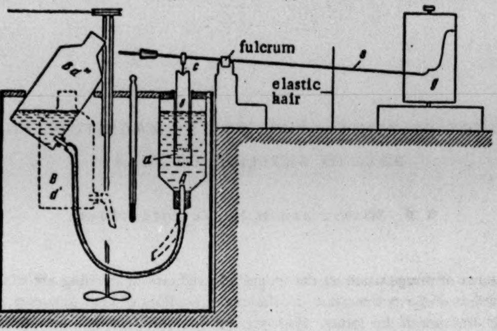

Fig. 1. Automatic recording apparatus for measurement of volume increase: A) glass vessel 300-400 ml in capacity; B) bottle with tube (d' – position before experiment; d" – position during experiment); a) small glass vessel with perforated bottom; b) hollow glass cylinder with perforated bottom and a depression at the top end; c) metal rod; e) pen; g) rotating drum.

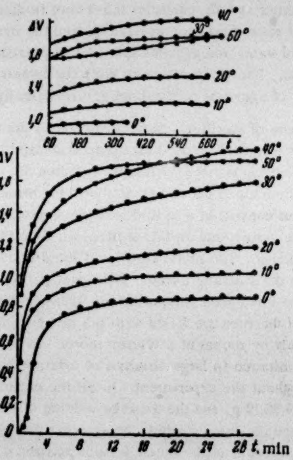

Fig. 2. Curves for the swelling of agar in water at various temperatures.

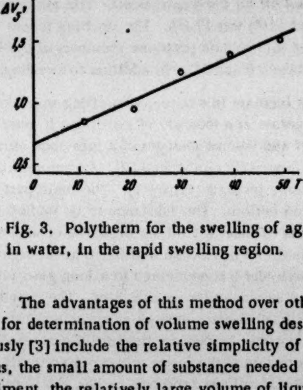

Fig. 3. Polytherm for the swelling of agar in water, in the rapid swelling region.

The advantages of this method over other methods for determination of volume swelling described previously [3] include the relative simplicity of the apparatus, the small amount of substance needed for the experiment, the relatively large volume of liquid in which the swelling occurs, automatic continuous recording of the volume increase, and the possibility of determining the swelling of any substance which can be obtained in finely divided form. It should be noted that the values measured by means of this apparatus are not the true changes in the volume of the swelling substance, as a certain volume of the "dead" space between the particles is added to the volume of the particles themselves. However, this presents no obstacle in comparative studies of the swelling of substances under different conditions, if the original degree of dispersion of the substance and the packing density of its particles under a small and

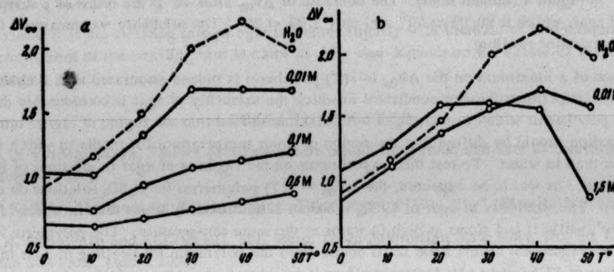

Fig. 4. Polytherms for the swelling of agar in water and: a) in 0.5 M; 0.1 M; 0.01 M solutions of K_2SO_4; b) in 1.5 M and 0.01 M solutions of KCNS.

constant pressure (0.004 atmos) exerted by a piston are the same in all the experiments. If necessary, the apparent volume increments can be converted into the true values with the aid of a calibration curve showing the relationship between the apparent and true volume increments. Such a curve can be found by determination of the true volume of a substance at different stages of swelling by the method of weighing in two liquids of different densities, proposed by one of us [4].

Each experimental curve (examples of such curves are given in Figure 2) has three characteristic regions: a region of rapid swelling, with a rapid rise of the curve, corresponding to the time interval of 0-10 minutes, irrespective of the temperature; a region of slow swelling with retarded ascent of the curve; and the region of maximum swelling, reached after prolonged times, different for different temperatures, in which the curve is practically parallel to the abscissa axis. At low temperatures the swelling rate during the time interval of about 0-0.5 minute is low. The probable explanation is that after the liquid comes into contact with the particles of the substance some time is required for their complete wetting. This time decreases with increase of temperature, and the region of the curve with a low swelling rate disappears. None of the equations for the kinetics of swelling known to us completely covers the whole $\Delta V = f(t)$ curve. The best of these equations are: the Rotinyan equation [5]

$$\frac{1}{t}\ln\frac{1}{1-i'}-\beta\frac{i'}{t}=M,$$

where $i' = i/i_\infty$; i is the swelling at time t; i_∞ is the maximum swelling; β and M are constants which satisfactorily fits the experimental data for the slow swelling region, and our proposed equation

$$\Delta V_t=\frac{\Delta V_\infty t}{K+t},$$

where ΔV_∞ is the maximum swelling; ΔV_t is the swelling at time t; K is a constant equal to the time at which

$$\Delta V_t=\frac{1}{2}\Delta V_\infty.$$

The last equation satisfactorily fits the region of rapid swelling, and partly the region of slow swelling.

As regards the effect of temperature on the swelling of agar, in all cases in which the swelling process was not complicated by solution the degree of swelling increased with increase of temperature. When the solubility of agar increased considerably with temperature, the $\Delta V_\infty = f(T)$ polytherms had maxima. A comparison of the values for the swelling of agar in water denoted by ΔV_5, found in the rapid swelling region in 5 minutes from the start of the process [6] shows, as illustrated in Figure 3, that the degree of swelling increases practically linearly with temperature, while the polytherm for the maximum swelling ΔV_{∞} passes through a maximum, found at 40° in Figure 4 (broken lines). The decrease of ΔV_{∞} after 40° is the result of a sharp increase of the solubility of agar, which is 20.7% at 50°, and only 2.6% at 20°. The solubility was measured for the time required to reach maximum swelling.

If the presence of a maximum on the $\Delta V_{\infty} = f(T)$ polytherm is indeed associated with a change of solubility, then experiments performed under conditions in which the solubility of agar is considerably decreased should give rise to polytherms without maxima, or with maxima shifted into the region of higher temperatures. Conversely, the maxima should be shifted into the region of lower temperatures for media in which the solubility of agar is higher than in water. To test this, experiments on the swelling of agar in solutions of K_2SO_4 and KCNS were carried out. As was to be expected, the $\Delta V_{\infty} = f(T)$ polytherms for K_2SO_4 solutions do not show maxima (Figure 4a). The solubility of agar in K_2SO_4 solutions is considerably lower than in water; it is 5% in 0.5 M solution at 50°, while it is 4 times as high in water at the same temperature. The polytherm for a very dilute KCNS solution (Figure 4b) differs little in its course from the polytherm for swelling of agar in water, but at high concentrations of KCNS, when its lyotropic effect is prominent, the $\Delta V_{\infty} = f(T)$ polytherm has a maximum at a lower temperature than for water. The solubility of agar in 1.5 M KCNS solution, even at 20°, is 13.5%, which is 5.2 times the solubility in water at the same temperature. It is interesting to note that the position of a salt in the lyotropic series, as is shown by the polytherms given, is determined not only by the nature of the salt but also by its concentration and the swelling temperature.

Temperature Coefficient of the Swelling Rate I

Temperature, °C	In H_2O	In solution of K_2SO_4			In solution of KCNS			
		0.01*M*	0.1*M*	0.5*M*	0.01*M*	0.1*M*	0.5*M*	1.5*M*
0—10	1.80	1.16	1.24	1.22	3.90	1.36	1.18	1.19
10—20	1.14	1.22	1.25	1,04	1.21	1.19	1.16	1.25
20—30	1.30	1.27	1.08	1.24	1.04	0.99	1.03	1.09
30—40	1.05	1.00	1.09	1.02	1.12	1.11	1.12	0.99
40—50	1.10	1.10	1,03	1.08	1.08	1.11	1.06	0,69

The authors [7-11] of a number of well-known books on colloid chemistry take into account the exothermic character of the swelling process and apply the Le Chatelier principle to it, reaching the conclusion that the degree of swelling should decrease with increasing temperature. Our data on the swelling of agar in various media, and also earlier data on the swelling of gelatin in water [12-14] and of rubbers in organic solvents [15-17], do not confirm this conclusion. In all instances when the swelling of agar is not appreciably complicated by solution we found that the maximum swelling increases with increasing temperature. The Le Chatelier principle cannot be applied in this way to the complicated process of swelling, since most of the liquid is absorbed osmotically by the swelling substance, and this absorption occurs without any appreciable heat effect.

In studies of the influence of temperature on the rate of swelling the rapid swelling region is of the most interest. The table contains data on the temperature coefficient I, which represents the change of the average rate of swelling during two minutes from the start of the process, when the temperature is changed by 10°.. It is seen that I is not constant, but depends on a number of factors, the most important of which are: the temperature range over which the swelling is studied, the nature and the concentration of the dissolved salt. In most cases the coefficient I is close to unity, which indicates a relatively small change of the swelling rate with temperature. The value of I becomes fairly large only for dilute solutions of KCNS and for water in the region of low temperatures, when the swelling process is not complicated by solution.

SUMMARY

1. An automatic recording instrument has been used to study the variations of the magnitude and rate of swelling of agar in water and in solutions of salts of the lyotropic series with the temperature.

2. It is shown that if the swelling of agar is not complicated by solution, the degree of swelling increases with temperature, while otherwise the $\Delta V_{\infty} = f(T)$ polytherm passes through a maximum which shifts in the di-

rection of lower temperatures for media in which the temperature coefficient of solubility of the swelling substance is greater.

3. It is shown that the swelling rate of agar increases slightly with increase of temperature and that the temperature coefficient of the swelling rate is close to unity and depends on the nature of the liquid and the temperature range.

LITERATURE CITED

[1] N.D. Verderevskaya, "Effect of Temperature on the Magnitude and Rate of Swelling" Dissertation (1 MOLMI, Moscow 1956).

[2] V.K. Tile, "Methods for Determination of the Degree of Swelling" (Dissertation, Moscow 1955).

[3] I.N. Ermolenko and M.I. Mazel, Sci. Mem. Lenin Belorussian State Univ. No. 20, Chem. Ser. (Acad. Sci. Belorussian SSR Press, Monsk 1954).

[4] Ya.S. Przheborovsky and V.K. Tile, Colloid J. 16, 304 (1954) (T.p. 297).*

[5] A.L. Rotinyan, Colloid J. 11, 431 (1949).

[6] A.A. Tager, Solutions of High Polymers (Goskhimizdat, Moscow-Leningrad 1951).

[7] H. Freundlich, Kapillarchemie B. 2 (1932).

[8] V.A. Naumov, Colloid Chemistry (State Chem. Tech. Press, Leningrad 1932).

[9] D.L. Rubinshtein, Physical Chemistry (Izd. AN SSSR, Moscow-Leningrad 1940).

[10] I.A. Izgaryshev, Course of Colloid Chemistry (Art. Acad. Press, 1944).

[11] N.P. Peskov and E.M. Aleksandrova-Preis, Course of Colloid Chemistry (Goskhimizdat, Moscow-Leningrad 1948).

[12] D.J. Lloyd and B. Pleass, Biochem. J. 21, 135 (1927); 23, 358 (1929); 24, 1472 (1930); 25, 1943 (1931).

[13] S.M. Lipatov, Colloid J. 5, 615 (1939).

[14] A.A. Bromberg and S.A. Merikalov, J. Appl. Chem. 23, 1280 (1950).

[15] F. Kirchof, Kolloid. Beih. 6, 1 (1914).

[16] P. Powers and B. Billmeyer, Ind. Eng. Chem. 37, 64 (1945).

[17] V.E. Gul and A.G. Shvarts, Colloid J. 17, 24 (1955).(T.p. 21).*

Received July 15, 1956

The I.M. Sechenov First Medical
Institute, Moscow
Chair of General Chemistry

---

*T.p. = C.B. Translation pagination.

INVESTIGATION OF THE STRUCTURE AND PROPERTIES OF CARBON CHAIN POLYMERS IN DILUTE SOLUTIONS

3. MIXTURES OF POLYVINYL CHLORIDE AND POLYACRYLONITRILE

N.V. Mikhailov and S.G. Zelikman

For production of polymeric materials with a great variety of properties, the method of molecular mixing of polymers with the aid of common solvents or in melts is used, in addition to copolymerization reactions. Plasticizers of high molecular weight are becoming increasingly important [1]. Studies of the properties of polymer mixtures have therefore become necessary for the proper practical utilization of high polymers and for further development of our theoretical knowledge of the relationship between the structure and properties of polymers.

Some data on the properties of polymer mixtures have been obtained in the course of selection of materials for particular practical purposes. The thermodynamic, mechanical and optical properties of polymer mixtures have been described in a number of publications [1, 2]. The basic laws of the phase state of polymer mixtures have been noted in a number of papers [3-5], in which it is established that the compatibility of polymers depends on the molecular weight and relative proportions of the polymers, solution concentration, and a number of other factors. Some workers [6] use a simpler approach to polymer compatibility, and evaluate it from mechanical data. The view has been put forward [7] that mutual solubility of polymers is determined principally by enthalpy changes in the system, and on this basis the following criterion of polymer compatibility has been suggested: polymers are mutually soluble if the heat effect of mixing $\Delta H < 0$. This criterion was experimentally confirmed by Strumynsky [2], attention being drawn to the importance of volume contraction when certain polymers are mixed. It follows from these data that the energy factor plays a predominant role in the compatibility of polymers, especially polar polymers.

Morawetz and Gobran [8] studied the influence of intermolecular forces in solutions of polymer mixtures; they measured the osmotic pressure of solutions of mixtures containing acidic (copolymer of methyl methacrylate with methacrylic acid) and basic (copolymer of methyl methacrylate with dimethylaminomethyl methacrylate) copolymers. Fairly stable aggregates are present even in very dilute solutions of such mixtures. The maximum degree of association is found in mixtures consisting of 50% of acidic and 50% of basic copolymer; its value is 5.43 at 30° and 3.2 at 50°.

In our earlier publications [9] certain properties of solutions of polyvinyl chloride, polyacrylonitrile, and copolymers based on them were described. It seemed of considerable interest to compare such "chemical mixtures" as copolymers with model systems consisting of molecular mixtures of the polymers of the equivalent chemical composition, and to compare their behavior in solution with that of the pure polymers.

The present communication contains the results of an investigation of the viscosities and osmotic pressures of such molecular mixtures of polymers. Since it was necessary to examine simultaneously the corresponding data on pure polymers, their copolymers, and molecular mixtures, the components were chosen to be as close as possible to each other in molecular weight; this was achieved by careful fractionation of the starting materials. Three mixtures of polyvinyl chloride and polyacrylonitrile were prepared, in the following proportions: 13 : 87; 29 : 81 and 40 : 60 by weight. The reason for these proportions was the composition of the copolymers described previously. The methods used for viscosity and osmotic pressure determinations were described in the earlier communications [9].

EXPERIMENTAL

The variation of viscosity with concentration in the 0.25-0.85% range, and the variation of viscosity with temperature in the 20-60° range, was studied for all the mixtures. The osmotic pressure was determined at 20, 35 and 50°.

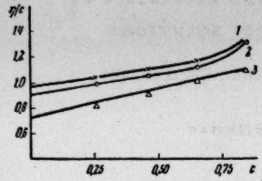

Fig. 1. Variation of reduced viscosity of polymer mixtures with concentration: 1) 40:60 mixture; 2) 29:71 mixture; 3) 13:87 mixture.

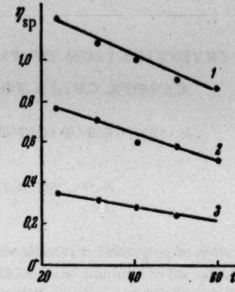

Fig. 2. Variation of viscosity with temperature for the 40:60 mixture; solution concentrations: 1) 0.85%; 2) 0.65%; 3) 0.45%.

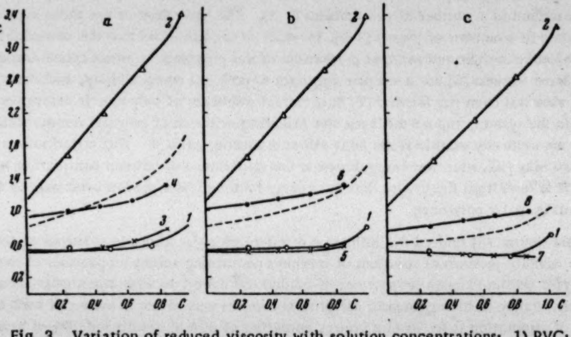

Fig. 3. Variation of reduced viscosity with solution concentrations: 1) PVC; 2) PAN; 3, 5, 7) copolymers; 4, 6, 8) mixtures. Ratios of PVC to PAN in the copolymers and mixtures: a) 40:60; b) 29:71; c) 13:87.

Variations of the reduced viscosity for the three mixtures are plotted in Figure 1, while variation of viscosity of the 40:60 mixture with temperature is shown in Figure 2. As for copolymers and pure polymers, the specific viscosity of polymer mixtures is a linear function of the temperature. For comparison, Figure 3 shows variations of the reduced viscosity with concentration for the copolymers, mixtures, and pure polymers. The broken lines represent the reduced viscosities calculated additively from the viscosities of the pure polymers. Figure 4 shows the variation of reduced osmotic pressure with solution concentration for all the polymer mixtures at 20, 35 and 50°. For comparison, Figure 5 shows the variation of the osmotic pressure of polyvinyl chloride, polyacrylonitrile and polymer mixtures at 20°.

A curious feature is that, in contrast to the pure polymers, the apparent molecular weight of the polymers in mixtures decreases with increase of temperature (Table 1).

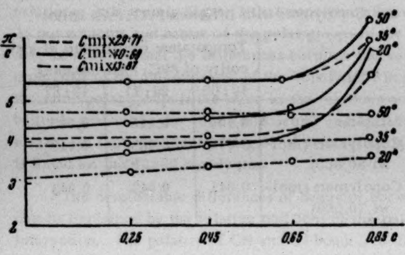

Fig. 4. Variation of reduced osmotic pressure of polymer mixtures with concentration.

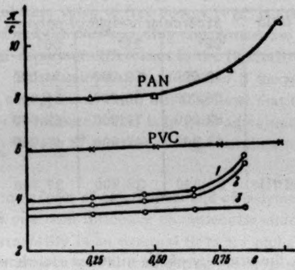

Fig. 5. Variation of osmotic pressure with concentration of PAN, PVC, and mixtures of the polymers at 20°; PVC : PAN ratios in mixtures: 1) 40 : 60; 2) 29 : 71; 3) 13 : 87.

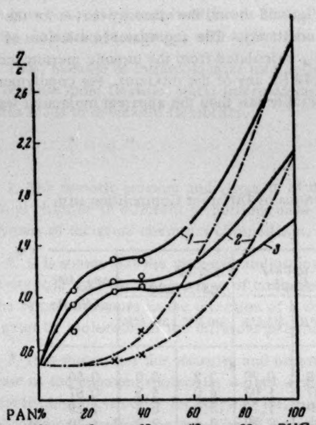

Fig. 6. Variation of viscosity with composition of mixtures (continuous lines) and copolymers (broken lines). Solution concentrations: 1) 0.85%; 2) 0.65%; 3) 0.25%.

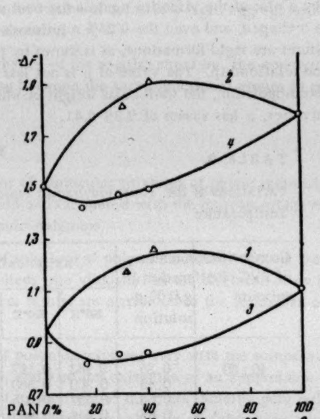

Fig. 7. Variation of free energy with composition. Copolymer solutions: 1) 0.45%; 2) 0.85%. Solutions of mixtures: 3) 0.45%; 4) 0.85%.

It must also be borne in mind that these apparent molecular weights of the polymers in the mixtures are considerably higher than the molecular weights of the pure polymers used for making the mixtures. This suggests that aggregates are formed as the result of intermolecular interaction in solutions of polymer mixtures. The degree of association calculated from the above data at 20° is in the range of 1.6-1.8. The intermolecular forces are weakened with increase of temperature, but even at 50° the degree of association is still 1.2-1.3, so that the aggregates are not completely destroyed. Molecular mixtures of the polymers also differ sharply from the corresponding copolymers in solution viscosity. With equal contents of functional groups in the mixtures and copolymers, and with almost equal molecular weights, the intrinsic viscosity of the mixtures is approximately double that of the corresponding copolymers, for all ratios.

TABLE 1

Variation of Molecular Weight with Temperature

PVC : PAN ratio in mixture	Molecular weight of polymer at 20°	35°	50°
40 : 60	73,000	63,000	54,000
29 : 71	66,000	58,000	54,000
13 : 87	82,000	71,000	62,000
Polyvinyl chloride	47,000	47,000	47,000
Polyacrylonitrile	39,000	38,800	37,700

TABLE 2

Temperature Coefficients of Viscosity for Mixtures and Copolymers with Different PVC : PAN Ratios

	Temperature coefficients of viscosity of PVC : PAN mixtures		
	40 : 60	29 : 71	13 : 87
Mixtures	0.100	0.125	0.083
Copolymers (mol wt 50,000)	0.076	0.063	0.043
Copolymers (mol wt 30,000)	0.041	0.043	0.043

Thus, the viscosity of the mixtures also shows that aggregation in solutions of polymer mixtures occurs even at low concentrations. It is very interesting to compare the viscosities of the mixtures with the calculated values based on additivity of the corresponding values for the pure polymers. As is to be expected from the osmotic pressure data, the observed interaction between unlike macromolecules in solutions of polymer mixtures should result in nonadditivity of the viscosity. Such deviations from additivity are demonstrated especially clearly by a plot of the viscosity against the composition. As Figure 6 shows, the viscosity curves for the mixtures are S-shaped, and even the 0.25% solution deviated from additivity. The aggregates in solutions of polymer mixtures are rigid formations, as is shown by the values of μ calculated from the osmotic pressure-concentration relationship. The value of μ is not less than 0.47-0.48 for any of the mixtures. For copolymers of the same composition, the molecular weight of which is considerably less than the apparent molecular weight of the mixtures, μ has values of 0.38-0.41.

TABLE 3

Variations of the Thermodynamic Functions of Mixtures of Different Composition with Temperature

Composition of PVC : PAN mixture	Concentration in g/100 g solution	$\Delta F_1 \cdot 10^6$ cal/mole			$\Delta H_1 \cdot 10^6$ cal/ /mole		$\Delta S_1 \cdot 10^5$ cal/mole		$\Delta S_{id} \cdot 10^6$ cal/mole
		295°K	308°K	325°K	300,5°K	315,5°K	300,5°K	315,5°K	
40 : 60	0.25	0.163	0.197	0.240	0.48	0.70	2.2	3.0	0.50
	0.45	0.300	0.360	0.428	0.87	1.03	4.0	4.5	0.87
	0.65	0.437	0.525	0.608	1.29	1.20	5.9	5.6	1.29
	0.85	0.942	0.993	1.027	0.05	—0.29	3.4	2.3	1.70
29 : 71	0.25	0.171	0.205	0.240	0.48	0.51	2.2	2.3	0.55
	0.45	0.325	0.368	0.419	0.53	0.66	2.9	3.3	1.01
	0.65	0.470	0.531	0.599	0.72	0.87	4.1	4.5	1.47
	0.85	0.856	0.976	0.950	1.48	—	8.0	—	1.89
13 : 87	0.25	0.145	0.171	0.205	0.36	0.53	1.7	2.3	0.46
	0.45	0.274	0.317	0.368	0.56	0.73	2.8	3.4	0.78
	0.65	0.394	0.462	0.539	0.93	1.10	4.5	5.1	1.15
	0.85	0.531	0.616	0.702	1.11	1.15	5.6	5.8	1.52

As the specific viscosity is a linear function of the temperature, the temperature coefficient of viscosity remains constant over the whole temperature range of 20-60°.

The variations of viscosity when the temperature of 0.85% solution is raised by 10° are given in Table 2. Table 2 shows that the temperature coefficient of viscosity for the mixtures is nearly double the corresponding value for the copolymers. For comparison it may be noted that the temperature coefficient of viscosity of 0.85% polyvinyl chloride solution is 0.040, and of polyacrylonitrile solution, 0.170.

The results for the osmotic pressure-temperature relationship were used to calculate the thermodynamic functions (Table 3).

The change of free energy as a function of composition is shown graphically in Figure 7 for 0.45 and 0.85% solutions. It is seen in Figure 7 that copolymers have the minimum value of free energy ($-\Delta F$ is maximum). As the contents and nature of the polar groups in the mixtures and the corresponding copolymers are the same, it may be assumed that the differences between the values of ΔF represent differences in the flexibility of the molecules of the mixtures and of the copolymers in solution. This assumption is admissible if the solvation of the same polar groups is the same in the mixtures and in the copolymers. From this it follows that the flexibility is greatest in the 40 : 60 copolymer and least in the 13 : 87 mixture. This is in good agreement with other results. In fact, the greatest degree of association is found in the 13 : 87 mixture, and the minimum value of μ is found for the 40 : 60 copolymer.

The considerable differences of behavior between the molecules of copolymers and of polymer mixtures can be explained by the relative positions of the polar groups and their influence on molecular structure and interaction. The polarity of CN and Cl bonds and their polarizability in an external field are probably the decisive influences with regard to the flexibility of the polymer molecules. In considering the properties of the copolymers, the mutual influence of the polymer groups in the copolymer chain itself must be primarily taken into account. This influence leads to mutual intramolecular saturation of the polar groups, probably resulting in some globulization of the molecules, owing to which the intermolecular interaction is weakened. In consequence, the copolymers are more readily soluble, have lower solution viscosity, etc. In mixtures, interaction occurs between polar groups in different chains; this leads to formation of relatively rigid aggregates of unlike polymer molecules in solution, with an increase of solution viscosity.

Thus, because of intramolecular interaction and disturbance of the regular structure, the copolymer molecules become more flexible, while intermolecular interaction between the same functional groups in polymer mixtures leads to decreased flexibility.

SUMMARY

1. The osmotic pressure and viscosity of dilute solutions of molecular mixtures of polyacrylonitrile and polyvinyl chloride in different proportions have been measured and compared with the corresponding values for copolymers of the same chemical composition, and for the pure polymers.

2. It is shown that the viscosity and osmotic pressure of solutions of polymer mixtures deviate from the additivity rule over the whole range of component ratios studied: the viscosity, in the direction of an increase, and the osmotic pressure in the direction of a decrease. These results are attributed to the formation of stable aggregates by molecules of the different polymers.

3. It is shown that the viscosity and osmotic pressure of polymer mixtures vary with the temperature. The decrease of the apparent molecular weight with temperature, and also the existence of an appreciable temperature coefficient of viscosity for polymer mixtures, in contrast to solutions of the corresponding pure polymers and copolymers, confirm the presence of aggregates of unlike molecules in solutions of polymer mixtures.

4. A comparison of data on molecular mixtures and on copolymers shows that they differ sharply in their behavior; this is attributed to intramolecular interaction between the polar CN and Cl groups in copolymers, and intermolecular interaction in polymer mixtures.

LITERATURE CITED

[1] R.A. Reznikova, A.D. Zaionchkovsky and S.S. Voyutsky, Colloid J. 15, 108 (1953) (T.p. 111)*; S.E. Bolam, Rubb. Age Synth. 34, No. 10, 436 (1953); V.I. Alekseenko and I.U. Mishustin, Colloid J. 18, No. 3, 257 (1956)(T.p. 247).*

[2] G.V. Struminsky, Dissertation (Moscow, 1953); R.A. Reznikova, Dissertation (Moscow, 1952).

[3] A. Dobry and F. Boyer Kawenoki, J. Pol. Sci. 2, 90 (1947).

[4] H. Tompa, Trans. Faraday Soc. 45, 1142 (1949).

---

*T.p. = C.B. Translation pagination.

[5] N.V. Mikhailov, Z.V. Ukhanova, V.S. Klimenkov and E.A. Kurilchikov, Text. Ind. 14, No. 9, 11 (1954).

[6] V.I. Alekseenko, I.U. Mishustin and S.S. Voyutsky, Proc. Acad. Sci. USSR 95, No. 1, 93 (1954).

[7] M.F. Komskaya, Dissertation (Moscow, 1952).

[8] H. Morawetz and R.H. Gobran, J. Pol. Sci. 12, No. 1, 133 (1954).

[9] N.V. Mikhailov and S.G. Zelikman, Colloid J. 18, No. 6, 717 (1956) (T.p. 715)*; S.G. Zelikman and N.V. Mikhailov, Colloid J. 19, No. 1, 35 (1957) (T.p. 37).*

Received September 7, 1956

All-Union Scientific Research Institute
for Artificial Fibers, Mytishchi

---

*T.p. = C.B. Translation pagination.

ALTERATION OF THE INTERMOLECULAR STRUCTURE OF CAPRON FIBER AS THE RESULT OF HEAT TREATMENT*

L.I. Pokrovsky and A.B. Pakshver

Capron fibers are subjected to various kinds of heat treatment in the course of production and during subsequent processing, in order to improve the performance characteristics of the articles made from them. Heat treatment of the fibers in the free state, known as heat shrinking, results in a considerable increase of the extensibility without appreciable decrease of tenacity, and an improvement of the elastic properties. Heat treatment of the fibers or articles on rigid forms, in the stretched state, known as heat setting, fixes the geometrical dimensions and stabilizes them against subsequent heat treatment. Despite the extensive use of a great variety of heat treatments, the literature contains no reports of systematic investigations of the mechanism of this process or of the structural changes which occur as the result of heat setting and heat relaxation.

Mikhailov and Fainberg [1], who studied the sorption of water vapor and determined the heats of wetting and solution of undrawn and drawn capron fibers, showed that drawing of capron fibers causes only slight changes in the energy of intermolecular interaction.

Data on the sorption of phenols by capron fibers [2] also showed that equilibrium sorption changes little as the result of drawing. However, it is well known that the mechanical properties of undrawn and drawn capron fibers and of fibers subjected to heat treatment vary very considerably, and the rates of various sorption processes vary to an equal extent [3]. Evidently the intermolecular structure undergoes further condensation during drawing or heat treatment of capron fibers. This increase of the density of the structure has little influence on the aggregate, equilibrium processes, but the kinetic processes, which are primarily associated with the loose portion of the material, are very greatly changed.

Therefore, for evaluation of changes in the intermolecular structure of capron fibers, as the result of various heat treatments, we determined the kinetic heat of solution, i.e., the quantity of heat liberated in a calorimeter in 15 minutes, which characterizes the solution rate of the macromolecules in the loose structure of the fibers. It was presumed that this would give greater differences of the heat effects than are found in determinations of total heats of solution [4].

For a fuller characterization of the changes of molecular structure, the densities of the fibers were determined at the same time, Such data are also lacking at the present time. The literature only contains data on densities of undrawn and drawn nylon fibers and nylon plates [5].

EXPERIMENTAL

The kinetic characteristics of the heat of solution of capron fibers were determined by means of an isothermal microcalorimeter of the Schottky type [6]. With this calorimeter it is possible to measure small heat effects with good reproducibility and with small relative errors. The heat effects were measured to within 0.3 cal. The duration of the determinations was 15 minutes. During this time the solution became quite clear, and the subsequent change of temperature was much slower.

In order to find the most suitable solvent, preliminary experiments were carried out with an ordinary calor-

---

*23rd communication in the series of investigations on the intermolecular structure of high polymers.

TABLE 1

Kinetic Characteristics of the Heats of Solution of Undrawn and Drawn Capron Fibers in Various Solvents

Solvents	Undrawn fiber, Q'_K	Drawn fiber, Q''_K
20% HCl solution	5.9	4.9
40% H_2SO_4 solution	8.3	6.5
85% HCOOH solution	10.8	8.3
85% phenol solution	19.6	15.5

Note: The accuracy of the determinations was ± 0.5 cal/g.

imeter to determine the kinetic characteristics of the heats of solution of undrawn and drawn capron fibers in 20% HCl, 40% H_2SO_4, 85% HCOOH, and 85% phenol.

The results of these determinations are given in Table 1.*

Visual observations showed that the rate of solution of capron fibers decreases in these solvents in the following sequence: 20% HCl, 40% H_2SO_4, 85% HCOOH, 85% phenol. The differences of the kinetic heats of solution ($Q'_K - Q''_K$) between undrawn and drawn fibers decrease in the opposite sequence. It seems that in 20% HCl solution the solution process is more rapid and the measured heat effect of solution approximates to the limiting value Q_0, and therefore in 20% HCl the difference between the heats of solution of the undrawn and drawn fibers ($Q'_K - Q''_K$) is not large. When 85% HCOOH or 85% phenol are used as solvents, in which the solution rate is considerably lower, only the heat effects of solvation of the more loose domains is measured, and the difference between the heat effects $Q'_K - Q''_K$ for undrawn and drawn fibers becomes considerably greater.

Maximum solvation, i.e., the passage of all the macromolecules into solution, occurs very slowly, during several hours, with only a small additional heat effect, which can be determined with sufficient accuracy only by an adiabatic calorimeter [1].

As the result of the preliminary experiments, 85% solution of chemically pure HCOOH and 85% aqueous solution of phenol were used as the solvents in the subsequent experiments. The fibers studied were: samples of capron yarn No. 34, the same yarn subjected to dry heat in skeins and on bobbins for 5, 20 and 70 minutes, samples of yarn boiled in water in skeins and on bobbins for 0.5, 1 and 3 hours, samples of yarn steamed in an autoclave in skeins and on bobbins at 140° for 0.5, 1 and 3 hours, and samples of yarn additionally stretched in the heated state.

The results of measurements of the kinetic characteristics of the heats of solution, in the form of average values for 3-4 experiments, are given in Table 2. The solution concentration was approximately the same, 0.5-0.6%, in all cases. Table 2 shows that the kinetic characteristic of the heat of solution Q_k is lower for capron yarns subjected to various heat treatments than for the original No. 34 yarn. Therefore heat treatment of capron yarn produces denser molecular packing.

The greatest change in structure is produced by the action of steam on the fibers. It seems that with the high mobility of the molecular segments which results from the high temperature and the action of steam the macromolecules become rearranged into a denser form of packing in the fiber. It must also be pointed out that heat treatment of the fibers in the free state not only does not decrease the molecular density, as might have been expected, but increases it still more than does treatment on a rigid bobbin, especially by steaming. This is in good agreement with the results obtained by Lipatov [7] and Rogovin and Zazulina [8], who showed that in a number of cases changes of the degree of orientation on relaxation do not follow the same course as the total intermolecular interaction. Equal values were obtained for the kinetic characteristics of the heat of solution of fibers subjected to the same kind of heat treatment but for different times. The condensation of the molecular structure therefore proceeds very rapidly.

The Q_k values for the fibers studied are in good agreement with the results of density determinations for the same fibers.

The densities were determined as follows: a small skein of the yarn to be tested was placed in a bulb which was then evacuated down to $(1.25\text{-}1.34) \cdot 10^{-3}$ mm Hg and sealed. The sealed bulb was transferred to a cylinder containing a mixture of benzene and nitrobenzene, and broken. The cylinder with the fibers was placed in a thermostat maintained at 25 ± 0.005°. The mixture in the cylinder was occasionally stirred by hand. Ben-

---

*The results given in Table 1 were obtained by A.F. Kolbashova. The measurements were also continued for 15 minutes, to complete visible solution of the fibers.

TABLE 2

Kinetic Characteristics of the Heats of Solution of Capron Fibers Subjected to Various Heat Treatments

Fibers	Q_k cal/g	
	85% HCOOH	85% phenol
Undrawn yarn (old)	8.5	–
Drawn capron yarn No. 34	6.6	20.2
Ditto, heated on bobbin at 160°, 5 minutes	5.9	–
" , heated on bobbin at 160°, 20 minutes	5.9	–
" heated on bobbin at 160°, 70 minutes	5.9	19.2
" heated in skein at 160°, 5 minutes	5.9	–
" heated in skein at 160°, 70 minutes	6.0	19.1
" additionally stretched at 160°	5.5	18.7
" boiled in water on bobbin, 0.5 hour	5.7	–
" boiled in water on bobbin, 3 hours	5.6	18.6
" boiled in water in skein, 0.5 hour	5.1	–
" boiled in water in skein, 3 hours	5.1	17.5
" steamed on bobbin in autoclave at 140°, 0.5 hour	4.5	–
" steamed on bobbin in autoclave at 140°, 1 hour	3.8	–
" steamed on bobbin in autoclave at 140°, 3 hours	4.0	14.9
" steamed in skein in autoclave at 140°, 0.5 hour	2.5	–
" steamed in skein in autoclave at 140°, 3 hours	2.5	13.4

Note: The accuracy of the determinations was ± 0.2 cal/g.

TABLE 3

Densities of Fibers after Various Types of Heat Treatment

Fibers	Density in g/cc
Undrawn yarn No. 34	1.1303
Drawn yarn No. 34	1.1449
Ditto, additionally stretched at 160°	1.1437
" heated on bobbin at 160°, 70 minutes	1.1456
" heated in skein at 160°, 70 minutes	1.1471
" boiled in water on bobbin, 3 hours	1.1464
" boiled in water in skein, 3 hours	1.1479
" steamed in autoclave on bobbin at 140°, 3 hours	1.1533
" steamed in autoclave in skein at 140°, 3 hours	1.1598

Note: The accuracy was ± 0.00042 g/cc.

zene or nitrobenzene was added until the skein began to float within the liquid. The density of the benzene-nitrobenzene mixture was then determined pycnometrically; this was equal to the density of the fiber specimen.

The results of the density determinations, which are the average values of three separate experiments, are given in Table 3. As was stated earlier, the density data in Table 3 are in good agreement with the kinetic characteristics of the heat of solution, Q_k, thereby confirming that heat treatment results in an increase of the molecular packing density in the fibers.

SUMMARY

1. The kinetic characteristics of the heat of solution of capron fibers after different types of heat treatment differ considerably. These results are in agreement with other kinetic data and are a good measure of the change in the molecular structure of capron fibers caused by heat treatment.

2. Heat treatment of capron fibers on bobbins or in the free state results in a denser packing of the intermolecular fiber structure.

LITERATURE CITED

[1] N.V. Mikhailov, E.Z. Fainberg and S.M. Skuratov, Colloid J. 15, 271 (1953) (T.p. 279)*; S.M. Skuratov, N.V. Mikhailov and E.Z. Fainberg, Colloid J. 16, 58 (1954) (T.p. 65)*; N.V. Mikhailov and E.Z. Fainberg, Colloid J. 18, 44 (1956) (T.p. 41).*

[2] V.D. Tetyushkina, A.N. Pkashver and S.S. Frolov, Colloid J. 17, 63 (1955) (T.p. 57).*

[3] A.B. Pakshver and E.K. Mankash, J. Appl. Chem. 24, No. 2, 182 (1954); E.K. Mankash and A.B. Pakshver, Colloid J. 16, 451 (1954) (T.p. 429)*; V.A. Myagkov and A.B. Pakshver, Colloid J. 17, 120 (1955) (T.p. 109).*

[4] E.K. Mankash, Trans. Ivanovo Inst. Chem. Technol. 5, 127 (1956).

[5] G. Clark, M. Mueller and L. Scott, Ind. Eng. Chem. 42, No. 5, 831 (1950); N. Abbot and A. Gottings, J. Text. Inst. 40, No. 4, 232 (1949).

[6] H. Schottky, Z. Phys. Chem. 64, 425 (1908); K.P. Mishchenko, M.Z. Pronina and A.M. Sukhotin, J. Appl. Chem. 27, No. 9, 1003 (1954).

[7] Yu.S. Lipatov, Candidate's Dissertation (1954).

[8] Z.A. Zazulina and Z.A. Rogovin, Colloid J. 17, 343 (1955) (T.p. 327).*

Received November 6, 1956

The Ivanovo Institute of Chemical Technology
The All-Union Correspondence Institute for the Textile and Light Industries

---

*T.p. = C.B. Translation pagination.

PERIODIC DEFORMATION OF COLLAGEN IN SOLUTIONS OF ELECTROLYTES AND TANNING AGENTS

A.G. Pasynsky and A.M. Tongur

The technical raw hide of the leather industry is a complex histological structure formed from bundles of collagen fibers (from 30 to 130μ in diameter) consisting consecutively, of collagen fibers (7-10μ), fibrils (tenths of a micron) and finally protofibrils (50-100 mμ), each containing some dozens of molecular chains. The interstices between the structural elements of the hide (up to several microns in size) are filled with interstitial materials (albumins, globulins, mucins, extractable matter) which are removed from the hide during the processes which precede tanning [1].

The permeability of hide to tanning agents largely depends on the histological rather than the molecular structure of the hide. Therefore, to accelerate penetration of tanning agents into hide, a suitable procedure seemed to be to influence the histological structure by periodic mechanical deformation of the hide. For this, a more detailed study of its relaxation properties was needed.

Zubov, Zhurkina and Kargin [2] discovered only short relaxation times for elastic gelatin gels (up to 20-30% gels); long relaxation times were found only under conditions in which some of the cross links of the network were broken and relative displacement of the molecules became possible. Gelatin gels are examples of histologically uniform structure, formed by molecular protein chains. Therefore, the variation of the deformation of raw hide in various media with the deformation frequency was also of interest in relation to the special deformation characteristics of histologically inhomogeneous structures, in the case of such a material as collagen (which comprises up to 98% of the fibrous protein of hide) [1]. In the present investigation a study was made of these characteristics, in order to determine the possibility of using them for acceleration of the tanning process.

EXPERIMENTAL

The relaxation properties of collagen were studied with the Aleksandrov-Kargin apparatus [2], at deformation frequencies from 1 to 1000 cycles per minute. Heavy cowhide specimens ~6 mm thick were used for the tests.

The clean hide (inner layer of fresh hide, with flesh side scraped and hair mechanically removed), in the loose and dense regions, behaves like an elastic gel up to 60°, with only short relaxation times in this range (Figure 1). Long relaxation times are found only at higher temperatures, corresponding to partial "fusion" of the hide structure. This behavior is similar to the properties of 30-40% gelatin gels [2], which have a similar content of dry protein (~35%) [1], but a sharp increase in the deformation of hide occurs at 60° (Figure 1), while for gelatin gels it occurs at 30°, which shows that the cross links of the network are stronger in collagen. At the same time, the existence of only short relaxation times below the "fusion" point of the gels indicates that the interaction between the chain segments between the cross links in the network is weak in both systems.

Alteration of the interchain bonding in the collagen structure may occur both as the result of temperature changes, and in presence of various dissolved substances. The effects of solutions of: KCNS, NaCNS, LiCl, KCl, $(NH_4)_2SO_4$ and urea, of various concentrations on periodic deformation behavior at different temperatures were therefore studied. Sets of curves similar to those shown in Figure 1 were obtained; the inflexion points on these curves varied for media of different composition, in general accordance with the thermal shrinkage temperatures in the same solvents. For example, after the hide specimens had been kept for 12 hours in the solutions, the

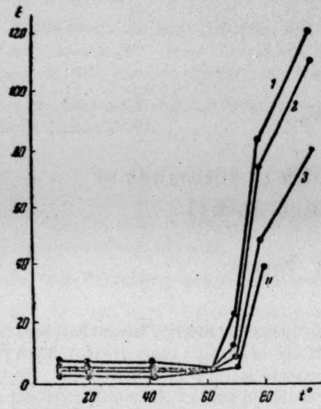

Fig. 1. Deformation-temperature curves for clean hide, for various frequencies: 1) 1 cycle/minute; 2) 10 cycles/minute; 3) 100 cycles/minute; 4) 1000 cycles/minute.

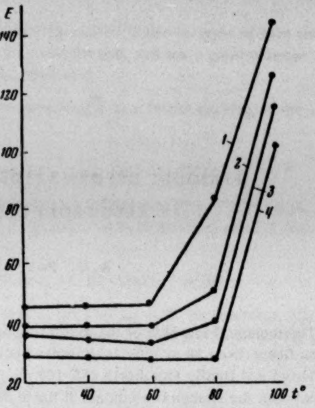

Fig. 3. Deformation-temperature curves for hide at the liming stage, for various frequencies: 1) 1 cycle/minute; 2) 10 cycles/minute; 3) 100 cycles/minute; 4) 1000 cycles/minute.

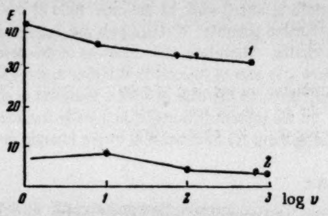

Fig. 2. Deformation of hide as a function of frequency, at the liming stage: 1) dense; 2) loose region of hide.

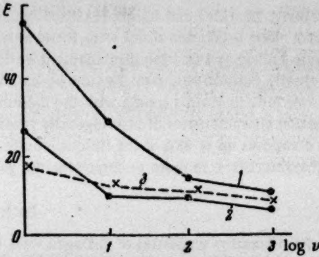

Fig. 4. Deformation of hide as a function of frequency, at the chroming stage: 1) dense region; 2) loose region; 3) deformation-frequency curve for leather.

points of inflexion on the curves were shifted to 20-22° in 2 M NaCNS and KCNS, to 38-40° in 5 M urea, were unchanged in 2 M LiCl, and were shifted by 10-20° in the direction of higher temperatures (i.e., up to 70-80°) in 2 M KCl and 25% solution of $(NH_4)_2SO_4$. The shrinkage temperature of the collagen was marked in all cases by a sharp increase of deformation (as shown in Figure 1) and the appearance, beyond the inflexion point, of long relaxation times, which are detected by the clear dependence of the magnitude of deformation on the temperature. As was to be expected, the greatest increase of deformation is found at low vibration frequencies. At temperatures below 40°, at which tanning of collagen is usually carried out, clean hide shows only short relaxation times.

The relaxational properties of hide change in the course of technological processing. At the liming stage,

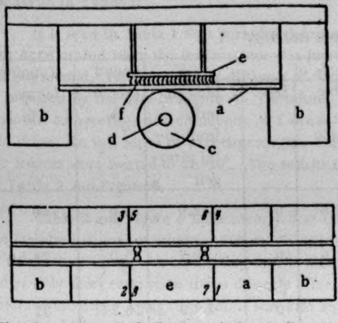

Fig. 5. Diagram of vibrator; below – diagram of control points.

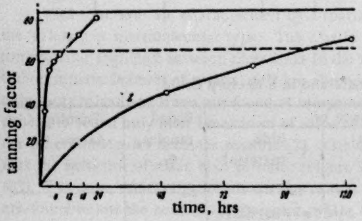

Fig. 6. The dynamics of tanning heavy hides: 1) during periodic compression 80 cycles/min; 2) in factory drum.

with the use of $Ca(OH)_2$ and Na_2S solutions, the deformation at 20° becomes almost independent of the frequency (Figure 2), but the deformation-temperature curves (Figure 3) begin to differ appreciably from the curves in Figure 1, both in the magnitude of deformation, and in the position of the inflexion points for various frequencies. At the liming and pickling stages (treatment with hydrochloric acid solution), deformation at 20° was almost independent of the frequency, both for the elastic and the soft portions of the hide, but at the liming stage the inflexion points on the deformation-temperature curves lay in the range of 60 to 90°, while at the pickling stage these curves again became similar to those shown in Figure 1, with a common inflexion point at 60°. It seems that at the liming and deliming stages additional stable bonds are formed in the collagen structure (possibly by calcium), which are completely destroyed in pickling.

At the chrome tanning stage the picture changes; as is seen in Figure 4 (Curves 1 and 2) the deformation of both the dense and the loose regions of the hide at 20° clearly depends on the frequency, especially at frequencies below 100 cycles/minute. This indicates that the hide has special mechanical properties at the chrome tanning stage, and it is significant that long relaxation times are found in this instance for the system in which relative displacement of the molecules is completely excluded as the result of a superposition of a network of additional stable bonds during chrome tanning, which results in a shift of the thermal shrinkage temperature to above 100°. An interesting fact is that even in the next operation (vegetable tanning in standard oak extract and syntans) the deformability of the leather again decreases considerably and the deformation becomes much less dependent on frequency (Figure 4, Curve 3).

We took advantage of the appearance of long relaxation times at the chrome tanning stage, before vegetable tanning, to influence the kinetics of the tanning process , the duration of which is determined primarily by the low rate of diffusion of the tanning solution into the hide. In our opinion, by means of periodic deformations of the hide, accompanied by contractions and extensions of the collagen fibers, equivalent to alternate condensation and rarefaction of the structure, it should be possible to accelerate the penetration of the tanning liquor into the hide. Naturally, this result could be expected only at deformation frequencies corresponding to long relaxation times, as at very high deformation frequencies the penetration of the tanning liquor into the structure could not keep pace with the changes in the field. As has been shown, at most stages in the production of leather, from the fresh hide up to the pickling stage, the hide has only short relaxation times at low temperatures, and it is only at the chroming stage, just before vegetable tanning, that the long relaxation times appear which could be used for accelerating the tanning process.

This possibility was explored in experiments on tanning of heavy and medium chromed hide (3 to 10 mm thick) with periodic deformation of the hide in the tanning liquor.

First we used vibrators operating at frequencies between 10 and 100 cycles/second. The vibrator (Figure 5) consists of two concrete supports b, with a plate a resting upon them, with an off-balance motor c attached to its under side. Vibrations of the body of the motor, induced by rotation of the eccentric pulley d mounted on the rotor, are transmitted to the plate a. The vibration conditions were controlled by means of an "Askania" recording dynamometer, which recorded the vibration amplitude and frequency at eight points in the vibrator,

TABLE 1

Results of Tanning in a Vibrator and in a Laboratory Drum (Without Heating)

Specimen No.	Tanning conditions	Moisture, %	% Contents in dry substance of					Bound tannins, %	Tanning factor, %
			ash	water-extractable substances		fats	hide material, from total nitrogen		
				inorganic	organic				
I	Vibrator, 50 cycles/ /sec, 6 hours	12.0	10.5	9.6	22.5	0	48.0	19.0	40
	Laboratory drum, 24 hours	13.8	10.7	9.0	21.6	0	52.7	15.0	28.5
II	Vibrator, 50 cycles /sec, 5 hours	12.7	7.6	6.8	14.7	0	59.9	18.2	31
	Laboratory drum, 5 hours	15.0	5.7	3.5	14.0	0	66.4	15.6	20

TABLE 2

Results of Tanning Under Periodic Compression at 80 cycles/minute and in a Factory Drum

Tanning time, hrs.	Moisture, %	% Contents in dry substance of					Bound tannins, %	Tanning factor, %
		ash	water-extractable substances		fats	hide material		
			inorganic	organic				
		Periodic compression at 80 cycles/minute						
2	11.2	10.2	9.3	29.8	0	44.5	15.5	35
4	12.0	9.1	8.7	26.3	0	41	23.7	57.7
6	10.6	9.7	8.8	24.6	0	41	24.7	60
12	10.15	9.85	9.0	29.2	0	37.4	23.55	63
18	10.0	9.9	9.05	28.6	0	35.4	26.1	74
24	9.7	9.3	8.35	27.8	0	35.0	27.9	80
		Factory drum						
48	12.8	6.7	6.0	11.5	0	56.5	27.4	45.0
82	12.2	7.8	6.9	11.8	0	53.0	25.3	52.0
125	11.7	6.9	5.0	10.8	0	49.2	33.1	67

indicated in the lower part of Figure 5. Specimens of chromed hide (6 × 6 cm) with tanning liquor were put into a thin rubber bag _f_ (made from a surgical glove), placed between the vibrating plate _a_ and the pressure plate _e_. The vibration amplitude of the pressure plate was considerably less than that of the vibrating plate (for example, 0.02 and 0.21-0.27 mm) in order to increase the relative deformation of the hide, and the deforming force was applied directly to the hide in order to create a vibration phase difference between the solid and the liquor. Simultaneously with the tanning in the vibrator, a specimen cut from the same portion of hide was tanned in a laboratory drum in standard oak tannin extract with additions of up to 20% of syntans, at a 1 : 4 ratio between the tanning agents in the volume of liquor used and the weight of the hide, and at pH of 4.25 to 4.5 of the diluted extract. The tanning was carried out at room temperature in both cases. The leather samples after tanning were analyzed according to GOST 938-45 for percentage fat, moisture, ash, easily removable low molecular substances, ash content of the extractable substances, and total nitrogen. The analytical data were used to calculate the total contents of nonhide material (percentage of bound tannins) and the tanning factor (ratio of bound tannins to total nitrogen in percent). The results for two heavy hide specimens (of the shoe sole type) are given in Table 1.

It is seen in Table 1 that periodic deformations accelerate the tanning of hide, and the process was further accelerated when the temperature was increased to 40° and the deformation frequency decreased to 25 cycles/second. However, it was difficult to reduce the frequency on the vibrator to below 100 cycles/minute, as required by the data in Figure 4. Therefore, in the following experiments the tanning was performed under periodic compression at a frequency of 1 cycle/second, effected by means of a plate with a rod with an eccentric drive. In this series of experiments (the control experiments for which were carried out in a factory drum) the liquors were heated to 38-40°. The results for the elastic region of heavy oxhide (5 mm thick) are given in Table 2 and Figure 6.

Table 2 and Figure 6 show clearly that tanning is accelerated on periodic compression of chromed hide, the standard degree of tanning (65% by GOST) being replaced in 12-13 hours instead of the 125 hours required in the factory drum. An interesting fact is that in experiments on vegetable tanning of unchromed hide, which shows only short relaxation times directly after pickling (see above), periodic deformation was found not to accelerate tanning. A negative result was also obtained in an experiment on vegetable tanning of a 15% chrome-treated gelatin gel, the deformation of which does not depend on the frequency..

DISCUSSION OF RESULTS

Gel structures are characterized by a spatial macromolecular network, cross linked by means of bonds of the valency or intermolecular type. The elastic properties of gels are determined by the flexibility of the macromolecular segments between cross links in the network, which fix the relative positions of the macromolecules. Characteristic features of typical gels are absence of fluidity and presence of elastic properties; in these gels only short relaxation times are found at temperatures below the gelation point. In such gels large relaxation times are found only after breakdown of some of the cross links of the network, when relative displacement of the macromolecules becomes possible [2]. Our data on the effect of frequency on the deformation of hide showed that the behavior of clean hide in water (Figure 1) and in various media (2 M solutions of KCNS, NaCNS, LiCNS, KCl, 5 M urea, 25% $(NH_4)_2SO_4$) is similar to that of an elastic protein gel, in which only short relaxation times are found below the heat shrinkage point, while the position of the inflexion points on the deformation-temperature curves (i.e., the appearance of long deformation times) is displaced in accordance with changes in the heat shrinkage temperature.

Interesting behavior is shown by chrome-tanned hide (Figure 4), in which long relaxation times are found in the gel state in presence of a network of additional bonds in the collagen structure, i.e., in conditions in which relative displacement of the macromolecules is excluded. This is not the consequence of an increased number of cross links in the network and interaction between the chains, as is shown by the fact that after vegetable tanning, during which the chrome cross links are retained and the absorption of vegetable tannins is added, long relaxation times are not found (Figure 4, Curve 3); neither are they found for chrome-treated gelatin gels. Therefore, the appearance of long relaxation times for chrome-tanned hide must depend on certain structural characteristics of the hide at this stage of treatment.

The characteristic in question is probably increased porosity of the structure. Owing to the removal of interstitial substances at the stages preceding tanning, the permeability of the hide increases sharply as has been shown by Frenkel and Mihailov [3], at the chroming stage, while during the subsequent vegetable tanning the permeability decreases again because the pores become filled with tannin particles [1]. Thus, at the chroming stage the structure of the leather acquires a peculiar character, which distinguishes it from the ordinary microscopically homogeneous gels, of the gelatin gel type, studied by Zubov, Zhurkina and Kargin [2].

In a histologically inhomogeneous porous structure, deformation of bundles of fibers or fibrils, even if the gel network is retained, leads to the appearance of longrelaxation times, associated with the deformed fibers entering and leaving the pores. This is the way in which the deformation of histologically porous structures differs in principle from the deformation of histologically homogeneous gels (such as gelatin gels), the heterogeneity of which is at the molecular structure level. This new effect in the deformation of collagen will probably be found in other polymeric substances with a submicroscopically heterogeneous structure. This effect disappears in collagen when the pores are filled with interstitial matter (in the raw hide) or with tannin (in vegetable tanning), on decrease of porosity as the result of fiber swelling (in unchromed hide) etc.

The appearance of long relaxation times in chromed hide is not only of theoretical but also of practical interest, in view of the possibility of accelerating the vegetable tanning stage, which is normally limited by the low rate of penetration of the tanning agent into the hide. It was to be expected that, on periodic deformation of chromed hide in tanning liquors at a frequency corresponding to its long relaxation periods, the alternating filling and emptying of the pores in the course of deformation of the collagen fibers should accelerate the penetration of the tanning liquor into the hide and assist repeated filling of the pores with fresh tanning liquor. We therefore carried out tanning tests in vibrators at frequencies from 25 to 100 cycles/second, and also under periodic compression at a frequency of 1 cycle/second, i.e., at fairly low deformation rates. Specimens of chromed hide were treated directly in the tanning liquor. Tables 1 and 2 and Figure 6 show that this method results in considerable acceleration of the tanning process in comparison with tanning either in a laboratory or in a factory drum. However, for materials which do not show long relaxation times – unchromed hide, chromed gelatin gel – periodic deformation does not accelerate tanning. It is possible that the use of periodic deformation at frequencies close to the long relaxation periods of the material in question may serve as a general method for accelerating the diffusion of liquids into materials of histologically inhomogeneous structure.

SUMMARY

1. The effect of frequencies from 1 to 1000 cycles/minute on the deformation of collagen (hide) in water and various media (2M solutions of KCNS, NaCNS, LiCl, KCl, 5M urea, 25% $(NH_4)_2SO_4$) has been studied at various temperatures and at different stages of the technological process. It is shown that with the exception of the chrome tanning stage (before vegetable tanning) hide has only short relaxation periods and shows behavior similar to that of an elastic protein gel.

2. In chromed hide, which has a histologically inhomogeneous porous structure, a new effect has been discovered; the appearance of long relaxation times in a polymeric material in absence of relative displacements of the molecules.

3. This effect was used to accelerate penetration of tanning agents into collagen by periodic deformation of chromed hide in tanning liquor at a frequency corresponding to the long relaxation times of the material. It is shown that by this method it is possible to accelerate the tanning of chromed hide considerably in comparison with tanning in a factory drum.

This work was performed in scientific cooperation with the Central Research Institute for the Leather Industry. The authors express their deep gratitude to Prof. A.N. Mikhailov and A.L. Zaides, and also to Academician V.A. Kargin and Z.N. Zhurkina for much valuable advice and help in this work.

LITERATURE CITED

[1] A.N. Mikhailov, Chemistry of Tanning Agents and Tanning Processes (State Light Industry Press, 1953), p. 794.

[2] P.I. Zubov, Z.N. Zhurkina and V.A. Kargin, Colloid J. 9, 109, 367 (1947).

[3] P.Ya. Frenkel and A.N. Mikhailov, Collected Papers of the Central Sci. Res. Inst. Leather Ind. No. 17, 50 (1950).

Received September 13, 1956

The A.N. Bakh Institute of Biochemistry
Academy of Sciences, USSR - Moscow

EFFECT OF ATMOSPHERIC TURBULENCE ON THE KINETICS OF AEROSOL COAGULATION

O.M. Todes and A.A. Chekunov

Turbulent pulsations in the atmosphere continuously decrease the particle concentration of an aerosol cloud for two reasons. Small scale pulsations intensify the chaotic motion of the particles and accelerate their coagulation. Large scale pulsations dilute the cloud and increase the volume occupied by the aerosol particles. The first of these factors decreases the particle concentration by a simultaneous increase of the particle size, while the latter does not affect the particle size.

The constant of turbulent coagulation. The influence of mass flow on the coagulation rate was considered even by Smoluchowski [1] and Muller [2]. Coagulation in turbulent flow was studied by Wigand and Frankenberger [3], Tunitsky [4], Teverovsky [5] and Levich [6, 7]. As the result of all these investigations it may be regarded as established that the influence of turbulence on coagulation rate increases very sharply with increasing particle size. In the case of aerosols with particles of the order of 10^{-6} to 10^{-5} cm turbulent diffusion does not play any important part, and the coagulation rate is determined entirely by the laws of Brownian movement. This view is challenged only by Teverovsky. However, Teverovsky's interpretation of his experimental data gives rise to a number of serious objections. Let us consider this important question in greater detail.

It was shown by Smoluchowski [8, 9] that in coagulation resulting from collisions between particles in Brownian movement the rate of change of the particle concentration N with time t is given by the expression

$$-\frac{dN}{dt} = KN^2 . \qquad (1)$$

The coagulation rate constant in this case is $K = \frac{8}{3}\frac{kT}{\eta}$, where η is the viscosity of air; k is the Boltzmann constant; and T is the absolute temperature. Integration of Equation (1) gives the well known law for the linear increase of the particle volume with time

$$\frac{1}{N} = \frac{1}{N_0} + K \cdot t. \qquad (2)$$

Equations (1) and (2) remain valid even if the polydispersity of the coagulating sol is taken into account, and only the coagulation rate constant is about 10% greater than the value calculated by the Smoluchowski equation [10, 11].

The theory of turbulent scattering of impurities in the atmosphere has been developed fairly fully by Laikhtman [12] and others. In the case of a linear source perpendicular to the wind direction, the volume of the aerosol cloud increases in direct proportion to the distance x from the source. Hence it may be concluded that 1/N increases linearly with x and that

$$-\frac{dN}{dx} = \frac{1}{\Lambda} N^2, \qquad (3)$$

where

$$A = \frac{Q}{\frac{2}{3}\pi^{1/2} S_z \delta r^3 u}. \tag{4}$$

Q is the output of the source per unit length (in g/m · second); r is the particle radius (in m); δ is the density of the particles (in g/m³); S_z is the vertical component of the turbulent diffusion coefficient (in m²/second); u is the wind velocity (in m/second); and N is the particle concentration of the aerosol (1/m³).

When the aerosol cloud is moved by the wind, x = ut and the coagulation rate Equation (1) can be written in the form

$$-\frac{dN}{dx} = \frac{K}{u} N^2. \tag{5}$$

Assuming that coagulation in the atmosphere is wholly determined by turbulent pulsations, Teverovsky replaces Equation (5) by the analogous equation

$$-\frac{dN}{dx} = \frac{K_T}{u} N^2 \tag{6}$$

and introduces, for the turbulent coagulation constant K_T, the relationship

$$K_T = 4\pi r \left(\frac{\lambda'}{l}\right)^4 \left(\frac{Lu}{\nu^2}\right)^3, \tag{7}$$

where L is the turbulence scale; l is the length of the path of mixing; λ' is the average free path of the particles coagulating on collision; D = Lu is the coefficient of turbulent diffusion, and ν is the kinematic viscosity of the air.

If both turbulent coagulation and scattering are present, Teverovsky considers the two factors to be additive, and proposes the following equation for the rate of change of the particle concentration during motion of the cloud:

$$-\frac{dN}{dx} = \left(\frac{K_T}{u} + \frac{1}{A}\right) N^2. \tag{8}$$

Integrating this equation, he finds that

$$\frac{1}{N} = \frac{1}{N_0} + \left(\frac{K_T}{u} + \frac{1}{A}\right) x \tag{9}$$

and compares the resultant theoretical N(x) relationship with his experimental determinations of the particle concentration at various distances from the source. Hence he calculates the value of K_T and compares it with the value calculated from Equation (7), obtaining satisfactory agreement between the theory and the experimental results. However, this agreement is purely apparent. The reason is that in the integration of Equation (8) the turbulent coagulation constant was assumed to retain a constant value. In fact, however, the values of λ' and r contained in it increase with decreasing particle concentration as follows:

$$\lambda' = N^{-1/3} \text{ and } r = \sqrt[3]{\frac{3c}{8\pi\delta}} N^{-1/3}. \tag{10}$$

Consequently

$$K_T = 4\pi \sqrt{\frac{5c}{8\pi\delta} \frac{D^3}{l^4 \gamma^3}} N^{-5/3} = BN^{-5/3}.$$

Substituting (10) into (8), and assuming, with Teverovsky, that $K_T/u \gg 1/A$, we find

$$-\frac{dN}{dx} = \frac{K_T}{u} N^2 = BN^{1/3}. \tag{11}$$

Integration of Equation (11) leads to a totally different expression for the particle concentration as a function of distance

$$N^{2/3} = N_0^{2/3} - \frac{2}{3} \cdot \frac{B}{u} x. \tag{12}$$

It follows from Equation (12) that at a certain distance

$$x_{\max} = \frac{3}{2} \cdot \frac{u}{B} N_0^{2/3} \tag{13}$$

coagulation ceases completely and the particle concentration N becomes zero. Substitution of the numerical values given by Teverovsky into Equation (13) gives $x_{\max} \approx 150$ m. This was not the case in reality, and in Teverovsky's experiments the aerosol continued to coagulate at considerably greater distances, and the coagulating particles, when conveyed by wind of $u \approx 3$ m/second to a distance of 1000 m, increased in size from $2 \cdot 10^{-5}$ to $4 \cdot 10^{-5}$ cm. Thus, Teverovsky's experiments do not provide convincing proof of his theory concerning the significant influence of atmospheric turbulence on coagulation, and we may, together with the other authors cited earlier, assume that for particles of the order of 10^{-5} cm, $K_T \ll K$.

Kinetics of the variation of particle concentration. For the derivation of a fundamental equation for the coagulation kinetics of a scattering cloud it is also necessary to examine critically Teverovsky's second assumption concerning the additivity of the coagulation and scattering processes. Consider a certain isolated volume V of the moving cloud and denote the total number of particles in it by n; then the particle concentration N in this volume will be

$$N = n/V. \tag{14}$$

If the cloud does not expand (V = const), N and n will vary synchronously; multiplying both sides of Equation (1) by V, we have:

$$-\frac{dn}{dt} = \frac{K}{V} n^2 . \tag{15}$$

Equation (15) gives the change in the total number of particles in the cloud caused by coagulation, and it remains valid if the volume of the cloud changes with time. On the other hand, Equation (1) ceases to be valid when $V \neq$ const. To find the rate of change of the particle concentration we must differentiate Equation (14)

$$-\frac{dN}{dt} = -\frac{d}{dt}\left(\frac{n}{V}\right) = -\frac{1}{V}\frac{dn}{dt} + \frac{n}{V^2}\frac{dV}{dt} . \tag{16}$$

Substituting the value of dn/dt from Equation (15) into Equation (16), and replacing the time of existence of the cloud t by the distance traversed by it, x = ut, we have

$$-\frac{dN}{dx} = \frac{K}{u} \cdot N^2 + \frac{1}{V}\frac{dV}{dx} N. \tag{17}$$

For a linear source the volume V of the cloud increases linearly with the distance x. Since near the source the concentration changes in the cloud should be determined by more complex relationships, we introduce an interpolation formula

$$V = c \cdot (x + x_0), \tag{18}$$

valid only for a certain distance $x > x_0$ from the origin of the cloud. Taking logarithms and differentiating Equation (18) we have

$$\frac{1}{V}\frac{dV}{dx} = \frac{1}{x + x_0}, \tag{19}$$

and the final equation for the process involving coagulation and scattering takes the form

$$-\frac{dN}{dx}=\frac{K}{u}N^2+\frac{N}{x_0+x}. \tag{20}$$

This equation is easily integrated by separation of the variables. The general integral of Equation (20) has the form

$$\frac{1}{N}=\frac{1}{N_0}+\frac{x}{N_0x_0}+\frac{K}{u}(x+x_0)\ln\frac{x+x_0}{x_0}. \tag{21}$$

Analysis of Equation (21). For analysis of the relationship derived in the form of Equation (21) let us consider the limiting cases of small and large distances.

1. For small distances when $x \ll x_0$ it is possible to resolve the logarithm into series and to use only the first term $\ln(1+x/x_0) \approx x/x_0$. Then, with an accuracy up to terms of the second order, we have from Equation (21) that

$$\frac{1}{N}=\frac{1}{N_0}+\left(\frac{K}{u}+\frac{1}{N_0x_0}\right)x. \tag{22}$$

It is thus seen that Teverovsky's assumption of the additive influence of coagulation and scattering on the particle concentration is valid only for very small distances, when the dimensions of the cloud are only slightly greater than the original.

2. At large distances when $x \gg x_0$ we may replace $x + x_0$ by x, and Equation (2) takes the form

$$\frac{1}{N}=\frac{1}{N_0}\cdot\frac{x}{x_0}\left(1+\frac{Kx_0N_0}{u}\cdot\ln\frac{x}{x_0}\right). \tag{23}$$

In this case simple additivity no longer applies and the variation of the particle concentration with distance depends considerably on the dimensionless parameter

$$\frac{KN_0x_0}{u}=\frac{KN_0}{u/x_0}, \tag{24}$$

which represents the ratio of the coagulation rate to the rate of scattering.

When $u = 5$ m/second and $x_0 \approx 50$ m, the rate of scattering $u/x_0 \approx 10^{-1}$ sec^{-1}. The coagulation constant $K = 3\cdot10^{-10}$ cc/second, at a low initial concentration $N_0 = 10^6$ cm^{-3}, the rate of scattering $KN_0 \approx 3\cdot10^{-4}$ sec^{-1} and the ratio of the rates $\frac{KN_0}{u/x_0} \approx \frac{1}{300} \ll 1$. In this case, even when $x/x_0 \approx 1000$ the value of $\ln x/x_0$ does not exceed 7 and coagulation may be neglected with an error of 2%; from Equation (23) we have that

$$N = N_0\cdot x_0/x. \tag{25}$$

Consequently, at low initial concentrations of the aerosol cloud the decrease of particle concentration is mainly determined by scattering of the cloud, and coagulation, even at large distances, produces not more than ~0.5% increase in the average particle size.

At a higher initial aerosol concentration, $N_0 \approx 10^9$ cm^{-3}, the ratio $\frac{KN_0}{u/x_0} \approx 3$ and at large distances the digit 1 in the parenthesis of Equation (23) may be neglected in comparison with the second term. In this case

$$\frac{1}{N}\approx\frac{1}{N_0}\frac{x}{x_0}\frac{Kx_0N_0}{u}\ln\frac{x}{x_0}=\frac{K}{u}x\cdot\ln\frac{x}{x_0}. \tag{26}$$

Comparison of Equations (26) and (2) shows that even if the rate of scattering is low in comparison with the coagulation rate ($u/x_0 < KN_0$), nevertheless at large distances scattering has a significant influence on the particle concentration N, which decreases $\ln x/x_0$ times as rapidly as in an enclosed space.

Since at large distances the volume of the cloud increases in direct proportion to the distance

$$V \approx V_0 \cdot x/x_0, \tag{27}$$

the total number of particles in the cloud will decrease according to the law

$$n = NV = \frac{uV_0}{Kx_0} \cdot \frac{1}{\ln (x / x_0)} \approx \frac{n_0}{\ln (x / x_0)}, \tag{28}$$

i.e., relatively slowly. Since the average radius of the particles is inversely proportional to the cube root of their number ($\bar{r} \sim n^{-1/3}$), as coagulation proceeds and the cloud expands, $\bar{r}$ will increase still more slowly with the distance, according to the relationship

$$\frac{\bar{r}}{r} = \sqrt[3]{\ln \frac{x}{x_0}}. \tag{29}$$

If, for instance, $x/x_0 = 1000$ and $\ln x/x_0 \approx 7$, the total number of particles n will decrease by a factor of 7, and the particle concentration N will decrease by a factor of 7000, while the average radius of the particles will become only $(7)^{1/3} \approx 2$ times as large. In the case of a point source, scattering of an aerosol cloud in the atmosphere occurs not only in a vertical but also in a horizontal direction at right angles to the wind. The particle concentration then decreases still more rapidly, while the particle size increases more slowly.

SUMMARY

1. In the motion of an aerosol cloud consisting of small particles of the order of 10^{-6} to 10^{-5} cm in size, small scale turbulent pulsations do not significantly increase the coagulation rate constant.

2. Large scale turbulent pulsations scatter and extend the cloud and thereby decrease the absolute rate of coagulation. Therefore, the particle size in an aerosol cloud in the atmosphere increases much more slowly than in an enclosed space.

LITERATURE CITED

[1] M. Smoluchowski, Zeit. Phys. Chem. 92, 129 (1917).

[2] H. Muller, Koll. chem. Beih. 27, 223 (1928).

[3] A. Wigand and E. Frankenberger, Phys. Zeit. 31, 204 (1930).

[4] N.N. Tunitsky, J. Phys. Chem. 20, 1137 (1946).

[5] E.N. Teverovsky, Symposium, New Ideas in the Study of Aerosols (1949), p. 108.

[6] V.G. Levich, Proc. Acad. Sci. USSR 94, No. 5, 809 (1954).

[7] V.G. Levich, Proc. Acad. Sci. USSR 94, No. 6, 1041 (1954).

[8] M. Smoluchowski, Phys. Zeit. 17, 587 (1916).

[9] M. Smoluchowski, Zeit. Phys. Chem. 92, 129 (1917).

[10] O.M. Todes, Coll. Papers Phys. Chem. 138 (1948).

[11] O.M. Todes, Symposium, Problems of Kinetics and Catalysis 7, 137 (1949).

[12] D.L. Laikhtman, Bull. Acad. Sci. USSR, Ser. Geog. and Geophys. 8, No. 1 (1944).

Received July 9, 1956 Leningrad

SETTLING OF AEROSOL PARTICLES ON THE WALLS OF AN ENCLOSED SPACE

I. Todorov and A. Sheludko

The settling of aerosol particles from the volume of a sphere on its walls is theoretically considered in this paper. It is assumed that the aerosol particles approach the walls by diffusion and sedimentation, and that no convection occurs in the gas. The coefficient of adhesion of the particles to the walls is assumed to be less than unity. This value is probably close to unity [1], but it nevertheless depends on the presence of surface-active substances [2], so that there are no grounds for assuming that it is equal to unity.

Our chosen model of a spherical space, with convection ignored, is of practical significance, for example, in calculations relating to dust removal by foam, and also as the limiting case of dust removal by filtration of aerosols through porous filters at a low rate of flow. In the latter instance, with a random arrangement of capillaries in the filter, such a filter will correspond to a certain spherical space the effective radius of which is determined by the capillary diameters. The question of the exact relationship between this effective radius and the actual capillary diameter is not considered here.

The following simplifying assumptions are made in solving the problem.

a) The aerosol concentration is taken to be fairly low, so that the coagulation rate is low in comparison with the rate of settling on the walls. This is a significant case, because if coagulation prevailed the walls would not influence the rate at which the aerosol particles are removed from the space. For a low particle concentration it can be assumed that the behavior of any given particles does not depend on the presence of other particles in the system, and also that the particles always settle on unoccupied regions of the wall surface and the adhesion coefficient does not change with time.

b) The adhesion coefficient is assumed to be independent of particle size.

c) The spherical space is fairly large relative to the free path of the gas molecules, so that it is possible to use the ordinary diffusion equations and to assume that the velocities of the aerosol particles throughout the volume, right up to the walls, have a Maxwellian distribution.

A preliminary qualitative examination of the problem on the assumption that the adhesion coefficient $\alpha = 1$ shows that particles of medium size will be the slowest to settle. Larger particles will mainly settle by sedimentation to the bottom under the force of gravity, and the smaller particles, by diffusion to the walls. The maximum time t_s in which a particle will settle to the bottom is evidently given by the expression $t_s = 2aB/P$, where a is the radius of the sphere; B is the coefficient of friction of the particle; P is its weight. The order of magnitude of the maximum time t_d in which a particle will reach the wall by diffusion can be calculated from its mean square displacement $\overline{\Delta}^2 = 2Dt$, if we assume that $\overline{\Delta}^2 = a^2$, so that $t_d = a^2B/2kT$, as

$$D = kT/B, \tag{1}$$

where k is the Boltzmann constant and T is the absolute temperature. It is obvious that t_s decreases and t_d increases with increasing particle size. Therefore, for the smaller particles the time for settling by diffusion is less than the time for settling by gravitation, while the converse is true for the larger particles. Particles for which $t_s \approx t_d$ will remain longest in the suspended state. It follows from this approximate condition that the weight of the most "stable" aerosol particles will be

$$P_0 = 4kT/a. \tag{2}$$

It is interesting to note that P_0 is determined only by the mean kinetic energy of the particles and the size of the space from which they are removed, and is independent of the viscosity of the gas. The time during which the suspended particles will be removed by the walls is determined by the time for the removal of particles with $P = P_0$, and is given by the expression $t_0 = a^2B_0/2kT$, where B_0 is calculated from P_0 for a given shape of the aerosol particles. Thus, the rate of settling of aerosol particles in an enclosed space depends on the behavior of particles with $P = P_0$. The order of magnitude of these particles can be determined from Equation (2). For example, for $a \geq 10^{-2}$ cm the effective radius of these particles R_0 is comparable to the mean free path of air molecules under atmospheric pressure and at room temperature. Therefore the Cunningham-Millikan equation should be used for B:

$$B = \frac{6\pi\eta R}{1 + A\lambda / R}. \tag{3}$$

The quantitative treatment of the problem is as follows: suppose the aerosol is contained in an enclosed spherical space of radius $\underline{a}$. We use a system of coordinates with the origin in the center of the sphere and the OZ axis directed downward. The particles fall under the action of their own weight at constant velocity $\underline{v}$ according to Stokes' law

$$v = P/B \tag{4}$$

and undergo random thermal motion. The weight of a spherical particle will be

$$P = \frac{4\pi}{3} \cdot R^3\rho g, \tag{5}$$

where $\rho = \rho_1 - \rho_2$ is the difference between the density of the particle ρ_1 and of the gas ρ_2; $\underline{g}$ is the acceleration due to gravity. Let $U(r, t) = U(x, y, z, t)$ be the concentration of the aerosol particles. By condition (c) the average number of particles meeting unit surface per second is $\sqrt{kT/2\pi m}\,U(r, t)$, where $m = 4\pi/3\, R^3\rho$. $U(r, t)$ for particles of one type satisfies the forced diffusion equation

$$\frac{\partial U}{\partial t} = D\Delta U - v\frac{\partial U}{\partial z}. \tag{6}$$

At the surface of the sphere ($\sqrt{x^2 + y^2 + z^2} = r = a$) the following boundary condition is satisfied

$$-D\frac{\partial U}{\partial n} = \alpha\sqrt{\frac{kT}{2\pi m}}\,U(r, t).$$

If we put

$$\varkappa = \sqrt{\frac{2\pi m}{kT}}\,\frac{D}{a} = \frac{\sqrt{2\pi mkT}}{Ba}, \tag{7}$$

the boundary condition is written in the form

$$U = -\varkappa\frac{\partial U}{\partial r}. \tag{8}$$

Suppose at instant $t = 0$ the initial concentration distribution is symmetrical with respect to $\underline{z}$

$$U(r, 0) = U_0(r) = U_0(r, \theta). \tag{9}$$

We can put $U_0(r) = c_0$ or

$$U_0(r) = c_0e^{k_1z}, \quad (k_1 \geqslant 0). \tag{10}$$

We first solve Equation (6) for the boundary Conditions (8-10), and then show how it can be used for approximate solutions. We solve the problem, in the first approximation, for small values of κ. We determine the settling rate for this approximation and find the weight P_α and the corresponding radius R_α of the most "stable" particles.

a) By the substitution

$$U(\mathbf{r}, t) = V(\mathbf{r}, t)\, e^{-\frac{v^2}{4D}t + \frac{v}{2D}z} \tag{11}$$

Equation (6) becomes

$$\frac{\partial V}{\partial t} = D\Delta V. \tag{6'}$$

In spherical coordinates $\underline{r}$, θ, φ (θ is the angle included between $\underline{r}$ and $\underline{z}$), on the assumption that axial symmetry is maintained ($\partial V/\partial\varphi = 0$),

$$\Delta V = \Delta_{r\theta} V = \frac{1}{r^2}\frac{\partial}{\partial r}\left(r^2\frac{\partial V}{\partial r}\right) + \frac{1}{r^2\sin^2\theta}\frac{\partial}{\partial\theta}\left(\sin\theta\frac{\partial V}{\partial\theta}\right).$$

Equation (8) is obtained in the form $\quad \varkappa\frac{\partial V}{\partial r} = -\left(1 + \frac{\varkappa v}{2D}\cos\theta\right)V$

Separation of the variables gives the auxiliary equation

$$\Delta_{r\theta} g_\lambda(r, \theta) + \lambda^2 g_\lambda(r, \theta) = 0; \tag{12}$$

for the boundary condition

$$\varkappa\frac{\partial g_\lambda}{\partial r} = -\left(1 + \frac{\varkappa v}{2D}\cos\theta\right) g_\lambda, \quad (r = a). \tag{13}$$

The solution of Equation (12), corresponding to its proper value of λ, has the form [3]:

$$g_\lambda(r, \theta) = \sum_{n=0}^{\infty} C_n^\lambda S_n(\lambda r) P_n(\cos\theta), \tag{14}$$

where $S_n(z) = \sqrt{\frac{\pi}{2}}\frac{I_{n+\frac{1}{2}}(z)}{\sqrt{z}}$; $I_k(z)$ is the k-th Bessel function

$$I_{\frac{1}{2}}(z) = \sqrt{\frac{2}{\pi z}}\sin z; \quad I_{\frac{3}{2}}(z) = \sqrt{\frac{2}{\pi z}}\left(\frac{\sin z}{z} - \cos z\right);$$

$$I_{p+1}(z) = \frac{2p}{z} I_p(z) - I_{p-1}(z) \ ([3]);$$

$P_n(z)$ are Legendre polynomials.

The Boundary Condition (13) gives:

$$\varkappa\sum_n C_n^\lambda \lambda S_n'(\lambda a) P_n(\cos\theta) =$$

$$= -\sum_n C_n^\lambda\left[S_n(\lambda a) + \frac{v\varkappa}{2D} S_n(\lambda a)\cos\theta\right] P_n(\cos\theta).$$

With the aid of the identity $zP_n(z) = \frac{n}{2n-1}P_{n-1}(z) + \frac{n+1}{2n+1}P_{n+1}(z)$ [3] the boundary condition may be written in the form:

$$C_0^\lambda[\varkappa\lambda S_0'(\lambda a)+S_0(\lambda a)]+C_1^\lambda\frac{\varkappa v}{6D}S_1(\lambda a)+$$

$$+\sum_{n=1}^{\infty}\left\{C_{n-1}^\lambda\frac{n}{2n-1}\frac{\varkappa v}{2D}S_{n-1}(\lambda a)+C_n^\lambda[\varkappa\lambda S_n'(\lambda a)+S_n(\lambda a)]+\right.$$

$$\left.+C_{n+1}^\lambda\frac{n+1}{2n+3}\frac{\varkappa v}{2D}S_{n+1}(\lambda a)\right\}P_n(\cos\theta).$$

Since this equation is identical with respect to θ, all the coefficients before $P_n(\cos\theta)$ are equal to zero:

$$\left.\begin{array}{c}
[\varkappa\lambda S_0'(\lambda a)+S_0(\lambda a)]\,C_0^\lambda+\frac{1}{3}\frac{\varkappa v}{2D}S_1(\lambda a)\,C_1^\lambda=0\\
\frac{\varkappa v}{2D}S_0(\lambda a)\,C_0^\lambda+[\varkappa\lambda S_1'(\lambda a)+S_1(\lambda a)]\,C_1^\lambda+\frac{2}{5}\frac{\varkappa v}{2D}S_2(\lambda a)\,C_2^\lambda=0\\
\cdots\cdots\cdots\cdots\cdots\cdots\cdots\cdots\cdots\cdots\\
\frac{n}{2n-1}\frac{\varkappa v}{2D}S_{n-1}(\lambda a)\,C_{n-1}^\lambda+[\varkappa\lambda S_n'(\lambda a)+S_n(\lambda a)]\,C_n^\lambda+\\
+\frac{n+1}{2n+3}\frac{\varkappa v}{2D}S_{n+1}(\lambda a)\,C_{n+1}^\lambda=0\\
\cdots\cdots\cdots\cdots\cdots\cdots\cdots\cdots\cdots\cdots
\end{array}\right\} \tag{15}$$

The Expression (15) is an infinite linear homogeneous system for unknown coefficients C_n^λ. From the condition that the system (15) has a nontrivial solution we determine the proper values λ_k of the parameter λ. We shall denote the coefficients $C_n^{\lambda_k}$ by C_n^k and the proper function, corresponding to the proper values of λ_k, by $g_k(r,\theta)$. It is convenient to represent $g_k(r,\theta)$ by the standardized condition

$$\int_0^\pi\int_0^a g_k^2(r,\theta)\,r^2\sin\theta\,dr\,d\theta=1.$$

The solution of Equation (6') is obtained in the form:

$$V(r,\theta;t)=\sum_k B_k g_k(r,\theta)\,e^{-D\lambda_k^2 t}. \tag{16}$$

The coefficients B_k are determined by the initial condition. According to Equations (9) and (11), $V(r,\theta;0)=$ $=U_0(r,\theta)\,e^{-\frac{v}{2D}r\cos\theta}$, so that

$$B_k=\int_0^\pi\int_0^a U_0(r,\theta)\,e^{-\frac{v}{2D}r\cos\theta}g_k(r,\theta)\,r^2\sin\theta\,dr\,d\theta. \tag{17}$$

Especially, if $U_0(r,\theta)=C_0e^{k_1r\cos\theta}$ (10), i.e., $V(r,\theta;0)=C_0e^{k_2r\cos\theta}$, ($k_2=k_1-v/2D$), then according to Equations (14) and (4),

$$B_k=2C_0\sum_n C_n^k(i)^n\int_0^a S_n(\lambda_k r)\,S_n(-ik_2r)\,r^2dr.$$

From Equation (11) we have for the required concentration:

$$U(r,t)=\sum_k B_k g_k(r,\theta)\,e^{-D\lambda_k^2 t}e^{-\frac{v^2}{4D}t+\frac{v}{2D}r\cos\theta} \tag{18}$$

b) We break off Equation (14) at the p-th term: $g_k(r, \vartheta) = \sum_{n=0}^{p} C_n^k S_n(\lambda_k r) P_n(\cos\theta)$. The boundary condition is then obtained in the form:

$$
\begin{gathered}
[\varkappa\lambda_k S_0'(\lambda_k a) + S_0(\lambda_k a)]\, C_0^k + \frac{1}{3}\frac{\varkappa v}{2D} S_1(\lambda_k a)\, C_1^k = 0 \\
\frac{\varkappa \iota}{2D} S_0(\lambda_k a)\, C_0^k + [\varkappa\lambda_k S_1'(\lambda_k a) + S_1(\lambda_k a)]\, C_1^k + \frac{2}{5}\frac{\varkappa v}{2D} S_2(\lambda_k a)\, C_2^k = 0 \\
\cdots\cdots\cdots\cdots\cdots\cdots\cdots\cdots\cdots\cdots \\
\frac{p}{2p-1}\frac{\varkappa r}{2D} S_{p-1}(\lambda_k a)\, C_{p-1}^k + [\varkappa\lambda_k S_p'(\lambda_k a) + S_p(\lambda_k a)]\, C_p^k = 0
\end{gathered}
$$

the term $\frac{p+1}{2p+1}\frac{\varkappa v}{2D} S_p(\lambda_k a) P_{p+1}(\cos\theta)\, C_p^k$ is neglected .

Cancellation of the coefficient determinant is necessary, and it is sufficient that this system of p + 1 equations with p + 1 unknowns C_n^k should have a nontrivial solution:

$$
\begin{vmatrix}
\varkappa\lambda_k S'_0(\lambda_k a) + S_0(\lambda_k a) & \frac{1}{3}\frac{\varkappa v}{2D} S_1(\lambda_k a) & 0 & \ldots 0 \\
\frac{\varkappa v}{2D} S_0(\lambda_k a) & \varkappa\lambda_k S_1'(\lambda_k a) + S_1(\lambda_k a) & \frac{2}{5}\frac{\varkappa v}{2D} S_1(\lambda_k a) & \ldots 0 \\
\cdots\cdots & \cdots\cdots & \cdots\cdots & \cdots\cdots \\
0 & 0 \quad \ldots & \frac{p}{2p-1}\frac{\varkappa v}{2D} S_{p-1}(\lambda_k a) & \varkappa\lambda_k S_p'(\lambda_k a) + S_p(\lambda_k a)
\end{vmatrix} = 0 \tag{19}
$$

The approximation made gives reason to assume that from the system of Equations (19) it is possible to determine the first p + 1 proper values (in order of increasing modulus) and consequently expansion of Equation (18) can be appropriately stopped at the (p + 1)-th term.

c) In order to find an expression for the aerosol concentration which is more convenient for calculations, we make the simplifying assumption

$$\varkappa \ll a, \tag{20}$$

which, as will be shown, is justified for the cases with which we are concerned.

We solve the problem in the first approximation, taking the first terms from the expansion of Equations (14) and (18). If we limit ourselves to accuracy of the first order with respect to κ, then the proper values of λ_k are determined from the System (19) as the roots of the equations $\kappa\lambda_k S'_n(\lambda_k a) + S_n(\lambda_k a) = 0$ [the Determinant (19) tends to zero together with κ^2 if at least one of the terms along the main diagonal cancels].

Suppose, for first orientation that $\kappa = 0$. The smallest positive root of the equations $S_n(\lambda a) = 0$, $n = 0, 1, 2 \ldots$ will be $\lambda_1 = \pi/a$ (root of the equation $S_0(\lambda'_1 a) \equiv \sin\lambda_1 a/\lambda_1 a = 0$ [4]). In the general case the least proper value is determined from the equation $\kappa\lambda_1 S_0(\lambda_1 a) + S_0(\lambda_1 a) = 0$, or

$$\frac{\varkappa}{a} = \frac{\sin\lambda_1 a}{\sin\lambda_1 a - \lambda_1 a\cos\lambda_1 a}. \tag{21}$$

Since according to the Assumption (20), κ/a is small, $\lambda_1 a$ is close to π. ($\lambda_1 a < \pi$). Expansion of $\lambda_1 a$ by powers of κ/a gives

$$\lambda_1 a = \pi - \pi\frac{\varkappa}{a} + \frac{\pi^3}{3}\frac{\varkappa^3}{a^3} + \ldots$$

We confine ourselves to terms of the first degree with respect to κ/a, as terms of higher degrees have already been omitted (19); this gives:

$$\lambda_1 \approx \frac{\pi}{a}\left(1 - \frac{\varkappa}{a}\right). \tag{22}$$

From Equations (14), (17) and (18) we have in the first approximation

$$U(r, t) = c_0 \frac{\sin \lambda_1 r}{\lambda_1 r} e^{\frac{v}{2D} r \cos \theta} e^{-\left(\frac{v^2}{4D} + D\lambda_1^2\right) t}, \tag{23}$$

where c_0 is a measure of the initial concentration of the aerosol particles. It is seen from Equation (23) that in the first approximation the concentration distribution at time t does not depend on the exact form of the initial Distribution (9). Equation (23) is the exact solution of the problem for the initial condition $U(r, 0) =$ $= c_0 \frac{\sin \lambda_1 r}{\lambda_1 r} e^{\frac{v}{2D} r \cos \theta}$, which corresponds to an axial symmetry of distribution of the aerosol with the center of gravity displaced downward along the OZ axis. The fact that even this approximation has a physical basis and is nontrivial is evidence that the general form of solution is acceptable. The subsequent calculations are based on Equation (23).

d) According to Equation (23), the value

$$K = \frac{v^2}{4D} + D\lambda_1^2 \tag{24}$$

can be regarded as a measure of the settling rate. By means of Equations (1, 3, 4, 5, 7 and 22) it is possible to express this rate as a function of the radius R of the aerosol particles and of the parameters T, a, ρ and η. Replacing v, D and λ_1 by the quantities equal to them as given by these relationships, we have

$$K = \frac{\pi kT}{6\eta a}\left[\left(\frac{2\rho g a}{3kT}\right)^2 (R^5 + A\lambda R^4) + \right.$$
$$\left. + \left(\frac{1}{R} + \frac{A\lambda}{R^2}\right)\left(1 - \frac{2\sqrt{R}}{3\eta a \alpha}\sqrt{\frac{2kT\rho}{3}}\left(1 + \frac{A\lambda}{R}\right) + \frac{2kT\rho}{27\eta^2 a^2 \alpha^2}\left(1 + \frac{A\lambda}{R}\right)^2\right)\right],$$

where $K \rightarrow \infty$ when $R \rightarrow 0$ or $R \rightarrow \infty$, so that for a certain radius $R_\alpha > 0$ we have maximum stability. To find R_α, we first assume as an approximation that $\varkappa = 0$. When $\alpha = 1$, $\varkappa$ is very small, as will be shown later. Then $K = \frac{\pi kT}{6\eta a^2}\left[\left(\frac{2\rho g a}{3kT}\right)^2 (R^5 + A\lambda R^4) + \frac{1}{R} + \frac{A\lambda}{R^2}\right]$: . Put

$$\mu = \frac{2\rho g a}{3kT}. \tag{25}$$

After simple transformations of the equation $\partial K/\partial R = 0$ we have

$$5\mu^2 R^7 + 4\mu^2 A\lambda R^6 - R - 2A\lambda = 0. \tag{26}$$

Introducing also the shortened forms

$$f = (\sqrt{5} \cdot \mu)^{\frac{1}{3}} R \tag{27}$$

and

$$\tau = \frac{2}{5} A\lambda (\sqrt{5}\, \mu)^{\frac{1}{3}}, \tag{28}$$

we obtain Equation (26) in the form $\tau = \frac{f^6 - 1}{5 - f^6} f$. The analytical expression for $f(\tau)$ will be

$$f(\tau) = \sqrt[6]{\frac{1+5\tau}{1+\tau}}\,(1 - g(\tau)), \tag{29}$$

where, approximately (we make use of the fact that $g(\tau)$ is small)

$$g(\tau) = \tau \frac{1 - \sqrt[6]{\frac{1+\tau}{1+5\tau}}}{{}^{3}/_{2} + 10\tau + {}^{13}/_{2}\tau^{2}}\,. \tag{30}$$

The function $f(\tau)$ increases and $f(0) = 1;\ \lim f(\tau) = \sqrt[6]{5} = 1{,}308..$ Detailed investigation, omitted here, shows that Equations (29) and (30) are exact. The correction for $g(\tau) < 1/10$.

Finally, for the radius of the most "stable" particles we have, according to Equation (27)

$$R_0 = \left(\frac{3}{2\sqrt{5}}\,\frac{kT}{\rho g a}\right)^{\frac{1}{3}} \left(\frac{1+5\tau}{1+\tau}\right)^{\frac{1}{6}} [1 - g(\tau)] \tag{31}$$

where τ is given by Equation (28). The weight of these particles will be

$$P_0 = \frac{4\pi}{3} R_0^3 \rho g = 2{,}81 \sqrt{\frac{1+5\tau}{1+\tau}}\,[1 - 3g(\tau) + 3g^2(\tau)]\,\frac{kT}{a}\,. \tag{32}$$

The coefficient of kT/a depends little on T or a. In fact, $\tau \sim (a/T)^{1/3}$ while $f^3(\tau)$ increases very slowly with τ: for $0 < \tau < 2$; $1 < f^3(\tau) < 1.81$.

Let us now consider the more general case when $\kappa \neq 0$, but small. The condition for the minimum rate of settling is obtained in the form

$$(5\mu^2 R^7 + 4\mu^2 A\lambda R^6 - R - 2A\lambda) + \frac{\varepsilon}{\alpha\sqrt{R}}(R^2 + 6A\lambda R + 5A^2\lambda^2) = 0, \tag{33}$$

where

$$\varepsilon = \sqrt{\frac{2kT}{3}\rho}\,\frac{1}{3\eta a}\,. \tag{34}$$

The term in the first set of parentheses coincides with the left side of Equation (26), while the second term represents a small correction, as κ/a is small relative to $\epsilon\sqrt{R}/\alpha$. We can therefore put for the radius of the most "stable" particles

$$R_\alpha = R_0(1 - \xi), \tag{35}$$

where R_0 is given by Equation (31) and ξ is a small correction. For approximate calculations we neglect the terms ξ^2 and $\xi\epsilon$, which corresponds to the approximations in calculation of λ_1; from the Condition (33) we have

$$-7R_0 f^6(\tau)\xi - \frac{24}{5} A\lambda f^6(\tau)\xi + R_0\xi + \frac{\varepsilon\sqrt{R_0}}{\alpha}\left(R_0 + 6A\lambda + 5\frac{A^2\lambda^2}{R_0}\right) = 0,$$

i.e.,

$$\xi = \frac{\varepsilon\sqrt[6]{R_0}}{\alpha}\,\frac{R_0 + 6A\lambda + 5A^2\frac{\lambda^2}{R_0}}{\left(7P_0 + \frac{24}{5}A\lambda\right) f^6(\tau) - R_0}\,. \tag{36}$$

Finally

$$R_\alpha = R_0(1-\xi) = R_0\left(1 - \frac{\sqrt{2kT\rho}}{3\sqrt{3}\eta a}\frac{R_0 + 6A\lambda + 5\frac{A^2\lambda^2}{R_0}}{\left(7R_0 + \frac{24}{5}A\lambda\right)f^6(\tau) - R_0}\frac{1}{\alpha}\right) \tag{37}$$

and correspondingly:

$$P_\alpha = P_0(1-\xi)^3 \approx P_0(1-3\xi) \equiv P_0\left(1 - \frac{\zeta}{\alpha}\right), \tag{38}$$

where P_0 is given by (32) and ξ by (36);

$$\zeta = 3\frac{R_0 + 6A\lambda + 5\frac{A^2\lambda^2}{R_0}}{\left(7R_0 + \frac{24}{5}A\lambda\right)f^6(\lambda) - R_0}\sqrt{R_0}\varepsilon \tag{39}$$

together with $\sqrt{R_0\epsilon}$, a small quantity.

Let us consider the concrete example of the settling of quartz dust ($\rho = \rho_1 - \rho_2 = 3$ g/cm^3) in air at atmospheric pressure and room temperature [$\lambda = 10^{-5}$ cm; $A = 0.9$; $\eta = 1.816 \cdot 10^{-4}$ (g cm/second)]. Let $a = 2 \cdot 10^{-2}$ cm; then we have

$$(\sqrt{5}\mu)^{\frac{1}{3}} = \left(2.236\,\frac{2}{3}\,\frac{\rho g a}{kT}\right)^{\frac{1}{3}} = 1.27 \cdot 10^5 \text{ cm}^{-1}$$

$$\tau = \frac{2}{5}A\lambda(\sqrt{5}\mu)^{\frac{1}{3}} = 0{,}457,$$

$$f(\tau) = \left(\frac{1+5\tau}{1+\tau}\right)^{\frac{1}{6}}\left(1 - \tau\frac{1 - \left(\frac{1+\tau}{1+5\tau}\right)^{\frac{1}{6}}}{{}^3/_2 + 10\tau + {}^{15}/_2\,\tau^2}\right) = 1{,}136,$$

$$R_0 = \frac{f(\tau)}{(\sqrt{5}\mu)^{\frac{1}{3}}} = 0.894 \cdot 10^{-5} \text{ cm}$$

$$P_0 = \frac{4}{3}\pi R_0^3\rho g = 8.8 \cdot 10^{-12} \text{ dyne}$$

and, approximately, at a and T close to those used

$$P_0 = \frac{2\pi}{\sqrt{5}}f^3(\tau)\frac{kT}{a} \approx 4{,}12\,\frac{kT}{a}$$

(this is in almost complete agreement with Equation (2) derived by a semiquantitative method).

When $\alpha = 1$ $\varkappa_0 = \frac{1}{3\eta}\sqrt{\frac{2kT\rho}{3}}\left(\sqrt{R_0} + A\frac{\lambda}{\sqrt{R_0}}\right) = 3{,}23 \cdot 10^{-6}$ cm.

Therefore, in this instance Assumption (20) is justified, as $\kappa_0/a = 1.615 \cdot 10^{-4}$ is small.

$$\sqrt{R_0}\cdot\varepsilon = \frac{\varkappa_0}{a}\frac{1}{1 + A\frac{\lambda}{R_0}} = 0{,}805 \cdot 10^{-4} \text{ and } \alpha\xi = \frac{\zeta}{3} = 4{,}02 \cdot 10^{-5}.$$

The coefficients of $1/\alpha$ in (37) and (38) are small, so that this is not a convenient way of calculating the adhesion coefficient α.

The fact that R_α or P_α depend little on α, at approximately $\alpha > 0.1$, justifies the approximations Ia and Ib. Our chosen value for a corresponds in order of magnitude to the dimensions of the capillaries in the lungs. Consequently, when air containing quartz dust is breathed in, particles $2 \cdot 10^{-5}$ cm in diameter are retained least effectively in the lung capillaries and penetrate into the depth of the lung. It is interesting to note that according to some reports particles of this size are met most frequently in the lungs of silicosis victims. This result confirms the views of Vigdorchik [5] on the absorption of dust by the lungs. It should also be pointed out that the formulas derived by Buchwald [6] are readily obtained from our Equation (18) if sedimentation is ignored ($v = 0$) and the concentration at the walls is assumed to be vanishingly small ($\kappa = 0$).

SUMMARY

1. It is shown theoretically that the settling rate of aerosol particles on the walls of an enclosed space containing them depends on the particle size and reaches a minimum value for an optimum particle size. A relationship has been derived between the optimum particle size and the temperature, radius of the enclosed spherical space, adhesion coefficient, and viscosity of the gas.

2. It is proved that the distribution of settling rates according to particle size depends little on the adhesion coefficient if this coefficient is not too small.

3. It is proved that the weight of the particles settling at the lowest rate can be calculated fairly accurately by the approximate equation $P_0 = 4kT/a$, where a is the radius of the spherical space.

In conclusion, we wish to thank Professor Khr.Ya. Khristov for much valuable advice.

LITERATURE CITED

[1] N.A. Fuks, Mechanics of Aerosols (Moscow, 1955), p. 175.

[2] P.A. Rebinder, N.N. Serb-Serbina and S.A. Kordyukova, The Struggle Against Silicosis, Collected papers, Vol. 1 (Moscow, 1953), p. 57.

[3] R. Courant and D. Hilbert, Methods of Mathematical Physics, Vol. 1 (Moscow-Leningrad, 1951), pp. 80, 269, 413.[Russian translation.]

[4] V.I. Smirnov, Course of Higher Mathematics, Vol. 3, Pt. 2 (Moscow-Leningrad, 1951), pp. 527, 563.

[5] E. Vigdorchik, Retention of Aerosols in Respiration (Leningrad Sci. Res. Inst. Labor Organization and Industrial Safety, Leningrad 1948).

[6] E. Buchwald, Ann. Phys. 66, 1 (1921).

Received October 3, 1956

Institute of Physical Chemistry
Sofia State University

APPLICATION OF THE METHOD OF APPROXIMATIONS TO CALCULATIONS OF FLOW OF DISPERSE SYSTEMS

N.V. Tyabin and G.V. Vinogradov

The advantage of the method of approximations for technical calculations of flow processes in disperse systems lies in the fact that it is not necessary to know the law of flow in the form of a continuous relationship between the true velocity gradient (D) and the shearing stress (τ), $D = \varphi(\tau)$, and it is possible to perform calculations on the basis of viscosimetric data obtained by direct experiments.

In the previous communication [1] examples were given of the approximation of flow curves for solid greases, with variations of the velocity gradient over a range of five tenth-powers, in the form of three or four straight lines corresponding to Shvedov-Bingham equations. However, the number of Shvedov-Bingham equations approximating to the flow curve for a plastic disperse system can be decreased considerably if the actual flow conditions of the disperse system are taken into account. It is first necessary to select the scale of the graph used for approximation of the flow curves. The choice of the scale should be based on the values of the maximum velocity gradients and tangential stresses in the flow zone. We shall consider, as examples, approximation of the flow curves for a plastic grease and bitumen.

Plastic greases are widely used for lubrication of sliding bearings, when the flow velocity gradients reach high values (10^5-10^6 sec^{-1}). A consecutive approximation to the flow equation for solidol grease at 20° [2]: $\tau_R = 3500 + 6\overline{D} + 2800\,\overline{D}^{1/3}$ was given in the previous communication [1].

If the graphical scale chosen for the approximation corresponds to a velocity gradient of $\sim 10^5$ sec^{-1}, and the experimental error is assumed to be 5%, it is seen (Figure 1, where the error zone is indicated by broken lines) that the flow curve for solidol in the zone of high velocity gradients can be fairly satisfactorily approximated by one Shvedov-Bingham equation:

$$\tau = \pm\,\theta + \eta D, \tag{1}$$

where $\theta = 7.9 \cdot 10^4$ dynes/cm^2; $\eta = 5.2$ poises.

A plastic grease in the low velocity gradient region, where the nonlinear relationship $D = \varphi(\tau)$ is most pronounced, can for simplicity be regarded as a "continuous" solid body, while the flow of the grease in the bearing should be calculated on the basis of the Shvedov-Bingham Equation (1). There is no doubt that relative flow will occur in the continuous "solid" body region, but at a velocity 3-4 orders of magnitude lower than in the main mass of the grease, and it may be neglected. Thus, for describing the "deformation" process in the zone in which the tangential stress is less than the limiting (yield) stress which follows from the Shvedov-Bingham equation, it is not admissible to apply formally the theory of elasticity, as flow at very low velocity gradients occurs in this zone.

As a second example of the method of approximations, this time for a zone of low velocity gradients, let us consider the approximation of the curve for the flow of bitumen [3]. Bitumens and materials based on them are used for construction of hydroinsulation covers and roofs. The durability of such a covering depends on the ability of a thin layer of bitumen (2-3 mm) to resist flow down inclined surfaces when the air temperature rises [4]. To select the graphical scale for approximation of the flow curves for bitumen, we determine the maximum tangential stress at the roof surface:

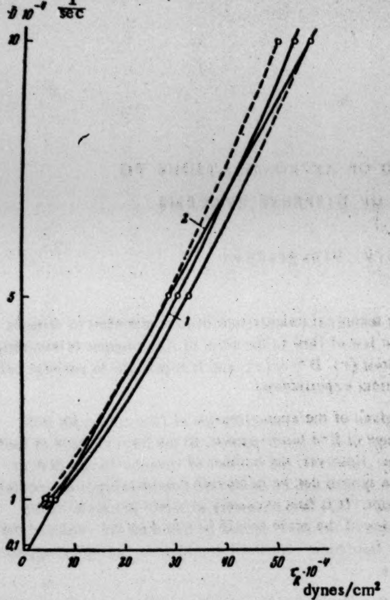

Fig. 1. Graph for the approximation of the flow behavior of solidol at 20° in the high velocity gradient region: 1) flow curve for solidol; 2) approximating straight line.

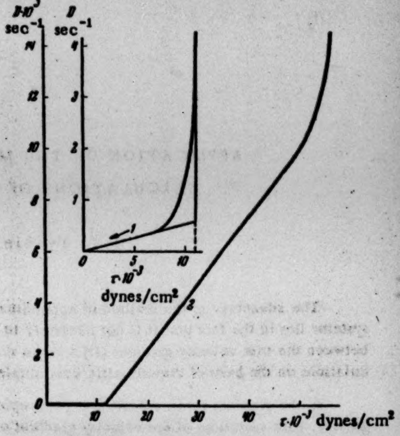

Fig. 2. Approximation curves for experimental data on the flow of bitumen III at 20° in the region of low tangential shearing stresses: 1) Newtonian straight line; 2) Shvedov-Bingham line.

$$\tau_{\max} = \gamma h (\sin\alpha)_{\max}, \tag{2}$$

where γ is the density of the bitumen; h is the thickness of the layer; α is the slope of the surface. Assuming $\gamma = 1000$ kg/m³ and $\alpha = 90°$, we find $\tau_{\max} \sim 10^3 \cdot h$ dynes/cm². Thus, a thin layer of bitumen on the surface of a roof is subjected to maximum tangential stresses of $\sim 10^2$-10^3 dynes/cm².

Approximation of the flow curve for bitumen at 20° [3, 5], shown on two scales in Figure 2, leads to two equations:

$$\tau = \eta_0 D\,(\tau < \tau_{01}) \text{and } = \theta_1 + \eta_1 D \quad (\tau_{01} \leqslant \tau \leqslant \tau_{02}), \tag{3}$$

where $\eta_0 = 1.25 \cdot 10^{11}$ poises; $\tau_{01} = 1.1 \cdot 10^4$ dynes/cm²; $\theta_1 = 1.1 \cdot 10^4$ dynes/cm²; $\eta_1 = 3.9 \cdot 10^6$ poises; $\tau_{02} = 5 \cdot 10^4$ dynes/cm². It is seen that η_0 is greater than η_1 by five tenth-powers, and therefore in layers in which $\tau < \tau_{01}$ the bitumen will move as a continuous body, and its flow in the zone of small tangential stresses should be calculated by Equation (3).

As examples of application of the method of approximation of flow curves for plastic disperse systems, let us consider the flow in the gap between two coaxial cylinders and along an inclined plane under the force of gravity.

Let a plastic disperse system, the flow curve of which is approximated by n Shvedov-Bingham equations, flow in the gap between two coaxial cylinders as the result of rotation of the inner cylinder of radius R_1 at angular velocity ω_0. The tangential stress in the medium will be $\tau = M/2\pi hr^2$, where M is the torque; h is the height of the cylinders; r is the current radius of the cylindrical coordinate system (Figure 3). In the gap n coaxial layers are formed, and the radii of the surfaces of the limiting and boundary shearing stresses are given by the expressions

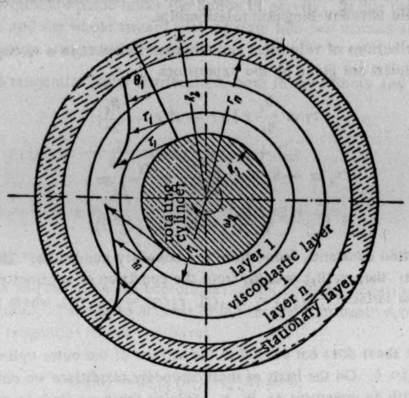
θ1
τ1
r1
r2
rn
rotating cylinder
layer 1
viscoplastic layer
layer n
stationary layer

Fig. 3. Flow of a plastic disperse system in the gap between two coaxial cylinders.

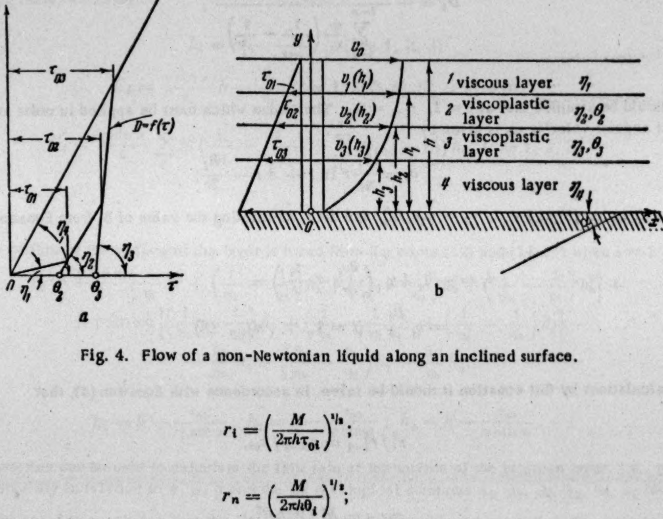
D
τ03
τ02
τ01
D=f(τ)
η4
η2
η3
0
η1
θ2
θ3
τ
a
y
v0
τ01
v1(h1)
1 viscous layer η1
τ02
v2(h2)
2 viscoplastic layer η2, θ2
τ03
v3(h3)
3 viscoplastic layer η3, θ3
4 viscous layer η4
h
h1
h2
h3
0
x
b

Fig. 4. Flow of a non-Newtonian liquid along an inclined surface.

$$r_i = \left(\frac{M}{2\pi h \tau_{0i}}\right)^{1/2}; \tag{4}$$

$$r_n = \left(\frac{M}{2\pi h \theta_i}\right)^{1/2}; \tag{5}$$

$$\tau_{0i} = \frac{\theta_i \eta_{i+1} - \theta_{i+1}\eta_i}{\eta_{i+1} - \eta_i}, \quad (i = 1, \ldots, n-1), \tag{6}$$

where τ_{0i} are the boundary shearing stresses; θ_1, θ_i, η_i are the limiting shearing stresses and plastic viscosities according to the approximate Shvedov-Bingham relationships.

As is known, the distributions of velocities and tangential stresses in a viscoplastic medium flowing in the space between coaxial cylinders are given by the expressions

$$v_i = \frac{\theta_i}{\eta_i} r \ln r + A r - \frac{B_i}{2r}; \tag{7}$$

$$\tau_i = -\theta_i + \eta_i \left(\frac{\partial v_i}{\partial r} - \frac{v_i}{r} \right) = \eta_i \frac{B_i}{r^2}, \quad (i = 1, \ldots, n), \tag{8}$$

where A_i and B_i are integration constants, found from the boundary conditions. The medium adheres to the surface of the rotating cylinder; then $v_1(R_1) = \omega_0 R_1$, from the condition of continuity of velocities and tangential stresses at the boundary stress surfaces – $v_i(r_i) = v_{i+1}(r)$, $\tau_i(r_i) = \tau_{i+1}(r_i)$, where $(i = 1, \ldots, n-1)$, $\tau_n(r_n = -\theta_1$.

Let us assume that the shear does not extend to the surface of the outer cylinder; then at the limiting shearing stress surface $v_n(r_n) = 0$. On the basis of these boundary conditions we obtain, from Equations (7) and (8), a system of equations with 3n unknowns A_i, B_i, r_i. Solving these we find, in particular, that

$$B_1 = -\frac{2\omega_0 + 2 \sum\limits_{i=1}^{i=n} \frac{\theta_i}{\eta_i} \ln \frac{r_i}{r_{i-1}}}{\sum\limits_{i=1}^{i=n} \frac{\eta_1}{\eta_i} \left(\frac{1}{r_{i-1}^2} - \frac{1}{r_i^2} \right)}, \tag{9}$$

where it should be assumed that at $i = 1$, $r_{i-1} = R_1$. The torque which must be applied in order to rotate the cylinder at angular velocity ω_0 is given by

$$v_i = \frac{\theta_i}{\eta_i} r \ln r + A r - \frac{B_i}{2r}; \tag{10}$$

From Equation (8) at $i = 1$, $\tau_1 = \eta_1 B_1 / R_1^2$, and then, substituting the value of B_1 from Equation (9), we find

$$\tau_i = -\theta_i + \eta_i \left(\frac{\partial v_i}{\partial r} - \frac{v_i}{r} \right) = \eta_i \frac{B_i}{r^2}, \quad (i = 1, \ldots, n), \quad (8) \tag{11}$$

In calculations by this equation it should be taken, in accordance with Equation (4), that

$$r_i^2 / r_{i-1}^2 = \tau_{0i-1} / \tau_{0i},$$

while

$$\tau_{0i-1} = M / 2\pi h R_1^2.$$

If the shear extends to the outer cylinder, then at $i = n$, $r_n = R_2$. When $i = 1$, then the medium flowing in the gap between the cylinders obeys a single Shvedov-Bingham equation, Equation (11) gives the known Reiner-Rivlin equation.

Bitumens at temperatures between 40 and 140° are typical non-Newtonian liquids [4, 5], the flow curves for which can be approximated by two Newton equations and two Shvedov-Bingham equations (Figure 4a) [6].

For calculations of the thermostability of bitumens and materials based on them, let us consider the flow of a non-Newtonian liquid along an inclined plane under the action of gravity. In this instance the stress will be greatest at the inclined surface and the whole stream will separate into two viscous and two viscoplastic layers. The coordinate system and notation are given in Figure 4b.

The laws of velocity and tangential stress distributions, both in the viscous and the viscoplastic layers, are given by the expressions:

$$v_i(y) = -\frac{\gamma}{2\eta_i}\sin\alpha y^2 + C'_i y + C''_i; \tag{12}$$

$$\tau_i(y) = -\theta_i + \eta_i\frac{\partial v_i}{\partial y} = -\theta_i - \gamma\sin\alpha y + C'_i\eta_i, \tag{13}$$

where $(i = 1, \ldots, 4)$, $\theta_1 = \theta_4 = 0$.

The integration constants and the unknown coordinates of the boundary shearing stream surfaces h_i are found from the boundary conditions. The liquid adheres to the inclined surface: $v_4(0) = 0$; from the condition of continuity of velocities and tangential stresses we have:

$$v_i(h_i) = v_{i+1}(h_i),\ \tau_1(h) = 0;$$
$$\tau_i(h_i) = \tau_{i+1}(h_i) = -\tau_{0i},\ (i = 1, 2, 3),$$

where τ_{0i} are the boundary shearing stresses determined by Equation (6), if it is assumed that $\theta_1 = \theta_4 = 0$. On the basis of the boundary conditions, we obtain, from Equations (12) and (13), eleven equations with eleven unknowns; solving these, we have:

$$h_i = h - \frac{\tau_{0i}}{\gamma\sin\alpha},\ (i = 1, 2, 3) \tag{14}$$

$$C'_i = \frac{\gamma\sin\alpha}{\eta_i}h - \frac{\theta_i}{\eta_i},\ (i = 1, 2, 3, 4);\ (\theta_1 = \theta_4 = 0) \tag{15}$$

$$C''_i = \frac{\gamma\sin\alpha}{2}\sum_1^3 h_i^2\left(\frac{1}{\eta_i} - \frac{1}{\eta_{i+1}}\right) + \sum_i^3 (C_{i+1} - C'_i)h_i,\ (i = 1, 2, 3) \tag{16}$$

$$C''_4 = 0. \tag{17}$$

The rate of flow at the surface of the layer is found from Equations (12) and (14-17) when $i = 1$

$$v_0 = \frac{\gamma\sin\alpha}{2}\left[\frac{1}{\eta_1}h^2 + \left(\frac{1}{\eta_1} - \frac{1}{\eta_2}\right)h_1^2 + \left(\frac{1}{\eta_2} - \frac{1}{\eta_3}\right)h_2^2 + \left(\frac{1}{\eta_3} - \frac{1}{\eta_4}\right)h_3^2\right] +$$
$$+ \gamma\sin\alpha h\left[\left(\frac{1}{\eta_2} - \frac{1}{\eta_1}\right)h_1 + \left(\frac{1}{\eta_3} - \frac{1}{\eta_2}\right)h_2 + \left(\frac{1}{\eta_4} - \frac{1}{\eta_3}\right)h_3\right] -$$
$$- \frac{\theta_2}{\eta_2}h_1 - \left(\frac{\theta_3}{\eta_3} - \frac{\theta_2}{\eta_2}\right)h_2 - \frac{\theta_3}{\eta_3}h_3,$$

where $h_1 = h - \frac{\tau_{01}}{\gamma\sin\alpha};\ h_2 = h - \frac{\tau_{02}}{\gamma\sin\alpha};\ h_3 = h - \frac{\tau_{03}}{\gamma\sin\alpha}.$

This expression can be used to calculate the flow rate at the surface of the bitumen layer, i.e., to evaluate its thermostability in relation to γ, α, $\underline{h}$ and the six rheological constants η_1, η_2, θ_2, η_3, θ_3, η_4 (Figure 4b).

It must be noted in conclusion that the flow curves can be approximated not only in the form of Shvedov-Bingham equations in the usual coordinate system, but also in the form of exponential functions $D = k\tau^N$ in logarithmic coordinates, when these functions are represented by linear intercepts.

SUMMARY

1. The flow of plastic greases in sliding bearings, and of bitumens along inclined planes, has been used to demonstrate the necessity of evaluating the actual values of the maximum tangential stresses and velocity

gradients in approximating the flow curves for disperse systems.

2. An expression has been derived for the torque as a function of the angular velocity of rotation in the flow of a plastic disperse system in an annular gap between coaxial cylinders, when the flow curve can be approximated by n Shvedov-Bingham equations.

3. The flow of a layer of non-Newtonian liquid along an inclined surface has been considered. The laws governing the flow velocity distributions in the layers and on the surface of a non-Newtonian liquid have been determined; the flow curves can be approximated by two Newton equations and two Shvedov-Bingham equations.

LITERATURE CITED

[1] N.V. Tyabin and G.V. Vinogradov, Colloid J. 19, 352 (1957) (T.p. 353)*

[2] V.P. Pavlov, Candidate's Dissertation (Moscow, 1948).

[3] N.V. Mikhailov, Doctorate Dissertation (Moscow, 1955).

[4] N.V. Mikhailov, Roof and Hydroinsulation Coverings (Machinery Constr. Press, 1950).

[5] S.Ya. Shalyt, Candidate's Dissertation (Moscow, 1955).

[6] N.V. Tyabin, J. Tech. Phys. 26, 1994 (1956).

Received June 19, 1956

Institute of Petroleum
Academy of Sciences, USSR - Moscow

---

* T. p. = C. B. Translation pagination.

EFFECT OF ELECTROLYTES ON THE STRUCTUROMECHANICAL PROPERTIES OF BENTONITE SUSPENSIONS

I.A. Uskov

Despite the large number of rheological studies of structure formation in bentonite suspensions [1], some important questions still remain unsolved. In particular, the mechanism of the action of electrolytes present in the dispersion medium is not clear; the influence of these electrolytes is often attributed to cation exchange effects [2], although there are no convincing grounds for this.

The present paper reports a study of the variations of the structuromechanical properties of aqueous askangel (a bentonite of Caucasian origin) suspensions under the action of various electrolytes. The purified material contained particles $< 50\mu$ in diameter. Most of the insoluble impurities were removed by dialysis through a collodion membrane at 50-70°. The electrical conductivity of a 6.91% suspension was $1 \cdot 10^{-4}$ ohm^{-1} cm^{-1}. To eliminate aging effects, the original 6.91% suspension was kept for 6 months; it was subsequently diluted with water or the appropriate electrolyte solution down to 3.12% concentration.

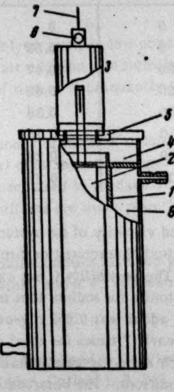

Fig. 1. Diagram of the main part of the instrument used for studying structuromechanical properties: 1) outer cylinder; 2) inner cylinder; 3) load on inner cylinder; 4) annular space for excess liquid displaced by immersion of the inner cylinder; 5) hydraulic seal to prevent evaporation during the experiment; 6) mirror; 7) torsion wire; 8) thermostat liquid.

The structuromechanical properties of the suspensions were studied by means of a coaxial cylinder instrument (Figure 1) of the Shvedov type [3]. Measures were taken to prevent evaporation of the suspension during the experiments and to ensure a constant liquid level in the outer cylinder. The temperature was kept constant by means of a circulating thermostat set to 25°.

The method for obtaining a group of deformation-time curves, developed by Rebinder and his associates [4], requires several hours for each experiment; this restricts its use to systems in which no appreciable changes occur during this time. This method is not applicable in this form to askangel suspensions containing considerable amounts of electrolytes, when syneresis effects hinder the experiment. However, it is possible to shorten the time required for obtaining the groups of deformation curves. Trapeznikov [5] made a detailed study of the effect of a constant load on deformation of adsorption layers of saponin; it follows from his results that the time required to reach a constant deformation rate is shortened tens of times as stresses corresponding to breakdown of the structure are approached. We obtained similar results for bentonite suspensions. It was found experimentally that at stresses close to the strength limit of the

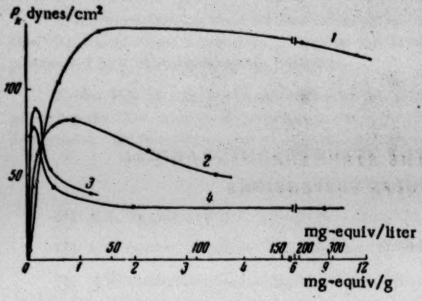

Fig. 2. Variations of the limiting shearing stress (yield value) of a 3.12% askangel suspension with electrolyte concentration: 1) sodium chloride; 2) sodium sulfate; 3) calcium sulfate; 4) calcium chloride.

structure practically steady flow is established in 1-2 minutes. The approximate strengths of the structure were first determined in the experiments, and the exact values of the structuromechanical constants were then calculated from curves plotted for fresh samples of the suspensions. The time of structural buildup in the suspensions (after filling of the instrument) was 1 hour in all experiments. The average deviations in repeated experiments from the average values of the measured quantities did not exceed 7%.

The effects of electrolytes most commonly met in oil well drilling – sodium and calcium chlorides and sulfates – were studied. It was found by preliminary experiments that the variation of the structuromechanical properties of the suspensions under the influence of added electrolytes continues for a long time. This effect was quantitatively studied for a suspension containing 0.053 mg-equiv sodium chloride per 1 g of bentonite (see table).

Variations of the Structuromechanical Properties of an Askangel Suspension after Addition of Sodium Chloride

Time in hours after addition of electrolyte	E_0 dynes/cm²	E_r dynes/cm²	P_k dynes/cm²	η_r poises	$\lambda = E_0/E$
0.02	0	0	0	0	0
0.1	1.6	1.5	0	0	0.52
1.0	5.2	5.8	0.7	600	0.47
4.5	15.5	21	2.4	3400	0.42
16.5	30	54	5.8	6050	0.36
25	33	78	6.4	6950	0.30
300	51	146	9.5	9000	0.26
576	55	151	11.5	9800	0.27

It is seen from these results that during the first day the elasticity and viscosity of the system show very large increases. Subsequently, the rate of increase of the structuromechanical characteristics diminishes, but they continue to increase even a month after addition of the electrolyte. The possibility is not excluded that in our experiments partial exchange of the calcium ions sorbed by the bentonite for sodium ions took place, but this exchange could not have been considerable. The amount of NaCl added was 0.053 mg-equiv per 1 g of bentonite containing 0.354 mg-equiv of adsorbed calcium, which was nearly 7 times the total amount of sodium added. If, moreover, it is considered that calcium is adsorbed much more vigorously than sodium [6], it becomes evident that practically no cation exchange occurs in these conditions. The observed changes in the mechanical properties of the suspensions were caused by the coagulating action of the electrolyte present in the dispersion medium, resulting in coagulational structure formation.

The increase of all the structuromechanical constants is accompanied by a decrease of the elasticity of the system, indicating strengthening of the structural bonds between the particles. Not all the bonds between the particles which arise in the course of thixotropic structure formation are broken down when the suspension is shaken. The number of such bonds of higher strength increases with increasing time of electrolyte action.

The influence of the concentration and nature of the electrolytes was studied 46-48 hours after addition of the electrolytes to the askangel suspension. Figure 2 shows the variation of the most important constant, P_k, with salt concentration. The other structuromechanical constants varied in the same way as P_k and are therefore not given. The system was not structurized before addition of the electrolytes. All the electrolytes studied caused structure formation even at very low concentrations. Coagulational structure formation greatly increased with additions of successive amounts of electrolytes.

As the salt concentration increases, P_k increases at first, reaches a maximum, and then decreases. The amounts of added sodium salts in the region of the maximum – 1.4 mg-equiv/g of NaCl and 0.9 mg-equiv/g of Na_2SO_4 – are sufficient for appreciable changes to take place in the composition of the adsorbed cations. However, here also the determining role is played by the coagulating action of the electrolyte, increasing concentration of which may lead to formation of a compact coagulate with lower mechanical characteristics.

The hypothesis that cation exchange plays a decisive role in processes involving the action of nonhydrolyzing electrolytes is entirely unsubstantiated in relation to calcium salts. The development of elasticity on addition of negligibly small amounts (relative to the capacity of the exchange complex) of calcium salts and the extremely rapid increase of P_k with increasing concentration of added electrolytes cannot be attributed to cation exchange.

The proportions of electrolyte concentrations required to produce equal degrees of structure formation in the ascending branches of the curves are in qualitative agreement with the Schulze-Hardy rule. Bentonite particles are negatively charged, and therefore the effects produced by salts depend on their cations. Calcium salts have 3-5 times the coagulational structure formation effect of the corresponding sodium salts. The effects of anions on the structuromechanical properties of bentonite suspensions can be judged by the effects of the different electrolytes studied. The data for calcium salts, for which the difference between the anions is masked by the strong bivalent cation, are not convenient for judging this effect. Sodium salts are more suitable in this respect. Sodium chloride at low concentrations causes less strengthening of the structure than sodium sulfate, but starting with 15 mg-equiv/liter it assists the formation of a stronger structure than that produced by the action of other electrolytes. The concentration corresponding to the strength maximum is considerably higher for sodium chloride than for the corresponding sulfate, so that the sulfate ion can be regarded as the more powerful coagulant.

SUMMARY

1. Electrolytes,even at low concentrations, cause structurization of aqueous askangel suspensions. During the first day after addition of electrolytes to the suspension, the strength, elasticity and viscosity characteristics increase tens of times, Subsequently these characteristics increase less rapidly, but continue to change even after a month.

2. Low concentrations of calcium and sodium chlorides and sulfates produce sharp increases in the structuromechanical constants of askangel suspensions owing to formation of coagulation structures. The electrolyte concentrations required to produce equal degrees of structurization conform to the Schulze-Hardy rule. Sodium and calcium sulfates are more powerful agents of coagulational structure formation than the corresponding chlorides.

The author expresses his deep gratitude to A.V. Dumansky for his guidance, and thanks to F.D. Ovcharenko, I.A. Dumansky and R.V. Voitsekhovsky for discussion of the work and critical comments.

LITERATURE CITED

[1] N.N. Serb-Serbina, In Viscosity of Liquids and Colloidal Solutions, Vol. 1 (1941); N.N. Serb-Serbina and P.A. Rebinder, Colloid J. 9, 381 (1947); H. Braune and J. Richter, Koll.-Z. 113, 20 (1949); N.N. Serb-Serbina and T.M. Polonsky, Proc. Acad. Sci. USSR 96, 103 (1954).

[2] P. Vageler, Cations and Water in Mineral Soils (Agric. Press, 1938); I.V. Popov, Fundamentals of Engineering and Geological Soil Science (State Geol. Press, 1941).

[3] F.N. Shvedov, J. phys. theori et appl. 2, 341 (1889).

[4] E.E. Segalova and P.A. Rebinder, Colloid J. 10, 223 (1948); P.A. Rebinder, In New Methods of Physicochemical Investigations of Surface Phenomena (Izd. AN SSSR, 1950), p. 3.

[5] A.A. Trapeznikov, In New Methods of Physicochemical Investigations of Surface Phenomena (Izd.

AN SSSR, 1950) p. 20; Trans. All-Union Conf. on Colloid Chem. (Acad. Sci. Ukrainian SSR Press, 1952), p. 175.

[6] K.K. Gedroits, The Absorptive Capacity of Soils (Agric. Press, 1933).

Received June 3, 1956

The T.G. Shevchenko State University
Kiev

RELATIONSHIP BETWEEN THE INTRINSIC VISCOSITY AND MOLECULAR WEIGHT OF BUNA S RUBBER*

Chien Jen-Yuan, Ching Wen and Cheng Yung-Shih

The intrinsic viscosity-molecular weight relationship for Buna S rubber has been studied by numerous workers [1-5] (Table 1). However, hitherto it was not taken into account that the fractions used for the viscosity and osmotic pressure determinations might contain branched macromolecules, which would result in a $[\eta]-M$ relationship different from the relationship for linear molecules. The presence of branched molecules, formed in high temperature polymerization at high degrees of conversion, or during fractionation, influences the viscosity [6, 7], and increases the value of the Huggins constant k', which represents the slope of the $[\eta]$ line relative to the abscissa axis [8, 9].

TABLE 1

Relationship Between Intrinsic Viscosity and Molecular Weight of Buna S; $[\eta] = KM^{\alpha}$

Polymerization temperature	K x 10^4	α	Solvent	Temperature in °C	Reference
50	5.4	0.66	Toluene	30	[1]
50	5.4	0.66	Benzene	25	[2]
50	5.25	0.67	Toluene	25	[3]
Low-temperature (SKS-30A)	2.96	0.71	Benzene	25	[4]
5	1.8*	0.76*	Benzene	25	[5]

*Estimated from the influence of polymerization temperature on the value of α for polybutadiene and chloroprene.

The viscosity of Buna S polymerized at lower temperatures, with molecules of a lower degree of branching [4, 5], also has high values owing to increases of the value of α in the equation $[\eta] = KM^{\alpha}$. Moreover, in the published papers on the osmotic pressure of Buna S solutions in toluene or benzene use was made of linear extrapolation of the $\pi/c - c$ relationship. It is shown in the present paper that the $\pi/c - c$ relationship is represented by curves convex toward the concentration axis, and therefore linear extrapolation gives incorrect molecular weight values.

Data on the viscosity and osmotic pressure of 9 Buna S fractions are given in Tables 2 and 3. The curves for the $\pi/c - c$ relationship (Figure 1a) are represented by the equation

$$\pi / c = RT\,(1/M_n + A_2 c + A_3 c^2), \qquad (1)$$

or, according to Flory,

---

*This paper was published in Chinese in Acta Chimica Sinica 22, 249 (1956).

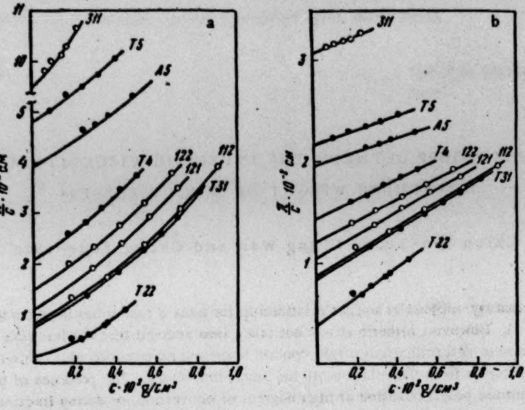

Fig. 1. $\pi/c - c$ (Figure a) and $(\pi/c)^{1/2} - c$ (Figure b) curves for Buna S fractions in toluene at 25°.

TABLE 2

Viscosity Data for Buna S Fractions in Toluene at 30°

$$\frac{\eta_r - 1}{c} = [\eta] + k'[\eta]^2 c; \quad \frac{\ln \eta_r}{c} = [\eta] - \beta [\eta]^2 c$$

Buna S fraction	Range of η_r	$[\eta]$	k'	β	$k' + \beta$
T22	1.80—1,20	4.76	0.76	—0.17	0.59
T31	2.48—1,49	2.72	0.52	0.05	0.57
T4	2.02—1,28	1.54	0.41	0,12	0.53
A5	1.99—1,37	0.92	0.40	0.14	0.54
T5	1.92—1,34	0.76	0.39	0.14	0.53
112	1.52—1,15	3,21	0.46	0.06	0.52
121	1.63—1,18	2.46	0.42	0.09	0.51
122	1.67—1,19	1.97	0.37	0.13	0.50
311	1.49—1,15	0.50	0.34	0.17	0.51

(2)

If we take $\Gamma_3 = g\Gamma_2^2$ at $g = \frac{1}{4}$, then a graphical plot of $(\pi/c)^{1/2}$ will also be linear [10]. This is confirmed by Figure 1b. Values of $(\pi/c)_0$, $\overline{M}_n$, Γ_2 and RTA_2 obtained in this way are given in Table 3.

Cassasa [11] considered that polymer molecules dissolved in a good solvent the value of $A_2\overline{M}_w/[\eta]$ should be constant and independent of M. Schultz [12] obtained the value $A_2\overline{M}_w/[\eta] = 1.39$ for polyvinyl acetate in butanol at 25°. From the data obtained in the present investigation, the value of $A_2\overline{M}_w/[\eta]$ for Buna S in toluene at 30° (Figure 2) is 0.87. Apart from fractions T22 and T31, the molecules of which are apparently strongly branched, the $[\eta] - M$ relationship is represented by the equation (Figure 3):

TABLE 3

Osmotic Pressure Data for Buna S Fractions in Toluene at 25° (π in g/cm^2; c in g/cc)

Buna S fraction	$c \times 10^2$	h, cm		$\pi/c \times 10^{-3}$	$(\pi/c)_0$	$\overline{M}_n \times 10^{-4}$	$\Gamma_2 \times 10^{-3}$	$RTA_2 \times 10^{-4}$
T22	0.1809	0.10	0.10	0.48	0.15	174	7.5	1.12
	0.2262	0.12	0.13	0.48				
	0.2714	0.18	0.19	0.60				
	0.3393	0.30	0.28	0.75				
	0.3619	0.34	0.32	0.80				
	0,4524	0.56	0.57	1.08				
T31	0.2609	0.40	0.42	1.36	0.71	34.9	2.9	2.06
	0.4170	0.87	0.89	1.82				
	0.5415	1.40	1.42	2.24				
	0.6256	1.86	1.89	2.58				
	0.7089	2.37	2.41	2.91				
	0.8160	3.17	3.24	3.39				
T4	0.1687	0.50	0.50	2.54	2.02	12.5	1.38	2.79
	0.2531	0.82	0.81	2.78				
	0.3375	1.20	1.21	3,07				
	0.5218	1.67	1.68	3.42				
	0.5062	2.17	2.17	3.70				
A5	0.2495	1,34	—	4.61	3.84	6.6	0.69	2.65
	0.3125	1.72	—	4.72				
	0.375	3.13	—	4.88				
	0.499	3.06	—	5.27				
T5	0.0817	0.46	0.49	4.99	4.75	5.3	0.61	2.90
	0.1634	0.99	1.02	5.29				
	0.2451	1.53	1.59	5.47				
	0.3268	2.15	2.21	5.72				
	0.4085	2.84	2.90	6.03				
112	0.1807	0.27	—	1.30	0.76	33.4	3.13	2,37
	0.3614	0.71	—	1.70				
	0,5420	1.45	—	2.33				
	0.7227	2.54	—	3.05				
	0.9034	4.01	—	3.86				
121	0.2849	0.62	—	1.88	1.10	23.0	2.17	2.39
	0.4273	1.16	—	2.37				
	0.5698	1.91	—	2.90				
	0.7123	2,83	—	3.45				
122	0.1704	0.38	—	1.95	1.47	17.2	1.72	2.53
	0,2922	0,78	—	2,31				
	0.4260	1.34	—	2,73				
	0.5453	1,99	—	3,16				
	0,6816	2,94	—	3,74				
311	0.0562	0,64	—	9.80	9.49	2.67	0.49	4.62
	0.0964	1.07	1.15	9.98				
	0.1406	1.63	1.66	10.09				
	0,1799	2.12	2.14	10.23				
	0.2249	2.75	2.78	10,62				

The higher value of α indicates that the fractions studied contain molecules of a lower degree of branching, as is shown by the values of α for polybutadiene samples polymerized at the same temperature but with different degrees of conversion [13]. The linear extrapolation of the $\pi/c - c$ relationship used by some workers would give high values of M. The higher the molecular weight, the greater would be the deviations of c and the lower the value of α.

EXPERIMENTAL

Fractionation. The material studied was emulsion-polymerized butadiene-styrene copolymer obtained at 50° with 80% conversion, with 71 : 29 butadiene : styrene ratio. The sample was extracted with acetone and fractionated three times by toluene-methanol mixture. Fractions T22, T31, T4, A5 and T5 were obtained from a sample which was dried under vacuum at 50° for 8.5 hours after acetone extraction. The fractions ob-

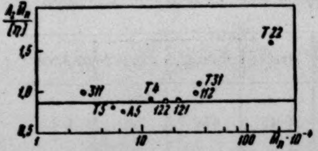

Fig. 2. Values of $A_2\overline{M}_n/[\eta]$ for Buna S fractions in toluene.

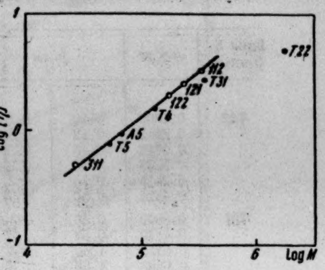

Fig. 3. log[η] – log M curves for Buna S in toluene.

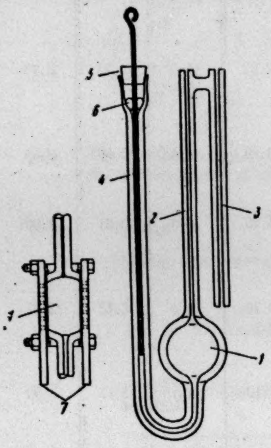

Fig. 4. Osmometer: 1) osmometric cell; 2) osmometric cell capillary; 3) reference capillary; 4) stainless steel wire; 5) bung; 6) mercury seal; 7) bronze plates.

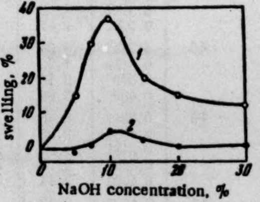

Fig. 5. Swelling of cellophane film in solutions: 1) parallel; 2) at right angles to the direction of winding.

tained after the second fractionation were kept in darkness in a nitrogen atmosphere for over seven months before the last fractionation. The final fractions were dried under vacuum at 30° for 8 hours, and then dissolved in toluene. Fractions 112, 121, 122 and 311 were not dried during purification and fractionation, and the precipitant-solvent mixture was driven off under vacuum. The viscosity and osmotic pressure were measured immediately after preparation of the solutions.

Osmotic pressure measurements. The osmometer used [14] (Figure 4) was a modification of the Zimm-Meyerson osmometer [15]. The measuring and control capillaries were chosen so that the difference of the capillary rise of the solvent did not exceed 0.015 cm. The semipermeable membrane was a cellophane film which had been consecutively swollen for half a minute in 20, 10 and 5% NaOH solutions. The film was then washed in water and kept for 2 hours in 50 and 95% ethanol solutions, 1 hour in absolute alcohol, and 2 hours in anhydrous ethanol-toluene mixture (50 : 50). As the film must not be allowed to dry, it was kept in toluene before use.

The swelling of cellophane film in NaOH solutions of various concentrations was studied. Figure 5 shows swelling curves for the film. It is seen that the swelling of the film is considerably greater in the longitudinal direction than at right angles to the direction of winding. The maximum swelling occurred in 10% NaOH solution. Equilibrium swelling was reached after several hours. The semipermeable membrane prepared in this way

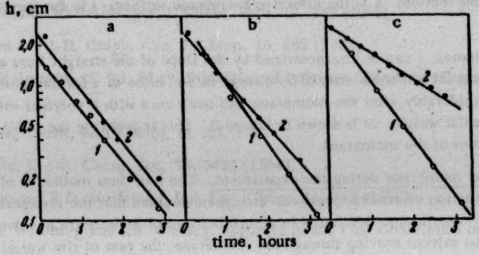

Fig. 6. Permeability of the membrane to the solvent after repeated use: a) kept in solvent; b) after use with sample of $\overline{M}_n = 7.5 \times 10^4$; c) the same, with sample of $\overline{M}_n = 3.3 \times 10^4$; 1) osmometer immediately after assembly; 2) after use during three months.

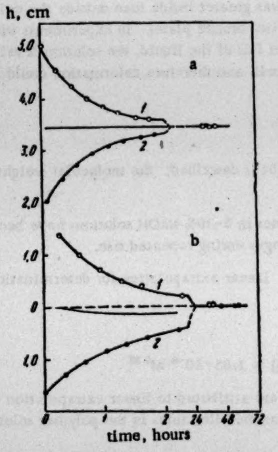

Fig. 7. Determination of osmotic pressure (a) and membrane asymmetry (b) by the half-sum method: 1) descending curve; 2) ascending curve.

showed appreciable asymmetry at first, up to several millimeters of solvent column, but after the membrane had been kept in the solvent for a week the asymmetry did not exceed 0.02 cm. The membrane was tested for Buna S fractions of $\overline{M}_\eta = 33{,}000$ and 22,000. In the former case the osmotic pressure did not decrease for 5 days, while in the latter case it fell by 5% in the first day and then continued to decrease, but at a lower rate. Evidently membranes prepared in this way can be used for determination of molecular weights above 30,000.

7-11 osmometers were put into a thermostat at 25°, ± 0.01°. The osmotic pressure was measured by the static method. The difference between the heights of the liquid columns in the capillaries was read off by means of a cathetometer with an accuracy of 0.01 cm. Equilibrium became established in 24-48 hours, after which the liquid levels in the capillaries varied only as the result of temperature fluctuations, within ± 0.01-0.02 cm. Most of the readings were taken after equilibrium had been reached. In the molecular weight determinations the osmometers were first filled with the less concentrated solutions. When the solution was changed, the osmometer was rinsed out with the next more concentrated solution and kept in it for 15 minutes. When the fraction was changed, the osmometer was placed in the solvent for 2-3 days, the solvent being changed 3-4 times, until the asymmetry did not exceed 0.02 cm.

Variation of membrane permeability during use. The permeability of the membrane to a solvent may be represented by the equation [16]

$$a\,dh/dt = sAh,$$

or

$$\ln h = A/a \cdot st + \text{const},$$

where h is the difference between the liquid column heights in the measuring and control capillaries for time t; a is the capillary cross section; A is the effective membrane surface; s is the permeability constant for the membrane.

For a given osmometer, s can be characterized by the slope of the straight lines on $\ln h - t$ plots. An osmometer kept in a solvent for 3 months showed no change in the value of s for the membrane. However, the value of s decreased considerably after the membrane had been used with a polymer solution, especially with fractions of lower molecular weight, as is shown in Figure 6. This is probably the result of adsorption of polymer molecules in the pores of the membrane.

Deformation of the membrane during the experiment. The half-sum method is often cited in the literature [17] for the determination of osmotic pressure. It is then assumed that the semipermeable membranes are not deformed during the experiment. We found in determinations of asymmetry in solvents that, for the same difference of levels of the solvent moving through the membrane, the rate of rise was always greater than the rate of fall, although ultimately the rise and fall curves always met at the same equilibrium height. This shows that if the half-sum method is used for evaluation of membrane asymmetry a negative value would always be obtained as shown in Figure 7, and the osmotic pressure values would increase with increasing difference between the initial levels. However, in measurements of the osmotic pressure of polymer solutions both the half-sum method and the statistical method gave the same results; this can be explained by deformation of the membrane during the experiment. If the hydrostatic pressure outside the cell was higher than inside, the membrane could be bent into the cell. Thus, as the liquid level rose within the cell, the membrane would gradually expand with decrease of the rate of rise. If the hydrostatic pressure was greater inside than outside the cell, the membrane could not be deformed, as the cell was clamped between two bronze plates. In experiments with polymer solutions, although equilibrium was reached with rise and not fall of the liquid, the solution level within the cell was always higher than the solvent level outside the cell, and therefore deformation could not occur.

SUMMARY

1. An osmometric method for determination of molecular weight is described; the molecular weights of nine Buna S fractions have been determined.

2. The kinetics and maximum swelling of Cellophane membranes in 5-30% NaOH solutions have been determined. It is shown that the permeability of the membranes changes during repeated rise.

3. The $\pi/c - c$ relationship for the system studied is nonlinear. Linear extrapolation for determination of $\overline{M}_n$ and A_2 is possible if $(\pi/c)^{1/2}$ curves are plotted.

The $A_2 M_n/\eta$ ratio for Buna S is constant, irrespective of M.

4. The variation of $[\eta]$ with M is represented by the equation $[\eta] = 1.65 \cdot 10^{-4} M^{0.78}$.

The somewhat higher values of α obtained by previous workers are attributed to linear extrapolation of the $\pi/c - c$ plots, which does not take into account the presence of branched structures in the polymer solutions.

LITERATURE CITED

[1] D.M. French and R.H. Ewart, Ind. Eng. Chem. Anal. Ed. 19, 165 (1947).

[2] J.A. Yanko, J. Polymer Sci. 3, 576 (1948).

[3] R.L. Scott, W.C. Carter and M. Magat, J. Am. Chem. Soc. 71, 220 (1949).

[4] A.S. Novikov, M.B. Khaikina, T.V. Dorokhina and M.I. Arkhangelskaya, Colloid J. 15, 51 (1953) (T.p. 55).*

[5] W.C. Mochel and J.B. Nichols, Ind.Eng. Chem. 43, 154 (1951).

[6] L.H. Cragg and A.T. Brown, Can. J. Chem. 30, 1033 (1952).

---

*T.p. = C.B. Translation pagination.

[7] L.H. Cragg and G.R.H. Fern, J. Polymer Sci. 10, 2 (1953).

[8] R. Speiser and R. Whittenberger, J. Chem. Phys. 13, 349 (1945).

[9] J.A. Manson and L.H. Cragg, Can. J. Chem. 30, 482 (1952).

[10] U. Berglund-Larssen, cf. P.J. Flory, Principles of Polymer Chemistry (Cornell Univ. Press, Ithaca, 1953), p. 280.

[11] E.F. Cassasa, Thesis, MIT (1953), cf. ref. 12.

[12] A.R. Schultz, J. Am. Chem. Soc. 76, 3422 (1954).

[13] B.L. Johnson and R.D. Wolfangel, Ind. Eng. Chem. 44, 752 (1952).

[14] J.Y. Chien, W. Ching and I.H. Chuang, Reported in the First Conference on High Polymer Chemistry (Peking, October 1954).

[15] B.H. Zimm and I. Meyerson, J. Am. Chem. Soc. 68, 911 (1946).

[16] H.J. Philipp and C.F. Bjork, J. Polymer Sci. 6, 383 (1951).

[17] R.M. Fuoss and D.J. Mead, J. Phys. Chem. 47, 59 (1943).

Received November 2, 1956

Institute of Applied Chemistry
Academy of Sciences, China
Changchun

LETTERS TO THE EDITOR

THE EXTERNAL FRICTION OF RUBBER

V.V. Lavrentyev

There is no agreed opinion on the nature of the friction of rubber and the laws of friction.

Ratner and Sokolskaya [1] use the relationship:

$$F = \mu_\infty P + BP^{1-h}, \tag{1}$$

based on Deryagin's binomial law for solids. In Equation (1) F is the frictional force; P is the normal pressure; μ_∞ and B are constants; μ_∞ depends only on the micro- and macroroughness of the surface. The term h accounts for the hardness of the rubber. Ratner assumes that Equation (1) is valid for any normally applied loads; he determines the coefficient μ_∞ by extrapolation of the $\mu - 1/P$ plot to $1/P \rightarrow 0$.

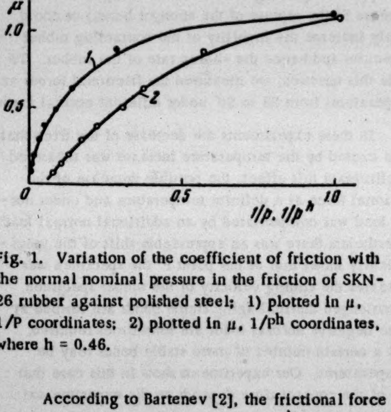

Fig. 1. Variation of the coefficient of friction with the normal nominal pressure in the friction of SKN-26 rubber against polished steel; 1) plotted in μ, $1/P$ coordinates; 2) plotted in μ, $1/P^h$ coordinates, where $h = 0.46$.

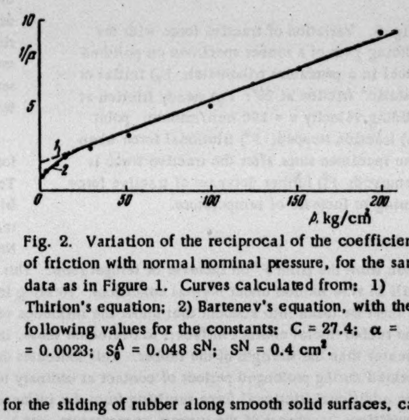

Fig. 2. Variation of the reciprocal of the coefficient of friction with normal nominal pressure, for the same data as in Figure 1. Curves calculated from: 1) Thirion's equation; 2) Bartenev's equation, with the following values for the constants: $C = 27.4$; $\alpha = 0.0023$; $S_0^A = 0.048\ S^N$; $S^N = 0.4\ \text{cm}^2$.

According to Bartenev [2], the frictional force F for the sliding of rubber along smooth solid surfaces, calculated with the actual contact area S^A taken into account, is given by the following expression:

$$F = CS^A = CS^N(\nu_0 + \alpha P)/(1 + \alpha P). \tag{2}$$

where C, ν_0 and α are constant, and $\nu_0 = S_0^A/S^N$, P is the normal pressure in kg/cm²; S^N is the nominal contact area in cm². This equation for a residual contact area S_0^A after removal of the load, becomes the Thirion equation [3].

It follows from Equation (1) that the experimental data* should lie on a straight line, whereas the corresponding experimental relationship is nonlinear (Figure 1). Consequently the coefficients μ_∞ and B in Equation (1) are not constants.

---

*The testing method is described in [1]. In this method the force of initial friction is measured after a definite time of static contact.

By the Thirion equation

$$1/\mu_\infty = a + bP. \tag{3}$$

a straight line should be obtained in $1/\mu$, P coordinates. Figure 2 shows that deviations from linearity are found only at small loads. The theoretical Curve (2) corresponds to Equation (2); it describes the data over the whole range of loads. Therefore, the Thirion equation is in agreement with experimental data over a wide load range. The deviations at low loads are explained by the influence of the residual area of actual contact S_0^A, taken into account in Bartenev's equation.

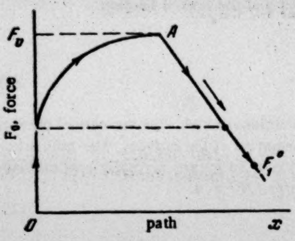

Fig. 3. Variation of tractive force with the sliding path of a rubber specimen on polished steel in a pendulum tribometer: F_0) initial or "static" friction at 20°; F_v) steady friction at sliding velocity v = 100 mm/minute; point A) traction stopped; F^0) frictional force when the specimen stops after the tractive force is removed; F_1^0) further decrease of tractive force owing to increase of temperature.

The molecular-kinetic nature of rubber friction is confirmed by our experiments on the influence of temperature on the force of friction on stopping. Figure 3 shows variations of tractive frictional force F as a function of the sliding path x (the experimental procedure is described in detail in [1]). At the point F^0 the solid support was heated above room temperature. The experiments showed that when the temperature was increased, even by 10°, the rubber specimen began to move with increased speed. At the point F^0 the specimen is either in very slow motion, or is retarded to a state of rest by the stronger bonds which arise between the rubber and the support on prolonged contact. Heating could either decrease F^0 (by rupture of the stronger bonds) or could simply increase the mobility of the contacting rubber molecules and hence the sliding rate of the rubber. To settle this question, we measured the frictional forces at temperatures from 23 to 90° under different normal loads.

In these experiments the decrease of the frictional force caused by the temperature increase was measured. To eliminate this effect, the possible decrease of the frictional force at a definite temperature and under normal load was compensated by an additional normal load. Nevertheless there was an appreciable shift of the specimen from the point F^0 on increase of temperature. This clearly shows that at the point F^0 the specimen was still in slow motion under normal conditions. Heating increases the sliding velocity of the rubber specimen. It must be taken into account that under the influence of prolonged thermal aging stable bonds are formed at the rubber-metal contact surface; to overcome these, large negative normal loads are sometimes required, greater than the strength of the rubber. This indicates that a certain number of more stable bonds may be formed during prolonged periods of contact at ordinary temperatures. Our experiments show in this case that the additional frictional force resulting from the influence of the contact time depends on the experimental conditions (roughness of the support, temperature, etc.).

The molecular nature of the friction of rubber and the conventional character of static friction are most predominantly seen at high temperatures (with short contact times) and under large normal loads. Formation of stable bonds on prolonged contact, and large amounts of filler in the rubber, mask the molecular nature of rubber friction.

LITERATURE CITED

[1] S.B. Ratner and V.D. Sokolskaya, Proc. Acad. Sci. USSR 99, 431 (1954).

[2] G.M. Bartenev, Proc. Acad. Sci. USSR 96, 1161 (1954); 103, 1017 (1953).

[3] P. Thirion, Rubb. Chem. Techn. 21, 505 (1948).

Received December 11, 1956

The V.M. Potemkin Moscow
Pedagogic Institute
Chair of Theoretical Physics

CURRENT EVENTS

NINTH CONFERENCE ON COMPOUNDS OF HIGH MOLECULAR WEIGHT

The Ninth Conference on Compounds of High Molecular Weight, devoted to general questions of chemistry and physics of high polymers, took place in Moscow from January 28 to February 1, 1957. The range of participants at the Conference, the diversity of the problems considered, and the depth of the discussions reflect not only the importance of the problems confronting polymer science, but also the broad sweep of the research which is proceeding in this field in our country.

About 1500 delegates took part in the Conference, including foreign scientists from the People's Republic of China, the German Democratic Republic, Poland, Rumania, Federal Republic of Germany, Israel, and Yugoslavia. Academician V.A. Kargin, in opening the Conference, reviewed the present state of polymer science and emphasized the urgent necessity for extending research work with the aim of finding new methods of polymer production and new classes of polymers, and of development of deep studies of the phenomena and mechanisms of processes which occur in the synthesis, conversion and utilization of polymeric materials.

About two hundred papers were presented at the meetings of six sections of the Conference.

The Section on Polymer Synthesis included 44 papers; in addition, 10 papers in the Section on Chemical Properties and Modification of Polymers also dealt with synthesis. A.N. Nesmeyanov, R.Kh. Freidlina and a group of their associates reported on the reaction of telomerization of CCl_4 and C_2H_4 and on new possibilities of obtaining monomers of great practical interest from the products of this reaction. In the paper by B.A. Dolgoplosk et al., a number of new systems which initiate polymerization reactions were described and the mechanism of their action examined. The papers by S.S. Medvedev et al., and by A.I. and S.T. Yurzhenko dealt with the mechanism of emulsion polymerization. A.N. Pravednikov and S.S. Medvedev gave convincing proofs for their proposed peculiar mechanism of the formation of the ω-polymer of chloroprene.

A.S. Semenova and E.V. Kuvshinsky reported the results of an investigation of the influence of pressure (up to 4000 kg/cm^2) on the polymerization kinetics of styrene. The paper by S.E. Bresler and his co-workers described the determination of free radical concentrations by means of the Hg^{203} radioactive isotope and by a radiospectroscopic method. Questions of diene hydrocarbon polymerization formed the subject of the papers by K.B. Piotrovsky and by teams of authors headed by A.A. Korotkov, N.I. Nikolaev and others. A.R. Gantmakher and S.S. Medvedev described in their paper the peculiarities of the kinetics of carbonium polymerization and copolymerization.

Interesting data on the synthesis and properties of certain polymers were reported in the papers by Yu.V. Mitin (on polymers containing aromatic rings in the chain), B.A. Dolgoplosk, E.I. Tinyakova, et al. (on carboxyl-containing rubbers), and I.A. Lifshits, S.I. Ilyina and V.N. Reikh (on piperylene polymers); the paper by S.A. Subbotin et al. gave the results of an investigation of isoprene rubber (synthesized under the guidance of A.A. Korotkov) similar to natural rubber in structure and properties. Polymerization of methyl methacrylate under the action of butyllithium yields a polymer of much higher heat stability than ordinary polymethyl methacrylate; this is the principal result of an investigation reported by A.A. Korotkov and his associates. Polymers (and copolymers) of certain unsaturated esters of phosphinic acids, described by G. Kamai and V.A. Kukhtin, have high flame resistance.

The papers by V.V. Korshak and his co-workers gave the results of studies of the polymerization and copolymerization of unsaturated organosilicon and organogermanium compounds, synthesis of polyesters of various dicarboxylic acids and glycols, and polycondensation of phosphine and phosphinic acid derivatives. M.F. Shostakovsky described methods of preparation and polymerization, and the properties of vinyl organosilicon compounds. The paper by O.Ya. Fedotova, M.A. Askarov and I.P. Losev dealt with synthesis and study of symmetrical diaminodiarylmethanes and polyamides derived from them. A.L. Klebansky and N.S. Vilesova reported interesting data on the synthesis of N-alkyl derivatives of hexamethylenediamine and their polycondensation with dibasic acids. T.S. Sogomonyants and M.V. Volkenshtein put forward experimental proofs of the influence of stereoisomerism on the properties of polymers (illustrated by certain polyamides and polyesters synthesized by them). Interesting papers were presented by the Czechoslovak scientists O. Wichterle and K. Vesely' on cationic polymerization of olefins.

At the Section entitled "Chemical Properties and Modification of Polymers" great interest and lively discussions were aroused by six papers on various aspects of rubber vulcanization (by B.A. Dogadkin and his co-workers, G.M. Bartenev, A.S. Priss and L.E. Vinnitsky); I.S. Okhrimenko reported some interesting results on the high pressure vulcanization of rubber. A.Ya. Drinberg and A.D. Yakovlev reported on the structurization of linear polymers. The paper by B.A. Dogadkin, A.V. Dobromyslova, et al. dealt with the influence of the structure of butadiene polymers on their chemical activity. Papers on various aspects of the chemistry and physical chemistry of cellulose and its derivatives comprised a considerable proportion of the Section (14 papers). These included descriptions of new derivatives of cellulose (papers by S.P. Danilov and A.A. Lopatenok, and by Z.A. Rogovin et al.) and of chitin (by E.A. Plisko); data were presented on the reactivity of primary and secondary hydroxyls (V.A. Derevitskaya et al., O.M. Klimova), and the results of studies of hydrolysis, oxidation, and thermal decomposition of cellulose and its derivatives were reported (V.I. Maiboroda and N.V. Mikhailov, O.P. Golova et al., O.P. Kozmina and V.I. Kurlyankina, M.M. Pavlyuchenko et al.). V.I. Ivanov and N.Ya. Lenshina reported on the properties of cellulose in relation to its use in chromatography.

Several papers dealt with polymer-analog conversions (of polyvinyl alcohol, by S.N. Ushakov and E.M. Lavrentyeva; of polyacrylonitrile, by A.A. Strepikheev, G.I. Kudryavtsev and E.A. Vasilyeva-Sokolova); E.A. Kurilchikov described the modification of certain fiber-forming polymers by proteins. Wan U Hey (People's Republic of China) gave an interesting paper on the study of caprolactam by end group titration.

The section on "Molecular Structure and Solutions of Polymers" contained papers giving the results of investigations of various materials by the most diverse methods. The paper by V.A. Kargin, S.Ya. Mirlina and N.F. Bakeev contained conclusions concerning the shape of the molecules of polyacrylic acid and its salts, based on electrochemical measurements and direct observations by means of the electron microscope. O.B. Ptitsyn reported on a detailed theory of light scattering by polymer solutions; the consequences of this theory are of considerable importance. Studies of light scattering, viscosity, diffusion, and flow birefringence of polymer solutions were described in a series of papers by V.N. Tsvetkov and his co-workers, and also by E.V. Frisman. The paper by I.Ya. Poddubnyi and E.G. Erenburg gave the results of a study of the connection between the conditions of rubber synthesis and the structure of the macromolecules formed, determined by studies of their solutions. S.M. Lipatov et al. and A.A. Tager reported results of thermodynamic investigations of polymer-solvent systems. In the paper by S.A. Glikman and L.A. Root reference was made to the possibility of studying intermolecular forces in polymer solutions by the dilatometric method. The paper by P.A. Rebinder and L.V. Ivanova-Chumakova was devoted to the general laws governing the viscoelastic properties of polymer solutions, and methods for studying them over a very wide concentration range – from very dilute solutions to the pure polymers. The papers presented by G.V. Vinogradov and his associates described methods and results of studies of the mechanical and optical polarization properties of concentrated polymer solutions.

In the paper by V.V. Korshak, S.A. Pavlova and G.L. Slonimsky a relationship was established between the molecular weight distribution function of polycondensation products and the polycondensation mechanism. I.Ya. Poddubnyi reported an investigation, which has practical significance, of the molecular weight distribution of divinyl-styrene rubbers. Teams of authors headed by V.V. Korshak and N.V. Mikhailov reported on the relationships between the properties and macromolecular structure of polyamides. S.S. Voyutsky et al. reported the results of a study of the relationship between the adhesive properties of polymers and macromolecular structure.

The controversial question of the structure of crystalline polymers was dealt with in papers by A.I. Kitaigorodsky and Yu.V. Mynukh, and by G.S. Markova and V.A. Kargin. Studies of internal rotation and rotational isomerism of polymeric molecules by the photoelastic method and by means of polarized infrared radiation were described in papers by teams headed by N.M. Bazhenov and V.N. Nikitin. Yu.Ya. Gotlib advanced a theory of birefringence in polymers and demonstrated that this theory is in satisfactory agreement with experimental data for several substances. Studies of dielectric properties were reported in papers by G.P. Mikhailov and T.I. Borisov (amorphous polymers), B.I. Sazhina (crystalline polymers), and O.D. Kurlienko (hydrophilic polymers). N.V. Mikhailov et al. reported the results of an investigation of polymer compatibility and the use of polymer mixtures for improving fiber properties. Several papers (S.N. Danilov and M.G. Okun, A.G. Pasynsky and A.M. Tongur, V.I. Kasatochkin, A.A. Alimov et al.) dealt with studies of natural compounds.

Interesting, but in many respects controversial views on the submicroscopic structure of polymers were advanced by K. Hess (Federal Republic of Germany). A.Katchalsky (Israel) gave two papers, on the principal properties of polyelectrolytes and on certain questions related to the direct conversion of chemical into mechanical energy.

At the Section entitled "Structure and Mechanics of Polymers" about thirty papers were presented and discussed. A very wide range of problems was covered by these papers. The papers by T.I. Sogolova and V.A. Kargin, and by A.A. Pozin et al., dealt with the mechanism and laws of the flow of polymers. High-elastic properties of polymers formed the subject of papers by G.M. Bartenev et al., G.L. Slonimsky, A.P. Kusov, G.A. Patrikeev, and E.V. Kuvhsinsky et al. The characteristics of relaxation processes in polymer glasses and the mechanical behavior of glassy polymers were discussed in the papers by M.V. Volkenshtein et al. and Yu.S. Lazurkin et al. Highly important questions of the strength and fatigue of polymer materials were considered in papers by A.A. Rogovina and V.A. Kargin, G.M. Bartenev et al., M.M. Reznikovsky et al., V.G. Epshtein, and V.E. Gul. S.B. Ratner and V.V. Lavrentyev reported the results of a study of the static friction of rubber. The value of the thermomechanical method of polymer investigation, in particular in relation to determination of the mechanism of hardening and the structure of three-dimensional polymers, was demonstrated in papers by L.A. Igonin and V.A. Kargin, B.M. Kovarskaya et al., and L.E. Kalinina, V.I. Alekseenko and S.S. Voyutsky. The paper by S.V. Vinogradov, G.L. Slonimsky and V.V. Korshak gave the results of a study of the mechanical properties of amorphous polyesters, and the relationship between the structure and molecular flexibility of these substances was discussed on the basis of the data obtained. V.P. Pavlov and G.V. Vinogradov described new apparatus by means of which it is possible to determine the instantaneous modulus and to study the relaxation behavior of easily deformed polymeric systems. N.A. Shchegolevskaya and S.N. Sokolov reported on the relationships established by them between the composition, structure and mechanical and optical (photoelastic) properties of certain multicomponent polymer systems. Chen Bao-Kun (People's Republic of China) devoted his paper to the viscoplastic properties of natural rubber. Prof. Porejko (Poland) dealt with some questions of the technology of polyvinyl chloride processing.

In the Section on "Aging and Degradation of Polymers" the papers reflected the attention paid by our investigators to studies not only of pure polymers but also of complex polymeric systems containing such components as solvents, fillers, etc. A series of papers dealt with questions of oxidation and photodegradation of vulcanizates and other systems containing rubber (by B.A. Dogadkin et al., T.G. Degteva and A.S. Kuzminsky, G.A. Patrikeev et al., Yu.S. Zuev and S.I. Pravednikova, N.N. Lezhnev,and A.S. Kuzminsky). The papers by V.V. Korshak et al., S.E. Bresler et al., N.V. Mikhailov et al., R.I. Gruz, and A.A. Vanshteidt gave the results of studies of the light and heat degradation of certain plastics and summarized work on the increase of their stability.

Papers by A.A. Berlin, G.L. Slonimsky et al., and N.K. Baramboim, dealing with problems of mechanochemistry, aroused great interest and lively discussions.

In the Section on "Applications and Methods of Polymer Control" more than 20 papers were presented. N.K. Moshchinskaya's paper dealt with the synthesis of diarylmethanes and the possibility of their use as plasticizers. S.A. Pavlov in his paper discussed the relationship between the chemical nature and properties of high polymers used in the production of artificial leather. Z.A. Rogovin and Z.A. Zazulina reported on a method for the production of a new fiber, ftorlon, which is of great practical interest. Several papers dealt with purification, utilization, and properties of cellulose and its derivatives and of starch. Interesting data on the sorption of dipolar ions by ion exchange resins were given by G.V. Samsonov and his associates. V.D. Bezuglyi and V.I. Dmitrieva reported on the successful use of a polarographic method in studying the production and processing of various plastics. G.N. Kukin devoted his paper to studies of the mechanical properties of textile materials, and B.I. Gengrinovich dealt with the plasticoelastic properties of rubbers and raw rubber compositions. L.A. Igonin and E.E. Glukhov described their new instruments, of great interest for studying the mechanical properties of polymeric materials. H. Klare (German Democratic Republic) presented interesting data obtained in studies of certain cellulose derivatives and viscose fibers. E. Correns (German Democratic Republic) devoted his paper to the reactivity of wood; C. Simionescu (Rumania) dealt with fractionation of cellulose. T. Rabek (Poland) reported the results of studies of the properties of ion exchange resins.

The participants at the Conference expressed the desire for the organization of a future series of meetings on individual questions — heat stability of polymers, some physical properties of polymer systems (viscosity and elasticity, thermodynamics of solutions, dielectric properties), aging and stabilization, mechanochemistry, artificial leather, polymerization and hardening at room temperatures, and apparatus for mechanical testing.

In closing the Conference, V.A. Kargin announced that, by the decision of the Commission on High Polymers of the Academy of Sciences USSR the next, 10th Conference, which is to be called in a year's time, will be devoted to biologically active polymers (proteins, nucleoproteins) and to models of such polymers.

Yu.M. Malinsky.

DEVELOPMENT OF COLLOID CHEMISTRY IN THE USSR

Prior to the Great October Socialist Revolution, only a relatively small number of people carried on systematic research in the field of colloid chemistry in Russia (A.V. Dumansky, V.V. Kurilov, P.P. Weimarn, N.P. Peskov, and N.A. Shilov. There were hardly any scientific institutions dealing with problems of colloid chemistry. Lectures in colloid chemistry were first given in 1912 by A.V. Dumansky in the University of Kiev. However, views on colloidal systems and their characteristics were advanced in Russia even in the earliest days of the science. For example, as long ago as 1869, Prof. I.G. Borshchov of Kiev University devised a more complete characterization of colloidal systems than had been produced abroad. The rheological properties of colloid solutions were studied in 1889 by Prof. F.N. Shvedov of Odessa University, who showed that dilute gelatin solutions do not obey the Maxwell relaxation equation but, in contrast to true viscous liquids, have a region of elastic deformations which persist for considerable periods.

After the October Socialist Revolution, the scientists of the Soviet Union were confronted with wide possibilities for free and full creative activity. Several scientific research institutes were established for rapid development of research and for training numerous scientific workers. The first Soviet groups of research workers in various branches of colloid chemistry were formed in the laboratories of N.A. Shilov, A.V. Dumansky, N.P. Peskov, A.I. Rabinovich, I.I. Zhukov, P.A. Rebinder and S.M. Lipatov. These laboratories were centers for the training of young specialists, many of whom became eminent scientists (V.A. Kargin, L.K. Lepin, and others). Simultaneously with this, numerous centers of research into topical problems directly related with the theory of colloid chemistry arose in many Universities and industrial undertakings of the Soviet Union (V.A. Naumov, S.I. Sokolov, B.A. Dogadkin, M.P. Volarovich, I.N. Antipov-Karataev, A.G. Pasynsky, A.I. Rabinerson, S.A. Voznesensky, V. I. Nazarov, S.G. Mokrushin, N. F. Ermolenko, S. S. Voyutsky, S. A. Glikman, and others).

The number of published papers on colloid chemistry rose sharply; between 1869 and 1917 only 234 papers were published by 50 authors, whereas between 1917 and 1952 6410 papers by nearly 1000 authors were published.

The most vigorous development of colloid chemistry in the Soviet Union was seen during the period of industrialization and during the early Five-Year Plans. During this period a number of applied problems of colloid chemistry was studied in addition to theoretical work. The number of laboratories increased both in the applied and in the fundamental scientific institutes.

In 1929 V.A. Kistyakovsky organized a colloido electrochemical laboratory, which was reorganized in 1935 as an institute under the same title. The extensive work of P.A. Rebinder on the physical chemistry of surface layers and disperse systems, and of B. V. Deryagin on the properties of thin liquid films and surface forces, has been developed in this institute.

The growth of the Colloid Chemistry Laboratory of the Voronezh Agricultural Institute was such that in 1932 it was reorganized as the All-Union Scientific Research Institute for Colloid Chemistry (Director A. V. Dumansky). The first All-Union Conference on the physical chemistry of colloids was held in 1934 in Voronezh at this Institute. The Conference indicated the course of the further development of colloid chemistry in the USSR, and approved A. V. Dumansky's proposals that a special colloid journal should be produced (this commenced publication in 1935) and that All-Union Conferences on colloid chemistry should be held periodically.

At that time the new synthetic rubber industry was beginning to develop in the Soviet Union. The first factory in the world for the production of sodium butadiene rubber, based on the classic researches of S. V. Lebedev, commenced production. Development of the synthetic rubber industry and of a number of other branches of industry (rubber, plastics, synthetic fibers and films) stimulated extensive colloidochemical and physicochemical researches on high polymers and their solutions.

In May 1937 a conference on lyophilic colloids was held in Moscow; attention was drawn to the importance of research on lyophilic systems, studies of interactions between the disperse phase and the medium, the structure of high polymers, and to the need for close coordination between physicochemical research on high polymers and the problems of organic chemistry and physics in this field.

The XVIIIth Congress of the All-Union Communist Party (Bolsheviks) presented the Soviet people with new important tasks for the further mighty development of the productive forces of the country. In consequence, numerous research institutes and universities, with highly qualified staffs available, directed their efforts to the solution of the most important theoretical and practical scientific problems. From that time research on colloid chemistry became increasingly closely associated with the demands of the national economy. New theoretical problems were studied in order to fulfill successfully the practical tasks of socialist industry.

During the years of the Great Patriotic War, Soviet scientists carried out numerous investigations relating to the defense industries and military needs.

After the end of the War, the scientific institutions for colloid chemistry started work on current problems directly related to restoration of the national economy. In 1945 a scientific conference on colloid chemistry in the food industry was held in Moscow. The number of publications grew rapidly. Colloid Journal, the publication of which was suspended during the War, resumed publication in 1946, under the Academy of Sciences USSR Press.

The organization of colloid and high polymer sections of the Moscow Section of the D.I. Mendeleev All-Union Chemical Society helped to unite scientists working in these respective fields.

In 1950 the Second All-Union Conference on Colloid Chemistry was held in Kiev; numerous papers were presented, mainly on the mechanical properties of disperse systems, the structure and properties of high polymers, solvation, properties of solvate layers, intermolecular forces, and stability of lyophobic colloids and suspensions. Conferences on high polymers, both on special aspects and on general questions of polymer chemistry, physics, and technology, have been regularly held.

The Third All-Union Conference on Colloid Chemistry was held in 1953 in Minsk. 62 papers were discussed, mainly on the following principal topics: the structure of disperse systems and their rheological properties, the stability of colloidal solutions, suspensions, and emulsions, the properties of thin layers at interphases, the properties of high polymers, and various applications of colloid chemistry in the national ecomy.

The successful development of colloid chemistry in the USSR is helped by direct contacts between many specialists in this field and industry, and the wide adoption of the results of scientific research in the national economy. In the place of the few laboratories of the prerevolutionary era, there are numerous laboratories in the universities and scientific research institutes in which vigorous work is done on colloid chemistry.

Let us examine some of the problems studied during the 40 years of Soviet power.

Most of our scientists were interested in the fundamental question of the stability of colloid systems. N. P. Peskov studied coagulation and aging of sols. He introduced the concepts of kinetic and aggregative stability. N. P. Peskov also attached great importance to questions of solvation. The problem of the stability of colloid systems was extensively studied by P. A. Rebinder and B. V. Deryagin.

A. V, Dumansky established that in the production of sols in chemical reactions micelle formation is preceded by formation of complex compounds, and that the micelle formed has an ionogenic complex based on these complex compounds. For a study of colloid systems from this viewpoint, a detailed investigation was made of the formation of hydrosols of heavy metal hydroxides in presence of hydroxy compounds and alkalies. A number of scientists cooperated in this research; S. I. Dyachkovsky, A. P. Buntin, A. G. Kniga, and S. E. Kharin worked in their respective departments on the stability and structure of sols. Several quantitative determinations of the water bound with the disperse phase were made, and the mechanism of water binding was examined. The heats of wetting (E.F. Nekryach, F. D. Ovcharenko), variations of dielectric constant (O. D. Kurilenko), and effects associated with the lyophilic properties of colloids were also studied. Original methods for preparation of metal organosols were developed, and the conditions for their stability were studied (E. M. Natanson).

Extensive work was done at the L. Ya. Karpov Physicochemical Institute by A. I. Rabinovich, V. A. Kargin, and their associates. The studies dealt mainly with electrochemical processes in lyophobic sols. This work led to a better understanding of the structure of micelles, and helped to develop the theory of coagulation in presence of electrolytes. A. I. Rabinovich and V. A. Kargin used the potentiometric titration method to make a detailed study of the coagulation mechanism of hydrophobic sols, and advanced and confirmed the view that the stability of hydrophobic sols and their selective sensitivity to different electrolytes are difficult to explain by physical models only; it is necessary to study chemical processes occurring between the disperse phase and the electrolytes of the dispersion medium during coagulation.

Interesting work has been done on highly purified sols and on electron microscopy of micelle structure at the instant of formation. It was shown that the particles of the disperse phase of a number of inorganic compounds originate from solutions in the form of amorphous spherical relatively large formations; these crystallize only later, and disintegrate into particles of colloidal dimensions.

V. A. Kargin, S. M. Lipatov, and B. A. Dogadkin began their investigations of the physicochemical properties of high polymers in the 1930 's.

I. I. Zhukov organized a scientific research laboratory for colloid chemistry in Leningrad University, and from 1926 he worked there with his pupils on the emulsifying properties of gelatin. Subsequent investigations dealt with synthetic rubbers, alginic acid, and its derivatives. The extensive work of Zhukov and his school on electrokinetic phenomena is particularly important.

S. M. Lipatov has worked systematically on problems of the lyophilic nature of disperse systems since 1925. It was shown that the syneresis effect is associated with a tendency of the system to reach a state of thermodynamically stable equilibrium. The work of S. M. Lipatov and his associates (A. A. Morozov, I. N. Putilova) has provided explanations for many processes of gel formation and gel structure. These authors consider that lyophilic colloidal systems –high polymers – are complex polydisperse systems consisting of a number of adsorptively interacting fractions.

The work of N. F. Ermolenko on swelling in high polymer systems should also be mentioned.

It was later established, by the work of B.A. Dogadkin, V.A. Kargin and their associates (A. A. Tager and S. P. Papkov)that polymers form true solutions which are thermodynamically stable systems.

P. A. Rebinder and his associates (A. B. Taubman, E. K. Venstrem, K. F. Zhigach, N. N. Serb-Serbina, and others) have carried out numerous important investigations in a variety of directions; in general these are all associated with the influence of surface phenomena on disperse systems and their stability. Extensive investigations on the wetting of solid surfaces have led to the concept of selective wetting, and have shown that this quantity is a quantitative characteristic of the molecular nature of the solid phase. Investigations of all aspects of the influence of surface layers on the properties of suspensions, emulsions, foams, and colloidal systems, carried out by means of new methods, were used for stydying the possibility of regulating technological processes. Studies of the influence of the medium on the mechanical properties of solids have great significance. In this field, the effect of adsorptional decrease of strength was discovered. In recent years, the work of P.A. Rebinder and his school (N.E. Segalova, N. N. Serb-Serbina, B. Ya. Yampolsky) has been directed toward studies of the eleasticoplastic properties of a great variety of structurized systems.

Mention should be made of the work of A.A. Trapeznikov on the elasticoviscous properties of monolayers of various compounds and the effects of various factors on their structural and mechanical properties.

N. A. Figurovsky developed convenient methods of sedimentation analysis, which have been extensively adopted.

In the field of rheology, mention must be first made of the investigations of M.P. Volarovich and his associates (D. M. Tolstoi, A. M. Gutkin, V. L. Valdman, and others), who developed new methods for measurement of viscosity and flow limit of highly viscous and viscoplastic bodies, and studied the structuromechanical properties of a number of different disperse systems. Their methods have been widely adopted.

B. A. Dogadkin and his associates (M. M. Reznikovsky, K. A. Pechkovskaya, Z. N. Tarasova, A. S. Novikov, V. E. Gul) have carried out investigations on rubber. The viscosity, structure formation, and structuromechanical properties of rubbers with and without fillers have been studied in detail.

G. V. Vinogradov and his associates designed original instruments for studying flow processes in lubricant greases at various velocities and temperatures, and also hydrophobization of clays and other mineral adsorbents. D. S. Velikovsky, M. P. Volarovich, G. I. Fuks, and others studied colloidochemical processes in lubricating materials. Problems of adsorption have been successfully studied by M.M. Dubinin and his school and by A. V. Kiselev.

The large number of investigations on high polymers has already been mentioned. Here we will refer only to certain studies of latexes, of general significance in colloid chemistry (B. A. Dogadkin, S. S. Voyutsky, D. M. Sandomirsky, A. A. Yurzhenko). Extensive work on rubber and other polymers has been done by P. P. Kobeko, A. P. Aleksandrov, Ya. I. Frenkel, S. E. Bresler, and others. Soil colloids have been studied by I. N. Antipov-Karataev, A. F. Tyulin, and others.

B. V. Deryagin's studies, commenced in 1932, on liquid films at solid surfaces are of great significance for colloid chemistry. These studies provide explanations of the stability of sols, emulsions, and suspensions. In his study of the so-called disjoining action effect (discovered jointly with E. V. Obukhov, M. M. Kusakov, and others), Deryagin concluded that a solid surface exerts an influence at a considerable distance on the properties and thermodynamic state of adjacent liquid layers. In particular, Deryagin and Landau jointly developed a theory of the stability of lyophobic sols, which has gained wide acceptance. It was applied by Yu. M. Glazman and I. M. Dykman to the problem of ionic antagonism. Direct determinations of molecular forces, carried out by B. V. Deryagin and I. I. Abrikosova, confirmed the validity of the physical principles of Im. M. Lifshits's theory of molecular forces. Original methods for measuring forces and energy of adhesion have been developed, and an electrical theory of adhesion was put forward (jointly with N. A. Krotova). Interesting work has been done by S. G. Mokrushin and N. Demenev on the formation of solid films on the surfaces of aqueous solutions.

During the period under review, estensive and important work on aerosols was initiated and continued by N. A. Fuks and I. V. Pteryanov, and by B. V. Deryagin and his associates (I. S. Artemova, P. S. Prokhorov, G. Ya. Vlasenko, A. G. Amelin, O. M. Todes, and G. L. Natanson).

The above far from complete review* shows that dozens of scientific research institutes, and hundreds of laboratories in the universities and technical colleges, opened and equipped for research by the Soviet Government, have attracted thousands of scientists, and have helped to establish important scientific schools and to raise work on colloid chemistry to a level which has given a leading position to Soviet colloid chemistry.

A. V. Dumansky

---

* A more detailed review will be found in A. V. Dumansky's published monograph: "Bibliographical Review of the Development of Russian Colloid Chemistry", in three parts, published by the Academy of Sciences, Ukrainian SSR.

ANTIFRICTIONAL PROPERTIES OF DISPERSE PHASES OF METAL ORGANOSOLS

M. L. Barabash and E. M. Natanson

It has been established by a series of investigations that the antifrictional properties of many metals and alloys are primarily determined by the fact that at the time of first contact highly disperse particles are liberated at the points of friction and form a more or less stable suspension in the lubricating oil. When such a suspension is formed in the gap at the point of friction, the wear and the coefficient of friction of the contacting metallic surfaces are sharply diminished [1-3].

On this basis, we suggested [4] the introduction of lubricating oils containing colloidal metal additives into the gaps at points of friction. Use was made of the principle that the antifrictional properties of rubbing surfaces largely depend on the physicochemical state of these surfaces and of the layer of oil in the gap at the point of friction. In absence of colloidal metal additives, a lubricating oil usually forms adsorbed solvate layers only on the surfaces of contacting metals [5-7]. In such cases the lubricating oil interlayer consists only of two solvate layers and a thin interlayer of free oil between them. On addition of a colloidal metal, nearly all the lubricating oil is in a solvated state owing to the formation of a solvate layer on the surface of each particle. Thus, if a colloidal metal is present in the lubricant, instead of two solvate layers of oil, polysolvate layers appear in the gap, which should have a favorable effect in lowering the coefficient of friction and wear of the metals.

The organosols of iron, bismuth, and other metals in various lubricating oils, which were subsequently named metallocolloidal lubricants, have been studied in many scientific research institutions and undertakings. Some of the results are given in the present communication.

Tests of wear with various frictional pairs were made with a disk friction machine of special design, in which it was possible to measure the frictional moment, the temperature of friction, the rotational speed, the frictional path, and the current consumption of the machine motor (Fig. 1). The operating time of the machine could be automatically varied between 30 seconds and 12 minutes. A frequent start-stop procedure was used in the experiments. In such "impulse" conditions it is possible to shorten considerably the testing time, which is usually very long in presence of high-quality lubricants. The effects of pressure variations (between 6 and 60 kg/cm^2), sliding velocity (from 0.67 to 7.5 m/second), friction path (from 2,000 to 30,000 m), and of an electric current passing through the friction pair were studied. The wear was estimated from the change in weight, the running-in time being deducted.

Four friction pairs were chosen for study: 1) bronze OTsS on steel 45; 2) globular gray iron on steel 45; 3) metal compact (based on iron powder) on steel 45; 4) the same metal compact on globular gray iron. The first two pairs are often used at points of friction, while the two latter are of definite interest in relation to the prospects of their wide adoption in machine construction.

In addition, specimens of conducting contacts used in town trolley cars were studied: aluminum, a copper-graphite composition, and a metal compact, both with and without graphite and sulfur. The wear resistance of all the specimens was studied in presence of a number of lubricating oils in pure form and in the form of organosols of iron and other metals. The latter were made by the electrolytic [8] and flotation [9] methods, based on formation of colloidal metal particles in an aqueous medium followed by their transfer into an organic medium by means of surface active substances.

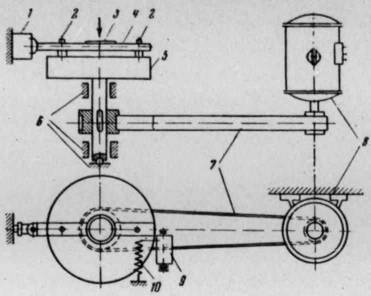

Fig. 1. Diagram of KADI-02 machine for studying friction and wear; 1) universal joint for machine arm; 2) specimen holders; 3) load pan; 4) arm carrying the specimen holders; 5) machine disk and shaft; 6) shaft bearigns; 7 belt drive; 8) electric motor; 9) recording device; 10) spring dyanmometer.

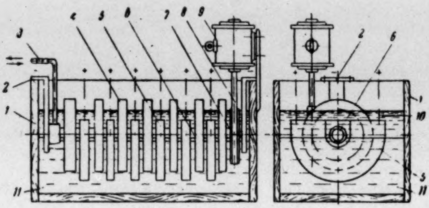

Fig. 2. Electrolytic cell with rotating cathode, for production of iron organosols on the semimanufacturing scale; 1) cell casing; 2) cathode shaft supports; 3) inlet and outlet tubes for water cooling the cathode shaft; 4) internally cooled cathode disk; 5) anode plates; 6) hollow cathode shaft; 7) worm gear; 8) worm shaft; 9) electric motor; 10) organic medium; 11) electrolyte.

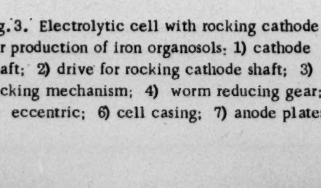

Fig. 3. Electrolytic cell with rocking cathode for production of iron organosols; 1) cathode shaft; 2) drive for rocking cathode shaft; 3) rocking mechanism; 4) worm reducing gear; 5) eccentric; 6) cell casing; 7) anode plates.

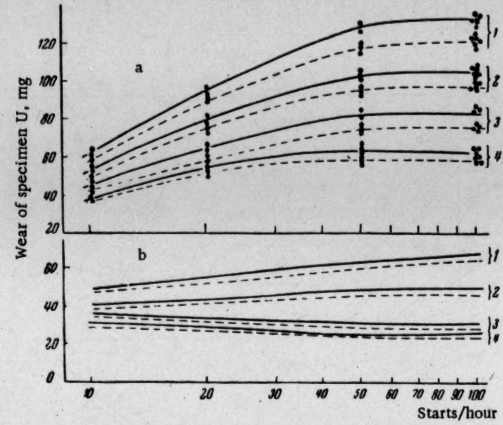

Fig. 4. Effect of the number of starts and stops of the testing machine on wear: a) with lubrication by a mixture of Avtol 10 (50%) and Solidol T (50%); b) with the same lubricant with addition of 2% iron organosol in Avtol 10. Friction pairs: 1) bronze OTsS on steel 45; 2) globular gray iron on steel 45; 3) metal compact on steel 45; 4) metal compact on globular gray iron. Continuous lines – with removal of products of wear; broken lines – without removal of products of wear. Test conditions: pressure 60 kg/cm^2; sliding velocity 0.67 m/second; sliding path 5000 m.

The electrolysis was usually carried out in a two-layer electrolytic bath, the lower layer of which was an aqueous solution of a salt of the metal in question, and the upper layer consisted of various lubricating oils containing small amounts of surface active agents. The cathode was a rotating horizontal shaft with a system of disks at the boundary between the oil and water phases. The anodes (fixed) were plates of the appropriate metals.

This principle was the basis for the design of electrolytic cells of various types, suitable for production of metal organosols in lubricating oils on the semimanufacturing scale and under factory conditions. After tests of a number of the most suitable cells for this purpose, we chose a cell with a cathode internally cooled (Fig. 2) by running water, so that it was possible to perform the electrolysis at relatively high current densities without any great increase of the cell temperature. It was found, however, that cells with rotating cathodes have a considerable disadvantage owing to the presence of a sliding contact in the cathode circuit, causing sparking and undesirable loss of potential. To avoid this fault, we designed a cell with a rocking cathode (Fig. 3), to operate at 1500 amp. One such cell is used as the main unit in the section producing metallocolloidal lubricants based on iron organosols.

The results of tests on the above systems are given in Figs. 4 and 5. It is seen in Fig. 4, a and 4, b that the wear of the specimen pairs is proportional to the number of starts of the machine, between 10 and 50 starts per hour. The wear is less with a lubricant containing 2% disperse iron organosol. A decrease of wear was also found when the products of wear were not removed from the friction surface of the machine disk.

The best results were obtained for the powdered metal compact against a disk of globular gray iron. This pair was subjected to further tests in order to study the effects of pressure, sliding velocity, and sliding path on wear. In all these experiments the number of stops and starts of the machine was automatically kept at 20 starts per hour.

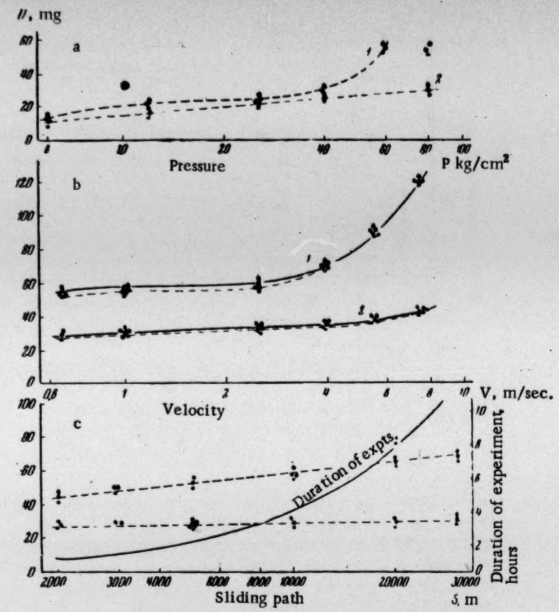

Fig. 5. Effects of pressure (a), sliding velocity (b) and sliding path (c) on wear of powdered metal compacts rubbed against globular gray iron: 1) lubricant – Avtol 10 and Solidol T (1:1); 2) the same, with addition of 2% iron organosol. Continuous lines – with removal; broken lines – without removal of the products of wear.

Test conditions: a) sliding velocity 0.67 m/second; sliding path 5000 m with 20 starts of the machine per hour; b) pressure 60 kg/cm²; sliding velocity 0.67 m/second with 20 starts of the machine per hour.

The results of these investigations, presented in graphical form (Fig. 5) show that addition of 2% iron organosol in Avtol decreases the wear in this pair considerably. Verification of these results under industrial conditions is of considerable interest. A study of the effects of additions of organosols to lubricating oils on the wear resistance of a worm wheel and crown wheel – the principal parts of the reducing gear on the rear platform of a trolley car – was carried out on a special test stand constructed to the design of M. L. Barabash, B. S. Veneraki, A. A. Ruklyadev, G. P. Litvak, and others. The results of these tests, shown in Fig. 6, confirm the great effectiveness of additions of iron and especially of bismuth organosols to lubricants, in lowering wear in these machine parts.

Similar results were obtained in a study of the wear resistance of sliding contacts, widely used in electrical transport (trolley cars, etc.). Experiments showed that additions of iron organosol to the lubricant used for impregnation of the metal compact inserts increase their wear resistance 2 to 3-fold.

Valchuk's investigations [10] have shown that additions of colloidally dispersed metals to MS-20 lubricating oil decrease wear, coefficient of friction, (= C of F) and specific work of friction over a definite range of pressures and friction paths. Some of these results are given in Fig. 7.

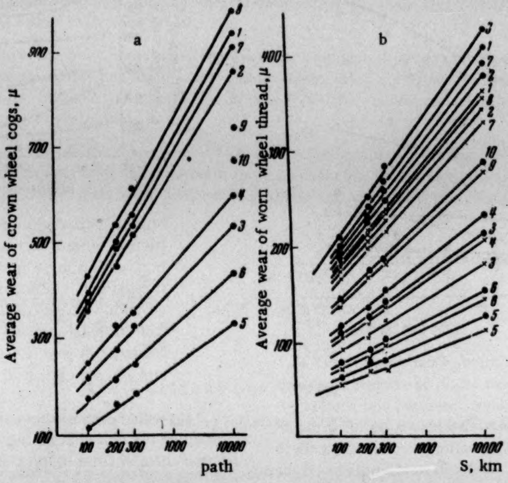

Fig. 6. Effect of type of lubricant on the wear of reducing gear crown wheel cogs a) and of thread of reducing gear worm wheel (b) of a trolley car : 1-6) bronze crown wheel; 7-8) ditto, cast iron; 9-10) Rusanov's data.

1) cylinder oil;
2,10) EZN-2 oil;
3,7) ditto + 0.1% colloidal iron;
4,8) ditto + 0.2% " " ;
5) ditto + 0.25% " bismuth;
6) cylinder oil + 0.25% "
9) EZN-3 oil.

Fig. 7 shows that at a pressure P = 25 kg/cm^2 the least wear was found with the use of MS-20 oil with added colloidal bismuth. Additions of colloidal iron or graphite had less effect. Under a pressure P = 100 kg/cm^2 the least wear is again found with additions of colloidal bismuth. In this case colloidal iron and graphite accelerate running-in.

Variations of the C. of F. of steel 45 against cast iron MSCh 38-60 with different types of lubricants, pressure, and friction path are shown in Fig.8. It is seen that under a pressure P = 25 kg/cm^2 the lowest C. of F. is found for a lubricant containing colloidal iron. It is significant that the C. of F. remains almost unchanged for 200,000 cycles. Additions of colloidal bismuth at this pressure result in a higher C. of F. than is found for oil with added colloidal iron. The situation changes when the pressure is increased to P = 100 kg/cm^2: the lowest C. of F. is found with additions of colloidal bismuth; additions of colloidal iron and graphite give approximately the same C's. of F., somewhat higher than for pure MS-20 oil. It is interesting to note that addition of colloidal graphite to MS-20 oil gives the highest C. of F., higher than for pure MS-20 oil, at P = 100 kg/cm^2. It is also noteworthy that the C. of F. is decreased for the lubricant containing colloidal bismuth when the pressure is raised from 25 to 100 kg/cm^2 .

Fig. 9 shows variations of the specific work of friction for some of the pairs studied (steel 45 on steel 45 and MSCh 38-60 on MSCh 38-60 cast iron) with lubrication by pure MS-20 oil and the same oil with additions of colloidal brass. In the latter case the addition of the colloidal metal decreases the specific work of friction sharply as compared with the value found for pure MS-20 oil, for the whole pressure range from 25 to 112.5 kg/cm^2.

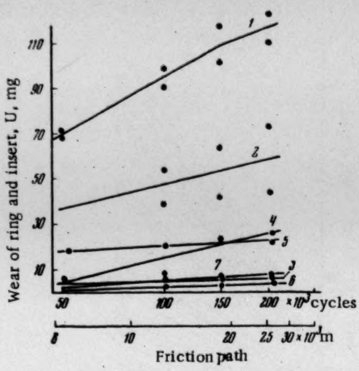

Fig. 7. Variation of the wear of steel 45, rubbed against MSCh 38-60 cast iron, with type of lubricant, pressure, and friction path. Lubrication with MS-20 oil with additions of: 1,4) colloidal iron; 2,5) colloidal graphite; 3,6) colloidal bismuth; 7) pure MS-20 oil; 1-3 and 7) pressure 100 kg/cm²; 4-6) pressure 25 kg/cm².

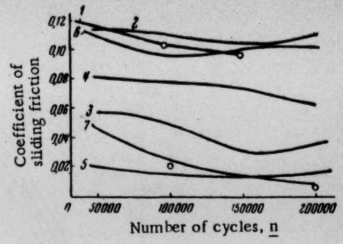

Fig. 8. Variation of the coefficient of friction of steel 45 on MSCh 38-60 cast iron, with type of lubricant, pressure, and friction path. Lubrication with MS-20 oil with additions of: 1,5) colloidal iron; 2,6) colloidal graphite; 3,7) colloidal bismuth; 4) pure MS-20 oil; 1-4) pressure 100 kg/cm²; 5-7) pressure 25 kg/cm².

It should be noted that with the use of a lubricant containing the colloidal metal, the specific work of friction changes little in the course of the tests for both pairs, whereas with the use of pure MS-20 oil in prolonged trials it shows a tendency to continuous increase over more than 500,000 cycles.

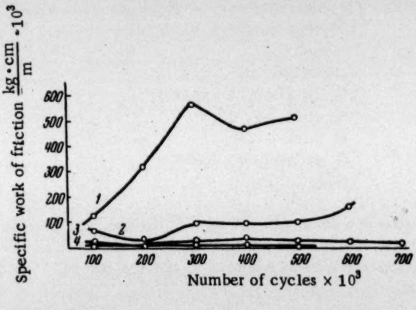

Fig.9. Variation of the specific work of friction of steel 45 on steel 45 (2), and cast iron MSCh 38-60 on cast iron MSCh 38-60 (1,3,4), with type of lubricant, pressure, and friction path. Lubrication with MS-20 oil (1,3); lubrication with MS-20 oil with addition of colloidal brass (2, 4); 1, 2, 4) pressure 112.5 kg/cm²; 3) pressure 25 kg/cm².

SUMMARY

1. The antifriction properties of organosols of iron, bismuth, and other metals in ordinary lubricating oils have been studied, and the technology of their preparation is briefly described.

2. Laboratory tests have shown the high effectiveness of these systems in increasing the wear resistance of the following friction pairs:

a) steel 45 on bronze OTsS; b) steel 45 on globular gray iron; c) powdered iron compact on steel 45; d) powdered iron compact on globular gray iron; e) steel 45 on modified gray iron MSCh 38-60; f) modified gray iron MSCh 38-60 on MSCh 38-60, and others.

3. Tests of these results under operational conditions in a number of points of friction: reducing worm gear in the rear platform of a trolley car, conducting contact inserts, etc., confirmed the suitability of organosols of certain metals (iron, bismuth, and others) for increasing the wear resistance at a number of points under heavy frictional load in modern machines.

We express our gratitude to the management of the Kiev Trolleybus and Trolley Car Administration and of the Dzerzhinsky factory for their cooperation in the tests under operational conditions, for organization of the experimental production of metallocoloidal lubricants, and active participation in work on adoption of the materials.

Institute of General and Inorganic Chemistry
Academy of Sciences, Ukrainian SSR, Kiev
The Kiev Automobile and Road Institute

Received July 4, 1956.

LITERATURE CITED

[1] M.P. Slavyansky and R.N. Bordovsky, in Symposium, "Tin-Free and Low-Tin Babbitts", No. 1 1935; No. 2 1937.

[2] G.A. Kashchenko, Principles of Metallography (Metallurgy Press, Leningrad-Moscow, 1950) p. 640.

[3] M. L. Barabash, in Symposium "Increase of Wear Resistance and Service Life of Machines" (Mashgiz, Kiev 1953) p. 352.

[4] M. L. Barabash, and E. M. Natanson, Authors' Certif. No. 104098.

[5] P.A. Rebinder and N.A. Kalinovskaya, in Symposium "Investigations in the Field of Applied Physical Chemistry of Surface Phenomena"(Izd. AN SSSR, Moscow-Leningrad 1936); P. A. Rebinder and N. N. Petrova, in Symposium "Friction and Wear in Machines" vol. 1, (Izd. AN SSSR, Moscow 1939).

[6] B. V. Deryagin, in Symposium "Friction and Wear in Machines" vol. 4, (Izd. AN SSSR, Moscow -Leningrad, 1951).

[7] A. S. Akhmatov, in Symposium "Friction and Wear in Machines", vol. 3, (Izd. AN SSSR, Moscow -Leningrad, 1949).

[8] E.M. Natanson, Mem. Inst. Chem. Acad. Sci. Ukrainian SSR, 7, 311 1040; Colloid J., 9, 191 1947; Authors' Certif. No. 538521.

[9] E. M. Natanson, Colloid J., 9, 428 1947.

[10] M. L. Barabash, G. I. Valchuk, and E. M. Natanson, Trans. Inst. Constr. Mechanics Acad. Sci. Ukrainian SSR, No. 22 1956.

MODIFICATION OF POLYAMIDE PROPERTIES BY THE INCLUSION METHOD*

A.N. Bykov, M.I. Ivanova and A.B. Pakshver

It was shown in the previous communication [1] that by means of inclusion it is possible to change the properties of high polymers, and in particular to increase their reactivity.

Recently a single paper has been published [2] on the effect of "intermediate swelling" on the sorptive properties of cellulose. The term "intermediate swelling" was applied to preliminary treatment of cellulose with alkali with subsequent replacement of the alkali by water and alcohol, i.e., inclusion. The molecular structure of the cellulose, loosened by swelling in alkali, became fixed by the alcohol. After such treatment the cellulose had a considerably higher sorptive power for dyes and iodine.

The present paper deals with modification of the properties of polyamide fibers by the inclusion method, and in particular the increase of polyamide reactivity in sorption of dyes, acids, and phenol. The effects of the degree of drying of the treated specimen, and of the duration and temperature of the inclusion treatment on fiber reactivity were also studied. The rate of restoration of the polyamide structure after swelling, the equilibrium sorption of phenol after inclusion treatment, and the kinetics of sorption of phenol by treated specimens were studied.

Drawn and undrawn capron yarn was used for the experiments. Benzene was used as the inclusion substance. The results of the inclusion treatment were studied by experiments on the sorption of 0.01 N acetic acid, acid chrome brown dye at pH 3.0, and phenol from solutions of various concentrations, by the polyamide fibers. The amounts of acid, dye, and phenol taken up were determined as follows: for acid, from the decrease of the acid concentration, found by titration with 0.01 N NaOH solution before and after the sorption; for the dye, by means of the Kol-1 M concentration colorimeter; and for phenol, iodometrically by the bromide–bromate method.

The inclusion treatment was performed as follows: a 2.0 g sample of the fiber was treated for 15 minutes with a substance which causes swelling and weakens interaction between the polymer macromolecules. A solution of phenol, at a concentration of 20 g/liter, was used for this purpose. The sample was pressed out after the treatment, and the swelling liquid was replaced by the inclusion substance–benzene. The replacement was effected consecutively in the sequence: phenol → water → alcohol → benzene.

Effect of the degree of drying of the inclusion-treated sample on the reactivity of the polyamide. The sorption of acid and dye by inclusion-treated drawn capron yarn was determined under the following conditions: without drying, after drying in air for 1 hour, after drying in a drying oven for 1 hour, and after drying in a drying oven to constant weight. The oven drying was effected at 60-70°.

The results are given in Table 1 (the sorption of the untreated sample is taken as 100%).

These results show that the drying conditions after the inclusion treatment do not affect the change of reactivity which results from swelling and treatment with the inclusion substance. The samples remain highly reactive even when dried to constant weight.

Effect of duration of inclusion treatment. The results of a study of the effect of duration of the inclusion treatment on the sorption of acid and dye by inclusion-treated capron fiber are given in Table 2.

---

[*] Communication 2 in the series on inclusion processes in high polymers.

TABLE 1

Effect of Degree of Drying of Inclusion-Treated Polyamide on the Sorption of Acid and Dye*

Degree of drying of inclusion-treated polyamide	Sorption of acid, %	Sorption of dye, %
Without drying	149	198
After drying for 1 hour in air	148	192
After drying for 1 hour in drying oven	146	201
After drying to constant weight	151	199

---

* The sorption of acid and dye by an untreated sample was taken as 100%.

TABLE 2

Effect of Duration of Inclusion Treatment on Polyamide Reactivity

Duration of inclusion treatment, min.	Sorption of acid, %	Sorption of dye, %
10	145	198
30	148	198
60	146	198
180	—	193

TABLE 3

Effect of Temperature of Inclusion Treatment on Polyamide Reactivity

Treatment temperature, °C	Sorption of acid, %	Sorption of dye, %
20	158	198
25	158	195
30	159	200
35	159	199
40	160	198

It is seen from Table 2 that increase of the inclusion treatment time does not affect the sorption of acid or dye by the treated fiber. 10 minutes is sufficient for the inclusion substance to penetrate into the loosened structure and fix it.

The reactivity is largely determined by the degree of swelling, i.e., loosening of the intermolecular structure of the polymer, as was shown previously [1].

Effect of temperature of the inclusion treatment. The treatment was carried out at different temperatures in order to find whether the treatment temperature has any effect on the increased reactivity of the polyamide resulting from inclusion treatment (Table 3).

It follows from Table 3 that the temperature, like the duration of the inclusion treatment, does not influence the increased reactivity of the treated polyamide. The inclusion substance is already able at 20° to replace the swelling substance and to fix the structure at an adequate rate.

Restoration of polyamide structure after swelling. Throughout the investigation the treatment was carried out in the following sequence:

phenol ⟶ water ⟶ alcohol ⟶ benzene*

Parallel experiments were carried out on the replacement of water and alcohol by benzene in the sequence:

phenol ⟶ acetone ⟶ benzene

---

* The mechanical properties of treated and untreated fiber samples were determined. The tensile strength decreased by 3% and the elongation at break increased by 3% as the result of the treatment of capron yarn; thus, the mechanical properties changed little.

The purpose of this substitution was the better preservation of the increased reactivity of the inclusion-treated polyamide, since the more rapid the replacement of the swelling substance by the inclusion substance, the higher should be its reactivity. This is confirmed by the data in Tables 4 and 5.

TABLE 4

Influence of Intermediate Steps in Inclusion Treatment on Polyamide Reactivity

Treatment sequence	Sorption of acid, %	Sorption of dye %
Phenol — water — alcohol — — benzene	148	190
Phenol — acetone — benzene	157	202

TABLE 5

Restoration of Polyamide Structure After Swelling

Treatments	Sorption of phenol %	Sorption of dye, %
Swelling in phenol solution for 15 min. without washing	—	231
Swelling for 15 min., 3 water washings in 30 min., drying	158	216
Inclusion treatment and drying	172	228
Inclusion treatment after three days of storage	175	—

The data in Tables 4 and 5 show that the reactivity increases with increasing speed with which the swelling substance is replaced by the inclusion substance. Any additional operations which prolong the interval between the state of maximum loosening of the structure and the instant of fixation decrease fiber reactitivity. The highest reactivity is found when the sorption of the dye takes place immediately after swelling.* Washing with water does not retard the formation of new intermolecular bonds, broken during swelling, and the reactivity decreases. Inclusion treatment with nonpolar or weakly polar liquids halts the formation of intermolecular bonds, fixing the loosened structure, and the reactivity is therefore higher.

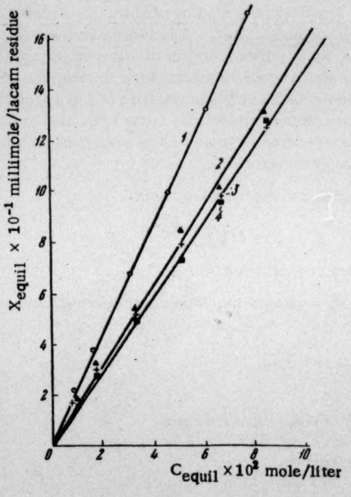

Fig. 1. Sorption isotherms for capron yarn: 1) original undrawn; 2) inclusion-treated drawn; 3) swollen and washed, drawn; 4) original drawn.

The inclusion-treated fibers retain their high reactivity even after three days of storage, i.e., after the inclusion treatment the fixed loosened structure does not become dense again, at least for a considerable time. To determine the degree of change of the polyamide fiber structure by inclusion treatment, experiments were carried out on the equilibrium sorption of phenol and on the kinetics of phenol sorption.

Equilibrium sorption of phenol. For determination of the equilibrium sorption of phenol, 0.5 g samples of polyamide fiber were placed in 25 ml lots of phenol solution, of 1, 2, 4, 6, 8, and 10 g/liter. The flasks were firmly stoppered and held at 20° in a thermostat until equilibrium was reached. The state of equilibrium was indicated by equal values for the sorption by three samples after different times in the thermostat. Sorption isotherms were plotted for the original drawn and undrawn capron yarn, inclusion-treated samples, and fibers swollen and washed in water (Fig. 1).

Fig. 1 shows that undrawn yarn has a higher value than drawn yarn for the equilibrium sorption of phenol; this is explained by differences in their structure. The values for the equilibrium sorption by the original untreated, swollen and washed, and inclusion-treated samples are practically the same. This is explained by the fact that the changes occurring in the structure of the polyamide as the result of inclusion treatment are not as deep as those produced by drawing.

---

* In these conditions the dye is sorbed only by the end groups, while phenol interacts with the amide groups of the polyamide.

The integral heats of solution of untreated and inclusion-treated polyamide fiber samples were also practically equal, confirming the above supposition.

Integral heat of solution in cal./g	
Untreated yarn	14.70
Inclusion-treated yarn	14.66

TABLE 6

Values of k and Diffusion Coefficient D for Different Samples of Polyamide Fibers

Fiber sample	$k\cdot10^2$	$D\cdot10^{12}$
Not treated	1.82	147.0
Swollen and washed	2.58	295.0
Inclusion-treated	4.00	710.0

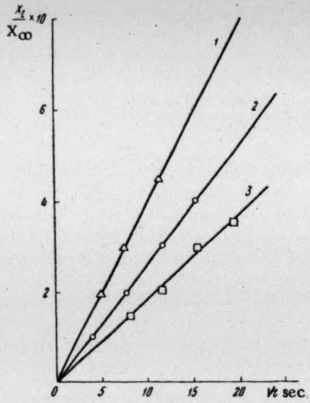

Fig. 2. Kinetics of sorption by capron yarn: 1) inclusion-treated; 2) swollen and washed; 3) original.

Kinetics of the sorption of phenol by inclusion-treated polyamide fiber. The kinetic studies were carried out as follows: samples of drawn capron yarn (0.5 g) after various treatments were immersed in 25 ml of phenol solution at a concentration of 1 g/liter at 20°. The time from the immersion to the extraction of the sample was noted. The amount of sorbed phenol was determined iodometrically.

Fig. 2 shows the relationship

$$x_t/x_\infty = f(\sqrt{t}),$$

where x_t is the sorption of phenol at time t; x_∞ is the sorption at equilibrium.

For diffusion processes, this relationship is represented by a straight line, from the slope of which it is possible to determine the value of k in the equation.

$$x_t/x_\infty = k\sqrt{t}, \quad k = 4/r\sqrt{D/\pi},$$

where r is the fiber radius.
This method was used to calculate the coefficients of diffusion of phenol into the fibers

$$D = k^2r^2\pi/16; \; r = 1{,}5\cdot10^{-3} \text{ cm}.$$

The applicability of this equation to the sorption of phenol by polyamide fibers was demonstrated earlier by Pakshver and Mankash [3], who showed that the sorption of phenol by capron is determined mainly by internal diffusion of phenol into the fiber.

Values of k and the diffusion coefficient D are given in Table 6.

These values show that diffusion of phenol into inclusion-treated yarn proceeds at almost 5 times the rate for the original, untreated yarn. Previous swelling of the polyamide fibers, without fixation of the loosened structure, only doubles the diffusion rate. The inclusion treatment is therefore of special significance in processes the rate of which is determined by internal diffusion, such as dyeing.

SUMMARY

1. The increase of polyamide reactivity produced by inclusion treatment does not depend on the time of drying of the inclusion-treated fiber for given conditions, time, and temperature of the treatment.

2. The more rapid the replacement of the substance causing swelling by the inclusion substance, the higher is the reactivity of the treated fiber.

3. Inclusion treatment results in a several-fold increase of the rate of diffusion of reagents into the fibers, and is especially important for acceleration of processes determined by internal diffusion.

The Ivanovo Institute of Chemical Technology

Received October 13, 1956

LITERATURE CITED

[1] A. N. Bykov and A. B. Pakshver, Colloid J., 19, 27 1957.*

[2] Messik Klara, Szabo Kalman, Faserforshchung und Textiltechnik 2, 89 1956.

[3] A. B. Pakshver and E. K. Mankash, J. Phys. Chem., 25, No. 4, 468 1951; J. Appl. Chem., No. 10, 1200, 1953.

---

* Original Russian pagination. See C. B. translation.

STUDIES OF ELECTROOSMOSIS IN BINARY POWDER MIXTURES CONSISTING OF PARTICLES OF DIFFERENT CHEMICAL NATURE

O.N. Grigorov and K.P. Tikhomolova

Investigations of electroosmosis in complex capillary sustems heterogeneous in composition and structure are of considerable interest in relation to extension of the field of application of this method. In many instances of the use of electroosmosis as a method for determining zeta potential or for removal of water from various comminuted substances one deals with materials containing particles of different chemical nature. The known laws for electroosmotic effects in homogeneous capillary systems may prove inapplicable to systems of this type. Unfortunately, very little information on this subject is available in the literature. The only work known to us on electroosmosis in mixed powder diaphragms consisting of different types of particles is that of Reshetnikov [1]. On the assumption that the electrokinetic potential should be definitely determined by the nature of the solid partition for a solution of given composition and concentration, Reshetnikov derived a number of relationships which aid in determining the specific surfaces of powders composed of different substances. In particular, for determining the specific surface of porous adsorbents, Reshetnikov finds it convenient to determine those surface properties of the adsorbent which would vary, when it was mixed with another adsorbent (with known specific surface), in the composition–property diagram additively with variations of the composition of the binary mixture. The property chosen by Reshetnikov is the electrokinetic potential, which depends on the nature of the surface in interaction with the liquid medium, and is independent of the total surface or mass of the substance. As a result, he derives the following equation for the zeta potential of the mixture:

$$\zeta_m = \frac{\zeta_1 x + \zeta_2 k (1 - x)}{x + k (1 - x)},$$

where $\underline{x}$ and $1 - \underline{x}$ are the fractions of the components present; k is the ratio of the specific surfaces of the components of the mixture; ζ_1 and ζ_2 are the zeta potentials of the individual components.

On the condition that the properties of the mixture are additive, the variation of the zeta potential of a binary mixture with the ratio of the components present should be represented on a composition – zeta potential diagram by a curve which satisfies the condition $\zeta_1 > \zeta_n > \zeta_2$ when k = constant. For the particular case, when k = 1, the curve becomes a straight line. Reshetnikov considers that the above equation can be used to determine the true specific surface of one component if the specific surface of the other is known or can be determined, and also to find the relative specific surface of oen of the components if the specific surface of the other is taken as unity. To confirm his views, Reshetnikov carried out a series of experiments on electroosmosis in mixtures; the substances used were ground quartz sand and Khotkovo tripoli earth roasted at various temperatures. The above equation proved to be valid for this mixture, and the nature of the zeta potential – composition curve was as predicted.

In our opinion, however, Reshetnikov's experiments do not provide a quantitative verification of his theory, since both tripoli and sand particles are irregular in shape, and moreover tripoli has a considerable internal surface owing to the fine pores permeating its particles. In other words, tripoli powder has two types of capillaries: within and between the particles. The conditions for motion of the liquid are different in these types of capillaries, and it is doubtful whether the foregoing theory is applicable in principle to the use of electroosmosis as a method for determining the electrokinetic potential.

To verify this view, we carried out experiments on mixed powders of spherical polystyrene particles in the pure state and with added Sudan III dye. The original powders in 0.01 N KCl solution ($\kappa - 9.3 \cdot 10^{-4}$ $ohm^{-1} \cdot cm^{-1}$) had zeta potentials of 15 mv for pure polystyrene and 33 mv for polystyrene with Sudan III. Fractions of the powders with narrow particle size ranges were obtained by prolonged sedimentation in distilled water; microscopical dispersion analysis was used as a check. The apparatus described in the previous communication [2] was used for the electroosmotic transport determinations. The apparatus was filled as follows; a definite fraction was first settled in it, and the height of its column was measured; it was then covered with another fraction, and the height of the column of the latter was measured. The percentage composition was found from the ratio of the column heights (the cross section of the apparatus was constant). The fractions were then mixed thoroughly and the electroosmotic transport determinations were carried out.

The results for mixtures of different compositions were represented graphically in the form of plots of the zeta potential, calculated by means of the usual Helmholtz-Smoluchowski equation, against the compositions of the binary mixtures.

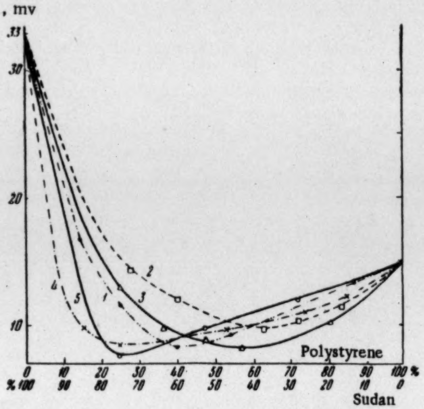

Variation of zeta potential with binary mixture composition

Particle diameter				Particle diameter
1) Polystyrene	8.3	μ +	polystyrene and Sudan	55 μ
2) "	34.1	μ +	" "	55 μ
3) "	53.7	μ +	" "	55 μ
4) "	53.7	μ +	" "	38.5 μ
5) "	53.7	μ +	" "	13 μ

The value of k for a system of spherical particles is easily calculated, as the ratio of the specific surfaces of the spheres in the mixture must be equal to the inverse ratio of their radii. However, if k is calculated from Reshetnikov's equation, not only is there no agreement with the experimental data, but for most values of the zeta potential of the above mixture such calculations cannot be made at all. The graph shows that the zeta potential of the mixture decreases sharply with small additions of the other component, and assumes values smaller than the electrokinetic potential of the less active component, in this instance pure polystyrene.

Comparison of Curves 1 and 2 shows that a decrease of the particle size of the less active component leads to a steeper descent of the curve in the region where the percentage content of the less active component is low. The position of the minima on the curves is also shifted into this region. If the particle size of the more active component is greater than that of the other component, a decrease of the particle size of the former results in a less steep descent of the curve (Curves 4 and 5).

The great discrepancy between the results for powder mixtures with spherical particles and the results which should be obtained on the basis of Reshetnikov's theory shows that this theory is erroneous. The zeta potential of binary mixtures determined by electroosmosis cannot be assumed to be an additive property. The electroosmotic transport effect in a real capillary system is much more complex than Reshetnikov assumes. In considerations of the mechanism of liquid flow in the pore channels of such mixed diaphragms the rate of liquid flow cannot be taken as constant, as the regions over which the flow conditons change are comparable in size to the lengths of the capillaries. Changes in the liquid flow rates along the pore channels, caused by variations in the mosaic structure of the walls, and also by possible changes in the direction of the flow, may result in disturbances of steady laminar flow in such a system, with a resultant decrease of the volume of liquid transported.

Therefore, Reshetnikov's views concerning the applicability of the additivity principle to variations of a definite surface property of a binary mixture of substances in the disperse state are not confirmed by the results of determinations of electroosmotic transport of a liquid.

SUMMARY

1. Electroosmotic transport values through powder diaphragms consisting of mixtures of spherical particles of pure polystyrene and of polystyrene with additions of Sudan III dye, having different zeta potentials, have been determined.

2. The values of the zeta potential plotted as functions of the binary mixture composition have sharply defined minima, owing to deviations from steady laminar flow of the liquid in such mixed systems.

3. The results show that the additivity principle is not applicable to variations of the electrokinetic potential (determined by electroosmosis) as a function of the composition of a binary mixture of particles with charges of different magnitudes.

The A. A. Zhdanov State University, Leningrad

Received November 6, 1956

LITERATURE CITED

[1] M. A. Reshetnikov, Colloid J., 7, 537 1941.

[2] O. N. Grigorov and K. P. Tikhomolova, Colloid J., 19, No. 4, 406 1957.*

---

* Original Russian pagination. See C. B. translation.

THE INFLUENCE OF INTERMOLECULAR INTERACTION ON THE PROPERTIES OF RUBBER SOLUTIONS

V.E. Gul and V.A. Berestnev

As has already been shown, the nature of the intermolecular interaction is one of the basic factors determining a number of properties of rubbers and vulcanizates [1]. The effects of intermolecular action on molecular light scattering in solutions of nitrile rubbers have also been studied [2]. In the present investigation, the influence of intermolecular interaction on the properties of polymer solutions has been studied by viscosimetric and swelling determinations* .

In order to study the influence of intermolecular interaction on the properties of polymers and their solutions, it is necessary to have a series of polymers which differ in the degree of intermolecular interaction but with all the other structural characteristics constant. For example, if the light scattering method is used, the chain length and branching should be the same for all the polymers. If the swelling method is used, the degree of cross linking should be the same in all the polymers. Finally, for viscosimetric determinations the polymers should also have the same molecular weight and degree of branching.

Four types of intermolecular interaction in polymer solutions are usually considered: 1) between regions of the same polymer chains; 2) between individual polymer molecules; 3) between molecules of the polymer and solvent; 4) between the solvent molecules.

The first and third of these types of interaction have the predominant influence on the viscous properties and molecular light scattering of rubber solutions, while in swelling the principal role is played by the second type of interaction. Thus, studies of the properties of polymers by light scattering, viscosimetry, and swelling provide a complete picture of the influence of intermolecular interaction on the properties of polymers and their solutions. Interaction between the solvent molecules does not seem to be significant in investigations like ours, although there are indications [3] that it must be taken into account in some cases.

Guided by the foregoing considerations, we chose standard butadiene – acrylonitrile copolymers (SKN-18, SKN-26, and SKN-40), containing different proportions of acrylonitrile, as the materials, and these were studied by the viscosimetric and swelling methods.

The polymers were purified and fractionated for the viscosimetric determinations. The purification was effected by double reprecipitation by dehydrated methyl alcohol from solutions in benzene, in an atmosphere of pure nitrogen. The fractionation consisted of fractional precipitation of the polymers from benzene solutions with cooling to 0°. The fractions were dried in nitrogen and dissolved in methyl ethyl ketone. These solutions were used for determinations of the molecular weights of the fractions and for the viscosimetric measurements. The molecular weights of the fractions were determined by the light scattering method described previously [2]. The results of these determinations are given in Table 1.

For studying intermolecular interaction by the swelling method, the polymers were converted into unfilled vulcanizates of the following composition (in parts by weight):

Rubber	100
Sulfur	2
Sulfenamide BT	1.8
Zinc oxide	5
Stearic acid	2
Neozone "D"	1

---

* The swelling data were obtained jointly with L. A. Oksentyevich.

The density ρ by the double weighing method, and the equilibrium elasticity modulus E_{∞} by a dynamometer of the Polanyi type, were determined for these vulcanizates, and the molecular weights of the chains M_c were then calculated by means of the equation [4]:

$$M_c = N_a \cdot 3k \cdot T\rho / E_{\infty}, \tag{1}$$

where N_a is the Avogadro number; k is the Boltzmann constant; T is the absolute temperature.

TABLE 1

Molecular Weights of Different Fractions of Nitrile Rubbers

Rubber	Molecular weights of fractions			
	I	II	III	IV
SKN-18	148 000	57 100	19 250	—
SKN-26	—	312 000	87 800	48 200
SKN-40	148 000	100 000	46 700	28 400

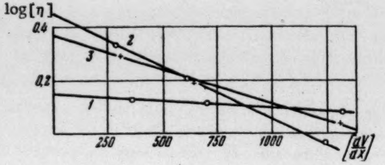

Fig. 1. Variation of intrinsic viscosity with limiting velocity gradient for fractions of similar molecular weight: 1) SKN-18 (M-57,000); 2) SKN-26(M--48,200); 3) SKN-40 (M-46,700)

The greatest deviation between the values of M_c was only 6%. Therefore the degree of cross linking was practically the same in all three vulcanizates; this satisfies the above condition for the applicability of the swelling method.

The viscosimetric determinations were carried out with three efflux velocity gradients in a special capillary viscosimeter [5], the measuring portion of which consisted of three balls arranged vertically. The efflux velocity gradient dv/dx is caluculated by means of the equation

$$\frac{\partial v}{\partial x} = \frac{A}{\eta / d}, \tag{2}$$

where A is a constant found by calculation; η / d is the kinematic viscosity, determined from the equation

$$\eta/d = \alpha\,(t - \beta/dt), \tag{3}$$

where α and β are constants for the apparatus; t is the efflux time.

The constants α and β were found by determinations of the viscosity of water; the efflux time was measured by a seconds clock to an accuracy of 0.2 second. The efflux times were used to calculate the specific viscosity η_{sp}, the reduced viscosity η_{sp}/c, and the velocity gradient. The following relationships were plotted for each ball of the viscosimeter, situated at a definite height:

1) η_{sp}/c against the concentration c. Extrapolation to $c \to 0$ gave the intrinsic viscosity $[\eta]$;

2) logarithm of the efflux velocity gradient against the concentration. This was also extrapolated to $c \to 0$ to determine the efflux velocity gradient at zero concentration [dv/dx].

The values found for $[\eta]$ and [dv/dx] were used to plot the logarithm of the intrinsic viscosity against the velocity gradient. Extrapolation of this graph to zero velocity gradient gave values for the viscosity at zero concentration and zero efflux velocity gradient, i.e., values which were entirely independent of the experimental conditions.

Fig. 1 shows log $[\eta]$ plotted against [dv/dx] for fractions of different nitrile rubbers of approximately the same molecular weight (Table 1). The relationships are linear, and conform to the equation:

$$\lg[\eta] = \lg[\eta]' - B\,[\partial v/\partial x], \tag{4}$$

where log $[\eta]'$ corresponds to the intrinsic viscosity at zero velocity gradient and zero concentration. The coefficient B differs for the different polymers used, and depends on the acrylonitrile content, i.e., on the intermolecular interaction (Table 2), characterized by the square root of the cohesive energy density [6]. The values of the slope factor (B) in Equation (4), the equilibrium swelling (Q), the slope factors of the molecular light scattering curves, taken from an earlier paper [2], and the cohesive energy densities ($\sqrt{E/V}$) for the rubbers studied are given in Table 2. The data in Table 2 show that the factor B does not vary steadily with $\sqrt{E/V}$. The probable reason is that changes of polymer polarity are accompanied by changes in the difference between the nature of intermolecular interaction in the solvent and in the polymer. The less this difference is, the stronger will be the polymer-solvent interaction. With increase of this interaction the polymer molecules become more flexible, the dependence of log $[\eta]$ on $[dv/dx]$ becomes more pronounced, and the absolute value of B in Equation (4) increases. If the polarity of the polymer is increased further, the nature of the interaction between the polymer molecules will change so much that it will again differ from the nature of the interaction between the solvent molecules. This will diminish polymer-solvent interaction and therefore decrease the absolute value of B, as the polymer molecules will become more rigid and will be deformed less by flow of the solution.

TABLE 2

Variation of Slope Factors of Viscosimetric and Light Scattering Curves and Equilibrium Swelling with Degree of Intermolecular Interaction

Polymer	$B \cdot 10^3$	Q in%	$B_\tau \cdot 10^3$	$\sqrt{\frac{F}{V}}$
SKN-18	1.12	210	0,67	8.86
SKN-26	4.89	215	3.86	9.22
SKN-40	3.24	207	1.94	9.52

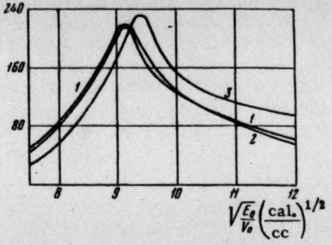

Fig. 2. Variation of degree of swelling of nitrile rubbers with cohesive energy density of the solvent: 1) SKN-18; 2) SKN-26; 3) SKN-40.

To estimate the energy of intermolecular interaction, the equilibrium swelling was found by extrapolation of the plot of the degree of swelling Q against time t to t ⟶ 0. Several solvents with increasing values of cohesive energy density were chosen for these experiments: ethyl ether, n-amyl acetate, n-propyl acetate, butyraldehyde, ethyl acetate, methyl ethyl ketone, ethyl formate; methyl acetate, acetone, and acetonitrile. The values of the cohesive energy density for the polymers studied were at about the middle of this series. The values for the cohesive energy densities of the solvents were taken from Gee's paper [6].

These values were used to plot the equilibrium swelling of the three polymers against the cohesive energy densities of the solvents, as shown in Fig. 2. These smoothed curves were used for determining the degree of swelling of nitrile rubbers in solvents with known values of $\sqrt{E_0/V_0}$. The results show that the maximum is displaced toward lower values of Q and $\sqrt{E_0/V_0}$ with decreasing $\sqrt{E/V}$ for the polymer.

It follows from the data in Table 2 that such properties as viscosity, swelling, and molecular light scattering of divinyl-acrylonitrile polymers in methyl ethyl ketone do not vary smoothly with intermolecular interaction, and vary with the polarity of the rubber, passing through a maximum.

SUMMARY

1. A study has been made of the viscosities of divinyl-acrylonitrile rubber solutions, and of the equilibrium swelling of vulcanizates of these rubbers with the same degree of cross linking, in various solvents.

2. It was found that the viscosity and light scattering characteristics of the solutions, and swelling of the vulcanizates of divinyl-acrylonitrille rubbers, are not steady functions of the degree of intermolecular interaction, represented by the difference of the square roots of the cohesive energy densities of the polymer and the solvent, and pass through a maximum with variations in the polarity of the rubber.

The M. V. Lomonosov Institute of Fine
Chemical Technology Moscow

Received September 5, 1956.

LITERATURE CITED

[1] B. A. Dogadkin and V. E. Gul, Proc. Acad. Sci. USSR, 70, 6, 1017 1950; V. E. Gul, Colloid J., 13, 2, 99 1951; V. E. Gul, T. V. Dorokhina, and B. A. Dogadkin, Colloid J., 13, 5, 339 1951; V. E. Gul, N. Ya. Sidneva, and B. A. Dogadkin, Colloid J., 13, 6, 422 1951.

[2] V. E. Gul and G. S. Klitenik, Colloid J., 16, 3, 37 1954.*

[3] J. G. Kirkwood, R. J. Goldberg, Chem. Phys. 18, 1, 54 1950.

[4] G. M. Bartenev and L. A. Vishnitskaya, J. Tech. Phys., 20, 7, 858 1950.

[5] Krigbaum, P. Flory, J. Pol. Sci. 11, 1, 37 1953.

[6] G. Gee, Chemistry of Large Molecules, Vol. 1, (IL, 1948).

---

* Original Russian pagination. See C. B. translation.

THE POSSIBILITY OF SURFACE ACTIVATION AND PASSIVATION OF NUCLEI IN WATER VAPOR CONDENSATION

G.I. Izmailova, P.S. Prokhorov, and B.V. Deryagin

It is known that atmospheric condensation nuclei play the principal role in processes of cloud and mist formation, and therefore in precipitation. By artificially introducing hygroscopic $CaCl_2$ nuclei into clouds, Fedoteev succeeded, for the first time in history, in inducing artificial precipitation. Studies of the activity of different kinds of atmospheric condensation nuclei should assist in the development of the theory of cloud formation and precipitation. It appears even more attractive to develop means for varying the activity, and hence the "activity spectrum", of atmospheric condensation nuclei, as this may make it possible to influence the dispersivity of the forming cloud, and hence the precipitation conditions.

For a study of this range of problems, we began by developing a method for estimation of the activity of condensation nuclei by measurement of the degree of supersaturation at which the condensation nuclei "appear", i.e., can be observed visually. This degree of supersaturation can be termed the "nominal critical supersaturation", as it depends to a considerable extent on the experimental and observation conditions*.

The most convenient of the very few existing methods for determining the critical supersaturation is Amelin's flow method [2]. The principle of this method is that when a free vapor-air stream mixes with the surrounding air (or in general, when any gases differing considerably in temperature and humidity are mixed), there is a definite optimum mixing ratio n, which depends only on the temperatures and humidities of the mixing gases, and which corresponds to the maximum supersaturation given by:

$$S = \frac{p_1 + p_2 bn}{(1 + bn)\, p_s}, \tag{1}$$

where p_1 and p_2 are the water vapor pressures in the stream and the air volume; b is the ratio of the molecular weights of the vapor-air mixture in the stream and the volume, M_1/M_2; n is the mixing ratio, equal to the ratio of the weights of the mixing volumes, g_2/g_1; p_s is the saturated vapor pressure of water at the temperature of mixing.

By gradually varying the temperature of the stream and recording the temperatures and moisture contents of the mixing volumes at the instant of mist formation, it is possible to use the above equation to calculate the corresponding supersaturation, which is also the critical value. If condensation could be observed at the first instant of new phase formation, this method would give quite exact results. In fact, however, there is some lag in recording the start of condensation. It may happen that before this occurs some droplets will leave the zone of maxium supersaturation, at which condensation began, and will start to evaporate; this will evidently give a high value for the measured critical supersaturation. This disadvantage may be avoided by mixing two streams, with a volume flow ratio exactly equal to the optimum mixing ratio n_{opt} which gives the maximum supersaturation S_{max} at the given temperatures and moisture contents of the streams. In such a case, if the corresponding S_{max} is equal to the critical supersaturation for the condensation nuclei introduced into one of the streams, droplet growth will not cease even after complete mixing, once it has started. At the same time there is no longer any risk that the measured critical supersaturation is below the true value, as it is impossible for a region to be formed in the mixing zone where the supersaturation is greater than it would be on complete mixing, and accordingly greater than S_{max}. To diminish errors due to condensation of moisture on the walls, the mixing streams can be directed countercurrent, as the supersaturation zone is then formed in the central region of the cell.

---

* It may be noted, however, that the theoretical value of the critical supersaturation in the theories of Volmer, Beaker and Doring, Zeldovich, Frenkel [1] and others also depends on an arbitrary boundary value of the rate of formation of viable nuclei, although in practice this uncertainty is not very important.

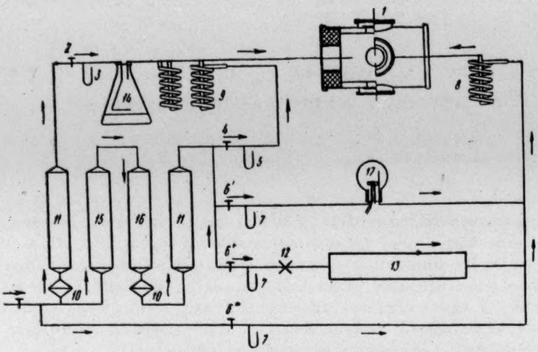

Fig. 1. Diagram of apparatus for measurement of critical supersaturation: 1) cell; 2-4-6^{I}-6^{II}-6^{III}) micro-taps; 3-5-7) flow meters; 8-9) thermostats; 10) glass gas filter; 11) filter filled with absorbed degreased cotton wool; 12) atomizer; 13) oven with drying agent; 14) humidifier for hot stream; 15) $CaCl_2$ column; 16) activated alumina column; 17) device for sublimated nuclei.

The apparatus is shown schematically in Fig. 1. Two streams are mixed in the cell 1; one is a hot stream of variable moisture content, passing through the micro-taps 2 and 4, and flow meters 3 and 5, where the flow rate is measured. The second is a dry cold stream, with condensation nuclei introduced into it; this passes through the micro-tap 6 and is measured in the flow meter 7. The temperature of the cold stream is regulated by means of the thermostat 8. The hot stream is humidified in the evaporator 14. Condensation nuclei are fed into the cold stream as required; atmospheric nuclei (micro-tap 6^{III}), by sublimation (micro-tap 6^{I}), and from a solution atomized in the atomizer 12 (micro-tap 6^{II}), the solvent being absorbed in the drying oven 13. The air is filtered through glass and cotton wool gas filters. Moisture is absorbed from the air in calcium chloride and activated alumina to a dew point ≈ - 50°.

The determination procedure is as follows: n_{opt} * corresponding to the given characteristics of the cold and hot streams is calculated. The cold dry stream containing the condensation nuclei, and the warm stream of variable humidity, are then fed into the cell in a ratio equal to n_{opt}. The moisture content of the warm stream is then smoothly varied by addition of a stream saturated with water vapor to it, at a constant total flow rate. At the instant of visible mist formation in the cell the moisture content of the warm stream and the temperature of the mixture are recorded, and the results are used to calculate the critical supersaturation from Equation (1).

It should be noted that n_{opt} does not remain constant with increase of the moisture content of the warm stream, as the specific heat and molecular weight vary accordingly. However, it is easy to make the appropriate corrections.

---

* If the first derivative of S with respect to n is equated to zero and the equation solved for n, we have:

where $a = \frac{C_2}{C_1}$ is the specific heat ratio; L is the latent heat of vaporization in cal./g.

TABLE 1

Critical Supersaturation (S_c) as a Function of the Size of the Condensation Nuclei

Weight concentration of solution in g per 100 g of solution	Area of rectangle, $cm^2 \cdot 28{,}000$	Nominal radius, cm	S_c, experimental	S_c' theoretical, calculated by[2]
0.3	0.96	$2 \cdot 10^{-5}$	0.84	1.000
$0.3 \cdot 10^{-2}$	0.34	$1 \cdot 10^{-5}$	0.92	1.001
$0.3 \cdot 10^{-4}$	0.1	$6 \cdot 10^{-6}$	1.1	1.002
$0.3 \cdot 10^{-6}$	0.04	$3.6 \cdot 10^{-6}$	1.33	1.005

TABLE 2

Critical Supersaturation for NaCl Nuclei Modified by Vapors of Surface Active Substances

Surface active substance	Critical supersaturation			$\frac{\bar{S}_c^{\times}}{\bar{S}_c}$
	before modification $\bar{S}_c$	modified $\bar{S}_c^{\times}$	after modification $\bar{S}_c$	
Formaldehyde	1.6	2.38	1.77	1.4
$Si(C_2H_5)_2$	1.34	1.25	1.38	0.9
$[(C_2H_5)_3Si]_2O$	1.33	1.15	1.33	0.82
Acetone	1.16	0.9	1.16	0.8
Isoamyl alcohol	1.47	1.09	1.47	0.7

The method described above was used to determine the critical supersaturation for small (average radius $r = 3.6 \cdot 10^{-6}$ cm) crystals of sodium chloride as a function of crystal size. A solution of NaCl in distilled water was atomized by a dry filtered stream of air in a glass atomizer. The resultant fairly monodisperse mist, with droplet size $\sim 0.1\,\mu$ was first passed through a heated tube, where the drops dried and the water vapor was then absorbed in phosphoric anhydride, while the air stream containing the crystals was cooled in a thermostat and entered the cell. The crystal size can be regulated by variation of the solution concentration. At the entry into the cell the crystals were caught on a gauze and then photographed under the electron microscope after chrome shadowing*. The photographs were used to determine the crystal size in mutually perpendicular directions, and the nominal radius of a nucleus was calculated from the average of several such measurements. Nuclei consisting of silica were studied next. The starting material was silica powder of the following chemical composition:

$$Na_2CO_3 \text{ not } > 2\%$$
$$CaCO_3 \text{ not } > 8\%$$
$$SiO_2 \text{ and } H_2O \text{ not } < 90\%$$

The specific surface of the powder was 100 m^2/g.

The SiO_2 nuclei were fed in by the same procedure as the NaCl nuclei, the only difference being that a suspension of SiO_2 in distilled water was atomized rather than a solution.

The results obtained for NaCl nuclei are given in Table 1.

The activity of the condensation nuclei – NaCl crystals – was modified by the action of vapors of certain surface active substances. To a stream containing the nuclei a small amount of vapors of the surface active substances. To a stream containing the nuclei a small amount of vapors of the surface active substances was added, penetrating into the system by diffusion from a vessel connected by a tap, and the surface active substances were adsorbed on the nuclei. The accuracy of the determinations was checked by comparison of the values for the critical supersaturation at the nuclei before introduction of the vapors, and after their supply had been cut off. If these values agreed, there were no errors in the determination. The results are given in Table 2.

---

* The electron micrographs were kindly taken by Yu. M. Polukarov, to whom we express our gratitude.

Silica was chosen as a material for study as its surface properties can be easily modified by heat treatment [3]. The SiO_2 nuclei were modified in a tubular quartz furnace through which they were passed, and the temperature of which could be varied by variation of the heater voltage. The treatment time was 2-3 minutes. The temperature, which was varied between 120 and 732°, was measured by means of a thermocouple placed in the aerosol stream at the furnace exit.

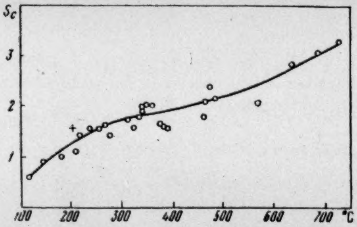

Fig. 2. Variation of the critical supersaturation for SiO_2 condensation nuclei with the temperature of heat treatment.

The relationship obtained between S_c for water vapor and the temperature of heat treatment of the condensation nuclei is shown graphically in Fig. 2. To test whether the thermal modification was reversible, SiO_2 powder was heated in a muffle furnace at 750° for 4 hours, cooled, introduced into the cell by the usual method, and S_c for it was determined (the result is indicated on the graph by a cross). It is seen that the thermal modification is reversible, the initial surface properties being restored.

DISCUSSION OF RESULTS

Our experimental values of S_c for different sizes of the NaCl nuclei were compared with theoretical values of S_c' calculated with the influence of curvature (Kelvin) and of vapor pressure variations over solutions of variable concentrations (Raoult) taken into account [4]. The values found for S_c' are given in Table 1.

The experimental values for condensation nuclei 0.1-0.2 μ in size are rather lower than the calculated values, which is probably because the large nuclei can reach 0.4 μ in diameter, which corresponds to the threshold of visibility by equilibrium humidification before the maximum on the supersaturation – droplet size curve is reached.

For nuclei of the order of 10^{-6}cm the deviations between the experimental and theoretical values are considerable. The probable reason for this discrepancy is that the theoretical calculations are primarily based on the assumption that the condensation process is fairly slow, whereas in our case the process is very rapid. In consequence, our measured values must be regarded as nominal supersaturation.

Calculations show that in our apparatus the droplets should grow to 0.4μ in 0.5 second, and the mist formed can then be observed visually. It is interesting to compare our values of S_c for NaCl with previously published data [5].

In the investigation cited, the authors used a diffusion chamber and obtained a value of 1.09-1.2 for S_c for NaCl nuclei with minimum diameter 10^{-6} cm, which is fairly close to our value for $6 \cdot 10^{-6}$ cm nuclei (see Table 1). However, the kinetic factor to which reference was made earlier should have an effect in this case also.

The results of experiments on modification of the condensation nuclei, either by vapors of surface active substances in the case of NaCl, or by heat treatment, show that it is possible in practice to vary the measured nominal critical supersaturation at condensation nuclei.

The dehydration mechanism of the SiO_2 surface (as a result of modification) probably involves impedance to the formation of donor-acceptor bonds between molecules on the surface and molecules of condensing water [3], which evidently influences the condensation process. The results obtained for NaCl nuclei modified by surface active vapors indicate that the surface of the condensation nuclei is changed owing to formation of adsorption layers. The formation of adsorption layers is accompanied by a change in the interaction between the surfaces of the condensation nuclei and the molecules of condensing water, i.e., in the general case the hydrophilic nature of the surface is changed and it may become hydrophobic.

SUMMARY

1. It is shown that it is possible to vary the "activity" of NaCl and SiO_2 condensation nuclei toward water vapor, as shown by increase or decrease of the nominal critical supersaturation S_c.

2. The change of "activity" can be effected by adsorption of vapors of surface active substances on the nuclei in the case of NaCl, or by dehydration in the case of SiO_2.

3. The mechanism of this effect probably consists of modification of the surface properties of the condensation nuclei, leading to changes in the condensation rate owing to variation of the accommodation coefficient.

Institute of Physical Chemistry Academy of Sciences
USSR Moscow

Received January 24, 1957

LITERATURE CITED

[1] M. Volmer, Kinetic der Phasenbildung, Leipzig, 1939; Beaker, Doring., Ann. Phys. 24, 719 1935; Ya. B. Zeldovich, J. Exp. Theoret. Phys., 12, 525 1942; Ya. I. Frenkel, The Kinetic Theory of Liquids (Izd. AN SSSR 1945).

[2] A. G. Amelin, Theoretical Principles of Mist Formation in Chemical Industries (Goskhimizdat, 1951).

[3] S. P. Zhdanov, Proc. Acad. Sci. USSR, 68, 99; 100, 1115 1955.

[4] W. E. Howell, J. Meteorol., 6, 134-149 1949; B. V. Kiryukhin, Trans. Chief Geophys. Observatory, No. 24, 86 1950; B. V. Deryagin, S. S. Dukhin, M. L. Mikelson, and V. I. Kagener, The Struggle Against Silicosis (Izd. AN SSSR 1955) p. 22.

[5] D. Schiff, H. J. Schilf, P. R. Gendron, Canad. J. Chem. 31, No. 11, 1108 1953.

ADSORPTION OF WATER VAPOR BY SILICA AND HYDRATION OF ITS SURFACE*

A.V. Kiselev and G.G. Muttik

Investigations of the adsorptive properties of coarsely porous silica gels and various specimens of quartz show that the adsorptive properties per unit surface of these adsorbents are similar [2-7]. This is the consequence of the similarity of the chemical surface structure of these substances if their degrees of hydration are similar. Differences in the packing of the silicon-oxygen tetrahedra in the amorphous particles of the silica gel skeleton and in quartz crystals have no significant influence on the adsorptive properties. Silica xerogels, since they originate from hydrogels, carry silicic acid hydroxyls on the surface. These hydroxyls can be removed by calcination [8, 9]. Hydration of the surface of calcined silica gels again leads to formation of surface hydroxyls, bound to the skeleton by valency bonds [10-12]. These acid hydroxyl groups act as electron acceptor centers of the surface, and may form donor-acceptor bonds with molecules having electron donor properties [5, 7, 13, 14]; water molecules are bound to the surface hydroxyl groups by hydrogen bonds, and these are the bonds which primarily determine adsorption on hydrated silica gel and quartz surfaces. It is therefore of interest to study the concentration of hydroxyl groups on silica gel surfaces, and the bonds between adsorbed molecules and these groups. In adsorption of water vapor, each molecule can be bound to the surface hydroxyls by means of one or of two hydrogen bonds. Electrostatic and dispersional interaction also depend on the degree of hydration, as the electostatic field of the surface and the distances between the adsorbed molecules and the atoms of the lattice vary with changes in the concentration of the hydroxyl groups. On the other hand, the view has been put forward that other adsorption centers are present on silica gels, differing from hydroxyl groups by having considerably higher activity in adsorption of water and alcohol vapors [15].

Most workers who studied adsorption on silica gel and quartz used adsorbents with surfaces hydrated to various extents. In the case of silica gels, the surface hydration depends on the method used for their preparations from hydrogels; the various specimens of quartz, rock crystal, porous glass, and other silica specimens were usually subjected to prolonged contact with water and their surfaces were hydrated. However, in most of the cases described in the literature** the adsorbents were heated in vacuum at 150-500°, and were thereby dehydrated to various extents; this affected the adsorptive surface properties. It has been established [10-12] that after adsorption of water vapor followed by evacuation at temperatures not higher than 200° the surfaces of different specimens of silica gel and quartz are hydrated to approximately the same extent. The isotherms for adsorption of water vapor per unit area of such similar surfaces coincide [5, 11, 12]. The surfaces of such specimens are almost completely hydrated, i.e., all the silicon atoms on the surfaces are bound to hydroxyl groups. Heating in a vacuum at 200-300° has little effect on the degree of surface hydration. At maximum hydration, all the silicon atoms emerging on the surface are bound with one or two hydroxyl groups [5, 12].

In the present investigation the adsorption of water vapor was studied on a silica specimen which did not come into contact with water during preparation, and which was therefore not so strongly hydrated as silica gels.

---

*A preliminary communication of the results of this investigation was made at the Jubilee Conference of the Moscow State University, April 20, 1955 [1].

** See [11, 12] for the literature.

Specimens and Determinations

Silica. The starting specimen of silica was prepared by G. V. Vinogradov, by combustion of organosilicon compounds; to remove residual carbon the specimen was heated at 900-1000° for several hours* ; its specific surface was 185 m^2/g [16]. A part of the original specimen was covered with water and dried at 90-100° after 6.5 months of exposure to water. The specific surface of this hydrated specimen, also determined by nitrogen adsorption, was 135 m^2/g** . Investigations of the adsorption-desorption isotherms for benzene vapor on these specimens showed that they are heterogeneously porous [19]; combustion and calcination resulted in irregular sintering, but the surfaces of the specimens were quite accessible even to benzene molecules. The hydroxyl group contents on the surfaces of the evacuated specimens were determined from the weight loss after calcination at 1100°. For the original specimen, evacuated at 200°, the hydroxyl group content was 3 micromoles/ m^2, while for the specimen hydrated by exposure to water and then evacuated at 115° it was 11 micromoles/ m^2. This latter value is close to the limiting hydroxyl content on silica surfaces, which is ~ 13 micromoles/ m^2 [12].

Adsorption determinations. The choice of the method of adsorption determination was guided by the following considerations: 1) it was necessary to determine with fair accuracy very small values of adsorption with small degrees of surface filling, especially on dehydrated specimens; 2) it was also necessary to determine very large values of adsorption on the same specimens at high relative pressures of water vapor; 3) it was very desirable to follow the course of slow hydration of the surface of the original specimen. To satisfy these requirements, we used an automatic recording vacuum balance specially designed for such determinations [20]. To ensure a fairly large total surface of the specimen, the balance takes loads up to 10 g; the weighing range is 1.2 g; the sensitivity over the whole weighing range is at least $1 \cdot 10^{-4}$ g. The zero position should not be appreciably displaced during an adsorption – desorption experiment, which usually lasted several months.***

A diagram of the vacuum adsorption apparatus with the recording balance, used in our investigation, is shown in Fig. 1.

The specimen is placed in the bucket 1, suspended from the front end of the beam 2 by means of a tungsten wire 18 μ in diameter. The beam is suspended, from similar vertical tungsten wires 3, inside the glass T-tube 4. The opposite end of the beam carries an iron core 5. By varying the current strength in the electromagnet 6 by means of the rheostats R_1 and R_2 the beam may be brought into the horizontal position. Changes in the weight of the specimen can be found from changes in the current strength, measured by the milliammeter 7. The horizontal position of the beam is indicated by the position of the end of the pointer 8. By varying the current in the electromagnet 6 between 0 and 30 ma, an increase of 0.1 g in the weight of the specimen can be compensated; if the weight increase is greater than this, the rider 9 is moved along the notches of the beam with the aid of an auxiliary magnet****. For each of the 12 positions of the rider, a calibration curve is plotted showing the current strength in the coil of the electromagnet 6 as a function of the load on the front end of the beam; the calibration is carried out with the aid of microanalytical weights and by an aerostatic method [25].

Changes in the weight of the specimen can be recorded automatically. A light beam from the source 10 is directed on the mirror 11, attached to the beam. The reflected light is distributed between the photocells of the differential photorelay***** in a manner which depends on the deflection of the beam; the amplifier 13 receives a positive or negative signal, and the pen of the recording device moves to the right or left, simultaneously displacing the sliding contact of the rheostat. As a result the current strength in the electromagnet 6 is altered, and the beam again assumes the horizontal position*.

---

* We take this opportunity to thank G. V. Vinogradov for supplying this specimen.

** The decrease of specific surface after exposure to water is probably the consequence of reconstruction of the silica particles owing to solution of the smallest particles, which comprise an appreciable fraction of the total surface. A similar change of specific surface on treatment of xerogels by hot water vapor occurs very rapidly (see [17, 18]).

*** The vacuum balances described in the literature do not satisfy all the above requirements. The most sensitive vacuum balances [21-23] can only take considerably smaller loads, and their weighing range is considerably narrower. Gregg's balance [24] is free from these faults, but is too complicated.

**** Displacement of the rider by one notch corresponds to 0.1 g change in weight.

***** For the photorelay circuit, see [26].

The glass T-tube of the balance is separated from the ampoule containing the adsorbate by an electromagnetic valve 14, which admits the adsorbate vapor into the working part of the apparatus. The construction of the valve is shown in Fig. 1. A moving iron core 23 with a Teflon lining is pressed against the central opening by the spring 24 – in the normal position the valve is shut. If a current is passed through the electromagnet 25, the core 23 is attracted to the stationary part 26, and the tubes 27 become connected. The coil of the electromagnet is enclosed in the iron yoke 28 in order to increase the magnetic flux in the gap between cores 23 and 26.

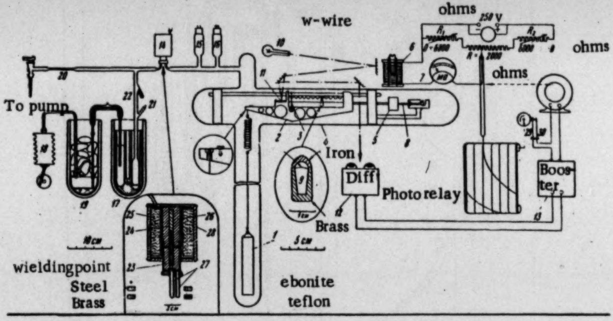

Fig. 1. General diagram of apparatus: 1) specimen; 2) balance beam; 3) tungsten suspensions; 4) glass T-tube; 5) iron core; 6) electromagnet; 7) milliammeter of 0.1 class; 8) pointer; 9) rider; 10) light source; 11) beam mirror; 12) photorelay; 13) booster for recording EPP-09 potentiometer; 14) electromagnetic valve; 15) tube of LT-1 thermocouple vacuum gauge; 16) tube of LM-2 ionization manometer; 17) aluminum block; 18) pneumatic pump; 19) cold storage cell of cryostat; 20) capillary tube; 21) branch tube; 22) glass membrane; 23) core of valve; 24) spiral spring; 25) electromagnet winding (wire 0.3 mm in diameter); 26) stationary iron core of valve; 27) outlet tubes; 28) yoke of electromagnet; 29, 30) cut-out contacts.

The vacuum is measured during evacuation of the adsorbent by means of a Pirani manometer 15 and an ionization manometer 16. The ampoule with the absorbent is placed in a K-1 cryostat**. The aluminum block 17 of the cryostat is cooled at a temperature of +20 to -60° by methanol, which is pumped by the pump 18 from the cold storage cell 19, where it is cooled by solid carbon dioxide. At lower temperatures, liquid nitrogen is used for cooling. In such cases the cold storage cell 19 is replaced by a Dewar flask (Fig. 2) 1 liter in capacity. The block 17 is then cooled by liquid nitrogen entering along the tube 2, as in Henning's cryostat [28, 29]. Instead of a contact thermometer, a resistance thermometer 3, which is an arm of a Wheatstone bridge supplied by an alternating current at 2 v through the transformer 12, is inserted into the block 17. The disbalance potential is fed from the bridge to the booster 4 of an EPD-17 recording potentiometer***. A variable resistance R_1 (type SP-2) and a mercury valve 5 are attached along the axis of the recording instrument slide wire. The cryostat is regulated to the required temperature by means of the resistance box R_2. If the temperature of the block 17 is higher than required, the bridge is out of balance, and the recorder motor closes the valve 5.

---

* For a more detailed description of the vacuum balance, see [20].

** Described in [27], manufactured by the "Platinopribor" works.

*** EPD-07 or EPP-09 may be used, or balanced bridges with electronic boosters.

Evaporating nitrogen cannot then escape from the vessel 7 and liquid nitrogen therefore passes along the tube 2 into the block 17 and cools it. When the block has reached the required temperature, the sign of disbalance in the bridge changes, the motor opens the valve 5, and flow of nitrogen into the block 17 stops. This low-temperature cryostat was used at temperatures below – 60°, down to – 195°, with a thermostatic accuracy of ± 1°.

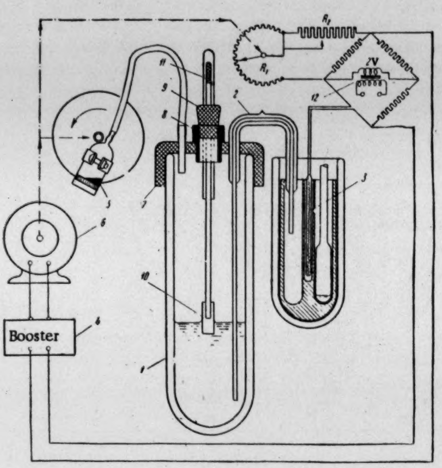

Fig. 2. Cryostat for temperatures between – 60 and – 195°: 1) cold storage cell with liquid nitrogen; 2) siphon tube; 3) resistance thermometer (nickel wire 0.07 mm in diameter); 4) booster of EPD-17 recording instrument; 5) mercury valve with porous glass partition (No.2 filter); 6) motor; 7) rubber cover; 8) tube for adding nitrogen; 9) bung; 10) float; 11) nitrogen level indicator; 12) transformer.

By keeping the block 17 at the required temperature by means of one of these cryostats, the desired vapor pressure of the adsorbate can be maintained in the apparatus. The apparatus therefore has no greased taps (the constriction 20 is sealed off after evacuation of the apparatus), mercury seals, or mercury manometers, so that it is possible to work with organic vapors soluble in vacuum grease, and no mercury vapor is present.

The evacuation is effected by an MM-40A oil diffusion pump and a VN-494 rotary pump. The apparatus was separated from the pumps by a trap with liquid nitrogen. Dissolved gases were removed from the adsorbate through the side tube 21 in a separate apparatus. After evacuation of the apparatus the ampoule membrane 22 was broken, and the adsorbate vapor was able to enter the intermediate part of the apparatus. A thermostat was placed under the lower end of the glass T-tube 4 (see Fig. 1), by means of which the specimen could be thermostatically controlled between 10 and 450° to an accuracy of ± 0.1°.

DISCUSSION OF RESULTS

Adsorption of water vapor on the original silica specimen. Fig. 3 shows the isotherm for adsorption of water vapor on the original specimen, after evacuation at $2\text{–}5 \cdot 10^{-5}$ mm Hg and 200° for 20 hours. The weight loss was small ($<$ 3 mg per 1 g silica) although the original specimen was exposed to air after preparation.

Despite the large specific surface of the original specimen (185 m^2/g), the adsorption is very slight in the initial part of the isotherm, indicating that the activity of this silica specimen in adsorption of water vapor

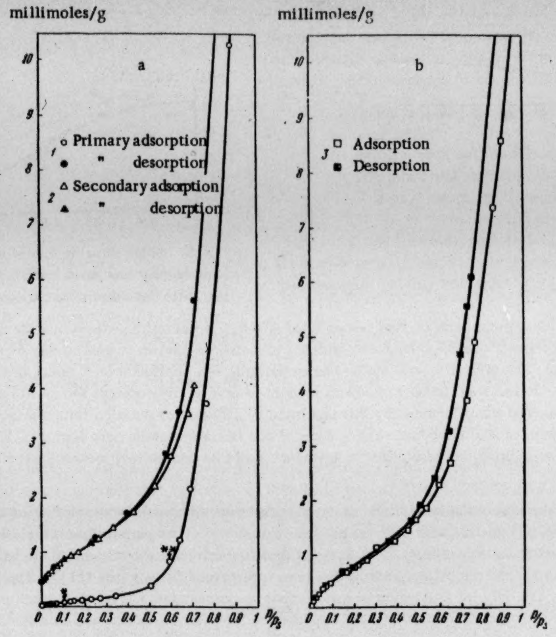

Fig. 3. Isotherms for adsorption and desorption of water vapor: 1) on the original specimen; 2) specimen hydrated in water vapor; 3) specimen hydrated in liquid water.

is very low in comparison with silica gels. At a relative water vapor pressure $p/p_s = 0.2$ the specimen adsorbed only 0.6 micromole/m^2, whereas a silica gel with a hydrated surface at the same p/p_s adsorbed 6.5 micromoles/m^2, [11]. The initial region of the isotherm for this specimen is concave; equilibrium was established rapidly (within 1-2 hours) in this region. This indicates that the interaction is confined to physical adsorption of water vapor. However, at relative pressure of 0.4-0.6 and over, the amount of adsorbed water increased sharply, and equilibrium at each point of this region of the isotherm was only reached after 30-60 hours*. Fig. 4 shows the corresponding kinetic curves for the original specimen at $p/p_s \approx 0.1$ and at $p/p_s \approx 0.6$. The nature of the curves in Figs. 3 and 4 indicates that in the region of high p/p_s slow chemisorption leading to hydration of the silica surface takes place in the original specimen, in addition to capillary condensation and physical adsorption.

2.5 months was necessary for studying the region of the isotherm in the p/p_s range between 0.4 and 0.95. Thus for ~ 1800 hours the specimen was in an atmosphere of water vapor at relative pressures between 0.4 and 0.95. Total saturation ($p/p_s = 1.0$) was not reached in this experiment, but despite this, as Fig. 5 shows, the desorption and adsorption branches did not coincide down to the lowest water vapor pressures. After evacuation at 25° for 2 weeks, ~ 0.42 micromole of water per 1 g, or 1.8 micromole/m^2, remained bound with the silica surface. The secondary adsorption branch determined after this coincided with the desorption branch up to $p/p_s = 0.3$ (to the start of capillary condensation); it resembles in shape the usual convex isotherm for adsorption of water vapor on silica gels and quartz. Thus, after prolonged exposure of the specimen to water vapor at high values of p/p_s, when a liquid water film accelerating hydration was formed on the surface, the isotherm became reversible.

---

* In analogous cases capillary condensation on silica gels with hydrated surfaces is much more rapid.

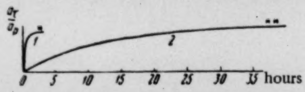

Fig. 4. Comparison of the kinetics of water vapor adsorption at low and high relative pressures. The curves lead to the equilibrium points marked by asterisks in Fig. 3: 1) one asterisk; 2) two asterisks.

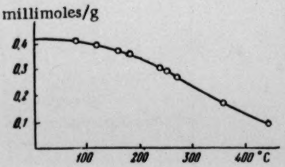

Fig. 5. Graph showing loss of weight on heating of a specimen hydrated in vapor, i.e., after an adsorption-desorption cycle.

After a second adsorption was carried out up to $p/p_s = 0.7$, a desorption experiment demonstrated the reversibility of the isotherm. The specimen was further evacuated on heating consecutively to temperatures of 80, 120, 160, 180, 240, 250, 270, 360 and 450°. The evacuation was continued for 6 hours at each temperature, with 20 hours at 450°. In this way the specimen was brought to practically constant weight at each temperature. Fig. 5 shows the amounts of water retained by this specimen at different evacuation temperatures. It is seen that heating in a vacuum to 200° dehydrates the surface of this silica specimen only slightly. The water adsorbed by the original specimen during the adsorption experiment cannot be completely removed even by heating to 450° in vacuum.

The fact that the desorption branch and the primary adsorption branch for adsorption of water vapor do not coincide in the initial region of the isotherm has been noted earlier for porous glasses and silica gels heated to 300° before the adsorption experiments. However, in these experiments the amount of irreversibly bound water was relatively small and the primary adsorption branch remained convex (see [11]). The primary adsorption isotherm was concave only for adsorption of water vapor by porous glass and silica gel heated at 650° in vacuum [12, 30]. In such cases the action of capillary-condensed water on the surface freshly dehydrated by heating also restored the original convex form of the isotherm, and ~ 5 micromoles/ m² of water again remained irreversibly bound to the surface.

In our case the adsorption took place on a specimen which was still less hydrated, and therefore the amount of irreversibly bound water proved very large.

Adsorption of water vapor on a hydrated silica specimen. Isotherms for adsorption and desorption of water vapor on a silica specimen kept under water for 6.5 months are given in Fig. 3, b. The specimen was evacuated at 115° before the experiment. The initial region of the isotherm for primary adsorption of water vapor is convex in this instance, and differs sharply in this respect from the concave initial region of the isotherm for the original specimen (Fig. 3, a). The isotherm in Fig. 3, b resembles the isotherms for adsorption of water vapor on silica gels [11]. The secondary adsorption branch is close to the primary adsorption branch.

The initial regions of the adsorption isotherms, calculated per unit surface, are compared in Fig. 6. These graphs show that hydration of the original sample during sorption of water vapor (see Fig. 3, a) increased 6-fold its adsorptive activity at $p/p_s = 0.1$, while exposure to water produced an 8-fold increase. Comparison with the isotherm for adsorption of water vapor in silica gels (curve without points in Fig. 6 [11]) shows that adsorption of water vapor by a specimen of silica prepared by combustion of organosilicon compounds and hydrated by exposure to liquid water approaches the adsorption of water by silica gel. The absolute values of adsorption for the hydrated specimen are only 20% lower than for silica gel. As the result of prolonged action of liquid water, the surface state of this silica became similar to the state of the hydrated silica gel surface. The somewhat lower values for the adsorption are probably the consequence of a lower (by about 8%) hydroxyl content on the surface of this hydrated silica specimen (11 micromoles/ m²) in comparison with the silica gel surface (~ 13 micromoles/ m²).

Thus, the surface of silica obtained from organosilicon compounds is hydrated much less rapidly (some tens of times) in water vapor than silica gel or porous glass after dehydration by heat at temperatures up to 650° [12]; even prolonged exposure (more than half a year) of this silica to liquid water hydrates its surface less than the surface of silica gel.

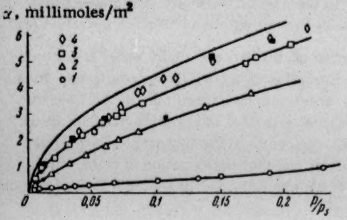

Fig. 6. Initial regions of isotherms for adsorption of water vapor (α-adsorption on 1 m²): 1) on original silica; 2) on silica hydrated in vapor; 3) on silica hydrated in water; 4) ditto, secondary adsorption. Curve without points represents the absolute reversible isotherm for adsorption of water vapor on silica gels [11].

Possible forms of hydration of the silica surface. Silica gels are formed by polymerization of orthosilicic acid in aqueous solution, and therefore they can have at least two different types of bonds with surface hydroxyls

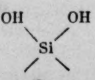

(I)

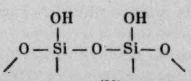

(II)

[8, 11, 12]. Such surface groups yield anhydride groups* on thermal dehydration of the silica gel, the anhydride groups also being of two different types** [5, 12]:

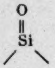

(III)

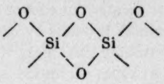

(IV)

Under the action of water vapor groups of Type (III) are probably hydrated more easily, becoming hydrate forms of type (I). It seems likely that hydration of anhydride groups of Type (IV) to give hydrate groups of Type (II) is slower, as this requires a greater activation energy. Thre presence of liquid water is probably necessary for this reaction to take place, i.e., this reaction occurs predominantly only in the capillary condensation region (at $p/p_s = 0.4$ and over). On thermal treatment of silica gels and silica, these reactions proceed in the reverse direction.

The relative content of Type (I) groups is probably higher in hydrated silica gels than in silica prepared from organosilicon compounds and then hydrated. Therefore the action of water vapor on silica gels thermally dehydrated at temperatures below 650° and on porous glasses [12] leads to hydration of a considerable number of Type (III) (siloxane) groups. These reactions take place on adsorption of water vapor even at relatively low p/p_s [5, 11].

Silica prepared by combustion of organosilicon compounds followed by heating to 1000° apparently has a predominance of Type (IV) anhydride groups on its surface. In particular, a recent investigation [31] indicates that the formation of these groups is probable. As this silica was not formed from the hydrate, as is the case with silica gel, the anhydride bonds are more stable than in dehydrated silica gel. Therefore the cleavage of such bonds in the silica used in our investigation occurs more slowly, i.e., requires a greater activation energy than in dehydrated silica gel.

Comparison of Silica Specimens and Silica Gel

Specimen	Treatment temperature, °C	Specific surface, m²/g	Water content, millimoles/g	OH group concentration α, micromoles/m²	$\omega_{OH} = \frac{1}{\alpha}$ in Å²
Original	200	195	0.3	3	50
Hydrated in vapor	25	185	0.75	8	21
Hydrated in water	115	135	0.75	11	16
Silica gel	20	320	1.7	12	14

---

* The hydrated forms are sometimes termed silanols, and the anhydrides, siloxanes [31].

** Type IV anhydride groups are formed in fibrous silica; see [32].

Thus, the sorption of water vapor by this silica at low relative pressures (up to $p/p_s = 0.4$) is mainly reversible adsorption, effected by ordinary van der Waals forces. In the case of thermally dehydrated silica gel, even at lower values of p/p_s, physical adsorption is followed by chemisorption and surface hydration [11].

At relative pressures above 0.4-0.6, vigorous chemical action occurs between liquid water and the surface of the original silica specimen, leading in all probability to formation of Type (II) hydrate forms. Increase of the temperature at which the water acts should correspondingly accelerate hydration, but in this case the changes in the geometrical structure of the silica: surface contraction, growth of the primary particles in the skeleton, and pore expansion [16, 17] are also accelerated. Thus, the course of the hydration of the silica surface varies according to its origin, both with regard to the kinetics and the concentration of water vapor required for hydration, and with regard to the maximum number of hydroxyl groups bound by the surface silicon atoms, although the latter differences are small.

The following tabulated values of the hydroxyl group contents retained on the surface after evacuation at 200°, compared with the values for silica gel, show that the differences between the final states are not large.

It was pointed out earlier (see Fig. 6) that the reversible absolute isotherm for adsorption of water vapor on a silica sample hydrated by exposure to liquid water does not lie, in its initial region, far below the curve for similarly treated silica gel. After reproducible adsorption-desorption cycles had been carried out, the mechanism of water vapor adsorption on hydrated silica and hydrated silica gel in all probability becomes the same, and the small difference between the absolute values of the adsorption is merely the consequence of somewhat different concentrations and forms of bonding of the hydroxyl groups on the silica and silica gel surfaces.

SUMMARY

1. The isotherms for the kinetics and equilibrium adsorption of water vapor on three specimens of silica prepared by combustion of organosilicon compounds have been studied: the original specimen, after hydration in water vapor, and after hydration in liquid water.

2. The adsorption isotherm for the original specimen is concave: in the region of low relative pressures the adsorption is small, and the interaction is predominatly physical in character. At higher pressures slow chemisorption also occurs, leading to hydration of the surface.

3. The isotherm for adsorption of water vapor on the specimen hydrated in liquid water is very similar to the isotherm for adsorption of water vapor on hydrated silica gel. The small differences are due to differences in concentration and types of hydrate forms on the surfaces of these adsorbents.

The authors express their gratitude to V. S. Bronshvager for his assistance in the construction of the vacuum balance used in this investiagion.

The M. V. Lomonosov State University, Moscow
Adsorption Laboratory

Received February 21, 1957

LITERATURE CITED

[1] A. V. Kiselev, in Symposium: "Surface Chemical Compounds and Their Role in Adsorption Phenomena" (Izd. MGU, 1957) p. 199.

[2] N. N. Avgul, O. M. Dzhigit, V. P. Dreving, M. V. Guryev, and O. A. Likhacheva, Proc. Acad. Sci. USSR, 77, 77 1951.

[3] N. N. Avgul, O.M. Dzhigit, A. A. Isirikyan, A. V. Kiselev, and K. D. Shcherbakova, Proc. Acad. Sci. USSR, 77, 625 1951.

[4] A. P. Karnaukhov, A. V. Kiselev, and E. V. Khrapova, Proc. Acad. Sci. USSR, 94, 915 1954.

[5] A. V. Kiselev, in Symposium: "Surface Chemical Compounds and Their Role in Adsorption Phenomena" (Izd. MGU, 1957) p. 90.

[6] A. V. Kiselev and Yu. A. Eltekov, J. Phys. Chem., 31, 250 1957.

[7] A. V. Kiselev, Progr. Chem., 25, 705 1956.

[8] A. V. Kiselev, Colloid J., 2, 17 1936.

[9] N. G. Yaroslavsky, J. Phys. Chem., 24, 68 1950.

[10] S. P. Zhdanov, Proc. Acad. Sci. USSR, 100, 1115 1955.

[11] L. D. Belyakova, O. M. Dzhigit, and A. V. Kiselev, J. Phys. Chem., 31, 1577 1957.

[12] S. P. Zhdanov and A. V. Kiselev, J. Phys. Chem., 31, No. 10 1957.

[13] A. V. Kiselev, Proc. Acad. Sci. USSR, 106, 1046 1956.

[14] A. N. Terenin, in Symposium: "Surface Chemical Compounds and Their Role in Adsorption Phenomena" (Izd. MGU, 1957) p. 206.

[15] V. A. Nikitin, A. N. Sidorov, and A. V. Karyakin, J. Phys. Chem., 30, 117 1956.

[16] A. V. Kiselev and E. V. Khrapova, Colloid J., 19, 572 1957.*

[17] A. V. Kiselev, E. A. Leontyev, V. M. Lukyanovich, and Yu. S. Nikitin, J. Phys.Chem.,30, 2149, 1956.

[18] H. Ries, in Catalysis. Catalysis for Organic Reactions (IL, 1955) p. 37.

[19] A. V. Kiselev and A. A. Isirikyan, Proc. Acad. Sci. USSR, 115, 244 1957.

[20] G. G. Muttik, J. Phys. Chem., 31, 263 1957.

[21] G. Rodin, in Catalysis. Investigations of Heterogeneous Processes (IL, 1956), p. 45.

[22] B. P. Bering and V. V. Serpinsky, Proc. Acad. Sci. USSR, 94, 497 1954.

[23] A. I. Sarakhov, Bull. Acad. Sci. USSR, Div. Chem. Sci., No. 1, 5 1956.

[24] S. J. Gregg, J. Chem. Soc., No. 5, 1438 1955.

[25] Steele, Grant, Proc. Roy. Soc. 82, 580 1909.

[26] A. V. Kiselev, V. F. Kiselev, N. N. Mikos, G. G. Muttik, A. D. Runov, and K. D. Shcherbakova, J. Phys. Chem., 23, 577 1949.

[27] G. G. Muttik, Factory Labs., 17, 1403 1951.

[28] F. Henning, Z. Instrumentenkunde 33, 33, 1913.

[29] K. V. Chmutov, Techniques of Physicochemical Research (Goskhimizdat 1954) p. 70.

[30] S. P. Zhdanov, Proc. Acad. Sci. USSR, 68, 99 1949.

[31] S. Brunauer, D. L. Kantro, C. H. Weise, Can. J. Chem. 34, 1438 1956.

[32] A. Weiss, Z. anorg. Chem. 276, 95 1954.

---

* Original Russian pagination. See C. B. translation.

INFLUENCE OF PORE SIZE AND SURFACE HYDRATION OF SILICA ON ADSORPTION OF NITROGEN VAPOR

A. V. Kiselev and E. V. Khrapova

It has been shown [1] that there are no significant differences between quartz and coarsely porous silica gels in absolute (i.e. calculated per unit surface) adsorption isotherms for nitrogen vapor. For adsorption on a finely porous silica gel specimen with effective pore diameter of ~ 25 A, the adsorption potential was found to be higher, and the isotherm was more convex. There were similar increases of the adsorption potential on silica gels of larger pore size for saturated hydrocarbons with large molecules, containing from 4 to 7 carbon atoms [2, 3], and for benzene [4-6]. The increased adsorption found for nitrogen and hydrocarbons [1] in fine silica gel pores is caused by an increase of the dispersional portion of the adsorption potential, which is additive. On the other hand, adsorption of nitrogen vapor depends on the nature of the adsorbent [7]. It has been shown [8-14] that the adsorptive properties of silica gels change, as the result of surface dehydration, esterification, and halogenation reactions, toward substances which are adsorbed not only by nonpolar van der Waals interaction, but are also capable of forming additional, closer bonds of the acid-base type with the acid hydroxyls of the silica gel surface [8, 15, 16]. This includes the adsorption of water vapor [17, 18], methanol [19, 20], and benzene [19, 21, 22]. The adsorption of saturated hydrocarbons, such as n-pentane [3] and n-hexane [22] is not very sensitive to dehydration of the silica surface. It was of interest to study the adsorption of nitrogen vapor in this respect. The nitrogen molecule has two free pairs of electrons [23] and therefore its adsorption should depend on the degree of hydration of acid adsorbents, including silica gels.

The adsorption of nitrogen vapor has usually been studied for determinations of specific surface by the BET (Brunauer, Emmett, and Teller) method, so that the measurements were carried out only in the region of high degrees of surface filling, $\theta > 1$. Therefore the question of the influence of the degree of surface hydration on the adsorption of nitrogen vapor remains unanswered. In the present investigation the effects of narrowing of the pores in silica, and of the degree of surface hydration, were studied, starting with very low degrees of surface filling.

Specimens and Determinations

Adsorbents. The influence of silica structure on adsorption of nitrogen vapor was studied with silica gel No. 3 of the standard series [24] and two purified commercial specimens, KSK-2 and KSM-2, described previously [17]. The adsorption of nitrogen vapor on silica gels No.5 and No. 8 of the standard series and on a specimen of ground quartz was studied by us earlier [1]. It was therefore possible to evaluate the effects of constriction of pore dimensions (d) between approximately 100 and 25 A. Before the determinations all the specimens were evacuated at 280° down to a pressure $p < 10^{-5}$ mm Hg.

The following specimens were used for studying the effects of the degree of surface hydration of silica. The nonporous specimen used was quartz, hydrated by exposure to liquid water for one month; before the adsorption determinations this hydrated quartz specimen was dried at 100° and evacuated at 200° (a quartz specimen evacuated at 280° was used in the earlier investigation [1]). The next specimen was quartz evacuated for a long time at 430°. All these specimens were different fractions of the same portion of ground quartz. In addition, adsorption of nitrogen vapor was studied on an original and a hydrated specimen of silica prepared by G. V. Vinogradov by combustion of organosilicon compounds followed by heating of the fine powder at 800-1000°*. This method of preparation eliminated the possibility of formation of a dense layer of silicic acid hydroxyl groups on the surface (in contrast to silica gels made from hydrogels [8, 25]). The hydrated specimen was prepared by exposure of the original specimen to liquid water for six months, followed by drying at 120° [22, 26]. The effect of increasing the vacuum heating temperature from 280 to 400° was also studied for the finely porous silica gel specimen No. 28 [24]. The adsorption isotherms were determined with the use of a volumetric gas apparatus as previously [1, 27].

---

* The authors take this opportunity to thank G. V. Vinogradov for supplying this silica.

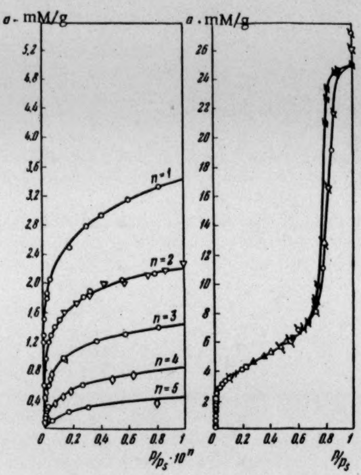

Fig. 1. Isotherm for the adsorption of nitrogen vapor on silica gel KSK-2. Here and subsequently different signs represent points obtained in different series of determinations; black points correspond to desorption.

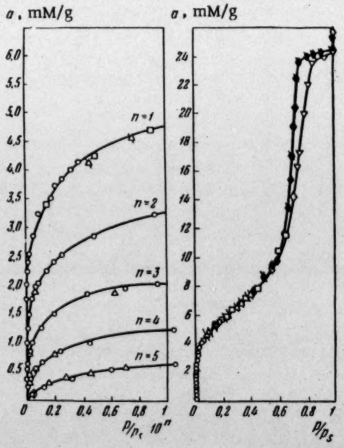

Fig. 2. Isotherm for adsorption of nitrogen vapor on silica gel No. 3 of the standard series.

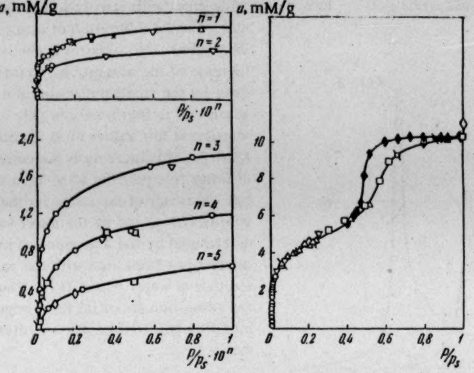

Fig. 3. Adsorption isotherm for nitrogen vapor on silica gel KSM-2. The scale along the ordinate axis is 5 times greater for the curves n = 1 and n = 2 than for the curves n = 3, n = 4, and n = 5.

Effect of Pore Size

Relative values of adsorption (per gram of adsorbent). Figs. 1-3 show isotherms for the adsorption of nitrogen vapor on silica gels KSK-2, No. 3, and KSM-2. The adsorption isotherms for silica gels No. 5 and No. 8 and for quartz heated at 280° are given in an earlier paper [1], and are used here for comparison only.

TABLE 1

Structural Characteristics of Silica Specimens Used for Studying the Effect of Pore construction on Adsorption of Nitrogen Vapor

Specimen	Total pore volume V_s in cm^2/g	Pore neck diameter * $d_T + 2\tau$	Specific surface s in cm^2/g	
			for nitrogen	for water [24]
Quartz	—	—	0.58	—
Silica gels:				
KSK-2	0.870	110	330	340
No. 3	0.843	70	460	430
No. 5	0.495	38	600	566
SKM-2	0.356	38	360	≈500
No. 8	0.262	24 **	510	800

*With a correction for the thickness of the adsorption film formed by the start of hysteresis.

** From water vapor adsorption data.

The adsorption isotherms for nitrogen vapor were used to calculate the specific surface s by the BET equation for the range of relative vapor pressures p/p_s from 0.01-0.2 to 0.30-0.35. The same isotherms were use to determine the effective pore neck diameters [8] (in the same way as in [24]). The data so found for the silica samples are given in Table 1, and curves for the distribution of pore volumes by their neck diameters [8] are given in Fig. 4.

Absolute and reduced adsorption isotherms. For comparison of the isotherms for adsorption of nitrogen vapor on specimens of different porosity, the adsorption values were recalculated per unit surface, determined by the BET method from these isotherms. This comparison is made in Fig. 5, which shows adsorption isotherms for five silica gels and for quartz, starting from θ = 0.01-0.03, over a range of p/p_s values covering 5 tenth-

-powers. The absolute adsorption isotherms for nitrogen vapor in quartz and on silica gels No. 3, No. 5, and KSK-2 are similar, as these silica gels have fairly wide pores with respect to adsorption of nitrogen molecules. For the adsorption of nitrogen vapor on silica gel No. 8 ($d \approx 25$A) the isotherm is obviously distorted owing to the increase of the adsorption potential in these very fine pores, even for the small molecules of nitrogen. This makes the adsorption isotherm steeper [1]. A small increase of adsorption at low values of θ is also found with silica gel KSM-2. This increase is the consequence of the presence of fairly fine pores in KSM-2, as shown by the more diffuse character of the curve for the distribution of pore volumes by $\underline{d}$, and by the lower value for the specific as determined by the adsorption of nitrogen vapor by the BET method in comparison with the value found from the adsorption of water vapor [17]. Thus the higher value of the adsorption potential for nitrogen, found previously [1] for silica gels with small pore diameters, conforms to theory[*].

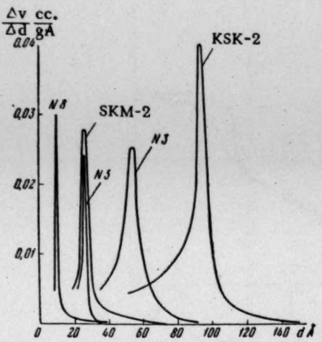

Fig. 4. Curves for pore volume distribution by pore neck diameters for silica gels: KSK-2, KSM-2, No. 3, No. 5, and No. 8 of the standard series.

Distortion of the shape of the isotherms for adsorption of nitrogen vapor on finely porous silica gels suggests that values found for their surface from these isotherms by the BET method should be regarded with caution. Indeed, in this case deviations from a layer covering of the surface in accordance with the usual BET scheme may become very prominent in the pore constrictions (gaps between the globular particles forming the silica gel skeleton) even for these small molecules. The BET equation in this case may be satisfied, but its constant a_m will not have the value of the capacity of a dense monolayer. For silica gel No. 8 the value of a_m determined by the BET method is 70% of the limiting value $a_s = 7.55$ millimoles/g at $p/p_s = 1$, i.e., of the total filling of all the pores of this silica gel. It has been reported [5, 21] that adsorption of hexane, heptane, and benzene vapors by this silica gel formally obeys the BET equation, but the value of a_m given by the BET equation is even greater than a_s.

Therefore, in the case of adsorption of nitrogen vapor on finely porous silica gels, as on carbons [27], the influence of pore constriction should be determined by reduction of the adsorption isotherms to the absolute isotherm, derived by us for quartz and coarsely porous silica gels.

For quartz and for silica gels with fairly large pores ($d > 40$ A) the isotherms for nitrogen vapor adsorption are not distorted and the absolute isotherms are satisfactorily reproduced by an interpolation curve. An interpolated absolute isotherm of this type, together with an isotherm based on the BET equation, is shown in Fig. 6. The BET isotherm in the p/p_s range between 10^{-6} and $1 \cdot 10^{-3}$, i.e., in the monomolecular region, in contrast to the isotherm for adsorption of nitrogen vapor on graphitized carbon blacks with nonporous homogeneous surfaces [27] at low pressures, deviates considerably from the experimental isotherm; it lies considerably lower and is more linear. The isotherm calculated by the BET equation coincides with the experimental curve only in the p/p_s range between 0.1 and 0.3, and then, as usual, it deviates upward from it. The higher adsorption of nitrogen than that given by the BET equation in the initial region is probably caused by chemical heterogeneity of the surface of the hydrated silica. The deviation of the isotherm calculated by the BET equation from the experimental curve at high p/p_s is the consequence of the considerable influence of small differences in the energies of adsorption in the second and subsequent layers, which is not taken into account in the BET theory [31].

---

[*] These results are in agreement with earlier data [28, 29] for a finely porous silica gel (Specimen A). In these papers [28, 29] the pore diameter of this specimen (20 A), as was pointed out in [30], was given without a correction for the thickness of the adsorbed film. Introduction of the appropriate correction increases the pore diameter to about 28 A. In one of these investigations [29] this silica gel specimen was also found to have a higher adsorption potential for nitrogen. This effect was distinctly observed at $p/p_s < 5 \cdot 10^{-3}$.

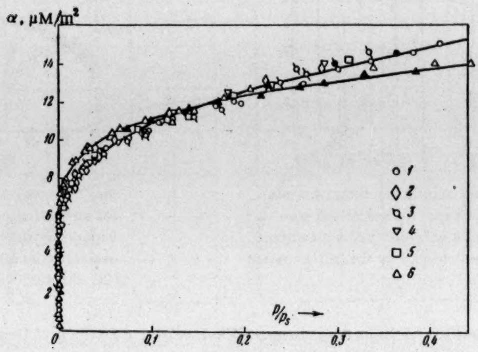

Fig. 5.
Absolute isotherms for adsorption of nitrogen vapor on quartz (1) and on silica gels: KSK-2 (2), No. 3 (3), No. 5 (4), KSM-2 (5), and No. 8 (6).

Effect of the nature of the surface.

As has already been stated, we studied the adsorption of nitrogen vapor on silica specimens of different degrees of hydration. The characteristics of the specimens used are given in Table 2. The specific surfaces were determined by the BET method from the experimental isotherms.

Fig. 7. shows the absolute isotherms for adsorption of nitrogen vapor on three quartz specimens, exposed to liquid water and evacuated at 200, 280 and 430°. In the monomolecular region ($p/p_s < 0.1$) the adsorption of nitrogen vapor on these quartz specimens decreases with increasing evacuation temperature. As θ increases, the difference decreases, and in the $p/p_s > 0.1$ range, i.e., in the multimolecular region, all three isotherms coincide.

The difference between the adsorptions of nitrogen vapor on the original and hydrated silica prepared from organosilicon compounds is particularly large. In Fig. 8 these isotherms are compared with the absolute isotherm for hydrated quartz. In the initial p/p_s region (Fig. 8, a, b) the adsorption on the original, low-

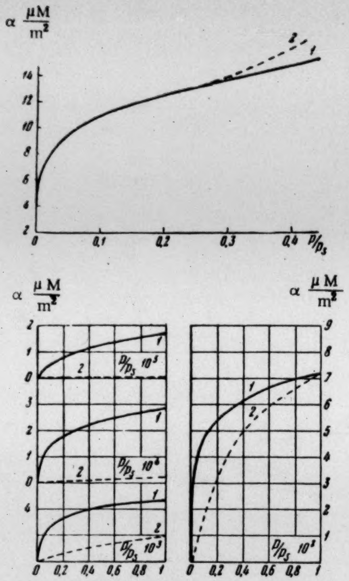

Fig. 6. Interpolated absolute isotherm for adsorption of nitrogen vapor on quartz and on coarsely porous silica gels with hydrated surface (1), and isotherm calculated by the BET equation (2).

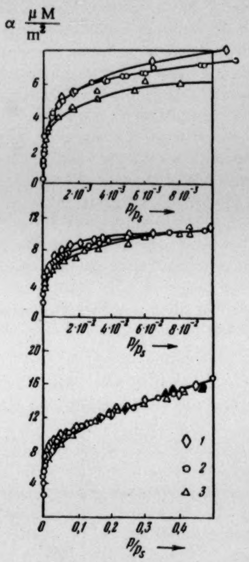

Fig. 7. Absolute isotherms for adsorption of nitrogen vapor on hydrated quartz, evacuated at 200° (1), 280° (2), and 430° (3).

TABLE 2

Structural Characteristics of Silica Specimens Used for Studying the Effects of Degree of Surface Hydration on the Adsorption of Nitrogen Vapor

Specimen	Evacuation temperature before adsorption determinations, °C	Specific surface s, m²/g	Contents of "structural" water, %	Surface concentration of hydroxyl groups, micromoles/m²
Silica gel KSK-2	280	330	3.0	12.0
Quartz, Fraction I	200	0.45	—	—
Quartz, Fraction III	280	5.8	—	—
Quartz, Fraction II	430	0.48	—	—
Silica from organosilicon compounds				
Silica hydrate in liquid water	200	135	1.32[22.26]	11
Silica hydrated in vapor and evacuated at 450°	200	145	0.66	5.0
Original silica	200	185	0.6[22.26]	3.0
Silica gel No. 8	280	510	4.6	(10.0)
Silica gel No. 8	400	495	3.3	(7.5)

-hydrated silica is less than half that on the hydrated silica. The absolute isotherm for quartz with hydrated surface lies even higher. This is in accordance with the fact that hydration of silica from organosilicon compounds had not yet reached the limit after prolonged exposure to water (see Table 2 and [26]). The difference between

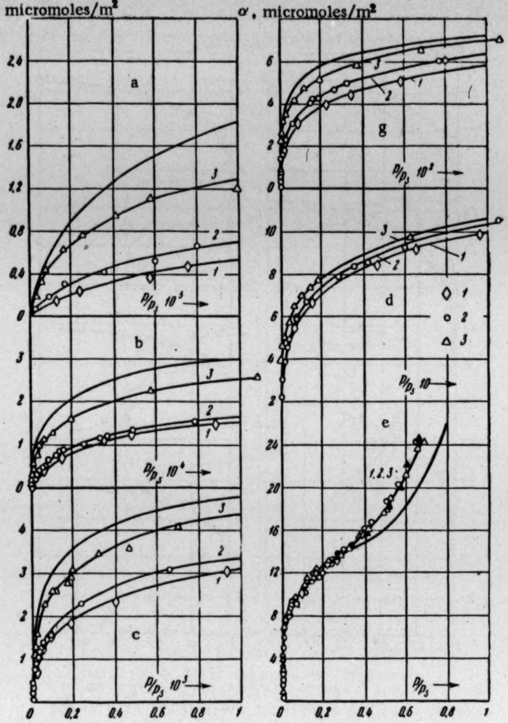

Fig. 8. Absolute isotherms for the adsorption of nitrogen vapor on silica specimens prepared from organosilicon compounds: original (1), evacuated at 450° after hydration of the original specimen in vapor (2), and hydrated in liquid water (3). Curve without points is the isotherm for adsorption on coarsely porous silica gels and on quartz (see Fig. 6, Curve 1).

the absolute isotherms for adsorption on silica hydrated in water vapor and then evacuated at 450°, and on the original silica is not large, in accordance with the similar values for the concentrations of surface hydroxyl groups, which are 3 and 5 micromoles/m² respectively. With increasing p/p_s the isotherms for adsorption of nitrogen vapor on all these specimens come closer together, and practically coincide in the p/p_s range between 0.1 and 0.25. In the region of higher p/p_s the isotherms for adsorption of nitrogen vapor on silica specimens made from organosilicon compounds deviate upward owing to the start of capillary condensation (it has been shown [22] that these specimens are not homogeneously porous).

Fig. 9 shows the reduced isotherms, at $p/p_s = 1$, for adsorption of nitrogen vapor on finely porous silica gel No. 8, evacuated at 280 and 400°. In the $p/p_s < 1 \times 10^{-4}$ and $\theta < 0.5$ range the isotherm for the dehydrated specimen lies below the other. As p/p_s increases the isotherms come closer together, and coincide in the p/p_s range between $1 \cdot 10^{-4}$ and 1*.

---

*It has been shown [32] that the absolute isotherms for adsorption of nitrogen vapor at high p/p_s (from 0.05 to 0.2) on silica gels dehydrated at higher temperatures (above 400°) also coincide. However, the authors of the paper [32] did not investigate the monomolecular filling region and therefore did not observe the influence of dehydration on the adsorption of nitrogen vapor.

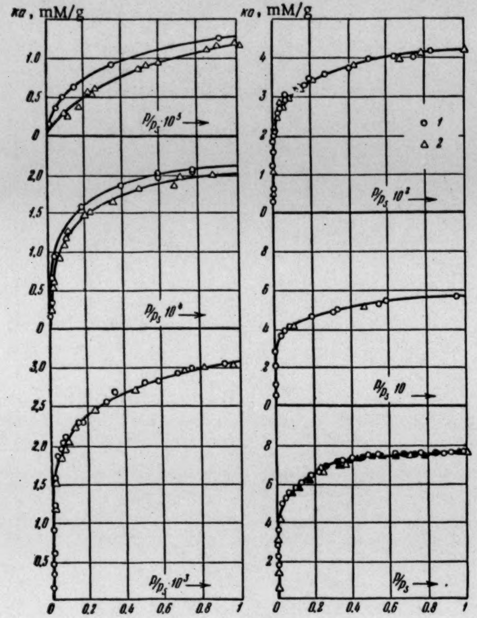

Fig. 9. Reduced isotherms for adsorption of nitrogen vapor on finely porous silica gel No. 8, evacuated at 280° (1) and 400° (2).

Therefore dehydration of the silica surface results in a quite distinct decrease of adsorption of nitrogen vapor in the monomolecular region. Whereas the increase of adsorption with constriction of the pores to $d < 38$ A indicates the important role of additive dispersional interaction of nitrogen molecules with silica, the decrease of adsorption on hydration also indicates the considerable contribution of interactions with acid hydroxyl groups. These interactions are probably effected by donor-acceptor bonding between the free electron pairs of the nitrogen molecules and the partially protonized hydrogen of the acid hydroxyl groups of silicic acid [15, 16]. The quadrupole moment of the nitrogen molecules may also have an influence.

It is also of interest to compare the absolute isotherms for adsorption of nitrogen vapor on silica with isotherms for adsorbents the whole skeleton of which has a different chemical nature. Fig. 10 shows absolute isotherms for adsorption of nitrogen vapor on barium sulfate [7], hydrated quartz [1], carbon black P-33 graphitized at 1700° [27], and metallic tungsten. Over the p/p_s range between 10^{-5} and $1 \cdot 10^{-4}$ the isotherm for adsorption on the homogeneous graphitized carbon black surface lies below the isotherm for the less homogeneous quartz surface covered with hydroxyl groups, and subsequently the increase of adsorption on quartz with increase of p/p_s is retarded and with further increase of p/p_s the isotherm for adsorption on quartz lies below that for carbon black. The isotherms for tungsten and barium sulfate occupy an intermediate position in the initial region. In the multimolecular adsorption region the difference between the absolute values of adsorption of nitrogen vapor on different adsorbents diminishes, and the isotherms come closer together. Thus, in the region of monolayer filling, the differences between the absolute isotherms for adsorbents of different chemical nature are large, especially at low θ. These differences diminish only in the transition to adsorption in the multimolecular region;

this is in agreement with earlier findings [7, 33]. It may be noted that near $\theta = 1$ the absolute values for the adsorption of nitrogen vapor probably differ somewhat for different adsorbents because of the influence of the energy of adsorption on the area ω_0 occupied by molecules of a given adsorbate in a dense monolayer. In our specific surface determinations, however, we assumed the same value $\omega_0 = 16.2\ A^2$ per molecule of nitrogen for all the specimens*.

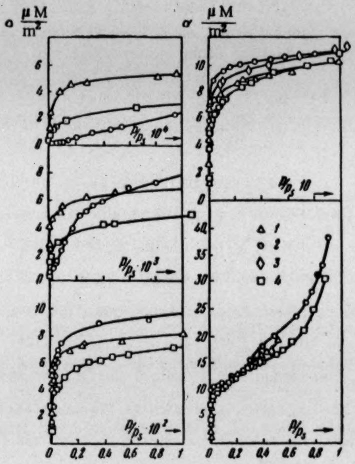

Fig. 10. Absolute isotherms for adsorption of nitrogen vapor on barium sulfate (1), graphitized carbon black (2), metallic tungsten (3), and hydrated quartz (4).

---

* The authors of [32] consider that adsorption of nitrogen vapor is not sensitive to the degree of hydration of silica gels and even to the chemical nature of the absorbent surface in general; however, this is not supported by theory, as calculation of the energy of adsorption includes specific constants not only for the adsorbate but also for the adsorbent (its electrical, magnetic, and structural properties). In support of their views these authors refer to papers [34, 35] on heats of wetting by liquid nitrogen. However, the heat of wetting is only a very rough integral characteristic of the energy of adsorption of a liquid, and similar values for it cannot be used as an indication of the sensitivity or insensitivity of the energy of adsorption of a vapor to the chemical state of the surface. For example, the heats of wetting of original and graphitized channel blacks by nitrogen [34], hexane [31], and benzene [36] are similar, whereas the differential heats of adsorption of these vapors in the region of monolayer filling differ very much [37, 31, 36]. The reason is that the authors of the paper [32] measured the adsorption of nitrogen vapor largely in the multimolecular region (in the p/p_s range between 0.05 and 0.2), when the adsorbent surface is shielded by a layer of previously adsorbed nitrogen molecules.

The difference between the absolute isotherms for adsorption of nitrogen vapor on barium sulfate, silica gel, and carbon black has already been demonstrated [7, 38]. The similarity which has been reported [7] between the absolute isotherms for adsorption of nitrogen vapor on hydrated surfaces of silica gel and aluminosilica gel with a low alumina content can be explained by the similarity of the chemical structure of surfaces of these xerogels, and is in accordance with the similarity of their adsorptional properties toward other adsorbates [39, 40].

SUMMARY

1. The isotherms for adsorption of nitrogen vapor on a number of silica specimens of different pore size and with different degrees of surface hydration have been studied.

2. The isotherms for nitrogen vapor adsorption on silica gels with effective pore diameters greater than ~ 40 A coincide, while in presence of smaller pores the adsorption potential for nitrogen increases.

3. Dehydration of the silica surface decreases the adsorption of nitrogen vapor at low degrees of filling.

4. For adsorbents of different chemical nature, the differences between the absolute values for the adsorption of nitrogen vapor at low degrees of surface filling are very large.

The M. V. Lomonosov State University, Moscow

Received March 21, 1957

LITERATURE CITED

[1] A. V. Kiselev, A. P. Karnaukhova, E. V. Khrapova, Proc. Acad. Sci. USSR, 94, 915 1954.

[2] A. V. Kiselev and Yu. A. Eltekov, J. Phys. Chem., 29, 904 1955.

[3] A. V. Kiselev and Yu. A. Eltekov, J. Phys. Chem., 31, 250 1957.

[4] A. V. Kiselev and Yu. A. Eltekov, Proc. Acad. Sci. USSR, 100, 107 1955.

[5] A. A. Isirikyan and A. V. Kiselev, J. Phys. Chem., 31, No. 9 1957.

[6] A. V. Kiselev, Trans. Commission Anal. Chem., 6 (9), (Izd. AN SSSR, 1955) p. 46.

[7] V. P. Dreving, A. V. Kiselev, and O. A. Likhacheva, Proc. Acad. Sci. USSR, 82, 277 1952.

[8] A. V. Kiselev, in Symposium: "Surface Chemical Compounds and Their Role in Adsorption Phenomena" (Izd. MGU, 1957) pp. 90 and 199.

[9] S. P. Zhdanov, Proc. Acad. Sci. USSR, 68, 99 1949.

[10] O. M. Dhzigit, A. V. Kiselev, N. N. Mikos-Avgul, and K. D. Shcherbakova, Proc. Acad. Sci. USSR, 70, 441 1950.

[11] A. V. Topchieva and A. P. Ballod, Proc. Acad. Sci. USSR, 75, 247 1950.

[12] A. P. Ballod and A. V. Topchieva, in Symposium "Surface Chemical Compounds and Their Role in Adsorption Phenomena Izd. MGU, 1957) p. 146.

[13] I. E. Neimark, R. Yu. Sheinfain, and L. G. Svintsova, Proc. Acad. Sci. USSR, 108, 871 1956.

[14] K. D. Shcherbakova and K. I. Slovetskaya, Proc. Acad. Sci. USSR, 111, 855 1956.

[15] A. V. Kiselev, Proc. Acad. Sci. USSR, 106, 1046 1956.

[16] A. V. Kiselev, Progr. Chem., 25, 705 1956.

[17] L. D. Belyakova, O. M. Dzhigit, and A. V. Kiselev, J. Phys. Chem., 31, 1577 1957.

[18] S. P. Zhdanov and A. V. Kiselev, J. Phys. Chem., 31 1957.

[19] A. V. Kiselev, K. G. Krasilnikov, and L. N. Soboleva, Proc. Acad. Sci. USSR, 94, 25 1954.

[20] L.N. Soboleva and A. V. Kiselev, J. Phys. Chem., 31 1957.

[21] A. A. Isirikyan and A. V. Kiselev, J. Phys. Chem., 31 1957.

[22] A. A. Isirikyan and A. V. Kiselev, Proc. Acad. Sci. USSR, 115, 244 1957.

[23] J. Lennard-Jones, J.A. Pople, Proc. Roy. Soc., 205, 155 1951.

[24] O. M. Dzhigit, A. V. Kiselev, and I. E. Neimark, J. Phys. Chem., 28, 1804 1954.

[25] A. V. Kiselev, Colloid J., 2, 17 1936.

[26] A. V. Kiselev and G. G. Muttik, Colloid J., 19, 562 1957.*

[27] A. V. Kiselev and E. V. Khrapova, Bull. Acad. Sci. USSR, Div. Chem. Sci. 1957.

[28] N. N. Avgul, O. M. Dzhigit, V. P. Dreving, M. V. Guryev, A. V. Kiselev, and O. A. Likhacheva, Proc. Acad. Sci. USSR, 77, 77 1951.

[29] O. A. Likhacheva, Dissertation (Moscow State Univ. 1952).

[30] A. V. Kiselev, in Symposium: "Methods for Studying the Structure of Highly Disperse and Porous Bodies (Izd. AN SSSR, Div. Chem. Sci., 1953) p. 86.

[31] N. N. Avgul, G. I. Berezin, A. V. Kiselev, and I. A. Lygina, J. Phys. Chem., 30, 2106 1956.

[32] G. I. Aleksandrova, V. F. Kiselev, K. G. Krasilshchikov, V. V. Murina, E. A. Sysoev (Proc. Acad. Sci. USSR, 108, 283 1956.

[33] C. Shuell, J. Am. Chem. Soc., 70, 1405 1948.

[34] J. J. Chessick, G. J. Joung, A. C. Zettlemoyer, Trans. Farad. Soc., 50, 587 1954.

[35] G. Kraus, J. Phys. Chem. 59, 343 1955.

[36] N. N. Avgul, G. I. Berezin, A. V. Kiselev, and I. A. Lygina, Bull. Acad. Sci. USSR, Div. Chem. Chem. Sci., 1304 1956.

[37] R. A. Beebe, J. Biscoe, W. R. Smith, C. B. Wendell, J. Am. Chem. Soc., 69, 95 1947.

[38] A. P. Karnaukhov, A. V. Kiselev, and E. V. Khrapova, Proc. Acad. Sci. USSR, 92, 361 1953.

[39] M. A. Romanchuk, Dissertation (Moscow State Univ., 1946).

[40] A. V. Kiselev and N. M. Kamakin, Proc. Acad. Sci. USSR, 80, 393 1951.

---

* This issue, p. 563.

THE SPECIFIC HEAT OF BOUND WATER

O.D. Kurilenko

The data available in the literature on the specific heat of bound water are highly contradictory [1]. Some authors found that the specific heat of bound water is less than unity. For example, values of less than unity for the specific heat of bound water were found by Andrianov, Kotukov, and Smolina [2]. At the same time there are convincing data indicating that the specific heat of water is unchanged by binding. For example, Dumansky and Ponomarev, with Skuratov's assistance [1] obtained a value near to unity for the specific heat of water bound by starch. A similar result was obtained by Porter and Swain [3] in a study of the adsorption of water on carbon.

Finally, careful experiments led Skuratov [4] to the conclusion that the specific heat of water is not changed by binding.

It must be remembered, however, that, as Dumansky [1] points out, only the experimentally determined specific heat of the whole system is unquestionable. The specific heats of the components are determined by the additivity rule. Dumansky states that the calculation of the specific heat of bound water will be correct if the specific heat of the other component is known. If during the wetting process the specific heat of the wetted object changes, then calculations based on the additivity rule cannot be correct. This can be convincingly demonstrated as follows.

As is known, the heat of wetting of hydrophilic substances is practically independent of the temperature, so that

$$\frac{dQ}{dT} = 0. \tag{1}$$

where Q is the heat of wetting of 1 g of the hydrophilic substance. By Kirchhoff's law

$$\frac{dQ}{dT} = \Sigma C. \tag{2}$$

Here ΣC is the algebraic sum of the specific heats of all the substances taking part in a reaction.

From Equations (1) and (2) it follows that

$$\Sigma C = 0 \text{ or } C_k + G_b' C_w - C_k' - G_b C_b = 0, \tag{3}$$

where C_k and C'_k are the specific heats of the hydrophilic substance before and after wetting, C_w and C_b are the specific heats of water before and after wetting (C_b is the specific heat of bound water). G_b is the amount of water bound by 1 g of the substance in question.

It follows directly from Equation (3) that if C_k is equal to C'_k, C_w must be equal to C_b. Thus the heat of wetting – temperature relationship leads to the conclusion reached by Skuratov. This conclusion will be incorrect if the specific heat of the substance changes during wetting. It is then possible, for example, that $C_k < C'_k$ and $C_w > C_b$ or vice versa. There are reasons for believing that the specific heat of a wetted substance remains practically constant during wetting. Experiments show that the heats of wetting are independent of the temperature for substances of the most diverse origins; this is found to be the case for starch, silica gel, carbon, bentonite, and other substances; if their specific heats changed during wetting, the changes could not be equal. Consequently, the heat of wetting – temperature relationship for different substances could not remain equally constant. The more likely conclusion is that $C_k = C'_k$ and $C_w = C_b$, i.e., that the specific heat of bound water is equal to the specific heat of ordinary water. This same conclusion is reached both from Skuratov's data and from an analysis of values for the heats of wetting. Nevertheless, it is difficult to agree with the view that the specific heat of water does not change during binding.

When water passes from the free into the bound state, there are abrupt changes in its thermodynamic properties such as enthalpy, entropy, density etc. In other words, transition of water into the bound state is formally analogous to phase transation; the specific heat cannot then remain constant. This apparent contradiction is easily resolved as follows. A state of equilibrium exists between bound and ordinary water. When the system is heated, this equilibrium is displaced in the direction of desorption of water. In other words, the amount of bound water decreases with increase of temperature. This follows from the Le Chatelier principle. There is also direct experimental evidence for this [5]. In experimental determinations of specific heat, the added heat is used not only to heat the system, but also to displace the equilibrium in it. In such cases Equation (3) cannot be used for calculations. It is necessary to take into account the heat which is expended in displacement of the equilibrium in addition to the heat required to heat the system. Simple thermodynamic calculations show [6] that if it is assumed that $C_k = C'_k$, Equation (3) becomes:

$$C_b = C_w - \frac{Q}{T}, \tag{4}$$

where Q is the heat of addition (binding) of one gram of water; T is the absolute temperature.

By Dumansky's data, the heat of wetting per 1 g of bound water is approximately 80 calories for many hydrophilic substances. Then for experiments at room temperature we have:

$$C_b = 1 - \frac{80}{293} = 0.73.$$

It is known that the addition of the earliest portions of water is accompanied by a larger heat effect. This means that the specific heat of bound water will be less if the wetted substance is not completely saturated with water.

SUMMARY

1. Calculations of the specific heat of bound water by the additivity rule give a high value.
2. The specific heat of bound water is less than unity.

The Kiev Technological Institute for the
Food Industry

Received March 12, 1957

LITERATURE CITED

[1] A. V. Dumansky, Colloid J., 8, 133 1946.

[2] P. I. Andrianov, Koll. -Z., 107 1937; A. Z. Kotikov, Colloid J., 2, 293 1936; L. B. Smolina, Colloid J., 7, 459 1941.

[3] J. Porter, R.C. Swain, J. Am. Chem. Soc. 55, 2792 1933.

[4] S. M. Skuratov, Colloid J., 9, 133 1947.

[5] T. A. Granskaya and N. E. Sakun, Colloid J., 3, 117 1937.

[6] M. Kh. Karapetyants, Chemical Thermodynamics (Goskhimizdat, 1953) p. 212.

VARIATIONS OF THE SPECIFIC VOLUME OF RUBBER DURING STRETCHING

A.B. Kusov, V.I. Trofimova, and Yu. I. Nilova

Studies of volume changes during the stretching of rubber, apart from their practical significance, are of considerable theoretical interest. Experimental data obtained in such studies may be applied to considerations of the structural changes which occur during deformation, and of the nature of the forces involved in this process.

The first investigations of the volume changes in rubber were probably those of Joule [1] who found that when rubber is stretched 100-150% there is a density decrease of up to 0.2%. An increase of volume during stretching of rubber was also observed by Villari [2]; he found that the volume increase is retarded with increasing extension. In contrast to others, Thomas [3] did not observe an increase in the volume of rubber during stretching. As Whitby [3] points out, this is perhaps because Thomas used previously deformed specimens. Lundal [4] observed volume increases of up to 0.45% when rubber was stretched by 23%. Schippel [5], who studied the behavior of loaded mixtures, concluded that increase of volume on stretching greatly increases with increasing amounts of filler. The nature of the filler also influences the magnitude of the effect. Schippel was the first to advance the view that when rubber is stretched, vacuoles are formed near the filler particles in the direction of the extension, in consequence of detachment of rubber from the particles. Hol' and MacPherson [6] studied loaded (with carbon black and chalk) and unloaded mixtures. With the exception of the mixture with chalk, which showed a volume increase on stretching, the volumes of the other mixtures remained unchanged up to 200 or 300% extensions. Above this limit, the volume decreased, the decrease being greater with greater extensions, lower temperatures, and longer times during which the rubber was kept in the stretched state. Increase of the degree of vulcanization in general decreases volume changes on stretching. The volume decrease in these experiments reached 2%.

Gee, Stern, and Treloar [7] studied volume changes during stretching of natural rubber vulcanizates entirely free of filler particles or of other particles not dissolved in the rubber; they found that the volume increases by 0.01-0.02% at extensions up to 100%. There is a correlation between volume (V) – extension (ϵ) and stress (σ) – extension (ϵ) curves. The authors attribute the volume increase to the hydrostatic pressure which arises in any isotropic body on stretching. If the compressibility of the material and the degree of elongation are known, the volume increase can be calculated. The authors carried out such calculations for their specimens and obtained values in close agreement with the experimental data.

The objects of the present investigation included: a) a study of volume changes during stretching of synthetic rubber vulcanizates, which have not been studied previously; b) experiments at large deformations; c) attempts to establish a correlation between volume changes during deformation and the stress.

The procedure used was based on a hydrostatic weighing method similar to that used by Gee, Stern, and Treloar [7].

Rings of 25 mm internal and 28 mm external diameter were cut by a special knife from vulcanized rubber plates. A special steel plate was drilled with holes into which steel rods could be inserted at various distances apart. The rubber rings were stretched on the steel rods on both sides of the plate. In this way extensions from 0 to 700% or over, with 50% intervals, could be produced. This device with the specimens was weighed on an analytical balance in air and in distilled water at various extensions, starting from zero. The data were used to calculate volume changes. All the necessary precautions were taken to maintain a constant temperature and to obtain reproducible results. For better wetting of the rubber and avoidance of air bubbles, several drops of ethyl alcohol were added to the water. The experiments were carried out with vulcanizates based on natural, sodium–butadiene, butadiene–styrene, nitrile, chloroprene, and butyl rubbers. Both unloaded mixtures and mixtures containing carbon black, with different degrees of loading and vulcanization, were studied. Extension–load curves were also plotted for all the rubbers, with the use of spade-shaped specimens cut from the plates which were used for the volume determinations. The formulations of the mixes were similar to the standard, and are therefore not given. Only the degree of loading is given in the graphs.

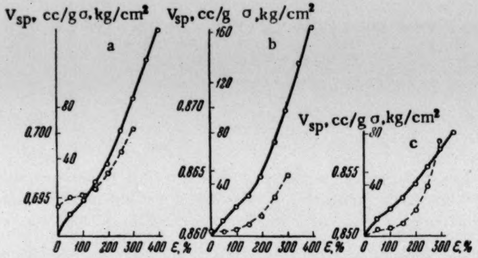

Fig. 1. Variations of stress and specific volume with extension for vulcanizates based on a) chloroprene; b) butadiene–styrene (SKS-30); c) sodium–butadiene rubbers; –) stress; – – –) specific volume.

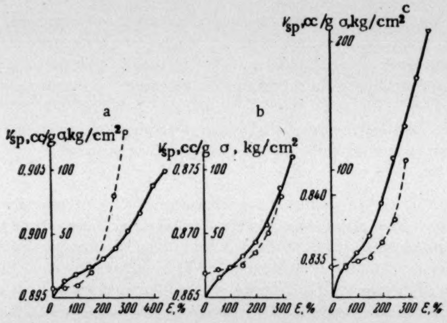

Fig. 2. Variations of stress and specific volume with extension for SKS-30 vulcanizates containing: a) 30; b) 45; c) 60 parts of carbon black; –) stress; – – –) specific volume.

The experiments showed that extension of the various rubbers is accompanied by volume increase, reaching 1.7-1.8% at maximum extension in some cases. The specific volume – extension curve is in general S-shaped; at first the volume increase per unit extension decreases, and then (after the point of inflection on the curve has been reached) the volume begins to increase strongly with extension (see Figs. 1 and 2). In some cases the S-shaped is weak or absent, but in the majority of cases it is pronounced. This is found for all vulcanizates except natural rubber; for the latter, at a certain extension, which is higher at higher degrees of vulcanization, the volume increase is replaced by a decrease, slight at first and then very rapid. Fig. 3 gives specific volume – extension curves for natural rubber vulcanizates based on the same formulation but with different vulcanization times. It is seen that these curves also have inflection points at extensions of ~ 100%, but these are followed by breaks indicating the start of an increase in density (decrease of volume). Fig. 4 shows the

the degree of vulcanization of the specimens, represented by the vulcanization time, plotted against the extension at which the volume increase is replaced by a decrease (the inversion point). This graph shows that at a certain degree of vulcanization, in our case for 15 minutes of vulcanization, the maximum extension corresponding to the inversion point is reached. Fig. 5 shows the critical extension (when the density of the rubber begins to increase) plotted against the bound sulfur content. The latter was determined from the difference between total and free sulfur.

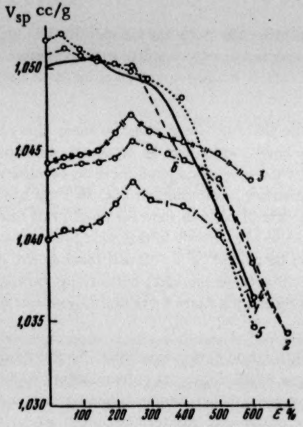

Fig. 3. Specific volume – extension curves for natural rubber vulcanized for : 1) 15; 2) 30; 3) 90; 4) 10; 5) 7.5 and 6) 6 minutes.

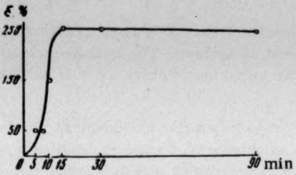

Fig. 4. Extension corresponding to the start of density increase in natural rubber vulcanizates, as a function of the vulcanization time.

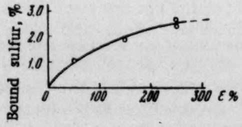

Fig. 5. Extension corresponding to the start of density increase in natural rubber vulcanizates, as a function of the bound sulfur content.

In Figs. 1 and 2, load-extension curves are given together with the specific volume – extension curves. A correlation between the two relationships is clearly seen. The inflections in the curves are found at the same extensions (from 75 to 150%). These plots are typical for most rubber mixes. The different relationships found for natural rubber mixes can probably be ascribed to crystallization. An attempt was made to find a volume decrease in chloroprene and butyl rubber mixes, which can also crystallize on stretching. A volume decrease was observed only after the specimens had been kept for a long time (for 7 days) in the stretched state. The volume of the chloroprene rubber decreased by 0.66% at 300 extension, and that of the butyl rubber by only 0.09% at 250 % extension. Greater extensions could not be reached in these periods.

The specimens used in these experiments had not been fatigued. It was of interest to study the behavior of rubber after repeated deformations. For this, ring-shaped specimens cut from the plates were stretched to 300% several times and then tested at several extensions as previously. Preliminary tenfold extension nearly always resulted in practically the limiting value of volume change.

These experiments showed that the nature of the volume-extension curves of such fatigued rubbers remains the same as before, and only the volume increase changes. Thus, in rubbers based on SKB, tenfold stretching increased the volume in the extension range up to 300% from 0.04 to 0.15% in comparison with unstretched specimens. SKN-26 mixtures showed somewhat larger changes in this extension range from 0.4 to 0.7%).

It is interesting to note that in a relatively few cases the volume-extension curves had a second inflection point in the region close to breaking extensions, indicating a gradual cessation of the volume increase. A similar inflection point can sometimes be seen in stress— extension curves in the higher extension region, predominantly in strongly loaded mixtures.

These results leave no doubt that an increase of volume during extension, up to failure of the specimen, is a common property of vulcanizates. The decrease of volume observed in natural rubber after a definite extension is in all probability the result of crystallization superposed on the primary effect. The magnitude of the observed volume increase indicates that it cannot be caused by the hydrostatic component of the stress only. It is highly probable that deformation results in destruction of the material at the inner surfaces of the rubber itself and at the rubber – added particle interfaces. The possibility of destruction of the added particles, i.e., loosening with formation of vacuoles within them, is also not excluded. Not all these effects are equally probable, but because of the lack of exact information we can only speak of the combined effects of different factors.

However, there is one striking fact – the existence of an inflection point on the specific volume – extension curve, its S-shape. The increase of volume might be expected to vary steadily with extension. The fact that the inflection points on the volume-extension and the stress-extension curves coincide is very interesting.

It might be possible to explain this fact on the assumption that the rubber contains some kind of an unstable spatial network, formed by different types of secondary bonds, which can be broken by deformation. Destruction of the network will be accompanied by a decrease of the modulus and an increase of volume owing to increased chain vibration and decreased steric hindrance. However, as the number of cross links capable of being broken decreases (the chains being already oriented), the rate of volume increase should fall to a minimum, corresponding to the inflection point on the curve. This also corresponds to the maximum decrease of the extensibility modulus. The subsequent volume increase may be caused by a different mechanism, or more accurately by the predominance of another component of the total volume increase, possibly by vacuole formation. Incidentally, this deformation stage is usually characterized by a sharp increase of hysteresis loss, indicating considerable structural breakdown.

The behavior of natural rubber definitely points to crystallization during extension. In this case the volume decrease reaches 1.5-1.7%. It is significant that increase of the degree of vulcanization, which decreases the distances between the points of cross linking, does not alter the extension, beyond a certain value, at which crystallization begins. The crystallization occurs more easily with greater "freedom" of the molecular chains (at lower degrees of vulcanization).

SUMMARY

1. It is shown that volume increases during extension occur both in loaded and unloaded vulcanizates of different rubbers, reaching 2% at maximum extension.

2. The specific volume – extension curves are in general S-shaped, and the inflection points on these curves correspond to the same extensions as the inflection points on stress-extension curves.

3. Vulcanizates based on natural rubber show volume decreases, caused by crystallization of the rubber, at a certain degree of extension, which is higher for higher degrees of vulcanization.

The Lensoviet Technological Institute Leningrad
Chair of Rubber Technology

Received November 3, 1956.

LITERATURE CITED

[1] J. P. Joule, Phil. Trans. 149, 104, 1859 (see [3], p. 490).

[2] E. Villari, Ann. Physik 143, 88, 290 1871.

[3] G. S. Whitby, Plantation rubber and the testing of Rubber, London 1920.

[4] A. E. Lundal, Ann. Physik 66, 741 1898.

[5] H. F. Schippel, Ind. Eng. Chem. 12, 33 1920.

[6] W. L. Holt, A. T. MacPherson, J. Res. Nat. Bur. Stand. 17, 657 1936.

[7] G. Gee, H.J. Stern, L. Treloar, Trans. Faraday Soc. 46, 1101 1950.

EFFECT OF THE NATURE OF THE EMULSIFIER ON THE THERMAL DECOMPOSITION OF CUMENE AND 1,1-DIPHENYLETHANE HYDROPEROXIDES IN AN AQUEOUS MEDIUM

R.V. Kucher and S.D. Kazmin

The influence of an emulsifier on reaction rates in emulsion systems is associated to a considerable extent with its effect on the rate of free radical formation during the thermal decomposition of hydroperoxide reaction initiators. Despite the fact that we have already carried out some investigations of this question [1, 2], the effects of emulsifiers on the thermal stability of hydroperoxides are not yet fully understood. The rate and mechanism of hydroperoxide decomposition in aqueous media primarily depend on the pH. In a strongly acid medium the decomposition of isopropylbenzene hydroperoxide proceeds at a very high rate with formation of phenol and acetone as the primary products. In an alkaline medium different decomposition products are formed (acetophenone, tertiary carbinol). However, the data on the influence of the emulsifier, and in particular of its colloidal nature, are very limited, and this question still remains obscure. Investigations of the influence of the nature of the emulsifier on the rate of thermal decomposition of hydroperoxides are of considerable interest in this connection. Studies of the thermal stability of tertiary hydroperoxides are also of interest, as these compounds can be prepared relatively easily by oxidation of the corresponding hydrocarbons. The stability of these hydroperoxides depends on the nature of the substituents at the third carbon atom [3]. This also influences the initiating activity of the hydroperoxides [4]. However, such data are at present lacking with regard to the aqueous phase.

The purpose of the present investigation was a study of the thermal decomposition of cumene and 1,1-diphenylethane hydroperoxides in an aqueous medium in presence of different types of emulsifiers. The effects of certain sulfonates and of a number of higher fatty acid salts on the thermal stability of these hydroperoxides were studied. This work is therefore a continuation of our earlier investigation [2].

EXPERIMENTAL

The thermal decomposition of cumene hydroperoxide (CHP, 100% pure) and 1,1-dipehnylethane hydroperoxide (DEH, 100% pure) was effected in sealed tubes in an atmosphere of pure nitrogen in a thermostat at 98.5 and 80°. The tubes were taken out of the thermostat at definite invervals, opened, and their contents analyzed for hydroperoxide. The analysis was carried out by the iodometric method [5].

The decomposition of CHP and DEH was studied in an aqueous medium at pH 9.9 in 0.1 N sodium carbonate solution, in presence of different types of emulsifiers. The emulsifiers used were Aerosols OT and IB (sodium salts of the dioctyl and dibutyl esters of sulfosuccinic acid), Alkanol S (imported sodium tetralinsulfonate [6]), sodium tetralinsulfonate synthesized by ourselves [7], Nekal, Leukanol [8], and sodium soaps of fatty acids – caproate, caprylate, and palmitate, free from unsaturated impurities; we also used a cation-active colloidal electrolyte, cetylpyridinium bromide, and Igepon T (a condensation product of oleyl chloride with methyltaurine [7]), containing a double bond in the molecule. The initial concentration of CHP was 1.4%, and of DEH, of the order of 10^{-3} mole/liter.

Data on the rate of the thermal decomposition of CHP in presence of a number of emulsifiers at 98.5° are shown in Fig. 1. It is seen that the rate of hydroperoxide decomposition decreases in presence of sulfonates. The small increase of the thermal stability of the hydroperoxide cannot, however, be attributed only to the "colloidality" (micelle size) of the emulsifier used, as with emulsifiers of the same type, one of which has a greater tendency to micelle formation in aqueous solutions (for example, Aerosols IB and OT, the micellar weight of the latter being considerably greater), the latter has the higher rate of thermal decomposition. Increase of micelle size of the emulsifier thus favors an increase in the rate of thermal decomposition of the hydroperoxide. The decrease of the rate of hydroperoxide decomposition in presence of sulfonates must be attributed to the specific action of these emulsifiers on the decomposition of CHP.

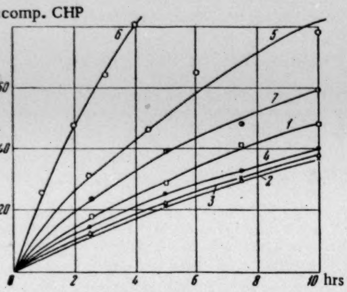

Fig. 1. Curves for the decomposition of CHP at 98.5° and pH 9.9 in presence of 2% of various emulsifiers: 1) Aerosol OT; 2) Aerosol IB; 3) sodium tetralinsulfonate; 4) Alkanol S; 5) Igepon T; 6) cetylpyridinium bromide; 7) without emulsifier.

As regards the action of Igepon T, the considerable increase of the rate of hydroperoxide decomposition in presence of this colloidal electrolyte can be attributed to partial interaction of the hydroperoxide with the emulsifier molecules at the double bond. A similar effect was observed in the influence of sodium oleate on the thermal stability of CHP [2].

It should also be noted that the thermal decomposition of CHP is accelerated considerably in presence of cation-active cetylpyridinium bromide. A curious feature is that in this case the rate of decomposition is much higher than in presence of other emulsifiers. When the temperature is decreased to 20° the decomposition of CHP still proceeds at an appreciable rate in presence of cetylpyridinium bromide, while in presence of the others emulsifiers no appreciable decomposition of CHP was observed during several days at room temperature. This effect of cetylpyridinium bromide must be attributed to its chemical nature and not to the colloidal nature (micelle formation) of this colloidal electrolyte. One probable explanation of the action of cetylpyridinium bromide is oxidation-reduction interaction between the hydroperoxide molecules and the nitrogen of the pyridine ring. Evidence for this interaction is provided by the behavior of this colloidal electrolyte in emulsion polymerization; experiments in our laboratory showed that this emulsifier acts in this case as an activator (reducing agent).

The influence of colloidal character on the decomposition rate of CHP is clearly seen in the results of experiments with sodium soaps of fatty acids. These results are given in Fig. 2. It is seen that the presence of fatty acid soaps in solution accelerates the thermal decomposition of CHP. In this case it proved possible to formulate a quantitative empirical relationship between the decomposition rate constant for CHP (calculated from a first-order equation) and the number of carbon atoms in the soap molecule. This relationship is presented graphically in Fig. 2, and is given by the equation:

$$k = 0{,}432\, n_c + 1{,}63 \cdot 10^{-3},$$

where k is the rate constant for hydroperoxide decomposition; n_C is the number of carbon atoms in the soap molecule. The size of the soap molecule may be a measure of the colloidal character of the solutions, as according to MacBain [9] the micelle size in soaps of the same nature is determined by the molecular weight of the soap.

The intercept cut off by the straight line along the ordinate axis corresponds to the rate constant for decomposition of CHP in absence of soap. It may be noted that the decomposition rate constant in absence of colloidal electrolytes fits exactly into this relationship.

As was noted in paper by Yurzhenko et al. [3], 1,1-diphenylethane hydroperoxide is less stable than isopropylbenzene hydroperoxide in a hydrocarbon medium. It was therefore interesting to investigate this relationship in an aqueous medium. Study of the decomposition of DEH in such conditions is difficult owing to the very low solubility of this compound in water ($3.75 \cdot 10^{-4}$ mole/liter at 20°). However, in presence of soaps the solubility of this hydroperoxide is increased considerably. Therefore in studies of the thermal decomposition of DEH in an aqueous medium the solutions were first saturated with the hydroperoxide.

The results of the study of the rate of thermal decomposition of DEH in an aqueous medium are given in Fig. 3. It follows from a comparison of the data in Fig. 1 and Fig. 3 that the thermal decomposition of DEH

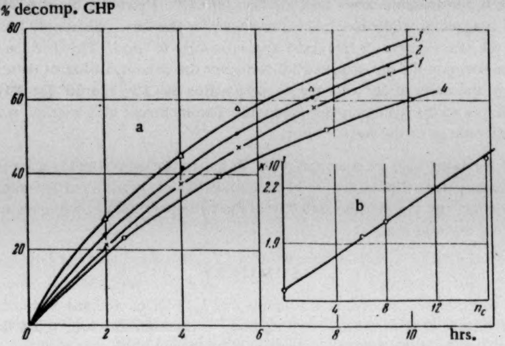

Fig. 2. Curves for the decomposition of CHP in presence of 2% of emulsifiers: (a): 1) Na caproate; 2) Na caprylate; 3) Na palmitate; 4) without emulsifier; decomposition rate constant for CHP as a function of the number of carbon atoms in the soap molecule (b).

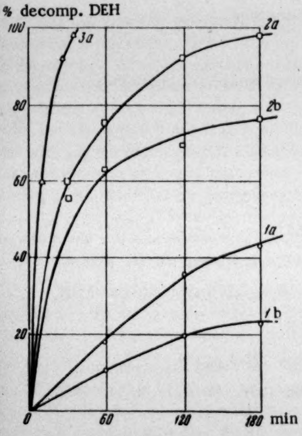

Fig. 3. Curves for the decomposition of DEH at 98.5° (a) and 80° (b) at pH 9.9 in presence of 2% of emulsifiers: 1) Nekal; 2) Na tetralinsulfonate; 3) Leukanol.

Rate Constants at 98.5 and 80°, and Activation Energies for the Decomposition of CHP and DEH in an Aqueous Medium

Emulsifier (c = 2%)	$k_{80°} \cdot 10^3$ min.$^{-1}$	$k_{98.5°} \cdot 10^3$ min.$^{-1}$	E (kcal./mole
CHP			
Soda without emulsifier	0.334	1.63	22.3
Aerosol IB	0.180	0.835	21.5
Aerosol OT	0.273	1.271	21.6
Alkanol S	0.187	0.842	21.1
Na caproate	0.366	1.927	23.3
Na palmitate	0.451	2.340	23.1
DEH			
Na tetralinsulfonate	11.2	23.3	10.3
Nekal	1.65	3.34	9.9

is considerably more rapid than that of CHP. This is in agreement with the data obtained by T.I. Yurzhenko et al. [3] for a hydrocarbon medium. The effects of the nature of the emulsifier on the decomposition of DEH in an aqueous medium are similar to those in the thermal decomposition of CHP.

From the results of experiments at 98.5 and 80° it was possible to calculate the activation energy of the thermal decomposition of the hydroperoxide by means of the Arrhenius equation. The rate constants were calculated for a reaction of the first order. The results of these calculations are given in the Table.

It should first be noted that the activation energy shows only small variations in presence of different emulsifiers for the same hydroperoxide (CHP). The data in the table also show that the activation energy of thermal decomposition is considerably lower for DEH than for CHP. However, the activation energy for the decomposition of DEH is approximately 10-12 kcal. less than for the first; this should lead to a $\sim 10^5$-fold increase of k. In fact the reaction rate is increased approximately 60-fold. This is to be explained by the considerable difference between the pre-exponential terms for the decomposition of these two hydroperoxides; these are respectively of the order of 10^{10} for the decomposition of CHP, and 10^4 for DEH. This, in turn, is determined by the structure of the hydroperoxide molecule (replacement of a methyl by a phenyl radical), resulting in a considerable change of the steric factor.

In summing up the foregoing, we may note that, in the initiation of liquid-phase reactions in emulsions by means of hydroperoxides, the colloidal nature of the emulsifier plays an important role, in addition to the nature of the hydroperoxide, and the thermal stability of the hydroperoxides in an aqueous medium decreases somewhat with increasing micelle size.

SUMMARY

1. The rate of thermal decomposition of cumene and 1,1-diphenylethane hydroperoxides in an aqueous medium in presence of various emulsifiers has been studied. Sulfonates decrease, while fatty acid soaps and cetylpyridinium bromide increase the decomposition rate of hydroperoxides.

2. Increase of the "colloidality" (micelle formation) of the emulsifier results in an increase in the rate of thermal decomposition of cumene hydroperoxide. In the case of fatty acid soaps this increase is a linear function of the number of carbon atoms in the colloidal electrolyte molecule.

3. The rate of thermal decomposition of 1,1-diphenylethane hydroperoxide in an aqueous medium is considerably higher than the rate of decomposition of isopropylbenzene (cumene) hydroperoxide, i.e., the relative stability of these hydroperoxides is the same as in a hydrocarbon medium.

The I. Franko State University, Lvov
Chair of Physical and Colloid Chemistry

Received September 14, 1956.

LITERATURE CITED

[1] A. I. Yurzhenko and F. I. Grobshtein, Ukrain. Chem. J., 20, 373 1954.

[2] R. V. Kucher and A. I. Yurzhenko, Colloid J., 18, 555 1956.*

[3] T. I. Yurzhenko, D. K. Tolopko, and V. A. Puchin, Proc. Acad. Sci. USSR, 74, 85 1950.

[4] T. I. Yurzhenko, V. A. Puchin, and K. S. Grigoryeva, Proc. Acad. Sci. USSR, 75, 547 1950.

[5] V. Kokatnur, M. Jelling, J. Am. Chem. Soc. 63, 1432 1941.

[6] A. Schwartz and J. Perry, Surface Active Agents (IL, Moscow 1953) p. 124.

[7] R. V. Kucher and S. D. Kazmin, Proc. and Comm. Lvov State Univ., No. 6, pt. 2, 140 1955.

[8] R. V. Kucher and M. A. Kovbuz, Colloid J., 18, 193 1956.*

[9] J. W. MacBain, J. Phys. Coll. Chem., 51, 286 1947.

---

* Original Russian pagination. See C. B. translation.

THE STRUCTURE OF THIN COPPER SULFIDE FILMS AT THE SOLUTION–GAS INTERFACE

S.G. Mokrushin, Yu. D. Tkachev and O.K. Shabalina

Devaux [1] put forward the view that sulfide films formed on the surface of solution of the salts of copper and other metals by chemical reactions between the salts and hydrogen sulfide are, in the limit, monomolecular layers. The subsequent increase of the film thickness was regarded by Devaux as the result of stratification of a number of monomolecular layers. Similar views were advanced by Perrin [2] for explaining the structure of thin soap films, the thickness of which, according to Perrin, is a multiple of the thickness of a bimolecular film. These views were accepted by Mokrushin et al. [3], but subsequent experimental work [4] showed that Devaux's views on the monomolecular and polymolecular structure of metal sulfide films are not in agreement with the experimental data.

It was shown by Mokrushin et al. [5] that very thin films are capable of spontaneous contraction; this is seen especially clearly if the films are compressed in Marcelin's apparatus. These experimental results led to the adoption of another concept of film formation, according to which the sulfide films are not mono- or polymolecular, but are surface colloidal solutions, which coagulate into surface networks of varying degrees of porosity, depending on the concentration of the colloidal solution. It followed from these investigations that the films must be regarded as being mono- and polymicellar, i.e., the structural elements in them are colloidal particles and not molecules. A similar conclusion was reached by Demenev [6] from the results of microscopical and electron-microscopical studies of thin metal films formed on surfaces of solutions by the action of reducing gases. Although the formation of metallic films as the result of coagulation was proved experimentally by Demenev et al. [7], only indirect proof was available with regard to the formation of sulfide films. It should be noted that it has been shown by electron microscopy that copper hydroxide films formed on solution surfaces as the result of hydrolysis consist of colloidal hydroxide particles [8].

The films of copper sulfide, electron micrographs of which (magnification 12,000) are given below, were prepared by the action of hydrogen sulfide gas (0.05% by volume) on 0.2 and 2.0 N solutions of copper sulfate. The time of action of the hydrogen sulfide was between 15 and 600 seconds.

The micrographs of the films formed on 0.2 N copper sulfate solution by the action of hydrogen sulfide for 15 seconds (Photo 1, a) and 150 seconds (Photo 1, b) show that the sulfide particles are typical secondary colloidal particles formed by coagulation. As far as can be seen from the photographs, the primary sulfide particles are probably globular. As was shown by Kargin and Berestneva [9], this form is found in the formation of many kinds of colloidal particles. It must be pointed out that the colloidal particles formed during a brief action of the gas (Photo 1,a) are not interconnected and exhibit Brownian movement, whereas after 150 seconds of the action of hydrogen sulfide (Photo 1, b) the particles form a network with large gaps of free surface. The photographs also show that the secondary particles were formed by surface (two-dimensional) coagulation.

The colloidal particles were compressed by the Langmuir-Blodgett "oil piston" method [10]. However, a film compressed by castor oil is still very porous (see Photo 2).

Films formed by the action of hydrogen sulfide for 10 minutes (Photo 3) at first sight resemble films compressed by castor oil, but the former differ from the latter in that, in the gaps between the colloidal particles, thin dendritic formations can be seen along the particle boundaries; these are oriented microcrystalline products of the crystallization or recrystallization of the copper sulfide particles. By addition of gelatin to the copper sulfate solution it is possible to prevent completely the formation of secondary colloidal particles, so that the film consists of primary globular colloidal particles. An example of such a film is shown in Photo 4. The film was prepared from a solution of copper sulfate to which 0.2% gelatin had been added.

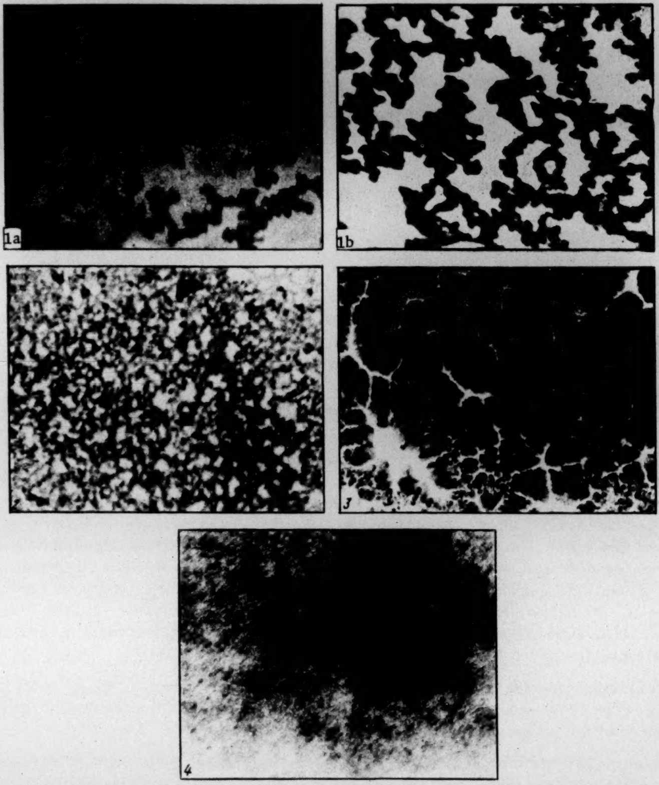

Electron micrographs of films on 0.2 N copper sulfate solution (magnification x 12,000) formed: 1) by action of H_2S for 15 seconds; 1,b) ditto, 150 seconds; 3) ditto, 10 minutes; 2) film compressed by castor oil; 4) with addition of 0.2% gelatin.

SUMMARY

Films of copper sulfide, and probably of other sulfides, like metallic and hydroxide films, consist of secondary colloidal particles formed by coagulation of primary sulfide particles and attached, owing to their hydrophobic nature, at the solution–gas interface.

The S. M. Kirov Polytechnic Institute, Urals
Sverdlovsk

Received April 28, 1956.

LITERATURE CITED

[1] H. Devaux, Koll.-Z 58, 129 1932.

[2] J. Perrin, Koll.-Z. 51, 5 1930.

[3] S. G. Mokrushin and A. M. Demyanova, J. Phys. Chem., 5, 1092 1934.

[4] S. G. Mokrushin and R. B. Ginzburg, Colloid J., 5, 5, 818 1939.

[5] S. G. Mokrushin, V. A. Kozheurov, and I. A. Blum, Colloid J., 6, 119 1940.

[6] N. V. Demenev, Trans. Inst. Chemistry and Metallurgy, Urals Branch, Acad. Sci. USSR, No. 1, 10 1948.

[7] N. V. Demenov, N. N. Buinov, and M. I. Milyutina, Colloid J., 12, 252 1950.

[8] S. G. Mokrushin, G. A. Kitaev, and O. K. Shabalina, Proc. Acad. Sci. USSR, 94, 1109 1954.

[9] Z. Ya. Berestneva, T. A. Koretskaya, and V. A. Kargin, Colloid J., 13, 323 1951.

[10] I. Langmuir, Progr. Chem., 8, 1195 1939; I.Langmuir and V. Schaefer, Colloid J., 8, 1231 1939.

THE EFFECT OF STRUCTURE ON THE VISCOSITY OF BUTADIENE –STYRENE RUBBERS

A.S. Novikov and F.S. Tolstukhina

Relative few investigations have dealt with the influence of molecular structure on the viscous flow of polymers. These studies have been carried out with polymers with molecules of simple linear structure, resistant to oxidation. In an investigation of the viscosity of polyester melts, a linear relationship was found between the logarithm of the viscosity and the square root of the molecular weight [1]:

$$\log \eta = A + CM^{1/2}.$$

Similar relationships have been found for butyl rubber [2] and polyethylene [3]. Recently the following equation was derived for a number of polymers with long flexible molecular chains:

$$\log \eta = A \log z + B,$$

where z is the number of atoms in the chain; A and B are constants. This empirical law of flow proved to be valid for polyisobutylene and polystyrene [4], polymethyl methacrylate [5], and butadiene-styrene polymers [6].

The viscosity of butadiene-styrene copolymers has been studied as a function of the molecular structure in the present investigation. It was desired to correlate the structure of the polymer with its viscous properties in solution and in bulk under steady flow conditions. The copolymers taken for the work were SKS-30 and SKS-30A, polymerized at +50 and +5° respectively. The structure of the copolymer fractions was characterized by the molecular weight, intrinsic viscosity, and the Huggins constant K'. The viscosity of the polymers was measured by means of Tolstoi's plastoelastometer [7] in shearing deformation conditions.

Fractionation. Specimens of the rubbers with different molecular weights were obtained by fractionation. The rubber was extracted with acetone in a nitrogen atmosphere before fractionation, at room temperature in darkness, over a period of two days. After extraction the rubber was dissolved in benzene (thiophene-free), with the addition of 3 parts by weight of recrystallized phenyl-β-naphthylamine (P-β-NA) per 100 parts of rubber. The solutions were filtered twice through a double layer of silk.

The fractionation was effected from 1.6% solutions by decrease of temperature. Methyl alcohol was used as precipitant. The fractions were dissolved, without drying, in benzene with P-β-NA (2 parts by weight per 100 parts of rubber) and kept under nitrogen in the dark. SKS-30A was separated into 7 fractions, the first of which was insoluble after the separation. SKS-30 was separated into fractions, of which the first and second were insoluble after the separation. The insoluble gel fractions were not studied.

For characterization of the molecular structure of the soluble sol fractions, a part of the solution was taken, and methyl alcohol was distilled off under vacuum at room temperature. The distillation was stopped when the refractive index of the distillate coincided with that of pure benzene. The molecular weights of the SKS-30A fractions were found from the intrinsic viscosity of solutions in benzene, determined at 25°.

The calculations were based on the equation

The molecular weights of the SKS-30 fractions were determined by the osmotic method by means of Digadkin's osmometers [8]. The degree of molecular chain branching was characterized by the Huggins constant K', which was determined for each fraction from the corresponding reduced specific viscosity – concentration relationship (Table 1, Figs. 1 and 2.) The values of K' for the fractions of low molecular weight are not given, as the slope of the reduced specific viscosity – concentration lines was very small and the accuracy of K' determined in this way was doubtful.

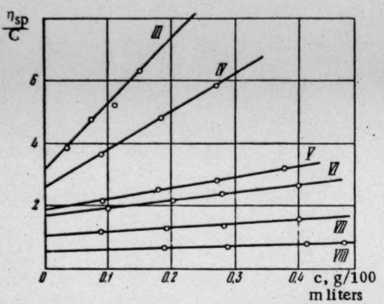

Fig. 1. Reduced specific viscosity – concentration relationships for solutions of SKS-30A fractions.

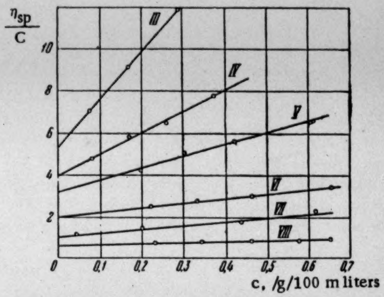

Fig. 2. Reduced specific viscosity – concentration relationships for solution of SKS-30 fractions.

Increase of the constant K' indicates increased molecular chain branching. It is seen from the data in Table 1 that the degree of branching increases with molecular weight for both rubbers. The SKS-30 fractions have lower intrinsic viscosities in solution and a more branched molecular structure than the SKS-30A fractions. For example, for the SKS-30 fraction of molecular weight 900,000, $[\eta]$ = 2.6; K' = 1.80, and for the SKS-30A fraction of molecular weight 775,000, $[\eta]$ = 5.24; K' = 0.845.

Preparation of the specimens. The specimens were prepared in the form of plates 1.5-1.7 mm thick by consecutive pouring of small amounts of solutions of the fractions into chrome plated molds. The benzene solvent was evaporated at 30°; the plates were then taken to constant weight under a residual pressure of 10^{-3} mm Hg at room temperature.

TABLE 1

Principal Molecular Characteristics of the Butadiene – Styrene Rubber Fractions

Fractions	SKS-30A			SKS-30		
	Molecular wt. of fraction	K'	$[\eta]$	Molecular wt. of fraction	K'	$[\eta]$
I	Insoluble gel fraction			Insoluble gel fraction		
II	775 000	0.845	5.24	»	»	
III	515 000	0.725	3.92	1 000 000	2.38	3.2
IV	377 000	0.589	3.14	901 000	1.80	2.6
V	199 500	0.535	2.00	257 000	0.92	1.92
VI	75 200	—	1.00	180 300	0.70	1.76
VII	40 100	—	0.64	97 400	—	1.12
VIII	—	—	—	48 000	—	0.60

Determination of the viscosity of polymer fraction melts. The Tolstoi plastoelastometer was used to determine, at constant stress, the shear deformation kinetics of the polymer placed between two plane parallel plates. The apparatus is shown diagrammatically in Fig. 3.

The essential parts of the apparatus are two metal plates with straight grooves on their inner sides, cut in at right angles to the displacement of the plates. The grooves provide a better grip between the rubber and

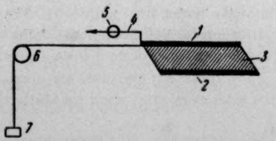

Fig. 3. Diagram of apparatus for measurement of shearing deformation in a polymer layer between two plane parallel plates: 1,2) steel plates; 3) polymer; 4) microphotographic scale; 5) cathetometer; 6) pulley; 7) load.

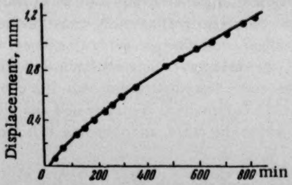

Fig. 4. Variation of shearing deformation with time for butadiene – styrene rubber.

the metal plates and eliminate the risk of slippage. The bottom plate is fixed, while the top plate is displaced by means of a load attached to a thread passing over a pulley resting on needle bearings. The action of an applied load causes horizontal displacement of the top plate and of the microphotographic scale fixed rigidly to it. The displacements were measured to an accuracy of 0.00025 cm by means of a cathetometer. The apparatus was placed in an air thermostat, the temperature in which was kept constant by means of an ultrathermostat. The test specimen, in the form of a plate, was clamped between the plane parallel plates in a press. The rubber filled the grooves under pressure; after subsequent relaxation of internal stresses it acquired residual deformation. The press was placed in a thermostat at 70°. The time required for stress relaxation varied with the molecular weight. The correct choice of the relaxation time was confirmed by the kinetics of the developing deformation, and also by absence of changes in the height of the specimen during the relaxation process.

A typical deformation-time curve is shown in Fig. 4. At the start of the process the deformation rate decreases at constant temperature and constant stress, gradually approaching a certain constant value. The curve then passes into a straight line. The slope of this linear region represents the rate of increase of irreversible deformation. When steady flow occurs under constant stress, the viscosity can be calculated by the simple formula

where η is the viscosity in poises; σ is the stress in dynes/cm²; h is the thickness of the specimen in cm; ϵ is the displacement in cm; t is the time in seconds.

TABLE 2

Determinations of the Viscosity of Butadiene–Styrene Polymer Fractions in the Solid Phase at 82°

Fraction	Stress in dynes/cm²	Layer thickness, cm	Velocity gradient in sec.⁻¹	Viscosity in poises
		SKS-30A		
III	67 590	0.1583	$3.67\cdot10^{-7}$	$1.85\cdot10^{11}$
IV	67 590	0.1377	$5.76\cdot10^{-7}$	$1.17\cdot10^{11}$
V	67 590	0.1814	$8.82\cdot10^{-6}$	$7.66\cdot10^{10}$
VI	23 838	0.1332	$4.71\cdot10^{-6}$	$5.08\cdot10^{9}$
VII	23 838	0.1229	$1.88\cdot10^{-3}$	$1.26\cdot10^{7}$
VIII	4905	0.1125	$1.72\cdot10^{-2}$	$2.84\cdot10^{5}$
		SKS-30		
IV	67 590	0.1400	$3.62\cdot10^{-6}$	$1.86\cdot10^{10}$
V	23 838	0.1158	$2.61\cdot10^{-4}$	$9.11\cdot10^{7}$
VI	23 838	0.1071	$2.98\cdot10^{-3}$	$7.50\cdot10^{6}$
VII	4905	0.0975	$2.10\cdot10^{-2}$	$2.33\cdot10^{5}$

In determinations of polymer viscosity, the question arises as to what is to be regarded as viscosity; the ratio of the total tangential stress to the velocity gradient, or the ratio of only the viscosity component of the stress to the velocity gradient. Here it is necessary to examine the molecular mechanism of polymer deformation, the physical origin of different forms of resistance to shear in the deformed system. Plastic and elastic deformations develop simultaneously under the action of an applied stress. At the start of the process the rate of plastic deformation changes owing to changes in the configuration of the molecular chains [9]. Then, after some time, the molecular chain configuration reaches a state of equilibrium for the given stress and temperature, and the subsequent deformation proceeds at a constant rate. Under the action of a constant stress the fully developed elastic deformation is maintained and plastic flow occurs. Thus, these two processes are inseparable, one accompanies the other, and therefore it is more correct to use the total tangential stress for viscosity calculations.

Variation of viscosity of the fractions with molecular weight. The viscosities of SKS-30 and SKS-30A fractions were measured at 82° in the stress region of 10^3 - 10^4 dynes/cm^2 (Table 2), where the flow remains practically Newtonian* [4,10]. Constancy of the molecular structure of the fractions in the course of the experiments was checked by determinations of solubility and intrinsic viscosity. These determinations showed that 2% (calculated on the rubber) of P- β -NA ensures stability of SKS-30 and SKS-30A rubbers under the experimental conditions (up to 5 days at 82°). However, the fractions of high molecular weight, which were soluble immediately after fractionation, partially lost solubility after preparation of the films. This was found for Fractions III and IV of SKS-30A and Fraction III of SKS-30.

It is seen in Table 2 that the viscosity varies over a range of 5-6 tenth-powers with molecular weight. With a variation of the molecular weight of SKS-30A from 40,000 to 800,000, the viscosity increased from $2.84 \cdot 10^5$ to $1.85 \cdot 10^{11}$ poises, and for SKS-30, as the molecular weight varied form 48,000 to 900,000 the viscosity varied from $2.33 \cdot 10^3$ to $1.86 \cdot 10^{10}$ poises. This viscosity variation resulted in a change in the duration of the experiments from a few seconds for the low molecular weight fractions to several days for the high fractions.

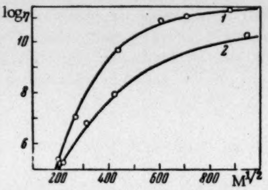

Fig. 5. Variation of the viscosity of fraction melts with the molecular weight: 1) SKS-30A; 2) SKS-30.

Fig. 5 shows the viscosities of the fractions plotted against the square root of the molecular weight. SKS-30 fractions, which have greater chain branching and lower intrinsic viscosities in solution than SKS-30A fractions, also have lower viscosities in the solid phase in steady flow

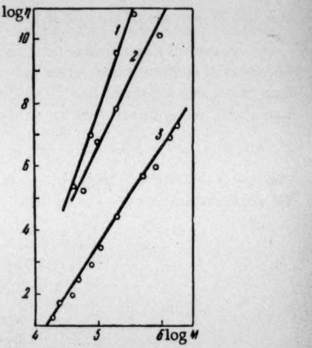

Fig. 6. Variation of log η with log M: 1) SKS-30A; 2) SKS-30; 3) polyisobutylene from the data of Fox and Flory.

---

* We showed for polyisobutylene that with a 30-fold change of stress from $5 \cdot 10^3$ to $1.5 \cdot 10^5$ dynes/cm^2 the viscosity decreased by 12%. The fact that at 82° the viscosity is independent of the stress in the low stress region for butadiene-styrene copolymer is seen from the following table:

Stress, dynes/ /cm^2	Layer thickness, cm	Displacement rate	Viscosity, poises
45 710	0.1304	$1.07 \cdot 10^{-6}$	$5.57 \cdot 10^{9}$
23 840	0.1414	$6.07 \cdot 10^{-7}$	$5.55 \cdot 10^{9}$

conditions. The difference between the viscosities of SKS-30 and SKS-30A melts diminishes with decreasing molecular weight; this is consistent with the simultaneous equalization of the constants K'. Thus, both in solutions and in melts under steady flow conditions the viscosity decreases with increasing degree of branching, which is probably the consequence of higher packing density for the branched polymer chains. This is based on the known fact that branched structure in a molecular chain decreases its geometrical dimensions [11, 12].

It follows from the data in Fig. 6 for fractions the molecular structure of which did not change during the experiments that a linear relationship between log η and log M holds for butadiene-styrene polymers over a wide molecular weight range.

For comparison, the results obtained by Fox and Flory [4] for polyisobutylene are also shown in Fig. 6. The linear relationships give the following expressions:

For SKS-30. . . . . log η = 4 logM − 13.2
For SKS-30A . . . . log η = 6.94 logM − 26.7
For polyisobutylene . . . log η = 3.17 logM − 12.37

TABLE 3

Effect of Temperature on the Viscosity of Butadiene-Styrene Polymers

Temperature, °C	Stress, dynes/cm²	Displacement rate, cm/sec.	Thickness of plate, cm	Velocity gradient, sec.⁻¹	Viscosity, poises
SKS-30 [η] = 1.12; mol. wt. 97,400					
24	23 838	$2.31 \cdot 10^{-5}$	0.1084	$0.213 \cdot 10^{-3}$	$1.11 \cdot 10^{8}$
40	23 838	$5.70 \cdot 10^{-5}$	0.1085	$0.543 \cdot 10^{-3}$	$4.53 \cdot 10^{7}$
60	23 838	$1.29 \cdot 10^{-4}$	0.1092	$1.18 \cdot 10^{-3}$	$2.01 \cdot 10^{7}$
82	23 838	$2.666 \cdot 10^{-4}$	0.1086	$2.45 \cdot 10^{-3}$	$9.73 \cdot 10^{6}$
SKS-30A [η] = 1.00; mol. wt. 75,000					
24.5	23 838	$1.08 \cdot 10^{-5}$	0.1162	$0.93 \cdot 10^{-4}$	$2.56 \cdot 10^{8}$
45	23 838	$2.11 \cdot 10^{-5}$	0.1169	$1.80 \cdot 10^{-4}$	$1.32 \cdot 10^{8}$
60	23 838	$7.60 \cdot 10^{-5}$	0.1172	$6.49 \cdot 10^{-4}$	$3.63 \cdot 10^{7}$
82	23 838	$3.32 \cdot 10^{-4}$	0.1229	$1.886 \cdot 10^{-3}$	$1.261 \cdot 10^{7}$
SKS-30A; mol. wt. 199,500					
41.5	67 590	$2.59 \cdot 10^{-7}$	0.1104	$2.34 \cdot 10^{-6}$	$2.88 \cdot 10^{10}$
60	67 590	$1.09 \cdot 10^{-6}$	0.1263	$8.59 \cdot 10^{-6}$	$7.00 \cdot 10^{9}$
70	67 590	$1.38 \cdot 10^{-6}$	0.1230	$1.12 \cdot 10^{-5}$	$6.02 \cdot 10^{9}$
82	23 838	$6.41 \cdot 10^{-7}$	0.1362	$4.70 \cdot 10^{-6}$	$5.06 \cdot 10^{9}$

The variations of viscosity with molecular weight for these butadiene-styrene polyemers are analogous to those for polyisobutylene and polystyrene [4]. The viscosity first rises sharply with molecular weight, and then from molecular weights of 300,000-400,000 onward, the viscosity increases much more slowly. It is probable that in the molecular weight range studied this relationship applies to all polymers. An analogous relationship between the mechanical properties of vulcanizates and the molecular weight of butadiene-styrene rubber was discovered earlier [13]. It is significant that the limiting molecular weight at which the change in the property in question begins to occur at a lower rate is the same for vulcanizates and raw rubbers. This type of variation of polymer properties with molecular weight can probably be atributed to tangling of molecular chains with formation of knots and loops, which behave similarly to chemical cross links, from the mechanical aspect, under the action of external stresses.

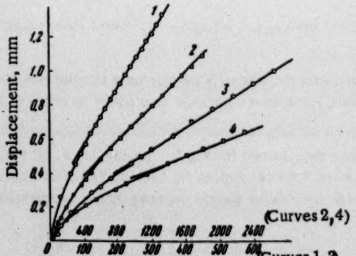

Fig. 7. Deformation–time relationship for SKS-30 of molecular weight 97,400 at various temperatures: 1) 82°; 2) 40°; 3) 60°; 4) 24°

Effect of temperature on the viscosity of butadiene-styrene rubbers. The viscosity of fractionated specimens of SKS-30 and SKS-30A was measured at four temperatures between 24 and 82°. The determinations were carried out under equal stresses (Table 3).

Deformation–time curves for different temperatures are shown in Fig. 7. It follows from Fig. 7 and Table 3 that increase of temperature results in earlier completion of high-elastic deformation, when the linear portion of the curve is reached, and in increase of the rate of plastic deformation. As the temperature increases from 24 to 82°, the viscosity decreases more than tenfold: from $1.11 \cdot 10^8$ to $9.73 \cdot 10^6$ poises for SKS-30 and from $2.56 \cdot 10^8$ to $1.26 \cdot 10^7$ poises for SKS-30 A.

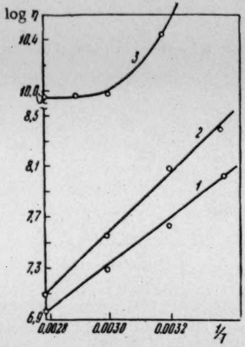

Fig. 8. Log η – 1/ T relationship for: 1) SKS-30, mol. wt. 7.400; 2) SKS--30A, mol. wt. 75,200; 3) SKS-30A, mol. wt. 199,500.

The data of Table 3 are plotted in log η – 1/ T coordinates in Fig. 8. The log η – 1/ T relationship for fractions of low molecular weight (Curves 1 and 2) is linear, i.e., the activation energy does not change with temperature in the 24-82° range. The corresponding values of the activation energy E are 10.8 kcal./ mole for SKS--30A and 7.8 kcal./ mole for SKS-30. The reason why the branched polymer gave a lower value of E is probably that the segments near the chain ends are capable of moving more freely than segments far from the chain ends, and the number of free ends is greater in branched polymers.

The equation

$$\eta = Ae^{E/RT}$$

is not applicable to fractions of higher molecular weight (Curve 3), as the log η – 1/ T relationship is nonlinear. The variation of the activation energy with temperature for a specimen of high molecular weight can probably be attributed to changes of the degree of the nearest order and of the intermolecular forces. The constancy of the activation energy for fractions of low molecular weight can be explained by the looseness of the structure.

SUMMARY

1. The viscosities of melts of fractions of butadiene-styrene rubbers SKS-30 and SKS-30A have been measured.

2. The degree of molecular chain branching in SKS-30 and SKS-30A fractions has been estimated by the Huggins constant K', and it is shown that the degree of branching increases with molecular weight for both rubbers. The molecules of SKS-30 fractions have a more branched structure than the molecules of SKS-30A fractions of the same molecular weight.

3. SKS-30 and SKS-30A rubbers conform to the flow law $\log \eta = A \log M + B$, over a wide range of molecular weights.

4. The degree of molecular chain branching influences the viscosity of polymers in solutions and melts. SKS-30 fractions, with a more branched molecular structure, have lower intrinsic viscosities in solution and, under steady flow conditions, lower melt viscosities.

5. The activation energy of viscous flow E has been determined for the low molecular weight fractions of SKS-30 and SKS-30A in the 24-82° range; the values were 7.8 kcal./ mole for SKS-30 and 10.8 kcal./ mole for SKS-30A. The activation energy for the fraction of high molecular weight depends on the temperature in this temperature range.

Scientific Research Institute for the Rubber Industry.
Moscow

Received November 23, 1956.

LITERATURE CITED

[1] Flory P., J. Am. chem. Soc. 62, 1057, 1940.

[2] Zapp, Baldwin, High Polymers, No. 8, (Goskhimizdat 1949).

[3] G. Diens, H. Klemm, J. Appl. Phys. 17, 458 1946.

[4] T. Fox, P. Flory, J. Am. chem. Soc. 70, 2384, 1948.

[5] F. Bueche, J. Appl. Phys. 26, 738 1955.

[6] A. S. Novikov and F. S. Tolstukhina, Proc. Acad. Sci. USSR, 109, 576 1956.

[7] D. M. Tolstoi, Colloid J., 10, 133 1948.

[8] B. Dogadkin, I.Soboleva and M. Arkhangelskaya, Investigations in the Field of High Polymers (Izd. AN SSSR, 1949) p. 253.

[9] G. M. Bartenev, J. Phys. Chem., 24, 10, 1210 1950.

[10] K. Van Holde, J.W. Williams, J. Pol. Sci. 11, 243 1953.

[11] V. N. Tsvetkov, Proc. Acad. Sci. USSR, 78, 1123 1951.

[12] I. G. Soboleva, N. V. Makletsova, A. V. Matveeva, and S. S. Medvedev, Colloid J., 18, 344 1956.*

[13] A. S. Novikov, M. B. Khaikina, and T. V. Dorokhina, Colloid J., 15, 1, 51 1953. *

---

* Original Russian pagination. See C. B. translation.

DEPENDENCE OF THE ELASTIC CONSTANT OF A VULCANIZATE ON THE MOLECULAR WEIGHT OF THE ORIGINAL RUBBER

L.S. Priss

By the kinetic theory of high elasticity, the equilibrium stress in a deformed vulcanizate without filler is

$$\sigma = C(\lambda^2 - 1/\lambda), \tag{1}$$

where $\lambda = l/l_0$ is the relative elongation, and

$$C = 2\nu_0 kT^*, \tag{2}$$

where ν_0 is the number of linkage points per unit volume of the material; T is the absolute temperature; k is the Boltzmann constant.

The latter expression is valid only if the average number of cross links per molecule of the original rubber is fairly large. We shall denote this number by γ. For sparse networks, when γ is a few units, Equation (2) requires modification. An approximate calculation for networks based on monodisperse linear polymers was made by Flory [1]; his result

$$C = 2\nu kT = 2\nu_0(1 - 2M_c/M) = n\gamma(1 - 2/\gamma) \tag{3}$$

(here ν and n are the numbers of "effective" network-forming cross links and original molecules per unit volume respectively; M_c and M are the molecular weights of the chain and the original rubber) should, according to Flory, be valid from $\gamma \approx 3$.

Since Equation (3) is sometimes very useful in certain physicochemical investigations of vulcanizates [4, 5], we decided to derive a more strict relationship between C and γ for networks formed from a monodisperse original rubber, and a rubber with a molecular weight distribution conforming to Poisson's law.

Considerable deviations from Equation (3) were found even at high values of γ. It was found that Flory's derivation contains an error, elimination of which leads to the expression

$$C = kT(2\nu_0 - n) = n\gamma kT(1 - 1/\gamma) = NkT \tag{4}$$

in agreement with the results (for large values of γ) of the calculations given below.

The following gives (4). Eq. (2) is valid for a network formed by cross linking of an infinitely long molecule. If n chains are broken in 1 cc of such a network, it will be equivalent to a network formed from a rubber containing $n + 1 \approx n$ molecules in 1 cc. The remaining chains number $2\nu_0 - n$, which leads to (4).

Flory's error is that he assumes the effective number of chains in 1 cc, N, to be twice the number of network-forming cross linkage points ν, defined as the difference $\nu_0 - n$. However, comparison of the number of cross linkage points per given molecule with the number of chains which results easily shows that $N = 2\nu + n$, and this leads to Equation (4).

Before we pass to a more rigid calculation, we shall consider the general structure of the network and introduce certain assumptions.

---

* Generally speaking, this relationship between C and ν_0 is not confirmed by experiment [2,3]. The reasons for this deviation will be discussed elswhere. Here we consider only the question of the dependence of C on the molecular weight of the original rubber.

Network structure. If the molecular weight of the original rubber has a finite value, then not all the molecules are incorporated in the network, and some of them form the soluble part of the vulcanizate, the sol fraction. The ratio between the soluble and insoluble (gel fraction) parts of vulcanizates has been calculated for different types of molecular weight distribution in the original rubber [6-8].

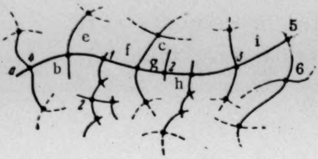

Fig. 1

The gel fraction can be mathematically defined as an entity of interconnected molecules of infinitely large molecular weight. Fig. 1 diagrammatically shows one of the original molecules contained in the gel fraction, and different types of attachment of other molecules to it. Chains which continue indefinitely are shown by broken lines.

As is seen from the diagram, in addition to the chains the network contains free ends of molecules of type a and b, and attachments, molecules c or groups of molecules d, attached to the network at single points. Points of type 1 and 2, to which groups of molecules of finite molecular weight are attached, will be regarded as inactive, and the chains e and f will be considered as a single chain; the same applies to chains g and h.

The network-forming points do not all lead to the formation of the same numbers of chains. For example, there are two chains corresponding to each point of type 3, which is a middle point for both the molecules joined there; for each point of type 4, which is a middle point for one molecule and an end point for another, there are 1.5 chains; while a junction of type 5, an end point for both molecules, does not lead to formation of new chains – the chains i and j constitute a single chain joining points 3 and 6. Thus, the total number of active chains in 1 cc of the network is

$$N = 2\nu_{mm} + 1{,}5\,\nu_{me} \tag{5}$$

where ν_{mm} and ν_{me} are the numbers of network-forming points of types 3 and 4 respectively (Fig. 1).

Apart from the above types of linkage, cross links can also be formed between two segments of the same molecule. If there are no other cross links between these segments, a point of this type, although it is network-forming and belongs to type 3 or 4 (Fig. 1) does not lead to chain formation. The probability of linkages of this type in not very dense networks is small and they will not be considered in the calculations below.

Network of molecules of equal length. Let us assume that 1 cc of the original rubber contains n molecules, each consisting of u units. Let q be the probability of the inclusion of a given unit in a cross link, i. e., double the ratio of the number of network points in 1 cc to the total number of reactive bonds nu (it is assumed that each monomer unit contains one reactive bond). Then the number of original molecules containing c monomer units entering the network points is

$$n(c) = nq^c(1-q)^{u-c}\frac{u!}{(u-c)!\,c!}, \tag{6}$$

and the ratio of the number of units entering the network points in these molecules to the total number of these units is

$$t(c) = \frac{cn(c)}{nuq} = \frac{c}{uq}\left(\frac{q}{1-q}\right)^c(1-q)^u\frac{u!}{(u-c)!\,c!}. \tag{7}$$

It is evident that t (c) will determine the probability that a molecule B, attached to a molecule A, will have c – 1 more cross links, which can continue the network. Thus, t (1) is the probability of the addition of a molecule containing no more cross links, t (2) is the probability of the addition of a molecule containing one cross link, etc.

If a molecule B, joined at some point to a molecule A, has limited continuation, such a point is conventionally taken to be non-network forming. Let the corresponding probability be represented by s. It is easily seen that

$$s = t(1) + t(2)s + t(3)s^2 + \ldots = \sum_{c=1}^{u} t(c)\,s^{c-1} = \frac{(1-q)}{suq}\sum_{c=1}^{u} c\left(\frac{qs}{1-q}\right)\frac{u!}{(u-c)!\,c!} =$$

$$= (1-q+qs)^{u-1} \approx e^{-\gamma(1-s)}, \qquad (8)$$

where $\gamma = uq$. The last equality in Equation (8) is valid only at high values of u, as is almost always the case.

It can be shown that s is equal to the relative content of the soluble fraction in the vulcanizate, and that the equation

$$s = e^{-\gamma(1-s)} \qquad (9)$$

can, by simple transformations, be reduced to the Flory equation derived for this particular case. Equation (9) has a solution other than the trivial $(s = 1)$ only if $\gamma \geq 1$, which corresponds to values of γ at which the network can exist.

The number of molecules containing c cross linkage points, of which r are network-forming, is:

$$v(c, r) = n(c)(1-s)^r s^{c-r}\frac{c!}{r!\,(c-r)!}. \qquad (10)$$

The total number of molecules in which r monomer units enter the network-forming points is found by summation of $v(c, r)$ for all values of c $(r \leqslant c < u)$:

$$v(r) = \sum_{c=r}^{u} v(r, c) = n\frac{(1-q)^u(1-s)^r}{s^r}\sum_{c=r}^{u}\left(\frac{qs}{1-q}\right)^c\frac{u!}{r!\,(c-r)!\,(u-c)!} = \qquad (11)$$

$$= nq^r(1-s)^r(1-q+qs)^{u-r}\frac{u!}{r!\,(u-r)!},$$

and the total number of monomer units entering the network-forming points, by summation of $rv(r)$ for all values of r from 2 to u:

$$l' = \sum_{r=2}^{u} rv(r) = n\gamma(1-s)^2; \qquad (12)$$

of these

$$l_m = \sum_{r=3}^{u}(r-2)\,v(r) = n(1-s)(\gamma - 2 + \gamma s) \qquad (13)$$

units enter network-forming points which are not at the ends of the given molecule, and

$$l_e = 2\sum_{r=2}^{u} v(r) = 2(1-s)(1-\gamma s) \qquad (14)$$

are at extreme network-forming points.

If l', l_m, and l_e are large enough (which is true even for very sparse networks), and the number of network points per molecule is small compared to the total number of such points, the probability that a given point is a middle one for the two molecules joined at it is l_m^2/l'^2. Similarly, for a point which is extreme for one and middle for the other, or extreme for both molecules, we have: $2\,l_e l_m/l'^2$ and $l_e^2\,l'^2$. The number of points of each of these types is found by multiplication of the corresponding probability by the total number of network points $(\nu = l'/2)$.

The number of active chains contained in unit volume of the network, according to Equation (5), is:

$$N = 2\nu_{mm} + 1{,}5\,\nu_{me} = l_m^2/l' + 1.5\,l_m l_e/l' = n(\gamma - 2 + \gamma s)(\gamma + 1 - 2\gamma s)/\gamma. \qquad (15)$$

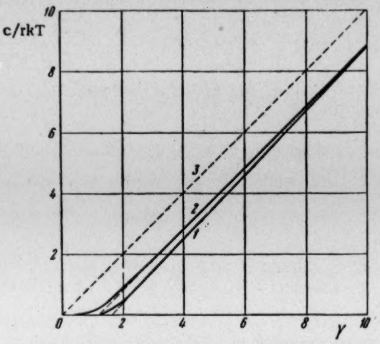

Fig. 2. Variation of the number of effective chains N with γ for a network formed in 1) a monodisperse rubber, Equation (15); 2) a rubber with a Poisson molecular weight distribution, Equation (24); 3) N/n = γ

The variation of N, a quantity proportional to the elastic constant C of the rubber, with γ, calculated by Equation (15), is shown in Fig. 2 (curve 1). It is seen that C = 0 at γ = 1, and then C gradually increases with γ, while from γ ≈ 2 its increase is approximately linear. Extrapolation of this plot to the abscissa axis gives an intersection point corresponding to γ ≈ 1.6. At high values of γ, Equation (15) reduces to the expression

$$N \approx n(\gamma - 1 - 2/\gamma) \approx n(\gamma - 1) \tag{16}$$

as stated at the beginning of this paper.

Network of molecules with size distribution conforming to Poisson's law. Suppose that the original rubber was formed by the random scission of an infinitely long molecule. Such a molecular weight distribution (or one similar to it) is found in real rubbers. In this case the number of molecules consisting of u monomer units is

$$m(u) = np(1-p)^{u-1} \approx npe^{-pu}/(1-p), \tag{17}$$

where n and u are the total numbers of molecules and monomer units per unit volume respectively; p = n/u. The rest of the notation used here is the same as before (γ = q/p).

The number of molecules containing c monomer units entering into cross links

$$n(c) = \frac{np}{1-p}\,\frac{1}{p+q-pq}\,A^c, \qquad A = (1-p)\,q/(p+q-pq) \tag{18}$$

was calculated by Charlesby [7].

From this it is not difficult to determine the number of molecules, containing r monomer units, entering the network-forming points:

$$v(r) = \sum_{c=r}^{\infty} v(c, r) = \frac{np}{1-p}\,\frac{(1-s)^r}{s^r(p+q-pq)} \sum_{c=r}^{\infty} A^c s^c \frac{c!}{r!\,(c-r)!} = \tag{19}$$

$$= \frac{np}{(1-p)(p+q-pq)}\,\frac{(1-s)^r A^r}{(1-As)^{r+1}},$$

where v (c, r) is expressed in terms of n (c), in accordance with Equation (10).

The values of l', l_m and l_e respectively are:

$$l' = \sum_{r=2}^{\infty} rv(r) = \frac{np}{(1-p)(p+q-pq)} A(1-s)\left[\frac{1}{(1-A)^2} - \frac{1}{(1-As)^2}\right] \approx \tag{20}$$

$$\approx n\gamma(1-s)^2. \tag{21}$$

$$l_e = 2\sum_{r=2}^{\infty} v(r) = \frac{2np}{1-p}\frac{(1-s)^2}{(p+p-pq)}\frac{A^2}{(1-A)(1-As)^2} \approx 2n\gamma^2(1-s)^2 s;$$
$$l_m = l' - l_e \approx n\gamma(1-s)^2(1-2\gamma s). \tag{22}$$

As an approximation, Charlesby's equation connecting γ and s [7] was used:

$$s = \frac{1}{(1+\gamma-\gamma s)^2}, \tag{23}$$

and it was assumed that q and p were negligible relative to unity.

The total number of active chains in unit volume, according to Equations (6) and (15) is

$$N = l_m^2/l' + 1.5\, l_m l_e/l' = n\gamma(1-s)^2(1-2\gamma s)(1+\gamma s). \tag{24}$$

The $N-\gamma$ relationship calculated by means of Equation (24) is also shown in Fig. 2. In this case N becomes zero at $\gamma = 0.5$ and Curve 2 at small values of γ lies somewhat above Curve 1. At high values of γ, N, expressed in accordance with Equation (24), is also approximately equal to $n(\gamma - 1)$. Extrapolation of the linear portion of the plot to the abscissa axis gives an intersection at $\gamma \approx 1.2$.

Some applications of the foregoing calculations. A comparison of the experimental relationships between the elastic constant C (number of active chains) and the original molecular weight, with Equations (15) and (24) may be used to estimate the number of cross linkage points per unit volume [4]. It follows from the foregoing that it is necessary to take into account the nature of the molecular weight distribution of the original rubber.

Horikx [5] has recently shown that studies of the relationship between the sol fraction content and the number of active chains in the gel fraction at different stages of oxidative degradation of vulcanizates can be used for elucidating the mechanism of this process. By comparing experimental data with theoretical relationships, derived on the assumption that oxidative degradation is accompanied by: 1) disintegration of cross linkage points, 2) random chain rupture, and 3) chain rupture near the cross linkage points, he concluded that disintegration of the network can be caused only by one of the two latter processes.

However, the relationship used by Horikx for the third case is not quite exact, as it was based on Equation (3). A more exact relationship can easily be derived from the results of the preceding section of this paper. Random chain rupture is equivalent to a decrease of the molecular weight of the original rubber, with a Poisson molecular weight distribution. If the number of cross linkage points per 1 cc remains unchanged during degradation, then $n\gamma = 2\nu_0$ = const, while γ decreases. Referring N in Equation (24) to the relative content of the insoluble fraction $1-s$, we find the number of active chains in 1 cc of the gel fraction:

$$N_2 = 2\nu_0(1-s)(1-2\gamma s)(1+\gamma s). \tag{25}$$

The plot of $1 - N_{22}/N_{21}$, calculated on the basis of Equation (25) (N_{22} and N_{21} are the numbers of active chains in 1 cc of the gel fraction of the degraded and original vulcanizate respectively) against s (the content of the soluble fraction) lies further away from the experimental points than the relationship calculated by Horikx. Thus, the assumption that in the oxidative degradation of natural rubber vulcanizates random chain rupture occurs is less probable than chain rupture near the cross linkage points, if the values of N_2 determined from maximum swelling can be taken as quantitatively significant.

Let us consider another application of these calculations. Chemical relaxation of stress in vulcanizates at high temperatures may in principle be determined by the same processes [9] as oxidative degradation. In this instance, in contrast to relaxation caused by rupture and rearrangement of cross links [10, 11] or by rupture of chains near cross linkage points, the relaxation resulting from random chain rupture should be nonexponential in character and should proceed at a rate inversely proportional to the density of the network. Indeed, on the assumption that rupture of monomer units is a reaction of the first order, we have:

$$p = 1 - (1 - p_0)\, e^{-kt} \approx p_0 + kt \tag{26}$$

or

$$\gamma = q/p = q_0/(p_0 + kt). \tag{27}$$

Here we confine ourselves to two terms in resolution of the exponent, as kt is always small. Substituting Equation (27) into (16), and taking into account that $n\gamma = 2\nu_0$ = const, we derive an approximate expression for N as a function of time at large values of γ (the first relaxation period)

$$N \approx 2\nu_0\,[(1 - 1/\gamma_0) - kt/q_0], \tag{28}$$

where terms with the subscript "$_0$" refer to the original vulcanizate.

A more exact relationship is obtained by substitution of Equation (27) into (24). The results of numerical calculations for $q_0 = 0.02$, $\gamma_0 = 40$ are shown graphically in Fig. 3 (Curve 1). This relationship differs from that derived by Berry and Watson [11] owing to the rougher concepts regarding the network structure. Comparison with an exponential relationship (Curve 2, Fig. 3) shows that in this instance stress relaxation should be more rapid than indicated by the exponential law.

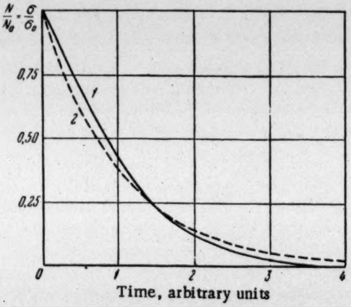

Fig. 3. Stress-time relationship during relaxation caused by random chain rupture (1), and the exponential relationship (2).

In comparisons of the equations given in this section with experimental data it should be remembered that secondary processes, which complicate the effect, may occur in oxidative degradation and chemical relaxation. We must also point out that these equations can be claimed to give only a qualitative description of the effect, as they were derived on the assumption that Equation (2) is valid, which is not the case.

SUMMARY

1. The elastic constant – initial molecular weight relationship has been calculated for monodisperse rubber and rubber with molecular weight distribution conforming to Poisson's law. It is found that the correction for the original molecular weight of the rubber depends on the type of distribution only for relatively sparse networks.

2. It is shown that Flory's calculation contains an error, and that the Flory equation $C = 2\nu_0\,(1 - 2\,M_c/M)$

should be replaced by $C = 2\nu_0(1 - M_c/M)$. The appropriate modifications must also be introduced into equations derived from the Flory equation.

3. Several applications of these calculations are illustrated by examples.

It is the author's pleasant duty to thank B.A. Dogadkin, who suggested the subject of this investigation.

Scientific Research Institute for the Tire Industry,
Moscow

Received April 12, 1957

LITERATURE CITED

[1] P. Flory J. Chem. Rev. 35, 51 1944.

[2] P. Flory, N. Rabjohn, M. Shaffer, J. Pol. Sci. 4, No. 3, 225 1949; Rub.Chim.Tech.19,522, 1956.

[3] A. M. Buche, J. Pol. Sci. 19, No. 92, 297 1956.

[4] P. Flory, J. Ind. Eng. Chem. 38, 417 1946; Rub. Chem. Technol. 19, 522 1946.

[5] M. H. Horikx, J. Pol. Sci. 19, No. 93, 445 1956; Rub. Chem. Technol. 29, No. 4, 1166 1956.

[6] P. Flory, J. Chem. Phys. 46, 132 1942.

[7] A. Charlesby, J. Pol. Sci. 11, No. 6, 513 1953.

[8] T. Alfrey, Mechanical Behavior of High Polymers, translation edited by M. V. Volkenshtein, (IL 1952) p. 310.

[9] A. V. Tobolsky, J. Appl. Phys. 27, No. 7, 673 1956.

[10] B. A. Dogadkin and Z. N. Tarasova, Colloid J., 15, No. 5, 347 1953.*

[11] J. P. Berry, W. F. Watson, J. Pol. Sci. 18, No. 88, 201 1955.

---

* Original Russian pagination. See C. B. translation

RECIPROCAL DISPLACEMENT OF COMPONENTS IN ION EXCHANGE CHROMATOGRAPHY

G.V. Samsonov and V.A. Orestova

In the movement of a mixed zone of two types of exchanging ions along a column filled with an ion exchange resin, separation of this zone into zones of the individual components should conform to the theory advanced by us earlier [1, 2]. If the exchanging ions are of equal valencies (with equal ionic charges) the conditions of ion displacement are completely determined by the ion exchange constant in the equation

$$\frac{m_1}{m_2} = K\frac{c_1}{c_2}, \tag{1}$$

where m_1 and m_2 are the quantities of ions of the first and second type in the adsorbed state on the resin, and c_1 and c_2 are the concentrations of these ions in solution. If $K > 1$, ions of the second type (c_2, m_2) form the leading zone, while ions of the first type (c_1,m_1) are in the second zone. When $K < 1$, the sequence of the zones should be reversed. If $K = 1$, the mixed ion zone moves without separation into zones of the individual components. Reciprocal displacement of the components can be observed most conveniently in dynamic sorption in a three-component system. If through a column filled with one type of ions a solution is passed containing exchanging ions of second and third types, then the moving mixed zone of the latter two components should be deformed in such a way as to form a sharp boundary between the zones of the ions contained in the mixed zone. This is possible only when ions of a particular type in a mixed zone form a separate zone of this component only, situated at the boundary between the zone of the displaced ion and the mixed zone, corresponding in composition to the solution continuously entering the column. The formation of a sharp boundary within the zone of the components entering the column and separation of a pure zone of one of them must evidently be accompanied by the formation of a maximum on the elution curve for the displaced component.

The presence of maxima on the elution curves in the exchange of three types of ions in dynamic conditions, when a solution containing two types of exchanging ions is introduced into the column, has been experimentally observed in a number of cases [3-6]. One of the components entering the column was displaced and formed a pure zone of the single component. As was already stated above, the conditions for the displacement of this component, which determine that one of the two components is displaced and forms a pure zone, depend entirely on the ion exchange constant in the exchange of ions of different valencies. This has been demonstrated experimentally. It follows from our theory of the dynamics of ion exchange [1, 2] that in the exchange of ions of different valencies in dynamic conditions the formation of a sharp boundary depends on a number of variables, including the solution concentration. In a two-component system a sharp boundary between zones of two types of ions is determined by the condition:

$$c_0 > c_{\text{cr}}, \text{ when } \quad z_1 < z_2 \tag{2}$$

or

$$c_0 < c_{\text{cr}}, \text{ when } \quad z_1 > z_2, \tag{3}$$

where c_0 is the aggregate concentration of the two types of exchanging ions.

$$c_{\text{cr}} = m/K^{\frac{z_1 \cdot z_2}{z_1 - z_2}}, \tag{4}$$

where m is the exchange capacity of the resin; K is the ion exchange constant in the equation

$$\frac{m_1^{1/z_1}}{m_2^{1/z_2}} = K\,\frac{c_1^{1/z_1}}{c_2^{1/z_2}}, \tag{5}$$

where z_1 and z_2 are the ionic charges (we are considering a process in which, in the separation of a mixed zone, the second component, with c_2 and m_2, is displaced by the first).

It follows from the theory that a mixed zone of two ions of different valencies can separate into zones containing the individual components in such a way that in one and the same two ions – resin system both ions of the higher and of the lower valencies can be displaced. It all depends on the aggregate concentration of the ions in the mixture. There is a certain critical concentration, readily calculated by means of Equation (4), on the two sides of which the sequence of the components in the ion exchange columns will be different. If the total solution concentration is greater than c_{cr}, ions of the lower valency should displace ions of the higher valency; at a concentration below c_{cr} the ion zones should move in the reverse sequence.

The method described above was used for experimental study of the reciprocal displacement of ions of different valencies. A solution of two components with respect to exchanging ions was passed through an ion exchange column containing a definite type of ions (sodium). As the result of formation of a sharp boundary between the ion zones, one of the ions should be displaced from the mixed zone with formation of a maximum on the elution curve.

In order that the critical concentration should not be too high (otherwise Equation (5) cannot be used, and moreover it is difficult to carry out the experiments at $c_0 > c_{cr}$), according to Equation (4) the constant for the exchange of the bivalent for the univalent ion must not be large.

In other words, the univalent ions chosen must interact vigorously with the resin. It is known [7] that quaternary ammonium ions have this property. Ions of calcium and trimethylbenzylammonium (chlorides) were therefore chosen for studying the sequence of ion motion in the chromatographic column. The cation exchange resin was SNF sulfonic resin. The exchange constant for calcium and the quaternary ammonium ions was 0.086; the critical concentration was 0.026 N.

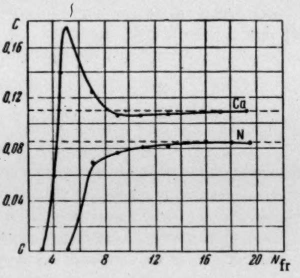

Fig. 1. Frontal sorption of calcium (Ca) and trimethylbenzylammonium (N) ions in the sodium form of SNF sulfophenolic resin at $c_0 > c_{cr}$. Initial concentrations of the ions: Ca – 0.1096 N $(CH_3)_3C_6H_5CH_2$ N – 0.0874 N; c_0 = 0.1953 N

In each experiment 1 g of the resin in sodium form was used, with grain size 60-150 mesh. The volumes of the fractions taken were 5 ml in the first experiment and 50 ml in the second. The solution flow rates were 20 and 50 ml/cm^2. hour respectively.

The elution curves in Fig. 2, obtained at $c_0 > c_{cr}$ and at $c_0 < c_{cr}$, show that in the first case trimethylbenzylammonium ions displace calcium ions, and in the second the position is reversed. As was predicted from our theory, the univalent ion is the displacing ion at high concentrations, and the multivalent ion at low. This transposition of the sequence of ionic motion in ion exchange chromatography by simple alteration of the solution concentration casts doubt on the value of sorption series of ions arranged in order of their reciprocal displacing power.

The reciprocal displacement of ions on ion exchange resins has been studied previously in relation to the statistical characteristics of ion exchange [3-6, 8, 9].

The effect of solution acidity on the sequence of the ion zones in chromatography has also recently been the subject of special investigations [10, 11]. It was found that changes in the sequence of the ion zones are in accordance with changes in the ion adsorbabilities, as was to be expected in systems in which the concentration of one type of exchanging ion is many times less than the concentration of the other.

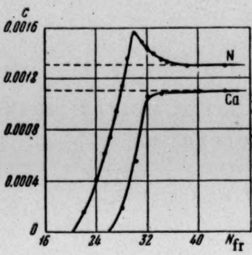

Fig. 2. Frontal sorption of calcium (Ca) and trimethylbenzylammonium (N) ions in the sodium form of SNF sulfophenolic resin at $c_0 < c_{cr}$. Initial concentrations of the ions: Ca – 0.00110 N; $(CH_3)_3C_6H_5CH_2$ N 0.00130 N; c_0 = 0.00240 N

Our results show that reciprocal displacement of ions under dynamic conditions, when the concentrations of the ions are comparable, is entirely determined by the laws of adsorption dynamics – by the conditions for the formation of sharp boundaries between the ion zones.

SUMMARY

1. It is shown that the sequence of the components in ion exchange chromatography involving ions of different valencies may change with changes in the concentration of the solution entering the column.

2. It is shown that the sequence of the ions in the column is determined by the conditions for formation of sharp ion zone boundaries.

Institute of High Molecular
Compounds, Leningrad

Received
February 9, 1957

LITERATURE CITED

[1] G. V. Samshonov, Proc. Acad. Sci. USSR, 97, 707 1954.

[2] G. V. Samsonov, in Symposium: "Chromatography" (Leningrad State Univ. Press 1956) p. 22.

[3] L. S. Aleksandrova, T. B. Gapon, N. V. Filatova, and K. V. Chmutov, Trans. Commission Anal. Chem., vol. 6 (9), 235 1955.

[4] O. Samuelson, Ion Exchangers in Analytical Chemistry (IL, 1955) p. 57.

[5] A. M. Trofimov, in Symposium: "Chromatography" (Leningrad State Univ. Press 1956) p. 15.

[6] G. V. Samsonov, S. F. Lavrentyeva, and M. P. Shesterikova, Antibiotics, No. 2 1957.

[7] T. R. Kressman, J. A. Kitscher, J. Chem. Soc. 1949, 1208.

[8] S. M. Partridge, R. C. Brimleg, Biochem. J. 44, 513 1949; S. M. Partridge, R. G. Westall, Biochem. J. 44, 418 1949.

[9] C. W. Davies, Biochem. J. 45, 38 1949.

[10] S. Yu. Elovich, Proc. Acad. Sci. USSR, 101, 293 1955.

[11] S. Yu. Elovich and L. T. Kuzmina, Colloid J., 18, 268 1956.*

---

* Original Russian pagination. See C. B. translation.

INVESTIGATION OF THE STRUCTURE OF BRANCHED POLYSTYRENE BY THE LIGHT SCATTERING METHOD

I.G. Soboleva, N.V. Maktletsova and S.S. Medvedev

It was shown in the previous paper [1] that the root mean square distance $\underline{h}$ between the chain ends, when the second virial coefficient is zero, is independent of the chemical nature of the solvent and is therefore a characteristic parameter of the polymer structure. This is in agreement with views on the configuration of polymer molecules in various solvents, based on the statistical physics of polymer molecules [2, 4]. On the basis of these views it seems likely that the most promising approach to evaluation of polymer chain structure is by studies of the behavior of the polymer molecules near the precipitation point.

The purpose of the present investigation was to establish the possibility, by using polystyrene of known degree of branching, of evaluating molecular chain structure from the absolute magnitude of the polymer molecules dissolved in different media.

Radical polymerization of styrene does not result in appreciable branching of the polymer, owing to the low rate of chain transfer to the polymer [5]. Branched polystyrene was prepared by photopolymerization of styrene in presence of a narrow fraction of brominated polystyrene of high molecular weight (graft polymerization). The active centers formed in the chain as the result of bromine removal serve as origins of side chain growth [6]. This was accompanied by polymerization of styrene, initiated by bromine atoms. The average length of the side chains formed could be deduced from the average molecular weight of this polymer.

The graft polymerization was carried out in benzene solution at 40°. The amount of brominated polystyrene added (containing 1.5-3.5% bromine) was 15% on the monomer; the initial concentration of the polymer in the reaction mixture was 7-9%. The irradiation was by means of ultraviolet light of wave length 3600 A and over; the irradiation intensity, determined by means of a uranyl oxalate actinometer, was $1.4 \cdot 10^{-8}$ einstein/sec.

Control experiments in absence of monomer showed that under such conditions only slight changes take place in the molecular characteristics of the original brominated polystyrene, indicating that the reaction of recombination of the polymer radicals formed by removal of bromine atoms has little effect. However, in presence of monomer, owing to the formation of growing polymer radicals, the probability of their recombination increases. The degree of branching cannot therefore be conclusively estimated from molecular weight data. To estimate the degree of branching of polystyrene, graft polymerization was carried out with styrene containing radioactive carbon.

Tagged styrene was prepared from ethyl alcohol containing C^{14} and benzene, by the following scheme: ethyl alcohol ⟶ ethylene; ethylene + benzene ⟶ ethylbenzene ⟶ styrene. The degree of branching of the graft polymers was calculated from the results of determinations of the radioactivity of narrow fractions of the graft polymers relative to the activity of polystyrene synthesized from tagged monomer without any additions. Isolation of the narrow fractions, not contamined with low molecular radioactive polymer, was carried out by precipitation with methyl alcohol from 0.25% solution, with subsequent fractionation from 0.1% solution. The fractions so obtained were reprecipitated from 0.05% solution. Table 1 gives the results of determinations for polymer P23, prepared by graft polymerization with linear brominated polystyrene L2 containing 3.5% bromine.

The molecular weight and molecular size determinations were carried out by the light scattering method with apparatus in which the determinations could be made at three angles [7]. The calculations were done by

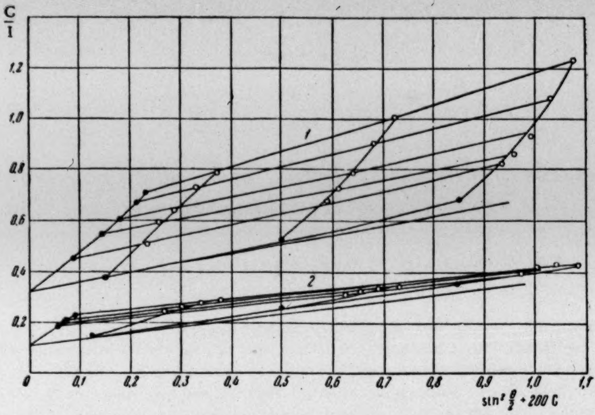

Fig. 1. Graphical determination of molecular weight and molecular size of L-1 polystyrene from light scattering data: 1) in toluene; 2) in cyclohexane; ordinate to double scale; arbitrary constant, 1.33.

TABLE 1

Relative Radioactivity and Degree of Branching of P23 Polystyrene Fractions

Fractions	Molecular wt. $M \cdot 10^{-3}$ by light scattering	Number of pulses per 3 minutes	Relative radioactivity	Wt. of branches in molecule $\times$ $\times 10^{-3}$	Number of branches per molecule
1					
2	6100	2227	0.372	2270	27.7
3	4350	1352	0.225	980	13.1
4	3250	1049	0.175	569	7.6
5	2500	1122	0.187	468	6.2
6	1600	1137	0.189	303	4.0
7	950	1832	0.305	—	—
8	620	3743	0.625	—	—
9	360	5092	0.850	—	—
10*	75	5323	0.887	—	—
Standard**	—	6000	1.000		

---

* Molecular weight determined from osmotic data.

** Polystyrene synthesized from tagged monomer.

TABLE 2

Effect of Bromine Content on the Molecular Size of Brominated Polystyrene in Solution

Bromine content of polystyrene, %	Mol. wt. $M \cdot 10^{-3}$	$h_T/M^{1/2}$* in toluene	Bromine content of polystyrene %	Mol. wt. $M \cdot 10^{-3}$	$h_T/M^{1/2}$* in toluene
0	1820	0.91	2.0	460	0.94
0	1500	0.95	3.0	1130	1.00
0	1070	0.98	5.5	1560	0.68
2.0	1060	0.93	5.5	715	0.65

---

* h_T is the root mean square distance between the chain ends.

Zimm's method [8] with approximate extrapolation to zero concentration and zero angle. The calculated data for the linear polymers did not differ from data calculated by Debye's method from the scattering asymmetry [9]. The data for the branched polymers were somewhat lower. The measurements were performed in toluene at room temperature and in cyclohexane at a temperature 3° above the precipitation point. The measurement temperature was 30-35°, depending on the molecular weight. The second virial coefficient in the osmotic pressure equation for solutions in cyclohexane was close to zero. Fig. 1 shows an example of a graphical determination of molecular weight and molecular size from light scattering data at three angles.

The intrinsic viscosity was measured in toluene, methyl ethyl ketone, and cyclohexane at the temperatures of the light scattering determinations. In order to determine the influence of molecular chain structure on the configuration of the molecules in solution, it was necessary to find the extent of the influence of the bromine present in the macromolecule on the molecular size. Table 2 gives the molecular parameters of polystyrene with different bromine contents.

TABLE 3

Molecular Characteristics of Linear and Branched Polystyrenes, Based on Light Scattering Data

Polymer	Mol. wt. $M \cdot 10^{-3}$	Number of branches per 3500 monomer units of principal chain	Root mean square distance between chain ends, A		$\frac{h_T}{M^{1/2}}$	$\frac{h_\theta}{M^{1/2}}$	Second virial coefficient in toluene $B \cdot 10^4$
			in toluene $[\eta]_T$	in cyclohexane $[\eta]_{ch}$			
L-1	1900	0	1900	810	0.94	0.59	1.9
L-2	1150	0	1150	670	0.92	0.64	3.6
P1-1	2400	0.5	1240	920	0.80	0.59	2.8
P2-1	2600	1.1	1200	720	0.74	0.45	3.2
P23-1	6100	3.0	1920	1130	0.78	0.46	1.2
P23-2	4350	1.3	1770	840	0.83	0.40	1.8
P23-3	3250	1.0	1300	860	0.72	0.47	1.9
P23-5	2500	1.1	1180	630	0.75	0.40	1.9
P23-6	1600	1.1	1030	570	0.82	0.45	5.0

TABLE 4

Intrinsic Viscosities of Linear and Branched Polystyrenes

Polymer	Mol. wt. $M \cdot 10^{-3}$	Branches / 3500 units of chain	Intrinsic viscosity $[\eta] \frac{100\ \text{ml}}{g}$			$\frac{(M[\eta_\theta])^{1/3}}{M^{1/2}}$		
			in toluene $[\eta]_T$	in methyl ethyl ketone $[\eta]_{mek}$	in cyclohexane $[\eta]_{ch}$	in toluene	in methyl ethyl ketone	in cyclohexane
L-1	1900	0	5.0	3.1	1.8	1.53	1.31	1.09
L-2	1150	0	4.0	2.2	1.1	1.55	1.27	1.02
P1-1	2400	0.5	4.6	—	1.4	1.44	—	0.97
P2-1	2600	1.0	4.0	2.3	1.45	1.36	1.11	0.960
P23-1	6100	3	7.0	3.8	1.70	1.43	1.16	0.90
P23-2	4350	1.3	4.5	—	—	1.29	—	—
P23-3	3250	1.0	3.9	2.5	1.5	1.295	1.12	0.94
P23-5	2500	1.1	3.4	—	1.3	1.29	—	0.93
P23-6	1600	1.1	2.65	—	1.0	1.28	—	0.92

It follows from Table 2 that an increase of the density of globularly coiled molecules is found at ~ 5% bromine content; lower contents of bromine do not affect the molecular configuration of polystyrene in solution. Therefore, with a total bromine content not greater than 3.5% in the polymers studied, small fluctuations of the bromine content as the result of partial removal in the course of photopolymerization could not influence the results of the molecular size determinations.

Table 3 contains the results of nephelometric determinations of the molecular characteristics of linear polystyrene fractions L-1 (the starting polymer used for preparation of brominated polystyrene L-2), L-2 (the starting polymer used for preparation of graft polymers P2 and P23), and branched polymers: the first fractions of polymers P1 and P2, and six fractions of polymer P23. The following three fractions of polymer P 23 were not investigated, as they were contaminated with low molecular radioactive polymer.

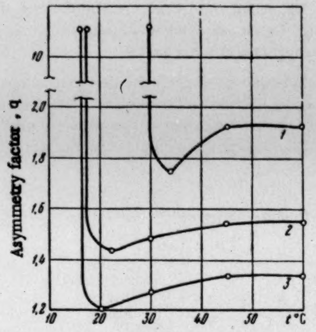

Fig. 2. Precipitation temperatures of polystyrenes with different chain structure. Solvent: toluene + 29 ml/100 ml of methyl alcohol; polymer concentration 0.02 g/100 ml; 1) linear polystyrene, M = $3 \cdot 10^6$; 2) branched polystyrene P2 = 1, M = 2, $6 \cdot 10^6$; 3) linear polystyrene L-2, M = $1.15 \cdot 10^6$

Examination of the data in Table 3 indicates that the parameter $h/M^{1/2}$ decreases with molecular chain branching by a factor of about 1.2 in a good solvent, and by 1.5 near the precipitation point. Further increase of the degree of branching of the polystyrene molecules could not be achieved, as increase of the bromine content led to structurization of the polymer. Jones et al. [6], in order to avoid gel formation in the synthesis of branched polystyrene, used carbon tetrachloride in graft polymerization; the rate of chain transfer to the polymer is then fairly high and indefinite amounts of chlorine were thereby introduced into the molecular chains. Naturally this made it difficult to draw conclusions concerning the influence of branching on the molecular configuration in solution.

The viscosimetric results are given in Table 4. The ratio of $(M[\eta])^{1/3}$, proportional to the size of the molecules in solution [2], to the root of the molecular weight, like the parameter $h/M^{1/2}$, decreases with increasing chain branching. The ratio in cyclohexane decreases somewhat less, as compared with the light scattering data.

It is seen that the second virial coefficients for branched polymers in toluene solutions are somewhat higher than for linear polymers (see Table 3). A comparison of the precipitation points of linear and branched polystyrenes from toluene solutions on addition of methyl alcohol also showed that the branched polystyrene is precipitated at lower temperatures (see Fig. 2). This is understandable if it is taken into account that cross linkage points and free chain ends influence entropy changes in opposite directions.

SUMMARY

1. Branched polystyrene was synthesized by grafting of side chains containing radioactive carbon C^{14} on brominated linear polystyrene.

2. The molecular size of the branched polystyrenes in solution is less than that of linear polymers. The changes in molecular size are more prominent near the precipitation point of the polymer.

3. Viscosimetric data are in agreement with light scattering data, confirming the validity of the Flory equation for the relationship between the size of polymer molecules and the intrinsic viscosity.

The L. Y. Karpov Physicochemical Scientific
Research Institute

Received July 2, 1956.

LITERATURE CITED

[1] I. G. Soboleva, N. V. Makletsova, and S. S. Medvedev, Proc. Acad. Sci. USSR, 106, No. 2, 303 1956.

[2] P. Flory, T. Fox, J. Am. Chem. Soc. 73, 1904 1951.

[3] M. V. Volkenshtein and O. B. Ptitsyn, Progr. Phys. Sci. 4, No. 4, 501 1953.

[4] O. B. Ptitsyn, J. Phys. Chem., 29, No. 2, 396 1955.

[5] J. C. Bevington, G. M. Guzman, H. W. Melville, Proc. Roy. Soc. 221, 453 1954.

[6] M. H. Jones, H. W. Melville, W.J.P. Robertson, Nature 174, 78, 1954.

[7] I. G. Soboleva, Inst. Tech. Econ. Inf. Acad. Sci. USSR, Instruments and Stands, Theme 8, No. 2, pp. 56-449 1956.

[8] B. Zimm, J. Chem. Phys., 16, 1099 1948.

[9] N. Z. Fattakhov, V. N. Tsvetkov, and O. V. Kallistov, J. Exp. Theoret. Phys., 26, No. 3, 345 1954.

THE EFFECT OF PLASTICIZERS ON THE HYDROGEN PERMEABILITY OF POLYVINYL CHLORIDE

S.I. Sokolov, S.A. Reitlinger and R.I. Feldman

Addition of plasticizers to high polymers weakesn intermolecular bonds, with a consequent lowering of the potential barriers which restrict flexibility, and a decrease of steric obstacles to the relative displacement of the segments of the polymer chains [1-3]. It follows from this that the structural changes caused by plasticizers should lead to an increase in the gas permeability of polymer systems [4]. In fact, it has been shown in earlier investigations that plasticization results in an increase of polymer permeability [5, 6] and in changes of the permeability activation energy [7]. However, the available data mainly refer to plasticized polymers in the high elastic state.

Investigations of the gas and vapor permeability of films in the temperature range covering the transition from the glassy to the high elastic state [8-10] have shown that the transition is accompanied by changes in the relationships between the temperature and the permeability and diffusion constants. Studies of the gas permeability of plasticized polymers, in different states of aggregation according to the plasticizer content, are of definite interest. In the present investigation the hydrogen permeability of polyvinyl chloride films has been studied over a wide range of plasticizer concentrations, covering all the states from the glassy to the viscofluid.

The hydrogen permeability (P) was determined by means of a thermostatically controlled Daynes-Shakespeare apparatus [5]. The gas pressures on both sides of the films were kept equal during the tests. The diffusion constants (D) were determined by the "lag" method, and the solubility constants (σ) were calculated from the values found for P and D [4]. The hydrogen used for the tests contained 99.8% H_2.

The films were made from polyvinyl chloride prepared by emulsion polymerization and extracted with alcohol, with molecular weight $6.2 \cdot 10^4$. The film specimens, in the form of circles ~0.5 mm thick and 80 mm in diameter, were made by hot pressing between sheets of aluminum foil in a hydraulic press. For films with high plasticizer contents, the polyvinyl chloride was dissolved by warming in the plasticizer, and a film was cast from the solution on silk gauze as a support.

The gas permeability constants were expressed in cubic centimeters (at 0° and 760 mm Hg) of gas which passed through a film 1 cm^2 in area and 1 cm thick per second, with a pressure drop of 1 atmosphere /$cm^2 \cdot sec.^{-1} \cdot atm.^{-1}$/; the diffusion constants were expressed in $cm^2 \cdot sec.^{-1}$, and the solubility constants in cc (at o° and 760 mm Hg) of gas dissolved in 1 cc of the polymer under a pressure of 1 atmosphere [$atm.^{-1}$].

Fig. 1 shows variations of the hydrogen permeability of plasticized polyvinyl chloride with dimethyl phthalate content. The plasticizer concentration is expressed in mole fractions; the molecular weight of the polymeric component is taken as 62.5, the weight of one monomer unit in the polyvinyl chloride molecule. The curve has three characteristic regions, corresponding to the known thermomechanical states: the glassy, high elastic, and viscofluid states of amorphous polymers [11]. The greatest increase of gas permeability with plasticizer content in the polymer ($\Delta P/\Delta N_2$) is found in the high elastic state. The transition of polyvinyl chloride from the glassy into the high elastic state occurs at a ratio of 1:12 – 1 : 14 dimethyl phthalate molecules to polyvinyl chloride monomer units, and the transition from the high elastic to the viscofluid state at a ratio of 1:3 – 1:4; this approximately corresponds to the ratios found in mechanical tests.

The gas permeability constant of plasticized polyvinyl chloride (P_{pp}) in the region of high elasticity can be approximately expressed, like the relationship for the mechanical characteristics [12], in terms of the gas permeability constants of the polymer (P_p) and plasticizer (P_{pl}) present in the same state in the mixture

$$P_{pp} = P_{p}^{N_1} \cdot P_{pl}^{N_2}$$

where N_1 and N_2 are the respective mole fractions of polymer and plasticizer in the system, such that $N_1 + N_2 = 1$. The values of P_p and P_{pl} calculated by means of this equation are given in the Table.

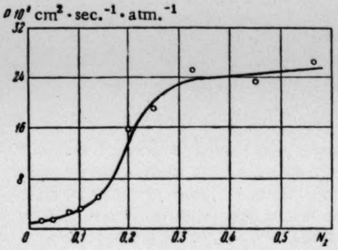

Fig. 1. Variation of the constant P with mole fraction of dimethyl phthalate N_2 in the binary system polyvinyl chloride – dimethyl phthalate at 20°.

Fig. 2 shows the results found for the constants P, D, and σ for hydrogen and polyvinyl chloride with dibutyl phthalate plasticizer. In the transition from the glassy to the high elastic state the ratio $\Delta D / \Delta N$ increases, while the solubility of hydrogen changes only slightly.

Fig. 3 shows variations of the logarithm of the permeability constant for plasticized polyvinyl chloride with contents of phthalate ester plasticizers.

The data obtained on the hydrogen permeability of films are of great interest, as they make it possible to regard gas permeability determination as a method for studying the states of aggregation of polymers [13] and variations of them under the action of plasticizers.

Plots of the gas permeability – composition relationship, if the composition of the mixture is expressed in mole fractions [14] give a clear picture of differences in the states of aggregations, which is evidence of the homogeneity of the systems in question. Essentially we are dealing with ternary systems: polymer-plasticizer-hydrogen. However, in view of the low solubility of hydrogen and of the constant permeation conditions (pressure and temperature), they may be regarded as binary polymer-plasticizer systems.

Calculated Values of P_p and P_{pl} for Polymer-Plasticizer Mixtures in the High Elastic State

Plasticizer	P_p	P_{pl}	$d \log P_{pp}/dN_2$
Dimethyl phthalate	$0.73 \cdot 10^{-8}$	$6.05 \cdot 10^{-3}$	6.00
Diethyl phthalate	$0.76 \cdot 10^{-8}$	$5.76 \cdot 10^{-1}$	7.88
Dibutyl phthalate	$0.79 \cdot 10^{-8}$	$1.86 \cdot 10^{-1}$	9.39
Diamyl phthalate	$0.75 \cdot 10^{-8}$	$1.61 \cdot 10^{3}$	11.33
Dioctyl phthalate	$0.76 \cdot 10^{-8}$	$8.52 \cdot 10^{4}$	13.05

In a binary mixture the distinction between solvent and solute is to some extent arbitrary. However, it is more rational to regard as the solvent the component which determines the state of aggregation of the mixture. If, for example, when a large amount of a crystalline substance is dissolved in a small amount of liquid a liquid solution is obtained, the second, liquid component should be regarded as the solvent. In the present instance before a mixture in the viscofluid state is obtained it is more correct to regard the polymer and not the plasticizer as the solvent.

On the other hand, after the mixture has been formed, both the components can be regarded as existing in the same state of aggregation as the mixture. The hydrogen dissolved in the mixture should be considered as being in the liquid state, despite the fact that the temperature of the mixture is considerably above its critical temperature. This may be extended to any state of aggregation, for example, the state of high elasticity [12]. Thus, both the plasticizer and the hydrogen dissolved in the mixture should be considered as if existing in the high elastic state, like the system as a whole. It follows that the values obtained by extrapolation for the pure components in the high elastic state cannot be compared with the properties which they have if taken in pure form, but not in the same state as the mixture.

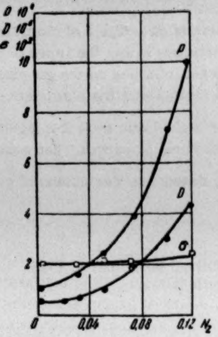

Fig. 2. Variations of the constants P, D, and σ with mole fraction of dibutyl phthalate in a system containing polyvinyl chloride, at 20°.

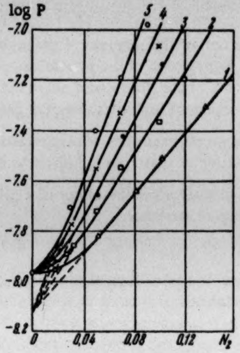

Fig. 3. Variations of the logarithm of the permeability constant for polyvinyl chloride with mole fractions of plasticizers at 20°: 1) dimethyl phthalate; 2) diethyl phthalate; 3) dibutyl phthalate; 4) diamyl phthalate; 5) dioctyl phthalate.

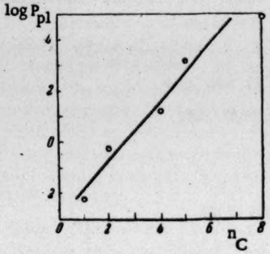

Fig. 4. Variation of the logarithms of the limiting permeabilities P_{pl} of plasticizers with n_C (n is the number of C atoms in the alkyl groups of the phthalate esters).

The large differences between the values of P_{pl} found by extrapolation for different plasticizers in the high elastic state do not correspond to the intrinsic properties of the pure plasticizers, but to the effects which they have in changing the properties of the system in the given state of aggregation. The limiting values of $P_{pl}^{N_2=1}$, found for the pure plasticizers by extrapolation, are characteristic constants, and, as Fig. 4 shows, their logarithms are a linear function of the number of carbon atoms in the alkyl groups of the phthalate esters used as plasticizers for polyvinyl chloride.

The results obtained show that additions of plasticizers to polyvinyl chloride influence the gas permeability to different extents, according to the state of aggregation of the polymer. Additions of plasticizer to the polyvinyl chloride in amounts which do not alter the glassy state have little influence on gas permeability, as the plasticizer molecules, becoming bound with individual groups along the chain, do not induce chain flexibility.

The hydrogen permeability of unplasticized polyvinyl chloride, determined experimentally at 20° (Fig. 3), is $1.06 \cdot 10^{-8}$ cm. sec.$^{-1}$. atm.$^{-1}$, as distinct from the corresponding average value $0.75 \cdot 10^{-8}$ found by extrapolation of the linear region of the plot to the ordinate axis. This discrepancy may be caused by fixation of the polymer structure at its glass transition temperature.

In the high elastic state the plasticizer molecules separate the polymer chains, with a consequent lowering of the potential barriers of chain rotation, favoring an increase of the gas permeability. It may be assumed that the action of plasticizer molecules is not confined only to interaction with polar groups, but affects a wider region of the polymer chains. Finally, in the viscofluid state an increase of the plasticizer content does not produce any significant changes in the intermolecular forces, as the separation of the chain molecules of polyvinyl chloride is largely complete. Accordingly, the viscofluid state is characterized by only a slow increase of the gas permeability of the films on addition of plasticizer.

SUMMARY

1. The rate of the increase of gas permeability of polyvinyl chloride on addition of plasticizers depend on the state of aggregation of the plasticized polymer. Additions of plasticizer within the limits of the glassy or viscofluid states of the plasticized polyvinyl chloride have no significant influence on the gas permeability, whereas in the region of high elasticity, the gas permeability increases rapidly with the plasticizer content.

2. The gas permeability of plasticized polyvinyl chloride in the high elastic state is a regular function of the mole fraction of plasticizer, similar to that found earlier for mechanical properties. The constant $P_{pl}^{N_2=1}$ which characterizes the effect of a given phthalate plasticizer, depends on the number of carbon atoms in the alkyl group of the ester.

The Moscow Technological Institute for the
Light Industries

Received November 3, 1956.

LITERATURE CITED

[1] V. A. Kargin and Yu. M. Malinsky, Proc. Acad. Sci. USSR, 73, 967 1950.

[2] P. V. Kozlov and E. F. Russkova, High Molecular Compounds, 12, 44 1952.

[3] S. I. Sokolov and R. I. Feldman, Investigations of High Molecular Compounds (Izd. AN SSSR, 1949) p. 329.

[4] S. A. Reitlinger, Progr. Chem., 20, 213 1951.

[5] S. A. Reitlinger, and L. A. Panyunina, J. Appl. Chem., 12, 886 1939.

[6] D. W. Brubaker, K. Kommermeyer, Ind. Eng. Chem. 45, 1148 1953.

[7] P. M. Doty, J. Chem. Phys. 14, 244 1946.

[8] P. Meors., J. Am. Chem. Soc. 76, 3415 1954.

[9] S. N. Zhurkov and G. Ya. Ryskin, J. Tech. Phys., 24, 797 1954.

[10] G. Ya. Ryskin, J. Tech. Phys., 24, 797 1954.

[11] V. A. Kargin and T. I. Sogolova, J. Phys. Chem., 23, 530 1949.

[12] R. I. Feldman, Proc. Acad. Sci. USSR, 97, 1033 (1954).

[13] R. I. Feldman and S. I. Sokolov, Chemistry and Physical Chemistry of High Molecular Compounds (Izd. AN SSSR, 1952) p. 159.

[14] S. I. Sokolov and R. I. Feldman, Summaries of Papers at the 3rd All-Union Conference on Physico-chemical Analysis (Izd. AN SSSR 1955) p. 160.

SPECIFIC HEATS OF AQUEOUS SOLUTIONS OF SOME SOAPS

V.I. Solnyshkin

The question of the micellar structure of colloidal soap solutions is of great theoretical significance, as definite conclusions cannot be drawn from the investigations which have been carried out in this field. Clearly defined association of molecules into micelles is observed at different concentrations of fatty acid salts.

The concentration region in which micelle formation takes place in aqueous soap solutions has been termed the "critical concentration of micelle formation" [1], below which soaps are in the ionic state, while above it colloidal solutions are formed. The work of Davies [2] on potassium n-caprylate solutions showed that measurements of the specific heats of such systems can provide additional information on micelle formation.

It was first shown by M. Fischer [3] that, in very dilute aqueous solutions, sodium salts of fatty acids are completely dissociated. Powney and Jordan [4], in a study of the hydrolysis of the salts of various fatty acids, discovered the existence of a minimum and a maximum at concentrations of the order 10^{-4} - 10^{-5} mole/liter. However, the suggested interpretation did not explain the changes in the minimum values of hydrolysis [4,5] with increasing temperature. Flockhart and and Graham [6] studied electrical conductivity and viscosity of sodium oleate solutions, and discovered sharp changes in the curves in this region. They cast doubt on the hypothesis that micelles are formed from the fatty acid molecules formed by hydrolysis of soaps, but did not examine the question in detail. The existence of aggregates of soap molecules at low concentrations is still a subject of controversy.

Hartley [1] stated that below "the critical concentration of micelle formation sodium salts of fatty acids behave like strong electrolytes" (Fig. 1, a). McBain [7] postulated the formation of ionic micelles in very dilute solutions until this concentration is reached. Ekwall discovered the existence of flat regions in electrical conductivity – concentration curves for sodium myristate solutions, while Hartley [1] postulated that this form of the conductivity curves is caused by micelle formation in the concentration region corresponding to the plateau.

It is difficult to believe that at normal temperatures the ions of a dissociated fatty acid soap, hydrated by associated water molecules and undergoing Brownian movement, can form aggregates. If this was the case, the Van-der Waals forces of the CH_2 groups would not be able to maintain such formations in equilibrium with the medium. The situation may change if the ions associate into molecules. The sharply decreasing degree of hydration would favor aggregation. Ekwall [5] and Steinsby and Alexander [8] showed that the observed changes on the hydrolysis curve [4] take place if molecular association occurs. They assumed that mixed micelles of fatty acid molecules and soap ions are formed. However, it is difficult to account for the hydrolysis minimum on this theory. If mixed micelles are formed, sodium ions remain in solution and a hydrolysis minimum cannot occur, as alkalies are completely dissociated in dilute solutions. The degree of hydrolysis corresponding to the minimum on the curve coincides with the degree of hydrolysis at high concentrations, which suggests that nonionic soap molecules are formed (Fig. 1, b). Further autoflocculation [9] of these (Fig. 1, c) leads to a sharp decrease in the concentration of soap in true solution, which naturally increases the degree of hydrolysis. The minimum value, according to the data of various authors, corresponds to the following concentrations:

Ulman [10]..........	$0.986 \cdot 10^{-3}$ M
Powney and Jordan [4]...	$0.1 \cdot 10^{-4}$ M
Flockhart and Graham [6]	$0.9 \cdot 10^{-3}$ M

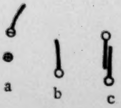

Fig. 1.

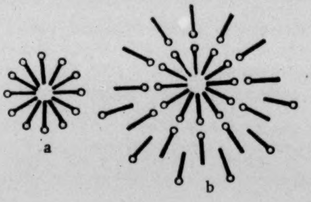

Fig. 2

However, the autoflucculated molecules are unstable and at a concentration of $1.5 \cdot 10^{-3}$ M, as indicated by the maximum on the viscosity curve for sodium oleate solutions [6], they may pass into a more stable form, which balances the van der Waals forces and confers stability to such "nuclei" in Brownian movement (Fig. 2,a). The greater the stability of such an aggregate, the higher is the degree of hydrolysis to which the maximum on the curve corresponds. The stability depends on the number of CH_2 groups in the molecular chain. The longer the molecule, the more stable is the nucleus formed and the lower is the concentration of soap in true solution. This explanation is supported by data on the hydrolysis of sodium oleate, laurate, myristate, palmitate, and stearate, as the maximum on the hydrolysis curve increases with increasing molecular length [4]. The position of the minimum on the hydrolysis curve does not remain constant with change of temperature; above 40° autoflocculates of two or three molecules may be formed, with the fatty acid playing an active role. Transition to the stable form, both at high and at normal temperatures, is associated with formation of aggregates from nonionic molecules which form layers around themselves and become the classical spherical associated micelles (Fig. 2,b).

Viscosity, electrical conductivity, and hydrolysis curves [4, 6] show that formation of initial nuclei in sodium oleate solutions at normal temperature is completed between $2.5 \cdot 10^{-3}$ and $3.0 \cdot 10^{-3}$ M. It is evident that the plateau on the conductivity curve is caused by dissociation of soap molecules together with their aggregation into autoflocculates, and hydrolysis of the soap only falls to low values again after the concentration has been reached at which nucleus formation is complete. Additions of oleic acid and caustic soda to the solutions during the determinations also indicate the predominant formation of nonionic molecules of sodium oleate. Addition of oleic acid leads to disappearance of the plateau on the conductivity curve, whereas caustic soda does not influence its course. It is evident that more nonionic molecules are formed in the first case, leading to a decrease in the degree of hydrolysis of the soap; little change in it is produced by addition of alkali.

For the specific heat determinations, sodium oleate and ricinoleate prepared by the Powney and Jordan method [4] in the form of dry neutral powders were dissolved in distilled water ($\kappa = 3.0 - 4.0 \cdot 10^{-6}\ \mathrm{ohm}^{-1} \cdot \mathrm{cm}^{-1}$) and then heated to 90-95°. The homogeneous solutions were cooled and analyzed by titration with 0.1 N HCl with phenolphthalein indicator [11].

The specific heats of the solutions were determined in a water-cooled adiabatic calorimeter at 20°. The heat capacity of the metallic parts of the inner calorimeter was $K_M = 47.8$ cal./deg. The specific heat was calculated by the formula:

$$c = \frac{191131\ Rg^2/\tau\Delta t - K_M}{s} \frac{\mathrm{cal}}{\mathrm{g} \cdot {}^{\circ}\mathrm{C}},$$

where R is the resistance of the heater in ohms (8.783Ω); g is the weight of silver deposited in the platinum basin, in g; τ is the time during which the current was passed, in seconds; Δt is the difference between the thermometer readings before and after passage of the current, in deg; s is the weight of the solution in grams.

The most reproducible results under our conditions were obtained at current strengths of 0.2-0.3 amp. The results are given in Figs. 3 and 4.

In both cases a plateau is found on the specific heat curves. For sodium oleate solutions the specific heat remains constant at concentrations between 0.25 and 0.65 M, and for sodium ricinoleate the corresponding region lies between 2.25 and 2.85 M.

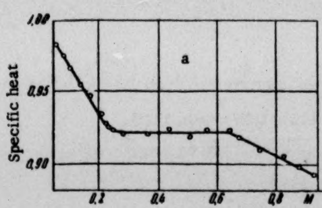

Fig. 3. Variation of specific heats of sodium oleate solutions with the molar concentration.

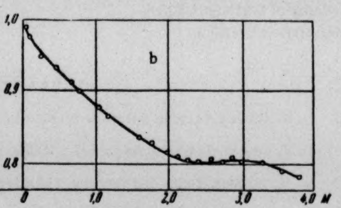

Fig. 4. Variation of specific heats of sodium ricinoleate solutions with the molar concentration.

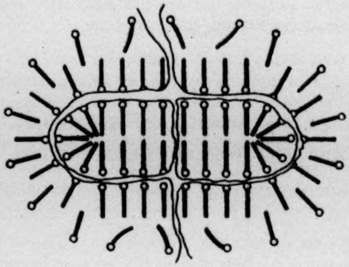

Fig. 5.

Further growth of the nuclei into micelles does not influence the steady increase of viscosity or decrease of specific heat, but at a concentration of 8 g / 100 ml or 0.26 M of sodium oleate [12], or at 0.25 M according to our determinations, the rate of change of the specific heat with concentration decreases sharply. At these concentrations formation of asymmetric micelles of the lamellar type begins (Fig. 5). The plateaus on the specific heat curves, first discovered by Davies for potassium caprylate solutions [2], and the plateaus on the conductivity curves in dilute solutions, are caused by the characteristics of micellar growth. The spherical micelles have all their degrees of freedom, and the specific heat of the solution decreases as the result of the increase in their size and numbers. Formation of the cylindrical form disturbs the thermodynamic equilibrium of the micellar motion, leading to vigorous rotation of the spherical micelles. This transition keeps the specific heat of the solution practically constant.

At concentrations above 0.65 M, when the transition to cylindrical micelles is complete, the formation of long micellar entanglements, causing gelation of the solution, can be postulated; the number of these increases with concentration, and in highly concentrated solutions soap crystals begin to form, consisting of oriented layers of soap molecules separated by interlayers of water. The final hydrated form of sodium oleate corresponds to the formula $NaOl \cdot 2H_2O$ [13].

In solutions of sodium ricinoleate the analogous, thermodynamically reversible process of micelle formation is shifted into the region of higher concentrations owing to the presence of a hydroxyl group in the molecular chain.

SUMMARY

1. The specific heats of aqueous solutions of sodium oleate and ricinoleate have been measured over a wide range of concentrations; plateaus have been found on the specific heat curves (Davies plateaus) in the concentration ranges from 0.25 to 0.65 M for sodium oleate solutions and from 2.25 to 2.85 M for sodium ricinoleate solutions.

2. Literature data and the experimental results are used to show the possible transition of sodium salts of fatty acids from the ionic state to the hydrated crystalline form through colloidal solutions.

Mining Institute
Academy of Sciences USSR
Beneficiation Division

Received October 12, 1956.

LITERATURE CITED

[1] G. S. Hartley, Aqueous Solutions of Paraffin-Chain Salts (Paris, 1936).

[2] D. S. Davies, J. Chem. Soc., 551 1933.

[3] M. H. Fischer, Soaps and Proteins (Moscow, 1932).

[4] I. Powney, D. O. Jordan Trans. Faraday. Soc. 34, 363 1938.

[5] P. Ekwall, Koll. Z. 101, 135 1942; Z. phys. Chem. A161, 195 1932.

[6] B. D. Flockhart, H. Graham, J. Coll. Sci. 8, 105 1953.

[7] M. N. Fineman, I. W. McBain, J. Phys. Coll. Chem. 52, 881 1948.

[8] G. Steinsby, A.E. Alexander, Trans. Faraday Soc. 45, 585 1949.

[9] B. V. Mokievsky and P. A. Rebinder, Proc. Acad. Sci. USSR, 26, 46 1940.

[10] M. Ulman, Z. phys. Chem. A182, 18 1938.

[11] I. V. Egorov, Technical Analysis (Kiev, 1926).

[12] Z. N. Markina, K. A. Pospelova, and P. A. Rebinder, Proc. Acad. Sci. USSR, 99, 121 1954.

[13] A. V. Dumansky, V. I. Solnyshkin, and P. A. Demchenko, Ukrain. Chem. J., 20, 635 1954.

LIGHT SCATTERING BY A COAGULATING AEROSOL

O.M. Todes and A.A. Chekunov

In many investigations of the scattering of light by suspended particles [1-3] this effect has been considered mainly with reference to monodisperse aerosol systems. It is known, however, that real mists, clouds, smokes, and similar systems consist of particles of different sizes; i.e., they are polydisperse. Moreover, because of sedimenation and other processes, the particle size distribution in these systems varies continuously with time. Because of these changes the optical properties of the systems also vary and these variations may be used to study the nature of the processes taking place in aerosol systems.

The literature contains solutions of particular problems on light scattering in polydisperse aerosol systems with definite particle size distributions. This problem was solved from the meteorological aspect by Foitzik [4], and it is presented in detail in Kondratyev's monograph [5]. Foitzik assumed a Gaussian particle size distribution in clouds and mists, introduced certain empirical constants, and calculated light scattering curves. Comparison of these curves with light scattering curves for monodisperse aerosols shows significant differences. In particular, the relationship between the scattering coefficient and the average particle size is of a more complex character, while the scattering coefficients themselves can exceed the corresponding values calculated for ideal monodisperse systems.

Scattering by rain droplets of different sizes has recently been studied by Polyakova and Shifrin [6]; they assumed an empirical particle size distribution of the rain droplets, in the form

$$\frac{dn}{dr} = A_1 r^2 e^{-\beta r}, \tag{1}$$

where n is the number of particles of radius greater than r per unit volume; A_1 and β are parameters determined by measurement of the integral characteristics of the rain – its optical transparency α and total intensity f.

Particles of the order of 10^{-5} cm show the greatest scattering in the visible region of the spectrum. The sedimentation rate of such particles is negligibly small (of the order of one micron per second) and changes in the aerosol cloud are primarily determined by coagulation processes. Calculations have been reported [7, 8] of the coagulation kinetics and changes of particle size distribution in coagulating clouds. We used the results of these investigations in a theoretical and experimental study of changes in the optical properties of a coagulating aerosol.

Interpolation formula for light scattering by a monodisperse smoke. If a beam of light of intensity I passes through an aerosol layer of thickness dx, part of the light is scattered by the suspended particles and the intensity of the original beam is diminished by

$$-dI = KI\,dx, \tag{2}$$

where K is the linear coefficient of extinction due to scattering, in cm^{-1}.

We denote the particle concentration of a monodisperse aerosol by N (cm^{-3}). At low weight concentrations of the aerosol multiple scattering may be neglected, and the coefficient of extinction will be directly proportional to the particle concentraion, i.e.

$$K = FN, \tag{3}$$

where $F = K/N(\mathrm{cm}^2)$ is the effective cross section of light scattering by a single aerosol particle.

For particles the radii of which are small relative to the wave length of the scattered light λ ($r \ll \lambda$), the effective scattering cross section is given by Rayleigh's law [9]:

$$F_p = \frac{24\pi^3}{\lambda^4}\left(\frac{4}{3}\pi r^3\right)^2\left(\frac{m^2-1}{m^2+2}\right)^2 = B\omega^2, \tag{4}$$

where $\underline{m}$ is the refractive index of the particle substance, $\omega = \frac{4}{3}\pi r^3$ is the volume of a particle, and B is a proportionality factor which depends on the properties of the particles (m) and of the scattered light (λ)

$$B = \frac{24\pi^3}{\lambda^4}\left(\frac{m^2-1}{m^2+2}\right)^2. \tag{5}$$

In the other extreme case, with particles large relative to the wave length ($r \gg \lambda$) purely geometrical scattering occurs by reflection of light from the particle surfaces. In this case the effective section [1] is equal to the lateral area of the front half of the particle, facing the incident light, i.e.

$$F = 2\pi r^2 = 2\pi\left({}^3/_4\pi\right)^{2/3}\left(\frac{4}{3}\pi r^3\right)^{2/3} = A\omega^{2/3}, \tag{6}$$

where $A = \sqrt[3]{9\pi/2}$ is a numerical term.

In the intermediate region of the greatest practical interest, with particles of a size comparable to the wave length of light ($r \approx \lambda$), diffraction scattering occurs. In this case the effective scattering cross section F_ω is a complex function of the particle volume ω, the refractive index $\underline{m}$, and the wave length λ. To simplify the calculations, we considered it suitable to derive a simple interpolation formula for F as a function of ω, which for large particles would pass into the limiting Equation (6) of geometrical optics, and for small particles, into the Rayleigh Equation (4). In its simplest form, this interpolation relationship can be written as

$$\frac{1}{F_\omega} = \frac{1}{F_p} + \frac{1}{F_r} = \frac{1}{B\omega^2} + \frac{1}{A\omega^{2/3}}. \tag{7}$$

when $\omega \gg \left(\frac{A}{B}\right)^{3/4} \cdots\cdots \frac{1}{B\omega^2} \ll \frac{1}{A\omega^{2/3}}$ и $F_\omega \approx F_p$.

when $\omega \ll \left(\frac{A}{B}\right)^{3/4} \cdots\cdots \frac{1}{B\omega^2} \gg \frac{1}{A\omega^{2/3}} u F_\omega \approx F_r$.

Transformation of Equation (7) gives the interpolation function in explicit form

$$F_\omega = \frac{AB\omega^2}{A + B\omega^{4/3}}. \tag{8}$$

To reduce Equation (8) to a dimensionless form, we introduce scales for the volume

$$\omega_0 = \left(\frac{A}{B}\right)^{3/4} = \frac{\lambda^3}{4\pi^2\sqrt[4]{12}}\left(\frac{m^2+2}{m^2-1}\right)^{3/2} \tag{9}$$

and the effective cross section

$$F_0 = \sqrt{\frac{A^3}{B}} = \frac{\sqrt{3}}{4\pi}\lambda^2\,\frac{m^2+2}{m^2-1}. \tag{10}$$

Putting $x = \frac{\omega}{\omega_0}$ and $\frac{F_\omega}{F_0}$, we reduce Equation (8) into the final form of the universal relationship

$$y = \frac{x^2}{1 + x^{4/3}}. \tag{11}$$

Fig. 1 shows a plot of Equation (11) in logarithmic coordinates. For comparison, the broken lines in the graph represent curves for diffraction scattering, taken from Rayleigh's paper [9].

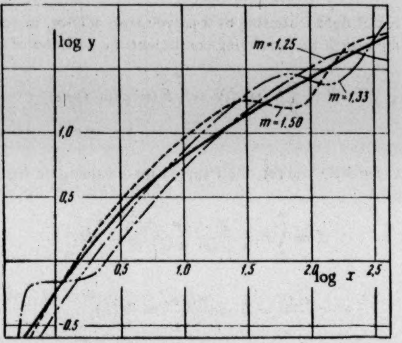

Fig. 1. Light scattering curves for a polydisperse smoke, based on diffraction scattering and Equation (11).

Fig. 1 shows that these points fit fairly satisfactorily on the plot of Equation (11). The interpolation Equation (11) is therefore suitable for approximate calculations of light scattering by monodisperse aerosols not only for the extreme cases of small and large particles, but also for the most interesting particle size range from the practical aspect, comparable with the wave length $r \approx \lambda$.

Light scattering by a coagulating aerosol. It has been shown [7, 8] that, in the coagulation of an aerosol with a fairly high initial particle concentration, a short time after the start of the process the particle size distribution function begins to vary asymptotically. We denote by dN the number of particles of size between ω and $\omega + d\omega$ per unit volume. The particle size distribution function $\rho(\omega, t)$ and dN are connected by the relationship

$$dN = \rho(\omega, t)\, d\omega. \tag{12}$$

With the coagulation process taking an asymptotic course, the function $\rho(\omega, t)$, varies with the time t according to the law

$$\rho(\omega, t) = \frac{P}{t^2} \varphi\left(\frac{Q\omega}{t}\right), \tag{13}$$

where $\varphi(u)$ is a certain function of the variable $u = Q\omega/t$, and P and Q are constants, respectively equal to

$$P = \frac{\delta}{M}\left(\frac{3\eta}{8kT}\right)^2 \text{and} Q = \frac{\delta}{M}\frac{3\eta}{8kT}, \tag{14}$$

where M is the weight concentration of the aerosol; δ is the density of the particles themselves; η is the viscosity of the surrounding medium; k is the Boltzmann constant; T is the absolute temperature.

The function $\varphi(u)$ can be found from a fairly complex differential equation to various degrees of accuracy. In the first approximation $\varphi(u)$ can be found from Smoluchowski's approximate solution [10]

$$\varphi_0(u) = 4e^{-2u}, \tag{15}$$

where e is the base of natural logarithms.

As was shown in our papers, the further refinements introduced by Phsenai-Severin [11] do not change significantly the integral characteristics of the coagulation process. Therefore in the subsequent calculations we shall only use the first approximation (15).

The linear coefficient of light scattering by a polydisperse aerosol, in accordance with Equations (3) and (12), will be given by the sum of the scattering coefficients for particles of different sizes, i.e.

$$K=\int F(\omega)\,dN=\int\limits_{1}^{\infty}F(\omega)\,\rho(\omega,\,t)\,d\omega, \tag{16}$$

substituting, instead of Equations (10) and (6), their approximate values, we find

$$K=\int\limits_{0}^{\infty}F_0\frac{x^2}{1+x^{4/3}}\,\frac{4P}{t^2}\,e^{-\frac{2Q\omega_0}{t}x}\,dx. \tag{17}$$

Putting

$$\frac{2\omega_0 Q}{t}=h\text{ and}\frac{KQ^2\omega_0}{PF_0}=\Phi(h),$$

we reduce Equation (17) to the form

$$\Phi(h)=h^2\int\limits_{0}^{\infty}\frac{x^2}{1+x^{4/3}}\,e^{-hx}dx. \tag{18}$$

When h >> 1 (small times) the function e^{-hx} diminishes very rapidly with x, and in calculations of the integral in the right hand side of Equation (18) the integrand is of primary importance at low values of x. Assuming that $\frac{x^2}{1+x^{4/3}}\approx x^2$, we can find the approximate value of the required integral

$$\Phi_1(h)\approx h^2\int\limits_{0}^{\infty}e^{-hx}\,dx=\frac{\Gamma(2+1)}{h}=\frac{2}{h}. \tag{19}$$

In the opposite extreme case the large values of the variable x = 1/h are of primary importance in calculation of the integral. Here the integrand at large values of this variable can be replaced by an asymptotic expression, by putting $x^2/(1+x^{4/3})\approx x^{2/3}$; the approximate value of the required integral will then be

$$\Phi_2(h)=h^2\int\limits_{0}^{\infty}x^{2/3}e^{-hx}\,dx=\Gamma\left(\frac{5}{3}\right)h^{1/3}=0{,}90\,h^{1/3}. \tag{20}$$

To find the function Φ (h) at intermediate values of the variable (h ≈ 1) we replace it by an interpolation formula, which at large values of h passes into Equation (19), and at small values of h, into Equation (20). The simplest interpolation formula to satisfy these conditions will be an expression of the type

$$\frac{1}{\Phi(h)}=\frac{1}{\Phi_1(h)}+\frac{1}{\Phi_2(h)}=\frac{1+0.45\,h^{1/3}}{0.90\,h^{1/3}}. \tag{21}$$

By replacing h and Φ (h) by their values (see above), Equation (21) can be reduced to the form

$$\frac{K}{M}=\frac{11.1}{\delta\lambda}\sqrt{\frac{m^2-1}{m^2+2}}\cdot\frac{\tau}{1+\tau^{4/3}}. \tag{22}$$

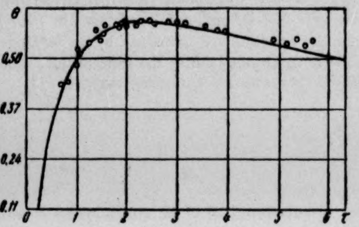

Fig. 2. Variation of the hiding power of a polydisperse aerosol with time.

The quantity K/ M represents the weakening of the light per unit length at unit weight concentration of the aerosol; it is known in the literature as the "hiding power" of a given smoke. The dimensionless time τ depends on the aerosol concentration, its optical properties at the particular wave length, and the coagulation rate; it is determined by the expression:

$$\tau = 30.2\frac{M}{\delta}\frac{kT}{\eta\lambda^3}\sqrt{\frac{m^2-1}{m^2+2}}. \qquad (23)$$

The dimensionless extinction (light weakening) coefficient, which represents the hiding power

$$\theta = \frac{K\delta\lambda}{11.1\,M}\sqrt{\frac{m^2+2}{m^2-1}} \qquad (24)$$

varies with the dimensionless time τ according to the law

$$\theta = \frac{\tau}{1+\tau^{4/3}}. \qquad (25)$$

a plot of which is given in Fig. 2.

It is seen in Fig. 2 and Equation (25) that the power of an aerosol first increases relatively rapidly with particle size, and then decreases slowly and gradually.

The maximum value of K/ M can be found by the usual differential calculation rules

$$\left(\frac{K}{M}\right)_{\max} = \frac{6.36}{\delta\lambda}\sqrt{\frac{m^2-1}{m^2+2}} \qquad (26)$$

and the time to reach this maximum is

$$\tau_{\max} = \frac{0.0235\,\delta\lambda^3\eta}{MkT}\left(\frac{m^2+2}{m^2-1}\right)^{1/2}. \qquad (27)$$

It follows from Equations (22) and (27) that the masking power (K/ M) of a particular aerosol is not a constant for the substance (one which depends only on its refractive index m at the given wave length λ), but varies continuously with time. Only the maximum hiding power of the aerosol, given by Equation (26) can be regarded as such a constant. Under otherwise equal conditions, increase of the weight concentration results in a decrease of the time required to reach the maximum K/ M and in accelerated decrease of K/ M after the maximum has been reached, as shown in Fig. 3. The maximum value of K/ M increases with the refractive index m, but the time required to reach this maximum and the duration of its existence are diminished to a greater extent, as is shown in Fig. 4.

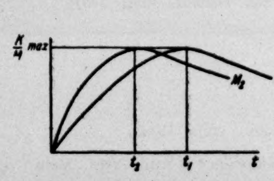

Fig. 3. Variation of the time required to reach maximum hiding power with varying aerosol concentration.

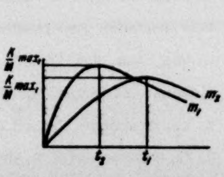

Fig. 4. Variation of maximum hiding power and of the time required to reach it with varying refractive index of a smoke.

Experimental verification of Equation (25). An experimental investigation was carried out to test the theoretically derived Equation (25). A heavy oil aerosol was prepared by the condensation method and introduced into a smoke chamber (average b.p. of the oil was 360°, density $\gamma = 0.95\ \text{g/cm}^3$, refractive index $m = 1.50$). The weight concentration M of the smoke and the light extinction coefficient K, measured by the readings I of a photocell at a distance l from a standard light source, were determined during the experiments. The extinction coefficient was calculated by the equation

$$K = \frac{2.3}{l} \log \frac{I_0}{I}. \tag{28}$$

where I_0 is the photocell reading in absence of the aerosol.

The experimental data were plotted in the form of the relationship (25) in the dimensionless coordinates θ and τ. For the experimental values of γ and m for the most perceptible wave length $\lambda = 555$ mμ the values of θ and τ were calculated from the expressions

$$\theta = 0.097 \frac{\text{g}}{\text{m}^2} \frac{K}{M}. \tag{29}$$

$$\tau = 2.10^6 \frac{\text{cm}^3}{\text{g sec}} Mt. \tag{30}$$

It was assumed in the calculations that the true value of K is 10% lower than that given by Equation (28) owing to absorption of light by the aerosol particles [12].

As is seen in Fig. 2, the experimental data fit satisfactorily on the theoretical curve for Equation (25). As a rule, at the end of the experiment the theoretical curve descends more steeply than the experimental. However, these deviations are not large, and do not exceed 30% within the limits of a 30-minute exposure. The probable cause of these systematic deviations is that coagulation is accompanied by evaporation of the oil particles; this somewhat decreases the particle size and increases the content of fractions with a higher refractive index, and therefore with better hiding properties.

SUMMARY

The optical properties of aerosols depend on the scattering of light by the particles and on the particle size distribution. A simple interpolation Equation (11), which smooths out the diffraction peaks somewhat, is given for calculation of light scattering by particles comparable in size to the wave length. On the basis of this equation and the asymptotic character of coagulation, an interpolation Equation (25) has been derived for determination of the extinction of light by aerosols; this equation was verified by an experimental study of heavy oil mist.

Leningrad

Received July 9, 1956.

LITERATURE CITED

[1] K. S. Shifrin, Light Scattering by Turbid Media (State Tech. Theoret. Press, 1951).

[2] V. V. Shuleikin, Physics of the Sea (Izd. AN. SSSR, 1953).

[3] G. Mie, Ann. Phys. 25, 377 1908.

[4] L. Foitzik, Z. Meteor. 4, No. 10, 11 1950.

[5] K. Ya. Kondratyev, Radiant Energy of the Sun (Hydrometeor. Press, 1954).

[6] E. Ya. Polikova and K. S. Shifrin, Microstructure and Transparency of Rain, Trans. Main Geophysical Observatory, No. 26, 88 1951.

[7] O. M. Todes, Physical Chemistry Symposium, p. 138 1948.

[8] O. M. Todes, Problems of Kinetics and Catalysis, 7, 157 1949.

[9] Rayleigh, Phil. Mag. (5) 47, 375, 1899

[10] Smoluchowski Z. Phys. Chem. 92, 129 1917.

[11] Pshenai-Severin, Proc. Acad. Sci. USSR, 94, 865 1954.

[12] Yu. M. Veitser and G. P. Luchinsky, Chemistry and Physics of Masking Smokes (Moscow-Leningrad, 1939).

ORIENTATION OF CLAY PARTICLES DURING DEFORMATION OF A CLAY BODY

V.S. Fadeeva

When plastic clay bodies are molded into ware, in some cases a stratified structure is formed (Fig. 1), sometimes right through the thickness of the specimen and sometimes only in isolated regions. There is reason to believe that orientation of the clay particles during deformation of the body may play a part in this effect, as deformation of a disperse system is accompanied by definite spatial orientation of its particles [1-4].

In order to study the relationship between a stratified structure in a clay body and the orientation of its particles during molding of ceramic ware, we carried out a number of experiments on the deformation of a clay body based on highly plastic Chasov Yar clay with addition of 5% biotite. The biotite was first finely ground in a vibratory mill in order that the biotite particles should be of comparable size to the clay particles and undergo orientation with them. The dark biotite scales were easily distinguishable in the pale clay mass, making it possible to observe orientation of the particles during deformation of the clay body. The clay body was deformed in conditions of pure compression and under complex shearing deformation along a compression plane under the simultaneous action of compressing loads.

Three series of specimens, A, B, and C, 2 cm in height and in diameter, were made from an experimental paste with 38% moisture (the normal molding consistency). Specimens of Series A were subjected to a pressure of 1 kg/cm^2 for 24 hours; specimens of Series B were subjected to a pressure of 10 kg/cm^2 for 15 minutes; this resulted in extrusion of the body into the gap between the ring and the die. Specimens of Series C were compressed under a load of 1 kg/cm^2 for an hour (this time was sufficient to confer a uniform structure on the specimens) and were then sheared along the compression plane. The shearing was effected slowly, at 1-2 cm/minute, and was continued to various degrees of deformation, in some cases to total destruction.

Transparent sections were prepared from all three series of specimens. The sections were cut in a plane through the centers of the specimens at right angles to the base; they were dried in air and boiled in Canada balsam. Figs. 2,3 and 4 show micrographs of the sections. The structure seen in the section of a specimen of Series A (Fig. 2) is completely similar to the structure of the body before deformation, and is characterized by a random distribution of the biotite particles. The section of the specimen of Series B shows a definite orientation of the biotite particles, namely: in the region immediately under the die they tend to be oriented perpendicularly to the acting load (Fig. 3,a), and at the ring walls they tend to lie parallel to the walls, in the direction of the shearing force in the body relative to the walls (Fig.3,b). In the center of the specimen the particles of biotite had a random distribution. In the section of a specimen of Series C (Fig. 4) a tendency is seen for the biotite particles to be oriented parallel to the shear plane. In some parts of the shearing region, destruction was observed (longitudinal cracks). Investigation of the specimens of this series showed that destruction of the specimens in the shearing region does not occur before complete orientation of the particles. This is confirmed by the results of our investigations of the physicomechanical properties of plastic clay bodies based on clays of different mineralogical composition [5]. These properties were found to depend to a considerable extent on the spatial configuration of the clay mineral, determining its tendency to orientation under pressure. It may be noted that in the original body and in specimens of Series A (Fig.2) the biotite particles are larger than in the shearing region (Fig.4).

Observations were also made of the orientation of the particles in the surface layer of a specimen of the same body after sliding along a solid surface — the steel table of an instrument for determination of external friction. In this case the sections were cut in a plane perpendicular to the sliding surface (Fig. 5). Orientation

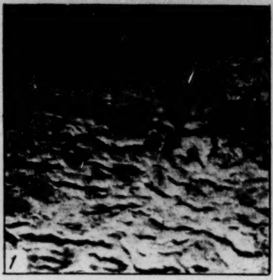

Fig. 1. Micrograph of a transparent section of a fired block molded under high pressure. The block was rejected owing to low frost resistance and nonstandard bending strength (× 56).

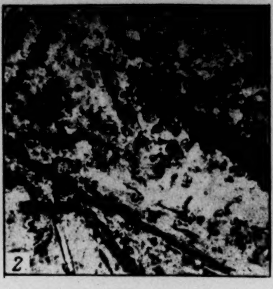

Fig. 2. Specimen after compression at 1 kg/cm² for 24 hours. The black elongated grains are biotite (× 56).

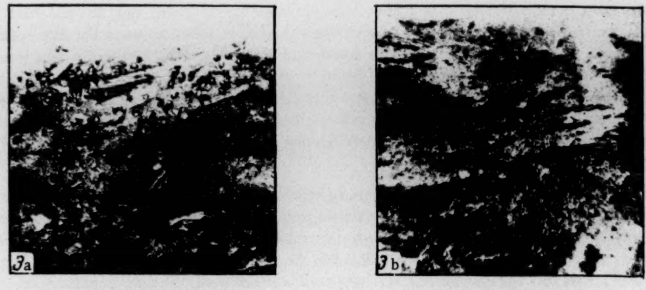

Fig. 3. Specimen after compression at 10 kg/cm² for 15 minutes (×56); 3a) pale field – boundary of die contact. Black elongated grains are biotite; 3b) pale field – boundary of ring walls, black elongated grains are biotite.

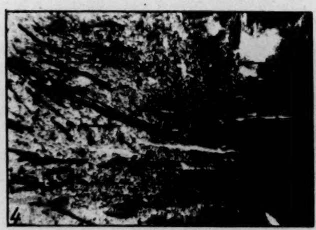

Fig. 4. Specimen after shear along a compression plane (shearing force near the limiting value) (× 56). Black elongated grains are biotite. The shearing region is marked by dotted lines. The pale stripes are cracks. The arrow indicates the direction of the shearing force.

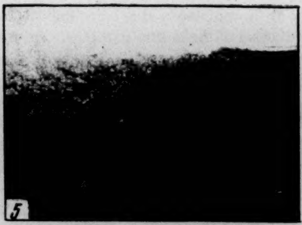

Fig. 5. Region of the friction surface of the specimen. Black lines are biotite grains. The pale field is the boundary of the friction surface (× 56).

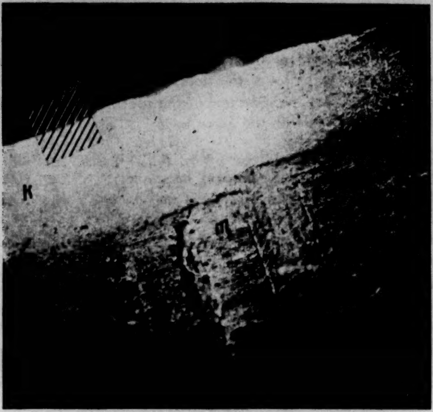

Fig. 6. Micrograph of a cross section of a clay specimen. The Zone k is a layer on the friction surface of the specimen. The square indicates the place shown in the transparent section in Fig. 5. The Zone m is the main mass of the specimen. The transverse stripes (furrows) are traces formed by sand grains during cutting of the moist specimen (x 15).

of the particles parallel to the friction surface can be seen in the photograph. The observations were hindered by the fact that sliding resulted in differentiation of the clay and biotite particles, as a result of which only the finest particles, difficult to distinguish in the prepared section, remained in the layer contiguous with the sliding plane. Examination of samples taken from the sliding surface under the electron microscope also showed them to be highly disperse. Fig. 6, which is a direct micrograph of a cross section of the specimen, shows that the surface sliding layer, Zone k, differs sharply in general strucutre from the rest of the specimen, Zone m. This accounts for the decrease of the coefficient of friction with increased normal load on the specimen, which has been observed in studies of the friction of clay specimens against solid surfaces, as the surface layer appears to act as a lubricant during movement of the specimen. It also explains why the coefficients of friction found in these investigations for bodies of molding consistency made from different clays were similar, as all clays have a highly disperse fraction which forms this layer. These results are in good agreement with Tolstoi's work [6] on the wall effect in disperse systems.

The formation of such a layer can be represented as follows: water containing minute clay particles, of colloidal dimensions passes from the interior of the specimen during its motion toward the sliding surface, which is a region under higher stress [7]; these clay particles are deposited on the sliding surface and oriented in the direction of the shearing force to form a layer consisting of very closely packed highly disperse particles. Observations showed that the friction surface of a clay specimen is similar in character to the surface of a deposit of a colloidal clay fraction on a filter; i.e., it is in the form of a dense, shining coating ("polished layer"). It is evident that the higher the pressure, the more rapidly is such a layer formed, and the higher will be its moisture content (of course, for the given sliding velocity, 2 cm/sec).

Under pure compression conditions, even under high pressures, particle orientation within a specimen of a plastic clay body occurs slowly, and probably has no appreciable influence on the formation of a stratified structure during molding of ware from these bodies. In compression with simultaneous shearing of a specimen of a plastic clay body the shearing force does not reach its limiting value (yield value) before complete orientation of the particles in the body in the shearing region. When orientation of the particles is complete further increase of the shearing force results in destruction of the specimen along the plane of the action of the maximum tangential stresses, leading to the formation of a stratified structure in the specimen. To prevent the formation of such a structure, it is necessary to vary the direction of the maximum tangential stresses during molding and not to exceed the maximum shearing stress for the given body.

When a clay specimen slides along a solid surface, a highly disperse fraction emerges toward the sliding surface, with simultaneous orientation of the particles in the direction of the frictional force. This leads to the formation of a layer, differing in structure from the rest of the specimen, on the sliding surface. Experiments showed that a similar process occurs in complex deformation of a clay specimen. Highly disperse clay fractions travel toward the planes of action of the maximum tangential stresses as these develop; this decreases the yield stress of the body and favors the formation of a heterogeneous stratified structure in the specimen. Each individual layer of such a structure is probably similar to the specimen shown in Fig. 6. The number of layers will depend on the homogeneity of the body, its degree of dispersion, and also on the homogeneity of stress distribution in it during deformation. It seems likely that the microstratified structure formed in clay specimens during molding is the result of the action of tangential stresses near or equal to the yield value of the body in these specimens; this is in agreement with the modern views on the destruction processes in such materials.

SUMMARY

1. Deformation of plastic clay bodies is accompanied by spatial orientation of the particles, mainly in the direction of the maximum shearing force. This is accompanied by differentiation of the particles in the body by size, with liberation of water containing minute particles (of colloidal dimensions) toward the shearing region.

2. Particle orientation precedes destruction of plastic clay body specimens.

3. Particle orientation and differentiation effects in plastic clay bodies occur also during slippage of specimens along solid surfaces; in consequence, the coefficient of surface friction of clays is a variable quantity.

We wish to express our gratitude to Prof. M. P. Volarovich for valuable advice in the course of this investigation.

Scientific Research Institute
for Construction Ceramics
Moscow

Received July 3, 1956

LITERATURE CITED

[1] A. Nadai, Plasticity (ONTI, 1933).

[2] K. Tertsagi, Building Mechanics of Soils on the Basis of their Physical Properties (State Constr. Press, 1933).

[3] M. P. Volarovich, Bull. Acad. Sci. USSR, Div. Math. Nat. Sci., 599 1938.

[4] M. P. Volarovich and I. S. Erokhin, J. Phys. Chem., 12, No. 2-3 1938.

[5] V. S. Fadeeva, Trans. Sci. Res. Inst. Constr. Ceramics No. 8, (Ind. Press, 1953).

[6] D. M. Tolstoi, Colloid J., 10, No. 2 1948.

[7] N. A. Nasedkin, J. Tech. Phys., 8, No. 3 1938.

EFFECTS OF THE TYPES OF RUBBER AND CARBON BLACK ON THE FORMATION OF CARBON-RUBBER GELS

Z.V. Chernykh and V.G. Epshtein

Addition of carbon black to rubber mixtures results in increased modulus and higher tensile, tearing, and abrasion strength. This effect is evidently determined to a considerable extent by the bonds formed between the rubber and carbon in the mixture.

In a number of recent investiagtions the bonding between rubber and carbon black has been studied by determinations of the so-called carbon-rubber gel, which is the portion of the nonvulcanized rubber mix insoluble in benzene. According to Dogadkin and Feldhstein [5], the proportion of the insoluble fraction depends on the activity of the filler. It has also been shown that the amount of carbon-rubber gel depends on the molecular weight of the rubber [1, 2], the type of carbon black (mainly its degree of dispersion) [2, 4], and on the compounding temperature [3, 6].

It is believed that the formation of a carbon–rubber gel is the result of formation of a carbon network (as was proved by Dogadkin [7]), of the considerable energy of intermolecular interaction between the rubber and the carbon, and of the entanglement of the flexible molecular chains of the rubber [1].

The formation of a carbon-rubber gel has been associated with rubber reinforcement in a number of papers [1, 2, 6, 8]. It has been shown that an increase in the amount of carbon-rubber gel corresponds to an increase in the modulus and the abrasion resistance of vulcanizates [6, 7].

Carbon-rubber gel determinations are not particularly accurate, but they may be used for estimating bond strengths in rubber-carbon black mixtures. For determining the nature of these bonds, we studied the formation of carbon-rubber gels in mixtures of natural and synthetic rubber with various carbon blacks, and estimated gel stability under various extraction conditions.

EXPERIMENTAL

The following rubbers were taken for the investigation: natural rubber (NR) (smoked sheet), SKB 50, SKBM 50, thermally plasticized SKS-10 and SKS-30 A with plasticity 0.5, and the following carbon blacks: channel, acetylene, nossle furnace, and thermal.

The molecular weights of the rubbers were calculated from viscosimetric data by the formulas:

For NR .... $[\eta] = 5.02 \cdot 10^{-4} . M^{0.67}$;
For SKS........ $[\eta] = 4.4 \cdot 10^{-4} . M^{0.67}$; [11]
For SKB and SKBM $[\eta] = 2.7 . 10^{-4} . 10 M^{0.725}$ [12]

the values veing 126,000 for NR, 85,500 for SKB, 106,200 for SKBM, 172,600 for SKS-10, and 102,000 for SKS-30A.

The characteristics of the carbon blacks are given in Table 1.

The mixtures were milled on laboratory rolls, with roll diameter 160 mm, at 20-30°, in the following formulation:

Rubber	100	parts by weight
Stearic acid	3.0	" " "
Rubrax	5.0	" " "
Carbon	from 10 to 180	" " "

The compounding time increased with the carbon black content, and ranged from 10 to 20 minutes.

TABLE 1

Characteristics of the Carbon Blacks [10]

Type of carbon	Average particle diameter, A	pH	Oil adsorption, ml/g
Channel	280	3.5—4.5	1.4
Acetylene	400	6.5—7.0	2.8
Furnace	640	9—10	0.8
Nozzle	1100	9—10	3.0
Thermal	1880	7—8	0.3

The compounded mixtures were left for 24 hours, and the rubber-carbon gel contents were then determined as follows: a weighed sample of 2.0 g of the finely shredded mixture was placed in a weighed textile cartridge. The cartridge was placed in a wide-necked Erlenmeyer flask and covered with benzene or carbon tetrachloride. The extraction was continued for 24 and 48 hours at 20°, and for 18 hours in boiling benzene at 78°. At the end of the extraction the solvent was decanted, the cartridge was washed once with ligroine, and dried in a thermostat at 60° to constant weight. The carbon-rubber gel content was determined as the ratio of the weight of the dry gel to the weight of the sample. The reproducibility of the results was within 2-3%. The carbon content of the carbon-rubber gels was determined by the method used for determination of carbon black in vulcanizates (by decomposition of the gel in nitric acid sp. gr. 1.37). The fraction of the rubber bound with carbon was calculated from the results.

The results of the carbon-rubber gel determinations for NR, SKB and SKS-30A rubbers are shown in the diagram. The following comments may be made on the results.

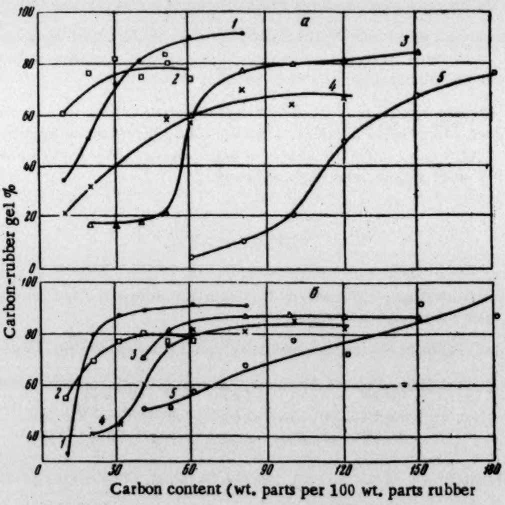

Contents of carbon-rubber gel in mixtures based on NR (a) and SKS-30A (b) with different carbon contents: 1) channel black; 2) acetylene black; 3) furnace black; 4) nossle black; 5) thermal black.

TABLE 2

Variations of Carbon-Rubber Gel Contents in Mixtures Based on NR with the Extraction Conditions

Type of carbon black	Wt. parts of carbon to 100 wt. parts rubber	Carbon-rubber gel, content, %			
		Benzene			CCl₄
		24 hrs. 20°	48 hrs. 20°	18 hrs. 78°	48 hrs. 20°
Channel	30	83.0	74.0	68.0	80.0
	80	92.0	83.0	82.0	—
Acetylene	20	77.0	67.0	63.0	79.0
	50	81.0	72.0	62.0	72.0
Furnace	80	79.0	78.0	72.0	84.0
Nozzle	80	70.0	61.0	60.0	75.0
Thermal	180	77.0	73.0	72.0	73.0

TABLE 4

Contents of Carbon Black and Rubber Bound with Carbon in Carbon-Rubber Gels in Mixtures Based on NR

Type of carbon black	Wt. parts carbon to 100 wt. parts rubber	Benzene				CCl₄	
		48 hrs. 20°		18 hrs. 78°		48 hrs. 20°	
		carbon content in gel, %	amount of rubber bound with carbon %	carbon content in gel, %	amount of rubber bound with carbon %	carbon content in gel, %	amount of rubber bound with carbon %
Channel	30	31.7	69.8	32.4	60.0	23.6	84
	80	68.5	48.0	57.6	64.0	48.6	—
Acetylene	20	47.0	45.4	32.5	44.3	27.0	52.0
	50	69.1	34.0	54.5	40.6	54.5	82.6
Furnace	80	77.6	33.0	62.0	48.3	63.4	72.2
Nozzle	80	84.0	18.5	75.5	26.2	56.0	51.6
Thermal	180	90.0	21.8	83.7	33.3	83.5	35.3

TABLE 3

Variations of Carbon-Rubber Gel Contents in Mixtures Based on SKB with the Extraction Conditions

Wt. parts carbon to 100 wt. parts rubber	Channel			Acetylene			Furnace			Nozzle			Thermal		
	Benzene		CCl₄	Benzene		CCl₄	Benzene		CCl₄	Benzene		CCl₄	Benzene		CCl₄
	24 hrs.	48 hrs.	48 hrs.	24 hrs.	48 hrs.	48 hrs.	24 hrs.	48 hrs.	48 hrs.	24 hrs.	48 hrs.	48 hrs.	24 hrs.	48 hrs.	48 hrs.
10	69.0	42.0	—	82.0	59.0	58.0	—	44.0	—	43.0	43.0	—	—	—	—
20	86.0	75.0	83.5	89.0	65.0	71.0	57.0	56.0	—	64.0	43.0	—	—	—	—
30	81.0	74.0	—	—	—	—	65.5	52.0	—	87.0	66.0	60.5	—	40.8	—
40	86.0	70.0	83.5	—	—	—	76.0	62.0	—	—	—	78.0	58.0	46.0	—
50	—	88.0	—	—	—	—	87.0	64.0	68.0	80.0	77.0	76.0	62.0	54.0	—
60	86.0	86.0	82.0	85.0	66.0	78.0	87.0	66.0	—	90.0	76.0	79.0	83.0	60.0	—
80	—	—	—	—	—	—	89.0	75.0	74.0	—	—	—	83.0	68.0	58.0
100	—	—	—	—	—	—	82.0	73.0	74.0	—	—	—	—	69.0	62.0
120	—	—	—	—	—	—	—	—	—	—	—	—	82.0	69.0	71.0
180	—	—	—	—	—	—	—	—	—	—	—	—	86.0	73.0	73.0

The carbon-rubber gel content increases with the amount of carbon black added. For example, thermal black, which does not form a gel when added in small amounts, forms a large amount of gel when added in 150-180 parts by weight. The carbon-rubber gel content for a definite amount of carbon depends on the type of carbon black added. At contents of 20-40 parts by weight, the carbons form the following sequence: acetylene, channel, nozzle, furnace, thermal. The carbon-rubber gel content depends on the type of rubber. In synthetic rubbers (SKB, SKS-30A) gel formation occurs to a greater extent and with smaller additions of carbon black than in natural rubber, despite the somewhat lower molecular weight of these rubbers.

The variations of the carbon-rubber gel content with extraction conditions are given in Tables 2 and 3.

It follows from Tables 2 and 3 that the more harsh conditions of benzene extraction (boiling, or increase of extraction time) do not cause decomposition of the carbon-rubber gel, but only decrease its content somewhat; this effect is more prominent in mixtures with small amounts of carbon black.

The amounts of gel formed when the mixtures are dissolved in carbon tetrachloride are somewhat greater than when they are dissolved in benzene for mixtures containing channel and acetylene blacks, approximately the same for mixtures with furnace and nozzle blacks, and less for mixtures with thermal black.

Table 4 contains data on the contents of carbon black in the carbon-rubber gels for different extraction conditions and types of carbon. These results show that: 1) the content of carbon in the gel increases with increasing amount of carbon added to the mixture; 2) in mixtures containing furnace and nozzle blacks, with a lower gel content (see Table 2) the carbon content of the gel is higher than in mixtures containing carbon black; 3) more harsh extraction conditions – the use of a more active solvent (CCl_4) or boiling – lead to a decrease of the carbon black content in the gel, i.e., carbon black is removed to a greater extent than rubber.

TABLE 5

Effects of Mastication on the Contents of Carbon-Rubber Gel and of Carbon in the Gel (Benzene Extraction for 24 hours at 20°)

Type of rubber	Type of carbon black	Wt. parts carbon to 100 wt. parts rubber	Contents of carbon–rubber gel, %		Contents of carbon in carbon–rubber gel, %	
			before treatment	after 20 minutes of mastication	before treatment	after 20 minutes of mastication
NK	Channel	60	92.0	83.0	43.6	46.0
	Furnace	100	86.0	86.0	53.0	57.3
SKB	Channel	60	89.0	90.0	40.0	40.7
	Furnace	100	90.0	88.0	60.0	53.5
SKBM	Channel	60	90.0	88.0	48.0	—
	Furnace	100	92.0	87.0	52.0	56.7
SKS-10	Channel	60	94.0	91.0	39.8	39.0
	Furnace	100	95.0	91.0	64.0	—
SKS-30A	Channel	60	95.0	91.0	—	40.9
	Furnace	100	86.0	85.0	56.3	61.0

The contents of carbon-rubber gel in mixtures based on various rubbers before and after additional mastication are given in Table 5. The mixture was masticated for 20 minutes on laboratory rolls at 20-30°. The gel contents are not appreciably affected by changes in the type of synthetic rubber (increased contents of butadiene residues in the 1-4 position or decreased contents of styrene residues). In the case of a mixture of NR with channel black the amount of gel decreases after mastication; this is possibly caused by degradation of the rubber. This effect is slight for other types of rubbers.

DISCUSSION OF RESULTS

The view has been put forward in a number of papers [2, 6] that formation of carbon-rubber gels can be largely attributed to the high stability of the bonds between the rubber molecules and the carbon black. It was considered that only active blacks form carbon-rubber gels [6]. It had also been suggested that chemical bonds may be formed between the rubber and the carbon black [9].

It is known that carbon blacks differ in their tendency to form carbon structures. Channel and acetylene blacks readily form continuous structures in rubber mixtures, consisting of chains of carbon particles. This property is not found in furnace and especially in thermal blacks [7]. According to our results, the ease of formation of a carbon-rubber gel depends on the tendency of the carbon black to form structures. In mixtures containing acetylene or channel blacks, appreciable amounts of gel are formed at lower carbon contents than in mixtures containing nozzle furnace, or thermal blacks. Acetylene black, which has a greater tendency to structure formation, forms large amounts of gel at lower contents than channel black, although the latter is highly disperse. The same applies to nozzle black. Though the particle size of nozzle black is greater than that of furnace black; the former forms appreciable amounts of gel at lower contents than does furnace black. On the other hand, on increase of the amount of semiactive or inactive (furnace or thermal) black, a gel is still formed. Therefore it may be assumed that all carbon blacks can form continuous structures when added in definite, large or small amounts.

Studies of the strength and stability of carbon-rubber gels, based on increasing the time and raising the temperature of extraction, or on using a more active solvent (carbon tetrachloride) showed that more harsh extraction conditions do not result in total disappearance or a substantial decrease of the carbon-rubber gel content. Moreover, it was found that on extraction with carbon tetrachloride or boiling benzene the gel contains less carbon black and more rubber than on extraction with benzene at 20°. Thus the amount of rubber bound with carbon increases in such conditions. Consequently, the action of a more active solvent or increase of temperature intensifies the separation of the carbon black particles from each other, with their subsequent elution, rather than the separation of rubber molecules from carbon particles. The action of carbon tetrachloride becomes more pronounced with decreasing strength of the bonds between the carbon particles (with decreasing tendency to structure formation). Therefore it seems probable that the strength of the bonds between the carbon black particles is one of the main factors in the stability of carbon-rubber gels.

The carbon black structure is reinforced with increasing carbon black content. At the same time the differences between the amounts of carbon-rubber under different extraction conditions decrease. Thus, in mixtures of SKB with 20 parts by weight of channel black the differences between the amounts of gel obtained by extraction with cold and with hot benzene is 11%, whereas with 60 parts by weight there is no longer any difference. This confirms once again that the gel stability depends on the formation of a carbon black structure at high loadings.

It should also be noted that formation of a carbon structure increases the cohesion between the rubber and the carbon. The carbon-rubber gel contains less carbon and more rubber in the case of structural blacks (channel and acetylene) than in the case of nonstructural blacks (furnace and thermal) (Table 4).

It is at present difficult to say what the nature of the forces is between the carbon black particles and between the carbon and the rubber. Further investigation is also needed of the reasons for the increased strength of the bonds between the rubber and the carbon if a structure is formed. The higher content of gel in synthetic rubbers as compared with natural rubber is of great interest. It is possible that the explanation lies in the larger cohesion forces between the molecules of natural rubber, associated with a tendency to crystallization, hindering adsorption of the rubber molecules on the carbon particles. The higher gel contents of synthetic rubber mixtures probably account for the higher abrasion resistance, reported in the literature, of synthetic rubber vulcanizates in comparison with natural rubber, despite the lower tensile strength of the former.

The results of our investigation show that the formation of a carbon-rubber gel is closely related to formation of carbon networks, i.e., the cohesion between the carbon black particles. The amount of carbon-rubber gel may be a measure of the tendency to carbon structure formation.

It is known that the carbon-rubber gel content determines the abrasion resistance and other properties of a vulcanizate. The fact that the gel content depends on the tendency to carbon structure formation indicates that there is a link between such structures and rubber reinforcement.

SUMMARY

1. Carbon-rubber gels are formed in mixtures containing all the types of carbon black tested (channel, acetylene, nozzle, furnace, thermal) and not only active carbons.

2. The amount of carbon-rubber gel formed depends on the amount of carbon black added. With carbon blacks which readily form continuous carbon structures (channel, acetylene) the amounts of gel are greater than with nonstructural blacks, for the same amount of black added.

3. The amount of gel is greater in synthetic than in natural rubber mixtures.

4. More harsh extraction conditions do not cause disappearance of the gel, but increase the amount of bound rubber and decrease the amount of carbon in the gel.

5. The carbon-rubber gels formed from structural carbons contain larger amounts of bound rubber.

6. It is suggested that bond stability between carbon black particles (characterized by the formation of a carbon black structure) is one of the basic causes of carbon-rubber gel formation.

Yaroslav Technological Institute

Received October 12, 1956.

LITERATURE CITED

[1] A. S. Novikov, M. B. Khaikina, T. V. Dorokhina, and M. I. Arkhangelskaya, Colloid J., 15, No. 1, 51 1953.*

[2] J. Duke, W. K. Taft, J.M. Kolthoff, Rubb. Chem. Techn. 25, No. 3, 500 1952.

[3] C. W. Sweitzer, W.C. Goodrich, K. A. Burgess, Rubb. Age (NJ) 65, No. 6, 651 1949.

[4] C. W. Sweitzer, Rubb. Age (NJ) 72, No. 1, 55 1952.]

[5] B. A. Dogadkin and M. S. Feldshtein, Caoutchouc and Rubber, No. 12, 12 1939.

[6] L. R. Sperberg, J.F. Svetlik, Ind. Eng. Chem. 41, No. 8, 1641, 1949.

[7] B. A. Dogadkin, K. A. Pechkovskaya, and V. V. Kuriyanova, Investigations of the Physics and Chemistry of Caoutchouc and Rubber (Goskhimizdat, 1950), p. 103.

[8] S. D. Gehman, Ind. Rubb. World. 128, No. 2, 129 1953.

[9] W. F. Watson, Ind. Eng. Chem. 47, 1281 1955.

[10] V. P. Zuev and V. V. Mikhailov, Production of Carbon Black (Goskhimizdat, 1953) p. 15.

[11] T. Alfrey, Mechanical Behavior of High Polymers (IL, 1950) p. 484.

[12] I. I. Zhukov, I. Ya. Poddubnyi, and A. V. Lebedev, Investigations in the Field of High Molecular Compounds (Izd. AN SSSR, 1949) p. 250.

---

* Original Russian pagination. See C. B. translation.

THE STRUCTURE OF GELS

11. EFFECT OF THE FORMATION CONDITIONS OF GELATIN FILMS ON BONDING STRENGTH

S.A. Shreiner and P.I. Zubov

It was shown in a study of the mechanism of protein gel formation that the physicochemical properties of such systems depend very largely on the conditions of the formation of their structure [1]. Since protein solutions are widely used for impregnation and gluing of various materials, it was of interest to determine how the formation conditions of an adhesive film (glue layer) affect the strength of the bond. The effects of the drying rate of the glue layer, concentration of the adhesive solution, and presence of low-molecular additives on bonding strength were studied.

The bonding strength was measured in terms of the average shearing force required to break down the bond between two overlapping optically polished steel plates, 10 mm thick and 20 mm wide, glued together.

The amount of gelatin in the glue layer was determined from the weights of the specimens, weighed on an analytical balance, before and after gluing, and the thickness of the layer was found by calculation. The plates were fixed in the dynamometer by means of a self-centering device. Before being joined, the plates were washed thoroughly in alcohol-ether mixture, dried, and rubbed with finely powdered active charcoal.

The adhesive solutions were prepared as follows. Weighed amounts of gelatin were mixed in flasks (with ground glass stoppers) with water, or with solutions of urea or acetamide, or other substances of known composition by weight, and after 4 hours of swelling were heated at 60° on a water bath until the gels were completely dissolved. A definite amount of the solution was then applied from a pipet to the surface of the plate intended to form the joint, and this was covered by the other plate. The joined plates were placed in holders and pressed in a spring screw press at 5-20 kg (according to the concentration of the adhesive solution and the thickness of the layer); they were left in this state during the whole hardening period of the adhesive layer. The very first experiments showed that the bonding strength depends on the rate of drying; the bonding strength is always less after rapid than after slow drying. Since slow drying is very inconvenient in experimental work, the rate of drying was accelerated by gradual increase of temperature as the solvent was removed.

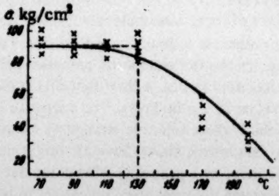

Fig. 1. Effect of temperature on the average shearing force (σ) required to separate glued polished steel surfaces.

The following drying procedure was adopted, as giving the most reproducible results in our experimental conditions. The drying was performed for three days at 30°, and for three days at 35°, with final drying of 8-hour periods at 60, 80, and 100°. It was found that with small amounts of water in the adhesive layer the drying can be done at even higher temperatures. Degradation of the adhesive film becomes appreciable only above 130° as can be seen from the experimental data in Fig. 1, where the average destroying shearing force is plotted against the drying temperature. The reproducibility of parallel experiments is indicated by the scatter of the experimental points in this and the other figures.

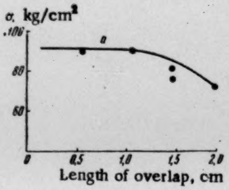

Fig. 2. Effect of length of overlap (in cm) of a joint glued by 20% gelatin solution on the average destroying force σ; thickness of adhesive layer $5 \cdot 10^{-4}$ cm.

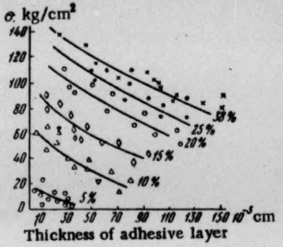

Fig. 3. Effect of thickness of adhesive layer and concentration of adhesive gelatin solution on bonding strength.

Fig. 2 shows the variation of the destroying force with the length of the overlap. It is seen in Fig. 2 that with overlaps up to ~ 1 cm the average destroying force is practically constant. Similar results have been obtained by others [2]. An overlap of 0.9 cm was used in the subsequent experiments.

Some workers found [3, 4] that bonding strength depends on the thickness of the adhesive layer. This was found to be the case in our experiments also; Fig. 3 shows that the bonding strength depends not only on the thickness of the adhesive layer, but also on the concentration of the adhesive solution. Under equal drying conditions and with equal layer thicknesses, the bonding strength increases with gelatin concentration. Change of concentration from 5 to 30% more than doubles the bonding strength.

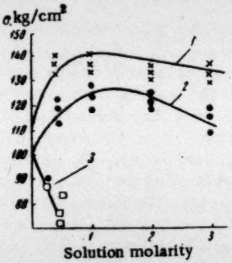

Fig. 4. Effect of additives on the bond strength between two steel plates glued by 20% gelatin solution based on solutions of different concentrations of: 1) urea, 2) acetamide, 3) sodium sulfate.

This effect, which is of interest and of practical importance, is in our opinion associated with the kinetics of relaxation of the internal stresses which arise during removal of solvents from dilute and concentrated adhesive solutions. As is known [1], relaxation effects and the nature of the internal stresses depend not only on gel concentration but also on the number of local intermolecular bonds. Increase of intermolecular interaction should retard while weakening accelerates relaxation processes [5]. The experimental data in Fig. 4 show that this is the case during formation of a glue layer. The curves in Fig. 4 show that the highest adhesive strength is found in adhesive films containing urea (Curve 1); this is probably because urea, by weakening intermolecular interaction, accelerates the relaxation processes. In presence of acetamide, which is a less active plasticizer, although the bond strength increases (Curve 2), the increase is considerably less than with urea.

Addition of sodium sulfate, which increases intermolecular interaction in gelatin solutions, decreases the bonding strength.

SUMMARY

1. The bonding strength between two lapped polished steel plates depends on the formation conditions of the adhesive film and the concentration of the gelatin solution.

2. Additives of low molecular weight, which weaken interaction between the polymer chains, increase the bonding strength; additives which intensify interaction between the macromolecules decrease it.

The L. Ya. Karpov Physicochemical Institute
The Leningrad Technological Institute
for the Food Industry

Received January 12, 1957

LITERATURE CITED

[1] P. I. Zubov, Z. N. Zhurkina, and V. A. Kargin, Colloid J. No. 2, 109 1947.

[2] N. A. de Bruyne, Aircraft Eng. 16, 115 140 1940.

[3] I. W. Mc Bain, W. B. Lee, J. Phys. Chem. 31, 1675 1927.

[4] O. Gerngross, Z. ang. Chem. 37, 847, 1924; 44, 232 1931.

[5] P. I. Zubov, Z. N. Zhurkina, and V. A. Kargin, Colloid J., 16, 109 1954.*

---

* Original Russian pagination. See C. B. translation.

LETTER TO THE EDITOR

THE TENSILE STRENGTH OF MIXTURES OF POLYETHYLENE AND POLYISOBUTYLENE

R.I. Feldman and A.K. Mironova

In studies of the mechanical properties [1, 2] and gas permeability [3] of systems consisting of polymers and low-molecular plasticizers, we established relationships between the conventional modulus conventional tensile strength, and gas permeability of mixtures in the high-elastic state, the corresponding characteristics of the constituents, and the composition expressed in mole fractions. The characteristics of the components were calculated in the form of limiting values by extrapolation of the linear plots of the logarithm of the property against the composition of a given system. It was reported [1] that for a system polymer I – polymer II the values of these characteristics at suitable temperatures can be found experimentally. The present communication deals with a study of the conventional (nominal) tensile strength of the system polyethylene-polyisobutylene in which polyisobutylene can be regarded as a polymeric plasticizer for polyethylene. Mixtures of the two polymers in different proportions were prepared by mixing on rolls with subsequent pressing. The polymers and mixtures were extended to break in a Polanyi dynamometer at 20° ± 0.5. The uniaxial extension rate was constant at 2 mm/minute.

Conventional Tensile Strengths of Polyethylene-Polysobutylene Mixtures, Determined Experimentally and Calculated by Equation (1). Extension Rate 2 mm/minute, t = 20°

Composition in mole fractions		Conventional tensile strength in kg/mm²	
polyethylene	polyisobutylene	experimental	calculated by Equation (1)
1.000	0	1.140	—
0.886	0.114	0.685	0.666
0.825	0.175	0.402	0.497
0.747	0.253	0.353	0.344
0.666	0.334	0.234	0.234
0.572	0.418	0.202	0.157
0.461	0.539	0.085	0.069
0.333	0.667	0.038	0.048
0.183	0.817	0.028	0.024
0	1.000	0.010	—

Plots of the logarithms of the conventional tensile strengths of the mixtures against the composition on mole fractions are linear. The mole fractions of polyethylene (N_{pe}) and polyisobutylene (N_{pib}) were calculated from the molecular weights of the monomer units C_2H_4 and C_4H_8 ($N_{pe} + N_{pib} = 1$).

The C_2H_4 group was taken as the unit in polyethylene, as the polyisobutylene unit corresponds to two carbon atoms in the principal macromolecular chain.

If the plot of log σ as a function of N is linear then the conventional tensile strengths of various polyethylene-polyisobutylene mixtures (σ_m) can be expressed in terms of the conventional tensile strengths of polyethylene (σ_{pe}) and polyisobutylene (σ_{pib}), in the first approximation as follows:

$$\sigma_m = \sigma_{pe}^{N_{pe}} \cdot \sigma_{pib}^{N_{pib}} . \qquad (1)$$

The Table gives the experimental values of σ_m and values calculated by Equation (1).

Because of the fairly good agreement between σ_m^{calc} and σ_m^{exp}, it is possible to calculate the conventional tensile strength of a mixture from experimentally determined tensile strengths of the constituent polymers for given extension conditions. The composition of a mixture of given properties can also be calculated.

The Moscow Technological Institute
for the Light Industry

Received June 2, 1957

LITERATURE CITED

[1] R. I. Feldman, Proc. Acad. Sci. USSR, 97, No. 6, 1033 1954.

[2] R. I. Feldman and A. K. Mironova, Colloid J., 17, No. 6, 465 1955.*

[3] S. I. Sokolov, S. A. Reitlinger and R. I. Feldman, Colloid J., 19, 624 1957.*

---

* Original Russian pagination. See C. B. translation.

SUBSCRIPTION PRICES SLASHED ON SOVIET CHEMISTRY TRANSLATIONS

Consultants Bureau is pleased to announce a major achievement in our program to reduce the prices of our cover-to-cover translations of Soviet scientific journals.

An arrangement with the National Science Foundation has made possible reductions of up to 90% in the annual subscription prices of 3 major Soviet chemical journals in complete translation. These price slashes, effective with the first issues of 1957, put these cover-to-cover translations well within the reach of even the most limited library and research laboratory budgets.

The journals affected are:	(Former price)	New price*	Non-profit research and academic institutions*
Journal of General Chemistry (*Zhurnal Obschei Khimii*). Oldest and major Soviet chemical journal—theoretical and experimental reports in organic, analytical and physical chemistry. 12 issues per year, approximately 3600 pages.	$170.00	**$90.00**	**$30.00**
Journal of Applied Chemistry (*Zhurnal Prikladnoi Khimii*). All aspects of applied chemical research. Reports from research institutes and USSR factory laboratories. 12 issues per year, approximately 2000 pages.	95.00	**60.00**	**20.00**
Bulletin of the Academy of Sciences USSR, Div. Chem. Sci. (*Izvestiya Akad. Nauk SSSR, Otdel. Khim. Nauk*). Research reports in all fields of chemistry, by leading members of the Soviet Academy of Sciences. General, organic, inorganic, physical and biological chemistry. 12 issues per year, approximately 1500 pages.	150.00	**45.00**	**15.00**

*Foreign subscriptions—$5.00 higher.

These cover-to-cover translations by Consultants Bureau bilingual chemists are clearly reproduced by the multilith process from IBM cold-type composition. All tabular material, diagrams and photographs are reproduced, integal with the text. Each issue is staple bound and is mailed to subscribers immediately on publication.

CONSULTANTS BUREAU, INC.
227 West 17th Street, New York 11, N. Y.
Telephone: ALgonquin 5-0713 **Cable: CONBUREAU NEWYORK**

THE COAGULATION MECHANISM OF BUTADIENE–STYRENE LATEX

S. A. Glikman and E. P. Korchagina

Most authors attribute the stability of synthetic latexes mainly to the presence on the globule surfaces of an electric double layer, formed as the result of ionization of adsorbed soap molecules [1]. It has been reported that the structural film formed by colloidal soaps has a protective action [2]. However, calculations based on data on globule size [3-5] show that the amounts of adsorbed substances are not enough to coat the globules even with a monomolecular layer. Data on the coagulation thresholds of latexes by various cations [1, 6] are in general agreement with typical data for lyophobic sols. At the same time the role of univalent cations, the action of which can be compared with the salting-out effect [7, 2], gives rise to doubt.

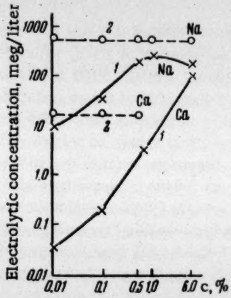

Fig. 1. Variation of coagulation thresholds (1) and complete coagulation concentration (2) with concentration of SKS-30A latex (logarithmic scale).

Extension of our knowledge of the nature of synthetic rubber latex coagulation by electrolytes, and of means of influencing the course of this process, is of theoretical and practical interest. In particular, in the production of butadiene–styrene rubber (SKS-30A) it would be desirable in many respects to replace calcium chloride, generally used for coagulation of the latex, by sodium chloride; but 40 times as much of the latter as of $CaCl_2$ is needed to coagulate the latex, and the resultant blanket is difficult to dry, owing to its structural peculiarities.

In order to investigate the nature of the action of mineral salts and certain other substances on the coagulation of SKS-30A latexes, we studied the effect of sodium and calcium chlorides and of certain nonelectrolytes on latexes at concentrations from 0.01 to 6%. The observations were carried out by means of a nephelometer 24 hours after preparation of the solutions. Aqueous solutions without added buffers were used, so that the influence of extraneous ions of buffer mixtures was excluded. The results are given in Fig. 1. Figure 1 shows that the coagulation thresholds of the diluted latexes are 200 times as high for NaCl as for $CaCl_2$. The coagulation thresholds increase with increasing latex concentration, and the difference between the effects of Na^+ and Ca^{2+} diminishes somewhat. At the same time, the complete coagulation concentrations remain unchanged at all latex concentrations, being 30 times greater for Na^+ than for Ca^{2+}. The absolute values of NaCl concentrations which cause complete coagulation even of concentrated latexes are several times less than the concentrations required for the salting-out effect. On the other hand, however, the fact that, for any latex concentration, equal amounts of Na^+ and Ca^{2+} are required for complete coagulation indicates that the role of electrolytes in latex coagulation is not confined to lowering the zeta potential. Our study [8] of the structural differences between the coagulation products obtained by the action of Na^+ and Ca^{2+}, and of the nature and porosity of the blankets formed from these products also indicates this. The nature of these differences is revealed by studies of the influence of certain nonelectrolytes on the course and character of the coagulation of SKS-30A latex.

Experiments showed that the coagulation threshold is not affected by addition of various amounts of hydroquinone to the latex. However, with an NaCl concentration which causes complete coagulation, the presence of 0.5% of hydroquinone in the latex gives a looser blanket, easier to dry. Addition of 2-5% hydroquinone to the latex makes blanket formation impossible, as with the amounts of NaCl used in the formulation a milky dispersion of very fine particles is formed, and visible coagulation does not occur at all. This dispersion, at a high degree of dilution with water, is as stable as the original latex; after it has been allowed to stand for many days not only does it show no signs of visible coagulation, but its turbidity remains quite unchanged.

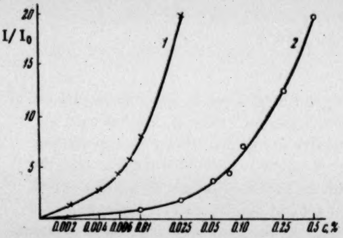

Fig. 2. Effect of rubber concentration on the relative light scattering of dispersion containing hydroquinone (1) and of latex (2).

Figure 2 shows the effect of concentration of rubber (in grams per 100 ml of liquid) on the relative light scattering (I/I_0, where I_0 is the light scattering of 0.01% latex) of dispersion with hydroquinone and of latex. These results show that at low concentrations of rubber in the latex light scattering is approximately proportional to the concentration, in accordance with Rayleigh's law; at higher concentrations the relationship is no longer linear. On the average, for equal concentrations of rubber in the latex and the dispersion, $I_{disp}/I_{lat} \sim 10$. This means that the volume of a particle of the dispersion is about 10 times the volume of a globule of the uncoagulated latex.

A latex dispersion diluted to a low concentration immediately after coagulation by NaCl, without additional hydroquinone, does not differ in any respect from a diluted dispersion of the coagulated latex containing 5% hydroquinone. In 0.005% dispersions of both types negligible amounts of NaCl and hydroquinone are present; they consist of particles about 10 times the size of the original latex particles. Visible coagulation of these dispersions requires the addition of 2.5% NaCl. Complete coagulation (with formation of flakes and a transparent serum) is caused by addition of 3.0% NaCl. However, if before addition of NaCl 5% of hydroquinone is added to 0.005% dispersion (made from latex coagulated by the usual formula), then after 24 hours of standing only reversible "creaming" occurs, whereas in control experiments (without hydroquinone) irreversible flakes are formed. All these experiments indicate that the size of the primary particles in latex coagulated by sodium chloride does not depend on the presence of hydroquinone in the latex.

It has been shown [8] that the difference between the blankets formed from latex coagulated by Na^+ and Ca^{2+} respectively lies in their macrostructure, in the volume and form of the intermediate pores, and the associated macrocavities. The specific surface, which is largely determined by the presence of micropores, is almost the same for both types of blanket. If this is considered in conjunction with the fact, noted above, that the dimensions of the primary aggregates of rubber globules remain constant, the idea of two stages in the coagulation process naturally arises. The first stage is the result of a fall of the zeta potential to the critical value, and consists of primary aggregate formation; the second stage consists of coalescence of these aggregates. This is evidently the stage which determines the difference between the structures of the blankets.

In the case of coagulation by calcium chloride, the fixation of molecules of insoluble Ca soaps on the globule surfaces should play an important role. Here not only the steric factor, which results in the formation of a looser structure, but also the energy factor, which consolidates this structure owing to interaction between the Ca soap molecules, may be of significance. In latexes coagulated by sodium salts the primary globule aggregates may be protected from coalescence by molecules of other constituents of the latex, including hydroquinone molecules, adsorbed on these particles.

After decrease of the zeta potential the surface soap film is not sufficient to protect the latex particles from coalescence resulting from autohesion, as this film does not completely cover the globule surface. On the contrary, the presence of such an incomplete film may sometimes intensify cohesion and coalescence of the particles, if, for example, this film is formed by soaps with bivalent cations, as is the case at a concentration of ~ 0.1% $CaCl_2$. Here, regardless of the latex concentration, the $CaCl_2$ concentration plays the dominant role, since exchange adsorption is the factor which determines the state of the system. Coagulation of the latex by calcium chloride is not only an autohesion effect, but is also ionic in character, and this leads to formation of loose coagulation products. The structure of the latter is determined by a combination of the steric and energy factors (ionic bonds).

The effect of sodium chloride on the coalescence of the primary aggregated latex particles is in fact analogous to (but not identical with) salting-out. The effect occurs at relatively high NaCl concentrations (of the order of 3%), and does not depend on the concentration of the latex. The coalescence which takes place at a definite ratio of the interaction energies of the primary aggregates of latex globules with each other and with water, occurs at a certain limiting concentration of NaCl, in presence of which the adhesive power of water is diminished. Since the coalescence of the primary particles in the coagulation of latexes by NaCl is primarily due to autohesion, the secondary structures formed are dense, and this leads in its turn to the formation of a compact blanket, difficult to dry, typical of these conditions. The molecules of "diphilic" substances, which are adsorbed more vigorously by rubber but are less hydrophilic than soaps, may protect the uncharged and partially "stripped" (owing to desorption of soaps) particles of the coagulated latex from coalescence. Hydroquinone is evidently such a substance. If the amount of hydroquinone is insufficient, coalescence is not excluded but merely hindered, and other steric conditions are set up, so that the coagulum is looser.

Certain other nonelectrolytes exert an influence analogous to that of hydroquinone on the second stage of coagulation. Especially interesting results were obtained with phenol. The action of the latter was even more dependent on the concentration than the action of hydroquinone, and it also greatly depended on the concentrations of the latex and NaCl. In particular, it was found that in presence of 0.8% of phenol (on the weight of the latex) complete coagulation of the latex can be effected by addition of one third of the amount of NaCl prescribed in the formulation, and the blanket formed from the coagulum is fully satisfactory and is dried more easily than the usual blanket obtained by NaCl coagulation of the latex.

The complex nature of the effects produced by the addition of different amounts of phenol to the latex can be explained by its twofold role. It seems that phenol, on the one hand, assists coagulation of the latex, and on the other, hinders coalescence of the coagulated particles. It seems possible that phenol molecules are not only adsorbed on the soap-free regions of the surface of the globules and their primary aggregates (or are solubilized in the soap film), but also partially displace the soap molecules from this surface. This is confirmed by variations of the soap concentration in the dispersion medium of the coagulated latex. It was shown by a conductometric titration method developed by Maron, et al. [9] that serums of latexes to which 0.8% phenol had been added before coagulation by NaCl contained much higher concentrations of soap than control serums, formed under the usual coagulation conditions.

SUMMARY

1. It is shown that the absolute values of the coagulation thresholds of SKS-30A latexes diluted down to 0.01% correspond to the usual values for lyophobic sols. The values for NaCl are 200 times those for $CaCl_2$, and increase with the latex concentration. The complete coagulation concentration for NaCl is 30 times that for $CaCl_2$, and does not depend on the dilution of the latex.

2. It was shown by a nephelometric method that the volume of the primary particles formed in coagulation of the latex by sodium chloride is about 10 times the volume of the uncoagulated latex globules, irrespective of the latex concentration.

3. Consideration of the experimental data, in conjunction with facts reported in the literature, leads to the concept of two stages in the coagulation of latex by electrolytes: the first is the consequence of a decrease of the zeta potential, leading to the formation of primary particles, and the second leads to coalescence of these particles. The secondary aggregation processes can be prevented or modified by introduction of certain additives (nonelectrolytes) into the latex.

4. In addition to an explanation of the mechanism of latex coagulation by electrolytes, and a demonstration that this process can be controlled, indications are given of means of an approach to development of conditions for the production of a good blanket by coagulation of latex by sodium chloride, with a much decreased consumption of the latter.

The Saratov State University

Received October 3, 1956.

LITERATURE CITED

[1] S. S. Voyutsky and R. M. Panich, Progr. Chem., 25, 57 (1956).

[2] E. M. Aleksandrova and P. V. Mochalov, Colloid J., 16, 161 (1954). *

[3] M. Ardenne and D. Beischer, Kautschuk 5, 55 (1940).

[4] A. Yurzhenko and S. Mints, Proc. Acad. Sci. USSR, 55, 339 (1947).

[5] B. Zwicker, Ind. Eng. Chem. 44, 774 (1952).

[6] V. Balandina, K. Berezan, A. Dobromyslova, B. Dogadkin and M. Lapuk, Bull. Acad. Sci. USSR, Chem. Ser., 2, 397 (1936).

[7] A. I. Yuzhenko and V. P. Gusyakov, Colloid J., 16, 72 (1954).*

[8] E. P. Korchagina and S. A. Glikman, Sci. Mem. Saratov State Univ. Chem. Ser. (in the press).

[9] S. H. Maron, I. N. Ulevitch and M. E. Elder, Anal. Chem. 21, 691 (1949).

---

* Original Russian pagination. See C. B. translation.

ANALYSIS OF THE FORMS OF MOISTURE BONDING IN POROUS ADSORBENTS WITH THE AID OF DRYING THERMOGRAMS

M. F. Kazansky

In Lykov's theory of drying [1] it is shown that the drying of colloidal capillary-porous bodies is a complex thermal and physicochemical process, the laws of which are determined by the forms of bonding of the moisture being removed, and its state within the pores of the body. By studies of the kinetics of the drying of moist porous bodies it is possible to carry out a quantitative analysis of the forms of moisture bonding. The present paper gives descriptions of experiments on the drying of powdered silica gels of various structural types and of activated charcoal, moistened with water and methyl alcohol, carried out in order to establish a new method for the analysis of the forms of moisture bonding in porous bodies. The experiments were carried out at constant surrounding air temperature.

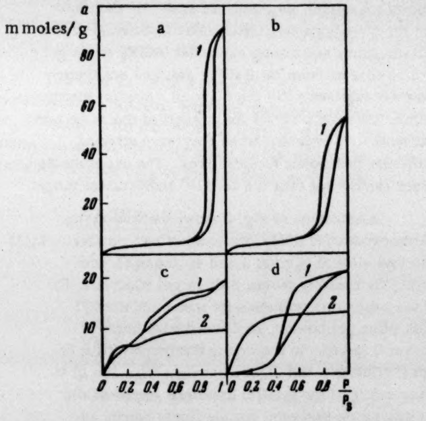

Fig. 1. Adsorption isotherms for water (1) and methyl alcohol (2) vapors on silica gels: a) E; b) VKhK$_2$ [6]; c) MSM; d) activated charcoal.

Of all the curves which illustrate graphically the kinetic relationships of the drying of porous bodies, in our opinion the most suitable for solution of the problem in question is the curve representing the temperature variations of a porous body during drying at constant surrounding air temperature. The important advantage of such a curve, which we have named the drying thermogram, is that it represents a direct experimental result and can be automatically recorded by means of suitable apparatus.

Silica gels and activated charcoal were chosen for the investigation because they are typical capillary-porous bodies, the structure of which have been studied fairly fully by a number of independent methods [2], while the contents of moisture bound in different forms can be determined from isotherms for water vapor adsorption.

With the aid of an automatic laboratory apparatus [3], the drying thermogram, the weight variation curve (drying curve), and a control curve for the surrounding air temperature were recorded automatically on the ribbon of a recording potentiometer. The experiments were performed with powder fractions > 0.25 mm of three silica gels: uniformly coarsely porous silica gel E, prepared in the Institute of Physical Chemistry, Academy of Sciences Ukrainian SSR; homogeneously coarsely porous silica gel VKhK$_2$; finely porous silica gel MSM from commercial samples of the Voskresensk Chemical Combine; the activated charcoal was a finely porous sample from the Molotov Chemical Works. The adsorption isotherms for water and methyl alcohol vapors are given in Fig. 1.

Before the experiment, the adsorbent powder was put into the cell of the laboratory apparatus [3] in a layer 1-2 mm thick. The cell was then put into the thermostat of the same apparatus, where the powder was dried at 110°. The cell was then placed in a desiccator where the powder was cooled over P_2O_5, and then moistened with water or methyl alcohol from a buret inserted in the neck of the desiccator lid.

The isothermal drying thermograms and the drying curves for the moistened adsorbent powders were recorded on the ribbon of a recording potentiometer while they were dried in the thermostat. The air temperature in the thermostat was kept constant by means of an electronic thermoregulator.

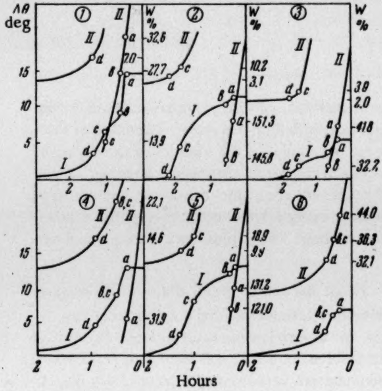

Fig. 2. Isothermal drying thermograms (I) and drying curves (II) at different temperatures for silica gel powders moistened with water: 1) MSM, 72°; 2) E, 75.4°; 3) activated charcoal, 51°, and moistened with methyl alcohol: 4) MSM, 75.4°; 5) E, 75.5°; 6) activated charcoal, 55.1°.

The powders were weighed automatically during the experiments by means of a photoelectric balance, the weight variations being recorded in the form of drying curves. The powder temperature was measured by means of a thermopile consisting of 32 thermocouples made from thin copper and constantan wires. One group of the thermopile junctions was in the cell with the adsorbent, and the other in the air over the powder. Thus the drying thermograms for the powders, recorded on the ribbon, show variations of the temperature difference between the powders and the constant temperature of the surrounding air during drying. The upper part of Fig. 2 shows thermograms(I) and drying curves (II) for MSM silica gel, E silica gel, and activated charcoal, moistened with water; in the lower part the corresponding thermograms and drying curves for the same adsorbents moistened with methyl alcohol are given. The graphs shown are copies, on a reduced scale, of the traces on the potentiometer ribbon. The isothermal drying thermograms and drying curves for VKhK$_2$ silica gel are similar to those for E silica gel, and are therefore not reproduced in the diagram. Similar thermograms and drying curves for powders of the same adsorbents were obtained when they were dried at different thermostat temperatures. The experiments were carried out over the 25-110° temperature range.

Examination of Fig. 2 shows that the drying thermograms for finely porous adsorbent powders – MSM silica gel and activated charcoal, moistened with water or methyl alcohol (Curves 1 and 4; 3 and 6), are similar in character, but differ from the drying thermograms for the coarsely porous E silica gel (Curves 2, 5). Corresponding to the presence of a large hysteresis region in the adsorption isotherms for water and methyl alcohol vapors on E silica gel, the drying thermograms for this silica gel powder, moistened with water or methyl alcohol, have considerable convex regions (b–c; Curves 2 and 5). In the drying thermograms for the finely porous adsorbents, MSM silica gel and activated charcoal (Curves 1 and 3), the convex region (b–c) is considerably smaller than in the curves for E silica gel, corresponding to the smaller hysteresis region of the water vapor adsorption isotherms. The methyl alcohol vapor adsorption isotherms for the finely porous adsorbents – MSM silica gel and activated charcoal – do not have a hysteresis region, and the thermograms for these powders, moistened with methyl alcohol (Curves 4 and 6) do not have a convex region (b–a); the point b on the thermogram coincides with the point c.

The moisture contents of the powders corresponding to the critical points a, b, c, and d on the thermograms, were determined from the drying curves. The moisture contents expressed as percentages on the weight of the dry powder, corresponding to the critical points on the thermograms, are indicated (in Fig. 2) for each adsorbent along the moisture axis.

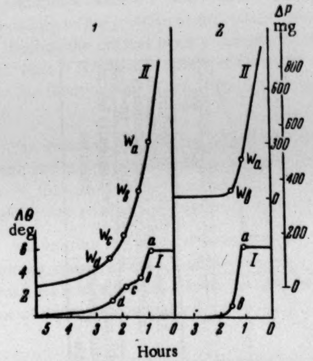

Fig. 3. Thermograms (I) and drying curves (II) at 50° for similar < 0.25 mm fractions of: 1) MSM silica gel powder; 2) quartz sand.

Figure 3 gives thermograms (1) and drying curves (II) at 50° for similar fractions of MSM silica gel powder (Fig. 3, 1) and quartz sand (Fig. 3, 2), moistened with water. The thermogram for quartz sand has two critical points, a and b, while the thermogram for the silica gel powder has four critical points, a, b, c and d. The upper part of the thermogram for the silica gel, above the point b, resembles the part of the thermogram for quartz sand above the point b.

We showed earlier [3] that the upper region of the drying thermogram for silica gel powder, limited by the position of the critical point b, and the corresponding region of the drying thermogram for sand, both correspond to the removal, from the macropores of the powder ($r > 10^{-5}$ cm), of capillary moisture in different states – capillary, "rope", and "joint".

Thus, the critical point b divides the drying thermograms for powdered adsorbents into two regions: the upper region corresponds to the period of moisture removal from the macropores of the body in the so-called moist state, and the lower, to the period of moisture removal from the body in the hygroscopic state from pores less than 10^{-5} cm radius, removed at relative vapor pressures less than unity.

The physicochemical nature of the points b, c and d on the drying thermograms was elucidated by comparison of the moisture contents, W_b, W_c, and W_d of the powders at the critical points of the thermograms, found from the drying curves, with the moisture contents of the same adsorbents at the inflection points of the adsorption isotherms at 20°.

The data in Table 1 show that the moisture content W_b of the adsorbents coincides, within the limits of experimental accuracy, with the moisture content P of the maximum hygroscopic state; the moisture content W_c coincides with the moisture content at the point of the start of the hysteresis region of the adsorption isotherm P_{sh} and it therefore equal to the amount of adsorbed water; and the moisture content W_d is equal to the moisture content P_{ma} of the adsorbent at the point at which monomolecular layer adsorption is completed.

TABLE 1

Adsorbent	Moistening agent	Moisture content, % of wt. of dry powder at 20°					
		P	W_b	P_{sh}	W_c	P_{ma}	W_d
MSM silica gel	Water	32.6	31.8	13.9	14.1	7.2	8.3
$VKhK_2$ silica gel	Water	93.6	87.0	7.0	6.6	2.6	3.0
E silica gel	Water	170.0	172.0	10.0	9.8	3.4	3.0
Activated charcoal	Water	37.8	35.2	3.6	4.5	—	—
MSM silica gel	Methyl alcohol	28.2	29.5	—	—	14.4	18.2

The moisture contents of the powders at all the critical points of the thermograms were determined for different temperatures from the thermograms and drying curves recorded during drying at different air temperatures. The results of these experiments were used to plot the curves in Fig. 4, which show the variations, with the temperature, of the moisture content at the maximum hygroscopic state (Curves 1b – 4b) and the amount of adsorbed water (Curves 1c – 4c) of MSM, $VKhK_2$, and E silica gel powders and of activated charcoal moistened with water, and of MSM silica gel (Curve 5bc) moistened with methyl alcohol.

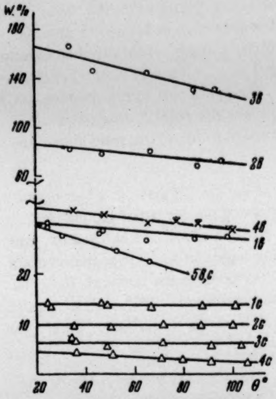

Fig. 4. Moisture contents at the critical points b and c of the isothermal drying thermograms for water-moist silica gel powders at various temperatures: 1b and 1c) MSM; 2b and 3c) VKhK$_2$; 3b and 2c) E; 4b and 4c) activated charcoal; 5b,c) MSM silica gel moistened with methyl alcohol.

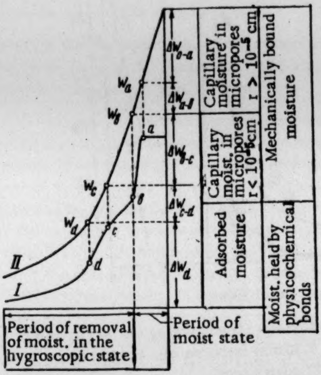
ΔW_{0-a}
W_a
ΔW_{a-b}
W_b
a
ΔW_{b-c}
W_c
b
ΔW_{c-d}
W_d
c
II
d
ΔW_d
I
Capillary moisture in micropores r > 10^{-5} cm
Capillary moist. in micropores r < 10^{-5}cm
Mechanically bound moisture
Adsorbed moisture
Moist. held by physicochemical bonds
Period of removal of moist. in the hygroscopic state
Period of moist state

Fig. 5. Diagram of the kinetics of the removal of moisture in different forms of bonding and states in the pores, during drying of fine capillary-porous bodies in isothermal conditions.

It is seen Fig. 4 that the moisture content of the maximum hygroscopic state of different silica gel powders decreases with increase of temperature, whereas the amounts of water adsorbed by silica gels remain constant; the amount of moisture in the hygroscopic state and the amount of adsorbed water in activated charcoal powder (Curves 4b and 4c) decrease with increasing temperature.

On the basis of the foregoing considerations concerning the nature of the critical points and the drying thermograms, in accordance with the modern theory of the drying of porous bodies, the kinetics of the consecutive removal of moisture during drying of adsorbent powders in isothermal conditions can be schematically represented as shown in Fig. 5. In Fig. 5, ΔW_{0-a} represents moisture in the capillary and "rope"* states, evaporating from a water-saturated surface; ΔW_{a-b} is moisture in the "joint"* state in the macropores, $r > 10^{-5}$ cm; ΔW_{b-c} is capillary condensation moisture in the pores, $r < 10^{-5}$ cm; ΔW_{c-d} is multimolecularly adsorbed moisture; ΔW_d is molecular adsorption moisture in monomolecular layers.

The diagram in Fig. 5 is based on the thermogram I and the drying curve II, for isothermal conditions, of a heterogeneously porous silica gel powder moistened with water to its full moisture capacity by contact with the liquid. By projecting the critical points of the thermogram I onto the drying curve II, and then projecting the corresponding points on the drying curve onto the moisture axis, we find the amounts of differently bonded moisture progressively removed during drying. In the interval from the start of drying to the critical point a, at constant temperature of the body and a constant drying rate, the moisture ΔW_{0-a} of the capillary and "rope" states is evaporated from the water-saturated surface of the porous body. In the time interval between the critical points a and b, moisture of the "joint" state ΔW_{a-b} is removed. Up to the critical point b moisture is evaporated at relative vapor pressure equal to unity; the porous body loses capillary moisture from the macropores, moisture of the so-called moist state of the body.

Starting from the critical point b, the body loses moisture of the hygroscopic state at a relative vapor pressure less than unity. Here, in the time interval between the critical points b and c the body loses capillary moisture present in pores of less than 10^{-5} cm radius, including moisture corresponding to the hysteresis loop of the adsorption isotherm. The moisture removed from the porous body from the start of drying to the instant corresponding to the position of the critical point c is moisture bound mechanically with the solid phase of the body. Beyond the critical point c removal of adsorbed moisture – moisture held by physicochemical bonds – occurs. First is removed moisture of the multimolecular layers ΔW_{c-d}, corresponding to the linear region c–d in the thermogram. Then, from the critical point d, moisture ΔW_d of the monomolecular layer is removed.

---

* [The significance of this terminology is not clear; it is apparently the terminology used in [3] – Translator].

The durations of these drying periods for thin specimens of porous bodies may vary according to the pore structure and the physicochemical properties of the body and of the liquid removed. If a particular bond form is absent, the corresponding section of the thermogram vanishes, as was the case for the drying of MSM silica gel and activated charcoal moistened with methyl alcohol.

We verified the above scheme in numerous experiments on the drying of other capillary-porous powders containing moisture bound in various forms to the solid phase. Therefore the scheme in Fig. 5 can be used as the basis for a new kinetic method for analyzing the forms of moisture bonding in capillary-porous bodies by means of drying thermograms for thin specimens.

SUMMARY

1. Thermograms and drying curves have been obtained for moistened silica gel powders of various types and for activated charcoal.

2. The moisture contents of powders at the critical points in the thermograms correspond to the limits of removal of moisture differing in the forms of bonding and state in the pores of the body during drying.

3. A kinetic scheme has been drawn up for the consecutive removal of moisture bound in different ways during drying of capillary-porous bodies; this is recommended as the basis for a new kinetic method of analyzing the forms of moisture bonding in porous bodies by the use of drying thermograms for thin specimens.

The A. M. Gorky State Pedagogic Institute, Kiev
Laboratory of Molecular Physics

Received September 8, 1957.

LITERATURE CITED

[1] A. V. Lykov, Colloid J., 10, 289 (1948).

[2] Coll.: Methods of Investigation of the Structure of Highly Disperse Bodies (Acad. Sci. USSR Press, Moscow, 1953).

[3] M. F. Kazansky, Sci. Mem., Phys.-Math. Ser., Kiev State Pedagogic Inst. 19, 155 (1956).

[4] O. M. Dzhigit, A. V. Kiselev, and I. E. Neimark, J. Phys. Chem., 28, 1804 (1954).

STUDY OF GELATION PROCESSES IN FRUIT CANDY MASSES BY MEANS OF THE CONE PLASTOMETER

L. S. Kuznetsova and A. L. Sokolovsky

For improving the technology of fruit gel production, it is important to develop an objective method for determining the gel strength and to establish the optimum gelation conditions. Our investigations have made it possible to determine the influence of a number of factors on gelation of candy masses containing pectin: sugar and moisture contents, pH, additions of various buffer salts. The gelling power of the raw fruit materials and confectionery masses was evaluated in terms of the strength of the gel, which depends on the presence of a structure in the gel. The strength was determined by means of the cone plastometer devised by Rebinder [1]. By means of this apparatus it was possible to study the kinetics of gel formation fairly simply, by the variation of the plastic strength with time. The cone plastometer is generally used for determining the least value of the acting force balanced by the plastic strength of the structure at the instant when the cone stops. In determinations of the plastic strength of candy jellies a creep effect was observed, consisting of a very slow immersion of the cone after it had apparently stopped. This shows that candy masses do not have true flow limit (elastic limit) forming a boundary between the regions of elastic and residual deformations. The stress corresponding to the abrupt change of the flow rate is the practical flow limit. Since we were interested in variations of the strength of confectionery jellies with time, the duration of the experiment had to be as short as possible. We selected a time interval of 1 minute, corresponding to immersion of the cone at the maximum speed.

Since it seems likely that the plastic strength values given by this method are too high, to determine the correction factor for conversion to true values the strength of the candy masses was determined by means of the Volarovich viscosimeter and by the plate shearing method.

In the first case the effective viscosity of the jellies was determined at various velocity gradients. Small forces, and therefore small velocity gradients, corresponded to high viscosities. Increase of the stress resulted in a decrease of effective viscosity owing to breakdown of the structure. The viscosity fell most sharply at stresses determined by extrapolation of the linear regions of the $\eta - P$ curves, indicating almost total breakdown of the structure. The stress determined in this way can be regarded as the strength of the gel. Comparison of the values for the strength of candy masses determined by this method ($5.05 \cdot 10^3$ and $2.54 \cdot 10^4$ dynes / cm^2) with the results found by means of the cone plastometer ($10 \cdot 10^3$ and $5 \cdot 10^4$ dynes/ cm^2) and by tangential displacement of a plate showed, as expected, that the cone plastometer gives high strength values. The factor for converting the plastic strengths to the true values is close to 0.5.

The nature of the strength increase in candy jellies as determined by these methods is the same in each case. The strength variation curves resemble the gel formation curves for pectin solutions. Therefore the cone immersion method, which gives the correct qualitative and quantitative characteristics of the strength properties of the structure (if the conversion factor is used), can be regarded as a convenient method both for studying the kinetics of gel formation in candy masses, and for production control.

By means of the cone immersion method it proved possible to determine the optimum strength of candy jelly over the range of $2 \cdot 10^4$ to $3 \cdot 10^4$ dynes/cm^2. The optimum strength of candy jellies is determined by correct formulation (contents of sugar, moisture, acid, and pectin). The data obtained on the effect of sugar on gelation processes in candy masses are of interest. Increase of the sugar content in fruit candy from 80 to 140 parts by weight (per 100 parts of fruit mixture) results in a decrease of jelly strength and a shorter gelation

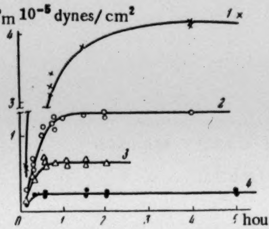

Fig. 1. Variation of candy jelly strength with moisture content: 1) moisture content 9.2%; 2) 14.0%; 3) 19.2%; 4) 23.6%.

time; this is in agreement with the existing views concerning the nature of sugar as a dehydrating agent in the formation of confectionery jellies, by decreasing solvation of the particles. The structural skeleton is formed by cohesion of individual pectin particles at regions free from solvate layers.

The strength of candy jellies is lowered not only by an increase of the sugar content but also by an increase of the moisture content, as is shown by the data in Fig. 1. (The recipe of the candy mass was sugar, plum puree, and apple puree in 1:0.7:0.3 ratio). In addition, the gelation time of candy masses is shortened with increase of moisture content. This is probably caused by accelerated orientation of the pectin chain molecules as the result of the decrease in the viscosity of the dispersion medium.

The active acidity plays a decisive role in the gelation of fruit candy masses. Two factors make it necessary to ensure the optimum active acidity in the gelation of candy masses: 1) at the optimum hydrogen ion concentration complete substitution of the metal ions in the carboxyl groups of the pectin molecules takes place, to give pectic acids, capable of gel formation; 2) increase of hydrogen ion concentration may lead to depolymerization of the pectin molecule, a decrease of the molecular weight of the pectin, and deterioration of its jellying power. The lower pH limit for a fruit candy jelly should be not less than 3.0, and the upper, ~ 4.

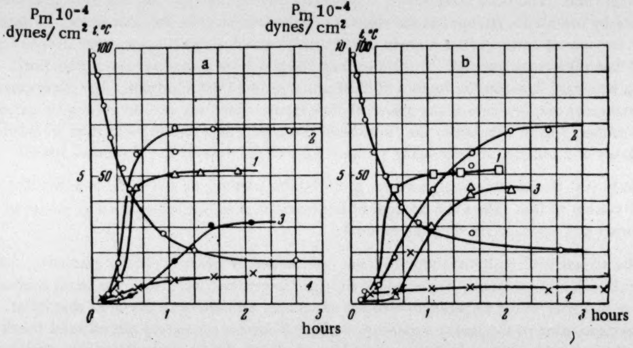

Fig. 2. Gelation kinetics of candy masses containing sodium tartrate (a) and sodium formate (b) in amounts: 1) 0%; 2) 0.2%; 3) 0.6%; 4) 1.0%.

The gelation processes can be regulated by addition to the candy masses of various buffer salts [2] of organic acids (tartaric, acetic, lactic, citric, and formic). Small amounts of the sodium salts of these acids (0.2% on the weight of the sugar and fruit puree) added to candy masses strengthen candy jellies (see Table). The sodium salts of the different organic acids can be arranged in the following sequence of their effects on the gelation of candy masses (increase of strength), which depend in this case on the anion: sodium citrate – sodium formate – sodium acetate – sodium tartrate – sodium lactate.

Small amounts (0.2%) of sodium tartrate and citrate accelerate the start of gelation (Fig. 2). On the

Effects of Sodium Salts of Organic Acids, and of Secondary and Tertiary Sodium Phosphates on the Physicochemical Properties of Candy Jellies.

Candy mass recipe	Salt	Salt, content, wt %of sugar – puree mixture	Moisture content, %	Acidity as % malic acid	pH	Reducing sugars, %	Jelly strength in dynes/cm²
Apricot puree, apple puree, sugar (0.5 : 0.5 : 1)	—	—	20.0	0.9	2.9	58.0	$5.2\cdot10^4$
Ditto	Sodium tartrate	0.2	20.0	0.9	3.3	54.75	$6.8\cdot10^4$
	Ditto	0.6	21.0	0.88	3.6	39.9	$3.1\cdot10^4$
		1.0	30.5	0.36	3.94	28.8	$1.0\cdot10^4$
	Sodium formate	0.2	20.0	0.86	3.5	41.25	$6.9\cdot10^4$
	Ditto	0.6	20.5	0.81	—	37.3	$4.5\cdot10^4$
		1.0	21.0	0.80	4.21	26.4	$6.0\cdot10^4$
	Sodium acetate	0.2	21.0	0.86	3.2	50.4	$6.8\cdot10^4$
	Ditto	1,0	20.0	0.79	3.5	37.2	$4.0\cdot10^4$
	Sodium lactate	0.2	19.8	1.06	—	—	$4.4\cdot10^4$
	Ditto	0,6	18.5	0.89	2.9	56.5	$4.6\cdot10^4$
		1.0	22.0	0.88	3.29	47.75	$7.4\cdot10^4$
Apricot puree, apple puree, sugar (0.7 : 0.3 : 1)	—	—	20.5	1.05	3.49	49.0	$2.8\cdot10^4$
Ditto	Sodium citrate	0.2	20.5	—	3.39	35.0	$1{,}07\cdot10^5$
	Ditto	0.6	20.7	0.74	—	34.5	$3.0\cdot10^5$
Apricot puree, apple puree, sugar (0.3 : 0.7 : 1)	—	—	20.0	0.92	3.22	65.7	$5.50\cdot10^4$
Ditto	Na_2HPO_4	0.4	19.6	0.9	3.47	55.8	$7.01\cdot10^4$
	Na_2HPO_4	0,6	19.4	0.87	3.49	44.2	$8.0\cdot10^4$
	Na_3PO_4	0.2	19.4	0.80	3.55	50,8	$8.0\cdot10^4$
	Na_3PO_4	0.5	17.4	0.77	4.09	38.5	$2.3\cdot10^4$
	Na_3PO_4	1.0	19.4	0.65	4.92	7.28	$0.8\cdot10^4$

other hand, sodium acetate, sodium lactate, and especially sodium formate retard gelation at the start, by lowering the temperature at which gelation begins. This makes it possible to extend the range of fruit materials used, and to make greater use of apple puree, which gives, under the ordinary boiling conditions without addition of salts, very viscous masses with a high temperature for the start of gelation. Secondary and normal sodium phosphates added to the candy masses in small amounts (0.2-0.6% on the weight of the puree and sugar) also have a favorable effect on gelation, increasing jelly strength.

Increase of the salt content, resulting in an increase of pH to 3.9-4.0 and over, has an adverse effect on the gelation of candy masses (the strength is decreased sharply). Not only salts containing the univalent Na^+ cation influence the formation of candy jellies. Several multivalent ions are known which have a favorable effect on the strength of pectin jellies; these include Ca^{2+}, Ba^{2+}, Al^{2+}; their role consists of the formation of new secondary bonds at the carboxyl groups of the polygalecturonic chains. This is fully confirmed by the results of our study of the effects of calcium lactate, chloride and phosphate; small additions (0.2-0.6%) of these salts increase gel strength and lower the gelation temperature. The quantitative differences between their effects are probably to be explained by the differences between the anions; these can be arranged in order of effectiveness as follows: PO_4, $CH_3CHOHCO_2$, Cl_2.

SUMMARY

1. It has been shown that the cone plastometer can be used for studying gelation processes of candy

masses and for control of the technological production processes.

2. The effects of the contents of sugar, moisture, active acidity, buffer salts, and salts containing multivalent ions on the gelation of fruit candy masses have been determined:

a) an increase of the sugar content from 80 to 140 parts by weight per 100 parts of the fruit mixture results in decreased jelly strength and a shorter gelation time;

b) increase of the moisture content of the jellies results in a decrease of strength and shortening of the gelation time;

c) an optimum active acidity must be maintained for normal gelation of fruit candy masses. The power pH limit of a fruit candy jelly must be not less than 3.0, and the upper limit, ~ 4;

d) addition various buffer salts to the candy masses results in changes of active acidity, and may be utilized for regulation of the gelation processes;

e) addition of small amounts of salts (lactates, chlorides, phosphates) containing bivalent ions (Ca^{2+}) has a favorable effect on the strength of candy jellies owing to formation of secondary bonds.

The Moscow Technological Institute for the
Food Industry

Received November 5, 1956.

LITERATURE CITED

[1] P. A. Rebinder, Summary of a General Course of Colloid Chemistry (Moscow State University Press, 1950). [In Russian].

[2] N. A. Gildebrandt, New Technology of Molded Marmalade Production (Food Industry Press, 1955). [In Russian].

THE ADSORPTIVE ACTIVITY OF CADMIUM HYDROXIDE IN RELATION TO THE CONDITIONS OF ITS FORMATION

S. A. Levina and N. F. Ermolenko

Of the papers which have been published in recent years on studies of the structure and the adsorptive and catalytic activity of metal hydroxides and oxides [1], only a few deal with cadmium oxide [2-3]. Nevertheless, studies of the influence of preparation conditions on the composition, structure, and adsorptive properties of cadmium hydroxide are of undoubted interest both in relation to the further conversion of the hydroxide into a more active catalyst, and for elucidation of the composition and structure of the hydroxide itself, prepared from different salts. The tendency of cadmium halides to complex formation is well known [4-7]. It is also known that when the hydroxide is precipitated from salts by the action of alkalies complexes are formed, the composition of which depend on the concentration of the components [8]. Iodine salts of cadmium have a considerable tendency to complex formation [9].

The purpose of the present work was to study the adsorptive activity of calcium hydroxide precipitated from the nitrate, and of the complex compounds of basic cadmium iodides formed by precipitation from cadmium iodide solutions at different pH values of the medium, in relation to their composition and structure.

Experimental procedure. Cadmium hydroxide was precipitated from cadmium nitrate solution by KOH solution. The precipitate was washed thoroughly and dried in air. To prepare basic cadmium salts, definite amounts of KOH solution were added to solutions of cadmium iodide. The precipitate was filtered off, washed with water to a negative reaction for I^- with $AgNO_3$, and dried in air. After the precipitate had been filtered off, the pH of the filtrate was determined (potentiometrically with a glass electrode) and a fresh portion of KOH was added. The precipitated fraction was again washed and dried in air. In this way the following 5 fractions were obtained in the air-dry state from 500 g of CdI_2:

Fraction No	I	II	III	IV	V
pH	4.22	6.25	7.20	8.20	11.24
Weight of precipitate,in g. .	7	10	11	70.0	32

The hydroxide samples and complex salt fractions were ground in a mortar and sifted through a sieve of 52 mesh. All the fractions were analyzed gravimetrically for moisture content and for cadmium and iodine. Cd was determined as the carbonate, and I as AgI. The particle size and surface were determined by Figurovsky's sedimentation method. The porosity was calculated from the apparent and true specific gravities. The adsorptive activity was determined from the adsorption of benzene vapor, of dyes from aqueous solutions, and of salicylic acid from benzene solutions.

Table 1 gives the analytical data for the moisture, cadmium, and iodine contents of the fractions.

These data show that the moisture contents of all the fractions are low, in contrast to the previously studied hydroxides of Al, Cr, and Fe, which contain from 25 to 37 % moisture in the air-dry state. The precipitation of the hydroxide by the action of alkali solution on cadmium nitrate solution differs from the precipitation of basic salts from cadmium iodide: in the former case it occurs at constant pH 6.44, while in the latter it begins at pH 4.2 and continues with considerable variation of the pH of the medium. During drying at 100° the basic salts do not decompose, but the hydroxide begins to turn brown, passing into CdO. The fairly high iodine content of the fractions obtained from CdI_2 should be noted. Spectroscopic data indicate absence of potassium in the fractions (the iodine was not adsorbed in the form of KI). Neither is the iodine adsorbed molecularly; this is shown by a negative reaction with starch even when the hydroxide is dissolved in dilute sulfuric or nitric acids. In view of the known ability of cadmium halides to form complexes [3-8], we believe that in this case complex formation occurs, analogous to that observed by Urazov and Kirakosyan [8] in the preparation of hydroxides from $CdSO_4$ by the action of alkali. The composition of the complex of the type $n\,Cd(OH)_2 \cdot CdSO_4 \cdot mH_2O$ varied, in the opinion of these authors, with the concentration of the components.

TABLE 1

Characteristics of the Individual Cadmium Hydroxide Fractions

Fractions	pH of medium	Moisture, %	% Cd	% I
Hydroxide	6.44	0.78	72.5	—
I	4.22	0.50	53.96	33.82
II	6.25	0.40	54.70	32.53
III	7.20	0.40	53.10	32.18
IV	8.20	0.10	54.70	32.07
V	11.24	0.70	65.60	16.2

The compositions of our fractions based on the analytical data are given in Table 2.

A complex in which there is one CdI_2 molecule per 8 $Cd(OH)_2$ molecules is formed only in an alkaline medium (pH 11.24). In the remaining cases, according to our analytical data, the complex consists of three molecules of $Cd(OH)_2$ to one molecule of CdI_2. However, further investigations showed that despite the same composition, the fractions differ in structure and adsorptive activity. Studies of the sedimentation of the hydroxide at the instant of formation showed that the content of particles between 5 and 8 μ in radius increases sharply when the reaction of the medium is changed from acid to neutral. Subsequent transition from a neutral to an alkaline medium is accompanied by an increase in the number of large particles, as is clearly seen in Fig. 1.

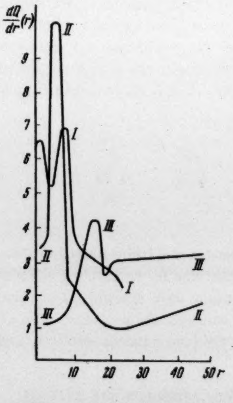

Fig. 1. Sedimenation analysis of calcium hydroxide suspensions at the instant of formation of different fractions: I) at pH 4.25; II) at pH 7.2; III) at pH 11.24.

The total surface area of the particles decreases in accordance with the increasing particle size as the pH of the medium rises. Table 3 gives the total surface areas of different cadmium hydroxide fractions, calculated from sedimentation analysis data obtained at the instant of formation of these fractions.

Sedimentation analysis of air-dry samples of the precipitated fractions also shows that the number of larger particles increases with rising pH of the medium.

The size of the precipitated particles depends to a considerable extent not only on the pH of the medium but also on the precipitation temperature. It is shown in Table 4 that, at a given solution pH (7.2-8), the content of larger particles increases with rise of temperature.

The porosity of the precipitates was determined from their apparent and true densities. The true and apparent densities and porosities of the precipitated fractions are given in Table 5.

The data in Table 5 show that Fractions I and IV have the highest true and apparent densities and also the lowest percentage porosities. They evidently have a dense structure of low porosity. It is to be expected that these fractions, especially Fraction IV, have a low adsorptive activity toward substances of high molecular weight. In fact, a study of

TABLE 2

Composition of Different Cadmium Hydroxide Fractions

Fraction	pH of medium	Composition of fractions	Calculated, %		Found, %	
			Cd	I	Cd	I
Hydroxide	6.44	2 $Cd(OH)_2 \cdot H_2O$	72.3	—	72.5	—
I	4.22	3 $Cd(OH)_2 \cdot CdI_2$	55,8	31.5	53.9	33.8
II	6.25	3 $Cd(OH)_2 \cdot CdI_2$	55.8	31.5	54.7	32.5
III	7.20	3 $Cd(OH)_2 \cdot CdI_2$	55.8	31.5	53,1	32.9
IV	8.20	3 $Cd(OH)_2 \cdot CdI_2$	55.8	31.5	54.7	32.0
V	11.24	8 $Cd(OH)_2 \cdot CdI_2$	65.8	16.5	65.6	16.2

TABLE 3

Total Surface Area of Particles in the Different Cadmium Hydroxide Fractions

Fraction No	I	II	III	IV	V
Total particle surface, in m^2	15	12	11	8	5

TABLE 4

Effect of Cadmium Hydroxide Precipitation Temperature on the Particle Size of the Main Bulk of the Sedimented Particles

Precipitation temperature, °C	5	10	20	25	30
Particle size, μ	2-8	3-10	3-12	4-8	4-11

TABLE 5

Variation of the Structure of Separate Fractions of Cadmium Hydroxide with the Precipitation Conditions

Fraction No.	Density		Porosity, %
	True	Apparent	
Hydroxide	4.8200	0.7746	83.9
I	5.4193	1.6398	69.8
II	4.3804	1.2978	70.6
III	4.8569	1.3246	72.7
IV	6.180	2.1694	64.9
V	4.4525	1.1728	73.6

the adsorption of dyes on the cadmium hydroxide fractions showed Fraction IV to be the least active.

The dyes used for the adsorption experiments differed both in nature and in degree of dispersion. The adsorption of the following dyes was studied: 1) methylene blue (a basic dye, molecularly dispersed); 2) Acid Blue (an anthraquinone dye), and 3) Congo Red (a coarsely disperse direct dye). In all cases normal adsorption isotherms were obtained, as shown in Fig. 2.

The values of the maximum surface saturation of the cadmium hydroxide fractions, calculated from the adsorption isotherms, are given in Table 6.

The data in Table 6 show that dye sorption depends not only on the structure of the adsorbent, but also on the nature and the degree of dispersion of the dye. Thus, the adsorption of the acid dye was greater than that of the basic dye in all cases.

Methylene blue is adsorbed better than the coarsely disperse Congo Red on all the fractions with the exception of cadmium hydroxide (which does not adsorb methylene blue at all) and Fraction V, where the basic nature of the compound evidently plays an important role in addition to the structure factor. The fact that Fraction IV has the lowest adsorptive power for the coarsely disperse Congo Red confirms that this fraction has a finely porous structure.

The active surface of the fractions was determined from the adsorption of benzene vapor and of salicylic acid from benzene solutions (Table 7).

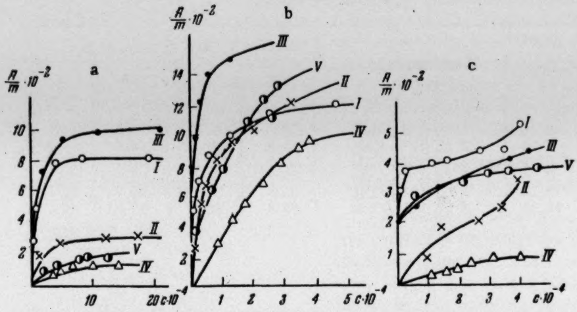

Fig. 2. Adsorption isotherms for methylene blue (a), Acid Blue (b), and Congo Red (c) on cadmium hydroxide fractions I-V.

The data in Table 7 show that the fractions have a fairly large active surface. As was to be expected, Fraction IV is the least active. It is interesting to note that nonpolar benzene is adsorbed very little on fractions containing iodine, and the value of the surface determined from benzene adsorption approaches to the value determined from adsorption of salicylic acid only for Fraction V and cadmium hydroxide. Fraction III is probably coarsely porous, and its active surface is therefore less than that of the other fractions (with the exception of IV). Owing to the presence of large pores, Fraction III adsorbs more of large dye molecules than do the other fractions. Therefore the adsorption of dyes is greater on this than on the other fractions.

TABLE 6

Maximum Surface Saturation of Cadmium Hydroxide Preparations by Dyes

Fraction No.	Amount of dye, in mg per g adsorbent		
	Methylene blue	Acid Blue	Congo Red
Hydroxide	—	86	57
I	90.9	142	45
II	50.0	125	55
III	108.0	180	55
IV	31.4	166	25
V	21.7	173	40

TABLE 7

Adsorptive Characteristics of Different Cadmium Hydroxide Fractions in Terms of the Active Surface

Fraction No.	Adsorbent surface, in m²/g	
	From adsorption of benzene vapor	From adsorption of salicylic acid
Hydroxide	385	426
I	77	399
II	110	366
III	110	320
IV	82	149
V	404	426

SUMMARY

1. The structure and composition of cadmium hydroxide and of complex compounds of cadmium hydroxide and iodide have been studied.

2. It is shown that the complex formed in an alkaline medium contains less iodine than the complexes formed in acid or neutral media.

3. Complexes of the same composition but precipitated at different pH differ in structure and therefore

in adsorptive activity.

4. The particle size of precipitated cadmium hydroxide fractions increases with increasing pH and precipitation temperature.

Institute of Chemistry, Academy of Sciences,
Belorussian SSR Minsk

Received November 19, 1956.

LITERATURE CITED

[1] Z. Ya. Berestneva, T. A. Koretskaya, and V. A. Kargin, Proc. Acad. Sci. USSR 70, 1121 (1948); Colloid J., 13, 323 (1951); 12, 338 (1950); 6, 369 (1949); N. F. Ermolenko and S. A. Levina, Bull. Acad. Sci. Belorussian SSR 1, 107 (1954); Colloid J. 17, 287 (1955);* Trans. 3rd All-Union Conf. Colloid Chem. (Izd. AN SSSR, 1956) p. 276.

[2] F. H. Healey, J. C. Fetsko, and A. C. Zettlemoyer, J. Phys. Chem. 57, 186 (1953).

[3] O. V. Krylov, S. Z. Roginsky and E. A. Forina, Proc. Acad. Sci. USSR 96, 1183 (1954).

[4] G. Urbain and E. Corner, Bull. Soc. Chim. 25, 131 (1919).

[5] P. Job, Ann. Chim. 9, 11 (1923).

[6] S. A. Shchukarev, L. S. Lilich and V. L. Latysheva, J. Inorg. Chem. 225 (1956).

[7] A. G. Bergman and E. L. Bakulskaya, J. Gen. Chem. 26, 625 (1956).*

[8] G. G. Urazov and A. K. Kirakosyan, Ann. Sector Phys.-Chem. Analysis, Inst. General and Inorganic Chem. Acad. Sci. USSR 25, 268 (1954).

[9] A. I. Golub, Ukrain. Chem. J., 19, 205 (1953).

---

* [Original Russian pagination. See C. B. translation].

A STUDY OF CHANGES IN THE STRUCTURAL AND MECHANICAL PROPERTIES OF PHOTOGRAPHIC EMULSIONS DURING DRYING

L. A. Lepilkina

Studies of the structural and mechanical properties of photographic emulsions are of great theoretical and practical importance, as in their physicochemical structure these emulsions constitute a new class of substances, distinct not only from such colloidal materials as clay and dough, but also from gelatin, which is one of the main constituents of photographic emulsions. The question involves the solution of a number of practical problems, foremost among which is the correct choice of optimum drying procedures and conditions. One of the causes of structural changes in photographic emulsions during drying is the stressed state resulting from irregular shrinkage which is the consequence of the existence of considerable moisture gradients along the surface and through the thickness of the emulsion layers. In consequence, stress concentration occurs at individual points of the emulsion layer during drying, leading to changes in the structure of the emulsion, pore formation, and warping of the layer.

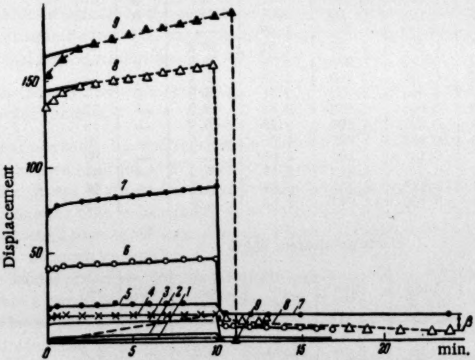

Fig. 1. Curves for the deformation kinetics of a positive emulsion at 450% moisture content and 18° at various stresses ($\tau \cdot 10^3$ kg/cm^2): 1) 0.160; 2) 0.323; 3) 0.668; 4) 1.18; 5) 1.68; 6) 3.06; 7) 6.07; 8) 11.6; 9) 17.3; ρ) degree of structural breakdown; β) degree of structural reinforcement.

The main purpose of the present investigation was to study the structural and mechanical properties of emulsion layers in order to reveal the peculiarities of their physicochemical structure and to determine the rheological characteristics necessary for calculation of the optimum drying conditions. Lykov's investigations [1] showed that the complex structural changes which occur during the drying of moist materials – local destruction, pore formation, changes in the forms of bonding between moisture and the material, transition of the structure from the amorphous into the crystalline state, and others – are caused by tangential stresses. For this reason the structural and mechanical properties of the emulsion layers were studied in shear conditions by means of a modified Gorazdovsky's apparatus [2]. The deformation kinetics under constant load, and the relationship between the tangential stresses and the relative shearing deformations under load applied according to a definite law were studied. The rheological characteristics were calculated by Rebinder's method [3, 4]. The following were studied: a diapositive emulsion with various contents of ammonium and potassium bromides, a positive emulsion, and an emulsion of the "ultrarapid" type with a high silver content. The rheological characteristics were determined at various moisture contents of the materials, from 1030 to 140% and at 18 and 25°. Figure 1 gives curves for the deformation kinetics at 18° of the positive emulsion at 450% moisture content, which are typical for all the emulsions studied. The rheological characteristics of the diapositive emulsion, determined at 18° and with 816 and 350% moisture contents are given in Table 1. Analysis of the experimental data shows that photographic emulsions are elasticoplastic bodies, with considerable elasticity.

TABLE 1

Variations of the Rheological Parameters of a Diapositive Emulsion with 816 and 350% Moisture Contents at 18°, with the Tangential Stress

τ, kg/cm^2	E_1, kg/cm^2	E_2, kg/cm^2	$\eta_1 \cdot 10^6$	θ, hours	ρ, 50 mm	β, 50 mm
Moisture content 816%						
0.160	0,046	0.069	—	—	4	4
0.276	0.027	0.118	—	—	4	—
0,669	0.038	0.286	—	—	0	—
1.175	0.063	0.503	—	—	0	—
3.090	0,059	0.885	1.58	—	0	—
4.160	0,068	1.780	4.97	20.2	2	—
5.550	0.079	2.370	5.70	20.0	0	—
8.260	0,058	7.110	1.69	8.1	14	—
10.800	0.064	1,160	1,11	4.8	0	—
13,500	0.061	1.650	3.48	15.9	—	27
16,300	0.073	1.990	4.20	16.0	—	18
19.200	0.083	5.820	1.65	5,5	—	20
22,100	0,137	3.160	2.84	5.7	—	80
25.300	0.136	4.350	2.17	4.4	—	84
28,300	0.123	2.700	3.64	8.3	—	46
34.400	0.150	1,970	2.52	4.6	—	38
Moisture content 350%						
3.08	0,266	0,88	—	—	3.5	—
5,99	0.342	2.57	—	—	0	—
8.65	0.370	4.90	—	—	2.0	—
12.80	0.305	3,65	—	—	2.0	—
22.40	0.305	3,19	5,74	5.3	—	1.0
32.40	0,327	3.46	2.08	1.8	—	4.0
42 80	0.307	18.40	2.45	2.2	—	2.0
53.50	0.327	6,54	3.92	3.4	—	0
64.00	0.320	6.85	2.19	2.0	—	8.0
75.00	0.316	9.20	2.56	2,3	—	0
86.50	0.316	14.90	1.27	1,1	—	26.0

At low loads, residual stresses arise in the emulsion layers and the diagrams do not coincide. The magnitude of the deviations, denoted here by ρ, represents the breakdown of the structure. In contrast to other colloidal materials, photographic emulsions have fairly large relaxation times. Consequently a considerable part of the energy used for deformation of the material is concentrated within the emulsion layer, causing complex structural changes. As a result, at certain tangential stresses not only is the emulsion structure completely restored, but it is also reinforced.

A characteristic feature of photographic emulsions is that at a definite stress and a definite moisture content they pass from the elasticoplastic into the elastic state. This indicates that under the influence of the stressed state a qualitatively different structure is formed. The elastic moduli of the emulsion in this new state are 5-10 times as high as in the original state; the relaxation time decreases considerably. The differences between the structures of the emulsion in these states are clearly seen in Fig. 2, which shows electron micrographs with × 10,000 magnification. Figure 2, b is a micrograph of the structure of a positive emulsion after a stressed state has been set up in it. This figure shows that under the influence of the stressed state an entirely new structure is formed in the emulsion layer, different from the original structure shown in Fig. 2,a. It seems likely that owing to the heterogeneous structure of the photographic emulsion stresses are concentrated at individual points in it during drying, leading to displacement of the silver halide grains with formation of groups containing from 2 to 10 grains. It is presumed that part of the moisture passes from the free into the bound state in the process. This new structure has not only different structural and mechanical properties, but evidently also different photographic properties. Similar studies of structural and mechanical properties were also carried out on diapositive emulsions with different ammonium and potassium bromide contents. Table 2 gives the rheological parameters of a diapositive emulsion containing excess potassium bromide at 18° with 400 % moisture content. It is seen from Table 2 that the strength and modulus of elasticity of this emulsion are much lower than those of an emulsion with lower ammonium and potassium bromide contents. With increase of ammonium and potassium bromide contents the structural transition from the elasticoplastic to the elastic state occurs at a higher moisture content. Consequently, these substances are surface-active, and as their content in the system increases the number of bonds at which adsorption of gelatin molecules occurs decreases, leading to weakening of the bonds between the silver bromide crystals and the dispersion medium. The emulsion with the higher potassium bromide content is nearer to gelatin in its structural and mechanical properties. Table 2 gives the rheological characteristics of an "ultrarapid" emulsion, calculated from data obtained at 330% moisture and 20°. Table 2 shows that the strength, elasticity, and plasticity moduli of the "ultrarapid" emulsion, containing 3 times as much silver as the diapositive emulsion, are one third of the corresponding values for the latter. This emulsion, in contrast to the diapositive and positive emulsions, does not show a transition of structure from the elasticoplastic to the elastic state with increase of tangential stress, at any moisture content. This emulsion shows considerable reinforcement at 430% moisture content.

Consequently, the bonds between the individual crystals and the dispersion medium are weaker in emulsions with higher silver bromide contents.

The structural and mechanical properties of these emulsions were also studied at 25°. The rheological characteristics of a diapositive emulsion at 25° and 930% moisture are given in Table 2. Increase of temperature results in a considerable change of the structural and mechanical properties; the elasticity moduli are decreased 3 to 5-fold, and the relaxation time is decreased 5 to 10-fold. The rheological characteristics of an emulsion previously held in the stressed state at 25° were also determined. The determinations were made at 18° and 785% moisture content. An emulsion which had previously been heated in the stressed state has considerably lower elasticity and a shorter relaxation time than an untreated emulsion. A characteristic feature of the diapositive emulsion is that β becomes zero with increase of temperature. The value of β characterizes reinforcement of the emulsion layer, probably by formation of groups of crystals of a complex compound of silver bromide. In this case reinforcement may occur under the influence of the stressed state by formation of a porous structure. A particularly large decrease of strength and elasticity with increase of temperature is found in the "ultrarapid" emulsion. For this emulsion the degree of structure reinforcement (β) at 25° is greater than the reinforcement at 20°. The probable explanation for this is that the mobility of the structure increases with rise of temperature, which leads to an increase in the number of possible groupings of silver bromide crystals when their content in the structure is high. To confirm the validity of the results obtained and to determine the rheological characteristics needed for calculation of the optimum drying conditions for emulsion layers, a study was made of the dependence of the tangential stress on the relative shearing deformation under definite loading conditions which apply during the drying of emulsion layers.

For the diapositive emulsion, the elasticity modulus increases with increasing stress down to 400% moisture content; this indicates considerable reinforcement of the structure. At lower moisture contents the reverse is

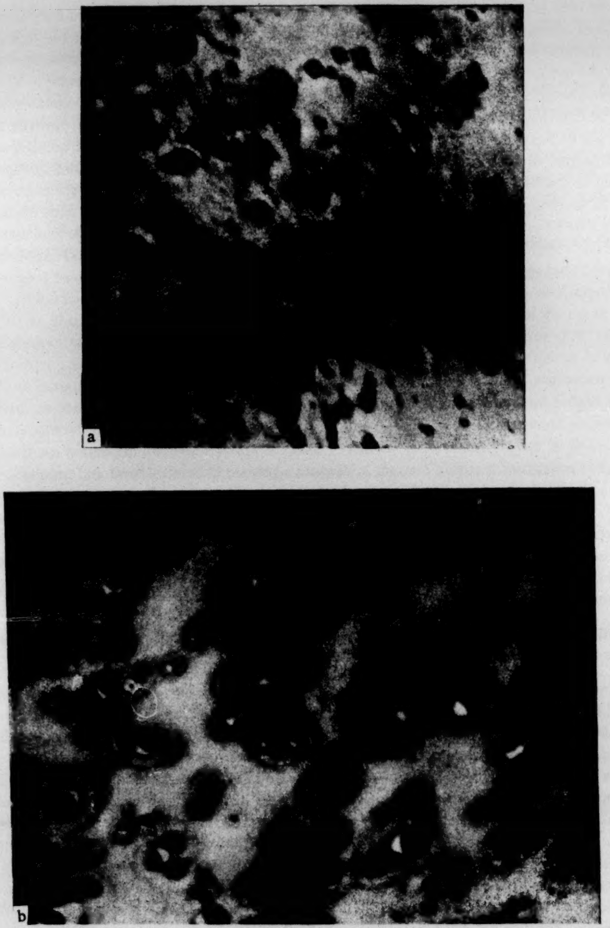

Fig. 2. Electron micrographs of the structure of a positive emulsion: a) before the stressed state; b) in the stressed state.

TABLE 2

Variations of the Rheological Parameters of Different Photographic Emulsions with the Tangential Stress

τ, kg/cm^2	E_1, kg/cm^2	E_2, kg/cm^2	$\eta_1 \cdot 10^6$	θ, hours	ρ 50 mm	β, 50 mm
Diapositive emulsion, 930% moisture at 25°						
0.16	0.0197	0.046	—	—	9	—
0.32	0.0106	0.145	—	—	12	—
0.88	0.0240	0.475	—	—	9	—
1.11	0.0227	0.472	—	—	0	—
2.31	0.0238	0.997	0.198	2.3	8	—
3.33	0.0200	2.840	0.189	2.6	20	—
4.82	0.0186	0.830	0.146	2.2	20	—
6.35	0.0171	0.410	0.146	3.3	5	—
7.85	0.0165	1.680	0.144	2.4	104	—
9.40	0.0159	0.672	0.342	5.9	12	—
Diapositive emulsion with excess potassium bromide, 400% moisture at 18°						
3.06	0.131	13.10	—	—	2	—
5.66	0.121	16.20	—	—	4	—
8.65	0.134	18.50	2.17	4.5	6	—
12.80	0.132	18.30	4.30	9.1	4	—
18.00	0.133	3.86	1.54	1.1	—	7
23.50	0.124	10.00	1.30	2.9	3	—
34.00	0.129	2.93	1.44	3.1	34	—
44.50	0.136	6.35	0.95	1.9	—	60
50.00	0.124	3.57	1.17	2.6	—	26
54:00	0.154	1.93	1.74	3.1	—	25
"Ultrarapid" emulsion, 330% moisture at 20°						
0.16	0.175	—	—	—	4	—
0.32	0.030	1.39	—	—	4	—
1.80	0.057	3.10	1.85	9.1	8	—
3.23	0.054	5.54	0.24	1.2	5	—
5.73	0,051	7.00	0.42	2.3	12	—
8.40	0.051	1.79	0.54	2.3	8	—
10.90	0.053	1.88	0.40	2.1	0	—
16.50	0.057	0.95	0.60	2.9	10	—
21.70	0.056	1.16	0.56	2.8	10	—

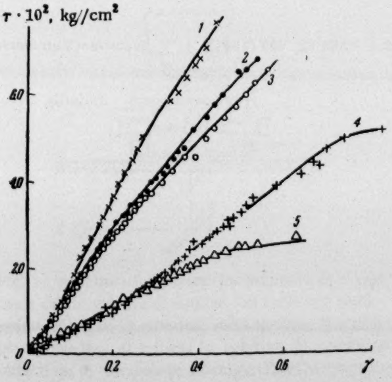

Fig. 3. Variation of tangential stress (τ) with relative shearing deformation (γ) for "ultrarapid" emulsion at 20° and at moisture contents: 1) 140%; 2) 229%; 3) 255%; 4) 440%; 5) 515%.

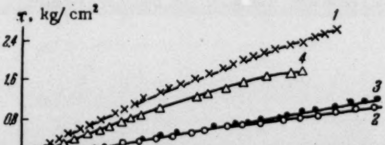

Fig. 4. Variation of tangential stress with relative shearing deformation for "ultrarapid" emulsion at 25° and at moisture contents: 1) 110%; 2) 180%; 3) 350%; 4) 500%.

the case. Figure 3 shows variations of the tangential stress with the relative shearing deformation for "ultrarapid" emulsion at 20° and various moisture contents. It is seen in Fig. 3 that the structure of this emulsion is reinforced only at 440% moisture content; on further decrease of the moisture content the elasticity modulus decreases with increasing stress. These results show that complex structural changes occur in the emulsion layers during the first period and at the start of the second period of drying. On further decrease of moisture content, probably with increasing local stresses, gradual breakdown of the structure takes place. The relationship between the tangential stresses and the relative shearing deformations was also studied for the above emulsions at 25° and with various moisture contents.

Such data for "ultrarapid" emulsion are given in Fig. 4. It is seen that at 25° the degree of structure reinforcement does not increase, as is the case at 18-20°, but decreases with increasing stress; a strength decrease is found even at relatively small loads. There is a sharp decrease of strength with increasing stress at moisture contents below 400%; this is a sign of breakdown in the structure formed at the beginning of the drying process.

SUMMARY

1. A new structure, different from the original structure, is formed during drying of emulsion layers under the influence of the stresses which arise. At a definite moisture content the formation of the new structure is accompanied by transition of the emulsion from the elasticoplastic into the elastic state, characterized by increased strength of the structure and different rheological properties.

2. The rheological characteristics necessary for calculation of the optimum drying conditions of emulsion layers have been determined.

In conclusion, the author expresses her gratitude to Professor A. V. Lykov for valuable guidance and advice during the work.

Scientific Research Institute of Motion
Picture Photography

Received October 1, 1956.

LITERATURE CITED

[1] A. V. Lykov, Heat and Mass Transfer in Drying Processes (State Power Press, 1956). [In Russian].

[2] L. A. Lepilkina, Colloid J. 18, 3, 302 (1956).*

[3] P. A. Rebinder et al., Proc. Acad. Sci. USSR, 72, 85 (1950); 49, 354 (1945); Colloid J., 9, 67, 381 (1947); 10, 223, 466 (1948); 12, 79 (1950).

[4] L. V. Chumakova and P. A. Rebinder, Proc. Acad. Sci. USSR 81, 239 (1951); L. V. Ivanova-Chumakova and P. A. Rebinder, Colloid J., 18, 540, 682 (1956).*

---

* [Original Russian pagination. See C. B. translation].

THE SWELLING OF ION EXCHANGE RESINS AND THE NATURE OF THEIR SELECTIVITY

V. P. Meleshko and O. N. Myagkoi

Studies of the ability of ion exchange resins to change their volume with changes of the ionic composition or concentration of the solution in contact with them are of undoubted interest in relation to the theory of ion exchange chromatography. Many papers published recently are devoted to this question.

The results of investigations carried out in order to determine the laws governing the swelling of ion exchange resins are given below. Variations in the specific volume of a cation exchange resin on swelling in solutions of hydrochloric acid and of alkali and alkaline earth chlorides were studied.

The investigations were carried out with SDV-3 cationic resin, which is a sulfonated polymer of styrene with divinylbenzene containing one type of functional group, SO_3H, in its structure. The specific volume of the swollen resin was determined by measurement of a spherical particle of the resin in contact with the solution in a special cell, with the aid of a microscope. The cell was a compartment made from transparent Plexiglas through which the liquid flowed. The grain of resin was fixed in the cell in a constant position by means of two nickel-plated needles which could be moved by means of screw threads. Grains of strictly spherical shape ~ 1.5 mm in diameter were chosen for the experiments. A diagram of the apparatus is shown in Fig. 1.

The saturating solution was passed slowly through the cell. The grain diameter was measured after a time interval sufficient for equilibrium to be established in the system; this was determined by experiments on swelling kinetics (Fig. 2). After each determination the cell was washed out with distilled water and a fresh portion of the saturating solution was passed through.

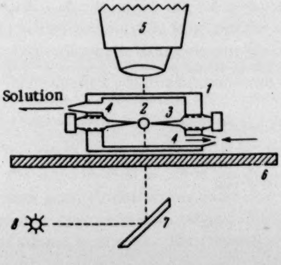

Fig. 1. Scheme of apparatus for microscopic measurement of the volume of swollen ion exchange resin grains: 1) cell; 2) spherical resin sample; 3) nickel-plated needles; 4) orifices for solution; 5) microscope objective; 6) microscope substage; 7) reflecting mirrors; 8) light source

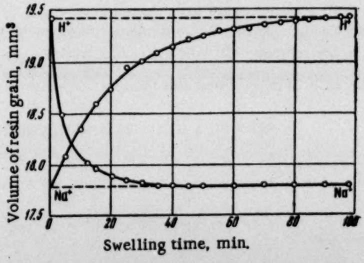

Fig. 2. Rate of swelling of spherical samples of SDV-3 cationic resin in relation to the initial and final ionic states.

All the determinations were performed with the cell in the same position and with a constantly focused microscope objective. The results of the measurements were checked by duplicate experiments, the average results being given in this paper.

Some of the experiments were conducted with artificial grains ~ 3 mm in diameter made from the same resin, which made greater accuracy possible. The grains were made by mixing the powdered resin with a small amount of adhesive made from butyl methacrylate film dissolved in a mixture of equal volumes of ligroin and benzene. It was shown in special experiments that the volume of a butyl methacrylate film remains unchanged even when immersed for a long time in water.

It was possible by the above method to carry out the measurements rapidly in conditions in which the resin is in contact with the saturating solution. This was expected to give results in closer agreement with the true state of the resin in use than any other method, including the pycnometric [1].

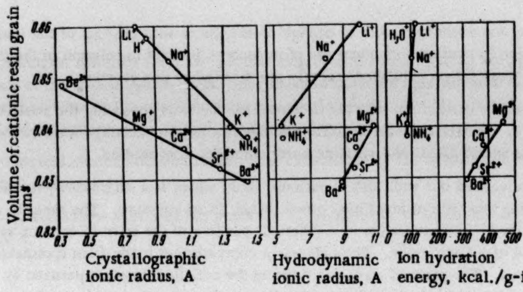

Fig. 3. Variation of the volume of a spherical sample of a swollen cationic resin with the radii of the saturating ions and their hydration energies.

The saturating solutions used for determinations of the effects of the kind of ion present on the volume of the swollen resin grain were 0.1 N solutions of alkali and alkaline earth metal chlorides. The grain volumes in different ionic forms were measured in the following sequence: R – Li, R – H, R – Na, R – K, R – NH_4, and the measurement sequence was then reversed: R – NH_4, R – K, R – Na, R – H, R – Li. The volumes of the cationic resin grain saturated with cations of bivalent metals: R – Be, R – Mg, R – Ca, R – Sr, R – Ba and R – Ba, R – Sr, R – Ca, R – Mg, R – Be, were determined in the same way. The reverse order of saturation served to check both the reproducibility of the results, and the reversibility of the volume change of the swollen resin.

The experiments showed that the specific volumes of the swollen resins form the following sequences:

$$RLi > RH > RNa > RK > RNH_4 \text{ and } RBe > RMg > RCa > RSr > RBa.$$

It is seen that these sequences are the reverse of the known adsorption series [1]:

$$Li^+ < H^+ < Na^+ < K^+ \text{ and } Mg^{2+} < Ca^{2+} < Sr^{2+} < Ba^{2+}.$$

The volume of the resin as a function of the crystallographic and hydrodynamic ionic radii and of the hydration energy of the saturating ions is shown graphically in Fig. 3. The cation hydration energies are taken from Mishchenko's data [2], the ionic radii from Goldschmidt's data [3], and the radii of the hydrated ions from Jenny's data [1]. It is seen from Fig. 3 that, in the alkali and alkaline earth metal series, the specific volume of the swollen resin is an inverse linear function of the radii of nonhydrated ions, and a direct linear function of their hydrodynamic radii and hydration energies.

This law for the volume change of the swollen resin, and its agreement with the adsorbability sequence of the cations studied, accounts for the affinity differences of these cations for a strongly acid cation exchanger such as SDV-3. It is evident that these differences are determined only to a small degree by the forces of chemical bonding between the cations and the active groups of the resin. In the present instance easily dissociated compounds are formed both in the resin phase and in the solution phase [4]. Consequently, the decisive role is played by the hydrated exchange ions.

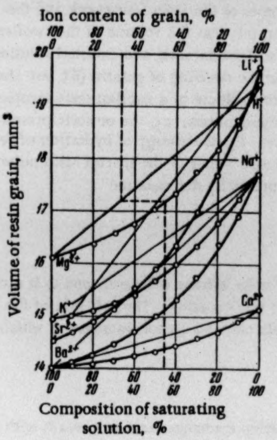

Fig. 4. Variation of the volume of a spherical sample of swollen resin with the composition of a solution of the chlorides of two cations.

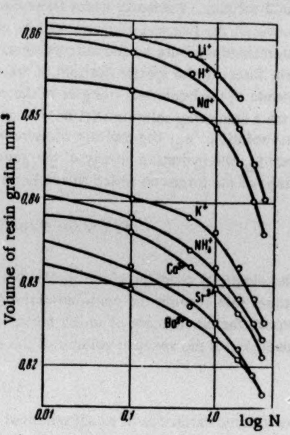

Fig. 5. Variation of the volume of a spherical sample of swollen resin with the concentration of the external solution.

In the absolutely dry resin the spatial network is in a state of least tension. Water entering the particle extends it. Entry of less hydrated ions into the resin is more favorable from the energy aspect than the entry of more highly hydrated ions. This is confirmed by the relationship between the volume of a resin particle in 0.1 N solutions of the chlorides of two cations and the composition of the mixture (Fig. 4). The concave curves in Fig. 4 show the variation of the volume of the swollen particle with the composition of the external solution. The straight lines correspond to the percentage contents of the ions in the resin phase at a given volume. The less the hydrate shell of the ion, the more of it enters into the resin phase. This is seen even more clearly by an examination of the kinetics of swelling of the resin in its conversion into various salt forms (Fig. 2). The process leading to a decrease in the volume of the resin is nearly three times as rapid in the system RH + Na^+ as in the saturation of the Na resin by hydrogen ions.

The effect of the concentration of the saturating solution on the volume of the swollen resin was studied next. The same method as before was used for these experiments. The curves in Fig. 5 show that the volume of the resin grain diminishes regularly with increasing concentration of the external solution. However, the differences between the specific volumes of the resin saturated with different cations persist even at high solution concentrations (up to 4 N). The sequence of the ions in order of their affinity for the resin also remains unchanged.

From the results of these investigations it is possible to draw conclusions concerning the nature of the forces acting in the resin–solution system.

As is known [5], the swelling of ion exchange resins is the result of hydration of active groups and of the gegenions neutralizing these groups, and also of the osmotic pressure which arises at the boundary between the resin particle and the solution. The swelling process and the behavior of the resin can be represented as follows. From the moment when water enters the resin phase, the particle begins to resemble a limited volume of electrolyte solution, and an osmotic pressure is set up between it and the free liquid. The organic framework of the resin, which retains the active groups in a limited volume, acts as a semipermeable membrane toward them, which is, however, permeable to other ions. The membrane action of the spatial resin network is analogous to the action of the semipermeable membranes in living cells, as its elastic forces restrict the amount of water entering the resin phase.

It is seen in Fig. 4 that equal volumes of particles saturated with different ions correspond to different concentrations of the external solutions. For example, the resin has a volume of 0-84 mm^3 in 0.1 N KCl solution and 3.0 N NaCl solution. Evidently under these conditions the elastic forces of the resin framework and the osmotic pressures of the internal solutions will be equal.• It follows from this that the volume of the swollen sample is determined not only by the magnitude of the osmotic pressures of the internal and external solutions and the elastic forces of the spatial network of the resin, as is the case in the swelling of gelatin [6], but also by the magnitude of the hydration energies of the adsorbed ions. Then the volume of a swollen resin sample in contact with a saturating solution will be the function of a number of parameters: π_i, the osmotic pressure of the internal solution; π_a, the osmotic pressure of the external solution; E_a, the energy of hydration of the active groups; E_u, the hydration energy of the gegenions; and u, the elastic forces of the spatial resin network. The distribution of the forces on which this volume will depend is determined by the equation

$$\pi_i + Q(E_a + E_u) = \pi_a + CV,$$

where C is the elasticity modulus of the spatial network of the resin; V is its volume increase; and Q is a constant which takes into account the commensurability of the quantities in this equation. The left side of the equation contains factors increase of which favors swelling; the right side contains factors increase of which results in a decrease of the specific volume of the swollen resin.

SUMMARY

1. The volume variations of small spherical samples of SDV-3 cation exchange resin in contact with solutions of alkali and alkaline earth metal chlorides of various concentrations have been studied.

2. It is shown that the volume of the swollen cation exchange resin increases regularly with decreasing crystallographic radii of the ions saturating the resin, and with increasing hydration energy of these ions. The action of the ions strictly corresponds to their positions in the adsorption series for strongly acid cation exchangers.

3. Curves for the variations in the volume of the cation exchange resin in contact with a solution (a mixture of two cations in various proportions) and curves for the rate of volume change in the conversion of the resin from one ionic form into another show that ions, the sorption of which leads to a decrease of volume of the swollen cation exchange resin, are the ions which are preferentially adsorbed.

4. The decreased differences between the volumes of the swollen resin with increasing concentration of the external solution correspond to the decreased selectivity of the ion exchangers found in such cases.

5. The investigations confirmed that the main cause of selectivity in the adsorption in the series of ions which form highly ionized compounds with the active groups of the resin lies in differences between the forces exerted from the exchanging ions against the elastic forces of the spatial resin network.

The Voronezh State University, Chair of
Inorganic Chemistry

Received November 26, 1956.

LITERATURE CITED

[1] R. Kunin and R. Myers, Ion Exchange Resins (IL, Moscow, 1952) [Russian translation].

[2] K. B. Yatsimirsky, Thermochemistry of Complex Compounds (Izd. AN SSSR, Moscow, 1954).

[3] Chemist's Reference Book, vol. 1 (State Chem. Press, Leningrad–Moscow, 1951) p. 288.

• Apart from certain concentration differences of the internal solutions with equal volumes of the sample, due to the Donnan effect.

[4] D. I. Ryabchikov, in coll.: Investigations in the Field of Chromatography (Izd. AN SSSR, Moscow, 1952) p. 234.

[5] H. P. Gregor, J. Am. Chem. Soc. 70, 1293 (1948).

[6] W. Bauman, in coll.: Ion Exchange (IL, Moscow, 1951) p. 49. [Russian translation].

[1] [illegible]

[2] [illegible]

[3] [illegible]

[illegible]

[illegible]

[illegible]

[illegible]

1. [illegible]

2. [illegible]

3. [illegible]

4. [illegible]

5. [illegible]

[illegible]

[illegible]

[1] [illegible]

[2] [illegible]

[3] [illegible]

[illegible]

THE SOLUTION STATE OF DIRECT DYES AND THEIR DIFFUSION IN A CELLOPHANE FILM

B. N. Melnikov and P. V. Moryganov

We have shown [1, 2] that the activation energy of diffusion of a number of direct dyes depends to a considerable extent on the neutral electrolyte concentration in the dye bath. For some dyes which tend to aggregate, there is an abrupt change in the activation energy in the transition from low temperatures (40-60°) to higher temperatures (70-100°). Addition of dispersing agents to the dye bath increases the diffusion coefficients and decreases the activation energy of diffusion, i.e., facilitates penetration of the dyes into the fiber. To explain these facts, we suggested that a relationship exists between the aggregation state of dyes in solution and their rate of penetration into the fiber. The purpose of the present investigation was to confirm this hypothesis experimentally. The work was accordingly divided into two parts:

1. Study of the diffusion of a number of direct dyes in solution over a wide range of temperatures and electrolyte concentrations.

2. Study of the diffusion of the same dyes in Cellophane in presence of dispersing agents in the system.

The diffusion of direct dyes in solution has been studied before [3, 4] for determination of particle size, but the investigations were mainly confined to 25°. At higher temperatures, diffusion in solution has been studied for five dyes: Benzopurpurine 4B and its meta isomer (Lenher and Smith [5]), Chicago Sky Blue 6B (Valko [6]), Chrysophenine, and Direct Fast Orange SE (Holmes and Standing [7]). It is difficult to use the results of these investigations for solving the present problem, owing to the great differences in the experimental procedures used.

We used the method of Northrop and Anson [8] for determining the diffusion coefficients of dyes in solution. In this method the two solutions between which diffusion occurs are separated by a porous sintered glass plate. If in the steady state the solution concentrations on the two sides of the porous plates are c_1 and c_2 respectively, the diffusion in this plate can be represented by the equation

$$\frac{dm}{dt} = {}_{c_2}\overline{D}_{c_1}\,\frac{\overline{A}}{L}\,(c_2 - c_1), \tag{1}$$

where $c_2\overline{D}c_1$ is the average coefficient of diffusion; L is the effective thickness of the plate; $\overline{A}$ is the effective average free surface of the plate.

In this method the diffusion coefficient is found from the increase in the dye solution concentration on one side of the plate, i.e., the dye concentration changes continuously during the experiment. A solution of Equation (1) with these concentration changes taken into account was given by Holmes and Standing [7]

$$\overline{D}\alpha = \frac{2\lambda}{(\lambda+1)\tau}\cdot\log\frac{c_1}{c_1-(\lambda+1)\,c_2}, \tag{2}$$

where α is a calibration constant for the diffusion cell; τ is the time during which the diffusion was observed; λ is the ratio of the solution volumes on the two sides of the plate; c_1 is the concentration of the dye in the inner vessel at the start of the experiment (when the dye concentration in the outer solution is zero); c_2 is the dye concentration in the outer solution after time τ.

In our studies of the effect of dispersing agents on the diffusion rates of direct dyes in Cellophane film in stationary conditions the diffusion coefficients were calculated from Fick's equation

$$\frac{ds}{dt}=DA\frac{dc}{dx} \tag{3}$$

or

$$D=\frac{bP}{A\,(c_2-c_1)}, \tag{4}$$

where P = ds/dt, the amount of dye in mg/minute diffusing through the film in unit time; b is the film thickness in cm; A is the area of the film in cm^2; c_2 and c_1 are the dye concentrations on either side of the film in mg/cc.

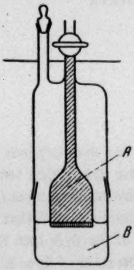

Fig. 1. Diagram of apparatus for determining the diffusion coefficients of dyes in solution.

The experiments on diffusion in solution were performed with three direct dyes; Direct Diazo Black C (CI 401), Direct Sky Blue K (CI 406), and Direct Diazo Black O (CI 395) at 25, 35, 60 and 80°. All the dyes were purified and analyzed by the method described previously [9]. The concentration of electrolyte, which was common salt, was varied from 0 to 20 g/liter for Diazo Black C and Sky Blue K, and from 0 to 0.5 g/liter for Diazo Black O. The reason for the lower electrolyte concentrations used for the latter dye is the possibility of its coagulation at high salt concentrations. The apparatus shown in Fig. 1 was used for determining the diffusion coefficients in solution.

The apparatus consists of the vessel A, terminating in a porous glass plate in the form of a disk 3 cm in diameter and ~ 0.2 cm thick. The approximate diameter of the pores in the plate is ~ 5-15 μ. The top part of vessel A is firmly closed by a well-ground stopcock. The vessel A was filled with the solution of dye and electrolyte and inserted into the vessel B, containing the electrolyte. The porous glass plate must only just touch the solution surface in vessel B. The whole apparatus was then put into a thermostat with the temperature kept constant to within ± 0.1°. At the end of a definite time, usually about 2-3 hours, required to establish thermal equilibrium and a concentration gradient in the plate, the solution was poured out of vessel B, and vessel A was very quickly transferred into another vessel B containing a solution of the same composition and temperature as in the first vessel B. The solution in vessel B was then analyzed at definite time intervals and the diffusion coefficients were calculated by means of Equation (2).

Equation (2) contains the calibration constant α, and therefore the apparatus was calibrated before the experiments with a substance of which the diffusion coefficient is well known. Chrysophenine dye was used for this purpose. The diffusion coefficients for this dye were determined very carefully by Holmes and Standing [7] who found, with the use of porous glass plates, that the calibration constants of the diffusion vessels changed gradually and irreversibly in the transition from lower to higher temperatures. We therefore repeated the calibrations by passing from lower to higher temperatures. However, we did not find any significant changes in the calibration constants. The changes did not exceed 5 % over the entire range studied. Some dyes, including Direct Diazo Black O, are adsorbed by the porous plate during the experiments. The apparatus was therefore washed thoroughly after each experiment. The results are given in Figs. 2, 3, and 4.

In studies of diffusion in Cellophane film, Direct Pure Blue (CI 518) was also used, in addition to the above dyes. The temperature in these experiments was varied from 25 to 85°. The dispersing agent used was pyridine, at concentrations of 80 and 200 g/liter. In addition, experiments were carried our for comparison

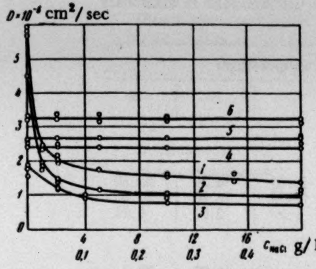

Fig. 2. Variation of the diffusion coefficients of direct dyes in solution with electrolyte concentration at 25°: 1) Direct Sky Blue K; 2) Direct Diazo Black C; 3) Direct Diazo Black O; 4,5,6) the same dyes, in presence of 200 g pyridine per liter.

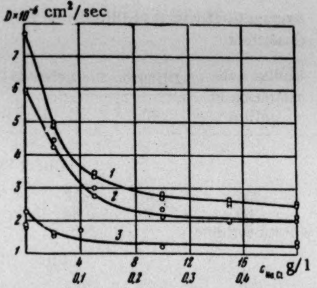

Fig. 3. Variation of the diffusion coefficients of direct dyes in solution with electrolyte concentration at 35°: 1) Direct Sky Blue K; 2) Direct Diazo Black C; 3) Direct Diazo Black O.

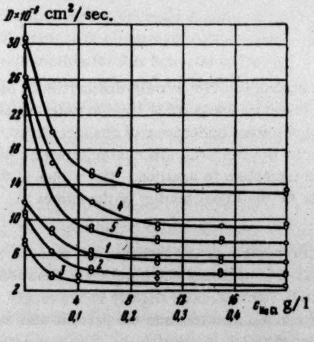

Fig. 4. Variation of the diffusion coefficients of direct dyes in solution with electrolyte concentration at 60 and 80°: 1,2, and 3) Direct Sky Blue K, Direct Diazo Black C, and Direct Diazo Black O at 60°; 4,5, and 6) the same, at 80°.

without addition of pyridine at 65, 75, and 85°. The experiments were carried out in U-shaped vessels, consisting of two parts separated by a Cellophane film. The thickness of the film was measured by means of a micrometer, and had the average value of 35 μ. The diameter of the film was 3.5 cm. Glycerol was carefully washed out of the film before the experiments. A solution containing the dye, common salt, and pyridine was put into one part of the vessel, and a solution containing the same components but without dye was put into the other. The apparatus was placed in a thermostat at a definite temperature. The temperature was controlled, as in the first series of experiments, to within ± 0.1°. The amounts of dye which passed through the membrane were then determined colorimetrically after definite time intervals. The time required to reach the steady state was determined by Barrer's method [10]. The diffusion coefficients of direct dyes in stationary conditions were calculated by means of Equation (4); the results are given in Table 1.

DISCUSSION OF RESULTS

The results in Figs. 2, 3, and 4 show that the coefficients of diffusion of direct dyes in solution greatly depend on the electrolyte concentration in the system. In pure water, owing to the action of the diffusion potential, the diffusion coefficients of dyes are abnormally high, and cannot be used for characterization of the state of dispersion of the system. Very small additions of electrolyte to the system greatly influence the diffusion potential and cause a sharp decrease in the diffusion coefficients of dyes. Increase of electrolyte concentration results in a further lowering of the diffusion potential and hence of the diffusion coefficients. However, as is seen in Figs. 2, 3, and 4, the subsequent fall of the diffusion coefficients is more gradual. This region of the curves can serve to characterize the dispersion state of dyes in solution, and can be used for calculations of the particle sizes of dyes by means

TABLE 1

Average Coefficients of Diffusion of Direct Dyes through Cellophane Film in Stationary Conditions

Pyrdine concentration in g/liter	Diffusion coefficient $D \cdot 10^{-7}$ cm²/min at temperatures						
	25°	35°	45°	55°	65°	75°	85°
				Direct Sky Blue K			
200	2.07	3.12	4.50	7.05	10.30	14.26	20.10
80	2.06	3.33	5.38	8.12	12.30	18.60	26.90
Without pyridine	—	—	—	—	1.22	2.80	6.11
				Direct Diazo Black C			
200	2.25	3.65	4.87	7.50	—	15.85	22.3
80	1.44	2.31	3.47	5.25	7.59	11.50	15.90
Without pyridine	—	—	—	—	1.02	2.57	5.50
				Direct Pure Blue			
200	—	3.32	4.96	7.50	10.90	14.90	21.11
80	2.46	3.47	—	9.30	14.40	19.90	30.00
				Direct Diazo Black O			
200	2.31	3.65	4.87	8.70	—	18.60	26.0
80	—	—	Coagulates		—	—	—
Without pyridine	—	—	Coagulates		—	—	—

of the Stokes–Einstein equation. The use of the Stokes–Einstein equation involves certain difficulties in this case because the dye particles are far from spherical in shape, and therefore the particle sizes as determined by this equation will not be absolute values, but can only serve as qualitative indications of changes in the degree of dispersion of dyes under particular experimental conditions. Nevertheless, this characterization of the dispersion state of the system is quite sufficient for solution of the problem in question. The values of the dye particle radii calculated from the average diffusion coefficients for the linear portion of the curves in Figs. 2, 3, and 4 are given in Table 2.

Table 2 shows that the dyes undergo progressive dispersion with increase of temperature, the process being fairly uniform over the whole temperature range studied in the case of Direct Sky Blue K and Diazo Black C. In contrast to this, in the case of Direct Diazo Black O the particle size decreases slightly in the range between 25 and 60°. At 60° the dispersion of the particles of this dye is accelerated, and the particle size is decreased sharply at 80°. It should be noted that the electrolyte concentration in solution at 80° in this case of this dye may be insufficient to eliminate the diffusion potential completely, and therefore the value of the diffusion coefficient in this case may be somewhat high. However, the fact that the diffusion coefficient of this dye increases sharply in the temperature range from 60 to 80° itself indicates that the particle size is sharply reduced as the result of the supply of heat from outside.

The results confirm our earlier hypothesis [1] that there is a relationship between the diffusion rate of a dye in the fiber and its state of aggregation in solution. Thus, we have shown [1] that in the temperature range between 70 and 100° there is a sharp increase of the coefficients of diffusion of Direct Diazo Black O in the fiber. For Direct Sky Blue K and Diazo Black C the coefficients of diffusion in the fiber increase without abrupt jumps, which is in full agreement with the observed behavior of these dyes in solution; the changes in their particle size occur smoothly and uniformly with a continuous reduction as the temperature increases. This is in all probability due to the higher degree of hydration of the anions of these dyes and hence to their greater stability in solution even at low temperatures.

The behavior of all these dyes in pyridine solution is somewhat different (Fig. 2). In this case the diffusion

TABLE 2

Effect of Temperature and Additions of Pyridine on the Particle Size of Direct Dyes in Solution

Dye	Temperature, °C	Particle radius $\times 10^8$cm	
		Without pyridine	In presence of pyridine
Direct Sky Blue K	25	15.90	9.62
	35	11.95	–
	60	9.75	–
	80	8.51	–
Direct Diazo Black C	25	21.81	8.75
	35	15.50	–
	60	12.80	–
	80	10.35	–
Direct Diazo Black O	25	26.80	7.15
	35	21.90	–
	60	20.40	–
	80	5.98	–

coefficients do not decrease sharply on addition of electrolyte to the solution. The variation of the diffusion coefficients with electrolyte concentration remains linear over the whole range of NaCl concentrations studied. An explanation for this behavior of the dyes in presence of pyridine in solution is that in this case the influence of the diffusion potential is diminished by the cations of pyridine itself, and therefore when common salt is added to the solution the diffusion coefficients do not decrease as sharply as in experiments without pyridine.

Another interesting fact revealed in the study of dye diffusion in pyridine solutions is that the diffusion coefficients of all the dyes are increased sharply in this case. The size of the dye particles decreases accordingly, i. e., pyridine acts in the same direction as increase of temperature. The results once again confirm that there is a relationship between the diffusion rates of dyes within the fiber and their state of dispersion in solution. Thus, the experiments on the diffusion of dyes through Cellophane films (see Table 1) show clearly that when pyridine is present in solution the diffusion of dyes in the film is accelerated approximately 10-fold. It must be pointed out that in absence of pyridine the dyes do not diffuse through the film at all at temperatures below 65°, and therefore the difference between the diffusion rates will be very great. As the temperature increases, this difference diminishes and at 85° the diffusion rates of the dyes differ only by a factor of 2 to 3. The reason is that the effect of temperature on changes of the degree of dispersion of the dyes, and therefore on their rates of diffusion in the film, is most pronounced when pyridine is not present in the solution. The addition of pyridine itself greatly favors disaggregation of the dye particles, and therefore the influence of temperature is less pronounced in this case.

Fig. 5 gives the relationship between the temperature and the rates of diffusion of dyes through the film in log D – 1/T coordinates, in accordance with the Arrhenius equation

$$\log D = B - A/T.$$

The activation energies of diffusion of the dyes in the film, determined from the slopes of the straight lines in Fig. 5, are given in Table 3.

In full agreement with the foregoing, the activation energy of diffusion in presence of pyridine in the solution is only about one half of the activation energy of diffusion in absence of pyridine.

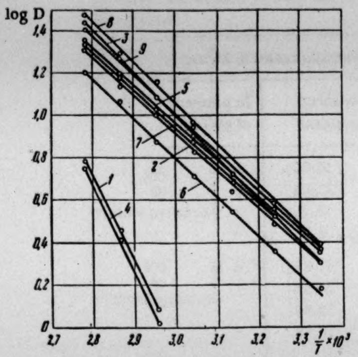

Fig. 5. Logarithmic relationship between the diffusion coefficients of direct dyes in the film and the reciprocal of the absolute temperature: 1) Direct Sky Blue K; 2) the same, with 200 g/liter of pyridine; 3) the same, with 80 g/liter of pyridine; 4) Direct Diazo Black C; 5) the same, with 200 g/liter of pyridine; 6) the same, with 80 g/liter of pyridine; 7) Direct Pure Blue with 200 g/liter of pyridine; 8) the same, with 80 g/liter of pyridine; 9) Direct Diazo Black O with 200 g/liter of pyridine.

TABLE 3

Energy of Activation of Diffusion of Direct Dyes in kcal/mole

Dye	Activation energy of diffusion at pyridine concentration		
	200 g/l	80 g/l	without pyridine
Direct Sky Blue K	8.09	9.20	18.70
Direct Diazo Black C	8.15	8.55	19.60
Direct Pure Blue	8.22	8.43	–
Direct Diazo Black O	8.38	–	–

A very remarkable fact is that the diffusion coefficients in the film of such dyes as Direct Sky Blue K and Direct Pure Blue are somewhat higher at pyridine concentration of 80 g/liter than at 200 g/liter. This indicates that the increase of the diffusion coefficients of dyes with increasing pyridine concentration in the bath is not unlimited, but passes through a maximum, after which the diffusion coefficients begin to decrease with increasing pyridine concentration. This relationship between the diffusion coefficients and the pyridine concentration in solution is probably the consequence of a decrease in the concentration of active water molecules at high pyridine concentrations in solution. The degree of hydration of the dye particles is therefore decreased, and their stability in solution is therefore less. These results show that by addition of suitable dispersing agents to the dye bath it is possible, without risk of aggregation, to increase very sharply the concentrations of the dye and neutral electrolyte and consequently to raise the dyeing rate. This is especially important in relation to acceleration of high-speed continuous dyeing processes.

SUMMARY

1. The coefficients of free diffusion in solution for three dyes over a wide range of temperatures and electrolyte concentrations, and also the diffusion coefficients of four dyes in Cellophane film with varying degrees of dispersion of the dyes in solution, have been determined.

2. A definite relationship exists between the degree of dispersion of the dyes in solution and their coefficients of diffusion in the film; in all cases the rate of penetration of the dyes through the film increases and the activation energy of diffusion diminishes with increasing degree of dispersion of the dyes in solution.

3. By addition of dispersing agents to the dye bath it is possible to increase considerably the concentrations of the dye and neutral electrolyte, and hence to raise the dyeing rate without the risk of producing surface dyeings which are not fast to rubbing.

The Ivanov Institute of Chemical Technology
Laboratory of the Chemical Technology of Fibrous Materials

Received November 2, 1956.

LITERATURE CITED

[1] B. N. Melnikov and P. V. Moryganov, Colloid J., 18, 566 (1956).*

[2] B. N. Melnikov and P. V. Moryganov, Colloid J., 18, 711 (1956).*

[3] E. Valko, Colloidochemical Principles of Textile Technology (State Light Industry Press, 1940) p. 369. [In Russian].

[4] T. Vickerstaff, The Physical Chemistry of Dyeing, (1954) p. 68.

[5] S. E. Lenher and J. E. Smith, J. Am. Chem. Soc. 57, 497 (1935).

[6] E. Valko, J. Soc. Dyers Col. 55, 173 (1939).

[7] F. H. Holmes and H. A. Standing, Trans. Faraday Soc. 41, 542 (1945).

[8] J. H. Northop and M. L. Anson. J. Gen. Physiol. 12, 543 (1929).

[9] P. V. Moryganov and B. N. Melnikov, Colloid J., 18, 49 (1956).*

[10] R. Barrer, Diffusion in and Through Solids (IL, Moscow, 1948) p. 33. [Russian translation].

---

* Original Russian pagination. See C. B. translation.

ELECTRON MICROSCOPE STUDY OF THE STRUCTURE OF ALUMINOSILICATE HYDROGELS BY THE REPLICA METHOD

Ya. V. Mirsky

Many adsorbents and catalysts pass through the hydrogel stage in the course of preparation. Studies of the structure of such systems are of great interest, as they can yield data characterizing the formation of adsorbents and catalysts. Several papers dealing with electron microscopy of hydrogels have been published in recent years. Berestneva, Koretskaya, and Kargin [1] studied colloidal silicic acid; Ashley and Innes [2] investigated aluminum hydroxide and an aluminosilicate catalyst; and Levina and Ermolenko [3] studied the hydroxides of aluminum, chromium, and iron. All these investigations were carried out by direct observation of hydrogel samples in the electron microscope; the shape and size of the gel particles could be observed.

Nevertheless, the potentialities of electron microscopy for studies of hydrogel structure, i.e., of relative disposition and character of the bonds between the hydrogel particles, are limited, as the hydrogel undergoes shrinkage and deformation owing to drying of samples while the observations are being made and the photographs taken.

It is known that in studies of the structure of rubber mixtures [4] and collagen [5] it proved possible to obtain replicas reproducing the structure of the colloidal substances under investigation. It was therefore of interest to apply the replica method for studying the structure of hydrogels; this was done in the present investigation with a sample of pelleted aluminosilicate catalyst.

The procedure was as follows: the pellets of the aluminosilicate catalyst hydrogel, washed free from salts, were split into halves under slight compression; the cleavage surface was covered with a drop of a solution of nitrocellulose in amyl acetate, which flowed in an even and thin layer over the surface; after drying, the lacquer replica was cut along the edges and separated by immersion of the hydrogel into water; the replica was taken out of the water by means of the specimen holder screen of the electron microscope, shadowed with gold, and investigated.

It is known that amyl acetate has very low surface tension at interfaces with water; this is used in electron microscopy for production of structureless films from nitrocellulose solutions on water surfaces. It was therefore to be expected that amyl acetate lacquer would give a high degree of definition in the reproduction of the surface details on the replica. In all probability the nature of the microreliefof the split hydrogel surface is determined by the presence of a hydrogel framework and by the form in which water is bound to the gel substance; in particular, it is evident that free water cannot give rise to a microrelief. It is also quite probable that variations of the distance between individual elements of the hydrogel framework and the amount of adsorbed water should influence the dimensions of the microrelief details.

The replica method was used to study changes in the structure of the aluminosilicate catalyst during drying; replicas of the original hydrogel and of partially dried specimens were made.

Micrograph 1 is an electron micrograph of a replica from the surface of the original specimen, and 2, of a specimen formed by removal of ~ 75% of the water initially present in the hydrogel. Both replicas show a microrelief on the hydrogel surface, which is evidence for the existence of a hydrogel framework, to a certain extent differentiated from the intermicellar liquid. The details of the surface relief do not have clearly defined boundaries; this is probably due to the absence of a sharp boundary between the water of the hydrate shells of the micelles forming the hydrogel framework and the free water in the interstices of the framework.

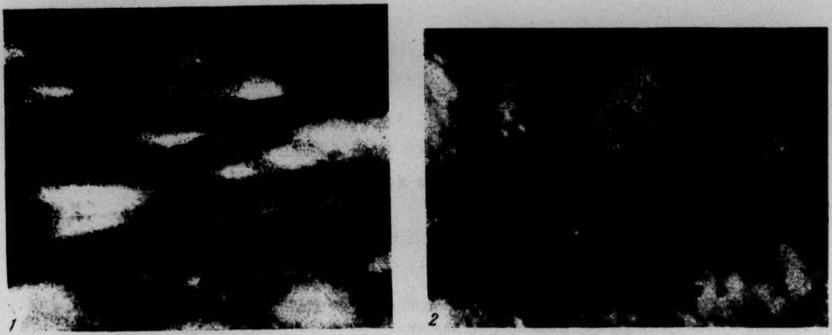

Electron micrographs (colloidion replica, magnification 15,000) of pelleted aluminosilicate catalyst with 90% moisture (1), and of the same specimen after removal of 75% of the water present (2).

Comparison of the two micrographs shows that the surface microrelief becomes finer and more complex as the hydrogel is dehydrated. While in Micrograph 1 considerable regions of the surface are almost entirely smooth (of the same shade), Micrograph 2 clearly shows an extensive microrelief structure, with individual details of several hundred angstroms in size. Replicas made from specimens with moisture contents intermediate between those of the specimens studied show an intermediate character of the hydrogel structure.

The closer approach of the micellar groups resulting from dehydration of the hydrogel cannot in itself be the cause of the observed structural changes. A change in the dimensions of the hydrate shells is also necessary. If this was not the case, the hydrogel surface would become smoother than before as the result of partial dehydration.

SUMMARY

1. Investigations of the structure of aluminosilicate hydrogel by means of the electron microscope showed the hydrogel has a microheterogeneous structure; this is direct evidence that it contains a micellar framework differentiated to some extent from the intermicellar liquid.

2. The micellar groups come closer together and the dimensions of the hydrate shells decrease with dehydration of the hydrogel.

The Grozny Petroleum Scientific Research Institute

Received July 23, 1956.

LITERATURE CITED

[1] Z. Ya. Berestneva, T. A. Koretskaya, and V. A. Kargin, Proc. Acad. Sci. USSR, 70, 1121 (1948); Colloid J. 13, 323 (1951).

[2] K. D. Ashley, and W. B. Innes, Ind. Eng. Chem. 44, 2857 (1952).

[3] S. A. Levina and N. F. Ermolenko, Colloid J. 17, 487 (1955).*

[4] K. A. Pechkovskaya, S. L. Pupko and B. A. Dogadkin, Colloid J. 12, 367 (1950).

[5] A. L. Zaides and S. L. Pupko, Proc. Acad. Sci. USSR 73, 379 (1950).

---

* Original Russian pagination. See C. B. translation.

GENERAL PRINCIPLES OF FORMATION OF METAL ALLOY ORGANOSOLS AT THE CATHODE IN A TWO-LAYER BATH

E. M. Natanson and N. N. Kozachek

It is known that simultaneous liberation of different metals at the cathode is possible only if their deposition potentials differ only slightly. Formation of alloys at the cathode then occurs mainly at fairly high cathode polarizations. Various surface-active agents, either of low or of high molecular weight, are usually added to the electrolyte in order to bring the deposition potentials of different metals closer together and to raise cathode polarization. The number of such additions is fairly large, and their effects on metal deposition and alloy formation at the cathode have been studied in detail.

However, no general laws have yet been established which would make it possible to classify the very considerable number of such substances into groups according to the nature of their action on electrode processes. Therefore at present they are usually selected on an empirical basis.

The formation of saturated layers of adsorbed surface-active substances on the cathode retards the discharge of predominantly those metal ions the equilibrium potentials of which correspond to the stability of these adsorbed layers. It is also necessary to take into account the depolarizing action of electropositve metals, which often decreases the deposition potentials of other, less positive components of the mixture.

The electrolyte composition has a significant influence on the deposition of alloys, Solutions of complex salts of the corresponding metals are generally used. This brings the equilibrium potentials of the different metals closer together. The proportions of the components in the alloy greatly depend on the nature and configuration of the polarization curve for each individual metal under the particular electrolysis conditions, and on the concentrations of these components in the electrolyte.

Apart from the above general considerations, in the electrolytic production of metal alloy organosols [1] it is also necessary to take into consideration the special circumstances when the electrolysis is carried out in a two-layer bath. The cathode which rotates horizontally in the upper oil layer touches the lower aqueous layer – the electrolyte solution – by only a part of its surface. Therefore the crystallization centers which form on its surface are rapidly transferred into the organic medium, which washes them off the cathode surface owing to the presence of surface-active substances. The cathode surface is thus continuously renewed and becomes coated with an adsorbed layer of surface-active substances and of the organic medium, which results in very strong cathode polarization, reaching 4-5 v in some cases. In such conditions the deposition potentials of a number of electropositive metals are increased so much that they become equal to or often even exceed the deposition potentials of typical electronegative metals (Zn, etc).

This sharp increase of cathode polarization in a two-layer bath occurs under the influence of a number of factors which cause continuous passivation of its surface. Thus, the discharge of ions on the cathode surface occurs at a considerable overvoltage, and only at individual places of the cathode surface, which are not covered with an insulating layer of surface-active substances and dispersion medium.

Electrocapillary effects [2] play a considerable role in electrolysis in a two-layer bath; they cause desorption of molecules of the surface-active agents and dispersion medium from the cathode surface when it is in the aqueous layer, and readsorption of these substances when this surface reenters the organic layer and leaves the zone in which metal ions are discharged. The ratio of the rates of these two processes determines the total cathode area at which metal ions are discharged during motion of the cathode. Under such conditions the true current density at individual regions of the moving cathode surface becomes especially high. In such regions the rate of metal ion discharge is very high; this greatly favors the formation of highly disperse particles of metal alloys. Adsorption of surface-active substances on the surface of such particles assists their removal from the cathode surface, protects them against aggregation, and to a considerable extent retards their oxidation.

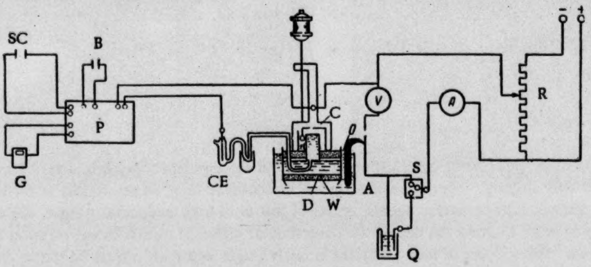

Fig. 1. Diagram of apparatus: C) rotating roller cathode; A) anode; O) upper organic layer; W) lower aqueous layer; D) ceramic diaphragm; CE) calomel electrode; P) potentiometer; B) battery; SC) standard cell; G) galvanometer; Q) coulometer; S) commutator switch; R) potential distributor.

In the preparation of alloys we were guided by the extensive experimental data accumulated in our laboratory (Institute of General and Inorganic Chemistry of the Academy of Sciences, Ukrainian SSR) over a number of years, on the cathodic deposition of colloidally disperse metal powders and on the formation of metal organosols.

In this paper we give the results of an experimental study of the cathodic formation of lead–tin, nickel–chromium, and nickel–iron alloys in a two-layer electrolytic bath, the upper layer of which is an organic medium containing dissolved surface-active substances, and the lower layer is an aqueous electrolyte solution. The apparatus is shown schematically in Fig. 1, and was described in detail in earlier publications [3].

Organosols of lead–tin alloys. In the electrolytic deposition of lead–tin alloys considerable difficulties arise mainly because of the limited number of anions which form soluble salts in the simultaneous presence of the cations of both metals. Fluoborate and fluosilicate electrolytes are the most commonly used. Deposition of lead–tin alloys has been studied by a number of authors [4, 5,-9], but all these studies dealt with the formation of dense compact deposits of lead–tin alloy at the cathode. The literature contains no data on the conditions for electrolytic deposition of highly disperse powders of these alloys.

As the result of numberous experiments on the selection of a suitable composition of the lower aqueous layer, we chose an alkaline electrolyte – a solution containing a mixture of plumbite, stannate, and stannite.

A production of powdered lead–tin alloys of a high degree of dispersion from electrolytes of this type does not present any special difficulties. In preparation of the plumbite we used the concentrations and lead oxide – caustic soda ratio established previously [10] (34 g of lead and 100 g of caustic soda per liter). The stannite was prepared from stannous chloride, 1 liter of the solution containing 36.2 g of $SnCl_2 \cdot 2H_2O$ and 100 g of caustic soda. The plumbite and stannite were kept separately and mixed in the required proportions immediately before electrolysis. The upper organic layer consisted of toluene with added surface-active agents. Considerable difficulties arose in selection of the composition of the upper organic layer owing to the presence of excess alkali in the aqueous layer. This reduced considerably the number of surface-active agents suitable for production of metal organosols without causing emulsification of the organic layer in the lower, strongly alkaline electrolyte layer.

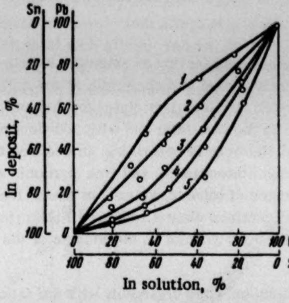

Fig. 2. Variation of the composition of the disperse phases of lead–tin organosols with the ratio of the component metals in the electrolyte. Current density: 1) 3; 2) 10; 3) 15; 4) 20; 5) 30 amp./dm^2.

Our selection of surface-active substances was based on the fundamental principles of lyophilization of disperse phases of metal organosols which had been established by one of us [3, 11]. Of the relatively large number of the substances surface-active with respect to the metal–organic medium interface, which were studied, the most suitable proved to be lead and tin oleates in the presence of a little octyl alcohol in the organic layer. The octyl alcohol plays a particularly important role in this case: it seems that its molecules interact with the hydrophilic groups of the lead oleate molecules dissolved in the organic phase (toluene) and adsorbed on the surface of the colloidal alloy particles, to form strongly hydrophobic compounds. This greatly diminishes the emulsifying power of lead oleate with respect to toluene and, despite the rotation of the cathode, toluene is not emulsified in the lower alkaline electrolyte layer.

In order to determine the optimum concentrations of these components in the organic layer, we made a more detailed study of the effects of lead oleate and octyl alcohol on the formation of cathode deposits of lead–tin alloys. The results of these experiments showed that the optimum concentration of lead oleate in toluene is in the range of 0.2 to 0.3% and cessation of emulsification and good peptization of the deposit commence at 3% octyl alcohol concentration. Excess of octyl alcohol does not have any significant effects on these processes. The variations of the composition of tin–lead alloy cathode deposits and of the current efficiency with: a) the ratio of the components in the aqueous electrolyte solution under constant conditions of electrolysis, and b) current density at constant electrolyte composition, were determined. These results are given in Fig. 2. It is seen that as the current density increases from 3 to 30 amp./dm^2, the lead–tin ratio in the disperse phases of the organosols decreases in comparison with the value of this ratio in the electrolyte; at the beginning, at current densities from 3 to 10 amp./dm^2, it is higher than in the electrolyte; at 10 amp./dm^2 it becomes equal to the latter, and at higher current densities it is considerably less. The current efficiency with respect to the yield of powdered lead–tin alloy varied between 30 and 60%.

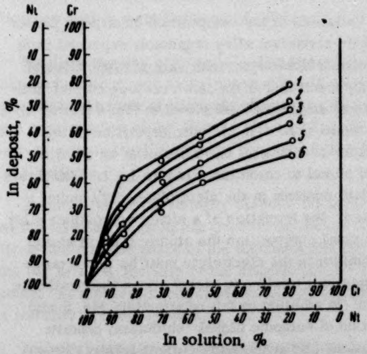

Fig. 3. Variation of the composition of disperse phases of nickel–chromium organosols with the ratio of the component metals in the electrolyte. Current density: 1) 5; 2) 10; 3) 20; 4) 30; 5) 40; 6) 50 amp./dm^2.

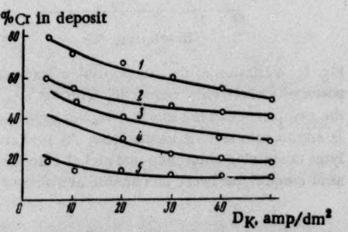

Fig. 4. Variation of the composition of disperse phases of nickel – chromium organosols with current density. Ratio of nickel to chromium in the disperse phase: 1) 1:5; 2) 1:1; 3) 2:1; 4) 5:1; 5) 10:1.

The results of detailed electron microscope and x-ray investigations of the disperse phases of lead–tin organosols obtained at various cathode current densities and with different component ratios in the aqueous layer of the electrolyte bath were published by us earlier [12].

Organosols of nickel–chromium alloys. As the result of a detailed examination of extensive experimental data on the question of the simultaneous electrolytic deposition of nickel and chromium at the cathode, and after numerous experiments, we reached the conclusion that the most suitable electrolytes for this purpose contain mixtures of nickel, chromium, and ammonium chlorides in the pure form and with additions of urea (30 g/liter) and hydrochloric acid (10-12 g/liter). Ammoniacal electrolytes containing, in addition to nickel and trivalent chromium salts, also ammonium tartrate, ammonium thiocyanate, and free ammonia are also of interest. With acid electrolytes, the upper organic layers consisted of toluene, xylene, or Diesel fuel, containing 0.5% oleic acid, while with ammoniacal electrolytes they contained oleates of heavy metals (lead, nickel, etc.) in concentrations from 0.25 to 0.5%. In the latter case 5% octyl alcohol on the volume of the upper layer was added to avoid emulsification.

Variations of the composition of the disperse phase of nickel–chromium alloy organosols with the ratio of the components in the acid electrolyte and cathode current density are shown graphically in Figs. 3 and 4. These results show that the chromium content of the disperse organosol phases increases with its content in the electrolyte. This is especially clearly seen for chromium concentrations not exceeding 50% in the electrolyte. With further increase of chromium concentration, its contents in the cathode deposits increase more slowly, especially at high current densities. For example, at D_k = 50 amp./dm^2 an increase of the chromium–nickel ratio in the electrolyte from 1 : 1 to 4 : 1 results in an increase of only 5-6% in the chromium contents of the deposits.

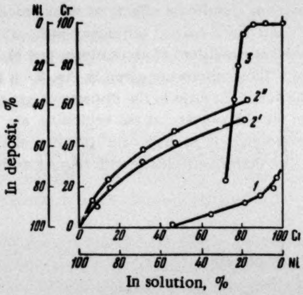

Fig. 5. Variation of the composition of cathode deposits of nickel–chromium alloy with the ratio of the components in the electrolyte, deposited from: 1) ammonium tartrate electrolytes; 2) acid electrolytes containing chromium and nickel chlorides; 3) acid electrolytes based on chromic anhydride [14].

Curves for the variation of chromium contents of the disperse phases of the organosols with the current density for given component ratios in the electrolyte, $c_{Cr} = f(D_k)$, show that a decrease of the chromium content occurs mainly as the current density increases from 5 to 30 amp./dm^2. Higher current densities (from 30 to 50 amp./dm^2) have no significant influence on the composition of the cathode deposits. The current efficiency in respect to the disperse organosol phases reaches 20% for these electrolytes; this can no doubt be increased if the experiments are carried out on a larger scale.

Variations of the composition of disperse phases of nickel–chromium alloy organosols deposited from ammoniacal electrolytes with various proportions of the components and at the same cathode current density (30-40 amp./dm^2) are shown in Fig. 5 (Curve 1). These results show that cathodic deposition of the alloy from ammoniacal baths begins at an atomic ratio of nickel to chromium close to 1 : 1. With lower chromium contents in the electrolyte, only nickel is deposited. For formation of a nickel–chromium alloy of the usual composition the atomic ratio of nickel to chromium in the electrolyte must be in the range between 1 : 20 and 1 : 50. It is probable that the excess of chromium relative to nickel brings their cathodic deposition potentials closer together and favors alloy formation. In addition to this relationship, Fig. 5 also shows, for comparison, curves for the variation of the composition of cathodic nickel–chromium deposits formed from acid electrolytes with various ratios of the components and at the same current density (30-40 amp./dm^2) (Curves 2 and 3). Comparison of these results shows that in the cathodic deposition of colloidally disperse nickel–chromium alloy powders, electrolytes based on nickel and chromium chlorides have considerable advantages with regard to composition variability and current efficiency.

Organosols of nickel–iron alloy. The electolytic production of nickel–iron alloys in compact form has been studied by many authors. However, very little information is available in the literature on the cathodic deposition of nickel–iron alloys of a colloidal degree of dispersion. We used the following electrolytes for the production of such alloys: ferrous chloride and nickel chloride in various proportions; ammonium chloride, 25 g/liter; urea, 30 g/liter; hydrochloric acid, 10-12 ml/liter; electrolyte pH 1.4-1.5. The use of such an acid electrolyte considerably simplifies the selection of the upper organic layer. For the latter, 0.5% solutions of oleic acid in toluene, xylene, Diesel fuel, MK oil, etc. were used.

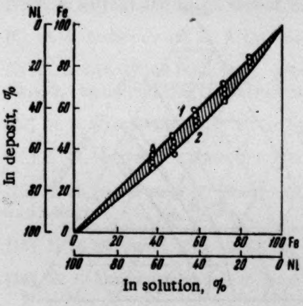

Fig. 6. Variation of the composition of disperse phases of iron–nickel organosols with the ratio of these components in the electrolyte. Current density: 1) 5; 2) 40 amp./dm².

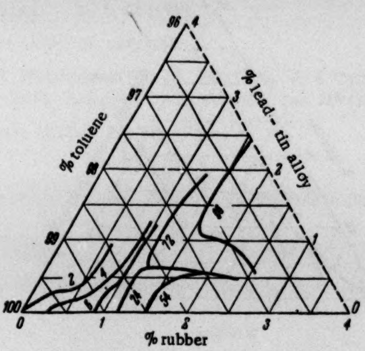

Fig. 7. Variations of the stability of lead–tin alloy organosols stabilized by rubber. Numbers on the curves represent hours.

Variations of the composition of disperse phases of nickel–iron organosols with the ratio of these components in the original electrolyte and with the cathode current density are shown in Fig. 6. In this case there is almost direct proportionality between the composition of the highly disperse cathode deposits and the electrolyte composition over a fairly wide range of current densities, from 3 to 40 amp./dm². The current efficiency with respect to the yield of nickel–iron alloy organosol varied from 60 to 80% in these experiments.

Stability of alloy organosols. The results of a study of the stability variations of organosols of lead–tin, nickel–chromium, and nickel–iron alloys in toluene in presence of a high polymer – rubber – are given in Figs. 7-9 in the form of triangular diagrams. The criterion of stability used was the time required for complete precipitation of the disperse phase of the alloy organosol from these systems at rest. Each system was observed systematically until the boundary of the disperse phase completely ceased to move toward the bottom of the cylinder.

Examination of the stability diagram for lead–tin alloy organosols stabilized with rubber (Fig. 7) shows that the stability of these sols depends on the concentration of the protective polymer (rubber) and on the ratio of the disperse phase of the organosol and the amount of rubber. At protective polymer concentrations from 0.1 to 1.2%, increase of the disperse phase – rubber ratio results in decreased stability of the organosols studied. At rubber concentrations from 1.2 to 1.8% increase of this ratio results in a considerable increase of the stability of these systems.

A similar situation is found in the stability diagrams for nickel–chromium and nickel–iron alloys stabilized by rubber (Figs. 8 and 9). This is especially pronounced when the nickel–chromium alloy concentration in the organosols is between 0.5 and 1.5%. In this case the stability increases from 3 hours for rubber concentrations of 0.1-0.4%, to 300-350 hours for rubber concentrations of 1.5-1.8%. With nickel–chromium alloy concentrations between 0.1 and 0.3%, the variations of stability with rubber concentration are less pronounced. The stability of nickel–chromium alloy organosols stabilized by rubber also depends on the quantitative ratio of the disperse phase of the organosol to the amount of rubber in these systems. As regards nickel–iron alloy organosols, the stability of these systems depends little on this ratio.

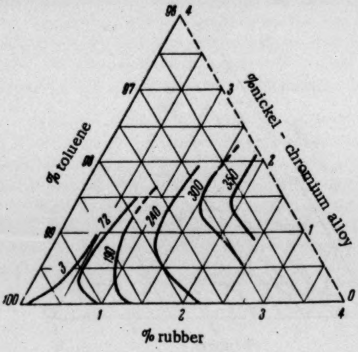

Fig. 8. Variations of the stability of nickel–chromium alloy organosols stabilized by rubber. Numbers on the curves represent hours.

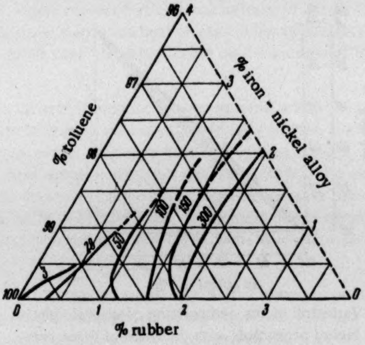

Fig. 9. Variations of the stability of iron–nickel alloy organosols stabilized by rubber. Numbers on the curves represent hours.

These results confirm the views, put forward by us earlier, concerning the significant influence of the quantitative ratio between the disperse phase and the protective polymer in a hydrophobic sol on the stability of such a sol [13].

The increase in the stability of the alloy organosols studied, found at higher concentrations of the protective polymer, is probably the result of the formation of a stable structural network from the rubber macromolecules and the colloidal alloy particles, which serve as the nodal points in such a network.

SUMMARY

1. The optimum conditions for formation of organosols of lead–tin, nickel–chromium, and nickel–iron alloys at a horizontal rotating cathode in a two-layer electrolytic bath have been determined.

2. The compositions of the disperse phases of organosols of these alloys have been studied in relation to the ratios of the component metals in the electrolyte and the cathode current density.

3. The stability of the organosols has been studied in presence of rubber, in relation to the concentration of the latter and to its quantitative ratio to the disperse phase of the organosol.

Institute of General and Inorganic Chemistry
Academy of Sciences Ukrainian SSR Kiev

Received May 24, 1956.

LITERATURE CITED

[1] E. M. Natanson, Colloid J. 9, 191 (1947).

[2] A. N. Frumkin, Electrocapillary Curves and Electrode Potentials (Odessa, 1919) ;* Naturwiss. 7, 235 (1928). A. N. Frumkin, V. S. Bagotsky, Z. A. Iofa and B. M. Kabanov, Kinetics of Electrode Processes (1952).*

[3] E. M. Natanson, Trans. 2nd All-Union Conf. on Colloid Chemistry, 1950, p. 113.*

[4] W. Blum and E. Haring, Trans. Amer. Electr. Soc. 40, 287 (1921).

[5] E. Raub and W. Blum, Metalloberflache 9, 4, A54 (1955).

[6] P. P. Belyaev and L. M. Berman, Technical News, No. 10 (1933).

[7] P. P. Belyaev and Ya. N. Birman, Bull. Metal Industry, No. 9, 88 (1937).

[8] M. A. Loshkarev and M. P. Grechukhina, J. Phys. Chem. 24, 1502 (1950).

[9] A. E. Carlson and J. M. Kane, Monthly Rev. Am. Electroplaters Soc. 33, 255 (1946); A. E. Carlson and C. Struyk, Metal Finishing Guide Book Directory, 24 (1956); N. J. Westwood, Finish Publ. Inc. 317 (1955).

[10] N. N. Gratsiansky and P. F. Kalyuzhnaya, Ukrain. Chem. J. 19, 380 (1953).

[11] E. M. Natanson, Colloid J. 9, 428 (1947).

[12] E. M. Natanson, V. P. Chalyi, N. N. Kozachek and A. P. Kaban, Colloid J. 19, 319 (1957). [See C. B. translation].

[13] E. M. Natanson, Proc. Acad. Sci. USSR 74, 517 (1950).

[14] M. F. Skalozubov and A. S. Vlasova, Bull. Novocherkassk Industrial Inst. Chem. Ser. 6, 15 (1940).

---

* In Russian.

INFLUENCE OF THE REACTION OF THE PRECIPITATION MEDIUM AND OF THE pH OF THE WASH WATER ON THE STRUCTURE OF CHALKY SILICA GELS

I. E. Neimark and I. B. Slinyakova

Silica gels prepared from solutions of sodium silicate and easily hydrolyzed salts are opaque or chalky. In contrast to glassy silica gels, in the precipitation of which silicic acid sols are first formed and then pass into gels, the formation of a chalky silica gel is accompanied by instantaneous formation of a flocculent precipitate consisting of silicic acid, metallic hydroxide, and possibly also of complex compounds. In addition, during the precipitation of a chalky silica gel the pH of the mixture varies over wide limits as the result of mixing of alkaline and acid components, and therefore the precipitate is heterogeneous in composition and degree of dispersion; this must undoubtedly influence the final pore structure of the chalky silica gel.

Therefore the formation of the pore structure of chalky silica gels (coagels) should be somewhat different from the structure formation of glassy silica gels (xerogels). While the pore structure of silicic acid xerogels does not depend on the history of the hydrogel formation, but is determined by the subsequent treatment and the dehydration conditions of the hydrogels [1], the porosity of coagels should depend on the conditions of their precipitation.

It was shown in our paper [2] that the reaction of the medium in a suspension formed from solutions of sodium silicate and nickel chloride has a considerable influence on the porosity of chalky silica gels. As the alkalinity of the medium decreases, the volume of the sorptional pores increases and the volume of the macropores diminishes. The purpose of the present investigation was to verify the applicability of these results to chalky silica gels precipitated from sodium silicate solutions by ferric chloride. We studied the influence of the precipitation medium and of the pH of the wash waters on the structure of chalky silica gels made from water glass and ferric chloride. An attempt was also made to elucidate the chemistry of chalky silica gel formation.

RESULTS AND DISCUSSION

Method. The method used for preparation of chalky silica gels from sodium silicate and ferric chloride was similar to that used previously [2]. A solution of $FeCl_3$ was added slowly, with vigorous stirring, to sodium silicate solution; an flocculent precipitate was instantly formed. This was aged for two days, filtered off, and molded into small cylinders. The cylinders were partially dried at room temperature for 18-20 hours to 70-80% moisture content. They were then treated with 6N HCl solution to remove ferric hydroxide, the acid was decanted off, and the gel washed with distilled water to a negative reaction for Cl^-. The hydrogel was dried for 24 hours at room temperature, for 6 hours at 100°, and for 6 hours at 200°.

The following were determined in order to obtain the structural and adsorptive characteristics of the chalky silica gels: bulk density, true and apparent densities from which the total pore volume was calculated, the maximum sorption volume of the pores for benzene at $p/p_s = 1$; methyl alcohol sorption isotherms were determined at 20° in a high vacuum apparatus with the aid of a quartz spring balance.

Influence of the reaction of the medium during precipitation of coagels on the structure of chalky silica gels. Several specimens were prepared, with different pH values of the suspension medium. In order to exclude the influence of silicic acid concentration, the sodium silicate solution used had the same density and the same modulus (d = 1.12, modulus 3.5), and was used in the same amounts in all the experiments. To obtain suspensions with different pH, the amounts of the 2N $FeCl_3$ solution added were varied. Specimens of the third series were prepared from more dilute water glass, sp.gr. 1.045 g/cc.

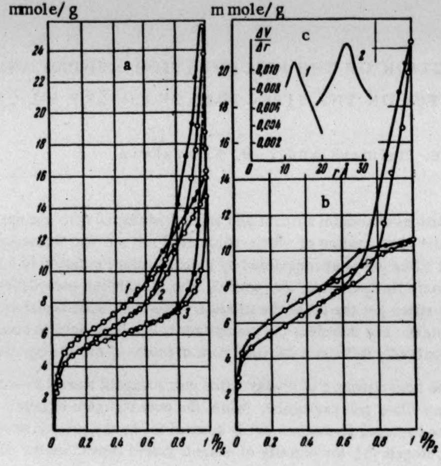

Fig. 1. Sorption isotherms for methyl alcohol vapor on chalky silica gels precipitated by $FeCl_3$ with different suspension pH: a. 1) pH 0.43; 2) pH 8.2; 3) pH 10.9; b. 1) pH 0.44; 2) pH 10.9; c. pore volume – effective radius distribution curves.

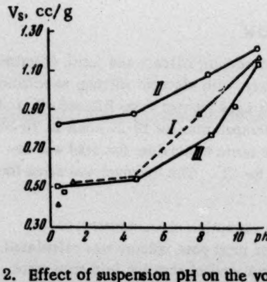

Fig. 2. Effect of suspension pH on the volume of benzene adsorbed by chalky silica gels from saturated vapor (I, II and III are series of experiments): I) Specimens 1-4; II) Specimens 5-9; III) Specimens 10-16 (see Table 1).

Table 1 gives the conditions for the preparation of three series of chalky silica gels specimens, and their sorption characteristics, and Fig. 1 shows isotherms for sorption of methyl alcohol vapor at 20° on specimens of the first (1, a) and second (1, b) series of experiments.

The variations of the volume of benzene taken up from saturated vapor with pH of the suspension are given in Fig. 2.

It follows from the data in Table 1 that the total pore volume, the limiting sorption volume of benzene at $p/p_s = 1$, and the volume of the macropores of chalky silica gels obtained from silicate and $FeCl_3$ increase with increasing pH of the suspension. Comparison of the sorption isotherms for specimens formed from an acid medium (Curves 1 in Fig. 1) with isotherms for silica gels precipitated in an alkaline medium (Curves 2 and 3 in Fig. 1) reveals considerable differences in the character of their porosity. In the first case the hysteresis loop is not large, indicating that the volume of the intermediate pores is not great. At low and moderate relative pressures Curves 1 lie above Curves 2 and 3. The specimens precipitated in an alkaline medium have a more coarsely porous structure. The isotherms show large hysteresis loops. The limiting sorptional volume of the pores of these silica gels at $p/p_s = 1$ is large.

TABLE 1

Preparation Conditions and Structural and Sorption Characteristics of the Silica Gels Studied

Series	Specimens	pH of suspension	$FeCl_3/Na_2SiO_3$ (by volume)	Apparent sp. gr. in g/cc	Total pore volume in cc/g	Benzene adsorbed at $p/p_s = 1$, in cc/g	Volume of macropores, cc/g	Specific surface, m^2/g
I	1	0.37	1:1	0.90	0.66	0.42	0.24	689
	2	1.2	3:4	0.76	0.85	0.52	0.33	—
	3	7.8	1:2	0,50	1.55	0.88	0.67	660
	4	11.0	1:3.3	0.39	2.11	1.16	0.95	638
II	5	0.43	1:1	0,40	2.05	0.84	—	762
	6	2,4	3:4	0.52	1.48	0.75	0.73	—
	7	4.4	3:5	0,48	1,63	0.88	0.75	732
	8	8,2	1:2	0,34	2.50	1.08	1,42	660
	9	10.94	1:3,3	0.31	2.75	1.21	1.54	682
III	10	0.44	1:2	1.12	0.44	—	—	768
	11	0,6	1:2.6	1.09	0.47	0.48	—	—
	12	2.5	1:3,3	0.96	0.59	0,65	—	—
	13	4.5	1:4	1.01	0.64	0,54	—	—
	14	8.4	1:5	0.86	0.71	0.77	—	—
	15	9.7	1:6	0.69	1.00	0.92	0,08	—
	16	10.9	1:8	0.54	1.40	1,06	0.36	688

Consequently, an acid medium leads to formation of chalky silica gels with highly developed microporosity, giving a large specific surface. These gels are either without macropores, or their macropore volume is low. The limiting sorptional volume of the pores (at $p/p_s = 1$) is 2-2.5 times smaller than that of specimens obtained from an alkaline medium.

For comparison, chalky silica gels were also precipitated by nickel chloride in the same conditions as the silica gels from $FeCl_3$, and their structure and sorptional properties were studied. The isotherms for sorption of methyl alcohol vapor on these specimens are given in Fig. 3. It follows from Fig. 3 that the sorption isotherms for chalky silica gels precipitated by $NiCl_2$ from acid media lie above the isotherms for silica gels prepared from alkaline media. The macropore volume of silica gels precipitated by $NiCl_2$ solution increases from 0.23 to 0.88 cc/g as the suspension pH increases from 0.5 to 10.5. However, in contrast to the silica gels precipitated by $FeCl_3$, the limiting sorptional volume of the pores decreases. The ratio of the sorptional pore volume to the macropore volume, V_s/V_{ma}, falls from 7.4 to 1.4. It seems that the increase of the total pore volume in silica gels precipitated by $NiCl_2$ is due to increased macropore volume, and in silica gels precipitated by $FeCl_3$ it is due to increased intermediate pore volume.

All the gels described above, precipitated at different pH values of the medium, were washed for prolonged periods with distilled water before being dried. It was of interest to determine the effect of the pH of the wash waters on the structure of chalky silica gels.

Influence of the pH of the wash water on the structure of chalky silica gels. Precipitates washed with distilled water to a negative reaction for Cl^- were divided into three portions; one was covered with a solution of pH 2.6, another, with a solution of pH 6.5, and the third, with a solution of pH 10.4; the specimens were then dried in a drying oven at 120°.

The structural and sorptional characteristics of these silica gels are given in Table 2, and isotherms for the sorption of methyl alcohol vapor on these specimens are shown in Fig. 4.

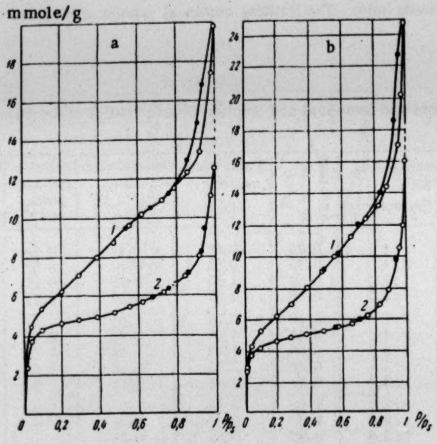

Fig. 3. Sorption isotherms for methyl alcohol vapor on chalky silica gels precipitated by $NiCl_2$ with different suspension pH: a. 1) pH 0.5; 2) pH 10.5; b. 1) pH 0.6; 2) pH 11.2.

TABLE 2

Structural and Sorptional Characteristics of the Silica Gels Studied

Specimen	pH of suspension	pH of wash water	Total pore volume, cc/g	Sorptional pore volume, cc/g	Volume of macropores, cc/g	Specific surface, m²/g
17	8.5	2.6	2.50	0.78	1.72	464
18	8.5	6 5	2.50	1.05	1.45	624
19	8.5	10.4	2.75	1.15	1.60	435
20	6.2	2.6	2.16	0.75	1.41	—
21	6.2	6.5	2.16	0.81	1.35	—
22	3.3	2.6	2.05	0.80	1.25	631
23	3.3	6.5	2.68	0.97	1.71	574
24	3.3	10.4	3.12	1.09	2.03	580

Comparison of the structural and sorptional characteristics of chalky silica gels covered with solutions of different pH values (see Table 2 and Fig. 6) showed that drying of precipitates at different pH values merely leads to some changes in the character of the pore distribution, and the structural differences consist only of changes in the volumes of the intermediate pores and macropores. The sorptional volume of the silica gel pores increases from 0.78 to 1.15 cc/g as the pH of the precipitate is increased from 2.6 to 10.4. The specific surfaces of these specimens have similar values, 500-600 m²/g. It is evident that this method cannot be used for varying the porous structure of chalky silica gels over a wide range.

Some considerations of the chemistry of chalky silica gel formation. The chemistry of the formation of chalky silica gels from water glass and easily hydrolyzable salts is still obscure. Holmes [3] presumed that in the first instant of the reaction the heavy metal salt is hydrolyzed with formation of acid; the latter reacts with sodium silicate, forming silicic acid:

$$\begin{array}{c} MeCl_2 + 2H_2O = Me(OH)_2\downarrow + 2HCl \\ Na_2SiO_3 + 2HCl = H_2SiO_3\downarrow + 2NaCl \\ \hline MeCl_2 + Na_2SiO_3 + 2H_2O = Me(OH)_2\downarrow + H_2SiO_3\downarrow + 2NaCl. \end{array}$$

Patrick [3] showed, however, that a precipitate is not formed if hydrochloric acid is added to sodium silicate in an amount equal to the amount of acid liberated by hydrolysis of the salt. Therefore Holmes' scheme does not appear to be consistent with the facts.

Dubinin [4] assumed that sodium silicate is first hydrolyzed to form silicic acid and alkali, and the latter then reacts with the heavy metal salt, giving the hydroxide according to the scheme:

$$\begin{array}{c} Na_2SiO_3 + H_2O = H_2SiO_3\downarrow + 2NaOH \\ 2NaOH + MeCl_2 = Me(OH)_2\downarrow + 2NaCl \\ \hline NaSiO_3 + MeCl_2 + H_2O = Me(OH)_2\downarrow + H_2SiO_3\downarrow + 2NaCl. \end{array}$$

However, it is difficult to imagine that the metal hydroxide and silicic acid can be present in an unbound state in the precipitate in an alkaline medium. They are most likely to form complex compounds.

To verify this hypothesis, we prepared ferric hydroxide by the action of ammonia on $FeCl_3$ solution, and, for comparison, we precipitated a chalky gel by mixing solutions of sodium silicate and $FeCl_3$. In order to determine whether this precipitate contains $Fe(OH)_3$ in pure form, or whether it is chemically combined with H_2SiO_3, we tested the solubility of pure $Fe(OH)_3$ and of the chalky gel precipitate in acids.

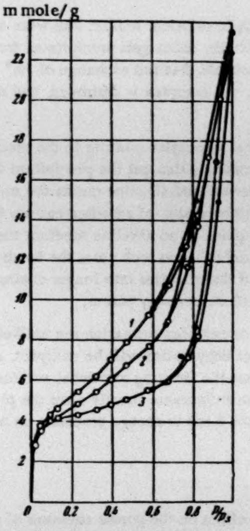

Fig. 4. Sorption isotherms for methyl alcohol vapor on chalky silica gels washed with solutions of different pH: 1) pH 2.8; 2) pH 6.5; 3) pH 10.4.

It was found that fresh $Fe(OH)_3$ dissolved readily in 6 N hydrochloric and 8 N acetic acids, and with difficulty in 4 N acetic acid. The iron in the precipitate formed when $FeCl_3$ and Na_2SiO_3 solutions were mixed dissolved in 6 N HCl but was entirely insoluble in 6N acetic acid. It is likely that, in addition to $Fe(OH)_3$ in the pure form, the precipitate contains iron combined with silicic acid. After treatment of the precipitate with 6N HCl this compound is destroyed and only silicic acid gel remains in the precipitate. It is probable that Dubinin's scheme also fails to conform to reality.

Ray and Ganguly [5] measured the quantity of heat evolved in complete reaction of one mole of $FeCl_3$ with various solutions of alkali metal silicates; they found that the quantity of heat evolved per mole of $FeCl_3$ falls appreciably with increasing contents of silicic acid and constant Na_2O content in the solutions. If the only reaction product was $Fe(OH)_3$, the heat of reaction should be constant, and close to the heat of reaction between $FeCl_3$ and NaOH. The gradual decrease of the heat effects observed by these authors indicates the formation of complex silicate ions with increasing contents of silica in solution.

In our opinion, Grigorjew [6] was nearer to a correct view of the chemistry of chalky silica gel formation; he assumed that the reaction proceeds according to the equation:

$$MeCl_2 + Na_2SiO_3 = 2NaCl + MeO \cdot n\,SiO_2.$$

It is difficult to believe, however, that in an alkaline medium the sodium ions present will not take part in complex formation.

We represent the general reaction scheme as follows:

$$Na_2SiO_3\,(SiO_2)_n + aMeCl_2 = Na_2O \cdot a\,MeO \cdot b\,SiO_2 \cdot mH_2O + nNaCl.$$

Evidence in favor of this scheme is provided by our quantitative determinations of Na and Fe in ferrosilica gels prepared from alkaline media.

When the ferrosilica gels were precipitated with excess of Na_2SiO_3 in solution, sodium ions were always present in the finished dry ferrosilica gel. Na^+ ions were not found in chalky silica gels precipitated from alkaline media if the hydrogels had been treated with 2N HCl. It is probable that ion exchange of Na^+ for H^+ takes place in such treatment. If the gels are treated with 6N HCl, the complex is destroyed, and neither Fe^{3+} ions nor Na^+ ions can be detected in the silica gel.

Our results are in good agreement with the fundamental theoretical principles relating to the mechanism of hydrophilic adsorbent structure formation [7]. In precipitation of a chalky silica gel the precipitate is formed instantaneously as the precipitant is added to the sodium silicate. In neutral and alkaline media the most probable result is formation of silicic acid micelles, the outer layers of which consist of adsorbed cations from the solution. The possibility is not excluded that if the precipitation takes place in an alkaline medium the cations will also be present within the micelles, forming complexes. It is probable that in such cases the bonds between the micelles and water are weakened, resulting in further aggregation of the micelles into longer chains and clusters. Dehydration will result in a loose texture and the silica gel will be coarsely porous.

In an acid medium, adsorption processes involving ion exchange or complex formation are unlikely, the micelles will be hydrophilic, the packing of the particles as the result of dehydration will be compact, and the resultant silica gel will be finely porous. It is interesting to note that the limiting sorptional volume of the pores of chalky silica gels, like that of glassy silica gels, only begins to increase sharply after the pH of the precipitation medium exceeds 5 (see Fig. 2). It is probable that up to pH 5 ion exchange processes do not take place on the micelle surfaces.

SUMMARY

1. The reaction of the medium in precipitation has an important effect on the porous structure of chalky silica gels. The total pore volume and the macropore volume increase with increasing pH.

2. The effect of the reaction of the precipitation medium is largely independent of the nature of the easily hydrolyzed salt.

3. Adsorption processes associated with ion exchange on the surfaces of the silicic acid micelles do not take place in an acid medium. In an alkaline medium the outer shell of the micelles consists of adsorbed cations.

4. The chemistry of chalky silica gel formation is discussed.

The L. V. Pisarzhevsky Institute of Physical Chemistry
Academy of Sciences, Ukrainian SSR, Kiev

Received March 29, 1957.

LITERATURE CITED

[1] I. E. Neimark, M. A. Piontkovskaya and I. B. Slinyakova, Colloid J. 18, 61 (1956).*

[2] I. E. Neimark and I. B. Slinyakova, Colloid J. 15, 277 (1953).*

[3] H. Holmes and J. Anderson, Ind. Eng. Chem. 17, 280 (1925).**

[4] M. M. Dubinin, Physicochemical Principles of Sorption Technology [In Russian] (Goskhimizdat, 1932).

[5] R. Ray and B. Ganguly, J. Phys. Chem. 2, 396 (1931).

[6] P. N. Grigorjew, J. prakt. Chem. 118, 91 (1928).

[7] I. E. Neimark, Progr. Chem. 25, 748 (1956).

---

* Original Russian pagination. See C. B. translation.

** [The original did not contain any reference by Patrick, as cited in the text – Publisher].

[illegible]

(6) M. M. Dubinin, [illegible]

[5] A. Ray and [illegible] J. Phys. Chem. [illegible]

[6] [illegible]

[7] [illegible]

[illegible]

GELATIN–GLYCEROL GELS AS MATERIALS FOR STUDYING STRESSES BY THE OPTICAL POLARIZATION METHOD

D. N. Osokina

Gelatin–glycerol gels are widely used for optical polarization studies of stresses in models in relation to problems of mining [1], soil mechanics [2, 3], geotectonics [4], etc.

Gelatin gels have not been sufficiently studied as optically active materials, although there have been numerous investigations of their properties. These investigations have followed two unrelated directions. In one type of investigation [5-10], purely physical and physicochemical, gelatin gels were studied for purposes which had nothing to do with modeling. In the second type [1-3, 11] gelatin gels were used as optically active materials for modeling phenomena in which volume forces play an important role. The most complete quantitative studies of gelatin gels as optically active materials were those carried out by Trumbachev [1].

Researches of the first type lead to the following conclusions:

1. The elasticity modulus of gelatin gels greatly decreases with increase of temperature and increases with the time which elapses after casting of the gel.

2. The temporary birefringence and deformation in a gel under constant load increase with time, at least for 20-30 minutes.

3. The magnitude of the temporary birefringence (optical effect) is evidently associated with the deformation and not with the stress acting on the specimen.

It has been shown [6, 13, 14] that Poisson's ratio for gelatin gels is 0.5. It should be pointed out that in studies of the mechanical properties of gelatin gels most authors referred to $E = \sigma/\epsilon$ (where σ is the applied force and ϵ is the deformation produced in the specimen) as Young's modulus or elasticity modulus, by analogy with ordinary solids. In the modern view [12], the elastic deformation produced in a gelatin gel at room temperature consists of a conventionally instantaneous component (ϵ_{ci}), and a high-elastic component (ϵ_e) which has developed at the instant of the determination, and hence

$$\frac{1}{E}=\frac{\epsilon}{\sigma}=\frac{\epsilon_{ci}+\epsilon_e}{\sigma}=\frac{1}{E_1}+\frac{1}{E_e},$$

where E_1 is the conventionally instantaneous modulus; E_e is the elasticity modulus.

Since several days are required before equilibrium high-elastic deformation is reached in gelatin gels, generally not the total elastic deformation is measured, but only a certain part of it, and accordingly E_e is greater than the equilibrium elasticity modulus, and E is greater than the total equilibrium elasticity modulus. In this paper, for brevity, we term E the elasticity modulus, remembering that this is not the total modulus but an intermediate value between the conventionally instantaneous and the total equilibrium modulus.

Most of the investigators in the second type of studies ignored the specific nature of the high-elastic state of gelatin gels, and regarded them as ordinary photoelastic materials in which the optical effect (optical path difference) is a linear function of the principal stress difference; i.e., they did not take into account the variations of the gel properties with the time of action of the load, temperature of the experiment, and "age" of the material.

The investigations cited above provide much important and necessary information on the properties of gelatin gels. However, before gels can be used for stress investigation with all the factors influencing the experimental results taken into account, the following questions remain to be answered: 1) for how long do the optical path difference and deformation continue to increase under constant load, and do these quantities reach equilibrium values within a period of time suitable for carrying out the experiments, i.e., within the first few hours after application of the load (since gelatin models are very susceptible to drying, it is undesirable to keep them under load for longer than this before the start of the experiment); 2) can the material be characterized by an elasticity modulus and an optical stress coefficient, constant for all stresses, at any time after application of the load; 3) how do the stress-optical coefficient and the elasticity modulus of a gelatin gel vary with the preparation conditions and the nature of the test.

Methods of specimen preparation and measurements of deformation and optical effect. The specimens for compression tests were made in the form of prisms (5 × 3 × 2 cm), and for extension tests in the form of strips (11 × 1.6 × 1 cm) of rectangular section and with mirror-smooth faces, so that the specimens could be investigated in polarized light. For the extension tests, two horizontal lines 2 cm apart were marked with India ink in the middle of the strip. The ends of the strip were fixed in two clamps, the top one being connected to a stand, and a light pan for weights being attached to the lower one. The distance between the marks was measured to an accuracy of 0.1 mm by means of a traveling microscope rigidly connected to a vernier moving along a vertical steel scale fixed on the same base as the stand.

For compression tests, the prismatic specimen was placed between circular plates of a small press in which a load between 5 g and 5 kg, with an accuracy of 2-3 g, could be applied to the specimen. The deformations were read off to an accuracy of 0.1 mm from the displacement of a vernier pointer attached to the upper plate of the press, along a scale. The interference colors of the specimens indicated that the stress distribution within them was fairly homogeneous.

For the birefringence determinations, the specimen fixed in the loading device was placed between the polaroids of a coordinated synchronous KSP-5 polarimeter. The path difference in the region of the specimen between the marks was measured by means of Krasnov's compensator. To avoid drying of the specimens, they were removed from the molds immediately before the start of the experiments, while during lengthy tests they were placed in a transparent hermetically sealed box.

Behavior of the specimen with time under constant load. Figure 1 shows the variations of the path difference R in mμ, and of the relative deformation ϵ arising in the specimen under a constant tensile force, with time from the application of the load. The determinations were made both with the specimen under load, and after release of the load. The composition of the gel was 30% gelatin, 30% glycerol, and 40% water; the temperature was 21-22°; the time of action of the load was 3 hours 50 minutes. The longest period of action of the load in experiments of this type was 70 hours. It follows from these experiments that the path difference and deformation under constant load at room temperature increase with time, at a diminishing rate; they do not reach equilibrium values in 60-70 hours. On removal of the load, part of the path difference and deformation disappears abruptly; the remainder diminishes at a continuously decreasing rate. If the specimen is heated through a frew degrees, the rate of decrease of the "residual" path difference and deformation rises sharply, and these value drop almost to zero. All the deformation remaining after application of the load can therefore be regarded as reversible and elastic, and it may be assumed that plastic deformation of the gel in these conditions (temperature 22°, small stresses of 0.1-0.2 kg/cm^2) is negligible or entirely absent.

Consequently the deformation and path difference do not reach constant values in the time which can be devoted to experiments with models. It is therefore necessary to carry out the measurements before equilibrium deformation becomes established.

Variations of the birefringence and deformation with the stress with the determinations carried out immediately after application of the load (1-1.5 minutes after loading) were determined in extension and compression experiments. The load on the specimen was increased by 50 g steps; before each successive i-th loading the specimen was released and the distance L_{i0} between the lines (in compression experiments, the height of the specimen) and the path difference R_{i_0} were measured. The load P_i was then applied, and the following were measured: L_i, the distance between the lines in extension experiments (or the height of the specimen in compression experiments), and the path difference R_i.

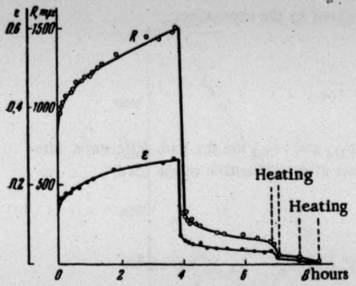

Fig. 1. Variations of the optical path difference R and relative deformation ε with time.

In the calculations, stress increases of $\sigma_i (\sigma_i = P_i / S_i)$, where S_i is the area of the specimen deformed under the action of the load (P_i), were correlated with $R = R_i - R_{i_0}$ and $L = L_i - L_{i_0}$, i.e., the increments of the path difference and of the length of the portion of the specimen in question, produced by the given stress increase. It was necessary to remove the load and to subtract R_{i_0} and L_{i_0} from the corresponding values of R_i and L_i in order to eliminate the influence of increases of R and L with time, which could distort the results of the determinations.

When the path difference changes by the value R, the difference between the principal refractive indices $\Delta n = n_1 - n_2$ changes by the value $\Delta n = R / d_i$, where d_i is the thickness of the specimen deformed by the load P_i; d_i was calculated on the assumption that the volume was constant

$$d_i = d_0 \sqrt{L_0 / L_i};$$

S_i was calculated on the same assumption: $S_i = S_0 L_0 / L_i$; the relative deformation ε was determined as

$$\epsilon = (L_i - L_{i_0}) / L_{i_0}.$$

Figure 2 shows variations of Δn and ε with the stress in extension and compression (1-1.5 minutes after

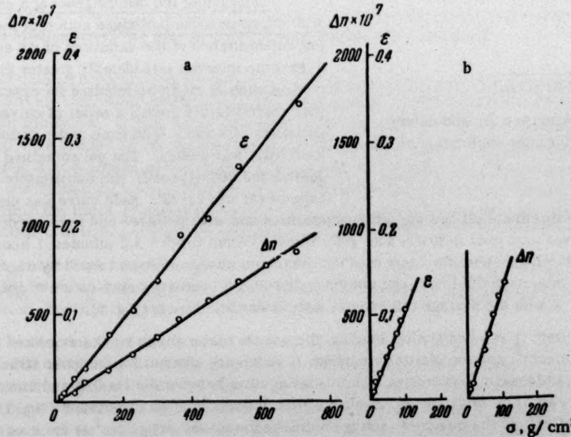

Fig. 2. Variations of birefringence Δn and relative deformation ε with stress: a) in extension (gel composition: 40% gelatin, 30% glycerol, 30% water); b) in compression (gel composition: 25% gelatin, 30% glycerol, 45% water).

application of the load); it is seen that at deformations not exceeding 25-30% Δn and ϵ are linear functions of σ.

It follows from the linear relationships between Δn and σ, and ϵ and σ, that 1-1.5 minutes after loading gelatin gels can be characterized by the optical coefficient C_{1M} and the elasticity modulus E_{1M}, constant for all stresses (at deformations not exceeding 25-30%). Since under uniaxial extension or compression $\sigma_1 = \sigma$, $\sigma_2 = 0$, $\sigma_1 - \sigma_2 = \sigma$, the values of C_{1M} and E_{1M} are given by the expressions

$$C_{1M} = \frac{R_{1M}}{\sigma d} = \frac{\Delta n_{1M}}{\sigma}, \; E_{1M} = \frac{\sigma}{\varepsilon_{1M}},$$

where d is the thickness of the deformed specimen, and R_{1M}, Δn_{1M} and ϵ_{1M} are the path difference, birefringence, and deformation arising in the specimen 1-1.5 minutes after application of the load.

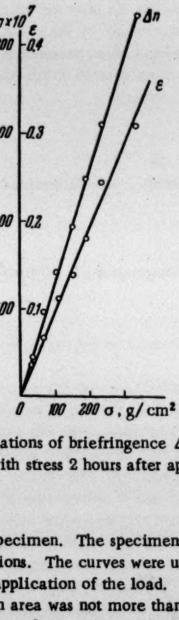

Fig. 3. Variations of briefringence Δn and deformation ϵ with stress 2 hours after application of the load.

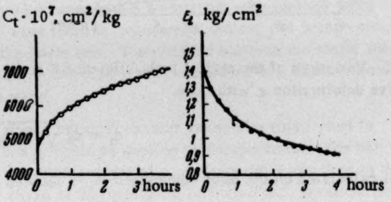

Fig. 4. Variation of the stress-optical coefficient C and elasticity modulus E with time under constant load.

Variations of the birefringence and deformation with the stress under prolonged action of the load. For determination of the variations of Δn and ϵ with σ for time intervals considerably greater than 1 minute, such as might be required for experiments with models (1.5-2 hours), a series of curves for the variations of R and ϵ with time under various constant loads was plotted. The gel contained 30% gelatin and 30% glycerol; the temperature of the experiment was 21-22°. Each curve was plotted for a separate specimen. The specimens all had the same composition and were prepared and tested under the same conditions. The curves were used to find R and ϵ for three different times – 1.5 minutes, 1 hour, and 2 hours after application of the load. With the loads used the maximum change of stress caused by decrease of the specimen area was not more than 6% 1 hour and not more than 10% 2 hours after application of the load. The variations of Δn and ϵ with the average true stresses were linear in all cases (Fig. 3).

Thus, at any time instant ($t \leq 2$ hours) after loading, the gelatin material can be characterized by values of the stress-optical coefficient C_t and the elasticity modulus E_t which are constant for the given time interval. The value of C_t increases, and that of E_t decreases with increasing time between the loading and measurement. Figure 4 shows variations, with time, of C_t and E_t calculated from the results of an experiment (Fig. 1) carried out under a constant load of 311 g; the true stress acting on the specimen was 229 g/cm² at the start and 251 g/cm² at the end of the experiment. The greatest changes in the values of C_t and E_t occur during the first hour, and subsequently the rate of change decreases considerably with time. During the whole time of action of the stress (3 hours 50 minutes) C_t increased by about 50%, while E_t decreased by 35% relative to the values of C_t and E_t 3 minutes after application of the load. During the same time the stress increased by only

10%. Therefore the increase of C_t cannot be attributed to increase of the stress. Thus, in determinations of stresses in gelatin models it must be taken into account that the stress-optical coefficient depends on the time elapsing after application of the load.

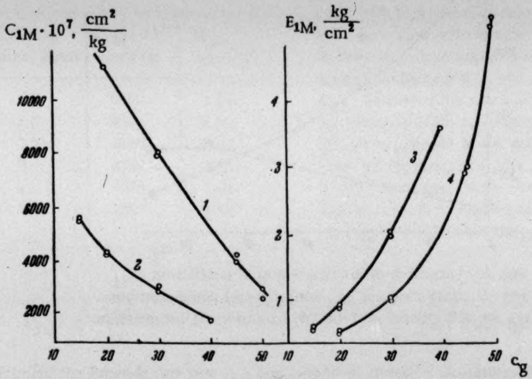

Fig. 5. Variations of the stress optical coefficient C_{1M} (1, 2) and elasticity modulus E_{1M} (3, 4) with gelatin concentration c_g at constant concentration of glycerol: 1 and 4) 10% glycerol; 2 and 3) 45% glycerol.

When the usual photoelasticity equation: $R = C(\sigma_1 - \sigma_2)d$ is applied to gelatin gels, the constant C must be replaced by the variable C(t), which depends on the time. For calibration of the material to be used for a model, curves for the variation of R and ϵ with time under constant load should be plotted for three or four different stresses; the results should then be used to calculate the values of C and E of the material for the time after application of the load at which the experiment was carried out.

Effect of gelatin concentration in the gel on optical activity and elasticity modulus. Specimens containing pregressively increasing amounts of gelatin were tested. All the specimens were made and tested under the same conditions. Graphs for the variation of Δn and ϵ with σ (time after application of the load, 1-1.5 minutes) were plotted for all the specimens. The values of C_{1M} and E_{1M} determined from these graphs are shown in Fig. 5 as functions of the gelatin concentration in the gels. In another series of experiments (30% glycerol) the determinations were carried out under compression as well as under extension. It follows from the results that within the limits of experimental error $C_{1M} = E_{1M}$* for compression and extension; C_{1M} decreases and E_{1M} increases with increasing gelatin concentration (c_g) (Fig. 5).

In the c_g range from 15 to 35% the variations of C_{1M} and E_{1M} can be approximately represented by the expressions $C_{1M} = A/c_g$ and $E_{1M} = Bc^2_g$. Here A and B are constants for each curve, but their values vary with the glycerol concentration (see Leik's paper [7]).

It must be noted that specimens made from the same solution show small variations of C_{1M} and E_{1M} (on the average 5-6%) which may be wholly attributed to experimental error. Values of C_{1M} and E_{1M} for the same specimens made from different solutions sometimes differ by as much as 40%, which is several times the mean experimental error. These large differences must be ascribed to differences in the thermal history of these specimens. Therefore for calibration of the material the thermal conditions for the preparation of the model and the specimen must be identical.

---

* [As in original – Publisher].

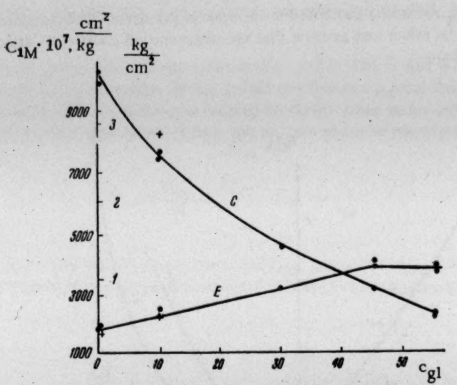

Fig. 6. Variations of the stress-optical coefficient C_{1M} and elasticity modulus E_{1M} with glycerol concentrations c_{gl} for 30% gelatin content. ●) extension, +) compression.

Effect of glycerol concentration. Variations of C_{1M} and E_{1M} with the glycerol concentration (c_{gl}) are shown in Fig. 6. It is seen that C_{1M} decreases while E_{1M} increases with increasing glycerol content. The decrease of C_{1M} is slower than that caused by increase of the gelatin content. As regards the value of E_{1M}, this increases almost linearly with c_{gl} up to about 40%, and then remains constant.

Effect of swelling time. The results of experiments with specimens differing only in the swelling time of the gelatin in the water–glycerol mixture showed that for specimens of two different compositions (30% gelatin and 30% glycerol, and 25% gelatin and 30% glycerol) the values of C_{1M} and E_{1M} remain unchanged, within the limits of experimental error, with increase of swelling time from a few minutes to 48 hours.

Effect of the dissolving time of gelatin in the water–glycerol mixture (heating time). Tests on specimens which differed only in the time during which they were "cooked" on the water bath showed that the stress-optical coefficient C_{1M} increases while the elasticity modulus E_{1M} decreases with increasing cooking time. The results are given in the Table. The specimens contained 30% gelatin and 30% glycerol; the "age" was 42 and 90 hours, and the test temperature was 19°.

It is seen from the Table that when the cooking time is increased from 2 to 7 hours C_{1M} increases by 20%, while E_{1M} decreases to about the same extent. A decrease of E_{1M} was observed previously by Fraas [6]; it can be attributed to degradation of the macromolecules during prolonged heating. Fraas recommended a cooking temperature of 60-70° in order to decrease degradation.

Effect of time elapsing after casting of the specimen (age). The test specimens differed only by the time they were left in the molds after casting. The tests were performed under compression. The gel contained 25% gelatin and 30% glycerol. The results in Fig. 7 show that E_{1M} increases and C_{1M} decreases with increasing time after casting. After four days C_{1M} diminished by nearly 20%, while E_{1M} increased by nearly 50%.

Variations of C_{1M} and E_{1M} during the first 20 hours after gelation are shown in Fig. 7,b. The less the "age" of the specimen, the higher is the rate of change of C_{1M} and E_{1M}. This change is especially rapid during the first 40 hours after casting. Therefore gels should not be used during the first few hours after gelation, when their properties change very rapidly; it is best to use them on the second day, 35-40 hours after casting.

Variation of birefringence with deformation. In publications [5] and [15] dealing with gelatin gels it has been suggested that the optical effect in gelatin gels is directly related to deformations and not to stresses.

TABLE

Variations of the Stress-Optical Coefficient C_{1M} and Elasticity Modulus E_{1M} in Extension with Cooking Time for Two Gel Specimens

Age of gel, hours	Cooking time, hours	$C_{1M} \cdot 10^7$ cm^2/kg	E_{1M}, kg/cm^2
42	2.7	3600	1.91
42	5.5	4200	1.70
42	7.7	4550	1.59
90	2	3750	2.21
90	5	4030	1.81
90	7	4280	1.65

The present investigation confirms this view by a number of facts: 1) the increase of the optical path difference with time under constant load (and almost constant stress) proceeds simultaneously with increase of the high-elastic deformation; 2) simultaneously with high-elastic after-effects there are path difference after-effects after removal of the load; 3) there is a close connection between the stress-optical coefficient C_{1M} and the elasticity modulus E_{1M}. Whenever the elasticity modulus E_{1M} of the gel increases (with increasing concentrations of gelatin or glycerol in the gel, and with increasing "age" of the specimen), the stress-optical coefficient decreases. If the elasticity modulus E_{1M} decreases (with increasing cooking time), the stress-optical coefficient C_{1M} increases.

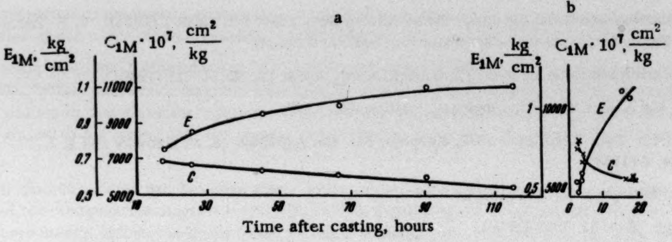

Fig. 7. Variations of the stress-optical coefficient C_{1M} and elasticity modulus E_{1M} with time after gelation at 22° ± 1°; a) during 5 days after casting; b) during the first 20 hours after casting.

All these facts can be satisfactorily explained on the hypothesis that the optical effect is directly related to the magnitude of the reversible elastic deformation, and therefore an increase of the modulus E_{1M}, which leads to a decrease of the deformation under a given stress, results in a decrease of the stress-optical coefficient.

The ratio of the birefringence Δn to the deformation ϵ may be termed the optical coefficient of deformation C_ϵ. The value of C_ϵ is obtained by multiplication of C by E

$$C \cdot E = \frac{\Delta n}{\sigma} \frac{\sigma}{\epsilon} = \frac{\Delta n}{\epsilon} = C_\epsilon.$$

The behavior of C_ϵ differs in many respects from the behavior of C. When deformation and optical path difference increase with time under constant load, C_ϵ remains practically constant, decreasing by not more than 5-6% while C increases by nearly 50%. C_ϵ increases almost linearly with increasing gelatin content in the gel, and decreases linearly with increasing glycerol content. C_ϵ increases with increasing age of the specimen, the increase being particularly rapid during the first 20-40 hours after gelation.

SUMMARY

1. The value of the artifical birefringence and deformation produced under constant load at 22° in highly concentrated gelatin—glycerol gels increase with time for a least 60-70 hours.

2. The stress-optical coefficient C and the elasticity modulus E of the gels remain constant at different

stresses for equal times after application of the load (this has been demonstrated for time intervals of 1 minute to 2 hours after application of the load).

3. Variations C_{1M} and E_{1M} with the composition of the material and the preparation conditions have been studied.

4. The earlier view is confirmed that the birefringence depends directly on the deformation and not on the stress. The concept of the optical coefficient of deformation of gelatin gels is discussed and its behavior under the influence of various factors is shown.

5. The great influence of "thermal history" on the values of C_{1M} and E_{1M} has been confirmed.

In conclusion, the author expresses her deep gratitude to M. V. Gzovsky who supervised, to M. P. Volarovich and V. F. Trumbachev for guidance, to Yu. S. Lazurkin for valuable advice, and to V. V. Fedorova, who took part in the experimental work and analysis of the results.

Institute of Soil Physics Academy of
Sciences USSR Moscow

Received September 24, 1956.

LITERATURE CITED

[1] V. F. Trumbachev and N. A. Suvorov, Trans. Mining Inst. Acad. Sci. USSR 1 (1954); V. F. Trumbachev, ibid; G. A. Krupennikov and V. F. Trumbachev, Coal, No 3 (1954).

[2] F. B. Farquharson and R. G. Hennes, Civil Engineering, April, 10, No. 4, 211 (1940).

[3] D. C. John and B. C. Crisp, The Engineer, March, 465 (1953).

[4] M. V. Gzovsky, Bull. Acad. Sci. USSR, Geophys. Ser. No. 6 (1954); M. V. Gzovsky and E. I. Chertkova, op. cit. No. 6 (1953).

[5] P. Bjerken, Ann. phys. 43, 808 (1891).

[6] E. Fraas, Ann. phys. 53, 1074 (1894).

[7] A. Leik, Ann. phys. 14, 139 (1904).

[8] H. J. Pool, Trans. Faraday Soc. 21, 114 (1926).

[9] E. Hatschek, Trans. Faraday Soc. 29, 1109 (1933).

[10] R. I. Dulitskaya and S. I. Sokolov, Collected Papers of the Physicochemical Section of TsNIKL (1927) p. 138.

[11] L. D. Prokofyeva-Mikhailovskaya, Trans. Conf. on Control of Rock Pressure (Izd. AN SSSR, 1938).

[12] N. A. Mikhailov and P. A. Rebinder, Colloid J. 17, 107 (1955). [See C. B. translation].

[13] R. Maurer, Wied. Ann. 28, 628 (1886).

[14] E. Wiedemann, Verhandl. phys. Gesellschaft, Berlin, 24 October, 1884, p. 45.

[15] E. Coker and L. Filon, Optical Method of Stress Investigation (Leningrad–Moscow, 1936). [Russian translation].

THE SELECTION OF PLASTICIZERS FOR HIGH POLYMERS*

S. P. Papkov

The purpose of the present paper is to examine certain general principles of the selection of plasticizers for high polymers in relation to phase equilibrium in the plasticizer–polymer system. It is necessary to take this equilibrium into account because in most cases plasticizers, being solvents of low activity, are incompletely compatible with polymers. At definite component ratios and definite temperatures considerable changes occur in the properties of the systems as the result of microseparation which may sometimes go as far as macroseparation of one of the phases ("bleeding" of the plasticizer).

Some questions of plasticization of high polymers were considered in one of our earlier papers [1]. In particular, phase equilibrium diagrams were used for explaining the plasticizer–polymer compatibility limits, and it was shown that plasticizer–polymer compatibility is determined by the position of the equilibrium curve for separation of the system into two phases. Later, similar views were advanced by Spurlin [2] and Colborne [3].

It must be pointed out, however, that examination of the position of the phase equilibrium curve on the composition–temperature diagram is not sufficient for explaining the properties of a polymer–plasticizer system. This curve merely defines the limits of the permissible plasticizer concentrations, but does not show variations of the mechanical properties of the plasticized product at various component ratios. In Colborne's paper cited above, a curve for variations of the "melting" temperature as a function of composition is drawn on the phase equilibrium diagram, as a characterization of the mechanical properties. However, this curve by no means represents the principal properties of the plasticized polymer from the practical aspect. Moreover, Colborne's paper contains an error of principle; the point of intersection of the "melting" curve with the compatibility curve is taken as the critical temperature of mixing. It is known that phase equilibrium is not related to transitions of this type. As Kobeko [4] correctly pointed out, gradual softening of polymers cannot be regarded as a phase transition.

For a more complete characterization of the properties of a polymer–plasticizer system a suitable form of temperature–composition diagram is one which shows, together with a phase equilibrium curve for the components, a family of curves for isoviscous solutions. Additional justification for this is that the principal purpose of polymer plasticization is modification of its viscous properties so that the system is not prone to brittle fracture at a given frequency of load variation. As is known, brittleness depends mainly on viscosity. Under normal use conditions the viscosity limit of plasticized polymers (above which brittle fracture occurs) is of the order of 10^{10} - 10^{13} poises. Additions of plasticizers (formation of polymer solutions) lowers the viscosity of brittle polymers down to the limits set by the use conditions.

Figure 1 is a generalized diagram of this type for a polymer–plasticizer system. Before consideration of variations in the properties of the system, it is necessary to comment briefly on the general nature of the curves in the diagram.

The phase equilibrium curve ABC lies far on the side of high plasticizer concentrations; this is in accordance with practical data on equilibria in polymer–solvent systems [5]. In a plasticized polymer, the composition of one of the coexisting phases differs very little from that of the pure plasticizer; it is therefore sometimes justifiable to speak of the separation ("bleeding") of pure plasticizer in the case of a system which lies in the region of phase separation, although in theory the concentration of the high polymer in the separating liquid phase is not zero. The maximum on the curve also lies in the region of low polymer concentrations, whereas the second branch of the curve can lie at low temperatures, according to practical data on plasticizer–polymer compatibility, in the region of 25-75% plasticizer concentration (by weight).

---

* Communication II in the series "Phase Equilibria in Colloid Systems."

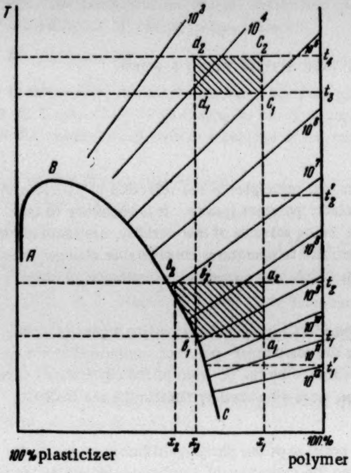

Fig. 1: Phase equilibrium diagram for a polymer–plasticizer system.

The position and form of the group of curves for isoviscous solutions as shown in the diagram are to some extent arbitrary, but they conform to the known fact that for solutions of equal concentration the viscosity increases with decrease of temperature according to an exponential law, the exponent being greater than unity. Nevertheless, the exact nature of the isoviscous curves is not important for the subsequent discussion. It is only important to note that these curves do not intersect. For convenience of analysis, these curves have been given values from 10^{12} to 10^3 poises, which represent the practical limits within which the viscosity of plasticized polymers varies during molding and in use.

Let us consider an example of the choice of the quantitative polymer–plasticizer ratio on the basis of this diagram. If the temperature range in which the polymer products are to be used is t_1-t_2, then the diagram shows that the unplasticized polymer will be unsuitable for use, as the brittle limit (viscosity 10^{10} poises) for the pure polymer lies within this temperature range. Addition of plasticizer to the polymer lowers its viscosity. We follow the dash line corresponding to the temperature t_1 (the lower temperature limit for use of the product) in the diagram until we reach the point a_1, at which the viscosity of the plasticized polymer is 10^{10} poises. This point corresponds to the composition x_1. This is the lower limit for the amount of plasticizer which must be added to the polymer. With lower plasticizer contents the product will not have the necessary plasticity in the conditions of use.

The upper limit for the plasticizer content can also be determined from the viscosity of the plasticized polymer. If the product is under load for considerable periods at the highest use temperature, the possibility of considerable irreversible deformations must be taken into account. Let us assume that on practical grounds the viscosity of the product must not be less than 10^7 poises to avoid appreciable residual deformations. Then the maximum permissible amount of plasticizer is determined by the position of the point b_2 (intersection of the t_2 temperature line with the 10^7 poise viscosity curve), which corresponds to the composition x_2. It is found, however, that for the case shown in this diagram this upper limit of plasticizer concentration is unacceptable, as with the composition x_2 the system enters the region of separation into two phases when the temperature falls to the lower limit t_1. If the product is used in the low temperature region, the plasticizer–polymer compatibility limit will be passed; this will influence the properties of the product and will result in "bleeding" of the plasticizer. The compatibility limit is determined by the phase equilibrium curve, and for temperature t_1 (point b_1) it corresponds to the composition x_3. The plasticizer content of the system cannot exceed this limit. Thus the region of temperatures and compositions satisfying the given brittleness and flow conditions lies within the limits of the shaded area. In practice only the area confined between the points a_1, a_2, b_2, b_1 is used.

Let us consider other possible limitations in the selection of plasticizers. Suppose that the lower temperature limit for use of the product is t_1', while the character of the mechanical stresses remains the same, so that brittle fracture corresponds to a viscosity of 10^{10} poises. Examination of the diagram shows that the required degree of plasticization cannot be attained in this system, as with an increase of the plasticizer content at temperature t_1' the compatibility limit is reached before the required plasticity. It is therefore necessary to choose another plasticizer, with the phase equilibrium and isoviscosity curves in other positions, such that the region of the required viscosities of the product does not overlap the region of phase separation of the system.

On the other hand, if the use temperature range is extended in the direction of higher temperatures and lies, for example, between t_1 and t_2', then it is impossible to use the particular plasticizer if the minimum viscosity is 10^7 poises (to avoid irreversible deformation), since at temperature t_2' and the lower plasticizer concentration limit the viscosity of the product will be below 10^7 poises. It is therefore necessary to choose another plasticizer, with a smaller change of viscosity with temperature.

Yet another limitation in the choice of plasticizers is the molding temperature. If the molding is effected by the casting process with subsequent evaporation of volatile solvent from the solution, the stability of the plasticizer and polymer at high temperatures is not significant. However, if the molding is a mechanical process involving heating, the temperature at which the system reaches the required viscosity must not exceed the decomposition temperature of the polymer or plasticizer. The temperature range for mechanical molding is determined by the lower and upper viscosity limits. If, for example, the lower viscosity limit is 10^5 poises, and the upper limit must not exceed $5 \cdot 10^3$ poises, the molding temperature range for the case considered above will be $t_3 - t_4$, which corresponds to the shaded area c_1, c_2, d_1, d_2 in the diagram. The plasticizer can be regarded as suitable if the system does not undergo thermal decomposition at temperature t_4.

It is of interest to follow the changes in the mechanical properties of a plasticized polymer with variations of composition and temperature. For this it is most convenient to determine total deformations under loads acting for relatively short times, as this corresponds to the most usual conditions in which plasticized products are used. In this paper we shall confine ourselves to consideration of "rigid" polymers, in view of the fact that plasticization of this group of polymers presents the greatest practical interest. Such polymers include cellulose esters or ethers, which do not have rubberlike elasticity under normal conditions.

Figure 2 shows, in simplified form, a phase equilibrium diagram for a polymer–plasticizer system with two isoviscosity lines: the lower line corresponds to transition of the system into the glassy (brittle) state, and the upper corresponds to transition into a state of high fluidity. As is known, both these limits are arbitrary, and in practice they cover viscosity ranges of $10^{10} - 10^{13}$ poises (glass transition) to $10^3 - 10^5$ poises (high fluidity).

Let us consider variations of the total deformation with the temperature at constant polymer : plasticizer ratio. At concentration x_1, which is beyond the limit of phase separation, increase of temperature should produce a gradual increase of deformation (Curve 1, Fig. 2,a); until the glass transition limit is reached the deformation is elastic in character and does not exceed 1-2%, while above this limit irreversible deformation should increase considerably, and should reach very high values (flow) at the second viscosity boundary (temperature t_4).

The following situation should be found for a concentration x_2 lying in the region of phase separation of the system. The system separates into two phases; one of these, which determines the principal mechanical properties of the system, is a concentrated solution of the polymer in the plasticizer, and the other is the practically pure plasticizer. In most cases the conditions for separation of high polymer systems into two phases are such that the low-viscosity phase is liberated in the form of micro-inclusions in a continuous high-viscosity phase. The resulting system, with incomplete macroscopic separation, is a gel and therefore has increased elasticity [6]. With increase of temperature, when the viscosity of the concentrated phase passes beyond the brittle fracture limit, i.e., at t_1, this peculiar structure of the two-phase system begins to have an effect. Elastic bending of the thin "walls" (interlayers) of the viscous phase leads to a sharp increase of reversible deformation. This reversible deformation of a laminar system differs in principle, on the one hand, from the elastic deformation of a continuous solid, where changes of interatomic distances within the limits of the potential barriers play the principal role, and on the other, from rubberlike elasticity, in which the principal role is played by changes in the equilibrium length of the curved macromolecules. This type of reversible deformation could be conventionally termed the elasticity of a gel system, in contrast to rubberlike elasticity. As has already been stated [6], gel system elasticity is characteristic not only of high polymers, but of any substances which form gels. The maximum value of this type of deformation cannot in theory exceed 57% of the original length of the specimen.

The curve for variations of the total deformation for the concentration x_2 will have the following form (Curve 2, Fig. 2,a). Up to temperature t_1 elastic deformation will prevail; this will not exceed 1-2%, as the viscosity of the concentrated phase lies above the glass transition limit. The concentration of this phase varies along the phase equilibrium curve BCDE. At temperature t_2 the composition of the second phase will correspond to concentration x'_2 (point D) while its viscosity will reach the limit at which gel system elasticity begins to appear. At this point in Curve 2 (Fig. 2,a) there will be a sharp increase of total deformation, the greater part of which will consist of the gel system elasticity, since elastic deformation does not change greatly with temperature, while plasticity does not have time to develop to any appreciable extent during the brief action of the load. With further increase of temperature the system still consists of two phases, but the composition of the second phase shifts in the direction of lower polymer concentrations, and its plasticity begins to increase appreciably. Deformation due to plastic flow of the system begins to predominate in the total deformation. At the point C, a single phase is formed. Elasticity due to the gel structure of the system disappears at this point, but plasticity (fluidity) becomes considerable. Finally, at temperature t_3 a viscosity is reached at which the product becomes a liquid of relatively low viscosity. The general form of Curve 2 is characterized by the presence of a "plateau" which corresponds to the region of high reversible deformation.

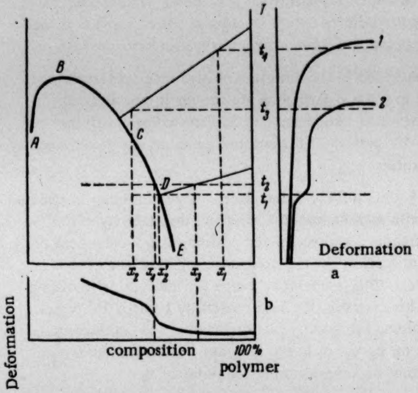

Fig. 2. Variations of the mechanical properties of a plasticized polymer with temperature (a) and composition (b).

As an example, let us consider the experimental data obtained by Kozlov and Russkova [7] for the system nitrocellulose–dibutyl phthalate. Figure 3 shows one of their curves for the variations of the total deformation, over a wide temperature range, of a nitrocellulose–dibutyl phthalate composition in a molar ratio of 1:0.75. The general form of this curve is in agreement with the form of the schematic curve in Fig. 2,a (Curve 2).

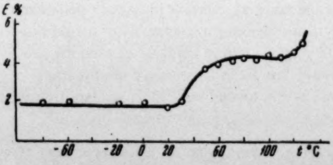

Fig. 3. Variation of deformation with temperature in the system nitrocellulose–dibutyl phthalate (after Kozlov and Russkova).

Let us now consider in a similar way the variations of deformation with composition of the plasticized product at constant temperature. A schematic curve for the variation of total deformation at temperature t_2 is given in Fig. 2,b. It is seen in Fig. 2,b that the deformation remains practically constant and corresponds to the elastic deformation of an amorphous solid up to the composition x_3, which represents the limit of brittleness. With further increase of plasticizer content the viscosity of the system gradually decreases; this leads to some increase of total deformation owing to an increase of its irreversible component. At the point corresponding to composition x_4 the system separates into two phases with formation of a gel, and accordingly the total deformation increases considerably on account of an additional component – gel system elasticity. Further increase of plasticizer content produces an increase of total deformation because the amount of the second phase diminishes while the specific load on the specimen remains constant. No increase of the plastic component should be found above the concentration x_4. The deformation of the system will be predominantly reversible up to concentrations corresponding to the solubility limit of the polymer in the plasticizer (limit of gel formation). This region is not shown on the curve, as the deformation (fluidity) of plasticizer with low polymer content has very high values.

An experimental example is provided by data for the system nitrocellulose–dibutyl phthalate, taken from the paper by Kozlov and Russkova [8]. For temperatures of 40 and 60°, the total deformation curves show sudden rises at dibutyl phthalate–nitrocellulose ratios between 0.50-0.75:1 (Fig. 4). The dash line represents elastic and plastic deformations, extrapolated from the initial points. This curve also coincides in principle with the schematic curve in Fig. 2,b. Unfortunately, the paper [8] does not give points between 0.50 and 0.75 mole of plasticizer, which would make the curve more precise. However, its general nature is evident. *

A similar high elasticity effect for the same nitrocellulose–dibutyl phthalate system was found by Wadano [9], who found that at plasticizer concentrations above 40% (approximately 0.6 mole per 1 mole of nitrocellulose) the plasticized specimen tends to return to its original cross section after rupture under tension. At lower plasticizer concentrations the specimen exhibits ordinary plastic flow at break. Figure 5 gives a curve for the variation of the cross section of the specimen at break with the component ratio, based on Wadano's data.

It follows from this scheme for the variations of the mechanical properties of a polymer with additions of substances of low molecular weight that the same substance may produce both an increase of plasticity and large reversible deformations, according to the amount added. Until the compatibility limit is reached, a low-molecular substance increases the plasticity of the polymer; above this limit the plasticity of the system does not increase, but large reversible deformations arise.

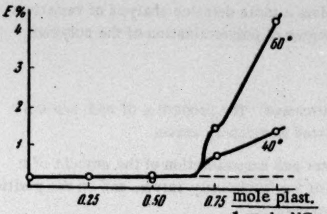

Fig. 4. Variations of deformation with nitrocellulose–dibutyl phthalate ratio (after Kozlov and Russkova).

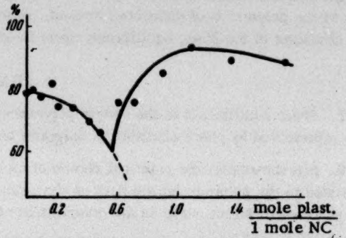

Fig. 5. Cross section of specimen at break (as % of original cross section) for the system nitrocellulose–dibutyl phthalate (after Wadano).

On these grounds, classification of low-molecular substances into plasticizers and elasticizers [10] according to their effects on the mechanical properties of polymers is inappropriate. By this classification a substance such as dibuyl phthalate is both a plasticizer and an elasticizer for nitrocellulose, since limited amounts of it decrease the viscosity of the system, while large amounts give rise to considerable reversible deformations.

In introducing the concept of elasticizers, Kozlov and Russkova assumed that certain substances can increase the flexibility of polymer macromolecules and thereby confer rubberlike properties to "rigid" polymers. It is difficult to believe, however, that the polar groups which hinder free rotation of adjacent polymer segments are shielded only when very large amounts of low-molecular substances are added, and that the effect is not produced by moderate additions. In fact, experimental data show that high reversible deformations in polymer–plasticizer systems are found only with considerable amounts of plasticizers, and the effect arises abruptly.

Moreover, the interacting polar groups which are the cause of polymer "rigidity" are situated at distances of the same order of magnitude as interatomic distances. Accordingly, increases of macromolecular flexibility should be more likely on addition of substances with small molecules, and in particular, on addition of the lower members of a homologous series. However, the "elasticization" effect is found primarily with the higher members of homologous series. For example, according to the data of Kozlov and Russkova, this effect is produced by dibutyl phthalate but not by dimethyl phthalate.

---

* The paper by Kargin et al. [11] contains an analogous diagram for the system polyvinyl chloride–dibutyl phthalate, which coincides in form with the schematic curve in Fig. 2,b.

According to the concepts of the mechanism by which the properties of a polymer are changed in plasticization, as developed in this paper, the difference between the behavior of dimethyl and dibutyl phthalates is entirely due to the higher compatibility of dimethyl phthalate with nitrocellulose. With very large additions of dimethyl phthalate, large reversible deformations should also be found; evidence for this is the formation of elastic gels with nitrocellulose concentrations of the order of 2-5% in dimethyl phthalate. On the other hand, solvents do not produce the "elasticization" effect.

In conclusion, let us consider possible practical methods for determining the limits of plasticizer–polymer compatibility. The plotting of phase equilibrium curves is made very difficult by the very high viscosity of one of the phases formed, so that complete hydrostatic phase separation is not attained in finite periods. Sorption of a plasticizer by a polymer is equally slow, and it is impossible to obtain equilibrium values in practice. Spurlin [2] refers to Mark's proposed method for determination of equilibrium concentrations in such systems from the vapor pressures of the low-molecular substances over the solutions. However, this method also involves exceptionally great experimental difficulties.

A suitable method for practical purposes is to make use of the fact, described above, that large reversible deformations arise at the point of phase separation of the system, for plotting phase equilibrium curves. The similarity of independent data obtained by Wadano (0.6 mole plasticizer per 1 mole nitrocellulose) on the one hand, and by Kozlov and Russkova (0.50-0.75 mole) on the other, shows that this is a suitable method for determining the approximate position of the phase equilibrium curve.

Examination of the relationship between the properties of the plasticized product and the molecular weight of the polymer is of undoubted interest. However, this involves a more detailed analysis of variations in the character of the phase equilibrium curve in relation to the degree of polymerization of the polymer.

SUMMARY

1. Phase equilibrium in the system polymer–plasticizer is discussed. The properties of such systems can be represented by phase equilibrium diagrams on which are plotted isoviscosity curves.

2. It is shown that the practical choice of an actual plasticizer and determination of the amount of it to be added to the polymer depend both on the nature of the group of the isoviscosity curves, and on the position of the phase equilibrium curve on the composition–temperature diagram.

3. Variations of the mechanical properties of plasticized polymers with the temperature and plasticizer content are briefly discussed. An attempt is made to explain the appearance of large reversible deformations at definite temperatures and polymer–plasticizer ratios; this is attributed to transition of the system into the region of separation into two equilibrium phases, with incomplete separation (gel formation).

4. It is pointed out that the same low-molecular substance can change both the plasticity and the elasticity of a polymer, depending on whether the amount of it is below or above the compatibility limit. Accordingly, the classification of low-molecular substances by their effects on polymers into plasticizers and elasticizers has no adequate basis.

5. The principle is proposed of a method for determining the phase equilibrium curve for a polymer–plasticizer system from the points at which increased reversible deformation begins to occur in the plasticized polymer.

Moscow

Received November 17, 1956.

LITERATURE CITED

[1] S. Papkov, Org. Chem. Ind. 6, 240 (1939).

[2] H. M. Spurlin, A. F. Martin and H. G. Tennet, J. Pol. Sci. 1, 63 (1947).

[3] R. S. Colborne, Brit. Plastics 20, 346 (1948).

[4] P. P. Kobeko, Amorphous Substances (Izd. AN SSSR, Moscow–Leningrad, 1952).

[5] S. P. Papkov, V. A. Kargin and Z. A. Rogovin, J. Phys. Chem. 10, 157,607 (1937); A. Dobry, J.

chim. phys. 35, 397 (1938); A. R. Schultz and P. J. Flory, J. Am. Chem. Soc. 75, 3888 (1953).

[6] S. P. Papkov, Colloid J. 19, 333 (1957).*

[7] P. V. Kozlov and E. F. Russkova, Proc. Acad. Sci. USSR 99, 105 (1954).

[8] P. V. Kozlov and E. F. Russkova, Proc. Acad. Sci. USSR 95, 583 (1954).

[9] M. Wadano, Koll.-Z. 93, 103 (1940).

[10] P. V. Kozlov and E. F. Russkova, High Polymers, No. 12, 44 (State Chemistry Press, 1952).

[11] V. A. Kargin, G. L. Slonimsky and L. Z. Rogovina, Colloid J. 19, 142 (1957).*

---

* Original Russian pagination. See C. B. translation.

EXCHANGE OF SODIUM AND CALCIUM IONS ON SWELLING SULFONIC AND CARBOXYLIC RESINS

G. V. Samsonov, A. A. Vasilyev and V. A. Orestova

It was established by a thermodynamic method [1] that in the exchange of ions of any valency the selectivity of ion sorption (determined by the exchange constant) should diminish with increasing swelling of the resins.

The ion exchange constant in the equation

$$\frac{m_1^{1/z_1}}{m_2^{1/z_2}} = K \frac{c_1^{1/z_1}}{c_2^{1/z_2}} \tag{1}$$

(where m_1 and m_2 are the amounts of sorbed ions in mg-equiv./g; c_1 and c_2 are the concentrations of the ions in solution; z_1 and z_2 are the ionic charges) for resins of different degrees of swelling depends on the change of thermodynamic potential ($n_s \Delta \Phi_s$) during swelling or shrinkage of the resin during ion exchange

$$K = e^{r - n_s \Delta \Phi_s}, \tag{2}$$

where $\underline{r}$ can be regarded as a constant for any given pair of exchanging ions; n_s is the number of moles of solvent transferred into or out of the resin in the exchange of 1 mg-equivalent of ions.

Since $n_s \Delta\Phi_s > 0$ if sorption of the first component (see Equation (1)) leads to shrinkage of the resin, it follows, according to Equation (2), that the ion exchange constant will decrease with increasing swelling of the resins. If, in addition, the component the sorption of which causes shrinkage of the resin is sorbed more selectively, it follows that selectivity of ion sorption diminishes with increasing degree of swelling of the resins.

Since these relationships are of considerable theoretical interest, it was desired to verify them experimentally by a study of the exchange of metal ions on swelling resins.

The swelling resins used were KFU carboxylic resins supplied to us by A. A. Vansheidt and N. N. Kuznetsova, and SNF sulfonic phenolic resins prepared by us by the method described by A. A. Vansheidt and A. A. Vasilyev.

The carboxylic resins are polymers of phenoxyacetic acid

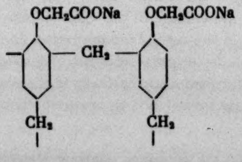

The structure of the SNF cation exchange resins can be represented as

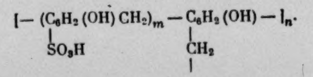

$$[-(\underset{|\atop \mathrm{SO_3H}}{\mathrm{C_6H_2}}(\mathrm{OH})\,\mathrm{CH_2})_m - \underset{|\atop \mathrm{CH_2}\atop |}{\mathrm{C_6H_2}}(\mathrm{OH}) -]_n.$$

The sulfo group content of the resin was determined by the action of an excess of neutral salt solution on the resin in hydrogen form, followed by titration of the solution in presence of the resin, with methyl orange indicator [2].

The total sulfur found in SNF resins by elementary analysis is usually somewhat greater than the "active sulfur" content of the sulfo groups. The "inactive" sulfur is most probably present in the form of sulfones, which can also take part in cross bonding.

The degree of swelling of a cation exchange resin depends on the amount of formaldehyde present and on the heat treatment conditions of the insoluble sulfonation product. SNF sulfonic resins can be recommended as cation exchangers of fairly high exchange capacity with considerable swelling coefficients, which retain satisfactory mechanical strength.

The action of formaldehyde on the soluble sulfonation products is accompanied by a decrease of sulfo group content and additional cross bonding. An increase of the amount of added formaldehyde produces a considerable decrease of the swelling coefficient and exchange capacity and a further increase of the mechanical strength of SNF resins.

The substances chosen for the investigation were three samples of SNF resins based on the same starting material with different amounts of cross-linking agent (formaldehyde). The properties of the SNF resin samples are given in Table 1.

TABLE 1

Properties of Samples of SNF Sulfonic Resins

Sample No.	g formaldehyde per 100 g of starting material	Coefficient of swelling of resin in H form	Exchange capacity (by titration of resin in presence of NaCl) in mg-equiv./g	Sulfur content, %	
				By titration	By elementary analysis
1	21.5	2.4	2.78	8.91	10.60
2	6.5	4.2	3.53	11.29	11.24
3	4.6	9.7	3.81	12.22	12.74

Determination of exchange constants for sodium and calcium ions on KFU carboxylic resins. Ion exchange was studied by the dynamic method. A solution containing sodium chloride and calcium chloride in known concentrations was passed through a column containing KFU resin previously converted into the sodium form. Two methods were used for determining the amounts of ions taken up.

The first method involved the plotting of an elution curve, i.e., the relationship between the ion concentration at the exit from the column and the volume of the solution passed through. These curves were used to calculate the amounts of ions taken up. In the second method, after complete saturation of the column, when the resin had reached equilibrium with the original solution, sodium and calcium were displaced from the resin by hydrochloric acid solution and determined quantitatively in the eluate. The results are given in Table 2. The total exchange capacity was also determined by a dynamic method, from the displacement of sodium ions by calcium ions.

It is clear from Fig. 1 and Table 2 that the exchange constant K decreases with increasing swelling of the resins. This is in agreement with the theory put forward earlier [1], as sorption of the first type of ions –

calcium ions – leads to shrinkage of the resins. The exchange constant decreases only slightly with a small increase of the swelling coefficient of KFU resins from 2 to 3.3. With a very strongly swelling KFU resin ($K_s = 11$) the exchange constant decreases sharply. It must be pointed out that the exchange constants were determined over a very wide range of sodium ion concentrations, up to 1 N. At the same time, the ion exchange law without activity coefficients taken into account, as expressed by Equation (1), was very strictly obeyed.

TABLE 2

Exchange of Sodium and Calcium Ions on KFU Carboxylic Resins with Different Degrees of Swelling (K_s); m is Total Exchange Capacity

K_g	m in mg-equiv/g	c_{Ca} in mg-equiv.	c_{Na} in mg-equiv.	m_{Ca} in mg-equiv/g	m_{Na} in mg-equiv/g	K
2.0	4.37	0.0050	0.50	2.56	1.81	6.25
2.0	4.37	0.0024	0.25	2.92	1.45	6.02
2.0	4.37	0.00108	0.10	3.45	0.92	6.16
2.0	4.37	0.00052	0.05	3.68	0.69	6.11
3.3	4.47	0.0107	1.00	2.15	2.32	6.11
3.3	4.47	0.00535	0.50	2.58	1.89	5.81
3.3	4.47	0.0026	0.25	3.0	1.47	5.75
3.3	4.47	0.00115	0.10	3.53	0.94	5.90
11	4.10	0.0108	1.0	1.23	2.87	3.72
11	4.10	0.00526	0.50	1.79	2.31	4.00
11	4.10	0.00206	0.25	2.24	1.86	3.90
11	4.10	0.00095	0.10	2.70	1.40	3.91

All the determinations with KFU carboxylic resins were carried out at a constant concentration ratio of the exchanging ions, $c_{Na}/c_{Ca} = 100$. Table 2 shows that dilution of the solution leads to an increase in the sorbability of ions with the higher charge – calcium ions; this has been shown by a number of workers [3] for other systems.

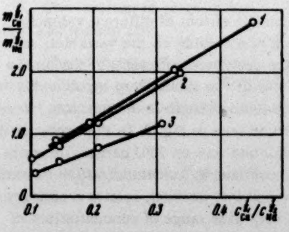

Fig. 1. Exchange of calcium ions with sodium ions on KFU carboxylic resins with different swelling coefficients: 1) 2; 2) 3.3; 3) 11.0.

Determination of the exchange constants of sodium and calcium ions on SNF sulfonic resins. The exchange constants of sodium and calcium ions on sulfonic phenolic resins with swelling coefficients 2.64, 4.44, and 10 were determined by the dynamic method described above. The results of determinations of the exchange capacity of the sulfonated resins (at the sulfo groups only – the exchange of Na^+ and Ca^{2+} ions took place in neutral solutions) and of the sorption capacity for sodium and calcium ions at definite equilibrium concentrations of the ions in solution are given in Table 3.

Comparison of the exchange constants of resins of different degrees of swelling (Table 3 and Fig. 2) shows that the exchange constant for calcium and sodium ions decreases with increasing degree of swelling of the resin, as sorption of calcium ions leads to a decrease in the degree of swelling of the resin. The exchange constant can be either greater or less than unity for resins of different degrees of swelling. Calcium ions are selectively sorbed on weakly swelling resins, and sodium ions on strongly swelling resins. Sulfonation is more complete at low degrees of cross linkage of the resin, which leads to an increase of the exchange capacity. However, this increase of the exchange capacity of swelling resins is not sufficient, as a sole factor, for practical utilization of strongly swelling resins for water softening, as the selectivity of calcium sorption and the total exchange capacity per unit volume decrease simultaneously with it.

TABLE 3

Exchange of Sodium and Calcium Ions on SNF Sulfonic Phenolic Resins with Different Degrees of Swelling (K_s); m is Total Exchange Capacity

K_s	m in mg-equiv/g	c_{Ca} in mg-equiv	c_{Na} in mg-equiv	m_{Ca} in mg-equiv/g	m_{Na} in mg-equiv/g	K
2.64	2.70	0.030	0.050	2.30	0.40	1.09
2.64	2.70	0.0100	0.050	2.02	0.68	1.05
2.64	2.70	0.0050	0.050	1.82	0.88	1.08
4.44	3.67	0.030	0.050	3.04	0.63	0.799
4.44	3.67	0.0100	0.050	2.60	1.07	0.753
4.44	3.67	0.0050	0.050	2.32	1.35	0.798
10.0	4.02	0.030	0.050	3.16	0.86	0.596
10.0	4.02	0.0100	0.050	2.64	1.38	0.590
10.0	4.02	0.0050	0.050	2.22	1.80	0.585

Laws governing exchange of sodium and calcium ions on ion exchange resins in concentrated solutions. Ion exchange over a wide range of ion concentrations conforms to Nikolsky's equation [4], which has the form:

$$\frac{m_1^{1/z_1}}{m_2^{1/z_2}} \cdot \frac{\overline{f}_1^{1/z_1}}{\overline{f}_2^{1/z_2}} = K^x \frac{c_1^{1/z_1}}{c_2^{1/z_2}} \frac{f_1^{1/z_1}}{f_2^{1/z_2}}, \tag{3}$$

where f_1 and f_2 are the activity coefficients of the ions in solution and on the resin respectively.

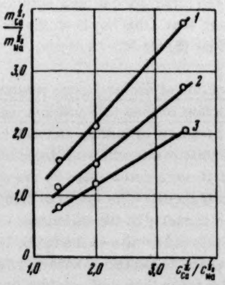

Fig. 2. Exchange of calcium ions with sodium ions on SNF sulfonated resins with different swelling coefficients: 1) 2.64; 2) 4.44; 3) 10.0.

For exchange of ions of different valencies, Equation (3) should include all the variables, and the ratio of the activity coefficients of the ions in solution, $f_1^{1/z_1}/f_2^{1/z_2}$, should vary considerably with changes in the ionic strength of the solution. Nevertheless, as can be seen in Fig. 3, in the exchange of sodium and calcium ions on KFU carboxylic resins the exchange constant K, calculated without activity coefficients taken into account, retains a constant value over a very wide range of concentrations of the ions in solution.

The data given in the beginning of this paper, showing that the ion exchange law is obeyed for the same system of ions on sulfonated resins, are related to low ion concentrations. In such conditions the exchange constant K was independent of the ion concentrations. The exchange constant for Ca^{2+} and Na^+ ions was then determined for solutions of higher ionic strengths.

It is seen in Fig. 3 that in this case the ion exchange constant increases considerably. These results can be interpreted as follows.

The following conditions should be satisfied in the exchange of calcium and sodium ions on carboxylic resins:

$$\frac{\bar{f}_1^{1/z_1}}{\bar{f}_2^{1/z_2}} = \frac{f_1^{1/z_1}}{f_2^{1/z_2}}. \qquad (4)$$

This condition is not satisfied in the exchange of the same ions on sulfonic resins. It is possible that Equation (4) is valid if the resin swells strongly. In that case the ions present in the resin are surrounded by a solution which exerts the same electrostatic action on the ions as is exerted by the solution outside the resin on the ions present in the solution.

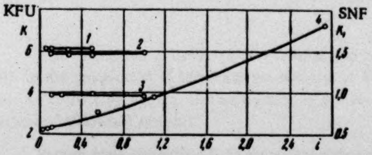

Fig. 3. Variation of the exchange constants for calcium and sodium ions on carboxylic and sulfonic resins with ionic strength of the solution: 1) KFU, $K_s = 2.0$; 2) KFU, $K_s = 3.3$; 3) KFU, $K_s = 11.0$; 4) SNF, $K_s = 10.0$.

It is probable that a significant role is also played by the weakness of the interaction of the ions with the carboxylic resin polymer, so that the solvate shell surrounding the ion is not changed substantially. The validity of Equation (4) depends on the presence of two factors – swelling of the resin and weak interaction between the ions and the resin. In such cases ion exchange conforms to the following equation over a wide range of concentrations:

$$\frac{m_1^{1/z_1}}{m_2^{1/z_2}} = K\,\frac{c_1^{1/z_1}}{c_2^{1/z_2}}.$$

SUMMARY

1. The exchange of sodium and calcium ions on KFU carboxylic resins and SNF sulfonic resins of various degrees of swelling has been studied. The selectivity of ion sorption diminishes with increasing degree of swelling.

2. The sorption of calcium ions by KFU resins increases with increasing dilution of solutions containing calcium and sodium ions.

3. The exchange of sodium and calcium ions on carboxylic resins obeys the ion exchange equation in which the activity coefficients of the ions are not taken into account, over a wide concentration range. Exchange of these ions on the sulfonic resins does not conform to this equation at high ionic strengths of the solution.

Institute of High Molecular Compounds
Leningrad

Received November 19, 1956.

LITERATURE CITED

[1] G. V. Samsonov, Colloid J. 18, 592 (1956).*

[2] A. A. Vansheidt, A. A. Vasilyev, and O. I. Okhrimenko, Theory and Practice of Ion Exchange Materials, Collected Papers (Izd. AN SSSR, Moscow, 1955) p. 110.

[3] K. K. Gedroits, The Sorption Capacity of Soils (1933); E. N. Gapon and A. O. Pryanishnikov, Colloid J. 3, 347 (1937); E. N. Gapon and A. I. Ivanov, Colloid J. 3, 443 (1937); E. N. Gapon and N. I. Gorbunova, Colloid J. 3, 447 (1937); K. M. Saldadze and E. D. Bozhevolnov, Colloid J. 16, 387 (1954);* G. V. Samsonov and S. E. Bresler, Colloid J. 18, 88 (1956);* G. V. Samsonov and S. E. Bresler, Colloid J. 18, 337 (1956).*

[4] B. P. Nikolsky and V. I. Paramonova, Progr. Chem. 8, 1539 (1939).

---

* [See C. B. translation].

This condition is not fulfilled in the [illegible] of [illegible] [illegible] [illegible] equation (5) is valid if the [illegible] [illegible] [illegible] [illegible] [illegible] a solution which [illegible] [illegible] [illegible] [illegible] on the bond present in the [illegible].

[illegible]

Fig. 3. Variation of the exchange constant for [illegible] [illegible] and sodium [illegible] [illegible] [illegible] with [illegible] [illegible] [illegible] [illegible]

[illegible]

[illegible] on KU-2 cation-exchanger and [illegible] [illegible] [illegible] [illegible] [illegible] [illegible] with increase in degree of [illegible].

2. The sorption [illegible] by KU-2 [illegible] [illegible] [illegible] calcium and sodium ions.

3. [illegible] which the [illegible] coefficients of the [illegible] are [illegible] [illegible] [illegible] [illegible].

[illegible]

[illegible]

[1] [illegible]

[2] A. N. [illegible] [illegible] [illegible]

[3] [illegible]

[4] [illegible]

---

* [illegible]

HYDRATES OF THE CALCIUM SALTS OF CERTAIN FATTY ACIDS

V. I. Solnyshkin

The formation of hydrates of saturated and unsaturated salts of fatty acids (soaps) plays an important role in the production of lubricant greases and in flotation processes of ore beneficiation, in which soaps are used as collecting agents, and especially in the use of these substances as stabilizing and peptizing agents in disperse (colloidal) systems.

Earlier investigations [1, 2] show that soaps can be obtained in hydrated form under certain conditions, while determinations of the heats of wetting of the water-insoluble calcium salts of stearic, oleic, and ricinoleic acids may give an indication of the amounts of water coordinated by the polar groups.

The calcium salts of stearic and oleic acids were prepared by two methods: by Trapeznikov's method [3], based on direct reaction of the fatty acid with Ca^{2+} ions, which ensures that the final product is free from univalent metals which may enter it in exchange reactions with sodium salts. The product was then treated, in powder form, with 96% ethyl alcohol and then dried in ampoules under vacuum. Calcium oleate and ricinoleate were also prepared by neutralization of alcoholic solutions of the fatty acids with calcium oxide.

The following method was used for neutralization of fatty acids in alcoholic solution: a weighed sample of oleic acid was dissolved in 3-4 times its own volume of alcohol and heated to boiling in a flask under reflux. Finely divided chemically pure calcium oxide, previously heated at 800°, was then added in 0.5-0.6 g portions to the solution in the flask. When all the calculated amount of calcium oxide had been added, the calcium soap, which is insoluble in the alcohol–water mixture, settled on the bottom of the flask. The neutral soap was boiled for 12-20 hours in the aqueous alcohol mixture until the calcium oleate melt changed from a turbid white into a pale yellow clear layer. The aqueous alcohol solution was decanted hot from the flask, as at temperatures below 40° the formation of an acid soap in the surface layer is possible [4].

The preparation of calcium ricinoleate is made difficult by its good solubility in alcohol. Therefore the neutralization must be carried out in absolute alcohol. The solubility of calcium ricinoleate in alcohol is probably due to the presence of a hydroxyl group in its molecule, situated at the 12th carbon atom from the acid group. The method of preparation was as before, but instead of 96% ethyl alcohol anhydrous rectified spirit prepared by boiling with CaO was used. The end of the reaction was indicated by the appearance of a pale pink color with phenolphthalein. A few drops of ricinoleic acid were added to take the pH of the solution to 7. At the end of the reaction the aqueous alcohol was distilled off; the temperature was then raised sharply to 120° and the residual alcohol was distilled off under vacuum. Slow heating of the calcium ricinoleate mass leads to formation of a plastic modification of the soap [5].

The products were ground, sifted through a sieve of 0.1 mm^2 mesh, and packed into ampoules.

The temperature of the vacuum drying in ampoules depended on the melting points of the fatty acid salts. Fusion of calcium oleate and ricinoleate began at 69.2 and 64.6° respectively. The drying temperature used was therefore 55°. The calcium stearate powder was heated under vacuum at 110° under a residual pressure of 10^{-2} mm.

The heats of wetting of the calcium soaps by water were determined in an adiabatic calorimeter, which is more correctly described as a calorimeter with equivalent heat transfer, as in this case heat transfer between the calorimetric beaker and the water is not zero. This heat transfer must be taken into account, as the calorimeter contains constant heat transferrers: the stirrer and the basket (if the temperature of the surrounding medium is higher than the temperature of the experiment). Therefore the water jacket of the calorimeter is maintained at a higher temperature when the temperature of the surrounding air is below the temperature of the experiment, and at a lower temperature when the air temperature is higher than the experimental temperature. If the water jacket and beaker temperatures are equal, the initial period may take a positive or a negative course, depending on the temperature of the surrounding medium, as the projecting portions – the stirrer, crusher, and thermometer– absorb or give up a definite quantity of heat. The main difficulty therefore lies in strict maintenance of constant heat transfer between the calorimetric beaker and the water jacket; this is controlled by means of the external Beckmann thermometer.

The average results of the determinations are given in the Table.

TABLE

Heats of Wetting of Soaps and Numbers of Coordinated Molecules of Water

Fatty acid salt	Method of preparation	q_C in cal./g	n			Hydrate forms
			Calorimetric	Solution of hydrate in oil	Saturation in aqueous xylene	
Calcium stearate	A. A. Trapeznikov's	—	—	—	1.81	$CaSt_2 \cdot 2H_2O$
Ditto	Ditto	8.4	3.6	3.84	—	$CaSt_2 \cdot 4H_2O$
Calcium oleate	Ditto	13.8	5.8	—	—	$CaOl_2 \cdot 6H_2O$
Ditto	Neutralization of fatty acid by CaO in ethyl alcohol	13.9	5.8	—	—	$CaOl_2 \cdot 6H_2O$
Calcium ricinoleate	Ditto	17.9	7.9	—	—	$CaRz_2 \cdot 8H_2O$
Calcium stearate	Neutralization of fatty acid by 50% aqueous solution of NaOH in alcohol	4.3	0.92	0.96	—	$NaSt \cdot H_2O$

The number of coordinated water molecules was calculated by means of the equation [1]

$$n = \frac{q_C M_S}{K_W M_W}. \qquad (1)$$

where q_c is the heat of wetting in cal./g; n is the number of water molecules coordinated by one soap molecule; K_W is a quantity of the order of 80 cal / g; M_s and M_W are the molecular weights of the soap and water.

The data on calcium stearate were verified by other methods: by saturation of weighed samples with different amounts of water followed by wetting in the calorimeter. The heat effect in the wetting of calcium stearate containing water in 1:4 molar ratio is within the limits of experimental error. The saturation curve is given in Fig. 1. It must be noted that the measurements of the heats of wetting and the saturation of the calcium stearate samples were carried out immediately after drying. If the samples are kept in the anhydrous state the heat effects decrease, probably owing to intracrystalline transformations of the hydrophilic surface.

The amounts of water coordinated by the polar groups were also determined by solution of the soap hydrates in vaseline oil, as follows: a weighed sample of the dry soap, saturated with water vapor for 25-30 hours, was mixed with vaseline oil (10-12 times its own volume). The suspension of the hydrated calcium stearate in the oil was heated at 125-130° until the soap was completely dissolved and foaming ceased. In these experimental conditions water is removed, as the most rapid evaporation of vaseline oil (GOST 3164–46) commences at about 185° [6]. With the weights of the soap hydrate and vaseline oil known, the difference between the weights before and after heating is determined and the number of water molecules removed per one soap molecule is calculated from the equation

$$n = \frac{xM_S}{(g-x)\,M_W}, \qquad (2)$$

where g is the weight of soap hydrate, in grams; x is the amount of water removed, in grams (the difference between the weights before and after heating).

This method was used to check the amount of water coordinated by the polar groups of sodium and calcium stearates. The amount of water coordinated by the polar groups of calcium stearate was also determined by saturation of a weighed sample in aqueous xylene [7]. The results are given in Table 1; the number n was calculated from the equation

$$n = \frac{x_1 M_S}{m M_W}, \qquad (3)$$

where x_1 is the amount of water in cubic centimeters, distilled off in the Dean and Stark apparatus; m is the weight of dry soap in grams.

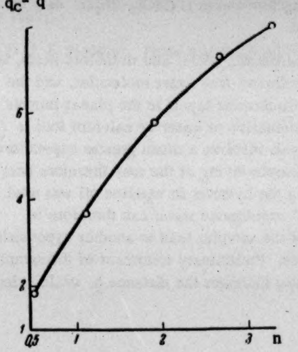

Fig. 1. Curve for saturation of calcium stearate with water (from heats of wetting).

DISCUSSION OF RESULTS

The physicochemical concepts of the surface forces whereby water molecules are coordinated are based on the formation of two layers in dynamic equilibrium. A monomolecular water layer directly balances the greater part of these forces, being in a strictly oriented position. The diffuse layer balances the remainder and thus in the first case, when a free surface is present, water dipoles are adsorbed by two layers (Fig. 2, I).

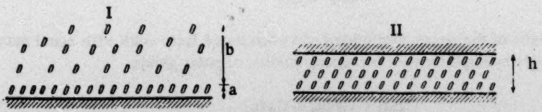

Fig. 2. Surface adsorption of water molecules (I): a) monomolecular layer; b) diffuse layer; formation of multimolecular layers (II).

The distribution of the forces is somewhat different from this if these surfaces approach each other to within a few angstroms. Then, on complete contact, a cleavage plane of a soap crystal is formed. However, mechanical, thermal, and chemical influences on the crystal split it along the planes and give rise to planar tunnels which adsorb polar substances. Planes in this position are shown in Fig. 2, II; different numbers of molecules of the polar substance will be adsorbed in the tunnel, according to the distance h.

An analogous situation is found when water is adsorbed by polar groups of soap molecules. The adsorbing planes are formed from rows of mutually oriented acid groups of the soap molecules [5].

It follows from the experimental data that the amounts of water adsorbed by the planar polar group tunnels vary. Calcium stearate forms the following hydrates [8]:

$$CaSt_2 \cdot 4H_2O,\ CaSt_2 \cdot 2H_2O \text{ and } CaSt_2 \cdot H_2O.$$

Sodium stearate forms the same number of hydrates:

$$8NaSt \cdot H_2O, \; 2NaSt \cdot H_2O, \; [9]$$

and also $NaSt \cdot H_2O$ [10].

Our own data and data from the literature suggest that for the formation of hydrated forms of soaps there are quite definite discrete values of h at which hydrate formation is possible; phase transitions in soaps depend on these as much as on the slope of the hydrocarbon chains relative to the basal planes. A similar conclusion follows from Hoppler's data [11]; he found that the hydrate form of calcium oleate is $CaOl_2 \cdot 2H_2O$; data on heats of wetting indicate that the hexahydrate, $CaOl_2 \cdot 6H_2O$ is formed.

The numbers of water molecules coordinated by calcium salts of stearic, oleic, and ricinoleic acids, in relation to the structure of the latter, confirm that the acid group coordinates four water molecules, and the double bond and the hydroxyl group, one each [2]. The formation of bimolecular layers in the planar tunnels formed by hydrophilic groups is most likely, but the possibility of coordination of water by calcium ions is not excluded. The removal of coordinated water from the planar tunnels involves a much greater expenditure of energy than removal of water from an open hydrophilic surface. Simple drying of the soap therefore does not give the desired result, and for this reason the method of dissolving the hydrates in vaseline oil was used. In such conditions the planar tunnels are destroyed, and the amount of coordinated water can therefore be determined much more completely. The conditions for preparation of the samples lead to another hypothesis which, in our opinion, characterizes the state of the hydrophilic surface. Preliminary treatment of the samples with alcohol not only clears the basal plane of the polar groups, but also increases the distance h, while xylene treatment diminishes it.

SUMMARY

1. It is shown that the calcium salts of stearic, oleic, and ricinoleic acid may exist in the following hydrated forms after alcohol treatment followed by drying:

$$CaSt \cdot 4H_2O, \; CaOl_2 \cdot 6H_2O, \; CaRz_2 \cdot 8H_2O.$$

2. Saturation of dry calcium stearate in aqueous xylene resulted in formation of a soap dihydrate:

$$CaSt_2 \cdot 2H_2O.$$

3. The calcium salts of the series of saturated and unsaturated fatty acids with equal numbers of carbon atoms become increasingly hydrophilic with increasing number of polar groups:

$$CaSt_2 < CaOl_2 < CaRz_2.$$

An acid group can coordinate four molecules of water, and double bonds and hydroxyl groups one each.

4. It is suggested that the formation of several hydrate forms is possible owing to the existence of discrete distances between the basal planes of the acid groups in the soaps.

Institute of Mining, Academy of Sciences
USSR Moscow

Received October 5, 1956.

LITERATURE CITED

[1] V. I. Klassen and V. A. Mokrousov, Introduction to Flotation Theory (Metallurgy Press, 1953).*

[2] A. V. Dumansky, V. I. Solnyshkin and P. A. Demchenko, Ukrain. Chem. J. 20, 635 (1954).

[3] A. A. Trapeznikov and S. Kh. Zakieva, Colloid J. 8, 429 (1946).

[4] E. Lederer, Colloid Chemistry of Soaps (Moscow, 1934).*

---

* [In Russian].

[5] A. A. Trapeznikov and E. M. Shlosberg, Colloid J. 8, 421 (1946).

[6] R. G. Ivanov et al., Lubricating Oils and Greases (Standards State Press, Moscow, 1949).*

[7] R. V. Voitsekhovsky and P. A. Demchenko, Colloid J. 17, 261 (1955).**

[8] M. J. Vold, C. S. Hattiangdi and R. D. Vold, J. Colloid Sci. 4, 93 (1949).

[9] M. J. Buerger, Proc. Natl. Acad. Sci. 28, 526 (1942).

[10] P. A. Demchenko, Dissertation, Inst. General and Inorganic Chemistry Acad. Sci. Ukrainian SSR (Kiev, 1952).

[11] F. Hoppler, Fette und Seife 49, 700 (1942).

---

* [In Russian].

** Original Russian pagination. See C. B. translation.

THE SHRINKAGE OF COLLAGEN

N. N. Stefanovich and A. N. Mikhailov

The alteration which collagen undergoes on heating, known as shrinkage, is usually compared with the fusion of crystalline substances [1-4], denaturation of proteins [5], or changes in the state of aggregation of high polymers under the influence of heat [6]. These three types of transitions have different mechanisms. Fusion is accompanied by considerable absorption of heat, whereas the two latter processes usually involve absorption of small amounts of heat.

Investigations of the heat of shrinkage of collagen have been carried out by Wöhlisch [2, 3] and by Küntzel [4]. However, there are objections to the methods used by them, as they are based on a wrong concept of the reversibility of the shrinkage process. Moreover, the results obtained by these two authors differ greatly. Determinations of the heat of shrinkage may assist in elucidation of the mechanism of the process, and we therefore determined the heats of shrinkage of collagen.

All the experiments were carried out with specimens from the same raw cowhide. The specimens were cut in the form of an asymmetric fringe from the middle layer (derma) of the saddle region of the hide. Specimens of the untreated raw material, limed material (after treatment with $Ca(OH)_2$), and leather tanned with quinone and phosphotungstic acid, were tested in the form of small pieces 2 x 2 mm in size. All the specimens were thoroughly washed after treatment, dialyzed against distilled water, and dehydrated with acetone. Half of the total number of each kind of specimens were treated in boiling water for 10 minutes.

The characteristics of the specimens are given in Table 1.

TABLE 1

Characteristics of the Specimens

Specimens	Moisture, %	Protein (derma substance) as % on absolutely dry weight	Shrinkage temperature, °C
Raw derma	15.1	98.6	66
Shrunken raw derma	12.8	97.9	–
Limed derma	18.5	98.9	66
Shrunken limed derma	14.3	97.2	–
Leather, phosphotungstate-tanned	12.4	70.2	63
Leather, quinone-tanned	–	–	90

The heat of shrinkage was determined by two methods – calorimetrically and thermographically. A variable-temperature calorimeter with an isometric jacket was used for the calorimetric analysis. The temperature in the calorimeter was kept constant with the aid of anultrathermostat, and was measured to an accurary of 0.003° with a Beckmann thermometer.

Prior to the determinations of the heats of shrinkage, the specific heats of the shrunken and raw derma were determined. For the specific heat determinations, previously soaked weighed samples of the derma were heated through 1.0-1.5°. The heating was carried out in water. To prevent strong evaporation, the water was covered with a layer of mineral oil. The usual heat balance equation was used for the calculations.

The results of the specific heat determinations are given in Table 2.

TABLE 2

Specific Heats of Shrunken and Raw Derma

Temperature, °C	Specific heat in cal / g. degree	
	Shrunken derma	Raw derma
20	0.33 ± 0.04	0.32 ± 0.04
30	0.38 ± 0.02	0.31 ± 0.02
40	0.42 ± 0.03	0.41 ± 0.04
50	0.42 ± 0.04	0.43 ± 0.02
60	0.44 ± 0.04	0.33 ± 0.02
70	0.48 ± 0.07	—

The specific heat – temperature relationship conforms to the equation $C_p = 2.2 \cdot 10^{-7} T^{2.5}$.

For determination of the heats of shrinkage, specimens of the shrunken and unshrunken material were introduced into the calorimeter at 74°. To eliminate the effect of wetting, the specimens were first moistened. Excess water was removed by means of filter paper before the experiments. The heat of shrinkage is the difference between the heat effects produced when unshrunken and shrunken material is introduced into the calorimeter; these heat effects were calculated by the heat balance equation. The calculated values for the heats of shrinkage are given in Table 3.

TABLE 3

Heats of Shrinkage of Various Collagen Specimens

Specimen	Heat effect in cal / g on introduction of		Heat of shrinkage in cal / g	
	Unshrunken material	Shrunken material	Absolutely dry material	Protein
Derma	10.3 ± 0.1	8.4 ± 0.2	1.9 ± 0.3	1.9 ± 0.3
Limed derma	12.8 ± 0.2	9.2 ± 0.2	3.6 ± 0.4	3.6 ± 0.4
Phosphotunstate-tanned leather	3.8 ± 0.3	0	3.8 ± 0.3	5.4 ± 0.3

According to the calorimetric data, the heat of shrinkage of collagen is small, of the order of 2.0-5.4 cal / g.

Specimens of unlimed derma were used for the thermographic investigations. The comparison standard was shrunken derma. Specimens of the unlimed and shrunken dermas were shredded and kept in water for 12-16 hours. Equal amounts of the unlimed and shrunken materials were then placed in crucibles. The specimens were heated in water. To prevent evaporation, the contents of the crucibles were covered with a few drops of mineral oil. The thermograms in Fig. 1 show an endothermic heat effect at 65-70°. Moreover, this effect is small, as the ordinary trace does not show a halt in the temperature rise, and the jump in the differential curve is small.

Cooling and repeated heating curves (Fig. 2) show that the shrinkage is irreversible, as these curves do not show the corresponding jumps.

These thermograms show that shrinkage is an endothermic irreversible process which takes place at a definite temperature with absorption of a small quantity of heat. An approximate quantitative estimate of the shrinkage heat effect was obtained by simultaneous heating of derma with substances of known heats of transition. The standard, as in the previous experiments, was shrunken derma.

The substances used for comparison were sodium sulfate decahydrate (mirabilite), $Na_2SO_4 \cdot 10H_2O$, which has

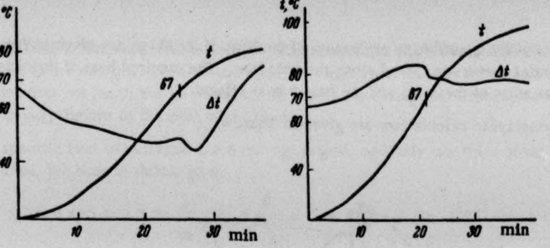

Fig. 1. Heating thermograms for two specimens of derma.

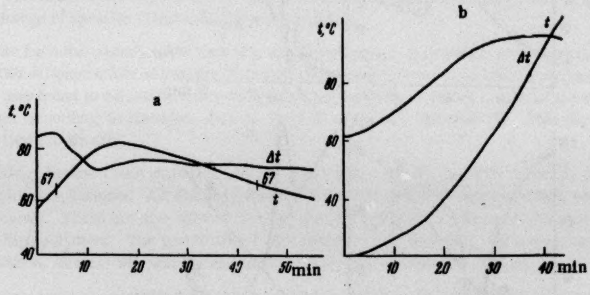

Fig. 2. Cooling (a) and repeated heating (b) thermograms for derma.

a transition at 32°, and potassium palmitate $C_{15}H_{31}CO_2K$, with a transition at 63°. The heat of transition of mirabilite is 57.36 cal / g, and of potassium palmitate, 5.46 cal / g.

TABLE 4

Thermographic Calculations

Specimens	Standard	m_2 in g	m_1 in g	l_1 in cal./g	S_1	S_2	$l_2 = \frac{S_2 m_1}{S_1 m_2} l_1$ in $\frac{\text{cal}}{\text{g}}$
Unshrunken derma in water	Potassium palmitate	0.14	0.69	5.46	15	3	5.4
Unshrunken derma and mirabilite	Shrunken derma	0.20	0.46	57.36	258	10.4	5.3
Unshrunken derma and mirabilite	Al_2O_3	0.26	0.22	57.36	254	3	0.5
Unshrunken derma in water	Shrunken derma and mirabilite	0.46	0.14	57.36	81.2	2.86	0.6

Note. m_1, l_1, and S_1 are the weight in g, the heat of transition in cal./g, and the area of the loop on the differential curve in arbitrary units due to the heat of transition of mirabilite or potassium palmitate. m_2, l_2, and S_2 are the weight in g (on the absolutely dry substance), the heat of shrinkage, and the area of the loop due to the heat of shrinkage.

The thermograms recorded for quantitative evaluation of the heat of shrinkage are given in Fig. 3. The loops formed by the differential curves are closed along the zero line. The required heat of shrinkage is calculated from the ratio of the areas of the loops and the known heat effects.

The results of the thermographic calculations are given in Table 4.

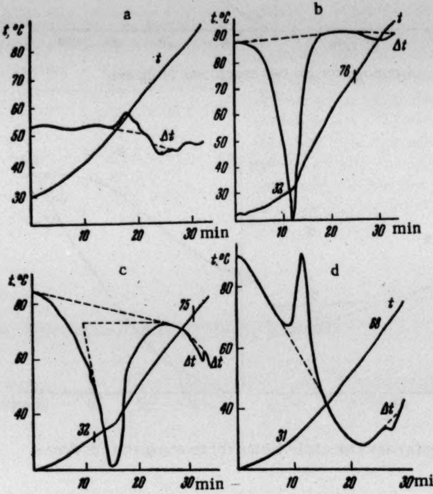

Fig. 3. Heating thermograms for derma; standards: K palmitate (a), shrunken derma (b), Al_2O_3 (c), shrunken derma and mirabilite (d).

In view of the fact that the heating was performed in water, the accuracy of the determinations was very low. However, the results of thermographic analysis do not contradict the calorimeteric data, and confirm that the heat of shrinkage is very small, between 0.5 and 5.4 cal. per g of derma.

DISCUSSION OF RESULTS

The absence of a difference between the specific heats of the shrunken and unshrunken material, the low value of the heat of shrinkage, and the irreversibility of the process suggest that it is necessary to revise the existing views of the shrinkage process. In our opinion, the interpretation of shrinkage as a phase transition of the fusion type must be abandoned. The analogy between shrinkage and the melting of crystals is largely based on the fact that Wöhlisch [2, 3] found a large heat effect on shrinkage, comparable with the heats of fusion of other organic compounds (16.8 cal per g of collagen). However, Wöhlisch wrongly assumed that the shrinkage is reversible, and took the sum of the heat of shrinkage and the heat of isothermal contraction to be the heat of shrinkage. Recalculation of Wöhlisch's data with the heat of isothermal contraction taken into account leads to a different result. This recalculation is given below. Wöhlisch found the following temperature changes during isothermal contraction and extension at 76° for three specimens of previously stretched tendons:

	t°C		
Isothermal contraction and heat shrinkage . . .	— 3.48	— 3.36	— 3.12
Isothermal extension.	+ 2.16	+ 1.75	+ 1.15
Temperature change due to absorption of heat during heat shrinkage (Δ T)*	— 1.32	— 1.61	— 1.97

---

* Calculated by us.

When the load is removed from stretched specimens, isothermal contraction and heat shrinkage occur: the temperature of the specimens falls as the result of these processes. On subsequent extension the temperature rises again, but does not reach the intial value. In our opinion, only this irreversible change must be taken into account in calculations of the heat of shrinkage.

As the specific heat of collagen is 0.4 cal / g· degree, and only one third of the weight of wet tendon is organic substance, the heat of shrinkage is:

$$1.32 \cdot 0.4 \cdot 3 = +1.58 \text{ cal / g}; \quad 1.6 \cdot 0.4 \cdot 3 = 1.93 \text{ cal / g}; \quad 1.97 \cdot 0.4 \cdot 3 = 2.36 \text{ cal / g}.$$

The values so obtained are of the same order as found in our experiments.

The criteria of fusion regarded as a phase transition are: 1) a difference between the specific heats of the substance before and after the transition; 2) a heat effect comparable in magnitude to heats of fusion of crystals; 3) change of specific volume during the transition.

It follows from the experimental data that the specific heats of shrunken and unshrunken derma differ very little. The difference lies within the limits of experimental error. The heat of shrinkage, determined by two methods, was found to be small, not comparable with the heats of fusion of crystalline substances. The volume change, according to literature data [2, 7, 8] is very small, not over 1%. Thus the above criteria of a phase transition are absent.

The analogy between heat shrinkage and fusion is confined to the factthat shrinkage and fusion both take place at definite temperatures. All this suggests that the nature of heat shrinkage differs from that of phase transition processes. There are also objections to an analogy between shrinkage of collagen and aggregative transitions of high polymers. The transitions of high polymers are reversible, and are accompanied by changes of specific volume, whereas the heat shrinkage of collagen is an irreversible process.

In our view there is a sounder basis for an analogy between heat shrinkage and denaturation of proteins. Most of the changes in proteins during heat shrinkage of collagen and in the heat denaturation of proteins occur in one direction. In both cases the water absorption of the protein decreases after heat treatment. The isoelectric point is shifted in the direction of higher pH values, the stability to enzymes decreases, and the reactivity increases [1]. The heat of shrinkage determined in the present investigation is close in value to the heats of denaturation of globular proteins.

The heat of shrinkage is 1-3 cal / g of protein; the heat of denaturation is ~ 1 cal / g of protein [9]. Protein denaturation and shrinkage of collagen both occur abruptly. However, in denaturation of globular proteins the asymmetry of the particles increases. The reverse is found in the heat shrinkage of collagen – the molecular chains become coiled. This difference in behavior can be ascribed to differences in the native structure of collagen and globular proteins. Both types of proteins approach the same equilibrium state on denaturation.

Moreover, the denaturation of globular proteins is in principle regarded as a reversible process. However, research on the regeneration of denatured proteins has shown that the native properties are not fully restored [10].

SUMMARY

1. The specific heat of shrunken and unshrunken collagen is ~ 0.4 cal / g in the 20-70° range. The heat of shrinkage has an average value of 2-5 cal / g of collagen.

2. Heat shrinkage differs substantially from phase transition of the fusion type and from aggregative transitions of high polymers. The heat shrinkage process must be regarded as denaturation of the fibrous protein.

The authors are deeply grateful to Professor A. V. Nikolaev and to Cand. Chem. Sci. I. S. Rassonskaya for interest in the work and for assistance in the thermographic analysis.

Central Scientific Research Institute for the
Leather and Footwear Industry, Moscow

Received October 7, 1956.

LITERATURE CITED

[1] A. N. Mikhailov, Physicochemical Principles of Leather Technology (State Light Industry Press, 1949).*

[2] E. Wöhlisch, René du Mesnil de Rochemont Z. für Biologie, 85, 406 (1927).

[3] E. Wöhlisch, Biochem. Z. 247, 329 (1932).

[4] A. Küntzel, Angew. Chem. 52, 175 (1939).

[5] A. G. Pasynsky, Proteins in Industry and Agriculture (Izd. AN SSSR, 1952)* p. 85.

[6] G. I. Kutyanin, Proc. Acad. Sci. USSR 82, 405 (1952).

[7] V. D. Chater, Heat Shrinkage of Tanned Leather (State Light Industry Press, 1932).*

[8] C. Weir, J. Soc. Leather Trades Chem. 36, 155 (1952).

[9] F. Haurowitz, Chemistry and Biology of Proteins (IL, 1953). [Russian translation].

[10] V. S. Tongur, Colloid J. 11, 274 (1949); Doctorate Dissertation, Institute of Nutrition (Moscow, 1951).

---

* [In Russian].

THE HYDROPHILIC PROPERTIES OF CLAYS OF THE KAOLINITE GROUP

E. T. Uskova

It is known that the hydrophilic nature of clays depends on their mineralogical composition, the degree of dispersion, and the composition of adsorbed cations [1]. The electrokinetic potentials of clays should also have a considerable influence on their hydrophilic properties [2]. However, very few experimental data are available on the relationship between the zeta potential and the hydrophilic character of clays [3].

In the present work the variations of the hydrophilic nature of a kaolinite clay with different proportions of bivalent and univalent ions, and with the zeta potential, were studied.

The material used for the study was Chasov Yar clay No. 5. The test samples were prepared as follows. The clay was covered with five times its own bulk of distilled water for 24 hours. The resultant suspension was rubbed through a sieve of 4900 mesh per cm^2. It was then allowed to settle for 24 hours, the water over the sediment was decanted off, and the sediment was treated with 1 N sodium chloride solution to a negative reaction for Ca^{2+}. Excess electrolyte was removed by washing with decantation. During washing of the sodium clay two clearly distinct layers were formed in the deposit: a lower pale, almost white layer of a coarse fraction, and an upper gray-pink layer of a fine fraction. These fractions were separated, and treated and studied separately. The washed sodium clay was dried at 105°, ground, and sifted without residue. Weighed samples of the Na clay were covered with solutions of calcium or magnesium chloride of various concentrations in 1:5 ratio, stirred, and left to stand for 24 hours. Complete saturation with Ca and Mg was effected by threefold treatment with 1 N solutions of the corresponding chlorides. The samples were washed free of electrolyte, until the suspensions had a conductivity of 10^{-4} ohm^{-1} cm^{-1}. After settling, the sediments in the suspensions were reduced to equal volumes by decantation of the liquid, and dried at 105°.

The amounts of adsorbed calcium and magnesium in the samples were determined by K. K. Gedroits' ammonium chloride method. The analytical results are given in the Table.

It follows from the tabulated data that the exchange capacity depends on the degree of dispersion of the clay particles and on the nature of the sorbed cation; it is almost twice as high for the fine as for the coarse fraction; magnesium is adsorbed more actively than calcium.

The hydrophily was characterized by the amount of water bound by the surface of 1 g of the clay sample [4]. The amount of bound water was determined by Dumansky's indicator method [5]. The calculations were based on the Dumansky–Voitsekhovsky equation with soluble substances taken into account [5]. The indicator used was sucrose of analytical purity grade. The solution concentration was of the order of 13-15%, at which the amount of bound water determined by the indicator method is approximately equal to the amount found by the heat of wetting method [6]. Changes of sucrose concentration were determined by means of a Zeiss interferometer for liquids, with a cell 20 mm long, calibrated against sucrose. For determination of the bound water, two weighed samples of the material, previously dried for 12 hours at 110°, were put into weighing bottles; one sample was covered with sucrose solution, and the other with distilled water. After thorough stirring with a rod, the suspensions were left in the stoppered bottles for 15 minutes to reach equilibrium. The samples were then centrifuged for 15 minutes in closed centrifuge tubes.

It was assumed in the investigations that the degree of dispersion of the clay samples within the experimental series remains unchanged (this applies to primary particles; the size of secondary formations should not have any significant effect on the amount of bound water). Formation of microaggregates occurs by contact

Adsorption of Ca^{2+} and Mg^{2+} by Chasov Yar Coarsely and Finely Disperse Clay in the Sodium Form as a Function of Electrolyte Concentration

Calcium chloride			Magnesium chloride		
Concentration in g-equiv./liter	Adsorption in micro-equiv./g	Substitution, %	Concentration in g-equiv./liter	Adsorption in micro-equiv./g	Substitution, %
Coarsely disperse clay					
0.005	20	19	0.002	19	16
0.01	33	31	0.005	36	31
0.02	50	47	0.01	60	52
0.05	75	71	0.02	84	75
0.1	84	80	0.1	95	83
0.5	95	90	0.5	105	92
1.0	105	100	1.0	111	100
Finely disperse clay					
0.005	48	25	0.002	23	11
0.01	62	32	0.005	65	32
0.02	126	65	0.01	103	51
0.1	158	82	0.02	139	69
0.5	170	88	0.1	168	83
1.0	193	100	0.5	181	89
			1.0	202	100

between the primary particles over small regions of their surface. Water molecules can easily penetrate into the micropores, and therefore the surface of the sample accessible to water does not change appreciably in the presence of aggregates.

The results of the determinations are given in Fig. 1; it is seen that introduction of bivalent ions into the exchange complex makes the clay more hydrophilic. However, this increase is not linear, or even continuous. With gradual increase of the content of bivalent ions in the exchange complex, the clays at first rapidly become more hydrophilic; a maximum is reached when the contents of adsorbed calcium or magnesium ions reach 30-35% of the capacity, and there is then a rapid decrease in the hydrophily. Despite this, samples containing between 50 and 80% of the maximum capacity values of adsorbed bivalent ions (the region in which they are least hydrophilic) are still more hydrophilic than the pure sodium clay. The minimum is followed by a new rise, smaller than that found on addition of small amounts of bivalent cations, in the hydrophilic properties.

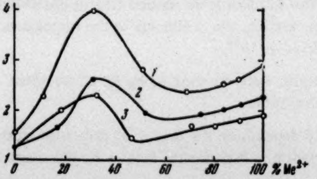

Fig. 1. Variation of the amount of bound water with the degree of substitution of sodium in a sample of Chasov Yar clay in sodium form; 1) fine fraction, substitution by magnesium; 2) coarse fraction, by magnesium; 3) coarse fraction, by calcium.

The appearance of the hydrophily maximum cannot be attributed to a higher degree of hydration of the introduced bivalent ion than that of the sodium ion. The mineralogical composition and active surface of the particles remain unchanged. It is evident that some other factors influence the hydrophilic properties of the clays. Changes of the zeta potantial may have an effect. To test this supposition, the zeta potentials of the clays were determined.

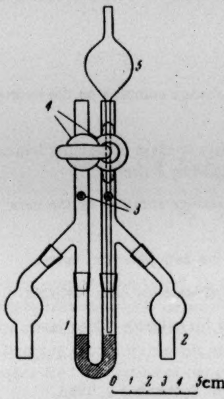

Fig. 2. Apparatus for determination of zeta potential by the electroosmotic method: 1) U-tube; 2) siphon filled with agar; 3) measuring capillaries; 4) stopcocks for meniscus regulation in the measuring capillaries; the right stopcock is open; 5) pipet.

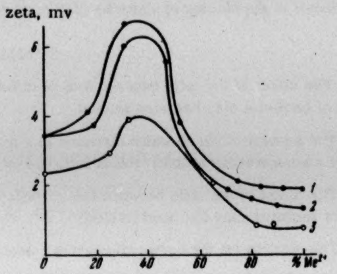

Fig. 3. Variations of zeta potential of Chasov Yar clay samples with different degrees of substitution of sodium in sodium clays: 1) coarse fraction, substitution by magnesium; 2) coarse fraction, by calcium; 3) fine fraction, by magnesium.

The zeta potential determinations were carried out by the electroosmotic method with the aid of apparatus based on Gortikov's design [7]. We met a number of inconveniences in work with Gortikov's apparatus, and therefore the latter was modified in some respects. The siphon tubes were placed at an acute angle, to prevent formation of air bubbles in them. Meniscus regulation in the measuring capillaries can be conveniently carried out with the aid of stopcocks with 1.5-2 mm openings, through which the apparatus is filled with the intermicellar liquid by means of a pipet with a drawn-out tip (Fig. 2). The U-tube of the instrument was kept at constant temperature by means of a circulating termostat. The thermostatic vessel with the U-tube was fixed in a special clamp with a device for tilting in two mutually perpendicular directions. The diaphragm was made by centrifugation of the suspension in the U-tube; the centrifugate served as the intermicellar liquid.

The electrokinetic potential was calculated by the Helmholtz–Smoluchowski equation.

Figure 3 gives the variations of zeta potential of sodium Chasov Yar clay samples with the degree of substitution of sodium by calcium or magnesium.

Introduction of calcium or magnesium ions into the exchange complex of Chasov Yar sodium clay does not produce a steady decrease of zeta potential. There is a considerable increase of zeta potential in samples with low contents (up to 30%) of Ca^{2+} or Mg^{2+}. The maximum is followed by a decrease of zeta potential, but the value of the latter when the content of adsorbed bivalent cations is in the region of 30-50% remains higher than for the sodium clay. At higher contents (70%) of Ca^{2+} or Mg^{2+} the zeta potential becomes less than for the sodium clay.

A comparison of the curves for variations of the hydrophily and zeta potential with the composition of the exchange cations shows that maxima in the region of 30-35% substitution by bivalent cations coincide in the two types of curves. This confirms our supposition that the hydrophily maximum has its origin in the value of the zeta potential. The sharp increase of zeta potential produced by the introduction of the first portions of bivalent ions increases the hydrophily. It is evident that increased diffuseness of the electric double layer leads to thickening of the hydrate shells of the particles.

The zeta potential of samples with high contents of bivalent ions is low, and therefore its relative influence on the binding of water is less. The influence of the higher hydration of the bivalent ions becomes predominant in this case. However, the absolute value of the increase of hydrophily caused by the adsorbed cations is less than in samples with the maximum value of the zeta potential. Thus, the zeta potential is a powerful factor in the binding of water by clay particles.

SUMMARY

1. The effect of the ratio between ions of different valencies in the exchange complex on the hydrophilic properties of kaolinite clay has been studied.

2. The amount of bound water increases to a maximum from sodium clays to clays containing increasing amounts of adsorbed bivalent ions; this is followed by a minimum and then again by a rise.

3. The effect of the ratio between ions of different valencies in the exchange complex on the zeta potential of kaolinite clay has been studied.

4. The maxima on the hydrophily curves coincide with the maxima on the zeta potential curves.

5. The value of the zeta potential is an important factor in the binding of water by clay particles.

In conclusion, the author expresses her deep gratitude to A. V. Dumansky for valuable advice and guidance.

The Ukrainian Academy of Agricultural
Sciences Kiev

Received September 2, 1956.

LITERATURE CITED

[1] L. G. Kapp, Soil Sci. 29 (1930); A. A. Rode, Soil Moisture (Izd. AN SSSR, 1952); E. M. Sergeev, General Soil Sciences (Izd. MGU, 1952); P. F. Melnikov, Sci. Mem. MGU 133, 1, 39 (1949); V. S. Sharov, Colloid J. 5, 521 (1939); K. K. Gedroits, Communications of the Bureau of Agriculture and Soil Science 15, 36 (1914).

[2] E. M. Sergeev, General Soil Science (1952); V. A. Priklonsky, Soil Science, pt. 1 (State Geol.-Tech. Press, 1955); I. V. Popov, Principles of Engineering and Geological Soil Science (Moscow—Leningrad, 1941); L. G. Melnichenko, Refractories 2, 81 (1951); N. Ya. Denisov, Colloid J. 6, 835 (1940); S. S. Filatov, Bentonites of the Georgian SSR (Izd. AN SSSR, 1943).

[3] F. I. Arkhipov, Colloid J. 6, 241 (1940).

[4] A. V. Dumansky, Lyophily of Disperse Systems (Voronezh University Press, 1940).

[5] A. V. Dumansky, Koll.-Z. 65, 178 (1933); A. V. Dumansky and O. V. Neiman, Colloid J. 2, 625 (1936); A. V. Dumansky and R. V. Voitsekhovsky, Colloid J. 10, 413 (1948).

[6] A. V. Dumansky and M. V. Chapek, Colloid J. 2, 95 (1936); F. D. Ovcharenko, Ukrain. Chem. J. 19, 139 (1953).

[7] V. N. Gortikov, Colloid J. 1, 233 (1935).

DISCUSSION

MORE ON THE SUBJECT OF THERMOMECHANICAL CURVES

E. I. Regirer and M. S. Kalantarova

Kargin and Malinsky [1], in their discussion of our paper [2], consider that this paper "in addition to views and generalizations which are worthy of attention, contains certain incorrect deductions based on an erroneous concept of the nature of the measurements made for the plotting of thermomechanical curves". Unfortunately, in challenging us to a discussion, the authors did not state with which views and generalizations they agree; this makes the formulation of our reply difficult.

We shall confine ourselves to the three aspects of thermomechanical curves (TM curves) touched upon by our critics.

The nature of the measurements carried out for the plotting of thermomechanical curves. It is clear from our paper that in our view the plotting of TM curves is not an isolated technique, but is one of the methods of physicochemical analysis. Since it is not clear whether our critics accept this, we shall attempt to answer possible objections.

It might be objected that Kurnakov [3] regarded physicochemical analysis as a science of phases, not applicable to amorphous polymers.

However, modern views on different states of aggregation do not discard the concept of phases, but extend it, as within the limits of the same (liquid) phase three states of aggregation are postulated – glassy, highelastic, and viscofluid.

A further possible objection is that the fundamental method of physicochemical analysis is the measurement (over a wide temperature range) of heat effects; this is not applicable to studies of transitions from one state of aggregation into another. However, in addition to heat effects, physicochemical analysis involves the study of such properties as fusibility, relaxation time, the coefficient of thermal expansion, and also properties characterized by susceptibility to external forces – hardness, efflux pressure, viscosity, elasticity moduli, etc. [4]. It is therefore quite reasonable to include the curves plotted for vitrified rosin by Tamman, a disciple of physicochemical analysis, in the category of TM curves.

Finally, another possible objection is that, in contrast to TM curves, the diagrams obtained as the result of physicochemical analysis are usually plotted in "composition–property" coordinates. However, are the final diagrams obtained as the result of TM measurements not plotted in these usual physicochemical coordinates? As an example, we may cite Fig. 2 in the article [5], obtained by TM measurements, which is a typical physicochemical analysis diagram.

On the above considerations we believe that it would be correct to define TM curves as those special cases of primary physicochemical analysis curves (of the property–temperature type) in which the given substances in different states of aggregation are characterized by the influence of temperature on susceptibility to changes of form (in other words, on mechanical properties).

The definition given by our critics: "A thermomechanical curve should be understood to mean a curve which expresses the variation of deformation with temperature over a fairly wide temperature range, when the deformation is produced by an external force" appears to us inappropriate in the following respects:

1. There are no grounds for restricting the evaluation of the effects of temperature on mechanical

properties to deformation only (several physicochemical characteristics of susceptibility are given above). To emphasize more clearly that this restriction is not essential, we may note that, with some modification of the method, a TM curve may be plotted as a curve for the varying force required to produce a constant deformation over a wide temperature range – the experimental technique would be different, but essentially the method would be the same.

2. Under practical conditions it is difficult to eliminate completely the influence of internal factors on deformation, and therefore in practice a pure picture of the action of external forces only is not usually obtained. Apart from the external forces, the deformation of a specimen is also determined by "internal factors", such as chemical processes within it. Our critics state that dimensional changes of the specimen caused by internal factors "must not be regarded in this case as deformation"; nevertheless, it is difficult in practice to separate the two kinds of deformation, since internal changes may take place even during the relatively short time (of the order of two hours) required for plotting a TM curve (this is sometimes seen in differences between TM curves plotted for the same specimen). The desire to distinguish between these two forms of deformation is understandable, but it is necessary to make the definition more precise so that it cannot be taken as meaning that the field of application of TM curves excludes the investigation of internal factors, as this exclusion would impoverish the TM method of investigation. We therefore drew attention in our paper to the possibility of using TM curves for studying "thermoreactive" changes in polymers, i.e., chemical processes of oxidation, condensation, and so forth, in them which are not induced by external mechanical forces. As was made known later, Kargin and Shteding [6] made effective use of TM curves for the same purpose. It would therefore be erroneous to suppose that TM investigations should be restricted to studies of the action of external forces only. On the contrary, it must be emphasized that the action of an external force is merely a method of detecting internal changes.

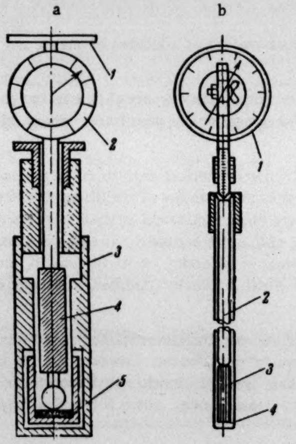

a) Zhurkov's apparatus: 1) platform for a constant load; 2) scale for measurement of deformation; 3) outer case; 4) insulating ebonite cylinder; 5) specimen. b) Quartz dilatometer; 1) graduated dial; 2) insulating quartz tube; 3) specimen; 4) outer case.

Our critics saw fit to put forward yet another consideration, also in the form of a definition of TM curves: "the term 'thermomechanical curves' should be applied only to curves for the dependence of the difference between the deformations of the specimen under two loads on the temperature, with the smaller load so chosen that the specimen undergoes practically no deformation". This, an even narrower definition, is also difficult to accept:

1. It is possible to use only one (working) load, if: 1) this load is not too large, so that the specimen should retain a reserve amount of height over which its deformability could be manifested further, in measurements over the entire temperature range; 2) the temperature is raised rapidly provided that a homogeneous temperature field is maintained through the whole volume of the specimen. If one of these conditions is satisfied, it is possible to eliminate entirely the use of small (preliminary) loads, which serve as "pauses" to protect the specimen from the action of large loads between readings. Although there are practical difficulties in satisfying these requirements, that is not a reason for considering the use of two loads necessary in principle and for raising this requirement to the rank of a definition by which curves plotted without the use of small loads are not to be termed TM curves, but are to be given some other name, although they are similar in appearance and reveal the same characteristics, corresponding to transitions from one state of aggregation into another.

2. The selection of the smaller (preliminary) load which produces practically no deformation in the specimen is difficult to achieve if it is considered that the determinations are carried out over a wide temperature range and that a small load, which does not deform the specimen at low temperatures, may produce appreciable deformations at high temperatures. However, the deformation of the specimen under the small load, although it is technically inconvenient, is not decisive, since differences of deformation are measured.

Explanation for the S-shaped course of certain curves. As has already been stated, internal factors the influence of which increases with the temperature are added to various extents to the external forces. Therefore the resultant curve may represent the aggregate course of these superposed effects. We observed one instance in which such superposition caused the curve to be S-shaped (this was because the specimens were molded at an insufficiently high temperature). As such an instance is possible, if an S-shaped curve is obtained it is necessary to prove that it is not the consequence of such an extraneous factor. Otherwise, the S-shape may be attributed to the presence of a plasticizer; this is evidently not applicable for interpretation of results obtained with unplasticized polymers. The curves taken from the paper [5]* include an example of an S-shaped curve, which the authors attribute to separation of the polymer molecules at high plasticizer contents. As our observations showed that S-shaped curves may also be the consequence of test conditions which do not exclude undesirable "extraneous" deformations, we put forward views which explained why this effect may be particularly prominent in highly plasticized specimens. We are not able to verify the effect of molding conditions in the case of tributyrin, but we do not believe that the cause of the S-shape observed for polyvinyl chloride and Vinylite cannot be impossible in principle for tributyrin. We did not assert, of course, that the cause of the S-shape found by us is the only one possible, and we think that such assertions should not be made with regard to any other cause of the S-shape.

Relationship between methods for plotting TM curves and methods for the contact measurement of linear thermal expansion. As our critics did not agree with our view that these methods are identical, but did not put forward any special considerations on the subject, we wish to explain our assertions by comparing concrete examples of both methods.

The Fig. (1,a) shows Zhurkov's apparatus [7], which has proved fully suitable for the plotting of TM curves, while Fig. (1,b) shows the "quartz dilatometer" [8], used in the United States as a standard instrument for determination of the coefficients of linear expansion of plastics. These two instruments are quite different in name and purpose. Nevertheless, the acting factor in both instruments is temperature, measured by its function, dimensional change. It is readily seen that even the design details of the two instruments are similar (in both instruments a cylindrical specimen is gradually heated and changes in its height are measured). Therefore the assumption that we are dealing here not with one but two characteristics of the material would imply that a specimen, placed under similar conditions and unaware of the operator's intentions is able to exhibit different properties in the two cases. It is surely more correct to say that the same is done in both cases, namely, a TM curve is plotted, showing variations of the linear dimensions of the specimen, found by contact measurement (i.e. with application of an external load), in the direction of the applied mechanical force. We therefore consider that the contact method for measurement of coefficients of linear thermal expansion is, in implicit form, a method for the plotting of TM curves; for example, there is nothing to prevent us "switching these instruments over" — by using Zhurkov's apparatus for carrying out tests by the American standard method for determination of the "coefficient of thermal expansion of plastics", and using the quartz dilatometer for the plotting of TM curves; if the tests are carried out in the same temperature region on the same specimens, similar TM curves will be obtained in both cases. This surely shows that the two are identical. Therefore there is nothing strange in the fact that determinations of uniaxial deformation (in the direction of the load) by means of the contact dilatometer can yield typical TM curves, as the measuring pressure can serve as the load. Hence follows our suggestion that the coefficients of linear thermal expansion of polymers should not be determined by contact methods.

We offered our paper on the methods of plotting and interpreting TM curves in the belief that discussion of a number of methodological questions would assist the wide adoption of the method, We became convinced that a paper on this subject is of topical interest when, after our paper had already been accepted by "Colloid

---

* By an error, the number of the next literature citation was given in the caption to Fig. 4 in the paper [2], which gave the critics cause to state that we attribute this figure to Kobeko, although in the text (p. 442) the number of the citation is given correctly.

Journal", an interesting article [9] of similar nature was published; unfortunately, the question of instruments used for TM determinations was not discussed in this paper. Yet there are still instances of not fully realized use of different instruments for the plotting of TM curves (for example, TM curves can be plotted with the aid of the Höppler consistometer [10] with a flat tip, this version being very similar to Zhurkov's apparatus).

If too narrow a definition of TM curves is adopted, there would be a tendency to regard any such instrumental modification as a new method, and not as a special case of the general TM method. This may even lead to TM curves being "discovered" again, and studied independently of V. A. Kargin's fundamental investigations. An example is provided by a paper [11] (based on differences of apparatus and method), which gives TM curves, not only not described as such, but not subjected to any deep analysis of their nature.

We therefore felt obliged to enter into the proposed discussion and to defend the wider definition of TM curves.

Received March 27, 1957.

LITERATURE CITED

[1] V. A. Kargin and Yu. M. Malinsky, Colloid J. 18, 372 (1956).*

[2] E. I. Regirer and M. S. Kalantarova, Colloid J. 17, 439 (1955).*

[3] N. S. Kurnakov, Introduction to Physicochemical Analysis, 3rd Ed. (ONTI, Leningrad, 1935) p. 91.

[4] Ibid, p. 92.

[5] V. A. Kargin and Yu. M. Malinsky, Collected Papers "Chemistry and Physical Chemistry of High Polymers" (Izd. AN SSSR, Moscow, 1952) p. 256.

[6] V. A. Kargin and M. N. Shteding, Chemical Industry 3, 137 (1955).

[7] S. N. Zhurkov, Trans. 1st and 2nd Conf. on High. Mol. Compds. (Izd. AN SSSR, 1945) p. 68.

[8] "Coefficient of Linear Thermal Expansion of Plastics", Appendix to ASTM D 696-44.

[9] V. A. Kargin and M. N. Shteding, Chemical Industry 2, 74 (1955).

[10] F. Höppler, Forschungsberichte des Prüfgerätewerkes Madingen (1940) N. 5.

[11] W. H. Willert, Ind. Rubber World 124, 324 (1951).

---

* [Original Russian pagination. See C. B. translation].

LETTERS TO THE EDITOR

KINETICS OF THE SPRAYING OF WATER DROPS IN AN ELECTRIC FIELD

V. I. Arabadzhi

The question of the spraying of water drops in an electric field is of considerable importance for understanding processes occurring in thunderstorms. Some authors even consider that the spraying of drops in an electric field is a necessary condition for further intensification of the field and development of electric discharge. To investigate the influence of a vertical electric field on water drops, we took motion pictures of the emergence of water drops from a capillary of 1 mm internal diameter. Photograph 1,a shows the emergence of drops 2.7-3 mm in radius without the influence of an electric field, and Photograph 1,b shows the influence of a vertical electric field of 2.5 kv/cm on the process. The field was created by an electrostatic machine, one electrode of which was introduced into the upper part of the capillary and the other was connected to the water surface under the capillary, onto which the drops fell. The emergence of the drops from the capillary, with and without the field, was photographed at 200 frames per second. Apart from the field, all the experimental conditions were the same in both cases. It is seen from the photographs that under the action of the field a stream of water with a sharp tip was drawn out of the capillary; this stream then began to break up in the middle. This resulted in the formation of much smaller drops than those obtained in absence of a field. Photograph 1, c shows the deformation of a drop passing through a vertical electric field of 3.5 kv/cm, photographed at 1500 frames per second. In more powerful fields, according to Mecky [1], the drops should become drawn out into thin threads and, starting from the tail, should disintegrate into numerous small droplets.

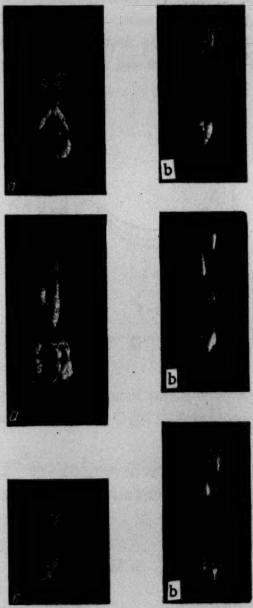

Deformation of drops in an electric field: a) emergence of a drop from a capillary without the action of a field; b) the same, in a field of 2.5 kv/cm; c) deformation of a drop in a field of 3.5 kv/cm.

In our view, drops play the following role in the development of discharge: as is known from electrostatics, the field strength at the opposite ends of a drop reaches a value three times that of the external polarizing field strength; this greatly favors the development of discharge.

SUMMARY

1. Under the action of a 2.5 kv/cm electric field, a stream of water with a sharp tip emerges, instead of a drop, from a capillary of 1 mm internal diameter; this stream begins to break up in its middle portion.

2. When a field of 3.5 kv/cm acts on a falling drop, the drop becomes thickened at the base; a

tail is formed at the upper end and becomes thinner during flight of the drop.

Received October 24, 1956.

LITERATURE CITED

[1] Mecky, Proc. Roy. Soc. 133, 565 (1931).

THE DEVELOPMENT OF A KINETIC THEORY OF GELATION

I. F. Efremov and S. V. Nerpin

The publication of the letter by Hamilton and Hamm [1] concerning the distant-packing mechanism of colloid particles and the formation of a quasicrystalline lattice has prompted us to publish this communication. The letter cited above contains certain elements of our kinetic theory of gelation, based on a series of papers published by one of us [2], the general principles of which are presented below.

1. The existence, under certain conditions, of a resemblance between the potential curve of molecular interaction and the potential curve of colloid particle interaction makes it possible to draw an analogy between the transition of substances with a molecular structure from the liquid into the solid state, and some instances of transition of a colloid system from a sol into a gel. In the latter case, instead of attraction and repulsion forces between individual molecules, forces of molecular attraction and ionic electrostatic repulsion between the colloid particles come into play. In this case the fixation of particles is determined by the presence of potential pits, the depth of which should be found with the collective interaction of the particles taken into account. Numerical calculations may be based on previous publications [3, 4].*

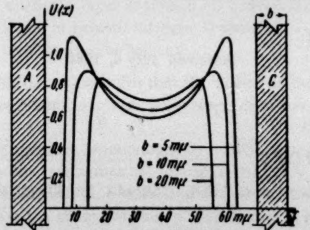

Total potential curves of interaction of a "test" particle with particles A and C (of different thicknesses b).

2. The occurrence of shearing elasticity G in a system of fixed particles, which is a characteristic sign of gel formation, is determined by the expression:

$$G = \frac{d^2F}{d\varphi^2}, \tag{1}$$

where F is the free energy of the system and φ is the angle of shear. The system will then act as a gel provided that the relaxation time of the colloid particles, both in cohesion processes and in transitions into vacant spaces of the quasicrystalline lattice, considerably exceeds the time of action of external influences. If these conditions are not satisfied, either the system will age rapidly or its elastic properties will be masked by fluidity.

3. The conditions of fixation of the particles are considerably influenced by their shape and dimensions. For example, the interaction energy of two plates can be represented by the following approximate expression:

$$U = \frac{\pi}{2} D\left(\frac{kT}{ze}\right)^2 \cdot 1/H - \frac{\zeta\delta^2\sigma}{H^2}\left[1 - \frac{2}{(1+b/H)^2} - \frac{1}{(1+2b/H)^2}\right], \tag{2}$$

---

* Hamilton and Hamm wrongly consider that the theory of Levine and Dube, which was shown by Deryagin [4, 5] to be erroneous, is applicable, and do not mention publications [4-6] in which the theory of the ionic electrostatic interaction of colloid particles was first developed.

where D is the dielectric constant of the medium; z is the electrovalency of the gegenion; e is the electron charge; ζ is a constant near to unity; b is the thickness of the plate; δ is the size of the molecules in the plate; σ is the surface tension at the plate–solution interface; H is the distance between the plates; kT has the usual meaning.

Equation (2) can be easily used to find the value of the potential energy of interaction between a "test" particle and its neighboring particles A and C. The diagram shows U(x) curves for different thicknesses of the interacting particles; it is seen that as the particle thickness is decreased from 20 to 5 mμ the depth of the potential pit is approximately trebled; therefore fixation of thin particles will be more rigid and the system will age more slowly than if particles of greater thickness are present.

4. The above considerations, which relate to the nature of gelation processes, may be extended in their entirety to such systems as highly concentrated emulsions and foams. In the latter case the equilibrium state of the layer separating the gas bubbles is determined by the algebraic sum of the molecular component of the disjoining pressure, which is in this case negative (corresponding to a tendency of the bubbles or droplets to come closer together), and the ionic electrostatic component of this pressure, which is positive in sign.

A distinguishing feature of foamlike systems is that shear in these systems is accompanied not only by deformation of the layers separating the particles, but also by changes in the specific surface of the latter. In the simplest case, when the potential energy of interaction between the molecules within the layer separating the bubbles remains unchanged during shearing of the system, we may write the following expressions for the shearing force and the shear modulus G:

$$\tau = \frac{2\varphi}{d}\left(\sigma + \frac{d\sigma}{d\omega}\,\omega\right), \tag{3}$$

$$G = \frac{d\tau}{d\varphi} = \frac{2}{d}\left(\sigma + \omega\,\frac{d\sigma}{d\omega}\right), \tag{4}$$

where d is the size of a bubble; ω is the specific surface, and σ is the surface tension.

The Lensoviet Technological Institute Leningrad

Received July 4, 1956.

LITERATURE CITED

[1] J. E. Hamilton and F. A. Hamm, J. Appl. Phys. 27, 190 (1956).

[2] I. F. Efremov, Trans. Leningrad Inst. of Soviet Trade (Leningrad, 1950); Colloid J. 10, 337 (1948); 15, 429 (1953);* 16, 4, 264 (1954);* 18, 3 (1956).*

[3] S. V. Nerpin, Dissertation** (Leningrad, 1956).

[4] B. Deryagin and L. Landau, J. Exp. Theoret. Phys. 11, 802 (1941) (reprinted 15, 662 (1945)); Acta Phys. Chim. 14, 633, 1941.

[5] B. Deryagin, Trans. Faraday Soc. 36, 203, 1940; 36, 730 1940; Colloid J. 6, 291 (1940); 7, 285 (1941).

[6] B. V. Deryagin, Bull. Acad. Sci. USSR, Chem. Ser. 5, 1153 (1937); Acta Phys. Chim. 10, 333 (1939); E. J. W. Verwey and J. Th. C. Overbeek, Koll.-Z. 141, 44, (1955); Coll. Sci. 10, 224 (1955).

---

* [Original Russian pagination. See C. B. translation].

** [In Russian].

THE NATURE OF THE CHROMATOGRAPHIC METHOD

S. G. Mokrushin

The principles of chromatography have been considered in a number of publications. In particular, Rachinsky [1] states the "fundamental law of chromatography" as follows: "Any liquid or gaseous mixture is separated when passing through a layer of sorbent if there are differences in the sorptional interaction between the components of the mixture and the sorbent". If follows from this definition that the sorbent (solid phase) is the stationary portion of a chromatographic system, while the liquid or gaseous mixture is the motile phase. This definition of the nature of chromatography fully conforms to Tswett's classical chromatographic method [2].

It is the present author's view that Tswett's method should be given a wider intepretation, namely: it should not be confined to the motion of a liquid or gaseous phase through a solid sorbent, but the concept of relative motion should be accepted; i.e., the motion of a disperse sorbent through a stationary liquid or gaseous phase should be included in the concept. This second case may be regarded as an inversion of Tswett's classical method.

If the condition of relative directed motion is accepted, the above formulation of the fundamental law of chromatography is extended to the following form: "Any liquid or gaseous mixture is separated when it moves through a layer of sorbent or, conversely, in the directed movement of a disperse sorbent through a layer of the liquid or gaseous mixture, if there are differences in the sorptional interaction between the components of the mixture and the sorbent".

If follows from this that the Tswett method should include three other forms in addition to the generally accepted forms, namely: suspension, emulsion and foam chromatography.

Suspension chromatography takes place when particles of a finely divided solid sorbent are in directed motion (by sedimentation) through a stationary layer of liquid (or gas). As the result of selective sorption, the components will be consecutively sorbed from the liquid as the solid settles and new portions of it are added. Ultimately a chromatogram will be formed, i.e., the lowest layer of the settled sorbent will contain the most sorbable, and the topmost layer will contain the least sorbable component.

At the author's suggestion, Shveikina carried out experiments on the separation of ferric chloride (2%) and nitrates of copper (3%) and cobalt (2%) dissolved in water. Into a tube (31 cm high, 1.5 cm in diameter) containing 15 ml of the solution, 33 g of aluminum oxide was added. After 1 hour 15 minutes the salts had been completely sorbed from solution, and the sediment consisted of three distinct layers: a bottom brown layer (ferric chloride), a middle blue layer (copper nitrate), and a top pink layer (cobalt nitrate). The cobalt, copper, and iron salts were succesively isolated from the sediment by elution with water.

This experiment shows that the method of suspension chromatography is analogous to Tswett's classical method, being an inversion of the latter with respect to the relative and directed phase motion. The suspension method was used by Aleskovsky [3] for low concentrations. It must be noted that suspension chromatography is considerably more rapid than Tswett's classical method.

In emulsion chromatography the sorbent consists of liquid droplets ascending through the layer of liquid to be separated. As Shedlovsky [4] points out, this method has been developed very little as yet.

In foam chromatography small air bubbles ascend through the liquid layer. The term "foam chromatography* was used by Ermolenko [5]. The isolation of surface-active substances from solutions with the aid of foam was suggested by Dumansky [6], Ostwald and Siehr [7], and Schutz [8], while Mokrushin [9] proposed the use of the method for separation of colloids.

On the basis of the foregoing, all chromatographic methods may be divided into two groups: 1) the classical method of Tswett, in which a liquid or gas flows through a porous sorbent, and 2) inversion of the classical Tswett method, or sedimentation (or ascent) of solid, liquid, or gaseous sorbent particles through a stationary layer of a solution of the components to be separated.

The S. M. Kirov Polytechnic Institute of the
Urals, Sverdlovsk

Received July 25, 1955.

LITERATURE CITED

[1] V. V. Rachinsky, Trans. Commission on Analytical Chem. 6 (9), 21 (1955).

[2] M. S. Tswett, Selected Works (Izd. AN SSSR, 1946) p. 141.

[3] V. B. Aleskovsky, Summaries of Papers at the Scientific-Technical Conference of the Lensoviet Technological Institute, Leningrad (Goskhimizdat, Leningrad, 1955) p. 27.

[4] L. Shedlovsky, Chromatography, Coll. edited by Academician M. M. Dubinin (Moscow, 1949) pp. 178, 186.

[5] A. F. Ermolenko, Chromatographic Adsorption Analysis and its Development (Acad. Sci. Belorussian SSR Press, Moscow, 1956) p. 81.

[6] A. V. Dumansky, J. Sugar Ind. 4, 427, 440 (1930).

[7] Wo. Ostwald and A. Siehr, Koll.-Z. 76, 33 (1936).

[8] F. Schutz, Trans. Faraday Soc. 42, 437 (1946).

[9] S. G. Mokrushin, Summaries of Papers at the Conference on the Use of M. S. Tswett's Chromatographic Method in Chemical Analysis (Izd. AN SSSR, 1953) p. 14.

THE ROLE OF FILLER GRAIN STRUCTURE IN THE FORMATION OF STRUCTURES IN BITUMEN SUSPENSIONS

L. S. Terletskaya

Addition of fillers to bitumen leads, at definite concentrations, to formation of a structural network and its reinforcement. The strength of the structure formed is determined to a considerable extent by the properties of the filler [1]. Our investigations have shown that, in addition to the magnitude and nature of the surface and the mineralogical composition, special importance attaches to the porous structure of the filler grains, characteristic of both natural and artifical finely divided materials used as fillers. When such fillers are introduced into bitumen, the structure of the filler grains may change significantly the properties of the whole system and of the structure formed in it [3].

In the present investigation, a study was made of the pore structure of mineral grain fillers, and its effects on bitumen–filler interaction and on the mechanical properties of the system formed. Two types of mineral fillers, differing in chemical composition, were chosen for the study:

1. Carbonate rocks – calcite, marble, limestones of different structures, and chalk.
2. Rocks consisting mainly of silica – quartzite, tripoli, opoka, and quartz sand.

Investigations of the structure of these fillers by means of electron microscopy in conjunction with dye adsorption showed that they have different internal structures – compact, finely porous, porous, and coarsely porous. Filler– bitumen interaction was studied by adsorption and luminescence methods. The physicochemical characteristics of the fillers are given briefly in the Table.

Luminescence analysis showed that the bitumen components are zonally distributed over the cross sections of grains of the finely porous fillers (tripoli, opoka, limestone I) extracted from mixtures with bitumen. Oils, followed by tars, are ranged from the grain center to the periphery. Asphaltenes do not penetrate into the grains at all, and gradually merge with the free bitumen. The same is found in porous fillers (limestone II, marble, chalk) but the luminescence is less intense, and the above-named bitumen components penetrate deeper into the grains. Coarsely porous specimens do not show the characteristic luminescence, as the bitumen penetrates completely into the pores, without fractionation. In compact fillers bitumen does not penetrate through the whole bulk of the grain, but only along the microcrevices and faulty cleavage planes of the crystals. Thus, the structure of the filler grains participates in different ways in filler– bitumen interaction processes.

A finely porous grain structure causes fractionation of the bitumen as the result of selective capillary suction of the least viscous components of the dispersion medium of the bitumen. In consequence the bitumen becomes richer in structure-forming components, so that its interlayers acquire higher mechanical strength, viscosity, and shear modulus.

Moreover, selective removal (mainly of surface-inactive oils) by capillary suction may raise the concentration of high-molecular and colloidally dispersed surface-active components in the layers between the external surfaces of the particles, aiding adsorptive saturation and hence oleophilization of the external surfaces of the filler grains, and so causing greater adhesion of bitumen to these surfaces.

The mechanical strength of the bitumen interlayers is the principal factor in the mechanical strength of the system as a whole. Structurized bitumen– filler systems are densely packed plastic systems in which the solid phase particles are separated by thin layers of bitumen. It has been shown by Rebinder and his

Some Physicochemical Properties of the Fillers

Filler	Chemical composition, %					Loss on ignition	Specific surface in cm²/g		Adsorption in mg/g	Type of structure
	SiO_2	Al_2O_3	Fe_2O_3	CaO	MgO		total	internal		
Tripoli	83.08	7.61	0.19	1.18	0,87	4.0	287500	285300	10.0	Finely porous
Opoka	85.86	4.13	1.07	1.35	0.96	6.63	145000	142580	9.5	Ditto
Quartz sand	99.38	0.39	0.04	0,06	0.05	0.28	8300	4070	0.65	Compact
Quartzite	—	—	—	—	—	—	6400	3010	0.40	Compact
Limestone I	1.02	0.07	0.39	55.22	0.36	43 28	21400	18210	5.0	Porous
Limestone II	0.79	0.64	0.84	55.92	0.55	43.09	15500	12290	3.70	Porous
Chalk	0.48	0.08	0.1	55.63		43.71	17800	15690	—	Ditto
Marble	0.16	0.03	0.09	55,59	0.38	44.05	16700	13080	5 90	"
Calcite	0.43	0.05	0.5	55.8		43.42	10500	6720	2.80	Compact

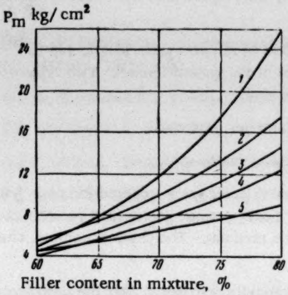

Variations of plastic strength of filler–bitumen mixtures with filler concentration: 1) tripoli; 2) limestone; 3) marble; 4) chalk; 5) quartz sand.

associates [2] that the susceptibility of such systems to plastic deformation is caused by the fact that the particles are not connected directly, but are joined through thin solvate layers of the medium, which allow free relative slippage of the particles. The mechanical strength of such systems depends on the properties of the layers separating the particles.

Structure formation in thin adsorbed solvate layers of bitumen, caused by removal of oils by capillary suction, leads to their reinforcement and an increase of the mechanical strength of the whole system. To verify the above views, the structural and mechanical properties of mixtures of bitumen containing from 60 to 80% of the fillers were studied. As a measure of the mechanical strength, the limiting shear stress (plastic strength P_m) was determined by the cone plastometer method [2, 3]. As the filler content approaches the concentration at which a structure is formed, differences between the properties of the fillers become prominent (see Fig.). Mineral fillers with a finely porous structure, which give rise to strong bitumen films, form mixtures of high mechanical strength. On the other hand, compact and coarsely porous fillers give mixtures of low plastic strength.

Thus an important property of mineral filler grains, in addition to their molecular nature and the total specific surface, is the nature of the pore structure.

The Kharkov Automobile Road Institute
Department of Chemistry

Received February 1, 1957.

LITERATURE CITED

[1] P. A. Rebinder, G. A. Ab, and S. Ya. Veiler, Proc. Acad. Sci. USSR 31, No. 5, 444 (1941); Ya. T. Aron and P. A. Rebinder, Proc. Acad. Sci. USSR 52, 235 (1946).

[2] E. E. Segalova and P. A. Rebinder, Colloid J. 10, 223 (1948).

[3] P. A. Rebinder and N. A. Semenenko, Proc. Acad. Sci. USSR 64, 835 (1949).

AUTHOR INDEX

1957

Agranat, N.N., and M. F. Shirokov. Theory of the cone immersion method for determination of the yield values of disperse systems, 9.
Agranat, N.N., and M.P. Volarovich. Calculation of the limiting shear stress (yield value) of disperse systems in experiments with the cone plastometer, 1.
Akhmedov, K.S., and S.M. Lipatov. Heats of swelling and solution of polymers in relation to molecular weights and temperature, 263.
Akutin, M.S. The seventieth anniversary of the birth and fifty years of the scientific activity of Grigory Semenovich Petrov, 137.
Aleksandrova, E.M. and N.S. Razumikhina. Adsorption of polystyrene latexes in relation to the sign of the particle charge and the sorbent, 159.
Alekseenko, V.L., see Kalinina, L.E.
Apukhtina, N.P., and A.M. Lyagalova. The relationship between the structure of emulsifiers of the alkylaromatic acid type and the polymerization of unsaturated compounds. 4. Salts of di-sec-butylnaphthalenesulfonic acid with univalent cations, 165.
Arabadzhi, V.I. Kinetics of the spraying of water drops in an electric field, 757.
Aripov, E., Z.Ya. Berestneva and V.A. Kargin. An electron microscope study of structure formation in loess. I. Influence of the dispersion medium, 15.
Aripov, E., Z.Ya. Berestneva and V.A. Kargin. An electron microscope study of structure formation in loess. 2. Influence of loess components on structure formation, 19.

Bakeev, N.F., see Kargin, V.A.
Barabash, M.L., and E.M. Natanson. Antifrictional properties of disperse phases of metal organosols, 535.
Bartenev, G.M. Concerning the discussion of the friction of rubber, 399.
Bartenev, G.M. Two stages of the network formation process in polymers, 267.
Batalova, L.G., see Kanavets, L.F.
Belyaeva, I.I., A.E. Mikirov and N.S. Smirnov. The effect of air ionization on the disperse phase of aero colloids, 25
Berestnev, V.A., see Gul, V.E.
Berestneva, Z.Ya., see Aripov, E.
Berestneva, Z.Ya., M.B. Konstantinopolskaya and V.A. Kargin. The formation of crystalline aluminosilicates, 149.
Berestneva, Z.Ya., and G.L. Slonimsky. On the fiftieth birthday of Valentin Alekseevich Kargin, 139.
Bykov, A.N., M L Ivanova and A.B. Pakshver. Modification of polyamide properties by the inclusion method, 543.
Bykov, A.N., and A.B. Pakshver. Intermolecular structure of high polymers. Communication 22. Modification of the molecular structure of high polymers by the inclusion method, 29.

Chalyi, V.P., see Natanson, E.M.
Chekunov, A.A., see Todes, O.M.
Chernykh, Z.V., and V.G. Epshtein. Effects of the types of rubber and carbon black on the formation of carbon-rubber gels, 645.
Chmutov, K.V., and O. G. Larionov. Use of ion exchange resins for purifying quartz suspensions, 403.
Churaev, N.V., see Volarovich, M.P.

Davydov, A.T., and R.F. Skoblionok. Dependence of the exchange adsorption of ions on their structure. 2. Adsorption of bivalent amines, 193.
Deryagin, B.V. Applicability of the binomial law of friction to the friction of rubber, 401.
Deryagin, B.V., see Izmailova, G.L
Deryagin, B.V., see Medvedeva, A.M.
Dobromyslova, A., see Dogadkin, B.
Dobromyslova, A.V., see Dogadkin, B.A.
Dogadkin, B., A. Dobromyslova, L. Sapozhkova and I. Tutorsky. Effect of mercaptobenzothiazole on structural changes in rubber on oxidation, heating and plasticization, 425.
Dogadkin, B.A., A.V. Dobromyslova, F.S. Tolstukhina and N.G. Samsonova. The influence of structure on the chemical activity and vulcanizability of butadiene polymers, 199.
Dogadkin, B.A., D.L. Fedyukin and V.E. Gul. The effect of swelling on the strength of vulcanizates, 291.
Dumansky, A.V. Development of colloid chemistry in the USSR, 531.

Efremov, I.F. and S.V. Nerpin. The development of a kinetic theory of gelation, 759.
Epshtein, V.G., see Chernykh, Z.V.
Ermakov, V.I., V.N. Maslov and O.G. Stolyarov. The use of high frequency analysis in colloidochemical investigations, 207.
Ermolenko, N.F., see Levina, S.A.

Fadeeva, V.S. Orientation of clay particles during deformation of a clay body, 641.